ARMY TM 5-1300
NAVY NAVFAC P-397
AIR FORCE AFR 88-22

STRUCTURES TO RESIST THE EFFECTS OF ACCIDENTAL EXPLOSIONS

"Approved for public release; distribution is unlimited"

DEPARTMENTS OF THE ARMY, THE NAVY, AND THE AIR FORCE
NOVEMBER 1990

Report Documentation Page

Form Approved
OMB No. 0704-0188

Public reporting burden for the collection of information is estimated to average 1 hour per response, including the time for reviewing instructions, searching existing data sources, gathering and maintaining the data needed, and completing and reviewing the collection of information. Send comments regarding this burden estimate or any other aspect of this collection of information, including suggestions for reducing this burden, to Washington Headquarters Services, Directorate for Information Operations and Reports, 1215 Jefferson Davis Highway, Suite 1204, Arlington VA 22202-4302. Respondents should be aware that notwithstanding any other provision of law, no person shall be subject to a penalty for failing to comply with a collection of information if it does not display a currently valid OMB control number.

1. REPORT DATE	2. REPORT TYPE	3. DATES COVERED
01 NOV 1990	**N/A**	**-**

4. TITLE AND SUBTITLE	5a. CONTRACT NUMBER
Structures to Resist the Effects of Accidental Explosions	5b. GRANT NUMBER
	5c. PROGRAM ELEMENT NUMBER
6. AUTHOR(S)	5d. PROJECT NUMBER
	5e. TASK NUMBER
	5f. WORK UNIT NUMBER
7. PERFORMING ORGANIZATION NAME(S) AND ADDRESS(ES) **Department of Defense Explosives Safetyboard Alexandria, VA**	8. PERFORMING ORGANIZATION REPORT NUMBER
9. SPONSORING/MONITORING AGENCY NAME(S) AND ADDRESS(ES)	10. SPONSOR/MONITOR'S ACRONYM(S)
	11. SPONSOR/MONITOR'S REPORT NUMBER(S)

12. DISTRIBUTION/AVAILABILITY STATEMENT
Approved for public release, distribution unlimited

13. SUPPLEMENTARY NOTES
See also ADM000097.

14. ABSTRACT

15. SUBJECT TERMS

16. SECURITY CLASSIFICATION OF:			17. LIMITATION OF ABSTRACT	18. NUMBER OF PAGES	19a. NAME OF RESPONSIBLE PERSON
a. REPORT	b. ABSTRACT	c. THIS PAGE			
unclassified	**unclassified**	**unclassified**	**UU**	**1796**	

FOREWORD

"STRUCTURES TO RESIST THE EFFECTS OF ACCIDENTAL EXPLOSIONS"
Revision 1

Revision 1 is a significant change to this tri-Service manual. It supersedes Change 1 of 17 March 1971 and provides design criteria for a wide assortment of construction materials. Blast resistant capacities of selected, pre-engineered facilities and suppressive shields are now formally recognized. Significant changes are made in design criteria for stirrups. Single leg stirrups with 135 degree bends are permitted for rotations up to eight degrees for Category 2 protection. Membrane stresses are recognized for the reserve strength they provide as dynamic rotations increase. Capacities and design procedures for blast resistant windows are addressed.

Many individuals contributed to this manual and all such contributions are appreciated. Contributions from Mr. Norval Dobbs, Dr. Wilfred Baker and Dr. Thomas Zaker are particularly worthy of note.

Design procedures in this manual are recognized by DOD 6055.9-STD, "Ammunition and Explosives Safety Standards" and are intended for use in the design and analysis of protective constructions intended to control the effects of accidental explosions. The design procedures provide a basis for quantitative protection against propagation of explosions, damage to facilities, and loss of life. Nevertheless, in a work of this magnitude it is expected that there may be points which require further verification or modification as a result of future tests and experience. Recommendations for change or comments with regard to the usefulness of the manual may be submitted to:

Chairman
Department of Defense Explosives Safety Board
2461 Eisenhower Avenue
Room 856C, Hoffman Building #1
Alexandria, VA 22331-0600

REPRODUCTION AUTHORIZATION/RESTRICTIONS

This manual has been prepared by or for the Government and, except to the extent indicated below, is public property and not subject to copyright.

Reprints or republications of this manual should include a credit substantially as follows: "Joint Departments of the Army, the Navy, and the Air Force, Structures to Resist the Effects of Accidental Explosions, TM 5-1300/NAVFAC P-397/AFR 88-22."

If the reprint or republication contains copyrighted material, the credit should also state: "Anyone wishing to make further use of copyrighted material, by itself and apart from this text, should seek necessary permission directly from the proprietors."

*TM 5-1300
*NAVFAC P-397
*AFR 88-22

ARMY MANUAL
No. 5-1300
NAVY MANUAL
No. NAVFAC P-397
AIR FORCE REGULATION
No. 88-22

HEADQUARTERS
DEPARTMENTS OF THE ARMY, THE
NAVY, AND THE AIR FORCE
WASHINGTON, DC, 19 NOVEMBER 1990

STRUCTURES TO RESIST THE EFFECTS OF ACCIDENTAL EXPLOSIONS

CHAPTER 1. INTRODUCTION

SECTION		PAGE
1-1	Purpose	1-1
1-2	Objective	1-1
1-3	Background	1-1
1-4	Scope	1-2
1-5	Format	1-3
1-6	General	1-4
1-7	Safety Factor	1-4
1-8	System Components	1-4
	1-8.1 General	1-4
	1-8.2 Donor System	1-4
	1-8.3 Acceptor System	1-6
1-9	Protection Categories	1-8
1-10	Protective Systems	1-9
	1-10.1 Protective Structures	1-9
	1-10.2 Containment Type Structures	1-10
	1-10.3 Shelters	1-11
	1-10.4 Barriers	1-11
1-11	Human Tolerance	1-11
	1-11.1 Blast Pressures	1-11
	1-11.2 Structural Motion	1-12
	1-11.3 Fragments	1-14
1-12	Equipment Tolerance	1-14
	1-12.1 Blast Pressures	1-14
	1-12.2 Structural Motion and Shock	1-15
	1-12.3 Fragments	1-16
1-13	Tolerance of Explosives	1-16
	1-13.1 General	1-16
	1-13.2 Blast Pressures	1-16
	1-13.3 Structural Motions	1-17
	1-13.4 Fragments	1-17
1-14	Structural Response	1-29
	1-14.1 General	1-29
	1-14.2 Pressure Design Ranges	1-29
	1-14.3 Analyzing Blast Environment	1-30
APPENDIX 1A	List of Symbols	
APPENDIX 1B	Bibliography	

"Approved for public release; distribution is unlimited"

*This manual supersedes TM 5-1300/NAVFAC P-397/AFM 88-22, dated 15 June 1969.

CHAPTER 2. BLAST, FRAGMENT, AND SHOCK LOADS

Section			PAGE
2-1	Purpose		2-1
2-2	Objective		2-1
2-3	Background		2-1
2-4	Scope		2-2
2-5	Format		2-3
2-6	General		2-4
2-7	Effects of Explosive Output		2-5
2-8	Blast Phenomena		2-6
	2-8.1 General		2-6
	2-8.2 Explosive Materials		2-6
2-9	TNT Equivalency		2-7
2-10	Blast-Loading Categories		2-8
	2-10.1	Unconfined Explosion	2-8
	2-10.2	Confined Explosion	2-8
2-11	Blast Loading Protection		2-9
2-12	Blast-Wave Phenomena		2-10
2-13	Unconfined Explosions		2-11
	2-13.1	Free Air Burst	2-11
	2-13.2	Air Burst	2-12
	2-13.3	Surface Burst	2-13
	2-13.4	Multiple Explosions	2-14
2-14	Confined Explosions		2-15
	2-14.1	Effects of Confinement	2-15
	2-14.2	Shock Pressures	2-17
	2-14.3	Gas Pressures	2-23
	2-14.4	Leakage Pressures	2-26
2-15	External Blast Loads on Structures		2-29
	2-15.1	General	2-29
	2-15.2	Forces Acting on Structure	2-30
	2-15.3	Above-Ground Rectangular Structure Without Openings	2-31
	2-15.4	Above Ground Rectangular Structures with Openings	2-35
	2-15.5	Pressure Buildup In Structures	2-41
2-16	General		2-287
2-17	Primary Fragments		2-287
	2-17.1	General	2-287
	2-17.2	Initial Fragment Velocity	2-288
	2-17.3	Fragment Mass Distribution	2-289
	2-17.4	Variation of Fragment Velocity with Distance	2-292
	2-17.5	Primary Fragments - Shape, Caliber Density and Impact Angle	2-294
2-18	Secondary Fragments		2-296
	2-18.1	General	2-296
	2-18.2	Velocity of Unconstrained Secondary Fragments	2-297
	2-18.3	Velocity of Constrained Secondary Fragments	2-300
2-19	Fragment Trajectories		2-301
2-20	Introduction		2-326
2-21	Ground Shock		2-326
	2-21.1	Introduction	2-326
	2-21.2	Air Blast-Induced Ground Shock	2-327
	2-21.3	Direct-Induced Ground Motion	2-329
2-22	Air Shock		2-330
	2-22.1	Introduction	2-330
	2-22.2	Method of Analysis	2-330

2-23 Structure Motions 2-332
2-23.1 Introduction 2-332
2-23.2 Net Ground Shock 2-332
2-23.3 Maximum Structure Motion 2-333
2-24 Shock Response Spectra 2-334
2-24.1 Introduction 2-334
2-24.2 Definition of Shock Spectra Grid 2-334
2-24.3 Response Spectra 2-335
APPENDIX 2A Illustrative Examples
APPENDIX 2B List of Symbols
APPENDIX 2C Bibliography

CHAPTER 3. PRINCIPLES OF DYNAMIC ANALYSIS
3-1 Purpose 3-1
3-2 Objective 3-1
3-3 Background 3-1
3-4 Scope 3-2
3-5 Format 3-3
3-6 General 3-4
3-7 General 3-5
3-8 Introduction 3-7
3-9 Ultimate Resistance 3-8
3-9.1 General 3-8
3-9.2 One-Way Elements 3-8
3-9.3 Two-Way Elements 3-9
3-9.4 Openings in Two-Way Elements 3-13
3-10 Post-Ultimate Resistance 3-14
3-11 Partial Failure and Ultimate Deflection 3-14
3-12 Elasto-Plastic Resistance 3-15
3-13 Elasto-Plastic Stiffnesses and Deflections 3-16
3-14 Resistance-Deflection Functions for Design 3-17
3-14.1 General 3-17
3-14.2 Limited Deflections 3-18
3-14.3 Large Deflections 3-18
3-15 Support Shears or Reactions 3-18
3-16 Introduction 3-72
3-17 Dynamic Design Factors 3-73
3-17.1 Introduction 3-73
3-17.2 Load, Mass, and Resistance Factors 3-74
3-17.3 Load-Mass Factor 3-77
3-17.4 Natural Period of Vibration 3-79
3-18 Introduction 3-85
3-19 Elements Which Respond to Pressure Only and Pressure-Time Relationship 3-85
3-19.1 General 3-85
3-19.2 Analysis by Numerical Methods 3-85
3-19.3 Design Charts for Idealized Loadings 3-90
3-20 Elements Which Respond to Impulse 3-98
3-20.1 General 3-98
3-20.2 Determination of Time to Reach Maximum Deflection . . 3-101
APPENDIX 3A Illustrative Examples
APPENDIX 3B List of Symbols
APPENDIX 3C Bibliography

CHAPTER 4. REINFORCED CONCRETE DESIGN

4-1 Purpose 4-1
4-2 Objective 4-1
4-3 Background 4-1
4-4 Scope 4-2
4-5 Format 4-3
4-6 General 4-4
4-7 General 4-5
4-8 Modes of Structural Behavior 4-5
4-9 Structural Behavior of Reinforced Concrete 4-5
4-9.1 General 4-5
4-9.2 Ductile Mode of Behavior in the Far Design Range 4-6
4-9.3 Ductile Mode of Behavior in the Close-in Design Range . . . 4-7
4-9.4 Brittle Mode of Behavior 4-7
4-10 Introduction 4-16
4-11 Stress-Strain Curve 4-16
4-12 Allowable Material Strengths 4-17
4-12.1 General 4-17
4-12.2 Reinforcement 4-17
4-12.3 Concrete 4-18
4-13 Dynamic Design Stresses for Reinforced Concrete 4-18
4-13.1 General 4-18
4-13.2 Dynamic Increase Factor 4-18
4-13.3 Dynamic Design Stresses 4-20
4-14 Modulus of Elasticity 4-27
4-14.1 Concrete 4-27
4-14.2 Reinforcing Steel 4-27
4-14.3 Modular Ratio 4-27
4-15 Moment of Inertia 4-27
4-16 Introduction 4-32
4-17 Ultimate Moment Capacity 4-33
4-17.1 Cross Section Type I 4-33
4-17.2 Cross Section Types II and III 4-34
4-17.3 Minimum Flexural Reinforcement 4-35
4-18 Ultimate Shear (Diagonal Tension) Capacity 4-35
4-18.1 Ultimate Shear Stress 4-35
4-18.2 Shear Capacity of Unreinforced Concrete 4-36
4-18.3 Design of Shear Reinforcement 4-37
4-18.4 Minimum Shear Reinforcement 4-38
4-19 Direct Shear Capacity 4-39
4-19.1 General 4-39
4-19.2 Direct Shear Capacity of Concrete 4-39
4-19.3 Design of Diagonal Bars 4-40
4-20 Punching Shear 4-40
4-20.1 Ultimate Punching Shear Stress 4-40
4-20.2 Punching Shear Capacity of Concrete 4-40
4-21 Development of Reinforcement 4-41
4-21.1 General 4-41
4-21.2 Provisions for Conventionally Reinforced Concrete Elements 4-41
4-21.3 Provisions for Laced Reinforced Concrete Elements . . 4-42
4-21.4 Development Length for Reinforcement in Tension 4-43
4-21.5 Development Length for Reinforcement in Compression . . 4-43
4-21.6 Development Length of Hooked Bars 4-44
4-21.7 Lap Splices of Reinforcement 4-44
4-21.8 Mechanical Splices of Reinforcement 4-45

4-21.9 Welding of Reinforcement 4-45
4-21.10 Bundled Reinforcing Bars 4-45
4-22 Introduction 4-52
4-23 Distribution of Flexural Reinforcement 4-53
4-23.1 General 4-53
4-23.2 Optimum Reinforcement Distribution 4-53
4-23.3 Optimum Total Percentage of Reinforcement 4-54
4-24 Flexural Design for Small Deflections 4-54
4-25 Design for Large Deflections 4-55
4-25.1 Introduction 4-55
4-25.2 Lateral Restraint 4-55
4-25.3 Resistance-Deflection Curve 4-56
4-25.4 Ultimate Tensile Membrane Capacity 4-56
4-25.5 Flexural Design 4-57
4-26 Dynamic Analysis 4-58
4-26.1 Design for Shock Load 4-58
4-26.2 Design for Rebound 4-59
4-27 Design for Shear 4-60
4-27.1 General 4-60
4-27.2 Ultimate Shear Stress at d_e from the Support 4-60
4-27.3 Ultimate Support Shear 4-62
4-28 Introduction 4-69
4-29 Distribution of Flexural Reinforcement 4-70
4-29.1 General 4-70
4-29.2 Elastic Distribution of Moments According to the ACI Building Code 4-70
4-29.3 Design for Small Deflections 4-73
4-29.4 Design for Large Deflections 4-73
4-29.5 Minimum Reinforcement 4-74
4-30 Dynamic Analysis 4-74
4-30.1 General 4-74
4-30.2 Ultimate Flexural Resistance 4-75
4-30.3 Ultimate Tension Membrane Capacity 4-78
4-30.4 Elastic Deflections 4-79
4-30.5 Load-Mass Factors 4-80
4-30.6 Dynamic Response 4-81
4-31 Dynamic Design 4-82
4-31.1 Flexural Capacity 4-82
4-31.2 Shear Capacity 4-82
4-31.3 Columns 4-83
4-32 Introduction 4-94
4-33 Flexural Design for Large Deflections 4-95
4-33.1 General 4-95
4-33.2 Impulse Coefficients 4-96
4-33.3 Design Equations for Deflections X_1 and X_u 4-99
4-33.4 Optimum Reinforcement 4-99
4-33.5 Design Equation for Deflections Less than X_1 or X_u 4-102
4-33.6 Design Equations for Unspalled Cross Sections 4-103
4-34 Flexural Design for Limited Deflections 4-103
4-35 Design for Shear 4-104
4-35.1 General 4-104
4-35.2 Ultimate Shear Stress 4-105
4-35.3 Ultimate Support Shears 4-106
4-36 Composite Construction 4-143
4-36.1 General 4-143

4-36.2 Blast Attenuation Ability of Sand Fill 4-143
4-36.3 Procedure for Design of Composite Elements 4-145
4-37 Introduction 4-149
4-38 Ultimate Moment Capacity 4-150
4-38.1 Tension Reinforcement Only 4-150
4-38.2 Tension and Compression Reinforcement 4-151
4-38.3 Minimum Flexural Reinforcement 4-152
4-39 Ultimate Shear (Diagonal Tension) Capacity 4-152
4-39.1. Ultimate Shear Stress 4-152
4-39.2 Shear Capacity of Unreinforced Concrete 4-153
4-39.3 Design of Shear Reinforcement 4-153
4-39.4 Minimum Shear Reinforcement 4-153
4-40 Direct Shear 4-154
4-41 Ultimate Torsion Capacity 4-155
4-41.1 General 4-155
4-41.2 Ultimate Torsional Stress 4-155
4-41.3 Capacity of Unreinforced Concrete for Combined Shear and Torsion 4-156
4-41.4 Design of Torsion Reinforcement 4-157
4-41.5 Minimum Torsion Reinforcement 4-159
4-42 Flexural Design 4-160
4-42.1 Introduction 4-160
4-42.2 Small Deflections 4-160
4-42.3 Large Deflections 4-160
4-43 Dynamic Analysis 4-162
4-43.1 Design for Shock Load 4-162
4-43.2 Design for Rebound 4-163
4-44 Introduction 4-166
4-45 Strength of Compression Members (P-M Curve) 4-166
4-45.1 General 4-166
4-45.2 Pure Compression 4-166
4-45.3 Pure Flexure 4-167
4-45.4 Balanced Conditions 4-167
4-45.5 Compression Controls 4-168
4-45.6 Tension Controls 4-169
4-46 Slenderness Effects 4-170
4-46.1 General 4-170
4-46.2 Slenderness Ratio 4-170
4-46.3 Moment Magnification 4-171
4-47 Dynamic Analysis 4-173
4-48 Design of Tied Columns 4-174
4-48.1 General 4-174
4-48.2 Minimum Eccentricity 4-175
4-48.3 Longitudinal Reinforcement Requirements 4-175
4-48.4 Closed Ties Requirements 4-175
4-49 Design of Spiral Columns 4-176
4-49.1 General 4-176
4-49.2 Minimum Eccentricity 4-176
4-49.3 Longitudinal Reinforcement Requirements 4-176
4-49.4 Spiral Reinforcing Requirements 4-176
4-50 Introduction 4-180
4-51 Design of Exterior Columns 4-180
4-52 Introduction 4-181
4-53 Direct Spalling 4-181
4-54 Scabbing 4-182

4-55 Prediction of Concrete Spalling 4-182
4-56 Minimization of Effects of Spalling and Scabbing 4-183
4-56.1 Design parameters 4-184
4-56.2 Composite Construction 4-184
4-56.3 Fragment Shields 4-185
4-57 Post-Failure Concrete Fragments 4-187
4-58 Post-Failure Impulse Capacity 4-188
4-58.1 General 4-188
4-58.2 Laced Elements 4-188
4-59 Introduction 4-205
4-59.1 Fragment Characteristics 4-205
4-59.2 Velocity and Impact Limitations 4-205
4-60 Fragment Impact on Concrete 4-205
4-60.1. General 4-205
4-60.2 Penetration by Armor-Piercing Fragments 4-206
4-60.3 Penetration of Fragments Other than Armor-Piercing . 4-207
4-60.4 Perforation of Concrete 4-208
4-60.5 Spalling due to Fragment Impact 4-209
4-61 Fragment Impact on Composite Construction 4-209
4-61.1 General 4-209
4-61.2 Penetration of Composite Barriers 4-210
4-62 Introduction 4-219
4-63 Concrete 4-219
4-64 Flexural Reinforcement 4-220
4-65 Construction Details for "Far Range" Design 4-221
4-65.1 General 4-221
4-65.2 Elements Designed for Limited Deflections 4-221
4-65.3 Elements Designed for Large Deflections 4-222
4-65.4 Column Details 4-222
4-66 Construction Details for "Close-In Design" 4-223
4-66.1 General 4-223
4-66.2 Laced Elements 4-224
4-66.3 Elements Reinforced with Single Leg Stirrups 4-227
4-67 Composite Construction 4-229
4-68 Single and Multicubicle Structures 4-230
4-69 Sequence of Construction 4-231
APPENDIX 4A Illustrative Examples
APPENDIX 4B List of Symbols
APPENDIX 4C Bibliography

CHAPTER 5. STRUCTURAL STEEL DESIGN
5-1 Purpose 5-1
5-2 Objective 5-1
5-3 Background 5-1
5-4 Scope 5-2
5-5 Format 5-3
5-6 General 5-4
5-7 Differences Between Steel and Concrete Structures in Protective Design 5-5
5-8 Economy of Design of Protective Structures in the Inelastic Range . 5-6
5-9 Applications of Steel Elements and Structures In Protective Design 5-6
5-10 Application of Dynamic Analysis 5-6
5-11 General 5-8

5-12 Mechanical Properties 5-8
5-12.1 Mechanical Properties Under Static Loading. Static Design Stresses 5-8
5-12.2 Mechanical Properties Under Dynamic Loading, Dynamic Increase Factors 5-9
5-13 Recommended Dynamic Design Stresses 5-10
5-13.1 General 5-10
5-13.2 Dynamic Design Stress for Ductility Ratio $\mu \leq 10$ . . . 5-10
5-13.3 Dynamic Design Stress for Ductility Ratio, $\mu > 10$ . . . 5-11
5-13.4 Dynamic Design Stress for Shear 5-11
5-14 Plastic Behavior of Steel Structures 5-16
5-15 Relationship Between Structure Function and Deformations 5-16
5-15.1 General 5-16
5-15.2 Acceptor-type Structures in the Low Pressure Ranges . . 5-16
5-15.3 Acceptor- or Donor-type Structures in the High Pressure Range 5-16
5-16 Deformation Criteria 5-17
5-16.1 General 5-17
5-16.2 Structural Response Quantities 5-17
5-16.3 Ductility Ratio, μ 5-17
5-16.4 Support Rotation, θ 5-18
5-16.5 Limiting Deformations for Beams 5-18
5-16.6 Application of Deformation Criteria to a Frame Structure 5-18
5-16.7 Limiting Deformations for Plates 5-19
5-17 Rebound 5-20
5-18 Secondary Modes of Failure 5-20
5-18.1 General 5-20
5-18.2 Instability Modes of Failure 5-20
5-18.3 Brittle Modes of Failure 5-21
5-19 General 5-26
5-20 Dynamic Flexural Capacity 5-26
5-20.1 General 5-26
5-20.2 Moment-curvature Relationship for Beams 5-27
5-20.3 Design Plastic Moment, M_p 5-27
5-21 Resistance and Stiffness Functions 5-28
5-21.1 General 5-28
5-21.2 Single-span Beams 5-28
5-21.3 Multi-span Beams 5-28
5-22 Design for Flexure 5-29
5-22.1 General 5-29
5-22.2 Response Charts 5-29
5-22.3 Preliminary Dynamic Load Factors 5-29
5-22.4 Additional Considerations in Flexural Design 5-30
5-23 Design for Shear 5-30
5-24 Local Buckling 5-31
5-25 Web Crippling 5-32
5-26 Lateral Bracing 5-32
5-26.1 General 5-32
5-26.2 Requirements for Members with $\mu \leq 3$ 5-33
5-26.3 Requirements for Members with $\mu > 3$ 5-33
5-26.4 Requirements for Elements Subjected to Rebound 5-34
5-26.5 Requirements for Bracing Members 5-34
5-27 General 5-39
5-28 Dynamic Flexural Capacity 5-39

5-29 Resistance and Stiffness Functions 5-39
5-30 Design for Flexure 5-40
5-31 Design for Shear 5-40
5-32 Unsymmetrical Bending 5-44
5-32.1 General 5-44
5-32.2 Elastic and Plastic Section Modulus 5-44
5-32.3 Equivalent Elastic Stiffness 5-45
5-32.4 Lateral Bracing and Recommended Design Criteria 5-45
5-32.5 Torsion and Unsymmetrical Bending 5-45
5-33 Steel Joists and Joist Girders (Open-web Steel Joists) 5-46
5-34 Blast Resistant Design of Cold-Formed Steel Panels 5-48
5-34.1 General 5-48
5-34.2 Resistance in Flexure 5-48
5-34.3 Equivalent Elastic Deflection 5-50
5-34.4 Design for Flexure 5-50
5-34.5 Recommended Ductility Ratios 5-50
5-34.6 Recommended Support Rotations 5-51
5-34.7 Rebound 5-51
5-34.8 Resistance in Shear 5-51
5-34.9 Web Crippling 5-52
5-35 Summary of Deformation Criteria for Structural Elements 5-54
5-36 Blast Door Design 5-64
5-36.1 General 5-64
5-36.2 Functions and Methods of Opening 5-64
5-36.3 Design Considerations 5-64
5-36.4 Examples of Blast Door Designs 5-66
5-36.5 Blast Door Rebound 5-67
5-36.6 Methods of Design 5-68
5-37 Plastic Design Criteria 5-76
5-37.1 General 5-76
5-37.2 In-plane Loads 5-76
5-37.3 Combined Axial Loads and Biaxial Bending 5-76
5-38 Effective Length Ratios for Beam-columns 5-77
5-39 Effective Length Factor, K 5-78
5-40 General 5-81
5-41 Trial Design of Single-Story Rigid Frames 5-82
5-41.1 Collapse Mechanisms 5-82
5-41.2 Dynamic Deflections and Rotations 5-83
5-41.3 Dynamic Load Factors 5-83
5-41.4 Loads in Frame Members 5-83
5-41.5 Sizing of Frame Members 5-83
5-41.6 Stiffness and Deflection 5-84
5-42 Trial Design of Single-Story Frames with Supplementary Bracing . . 5-85
5-42.1 General 5-85
5-42.2 Collapse Mechanisms 5-85
5-42.3 Bracing Ductility Ratio 5-85
5-42.4 Dynamic Load Factor 5-86
5-42.5 Loads in Frame Members 5-86
5-42.6 Stiffness and Deflection 5-87
5-42.7 Slenderness Requirements for Diagonal Braces 5-87
5-42.8 Sizing of Frame Members 5-87
5-43 General 5-96
5-44 Types of Connections 5-96
5-45 Requirements for Main Framing Connections 5-97
5-46 Design of Connections 5-97

5-47 Dynamic Design Stresses for Connections 5-98
5-48 Requirements for Floor and Wall Panel Connections 5-98
5-49 Penetration of Fragments into Steel 5-102
5-49.1 Failure Mechanisms 5-102
5-49.2 Primary Fragment Penetration Equations 5-102
5-49.3 Residual Velocity After Perforation of Steel Plate . 5-103
5-50 General 5-107
5-51 Steel Framed Buildings 5-107
5-52 Cold-formed, Light Gage Steel Panels 5-107
5-53 Blast Doors 5-108
APPENDIX 5A Illustrative Examples
APPENDIX 5B List of Symbols
APPENDIX 5C Bibliography

CHAPTER 6. SPECIAL CONSIDERATIONS IN EXPLOSIVE FACILITY DESIGN
6-1 Purpose 6-1
6-2 Objective 6-1
6-3 Background 6-1
6-4 Scope 6-2
6-5 Format 6-3
6-6 General 6-4
6-7 Application 6-5
6-8 Design Criteria for Reinforced Masonry Walls 6-6
6-8.1 Static Capacity of Reinforced Masonry Units 6-6
6-8.2 Dynamic Strength of Material 6-7
6-8.3 Ultimate Strength of Reinforced Concrete Masonry Walls . . . 6-7
6-8.4 Dynamic Analysis 6-9
6-8.5 Rebound 6-10
6-9 Non-Reinforced Masonry Walls 6-10
6-9.1 Rigid Supports 6-10
6-9.2 Non-rigid Supports 6-12
6-9.3 Simply Supported Walls 6-13
6-10 Applications 6-26
6-11 Static Strength of Materials 6-26
6-11.1 Concrete 6-26
6-11.2 Reinforcing Bars 6-26
6-11.3 Welded Wire Fabric 6-27
6-11.4 Prestressing Tendons 6-27
6-12 Dynamic Strength of Materials 6-27
6-13 Ultimate Strength of Precast Elements 6-27
6-13.1 Ultimate Dynamic Moment Capacity of Prestressed Beams . 6-28
6-13.2 Diagonal Tension and Direct Shear of Prestressed Elements 6-31
6-14 Dynamic Analysis 6-31
6-15 Rebound 6-32
6-15.1 Non-prestressed elements 6-32
6-15.2 Prestressed elements 6-32
6-16 Connections 6-33
6-16.1 General 6-33
6-16.2 Column-to-Foundation Connection 6-34
6-16.3 Roof Slab-to-Girder Connection 6-34
6-16.4 Wall Panel-to-Roof Slab Connection 6-34
6-16.5 Wall Panel-to-Foundation Connection 6-34
6-16.6 Panel Splice 6-34

6-16.7 Reinforcement Around Door Openings 6-34
6-17 General 6-42
6-18 General Layout 6-42
6-18.1 Structural Steel 6-42
6-18.2 Foundations 6-43
6-18.3 Roof and Walls 6-43
6-18.4 Connections for Roof and Wall Coverings 6-43
6-19 Preparation of Partial Blast Analysis 6-44
6-20 Pre-Engineered Building Design 6-44
6-21 Blast Evaluation of the Structure 6-45
6-22 Recommended Specification for Pre-Engineered Buildings 6-45
6-23 General 6-55
6-24 Application 6-55
6-24.1 Safety Approved Suppressive Shields 6-56
6-24.2 New Shield Design 6-56
6-25 Design Criteria 6-57
6-26 Design Procedures 6-58
6-26.1 Space Requirements 6-58
6-26.2 Charge Parameters 6-58
6-26.3 Fragment Parameters 6-58
6-26.4 Structural Details 6-59
6-26.5 Access Penetrations 6-59
6-27 Introduction 6-73
6-28 Background 6-73
6-29 Design Criteria for Glazing 6-74
6-29.1 Specified Glazing 6-74
6-29.2 Design Stresses 6-75
6-29.3 Dynamic Response to Blast Load 6-75
6-29.4 Design Charts 6-75
6-29.5 Alternate Design Procedure 6-76
6-30 Design Criteria for Frames 6-78
6-30.1 Sealants, Gaskets, and Beads 6-78
6-30.2 Glazing Setting 6-78
6-30.3 Frame Loads 6-78
6-30.4 Rebound 6-80
6-31 Acceptance Test Specification 6-80
6-31.1 Test Procedure - Window Assembly Test 6-80
6-31.2 Acceptance Criteria 6-81
6-31.3 Certification for Rebound 6-82
6-32 Installation Inspection 6-82
6-33 Introduction 6-134
6-34 Design Loads for Underground Structures 6-134
6-34.1 General 6-134
6-34.2 Roof Loads 6-135
6-34.3 Wall Loads 6-135
6-35 Structural Design 6-136
6-35.1 Wall and Roof Slabs 6-136
6-35.2 Burster Slab 6-136
6-36 Structure Motions 6-137
6-36.1 Shock Spectra 6-137
6-36.2 Shock Isolation Systems 6-137
6-37 General 6-142
6-38 Description of Earth-Covered Arch-Type Magazines 6-142
6-39 Separation Distances of Standard Magazines 6-143
6-40 Design 6-143

6-41 Construction 6-144
6-42 Non-Standard Magazines 6-144
6-43 General 6-147
6-43.1 Applications 6-147
6-43.2 Remote-Actuated valves 6-147
6-43.3 Blast-Actuated Valves 6-148
6-43.4 Plenums 6-148
6-43.5 Fragment Protection 6-149
6-44 Types of Blast Valves 6-149
6-44.1 General 6-149
6-44.2 Blast Shield 6-149
6-44.3 Sand Filter 6-149
6-44.4 Blast Resistant Louvers 6-150
6-44.5 Poppet Valves 6-150
6-45 Introduction 6-164
6-46 Objectives 6-164
6-47 Structure Motions 6-165
6-48 Shock Tolerance of Personnel and Equipment 6-165
6-48.1 Personnel 6-165
6-48.2 Equipment 6-165
6-49 Shock Isolation Principles 6-166
6-49.1 General Concepts 6-166
6-49.2 Single-Mass Dynamic Systems 6-167
6-49.3 Shock Isolation Arrangements 6-169
6-50 Shock Isolation Devices 6-173
6-50.1 Introduction 6-173
6-50.2 Helical Coil Springs 6-174
6-50.3 Torsion Springs 6-175
6-50.4 Pneumatic Springs 6-175
6-50.5 Liquid Springs 6-176
6-50.6 Other Devices 6-177
6-51 Hardmounted Systems 6-178
6-52 Attachments 6-178
6-52.1 Introduction 6-178
6-52.2 Design Loads 6-179
APPENDIX 6A Illustrative Examples
APPENDIX 6B List of Symbols
APPENDIX 6C Bibliography

LIST OF TABLES

TABLE		PAGE
1-1	Blast Effects in Man Applicable to Fast-Rising Air Blasts of Short Duration (3-5 ms.)	1-23
1-2	50 Percent Probability of Penetrating Human Skin	1-23
1-3	Threshold of Serious Injury to Personnel Due to Fragment Impact	1-24
1-4	Examples of Equipment Shock Tolerances	1-24
1-5	Safe Separation Distance (bulk explosives)	1-25
1-6	Safe Separation Distance (munitions)	1-26
2-1	Heat of Detonation and Heat of Combustion	2-278
2-2	List of Illustrations of Peak Incident Pressure and Impulse Produced by Surface Detonation of Various Explosives	2-279
2-3	List of Illustrations for Average Peak Reflected Pressure and Scaled Average Unit Reflected Impulse	2-285
2-4	List of Illustrations for Interior Side Wall Idealized Times T_3 and T_4	2-286
2-5	Specific Weight and Gurney Energy Constant for Various Explosives	2-321
2-6	Initial Velocity of primary fragments for various geometries.	2-322
2-7	Mott Scaling Constants for Mild Steel Casings and Various Explosives	2-323
2-8	Drag Coefficient, C_D, for various shapes	2-324
2-9	Steel Toughness	2-325
2-10	Mass Density for Typical Soils and Rocks	2-338
2-11	Typical Seismic Velocities for Soils and Rocks	2-338
2-12	Coefficient of Friction for Concrete Foundation and Underlying Soils	2-339
3-1	Ultimate Unit Resistance for One-Way Elements	3-61
3-2	Ultimate Unit Resistance for Two-Way Elements (Symmetrical Yield Lines)	3-62
3-3	Ultimate Unit Resistance for Two-Way Elements (Unsymmetrical Yield Lines)	3-63
3-4	Post Ultimate Unit Resistances for Two-Way Elements	3-64
3-5	General and Ultimate Deflections for One-Way Elements	3-65
3-6	General, Partial Failure, and Ultimate Deflections for Two-Way Elements	3-66
3-7	Elastic and Elasto-Plastic Unit Resistances for One-Way Elements	3-67
3-8	Elastic, Elasto-Plastic and Equivalent Elastic Stiffnesses for One-Way Elements	3-68
3-9	Support Shears for One-Way Elements	3-69
3-10	Ultimate Support Shears for Two-Way Elements (Symmetrical Yield Lines)	3-70
3-11	Ultimate Support Shears for Two-Way Elements (Unsymmetrical Yield Lines)	3-71
3-12	Transformation Factors for One-Way Elements	3-83
3-13	Load-Mass Factors in the Elastic and Elasto-Plastic Ranges for Two-Way Elements	3-84
3-14	Details of computation by acceleration impulse extrapolation method	3-328
3-15	Figure numbers corresponding to various combinations of C_1 and C_2	3-329
3-16	Response Chart Interpolation	3-330
4-1	Dynamic Increase Factor (DIF) for Design of Reinforced Concrete Elements	4-25

4-2 Dynamic Design Stresses for Design of Reinforced Concrete Elements 4-26
4-3 Minimum Area of Flexural Reinforcement 4-50
4-4 Minimum Design Shear Stresses for Slabs 4-51
4-5 Restraint and Aspect Ratio Requirements of Tension Membrane Behavior 4-66
4-6 Ultimate Shear Stress at Distance d_e from Face of Support for One-Way Elements 4-67
4-7 Ultimate Shear Stress at Distance d_e from Face of Support for Two-Way Elements 4-68
4-8 Deflection Coefficients for Interior Panels of Flat Slabs 4-93
4-9 Impulse Coefficient C_1 for Two-Way Elements 4-136
4-10 Impulse Coefficient C_u for Two-Way Elements 4-137
4-11 Impulse Coefficient C_u for One-Way Elements 4-138
4-12 Shear Coefficients for Ultimate Shear Stress at Distance d_c from the Support for One-Way Elements (Cross Section Type II and III) 4-139
4-13 Shear Coefficients for Ultimate Shear Stress at Distance d_c from the Support for Two-Way Elements (Cross Sections Type II and III) 4-140
4-14 Shear Coefficients for Ultimate Shear for One-Way Elements (Cross Section Type II and III) 4-141
4-15 Shear Coefficients for Ultimate Support Shear for Two-Way Elements (Cross Section Type II and III) 4-142
4-16 Relative Penetrability Coefficients for Various Missile Materials 4-218

5-1 Static Design Stresses for Materials 5-14
5-2 Dynamic Increase Factor, c, for Yield Stress of Structural Steels . 5-15
5-3 Dynamic Increase Factor, c, for Ultimate Stress of Structural Steels 5-15
5-4 Preliminary Dynamic Load Factors for Plates 5-43
5-5 Dynamic Design Shear Stress for Webs of Cold-formed Members (f_{ds} = 44 ksi) 5-60
5-6 Dynamic Design Shear Stress for Webs of Cold-formed Members (f_{ds} = 66 ksi) 5-61
5-7 Dynamic Design Shear Stress for Webs of Cold-formed Members (f_{ds} = 88 ksi) 5-62
5-8 Summary of Deformation Criteria 5-63
5-9 Design Requirements for Sample Blast Doors 5-75
5-12 Effective Length Factors for Columns and Beam-Columns. 5-80
5-13 Collapse Mechanisms for Rigid Frames with Fixed and Pinned Bases. . 5-92
5-14 Stiffness Factors for Single Story, Multi-Bay Rigid Frames Subjected to Uniform Horizontal Loading. 5-93
5-15 Collapse Mechanisms for Rigid Frames with Supplementary Bracing and Pinned Bases. 5-94
5-16 Collapse Mechanisms for Frames with Supplementary Bracing, Nonrigid Girder-to-Column Connections and Pinned Bases. 5-95

6-1 Properties of Hollow Masonry Units 6-24
6-2 Deflection Criteria for Masonry Walls 6-24
6-3 Moment of Inertia of Masonry Walls 6-25
6-4 Summary of Suppressive Shield Groups 6-71
6-5 Charge Parameters for Safety Approved Shields 6-72
6-6 Static Design Strength r_u (psi), for Tempered Glass* [a = long dimension of glass pane (in.); b = short dimension of glass pane (in.)] 6-109
6-7 Minimum Design Thickness, Clearances, and Bite Requirements 6-116

6-8 Maximum (b/t) Ratio for Linear Plate Behavior Under Blast Load and Coefficients for Resistance and Deflection and Fundamental Period of Simply Supported Glass Plates Based on Small Deflection Theory (No Tensile Membrane Behavior) 6-117
6-9 Coefficients for Frame Loading 6-118
6-10 Statistical Acceptance and Rejection Coefficients 6-119
6-11 Fundamental Period of Vibration, T_n, for Monolithic Tempered Glass 6-120
6-12 Effective Elastic Static Resistance, r_{eff} 6-127
6-13 Blast Valves 6-163

LIST OF FIGURES

FIGURE		PAGE
1-1	Explosive Protection System	1-7
1-2	Survival curves for lung damage	1-19
1-3	Human ear damage due to blast pressure	1-20
1-4	Example of safe separation tests	1-21
1-5	Safe separation test shields	1-22
1-6	Variation of structural response and blast loads	1-32
1-7	Parameters defining pressure design ranges	1-33
1-8	Design ranges corresponding to location of the structural elements relative to an explosion	1-34
2-1	Blast loading categories	2-43
2-2	Free-field pressure-time variation	2-44
2-3	Peak incident pressure versus peak dynamic pressure, density of air behind shock front and particle velocity	2-45
2-4	Free-air burst environment	2-46
2-5	Pressure-time variation for a free-air burst	2-47
2-6	Peak incident pressure versus the ratio of normal reflected pressure/incident pressure for a free air burst	2-48
2-7	Positive phase shock wave parameters for a spherical TNT explosion in free air at sea level	2-49
2-8	Negative phase shock wave parameters for a spherical TNT explosion in free air at sea level	2-50
2-9	Variation of reflected pressure as a function of angle of incidence	2-51
2-10	Variation of scaled reflected impulse as a function of angle of incidence	2-52
2-11	Air burst environment	2-53
2-12	Pressure-time variation for air burst	2-54
2-13	Scaled height of triple point	2-55
2-14	Surface bust blast environment	2-56
2-15	Positive phase shock wave parameters for a hemispherical TNT explosion on the surface at sea level	2-57
2-16	Negative phase shock wave parameters for a hemispherical TNT explosion on the surface at sea level	2-58
2-17	Explosive shapes	2-59
2-18	Peak positive incident pressure and scaled impulse for an explosion on the surface at sea level	2-60
2-19	Peak positive incident pressure and scaled impulse for an explosion on the surface at sea level	2-61
2-20	Peak positive incident pressure and scaled impulse for an explosion on the surface at sea level	2-62
2-21	Peak positive incident pressure and scaled impulse for an explosion on the surface at sea level	2-63
2-22	Peak positive incident pressure and scaled impulse for an explosion on the surface at sea level	2-64
2-23	Peak positive incident pressure and scaled impulse for an explosion on the surface at sea level	2-65
2-24	Peak positive incident pressure and scaled impulse for an explosion on the surface at sea level	2-66
2-25	Peak positive incident pressure and scaled impulse for an explosion on the surface at sea level	2-67
2-26	Peak positive incident pressure and scaled impulse for an explosion on the surface at sea level	2-68

2-27 Peak positive incident pressure and scaled impulse for an explosion on the surface at sea level 2-69
2-28 Peak positive incident pressure and scaled impulse for an explosion on the surface at sea level 2-70
2-29 Peak positive incident pressure and scaled impulse for an explosion on the surface at sea level 2-71
2-30 Peak positive incident pressure and scaled impulse for an explosion on the surface at sea level 2-72
2-31 Peak positive incident pressure and scaled impulse for an explosion on the surface at sea level 2-73
2-32 Peak positive incident pressure and scaled impulse for an explosion on the surface at sea level 2-74
2-33 Peak positive incident pressure and scaled impulse for an explosion on the surface at sea level 2-75
2-34 Peak positive incident pressure and scaled impulse for an explosion on the surface at sea level 2-76
2-35 Peak positive incident pressure and scaled impulse for an explosion on the surface at sea level 2-77
2-36 Peak positive incident pressure and scaled impulse for an explosion on the surface at sea level 2-78
2-37 Peak positive incident pressure and scaled impulse for an explosion on the surface at sea level 2-79
2-38 Peak positive incident pressure and scaled impulse for an explosion on the surface at sea level 2-80
2-39 Peak positive incident pressure and scaled impulse for an explosion on the surface at sea level 2-81
2-40 Peak positive incident pressure and scaled impulse for an explosion on the surface at sea level 2-82
2-41 Peak positive incident pressure and scaled impulse for an explosion on the surface at sea level 2-83
2-42 Peak positive incident pressure and scaled impulse for an explosion on the surface at sea level 2-84
2-43 Peak positive incident pressure and scaled impulse for an explosion on the surface at sea level 2-85
2-44 Peak positive incident pressure and scaled impulse for an explosion on the surface at sea level 2-86
2-45 Peak positive incident pressure and scaled impulse for an explosion on the surface at sea level 2-87
2-46 Peak positive incident pressure and scaled impulse for an explosion on the surface at sea level 2-88
2-47 Peak positive incident pressure and scaled impulse for an explosion on the surface at sea level 2-89
2-48 Peak positive incident pressure and scaled impulse for an explosion on the surface at sea level 2-90
2-49 Peak positive incident pressure and scaled impulse for an explosion on the surface at sea level 2-91
2-50 Confined explosion structures 2-92
2-51 Barrier and cubicle configurations and parameters 2-93
2-52 Average peak reflected pressure (N = 1, P/L = 0.10, h/H = 0.10) . . . 2-94
2-53 Average peak reflected pressure (N = 1, P/L = 0.25 and 0.75, h/H = 0.10) 2-95
2-54 Average peak reflected pressure (N = 1, P/L = 0.50, h/H = 0.10) . . 2-96
2-55 Average peak reflected pressure (N = 1, P/L = 0.10, h/H = 0.25) . . 2-97
2-56 Average peak reflected pressure (N = 1, P/L = 0.25 and 0.75, h/H = 0.25) 2-98

2-57 Average peak reflected pressure (N = 1, P/L = 0.50 h/H = 0.25) . . 2-99
2-58 Average peak reflected pressure (N = 1, P/L = 0.10; h/H = 0.50) . 2-100
2-59 Average peak reflected pressure (N = 1, P/L = 0.25 and 0.75, h/H = 0.50) 2-101
2-60 Average peak reflected pressure (N = 1, P/L = 0.50, h/H = 0.50) . 2-102
2-61 Average peak reflected pressure (N = 1, P/L = 0.10, h/H = 0.75) . 2-103
2-62 Average peak reflected pressure (N = 1, P/L = 0.25 and 0.75, h/H = 0.75) 2-104
2-63 Average peak reflected pressure (N = 1, P/L = 0.50, h/H = 0.75) . 2-105
2-64 Average peak reflected pressure (N = 2, P/L = 0.10, h/H = 0.10) . 2-106
2-65 Average peak reflected pressure (N = 2, P/L = 0.25, h/H = 0.10) . 2-107
2-66 Average peak reflected pressure (N = 2, P/L = 0.50, h/H = 0.10) . 2-108
2-67 Average peak reflected pressure (N = 2, P/L = 0.75, h/H = 0.10) . 2-109
2-68 Average peak reflected pressure (N = 2, P/L = 0.10, h/H = 0.25) . 2-110
2-69 Average peak reflected pressure (N = 2, P/L = 0.25, h/H = 0.25) . 2-111
2-70 Average peak reflected pressure (N = 2, P/L = 0.50, h/H = 0.25) . 2-112
2-71 Average peak reflected pressure (N = 2, P/L = 0.75, h/H = 0.25) . 2-113
2-72 Average peak reflected pressure (N = 2, P/L = 0.10, h/H = 0.50) . 2-114
2-73 Average peak reflected pressure (N = 2, P/L = 0.25, h/H = 0.50) . 2-115
2-74 Average peak reflected pressure (N = 2, P/L = 0.50, h/H = 0.50) . 2-116
2-75 Average peak reflected pressure (N = 2, P/L = 0.75, h/H = 0.50) . 2-117
2-76 Average peak reflected pressure (N = 2, P/L = 0.10, h/H = 0.75) . 2-118
2-77 Average peak reflected pressure (N = 2, P/L = 0.25, h/H = 0.75) . 2-119
2-78 Average peak reflected pressure (N = 2, P/L = 0.50, h/H = 0.75) . 2-120
2-79 Average peak reflected pressure (N = 2, P/L = 0.75, h/H = 0.75) . 2-121
2-80 Average peak reflected pressure (N = 3, P/L = 0.10, h/H = 0.10) . 2-122
2-81 Average peak reflected pressure (N = 3, P/L = 0.25 and 0.75, h/H = 0.10) 2-123
2-82 Average peak reflected pressure (N = 3. P/L = 0.50, h/H = 0.10) . 2-124
2-83 Average peak reflected pressure (N = 3, P/L = 0.10, h/H = 0.25) . 2-125
2-84 Average peak reflected pressure (N = 3, P/L = 0.25 and 0.75, h/H = 0.25) 2-126
2-85 Average peak reflected pressure (N = 3, P/L = 0.50, h/H = 0.25) . 2-127
2-86 Average peak reflected pressure (N = 3, P/L = 0.10, h/H = 0.50) . 2-128
2-87 Average peak reflected pressure (N = 3, P/L = 0.25 and 0.75, h/H = 0.50) 2-129
2-88 Average peak reflected pressure (N = 3, P/L = 0.50, h/H = 0.50) . 2-130
2-89 Average peak reflected pressure (N = 3, P/L = 0.10, h/H = 0.75) . 2-131
2-90 Average peak reflected pressure (N = 3. P/L = 0.25 and 0.75, h/H = 0.75) 2-132
2-91 Average peak reflected pressure (N = 3. P/L = 0.50, h/H = 0.75) . 2-133
2-92 Average peak reflected pressure (N = 4, P/L = 0.10, h/H = 0.10) . 2-134
2-93 Average peak reflected pressure (N = 4, P/L = 0.25 and 0.75, h/H = 0.10) 2-135
2-94 Average peak reflected pressure (N = 4, P/L = 0.50, h/H = 0.10) . 2-136
2-95 Average peak reflected pressure (N = 4, P/L = 0.10, h/H = 0.25 and 0.75) 2-137
2-96 Average peak reflected pressure (N = 4, P/L = 0.25 and 0.75, h/H = 0.25 and 0.75) 2-138
2-97 Average peak reflected pressure (N = 4, P/L = 0.50, h/H = 0.25 and 0.75) 2-139
2-98 Average peak reflected pressure (N = 4, P/L = 0.10, h/H = 0.50) . 2-140
2-99 Average peak reflected pressure (N = 4, P/L = 0.25 and 0.75, h/H = 0.50) 2-141
2-100 Average peak reflected pressure (N = 4, P/L = 0.50, h/H = 0.50) . 2-142

2-101 Scaled average unit reflected impulse (N = 1, P/L = 0.10, h/H = 0.10) 2-143
2-102 Scaled average unit reflected impulse (N = 1, P/L = 0.25 and 0.75, h/H = 0.10) 2-144
2-103 Scaled average unit reflected impulse (N = 1, P/L = 0.50, h/H = 0.10) 2-145
2-104 Scaled average unit reflected impulse (N = 1, P/L = 0.10, h/H = 0.25) 2-146
2-105 Scaled average unit reflected impulse (N = 1, P/L = 0.25 and 0.75, h/H = 0.25) 2-147
2-106 Scaled average unit reflected impulse (N = 1, P/L = 0.50, h/H = 0.25) 2-148
2-107 Scaled average unit reflected impulse (N = 1, P/L = 0.10, h/H = 0.50) 2-149
2-108 Scaled average unit reflected impulse (N = 1, P/L = 0.25 and 0.75, h/H = 0.50) 2-150
2-109 Scaled average unit reflected impulse (N = 1, P/L = 0.50, h/H = 0.50) 2-151
2-110 Scaled average unit reflected impulse (N = 1, P/L = 0.10, h/H = 0.75) 2-152
2-111 Scaled average unit reflected impulse (N = 1, P/L = 0.25 and 0.75, h/H = 0.75) 2-153
2-112 Scaled average unit reflected impulse (N = 1, P/L = 0.50, h/H = 0.75) 2-154
2-113 Scaled average unit reflected impulse (N = 2, P/L = 0.10, h/H = 0.10) 2-155
2-114 Scaled average unit reflected impulse (N = 2, P/L = 0.25, h/H = 0.10) 2-156
2-115 Scaled average unit reflected impulse (N = 2. P/L = 0.50, h/H = 0.10) 2-157
2-116 Scaled average unit reflected impulse (N = 2, P/L = 0.75, h/H = 0.10) 2-158
2-117 Scaled average unit reflected impulse (N = 2, P/L = 0.10, h/H = 0.25) 2-159
2-118 Scaled average unit reflected impulse (N = 2, P/L = 0.25, h/H = 0.25) 2-160
2-119 Scaled average unit reflected impulse (N = 2. P/L = 0.50, h/H = 0.25) 2-161
2-120 Scaled average unit reflected impulse (N = 2, P/L = 0.75, h/H = 0.25) 2-162
2-121 Scaled average unit reflected impulse (N = 2, P/L = 0.10, h/H = 0.50) 2-163
2-122 Scaled average unit reflected impulse (N = 2, P/L = 0.25, h/H = 0.50) 2-164
2-123 Scaled average unit reflected impulse (N = 2, P/L = 0.50, h/H = 0.50) 2-165
2-124 Scaled average unit reflected impulse (N = 2, P/L = 0.75, h/H = 0.50) 2-166
2-125 Scaled average unit reflected impulse (N = 2, P/L = 0.10, h/H = 0.75) 2-167
2-126 Scaled average unit reflected impulse (N = 2, P/L = 0.25, h/H = 0.75) 2-168
2-127 Scaled average unit reflected impulse (N = 2, P/L = 0.50, h/H = 0.75) 2-169

2-128 Scaled average unit reflected impulse (N = 2, P/L = 0.75, h/H = 0.75) 2-170
2-129 Scaled average unit reflected impulse (N = 3, P/L = 0.10, h/H = 0.10) 2-171
2-130 Scaled average unit reflected impulse (N = 3, P/L = 0.25 and 0.75, h/H = 0.10) 2-172
2-131 Scaled average unit reflected impulse (N = 3, P/L = 0.50, h/H = 0.10) 2-173
2-132 Scaled average unit reflected impulse (N = 3, P/L = 0.10, h/H = 0.25) 2-174
2-133 Scaled average unit reflected impulse (N = 3, P/L = 0.25 and 0.75, h/H = 0.25) 2-175
2-134 Scaled average unit reflected impulse (N = 3, P/L = 0.50, h/H = 0.25) 2-176
2-135 Scaled average unit reflected impulse (N = 3. P/L = 0.10, h/H = 0.50) 2-177
2-136 Scaled average unit reflected impulse (N = 3, P/L = 0.25 and 0.75. h/H = 0.50) 2-178
2-137 Scaled average unit reflected impulse (N = 3. P/L = 0.50, h/H = 0.50) 2-179
2-138 Scaled average unit reflected impulse (N = 3, P/L = 0.10, h/H = 0.75) 2-180
2-139 Scaled average unit reflected impulse (N = 3, P/L = 0.25 and 0.75, h/H = 0.75) 2-181
2-140 Scaled average unit reflected impulse (N = 3, P/L = 0.50, h/H = 0.75) 2-182
2-141 Scaled average unit reflected impulse (N = 4, P/L = 0.10, h/H = 0.10) 2-183
2-142 Scaled average unit reflected impulse (N = 4, P/L = 0.25 and 0.75, h/H = 0.10) 2-184
2-143 Scaled average unit reflected impulse (N = 4, P/L = 0.50, h/H = 0.10) 2-185
2-144 Scaled average unit reflected impulse (N = 4, P/L = 0.10, h/H = 0.25 and 0.75) 2-186
2-145 Scaled average unit reflected impulse (N = 4, P/L = 0.25 and 0.75, h/H = 0.25 and 0.75) 2-187
2-146 Scaled average unit reflected impulse (N = 4, P/L = 0.50, h/H = 0.25 and 0.75) 2-188
2-147 Scaled average unit reflected impulse (N = 4, P/L = 0.10, h/H = 0.50) 2-189
2-148 Scaled average unit reflected impulse (N = 4, P/L = 0.25 and 0.75, h/H = 0.50) 2-190
2-149 Scaled average unit reflected impulse (N = 4, P/L = 0.50, h/H = 0.50) 2-191
2-150 Reflection factor for shock loads on frangible elements. 2-192
2-151 Pressure-time variation for a partially vented explosion. 2-193
2-152 Peak gas pressure produced by a TNT detonation in a partially contained chamber. 2-194
2-153 Scaled gas impulse (W/V_f = 0.002, $i_r/W^{1/3}$ = 20) 2-195
2-154 Scaled gas impulse (W/V_f = 0.002, $i_r/W^{1/3}$ = 100) 2-196
2-155 Scaled gas impulse (W/V_f = 0.002, $i_r/W^{1/3}$ = 600) 2-197
2-156 Scaled gas impulse (W/V_f = 0.015, $i_r/W^{1/3}$ = 20) 2-198
2-157 Scaled gas impulse (W/V_f = 0.015, $i_r/W^{1/3}$ = 100) 2-199
2-158 Scaled gas impulse (W/V_f = 0.015, $i_r/W^{1/3}$ = 600) 2-200
2-159 Scaled gas impulse (W/V_f = 0.15, $i_r/W^{1/3}$ = 20) 2-201

2-160 Scaled gas impulse ($W/V_f = 0.15$, $i_r/W^{1/3} = 100$) 2-202
2-161 Scaled gas impulse ($W/V_f = 0.15$, $i_r/W^{1/3} = 600$) 2-203
2-162 Scaled gas impulse ($W/V_f = 1.0$, $i_r/W^{1/3} = 100$) 2-204
2-163 Scaled gas impulse ($W/V_f = 1.0$, $i_r/W^{1/3} = 600$) 2-205
2-164 Scaled gas impulse ($W/V_f = 1.0$, $i_r/W^{1/3} = 2000$) 2-206
2-165 Combined shock and gas pressures. 2-207
2-166 TNT conversion factor for charges. 2-208
2-167 Fully vented three-wall cubicles and direction of blast wave propagation. 2-209
2-168 Envelope curves for peak positive pressure outside three-wall cubicles without a roof 2-210
2-169 Envelope curves for peak positive pressure outside three-wall cubicles with a roof 2-211
2-170 Envelope curves for maximum peak pressure outside three-wall cubicles 2-212
2-171 Scaled peak positive impulse out the open front of cubic three-wall cubicle without a roof 2-213
2-172 Scaled peak positive impulse out the open front of rectangular three-wall cubicle without a roof 2-214
2-173 Scaled peak positive impulse behind sidewall of cubic three-wall cubicle without a roof 2-215
2-174 Scaled peak positive impulse behind sidewall of rectangular three-wall cubicle without a roof 2-216
2-175 Scaled peak positive impulse behind backwall of cubic three-wall cubicle without a roof 2-217
2-176 Scaled peak positive impulse behind backwall of rectangular three-wall cubicle without a roof 2-218
2-177 Scaled peak positive impulse out the open front of cubic three-wall cubicle with a roof 2-219
2-178 Scaled peak positive impulse out the open front of rectangular three-wall cubicle with a roof 2-220
2-179 Scaled peak positive impulse behind sidewall of cubic three-wall cubicle with a roof 2-221
2-180 Scaled peak positive impulse behind sidewall of rectangular three-wall cubicle with a roof 2-222
2-181 Scaled peak positive impulse behind backwall of cubic three-wall cubicle with a roof 2-223
2-182 Scaled peak positive impulse behind backwall of rectangular three-wall cubicle with a roof 2-224
2-183 Four wall cubicle vented through its roof 2-225
2-184 Peak positive pressure outside of a four-wall cubicle vented through its roof 2-226
2-185 Scaled positive impulse outside of a four-wall cubicle vented through its roof 2-227
2-186 Four wall cubicle vented through a wall and direction of blast wave propagation 2-228
2-187 Peak positive pressure at the front of a partially vented four-wall cubicle 2-229
2-188 Peak positive pressure at the side of a partially vented four-wall cubicle 2-230
2-189 Peak positive pressure at the back of a partially vented four wall cubicle 2-231
2-190 Idealized pressure-time variation. 2-232
2-191 Front wall loading. 2-233

2-192 Velocity of sound in reflected overpressure region versus peak incident overpressure. 2-234
2-193 Reflected pressure coefficient versus angle of incidence. 2-235
2-194 Reflected scaled impulse versus angle of incidence. 2-236
2-195 Roof and side wall loading. 2-237
2-196 Peak equivalent uniform roof pressures. 2-238
2-197 Scaled rise time of equivalent uniform positive roof pressures. . 2-239
2-198 Scaled duration of equivalent uniform roof pressures. 2-240
2-199 Rear wall loading. 2-241
2-200 Idealized structure configuration for interior blast loads. . . . 2-242
2-201 Idealized interior blast loads. 2-243
2-202 Sub-division of typical front wall with openings. 2-244
2-203 Maximum average pressure on interior face of front wall (W/H = 3/4). 2-245
2-204 Maximum average pressure on interior face of front wall (W/H = 3/2). 2-246
2-205 Maximum average pressure on interior face of front wall (W/H = 3). 2-247
2-206 Maximum average pressure on interior face of front wall (W/H = 6). 2-248
2-207 Arrival time, T_1, for interior front wall blast load (W/H = 3/4 and 3/2) 2-249
2-208 Arrival time, T_1, for interior front wall blast load (W/H = 3 and 6) 2-250
2-209 Idealized rise time, $T_2 - T_1$, for interior front wall blast load (W/H = 3/4 and 3/2) 2-251
2-210 Idealized rise time, $T_2 - T_1$, for interior front wall blast load (W/H = 3 and 6) 2-252
2-211 Idealized duration, $T_3 - T_1$, for interior front wall blast load (W/H = 3/4 and 3/2) 2-253
2-212 Idealized duration, $T_3 - T_1$, for interior front wall blast load (W/H = 3 and 6) 2-254
2-213 Idealized times T_1 and T_2 for interior side wall blast load . . 2-255
2-214 Idealized times T_3 and T_4 for interior side wall blast load (L/H = 1, W/H = 3/4) 2-256
2-215 Idealized times T_3 and T_4 for interior side wall blast load (L/H = 1, W/H = 3/2) 2-257
2-216 Idealized times T_3 and T_4 for interior side wall blast load (L/H = 1, W/H = 3) 2-258
2-217 Idealized times T_3 and T_4 for interior side wall blast load (L/H = 1, W/H = 6) 2-259
2-218 Idealized times T_3 and T_4 for interior side wall blast load (L/H = 2, W/H = 3/4) 2-260
2-219 Idealized times T_3 and T_4 for interior side wall blast load (L/H = 2, W/H = 3/2) 2-261
2-220 Idealized times T_3 and T_4 for interior side wall blast load (L/H = 2, W/H = 3) 2-262
2-221 Idealized times T_3 and T_4 for interior side wall blast load (L/H = 2, W/H = 6) 2-263
2-222 Idealized times T_3 and T_4 for interior side wall blast load (L/H = 4, W/H = 3/4) 2-264
2-223 Idealized times T_3 and T_4 for interior side wall blast load (L/H = 4, W/H = 3/2) 2-265
2-224 Idealized times T_3 and T_4 for interior side wall blast load (L/H = 4, W/H = 3) 2-266

2-225 Idealized times T_3 and T_4 for interior side wall blast load (L/H = 4, W/H = 6) 2-267
2-226 Idealized times T_3 and T_4 for interior side wall blast load (L/H = 8, W/H = 3/4) 2-268
2-227 Idealized times T_3 and T_4 for interior side wall blast load (L/H = 8, W/H = 3/2) 2-269
2-228 Idealized times T_3 and T_4 for interior side wall blast load (L/H = 8, W/H = 3) 2-270
2-229 Idealized times T_3 and T_4 for interior side wall blast load (L/H = 8, W/H = 6) 2-271
2-230 Idealized pressure coefficient for back wall interior blast load (L/H = 1 and 2) 2-272
2-231 Idealized pressure coefficient for back wall interior blast load (L/H = 4 and 8) 2-273
2-232 Arrival time, T_1, for interior back wall blast load (W/H = 3/4 and 3/2) 2-274
2-233 Arrival time, T_1, for interior back wall blast load (W/H = 3 and 6) 2-275
2-234 Idealized time T_2 and T_1 for interior back wall blast load 2-276
2-235 Leakage pressure coefficient vs. pressure differential 2-277
2-236 Explosive outer casing separated by incompressible fluid 2-304
2-237 Initial velocity of primary fragments for various geometries . . 2-305
2-238 M_A/B versus cylindrical casing geometry 2-306
2-239 Design fragment weight versus design confidence level ($0.3<C_L<1$) 2-307
2-240 Design fragment weight versus design confidence level ($0.986<C_L<1$) 2-308
2-241 $B^2/N_T/W_c$ versus casing geometry 2-309
2-242 Equivalent cylindrical explosive casings 2-310
2-243 Variation of primary fragment velocity with distance 2-311
2-244 Primary fragment shapes 2-312
2-245 Relationship between fragment weight and fragment diameter . . . 2-313
2-246 Interaction of blast wave with an irregular object 2-314
2-247 Idealized pressure-time loading in an irregular fragment 2-315
2-248 Nondimensional object velocity, V, as a function of pressure and impulse 2-316
2-249 Target shape factor for unconstrained fragments 2-317
2-250 Specific acquired impulse versus distance 2-318
2-251 Scaled fragment velocities for constrained fragments 2-319
2-252 Fragment range prediction 2-320
2-253 Net ground motions produced by an explosion at the ground surface 2-336
2-254 Typical response shock spectra. 2-337

3-1 Typical resistance-deflection for two-way element 3-20
3-2 Idealized yield line locations for several two-way elements 3-21
3-3 Determination of ultimate unit resistance. 3-22
3-4 Location of yield lines for two-way element with two adjacent edges supported and two edges free (values of x) 3-23
3-5 Location of yield lines for two-way element with two adjacent edges supported and two edges free (values of y) 3-24
3-6 Location of symmetrical yield lines for two-way element with three edges supported and one edge free (values of y) 3-25
3-7 Location of unsymmetrical yield lines for two-way element with three edges supported and one edge free ($x_2/x_1 = 0.1$) 3-26
3-8 Location of unsymmetrical yield lines for two-way element with three edges supported and one edge free ($x_2/x_1 = 0.3$) 3-27

3-9 Location of unsymmetrical yield lines for two-way element with three edges supported and one edge free ($x_2/x_1 = 0.5$) 3-28
3-10 Location of unsymmetrical yield lines for two-way element with three edges supported and one edge free ($x_2/x_1 = 0.75$) 3-29
3-11 Location of unsymmetrical yield lines for two-way element with three edges supported and one edge free ($x_2/x_1 = 1.0$) 3-30
3-12 Location of unsymmetrical yield lines for two-way element with three edges supported and one edge free ($x_2/x_1 = 1.25$) 3-31
3-13 Location of unsymmetrical yield lines for two-way element with three edges supported and one edge free ($x_2/x_1 = 1.5$) 3-32
3-14 Location of unsymmetrical yield lines for two-way element with three edges supported and one edge free ($x_2/x_1 = 1.75$) 3-33
3-15 Location of unsymmetrical yield lines for two-way element with three edges supported and one edge free ($x_2/x_1 = 2.0$) 3-34
3-16 Location of unsymmetrical yield lines for two-way element with three edges supported and one edge free (values of y) 3-35
3-17 Location of symmetrical yield lines for two-way element with four edges supported 3-36
3-18 Location of unsymmetrical yield lines for two-way element with four edges supported (values of x_1) 3-37
3-19 Location of unsymmetrical yield lines for two-way element with four edges supported (values of y_1) 3-38
3-20 Location of unsymmetrical yield lines for two-way element with four edges supported values of x/L and y/H) 3-39
3-21 Effects of openings on yield lines locations 3-40
3-22 Deflection of two-way element 3-41
3-23 Graphical summary of two-way elements 3-42
3-24 Moment and deflection coefficients for uniformly loaded, two-way element with two adjacent edges fixed and two edges free 3-43
3-25 Moment and deflection coefficients for uniformly loaded, two-way element with one edge fixed, an adjacent edge simply supported and two edges free 3-44
3-26 Moment and deflection coefficients for uniformly loaded, two-way element with two adjacent edges simply supported and two edges free 3-45
3-27 Moment and deflection coefficients for uniformly loaded, two-way element with three edges fixed and one edge free 3-46
3-28 Moment and deflection coefficients for uniformly loaded, two-way element with two opposite edges fixed, one edge simply supported and one edge free 3-47
3-29 Moment and deflection coefficients for uniformly loaded, two-way element with two opposite edges simply supported, one edge fixed, and one edge free 3-48
3-30 Moment and deflection coefficients for uniformly loaded, two-way element with three edges simply supported and one edge free 3-49
3-31 Moment and deflection coefficients for uniformly loaded, two-way element with two adjacent edges fixed, one edge simply supported, and one edge free 3-50
3-32 Moment and deflection coefficients for uniformly loaded, two-way element with two adjacent edges simply supported, one edge fixed, and one edge free 3-51
3-33 Moment and deflection coefficients for uniformly loaded, two-way element with all edges fixed 3-52

3-34 Moment and deflection coefficients for uniformly loaded, two-way element with two opposite edges fixed and two edges simply supported 3-53
3-35 Moment and deflection coefficients for uniformly loaded, two-way element with three edges fixed and one edge simply supported . . . 3-54
3-36 Moment and deflection coefficients for uniformly loaded, two-way element with all edges simply supported 3-55
3-37 Moment and deflection coefficients for uniformly loaded, two-way element with two adjacent edges fixed, and two edges simply supported 3-56
3-38 Moment and deflection coefficients for uniformly loaded, two-way element with three edges simply supported and one edge fixed . . . 3-57
3-39 Resistance-deflection functions for limited deflections 3-58
3-40 Resistance-deflection functions for large deflections 3-59
3-41 Determination of ultimate support shear 3-60
3-42 Typical single-degree-of-freedom system 3-80
3-43 Determination of load-mass factor in the plastic range 3-81
3-44 Load-mass factors in plastic range for two-way elements 3-82
3-45 Acceleration-impulse extrapolation method 3-102
3-46 Discontinuities in the acceleration curve 3-103
3-47 Pressure-time function with two different time intervals 3-104
3-48 A two-degrees-of-freedom system 3-105
3-49 Maximum response of elastic, one-degree-of-freedom system for triangular load 3-106
3-50 Maximum response of elastic, one-degree-of-freedom system for rectangular load 3-107
3-51 Maximum response of elastic, one-degree-of-freedom system for gradually applied load 3-108
3-52 Maximum response of elastic, one-degree-of-freedom system for triangular pulse load 3-109
3-53 Maximum response of elastic, one-degree-of-freedom system for sinusoidal pulse load 3-110
3-54 Maximum deflection of elasto-plastic, one-degree-of-freedom system for triangular load 3-111
3-55 Maximum response time of elasto-plastic, one-degree-of-freedom system for triangular load 3-112
3-56 Maximum deflection of elasto-plastic, one-degree-of-freedom system for rectangular load 3-113
3-57 Maximum response time of elasto-plastic, one-degree-of-freedom system for rectangular load 3-114
3-58 Maximum deflection of elasto-plastic, one-degree-of-freedom system for gradually applied load 3-115
3-59 Maximum response time of elasto-plastic, one-degree-of-freedom system for gradually applied load 3-116
3-60 Maximum deflection of elasto-plastic, one-degree-of-freedom system for triangular pulse load 3-117
3-61 Maximum response time of elasto-plastic, one-degree-of-freedom system for triangular pulse load 3-118
3-62 Various bilinear-triangular loads 3-119
3-63 Regions of figures 3-64 through 3-266, labeling of axis and curves 3-120
3-64a Maximum response of elasto-plastic, one-degree-of-freedom system for bilinear-triangular pulse (C_1 = 1.000, C_2 = 1.0) 3-121
3-64b Maximum response of elasto-plastic, one-degree-of-freedom system for bilinear-triangular pulse (C_1 = 1.000, C_2 = 1.0) 3-122

3-65 Maximum response of elasto-plastic, one-degree-of-freedom system for bilinear-triangular pulse (C_1 = 0.681, C_2 = 1.7) 3-123
3-66 Maximum response of elasto-plastic, one-degree-of-freedom system for bilinear-triangular pulse (C_1 0.464, C_2 = 1.7) 3-124
3-67 Maximum response of elasto-plastic, one-degree-of-freedom system for bilinear-triangular pulse (C_1 = 0.316, C_2 = 1.7) 3-125
3-68 Maximum response of elasto-plastic, one-degree-of-freedom system for bilinear-triangular pulse (C_1 = 0.215, C_2 = 1.7) 3-126
3-69 Maximum response of elasto-plastic, one-degree-of-freedom system for bilinear-triangular pulse (C_1 = 0.147, C_2 = 1.7) 3-127
3-70 Maximum response of elasto-plastic, one-degree-of-freedom system for bilinear-triangular pulse (C_1 = 0.100, C_2 = 1.7) 3-128
3-71 Maximum response of elasto-plastic, one-degree-of-freedom system for bilinear-triangular pulse (C_1 = 0.056, C_2 = 1.7) 3-129
3-72 Maximum response of elasto-plastic, one-degree-of-freedom system for bilinear-triangular pulse (C_1 = 0.032, C_2 = 1.7) 3-130
3-73 Maximum response of elasto-plastic, one-degree-of-freedom system for bilinear-triangular pulse (C_1 = 0.018, C_2 = 1.7) 3-131
3-74 Maximum response of elasto-plastic, one-degree-of-freedom system for bilinear-triangular pulse (C_1 = 0.010, C_2 = 1.7) 3-132
3-75 Maximum response of elasto-plastic, one-degree-of-freedom system for bilinear-triangular pulse (C_1 = 0.681, C_2 = 3.0) 3-133
3-76 Maximum response of elasto-plastic, one-degree-of-freedom system for bilinear-triangular pulse (C_1 = 0.464, C_2 = 3.0) 3-134
3-77 Maximum response of elasto-plastic, one-degree-of-freedom system for bilinear-triangular pulse (C_1 = 0.316, C_2 = 3.0) 3-135
3-78 Maximum response of elasto-plastic, one-degree-of-freedom system for bilinear-triangular pulse (C_1 = 0.215, C_2 = 3.0) 3-136
3-79 Maximum response of elasto-plastic, one-degree-of-freedom system for bilinear-triangular pulse (C_1 = 0.147, C_2 = 3.0) 3-137
3-80 Maximum response of elasto-plastic, one-degree-of-freedom system for bilinear-triangular pulse (C_1 = 0.100, C_2 = 3.0) 3-138
3-81 Maximum response of elasto-plastic, one-degree-of-freedom system for bilinear-triangular pulse (C_1 = 0.056, C_2 = 3.0) 3-139
3-82 Maximum response of elasto-plastic, one-degree-of-freedom system for bilinear-triangular pulse (C_1 = 0.032, C_2 = 3.0) 3-140
3-83 Maximum response of elasto-plastic, one-degree-of-freedom system for bilinear-triangular pulse (C_1 = 0.018, C_2 = 3.0) 3-141
3-84 Maximum response of elasto-plastic, one-degree-of-freedom system for bilinear-triangular pulse (C_1 = 0.010, C_2 = 3.0) 3-142
3-85 Maximum response of elasto-plastic, one-degree-of-freedom system for bilinear-triangular pulse (C_1 = 0.750, C_2 = 5.5) 3-143
3-86 Maximum response of elasto-plastic, one-degree-of-freedom system for bilinear-triangular pulse (C_1 = 0.562, C_2 = 5.5) 3-144
3-87 Maximum response of elasto-plastic, one-degree-of-freedom system for bilinear-triangular pulse (C_1 = 0.422, C_2 = 5.5) 3-145
3-88 Maximum response of elasto-plastic, one-degree-of-freedom system for bilinear-triangular pulse (C_1 = 0.316, C_2 = 5.5) 3-146
3-89 Maximum response of elasto-plastic, one-degree-of-freedom system for bilinear-triangular pulse (C_1 = 0.237, C_2 = 5.5) 3-147
3-90 Maximum response of elasto-plastic, one-degree-of-freedom system for bilinear-triangular pulse (C_1 = 0.178, C_2 = 5.5) 3-148
3-91 Maximum response of elasto-plastic, one-degree-of-freedom system for bilinear-triangular pulse (C_1 = 0.133, C_2 = 5.5) 3-149

3-92 Maximum response of elasto-plastic, one-degree-of-freedom system for bilinear-triangular pulse (C_1 = 0.100, C_2 = 5.5) 3-150
3-93 Maximum response of elasto-plastic, one-degree-of-freedom system for bilinear-triangular pulse (C_1 = 0.068, C_2 = 5.5) 3-151
3-94 Maximum response of elasto-plastic, one-degree-of-freedom system for bilinear-triangular pulse (C_1 = 0.046, C_2 = 5.5) 3-152
3-95 Maximum response of elasto-plastic, one-degree-of-freedom system for bilinear-triangular pulse (C_1 = 0.032, C_2 = 5.5) 3-153
3-96 Maximum response of elasto-plastic, one-degree-of-freedom system for bilinear-triangular pulse (C_1 = 0.022, C_2 = 5.5) 3-154
3-97 Maximum response of elasto-plastic, one-degree-of-freedom system for bilinear-triangular pulse (C_1 = 0.015, C_2 = 6.) 3-155
3-98 Maximum response of elasto-plastic, one-degree-of-freedom system for bilinear-triangular pulse (C_1 = 0.010, C_2 = 6.) 3-156
3-99 Maximum response of elasto-plastic, one-degree-of-freedom system for bilinear-triangular pulse (C_1 = 0.750, C_2 = 10.) 3-157
3-100 Maximum response of elasto-plastic, one-degree-of-freedom system for bilinear-triangular pulse (C_1 = 0.648, C_2 = 10.) 3-158
3-101 Maximum response of elasto-plastic, one-degree-of-freedom system for bilinear-triangular pulse (C_1 = 0.562, C_2 = 10.) 3-159
3-102 Maximum response of elasto-plastic, one-degree-of-freedom system for bilinear-triangular pulse (C_1 = 0.422, C_2 = 10.) 3-160
3-103 Maximum response of elasto-plastic, one-degree-of-freedom system for bilinear-triangular pulse (C_1 = 0.316, C_2 = 10.) 3-161
3-104 Maximum response of elasto-plastic, one-degree-of-freedom system for bilinear-triangular pulse (C_1 = 0.237, C_2 = 10.) 3-162
3-105 Maximum response of elasto-plastic, one-degree-of-freedom system for bilinear-triangular pulse (C_1 = 0..178, C_2 = 10.) 3-163
3-106 Maximum response of elasto-plastic, one-degree-of-freedom system for bilinear-triangular pulse (C_1 = 0..133, C_2 = 10.) 3-164
3-107 Maximum response of elasto-plastic, one-degree-of-freedom system for bilinear-triangular pulse (C_1 = 0..100, C_2 = 10.) 3-165
3-108 Maximum response of elasto-plastic, one-degree-of-freedom system for bilinear-triangular pulse (C_1 = 0.068, C_2 = 10.) 3-166
3-109 Maximum response of elasto-plastic, one-degree-of-freedom system for bilinear-triangular pulse (C_1 = 0.046, C_2 = 10.) 3-167
3-110 Maximum response of elasto-plastic, one-degree-of-freedom system for bilinear-triangular pulse (C_1 = 0.032, C_2 = 10.) 3-168
3-111 Maximum response of elasto-plastic, one-degree-of-freedom system for bilinear-triangular pulse (C_1 = 0.022, C_2 = 10.) 3-169
3-112 Maximum response of elasto-plastic, one-degree-of-freedom system for bilinear-triangular pulse (C_1 = 0.015, C_2 = 10.) 3-170
3-113 Maximum response of elasto-plastic, one-degree-of-freedom system for bilinear-triangular pulse (C_1 = 0.010, C_2 = 10.) 3-171
3-114 Maximum response of elasto-plastic, one-degree-of-freedom system for bilinear-triangular pulse (C_1 = 0.909, C_2 = 30.) 3-172
3-115 Maximum response of elasto-plastic, one-degree-of-freedom system for bilinear-triangular pulse (C_1 = 0.866, C_2 = 30.) 3-173
3-116 Maximum response of elasto-plastic, one-degree-of-freedom system for bilinear-triangular pulse (C_1 = 0.825, C_2 = 30.) 3-174
3-117 Maximum response of elasto-plastic, one-degree-of-freedom system for bilinear-triangular pulse (C_1 = 0.750, C_2 = 30.) 3-175
3-118 Maximum response of elasto-plastic, one-degree-of-freedom system for bilinear-triangular pulse (C_1 = 0.715, C_2 = 30.) 3-176

3-119 Maximum response of elasto-plastic, one-degree-of-freedom system for bilinear-triangular pulse (C_1 = 0.681, C_2 = 30.) 3-177
3-120 Maximum response of elasto-plastic, one-degree-of-freedom system for bilinear-triangular pulse (C_1 = 0.648, C_2 = 30.) 3-178
3-121 Maximum response of elasto-plastic, one-degree-of-freedom system for bilinear-triangular pulse (C_1 = 0.619, C_2 = 30.) 3-179
3-122 Maximum response of elasto-plastic, one-degree-of-freedom system for bilinear-triangular pulse (C_1 = 0.562, C_2 = 30.) 3-180
3-123 Maximum response of elasto-plastic, one-degree-of-freedom system for bilinear-triangular pulse (C_1 = 0.511, C_2 = 30.) 3-181
3-124 Maximum response of elasto-plastic, one-degree-of-freedom system for bilinear-triangular pulse (C_1 = 0.464, C_2 = 30.) 3-182
3-125 Maximum response of elasto-plastic, one-degree-of-freedom system for bilinear-triangular pulse (C_1 = 0.383, C_2 = 30.) 3-183
3-126 Maximum response of elasto-plastic, one-degree-of-freedom system for bilinear-triangular pulse (C_1 = 0.316, C_2 = 30.) 3-184
3-127 Maximum response of elasto-plastic, one-degree-of-freedom system for bilinear-triangular pulse (C_1 = 0.261, C_2 = 30.) 3-185
3-128 Maximum response of elasto-plastic, one-degree-of-freedom system for bilinear-triangular pulse (C_1 = 0.215, C_2 = 30.) 3-186
3-129 Maximum response of elasto-plastic, one-degree-of-freedom system for bilinear-triangular pulse (C_1 = 0.178, C_2 = 30.) 3-187
3-130 Maximum response of elasto-plastic, one-degree-of-freedom system for bilinear-triangular pulse (C_1 = 0.147, C_2 = 30.) 3-188
3-131 Maximum response of elasto-plastic, one-degree-of-freedom system for bilinear-triangular pulse (C_1 = 0.121, C_2 = 30.) 3-189
3-132 Maximum response of elasto-plastic, one-degree-of-freedom system for bilinear-triangular pulse (C_1 = 0.100, C_2 = 30.) 3-190
3-133 Maximum response of elasto-plastic, one-degree-of-freedom system for bilinear-triangular pulse (C_1 = 0.075, C_2 = 30.) 3-191
3-134 Maximum response of elasto-plastic, one-degree-of-freedom system for bilinear-triangular pulse (C_1 = 0.056, C_2 = 30.) 3-192
3-135 Maximum response of elasto-plastic, one-degree-of-freedom system for bilinear-triangular pulse (C_1 = 0.042, C_2 = 30.) 3-193
3-136 Maximum response of elasto-plastic, one-degree-of-freedom system for bilinear-triangular pulse (C_1 = 0.032, C_2 = 30.) 3-194
3-137 Maximum response of elasto-plastic, one-degree-of-freedom system for bilinear-triangular pulse (C_1 = 0.026, C_2 = 30.) 3-195
3-138 Maximum response of elasto-plastic, one-degree-of-freedom system for bilinear-triangular pulse (C_1 = 0.018, C_2 = 30.) 3-196
3-139 Maximum response of elasto-plastic, one-degree-of-freedom system for bilinear-triangular pulse (C_1 = 0.013, C_2 = 30.) 3-197
3-140 Maximum response of elasto-plastic, one-degree-of-freedom system for bilinear-triangular pulse (C_1 = 0.010, C_2 = 30.) 3-198
3-141 Maximum response of elasto-plastic, one-degree-of-freedom system for bilinear-triangular pulse (C_1 = 0.909, C_2 = 100.) 3-199
3-142 Maximum response of elasto-plastic, one-degree-of-freedom system for bilinear-triangular pulse (C_1 = 0.866, C_2 = 100.) 3-200
3-143 Maximum response of elasto-plastic, one-degree-of-freedom system for bilinear-triangular pulse (C_1 = 0.825, C_2 = 100.) 3-201
3-144 Maximum response of elasto-plastic, one-degree-of-freedom system for bilinear-triangular pulse (C_1 = 0.787, C_2 = 100.) 3-202
3-145 Maximum response of elasto-plastic, one-degree-of-freedom system for bilinear-triangular pulse (C_1 = 0.750, C_2 = 100.) 3-203

3-146 Maximum response of elasto-plastic, one-degree-of-freedom system for bilinear-triangular pulse (C_1 = 0.715, C_2 = 100.) 3-204
3-147 Maximum response of elasto-plastic, one-degree-of-freedom system for bilinear-triangular pulse (C_1 = 0.681, C_2 = 100.) 3-205
3-148 Maximum response of elasto-plastic, one-degree-of-freedom system for bilinear-triangular pulse (C_1 = 0.648, C_2 = 100.) 3-206
3-149 Maximum response of elasto-plastic, one-degree-of-freedom system for bilinear-triangular pulse (C_1 = 0.619, C_2 = 100.) 3-207
3-150 Maximum response of elasto-plastic, one-degree-of-freedom system for bilinear-triangular pulse (C_1 = 0.590, C_2 = 100.) 3-208
3-151 Maximum response of elasto-plastic, one-degree-of-freedom system for bilinear-triangular pulse (C_1 = 0.562, C_2 = 100.) 3-209
3-152 Maximum response of elasto-plastic, one-degree-of-freedom system for bilinear-triangular pulse (C_1 = 0.511, C_2 = 100.) 3-210
3-153 Maximum response of elasto-plastic, one-degree-of-freedom system for bilinear-triangular pulse (C_1 = 0.464, C_2 = 100.) 3-211
3-154 Maximum response of elasto-plastic, one-degree-of-freedom system for bilinear-triangular pulse (C_1 = 0.422, C_2 = 100.) 3-212
3-155 Maximum response of elasto-plastic, one-degree-of-freedom system for bilinear-triangular pulse (C_1 = 0.365, C_2 = 100.) 3-213
3-156 Maximum response of elasto-plastic, one-degree-of-freedom system for bilinear-triangular pulse (C_1 = 0.316, C_2 = 100.) 3-214
3-157 Maximum response of elasto-plastic, one-degree-of-freedom system for bilinear-triangular pulse (C_1 = 0.274, C_2 = 100.) 3-215
3-158 Maximum response of elasto-plastic, one-degree-of-freedom system for bilinear-triangular pulse (C_1 = 0.261, C_2 = 100.) 3-216
3-159 Maximum response of elasto-plastic, one-degree-of-freedom system for bilinear-triangular pulse (C_1 = 0.237, C_2 = 100.) 3-217
3-160 Maximum response of elasto-plastic, one-degree-of-freedom system for bilinear-triangular pulse (C_1 = 0.215, C_2 = 100.) 3-218
3-161 Maximum response of elasto-plastic, one-degree-of-freedom system for bilinear-triangular pulse (C_1 = 0.178, C_2 = 100.) 3-219
3-162 Maximum response of elasto-plastic, one-degree-of-freedom system for bilinear-triangular pulse (C_1 = 0.147, C_2 = 100.) 3-220
3-163 Maximum response of elasto-plastic, one-degree-of-freedom system for bilinear-triangular pulse (C_1 = 0.121, C_2 = 100.) 3-221
3-164 Maximum response of elasto-plastic, one-degree-of-freedom system for bilinear-triangular pulse (C_1 = 0.100, C_2 = 100.) 3-222
3-165 Maximum response of elasto-plastic, one-degree-of-freedom system for bilinear-triangular pulse (C_1 = 0.075, C_2 = 100.) 3-223
3-166 Maximum response of elasto-plastic, one-degree-of-freedom system for bilinear-triangular pulse (C_1 = 0.056, C_2 = 100.) 3-224
3-167 Maximum response of elasto-plastic, one-degree-of-freedom system for bilinear-triangular pulse (C_1 = 0.042, C_2 = 100.) 3-225
3-168 Maximum response of elasto-plastic, one-degree-of-freedom system for bilinear-triangular pulse (C_1 = 0.032, C_2 = 100.) 3-226
3-169 Maximum response of elasto-plastic, one-degree-of-freedom system for bilinear-triangular pulse (C_1 = 0.026, C_2 = 100.) 3-227
3-170 Maximum response of elasto-plastic, one-degree-of-freedom system for bilinear-triangular pulse (C_1 = 0.018, C_2 = 100.) 3-228
3-171 Maximum response of elasto-plastic, one-degree-of-freedom system for bilinear-triangular pulse (C_1 = 0.013, C_2 = 100.) 3-229
3-172 Maximum response of elasto-plastic, one-degree-of-freedom system for bilinear-triangular pulse (C_1 = 0.010, C_2 = 100.) 3-230

3-173 Maximum response of elasto-plastic, one-degree-of-freedom system for bilinear-triangular pulse (C_1 = 0.909, C_2 = 300.) 3-231
3-174 Maximum response of elasto-plastic, one-degree-of-freedom system for bilinear-triangular pulse (C_1 = 0.866, C_2 = 300.) 3-232
3-175 Maximum response of elasto-plastic, one-degree-of-freedom system for bilinear-triangular pulse (C_1 = 0.825, C_2 = 300.) 3-233
3-176 Maximum response of elasto-plastic, one-degree-of-freedom system for bilinear-triangular pulse (C_1 = 0.787, C_2 = 300.) 3-234
3-177 Maximum response of elasto-plastic, one-degree-of-freedom system for bilinear-triangular pulse (C_1 = 0.750, C_2 = 300.) 3-235
3-178 Maximum response of elasto-plastic, one-degree-of-freedom system for bilinear-triangular pulse (C_1 = 0.715, C_2 = 300.) 3-236
3-179 Maximum response of elasto-plastic, one-degree-of-freedom system for bilinear-triangular pulse. (C_1 = 0.681, C_2 = 300.) 3-237
3-180 Maximum response of elasto-plastic, one-degree-of-freedom system for bilinear-triangular pulse (C_1 = 0.648, C_2 = 300.) 3-238
3-181 Maximum response of elasto-plastic, one-degree-of-freedom system for bilinear-triangular pulse (C_1 = 0.619, C_2 = 300.) 3-239
3-182 Maximum response of elasto-plastic, one-degree-of-freedom system for bilinear-triangular pulse (C_1 = 0.590, C_2 = 300.) 3-240
3-183 Maximum response of elasto-plastic, one-degree-of-freedom system for bilinear-triangular pulse (C_1 = 0.562, C_2 = 300.) 3-241
3-184 Maximum response of elasto-plastic, one-degree-of-freedom system for bilinear-triangular pulse (C_1 = 0.536, C_2 = 300.) 3-242
3-185 Maximum response of elasto-plastic, one-degree-of-freedom system for bilinear-triangular pulse (C_1 = 0.511, C_2 = 300.) 3-243
3-186 Maximum response of elasto-plastic, one-degree-of-freedom system for bilinear-triangular pulse (C_1 = 0.487, C_2 = 300.) 3-244
3-187 Maximum response of elasto-plastic, one-degree-of-freedom system for bilinear-triangular pulse (C_1 = 0.464, C_2 = 300.) 3-245
3-188 Maximum response of elasto-plastic, one-degree-of-freedom system for bilinear-triangular pulse (C_1 = 0.422, C_2 = 300.) 3-246
3-189 Maximum response of elasto-plastic, one-degree-of-freedom system for bilinear-triangular pulse (C_1 = 0.383, C_2 = 300.) 3-247
3-190 Maximum response of elasto-plastic, one-degree-of-freedom system for bilinear-triangular pulse (C_1 = 0.365, C_2 = 300.) 3-248
3-191 Maximum response of elasto-plastic, one-degree-of-freedom system for bilinear-triangular pulse (C_1 = 0.348, C_2 = 300.) 3-249
3-192 Maximum response of elasto-plastic, one-degree-of-freedom system for bilinear-triangular pulse (C_1 = 0.316, C_2 = 300.) 3-250
3-193 Maximum response of elasto-plastic, one-degree-of-freedom system for bilinear-triangular pulse (C_1 = 0.287, C_2 = 300.) 3-251
3-194 Maximum response of elasto-plastic, one-degree-of-freedom system for bilinear-triangular pulse (C_1 = 0.274, C_2 = 300.) 3-252
3-195 Maximum response of elasto-plastic, one-degree-of-freedom system for bilinear-triangular pulse (C_1 = 0.261, C_2 = 300.) 3-253
3-196 Maximum response of elasto-plastic, one-degree-of-freedom system for bilinear-triangular pulse (C_1 = 0.237, C_2 = 300.) 3-254
3-197 Maximum response of elasto-plastic, one-degree-of-freedom system for bilinear-triangular pulse (C_1 = 0.215, C_2 = 300.) 3-255
3-198 Maximum response of elasto-plastic, one-degree-of-freedom system for bilinear-triangular pulse (C_1 = 0.198, C_2 = 300.) 3-256
3-199 Maximum response of elasto-plastic, one-degree-of-freedom system for bilinear-triangular pulse (C_1 = 0.178, C_2 = 300.) 3-257

3-200 Maximum response of elasto-plastic, one-degree-of-freedom system for bilinear-triangular pulse (C_1 = 0.162, C_2 = 300.) 3-258
3-201 Maximum response of elasto-plastic, one-degree-of-freedom system for bilinear-triangular pulse (C_1 = 0.147, C_2 = 300.) 3-259
3-202 Maximum response of elasto-plastic, one-degree-of-freedom system for bilinear-triangular pulse (C_1 = 0.133, C_2 = 300.) 3-260
3-203 Maximum response of elasto-plastic, one-degree-of-freedom system for bilinear-triangular pulse (C_1 = 0.121, C_2 = 300.) 3-261
3-204 Maximum response of elasto-plastic, one-degree-of-freedom system for bilinear-triangular pulse (C_1 = 0.110, C_2 = 300.) 3-262
3-205 Maximum response of elasto-plastic, one-degree-of-freedom system for bilinear-triangular pulse (C_1 = 0.100, C_2 = 300.) 3-263
3-206 Maximum response of elasto-plastic, one-degree-of-freedom system for bilinear-triangular pulse (C_1 = 0.091, C_2 = 300.) 3-264
3-207 Maximum response of elasto-plastic, one-degree-of-freedom system for bilinear-triangular pulse (C_1 = 0.083, C_2 = 300.) 3-265
3-208 Maximum response of elasto-plastic, one-degree-of-freedom system for bilinear-triangular pulse (C_1 = 0.075, C_2 = 300.) 3-266
3-209 Maximum response of elasto-plastic, one-degree-of-freedom system for bilinear-triangular pulse (C_1 = 0.068, C_2 = 300.) 3-267
3-210 Maximum response of elasto-plastic, one-degree-of-freedom system for bilinear-triangular pulse (C_1 = 0.056, C_2 = 300.) 3-268
3-211 Maximum response of elasto-plastic, one-degree-of-freedom system for bilinear-triangular pulse (C_1 = 0.046, C_2 = 300.) 3-269
3-212 Maximum response of elasto-plastic, one-degree-of-freedom system for bilinear-triangular pulse (C_1 = 0.042, C_2 = 300.) 3-270
3-213 Maximum response of elasto-plastic, one-degree-of-freedom system for bilinear-triangular pulse (C_1 = 0.032, C_2 = 300.) 3-271
3-214 Maximum response of elasto-plastic, one-degree-of-freedom system for bilinear-triangular pulse (C_1 = 0.026, C_2 = 300.) 3-272
3-215 Maximum response of elasto-plastic, one-degree-of-freedom system for bilinear-triangular pulse (C_1 = 0.022, C_2 = 300.) 3-273
3-216 Maximum response of elasto-plastic, one-degree-of freedom system for bilinear-triangular pulse (C_1 = 0.018, C_2 = 300.) 3-274
3-217 Maximum response of elasto-plastic, one-degree-of-freedom system for bilinear-triangular pulse (C_1 = 0.015, C_2 = 300.) 3-275
3-218 Maximum response of elasto-plastic, one-degree-of-freedom system for bilinear-triangular pulse (C_1 = 0.013, C_2 = 300.) 3-276
3-219 Maximum response of elasto-plastic, one-degree-of-freedom system for bilinear-triangular pulse (C_1 = 0.010, C_2 = 300.) 3-277
3-220 Maximum response of elasto-plastic, one-degree-of-freedom system for bilinear-triangular pulse (C_1 = 0.909, C_2 = 1000.) 3-278
3-221 Maximum response of elasto-plastic, one-degree-of-freedom system for bilinear-triangular pulse (C_1 = 0.866, C_2 = 1000.) 3-279
3-222 Maximum response of elasto-plastic, one-degree-of-freedom system for bilinear-triangular pulse (C_1 = 0.825, C_2 = 1000.) 3-280
3-223 Maximum response of elasto-plastic, one-degree-of-freedom system for bilinear-triangular pulse (C_1 = 0.787, C_2 = 1000.) 3-281
3-224 Maximum response of elasto-plastic, one-degree-of-freedom system for bilinear-triangular pulse (C_1 = 0.750, C_2 = 1000.) 3-282
3-225 Maximum response of elasto-plastic, one-degree-of-freedom system for bilinear-triangular pulse (C_1 = 0.715, C_2 = 1000.) 3-283
3-226 Maximum response of elasto-plastic, one-degree-of-freedom system for bilinear-triangular pulse (C_1 = 0.681, C_2 = 1000.) 3-284

3-227 Maximum response of elasto-plastic, one-degree-of-freedom system for bilinear-triangular pulse (C_1 = 0.648, C_2 = 1000.) 3-285
3-228 Maximum response of elasto-plastic, one-degree-of-freedom system for bilinear-triangular pulse (C_1 = 0.619, C_2 = 1000.) 3-286
3-229 Maximum response of elasto-plastic, one-degree-of-freedom system for bilinear-triangular pulse (C_1 = 0.590, C_2 = 1000.) 3-287
3-230 Maximum response of elasto-plastic, one-degree-of-freedom system for bilinear-triangular pulse (C_1 = 0.562, C_2 = 1000.) 3-288
3-231 Maximum response of elasto-plastic, one-degree-of-freedom system for bilinear-triangular pulse (C_1 = 0.536, C_2 = 1000.) 3-289
3-232 Maximum response of elasto-plastic, one-degree-of-freedom system for bilinear-triangular pulse (C_1 = 0.511, C_2 = 1000.) 3-290
3-233 Maximum response of elasto-plastic, one-degree-of-freedom system for bilinear-triangular pulse (C_1 = 0.487, C_2 = 1000.) 3-291
3-234 Maximum response of elasto-plastic, one-degree-of-freedom system for bilinear-triangular pulse (C_1 = 0.464, C_2 = 1000.) 3-292
3-235 Maximum response of elasto-plastic, one-degree-of-freedom system for bilinear-triangular pulse (C_1 = 0.422, C_2 = 1000.) 3-293
3-236 Maximum response of elasto-plastic, one-degree-of-freedom system for bilinear-triangular pulse (C_1 = 0.383, C_2 = 1000.) 3-294
3-237 Maximum response of elasto-plastic, one-degree-of-freedom system for bilinear-triangular pulse (C_1 = 0.365, C_2 = 1000.) 3-295
3-238 Maximum response of elasto-plastic, one-degree-of-freedom system for bilinear-triangular pulse (C_1 = 0.348, C_2 = 1000.) 3-296
3-239 Maximum response of elasto-plastic, one-degree-of-freedom system for bilinear-triangular pulse (C_1 = 0.316, C_2 = 1000.) 3-297
3-240 Maximum response of elasto-plastic, one-degree-of-freedom system for bilinear-triangular pulse (C_1 = 0.287, C_2 = 1000.) 3-298
3-241 Maximum response of elasto-plastic, one-degree-of-freedom system for bilinear-triangular pulse (C_1 = 0.274, C_2 = 1000.) 3-299
3-242 Maximum response of elasto-plastic, one-degree-of-freedom system for bilinear-triangular pulse (C_1 = 0.261, C_2 = 1000.) 3-300
3-243 Maximum response of elasto-plastic, one-degree-of-freedom system for bilinear-triangular pulse (C_1 = 0.237, C_2 = 1000.) 3-301
3-244 Maximum response of elasto-plastic, one-degree-of-freedom system for bilinear-triangular pulse (C_1 = 0.215, C_2 = 1000.) 3-302
3-245 Maximum response of elasto-plastic, one-degree-of-freedom system for bilinear-triangular pulse (C_1 = 0.198, C_2 = 1000.) 3-303
3-246 Maximum response of elasto-plastic, one-degree-of-freedom system for bilinear-triangular pulse (C_1 = 0.178, C_2 = 1000.) 3-304
3-247 Maximum response of elasto-plastic, one-degree-of-freedom system for bilinear-triangular pulse (C_1 = 0.162, C_2 = 1000.) 3-305
3-248 Maximum response of elasto-plastic, one-degree-of-freedom system for bilinear-triangular pulse (C_1 = 0.147, C_2 = 1000.) 3-306
3-249 Maximum response of elasto-plastic, one-degree-of-freedom system for bilinear-triangular pulse (C_1 = 0.133, C_2 = 1000.) 3-307
3-250 Maximum response of elasto-plastic, one-degree-of-freedom system for bilinear-triangular pulse (C_1 = 0.121, C_2 = 1000.) 3-308
3-251 Maximum response of elasto-plastic, one-degree-of-freedom system for bilinear-triangular pulse (C_1 = 0.110, C_2 = 1000.) 3-309
3-252 Maximum response of elasto-plastic, one-degree-of-freedom system for bilinear-triangular pulse (C_1 = 0.100, C_2 = 1000.) 3-310
3-253 Maximum response of elasto-plastic, one-degree-of-freedom system for bilinear-triangular pulse (C_1 = 0.091, C_2 = 1000.) 3-311

3-254 Maximum response of elasto-plastic, one-degree-of-freedom system for bilinear-triangular pulse (C_1 = 0.083, C_2 = 1000.) 3-312
3-255 Maximum response of elasto-plastic, one-degree-of-freedom system for bilinear-triangular pulse (C_1 = 0.075, C_2 = 1000.) 3-313
3-256 Maximum response of elasto-plastic, one-degree-of-freedom system for bilinear-triangular pulse (C_1 = 0.068, C_2 = 1000.) 3-314
3-257 Maximum response of elasto-plastic, one-degree-of-freedom system for bilinear-triangular pulse (C_1 = 0.056, C_2 = 1000.) 3-315
3-258 Maximum response of elasto-plastic, one-degree-of-freedom system for bilinear-triangular pulse (C_1 = 0.046, C_2 = 1000.) 3-316
3-259 Maximum response of elasto-plastic, one-degree-of-freedom system for bilinear-triangular pulse (C_1 = 0.042, C_2 = 1000.) 3-317
3-260 Maximum response of elasto-plastic, one-degree-of-freedom system for bilinear-triangular pulse (C_1 = 0.032, C_2 = 1000.) 3-318
3-261 Maximum response of elasto-plastic, one-degree-of-freedom system for bilinear-triangular pulse (C_1 = 0.026, C_2 = 1000.) 3-319
3-262 Maximum response of elasto-plastic, one-degree-of-freedom system for bilinear-triangular pulse (C_1 = 0.022, C_2 = 1000.) 3-320
3-263 Maximum response of elasto-plastic, one-degree-of-freedom system for bilinear-triangular pulse (C_1 = 0.018, C_2 = 1000.) 3-321
3-264 Maximum response of elasto-plastic, one-degree-of-freedom system for bilinear-triangular pulse (C_1 = 0.015, C_2 = 1000.) 3-322
3-265 Maximum response of elasto-plastic, one-degree-of-freedom system for bilinear-triangular pulse (C_1 = 0.013, C_2 = 1000.) 3-323
3-266 Maximum response of elasto-plastic, one-degree-of-freedom system for bilinear-triangular pulse (C_1 = 0.010, C_2 = 1000.) 3-324
3-267 Graphical interpolation 3-325
3-268 Elastic rebound of simple spring-mass system 3-326
3-269 Pressure-time and resistance-time curves for elements which respond to impulse 3-327

4-1 Typical resistance-deflection curve for flexural response of concrete elements 4-9
4-2 Single leg stirrups 4-10
4-3 Lacing reinforcement 4-11
4-4 Typical resistance-deflection curve for tension membrane response of concrete 4-12
4-5 Typical laced wall 4-13
4-6 Failure of a laced element 4-14
4-7 Failure of an unlaced element 4-15
4-8 Typical stress-strain curves for concrete and reinforcing steel . . 4-22
4-9 Design curve for DIF for ultimate compressive strength of concrete 4-23
4-10 Design curve for DIF for yield stress of ASTM A 615 grade 60 reinforcing steel 4-24
4-11 Coefficient for moment of inertia of cracked sections with tension reinforcement only 4-30
4-12 Coefficient for moment of inertia of cracked sections with equal reinforcement on opposite faces 4-31
4-13 Typical reinforced concrete cross sections 4-46
4-14 Location of critical sections for diagonal tension 4-47
4-15 Angle of inclination of lacing bars 4-48
4-16 Geometry for standard hooked reinforcement 4-49
4-17 Relationship between design parameters for unlaced elements 4-63
4-18 Idealized resistance-deflection curve for large deflections 4-64

4-19 Determination of ultimate shears 4-65
4-20 Typical flat slab structure 4-84
4-21 Relationship between design parameters for flat slabs 4-85
4-22 Unit moments 4-86
4-23 Typical resistance-deflection functions for flat slabs 4-87
4-24 Yield line pattern for multi-panel flat slab 4-88
4-25 Quarter panel of flat slab 4-89
4-26 Dynamic resistance-deflection curve 4-90
4-27 Critical locations for shear stresses 4-91
4-28 Typical column loads 4-92
4-29 Relationship between design parameters for laced elements 4-108
4-30 Impulse coefficient C_1 for an element with two adjacent edges fixed and two edges free 4-109
4-31 Impulse coefficient C_1 for an element with three edges fixed and one edge free 4-110
4-32 Impulse coefficient C_1 for an element with four edges fixed . . . 4-111
4-33 Impulse coefficient C_u for an element with two adjacent edges fixed and two edges free 4-112
4-34 Impulse coefficient C_u for an element with three edges fixed and one edge free 4-113
4-35 Impulse coefficient C_u for an element with four edges fixed . . . 4-114
4-36 Determination of optimum ratio of p_V/p_H for maximum impulse capacity 4-115
4-37 Optimum ratio of p_V/p_H for maximum capacity at partial failure deflection, X_1 4-116
4-38 Optimum ratio of p_V/p_H for maximum capacity at incipient failure, X_u 4-117
4-39 Vertical shear coefficients for ultimate shear stress at distance d_c from the support (cross section type II and III) 4-118
4-40 Horizontal shear coefficients for ultimate shear stress at distance d_c from the support (cross section type II and III) 4-119
4-41 Vertical shear parameters for ultimate shear stress at distance d_c from the support (cross section type II and III) 4-120
4-42 Vertical shear coefficient ratios for ultimate shear stress at distance d_c from the support (cross section type II and III) . . 4-121
4-43 Horizontal shear parameters for ultimate shear stress at distance d_c from the support (cross section type II and III) 4-122
4-44 Horizontal shear coefficient ratios for ultimate shear stress at distance d_c from the support (cross section type II and III) . . 4-123
4-45 Vertical shear parameters for ultimate shear stress at distance d_c from the support (cross section type II and III) 4-124
4-46 Vertical shear coefficient ratios for ultimate shear stress at distance d_c from the support (cross section type II and III) . . 4-125
4-47 Horizontal shear parameters for ultimate shear stress at distance d_c from the support (cross section type II and III) 4-126
4-48 Horizontal shear coefficient ratios for ultimate shear stress at distance d_c from the support (cross section type II and III) . . 4-127
4-49 Vertical shear parameters for ultimate shear stress at distance d_c from the support (cross section type II and III) 4-128
4-50 Vertical shear coefficient ratios for ultimate shear stress at distance d_c from the support (cross section type II and III) . . 4-129
4-51 Horizontal shear parameters for ultimate shear stress at distance d_c from the support (cross section type II and III) 4-130
4-52 Horizontal shear coefficient ratios for ultimate shear stress at distance d_c from the support (cross section type II and III) . . 4-131

4-53 Shear coefficients for ultimate support shear (cross section type II and III) 4-132
4-54 Shear coefficients for ultimate support shear (cross section type II and III) 4-133
4-55 Shear coefficients for ultimate support shear (cross section type II and III) 4-134
4-56 Shear coefficients for ultimate support shear (cross section type II and III) 4-135
4-57 Attenuation of blast impulse in sand and concrete, w_s = 85 pcf . 4-147
4-58 Attenuation of blast impulse in sand and concrete, w_s = 100 pcf . 4-148
4-59 Relationship between design parameters for beams 4-164
4-60 Arrangement of reinforcement for combined flexure and torsion . . 4-165
4-61 Column interaction diagram 4-178
4-62 Typical interior column sections 4-179
4-63 Direct spalled element 4-192
4-64 Scabbed element 4-193
4-65 Spall threshold for blast waves loading walls 4-194
4-66 Unspalled panel of composite panel 4-195
4-67 Shielding systems for protection against concrete fragments . . . 4-196
4-68 Rigid attachment of fragment shield to barrier 4-197
4-69 Failure of an unlaced element 4-198
4-70 Failure at plastic hinges of laced elements 4-199
4-71 Backwall failure of cubicle with laced reinforcement 4-200
4-72 Idealized curves for determination of post-failure fragment velocities 4-201
4-73 Post-failure coefficient C_f for an element fixed on two adjacent edges and two edges free 4-202
4-74 Post-failure coefficient C_f for an element fixed on three edges and one edge free 4-203
4-75 Post-failure coefficient C_f for an element fixed on four edges . . 4-204
4-76 Perforation and spalling of concrete due to primary fragments . . 4-212
4-77 Shape of standard primary fragments 4-213
4-78 Concrete penetration chart for armor-piercing steel fragments . . 4-214
4-79 Residual fragment velocity upon perforation of concrete barriers (for cases where $x < 2d$) 4-215
4-80 Residual fragment velocity upon perforation of: (1) Concrete barriers (for cases where $x > 2d$) (2) Sand layers 4-216
4-81 Depth of penetration into sand by standard primary fragments . . . 4-217
4-82 Typical flexural reinforcement splice pattern for close-in effects 4-234
4-83 Typical section through conventionally reinforced concrete wall . 4-235
4-84 Floor slab-wall intersections 4-236
4-85 Typical horizontal corner details of conventionally reinforced concrete walls 4-237
4-86 Preferred location of lap splices for a two-way element fixed on four edges 4-238
4-87 Splice locations for multi-span slab 4-239
4-88 Section through column of flat slab 4-240
4-89 Laced reinforced element 4-241
4-90 Typical lacing bend details 4-242
4-91 Typical methods of lacing 4-243
4-92 Typical location of continuous and discontinuous lacing 4-244
4-93 Typical details for splicing of lacing bars 4-245
4-94 Length of lacing bars 4-246
4-95 Reinforcement details of laced concrete walls 4-247

4-96 Typical detail at intersection of two continuous laced walls . . . 4-248
4-97 Typical detail at intersection of continuous and discontinuous laced walls . . . 4-249
4-98 Typical detail at corner of laced walls . . . 4-250
4-99 Intersection of continuous and discontinuous laced walls without wall extensions . . . 4-251
4-100 Corner details for laced walls without wall extensions . . . 4-252
4-101 Element reinforced with single leg stirrups . . . 4-253
4-102 Typical detail at corner for walls reinforced with single leg stirrups . . . 4-254
4-103 Reinforcement detail of wall with single leg stirrups . . . 4-255
4-104 Typical composite wall details . . . 4-256
4-105 Typical single-cell structures . . . 4-257
4-106 Typical multicubicle structures . . . 4-258
4-107 Pouring sequence . . . 4-259

5-1 Typical stress-strain curves for steel. . . . 5-12
5-2 Dynamic increase factors for yield stresses at various strain rates for ASTM A-36 and A-514 steels. . . . 5-13
5-3 Member end rotations for beams and frames. . . . 5-23
5-4 Relationships between design parameters for beams. . . . 5-24
5-5 Relationships between design parameters for plates. . . . 5-25
5-6 Theoretical stress distribution for pure bending at various stages of dynamic loading. . . . 5-35
5-7 Moment-curvature diagram for simple-supported, dynamically loaded, I-shaped beams. . . . 5-36
5-8 Values of ß for use in equations 5-20 and 5-21. . . . 5-37
5-9 Typical lateral bracing details. . . . 5-38
5-10 Moment-curvature diagram for dynamically loaded plates and rectangular cross section beams. . . . 5-41
5-11 Biaxial bending of a doubly-symmetric section. . . . 5-42
5-12 Resistance-deflection curve for a typical cold-formed section. . . . 5-55
5-13 Elastic rebound of single-degree-of-freedom system. . . . 5-56
5-14 Allowable dynamic (design) shear stresses for webs of cold- . . . 5-57
5-15 Maximum end support reaction for cold-formed steel sections . . . 5-58
5-16 Maximum interior support reaction for cold-formed steel . . . 5-59
5-17 Gasket detail for blast door. . . . 5-69
5-18 Built-up double-leaf blast door with frame built into concrete. . . . 5-70
5-19 Horizontal sliding blast door. . . . 5-71
5-20 Single-leaf blast door with fragment shield (very high pressure). . . . 5-72
5-21 Single-leaf blast door (high pressure). . . . 5-73
5-22 Bilinear blast load and single-degree-of-freedom response for determining rebound resistance. . . . 5-74
5-23 Orientation of roof purlins with respect to blast load direction for frame blast loading. . . . 5-89
5-24 Estimates of peak shears and axial loads in rigid frames due to horizontal loads. . . . 5-90
5-25 Estimates of peak shears and axial loads in braced frames due to horizontal loads. . . . 5-91
5-26 Corner connection behavior. . . . 5-100
5-27 Typical connections for cold-formed steel panels. . . . 5-101
5-28 Steel penetration design chart - AP steel fragments penetrating mild steel plates. . . . 5-104
5-29 Steel penetration design chart - mild steel fragments penetrating mild steel plates. . . . 5-105

5-30 Residual fragment velocity upon perforation of steel barriers. . 5-106
5-31 Typical framing plan for a single-story blast-resistant steel structure. 5-109
5-32 Typical framing detail at interior Column 2-C. 5-110
5-33 Typical framing detail at end Column 1-C. 5-111
5-34 Typical framing detail at side column 2-D. 5-112
5-35 Typical framing detail at corner Column 1-D. 5-113
5-36 Typical details for cold-formed, light gage steel paneling. . . . 5-114
5-37 Typical welded connections for attaching cold-formed steel panels to supporting members. 5-115
5-38 Typical bolted connections for attaching cold-formed steel panels to supporting members. 5-116
5-39 Details of typical fasteners for cold-formed steel panels. . . . 5-117
5-40 Single-leaf blast door installed in a steel structure. 5-118
5-41 Double-leaf blast door installed in a concrete structure. 5-119
5-42 Compression-arch and tension-arch blast doors. 5-120

6-1 Masonry wall with flexible support 6-14
6-2 Masonry wall with rigid support 6-15
6-3 Concrete masonry walls 6-16
6-4 Typical joint reinforced masonry construction 6-17
6-5 Special masonry unit for use with reinforcing bars 6-18
6-6 Arching action of non-reinforced masonry wall 6-19
6-7 Typical concrete masonry units 6-20
6-8 Connection details for rebound and/or negative overpressures . . . 6-21
6-9 Deflection of non-reinforced masonry walls 6-22
6-10 Structural behavior of non-reinforced solid masonry panel with rigid supports 6-23
6-11 Common precast elements 6-36
6-12 Typical stress-strain curve for high strength wire 6-37
6-13 Roof slab-to-girder connection 6-38
6-14 Typical wall panel-to-roof slab connection 6-39
6-15 Wall panel-to foundation connection 6-40
6-16 Typical panel splice 6-41
6-17 General layout of pre-engineered building 6-53
6-18 Recommended pre-engineered building design loads 6-54
6-19a General configuration of suppressive shield groups 6-62
6-19b General configuration of suppressive shield groups (continued) . . 6-63
6-20 Typical utility penetration 6-64
6-21 Typical location of utility penetration in shield groups 4, 5, and 81 mm 6-65
6-22 Typical location of utility penetrations in shield group 3 6-66
6-23 Typical vacuum line penetration 6-67
6-24 Sliding personnel door 6-68
6-25 Door - group 3 shield 6-69
6-26 Rotating product door 6-70
6-27 Characteristic Parameters for Glass Pane, Blast Loading, Resistance Function and Response Model 6-83
6-28 Peak Blast Pressure Capacity for Tempered Glass Panes (a/b = 1.00, t = 1/4 and 5/16 in) 6-84
6-29 Peak Blast Pressure Capacity for Tempered Glass Panes (a/b = 1.00, t = 3/8 and 1/2 in) 6-85
6-30 Peak Blast Pressure Capacity for Tempered Glass Panes (a/b = 1.00, t = 5/8 and 3/4 in) 6-86

6-31 Peak Blast Pressure Capacity for Tempered Glass Panes (a/b = 1.25, t = 1/4 and 5/16 in) 6-87
6-32 Peak Blast Pressure Capacity for Tempered Glass Panes (a/b = 1.25, t = 3/8 and 1/2 in) 6-88
6-33 Peak Blast Pressure Capacity for Tempered Glass Panes (a/b = 1.25, t = 5/8 and 3/4 in) 6-89
6-34 Peak Blast Pressure Capacity for Tempered Glass Panes (a/b = 1.50, t = 1/4 and 5/16 in) 6-90
6-35 Peak Blast Pressure Capacity for Tempered Glass Panes (a/b = 1.50, t = 3/8 and 1/2 in) 6-91
6-36 Peak Blast Pressure Capacity for Tempered Glass Panes (a/b = 1.50, t = 5/8 and 3/4 in) 6-92
6-37 Peak Blast Pressure Capacity for Tempered Glass Panes (a/b = 1.75, t = 1/4 and 5/16 in) 6-93
6-38 Peak Blast Pressure Capacity for Tempered Glass Panes (a/b = 1.75, t = 3/8 and 1/2 in) 6-94
6-39 Peak Blast Pressure Capacity for Tempered Glass Panes (a/b = 1.75, t = 5/8 and 3/4 in) 6-95
6-40 Peak Blast Pressure Capacity for Tempered Glass Panes (a/b = 2.00, t = 1/4 and 5/16 in) 6-96
6-41 Peak Blast Pressure Capacity for Tempered Glass Panes (a/b = 2.00, t = 3/8 and 1/2 in) 6-97
6-42 Peak Blast Pressure Capacity for Tempered Glass Panes (a/b = 2.00, t = 5/8 and 3/4 in) 6-98
6-43 Peak Blast Pressure Capacity for Tempered Glass Panes (a/b = 3.00, t = 1/4 and 5/16 in) 6-99
6-44 Peak Blast Pressure Capacity for Tempered Glass Panes (a/b = 3.00, t = 3/8 and 1/2 in) 6-100
6-45 Peak Blast Pressure Capacity for Tempered Glass Panes (a/b = 3.00, t = 5/8 and 3/4 in) 6-101
6-46 Peak Blast Pressure Capacity for Tempered Glass Panes (a/b = 4.00, t = 1/4 and 5/16 in) 6-102
6-47 Peak Blast Pressure Capacity for Tempered Glass Panes (a/b = 4.00, t = 3/8 and 1/2 in) 6-103
6-48 Peak Blast Pressure Capacity for Tempered Glass Panes (a/b = 4.00, t = 5/8 and 3/4 in) 6-104
6-49 Nondimensional Static Load-Stress Relationships for Simply Supported Tempered Glass 6-105
6-50 Nondimensional Static Load-Crater Deflection Relationships for Simply Supported Tempered Glass 6-106
6-51 Edge, Face, and Bite Requirements 6-107
6-52 Distribution of Lateral Load Transmitted by Glass Pane to the Window Frame 6-108
6-53 Geometry of a buried structure 6-138
6-54 Typical roof panel load 6-139
6-55 Contribution of three pressure waves on a wall 6-140
6-56 Spall plate 6-141
6-57 Typical earth-covered steel-arch magazine 6-145
6-58 Minimum separation distances of standard magazine 6-146
6-59 Sketch of 300 cfm sand filter 6-157
6-60 Blast-actuated louver 6-158
6-61 Arrangement of multiple louvers for a large volume of air 6-159
6-62 Typical blast-actuated poppet valve 6-160
6-63 Time delay path 6-161

6-64 Idealized model of shock isolated mass 6-162
6-65 Shock isolation system 6-180
6-66 Base-mounted isolation systems configuration 6-181
6-67 Overhead pendulum shock isolation systems using platforms 6-182
6-68 Helical compression spring mounts 6-183
6-69 Typical torsion spring shock isolation system 6-184
6-70 Schematic of single and double action pneumatic cylinders 6-185
6-71 Schematic of liquid springs 6-186
6-72 Belleville springs 6-187

CHAPTER 1. INTRODUCTION

CHAPTER 1

INTRODUCTION

INTRODUCTION

1-1. Purpose

The purpose of this manual is to present methods of design for protective construction used in facilities for development, testing, production, storage, maintenance, modification, inspection, demilitarization, and disposal of explosive materials.

1-2. Objective

The primary objectives are to establish design procedures and construction techniques whereby propagation of explosion (from one structure or part of a structure to another) or mass detonation can be prevented and to provide protection for personnel and valuable equipment.

The secondary objectives are to:

(1) Establish the blast load parameters required for design of protective structures.
(2) Provide methods for calculating the dynamic response of structural elements including reinforced concrete, and structural steel.
(3) Establish construction details and procedures necessary to afford the required strength to resist the applied blast loads.
(4) Establish guidelines for siting explosive facilities to obtain maximum cost effectiveness in both the planning and structural arrangements, providing closures, and preventing damage to interior portions of structures because of structural motion, shock, and fragment perforation.

1-3. Background

For the first 60 years of the 20th century, criteria and methods based upon results of catastrophic events were used for the design of explosive facilities. The criteria and methods did not include a detailed or reliable quantitative basis for assessing the degree of protection afforded by the protective facility. In the late 1960's quantitative procedures were set forth in the first edition of the present manual, "Structures to Resist the Effects of Accidental Explosions". This manual was based on extensive research and development programs which permitted a more reliable approach to current and future design requirements. Since the original publication of this manual, more extensive testing and development programs have taken place. This additional research included work with materials other than reinforced concrete which was the principal construction material referenced in the initial version of the manual.

Modern methods for the manufacture and storage of explosive materials, which include many exotic chemicals, fuels, and propellants, require less space for a given quantity of explosive material than was previously needed. Such concentration of explosives increases the possibility of the propagation of accidental explosions. (One accidental explosion causing the detonation of

other explosive materials.) It is evident that a requirement for more accurate design techniques is essential. This manual describes rational design methods to provide the required structural protection.

These design methods account for the close-in effects of a detonation including the high pressures and the nonuniformity of blast loading on protective structures or barriers. These methods also account for intermediate and far-range effects for the design of structures located away from the explosion. The dynamic response of structures, constructed of various materials, or combination of materials, can be calculated, and details are given to provide the strength and ductility required by the design. The design approach is directed primarily toward protective structures subjected to the effects of a high explosive detonation. However, this approach is general, and it is applicable to the design of other explosive environments as well as other explosive materials as mentioned above.

The design techniques set forth in this manual are based upon the results of numerous full- and small-scale structural response and explosive effects tests of various materials conducted in conjunction with the development of this manual and/or related projects.

1-4. Scope

It is not the intent of this manual to establish safety criteria. Applicable documents should be consulted for this purpose. Response predictions for personnel and equipment are included for information.

In this manual an effort is made to cover the more probable design situations. However, sufficient general information on protective design techniques has been included in order that application of the basic theory can be made to situations other than those which were fully considered.

This manual is applicable to the design of protective structures subjected to the effects associated with high explosive detonations. For these design situations, the manual will apply for explosive quantities less than 25,000 pounds for close-in effects. However, this manual is also applicable to other situations such as far- or intermediate-range effects. For these latter cases the design procedures are applicable for explosive quantities in the order of 500,000 pounds which is the maximum quantity of high explosive approved for aboveground storage facilities in the Department of Defense manual, "Ammunition and Explosives Safety Standards", DOD 6055.9-STD. Since tests were primarily directed toward the response of structural steel and reinforced concrete elements to blast overpressures, this manual concentrates on design procedures and techniques for these materials. However, this does not imply that concrete and steel are the only useful materials for protective construction. Tests to establish the response of wood, brick blocks, and plastics, as well as the blast attenuating and mass effects of soil are contemplated. The results of these tests may require, at a later date, the supplementation of these design methods for these and other materials.

Other manuals are available to design protective structures against the effects of high explosive or nuclear detonations. The procedures in these manuals will quite often complement this manual and should be consulted for specific applications.

Computer programs, which are consistent with procedures and techniques contained in the manual, have been approved by the appropriate representative of the US Army, the US Navy, the US Air Force and the Department of Defense Explosives Safety Board (DDESB). These programs are available through the following repositories:

(1) Department of the Army
Commander and Director
U.S. Army Engineer
Waterways Experiment Station
Post Office Box 631
Vicksburg, Mississippi 39180-0631
Attn: WESKA

(2) Department of the Navy
Commanding Officer
Naval Civil Engineering Laboratory
Port Hueneme, California 93043
Attn: Code L51

(3) Department of the Air Force
Aerospace Structures
Information and Analysis Center
Wright Patterson Air Force Base
Ohio 45433
Attn: AFFDL/FBR

If any modifications to these programs are required, they will be submitted for review by DDESB and the above services. Upon concurrence of the revisions, the necessary changes will be made and notification of the changes will be made by the individual repositories.

1-5. Format

This manual is subdivided into six specific chapters dealing with various aspects of design. The titles of these chapters are as follows:

Chapter 1	Introduction
Chapter 2	Blast, Fragment, and Shock Loads
Chapter 3	Principles of Dynamic Analysis
Chapter 4	Reinforced Concrete Design
Chapter 5	Structural Steel Design
Chapter 6	Special Considerations in Explosive Facility Design

When applicable, illustrative examples are included in the Appendices.

Commonly accepted symbols are used as much as possible. However, protective design involves many different scientific and engineering fields, and, therefore, no attempt is made to standardize completely all the symbols used. Each symbol is defined where it is first used, and in the list of symbols at the end of each chapter.

CHAPTER CONTENTS

1-6. General

This chapter presents a qualitative description of an explosive protective system, and addresses acceptor system tolerances, and the basis for structural design.

SAFETY FACTOR

1-7. Safety Factor

Simplifications leading to safety conservative structural designs are made in the design procedures of this manual. However, unknown factors can still cause an overestimation of a structure's capacity to resist the effects of an explosion. Unexpected shock wave reflections, construction methods, quality of construction materials, etc., vary for each facility. To compensate for such unknowns it is recommended that the TNT equivalent weight be increased by 20 percent. This increased charge weight is the "effective charge weight" to be used for design. Departures from this recommendation must be approved by the responsible agency.

All charts pertaining to explosive output in this manual are for readings at sea level.

EXPLOSION PROTECTION SYSTEM

1-8. System Components

1-8.1. General

Explosive manufacturing and storage facilities are constructed so that they provide a predetermined level of protection against the hazards of accidental explosions. These facilities consist of three components: (1) the donor system (amount, type and location of the potentially detonating explosive) which produces the damaging output, (2) the acceptor system (personnel, equipment, and "acceptor" explosives) which requires protection, and (3) the protection system (protective structure, structural components or distance) necessary to shield against or attenuate the hazardous effects to levels which are tolerable to the acceptor system. The flow chart in Figure 1-1 briefly summarizes the protective system and relates the individual components to each other.

1-8.2. Donor System

The donor system includes the type and amount of the potentially detonating explosive as well as materials which, due to their proximity to the explosive, become part of the damaging output. The output of the donor explosive includes blast overpressures (hereafter referred to as blast pressures or pressures), primary fragments resulting from cased explosives and secondary fragments resulting from materials in the immediate vicinity of the donor explosive. Other effects from the donor include ground shock, fire, heat, dust, electromagnetic pulse, etc. For the quantities of explosives considered in this manual, blast pressures constitute the principal parameter governing the design of protective structures. However, in some situations, primary

and/or secondary fragments and ground shock may assume equal importance in the planning of the protection system. The other effects mentioned are usually of concern in specific types of facilities, and their influence on the overall design can usually be met with the use of standard engineering design procedures. Except for very large quantities of explosives, ground shock effects will usually be small and, in most cases, will be of concern when dislodging of components within the protective structure is possible.

The chemical and physical properties of the donor explosive determine the magnitude of the blast pressures whereas the distribution of the pressure pattern is primarily a function of the location of the donor explosive relative to the components of the protective facility. The mass-velocity properties of the primary fragments depend upon the properties of the donor explosive and the explosive casing, while, for secondary fragments, their mass-velocity properties are functions of the type of fragment materials (equipment, frangible portions of the structure, etc.), their relative position to the donor explosive, and the explosive itself.

The explosive properties, including the molecular structure (monomolecular, bimolecular, etc.) of the explosive, shape and dimensional characteristics, and the physical makeup (solid, liquid, gas) of the charge, determine the limitation of the detonation process. These limitations result in either a high- or low-order detonation. With a high-order detonation, the process is generally complete and results in the maximum pressure output for the given type and amount of material. On the other hand, if the detonation is incomplete with the initial reaction not proceeding through the material mass, then a large quantity of the explosive is consumed by deflagration and the blast pressure is reduced.

Primary fragments are produced by the explosion of a cased donor charge. They result from the shattering of a container which is in direct contact with the explosive material. The container may be the casing of conventional munitions, the kettles, hoppers, and other metal containers used in the manufacture of explosives, the metal housing of rocket engines, etc. Primary fragments are characterized by very high initial velocities (in the order of thousands of feet per second), large numbers of fragments, and relatively small sizes. The heavier fragments may penetrate a protective element depending upon its composition and thickness. The lighter fragments seldom achieve perforation. However, in certain cases, primary fragments may ricochet into the protected area and cause injury to personnel, damage to equipment, or propagation of acceptor explosives. For protection against primary fragments, sufficient structural mass must be provided to prevent full penetration, and the configuration of the components of the protective facility must prevent fragments from ricocheting into protected areas.

Secondary fragments are produced by the blast wave impacting objects located in the vicinity of the explosive source. At these close distances, the magnitude of the shock load is very high and objects can be broken up and/or torn loose from their supports.

Pieces of machinery, tools, materials such as pipes and lumber, parts of the structure (donor structure) enclosing the donor explosive, large pieces of equipment, etc. may be propelled by the blast. Secondary fragments are characterized by large sizes (up to hundreds of pounds) and comparatively low velocities (hundreds of feet per second). These fragments may cause the same

damage as primary fragments, that is, injury to personnel, damage to equipment or detonation of acceptor explosives. However, protection against secondary fragments is slightly different than for primary fragments. While preventing perforation by primary fragments is important, secondary fragments pose additional problems due to their increased weight. The protective structure must be capable of resisting the large impact force (momentum) associated with a large mass travelling at a relatively high velocity.

1-8.3. Acceptor System

The acceptor system is composed of the personnel, equipment, or explosives that require protection. Acceptable injury to personnel or damage to equipment, and sensitivity of the acceptor explosive(s), establishes the degree of protection which must be provided by the protective structure. The type and capacity of the protective structure are selected to produce a balanced design with respect to the degree of protection required by the acceptor and the hazardous output of the donor.

Protection in the immediate vicinity of the donor explosive is difficult because of high pressures, ground shock, fire, heat, and high speed fragments generally associated with a detonation. Protection can be afforded through the use of distance and/or protective structures. Personnel may be subjected to low blast pressures and/or small ground motions without direct injury. However, injury can be sustained by falling and impacting hard surfaces.

In most explosive processing facilities, equipment is expendable and does not require protection. Equipment which is very expensive, difficult to replace in a reasonable period of time, and/or must remain functional to insure the continuous operation of a vital service may require protection. The degree of protection will vary depending upon the type and inherent strength of the equipment. In general, equipment and personnel are protected in a similar manner. However, equipment can usually sustain higher pressures than personnel, certain types of equipment may be able to withstand fragment impact whereas personnel can not, and lastly, equipment can sustain larger shock loads since it can be shock isolated and/or secured to the protective structure.

The degree of protection for acceptor explosives range from full protection to allowable partial or total collapse of the protective structure. In order to prevent detonation, sensitive acceptor explosives must be protected from blast pressures, fragment impact, and ground shock whereas "insensitive" explosives may be subjected to these effects in amounts consistent with their tolerance. The tolerances of explosives to initial blast pressures, structural motions, and impact differ for each type of explosive material with pressure being the lesser cause of initiation. Impact loads are the primary causes of initiation of acceptor explosives. They include primary and secondary fragment impact as well as impact of the explosive against a hard surface in which the explosive is dislodged from its support by pressure or ground shock and/or propelled by blast pressures.

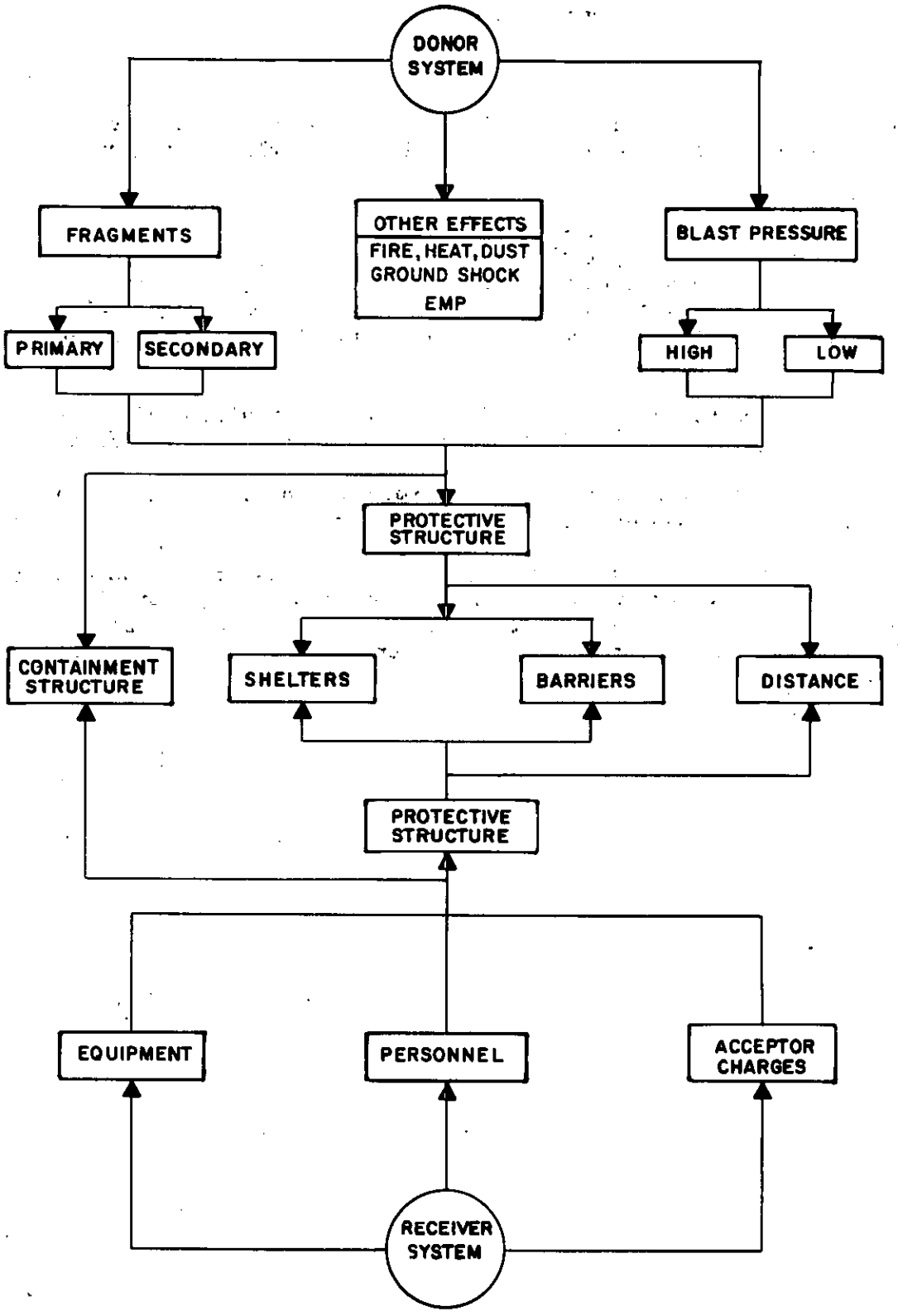


Figure 1-1 Explosive protective system

PROTECTION CATEGORIES

1-9. Protection Categories

For the purpose of analysis, the protection afforded by a facility or its components can be subdivided into four protection categories as described below:

1. Protection Category 1 - Protect personnel against the uncontrolled release of hazardous materials, including toxic chemicals, active radiological and/or biological materials; attenuate blast pressures and structural motion to a level consistent with personnel tolerances; and shield personnel from primary and secondary fragments and falling portions of the structure and/or equipment;

2. Protection Category 2 - Protect equipment, supplies and stored explosives from fragment impact, blast pressures and structural response;

3. Protection Category 3 - Prevent communication of detonation by fragments, high-blast pressures, and structural response; and

4. Protection Category 4 - Prevent mass detonation of explosives as a result of subsequent detonations produced by communication of detonation between two adjoining areas and/or structures. This category is similar to Category 3 except that a controlled communication of detonation is permitted between defined areas.

ACCEPTOR SYSTEMS TOLERANCES

1-10. Protective Systems

1-10.1. Protective Structures

Personnel, equipment or explosives are protected from the effects of an accidental explosion by the following means: (1) sufficient distance between the donor and acceptor systems to attenuate the hazardous effects of the donor to a level tolerable to the acceptor, (2) a structure to directly protect the acceptor system from the hazardous output of the donor system, (3) a structure to fully contain or confine the hazardous output of the donor system, and (4) a combination of the above means. While large distances may be used to protect acceptor systems, a protective facility is the most common method employed when limited area is available. In general, separation distances are used as a means of attenuating the hazardous effects of the donor to a level which makes the design of a protective facility feasible, practical and cost effective.

Protective structures can be classified as shelters, barriers or containment structures. Protection is provided by each structure in three distinct manners. Shelters are structures that fully enclose the acceptor system with hardened elements. These elements provide direct protection against the effects of blast pressures, primary and secondary fragments and ground shock. Containment structures are buildings which fully or near fully enclose the donor system with hardened elements. They protect the acceptor system by confining or limiting the damaging output of the donor system. A barrier acts as a shield between the donor and acceptor systems. They attenuate the damaging output of the donor system to a level which is tolerable to the acceptor system.

Shelters are fully enclosed structures and are used to protect personnel from injury, prevent damage to valuable equipment, and prevent detonation of sensitive explosives. The exterior of the structure is composed of hardened elements which must be designed to resist the effects of blast pressures and both primary and secondary fragment impact and the interior must be arranged to shock isolate the acceptor system. Entrances must be sealed by blast doors, and depending upon the amount of usage and/or the potential explosive hazard, may also require blast locks (an entrance containing a blast door followed by a second blast door; one of which is always closed). Other openings required for facility operations, such as ventilation passages, equipment access openings, etc., may be sealed by blast valves or blast shields. Design criteria for these protective closures are governed by their size and location and the magnitude of the blast pressure and fragment effects acting on them. Small openings may be permitted if the magnitude and rate of pressure buildup within the structure is tolerable to the occupants and contents of the shelter. Specific provisions may also be necessary to insure that partitions, hung ceilings, lighting fixtures, equipment, mechanical and electrical fixtures, piping, conduits, etc., are not dislodged as a result of structure motions or leakage pressures and become a hazard to the building's occupants and contents.

Barriers are generally used to prevent propagation of explosions. They act as a shield between two or more potentially detonating explosives. Their main purpose is to stop high speed fragments from impacting acceptor explosives.

In addition, they reduce secondary fragments striking the acceptor. They can also reduce blast pressures in the near range (at a distance up to ten times barrier height) but have little or no effect on the far range. Barriers can be either barricades (revetted or unrevetted earth barricades), simple cantilever walls, etc., or cubicle-type structures where one or more sides and/or the roof are open to the atmosphere or enclosed by frangible elements. Igloos (earth covered magazines), below ground silos, and other similar structures with open or frangible surfaces can also be classified as barriers. They are usually used in storage, manufacturing, or processing of explosives or explosive materials. The explosives are usually located close to the protective element. Consequently, the barrier is subjected to high intensity blast loads and the acceptor explosive is subjected to comparatively high leakage pressures.

Containment structures are generally used for high hazard operations and/or operations involving toxic materials. These operations must be remotely controlled since operating personnel should not be located within the structure during hazardous operation. All entrances must be sealed with blast doors. Other openings required for facility operations such as ventilation passages, equipment and/or product access openings, etc., must be sealed by blast valves or blast shields. For operations not involving toxic materials, blast pressures may be released to the atmosphere. However, this pressure release must be controlled both in magnitude and direction either by mechanical means (through blast valves or shields) or by limiting the size of the openings and/or directing the leakage pressures to areas where personnel, equipment and acceptor explosives will be protected.

The various components of a protective facility must be designed to resist the effects of an explosion. The exterior walls and roof are the primary protective elements. These elements are said to be "hardened" if they are designed to resist all the effects associated with an explosion (blast pressures, primary and secondary fragments, structure motions). On the other hand, a blast resistant element is designed to resist blast pressure only. While a blast resistant element is not designed specifically to resist fragments, the element has inherent fragment resistance properties which increases with increasing blast resistant capabilities. In many parts of this manual, the term "blast resistant" is used synonymously with "hardened."

1-10.2. Containment Type Structures

The first three protection categories can apply to structures classified as containment structures when these structures are designed to prevent or limit the release of toxic or other hazardous materials to a level consistent with the tolerance of personnel. These structures generally are designed as donor structures and can resist the effects of "close-in" detonations (detonations occurring close to the protective structures). Added protection is accomplished by minimizing the pressure leakage to the structures exteriors, by preventing penetration to the exterior of the structure by primary fragments and/or formation of fragments from the structure itself. Quite often, containment structures may serve as a shelter as described below. Procedures for designing reinforced concrete containment structures are contained in Chapter 4. A design ratio of weight to volume of $W/V < .15$ lb/ft^3 is a practical range for reinforced concrete containment structures.

1-10.3. Shelters

The first three protection categories apply to shelters which provide protection for personnel, valuable equipment, and/or extremely sensitive explosives. Shelters, which are usually located away from the explosion, accomplish this protection by minimizing the pressure leakage into a structure, providing adequate support for the contents of the structure, and preventing penetration to the interior of the structure by high-speed primary fragments, and/or by the impact of fragments formed by the breakup of the donor structure. Protection against the uncontrolled spread of hazardous material is provided by limiting the flow of the dangerous materials into the shelter using blast valves, filters, and other means. Procedures for designing concrete and structural steel buildings are contained in Chapters IV and V, respectively.

1-10.4. Barriers

Although the first three protection categories of protection can be achieved with the use of a shelter, the last two protection categories (para. 1-9) pertain to the design of barriers where protection of explosives from the effects of blast pressures and impact by fragments must be provided. For the third protection category, the explosion must be confined to a donor cell, whereas in the fourth protection category, propagation between two adjoining areas is permitted. However, the communication of detonation must not extend to other areas of the facility. This situation may arise in the event of the dissimilarity of construction and/or explosive content of adjacent areas. Procedures for designing reinforced concrete barriers are contained in Chapter 4.

1-11. Human Tolerance

1-11.1. Blast Pressures

Human tolerance to the blast output of an explosion is relatively high. However, the orientation of a person (standing, sitting, prone, face-on or side-on to the pressure front), relative to the blast front, as well as the shape of the pressure front (fast or slow rise, stepped loading), are significant factors in determining the amount of injury sustained. Shock tube and explosive tests have indicated that human blast tolerance varies with both the magnitude of the shock pressure as well as the shock duration, i.e., the pressure tolerance for short-duration blast loads is significantly higher than that for long-duration blast loads.

Tests have indicated that the air-containing tissues of the lungs can be considered as the critical target organ in blast pressure injuries. The release of air bubbles from disrupted alveoli of the lungs into the vascular system probably accounts for most deaths. Based on present data, a tentative estimate of man's response to fast rise pressures of short duration (3 to 5 ms.) is presented in Figure 1-2. The threshold and severe lung-hemorrhage pressure levels are 30 to 40 psi and above 80 psi, respectively, while the threshold for lethality due to lung damage is approximately 100 to 120 psi (Table 1-1). On the other hand, the threshold pressure level for petechial hemorrhage resulting from long-duration loads may be as low as 10 to 15 psi, or approximately one-third that for short duration blast loads. Since survival is dependent on the mass of the human, the survival for babies will be different than the survival for small children which will be different from

that for women and men. These differences have been depicted in Figure 1-2 which indicates that the survival scaled impulse depends on the weight of the human. It is recommended that 11 lb. be used for babies, 55 lb. for small children, 121 lb. for adult women and 154 lb. for adult males.

A direct relationship has been established between the percentage of ruptured eardrums and maximum pressure, i.e., 50 percent of exposed eardrums rupture at a pressure of 15 psi for fast rising pressures while the threshold of eardrums rupture for fast rising pressure is 5 psi. Temporary hearing loss can occur at pressure levels less than that which will produce onset of eardrum rupture. This temporary hearing loss is a function of the pressure and impulse of a blast wave advancing normal to the eardrum. The curve which represents the case where 90 percent of those exposed are not likely to suffer an excessive degree of heating loss, is referred to as the temporary threshold shift. The pressures referred to above are the maximum effective pressures, that is, the highest of either the incident pressure, the incident pressure plus the dynamic pressures, or the reflected pressure. The type of pressure which will be the maximum effective depends upon the orientation of the individual relative to the blast as well as the proximity of reflecting surfaces and the occurrence of jetting effects which will cause pressure amplification as the blast wave passes through openings. As an example, consider the pressure level which will cause the onset of lung injury to personnel in various positions and locations. The threshold would be 30 to 40 psi reflected pressure for personnel against a reflector (any position), 30 to 40 psi incident plus dynamic pressure; 20 to 25 psi would be the incident pressure plus 10 to 15 psi dynamic pressure for personnel in the open, either standing or prone-side-on, and 30 to 40 psi incident pressure for personnel in the open in a prone-end-on position.

However, the above pressure level assumes that an individual is supported and will not be injured due to being thrown off balance and impacting a hard and relatively non-yielding surface. In this case, pressure levels which humans can withstand are generally much lower than those causing eardrum or lung damage. For this case, one publication has recommended that tolerable pressure level of humans not exceed 2.3 psi which is higher than temporary threshold shift of temporary hearing loss (Figure 1-3) and probably will cause personnel, which are located in the open, to be thrown off balance.

Structures can be designed to control the build-up of internal pressure, however, jetting effect produced by pressure passing through an opening can result in amplification of the pressures at the interior side of the opening. The magnitude of this increased pressure can be several times as large as the maximum average pressure acting on the interior of the structure during the passage of the shock wave. Therefore, openings where jetting will occur should not be directed into areas where personnel and valuable equipment will be situated.

1-11.2. Structural Motion

It is necessary that human tolerance to two types of shock exposure be considered:

1. Impacts causing body acceleration/deceleration, and

2. Body vibration as a result of the vibratory motion of the structure.

If a subject is not attached to the structure, he may be vulnerable to impact resulting from collision with the floor due to the structure dropping out beneath him and/or the structure rebounding upward towards him. However, the more plausible means of impact injury results from the subject being thrown off balance because of the horizontal motions of the structure, causing him to be thrown bodily against other persons, equipment, walls and other hard surfaces.

Studies have indicated that a probable safe impact tolerance velocity is 10 fps. At 18 fps there is a 50 percent probability of skull fracture and at 23 fps, the probability is nearly 100 percent. This applies to impact with hard, flat surfaces in various body postures. However, if the line of thrust for head impact with a hard surface is directly along the longitudinal axis of the body (a subject falling head first), the above velocity tolerance does not apply since the head would receive the total kinetic energy of the entire body mass. Impacts with corners or edges are also extremely critical even at velocities less than 10 fps. An impact velocity of 10 fps is considered to be generally safe for personnel who are in a fairly rigid posture; therefore, greater impact velocities can be tolerated if the body is in a more flexible position or if the area of impact is large.

The effect of horizontal motion on the stability of personnel (throwing them off balance or hurling them laterally) depends on the body stance and position, the acceleration intensity and duration, and the rate of onset of the acceleration. An investigation of data concerning sudden stops in automobiles and passenger trains indicates that personnel can sustain horizontal accelerations less than 0.44 g without being thrown off balance. These accelerations have durations of several seconds; hence, the accelerations considered in this manual required to throw personnel off balance are probably greater because of their shorter durations. Therefore, the tolerable horizontal acceleration of 0.50 g required to provide protection against ground-shock effects resulting from nuclear detonations should be safe for non-restrained personnel (standing, sitting, or reclining).

If the vertical downward acceleration of the structure is greater than 1 g, relative movement between the subject and the structure is produced. As the structure drops beneath him, the subject begins to fall until such time that the structure slows down and the free falling subject overtakes and impacts with the structure. The impact velocity is equal to the relative velocity between the structure and the subject at the time of impact, and to assure safety, it should not exceed 10 fps.

To illustrate this vertical impact, a body which free falls for a distance equal to 1.5 feet has a terminal or impact velocity of approximately 10 fps against another stationary body. If the impacted body has a downward velocity of 2 fps at the time of impact, then the impact velocity between the two bodies would be 8 fps.

Based on the available personnel vibration data, the following vibrational tolerances for restrained personnel are considered acceptable: 2g for less than 10 Hz, 5g for 10-20 Hz, 7g for 20-40 Hz; and 10g above 40 Hz. However, the use of acceleration tolerances greater than 2g usually requires restrain-

ing devices too elaborate for most explosive manufacturing and testing facilities.

1-11.3. Fragments

Overall, human tolerance to fragment impact is very low; however, certain protection can be provided with shelter type structures. Fragments can be classified based on their size, velocity, material and source, i.e.:

1. Primary fragments, which are small, high-speed missiles usually formed from casing and/or equipment located immediately adjacent to the explosion, and

2. Secondary fragments, which are generated from the breakup of the donor building, equipment contained within the donor structure and/or acceptor buildings which are severely damaged by an explosion.

Discussion of human tolerance of both of these types of fragment overlap, since the basic differences between these fragments are their size and velocity. Impact of primary fragments can be related to an impact by bullets where the fragment is generally small, usually of metal and traveling at high velocities. A great deal of research has been conducted for the military; however, most of the data from these tests is not available. Some fragment-velocity penetration data of humans has been developed for fragment weights equal to or less than 0.033 pounds, and indicates that, as the ratio of the fragment area to weight increases, the velocity which corresponds to a 50 percent probability of penetrating human skin will increase. This trend is illustrated in Table 1-2 where the increase in velocity coincides with the increase of area of the fragment.

Secondary fragments, because they have a large mass, will cause more serious injuries at velocities significantly less than caused by primary fragments. Table 1-3 indicates the velocity which corresponds to the threshold of serious human injury. As mentioned in 1-11.2 above, the impact of a relatively large mass with a velocity less than 10 fps against a human can result in serious bodily injury. Also, the impact of smaller masses (Table 1-3) with higher velocities can result in injuries as severe as those produced by larger masses. See applicable Safety Manual for fragment criteria.

1-12. Equipment Tolerance

1-12.1. Blast Pressures

Unless the equipment is of the heavy-duty type (motor, generators, air handlers, etc.), equipment to be protected from blast pressures must be housed in shelter-type structures similar to those required for the protection of personnel. Under these circumstances, the equipment will be subjected to blast pressures which are permitted to leak into the shelter through small openings. If the magnitude of these leakage pressures is minimized to a level consistent with that required for personnel protection, then in most cases protection from the direct effects of the pressures is afforded to the equipment. However, in some instances, damage to the equipment supports may occur which, in turn, can result in damage to the equipment as a result of falling. Also, if the equipment is located immediately adjacent to the shelter open-

ings, the jetting effects of the pressures entering the structure can have adverse effects on the equipment. In general, equipment should be positioned away from openings and securely supported. However, in some cases, equipment such as air handling units must be positioned close to the exterior openings. In this event, the equipment must be strong enough to sustain the leakage pressures (pressures leaking in or out of openings) or protective units such as blast valves must be installed.

1-12.2. Structural Motion and Shock

Damage to equipment can result in failures which can be divided into two classes; temporary and permanent. Temporary failures, often called "malfunctions," are characterized by temporary disruption of normal operation, whereas permanent failures are associated with breakage, resulting in damage so severe that the ability of the equipment to perform its intended function is impaired permanently or at least over a period of time.

The capacity of an item of equipment to withstand shock and vibration is conventionally expressed in terms of its "fragility level" which is defined as the magnitude of shock (acceleration) that the equipment can tolerate and still remain operational. The fragility level for a particular equipment item is dependent upon the strength of the item (frame, housing, and components) and, to some extent, the nature of the excitation to which it is subjected. An equipment item may sustain a single peak acceleration due to a transient input load, but may fail under a vibration-type input having the same peak acceleration amplitude. Also the effects of the occurrence of resonance may be detrimental to the item functioning. For these reasons, fragility data should be considered in connection with such factors as the natural frequencies and damping characteristics of the equipment and its components, as well as the characteristics of the input used to determine the tolerance as compared to the motion of the structure which will house the equipment.

The maximum shock tolerances for equipment vary considerably more than those for personnel. To establish the maximum shock tolerance for a particular item, it is necessary to perform tests and/or analyses. Only selected items of equipment have been tested to determine shock tolerances applicable for protection from the damage which may be caused by structural motions.

Most of this data resulted from tests to sustain ground-shock motions due to a nuclear environment, which will have a duration considerably longer than that associated with a HE explosion. However, the data which are available concerning shock effects indicate strength and ruggedness or sensitivity of equipment. These data, which are based primarily on transportation and conventional operational shock requirements, indicate that most commercially available mechanical and electrical equipment are able to sustain at least 3g's, while fragile equipment (such as electronic components) can sustain approximately 1.5g's.

The above tolerances are safe values, and actual tolerances are, in many cases, higher than 3g's, as indicated in Table 1-4. However, the use of such acceleration values for particular equipment require verification by shock testing with the induced motions (input) consistent with expected structural motions.

The above tolerances are applicable to equipment which is mounted directly to the sheltering structure. For the equipment to sustain shock accelerations in the order of magnitude of their tolerances, the equipment item must be "tied" down to the structure, that is, the equipment stays attached to the structure and does not impact due to its separation. In most cases, shock isolation systems will be needed to protect the equipment items. The shock isolation systems will consist of platforms which are supported by a spring assembly for large motion and/or cushioning material when the motions are small. These systems should be designed to attenuate the input accelerations to less than 1g in order that separation between the equipment and support system does not occur. If the spring systems are designed to be "soft" (less than 1/2 g) then, depending on the mass of the equipment, vibratory action of the system could occur due to individuals walking on the platforms.

1-12.3. Fragments

Susceptibility of an item of equipment to damage from fragment impact depends upon the ruggedness of its components, its container, if any, and upon the size and velocity of the fragment at the time of impact.

Some heavy equipment (motors, generators, etc.) may sustain malfunctions as a result of the severing of electrical or mechanical connections, but seldom are destroyed by the impact of primary fragments. On the other hand, this heavy equipment can be rendered useless by secondary fragment impact. Fragile equipment (electronic equipment, etc.) will generally be inoperable after the impact of either primary or secondary fragments. The impact force and penetration capability of light fragments may perforate sensitive portions of heavy equipment (fuel tank of generators, etc.). Low-velocity light fragments seldom result in severe damage. These fragments usually ricochet beyond the equipment unless the component part of the equipment it strikes is glass or other fragile material, in which case, some damage may be inflicted.

Although the damage to the equipment of a structure can be great as a result of falling or flying debris, the increased cost of strengthening walls and other portions of the protective shelter is usually not warranted unless personnel or acceptor charge protection is also required and/or the cost of the equipment item lost exceeds the increased construction costs. Even in this latter situation, a probability analysis of the occurrence of an incident should be made prior to incurring additional construction costs.

1-13. Tolerance of Explosives

1-13.1. General

The tolerances of explosives to blast pressure, structural motion, and impact by fragments differ for each type of explosive material and/or item. Generally, fragment impact is the predominant cause of detonation propagation.

1-13.2. Blast Pressures

Except in regions of extremely high pressure, most explosive materials are insensitive to the effects of blast pressures. In many instances, however, the secondary effects, such as dislodgement of the explosive from its support and propulsion of the explosive against hard surfaces, can result in a possible detonation depending upon the tolerance of the explosive to impact.

Results of several different types of sensitivity tests (drop test, card gap tests, friction tests, etc.) are presently available which will aid in the establishment of the tolerances of most explosive materials to impact.

1-13.3. Structural Motions

Structural motion effects on explosives are similar to the impact effects produced by blast pressures. The movement of the structure tends to dislodge the explosive from its support, resulting in an impact of the explosive with the floor or other parts of the structure. The distance the explosive falls and its sensitivity to impact and friction determine whether or not propagation occurs.

1-13.4. Fragments

Although blast pressures and structural motions can produce explosive propagation, the main source of communication of explosions is by fragments, principally primary fragments from the breakup of the donor charge casing, fragments produced by the fracture of equipment close to the explosion, disengagement of interior portions of the structure, and/or failure of the structure proper.

In recent years, an extensive test program has been performed which has provided a significant amount of information regarding explosive propagation by primary fragment impact. This program was conducted primarily to determine safe separation criteria for bulk explosives and munitions, mainly for the design and operation of conveyance systems. The individual test programs were predicated upon given manufacturing operations where improved safety criteria would lessen the probability of a catastrophic event. Individual test programs were performed in two stages, exploratory and confirmatory, where the safe separation was determined during the exploratory phase and confirmation was established on a 95 percent confidence level.

A typical test set-up is illustrated in Figure 1-4, while the results of the various test programs are listed in Table 1-5 for bulk explosives and in Table 1-6 for munitions. These Tables list the bulk explosives and munition types, the configurations examined and the established safe separation distances. For all items/configurations examined, unless specified, the test conditions were: 1) in free air (without tunnels), 2) open spaced (no shields), 3) in a vertical orientation, and 4) measured edge-to-edge. Inspection of Tables 1-5 and 1-6 reveal that minimum safe separation distances have not been established for some of the items listed. If specific safe separation distances are required, as will be for other items not listed, further tests will be required. A detailed compilation of the items and test procedures and methods are listed in the bibliography.

Several testing methods have been developed to determine the sensitivity of explosives to impact by secondary fragments. In one series of tests which utilized a catapult method for propelling approximately 70 pounds of concrete fragments, sand and gravel rubble, against lightly cased Composition B acceptor explosives indicated a boundary velocity on the order of approximately 400 fps. A second series of tests, which propelled concrete fragments as large as 1000 pounds against 155 mm projectiles (thick steel wall projectile), indicated that the projectile would not detonate with striking velocities of 500 fps. This latter test series also included acceptor items consisting of 155 projectiles with thin wall riser funnels, which detonated upon impact with the

concrete. Another series of fragment testing included the propelling of large concrete fragments against thin wall containers with molten explosive simulating typical melt-pour kettles in a loading plant. In all cases, the contents of the simulated kettle detonated. Although the results of these test series indicated that thick wall containers of explosive will prevent propagation, while thin wall containers will not, the number of tests performed in each series was relatively few. Additional tests are required to determine the extent that the variation of container thickness has on the magnitude of the mass/velocity boundary established to date.

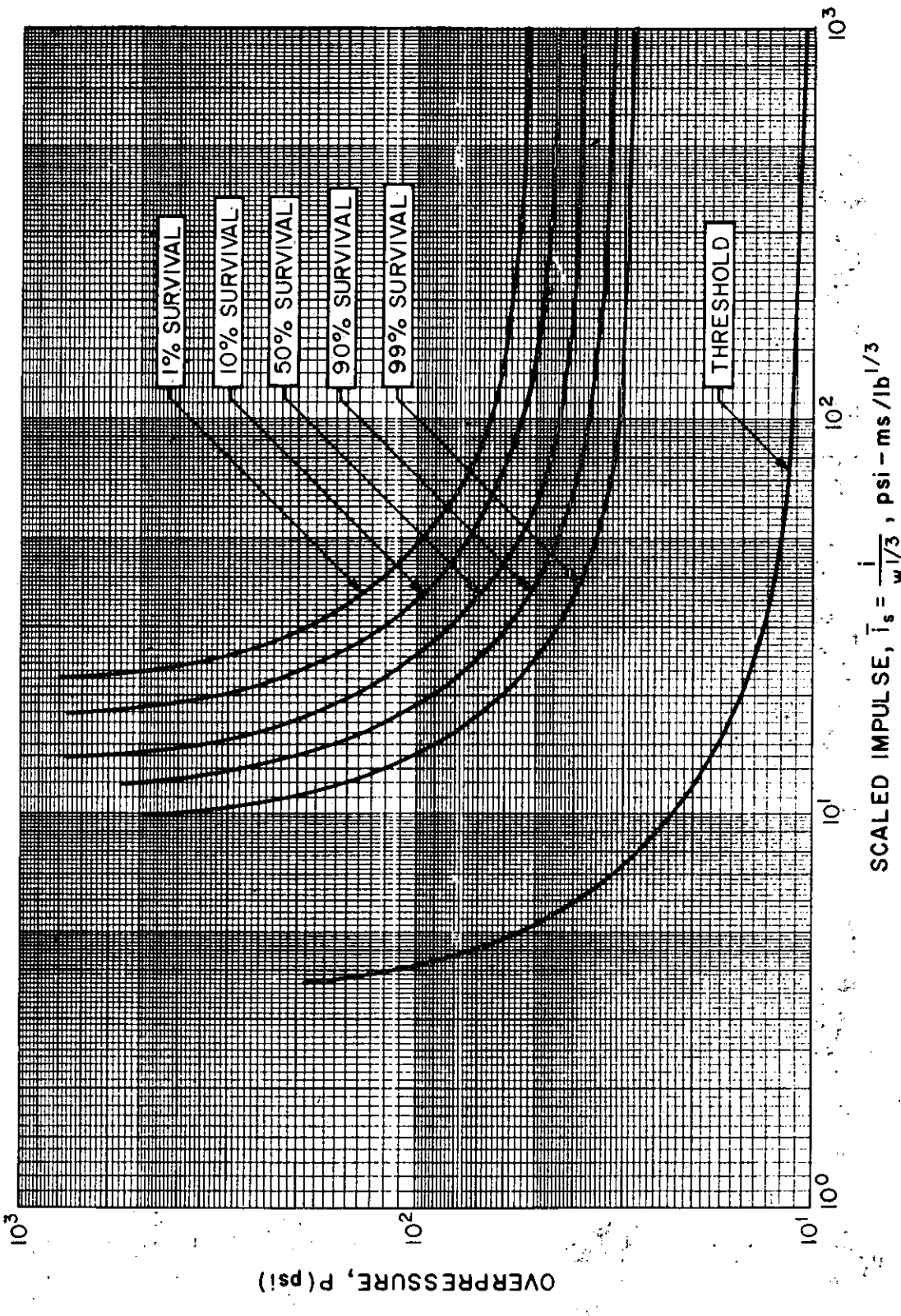


Figure 1-2 Survival curves for lung damage

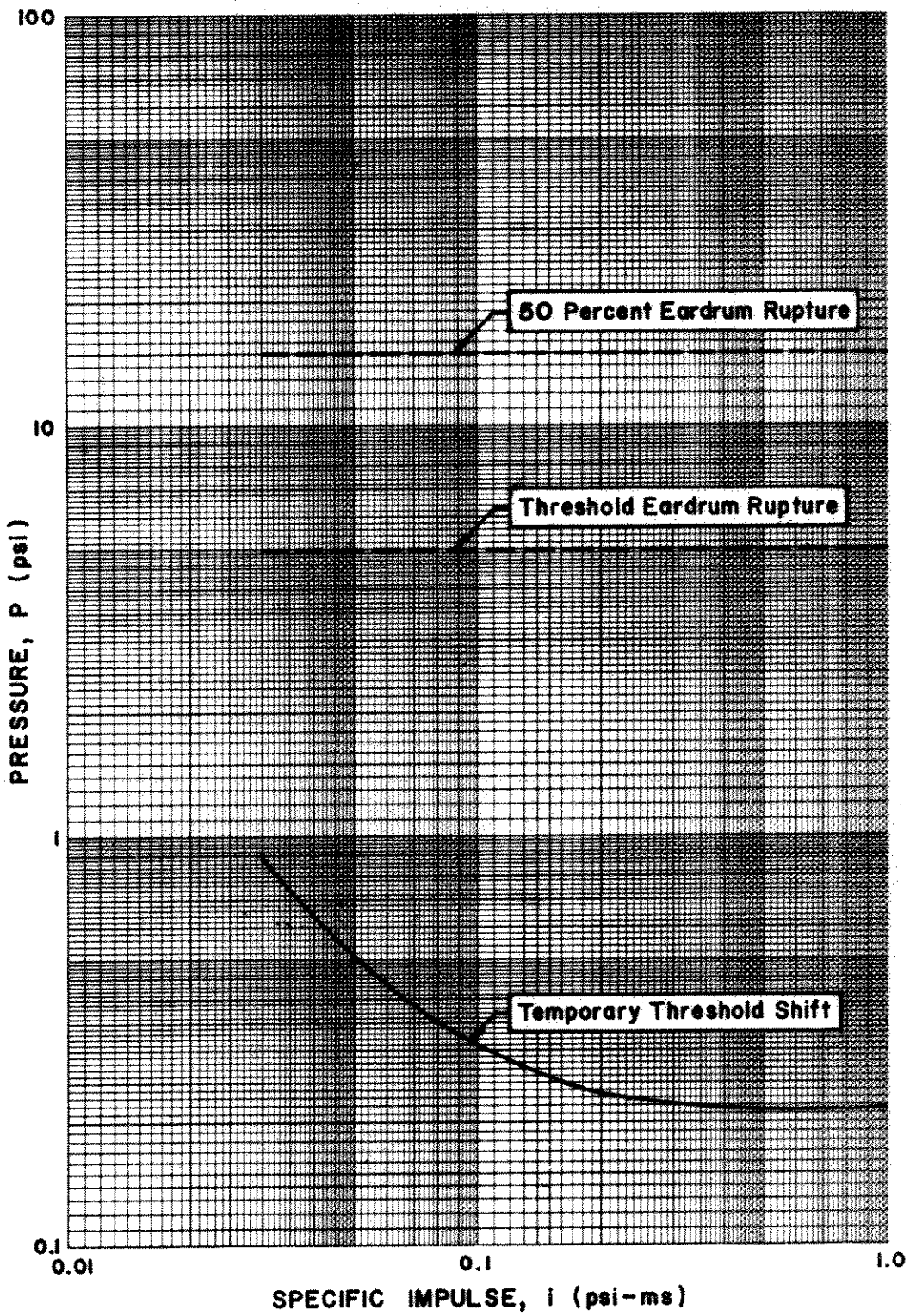


Figure 1-3 Human ear damage due to blast pressures

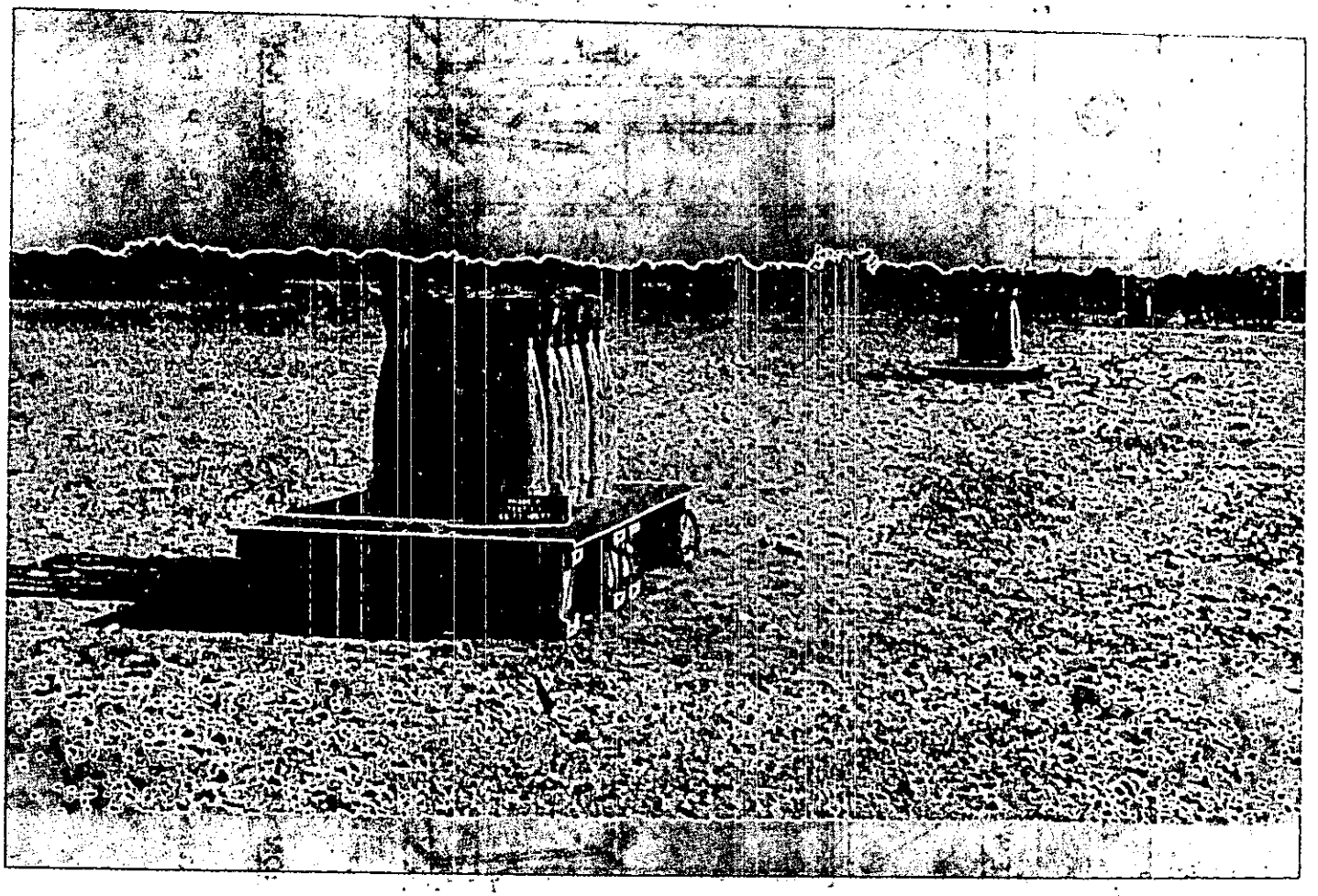


Figure 1-4 Example of safe separation tests

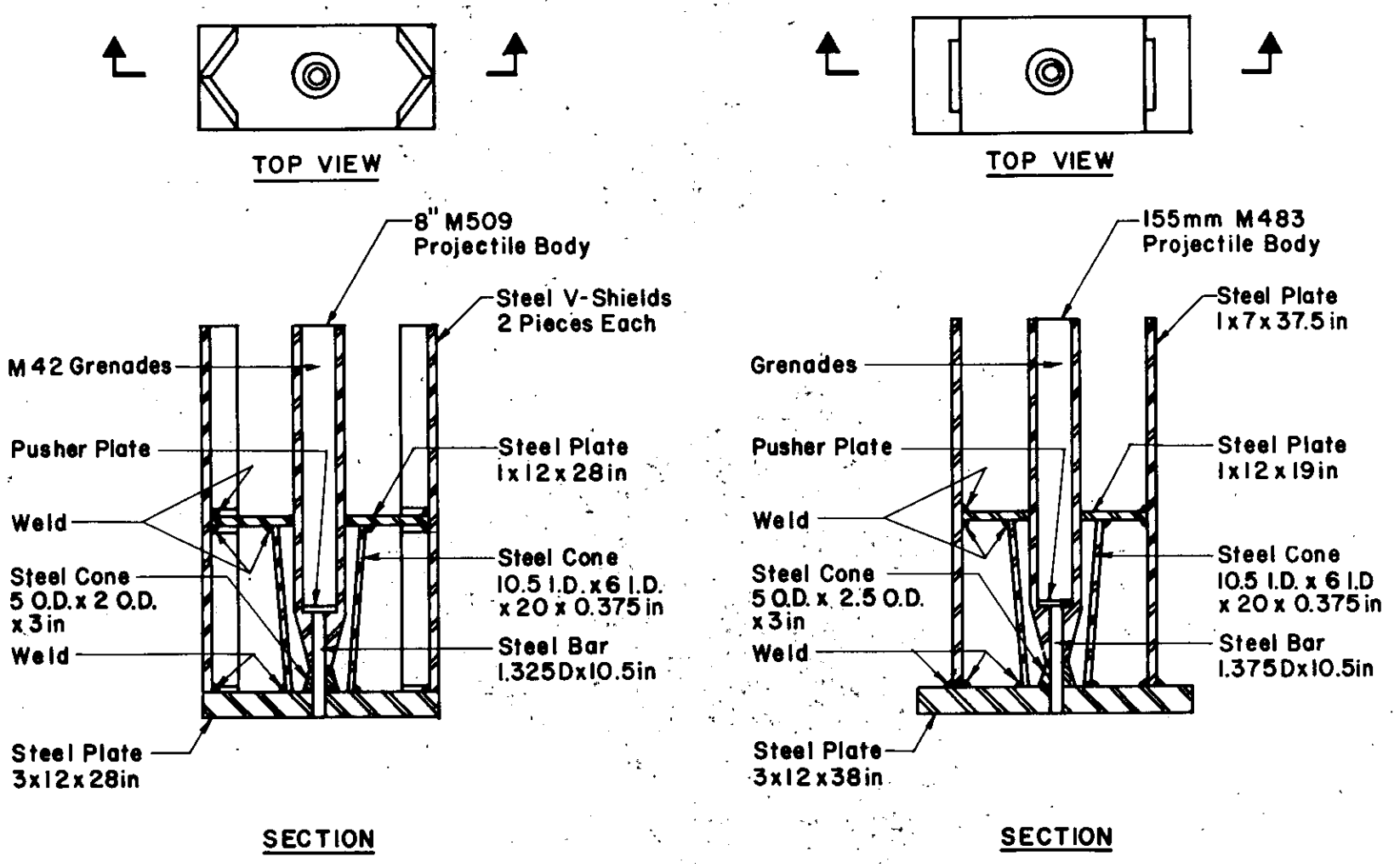


Figure I-5 Safe separation test shields

Table 1-1 Blast Effects in Man Applicable to Fast-Rising Air Blasts of Short Duration (3-5 ms.)

Critical Organ or Event	Maximum Effective Pressure (psi)*
Eardrum Rupture	
Threshold	5
50 percent	15
Lung Damage:	
Threshold	30-40
50 percent	80 and above
Lethality	
Threshold	100-120
50 percent	130-180
Near 100 percent	200-250

* Maximum effective pressure is the highest of incident pressure, incident pressure plus dynamic pressure, or reflected pressure.

Table 1-2 50 Percent Probability of Penetrating Human Skin

Ratio of Fragment area/weight (ft^2 /lb)	Fragment Area Based on 0.033 lb. fragment weight (ft^2)	Velocity (fps)	Threshold Energy (ft-lb.)
0.03	.00099	100	5
0.10	.00330	165	14
0.20	.00660	250	32
0.30	.00990	335	58
0.40	.01320	425	93

Table 1-3 Threshold of Serious Injury to Personnel Due to Fragment Impact

Critical Organ	Weight (lbs.)	Fragment Velocity(fps)	Energy (ft-lb.)
Thorax	>2.5	10	4
	0.1	80	10
	0.001	400	2.5
Abdomen and limbs	>6.0	10	9
	0.1	75	9
	0.001	550	5
Head	>8.0	10	12
	0.1	100	16
	0.001	450	3

Table 1-4 Examples of Equipment Shock Tolerances

Equipment	Peak Accelerations
Fluorescent light fixtures (with lamps)	20 to 30g
Heavy machinery (motor, generators, transformers, etc. > 4,000 lbs.)	10 to 30g
Medium-weight machinery (pumps, condensers, AC equipment, 1,000 to 4,000 lbs.)	15 to 45g
Light machinery (small motors <1,000 lbs.)	30 to 70g

Table 1-5 Safe Separation Distance (bulk explosives)

Bulk Explosive	Explosive Weight (lbs)	Test Configuration	Safe Separation (ft)
Composition A-5	10	Rubber buckets in tunnel	6.0
	15	Aluminum buckets in tunnel	20.0
Composition B	---	Flake, depth on 15 inch Serpentix conveyor	.17 (1)
	2.5	Riser scrap:2 pieces	1.5
	2.5	4 pieces	3.0
	2.5	2 pieces within funnels	2.0
	2.5	4 pieces within funnels	3.0
	60	Cardboard container in tunnel	12.0
	60	Plastic buckets	12.0 (2)
Composition C-4	35	Aluminum buckets in tunnel	20.0 (2)
	50	Aluminum buckets in tunnel	25.0 (2)
Cyclotol (75/25)	60	Aluminum box in tunnel & 0.38-in Kevlar shield.	24.0
	60	Cardboard box in tunnel.	18.0
Guanidine Nitrate	20	DOT-21C-60 Containers with tops on	3.8
	40	DOT-21C-60 Containers with tops on	4.8
	80	DOT-21C-60 Containers with tops on	5.5
Nitro-Guanidine (Powder)	25	DOT-21C-60 Containers with tops on	5.5
	50	DOT-21C-60 Containers with tops on	7.0
	450	DOT-21C-60 Containers with tops on	16.0
TNT, Type 1 Flake	---	Depth on 2-foot Serpentix conveyor	.08 (1)
	55	Cardboard box	12.0
	168	Aluminum tote bin, w/steel fiberglass in tunnel	60.0
	168	Aluminum tote bin in wooden tunnel	50.0

(1)Depth of material at which propagation is prevented is less than or equal to the value shown.

(2)Minimum distance tested. Actual safe separation distance less than or equal to that indicated. Further tests required to establish minimum safe separation distance.

Table 1-6 Safe Separation Distance (munitions)

Munition	Test Configuration	Safe Separation (ft)
8-inch M106 HE Projectile	Single round with 3-inch diameter aluminum bar shield	1.0
8 inch M509 HE Projectile	Single round with "VEE" shield Figure 1-5a)	2.7
155 mm M107 HE Projectile	Single round with one-inch thick aluminum or 1/2-inch thick steel plate shield	1.5
	24 per pallet	110.0
155 mm M483 HE Projectile	Single round with MS shield (Fig. 1-5b)	0
155 mm M795 HE Projectile (TNT, TYPE 1)	Single round	15.0
105 mm M1 HE Projectile	16 per pallet	30.0
	16 per pallet, with funnel and 3/4-inch thick steel plate shield	20.0
105 mm M456 HEAT-T Projectile	Primed cartridge cases	0
	Single round with 3-inch diameter aluminum bar shield	1.6
	Single round, horizontal with 3-inch diameter aluminum bar shield	0.91
81 mm M374A2E1 HE Cartridge	Single round with 1/4-inch thick Lexan plate extension to 2-inch thick aluminum brick shield	0.73 (1)

Table 1-6 (Cont'd.)

Munition	Test Configuration	Safe Separation (ft)
81mm M374 HE Projectile	Single round	2.0
	Single round with 2-inch thick aluminum brick shield	0.73 (1)
	72 per pallet	30.0
30 mm XM789 HEDP Projectile	2 each. PBXN-5 pellets	0.08
	Shell body with 2 pellets	0.08
	Loaded body assembly	0.08
	Heated loaded body assembly	0.25
	Fuzed projectile	0.25
25 mm XM792 HEI-T Cartridge	Type I pellets	0.08
	Type II pellets	0.04
	Loaded body assembly	0.17
	Fuzed projectile	0.17
	Complete cartridge	0.17
BLU-63 A/B Bomblet	Hemispheres	0.04
	Hemispheres in fixtures	0
	Hemispheres, 16 per tray	0
	Bomblet	0.17

Table 1-6 (Cont'd.)

Munition	Test Configuration	Safe Separation (ft)
BLU-97/B Submunition	16 per pallet with 1/2-inch thick aluminum plate shield	4.0
	16 per pallet with "airflow" shield (1/2-inch thick aluminum plates, cut in open "picket fence" design with one plate's spaces covered by the second plate's columns).	5.0
	Single bomblet with either 100% or 75% shield (1/2-inch thick aluminum plate).	0.75
M42/M46 GP Grenades (w/o fuzes)	Single grenade	0.17
	64 per tray	7.0
	768 per carrier, in tunnel	40.0
	8 per M483 Ring Pack	1.0
	15 per M509 Ring Pack	1.5
	32/64 per single/dual cluster tray	0
M56 Mine	Single mine	0.50 (1)
	2-mine canister	0.50 (1)
M74AP and M75 ATAV mines(w/o fuzes)	Single mine with 3-inch thick aluminum brick shield	0.25

(1) Minimum distance tested. Actual safe separation distance less than or equal to that indicated. Further tests required to establish minimum safe separation distance.

BASIS FOR STRUCTURAL DESIGN

1-14. Structural Response

1-14.1. General

Dynamic response criteria to be used in the design of a protective structure and its elements depend on: (1) the properties (type, weight, shape, casing, etc.) and location of the donor explosive, (2) the sensitivity (tolerance) of the acceptor system, and (3) the physical properties and configuration of the protective structure. In many situations, the acceptor system will control the overall required structural response.

1-14.2. Pressure Design Ranges

1-14.2.1. General

An engineering analysis of the blast pressure and fragments associated with high explosive detonations acting on protective structures must be made to describe the response of the protective structures to donor output. The response to the blast output is expressed in terms of design ranges according to the pressure intensity, namely, (1) high pressure, and (2) low pressure. As subsequently shown, these design ranges are related to the relative location of the protective structure to the explosion.

1-14.2.2. High-Pressure Design Range

At the high-pressure design range, the initial pressure acting on the protective structure are extremely high and further amplified by their reflections on the structure. Also the durations of the applied loads are short, particularly where complete venting of the explosion products of the detonation occurs. These durations are also short in comparison to the response time (time to reach maximum deflection) of the individual elements of the structures. Therefore, structures subjected to blast effects in the high-pressure range can, in certain cases, be designed for the impulse (area under the pressure-time curve, Chapter 2) rather than the peak pressure associated with longer duration blast pressures. If the acceptor system is comprised exclusively of explosives, the protective donor structure may be permitted to exceed incipient failure and produce "post failure" fragments provided that the fragment velocities are less than that which will initiate detonation of acceptor charges. This latter range of response is referred to as the "brittle mode of failure."

In the event personnel and/or expensive equipment is being protected or where containment type structures are providing the protection, then incipient failure design is not permitted. Here, the effects of the high pressure and the long duration pressures associated with contained products of the explosion must be accounted for in determining the protective structure response.

Fragments associated with the high-pressure range usually consist of high velocity missiles associated with casing breakup or acceleration of equipment positioned close to the explosion. For acceptors containing explosives, the velocities of primary fragments which penetrate the protective structure must be reduced to a level below the velocity which will cause detonation of the acceptor charges. For personnel or expensive equipment, the possibility of

fragment impact on the acceptor must be completely eliminated. Also associated with the "close-in" effects of a high-pressure design range are the possible occurrence of spalling of concrete elements. Spalling is generally associated with the disengagement of the concrete cover over reinforcement at the acceptor side of a protective element. Spalling can be a hazard to personnel and sometimes to equipment but seldom will result in propagation of explosion of an acceptor system.

1-14.2.3. Low-Pressure Design Range

Structures subjected to blast pressures associated with the low-pressure range sustain peak pressures of smaller intensity than those associated with the high-pressure range. However, the duration of the load can even exceed the response time of the structure. Structural elements designed for the low-pressure range depend on both pressure and impulse.

In cases where the peak pressure is relatively low and the explosive charge is very large (several hundred thousand pounds of explosive) the duration of blast pressures will be extremely long in comparison to those of smaller explosive weights. Here the structure responds primarily to the peak pressure in a manner similar to those structures designed to resist the effects of nuclear detonations. This latter case, although seldom encountered, is sometimes referred to as the "very low-pressure range."

Since the low-pressure design range is involved in the design of shelter type structures, donor fragmentation is of concern. Secondary fragments formed from the break-up of donor structures can produce minor damage to a shelter. These fragments generally have a large mass but their velocities are generally much less than those of primary fragments.

1-14.3. Analyzing Blast Environment

Although each design pressure range is distinct, no clear-cut divisions between the ranges exist; therefore, each protective structure must be analyzed to determine its response.

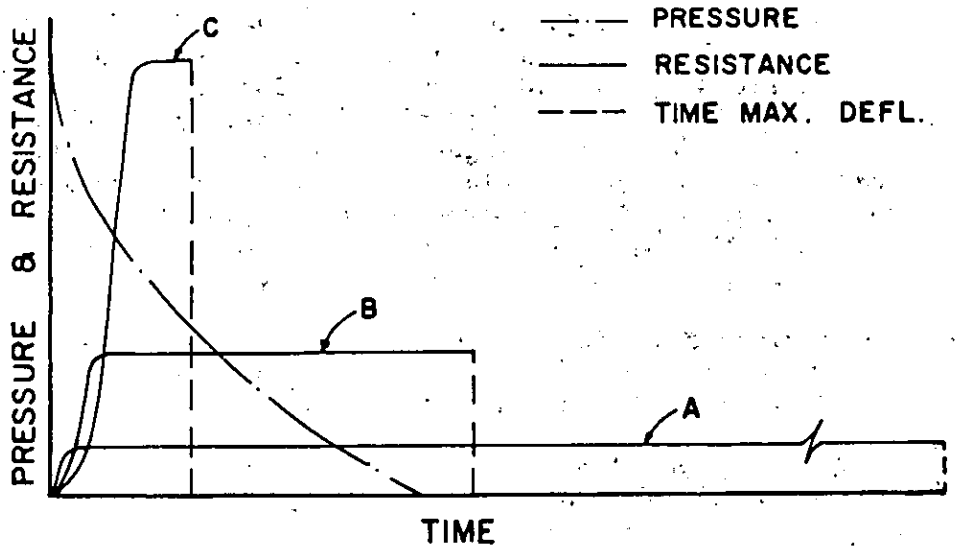
Structural response depends on design and load. Three possible designs, resulting in three distinct resistance-time responses are illustrated in Figure 1-6. Curve A represents the resistance-time function of an element which responds to the impulse; the time to reach maximum deflection is very long in comparison to the load duration. The low-pressure range is represented by Curve B where the element's response depends on both pressure and impulse. Here and dependent on design, the response time of an element can be less than, equal to, or greater than the load duration (Figure 1-6). Curve C illustrates the very low-pressure design range where the element responds to pressure. The required peak resistance is in the order of magnitude of the peak pressure, while the duration of the load is extremely long compared to the time to reach maximum deflection. Although the required maximum resistance will vary in comparison to the peak pressure, the variation will be slight and, in general, the required maximum resistance of an element to resist long duration loads will be only slightly larger (5 to 10 percent) than the peak pressure.

Figure 1-7 indicates semi-quantitatively the parameters which define the design ranges (including the very low range) of an element, along with the

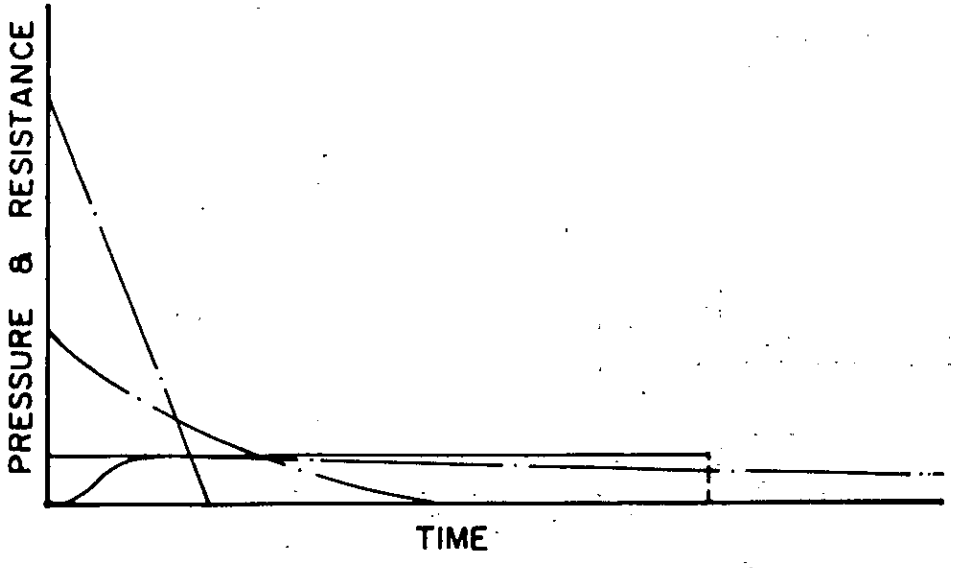
approximate relationship between the time to reach maximum deflection and the load duration.

It was indicated earlier that the design range of an element is related to the location of the element relative to the explosion. For the quantity of explosives considered in this manual, an element designed for the high-pressure range is usually situated immediately adjacent to the explosion, and its exposed surfaces facing the explosion are oriented normal or nearly normal to the propagation of the initial pressure wave (Figure 1-8, cases I through IV). On the other hand, elements which are located close to the explosion and are positions parallel to the path of the wave propagation may respond to the blast effects associated with the low pressure design range. Elements located close to a detonation seldom respond solely to a peak pressure.

Certain elements of a protective structure located a distance from the explosion may respond to the impulse (high-pressure range) even though they are located at the low-pressure range while other structures located near the explosion will respond to the low-pressure design range. In the former case, the structure will not contain personnel or expensive equipment and will primarily serve as a barrier structure. In the latter case, the structure will serve as a shelter (Case I, Figure 1-8).

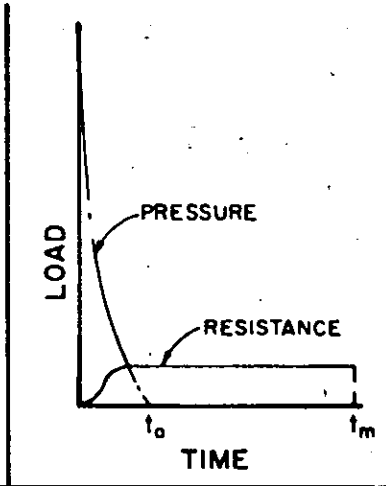


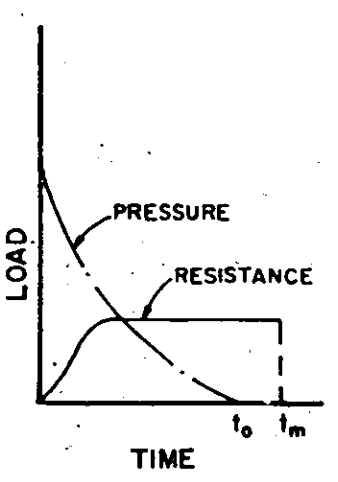
a) VARIABLE RESISTANCE – TIME CURVES

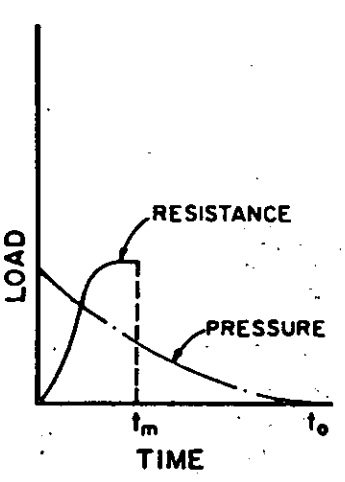


b) VARIABLE PRESSURE – TIME CURVES

Figure 1-6 Variation of structural response and blast loads







PRESSURE DESIGN RANGE	HIGH	LOW	VERY LOW
DESIGN LOAD	IMPULSE	PRESSURE-TIME	PRESSURE
INCIDENT PRESSURE	$\gg$ 100 psi	$<$ 100psi	$<$ 10 psi
PRESSURE DURATION	SHORT	INTERMEDIATE	LONG
RESPONSE TIME	LONG	INTERMEDIATE	SHORT
RELATIONSHIP OF t_m/t_o	$t_m/t_o > 3$	$3 > t_m/t_o > 0.1$	$t_m/t_o < 0.1$

Figure 1-7 Parameters defining pressure design ranges

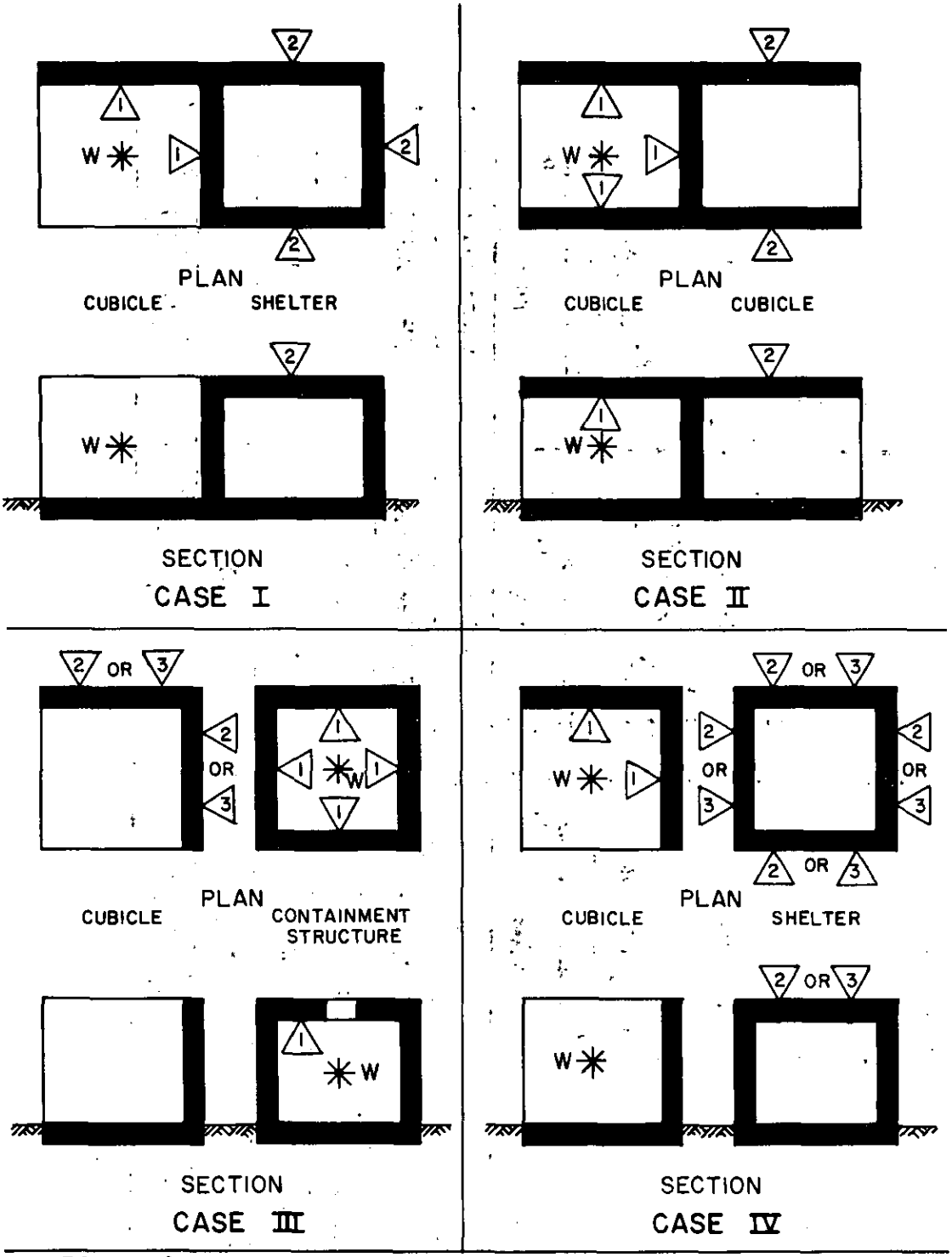


Figure 1-8 Design ranges corresponding to location of the structural elements relative to an explosion

APPENDIX 1A

LIST OF SYMBOLS

g	acceleration due to gravity (ft/sec^2)
i	unit positive impulse (psi-ms)
$\bar{i}_s$	unit scaled impulse for use in figure 1-2 ($psi\text{-}ms/lb^{1/3}$)
p	pressure (psi)
t_m	time at which maximum deflection occurs (ms)
t_o	duration of positive phase of blast pressure (ms)
V	volume of containment structure (ft^3)
w_h	weight of human being (lbs)
W	charge weight (lbs)

APPENDIX 1B

BIBLIOGRAPHY

1. Structures to Resist the Effects of Accidental Explosions (with Addenda), Department of the Army Technical Manual (TM5-1300), Department of the Navy Publication (NAVFAC P-397), Department of the Air Force Manual (AFM 88-22), Washington, D.C., June 1969.
2. Dobbs, N., Structures to Resist the Effects of Accidental Explosions, Volume I, Introduction, Special Publication ARLCD-SP-84001, Prepared by Ammann & Whitney Consulting Engineers, New York, N.Y., for U.S. Army Armament Research, Development and Engineering Center, Armament Engineering Directorate, Picatinny Arsenal, Dover, New Jersey, December 1987.
3. Ayvazyan, H., et al., Structures to Resist the Effects of Accidental Explosions, Volume II, Blast, Fragment, and Shock Loads, Special Publication ARLCD-SP-84001, Prepared by Ammann & Whitney Consulting Engineers, New York, N.Y., in association with Southwest Research Institute, San Antonio, TX, for U.S. Army Armament Engineering Directorate, Picatinny Arsenal, Dover, New Jersey, December 1986.
4. Dede, M., et al., Structures to Resist the Effects of Accidental Explosions, Volume III, Principles of Dynamic Analysis, Special Publication ARLCD-SP-84001, Prepared by Ammann & Whitney Consulting Engineers, New York, N.Y., for U.S. Army Armament Research and Development Center, Large Caliber Weapon systems Laboratory, Dover, New Jersey, June 1984.
5. Dede, M., and Dobbs, N., Structures to Resist the Effects of Accidental Explosions, Volume IV, Reinforced Concrete Design, Special Publication ARLCD-SP-84001, Prepared by Ammann & Whitney Consulting Engineers, New York, N.Y., for U.S. Army Armament Research, Development and Engineering Center, Armament Engineering, Directorate, Picatinny Arsenal, Dover, New Jersey, April 1987.
6. Kossover, D., and Dobbs, N., Structures to Resist the Effects of Accidental Explosions, Volume V, Structural Steel Design, Special Publication ARLCD-SP-84001, Prepared by Ammann & Whitney Consulting Engineers, New York, N.Y., for U.S. Army Armament Research, Development and Engineering Center, Armament Engineering Directorate, Picatinny Arsenal, Dover, New Jersey, May 1987.
7. Dede, M., Lipvin-Schramm, S., and Dobbs, N. Structures to Resist the Effects of Accidental Explosions, Volume VI, Special Conditions in Explosive Facility Design, Special Publication ARLCD-SP-84001, Prepared by Ammann & Whitney Consulting Engineers, New York, N.Y. for U.S. Army Armament Research and Development Center, Large Caliber Weapon System Laboratory, Dover, New Jersey, April 1985.
8. Safety Manual, AMC-R 385-100, Department of the Army, Headquarters U.S. Army Materiel Command, Alexandria, Virginia, August 1985.
9. A Manual for the Prediction of Blast and Fragment Loadings on Structures, DOE/TIC-11268, Prepared by Southwest Research Institute, San Antonio, TX, for U.S. Department of Energy, Albuquerque Operations Office, Amarillo Area Office, Pantex Plant, Amarillo, Texas, November 1980.
10. White, C.S., The Scope of Blast and Shock Biology and Problem Areas in Relating Physical and Biological Parameters, Lovelace Foundation for Medical Education and Research, Albuquerque, New Mexico, 1968.
11. Richmond, D.R., et al., The Relationship Between Selected Blast Wave Parameters and the Response of Mammals Exposed to Air Blast, Lovelace Foundation for Medical Education and Research, Albuquerque, New Mexico 1968.

12. Hirsch, F.G., Effects of Overpressure on the Ear - A Review, Lovelace Foundation for Medical Education and Research, Albuquerque, New Mexico, 1968.
13. Clemedson, C., Hellstrom, G. and Lingren, S., The Relative Tolerance of the Head, Thorax and Abdomen to Blunt Trauma, Defense Medical Board, Stockholm and Research Institute of National Defense, Sundbyberg, Sweden; Department of Surgery, University of Uppsala, Uppsala, Sweden; Department of Neurosurgery, University of Gothenburg, Gothenburg, Sweden, 1968.
14. Zaker, T.A., Fragment and Debris Hazards, Technical Paper No. 12, Department of Defense Explosives Safety Board, July 1975.
15. Zaker, T.A., Computer Program for Predicting Casualties and Damage from Accidental Explosions, Technical Paper No. 11, Department of Defense Explosives Safety Board, May 1975.
16. Cohen, and Dobbs, Prevention of and Protection Against Accidental Explosion of Munitions, Fuels and Other Hazardous Mixtures, Annals of the New York Academy of Science, October 1968.
17. Stirrat W., Compilation of Safe Separation Data on Bulk Explosives and Munitions, Technical Report ARAED-TR-87033, U.S. Army Armament Research, Development and Engineering Center, Dover, N.J., October, 1987.

CHAPTER 2. BLAST, FRAGMENT, AND SHOCK LOADS

CHAPTER 2

BLAST, FRAGMENT, AND SHOCK LOADS

INTRODUCTION

2-1. Purpose

The purpose of this manual is to present methods of design for protective construction used in facilities for development, testing, production, storage, maintenance, modification, inspection, demilitarization, and disposal of explosive materials.

2-2. Objective

The primary objectives are to establish design procedures and construction techniques whereby propagation of explosion (from one structure or part of a structure to another) or mass detonation can be prevented and to provide protection for personnel and valuable equipment.

The secondary objectives are to:

(1) Establish the blast load parameters required for design of protective structures.
(2) Provide methods for calculating the dynamic response of structural elements including reinforced concrete, and structural steel.
(3) Establish construction details and procedures necessary to afford the required strength to resist the applied blast loads.
(4) Establish guidelines for siting explosive facilities to obtain maximum cost effectiveness in both the planning and structural arrangements, providing closures, and preventing damage to interior portions of structures because of structural motion, shock, and fragment perforation.

2-3. Background

For the first 60 years of the 20th century, criteria and methods based upon results of catastrophic events were used for the design of explosive facilities. The criteria and methods did not include a detailed or reliable quantitative basis for assessing the degree of protection afforded by the protective facility. In the late 1960's quantitative procedures were set forth in the first edition of the present manual, "Structures to Resist the Effects of Accidental Explosions". This manual was based on extensive research and development programs which permitted a more reliable approach to current and future design requirements. Since the original publication of this manual, more extensive testing and development programs have taken place. This additional research included work with materials other than reinforced concrete which was the principal construction material referenced in the initial version of the manual.

Modern methods for the manufacture and storage of explosive materials, which include many exotic chemicals, fuels, and propellants, require less space for a given quantity of explosive material than was previously needed. Such concentration of explosives increases the possibility of the propagation of accidental explosions. (One accidental explosion causing the detonation of

other explosive materials.) It is evident that a requirement for more accurate design techniques is essential. This manual describes rational design methods to provide the required structural protection.

These design methods account for the close-in effects of a detonation including the high pressures and the nonuniformity of blast loading on protective structures or barriers. These methods also account for intermediate and far-range effects for the design of structures located away from the explosion. The dynamic response of structures, constructed of various materials, or combination of materials, can be calculated, and details are given to provide the strength and ductility required by the design. The design approach is directed primarily toward protective structures subjected to the effects of a high explosive detonation. However, this approach is general, and it is applicable to the design of other explosive environments as well as other explosive materials as mentioned above.

The design techniques set forth in this manual are based upon the results of numerous full- and small-scale structural response and explosive effects tests of various materials conducted in conjunction with the development of this manual and/or related projects.

2-4. Scope

It is not the intent of this manual to establish safety criteria. Applicable documents should be consulted for this purpose. Response predictions for personnel and equipment are included for information.

In this manual an effort is made to cover the more probable design situations. However, sufficient general information on protective design techniques has been included in order that application of the basic theory can be made to situations other than those which were fully considered.

This manual is applicable to the design of protective structures subjected to the effects associated with high explosive detonations. For these design situations, the manual will apply for explosive quantities less than 25,000 pounds for close-in effects. However, this manual is also applicable to other situations such as far- or intermediate-range effects. For these latter cases the design procedures are applicable for explosive quantities in the order of 500,000 pounds which is the maximum quantity of high explosive approved for aboveground storage facilities in the Department of Defense manual, "Ammunition and Explosives Safety Standards", DOD 6055.9-STD. Since tests were primarily directed toward the response of structural steel and reinforced concrete elements to blast overpressures, this manual concentrates on design procedures and techniques for these materials. However, this does not imply that concrete and steel are the only useful materials for protective construction. Tests to establish the response of wood, brick blocks, and plastics, as well as the blast attenuating and mass effects of soil are contemplated. The results of these tests may require, at a later date, the supplementation of these design methods for these and other materials.

Other manuals are available to design protective structures against the effects of high explosive or nuclear detonations. The procedures in these manuals will quite often complement this manual and should be consulted for specific applications.

Computer programs, which are consistent with procedures and techniques contained in the manual, have been approved by the appropriate representative of the US Army, the US Navy, the US Air Force and the Department of Defense Explosives Safety Board (DDESB). These programs are available through the following repositories:

(1) Department of the Army
Commander and Director
U.S. Army Engineer
Waterways Experiment Station
Post Office Box 631
Vicksburg, Mississippi 39180-0631
Attn: WESKA

(2) Department of the Navy
Commanding Officer
Naval Civil Engineering Laboratory
Port Hueneme, California 93043
Attn: Code L51

(3) Department of the Air Force
Aerospace Structures
Information and Analysis Center
Wright Patterson Air Force Base
Ohio 45433
Attn: AFFDL/FBR

If any modifications to these programs are required, they will be submitted for review by DDESB and the above services. Upon concurrence of the revisions, the necessary changes will be made and notification of the changes will be made by the individual repositories.

2-5. Format

This manual is subdivided into six specific chapters dealing with various aspects of design. The titles of these chapters are as follows:

Chapter 1	Introduction
Chapter 2	Blast, Fragment, and Shock Loads
Chapter 3	Principles of Dynamic Analysis
Chapter 4	Reinforced Concrete Design
Chapter 5	Structural Steel Design
Chapter 6	Special Considerations in Explosive Facility Design

When applicable, illustrative examples are included in the Appendices.

Commonly accepted symbols are used as much as possible. However, protective design involves many different scientific and engineering fields, and, therefore, no attempt is made to standardize completely all the symbols used. Each symbol is defined where it is first used, and in the list of symbols at the end of each chapter.

CHAPTER CONTENTS

2-6. General

This chapter contains the procedures for determining explosive output and associated structure loadings, fragment effects, and the structural motion effects associated with accidental explosions. These procedures are contained in the following sections: Sections 2-8 through 2-15 deals with the loadings associated with the blast phenomena. These data include, in addition to the determination of the effects of the explosive output, methods for determining blast loads acting on the exterior of and within structures. Sections 2-16 through 2-19 cover the formation of fragments which can be projected by an explosion and include both primary and secondary fragments effects. Sections 2-20 to 2-24 present the method for determining the structural motions, including both ground and air shock effects.

EXPLOSION EFFECTS

2-7. Effects of Explosive Output

In the design of protective structures to resist the effects of accidental explosions, the principal effects of the explosive output to be considered are blast overpressures (hereafter referred to as blast pressures or pressures), fragments generated by the explosion and the shock loads produced by the shock wave transmitted through the air or ground. Of these three parameters, the blast pressures are usually the governing factor in the determination of the structure response. However, in some situations, fragments and/or shock loads may be just as important as the pressures in determining the configuration of the facility.

Although the quantitative data presented pertain to the blast output of bare trinitrotoluene (TNT) spherical or hemispherical charges considered as point source explosions, and other explosives which have been specifically tested. These data can be extended by appropriate means including testing to include other potentially mass-detonating materials (solid, liquid, or gas) of varying shape.

BLAST LOADS

2-8. Blast Phenomena

2-8.1. General

Bare, solid explosives must detonate to produce any explosive effect other than a fire. The term detonation refers to a very rapid and stable chemical reaction which proceeds through the explosive material at a speed, called the detonation velocity, which is supersonic in the unreacted explosive. Detonation velocities range from 22,000 to 28,000 feet per second for most high explosives. The detonation wave rapidly converts the solid or liquid explosive into a very hot, dense, high-pressure gas, and the volume of this gas which had been the explosive material is then the source of strong blast waves in air. Pressures immediately behind the detonation front range from 2,700,000 to 4,900,000 psi. Only about one-third of the total chemical energy available in most high explosives is released in the detonation process. The remaining two-thirds is released more slowly in explosions in air as the detonation products mix with air and burn. This afterburning process has only a slight effect on blast wave properties because it is so much slower than detonation.

The blast effects of an explosion are in the form of a shock wave composed of a high-intensity shock front which expands outward from the surface of the explosive into the surrounding air. As the wave expands, it decays in strength, lengthens in duration, and decreases in velocity. This phenomena is caused by spherical divergence as well as by the fact that the chemical reaction is completed, except for some afterburning associated with the hot explosion products mixing with the surrounding atmosphere.

As the wave expands in air, the front impinges on structures located within its path and then the entire structure is engulfed by the shock pressures. The magnitude and distribution of the blast loads on the structure arising from these pressures are a function of the following factors: (1) explosive properties, namely type of explosive material, energy output (high or low order detonation), and weight of explosive; (2) the location of the detonation relative to the protective structures; and (3) the magnitude and reinforcement of the pressure by its interaction with the ground barrier, or the structure itself. The first of these three factors are discussed in Sections 2-8.2 and 2-9 below and the latter two factors are discussed throughout the remainder of this section.

2-8.2. Explosive Materials

Explosive materials may be classified according to their physical state: solids, liquids, or gases. Solid explosives are primarily high explosives; however, other materials such as flammable chemicals and propellants may also be classified as potentially explosive materials. Liquid and gaseous explosives encompass a wide variety of substances used in the manufacture of chemicals, fuels, and propellants. The blast pressure environment produced will vary not only among the different materials but may also differ for a particular material. Such factors as methods and procedures used in manufacturing, storage, and handling, in addition to specific individual physical and chemical characteristics, may alter the blast effects of an explosive material.

The blast effects of solid materials are best known. This is particularly true for high-explosive materials. The blast pressures, impulses, durations, and other blast effects of an explosion have been well established. These effects are contained in this chapter.

Unlike high-explosive materials, other solid, liquid, and gaseous explosive materials will exhibit a variation of their blast pressure output. An explosion of these materials is in many cases incomplete, and only a portion of the total mass of the explosive (effective charge weight) is involved in the detonation process. The remainder of the mass is usually consumed by deflagration resulting in a large amount of the material's chemical energy being dissipated as thermal energy which, in turn, may cause fires or thermal radiation damage.

2-9. TNT Equivalency

The major quantity of blast effects data presented in this manual pertains to the blast pressures output of bare spherical TNT explosive. These data can be extended to include other potentially mass-detonating materials (Class 1.1) by relating the explosive energy of the "effective charge weight" of those materials to that of an equivalent weight of TNT. In addition to the energy output, other factors may affect the equivalency of material compared to TNT. These factors include the material shape (flat, square, round, etc.), the number of explosive items, explosive confinement (casing, containers, etc.), and the pressure range being considered (close-in, intermediate or far ranges). These other factors will be discussed later in this manual

For blast resistant design, the effects of the energy output on explosive material, of a specific shape, relative to that of TNT, of similar shape, can be expressed as function of the heat of detonation of the various materials as follows:

$$W_E = \frac{H^d_{EXP}}{H^d_{TNT}} W_{EXP} \qquad 2\text{-}1$$

where

W_E = effective charge weight

W_{EXP} = weight of the explosive in question

H^d_{EXP} = heat of detonation of explosive in question

H^d_{TNT} = heat of detonation of TNT

The heat of detonation of some of the more commonly used explosives are listed in Table 2-1.

The above equation for the effective charge weight is related primarily to the blast output associated with the shock effects of unconfined detonations (Section 2-13). The effective charge weight produced by the confinement effects

of explosions (Section 2-14) will differ. These differences will be discussed later in this manual.

2-10. Blast-Loading Categories

Blast loads on structures can be divided into two main groups based on the confinement of the explosive charge (unconfined and confined explosions) and can be subdivided based on the blast loading produced within the donor structure or acting on acceptor structures. These blast loading categories are illustrated in Figure 2-1. Figure 2-1 gives the six blast loading categories possible. Figure 2-1 also shows the five possible pressure loads associated with the blast load categories, the location of the explosive charge which would produce these pressure loads, and the protective structures subjected to these loads.

The blast load categories and the resulting pressure loads listed in Figure 2-1 are qualitatively and quantitatively defined below and in subsequent sections, respectively.

2-10.1. Unconfined Explosion

2-10.1.1. Free Air Burst Explosion

An explosion, which occurs in free air, produces an initial output whose shock wave propagates away from the center of the detonation, striking the protective structure without intermediate amplification of its wave.

2-10.1.2. Air Burst Explosion

An explosion which is located at a distance from and above the protective structure so that the ground reflections of the initial wave occur prior to the arrival of the blast wave at the protective structure. As used in this manual, an air burst is limited to an explosion which occurs at two to three times the height of a one or two-story building.

2-10.1.3. Surface Burst Explosion

A surface burst explosion will occur when the detonation is located close to or on the ground so that the initial shock is amplified at the point of detonation due to the ground reflections.

2-10.2. Confined Explosion

2-10.2.1. Fully Vented Explosion

A fully vented explosion will be produced within or immediately adjacent to a barrier or cubicle type structure with one or more surfaces open to the atmosphere. The initial wave, which is amplified by the nonfrangible portions of the structure, and the products of detonation are totally vented to the atmosphere forming a shock wave (leakage pressures) which propagates away from the structure.

2-10.2.2. Partially Confined Explosion

A partially confined explosion will be produced within a barrier or cubicle type structure with limited size openings and/or frangible surfaces. The initial wave, which is amplified by the frangible and nonfrangible portion of the structure, and the products of detonation are vented to the atmosphere after a finite period of time. The confinement of the detonation products, which consist of the accumulation of high temperatures and gaseous products, is associated with a buildup of quasi-static pressure (hereafter referred to as gas pressure). This pressure has a long duration in comparison to that of the shock pressure.

2-10.2.3. Fully Confined Explosions

Full confinement of an explosion is associated with either total or near total containment of the explosion by a barrier structure. Internal blast loads will consist of unvented shock loads and very long duration gas pressures which are a function of the degree of containment. The magnitude of the leakage pressures will usually be small and will only affect those facilities immediately outside the containment structure.

2-11. Blast Loading Protection

Protection of personnel and valuable equipment (acceptor system) will usually involve protective shelters located away from the detonation. Their design may involve one or more of the following blast-loading categories: free-air burst, air burst, surface burst, and exterior or leakage pressures from either vented or partially confined explosions. These shelters are usually enclosed buildings located at pressure ranges of a few hundred pounds per square inch (psi) or less. Depending on the shelter design pressures, these structures can be either above, below, or at ground surface. In this manual, primary consideration is given to above-ground shelters. However, some consideration is given in Chapter VI regarding shelters positioned at other locations. For the third type of pressure loading of Figure 2-1 (interior shock pressure), protection is required when the shelter is located immediately adjacent to the explosion. The reflected pressure there may be in thousands of psi, but with pressure durations usually small. The acceptor portion of such an explosive system may include other explosive materials and/or personnel. The structure associated with the fifth pressure-loading type is a containment type building and is usually used to prevent escape of toxic chemicals, radiological and/or biological materials, or to limit blast pressures at the exterior to a level consistent with personnel protection.

Of the six categories, those from air bursts are seldom encountered and the free air burst is the least likely to occur. The possibility of such blast environments exists where potentially explosive materials are stored at heights adjacent to or away from protective structures such as in manufacturing (process or storage tanks) or missile sites. In the latter, the rocket propellant would be a source of explosive danger to the ground crew and control facilities.

The other four blast-loading categories can occur in most explosive manufacturing and storage facilities. In such installations, transportation of explosive materials between buildings either by rail, vehicle, or in the case of

liquid or gases, through piping, is a possibility. Also, storage and handling of explosives within buildings are common occurrences.

Although the blast-loading categories can be separated and classified individually, no clear-cut limits differentiate each category. In most explosive facilities, the various blast environments will overlap, and judgement should be used in the application of the following recommendations for determining the blast parameters consistent with the various blast-loading categories.

2-12. Blast-Wave Phenomena

The violent release of energy from a detonation converts the explosive material into a very high pressure gas at very high temperatures. A pressure front associated with the high pressure gas propagates radially into the surrounding atmosphere as a strong shock wave, driven and supported by the hot gases. The shock front, termed the blast wave, is characterized by an almost instantaneous rise from ambient pressure to a peak incident pressure P_{so} (Figure 2-2).

This pressure increase or shock front travels radially from the burst point with a diminishing shock velocity U which is always in excess of the sonic velocity of the medium. Gas molecules behind the front move at lower flow velocities, termed particle velocities u. These latter particle velocities are associated with the dynamic pressures, whose maximum values are denoted qo' or the pressures formed by the winds produced by the passage of the shock front. As the shock front expands into increasingly larger volumes of the medium, the peak incident pressures at the fronts decrease and the durations of the pressures increase. Those parameters which vary as the peak incident pressure varies are presented in Figure 2-3.

At any point away from the burst, the pressure disturbance has the shape shown in Figure 2-2. The shock front arrives at a given location at time t_A and, after the rise to the peak value, P_{so} the incident pressure decays to the ambient value in time to which is the positive phase duration. This is followed by a negative phase with a duration t_o^- that is usually much longer than the positive phase and characterized by a negative pressure (below ambient pressure) having a maximum value of P_{so}^- as well as a reversal of the particle flow. The negative phase is usually less important in a design than is the positive phase, and its amplitude P_s^- must, in all cases, be less than ambient atmosphere pressure p_o. The incident impulse density associated with the blast wave is the integrated area under the pressure-time curve and is denoted as i_s for the positive phase and i_s^- for the negative phase.

An additional parameter of the blast wave, the wave length, is sometimes required in the analysis of structures. The positive wave length L_w^+ is that length at a given distance from the detonation which, at a particular instant of time, is experiencing positive pressure. The negative wave length L_w^- is similarly defined for negative pressures.

The above treatment of the blast wave phenomena is general. In subsequent sections of this chapter, the magnitude of the various parameters is presented depending upon the category of the detonation as previously described: free air burst, surface burst, exterior or leakage pressures, or interior or high pressure blast loading.

2-13. Unconfined Explosions

2-13.1. Free Air Burst

When a detonation occurs adjacent to and above a protective structure such that no amplification of the initial shock wave occurs between the explosive source and the protective structure, then the blast loads acting on the structure are free-air blast pressures (Fig. 2-4).

As the incident wave moves radially away from the center of the explosion, it will impact with the structure, and, upon impact, the initial wave (pressure and impulse) is reinforced and reflected (Fig. 2-5). The reflected pressure pulse of Figure 2-5 is typical for infinite plane reflectors.

When the shock wave impinges on a surface oriented so that a line which describes the path of travel of the wave is normal to the surface, then the point of initial contact is said to sustain the maximum (normal reflected) pressure and impulse. Figure 2-6 presents the ratios of the normal reflected pressures to the incident pressures as a function of the incident pressures.

The peak pressure and impulse patterns on the structure vary with distance from a maximum at the normal distance R_A to a minimum (incident pressure) where the plane of the structure's surface is perpendicular to the shock front. The positive phase pressures, impulses, durations, and other parameters of this shock environment for a spherical TNT explosions are given in Figure 2-7 versus the scaled distance ($Z = R/W^{1/3}$).

The smallest scaled distance of 0.136 $ft/lb^{1/3}$ represents the radius of the spherical TNT explosive and, therefore, represents the surface of the explosive. Some parameters have been extrapolated to the charge surface which are shown as dashed portions of the curves. These dashed curves represent an upper limit of scatter in experimental data and variation in theoretical predictions, giving for design purposes conservative limits for these parameters.

In some blast loading situations, negative blast wave parameters (Fig. 2-8) are needed to predict the loading-time function of the blast wave acting on a structure. This is particularly true in flexible type protective structures (usually steel-frame structures) where the overall motion of the structure will be affected by the phasing of the blast loads acting on the various structure surfaces. The effects of the negative phase parameters are usually not important for the design of the more rigid type structures (reinforced concrete).

The curves presented in Figures 2-7 and 2-8 which give the blast wave parameters as a function of scaled distance, extend only to a scaled distance $Z = 100\ ft/lb^{1/3}$. For most protective structures, or even light structures, damage is relatively superficial beyond this scaled distance, consisting at most of broken windows or deformation of light panels or blow-out walls. But, the curves are also not extended beyond these levels because the blast wave properties start to be seriously affected by atmospheric conditions so that overpressures are very much less or very much more than the "ideal" parameters transmitted through a homogeneous atmosphere.

In the low pressure region, the pressure varies as a function of sound velocity with altitude above the ground surface. At very far distances from an explosion ($Z = 1000$ ft/lb$^{1/3}$, the peak pressures (really sound pressures at these levels) can be ten times greater or more than ten times less than the ideal pressures for a homogenous atmosphere.

Even with enhancement caused by real atmospheric conditions (also called blast focusing), the pressures are still quite low and structural damage should be superficial. If it is necessary to predict such low levels, one should obtain and study more detailed reports listed in the bibliography.

The variation of the pressure and impulse patterns on the surface of a structure between the maximum and minimum values is a function of the angle of incidence This angle is formed by the line which defines the normal distance R_A between the point of detonation and the structure, and line R (slant distance) which defines the path of shock propagation between the center of the explosion and any other point in question on the structure surface (Fig. 2-4).

The effects of the angle of incidence on the peak reflected pressure $P_{r\alpha}$ and the reflected impulse $i_{r\alpha}$ are shown in Figures 2-9 and 2-10, respectively. The figures are plots of the angle of incidence versus the peak reflected pressure or the reflected impulse as a function of the scaled normal distance between the charge and the surface in question. The usual load condition involves the ground surface and, therefore, this normal scaled distance is referred to as the scaled height of charge above the ground ($H_c/W^{1/3}$). All other blast parameters are obtained from Figures 2-7 and 2-8 for the scaled slant distance $R/W^{1/3}$ to the point in question.

2-13.2. Air Burst

The air burst environment is produced by detonations which occur above the ground surface and at a distance away from the protective structure so that the initial shock wave, propagating away from the explosion, impinges on the ground surface prior to arrival at the structure. As the shock wave continues to propagate outward along the ground surface, a front known as the Mach front (Fig. 2-11) is formed by the interaction of the initial wave (incident wave) and the reflected wave. This reflected wave is the result of the reinforcement of the incident wave by the ground surface.

Some variation of the pressures over the height of the Mach front occurs, but for design purposes, this variation can be neglected and the shock considered as a plane wave over the full height of the front. The blast parameters in the Mach front are calculated at the ground surface. The pressure-time variation of the Mach front (Fig. 2-12a) is similar to that of the incident wave except that the magnitude of the blast parameters are somewhat larger.

The height of the Mach front increases as the wave propagates away from the center of the detonation. This increase in height is referred to as the path of the triple point and is formed by the intersection of the initial, reflected, and Mach waves. A protected structure is considered to be subjected to a plane wave (uniform pressure) when the height of the triple point exceeds the height of the structure. The scaled height of the triple point $H_T/W^{1/3}$ versus scaled ground distance Z_G and scaled charge height $H_c/W^{1/3}$ is plotted in Figure 2-13.

If the height of the triple point does not extend above the height of the structure, then the magnitude of the applied loads will vary with the height of the point being considered. Above the triple point, the pressure-time variation consists of an interaction of the incident and reflected incident wave pressures resulting in a pressure-time variation (Fig. 2-12b) different from that of the Mach incident wave pressures. The magnitude of pressures above the triple point is smaller than that of the Mach front. In most practical design situations, the location of the detonation will be far enough away from the structure so as not to produce this pressure variation. An exception may exist for multistory buildings even though these buildings are usually located at very low-pressure ranges where the triple point is high.

In determining the magnitude of the air blast loads acting on the surface of an above-ground protective structure, the peak incident blast pressures in the Mach wave acting on the ground surface immediately before the structure are calculated first. The peak incident pressure $P_{r\alpha}$ is determined for this point from Figure 2-9 using the scaled height of charge above the ground $H_c/W^{1/3}$ and the angle of incidence α.

A similar procedure is used with Figure 2-10 to determine the impulse $i_{r\alpha}$ of the blast wave acting on the ground surface immediately before the structure. An estimate of the other blast parameters may be obtained from Figures 2-7 and 2-8 by setting the values of $P_{r\alpha}$ and $i_{r\alpha}$ equal to the values of the peak incident pressure P_{so} and incident impulse i_s of the mach wave, respectively. The scaled distances corresponding to P_{so} and i_s are determined from Figure 2-7. The scaled distance corresponding to P_{so} is used to obtain values of Pr, P_{so}^-, $t_A/W^{1/3}$, U, $L_W/W^{1/3}$ and $L_W^-/W^{1/3}$ while the scaled distance corresponding to i_s is used to obtain values of i_r, i_s^-, i_r^-, $t_o/W^{1/3}$ and $t_o^-/W^{1/3}$.

2-13.3. Surface Burst

A charge located on or very near the ground surface is considered to be a surface burst. The initial wave of the explosion is reflected and reinforced by the ground surface to produce a reflected wave. Unlike the air burst, the reflected wave merges with the incident wave at the point of detonation to form a single wave, similar in nature to the mach wave of the air burst but essentially hemispherical in shape (Fig. 2-14).

The positive phase parameters of the surface burst environment for hemispherical TNT explosions are given in Figure 2-15 while the negative phase parameters are given in Figure 2-16. A comparison of these parameters with those of free-air explosions (Fig. 2-7 and 2-8) indicate that, at a given distance from a detonation of the same weight of explosive, all of the parameters of the surface burst environment are larger than those for the free-air environment.

As for the case of air bursts, protected structures subjected to the explosive output of a surface burst will usually be located in the pressure range where the plane wave (Fig. 2-14) concept can be applied. Therefore, for a surface burst, the blast loads acting on structure surface are calculated as described for an air burst except that the incident pressures and other positive phase parameters of the free-field shock environment are obtained from Figure 2-15, and theoretical negative phase blast parameters are shown in Figure 2-16.

As for the case of an air burst, the curves presented in Figures 2-15 and 2-16 which give the blast wave parameters as a function of scaled distance, extend only to a scaled distance Z = 100 ft/lb$^{1/3}$ (see section 2-13.1).

Blast parameters for explosives detonated on the ground surface other than hemispherical TNT are listed in Table 2-2. These explosives include both uncased and cased high explosives, propellants and propelling charges as well as pyrotechnic mixtures. The various shapes of the explosive materials are given in Figure 2-17. The blast parameters for the various explosives are illustrated in Figures 2-18 through 2-49. For each explosive material considered, the peak incident pressure P_{so} and scaled incident impulse $i_s/W^{1/3}$ is presented as a function of the scaled ground distance $Z_G = R_G/W^{1/3}$ from the point of detonation. The charge weight W is equal to the actual weight of the explosive material under consideration increased by the required factor of safety (20 percent).

An estimate of the blast parameters other than incident pressure and impulse, may be obtained from Figures 2-15 and 2-16. The scaled ground distance corresponding to the incident pressure P_{so} is used to obtain the values of P_r, P_{so}^-, P_r^-, $t_A/W^{1/3}$, U, $L_w/W^{1/3}$ and $L_w^-/W^{1/3}$. In addition, this scaled ground distance $Z_G = R_G/W^{1/3}$ is used to calculate the equivalent TNT design charge weight W for pressure using the actual ground distance R_G. The absolute values of the scaled blast parameters are obtained by multiplying the scaled values by the equivalent TNT design charge weight.

The scaled ground distance corresponding to the incident impulse requires a graphical solution. The point corresponding to the scaled incident impulse and scaled ground distance for the explosive material in question is plotted on Figure 2-15. A 45 degree line is drawn through this point. The point where the line intersects the scaled impulse curve corresponds to the scaled impulse and scaled ground distance for the equivalent TNT charge. This scaled ground distance is then used to obtain the values of $i_r/W^{1/3}$, $i_s^-/W^{1/3}$, $i_r^-/W^{1/3}$, $t_o/W^{1/3}$ and $t_o^-/W^{1/3}$. In addition, this scaled ground distance and the actual ground distance is used to calculate the equivalent TNT design charge weight for impulse. The absolute values of the scaled blast parameters are obtained by multiplying the scaled values by the equivalent TNT design charge weight.

It may be noted that the above data for explosives other than TNT is limited to surface bursts with container shapes indicated in Figure 2-17. This data should not be extrapolated for scaled distances less than those indicated on Figures 2-18 through 2-49. In addition, the blast pressure and impulse for propellants and, in particular, the pyrotechnic mixtures were obtained from tests which utilized booster charges to initiate the explosive material. Therefore, the blast parameters for both of these materials should be considered as upper limits.

2-13.4. Multiple Explosions

When two or more explosions of similar material occur several milliseconds apart, the blast wave of the initial explosion will propagate ahead of the waves resulting from the subsequent explosions, with the phasing of the propagation of these latter waves being governed by the initiation time and orientation of the individual explosives. If the time delay between explosions is not too large, the blast waves produced by the subsequent explosions will

eventually overtake and merge with that of the initial detonation. The distance from the explosion at which this merger occurs will depend on: (1) the magnitude of the individual explosions, (2) the time delays between the initiation of the explosions, (3) the separation distances between and orientation of the explosives, and (4) obstructions between the explosives themselves and other obstructions between the explosives and other parts of the facility (buildings, walls, barricades, terrain, etc.) which will distort, hinder, and generally interfere with wave propagation.

The pressure time relationships associated with the wave propagation will depend upon the interaction of the individual waves themselves. After all the waves have merged, the pressures associated with the common or merged wave will have a pressure-time relationship which is similar to that produced by a single explosion (Fig. 2-12). However, at closer distances to the explosion, the pressure-time relationship will be more closely represented by a pressure-time curve with multiple peak pressures (similar to that occurring above the triple point (Fig. 2-12)). The multiple peak pressures represent the interaction as the various waves reach the point in question. At distances even closer to the explosion, the time history of the pressures acting on the ground surface may consist of a series of completely separate blast loads. This loading condition is a result of the arrival of the subsequent blast waves at a particular point during or after the occurrence of the negative phase pressures produced by the initial wave at that point.

The latter pressure-time relationship is probably most likely to occur at high pressures close to the explosions while the multiple peak pressure pulse is normally associated with low pressures at far distances. However, in many instances, the multiple peak pressure pulse will occur at high pressures, in particular where the individual explosives are positioned close together, e.g., in a cubicle or other storage facility.

2-14. Confined Explosions

2-14.1. Effects of Confinement

When an explosion occurs within a structure, the peak pressures associated with the initial shock front (free-air pressures) will be extremely high and, in turn, will be amplified by their reflections within the structure. In addition, and depending upon the degree of confinement, the effects of the high temperatures and accumulation of gaseous products produced by the chemical process involved in the explosion will exert additional pressures and increase the load duration within the structure. The combined effects of these pressures may eventually destroy the structure unless the structure is designed to sustain the effects of the internal pressures. Provisions for venting of these pressures will reduce their magnitude as well as their duration.

The use of cubicle-type structures (Fig. 2-50a) or other similar barriers with one or more surfaces either sufficiently frangible or open to the atmosphere will provide some degree of venting depending on the opening size. This type of structure will permit the blast wave from an internal explosion to spill over onto the surrounding ground surface, thereby, significantly reducing the magnitude and duration of the internal pressures. The exterior pressures are quite often referred to as "leakage" pressures while the pressures reflected and reinforced within the structure are termed interior "shock pressures". The pressures associated with the accumulation of the gaseous products and

temperature rise are identified as "gas" pressures. For the design of most fully vented cubicle type structures, the effects of the gas pressure may be neglected.

Detonation in an enclosed structure with relatively small openings (Fig. 2-50b) is associated with both shock and gas pressures whose magnitudes are a maximum. The duration of the gas pressure and, therefore, the impulse of the gas pressure is a function of the size of the opening. It should be noted that the onset of the gas pressure does not necessarily coincide with the onset of the shock pressure. Further, it takes a finite length of time after the onset for the gas pressure to reach its maximum value. However, these times are very small and, for design purposes of most confined structures, they may be treated as instantaneous.

The term "frangible" pertains to those elements of a protective structure which fail and whose strength and mass are such as to reduce the amplification of the shock pressures and the confinement of the explosive gases. To reduce the amplification of the shock pressures, frangible elements must fail so as to relieve quickly the interior pressures acting on those surfaces and minimize their reflection to the nonfrangible elements of the structure. Blast tests of glass panels have shown that a true frangible material does not exist and that some reflection of the initial blast pressures may be expected from very weak and light elements. Further, the buildup of gas pressures is a function of the ratio of the weight of the charge to the volume of the confining structure and the venting area. As stated, this pressure buildup will not begin until sometime after the onset of the shock pressures. Therefore, an element which is not considered frangible for the shock pressure may be frangible for gas pressures.

In addition to being dependent upon the physical properties of an element, frangibility will also be a function of the magnitude of the applied blast loads and, therefore, a function of the quantity of explosive being contained and the distance from the frangible element. Although frangibility is imperfectly understood and difficult to measure, in general, it can be assumed that if a closure's resistance to outward motion is equal to or less than 25 pounds per square foot of surface area, the resistance can be neglected since the time to reach failure is practically zero. In this case, frangibility can be stated solely in terms of the weight (inertial force) of the vent area closure. For resistances greater than 25 psf, the evaluation of frangibility must include the effects of resistance in addition to the weight of an element. The combined effects of the inertial force and the resistance can be accounted for by performing a dynamic analysis and determining the time to reach failure. However, if the blast pressure is very large in comparison to the resistance of the element, the effects of the resistance can be neglected without introducing significant errors. Therefore, it is advantageous to use vent closures that are light and inherently weak and/or weakly supported; such as, corrugated metal decking supported on steel joists, metal panels for walls, plexiglass or thin fiberglass panels supported by wood or lightweight steel frames or gypsum board panels.

In the following paragraphs of this section, a simple cantilever barrier as well as cubicle-type and containment type structures will be discussed. The cubicles are assumed to have one or more surfaces which are open or frangible while the containment structures are either totally enclosed or have small

size openings. The effects of the inertia of frangible elements of these structures will be discussed in subsequent sections.

2-14.2. Shock Pressures

2-14.2.1. Blast Loadings

When an explosion occurs within a cubicle or containment-type structure, the peak pressures as well as the impulse associated with the shock front will be extremely high and will be amplified by the confining structure. Because of the close-in effects of the explosion and the reinforcement of blast pressures due to the reflections within the structure, the distribution of the shock loads on any one surface will be nonuniform with the structural surface closest to the explosion subjected to the maximum load.

An approximate method for the calculation of the internal shock pressures has been developed using theoretical procedures based on semi-empirical blast data and on the results of response tests on slabs. The calculated average shock pressures have been compared with those obtained from the results of tests of a scale-model steel cubicle and have shown good agreement for a wide range of cubicle configurations. This method consists of the determination of the peak pressures and impulses acting at various points of each interior surface and then integrating to obtain the total shock load. In order to simplify the calculation of the response of a protective structure wall to these applied loads, the peak pressures and total impulses are assumed to be uniformly distributed on the surface. The peak average pressure and the total average impulse are given for any wall surface. The actual distribution of the blast loads is highly irregular, because of the multiple reflections and time phasing and results in localized high shear stresses in the element. The use of the average blast loads, when designing, is predicated on the ability of the element to transfer these localized loads to regions of lower stress. Reinforced concrete with properly designed shear reinforcement and steel plates exhibit this characteristic.

The parameters which are necessary to determine the average shock loads are the structure's configuration and size, charge weight, and charge location. Figure 2-51 shows many possible simple barriers, cubicle configurations, and containment type structures as well as the definition of the various parameters pertaining to each. Surfaces depicted are not frangible for determining the shock loadings. The effects of frangibility will be discussed later.

Because of the wide range of required parameters, the procedure for the determination of the shock loads was programmed for solutions on a digital computer. The results of these calculations are presented in Figures 2-52 through 2-100 for the average peak reflected pressures p_r and Figures 2-101 through 2-149 for the average scaled unit impulse $i_r/W^{1/3}$. These shock loads are presented as a function of the parameters defining the configurations presented in Figure 2-51. Each illustration is for a particular combination of values of h/H, l/L, and N reflecting surfaces adjacent to the surface for which the shock loads are being calculated. The wall (if any) parallel and opposite to the surface in question has a negligible contribution to the shock loads for the range of parameters used and was therefore not considered.

The general procedure for use of the above illustrations is as follows:

1. From Figure 2-51, select the particular surface of the structure which conforms to the protective structure given and note N of adjacent reflecting surfaces as indicated in parenthesis.

2. Determine the values of the parameters indicated for the selected surface of the structure in Item 1 above and calculate the following quantities:

$$h/H,\ l/L,\ L/H,\ L/R_A,\ \text{and}\ Z_A = R_A/W^{1/3}.$$

3. Refer to Table 2-3 for the proper peak reflected pressure and impulse charts conforming to the number of adjacent reflected surfaces and the values of l/L and h/H of Item 2 above, and enter the charts to determine the values of p_r and $i_r/W^{1/3}$.

In most cases, the above procedure will require interpolation for one or more of the parameters which define a given situation, in order to obtain the correct average reflected pressure and average reflected impulse. Examples of this interpolation procedure are given in Appendix 2A.

Because of the limitations in the range of the test data and the limited number of values of the parameters given in the above shock load charts, extrapolation of the data given in Figures 2-52 through 2-149 may be required for some of the parameters involved. However, the limiting values as given in the charts for other parameters will not require extrapolation. The values of the average shock loads corresponding to the values of the parameters, which exceed their limiting values (as defined by the charts), will be approximately equal to those corresponding to the limiting values. The following are recommended procedures which will be applicable in most cases for either extrapolation or establishing the limits of impulse loads corresponding to values of the various parameter which exceed the limits of the charts:

1. To extrapolate beyond the limiting values of Z_A, plot a curve of values of p_r versus Z_A for constant values of L/R_A, L/H, h/H and l/L. Extrapolate curve to include the value of p_r corresponding to the value of Z_A required. Repeat similarly for value of $i_r/W^{1/3}$.

2. To extrapolate beyond the limiting values of L/R_A, extrapolate the given curve of p_r versus L/R_A for constant values of Z_A, L/H, h/H and l/L to include the value of p_r corresponding to the value of L/R_A required. Repeat this extrapolation for value of $i_r/W^{1/3}$.

3. Values of p_r and $i_r/W^{1/3}$ corresponding to values of L/H greater than 5 shall be taken as equal to those corresponding to L/H = 6 for actual values of Z_A, h/H, and l/L but with a fictitious value of L/R_A in which R_A is the actual value and L is a fictitious value equal to 5H.

4. Values of p_r and $i_r/W^{1/3}$ corresponding to values of l/L less than 0.10 and greater than 0.75 shall be taken as equal to those corresponding to l/L = 0.10 and 0.75, respectively.

5. Values of p_r and $i_r/W^{1/3}$ corresponding to values of h/H less than 0.10 and greater than 0.75 shall be taken as equal to those corresponding to h/H = 0.10 and 0.75, respectively.

A computer program is available which executes the interpolation procedure using numerical tables equivalent to Figure 2-52 through 2-149. Availability of this program is listed in Section 2-4.

A protective element subjected to high intensity shock pressures may be designed for the impulse rather than the pressure pulse only if the duration of the applied pressure acting on the element is short in comparison to its response time. However, if the time to reach maximum displacement is equal to or less than three times the load duration, then the pressure pulse should be used for these cases. The actual pressure-time relationship resulting from a pressure distribution on the element is highly irregular because of the multiple reflections and time phasing. For these cases, the pressure-time relationship may be approximated by a fictitious peak triangular pressure pulse. The average peak reflected pressure of the pulse is obtained from Figures 2-52 through 2-100 and the average impulse from Figure 2-101 through 2-149 and a fictitious duration is established as a function of the reflected pressure p_r and impulse i_r acting on the element.

$$to = 2i_r / p_r \qquad 2\text{-}2$$

The above solution for the average shock load does not account for increased blast effects produced by contact charges. Therefore, if the values of the average shock loads given in Figures 2-52 through 2-149 are to be applicable, a separation distance between the element and explosive must be maintained. This separation is measured between the surface of the element and the surface of either the actual charge or the spherical equivalent, whichever results in the larger normal distance between the element's surface and the center of the explosive (the radius of a spherical TNT charge is $r = 0.136\ W^{1/3}$). For the purposes of design, the following separation distances are recommended for various charge weights:

Weight of Explosive (lb)	Separation Distance
up to 500	1.0
501 to 1,000	1.5
1,001 to 2,000	2.0
2,001 to 3,000	2.5
above 3,000	3.0

The above separation distances do not apply to floor slabs or other similar structural elements placed on grade. However, a separation distance of at least one foot should be maintained to minimize the size of craters associated with contact explosions.

It should be noted that these separation distances do not necessarily conform to those specified by other government regulations; their use in a particular design must be approved by the cognizant military construction agency.

Average shock loads over entire wall or roof slabs were discussed above. An approximate method may be used to calculate shock loads over surfaces other than an entire wall. These surfaces might include a blast door, panel, column, or other such items found inside any shaped structure.

The method assumes a fictitious strip centered in front of the charge having a width equal to the normal distance R_A and a height equal to that of the struc-

ture. This is the maximum representative area that may be considered. Average shock loads can be determined on entire area or any surface falling within the boundaries of the representative area.

The procedure for determining the shock loads consists of partitioning the surface under consideration into subareas. These subareas do not need to be the same size. The angle of incidence to the center of each subarea is calculated. The reflected pressure and scaled impulse are determined for each subarea using Figures 2-9 and 2-10 respectively. A weighted average with respect to area is taken for both pressure and scaled impulse.

Both the pressure and the impulse are multiplied by a factor of 1.75 to account for secondary shocks. Idealized duration is calculated using Equation 2-2.

2-14.2.2. Frangibility

A frangible element, as defined here, is an element that exhibits a resistance to internal shock loads equal to or less than 25 pounds per square foot and will undergo significant displacement during the loading time of the shock pressures and, thereby, reduce the effects of the shock pressures acting on both the frangible panel itself and reflections to other elements of the structure.

The following are design procedures for determining the magnitude of applied shock pressures which will contribute to the displacement of the frangible element:

(1) Determine the peak average reflected pressure P_r and average impulse i_r acting on the frangible element assuming that the element is rigid (Figures 2-52 through 2-149).

(2) Calculate the unit weight of the frangible element and divide this weight by the sixth root of charge weight, $W_F/W^{1/6}$.

(3) Determine the fictitious scaled distance Z from Figure 2-7, which corresponds to the average impulse determined in Step 1.

(4) Determine the value of the factor f_r, of average impulse by using the value of $W_F/W^{1/6}$ from Step 2 and the fictitious scaled distance of Step 3 and utilizing Figure 2-150, contributing to the translation of the frangible element (may require interpolation).

(5) Calculate the value of the average impulse contributing to the translation of the frangible element by multiplying the values of i_r and f_r of steps 1 and 4 respectively.

(6) Contribute the value of the peak average pressure to the translation of the frangible element that is assumed to be equal to the value of P_r of Step 1.

The step by step procedure for determining the shock loads being reflected from a frangible element to an adjacent element is to:

(1) Determine the average peak reflected pressure P_r and the average reflected impulse i_r acting on the element in question, assuming that the adjoining frangible element will remain in place (figs. 2-52 through 2-149).

(2) Determine the average impulse acting on the element in question assuming that the adjoining frangible element is removed (figs. 2-52 through 2-149).

(3) Subtract the average impulse determined in Step 2 from the average impulse determined in Step 1.

(4) Calculate the unit weight of the frangible element and divide this weight by the sixth root of the charge weight, $W_F/W^{1/6}$.

(5) Calculate the normal scaled distance Z between the center of the charge and the surface of the frangible element.

(6) Utilize Figure 2-150 to determine the value of the fraction f_r of the average impulse reflected to the element in question using the scaled weight density and scaled distance of Steps 4 and 5, respectively (may require interpolation).

(7) Determine the magnitude of the impulse load reflected to the element in question from the frangible element by multiplying the value of the average impulse of Step 3 by the value of f_r of Step 6.

(8) Determine the total impulse load acting on the element in question by adding the impulse loads determined in Steps 2 and 7.

(9) Calculate the peak average reflected pressure of the shock loads acting on the element in question making it equal to the value of P_r of Step 1.

In the above procedure, it is assumed that the frangible element will remain intact while being displaced away from the structure. If the element fails while being translated, then the portion of the shock pressure impulse displacing the element as well as that portion of the impulse being reflected to other elements will be reduced because of additional venting area produced by the element's "break up".

2-14.2.3. TNT Equivalency

The shock loads presented in Figure 2-52 through 2-149 pertain to the blast effects of bare spherical TNT explosives and must be extended to include other potentially mass-detonating materials. However, only a limited amount of testing has been performed to determine the TNT equivalency of confined explosives. Therefore, as an interim procedure, it is suggested that the determination of shock pressures for confined explosives other than TNT utilize equivalencies based on Equation 2-1.

The above relationship assumes that the explosive in question is a bare charge and spherical in shape. If the charge is not spherical, then it is suggested that the explosive be subdivided into several segments which will have approx-

imately equal dimensions and that the reflected impulse for any segment be calculated, as previously discussed. The reflected impulse of the total charge is then determined by multiplying the impulse of the individual segments by the total number of segments. The peak average reflected pressure is calculated by assuming the total charge as having a spherical shape. The impulse load for multiple explosives is obtained in a similar manner except that the locations of the individual charges are considered in calculating their individual impulse load. The impulse load of the total charge is determined by adding together the individual impulse loads. The average peak reflected pressure is calculated using the total weight of the explosive located at the centroid of the individual charges.

The explosive casing will have an effect on the magnitude of the shock pressures. These effects are dependent on the properties of the casing such as material, thickness, shape, etc. A review of a limited amount of surface detonated test data has indicated that the effects of the casing are not severe and, therefore, for design purposes it is recommended that casing effects be neglected.

2-14.2.4. Multiple Explosions

The blast pressures and impulse loads, acting on various elements of cubicle or other similar structures, which are produced by multiple explosions, will usually differ from those produced by a single explosion of the same amount of explosives.

Although the magnitude of the total combined impulse produced by the multiple explosions will usually be larger than that produced by the single explosion, the damage to a protective element due to the impulse of the multiple detonation may be either greater, equal to, or less than that produced by the impulse of the single explosion. For a given total impulse, the degree of damage to a protective element will be defined by the duration of the entire load relative to the response time of the element (time to reach maximum deflection).

A minimum amount of theoretical and experimental data is available concerning the degree of damage sustained by structural elements due to multiple explosions. However, results of response tests of reinforced concrete slabs have indicated that if the total combined duration of the blast loads produced by simultaneously or near simultaneously exploded charges is equal to or less than one-third the response time (time to reach maximum deflection) of the element, then the total combined impulse acting on the element can be estimated by numerically adding the impulse loads produced by the individual explosions. However, if the total combined duration of the blast loads is greater than one-third the response time, the actual pressure-time relationship of the combined loads approximated by a fictitious peaked triangular pressure pulse (similar to that of a single explosion) should be considered. The blast loads produced by charges that are not simultaneously or near simultaneously exploded may be considered as two or more impulse loads, two or more pressure-time loads, or a combination of impulse and pressure-time loads depending on the time delay and the duration of the individual loads compared to the response time of the element. A load or group of loads should be treated as an impulse load if the duration (one load or the combined duration of two or more loads) of the loading is less than one-third the time interval between the on-set of the load or group of loads and the response time of the member.

The duration of the blast loads due to multiple explosions may be approximated by considering the interrelationship between (a) the time intervals between individual explosions , (b) arrival times of the blast waves of the individual explosions at the element and (c) the fictitious duration of the pressure load from individual explosions. Because of the many variables involved, a relationship cannot be given to obtain the duration of the blast loads due to multiple explosions. Each situation will require a series of computations involving the time increments outlined above.

2-14.3. Gas Pressures

2-14.3.1. Blast Loadings

When an explosion occurs within a confined area, gaseous products will accumulate and a temperature within the structure will rise, thereby forming blast pressures whose magnitude is generally less than that of the shock pressure but whose duration is significantly longer. The magnitude of the gas pressures as well as their durations is a function of the size of the vent openings in the structure. For very small openings or no openings at all, the duration of the gas pressures will be very long in comparison to the fundamental periods of the structure's elements and, therefore, may be considered as a long duration load similar to that associated with a nuclear event.

These conditions usually occur in total or near containment type structures. In the former, the internal blast pressures must be contained because of the presence of toxic or other harmful materials in the structure. In near containment structures, the leakage of pressure flow out of the structure usually must be limited because of either personnel or frangible structure are located immediately adjacent to the donor structure. In other cases, however, openings in structures may be quite large, thereby minimizing the products' accumulation and limiting the temperature rise, hence producing gas pressures with limited duration or no duration at all. The structures without gas pressure buildup are referred to as fully vented structures.

A typical pressure-time record at a point on the interior surface of a partially vented chamber is shown in Figure 2-151. The high peaks are the multiple reflections associated with shock pressures. The gas pressure, denoted as p_g, is used as the basis for design and is a function of the charge weight and the contained net volume of the chamber.

Figure 2-152 shows an experimentally fitted curve based upon test results of partially vented chambers with small venting areas where the vent properties ranged between:

$$0 \leq A_f/V^{2/3} \leq 0.022 \qquad 2\text{-}3$$

The values of A and V_f are the chamber's total vent area and free volume which is equal to the total volume minus the volume of all interior equipment, structural elements, etc. The maximum gas pressure, P_g, is plotted against the charge weight to free volume ratio.

Figures 2-153 through 2-164 provide the relationship of the gas pressure scaled impulse $i_g/W^{1/3}$ as a function of the charge weight to free volume ratio

W/V_f, scaled value of the vent opening $A/V_f^{2/3}$, the scaled unit weight of the cover $W_f/W^{1/3}$ over the opening, and the scaled average reflected impulse $i_r/W^{1/3}$ of the shock pressures acting on the frangible wall (Section 2-14.2.2) or a non-frangible wall with a vent opening. (The curves in figures 2-153 through 2-164 for $W_F/W^{1/3} = 0$ were obtained from data with $A/V_f^{2/3} \leq 1.0$. Extrapolated values, for which there is less confidence, are dashed. Curves for $W_F/W^{1/3} > 0$ are not dashed at $A/V_f^{2/3} > 1.0$ because they are not strongly dependent on the extrapolated portion of the curve for $W_F/W^{1/3} = 0$. Even lightweight frangible panels displace slowly enough that the majority of the gas impulse is developed before significant venting ($A/V_f^{2/3} > 1$) can occur.) For a full containment type structure the impulse of the gas pressure will be infinite in comparison to the response time of the elements (long duration load). For near containment type structures where venting is permitted through vent openings without covers, then the impulse loads of the gas pressures are determined using the scaled weight of the cover equal to zero. The impulse loads of the gas pressures corresponding to scaled weight of the cover greater than zero relates to frangible covers and will be discussed later. The effects on the gas pressure impulse caused by the shock impulse loads will vary. The gas impulse loads will have greater variance at lower shock impulse loads than at higher loads. Interpolation will be required for the variation of gas impulse as a function of the shock impulse loads. This interpolation can be performed in a manner similar to the interpolation for the shock pressures.

A computer program is available which executes the interpolation procedure. Availability of this program is listed in Section 2-4.

The actual duration and the pressure-time variation of the gas pressures is not required for the analysis of most structural elements. Similar to the shock pressures, the actual pressure-time relationship can be approximated by a fictitious peak triangular pulse. The peak gas pressure is obtained from Figure 2-152 and the impulse from Figures 2-153 through 2-164 and the fictitious duration is calculated from the following:

$$t_g = 2i_g / P_g \qquad 2\text{-}4$$

Figure 2-165a illustrates an idealized pressure-time curve considering both the shock and gas pressures. As the duration of the gas pressures approach that of the shock pressures, the effects of the gas pressures on the response of the elements diminishes until the duration of both the shock and gas pressures are equal and the structure is said to be fully vented.

If a chamber is relatively small and/or square in plan area then the magnitude of the gas pressure acting on an individual element will not vary significantly. For design purposes the gas pressures may be considered to be uniform on all members. When the chamber is quite long in one direction and the explosion occurs at one end of the structure, the magnitude of the gas pressures will initially vary along the length of the structure. At the end where the explosion occurs, the peak gas pressure is P_{g1} (Fig. 2-165b) which after a finite time decays to P_{g2}, and finally decays to zero. The gas pressure P_{g2} is based on the total volume of the structure and is obtained from Figure 2-152 while the time for this pressure to decay to zero is calculated from Equation 2-4 where the impulse is obtained from Figures 2-153 through 2-164 again for the total volume of the structure. The peak gas pressure P_{g1} is obtained from Figure 2-152 based on a pseudo volume (Fig. 2-165b) whose length is equal to

its width and the height is the actual height of the structure. The time t_p for the gas pressure to decay from P_{g1} to P_{g2} is taken as the actual length of the structure minus the width divided by the velocity of sound (1.12 fpms). At the end where the explosion occurs, the peak gas pressures (P_{g1}, Figure 2-165b) will be a maximum and, after a finite time, they will decay to a value (P_{g2}, Figure 2-165b) which is consistent with full volume of the structure; after which they will decay to zero. The magnitude of the peak gas pressures (P_{g1}) may be evaluated by utilizing Figure 2-152 and a pseudo volume whose length is equal to its width and the height is the actual height of the chamber. The length of time t_p between the two peak gas pressures may be taken as the length minus the width of the structure divided by the velocity of sound (1 fpms).

2-14.3.2. Frangibility

Similar to shock pressures, an element can be considered frangible if it is designed such that its resistance to internal blast forces does not exceed 25 psf and that it will undergo significant displacement during the shock and gas loading phases. Figures 2-153 through 2-164 present the method for determining the gas pressure impulse acting on the interior surfaces of the donor structure. These impulse loads will vary as the mass of the cover over the vent opening varies; that is, the heavier the vent opening cover, the larger the gas pressure impulse. Like the vented structures, the internal gas pressure impulse loads produced by a frangible cover must be interpolated as a function of the shock pressure impulse loads.

2-14.3.3. TNT Equivalency

The data presented in Figure 2-152 and Figures 2-153 to 2-164 are for TNT only and must be extended to include other potentially mass-detonating materials. Similar to the shock pressures, only a limited amount of data is available regarding the TNT equivalency of confined explosions and in particular the effects produced on gas pressures. It has been suggested that the TNT equivalency of explosives relating to gas pressures is a function of both the heat of detonation as well as the heat of combustion, while for the shock pressures, the TNT equivalency is a function of the former only. A relationship has been developed based on a limited amount of testing as follows:

$$W_{E_g} = \frac{\phi\,[H^c_{EXP} - H^d_{EXP}] + H^d_{EXP}}{\phi\,[H^c_{TNT} - H^d_{TNT}] + H^d_{TNT}}\, W_{EXP} \qquad 2\text{-}5$$

where

W_{E_g} - effective charge weight for gas pressure

H^c_{TNT} - heat of combustion of TNT

H^c_{EXP} - heat of combustion of explosive in question

ϕ - TNT conversion factor (Figure 2-166)

H^d_{TNT} - heat of detonation of TNT

H^d_{EXP} - heat of detonation of explosion in question

W_{EXP} - weight of explosive in question

Gas pressures will be increased because of casings, in particular, if the casing is combustible. Since only unrelated data are available concerning the effects on gas pressures by the casing, a method of compensating for these effects is to adjust the heat of combustion of the given explosive material in Equation 2-5 to account for the heat of combustion of the casing material. This adjustment should be made by chemically combining the heat of combustion of the explosive and casing.

2-14.3.4. Multiple Explosions

The gas pressure produced by the release of the gaseous products of multiple explosions in a confined area may be approximated by considering the explosion to be produced by a single explosive whose weight is equal to the combined weights of the individual charges. This approximation is accurate if the individual charges are positioned in the immediate vicinity of one another and if near simultaneous detonation of the individual charges occurs. If the individual charges are not close to one another and/or positioned at one end of the structure, the magnitude of the gas pressures will initially vary along the length or width of the structure. This variation may be determined in a manner similar to that described in Section 2-14.3.1.

2-14.4. Leakage Pressures

2-14.4.1. Introduction

When an explosion occurs inside a vented chamber, shock pressures escape to the outside along with venting of the gas pressures. Trailing shocks overrun and coalesce with the lead shock at some distance to form a single diverging shock wave. Close to the structure, the blast pressures are affected by the structure itself as the shock pressures spill around the edges of the structure and form highly turbulent vortices. At further distances, this effect is no longer present and the shock pressure decreases with increasing distances. The leakage pressures are enhanced in the direction of venting (front) and reduced to the side and rear. The enhancement of pressures in the front and reduction of pressures to the side and rear are less extreme as the distance away from the structure is increased.

The blast environment outside of cubicle containing fully and partially vented explosions is presented in this section. Pressures and impulses acting on the ground surface are provided as a function of distance from the explosion, direction (front, side, back) relative to the vent opening in the structure, area of the vent opening and volume of the structure. For design purposes, the remaining blast parameters corresponding to the pressure and impulse acting on the ground surface may be obtained from Figure 2-15 and 2-16 in exactly the same manner as a surface burst of an explosive other than TNT.

Explosions in three and four wall cubicles are considered. Three wall cubicles are fully vented structures. The blast environment is furnished for cubicles with or without roofs. Four wall cubicles with a vent opening located either in the roof or one wall are considered. The size of the vent opening is varied from that of a fully vented cubicle through a full range of partially vented structures.

The data presented is based on tests in which the vent openings were completely open. There were no frangible covers over the vent area which might inhibit the pressure flow. Vent openings in protective structures are normally covered with frangible panels for weather protection, separation of operations, etc. These panels will affect the leakage pressures. However, it is assumed that these frangible panels will reduce the shock pressures leaking through the opening to a greater extent than the increase in the internal gas pressure buildup. Therefore, use of this data will predict conservative leakage pressures from cubicles with frangible covers.

2-14.4.2. Fully Vented Three Wall Cubicles

For cubicle-type structures where full venting is provided through the frangible or open portion of the structure, the resulting blast wave exterior of the cubicle will be appreciably modified as compared to an unbarricaded detonation. As the blast wave propagates out from the center of the explosion, the shock front will collide with the interior surfaces of the structure. These collisions will reflect and reinforce the initial loads (pressure and impulse). Eventually these pressures will spill over and around the blast walls, and in the event of rapid collapse of frangible walls, through the structure to the surrounding area. The exterior pressures will not initially have a definite shock front but will, at some distance from the structure, shock-up with frontal pressures similar to those produced by a surface burst. The pressure distance gradients away from the explosion will vary in all directions. This variation is defined by the configuration (shape, openings, etc.) of the protective structure containing the explosion.

A series of tests have been performed on three wall cubicle type structures illustrated in Figure 2-167. Cubic and rectangular three wall cubicles with and without a roof were tested. The results indicated that several parameters were important:

(1) Direction. Three directions illustrated in Figure 2-167 are considered. The direction normal to the open wall is called the front. The directions perpendicular to the front normal are called the sides. The direction opposite the normal to the open wall is called the back. The blast pressures out the front are greater than that to the side which, in turn, are greater than that to the back.

(2) Structure geometry. Differences were found in the blast environment depending upon whether the shape of the structure was cubic or rectangular. This was true for pressure and impulse measurements to the side and back, and only impulse to the front. There were no differences in pressure out the front for the cubicle and rectangular structures. The difference in pressures to the side and back occur only close to the structure. Far from the structure, there is no effect on pressure in any direction due to

structure shape. However, impulse does not converge with distance for differences in cubicle shape.

(3) Charge weight to volume ratio W/V and distance. The ratio W/V does not have an effect on the pressure to the front of any cubicle. There is an effect of W/V on pressure to the side and back of all cubicles, but only close to the structure. For a particular W/V, the pressure is affected differently for a cubic or rectangular structure. Thus, the effect on pressure close in depends both on structure size and W/V. But, for further out, neither affect the pressures. For all values of Z, there is a measured effect of W/V on impulse.

(4) Venting through the roof. For any direction, cubicle shape, and W/V value, there are differences in blast pressure and impulse based solely on whether or not venting could occur through the roof.

(5) Scaled distance Z. Both blast pressure and scaled impulse are affected by scaled distance from the explosion. This parameter is not independent of other factors.

The pressure variation in the front, side, and back direction of any three wall cubicle without a roof is given in Figure 2-168 while for a three wall cubicle with a roof the pressure variation is given in Figure 2-169. Due to interferences from the side and back walls which cause complex vortices near the structure and coalescence of shock waves in close, there is a maximum pressure produced in the side and back directions. These pressures are a function of the charge weight to cubicle volume ratio, W/V, and the configuration of the cubicle. The maximum peak pressure in the side or back direction of three wall cubicles with or without a roof are given in Figure 2-170.

The scaled peak positive impulse in the front, side, and back direction of three wall cubicles is given in Figures 2-171 through 2-182. The scaled impulse is given as a function of scaled distance from the explosion for various values of charge weight to structure volume ratio. The curves are presented in two groups; three wall cubicles without roofs and then cubicles with roofs. For each direction, the impulse is given for explosions in cubic and rectangular cubicles, respectively.

2-14.4.3. Partially vented four wall cubicles - vent opening in roof

Four wall cubicles with a vent openings located in the roof will produce blast pressures on the ground surface which are symmetric about the vent opening. Leakage pressures were determined for a below ground cubicle with its roof flush with the ground surface (Fig. 2-183a). Figure 2-183b shows the above-ground four wall cubicle. The vent opening was centrally located in the roof, and various vent areas were considered. The blast pressure was determined to be a strong function of the vent area divided by the structure volume to the two-thirds power ($A/V^{2/3}$) and the scaled distance, and a very weak function of the charge weight to volume ratio W/V which can be ignored with negligible error.

The leakage pressures resulting from an explosion in a partially vented below-ground cubicle with a vent opening in its roof is given in Figure 2-184, and

the impulse is given in Figure 2-185. The scaled ground distance as indicated in Figure 2-183a is used in these charts for the below-ground structures.

Figures 2-184 and 2-185 may also be used to determine the pressure and impulse acting on the ground surface for above-ground four wall cubicles (Fig. 2-183b). For an above-ground structure, the shock front must travel a longer distance than a below-ground structure. Therefore, the scaled distance that must be used in Figures 2-184 and 2-185 is approximated by the addition of the slant and horizontal distances indicated in Figure 2-183b.

The figures are useful in selecting the degree of venting required to limit leakage pressures outside roof-vented four wall cubicles to a specified safe level at safe given distance. From a knowledge of the pressure and impulse on the ground surface, the blast load acting on a structure may be obtained from the procedures given in this report. Thus, an adjacent structure may be designed to resist a blast load resulting from a given vent opening or the vent opening may be varied to suit the capacity of an adjacent structure.

2-14.4.4. Partially vented four wall cubicle - vent opening through wall

Leakage pressures resulting from an explosion in a partially vented four wall cubicle where the vent opening is located in a wall (Fig. 2-186) have not been documented. These leakage pressures have a variation in direction similar to a three wall cubicle with a roof and a variation with vent opening similar to a roof vented four wall cubicle. Extrapolation of the data for these types of cubicles have resulted in Figures 2-187 through 2-189. These figures present a reasonable estimate of the pressures produced in the front, side, and back directions (Fig. 2-186). In addition to direction, these pressures are a function of scaled distance and the vent area divided by the volume to the two-thirds power (A/V**(2/3)).

2-15. External Blast Loads on Structures

2-15.1. General

The blast loading on a structure caused by a high-explosive detonation is dependent upon several factors:

(1) The magnitude of the explosion.
(2) The location of the explosion relative to the structure in question (unconfined or confined).
(3) The geometrical configuration of the structure.
(4) The structure orientation with respect to the explosion and the ground surface (above, flush with, or below the ground).

The procedures presented here for the determination of the external blast loads on structures are restricted to rectangular structures positioned above the ground surface where the structure will be subjected to a plane wave shock front. The procedures can be extended to include structures of other shapes (cylindrical, arch, spherical, etc.) as well as structures positioned at and below the ground surface.

2-15.2. Forces Acting on Structure

The forces acting on a structure associated with a plane shock wave are dependent upon both the peak pressure and the impulse of the incident and dynamic pressures acting in the free-field. The peak pressures and impulses associated with the free-field shock wave have been presented for various explosives.

For each pressure range there is a particle or wind velocity associated with the blast wave that causes a dynamic pressure on objects in the path of the wave. In the free field, these dynamic pressures are essentially functions of the air density and particle velocity. For typical conditions, standard relationships have been established between the peak incident pressure (P_{so}), the peak dynamic pressure (q_o), the particle velocity, and the air density behind the shock front. The magnitude of the dynamic pressures, particle velocity and air density is solely a function of the peak incident pressure, and, therefore, independent of the explosion size. Figure 2-3 gives the values of the parameters versus the peak incident pressure. Of the three parameters, the dynamic pressure is the most important for determining the loads on structures.

For design purposes, it is necessary to establish the variation or decay of both the incident and dynamic pressures with time since the effects on the structure subjected to a blast loading depend upon the intensity-time history of the loading as well as on the peak intensity. The form of the incident blast wave (Fig. 2-190) is characterized by an abrupt rise in pressure to a peak value, a period of decay to ambient pressure and a period in which the pressure drops below ambient (negative pressure phase).

The rate of decay of the incident and dynamic pressures, after the passage of the shock front, is a function of the peak pressure (both positive and negative phases) and the size of the detonation. For design purposes, the actual decay of the incidental pressure may be approximated by the rise of an equivalent triangular pressure pulse. The actual positive duration is replaced by a fictitious duration which is expressed as a function of the total positive impulse and peak pressure:

$$t_{of} = 2i/p \qquad 2\text{-}6$$

The above relationship for the equivalent triangular pulse is applicable to the incident as well as the reflected pressures; however, in the case of the latter, the value of the pressure and impulse used with Equation 2-6 is equivalent to that associated with the reflected wave. The fictitious duration of the dynamic pressure may be assumed to be equal to that of the incident pressure.

For determining the pressure-time data for the negative phase, a similar procedure as used in the evaluation of the idealized positive phase may be utilized. The equivalent negative pressure-time curve will have a time of rise equal to 0.25 to whereas the fictitious duration t_{of}^- is given by the triangular equivalent pulse equation:

$$t_{of}^- = 2i^-/p^- \qquad 2\text{-}7$$

where i^- and p^- are the total impulse and peak pressure of the negative pulse of either the incident or reflected waves. The effects of the dynamic pressure in the magazine phase region usually may be neglected.

Since the fictitious duration of the positive phase will be smaller in magnitude than the actual duration, a time gap will occur between the fictitious duration and the onset of the negative phase. This time gap, which is illustrated in Figure 2-190, should be maintained in an analysis for consistency of the onset of the various load phasings.

2-15.3. Above-Ground Rectangular Structure Without Openings

2-15.3.1. General

For any given set of free-field incident and dynamic pressure pulses, the forces imparted to an above-ground structure can be divided into four general components: (a) the force resulting from the incident pressure, (b) the force associated with the dynamic pressures, (c) the force resulting from the reflection of the incident pressure impinging upon an interfering surface, and (d) the pressures associated with the negative phase of the shock wave. The relative significance of each of these components is dependent upon the geometrical configuration and size of the structure, the orientation of the structure relative to the shock front, and the design purpose of the blast loads.

The interaction of the incident blast wave with a structure is a complicated process. To reduce the complex problem of blast to reasonable terms, it will be assumed that (a) the structure is generally rectangular in shape, (b) the incident pressure of interest is 200 psi or less, (c) the structure being loaded is in the region of the Mach stem, and (d) the Mach stem extends above the height of the building.

2-15.3.2. Front Wall Loads

For a rectangular above-ground structure at low pressure ranges, the variation with time on the side facing the detonation (front face) when this side is parallel to the shock front (normal reflection) is illustrated in Figure 2-191a. At the moment the incident shock front strikes the front wall, the pressure immediately rises from zero to the normal reflected pressure, P_r, which is a function of the incident pressure (Fig. 2-15). The clearing time, t_c, required to relieve the reflected pressure is represented as:

$$t_c = \frac{4S}{(1 + R)\, C_r} \qquad 2\text{-}8$$

where

S = clearing distance and is equal to H or W/2 (Fig. 2-191a) whichever is the smallest

H = height of the structure

R = ratio of S/G where G is equal to H or W/2 (Fig. 2-191) whichever is larger

C_r = sound velocity in reflected region (Fig. 2-192)

The pressure acting on the front wall after time t_c is the algebraic sum of the incident pressure P_s and the drag pressure $C_D q$ or:

$$P = P_s + C_D q \qquad 2\text{-}9$$

The drag coefficient C_D gives the relationship between the dynamic pressure and the total translational pressure in the direction of the wind produced by the dynamic pressure and varies with the Mach number (or with the Reynold's number at low incident pressures) and the relative geometry of the structure. A value of C_D=1 for the front wall is considered adequate for the pressure ranges considered in this manual. At higher pressure ranges, the above procedure may yield a fictitious pressure-time curve because of the extremely short pressure pulse durations involved. Therefore, the pressure-time curve constructed must be checked to determine its accuracy. The comparison is made by constructing a second curve (dotted triangle as indicated in Fig. 2-191a) using the total reflected pressure impulse i_r from Figure 2-15 for a normal reflected shock wave (Fig. 2-191a). The fictitious duration t_{rf} for the normal reflected wave is calculated from:

$$t_{rf} = 2i_r / P_r \qquad 2\text{-}10$$

where P_r is the peak normal reflected pressure (Fig. 2-15). Whichever curve (Fig. 2-191a) gives the smallest value of the impulse (area under curve), that curve should be used in calculating the wall loading.

If the shock front approaches the structure at an oblique angle (Fig. 2-191b), then the peak pressure will be a function of the incident pressure and the incident angle between the front and the front wall and is obtained from Figure 2-193.

An equation similar to that used for the manual shock front may be used when the angle of obliquity is greater than zero as follows:

$$t_{rf} = 2i_{r\alpha} / P_{r\alpha} \qquad 2\text{-}11$$

where peak reflected impulse $i_{r\alpha}$ is obtained from Figure 2-194.

Usually only the positive pulse of the pressure-time relationship of Figure 2-191b is utilized for the front wall design since the negative pulse seldom affects the design. For determining the overall motion of the structure, the effects of negative pressures should be included. The peak negative reflected pressure (Fig. 2-190) and reflected impulse are obtained from Figure 2-16 and correspond to the peak incident pressure (Fig. 2-15) acting on the front wall. The rise time and decay of the negative pressures are similarly calculated as described in Section 2-15.2.

2-15.3.3. Roof and Side Walls

As the shock front traverses a structure a pressure is imparted to the roof slab, and side walls equal to the incident pressure at a given time at any specified point reduced by a negative drag pressure. The portion of the sur-

face loaded at a particular time is dependent upon the magnitude of the shock front incident pressure, the location of the shock front and the wavelength (L_w and L_w^-) of the positive and negative pulses.

To determine accurately the overall loading on a surface, a step-by-step analysis of the wave propagation across the surface should be made. This analysis includes an integration of the pressures at various points (Fig. 2-195a) on the surface and at various times to determine the equivalent uniform incident pressure acting on a span L as a function of time (Fig. 2-195b). Since the point of inflection of the element will vary as the shock front traverses the surface, in order to make the assumption of the uniform pressure valid, the reinforcement on both faces must be continuous across the span length.

As the shock wave traverses the roof, the peak value of the incident pressure decays and the wave length increases. As illustrated in Figure 2-195b, the equivalent uniform pressure will increase linearly from time t_f when the blast wave reaches the beginning of the element (point f) to time t_d when the peak equivalent uniform pressure is reached when the shock front arrives at point d. The equivalent uniform pressure will then decrease to zero where the blast load at point b on the element decreases to zero.

To simplify the calculations, the equivalent uniform pressure has been expressed as a function of the blast wave parameters at point f. The equivalent load factor C_E, the rise time, and duration of the equivalent uniform pressure are obtained from Figures 2-196, 2-197, and 2-198, as a function of the wave length-span ratio L_{wf}/L.

The peak value of the pressure acting on the roof P_R is the sum of contribution of the equivalent uniform pressure and drag pressure:

$$P_R = C_E P_{sof} + C_D q_{of} \qquad 2\text{-}12$$

where P_{sof} is the incident pressure occurring at point f and q_{of} is the dynamic pressure corresponding to $C_E P_{sof}$.

The drag coefficient C_D for the roof and side walls is a function of the peak dynamic pressure. Recommended values are as follows:

Peak dynamic pressure	Drag coefficient
0-25 psi	-0.40
25-50 psi	-0.30
50-130 psi	-0.20

The data presented above for the equivalent uniform roof and side wall blast pressures are used principally for the design of individual elements. For overall motions of a structure, the effects of the negative phase pressures should be included. The equivalent load factor C_E for the peak equivalent uniform negative pressure is obtained from Figure 2-196 as a function of the wavelength span ratio L_{wf}/L. The value of the negative pressure acting on the roof, P_R^- is equal to $C_E^- P_{sof}$ where the value of C_E^- is a minus value. The value of the equivalent negative pressure duration t_{of} is obtained from Figure 2-198. The value is not a function of the peak incident pressure at point f. The rise time of the negative phase is equal to 0.25 t_{of}.

If a side wall is positioned at an oblique angle to the shock front, then blast loads acting on the side wall are calculated in the same manner as that described for front walls.

2-15.3.4. Rear Wall

As the shock front passes over the rear edges of the roof and/or side walls the pressure front will expand, forming secondary waves which propagate over the rear wall. In the case of long buildings, the secondary wave enveloping the back wall essentially results from the spillover from the roof, and the side walls. In both cases, the secondary waves are reinforced due to their impingement with reflecting surfaces. The reinforcement of the spillover wave from the roof is produced by its reflection from the ground surface at the base of the rear wall, and the reinforcement of the secondary waves from the side walls is produced by their collision near the center of the wall and/or their interaction with the wave from the roof. Little information is available on the overall effects on the rear wall loading produced by the reflections of the secondary waves.

In most design cases, the primary reason for determining the blast loads acting on the rear wall is to determine the overall drag effects (both front and rear wall loadings) on the building. For this purpose, a procedure may be used where the blast loading on the rear wall Figure (2-199a) is calculated using the equivalent uniform method used for computing the blast loads on the roof and side walls. Here the peak pressure of the equivalent uniform pressure-time curve (Fig. 2-199b) is calculated using the peak pressure that would accrue at the back edge of the roof slab P_{sob}. The equivalent uniform load factors C_E and C_E^- are based on the wave length of the peak pressure above and the height of the rear wall H_s as are the time rises and duration of both the positive and negative phases.

Like the roof and side walls, the blast loads acting on the rear wall are a function of the drag pressures in addition to the incident pressure. The dynamic pressure of the drag corresponds to that associated with the equivalent pressure $C_E P_{sob}$, while the recommended drag coefficients are the same as used for the roof and side walls.

In the event that the back wall is positioned at an oblique angle to the shock front, peak incident pressure at point b should be calculated at the mid width.

2-15.3.5. Multiple Explosions

As previously mentioned, the blast loads, produced by multiple explosions, acting on structures located far from an explosion may consist of a series of separate pressure pulses rather than a single pulse blast load. However, the multiple pressure-pulse loading is usually associated with weights of explosives which are very small (several pounds) and, therefore, will not be the usual design situation. For large charge weights, however, the single pressure pulse loading with multiple peak pressures will occur. At the present time no specific method has been devised which will enable one to evaluate this type of blast loading. In the interim, it is suggested that the multiple peak pressure type loading be replaced by the pressure-pulse which is associated with the merged shock wave. The parameters of this shock wave and cor-

responding pressures are determined assuming a single explosion, the explosive weight of which is equal to the combined weight of the individual charges.

2-15.4. Above Ground Rectangular Structures with Openings.

2-15.4.1. General

Two structural configurations are usually encountered when blast loads are determined on structures with unsealed or unprotected openings in its exterior. The first configuration includes windows, doors or other openings located in both the front and rear walls as well as along the side walls of the structure. The second would include openings located only in the front face of the structure. The remaining surfaces are void of openings. The second configuration is the one most likely to be encountered since interior partitions will restrict the flow of the blast wave through the structure. Increased interior blast loads are produced due to the reflection of the blast wave on interior components. The blast loads associated with the second configuration are primarily discussed in this section with comments regarding the loads pertaining to the first configuration.

When a shock front strikes the front wall of a structure, the incident pressure is amplified. Windows and doors will fail almost immediately (approximately one millisecond) after the onset of the shock front unless they were designed to resist the applied load. As a result, blast pressures will flow into the structure through these openings. This sudden release of high pressure will cause a shock front to form inside of each opening. Each individual front will expand and tend to combine into a single front which will further expand throughout the structure's interior. This interior shock is initially weaker than the incident pressure at the building's exterior. However, the interior pressure will tend to get stronger due to reflections off interior building components.

An idealized structure configuration is shown in Figure 2-200. The incident shock front arriving at the front wall of the structure has an incident pressure P_{so} and wave length L_w. As the shock front sweeps across the structure, blast pressures enter the interior of the building through the opening in the front wall of area A_o. The area of multiple openings are added to obtain a fictitious single opening located at the center of the front wall. The blast pressures entering the building first load the interior surface of the front wall, followed by the interior surface of the side walls and roof, and finally the interior surface of the back wall. The idealized pressure-time load curves for these surfaces are presented in Figure 2-201. The procedures necessary to obtain the magnitude of the parameters given on the idealized load curves for a particular explosion are presented in the remainder of this section. Except for the front wall, the blast pressures acting on the exterior of the structure are not affected by the opening and are determined according to the procedures of the previous section.

The primary purpose of this section is to provide the blast loading on the interior surface of an exterior wall so that the maximum outward motion of the wall may be determined. It is not the intent to use these interior loads to reduce the exterior positive phase loading. Except for the front wall, accurate phasing of the interior and exterior blast loads are not possible. The interior loads will always lag the exterior positive phase loading and, due to reflections off interior components, the duration of the interior load is al-

ways longer. For design, the interior blast loads should be added to the negative phase exterior loading to obtain the maximum outward motion (negative response) of a side wall, roof or back wall. The maximum positive response should be determined for the exterior positive phase loading without any reductions due to internal pressures. In most instances, interior partitions are required to withstand the blast pressures leaking into a structure. The procedures presented in this section may be used to determine the design blast load acting on these elements. An interior partition located parallel to the front wall will reflect the shock front and, therefore, is considered as a back wall. The length of the side wall would then be taken as the distance between the front wall and this partition. An interior partition(s) perpendicular to and framing into the front wall may be considered as a side wall(s). The length of the front wall would then be taken as the distance between an interior partition and a side wall or between two interior partitions. In both cases, only the openings located between these partition walls would be considered as the vent opening.

The procedures presented in this section to determine interior blast loads acting on a structure with an opening in the front wall were developed for a shock front striking the front wall head-on. For the same size opening in a front wall, this orientation of the approaching shock front results in the most severe interior shock wave effects. The use of these procedures for shock fronts approaching at all other angles will result in conservative estimates of the blast loadings acting on the interior of the structure.

2-15.4.2. Exterior Front Wall Loads

The time required for reflected pressures to clear a solid front wall is expressed in multiples of the time necessary for a rarefaction wave to sweep the wall. When walls with openings are considered, clearing takes place ground the edges of the opening in addition to the edges of the wall. Depending upon the size of the overall wall and the openings, the clearing time of the reflected pressures may be significantly reduced.

The pressure-time relationship of the applied blast load acting on the front wall of a structure with openings is the same as that of a solid front wall (Fig. 2-191) except the clearing time will be reduced. To evaluate this reduced time, the value of S′ is introduced into Equation 2-8. This value is the weighted average distance that the rarefaction wave must travel to cover the wall assuming immediate access of the incident shock to the interior of the structure. If frangible covers (windows, doors) do not fail immediately, the clearing time should not be reduced.

The method for evaluating S′ is illustrated in Figure 2-202 where the face of the front wall is divided into rectangular areas. These areas are determined by the location and dimensions of the openings in the wall, and by consideration of the direction along which the reflected pressure clears around the area in the shortest possible time. The individual areas are labeled depending upon the number and location of the clearing sides of the individual areas. Clearing factors δ_n are established for these areas as follows:

Area	δ_n	Number of Clearing Sides
1	1.0	Two adjacent sides
2	0.5	Two opposite sides
3	1.0	One side
4	1.0	None

The weighted average clearing distance S′ is expressed as:

$$S' = \frac{\Sigma\, \delta_n\, h_n\, A_n}{A_f} \leq S \qquad 2\text{-}13$$

where

S' = weighted average clearing distance with openings

δ_n = clearing factor

h_n = average clearing distance for individual areas as follows:

Area 1 - width or height of area whichever is smaller
Area 2 - distance between opposite sides where clearing occurs
Area 3 - distance between side where clearing occurs and opposite side
Area 4 - same as Area 1

A_n = area of individual wall subdivision

A_f = net area of the wall excluding openings

The clearing time t'_c for a front wall with opening is calculated from Equation 2-8 in which S′ is substituted for S or

$$t'_c = \frac{4S'}{(1 + R)\, C_r} \qquad 2\text{-}14$$

where all components of Equation 2-14 have been previously defined. It should be realized that the load acting on the front wall with openings is still the same as that shown in Figure 2-191 except with the reduced clearing time, t'_c. The curve which represents the wall loading is still the curve which gives the lower impulse.

As previously stated, window breakage will require a finite length of time. This time may be evaluated using the resisting functions of Chapter VI and the dynamic procedures of Chapter 3. This time must be accounted for in determining the window contribution to the blast pressures acting on the wall.

2-15.4.3. Interior Front Wall Loads

The average pressure acting on the interior face of the front wall will initially build up in a similar manner as
the average pressure on the exterior back wall of a closed structure. However, vortices are located all around the interior edges of all openings in the front wall. The effect of these vortices, which tend to reduce the blast load, has been neglected.

The shock front entering through the opening in the front wall travels along the interior face of the front wall, thereby subjecting the wall to incident pressures. When the front reaches the side wall, it is reflected back. The length of wall loaded by this reflected wave is a function of the wave length, L_w. The average pressure acting on the wall is determined assuming a single opening of area A_o located at the center of the wall. In the case of multiple openings, a single opening equal to the combined area of all openings is located in the center of the front wall.

The idealized pressure-time blast load acting on the interior face of the front wall is shown in Figure 2-201a. The time at which the shock front arrives at the exterior surface of the front wall is taken as zero ($T_o = 0$). The blast load acting on the wall begins at time T_1. This time represents the time it takes for the shock front to enter the structure through the opening A_o. The pressure buildup is linear from time T_1 to a maximum pressure P_{max} at time T_2, and then it decays linearly to zero at time T_3.

The maximum average pressure P_{max} acting on the interior face of the front wall varies as a function of the incident pressure P_{so} and the wavelength L_w corresponding to that pressure, and the geometry of the wall. Figure 2-203 through 2-206 give the maximum pressure P_{max} acting on front walls having width to height ratios (W/H) equal to 3/4, 3/2, 3 and 6, respectively.

The idealized times T_1, T_2 and T_3 are also obtained from plots of front walls having width to height ratios W/H equal to 3/4, 3/2, 3 and 6. The arrival time T_1 of the load is given in Figures 2-207 and 2-208 as a function of the incident pressure acting on the exterior surface of the front wall P_{so} for various opening to wall area ratios A_o/A_w. The rise time of the load, $T_2 - T_1$ is given in Figures 2-209 and 2-210 as a function of P_{so} and various wave length to width of front ratios L_w/W. Finally, the duration of the load $T_3 - T_1$ is given in Figures 2-211 and 2-212 again as a function of P_{so} and L_w/W. The times T_2 and T_3 are obtained from subtracting T_1 from the rise time and duration, respectively.

Failure of the cover sealing openings in a building (windows, doors) will affect the onset of the blast load acting on the interior surface of the front wall. Due to the time required to cause failure of the covers, the onset of the interior pressures may not be in phase with the onset of the exterior blast load. Therefore, care must be taken to arrive at a combined loading for the structural element.

2-15.4.4. Interior Side Wall and Roof Loads

The blast pressures entering the interior of the building through the opening in the front wall (multiple openings are combined to form a single opening) must travel along the interior face of the front wall before arriving at the side wall. The incident pressures arriving at the side wall are increased due to reflection off the wall itself. The front expands and travels across the side wall until it reaches the back wall. It is then reflected off the back wall, and the reflected wave travels back across the side wall towards the front wall. The length of side wall loaded by this reflected wave is a function of the wave length L_w.

The idealized pressure-time blast load acting on the interior face of the side wall and roof is shown on Figure 2-201b. The same assumption is made for the

side wall and roof as for the interior front wall. That is, the time at which the shock front arrives at the front wall of the structure is taken as zero ($T_o = 0$). The time T_1 represents the time it takes the shock front to travel from the opening across the interior face of the front wall to the side wall (or roof). The pressure build up is linear from time T_1 to a maximum pressure Pmax at time T_2, remains constant until time T_3 and decays linearly to zero at time T_4. This idealized curve applies to both the side walls and roof. The structure configuration parameters as given in Figure 2-200 apply for side wall loadings. However, to determine the roof loading, the structure must be rotated 90 degrees so that the roof takes the position of a side wall. The width and height of the structure must be interchanged. All other parameters are not effected.

The maximum average pressure P_{max} acting on the interior face of the side wall (or roof) varies as a function of the incident pressure P_{so} acting on the exterior face of the front wall, the wavelength L_w corresponding to P_{so}, and the geometry of the structure. Since a large number of plots would be required to describe P_{max} for the blast and geometric parameters involved, an equation has been developed. The value of P_{max} is given by:

$$P_{max} = K/(L_w/L) \qquad 2\text{-}15$$

For $6 \geq W/H \leq 3/2$

$$K = (A + [B \times (L_w/L)^C]) \times D \times E \times P_{so}^{1.025} \qquad 2\text{-}16$$

where

$$A = [0.002\ (W/H)^{1.4467}] - 0.0213 \qquad 2\text{-}17$$

$$B = 2.2075 - [1.902\ (W/H)^{-0.085}] \qquad 2\text{-}18$$

$$C = 1.231 + [0.0008\ (W/H)^{2.678}] \qquad 2\text{-}19$$

$$D = [2.573\ (L/H)^{-0.444}] - 0.3911 \qquad 2\text{-}20$$

$$E = 0.4221 + [1.241\ (A_o/A_w)^{0.367}] \qquad 2\text{-}21$$

For $W/H = 3/4$

$$K = A \times B \times C^E \times F^H \times P_{so}^{0.9718} \qquad 2\text{-}22$$

where

$$A = [0.5422\ (L_w/L)^{1.2944}] - 0.001829 \qquad 2\text{-}23$$

$$B = [0.654 + 2.616\ (A_o/A_w) - 4.928\ (A_o/A_w)^2] \qquad 2\text{-}24$$
$$[2.209\ (L/H)^{-0.3451} - 0.739]$$

$$C = 0.829 + 0.104\ (L_w/L)^{1.6} \qquad 2\text{-}25$$
$$+ [0.00124 + 0.00414\ (L_w/L)^{3.334}]\ [L/H]^D$$

$$D = 2.579 - 0.0534\ (L_w/L)^{3.891} \qquad 2\text{-}26$$

$$E = 999\ (A_o/A_w)^{9.964} \qquad 2\text{-}27$$

$$F = 1.468 - 1.6627\ (A_o/A_w)^{0.7801} + [1.8692 - 1.1735\ (A_o/A_w)^{-0.2226}]\ [L_w/L]^G \qquad 2\text{-}28$$

$$G = 0.2979\ (A_o/A_w)^{-1.4872} - 0.8351 \qquad 2\text{-}29$$

$$H = (5.425 \times 10^{-4}) + (1.001 \times 10^{-9})\ (L/H)^{9.965} \qquad 2\text{-}30$$

For $3/2 > W/H > 3/4$, graphical interpolation is required to determine P_{max}. Several values of P_{max} are determined from Equation 2-15 for values of W/H equal to 3/4, 3/2, and preferably two values greater than 3/2. A plot of P_{max} versus W/H is prepared and the value of P_{max} is read for the required W/H.

The idealized times T_1 and T_2 are determined from Figure 2-213. These times are presented as a function of the incident pressure P_{so} arriving at the exterior of the building and the width to height ratio W/H of the front wall. Since the distance that the shock front must travel across the front wall is taken from the center of the opening, times T_1 and T_2 are not a function of the area of the opening. This assumption will not result in significant errors since the openings considered are comparatively small.

The idealized times T_3 and T_4 are determined from Figures 2-214 through 2-229. Each figure is prepared for a given structure configuration defined by the length to height ratio of the side wall L/H and the width to height ratio of the front wall W/H. The times T_3 and T_4 are given on each figure as a function of the incident pressure Pso and various values of the wave length to side wall length ratio L_w/L. As explained above, these times are not a function of the area of the opening. For ease of reference, these figures are listed in table 2-4 for the various L/H and W/H ratios provided. In most cases, interpolation will be required to obtain the correct values of T_3 and T_4 for the given structure configuration.

2-15.4.5. Interior Back Wall

The blast pressures entering the interior of the building through the opening in the front wall must travel the full length of the building before arriving at the back wall. The incident pressure arriving at the back wall is essentially uniform over the wall. This pressure is immediately increased to the normal reflected pressure when it strikes the back wall.

The idealized pressure-time blast load acting on the interior face of the back wall is shown in Figure 2-201c. Again, the time at which the shock front arrives at the front wall of the structure is taken as zero ($T_o = 0$). The time T_1 represents the time it takes the shock front to travel from the opening to the back wall. The pressure buildup is instantaneous to P_{RIB} due to the normal reflection of the shock front and then decays to zero at time T_2. This loading is similar to the loading of an exterior front wall except that clearing is not possible.

The maximum average pressure P_{RIB} acting on the back wall is obtained from Figures 2-230 and 2-231. Each figure is prepared for a given value of L/H. The ratio of the maximum average pressure on the back wall to the incident

pressure P_{RIB}/P_{so} is given as a function of P_{so} for various values of A_o/A_w. Interpolation between figures may be necessary for a given structural configuration.

The idealized time T_1 is determined from Figures 2-232 and 2-233. Each figure is prepared for a given value of the width to height ratio of the wall W/H. The time T_1 is given as a function of the incident pressure P_{so} for various values of the wall length to height ratio L/H and the ratio of the opening area to the wall area A_o/A_w. The duration of the load T_2-T_1 is determined from Figure 2-234. The time is given as a function of the incident pressure P_{so} for various values of A_o/A_w. Since the back wall is located at the greatest distance from the front wall, the area of the opening has a significant effect on these times and must be considered.

2-15.5. Pressure Buildup In Structures

2-15.5.1. General

The procedures in Section 2-15.4 are for determining the net effects of shock loads entering openings in structures from windows or doors which are not designed to withstand the applied blast loads. In certain cases, structures may have closures which are designed to resist the blast loading, but have very small openings due to vents and ducts, which will not withstand the blast. In this case, the small opening will not allow the shock front to develop inside the structure. However, the structure experiences an increase in its ambient pressure (a "filling" pressure) in a time that is a function of the structure volume, area of the openings, and applied exterior pressure and duration. Since personnel exhibit a tolerance limit to such pressure increases, a method of determining the average pressure inside the structure is needed. It should be noted that the interior pressures immediately adjacent to the openings will be higher than the average pressure.

2-15.5.2. Method of Calculation

The following procedure is applicable for structures with small area-volume ratios and applied blast pressures less than 150 psi. The change in pressure δP_i inside the structure within a time interval δt is a function of the pressure difference at the openings, $P-P_i$, and the area-volume ratio, A_o/V_o:

$$\delta P_i = C_L \, (A_o / V_o) \, \delta t \qquad 2\text{-}31$$

where

C_L = leakage pressure coefficient and a function of the pressure difference $P-P_i$ and is obtained from Figure 2-235

P = applied exterior pressure

P_i = interior pressure

δP_i = interior pressure increment

A_o = area of openings

V_o = structure volume

δt = time increment

The interior pressure-time curve is calculated as follows:

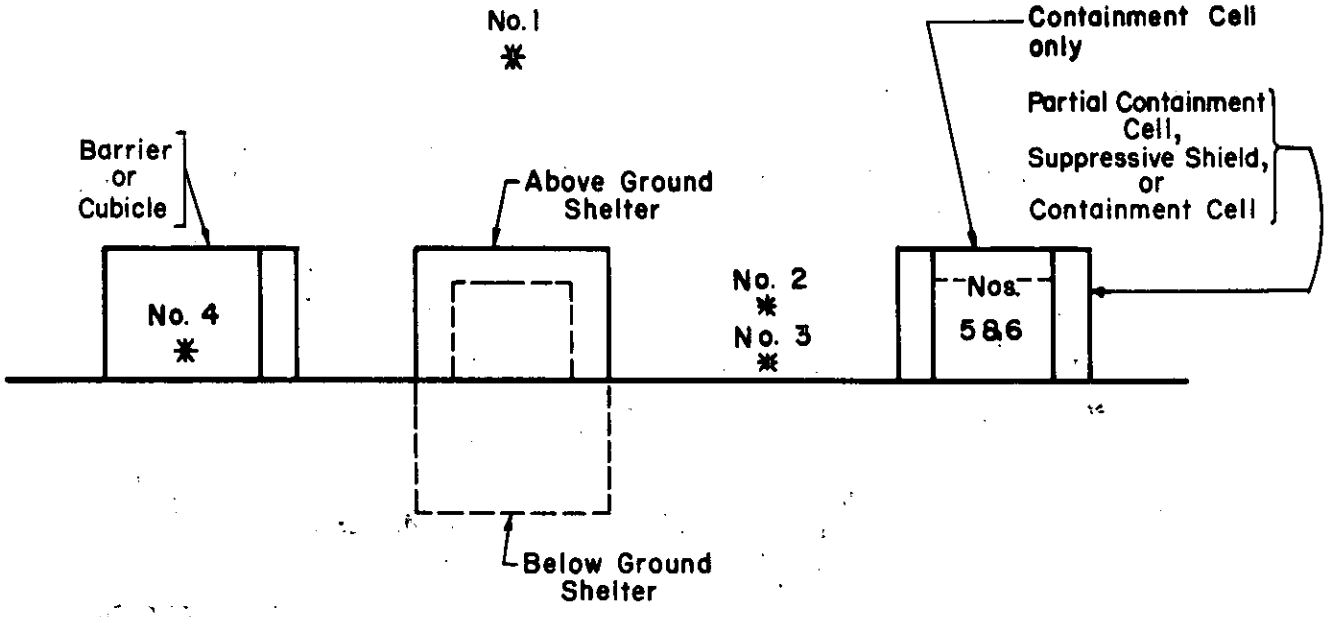
(1) Determine the pressure-time history of the applied blast pressures P acting on the surface surrounding the opening as presented in Section 2-15.3.

(2) Divide the duration to of the applied pressure into n equal intervals (δt), each interval being approximately $t_o/10$ to $t_o/20$, and determine the pressures at the end of each interval.

(3) Compute the pressure differential $P-P_i$ for each time interval, determine the corresponding value of C_L from Figure 2-235, and calculate δP_i from Equation 2-31 using the proper values of A_o/V_o and δt. Add δP_i to P_i for the interval being considered to obtain the new value of P_i for the next interval.

(4) Repeat for each interval using the proper values of P and P_i. When $P-P_i$ becomes negative during the analysis, the value of C_L must also be taken as negative.

The above procedure is most easily accomplished by using a tabular arrangement for the required computations. An illustrative example is presented in Appendix 2A.



BLAST LOADING CATEGORIES			
CHARGE CONFINEMENT	CATEGORY	PRESSURE LOADS	PROTECTIVE STRUCTURE
Unconfined Explosions	1. Free Air Burst 2. Air Burst 3. Surface Burst	a. Unreflected b. Reflected b. Reflected	Shelter
Confined Explosions	4. Fully Vented	c. Internal Shock d. Leakage	Cubicle
	5. Partially Confined	c. Internal Shock e. Internal Gas d. Leakage	Partial Containment Cell or Suppressive Shield
	6. Fully Confined	c. Internal Shock e. Internal Gas	Full Containment Cell

Figure 2-1 Blast loading categories

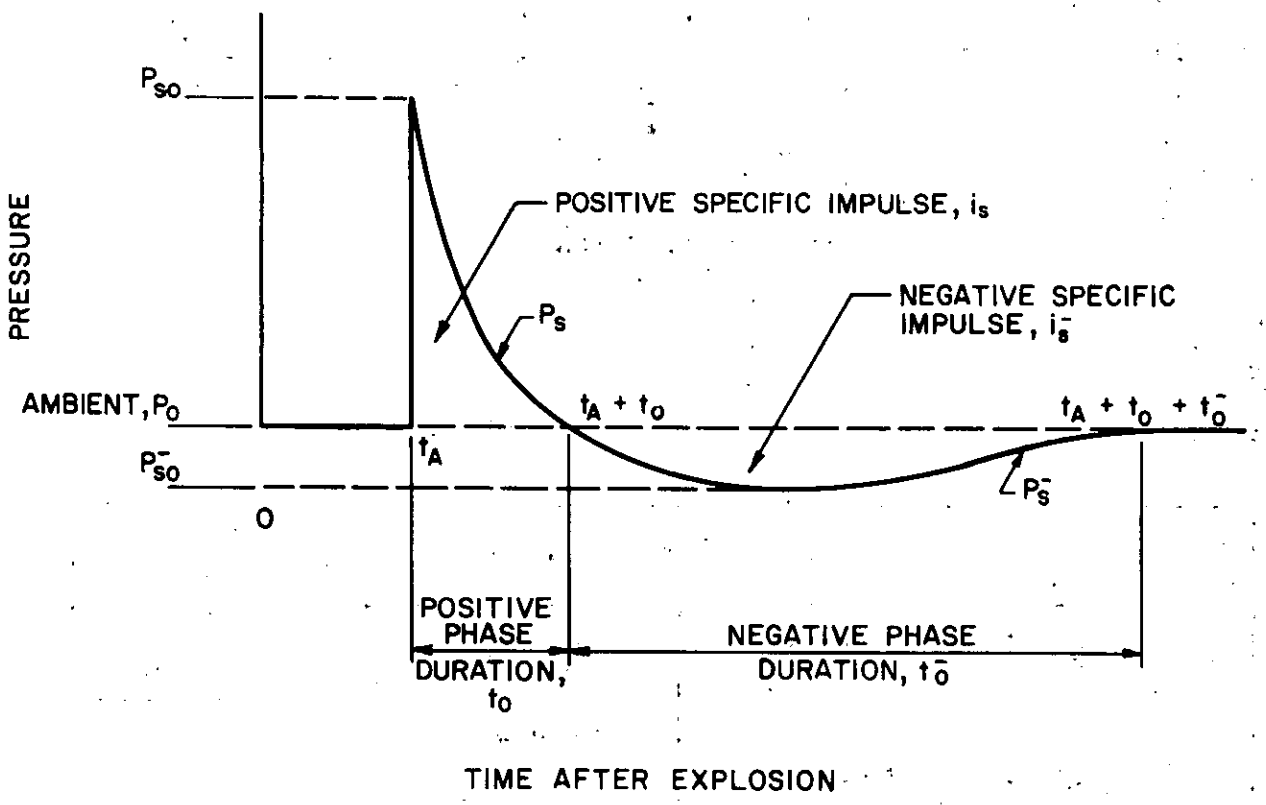


Figure 2-2 Free-field pressure-time variation

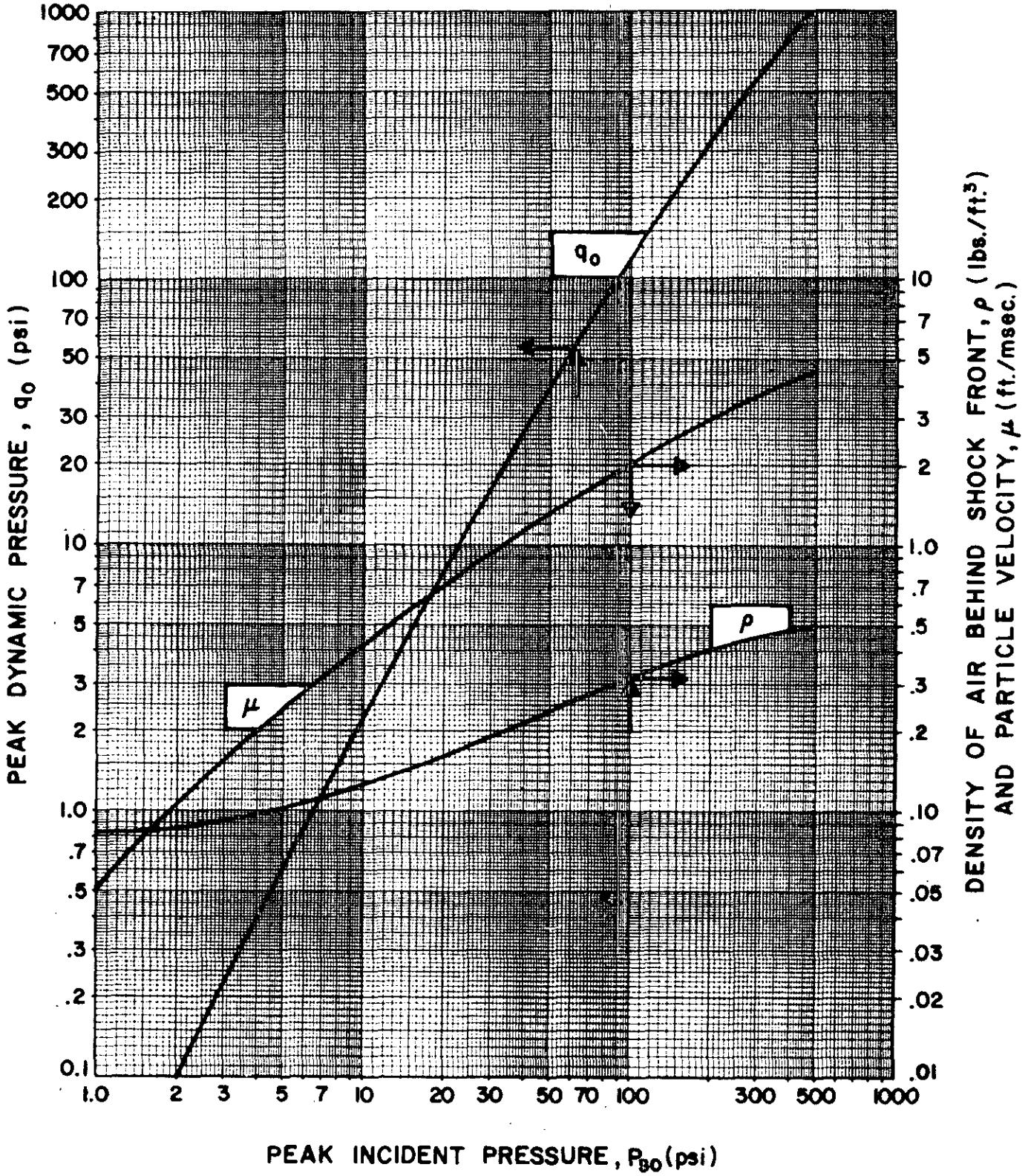


Figure 2-3 Peak incident pressure versus peak dynamic pressure density of air behind the shock front and particle velocity

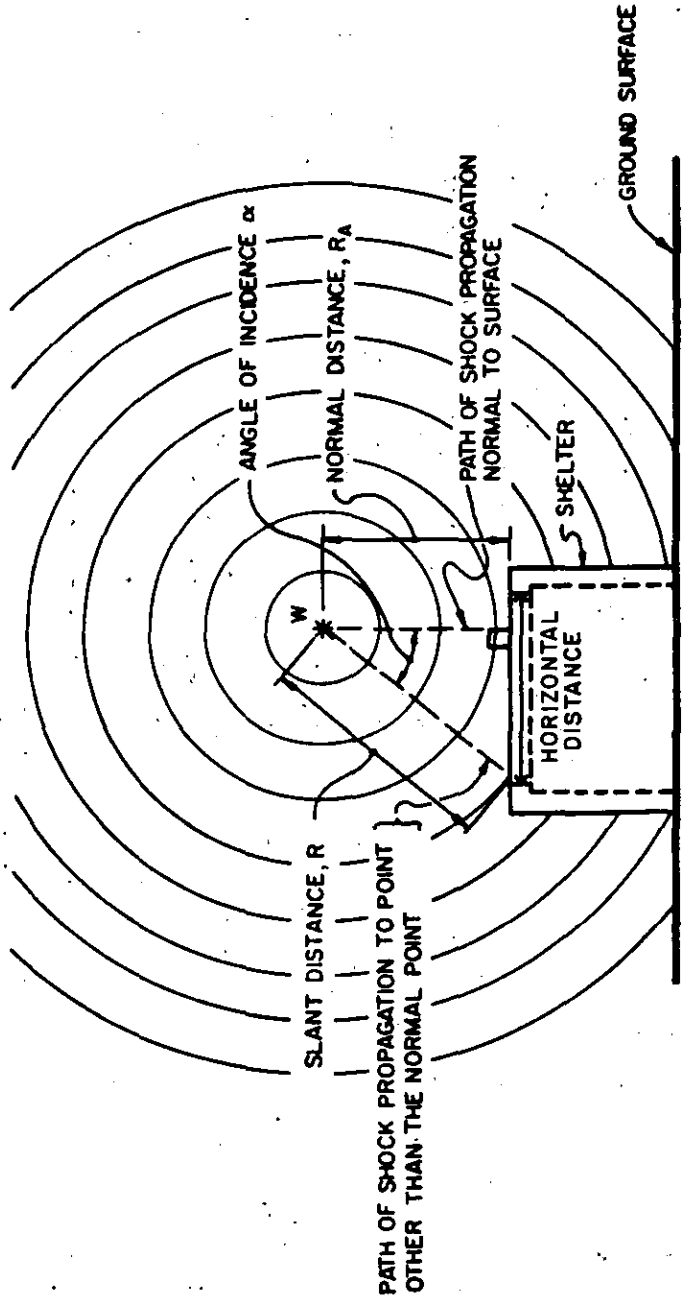


Figure 2-4 Free-air burst blast environment

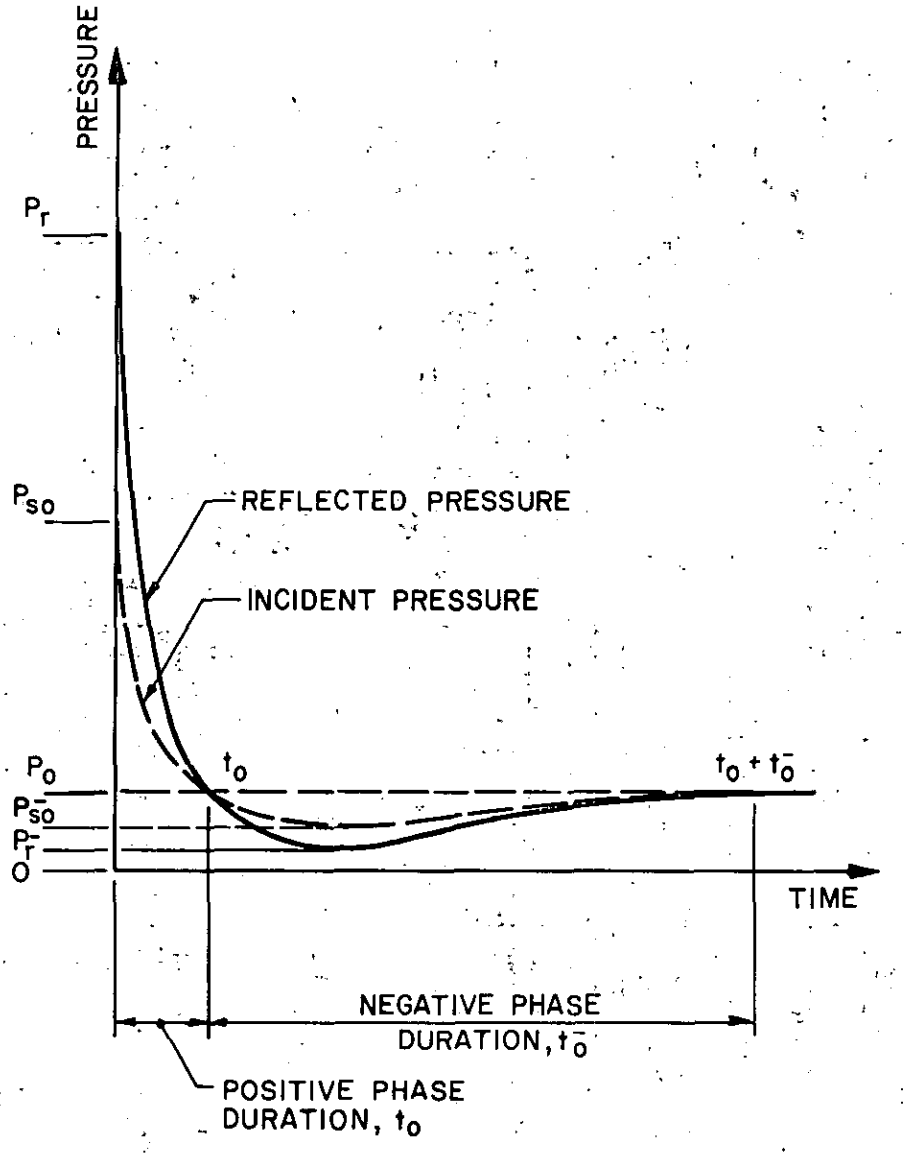


Figure 2-5 Pressure-time variation for a free-air burst

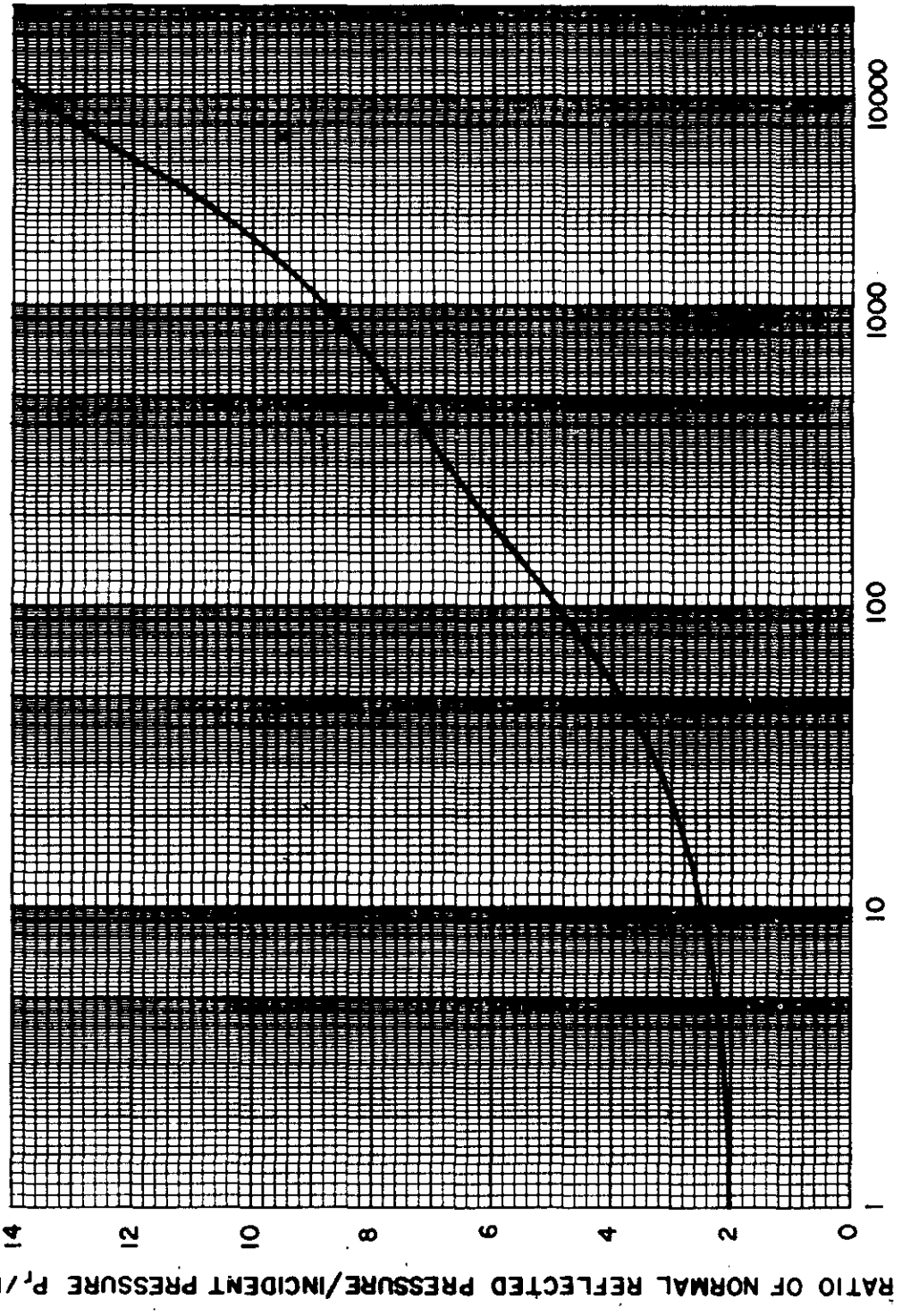
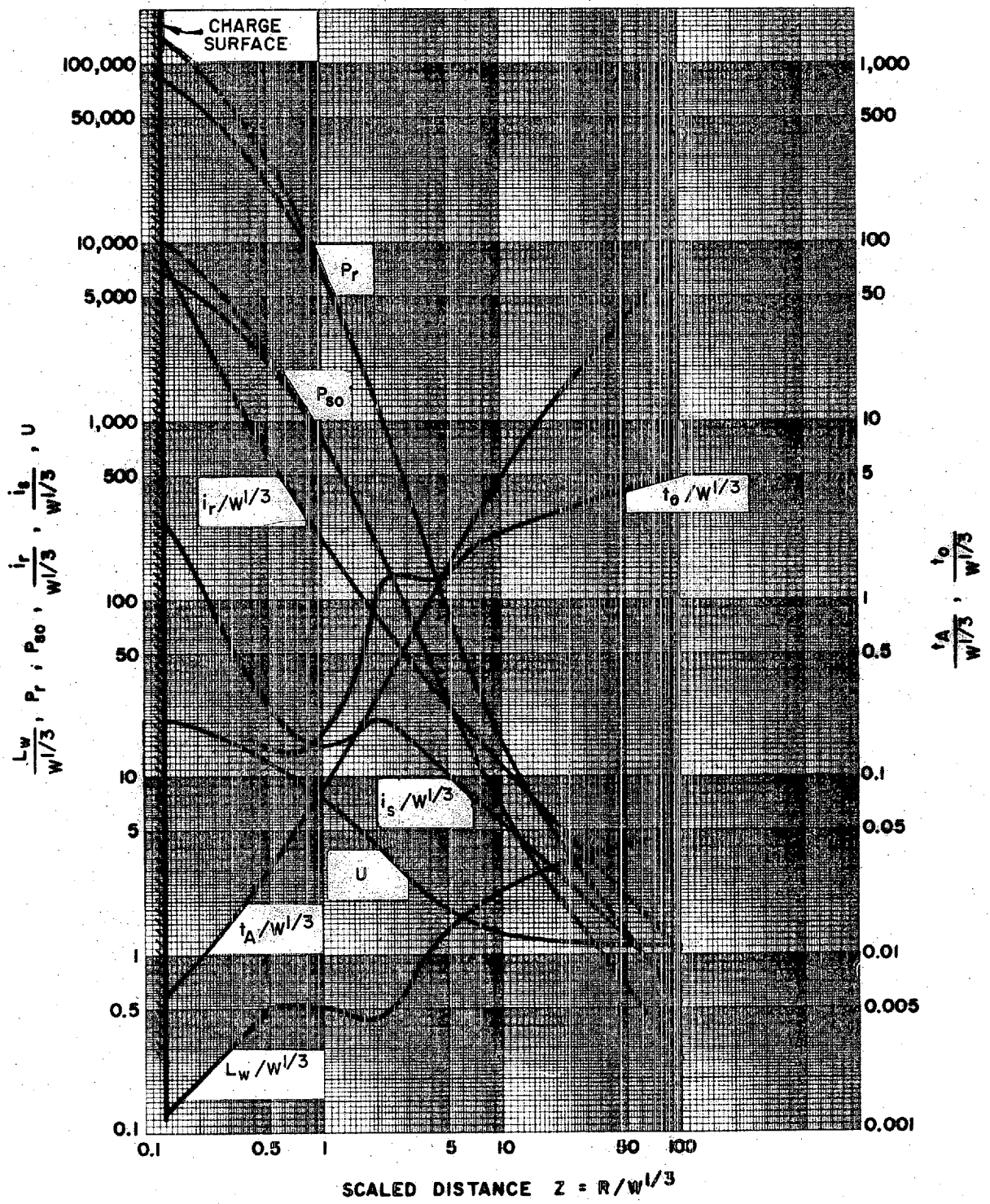
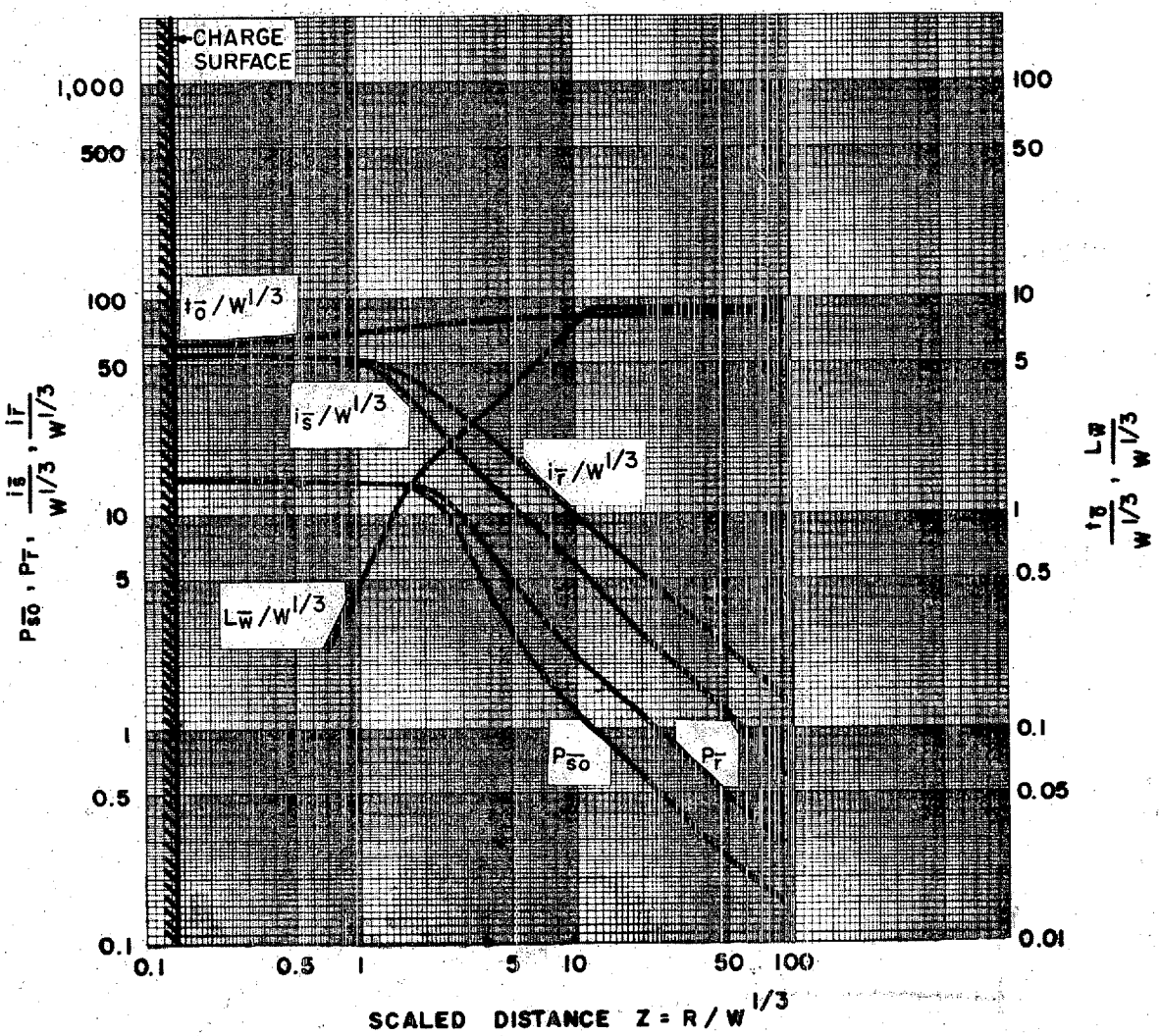


Figure 2-6 Peak incident pressure versus the ratio of normal reflected pressure/ incident pressure for a free air burst



P_{so} = PEAK POSITIVE INCIDENT PRESSURE, psi
P_r = PEAK POSITIVE NORMAL REFLECTED PRESSURE, psi
$i_s/W^{1/3}$ = SCALED UNIT POSITIVE INCIDENT IMPULSE, psi-ms/lb$^{1/3}$
$i_r/W^{1/3}$ = SCALED UNIT POSITIVE NORMAL REFLECTED IMPULSE, psi-ms/lb$^{1/3}$
$t_A/W^{1/3}$ = SCALED TIME OF ARRIVAL OF BLAST WAVE, ms/lb$^{1/3}$
$t_o/W^{1/3}$ = SCALED POSITIVE DURATION OF POSITIVE PHASE, ms/lb$^{1/3}$
U = SHOCK FRONT VELOCITY, ft/ms
W = CHARGE WEIGHT, lbs
$L_w/W^{1/3}$ = SCALED WAVE LENGTH OF POSITIVE PHASE, ft/lb$^{1/3}$

Figure 2-7 Positive phase shock wave parameters for a spherical TNT explosion in free air at sea level



$P_{\bar{so}}$ = PEAK NEGATIVE INCIDENT PRESSURE, psi

$P_{\bar{r}}$ = PEAK NEGATIVE NORMAL REFLECTED PRESSURE, psi

$i_{\bar{s}}/W^{1/3}$ = SCALED UNIT NEGATIVE INCIDENT IMPULSE, psi-ms/lb$^{1/3}$

$i_{\bar{r}}/W^{1/3}$ = SCALED UNIT NEGATIVE NORMAL REFLECTED IMPULSE, psi-ms/lb$^{1/3}$

$t_{\bar{o}}/W^{1/3}$ = SCALED DURATION OF NEGATIVE PHASE, ms/lb$^{1/3}$

$L_{\bar{w}}/W^{1/3}$ = SCALED WAVE LENGTH OF NEGATIVE PHASE, ft/lb$^{1/3}$

Figure 2-8 Negative phase shock wave parameters for a spherical TNT explosion in free air at sea level

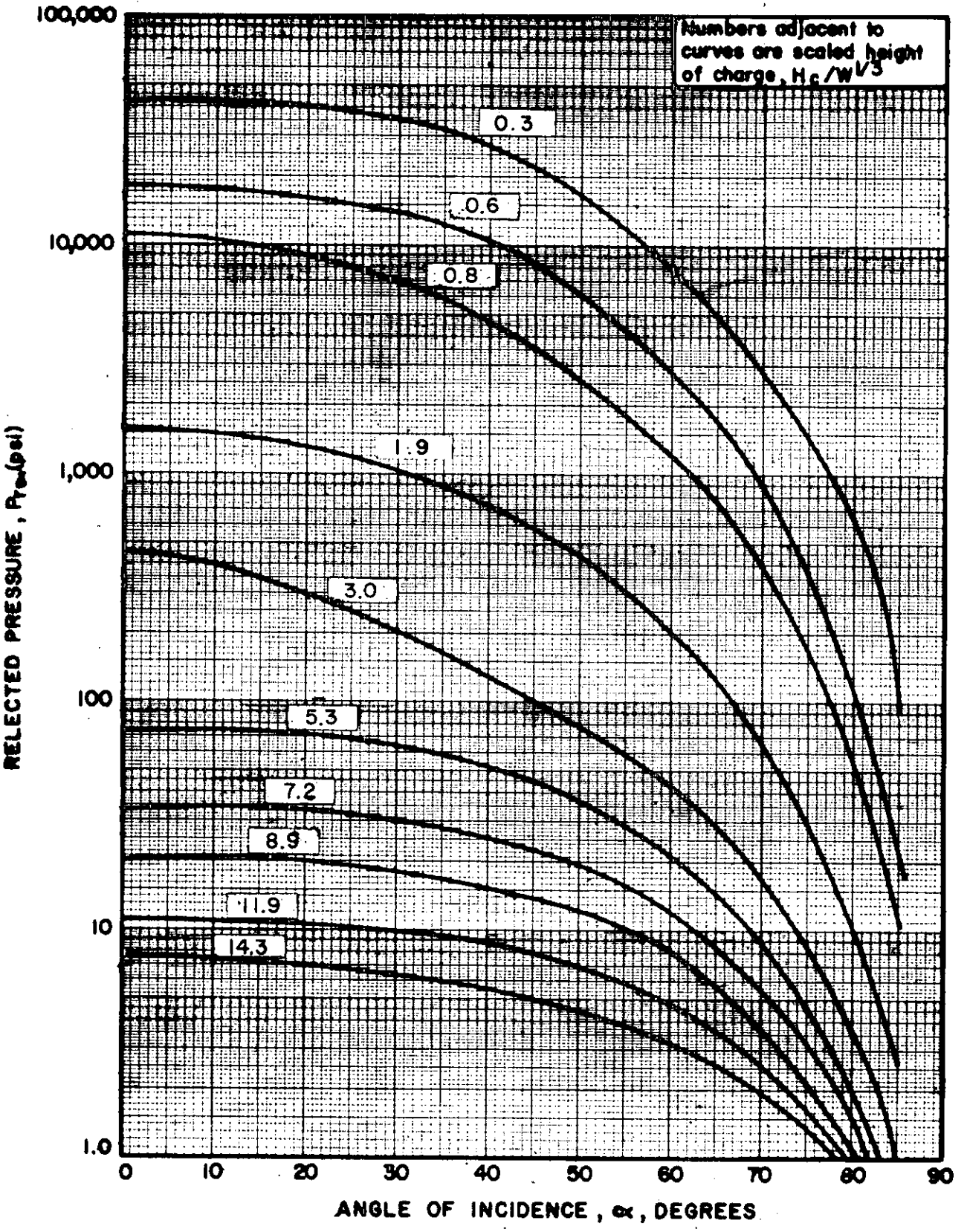


Figure 2-9 Variation of reflected pressure as a function of angle of incidence

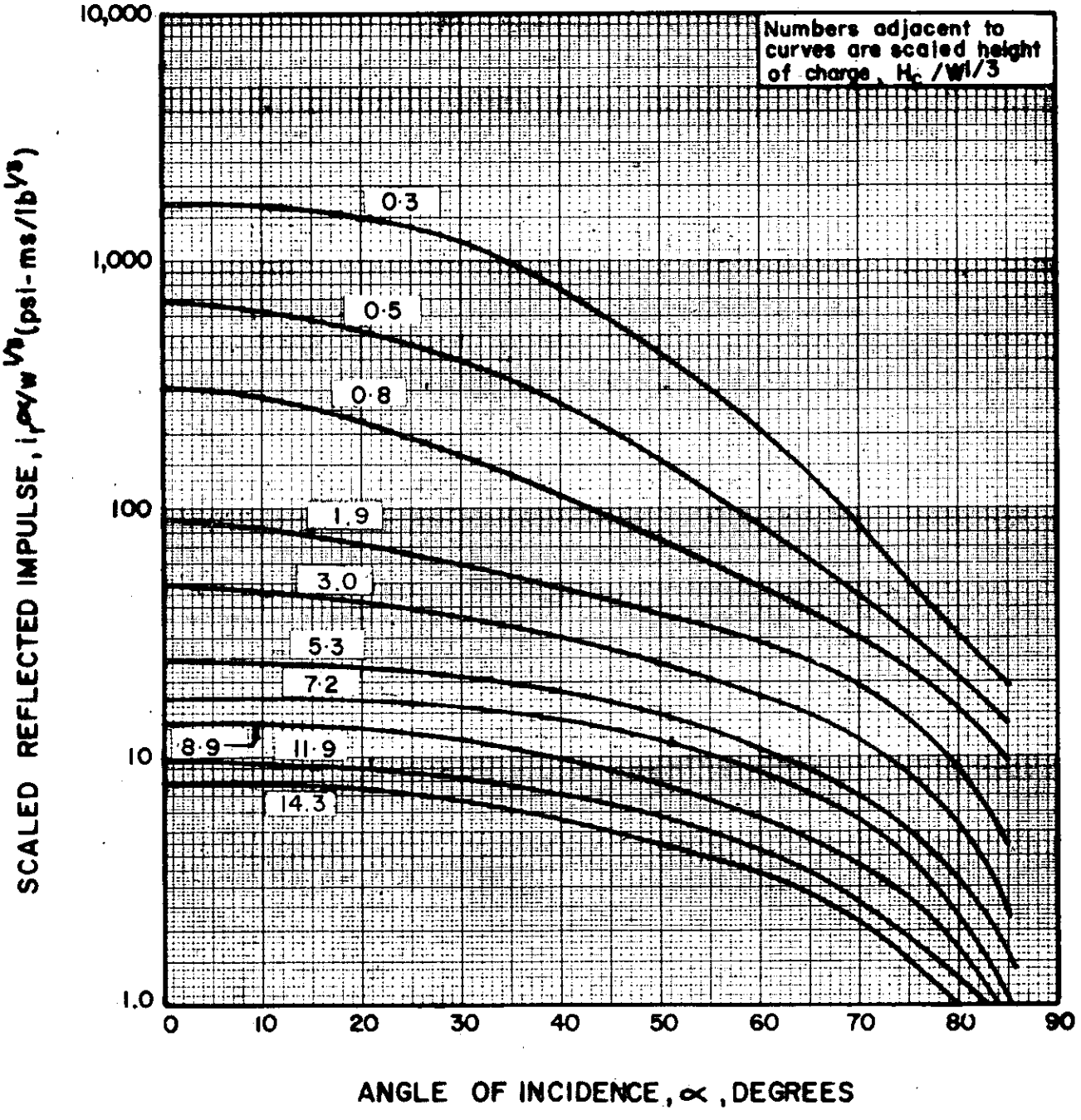


Figure 2-10 Variation of scaled reflected impulse as a function of angle of incidence

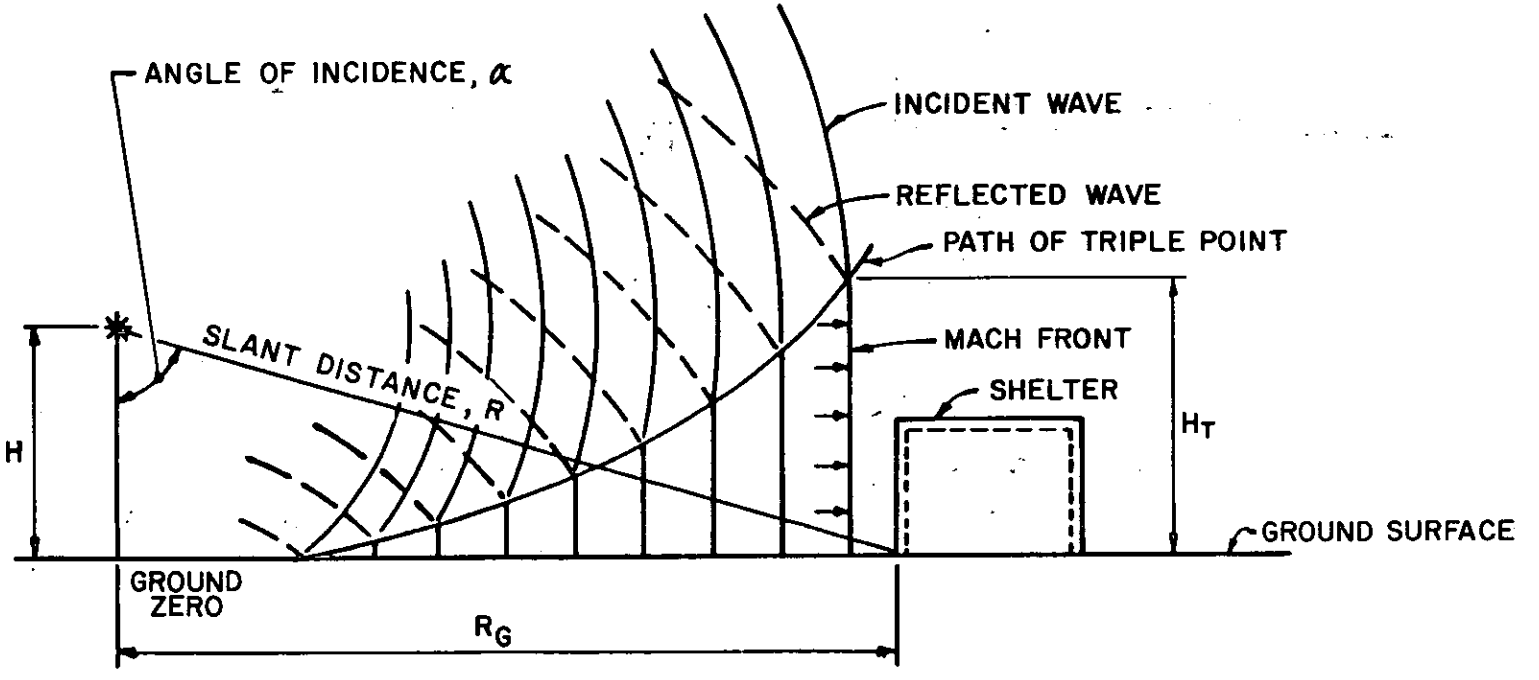


Figure 2-11 Air burst blast environment

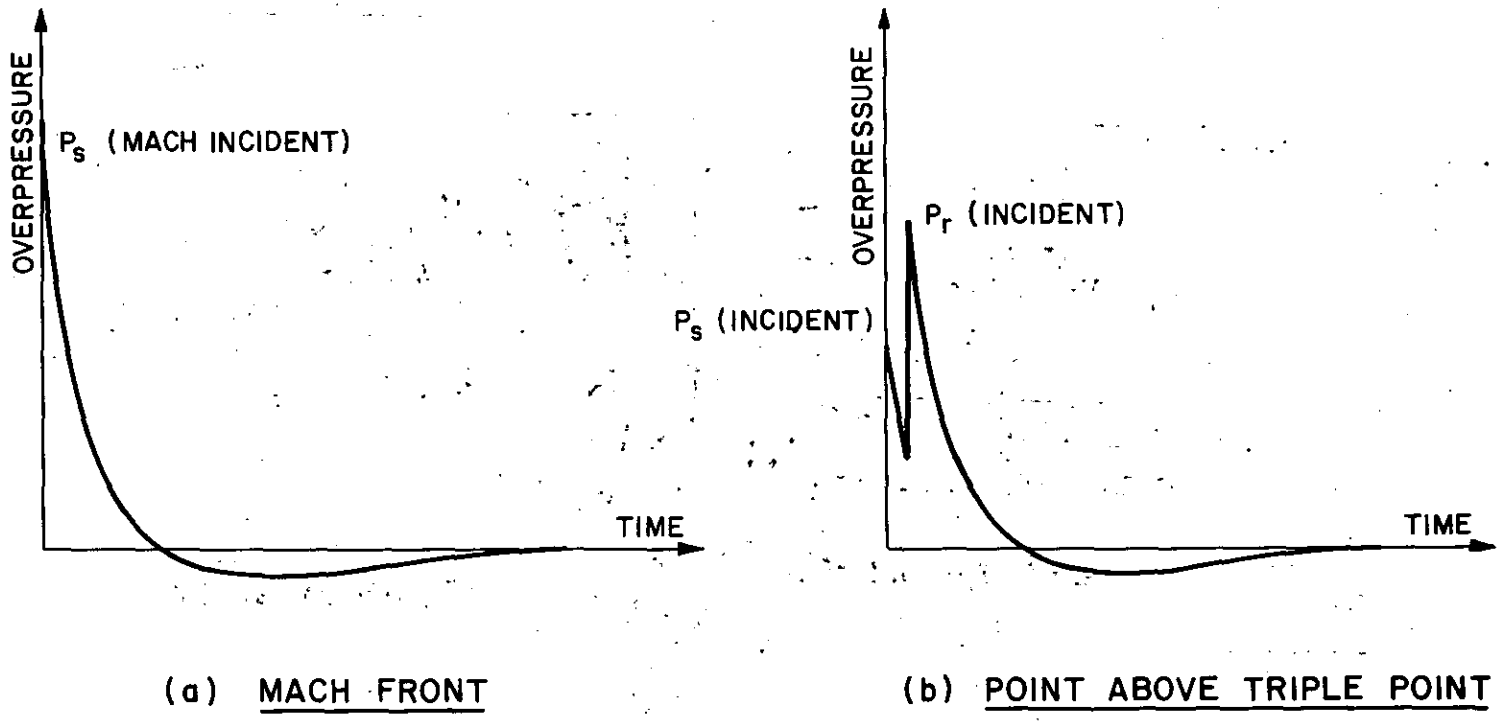


Figure 2-12 Pressure-time variation for air burst

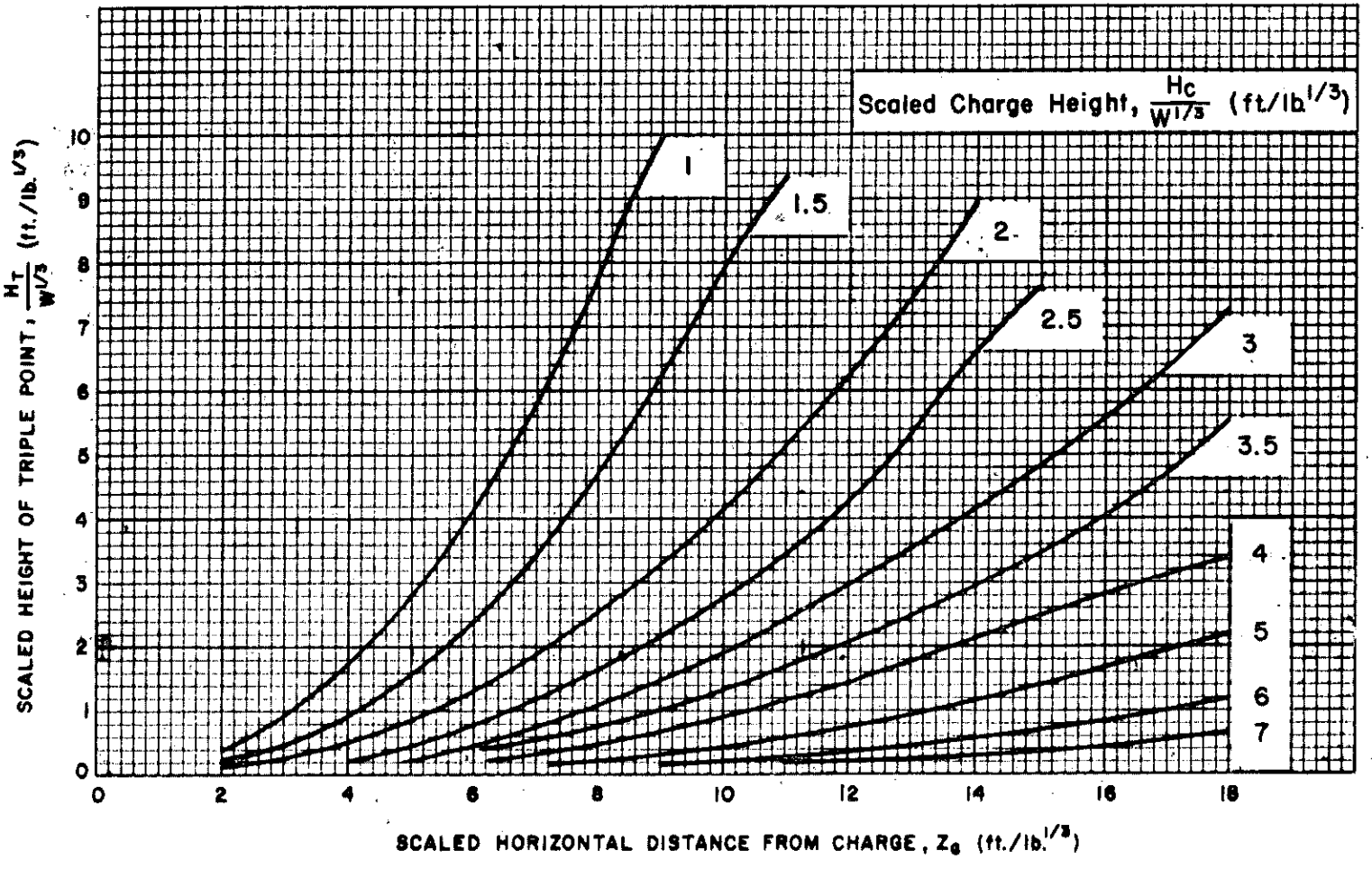


Figure 2-13 Scaled height of triple point

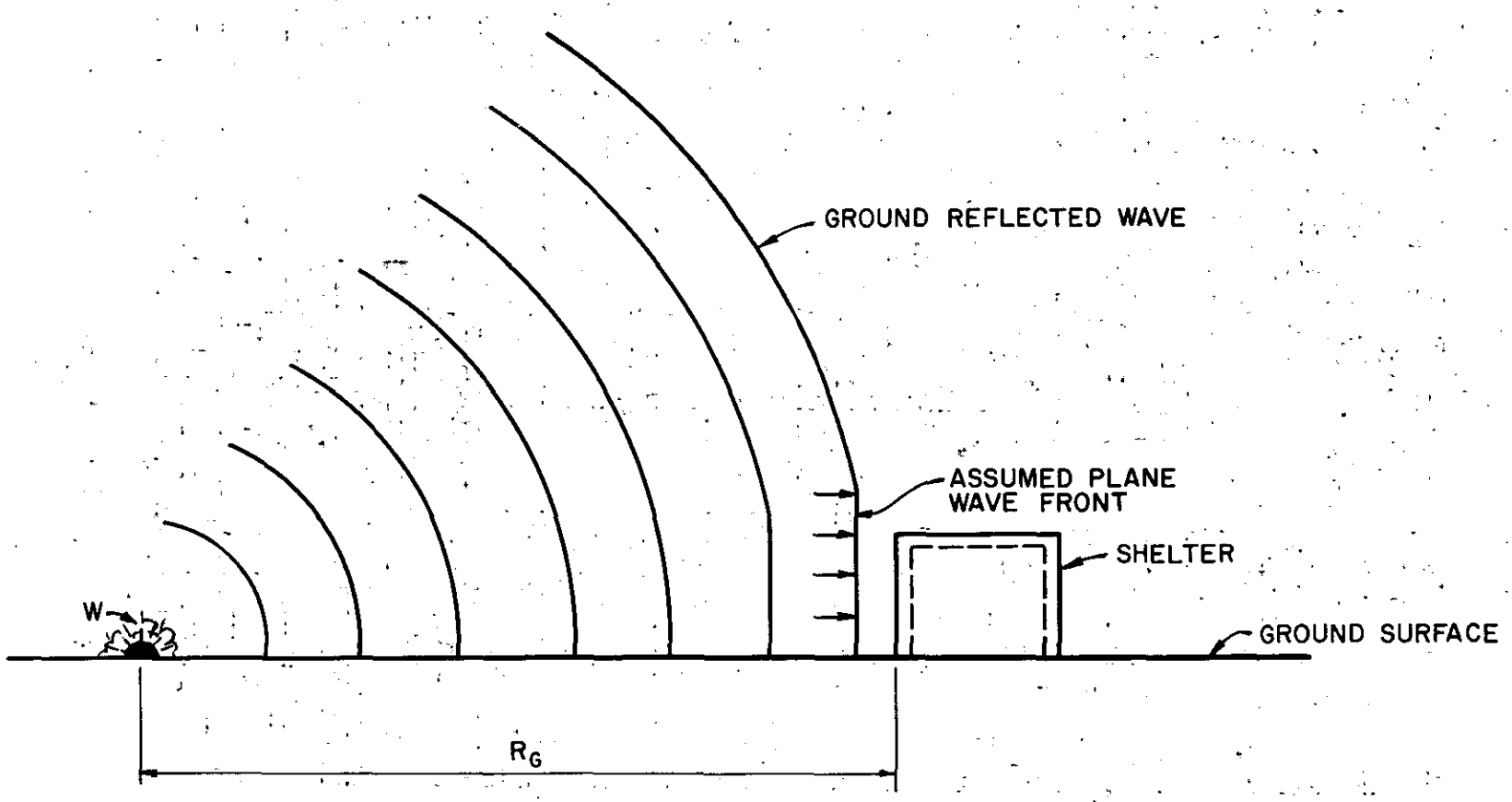
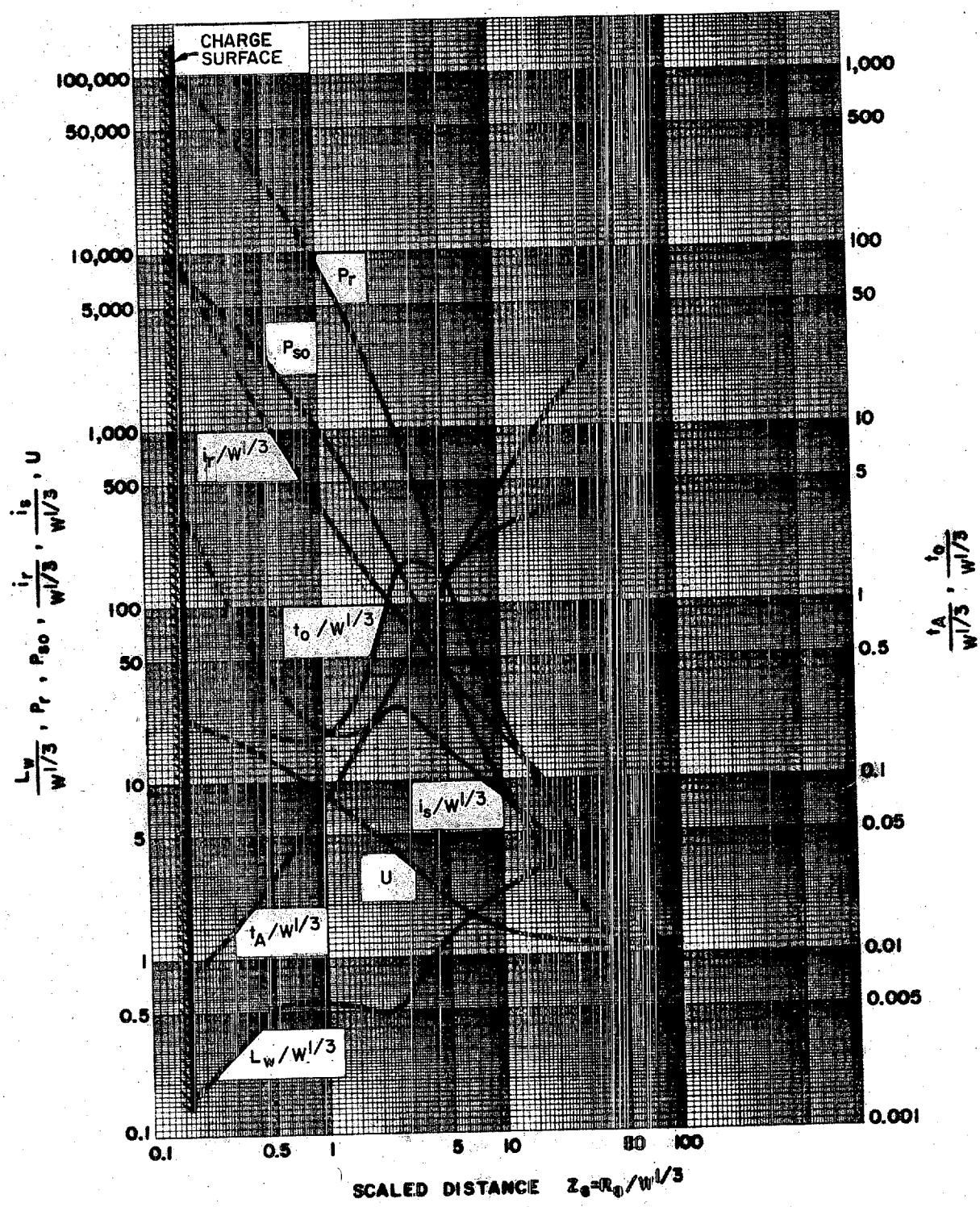
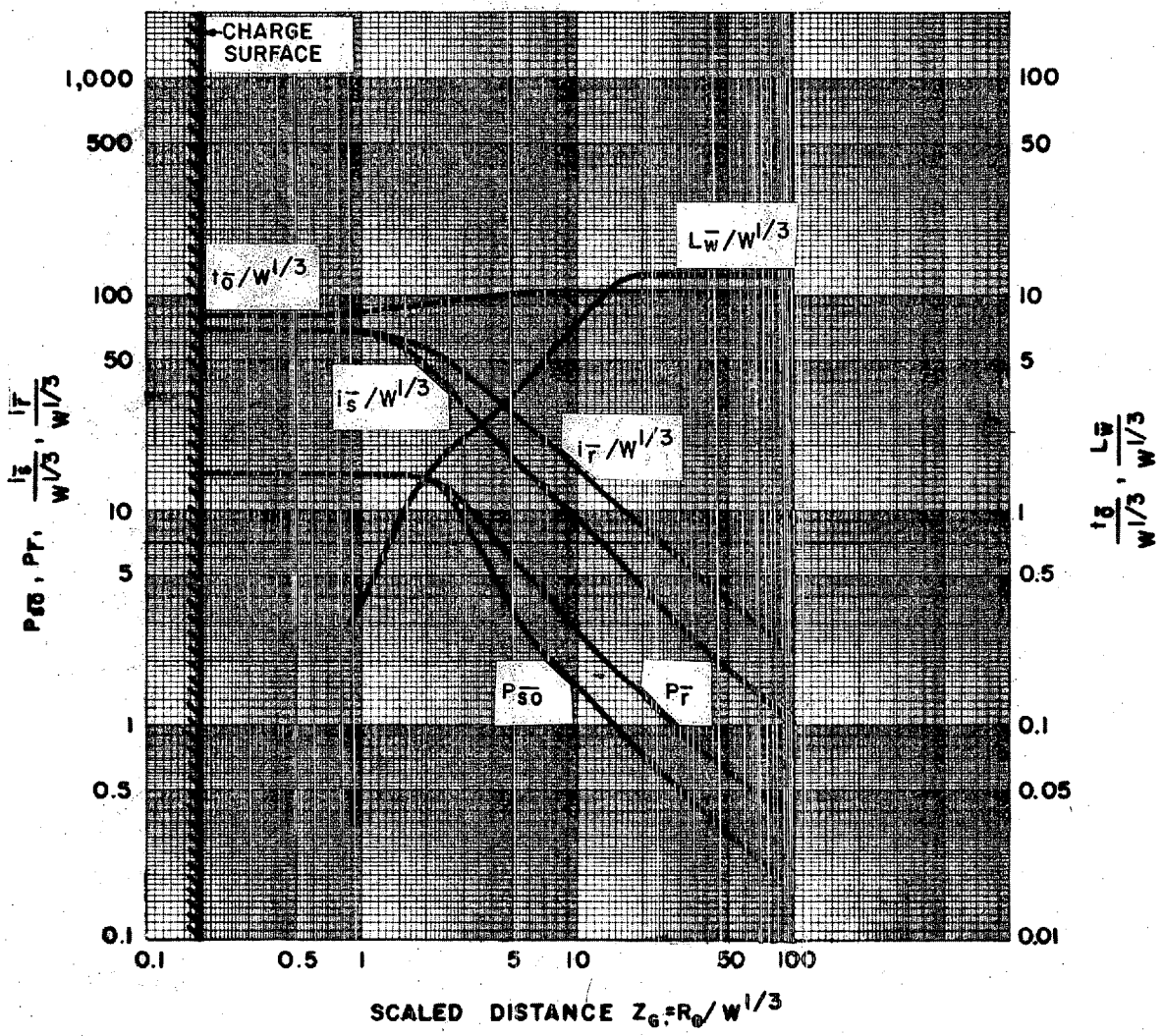


Figure 2-14 Surface burst blast environment



P_{so} = PEAK POSITIVE INCIDENT PRESSURE, psi
P_r = PEAK POSITIVE NORMAL REFLECTED PRESSURE, psi
$i_s/W^{1/3}$ = SCALED UNIT POSITIVE INCIDENT IMPULSE, psi-ms/lb$^{1/3}$
$i_r/W^{1/3}$ = SCALED UNIT POSITIVE NORMAL REFLECTED IMPULSE, psi-ms/lb$^{1/3}$
$t_A/W^{1/3}$ = SCALED TIME OF ARRIVAL OF BLAST WAVE, ms/lb$^{1/3}$
$t_o/W^{1/3}$ = SCALED POSITIVE DURATION OF POSITIVE PHASE, ms/lb$^{1/3}$
U = SHOCK FRONT VELOCITY, ft/ms
W = CHARGE WEIGHT, lbs
$L_w/W^{1/3}$ = SCALED WAVE LENGTH OF POSITIVE PHASE, ft/lb$^{1/3}$

Figure 2-15 Positive phase shock wave parameters for a hemispherical TNT explosion on the surface at sea level



$P_{\bar{so}}$ = PEAK NEGATIVE INCIDENT PRESSURE, psi

$P_{\bar{r}}$ = PEAK NEGATIVE NORMAL REFLECTED PRESSURE, psi

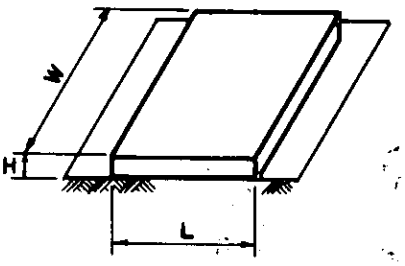
$i_{\bar{s}}/W^{1/3}$ = SCALED UNIT NEGATIVE INCIDENT IMPULSE, psi-ms/lb$^{1/3}$

$i_{\bar{r}}/W^{1/3}$ = SCALED UNIT NEGATIVE NORMAL REFLECTED IMPULSE, psi-ms/lb$^{1/3}$

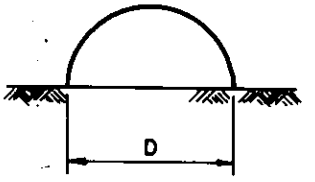
$t_{\bar{o}}/W^{1/3}$ = SCALED DURATION OF NEGATIVE PHASE, ms/lb$^{1/3}$

$L_{\bar{w}}/W^{1/3}$ = SCALED WAVE LENGTH OF NEGATIVE PHASE, ft/lb$^{1/3}$

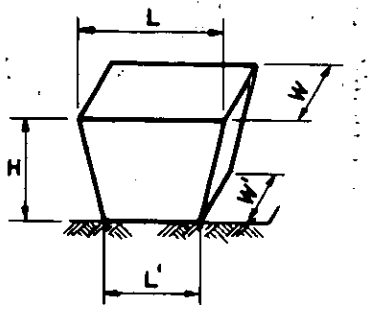
Figure 2-16 Negative phase shock wave parameters for a hemispherical TNT explosion on the surface at sea level



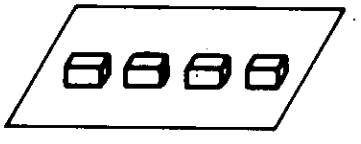
a. ORTHORHOMBIC



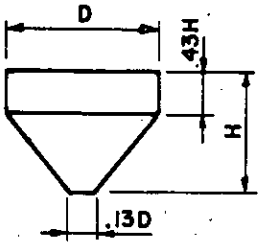
b. HEMISPHERICAL



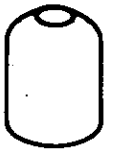
c. IN-PROCESS HOPPER



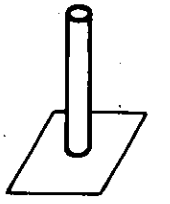
d. GRENADES IN-PROCESS



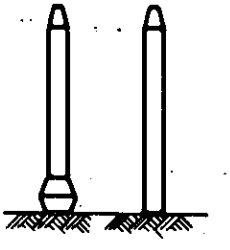
e. CLOSED-TOP HOPPER



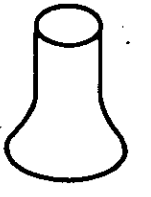
f. PRESSED BILLETS



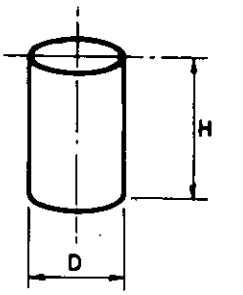
g. EXTRUDED ROD



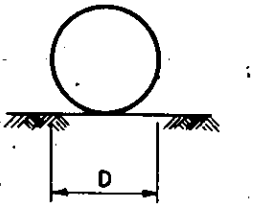
h. PROJECTILES



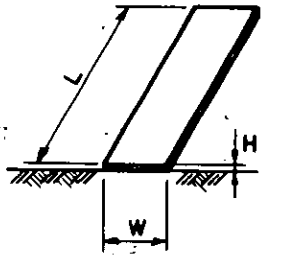
i. BEAKER



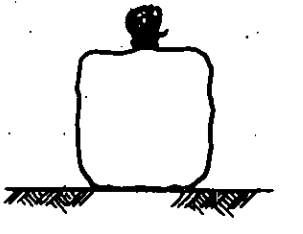
j. CYLINDRICAL



k. SPHERICAL

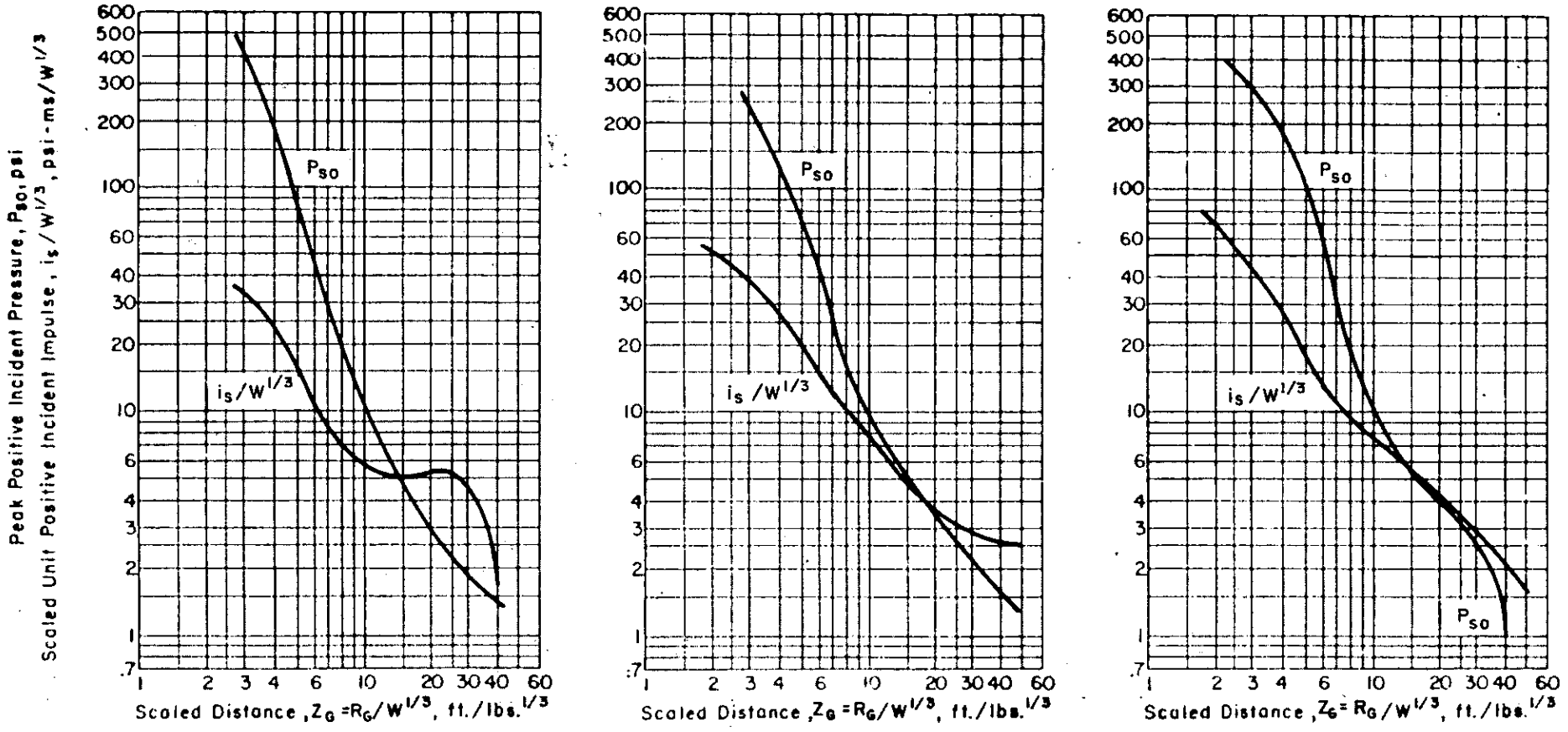


l. CARPET



m. BAG

Figure 2-17 Explosive shapes



a. Composition A-3
Rectangular Shape

b. Composition A-5
Rectangular Shape

c. Composition A-5
Cylindrical Shape

Figure 2-18 Peak positive incident pressure and scaled impulse for an explosion on the surface at sea level

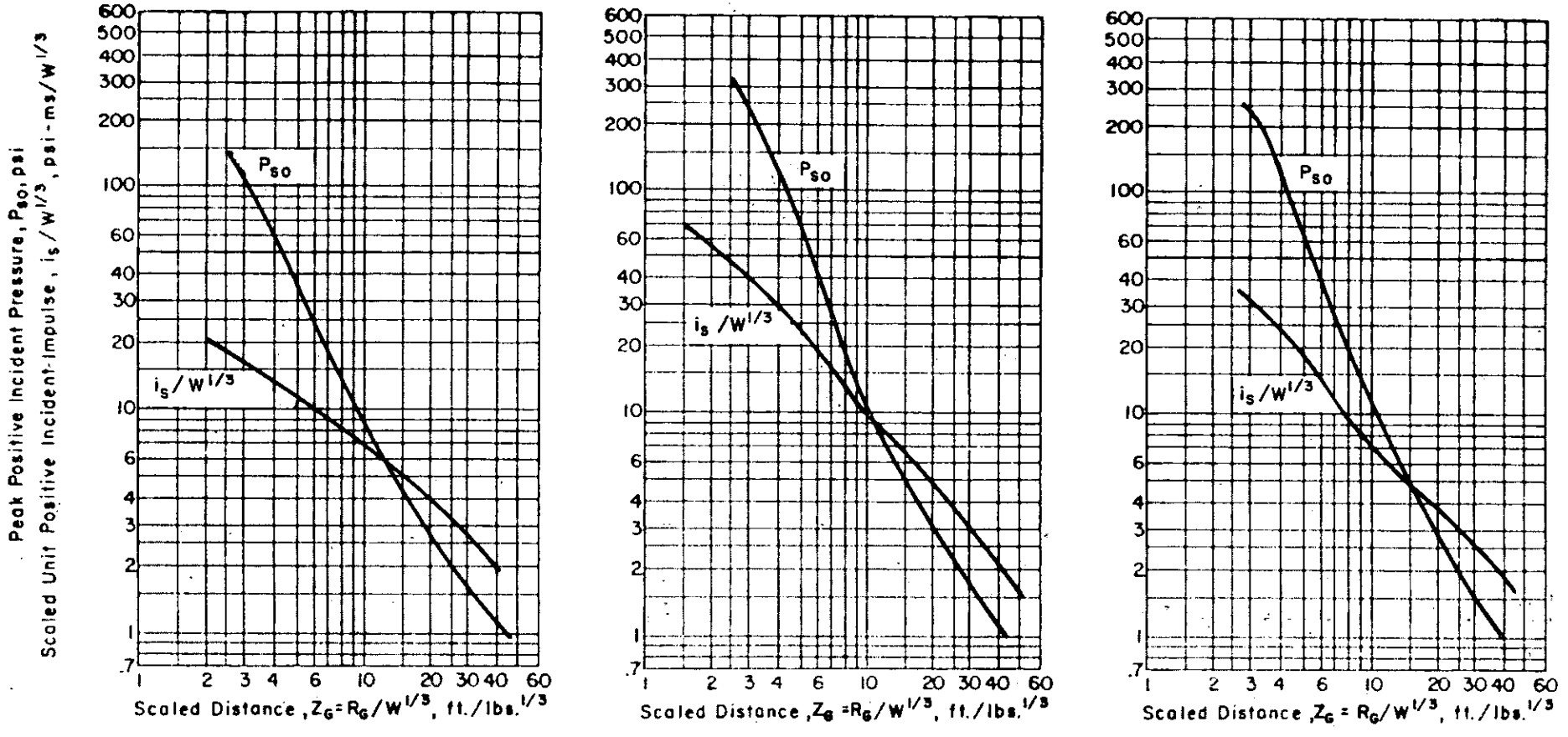
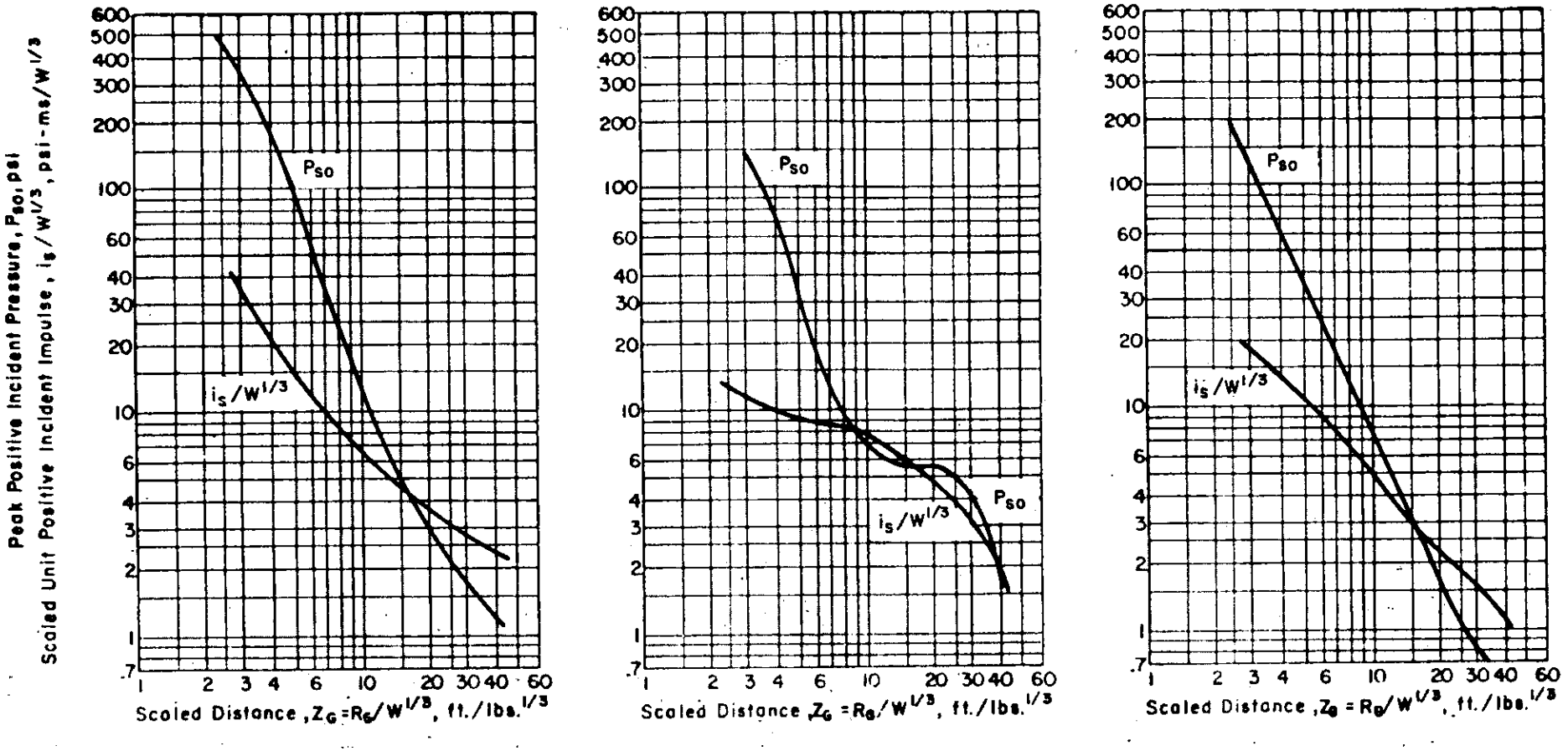


Figure 2-19 Peak positive incident pressure and scaled impulse for an explosion on the surface at sea level

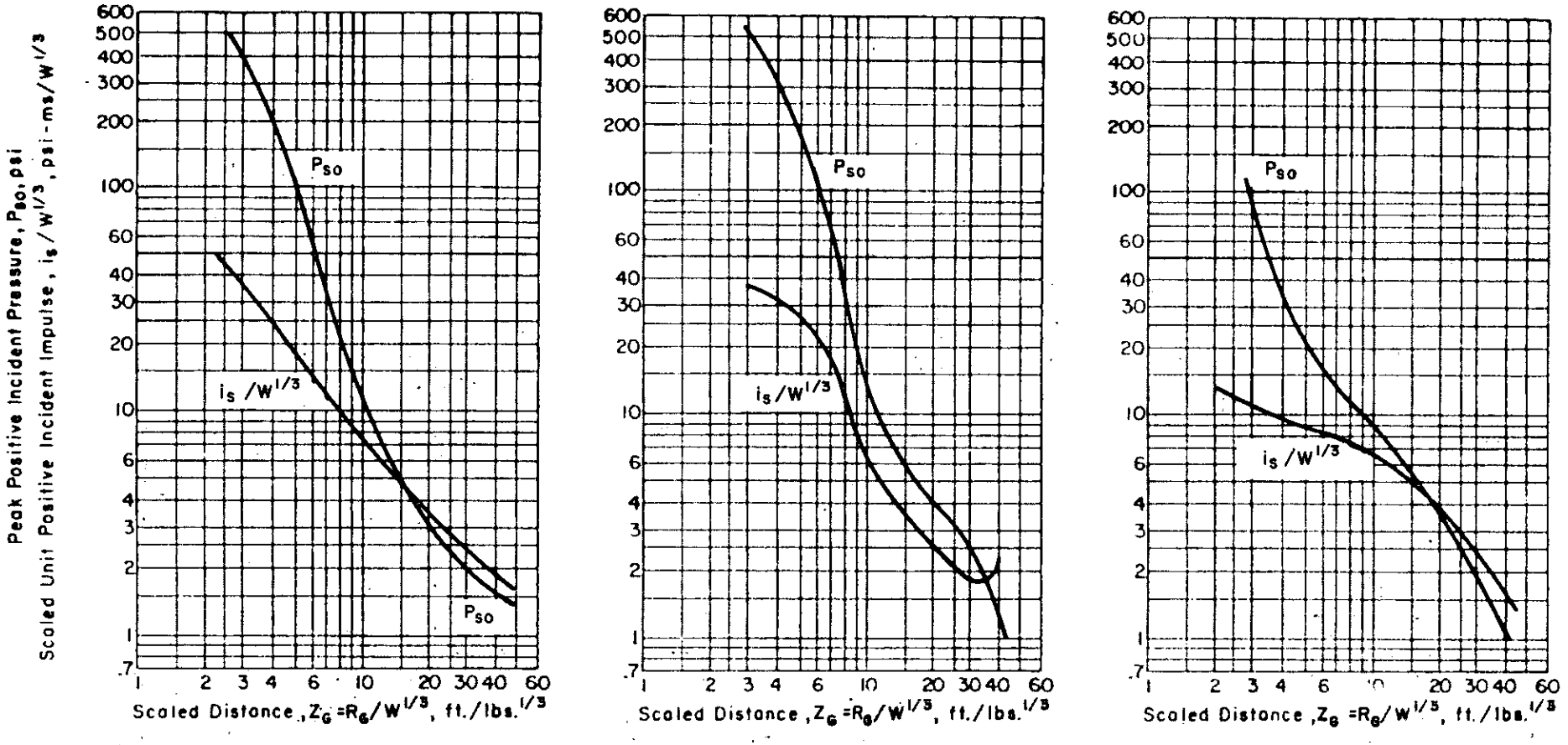


a. Composition C-4
Orthorhombic

b. Composition C-4
Orthorhombic

c. Guanidine Nitrate
Orthorhombic

Figure 2-20 Peak positive incident pressure and scaled impulse for an explosion on the surface at sea level

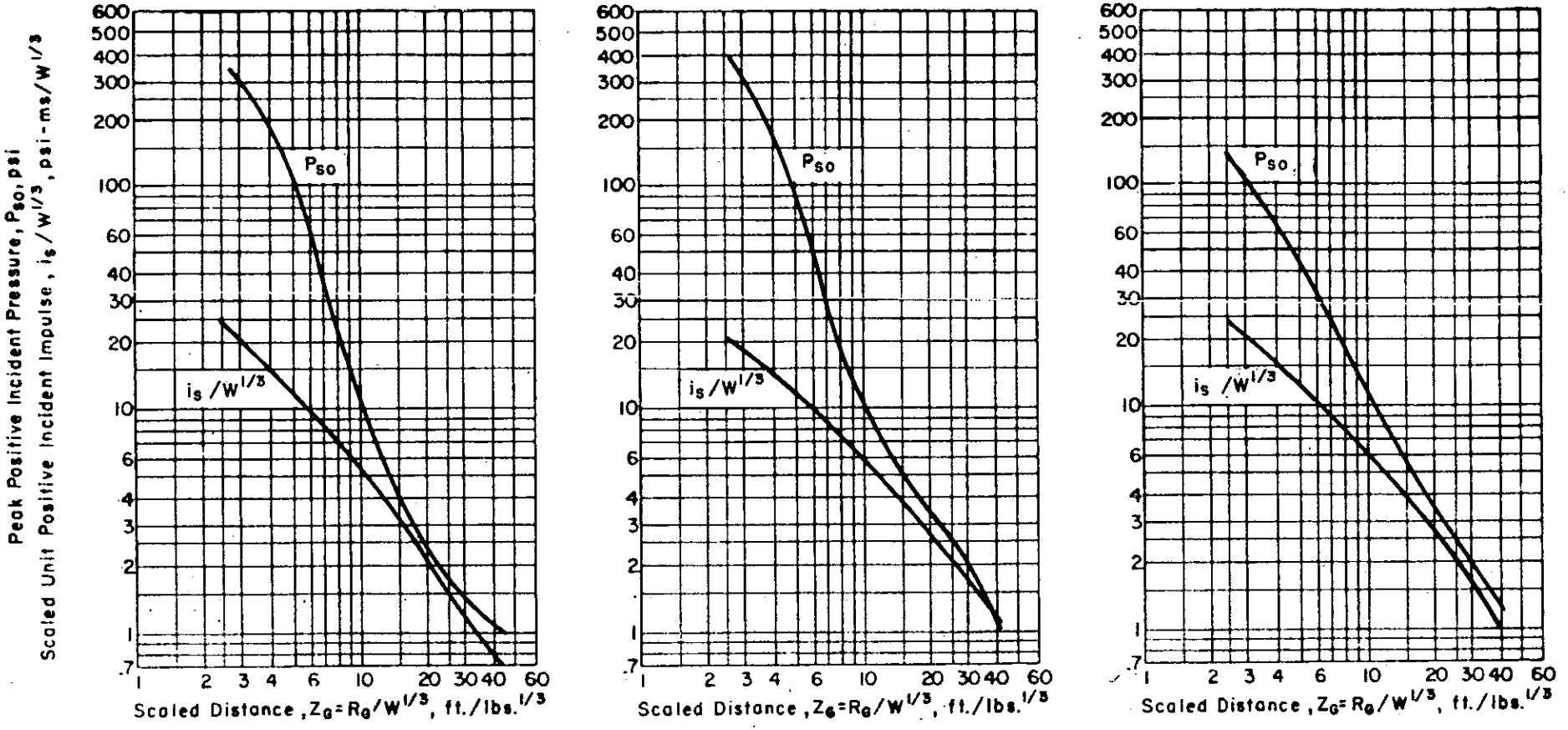


a. Cyclotol 70/30 Orthorhomic

b. Cyclotol 70/30 Hoppers

c. 64 M42 Grenades Tray of 64

Figure 2-21 Peak positive incident pressure and scaled impulse for an explosion on the surface at sea level



a. HMX
Orthorhombic

b. HMX
Cylindrical

c. M483 155mm ICM Projectile
Single Round

Figure 2-22 Peak positive incident pressure and scaled impulse for an explosion on the surface at sea level

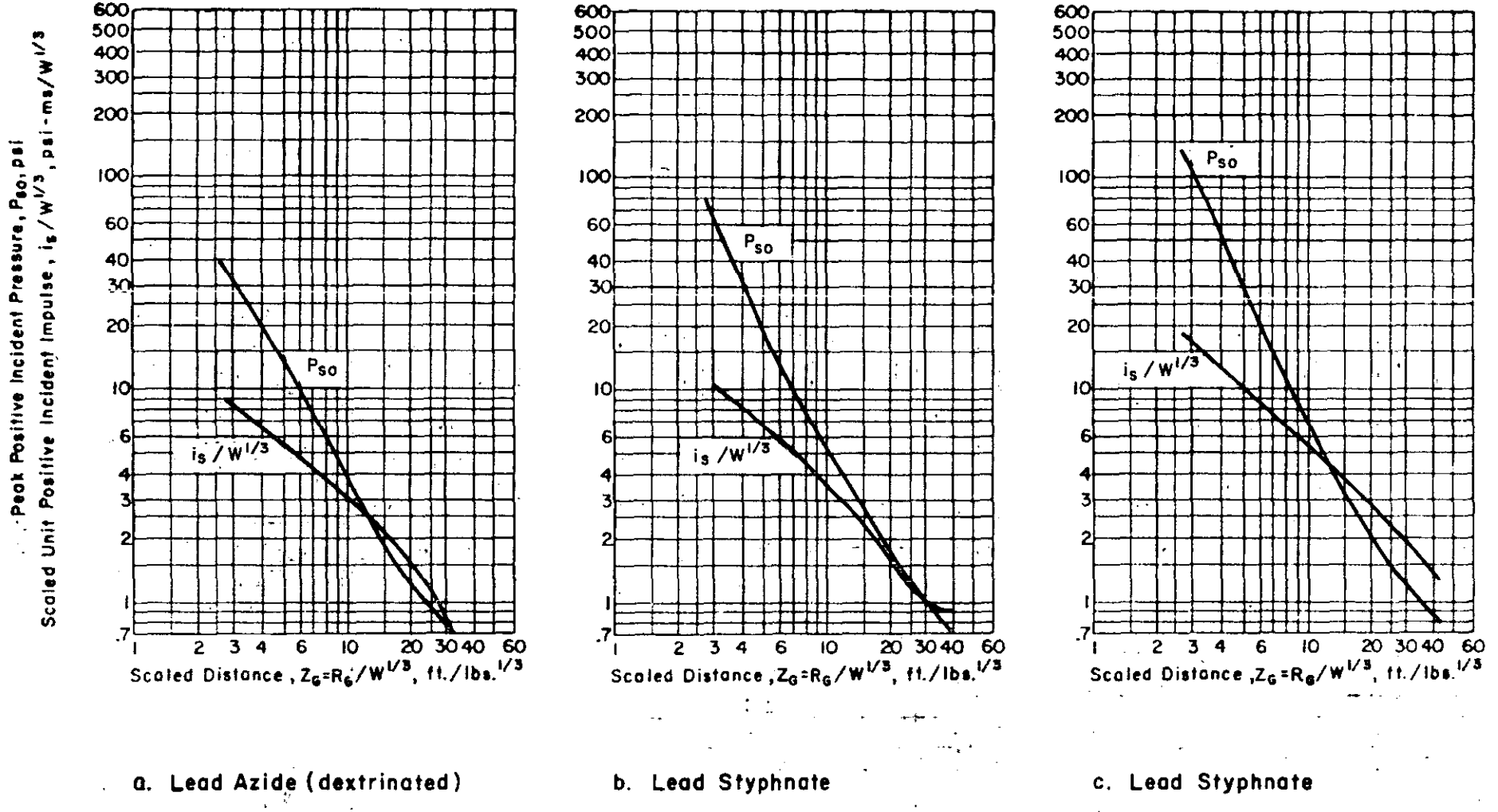
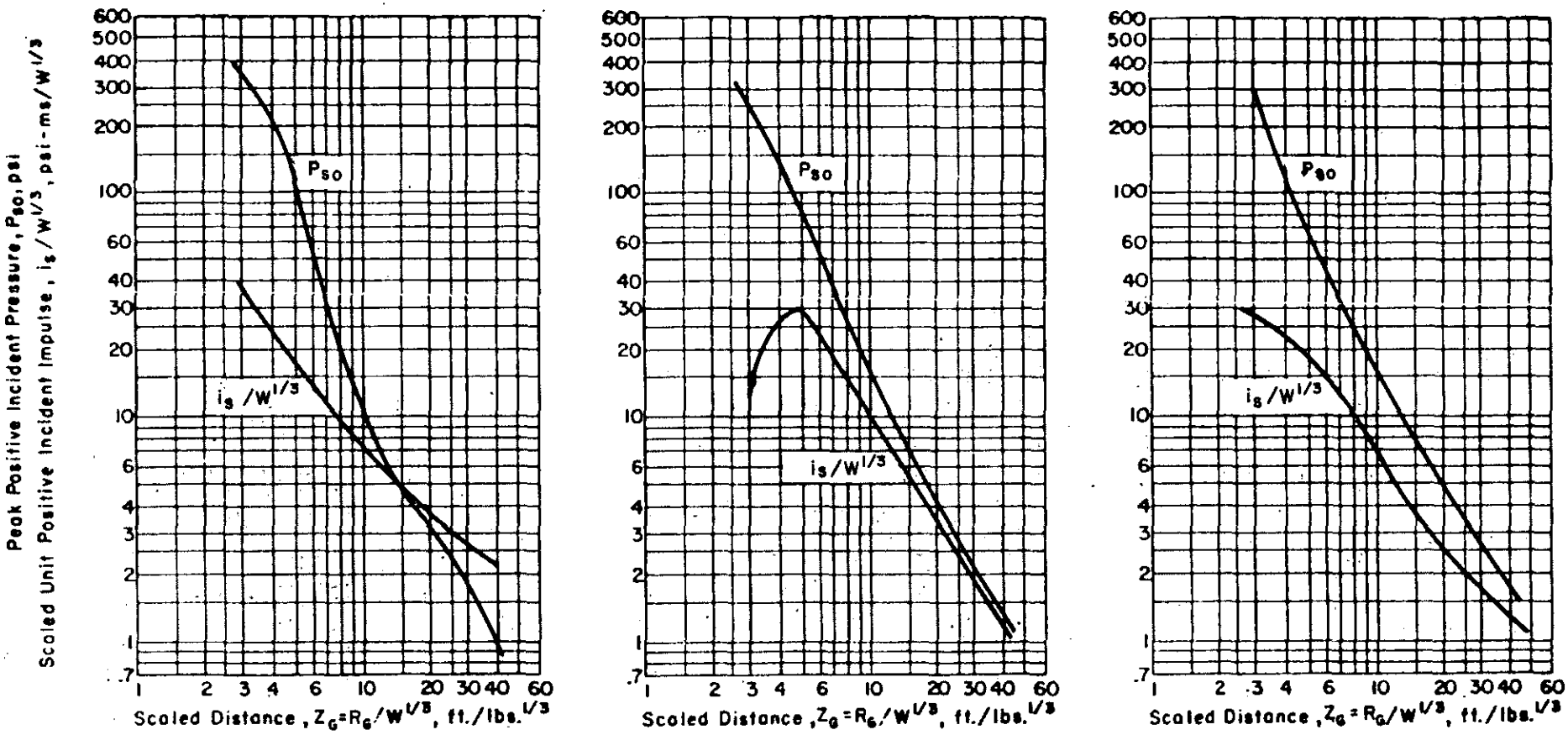


Figure 2-23 Peak positive incident pressure and scaled impulse for an explosion on the surface at sea level



a. LX-14
Orthorhombic

b. LX-14
Pressed billets

c. LX-14
Orthorhombic

Figure 2-24 Peak positive incident pressure and scaled impulse for an explosion on the surface at sea level

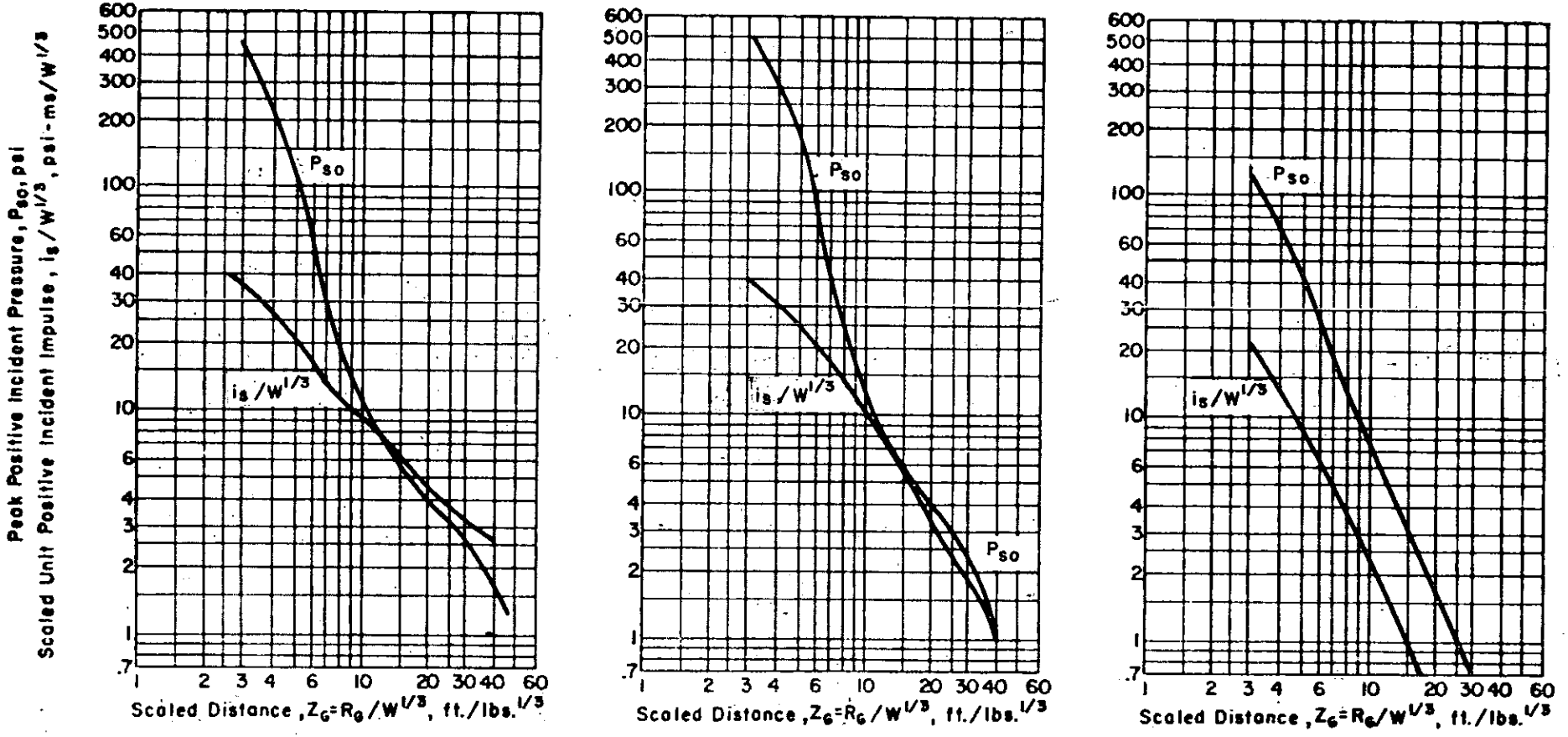


Figure 2-25 Peak positive incident pressure and scaled impulse for an explosion on the surface at sea level

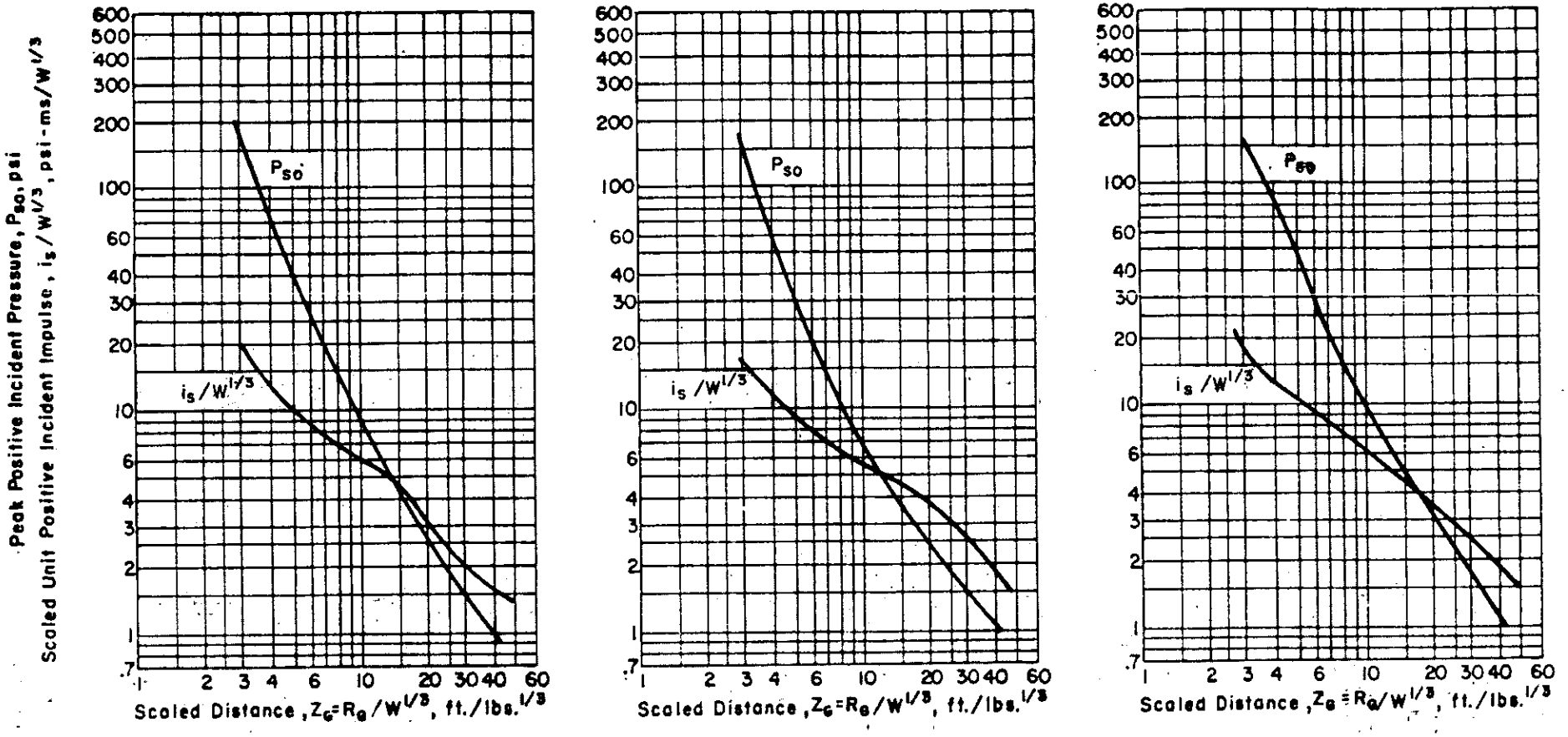


Figure 2-26 Peak positive incident pressure and scaled impulse for an explosion on the surface at sea level

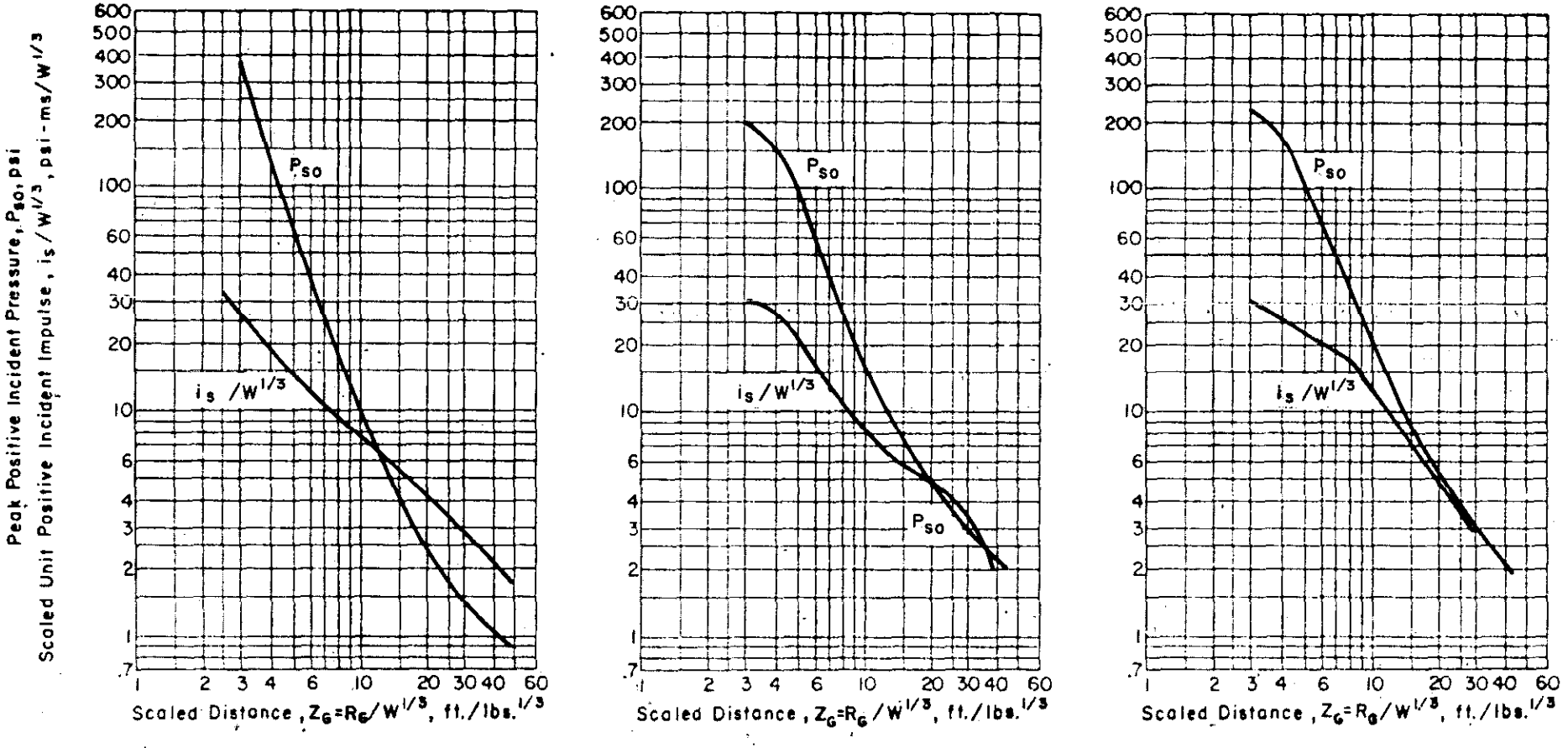


Figure 2-27 Peak positive incident pressure and scaled impulse for an explosion on the surface at sea level

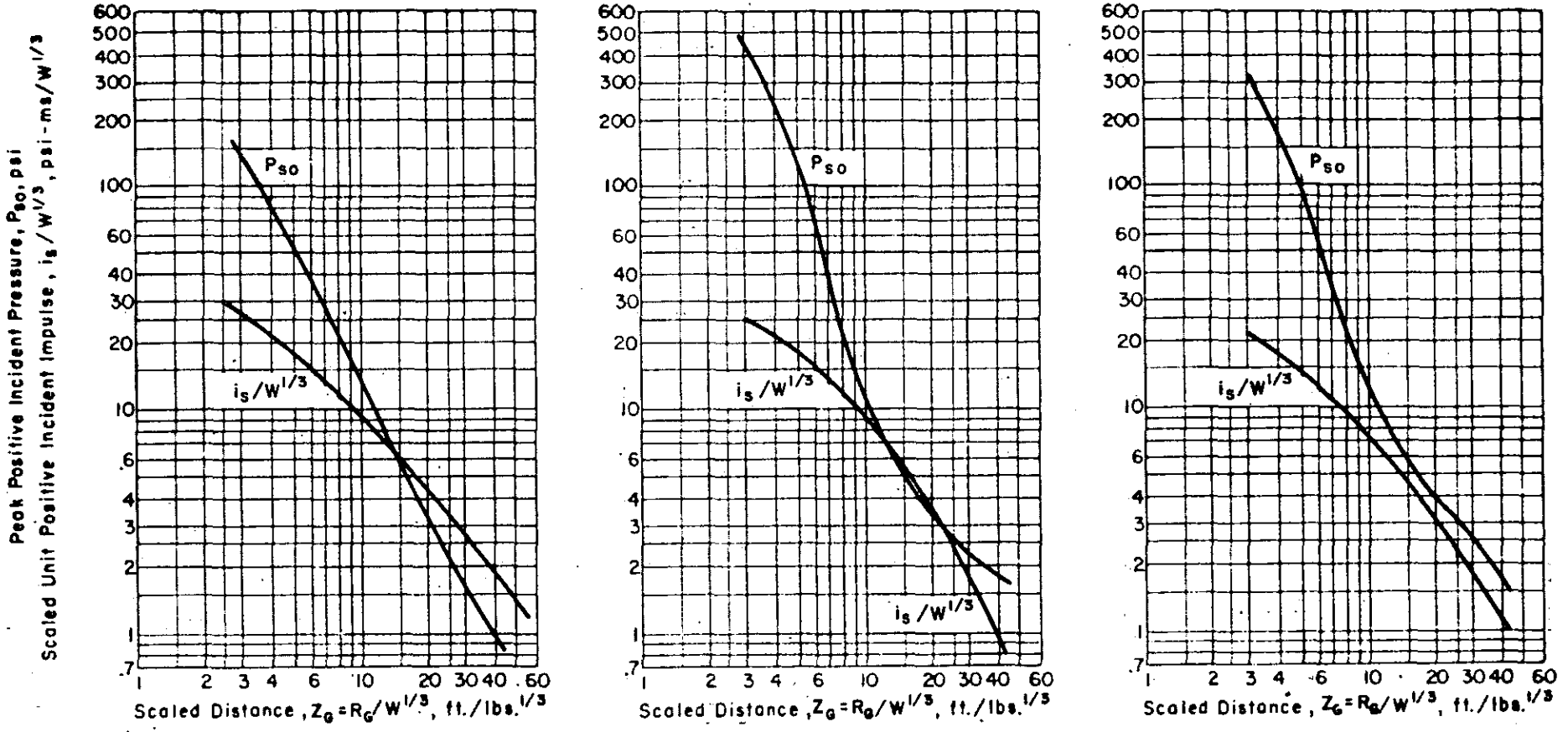


Figure 2-28 Peak positive incident pressure and scaled impulse for an explosion on the surface at sea level

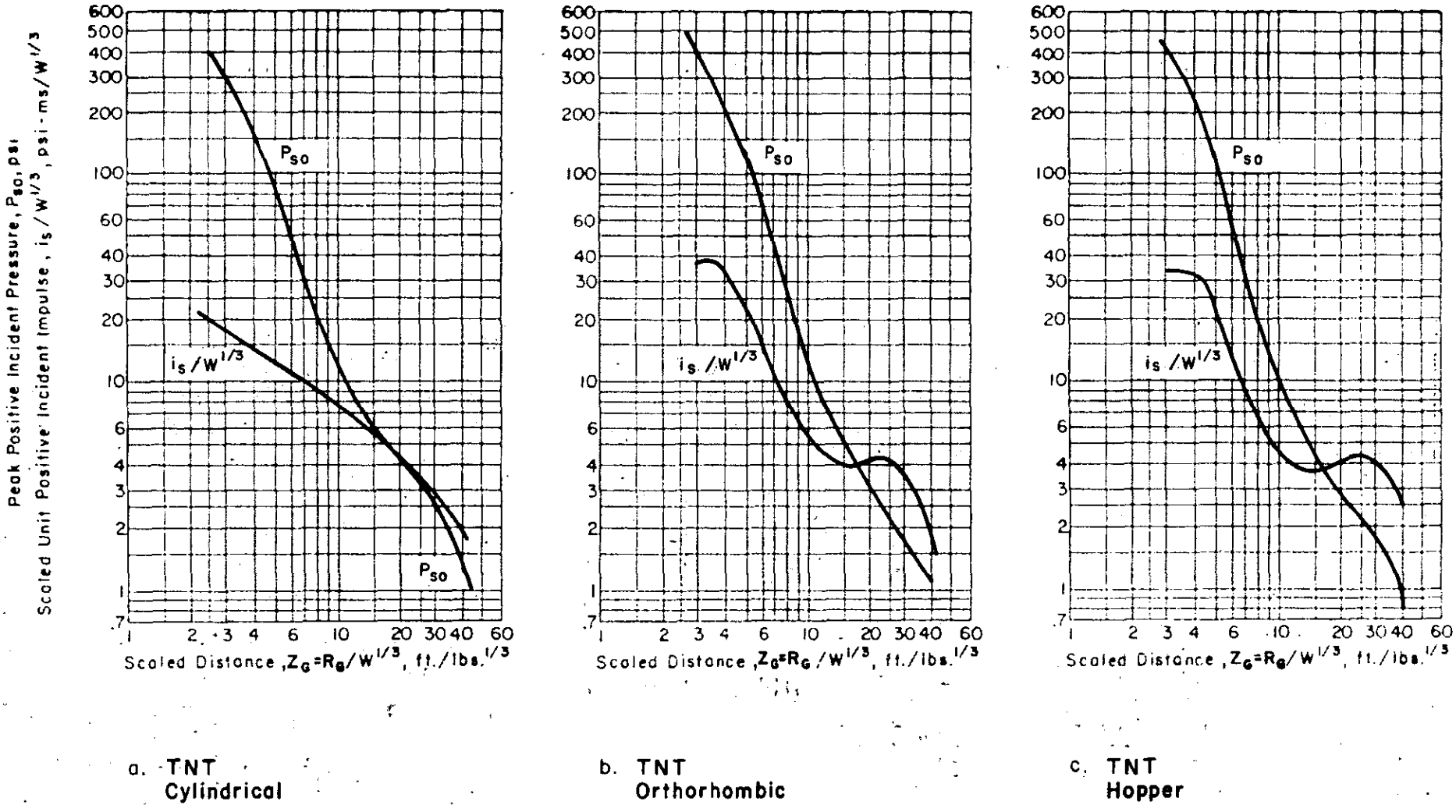


Figure 2-29 Peak positive incident pressure and scaled impulse for an explosion on the surface at sea level

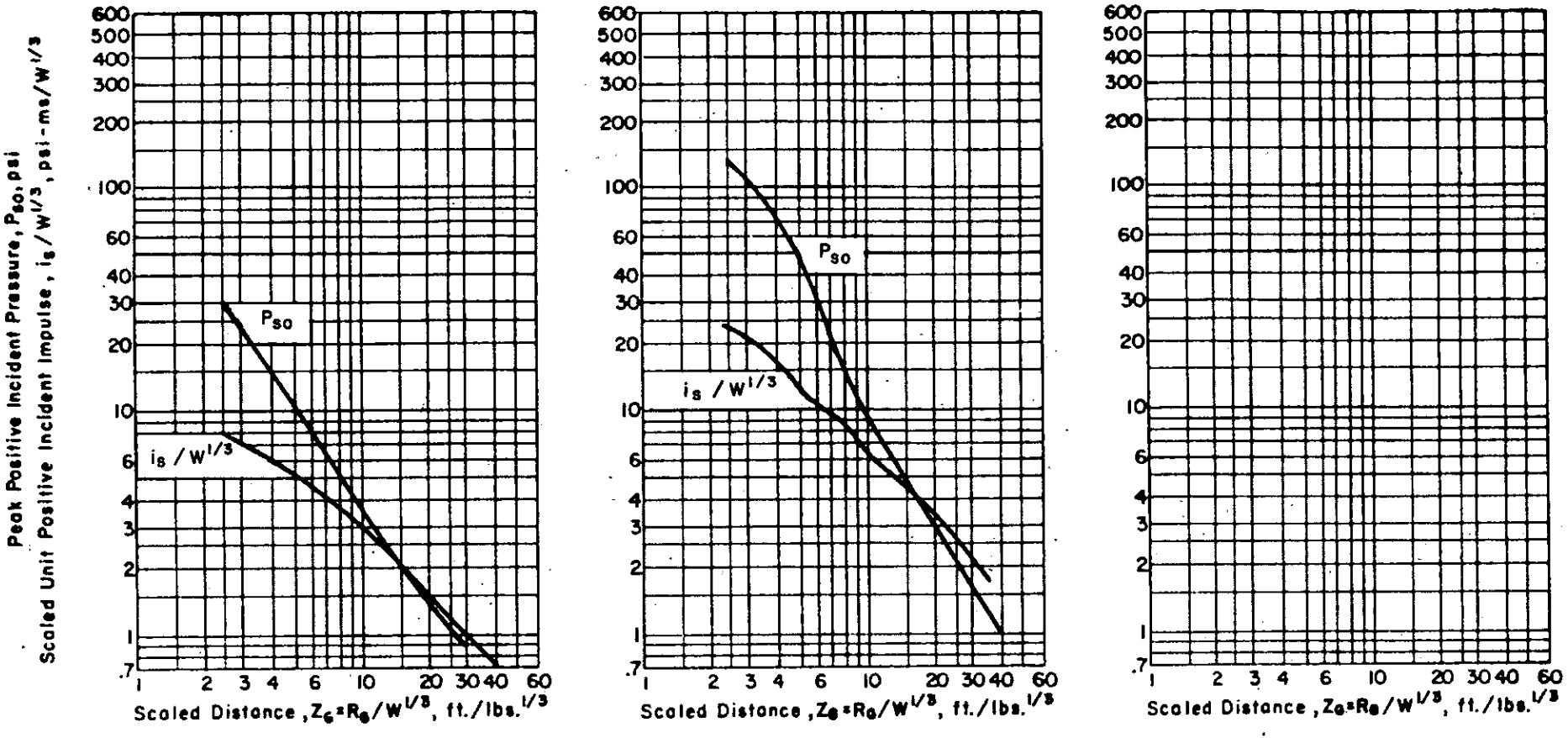


Figure 2-30 Peak positive incident pressure and scaled impulse for an explosion on the surface at sea level

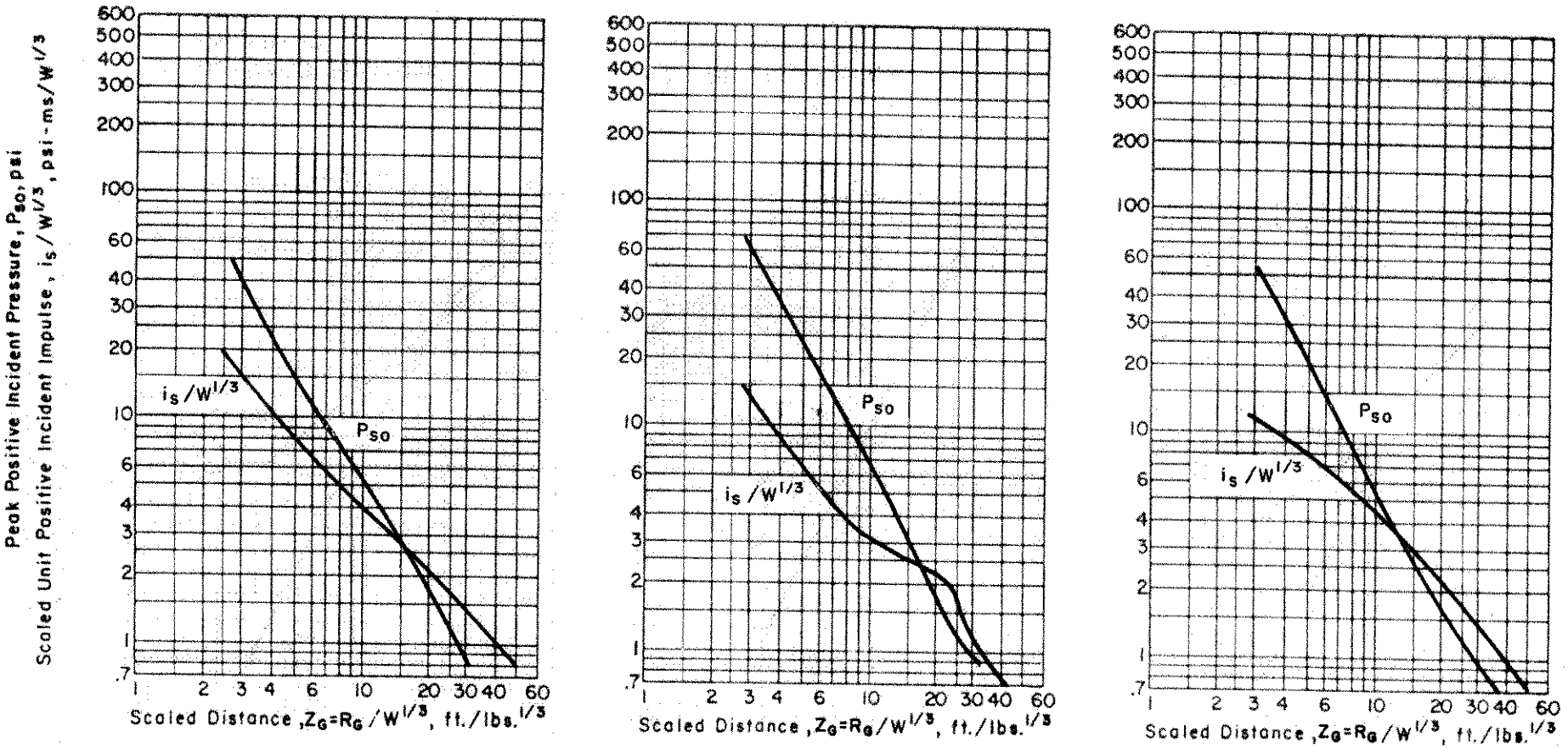
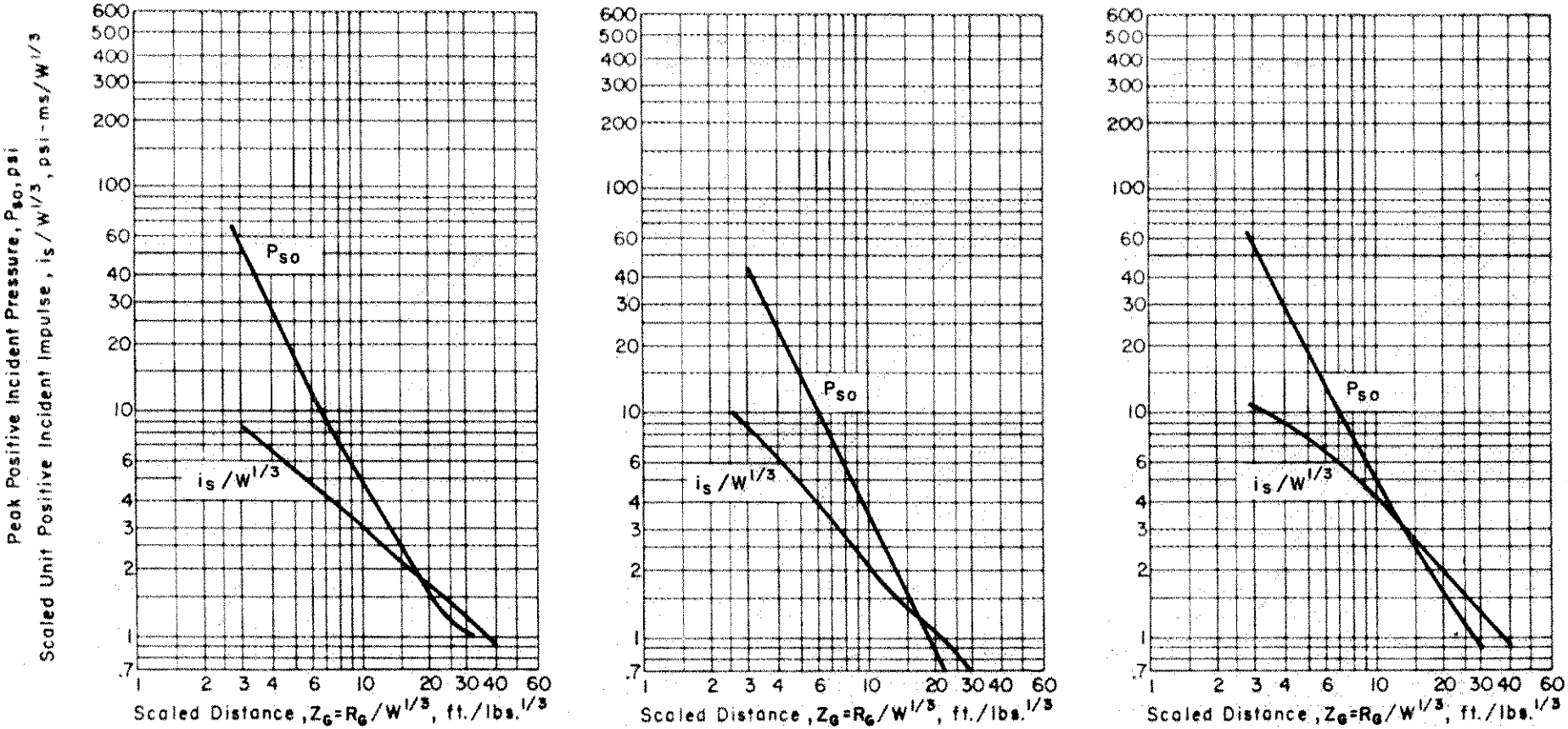


Figure 2-31 Peak positive incident pressure and scaled impulse for an explosion on the surface at sea level

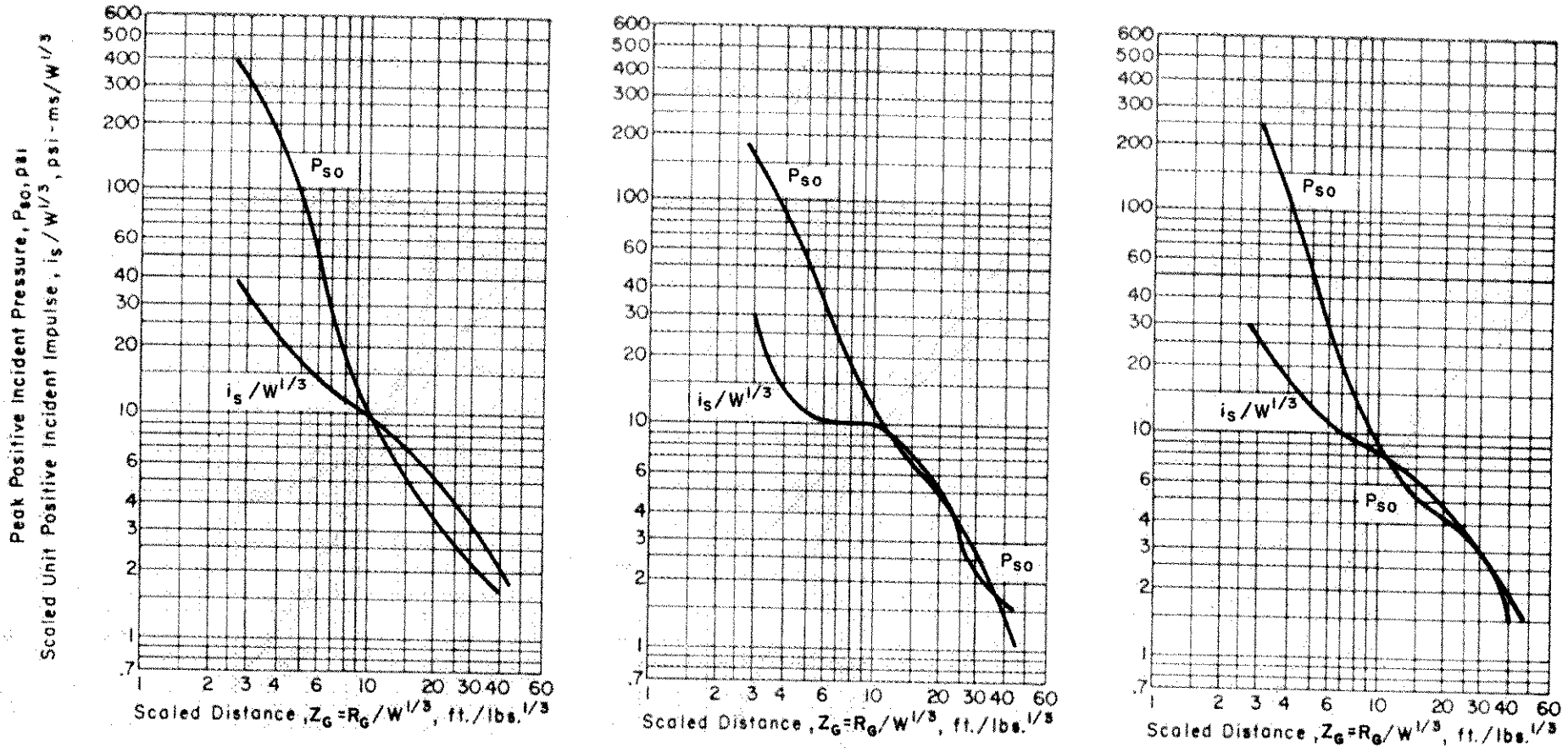


a. BS-NACO Propellant Cylindrical

b. BS-NACO Propellant Orthorhombic

c. BS-NACO Propellant Hoppers

Figure 2-32 Peak positive incident pressure and scaled impulse for an explosion on the surface at sea level

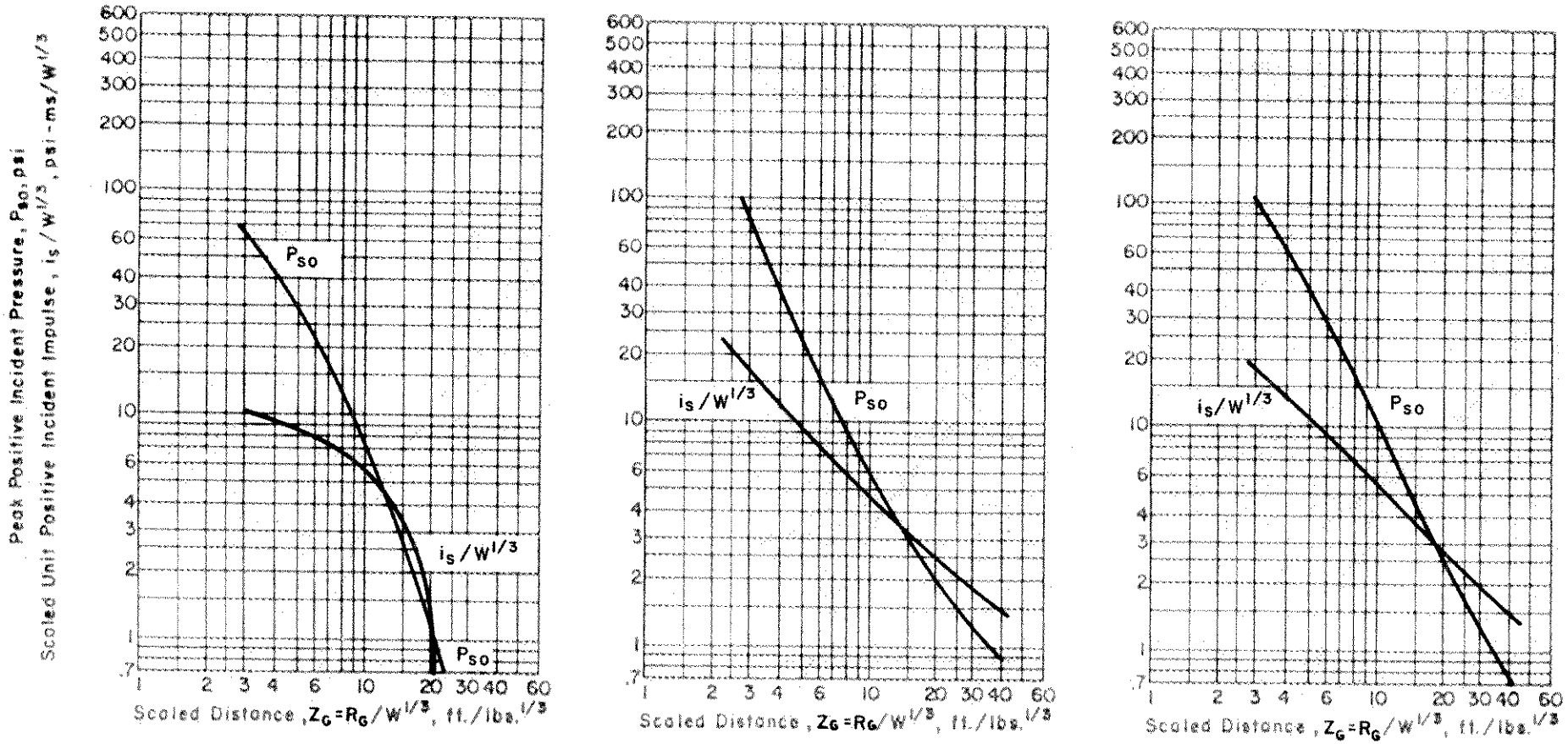


a. DIGL-RP I5420 Propellant Orthorhombic

b. DIGL-RP I5421 Propellant Cylindrical

c. DIGL-RP I5422 Propellant Orthorhombic

Figure 2-33 Peak positive incident pressure and scaled impulse for an explosion on the surface at sea level

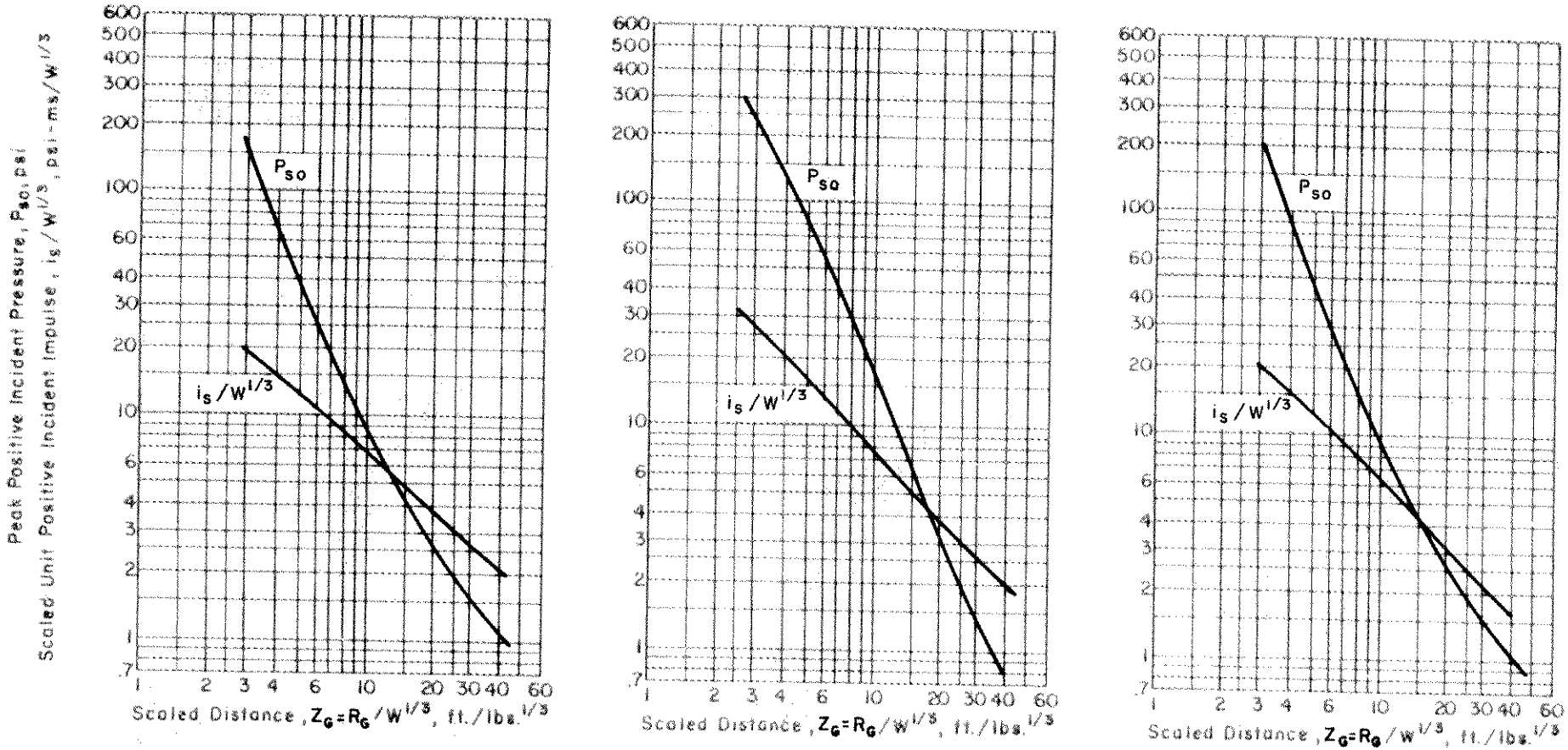


a. MI Propellant (Single perforated)

b. MI Propellant (Multi-perforated)

c. M26 EI Propellant (Multi-perforated) Blender barrel

Figure 2-34 Peak positive incident pressure and scaled impulse for an explosion on the surface at sea level

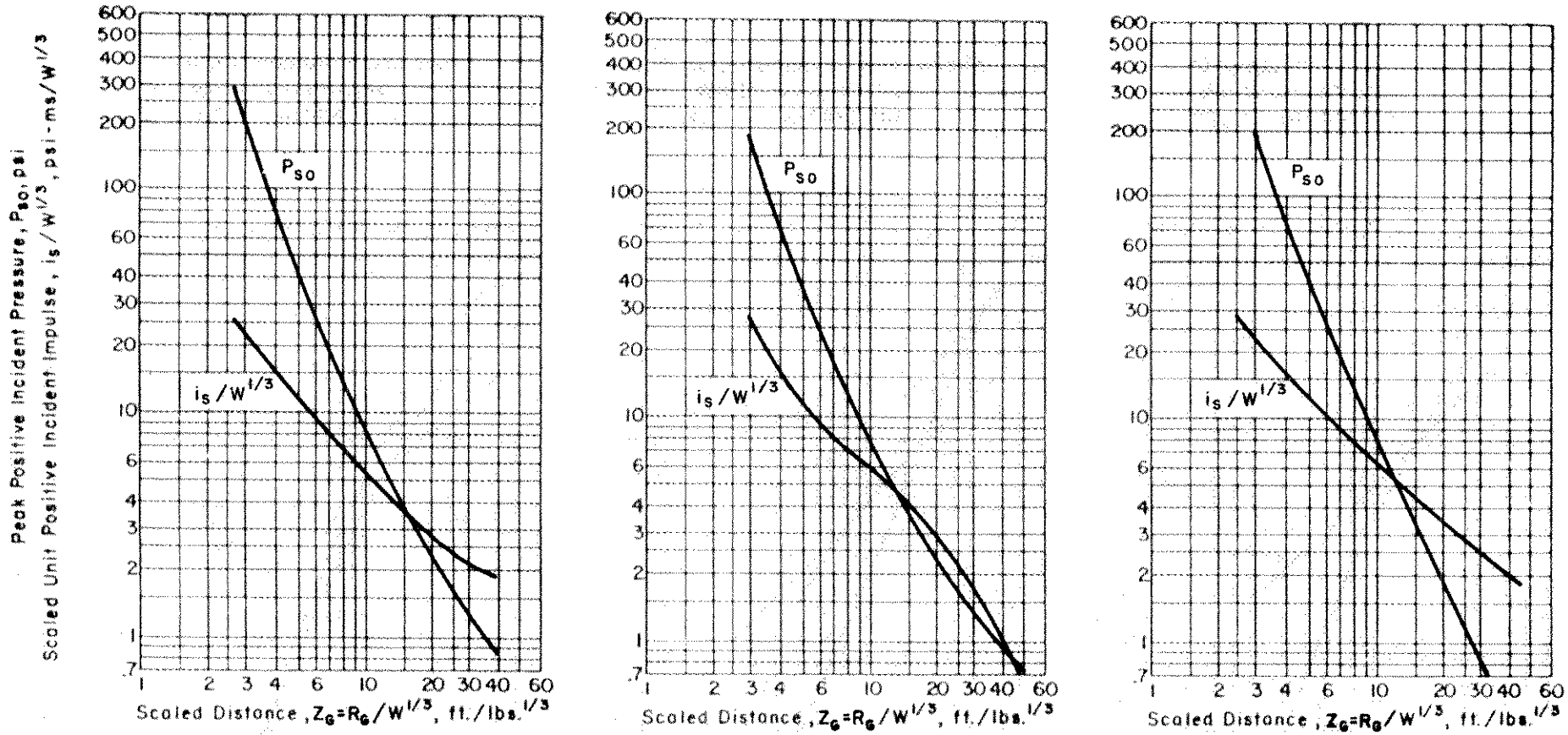


a. M26 E1 Propellant
(Multi-perforated)
Orthorhombic dryer bed

b. M26 E1 Propellant
(Multi-perforated)
Orthorhombic drop buggy

c. M26 E1 Propellant
(Multi-perforated)
Cylindrical

Figure 2-35 Peak positive incident pressure and scaled impulse for an explosion on the surface at sea level

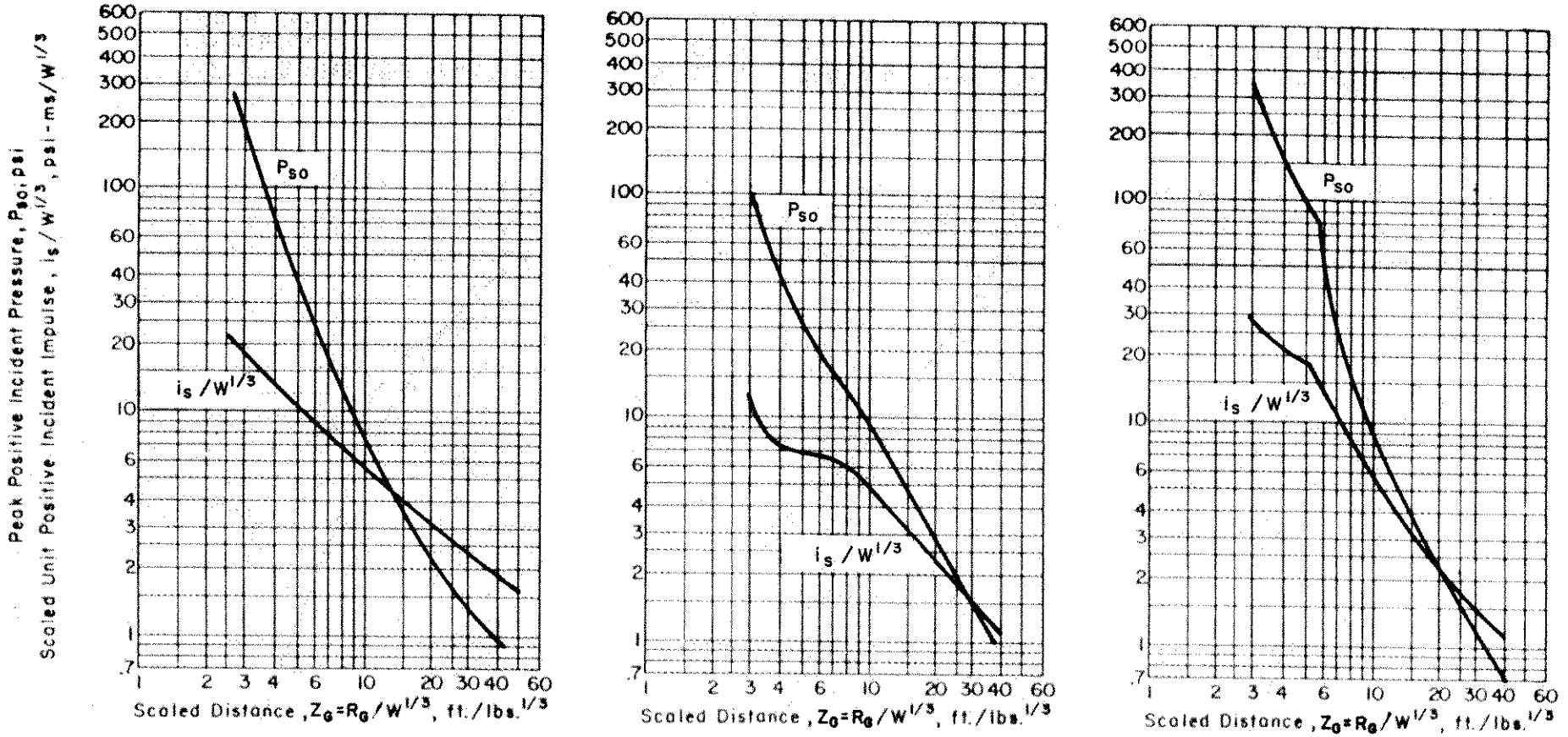


a. M30 Al Propellant (Single perforated) Cylindrical

b. M30 Al Propellant (Multi-perforated) Cylindrical

c. M30 Al Propellant (Single perforated) Orthorhombic dryer bed

Figure 2-36 Peak positive incident pressure and scaled impulse for an explosion on the surface at sea level

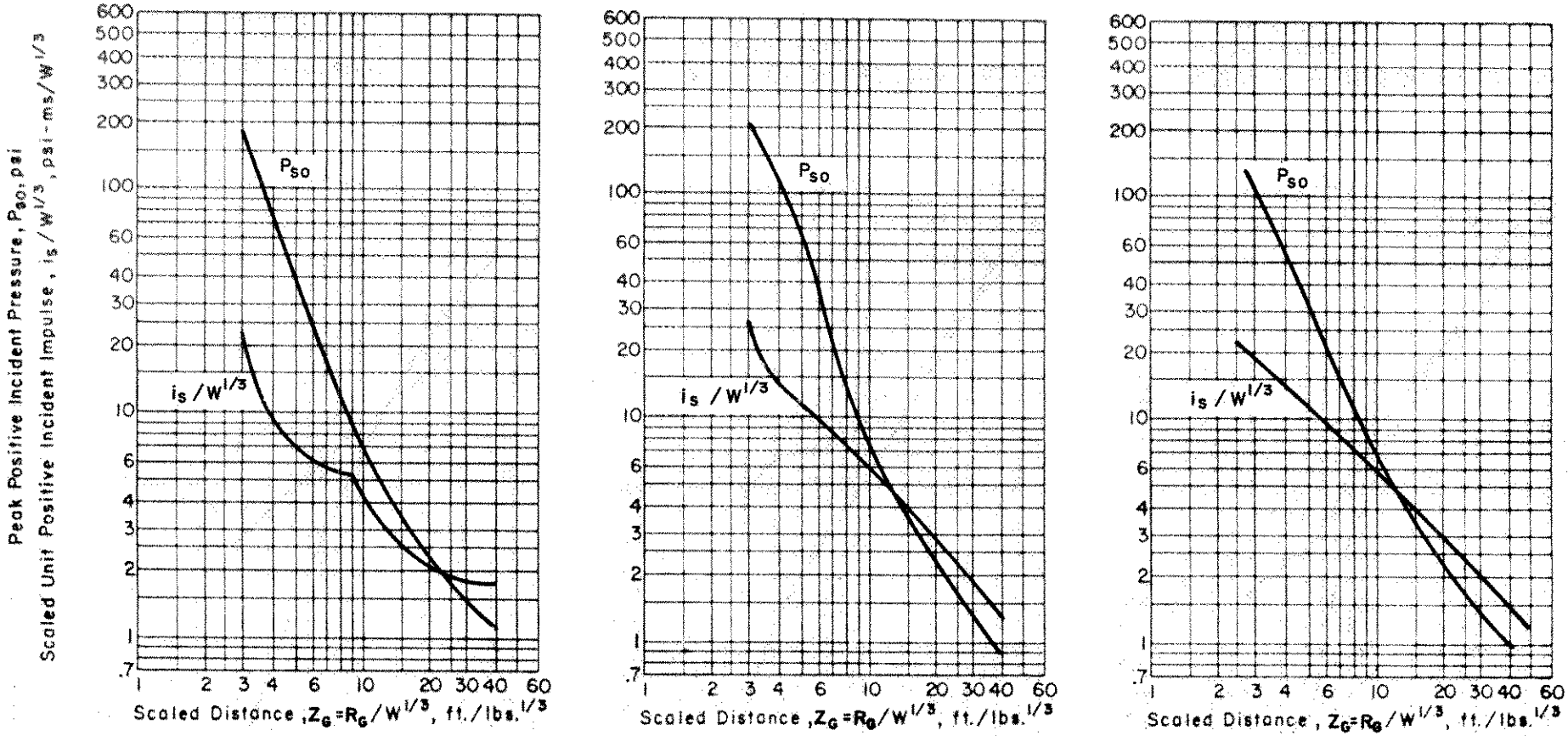


a. M30 Al Propellant
(Multi-perforated)
Orthorhombic dryer-bed

b. M31 Al El Slotted Stick Propellant
Orthorhombic
(Short Side)

c. M31 Al El Slotted Stick Propellant
Orthorhombic
(Long Side)

Figure 2-37 Peak positive incident pressure and scaled impulse for an explosion on the surface at sea level

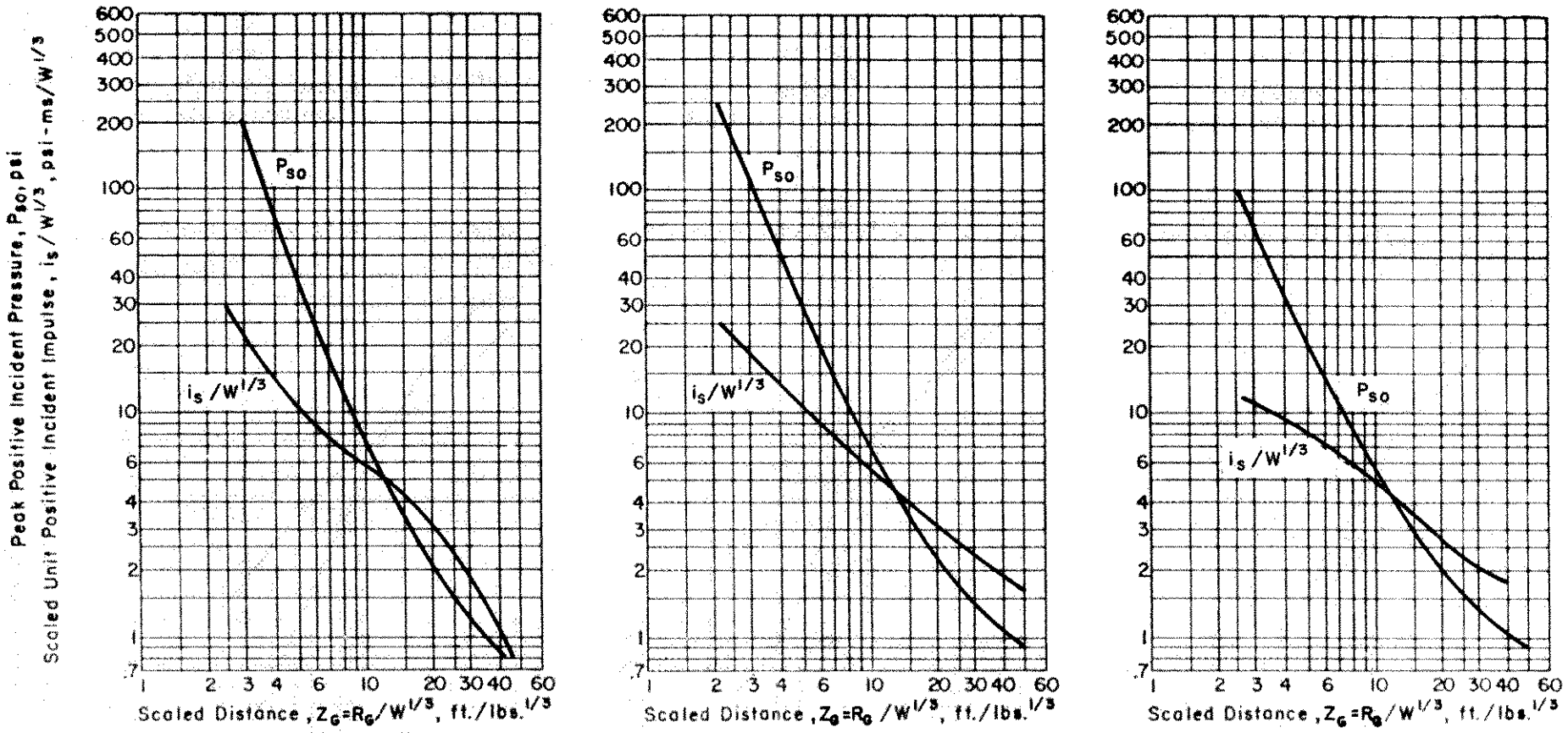


a. M31A1E1 Slotted Stick Propellant Orthorhombic (Short Side)

b. M31A1E1 Slotted Stick Propellant Orthorhombic (Long Side)

c. N5 Propellant Shipping containers

Figure 2-38 Peak positive incident pressure and scaled impulse for an explosion on the surface at sea level



a. N5 Propellant
Carpet rolls

b. N5 Propellant
Charge buckets

c. N5 Propellant
Conveyor belt configuration

Figure 2-39 Peak positive incident pressure and scaled impulse for an explosion on the surface at sea level

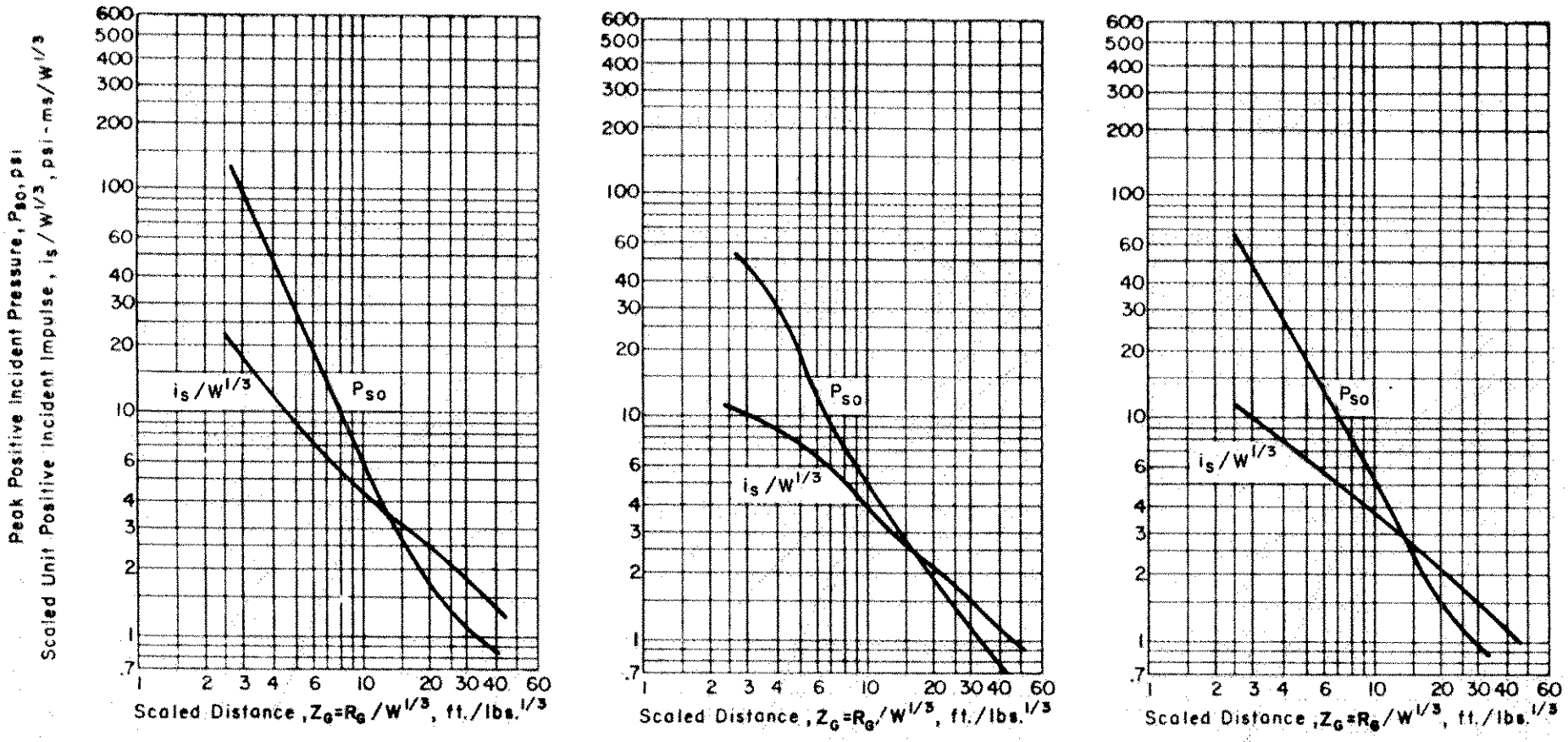


Figure 2-40 Peak positive incident pressure and scaled impulse for an explosion on the surface at sea level

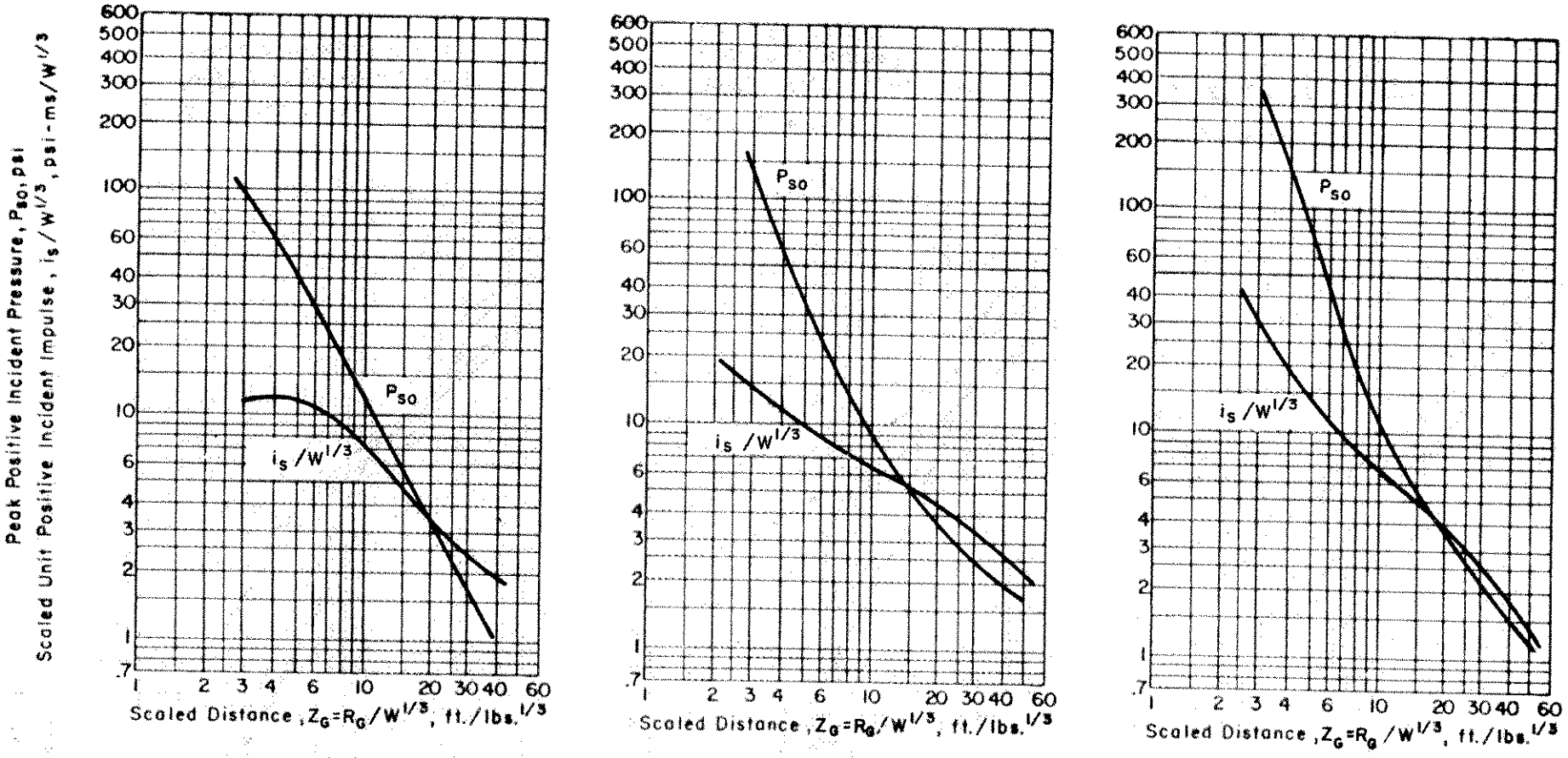
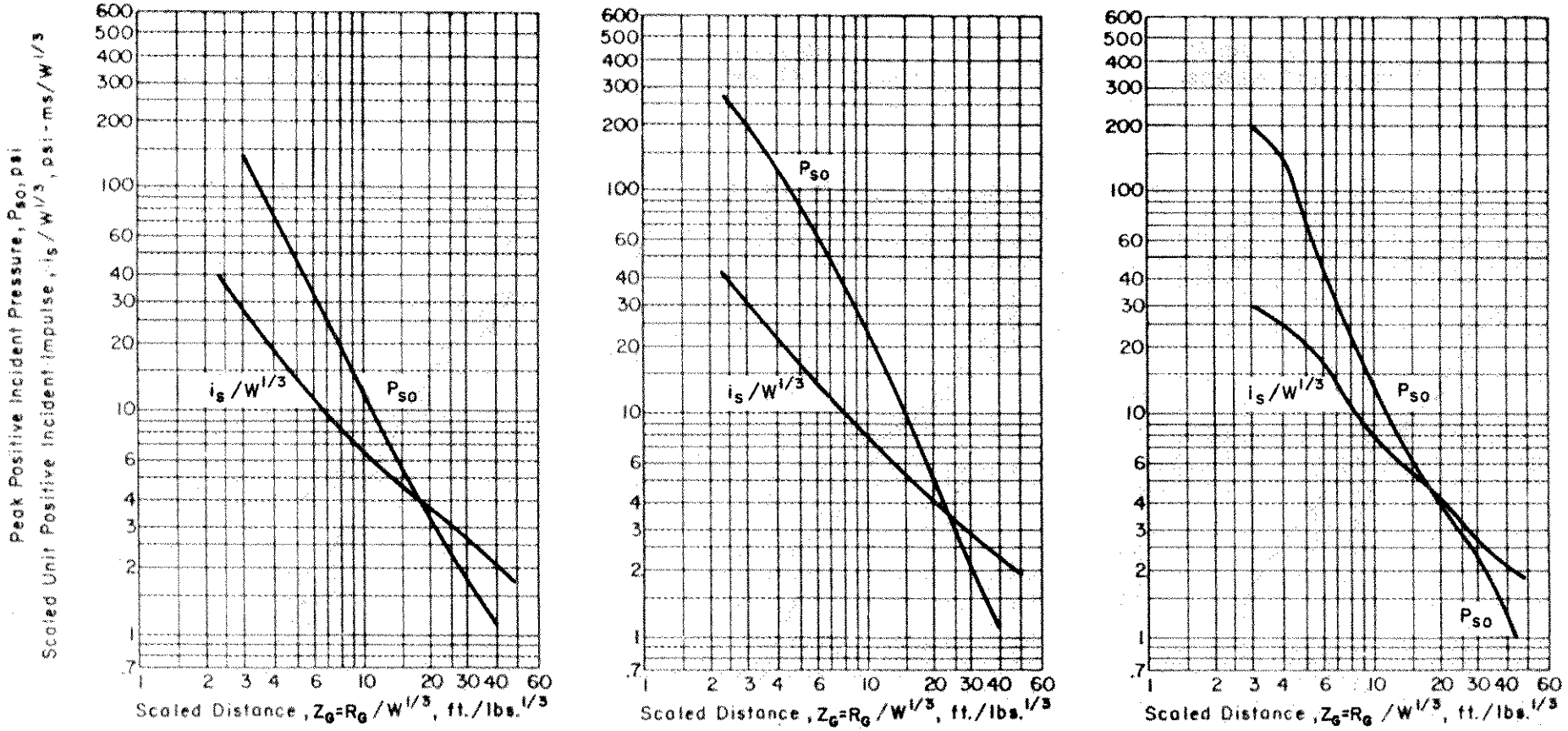


Figure 2-41 Peak positive incident pressure and scaled impulse for an explosion on the surface at sea level

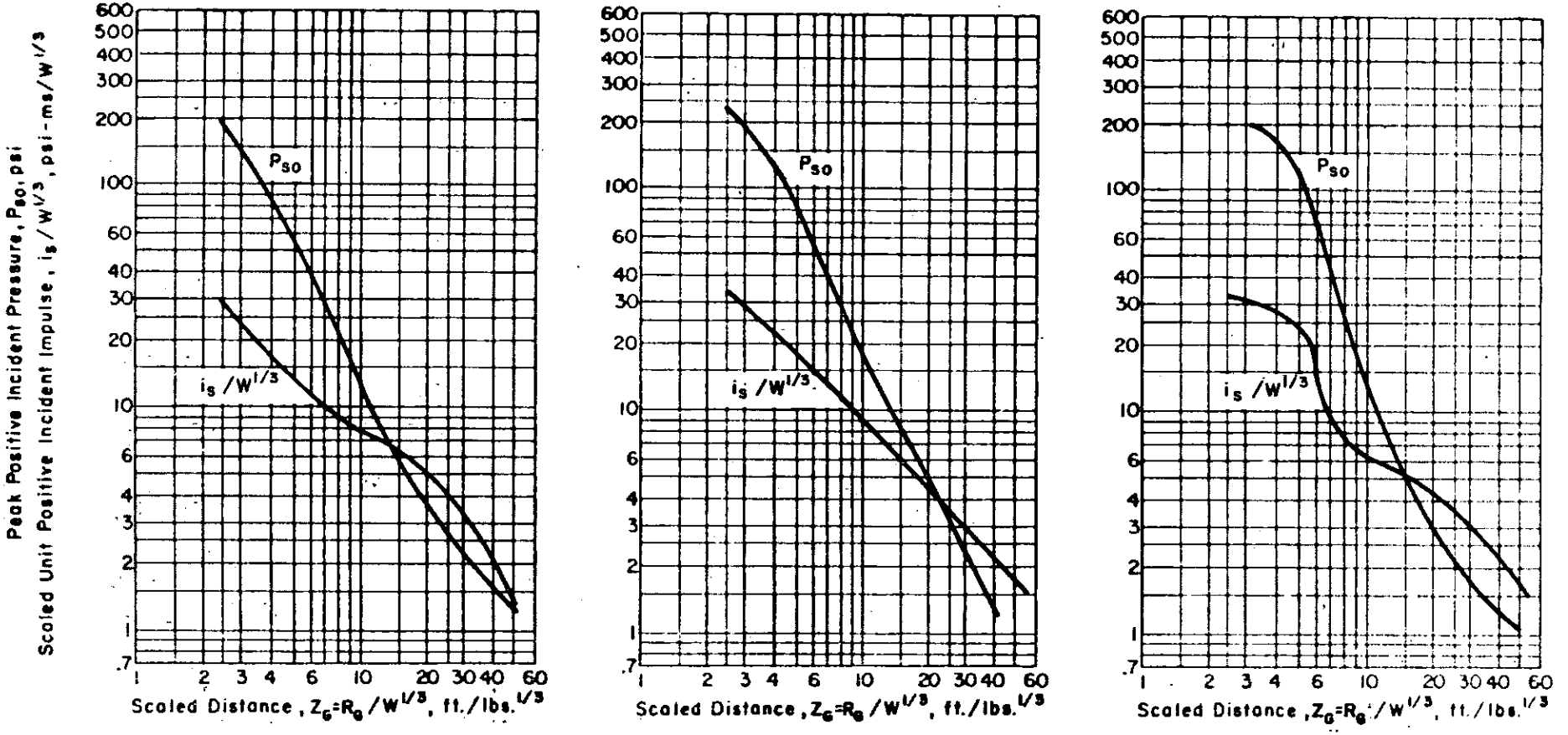


a. XM37 RAP Propellant (Single forward grain)

b. XM37 RAP Propellant (Forward grains) Extruded billet

c. XM37 RAP Propellant (Forward grains) Ro Con shipping containers

Figure 2-42 Peak positive incident pressure and scaled impulse for an explosion on the surface at sea level



a. XM37 RAP Propellant
(Single aft grain)

b. XM37 RAP Propellant
(Aft grain)
Extruded billets

c. XM37 RAP Propellant
(Aft grains)
Ro Con shipping containers

Figure 2-43 Peak positive incident pressure and scaled impulse for an explosion on the surface at sea level

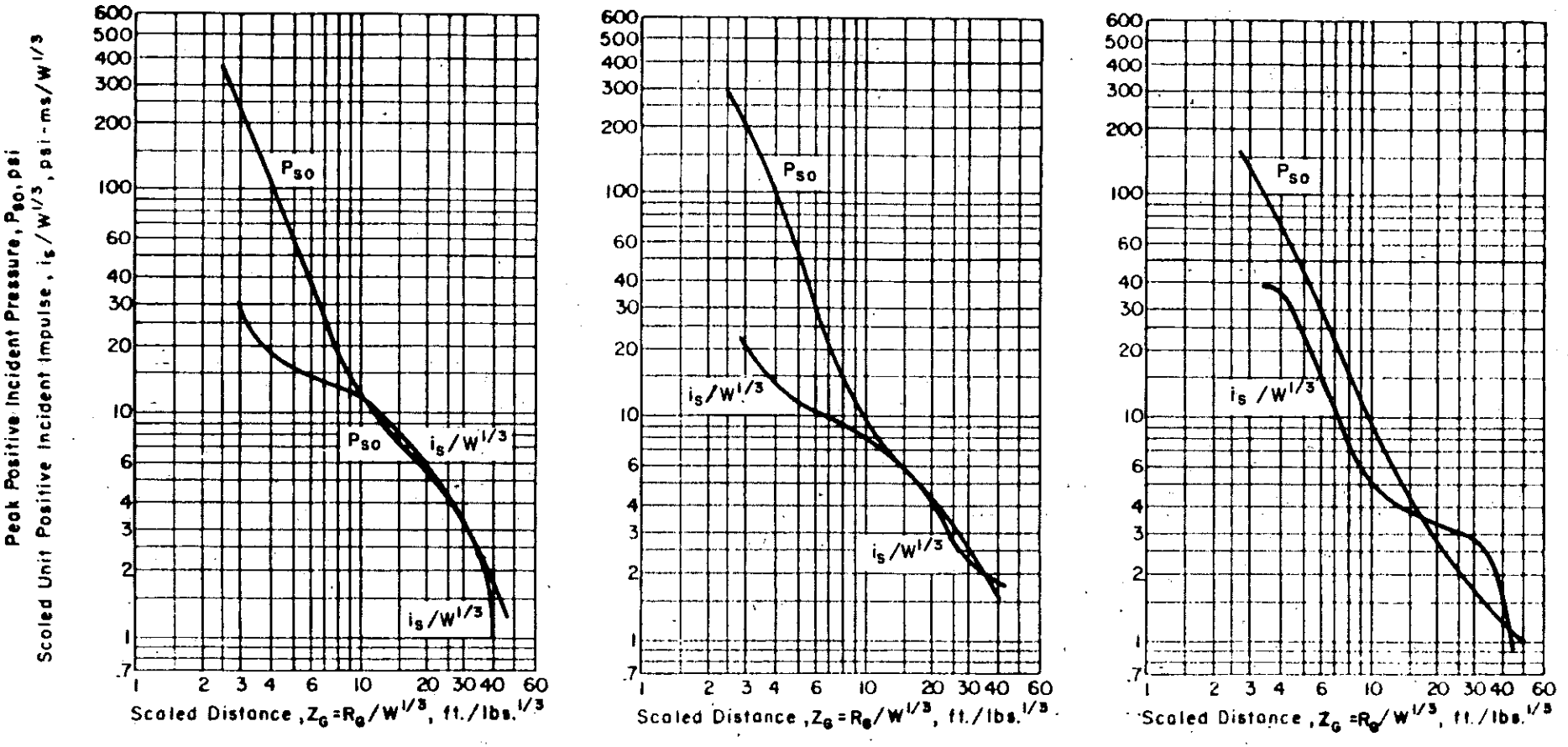
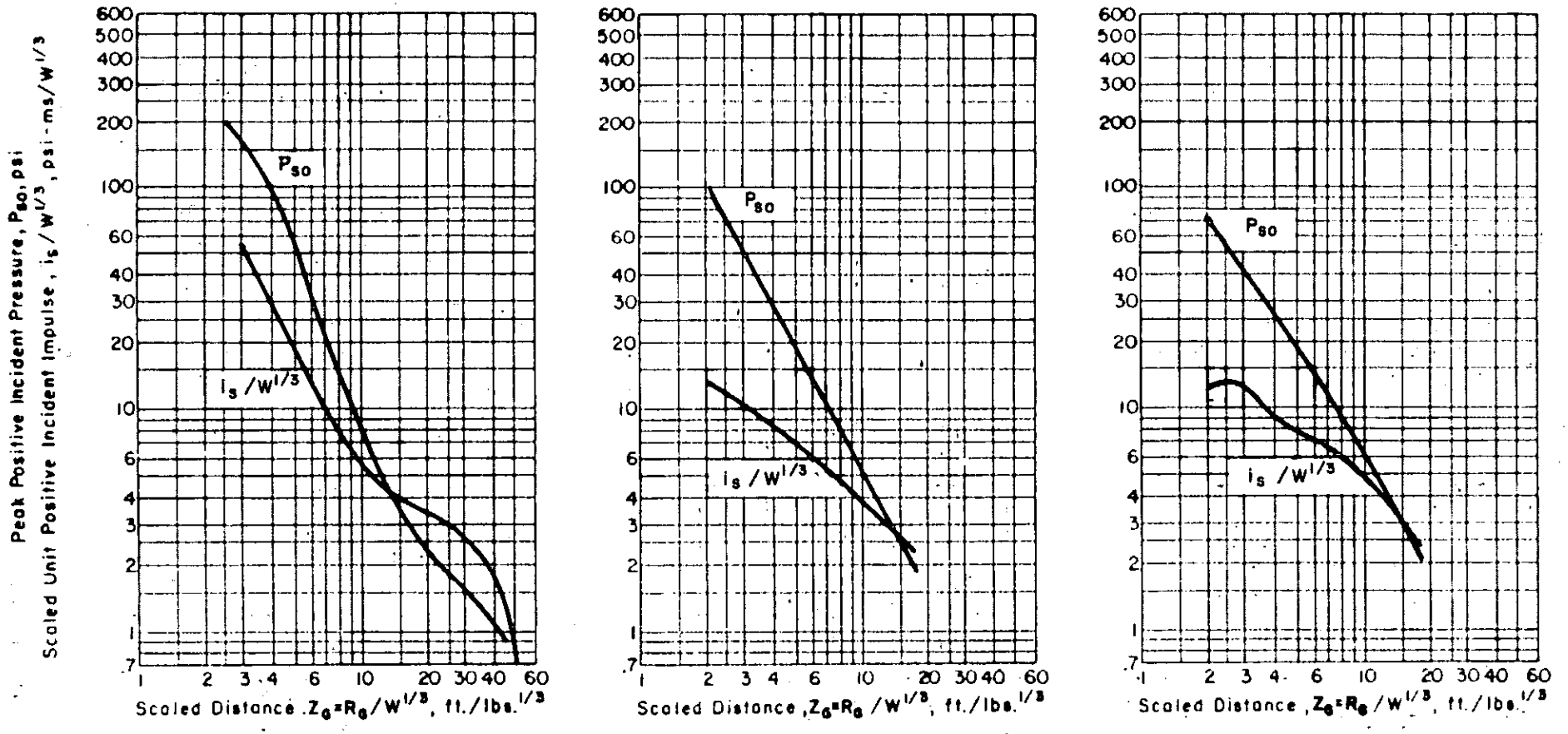


Figure 2-44 Peak positive incident pressure and scaled impulse for an explosion on the surface at sea level

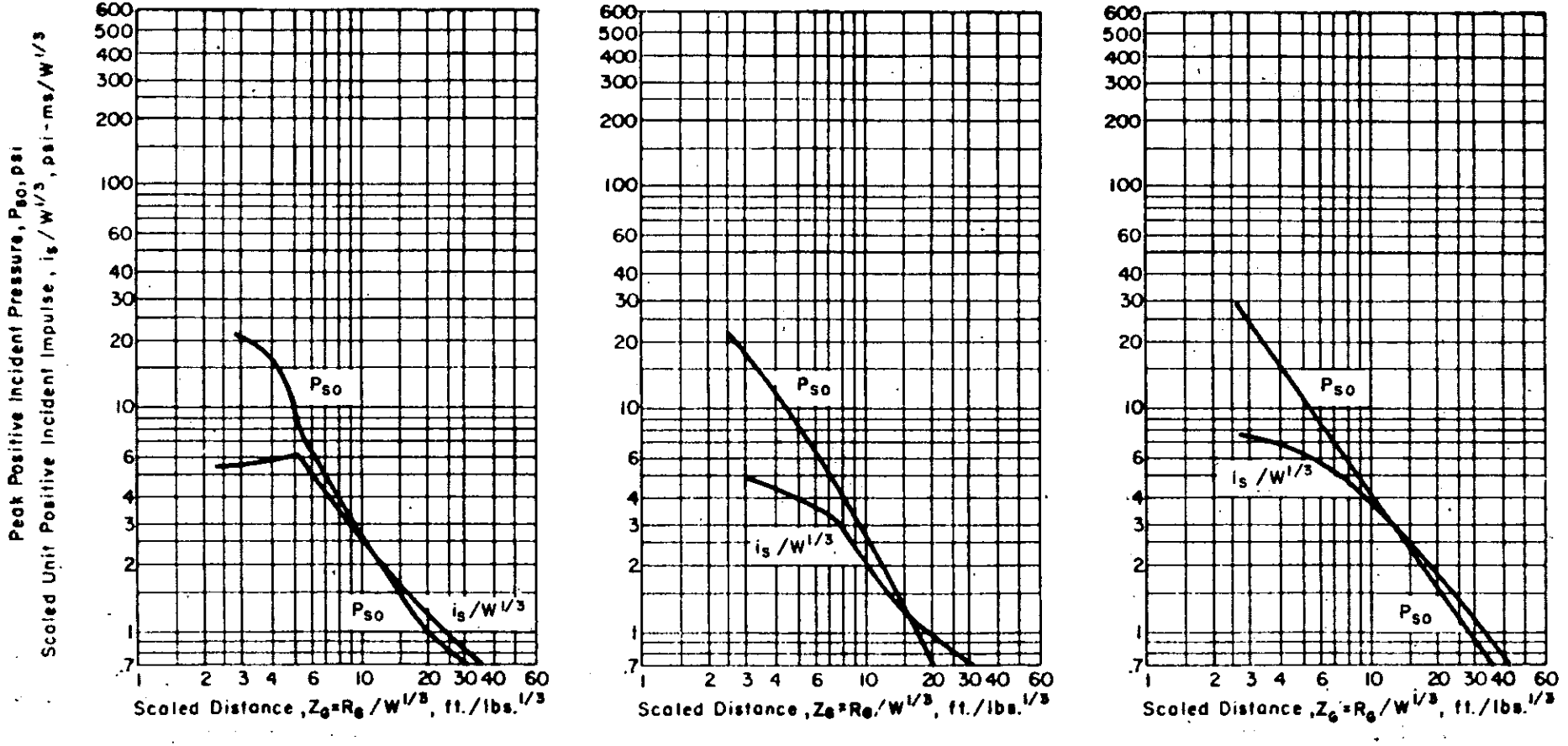


a. M10 Propellant Orthorhombic (H/W<1)

b. 105mm M314-A3 Illuminated Composition (Cylindrical)

c. 105mm M314-A3 Illuminated Composition (Cylindrical)

Figure 2-43 Peak positive incident pressure and scaled impulse for an explosion on the surface at sea level

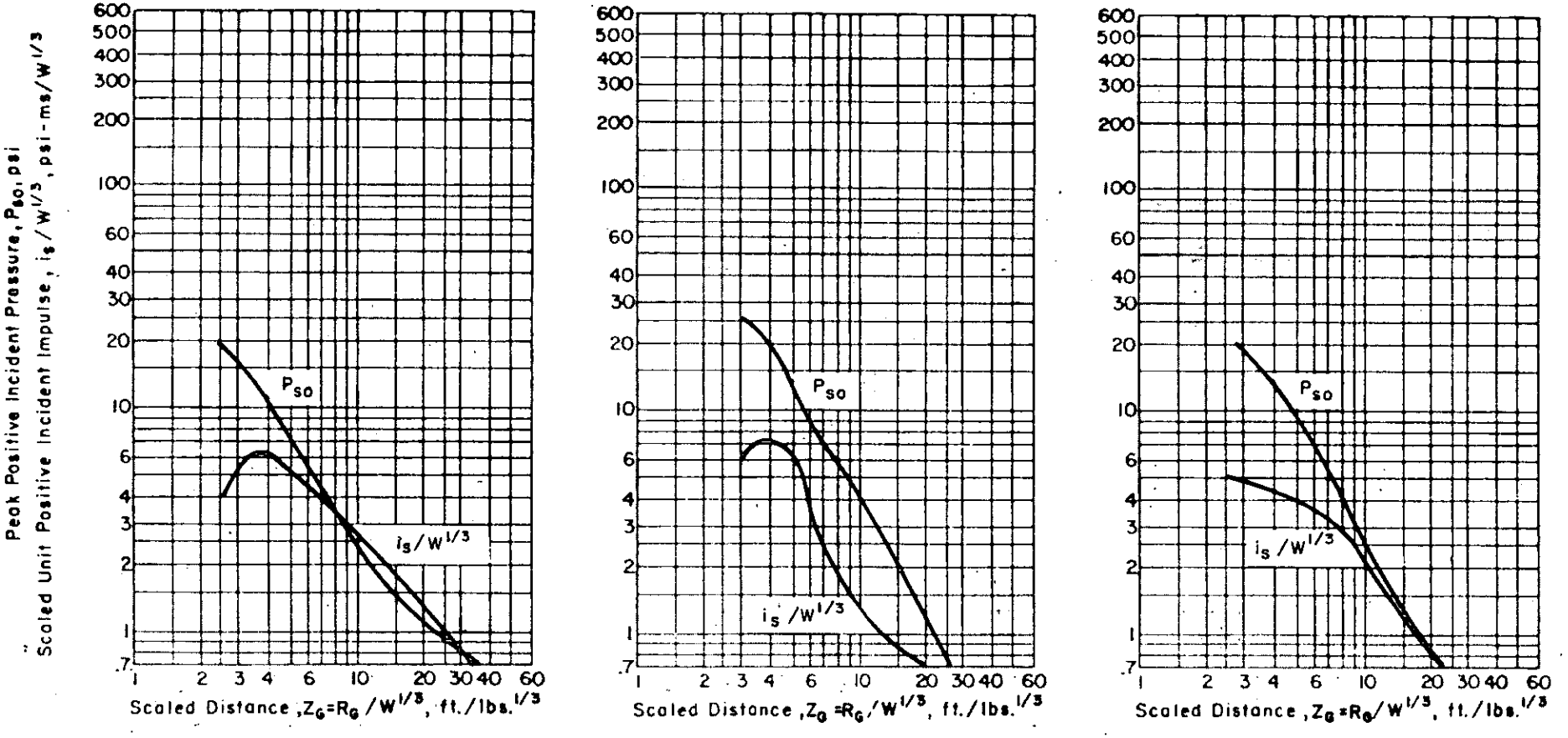


a. I559 Igniter Mixture Cylinder

b. I559 Igniter Mixture Cylinder

c. I560 Subigniter Mixture Cylinder

Figure 2-46 Peak positive incident pressure and scaled impulse for an explosion on the surface at sea level

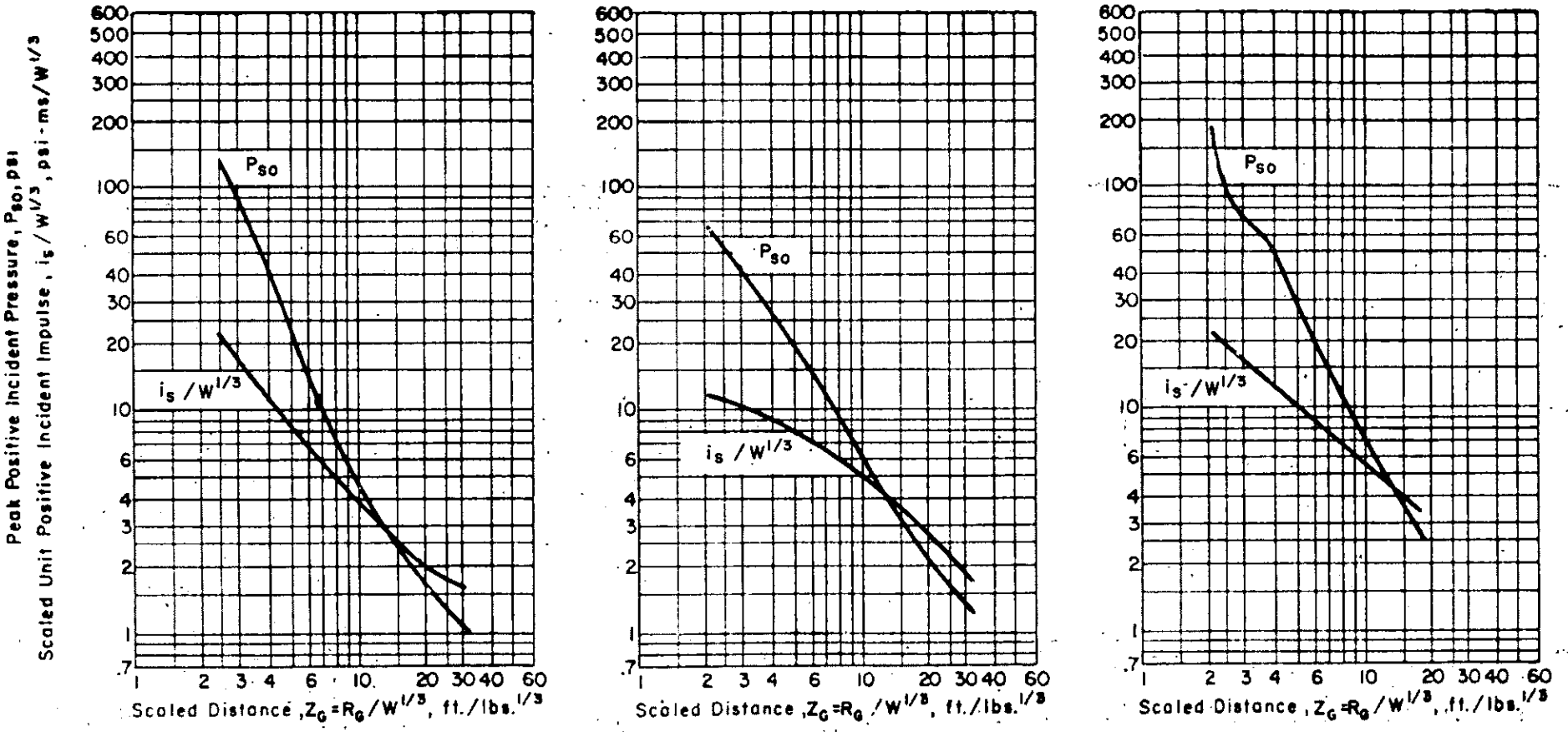


a. I560 Subigniter Mixture Cylinder

b. R284 Tracer Mixture Cylinder

c. R284 Tracer Mixture Cylinder

Figure 2-47 Peak positive incident pressure and scaled impulse for an explosion on the surface at sea level

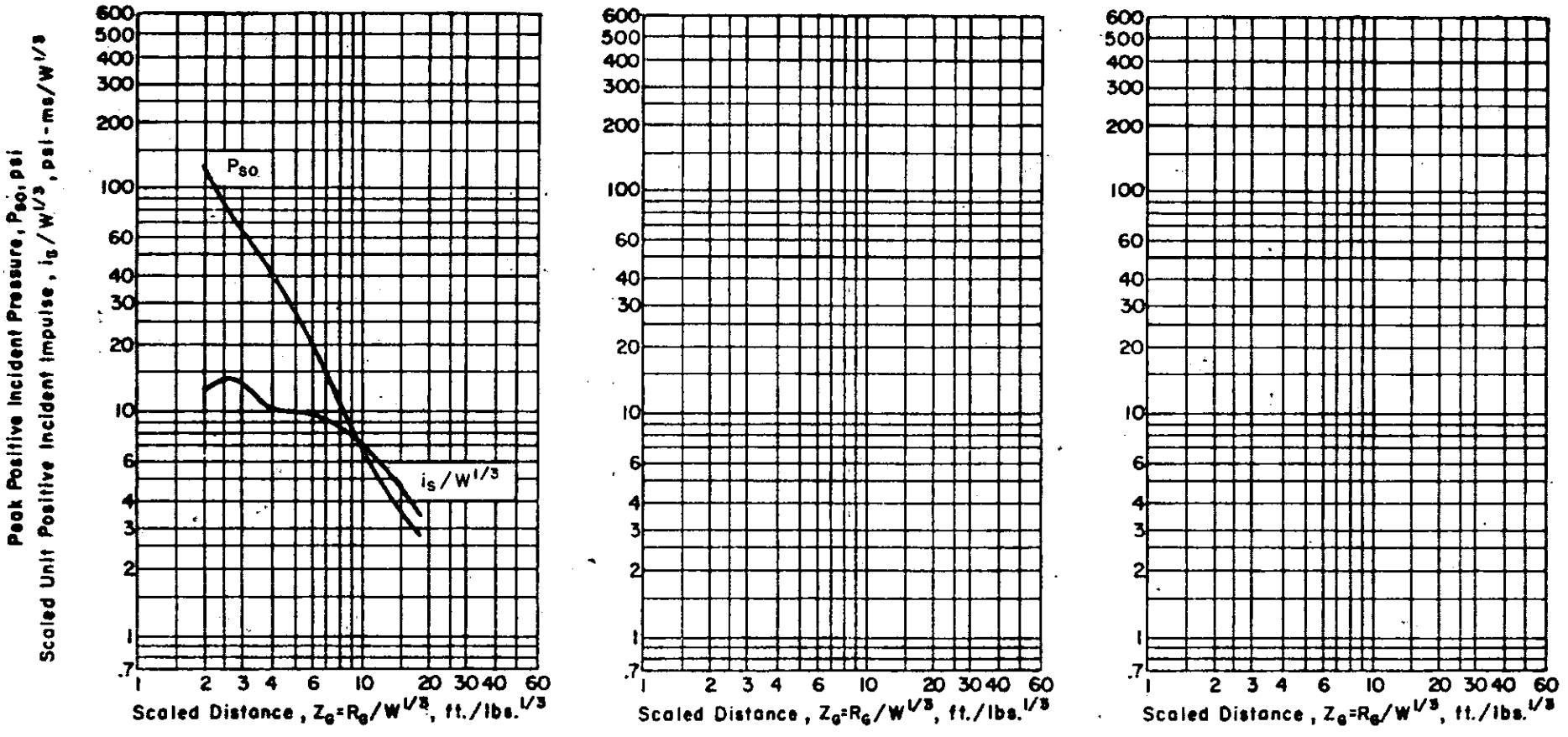


a. M314-A3 First Fire Composition Orthorhombic

b. M314-A3 First Fire Composition Cylinder

c. M49-A1 Trip Flare Composition Cylinder

Figure 2-48 Peak positive incident pressure and scaled impulse for an explosion on the surface at sea level

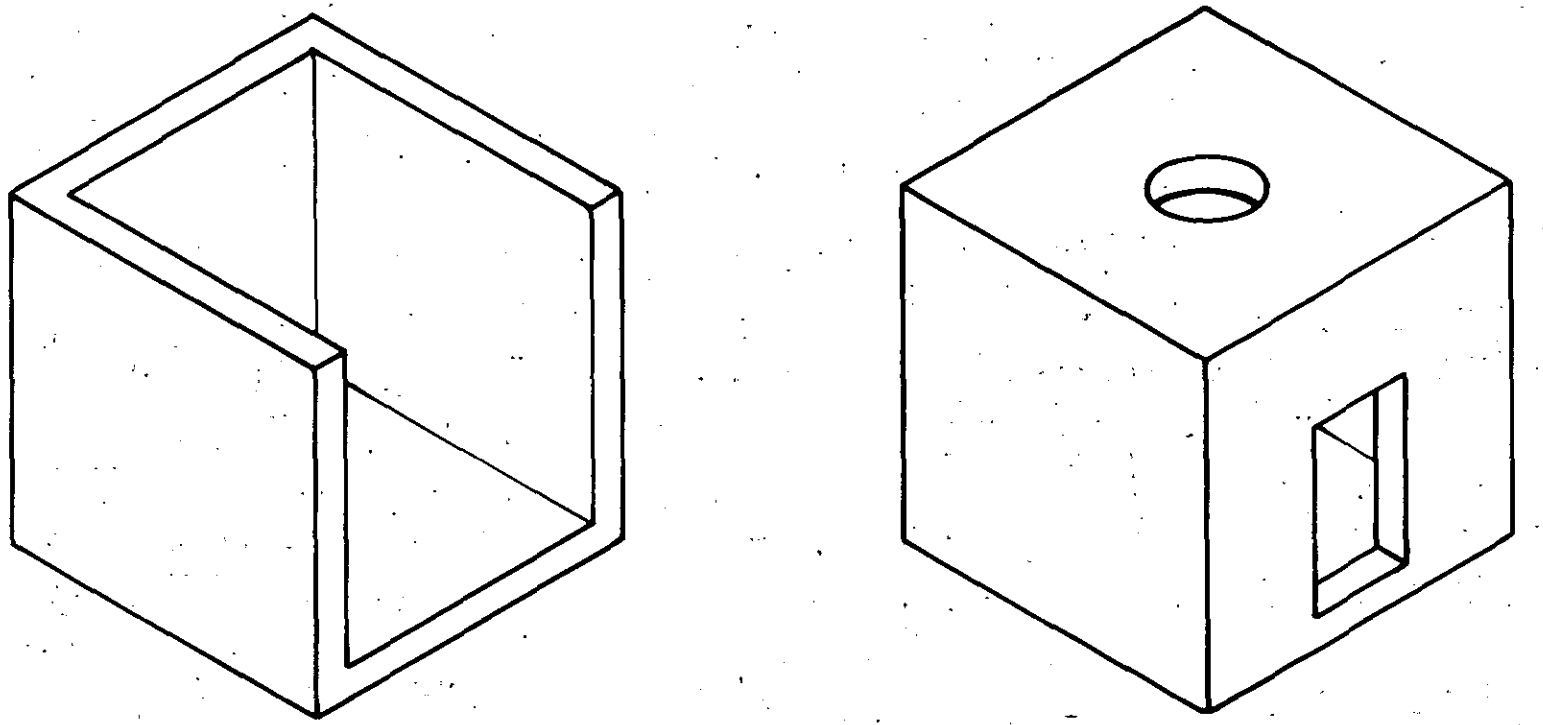


a. M49-A1 Trip Flare Composition Cylindrical

b.

c.

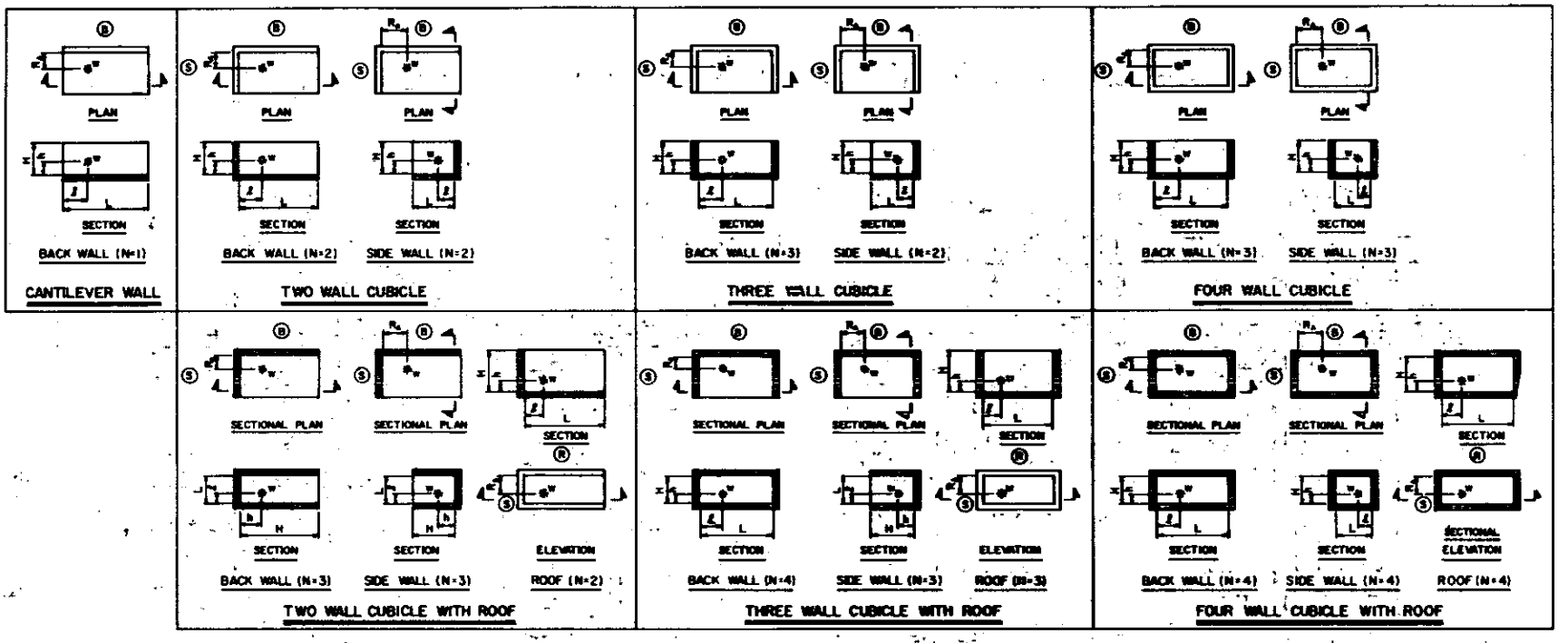
Figure 2-49 Peak positive incident pressure and scaled impulse for an explosion on the surface at sea level



a. Cubicle Structure

b. Enclosed Structure with Openings

Figure 2-50 Confined explosion structures



Notes:

1. B denotes Back Wall, S denotes Side Wall and R denotes Roof.
2. Numbers in parentheses indicate number, N, of reflecting surfaces adjacent to surface in question.
3. h is always measured to the nearest reflecting surface.
4. ℓ is always measured to the nearest reflecting surface except for the cantilever wall where it is measured to the nearest free edge.
5. For values of average peak pressures for barrier and cubicle arrangements shown, see Figures 2-52 to 2-100.
   For respective scaled average reflected impulses, see Figures 2-101 to 2-149.
   For reference list of above Figures for particular values of required parameters in Note 6, see Figure 2-3.
6. Required parameters: N, ℓ/L, h/H, L/H, L/R_A, $Z_A = R_A/W^{1/3}$

Figure 2-51 Barrier and cubicle configurations and parameters

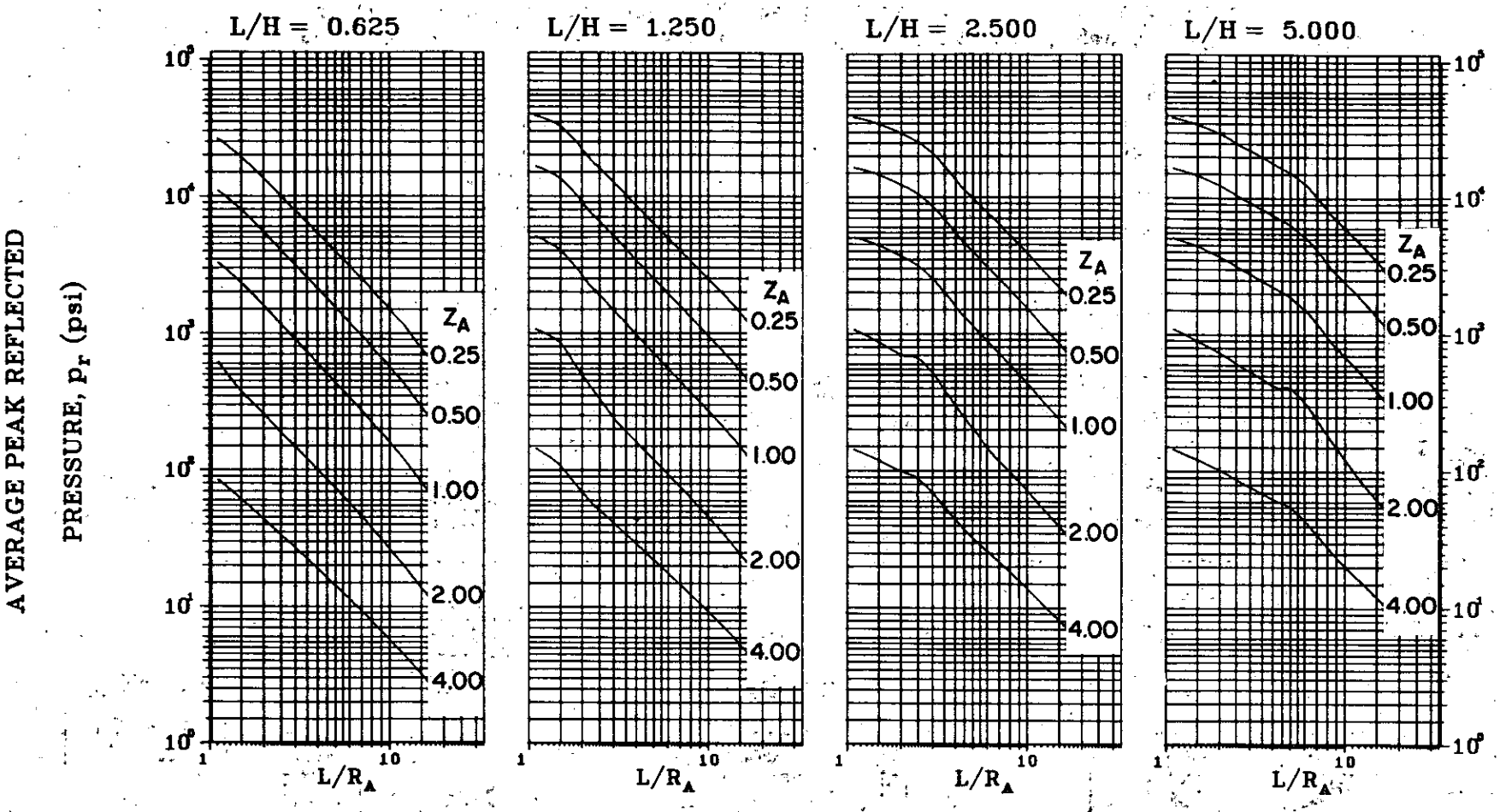


Figure 2-52 Average peak reflected pressure (N = 1, /L = 0.10, h/H = 0.10)

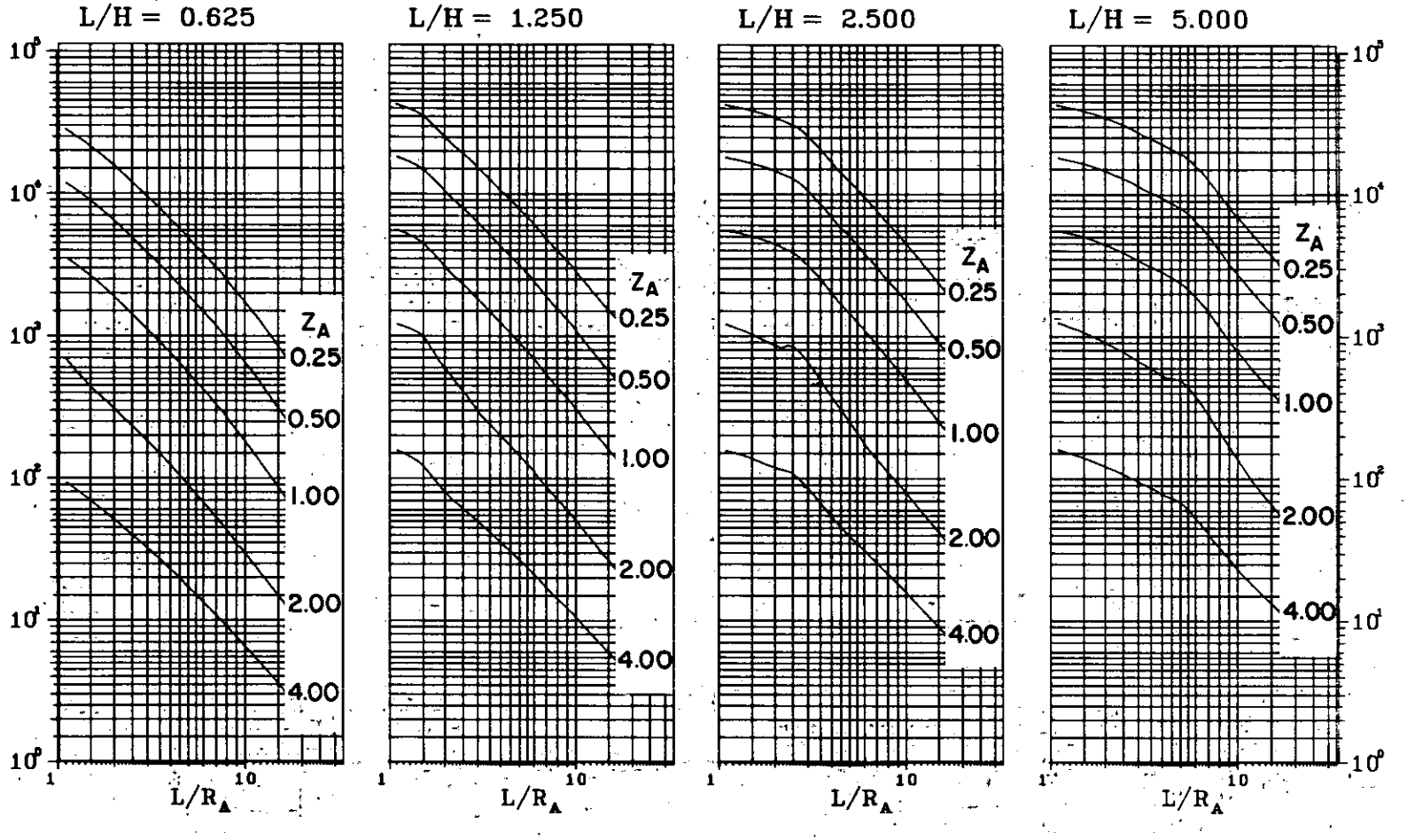


Figure 2-53 Average peak reflected pressure (N = 1, /L = 0.25 and 0.75, h/H = 0.10)

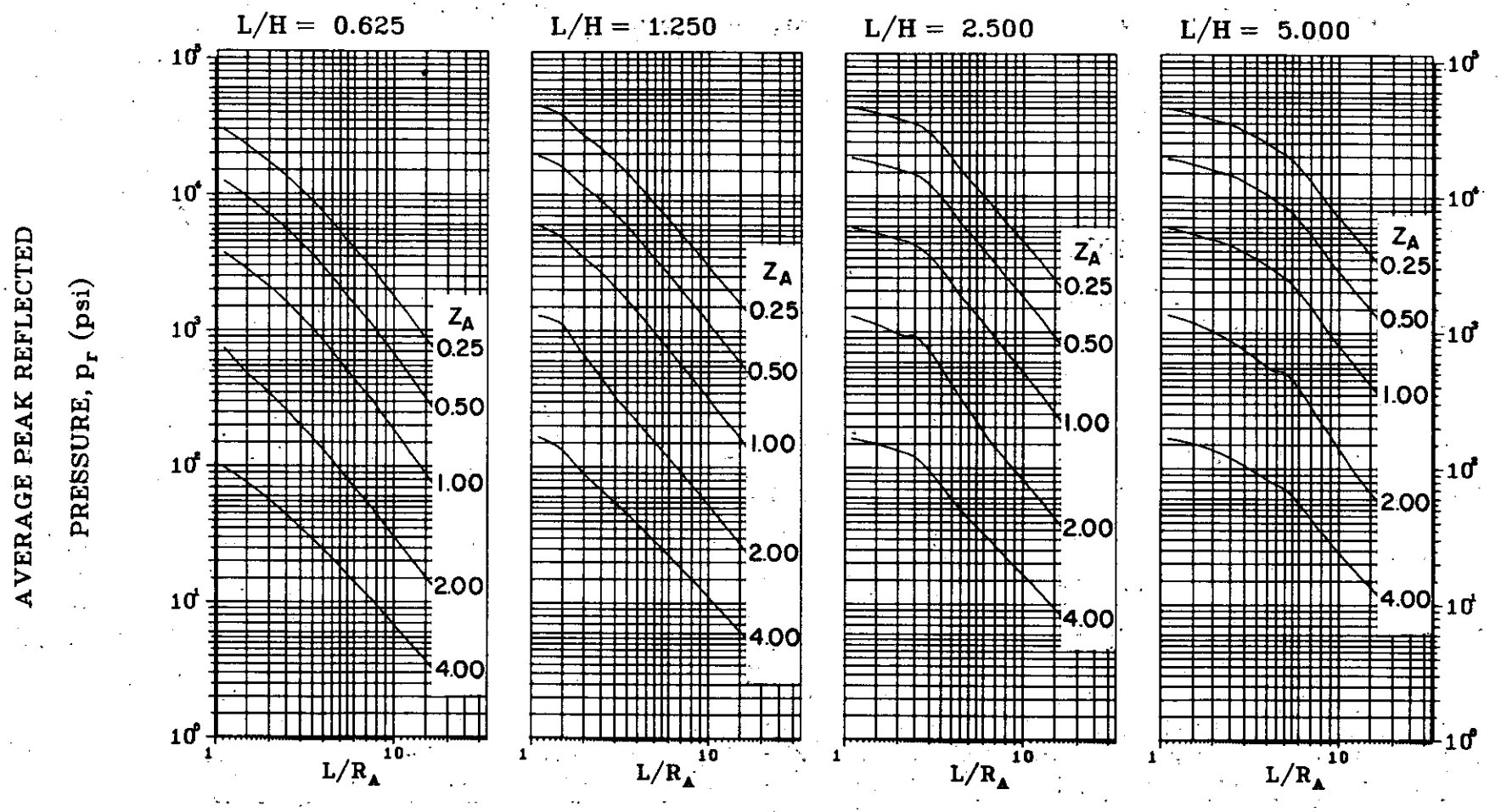


Figure 2-54 Average peak reflected pressure (N = 1, /L = 0.50, h/H = 0.10)

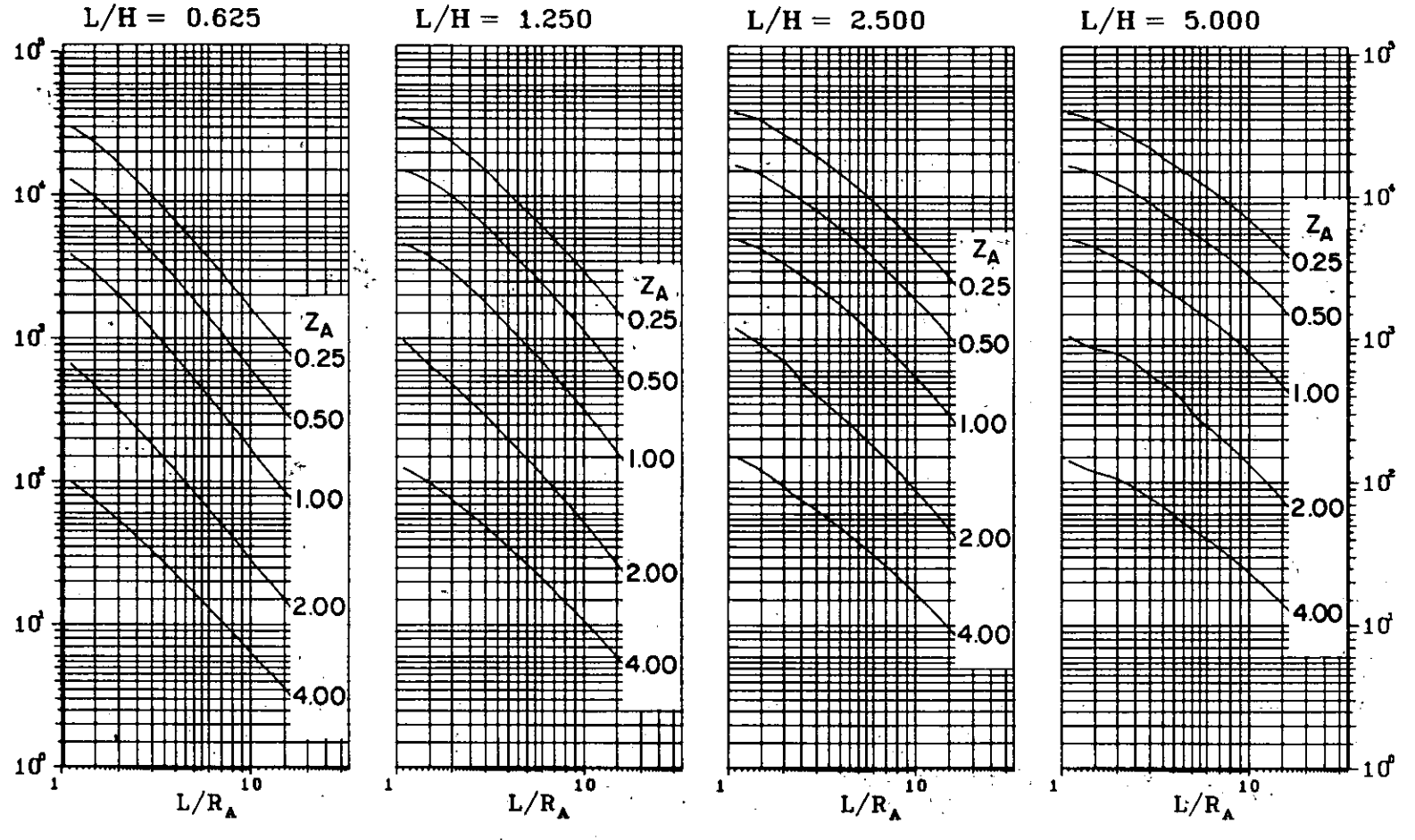


Figure 2-55 Average peak reflected pressure (N = 1, /L = 0.10, h/H = 0.25)

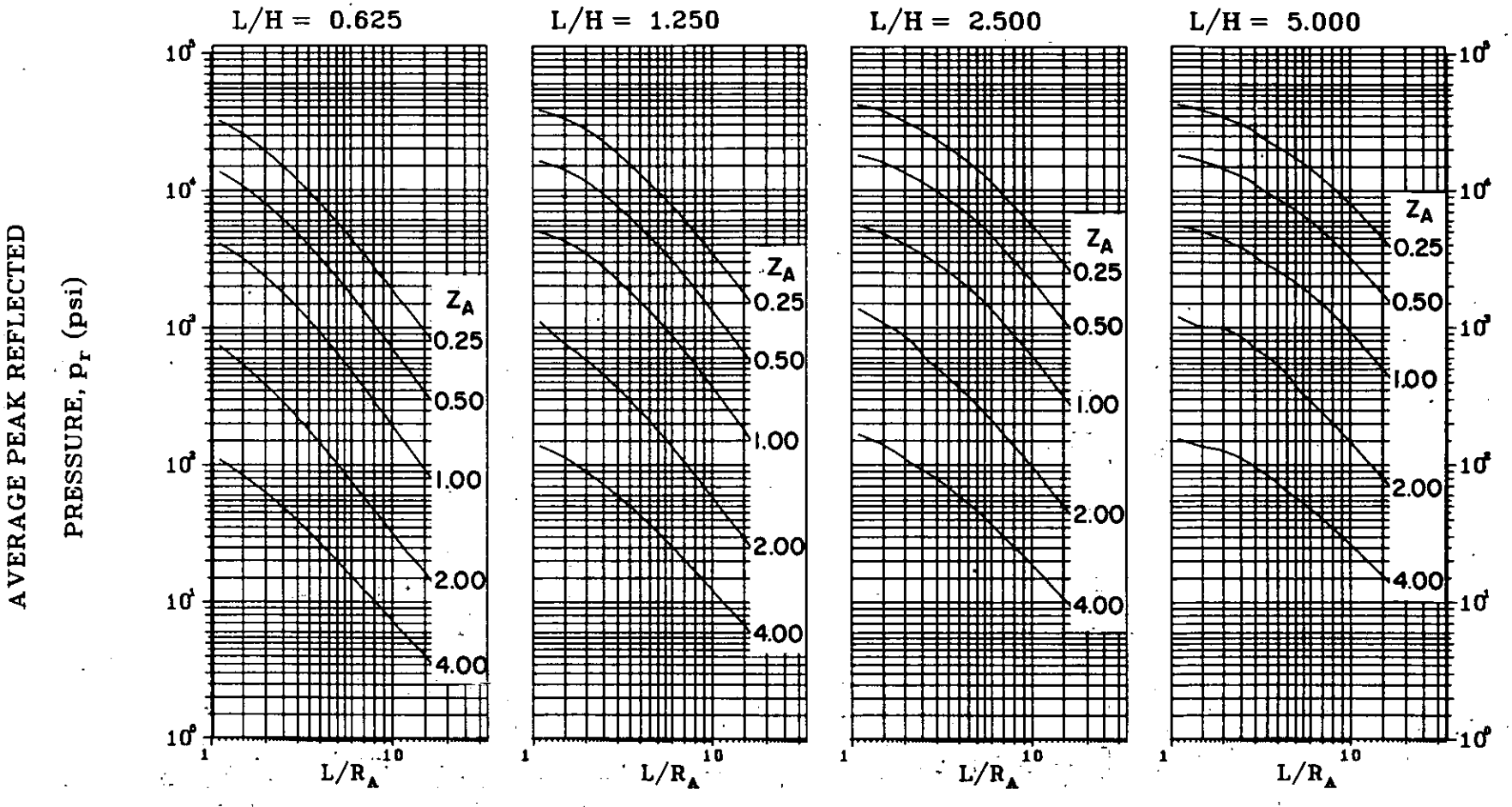


Figure 2-56 Average peak reflected pressure
(N = 1, ℓ/L = 0.25 and 0.75, h/H = 0.25)

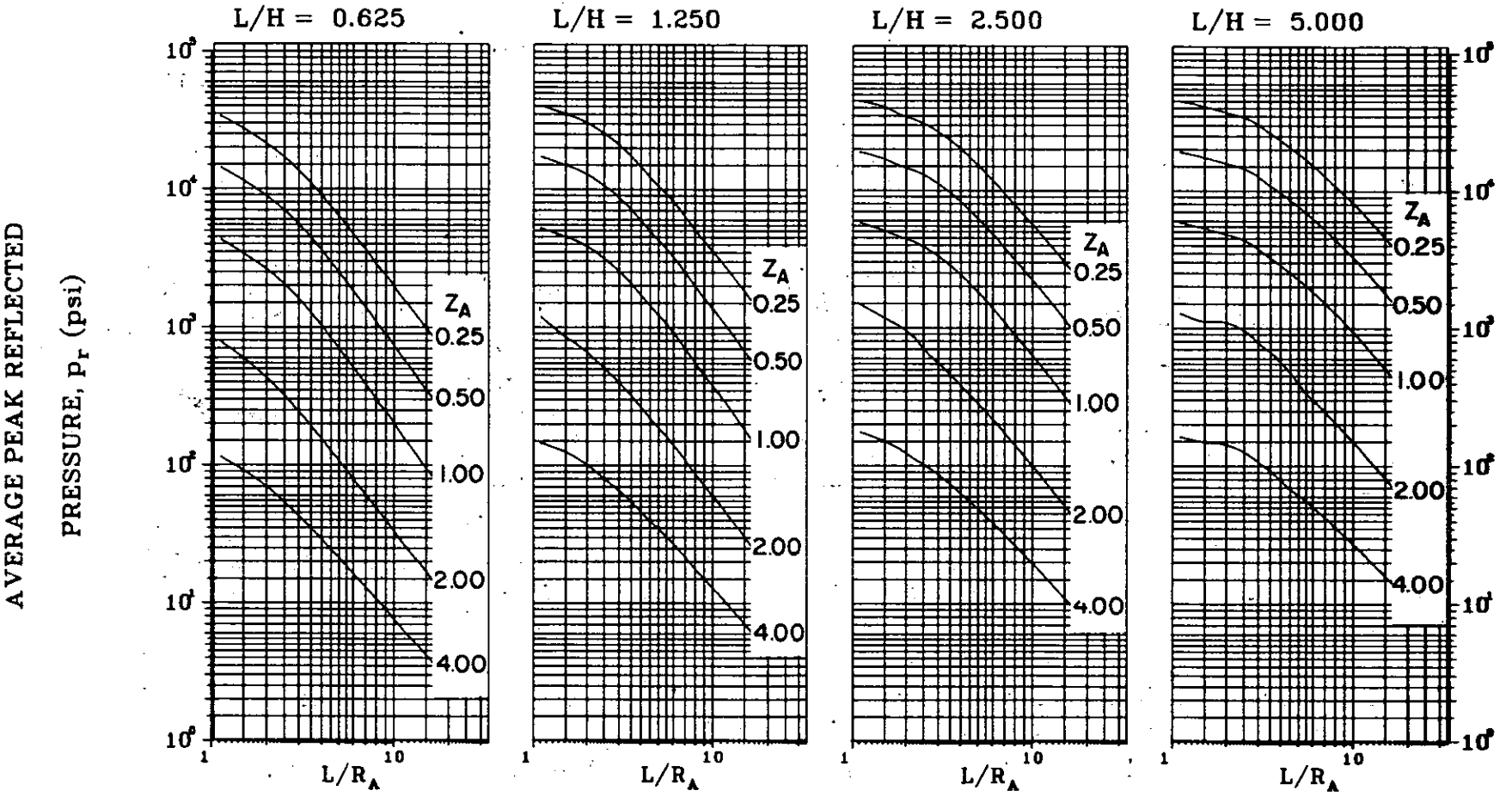
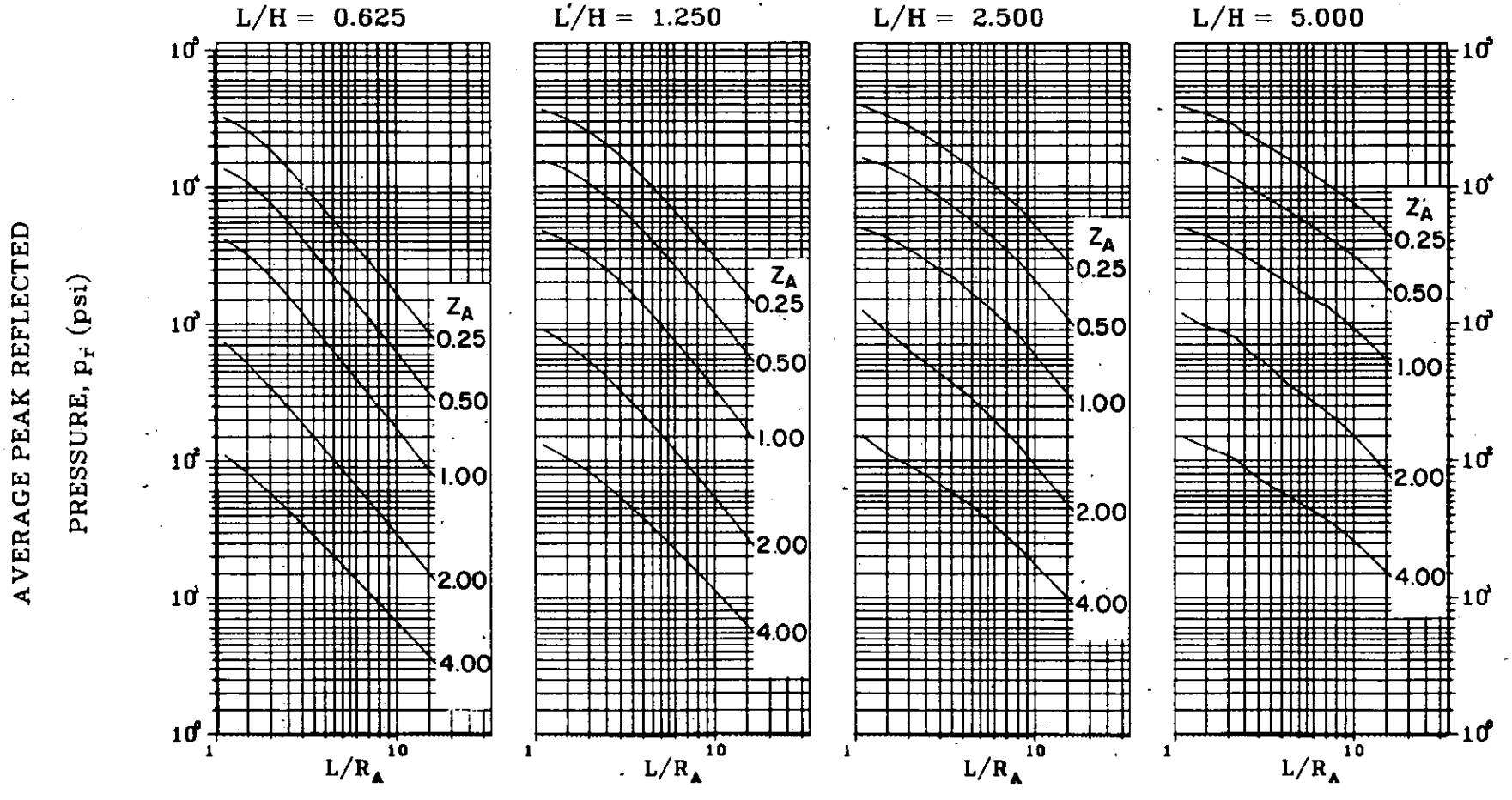


Figure 2-57 Average peak reflected pressure (N = 1, ℓ/L = 0.50, h/H = 0.25)



07B

Figure 2-58 Average peak reflected pressure (N = 1, ℓ/L = 0.10, h/H = 0.50)

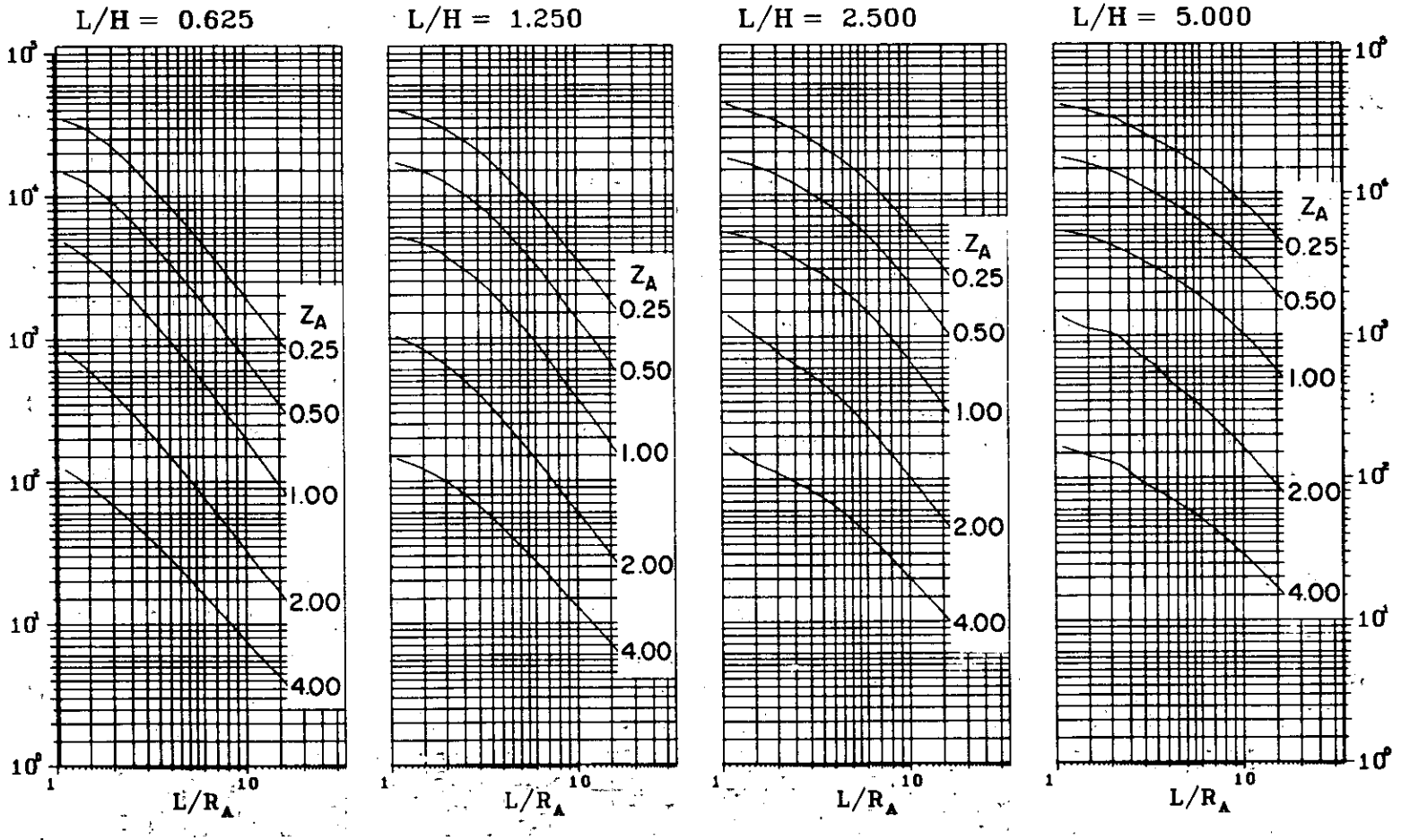


Figure 2-59 Average peak reflected pressure (N = 1, ℓ/L = 0.25 and 0.75, h/H = 0.50)

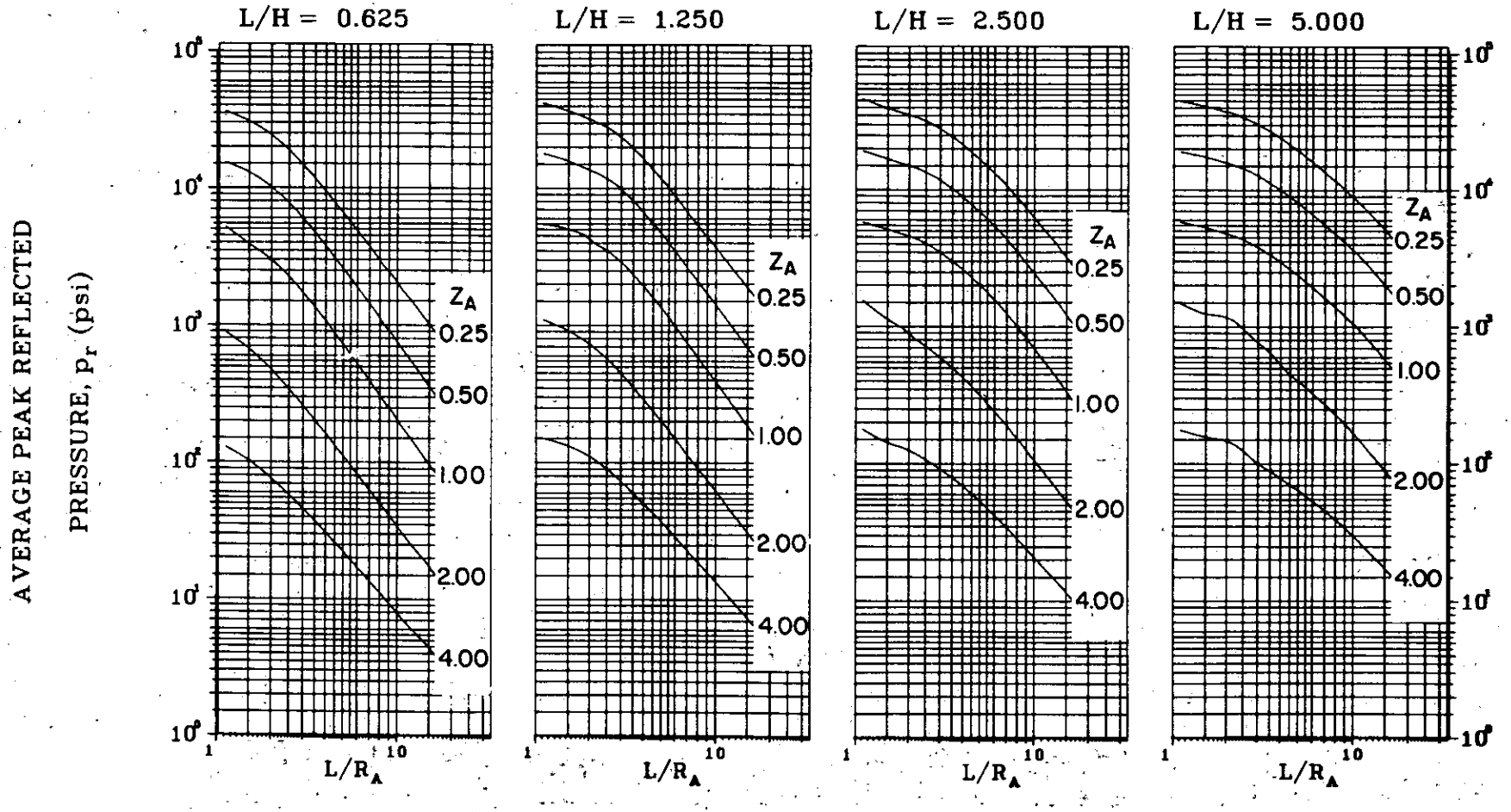


Figure 2-60 Average peak reflected pressure (N = 1, ℓ/L = 0.50, h/H = 0.50)

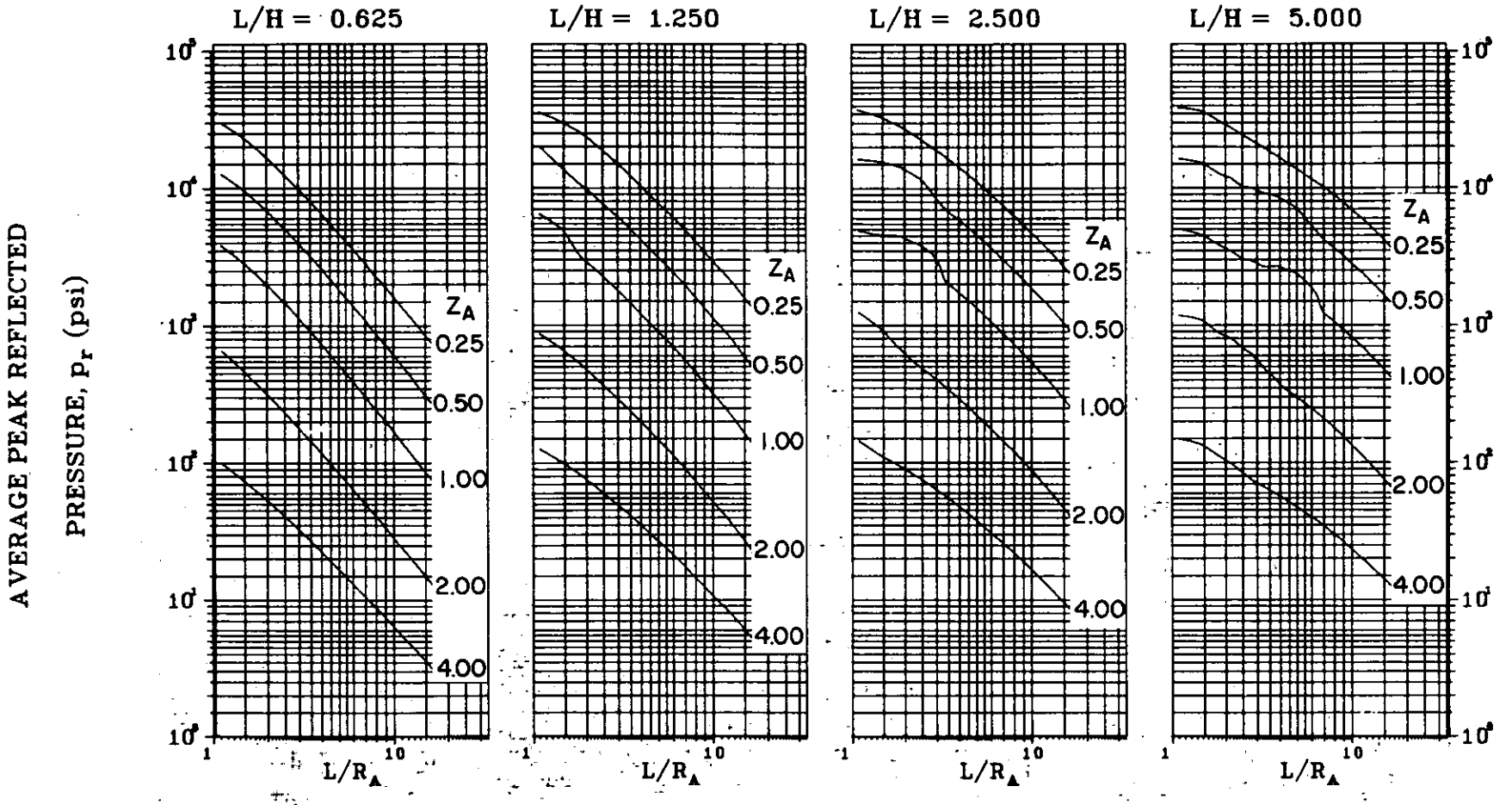


Figure 2-61 Average peak reflected pressure (N = 1, ℓ /L = 0.10, h/H = 0.75)

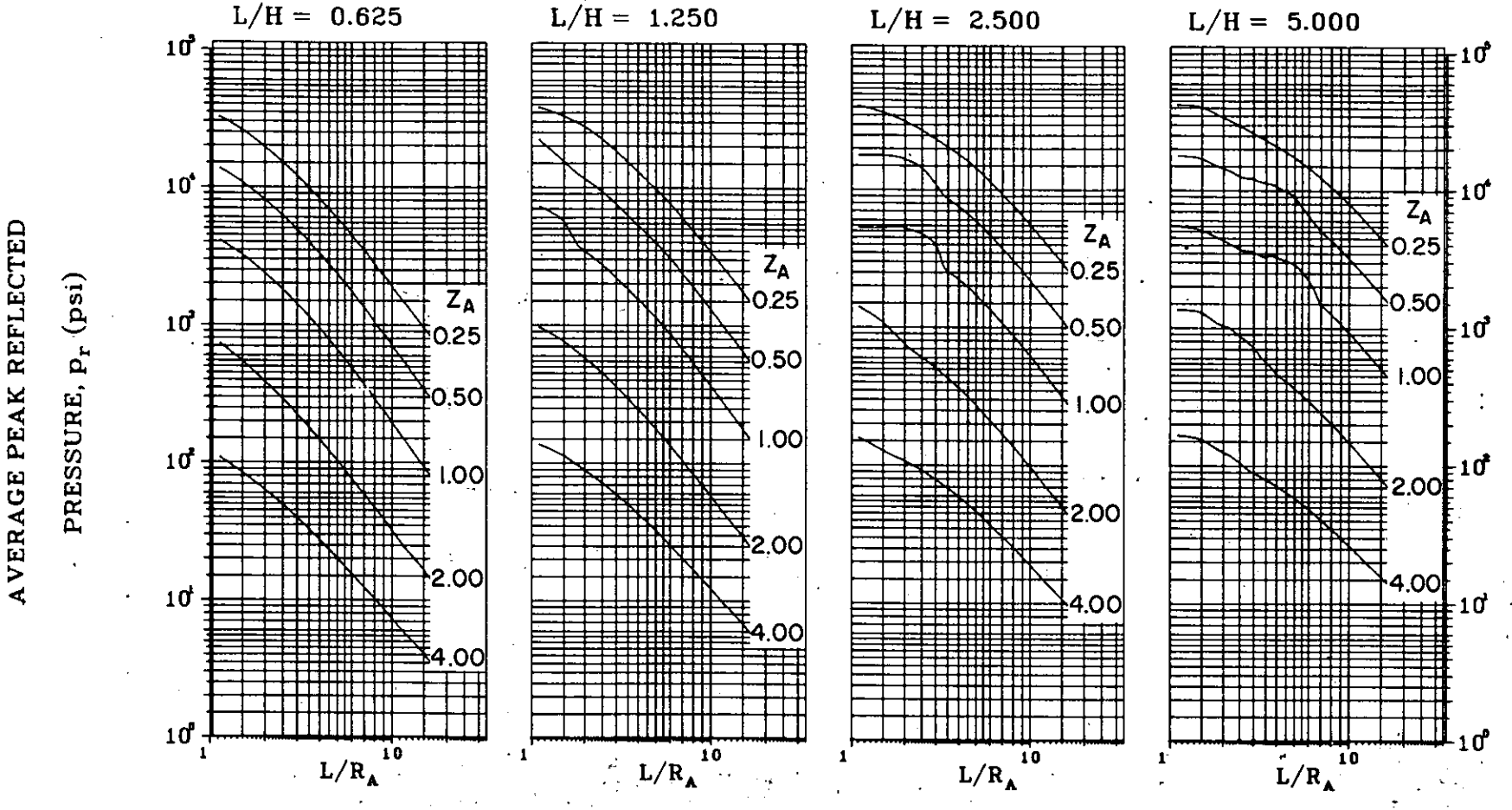


Figure 2-62 Average peak reflected pressure (N = 1, ℓ/L = 0.25 and 0.75, h/H = 0.75)

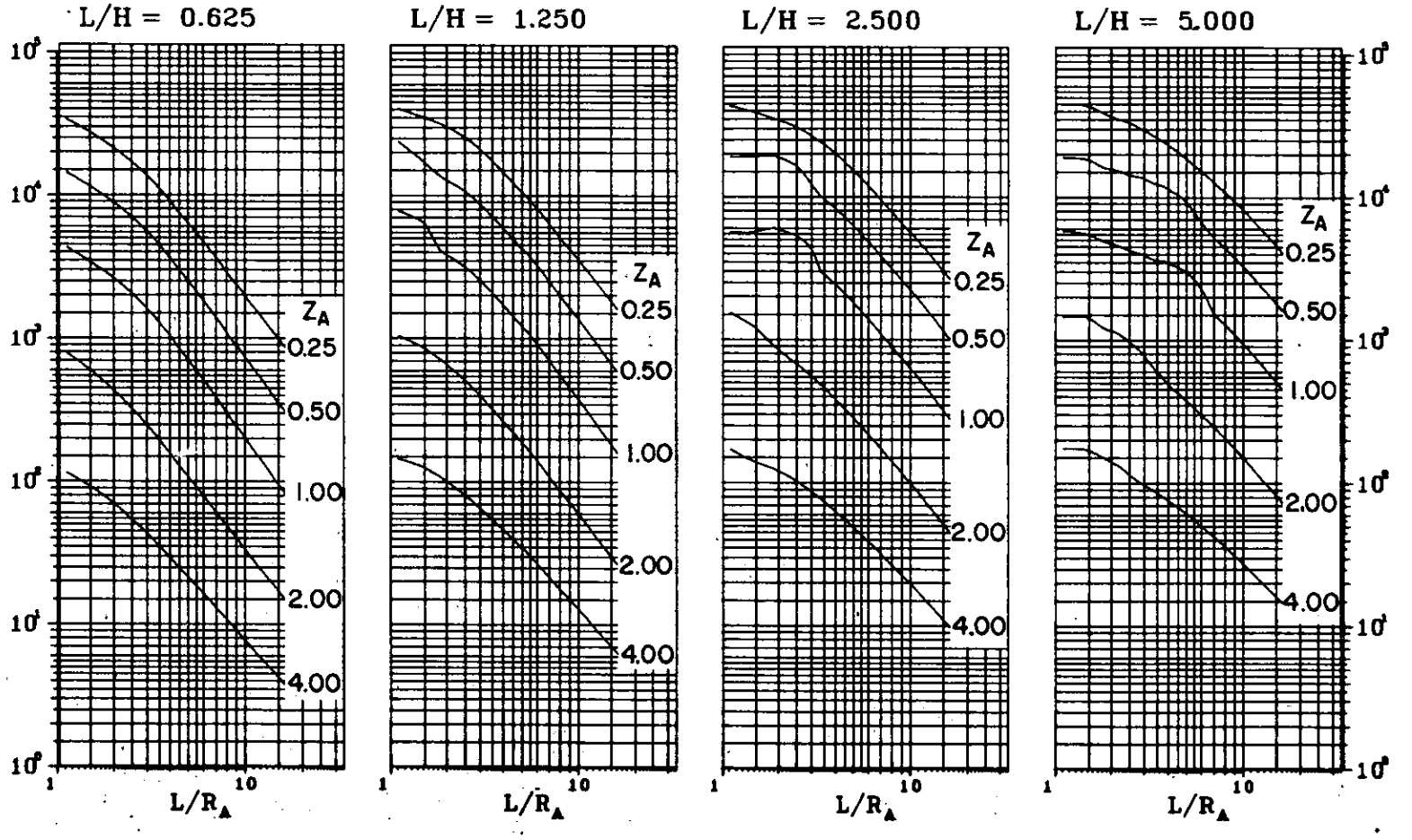
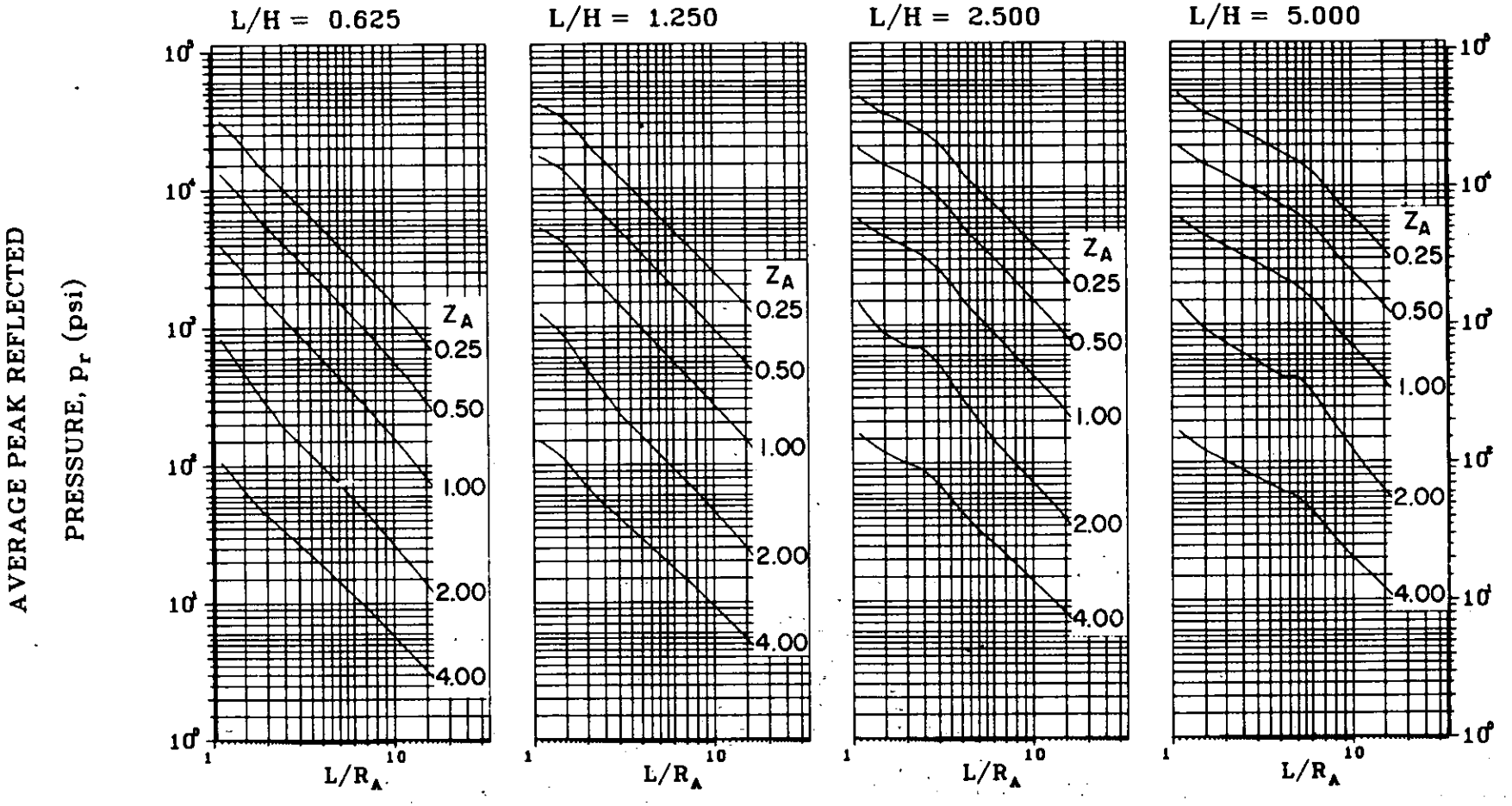


Figure 2-63 Average peak reflected pressure (N = 1, ℓ /L = 0.50, h/H = 0.75)



13B

Figure 2-64 Average peak reflected pressure (N = 2, ℓ/L = 0.10, h/H = 0.10)

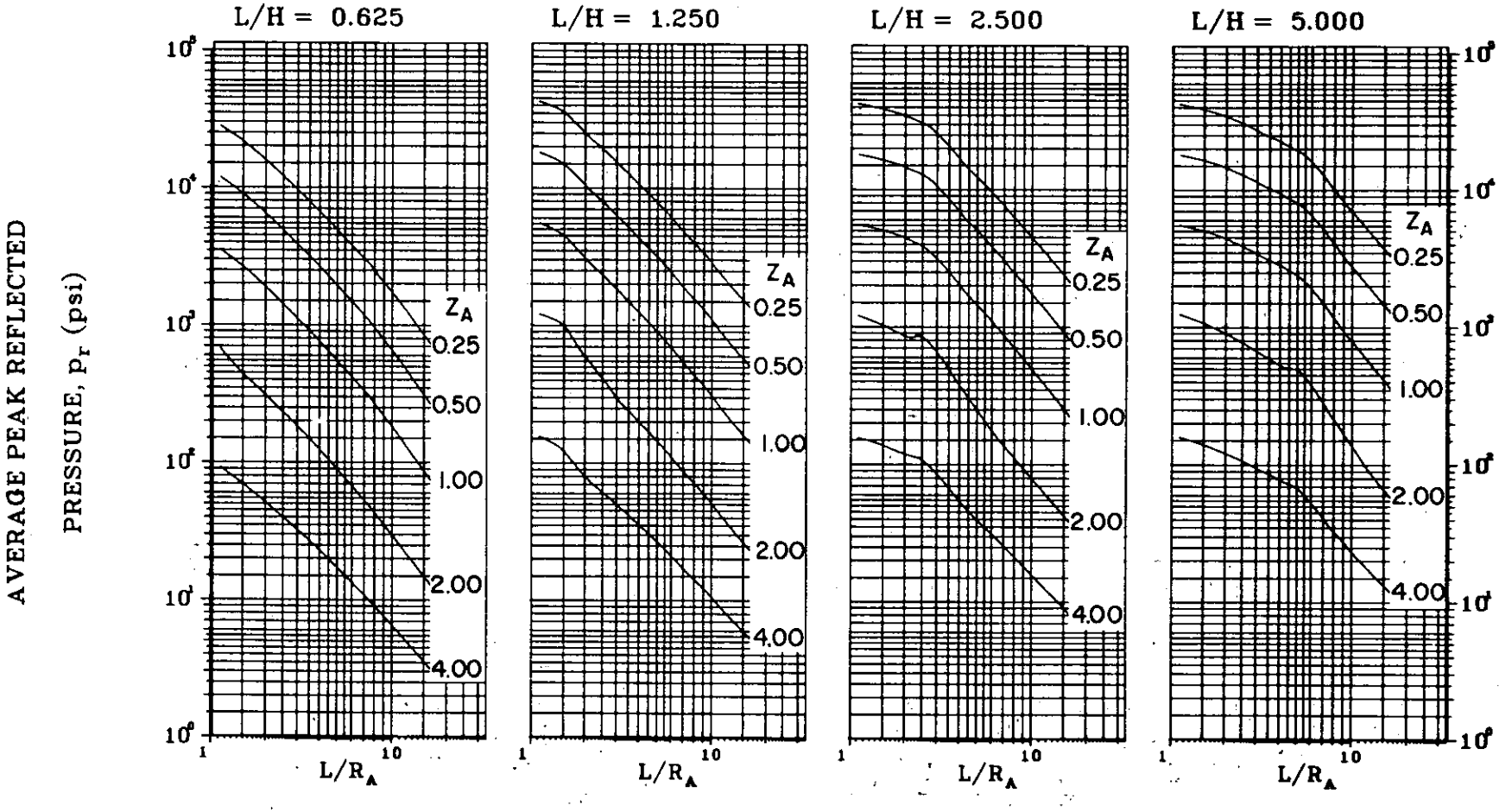


Figure 2-65 Average peak reflected pressure (N = 2, ℓ/L = 0.25, h/H = 0.10)

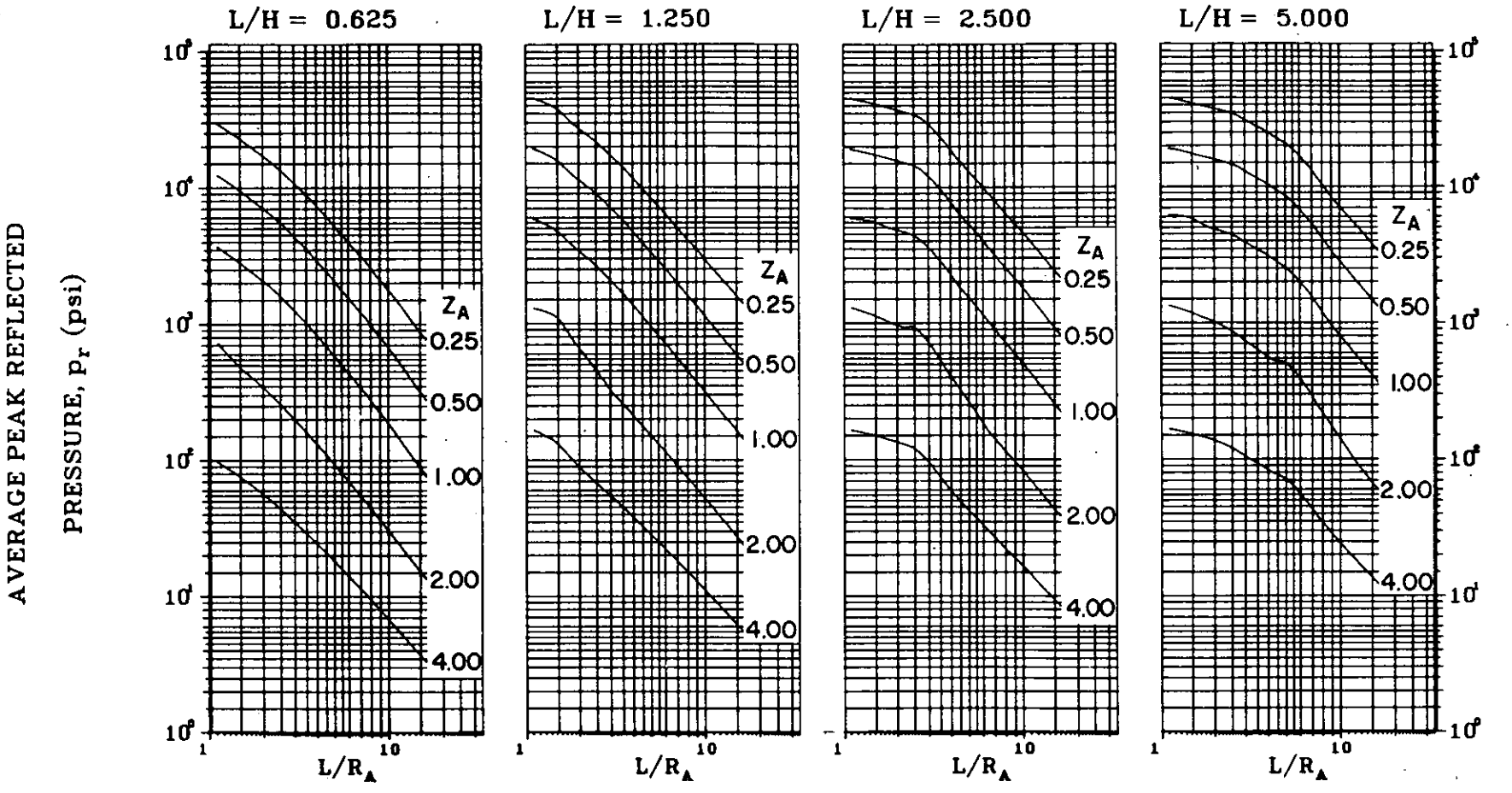


Figure 2-66 Average peak reflected pressure (N = 2, ℓ/L = 0.50, h/H = 0.10)

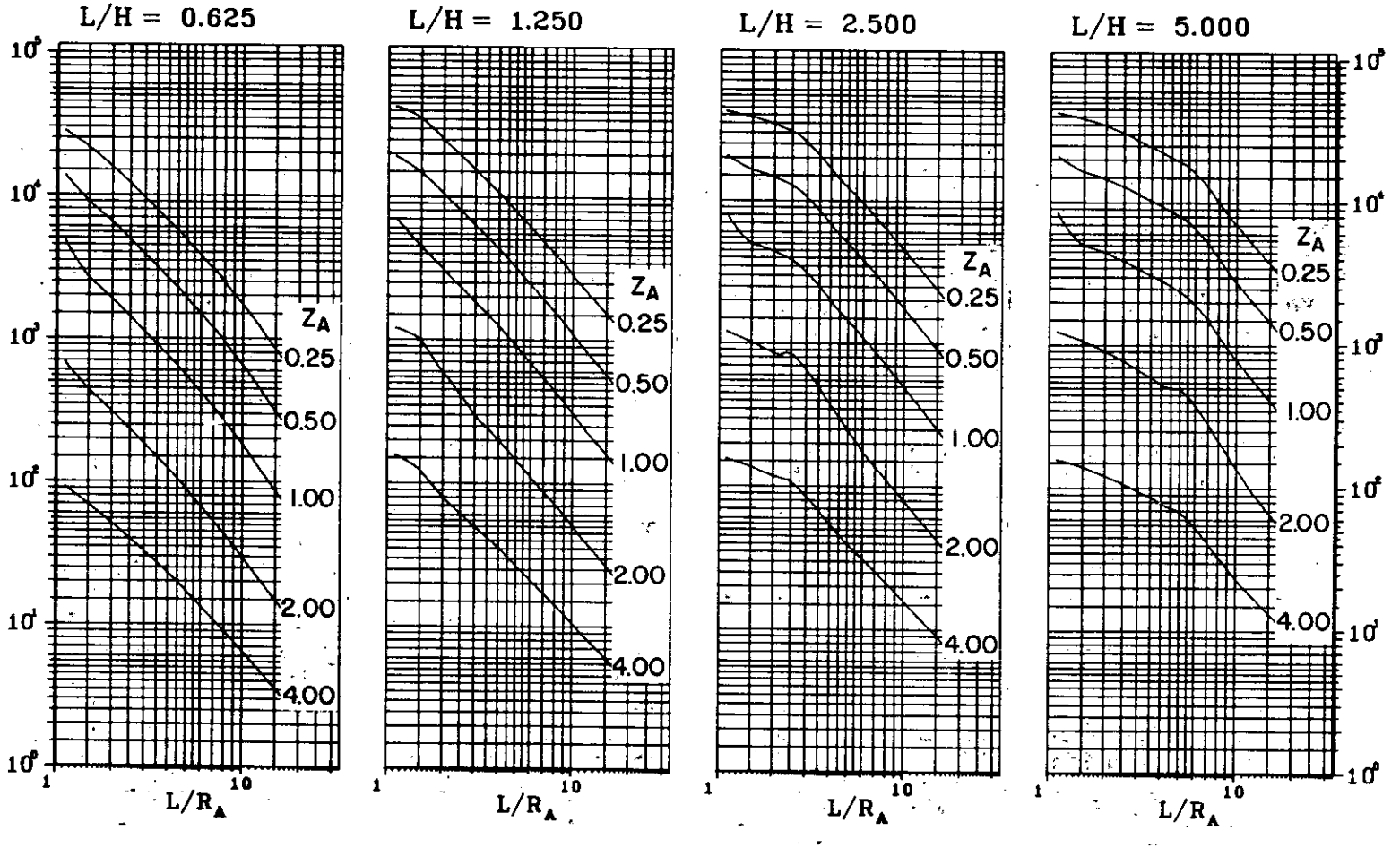


Figure 2-67 Average peak reflected pressure (N = 2, ℓ/L = 0.75, h/H = 0.10)

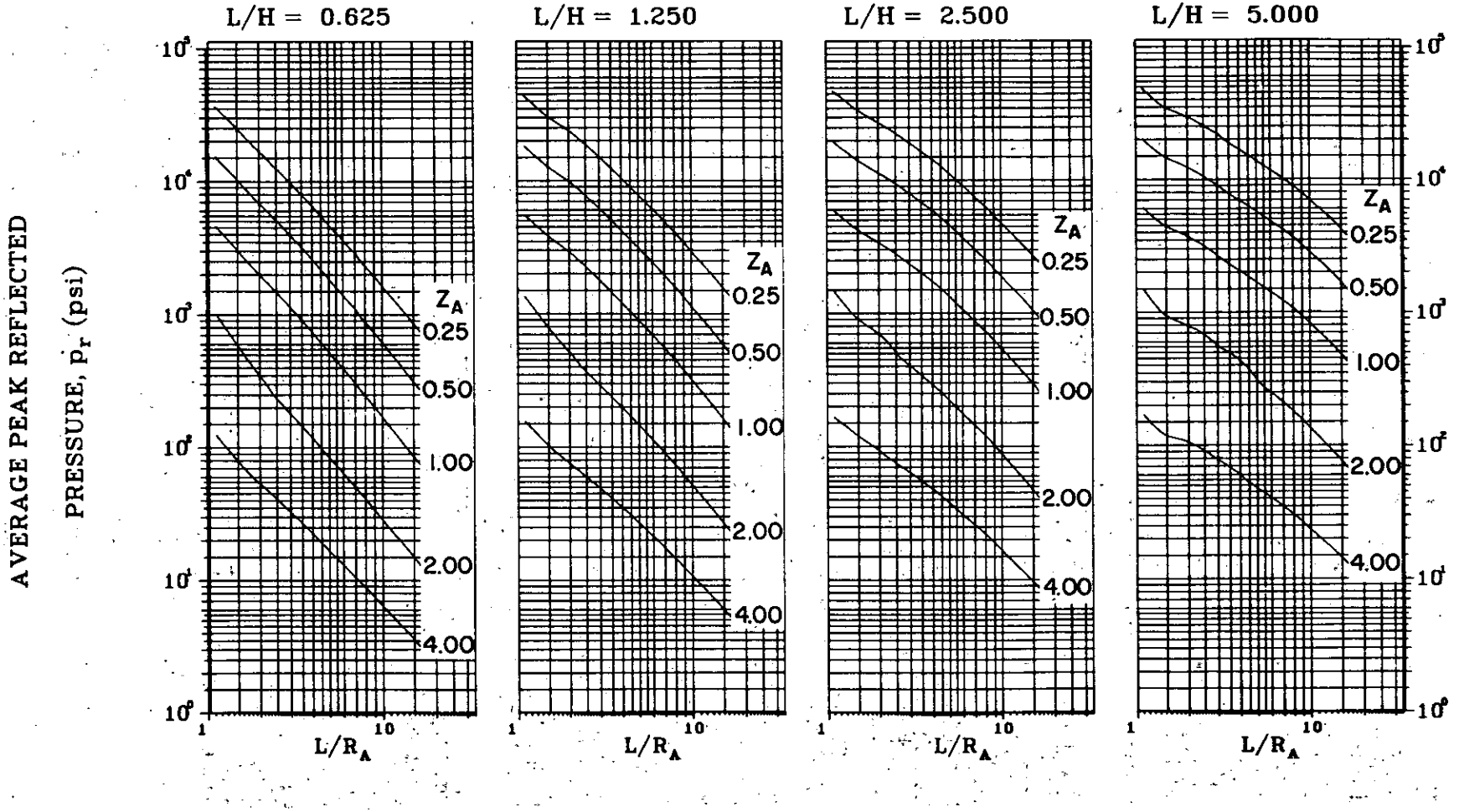


Figure 2-68 Average peak reflected pressure (N = 2, ℓ/L = 0.10, h/H = 0.25)

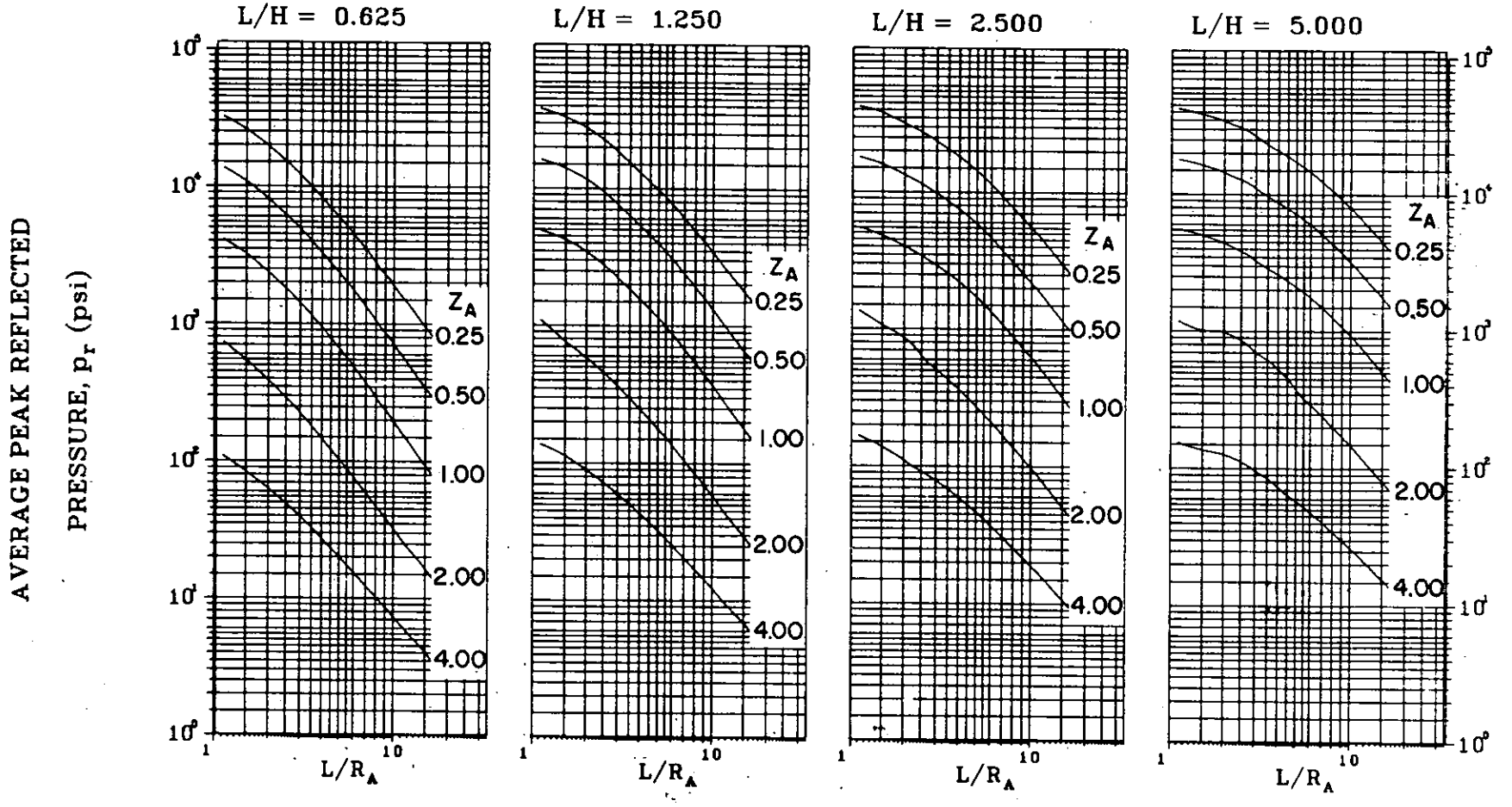


Figure 2-69 Average peak reflected pressure (N = 2, ℓ/L = 0.25, h/H = 0.25)

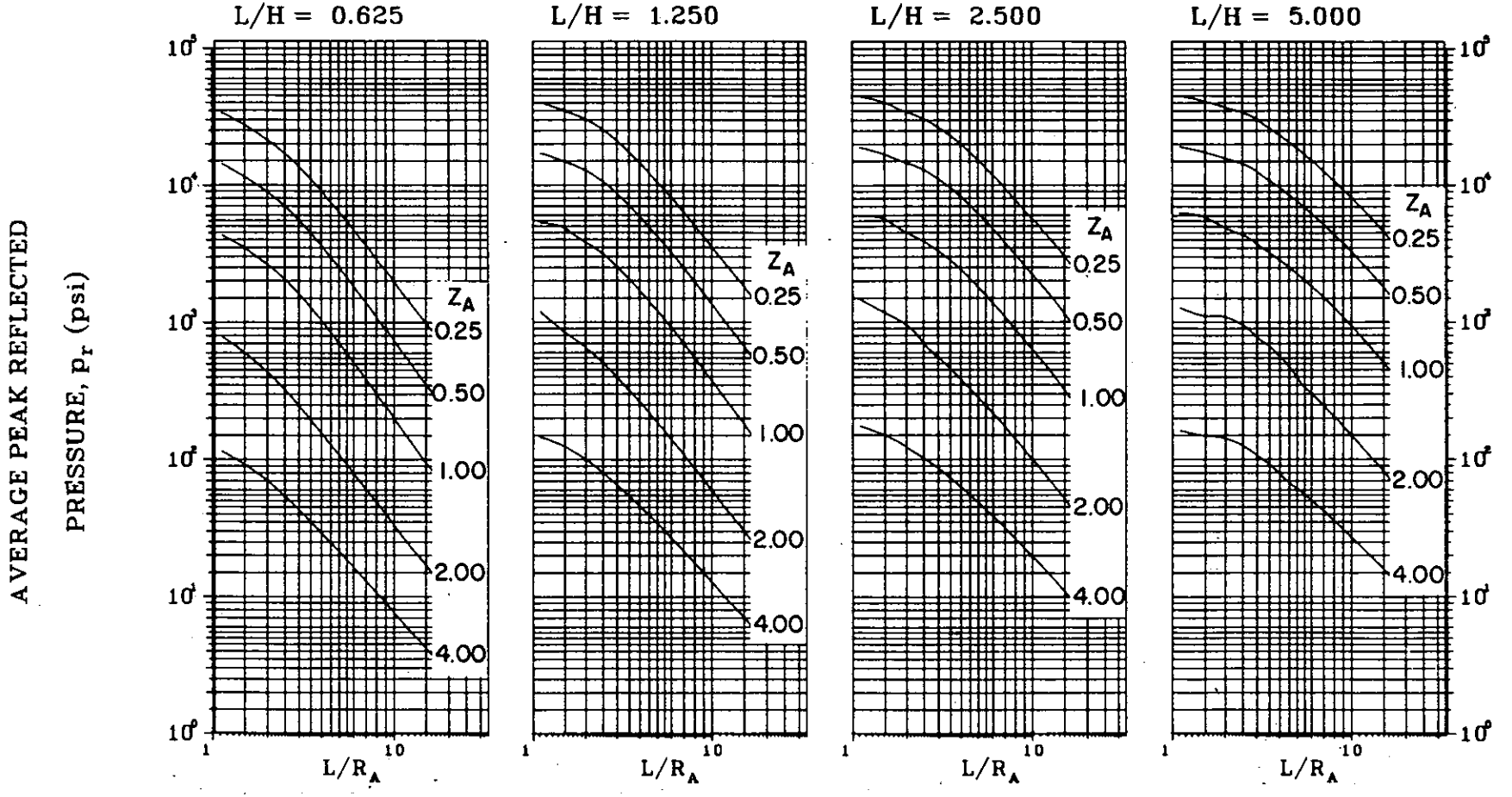


Figure 2-70 Average peak reflected pressure (N = 2, ℓ/L = 0.50, h/H = 0.25)

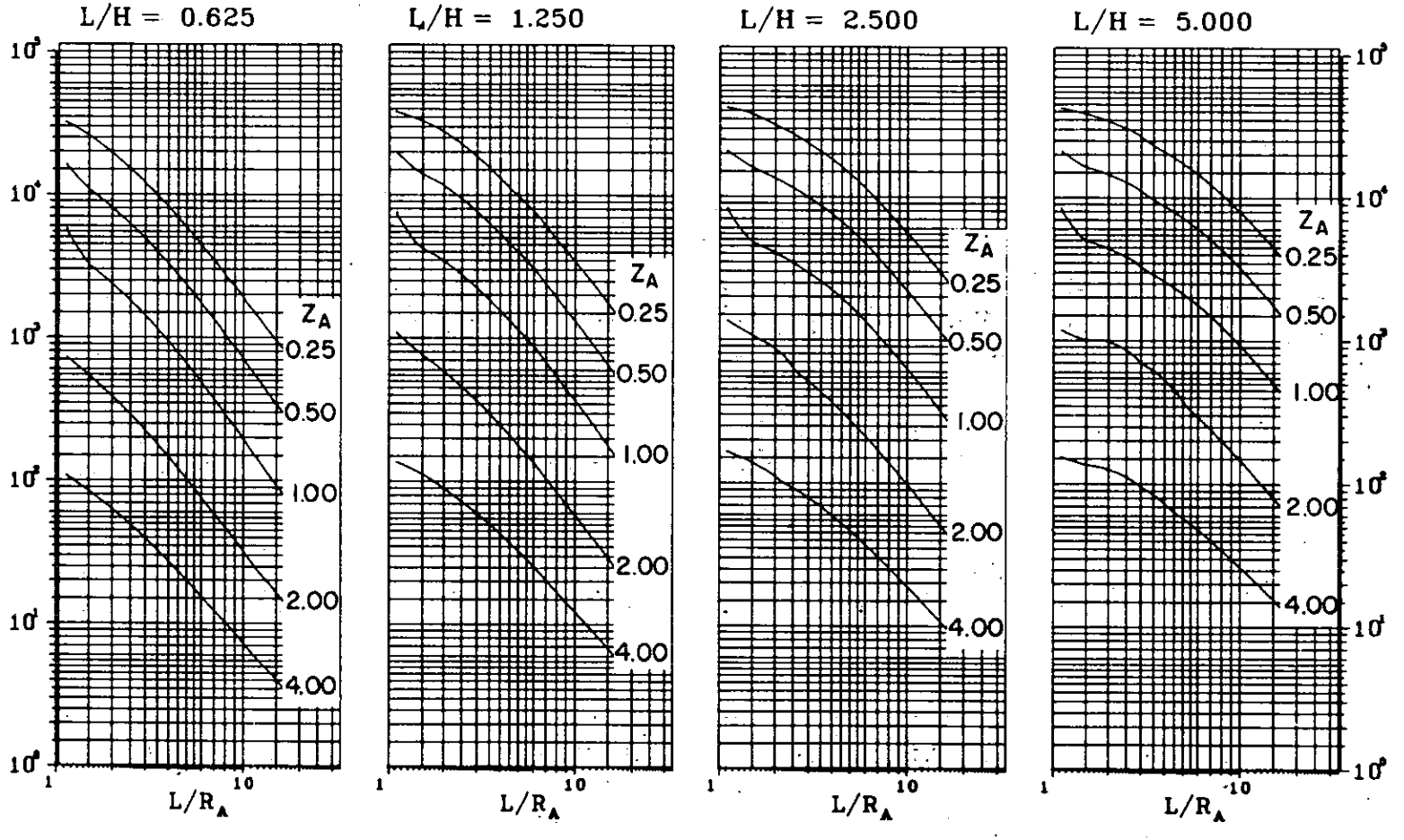


Figure 2-71 Average peak reflected pressure (N = 2, ℓ/L = 0.75, h/H = 0.25)

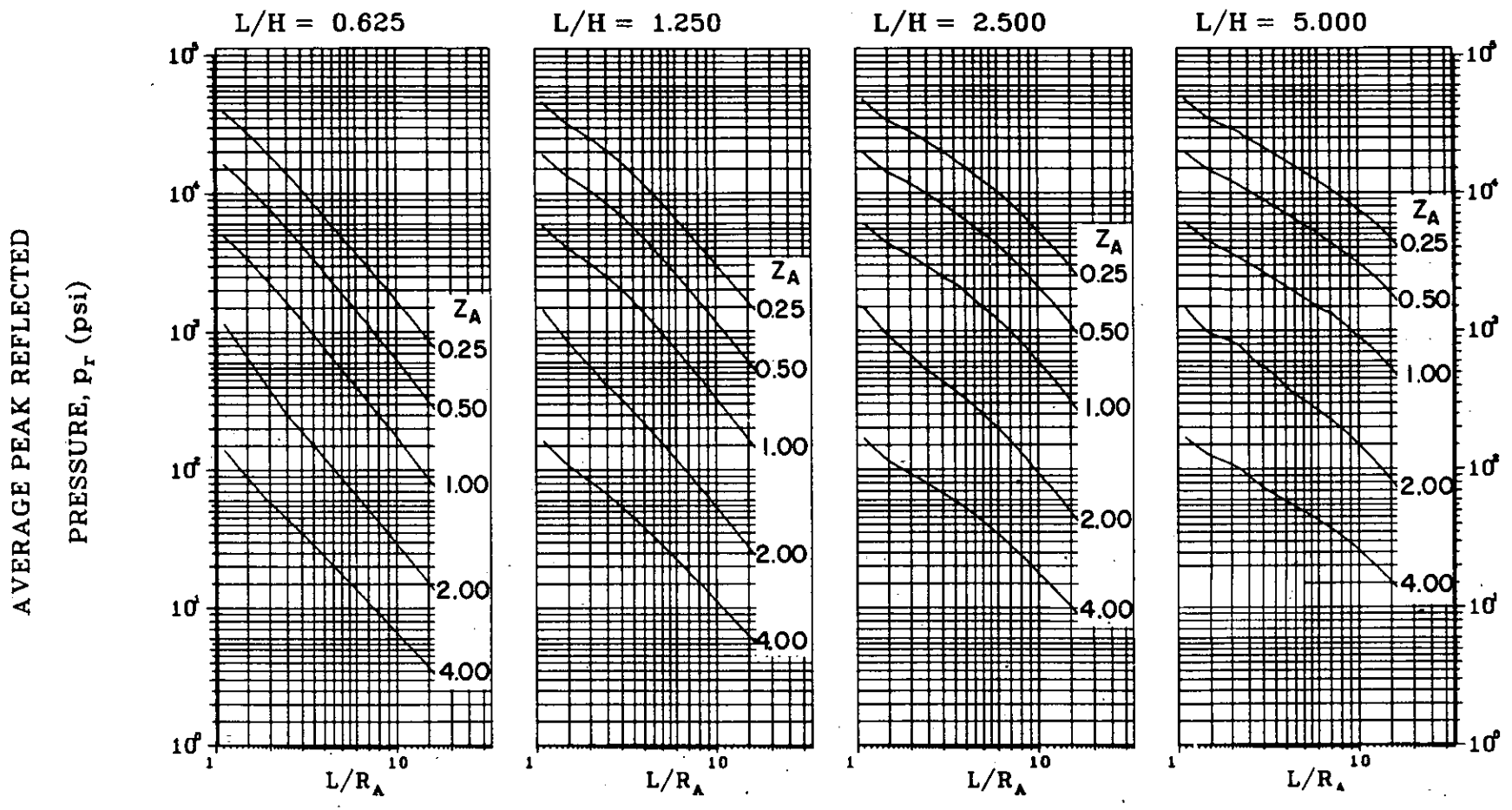


Figure 2-72 Average peak reflected pressure (N = 2, ℓ/L = 0.10, h/H = 0.50)

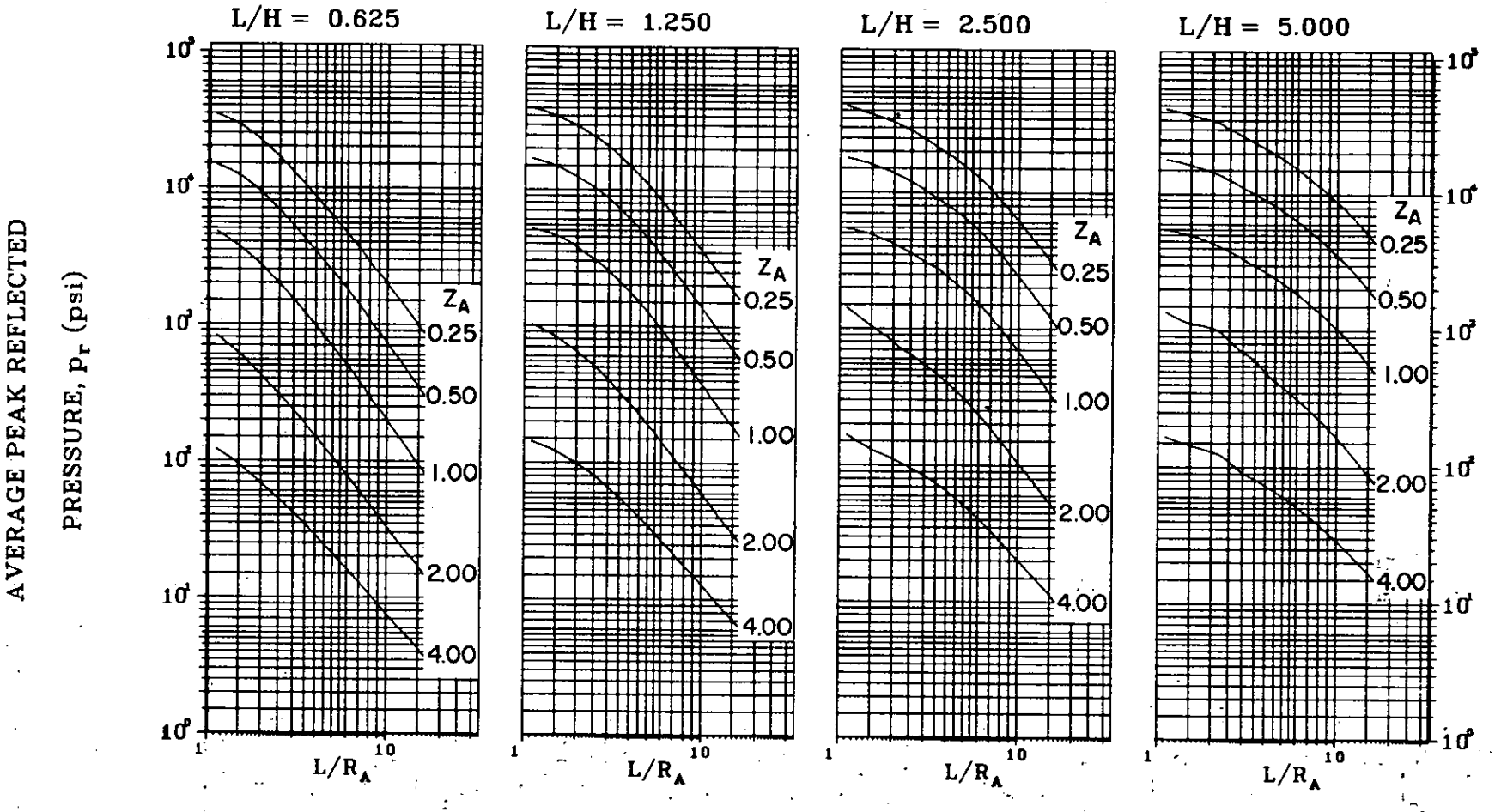


Figure 2-73 Average peak reflected pressure (N = 2, ℓ/L = 0.25, h/H = 0.50)

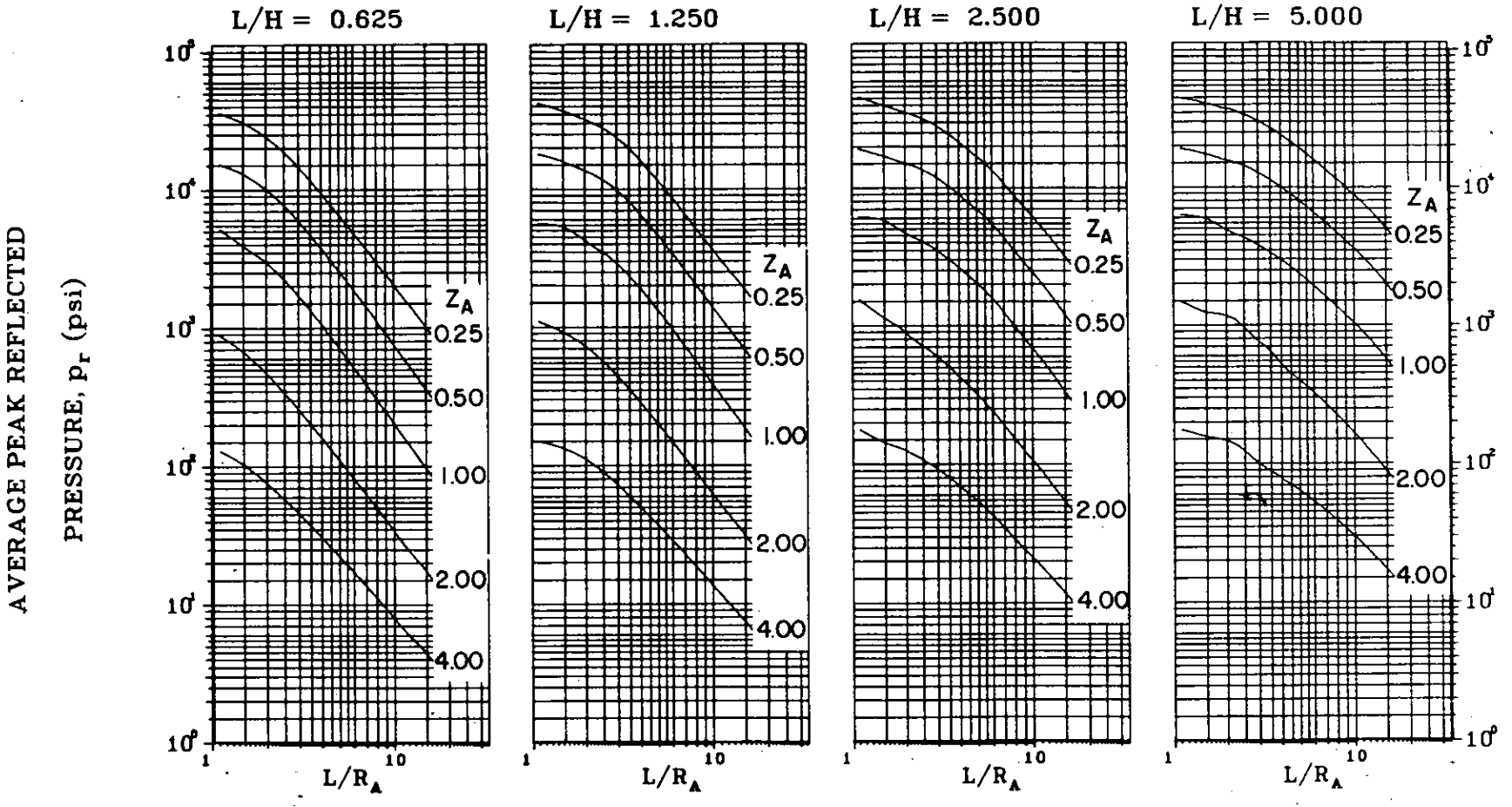


Figure 2-74 Average peak reflected pressure (N = 2, ℓ/L = 0.50, h/H = 0.50)

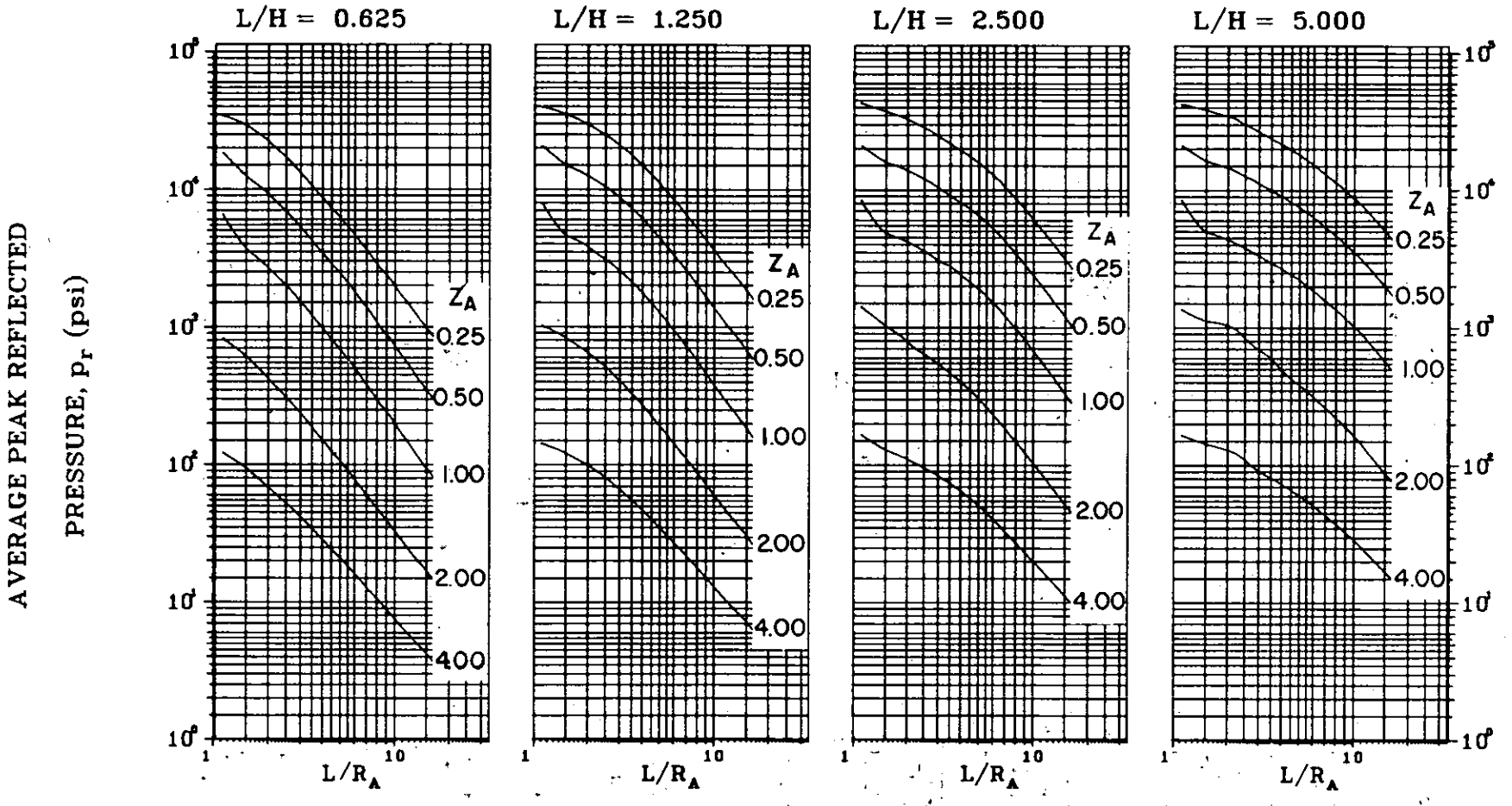


Figure 2-75 Average peak reflected pressure (N = 2, ℓ/L = 0.75, h/H = 0.50)

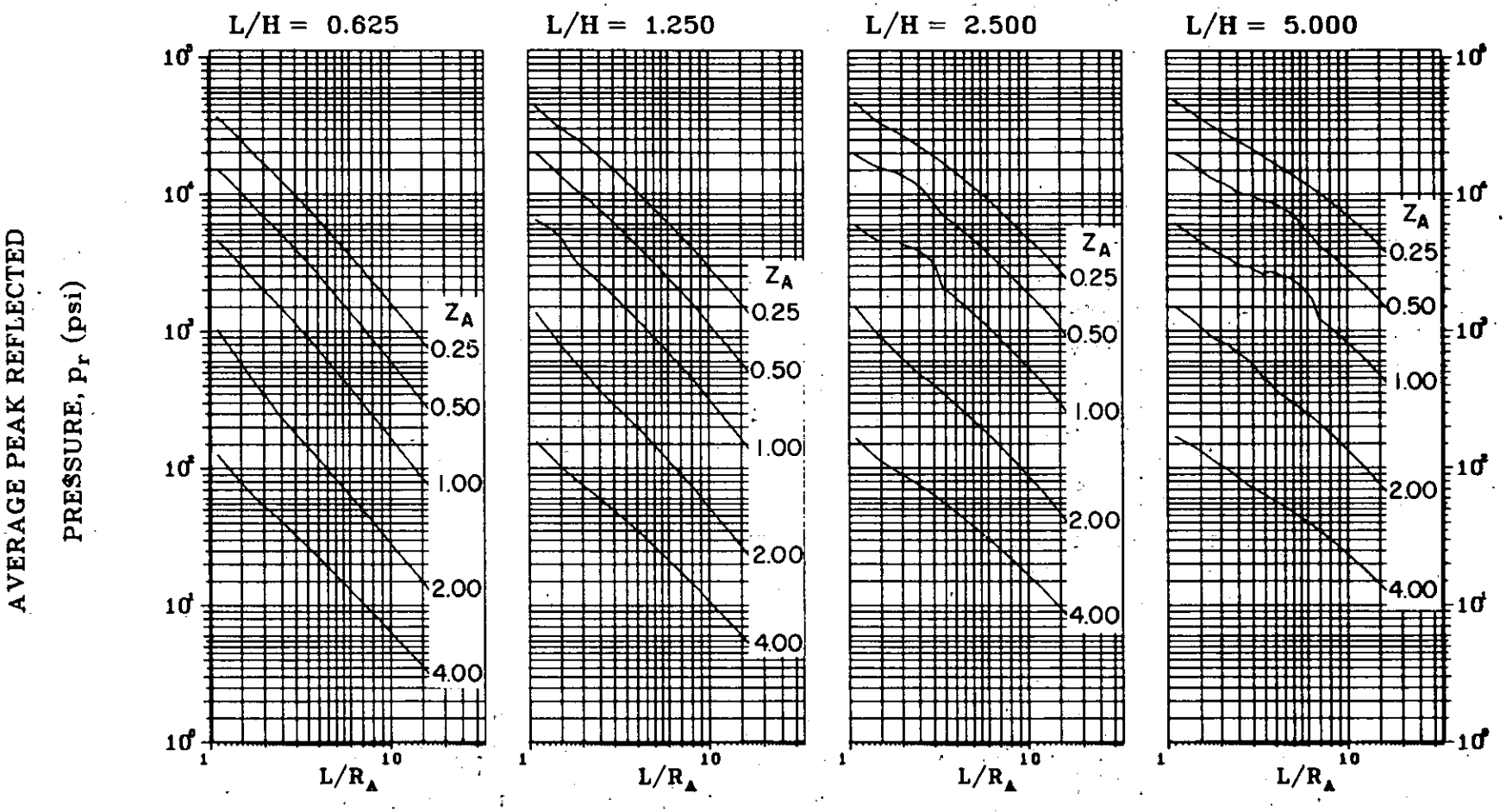


Figure 2-76 Average peak reflected pressure (N = 2, ℓ /L = 0.10, h/H = 0.75)

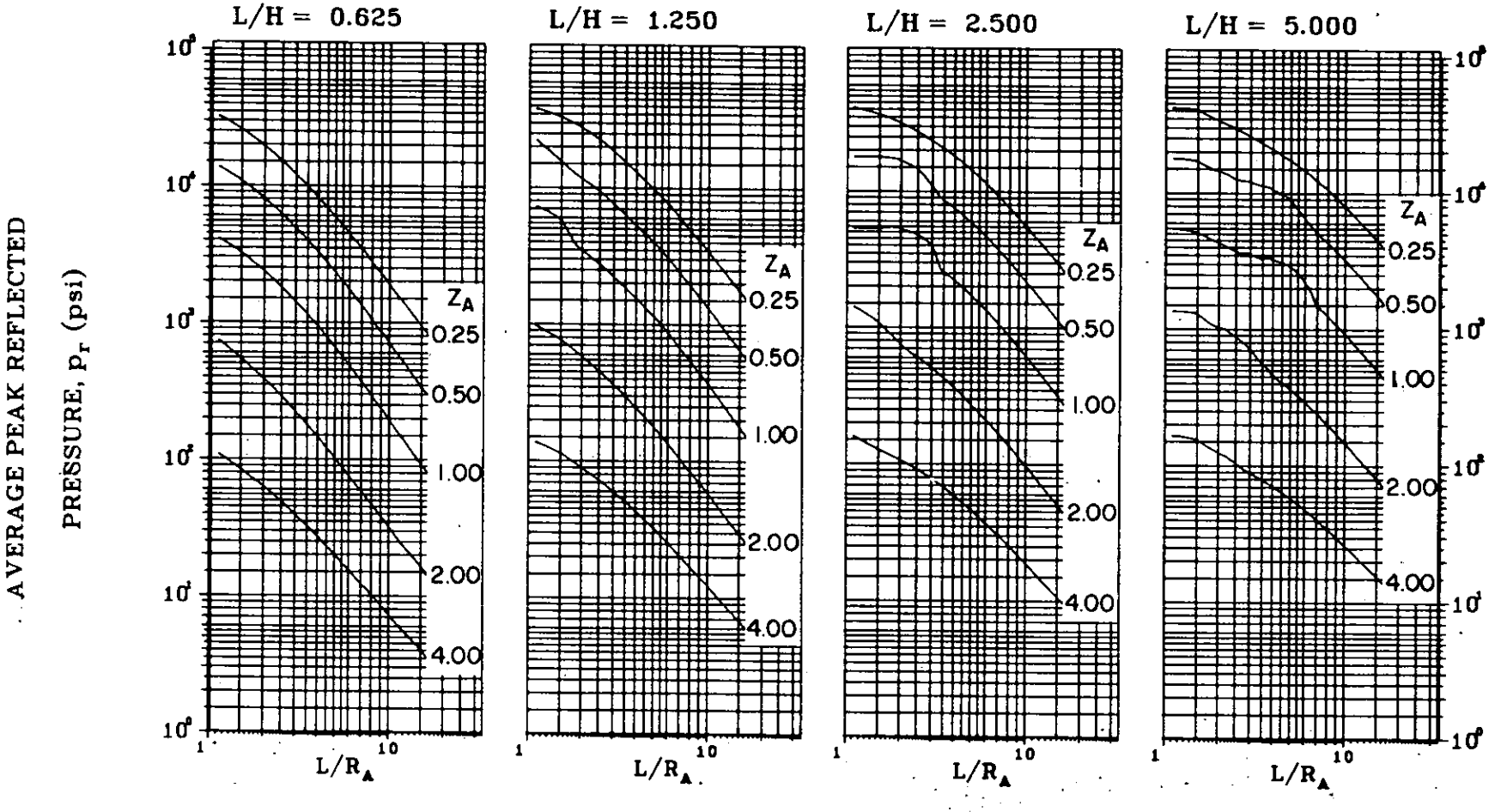


Figure 2-77 Average peak reflected pressure (N = 2, ℓ/L = 0.25, h/H = 0.75)

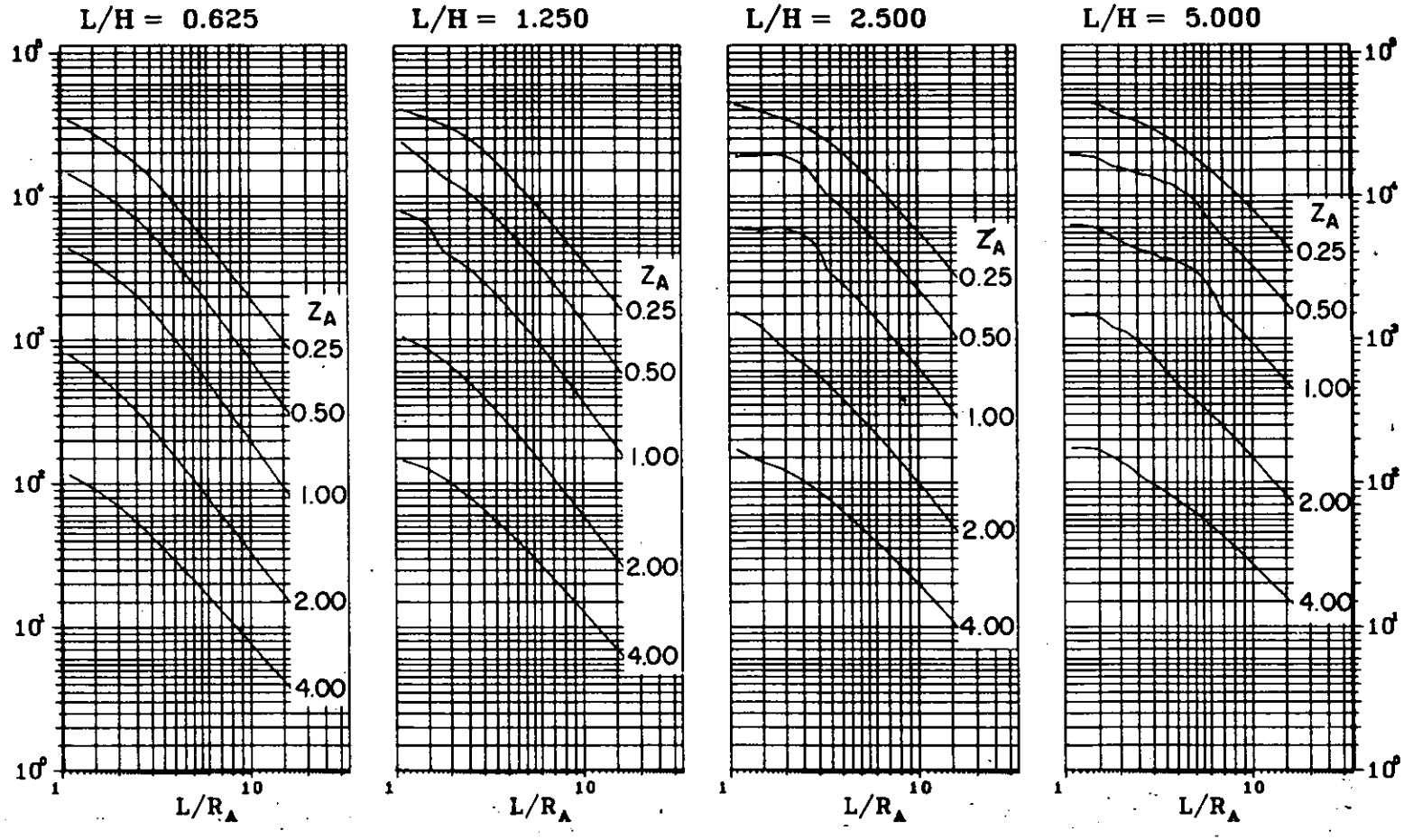


Figure 2-78 Average peak reflected pressure (N = 2, ℓ/L = 0.50, h/H = 0.75)

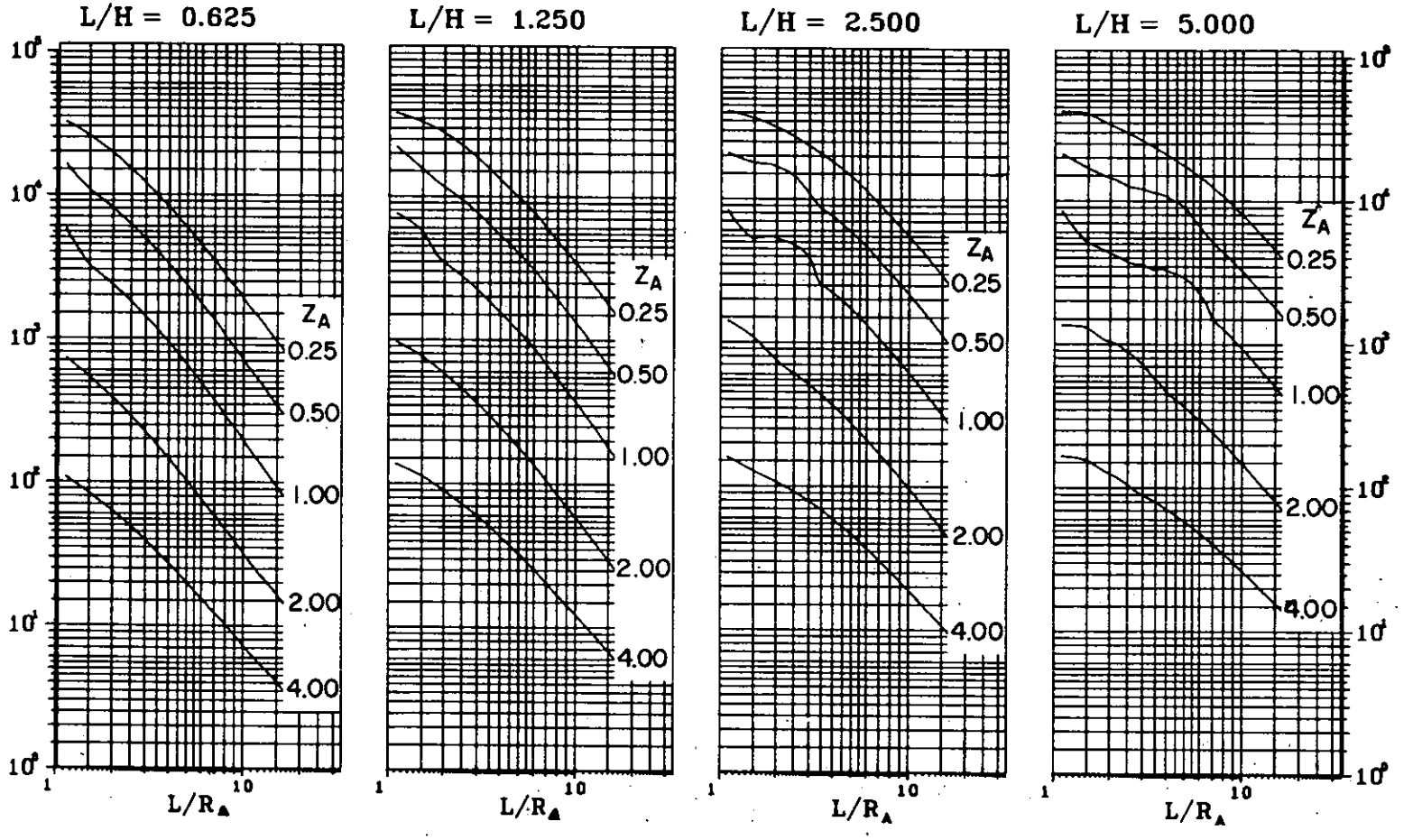


Figure 2-79 Average peak reflected pressure (N = 2, ℓ/L = 0.75, h/H = 0.75)

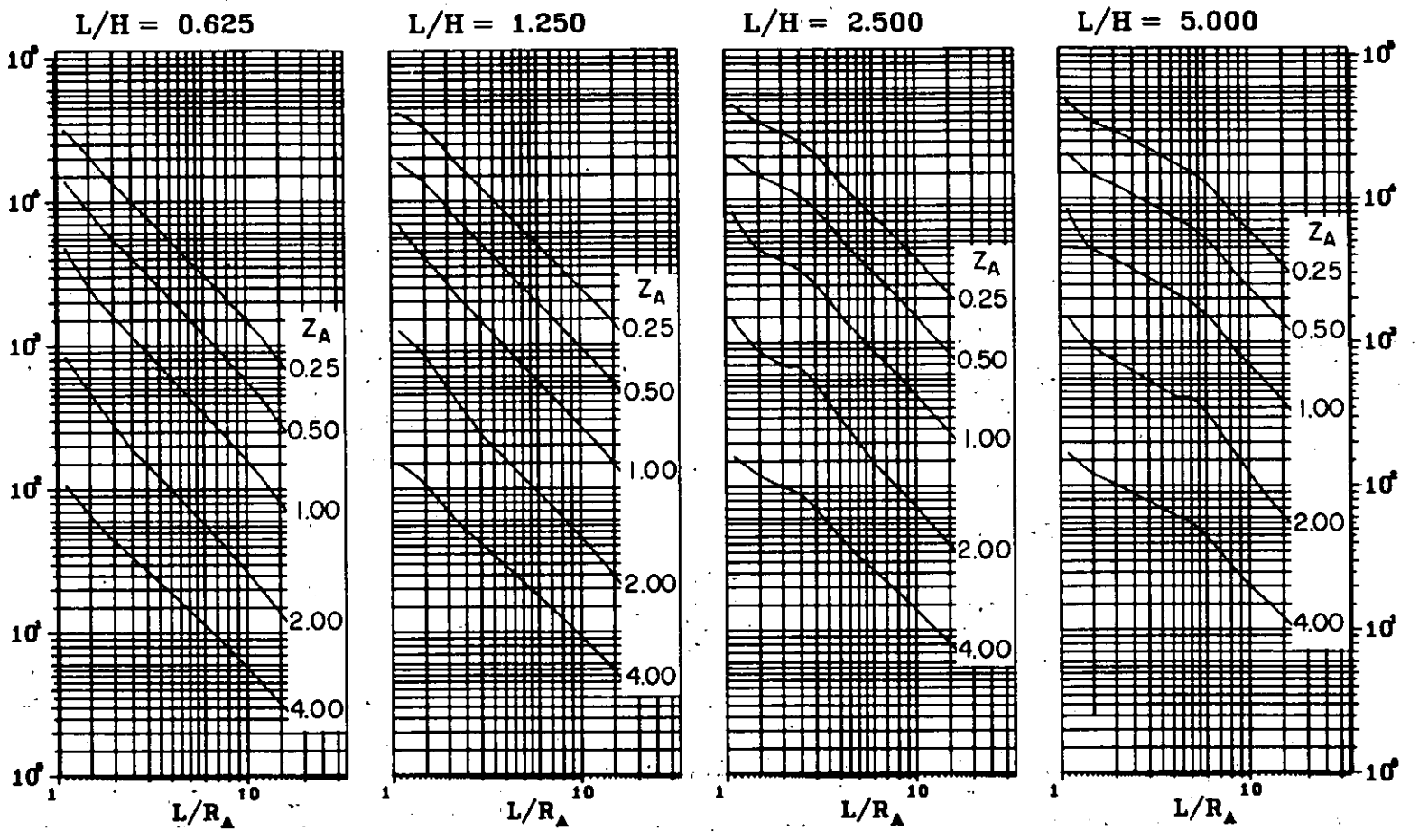


Figure 2-80 Average peak reflected pressure (N = 3, ℓ/L = 0.10, h/H = 0.10)

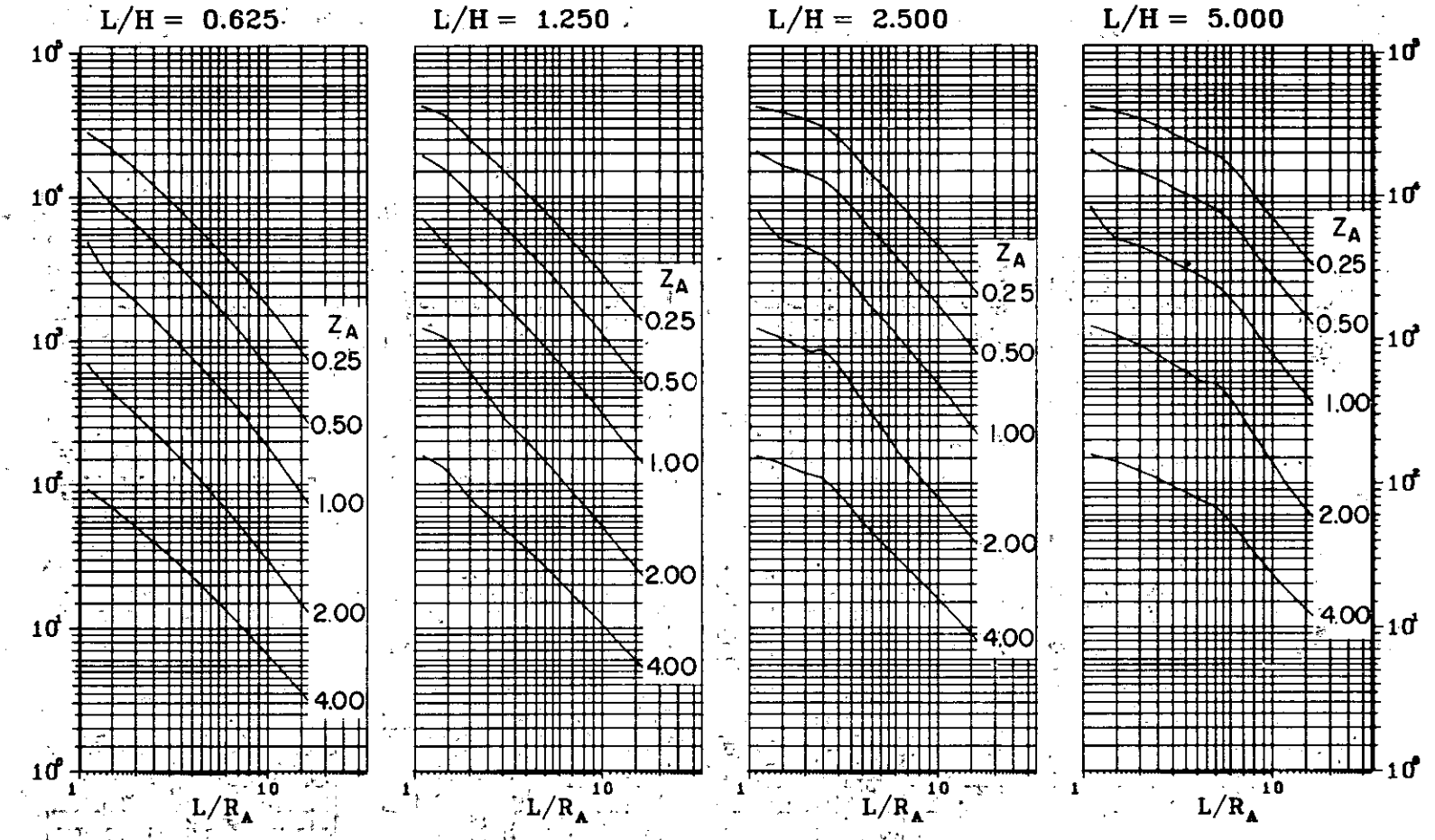


Figure 2-81 Average peak reflected pressure (N = 3, ℓ/L = 0.25 and 0.75, h/H = 0.10)

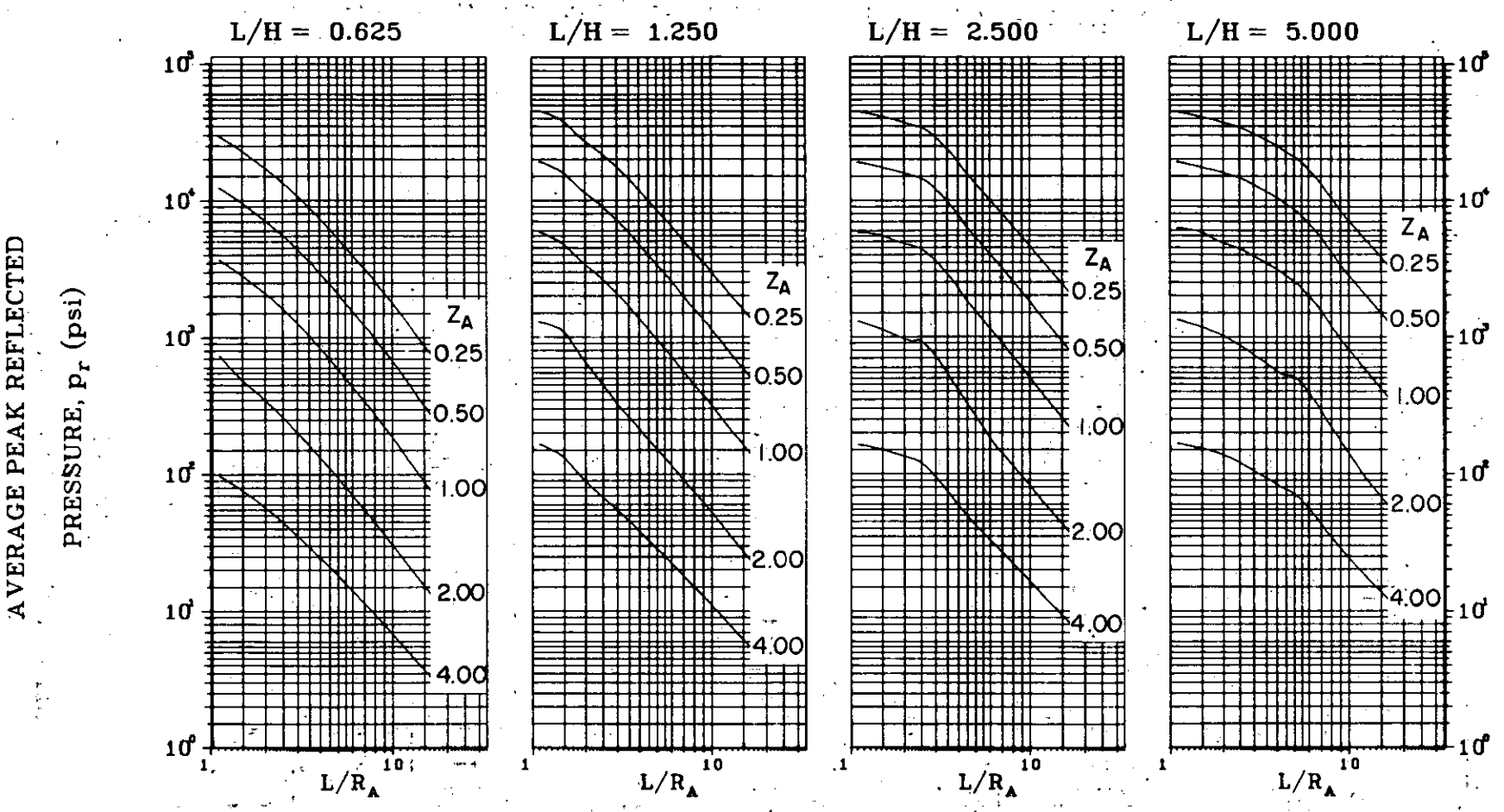


Figure 2-82 Average peak reflected pressure (N = 3, ℓ/L = 0.50, h/H = 0.10)

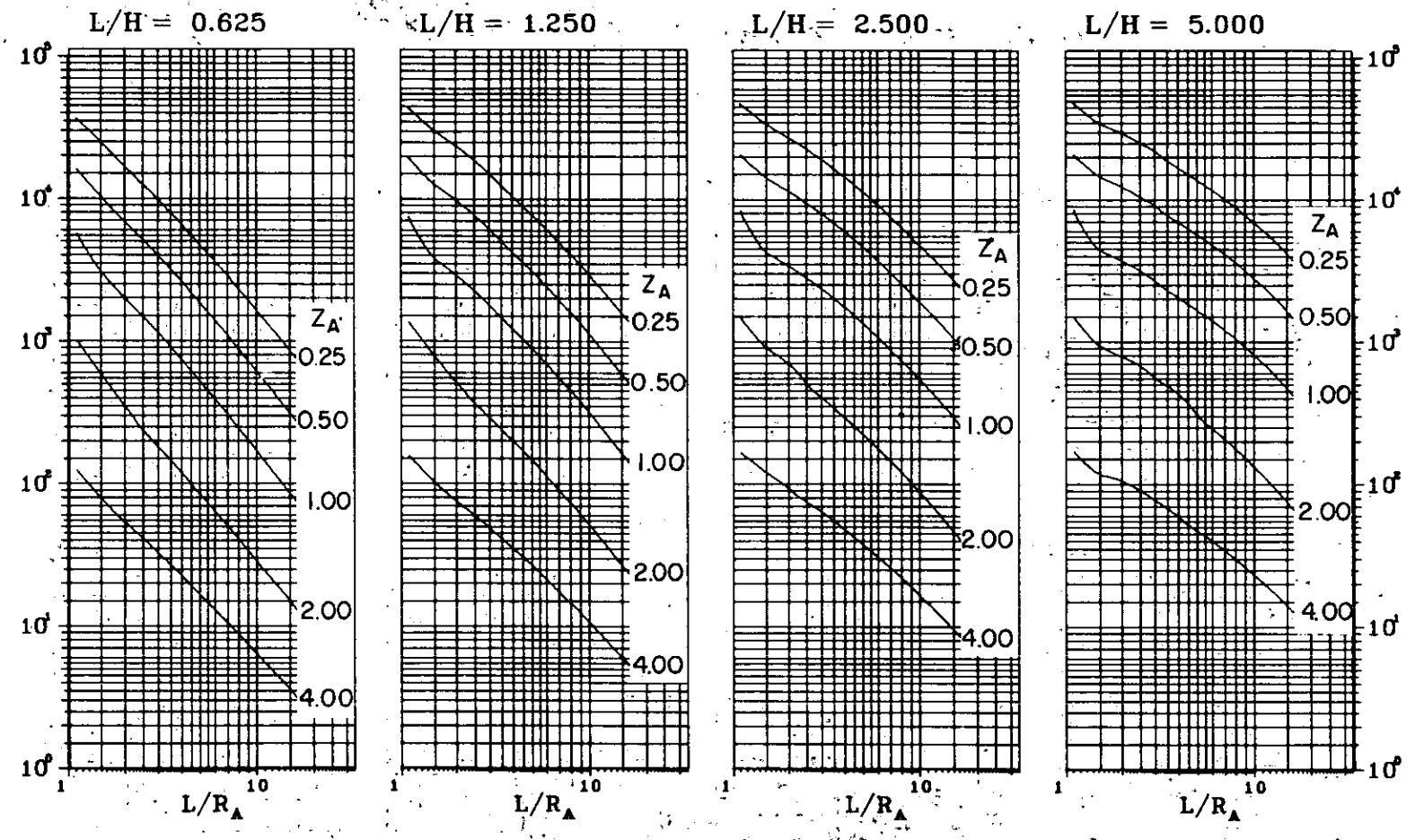


Figure 2-83 Average peak reflected pressure (N = 3, ℓ/L = 0.10, h/H = 0.25)

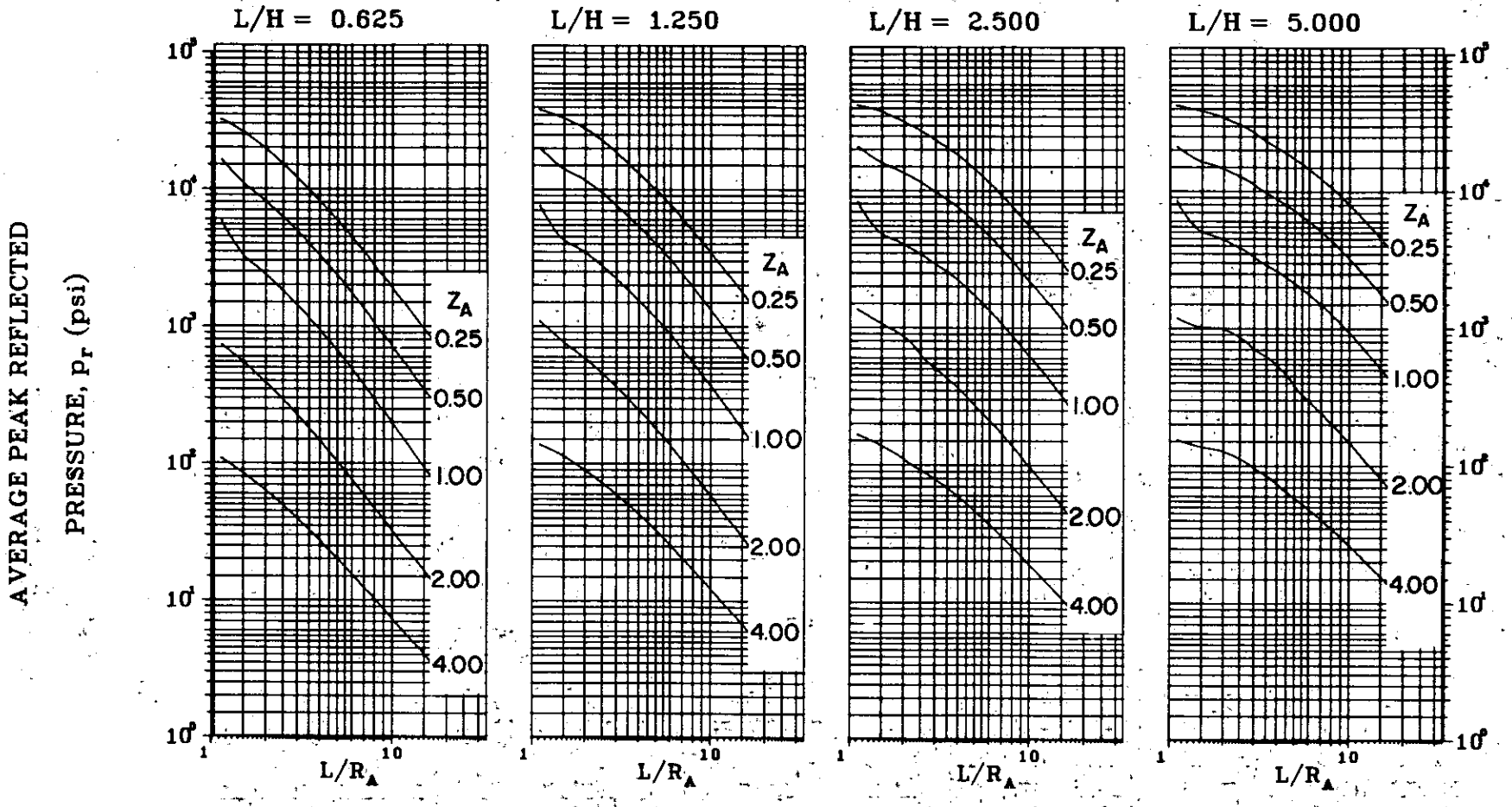


Figure 2-84. Average peak reflected pressure (N = 3, ℓ/L = 0.25 and 0.75, h/H = 0.25)

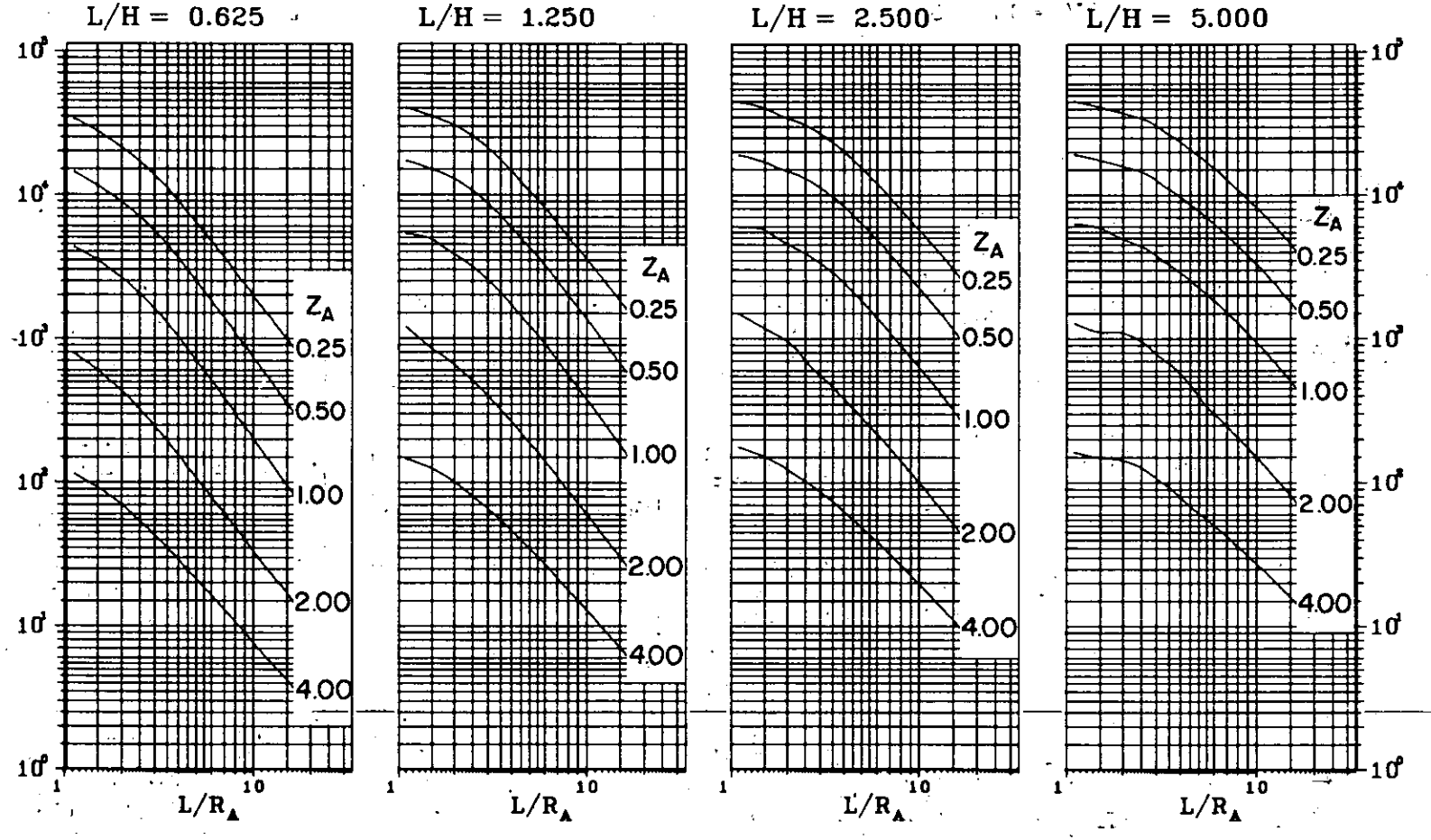


Figure 2-85 Average peak reflected pressure (N = 3, ℓ/L = 0.50, h/H = 0.25)

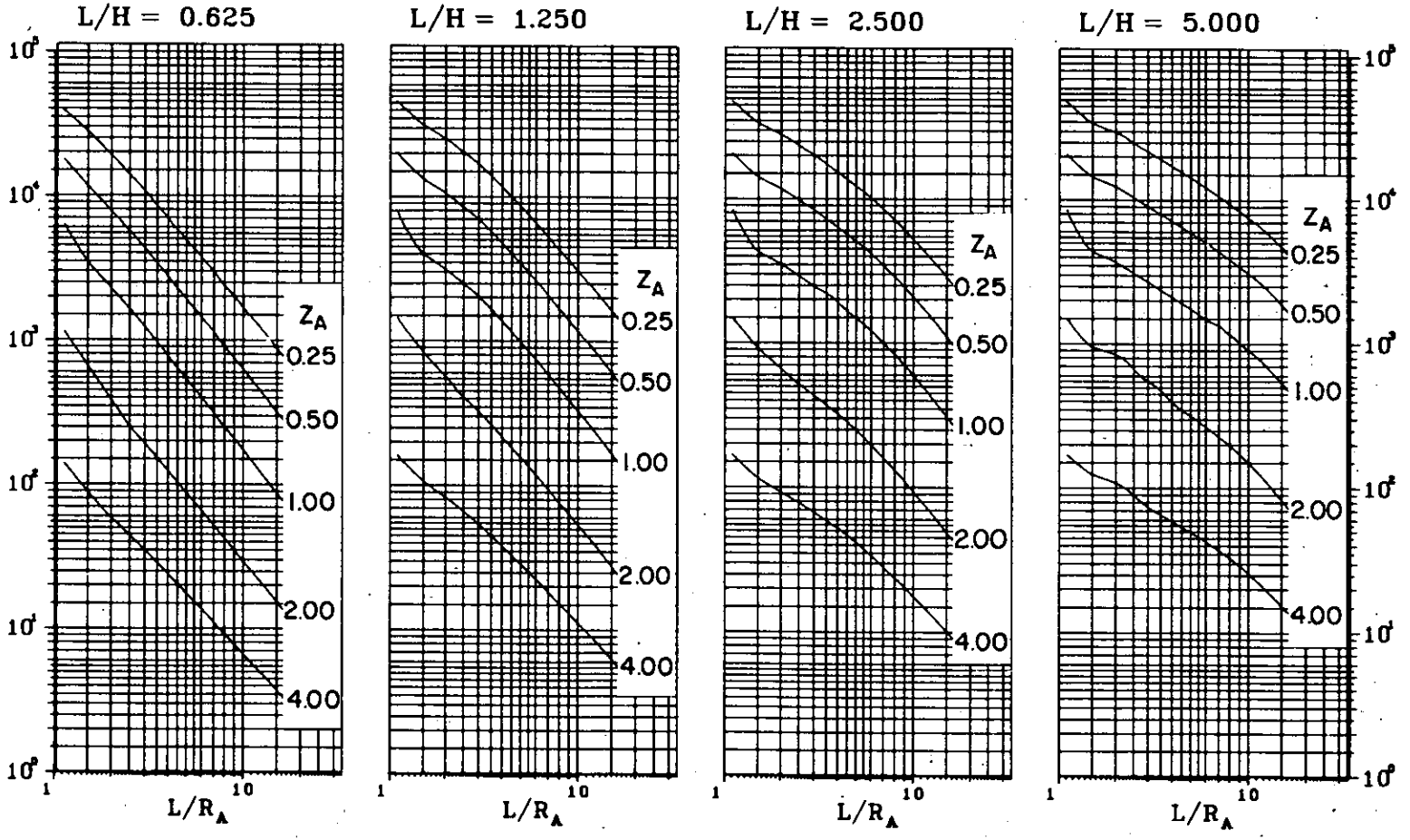


Figure 2-86 Average peak reflected pressure (N = 3, ℓ/L = 0.10, h/H = 0.50)

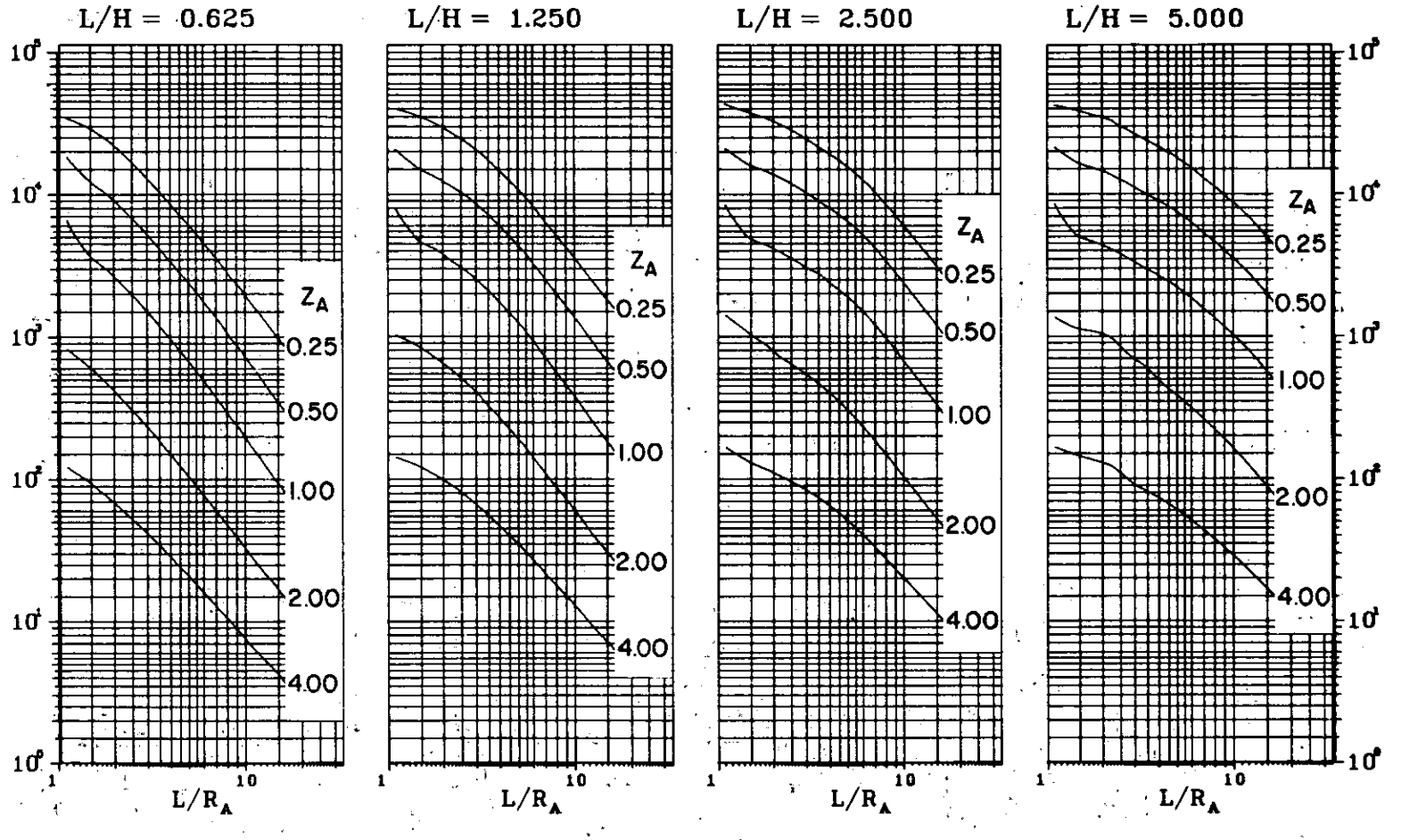


Figure 2-87 Average peak reflected pressure (N = 3, ℓ/L = 0.25 and 0.75, h/H = 0.50)

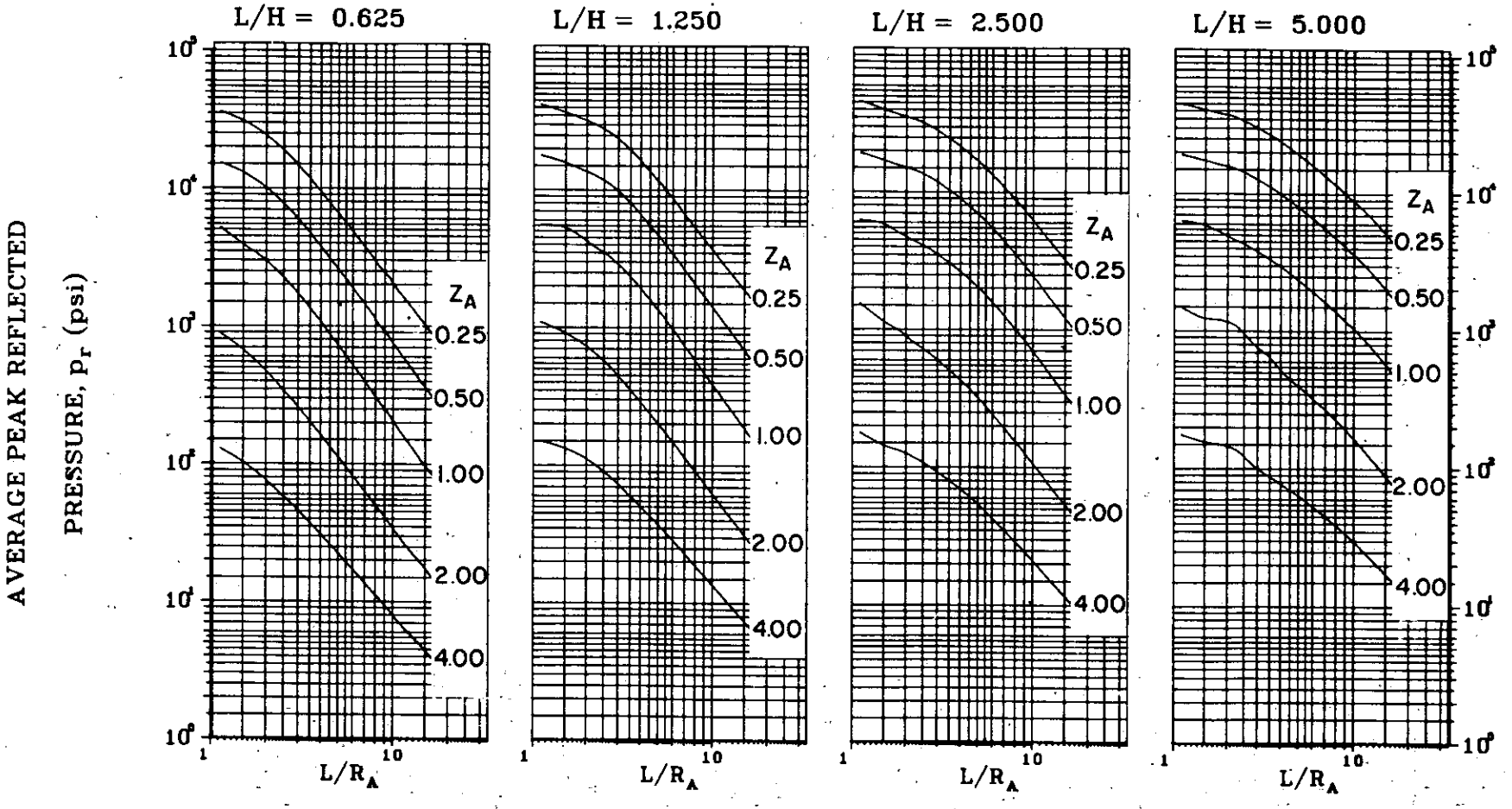


Figure 2-88 Average peak reflected pressure (N = 3, ℓ/L = 0.50, h/H = 0.50)

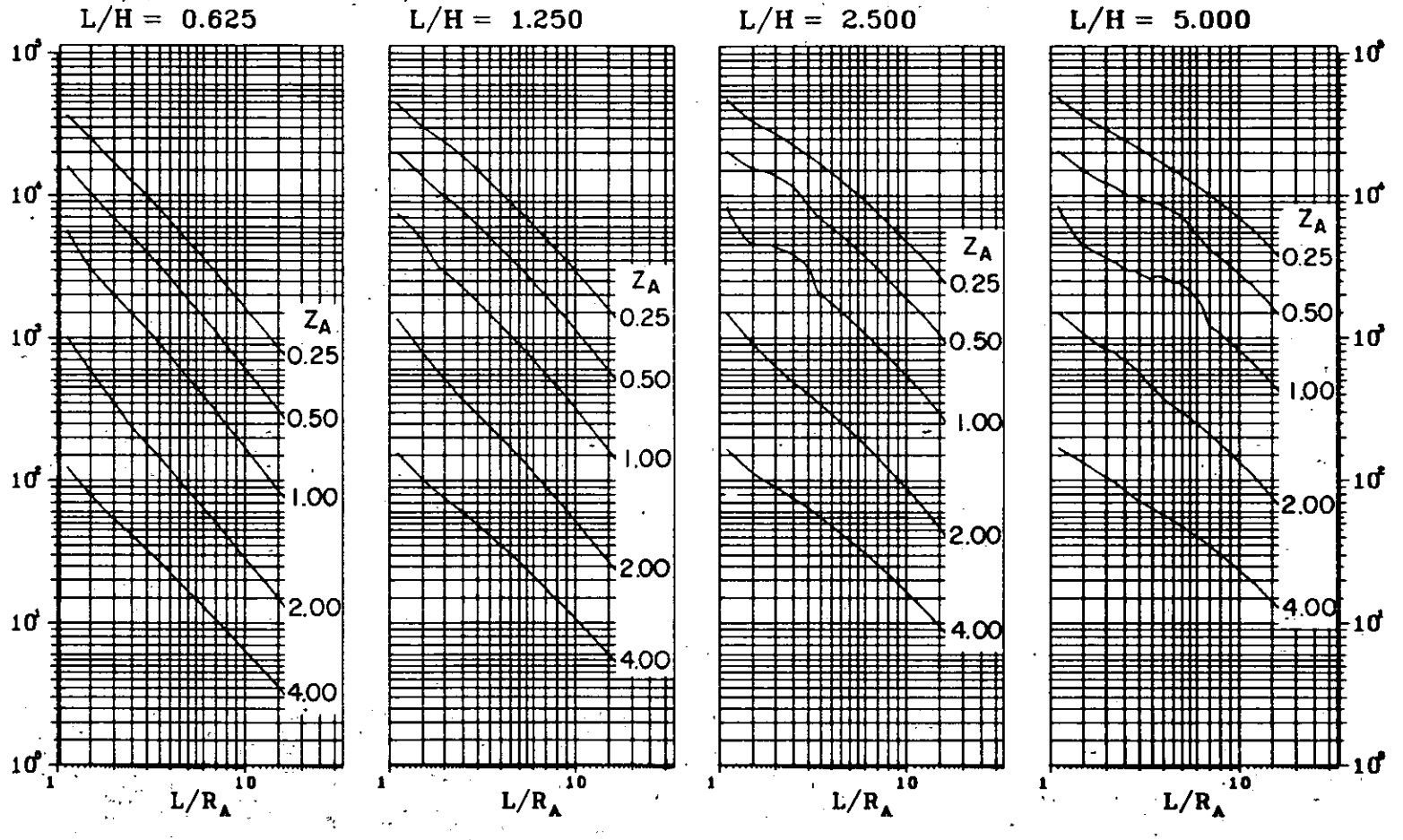


Figure 2-89 Average peak reflected pressure (N = 3, ℓ/L = 0.10, h/H = 0.75)

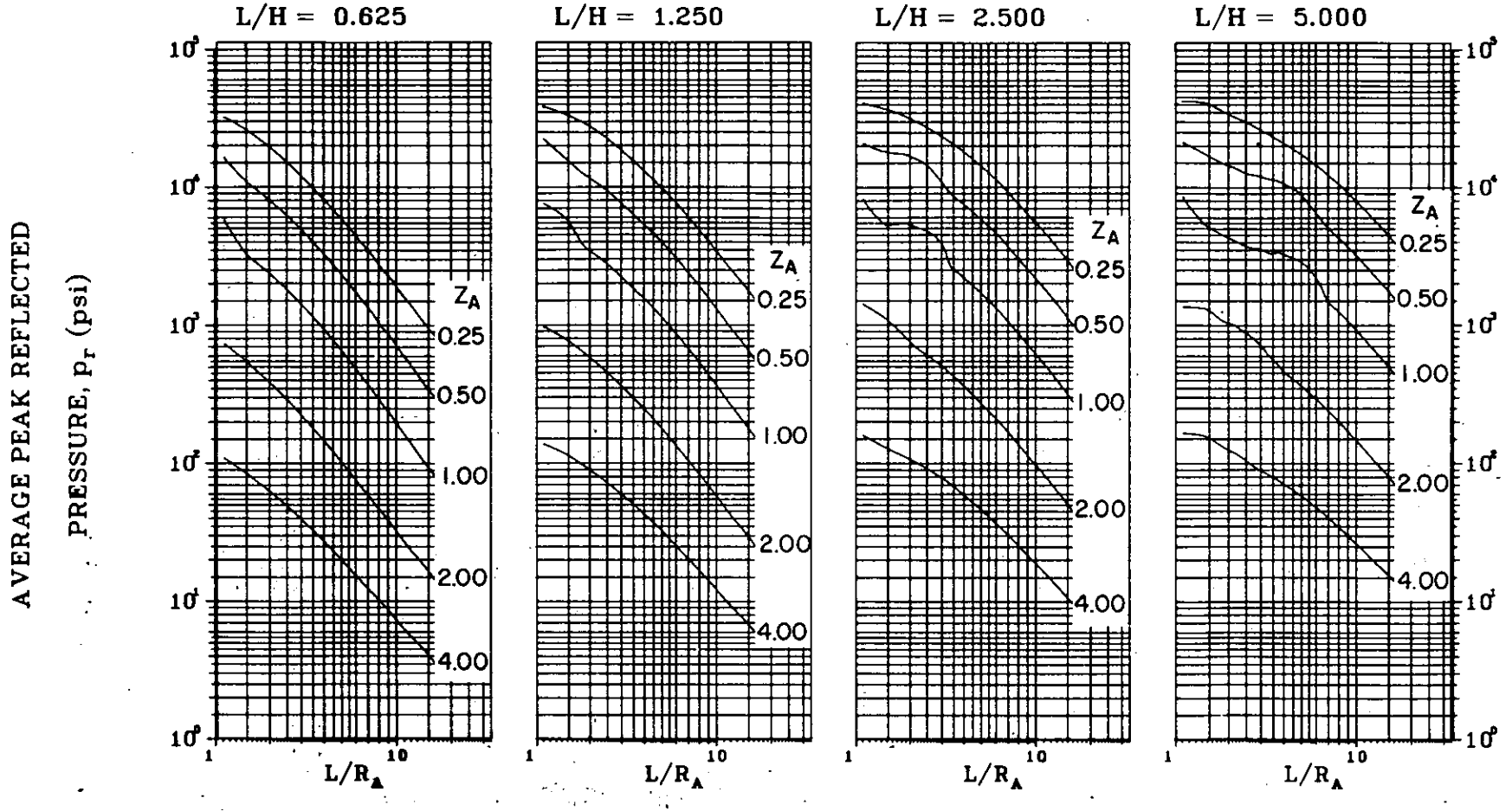


Figure 2-90 Average peak reflected pressure (N = 3, ℓ/L = 0.25 and 0.75, h/H = 0.75)

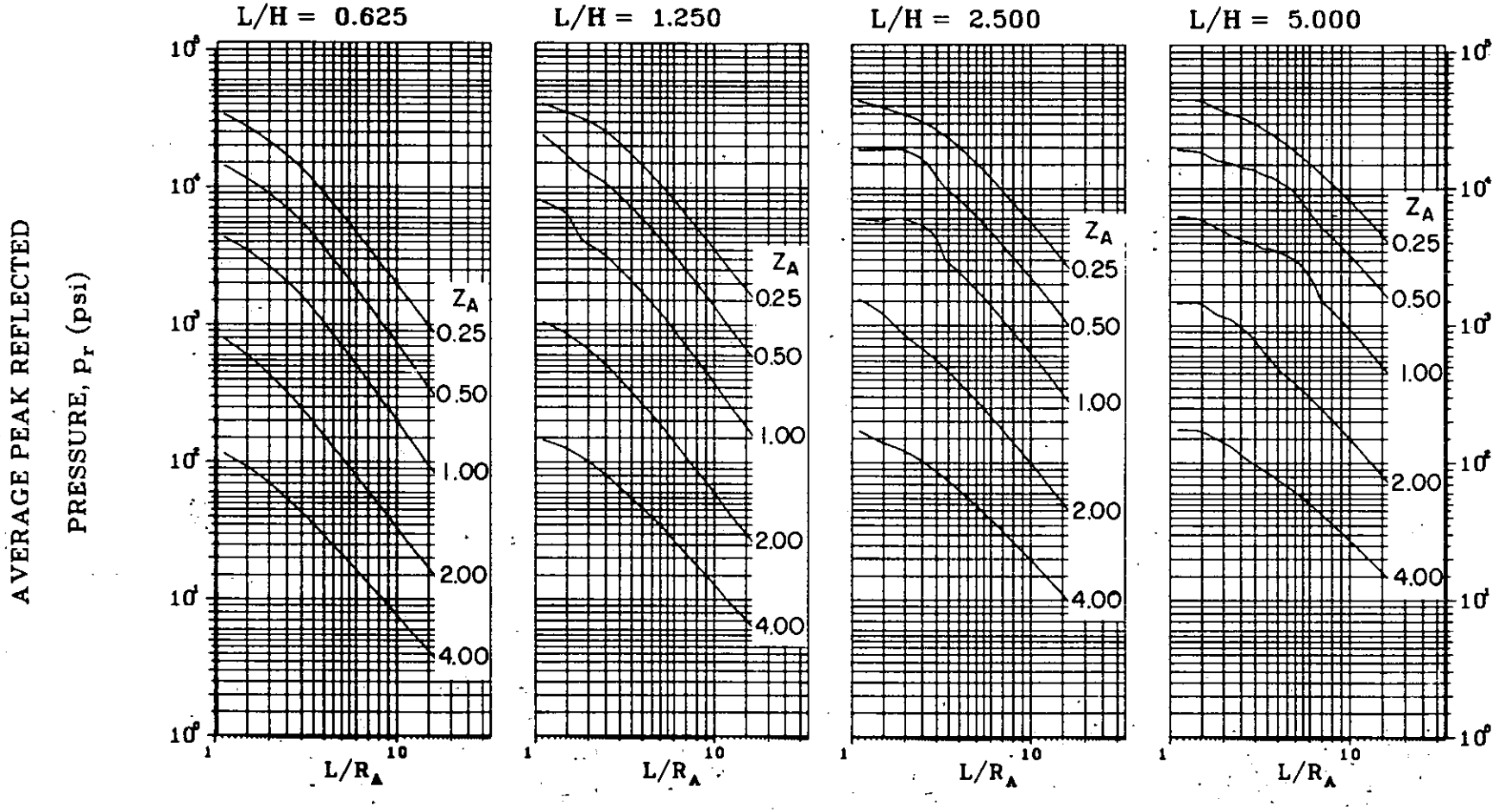


Figure 2-91 Average peak reflected pressure (N = 3, ℓ/L = 0.50, h/H = 0.75)

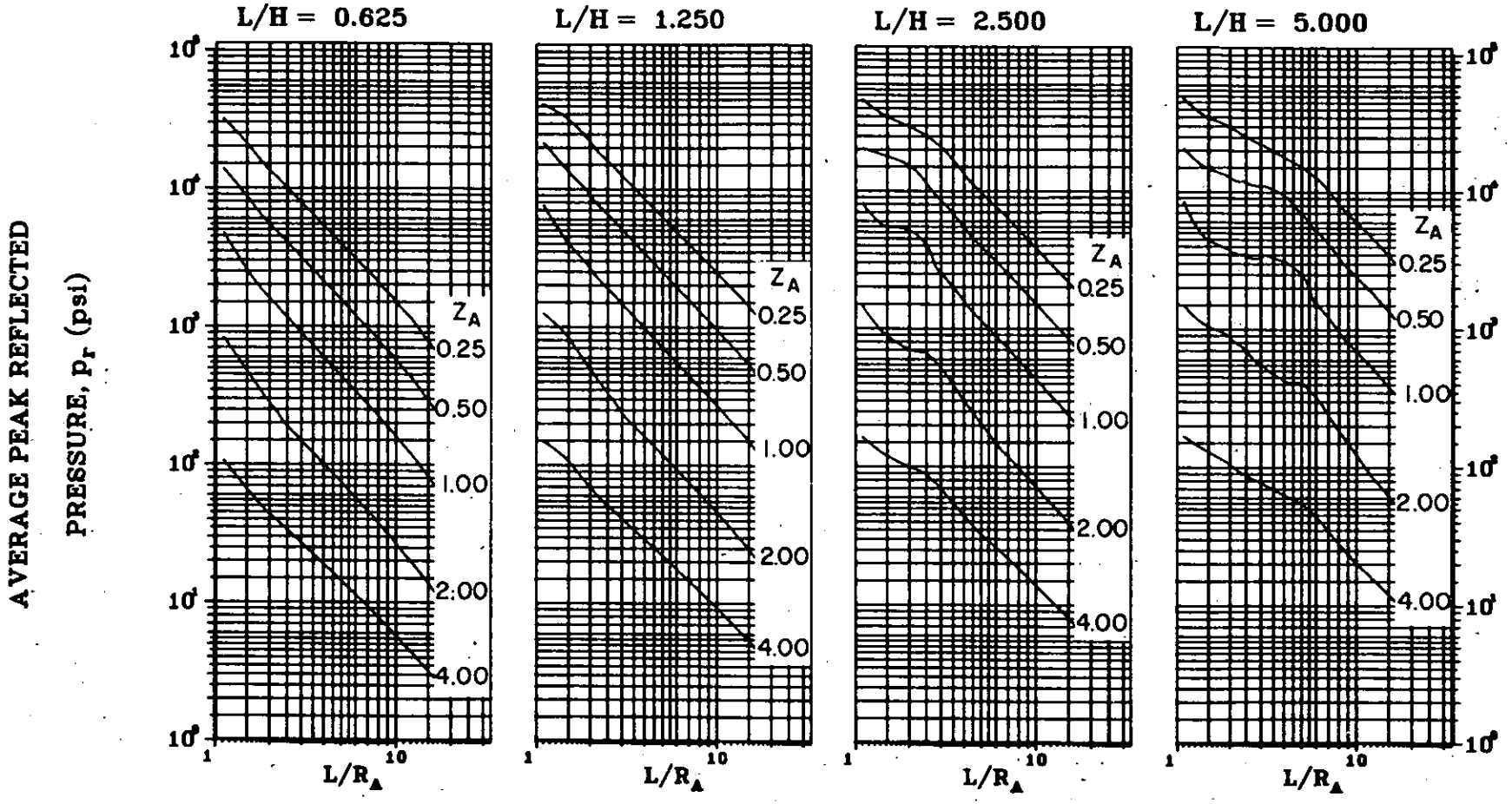


Figure 2-92 Average peak reflected pressure (N = 4, ℓ /L = 0.10, h/H = 0.10)

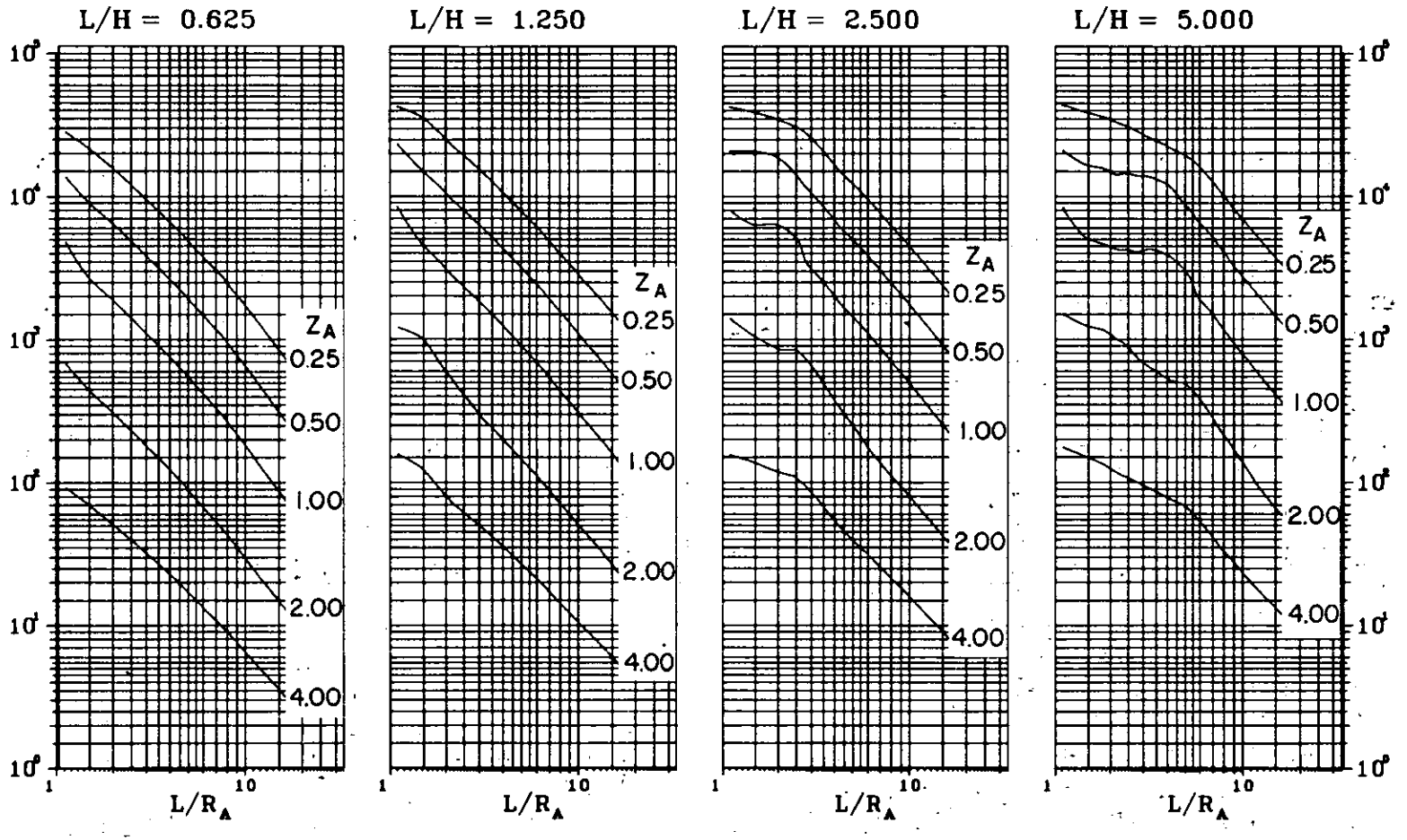


Figure 2-93 Average peak reflected pressure (N = 4, ℓ/L = 0.25 and 0.75, h/H = 0.10)

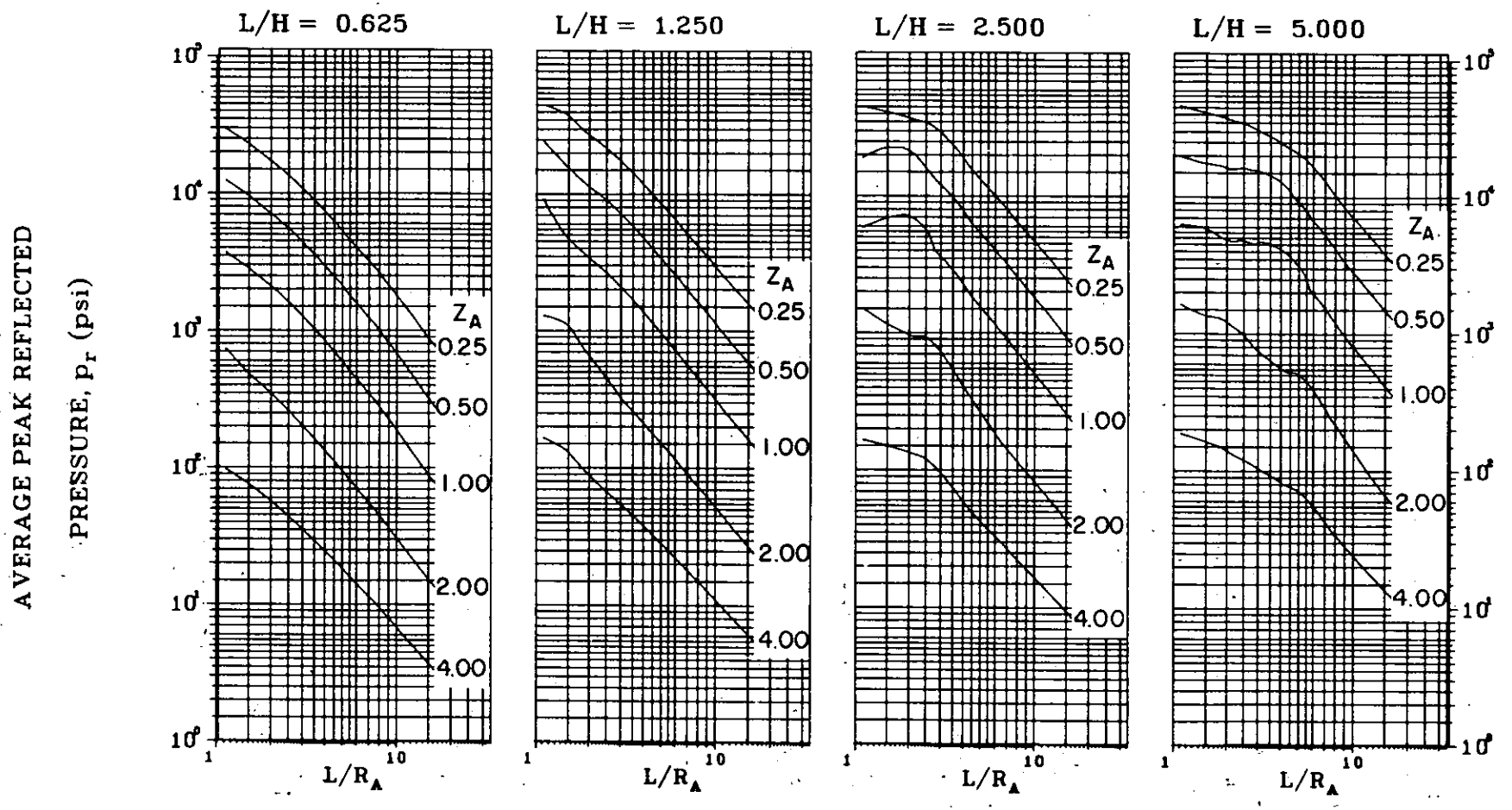


Figure 2-94 Average peak reflected pressure (N = 4, ℓ /L = 0.50, h/H = 0.10)

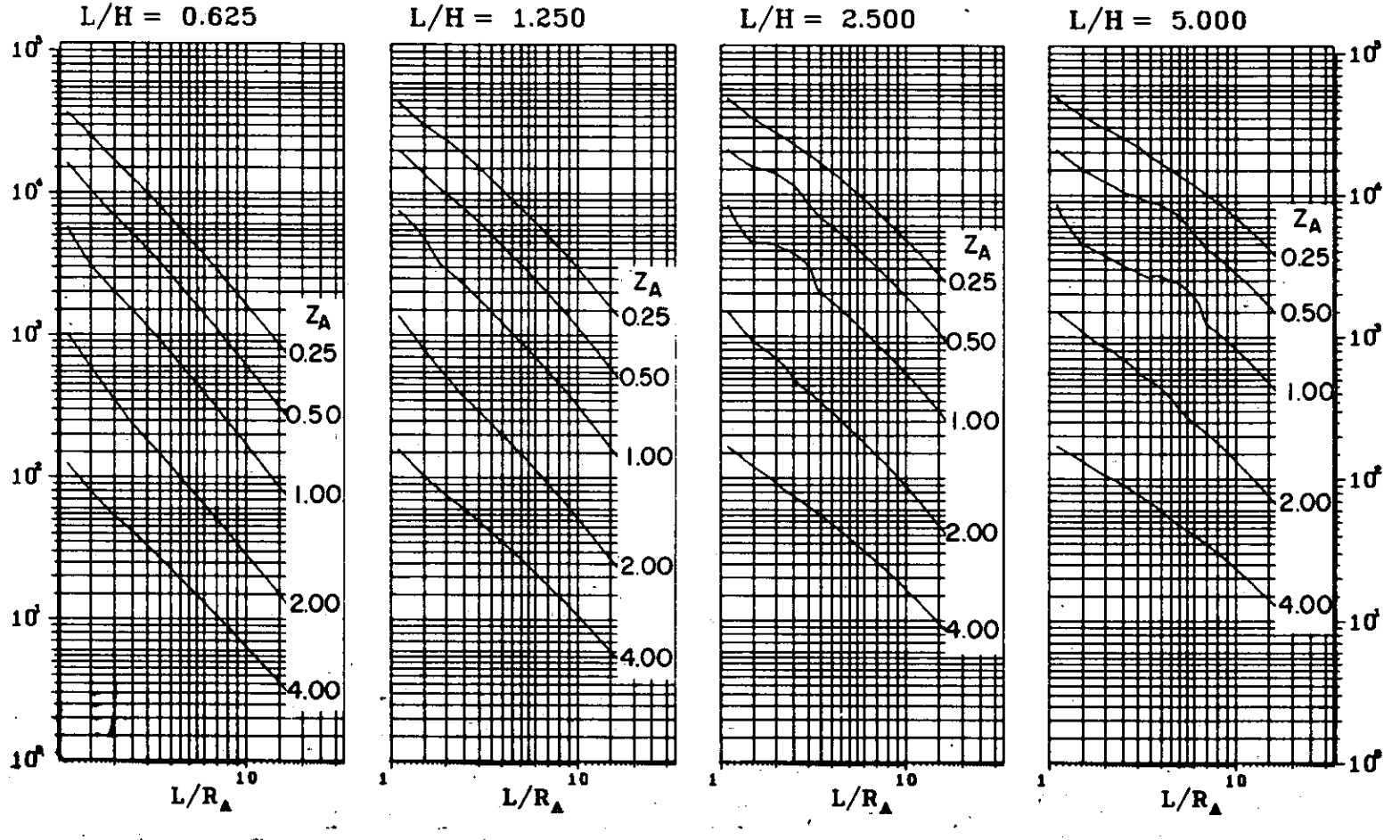


Figure 2-95 Average peak reflected pressure (N = 4, ℓ/L = 0.10, h/H = 0.25 and 0.75)

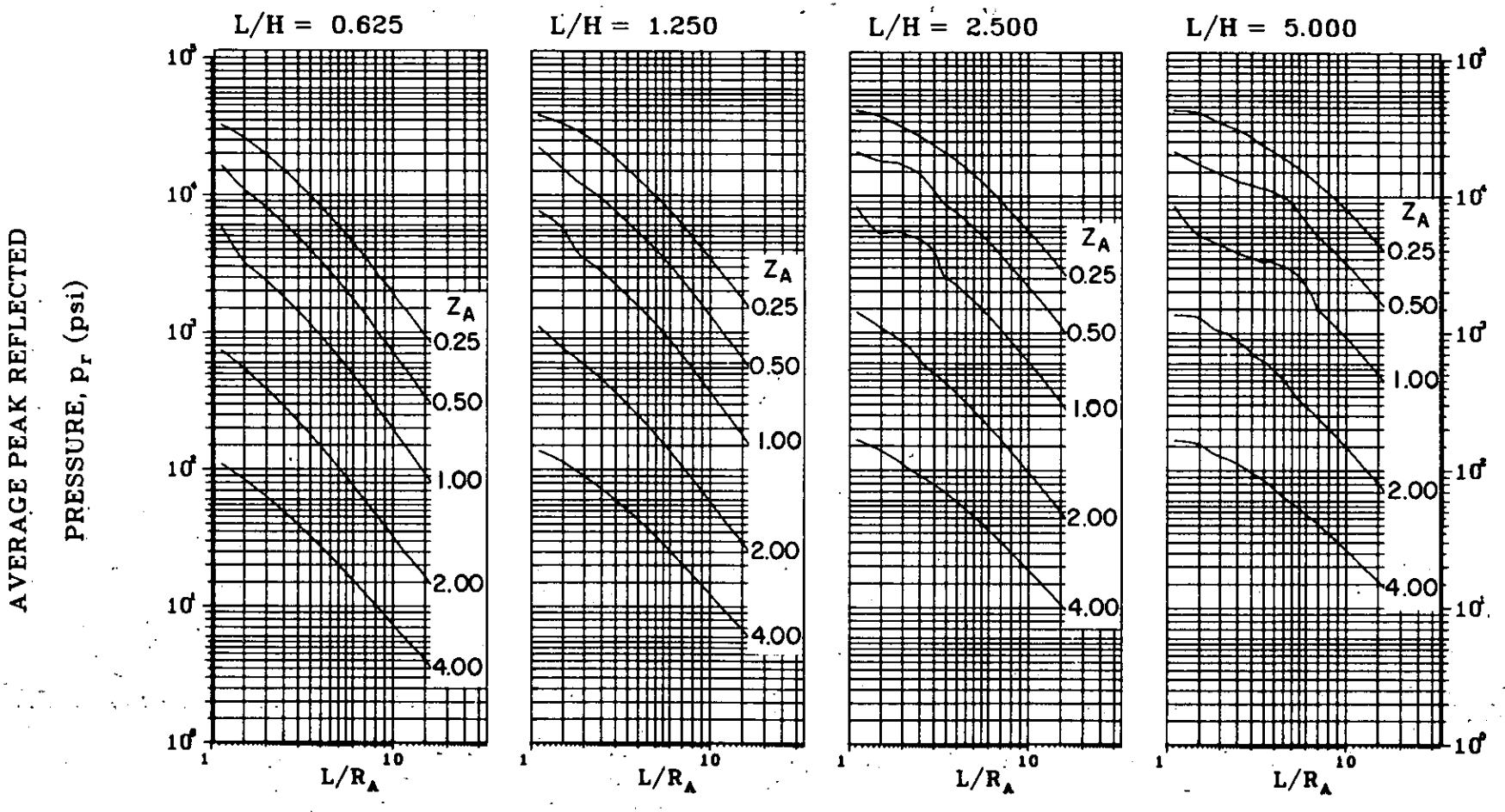


Figure 2-96. Average peak reflected pressure (N = 4, ℓ/L = 0.25 and 0.75, h/H = 0.25 and 0.75)

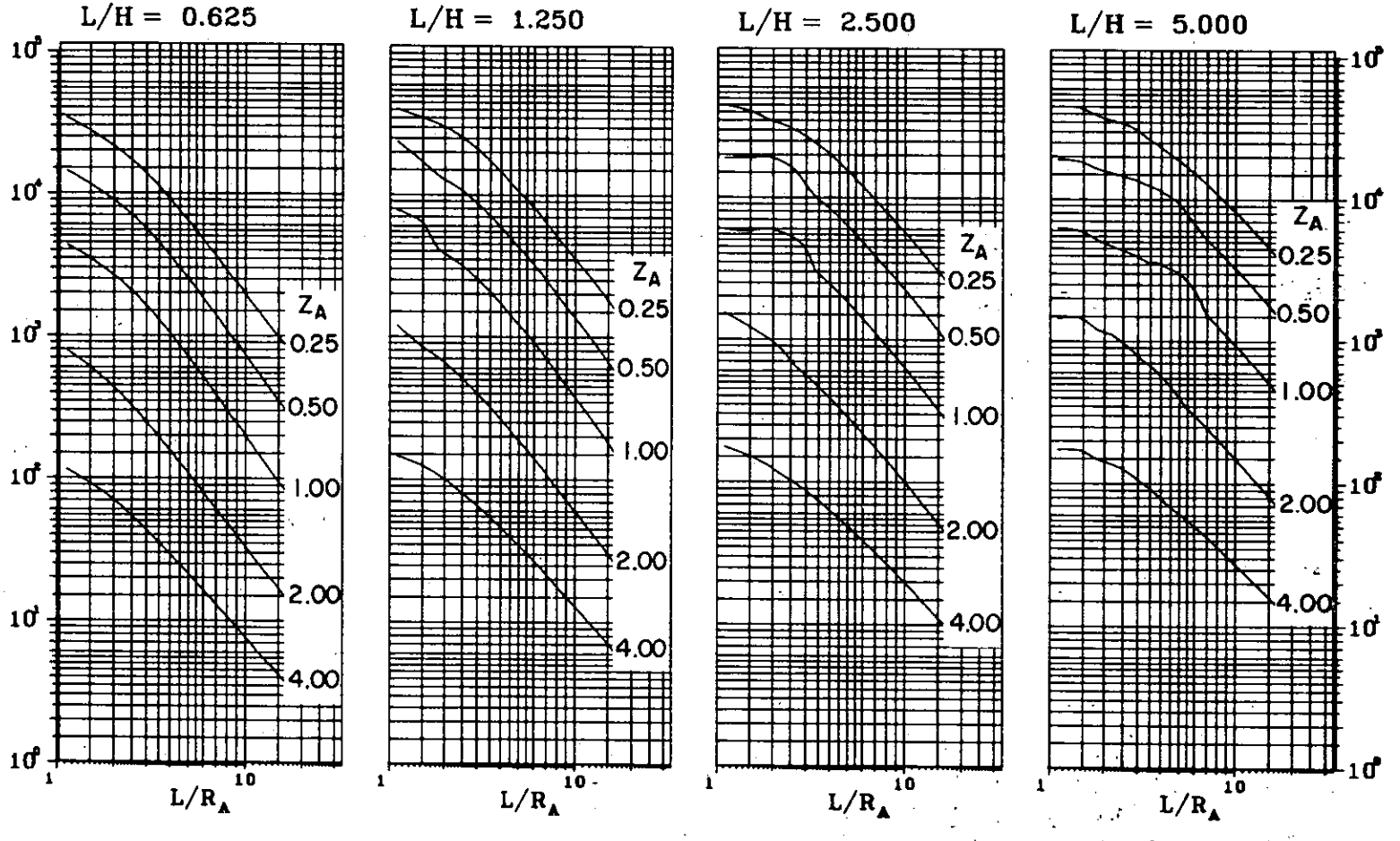


Figure 2-97 Average peak reflected pressure (N = 4, ℓ /L = 0.50, h/H = 0.25 and 0.75)

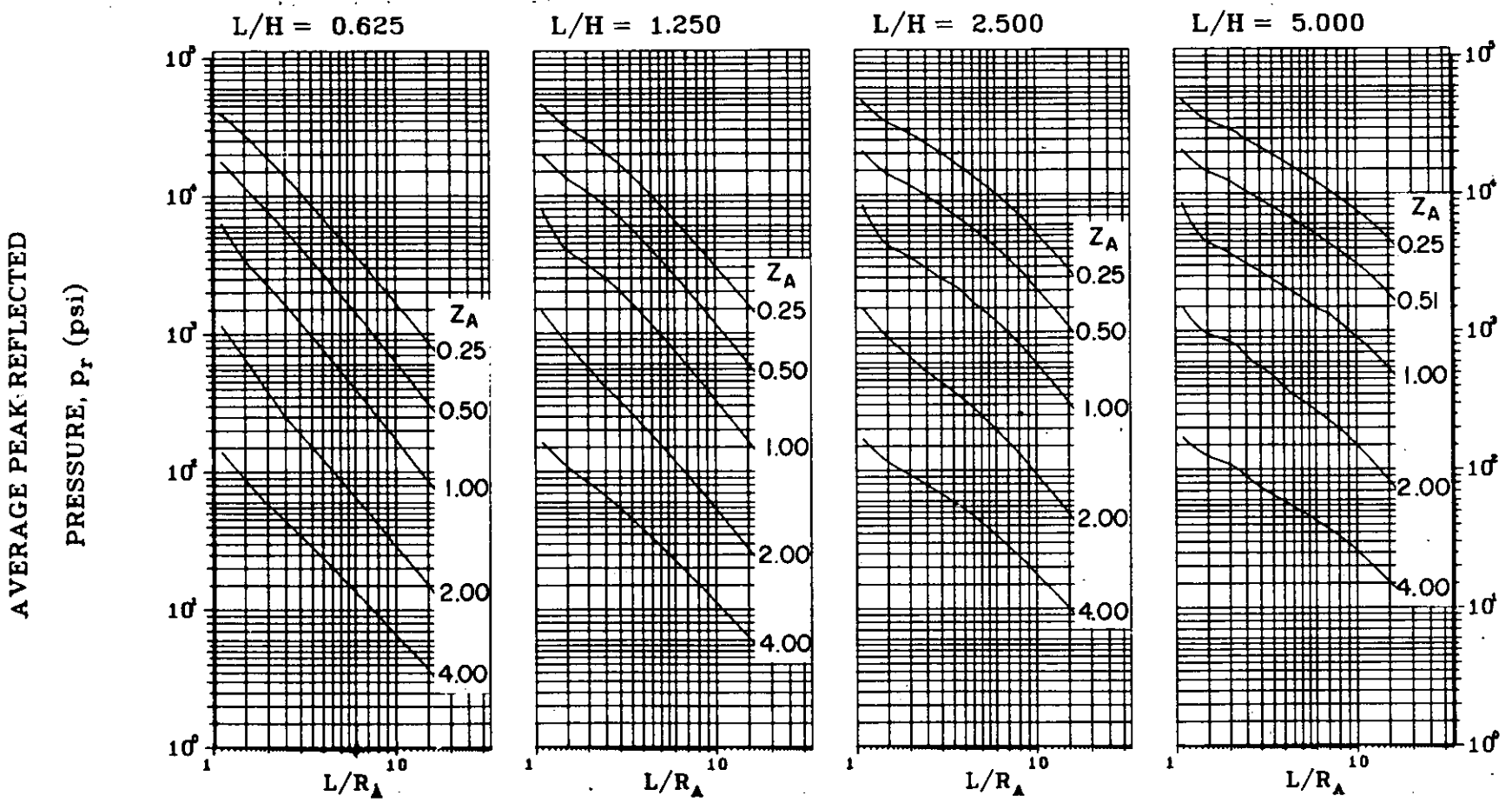


Figure 2-98 Average peak reflected pressure (N = 4, ℓ/L = 0.10, h/H = 0.50)

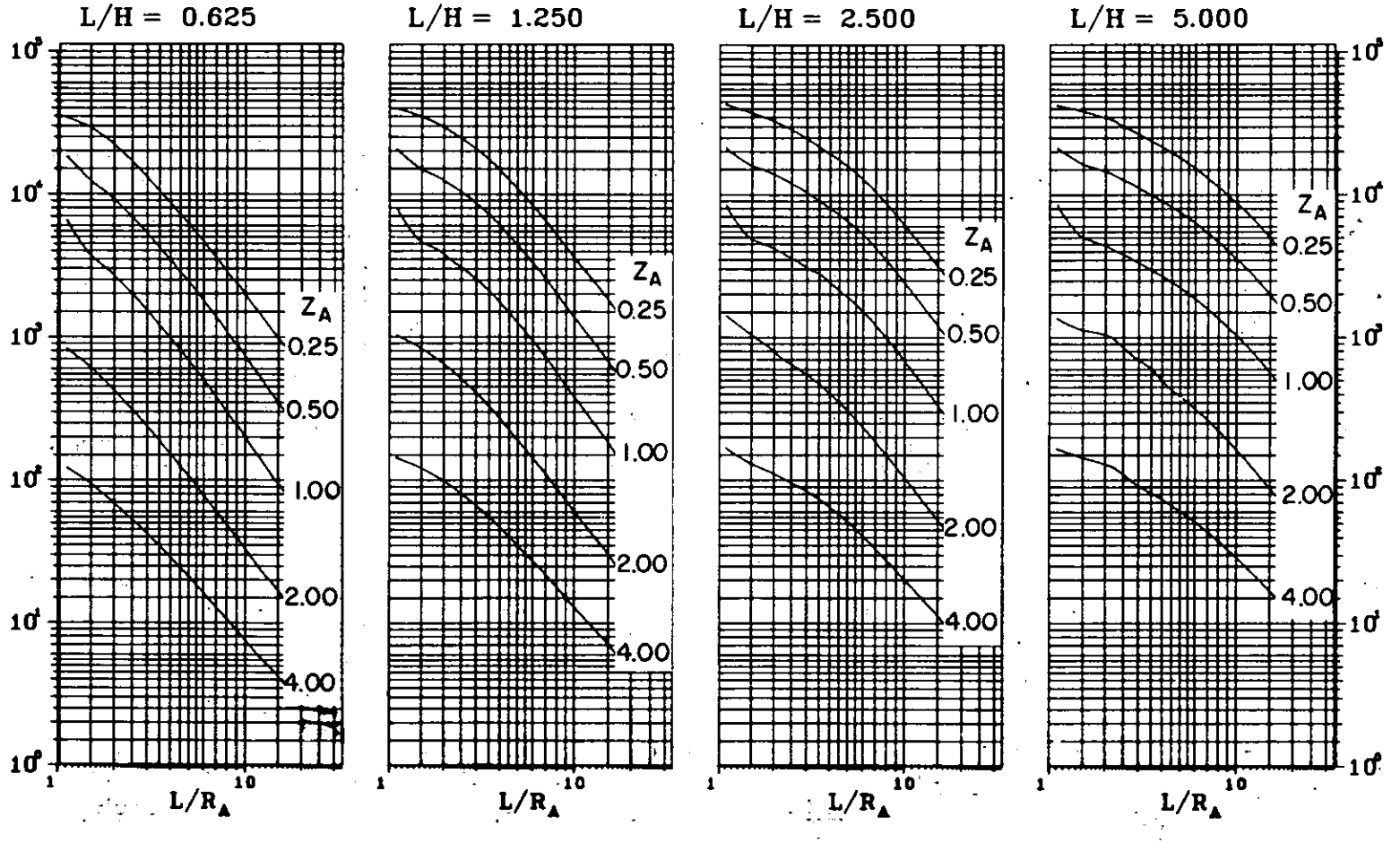


Figure 2-99 Average peak reflected pressure
(N = 4, ℓ/L = 0.25 and 0.75, h/H = 0.50)

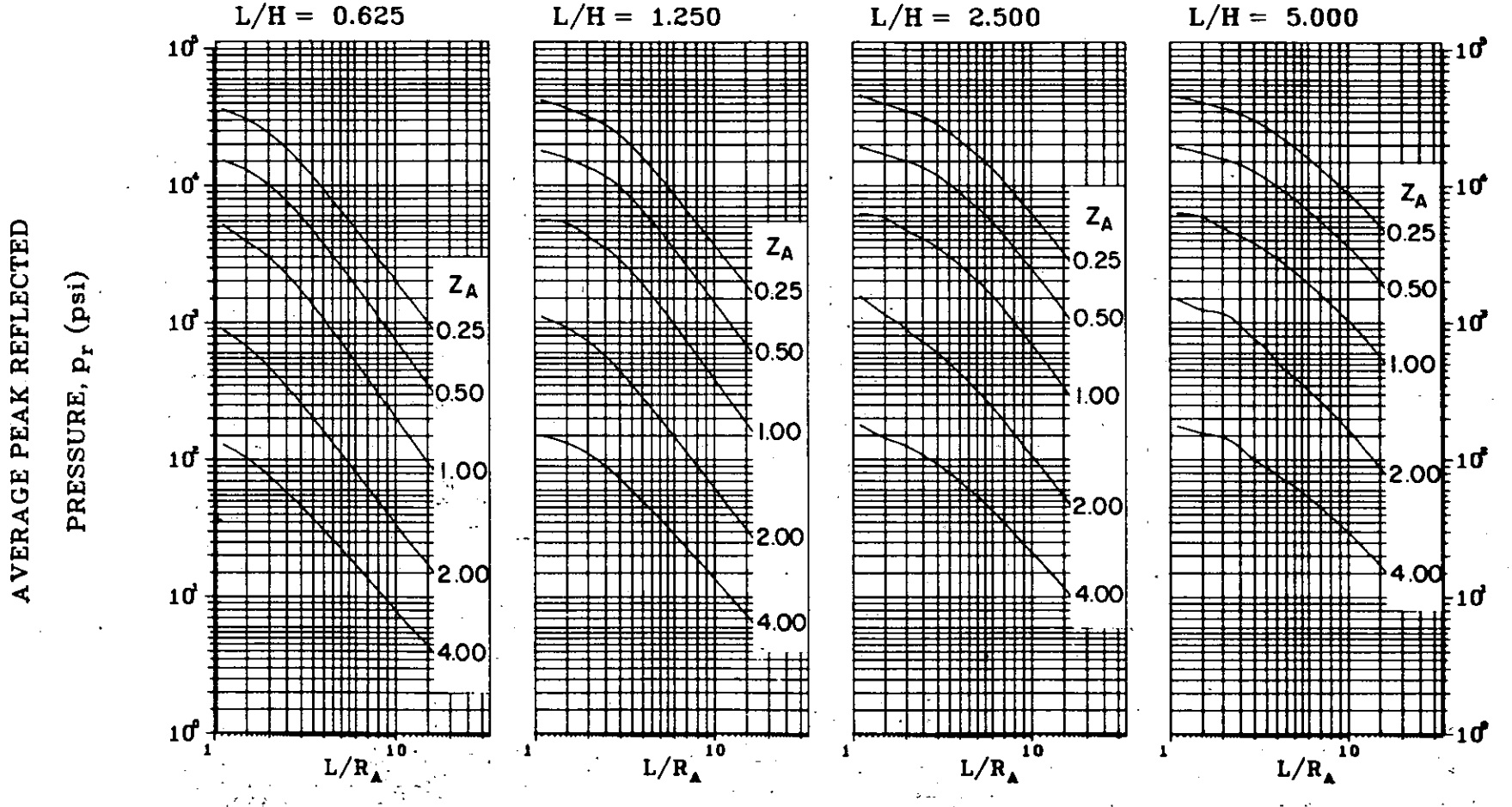


Figure 2-100 Average peak reflected pressure (N = 4, ℓ/L = 0.50, h/H = 0.50)

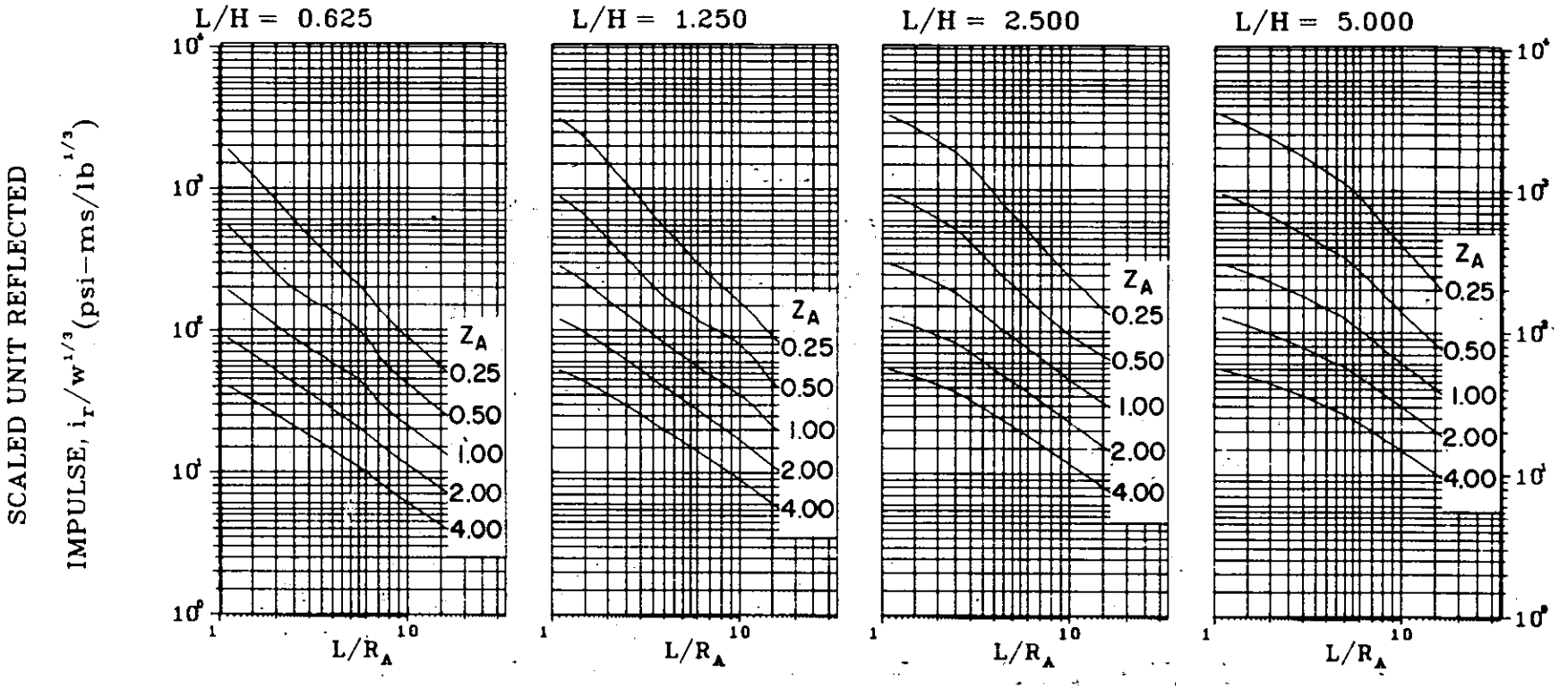


Figure 2-101 Scaled average unit reflected impulse
(N = 1, ℓ/L = 0.10, h/H = 0.10)

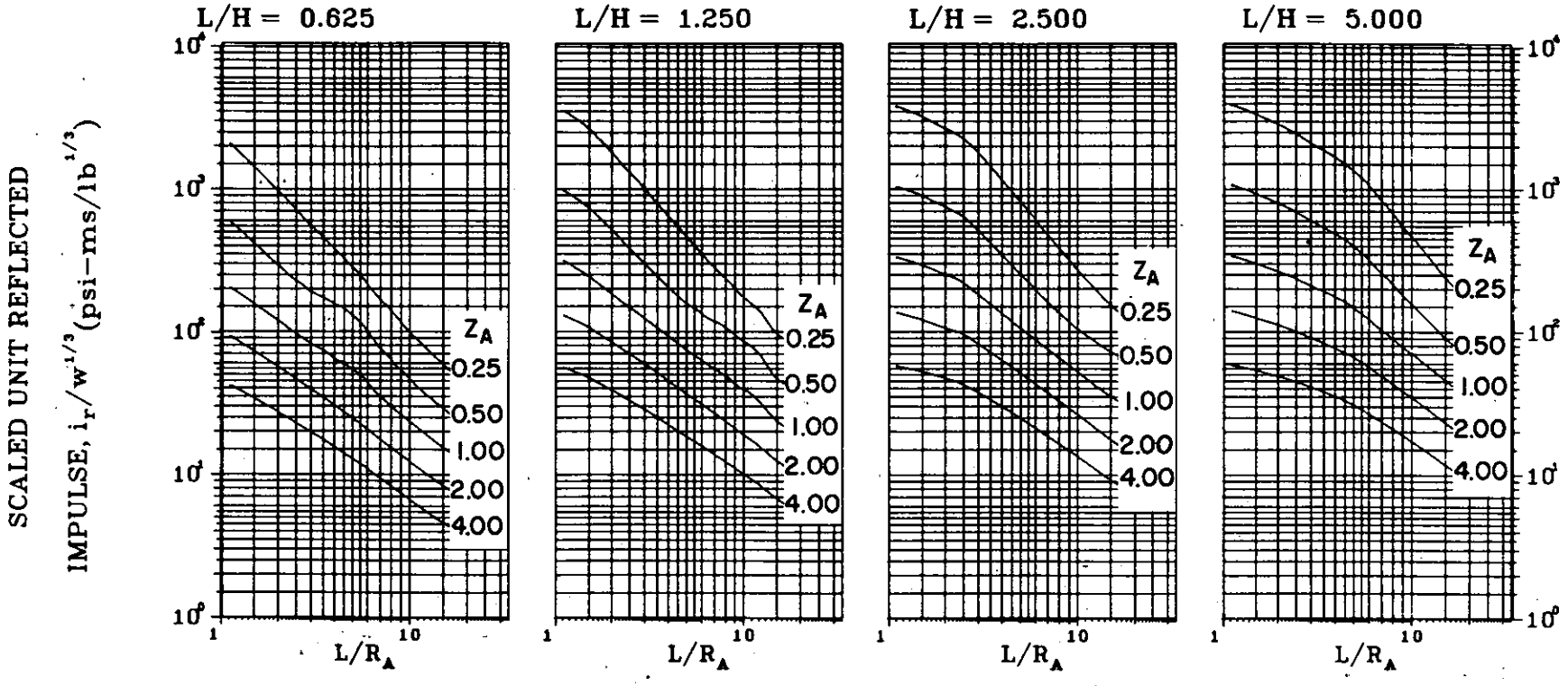


Figure 2-102 Scaled average unit reflected impulse
(N = 1, ℓ/L = 0.25 and 0.75, h/H = 0.10)

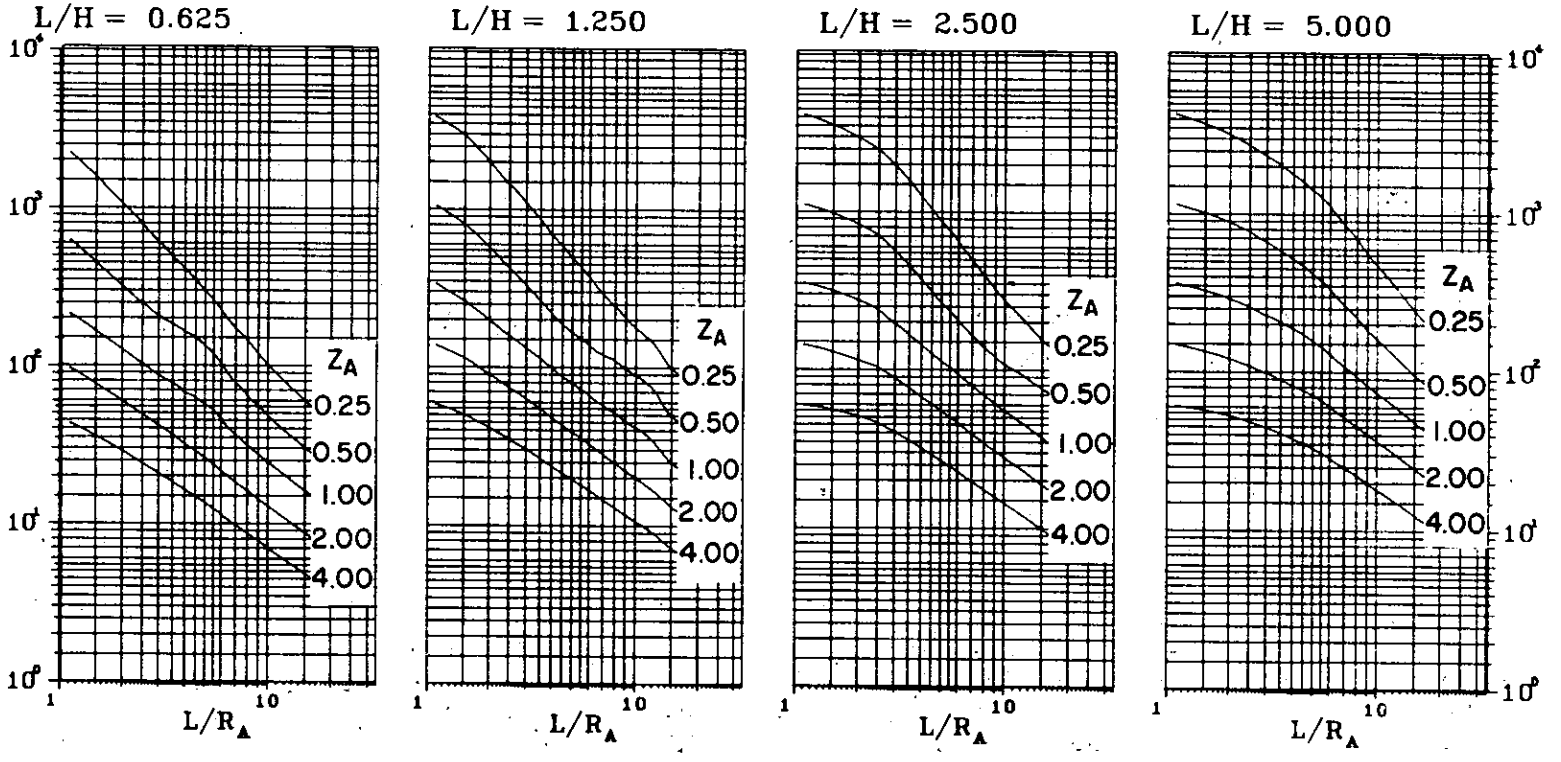


Figure 2-103 Scaled average unit reflected impulse
(N = 1, ℓ/L = 0.50, h/H = 0.10)

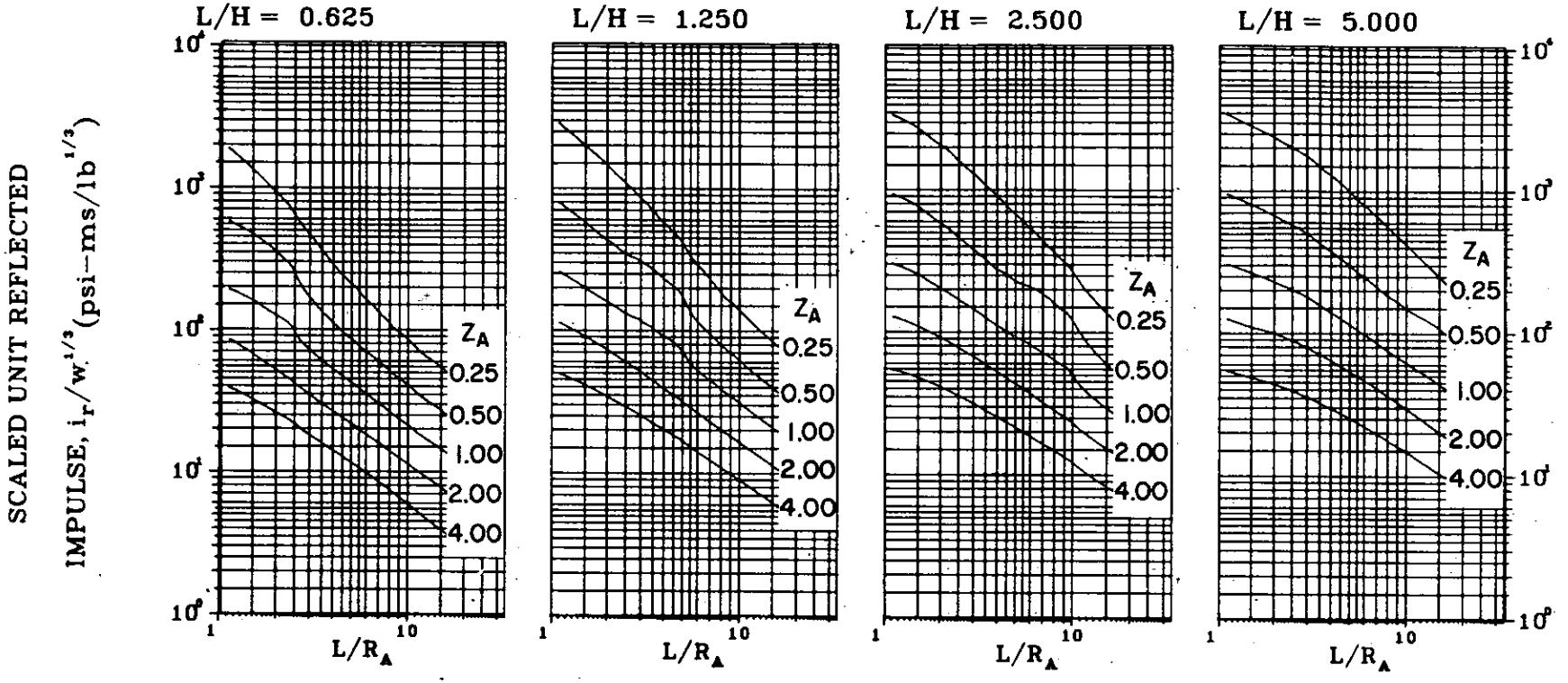


Figure 2-104 Scaled average unit reflected impulse
(N = 1, ℓ/L = 0.10, h/H = 0.25)

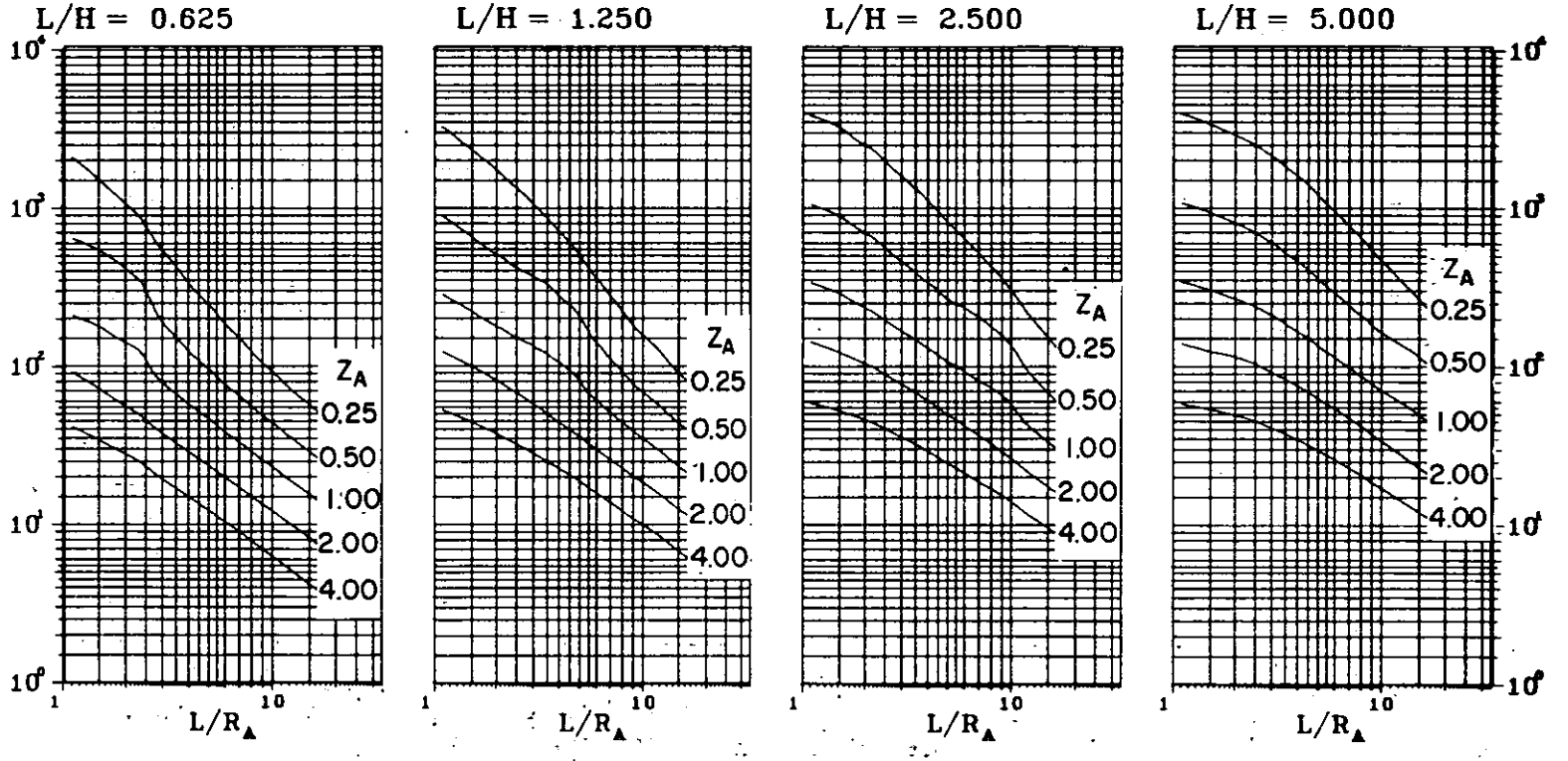


Figure 2-105 Scaled average unit reflected impulse
(N = 1, ℓ/L = 0.25 and 0.75, h/H = 0.25)

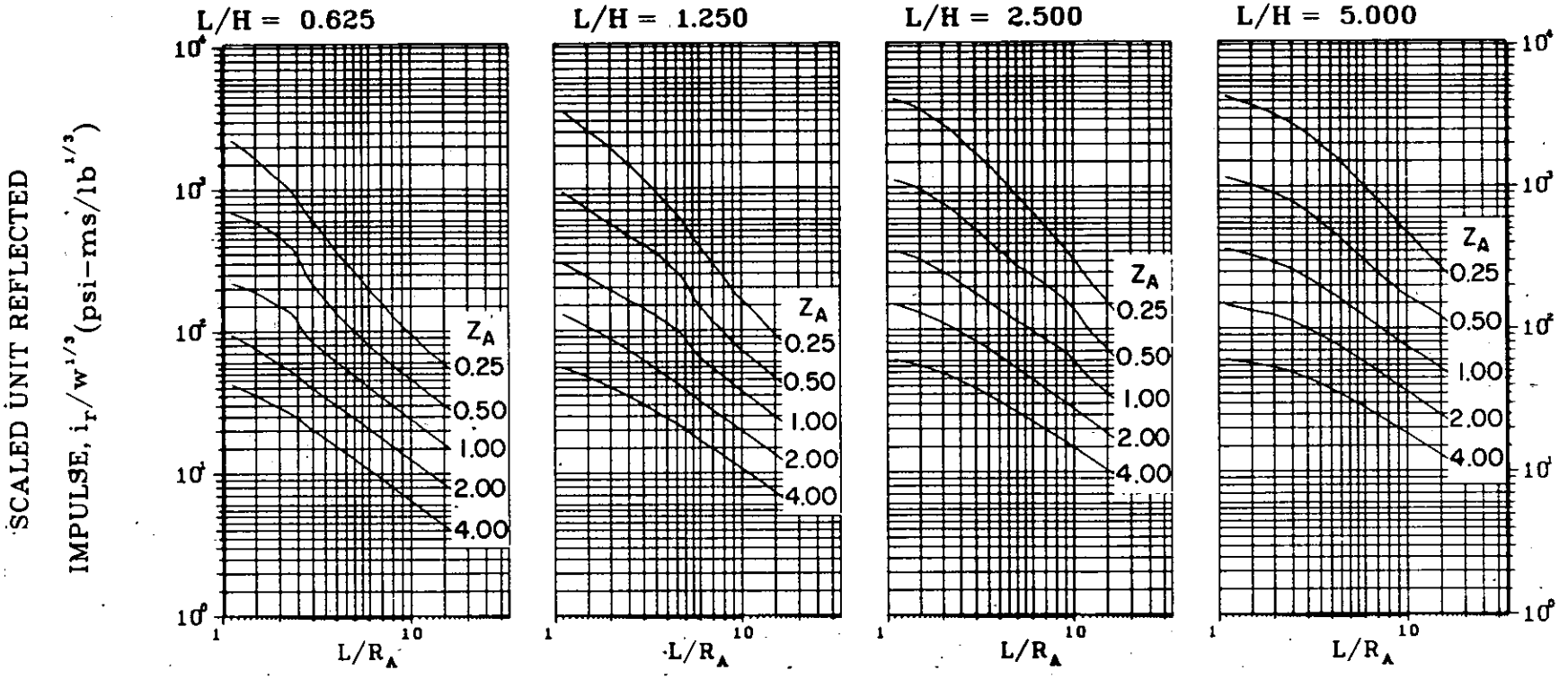


Figure 2-106 Scaled average unit reflected impulse
(N = 1, ℓ/L = 0.50, h/H = 0.25)

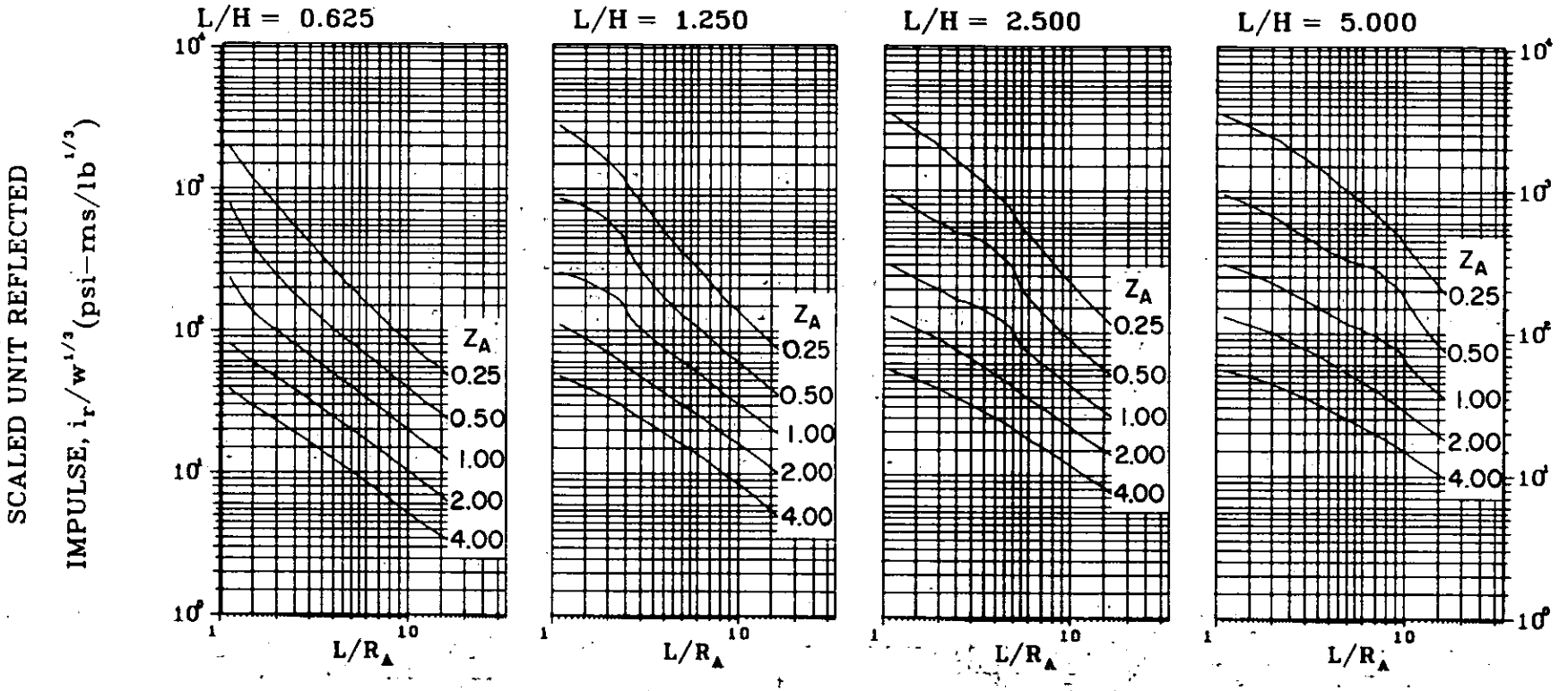


Figure 2-107 Scaled average unit reflected impulse
(N = 1, ℓ/L = 0.10, h/H = 0.50)

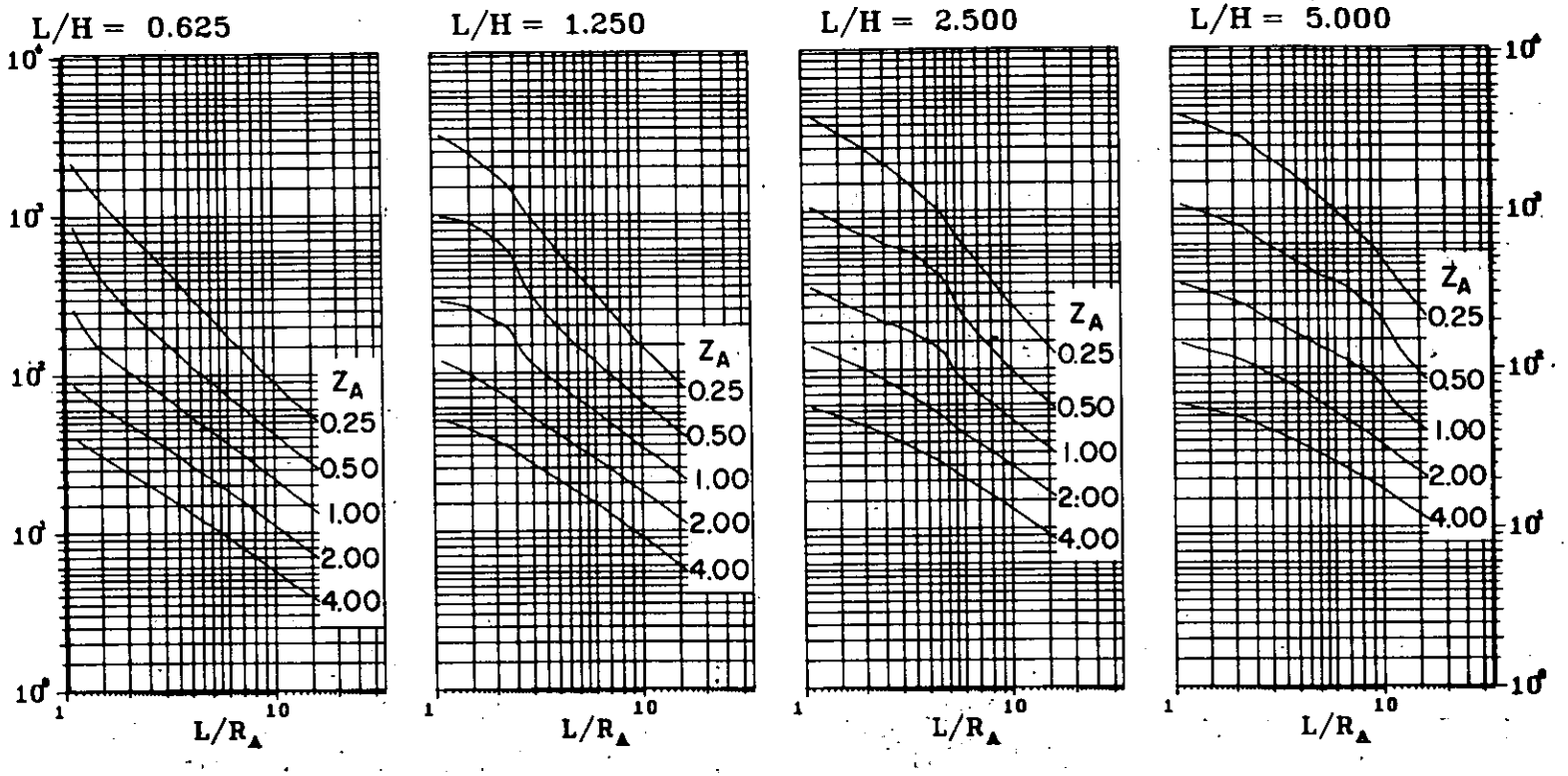


Figure 2-108 Scaled average unit reflected impulse
(N = 1, ℓ/L = 0.25 and 0.75, h/H = 0.50)

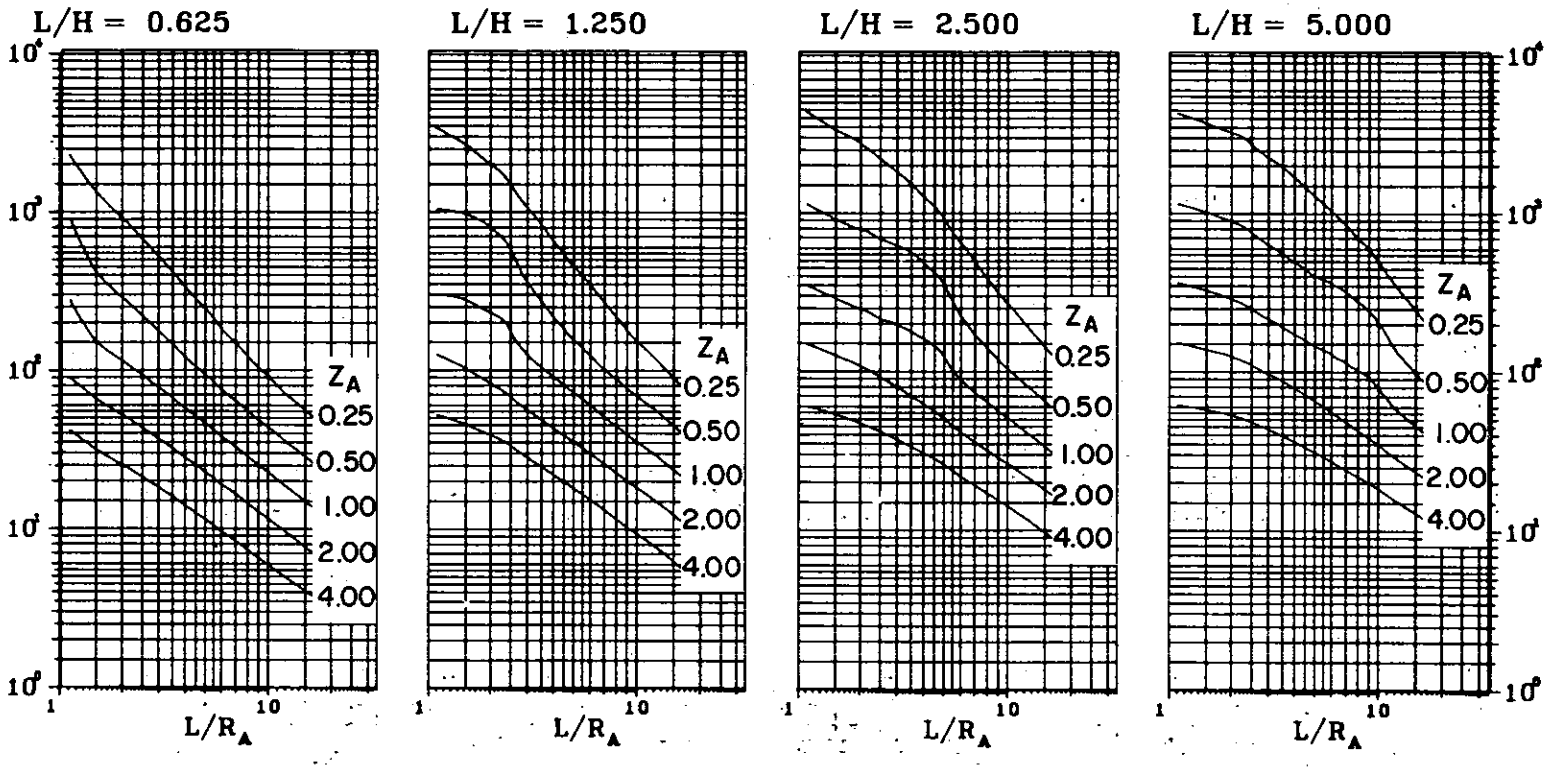


Figure 2-109 Scaled average unit reflected impulse
(N = 1, ℓ/L = 0.50, h/H = 0.50)

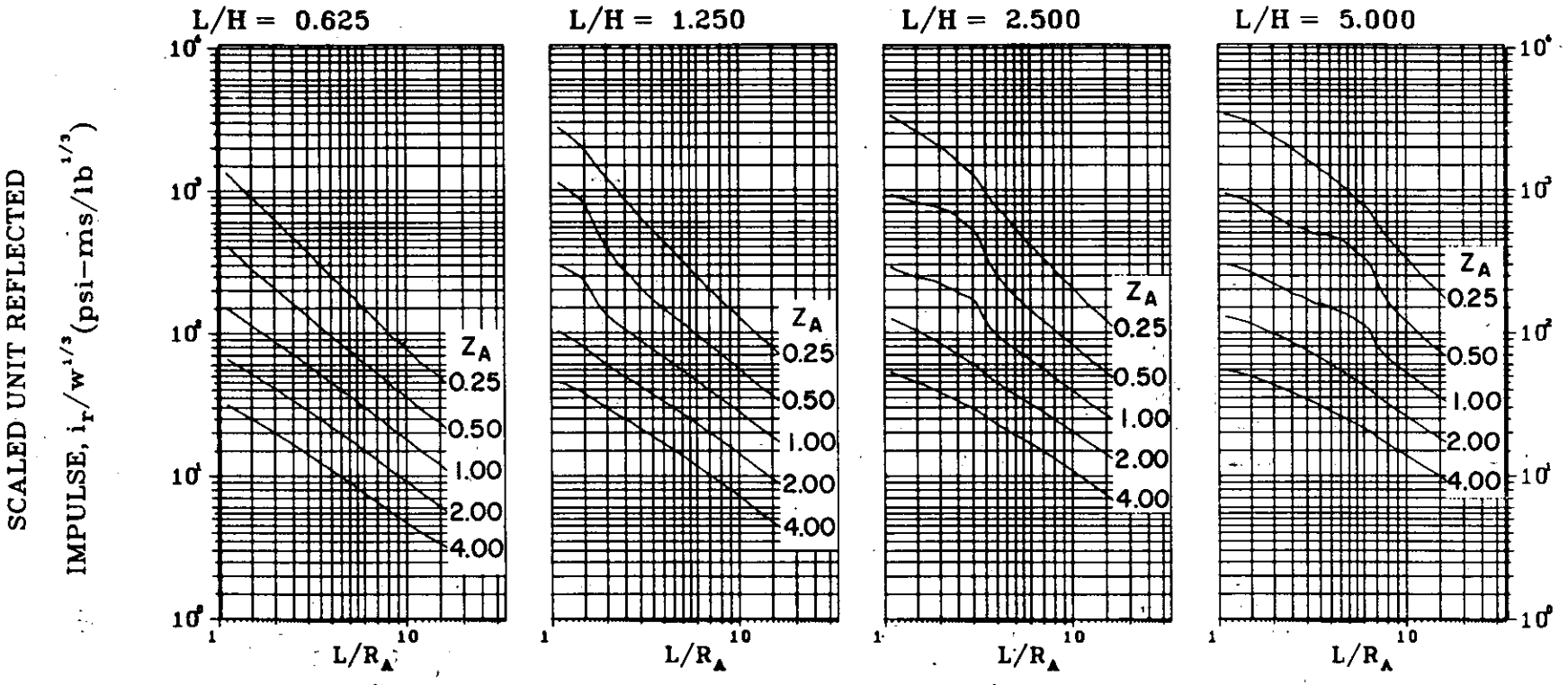


Figure 2-110 Scaled average unit reflected impulse
(N = 1, ℓ/L = 0.10, h/H = 0.75)

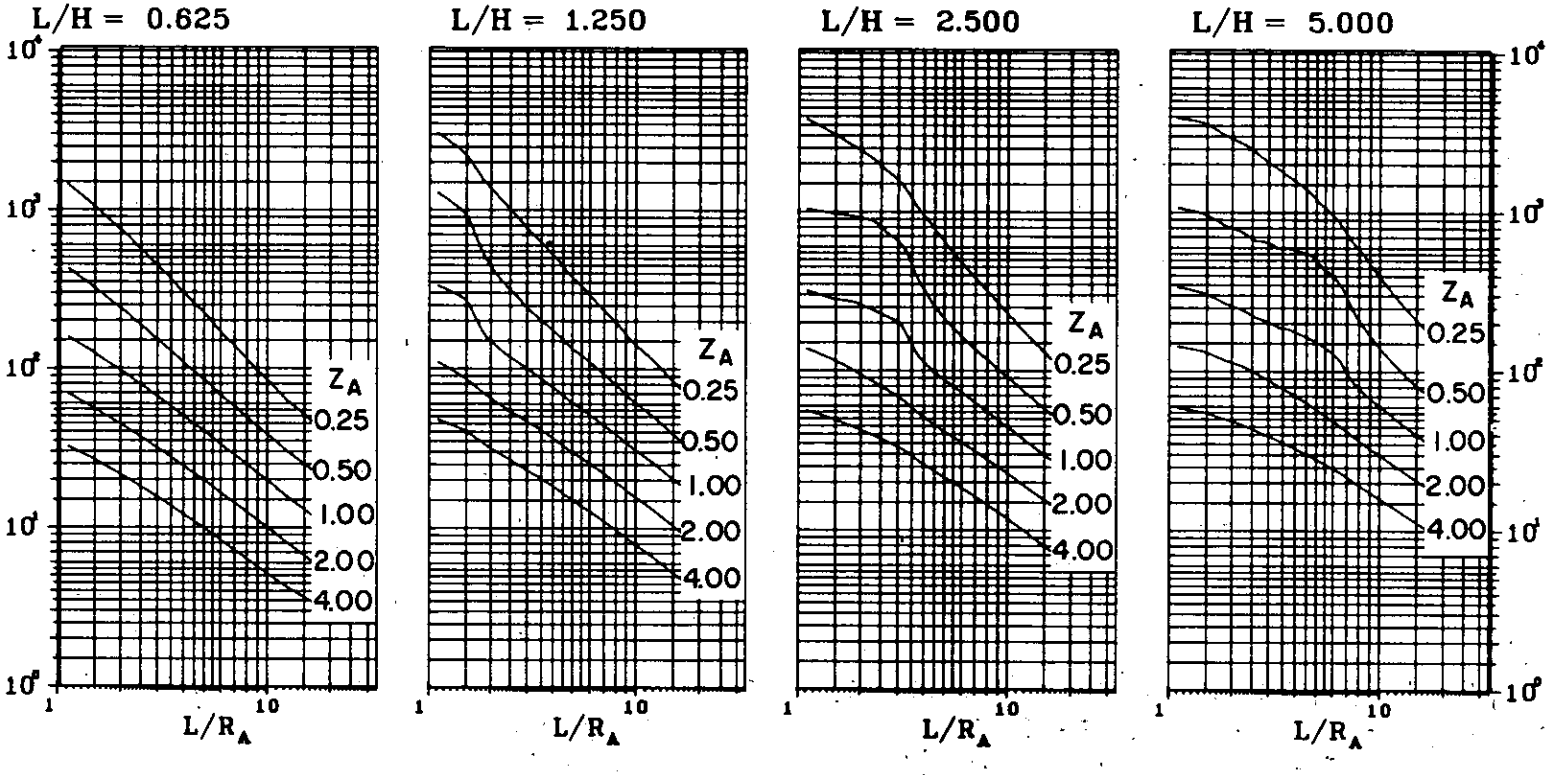


Figure 2-111 Scaled average unit reflected impulse
(N = 1, ℓ/L = 0.25 and 0.75, h/H = 0.75)

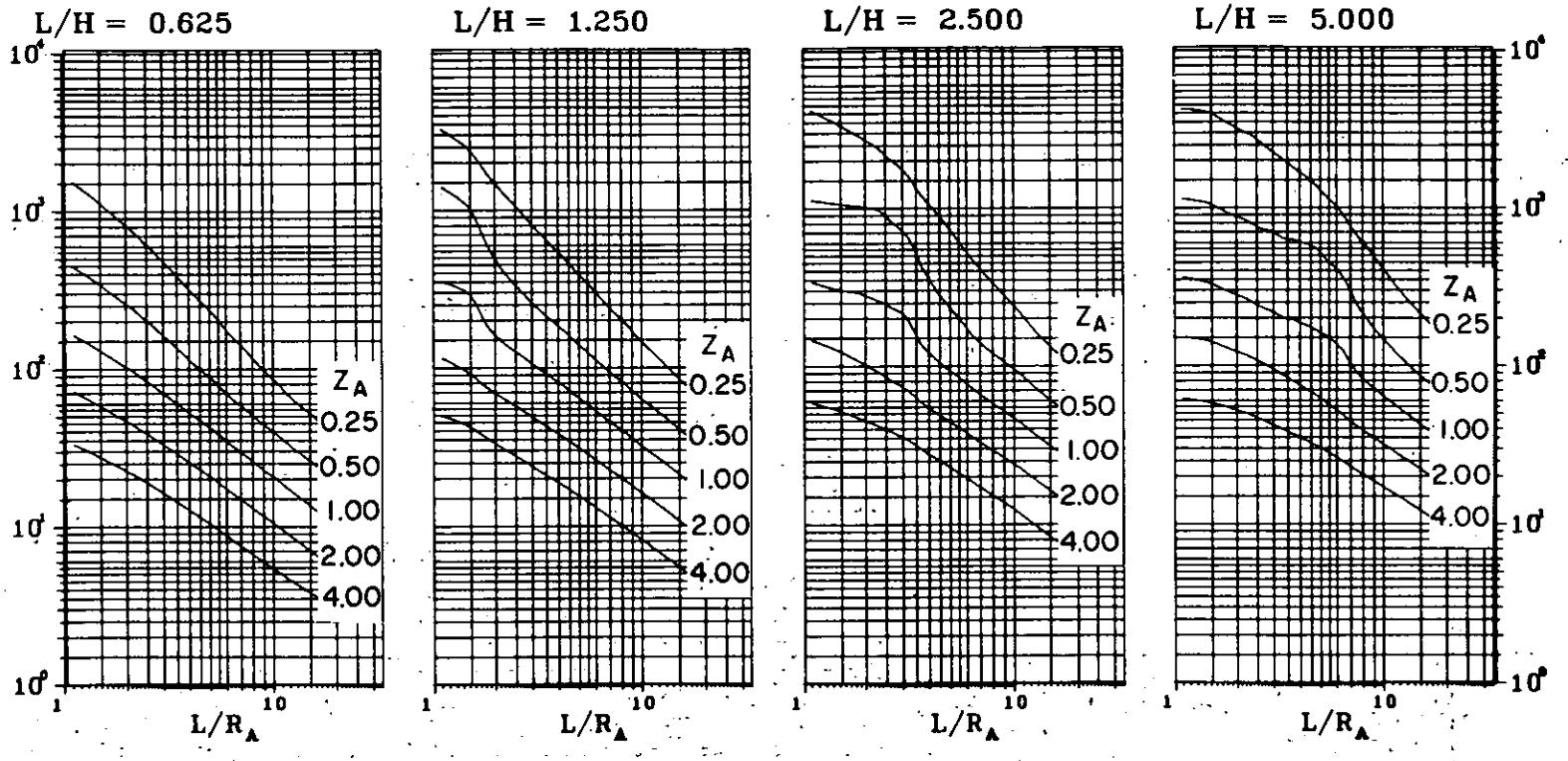


Figure 2-112 Scaled average unit reflected impulse
(N = 1, ℓ/L = 0.50, h/H = 0.75)

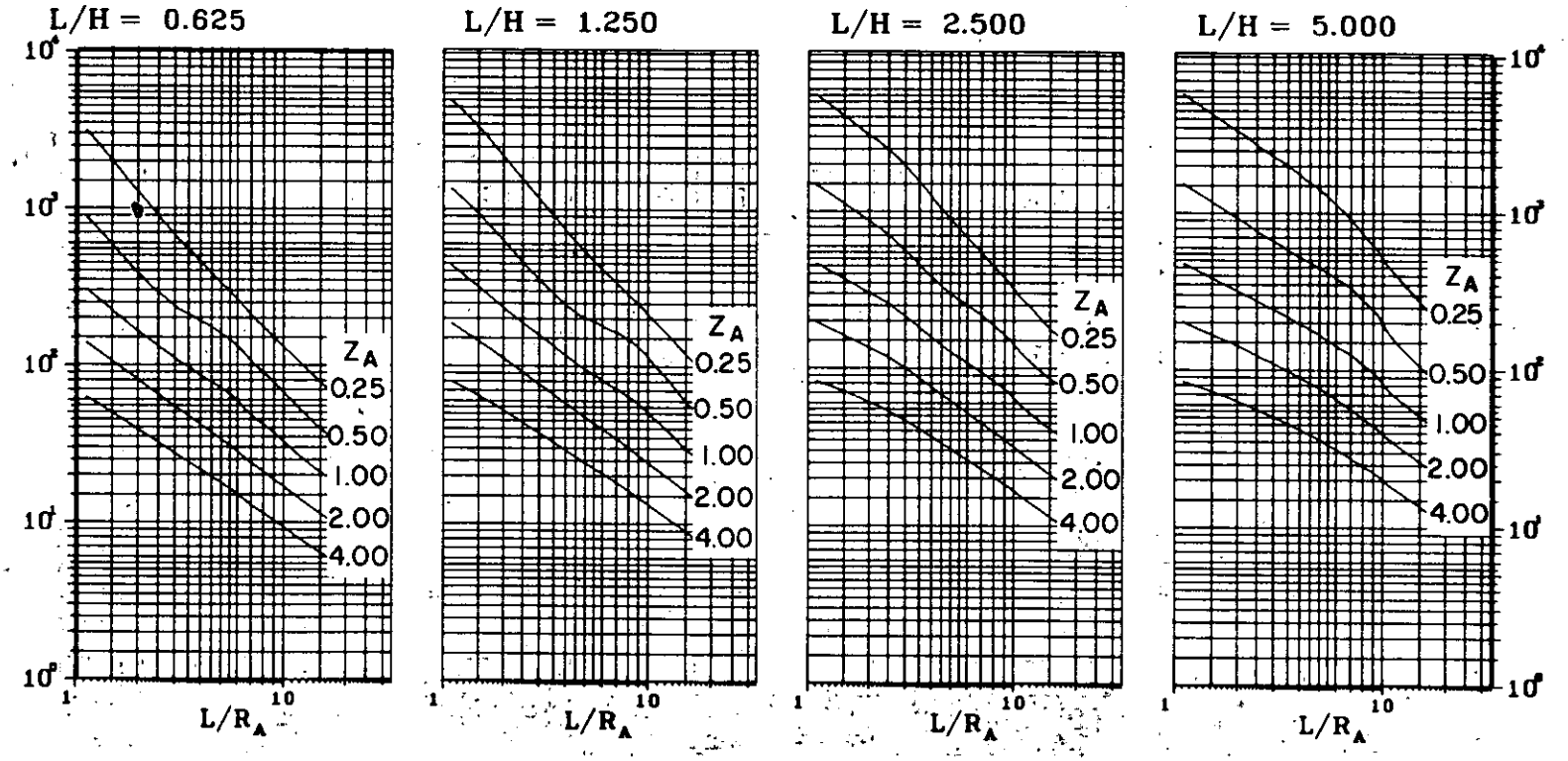


Figure 2-113 Scaled average unit reflected impulse
(N = 2, ℓ/L = 0.10, h/H = 0.10)

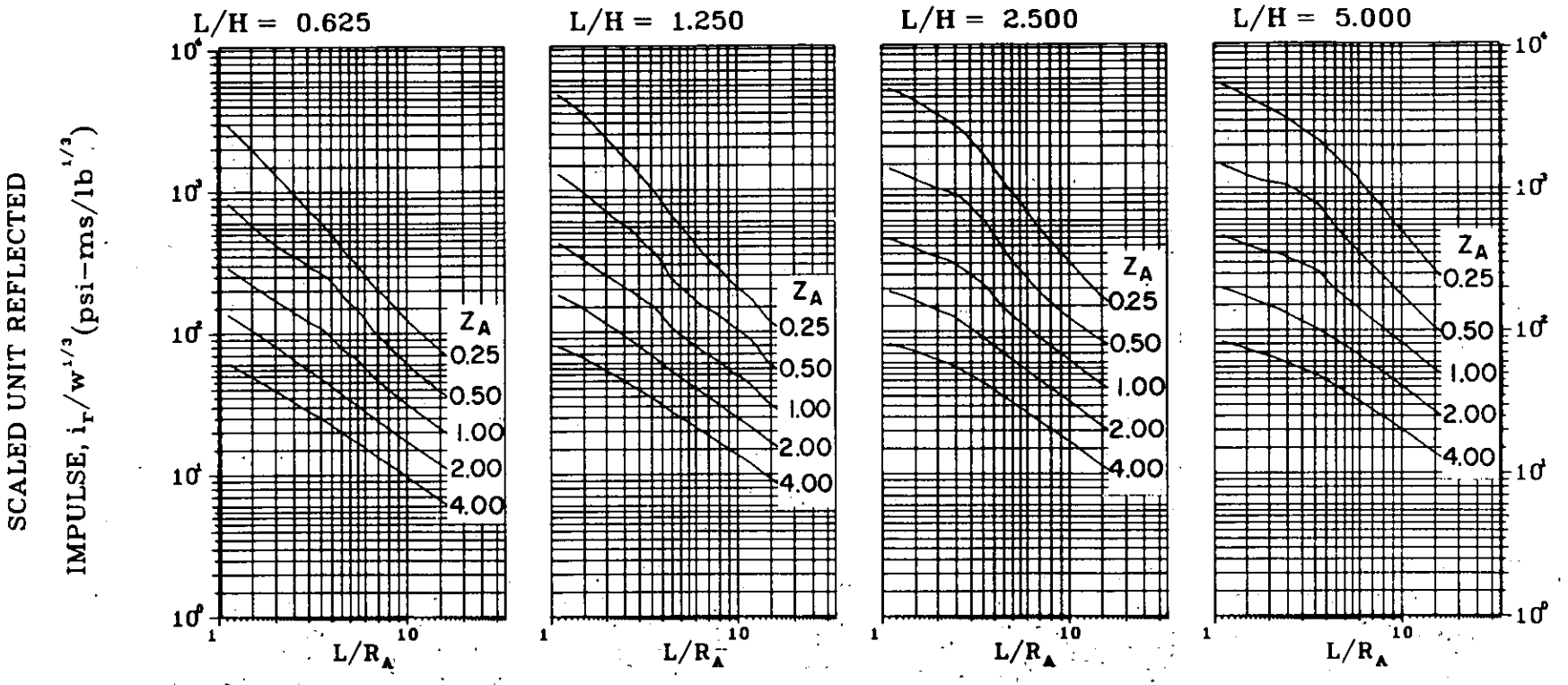


Figure 2-114 Scaled average unit reflected impulse
(N = 2, ℓ/L = 0.25, h/H = 0.10)

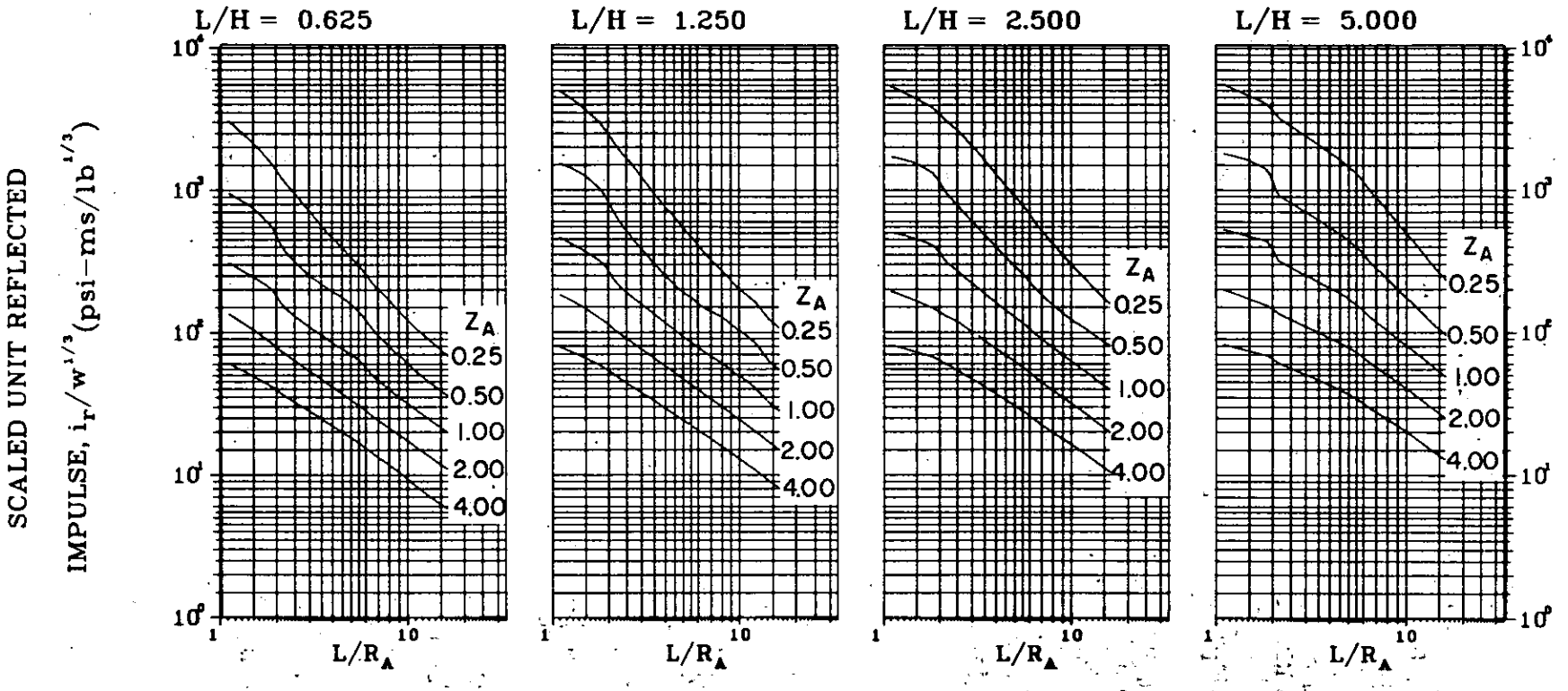


Figure 2-115 Scaled average unit reflected impulse
(N = 2, ℓ/L = 0.50, h/H = 0.10)

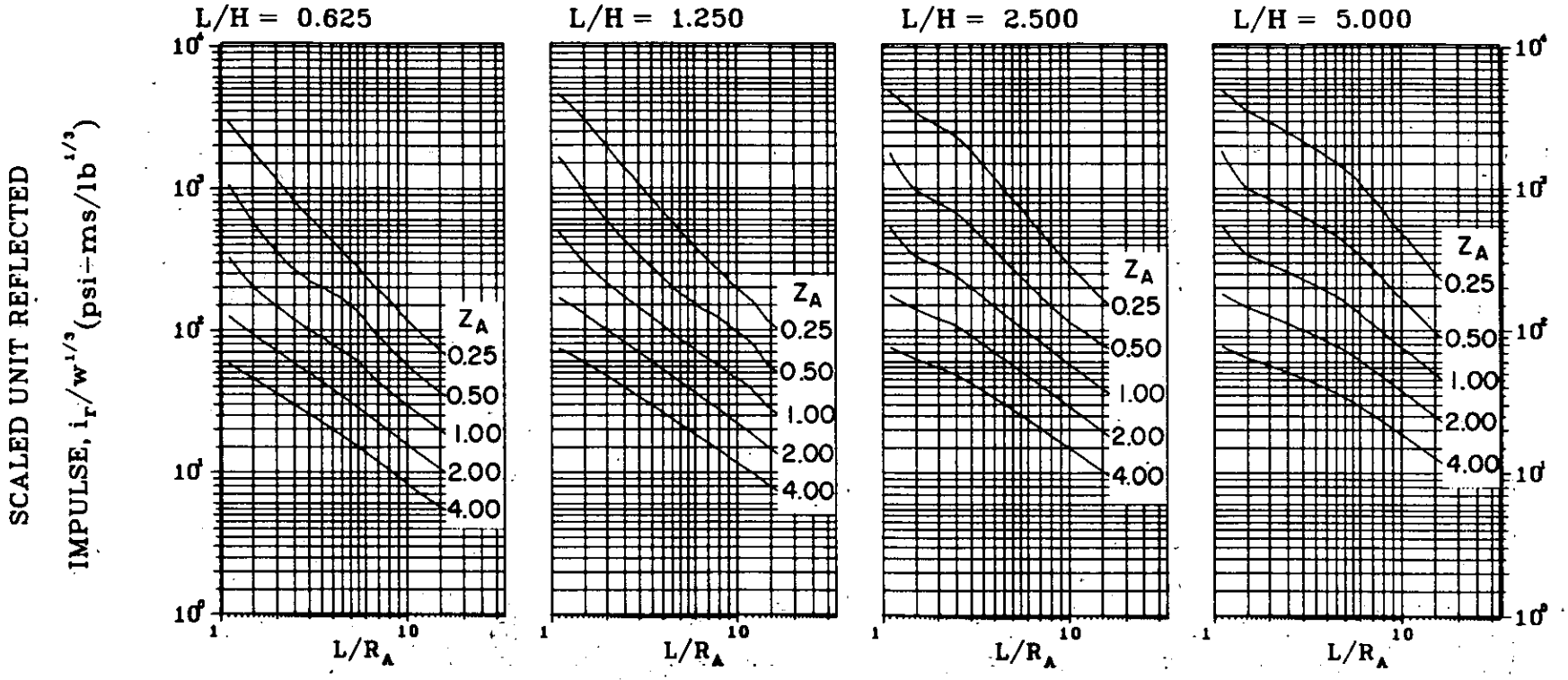
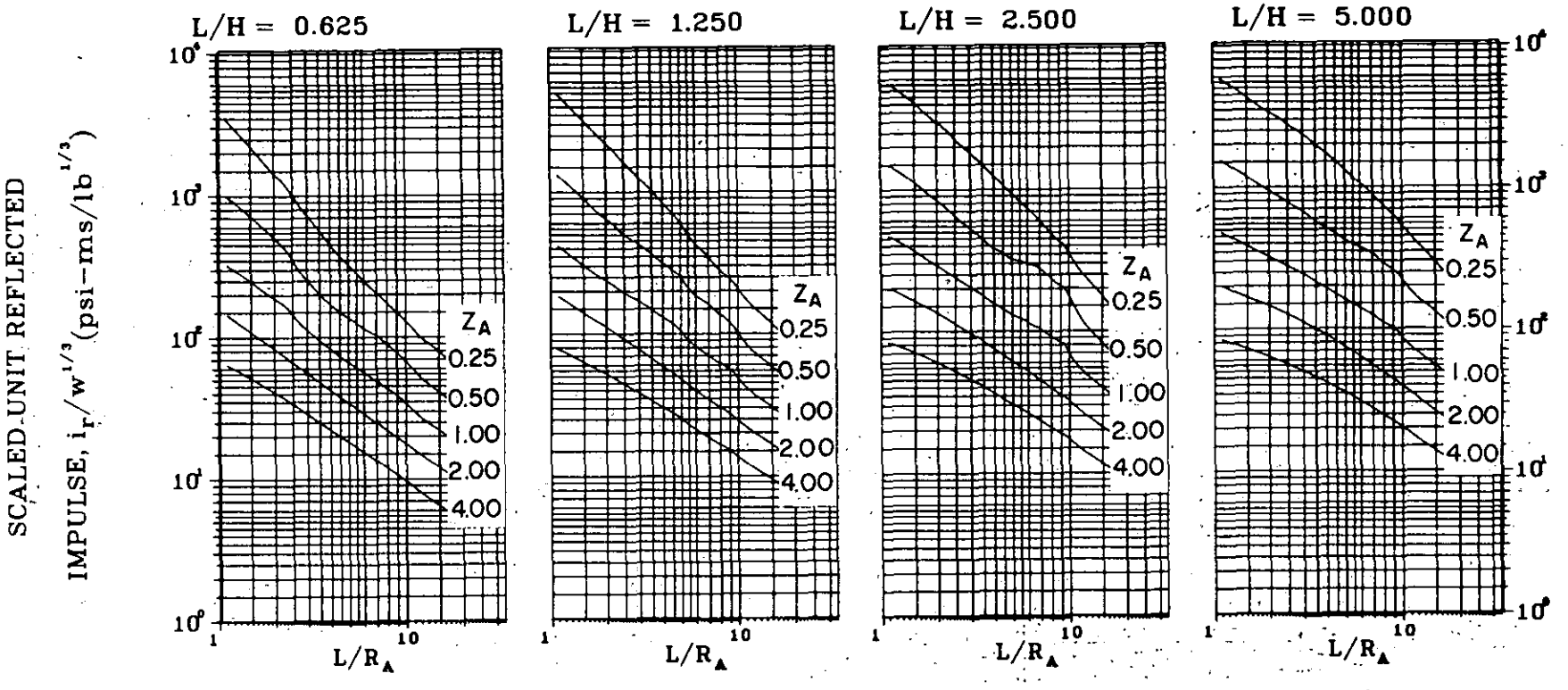


Figure 2-116 Scaled average unit reflected impulse
(N = 2, ℓ /L = 0.75, h/H = 0.10)



17A

Figure 2-117 Scaled average unit reflected impulse
(N = 2, ℓ/L = 0.10, h/H = 0.25)

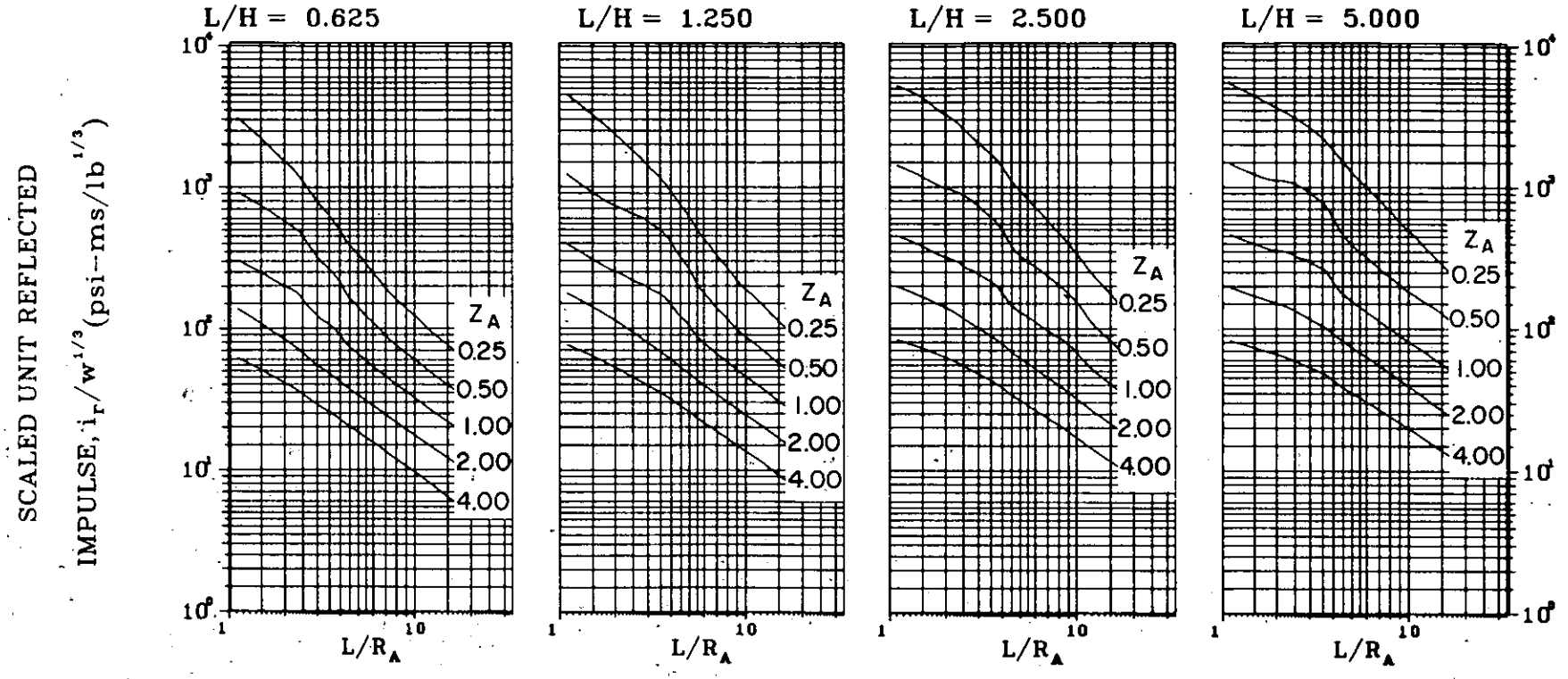


Figure 2-118 Scaled average unit reflected impulse
(N = 2. ℓ/L = 0.25. h/H = 0.25)

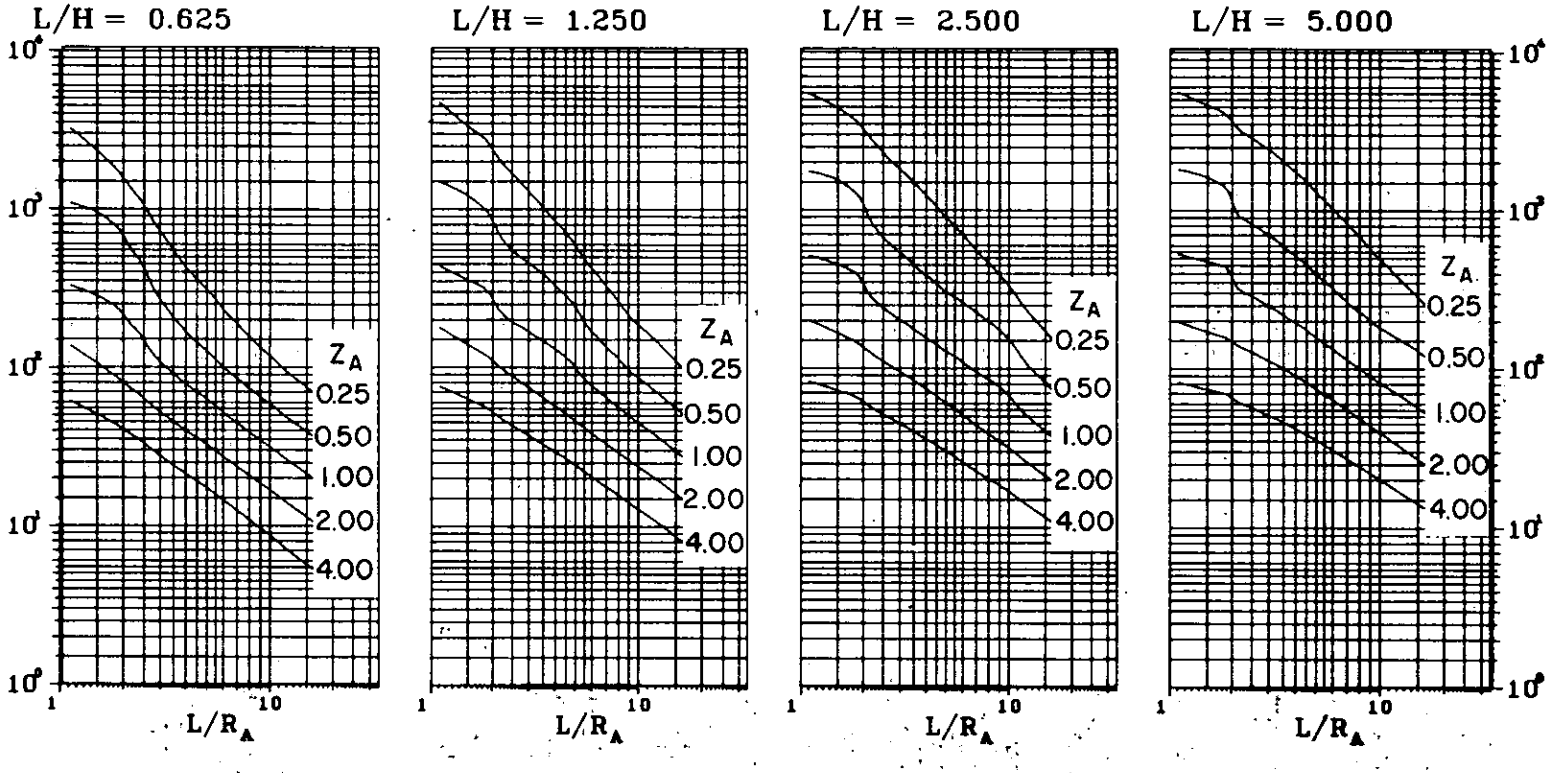


Figure 2-119 Scaled average unit reflected impulse
(N = 2, ℓ/L = 0.50, h/H = 0.25)

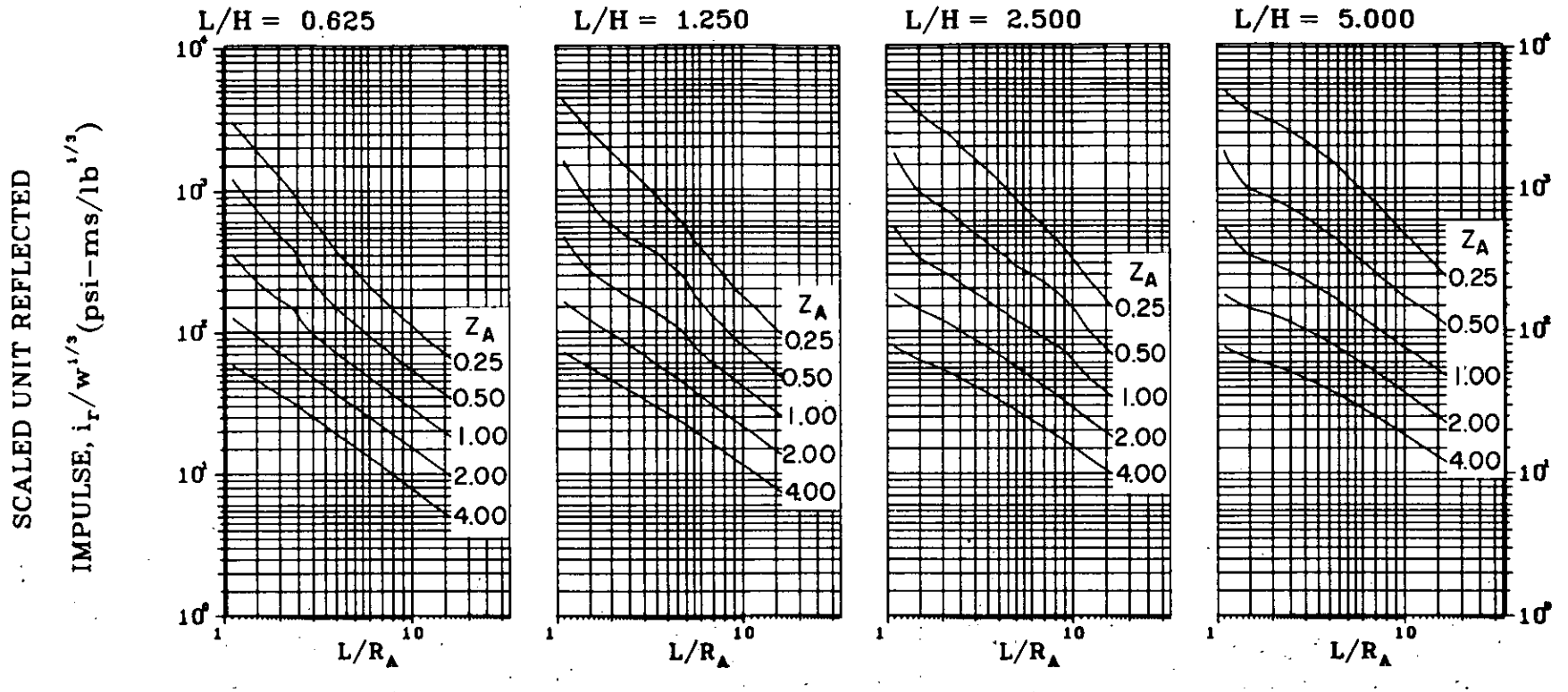


Figure 2-120 Scaled average unit reflected impulse
(N = 2, ℓ/L = 0.75, h/H = 0.25)

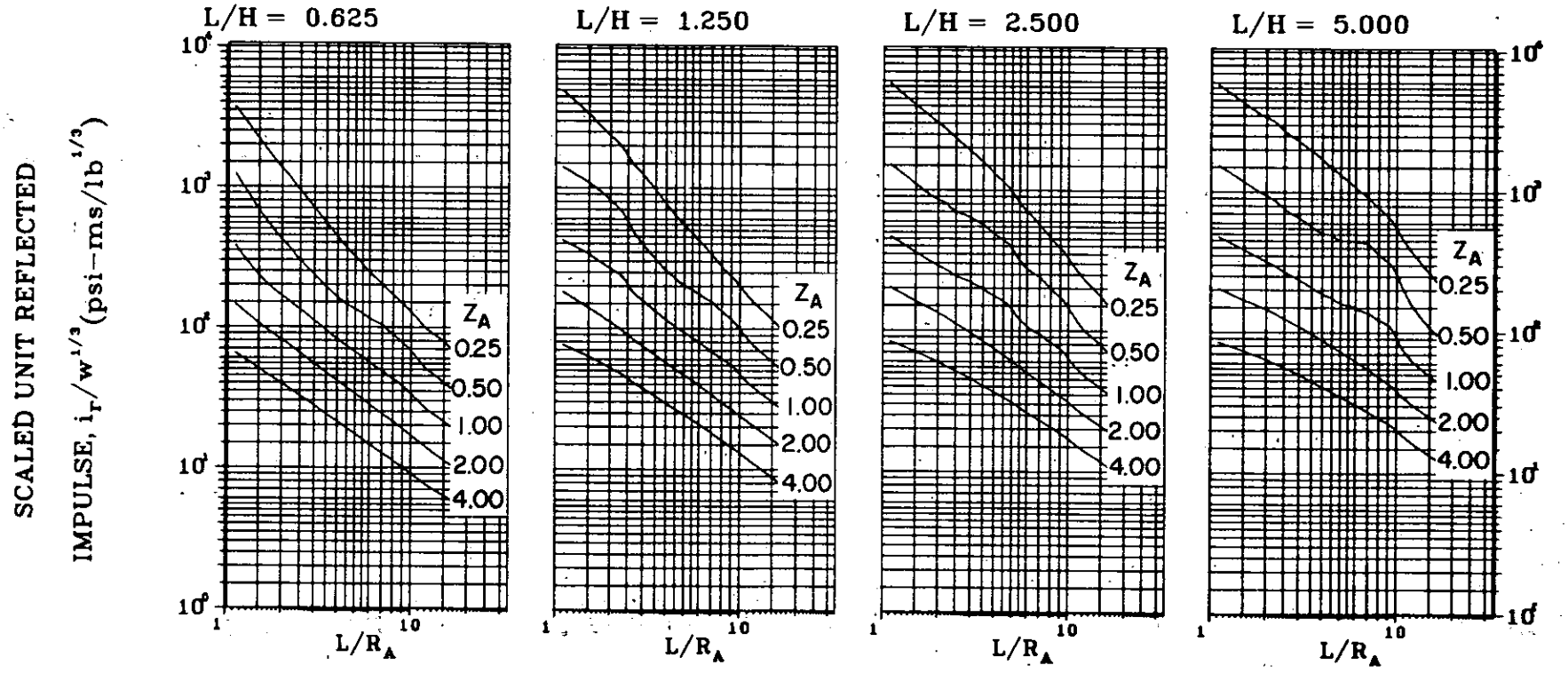


Figure 2-121 Scaled average unit reflected impulse
(N = 2, ℓ/L = 0.10, h/H = 0.50)

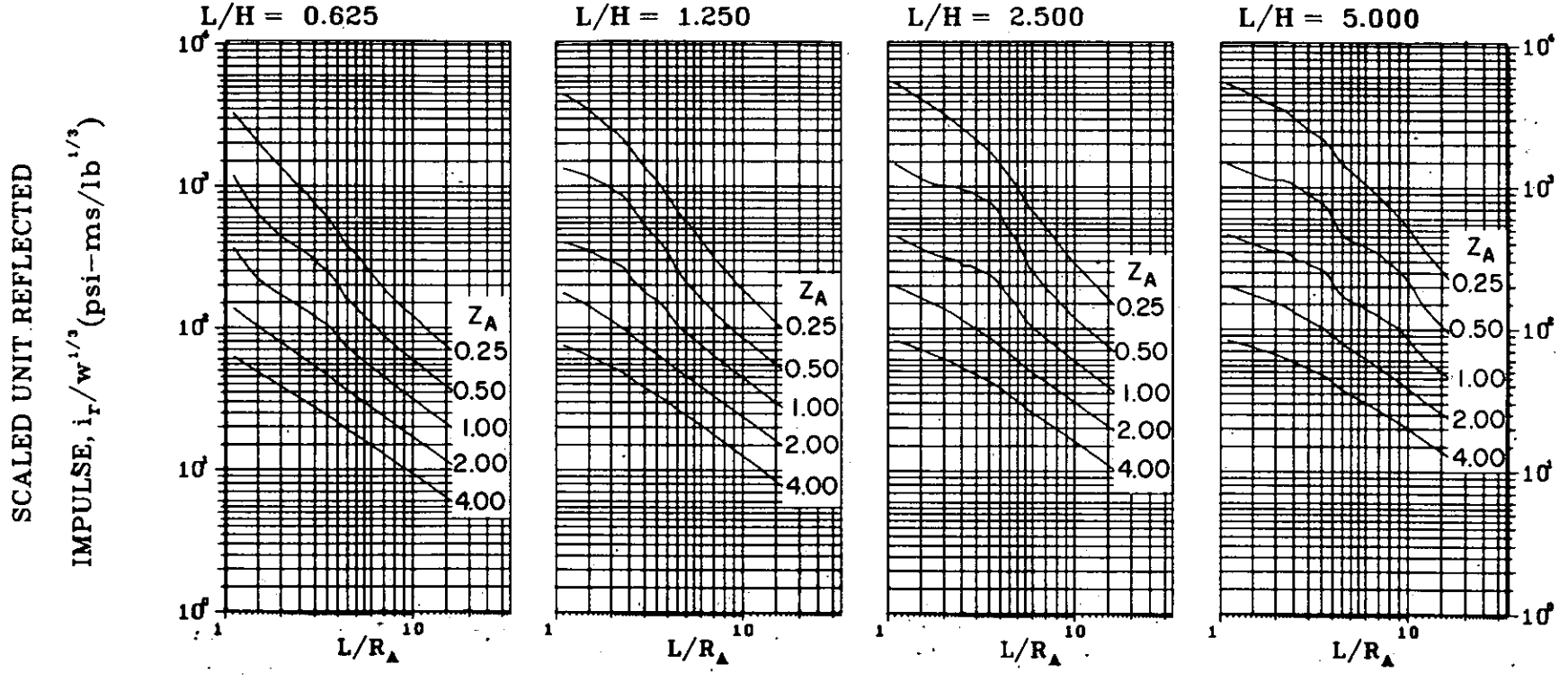


Figure 2-122 Scaled average unit reflected impulse
(N = 2, ℓ/L = 0.25, h/H = 0.50)

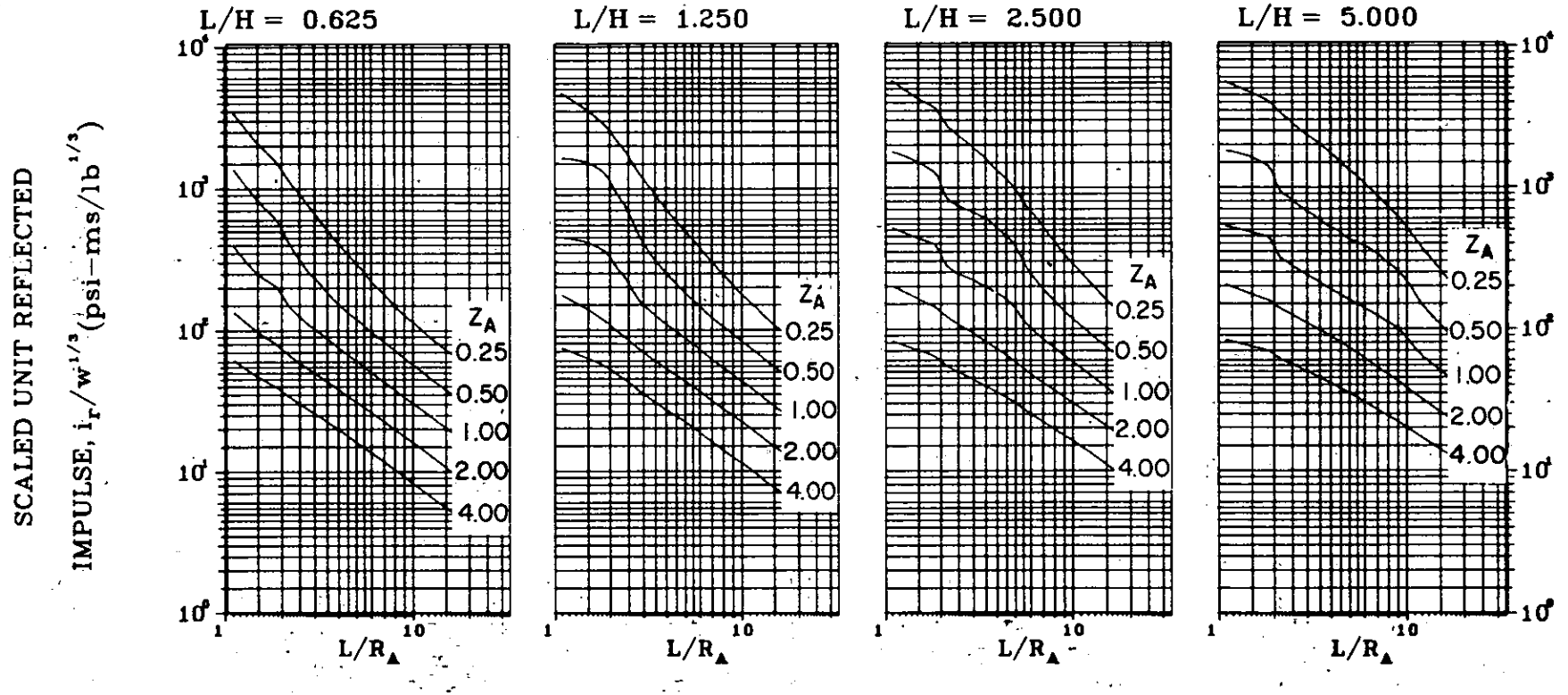


Figure 2-123 Scaled average unit reflected impulse
(N = 2, ℓ/L = 0.50, h/H = 0.50)

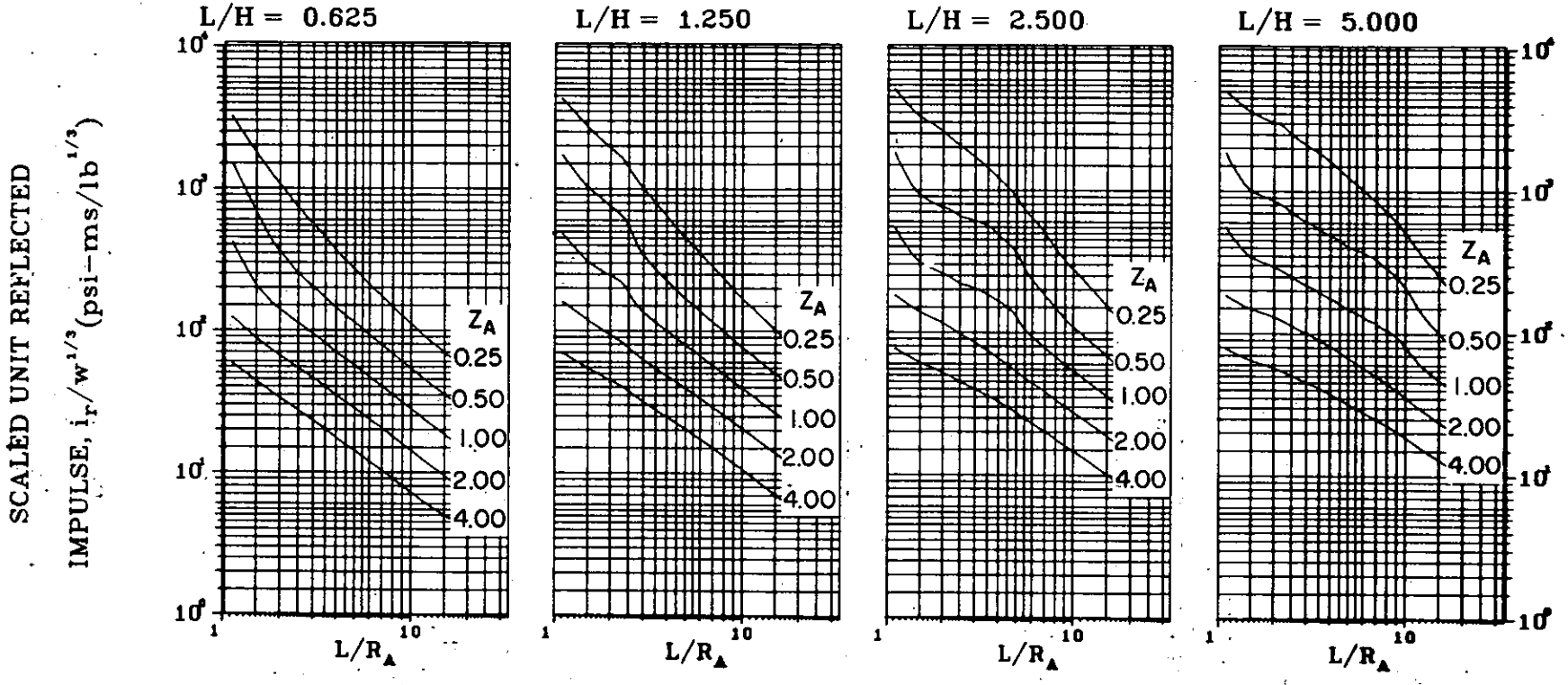


Figure 2-124 Scaled average unit reflected impulse
(N = 2, ℓ/L = 0.75, h/H = 0.50)

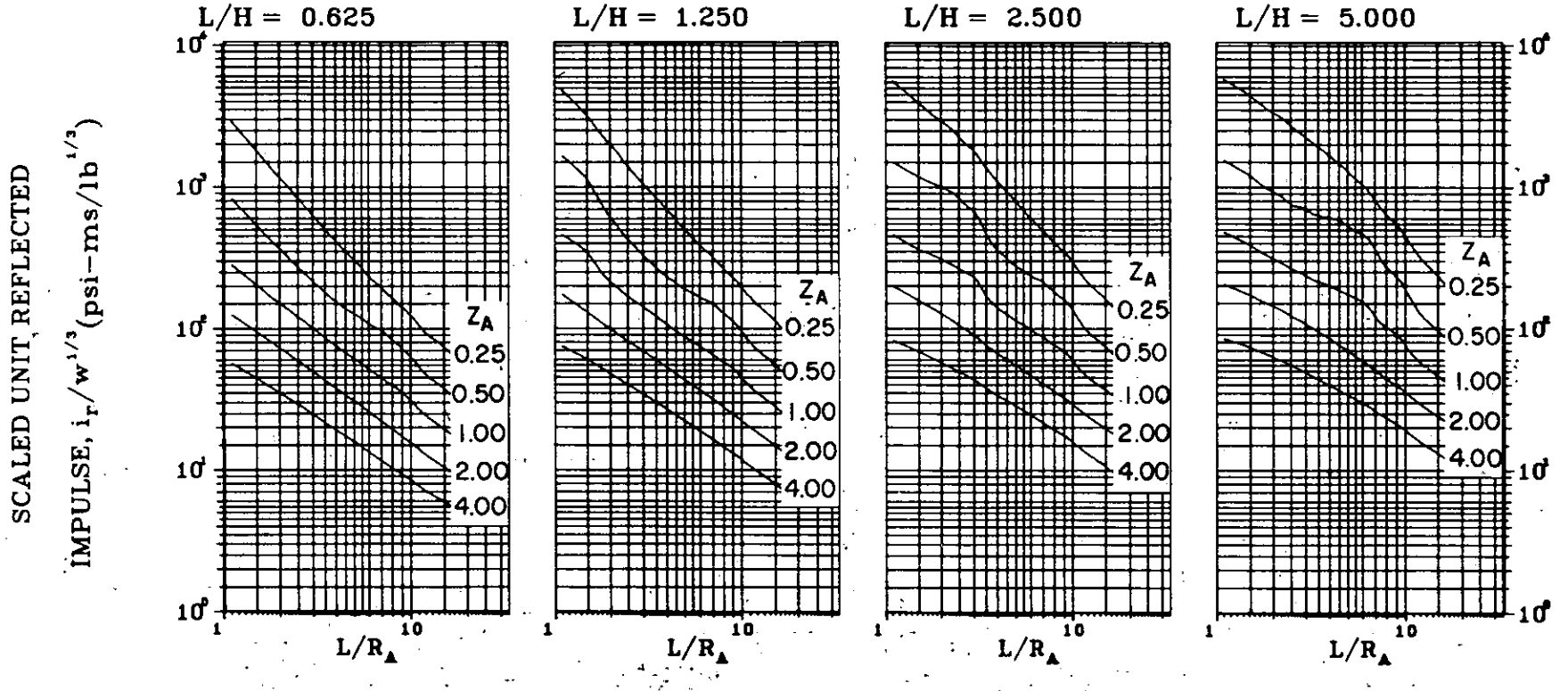


Figure 2-125 Scaled average unit reflected impulse
(N = 2, ℓ/L = 0.10, h/H = 0.75)

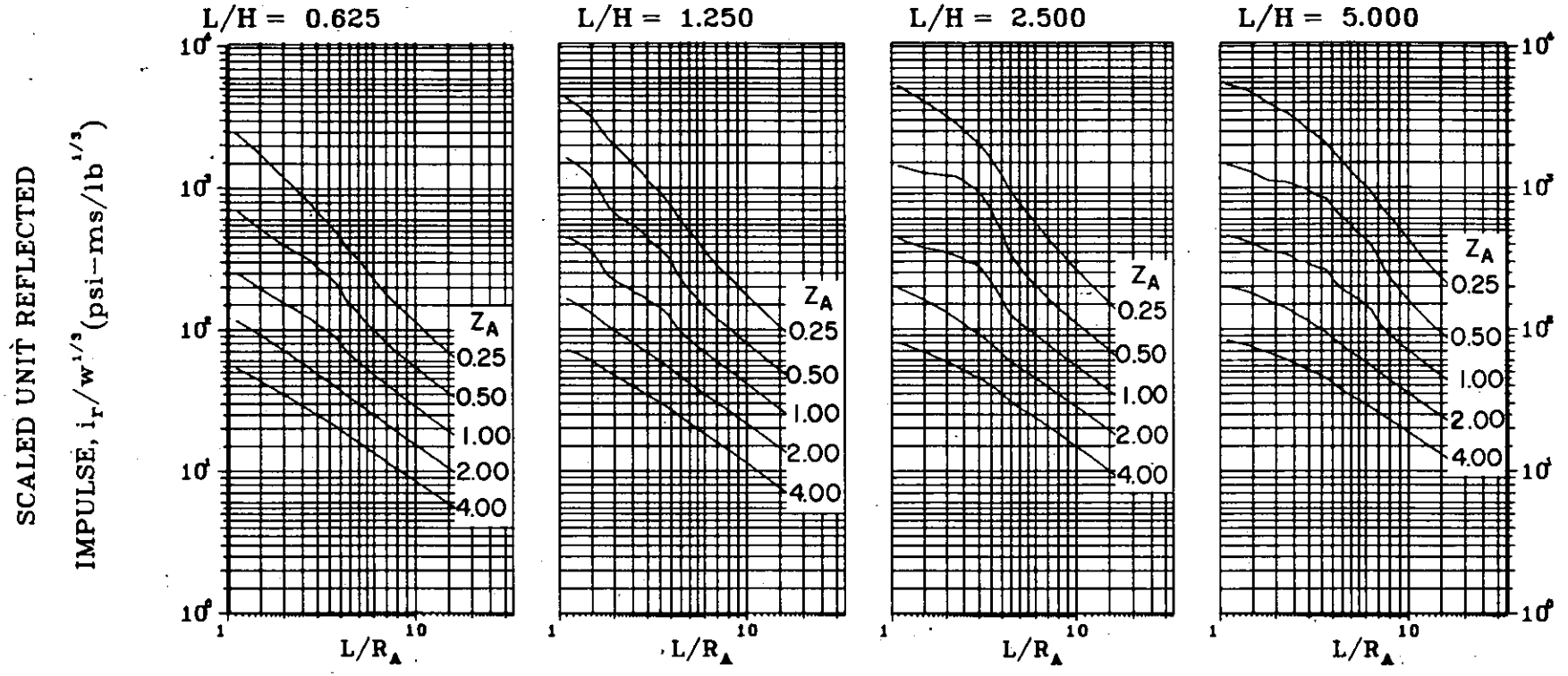


Figure 2-126 Scaled average unit reflected impulse
(N = 2, ℓ/L = 0.25, h/H = 0.75)

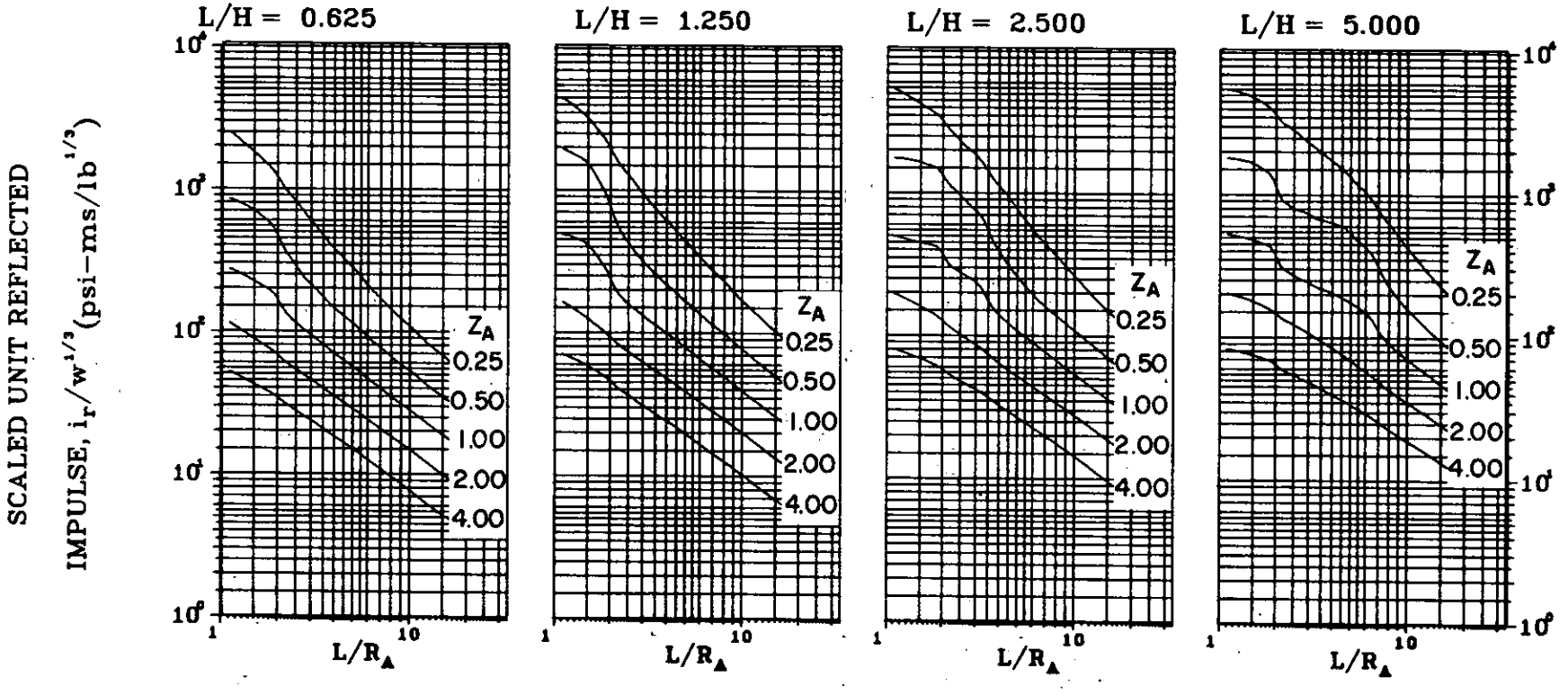


Figure 2-127 Scaled average unit reflected impulse
(N = 2, ℓ/L = 0.50, h/H = 0.75)

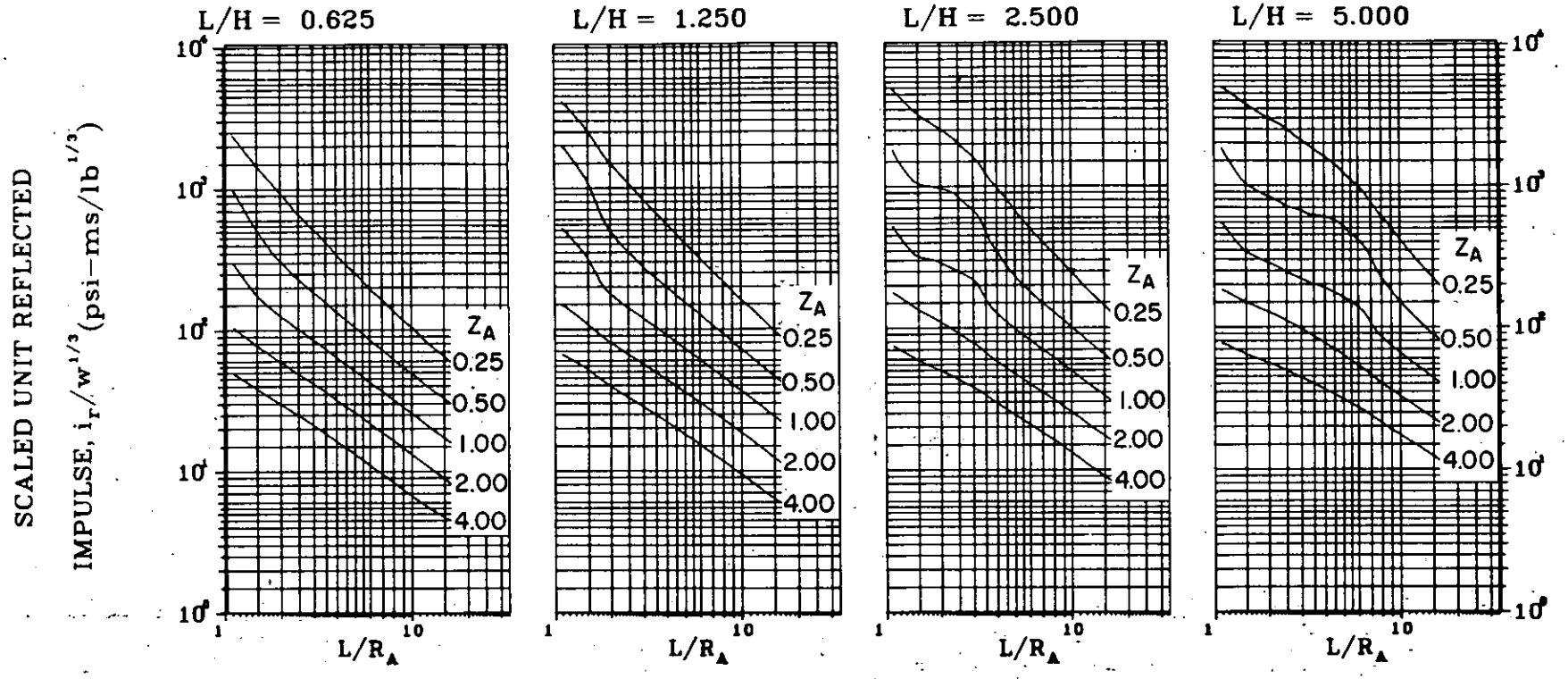


Figure 2-128 Scaled average unit reflected impulse
(N = 2, ℓ /L = 0.75, h/H = 0.75)

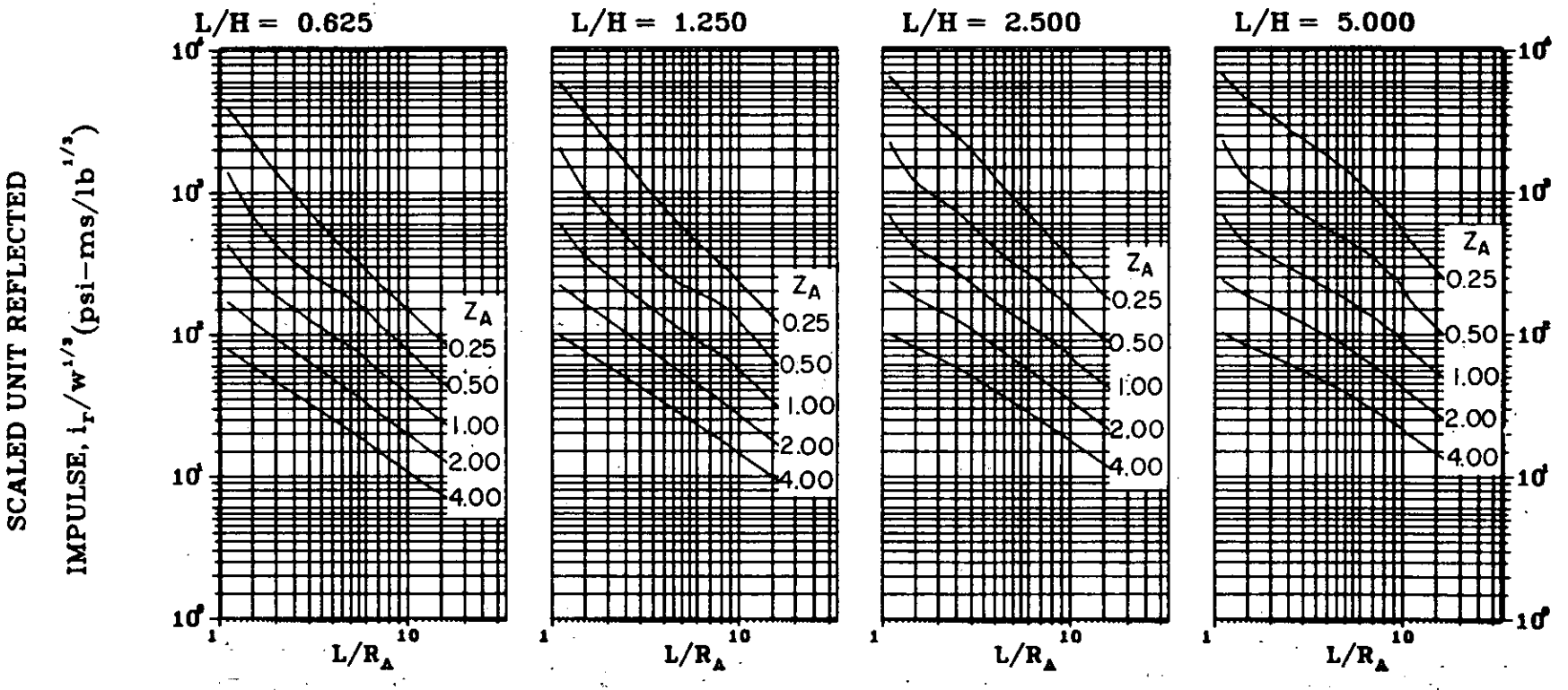


Figure 2-129 Scaled average unit reflected impulse

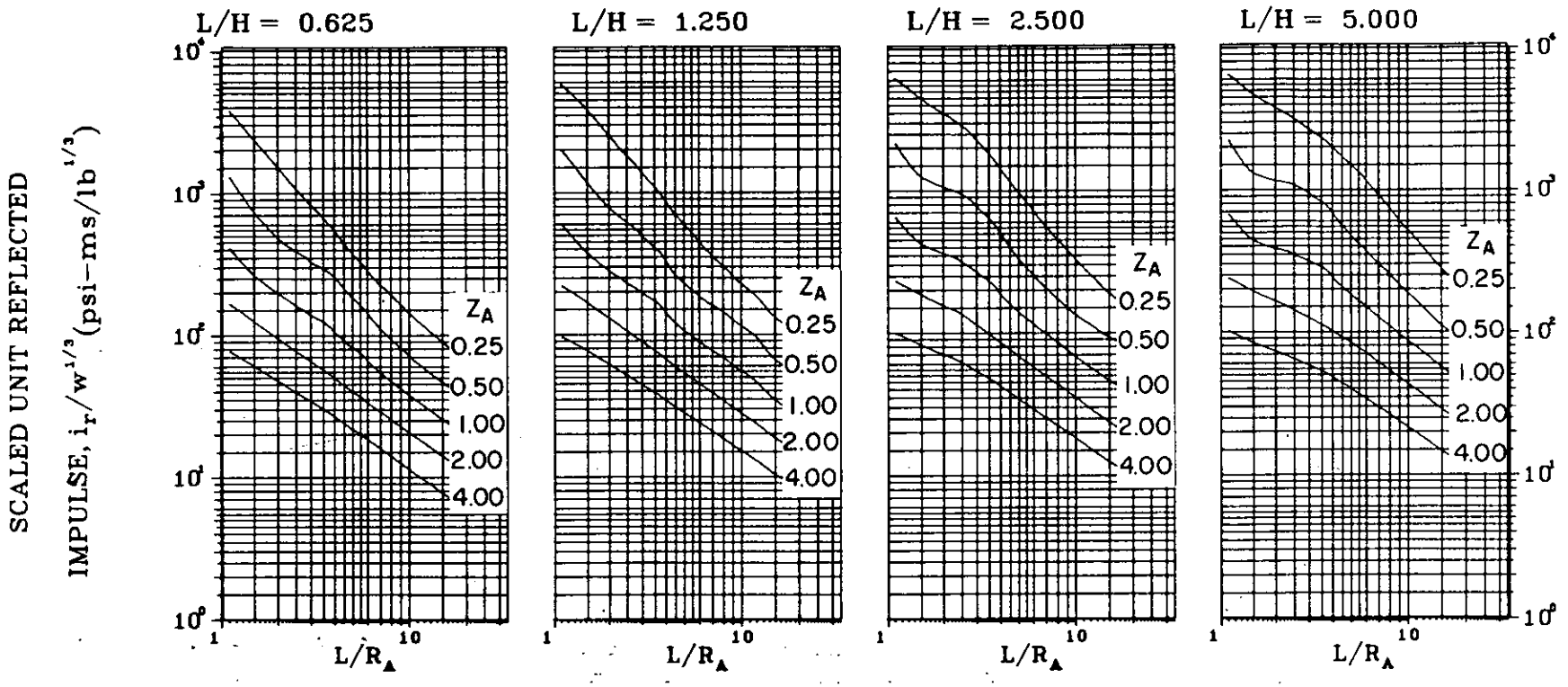


Figure 2-130 Scaled average unit reflected impulse
(N = 3, ℓ/L = 0.25 and 0.75, h/H = 0.10)

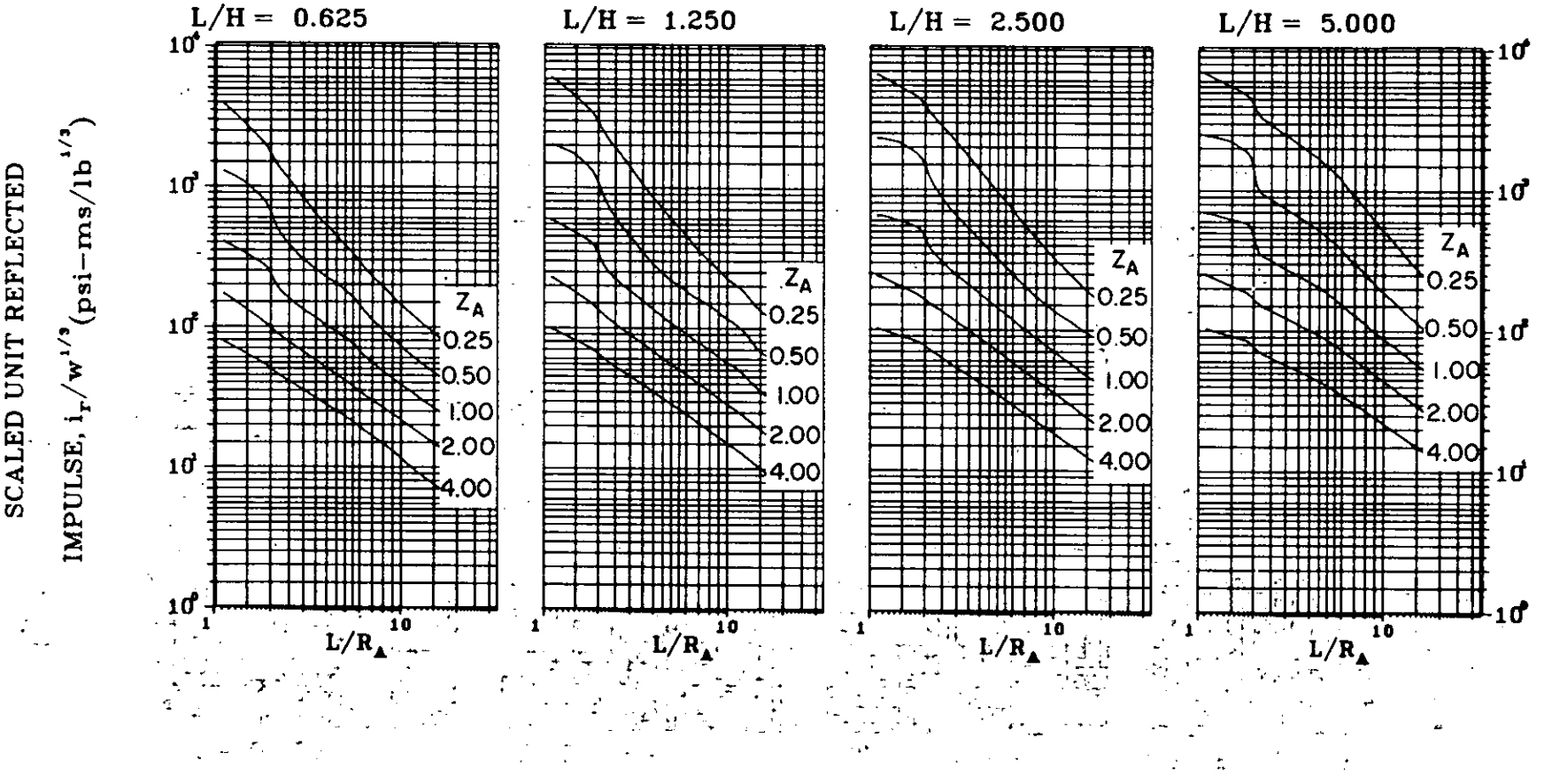


Figure 2-131 Scaled average unit reflected impulse
(N = 3, ℓ/L = 0.50, h/H = 0.10)

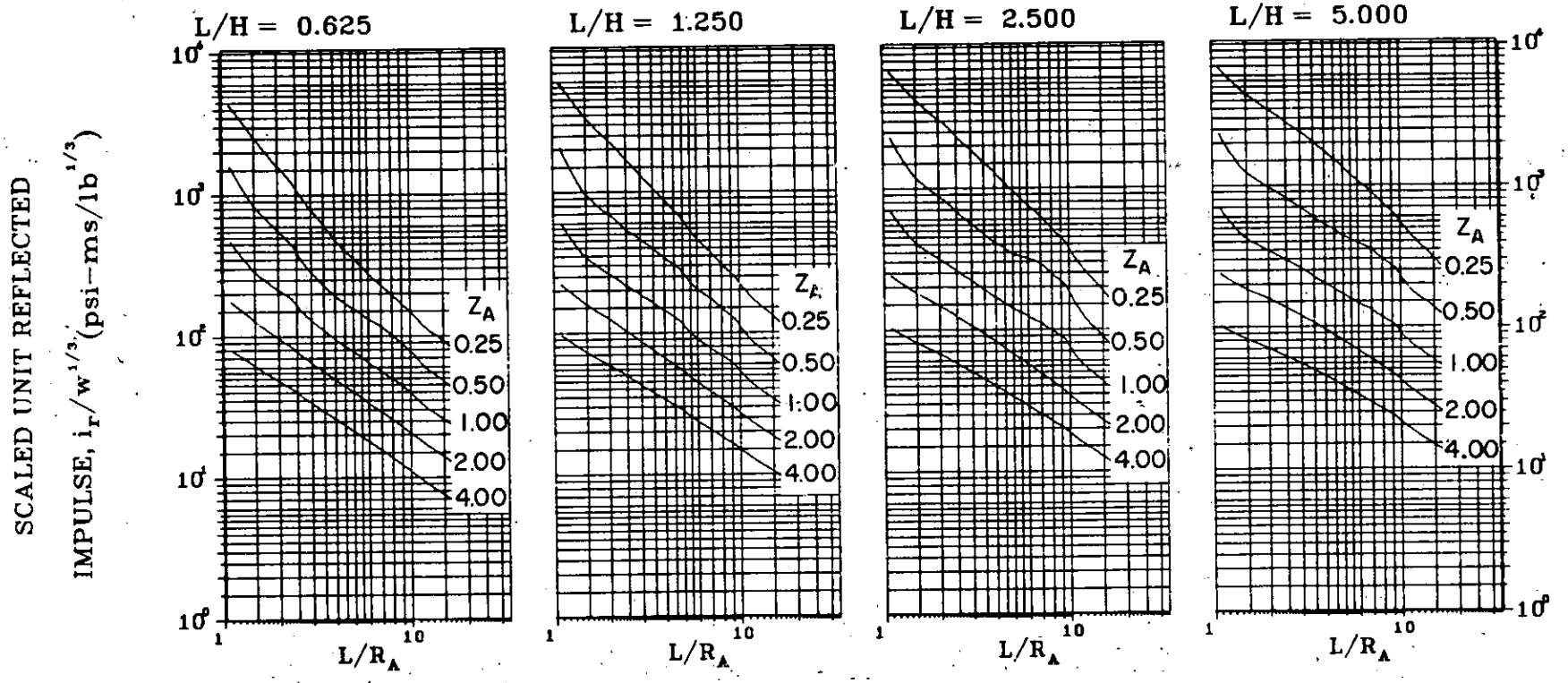


Figure 2-132 Scaled average unit reflected impulse
(N = 3, ℓ/L = 0.10, h/H = 0.25)

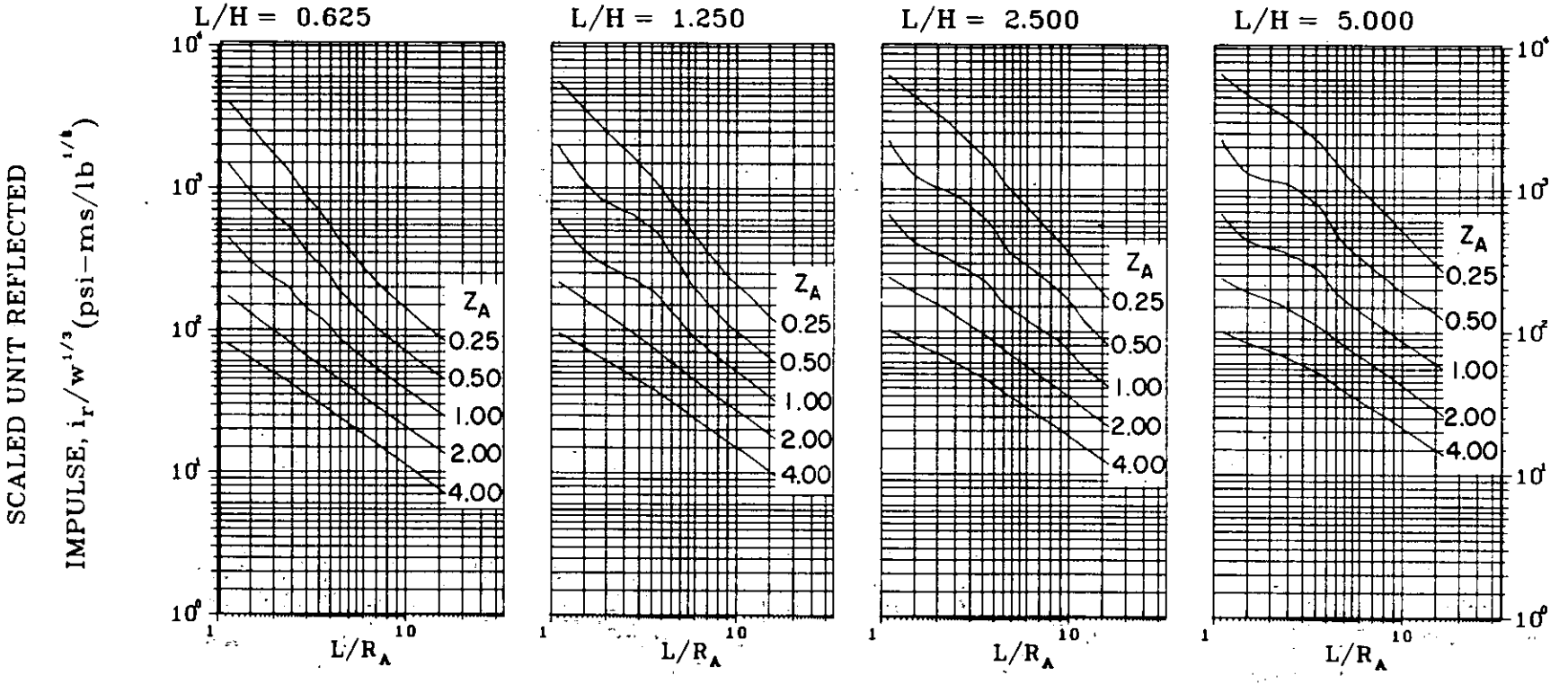


Figure 2-133 Scaled average unit reflected impulse
(N = 3, ℓ/L = 0.25 and 0.75, h/H = 0.25)

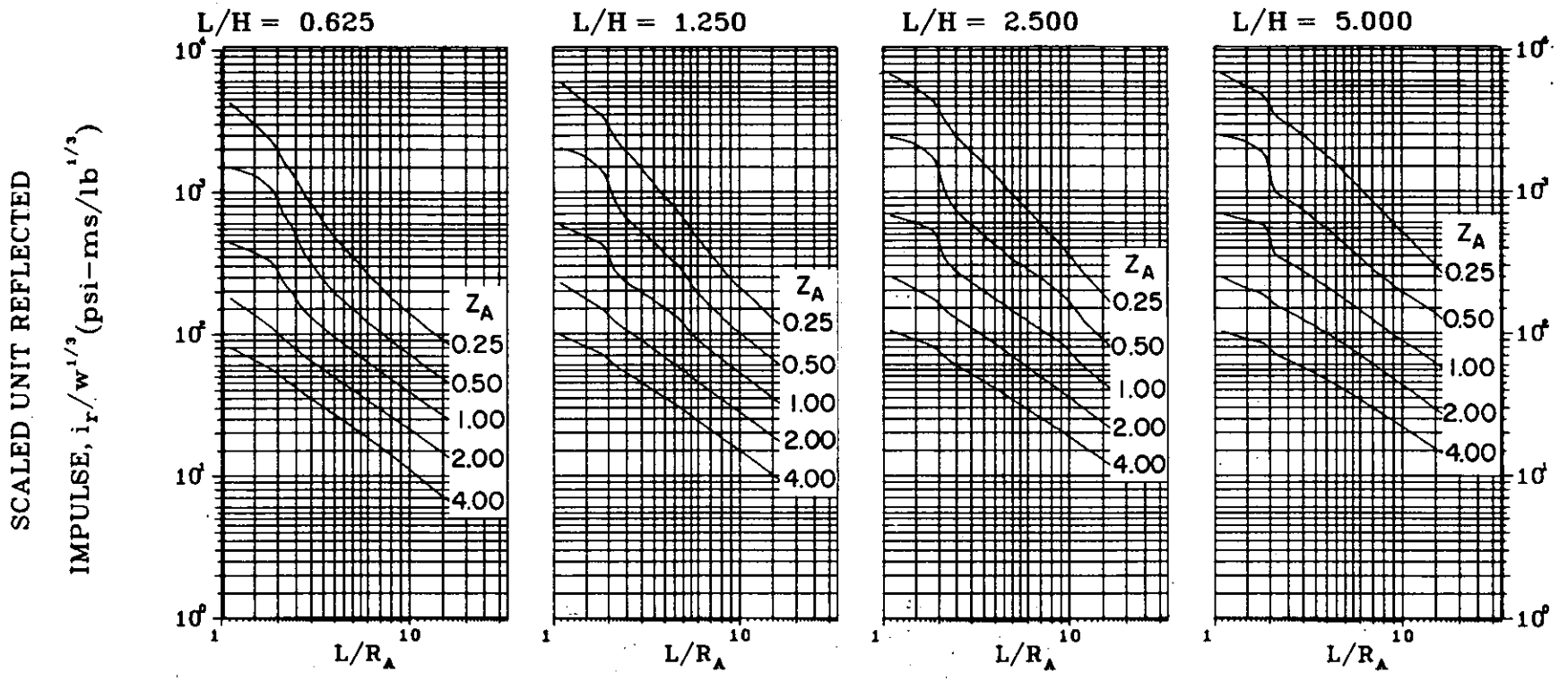


Figure 2-134 Scaled average unit reflected impulse
(N = 3, ℓ/L = 0.50, h/H = 0.25)

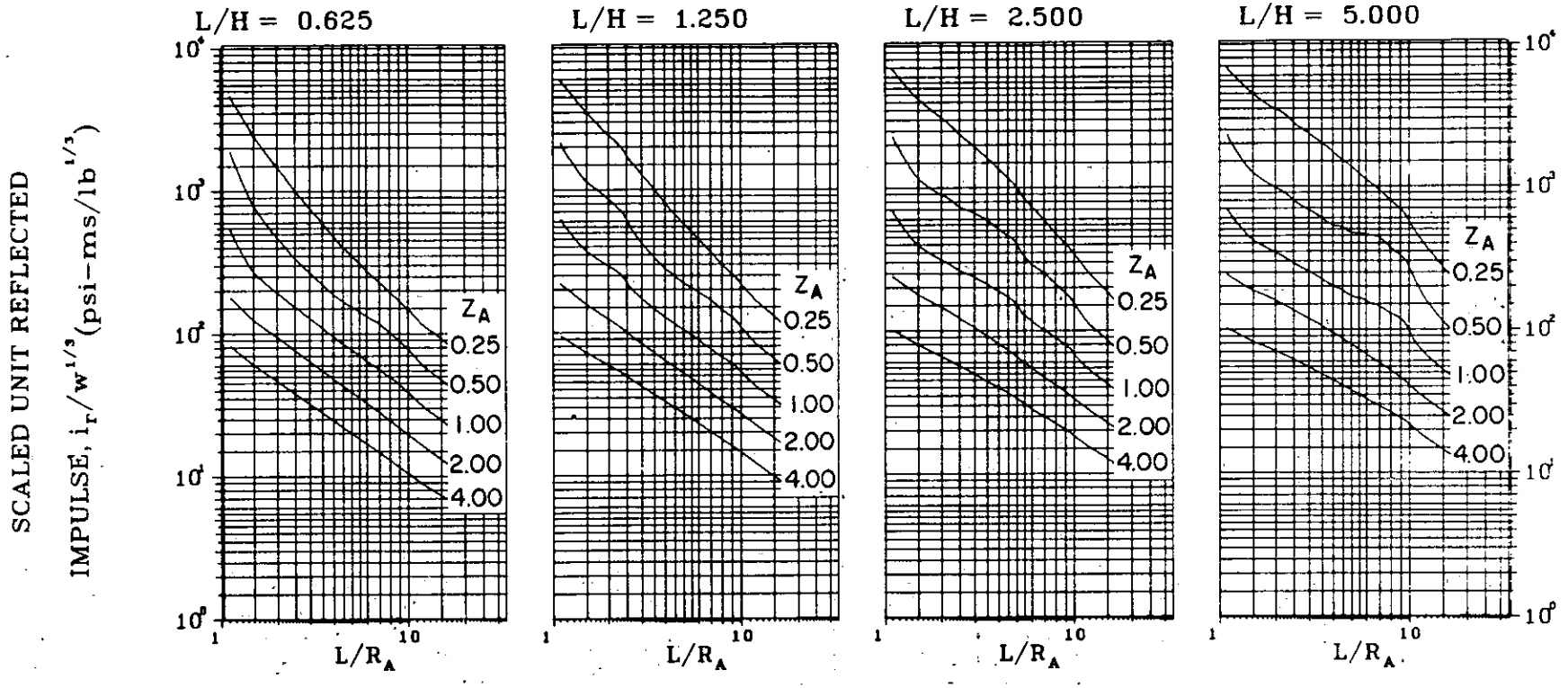


Figure 2-135 Scaled average unit reflected impulse
(N = 3, ℓ/L = 0.10, h/H = 0.50)

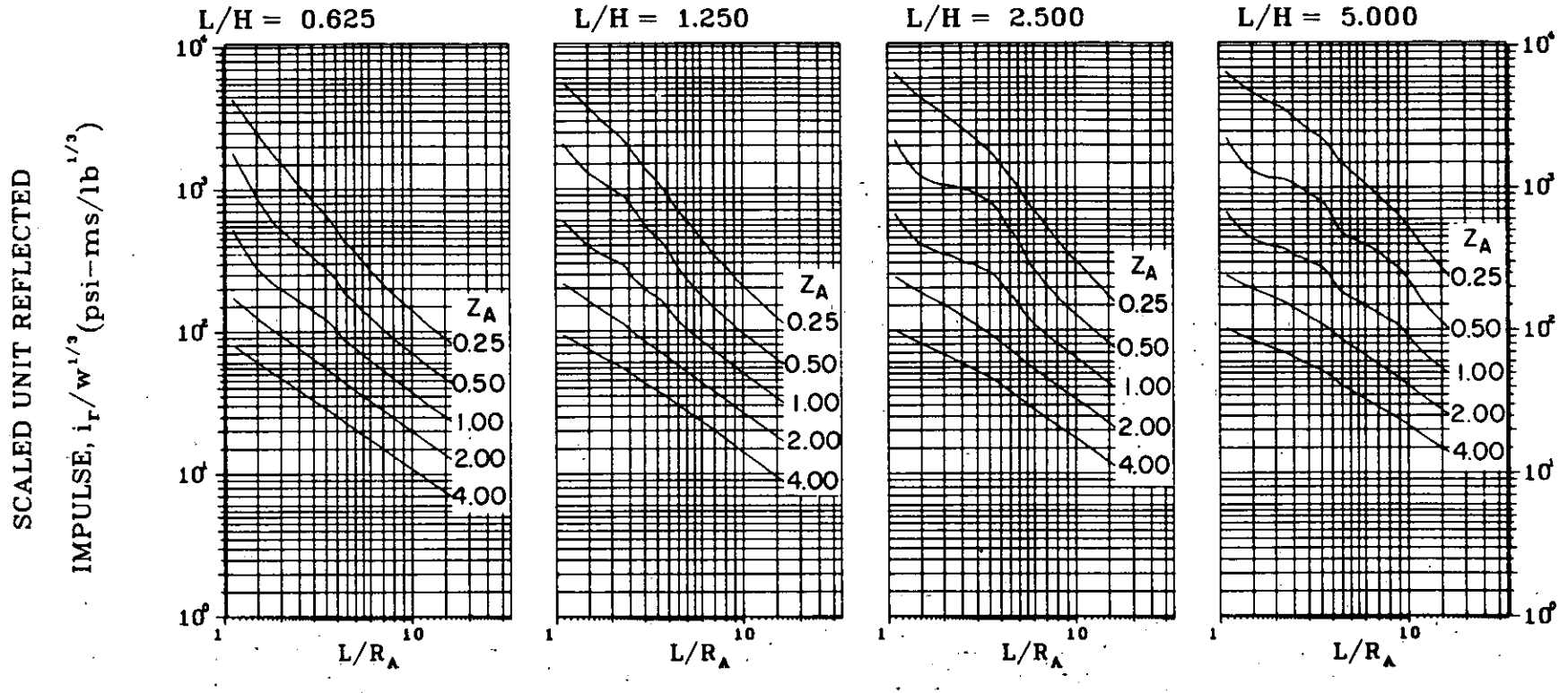


Figure 2-136 Scaled average unit reflected impulse
(N = 3, ℓ/L = 0.25 and 0.75, h/H = 0.50)

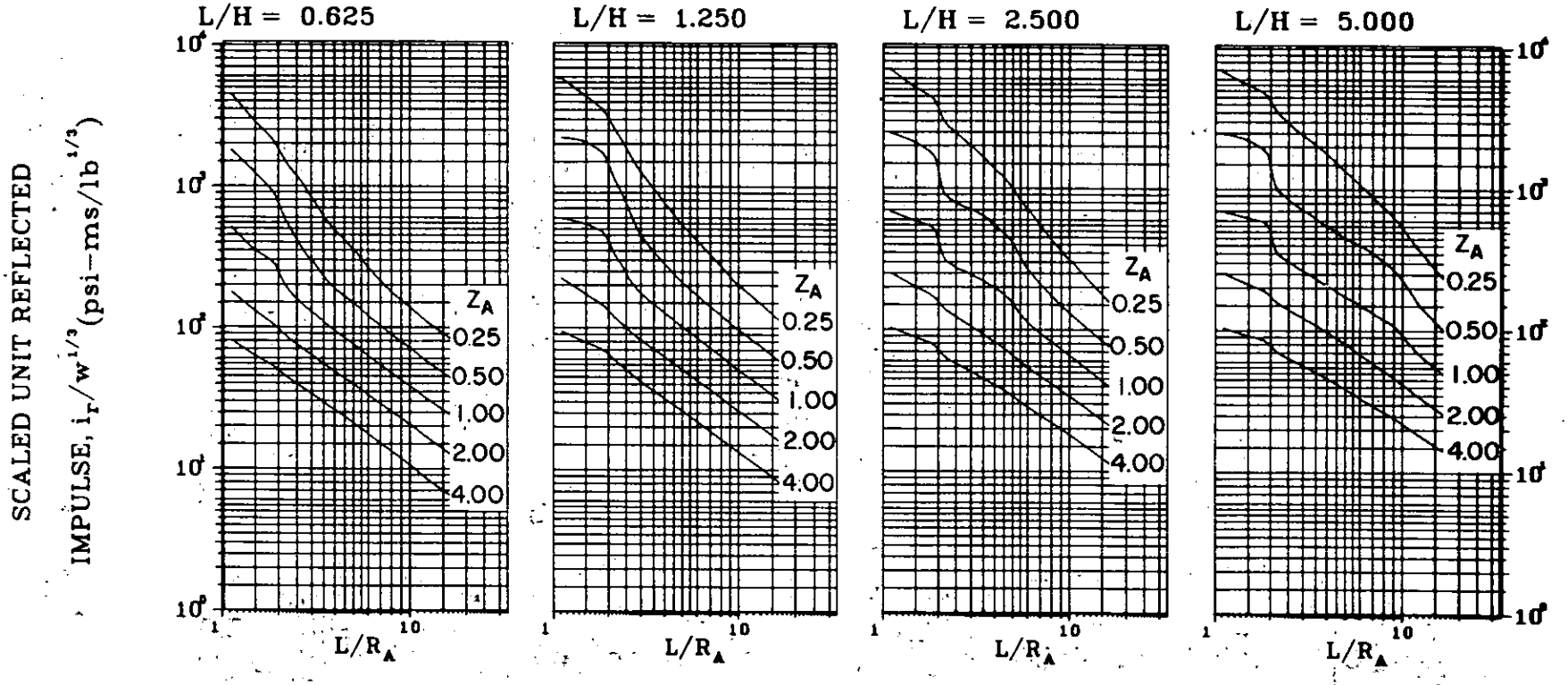


Figure 2-137 Scaled average unit reflected impulse
(N = 3, ℓ/L = 0.50, h/H = 0.50)

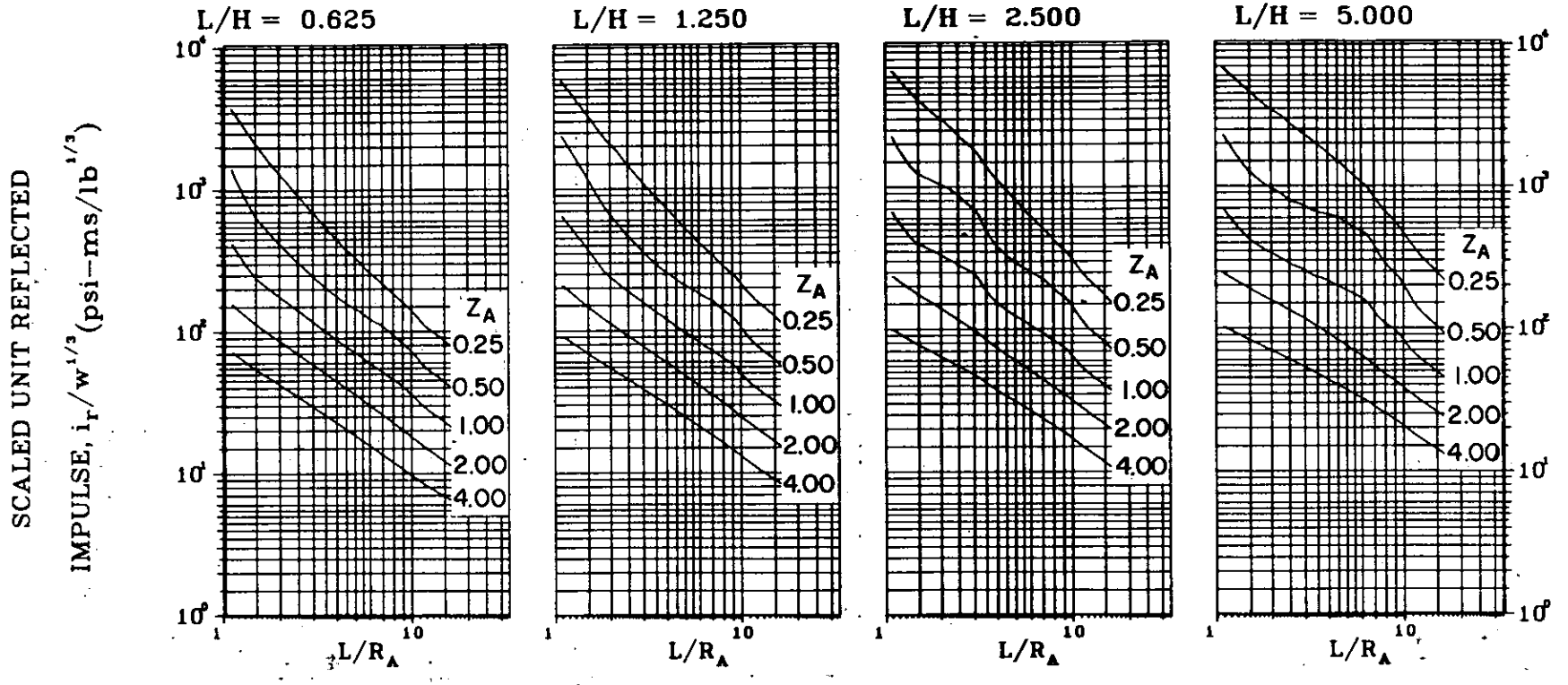


Figure 2-138 Scaled average unit reflected impulse
(N = 3, ℓ/L = 0.10, h/H = 0.75)

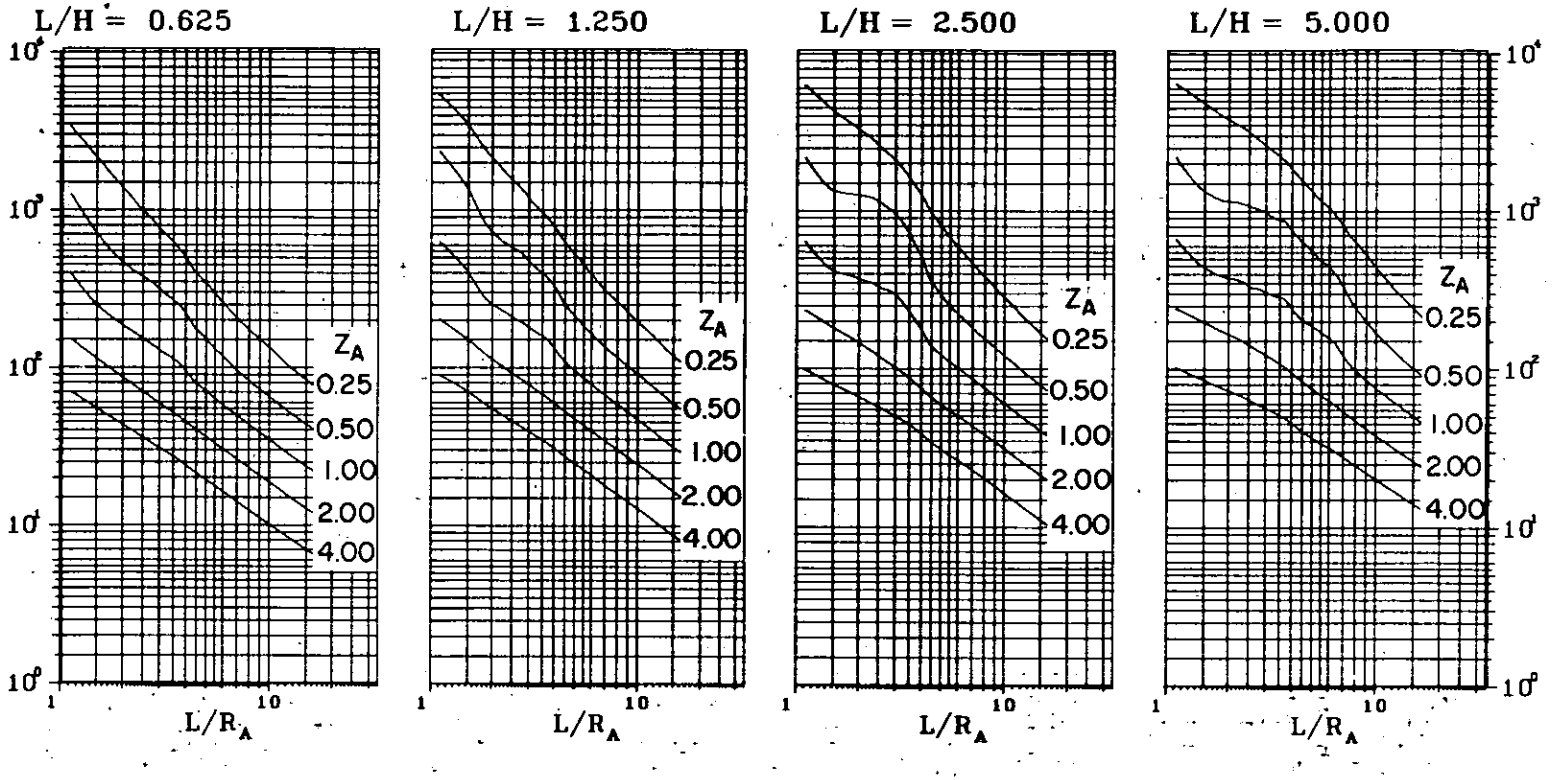


Figure 2-139 Scaled average unit reflected impulse
(N = 3, ℓ/L = 0.25 and 0.75, h/H = 0.75)

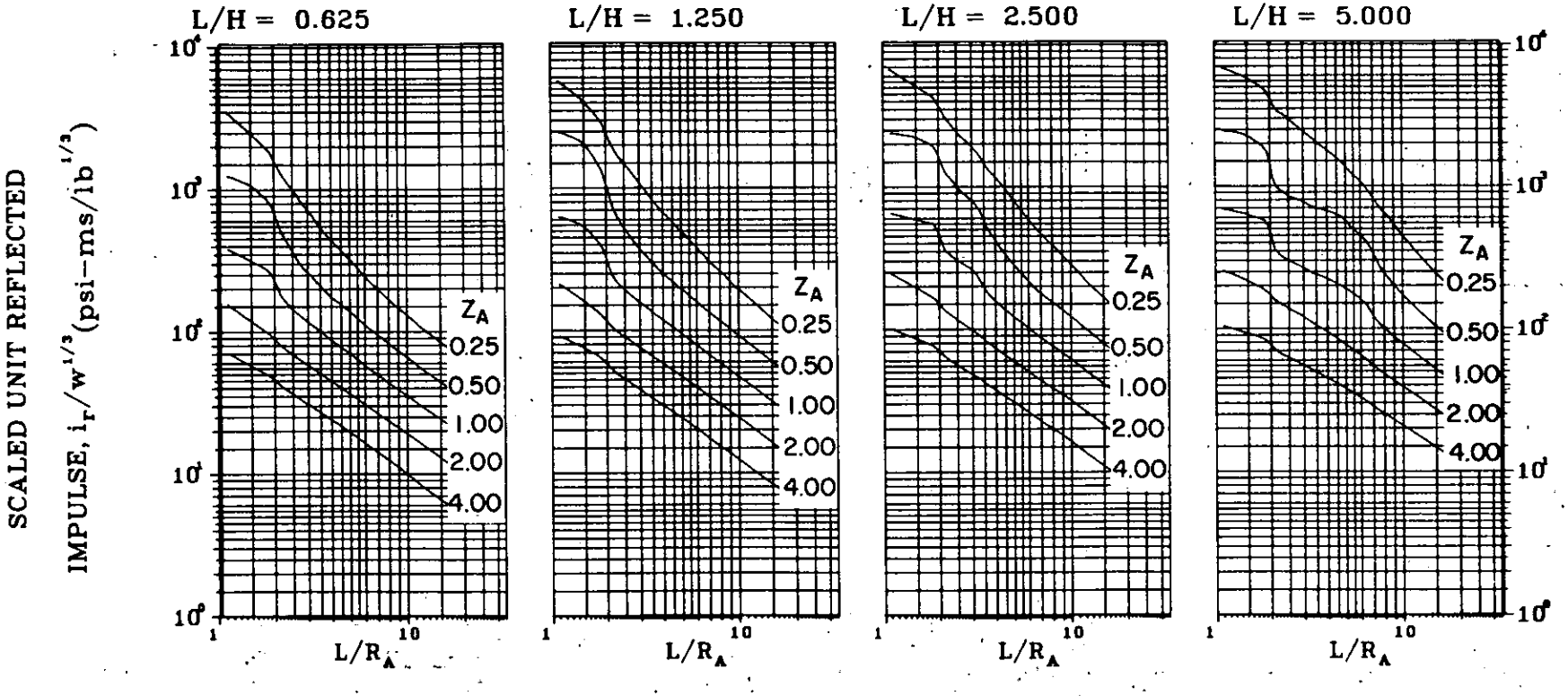


Figure 2-140 Scaled average unit reflected impulse
(N = 3, ℓ/L = 0.50, h/H = 0.75)

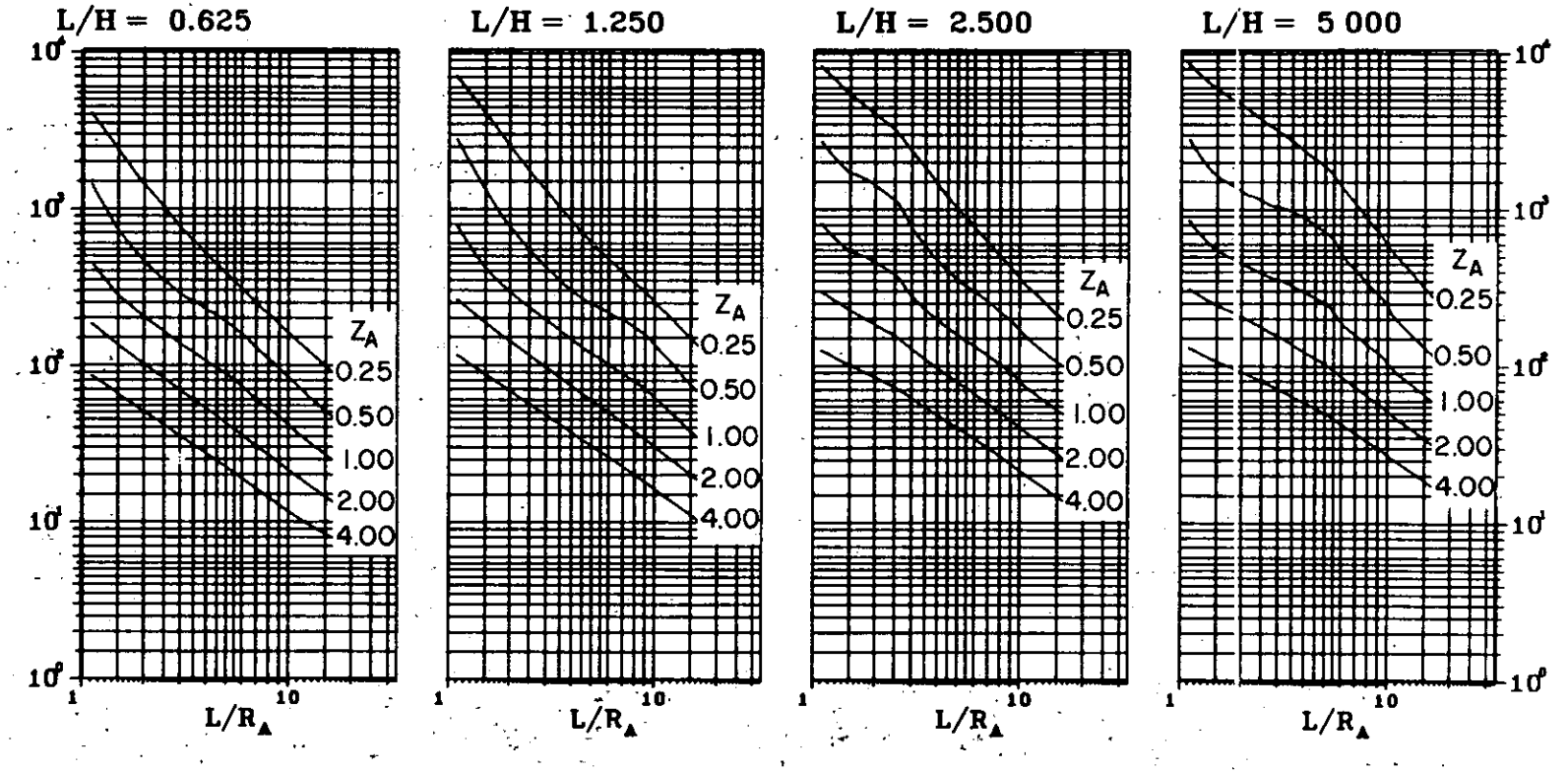


Figure 2-141 Scaled average unit reflected impulse
(N = 4, ℓ/L = 0.10, h/H = 0.10)

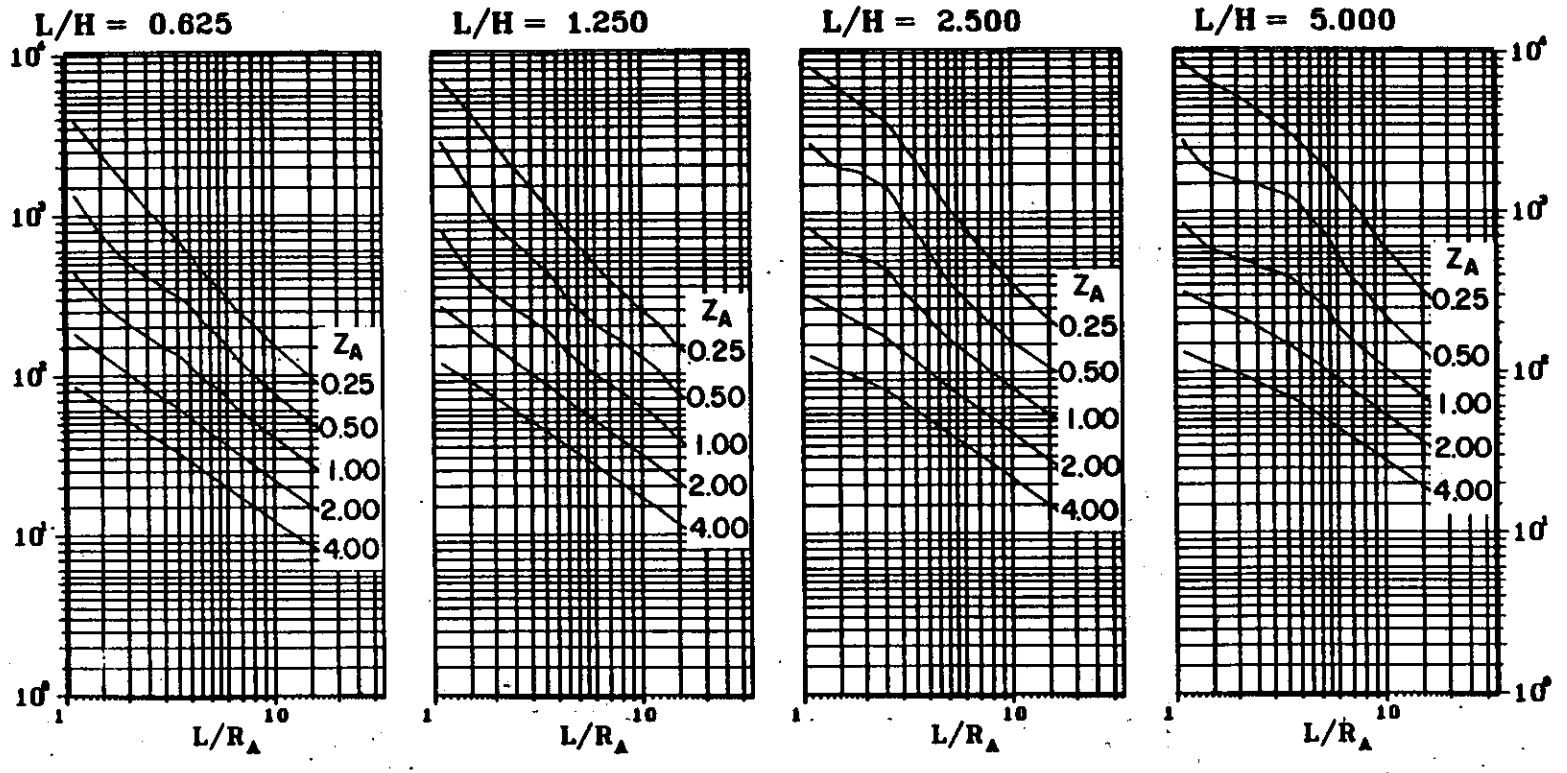


Figure 2-142 Scaled average unit reflected impulse
(N = 4, ℓ/L = 0.25 and 0.75, h/H = 0.10)

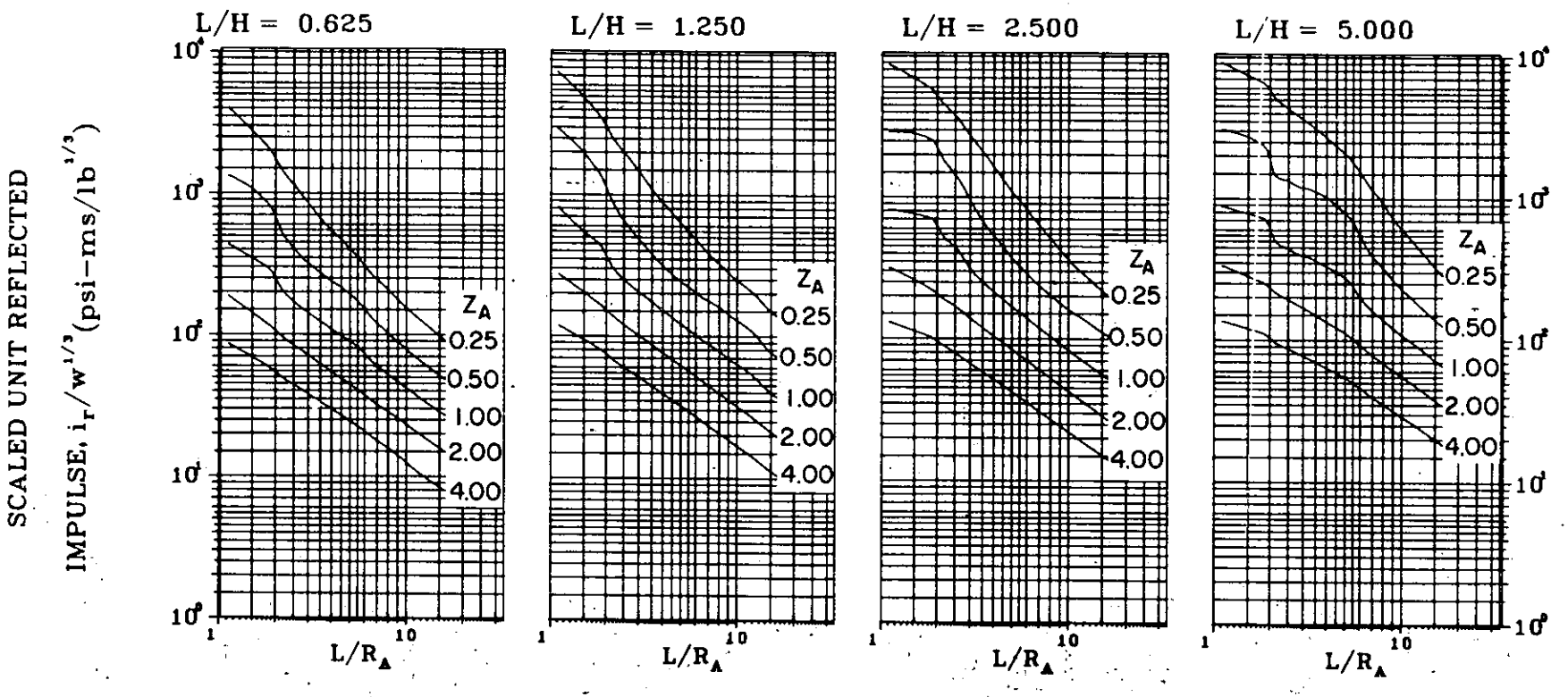


Figure 2-143 Scaled average unit reflected impulse
(N = 4, ℓ/L = 0.50 h/H = 0.10)

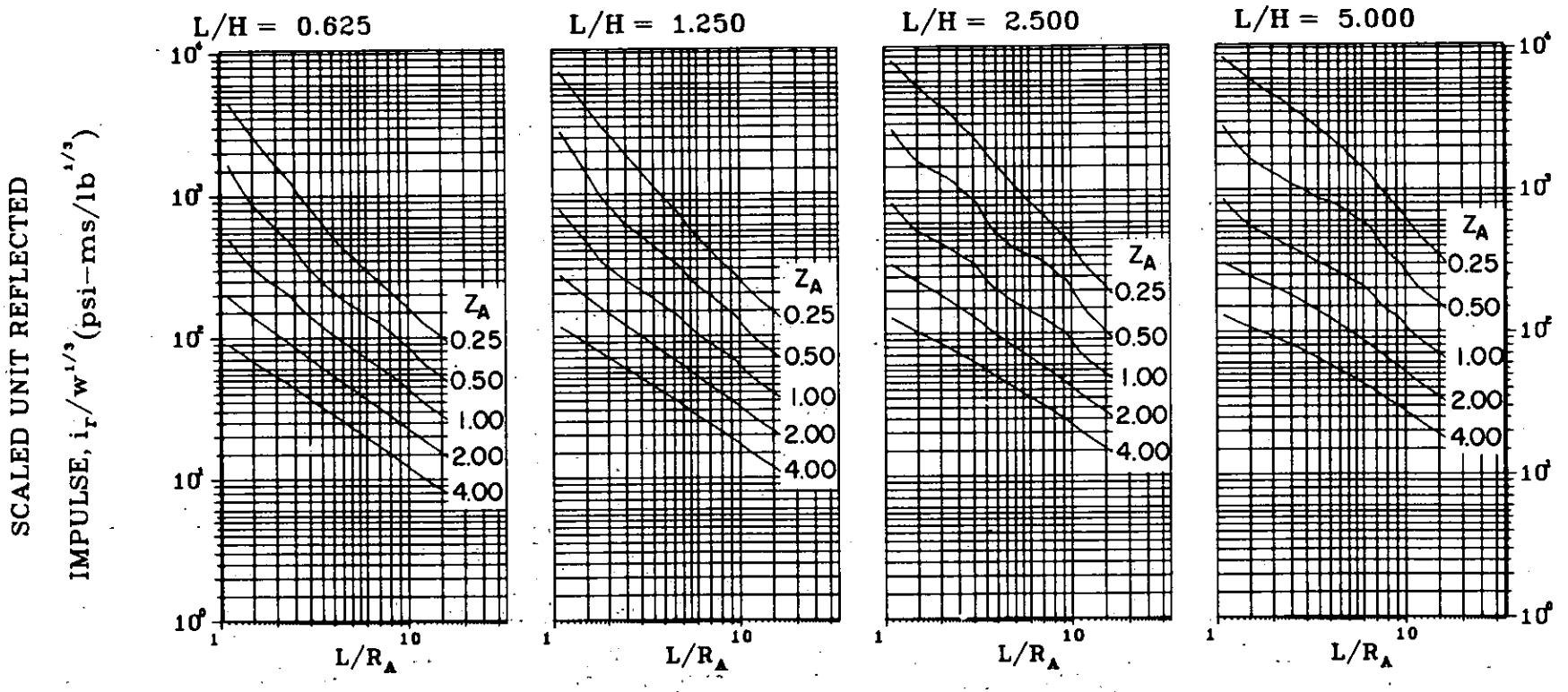


Figure 2-144 Scaled average unit reflected impulse
(N = 4, ℓ/L = 0.10, h/H = 0.25 and 0.75)

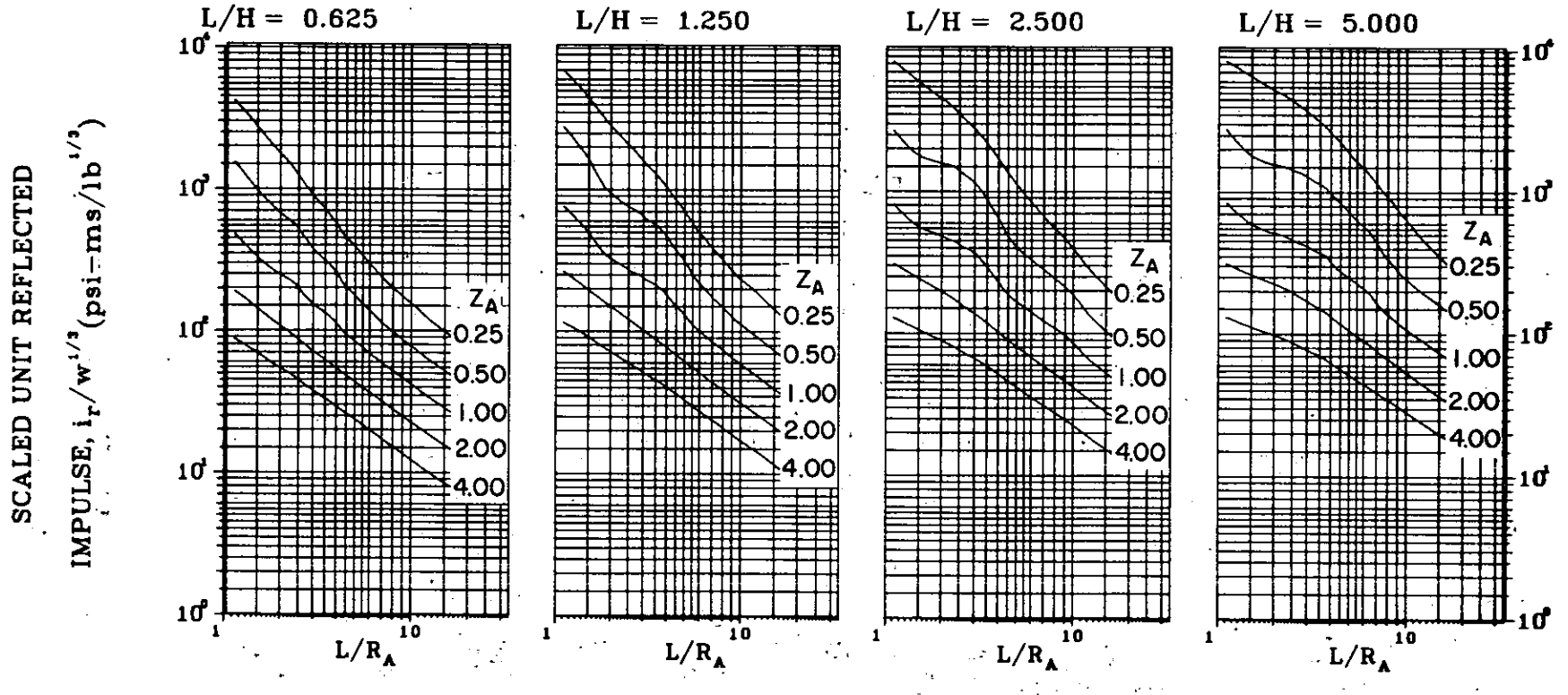


Figure 2-145 Scaled average unit reflected impulse
(N = 4, ℓ/L = 0.25 and 0.75, h/H = 0.25 and 0.75)

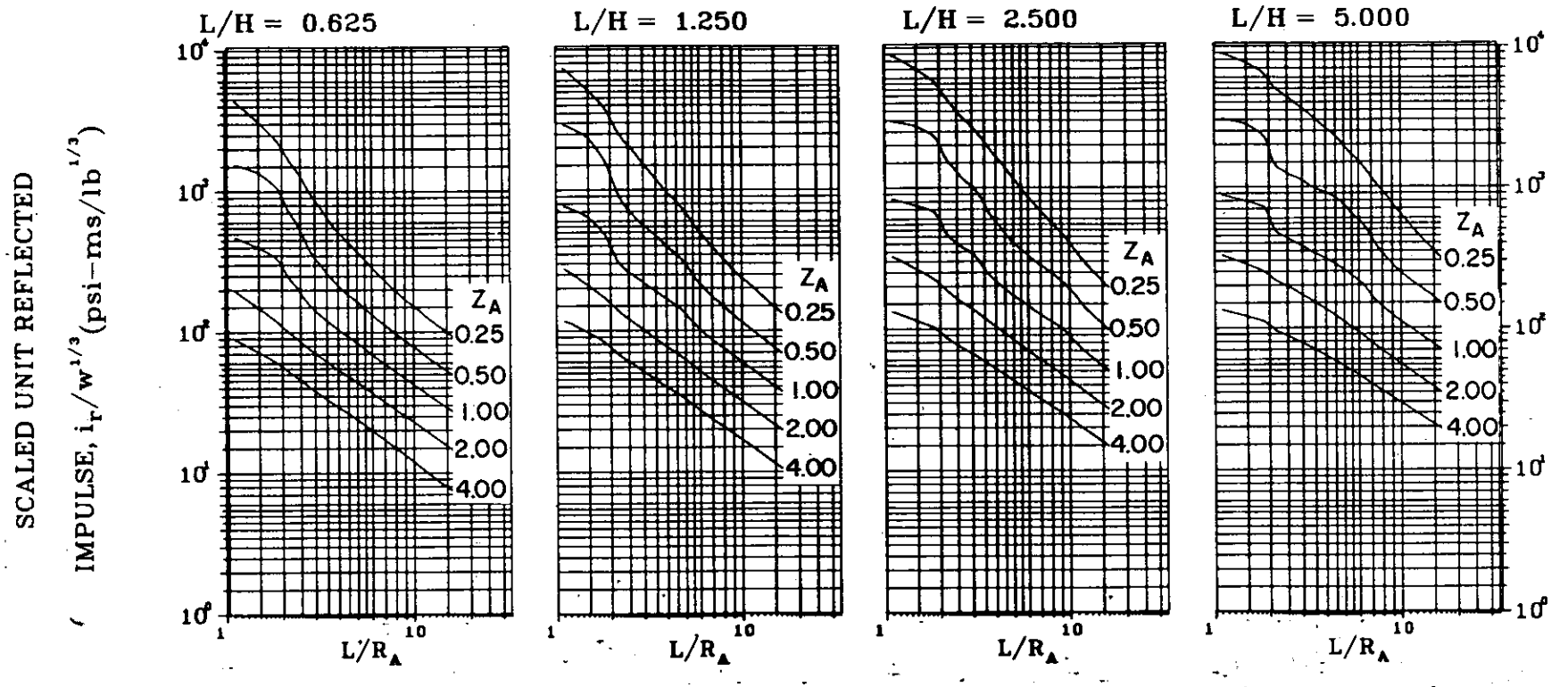


Figure 2-146 Scaled average unit reflected impulse
(N = 4, ℓ/L = 0.50, h/H = 0.25 and 0.75)

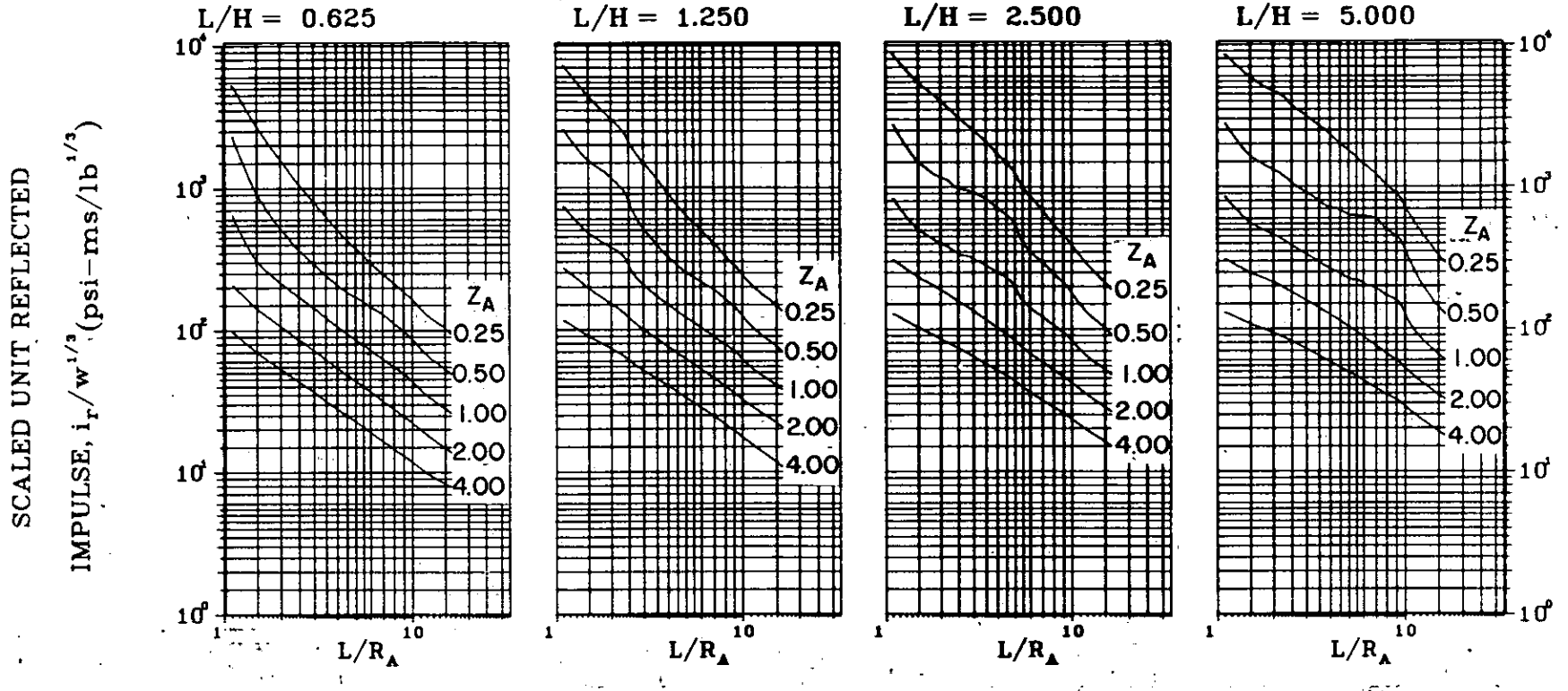


Figure 2-147 Scaled average unit reflected impulse
(N = 4, ℓ/L = 0.10, h/H = 0.50)

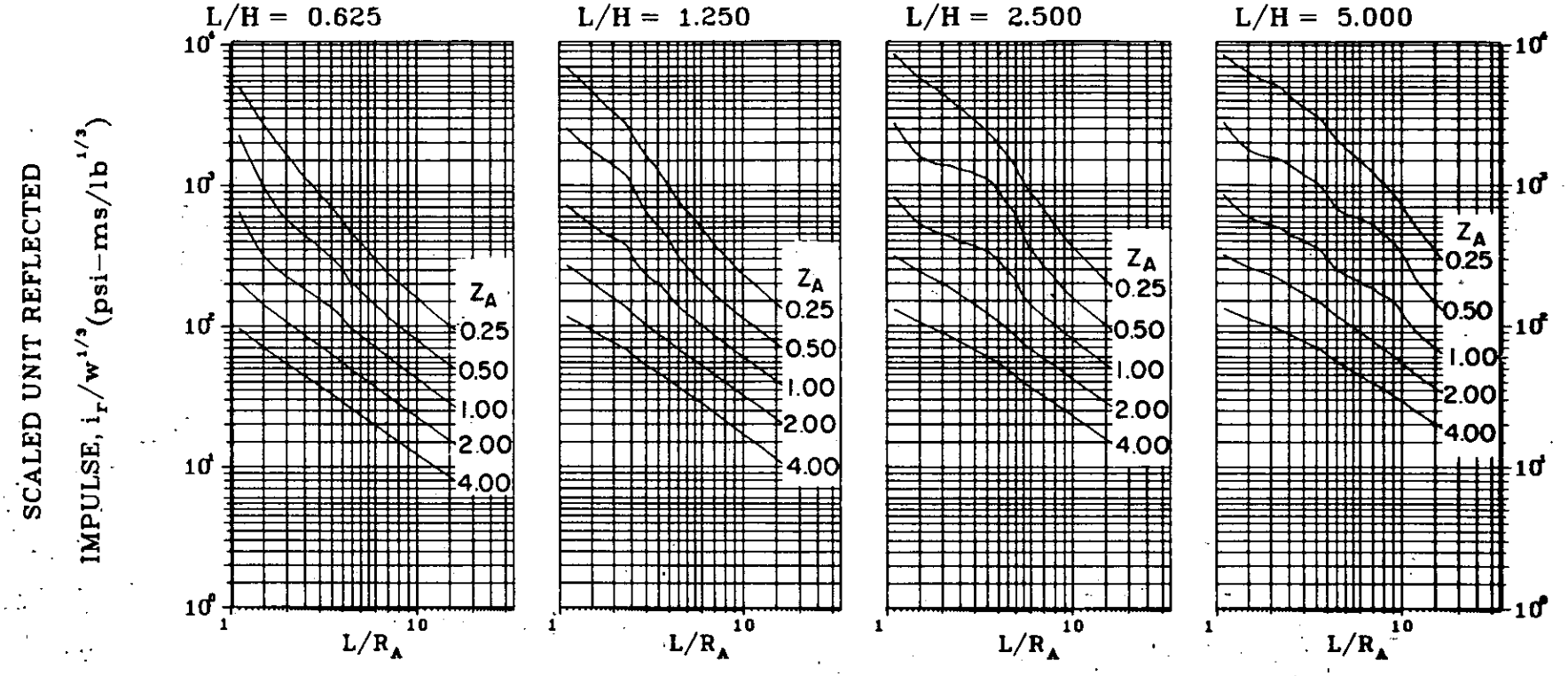


Figure 2-148 Scaled average unit reflected impulse
(N = 4, ℓ/L = 0.25 and 0.75, h/H = 0.50)

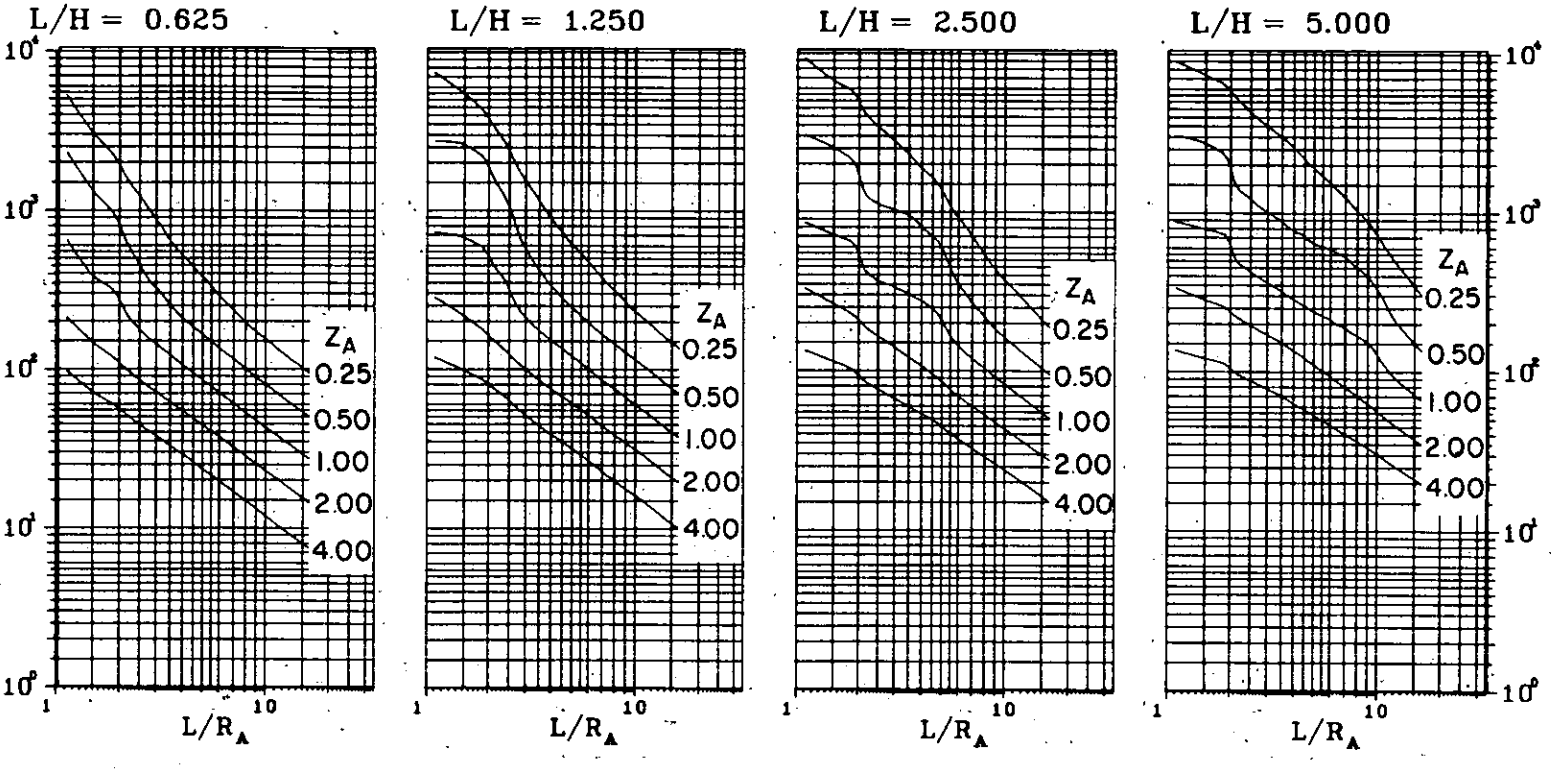


Figure 2-149 Scaled average unit reflected impulse
(N = 4, ℓ/L = 0.50, h/H = 0.50)

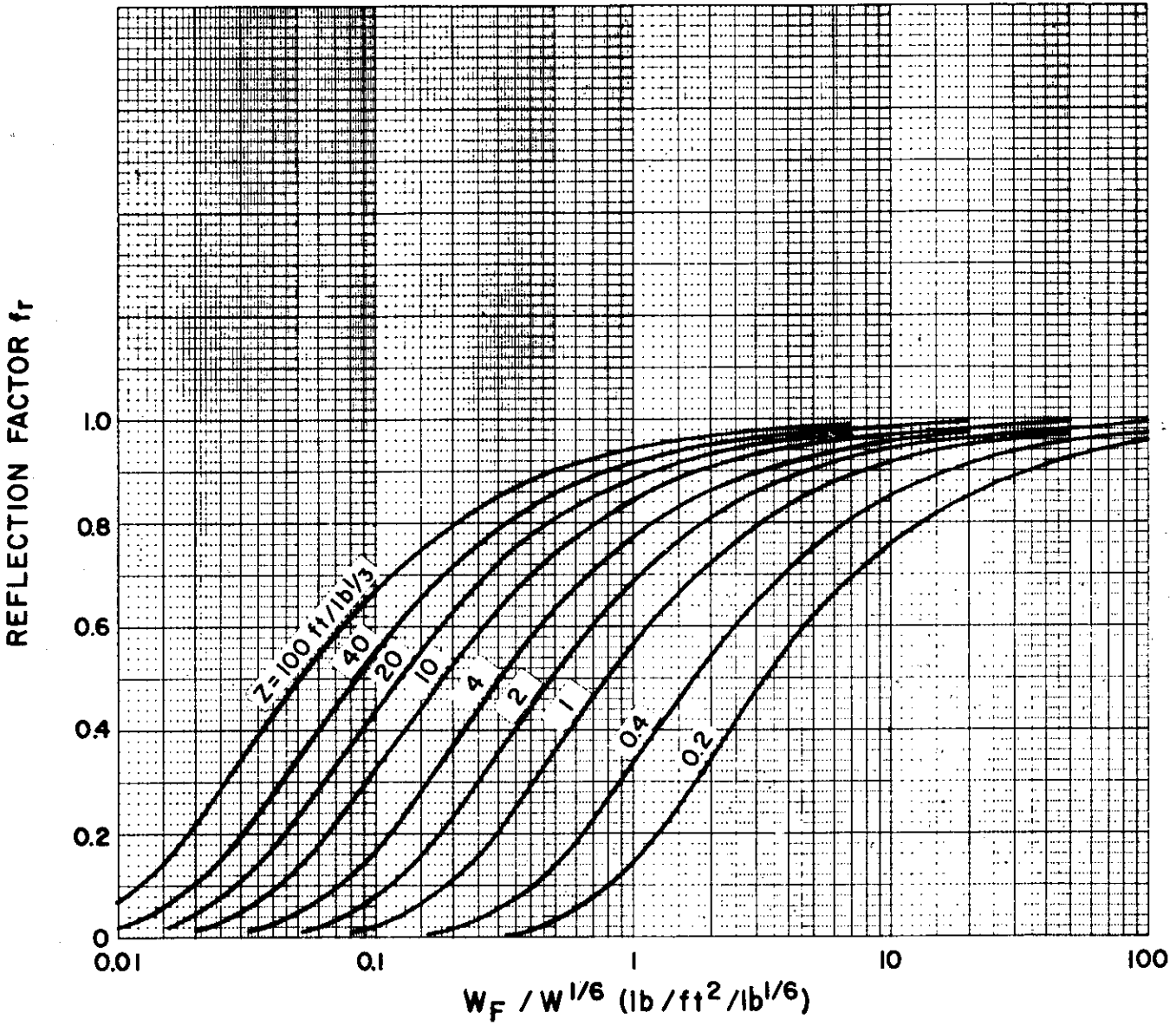


Figure 2-150 Reflection factor for shock loads on frangible elements

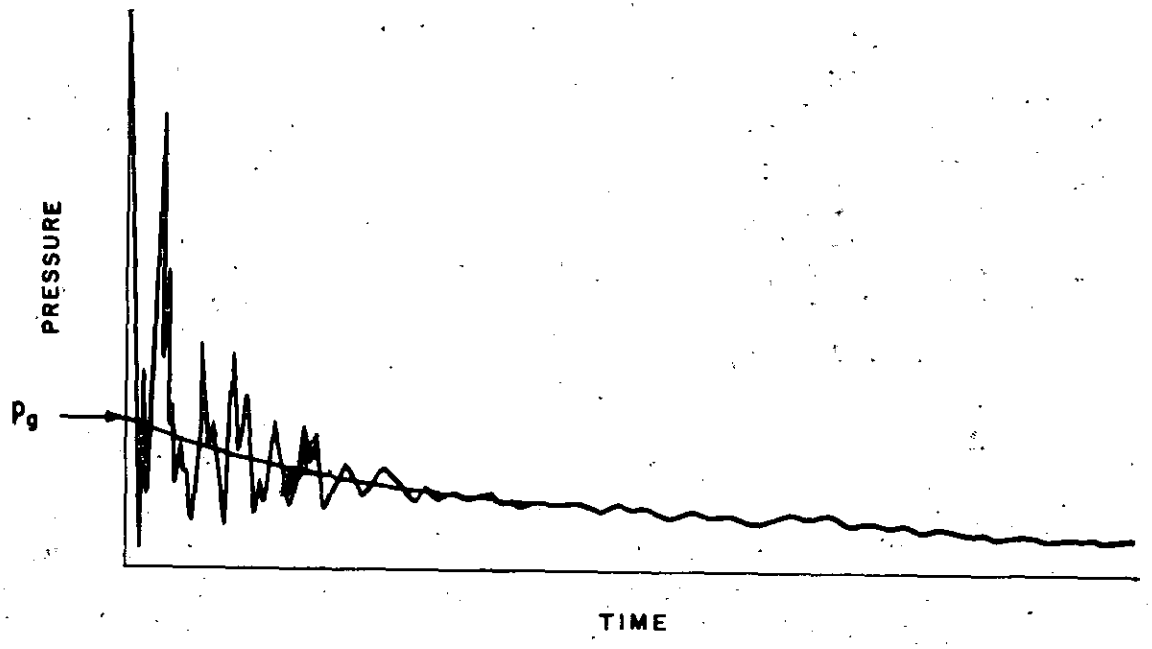


Figure 2-151 Pressure-time variation for a partially vented explosion

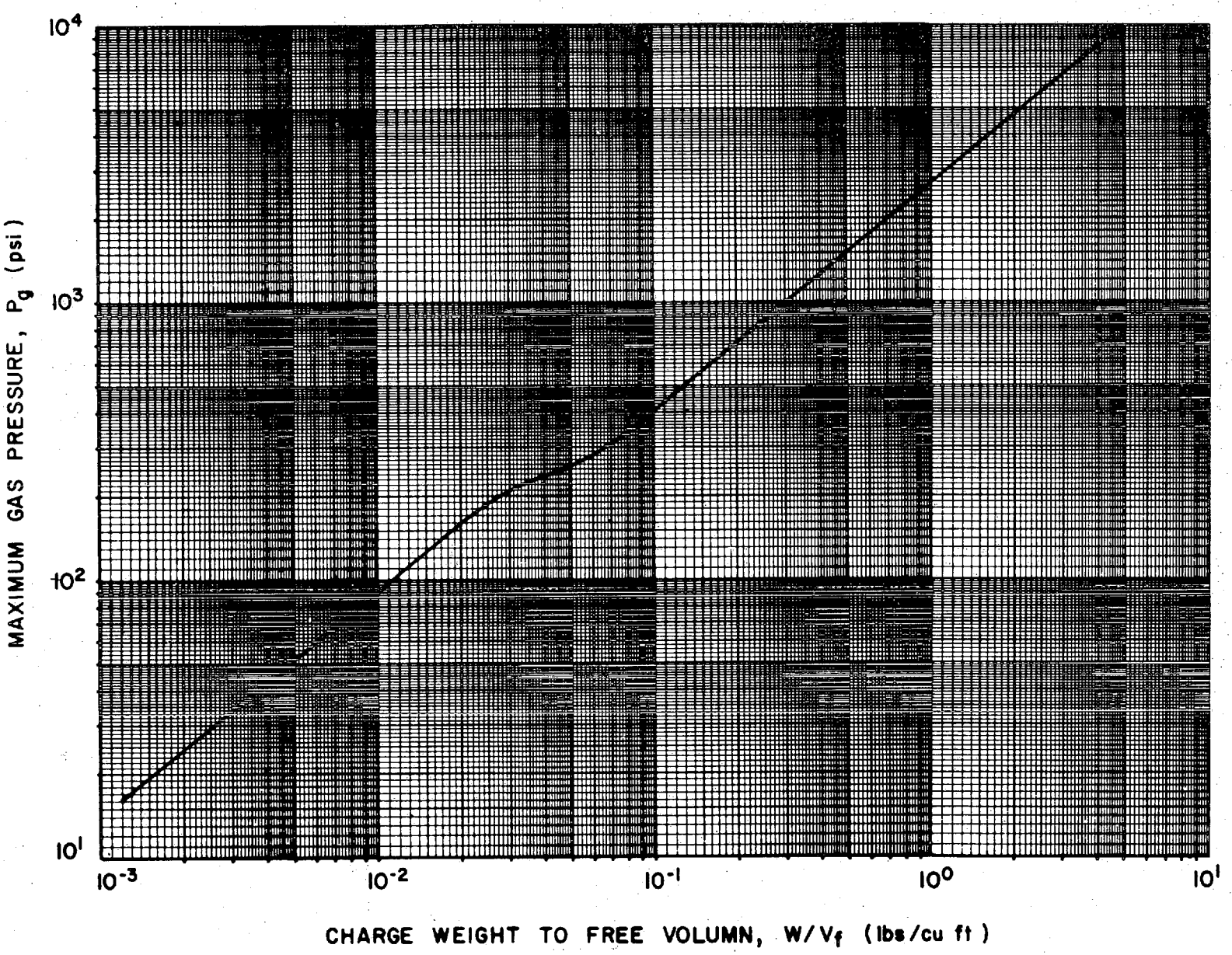


Figure 2-152 Peak gas pressure produced by a TNT detonation in a partially contained chamber

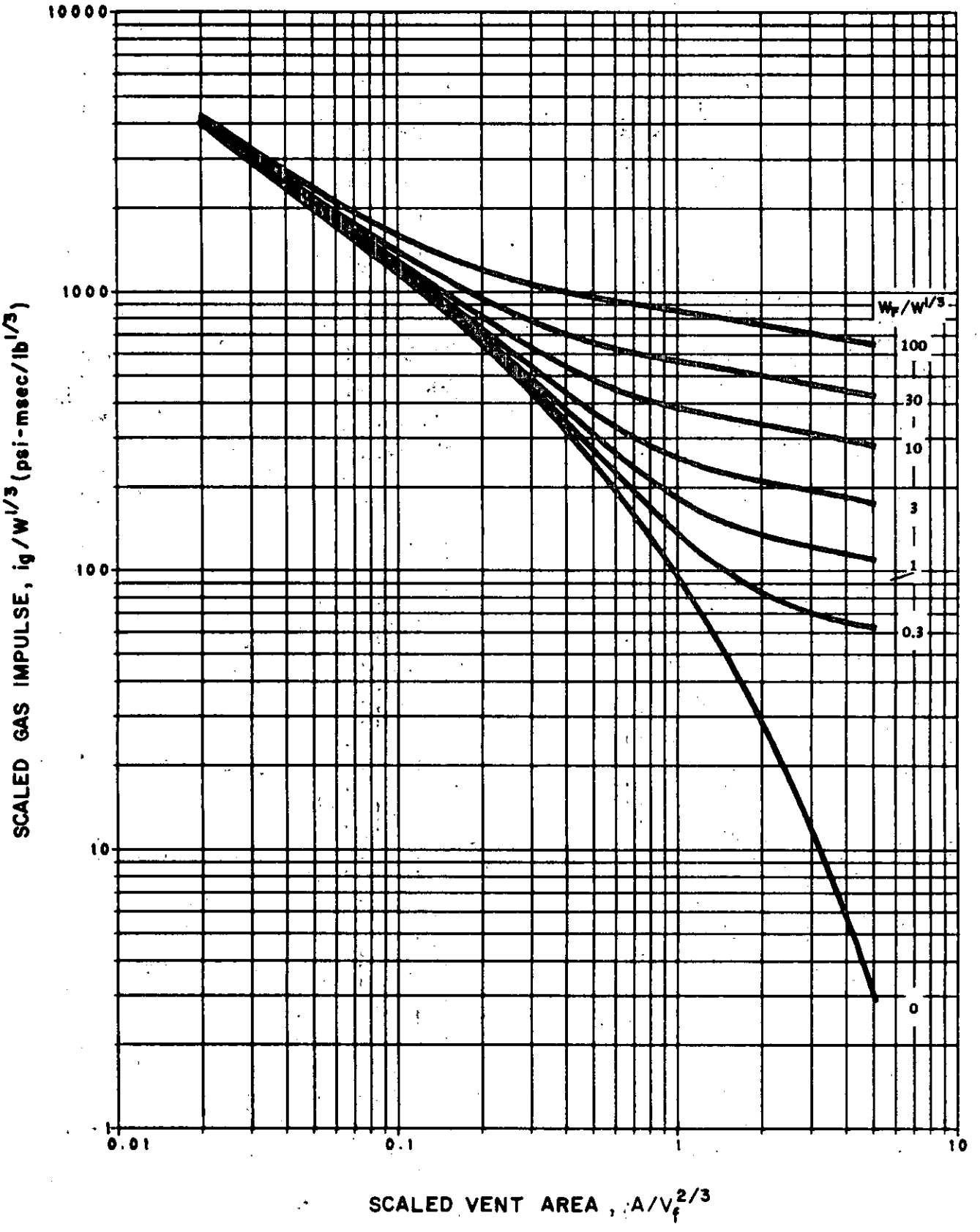


Figure 2-153 Scaled gas impulse (W/V_f = 0.002, $i_r/W^{1/3}$ = 20)

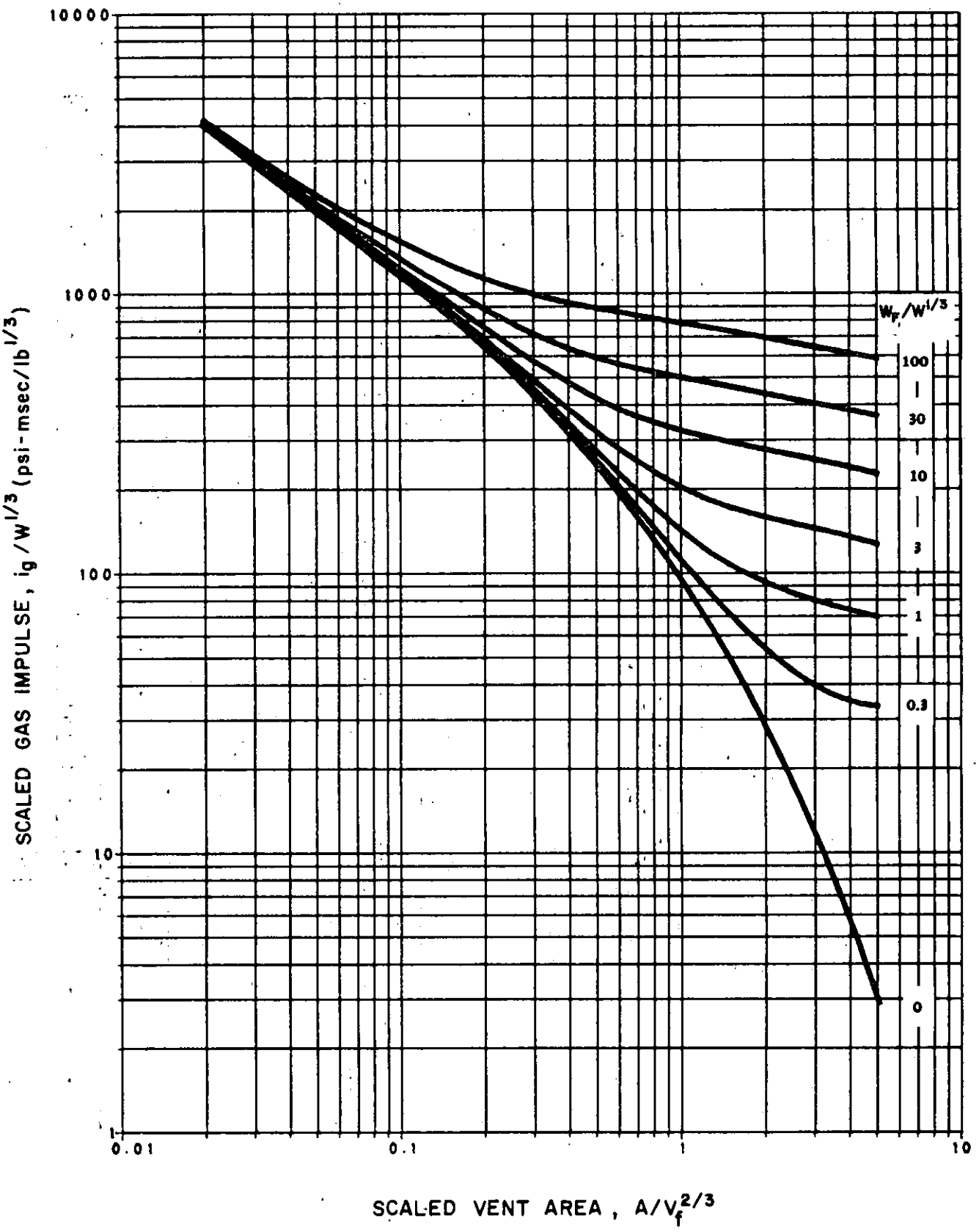


Figure 2-154 Scaled gas impulse ($W/V_f = 0.002$, $i_r/W^{1/3} = 100$)

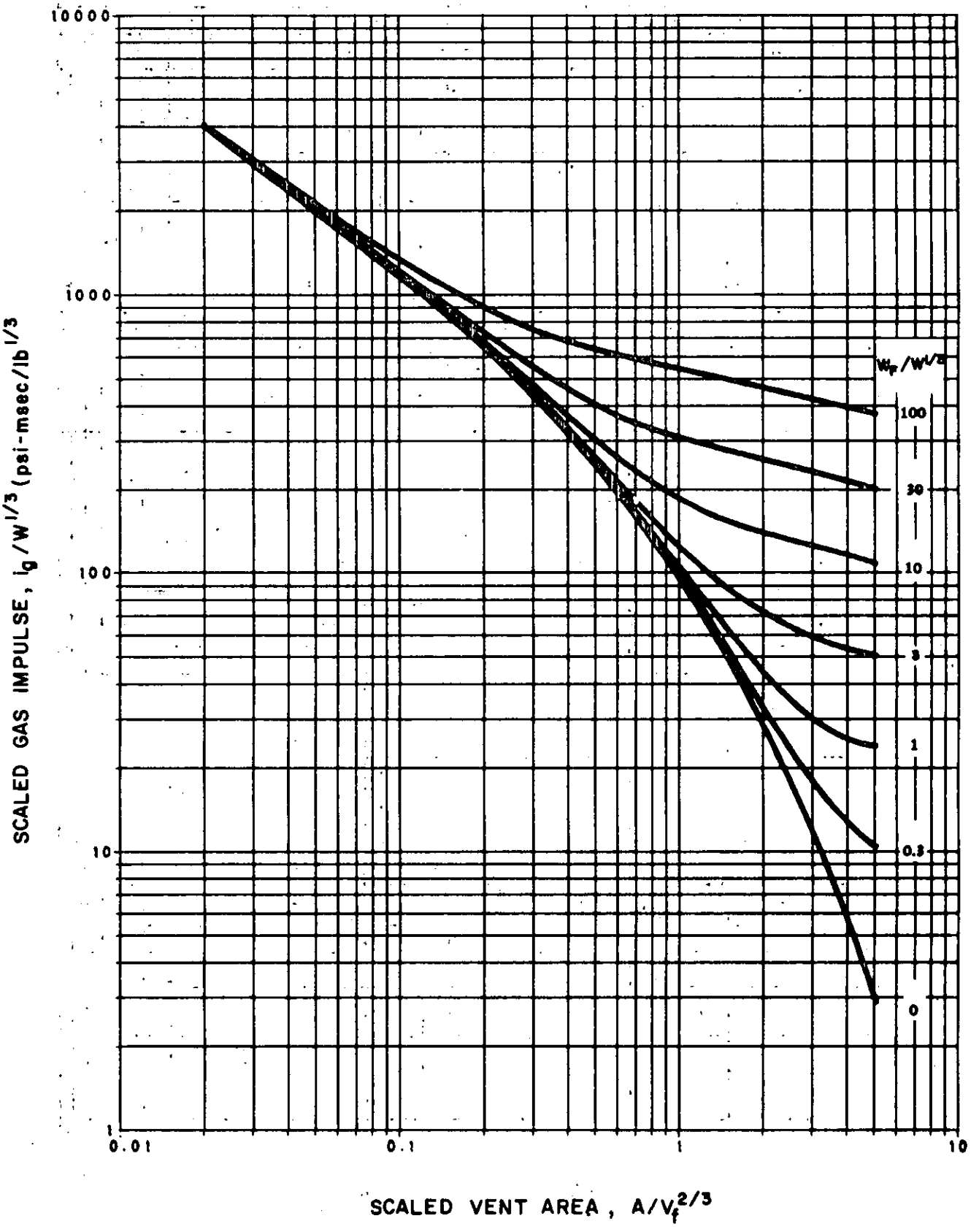


Figure 2-155 Scaled gas impulse (W/V_f = 0.002, $i_r/W^{1/3}$ = 600)

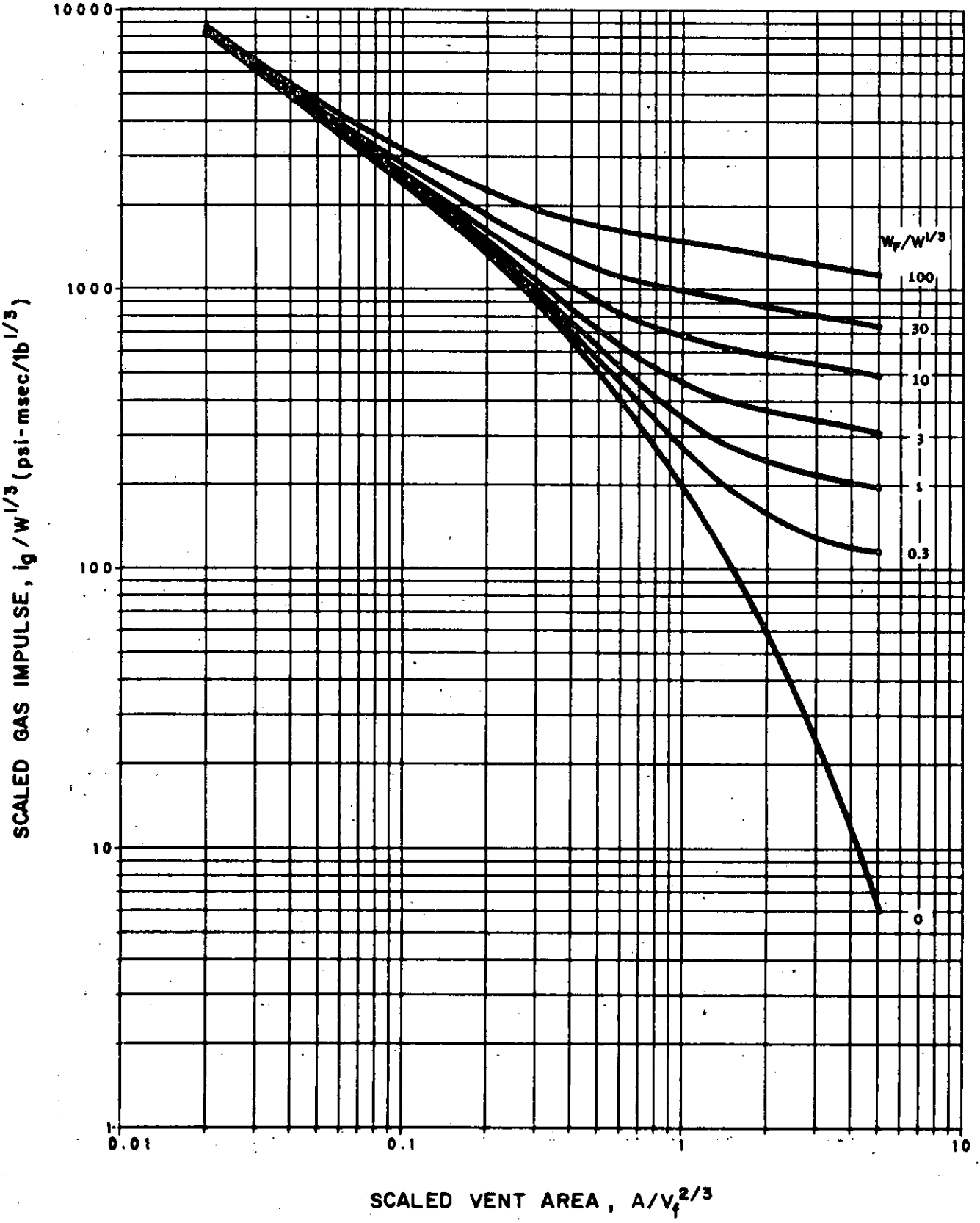


Figure 2-156 Scaled gas impulse ($W/V_f = 0.015$, $i_r/W^{1/3} = 20$)

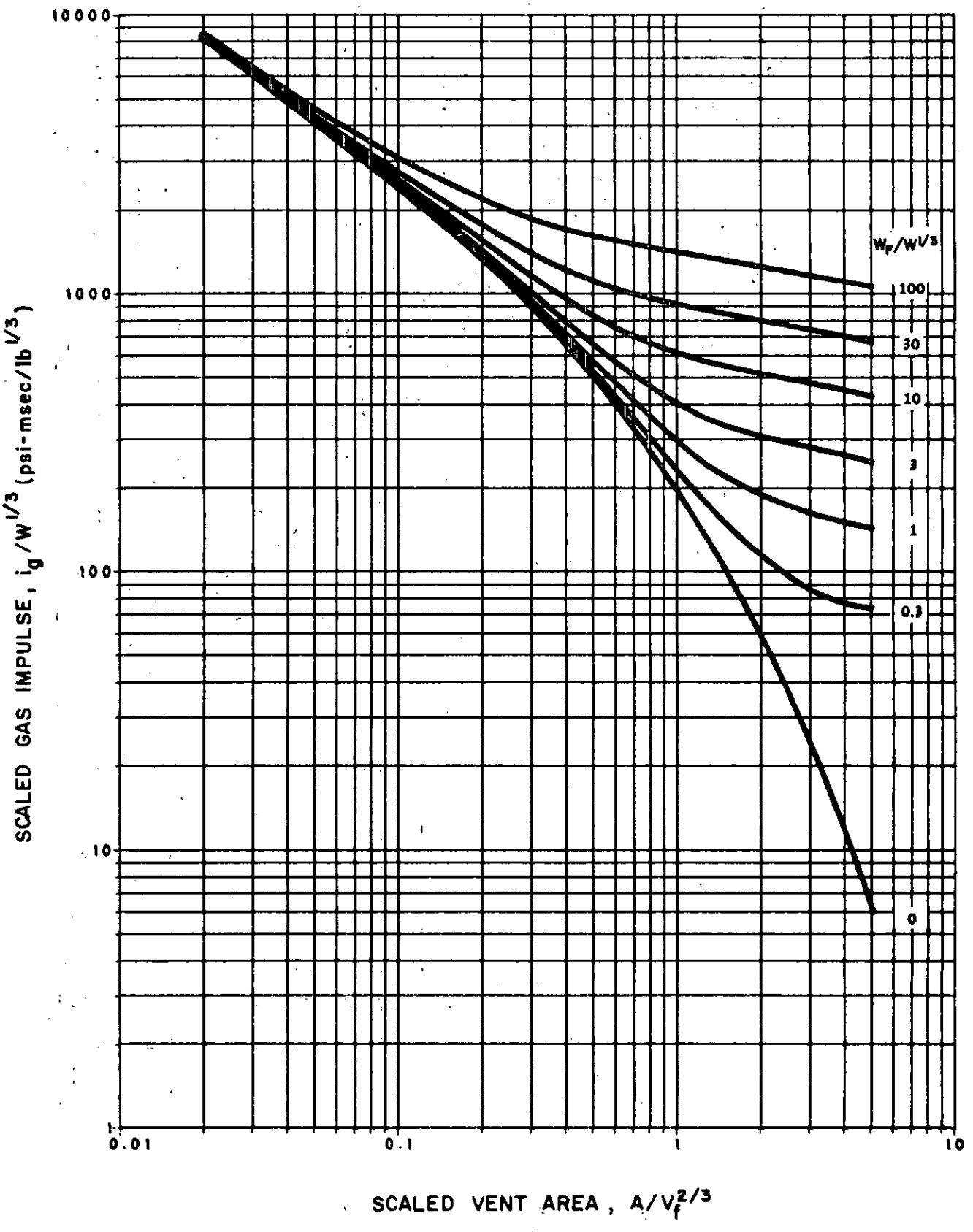


Figure 2-157 Scaled gas impulse ($W/V_f = 0.015$, $i_r/W^{1/3} = 100$)

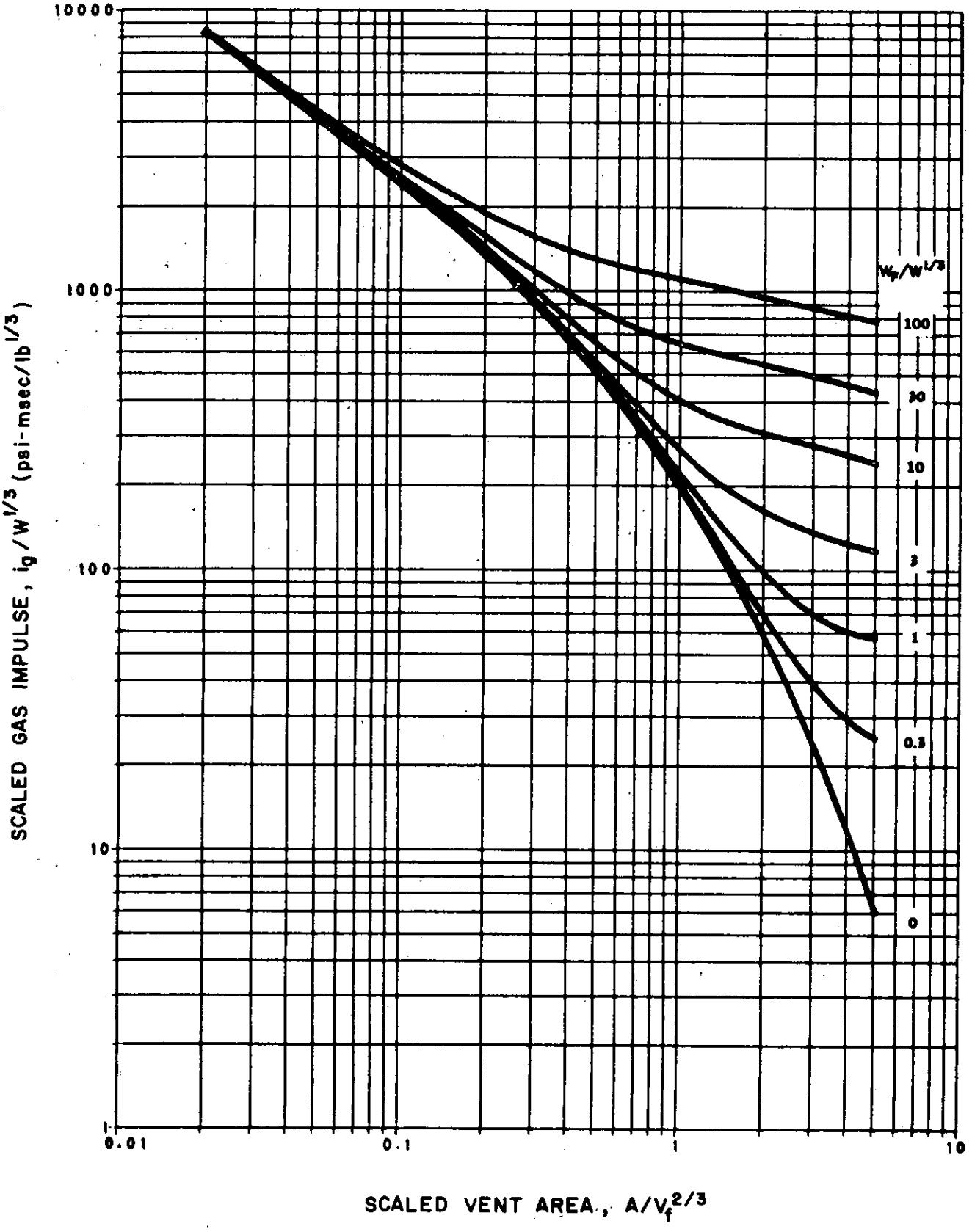


Figure 2-158 Scaled gas impulse (W/V_f = 0.015, $i_r/W^{1/3}$ = 600)

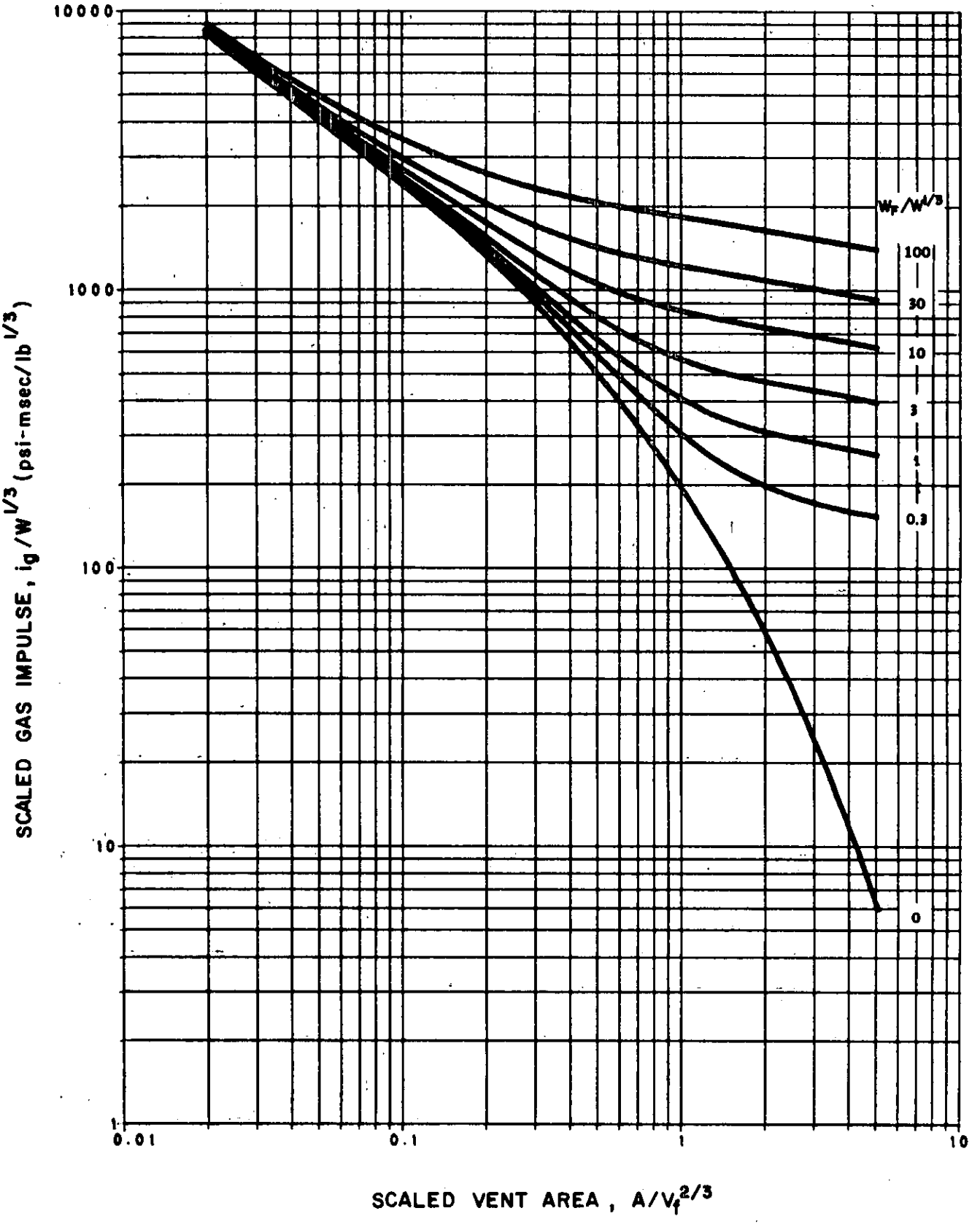


Figure 2-159 Scaled gas impulse ($W/V_f = 0.15$, $i_r/W^{1/3} = 20$)

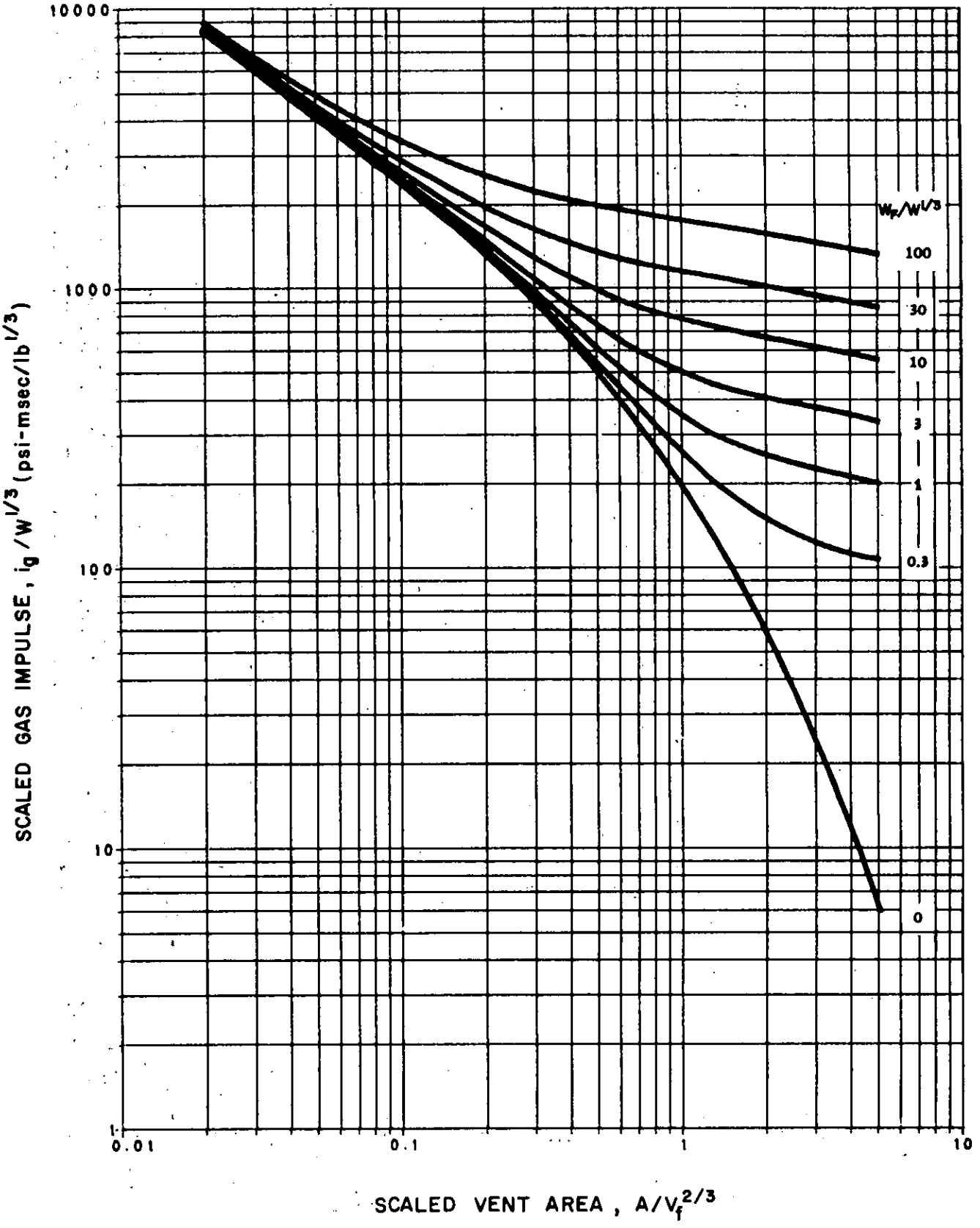


Figure 2-160 Scaled gas impulse ($W/V_f = 0.15$, $i_r/W^{1/3} = 100$)

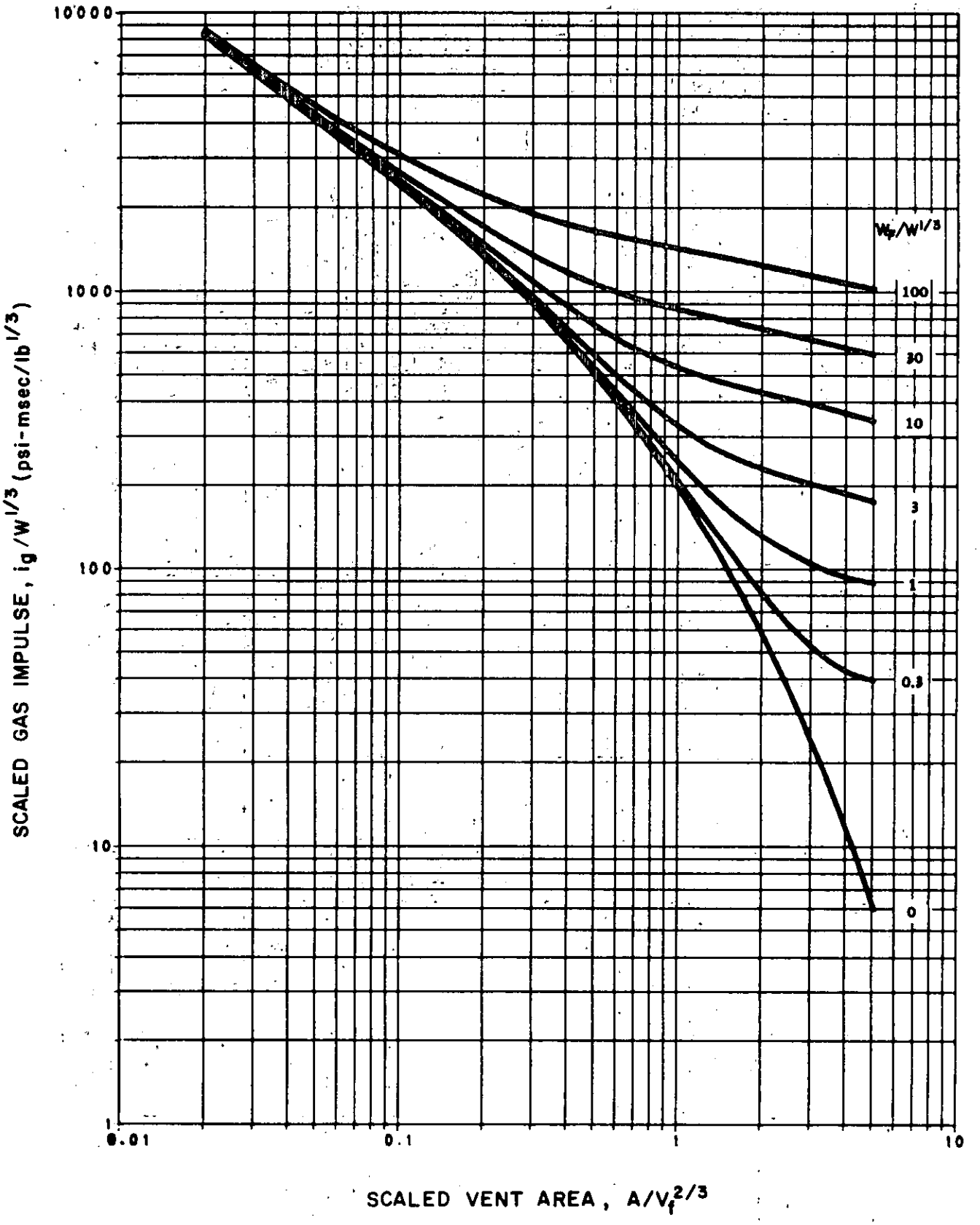


Figure 2-161 Scaled gas impulse (W/V_f = 0.15, $i_r/W^{1/3}$ = 600)

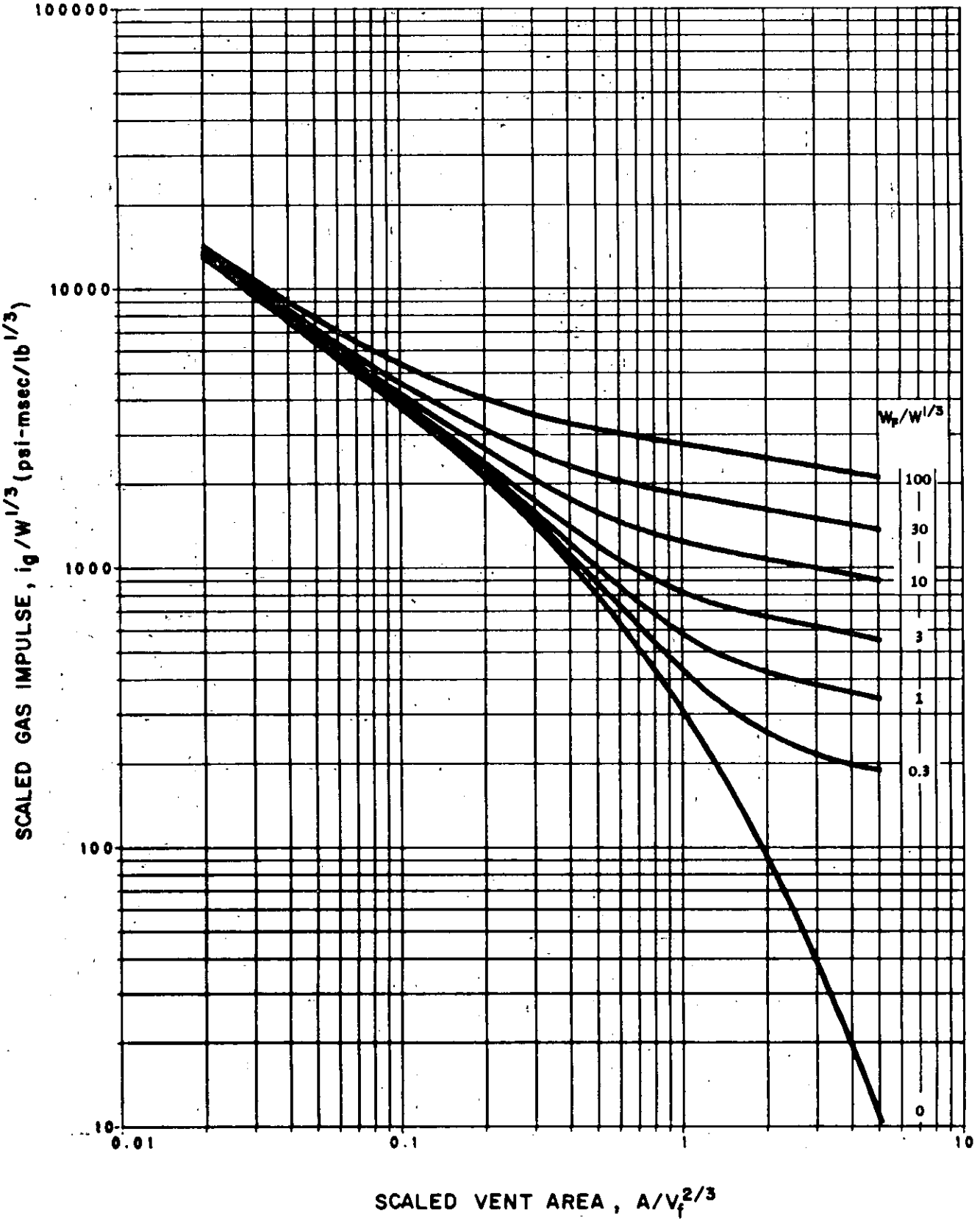


Figure 2-162 Scaled gas impulse (W/V_f = 1.0, $i_r/W^{1/3}$ = 100)

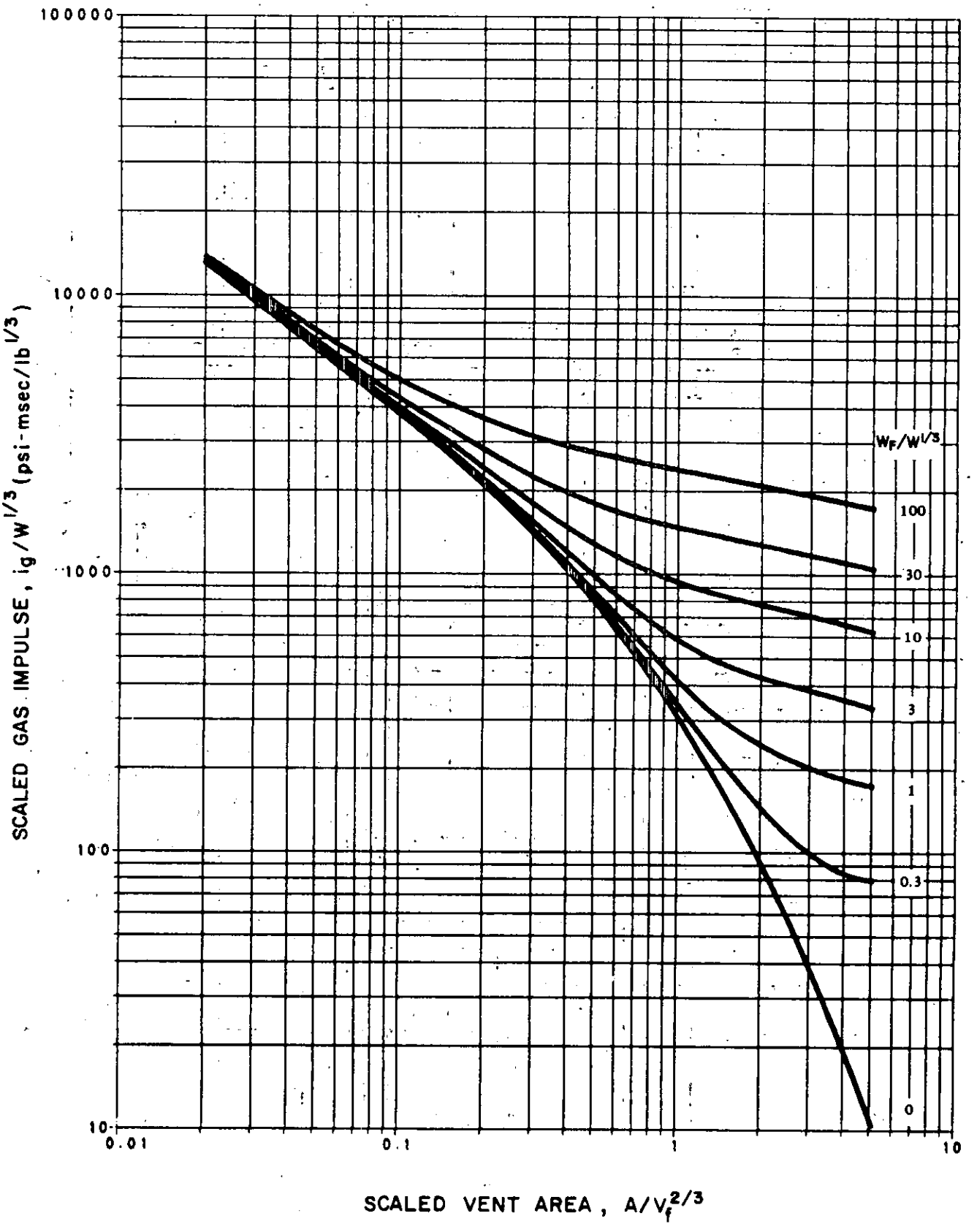


Figure 2-163 Scaled gas impulse (W/V_f = 1.0, $i_r/W^{1/3}$ = 600)

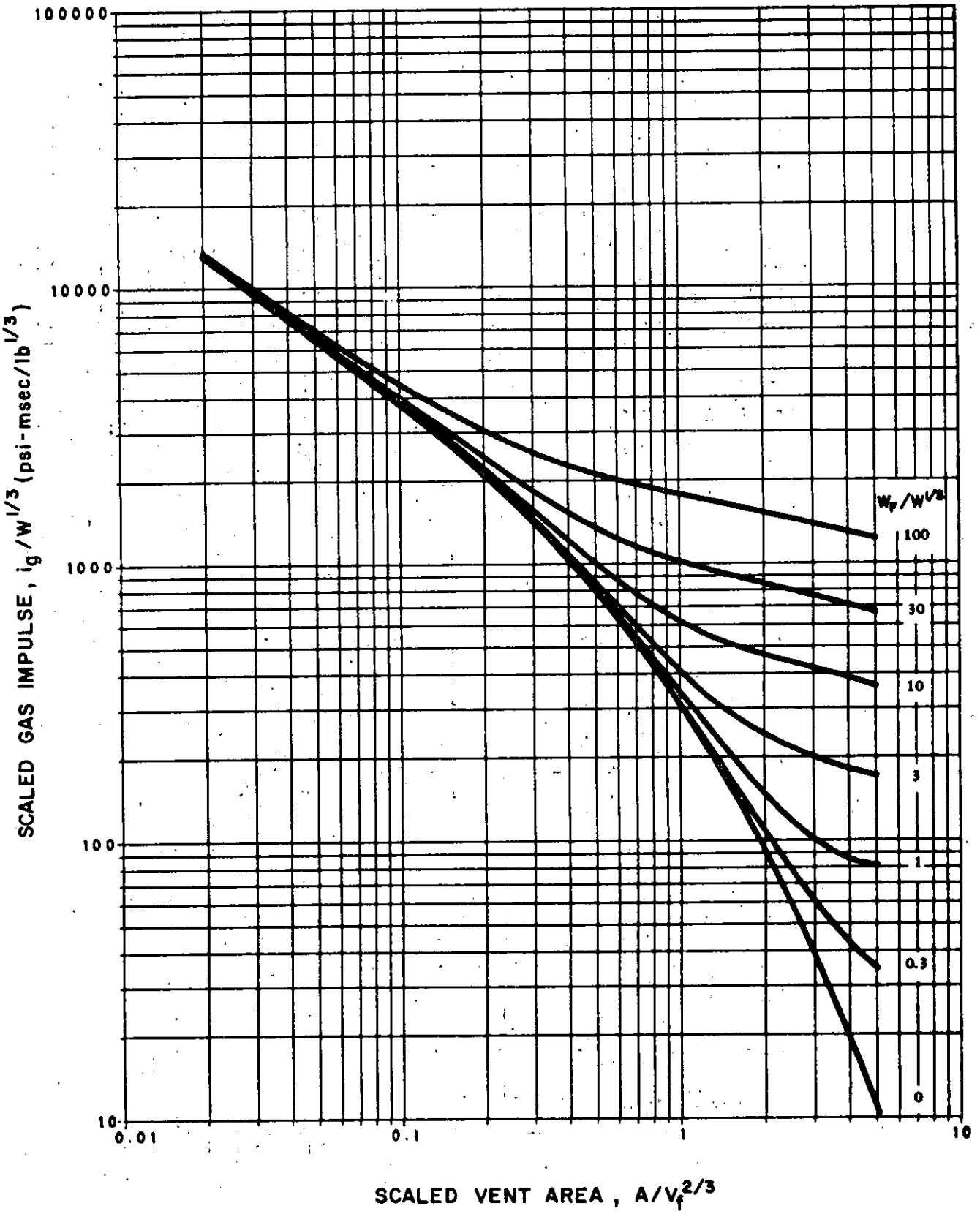
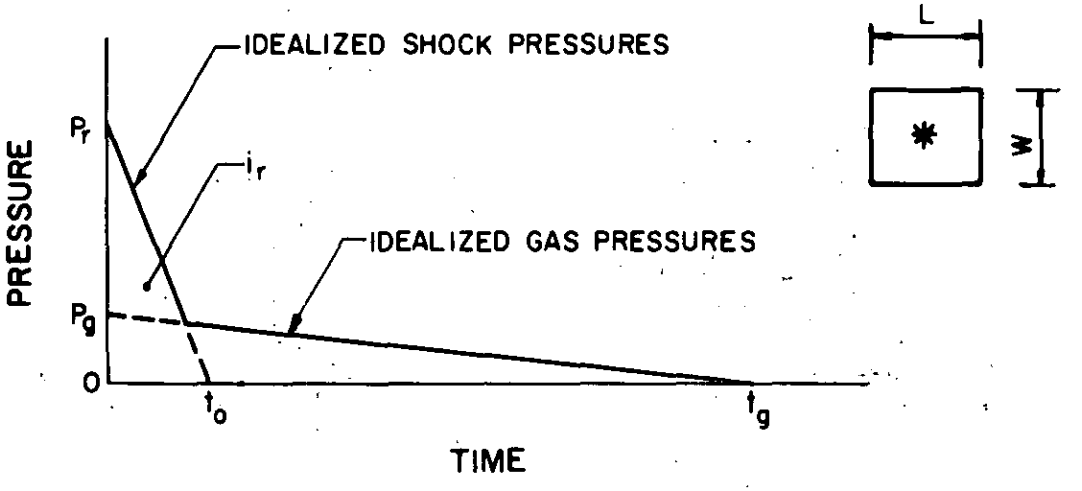
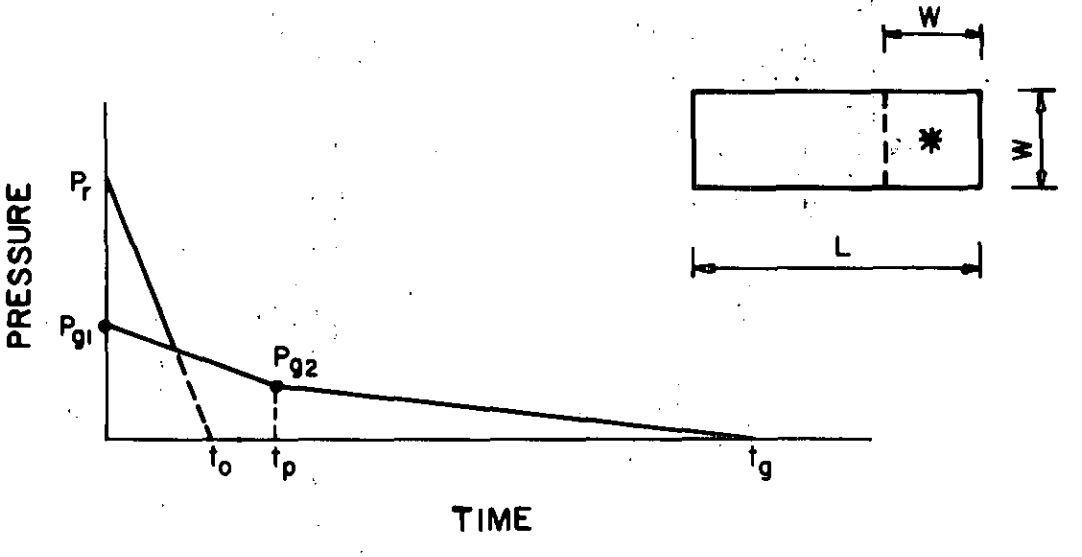


Figure 2-164 Scaled gas impulse (W/V_f = 1.0, $i_r/W^{1/3}$ = 2000)



a) SMALL AND/OR SQUARE CHAMBER



b) LONG RECTANGULAR CHAMBER

Figure 2-165 Combined shock and gas pressures

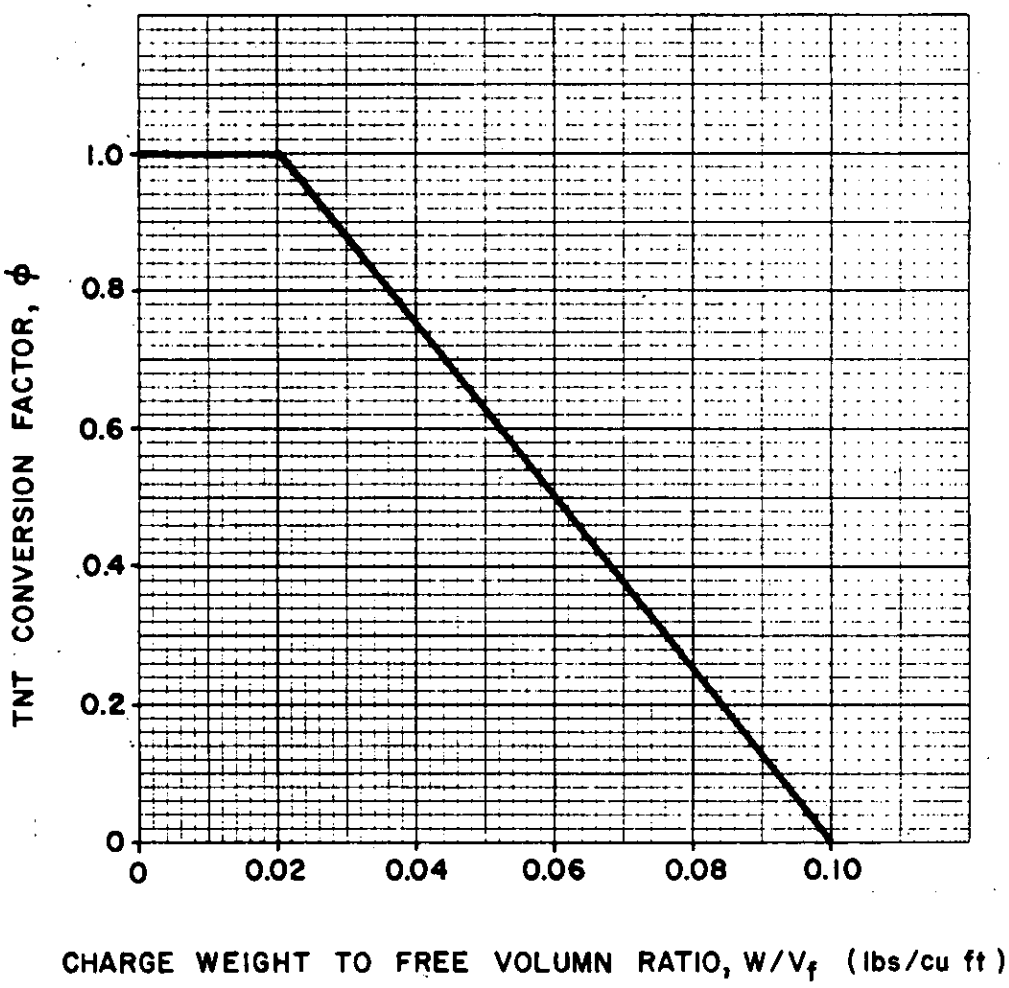
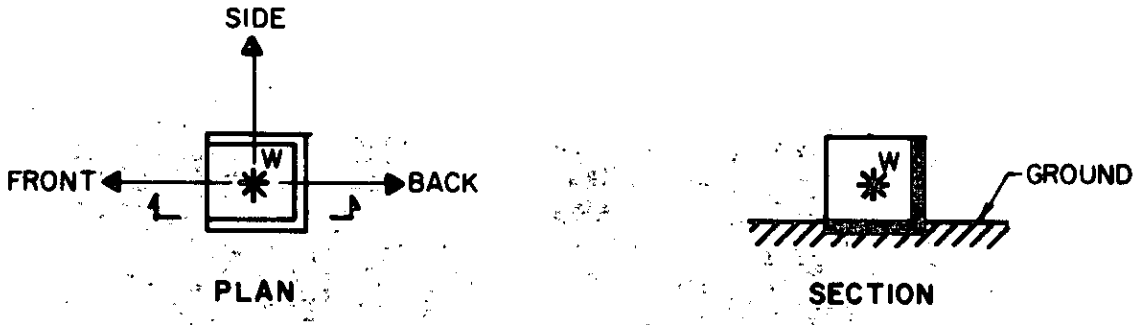
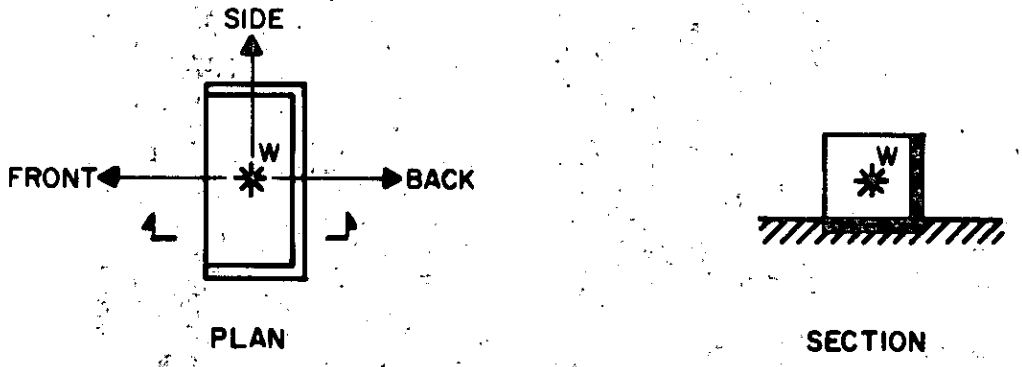


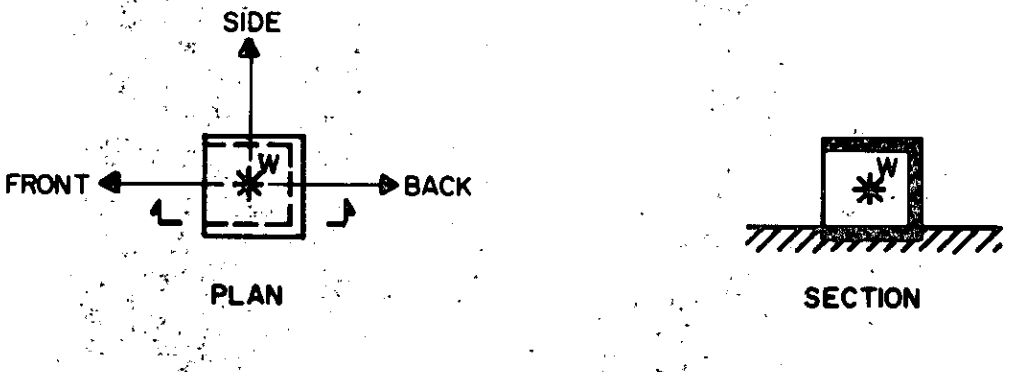
Figure 2-166 TNT conversion factor for charges



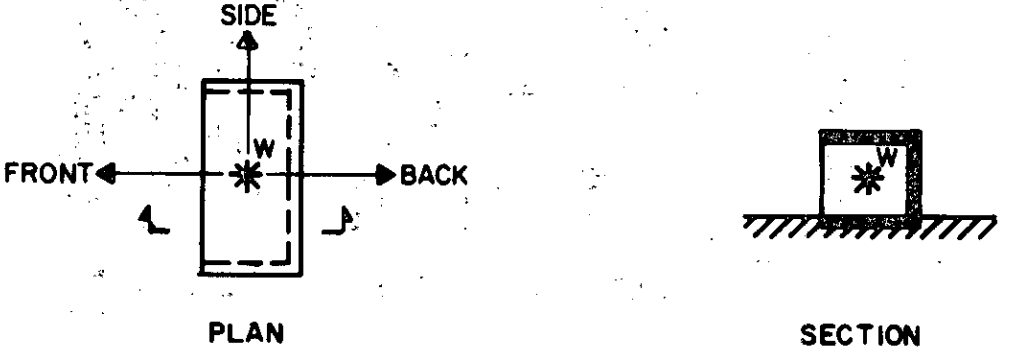
a) CUBIC THREE WALL CUBICLE WITHOUT A ROOF



b) RECTANGULAR THREE WALL CUBICLE WITHOUT A ROOF



c) CUBIC THREE WALL CUBICLE WITH A ROOF



d) RECTANGULAR THREE WALL CUBICLE WITH A ROOF

Figure 2-167 Fully vented three-wall cubicles and direction of blast wave propagation

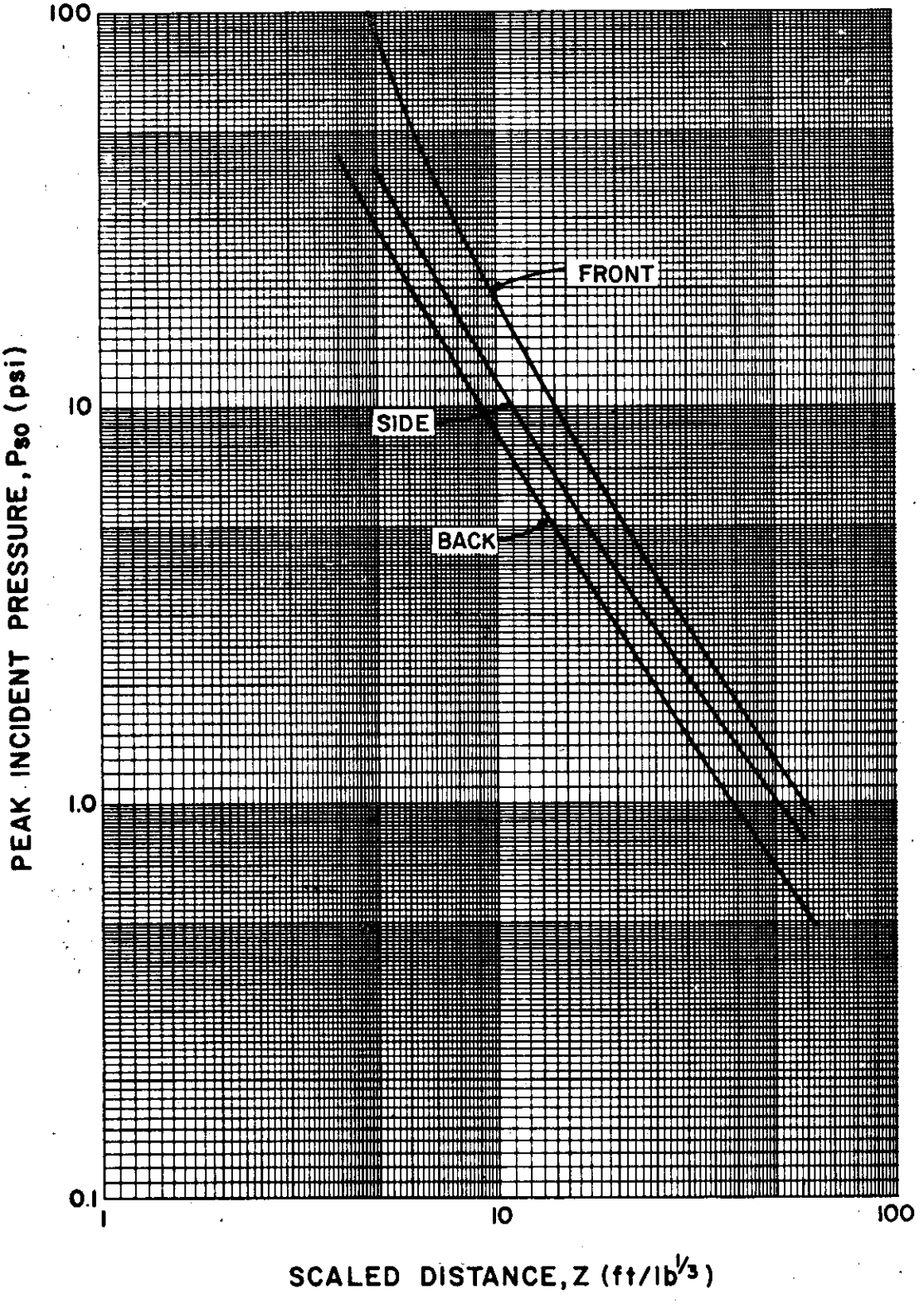


Figure 2-168 Envelope curves for peak positive pressure outside three-wall cubicles without a roof

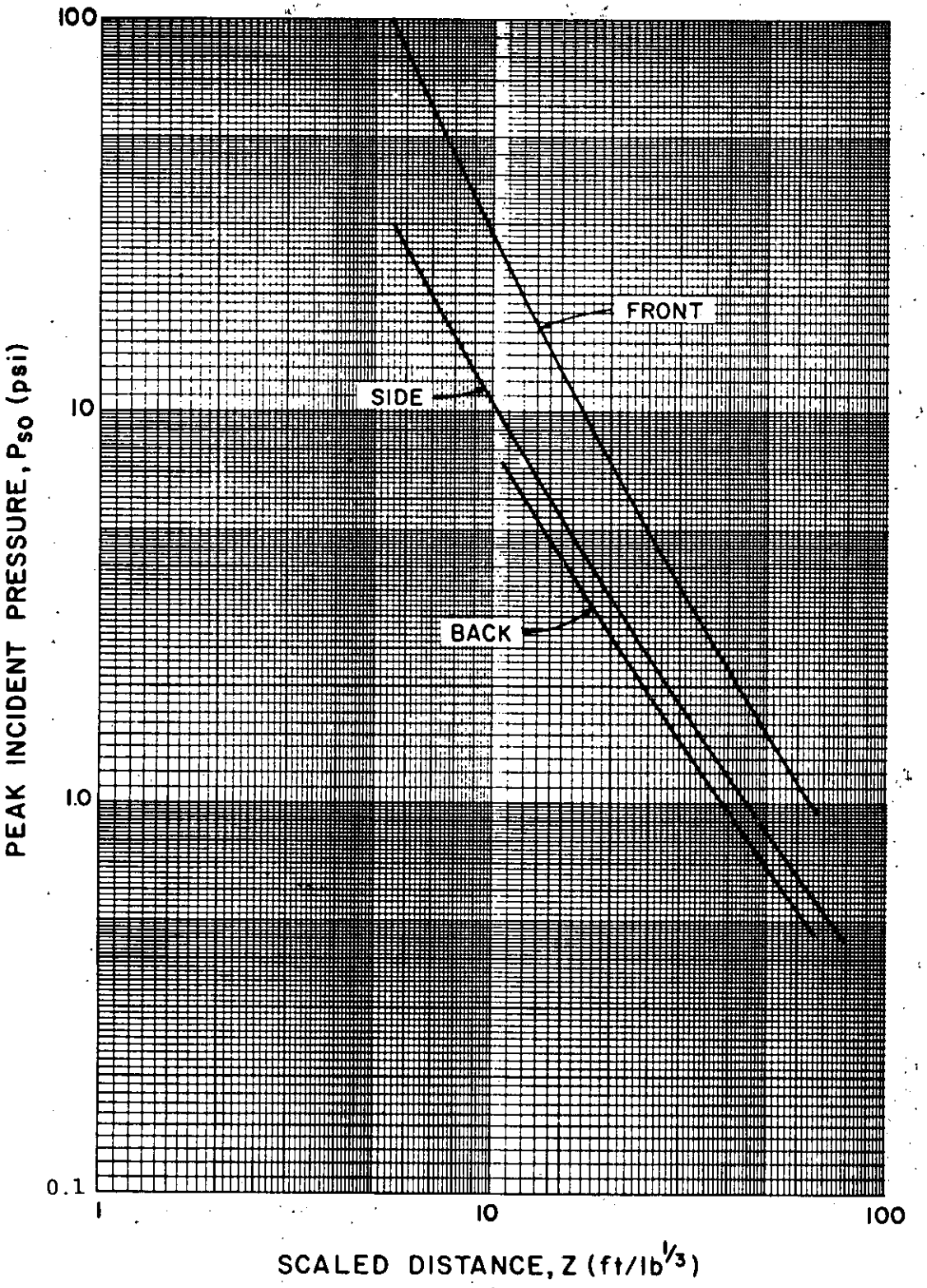


Figure 2-169 Envelope curves for peak positive pressure outside three-wall cubicles with a roof

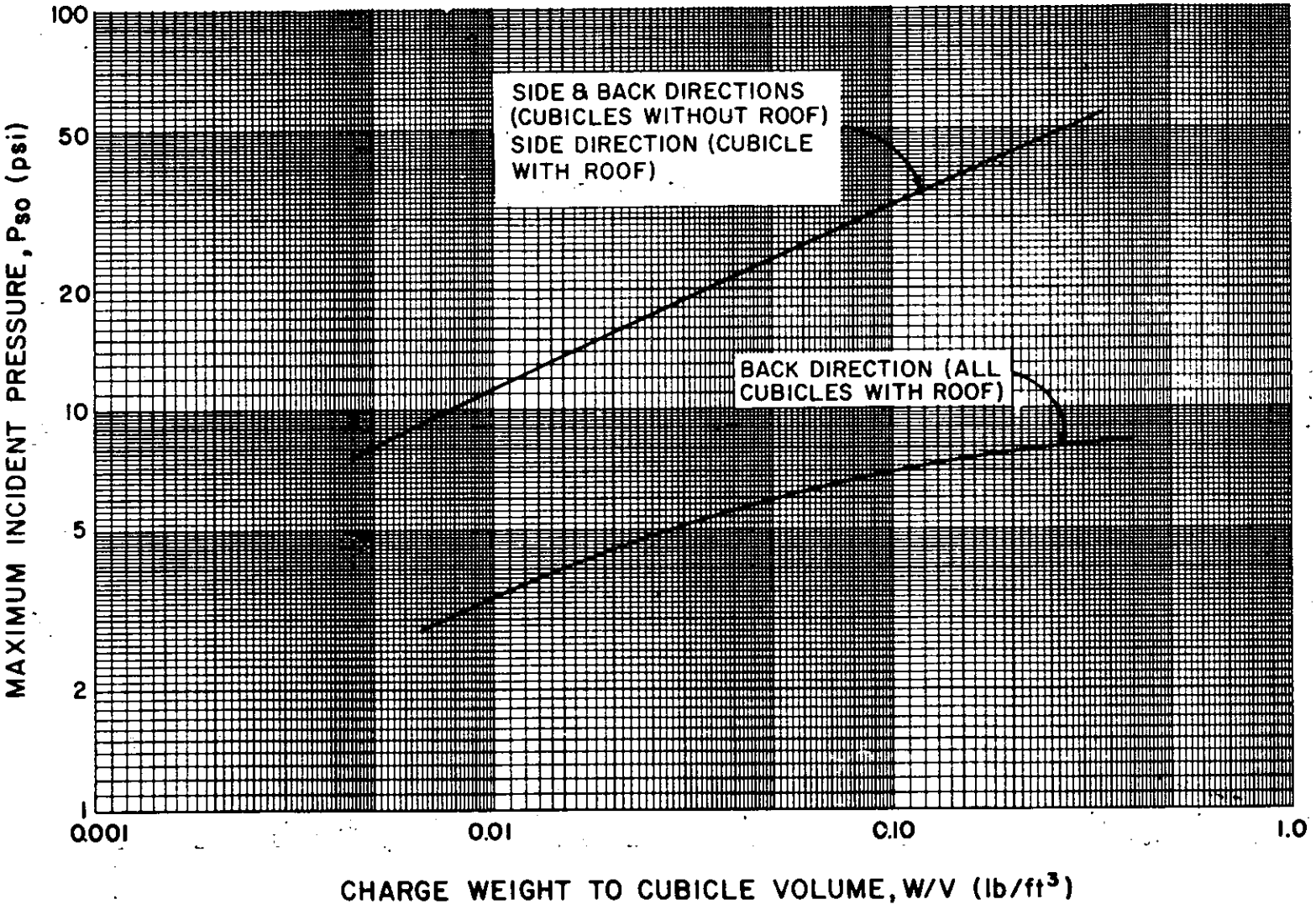


Figure 2-170 Envelope curves for maxium peak pressure outside three-wall cubicles

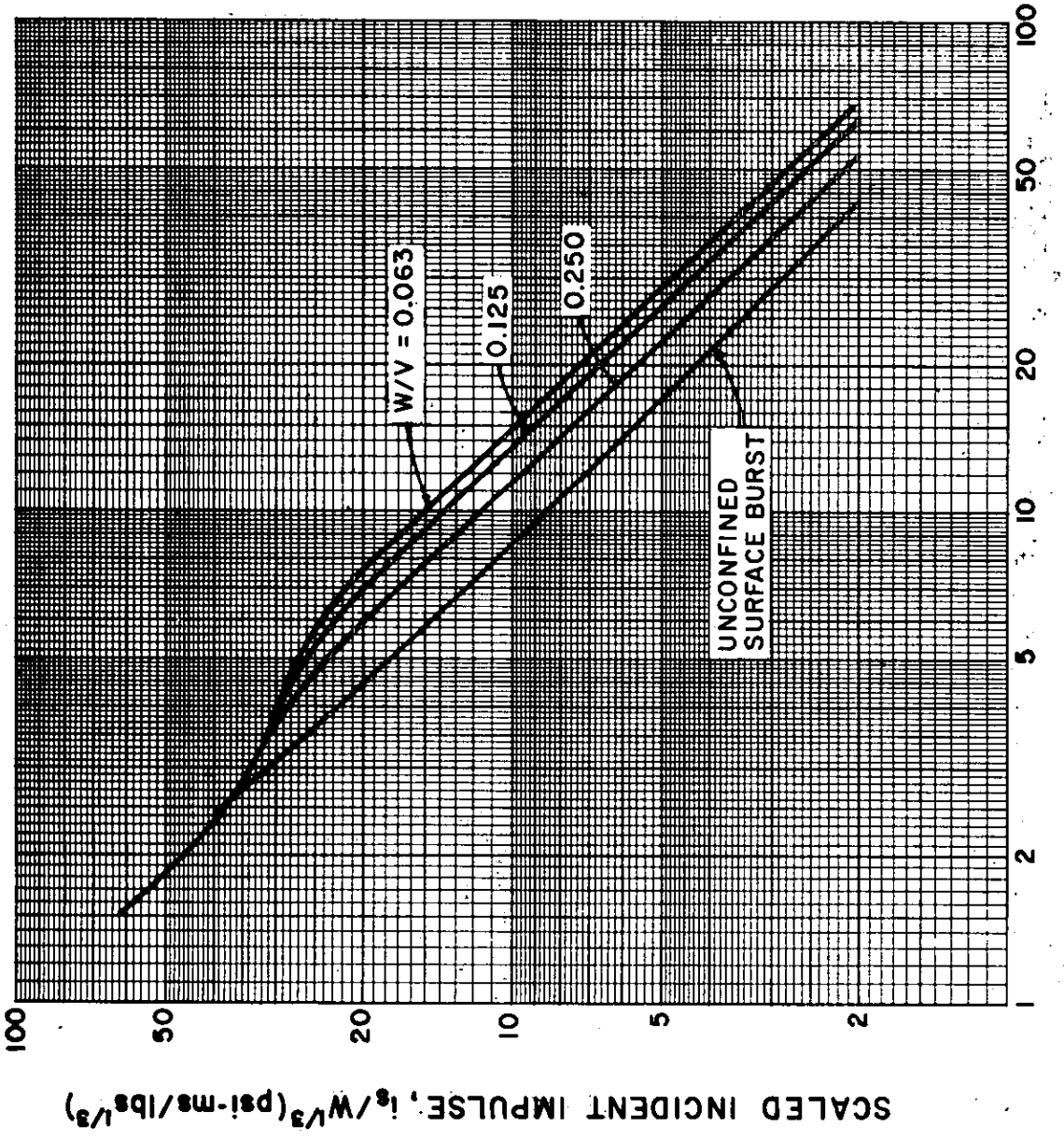


Figure 2-171 Scaled peak positive impulse out the open front of cubic three-wall cubicle without a roof

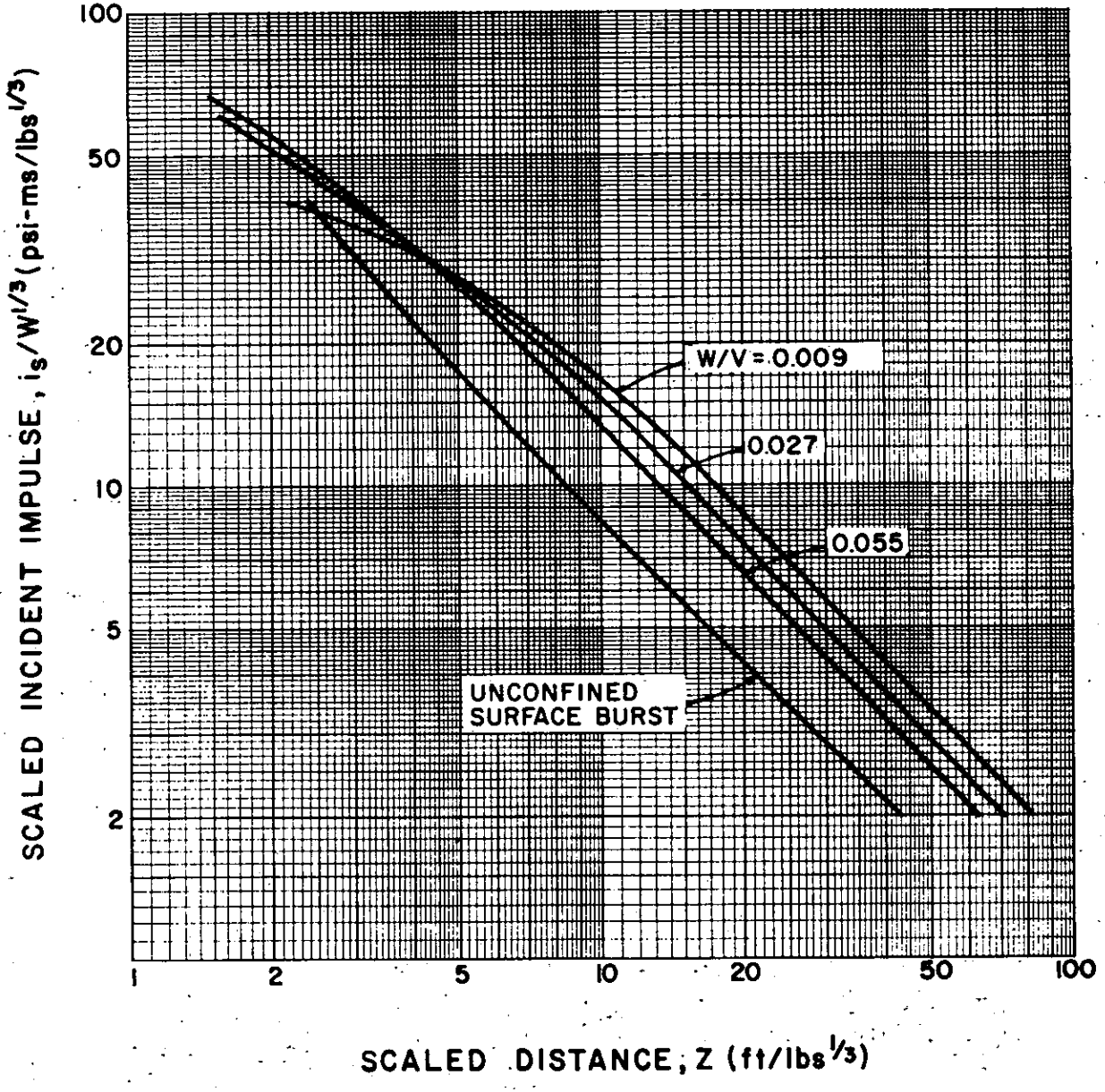


Figure 2-172 Scaled peak positive impulse out the open front of rectangular three-wall cubicle without a roof

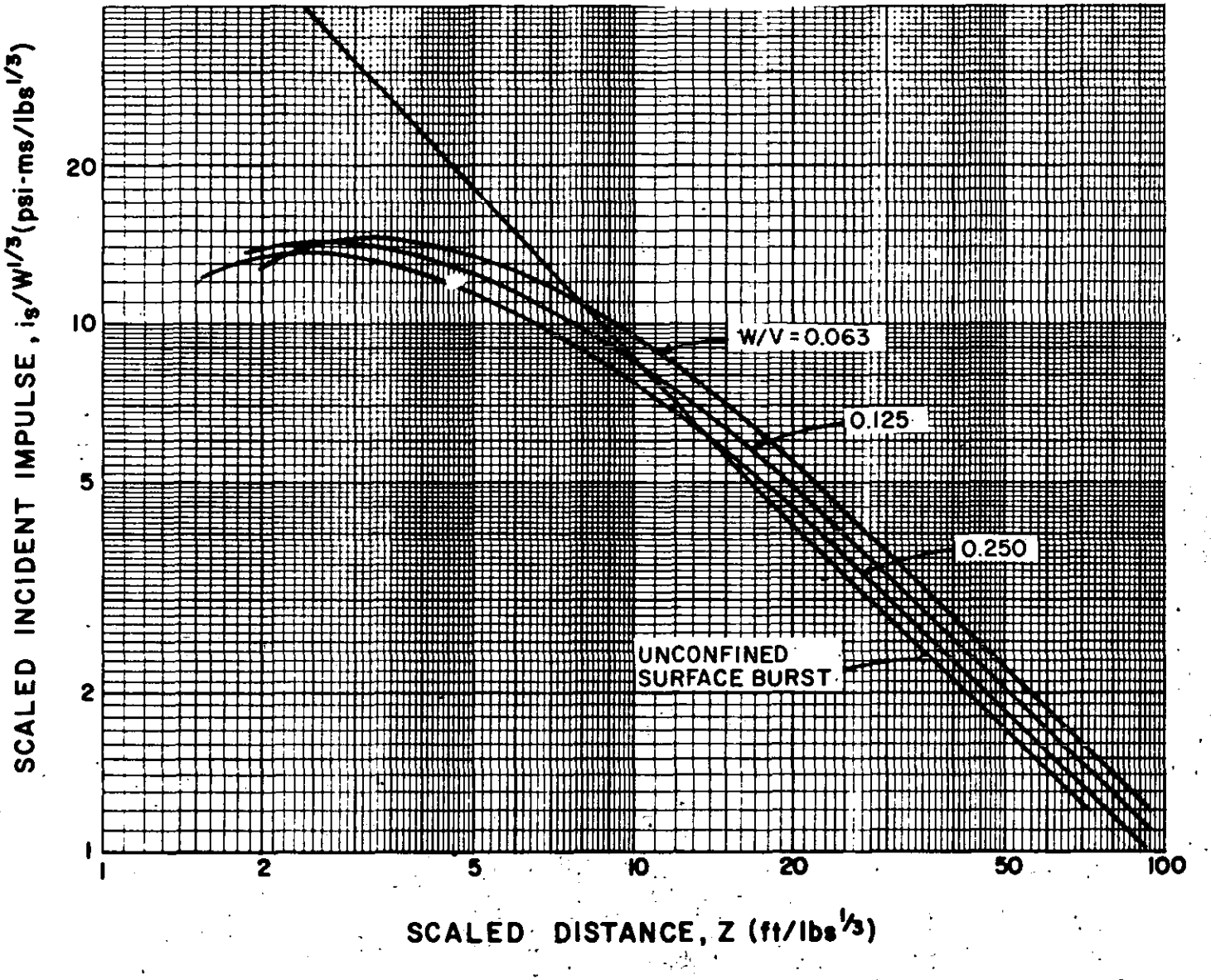


Figure 2-173 Scaled peak positive impulse behind sidewall of cubic three-wall cubicle without a roof

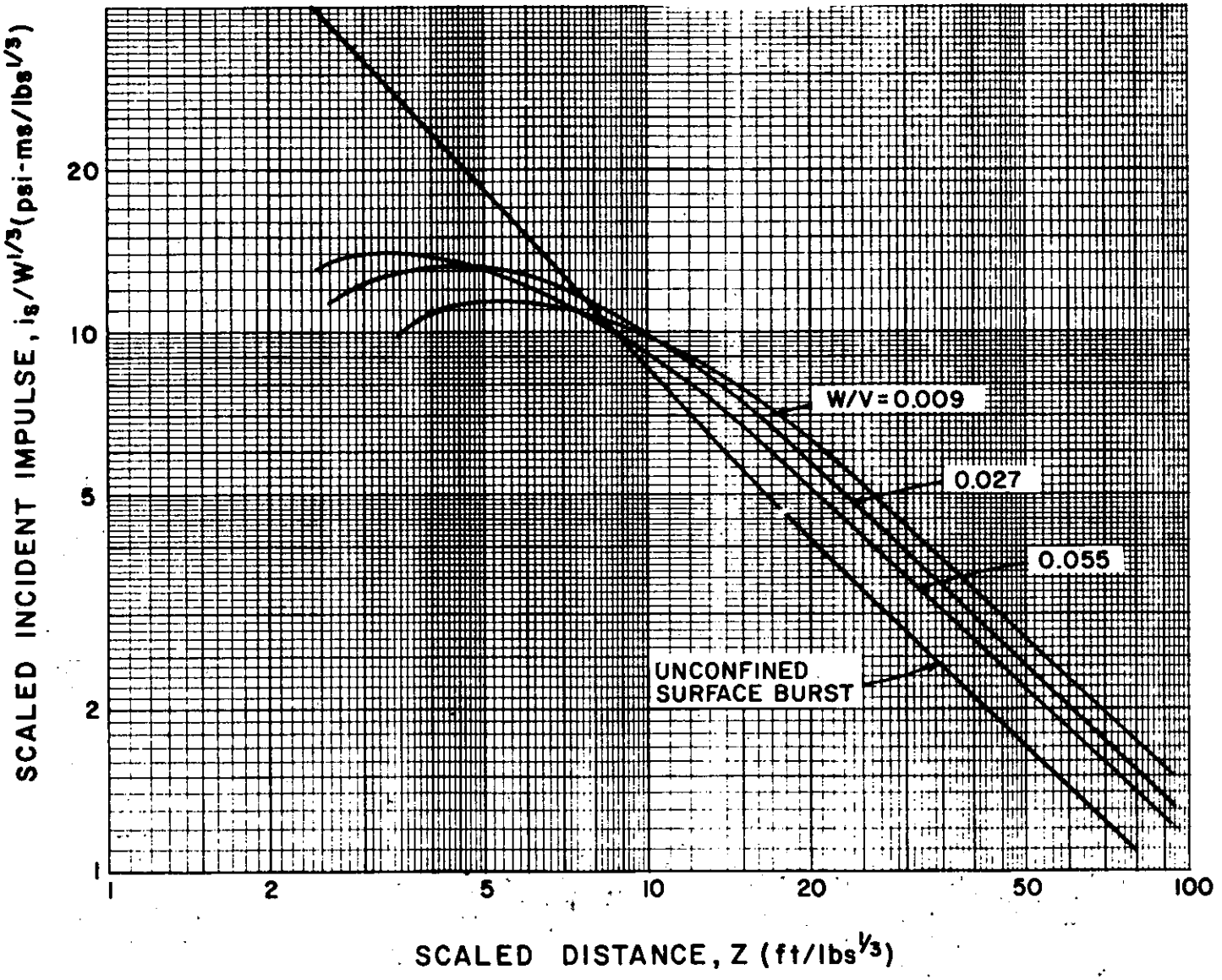


Figure 2-174 Scaled peak positive impulse behind sidewall of rectangular three-wall cubicle without a roof

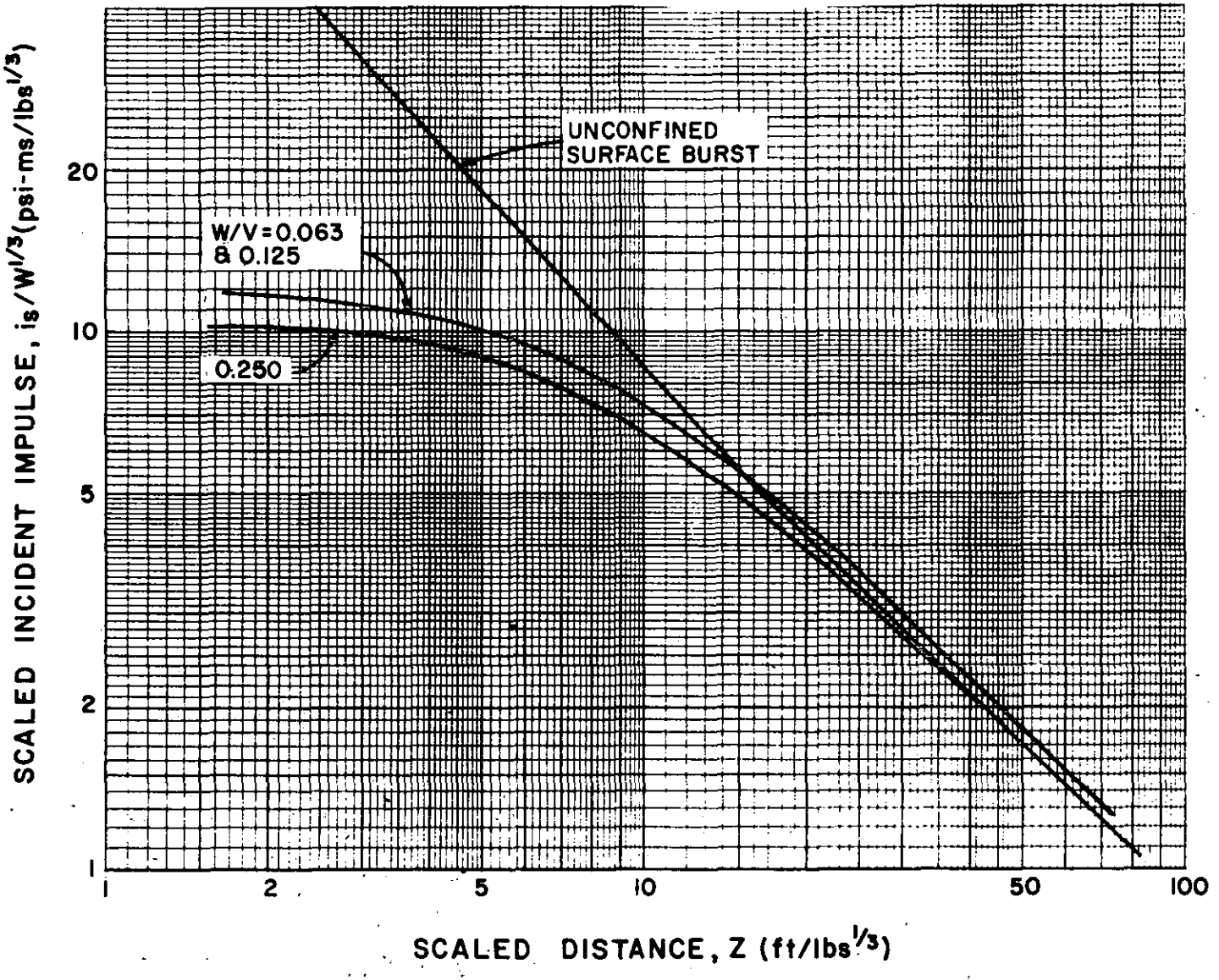


Figure 2-175 Scaled peak positive impulse behind backwall of cubic three-wall cubicle without a roof

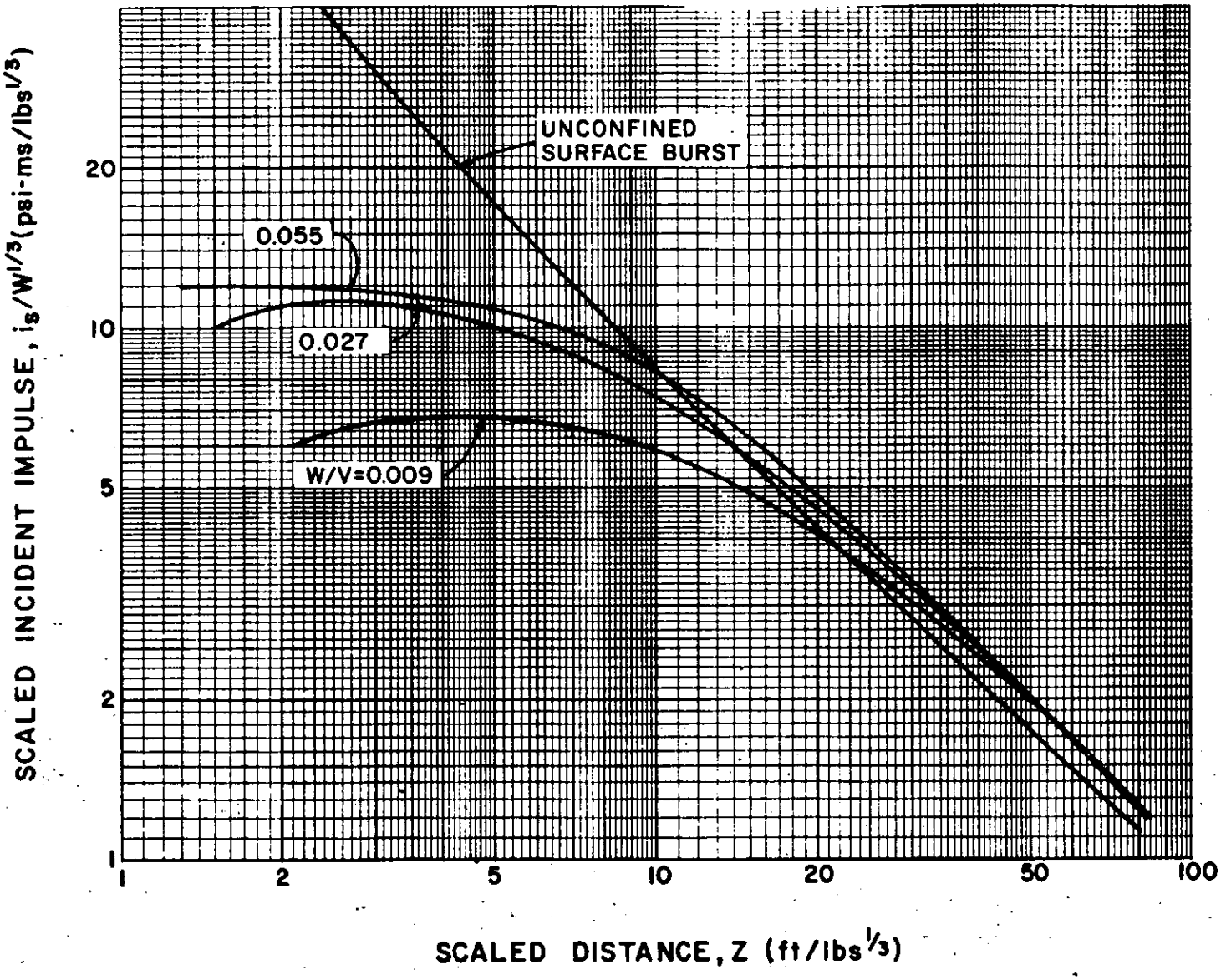


Figure 2-176 Scaled peak positive impulse behind backwall of rectangular three-wall cubicle without a roof

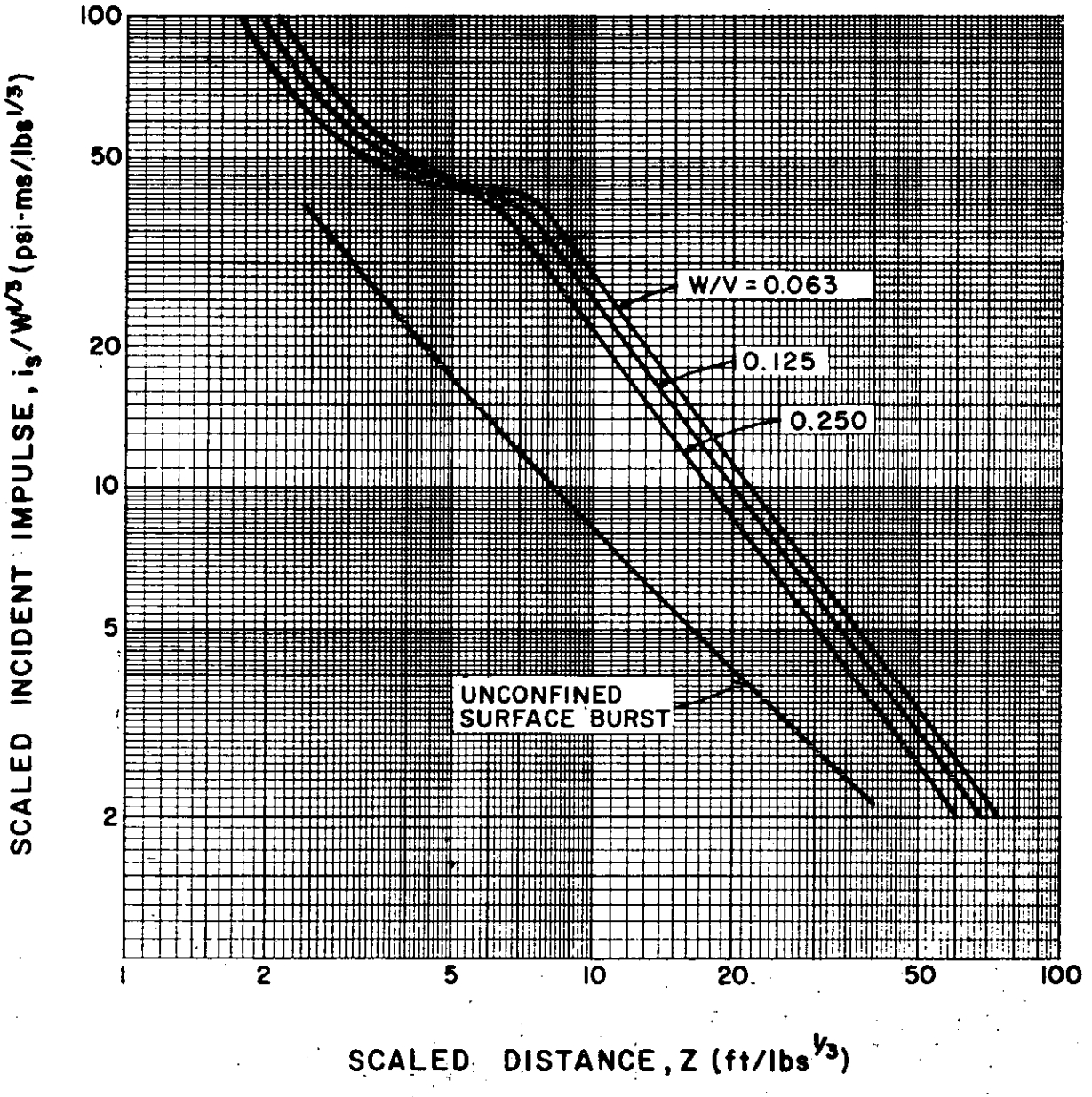


Figure 2-177 Scaled peak positive impulse out the open front of cubic three-wall cubicle with a roof

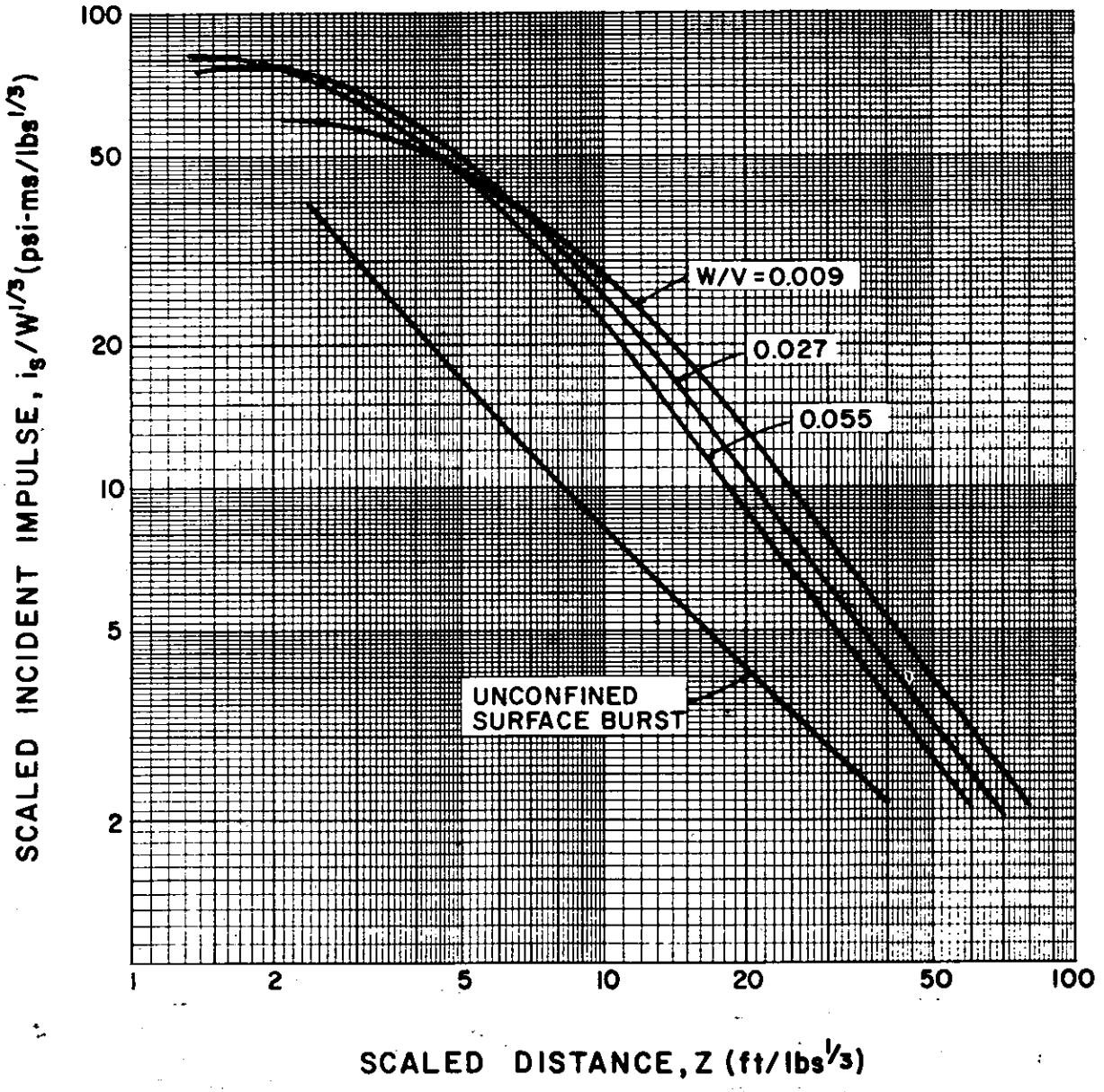


Figure 2-178 Scaled peak positive impulse out the open front of rectangular three-wall cubicle with a roof

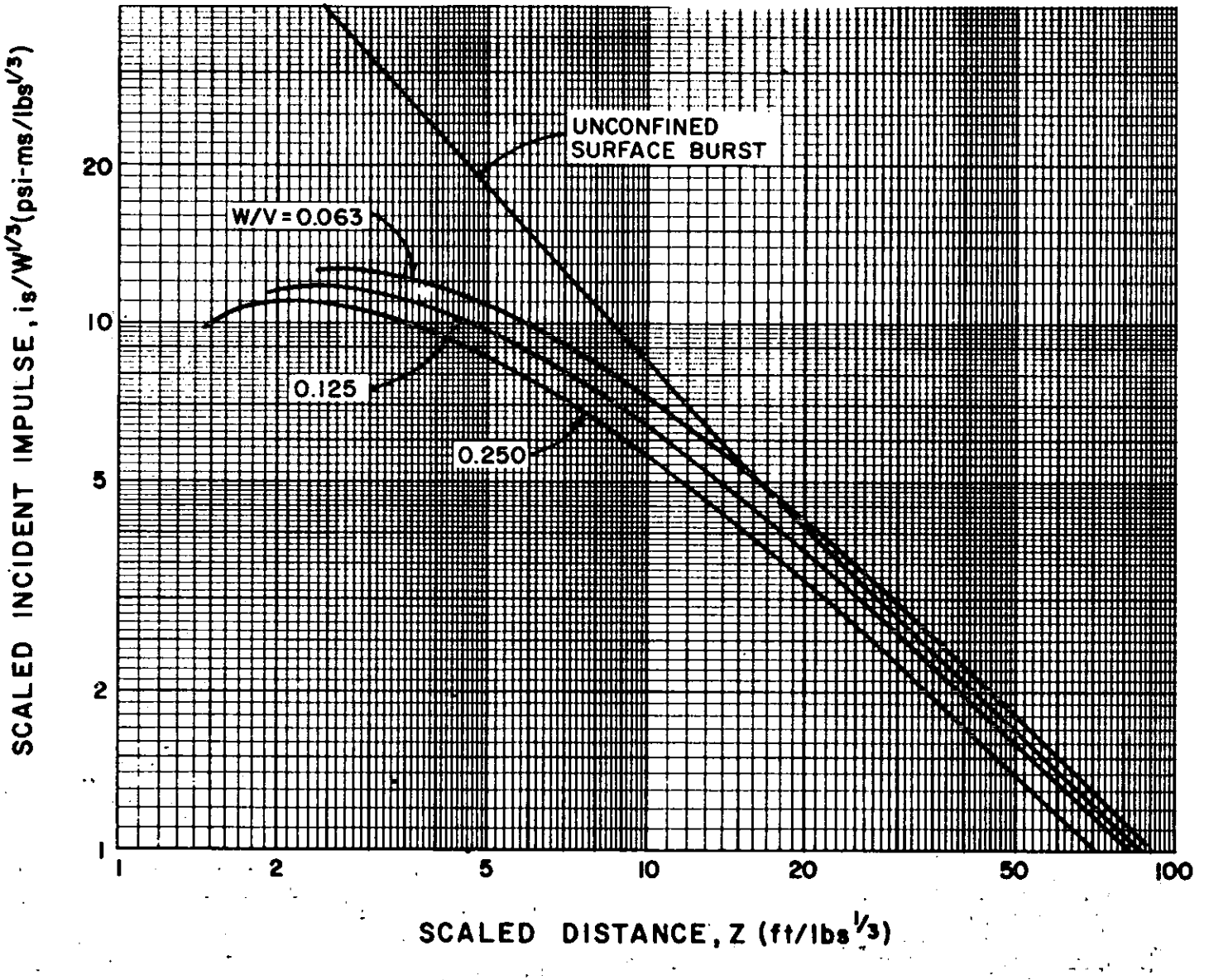


Figure 2-179 Scaled peak positive impulse behind sidewall of cubic three-wall cubicle with a roof

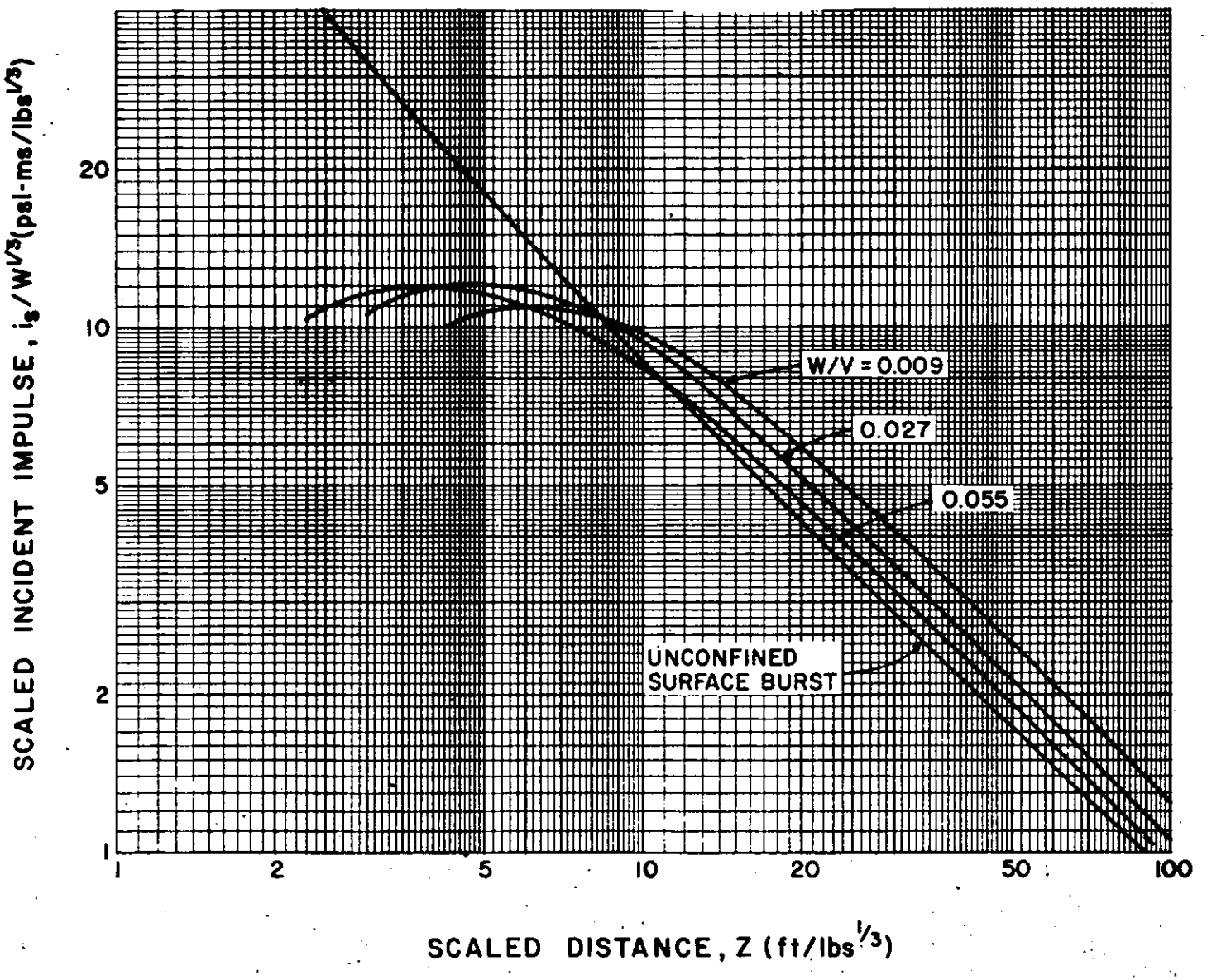


Figure 2-180 Scaled peak positive impulse behind sidewall of rectangular three-wall cubicle with a roof

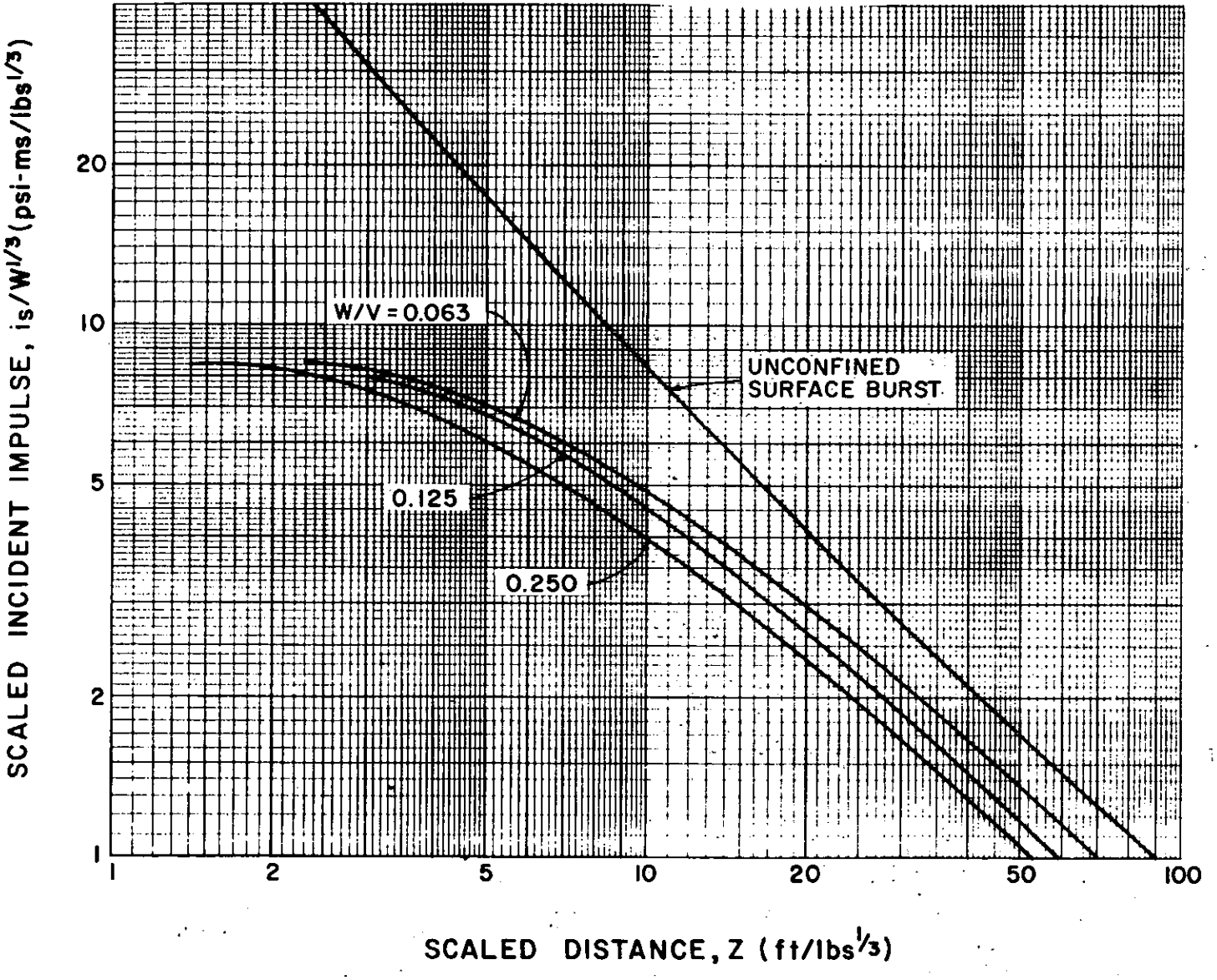


Figure 2-181 Scaled peak positive impulse behind backwall of cubic three-wall cubicle with a roof

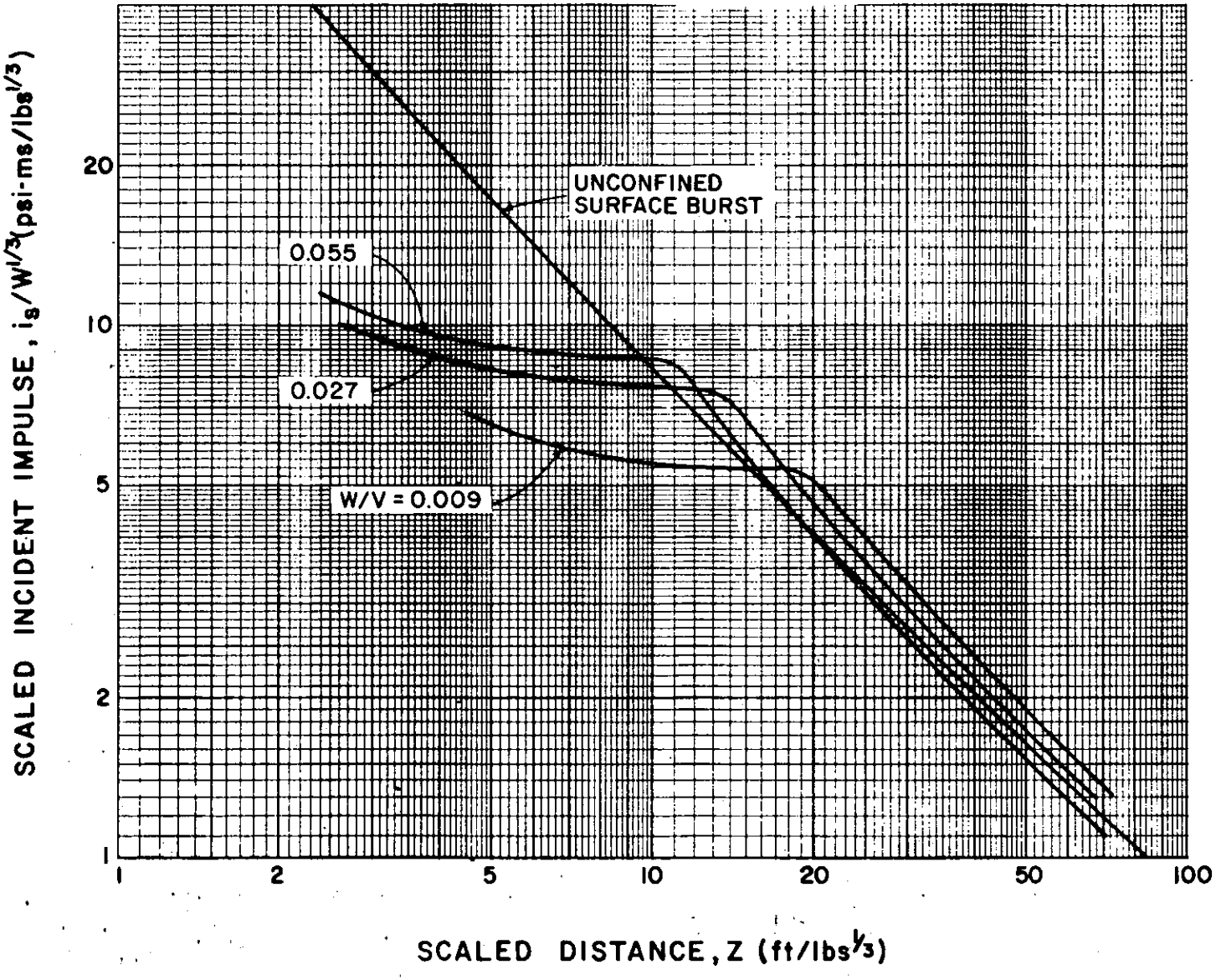
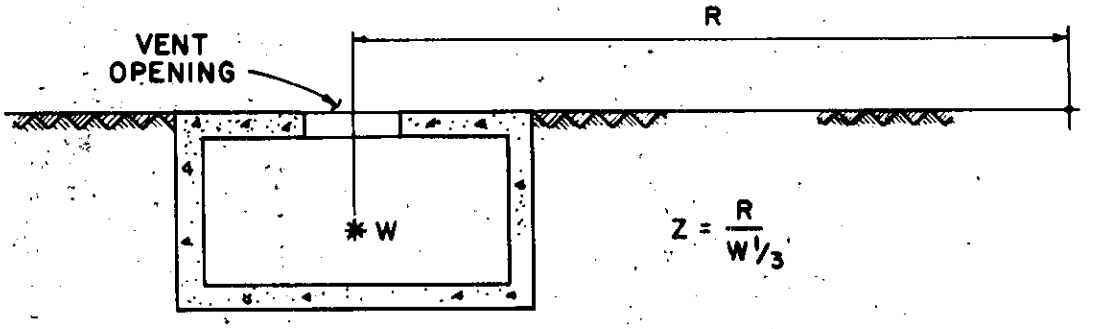
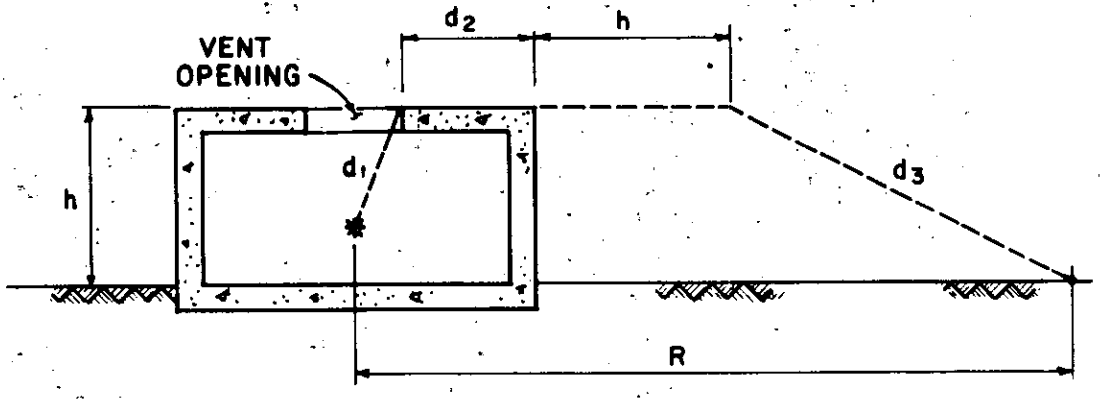


Figure 2-182 Scaled peak positive impulse behind backwall of rectangular three-wall cubicle with a roof



a) BELOW GROUND STRUCTURE WITH ROOF AT GROUND SURFACE



$$Z = \frac{d_1 + d_2 + h + d_3}{W^{1/3}}$$

b) ABOVE GROUND STRUCTURE

Figure 2-183 Four wall cubicle vented through its roof

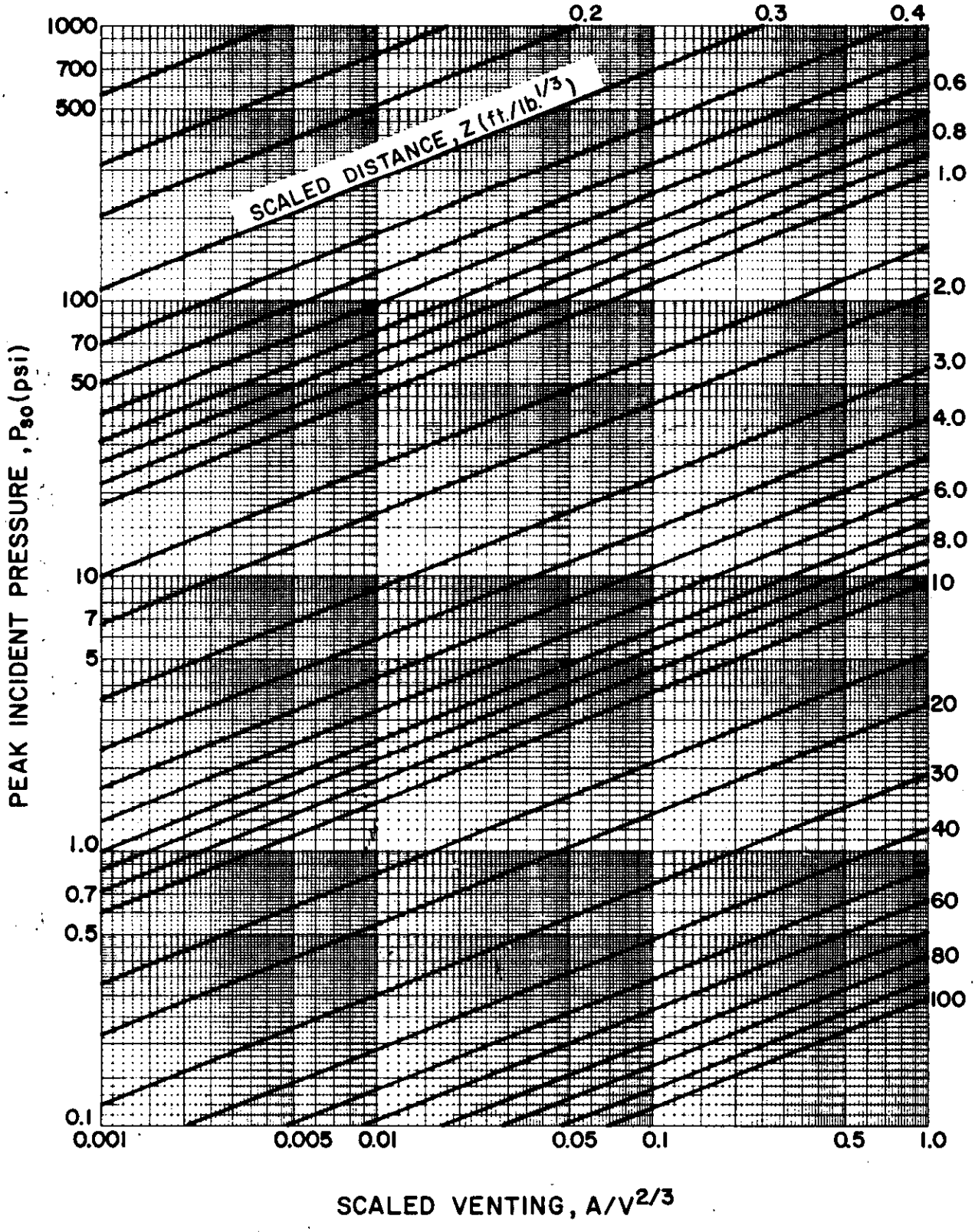


Figure 2-184 Peak positive pressure outside of a four-wall cubicle vented through its roof

Figure 2-185 Scaled positive impulse outside of a four-wall cubicle vented through its roof

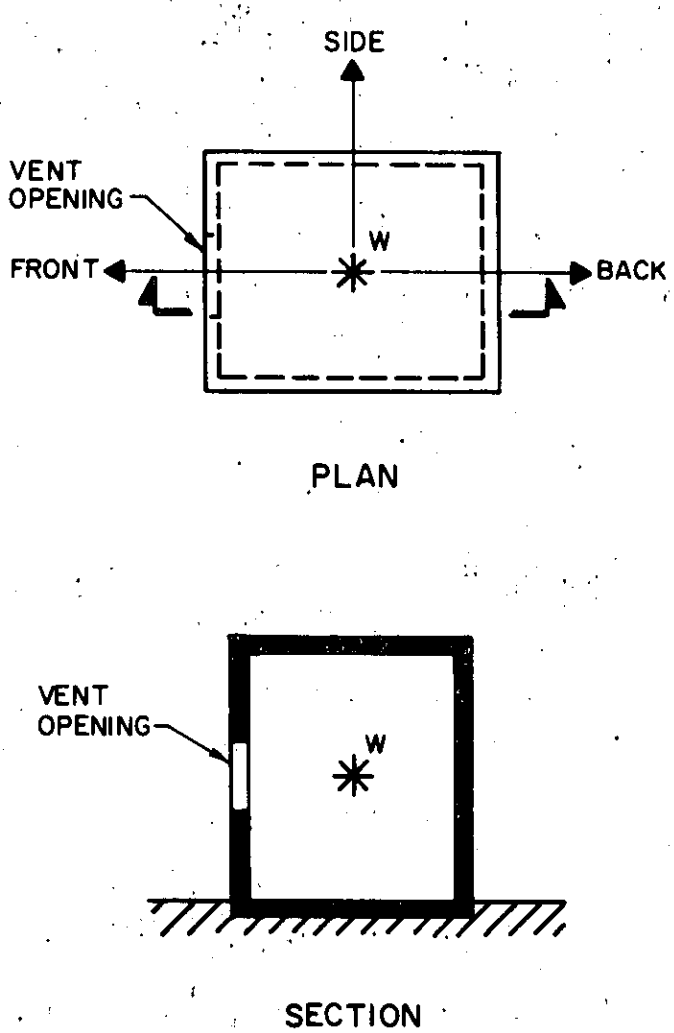


Figure 2-186 Four wall cubicle vented through a wall and direction of blast wave propagation

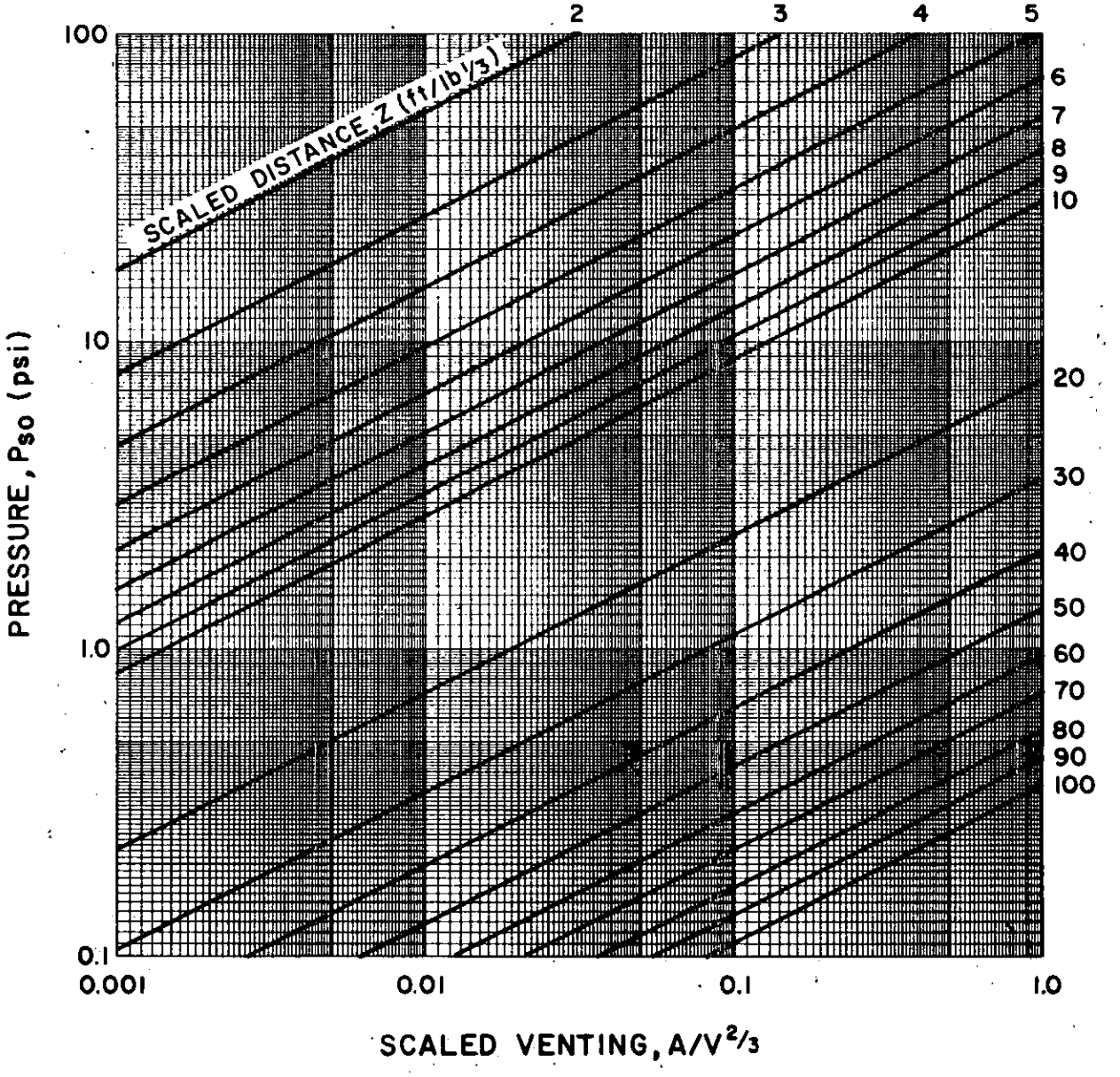


Figure 2-187 Peak positive pressure at the front of a partially vented four-wall cubicle

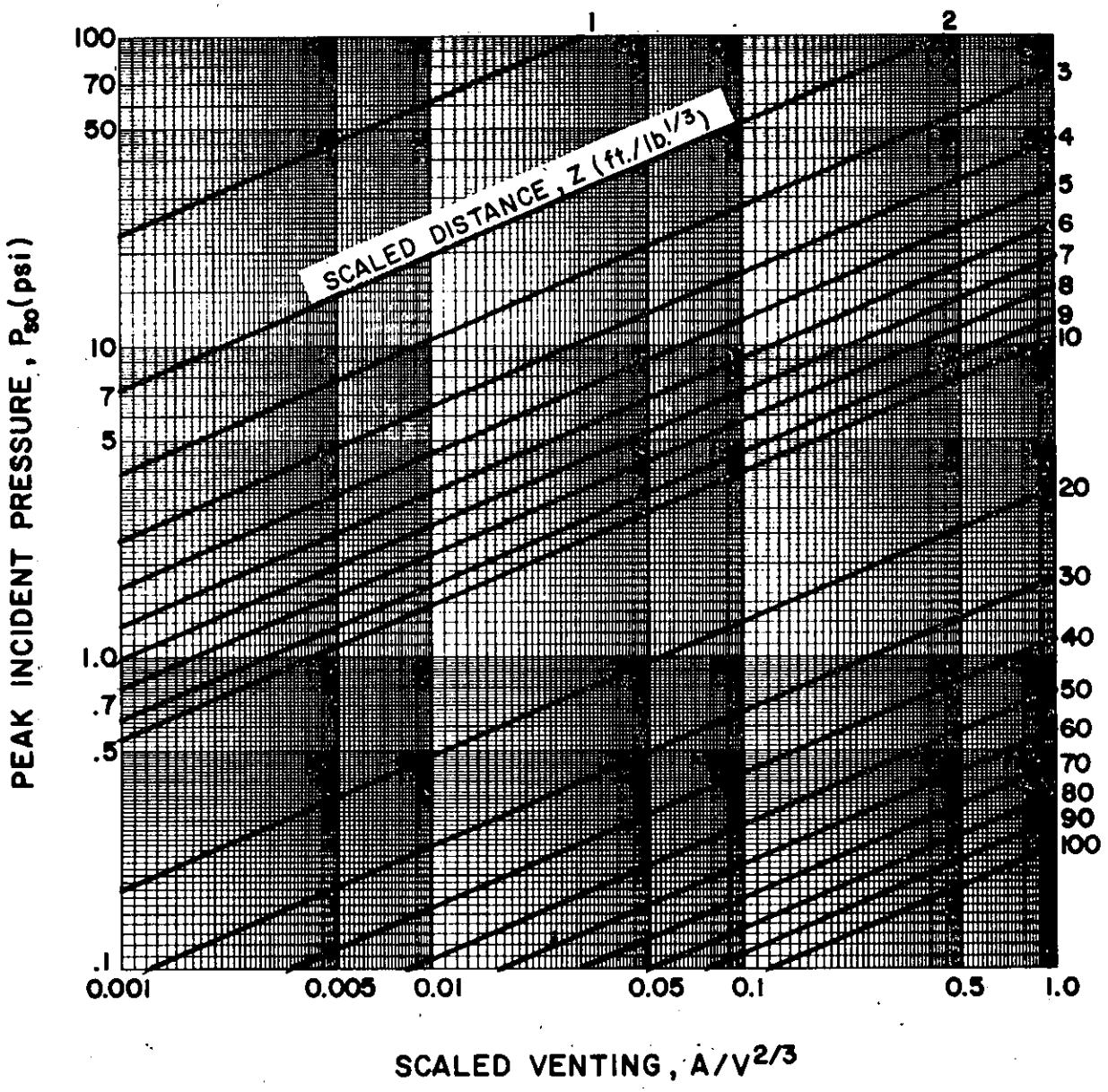


Figure 2-188 Peak positive pressure at the side of a partially vented four-wall cubicle

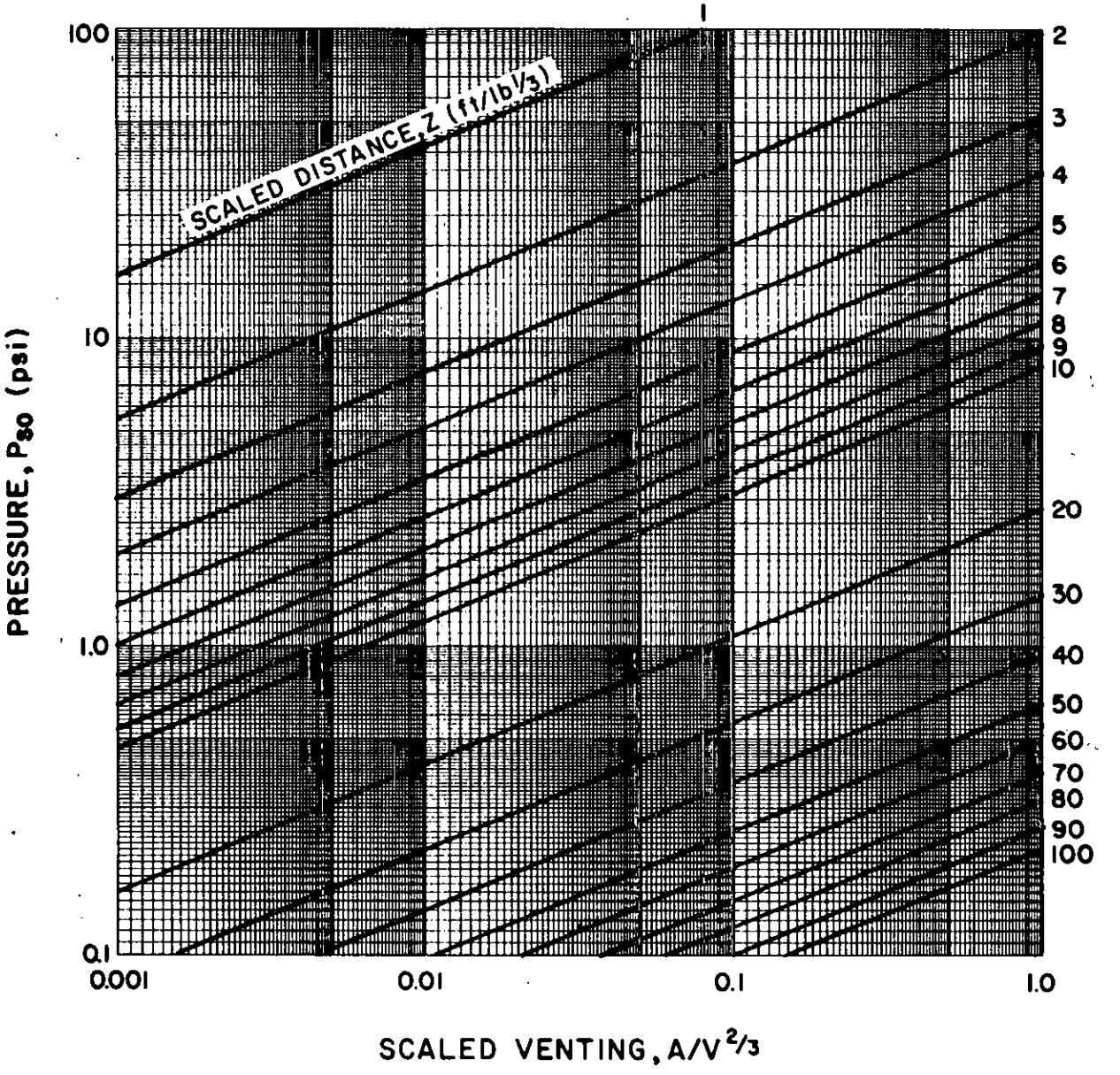


Figure 2-189 Peak positive pressure at the back of a partially vented four wall cubicle

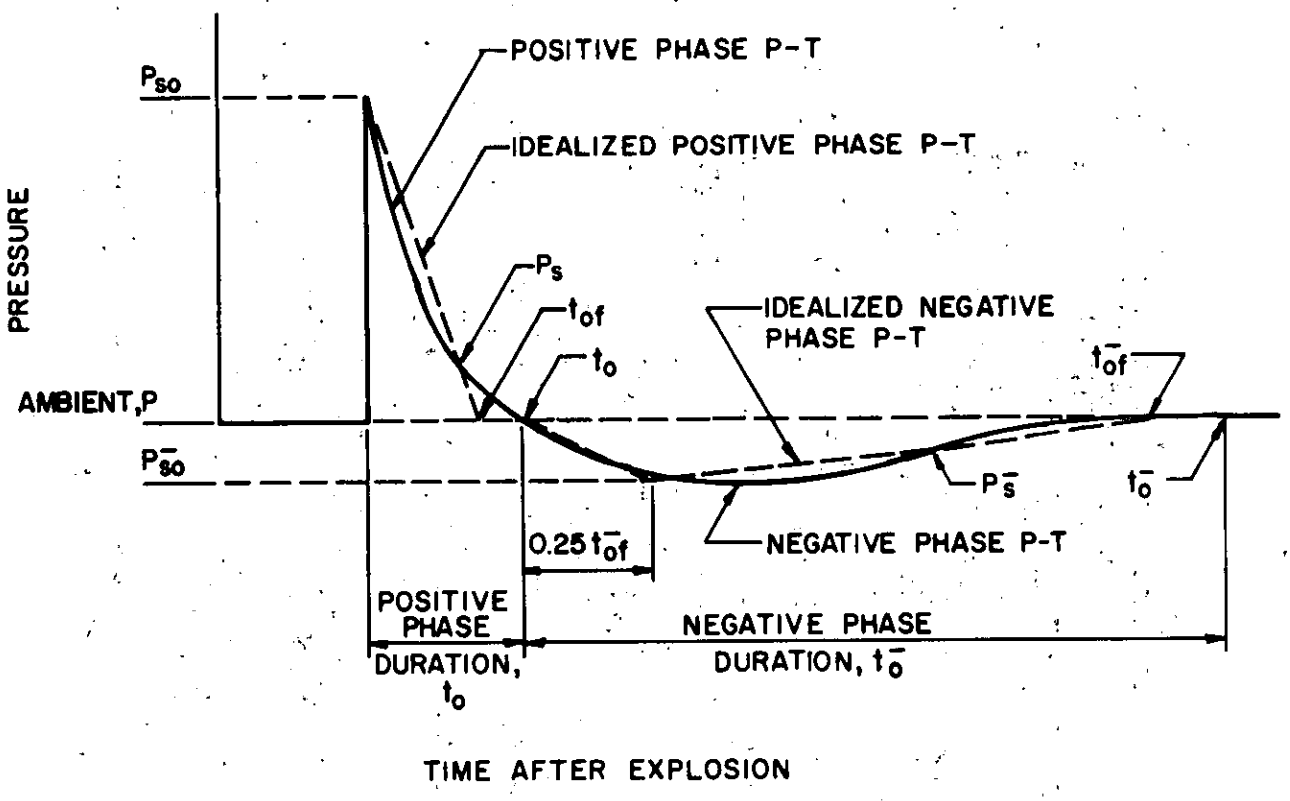
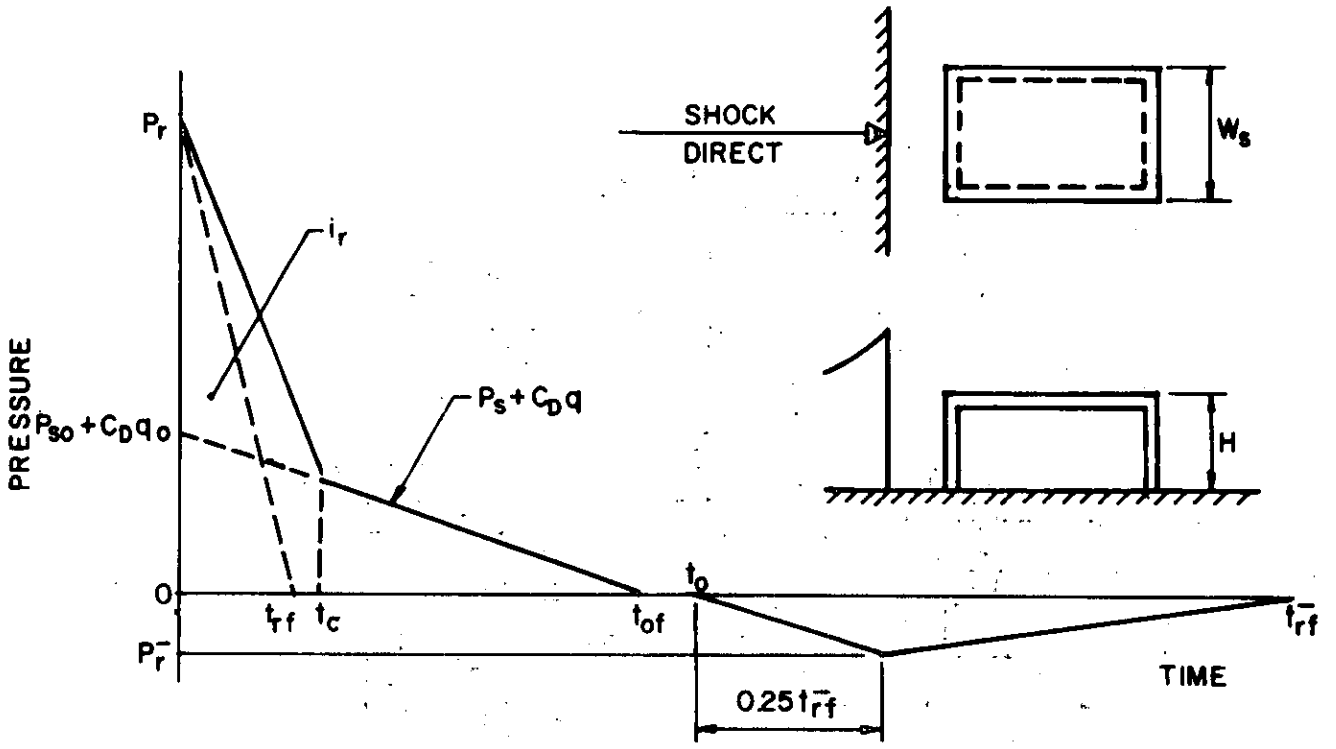
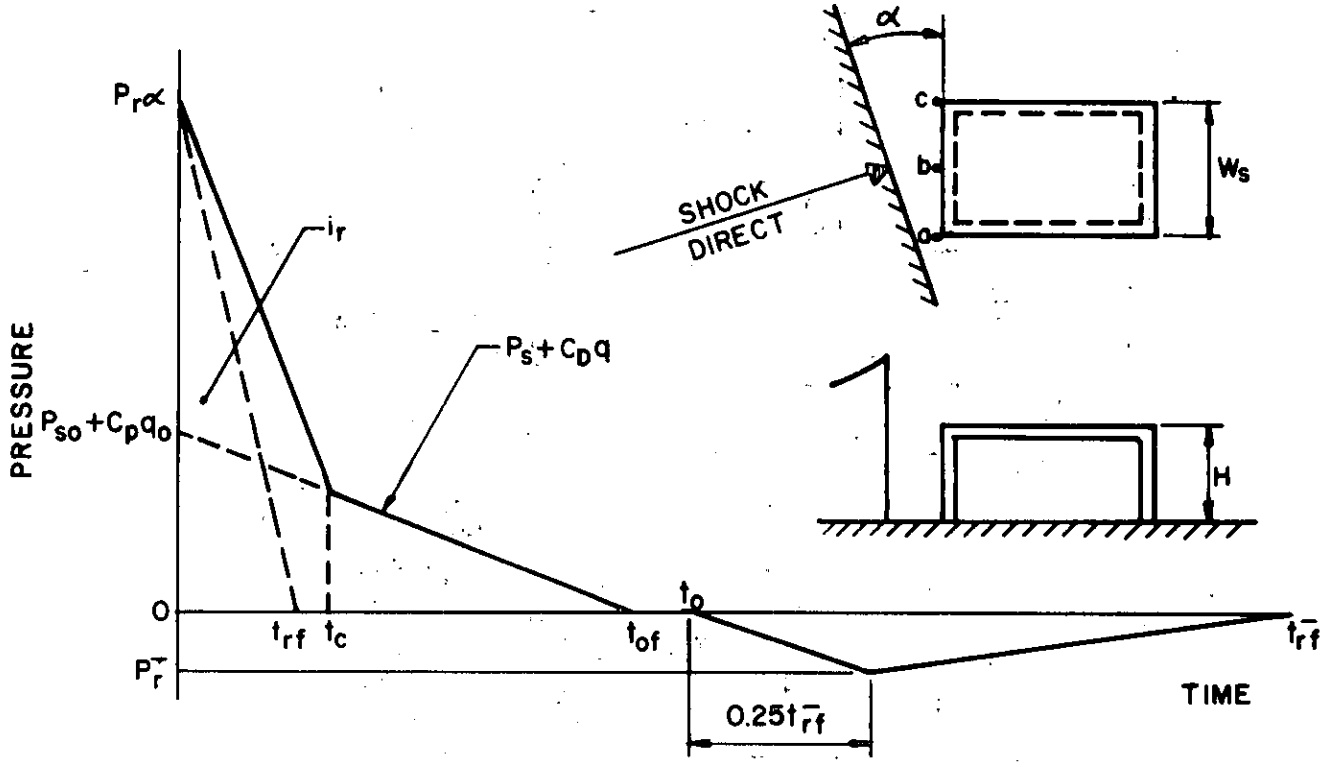


Figure 2-190 Idealized pressure-time variation



a. NORMAL REFLECTION



b. OBLIQUE REFLECTION

Figure 2-191. Front wall loading

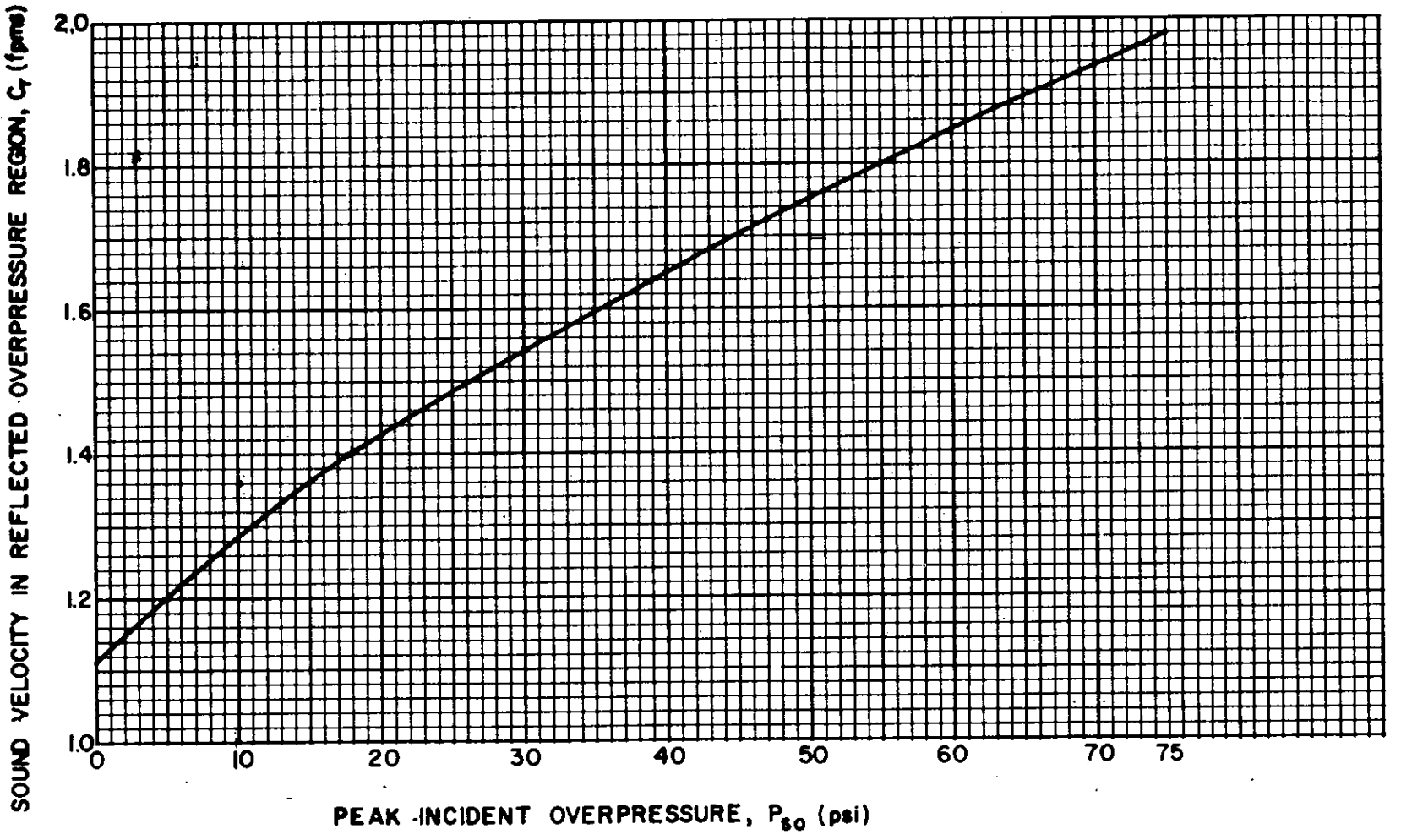


Figure 2-192 Velocity of sound in reflected overpressure region versus peak incident overpressure

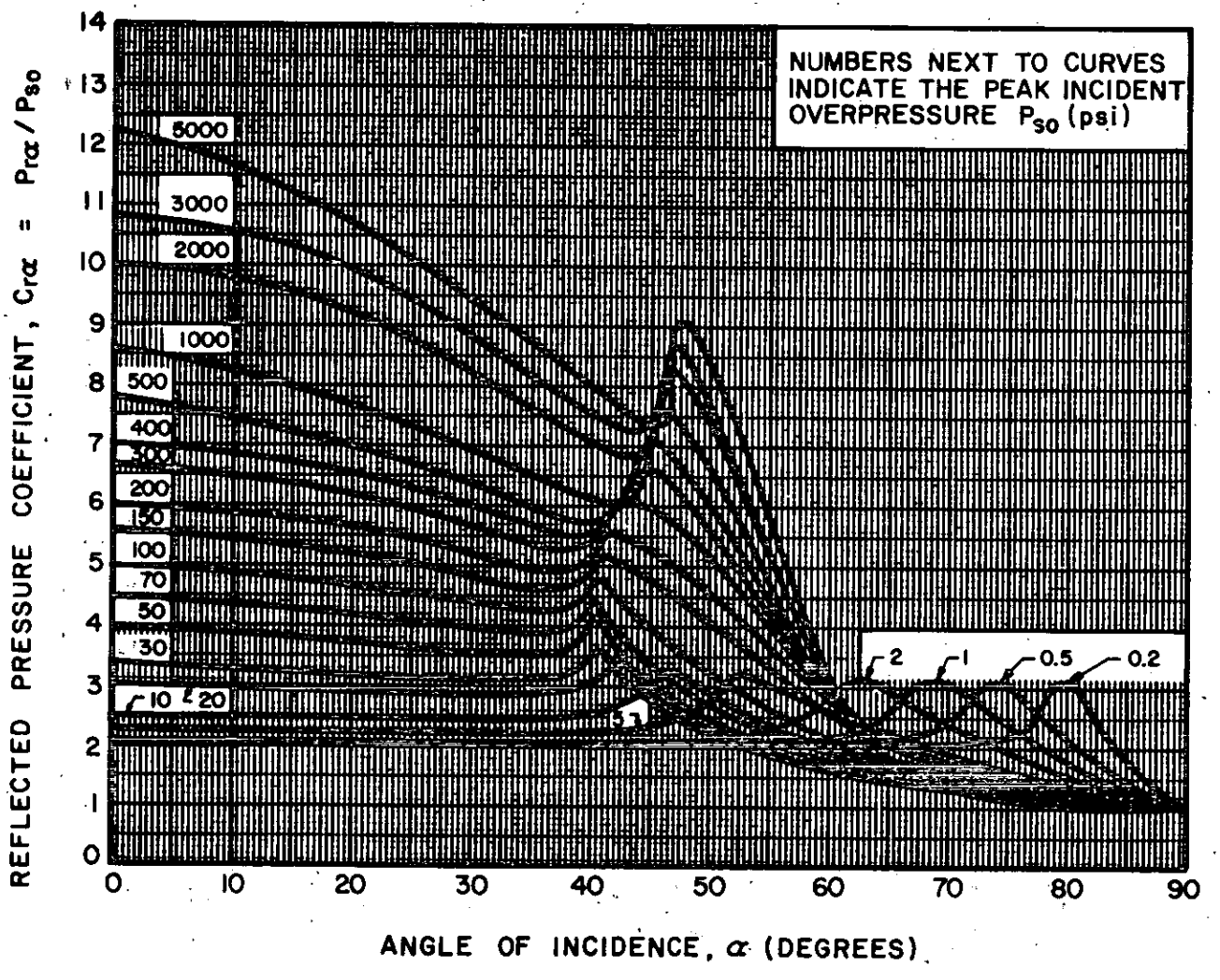


Figure 2-193 Reflected pressure coefficient versus angle of incidence

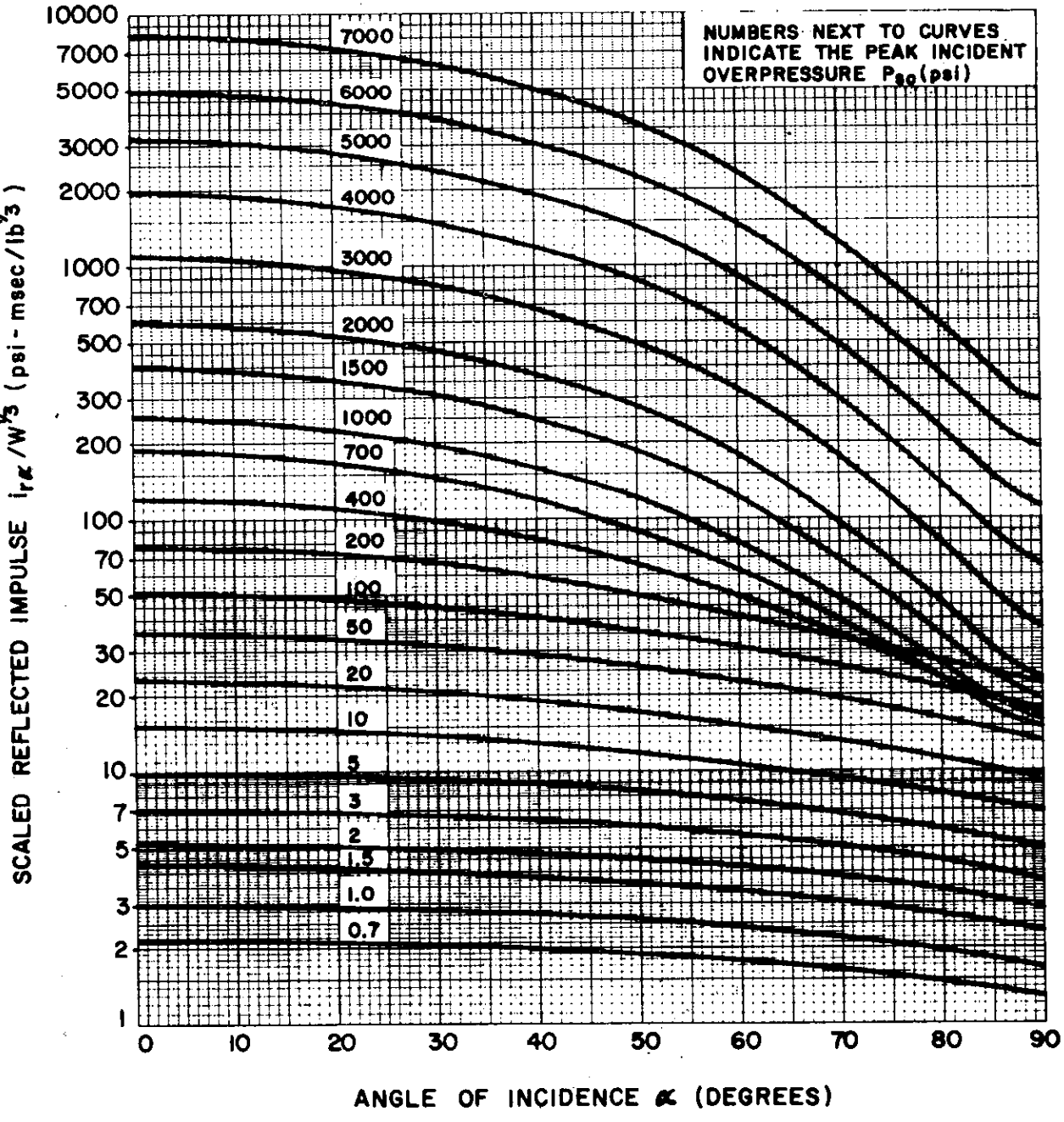


Figure 2-194 Reflected scaled impulse versus angle of incidence

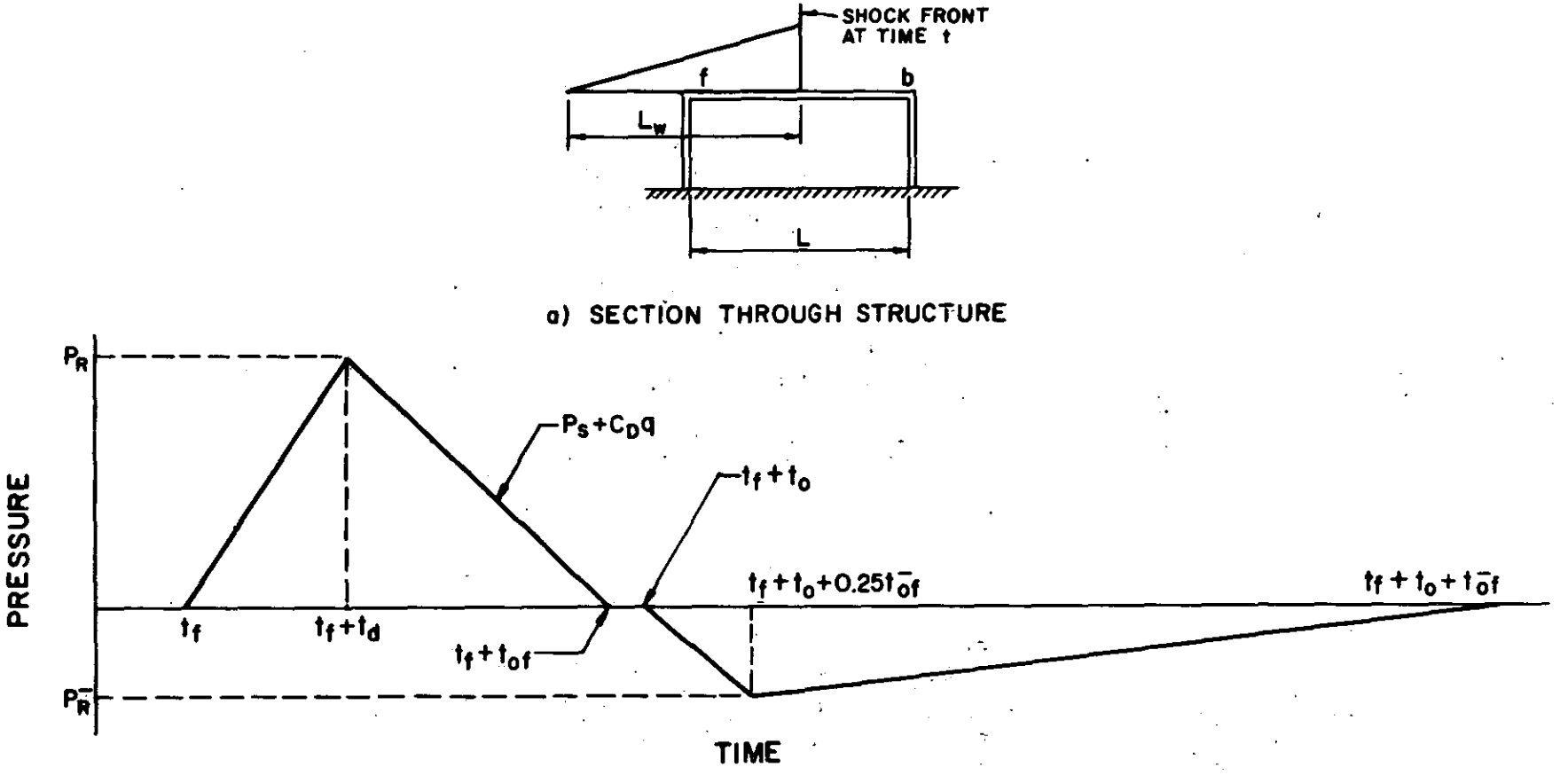


Figure 2-195 Roof and side wall loading

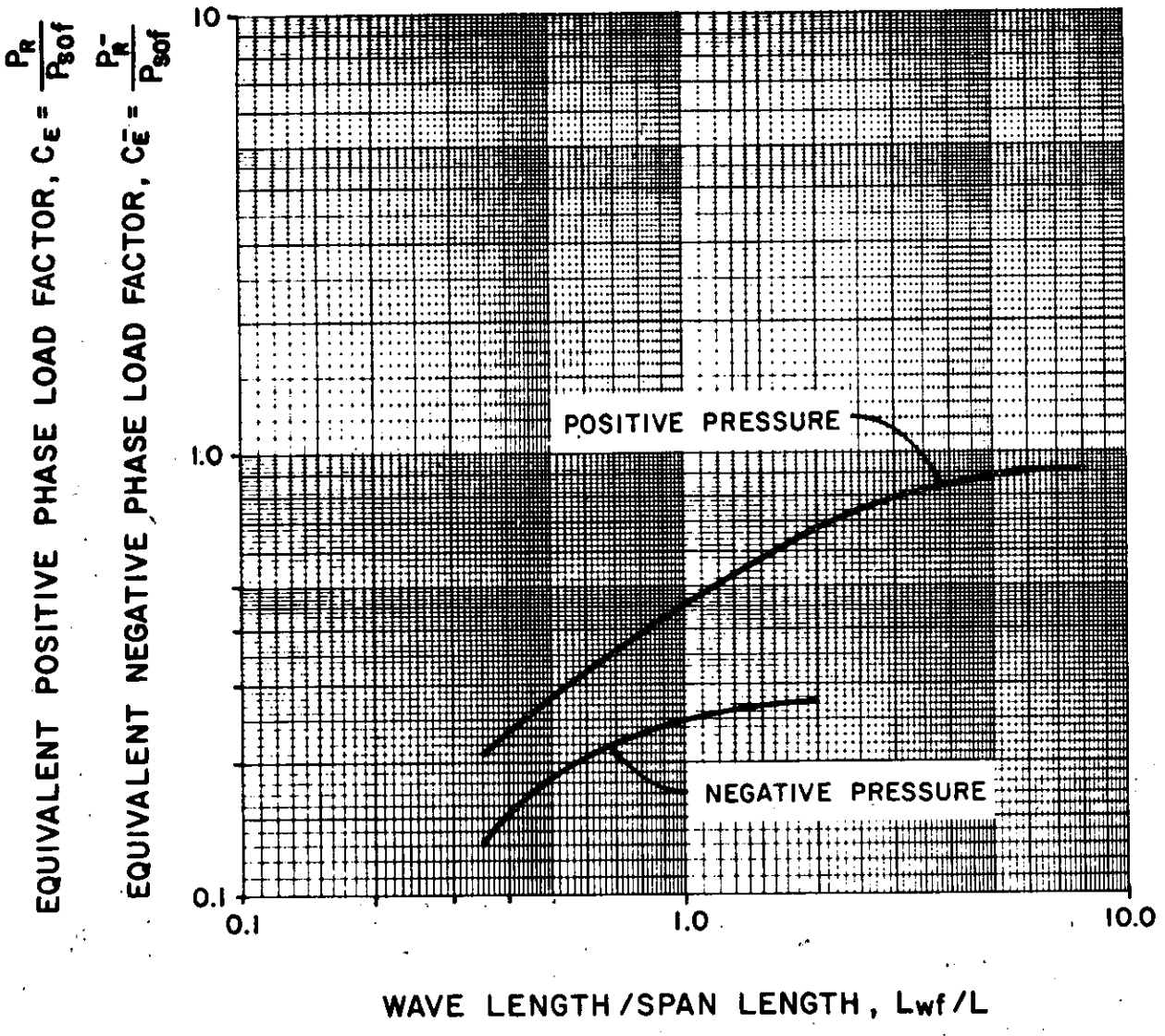
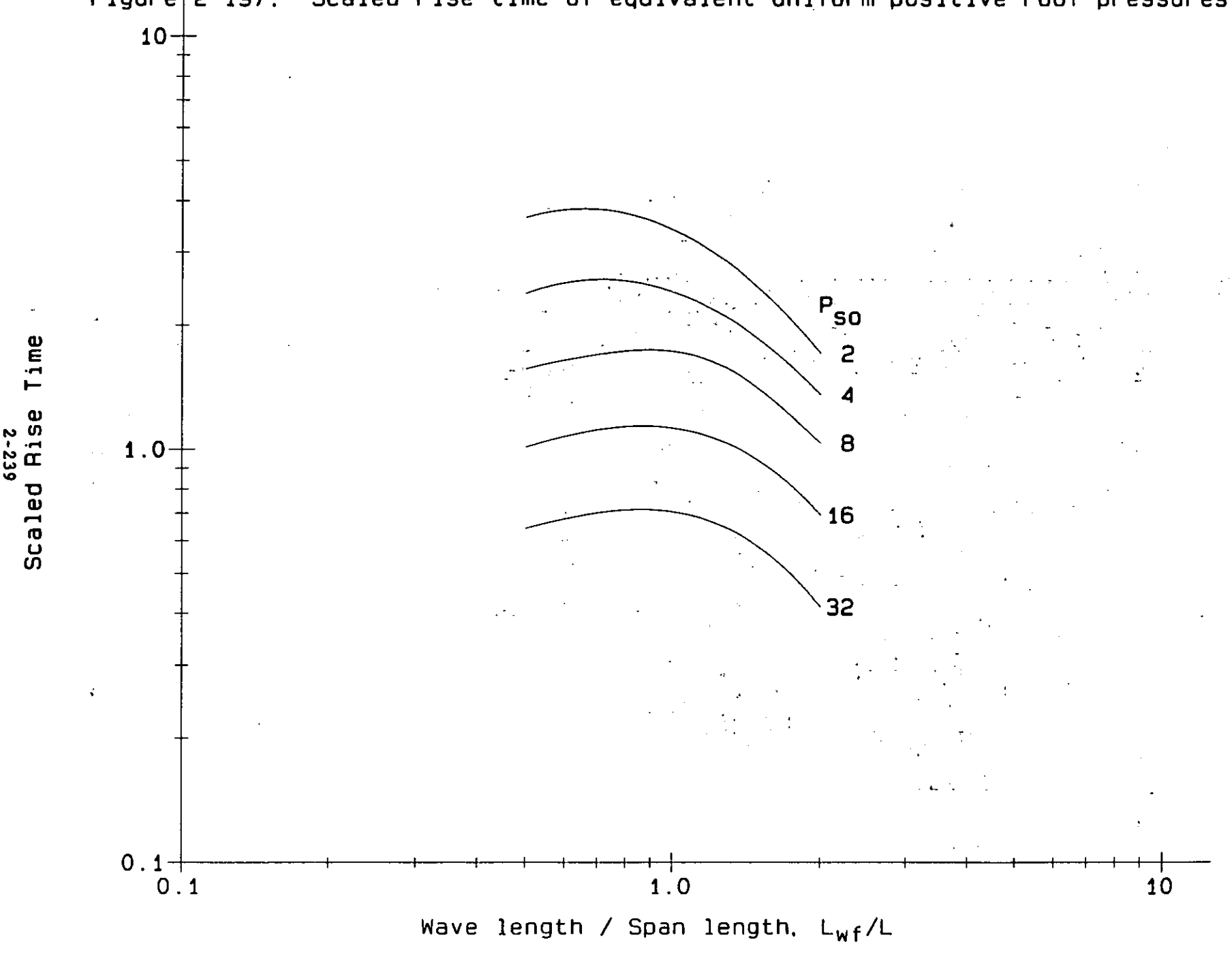


Figure 2-196 Peak equivalent uniform roof pressures

Figure 2-197. Scaled rise time of equivalent uniform positive roof pressures



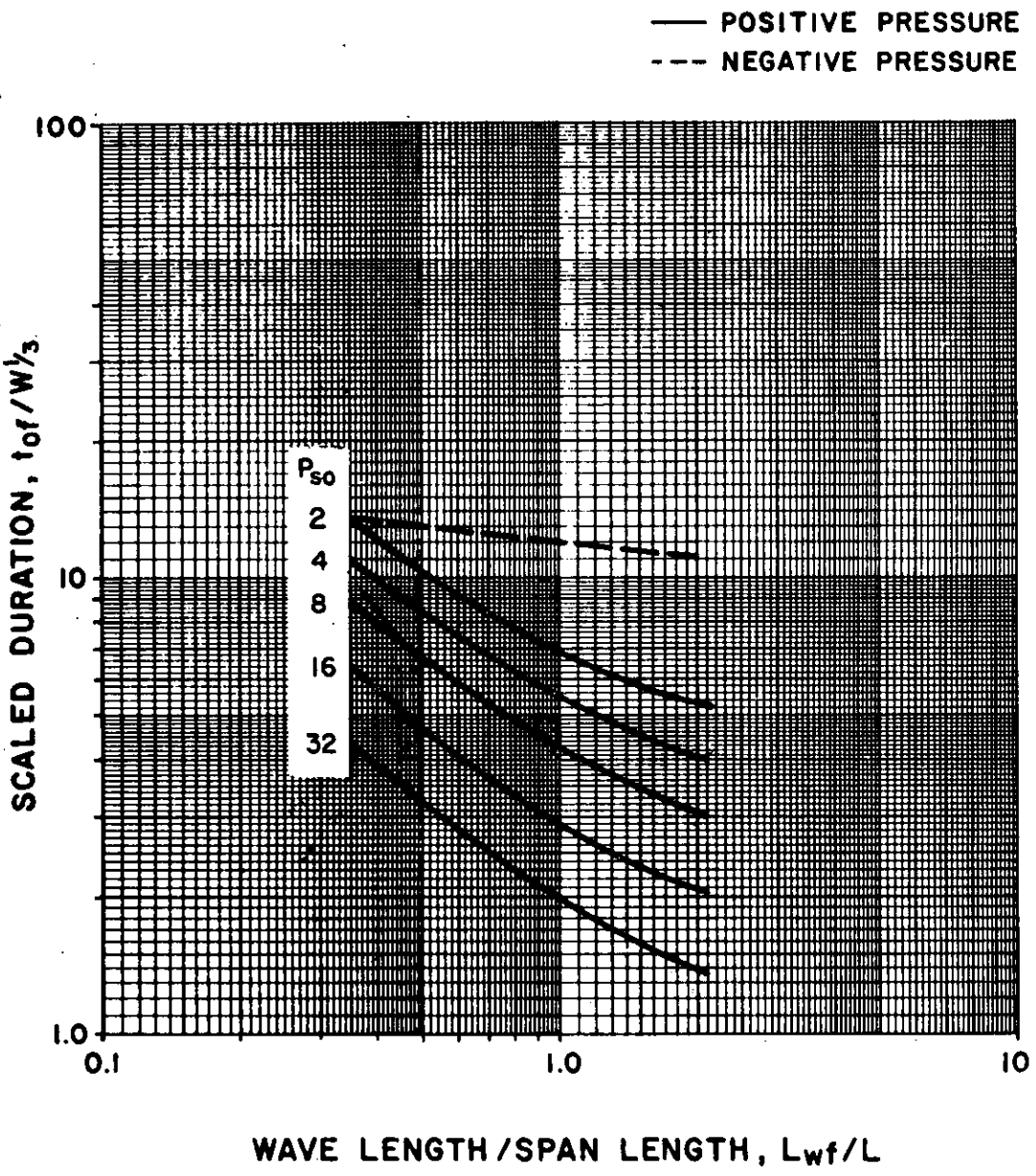
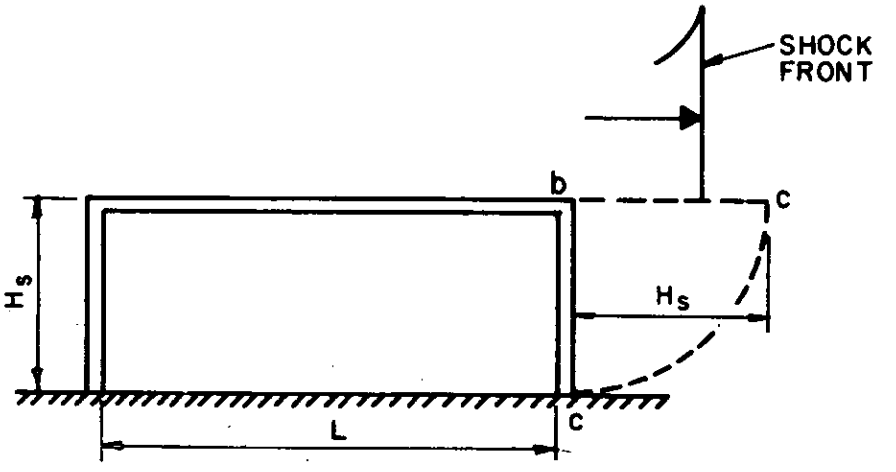
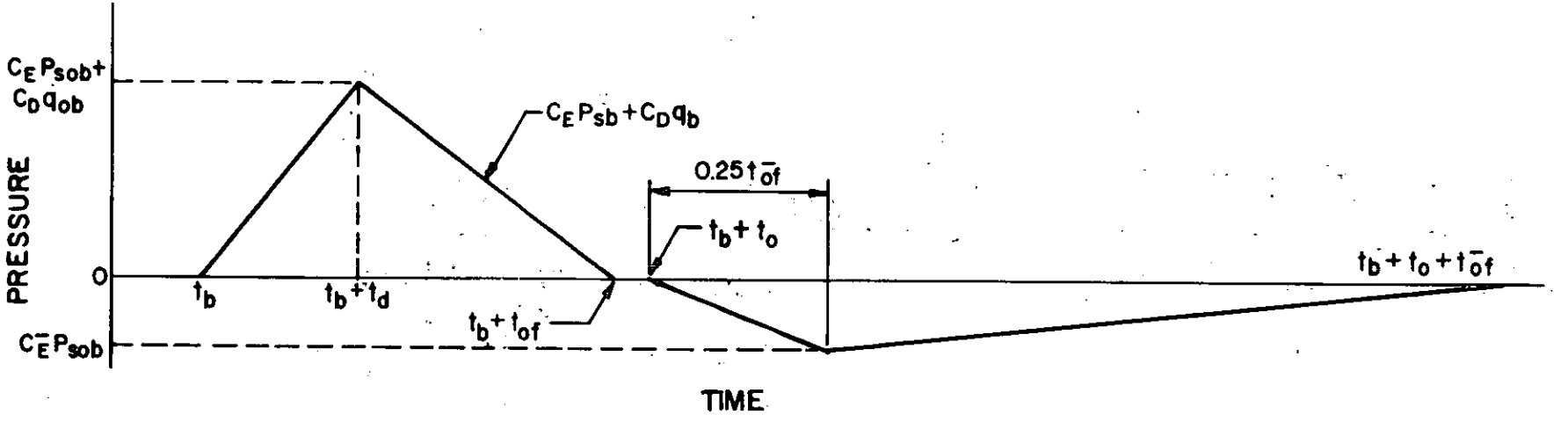


Figure 2-198 Scaled duration of equivalent uniform roof pressures

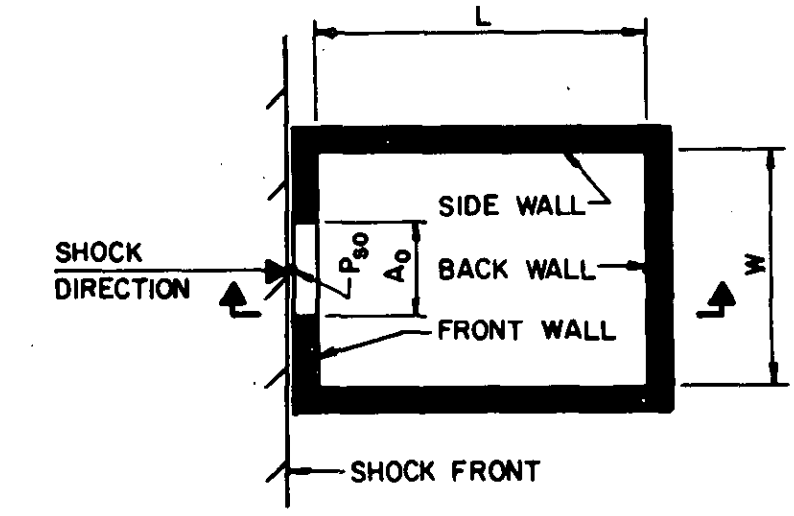


a) SECTION THROUGH STRUCTURE

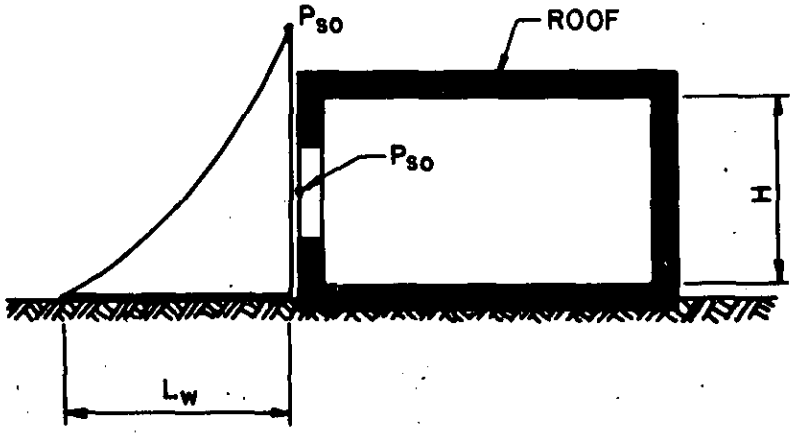


b) AVERAGE PRESSURE - TIME VARIATION

Figure 2-199 Rear wall loading



PLAN

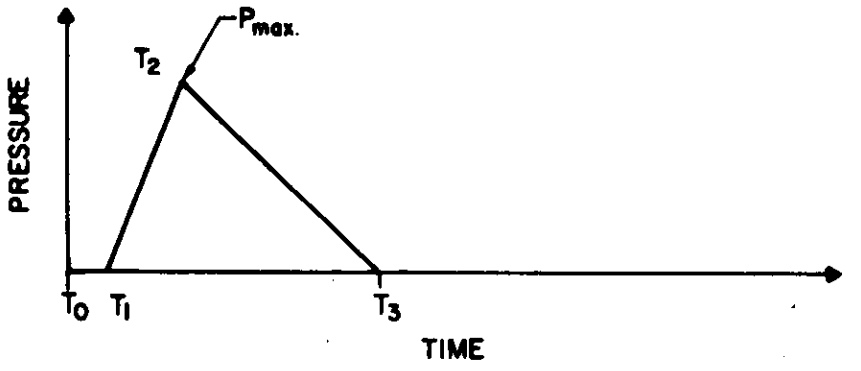


SECTION

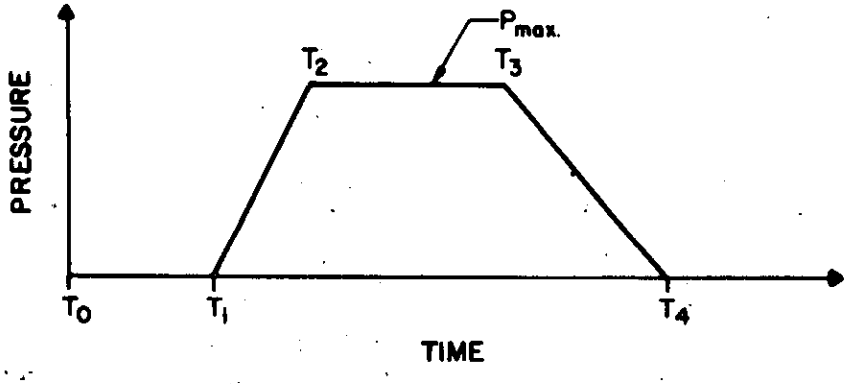
NOMENCLATURE:

L, LENGTH OF SIDE WALL
W, WIDTH OF BACK WALL AND FRONT WALL
H, HEIGHT OF ALL WALLS
A_o, AREA OF OPENING IN FRONT WALL
A_w, AREA OF BACK WALL
L_w, WAVE LENGTH OF SHOCK WAVE OF INCIDENT PRESSURE, P_{so}, AT EXTERIOR FACE OF FRONT WALL

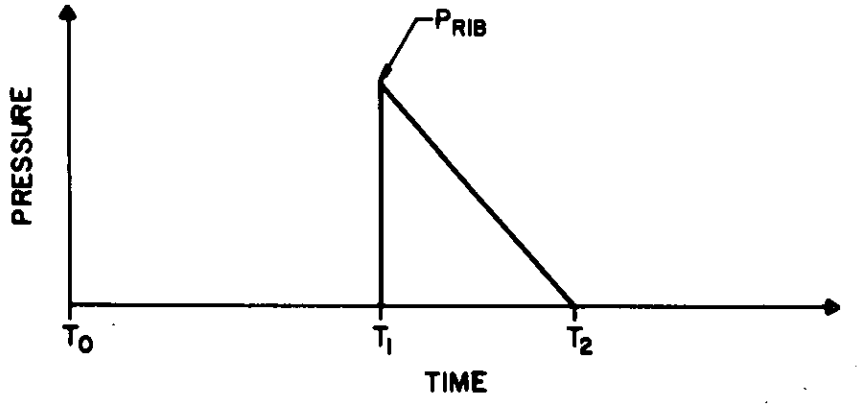
Figure 2-200 Idealized structure configuration for interior blast loads



a. INTERIOR FRONT WALL SURFACE



b. INTERIOR SIDE WALL OR ROOF SURFACE



c. INTERIOR BACK WALL SURFACE

Figure 2-201 Idealized interior blast loads

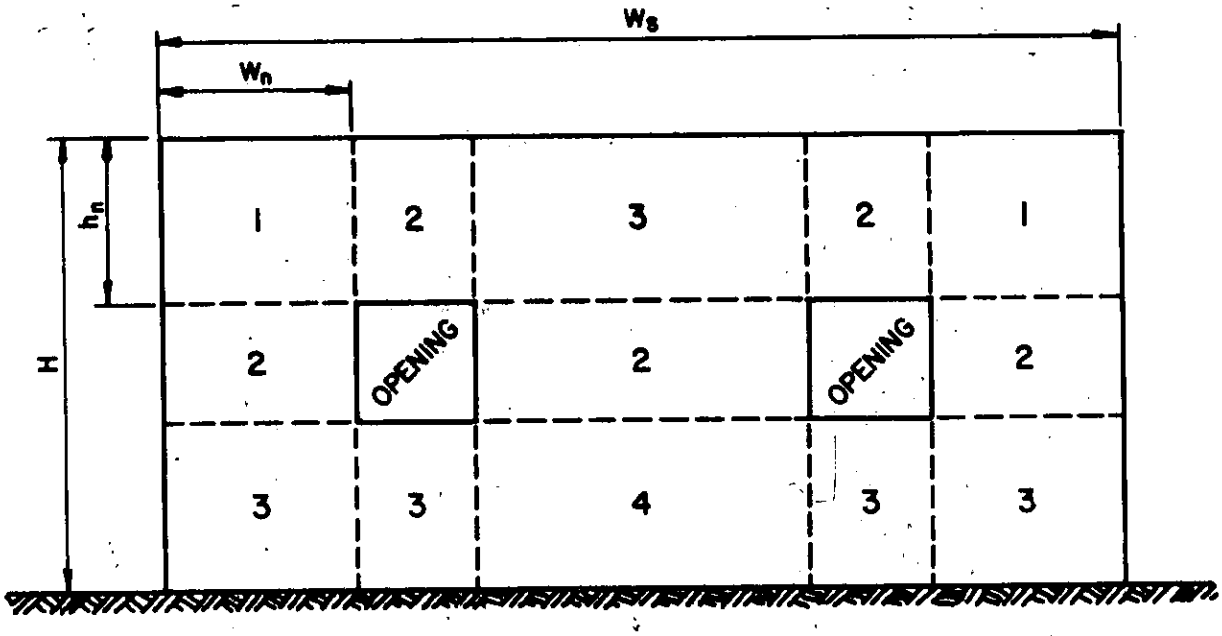


Figure 2-202 Sub-division of typical front wall with openings

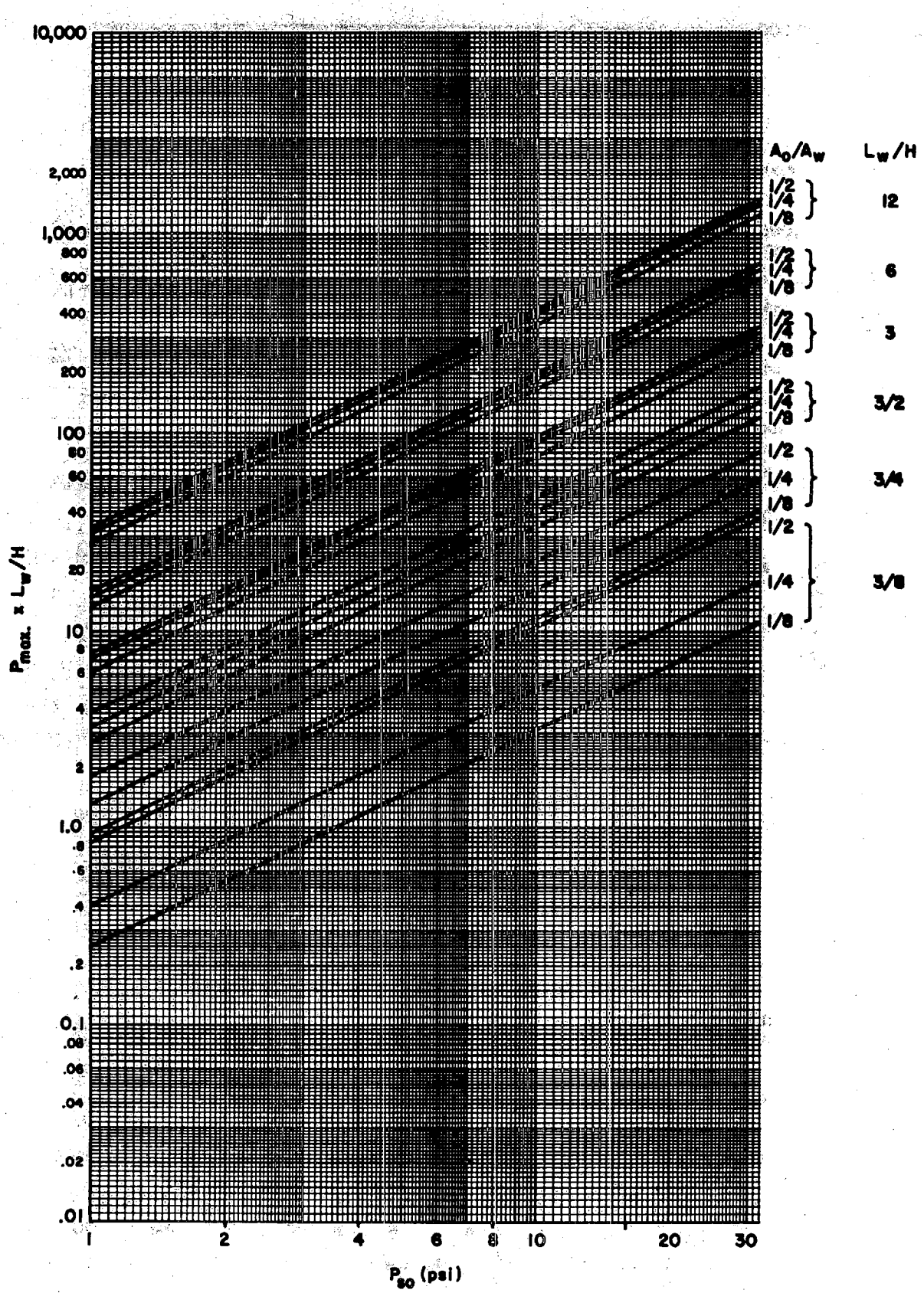


Figure 2-203 Maximum average pressure on interior face of front wall (W/H = 3/4)

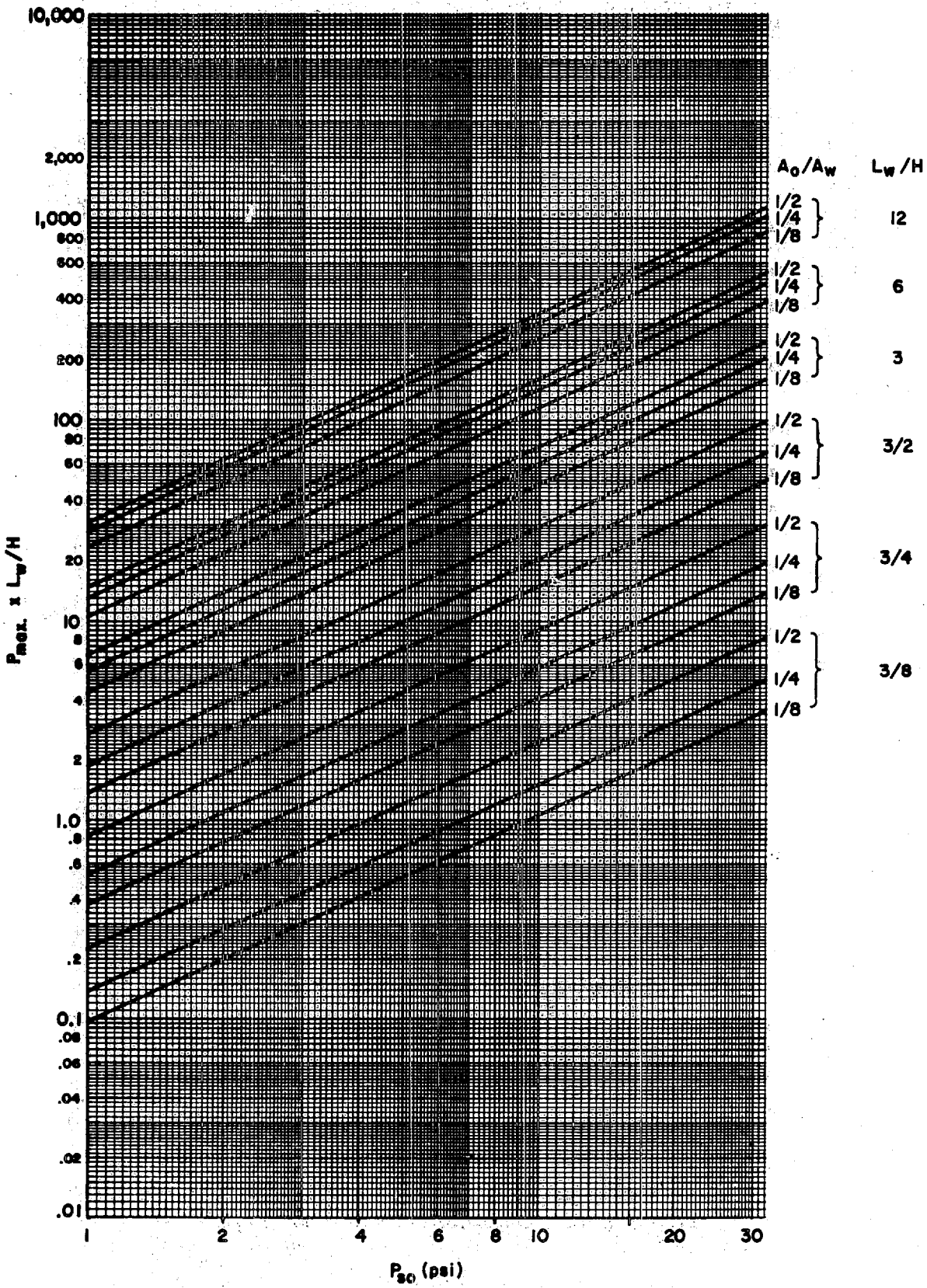


Figure 2-204 Maximum average pressure on interior face of front wall (W/H = 3/2)

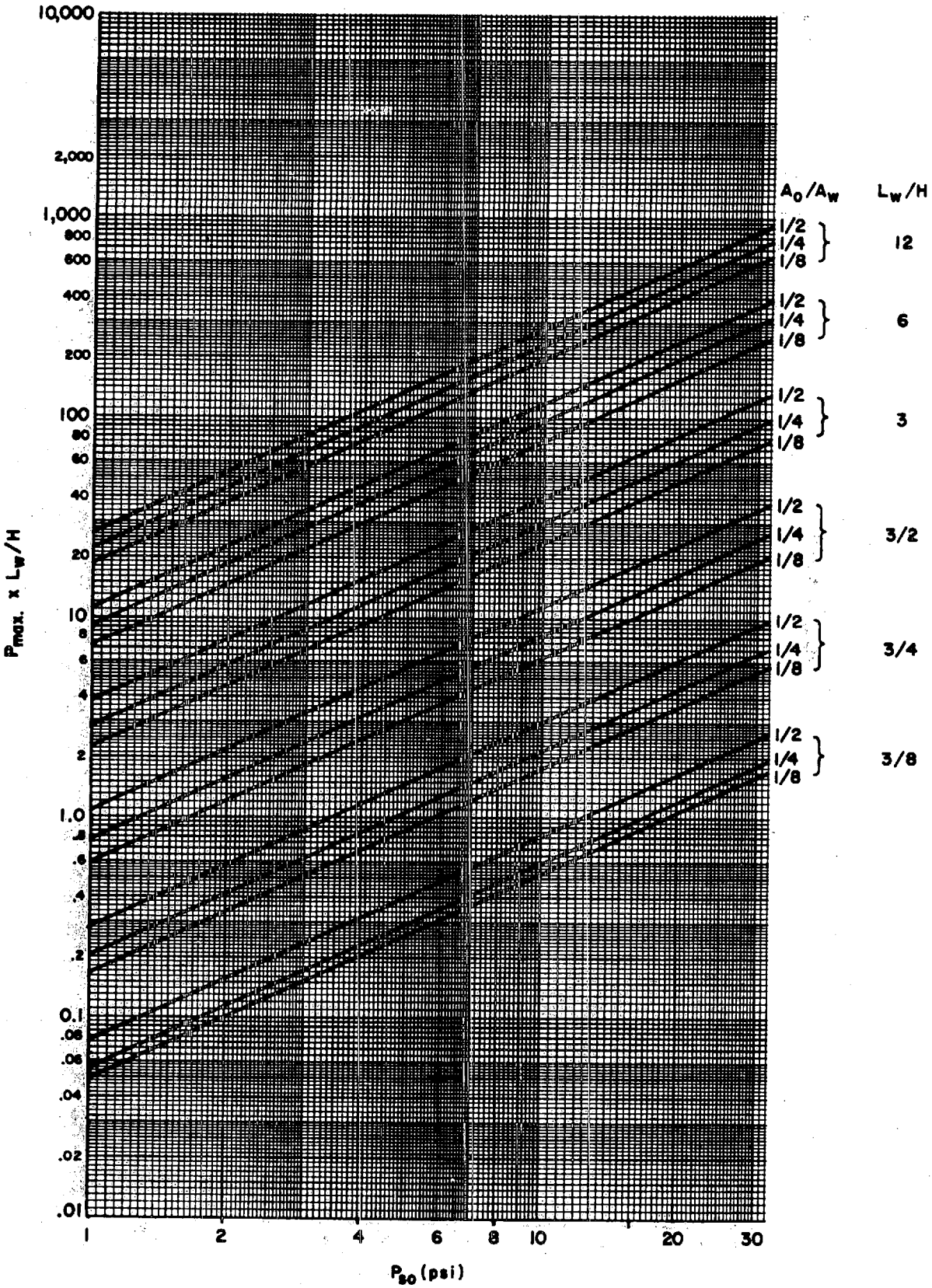


Figure 2-205 Maximum average pressure on interior face of front wall (W/H = 3)

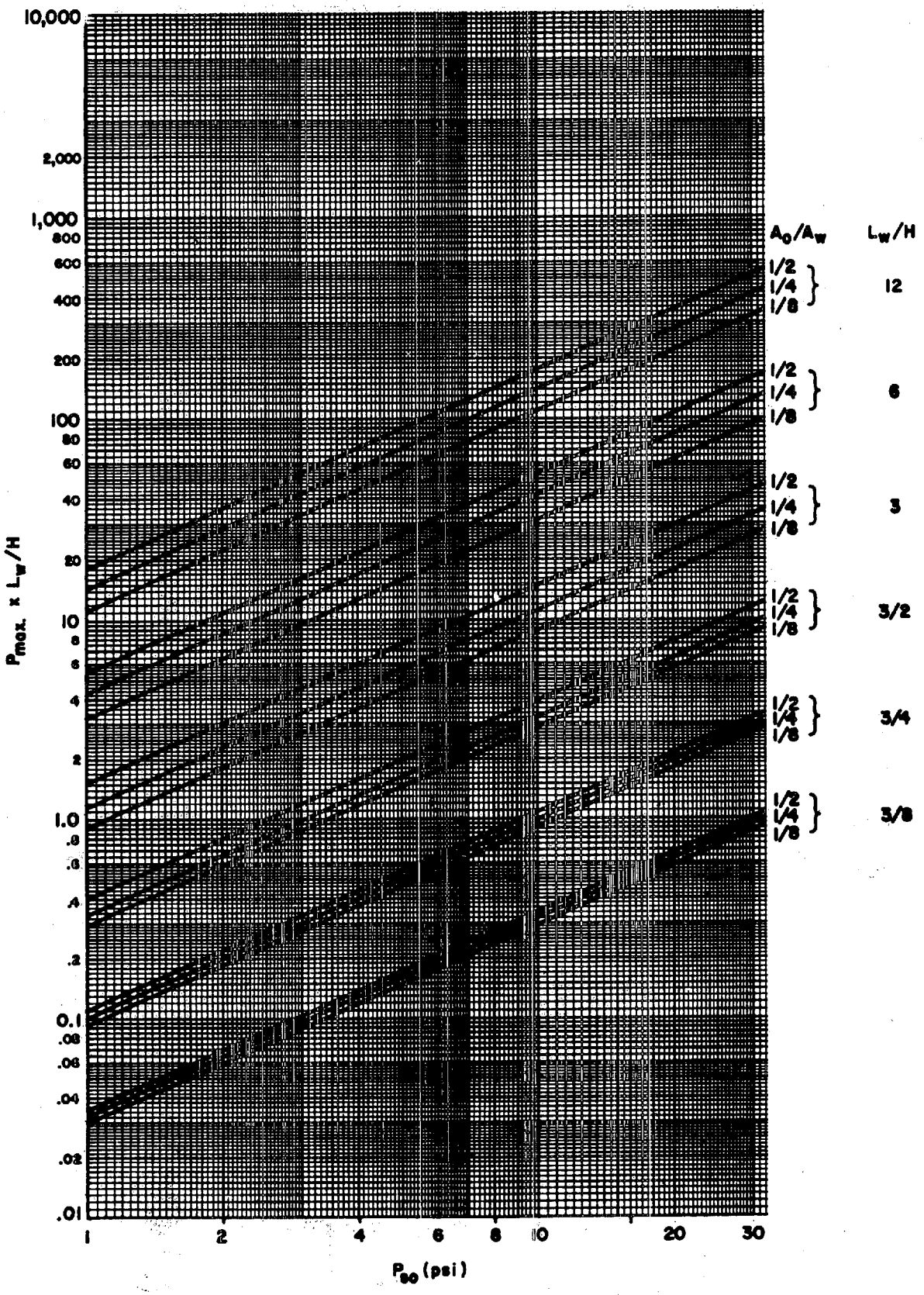


Figure 2-206 Maximum average pressure on interior face of front wall (W/H = 6)

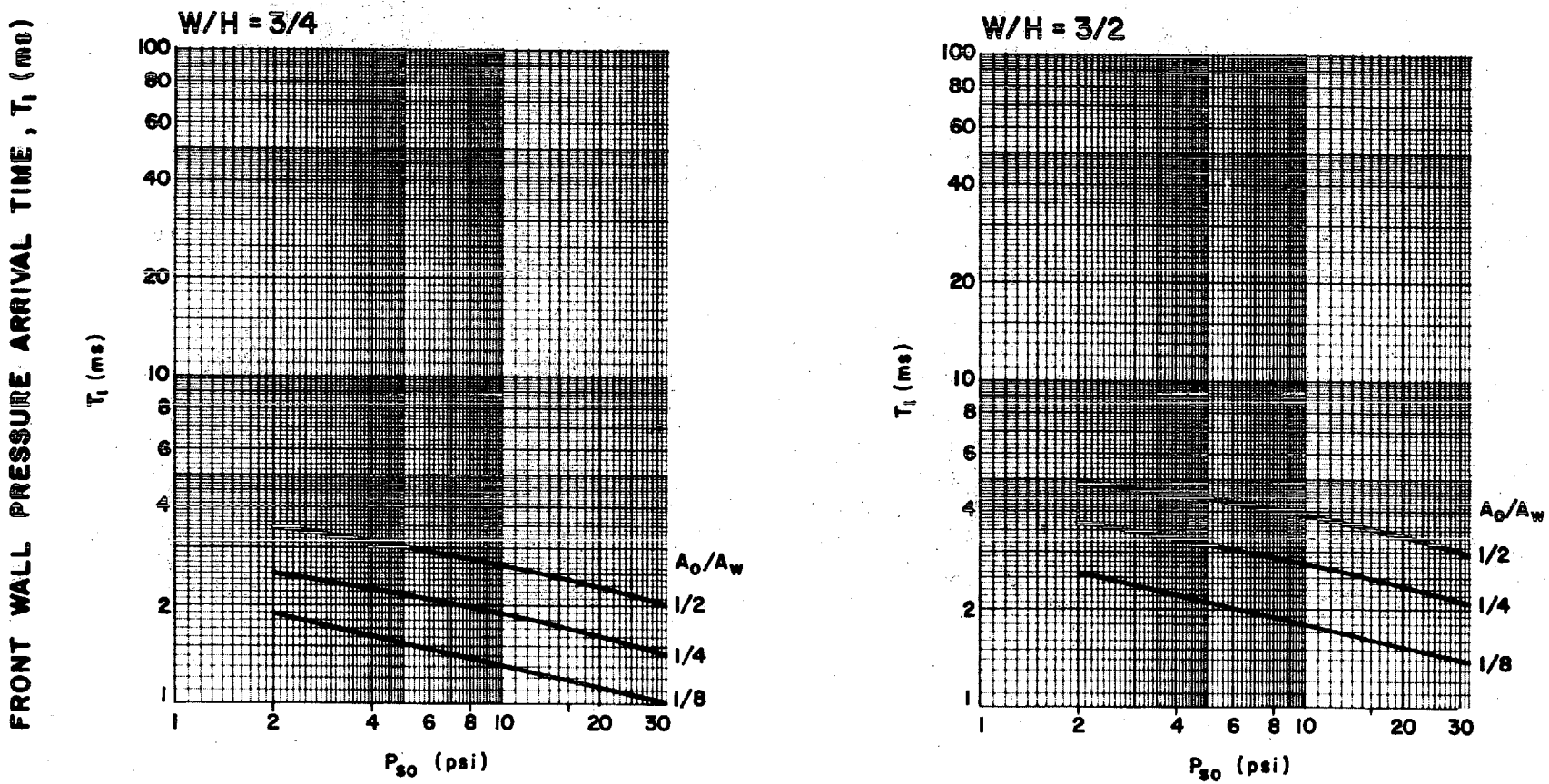


Figure 2-207 Arrival time, T_1, for interior front wall blast load (W/H = 3/4 and 3/2)

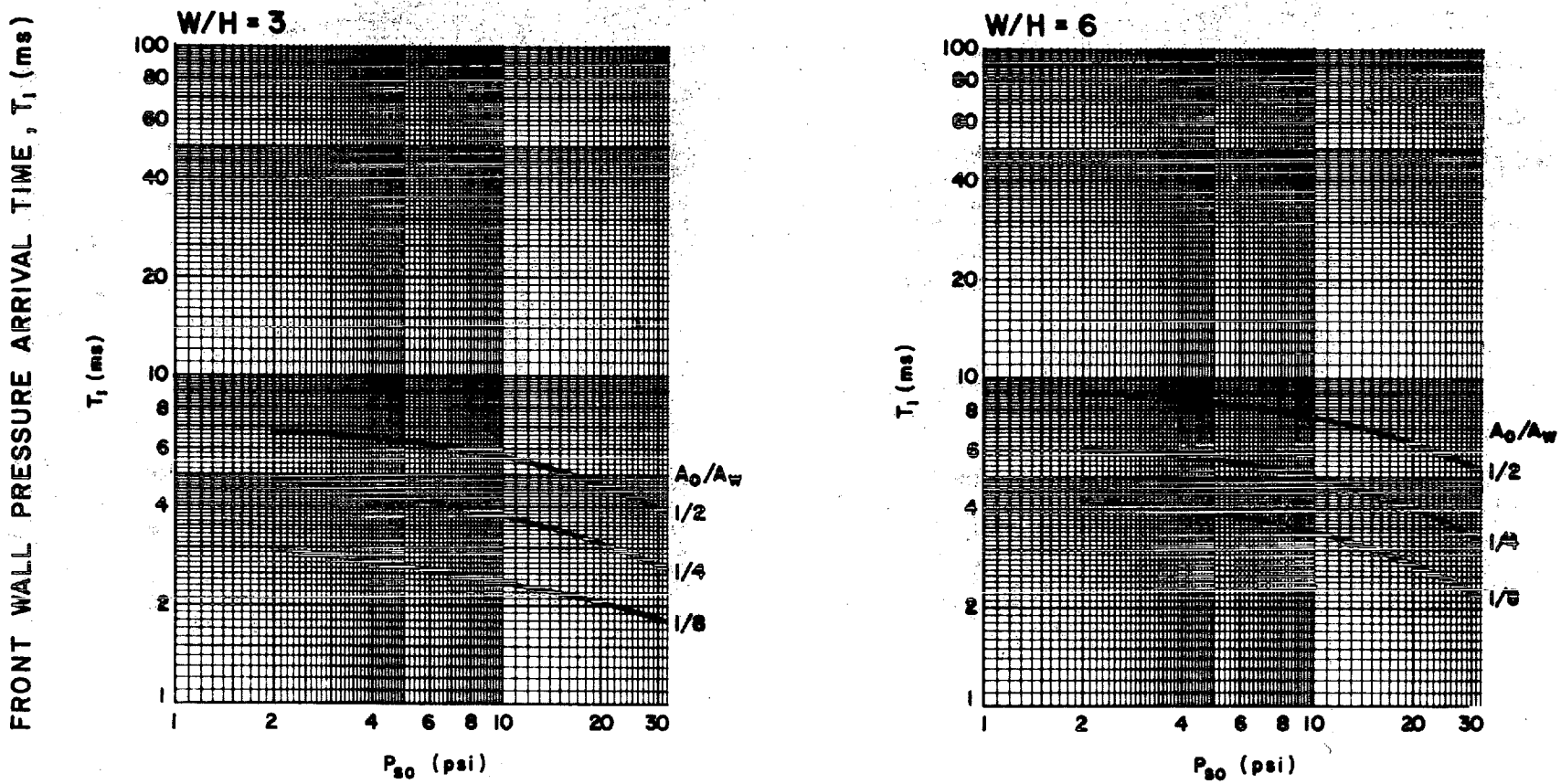


Figure 2-208 Arrival time, T_1, for interior front wall blast load (W/H = 3 and 6)

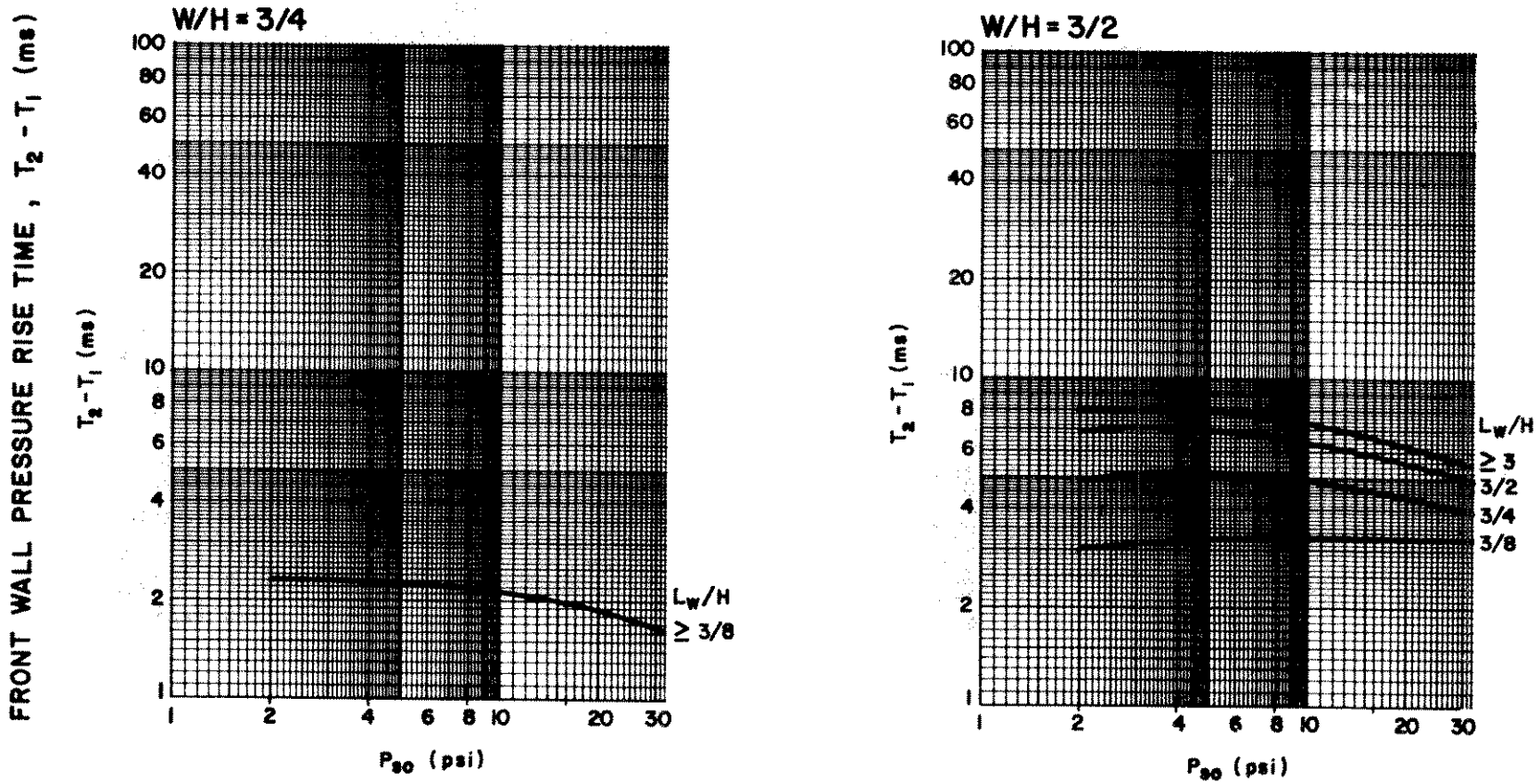


Figure 2-209 Idealized rise time, T_2 - T_1, for interior front wall blast load (W/H = 3/4 and 3/2)

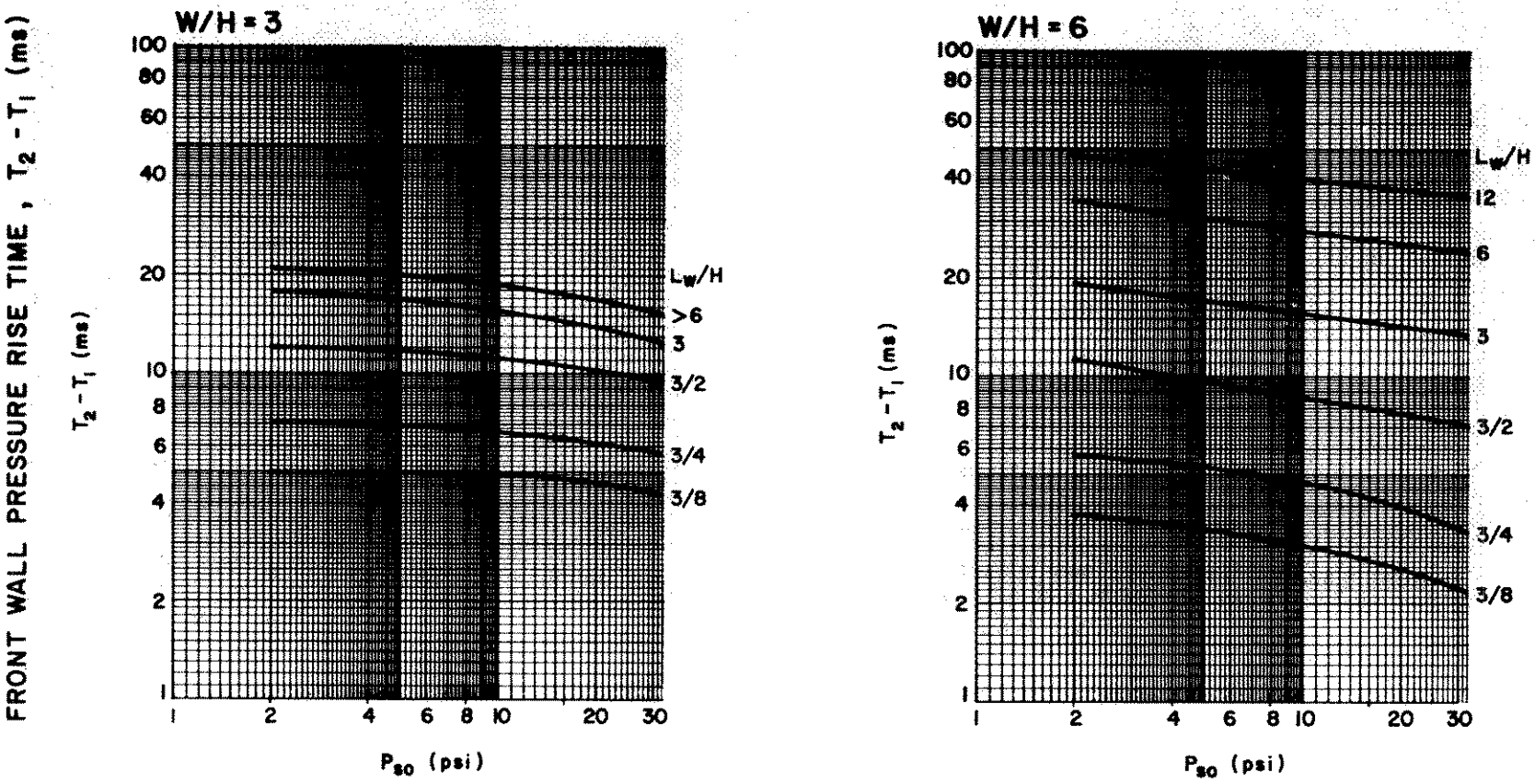


Figure 2-210 Idealized rise time, T_2 - T_1, for interior front wall blast load (W/H = 3 and 6)

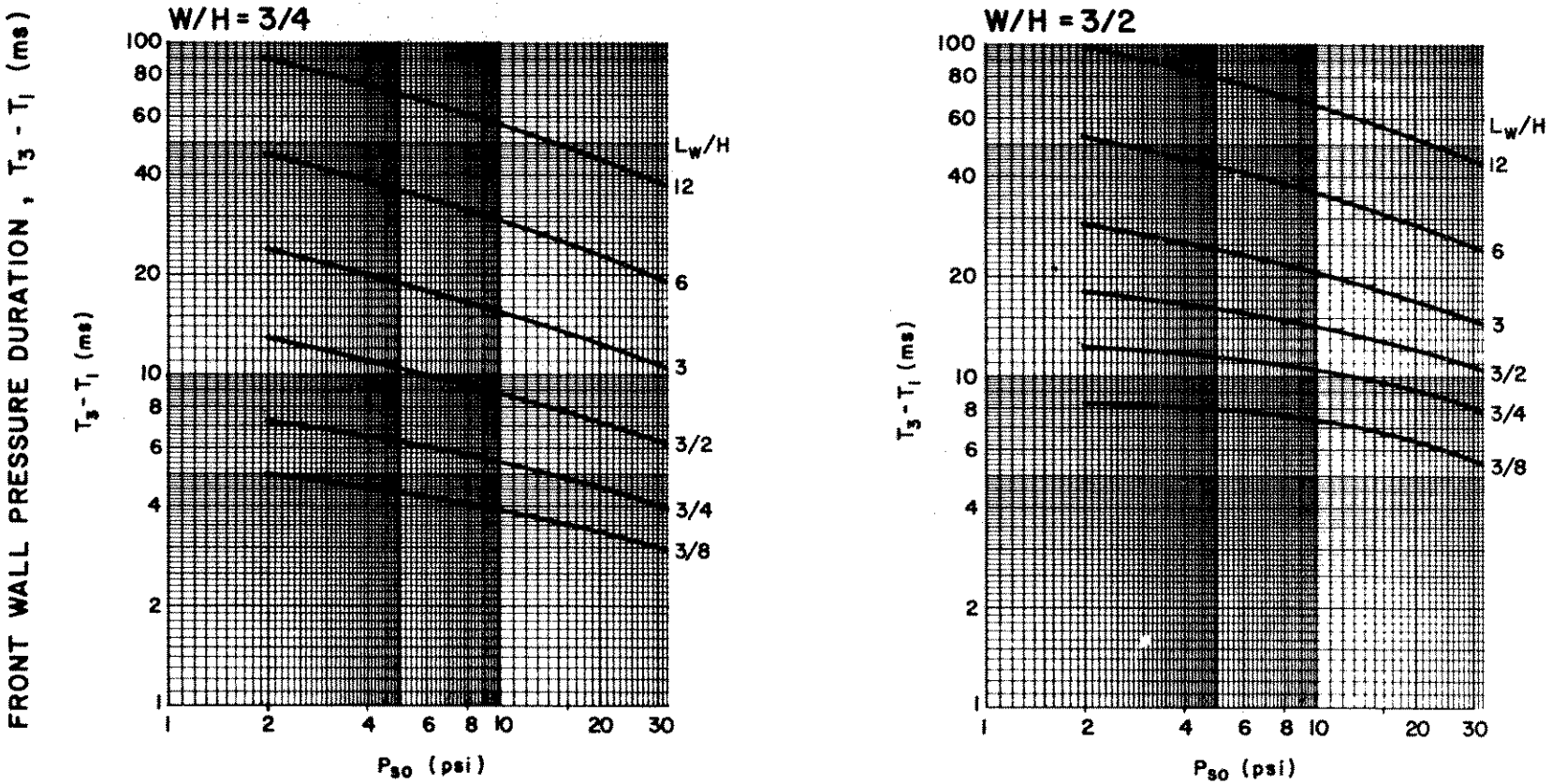


Figure 2-211 Idealized duration, $T_3 - T_1$, for interior front wall blast load (W/H = 3/4 and 3/2)

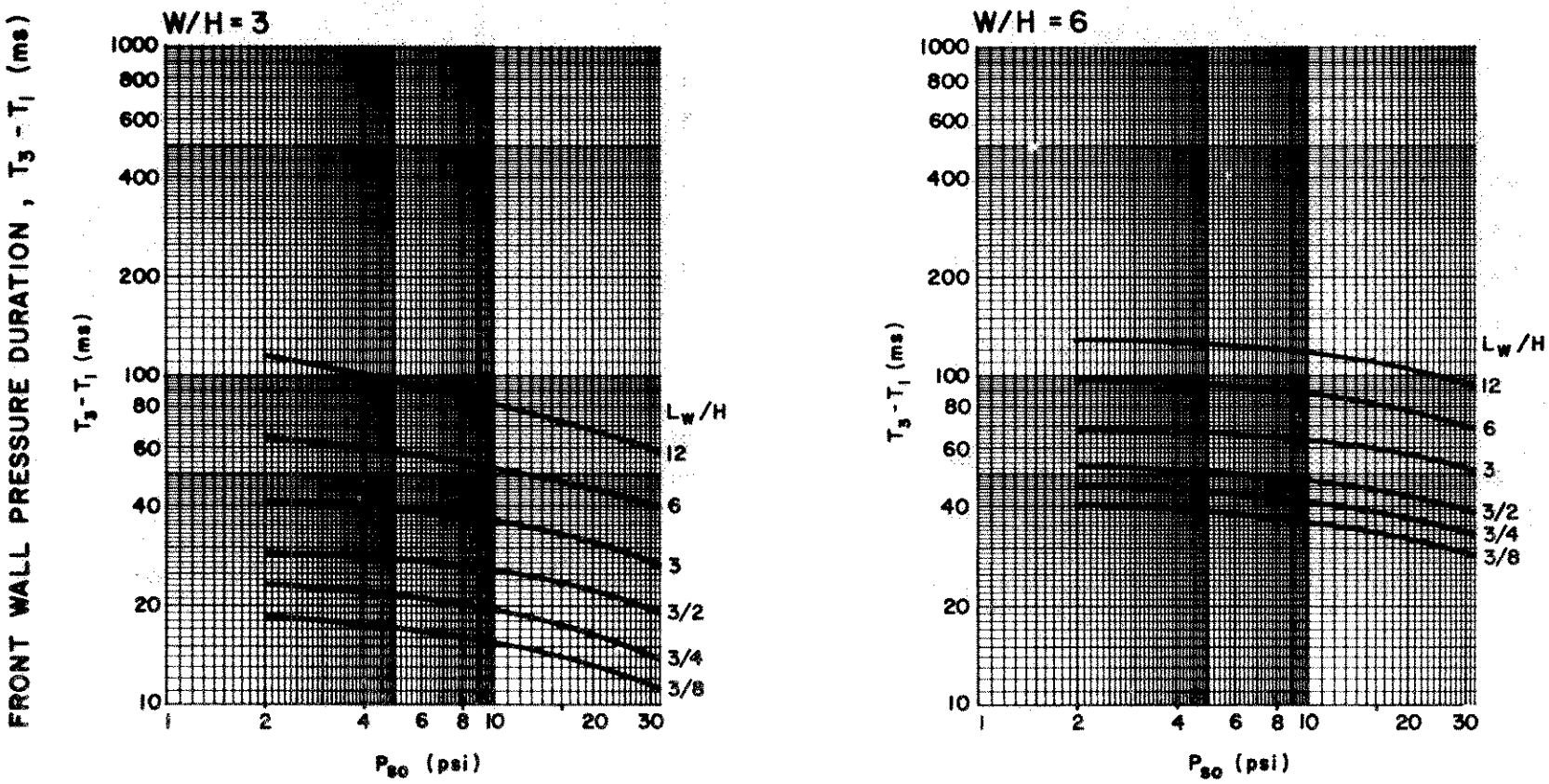


Figure 2-212 Idealized duration, $T_3 - T_1$, for interior front wall blast load (W/H = 3 and 6)

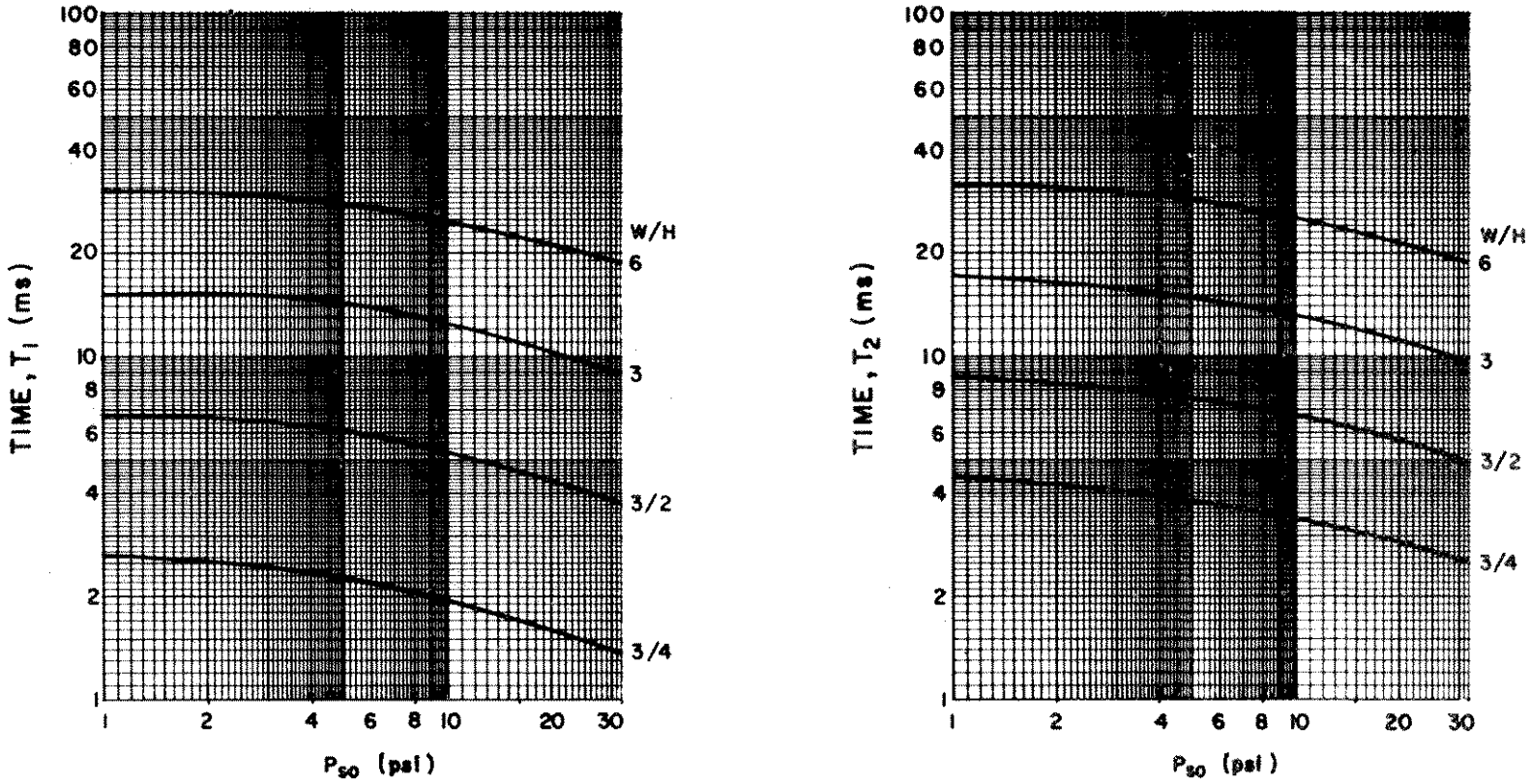


Figure 2-213 Idealized times T_1 and T_2 for interior side wall blast load

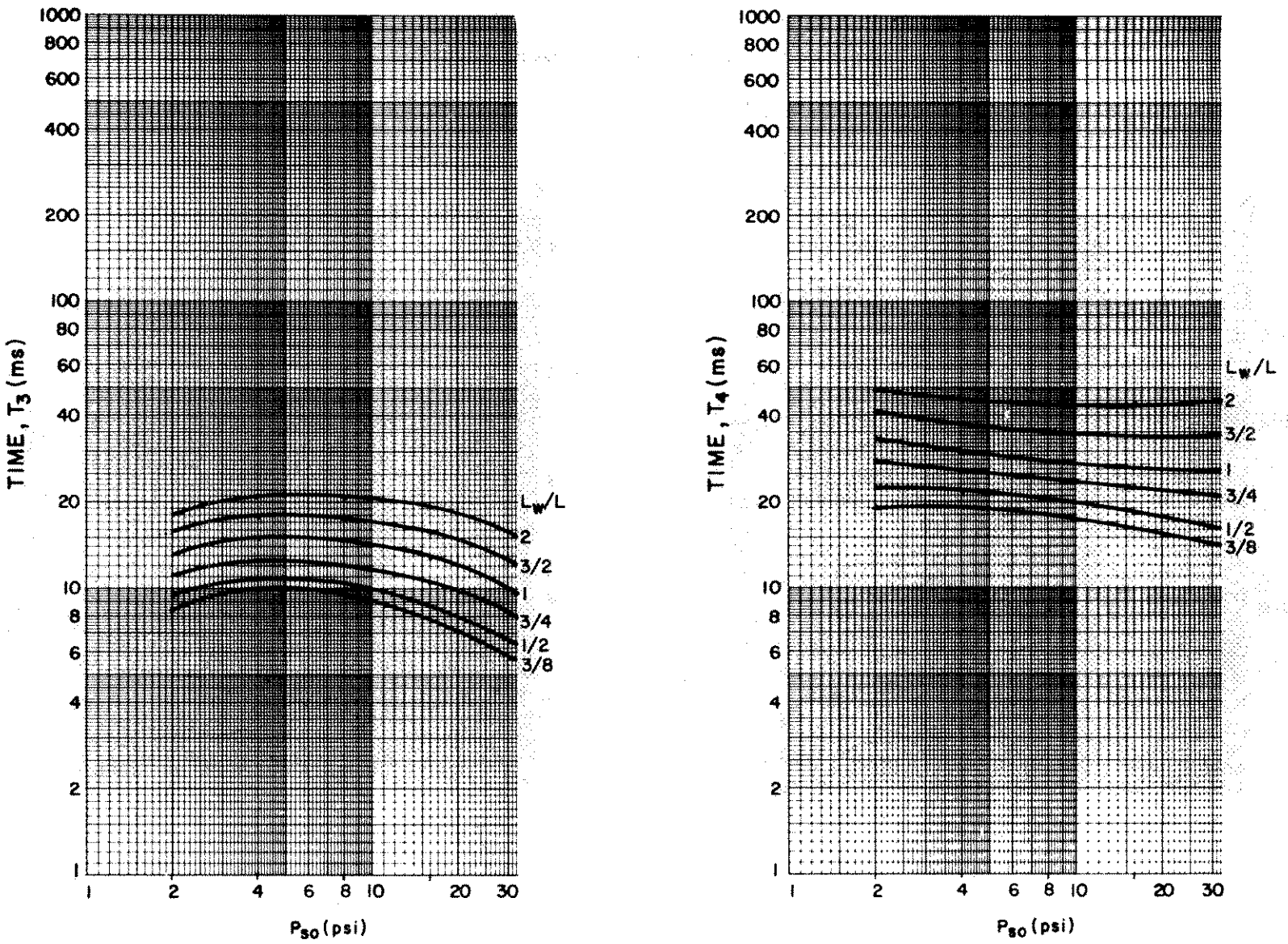


Figure 2-214 Idealized times T_3 and T_4 for interior side wall blast load (L/H = 1, W/H = 3/4)

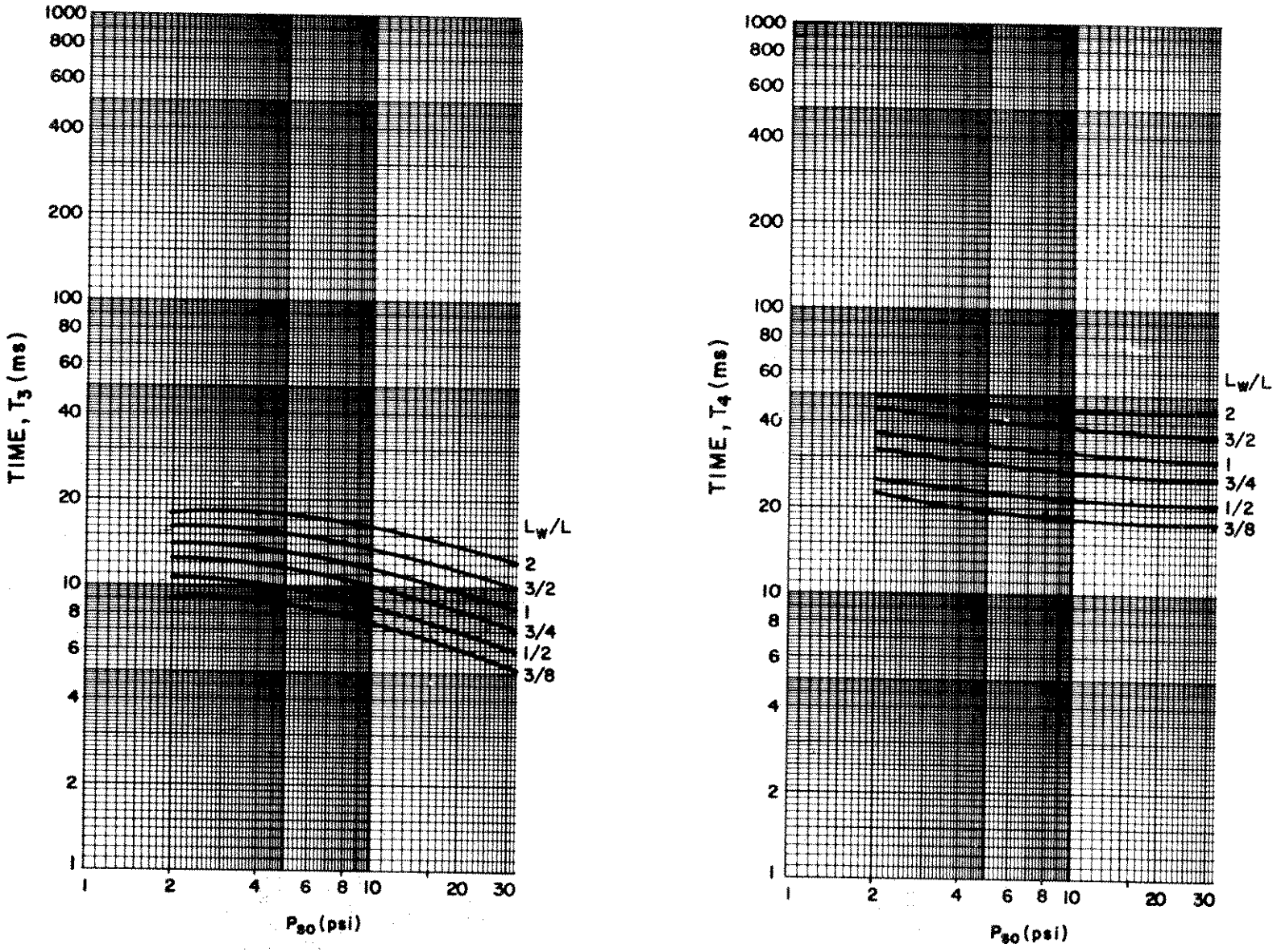


Figure 2-215 Idealized times T_3 and T_4 for interior side wall blast load (L/H = 1, W/H = 3/2)

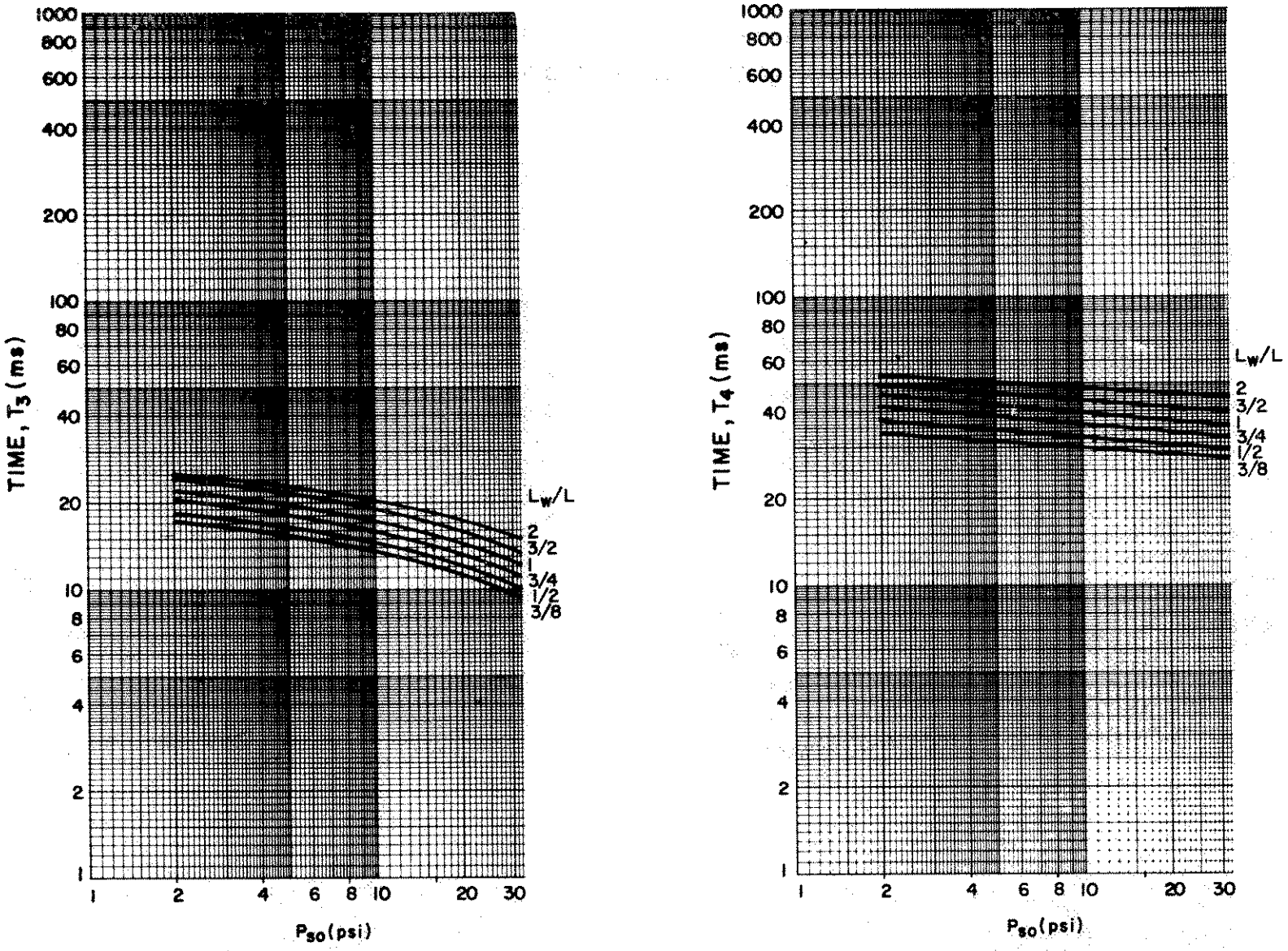


Figure 2-216 Idealized times T_3 and T_4 for interior side wall blast load (L/H = 1, W/H = 3)

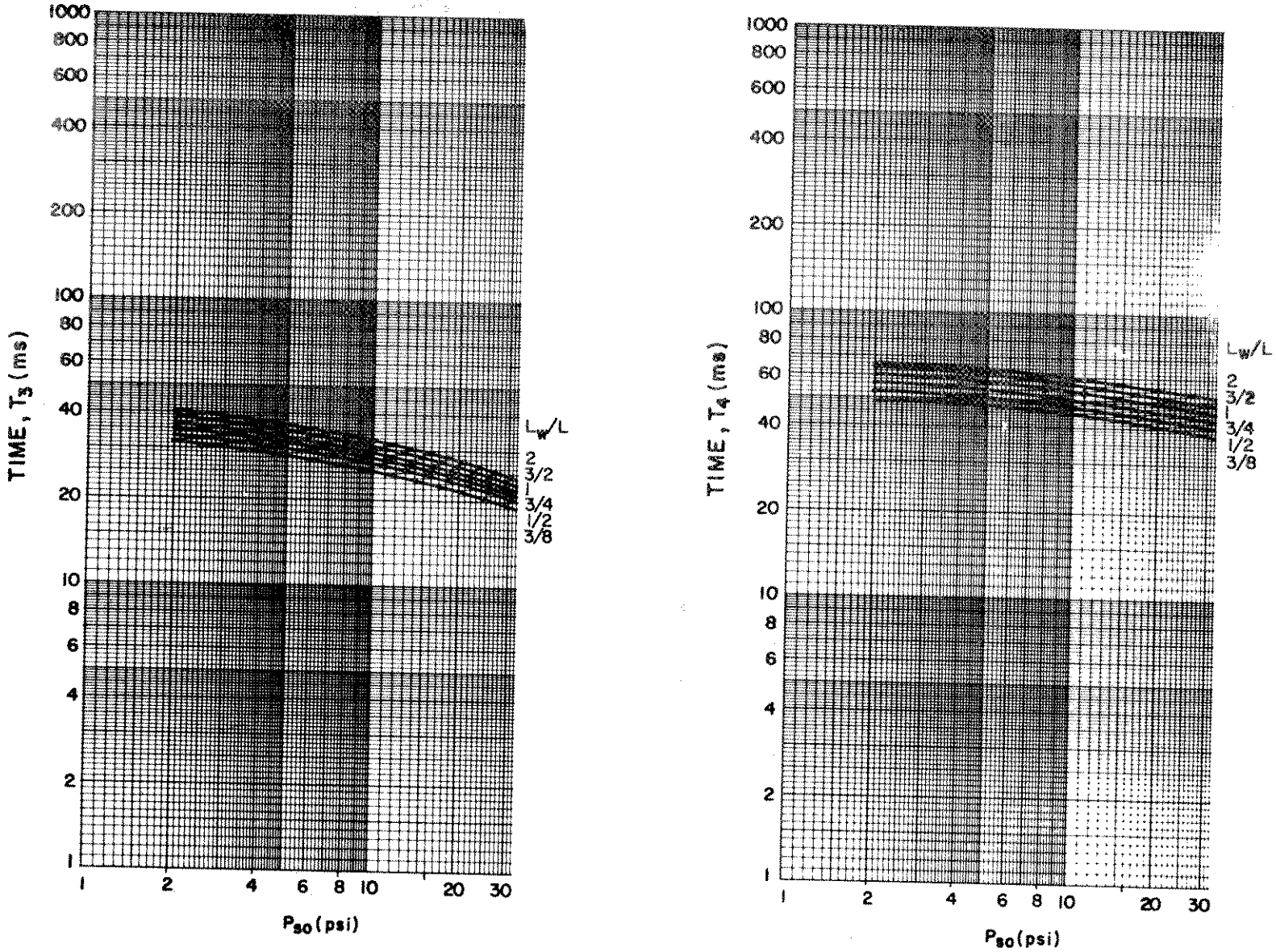


Figure 2-217 Idealized times T_3 and T_4 for interior side wall blast load (L/H = 1, W/H = 6)

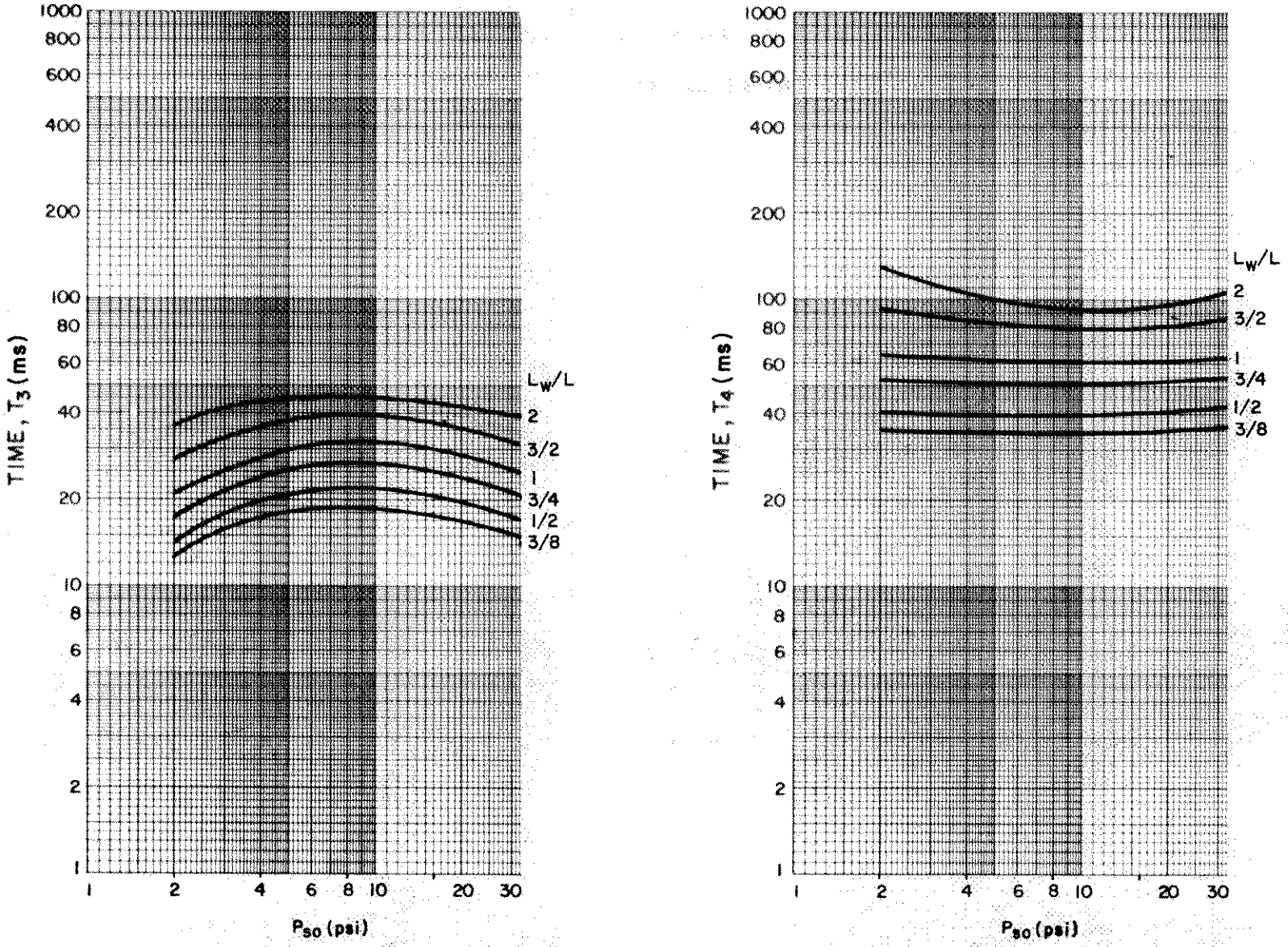


Figure 2-218 Idealized times T_3 and T_4 for interior side wall blast load (L/H = 2, W/H = 3/4)

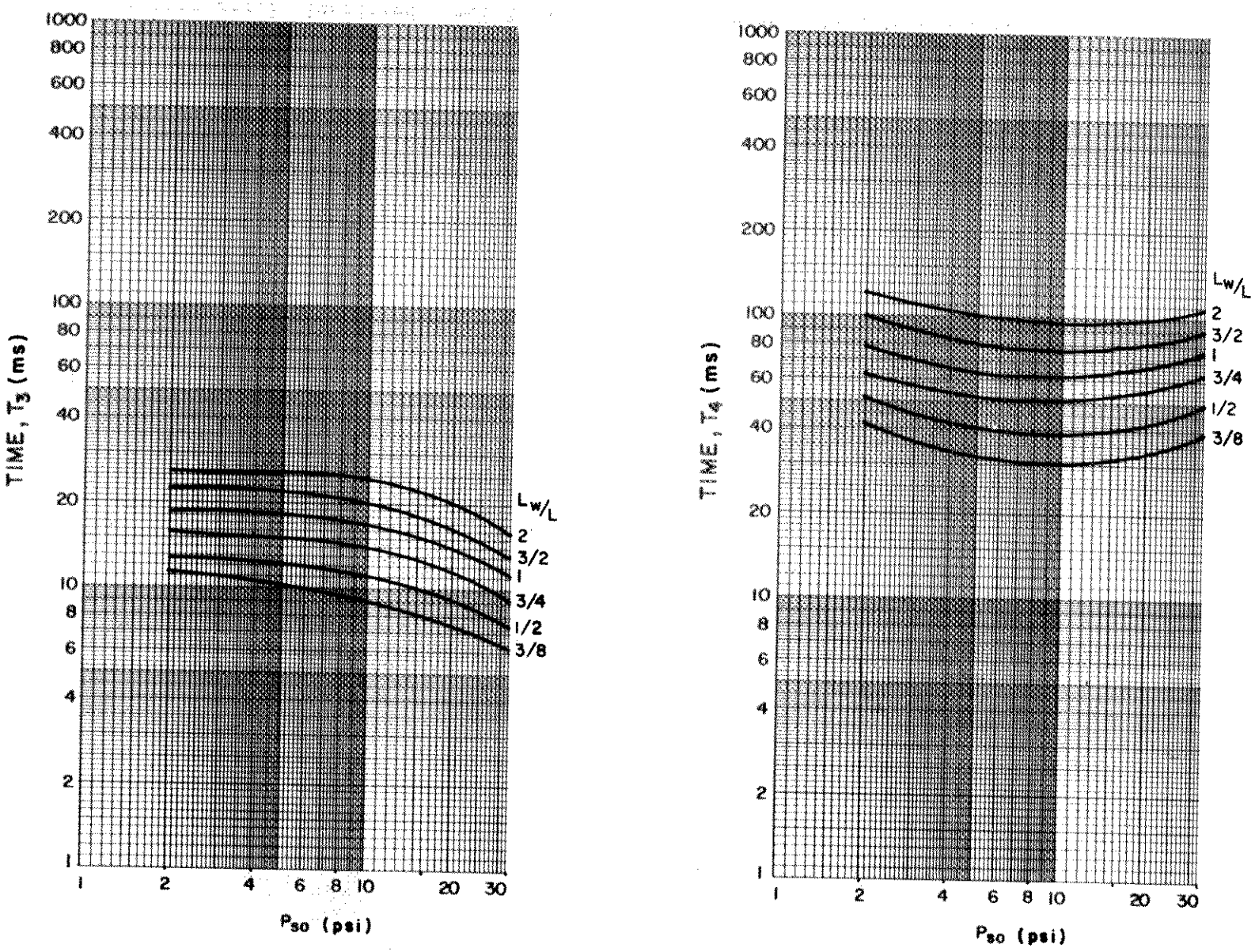


Figure 2-219 Idealized times T_3 and T_4 for interior side wall blast load (L/H = 2, W/H = 3/2)

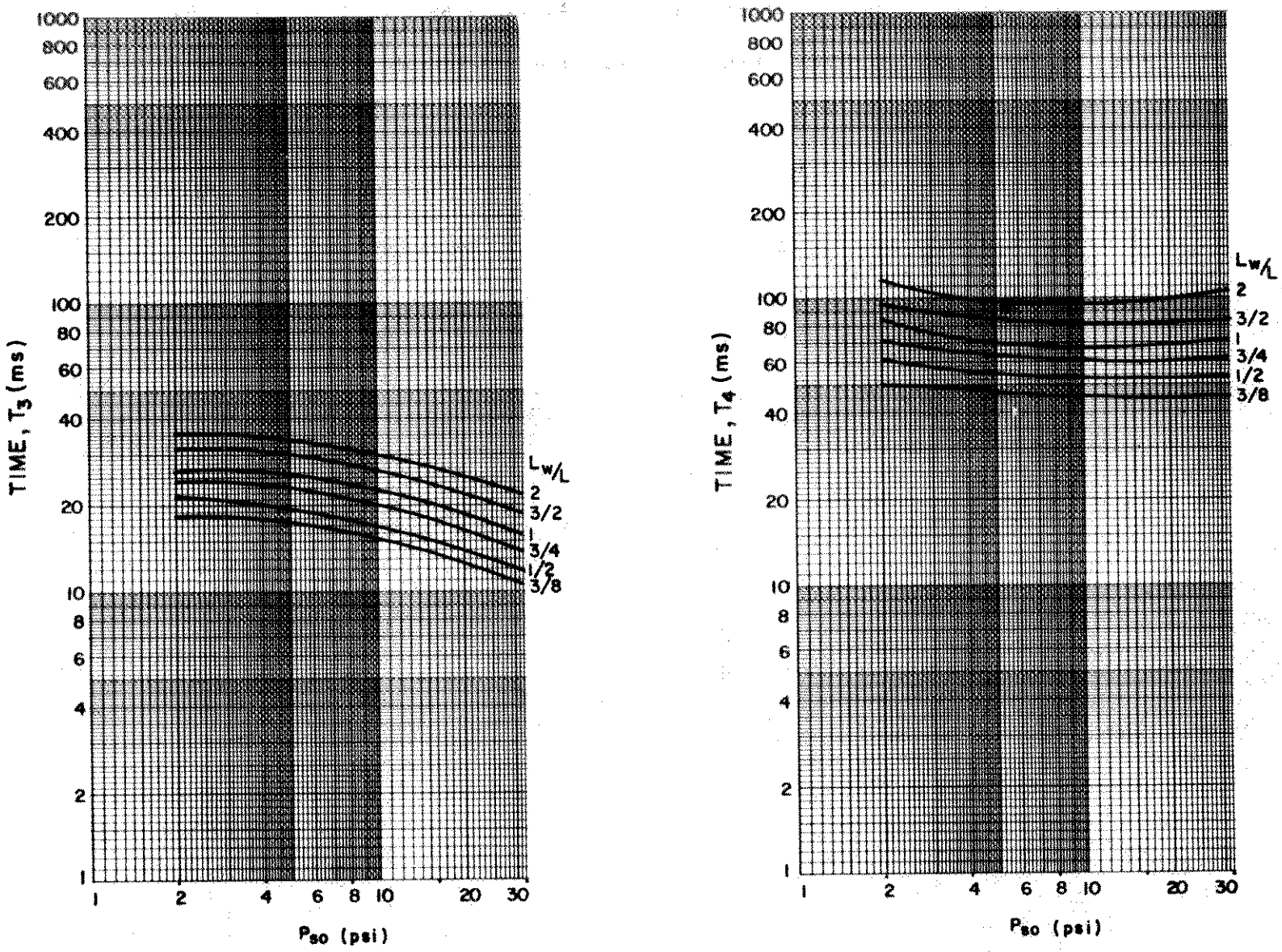


Figure 2-220 Idealized times T_3 and T_4 for interior side wall blast load (L/H = 2, W/H = 3)

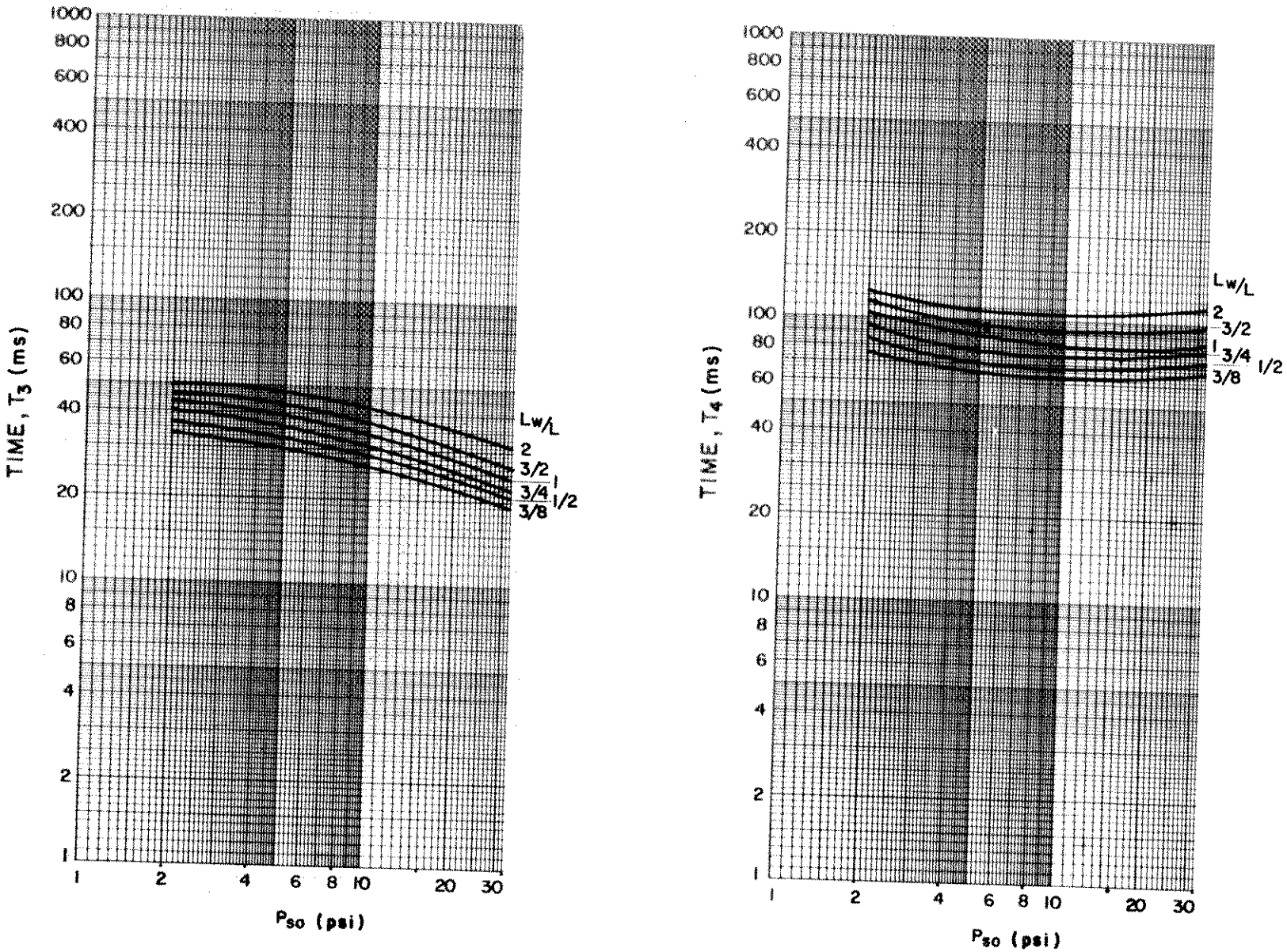


Figure 2-221 Idealized times T_3 and T_4 for interior side wall blast load (L/H = 2, W/H = 6)

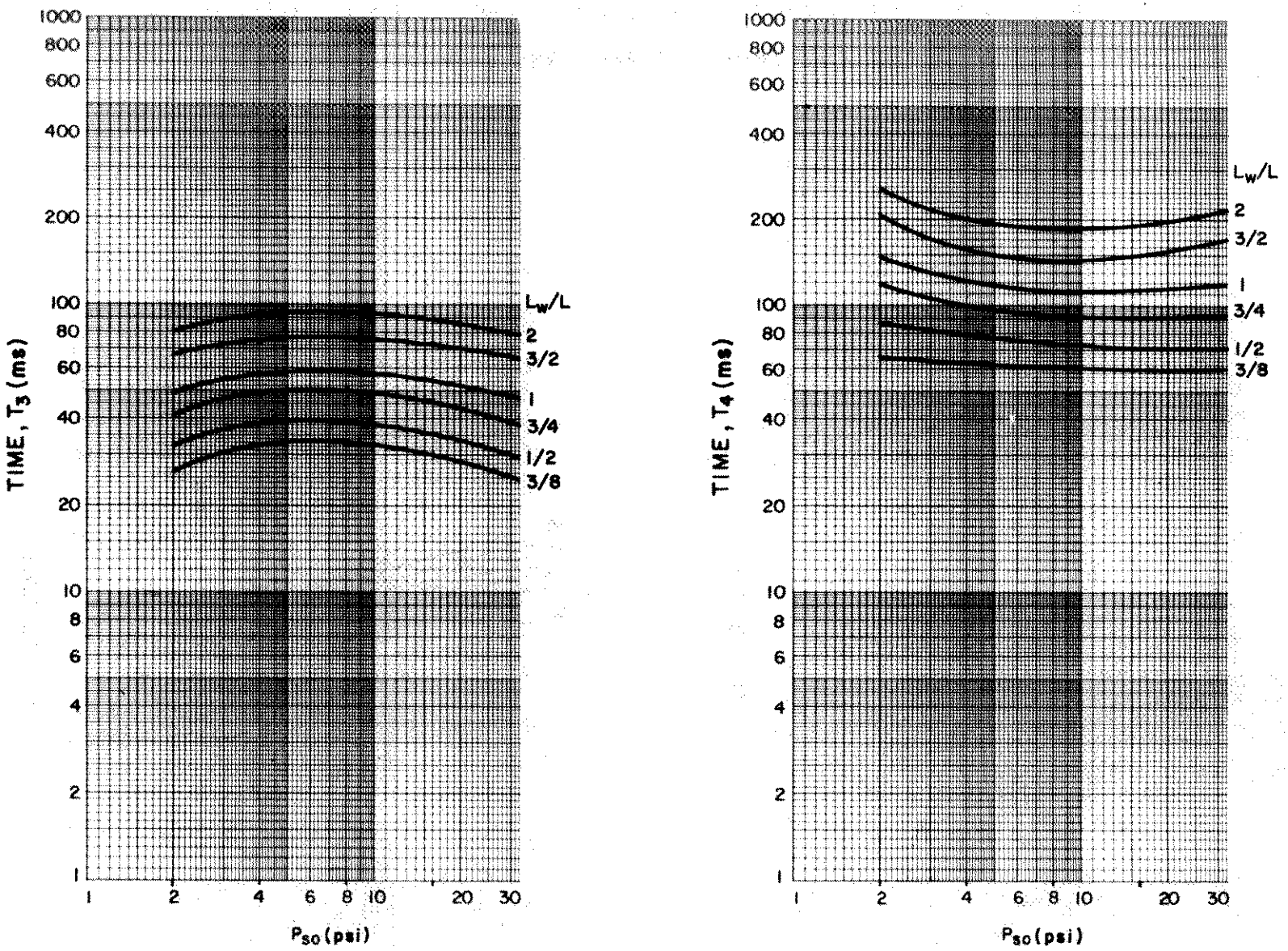


Figure 2-222 Idealized times T_3 and T_4 for interior side wall blast load (L/H = 4, W/H = 3/4)

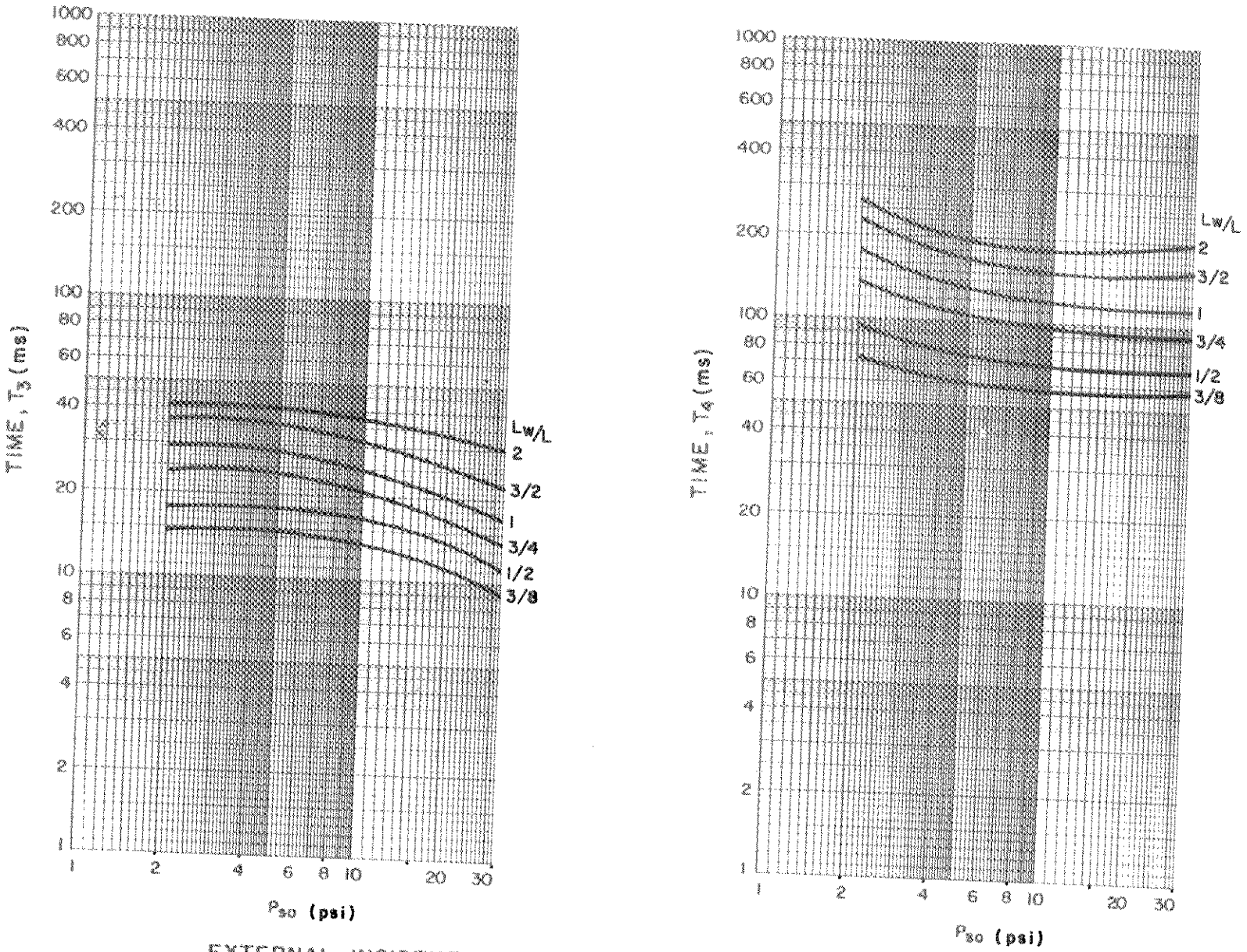


Figure 2-223 Idealized times T_3 and T_4 for interior side wall blast load (L/H = 4, W/H = 3/2)

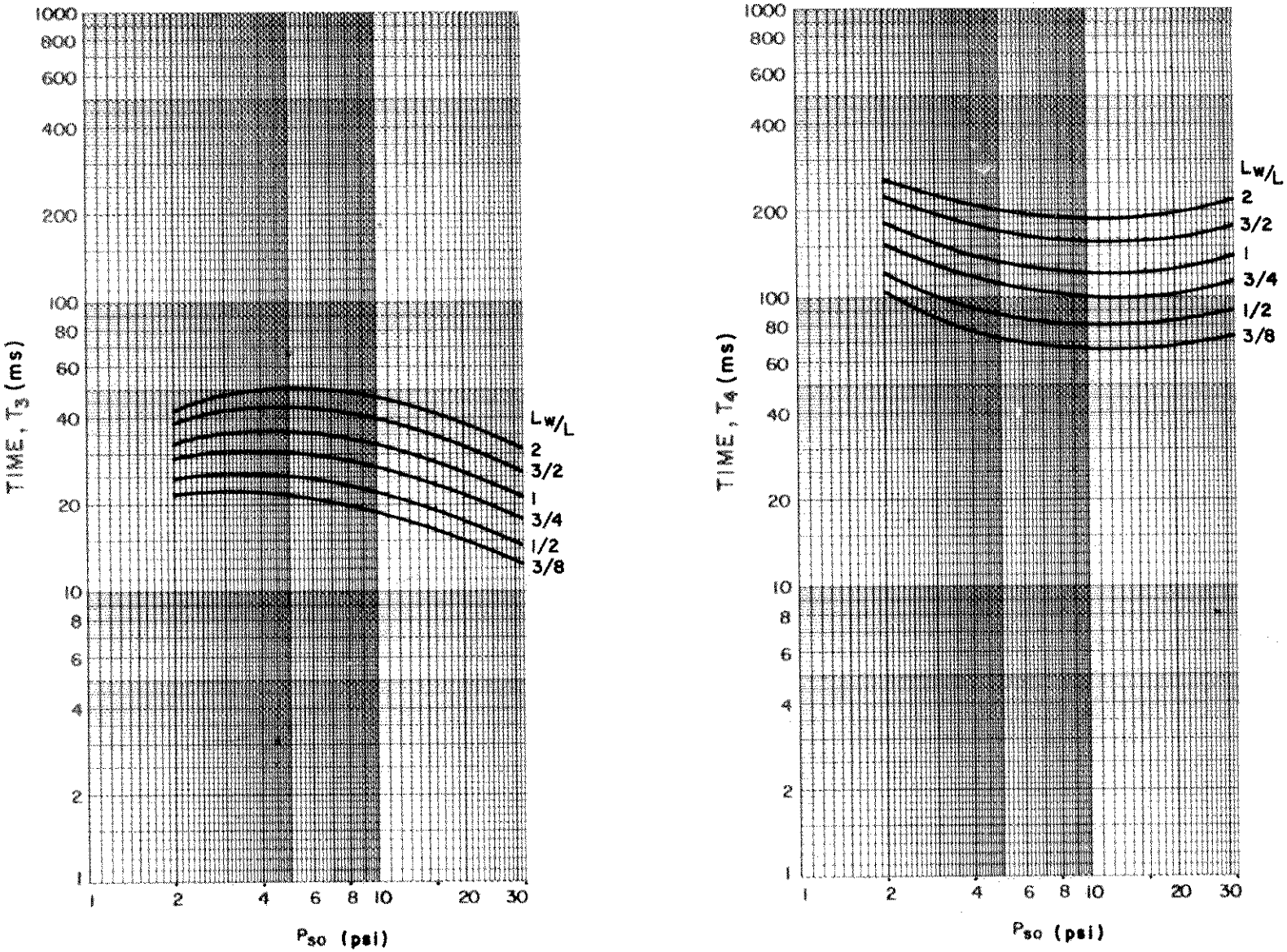


Figure 2-224 Idealized times T_3 and T_4 for interior side wall blast load (L/H = 4, W/H = 3)

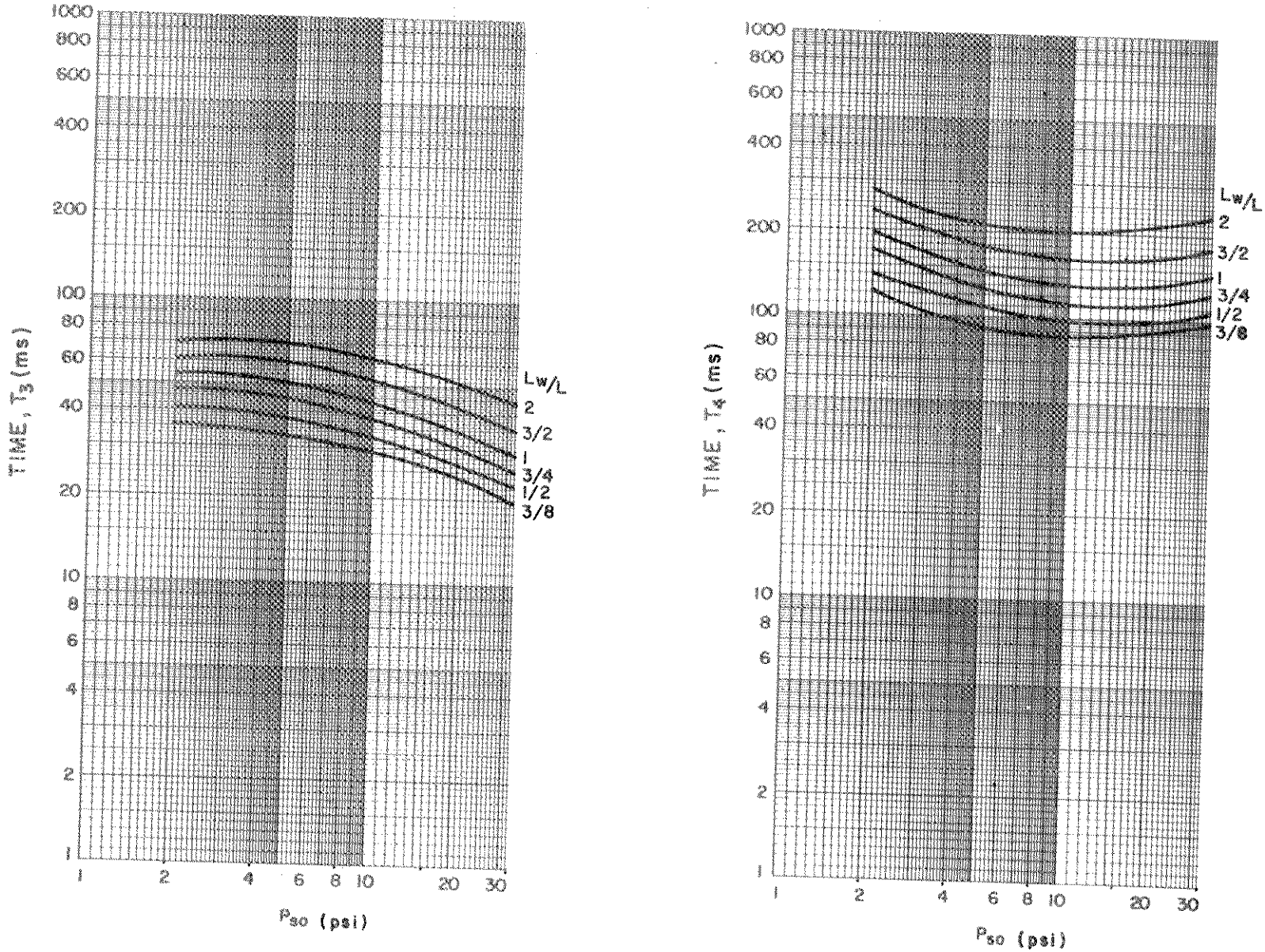


Figure 2-225 Idealized times T_3 and T_4 for interior side wall blast load (L/H = 4, W/H = 6)

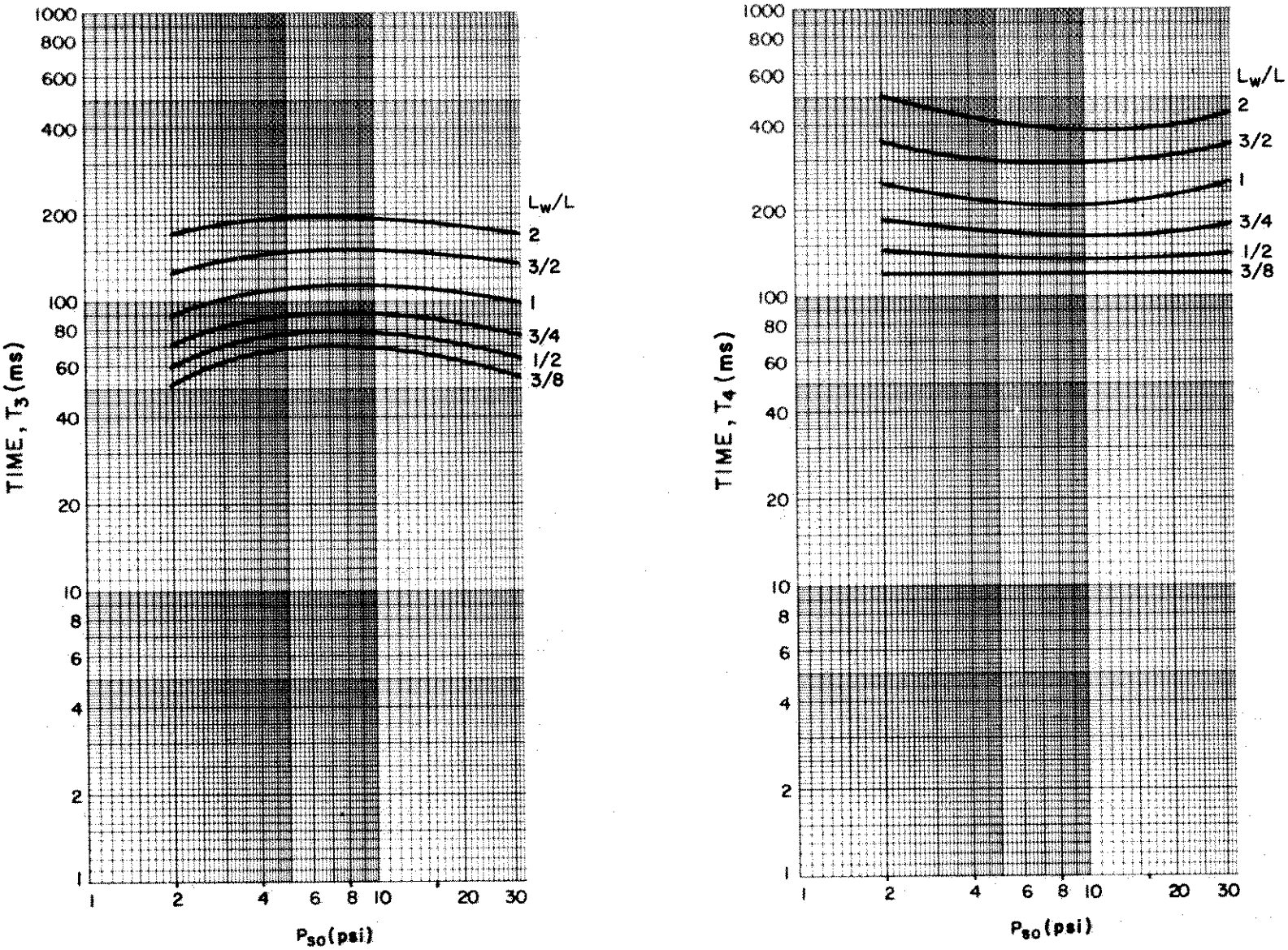


Figure 2-226 Idealized times T_3 and T_4 for interior side wall blast load (L/H = 8, W/H = 3/4)

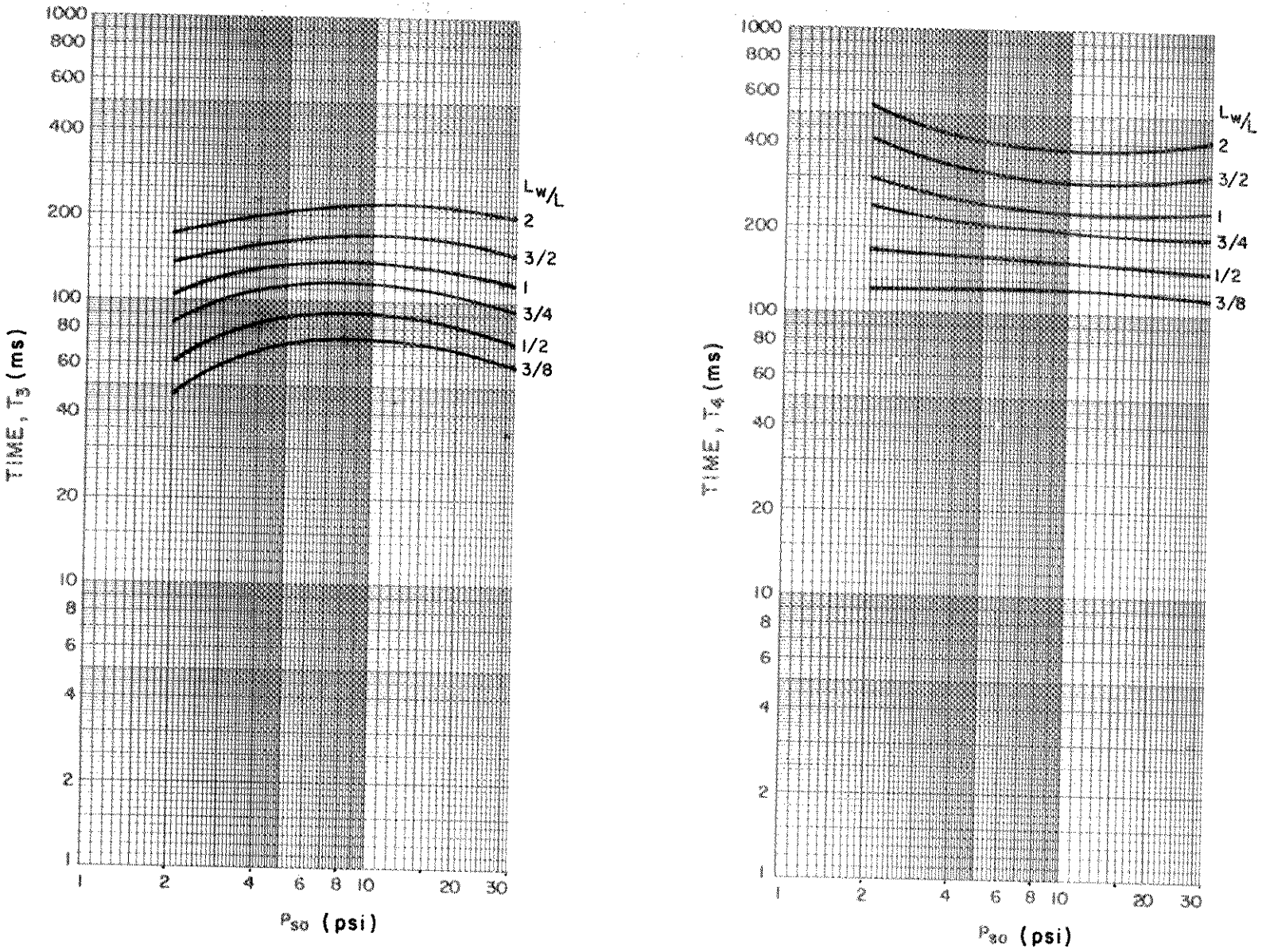


Figure 2-227 Idealized times T_3 and T_4 for interior side wall blast load (L/H = 8, W/H = 3/2)

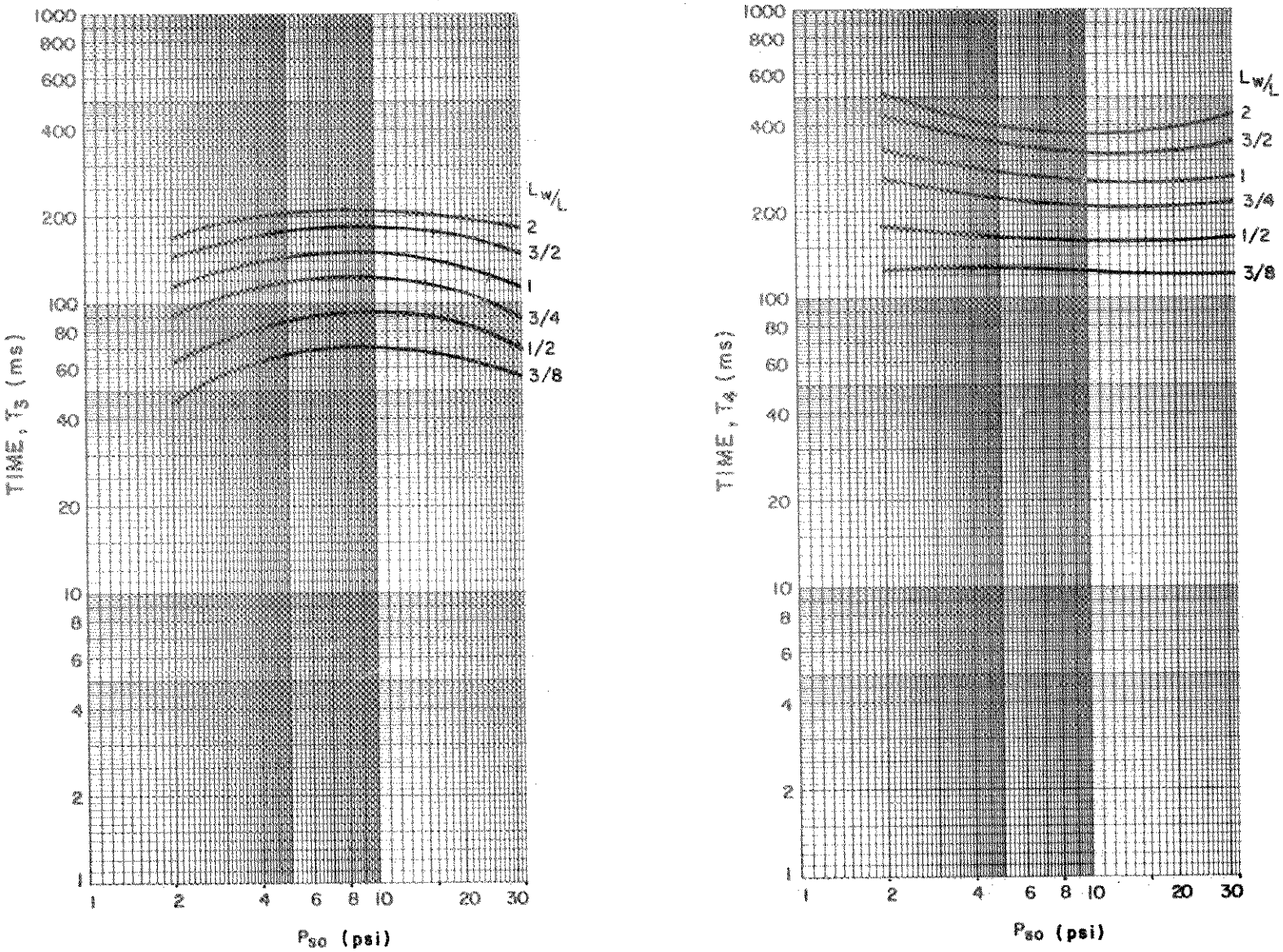


Figure 2-228 Idealized times T_3 and T_4 for interior side wall blast load (L/H = 8, W/H = 3)

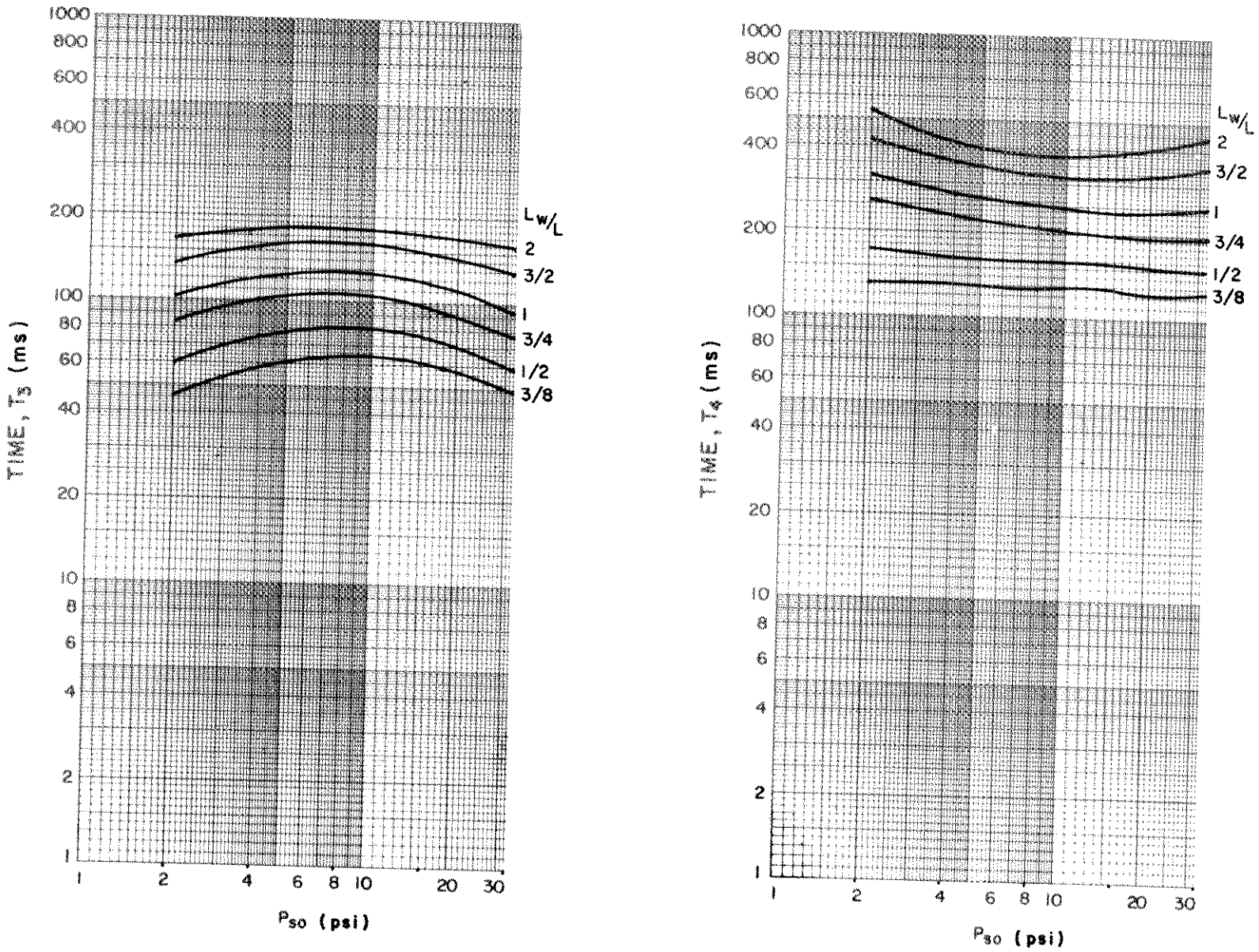


Figure 2-229 Idealized times T_3 and T_4 for interior side wall blast load ($L/H = 8$, $W/H = 6$)

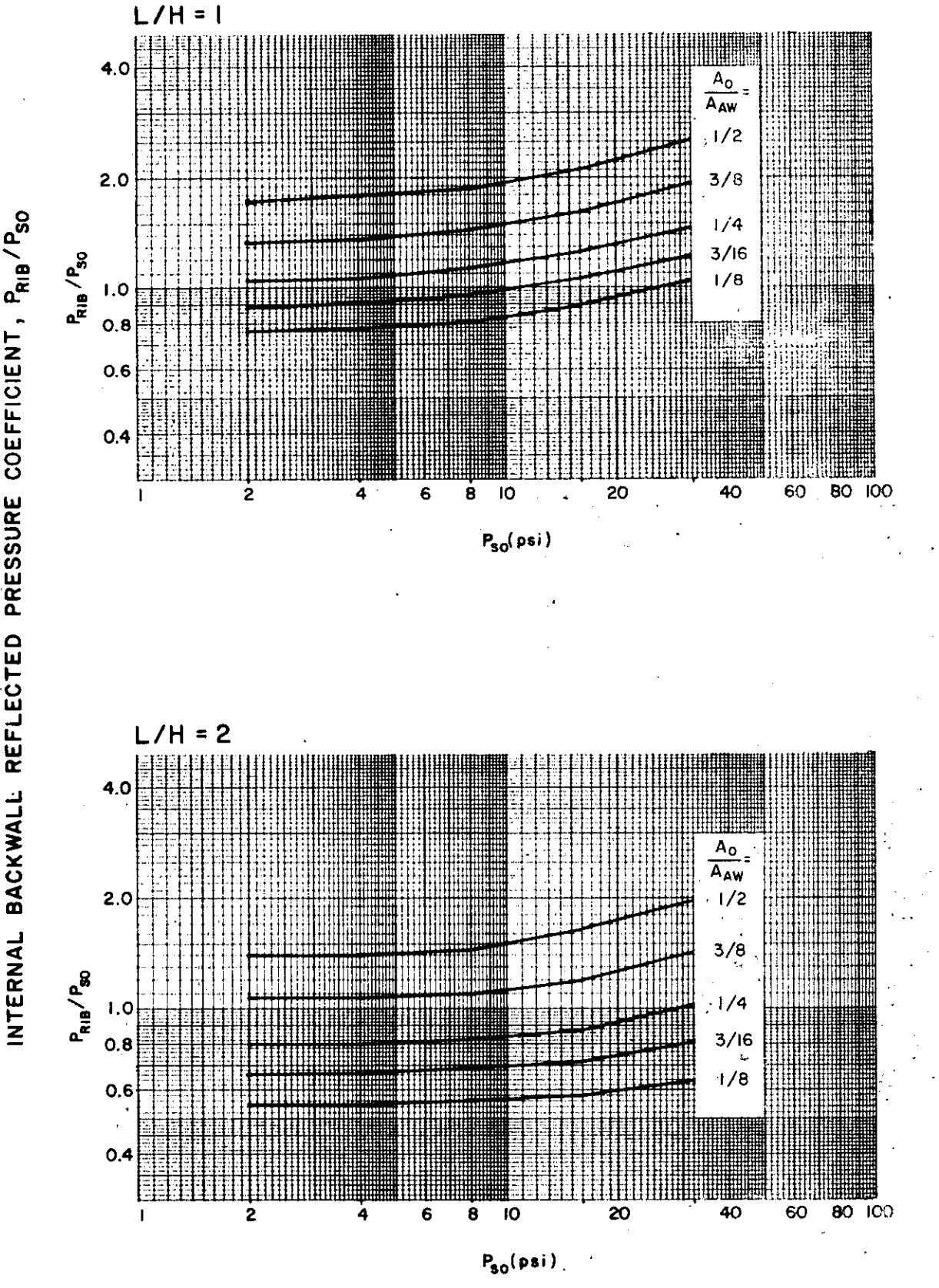


Figure 2-230 Idealized pressure coefficient for back wall interior blast load (L/H = 1 and 2)

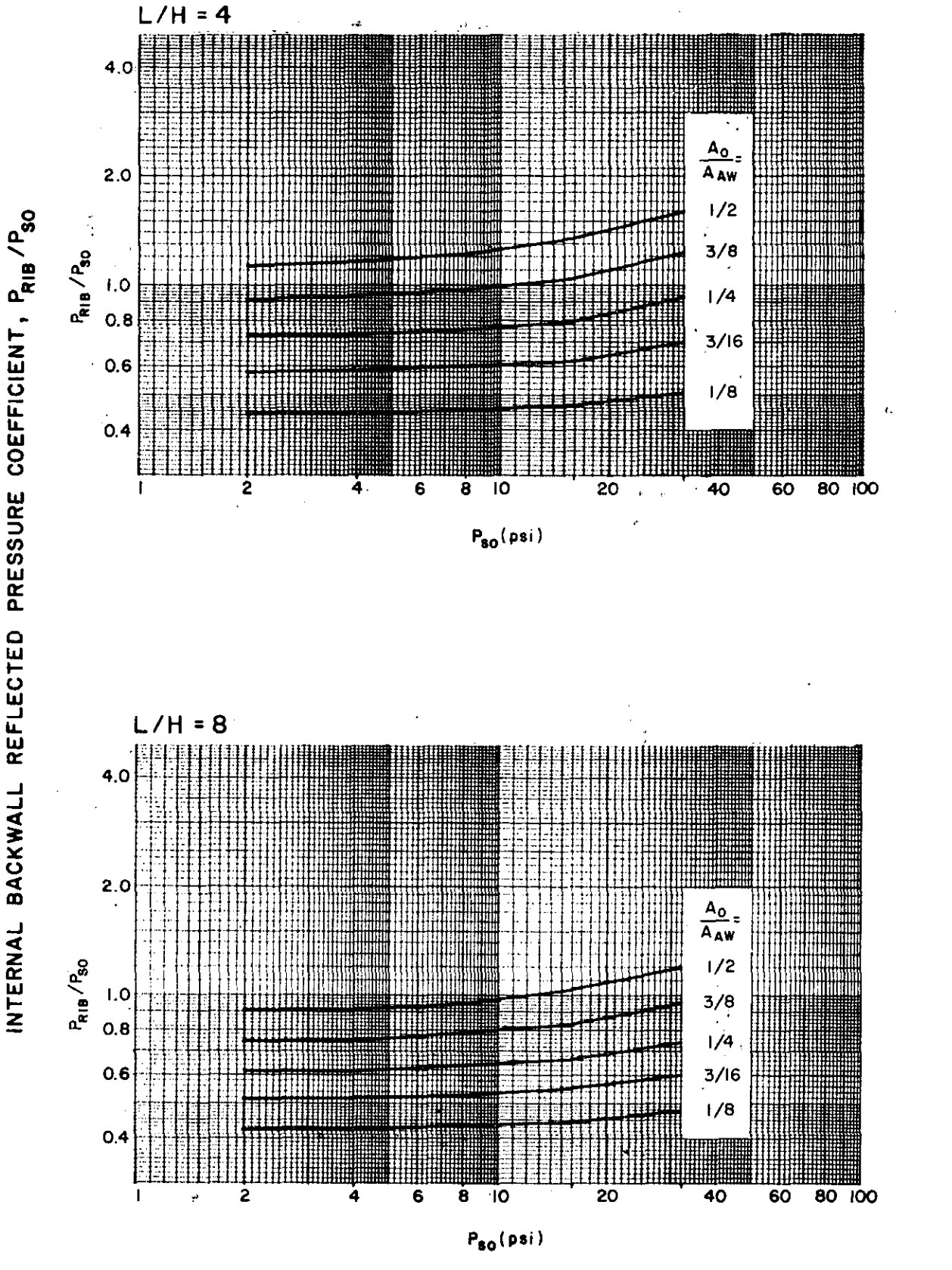
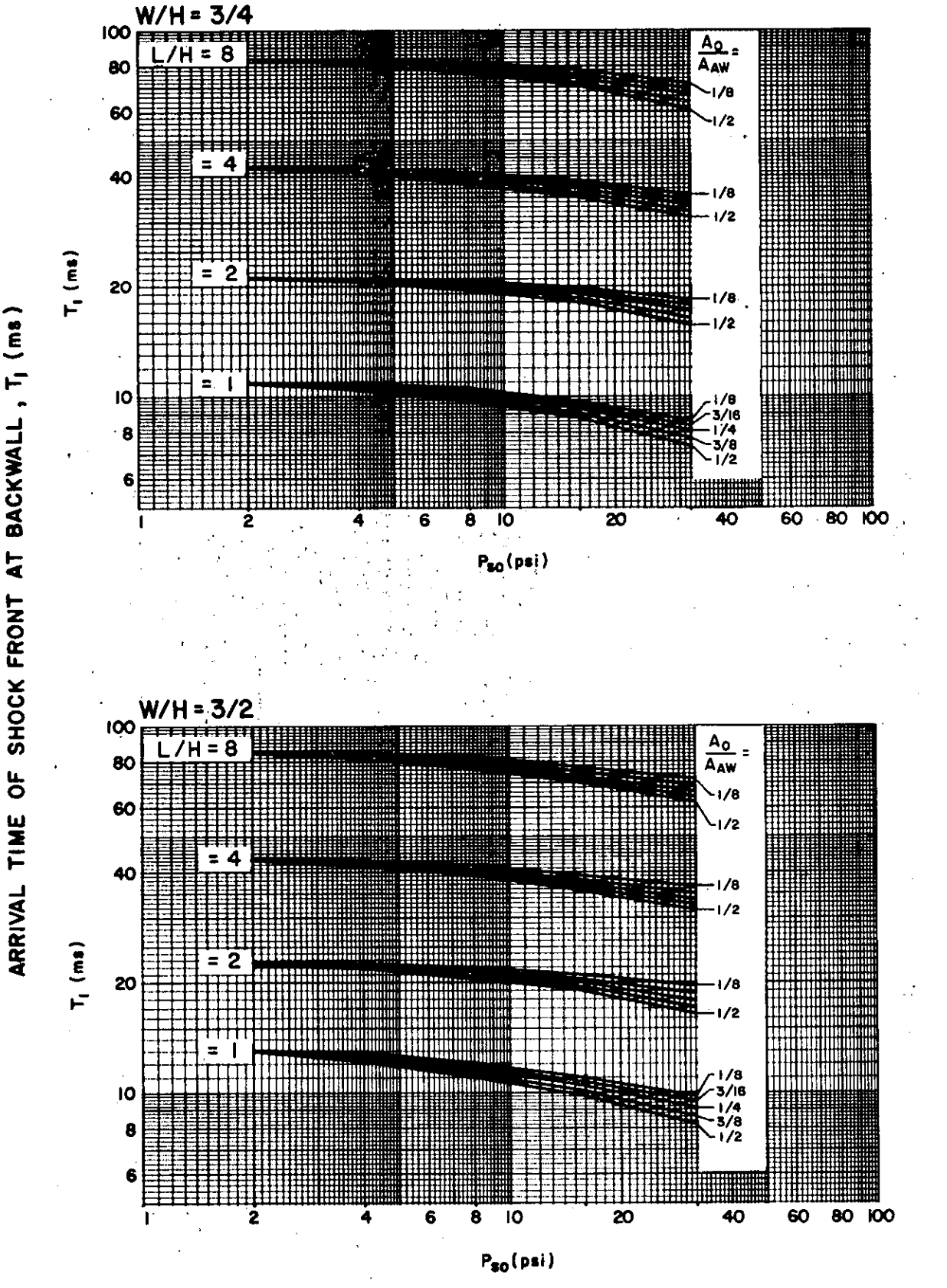


Figure 2-231 Idealized pressure coefficient for back wall interior blast load (L/H = 4 and 8)



ARRIVAL TIME OF SHOCK FRONT AT BACKWALL, T_1 (ms)

EXTERNAL INCIDENT PRESSURE AT FRONT FACE OF BUILDING, P_{so} (psi)

Figure 2-232 Arrival time, T_1, for interior back wall blast load (W/H = 3/4 and 3/2)

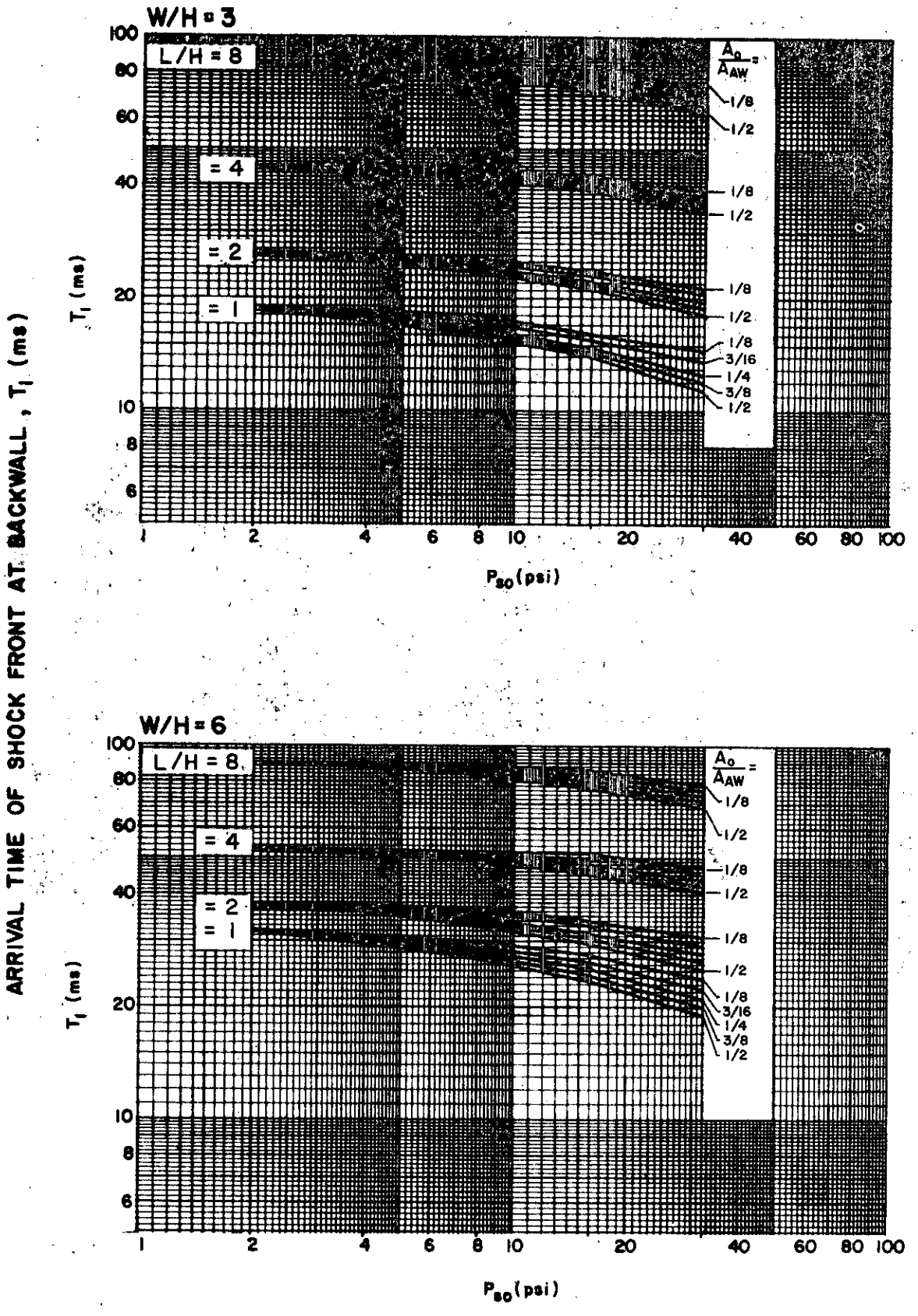


Figure 2-233 Arrival time, T_1, for interior back wall blast load (W/H = 3 and 6)

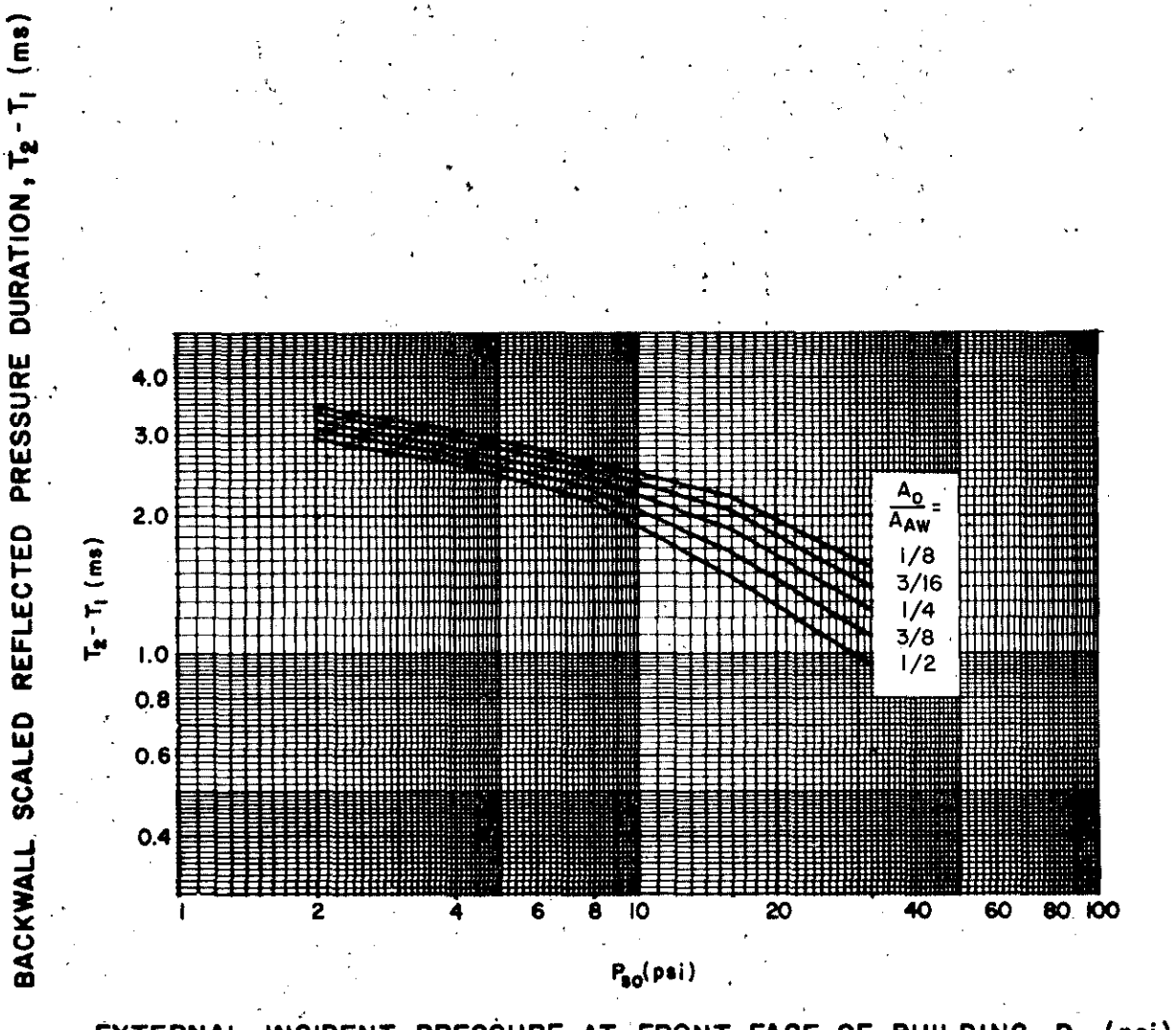


Figure 2-234 Idealized time T_2 - T_1 for interior back wall blast load

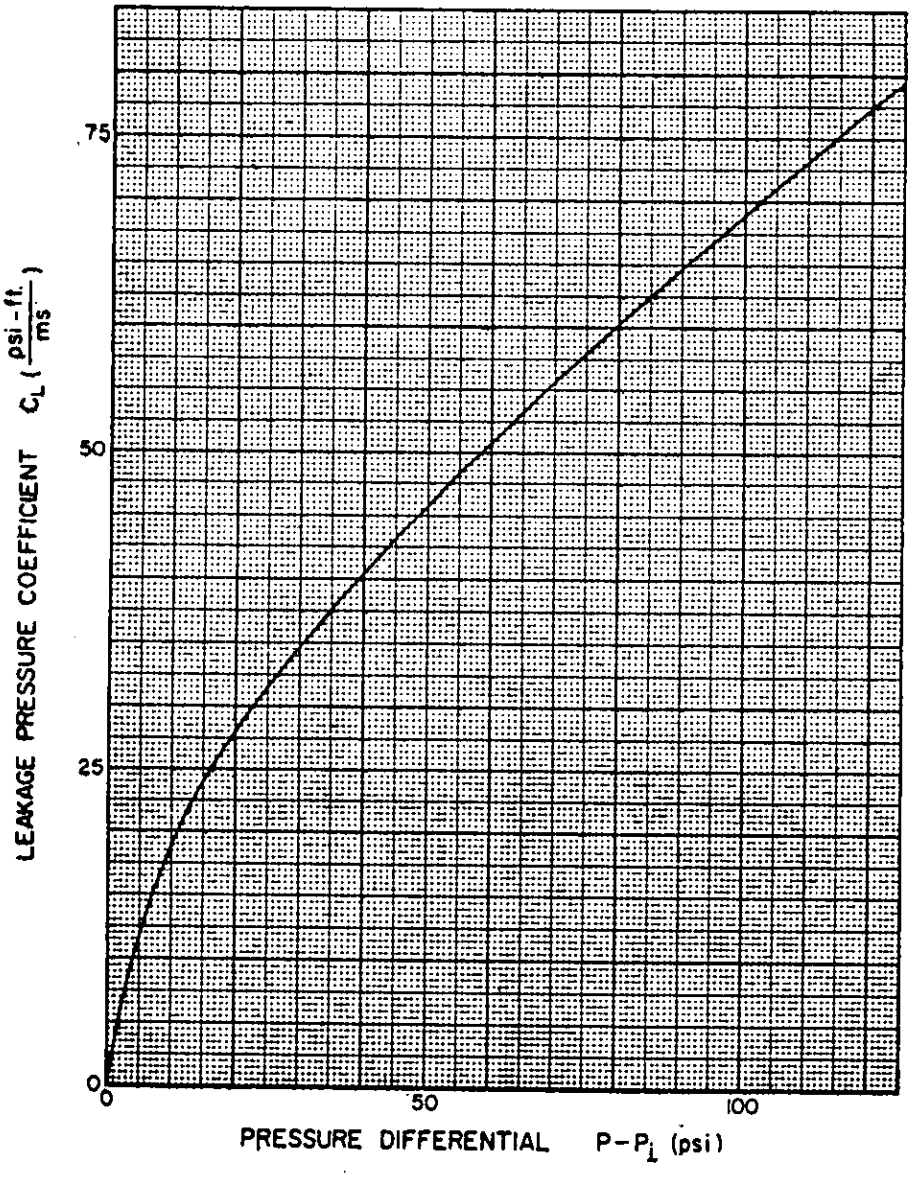


Figure 2-235 Leakage pressure coefficient vs. pressure differential

Table 2-1 Heat of Detonation and Heat of Combustion

Explosive Name	Symbol	Heat of Detonation (ft-lb/lb)	Heat of Combustion (ft-lb/lb)
Baratol	-	1.04 E+06	
Boracitol	-	5.59 E+06	
	BTF	2.37 E+06	
Composition B	Comp B	2.15 E+06	3.91 E+06
Composition C-4	Comp C-4	2.22 E+06	
Cyclotol 75/25	-	2.20 E+06	3.68 E+06
	DATB/DATNB	1.76 E+06	4.08 E+06
	DIPAM	1.89 E+06	
	DNPA	1.48 E+06	
	EDNP	1.72 E+06	
	FEFO	2.03 E+06	
	HMX	2.27 E+06	3.31 E+06
	HNAB	2.06 E+06	
	HNS	1.99 E+06	
	LX-01	2.41 E+06	
	LX-02-1	1.99 E+06	
	LX-04	1.99 E+06	
	LX-07	2.08 E+06	
	LX-08	2.77 E+06	
	LX-09-0	2.24 E+06	
	LX-10-0	2.17 E+06	
	LX-11	1.72 E+06	
	LX-14	2.20 E+06	
	NG	2.22 E+06	2.26 E+06
	NQ	1.49 E+06	2.79 E+06
Octol 70/30	-	2.20 E+06	3.81 E+06
	PBX-9007	2.18 E+06	
	PBX-9010	2.06 E+06	
	PBX-9011	2.14 E+06	
	PBX-9205	2.04 E+06	
	PBX-9404	2.18 E+06	
	PBX-9407	2.24 E+06	3.31 E+06
	PBX-9501	2.22 E+06	
Pentolite 50/50	-	2.14 E+06	
	PETN	2.31 E+06	2.70 E+06
	RDX	2.27 E+06	3.20 E+06
	TETRYL	2.11 E+06	4.08 E+06
	TNETB	2.34 E+06	
	TNT	1.97 E+06	5.05 E+06

Table 2-2 List of Illustrations of Peak Incident Pressure and Impulse Produced by Surface Detonation of Various Explosives

MATERIAL	FIGURE	DENSITY RANGE	SHAPE	CONFIGURATIONS L/H/W	L/L'	W/W'	H/D	REMARKS
Composition A-3	2-18a	1.59 to 1.91	2-17a	2.0/1.0/2.5 2.4/1.0/2.9 1.8/1.0/2.6	-	-	-	1) 91% RDX, 9% WAX 2) Fiberboard shipping containers
Composition A-5	2-18b	1.67 to 1.72	2-17a	2.5/1.0/2.0	-	-	-	1) 98.5% RDX, 1.5 ± 0.5% Stearic Acid
	2-18c	1.67 to 1.72	2-17j	-	-	-	1.7/1.0	2) Fiberboard shipping containers
Composition B	2-19a	1.65	2-17b	-	-	-	1.0/2.0	1) Mixture of RDX and TNT (60/40 percent, respectively) with 1% WAX added
	2-19b	1.65	2-17k	-	-	-	1.0/1.0	
	2-19c	1.65	2-17j	-	-	-	1.0/1.0	
Composition C-4	2-20a	1.52 to 1.61	2-17a	1.6/1.0/1.3	-	-	-	1) 91% RDX, 9% plasticizer (nonexplosive)
	2-20c	1.52 to 1.61	2-17a	2.5/1.0/2.0	-	-	-	
				9.0/1.0/9.0	-	-	-	2) Fiberboard shipping container and M112 extruded demolition blocks (Fig. 2-20a) 3) Dryer bed configuration (Fig. 2-20b)
Guanidine Nitrate	2-20c	0.72	2-17a	1.0/1.0/1.0	-	-	-	1) Bulk powder form 2) Tested in simulated storage bin configurations
Cyclotol 70/30	2-21a	1.71	2-17a	2.3/1.0/2.8	-	-	-	1) Type II, Class A
	2-21b	1.71	2-17c	2.0/1.0/2.5	1.2/1.0	2.5/1.0	-	2) Used primarily as a munition filler
				1.0/2.0/2.0	-	-	-	3) Fiberboard shipping containers and hopper
M42 Grenades	2-21c	-	2-17d	-	-	-	1.0/1.0	1) Each grenade is filled with .066 lb. of Composition A5 explosive. 2) A plywood tray filled with 64 M42 grenades
HMX	2-22a	1.87	2-17a	2.0/1.0/3.0	-	-	-	1) Plywood orthorhombic container
	2-22b	1.87	2-17j	-	-	-	1.0/1.2	2) Fiberboard cylindrical container 3) Wetted with isopropyl alcohol
M483 Projectile Single Round	2-22c	-	2-17h	-	-	-	4.0/1.0	1) A single full up M483 was placed vertically with the nose pointed downward

Table 2-2 List of Illustrations of Peak Incident Pressure and Impulse Produced by Surface Detonation of Various Explosives (Continued)

MATERIAL	FIGURE	DENSITY RANGE	SHAPE	CONFIGURATIONS L/H/W	L/L'	W/W'	H/D	REMARKS
Lead Azide	2-23a	-	2-17i	-	-	-	-	1) Wet dextrinated 2) Conductive rubber beaker/bag
Lead Styphnate	2-23b	-	2-17i	-	-	-	-	1) Conductive rubber beaker
	2-23c	-	2-17m	-	-	-	-	2) Test wet and dry state
LX-14	2-24a	-	2-17a	2.8/1.0/2.8	-	-	-	1) 95.5% HMX, 4.5% estane
	2-24b	-	2-17f	-	-	-	2.0/1.0	2) Aluminum orthorhomic container
	2-24c	-	2-17a	2.2/1.0/2.2	-	-	-	3) Pressed billets
Octol 75/25	2-25a	-	2-17a	1.2/1.0/1.2	-	-	-	1) 75% HMX, 25% TNT
		-		2.0/1.0/2.5	-	-	-	2) Received in flake form
	2-25b		2-17c	1.0/2.0/2.0	1.2/1.0	2.5/1.0	-	3) Fiberboard shipping container 4) Plywood truncated prism
M718/741 RAAM Projectile	2-25c	-	2-17h	-	-	-	2.0/1.0	1) Pallet of eight projectiles
Nitrocellulose	2-26a	-	2-17j	-	-	-	1.3/1.0	1) Dehydrated nitrocellulose (13.5% nitrogen) MIL-N-244A, Grade C 2) Standard shipping containers (Figure 2-26a,b) 3) Dryerbed (Fig. 2-26c)
	2-26b	-	2-17a	1.2/1.0/1.2	-	-	-	
	2-26c	-	2-17a	64.0/1.0/64.0	-	-	-	
Nitroglycerine	2-27a	-	2-17i	-	-	-	1.0/1.0	1) Liquid high explosive in polymethylpentene plastic laboratory beakers
PBXC-203	2-27b	1.6 ± 0.5	2-17j	-	-	-	2.0/1.0	1) Granular molding powder
	2-27c	1.6 ± 0.5	2-17g	-	-	-	20.0/1.0	2) Nominal composition by weight of 91% RDX and 9% ethylenevinyl acetate copolymer (EVA) 3) Cylindrical fiberboard container 4) Single, double, and triple extruded rods in varying lengths
RDX Slurry	2-28a	-	2-17j	-	-	-	3.7/1.0	1) Mixture consisted of RDX in a solution of 60% acetic acid, 32% water and 2% nitric acid. 2) Encased in polyethylene container
				-	-	-	2.4/1.0	

Table 2-2 List of Illustrations of Peak Incident Pressure and Impulse Produced by Surface Detonation of Various Explosives (Continued)

MATERIAL	FIGURE	DENSITY RANGE	SHAPE	CONFIGURATIONS L/H/W	L/L'	W/W'	H/D	REMARKS
RDX 98/2	2-28b	-	2-17a	1.7/1.0/2.6	-	-	-	1) High explosive received wet with isopropyl alcohol
	2-28c	-	2-17j	-	-	-	1.2/1.0	2) Plywood orthorhombic Nutsche container
				-	-	-	0.9/1.0	3) Fiberboard shipping containers
TNT (Flake)	2-29a	-	2-17j	-	-	-	1.8/1.0	1) Flake TNT bulk form
	2-29b	-	2-17a	1.2/1.0/1.2	-	-	-	2) Fiberboard cylindrical container
	2-29c	-	2-17c	1.0/2.4/2.0	1.25/1.0	2.5/1.0	-	3) Orthorhombic fiberboard container
								4) Hopper constructed from plywood
Tetracene	2-30a	-	2-17i	-	-	-	1.0/1.0	1) A primary explosive, was detonated in beakers in a dry state and in a wet state in storage bags
Nitroguanidine	2-30b	-	2-17j	-	-	-	1.0/1.0	1) Aluminum storage bin
								2) Bulk form
Benite Propellant	2-31a	-	2-17a	1.4/1.0/1.4	-	-	-	1) 40% nitrocellulose, 44.3% potassium nitrate, 6.3% sulfur, 9.4% charcoal and 0.5% ethyl centralite
	2-31b	-	2-17a	1.1/1.0/1.1	-	-	-	2) Container made of wood and fiberboard
Black Powder	2-31c	-	-	1.0/1.0/1.0	-	-	-	1) Class I, 4 by 8; Class 6, 20 by MIL-P-223B Grade A1, 4 by 8, Grade A3, 12 by 16; Grade A-3a
								2) Tested in loose powder form
								3) Storage bins and tote bins boxes were constructed from plywood
BS-NACO Propellant	2-32a	-	2-17j	-	-	-	1.7/1.0	1) Multi perforated
	2-32b	-	2-17a	1.6/1.0/2.9	-	-	-	2) Tested in cardboard drums (Fig. 2-32a), full-sized metal shipping containers (Fig. 2-32b) and aluminum hoppers (Fig. 2-32c)
	2-32c	-	2-17e	-	-	-	1.0/1.3	

Table 2-2 List of Illustrations of Peak Incident Pressure and Impulse Produced by Surface Detonation of Various Explosives (Continued)

MATERIAL	FIGURE	DENSITY RANGE	CONFIGURATIONS SHAPE	L/H/W	L/L'	W/W'	H/D	REMARKS
DIGL-RP Propellant	2-33a	-	2-17a	3.2/1.0/1.5	-	-	-	1) Composition of nitrocellulose, diethyleneglycol dinitrate, Akantite II Antralite I, magnesium oxide and graphite 2) Plywood containers (I5420 and I5422) 3) Cylindrical fiberboard container (I5421)
		-		1.9/1.0/3.2	-	-	-	
		-		1.4/1.0/2.2	-	-	-	
	2-33b	-	2-17j	-	-	-	1.0/1.0	
	2-33c	-	2-17a	2.2/1.0/2.7	-	-	-	
M1 Propellant	2-34a	-	2-17j	-	-	-	1.7/1.0	1) 84.2%, 13.15% N nitrocellulose; 9.9% dinitrotoluene; 4.9% dibutylphthalate; and 1.0% diphenylamine 2) Cylindrical drums, open hopper, closed feed hopper
	2-34b	-	2-17j	-	-	-	1.7/1.0	
	2-34a	-	2-17c	3.5/1.0/3.5	7.0/1.0	7.0/1.0	-	
	2-34a	-	2-17e	-	-	-	1.0/1.3	
	2-34b	-	2-17c	3.4/1.0/3.4	9.0/1.0	9.0/1.0	-	
	2-34b	-	2-17e	-	-	-	1.0/1.3	
M26 E1	2-34c		2-17j	-	-	-	1.0/1.5	1) Multi perforated propellant 2) Cylindrical fiberboard shipping containers, dryer bed configurations constructed from plywood; cylindrical container constructed from stainless steel (Fig. 2-35c)
	2-35a		2-17a	10.5/1.0/60.0	-	-	-	
	2-35b		2-17a	2.2/1.0/2.2	-	-	-	
	2-35c		2-17j	-	-	-	1.7/1.0	
M30 A1	2-36a	-	2-17j	-	-	-	1.5/1.0	1) Propellant single perforated and multi perforated 2) Cylindrical shipping drums and orthorhombic simulated dryers
	2-36b	-	2-17j	-	-	-	1.5/1.0	
	2-36c	-	2-17a	2.4/1.0/12.0	-	-	-	
	2-37a	-	2-17a	2.4/1.0/12.0	-	-	-	
M31 A1E1	2-37b	-	2-17a	3.1/1.0/1.0	-	-	-	1) Triple-base slotted stick propellant 2) Simulated fiberboard carton 3) Simulated wooden shipping/storage container 4) Short side (L) parallel to shock front, or 5) Long side (W) parallel to shock front
	2-37c	-	2-17a	3.1/1.0/1.0	-	-	-	
	2-38a	-	2-17a	3.8/1.0/2.0	-	-	-	
	2-38b	-	2-17a	3.8/1.0/2.0	-	-	-	

Table 2-2 List of Illustrations of Peak Incident Pressure and Impulse Produced by Surface Detonation of Various Explosives (Continued)

MATERIAL	FIGURE	DENSITY RANGE	SHAPE	CONFIGURATIONS L/H/W	L/L'	W/W'	H/D	REMARKS
N5 Propellant	2-38c	-	2-17j	-	-	-	1.5/1.0	1) Single base propellant
	2-39a	-	2-17j	-	-	-	1.0/2.0	2) Shipping drums with 10% moisture
							1.0/1.0	3) Carpet rolls cylindrically
							2.0/1.0	shaped
	2-39b	-	2-17a	1.4/1.0/6.8	-	-	-	4) N5 was loaded into charging buckets
	2-39c	-	2-17a	1.0/1.7/4.4	-	-	-	and conveyor belt configuration
M6 Propellant	2-40a	-	2-17j	-	-	-	1.7/1.0	1) Multi perforated propellant
		-		-	-	-	2.2/1.0	2) Cylindrical shipping drum
	2-40b	-	2-17e	-	-	-	1.0/1.3	3) Closed and open hoppers
	2-40c	-	2-17c	3.4/1.0/3.4	5.8/1.0	5.8/1.0	-	
2.75 in. Rocket Grain MK 43-1	2-41a	-	2-17g	-	-	-	-	1) N5 Propellant 2) Tested in shelves holding one, seven, and nine rocket grains
WC 844 Ball	2-41b	-	2-17a	16.5/1.0/70.0	-	-	-	1) Double base propellant
				3.8/1.0/35.0	-	-	-	2) Dryer bed constructed from plywood
	2-41c	-	2-17j	-	-	-	1.1/1.0	3) Cylindrical fiberboard containers
XM37 RAP	2-42a	-	2-17j	-	-	-	1.0/1.3	1) Consist of nitrocellulose 50%,
	2-42b	-	2-17g	-	-	-	9.0/1.0	nitroglycerine 36.2%, others 13.8%
	2-42c	-	2-17a	1.0/1.5/1.0	-	-	-	2) Forward and aft grains simulated
	2-43a	-	2-17j	-	-	-	1.0/1.6	extruded billet, Ro Con shipping
	2-43b	-	2-17g	-	-	-	10.0/1.0	drum
	2-43c	-	2-17a	1.2/1.0/1.2	-	-	-	
JA-2 (L5460)	2-44a	-	2-17j	-	-	-	1.0/1.0	1) Double base propellant
	2-44b	-	2-17a	10.0/1.0/10.0	-	-	-	2) 60% nitrocellulose, 24.6%
				5.0/1.0/5.0	-	-	-	diethylene glycol dinitrate, 15.4%
				2.5/1.0/2.5	-	-	-	others
								3) Fiberboard cylindrical container
								4) Orthorhombic fiberboard container
M10 Propellant	2-44c	-	2-17a	1.0/2.7/1.5	-	-	-	1) 98% nitrocellulose (13.5% N), 1%
				1.0/1.6/1.1	-	-	-	potassium sulfate and 1% dipheyla-
	2-45a	-	2-17a	2.1/1.0/1.3	-	-	-	mine
				1.5/1.0/1.2	-	-	-	2) Single perforated
								3) Fiberboard box, metal lined wooden boxes, orthorhombic stainless steel vented container

Table 2-2 List of Illustrations of Peak Incident Pressure and Impulse Produced by Surface Detonation of Various Explosives (Continued)

MATERIAL	FIGURE	DENSITY RANGE	SHAPE	CONFIGURATIONS L/H/W	L/L'	W/W'	H/D	REMARKS
105mm, M314 A3 Illuminant	2-45b	-	2-17j	-	-	-	1.0/1.4	1) 7.7% Luminac 4116 type A, 56% magnesium, 36% sodium nitrate 2) Fiberboard shipping drums (Fig. 2-45b) 3) Simulated steel mixer/muller (Fig. 2-45c)
	2-45c	-	2-17j	-	-	-	1.0/6.0	
I559 Igniter Mixture	2-46a	-	2-17j	-	-	-	1.8/1.0	1) I136 premix(90% strontiune nitrate and 10% calcium resinute) and a premix (23.3% lead dioxide and 77.7% magnesium) 2) Rubber and aluminum cylinder configurations (Fig. 2-46a and 2-46b respectively)
	2-46b	-	2-17j	-	-	-	1.0/1.8	
I560 Subigniter Mixture	2-46c	-	2-17j	-	-	-	2.1/1.0	1) Magnesium/strontium nitrate/ strontium peroxide/polyvinyl chloride 27.5/27.5/30/15% by weight respectively 2) Rubber (Fig. 2-46c) and aluminum (Fig. 2-47a) cylinder configurations
	2-47a	-	2-17j	-	-	-	1.0/1.1	
R284 Tracer Mixture	2-47b	-	2-17j	-	-	-	1.9/1.0	1) Strintium nitrate/polyvinyl chloride/(50/100 mesh) magnesium in 53.7/18.1/28.2% by weight, respectively 2) Rubber (Fig. 2-47b) and aluminum (Fig. 2-47c) cylinder configurations
	2-47c	-	2-17j	-	-	-	1.0/1.4	
M314-A3 First Fire Composition	2-48a	-	2-17a	1.0/1.17/1.0	-	-	-	1) 50% barium nitrate, 5% laminac Type B, 20% silicon, 15% zirconium hydrate, 10% tetranitro carbozole 2) Cardboard box (Fig. 2-48a) simulated mix/muller (Fig. 2-48b)
	2-48b	-	2-17j	-	-	-	1.0/1.8	
M49A1 Trip Flare Composition	2-48c	-	2-17j	-	-	-	1.0/1.4	1) Magnesium 36%, sodium nitrate 54%, binder 10% 2) Shipping drum fiberboard (Fig. 2-48c), simulated steel mixer/muller (Fig. 2-49a)
	2-49a	-	2-17j	-	-	-	1.0/6.0	

Table 2-3 **List of Illustrations for Average Peak Reflected Pressure and Scaled Average Unit Reflected Impulse**

h/H	l/L	Average Peak Reflected Pressure				Scaled Average Unit Reflected Impulse			
		Number of Adjacent Reflecting Surfaces							
		One	Two	Three	Four	One	Two	Three	Four
0.10	0.10	2-52	2-64	2-80	2-92	2-101	2-113	2-129	2-141
	0.25	2-53	2-65	2-81	2-93	2-102	2-114	2-130	2-142
	0.50	2-54	2-66	2-82	2-94	2-103	2-115	2-131	2-143
	0.75	2-53	2-67	2-81	2-93	2-102	2-116	2-130	2-142
0.25	0.10	2-55	2-68	2-83	2-95	2-104	2-117	2-132	2-144
	0.25	2-56	2-69	2-84	2-96	2-105	2-118	2-133	2-145
	0.50	2-57	2-70	2-85	2-97	2-106	2-119	2-134	2-146
	0.75	2-56	2-71	2-84	2-96	2-105	2-120	2-133	2-145
0.50	0.10	2-58	2-72	2-86	2-98	2-107	2-121	2-135	2-147
	0.25	2-59	2-73	2-87	2-99	2-108	2-122	2-136	2-148
	0.50	2-60	2-74	2-88	2-100	2-109	2-123	2-137	2-149
	0.75	2-59	2-75	2-87	2-99	2-108	2-124	2-136	2-148
0.75	0.10	2-61	2-76	2-89	2-95	2-110	2-125	2-138	2-144
	0.25	2-62	2-77	2-90	2-96	2-111	2-126	2-139	2-145
	0.50	2-63	2-78	2-91	2-97	2-112	2-127	2-140	2-146
	0.75	2-62	2-79	2-90	2-96	2-111	2-128	2-139	2-145

Table 2-4 List of Illustrations for Interior Side Wall Idealized Times T_3 and T_4

L/H	W/H			
	3/4	3/2	3	6
1	2-214	2-215	2-216	2-217
2	2-218	2-219	2-220	2-221
4	2-222	2-223	2-224	2-225
8	2-226	2-227	2-228	2-229

PRIMARY AND SECONDARY FRAGMENTS

2-16. General

Previous sections in this chapter have discussed explosive accident predictions in reference to studies of blast waves and their effects. Significant damage from accidental explosions can also be caused by the impact of fragments or objects which were generated during the explosions and hurled against structures or other receivers at high speed.

Fragments resulting from accidental explosions can be divided into two categories. The term "primary fragment" denotes a fragment from a casing or container of an explosive source or a fragment from an object in contact with an explosive. If the source is a true high explosive, the container or casing usually ruptures into a large number of small primary fragments which can be projected at velocities up to several thousand feet per second by the explosion. For bomb and shell casings, typical weights of damaging fragments recovered in field tests are about 0.032 oz. These primary fragments, though irregular, are usually of "chunky" geometry, i.e., all linear dimensions are of the same order.

Containers or casings which fragment or burst during explosions are not the only sources of fragments and missiles. Other potentially damaging objects, known as "secondary missiles" or "secondary fragments" can also be produced due to the blast wave interaction with objects or structures located near the explosive source. These objects can be torn loose from their moorings, if they are attached, and accelerated to velocities high enough to cause impact damage. The objects could be pieces of machinery, small tools, materials such as pipes and lumber, parts of buildings or other structures disrupted by the explosions, and large pieces of equipment. Characteristics of both primary and secondary fragments (often referred to as secondary "debris" to distinguish them from primary "fragments") will be discussed in this section.

2-17. Primary Fragments

2-17.1. General

The explosion of a cased donor charge results in the formation of primary fragments which are produced by the shattering of the explosive container. The container may be the casing of conventional munitions, the kettles, hoppers, and other metal containers used in the manufacture of explosives, metal housing of rocket engines.

Primary fragments are characterized by very high initial velocities (in the order of thousands of feet per second), a large number of fragments, and relatively small sizes in comparison to secondary fragments and concrete fragments formed due to partial failure or total collapse of protective elements. The initial velocity and size of the fragments are functions of the thickness of the metal container, the shape of the explosive as a whole (spherical, cylindrical, prismatic), and the sections of the container (ends and middle) from which the fragments are formed. The size and shape of the fragments will depend greatly on the metallographic history of the casing, its physical condition (such as dents, grooves, bends, or internal cracks or flaws), and the condition of joints, most notably welded joints.

Upon detonation of a cased explosive, the casing breaks up into fragments with varying weights and velocities. The destructive potential of these fragments is a function of their shapes, materials, momentum and kinetic energy distributions. Since only the larger fragments have the momentum necessary to perforate a barrier and/or cause propagation of explosions, they are usually the only fragments of concern in design of a protective system. Therefore, through testing or analysis, the velocity and weight of the "worst case" fragment must be determined and used as a design criterion.

2-17.2. Initial Fragment Velocity

2-17.2.1. Explosives with Uniform Cylindrical Containers

The most common technique for calculating the initial velocity of fragments in contact with an explosive charge is the Gurney method. The initial velocity of primary fragments resulting from the detonation of a cased explosive is a function of the explosive output and the ratio of the explosive charge weight to casing weight.

The initial velocity of primary fragments resulting from a high-order detonation of a cylindrical casing with evenly distributed explosives is expressed as:

$$v_o = (2E')^{1/2} \left[\frac{W/W_c}{1 + 0.5\ W/W_c} \right]^{1/2} \qquad 2\text{-}32$$

and, applying a 20 percent factor of safety, the design charge weight is:

$$W = 1.2W_{ACT} \qquad 2\text{-}33$$

where

v_o = initial velocity of fragments

$(2E')^{1/2}$ = Gurney Energy Constant from Table 2-5

W = design charge weight

W_c = weight of casing

W_{ACT} = actual quantity of explosive

The ratio of Gurney energy to the heat of detonation $E'/\delta H$, represents the conversion efficiency of chemical energy to "Gurney" energy. If E' is unknown for a particular explosive, and δH is known, $E'/\delta H$ may be determined for a similar explosive (i.e., similar heat of detonation) and the value used to estimate the Gurney energy.

2-17.2.2. Explosives with Non-Uniform Cylindrical Containers

Cylinders are the most common shape of cased explosives. Along the length of the cylinder, there may be a large variation in the thickness of the casing and its outside diameter. In such cases, the cylinder is divided into a

series of equivalent cylinders. This method is further discussed in Section 2-17.3.2.

Gurney's equations were developed for cased explosives where the explosive is in direct contact with the outer metal casing. Several conditions are illustrated in Figure 2-236 where the explosive and outer casing are separated by an incompressible fluid. The initial velocity of primary fragments resulting from the detonation of such items may be approximated by using the Gurney equations with slight modifications. The actual weight of the explosive is increased by the required 20 percent factor of safety. The design charge weight is:

$$W = 1.2\ W_{ACT} \qquad 2\text{-}34$$

and, the weight of the casing is increased to include the weight of the fluid and the weight of the inner casing which surrounds the explosive, if present, or:

$$W_c = W_{CO} + W_{CI} + W_A \qquad 2\text{-}35$$

where

W = design charge weight

W_{ACT} = actual quantity of explosive

W_c = total weight of casing

W_{CO} = weight of outer casing

W_{CI} = weight of inner casing

W_A = weight of fluid

2-17.2.3. Explosives with Non-Cylindrical Containers

Gurney formulas for some additional geometries are given in Table 2-6. A plot of velocity versus casing to charge weight ratio for various geometries is shown in Figure 2-237.

The shapes considered in Figure 2-237 are assumed to have an evenly distributed explosive and a uniform container (casing) or plate thickness. However, for those cases where the shape is slightly nonuniform, the initial velocity of the resulting fragments may be estimated by using the average cross-sectional dimensions.

2-17.3. Fragment Mass Distribution

2-17.3.1. Explosives with Uniform Cylindrical Containers

The fragmentation pattern and the weight of the largest fragment resulting from the high-order detonation of an evenly-distributed explosiv
drical metal case of uniform thickness have been calculated according t
tionships developed on the basis of theoretical considerations confirmed with

a large number of tests. The number of fragments produced by a cylindrical cased charge weighing more than a given design fragment is:

$$N_f = \frac{8W_c \, e^{-[W_f^{1/2} / M_A]}}{M_A^2} \qquad 2\text{-}36$$

and

$$M_A = B t_c^{5/6} d_i^{1/3} (1 + t_c / d_i) \qquad 2\text{-}37$$

where

N_f = number of fragments with weight greater than W_f

W_c = casing weight

W_f = design fragment weight

M_A = fragment distribution factor

B = explosive constant from Table 2-7

t_c = average casing thickness

d_i = average inside diameter of casing

The largest fragment produced by an explosion can be found by setting $N_f = 1$. Thus, the weight of the largest fragment is given by:

$$W_f = \left[M_A \ln (8W_c / M_A^2) \right]^2 \qquad 2\text{-}38$$

Setting the fragment weight W_f equal to zero, the following expression for the total number of fragments is obtained:

$$N_T = 8W_c / M_A^2 \qquad 2\text{-}39$$

where: N_T = total number of fragments

Hence, the average particle weight can be found:

$$W_f = 16W_c / N_T = 2M_A^2 \qquad 2\text{-}40$$

where

$\bar{W}_f$ = average fragment weight

For design purposes, a confidence level C_L, where $(0 < C_L < 1)$, can be defined as the probability that the weight, W_f, is the largest weight fragment released. The expression for the design fragment weight corresponding to a prescribed design confidence level (C_L) is given as:

$$C_L = 1 - N_f/N_T = 1 - e^{-[W_f^{1/2} / M_A]} \qquad 2\text{-}41$$

or rearranging terms:

$$W_f = M_A^2 \ln^2(1 - C_L) \qquad 2\text{-}42$$

Equation 2-42 can then be used to calculate the design fragment weight for a prescribed design confidence level. Note that Equation 2-42 uses an infinite distribution to describe a physical phenomenon which has a finite upper limit. Equation 2-42 may be used for CL ≤ 0.9999. If CL > 0.9999, use:

$$W_f = M_A^2 \ln^2 \left[1 - C_L(1 - e^{-[4(W_c)^{1/2} / M_A]})\right] \qquad 2\text{-}43$$

The number of fragments with weight greater than W_f is:

$$N_f = N_T (1 - C_L) \qquad 2\text{-}44$$

It should be noted that Equations 2-41 through 2-44 are not applicable to casings designed to fragment in a specific pattern.

In order to facilitate design calculations, Figure 2-238 is available for determining the quantity M_A/B for a given cylindrical casing geometry and Figures 2-239 and 2-240 provide the value of W_f/M_A corresponding to a specified confidence level. Figure 2-239 is applicable for a wide range of confidence levels $(0.3 \leq C_L < 1.0)$ whereas Figure 2-240 is applicable for high confidence levels $(0.986 \leq C_L \leq 1)$.

To calculate the actual number of fragments with a weight greater than the design fragment weight, Equation 2-36 can be applied directly. Alternatively, Figure 2-241 presents a plot of the quantity B^2N_T/W_c versus the casing geometry. The number of fragments with weight greater than W_f can then be calculated from Equation 2-44.

2-17.3.2. Explosives with Non-Uniform Cylindrical Containers

The equations in Section 2-17.3.1 were developed assuming a uniform cross-section along the axis of the cylinder with evenly distributed explosive in direct contact with the outer casing. Actual cased explosives rarely conform to these ideal conditions. If there is only slight variation in the casing thickness and/or casing diameter, the fragment weight may be estimated using an average casing thickness and diameter in Equation 2-37.

If the cross-section varies greatly, the container is treated as a series of equivalent cylinders representing the actual shape as closely as possible

(Fig. 2-242). Using the average casing thickness and diameter of each section, the velocity and weight of the design fragment must be determined for each section. The worst case fragment of the equivalent cylinders is then taken as the design fragment for the entire container.

Cylindrical explosives with steel and hollow cores are shown in table 2-6. The fragment mass distribution may be estimated for these shapes using the uniform cylinder equations of Section 2-17.3.1. In applying these equations, the same procedures as outlined above for nonuniform cylinders are employed, except that the steel or hollow cores are neglected in the calculations.

Figure 2-236 illustrates the cased explosive where the explosive and outer casing are separated by an incompressible fluid. The outer casing is much thicker than the inner casing which encloses the explosive. Here again, the fragment mass distribution may be estimated using the uniform cylinder equations of Section 2-17.3.1 except as indicated below. The heaviest fragment will fracture from the outer casing. Thus, W_c should be the weight of the outer casing only. The thin inner casing is neglected in the calculations. In addition, since the ratio of explosive weight to casing weight (W/W_c) is small, the fragment distribution factor (M_A) should be the larger of that given in Equation 2-36 and Equation 2-44 as follows:

$$M_A = At_c \frac{\left[d_i + t_c \right]^{3/2}}{d_i} \left[1 + \frac{W}{2W_c} \right]^{1/2} \qquad 2\text{-}45$$

where

A = explosive composition constant from table 2-7 and all other terms are as previously defined.

2-17.3.3. Explosives with Non-Cylindrical Containers

Information is not presently available for evaluating the number and weight of fragments from charges other than those having a cylindrical casing.

The equations of Section 2-17.3.1 can only be employed to calculate masses of primary fragments which evolve from accidents involving an explosive detonation within a container of some sort, such as a casing, a storage tank, or a confining piece of machinery such as a centrifuge or press. Weights of fragments created as a result of a given quantity of explosive detonating while being machined or in an unconfined space must be estimated using other methods.

2-17.4. Variation of Fragment Velocity with Distance

When an explosion is located close to an object (acceptor explosive or barrier), the velocity v_s at which a fragment strikes the object is approximately equal to the initial velocity v_o. However, if the detonation is located at a relatively large distance from the object, then the impact or striking velocity of the fragment may be substantially less than its velocity immediately after the explosion. This variation in velocities, which is primarily a re-

sult of air resistance, is also a function of the physical properties of the casing and the distance between the donor explosive and the object.

When the protective barriers are located 20 feet or less from a detonation, the variation between striking and initial velocities usually may be neglected. On the other hand, for determining the effects of primary fragment impact on structures further away from a detonation, the variation of fragment velocity with distance should be included in the design. The fragment velocity of major concern is the velocity with which the "design fragment(s)" (the worst case fragment(s) which the structure must be designed to withstand) strikes the protective structure. This striking velocity is expressed as:

$$v_s = v_o e^{-[12k_v R_f]} \qquad 2\text{-}46$$

and

$$k_v = (A/W_f)\ \rho_a\ C_D \qquad 2\text{-}47$$

where

v_s = fragment velocity at a distance R_f from the center of detonation

v_o = initial (maximum) fragment velocity

R_f = distance from the center of detonation

k_v = velocity decay coefficient

A = presented area of the fragment

W_f = fragment weight

A/W_f = fragment form factor

ρ_a = specific density of air

C_D = drag coefficient

The decay coefficient can be evaluated as:

$A/W_f = 0.78\ /W_f^{1/3}$ for a random mild steel fragment

$\rho_a = 0.00071$ oz/in^3

$C_D = 0.6$ for primary fragments

The resulting expression for the striking velocity is:

$$v_s = v_o e^{-[.004R_f/W_f^{1/3}]} \qquad 2\text{-}48$$

Figure 2-243 shows the variation of primary fragment velocity with distance. The term initial velocity refers to the maximum fragment velocity as the fragment is ejected from the charge. Due to the extremely high rates of fragment

acceleration, this velocity is considered to be attained by the fragment prior to moving appreciably from its initial position.

2-17.5. Primary Fragments - Shape, Caliber Density and Impact Angle

2-17.5.1. General

In order to determine the damage potential of primary fragments, it is necessary to evaluate the caliber density, shape and angle of obliquity of the fragments, and the previously described weight and striking velocity. When a container fragments, a random distribution of fragment shapes results. Section 2-17.3 contained a method for determining the weight distribution of primary fragments. From the weight of the fragment and shape of the containment vessel, one can estimate the size of individual fragments. This section discusses a method for performing an engineering estimate of a standard design fragment(s) for use in fragment impact damage.

2-17.5.2. Shape of Primary Fragments

Two possible fragment shapes are shown in Figure 2-244 for explosives in contact with the outer casing. The blunt fragment shape in Figure 2-244 is considered as the standard shape in the design charts presented in the following section. While the standard fragment has a milder nose shape than the alternate fragment, the standard fragment is generally considered appropriate for use in design since (1) only a small number of fragments will strike the structure nose-on, and (2) only a small fraction of these fragments will have a more severe nose shape than the standard fragment. In addition, the length-to-diameter ratio of these fragments is felt to be more representative of an average fragment configuration. For convenience, a plot of fragment weight versus fragment diameter for these two fragment shapes is given in Figure 2-245.

There is little data available concerning the shape of a fragment ejected from a cased explosive where the explosive is not in direct contact with the casing (Fig. 2-236). Consequently, the worst possible shape is assumed, a thin rectangular or circular rod. The diameter of the cross-section (the thickness of a rectangular cross-section) is equal to the casing thickness at rupture.

The fragmentation pattern of this type of cased explosive somewhat resembles that of a ruptured pressure vessel. The casing diameter typically expands before rupturing and, therefore, to conserve mass, the casing thickness must be decreased.

It is assumed that the outside diameter expands to 1.5 times the original diameter. Thus, the adjusted inside diameter is:

$$d_i' = \left[1.25 \, (d_i + 2t_c)^2 + d_i^2 \right]^{1/2} \qquad 2\text{-}49$$

where

d_i' = adjusted inside diameter of casing

d_i = original inside diameter of casing

t_c = original casing thickness

The adjusted or "necked-down" thickness is:

$$t_c' = 0.75\ (d_i + 2t_c) - 0.5d_i' \qquad 2\text{-}50$$

where

t_c' = adjusted casing thickness

Assuming a circular cross-section, the length of the fragment is:

$$L_f = \frac{4W_f}{\pi\rho_c(t_c')^2} \leq L_{cyl} \qquad 2\text{-}51$$

where

L_f = length of the fragment

W_f = weight of the fragment from Section 2-17.3

ρ_c = density of casing material

L_{cyl} = length of the cylinder or equivalent cylinder

If assuming a circular cross-section, the length L_f calculated is longer than the length of the cylinder, then a rectangular cross-section is assumed where the width is equal to:

$$b_f = \frac{W_f}{\rho_c t_c' L_{cyl}} \qquad 2\text{-}52$$

where

b_f = width of the fragment

2-17.5.3. Caliber Density

The influence of the fragment weight to fragment diameter ratio is expressed in terms of the caliber density of the fragment which is defined as:

$$D = W_f / d^3 \qquad 2\text{-}53$$

where

D = caliber density

d = fragment diameter

2-17.5.4. Nose Shape Factor

The nose shape factor expresses the influence of the shape of the primary fragment and is defined as:

For flat-nosed, solid fragments:

$$N = 0.72 \qquad 2\text{-}54$$

For fragments with special nose shapes:

$$N = 0.72 + 0.25\ (n - 0.2)^{1/2} < 1.17 \qquad 2\text{-}55$$

where

N = nose shape factor

n = caliber radius of the tangent ogive of the assumed fragment nose

2-17.5.5. Impact Angle

The angle of obliquity refers to the angle between the path of the fragment and a normal to the surface; thus, a normal impact corresponds to an angle of obliquity of zero degrees. A normal impact is usually assumed in penetration calculations in order to conservatively design for the worst case condition.

2-18. Secondary Fragments

2-18.1. General

The explosion of HE during some manufacturing or forming process (i.e., nitration, centrifuging, pressing, and machining on lathe) can result in a large number of secondary fragments which vary greatly in size, shape, initial velocity, and range. Each of these parameters affects the damage potential of an accidental explosion and, therefore, should be considered in the design of protective structures.

The current state-of-the-art for assessing damage potential requires that the design engineer estimate the conditions which are likely to exist at the time of the accident and perform a structural assessment of any equipment which will be involved. Some of the initial factors to consider are:

(1) Type and amount of HE.

(2) Configuration of HE (i.e., sphere, cylinder, cased, uncased).

(3) Location of HE (i.e., attached to lathe, resting on support table, contained in centrifuge, proximity to walls and other equipment).

(4) Type of propagation after initiation (i.e., high order, burning, partial detonation).

If the fragmentation pattern varies with the initial conditions, the Architectural Engineer must examine several likely scenarios to evaluate the damage potential.

To estimate the weight, shape, and velocity of fragments which result from detonation of an HE during a manufacturing or forming process, one would perform the following steps:

(1) Determine distance (R_i) from the center of the explosive to the i^{th} point of interest (refer to structural details of the machine and/or architectural drawings).

(2) Determine the size and shape of the expected fragment (refer to structural details of the machine).

(3) Determine the fragment velocity (refer to sections 2-18.2 and 2-18.3).

2-18.2. Velocity of Unconstrained Secondary Fragments

To predict velocities of objects accelerated by an explosion, the interaction of blast waves with solid objects must first be considered. Figure 2-246 shows the interaction of a blast wave with an irregular object. The interaction is shown in three phases as the wave passes over the object. As the wave first strikes the object, a portion is reflected from the front face, and the remainder diffracts around the object. In the diffraction process, the incident wave front closes in behind the object, greatly weakened locally, and a pair of trailing vortices is formed. Rarefaction waves sweep across the front face, attenuating the initial reflected blast pressure. After passage of the front, the object is immersed in a time-varying flow field. Maximum pressure on the front face during this "drag" phase of loading is the stagnation pressure.

To predict the effect of a blast wave on the object, it is necessary to examine the net transverse pressure on the object as a function of time. This loading, somewhat idealized, is shown in Figure 2-247. After the time arrival t_a, the net transverse pressure rises from zero to a maximum peak reflected pressure P_r in time $(T_1 - t_a)$. For an object with a flat face nearest the approaching blast wave, this time interval is zero. Pressure then falls linearly to drag pressure in time $(T_2 - T_1)$ and decays more slowly to zero in time $(T_3 - T_2)$.

The basic assumptions for unconstrained secondary fragments are (1) the object behaves as a rigid body, (2) none of the energy in the blast wave is absorbed in breaking the object loose from its moorings or deforming it elastically or plastically, and (3) gravity effects can be ignored during the acceleration phase of the motion. The equation of motion for the object is:

$$A\,p(t) = Ma \qquad 2\text{-}56$$

where

A = area of object presented to blast front

$p(t)$ = pressure-time history of blast wave acting on object

M = mass of object

a = acceleration of object

Rearranging terms and integrating:

$$v(T_3) = \int (T_3/t_a)\, a\,dt = \frac{A}{M} \int (T_3/t_a)\, p(t)\,dt = \frac{A}{M}\, i_d \qquad 2\text{-}57$$

where

$v(T_3)$ = initial velocity of the object

i_d = total drag and diffraction impulse

The integral in Equation 2-57 is the area under the curve of pressure-time relationship. Equation 2-57 can be integrated explicitly if the pressure-time history can be described by suitable mathematical functions or it can be evaluated graphically or numerically if p(t) cannot be easily written in function form.

For intermediate strength shocks, the solution of Equation 2-57 can be determined from a rather long equation. For computational purposes that equation is presented here in graphical form as Figure 2-248, where

P_{so} = peak incident overpressure

P_o = atmospheric pressure

C_D = drag coefficient

i_s = incident specific impulse

a_o = velocity of sound in air

K = constant (4 if object is on the ground or reflecting surface and 2 if object is in the air)

H = minimum transverse dimension of the mean presented area of object

X = distance from the front of the object to the location of its largest cross-section normal to the plane of the shock front

M = mass of object

A = mean presented area of object

v_o = initial velocity of object

The peak incident pressure P_s and the incident specific impulse i_s can be determined from Figure 2-7 knowing the scaled distance to the object. Values for the drag coefficient C_D for several common shapes are given in Table 2-8. This analysis is appropriate for objects "far" from the explosive charge; thus, the object is not in a high velocity flow field and C_D is essentially a constant. Figure 2-248 can be used in most cases where the distance from the object to the center of a spherical charge is greater than 20 charge radii, which is normally considered to be "far" from the charge. For objects close to a charge, the initial velocity is a function of the impulse on the target, and the actual pressure-time variation across the object is unimportant. For this close-in range the impulse acting on the object is equal to the applied momentum.

$$i = MV / A \qquad 2\text{-}58$$

Thus, the velocity in terms of the actual target shape is:

$$v_o = 1000 i \beta A / 12M \qquad 2\text{-}59$$

where

i = specific acquired impulse

β = target shape factor from Figure 2-249

A = area of the target

M = mass of the target

v_o = velocity of the target

To calculate the specific impulse imparted to a close-in target, the following equations were developed based on experimental data:

For spherical charges with $R/R_e \leq 5.07$:

$$\frac{i}{\beta R_{eff}} = \left[R_e / R_t \right]^{0.158} = 38{,}000 \left[R_e / R \right]^{1.4} \qquad 2\text{-}60$$

and

$$R_{eff} = R_e \qquad 2\text{-}61$$

For cylindrical charges with $R/R_e \leq 5.25$:

$$\frac{i}{\beta R_{eff}} = \left[R_e / R_t \right]^{0.158} = 46{,}500 \left[R_e / R \right] \qquad 2\text{-}62$$

For cylindrical charges with $5.25 < R/R_e \leq 10$:

$$\frac{i}{\beta R_{eff}} = \left[R_e / R_t \right]^{0.158} = 161{,}700 \left[R_e / R \right]^{1.75} \qquad 2\text{-}63$$

and:

$$R_{eff} = 0.909 \left[l_e / R_e \right]^{0.333} R_e \qquad 2\text{-}64$$

where

i = specific acquired impulse

β = nondimensional shape factor of the target from Figure 2-249

R_{eff} = effective radius

R_e = radius of the explosive

R = standoff distance

R_t = target radius

l_e = length of cylindrical explosive

The effective radius R_{eff} is the radius of an equivalent sphere of explosive which could be formed from a cylinder of radius R_e and length l_e.

The specific impulse imparted to a target, as given by Equations 2-60, and 2-62 and 2-63 for spherical and cylindrical charges, respectively, is plotted in Figure 2-250. This experimentally derived data should not be used beyond the distances shown in the figure. When these standoff distances are exceeded, the specific acquired impulse may be approximated by using the normal reflected impulse obtained from Figure 2-7.

2-18.3. Velocity of Constrained Secondary Fragments

The method used to predict initial velocities of a constrained secondary fragments close to an explosion must first consider the amount of energy applied to each fragment as well as the energy consumed in freeing the fragment from its support. This relationship can be expressed using the conservation of momentum and allowing the structural constraint to reduce the imparted impulse as follows:

$$I - I_{st} = mV_o \qquad 2\text{-}65$$

where

I = total impulse of the blast applied to the fragment

I_{st} = impulse consumed by the fragment support connection

m = mass of the fragment

V_o = velocity of the fragment after break away

The value of I_{st} must be established experimentally. Based on tests, an empirical expression has been developed for cantilever beams subjected to closein effects:

$$v_o = \frac{1000}{12}\left[\frac{T}{\rho_f}\right]^{1/2}\left[C_1 + C_2 ib_f \Big/ \left[A\left[a_f T\right]^{1/2}\right]\left[2L_f / b_f\right]^{0.3}\right] \qquad 2\text{-}66$$

where

T = toughness of material (area under the stress-strain curve) from Table 2-9

ρ_f = mass density of the fragment

C_1 = constant equal to -0.2369

C_2 = constant equal to +0.3931

i = unit impulse acting on the member

b_f = width of fragment exposed to the blast

A = cross-sectional area in the plan perpendicular to the long axis of the fragment

L_f = length of fragment exposed to the blast

Equation 2-66 is adequate for determining the fragment velocity when:

$$ib_f / \left[A \left[\rho_f T\right]^{1/2}\right] \left[2L_f / b_f\right]^{0.3} \geq 0.602 \qquad 2\text{-}67$$

When Equation 2-67 is less than 0.602, the magnitude of the velocity is equal to zero which indicates that disengagement of the fragment will not occur.

The constants in Equation 2-66 were derived from experimental data and can only be used for cantilevered beams of steel or aluminum.

An equation similar to that of Equation 2-66 has been developed for clamped-clamped fragments except that the value of C_1 is equal to -0.6498 and C_2 is equal to 0.4358.

A plot of Equation 2-66 for both cantilever and clamped-clamped fragments is presented in Figure 2-251.

2-19. Fragment Trajectories

Once primary fragments or secondary missiles have been formed and accelerated by an explosion, they will move along a specific trajectory until they impact a target (receiver), or the ground. The forces acting on the fragments and affecting their trajectories are inertia, gravitation, and fluid dynamic forces. The fluid dynamic forces are determined by the instantaneous velocity of the fragment at each instant in time. Generally, fragments are quite irregular in shape and may be tumbling, so a completely accurate description of the fluid dynamics forces during flight is difficult, if not impossible. In the trajectory analysis for fragment flight, one usually resorts to some simplified description of the fluid dynamic forces, and uses the concepts from aerodynamics of division of these forces into components called drag (along the trajectory or normal to the gravity vector) and lift (normal to the trajectory or opposing gravity). Then the force components are given at any instant by:

$$F_L = C_L A_L (1/2)\ \rho\ v^2 \qquad 2\text{-}68$$

and

$$F_D = C_D A_D (1/2)\ \rho\ v^2 \qquad 2\text{-}69$$

where

F_L = lift force

F_D = drag force

C_L = lift coefficient

C_D = drag coefficient

A_L = lift area

A_D = drag area

ρ = density of the medium through which the fragment is traveling

v = velocity of the fragment

The lift and drag coefficients are determined empirically as a function of shape and orientation with respect to the velocity vector, and the magnitude of the velocity v. Fragments discussed in sections 2-17 and 2-18 are generally of chunky shape, so that $C_D >> C_L$ for any flight orientation. Thus, they are called drag-type fragments. The lift force on drag-type fragments is very small and may be neglected.

In a simplified trajectory problem, where the fragment is considered to move in one plane, equations of motion can be written for acceleration in the X and Y directions.

The acceleration in the X direction (drag only) is:

$$a_x = A_D C_D \rho_o \left[v_x^2 + v_y^2 \right] \cos \alpha / 2M \qquad 2\text{-}70$$

and for the Y direction (drag only):

$$a_y = -1.2 \times 10^{-5} g - A_D C_D \rho_o \left[v_x^2 + v_y^2 \right] \sin \alpha / 2M \qquad 2\text{-}71$$

where:

a_x, a_y = acceleration in the X and Y directions, respectively

ρ_o = mass density of the medium through which the fragment travels

v_x, v_y = velocity in the X and Y directions, respectively

g = gravity force (32.2 ft./sec.^{2})

M = mass of the fragment

α = trajectory angle

At t = 0:

$$v_x = v_o \cos \alpha_o \qquad 2\text{-}72$$

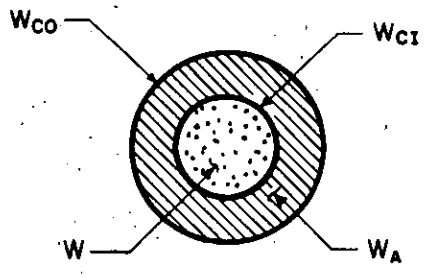
$$v_y = v_o \sin \alpha_o \qquad 2\text{-}73$$

where

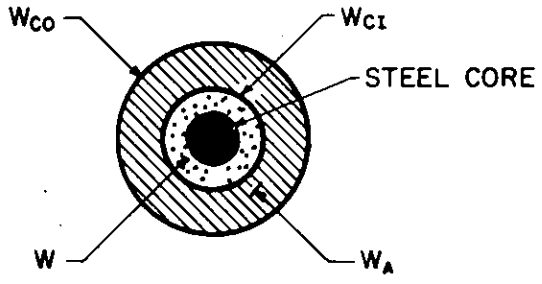
v_o = initial velocity

α_o = initial trajectory angle

The equations shown above can be solved simultaneously to eventually determine the distance traveled by the fragment. These equations are valid for fragment velocities up to Mach 1 for standard conditions. Figure 2-252 summarizes the results of fragment range R for numerous sets of initial conditions for fragments affected only by drag forces. It should be noted that, in this curve, several initial trajectory angles were used in the analysis to obtain the maximum range R for the respective fragments. Thus, one need not know the initial trajectory angle of a fragment in order to use Figure 2-252.



a. CYLINDER OR SPHERE



b. STEEL CORED CYLINDER

Figure 2-236 Explosive outer casing separated by incompressible fluid

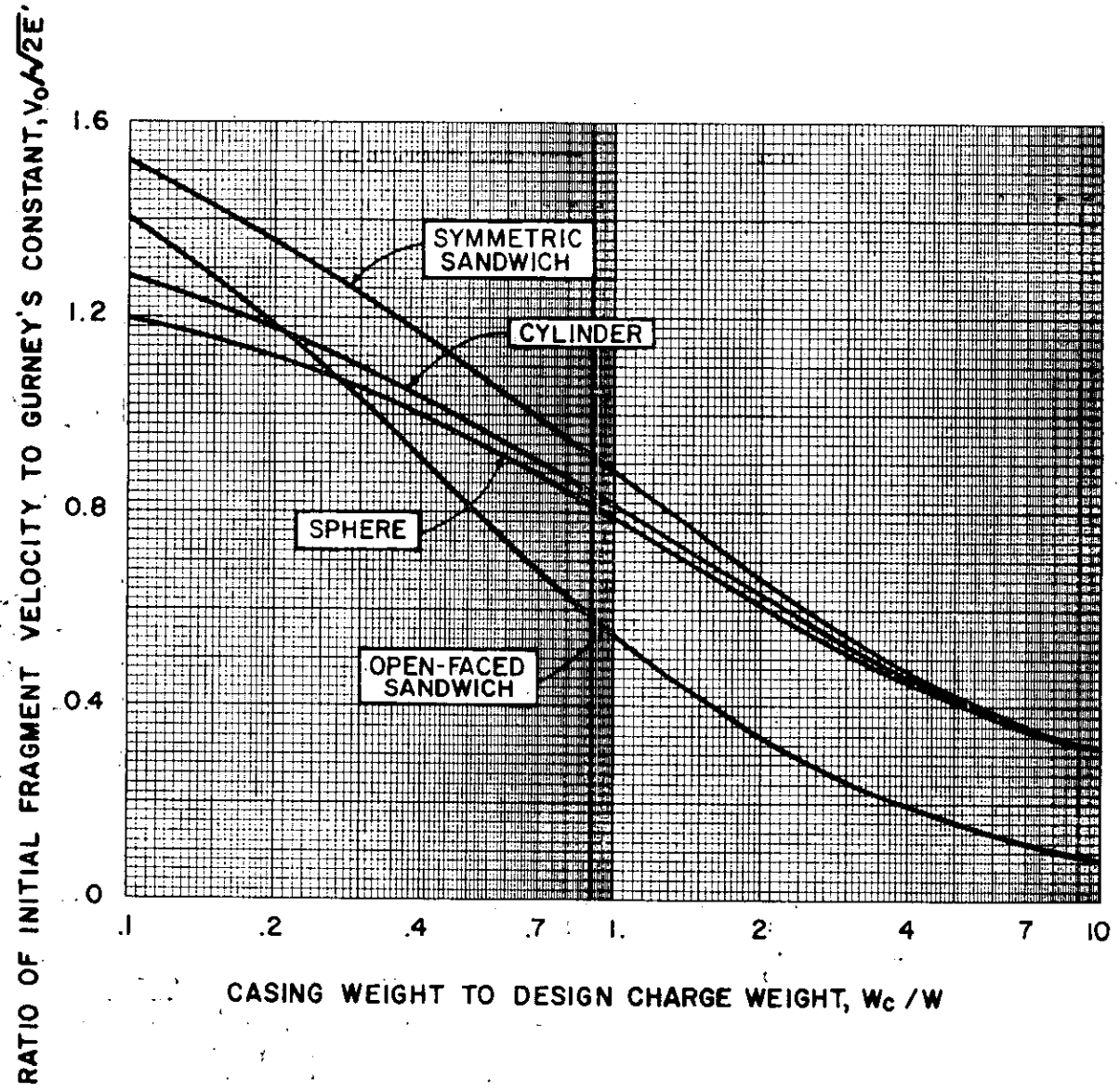


Figure 2-237 Initial velocity of primary fragments for various geometries

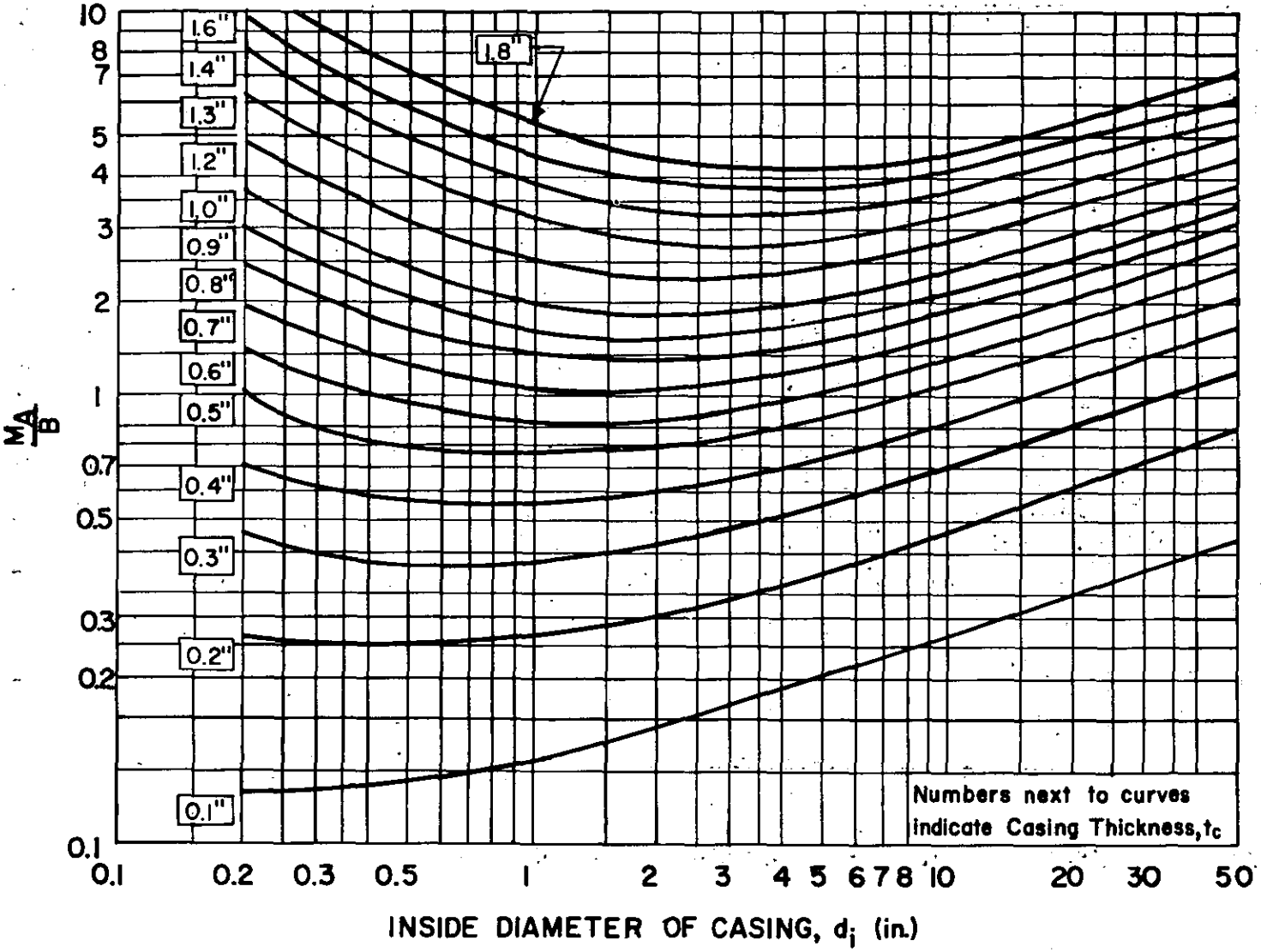


Figure 2-238 M_A/B versus cylindrical casing geometry

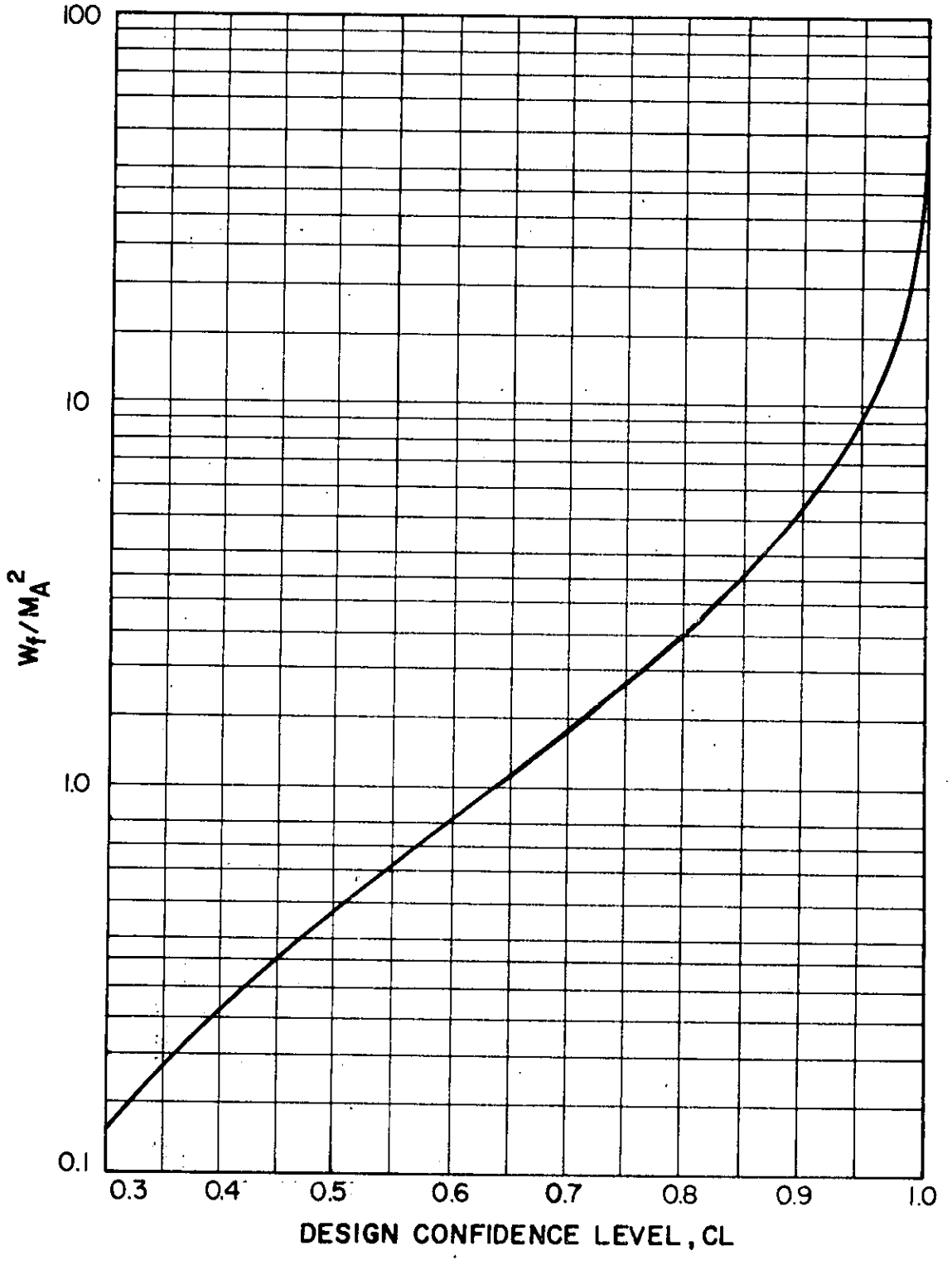


Figure 2-239 Design fragment weight versus design confidence level ($0.3 \leq CL \leq 1$)

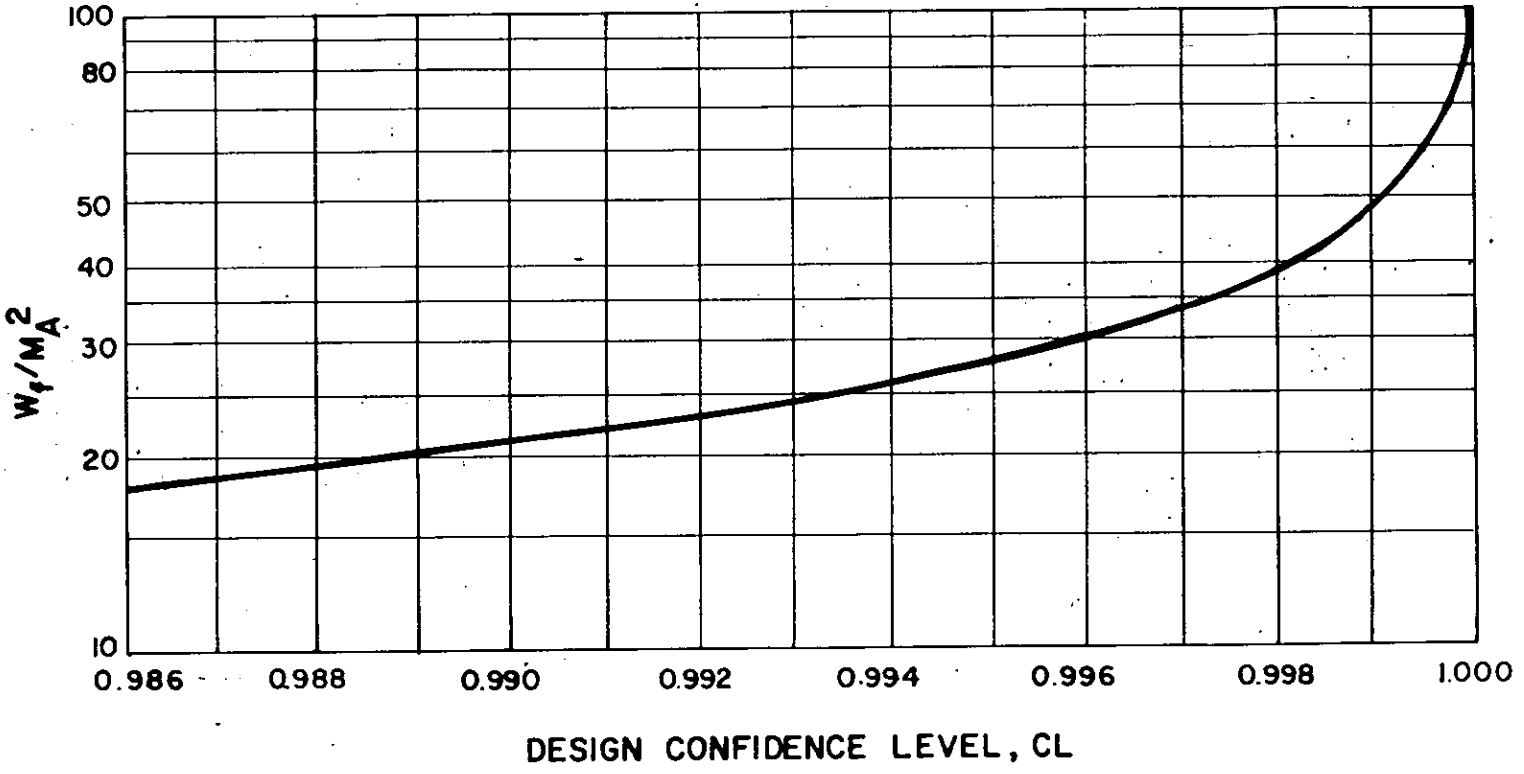


Figure 2-240 Design fragment weight versus design confidence level ($0.986 \leq CL \leq 1$)

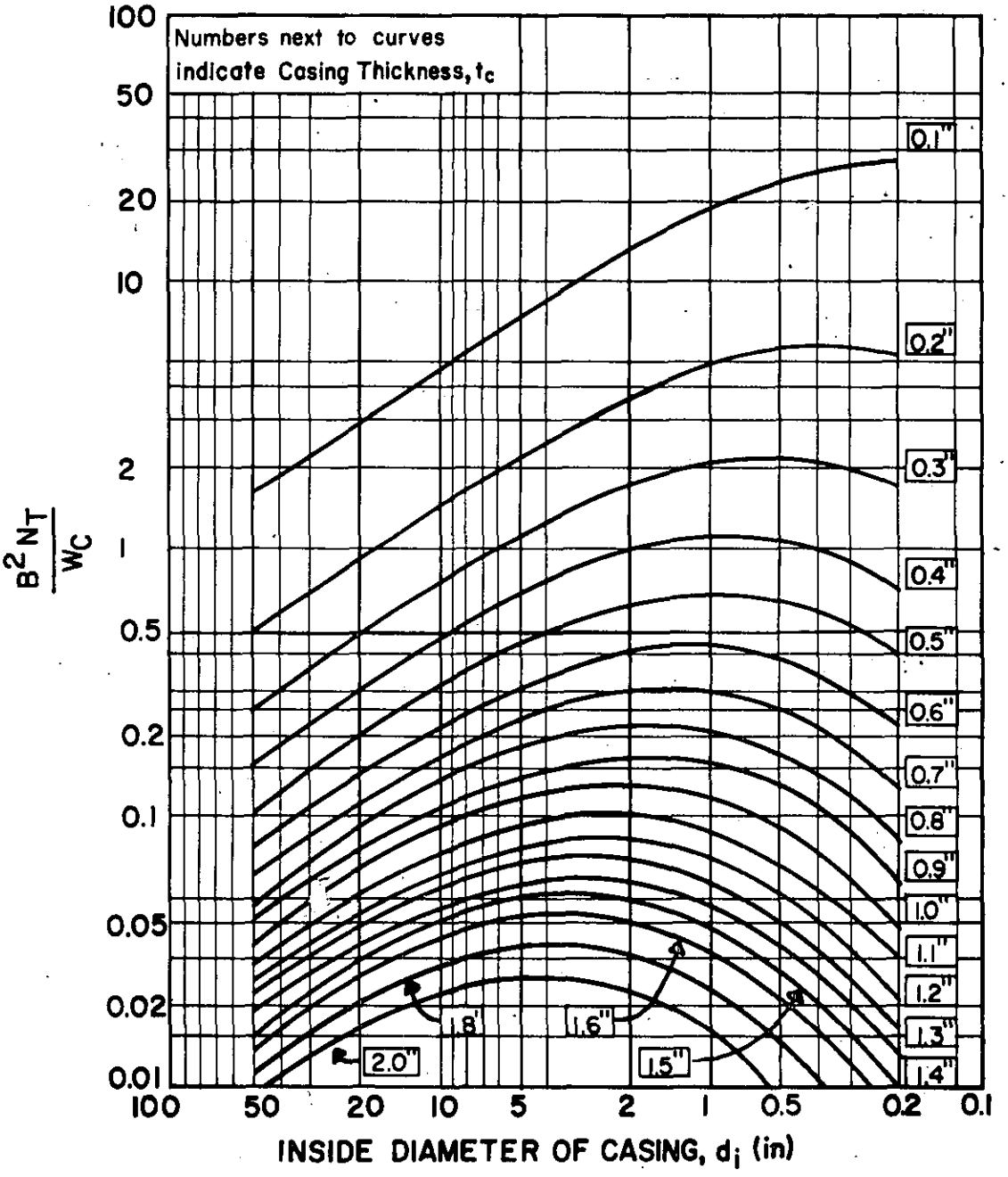
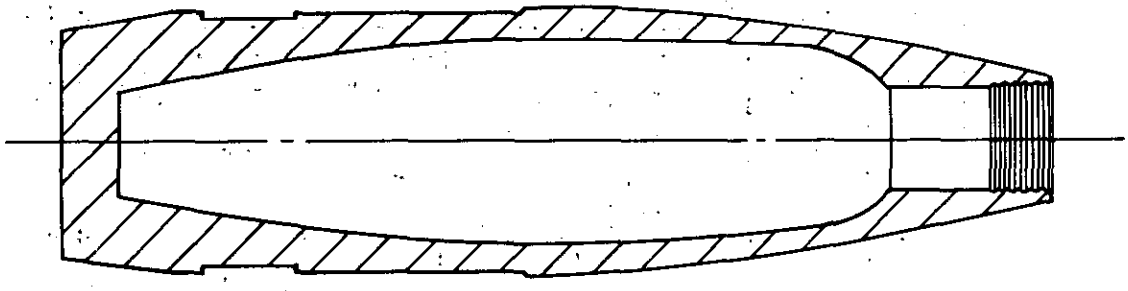
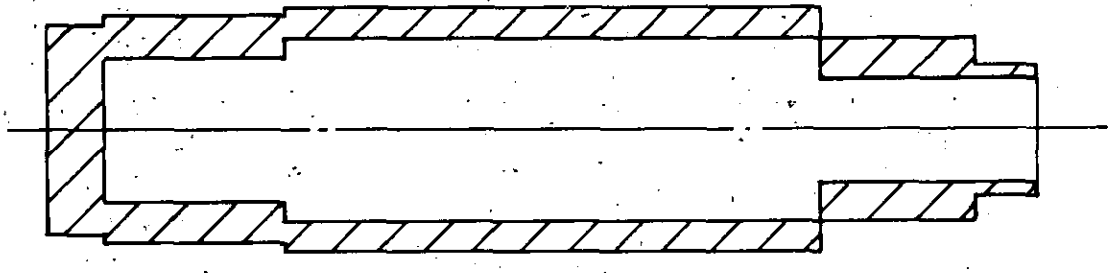


Figure 2-241 B^2N_T/W_c versus casing geometry



(a) ACTUAL CONFIGURATION



(b) IDEALIZED CONFIGURATION

Figure 2-242 Equivalent cylindrical explosive casings

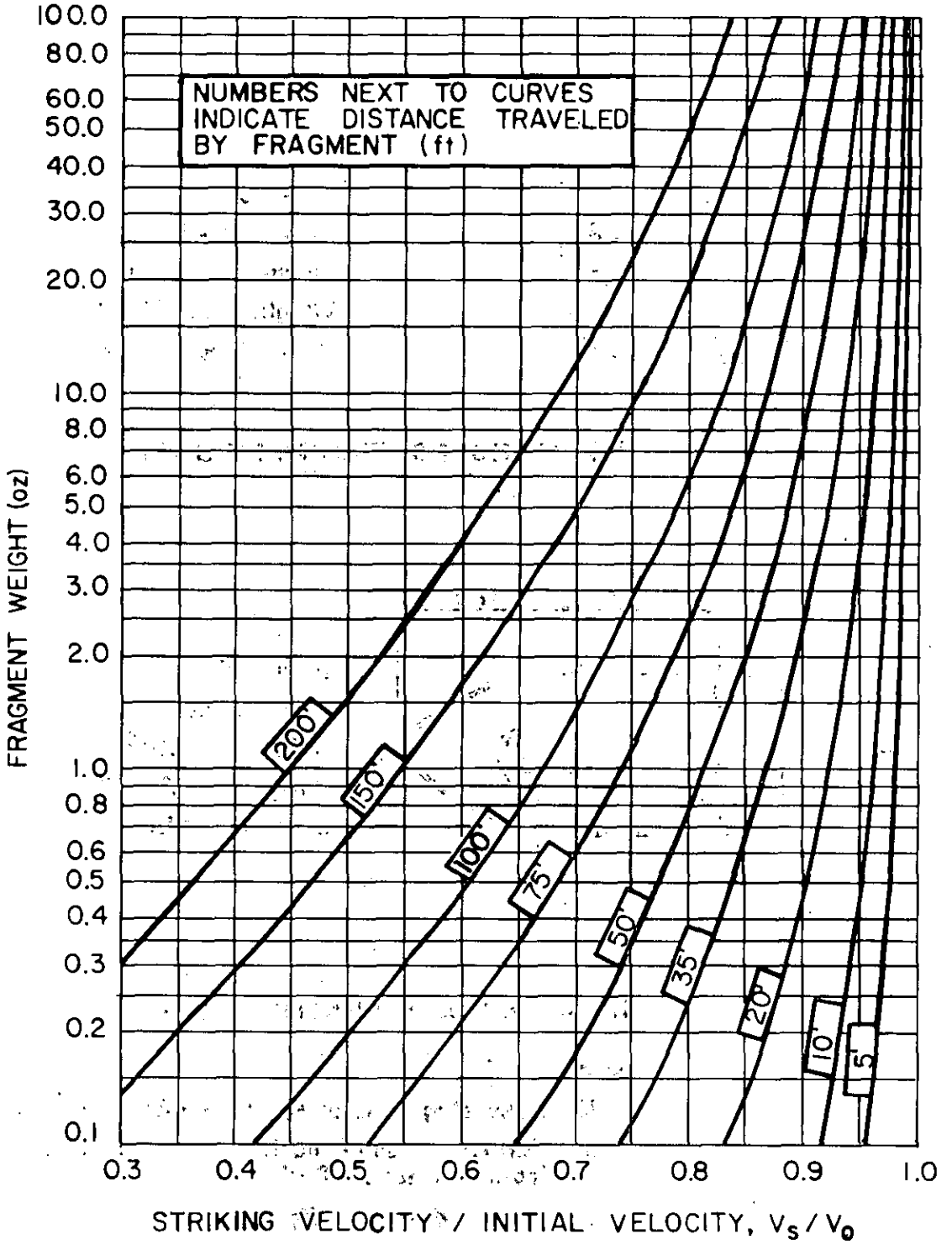
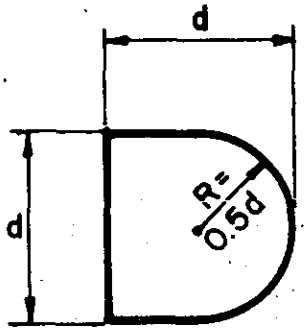
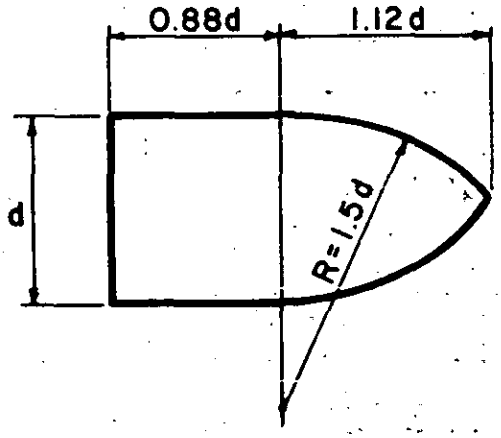


Figure 2-243 Variation of primary fragment velocity with distance



n = 0.5
N = 0.845
Volume = $0.654d^3$
Weight = $0.654d^3\gamma = 0.186d^3$
D = 0.186 lb./in.^{3}

(a) STANDARD FRAGMENT SHAPE



n = 1.5
N = 1.00
Volume = $1.2d^3$
Weight = $1.2d^3\gamma = 0.34d^3$
D = 0.34 lb./in.^{3}

(b) ALTERNATE FRAGMENT SHAPE

NOTE:

N = Nose shape factor = $0.72+0.25\sqrt{n-0.25}$

n = Caliber radius of the tangent ogive of the fragment nose = R/d

D = Caliber density = W_f/d^3

Figure 2-244 Primary fragment shapes

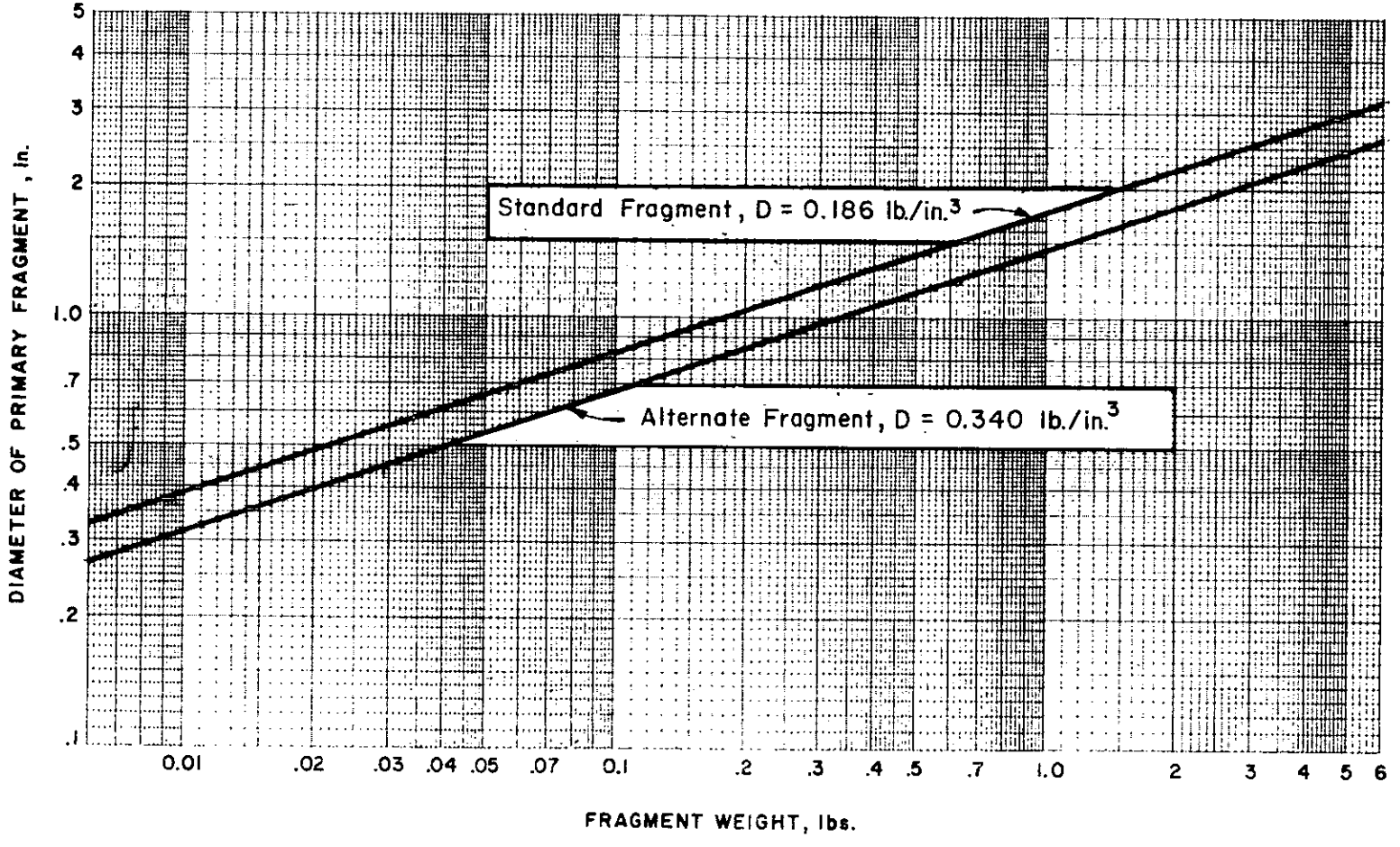


Figure 2-245 Relationship between fragment weight and fragment diameter

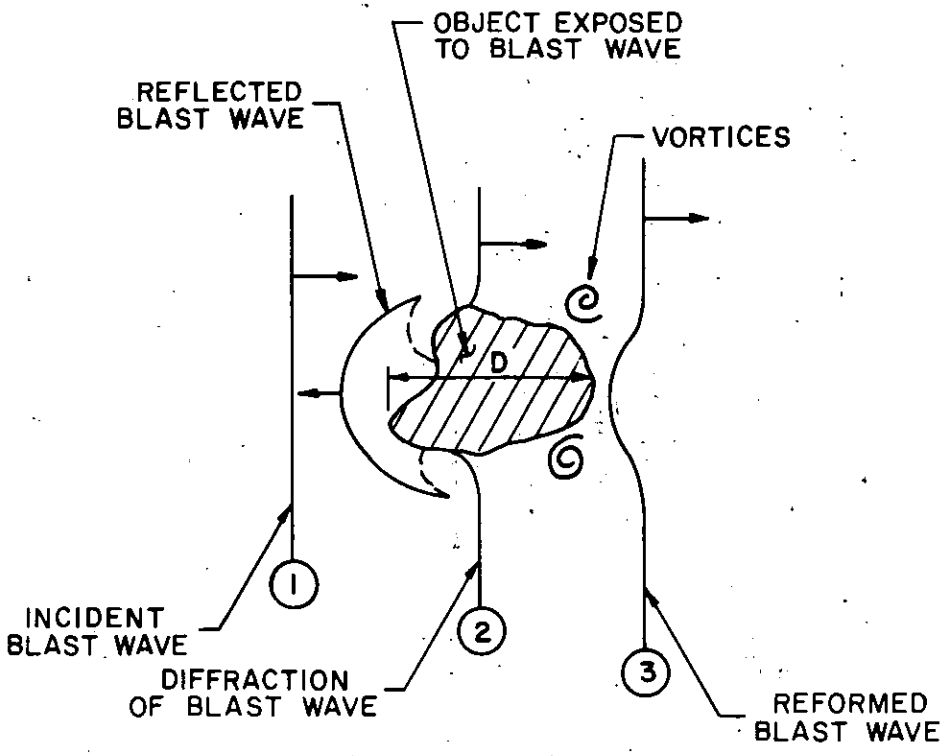


Figure 2-246 Interaction of blast wave with an irregular object

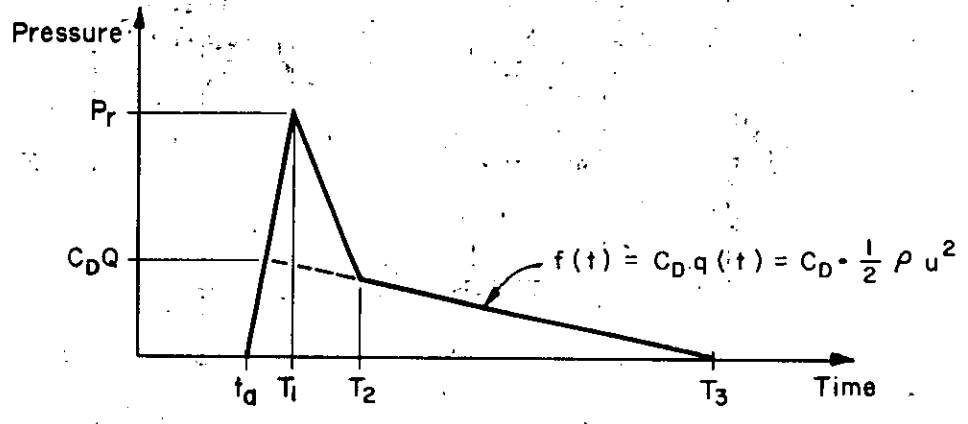


Figure 2-247 Idealized pressure-time loading on an irregular fragment

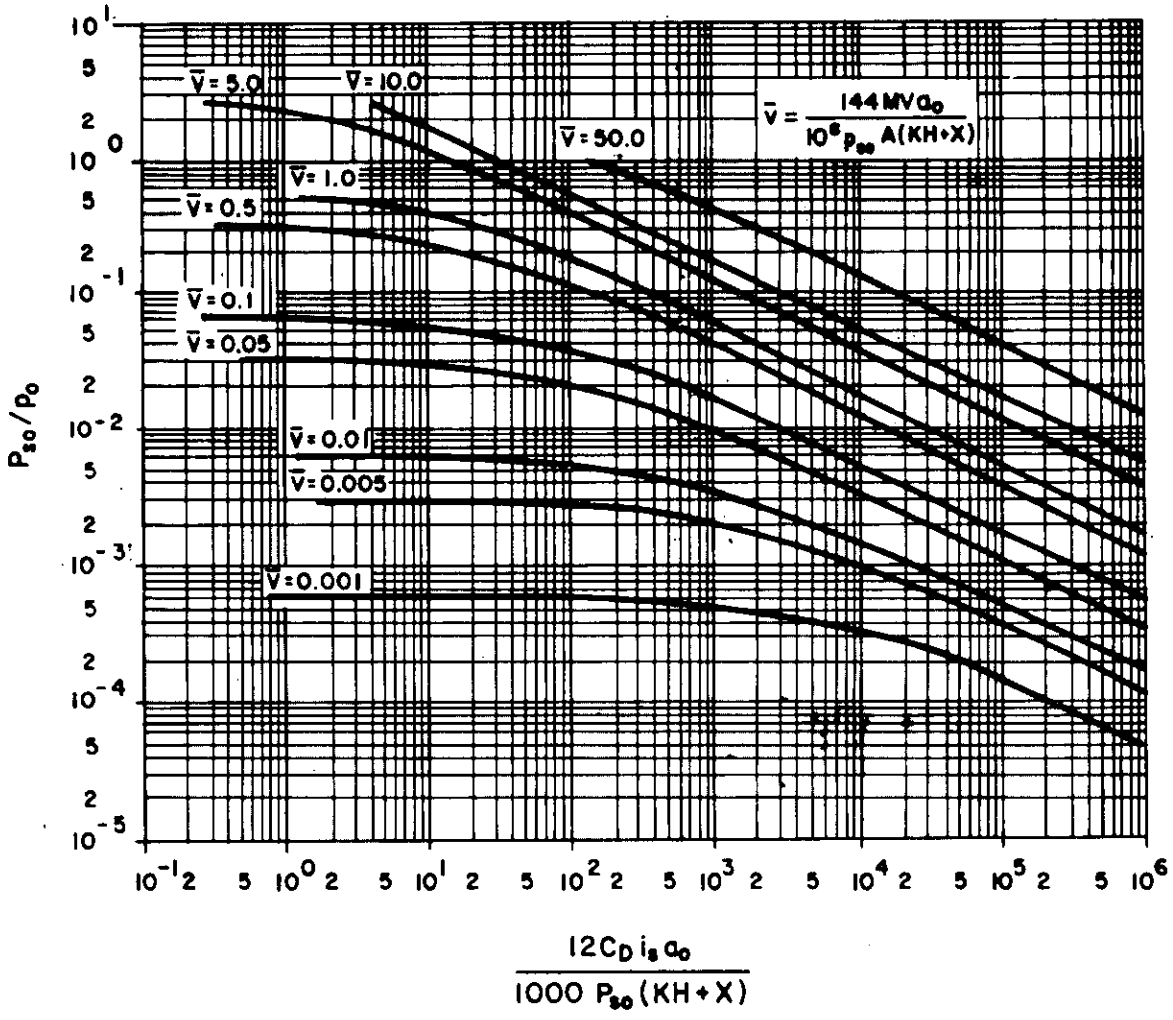
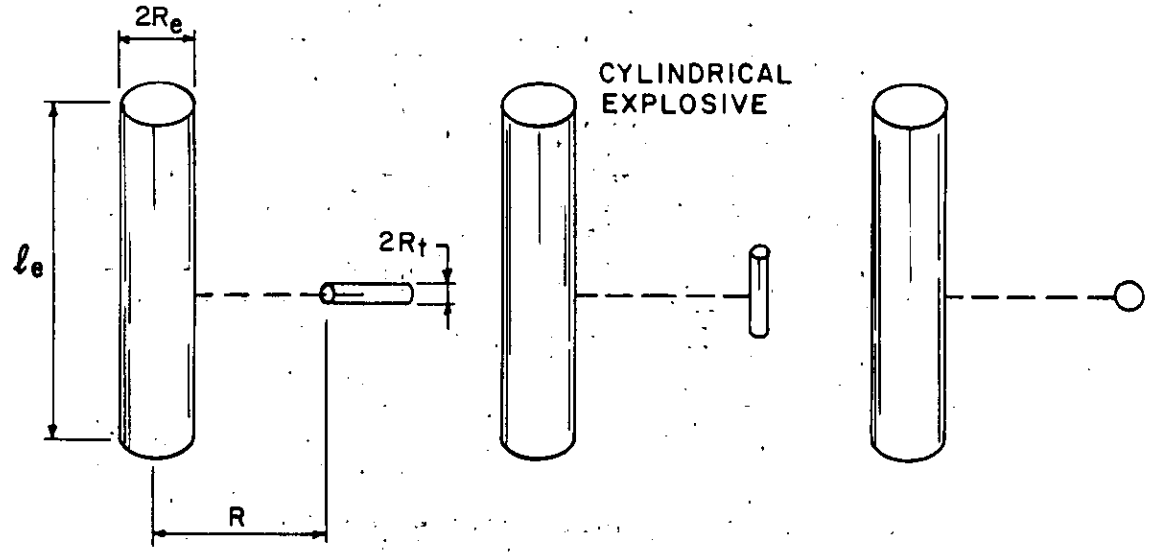


Figure 2-248 Nondimensional object velocity, $\bar{V}$, as a function of pressure and impulse



(a) EXPOSED FLAT FACE
$\beta = 1.0$

(b) EXPOSED CYLINDRICAL SURFACE
$\beta = \frac{\pi}{4}$

(c) EXPOSED SPHERICAL SURFACE
$\beta = \frac{2}{3}$

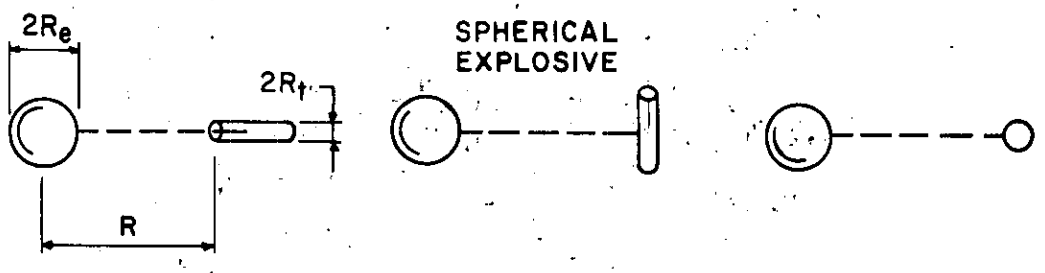


Figure 2-249 Target shape factor for unconstrained fragments

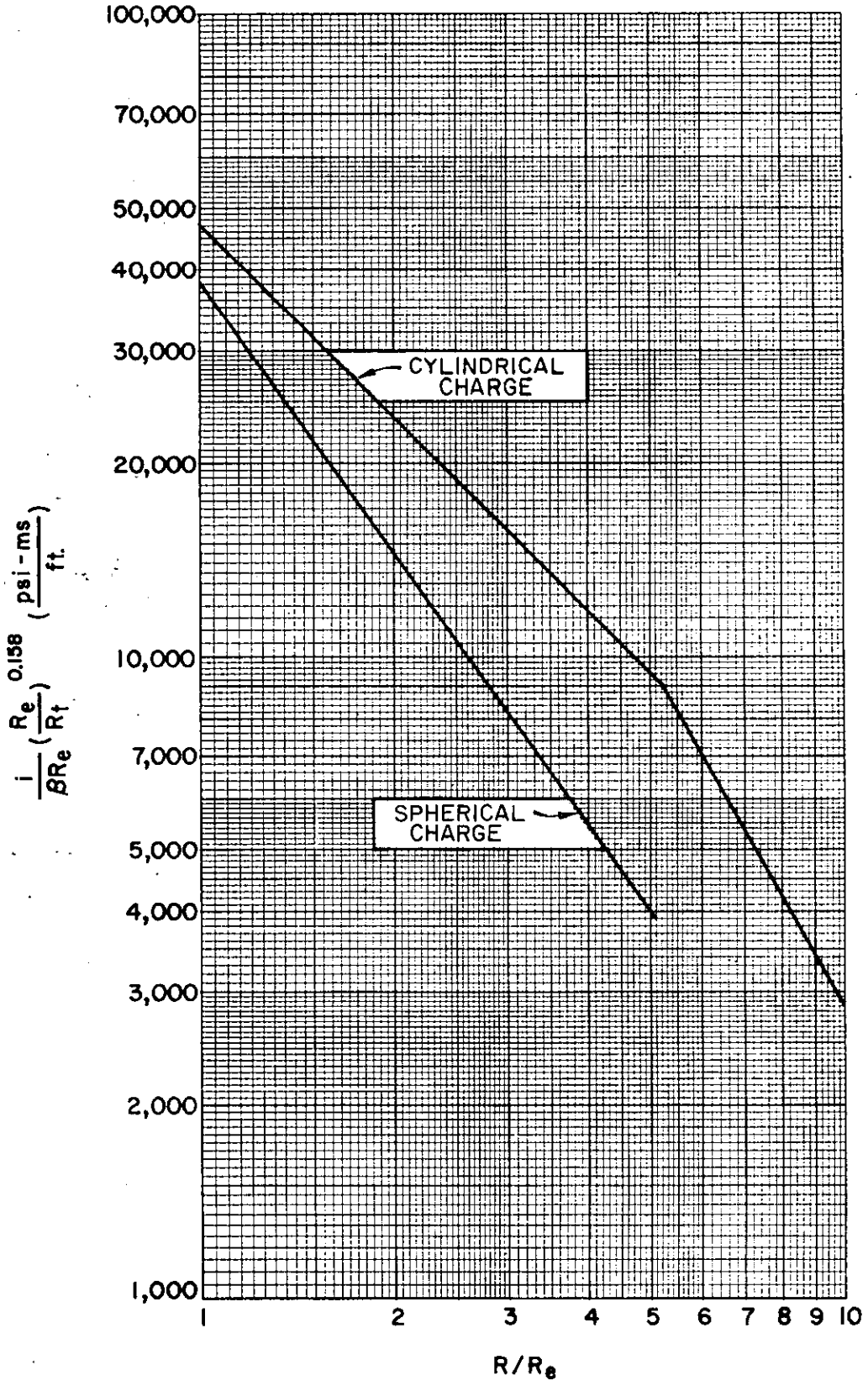


Figure 2-250 Specific acquired impulse versus distance

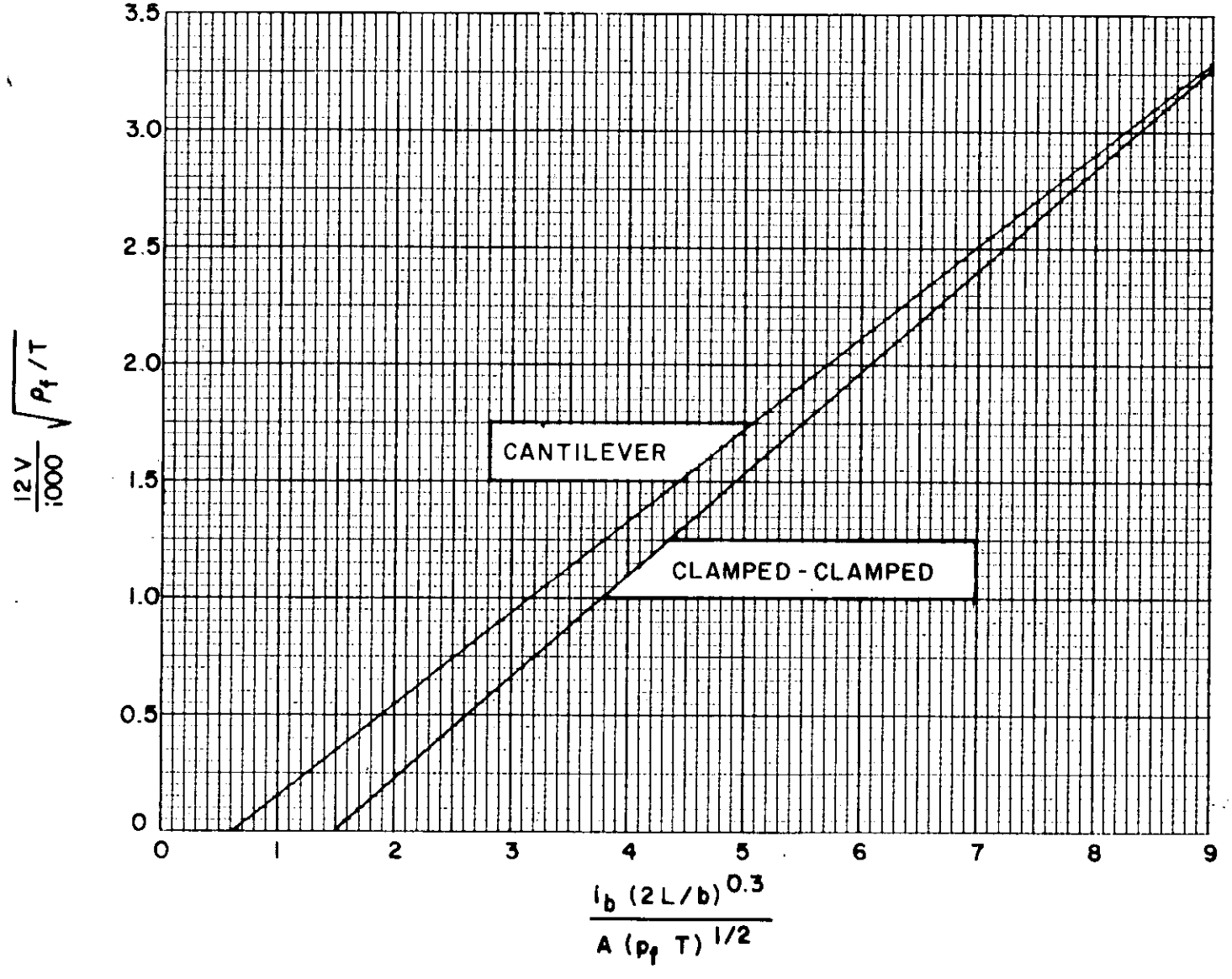


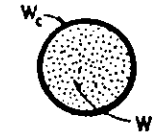
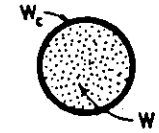
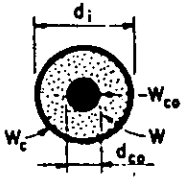
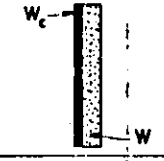
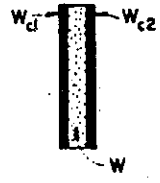
Figure 2-251 Scaled fragment velocities for constrained fragments

Figure 2-252 Fragment range prediction

Table 2-5 Specific Weight and Gurney Energy Constant for Various Explosives

Explosive	Specific Weight (lb/in^3)	$\sqrt{2E'}$ (ft/sec)
Composition B	0.0621	9100
Composition C-3	0.0578	8800
HMX	0.0682	9750
Nitromethane	0.0411	7900
PBX-9404	0.0664	9500
PETN	0.0635	9600
RDX	0.0639	9600
TACOT	0.0581	7000
Tetryl	0.0585	8200
TNT	0.0588	8000
Trimonite No. 1	0.0397	3400
Tritonal (TNT/Al = 80/20)	0.0621	7600

Table 2-6 Initial Velocity of Primary Fragments for Various Geometries

Type	Cross-sectional shape	Initial fragment velocity v_o	Maximum v_o	Remarks
Cylinder		$\sqrt{2E'}\left[\frac{\frac{W}{W_c}}{1+\frac{W}{2W_c}}\right]^{1/2}$	$\sqrt{2E'}\sqrt{2}$	See paragraph 2-17.2
Sphere		$\sqrt{2E'}\left[\frac{\frac{W}{W_c}}{1+\frac{3W}{5W_c}}\right]^{1/2}$	$\sqrt{2E'}\sqrt{1}$	
Steel cored cylinder		$\sqrt{2E'}\left[\frac{\frac{W}{W_c}}{1+\frac{(3+a)W}{6(1+a)W_c}}\right]^{1/2}$ where $a=\frac{d_{co}}{1.6d_i}$	$\sqrt{2E'}\sqrt{\frac{6(1+a)}{(3+a)}}$	If the steel core is many times more massive than the explosive, this expression for the initial velocity should be modified by multiplying it by the expression: $\sqrt{1-\frac{0.02W_{co}}{W}}$ where W_{co} is the weight of the steel core (lbs.).
Plate		$\sqrt{2E'}\left[\frac{\frac{3W}{5W_c}}{1+\frac{W}{5W_c}+\frac{4W_c}{5W}}\right]^{1/2}$	$\sqrt{2E'}\sqrt{3}$	This expression applies for a rectangular explosive in contact with a metal plate having the same surface area. It is assumed that the entire system is suspended in free air and its thickness is small in comparison to its surface area so that the resulting motions are essentially normal to the plane of the plate.
Hollow cylinder		—	—	Although an expression to predict the velocity of fragments is not available, an upper limit of the initial velocity may be obtained using the expression for a solid cylinder and a lower limit from the expression for a single plate. The ratio of the explosive weight to the casing weight (W/W_c) of the hollow cylindrical charge is used in both expressions.
Sandwich plates		if $W_{c1} \neq W_{c2}$ $\sqrt{2E'}\left[\frac{W}{W_{c1}+W_{c2}g+\frac{W}{3}(1-g+g^2)}\right]^{1/2}$ where $g=\frac{W_{c1}+\frac{W}{2}}{W_{c2}+\frac{W}{2}}$ if $W_{c1}=W_{c2}=W_c$ $\sqrt{2E'}\left[\frac{\frac{W}{2W_c}}{1+\frac{W}{6W_c}}\right]^{1/2}$	$\sqrt{2E'}\sqrt{3}$	This expression applies for a rectangular explosive sandwiched between two metal plates having the same surface area as the explosive. It is assumed that the entire system is suspended in free air and its thickness is small in comparison to its surface area so that the resulting motions are essentially normal to the plane of the plates.

Note:

W = E = Explosive weight

W_c = C = Casing weight

$W, W_c, W_{co}, W_{c1}, W_{c2}$ (lbs.)

d_i, d_{co} (lbs.)

$v_o, \sqrt{2E'}$ (ft./sec.)

Table 2-7 Mott Scaling Constants for Mild Steel Casings and Various Explosives

Explosive	A ($oz^{1/2}$ in.$^{-3/2}$)	B ($oz^{1/2}$ in.$^{-7/6}$)
Baratol	-	0.512
Composition A-3	-	0.220
Composition B	0.214	0.222
Cyclotol (75/25)	-	0.197
H-6	-	0.276
HBX-1	-	0.256
HBX-3	-	0.323
Pentolite (50/50)	0.238	0.248
PTX-1	-	0.222
PTX-2	-	0.227
RDX	0.205	0.212
Tetryl	0.265	0.272
TNT	0.302	0.312

Table 2-8 Drag Coefficient, C_D, for Various Shapes

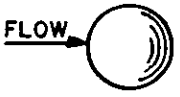
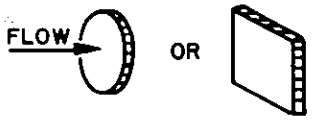
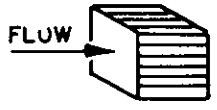
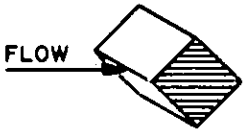
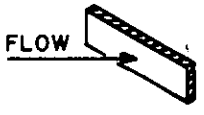
SHAPE	SKETCH	C_D
CIRCULAR CYLINDER (LONG ROD), SIDE-ON		1.20
SPHERE		0.47
ROD, END-ON		0.82
DISC, FACE-ON		1.17
CUBE, FACE-ON		1.05
CUBE, EDGE-ON		0.80
LONG RECTANGULAR MEMBER, FACE-ON		2.05
LONG RECTANGULAR MEMBER, EDGE-ON		1.55
NARROW STRIP, FACE-ON		1.98

Table 2-9 Steel Toughness

Steel	Toughness in-lb/cubic in.
ASTM A 36	12,000
ASTM A 441	15,000
ASTM A514 Grade F	19,000

SHOCK LOADS

2-20. Introduction

The strong air blast waves and high speed fragments are the primary hazards of accidental explosions. The exterior of a protective structure is designed primarily for the blast pressures. In some situations, the fragments may be just as important as the pressures in determining the configuration of a protective facility. While the contents of the structure are protected from the direct effects of blast pressures and fragments by the structure's exterior, the contents are subject to effects of the building's motion. These structure motions can cause injury to personnel, damage to equipment as well as dislodgement of the structure's interior components, including interior partitions, hung ceilings, light fixtures, ductwork, piping, and electrical lines.

Structure motions are caused by what is normally termed shock loads. These are loads which cause transient or short-duration vibratory motions of the ground surface and the structure. They do not cause significant structural damage but instead induce motion which, as stated above, can damage the structure's interior contents.

There are two distinct types of shock loads: ground shock and air shock. Ground shock results from the energy which is imparted to the ground by an explosion. Some of this energy is transmitted through the ground as direct-induced ground shock. Both of these forms of ground shock when imparted to a structure will cause the structure to move in both a vertical and horizontal direction. Air shock results from the blast overpressures striking the building. Vertical, horizontal and overturning motions result from the shock impact. The vertical and overturning motions are usually not significant and can be neglected while the horizontal motions must be considered. Large displacements can result when a structure slides relative to the ground surface.

The net motion of the structure is a combination of the motions due to the air induced and direct-induced ground shock, and the air shock. Curves which describe the ground motion (acceleration versus time, velocity versus time, and displacement versus time curves) are not readily calculated. However, these relationships are not required since the design of protective structures to resist shock loads is based on the peak values of the induced motion rather than the actual motion-time relationships.

The procedures presented in this section are applicable for uniform motions. The shock loads and resulting structure motions apply to rigid concrete structures located at the low- and intermediate-pressure design ranges. At distances corresponding to these pressures, the shock loads are uniform across the structure. A rigid concrete structure acts as a rigid body, that is, all components of the structure have essentially the same motion. The procedures can be applied to structures located close to an explosion and to non-rigid structures. However, the local effects associated with these conditions must be accounted for in the analysis.

2-21. Ground Shock

2-21.1. Introduction

When an explosion occurs at or near the ground surface, ground shock results from the energy imparted to the ground by the explosion. Some of this energy is transmitted through the air in the form of air-induced ground shock and some is transmitted through the ground as direct-induced ground shock.

Air-induced ground shock results when the air-blast shock wave compresses the ground surface and sends a stress pulse into the underlying media. The magnitude and duration of the stress pulse in the ground depend on the character of the air-blast pulse and the ground media. Generally, the air-induced ground motions are downward. They are maximum at the ground surface and attenuate with depth. However, the presence of a shallow water table, a shallow soil-rock interface, or other discontinuities can alter the normal attenuation process. The properties of the incident overpressure pulse and the surface soil layer usually determine the character of air-induced ground shock on above-ground structures.

Direct-induced ground shock results from the explosive energy being transmitted directly through the ground. This motion includes both the true direct-induced motions and cratering-induced motions. The latter generally have longer durations and are generated by the crater formation process in cratering explosions. The induced ground motion resulting from both types have a longer duration than air-blast-induced ground shock and the wave forms tend to be sinusoidal.

The net ground shock experienced by a point on the ground surface is a combination of the air-blast-induced and direct-induced shock. The relative magnitudes and sequencing of the motions are functions of the media (air and soil) through which the shock travels and the distance from the point of detonation. At ranges close to the blast, the highly compressed air permits the air-blast shock front to propagate at speeds greater than the seismic velocity of the ground. In this region, the super-seismic region, the air blast arrives at a given point before the direct-induced ground shock. As the air-blast shock front moves farther from the point of detonation, the shock front velocity decreases, and the direct-induced ground shock catches and "outruns" the air blast. This latter region is called the outrunning region. Wave forms in the outrunning region are generally a complex combination of both types of induced shock. The combined motion can be obtained from consideration of the arrival time of each wave. The arrival time of the air blast is determined from the data presented for unconfined explosions. Whereas, the arrival time of the direct-induced ground shock can be estimated by assuming that the ground shock travels at the seismic velocity of the ground media. The combined ground motion in both the superseismic and outrunning region are illustrated in Figure 2-253.

2-21.2. Air Blast-Induced Ground Shock

One-dimensional wave propagation theory is used to estimate air blast-induced ground shock. For surface structures located on ground media having uniform properties, the expressions to define this motion take very simple forms. Using this approach, the maximum vertical velocity at the ground surface, V_V, can be expressed as

$$V_v = P_{so} / \rho C_p \qquad 2\text{-}74$$

where

V_V = maximum vertical velocity of the ground surface

P_{so} = peak positive incident pressure (Fig. 2-15)

ρ = mass density of the soil

C_p = compression wave seismic velocity in the soil

The mass density, ρ, for typical soils and rock are presented in Table 2-10 and the seismic velocities are presented in Table 2-11.

The maximum vertical displacement, D_V, is obtained by integrating the above expression with respect to time. The integral of the pressure with respect to time is simply the total positive phase impulse so that:

$$D_V = i_s / 1{,}000\ \rho\ C_p \qquad 2\text{-}75$$

where

D_V = maximum displacement of the ground surface

i_s = unit positive incident impulse (Fig. 2-15)

The maximum vertical acceleration, A_V, is based on the assumption of a linear velocity increase during a rise time equal to one millisecond. The resulting acceleration is increased by 20 percent to account for nonlinearity during the rise time. Accelerations are expressed in multiples of the gravitational constant so that,

$$A_V = 100\ P_{so} / (\rho\ C_p\ g) \qquad 2\text{-}76$$

where

A_V = maximum vertical acceleration of the ground surface

g = gravitational constant equal to 32.2 ft/sec^2

The above equation is adequate for predicting the acceleration in dry soil. However, the equation underestimates the acceleration in saturated soils and rock. To approximate the acceleration of saturated soils and rock, it is recommended that the value of the acceleration obtained from the Equation 2-76 be doubled.

The maximum horizontal ground motions are expressed in terms of the maximum vertical motions as a function of the seismic velocity of the soil and the shock wave velocity so that

$$D_H = D_V \tan [\sin^{-1} (C_p / 12{,}000\ U)] \qquad 2\text{-}77$$

$$V_H = V_V \tan [\sin^{-1} (C_p / 12{,}000\ U)] \qquad 2\text{-}78$$

$$A_H = A_V \tan [\sin^{-1} (C_p / 12{,}000\ U)] \qquad 2\text{-}79$$

where U = shock front velocity (Fig. 2-15).

For (C_p/12,000 U) greater than one, horizontal and vertical motions are approximately equal. Therefore, it is recommended that for all values of the

above function greater than one, the horizontal motion is set equal to the calculated vertical motion.

The equations which describe the air-induced ground shock are a function of the density and seismic velocity of the soil. However, a wide range of seismic velocities is given in Table 2-11 for each of the soils listed. In a final design, soil tests are required to accurately determine the density and seismic velocity of the particular soil at the site. In lieu of tests, the mass density given in Table 2-10 may be used. However, since the range of seismic velocities given Table 2-11 is so large, it is recommended that the lower bound value of the velocity be used to produce a conservative estimate of the induced motion.

2-21.3. Direct-Induced Ground Motion

Empirical equations have been developed to predict direct-induced ground motions. The equations apply for TNT detonations at or near the ground surface. Three types of ground media have been considered; dry soil, saturated soil and rock. The ground shock parameters are expressed in terms of the charge weight and distance from the explosion.

The maximum vertical displacement (D_V) of the ground surface for a rock media is given by

$$D_V = 0.025\ R_G^{1/3}\ W^{1/3}\ /\ Z_G^{1/3} \qquad 2\text{-}80$$

in which

$$Z_G = R_G\ /\ W^{1/3} \qquad 2\text{-}81$$

where

R_G = ground distance from the explosion

W = weight of TNT charge

Z_G = scaled distance from the explosion

and the maximum horizontal displacement D_H of the ground surface is equal to one-half of the maximum vertical displacement or

$$D_H = 0.5\ D_V \qquad 2\text{-}82$$

When the ground media consists of either dry or saturated soil, the maximum vertical displacement is given by

$$D_V = 0.17\ R_G^{1/3}\ W^{1/3}\ /\ Z_G^{2.3} \qquad 2\text{-}83$$

while the maximum horizontal displacement D_H is equal to the maximum vertical displacement or,

$$D_H = D_V \qquad 2\text{-}84$$

The maximum vertical velocity (V_V) for all ground media is given by

$$V_V = 150 / Z_G^{1.5} \qquad 2\text{-}85$$

and the maximum horizontal velocity (V_H) is equal to the maximum vertical velocity for all ground media or

$$V_H = V_V \qquad 2\text{-}86$$

Finally, the maximum vertical acceleration (A_V) of the ground surface for all media is given by

$$A_V = 10{,}000 / (W^{1/3} Z_G^2) \qquad 2\text{-}87$$

while for dry soil, the maximum horizontal acceleration, A_H, is equal to one-half of the maximum vertical acceleration, or

$$A_H = 0.5 A_V \qquad 2\text{-}88$$

however, for a wet soil or a rock media, the horizontal and vertical acceleration is equal, or

$$A_H = A_V \qquad 2\text{-}89$$

2-22. Air Shock

2-22.1. Introduction

When an air blast strikes an aboveground protective structure, motions are imparted to the building. The most severe motion is due to the response of the individual elements which make up the exterior shell of the structure. Procedures for the design of these elements are presented in subsequent chapter of this manual. This section is concerned with the gross motion of the structure on its supporting soil due to the impact of the air blast. This gross motion is in addition to the ground induced motions.

Vertical, horizontal and overturning motions are imparted to the structure by the air blast. However, since the vertical motion of the structure is restricted by the ground which is already compressed due to the dead load of the structure and its contents, vertical motions must necessarily be small and can be safely neglected. Overturning motions are also neglected in this section. These motions are most significant in tall structures with small plan dimensions which are not common in protective construction. This section is concerned solely with horizontal sliding motions which can be quite significant.

Horizontal motion results from an unbalanced blast load acting on the structure. The tendency of the structure to slide is resisted by the friction forces developed between the foundation and the underlying soil. For structures with deep foundations, additional resistance to sliding is afforded by active and passive soil pressures developed at the leeward side of the structure.

2-22.2. Method of Analysis

The gross horizontal motion of a structure is computed in this manual using a method of numerical integration, namely, the acceleration-impulse extrapo-

lation method. This method of dynamic analysis is comprehensively presented in Chapter 3. Briefly, the equation of motion for a single-degree-of-freedom system is given as

$$F - R - D = Ma \qquad 2\text{-}90$$

where

F = applied blast load as a function of time
R = resistance of the system to motion as a function of displacement
D = damping force as a function of velocity
M = mass of the single-degree-of-freedom system
a = acceleration of the system

The numerical method of solving the equation of motion involves a step-by-step integration procedure. The integration is started at time zero where the displacement and velocity are known to be zero. The time scale is divided into small intervals. The values of F, R and M (D is not included) are calculated for each time step. The integration is started by first approximating the acceleration for the first time interval and progresses by successively calculating the acceleration at each time step. The change in velocity and displacement associated with each incremental acceleration is calculated. The accumulated velocity and displacement are obtained for each time step until the maximum values have been obtained.

The first step in the analysis is to describe the blast loads acting on the structure. The pressure-time variation of the blast load is computed as the shock front sweeps across the structure. The unbalanced load in the horizontal direction is computed as a function of the blast loads acting on the front and back walls (windward and leeward walls), respectively. The average blast load action of the roof of the structure is computed as the shock front traverses the building. The procedure used to describe these loading conditions have been presented in previous sections of this chapter.

The second step in the problem is the determination of the resistance of the building to horizontal motion. The tendency of the base of the structure to slide is resisted by friction forces on the foundation and earth pressure at the rear (leeward side) of the structure. For structures with shallow foundations, the resistance to sliding is afforded primarily by friction between the horizontal surfaces of the concrete foundation and underlying soil. The earth pressure resistance at the rear of the structure is small and can be conservatively neglected. For structures with deep foundations, the passive pressure at the rear of the structure is significant and greatly reduces the displacement of the building.

The friction force developed between the horizontal surfaces of the concrete foundation and underlying soil is given by

$$F_f = \mu F_N \qquad 2\text{-}91$$

where

F_f = frictional force resisting horizontal motion

μ = coefficient of friction between concrete and type of supporting soil

F_N = vertical load supported by the foundation

The coefficient of friction μ for the horizontal surface between the concrete foundation and the underlying soil is given in Table 2-12 for various types of soil. The coefficient is not a function of time or displacement. However, the structure must slide a finite amount before the frictional force is generated. The structure should slide approximately one-quarter of an inch before the frictional force is taken into account.

The vertical load F_N supported by the foundation consists of the dead weight of the structure, the weight of the building's interior contents, and the blast load acting on the roof of the structure. Since the blast load is a function of time, the building's resistance to sliding (frictional force F_f) is also a function of time. In addition, the blast load acting on the roof greatly increases the foundation loads, and consequently, significantly increases the building's resistance to sliding.

2-23. Structure Motions

2-23.1. Introduction

The net motion of a structure is a combination of the motions due to the air-induced and direct-induced ground shock, and the air shock. Since the methods of analysis described in this section are applicable to rigid concrete structures located at comparatively large distances from an explosion, the structure motions are taken equal to the ground motions in the vicinity of the building. In the case of air shock, the structure motions are computed directly.

The motion of structures located at comparatively close distances to an explosion as well as the motion of nonrigid structures may be determined. However, the local effects associated with these conditions such as motions due to cratering, fragment impact, etc. must be accounted for in the determination of the structure motions.

2-23.2. Net Ground Shock

The net ground shock associated with an accidental explosion is a combination of the air-induced and direct-induced ground shock. The time at which the shock is felt at adjacent structures and the magnitude and duration of the motion are a function of the quantity of explosives detonating, the absolute distance between the detonation and adjacent structure and the soil media at the site.

The air-induced ground shock is a function of the air blast. Consequently, the arrival time and duration of the ground shock may be taken equal to the arrival time t_A and duration to of the air blast. For an explosion occurring at or near the ground surface, the arrival time and duration are obtained from Figure 2-15 for the scaled ground distance Z_G between the explosion and the structure. Figure 2-15 provides the blast parameters associated with the detonation of hemispherical TNT charge located on the ground surface.

The direct-induced ground shock is a function of the soil media. The arrival time of the shock load at the structure is a function of the seismic velocity

in the soil and the distance from the explosion. The arrival time is expressed as

$$t_{AG} = 12{,}000\ R_G / C_p \qquad 2\text{-}92$$

where t_{AG} = arrival time of the ground shock

R_G = ground distance from the explosion

C_p = compression wave seismic velocity in the soil (table 2-11)

As previously explained, the seismic velocity of the soil should be obtained from soil tests for a final design. In lieu of tests, it is recommended that the entire range of velocities given in table 2-11 be investigated to determine if the direct-induced ground shock can be in phase with the air-induced ground shock.

The actual duration of the shock load is not readily available. However, it is sufficient to realize that the duration is long, that is, many times larger than the duration of the air-induced shock.

The net ground shock is obtained from consideration of the arrival time and duration of each type of induced shock. If $t_A + t_o$ is less than t, the structure is subjected to superseismic ground shock (Fig. 2-253). The air induced ground shock arrives at the structure first and is dissipated by the time that the direct-induced ground shock arrives. The structure feels the effect of each shock separately. If t_A is greater than t_{AG}, the structure is subjected to outrunning ground shock (Fig. 2-253). The direct-induced ground shock arrives at the structure first and, since its duration is long, the airinduced ground shock will arrive at the structure while the direct-induced ground shock is still acting. The structure feels the combined effects of the induced shocks. If t_A is slightly less than t_{AG} and $t_A + t_o$ is greater than t_{AG}, the air-induced ground shock will still be acting when the direct-induced ground shock arrives. For design purposes, this latter case should be treated as an outrunning ground shock.

2-23.3. Maximum Structure Motion

The design of protective structures to resist the effect of shock loads is based on the peak values of the induced motion rather than the actual motion-time relationships. In fact, the actual time history of the motion is not known nor can it be approximated with any degree of accuracy. Consequently, the phasing of the various shocks cannot be accomplished accurately. Therefore, for design purposes the peak values of the in-phase motions are added.

For the case of air-induced ground shock and air shock, the maximum values of horizontal displacement, velocity and acceleration are always added. These shock motions must be in phase since they are caused by the same source, namely, the air blast.

In the case of superseismic ground shock where the air-induced and direct-induced ground shock are completely separated, the maximum motion may be due to either source. The maximum value of displacement, velocity, or acceleration is the numerically larger value regardless of its source.

In the case of outrunning ground, the structure motion results from the combined effect of the air-induced and direct-induced ground shock as well as the air shock. The maximum motions in the vertical and horizontal direction is the algebraic sum of the maximum value of displacement, velocity, and acceleration from each source of motion in the vertical and horizontal directions.

2-24. Shock Response Spectra

2-24.1. Introduction

For the purposes of assessing the effects of shock on structures, one of the simplest interpretations of motion data involves the concept of the response spectrum. A response spectrum is a plot of the maximum response of a simple linear oscillator subjected to a given input motion against frequency. Hence, a response spectrum depicts only maximum response values, not a time-dependent history of the motion of the oscillator. The use of these maximum values is sufficient to ensure a reasonable and safe design for shock loads.

2-24.2. Definition of Shock Spectra Grid

Response spectra are constructed from consideration of the response of a simple linear oscillator. For a protective structure subjected to shock loads, a piece of equipment or any interior component can be considered as the mass of a simple oscillator. The load-deflection properties of the structural system which connects the component to the protective structure determine the spring constant of the oscillator.

The maximum displacement of the mass (building component) relative to the base (protective structure) is called the spectrum displacement (D), and the maximum acceleration of the mass is called the spectrum acceleration (A). The maximum velocity of the mass is approximately equal to the more useful quantity called the spectrum pseudo-velocity (V) which is given by

$$V = 2\pi f D \qquad 2\text{-}93$$

where V = velocity of the mass
f = natural frequency of vibration of the oscillator
D = displacement of the mass

For an undamped system, the displacement and acceleration are related by

$$A = \frac{(2\pi f)^2 D g}{387} \qquad 2\text{-}94$$

where A = acceleration of the mass in g's
g = gravitational constant

When damping is present, the above relationship between acceleration and displacement is approximate. However, the relationship may still be used to develop shock spectra.

Plots of the three quantities, displacement D, velocity V, and acceleration A, against frequency f, are then shock spectra. They may be plotted individually or, more conveniently, on a single plot by means of the type of chart shown in

Figure 2-254. Any point on this logarithmic grid represents a simultaneous solution to Equations 2-93 and 2-94. The log-log grid must be proportioned to satisfy the solution of the equations. The grid is constructed from standard log-log paper on which a second log-log grid is superimposed and rotated 45 degrees. The width of a log cycle on this rotated grid is 0.707 times the width of a cycle on the standard grid.

2-24.3. Response Spectra

A response spectrum is a plot of the maximum response of a single-degree-of-freedom system to a given input motion. The given input motions are the air shock and the air-induced and direct-induced ground shocks. Since the maximum values of the free-field displacement, velocity, and acceleration (input motion) are used to construct the spectra, a response spectrum envelope is produced. The spectrum takes a trapezoidal shape and is shown in Figure 2-254 by the lines labeled D, V and A. The three sides of this trapezoid can be related to the maximum free-field input motion parameters of displacement, velocity, and acceleration.

Relationships between the spectrum envelope bounds and the characteristics of the time dependent free-field input motions (displacements, velocities, and accelerations) clearly indicate that as the variation of the free-field motion parameters versus time is defined, the definition of the corresponding spectrum envelope can be refined. However, in the general case of blast-induced motions, the variation of the input motions with time cannot visually be described in significant detail. Consequently, it is recommended that for the elastic response of systems, the spectrum be defined by the following three straight lines as illustrated in Figure 2-254.

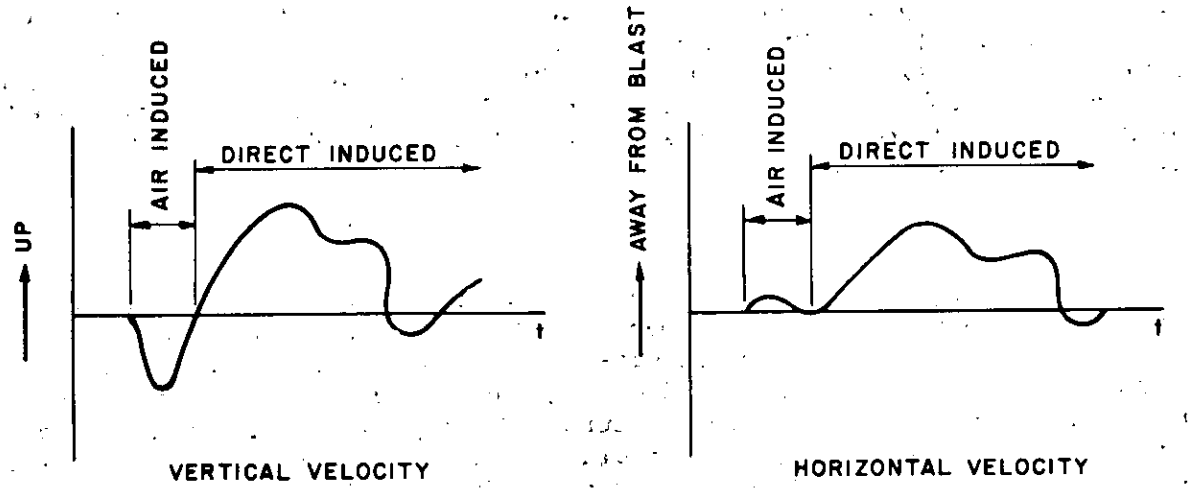
(1) Line "D" is drawn parallel to lines of constant displacement with a magnitude equal to the maximum free-field (building) displacement.

(2) Line "V" is drawn parallel to lines of constant velocity (actually pseudo velocity) with a magnitude equal to one and one-half (1.5) times the maximum free-field (building) velocity.

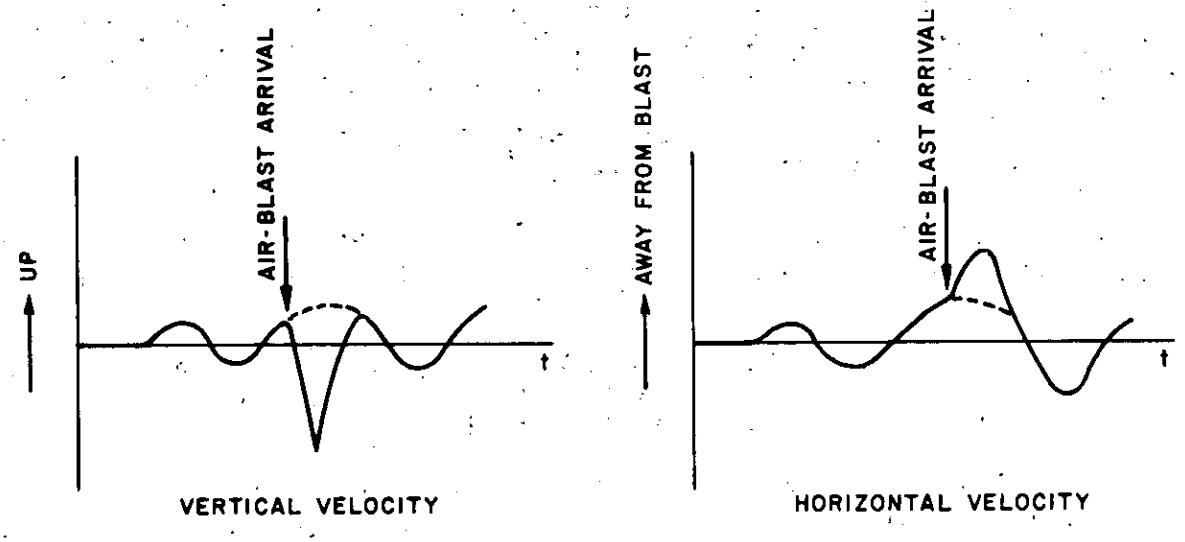
(3) Line "A" is drawn parallel to lines of constant acceleration with a magnitude equal to two (2) times the maximum free-field (building) acceleration.

A spectrum defined in this manner is clearly an approximation, however, its accuracy is considered to be consistent with the accuracy of the input free-field (building) motions on which it is based. In those cases where the input motions can be defined with greater confidence, the spectrum identified above can be defined to reflect the greater accuracy.

In most cases, interior components of the structure and/or equipment and equipment supports are designed elastically. Therefore, the shock spectra described above will suffice. However, when a very large explosion causes large structure motions, interior systems may require inelastic designs. These conditions will usually not arise for the charge capacities considered in this report. Therefore, methods for calculating inelastic shock spectra have not been presented. It is recommended that the bibliography given at the end of this chapter be consulted for further data on this subject.



(a) SUPERSEISMIC GROUND SHOCK



(b) OUTRUNNING GROUND SHOCK

Figure 2-253 Net ground motions produced by an explosion at the ground surface

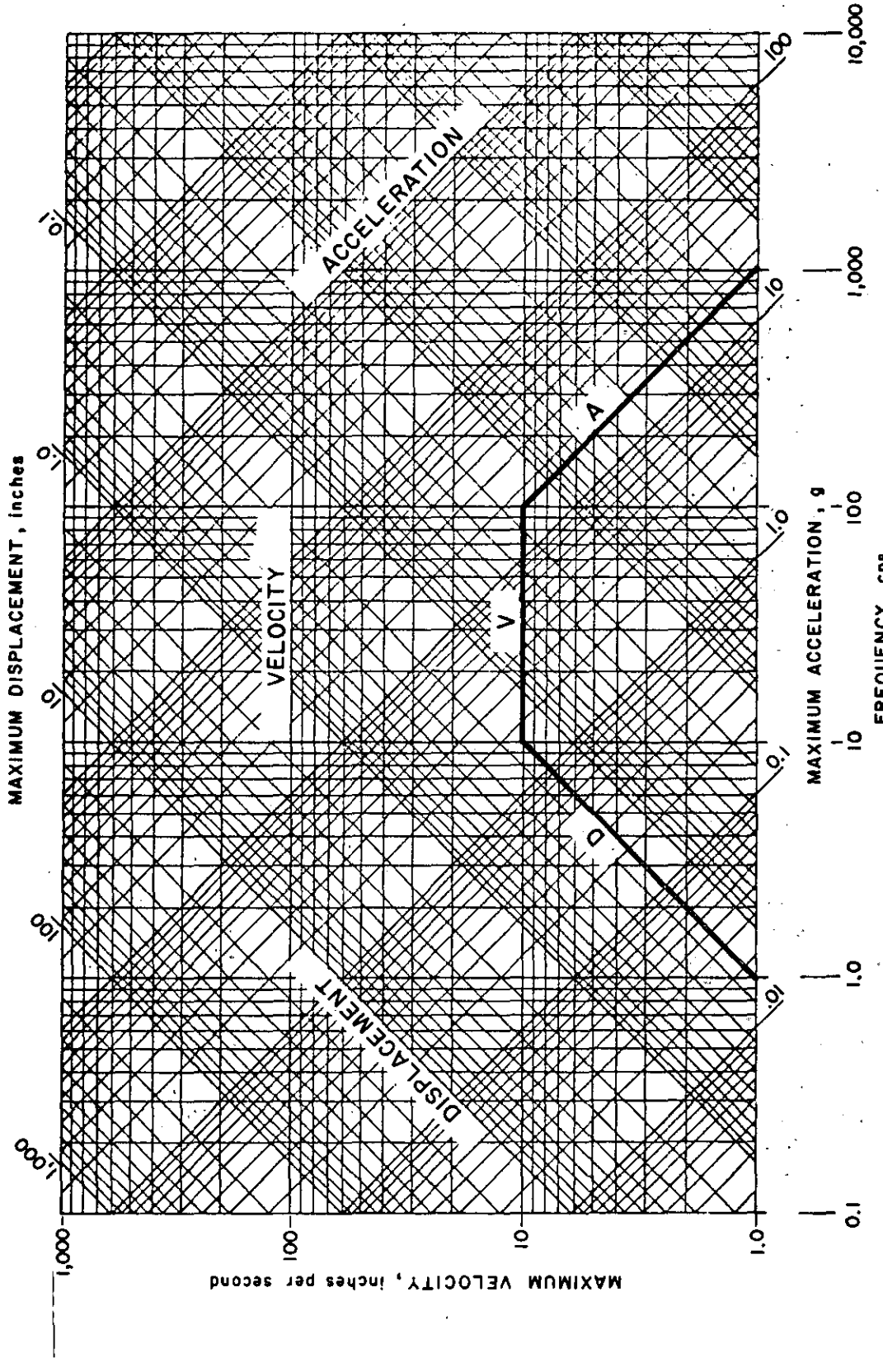


Figure 2-254 Typical response shock spectra

Table 2-10 Mass Density for Typical Soils and Rocks

Material	Mass Density, ρ $(lb\text{-}sec^2)/in.^4$
Loose, dry sand	1.42 E-04
Loose, saturated sand	1.79 E-04
Dense, dry sand	1.65 E-04
Dense, saturated sand	2.02 E-04
Dry clay	1.12 E-04
Saturated clay	1.65 E-04
Dry, sandy silt	1.57 E-04
Saturated, sandy silt	1.95 E-04
Basalt	2.56 E-04
Granite	2.47 E-04
Limestone	2.25 E-04
Sandstone	2.10 E-04
Shale	2.17 E-04
Concrete	2.25 E-04

Table 2-11 Typical Seismic Velocities for Soils and Rocks

Material	Seismic Velocity in./sec
Loose and dry soils	7,200 to 39,600
Clay and wet soils	30,000 to 75,600
Coarse and compact soils	36,000 to 102,000
Sandstone and cemented soils	36,000 to 168,000
Shale and marl	72,000 to 210,000
Limestone-chalk	84,000 to 252,000
Metamorphic rocks	120,000 to 252,000
Volcanic rocks	120,000 to 270,000
Sound plutonic rocks	156,000 to 300,000
Jointed granite	9,600 to 180,000
Weathered rocks	24,000 to 120,000

Table 2-12 **Coefficient of Friction for Concrete Foundation and Underlying Soils**

Soil Material	Coefficient of Friction, μ
Clean sound rock	0.70
Clean gravel, gravel-sand mixture, coarse sand	0.55 to 0.60
Clean fine to medium sand, silty medium to coarse sand, silty or clayey gravel	0.45 to 0.55
Clean fine sand, silty or clayey fine to medium sand	0.35 to 0.45
Fine sandy silt, nonplastic silt	0.30 to 0.35
Very stiff and hard residual or preconsolidated clay	0.40 to 0.50
Medium stiff and stiff clay and silty clay	0.30 to 0.35

APPENDIX 2A

ILLUSTRATIVE EXAMPLES

Problem 2A-1. Free-Air Burst

Problem: Determine incident blast wave parameters for a point of interest in the air for a free air burst.

Procedure:

Step 1. Determine the charge weight and height of burst H_c. Select point of interest in the air relative to the charge.

Step 2. Apply a 20% safety factor to the charge weight.

Step 3. For the point of interest, calculate slant distance R and scaled slant distance Z:

$$Z = R/W^{1/3}$$

Step 4. Determine incident blast wave parameters from Figures 2-7 and 2-8 for the calculated value of the scaled slant distance Z:

From Figure 2-7 read:

Peak positive incident pressure P_{so}

Shock front velocity U

Scaled unit positive incident impulse $i_s/W^{1/3}$

Scaled positive phase duration $t_o/W^{1/3}$

Scaled arrival time $t_A/W^{1/3}$

Scaled wave length of positive phase $L_w/W^{1/3}$

From Figure 2-8 Read:

Peak negative incident pressure P_{so}^-

Scaled unit negative incident impulse $i_s^-/W^{1/3}$

Scaled negative phase duration $t_o^-/W^{1/3}$

Scaled wave length of negative phase $L_w^-/W^{1/3}$

Multiply scaled values by $W^{1/3}$ to obtain absolute values.

Example 2A-1. Free-Air Burst

Required: Incident blast wave parameters P_{so}, $\bar{P_{so}}$, U, i_s, $\bar{i_s}$, t_o, $\bar{t_o}$, t_A, $\bar{L_w}$ at a point 30 ft. below and 45 ft. away in the air from an air burst of 290 lbs. at a height of burst of 60 ft. above the ground.

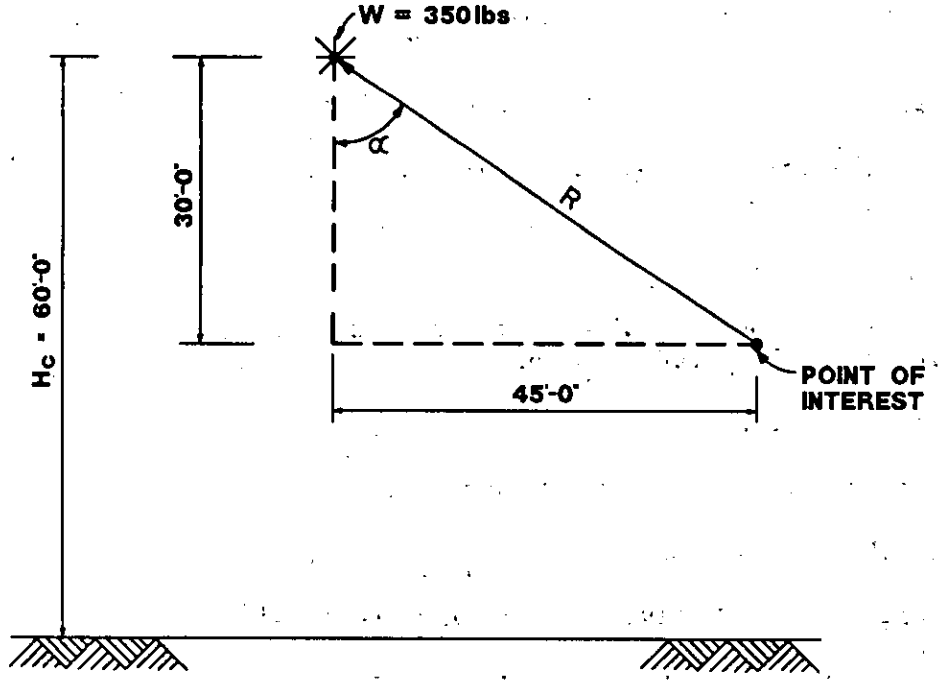


Figure 2A-1

Solution:

Step 1. Given: Charge weight = 290 lbs., H_c = 60 ft.

Step 2. W = 1.2 (290) = 350 lbs.

Step 3. For the point of interest:

$$R = \left[(45)^2 + (30)^2 \right]^{1/2} = 54.1 \text{ ft.}$$

$$Z = \frac{R}{W^{1/3}} = \frac{54.1}{(350)^{1/3}} = 7.67 \text{ ft./lb}^{1/3}$$

Step 4. Determine incident blast wave parameters for

$Z = 7.67$ ft./lb$^{1/3}$

From Figure 2-7:

P_{so} = 11.2 psi

U = 1.34 ft./ms

$i_s / W^{1/3}$ = 7.0 psi-ms/lb$^{1/3}$, i_s = 7.0 $(350)^{1/3}$ = 49.3 psi-ms

$t_o / W^{1/3}$ = 2.05 ms/lb$^{1/3}$, t_o = 2.05 $(350)^{1/3}$ = 14.45 ms.

$t_A / W^{1/3}$ = 3.15 ms/lb$^{1/3}$, t_A = 3.15 $(350)^{1/3}$ = 22.2 ms

$L_w / W^{1/3}$ = 2.0 ft/lb$^{1/3}$, L_w = 14.09 ft

From Figure 2-8:

P_{so} = 1.63 psi

$\bar{i}_s / W^{1/3}$ = 7.2 psi-ms/lb$^{1/3}$, $\bar{i}_s$ = 7.2 $(350)^{1/3}$ = 50.74 psi-ms

$\bar{t}_o / W^{1/3}$ = 8.4 ms/lb$^{1/3}$, $\bar{t}_o$ = 8.4 $(350)^{1/3}$ = 59.20 ms

$\bar{L}_w / W^{1/3}$ = 5.8 ft/lb$^{1/3}$, $\bar{L}_w$ = 5.8 $(350)^{1/3}$ = 40.87 ft.

Problem 2A-2. Air Burst

Problem: Determine free-field blast wave parameters at a point on the ground for an air burst.

Procedure:

Step 1. Select point of interest on the ground relative to the charge. Determine the charge weight, height of burst H_c, and ground distance R_G.

Step 2. Apply a 20% safety factor to the charge weight.

Step 3. Calculate scaled height of burst and angle of incidence α:

$H_c / W^{1/3}$

$$\alpha = \tan^{-1} (R_G/H_c)$$

Step 4. Determine peak reflected pressure $P_{r\alpha}$ and scaled unit positive reflected impulse $i_{r\alpha}/W^{1/3}$ in Mach front from Figures 2-9 and 2-10, respectively, for corresponding scaled height of burst and angle of incidence α:

Read $P_{r\alpha}$ and $i_{r\alpha}/W^{1/3}$

Multiply scaled value by $W^{1/3}$ to obtain absolute value.

Step 5. Read scaled distance Z from Figure 2-7 for corresponding peak incident pressure $P_{so} = P_{r\alpha}$ in the Mach front.

Step 6. Determine shock front velocity U and scaled time of arrival of blast wave $t_A/W^{1/3}$ from Figure 2-7 for value Z from step 5. Multiply scaled value of $W^{1/3}$ to obtain absolute value.

Step 7. Read scaled distance Z from Figure 2-7 for corresponding scaled unit positive incident impulse $i_s/W^{1/3} = i_{r\alpha}/W^{1/3}$ in the Mach front.

Step 8. Determine scaled positive duration of positive phase from Figure 2-7 for the value of Z from step 7. Multiply scaled value of $W^{1/3}$ to obtain absolute value.

Example 2A-2. Air Burst

Required: Free-field blast wave parameters P_{so}, U, i_s, t_o, t_A for an air burst of 20,800 lbs. at a ground distance of 300 ft. and a height of burst of 90 ft.

Solution:

Step 1. Given: Charge weight = 20,800 lb. R_G = 300 ft, H_c = 90 ft.

Step 2. W = 1.20 (20,800) = 25,000 lbs.

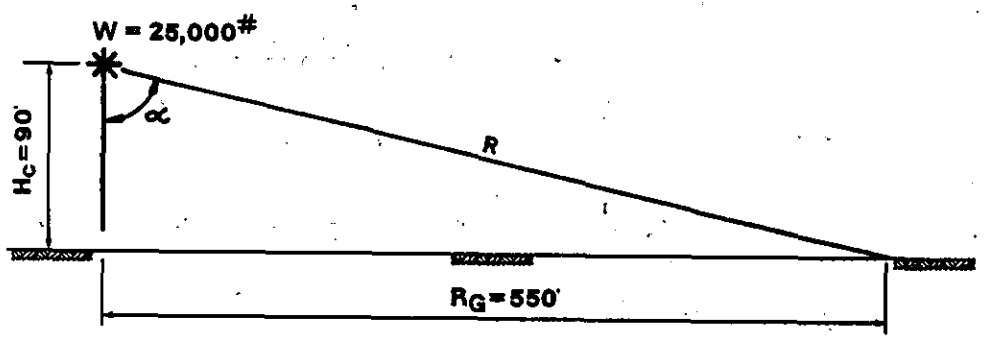


Figure 2A-2

Step 3. For point of interest

$$H_c/W^{1/3} = 90/(25,000)^{1/3} = 3.08 \text{ ft/lb}^{1/3}$$

$$\alpha = \tan^{-1}\left[\frac{R_G}{H_c}\right] = \tan^{-1}[300/90] = 73.3°$$

Step 4. Determine reflected pressure $P_{r\alpha}$ and reflected impulse in the Mach front from Figure 2-9 and 2-10.

$H_c/W^{1/3} = 3.08$ ft/lb$^{1/3}$ and $\alpha = 73.3°$

$P_{r\alpha} = 10.1$ psi

$$\frac{i_{r\alpha}}{W^{1/3}} = 9.2 \text{ psi-ms/lb}^{1/3}, \quad i_{r\alpha} = 9.2\ (25,000)^{1/3} = 269.0 \text{ psi-ms}$$

Step 5. Read scaled distance Z from Figure 2-7 corresponding to $P_{so} = P_{r\alpha} = 10.1$ psi

$Z = 7.8$ ft/lb$^{1/3}$

Step 6. Determine U and $t_A/W^{1/3}$ from Figure 2-7 corresponding to Z = 7.8 ft/lb$^{1/3}$.

$U = 1.38$ ft/ms

$t_A/W^{1/3} = 300$ ms/lb$^{1/3}$, $t_A = 300\ (25.000)^{1/3} = 8772.05$ ms.

Step 7. Read scaled distance Z from Fig. 2-7 corresponding to

$i_s/W^{1/3} = i_{r\alpha}/W^{1/3} = 9.2$ psi-ms/lb$^{1/3}$

$Z = 5.7$ ft/lb$^{1/3}$

Step 8. Determine $t_o/W^{1/3}$ from Figure 2-7 corresponding to

$Z = 5.7$ ft/lb$^{1/3}$

$t_o/W^{1/3} = 155$ ms/lb$^{1/3}$, $t_o = 155(25{,}000)^{1/3} = 4532.23$ ms

Problem 2A-3. Surface Burst

Problem: Determine free-field blast wave parameters for a surface burst.

Procedure:

Step 1. Select point of interest on the ground relative to the charge. Determine the charge weight, and ground distance R_G.

Step 2. Apply a 20% safety factor to the charge weight.

Step 3. Calculate scaled ground distance Z_G:

$$Z_G = \frac{R_G}{W^{1/3}}$$

Step 4. Determine free-field blast wave parameters from Figure 2-15 for corresponding scaled ground distance Z_G:

Read:

Peak positive incident pressure P_{so}

Shock front velocity U

Scaled unit positive incident impulse $i_s/W^{1/3}$

Scaled positive phrase duration $t_o/W^{1/3}$

Scaled arrival time $t_A/W^{1/3}$

Multiply scaled values by $W^{1/3}$ to obtain absolute values.

Example 2A-3. Surface Burst

Required: Free-field blast wave parameters P_{so}, U, i_s, t_o, t_A for a surface burst of 20,800 lbs at a distance of 530 ft.

Solution:

Step 1: Given: Charge weight = 20,800 lb. R_G = 530 ft.

Step 2. W = 1.20 (20,800) = 25,000 lbs.

Step 3. For point of interest:

$$Z_G = \frac{R_G}{W^{1/3}} = \frac{530}{(25,000)^{1/3}} = 18.1 \text{ ft/lb}^{1/3}$$

Step 4. Determine blast wave parameters from Figure 2-15 for

$Z_G = 18.1 \text{ ft/lb}^{1/3}$

$P_{so} = 3.45$ psi

U = 1.22 ft/ms

$$\frac{i_s}{W^{1/3}} = 4.7 \text{ psi-ms/lb}^{1/3}, \quad i_s = 4.7(25,000)^{1/3} = 137.4 \text{ psi-ms}$$

$$\frac{t_o}{W^{1/3}} = 3.3 \text{ ms/lb}^{1/3}, \quad t_o = 3.3(25,000)^{1/3} = 96.5 \text{ ms}$$

$$\frac{t_A}{W^{1/3}} = 10.6 \text{ ms/lb}^{1/3}, \quad t_A = 10.6(25.000)^{1/3} = 310 \text{ ms}$$

Problem 2A-4 Shock Loads on Cubicle Walls

Problem: Determine the average peak reflected pressure and average scaled reflected impulse acting on the wall of a cubicle from an internal explosion. The cubicle is fully vented.

Procedure:

Step 1. Select from Figure 2-51 the structural configuration which will define the number N and location of effective reflecting surfaces for the wall of the structure in question. Determine the charge weight, and, as defined by the structural configuration chosen above, the charge location parameters R_A, h, l and the structural parameters L, H.

Step 2. Apply a 20% safety factor to the charge weight.

Step 3. Calculate the chart parameters $\frac{h}{H}$, $\frac{l}{L}$, $\frac{L}{R_A}$, and the scaled distance Z_A.

Note:
Use of the average pressure and impulse charts may require interpolation in many cases. Interpolation may be achieved by inspection for the scaled distance Z_A and by a graphical procedure for the chart parameters L/H, l/L, and h/H using 2 cycle x 2 cycle logarithmic graph paper. The following procedure will illustrate the interpolation of all three chart parameters.

Step 4. From table 2-3 determine the appropriate pressure and impulse charts for the number of adjacent reflecting surfaces N. Determine and tabulate the values of the average pressure P_r and average scaled impulse $i_r/W^{1/3}$ from these charts for the required L/R_A and Z_A and the following variables:

L/H = 0.625, 1.25, 2.50, and 5.00

l/L = 0.10, 0.25. 0.50, and 0.75

h/H = 0.10, 0.25, 0.50, and 0.75

Step 5.

a. Prepare four 2-cycle log-log charts with L/H as the lower abscissa, l/L as the upper abscissa, and P_r as the ordinate (one chart for each of the h/H ratios). On each chart for constant h/H and Z_A, plot i_b versus L/H for all l/L values.

Repeat with the ordinate labeled as $i_r/W^{1/3}$.

b. Using chart for h/H = 0.10, read values of P_r and $i_r/W^{1/3}$ versus l/L for required L/H. Tabulate results.

c. Repeat step 5b for charts h/H = 0.25, 0.50, and 0.75. Tabulate results.

d. On each h/H chart, plot P_r and $i_r/W^{1/3}$ versus l/L from steps 5b and 5c.

e. On each h/H chart, read P_r and $i_r/W^{1/3}$ for required l/L ratio.

f. On a fifth chart, plot P_r and $i_r/W^{1/3}$ from step 5e versus h/H.

Step 6. For required h/H ratio, read P_r and $i_r/W^{1/3}$ from chart of step 5f.

Step 7. Calculate duration of load on element from equation 2-22

Example 2A-4 (A) Shock Loads on Cubicle Walls

Required: Average peak reflected pressure and average scaled reflected impulse on the side wall of a three-wall cubicle from an explosive charge of 205 lbs. The cubicle is fully vented.

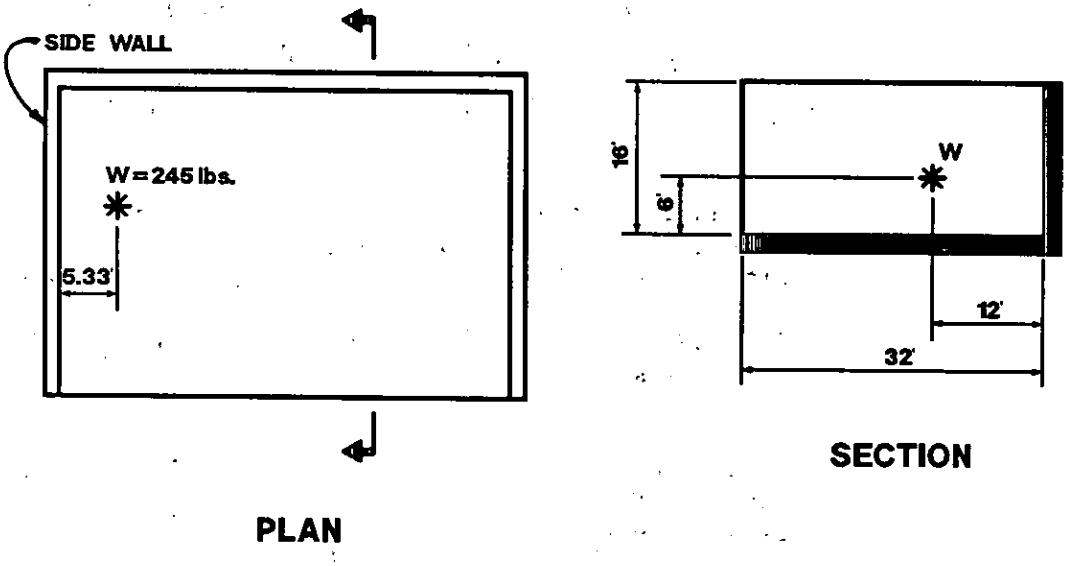


Figure 2A-3

Solution:

Step 1. H = 16 ft. L = 32 ft. Charge Weight = 205 lbs.

h = 6 ft. l = 12 ft. R_A = 5.33 ft.

Note:

For definition of terms, see Figure 2-51 (side wall of three wall cubicle, N = 2).

Step 2. $W = 1.20\ (205) = 245$ lbs.

Step 3. $h/H = 0.375$ $l/L = 0.375$ $L/R_A = 6.00$ $L/H = 2.00$

$$Z_A = \frac{R_A}{W^{1/3}} = \frac{5.33}{(245)^{1/3}} = 0.85 \text{ ft/lb}^{1/3}$$

Interpolation is required for Z_A, L/H, l/L, and h/H.

Step 4. Determine and tabulate the values of P_r and $i_r/W^{1/3}$ from pressure and impulse charts (see table 2-3 for N = 2) for:

$L/R_A = 6.00$, $Z_A = 0.85$

(interpolate by inspection) and for values given for L/H, l/L and h/H. The results are tabulated in tables 2A-1 and 2A-2.

Step 5.

a. Plot P_r and $i_r/W^{1/3}$ versus L/H for the values of l/L and constant h/H (fig. 2A-4 and 2A-5).

b. Determine P_r and $i_r/W^{1/3}$ for L/H = 2.00, h/H = 0.10, and various l/L ratios by entering Figure 2A-4a and 2A-5a with L/H = 2.00

c. Repeat above step for h/H = 0.25, 0.50, and 0.75 by entering Figures 2A-4b through d and 2A-5b through d with L/H = 2.00 (tabulation of results not shown).

d. On each h/H chart, plot P_r and $i_r/W^{1/3}$ (steps 5b and 5c) versus l/L (upper abscissa of Figures 2A-4a through d and 2A-5a through d).

e. Determine P_r and $i_r/W^{1/3}$ for l/L = 0.375 on each h/H chart of Figures 2A-4 and 2A-5 with l/L = 0.375 and reading curves plotted in step 5d.

Table 2A-1 Average Pressure
(Part 1)

h/H	0.10				0.25			
l/L	0.10	0.25	0.50	0.75	0.10	0.25	0.50	0.75
L/H 0.625	462	569	598	569	533	665	701	665
1.25	749	932	980	932	943	1178	1238	1178
2.50	1200	1488	1562	1488	1432	1796	1881	1796
5.00	2032	2519	2635	2519	1870	2334	2437	2334
Fig.	2-64	2-65	2-66	2-67	2-68	2-69	2-70	2-71

Table 2A-1 Average Pressure
(Part 2)

h/H	0.50				0.75			
l/L	0.10	0.25	0.50	0.75	0.10	0.25	0.50	0.75
L/H 0.625	546	681	718	681	533	665	701	665
1.25	1017	1267	1333	1267	943	1178	1238	1178
2.50	1609	2028	2120	2028	1432	1796	1881	1796
5.00	1987	2456	2563	2456	2623	3119	3210	3119
Fig.	2-72	2-73	2-74	2-75	2-76	2-77	2-78	2-79

Table 2A-2 Average Unit Impulses
(Part 1)

h/H	0.10				0.25			
l/L	0.10	0.25	0.50	0.75	0.10	0.25	0.50	0.75
L/H 0.625	73	71	70	66	65	61	59	55
1.25	96	92	90	84	96	92	90	83
2.50	126	121	121	111	139	131	129	120
5.00	172	164	164	153	167	153	154	143
Fig.	2-113	2-114	2-115	2-116	2-117	2-118	2-119	2-120

Table 2A-2 Average Unit Impulses
(Part 2)

h/H	0.50				0.75			
l/L	0.10	0.25	0.50	0.75	0.10	0.25	0.50	0.75
L/H 0.625	64	61	58	54	59	56	53	49
1.25	93	87	83	76	87	79	76	70
2.50	129	120	118	109	117	106	103	95
5.00	186	168	168	158	201	189	189	179
Fig.	2-121	2-122	2-123	2-124	2-125	2-126	2-127	2-128

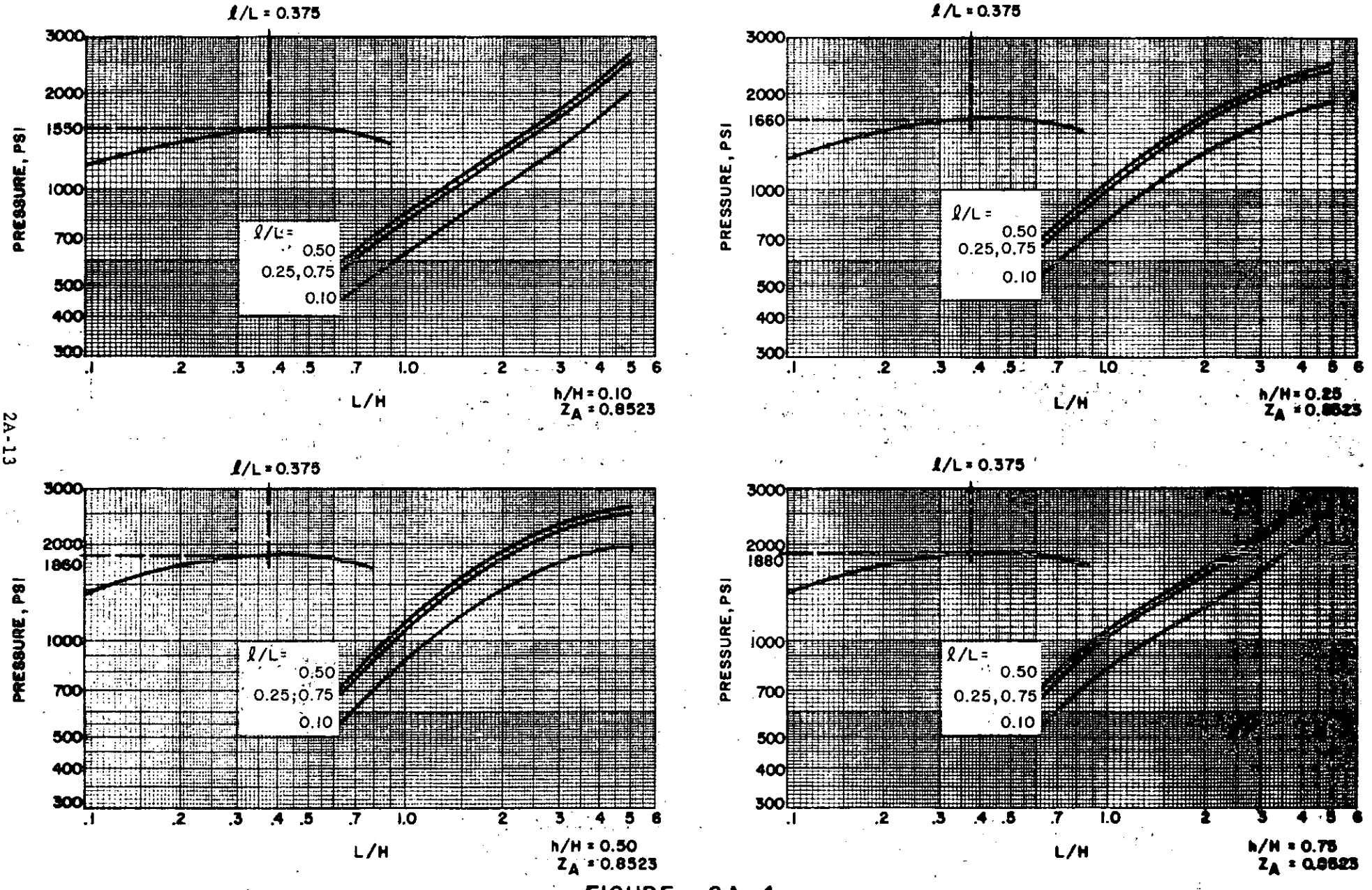
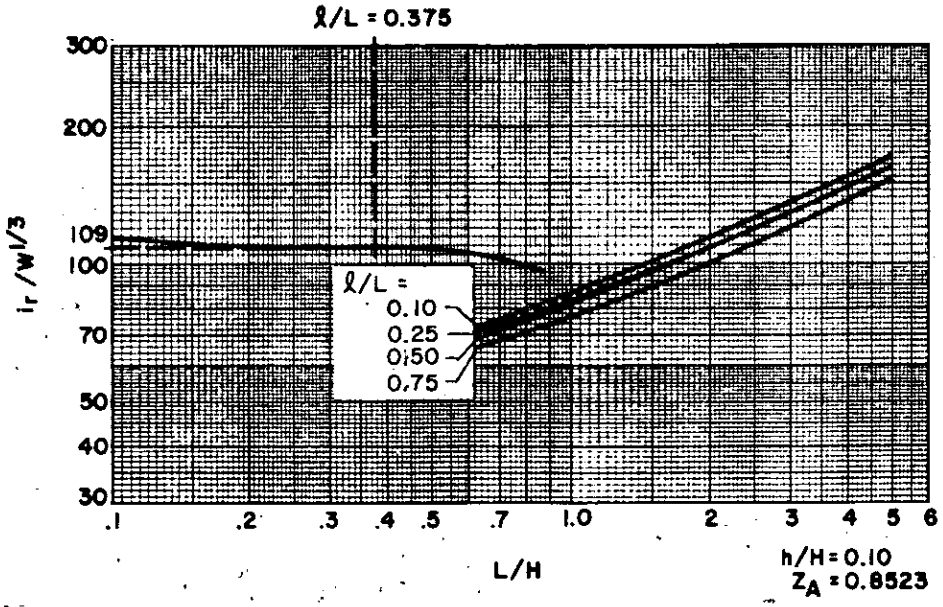
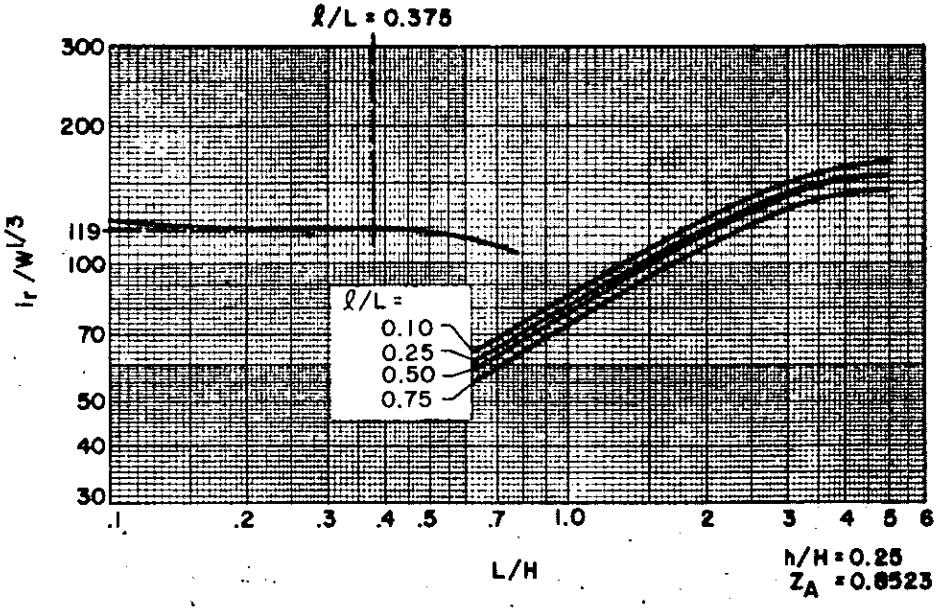
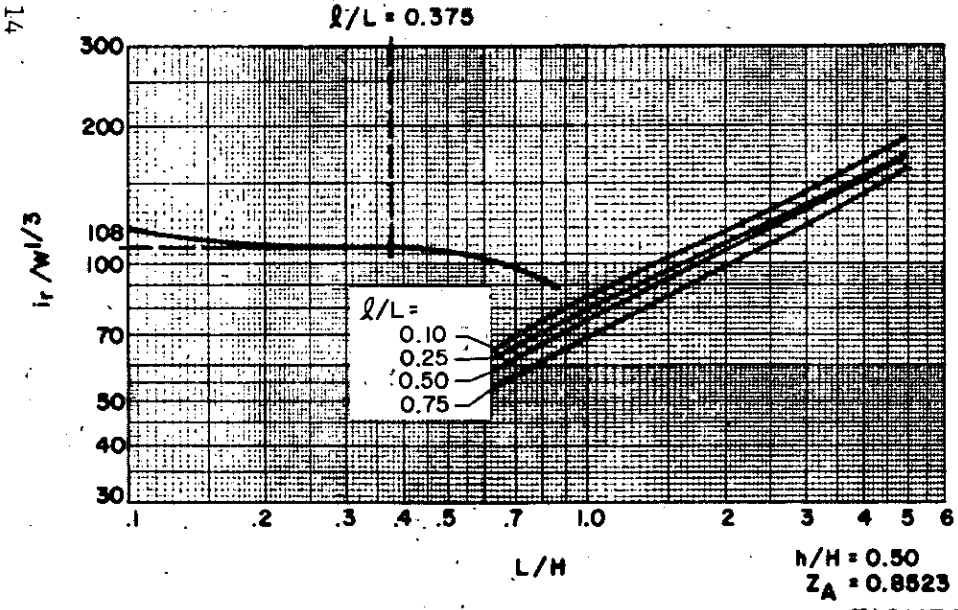

ℓ/L = 0.375
PRESSURE, PSI
3000
2000
1550
1000
700
500
400
300
.1
.2
.3
.4
.5
.7
1.0
2
3
4
5
6
L/H
ℓ/L =
0.50
0.25, 0.75
0.10
h/H = 0.10
Z_A = 0.8523
ℓ/L = 0.375
PRESSURE, PSI
3000
2000
1660
1000
700
500
400
300
L/H
ℓ/L =
0.50
0.25, 0.75
0.10
h/H = 0.25
Z_A = 0.8523
ℓ/L = 0.375
PRESSURE, PSI
3000
2000
1860
1000
700
500
400
300
L/H
ℓ/L =
0.50
0.25; 0.75
0.10
h/H = 0.50
Z_A = 0.8523
ℓ/L = 0.375
PRESSURE, PSI
3000
2000
1880
1000
700
500
400
300
L/H
ℓ/L =
0.50
0.25, 0.75
0.10
h/H = 0.75
Z_A = 0.8523

FIGURE 2A-4


ℓ/L = 0.375
300
200
109
100
70
50
40
30
.1
.2
.3
.4
.5
.7
1.0
2
3
4
5
6
ℓ/L =
0.10
0.25
0.50
0.75
L/H
h/H = 0.10
Z_A = 0.8523


ℓ/L = 0.375
300
200
119
100
70
50
40
30
.1
.2
.3
.4
.5
.7
1.0
2
3
4
5
6
ℓ/L =
0.10
0.25
0.50
0.75
L/H
h/H = 0.25
Z_A = 0.8523


ℓ/L = 0.375
300
200
108
100
70
50
40
30
.1
.2
.3
.4
.5
.7
1.0
2
3
4
5
6
ℓ/L =
0.10
0.25
0.50
0.75
L/H
h/H = 0.50
Z_A = 0.8523

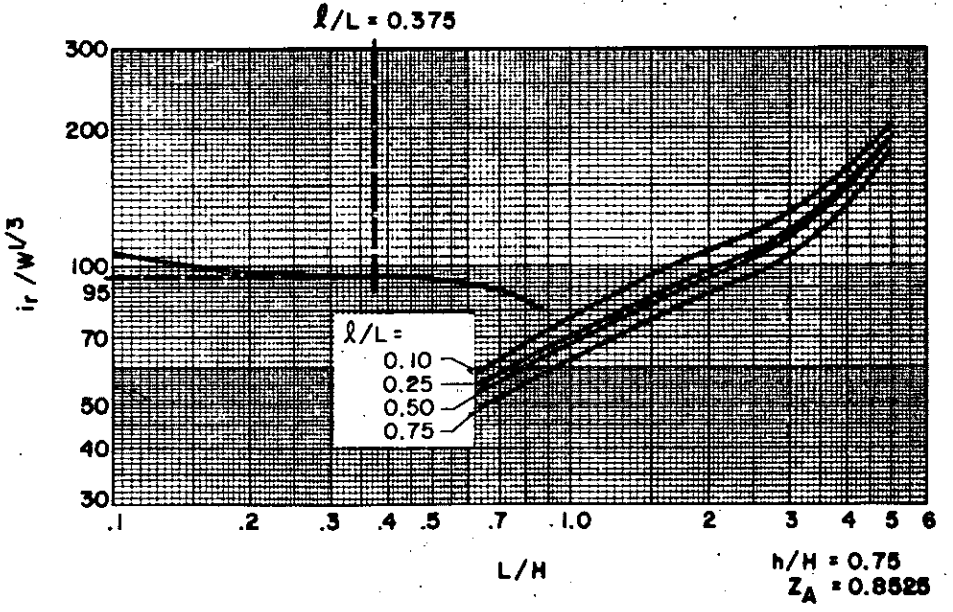

ℓ/L = 0.375
300
200
100
95
70
50
40
30
.1
.2
.3
.4
.5
.7
1.0
2
3
4
5
6
ℓ/L =
0.10
0.25
0.50
0.75
L/H
h/H = 0.75
Z_A = 0.8525

FIGURE 2A-5

h/H	P_r	$i_r/W^{1/3}$
0.10	1550	109
0.25	1660	119
0.50	1860	108
0.75	1880	95

f. Plot P_r and $i_r/W^{1/3}$ (step 5e) versus h/H (fig.2A-7).

Step 6. For h/H = 0.375 read P_r = 1800 psi on Figure 2A-7 and read $i_r/W^{1/3}$ = 115 psi-ms/$lb^{1/3}$ on Figure 2A-7

Step 7. Calculate duration of load on wall.

$$t_o = 2(i_r/W^{1/3})\ (W)^{1/3} / P_r = 2\ (115)\ (245)^{1/3} / 1800 = 0.80 \text{ ms}$$

Example 2A-4(B). Shock Loads on Cubicle Walls

Required: Average peak reflected pressure and average scaled reflected impulse on the back wall of a three-wall cubicle from an explosive charge of 3,750 lbs. The cubicle is fully vented and shown in Figure 2A-6.

Solution:

Step 1. H = 16 ft. L = 36 ft. Charge weight = 3,750 lbs.

h = 4 ft. l = 9 ft. R_A = 16.5 ft.

Note:

For definition of terms, see Figure 2-51 (back wall of three-wall cubicle, N = 3).

Step 2. W = 1.20 (3,750) = 4,500 lbs.

Step 3. h/H = 0.25 l/L = 0.25 L/R_A = 2.18 L/H = 2.25

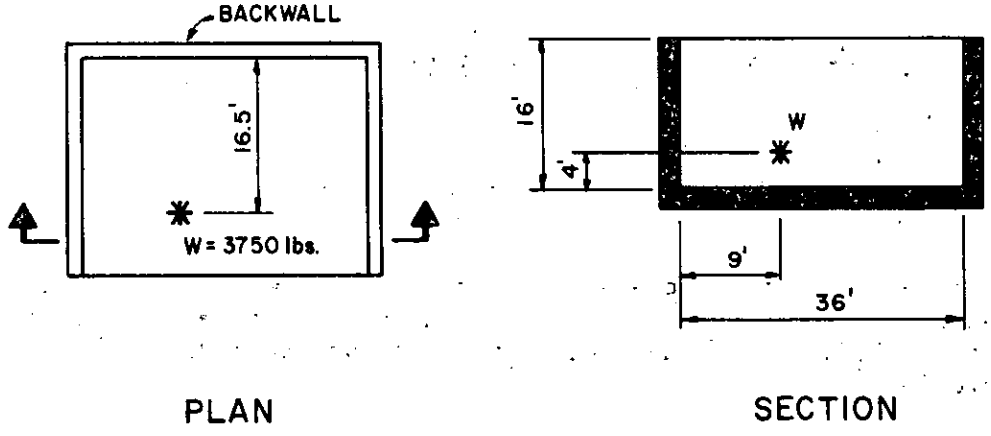
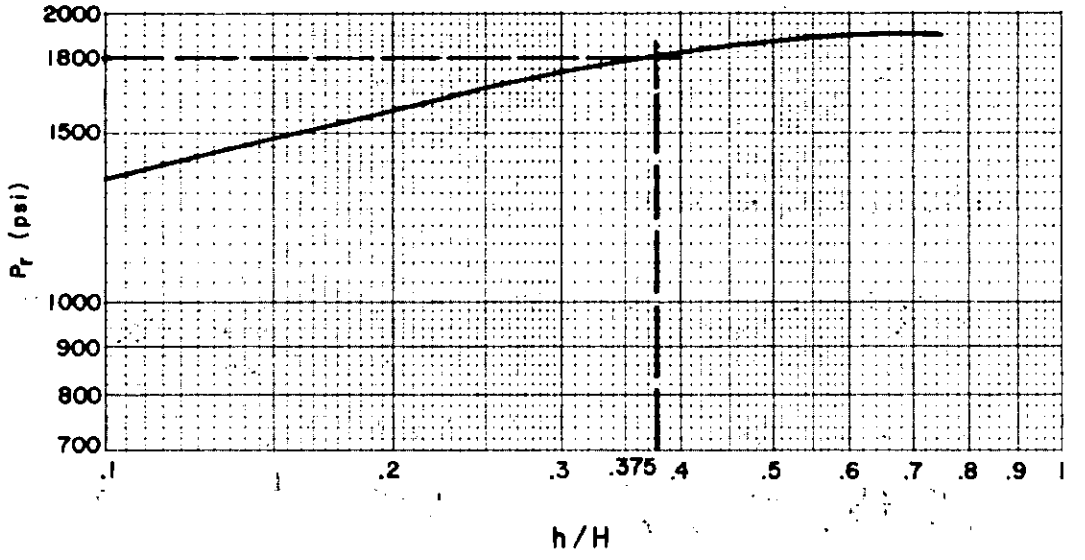
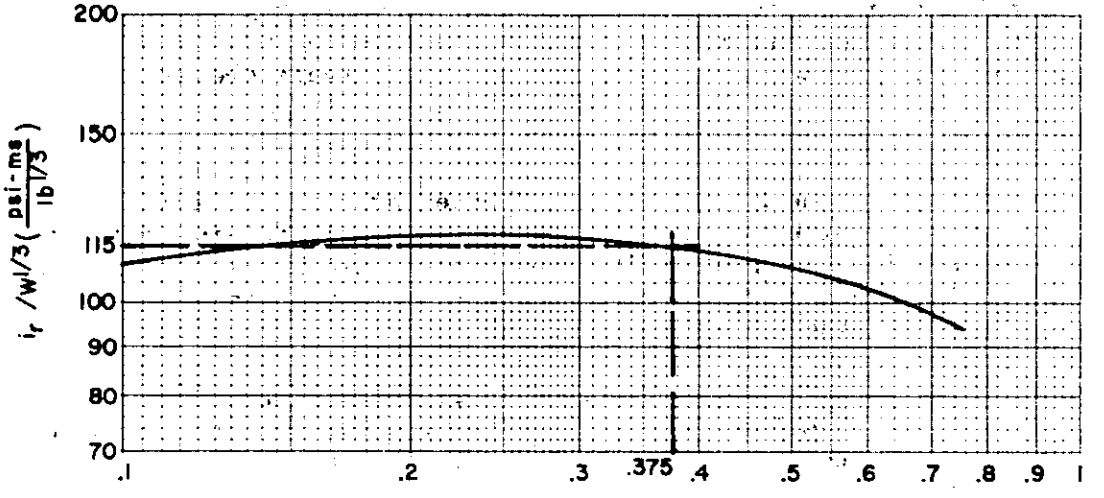


FIGURE 2A-6



(a)



(b)

R/A = 4.0
L/R = 6.0
Z/A = 0.85

L/H = 2.0
ℓ/L = 0.375
h/H = 0.375

FIGURE 2A-7

$$Z_A = \frac{R_A}{W^{1/3}} = \frac{16.5}{(4,500)^{1/3}} = 1.00 \text{ ft/lb}^{1/3}$$

Interpolation is required for L/H

Step 4. Determine the values of P_r and $i_r/W^{1/3}$ from Figures 2-84 and 2-133 (determined from table 2-3 for N = 3, h/H = 0.25, l/L = 0.25) for L/H ratios of 0.625, 1.25, 2.50 and 5.00.

Step 5. Plot P_r and $i_r/W^{1/3}$ versus L/H (fig. 2A-8).

Step 6. For L/H = 2.25 read, P_r = 3700 psi and $i_r/W^{1/3}$ = 295 psi-ms/lb$^{1/3}$ and on Figure 2A-8.

Step 7. Calculate duration of load on wall (equation 2-2).

$t_o = 2(i_r/W^{1/3})\ W^{1/3}/P_r = 2\ (295)\ (4500)^{1/3}/3700 = 2.63$ ms

Problem 2A-5 Effect of Frangibility on Shock Loads

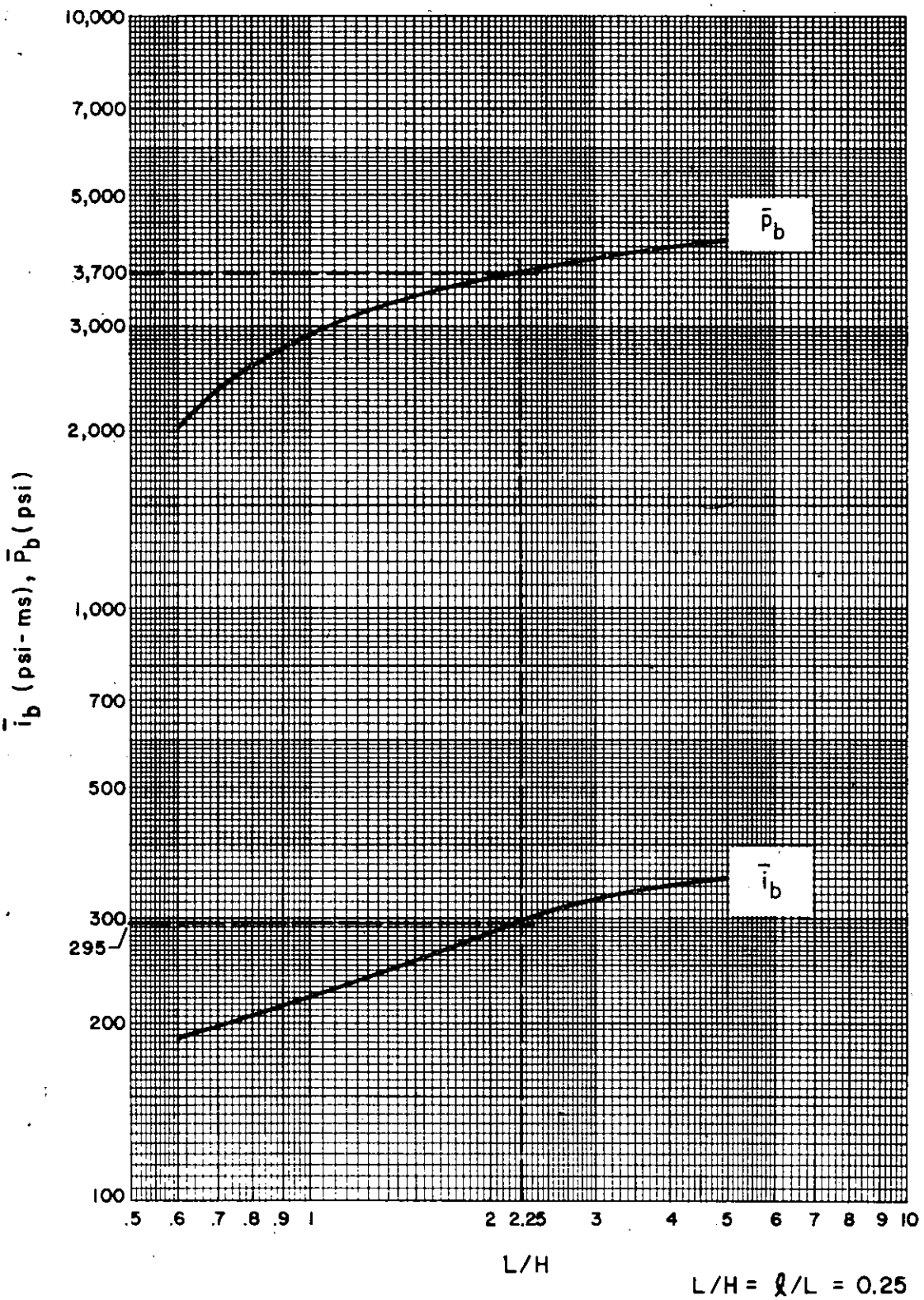
Problem: Determine average peak reflected pressure and average reflected impulse acting on the wall of a cubicle due to an internal explosion. One of the reflection surfaces is a frangible wall.

Procedure:

Step 1. Determine the average peak reflected pressure P_r and the average reflected impulse acting on the element in question according to the procedure in problem 2A-4 assuming that the adjoining frangible element will remain in place and provide full reflection.

Step 2. Determine the average reflected impulse acting on the element in question according to the procedure in problem A-4 assuming that the adjoining frangible element is not in place.

Step 3. Subtract the average impulse determined in step 2 from the one in step 1.



$L/H = \ell/L = 0.25$
$L/R_A = 2.1818$
$Z_A = \sim 1.0$

FIGURE 2A-8

Step 4. Calculate unit weight of the frangible element W_F and divide by the sixth root of the charge weight (apply a 20% factor of safety to the charge weight).

Step 5. Calculate the normal scaled distance Z between the center of the charge and the surface of the frangible element.

Step 6. Determine the reflection factor f_r from Figure 2-150 for the values of $W_F/W^{1/6}$ from step 4 and Z from step 5. Interpolate for value of Z if required.

Step 7. Determine the magnitude of the impulse load reflected from the frangible element to the element in question by multiplying the value of the average impulse from step 3 and f_r from step 6.

Step 8. a. Determine the total impulse load acting on the element in question by adding the impulse values from steps 2 and 7.

b. The peak average reflected pressure of the shock load is equal to the value of P_r in step 1.

c. Determine the duration of the load from equation 2-2.

Example 2A-5 Effect of Frangibility on Shock Loads

Required: Average peak reflected pressure and average reflected impulse on the back wall of the cubicle described in example 2A-4B except the left side wall is a 10 psf frangible element. The charge weight is 3,750 lbs (see Figure 2A-6).

Solution:

Step 1. Assuming the frangible side wall provides full reflection of the blast wave, P_r and i_r for the back wall according to the procedure in problem 2A-4 are:

P_r = 3700.0 psi

i_r = 4870.3 psi-ms

Step 2. Assuming no left side wall, the average reflected impulse on the back wall, according to procedure in problem 2A-4 is:

i_r = 3962.3 psi-ms

Step 3. Calculate the reflected impulse contributed by the left side wall by subtracting the impulse value of step 2 from step 1.

δi_r = 4870.3 - 3962.3 = 908.0 psi-ms

Step 4. a. W_F = 10 lb/ft^2 (given)

b. W = 3,750 x 1.20 = 4,500 lbs

c. Calculate $W_F/W^{1/6}$ ratio:

$W_F/W^{1/6} = 10/(4500)^{1/6} = 2.46$

Step 5. a. R = 9.0 feet (see Figure 2A-6)

b. Calculate normal scale distance Z:

$$Z = \frac{R}{W^{1/3}} = \frac{9}{(4500)^{1/3}} = 0.545 \text{ ft/lb}^{1/3}$$

Step 6. From Figure 2-150 where $W_F/W^{1/6} = 2.46$ and Z = 0.545 read: $f_r = 0.68$

Step 7. Determine the magnitude of the impulse reflected from the frangible left side wall, using $f_r = 0.68$ and the impulse from step 3.

i_r (left side wall) = 908 (0.68) = 617.4 psi-ms

Step 8. a. Calculate total reflected impulse on the back wall by adding impulse values from steps 2 and 7.

i_r (back wall) = 3962.3 + 617.4 = 4579.7 psi-ms

b. Peak reflected pressure from step 1:

P_r = 3700 psi

c. Calculate duration of load on wall:

$$t_o = \frac{2i_r}{P_r} = \frac{2\ (4579.7)}{3700} = 2.48 \text{ ms}$$

Problem 2A-6 Shock Loads on Frangible Elements

Problem: Determine the average peak reflected pressure and average reflected impulse acting on the frangible wall of a cubicle due to an internal explosion.

Procedure:

Step 1. Determine the average peak reflected pressure P_r and the average reflected impulse acting on the element in question according to the procedure in problem 2A-4, assuming that the wall will remain intact.

Step 2. Calculate the unit weight of the frangible element W_F and divide by the sixth root of the charge weight (apply a 20% factor of safety to the charge weight).

Step 3. From Figure 2-7 determine the fictitious scaled distance Z which corresponds to the average scaled impulse determined in step 1.

Step 4. Using the value of $W_F/W^{1/6}$ from step 2 and the Z from step 3. determine the reflection factor f_r from Figure 2-150. Interpolate for value of Z if required.

Step 5.
a. Calculate the value of the average impulse contributing to the translation of the frangible element by multiplying the values of i_r and f_r of steps 1 and 4 respectively.

b. The peak average reflected pressure of the shock load is equal to the value of P_r in step 1.

c. Determine the duration of the load from equation 2-2.

Example 2A-6 Shock Loads on Frangible Elements

Required: Average peak reflected pressure and average scaled reflected impulse on the back wall of the cubicle described in example 2A-4 except the back wall is a 10 psf frangible wall. The charge weight is 3,750 lbs (see Figure 2A-6).

Solution:

Step 1. P_r and i_r for the back wall, assuming it is a rigid element, according to procedure in problem 2A-4 are:

$P_r = 3700.0$ psi

$i_r/W^{1/3} = 295.0$ psi-ms/lb$^{1/3}$

$i_r = 4870.3$ psi-ms

Step 2. a. $W_F = 10.0$ lb/ft^2 (given)

b. $W = 3.750 \times 1.20 = 4{,}500$ lbs

c. Calculate $W_F/W^{1/6}$ ratio:

$W_F/W^{1/6} = 10/(4500)^{1/6} = 2.46$

Step 3. Read the fictitious scaled-distance Z corresponding to $i_r/W^{1/3} = 295$ from Figure 2-7.

$Z = 0.82$ ft/lb$^{1/3}$

Step 4. From Figure 2-150 where $W_F/W^{1/6} = 2.46$ and $Z = 0.82$ read:

$f_r = 0.74$

Step 5. a. Calculate reflected impulse on the frangible back wall by multiplying the value of impulse from step 1 and $f_r = 0.74$

i_r (frangible back wall) $= 4870.3\ (0.74) = 3604.0$ psi-ms

b. Peak reflected pressure from step 1.

$P_r = 3700$ psi

c. Calculate duration of load on wall.

$$t_o = \frac{2i_r}{P_r} = \frac{2\ (3604.0)}{3700} = 1.95 \text{ ms}$$

Problem 2A-7 Gas Pressure

Problem: Determine the gas pressure-time loading inside a cubicle, with a small vent opening, due to an internal explosion. The vent opening may be sealed or unsealed with a frangible panel or cover.

Procedure:

Step 1. Apply a 20% factor of safety to the charge weight.

Step 2. Calculate the free volume inside the cubicle V_f.

Step 3. Determine the charge weight to free volume ratio W/V_f.

Step 4. Determine the peak gas pressure P_g from Figure 2-152 using the value of W/V_f from step 3.

Step 5. Determine vent area A.

Step 6. Determine scaled value of the vent area $A/V^{2/3}$.

Step 7. a. Calculate the unit weight of the frangible panel W_F, if any.

b. Calculate the scaled unit weight of the frangible panel or cover $W_F/W^{1/3}$. Use $W_F/W^{1/3} = 0$ for no cover.

Step 8. Determine the scaled average reflected impulse on the element containing the vent opening with no cover according to the procedure outlined in Problem 2A-4 or on the frangible panel (cover) using the procedure of Problem 2A-6.

Step 9. Determine the scaled gas impulse from Figures 2-153 to 2-164. Use the values of W/V_f from step 3, $W_F/W^{1/3}$ from step 7, $A/V^{2/3}$ from step 6 and $i_r/W^{1/3}$ from step 8. Interpolate for values of W/V_f and $i_r/W^{1/3}$ if required. Multiply by $W^{1/3}$ to calculate gas impulse.

Step 10. Calculate the fictitious gas duration using equation 2-4 and values of P_g and i_g from steps 4 and 9 respectively.

Example 2A-7 (A) Gas Pressure (Small Vent Opening)

Required: Gas pressure-time loading inside a 10' x 10' x 10' cubicle with a 2' x 2' vent opening on the rear wall. The charge weight is 833.3 pounds.

Solution:

Step 1. Charge weight:

$W = 833.3 \times 1.20 = 1{,}000$ lbs

Step 2. Free volume inside the structure:

$V_f = 10' \times 10' \times 10' = 1{,}000\ ft^3$

Step 3. Charge weight to free volume ratio:

$W/V_f = 1000.0/1000.0 = 1.0$

Step 4. Read P_g from fig. 2-152 for $W/V_f = 1.0$.

$P_g = 2{,}650$ psi

Step 5. Vent area of 2' x 2' opening:

$A = 2' \times 2' = 4\ ft^2$

Step 6. Calculate scaled vent area:

$A/V^{2/3} = 4/1000^{2/3} = .04\ \ ft^2/ft^2$

Step 7. a. Vent has no cover.

b. Scaled weight of the cover:

$W_F/W^{1/3} = 0$

Step 8. Scaled average reflected impulse of the rear wall from procedure outlined in problem 2A-4:

$i_r/W^{1/3} = 1225$ psi-ms/lb$^{1/3}$

Step 9. Read scaled gas impulse from Figures 2-162 to 2-164 for $A/V^{2/3} = 0.04$ and $W_F/W^{1/3} = 0.0$. Interpolate for scaled impulse of

$i_r/W^{1/3} = 1225.$

$i_g/W^{1/3} = 7500$ psi-ms/lb$^{1/3}$

$\therefore\ i_g = 7{,}500 \times 1{,}000^{1/3} = 75{,}000.0$ psi-ms

Step 10. Calculate fictitious duration of gas load from equation 2-4.

$$t_g = \frac{2i_g}{P_g} = \frac{2 \times 75{,}000.0}{2{,}650} = 56.6 \text{ ms}$$

Example 2A-7 (B) Gas Pressure (Frangible Wall)

Required: Gas pressure-time loading inside a 10′ x 10′ x 10′ cubicle with a frangible wall of 10 psf as the rear wall. The charge weight is 833.3 pounds.

Solution:

Step 1. Charge weight:

$W = 833.3 \times 1.2 = 1{,}000$ lbs

Step 2. Free volume inside the structure:

$V_f = 10' \times 10' \times 10' = 1{,}000\ ft^3$

Step 3. Charge weight to free volume ratio:

$W/V_f = 1000/1000 = 1.0$

Step 4. Read P_g from fig. 2-152 for $W/V_f = 1.0$.

$P_g = 2650$ psi

Step 5. Vent area of frangible wall:

$A = 10' \times 10' = 100\ ft^2$

Step 6. Calculate scaled vent area:

$A/V^{2/3} = 100/1000^{2/3} = 1.0\ ft^2/ft^2$

Step 7. a. Unit density of the frangible wall:

$W_F = 10.0$ lbs/ft^2 (given)

b. Scaled weight of the frangible wall:

$W_F/W^{1/3} = 10/1000^{1/3} = 1.0$

Step 8. Scaled average reflected impulse of the rear frangible wall from procedure outlined in problem 2A-6:

$i_r/W^{1/3} = 784$ psi-ms/lb$^{1/3}$

Step 9. Read scaled gas impulse from Figures 2-162 to 2-164 for $A/V^{2/3} = 1.0$ and $W_F/W^{1/3} = 1.0$. Interpolate for scaled impulse of $i_r/W^{1/3} = 784$.

$$i_g/W^{1/3} = 400.0 \quad \text{psi-ms/lb}^{1/3}$$

$$\therefore \quad i_g = 400.0 \times 1000^{1/3} = 4000 \text{ psi-ms}$$

Step 10. Calculate fictitious duration of gas load from equation 2-4.

$$t_g = \frac{2i_g}{P_g} = \frac{2 \times 4000}{2650} = 3.02 \text{ ms}$$

Problem 2A-8 Leakage Pressures from Fully Vented Three Wall Cubicle

Problem: Determine free-field blast wave parameters at a distance from a fully vented explosion inside a three wall cubicle.

Procedure:

Step 1. Determine charge weight, distance in the desired direction and volume of structure.

Step 2. Apply a 20% safety factor to the charge weight.

Step 3. Calculate scaled distance and W/V ratio.

Step 4. Determine peak positive pressures using Figures 2-168 or 2-169.

Step 5. Determine maximum peak pressure for side and back directions from Figure 2-170 using W/V ratio.

Step 6. For W/V ratio determine scaled positive impulses using Figures 2-171 to 2-182. Multiply by $W^{1/3}$ to calculate actual value of impulses.

Step 7. Determine shock parameters from Figure 2-15 corresponding to the peak pressure from step 4, except for the normal reflected impulse where the scaled impulse from step 6 should be used.

Example 2A-8 Leakage Pressures from Fully Vented Three Wall Cubicle

Required: Blast wave parameters at a distance of 200 ft. from an explosion located at the center of a three wall cubicle with no roof. The charge weight is 833.3 lbs. and the interior dimensions of the cubicle are 17.5 ft. x 17.5 ft. x 13 ft. high. Calculate the parameters at the front, side and back of the cubicle.

Solution:

Step 1. Given:

a. Charge weight = 833.3 lbs.

b. R = 200 ft. in all directions.

c. $V = 17.5 \times 17.5 \times 13 = 3.980\ ft^3$

Step 2. Calculate W:

$W = 1.20 \times \text{Charge Weight} = 1.20 \times 833.3 = 1000$ lbs.

Step 3. Calculate:

a. Scaled distance Z,

$$Z = \frac{R}{W^{1/3}} = \frac{200}{(1000)^{1/3}} = 20\ ft/lbs^{1/3}$$

b. W/V ratio,

$W/V = 1000/3.980 = 0.25\ lbs/ft^3$

Step 4. Determine peak incident pressure from Figure 2-168:

P_{so} (front) = 5.5 psi

P_{so} (side) = 4.0 psi

P_{so} (back) = 2.8 psi

Step 5. For W/V = 0.25, read the maximum peak incident pressures from Figure 2-170:

$(P_{so})_{max}$ (back and side) = 47.0 psi > 4.0 > 2.8

Step 6. Scaled positive impulse, for $Z = 20\ ft/lb^{1/3}$ and $W/V = 0.25\ lbs/ft^3$

$i_s/W^{1/3}$ (front) = 5.5 psi-ms/$lb^{1/3}$ Figure 2-171

i_s (front) = 5.5 x $1000^{1/3}$ = 55 psi-ms

$i_s/W^{1/3}$ (side) = 4.5 psi-ms/$lb^{1/3}$ Figure 2-173

i_s (side) = 4.5 x $1000^{1/3}$ = 45 psi-ms

$i_s/W^{1/3}$ (back) = 3.8 psi-ms/$lb^{1/3}$ Figure 2-175

i_s (back) = 3.8 x $1000^{1/3}$ = 38 psi-ms

Step 7. For peak positive pressures (P_{so}) read shock parameters from Figure 2-15 at front, side and back directions.

a. For P_{so} (front) = 5.5 psi (Step 4)

U = 1.28 ft/ms

$t_o/W^{1/3}$ = 2.95 ms/$lb^{1/3}$

t_o = 2.95 x $1000^{1/3}$ = 29.5 ms

$t_A/W^{1/3}$ = 7.00 ms/$lb^{1/3}$

t_A = 7.00 x $1000^{1/3}$ = 70.0 ms

b. For P_{so} (side) = 4.0 psi (Step 4)

$U = 1.24$ ft/ms

$t_o/W^{1/3} = 3.20$ ms/lb$^{1/3}$

$t_o = 3.2 \times 1000^{1/3} = 32.0$ ms

$t_A/W^{1/3} = 9.30$ ms/lb$^{1/3}$

$t_A = 9.3 \times 1000^{1/3} = 93.0$ ms

c. For P_{so} (back) = 2.8 psi

$U = 1.20$ ft/ms

$t_o/W^{1/3} = 3.45$ ms/lb$^{1/3}$

$t_o = 3.45 \times 1000^{1/3} = 34.5$ ms

$t_A/W^{1/3} = 12.90$ ms/lb$^{1/3}$

$t_A = 12.9 \times 1000^{1/3} = 129.0$ ms

Problem 2A-9 Leakage Pressure from Partially Vented Four Wall Cubicle

Problem: Determine free-field blast wave parameters at a distance from a partially vented explosion inside a four wall cubicle.

Procedure:

Step 1. Determine charge weight, distance to point in question, vent area and volume of structure.

Step 2. Apply a 20% safety factor to the charge weight.

Step 3. Calculate distance Z, $A/V^{2/3}$ ratio and $AW^{1/3}/V$ ratio.

Step 4. Determine peak positive pressure using Figure 2-184.

Step 5. Determine scaled positive impulses using Figure 2-185. Multiply by $W^{1/3}$ to calculate actual value of impulses.

Step 6. Determine shock parameters from Figure 2-15. Use the peak pressure from step 4, except for normal reflected impulse where the scaled impulse(s) from step 5 should be used.

Example 2A-9 Leakage Pressure from Partially Vented Four Wall Cubicle

Required: Blast wave parameters at distance of 200 ft. from a charge located in an above ground four wall cubicle. The circular vent is located at the center of the roof and has a diameter of 4 ft. The charge is 833.3 lbs and located at the center of 17.5' x 17.5' x 13' cubicle. Top of the roof is 15 feet above the ground level.

Solution:

Step 1. Given (see Figure 2-183b for parameters):

a. Charge weight = 833.3 lbs.

b. R = 200 ft., h = 15 ft.

$$d_1 = \left[(4/2)^2 + (15 - 13/2)^2 \right]^{1/2} = 8.73 \text{ ft.}$$

$$d_2 = (17.5 - 4)/2 = 6.75 \text{ ft.}$$

$$d_3 = \left[(15)^2 + (200 - 4/2 - 6.75 - 15)^2 \right]^{1/2} = 176.89 \text{ ft.}$$

$$R' = d_1 + d_2 + h + d_3 = 8.73 + 6.75 + 15 + 176.89 = 207.37 \text{ ft.}$$

c. $A = \pi(2)^2 = 12.57 \text{ ft}^2$

d. $V = 17.5 \times 17.5 \times 13 = 3{,}980 \text{ ft}^3$

Step 2. Calculate W:

W = 1.20 x charge weight = 1.20 x 833.3 = 1000 lbs.

Step 3. Calculate:

a. Scaled distance Z.

$$Z = \frac{R'}{W^{1/3}} = \frac{207.37}{1000^{1/3}} = 20.7 \text{ ft/lb}^{1/3}$$

b. $A/V^{2/3} = 12.57/(3980)^{2/3} = 0.05$

c. $AW^{1/3}/V = 12.57\ (1000)^{1/3}\ /3,980 = 0.0316\ lb^{1/3}/ft$

Step 4. Peak positive pressure from Figure 2-184 for Z = 20.7 and $A/V^{2/3} = .050$.

$\therefore\ P_{so} = 0.95$ psi

Step 5. Peak positive pressure impulse from Figure 2-185 for Z = 20.7 and

$AW^{1/3}/V = .0316.$

$i_s/W^{1/3} = 1.80$ psi-ms/$lb^{1/3}$

$i_s = 1.8 \times 1000^{1/3} = 18.0$ psi-ms

Step 6. For peak positive pressure $P_{so} = .95$ psi, read shock parameters from Figure 2-15.

$U = 1.12$ ft/ms

$t_o/W^{1/3} = 4.5$ ms/$lb^{1/3}$

$t_o = 4.5 \times 1000^{1/3} = 45.0$ ms

$t_A/W^{1/3} = 35.0$ ms/$lb^{1/3}$

$t_A = 35.0 \times 1000^{1/3} = 350.0$ ms

Problem 2A-10 External Blast Loads on Structures

Problem: Determine the pressure-time blast loading curves on a rectangular structure from an external explosion.

Procedure:

Step 1. Determine the charge weight, ground distance R_G, height of burst H_c (for air burst) and structure dimensions.

Step 2. Apply a 20% safety factor to the charge weight.

Step 3. Select several points on the structure (front wall, roof, rear wall, etc.) and determine free-field blast wave parameters for each point. For air burst, follow the procedure outlined in problem 2A-2; a surface burst, problem 2A-3; and leakage pressures, problem 2A-8 or 2A-9.

Step 4. For the front wall:

a. Calculate peak positive reflected pressure $P_{r\alpha} = C_{r\alpha} \times P_{so}$. Read value of $C_{r\alpha}$ for P_{so} and α from Figure 2-193.

b. Read scaled unit positive reflected impulse $i_{r\alpha}/W^{1/3}$ from Figure 2-194 for P_{so} and α. Multiply scaled value by $W^{1/3}$ to obtain absolute value.

Note: If wave front is not plane, use average values.

Step 5. Determine positive phase of front wall loading.

a. Determine sound velocity in reflected overpressure region C_r from Figure 2-192 for peak-incident pressure P_{so}.

b. Calculate clearing time t_c:

$$t_c = \frac{4S}{(1 + R)\, C_r} \text{ (ms)} \qquad \text{(eq. 2-3)}$$

where:

S = height of front wall or one-half its width, whichever is smaller.

G = maximum of wall height or one-half its width

R = S/G

c. Calculate fictitious positive phase duration t_{of}:

$$t_{of} = \frac{2i_s}{P_{so}} \qquad \text{(eq. 2-6)}$$

d. Determine peak dynamic pressure q_o from Figure 2-3 for P_{so}.

e. Calculate $P_{so} + C_D q_o$. Obtain C_D from paragraph 2-15.3.2.

f. Calculate fictitious duration t_{rf} of the reflected pressure.

$$t_{rf} = \frac{2i_{r\alpha}}{P_{r\alpha}} \qquad \text{(eq. 2-11)}$$

g. Construct the positive pressure-time curve of the front wall similar to Figure 2-191. The actual loading is the smaller of the impulse (area under curve) due to reflected pressure or cleared reflected pressure plus incident pressure.

Step 6. Determine negative phase of the front wall loading.

a. Read the values of Z from Figure 2-15 for the value of $P_{r\alpha}$ from step 4a and $i_{r\alpha}/W^{1/3}$ from step 4b.

b. Determine $P_{r\alpha}^-$ and $i_{r\alpha}^-/W^{1/3}$ from Figure 2-16 for the corresponding values of Z from step 6a. Multiply scaled value of the negative impulse by $W^{1/3}$ to obtain absolute value.

c. Calculate the fictitious duration of the negative reflected pressure.

$$t_{rf}^- = 2i_{r\alpha}^-/P_{r\alpha} \qquad \text{(eq. 2-7)}$$

d. Calculate rise time of the negative pressure by multiplying t_{rf}^- by 0.27 (Section 2-15.3.2).

e. Construct the negative pressure-time curve similar to Figure 2-191.

Step 7. Determine positive phase of side wall loading.

a. Calculate the wave length to span length ratio L_{wf}/L at front of the span.

b. Read values of C_E, $t_d/W^{1/3}$ and $t_{of}/W^{1/3}$ from Figures 2-196, 2-197 and 2-198 respectively.

c. Calculate P_R, t_r and t_o.

d. Determine dynamic pressure q_o from Figure 2-3 for P_R.

e. Calculate $P_R = C_E P_{sof} + C_D q_o$ (eq. 2-12). Obtain C_D from paragraph ???

f. Construct positive phase pressure-time curve similar to Figure 2-195.

Step 8. Determine negative phase of side wall loading.

a. Determine value of C_E^- and $t_{of}^-/W^{1/3}$ for the value of L_{wf}/L from step 7a from Figures 2-196 and 2-198 respectively.

b. Calculate $P_r = C_E \times P_{sof}$ and t_{of}.

c. Calculate rise time of negative phase equal to 0.27 t_{of} (section 2-15.3.2).

d. Construct the negative pressure-time curve similar to Figure 2-195.

Step 9. Determine roof loading. Follow procedure outlined for side wall loading.

Step 10. Determine rear wall loading. Follow procedure outlined for side wall loading. For the purpose of calculations, assume that the back wall is rotated to a horizontal position (see Figure 2-199).

Example 2A-10 External Blast Loads on Structures

Required: Determine pressure-time blast loading curves for the front wall, roof, rear half of the side walls and rear wall of the structure shown in Figure 2A-9 for a surface burst of 5,000 lbs. at a distance from the front wall of 155 ft. Structure width is 30 ft. and the shock front is plane.

Step 1. Given: Charge weight = 5,000 lbs., R_G = 155 ft.

Step 2. W = 1.2 (5,000) = 6,000 lbs.

Step 3. Determine free-field blast wave parameters P_{so}, t_A, L_w and t_o at points 1 through 3 and i_s at point 1.

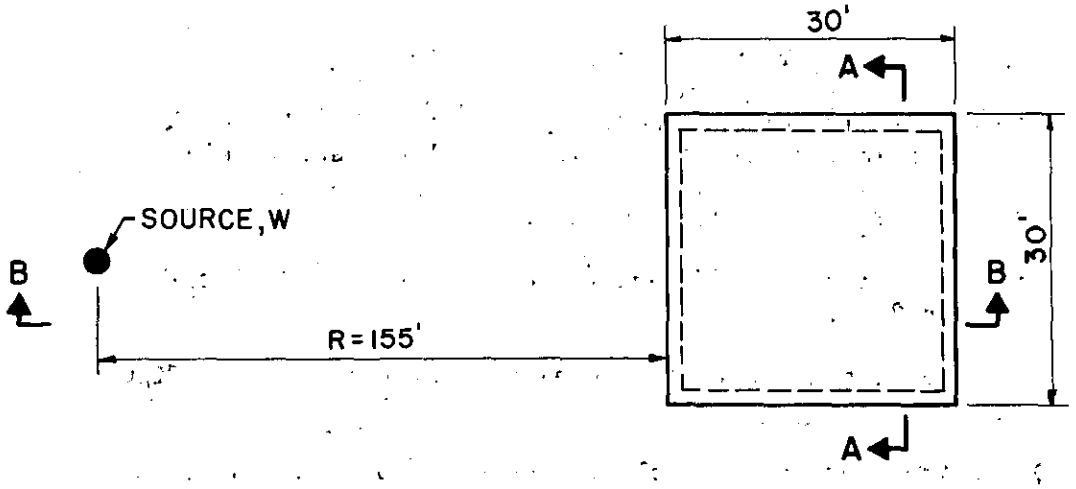
For point 1:

a. $$Z_G = \frac{R_G}{W^{1/3}} = \frac{155}{6000^{1/3}} = 8.53 \text{ ft/lb}^{1/3}$$

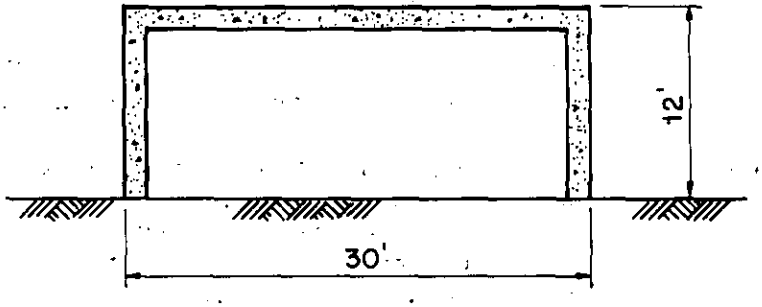
b. Determine free-field blast wave parameters from Figure 2-15 for $Z_G = 8.53$ ft/lb$^{1/3}$

$P_{so} = 12.8$ psi

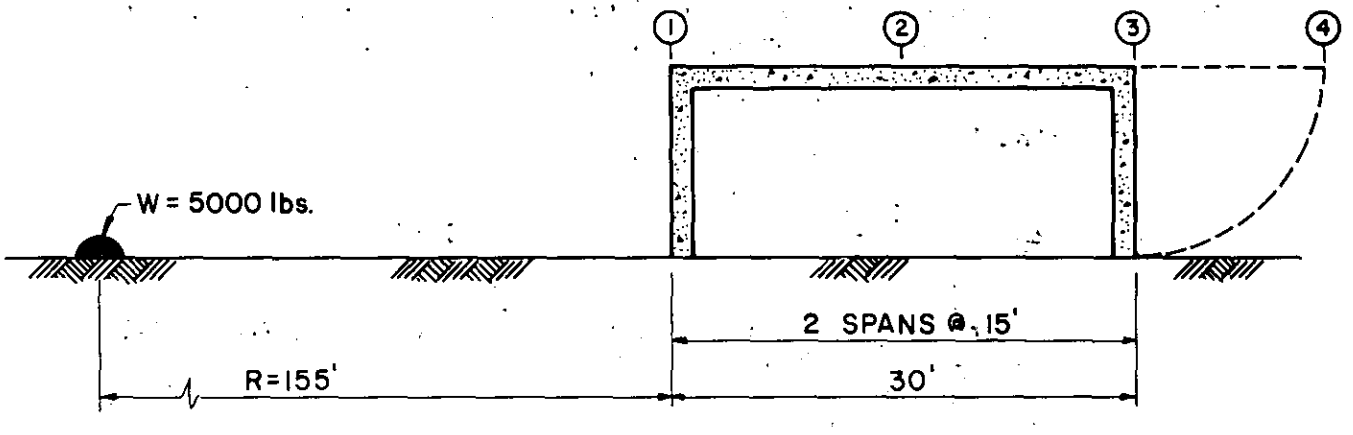
$t_A/W^{1/3} = 3.35$ ms/lb$^{1/3}$ $\therefore$ $t_A = 3.35\ (6000)^{1/3} = 60.9$ ms



PLAN



SECTION A-A



SECTION B-B

FIGURE 2A-9

$L_w/W^{1/3} = 2.10$ ft/lb$^{1/3}$ $\therefore$ $L_w = 2.10\ (6000)^{1/3} = 38.2$ ft

$t_o/W^{1/3} = 2.35$ ms/lb$^{1/3}$ $\therefore$ $t_o = 2.35\ (6000)^{1/3} = 42.7$ ms

c. Determine incident impulse from Figure 2-15 for $Z_G = 8.53$ ft/lb$^{1/3}$.

$$\frac{i_s}{W^{1/3}} = 9.0 \text{ psi-ms/lb}^{1/3} \quad \therefore \quad i_s = 9.0\ (6000)^{1/3} = 163.5 \text{ psi-ms}$$

d. Repeat steps 3a and 3b for points 2 and 3. Results are tabulated below.

Point No.	R_G (ft)	Z_G (ft/lb$^{1/3}$)	P_{so} (psi)	$t_A/W^{1/3}$ (ms/lb$^{1/3}$)	t_A (ms)
1	155.0	8.53	12.8	3.35	60.9
2	170.0	9.35	10.8	3.90	70.9
3	185.0	10.18	9.0	4.60	83.6

$L_w/W^{1/3}$ (ft/lb$^{1/3}$)	L_w (ft)	$t_o/W^{1/3}$ (ms/lb$^{1/3}$)	t_o (ms)	$i_s/W^{1/3}$ (psi-ms/lb$^{1/3}$)	i_s (psi-ms)
2.10	38.2	2.35	42.7	9.00	163.5
2.24	40.7	2.48	45.1	-	-
2.35	42.7	2.62	47.6	-	-

Step 4. Determine front wall reflected pressure and impulse.

a. Read $C_{r\alpha}$ for $P_{so} = 12.8$ psi and $\alpha = 0°$ from Figure 2-193 for point 1.

$C_{r\alpha} = 2.70$ then $P_{r\alpha} = C_{r\alpha} \times P_{so} = 2.70 \times 12.8 = 34.6$ psi

b. Read $i_{r\alpha}/W^{1/3}$ for $P_{so} = 12.8$ psi and $\alpha = 0°$ from Figure 2-194 for point 1.

$i_{r\alpha}/W^{1/3} = 17.0$ then $i_{r\alpha} = 17.0\ (6{,}000)^{1/3} = 308.9$ psi-ms

Step 5. Front wall loading, positive phase.

a. Calculate sound velocity in reflected overpressure region C_r from Figure 2-192 for P_{so} = 12.8 psi.

C_r = 1.325 ft/ms

b. Calculate clearing time t_c from eq. 2-3:

$$t_c = \frac{4S}{(1 + R)C_r} \qquad \text{(eq. 2-3)}$$

where:

S = 12.0 ft < 30./2.

G = 30./2 = 15.0 ft > 12.0 ft.

R = S/G = 12./15. = .80

then:

$$t_c = \frac{4 \times 12}{(1 + 0.80)\ 1.325} = 20.1 \text{ ms}$$

c. Calculate t_{of} from eq. 2-11. Use impulse from step 3c.

$$t_{of} = \frac{2i_s}{P_{so}} = \frac{2 \times 163.5}{12.8} = 25.5 \text{ ms}$$

d. Determine q_o from Figure 2-3 for P_{so} = 12.8 psi.

q_o = 3.5 psi

e. Calculate $P_{so} + C_D q_o$:

C_D = 1.0 from section 2-15.3.2

then,

$P_{so} + C_D q_o = 12.8 + (1.0 \times 3.5) = 16.3$ psi

f. Calculate t_{rf} from eq. 2-11 and results of step 4.

$$t_r = \frac{2i_{r\alpha}}{P_{r\alpha}} = \frac{2 \times 308.9}{34.6} = 17.9 \text{ ms}$$

g. Construct the pressure time curve. See Figure 2A-10.

Note: The reflected pressure-time curve is used for design since the reflected impulse is less than the impulse produced by the clearing time.

Step 6. Negative phase loading, front wall.

a. Read the values of Z corresponding to $P_{r\alpha} = 34.6$ (step 4a) and $i_{r\alpha}/W^{1/3} = 17.0$ (step 4b) from Figure 2-15.

$P_{r\alpha} = 34.6$ then, $Z\ (P_{r\alpha}) = 8.5$

$i_{r\alpha}/W^{1/3} = 17.0$ then, $Z\ (i_{r\alpha}/W^{1/3}) = 10.4$

b. Using the Z values from step 6a and Figure 2-16 determine values of $P_{r\alpha}^-$ and $i_{r\alpha}^-$ (Peak pressure and impulse in negative phase).

$Z(P_{r\alpha}) = 8.5$ then, $P_{r\alpha} = 3.25$ psi

$Z(i_{r\alpha}/W^{1/3}) = 10.4$ then, $i_{r\alpha}^-/W^{1/3} = 14.6$ psi-ms/lb$^{1/3}$

and

$$i_{r\alpha} = 14.6 \times (6{,}000)^{1/3} = 265.3 \text{ psi-ms}$$

c. Calculate fictitious duration t_{rf}^-.

$$t_{rf}^- = \frac{2\ i_{r\alpha}^-}{P_{r\alpha}^-}$$

$$t_{rf}^- = \frac{2 \times 265.3}{3.25} = 163.3 \text{ ms}$$

d. Calculate negative phase rise time:

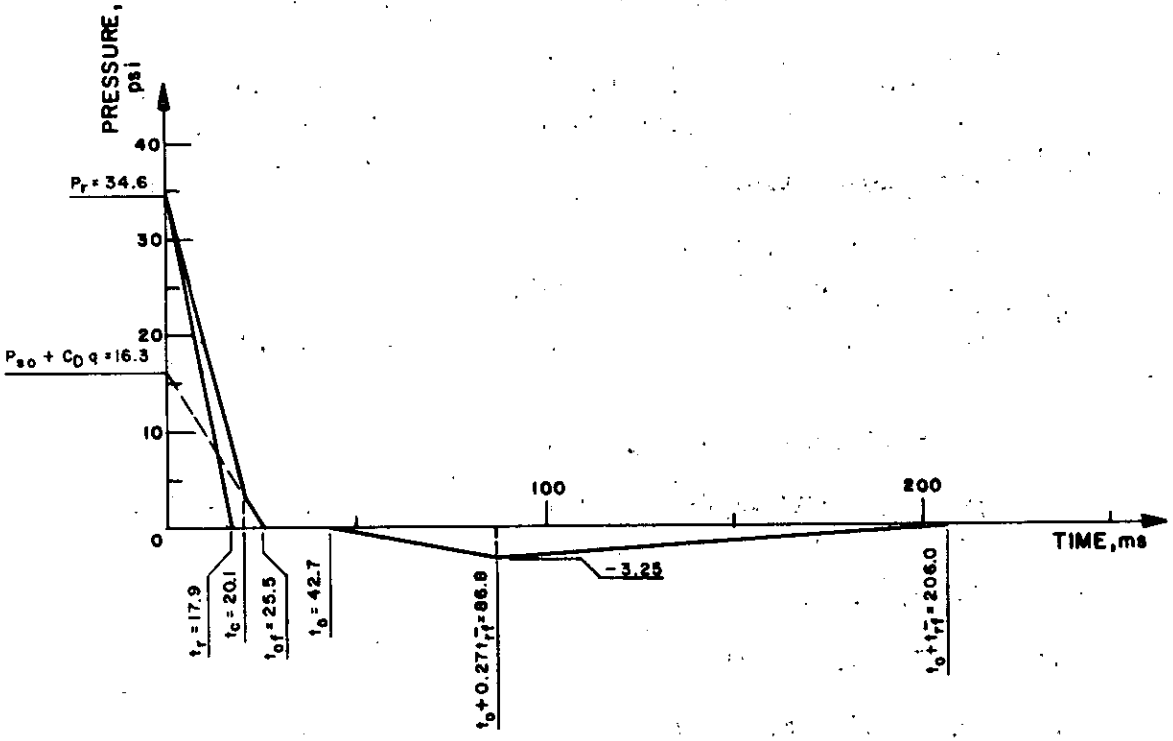

PRESSURE, psi
40
30
20
10
0
P_r = 34.6
$P_{so} + C_D q$ = 16.3
100
200
TIME, ms
-3.25
t_r = 17.9
t_c = 20.1
t_{of} = 25.5
t_o = 42.7
$t_o + 0.27 t_{rt}^2$ = 86.8
$t_o + t_{rt}^2$ = 206.0

FIGURE 2A-10

$0.27 \times t_{rf}^{-} = .27 \times 163.3 = 44.1$ ms

e. Construct the negative pressure-time curve.

$t_o = 42.7$ ms (Point 1, step 3d)

$t_o + 0.27\ t_{rf}^{-} = 42.7 + 44.1 = 86.8$ ms

$t_o = t_{rf}^{-} = 42.7 + 163.3 = 206.0$ ms

The negative pressure-time curve is plotted in Figure 2A-10.

Step 7. Side wall loading, positive phase, calculate the loading on the rear-half of the wall (Point 2 to 3, Figure 2A-9).

a. Calculate L_{wf}/L ratio:

$L = 15.0$ ft (Point 2 to 3)

$L_{wf} = 40.7$ ft (step 3d)

then,

$L_{wf}/L = 40.7 / 15.0 = 2.71$

b. Read $C_E, t_d/W^{1/3}$ and $t_{of}/W^{1/3}$ for $L_{wf}/L = 2.71$ and $P_{sof} = 10.8$ (step 3d, Point 2)

$C_E = .76$ fig. 2-196

$t_d/W^{1/3} = .66$ fig. 2-197

$t_{of}/W^{1/3} = 2.47$ fig. 2-198

c. Calculate $C_E P_{sof}$, t_d and t_{of} using results of step 7b.

$C_E P_{sof} = .76 \times 10.8 = 8.2$

$\therefore t_r = .66 \times (6{,}000)^{1/3} = 12.0$ ms

$\therefore t_{of} = 2.47 \times (6{,}000)^{1/3} = 44.9$ ms

d. Determine q_o from Figure 2-3 for $C_E P_{sof} = 8.2$ psi.

$q_o = 1.55$ psi

e. Calculate peak positive pressure from eq. 2-12.

$C_D = -0.40$ from section 2-15.3.2

$C_E P_{sof} + C_D q_o = .76 \times 10.8 + (-0.40 \times 1.55) = 7.6$ psi

f. Construct the pressure-time curve.

See Figure 2A-11 below.

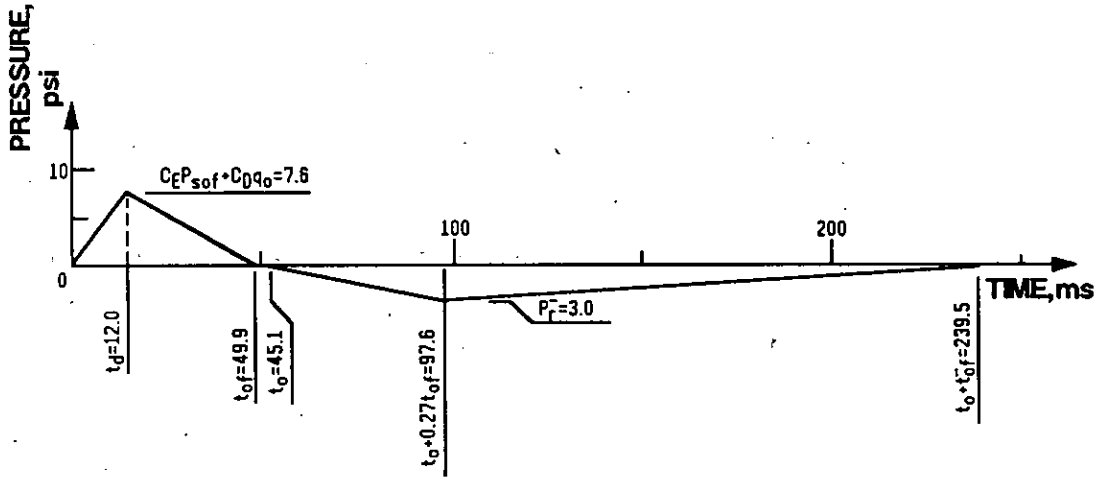


Figure 2A-11

Step 8. Negative phase loading on the rear-half of the side wall.

a. Read values of C_E^- and $t_{of}^-/W^{1/3}$ for $L_{wf}/L = 2.71$ (Step 7a) from Figures 2-196 and 2-198 respectively.

$C_E^- = .28$

$t_{of}^-/W^{1/3} = 10.7$ ms/lb$^{1/3}$

b. Calculate P_r^- and t_{of}^-:

$P_r^- = C_E^- \times P_{sof} = .28 \times 10.8 = 3.0$ psi

$t_{of}^- = 10.7 \times (6{,}000)^{1/3} = 194.4$ ms

c. Negative phase rise time:

$0.27\ t_{of}^- = .27 \times 194.4 = 52.5$ ms

d. Construct the negative pressure-time curve.

$t_o = 45.1$ ms (Point 2, step 3d)

$t_o + 0.27\ t_{of} = 45.1 + 52.5 = 97.6$ ms

$t_o + t_{of} = 45.1 + 194.4 = 239.5$ ms

The negative pressure-time curve is plotted in Figure 2A-11.

Step 9. Calculate roof loading. (Point 1 to 3, Figure 2A-9)

a. Calculate L_{wf}/L ratio:

$L = 30.0$ ft (Point 1 to 3)

$L_{wf} = 38.2$ ft (step 3d) then,

$L_{wf}/L = 38.2/30.0 = 1.27$

b. Read C_E, $t_d/W^{1/3}$ and $t_{of}/W^{1/3}$ for $L_{wf}/L = 1.27$ and $P_{sof} = 12.8$ psi (step 3d, Point 1) then,

$C_E = .52$ fig. 2-196

$t_d/W^{1/3} = 1.25$ fig. 2-197

$t_{of}/W^{1/3} = 3.10$ fig. 2-198

c. Calculate $C_E P_{sof}$, t_d and t_{of} using results of step 9b.

$C_E P_{sof} = .52 \times 12.8 = 6.66$

$t_d = 1.25 \times (6{,}000)^{1/3} = 22.7$ ms

$t_{of} = 3.10 \times (6{,}000)^{1/3} = 56.3$ ms

d. Determine q_o from Figure 2-3 for $C_E P_{sof} = 6.66$ psi.

$q_o = 1.05$ psi

e. Calculate maximum pressure from eq. 2-12:

$C_D = -0.40$ From section 2-15.3.2

$C_E P_{sof} + C_D q_o = .52 \times 12.8 + (-0.40 \times 1.05) = 6.24$ psi

f. Construct the pressure-time curve.

See Figure 2A-12 below.

g. Read values of C_E^- and $t_{of}^-/W^{1/3}$ for $L_{wf}/L = 1.27$ (step 9a) from Figures 2-196 and 2-198 respectively.

$C_E^- = .26$

$t_{of}^-/W^{1/3} = 11.7$ ms/lb$^{1/3}$

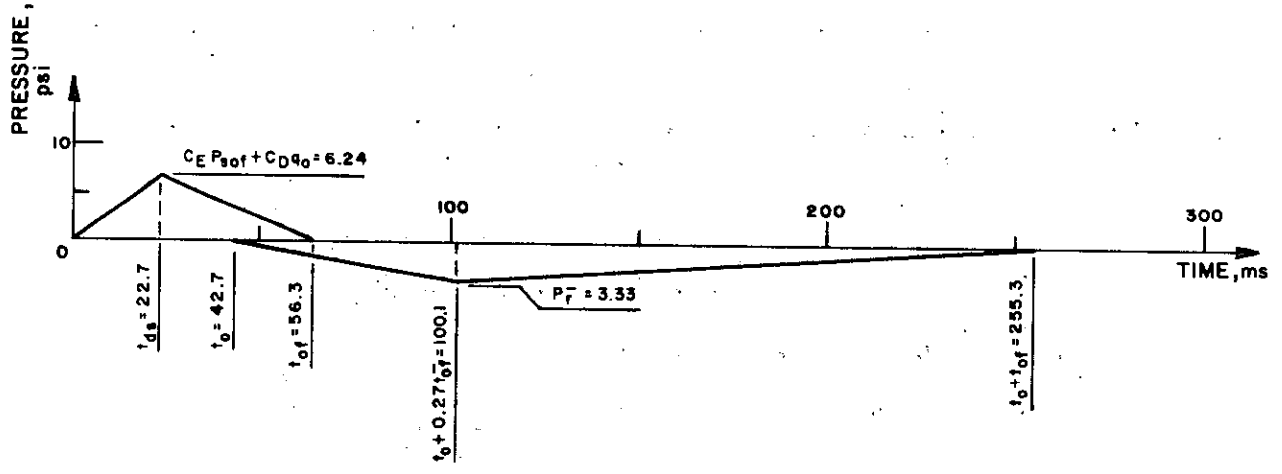

PRESSURE, psi
10
0
$C_E P_{sof} + C_D q_o = 6.24$
100
200
300
TIME, ms
$t_{ds} = 22.7$
$t_o = 42.7$
$t_{of} = 56.3$
$t_o + 0.27 t_{of} = 100.1$
$P_r = 3.33$
$t_o + t_{of} = 255.3$

FIGURE 2A-12

h. Calculate P_r^- and t_{of}^-:

$P_r^- = C_E^- \times P_{sof} = .26 \times 12.8 = 3.33$ psi

$t_{of}^- = 11.7 \times (6{,}000)^{1/3} = 212.6$ ms

i. Negative phase rise time:

$0.27\ t_{of}^- = .27 \times 212.6 = 57.4$ ms

j. Construct the negative pressure-time curve.

$t_o = 42.7$ ms (Point 1, step 3d)

$t_o + .27\ t_{of}^- = 42.7 + 57.4 = 100.1$ ms

$t_o + t_{of}^- = 42.7 + 212.6 = 255.3$ ms

The negative pressure-time curve is plotted in Figure 2A-12

Step 10. Calculate rear wall loading (Point 3 to 4, Figure 2A-9). Assume rear wall is rotated to a horizontal position.

a. Calculate L_{wf}/L ratio:

L = 12.0 ft (Point 3 to 4 or height of the structure)

$L_{wf} = 42.7$ ft (step 3d), then,

$L_{wf}/L = 42.7 / 12.0 = 3.56$

b. Read $C_E, t_d/W^{1/3}$ and $t_{of}/W^{1/3}$ for $L_{wf}/L = 3.56$ and $P_{sob} = 9.0$ psi (step 3d, point 3).

$C_E = .83$ fig. 2-196

$t_d/W^{1/3} = .51$ fig. 2-197

$t_{of}/W^{1/3} = 2.45$ fig. 2-198

c. Calculate $C_E P_{sob}$, t_r and t_o using results of step 10b.

$\therefore C_E P_{sob} = .83 \times 9.0 = 7.47$ psi

$\therefore t_d = .51 \times (6{,}000)^{1/3} = 9.3$ ms

$\therefore t_{of} = 2.45 \times (6{,}000)^{1/3} = 44.5$ ms

d. Determine q_o from Figure 2-3 for $C_E P_{sob} = 7.47$ psi

$q_o = 1.30$ psi

e. Calculate maximum pressure from eq. 2-12:

$C_D = -0.40$ from section 2-15.3.2

$C_E P_{sob} + C_D q_o = .83 \times 9.0 + (-0.40 \times 1.30) = 6.95$ psi

f. Construct the pressure-time curve.

See Figure 2A-13 below.

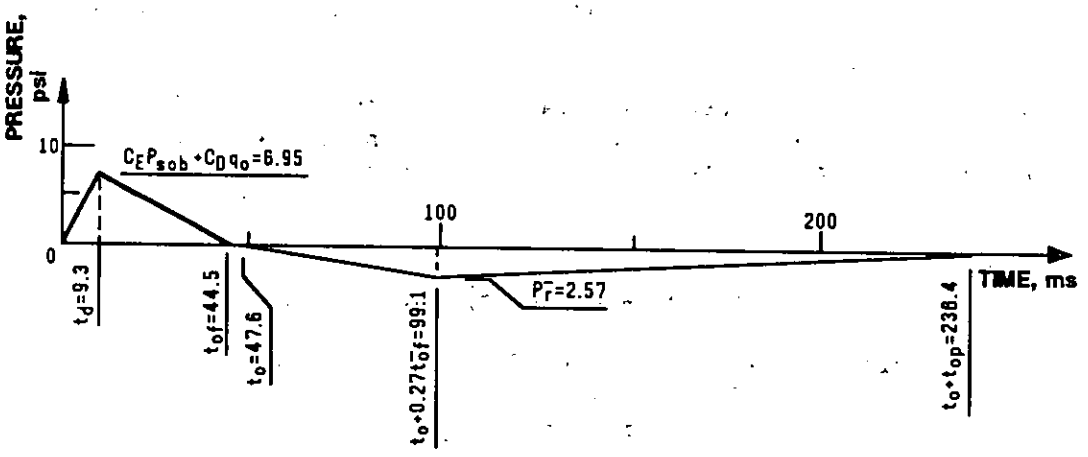


Figure 2A-13

g. Read values of C_E^- and $t_{of}^-/W^{1/3}$ for $L_{wf}/L = 3.56$ (step 10a) from Figures 2-196 and 2-198 respectively.

$C_E^- = .285$

$t_{of}^-/W^{1/3} = 10.5$ ms/lb$^{1/3}$

h. Calculate P_r^- and t_{of}^-:

$P_r^- = C_E^- \times P_{sob} = .285 \times 9.0 = 2.57$ psi

$t_{of}^- = 10.5 \times (6{,}000)^{1/3} = 190.8$ ms

i. Negative phase rise time:

$0.27\ t_{of}^- = .27 \times 190.8 = 51.5$ ms

j. Construct the negative pressure-time curve.

$t_o = 47.6$ ms (Point 3, step 3d)

$t_o + .27\ t_{of} = 47.6 + 51.5 = 99.1$ ms

$t_o + t_{of} = 47.6 + 190.8 = 238.4$ ms

The negative pressure-time curve is plotted in Figure 2A-13.

Problem 2A-11 Blast Loads on a Structure with Front Wall Openings

Problem: Determine the pressure-time loads acting on the exterior front wall and all interior surfaces of a rectangular structure with front wall openings due to an external shock load.

Step 1. Charge weight:

a. Determine TNT equivalent charge weight, W;

b. Increase charge weight by 20% safety factor, $W = 1.20 \times W$;

c. Determine charge weight scaling factor, $W^{1/3}$.

Step 2. Determine free field blast parameters:

a. For an air burst, use Problem 2A-2 procedure; for a surface burst, use Problem 2A-3 procedure; for leakage pressures, use Problem 2A-8 or 2A-9 procedures.

b. Evaluate the angle of incidence, α, as the angle between the ground distance from the charge to the center of the front wall, and the normal distance from the charge to the front wall.

Step 3. Front wall idealized pressure-time blast loads:

A. Exterior Blast Load:

a. Determine peak positive reflected pressure, P_r, as a function of P_{so} and α, using Figure 2-193.

b. Determine peak positive reflected scaled unit impulse, $i_{r\alpha}/(W^{1/3})$, as a function of P_{so} and α, using Figure 2-194.

c. Determine the absolute positive reflected impulse by multiplying the scaled unit impulse by $(W^{1/3})$.

d. Determine the sound velocity of the reflected pressure wave, C_r, as a function of P_{so}, using Figure 2-192.

e. Determine the reflected pressure clearing time, T'_c, from equation 2-14.

f. Construct the exterior blast pressure-time load. Follow the procedure in Problem 2A-10.

g. Determine the scaled wave length of the incident wave, $L_w/(W^{1/3})$ as a function of P_{so}, using Figure 2-15, irrespective of how the external incident wave was created.

h. Determine the absolute wave length by multiplying the scaled wave length by $(W^{1/3})$.

B. Interior Blast Load:

a. Determine the following parameters: L_w/L, L_w/H, A_o/A_w, W/H, and L/H, where A_o is the total area of openings in the front wall, and A_w is the area H by W.

b. Determine the idealized factored average peak pressure, (P_{max} x (L_w/H)), as a function of W/H, P_{so}, A_o/A_w, and L_w/H, using Figures 2-203 to 2-206. Calculate P_{max} = (P_{max} x L_w/H)/(L_w/H).

c. Determine the arrival time, T_1, as a function of W/H, P_{so}, and A_o/A_w, using Figures 2-207 and 2-208.

d. Determine the rise time, T_2 - T_1, as a function of W/H, P_{so}, and, L_w/H, from Figures 2-209 and 2-210.

e. Determine the duration time, T_3 - T_1, as a function of W/H, P_{so}, and L_w/H, from Figures 2-211 and 2-212.

f. Using times T_1, T_2 - T_1, T_3 - T_1, and P_{max}, construct the idealized pressure-time blast load. See Figure 2-201A for general configuration of this blast load.

Step 4. Side Wall Idealized Interior Pressure-Time Blast Load:

a. Determine the maximum average sidewall pressure, P_{max}, from equation 2-15.

b. Determine the idealized times T_1 and T_2 for W/H, using Figure 2-213.

c. Determine the idealized times T_3 and T_4 for W/H, using Figures 2-214 to 2-229.

d. Using times T_1, T_2, T_3, T_4, and P_{max}, construct the idealized pressure-time load. See Figure 2-201b for general configuration of this blast load.

Step 5. Back Wall Idealized Interior Pressure-Time Blast Load:

a. Determine the maximum average positive reflected pressure coefficient, P_{RIB}/P_{so}, as a function of L/H, P_{so}, and A_o/A_w, using Figures 2-233 and 2-234.

b. Determine the maximum average pressure, P_{RIB}, by multiplying the pressure coefficient, P_{RIB}/P_{so}, by P_{so}.

c. Determine the idealized time T_1 as a function of W/H, P_{so}, L/H, and A_o/A_w, using Figure 2-230.

d. Determine the idealized pressure duration, T_2 - T_1, as a function of P_{so}, and A_o/A_w, using Figure 2-232.

e. Using times T_1, $T_2 - T_1$, and P_{RIB}, construct the idealized pressure-time blast load. See Figure 2-201c for general configuration of this blast load.

Step 6. Roof Idealized Interior Pressure-Time Blast Load:

a. Determine the W/H ratio for the roof as the inverse of W/H ratio of the side wall.

b. Repeat Step 4 using the W/H ratio of the roof.

Example 2A-11 Blast Loads on a Structure with Front Wall Openings

Required: For the structure and charge as is shown in Figure 2A-14, determine the idealized positive external blast load on the front wall, and the idealized positive internal blast load on the front wall, side wall, roof and back wall.

Step 1. Charge weight

a. W = 5000 lbs. TNT

b. W = 1.20 x 5000 = 6000 lbs. TNT

c. $W^{1/3} = 18.1712$ $lbs^{1/3}$

Step 2. Free field blast parameters - surface burst

a. Procedure from Problem 2A-3.

Blast parameters: P_{so}, U, i_s, t_o, t_A, for W = 6000 lbs., R_G = 155' $Z_G = R_G/W^{1/3} = 155/18.1712 = 8.53$ (say 8.5)

From Figure 2-15 for hemispherical surface burst

$P_{so} = f_1(Z_G) = 12.6$ psi

$U = f_2(Z_G) = 1.46$ ft/ms

$i_s/W^{1/3}\ f_3(Z_G) = 9.0$ psi-ms/$lb^{1/3}$, $i_s = 163.54$ psi-ms

$t_o/W^{1/3} = f_4(Z_G) = 2.40$ ms/$lb^{1/3}$, $t_o = 43.61$ ms

$t_A/W^{1/3} = f_5(Z_G) = 3.40$ ms/$lb^{1/3}$, $t_A = 61.78$ ms

b. Charge to wall center ground distance = 155.0'
Charge to wall normal distance = 155.0'

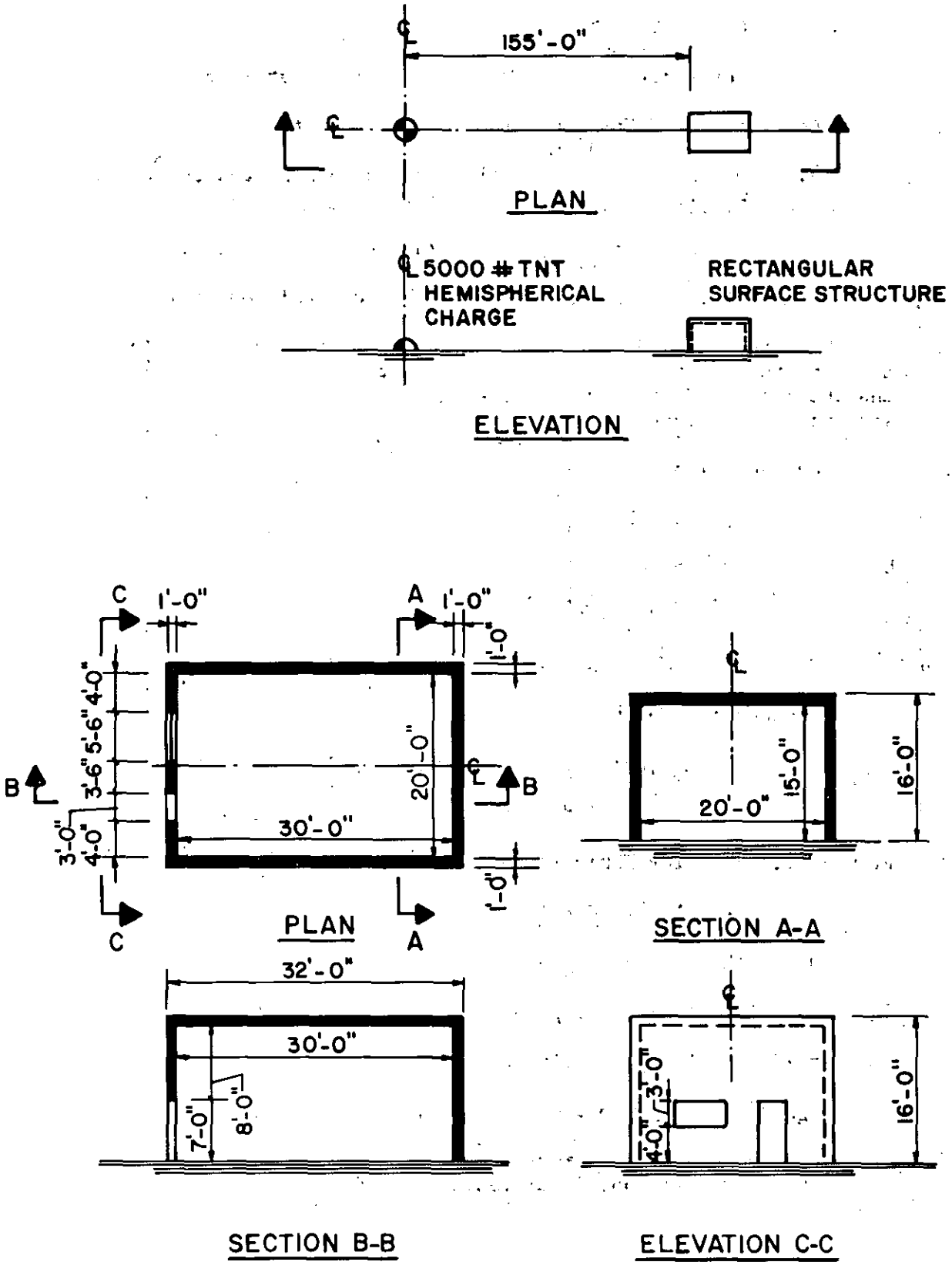
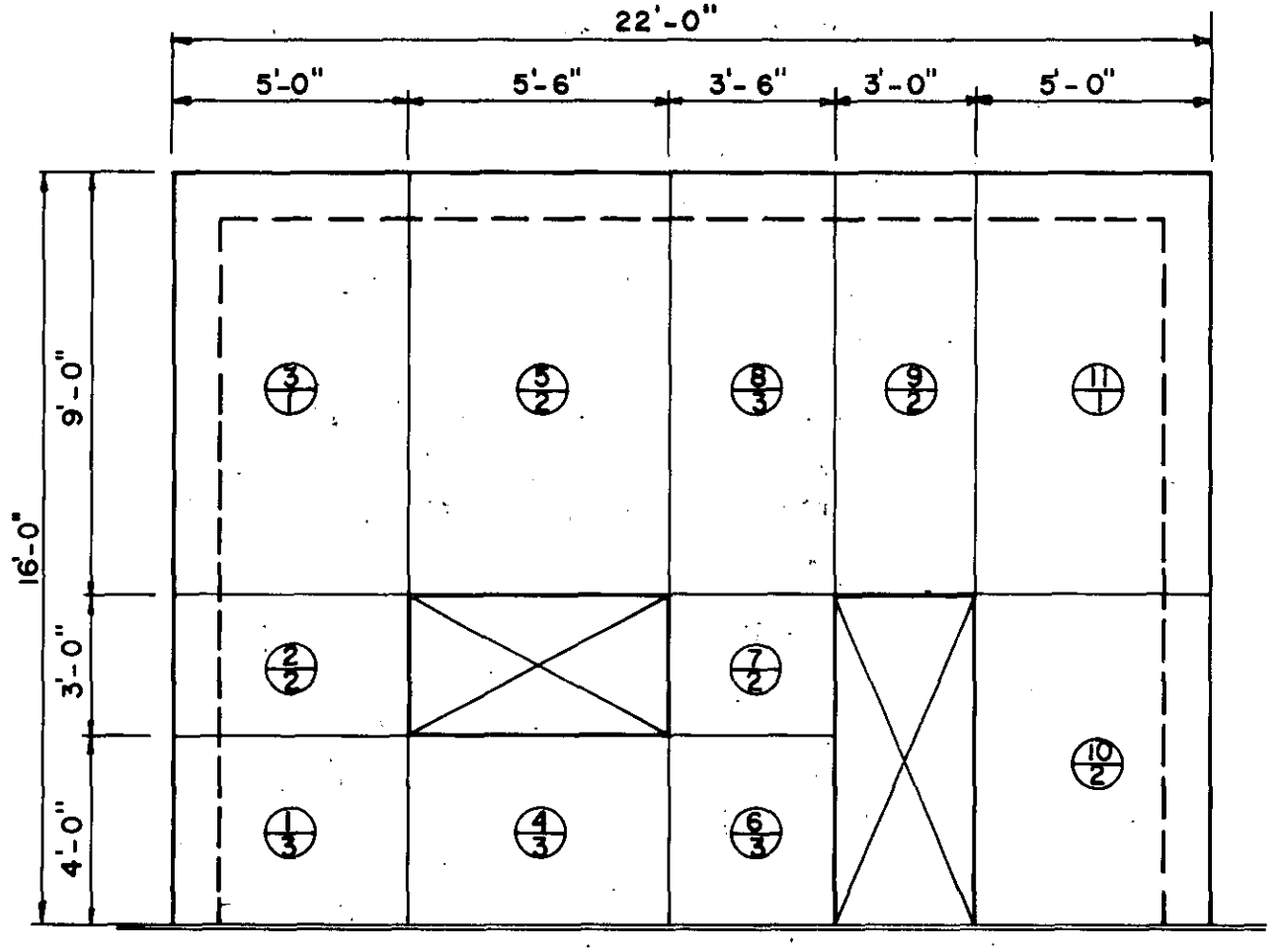
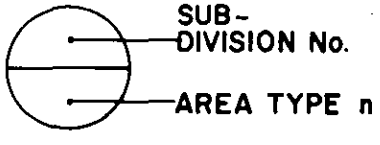

155'-0"
PLAN
5000 # TNT
HEMISPHERICAL
CHARGE
RECTANGULAR
SURFACE STRUCTURE
ELEVATION
C
1'-0"
A
1'-0"
B
3'-6"
5'-6"
4'-0"
3'-0"
4'-0"
20'-0"
30'-0"
1'-0"
PLAN
15'-0"
16'-0"
20'-0"
SECTION A-A
32'-0"
30'-0"
8'-0"
7'-0"
3'-0"
4'-0"
16'-0"
SECTION B-B
ELEVATION C-C

FIGURE 2A-14



ELEVATION



WALL SUB-DIVISION
NOMENCLATURE

FIGURE 2A-15

$\alpha = \cos^{-1}(155/155) = 0°$

Step 3. Front wall idealized pressure-time blast load

A. Exterior Blast Load

a. From Figure 2-193, for $\alpha = 0°$ and $P_{so} = 12.6$ psi, determine

$C_{r\alpha} = P_{r\alpha}/P_{so}$

P_{so}	10.0	12.6	20.0
$C_{r\alpha}$	2.40	?	2.90

$C_{r\alpha} = (2.9 - 2.4) \times (12.6 - 10.0) / (20.0 - 10.0) + 2.40$

$= 0.130 + 2.40 = 2.53$

$P_{r\alpha} = C_{r\alpha} \times P_{so} = 2.53 \times 12.6 = 31.878$ psi, say 31.9 psi

b. From Figure 2-194, for $\alpha = 0°$, read $i_{r\alpha}/W^{1/3}$ for $P_{so} = 10$ and 20 psi and interpolate for $i_{r\alpha}/W^{1/3}$ at $P_{so} = 12.6$ psi

P_{so}	$i_{r\alpha}/W^{1/3}$
psi	psi-ms/lb$^{1/3}$
10	15.2
12.6	?
20	23

$i_{r\alpha}/W^{1/3} = (23.0 - 15.2) \times (12.6 - 10.0)/$

$(20.0 - 10.0) + 15.2 = 2.028$

$+ 15.2 = 17.228$ psi-ms/lb$^{1/3}$

c. Determine absolute impulse,

$i_{r\alpha} = (i_{r\alpha}/W^{1/3}) \times (W^{1/3}) = 17.228 \times 18.1712 = 313.1$ psi-ms

d. For $P_{so} = 12.6$ psi, $C_r = 1.325$ ft/ms from Figure 2-192.

e. Using Figure 2A-15 as the front wall sub-divisioning, determine h_n, W_n, δ_n, h'_n, A_n, $\delta_n h'_n A_n$, $\Sigma \delta_n h'_n A_n$, A_f, S', S, R, and T'_c.

Subdivision No.	Type n	δ_n -	h'_n ft	h_n ft	W_n ft	A_n ft^2	$\delta_n h'_n A_n$ ft^3
1	3	1.0	5.0	4.0	5.0	20.0	100.0
2	2	0.50	5.0	3.0	5.0	15.0	37.50
3	1	1.0	5.0	9.0	5.0	45.0	225.0
4	3	1.0	4.0	4.0	5.5	22.0	88.0
5	2	0.50	9.0	9.0	5.5	49.50	222.750
6	3	1.0	3.50	4.0	3.5	14.0	49.0
7	2	0.50	3.50	3.0	3.5	10.5	18.375
8	3	1.0	9.0	9.0	3.5	31.5	283.50
9	2	0.50	9.0	9.0	3.0	27.0	121.50
10	2	0.50	5.0	7.0	3.0	35.0	87.50
11	1	1.0	5.0	9.0	3.0	45.0	225.0

$$\Sigma \delta_n h'_n A_n = \underline{1458.125}$$

$$A_f = (16 \times 32) - (3 \times 5.5) - (7.0 \times 3.0)$$

$$= 512 - 16.5 - 21.0$$

$$= 512 - 37.5$$

$$= 474.5 \text{ ft}^2$$

$$S' = \left(\sum_{1}^{11} \delta_n h'_n A_n\right)/A_f = 1458.1250/474.5 = 3.073 \text{ ft}$$

H = 15.0', W = 20.0', H < W . . S = H = 15.0', S' < S O.K.

W > H . . G = W = 20.0'

$$R = S/G = 15.0/20.0 = 0.75; C_r = 1.325 \text{ ft/ms}$$

$$t'_c = 4S'/\langle(1 + R) \times C_r\rangle = (4 \times 3.073)/(1.75 \times 1.325)$$

$$= 5.301 \text{ ms}$$

f. Following general procedure problem 2A-10, Step 5 required previously determined values are:

$$P_{so} = 12.6 \text{ psi}$$

$$i_s = 163.5 \text{ psi-ms}$$

$P_{r\alpha}$ = 31.9 psi

$i_{r\alpha}$ = 313.1 psi-ms

Determine

$t_{of} = 2i_s/P_{so}$ = 2 x 163.5/12.6 = 26 ms, Eq. 2-b,

$t_{rf} = 2i_{r\alpha}/P_{r\alpha}$ = 2 x 313.1/31.9 = 19.6 ms, eq. 2-11,

$q_o = f(P_{so})$ = 3.4 psi, Fig. 2-3

C_D = 1.0, Paragraph 2-15.3.2,

$P_{so} + C_D q_o$ = 16 psi, Paragraph 2-15.3.2

Construct infinite surface impulse and theoretic bi-linear actual surface impulse. Minimum value is design impulse.

Infinite surface fictitious impulse = $i_{r\alpha}$ = 313.1 psi-ms

Bi-linear theoretic actual surface impulse is area under curve $P_{r\alpha}$ to t'_c on line $P_{so} + C_D q_o$ to t_{of}

Let $P = (P_{so} + C_D q_o) < 1 - (t'_c/t_{of})>$

$= 16.0 < 1 - (5.3/26) > = 12.7$ psi

$i_{BL} = [<P_{r\alpha} - P><t'_c/2>] + <Pt'_c> + [<t_{of} - t'_c><P/2>]$

$= [(31.9 - 12.7)(5.3/2)] + (12.7 \times 5.3)$

$+ [<26 - 5.3><12.7/2>] = 50.9 + 67.3 + 131.4$

= 250 psi-ms

$i_{BL} < i_{r\alpha}$, use bi-linear pressure-time as design blast load.

See Figure 2A-16

g. For P_{so} = 12.6 psi, $L_w/W^{1/3}$ = 2.10 ft/lb$^{1/3}$, Fig 2-15

h. $L_w = (L_w/W^{1/3})(W^{1/3})$ = 2.10 x 18.1712 = 38.16, say 38.2 ft.

B. Interior Blast Load

a. From previous steps: L_w = 38.2 ft, L = 30 ft, H = 15 ft, W = 20 ft.

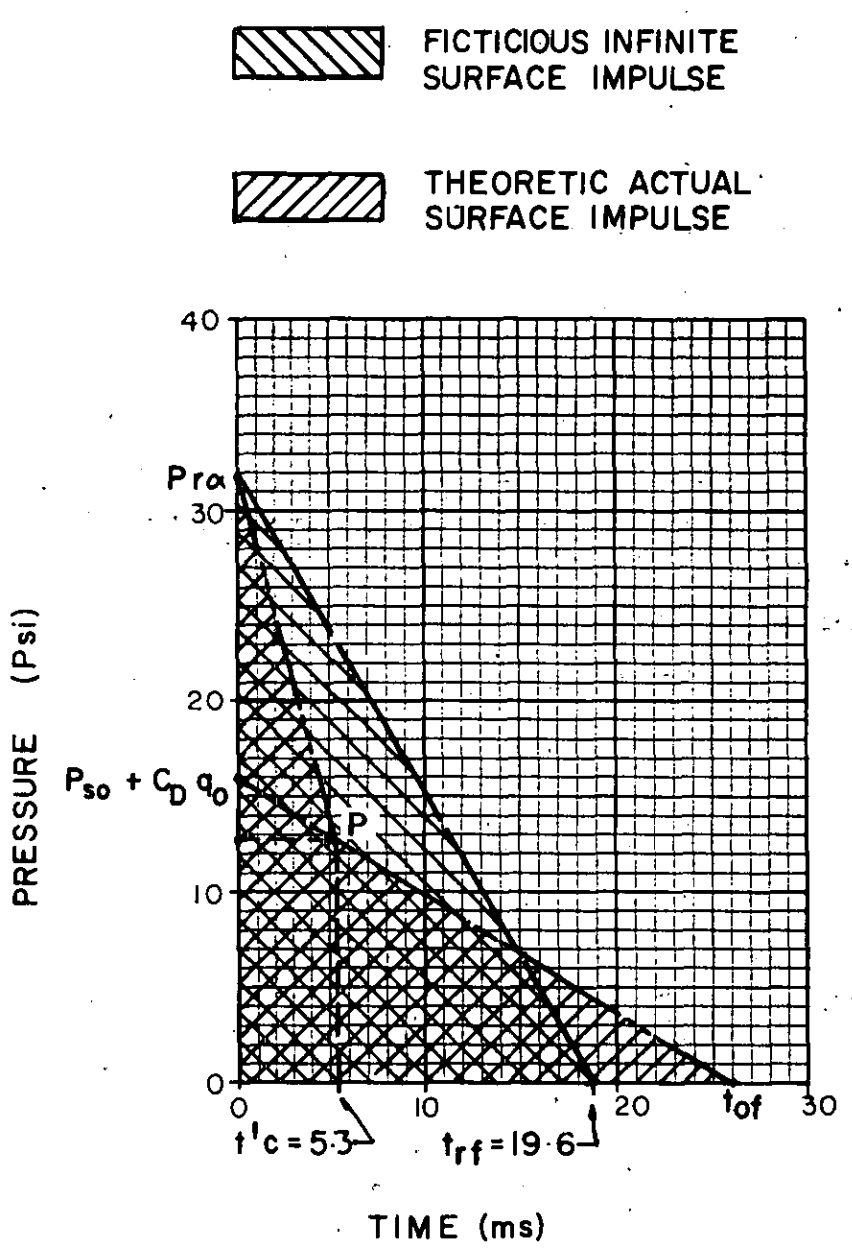

FICTICIOUS INFINITE SURFACE IMPULSE
THEORETIC ACTUAL SURFACE IMPULSE
PRESSURE (Psi)
40
30
20
10
0
Pra
Pso + CD qo
P
0
10
20
30
tof
t'c = 5.3
trf = 19.6
TIME (ms)

FIGURE 2A-16

A_o = Door opening area + window opening area

= (7 x 3) + (3 x 5.5) = 37.5 ft^2

A_w = H x W = 15 x 20 = 300 ft^2

A_o/A_w = 37.5/300 = 0.125

L_w/L = 38.2/30 = 1.27

L_w/H = 38.2/15 = 2.54

W/H = 20/15 = 1.33

L/H = 30/15 = 2.00

b. For W/H = 1.33, P_{so} = 12.6 psi, A_o/A_w = 0.125, and L_w/H = 2.54 summarize factored maximum average pressure, P_{max} x L_w/H, for W/H and L_w/H equal to .75, 1.5, 3 and 6.

Figure No.	W/H	L_w/H	P_{max} x L_w/H
2-203	0.75	0.75	15.0
		1.50	38.5
		3.0	88.0
		6.0	190.0
2-204	1.50	0.75	4.70
		1.50	17.0
		3.0	55.0
		6.0	131.0
2-205	3.0	0.75	2.0
		1.50	7.0
		3.0	27.0
		6.0	85.0
2-206	6.0	0.75	1.0
		1.50	3.20
		3.0	10.0
		6.0	35.0

Plot Figure 2A-17 (a), and interpolate to determine $P_{max} \times L_w/H$ at $L_w/H = 2.54$ for $W/H = .75$, 1.5, 3 and 6.

W/H	.75	1.5	3	6
$P_{max} \times L_w/H$	74	44	19	7.5

Plot Figure 2A-17 (b) from above values, and interpolate to determine $P_{max} \times L_w/H = 48$ for $W/H = 1.33$.

Determine $P_{max} = (P_{max} \times L_w/H)/(L_w/H) = 48/2.54 = 18.9$ psi.

c. For $P_{so} = 12.6$ psi and $A_o/A_w = 1/8$, determine T_1 for $W/H = .75$, 1.5, and 3. from Figures 2-207 and 2-208

W/H	.75	1.5	3
T_1	1.25	1.70	2.26

Plot Figure 2A-18 with above values, and determine $T_1 = 1.60$ for $W/H = 1.33$.

d. For $P_{so} = 12.6$ psi, determine $T_2 - T_1$ for W/H and $L_w/H = .75$, 1.5, and 3, from Figures 2-209 and 2-210

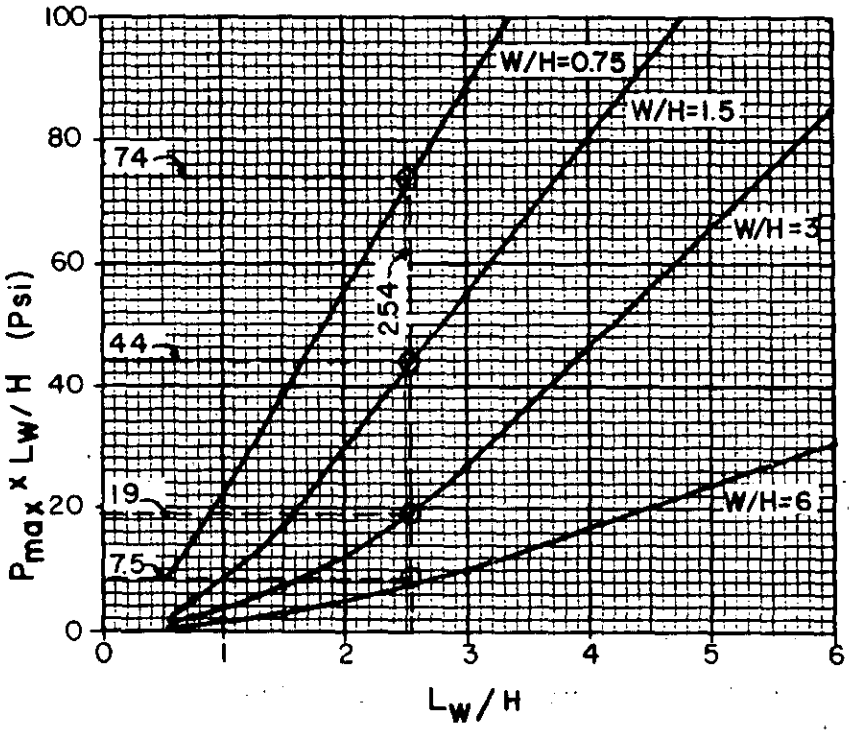
W/H	.75			1.5			3		
L_w/H	.75	1.5	3	.75	1.5	3	.75	1.5	3
$T_2 - T_1$	2.07	2.07	2.07	4.70	6.20	7.0	6.50	10.8	15.0

Plot Figure 2A-19 with above values, and interpolate to determine $T_2 - T_1$ at $L_w/H = 2.54$ for $W/H = .75$, 1.5 and 3, as summarized below.

W/H	.75	1.5	3
$T_2 - T_1$	2.07	6.75	14.0

Plot Figure 2A-19 with above values, and determine $T_2 - T_1 = 5.80$ ms for $W/H = 1.33$.

e. For $P_{so} = 12.6$ psi, determine $T_3 - T_1$ for $W/H = .75$, 1.5, and 3. and $L_w/H = .75$, 1.5, and 3, from Figures 2-211 and 2-212, as summarized below.

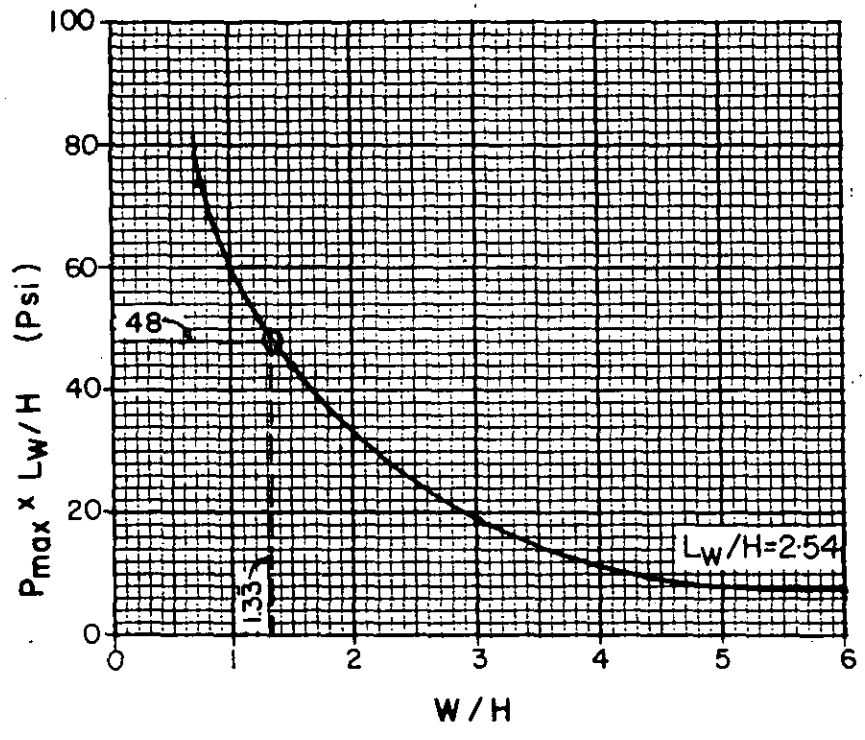


(a)

NOTE:
SEE EXAMPLE 2A-11, STEP 3, PART B, ITEM b

FOR $L_w/H = 2.54$ GRAPHIC INTERPOLATION YIELDS $P_{max}\ L_w/H = f.(W/H)$, AS SUMMARIZED BELOW.

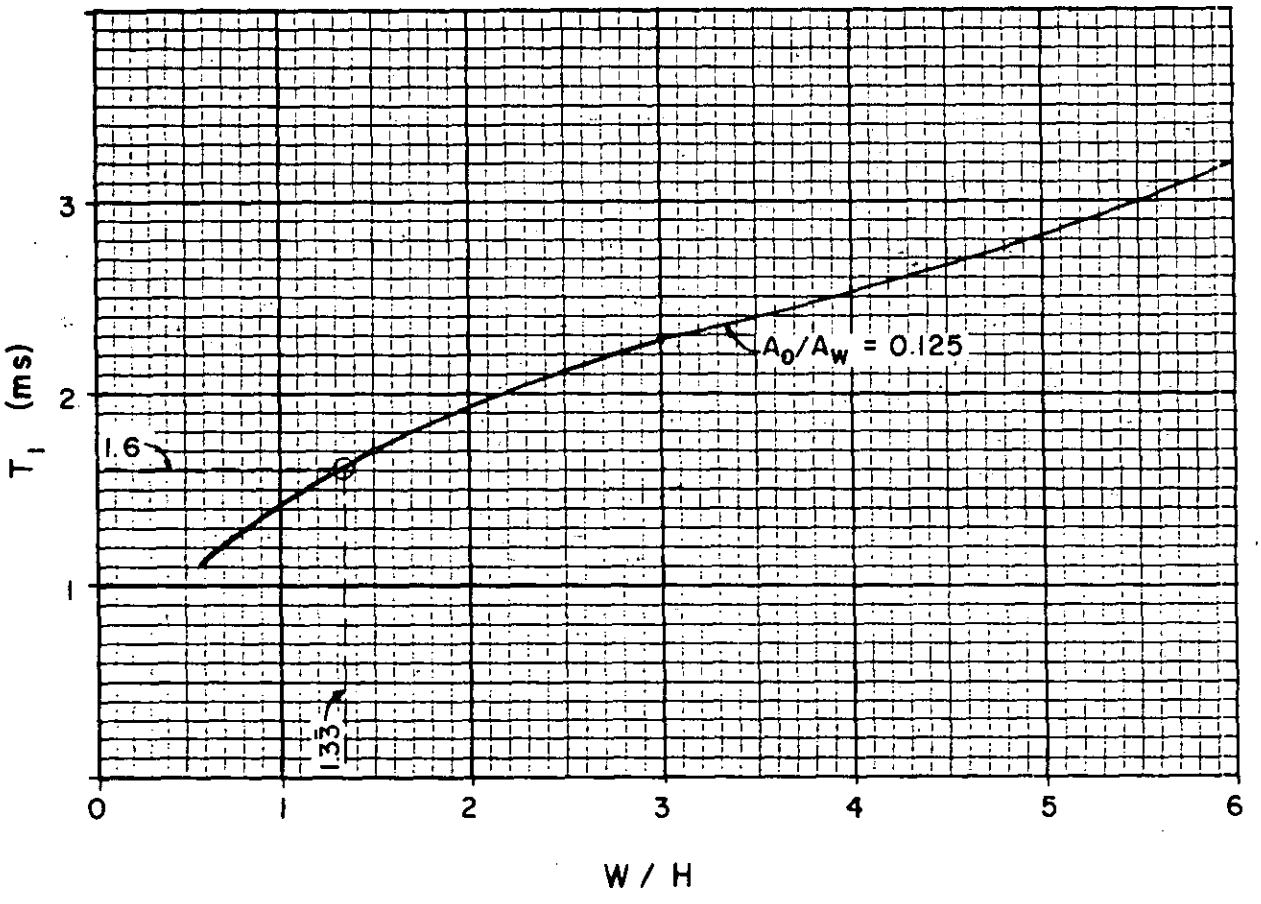
W/H	$P_{max}\ L_w/H$
0.75	74
1.5	44
3	19
6	7.5



(b)

FOR $L_w/H = 2.54$, AND $W/H = 1.33$, GRAPHIC INTERPOLATION YIELDS $P_{max}\ L_w/H = 48$

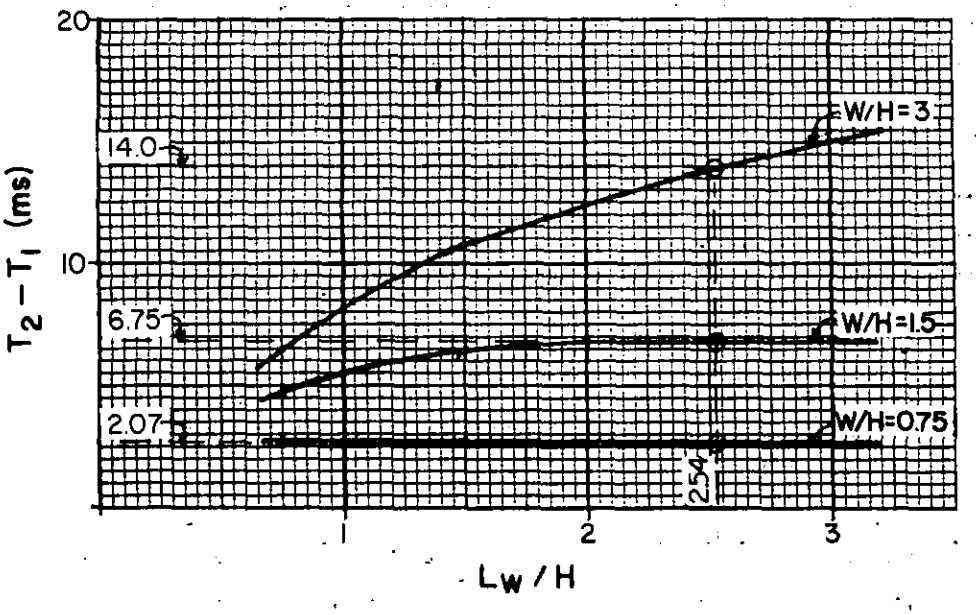
FIGURE 2A-17



NOTE:
SEE EXAMPLE 2A-11, STEP 3, PART B, ITEM c

FOR $A_0/A_W = 0.125$, FOR $W/H = 1.33$,
GRAPHIC INTERPOLATION YIELDS $T_1 = 1.60$ms

FIGURE 2A-18

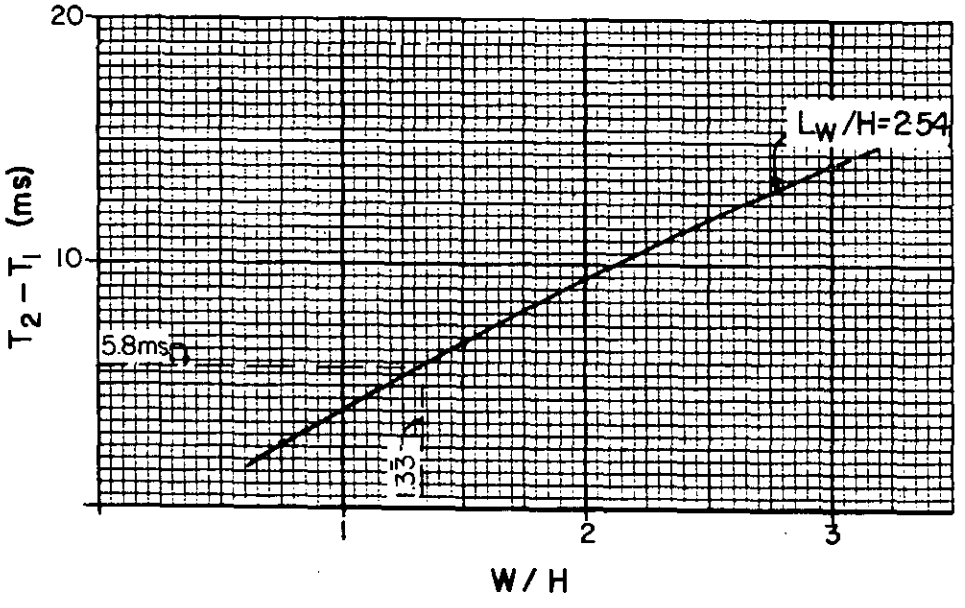


(a)

NOTE:

SEE EXAMPLE 2A-11 STEP 3, PART B, ITEM d. FOR $L_W/H = 2.54$, GRAPHIC INCORPORATION YIELDS $T_2 - T_1$ SUMMARIZED BELOW

W/H	$T_2 - T_1$
0.75	2.07
1.5	6.75
3	14.0



(b)

NOTE:

FOR W/H = 1.33
$T_2 - T_1$ = 5.8ms

FIGURE 2A - 19

W/H		.75			1.5			3	
L_w/H	.75	1.5	3	.75	1.5	3	.75	1.5	3
$T_3 - T_1$	5.2	8.2	14.5	10.0	13.5	19.5	18.6	24.8	34.8

Plot Figure 2A-20 with above values, and graphically interpolate to determine $T_3 - T_1$ at $L_w/H = 2.54$ for $W/H = .75$, 1.5, and 3, as summarized below.

W/H	.75	1.5	3
$T_3 - T_1$	12.8	17.5	31.7

Plot Figure 2A-20 with above values, and determine $T_3 - T_1 = 16.3$ ms at $W/H = 1.33$.

f. Determine times T_2 and T_3 from T_1, $T_2 - T_1$, and $T_3 - T_1$.

$T_1 = 1.60$ ms

$T_2 - T_1 = 5.80$ ms

$T_3 - T_1 = 16.30$ ms

$T_2 = 5.80 + 1.60 = 7.40$ ms

$T_3 = 16.30 + 1.60 = 17.9$ ms

Plot Figure 2A-23 using above values and $P_{max} = 18.9$ psi.

Step 4. Sidewall idealized interior pressure-time blast load.

a. Using equation 2-15, with $P_{so} = 12.6$ psi; $A_o/A_w = 1/8$, $L_w/L = 1.27$, $L/H = 2.0$, solve for P_{max} for $W/H = .75$, 1.5. and 3.

Equation 2-15: $P_{max} = K/(L_w/L)$

For $W/H = .75$, $K = A \times B \times C^E \times F^H \times P_{so}^{0.9718}$, where:

$A = [0.5422\ (L_w/L)^{1.2944}] - 0.001829 = 0.7385$

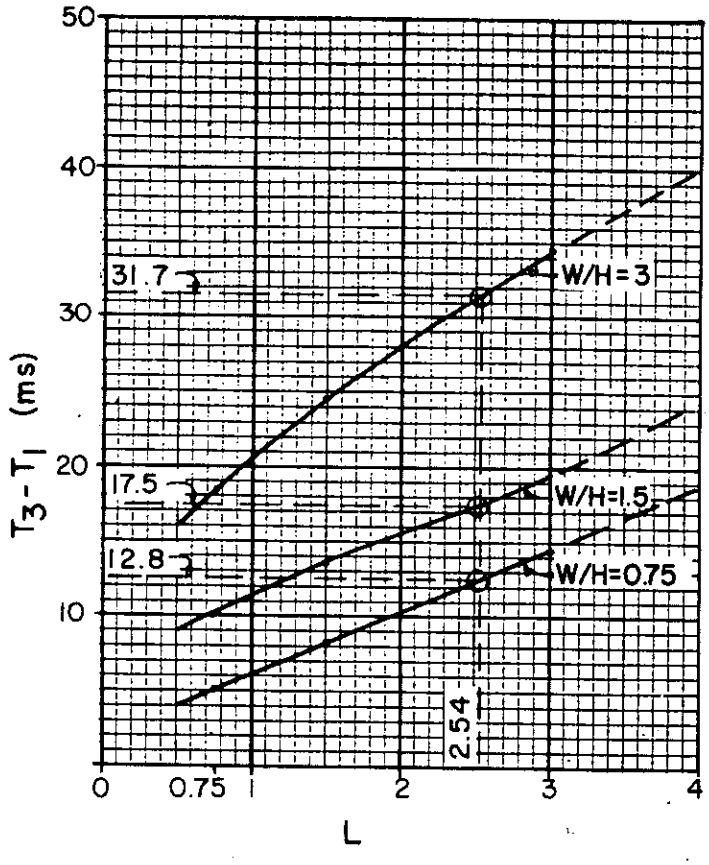
$B = [0.654 + 2.616\ (A_o/A_w) - 4.928\ (A_o/A_w)\ ]^2$

$\times\ [2.209\ (L/H)^{-0.3451} - 0.739] = 0.9040$

$C = [0.829 + 0.104\ (L_w/L)^{1.6}] + [0.00124 + 0.00414\ (L_w/L)^{3.334}]$

$\times\ [L/H]^D = 1.0388$

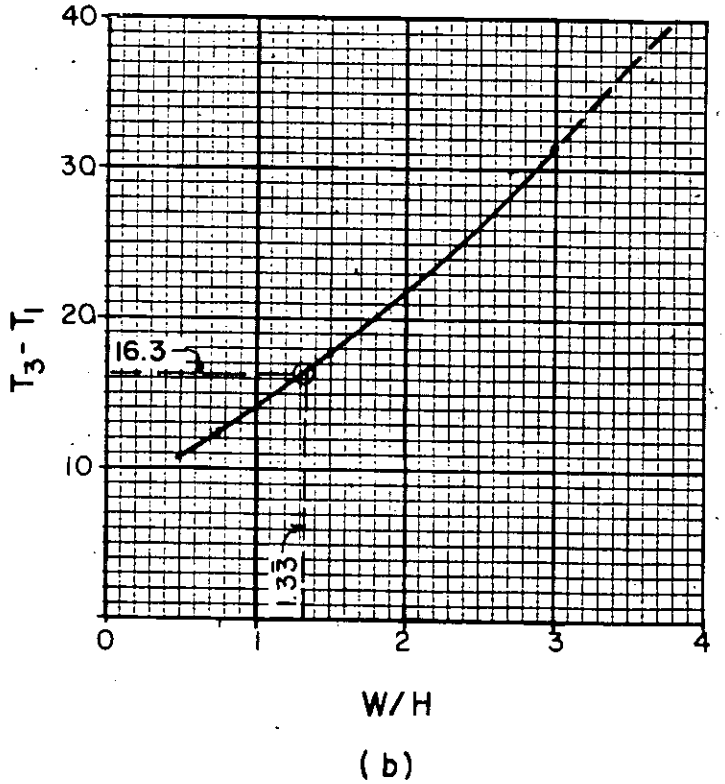
$D = 2.579 - .0534\ (L_w/L)^{3.891} = 2.4428$



(a)

NOTE:
SEE EXAMPLE 2A-11, STEP 3, PART B, ITEM e, FOR $L_W/H = 2.54$, GRAPHIC INTERPOLATION YIELDS $T_3 - T_1$ SUMMARIZED BELOW

W/H	$T_3 - T_1$
0.75	12.8
1.5	17.5
3	31.7
6	56.5



(b)

NOTE:
FOR $W/H = 1.3\bar{3}$
$T_3 - T_1 \simeq 16.3$ ms

FIGURE 2A - 20

$$E = 999\ (A_o/A_w)^{9.964} = 0.000001002$$

$$F = 1.468 - 1.6627\ (A_o/A_w)^{0.7801} + [1.8692 - 1.1735\ (A_o/A_w)^{-0.2226}] \times [L_w/L]^G = 1.1592$$

$$G = 0.2979\ (A_o/A_w)^{-1.4872} - 0.8351 = 5.7286$$

$$H = (5.425 \times 10^{-4}) + (1.001 \times 10^{-3})\ (L/H)^{9.965} = 0.0005435$$

$$K = 0.7385 \times 0.9040 \times 1.0388^{0.000001002} \times 1.1592^{0.0005435} \times 12.6^{0.9718} = 7.83$$

$P_{max} = 7.83/1.27 \approx 6.2$ psi, for $W/H = .75$

For $1.5 \leq W/H \leq 6$, $K = [A + [B \times (L_w/L)^C]] \times D \times E \times P_{so}^{1.025}$

where,

$$A = 0.002\ (W/H)^{1.4467} - 0.0213$$

$$B = 2.2075 - (1.902\ (W/H)^{-0.085})$$

$$C = 1.231 + (0.0008\ (W/H)^{2.678})$$

$$D = (2.573\ (L/H)^{-0.444}) - 0.3911$$

$$E = 0.4221 + (1.241\ (A_o/A_w)^{0.367})$$

For $W/H = 1.5$, 3, and 6, determine values for A to E, and K and P_{max}, as summarized below.

W/H	A	B	C	D	E	K	P_{max}
1.5	-0.0177	0.3700	1.2334	1.5003	1.0006	9.6743	7.60
3	-0.0115	0.4751	1.2462	1.5003	1.0006	12.690	9.98

Plot Figure 2A-21 with above values of P_{max} vs W/H = .75, 1.5, and 3, and determine P_{max} = 7.30 psi for W/H = 1.33.

b. For P_{so} = 12.6 psi, determine T_1 and T_2 for W/H = .75, 1.5, and 3 from Figure 2-213. as summarized below.

W/H	.75	1.5	3
T_1	1.82	4.95	11.7
T_2	3.20	6.50	12.5

Plot Figure 2A-21 using above values of W/H and T_1 and T_2, and determine T_1 = 4.4 ms and T_2 = 5.9 ms for W/H = 1.33.

c. For P_{so} = 12.6 psi and L/H = 2, determine T_3 and T_4 for W/H = .75, 1.5 and 3 and L_w/L = .75, 1, 1.5, and 2, from Figures 2-218 to 2-221, as summarized below:

Plot Figure 2A-21 with above values, and interpolate to determine T_3 and T_4, for $L_w/L \approx 1.27$ for W/H = .75, 1.5, and 3, as summarized below.

W/H	.75	1.5	3
T_3	35	18	24
T_4	71	71	74.5

Plot Figure 2A-21 with above values, and determine T_3 = 19 ms and T_4 = 71 ms, for W/H = 1.33.

d. For P_{max} = 7.3 psi, T_1 = 4.4 ms, T_2 = 5.9 ms, T_3 = 19 ms and T_4 = 71 ms plot Figure 2A-23.

Step 5. Back wall idealized interior pressure-time blast load.

a. For L/H = 2, P_{so} = 12.6 psi and A_o/A_w = 1/8, determine P_{RIB}/P_{so} = 0.575 from Figure 2-234.

b. $P_{RIB} = (P_{RIB}/P_{so}) \times P_{so} = 0.575 \times 12.6 = 7.5$ psi.

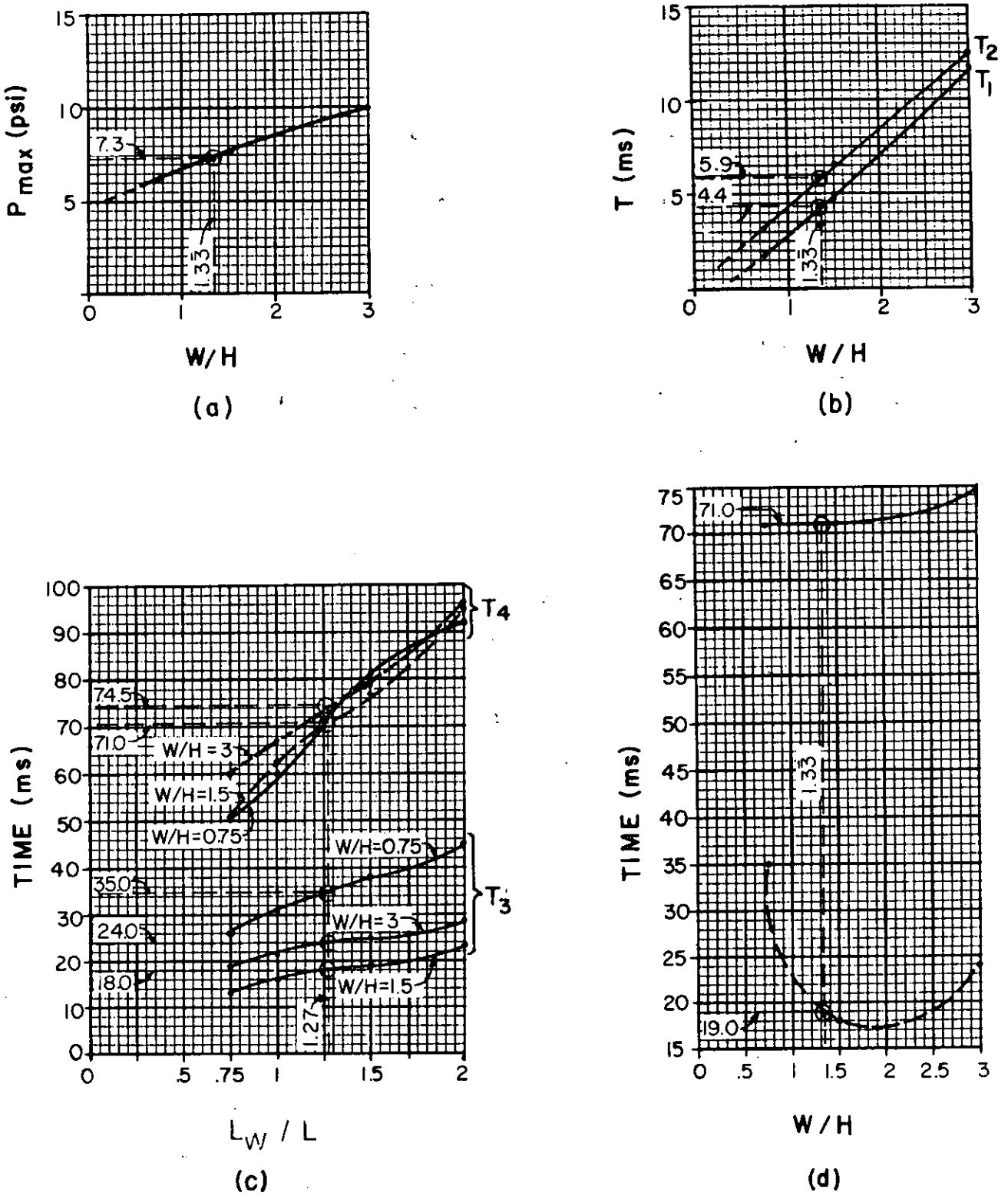

P max (psi)
15
10
5
7.3
1.33
0
1
2
3
W/H
(a)
T (ms)
15
10
5
T2
T1
5.9
4.4
1.33
0
1
2
3
W/H
(b)
TIME (ms)
100
90
80
70
60
50
40
30
20
10
0
74.5
71.0
W/H = 3
W/H=1.5
W/H=0.75
T4
T3
35.0
24.0
18.0
1.27
0
.5
.75
1
1.5
2
Lw / L
(c)
TIME (ms)
75
70
65
60
55
50
45
40
35
30
25
20
15
71.0
1.33
19.0
0
.5
1
1.5
2
2.5
3
W/H
(d)

FIGURE 2A-21

c. For P_{so} = 12.6 psi, L/H = 2, and A_o/A_w = 1/8, determine T_1 for W/H = .75, 1.5 and 3 from Figures 2-230 and 2-231, as is shown below.

W/H	.75	1.5	3
T_1	19.0	21.5	24.0

Plot Figure 2A-22 using above values, and determine T_1 = 21.1 ms for W/H = 1.33.

d. For P_{so} = 12.6 psi and A_o/A_w = 1/8, determine $T_2 - T_1$ = 2.35 ms from Figure 2-232.

Determine $T_2 = (T_2 - T_1) + T_1$ = 2.35 ms + 21.1 ms = 23.5 ms.

e. Plot Figure 2A-23 using P_{RIB} = 7.5 psi, T_1 = 21.1 ms and T_2 = 23.5 ms.

Step 6. Roof idealized interior pressure-time blast load

a. Sidewall W/H = 1-1/3 = 4/3

Roof W/H = 1/(4/3) = 3/4

b. Repeat Step 4 with W/H = 3/4

For W/H = 3/4, L/H = 2.0, A_o/A_w = 1/8, L_w/L = 1.272 and P_{so} = 12.6,

P_{max} = 6.2 psi

For W/H = 3/4 and P_{so} = 12.6 psi

T_1 = 1.82 and T_2 = 3.20 ms

For W/H = 3/4, P_{so} = 12.6 psi, and L_w/L = 1.27

T_3 = 35 and T_4 = 65 ms

Plot Figure 2A-23 with above values.

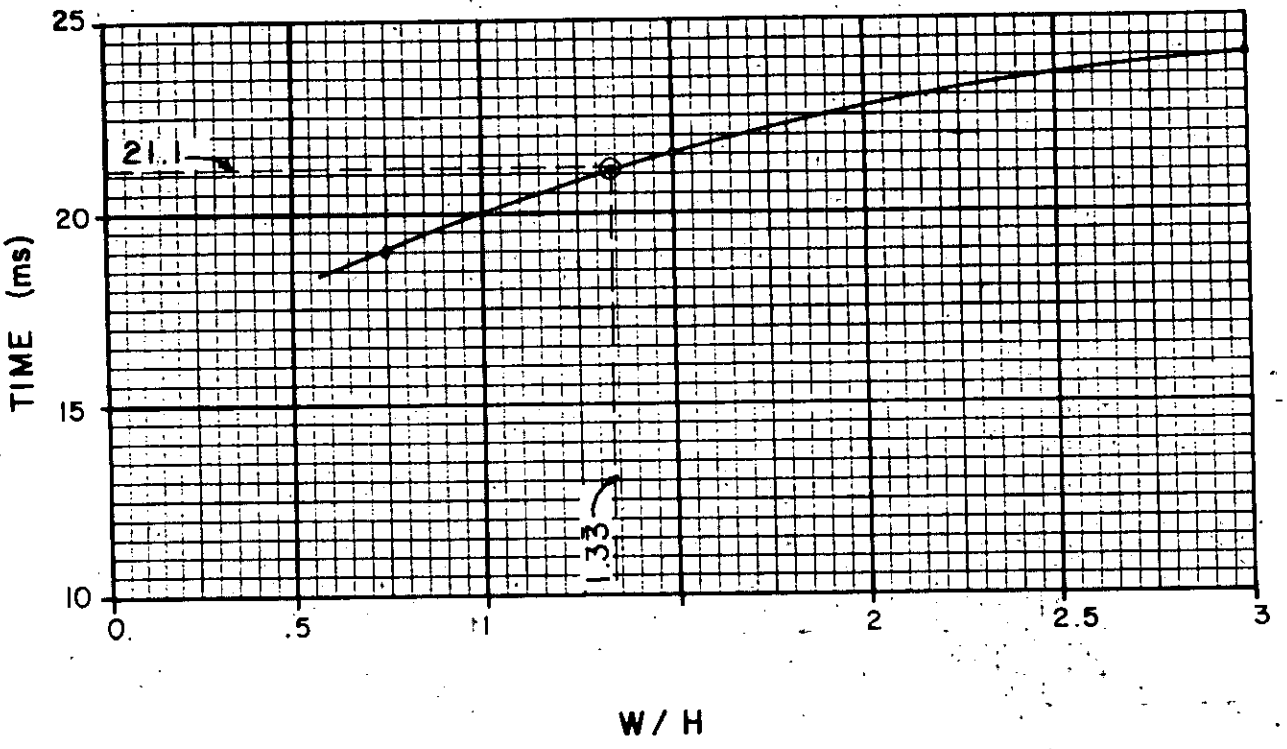
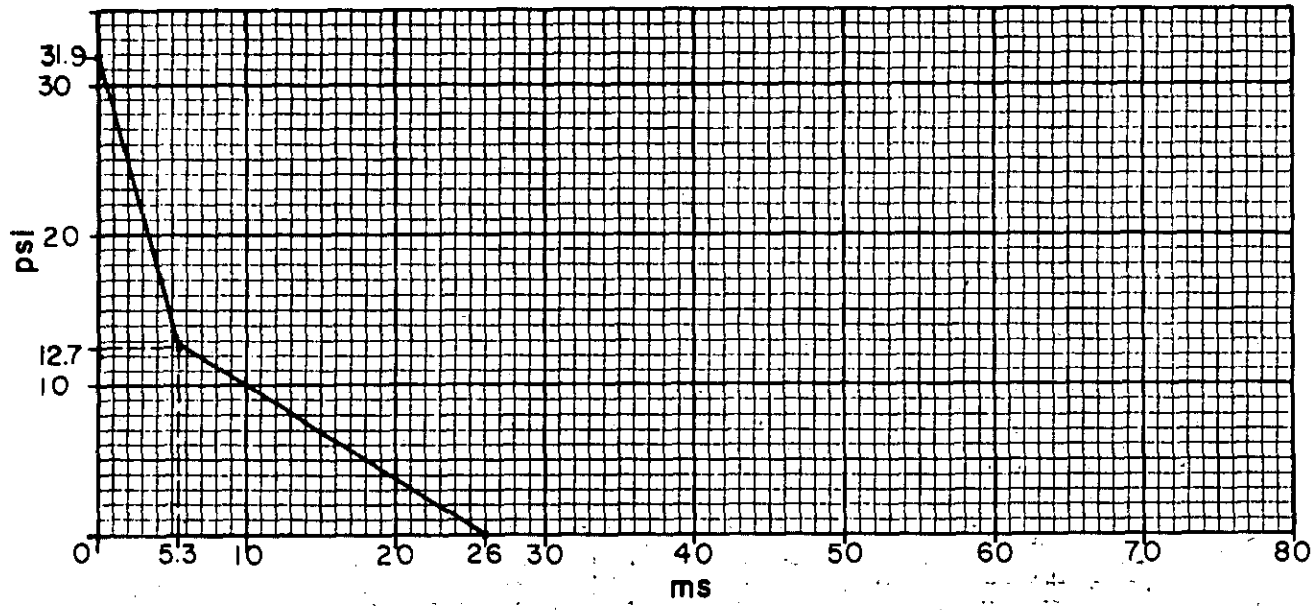
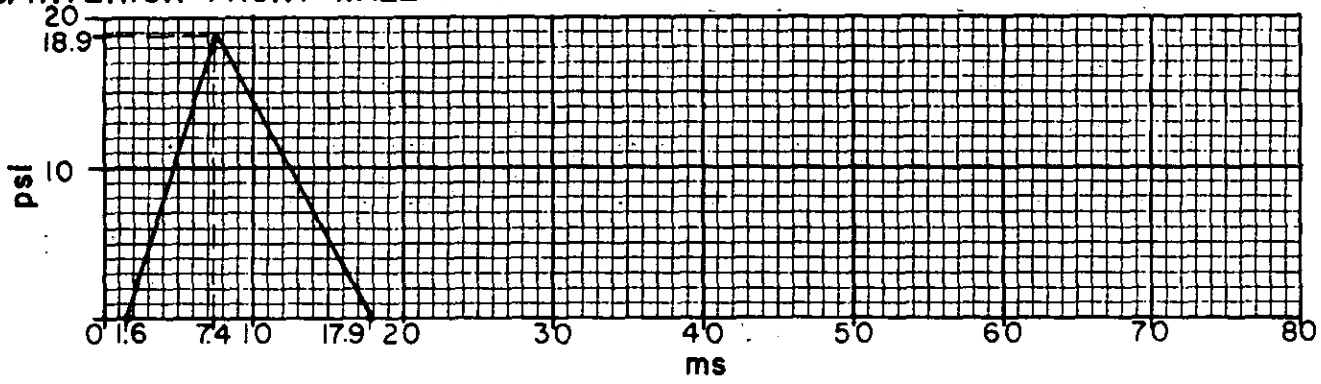


FIGURE 2A-22

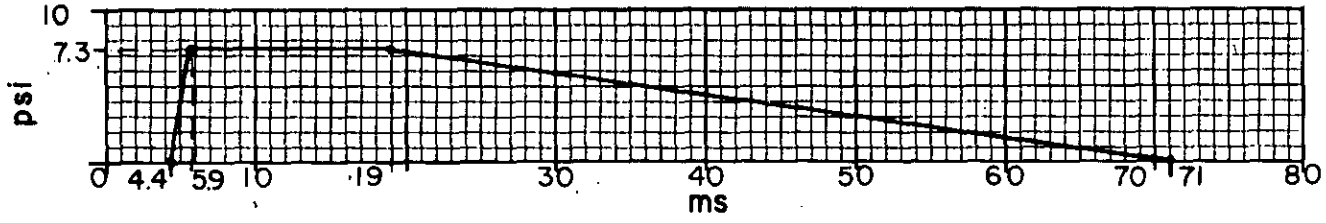
(a) EXTERIOR FRONT WALL



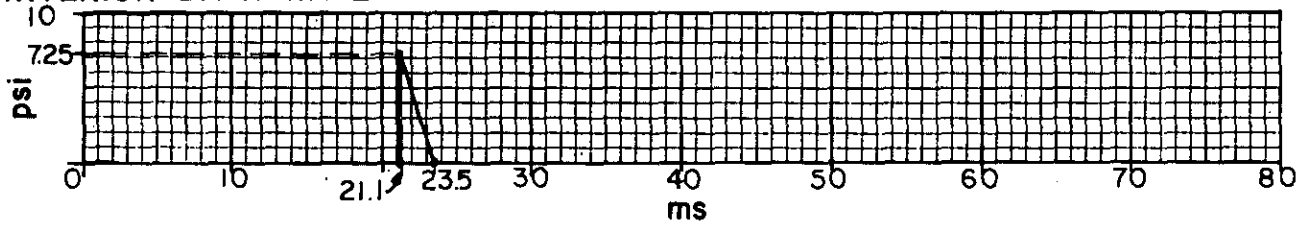
(b) INTERIOR FRONT WALL



(c) INTERIOR SIDE WALL



(d) INTERIOR BACK WALL



(e) INTERIOR ROOF

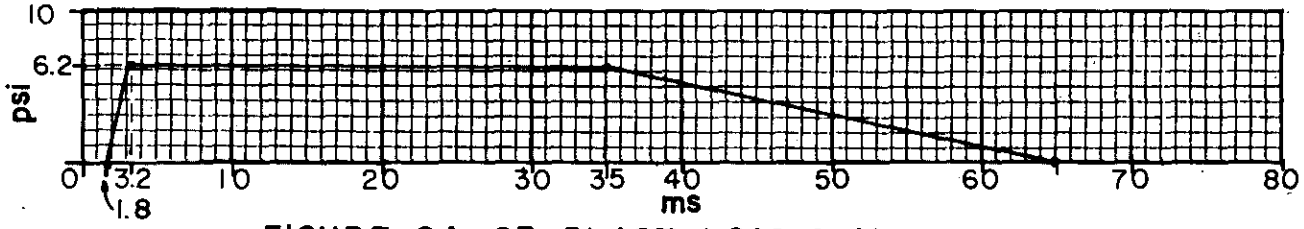


FIGURE 2A-23 BLAST LOAD SUMMARY

Problem 2A-12. Interior Pressure Buildup in a Structure

Problem: Determine the interior pressure-time curve for a structure with an opening in one of its walls and subjected to an applied blast pressure.

Procedure:

Step 1. Determine the pressure-time history of the applied blast pressure P acting on the wall surrounding the opening in the structure as presented in problem 2A-10. Also the area of the opening A_o and the volume of the structure V_o must be known.

Step 2. Divide the duration t_o of the applied pressure into n equal intervals δt, each interval being approximately $t_o/10$ to $t_o/20$, and determine the pressures at the end of each interval.

Step 3. Compute the pressure differential $P-P_i$ where P_i is the interior pressure. Obtain the leakage pressure coefficient C_L for each $P-P_i$ from Figure 2-235.

Step 4. Calculate δP_i from

$$\delta P_i = C_L \frac{A_o}{V_o} \delta t \qquad \text{(eq. 2-31)}$$

using the proper values for C_L and δt. Add δP_i to P_i for the interval being considered to obtain the new value of P_i for the next interval.

Step 5. Repeat steps 3 and 4 for each interval using the proper values of P and P_i. Plot curve of pressure buildup.

Note:
When $P-P_i$ becomes negative, the value of C_L must be taken as negative also.

Example 2A-12. Interior Pressure Buildup in a Structure

Required: Interior pressure-time curve for a structure with an opening in one of its walls and subjected to an applied blast pressure.

Solution:

Step 1. The curve of the applied blast pressure P for the wall in question is shown in Figure 2A-24. (Only the positive phase of the blast wave is considered in this example.)

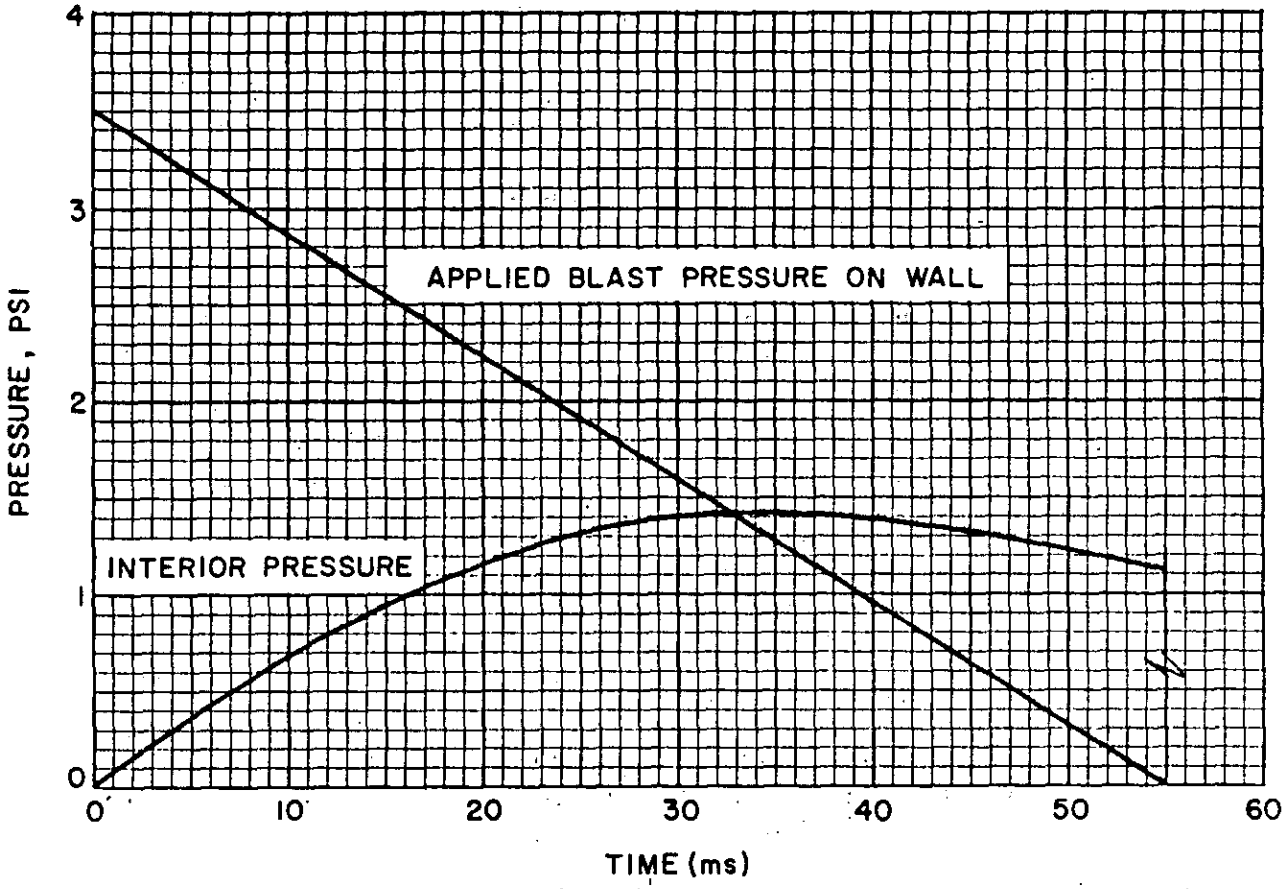

APPLIED BLAST PRESSURE ON WALL
INTERIOR PRESSURE
PRESSURE, PSI
TIME (ms)
0
1
2
3
4
0
10
20
30
40
50
60

FIGURE 2A-24

Area of opening $A_o = 3' \times 3' = 9$ sq ft.

Volume of structure $V_o = 10' \times 10' \times 10'$

$V_o = 1{,}000$ cu ft

Step 2. $t_o = 55$ ms

Use $n = 10$ $\delta t = 5.5$ ms

For the first interval, $P = 3.5$ psi at $t = 0$

Step 3. $P_i = 0$ for the first interval

$\therefore P - P_i = 3.50 - 0 = 3.50$ psi

$C_L = 8.75$ (fig. 2-235)

Step 4. $\delta P_i = C_L \frac{A_o}{V_o} \delta t$ (eq. 2-31)

$\delta P_i = 8.75\ (9.0 / 1000)\ (5.5) = 0.433$ psi

$\therefore$ new $P_i = 0 + 0.433 = 0.433$ psi

Step 5. The remainder of the analysis is presented in tabular form below and the pressure buildup within the structure is plotted in Figure 2A-24.

$t^{(1)}$	P	P_i	$P-P_i$	C_L	δP_i
(ms)	(psi)	(psi)	(psi)	(psi-ft/ms)	(psi)
0.	3.50	0.	3.50	8.75	0.433
5.5	3.15	0.433	2.72	7.00	0.347
11.0	2.80	0.780	2.02	5.45	0.270
16.5	2.45	1.05	1.40	3.78	0.187
22.0	2.10	1.24	0.86	2.32	0.115
27.5	1.75	1.36	0.39	1.05	0.052
33.0	1.40	1.41	-0.01	-0.027	-0.0013
38.5	1.05	1.41	-0.36	-0.972	-0.048
44.0	0.70	1.36	-0.66	-1.78	-0.088
49.5	0.35	1.27	-0.92	-2.48	-0.123
55.0	0.	1.14	-1.14	-3.50	-0.173
60.5	0.	.97	-0.97	-3.00	-0.148
66.0	0.	.82	-0.82	-2.50	-0.124
71.5	0.	.70	-0.70	-2.25	-0.111
77.0	0.	.59	-0.59	-2.00	-0.099
82.5	0.	.49	-0.49	-1.80	-0.089

$t^{(1)}$	P	P_i	$P-P_i$	C_L	δP_i
(ms)	(psi)	(psi)	(psi)	(psi-ft/ms)	(psi)
88.0	0.	.40	-.40	-1.60	-.079
93.5	0.	.32	-.32	-1.45	-.071
99.0	0.	.25	-.25	-1.30	-.064
104.5	0.	.19	-.19	-1.15	-.056
110.0	0.	.13	-.13	-1.0	-.050
115.5	0.	.08	-.08	-.85	-.042
121.0	0.	.04	-.04	-.05	-.025
126.5	0.	.01	-.01	-.2	-.01
132.0	0.	0.	0.	0.	0.

(1) Maximum P_i occurs between t = 27.5 and t = 33.0 ms

Problem 2A-13 Primary Fragments from Cased Cylindrical Charges

Problem: Determine the average fragment weight for a primary fragment ejected from a uniform cylindrical steel casing; the total number of fragments, the design fragment weight and the number of fragments weighing more than the design fragment.

Procedure:

Step 1. Establish design parameters:

a. type of explosive.

b. average casing thickness, t_c.

c. average inside diameter of casing, d_i.

d. total casing weight, W_c.

e. confidence level, C_L.

Step 2. Determine the value of the explosive constant B for the given type of explosive from table 2-6. With this value and the values of t_c and d_i from step 1, calculate the fragment distribution M_A from

$$M_A = Bt_c^{5/6}d_i^{1/3}\left[1 + (t_c/d_i)\right] \qquad \text{(eq. 2-37)}$$

Step 3. With the value of M_A from step 2, calculate the average weight of the fragments from

$$\bar{W}_f = 2M_A^2 \qquad \text{(eq. 2-40)}$$

Step 4. Calculate the total number of fragments using the value of W_c from step 1d and M_A from step 2 and equation 2-37.

$$N_T = 8W_c/M_A^2 \qquad \text{(eq. 2-39)}$$

or: With the values of d_i and t_c from step 1, enter Figure 2-241 and determine B^2N_T/W_c. From this value, the value of B from step 2 and W_c from step 1 find N_T.

Step 5. Find the design fragment weight for the confidence level C_L, given in step 1, using the value of M_A and

$$W_f = M_A^2 \ln^2(1 - C_L) \text{ for } C_L \leq 0.9999 \qquad \text{(eq. 2-42)}$$

or equation 2-43 if $C_L > 0.9999$

Step 6. Using the value of W_c from step 1, M_A from step 2 and W_f from step 5, determine the number of fragments which weigh more than the design fragment from

$$N_f = \frac{8W_c \; e^{-[(W_f)^{1/2}/M_A]}}{M_A^2} \qquad \text{(eq. 2-36)}$$

or: Calculate the number of fragments which weigh more than the design fragment using the confidence level of step 1, the total number of fragments from step 4 and equation 2-244.

Example 2A-13 Primary Fragments from Cased Cylindrical Charges

Required: The average fragment weight, the total number of fragments, the design fragment weight and the number of fragments weighing more than the design fragment.

Solution:

Step 1. Given:

a. type of explosive: Comp B

b. average casing thickness: $t_c = 0.50$ inch

c. average inside diameter of casing: $d_i = 12.0$ inches

d. total casing weight: $W_c = 65.0$ lbs

e. confidence level: $C_L = 0.95$

Step 2. For Comp B, $B = 0.22$ (table 2-7)

$$M_A = Bt_c^{5/6} d_i^{1/3} (1 + t_c/d_i) \qquad \text{(eq. 2-37)}$$

$$= 0.22\ (0.5)^{5/6}\ (12)^{1/3}\ (1 + 0.5/12) = 0.294$$

Step 3. Average weight of fragments.

$$\bar{W}_f = 2M_A^2 = 2 \times (0.294)^2 = 0.17 \text{ oz} \qquad \text{(eq. 2-40)}$$

Step 4. Total number of fragments.

$$N_T = 8W_c/M_A^2 = 8 \times 65/0.294^2 = 6016 \text{ fragments} \qquad \text{(eq. 2-39)}$$

or:
$$\frac{B^2 N_T}{W_c} = 0.28 \qquad \text{(fig. 2-37)}$$

$$N_T = 0.28 \times (65 \times 16)/.22^2 = 6016 \text{ fragments}$$

Step 5. Design fragment weight.

$$W_f = 2M_A^2 \ln^2(1 - CL) = 0.294^2 \ln^2(1 - 0.95) = 0.78 \text{ oz} \qquad \text{(eq. 2-42)}$$

Step 6. Number of fragments weighing more than $W_f = 0.78$ oz.

$$N_f = \frac{8W_c\, e^{-[(W_f)^{1/2}/M_A]}}{M_A^2} = \frac{(8 \times 65)\, e^{-(0.78)^{1/2}/0.294}}{(0.294)^2}$$

$$= 298 \text{ fragments} \qquad \text{(eq. 2-36)}$$

or: $C_L = 1 - N_f/N_T$ (eq. 2-44)

$N_f = N_T (1 - C_L) = 6016 (1 - 0.95) = 301$ fragments

Problem 2A-14 Primary Fragment Velocity

Problem: Determine the initial velocity of a primary fragment and its striking velocity.

Procedure:

Step 1. Establish design parameters.

a. shape of charge

b. dimensions of charge

c. type and density of explosive

d. type and density of casing

e. distance from center of charge to impact location

f. weight of fragment

Step 2. Calculate the total weight of the explosive W and increase it 20%. Find the weight of the casing W_c. Also calculate the ratio of the explosive weight to the casing weight W/W_c.

Step 3. Determine the Gurney Energy Constant $(2E')^{1/2}$ for the explosive charge from table 2-5. With this value and the value of W/W_c from step 2, calculate the initial v_o of the primary fragments from the equation chosen from table 2-6.

or: Calculate the casing to charge weight ratio W_c/W. With W_c/W, find the initial velocity from Figure 2-237 for proper shape.

Step 4. For the distance traveled by the fragment R_f, calculate the striking velocity v_s using the initial velocity from step 3, the weight of the fragment from step 1g and

$$v_s = v_o e^{-.004 R_f/W_f^{1/3}} \quad \text{(eq. 2-48)}$$

or: With the fragment weight W_f and striking distance R_f from step 1, enter Figure 2-243 and find the ratio of the striking velocity to initial velocity. Multiply the ratio by the initial velocity v_o from step 3 to find the striking velocity v_s.

Example 2A-14 Primary Fragment Velocity

Required: The initial velocity and striking velocity of a primary fragment.

Solution:

Step 1. Given:

a. spherical charge

b. inner diameter of charge: d_i = 6 inches

average casing thickness: t_c = 0.25 inches

c. type of explosive TNT

density of explosive = 0.0558 lb/in^3

d. mild steel casing

density of casing = 0.283 lb/in^3

e. striking distance R_f = 35 ft.

f. weight of fragment, W_f = 2 oz

Step 2.

a. weight of the explosive

$W = 4/3\ \pi\ (6/2)^3\ X\ 0.0558 = 6.31$ lbs

b. Increase weight of explosive 20 percent

$W = 1.20\ X\ 6.31 = 7.57$ lb

c. Weight of casing

$W_c = 4/3\ \pi\ (3.5^3 - 3^3)\ X\ 0.283 = 18.82$ lb

d. Explosive weight to casing weight ratio.

$W/W_c = 7.57/18.82 = 0.402$

Step 3. For TNT, $(2E')^{1/2} = 8000$ (table 2-5)

Initial velocity from table 2-6

$$v_o = (2E')^{1/2} \left[\frac{W/W_c}{1 + (3W/5W_c)}\right]^{1/2}$$

$$v_o = (8000) \left[\frac{0.40}{1 + 0.40\ (3/5)}\right]^{1/2} = 4500 \text{ ft/sec}$$

or: $W_c/W = 18.82/7.57 = 2.49$

from Figure 2-237

$v_o/(2E')^{1/2} = 0.56$

$v_o = 0.56 \times 8000 = 4500$ ft/sec

Step 4. Striking velocity

$$v_s = v_o e^{-0.004\ R_f/W_f^{1/3}} = 4500\ e^{-0.004 \times (35/2)^{1/3}} \quad \text{(eq. 2-48)}$$

$v_s = 4030$ ft/sec

or: from Figure 2-243

$v_s/v_o = 0.895$

$v_s = 0.895 \times 4500 = 4030$ ft/sec

Problem 2A-15. Unconstrained Secondary Fragments "Close" to a Charge

Problem: Determine the velocity of an unconstrained object close to an explosive charge and its maximum range.

Procedure:

Step 1. Establish design parameters

a. weight W and shape of TNT equivalent explosive

b. radius of explosive R_e

c. shape, dimensions and weight of target

d. distance from the center of the explosive charge to the surface of the target, R

e. orientation of target with respect to the explosive charge

f. mass density of air ρ_o

Step 2. Calculate the ratio of standoff distance to radius of the explosive R/R_e using the values from step 1.

Step 3. From Figure 2-249, determine target shape factor, ß.

Step 4.

a. If R/R_e is less than or equal to 10 for cylindrical charges, or less than equal to 5.0 for spherical charges, determine the specific acquired impulse either from Figure 2-250 or equations 2-60, or 2-61.

b. If $10 < R/R_e \leq 20$ for a cylindrical charge, or $5 < R/R_e \leq 20$ for a spherical charge, calculate the scaled standoff distance $Z_A = R/W^{1/3}$. With that value of Z_A, obtain the normal reflected impulse from Figure 2-7. The normal reflected impulse is then used as the specific acquired impulse.

Step 5. Calculate the mean presented area A of the target and the mass M using the values of step 1.

Step 6. With the area and mass from step 4, the target shape factor ß from step 2 and the impulse from step 3, calculate the velocity from

$$v_o = \frac{1000\ A\beta i}{12\ M} \qquad \text{(eq. 2-59)}$$

Step 7. Determine the drag coefficient C_D from table 2-8. Using that value of C_D, the area and mass of the target from step 5, the velocity from step 6 and the mass density of air from step 1f,

evaluate the term: $12\ \rho_o C_D A_D v_o^2/Mg$.

Step 8. With the term calculated in step 7, enter Figure 2-252 and read the value of 12 $\rho_o C_D A_D R/M$ from which the range R is calculated.

Example 2A-15 Unconstrained Secondary Fragments "Close" to a Charge

Required: The velocity and maximum range of a steel tool holder resting on a lathe when a charge being held by the lathe explodes.

Solution:

Step 1. Given:

a. spherical charge of TNT
W = 15 lbs

b. radius of explosive: $R_e = 0.33$ ft

c. cylindrical target; length = 8.0 in
$R_t = 1.0$ in = 0.083 ft

$W_t = 7.13$ lb

d. standoff distance: R = 1.0 ft

e. tool holder is resting so that its longitudinal axis is perpendicular to the radial line from the charge

f. mass density of air: $\rho_o = 0.115$ lb - ms^2/in^4

Step 2. Ratio of standoff distance to radius of explosive:

$R/R_e = 1.0/0.33 = 3.03$

Step 3. Target shape factor.

$\beta = \pi/4$ from Figure 2-512

Step 4. Determine specific acquired impulse

a. $$\frac{i}{\beta R_{eff}} \left[\frac{R_e}{R_t}\right]^{0.158} = 8000 \ \frac{\text{psi-ms}}{\text{ft}}$$ (fig 2-250)

b. $R_{eff} = R_e = 0.33$ ft (eq. 2-61)

c. $i = \pi/4\ (0.33\ ft)\ (0.083/0.33)^{0.158} \times 8000\ psi\text{-}ms/ft$

$i = 1667\ psi\text{-}ms$

Step 5. Calculate area and mass of target.

a. Mean presented area

$A = 2.0\ in \times 8.0\ in = 16\ in^2$

b. Mass

$$M = \frac{W_t}{g} = \frac{7.13\ lb}{32.2 \times 12 \times 10^{-6}\ in/ms^2} = 18{,}450\ \frac{lb\text{-}ms^2}{in}$$

Step 6. Find the velocity.

$$v_o = \frac{1000\ A\beta i}{12\ M} = \frac{1000 \times 16 \times (\pi/4) \times 1667}{12 \times 18450} \qquad \text{(eq. 2-59)}$$

$v_o = 95\ ft/sec$

Step 7. Evaluate the term $12\ \rho_o\ C_D A_D v_o^2/Mg$.

a. $C_D = 1.2$ (table 2-8)

b. $$\frac{12\rho_o C_D A_D V_o^2}{Mg} = \frac{0.115\ \ (1.2)\ (16)\ (95)^2\ 12}{18450 \times 32.2} = 0.40$$

Step 8. Calculate the range.

a. $$\frac{12\ \rho_o C_D A_D R}{M} = 0.33 \qquad \text{(fig. 2-252)}$$

b. $R = 0.33M/(12\rho_o C_D A_D)$

$= 0.33\ (18450)/[12\ (0.115)\ 1.2\ (16)] = 230\ ft.$

Problem: 2A-16 Unconstrained Secondary Fragments "Far" from a Charge

Problem: Determine the velocity of an unconstrained object "far" from an explosive charge.

Procedure:

Step 1. Establish design parameters:

a. weight W of TNT equivalent explosive

b. shape, dimensions and weight of target

c. distance from the center of explosive charge to surface of the target

d. orientation and location of target with respect to the explosive charge

e. velocity of sound in air, a_o

f. atmospheric pressure, p_o

Step 2. Calculate the scaled standoff distance from:

$$Z_A = R_A/W^{1/3}$$

From Figure 2-7. and the scaled distance find the peak incident overpressure and the incident specific impulse.

Step 3. Determine the drag coefficient C_D from table 2-8 based on the shape and orientation of target (step 1).

Step 4. Calculate the mass of the target. Determine the distance from the front of the target to the location of its largest cross-sectional area, X. Also, determine the minimum transverse distance of the mean presented area, H, and the presented area.

Step 5. Determine the constant K, which is equal to 4 if the object is on the ground or reflecting surface. If the target is in the air, K is equal to 2.

Step 6. With the peak incident overpressure P_{so} from step 2 and the atmospheric pressure p_o from step 1f, find P_{so}/p_o.

Step 7. Evaluate the term $12C_D i_s a_o/10^3[P_{so}(KH + X)]$ using i_s and P_{so} from step 2, C_D from step 3, a_o from step 1e, K from step 5 and H and X from step 4.

Step 8. With two terms calculated in steps 6 and 7 enter Figure 2-248 and read $144v_o Ma_o/[10^6 P_o A(KH + X)]$ from which the velocity is calculated.

Example 2A-16 Unconstrained Secondary Fragments "Far" from Charge

Required: The initial velocity of a steel tool holder resting on a nearby table, when a charge explodes.

Solution:

Step 1. Given:

a. weight of explosive: W = 15 lbs of TNT

b. cylindrical target: length = 8.0 in
R_t = 1.0 in
W_t = 7.13 lb

c. standoff distance: R = 10 ft

d. tool holder is resting on a table so that its longitudinal axis is perpendicular to the radial line from the charge

e. velocity of sound in air: a_o = 1100 ft/sec

f. atmospheric pressure: p_o = 14.7 psi

Step 2. Find the peak incident overpressure and the incident specific impulse.

a. Scaled distance

$$Z_A = R/W^{1/3} = 10/(15)^{1/3} = 4.05 \text{ ft/lb}^{1/3}$$

b. Peak incident overpressure.

P_{so} = 39 psi (fig. 2-7)

c. Incident specific impulse.

$i_s/W^{1/3}$ = 12 psi-ms/lb$^{1/3}$ (fig. 2-7)

$$i_s = 12\ (15)^{1/3} = 29.6 \text{ psi-ms}$$

Step 3. Drag coefficient.

$C_D = 1$ (from table 2-8 for cylinder loaded perpendicular to axis.)

Step 4. a. Mass of target.

$$M = \frac{W_t}{g} = \frac{7.13 \text{ lb}}{32.2 \times 12\text{x}10^{-6} \text{ in/ms}^2} = 18{,}450 \frac{\text{lb-ms}^2}{\text{in}}$$

b. Location of largest cross-section.

X = 1 in (radius of object in this case - see fig. 2A-21)

c. Transverse distance of presented area.

H = 2.0 in (diameter of object in this case - see fig. 2A-25).

d. Mean presented area.

$A = 2 \times 8 = 16 \text{ in}^2$

Step 5. Reflection constant.

Target is resting on table which is a reflecting surface so:

K = 4

Step 6. Evaluate P_{so}/p_o

$P_{so}/p_o = 39/14.7 = 2.65$

Step 7. Evaluate $12C_D i_s a_o/[10^3 P_{so} (KH + X)]$

$$\frac{12C_D i_s a_o}{10^3 P_{so} (KH + X)} = \frac{12 (1.2) (29.6) (1100)}{10^3 (39) (2 \times 4 + 1)} = 1.34$$

Step 8. Calculate the velocity.

$$\frac{144 \text{ v } M_o a_o}{10^6 \text{ p } A_o (KH + X)} = 6.0 \qquad \text{(fig. 2-248)}$$

$$v_o = \frac{6.0 \, p_o A (KH + X) \, 10^6}{144 \, Ma_o} = \frac{10^6 (6.0)(14.7)(16)(2 \times 4 + 1)}{(144)(18450)(1100)}$$

$v_o = 4.34$ ft/sec

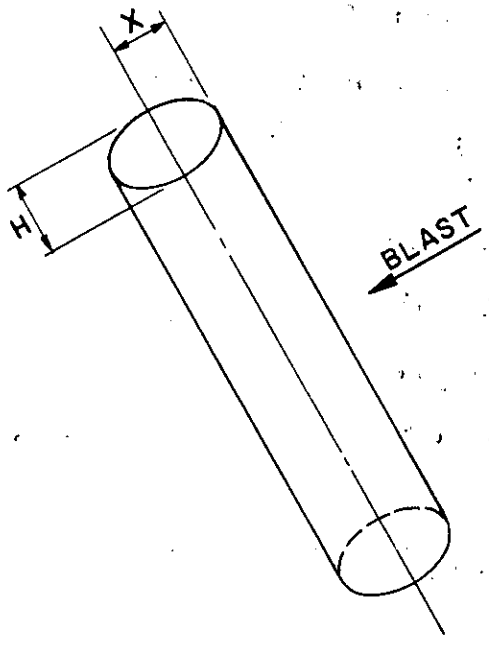


FIGURE 2A-25

Problem 2A-17 Constrained Secondary Fragments

Problem: Determine the velocity of a constrained object close to an exploding charge.

Procedure:

Step 1. Establish design parameters:

a. fragment material.

b. dimensions of object.

c. boundary condition, cantilever or fixed-fixed.

d. specific impulse imparted to object.

Step 2. Determine the fragment toughness T from table 2-9 and the fragment mass density ρ_f.

Step 3. Calculate the loaded area of the object.

Step 4. Evaluate the term $ib\,(2L/b)^{0.3}/[A(\rho_f\,T)^{0.5}]$, using the specific impulse and object dimensions from step 1, the fragment density and toughness from step 2 and the loaded area from step 3. With this term, enter Figure 2-251 and read the value of $12V/1000\,(\rho_f/T)^{0.5}$ from which the velocity is calculated.

or: Using the specific impulse and object dimensions from step 1, the fragment density and toughness from step 2, and the loaded area from step 3. calculate the velocity of the object from equation 2-66.

Example 2A-17 Constrained Secondary Fragments

Required: The velocity of a cylindrical tool holder after it breaks free of its moorings.

Solution:

Step 1. Given:

a. fragment material; A36 steel

b. dimensions of object: b = 2.0 inches
L = 8.0 inches

c. boundary conditions; cantilever

d. specific impulse: i = 1667 psi-ms (see step 4 of example 2A-15).

Step 2.

a. Fragment toughness.

$T = 12{,}000$ in-lb/in^3 (table 2-9)

b. Mass density of steel.

$$\rho_f = \frac{490 \text{ lb/ft}^3 \ (\text{ft}^3/1728 \text{ in}^3)}{32.2 \text{ ft/s}^2 \ (12 \text{ in/ft})(\text{s}^2/10^6 \text{ms}^2)} = 734 \frac{\text{lb-ms}^2}{\text{in}^4}$$

Step 3. Loaded area.

$$A = \pi r^2 = \pi \ (1.0)^2 = 3.14 \text{ in}^2$$

Step 4. Calculate the velocity.

$$\frac{ib}{A(\rho_f T)^{0.5}} \left[\frac{2L}{b}\right]^{0.3} = \frac{1667 \times 2.0}{3.14(734 \times 12{,}000)^{0.5}} \left[\frac{2 \times 8}{2}\right]^{0.3} = 0.668$$

from Figure 2-251

$12/1000 \ [\rho_f/T]^{1/2} V = 0.025$

so

$$V = \frac{1000}{12} \left[\frac{T}{\rho_f}\right]^{1/2} 0.025 = \frac{1000}{12} \left[\frac{12{,}000}{734}\right]^{1/2} 0.025 = 8.4 \text{ fps}$$

or from equation 2-66

$$V = \frac{1000}{12} \left[\frac{T}{\rho_f}\right]^{1/2} \left[-.2369 + 0.3931 \left[\frac{ib}{(\rho_f T)^{1/2} A}\right] \left[\frac{2L}{b}\right]^{0.3}\right]$$

$$= \frac{1000}{12} \left[\frac{12{,}000}{734}\right]^{1/2} (-.2369 + 0.3931 \times 0.668)$$

$V = 8.6$ fps

Problem 2A-18 Ground Shock Load

Problem: Determine the air blast and direct induced ground shock parameters.

Procedure: Air blast-induced ground shock.

Step 1. Determine the charge weight, ground distance R, height of burst H_c, if any, and structure dimensions.

Step 2. Apply a 20% safety factor to the charge weight.

Step 3. Calculate the scaled distance Z.

Read: From fig. 2-15

a. Peak positive incident pressure P_{so}.

b. Scaled unit positive incident impulse $i_s/W^{1/3}$. Multiply scaled value by $W^{1/3}$ to obtain absolute value.

c. Shock front velocity U.

Step 4. Determine the maximum vertical ground motions.

a. Calculate maximum vertical velocity.

$$V_V = \frac{P_{so}}{\rho\ C_p} \qquad \text{(eq. 2-74)}$$

where:

ρ = Mass density of soil (table 2-10)

C_p = Compression wave seismic velocity in the soil (table 2-11)

b. Calculate maximum vertical displacement

$$D_V = \frac{i_s}{1{,}000\ \rho\ C_p} \qquad \text{(eq. 2-74)}$$

c. Calculate maximum vertical acceleration of the ground surface.

$$A_V = \frac{100P_{so}}{\rho\ C_p g} \qquad \text{(eq. 2-76)}$$

where:

g = Gravitational constant equal to 32.2 ft/sec^2

Step 5. Determine the maximum horizontal ground motions parameters.

a. Check $C_p/12000\ U > .707$

b. Calculate maximum horizontal velocity.

$$V_H = V_V \tan\ [\sin^{-1}\ (C_p/12{,}000\ U)] \qquad \text{(eq. 2-77)}$$

c. Calculate maximum horizontal displacement.

$$D_H = D_V \tan\ [\sin^{-1}\ (C_p/12{,}000\ U)] \qquad \text{(eq. 2-78)}$$

d. Calculate maximum horizontal acceleration.

$$A_H = A_V \tan\ [\sin^{-1}(C_p/12{,}000\ U)] \qquad \text{(eq. 2-79)}$$

Step 6. Determine arrival time t_A and duration to:

a. Read from fig. 2-15.

$t_A/W^{1/3}$ scaled time of arrival of blast wave and,

$t_o/W^{1/3}$ scaled duration of positive phase.

b. Multiply scaled value by $W^{1/3}$ to obtain absolute value.

Direct-Induced Ground Shock

Step 7. Determine the maximum vertical ground motions.

a. Calculate maximum vertical displacement.

$$D_V = \frac{0.025\ R_G^{1/3} W^{1/3}}{Z_G^{1.3}}$$ (eq. 2-80, rock media)

or

$$D_V = \frac{0.17\ R_G^{1/3} W^{1/3}}{Z_G^{2.3}}$$ (eq. 2-83, dry or saturated soil)

b. Calculate the maximum vertical velocity.

$$V_V = 150/Z_G^{1.5}$$ (eq. 2-85)

c. Calculate the maximum vertical acceleration.

$$A_V = 10{,}000/W^{1/3} Z_G^2$$ (eq. 2-87)

Step 8. Determine the maximum horizontal ground motion parameters.

a. Calculate the maximum horizontal displacement.

$$D_H = 0.5\ D_V$$ (eq. 2-82, rock media)

or

$$D_H = D_V$$ (eq. 2-84, dry or saturated soil)

b. Calculate the maximum horizontal velocity.

$$V_H = V_V$$ (eq. 2-86, all ground media)

c. Calculate the maximum horizontal acceleration.

$$A_H = 0.5\ A_V$$ (eq. 2-88, dry soil)

$$A_H = A_V$$ (eq. 2-89, wet soil or rock media)

Step 9. Determine arrival time t_{AG}:

$$t_{AG} = 12000\ R_G/C_p \qquad \text{(eq. 2-92)}$$

Example 2A-18 Ground Shock Loads

Required: Maximum acceleration, velocity, and displacement at a point 155 ft. away from a surface burst of 5,000 lbs. Also required are: times of arrival and duration of air-blast induced ground shock.

Solution:

Air blast-induced ground shock.

Step 1. Given: Charge weight = 5,000 lbs., R = 155 ft., H_c = 12 ft.

Step 2. W = 1.2 (5,000) = 6,000 lbs.

Step 3. Calculate the scaled distance Z.

$$Z = \frac{R}{W^{1/3}} = \frac{155}{(6{,}000)^{1/3}} = 8.53\ \text{ft/lb}^{1/3}$$

Read from Figure 2-15.

a. P_{so} = 13 psi

b. $$\frac{i_s}{W^{1/3}} = 9\ \text{psi-ms/lb}^{1/3}$$

$$i_s = 9 \times W^{1/3} = 9 \times (6{,}000)^{1/3} = 163.54\ \text{psi-ms}$$

c. U = 1.5 ft/ms

Step 4. Determine the maximum vertical ground motion.

a. $$V_V = \frac{P_{so}}{\rho\ C_p} \qquad \text{(eq. 2-74)}$$

$$V_V = \frac{13}{1.65 \times 10^{-4} \times 70{,}000} = 1.125\ \text{in/sec}$$

b. $$D_V = \frac{i_s}{1{,}000\ \rho\ C_p} \qquad \text{(eq. 2-75)}$$

$$D_V = \frac{163.5}{1{,}000\ (1.65 \times 10^{-4})\ 70{,}000} = 0.0142 \text{ in}$$

c. $$A_V = \frac{100\ P_{so}}{\rho\ C_p g} \qquad \text{(eq. 2-76)}$$

$$A_V = \frac{100 \times 12.8}{(1.65 \times 10^{-4})\ 70{,}000 \times 32.2} = 3.44 \text{ g}$$

Step 5. Determine the maximum horizontal ground motion.

a. Check $C_p/12000\ U > .707$

$70{,}000/12{,}000 \times 1.5 = 3.89 > .707$

b. $V_H = V_V = 1.125$ in/sec

c. $D_H = D_V = 0.0142$ in

d. $A_H = A_V = 3.44$ g

Step 6. Arrival time t_A

a. Read from Figure 2-15.

$$\frac{t_A}{W^{1/3}} = 3.35 \text{ ms/lb}^{1/3}$$

$$t_o/W^{1/3} = 2.35 \text{ ms/lb}^{1/3}$$

b. $t_A = 3.35 \times W^{1/3} = 3.35\ (6{,}000)^{1/3}$

$t_A = 60.90$ ms

$t_o = 2.35 \times W^{1/3} = 2.35 \times (6{,}000)^{1/3}$

t_o = 42.70 ms

Direct-induced ground shock.

Step 7. Maximum vertical ground motions.

a. $$D_V = \frac{0.17\ R_G^{1/3}\ W^{1/3}}{Z_G^{2.3}}$$ (eq. 2-83)

$$= \frac{0.17\ (155)^{1/3}\ (6,000)^{1/3}}{(8.53)^{2.3}} = 0.1198 \text{ in}$$

b. $V_V = 150/Z_G^{1.5}$ (eq. 2-85)

$V_V = 150 / 8.53^{1.5} = 6.020$ in/sec

c. $A_V = 10,000 / W^{1/3}\ Z_G^2$ (eq. 2-87)

$A_V = 10,000 / [\ (6,000)^{1/3}\ (8.53)^2\ ] = 7.56$ g

Step 8. Horizontal ground motions.

a. $D_H = D_V$ (eq. 2-84)

$D_H = 0.1198$ in.

b. $V_H = V_V$ (eq. 2-86)

$V_H = 6.020$ in/sec

c. $A_H = 0.5\ A_V$ (eq. 2-88)

$A_H = 0.5\ (7.56)$

$A_H = 3.78\ g$

Step 9. Arrival time t_{AG}

$t_{AG} = 12{,}000\ R_G/C_p = (12{,}000 \times 155) / 70{,}000$ (eq. 2-92)

$t_{AG} = 26.6$ ms

Problem 2A-19 Structure Motion Due to Air Shock

Problem: Determine the maximum horizontal acceleration, displacement and velocity of an above ground structure subjected to air shock.

Procedure:

Step 1. Determine external loadings acting on the roof, front and rear walls according to the procedure outlined in problem 2A-10.

Step 2. Construct the horizontal force-time load curve by combining the front and rear wall loadings from step 1 applied over the area of front and rear walls. Use times of arrival to phase these two loads.

Step 3. Calculate the dead weight and mass of the structure.

Step 4. Construct the downward force-time curve by adding the weight of the structure and total roof load. The roof load is the pressure time loading from step 1 applied over the total area of the roof.

Step 5. Determine the coefficient of friction between soil and the structure from table 2-12.

Step 6. Determine maximum horizontal acceleration, displacement and velocity using the acceleration impulse extrapolation method outlined in Chapter 3, Article 3-19.2.1.2 of this manual. The resisting force at each time interval is equal to the value of downward force curve of step 4 multiplied by the coefficient of friction determined in step 5. The resisting force is assumed to be effective when the total horizontal movement is equal to or larger than 1/4 inch as mentioned in paragraph

Example 2A-19 Structure Motion Due to Air Shock

Required: Maximum horizontal acceleration, velocity and displacement of the square structure shown in Figure 2A-9 from problem 2A-10 for a surface burst of 5,000 lbs at a distance from the front wall of 155 ft. Assume a coarse and compact soil. Roof, floor slab and side walls are 1 foot thick reinforced concrete slabs and assume a 50 psf of internal dead load for the structure.

Step 1. External loadings on the structure are determined according to the procedure in example 2A-10. See Figures 2A-10, 2A-12 and 2A-13. The arrival time (t_A) for these loads are tabulated in step 3d of example 2A-10.

t_{Af} (front wall) = 60.9 ms

t_{Ab} (rear wall) = 83.6 ms

Step 2. a. Calculate area of front and rear walls.

Area (front and rear) = $30 \times 12 \times (12)^2 = 51840$ in^2

b. Calculate the time difference between the rear and front walls from step 1.

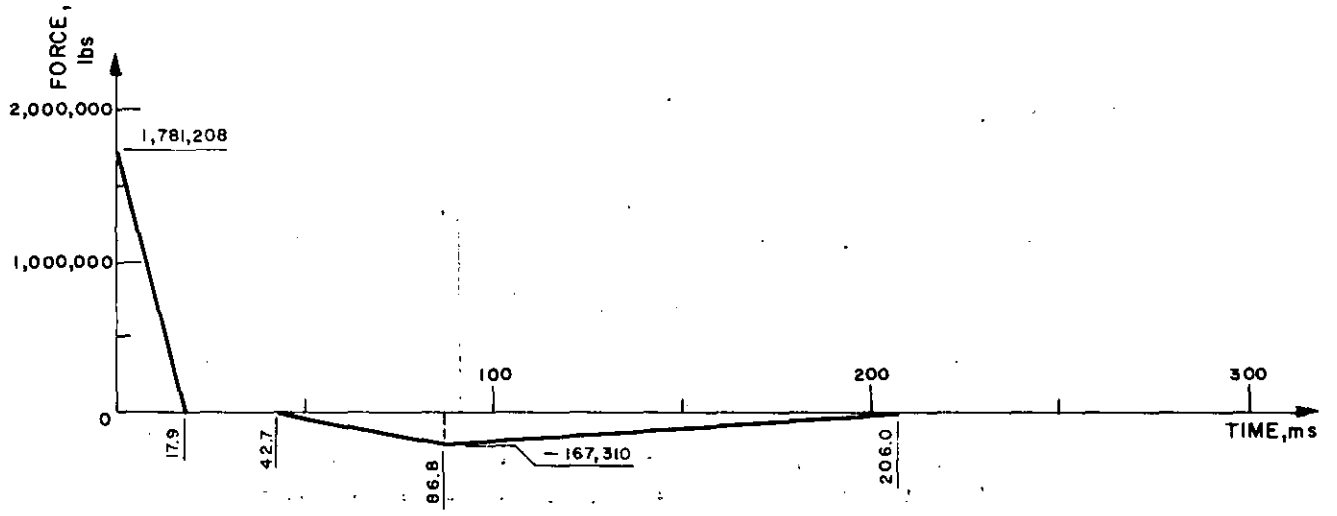
$\delta t = t_{Ab} - t_{Af} = 83.6 - 60.9 = 22.7$ ms

c. Construct the horizontal force-time load curve by multiplying the values of the front and rear wall curves from step 1 by the area from step 2a. Rear wall load starts at time equal to $\delta t = 22.7$ from step 2b. See Figure 2A-26.

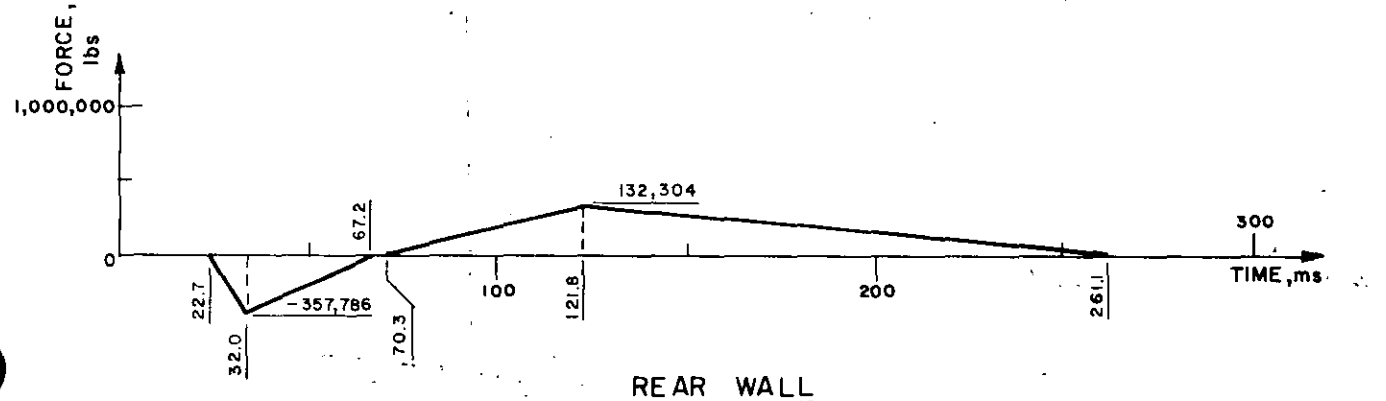
Step 3.

a. Calculate dead weight of structure W_d. Assume concrete weight is 150 psf.

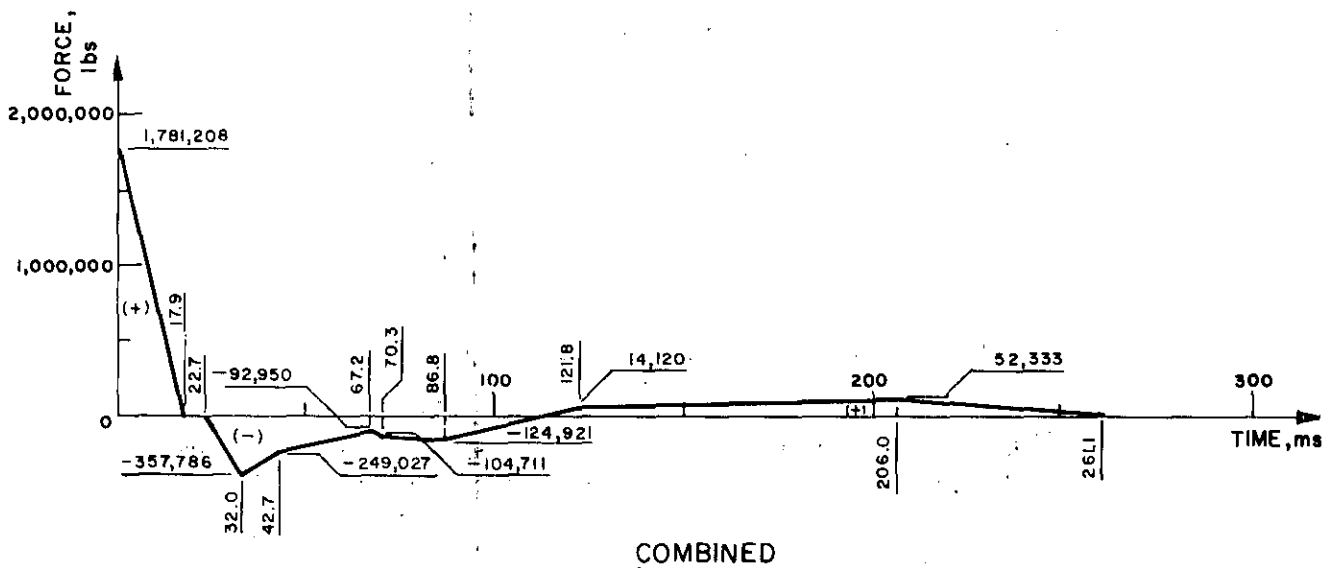
$W_d = 150\,[4\,(30 - 1)\,(12-1) + 2\,(30)^2] + 50\,(30-2)^2 = 500{,}600$ lbs



FRONT WALL



REAR WALL



COMBINED

FIGURE 2A-26

b. Calculate total mass.

$$m = \frac{W_d}{g} = \frac{500,600\ (1000)^2}{32.2 \times (12)} = 1295.55 \times 10^6 \quad \frac{\text{lb ms}^2}{\text{in}}$$

Step 4. a. Calculate area of the roof.

$$\text{Area (roof)} = 30^2 \times (12)^2 = 129,600\ \text{in}^2$$

b. Construct the downward force-time curve by multiplying the values of the roof curve from step 1 by the roof area from step 4a, and adding the dead weight of structure W_d = 500,600 lbs from step 3a. (If the resulting value is negative, assume zero). See Figure 2A-27 below.

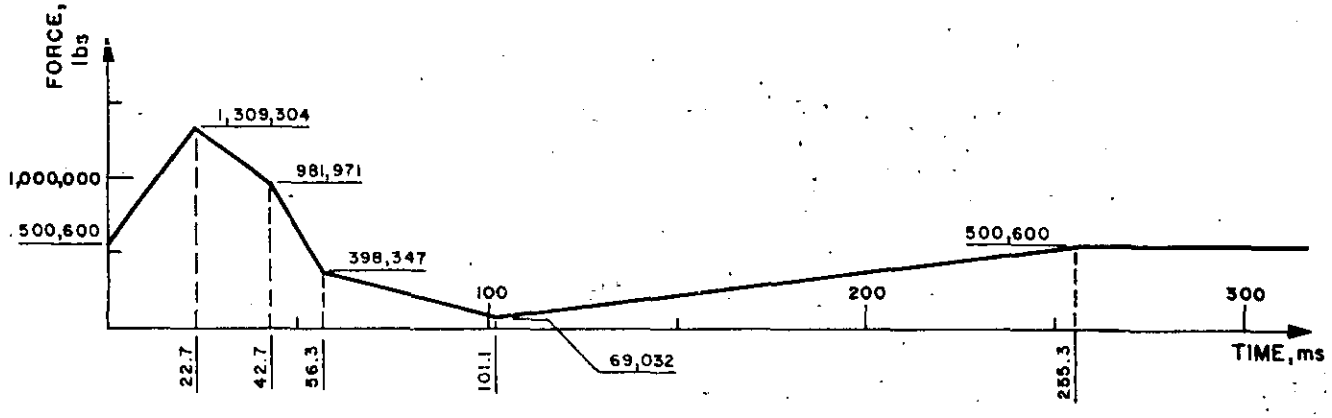


Figure 2A-27

Step 5. Coefficient of friction μ from table 2-12 for coarse and compact soil.

$\therefore \mu = 0.60$

Step 6. Using the acceleration impulse extrapolation method from Chapter 3 of this manual determine maximum horizontal acceleration, displacement and velocity of the structure due to load curve (P) from step 2c. Resisting force R is the friction force produced due to the downward load curve F from step 4b after an initial lateral translation of 1/4 inch. Use two ms time intervals for extrapolation. The following are the equations used in the extrapolation shown in Table 2A-3.

$$P_n - R_n = ma_n$$

$$R_n = \mu F_n$$

$$X_{n+1} = 2X_u - X_{n-1} + a_n (\delta t)^2$$

$$V_n = V_{n-1} + a_n (\delta t)$$

where

P_n = Load at time of step n (step 2c)

R_n = Resisting Friction Force at time step n

m = Mass from (step 3b)

a_n = Acceleration at time step n

μ = Friction coefficient (step 5)

F_n = Downward force at time step n (step 4b)

X_n = Deflection at time step n

V_n = Velocity at time step n

The maximum motions from Table 2A-3 are:

a_{max} = .00122 in/ms^2 << 101.67 ft/sec^2 << 3.16 g's

V_{max} = .01231 in/ms << 1.026 ft/sec

D_{max} = .355 in

Problem 2A-20 Shock Response Spectra

Problem: Construct the elastic shock response spectra for the interior components of an above ground structure subject to an external explosion.

Procedure:

Table 2A-3

n	t	P_n	R_n	P_n-R_n	$a_n = (P_n-R_n)/m$	$a_n(\delta t)^2$	$2X_n$	X_{n-1}	X_{n-1}	$a_n\delta t$	V_{n-1}	V_n	
	ms	lbs	lbs	lbs	in/ms²	in	in	in	in	in/ms	in/ms	in/ms	
0	0	1,781,208	0	1,781,208	(.00138)/2	(.00550)/2	0	0	.00275	(.00275)/2	0	.00138	
1	2	1,582,190	0	1,582,190	.00122	.00489	.00550	0	.01038	.00244	.00138	.00382	
2	4	1,383,173	0	1,383,173	.00107	.00427	.02077	.00275	.02229	.00214	.00382	.00596	
3	6	1,184,155	0	1,184,155	.00091	.00366	.04458	.01038	.03786	.00182	.00596	.00778	
4	8	985,137	0	985,137	.00076	.00304	.07571	.02229	.05646	.00152	.00778	.00930	
5	10	786,120	0	786,120	.00061	.00243	.11292	.03786	.07749	.00122	.00930	.01052	
6	12	587,102	0	587,102	.00045	.00181	.15497	.05646	.10032	.00090	.01052	.01142	
7	14	388,084	0	388,084	.00030	.00120	.20064	.07749	.12435	.00060	.01142	.01202	
8	16	189,067	0	189,067	.00015	.00058	.24870	.10032	.14896	.00029	.01202	.01231	
9	18	0	0	0	0	0	.29793	.12435	.17358	0	.01231	.01231	
10	20	0	0	0	0	0	.34716	.14896	.19820	0	.01231	.01231	
11	22	0	0	0	0	0	.39640	.17358	.22282	0	.01231	.01231	
12	24	-50,013	0	-50,013	-.00004	-.00015	.44564	.19820	.24728	-.00008	.01231	.01223	
13	26	-126,956	0	-126,956	-.00010	-.00039	.49456	.22282	.27135	-.00020	.01223	.01203	
14	28	-203,890	733,536	-937,426	-.00072	-.00289	.54270	.24728	.29253	-.00142	.01203	.01061	
15	30	-280,843	713,896	-994,739	-.00077	-.00307	.58505	.27135	.310629	-.00153	.01061	.00908	
16	32	-357,786	694,256	-1,052,042	-.00081	-.00325	.62126	.29253	.32548	-.00162	.00908	.00746	
17	34	-337,457	674,617	-1,012,074	-.00078	-.00312	.65096	.310629	.33721	-.00156	.00746	.00590	
18	36	-317,128	654,977	-972,105	-.00075	-.00300	.67441	.32548	.34593	-.00150	.00590	.00440	
19	38	-296,780	635,337	-932,117	-.00072	-.00288	.69186	.33721	.35177	-.00144	.0044	.00296	
20	40	-276,471	615,697	-892,168	-.00069	-.00275	.70354	.34593	.35486	-.00138	.00296	.00158	
21	42	-256,142	596,057	-852,199	-.00066	-.00263	.70972	.35177	.35532	-.00132	.00158	.00026	
22	44	-240,745	555,710	-796,455	-.00061	-.00244	.71064	.35486	.35332	-.00122	.00026	.00096	
23	46	-278,004	504,214				.70664	.35532					
24	48	-215,263	452,718				.35332						

Step 1. Determine maximum acceleration, velocity and displacement due to ground shock according to procedure outlined in Problem 2A-18.

Step 2. Determine maximum acceleration, velocity and displacement due to air shock according to the procedure outlined in Problems 2A-10 and 2A-19.

Step 3. Determine if the ground shock is outrunning or superseismic (paragraph 2-23.2). For outrunning ground shock the maximum values of displacement, velocity and acceleration in horizontal and vertical directions are the algebraic summation of the maximum motions from steps 1 and 2. Otherwise proceed to step 4.

Step 4. For superseismic ground shock the maximum values of displacement, velocity and acceleration are the numerically larger values of direct-induced ground shock or the algebraic sum of the maximum motions from air shock and airburst induced ground shock.

Step 5. Calculate the magnitude of acceleration, velocity and displacement for response spectra in horizontal and vertical directions by multiplying the maximum values of motions from step 3 or step 4 by their appropriate factor from paragraph 2-24.3.

Step 6. Draw the horizontal and vertical shock response spectras.

Example 2A-20 Shock Response Spectra

Required: Shock response spectra for the structure defined in Examples 2A-18 and 2A-19.

Solution:

Step 1. Maximum values of motion in vertical and horizontal directions due to ground shock according to the procedure outlined in Example 2A-18 are:

a. Air blast-induced

$A_H = A_V = 3.44$ g

$V_H = V_V = 1.125$ in/sec

$D_H = D_V = .014$ in

b. Direct-induced

$A_H = 3.78$ g

$A_V = 7.56$ g

$V_H = V_V = 6.02$ in/sec

$D_H = D_V = .120$ in

Step 2. Maximum horizontal acceleration, velocity and displacement due to air shock following the procedure outlined in Examples 2A-10 and 2A-19.

$A_{max} = 3.16$ g

$V_{max} = 12.31$ in/sec

$D_{max} = .355$ in

Step 3. a. Check for outrunning ground shock

$T_{AG} < T_A$:

From Example 2A-18

$T_{AG} = 26.6$ ms

$T_A = 60.9$ ms

$\therefore T_{AG} < T_A$ Outrunning ground shock

b. Add the values of maximum motions from step 1 and step 2.

$\therefore A_{H\ max} = 3.16 + 3.44 + 3.78 = 10.38$ g

$\therefore V_{H\ max} = 12.310 + 1.108 + 6.020 = 19.438$ in/sec

$\therefore D_{H\ max} = .355 + .014 + .120 = .489$ in

and

$\therefore A_{V\ max} = 3.44 + 7.56 = 11.00$ g

$\therefore V_{V\ max} = 1.108 + 6.020 = 7.128$ in/sec

$\therefore D_{V\ max} = .014 + .120 = .134$ in

Step 4. Does not apply, the ground shock is not superseismic.

Step 5. Magnitude of the motions for response spectra.

$A_H = 10.38 \times 2.0 = 20.76$ g

$V_H = 19.438 \times 1.5 = 29.157$ in/sec

$D_H = .489 \times 1.0 = .489$ in

and

$A_V = 11.00 \times 2.0 = 22.00$ g

$V_V = 7.128 \times 1.5 = 10.692$ in/sec

$D_V = .134 \times 1.0 = .134$ in

Step 6. See the shock response spectra for the values from step 6 in Figure 2A-28.

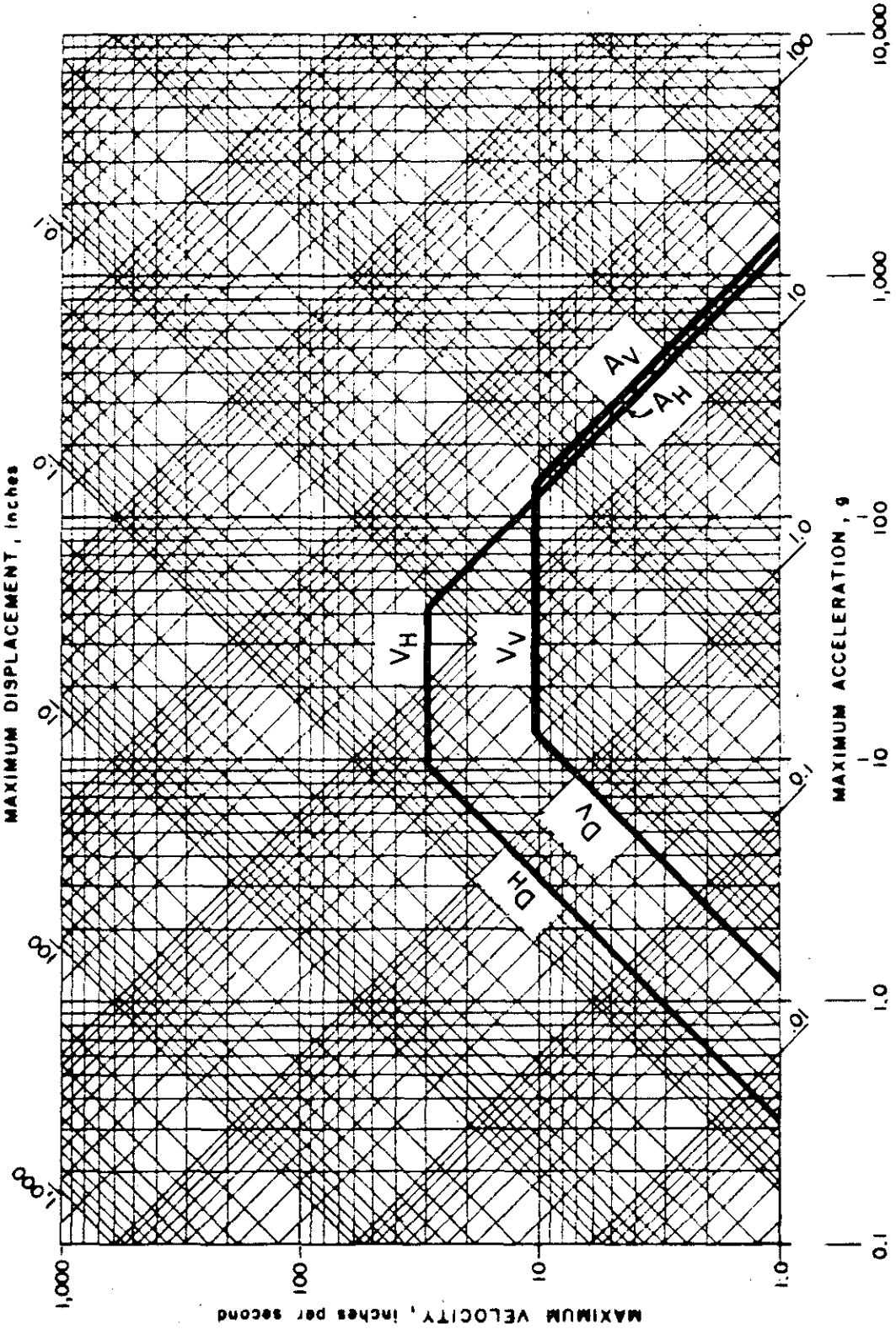

MAXIMUM VELOCITY, inches per second
MAXIMUM DISPLACEMENT, inches
MAXIMUM ACCELERATION, g
FREQUENCY, cps
AV
AH
VH
VV
DV
DH

FIGURE 2A-28

APPENDIX 2B

LIST OF SYMBOLS

a	(1) acceleration (in./ms^2) (2) depth of equivalent rectangular stress block (in.) (3) long span of a panel (in.)
a_o	velocity of sound in air (ft./sec.)
a_x	acceleration in x direction (in./ms^2)
a_y	acceleration in y direction (in./ms^2)
A	(1) area (in.^{2}) (2) explosive composition factor (oz.$^{1/2}$-in.$^{-3/2}$)
A_a	area of diagonal bars at the support within a width b (in.^{2})
A_b	area of reinforcing bar (in.^{2})
A_d	(1) door area (in.^{2}) (2) area of diagonal bars at the support within a width b (in.^{2})
A_D	drag area (in.^{2})
A_f	net area of wall excluding openings (ft.^{2})
A_g	area of gross section (in.^{2})
A_H	maximum horizontal acceleration of the ground surface (g's)
A_l	area of longitudinal torsion reinforcement (in.^{2})
A_L	lift area (in.^{2})
A_n	(1) net area of section (in.^{2}) (2) area of individual wall subdivision (ft.^{2})
A_o	area of openings (ft.^{2})
A_{ps}	area of prestressed reinforcement (in.^{2})
A_s	area of tension reinforcement within a width b (in.^{2})
A_s'	area of compression reinforcement within a width b (in.^{2})
A_s-	area of rebound reinforcement (in.^{2})
A_{sH}	area of flexural reinforcement within a width b in the horizontal direction on each face (in.^{2})*
A_{sp}	area of spiral reinforcement (in.^{2})
A_{st}	total area of reinforcing steel (in.^{2})
A_{sV}	area of flexural reinforcement within a width b in the vertical direction on each face (in.^{2})*

* See note at end of symbols

A_t area of one leg of a closed tie resisting torsion within a distance s ($in.^2$)

A_v total area of stirrups or lacing reinforcement in tension within a distance, s_s or s_l and a width b_s or b_l ($in.^2$)

A_V maximum vertical acceleration of the ground surface (g's)

A_w area of wall ($ft.^2$)

A_I, A_{II} area of sector I and II, respectively ($in.^2$)

b (1) width of compression face of flexural member (in.)
(2) width of concrete strip in which the direct shear stresses at the supports are resisted by diagonal bars (in.)
(3) short span of a panel (in.)

b_f width of fragment (in.)

b_s width of concrete strip in which the diagonal tension stresses are resisted by stirrups of area A_v (in.)

b_l width of concrete strip in which the diagonal tension stresses are resisted by lacing of area A_v (in.)

b_o failure perimeter for punching shear (in.)

b_t center-to-center dimension of a closed rectangular tie along b (in.)

B explosive constant defined in table 2-7 ($oz.^{1/2}$ $in.^{-7/6}$)

c (1) distance from the resultant applied load to the axis of rotation (in.)
(2) damping coefficient
(3) width of column capital (in.)

c_I, c_{II} distance from the resultant applied load to the axis of rotation for sectors I and II, respectively (in.)

c_s dilatational velocity of concrete (ft./sec.)

C (1) shear coefficient
(2) deflection coefficient for flat slabs

C_C deflection coefficient for the center of interior panel of flat slab

C_{cr} critical damping

C_d shear coefficient for ultimate shear stress of one-way elements

C_D drag coefficient

C_Dq drag pressure (psi)

C_{Dq_o} peak drag pressure (psi)

C_E equivalent load factor

C_f post-failure fragment coefficient (lb.^{2}-ms^4/in.^{8})

C_H shear coefficient for ultimate shear stress in horizontal direction for two-way elements*

C_L (1) leakage pressure coefficient from Figure 2-235
(2) deflection coefficient for midpoint of long side of interior flat slab panel
(3) lift coefficient

C_M maximum shear coefficient

C_m equivalent moment correction factor

C_p compression wave seismic velocity in the soil from Table 2-10 (in./sec.)

C_r sound velocity in reflected region from Figure 2-192 (ft./ms)

C_R force coefficient for shear at the corners of a window frame

$C_{r\alpha}$ peak reflected pressure coefficient at angle of incidence α

C_s shear coefficient for ultimate support shear for one-way elements

C_{sH} shear coefficient for ultimate support shear in horizontal direction for two-way elements*

C_{sV} shear coefficient for ultimate support shear in vertical direction for two-way elements*

C_S deflection coefficient for midpoint of short side of interior flat slab panel

C_u impulse coefficient at deflection X_u (psi-ms^2/in.^{2})

C_u' impulse coefficient at deflection X_m (psi-ms^2/in.^{2})

C_v shear coefficient for ultimate shear stress in vertical direction for two-way elements*

C_x shear coefficient for the ultimate shear along the long side of window frame

C_y shear coefficient for the ultimate shear along the short side of window frame

C_L confidence level

* See note at end of symbols

C_1 (1) impulse coefficient at deflection X_1 (psi-ms^2/in.^{2})
(2) ratio of gas load to shock load

C_1' impulse coefficient at deflection X_m (psi-ms^2/in.^{2})

C_2 ratio of gas load duration to shock load duration

d (1) distance from extreme compression fiber to centroid of tension reinforcement (in.)
(2) diameter (in.)
(3) fragment diameter (in.)

d' distance from extreme compression fiber to centroid of compression reinforcement (in.)

d_b diameter of reinforcing bar (in.)

d_c distance between the centroids of the compression and tension reinforcement (in.)

d_{cH} distance between the centroids of the horizontal compression and tension reinforcement (in.)

d_{co} diameter of steel core (in.)

d_{cV} distance between the centroids of the vertical compression and tension reinforcement (in.)

d_e distance from support and equal to distance d or d_c (in.)

d_i average inside diameter of explosive casing (in.)

d_i' adjusted inside diameter of casing (in.)

$d_{P_{normal}}$ distance between center lines of adjacent lacing bends measured to flexural reinforcement (in.)

d_p distance from extreme compression fiber to centroid of prestressed reinforcement (in.)

d_{sp} depth of spalled concrete (in.)

d_1 diameter of cylindrical portion of primary fragment (in.)

D (1) unit flexural rigidity (lb-in.)
(2) location of shock front for maximum stress (ft.)
(3) minimum magazine separation distance (ft.)
(4) caliber density (lb/in.^{3})
(5) overall diameter of circular section (in.)
(6) damping force (lb.)
(7) displacement of mass from shock load (in.)

D_E equivalent loaded width of structure for non-planar wave front (ft.)

D_H maximum horizontal displacement of the ground surface (in.)

DIF dynamic increase factor

D_s diameter of the circle through centers of reinforcement arranged in a circular pattern (in.)

D_{sp} diameter of the spiral measured through the centerline of the spiral bar (in.)

DLF dynamic load factor

D_V maximum vertical displacement of the ground surface (in.)

e (1) base of natural logarithms and equal to 2.71828...
(2) distance from centroid of section to centroid of prestressed reinforcement (in.)
(3) actual eccentricity of load (in.)

e_b balanced eccentricity (in.)

$2E'^{1/2}$ Gurney Energy Constant (ft./sec.)

E (1) modulus of elasticity
(2) internal work (in.-lbs.)

E_c modulus of elasticity of concrete (psi)

E_m modulus of elasticity of masonry units (psi)

E_s modulus of elasticity of reinforcement (psi)

f (1) unit external force (psi)
(2) frequency of vibration (cps)

f_c' static ultimate compressive strength of concrete at 28 days (psi)

f_{dc}' dynamic ultimate compressive strength of concrete (psi)

f_{dm}' dynamic ultimate compressive strength of masonry units (psi)

f_{ds} dynamic design stress for reinforcement (a function of f_y, f_u and θ) (psi)

f_{du} dynamic ultimate stress of reinforcement (psi)

f_{dy} dynamic yield stress of reinforcement (psi)

f_m' static ultimate compressive strength of masonry units (psi)

f_n natural frequency of vibration (cps)

f_{ps} (psi) average stress in the prestressed reinforcement at ultimate load

f_{pu} specified tensile strength of prestressing tendon (psi)

f_{py} yield stress of prestressing tendon corresponding to a 1 percent elongation (psi)

f_r reflection factor

f_s static design stress for reinforcement (psi)

f_{se} effective stress in prestressed reinforcement after allowances for all prestress losses (psi)

f_u static ultimate stress of reinforcement (psi)

f_y static yield stress of reinforcement (psi)

F (1) total external force (lbs.)
(2) coefficient for moment of inertia of cracked section
(3) function of C_2 and C_1 for bilinear triangular load

F_o force in the reinforcing bars (lbs.)

F_E equivalent external force (lbs.)

F_D drag force (lbs.)

F_F frictional force (lbs.)

F_L lift force (lbs.)

F_N vertical load supported by foundation (lbs.)

g acceleration due to gravity (32.2 ft./sec.^{2})

G shear modulus (psi)

h (1) charge location parameter (ft.)
(2) height of masonry wall

h_n average clearing distance for individual areas of openings from Section 2-15.4.2

h_t center-to-center dimension of a closed rectangular tie along h (in.)

h' clear height between floor slab and roof slab

H (1) span height (in.)*
(2) distance between reflecting surface(s) and/or free edge(s) in vertical direction (ft.)
(3) minimum transverse dimension of mean presented area of object (ft.)

H_c height of charge above ground (ft.)

* See note at end of symbols

H_s height of structure (ft.)

H_T height of triple point (ft.)

H_w height of wall (ft.)

H_c heat of combustion (ft.-lb./lb.)

H_d heat of detonation (ft.-lb./lb.)

i unit positive impulse (psi-ms)

i_a sum of blast impulse capacity of the receiver panel and the least impulse absorbed by the sand (psi-ms)

i_{ba} blast impulse capacity of receiver panel (psi-ms)

i^- unit negative impulse (psi-ms)

$\bar{i}_a$ sum of scaled unit blast impulse capacity of receiver panel and scaled unit blast impulse attenuated through concrete and sand in a composite element (psi-ms/lb.$^{1/3}$)

i_b unit blast impulse (psi-ms)

$\bar{i}_b$ scaled unit blast impulse (psi-ms/lb.$^{1/3}$)

$\bar{i}_{ba}$ scaled unit blast impulse capacity of receiver panel of composite element (psi-ms/lb.$^{1/3}$)

$\bar{i}_{bd}$ scaled unit blast impulse capacity of donor panel of composite element (psi-ms/lb.$^{1/3}$)

$\bar{i}_{bt}$ total scaled unit blast impulse capacity of composite element (psi-ms/lb.$^{1/3}$)

i_c impulse capacity of an element (psi-ms)

i_d total drag and diffraction impulse (psi-ms)

i_e unit excess blast impulse (psi-ms)

i_{fs} required impulse capacity of fragment shield (psi-ms)

i_g gas impulse (psi-ms)

i_r unit positive normal reflected impulse (psi-ms)

i_r^- unit negative normal reflected impulse (psi-ms)

$i_{r\alpha}$ peak reflected impulse at angle of incidence α (psi-ms)

i_s unit positive incident impulse (psi-ms)

i_s^- unit negative incident impulse (psi-ms)

i_{st} impulse consumed by fragment support connection (psi-ms)

I (1) moment of inertia ($in.^4$/in. for slabs) ($in.^4$ for beams)
(2) total impulse applied to fragment

I_a average of gross and cracked moments of inertia ($in.^4$/in. for slabs) ($in.^4$ for beams)

I_c moment of inertia of cracked concrete section ($in.^4$/in. for slabs) ($in.^4$ for beams)

I_{cH} moment of inertia of cracked concrete section in horizontal direction ($in.^4$/in.)*

I_{cV} moment of inertia of cracked concrete section in vertical direction ($in.^4$/in.)*

I_g moment of inertia of gross concrete section ($in.^4$/in. for slabs) ($in.^4$ for beams)

I_m mass moment of inertia (lb.-ms^2-in.)

I_n moment of inertia of net section of masonry unit ($in.^4$)

I_s gross moment of inertia of slab ($in.^4$/in.)

I_{st} impulse consumed by the fragment support connection (psi-ms)

I_w gross moment of inertia of wall ($in.^4$/in.)

j ratio of distance between centroids of compression and tension forces to the depth d

k (1) constant depending on the casing metal
(2) effective length factor

k_v velocity decay coefficient

K (1) unit stiffness (psi/in. for slabs) (lb./in./in. for beams) (lb./in. for springs)
(2) constant defined in paragraph 2-18.2

K_e elastic unit stiffness (psi/in. for slabs) (lb./in./in. for beams)

K_{ep} elasto-plastic unit stiffness (psi/in. for slabs) (lb./in./in. for beams)

K_E (1) equivalent elastic unit stiffness (psi/in. for slabs) (lb./in./ in. for beams)
(2) equivalent spring constant (lb./in.)

K_L load factor

* See note at end of symbols

K_{LM}	load-mass factor
$(K_{LM})_u$	load-mass factor in the ultimate range
$(K_{LM})_{up}$	load-mass factor in the post-ultimate range
K_M	mass factor
K_R	resistance factor
K_E	kinetic energy
l	charge location parameter (ft.)
l	(1) length of the yield line (in.) (2) width of 1/2 of the column strip (in.)
l_d	basic development length of reinforcing bar (in.)
l_{dh}	development length of hooked bar (in.)
l_c	length of cylindrical explosive (in.)
l_p	spacing of same type of lacing bar (in.)
l_s	span of flat slab panel (in.)
L	(1) span length (in.)* (2) distance between reflecting surface(s) and/or free edge(s) in horizontal direction (ft.)
L_{cyl}	length of cylinder (in.)
L_f	length of fragment (in.)
L_H	clear span in short direction (in.)
L_l	length of lacing bar requried in distance s_l (in.)
L_L	clear span in long direction (in.)
L_o	embedment length of reinforcing bars (in.)
L_u	unsupported length of column (in.)
L_w	wave length of positive pressure phase (ft.)
L_w^-	wave length of negative pressure phase (ft.)
L_x	clear span in long direction (in.)
L_y	clear span in short direction (in.)

* See note at end of symbols

L_{wb}, L_{wd} wave length of positive pressure phase at points b and d, respectively (ft.)

L_l total length of sector of element normal to axis of rotation (in.)

m (1) unit mass (psi-ms^2/in. for slabs) [beams, (lb./in-ms^2)/in.]
(2) ultimate unit moment (in.-lbs./in.)
(3) mass of fragment (lbs.-ms^2/in.)

m_a average of the effective elastic and plastic unit masses (psi-ms^2/in. for slabs) [beams, (lb./in-ms^2)/in]

m_e effective unit mass (psi-ms^2/in. for slabs) [beams, (lb/in-ms^2)/in]

m_{sp} mass of spalled fragments (psi-ms^2/in.)

m_u effective unit mass in the ultimate range (psi-ms^2/in. for slabs) [beams, (lb/in-ms^2]/in.]

m_{up} effective unit mass in the post-ultimate range (psi-ms^2/in.)

M (1) unit bending moment (in.-lbs./in. for slabs) (in.-lbs. for beams)
(2) total mass (lb.-ms^2/in.)
(3) design moment (in.-lbs.)

M_e effective total mass (lb.-ms^2/in.)

M_u ultimate unit resisting moment (in.-lbs./in. for slabs) (in.-lbs. for beams)

M_u^- ultimate unit rebound moment (in.-lbs./in. for slabs) (in.-lbs. for beams)

M_c moment of concentrated loads about line of rotation of sector (in.-lbs.)

M_A fragment distribution factor

M_E equivalent total mass (lb.-ms^2/in.)

M_{HN} ultimate unit negative moment capacity in horizontal direction (in.-lbs./in.)*

M_{HP} ultimate unit positive moment capacity in horizontal direction (in.-lbs./in.)*

M_{OH}, M_{OL} total panel moment for direction H and L respectively (in.-lbs.)

M_N ultimate unit negative moment capacity at supports (in.lbs./in. for slabs) (in.-lbs. for beams)

M_P ultimate unit positive moment capacity at midspan (in.-lbs./in. for slabs) (in.-lbs. for beams)

* See note at end of symbols

M_{VN} ultimate unit negative moment capacity in vertical direction (in.-lbs./in.)*

M_{VP} ultimate unit positive moment capacity in vertical direction (in.-lbs./in.)*

M_1 value of smaller end moment on column

M_2 value of larger end moment on column

n (1) modular ratio
(2) number of time intervals
(3) number of glass pane tests
(4) caliber radius of the tangent ogive of fragment nose

N (1) number of adjacent reflecting surfaces
(2) nose shape factor

N_f number of primary fragments larger than W_f

N_u axial load normal to the cross section

N_T total number of fragments

p reinforcement ratio equal to A_s/bd or A_s/bd_c

p' reinforcement ratio equal to A_s'/bd or A_s'/bd_c

p_b reinforcement ratio producing balanced conditions at ultimate strength

p_o ambient atmospheric pressure (psi)

p_p prestressed reinforcement ratio equal to A_{ps}/bd_p

p_m mean pressure in a partially vented chamber (psi)

p_{mo} peak mean pressure in a partially vented chamber (psi)

p_r average peak reflected pressure (psi)

p_H reinforcement ratio in horizontal direction on each face*

p_T total reinforcement ratio equal to $p_H + p_V$

p_V reinforcement ratio in vertical direction on each face*

p(x) distributed load per unit length

P (1) pressure (psi)
(2) concentrated load (lbs.)

P^- negative pressure (psi)

P_c critical axial load causing buckling (lbs.)

* See note at end of symbols

P_g maximum gas pressure (psi)

P_i interior pressure within structure (psi)

δP_i interior pressure increment (psi)

P_f fictitious peak pressure (psi)

P_{max} maximum average pressure acting on interior face of wall (psi)

P_o (1) peak pressure (psi)
(2) maximum axial load (lbs.)
(3) atmospheric pressure (psi)

P_r peak positive normal reflected pressure (psi)

P_r^- peak negative normal reflected pressure (psi)

$P_{r\alpha}$ peak reflected pressure at angle of incidence α (psi)

P_{RIB} maximum average pressure on backwall (psi)

P_s positive incident pressure (psi)

P_{sb}, P_{se} positive incident pressure at points b and e, respectively (psi)

P_{so} peak positive incident pressure (psi)

P_{so}^- peak negative incident pressure (psi)

P_{sob}, P_{sod}, P_{soe} peak positive incident pressure at points b, d, and e, respectively (psi)

P_u ultimate axial load at actual eccentricity c (lbs.)

P_x ultimate load when eccentricity e_x is present (lbs.)

P_y ultimate load when eccentricity e_y is present (lbs.)

q dynamic pressure (psi)

q_b, q_e dynamic pressure at points b and e, respectively (psi)

q_o peak dynamic pressure (psi)

q_{ob}, q_{oe} peak dynamic pressure at points b and e, respectively (psi)

r (1) unit resistance (psi)
(2) radius of spherical TNT [density equals 95 lb./ft.^{3}] charge (ft.)
(3) radius of gyration of cross section of column (in.)

r^- unit rebound resistance (psi, for slabs) (lb./in. for beams)

r_{avail} dynamic resistance available (psi)

δr change in unit resistance (psi, for slabs) (lb./in. for beams)

r_d radius from center of impulse load to center of door rotation (in.)

r_{DL} uniform dead load (psi)

r_e elastic unit resistance (psi, for slabs) (lb./in. for beams)

r_{ep} elasto-plastic unit resistance (psi, for slabs) (lb./in. for beams)

r_{fs} ultimate unit resistance of fragment shield (psi)

r_T tension membrane resistance (psi)

r_u ultimate unit resistance (psi, for slabs) (lb./in. for beams)

r_{up} post-ultimate unit resistance (psi)

r_1 radius of hemispherical portion of primary fragment (in.)

R
(1) total internal resistance (lbs.)
(2) slant distance (ft.)
(3) ratio of S/G
(4) standoff distance (ft.)

R_{eff} effective radius (ft.)

R_f
(1) distance traveled by primary fragment (ft.)
(2) distance from center of detonation (ft.)

R_g uplift force at corners of window frame (lbs.)

R_l radius of lacing bend (in.)

R_t target radius (ft.)

R_A normal distance (ft.)

R_E equivalent total internal resistance (lbs.)

R_G ground distance (ft.)

R_u total ultimate resistance (lb.)

R_I, R_{II} total internal resistance of sectors I and II, respectively (lbs.)

s
(1) sample standard deviation
(2) spacing of torsion reinforcement in a direction parallel to the longitudinal reinforcement (in.)
(3) pitch of spiral (in.)

s_s spacing of stirrups in the direction parallel to the longitudinal reinforcement (in.)

s_l spacing of lacing in the direction parallel to the longitudinal reinforcement (in.)

S height of front wall or one-half its width, whichever is smaller (ft.)

S' weighted average clearing distance with openings (ft.)

SE strain energy

t time (ms)

δt time increment (ms)

t_a any time (ms)

t_b, t_e, t_f time of arrival of blast wave at points b, e, and f, respectively (ms)

t_c (1) clearing time for reflected pressures (ms)
(2) average casing thickness of explosive charges (in.)

t_c' (1) adjusted casing thickness (in.)
(2) Clearing time for reflected pressures adjusted for wall openings (ms)

t_d rise time (ms)

t_E time to reach maximum elastic deflection (ms)

t_g fictitious gas duration (ms)

t_m time at which maximum deflection occurs (ms)

t_o duration of positive phase of blast pressure (ms)

t_o^- duration of negative phase of blast pressure (ms)

t_{of} fictitious positive phase pressure duration (ms)

t_{of}^- fictitious negative phase pressure duration (ms)

t_r fictitious reflected pressure duration (ms)

t_u time at which ultimate deflection occurs (ms)

t_y time to reach yield (ms)

t_A time of arrival of blast wave (ms).

t_{AG} time of arrival of ground shock (ms)

t_1	time at which partial failure occurs (ms).
T	(1) duration of equivalent triangular loading function (ms) (2) thickness of masonry wall (in.) (3) toughness of material (psi-in./in.)
T_c	thickness of concrete section (in.)
$\bar{T}_c$	scaled thickness of concrete section (ft./lb.$^{1/3}$)
T_g	thickness of glass (in.)
T_H	force in the continuous reinforcement in the short span direction (lbs.)
T_i	angular impulse load (lb.-ms-in.)
T_L	force in the continuous reinforcement in the long span direction (lbs.)
T_N	effective natural period of vibration (ms)
T_{pf}	minimum thickness of concrete to prevent perforation by a given fragment (in.)
T_r	rise time (ms)
T_s	(1) thickness of sand fill (in.) (2) thickness of slab (in.)
T_{sp}	minimum concrete thickness to prevent spalling (in.)
$\bar{T}_s$	scaled thickness of sand fill (ft./lb.$^{1/3}$)
T_u	total torsional moment at critical section (in.-lbs.)
T_w	thickness of wall (in.)
T_y	force of the continuous reinforcement in the short direction (lbs.)
u	particle velocity (ft./ms)
u_u	ultimate flexural or anchorage bond stress (psi)
U	shock front velocity (ft./ms)
U_s	strain energy
v	velocity (in./ms)
v_a	instantaneous velocity at any time (in./ms)
v_b	boundary velocity for primary fragments (ft./sec.)

v_c ultimate shear stress permitted on an unreinforced web (psi)

v_f maximum post-failure fragment velocity (in./ms)

$v_{f(avg.)}$ average post-failure fragment velocity (in./ms)

v_i velocity at incipient failure deflection (in./ms)

v_o initial velocity of primary fragment (ft./sec.)

v_r residual velocity of primary fragment after perforation (ft./sec.)

v_s striking velocity of primary fragment (ft./sec.)

v_{tc} maximum torsion capacity of an unreinforced web (psi)

v_{tu} nominal torsion stress in the direction of v_u (psi)

v_u ultimate shear stress (psi)

v_{uH} ultimate shear stress at distance d_e from the horizontal support (psi)*

v_{uV} ultimate shear stress at distance d_e from the vertical support (psi)*

v_x velocity in x direction (in./ms.)

v_y velocity in y direction (in./ms.)

V (1) volume of partially vented chamber ($ft.^3$)
(2) velocity of compression wave through concrete (in./sec.)
(3) velocity of mass under shock load (in./sec.)

V_d ultimate direct shear capacity of the concrete of width b (lbs.)

V_{dH} shear at distance d_e from the vertical support on a unit width (lbs./in.)*

V_{dV} shear at distance d_e from the horizontal support on a unit width (lbs./in.)*

V_f free volume ($ft.^3$)

V_H maximum horizontal velocity of the ground surface (in./sec.)

V_o volume of structure ($ft.^3$)

V_s shear at the support (lb./in., for panels) (lbs. for beam)

V_{sH} shear at the vertical support on a unit width (lbs./in.)*

V_{sV} shear at the horizontal support on a unit width (lbs./in.)*

V_u total shear on a width b (lbs.)

* See note at end of symbols

V_V maximum vertical velocity of the ground surface (in./sec.)

V_x unit shear along the long side of window frame (lb./in.)

V_y unit shear along the short side of window frame, (lbs./in.)

w applied uniform load (lbs.-in.^{2})

w_c (1) unit weight (psi, for panels) (lb./in. for beam)
(2) weight density of concrete (lbs./ft.^{3})

w_s weight density of sand (lbs./ft.^{3})

W (1) design charge weight (lbs.)
(2) external work (in.-lbs.)
(3) width of wall (ft.)

W_A weight of fluid (lbs.)

W_{ACT} actual quantity of explosives (lbs.)

W_c total weight of explosive containers (lbs.)

W_E effective charge weight (lbs.)

W_{Eg} effective charge weight for gas pressure (lb.)

W_{EXP} weight of explosive in question (lbs.)

W_f weight of primary fragment (oz.)

$\bar{W}_f$ average fragment weight (oz.)

W_F weight of frangible element (lb./ft.^{2})

W_{CI} weight of inner casing (lbs.)

W_{co} total weight of steel core (lbs.)

W_{CO} weight of outer casing (lbs.)

W_{c1}, W_{c2} total weight of plates 1 and 2, respectively (lbs.)

W_s width of structure (ft.)

W_D work done

x yield line location in horizontal direction (in.)*

X (1) deflection (in.)
(2) distance from front of object to location of largest cross section to plane of shock front (ft.)

X_a any deflection (in.)

* See note at end of symbols

X_c lateral deflection to which a masonry wall develops no resistance (in.)

X_{DL} deflection due to dead load (in.)

X_e elastic deflection (in.)

X_E equivalent elastic deflection (in.)

X_{ep} elasto-plastic deflection (in.)

X_f maximum penetration into concrete of armor-piercing fragments (in.)

X_f' maximum penetration into concrete of fragments other than armor-piercing (in.)

X_m maximum transient deflection (in.)

X_p plastic deflection (in.)

X_s (1) maximum penetration into sand of armor-piercing fragments (in.)
(2) static deflection (in.)

X_u ultimate deflection (in.)

X_1 (1) partial failure deflection (in.)
(2) deflection at maximum ultimate resistance of masonry wall (in.)

y yield line location in vertical direction (in.)*

y_t distance from the top of section to centroid (in.)

Z scaled slant distance (ft./lb.$^{1/3}$)

Z_A scaled normal distance (ft./lb.$^{1/3}$)

Z_G scaled ground distance (ft./lb.$^{1/3}$)

α (1) angle formed by the plane of stirrups, lacing, or diagonal reinforcement and the plane of the longitudinal reinforcement (deg)
(2) angle of incidence of the pressure front (deg)
(3) acceptance coefficient
(4) trajectory angle (deg.)

α_{ec} ratio of flexural stiffness of exterior wall to flat slab

α_{ecH}, α_{ecL} ratio of flexural stiffness of exterior wall to slab in direc-tion H and L respectively

* See note at end of symbols

β	(1) coefficient for determining elastic and elasto-plastic resistances (2) particular support rotation angle (deg) (3) rejection coefficient (4) target shape factor from Figure 2-212
β_1	factor equal to 0.85 for concrete strengths up to 4,000 psi and is reduced by 0.05 for each 1,000 psi in excess of 4,000 psi
γ	coefficient for determining elastic and elasto-plastic deflections
γ_p	factor for type of prestressing tendon
δ	moment magnifier
δ_n	clearing factor
δ	deflection at sector's displacement (in.)
ϵ_c'	average strain rate for concrete (in./in./ms)
ϵ_m	unit strain in mortar (in./in.)
ϵ_s'	average strain rate for reinforcement (in./in./ms)
ϵ_u	rupture strain (in./in./ms)
θ	(1) support rotation angle (deg) (2) angular acceleration (rad/ms^2)
θ_{max}	maximum support rotation angle (deg)
θ_H	horizontal rotation angle (deg)*
θ_V	vertical rotation angle (deg)*
μ	(1) ductility factor (2) coefficient of friction
v	Poisson's ratio
ρ	(1) mass density (lbs.-ms.^{2}/in.^{4}) (2) density of air behind shock front (lbs/ft.^{3})
ρ_a	density of air (oz./in.^{3})
ρ_c	density of casing (oz./in.^{3})
ρ_f	mass density of fragment (oz./in.^{3})
ρ_o	mass density of medium (lb.-ms.^{2}/in.^{4})
σ_u	fracture strength of concrete (psi)

* See note at end of symbols

Σ_o effective perimeter of reinforcing bars (in.)

ΣM summation of moments (in.-lbs.)

ΣM_N sum of the ultimate unit resisting moments acting along the negative yield lines (in.-lbs.)

ΣM_P sum of the ultimate unit resisting moments acting along the positive yield lines (in.-lbs.)

ϕ (1) capacity reduction factor
(2) bar diameter (in.)
(3) TNT conversion factor

ϕ_r assumed shape function for concentrated loads

$\phi(x)$ assumed shape function for distributed loads free edge

═══ simple support

$\overline{/////}$ fixed support

$\overline{XXXXX}$ either fixed, restrained, or simple support

* Note. This symbol was developed for two-way elements which are used as walls. When roof slabs or other horizontal elements are under consideration, this symbol will also be applicable if the element is treated as being rotated into a vertical position.

APPENDIX 2C - BIBLIOGRAPHY

Blast Loads

1. Armendt, B. R., Hippensteel, R. G., Hoffman, A. J., and Keefer, J. H., Project White Tribe: Air Blast From Simultaneously Detonated Large-Scale Explosive Charges, BRL Report 1145, Aberdeen Proving Ground, Maryland, September 1961.
2. Armendt, B. R., Hippensteel, R. G., Hoffman, A. J., and Kingery, C. N., The Air Blast From Simultaneously Detonated Explosive Spheres, BRL Report 1294, Aberdeen Proving Ground, Maryland, August 1960.
3. Armendt, B. R., Hippensteel, R. G., Hoffman, A. J., and Schlueter, S.D., The Air Blast From Simultaneously Detonated Explosive Spheres: Part II - Optimization, BRL Memorandum Report 1384, Department of the Army Project No. 503-04-002, Aberdeen Proving Ground, Maryland, January 1962.
4. Ayvazyan, H.E., Dobbs N., Computer Program-Impres, special publication ARLCD-SP-84001, prepared by Ammann and Whitney, New York, New York, for U.S. Army Armament Research and Development Center, Large Caliber Weapon Systems Laboratory, Dover, New Jersey.
5. Baker, W. E., Explosions in Air, University of Texas Press, Austin, Texas 1973.
6. Baker, W. E., Prediction and Scaling of Reflected Impulse From Strong Blast Waves, International Journal of Mechanical Science, 9, 1967, pp. 45-51.
7. Bleakney, W., The Diffraction of Shock Waves Around Obstacles and the Transient Loading of Structures, Princeton University, March 1950, (Published and Distributed by the Armed Forces Special Weapons Project).
8. Coulter, G.A., Air Shock and Flow in Model Rooms, BRL Memorandum Report 1987, Aberdeen Proving Ground, Maryland, June 1969.
9. Coulter, G. A., Air Shock Filling of Model Rooms, BRL Memorandum Report 1916, Aberdeen Proving Ground, Maryland, March 1968.
10. Coulter, G. A. and Peterson, R.L., Blast Fill Time of a One-Room Structure, Operation Prairie Flat Project Officers Report, Project LN 111 POR-2102, Ballistic Research Laboratory, Aberdeen Proving Ground, Maryland, November 1964.
11. Coulter, G. A., Bulmash G., and Kingery C., Feasibility Study of Shock Wave Modification in the BRL 2.44 m Blast Simulator, Memorandum Report ARBRL-MR-0339, prepared by U.S. Army Armament Research and Development Center, Ballistic Research Laboratory, Aberdeen Proving Ground, Maryland, March 1984.
12. Cranz, C., Lehrbuch der Ballistik, Springer-Verlag, Berlin, 1926.
13. Dewey, J.M., Johnson, O.T., and Patterson, J.D. II, Mechanical Impulse Measurements Close to Explosive Charges, BRL Report 1182, Aberdeen Proving Ground, Maryland, November 1962.
14. Dobratz, B.M., LLNL Explosives Handbook, Properties of Chemical Explosives and Explosive Simulants, URCL-52997, Lawrence Livermore National Laboratory, Livermore, California, March 1981.
15. Engineering Design Handbook, Principles of Explosive Behavior, AMCP 706-180, Headquarters, U.S. Army Material Command, Washington, D.C., April 1972.
16. Goodman, H. J., Compiled Free Air Blast Data on Bar Spherical Pentolite, BRL Report 1092, Aberdeen Proving Ground, Maryland, 1960.
17. Granstorm, S. A., Loading Characteristics of Air Blasts From Detonating Charges, Transactions of the Royal Institute of Technology, Stockholm, Sweden, Nr.100, 1956.
18. Hokanson, J.C., Esparza, E. D., and Wenzel, A. B., Blast Effects of Simultaneous Multiple-Charge Detonations, Contractor Report ARLCD-CR-78032, ARRADCOM, Dover, New Jersey, AD E400232, October 1978.

19. Hokanson, J.C., Esparza, E.D., Baker W.E., Sandoval, N.R. and Anderson, C.E., Determination of Blast Loads in the Damaged Weapons Facility, Vol 3, Final Report, Purchase Order F0913400, SwRI-6578, prepared by Southwest Research Institute, San Antonio, Texas, for Mason and Hanger - Silas Mason Company, Inc., Pantex Plant, Amarillo, Texas, July 1982.
20. Hokanson, J. C., Esparza, E. D., and Wenzel, A. B., Reflected Blast Measurements Around Multiple Detonating Charges, Minutes of the Eighteenth Explosives Safety Seminar, Volume I, September 1978, pp. 447-471.
21. Hokanson, J. C., Esparza, E. D., Wenzel, A. B. (Southwest Research Institute). Price, P. D. (ARRADCOM). Blast Effects of Simultaneous Multiple-Charge Detonations, Contractor Report ARLCD-CR-78032, prepared by U.S. Army Armament Research and Development Command, Large Caliber Weapon Systems Laboratory, Dover, New Jersey, October 1978.
22. Hopkinson, B. British Ordnance Board Minutes, 13565, 1915.
23. Iwanski, E. C., et al., Blast Effects on Buildings and Structures Operation of 6-Foot and 2-Foot Shock Tubes: High Pressure Tests on Simple Shapes, Report No. 54, Final Test Report No. 10, ARF Project No. D087, Armour Research Foundation of Illinois Institute of Technology.
24. Jack, W. H., Jr., Measurements of Normally Reflected Shock Waves From Explosive Charges, BRL Memorandum Report 1499, Aberdeen Proving Ground, Maryland, AD 422886, July 1963.
25. Jack, W. H., Jr. and Armendt, B. F., Jr., Measurements of Normally Reflected Shock Parameters Under Simulated High Altitude Conditions, BRL Report 1280, Aberdeen Proving Ground, Maryland, AD 469014, April 1965.
26. Johansson, C. H. and Persson, P.A., Detonics of High Explosives, Academic Press, London, England, and New York, New York, 1970.
27. Johnson, O.T., Patterson, J.D. II, and Olson, W.C., A Simple Mechanical Method for Measuring the Reflected Impulse of Air Blast Waves, BRL Report 1099, Aberdeen Proving Ground, Maryland, July 1957.
28. Kaplan, K., Lewis, K. S., and Morris, P. J., Blast Loading and Response of Military Equipment, Draft Final Report URS 7339-6, URS Research Company, San Mateo, California, Prepared for Ballistic Research Laboratory, December 1973.
29. Kaplan, K. and Price, P.D., Accidental Explosions and Effects of Blast Leakage Into Structures, Contractor Report ARLCD-CR-79009, U.S. Army ARRADCOM, Dover, New Jersey, AD E400320, June 1979.
30. Keenan, W. A., and Tancreto, J. E., Blast Environment From Fully and Partially Vented Explosions in Cubicles, Technical Report R 828, prepared by Civil Engineering Laboratory, Naval Construction Battalion Center, Port Hueneme, California, sponsored by Department of the Army Picatinny Arsenal, November 1975.
31. Keenan, W., Tancreto, J., Meyers, G., Johnson, F., Hopkins, J., Nickerson, H., and Armstrong, W., NCEL Products Supporting DOD Revision of NAVFAC P-397, Program No. Y0995-01-003-201, Technical Memorandum 2591TM, sponsored by Naval Facilities Engineering Command, Alexandria, Virginia, and Naval Civil Engineering Laboratory, Port Hueneme, California, March 1983.
32. Kingery, C.N., and Bulmash G., Airblast Parameters from TNT Spherical Air Burst and Hemispherical Surface Burst, Technical Report ARBRL-TR-02555, prepared by U.S. Army Armament Research and Development Center, Ballistic Research Laboratory, Aberdeen Proving Ground, Maryland, April 1984.
33. Kingery, C. N. and Coulter G. A., Reflected Overpressure Impulse on a Finite Structure, Technical Report ARBRL-TR-02537. prepared by U. S.

Army Armament Research and Development Center, Ballistic Research Laboratory, Aberdeen Proving Ground Maryland, December 1983.

34. Kingery, C. N. and Coulter G. A., Enhanced Blast as a Function of Multiple Detonations and Shape for Bare Pentolite Charges, Memorandum Report BRL-MR-3539, prepared by U.S. Army Ballistic Research Laboratory, Aberdeen Proving Ground, Maryland, July 1986.
35. Kingery, C. N., Bulmash G., and Muller P., Blast Loading on Above Ground Barricaded Munition Storage Magazines, Technical Report ARBL-TR-02557, prepared by U.S. Army Armament Research and Development Center, Ballistic Research Laboratory, Aberdeen Proving Ground, Maryland, May 1984.
36. Kriebel, A.R., Air Blast in Tunnels and Chambers, Final Report DASA 1200-11, Supplement 1, Prepared for Defense Civil Preparedness Agency, URS Research Company, San Mateo, California, September 1972.
37. Makino, R. The Kirkwood-Brinkley Theory of the Propagation of Spherical Shock Waves and Its Comparison With Experiment, BRL Report 750, Aberdeen Proving Ground, Maryland, April 1951.
38. McIntyre, F. L., TNT Equivalency Test Results of Selected High Explosives, Propellants, and Pyrotechnics in Surface Burst Configurations, Contractor Report, Prepared by Technical Services Laboratory, National Space Technology Laboratories , NSTL MS 39529, for U.S. Army Research and Development Engineering Center, Dover, New Jersey, Sponsored by U.S. Army - AMCCOM, July 1986.
39. Melichar, J. F., The Propagation of Blast Waves Into Chambers, BRL Memorandum Report 1920, Aberdeen Proving Ground, Maryland, March 1968.
40. Olson, W. C., Patterson, J. D. II, and Williams, J. S., The Effect of Atmospheric Pressure on the Reflected Impulse From Blast Waves, BRL Memorandum Report 1241, Aberdeen Proving Ground, Maryland, January 1960.
41. Reeves H., and Robinson W. T., Hastings Igloo Hazards Tests for Small Explosive Charges, Memorandum Report ARBL-MR-03356, prepared by U. S. Army Armament Research and Development Center, Ballistic Research Laboratory, Aberdeen Proving Ground, Maryland, May 1984.
42. Reisler, R. E., Kennedy, L. W., and Keefer, J. H., High Explosive Multi-Burst Air Blast Phenomena (Simultaneous and Non-Simultaneous Detonations), BRL Technical Report ARBRL-TR-02142, Aberdeen Proving Ground, Maryland, February 1979.
43. Sachs, R. G., The Dependence of Blast on Ambient Pressure and Temperature, BRL Report 466, Aberdeen Proving Ground, Maryland, 1944.
44. Shear, R. E., Incident and Reflected Blast Pressures for Pentolite, BRL Report 1262, Aberdeen Proving Ground, Maryland, September 1964.
45. Shear, R. E. and McCane, P., Normally Reflected Shock Front Parameters, BRL Memorandum Report 1273, Aberdeen Proving Ground, Maryland, May 1960.
46. Swisdak, M.M., Jr., Explosion Effects and Properties: Part I - Explosion Effects in Air, NSWC/WOL/TR 75-116, Naval Surface Weapons Center, White Oak, Silver Spring, Maryland, October 1975.
47. The Effects of Nuclear Weapons, S. Glastone, Editor, U. S. Atomic Energy Commission, Washington, D. C., (Revised Edition), 1964.
48. Voltz, R. D., and Kiger, S. A., An Evaluation of the Separated Bay Concept for a Munition Assembly Complex; An Experimental Investigation of the Department of Energy Building 12-64 Complex, Technical Report SL-83-6, prepared by Structures Laboratory, U.S. Army Engineer Waterways Experiment Station, Vicksburg, Mississippi, for Department of Energy, Albuquerque Operations, Amarillo, Texas, September 1983.
49. Ward, J. M. (DOD Explosives Safety Board), Swisdak, M. M., Jr., Peckham P. J., and Soper W. G. (NSWC), Lorenz R. A. (Boeing Military Aircraft Company), Modeling of Debris and Airblast Effects from Explosions

inside Scaled Hardened Aircraft Shelters, Final Report NSWC TR 85-470, prepared by Naval Surface Weapons Center, Silver Spring, Maryland, May 1985.

50. Warnecke, C. Data Report: Support Test Evaluation of a Pre-Engineered Building, TECOM Project No. 2-CO-PIC-004, U.S. Army Dugway Proving Ground, Dugway, Utah, June 1977.
51. Wenzel, A. B. and Esparza, E. D., Measurements of Pressures and Impulses at Close Distances From Explosive Charges Buried and in Air, Final Report on Contract No. DAAK02-71-C-0393 with U.S. Army MERDC, Fort Belvoir, Virginia, 1972.
52. Wilton, C. and Gabrielsen, B. L., Shock Tunnel Tests of Preloaded and Arched Wall Panels, Final Report URS 7030-10, prepared for Defense Civil Preparedness Agency, URS Research Company, San Mateo, California, June 1973.
53. Wilton, C. and Gabrielsen, B. L., Shock Tunnel Tests of Wall Panels, Technical Report, Volume I, Test Information and Analysis, URS 7030-7, prepared for Defense Civil Preparedness Agency, URS Research Company, San Mateo, California, January 1972.
54. Wilton, C., Kaplan, K., and Gabrielsen, B.L., The Shock Tunnel: History and Results, Volume II - Loading Studies, Final Report SSI 7618-1, prepared for Defense Civil Preparedness Agency, Scientific Service, Inc., Redwood City, California, March 1978.
55. Zaker, T. A., Blast Pressures From Sequential Explosions, Phase Report II, Project J6166, IIT Research Institute, Chicago, Illinois, March 25, 1969.

Primary and Secondary Fragments

56. Amos, C. W., Fragment Resistance of Martensitic Steel Sheets (U), AMRA TR-64-01, (CONFIDENTIAL), U.S. Army Materials Research Agency, Watertown, Massachusetts, January 1964.
57. Apgar, J. W., Reaction of Mild Steel Targets to Exploding Munitions (U), U.S. Army Ballistic Research Laboratories, Aberdeen Proving Ground, Maryland (CONFIDENTIAL), October 1967.
58. Baker, W. E., Non-Nuclear Weapons Effects on Protective Structures (U), AFWL-TR-67-133 (SECRET), Mechanics Research, Inc., Houston, Texas, for U.S. Air Force Weapons Laboratory, January 1969.
59. Beth, R. A., Final Report on Concrete Penetration, Report No A-388, National Defense Research Committee, Office of Scientific Research and Development, March 1946.
60. Bulmash, G., Kingery C.N., and Coulter, G.A., Velocity Measurements of Acceptor Wall Fragments From the Mass Detonation of Neighboring Above-Ground Barricaded Munition Storage Magazine Model, Technical Report BRL-TR-2719, prepared by U.S. Army Ballistic Research Laboratory, Aberdeen Proving Ground, Maryland, March 1986.
61. Cohen, E. and Dobbs N., Design Procedures and Details for Reinforced Concrete Structures Utilized in Explosive Storage and Manufacturing Facilities, Ammann and Whitney, Consulting Engineers, New York, New York, Annals of the New York Academy of Sciences, Conference on Prevention of and Protection Against Accidental Explosion of Munitions, Fuels and Other Hazardous Mixtures, Vol. 152, Art. 1, 1968.
62. Doyle, J.M., Klein, M.J. and Shah, H., Design of Missile Resistant Concrete Panels, Preprints of the 2nd International Conference on Structural Mechanics in Reactor Technology, Vol. 4, Commission of the European Communities, Brussels, 1973, Paper No. J 3/3.

63. Effects of Impact and Explosion, Volume 1, Office of Scientific Research and Development, National Defense Research Committee, Washington, D.C., 1946.
64. Fundamentals of Protective Design for Conventional Weapons, prepared by U.S. Army Engineer Waterways Experiment Station, Vicksburg, Mississippi, for Office, Chief of Engineers, U.S. Army, Washington, D.C., July 1984.
65. Gewaltney, R. C., Missile Generation and Protection in Light-Water-Cooled Power Reactor Plants, Nuclear Safety, 10(4): July-August 1969.
66. Giere, A. C., Calculating Fragment Penetration and Velocity Data for Use in Vulnerability Studies, NAVORD Report 6621, U.S. Naval Nuclear Evaluation Unit, Albuquerque, New Mexico, October 1959.
67. Gurney, R. W., The Initial Velocities of Fragments from Bombs, Shells and Grenades, Report No. 405, Ballistic Research Laboratories, Aberdeen Proving Ground, Maryland, September 1943.
68. Gurney, R. W., The Mass Distribution of Fragments from Bombs, Shells and Grenades, Report No. 448, Ballistic Research Laboratories, Aberdeen Proving Ground, Maryland, February 1944.
69. Healey, J. J., and Weissman, S., Primary Fragment Characteristics and Impact Effects in Protective Design, Minutes of the Sixteenth Explosive Safety Seminar, September 1974.
70. Hoffman, P. R., McMath, R.R., and Migotsky, E., Projectile Penetration Studies, AFWL Technical Report No. WL-TR-64-102, Avco Corporation for the Air Force Weapons Laboratory, Kirtland Air Force Base, December 1964.
71. Industrial Engineering Study to Establish Safety Design Criteria for Use in Engineering of Explosive Facilities and Operations; Ammann and Whitney, Consulting Engineers, New York, New York, Report for Picatinny Arsenal, Dover, New Jersey, April 1963.
72. Johnson, C. and Moseley, J.W., Preliminary Warhead Terminal Ballistic Handbook. Part 1: Terminal Ballistic Effects, NAVWEPS Report No. 7673, U.S. Naval Weapons Laboratory, Dahlgren, Virginia, March 1964.
73. Kolsky, H., Stress Waves in Solids, Dover Publications, New York, New York, 1963.
74. Kymer, J.R., Penetration Performance of Arrow Type Projectiles, Report R-1814, U.S. Army Frankford Arsenal, Philadelphia, Pennsylvania, May 1966.
75. Mott, R.I., A Theoretical Formula for the Distribution of Weights of Fragments, AC-3642 (British). March 1943.
76. Mott, R.I., A Theory of Fragmentation, Army Operational Research Group Memorandum, 113-AC-6427, Great Britain, 1943.
77. Non-Nuclear Weapons Effects on Protective Structures (U), Technical Report No. AFWL-TR-69-57, Air Force Weapons Laboratory, Kirtland Air Force Base, December 1964.
78. Non-Nuclear Weapons Effects on Protective Structures (U), Technical Report No. AFWL-TR-69-57, (SECRET), Mechanics Research, Inc., for the Air Force Weapons Laboratory, Kirtland Air Force Base, September 1969.
79. Recht, R., et al., Application of Ballistic Perforation Mechanics to Target Vulnerability and Weapons Effectiveness Analysis (U), NWC TR 4333 (CONFIDENTIAL), Denver Research Institute for the Naval Weapons Center, China Lake, California, October 1967.
80. Reeves H., and Robinson W. T., Hastings Igloo Hazards Tests for Small Explosive Charges, Memorandum Report ARBL-MR-03356, prepared by U.S. Army Armament Research and Development Center, Ballistic Research Laboratory, Aberdeen Proving Ground, Maryland, May 1984.

81. Rinehart, J. S. and Pearson, J., Behavior of Metals Under Impulsive Loads, The American Society of Metals, Cleveland, Ohio, 1954.
82. Robertson, H. P., Terminal Ballistics, Preliminary Report, Committee on Passive Protection Against Bombing, National Research Council, January 1941.
83. Sterne, T. E., A Note on the Initial Velocities of Fragments from Warheads, Report No. 648, Ballistic Research Laboratories, Aberdeen Proving Ground, Maryland, September 1947.
84. Thomas, L. H., Computing the Effect of Distance on Damage by Fragments, Report No. 468, Ballistic Research Laboratories, Aberdeen Proving Ground, Maryland, May 1944.
85. Voltz, R.D., and Kiger, S. A., An Evaluation of the Separated Bay Concept for a Munition Assembly Complex; an Experimental Investigation of the Department of Energy Building 12-64 Complex, Technical Report SL-83-6, prepared by Structures Laboratory, U. S. Army Engineer Waterways Experiment Station, Vicksburg, Mississippi, for Department of Energy, Albuquerque Operations, Amarillo, Texas
86. Ward, J. M. (DOD Explosives Safety Board), Swisdak, M. M., Jr., Peckham, P. J., and Soper, W. G. (NSWC), Lorenz, R. A. (Boeing Military Aircraft Company). Modeling of Debris and Airblast Effects from Explosions Inside Scaled Hardened Aircraft Shelters, Final Report NSWC TR 85-470, prepared by Naval Surface Weapons Center, Silver Spring, Maryland, May 1985.

Shock Loads

87. American Society of Civil Engineers (ASCE), A Comparative Study of Structural Response to Explosion-Induced Ground Motions, ASCE, New York, New York, 1975.
88. Auld, H. E., A Study of Air-Blast-Induced Ground Motions, Ph.D. Thesis, University of Illinois, May 1967.
89. Baladi, G. Y., and P. F. Hadala, Ground Shock Calculation Parameter Study Report I Effect of Various Nonlinear Elastic Plastic Model Formulations, Waterways Experiment Station Technical Report S-71-4, April 1971.
90. Ballard, R. F., R. E. Leach, Middle North Series, Mixed Company Event, Strong Motion Seismic Measurements, Defense Nuclear Agency Report POR-6746, July 25, 1973.
91. Barkan, D. D., Dynamics of Bases and Foundations, McGraw Hill Book Co., New York, New York 1962.
92. Baron, M. L., A Summary of Some Analytical Studies on Air Blast Induced Ground Motions, Defense Atomic Support Agency Report 2634, March 1971.
93. Baron, M. L., I. Nelson, and I. Sandler, Investigation of Air Induced Ground Shock Effect Resulting from Various Explosive Sources, Report 2 Influence of Constitutive Models on Ground Motion Predictions, Waterways Experiments Station Contract Report S-71-10, November 1971.
94. Batchelder, F. E., et al., Hardness Program - Non-EMP, Hardness Program Plan for Safeguard Ground Facilities, Vol. 1, Management and Technical Plan, U. S. Army Corps of Engineers, Huntsville Division, HNDDSP-73-153-ED-R, August 16, 1974.
95. Carder, D. S., and W. K. Cloud. Surface Motion from Large Underground Explosions, J. Geophys, Res., 64, 1471-1487, 1959.
96. Carnes, B. L., and J. A. Conway. Mine Throw I: Cratering Effects of a Multiton Near Surface Detonation in Desert Alluvium, Waterways Experiment Station Technical Report N-73-3, May 1973.

97. Christensen, W. J., Air Blast Induced Ground Shock, Navy Bureau of Yards and Decks Technical Study 27, September 1959.
98. Cooper, H. Jr., and J. L. Bratton, Calculation of Vertical Airblast-Induced Ground Motions from Nuclear Explosions in Frenchman Flat, Air Force Weapons Laboratory Report AFWL-TR-73-111, October 1973.
99. Cooper, H. F., Jr., Empirical Studies of Ground Shock and Strong Motions in Rock, Defense Nuclear Agency Report 3245F, October 1973.
100. Crandell, F. J., Ground Vibrations Due to Blasting and Its Effect Upon Structures, Journal Boston Soc., Civil Engineers, Vol. 36, p. 245, 1949.
101. Crandell, F. J., Transmission Coefficient for Ground Vibrations Due to Explosions, J. Boston Soc. Civil Engineering, 47, 152-168, 1960.
102. Crawford, R. E., C. J. Higgins, and E. H. Bultmann., Air Force Manual for Design and Analysis of Hardened Structures, Air Force Weapons Laboratory Report AFWL-TR-74-102, October 1974.
103. Day, J. D., H. J. Stout, and D. W. Murrell, Middle Gust Calibration Shots; Ground Motion Measurements, Waterways Experiment Station Technical Report N-75-1, February 1975.
104. Duvall, Wilbur I. and D. E. Fogelson, Review of Criteria for Estimating Damage to Residences from Blasting Vibrations, Bureau of Mines Report of Investigation 5968, 1962.
105. Dvorak, A., Seismic Effects of Blasting on Brick Houses, Proce Geofyrikeniha Ustance Ceskoslavenski Akademie, Vol. No. 169, Geofyskialni Sbornik, pp. 189-202, 1962.
106. Edwards, A. T. and T. D. Northwood, Experimental Studies of the Effects of Blasting on Structures, The Engineer, V. 210, pp. 538-546, September 30, 1960.
107. Eubanks, R. A. and B. R. Juskie, Shock Hardening of Equipment, Shock and Vibrations Bulletin, No. 32, Part III, December 1963.
108. Galbraith, F. W., Operation Distant Plain Final Report Proj. 3.02b Shock Spectrum Measurements, TRW Systems Group Report 05318-6001-R000, January 1968.
109. Galbraith, F. W., Operation Prairie Flat, Proj. LN-306 Shock Spectrum Measurements, Defense Atomic Support Agency Report POR-2107, February 1970.
110. Grubaugh, R. E., and L. E. Elliot, Scaling of Ground Shock Spectra, Defense Atomic Support Agency Report DASA-1921, February 1967.
111. Habberjam, G. M. and J. T. Whetton, On the Relationship Between Seismic and Amplitude and Charge of Explosive Fired in Routine Blasting Operations, Geophysics 17. 116-128, January 1952.
112. Hendron, A. J. Jr., Correlation of Operation Snowball Ground Motions with Dynamic Properties of Test Site Soils, Waterways Experiment Station Miscellaneous Paper I-745. October 1965.
113. Hoffman, H. V., F. M. Sauer, and B. Barclay, Operation Prairie Flat, Proj. LN-308 Strong Ground Shock Measurements, Defense Atomic Support Agency Report POR-2108, April 1971.
114. Hudson, D. E., J. L. Alford, and W. D. Iwan, Ground Accelerations Caused by Large Quarry Blasts, Bull. Seismic Soc., A, 51, 191-202, 1961.
115. Ichiro, I., On the Relationship Between Seismic Ground Amplitude and the Quantity of Explosives in Blasting, Reprint from Memoirs of the Faculty of Engineering, Kyoto University, 15, 579-587, 1953.
116. Ingram, J. K., Project Officer's Final Report Operation Distant Plain Events 1, 2A, 3, 4, and 5, Proj. 3.02A Earth Motion and Stress Measurements, Waterways Experiment Station Technical Report N-71-3, May 1971.
117. Ingram, L. F., Ground Motions from High Explosive Experiments, Waterways Experiment Station Miscellaneous Paper N-72-10, December 1972.

118. Jaramillo, E. E., and R. E. Pozega, Middle Gust Free-Field Data Analysis, Air Force Weapons Laboratory Report AFWL-TR-73-251, April 1974.
119. Joachim, C. E., Mine Shaft Series, Events Mine Under and Mine Ore; Ground Motion and Stress Measurements, Waterways Experiment Station Technical Report N-72-1, January 1972.
120. Kennedy, T. E., In-Structure Motion Measurements, Proj. LN-315 Operation Prairie Flat, Waterways Experiment Station Technical Report N-70-11, July 1970.
121. Kochly, J. A., and T. F. Stubbs, Mine Shaft Series, Mineral Rock Particle Velocity Measurements from a 100-ton TNT Detonation on Granite, Defense Nuclear Agency Report POR-2162, May 24, 1971.
122. Lamb, H., On the Propagation of Tremors Over the Surface of an Elastic Solid, Philosophical Transactions of Royal Society London, Series A, Volume 203, September 1904.
123. Langefors, Ulf, B. Kihlstron, and H. Westerberg, Ground Vibrations in Blasting, Water Power, pp. 335-338, 390-395, 421-424, February 1958.
124. Lockard, D. M., Crater Parameters and Material Properties, Air Force Weapons Laboratory Report AFWL-TR-74-200, October 1974.
125. Meireis, E. C. and A. R. Wright, Hardness Program - No-EMP, Hardness Program Plan for Safeguard Ground Facilities, Vol. 2, Safeguard Structures and TSE Description, U.S. Army Corps of Engineers, Huntsville Division, HNDDSP-73-153-ED-R, November 1973.
126. Morris, G., The Reduction of Ground Vibrations from Blasting Operations, Engineering, pp. 460-465, April 1957.
127. Morris, W. E., and others, Operation Jangle Blast and Shock Measurements I, Armed Forces Special Weapons Project Report WT 366, June 1952.
128. Murphey, B. F., Particle Motions Near Explosions in Halite, Journal of Geophysical Research, Vo. 66, No. 3, March 1961, pp. 947-958.
129. Murrell, D. W., Operation Mine Shaft, Mineral Rock Event, Far-out Ground Motions From a 100-ton Detonation on Granite, Waterways Experiment Station Technical Report N-72-6, April 1972.
130. Murrell, D. Operation SNOWBALL, Project 3.6 - Earth Motion Measurements, Waterways Experiment Station Technical Report TR 1-759. March 1967.
131. Newmark, N. M., and others, Air Force Design Manual Principles and Practices for Design of Hardened Structures, Air Force Special Weapons Center Report AFSWC-TDR-62-138, December 1962.
132. Nicholls, H. R., C. F. Johnson, and W. I. Duvall, Blasting Vibrations and Their Effects on Structures, Bureau of Mines Bulletin 656, 1971.
133. Odello, R. and P. Price, Ground Shock Effects from Accidental Explosions, Picatinny Arsenal Technical Report 4995, November 1976.
134. Palaniswamy, K., and J. L. Merritt, Evaluation of Middle Gust Data; Acoustic Path Length Scaling of Peak Velocities, Space and Missile Systems Organization Report 72-006-T4, November 1973.
135. Parsons, R. M., and others, Guide for the Design of Shock Isolation Systems for Underground Protective Structures, Air Force Special Weapons Center Report AFSWC-TDR-62-64, October 1962.
136. Phillips, B. R., and G. Y. Baladi, Results of Two Free-Field Code Calculations Versus Field Measurements for the Distant Plain 1A Event, Waterways Experiment Station Miscellaneous Paper S-73-21, April 1973.
137. Proceedings of the Mixed Company/Middle Gust Results Meeting 13-15 March 1973, Vol. II. Edited by General Electric-Tempo, Defense Nuclear Agency Report 3151-P2, May 1973.
138. Rausch, Maschinenfundamente Und Andere Dynamische Bauaufgaben, Vertrieb VDE Verlag G.M.B.H. (Berlin), 1943.

139. Reiher, H. and F. J. Meister, Die Empfindlichkeit der Menschen gegen Erschutterungen, Forsch. Gebiete Ingenieur wesen, Vol. 2, No. 11, pp. 381-386, 1931.
140. Richart, F. E. Jr., J. R. Hall, and R. D. Woods, Vibration of Soils and Foundations, Prentice-Hall, Inc., Englewood Cliffs, New Jersey, 1970.
141. Ricker, N., The Form and Nature of Seismic Waves and the Structure of Seismograms, Geophysics, 5, 348-366, 1940.
142. Sachs, D. C., and C. M. Swift, Small Explosion Tests, Project Mole, Armed Forces Special Weapons Project Report 291, Vols. I and II, December 1955.
143. Sager, R. A., Concrete Arch Studies, Proj. 3.2, Operation Snowball, Waterways Experiment Station Miscellaneous Paper I-736, August 1965.
144. Sandler, I.S., J. P. Wright, and M. L. Baron, Ground Motion Circulations for Events II and III of the Middle Gust Series, Defense Nuclear Agency Report DNA 3290T, April 1974.
145. Steffens, R. J., The Assessment of Vibration Intensity and its Application to the Study of Building Vibrations, National Building Studies Special Report No. 19, Department of Scientific and Industrial Research, Building Research Station, London, England, 1952.
146. Sauer, F. M., and C. T. Vincent, Ferris Wheel Series - Flat Top Event Earth Motion and Pressure Histories, Defense Atomic Support Agency Report Ferris Wheel POR-3002, April 1967.
147. Sauer, F. M., editor, Nuclear Geoplosics, A Sourcebook of Underground Phenomena and Effects of Nuclear Explosions, in 5 parts, Defense Atomic Support Agency Report DASA-1285, May 1964.
148. Sauer, F. M., Summary Report on Distant Plain Events 6 and 1a Ground Motion Experiments, Defense Atomic Support Agency Report DASA-2587, October 1970.
149. Teichmann, G. A. and R. Westwater, Blasting and Associated Vibrations, Engineering, pp. 460-465. April 1957.
150. Thoenen, J. R., and S. L. Windes, Seismic Effects of Quarry Blasting, Bureau of Mines Bulletin, 442, 83, 1942.
151. URS/John A. Blume and Associates, Seismic Hazard and Building Structure Behavior at the Pantex Facility, April 1976.
152. Vincent, C. T., Operation Prairie Flat, Proj. LN-304 Earth Pressure and Ground Shock Profile Measurements, Defense Atomic Support Agency Report POR-2113, May 1969.
153. Weidlinger, P., and A. Matthews, A Method for the Prediction of Ground Shock Phenomena in Soils, Air Force Special Weapons Center Report AFSWC-TDR-61-66, March 1962.
154. Westline, P. S., Esparza, E. D., and Wenzel, A. B., Analysis and Testing of Pipe Response to Buried Explosive Detonations, SwRI Final Report for American Gas Association, July 1978.
155. Willis, D. E. and J. T. Wilson, Maximum Vertical Ground Displacement of Seismic Waves Generated by Explosive Blasts, Bulletin Seismic Safety of America, 50, 455-459, 1960.
156. Zaccor, J. V., Procedures for Prediction of Ground Shock Phenomena Based on One-Dimensional Shock Propagation Considerations: Procedures and Applications, Waterways Experiment Station Contract Report 3-171. April 1967.
157. Zolasko, J. S., and G. Y. Baladi, Free-Field Code Predictions Versus Field Measurements: A Comparative Analysis for the Prairie Flat Event, Waterways Experiment Station Miscellaneous Paper S-71-6, March 1971.

CHAPTER 3. PRINCIPLES OF DYNAMIC ANALYSIS

CHAPTER 3

PRINCIPLES OF DYNAMIC ANALYSIS

INTRODUCTION

3-1. Purpose

The purpose of this manual is to present methods of design for protective construction used in facilities for development, testing, production, storage, maintenance, modification, inspection, demilitarization, and disposal of explosive materials.

3-2. Objective

The primary objectives are to establish design procedures and construction techniques whereby propagation of explosion (from one structure or part of a structure to another) or mass detonation can be prevented and to provide protection for personnel and valuable equipment.

The secondary objectives are to:

(1) Establish the blast load parameters required for design of protective structures.
(2) Provide methods for calculating the dynamic response of structural elements including reinforced concrete, and structural steel.
(3) Establish construction details and procedures necessary to afford the required strength to resist the applied blast loads.
(4) Establish guidelines for siting explosive facilities to obtain maximum cost effectiveness in both the planning and structural arrangements, providing closures, and preventing damage to interior portions of structures because of structural motion, shock, and fragment perforation.

3-3. Background

For the first 60 years of the 20th century, criteria and methods based upon results of catastrophic events were used for the design of explosive facilities. The criteria and methods did not include a detailed or reliable quantitative basis for assessing the degree of protection afforded by the protective facility. In the late 1960's quantitative procedures were set forth in the first edition of the present manual, "Structures to Resist the Effects of Accidental Explosions". This manual was based on extensive research and development programs which permitted a more reliable approach to current and future design requirements. Since the original publication of this manual, more extensive testing and development programs have taken place. This additional research included work with materials other than reinforced concrete which was the principal construction material referenced in the initial version of the manual.

Modern methods for the manufacture and storage of explosive materials, which include many exotic chemicals, fuels, and propellants, require less space for a given quantity of explosive material than was previously needed. Such concentration of explosives increases the possibility of the propagation of accidental explosions. (One accidental explosion causing the detonation of

other explosive materials.) It is evident that a requirement for more accurate design techniques is essential. This manual describes rational design methods to provide the required structural protection.

These design methods account for the close-in effects of a detonation including the high pressures and the nonuniformity of blast loading on protective structures or barriers. These methods also account for intermediate and far-range effects for the design of structures located away from the explosion. The dynamic response of structures, constructed of various materials, or combination of materials, can be calculated, and details are given to provide the strength and ductility required by the design. The design approach is directed primarily toward protective structures subjected to the effects of a high explosive detonation. However, this approach is general, and it is applicable to the design of other explosive environments as well as other explosive materials as mentioned above.

The design techniques set forth in this manual are based upon the results of numerous full- and small-scale structural response and explosive effects tests of various materials conducted in conjunction with the development of this manual and/or related projects.

3-4. Scope

It is not the intent of this manual to establish safety criteria. Applicable documents should be consulted for this purpose.. Response predictions for personnel and equipment are included for information.

In this manual an effort is made to cover the more probable design situations. However, sufficient general information on protective design techniques has been included in order that application of the basic theory can be made to situations other than those which were fully considered.

This manual is applicable to the design of protective structures subjected to the effects associated with high explosive detonations. For these design situations, the manual will apply for explosive quantities less than 25,000 pounds for close-in effects. However, this manual is also applicable to other situations such as far- or intermediate-range effects. For these latter cases the design procedures are applicable for explosive quantities in the order of 500,000 pounds which is the maximum quantity of high explosive approved for aboveground storage facilities in the Department of Defense manual, "Ammunition and Explosives Safety Standards", DOD 6055.9-STD. Since tests were primarily directed toward the response of structural steel and reinforced concrete elements to blast overpressures, this manual concentrates on design procedures and techniques for these materials. However, this does not imply that concrete and steel are the only useful materials for protective construction. Tests to establish the response of wood, brick blocks, and plastics, as well as the blast attenuating and mass effects of soil are contemplated. The results of these tests may require, at a later date, the supplementation of these design methods for these and other materials.

Other manuals are available to design protective structures against the effects of high explosive or nuclear detonations. The procedures in these manuals will quite often complement this manual and should be consulted for specific applications.

Computer programs, which are consistent with procedures and techniques contained in the manual, have been approved by the appropriate representative of the US Army, the US Navy, the US Air Force and the Department of Defense Explosives Safety Board (DDESB). These programs are available through the following repositories:

(1) Department of the Army
Commander and Director
U.S. Army Engineer
Waterways Experiment Station
Post Office Box 631
Vicksburg, Mississippi 39180-0631
Attn: WESKA

(2) Department of the Navy
Commanding Officer
Naval Civil Engineering Laboratory
Port Hueneme, California 93043
Attn: Code L51

(3) Department of the Air Force
Aerospace Structures
Information and Analysis Center
Wright Patterson Air Force Base
Ohio 45433
Attn: AFFDL/FBR

If any modifications to these programs are required, they will be submitted for review by DDESB and the above services. Upon concurrence of the revisions, the necessary changes will be made and notification of the changes will be made by the individual repositories.

3-5. Format

This manual is subdivided into six specific chapters dealing with various aspects of design. The titles of these chapters are as follows:

Chapter 1	Introduction
Chapter 2	Blast, Fragment, and Shock Loads
Chapter 3	Principles of Dynamic Analysis
Chapter 4	Reinforced Concrete Design
Chapter 5	Structural Steel Design
Chapter 6	Special Considerations in Explosive Facility Design

When applicable, illustrative examples are included in the Appendices.

Commonly accepted symbols are used as much as possible. However, protective design involves many different scientific and engineering fields, and, therefore, no attempt is made to standardize completely all the symbols used. Each symbol is defined where it is first used, and in the list of symbols at the end of each chapter.

CHAPTER CONTENTS

3-6. General

This chapter contains the procedures for analyzing structural elements subject to blast overpressures. These procedures are contained in the next eleven sections; Section 3-7 deals with a simplified discussion of the basic principles of dynamics as well as the procedures for calculating the various components used to perform the dynamic analyses. Presented in Sections 3-8 through 3-15 are resistance-deflection functions for various elements including both one- and two-way panels as well as beam elements. These functions include the elastic, elasto-plastic, and plastic ranges of response. In addition, a discussion of dynamic equivalent systems is presented in Sections 3-16 and 3-17. These include single- and multi-degree-of-freedom systems. Presented in this Section also are methods for calculating load and mass factors required to perform the dynamic analyses.

Sections 3-18 through 3-20 include both a step-by-step numerical integration of an element's motion under dynamic loads utilizing the Acceleration-Impulse-Extrapolation Method or the Average Acceleration Method and design charts for idealized loads. Presented also in these Sections are methods for analyzing elements subjected to impulse type loadings; that is, loadings whose durations are short in comparison to the time to reach maximum response of the elements.

BASIC PRINCIPLES

3-7. General

The principles used in the analysis of structures under static load will be reviewed briefly, since the same principles are used in the analysis and design of structures subjected to dynamic loads. Two different methods are used either separately or concurrently in static analysis: one is based on the principle of equilibrium, and the other on work done and internal energy stored.

Under the application of external loads, a given structure is deformed and internal forces developed in its members. In order to satisfy static equilibrium, the vector sum of all the external and internal forces acting on any free body portion of the structure must be equal to zero. For the equilibrium of the structure as a whole, the vector sum of the external forces and the reactions of the foundation must be equal to zero.

The method based on work done and energy considerations is sometimes used when it is necessary to determine the deformation of a structure. In this method, use is made of the fact that the deformation of the structure causes the point of application of the external load to be displaced. The force then does work on the structure. Meanwhile, because of the structural deformations, potential energy is stored in the structure in the form of strain energy. By the principle of energy conservation, the work done by the external force and the energy stored in the members must be equal. In static analysis, simplified methods such as the method of virtual work and the method of the unit load are derived from the general principle of energy conservation.

In the analysis of statically indeterminate structures, in addition to satisfying the equations of equilibrium, it is necessary to include a calculation of the deformation of the structure in order to arrive at a complete solution of the internal forces in the structure. The methods based on energy considerations such as the method of least work and the method based on Castigliano's theorems are generally used.

For the analysis of structures under dynamic loading, the same two methods are basically used; but the load changes rapidly with time and the acceleration velocity and, hence, the inertia force and kinetic energy are of magnitudes requiring consideration. Thus, in addition to the internal and external forces, the equation of equilibrium includes the inertia force and the equation of dynamic equilibrium takes the form of Newton's equation of motion:

$$F - R = Ma \qquad 3\text{-}1$$

where

F = total external force as a function of time
R = total internal force as a function of time
M = total mass
a = acceleration of the mass

As for the principle of conservation of energy, the work done must be equal to the sum of the kinetic energy and the strain energy:

$$WD = KE + SE \qquad 3\text{-}2$$

where WD = work done
KE = kinetic energy
SE = strain energy

and the strain energy includes both reversible elastic strain energy and the irreversible plastic strain energy. Thus, the difference between structures under static and dynamic loads is the presence of inertial force (Ma) in the equation of dynamic equilibrium, and of kinetic energy in the equation of energy conservation. Both terms are related to the mass of the structure; hence, the mass of the structure becomes an important consideration in dynamic analysis.

In the dynamic analysis of structures, both the energy balance equation and the force balance equation are applied with explicit description of the external forcing function F, and the internal resisting forcing function R. The difference between these forcing functions is the inertia force as described above. The following is a discussion of the details of how these forces are utilized in the design of structures which respond in the ductile mode.

In the design of a structure to resist the blast from an HE explosion, the total external force acting on the structure can be obtained by the principles discussed Chapter 2. The design method also consists of the determination of the total internal force, i.e. the resistance of the structure required to limit calculated deflections of the individual members and the structure as a whole under the external force (blast loading), to within prescribed maximum values. The determination of the resistance of the individual members of the structure is presented in Sections 3-8 through 3-17. Subsequent sections of this manual present the principles and methods of dynamic analysis and equations, charts, and procedures for design.

RESISTANCE - DEFLECTION FUNCTIONS

3-8. Introduction

Under the action of external loads, a structural element is deformed and internal forces set up. The sum of these internal forces tending to restore the element to its unloaded static position is defined as the resistance. The resistance of a structural element is a reactive force associated with the deflection of the element produced by the applied load. It is convenient to consider the resistance as an equivalent load in the same manner as the applied load, but opposite in direction. The variation of the resistance vs. displacement is expressed by a resistance-deflection function and may be represented graphically. An idealized resistance-deflection function for an element spanning in two directions and covering in the complete flexural range to incipient failure is shown in Figure 3-1.

As load is applied to a structural element, the element deflects and, at any instant, exerts a resistance to further deformation, which is a function of its units stiffness K, until the ultimate unit resistance r_u (total resistance is r_u where A is the element area) of the element is reached at deflection X_p. The initial portion of the resistance-deflection diagram is composed of the elastic and elasto-plastic ranges, each with its corresponding stiffness, the transition from one range to another occurring as plastic hinges are formed at points of maximum stress (yield lines). The number of elasto-plastic ranges required before the ultimate resistance of a particular element is reached depends upon the type and number of supports and the placement of reinforcing steel (in the case of reinforced concrete elements). For example a beam with simple supports subjected to uniformly distributed loads needs only one plastic hinge to develop the ultimate resistance (or full plastic strength) of the element; whereas for the same beam fixed at both ends, more than one plastic hinge is required.

In subsequent paragraphs, various procedures, equations and illustrations are presented to enable the designer to determine the resistances of both one- and two-way elements. The procedures outlined apply mainly to reinforced concrete elements and so do the equations appearing in the text, unless the equations are given as part of an illustrative example. However, they can also be used for structural steel elements as well as other structural elements such as aluminum, plastics, etc. Equations have been derived for specific cases most often encountered in practice. These are applicable for structural steel and reinforced concrete elements of uniform thickness in both the horizontal and vertical directions. Before the equations and figures can be used for reinforced concrete element, however, the reinforcing steel across any yield line must have a uniform distribution in both the vertical and horizontal directions; however, the reinforcement across the positive yield lines can be different from that across the negative yield lines and the reinforcing pattern in the vertical direction different from that in the horizontal direction.

Regardless of whether it is reinforced concrete or structural steel element, any opening in the element must be compact in shape and small in area, compared to the total area of the element.

3-9. Ultimate Resistance

3-9.1. General

The ultimate resistance of an element depends upon:

(1) The distribution of the applied loads.
(2) The geometry of the element (length and width).
(3) The number and type of supports.
(4) The distribution of the moment capacity or reinforcement in the case of reinforced concrete elements.

The distribution of the loads depends upon the design range of the element; i.e., high, intermediate or low pressure. For intermediate and low pressure ranges, it can be assumed that the pressure is uniform across the surface of the element although it varies with time. At high pressure ranges, however, the blast loads are variable across the surface of the element. However, for structural steel elements and concrete elements utilizing laced reinforcement, or for concrete elements with standard shear reinforcement which sustain relatively small deflections, a good estimate of the resulting deflections can be made using the resistance functions conforming to those of uniformly loaded elements.

The other factors that affect the ultimate resistance of an element are predetermined by the requirements of the protective structure (where the element is used) and the magnitude of the blast output.

3-9.2. One-Way Elements

The ultimate resistance of a one-way reinforced concrete element with an elastic distribution of its reinforcing steel is based on the moment capacity at first yield since all critical sections yield simultaneously. For one-way reinforced concrete elements (such as beams or slabs) with non-elastic distribution of reinforcing steel and for structural steel elements, the ultimate resistance is a function of the moment capacity at the first yield plus the added moment capacity due to subsequent yielding at other critical sections.

Values of the ultimate resistance for one-way elements are shown in Table 3-1 where the following symbols are used:

M_N = ultimate negative unit moment capacity at the support.
M_P = ultimate positive unit moment capacity at midspan.
L = length
r_u = ultimate unit resistance
R_u = total ultimate resistance

Table 3-1 applies to both beams and slabs. However, special attention must be paid to the units used for the respective element. The moment capacity of a slab is expressed for a unit strip of the slab (inch-pounds per inch) whereas the total moment capacity (inch-pounds) is considered for a beam. Consequently, the resistance of a slab is expressed in load per unit area (psi) where the resistance of a beam is expressed in load per length along the beam (pounds per inch).

3-9.3. Two-Way Elements

The amount of data available on the limit analysis of rectangular steel plates is very limited. However, an elementary approach imagines a mechanism formed of straight yield lines, as is customary in reinforced concrete. This approach for reinforced concrete elements will be considered appropriate for structural steel elements.

In the design of two-way reinforced concrete elements, it is not necessary to define accurately the stress distribution during the initial and intermediate stages of loading since the ultimate load capacity can be readily determined by the use of yield line procedures. The yield line method assumes that after initial cracking of the concrete at points of maximum moment, yielding spreads until the full moment capacity is developed along the length of the cracks on which failure will take place. Several illustrative examples of the simplified yield or crack lines for two-way elements are illustrated in Figure 3-2.

In using the yield line solution, the initial step is to assume a yield line pattern (as shown in Figure 3-2) applying the following rules:

(1) To act as plastic hinges of a collapse mechanism made up of plane segments, yield lines must be straight lines forming axes of rotation for the movements of the segments.

(2) The supports of the slabs will act as axes of rotation. A yield line may form along a fixed support and an axis of rotation will pass over a column.

(3) For compatibility of deformations, a yield line must pass through the intersection of the axes of rotation of the adjacent slab segments.

Tests indicate that the actual location and extent of these lines on reinforced concrete elements differ only slightly at failure from the theoretical ones. Use of the idealized yield lines results in little error in the determination of the ultimate resistance and the error is on the side of safety.

The corner sections of two-way elements are stiff in comparison to the remainder of the member; therefore, straining of the reinforcement which is associated with the reduced rotations at these sections will be less. To account for the corner effects, the design of any one particular section of a two-way element should consider a variation of the moment capacity along the yield lines rather than a uniform distribution.

This variation is approximated by taking the full moment capacity along the yield lines, except in the corners where two-thirds of the moment capacity over the lengths described in Figure 3-3 are used. The variation applies to both the negative moments along the supports and the positive moments at the interior. The ultimate unit resistance can be determined from the yield line pattern using either the principle of virtual work or the equations of equilibrium. Each approach has its advantages; in general, the virtual work method is easier in principle but difficult to manipulate algebraically since it involves differentiating a usually complex mathematical expression for a minimum value of resistance. The equilibrium method, which is used in this

manual, also has its disadvantages. Since equilibrium requires that the shear forces acting on each side of a yield line have to be equal and opposite, correction forces (also known as nodal forces) have to be introduced around openings in two-way members and at free edges, and these correction forces may not be available from simple analysis. However, in three of the six cases shown in Figure 3-2, (cases c, e, f), nodal forces exist; but their effects are negligible.

In order to calculate the ultimate unit resistance r_u of a two-way element, the equation of equilibrium of each sector formed by the yield lines is expressed in terms of the moments produced by the internal and external forces. The sum of the resisting moments acting along the yield lines (both positive and negative) of each sector is equated to the moment produced by the applied load about the axis of rotation (support of the sector), assuming that the shear forces are zero along the positive yield lines.

$$\Sigma M_N + \Sigma M_p = Rc = r_u Ac \qquad 3\text{-}3$$

where
- M_N = sum of the ultimate unit resisting moments acting along the support (negative yield lines)
- M_p = sum of the ultimate unit resisting moments acting along the interior failure lines (positive yield lines)
- R = total ultimate resistance of the sector
- c = distance from the centroid of the load to the line of rotation of the sector
- r_u = ultimate unit resistance of the sector
- m = area of the sector

Once the equations of equilibrium are known for all sectors, the ultimate resistance is obtained either by solving the equations simultaneously or by a trial and error procedure noting that the unit resistance of all sectors must be equal.

To illustrate the above procedure (Equation 3-3), consider the two-way concrete element shown in Figure 3-3 which is fixed on three edges and free on the fourth, and where the nomenclature is as follows:

- L = length of element
- H = height of element
- x = yield line location in horizontal direction
- y = yield line location in vertical direction
- M_{VN} = ultimate unit negative moment capacity in the vertical direction
- M_{VP} = ultimate unit positive moment capacity in the vertical direction
- M_{HN} = ultimate unit negative moment capacity in the horizontal direction
- M_{HP} = ultimate unit positive moment capacity in the horizontal direction

The nomenclature as stated in the paragraph above is strictly applicable to two-way elements which are used as walls. However, when roof slabs or other horizontal elements are under consideration, the preceding nomenclature will

also be applicable if the element is treated as being rotated into a vertical position.

The first step in the solution is to assume the location of the yield lines as defined by the coordinates x and y. It should be noted that in some cases, because of geometry, the value of x and y will be known and therefore need not be evaluated. In this example, the negative reinforcement in the horizontal direction at opposite supports is assumed to be equal; therefore, the vertical yield line is located at the center of the span and the value of x is numerically equal to L/2 (a, Figure 3-3). However, in other cases, neither the location of x nor y will be known, and the solution will require the determination of both coordinates.

Once the yield lines have been assumed, the distribution of the resisting moments along the yield lines is determined. In the case at hand, the reduced moments, as a result of the increased stiffness at the corners, act over lengths equal to x/2 and y/2 in the horizontal and vertical directions, respectively (a, Figure 3-3). The equations of equilibrium are then written for each sector with the use of the free body diagrams (b, Figure 3-3). For the triangular sector I:

$$M_{VN} = (2/3)M_{VN}\,(L/4 + L/4) + M_{VN}\,(L/2)$$

$$= (5/6)M_{VN}\,L \qquad 3\text{-}4$$

$$M_{VP} = (2/3)M_{VP}\,(L/4 + L/4) + M_{VP}\,(L/2)$$

$$= (5/6)M_{VP}\,L \qquad 3\text{-}5$$

$$C_I = y/3 \qquad 3\text{-}6$$

$$R_I = (M_{VN} + M_{VP})/C_I$$

$$= [5L(M_{VN} + M_{VP})]/2y \qquad 3\text{-}7$$

$$A_I = Ly/2 \qquad 3\text{-}8$$

$$r_u(\text{Sector 1}) = R_I/A_I$$

$$= [5(M_{VN} + M_{VP})]/y^2 \qquad 3\text{-}9$$

For the trapezoidal sector II, a similar procedure gives

$$M_{HN} = (2/3)M_{HN}\,(y/2) + M_{HN}\,(H - y/2)$$

$$= M_{HN}\,(H - y/6) \qquad 3\text{-}10$$

$$M_{HP} = (2/3)M_{HP}\,(y/2) + M_{HP}\,(H - y/2)$$

$$= M_{HP}\,(H - y/6) \qquad 3\text{-}11$$

$$C_{II} = (1/3)(L/2)[2(H-y) + H]/(H + H - y)$$

$$= [L(3H - 2y)]/6(2H - y) \qquad 3\text{-}12$$

$$R_{II} = (M_{HN} + M_{HP})/C_{II}$$

$$= [(6H - y)(2H - y)(M_{HN} + M_{HP})]/L(3H - 2y) \quad 3\text{-}13$$

$$A_{II} = (1/2)(L/2)(H + H - y)$$

$$= [L(2H - y)]/4 \quad 3\text{-}14$$

$$r_u(\text{Sector II}) = R_{II}/A_{II}$$

$$= [4(M_{HN} + M_{HP})(6H - y)]/L^2(3H - 2y) \quad 3\text{-}15$$

Equations 3-9 and 3-15 are the equations of equilibrium for the triangular (I) and the trapezoidal (II) sectors, respectively. As mentioned previously, these equations can be solved simultaneously or by a trial and error procedure. In the latter method, values of y are substituted into both equations until r_u (sector 1) is equal to r_u (sector II).

If a numerical solution based on the above procedure (Equation 3-3) yields negative values for either x, y or r then the assumed yield line location is wrong. In this example, the only other possible yield line pattern ($x \leq L/2$) would be as shown in Figure 3-2c.

The solution of Equation 3-3 is universally applicable for any two-way element. If the negative reinforcement in the horizontal direction had been unequal at the opposing supports, the value of $x = L/2$ would have changed, and all three sectors wold have had to be considered to determine x, y and hence, r_u.

Simultaneous solution of Equations 3-9 and 3-15 reveals that the locations of the yield lines are a function of the ratio of the spans L/H and the ratio of the sum of the unit vertical to horizontal moment capacities as follows:

$$r_u(\text{Sector I}) = r_u(\text{Sector II}) \quad 3\text{-}16$$

$$5(M_{VN} + M_{VP})/y^2 = [4(M_{HN} + M_{HP})(6H - y)]/L^2(3H - 2y) \quad 3\text{-}17a$$

$$L^2(M_{VN} + M_{VP})/H^2(M_{HN} + M_{HP}) =$$

$$[4y^2(6 - y/H)]/[5H^2(3 - 2y/H)] \quad 3\text{-}17b$$

$$(L/H)[(M_{VN} + M_{VN})/(M_{HN} + M_{HP})]^{1/2} =$$

$$(y/H)[(4(6 - y/H)/5(3 - 2y/H)]^{1/2} \quad 3\text{-}17c$$

Equation 3-17c, which relates the location of the yield lines to the moment capacity of the element, is used to plot Figure 3-6. Knowing the location of the yield lines, the resistance of the two-way element can be obtained from either Equation 3-9 or 3-15 which are also presented in Table 3-2.

Using the procedure outlined above, the values of the ultimate unit resistances for several two-way elements with various support conditions are given in Tables 3-2 and 3-3, the nomenclature confirming to that previously listed. Table 3-2 covers the special cases where opposite supports provide the same

degree of restraint thus resulting in symmetrical yield line patterns. Table 3-3 deals with the general cases when the yield line patterns are not symmetrical (that is, when opposite supports provide different restraints). Yield line location ratios x/L and y/H for the same elements are depicted in Figures 3-4 through 3-20.

Figures 3-4 and 3-5 show the location of the yield lines for two-way elements with two adjacent edges supported and the other two free. In each of these figures eight curves are shown which represent different ratios of the positive to the negative moment capacities in both the vertical and horizontal directions. Figures 3-6 through 3-16 illustrate the yield line location for two-way elements with three edges supported and one edge free. Figures 3-6 and 3-11 covers the case when the yield line pattern is symmetrical opposite supports provide the same degree of restraint). Figures 3-17 through 3-20 show the yield line location for two-way elements with four sides supported.

Figure 3-17 covers the special case when opposite supports provide the same degree of restraint thus resulting in a symmetrical yield pattern. An example illustrating the use of some of these figures is provided in Appendix A.

3-9.4. Openings in Two-Way Elements

The use of openings in two-way elements, whether for access as a door opening or for visual communication as in the case of observation ports, is permissible with certain reservations. It is difficult to state exact rules concerning openings, but their effect on the design is generally a function of location, size and shape.

Small compact openings with approximate areas of less than 5 percent of the panel area and located away from regions of high stress can usually be ignored in the design. However, as in the case of conventional design, reinforcement at least equal to the amount interrupted should be placed adjacent to the opening. For example, in Figure 3-21, the openings shown in (a) and (b) can be disregarded. If the opening in (b) were made more rectangular as in (c), then the design must be modified to account for the change in the yield lines and, hence, the change in the resistance. This change in resistance is a function of both the shape and the location of the opening.

Door openings invariably require special analysis because of their size. As depicted in (d), (e) and (f), Figure 3-21, the presence of door openings causes gross relocations of the yield lines which generally propagate from the corners of the openings. Since the door also sustains the blast loading, concentrated line loads are present around the periphery of such openings. These concentrated loads must be included in the analysis since they change the resistance. As previously outlined for solid elements and for this case also, the yield line locations are assumed and each sector is individually analyzed. The presence of line loads modifies Equation 3-3 to

$$\Sigma M_N + \Sigma M_p = r_u A_c + M_c \qquad 3\text{-}18$$

where M_c is the moment of the concentrated loads about the line of rotation of the sector being considered. Solution of elements with openings is most easily accomplished through a trial and error procedure by setting up the simultaneous equations for each sector and assuming various values of x and y until the several values of r_u agree to within a few percent.

3-10. Post-Ultimate Resistance

In general, the two-way elements described in this manual exhibit a post-ultimate resistance after initial failure occurs as indicated in Figure 3-1. Prior to this partial failure, the element is spanning in two directions with a resistance equal to the ultimate resistance r_u. At a particular deflection, denoted as X_1, failure occurs along one side or two opposite sides, and the element then spans in one direction with the reduced post-ultimate unit resistance r_{up} until complete failure occurs at deflection X_u. One-way elements do not exhibit this behavior.

The location of the yield lines determines the presence or absence of this range. If the yield lines emanating from the corners of the elements bisect the 90-degree corner angle, then all supports fail simultaneously and there is no post-ultimate range. As previously shown, the location of the yield lines for a particular element is a function of L/H and the ratio of the unit vertical to horizontal moment capacities. Post-ultimate resistances for two-way elements are shown in Table 3-4.

3-11. Partial Failure and Ultimate Deflection

Partial failure deflection X_1, for two-way elements and ultimate deflections X_u for both one-way and two-way elements are a function of the angle of rotation of the element at its supports and the geometry of the sectors formed by the position yield lines.

Once the ultimate resistance r_u is reached (full moment capacity developed along the yield lines), the structural element becomes a mechanism which rotates with no further increase in either the moment or curvature between the hinges. For one-way elements, the rotation continues and the deflection increases until either the maximum deflection X_m is reached or failure occurs at θ max. The equations for the maximum deflection X_m in the range $0 \leq X < X_u$ for several one-way elements as a function of the rotation angle θ and the ultimate deflection X_u are given in Table 3-5, when the values for X_u are based on the development of a maximum support rotation, θ max., prior to failure.

Actually, the maximum support rotation will vary with the material type and geometry of the element. The criteria for partial and incipient failure for concrete and structural steel elements can be found in Chapters 4 and 5 respectively.

For two-way elements, the rotations of all the sectors must be considered in order to define the deflections of partial and incipient failure. Prior to partial failure ($0 \leq X_m \leq X_1$), the maximum deflection is a function of the larger angle of rotation formed along either the vertical or horizontal supports. At deflection X_1, this larger angle equals θ max, and failure occurs along this support. Beyond this point, the element spans in one direction until the angle of rotation at the adjacent supports (in the direction opposite to that at which failure has already occurred) reaches θ at which time total collapse occurs ($X_m = X_u$).

To illustrate the above, consider a two-way element (Figure 3-22) which is fully restrained on four edges and whose positive yield lines are defined by $H/2 < x < L/2$ and $y = H/2$. Denoting θ_H as the angle of rotation in the

horizontal direction (along vertical supports) and θ_V as the vertical angle of rotation (along horizontal supports), the maximum deflection X_m at the center of the element prior to reaching the deflection X_1 is

$$X_m = (H \tan \theta_v)/2 \qquad 3\text{-}19$$

and at the partial failure deflection X_1 where θ_v max

$$X_1 = (H \tan \theta_{max})/2 \qquad 3\text{-}20$$

Referring to Figure 3-22, the deflected shape at deflection X_1 is indicated by the solid line and θ_H has value β which is defined as

$$\beta = \tan^{-1}(X_1/x) = \tan^{-1}(H \tan \theta_{max}/2x) \qquad 3\text{-}21$$

As the element continues to deflect the angle of rotation θ_H increases, its magnitude becoming equal to

$$\theta_H = \lambda + \beta \qquad 3\text{-}22$$

where λ is the angular rotation in excess of β. For a two-way element which undergoes partial failure but does reach incipient failure, the maximum deflection in the range $X_1 \leq X_m \leq X_u$ becomes

$$X_m = x \tan \theta_H + [(L/2) - x)] \tan (\theta_H - \beta) \qquad 3\text{-}23$$

When θ_H equal θ_{max}, the ultimate deflection X_u at incipient failure is

$$X_u = x \tan \theta_{max} + [(L/2 - x)] \tan [\theta_{max} - \tan^{-1} (H \tan \theta_{max}/2x)] \qquad 3\text{-}24$$

Equations 3-19 through 3-24 are specifically for two-way elements described in Figure 3-2 and will vary for other two-way elements with different material properties and geometry.

The maximum deflection X_m for several two-way elements in the ranges $0 \leq X_m \leq X_1$, and $X_1 < X_m \leq X_u$ as a function of the rotation angles θ_H and θ_V are given in Table 3-6 along with the values of partial failure (X_1) and ultimate (X_u) deflections. The support which fails at partial deflection X_1 is also indicated.

3-12. Elasto-Plastic Resistance

As stated in Section 3-8, the initial portion of the resistance function (Figure 3-1) generally is composed of an elastic and one or more elasto-plastic ranges. The elastic unit resistance r_e is defined as the resistance at which first yield occurs; similarly, the elasto-plastic unit resistance r_{ep} is the resistance at which second yields subsequently occur. Where all hinges form in a member at one time, r_e will be equal to the ultimate unit resistance r_u; where two or more hinges are formed at separate times, the maximum value of r_{ep} will be equal to r_u (depending upon the hinges formed, one or more values of r_{ep} may exist).

These resistances for one-way elements are listed in Table 3-7. In those cases where the elasto-plastic resistance is equal to the ultimate resistance, the value can be determined from Table 3-1.

The determination of the elasto-plastic resistances of two-way elements is more complicated than that for one-way elements, since the resistance varies with the span ratio and, in the case of reinforced concrete elements, with the placement of the reinforcement. Data for calculating the resistances of two-way elements during the elasto-plastic ranges (graphically summarized in Figure 3-23) are presented in Figures 3-24 through 3-38.

Figures 3-24 through 3-26 are for a two-way element supported on two adjacent sides and free at the others. Figures 3-27 through 3-32 are for a two-way element supported on three sides and free on the fourth, while Figures 3-33 through 3-38 are for elements fixed on four sides. The resistances in each range can readily be determined using the coefficients ß, the subscript referring to the points listed in the accompanying illustration.

For example, in Figure 3-27, for an element fixed on three sides and free on the fourth, if the ultimate unit resisting moments M_u are known for points 1, 2 and 3, a resistance r for each point can be calculated from

$$r = M_u / \beta H^2 \qquad 3\text{-}25$$

where the values of ß are found in Figure 3-27. The smallest value of resistance r, (say at point 2) corresponds to the first yield and is equal to r_e. Next, the moments at the remaining two points are computed for this value of r_e, and the differences between these and the ultimate values are determined. These differences represent the remaining moment capacities available for additional load. At r_e, the elements supports become free, fixed, and simply-supported on opposite sides. Using the moment differences and entering Figure 3-29 two values of the change in resistance can be calculated as above, the smaller being Δr and therefore:

$$r_{ep} = r_e + \Delta r \qquad 3\text{-}26$$

In similar fashion, the resistance at the end of each range can be determined until the ultimate unit resistance r_u is reached.

3-13. Elasto-Plastic Stiffnesses and Deflections

The slopes of the elastic and elasto-plastic ranges of the resistance function are defined by the stiffness K of the element:

$$K = r/X \qquad 3\text{-}27$$

where r is the unit resistance and X is the deflection corresponding to the value of r. The elastic range stiffness is denoted as K_e, the elasto-plastic range as K_{ep}, while in the plastic range the stiffness is zero.

Typical resistance-deflection functions used for design are shown in Figure 3-39. One- and two-step systems are generally used for one-way elements while two- and three-step systems are used for two-way elements. Two way elements fixed on all four sides will exhibit a four step system. As can be seen from the figure, the elastic range stiffness

$$K_e = r_e / X_e \qquad 3\text{-}28$$

the elasto-plastic stiffness for a two-step system

$$K_{ep} = (r_u - r_e) / (X_p - X_e) \quad 3\text{-}29$$

and for a three-step system, the elasto-plastic stiffnesses

$$K_{ep} = (r_{ep} - r_e) / (X_{ep} - X_e) \quad 3\text{-}30$$

and

$$K'_{ep} = (r_u - r_{ep}) / (X_p - X_{ep}) \quad 3\text{-}31$$

The elastic and elasto-plastic stiffnesses of one-way elements are given in Table 3-8 as a function of the modulus of elasticity E, moment of inertia I, and span length. Knowing the resistances and stiffnesses, the corresponding elastic and elasto-plastic deflections can be computed from the above equations.

The determination of the elasto-plastic stiffnesses and deflections of two-way elements is more complicated than for one-way elements since another variable, namely, the aspect ratio L/H, must be considered. For two-way elements, the deflections at the end of each range of behavior is obtained from the γ coefficients presented in Figures 3-24 through 3-38. The deflection for each range of behavior is obtained from

$$XD = \gamma r H^4 \quad 3\text{-}32$$

where D, the flexural rigidity of the element is defined as

$$D = EI/(1-\nu^2) \quad 3\text{-}33$$

E is the modulus of elasticity, I is the moment of inertia, and ν is Poisson's ratio. It must be realized that except for the elastic range, the values of X (the displacement) and r in Equation 3-32 represent change in deflection and resistance from one range of behavior to another. Therefore, for two-way members the change in deflection and resistance (as previously explained) is obtained from Figures 3-24 through 3-38 and the stiffnesses are computed from Equations 3-28 through 3-33.

3-14. Resistance-Deflection Functions for Design

3-14.1. General

The resistance-deflection function used for design depends upon the maximum permitted deflection according to the design criteria of the element being considered. This maximum deflection X_m can be categorized as either limited or large. In the limited deflection range, the maximum deflection of the system is limited to the elastic, elasto-plastic and plastic ranges. When the maximum deflection falls in the large deflection range, the response of the system is mainly within the plastic range and the elastic and elasto-plastic ranges need not be considered. The error resulting from the omission of the elastic and elasto-plastic portions in this analysis is negligible.

The support rotation that corresponds to limited deflection varies for the different materials used in protection design. The response criteria for each material is obtained from the chapter that describes the design procedures for that material.

3-14.2. Limited Deflections

When designing for limited deflections, the maximum deflection X_m of the element is kept within the elastic, elasto-plastic, and limited plastic ranges, and the resistance-deflection function for design takes the form shown in Figure 3-39 a, b, and c for a one-step system, a two-step system, and a three-step system, respectively. The design charts presented in Section 3-19.3 were established for a one-step system; for two- and three-step systems, these charts can be used if the resistance-deflection functions are replaced with equivalent elastic resistance-deflection functions defined by K_E and X_E as indicated by the dotted lines in Figure 3-39. The equivalent elastic stiffness K_E and the equivalent maximum elastic deflection X_E are calculated such that the area under the dotted curve is equal to the area under the solid curve, thereby producing the same potential energy in each system. The equivalent maximum elastic deflection X_E for the two-step and three-step systems shown is expressed by Equations 3-34 and 3-35, respectively.

$$X_E = X_e + X_p(1 - r_e/r_u) \qquad 3\text{-}34$$

$$X_E = x_e\ (r_{ep}/r_u) + X_{ep}(1 - r_e/r_u) + X_p(1 - r_{ep}/r_u) \qquad 3\text{-}35$$

The equivalent elastic stiffness K_E in each case is equal to

$$K_E = r_u/X_E \qquad 3\text{-}36$$

One-way elements exhibit one- and two-step resistance deflection curves depending on the type of supports. Consequently, the equivalent elastic stiffness K_E is given for one-way elements in Table 3-8. The equivalent elastic deflection can then be calculated from Equation 3-36. Two-way elements generally exhibit two- and three-step resistance-deflection curves which are a function of not only the type of supports but also of the aspect ratio L/H of the element. The equivalent elastic deflection X_E of the element under consideration must be calculated from Equations 3-34 and 3-35 for two- and three-step systems, respectively. The value of K_E for the system can then be obtained from Equation 3-36.

3-14.3. Large Deflections

When designing for a large deflection, it can be assumed without significant error that the resistance rises instantaneously from zero to its ultimate value r_u at the onset of the blast loading thus neglecting the elastic and elasto-plastic ranges. The design resistance function for one-way elements is approximated by a constant plastic range resistance as shown in Figure 3-40a, while for two-way elements, the resistance function becomes that shown in Figure 3-40b, where the maximum deflection X_m can be either smaller or larger than the partial failure deflection X_1.

3-15. Support Shears or Reactions

Support shears or reactions are a function the applied load and the maximum resistance attained by an element, its geometry and yield line location. However, for short duration blast loads, the support shears can be reasonably estimated by neglecting the applied load. Therefore, the ultimate support shear can be assumed to be developed when the resistance reaches the ultimate value, r_u.

Equations for the ultimate support shears V_s for one-way elements are given in Table 3-9. For those cases where an element does not reach its ultimate resistance, the support shears are obtained based upon elastic theory for the actual resistance r attained by the element.

For two-way elements, the ultimate shears acting at each section are calculated by use of the "yield line procedure" previously outlined for the determination of the ultimate resistance r_u. The shear along the support is assumed to vary in the same manner as the moment varies (2/3 V at the corners and V elsewhere) to account for the higher stiffness of the corners (Figure 3-41). Since the shear is assumed to be zero along the interior (usually positive) yield lines, the total shear at any section of a sector is equal to the resistance r_u times the area between the section being considered and the positive yield lines. Referring to Figure 3-41, the support shear V_{sV} for the triangular sector I is

$$(2/3)V_{sV}(L/4 + L/4) + V_{sV}(L/2) = r_u(Ly/2) \qquad 3\text{-}37$$

$$V_{sV} = 3r_u y/5 \qquad 3\text{-}38$$

and for the trapezoidal sector II

$$(2/3)V_{sH}(y/2) + V_{sH}(H - y/2) =$$

$$r_u(L/2)[(H - y + H)/2] \qquad 3\text{-}39$$

$$V_{sH} = [3r_u L(2-y/H)]/2(6 - y/H) \qquad 3\text{-}40$$

Values of the ultimate support shears V_{sH} and V_{sV} for several two-way elements derived as above are presented in Tables 3-10 and 3-11. Table 3-10 gives the ultimate support shears for the case where opposite supports provide the same degree of restraint resulting in symmetrical yield line patterns. Table 3-11 is for completely general situations where opposing supports provide different degrees of restraint and result in the formation of unsymmetrical yield lines. In these cases, the ultimate support shears are not equal at opposing supports.For the situations where the ultimate resistance of an element is not attained, the support shears are less than the ultimate value. The proportion of the total load along each support as well as the distribution of the shears along the support is assumed to be the same as previously cited for the ultimate support shear. Therefore, the support shears corresponding to the resistance r of the element is obtained from the equations presented in Tables 3-10 and 3-11 by replacing r_u with the actual resistance attained (r_e, r_{ep}, etc.).

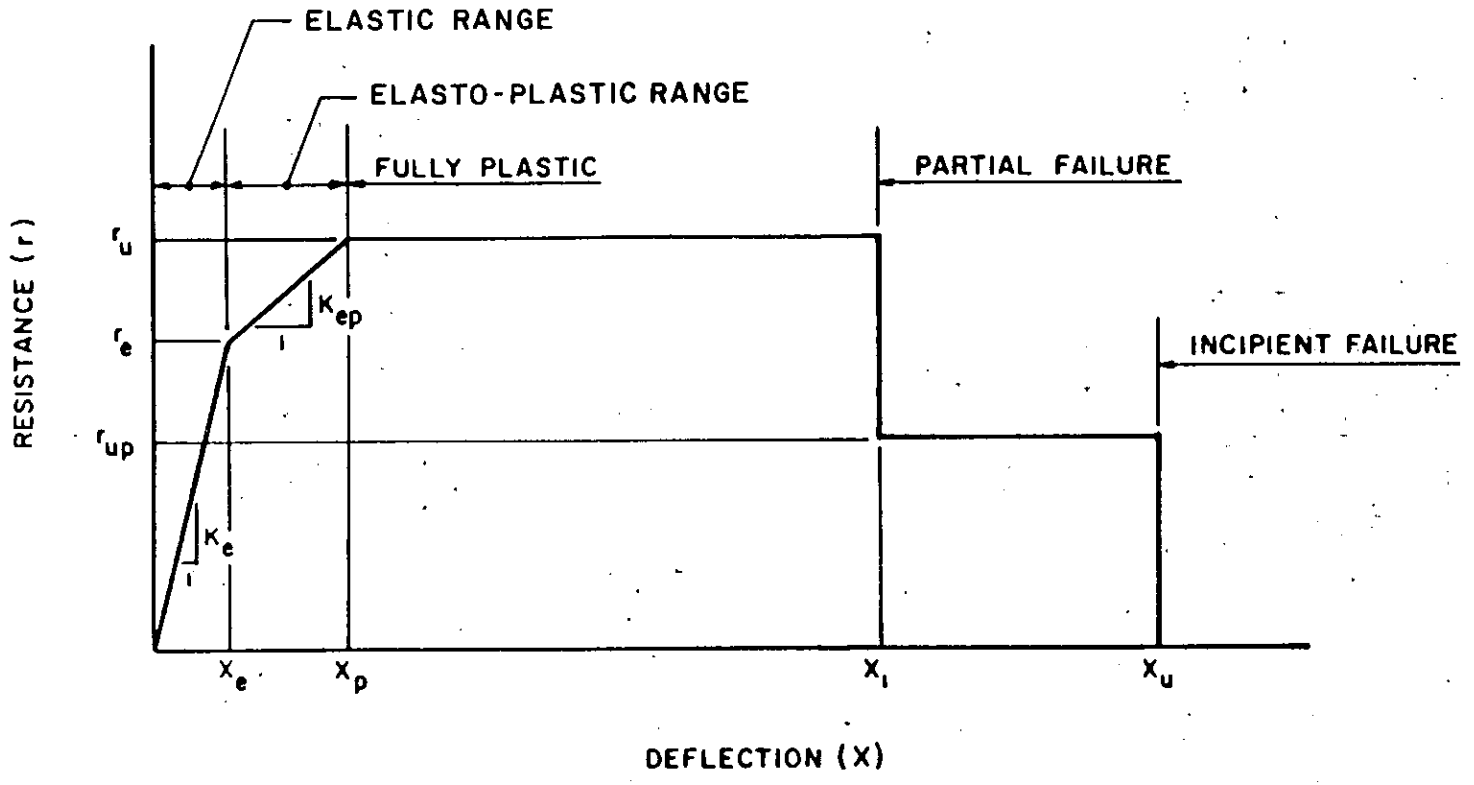


Figure 3-1 Typical resistance-deflection function for two-way element

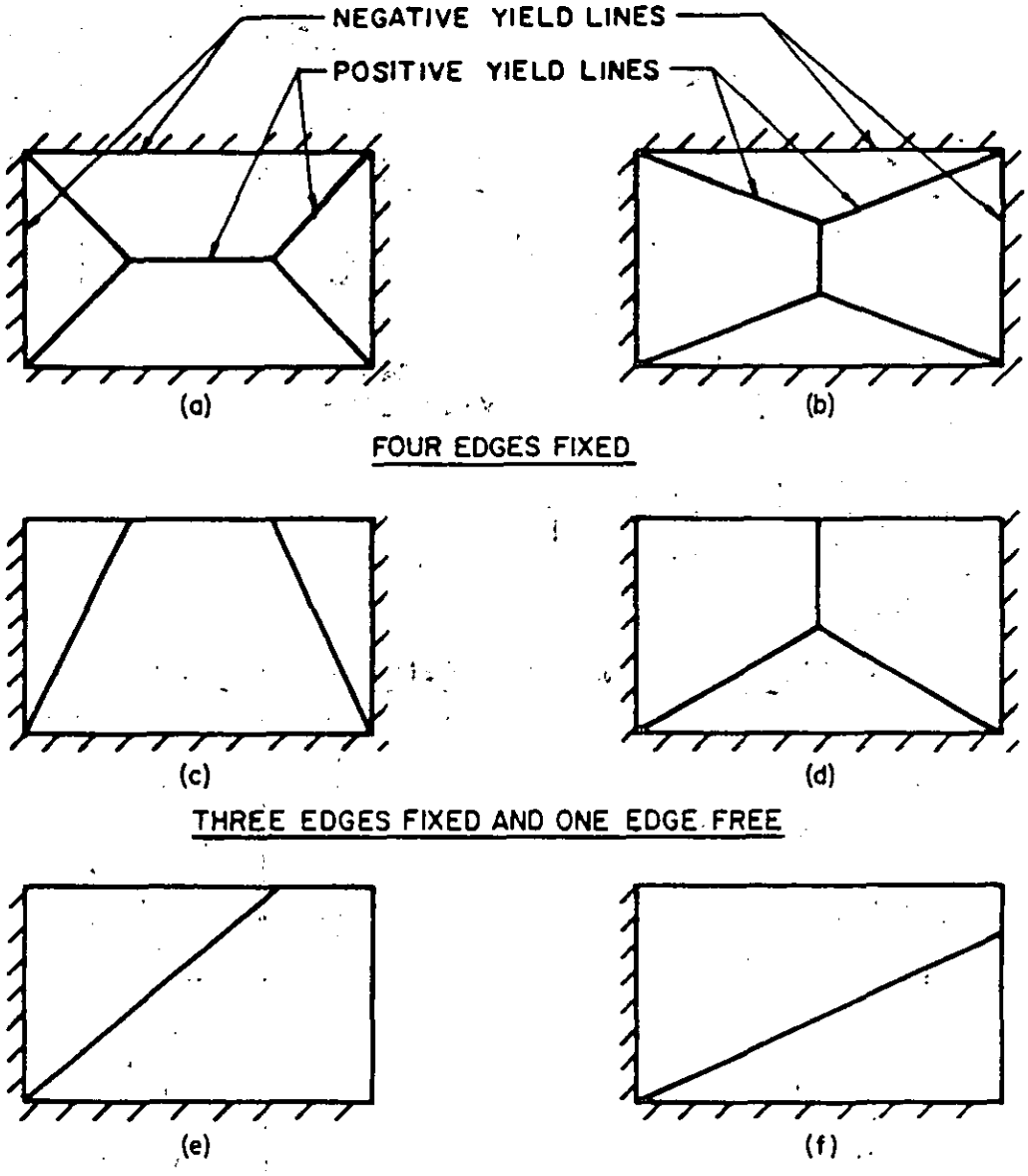
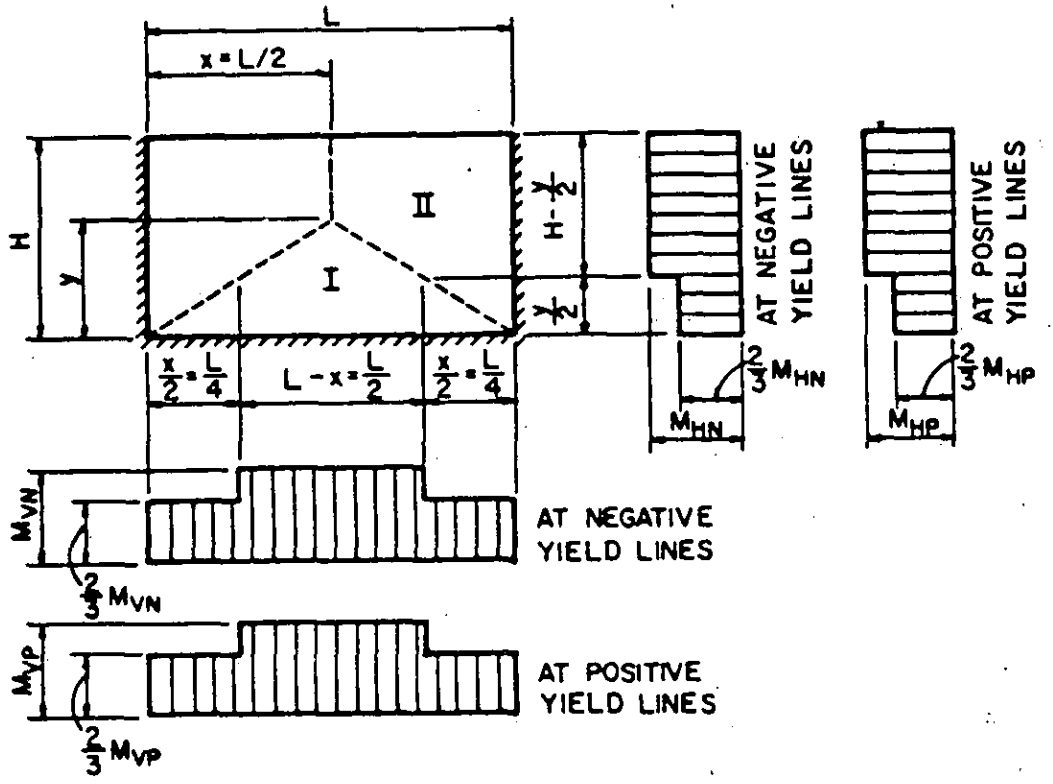
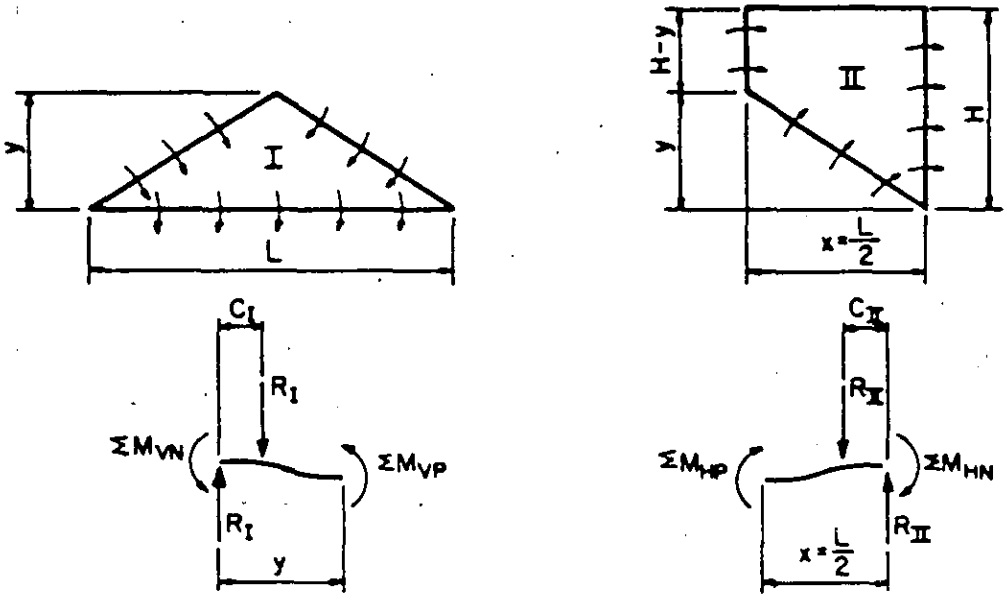


Figure 3-2 Idealized yield line locations for several two-way elements



a) YIELD LINES AND DISTRIBUTION OF MOMENTS



b) FREE-BODY DIAGRAMS FOR INDIVIDUAL SECTORS

Figure 3-3 Determination of ultimate unit resistance

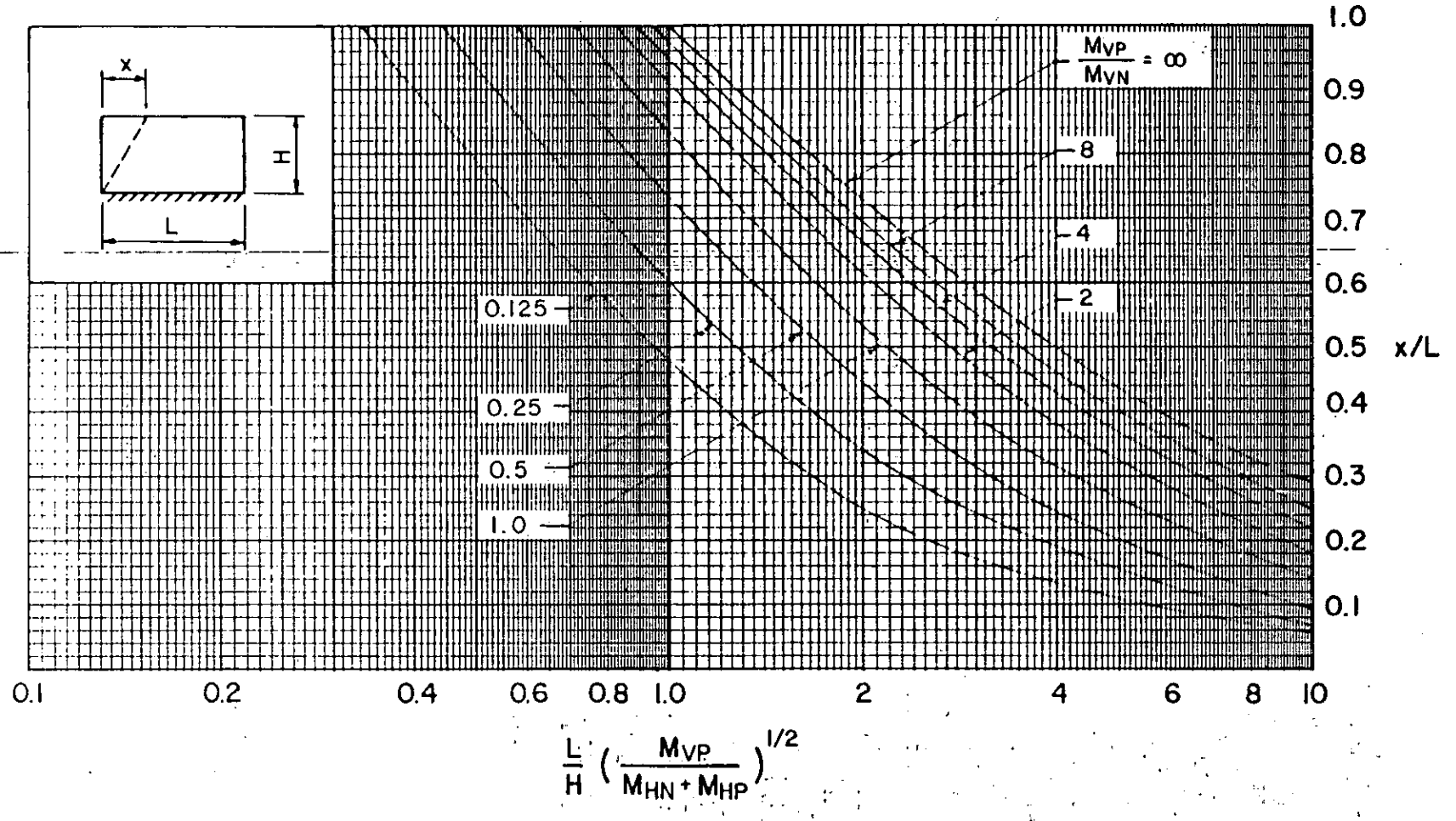


Figure 3-4 Location of yield lines for two-way element with two adjacent edges supported and two edges free (values of x)

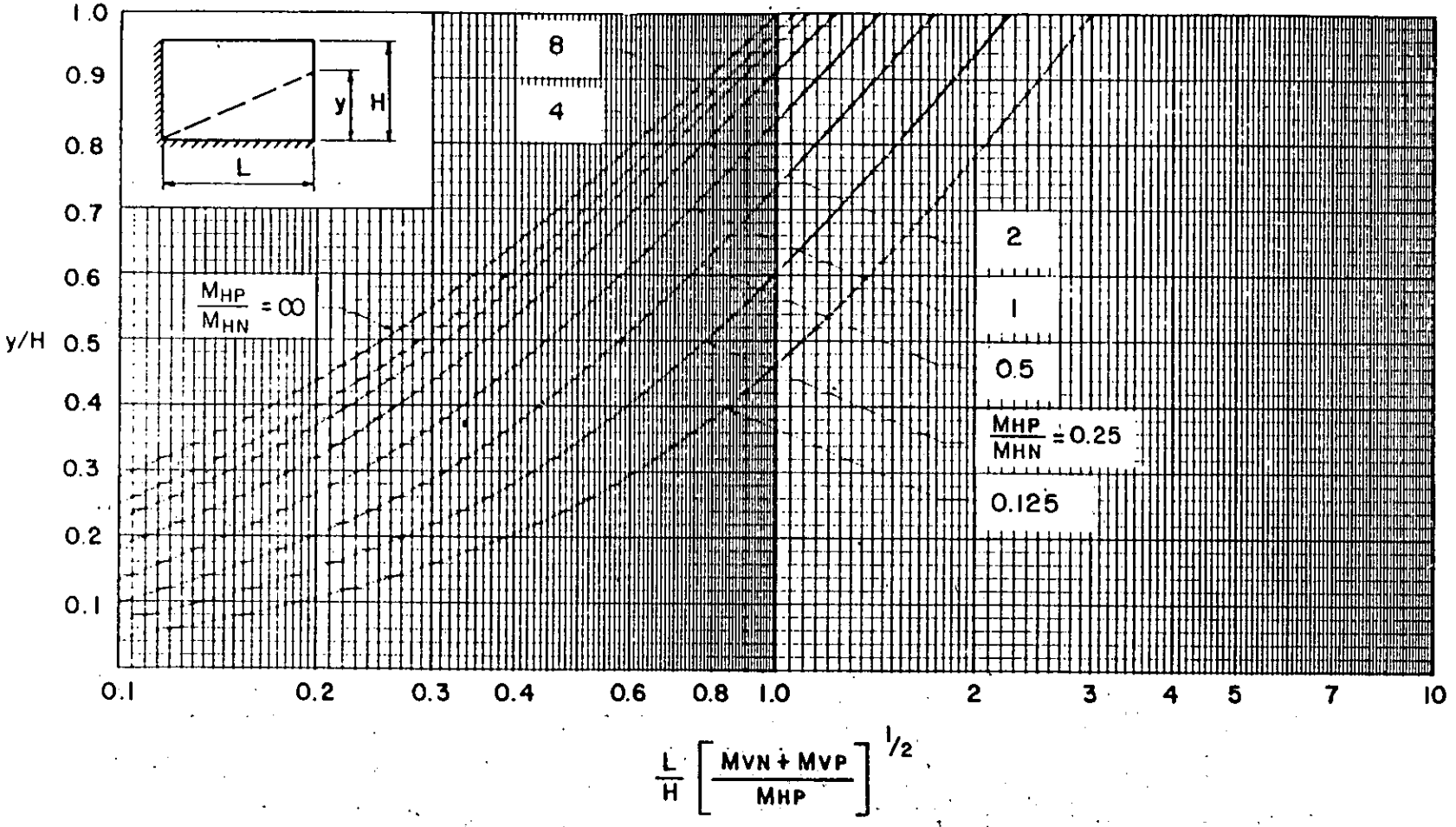


Figure 3-5 Location of yield lines for two-way element with two adjacent edges supported and two edges free (values of y)

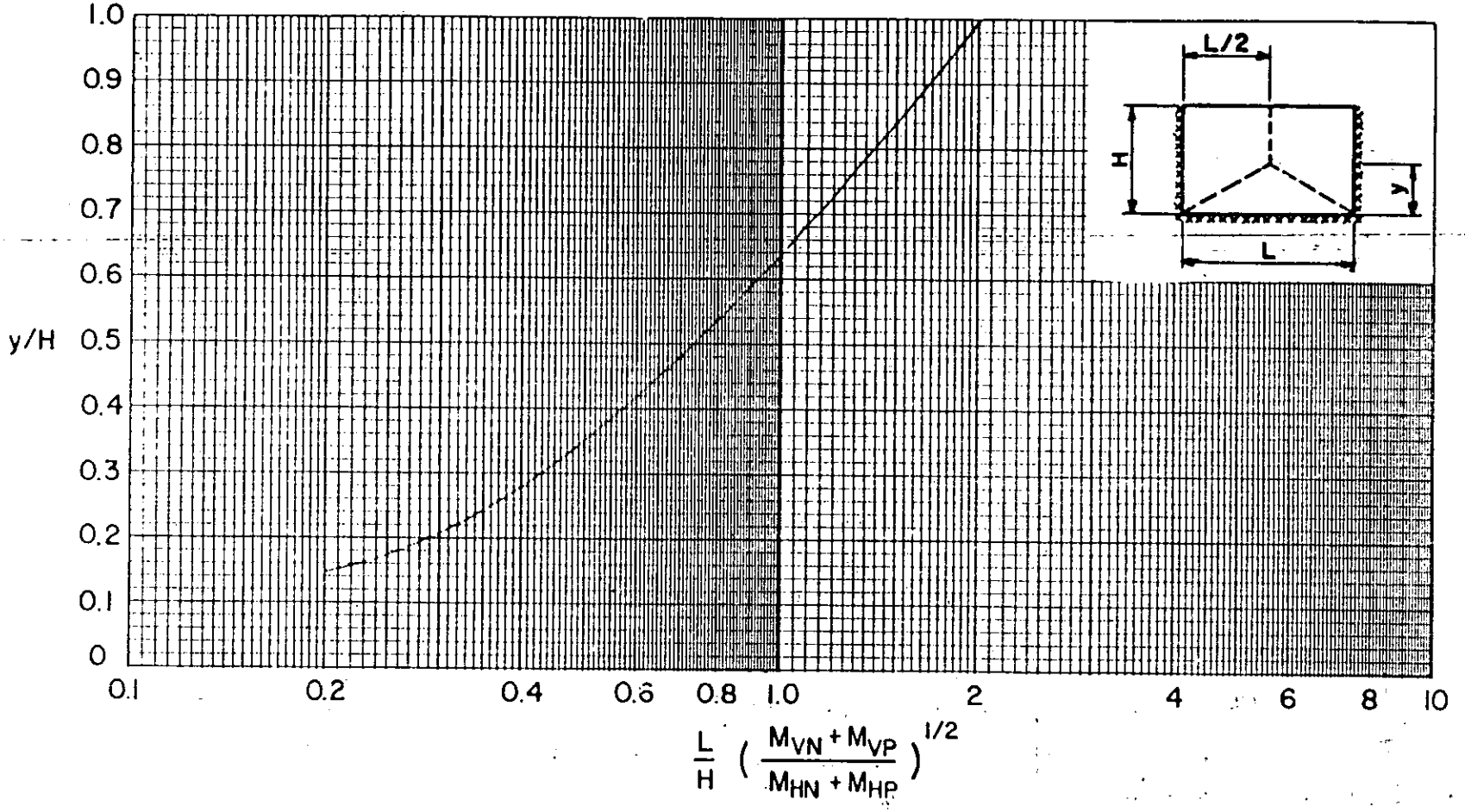


Figure 3-6 Location of symmetrical yield lines for two-way element with three edges supported and one edge free (values of y)

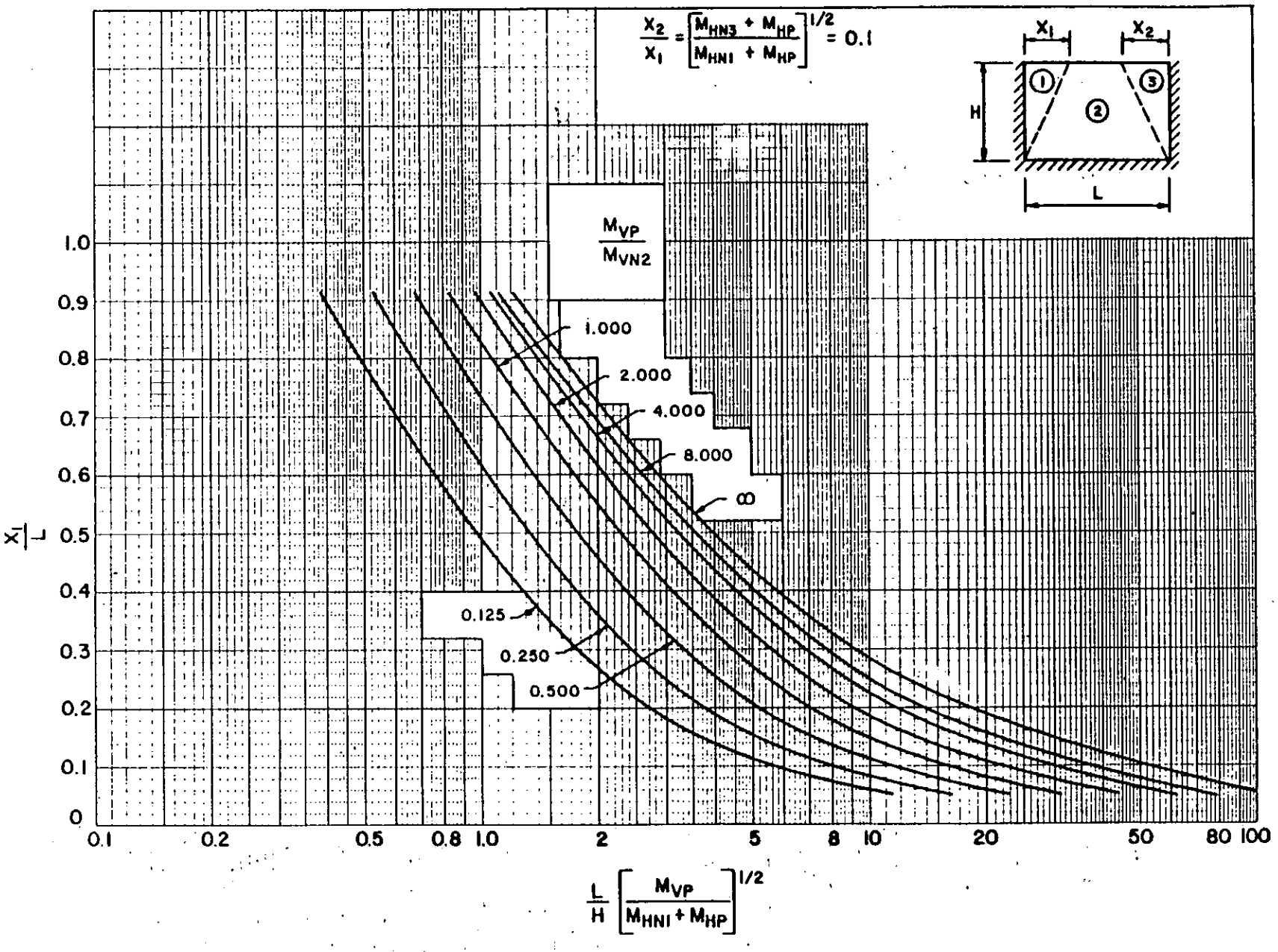


Figure 3-7 Location of unsymmetrical yield lines for two-way element with three edges supported and one edge free ($X_2/X_1=0.1$)

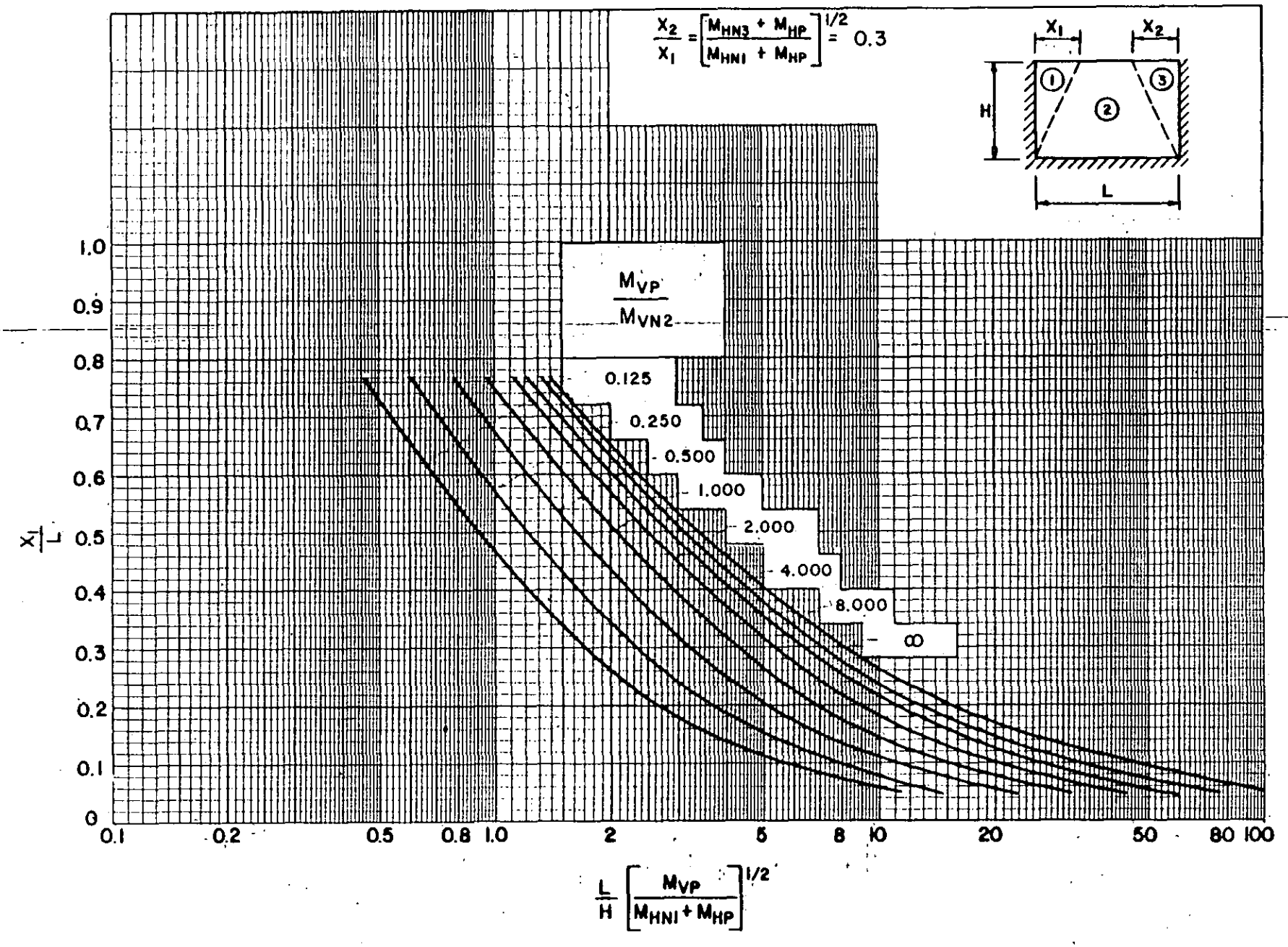


Figure 3-8 Location of unsymmetrical yield lines for two-way element with three edges supported and one edge free (X_2/X_1=0.3)

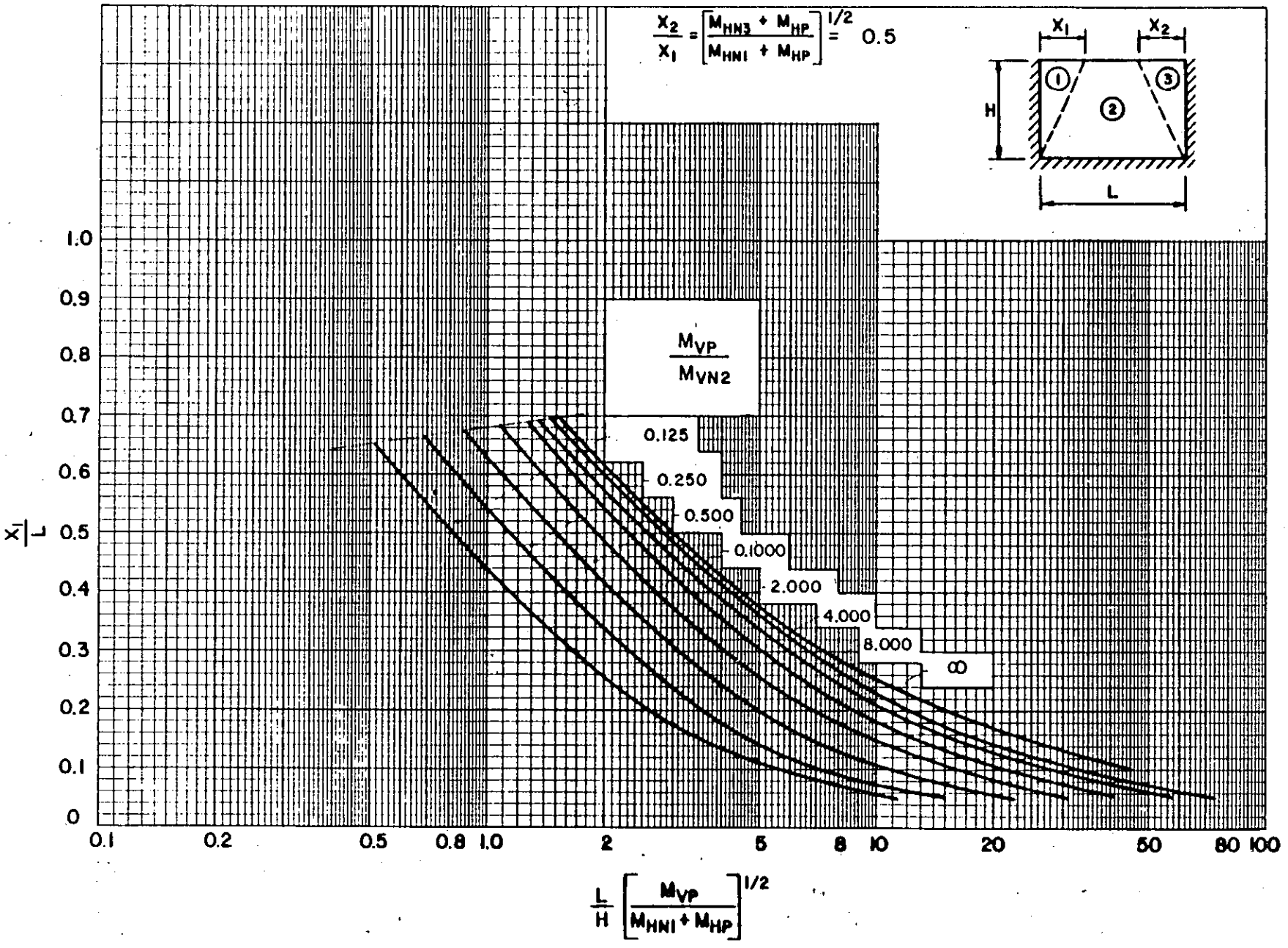


Figure 3-9 Location of unsymmetrical yield lines for two-way element with three edges supported and one edge free (X_2/X_1=0.5)

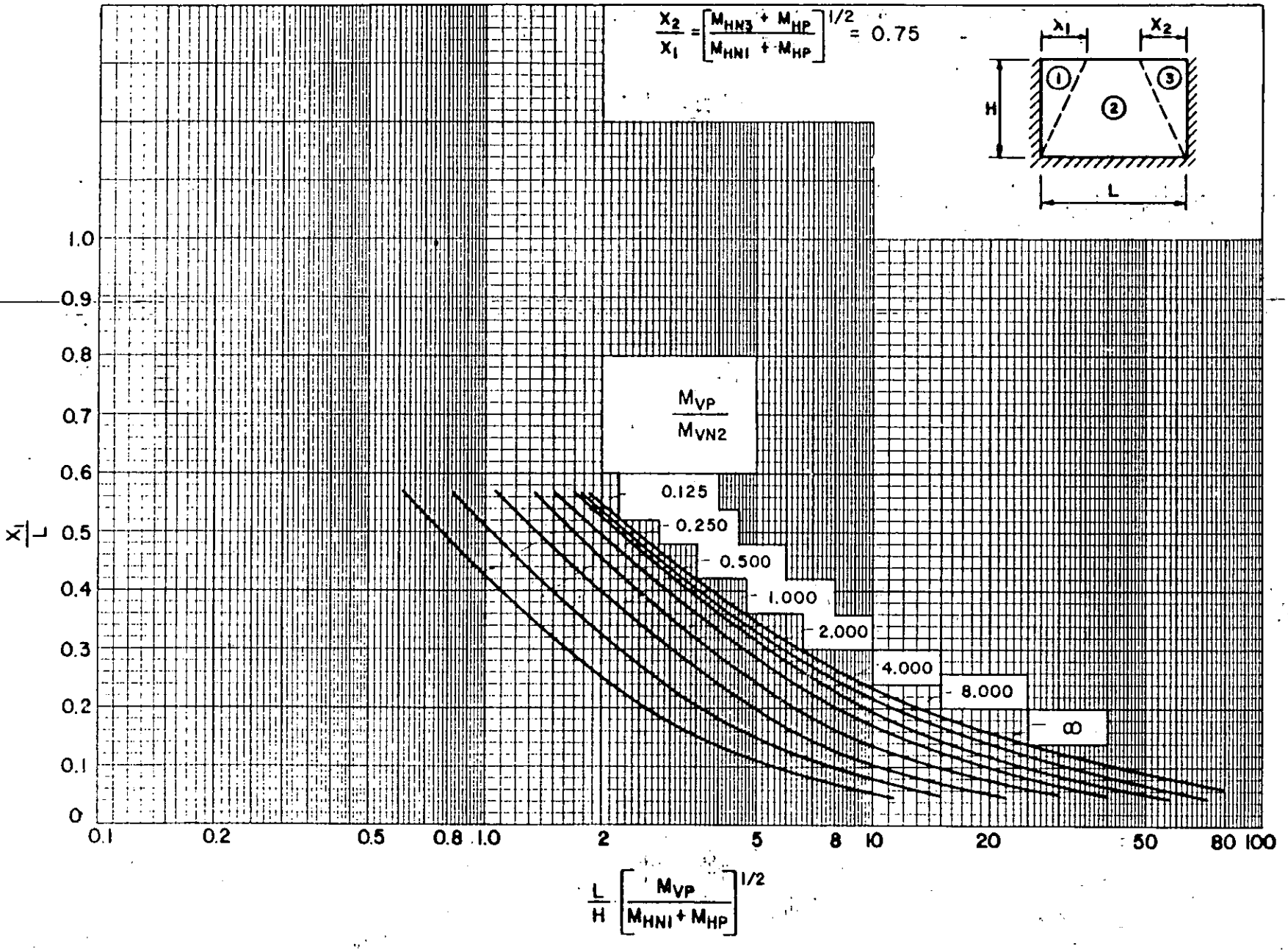


Figure 3-10 Location of unsymmetrical yield lines for two-way element with three edges supported and one edge free ($X_2/X_1=0.75$)

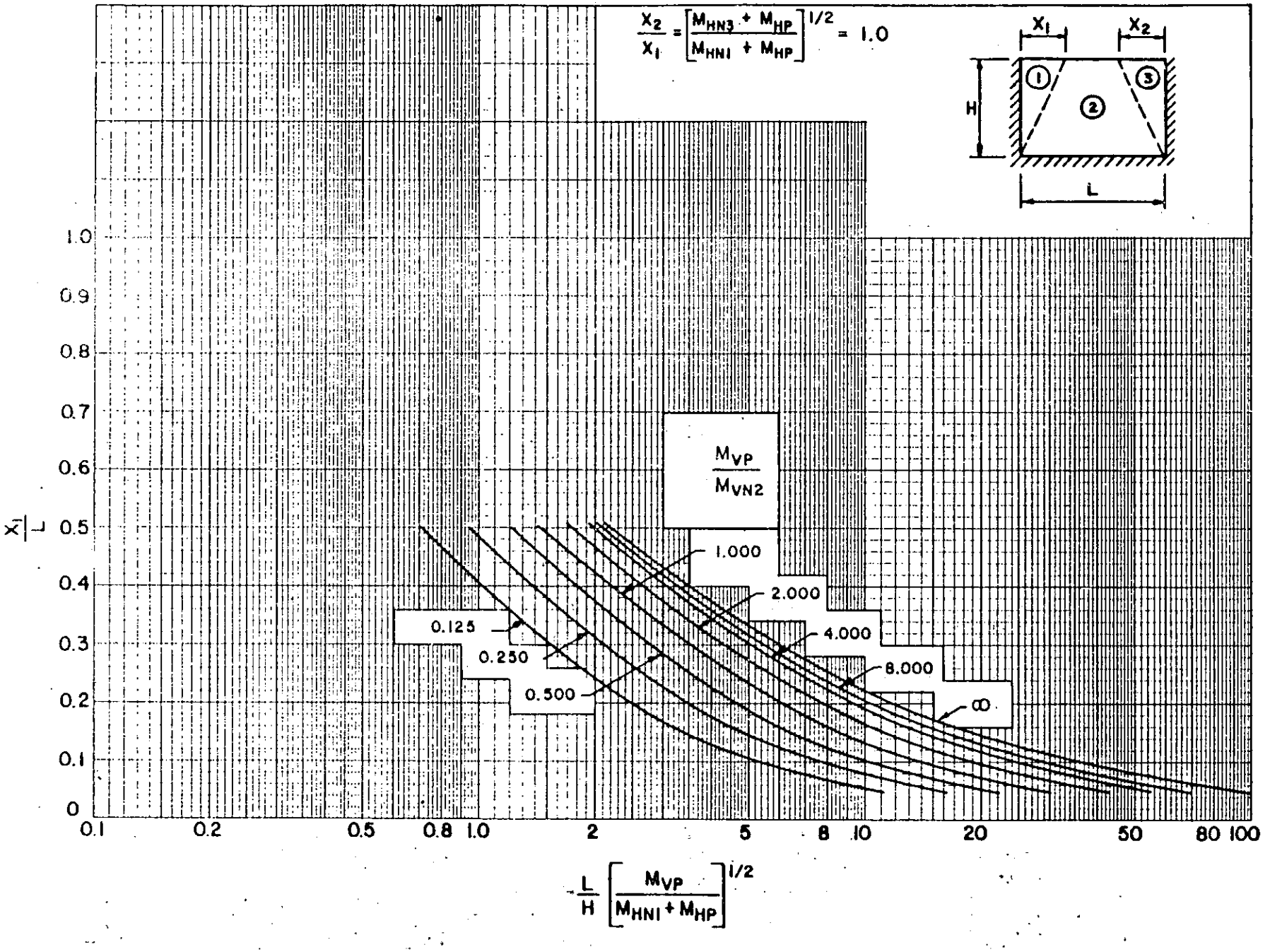


Figure 3-11 Location of unsymmetrical yield lines for two-way element with three edges supported and one edge free (X_2/X_1=1.0)

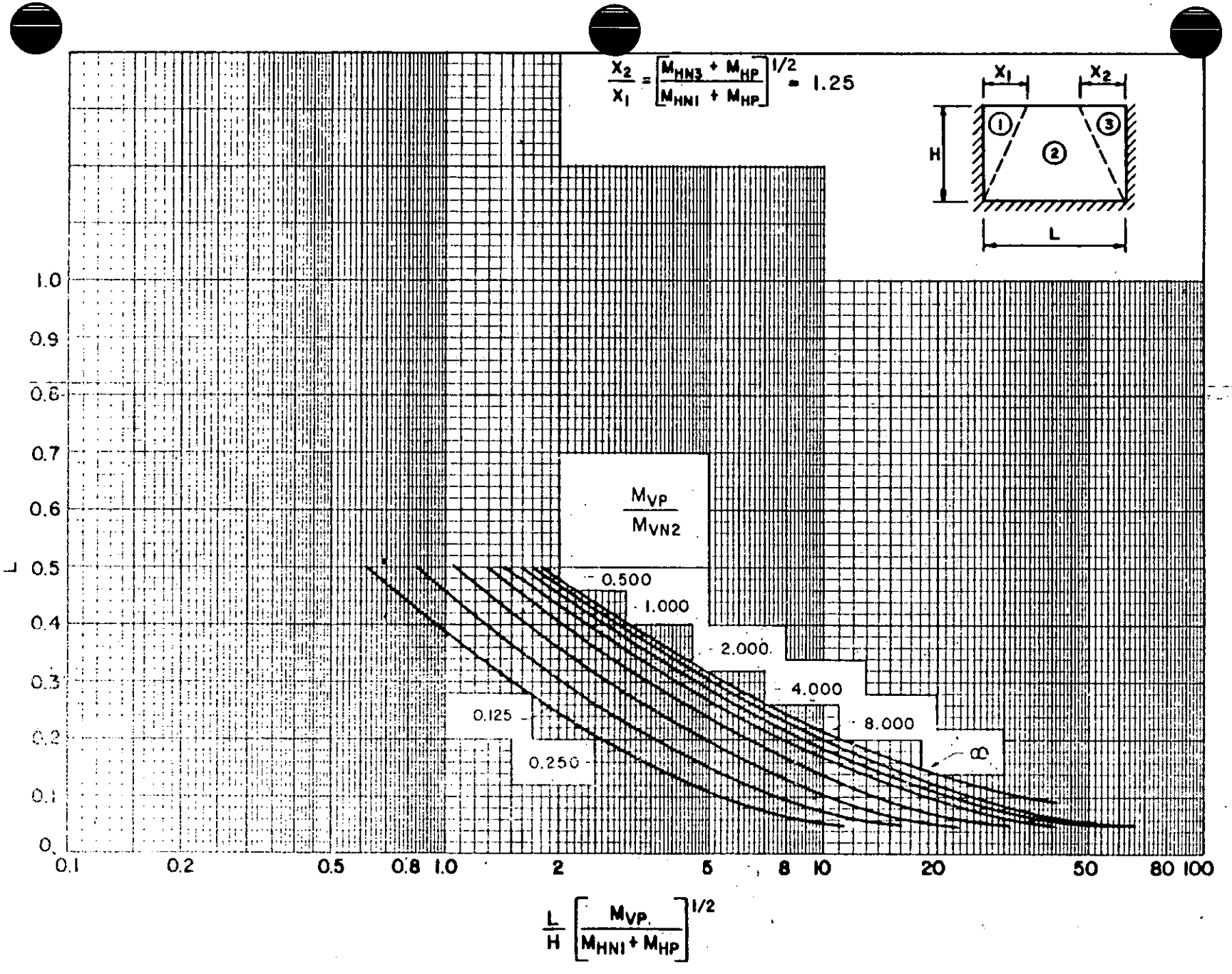


Figure 3-12 Location of unsymmetrical yield lines for two-way element with three edges supported and one edge free (X_2/X_1=1.25)

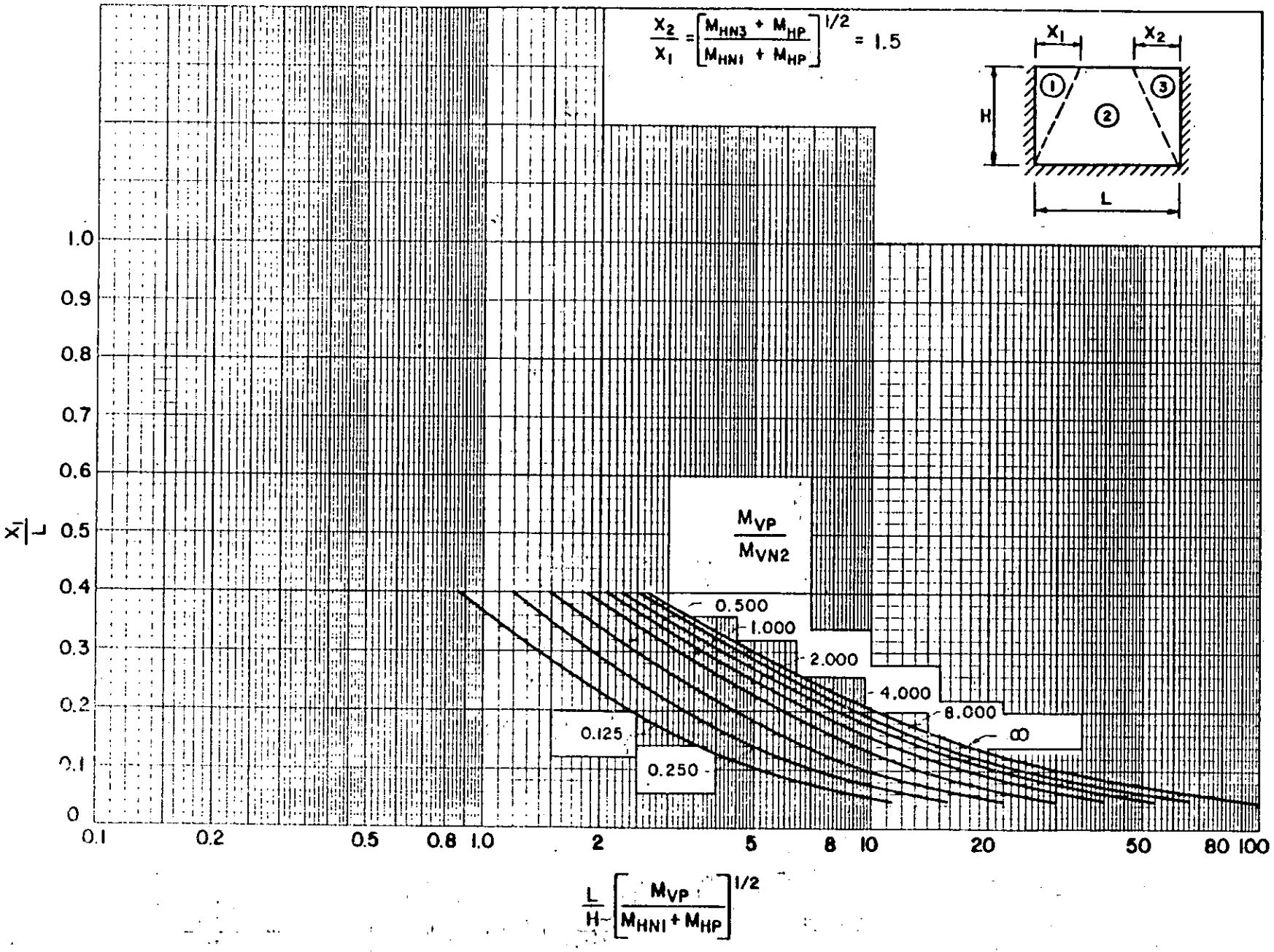


Figure 3-13 Location of unsymmetrical yield lines for two-way element with three edges supported and one edge free ($X_2/\ell_1 = 1.5$)

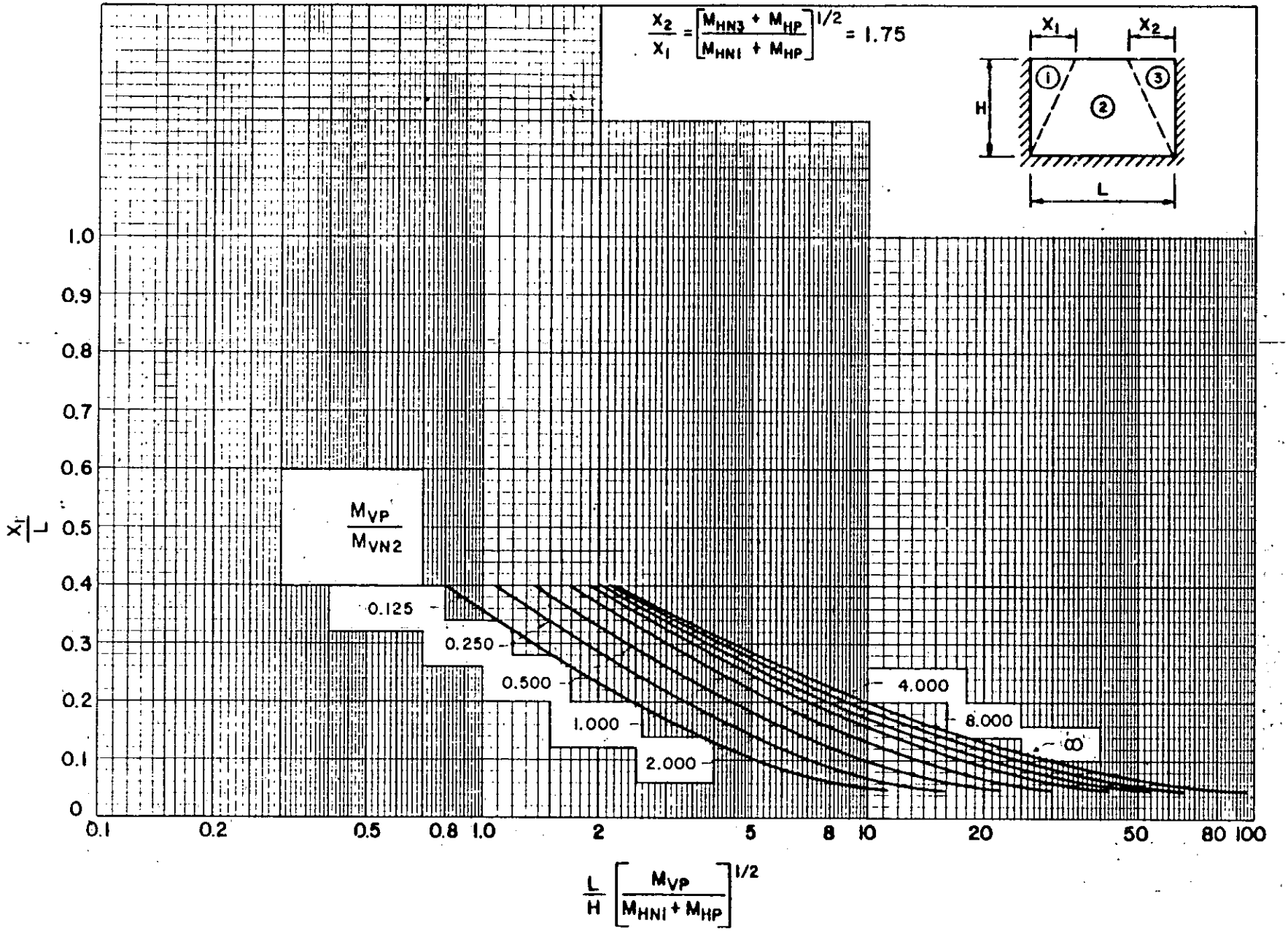


Figure 3-14 Location of unsymmetrical yield lines for two-way element with three edges supported and one edge free ($X_2/X_1 = 1.75$)

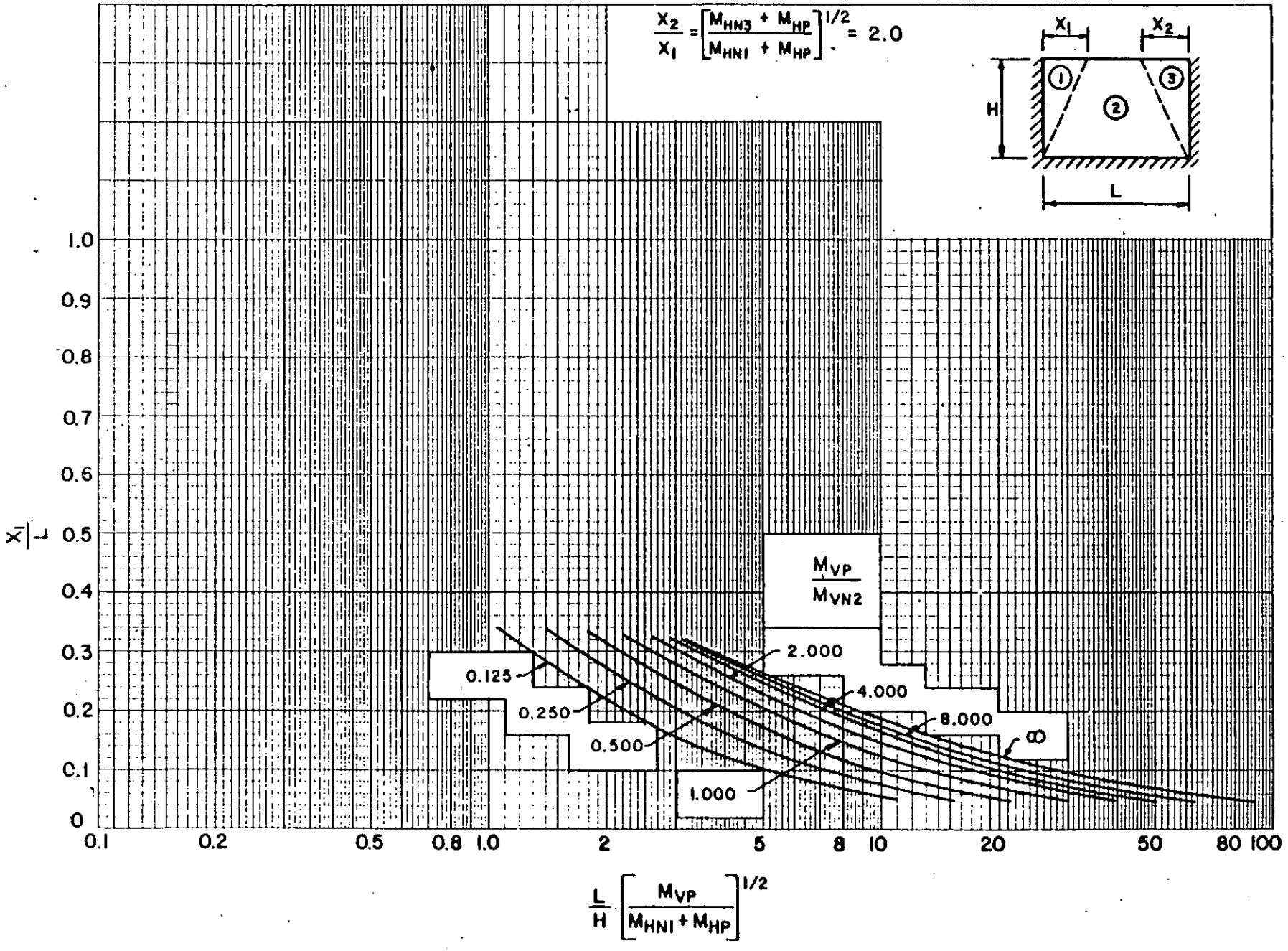


Figure 3-15 Location of unsymmetrical yield lines for two-way element with three edges supported and one edge free ($X_2/X_1 = 2.0$)

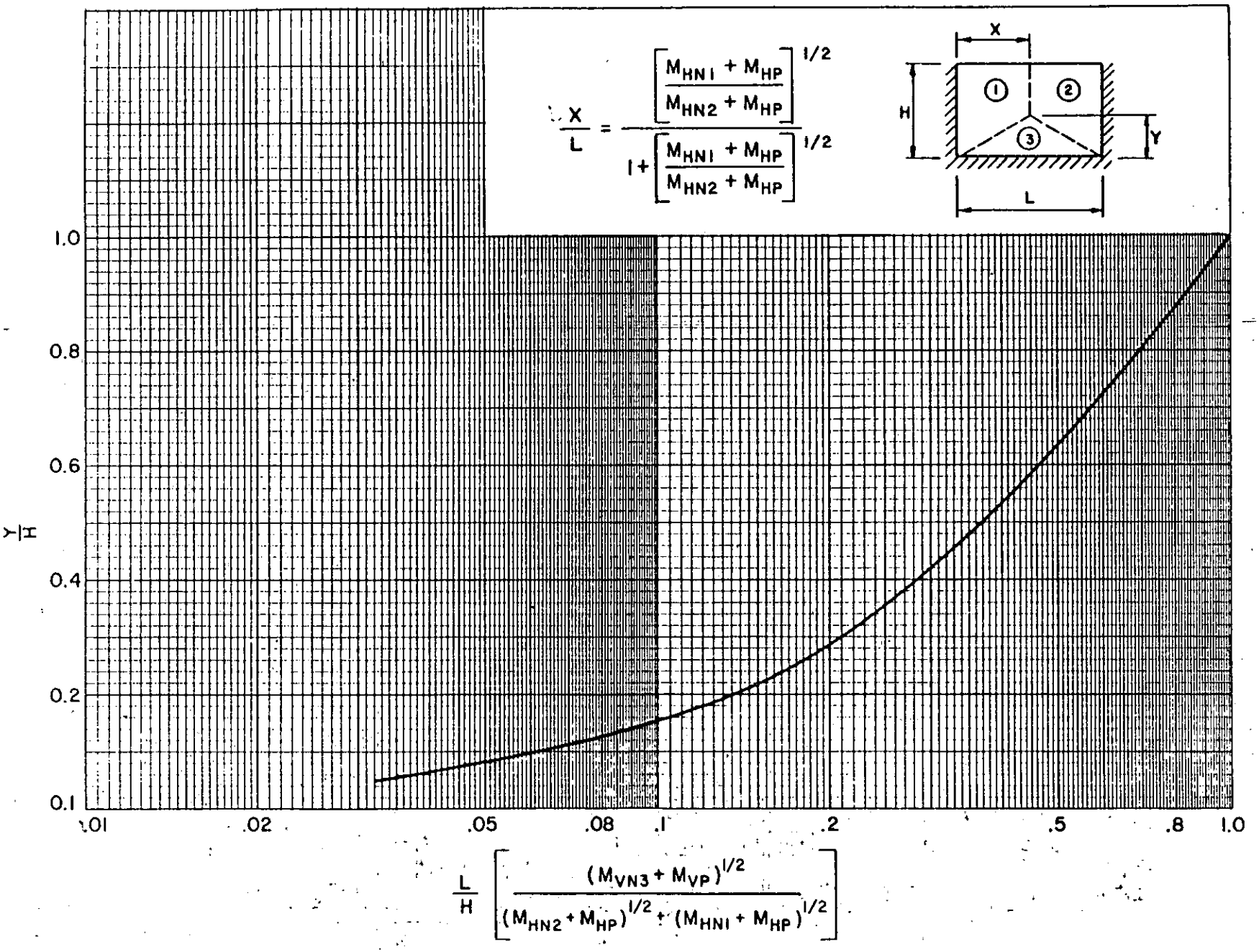


Figure 3-16 Location of unsymmetrical yield lines for two-way element with three edges supported and one edge free (values of y)

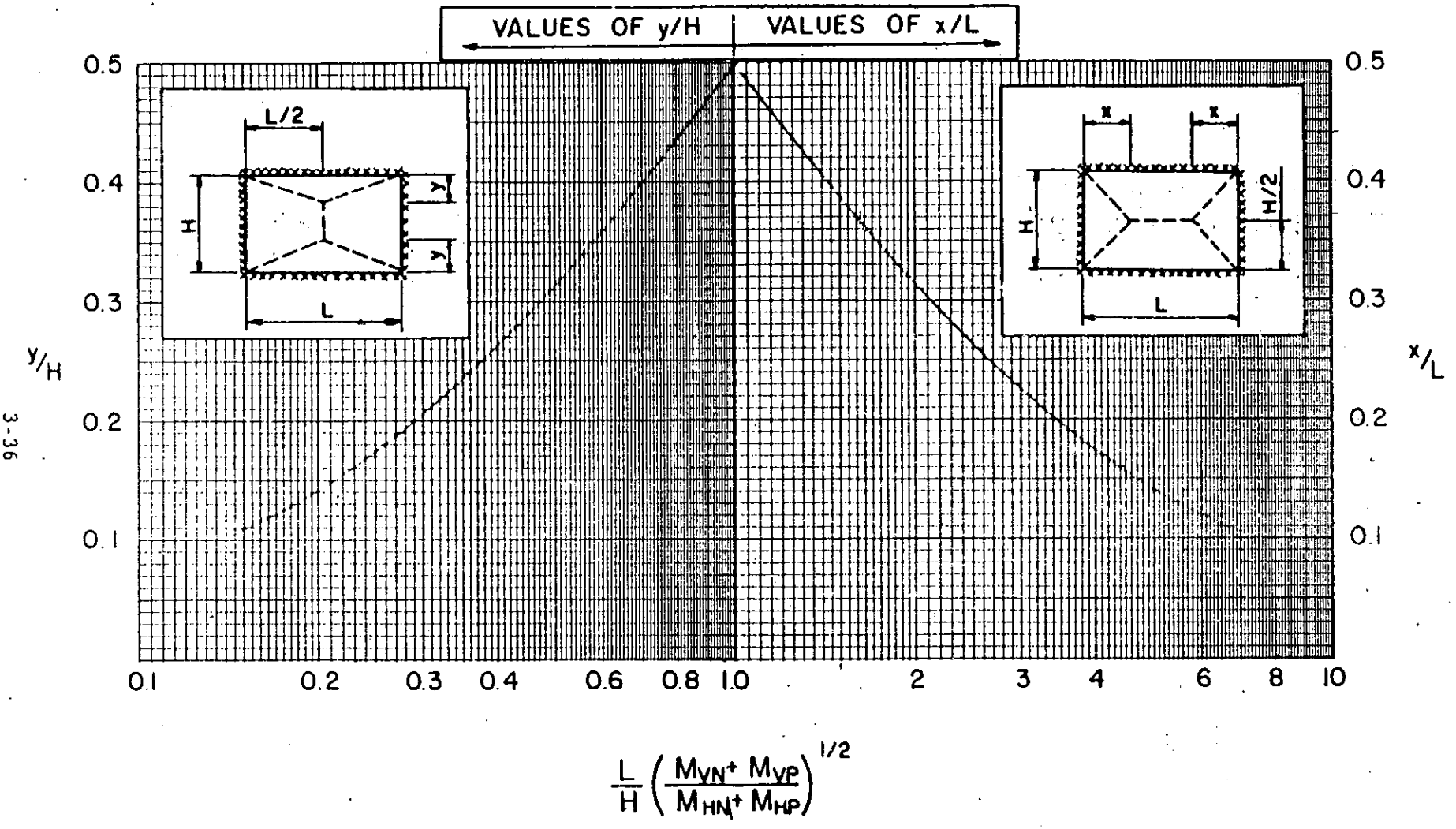


Figure 3-17 Location of symmetrical yield lines for two-way element with four edges supported

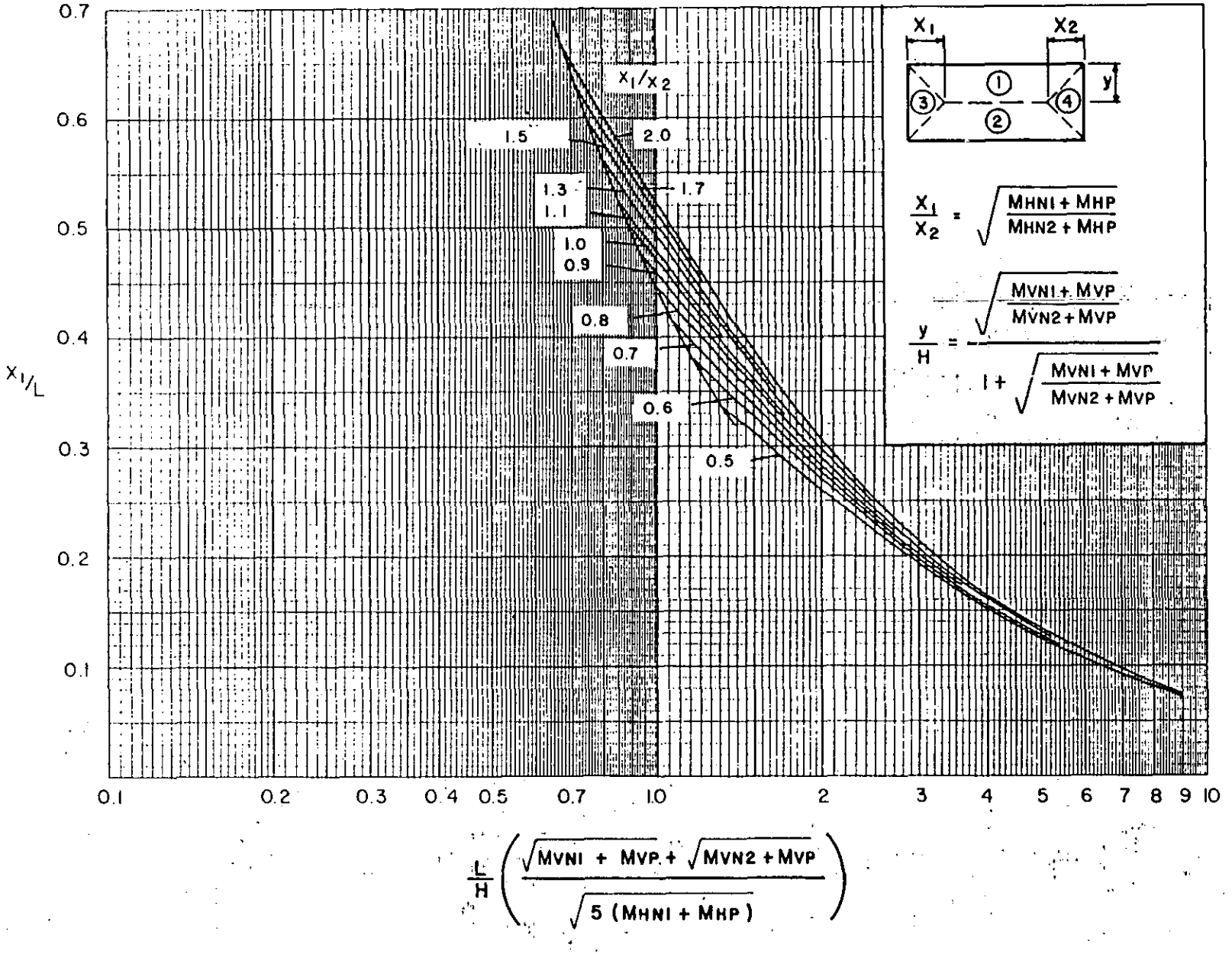


Figure 3-18 Location of unsymmetrical yield lines for two-way element with four edges supported (values of X_1)

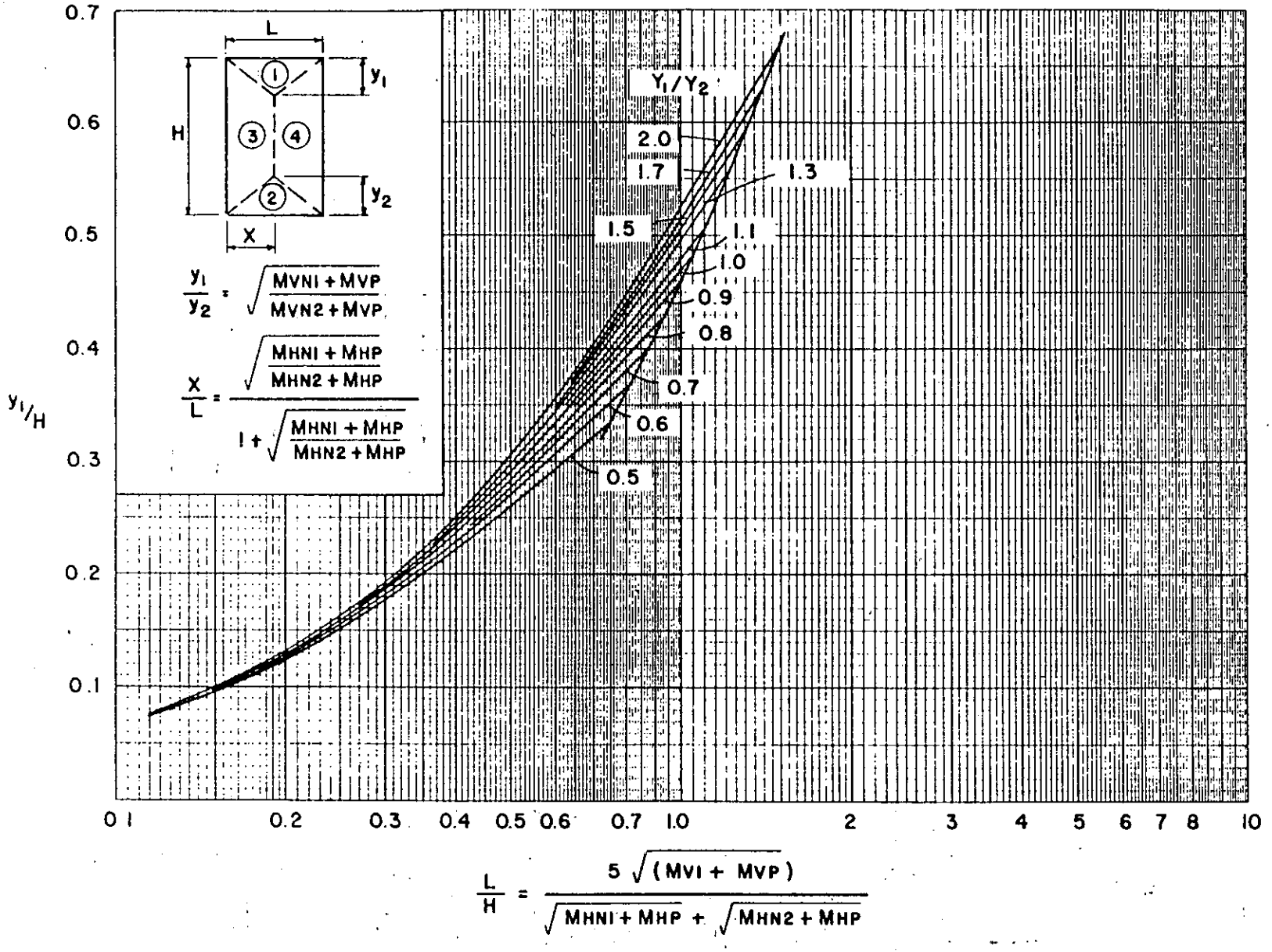


Figure 3-19 Location of unsymmetrical yield lines for two-way element with four edges supported (values of Y_1)

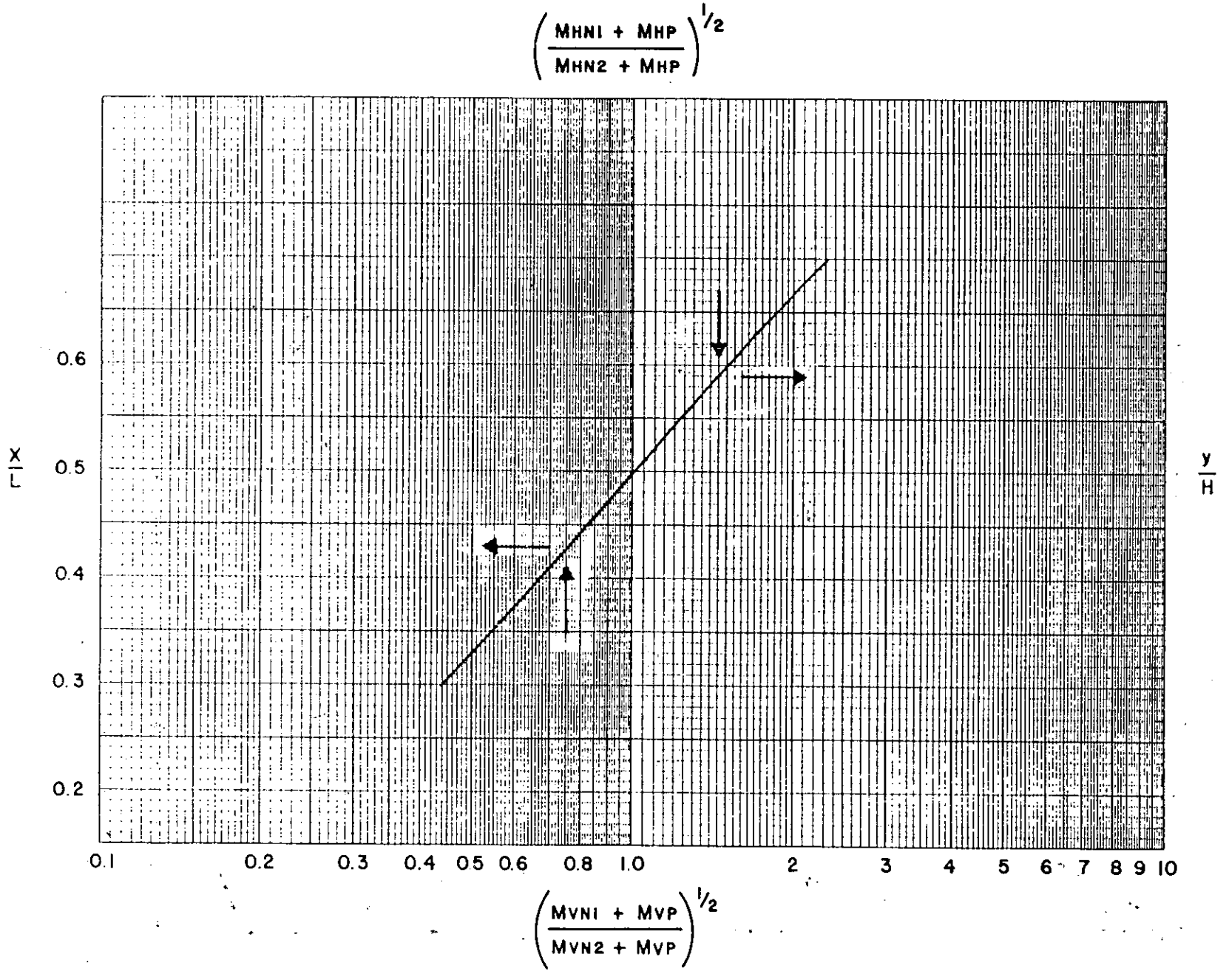


Figure 3-20 Location of unsymmetrical yield lines for two-way element with four edges supported (values of x/L and y/H)

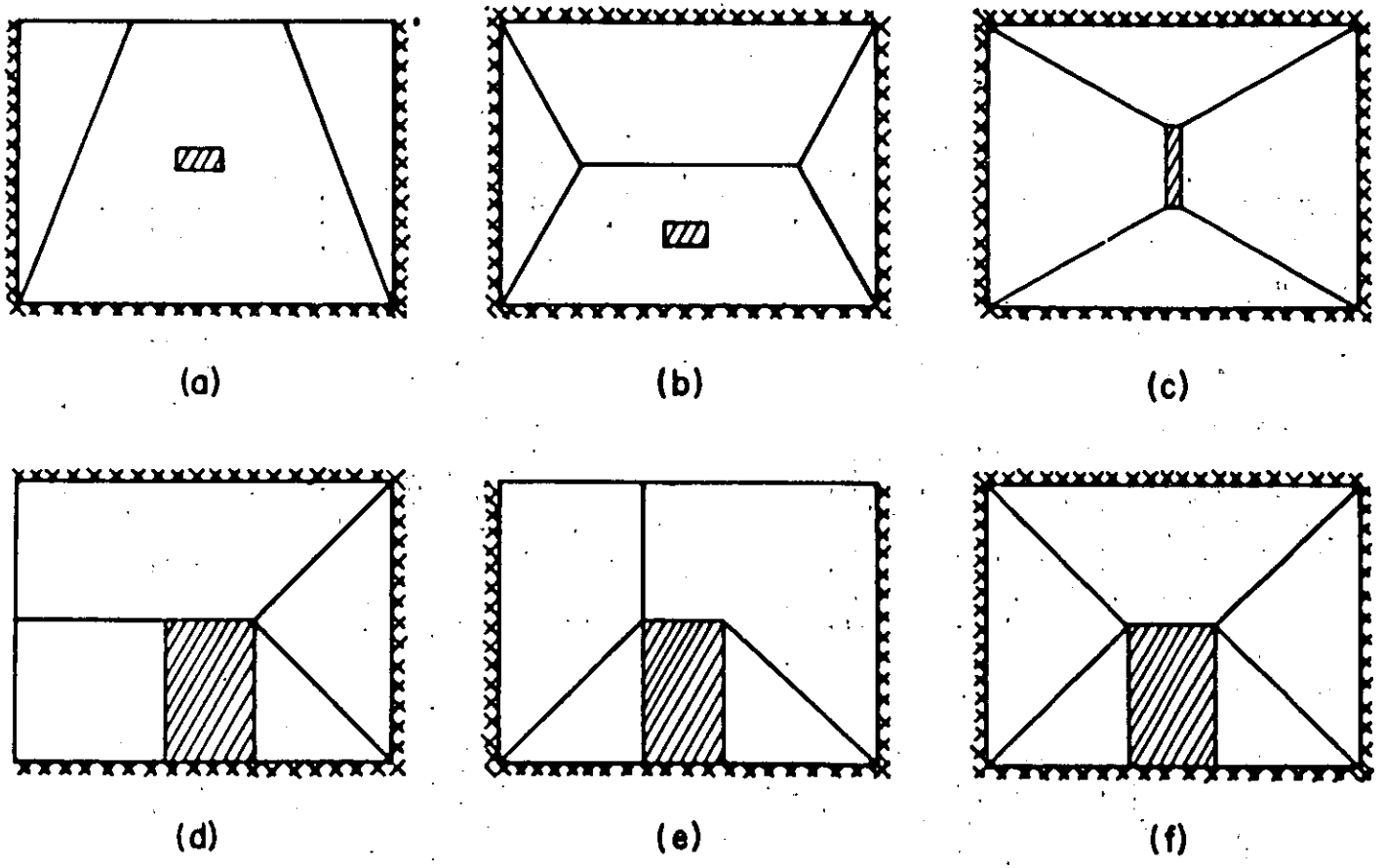
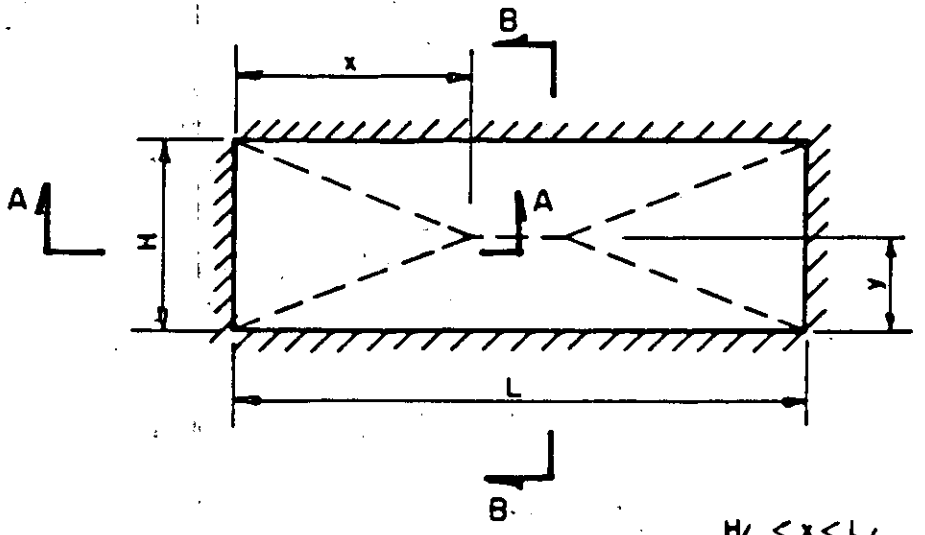


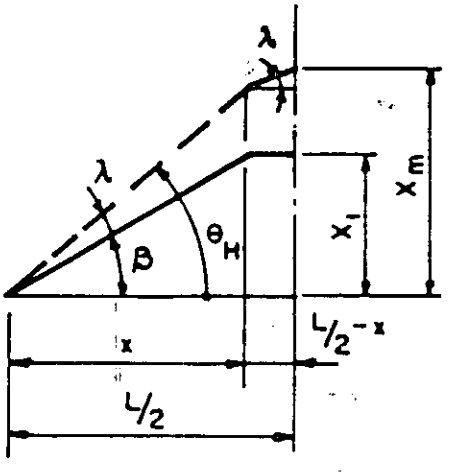
Figure 3-21 Effects of openings on yield lines locations



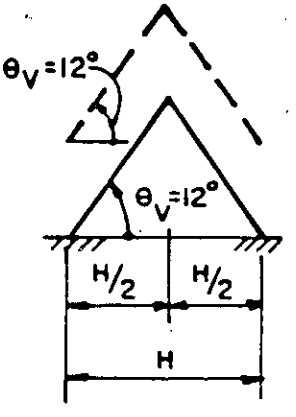
ELEVATION

$H/2 \leq x \leq L/2$

$y = H/2$



SECTION A-A



SECTION B-B

— PARTIAL FAILURE

--- INCIPIENT FAILURE

Figure 3-22 Deflection of two-way element

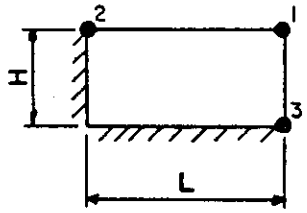


FIG. 3-24

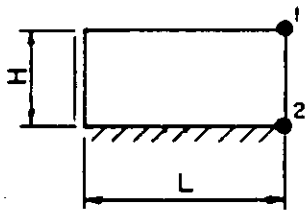


FIG. 3-25

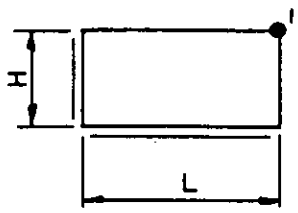


FIG. 3-26

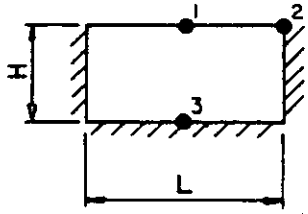


FIG. 3-27

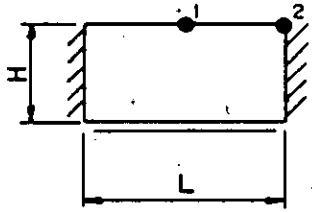


FIG. 3-28

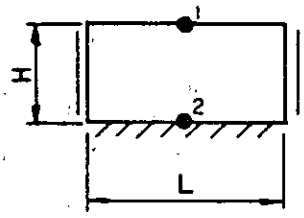


FIG. 3-29

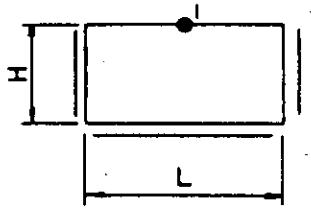


FIG. 3-30

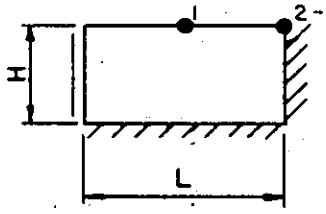


FIG. 3-31

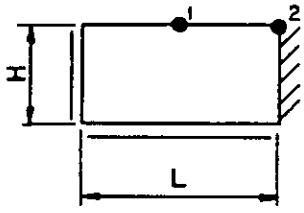


FIG. 3-32

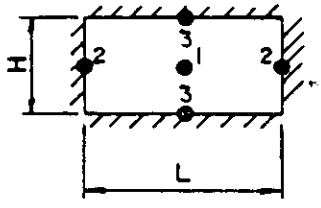


FIG. 3-33

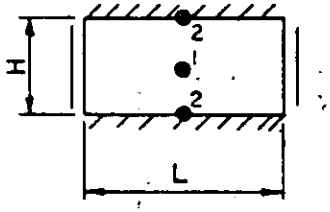


FIG. 3-34

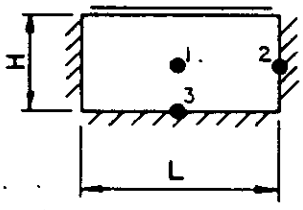


FIG. 3-35

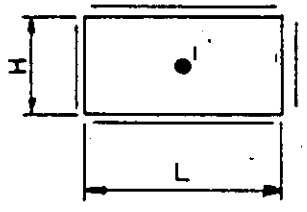


FIG. 3-36

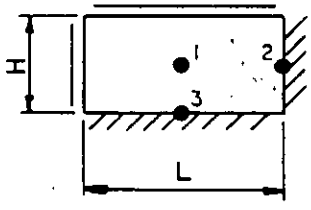


FIG. 3-37

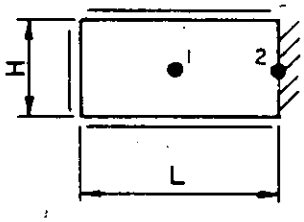
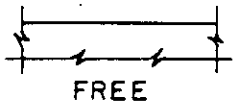
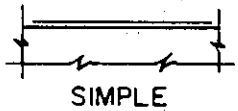


FIG. 3-38

LEGEND: EDGE CONDITIONS


FREE


SIMPLE

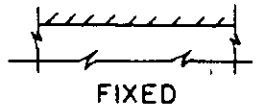

FIXED

Figure 3-23 Graphical summary of two-way elements

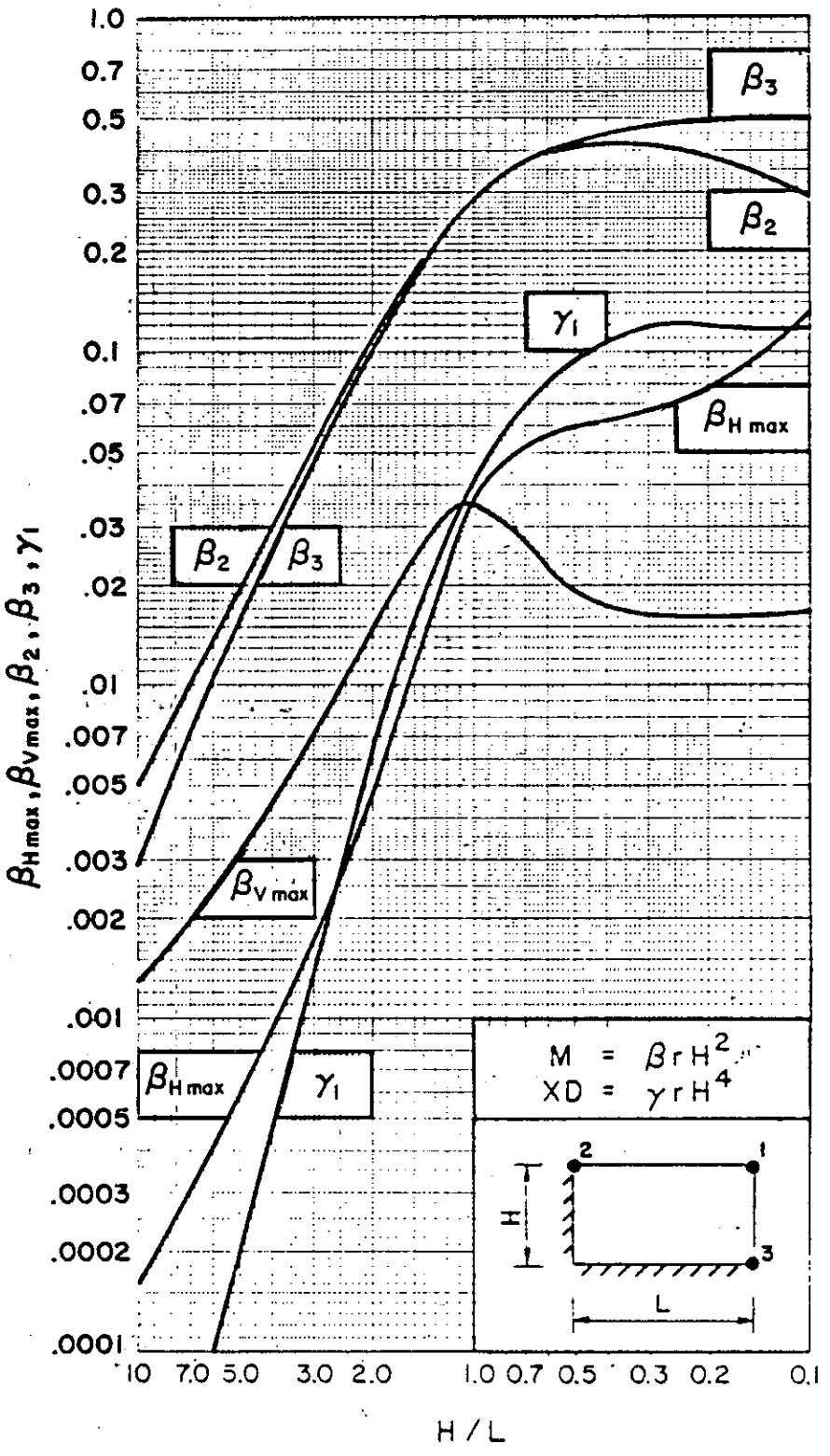


Figure 3-24 Moment and deflection coefficients for uniformly-loaded, two-way element with two adjacent edges fixed and two edges free

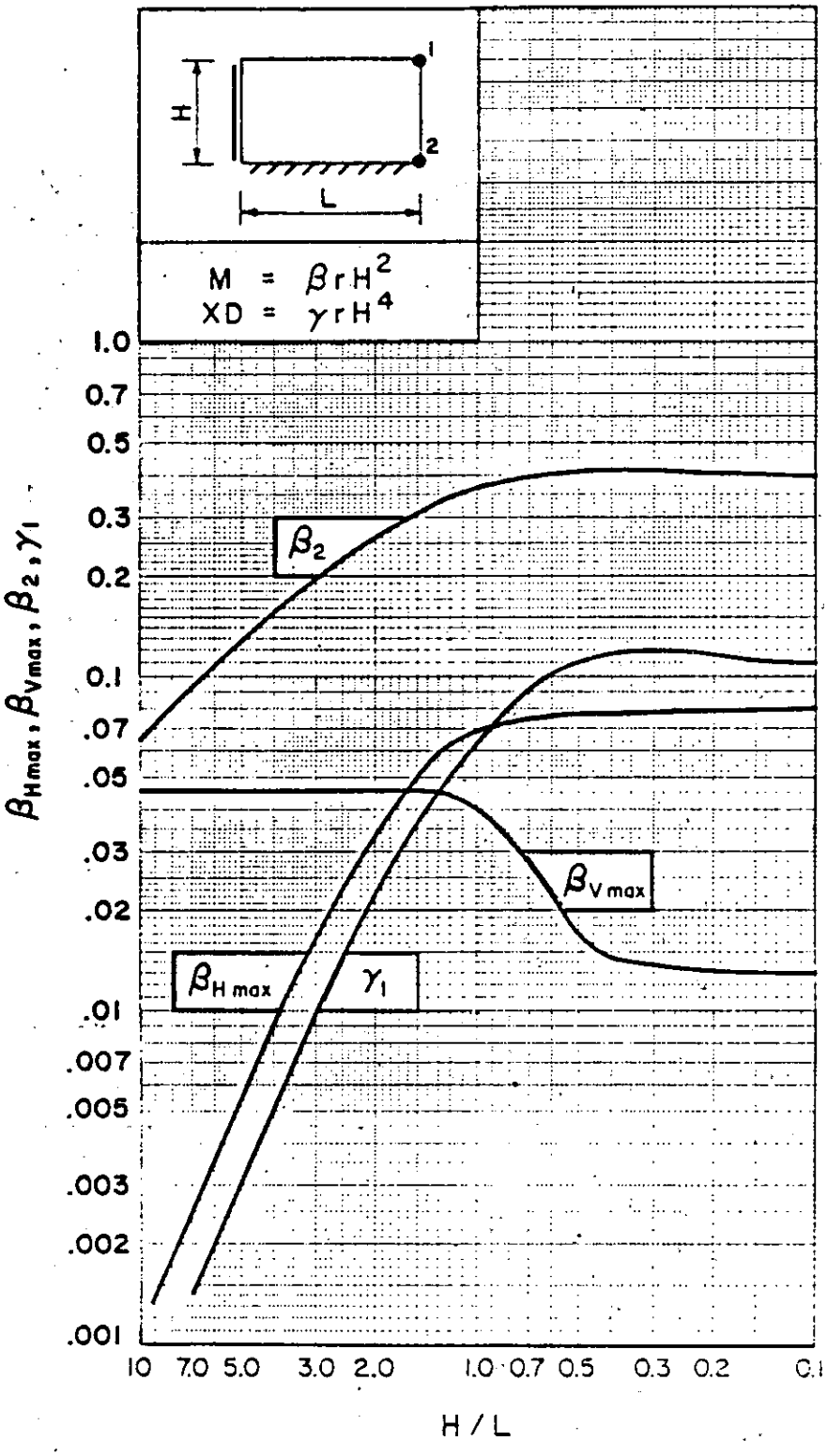


Figure 3-25 Moment and deflection coefficients for uniformly-loaded, two-way element with one edge fixed, an adjacent edge simply-supported and two edges free

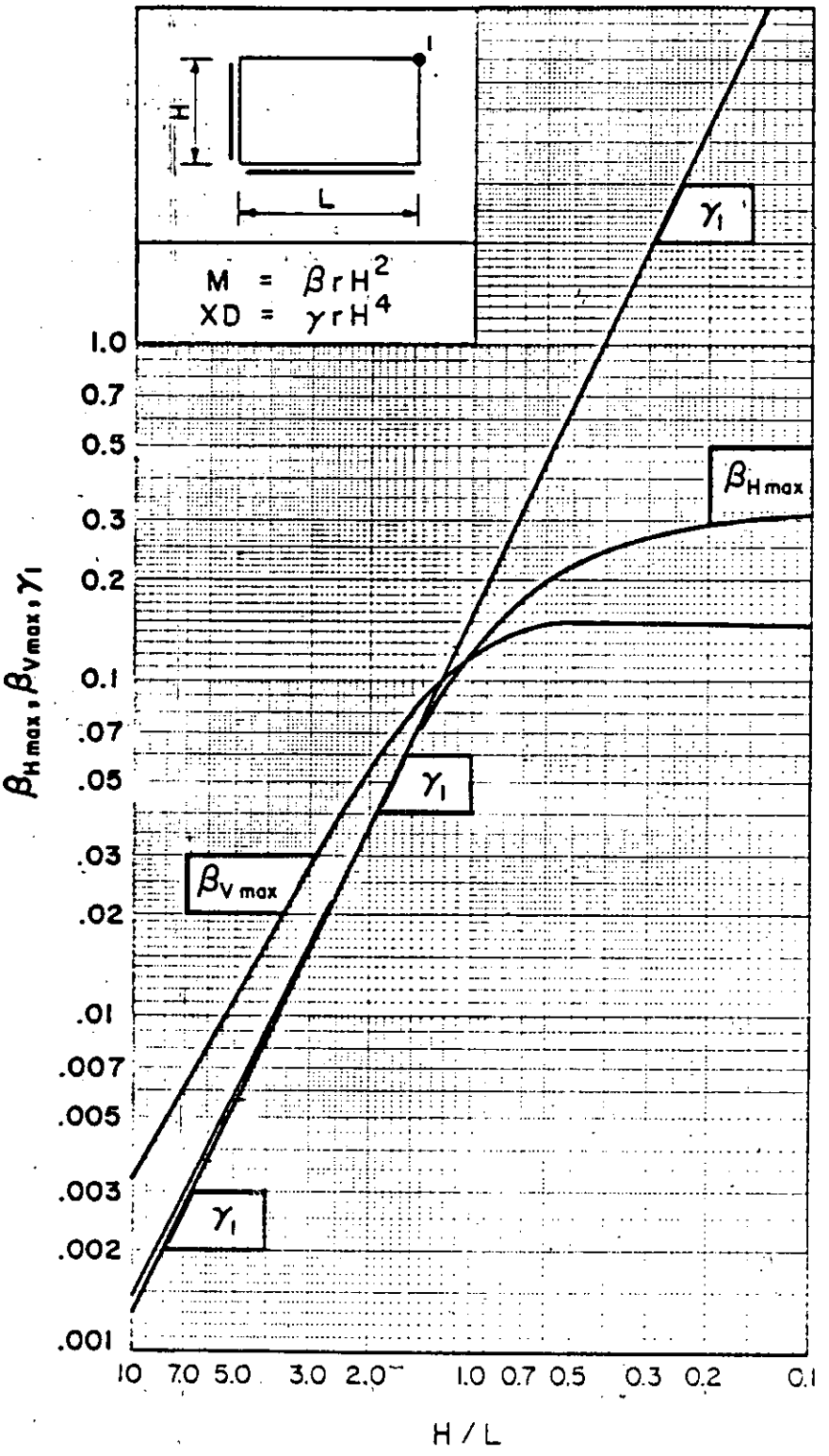


Figure 3-26 Moment and deflection coefficients for uniformly-loaded, two-way element with two adjacent edges simply-supported and two edges free

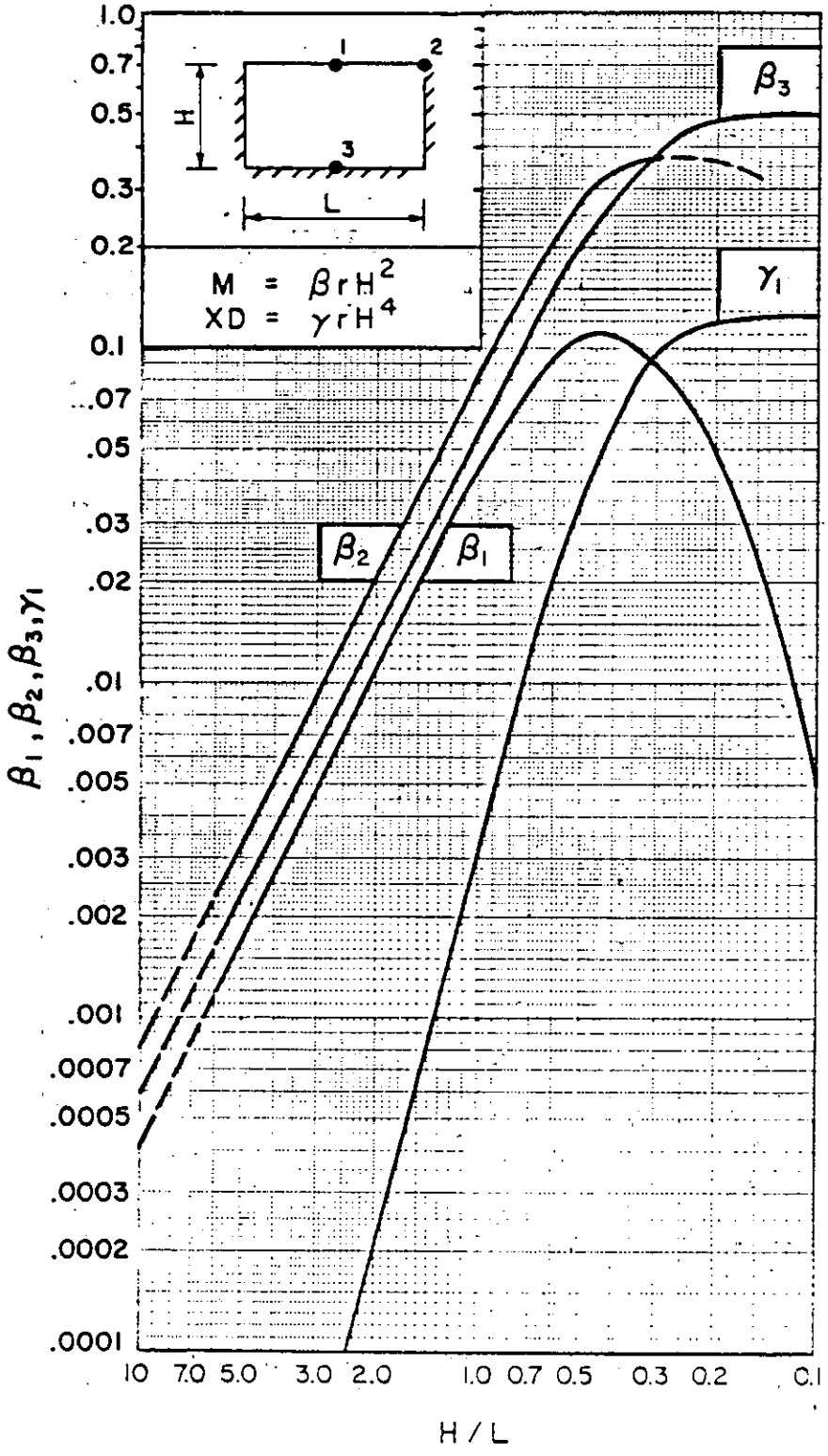


Figure 3-27 Moment and deflection coefficients for uniformly-loaded, two-way element with three edges fixed and one edge free

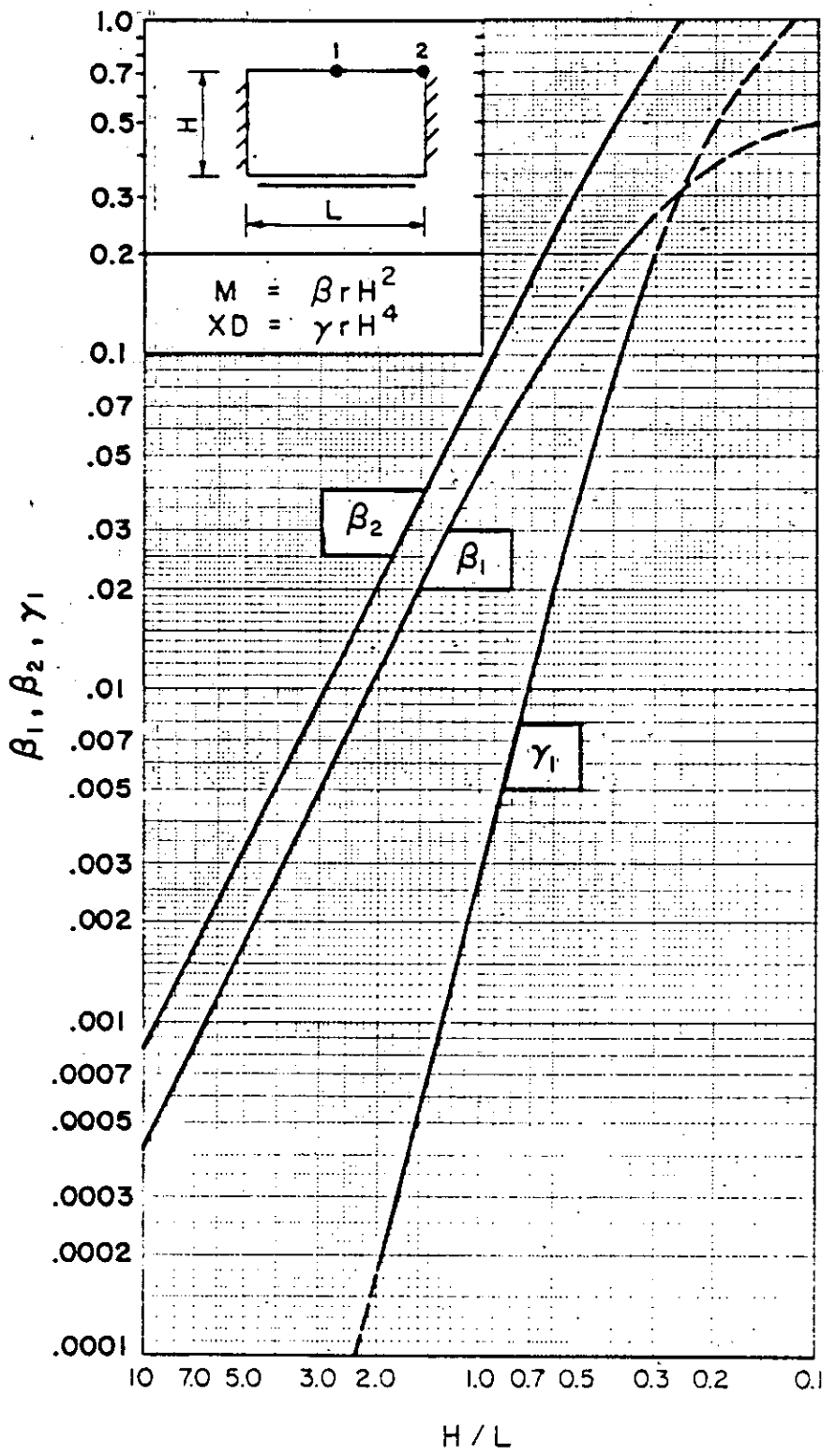


Figure 3-28 Moment and deflection coefficients for uniformly-loaded, two-way element with two opposite edges fixed, one edge simply-supported and one edge free

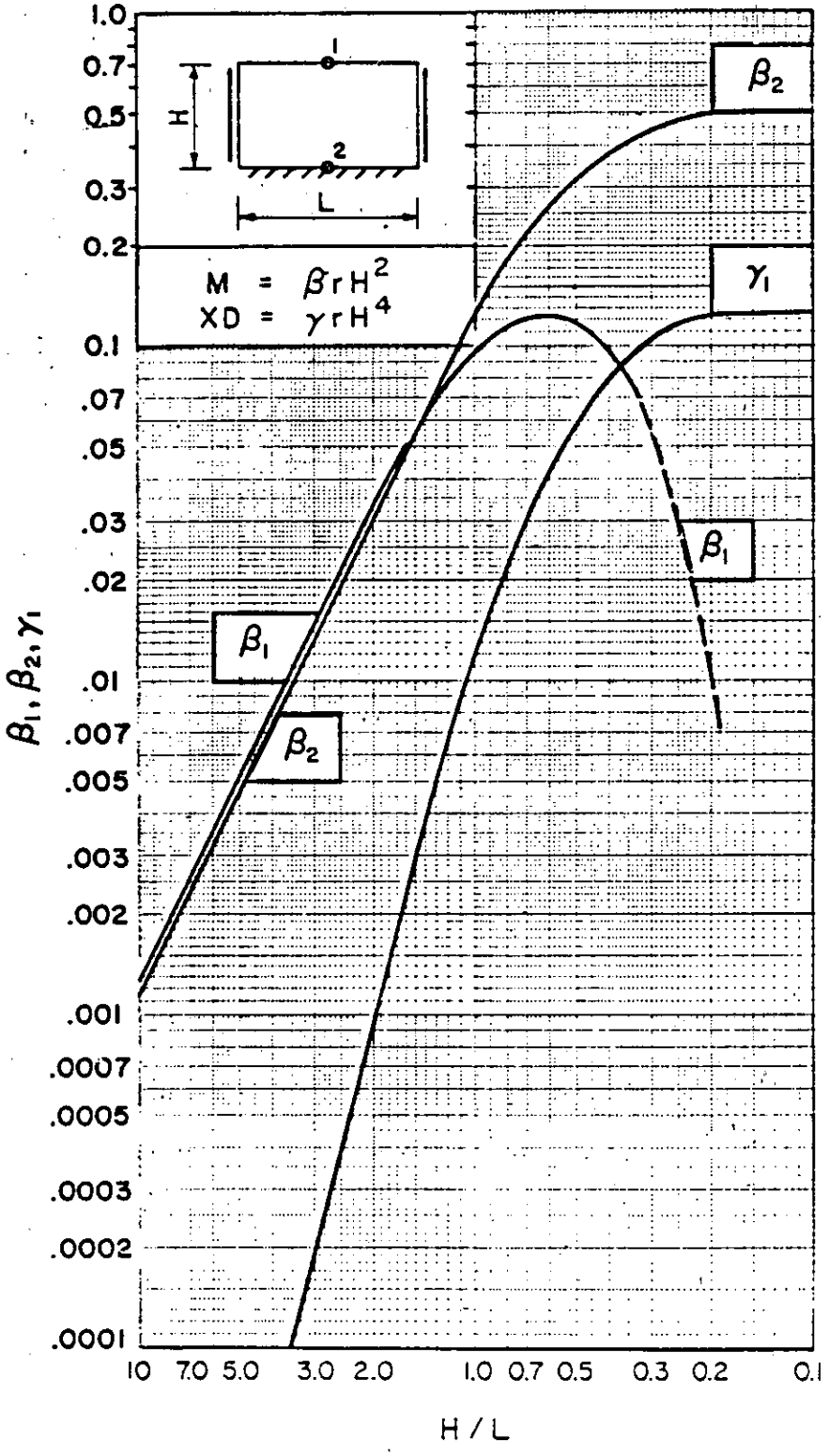


Figure 3-29 Moment and deflection coefficients for uniformly-loaded, two-way element with two opposite edges simply-supported, one edge fixed, and one edge free

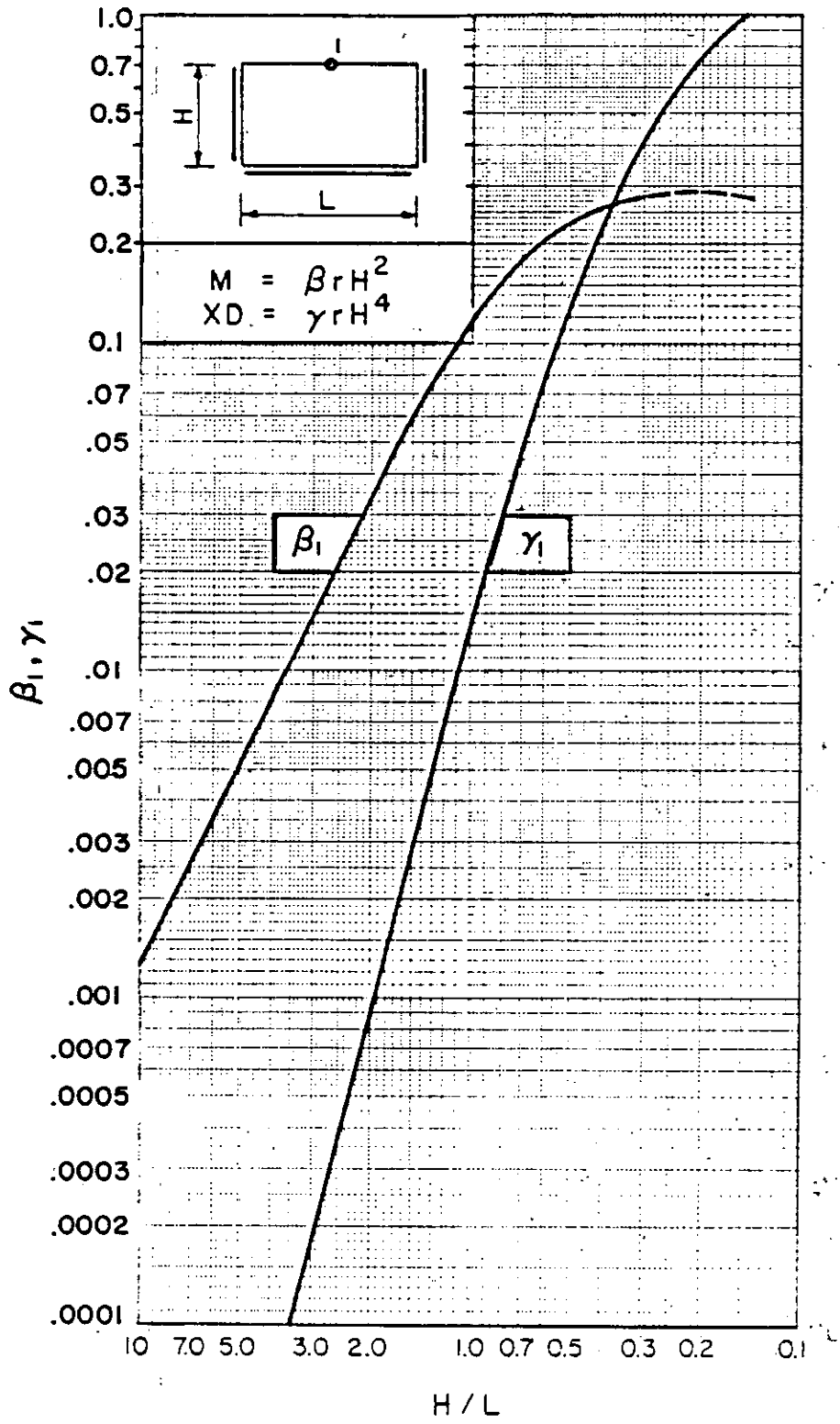


Figure 3-30 Moment and deflection coefficients for uniformly-loaded, two-way element with three edges simply-supported and one edge free

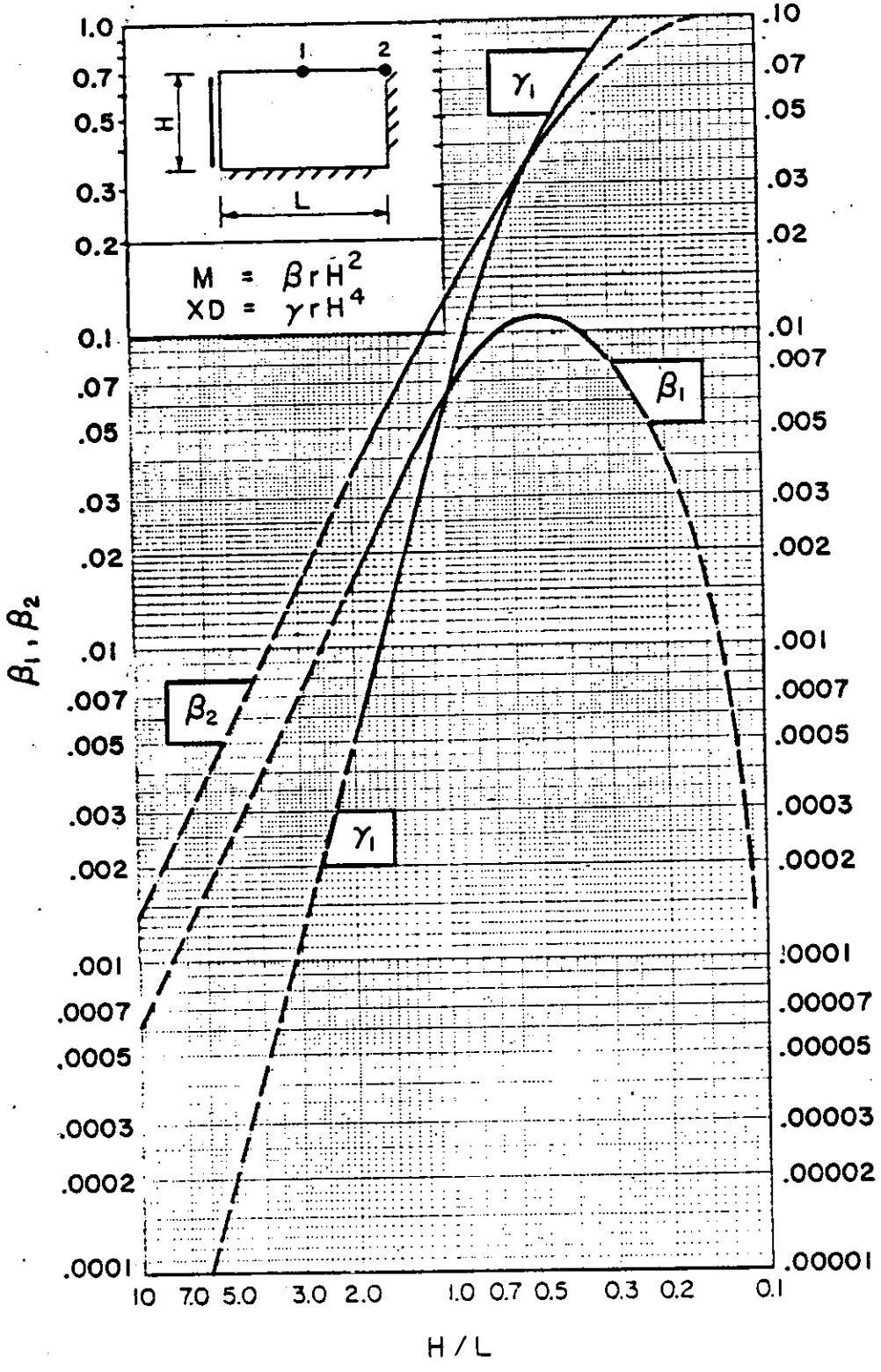


Figure 3-31 Moment and deflection coefficients for uniformly-loaded, two-way element with two adjacent edges fixed, one edge simply-supported, and one edge free

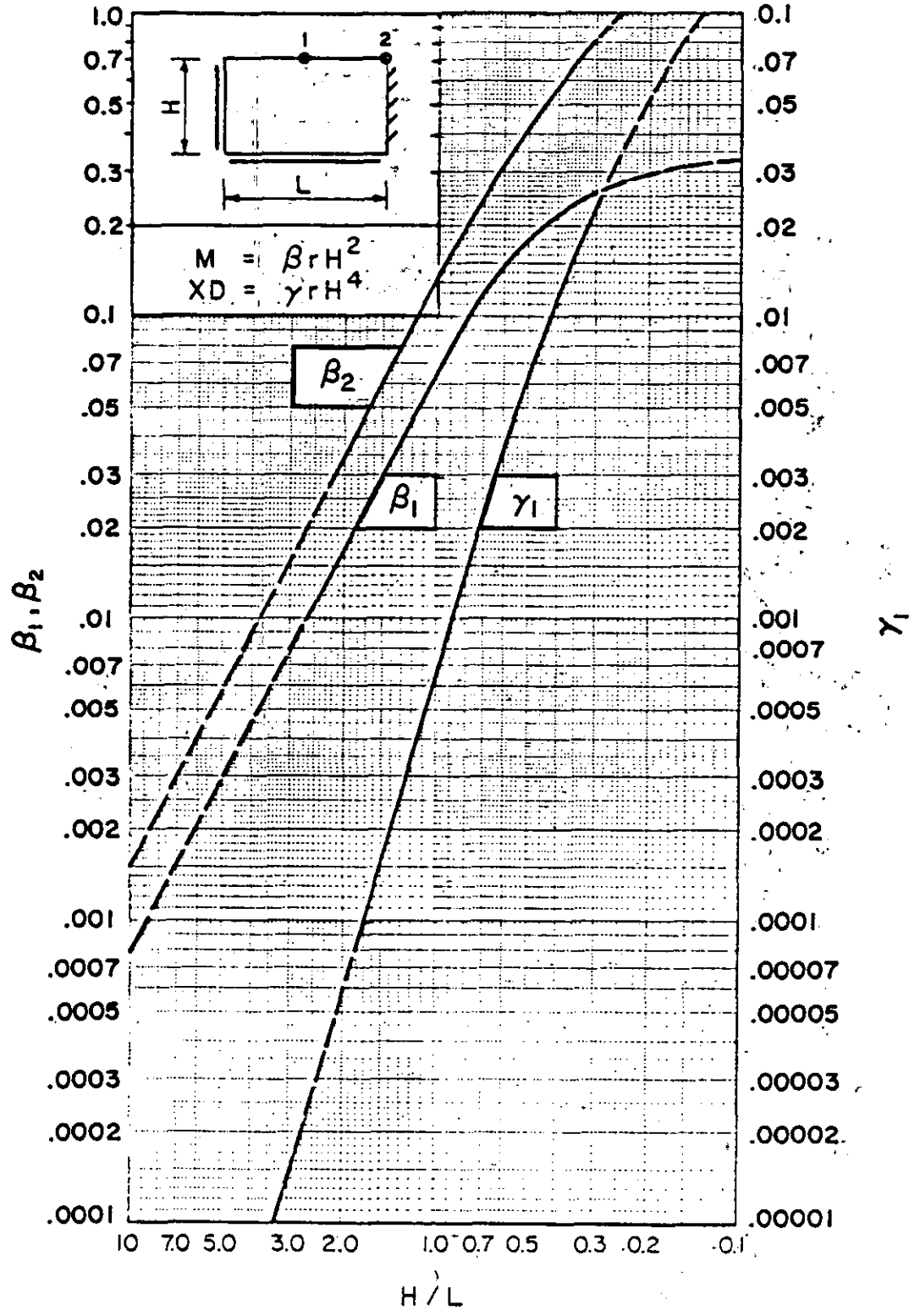


Figure 3-32 Moment and deflection coefficients for uniformly-loaded, two-way element with two adjacent edges simply-supported, one edge fixed, and one edge free

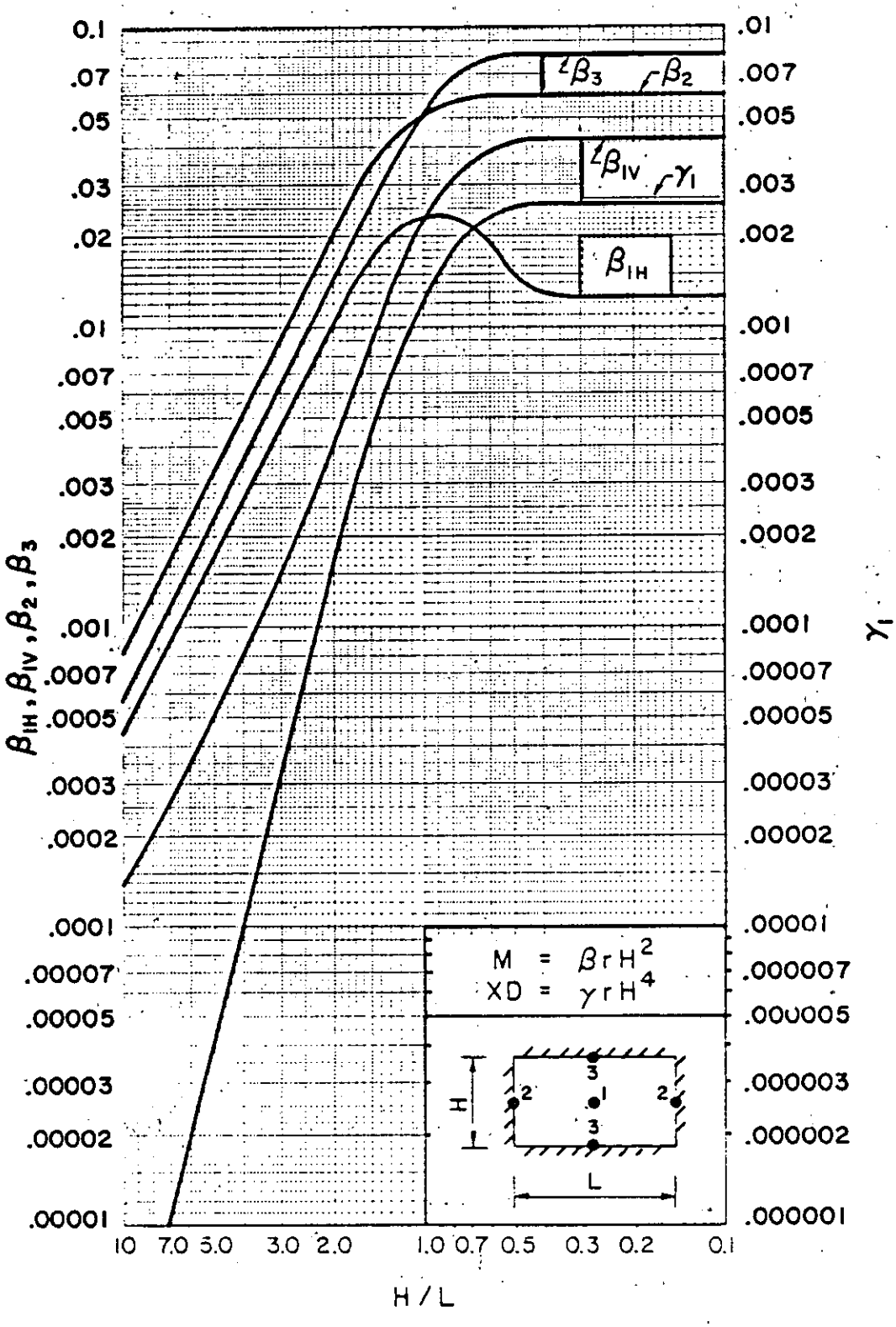


Figure 3-33 Moment and deflection coefficients for uniformly-loaded, two-way element with all edges fixed

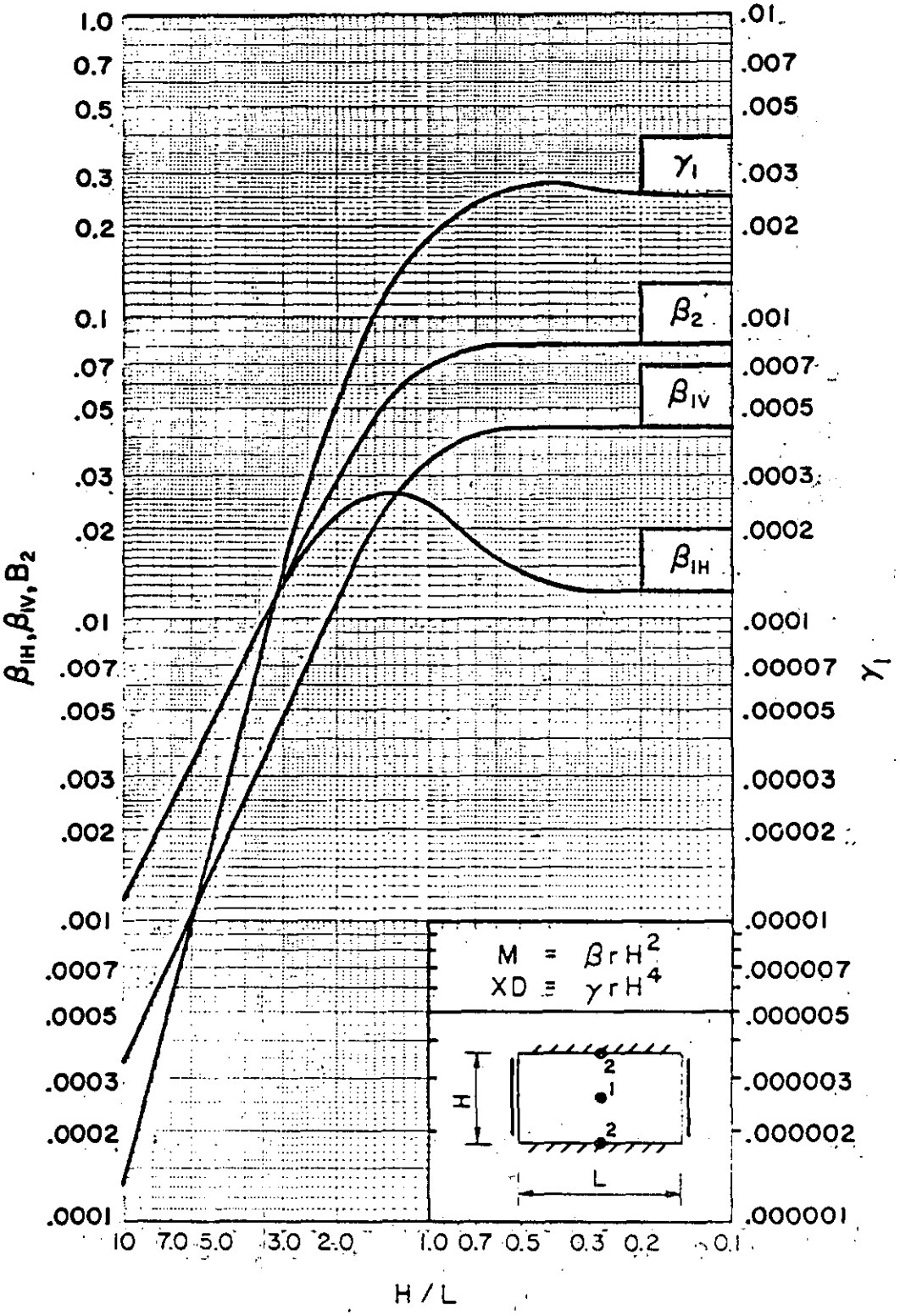


Figure 3-34 Moment and deflection coefficients for uniformly-loaded, two-way element with two opposite edges fixed and two edges simply-supported

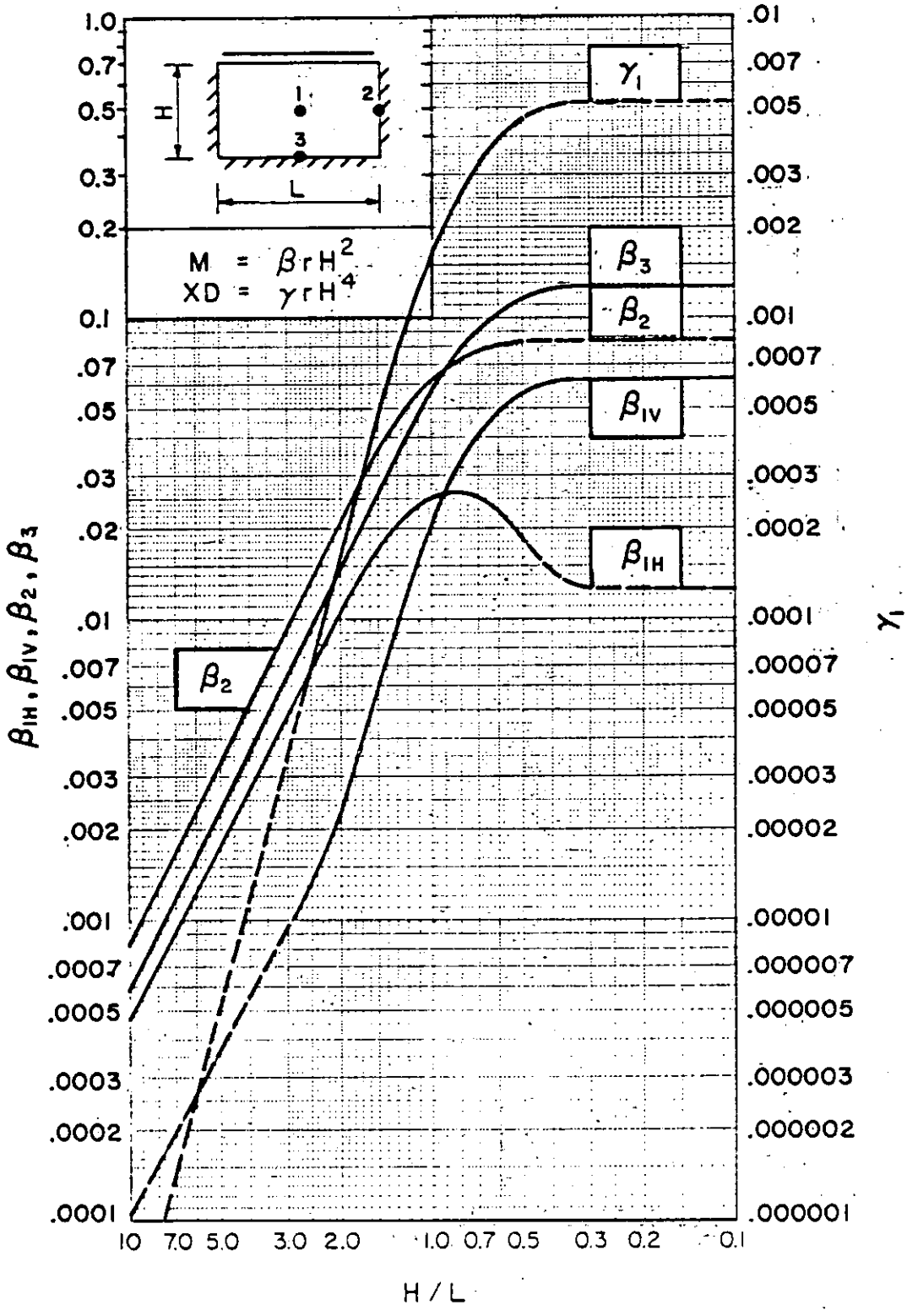


Figure 3-35 Moment and deflection coefficients for uniformly-loaded, two-way element with three edges fixed and one edge simply-supported

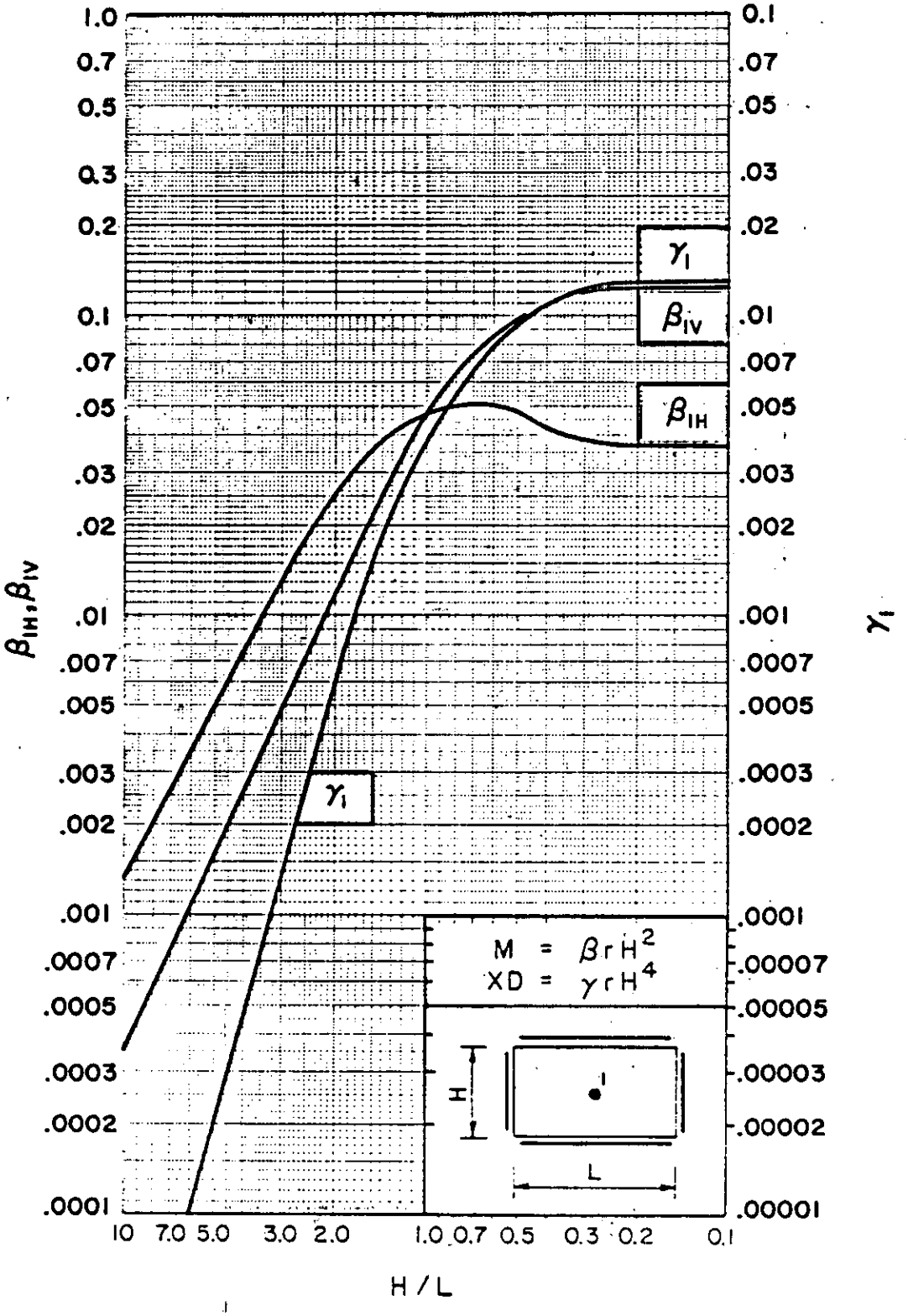


Figure 3-36 Moment and deflection coefficients for uniformly-loaded, two-way element with all edges simply-supported

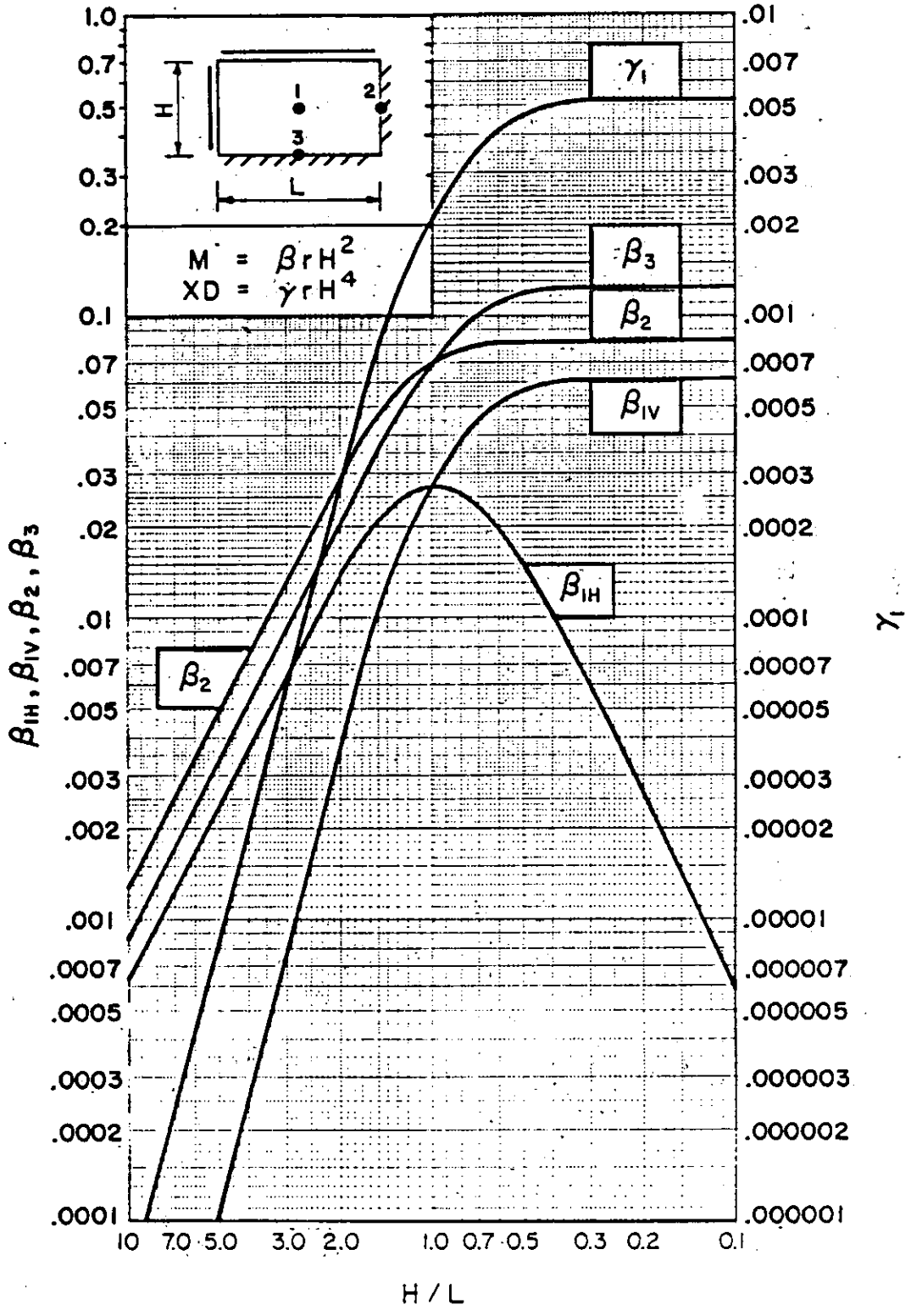


Figure 3-37 Moment and deflection coefficients for uniformly-loaded, two-way element with two adjacent edges fixed, and two edges simply-supported

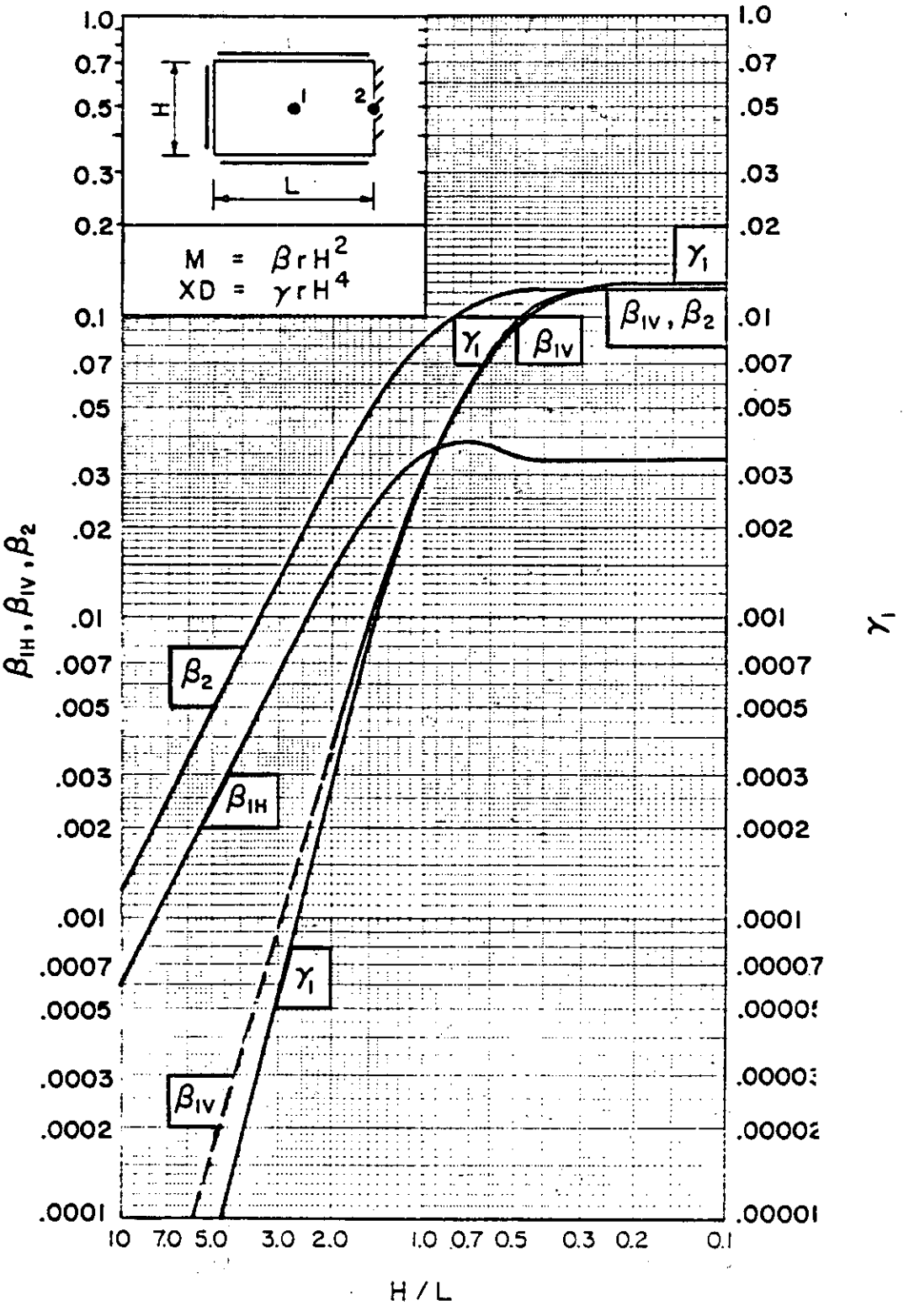
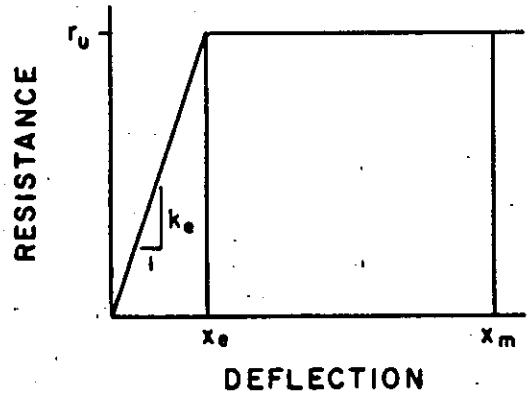
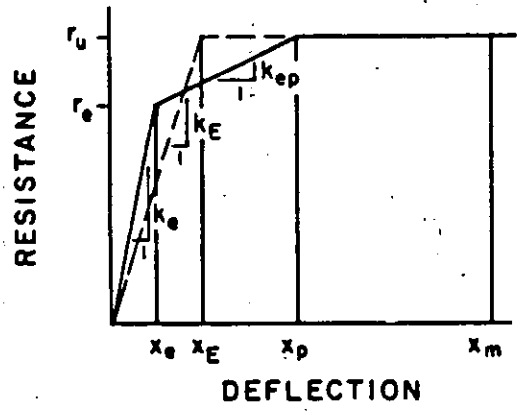


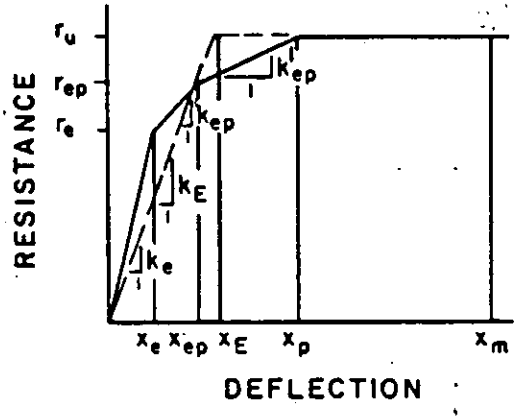
Figure 3-38 Moment and deflection coefficients for uniformly-loaded, two-way element with three edges simply-supported and one edge fixed



(a) ONE STEP ELASTO-PLASTIC SYSTEM

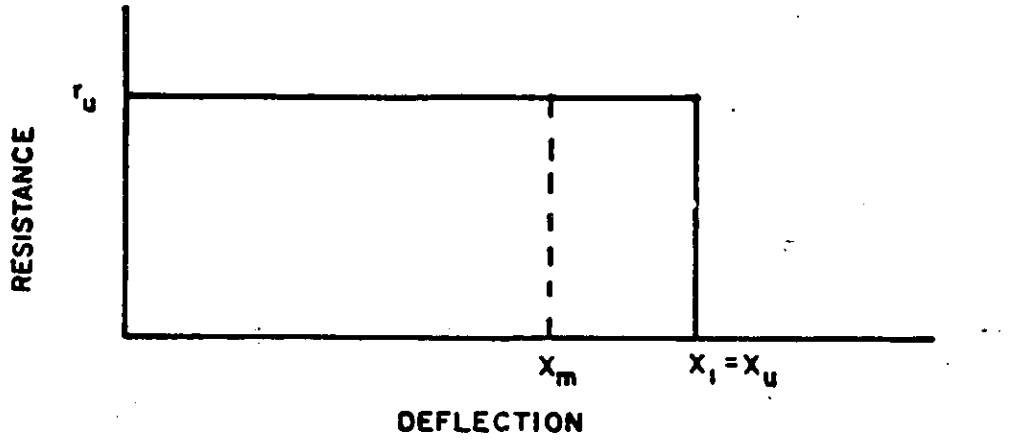


(b) TWO STEP ELASTO-PLASTIC SYSTEM

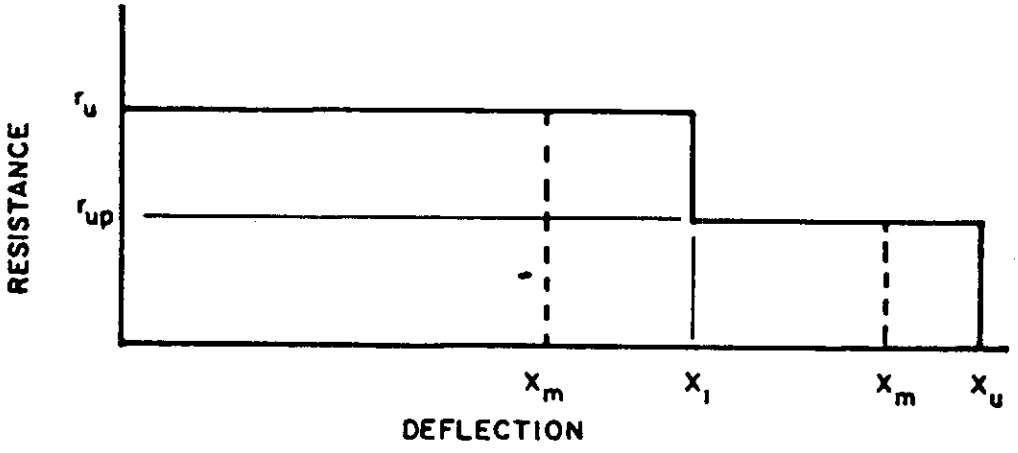


(c) THREE STEP ELASTO-PLASTIC SYSTEM

Figure 3-39 Resistance-deflection functions for limited deflections



a) ONE-WAY ELEMENT



b) TWO-WAY ELEMENT

Figure 3-40 Resistance-deflection functions for large deflections

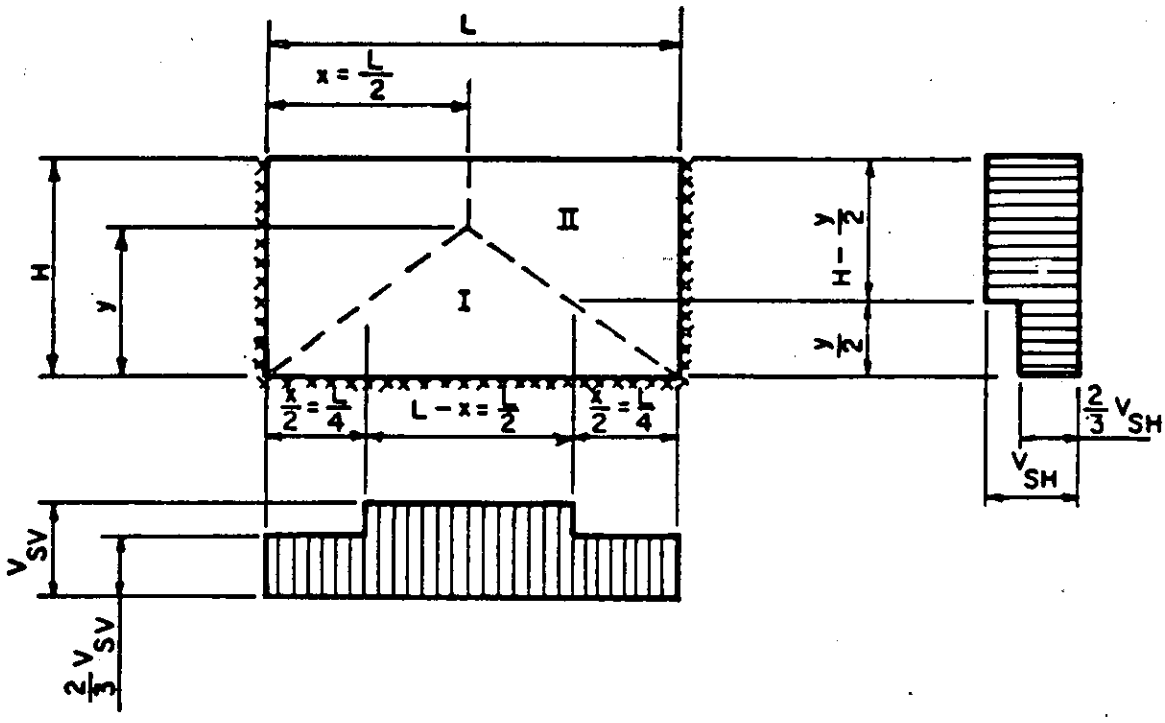


Figure 3-41 Determination of ultimate support shear

Table 3-1 Ultimate Unit Resistances for One-Way Elements

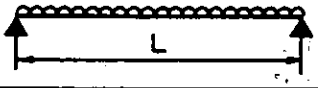
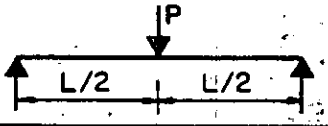
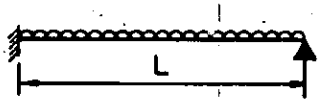
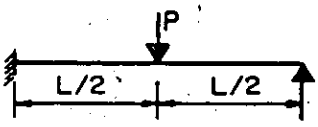
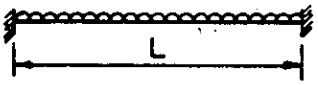
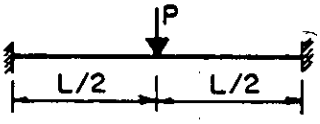
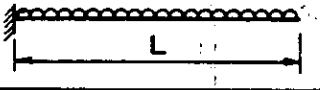
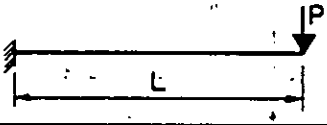
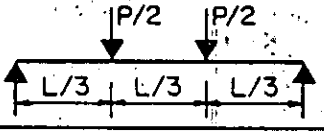
Edge Conditions and Loading Diagrams	Ultimate Resistance
	$r_u = \frac{8M_p}{L^2}$
	$R_u = \frac{4M_p}{L}$
	$r_u = \frac{4(M_N + 2M_p)}{L^2}$
	$R_u = \frac{2(M_N + 2M_p)}{L}$
	$r_u = \frac{8(M_N + M_p)}{L^2}$
	$R_u = \frac{4(M_N + M_p)}{L}$
	$r_u = \frac{2M_N}{L^2}$
	$R_u = \frac{M_N}{L}$
	$R_u = \frac{6M_p}{L}$

Table 3-2 Ultimate Unit Resistances for Two-Way Elements (Symmetrical Yield Lines)

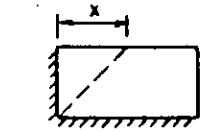
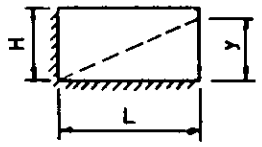
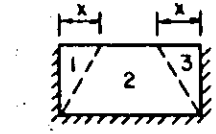
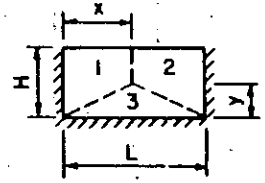
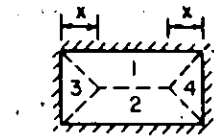
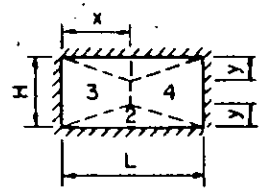
Edge Conditions	Yield Line Locations	Limits	Ultimate Unit Resistance
Two adjacent edges supported and two edges free		$x \le L$	$\frac{5(M_{HN}+M_{HP})}{x^2}$ OR $\frac{6L\,M_{VN}+(5M_{VP}-M_{VN})x}{H^2(3L-2x)}$
		$y \le H$	$\frac{5(M_{VN}+M_{VP})}{y^2}$ OR $\frac{6H\,M_{HN}+(5M_{HP}-M_{HN})y}{L^2(3H-2y)}$
Three edges supported and one edge free		$x \le \frac{L}{2}$	$\frac{5(M_{HN}+M_{HP})}{x^2}$ OR $\frac{2M_{VN}(3L-x)+10x\,M_{VP}}{H^2(3L-4x)}$
		$y \le H$	$\frac{5(M_{VN}+M_{VP})}{y^2}$ OR $\frac{4(M_{HN}+M_{HP})(6H-y)}{L^2(3H-2y)}$
Four edges supported		$x \le \frac{L}{2}$	$\frac{5(M_{HN}+M_{HP})}{x^2}$ OR $\frac{8(M_{VN}+M_{VP})(3L-x)}{H^2(3L-4x)}$
		$y \le \frac{H}{2}$	$\frac{5(M_{VN}+M_{VP})}{y^2}$ OR $\frac{8(M_{HN}+M_{HP})(3H-y)}{L^2(3H-4y)}$

Table 3-3 Ultimate Unit Resistances for Two-Way Elements (Unsymmetrical Yield Lines)

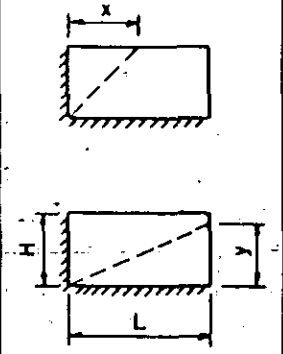
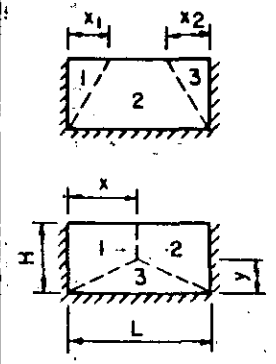
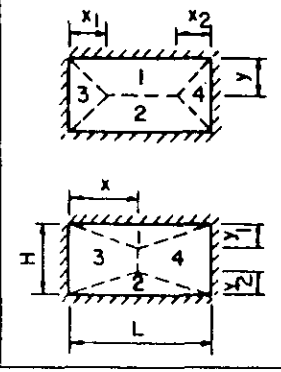
Edge Conditions	Yield Line Locations	Limits	Ultimate Unit Resistance
Two adjacent edges supported and two edges free		$x \le L$ $y \le H$	Same as in Table 3-2
Three edges supported and one edge free		$x \le \frac{L}{2}$ $y \le H$	$\frac{5(M_{HN1}+M_{HP1})}{X_1^2}$ OR $\frac{5(M_{HN3}+M_{HP})}{X_2^2}$ OR $\frac{(5M_{VP}-M_{VN2})(X_1+X_2)+6M_{VN2}L}{H^2(3L-2X_1-2X_2)}$ $\frac{(M_{HN1}+M_{HP})(6H-Y)}{X^2(3H-2Y)}$ OR $\frac{(M_{HN2}+M_{HP})(6H-Y)}{(L-X)^2(3H-2Y)}$ OR $\frac{5(M_{VN3}+M_{VP})}{Y^2}$
Four edges supported		$x \le \frac{L}{2}$ $y \le \frac{H}{2}$	$\frac{(M_{VN1}+M_{VP})(6L-X_1-X_2)}{Y^2(3L-2X_1-2X_2)}$ OR $\frac{(M_{VN2}+M_{VP})(6L-X_1-X_2)}{(H-Y)^2(3L-2X_1-2X_2)}$ $\frac{5(M_{HN1}+M_{HP})}{X_1^2}$ OR $\frac{5(M_{HN2}+M_{HP})}{X_2^2}$ $\frac{5(M_{VN1}+M_{VP})}{Y_1^2}$ OR $\frac{5(M_{VN2}+M_{VP})}{Y_2^2}$ $\frac{(M_{HN1}+M_{HP})(6H-Y_1-Y_2)}{X^2(3H-2Y_1-2Y_2)}$ OR $\frac{(M_{HN2}+M_{HP})(6H-Y_1-Y_2)}{(L-X)^2(3H-2Y_1-2Y_2)}$

Table 3-4 Post-Ultimate Unit Resistances for Two-Way Elements

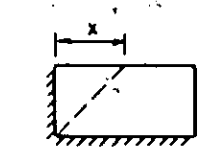
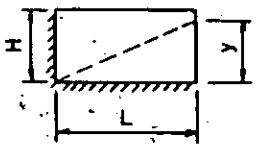
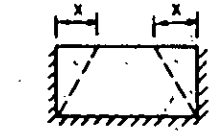
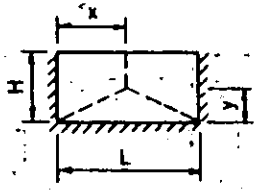
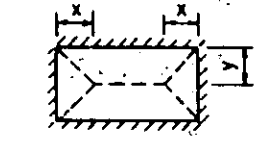
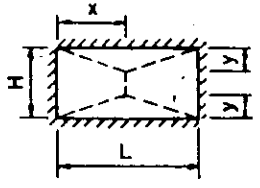
Edge Conditions	Yield Line Locations	Limits	Post - Ultimate Unit Resistance
Two adjacent edges supported and two edges free		$x < H$	$2 M_{VN}/H^2$
		$x > H$	$2 M_{HN}/L^2$
		$y < H$	$2 M_{HN}/L^2$
		$y > L$	$2 M_{VN}/H^2$
Three edges supported and one edge free		$x < H$	$2 M_{VN}/H^2$
		$x > H$	$8 (M_{HN} + M_{HP})/L^2$
		$y < L/2$	$8 (M_{HN} + M_{HP})/L^2$
		$y > L/2$	$2 M_{VN}/H^2$
Four edges supported		$x < H/2$	$8 (M_{VN} + M_{VP})/H^2$
		$x > H/2$	$8 (M_{HN} + M_{HP})/L^2$
		$y < L/2$	$8 (M_{VN} + M_{VP})/L^2$
		$y > L/2$	$8 (M_{HN} + M_{HP})/H^2$

Table 3-5 General and Ultimate Deflections for One-Way Elements

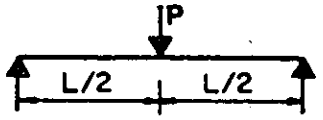
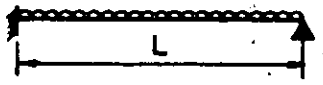
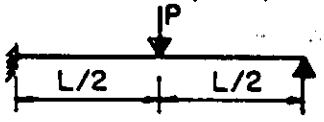
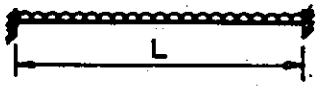
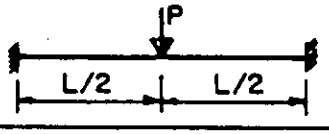
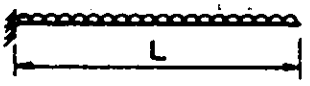
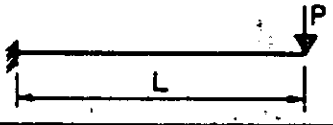
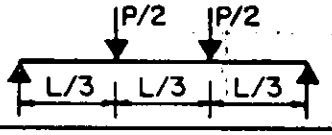
Edge Conditions and Loading Diagrams	Maximum Deflection, X_m	Ultimate Deflection, X_u
	$\frac{L}{2}\tan\theta$	$\frac{L}{2}\tan\theta_{max}$
	$(L/2)\tan\theta$	$(L/2)\tan\theta_{max}$
	$\frac{L}{2}\tan\theta$	$\frac{L}{2}\tan\theta_{max}$
	$(L/2)\tan\theta$	$(L/2)\tan\theta_{max}$
	$\frac{L}{2}\tan\theta$	$\frac{L}{2}\tan\theta_{max}$
	$(L/2)\tan\theta$	$(L/2)\tan\theta_{max}$
	$L\tan\theta$	$L\tan\theta_{max}$
	$L\tan\theta$	$L\tan\theta_{max}$
	$(L/3)\tan\theta$	$(L/3)\tan\theta_{max}$

Table 3-6 General, Partial Failure, and Ultimate Deflections for Two-Way Elements

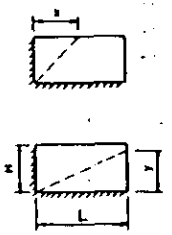
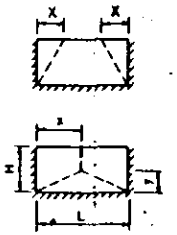
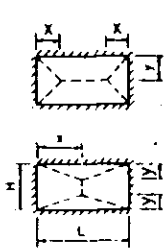
Edge Conditions	Yield Line Location	Limits	Maximum Deflection, X_m $(0 < X_m < X_l)$	Maximum Deflection, X_m $(X_l < X_m < X_u)$	Partial Failure Deflection X_l	Ultimate Deflection, X_u	Support Failing Deflection X_l
Two adjacent edges supported and two edges free		$x \le H$	$x \tan \theta_H$	$H \tan \theta_V$	$x \tan \theta_{max}$	$H \tan \theta_{max}$	H
		$x \ge H$	$H \tan \theta_V$	$x \tan \theta_H + (L-x) \tan \left[\theta_H - \tan^{-1}\left(\frac{\tan \theta_V}{x/H}\right)\right]$	$H \tan \theta_{max}$	$x \tan \theta_{max} + (L-x) \tan \left[\theta_{max} - \tan^{-1}\left(\frac{\tan \theta_{max}}{x/H}\right)\right]$	L
		$y \le L$	$y \tan \theta_V$	$L \tan \theta_H$	$y \tan \theta_{max}$	$L \tan \theta_{max}$	L
		$y \ge L$	$L \tan \theta_H$	$y \tan \theta_V + (H-y) \tan \left[\theta_V - \tan^{-1}\left(\frac{\tan \theta_H}{y/L}\right)\right]$	$L \tan \theta_{max}$	$y \tan \theta_{max} + (H-y) \tan \left[\theta_{max} - \tan^{-1}\left(\frac{\tan \theta_{max}}{y/L}\right)\right]$	H
Three edges supported and one edge free		$x \le H$	$x \tan \theta_V$	$H \tan \theta_V$	$x \tan \theta_{max}$	$H \tan \theta_{max}$	H
		$x \ge H$	$H \tan \theta_V$	$x \tan \theta_H + \left(\frac{L}{2} - x\right) \tan \left[\theta_H - \tan^{-1}\left(\frac{\tan \theta_V}{x/H}\right)\right]$	$H \tan \theta_{max}$	$x \tan \theta_{max} + \left(\frac{L}{2} - x\right) \tan \left[\theta_{max} - \tan^{-1}\left(\frac{\tan \theta_{max}}{x/H}\right)\right]$	L
		$y \le \frac{L}{2}$	$y \tan \theta_V$	$\frac{L \tan \theta_H}{2}$	$y \tan \theta_{max}$	$\frac{L \tan \theta_{max}}{2}$	L
		$y \ge \frac{L}{2}$	$\frac{L \tan \theta_H}{2}$	$y \tan \theta_V + (H-y) \tan \left[\theta_V - \tan^{-1}\left(\frac{\tan \theta_H}{2y/L}\right)\right]$	$\frac{L \tan \theta_{max}}{2}$	$y \tan \theta_{max} + (H-y) \tan \left[\theta_{max} - \tan^{-1}\left(\frac{\tan \theta_{max}}{2y/L}\right)\right]$	H
Four edges supported		$x \le \frac{H}{2}$	$x \tan \theta_H$	$\frac{H \tan \theta_V}{2}$	$x \tan \theta_{max}$	$\frac{H \tan \theta_{max}}{2}$	H
		$x \ge \frac{H}{2}$	$\frac{H \tan \theta_V}{2}$	$x \tan \theta_H + \left(\frac{L}{2} - x\right) \tan \left[\theta_H - \tan^{-1}\left(\frac{\tan \theta_V}{2x/H}\right)\right]$	$\frac{H \tan \theta_{max}}{2}$	$x \tan \theta_{max} + \left(\frac{L}{2} - x\right) \tan \left[\theta_{max} - \tan^{-1}\left(\frac{\tan \theta_{max}}{2x/H}\right)\right]$	L
		$y \le \frac{L}{2}$	$y \tan \theta_V$	$\frac{L \tan \theta_H}{2}$	$y \tan \theta_{max}$	$\frac{L \tan \theta_{max}}{2}$	L
		$y \ge \frac{L}{2}$	$\frac{L \tan \theta_H}{2}$	$y \tan \theta_V + \left(\frac{H}{2} - y\right) \tan \left[\theta_V - \tan^{-1}\left(\frac{\tan \theta_H}{2y/L}\right)\right]$	$\frac{L \tan \theta_{max}}{2}$	$y \tan \theta_{max} + \left(\frac{H}{2} - y\right) \tan \left[\theta_{max} - \tan^{-1}\left(\frac{\tan \theta_{max}}{2y/L}\right)\right]$	H

Table 3-7 Elastic and Elasto-Plastic Unit Resistances for One-Way Elements.

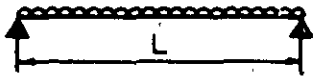
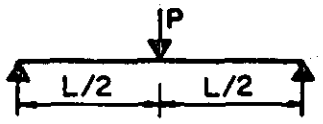
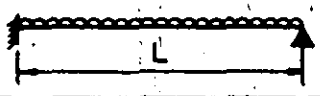
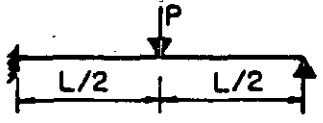
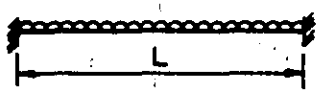
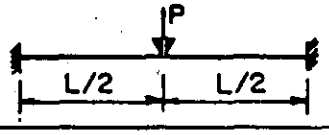
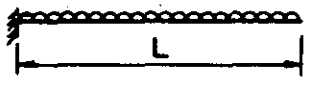
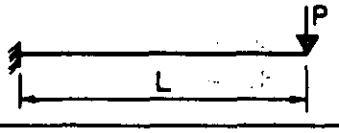
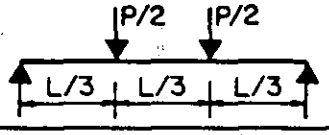
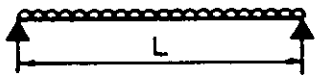
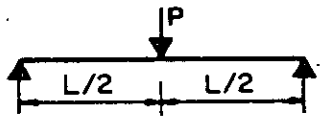
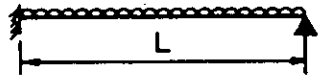
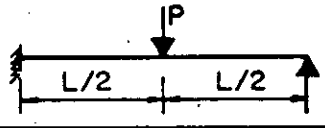
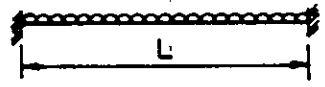
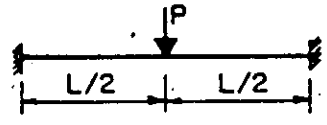
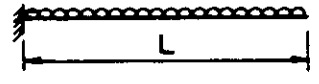
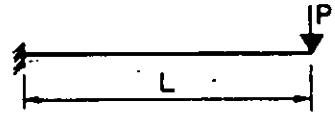
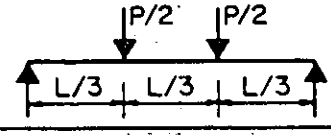
Edge Conditions and Loading Diagrams	Elastic Resistance, r_e	Elasto - Plastic Resistance, r_{ep}
	r_u	—
	R_u	—
	$\frac{8M_N}{L^2}$	r_u
	$\frac{16M_N}{3L}$	R_u
	$\frac{12M_N}{L^2}$	r_u
	$\frac{8M_N}{L}$	R_u
	r_u	—
	R_u	—
	R_u	—

Table 3-8 Elastic, Elasto-Plastic and Equivalent Elastic Stiffnesses for One-Way Elements

Edge Conditions and Loading Diagrams	Elastic Stiffness, K_e	Elasto-Plastic Stiffness, K_{ep}	Equiv. Elastic Stiffness, K_E
	$\frac{384EI}{5L^4}$	—	$\frac{384EI}{5L^4}$
	$\frac{48EI}{L^3}$	—	$\frac{48EI}{L^3}$
	$\frac{185EI}{L^4}$	$\frac{384EI}{5L^4}$	$\frac{160EI^*}{L^4}$
	$\frac{107EI}{L^3}$	$\frac{48EI}{L^3}$	$\frac{106EI^*}{L^3}$
	$\frac{384EI}{L^4}$	$\frac{384EI}{5L^4}$	$\frac{307EI^*}{L^4}$
	$\frac{192EI}{L^3}$	$\frac{48EI^{**}}{L^3}$	$\frac{192EI^*}{L^3}$
	$\frac{8EI}{L^4}$	—	$\frac{8EI}{L^4}$
	$\frac{3EI}{L^3}$	—	$\frac{3EI}{L^3}$
	$\frac{56.4EI}{L^3}$	—	$\frac{56.4EI}{L^3}$

* Valid only if $M_N = M_p$

** Valid only if $M_N < M_p$

Table 3-9 Support Shears for One-Way Elements

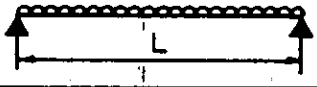
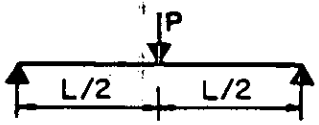
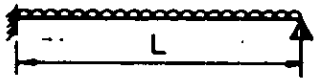
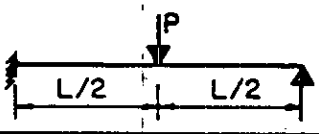
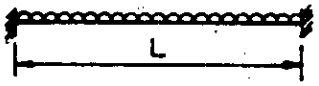
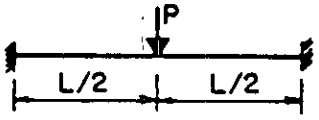
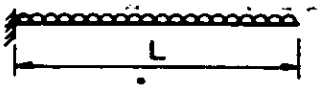
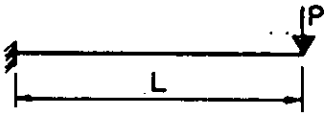
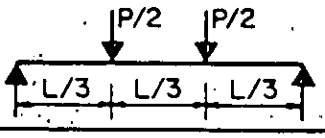
Edge Conditions and Loading Diagrams	Support Reactions, V_s
	$\frac{r_u L}{2}$
	$\frac{R_u}{2}$
	L. Reaction $\frac{5 r_u L}{8}$ R. Reaction $\frac{3 r_u L}{8}$
	L. Reaction $\frac{11 R_u}{16}$ R. Reaction $\frac{5 R_u}{16}$
	$\frac{r_u L}{2}$
	$\frac{R_u}{2}$
	$r_u L$
	R_u
	$\frac{R_u}{2}$

Table 3-10 Ultimate Support Shears for Two-Way Elements (Symmetrical Yield Lines)

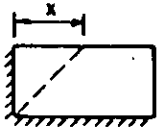
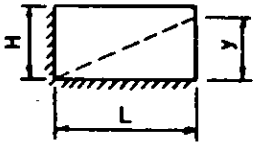
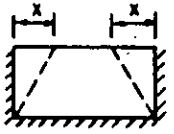
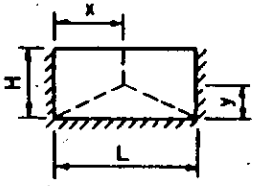
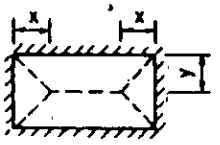
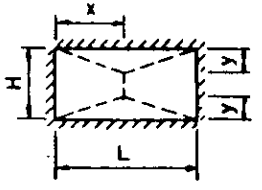
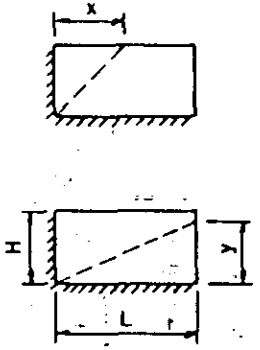
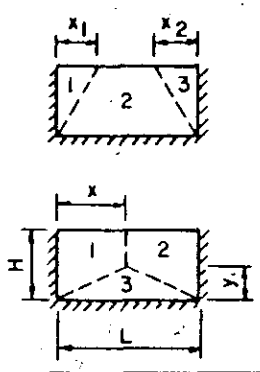
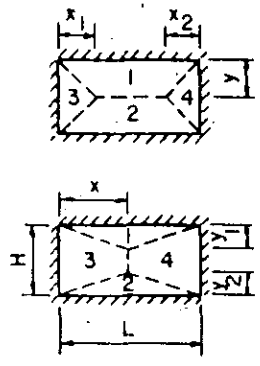
Edge Conditions	Yield Line Locations	Limits	Horizontal shear, V_{sH}	Vertical shear, V_{sV}
Two adjacent edges supported and two edges free		$x \le L$	$\frac{3r_u x}{5}$	$\frac{3r_u H\left(2-\frac{x}{L}\right)}{\left(6-\frac{x}{L}\right)}$
		$y \le H$	$\frac{3r_u L\left(2-\frac{y}{H}\right)}{\left(6-\frac{y}{H}\right)}$	$\frac{3r_u y}{5}$
Three edges supported and one edge free		$x \le \frac{L}{2}$	$\frac{3r_u x}{5}$	$\frac{3r_u H\left(1-\frac{x}{L}\right)}{\left(3-\frac{x}{L}\right)}$
		$y \le H$	$\frac{3r_u L\left(2-\frac{y}{H}\right)}{2\left(6-\frac{y}{H}\right)}$	$\frac{3r_u y}{5}$
Four edges supported		$x \le \frac{L}{2}$	$\frac{3r_u x}{5}$	$\frac{3r_u H\left(1-\frac{x}{L}\right)}{2\left(3-\frac{x}{L}\right)}$
		$y \le \frac{H}{2}$	$\frac{3r_u L\left(1-\frac{y}{H}\right)}{2\left(3-\frac{y}{H}\right)}$	$\frac{3r_u y}{5}$

Table 3-11 Ultimate Support Shears for Two-Way Elements
(Unsymmetrical Yield Lines)

Edge Conditions	Yield Line Locations	Limits	Horizontal shear, V_{sH}	Vertical shear, V_{sV}
Two adjacent edges supported and two edges free		$x \le L$ $y \le H$	Same as in Table 3-10	Same as in Table 3-10
Three edges supported and one edge free		$x_1 \le \frac{L}{2}$ $x_2 \le \frac{L}{2}$ $y \le H$	$\frac{3x_1 r_u}{5}$ $\frac{3x_2 r_u}{5}$ $\frac{3r_u x(2H-y)}{6H-y}$ $\frac{3r_u x(L-x)(2H-y)}{6H-y}$	$\frac{3r_u H(2L-x_1-x_2)}{6L-x_1-x_2}$ $\frac{3r_u y}{5}$
Four edges supported		$x_1 \le \frac{L}{2}$ $x_2 \le \frac{L}{2}$ $y_1 \le \frac{H}{2}$ $y_2 \le \frac{H}{2}$	$\frac{3r_u x_1}{5}$ $\frac{3r_u x_2}{5}$ $\frac{3r_u x(2H-y_1-y_2)}{6H-y_1-y_2}$ $\frac{3r_u(L-x)(2H-y_1-y_2)}{6H-y_1-y_2}$	$\frac{3r_u y(2L-x_1-x_2)}{6L-x_1-x_2}$ $\frac{3r_u(H-y)(2L-x_1-x_2)}{6L-x_1-x_2}$ $\frac{3r_u y_1}{5}$ $\frac{3r_u y_2}{5}$

DYNAMICALLY EQUIVALENT SYSTEMS

3-16. Introduction

In dynamic analysis, there are only three quantities to be considered: (1) the work done, (2) the strain energy, and (3) the kinetic energy. To evaluate the work done, the displacement at any point on the structure under externally distributed or concentrated loads must be known. The strain energy is equal to the summation of the strain energies in all the structural elements which may be in bending, tension, compression, shear or torsion. The kinetic energy involves the energy of translation and rotation of all the masses of the structure. The actual evaluation of these quantities for a given structure under dynamic load would be complicated. However, for practical problems, this can be avoided by using appropriate assumptions.

In most cases, a structure can be replaced by an idealized (or dynamically equivalent) system which behaves timewise in nearly the same manner as the actual structure. The distributed masses of the given structure are lumped together into a number of concentrated masses. The strain energy is assumed to be stored in several weightless springs which do not have to behave elastically; similarly, the distributed load is replaced by a number of concentrated loads acting on the concentrated masses. Therefore, the equivalent system consists merely of a number of concentrated masses joined together by weightless springs and subjected to concentrated loads which vary with time. This concentrated mass-spring-load system is defined as an equivalent dynamic system.

Although all structures possess many degrees of freedom, one mode usually predominates in the response to short duration loads; thus, for all practical purposes, this one mode may be considered to define the behavior of the structure and the problem can be simplified by considering a single-degree-of-freedom system whose properties are those of the fundamental mode of the structures. A single-degree-of-freedom system is defined as one in which only one type of motion is possible or, in other words, only one coordinate is required to define its motion. Such a system is shown in Figure 3-42 which consists of a concentrated mass on a frictionless surface attached to a weightless spring and subjected to a concentrated load. A single displacement variable x is sufficient to describe its motion. The material presented herein will be limited to single-degree-of-freedom systems only.

Many structures, however, exist which can not be adequately described by the first vibration, particularly when consideration of dynamic strain is necessary. For these situations, a two-(or more)-degree-of-freedom analysis may be required. Procedures are presented in section 3-19.2 for performing these analyses.

Two fundamental methods are available for treating simple systems subjected to dynamic forces. The first of these methods is concerned with solving the differential equations of the system by either classical, numerical or graphical means. The second method of analysis and chart solutions depend on solutions which have been determined by the use of the first method and are approximate solutions to the problems in hand. There is a third method which may also be very useful in vibrational problems; this involves the energy equation.

In the following paragraphs the design factors used to determine the equivalent dynamic system that is used to analyze structural elements are defined and the methods used to obtain these factors are discussed.

3-17. Dynamic Design Factors

3-17.1. Introduction

The values of the mass and external force used in the equation of motion (Equation 3-1) are the actual values only if all the elements of the mass of the structure experience the same force and, consequently, move as a unit, in which case, the entire mass may be assumed to be concentrated at its center of gravity. In other cases, the assumption of uniform motion of the entire mass cannot be made without introducing serious error. This is true for members with uniformly distributed mass which bend or rotate under load. In such cases, the motion of the particles of mass varies along the length of the member. Beams, slabs, etc., with such distributed mass actually have an infinite number of degrees of freedom; however, such structural elements can be represented by an equivalent single-degree-of-freedom system.

In order to define an equivalent one-degree system, it is necessary to evaluate the parameters of that system; namely, the equivalent mass M_E, the equivalent spring constant K_E and the equivalent load F_E. The equivalent system is selected usually so that the deflection of the concentrated mass is the same as that for a significant point of the structure. The single-degree-of-freedom approximation of the dynamic behavior of the structural element may be achieved by assuming a deflected shape for the element which is usually taken as the shape resulting from the static application of the dynamic loads. The assumption of a deflected shape establishes an equation relating the relative deflection of all points of the element.

The accuracy of the computed deformation of the single-degree-of-freedom system is dependent on the assumed deflected shape and the loading region. For example, in the impulsive loading realm, if the assumed deformed shape for a simply supported beam is taken to be a parabola, then the exact solution will be obtained for the deflection of the beam. In the quasi-static loading realm, however, the static deformed shape gives the exact answer. For blast resistance design, however, the differences in either a static deformed shape or a first mode approximation is negligible and thus either way is permissible. Usually, though, the static deformed shape is easier to use as it covers both symmetric and asymmetric deformation.

To permit rapid design of structural elements subjected to dynamic loads, it is convenient to introduce design or transformation factors. These factors are used to convert the real system to the equivalent system. To obtain them, it is necessary to equate the relations expressing the kinetic energy, strain and work done on the actual structural element deflecting according to the assumed deflected shape, with the corresponding relations for the equivalent mass and spring system.

3-17.2. Load, Mass, and Resistance Factors

3-17.2.1. Load Factor

The load factor is the design or transformation factor by which the total load applied on the structural element is multiplied to obtain the equivalent concentrated load for the equivalent single-degree-of-freedom system. If the actual total load on the structure is F and the equivalent load is F_E, the load factor K_L is defined by the equation

$$K_L = F_E / F \qquad 3\text{-}41$$

The load factor is derived by setting the external work done by the equivalent load F_E on the equivalent system equal to the external work done by the actual load F on the actual element deflecting to the assumed deflected shape.

For a structure with distributed loads;

$$WD = F_E \delta_{max} = \int_0^L p(x)\delta(x)\, dx \qquad 3\text{-}42a$$

where δ_{max} = maximum deflection of actual structure

$p(x)$ = distributed load per unit length

$\delta(x)$ = deflection at any point of actual structure

L = length of structure

rearranging terms

$$F_E = \int_0^L p(x)\phi(x)\, dx \qquad 3\text{-}42b$$

where $$\phi(x) = \delta(x)/\delta_{max} \qquad 3\text{-}43$$

and is called the shape function.

NOTE. The shape function, $\phi(x)$ is different for the elastic range and the plastic range and therefore the load factor, K_L, will be different.

For example; the shape factor for a simply supported beam with a uniformly distributed load, in the elastic rangers is defined as

$$\phi(x) = (16/5L^4)(L^3x - 2Lx^3 + x^4) \qquad 3\text{-}44a$$

while for the plastic range

$$\phi(x) = 2x/L \qquad x < L/2 \qquad 3\text{-}44b$$

For a structure with concentrated loads

$$WD = F_e\delta_{max} = \sum_{r=1}^{i} F_r\delta_r \qquad 3\text{-}45a$$

where F_r = r^{th} concentrated load

δ_r = deflection at load r

i = number of concentrated loads

rearranging terms

$$F_E = \sum_{r=1}^{i} F_r\phi_r \qquad 3\text{-}45b$$

where the shape factor is defined as

$$\phi_r = \sum_{r=1}^{i} \delta_r / \delta_{max} \qquad 3\text{-}46$$

Again there is a K_L for the elastic range and a K_L for the plastic range. However, for a single concentrated load located at the point of maximum deflection (i.e. the center of a simply supported or fixed-fixed beam, or the end of a cantilever beam) ϕ_r is equal to one for both the elastic and plastic ranges and therefore K_L is equal to one for both ranges.

Values for K_L for one-way elements are presented in Table 3-12. Equation 3-41 through 3-46 were used to calculate these values. An example calculating K_L is shown in Appendix A.

3-17.2.2. Mass Factor

The mass factor is the design or transformation factor by which the total distributed mass of an element is multiplied to obtain the equivalent lumped mass of the equivalent single-degree-of-freedom system. If the total mass of the actual element is M and the mass of the equivalent system is M_E, the mass factor K_M is defined by the equation

$$K_M = M_E / M \qquad 3\text{-}47$$

K_M can be obtained by setting the kinetic energy of the equivalent system equal to the kinetic energy of the actual structure as determined from its deflected shape.

For a structure with continuous mass

$$K_E = 1/2M_E(\omega\delta_{max})^2 = 1/2\int_0^L m(x)[\omega\delta(x)]^2\,dx \qquad 3\text{-}48a$$

where ω = natural circular frequency

$m(x)$ = distributed mass per unit length

rearranging terms

$$M_E = \int_0^L m(x)\phi^2(x)\,dx \qquad 3\text{-}48b$$

where the shape function $\phi(x)$ is based on the deflected shape of the element due to the applied loading and not to the distribution of the mass. Since the deflected shape of the element is different for the elastic and plastic ranges, $\phi(x)$, and therefore K_M, will also be different.

Using Equations 3-47 and 3-48, values for K_M were calculated for one-way elements with constant mass. These values are shown in Table 3-12.

For a concentrated mass system,

$$K_E = 1/2M_E(\omega\delta_{max})^2 = 1/2 \sum_{r=1}^{i} M_r(\omega\delta_r)^2 \qquad 3\text{-}49a$$

where

M_r = r^{th} mass

δ_r = deflection of mass r

i = number of lumped masses

rearranging terms

$$M_E = \sum_{r=1}^{i} M_r\phi_r^2 \qquad 3\text{-}49b$$

An example of calculations for finding K_M can be found in Appendix A.

3-17.2.3. Resistance Function

Resistance factor is the design factor by which the resistance of the actual structural element must be multiplied to obtain the resistance of the equivalent single-degree-of-freedom system. To obtain the resistance factor, it is necessary to equate the strain energy of the structural element, as computed from the assumed deflection shape, and the strain energy of the equivalent single-degree-of-freedom system. If the computed total resistance of the structural element is R and the equivalent total resistance of the equivalent system is R_E, then the resistance factor is defined by the equation

$$K_R = R_E / R \qquad 3\text{-}50$$

Since the resistance of an element is the internal force tending to restore the element to its unloaded static position, it can be shown that the resistance factor K_R must always equal the load factor K_L.

3-17.3. Load-Mass Factor

The load-mass factor is a factor formed by combining the two basic transformation factors, K_L and K_M. It is merely the ratio of the mass factor to the load factor, and it is convenient since the equation of motion may be written in terms of that factor alone. The equation of motion of the actual system is given as

$$F - R = Ma \qquad 3\text{-}51$$

and for the equivalent system:

$$K_L F - K_L R = K_M Ma \qquad 3\text{-}52a$$

which can be re-written as

$$F - R = (K_M / K_L)Ma \qquad 3\text{-}52b$$

or $$F - R = K_{LM}Ma = M_e a \qquad 3\text{-}52c$$

where K_{LM} = load-mass factor

$$= K_M / K_L \qquad 3\text{-}53$$

and M_e = effective total mass of the equivalent system

when expressed in terms of the unit area of the element, Equation 3-52c can be written as

$$f - r = K_{LM}ma = m_e a \qquad 3\text{-}54$$

Values of load, mass and load-mass factors are presented in Table 3-12. Equation 3-53 was used to calculate the load mass factor.

Instead of computing the several factors above, the load-mass factors in the elastic and elasto-plastic ranges can be determined by relating the primary mode of vibration of the member to that of an equivalent single-degree-of-freedom system. In the plastic range, it can be assumed that neither the moment nor the curvature changes between the plastic hinges under increasing deflection. This behavior results in a linkage action, consideration of which can be used to evaluate the effective plastic mass as follows:

In Figure 3-43, a portion of a two-way element bounded by the support and the yield line is shown. The equation of angular motion for this section is

$$\Sigma M = I_m \theta'' \qquad 3\text{-}55$$

where ΣM = summation of moments

I_m = mass moment of inertia about the axis of rotation

θ'' = angular acceleration

Substituting in equation

$$Fc - (\Sigma M_N + \Sigma M_p) = (I_m / L_1)a \qquad 3\text{-}56a$$

where a is the acceleration. Dividing through by c

$$F - (\Sigma M_N + \Sigma M_p)/c = (I_m / cL_1)a \qquad 3\text{-}56b$$

Since the second term is the resistance R

$$F - R = (I_m / cL_1)a = M_e a \qquad 3\text{-}56c$$

and the load-mass factor K_{LM} for the sector shown is

$$K_{LM} = I_m / cL_1 M \qquad 3\text{-}57$$

where c is the distance from the resultant applied load to the axis of rotation, L_1 is the total length of the sector normal to the axis of rotation and M is the total mass of the sector.

When the element is composed of several sectors, each sector must be considered separately and the contributions then summed to determine the load-mass factor for the entire element.

$$K_{LM} = \Sigma(I_m / cL_1)/M \qquad 3\text{-}58$$

For elements of constant depth and, therefore, of constant unit mass, the above equation can be written in terms of the area moment of inertia I and the areas A of the individual sectors.

$$K_{LM} = \Sigma(I/cL_1)/A \qquad 3\text{-}59$$

Table 3-13 gives the load-mass factors for the elastic and elasto-plastic response ranges for various two-way elements. The values given in the table apply for two-way elements of uniform thickness and supported as indicated. Also if there are openings in the element, they must be compact in shape and small in area compared to the total area of the element.

Figure 3-44 gives the load-mass factors for the plastic response of various two-way elements. The load-mass factors are a junction of support condition and yield line location. These two-way elements must conform to the following limitations:

(1) Element must be of constant thickness.

(2) Opposite support must provide the same restraint so that a symmetrical yield line pattern occurs.

(3) Any openings must be compact in shape and small in area compared to the total area of the element.

3-17.4. Natural Period of Vibration

To determine the maximum response of a system either by numerical methods or design charts (both methods are described in Section 3-19), the effective natural period of vibration is required. This effective natural period of vibration, when related to the duration of a blast loading of given intensity and a given structural resistance, determines the maximum transient deflection X_m of the structural element.

The effective natural period of vibration is

$$T_n = 2\pi(m_e/K_E)^{1/2} = 2\pi(K_{LM}m/K_E)^{1/2} \qquad 3\text{-}60$$

where m_e = the effective unit mass

K_E = the equivalent unit stiffness of system

The values used for the effective mass and stiffness for a particular element depends on the allowable maximum deflection. When designing for completely elastic behavior, the elastic stiffness is used. In all other cases the equivalent elasto-plastic stiffness, K_E, is used. The elastic value of the effective mass is used for the elastic range, while in the elasto-plastic range the effective mass is the average of the elastic and elasto-plastic values. For small plastic deflections ($\theta \leq 2°$), the value of the effective mass is equal to the average of the plastic value and the equivalent elastic value. The plastic effective mass is used for large plastic deflections.

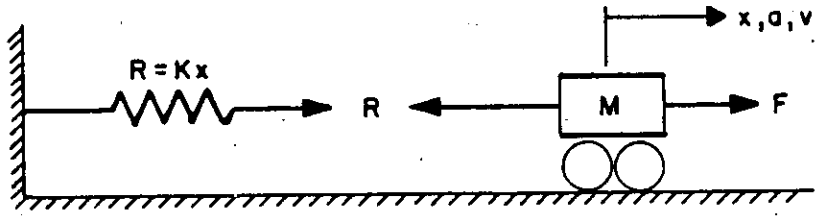


Figure 3-42 Typical single-degree-of-freedom system

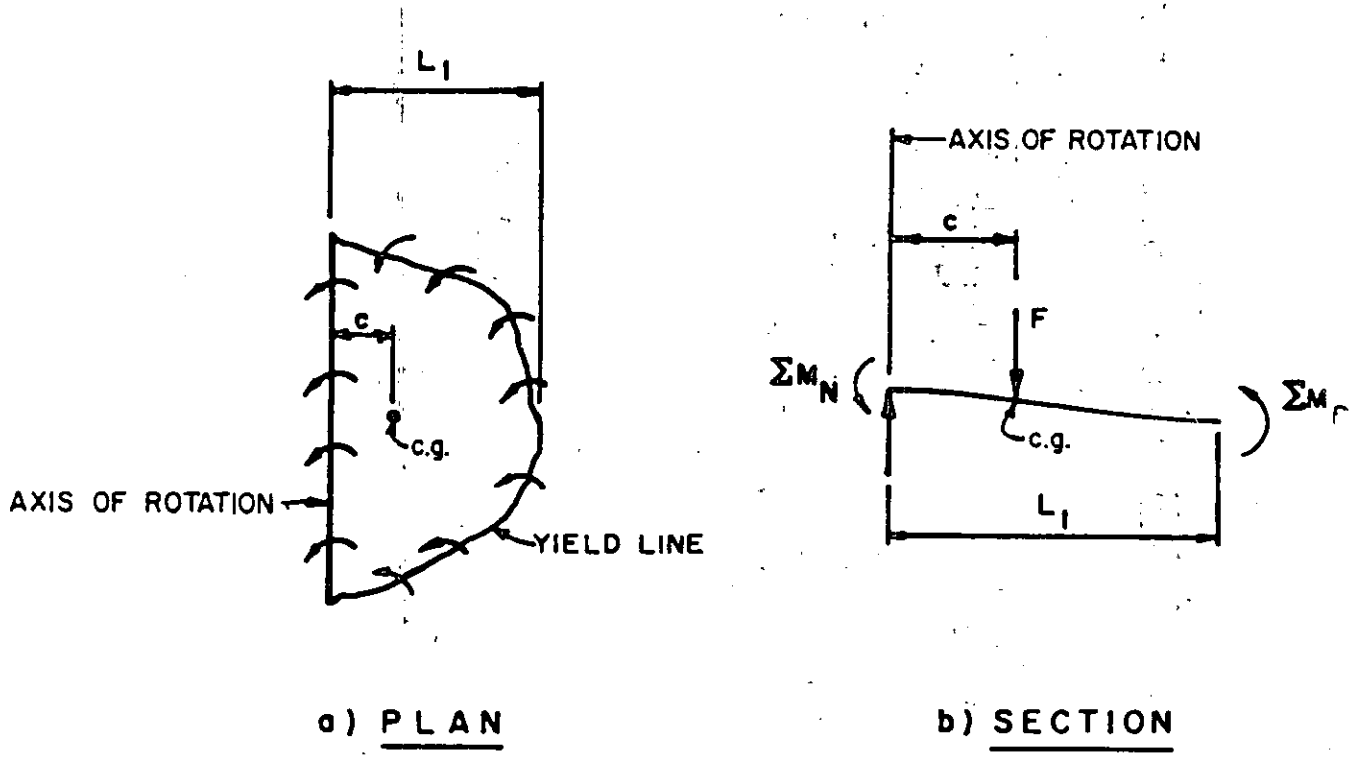


Figure 3-43 Determination of load-mass factor in the plastic range

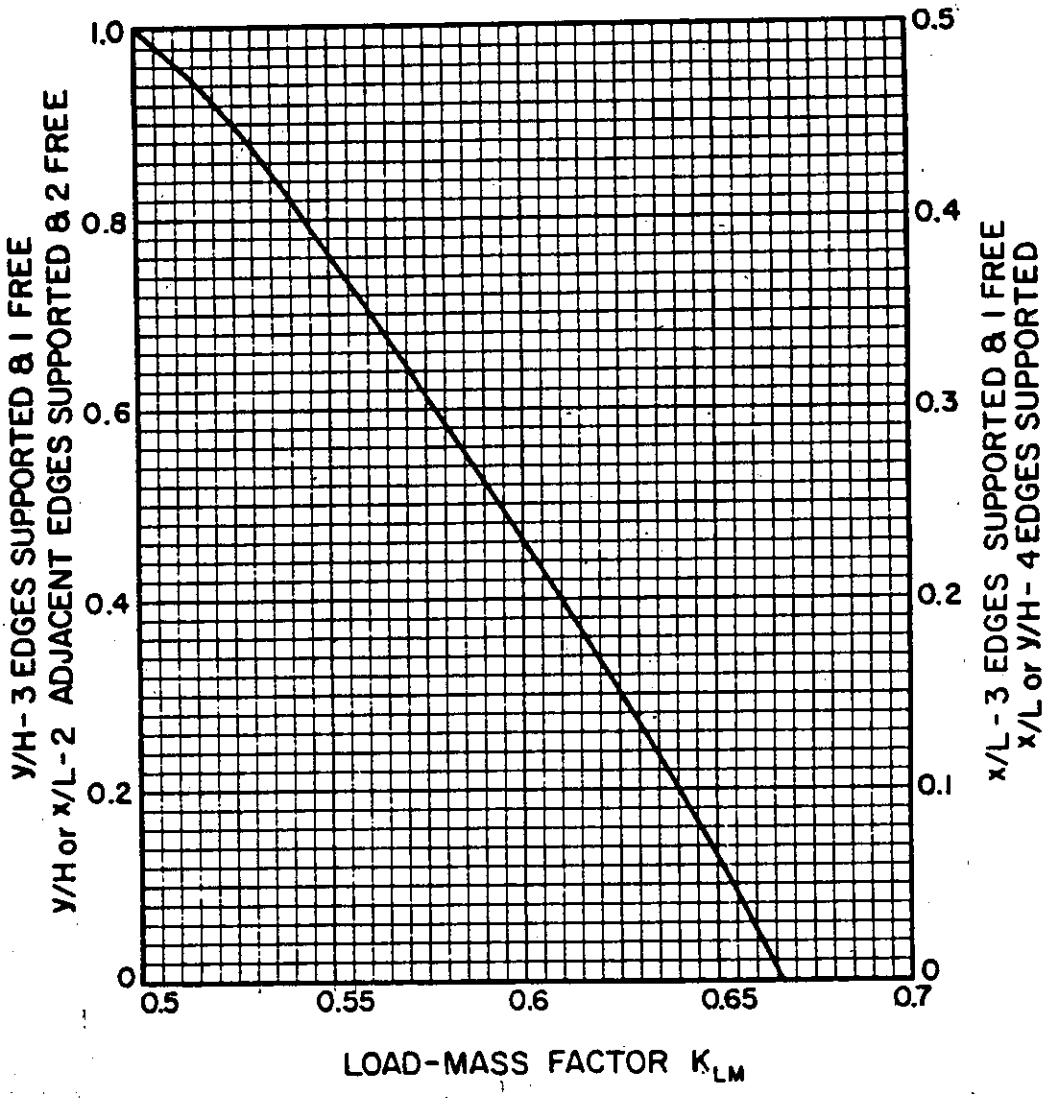


Figure 3-44 Load-mass factors in plastic range for two-way elements

Table 3-12 Transformation Factors for One-Way Elements

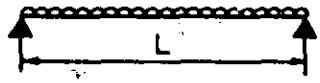
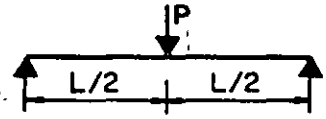
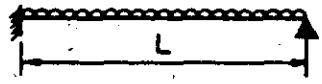
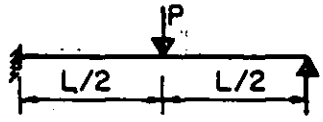
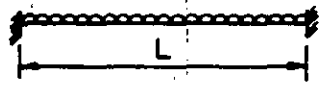
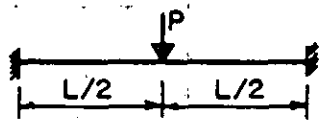
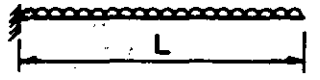
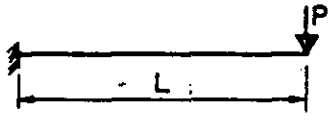
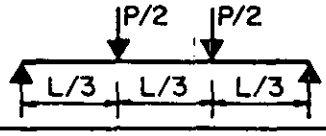
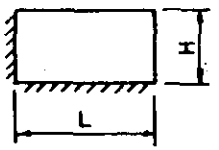
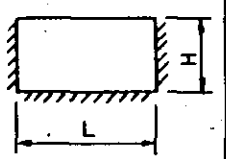
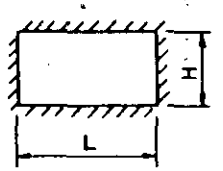
Edge Conditions and Loading Diagrams	Range of Behavior	Load Factor K_L	Mass Factor K_M	Load-Mass Factor K_{LM}
	Elastic	0.64	0.50	0.78
	Plastic	0.50	0.33	0.66
	Elastic	1.0	0.49	0.49
	Plastic	1.0	0.33	0.33
	Elastic	0.58	0.45	0.78
	Elasto-Plastic	0.64	0.50	0.78
	Plastic	0.50	0.33	0.66
	Elastic	1.0	0.43	0.43
	Elasto-Plastic	1.0	0.49	0.49
	Plastic	1.0	0.33	0.33
	Elastic	0.53	0.41	0.77
	Elasto Plastic	0.64	0.50	0.78
	Plastic	0.50	0.33	0.66
	Elastic	1.0	0.37	0.37
	Plastic	1.0	0.33	0.33
	Elastic	0.40	0.26	0.65
	Plastic	0.50	0.33	0.66
	Elastic	1.0	0.24	0.24
	Plastic	1.0	0.33	0.33
	Elastic	0.87	0.52	0.60
	Plastic	1.0	0.56	0.56

Table 3-13 Load-Mass Factors in the Elastic and Elasto-Plastic Ranges for Two-Way Elements

Support Conditions		Value of L/H	Elastic and Elasto-Plastic Ranges (Support Conditions)				
			All Supports Fixed	One Support Simple Other Supports Fixed	Two Supports Simple Other Supports Fixed	Three Supports Simple Other Supports Fixed	All Supports Simple
Two adjacent edges supported and two edges free		ALL	0.65	0.66	—	—	0.66
Three edges supported and one edge free		L/H<0.5	0.77	0.77	0.79	—	0.79
		.5≤L/H≤2	$0.65-0.16(\frac{L}{2H}-1)$	$0.66-0.144(\frac{L}{2H}-1)$	$0.65-0.186(\frac{L}{2H}-1)$	—	$0.66-0.175(\frac{L}{H}-1)$
		L/H ≥ 2	0.65	0.66	0.65	—	0.66
Four edges supported		L/H=1	0.61	0.61	0.62	0.63	0.63
		1≤L/H≤2	$0.61+0.16(\frac{L}{H}-1)$	$0.61+0.16(\frac{L}{H}-1)$	$0.62+0.16(\frac{L}{H}-1)$	$0.63+0.16(\frac{L}{H}-1)$	$0.63+0.16(\frac{L}{H}-1)$
		L/H ≥ 2	0.77	0.77	0.78	0.79	0.79

DYNAMIC ANALYSIS

3-18. Introduction

Structural elements must develop an internal resistance sufficient to maintain all motion within the limits of deflection prescribed for the particular design. The load capacity of the member depends on the peak strength developed by the specific member (see Chapters 4 and 5) and on the ability of the member to sustain its resistance for a specific though relatively short period of time. This section describes the methods used for the analysis of structural elements subjected to dynamic loads, and these elements are divided into three groups, namely: (1) elements which respond to the pressure only (low pressure range), (2) elements which respond to pressure-time relationship (intermediate-pressure design range) and (3) elements which respond to the impulse which corresponds to the high pressure design range.

The method of analysis is different for the groups of elements. Those elements that respond to pressure only (this is still a pressure-time relation) and those that respond to pressure-time relationship may be analyzed using either numerical methods or design charts, while elements that respond to the impulse are analyzed using either design charts for large deflection or an impulse method for designs with limited deflections.

The method of analysis employing numerical techniques provides a solution that is obtained by a step-by-step integration, and is generally applicable for any type of load and resistance function. This method of analysis is presented in this section. Also presented is the result of a systematic analysis of single-degree dynamic systems for several idealized loadings plotted in non-dimensional design charts.

3-19. Elements Which Respond to Pressure Only and Pressure-Time Relationship.

3-19.1. General

To analyze these elements, the true magnitudes for the pressure-time relationship of the applied blast loads must be known. The determination of the dynamic response of these systems is accomplished using numerical techniques or design charts which relate the dynamic properties of the element (natural period of vibration, resistance, and deflection) to those of the blast overpressures.

3-19.2. Analysis by Numerical Methods

The numerical method of analysis involves a step-by-step integration procedure, starting at zero time, when displacement and the velocity of the system are presumably known. The time scale is divided into several discrete intervals, and one progresses by successively extrapolating the displacement from one time station to the next. As the time interval in the sequence of time is reduced, i.e., as the number of discrete intervals is increased, the accuracy of the numerical method is improved.

3-19.2.1. Single-Degree-Of-Freedom Systems

As stated previously, a single degree of freedom system is one in which only one coordinate is essential to define its motion. The equation of motion for the single-degree-of-freedom system shown in Figure 3-42 can be expressed as:

$$F - kx - cv = Ma \qquad 3\text{-}61$$

when c = damping constant

There are several methods that can be used to numerically integrate Equation 3-61, but the two procedures applied to this problem will be the average acceleration, and the acceleration-impulse extrapolation methods.

3-19.2.1.1. Average Acceleration Method

In the average acceleration method, the velocity and displacement at any time t are expressed as

$$v_t = v_{t-1} + 1/2\ (a_t + a_{t-1})\Delta t \qquad 3\text{-}62$$

$$x = x_{t-1} + 1/2\ (v_t + v_{t-1})\ \Delta t \qquad 3\text{-}63$$

Substituting Equation 3-62 into Equation 3-63,

$$x = x_{t-1} + v_{t-1}\ \Delta t + 1/4\ (a_t + a_{t-1})\ \Delta t^2 \qquad 3\text{-}64$$

Substituting Equations 3-62 and 3-63 into Equation 3-61, we have

$$F - k\ [x_{t-1} + 1/2(v_t + v_{t-1})\Delta t] - c[v_{t-1} + 1/2\ (a_t + a_{t-1})\Delta t] = Ma \qquad 3\text{-}65$$

Equation 3-65 can be simplified to

$$a = \frac{1}{m + (1/2)c\ \Delta t + (1/4)k\ \Delta t^2}\ [F - k\ (x_{t-1} + v_{t-1}\ \Delta t + 1/4a_{t-1}\ \Delta t^2) - c\ (v_{t-1} + 1/2\ a_{t-1}\ \Delta t)] \qquad 3\text{-}66$$

The integrating procedure can be summarized as follows:

Step 1. At t = 0: Compute: a_o using Equation 3-61 and specified values for $x_o(t = o)$, $v_o(t = o)$, and $F(t = o)$.

Step 2. Increment time: $t = t + \Delta t$

Step 3. At $t = t + \Delta t$: Compute $a(t = t + \Delta t)$ using Equation 3-66, $v\ (t = t + \Delta t)$ using Equation 3-62 and $x\ (t = t + \Delta t)$ using Equation 3-63.

Step 4. Repeat steps 2 and 3 until some specified time or until the maximum displacement is reached.

It should be noted that if x (t = 0) and v (t = 0) are zero, then the system will not move as long as F (t = 0) is zero; however, if F (t = 0) is not zero, Equation 3-66 will give an acceleration and motion will start. Thus the system of equation is self-starting and requires no special starting provisions.

The procedure outlined above for an elastic single-degree-of-freedom system can be easily extended to accommodate elastic-plastic behavior. To do so, Equation 3-61 is re-written to include the restoring force R which replaces the spring restoring force kx, Equation 3-61 becomes

$$F - R - cv = ma \qquad 3\text{-}67$$

Substituting Equations 3-62 and 3-63 into Equation 3-67, the following equation for acceleration is obtained:

$$a_t = \frac{1}{m + (c\Delta t)/2} \left[F - R - c \left[v_{t-1} + \Delta t \, a_{t-1} / 2 \right] \right] \qquad 3\text{-}68$$

Unlike Equation 3-66, Equation 3-68 has a non-linear term R, and it depends on the displacement x at time t. Therefore, instead of using the direct integration approach as in the previous case, a predictor-corrector method is utilized. Briefly, the displacement x at time t is estimated (predicted) and then corrected and convergence of this procedure can be obtained in a single iteration if the value of Δt is small enough. The step-by-step procedure is outlined as follows:

Step 1. At t = 0: Compute at (t = t0) from Equation 3-67 and the initial conditions.

Step 2. Increment time: t = t + Δt

Step 3. At t = t + Δt: Set at = at-1 (t - 1 = 0, initially)

Step 4. Compute vt and xt from Equations 3-62 and 3-63

Step 5. Compute R

Step 6. Compute at from Equation 3-68

Step 7. If you are in the predicting pass, return to Step 4, if in the correcting pass, set xt-1 = xt, vt-1 = vt, at = at-1 and go to Step 2.

3-19.2.1.2. Acceleration Impulse Extrapolation Method

Suppose the acceleration of the system is defined by Figure 3-45a. The acceleration-impulse extrapolation method assumes that the actual acceleration curve can be replaced by a series of equally spaced impulses occurring at t_0, t_1, t_2, . . ., t_n, as shown in Figure 3-45b.

The magnitude of the acceleration impulse at t_n is given by

$$I(t_n) = a_n(\Delta t) \qquad 3\text{-}69$$

where $t_{-1} - t_0 = t_2 - t_1 = \ldots = t_n - t_{n-1}$. This is shown in Figure 3-45b. Since an impulse is applied at t_n, there is a discontinuity in the value of velocity at t_n. In the time interval from t to t_{n-1}, the velocity is constant and the displacement varies linearly with time. The velocity and displacement thus obtained are shown in Figures 3-45c and 3-45d.

Suppose t_n^- and t_n^+ indicate the time immediately before and after the application of the impulse at t_n, and let v_n^- and v_n^+ indicate respectively the velocity at t_n^- and t_n^+; these two velocities are related by the following equation:

$$v_n^+ = v_n^- + a_n(\Delta t) \qquad 3\text{-}70$$

The relationship between x_{n-1} and x_n, and between x_n and x_{n+1} are given by:

$$x_n - x_{n-1} = v_n^-(\Delta t) \qquad 3\text{-}71a$$

$$x_{n+1} - x_n = v_n^+(\Delta t) \qquad 3\text{-}71b$$

Combining Equations 3-70 and 3-71, the three successive displacements are related by:

$$x_{n+1} = 2x_n - x_{n-1} + a_n(\Delta t)^2 \qquad 3\text{-}72$$

This is the basic recurrence formula for the acceleration impulse extrapolation method. Once the values of x at t_{n-1} and t_n are known, the value at t_{n+1} can be directly computed without resorting to a trial and error procedure.

It is necessary, however, to use a special procedure in the first time interval because, at t = 0, no value of x_{n-1} is available. Two different procedures may be used. The first assumes the acceleration varies linearly up to the first time station, in which case, the displacement of the system at that time can be expressed as:

$$x_1 = (1/6)(2a_0 + a_1)(\Delta t)^2 \qquad 3\text{-}73$$

The second procedure assumes that the acceleration is constant during the first time interval and is equal to the initial value. This assumption results in the following expression for x_1:

$$x_1 = (1/2)a_0(\Delta t)^2 \qquad 3\text{-}74$$

It should be noted that Equation 3-73 has to be solved by trial and error since a_1 depends on x_1. This trial-and-error procedure can be avoided by taking the value of a_1 to be f(t)/m instead of the exact value of $[f(t_1) - R(t_1)]/m$. In Figure 3-46a if $a_o' = 0$, a_o is equal to $a_o'/6$ and in Figure 3-46b if a_o and a_1 are approximately equal to each other, the value $a_o'/2$ may be used for a_o. The recurrence formula is directly applicable for the evaluation of $x_2, x_3, \ldots, x_{n+1}$ whenever the acceleration is a continuous function. When there is a discontinuity in the acceleration, this equation can still be used but not before some modifications are made to reflect this discontinuity. In Figure 3-46a there is a discontinuity at t_4 which occurs at the end of the time interval Δt. Under this condition, the value of a_n used in the numerical

procedure is the average value at discontinuity, namely 1/2 (a_4' + a_4'') for a_4. In Figure 3-46b the discontinuity occurs within time interval, t. The correct value for a_3 in this procedure is:

$$a_3 = (1/2)[a_3 + a_3'' + (a_3' - a_3'')\ (\Delta t'/\Delta t)^2] \qquad 3\text{-}75$$

When there are more than two discontinuities, this procedure becomes cumbersome and it is more convenient to replace the given acceleration by a smooth curve. Equation 3-73 must be used if there is zero force (and hence zero acceleration) at zero time, for in no other way can x_1 be determined. If acceleration at t = 0 is not zero, Equation 3-74 may be used without appreciable error, provided the force does not change greatly in the first interval.

The tedious method of numerical analysis is made somewhat easier if the computation procedure is set up as shown in Table 3-14. In the first time interval, the value used for the acceleration, a_o, depends on the forcing function. If the value of the forcing function is zero at time zero, then a_o is taken as one-sixth of a_1, where a_1 is the ratio of the value of the forcing function at t, to the mass of the system [$a_o = f(t_1)/6m$]. When the value of the forcing function is not zero at time zero, and if the values of the forcing function at times t=0 and t=t_1 are approximately equal, then a_o may be taken as $(P_o-R_o)/2$. The recurrence formula (Equation 3-72) is used in the other intervals.

It may be necessary during the computational procedure, to increase the value of t so as to reduce the number of time intervals. In Figure 3-47, for example, the forcing function varies linearly after time j. For the next time station (j + 1)st, the value of Δt, can be increased ($\Delta t_2 = 2\Delta t_1$ for example) without introducing any errors in the computations. In such cases, caution has to be exercised when using the recurrence formula. In Table 3-14, the value of Δt changes after the jth step, to $\Delta t_2 = 2\Delta t_1$. In the (j + 1)st step, x_{n-1} should be the value of x for the (j-1)nd step and x_n will be the value of x_{n+1} for the (j-1)st step.

3-19.2.2. A Two-Degree-of-Freedom-System

A two-degree-of-freedom system is shown in Figure 3-48 where the coordinates defining the configuration of the system are X_1 and X_2. The equation of motion for each of the two masses can be expressed as follows:

$$F_1 + R_2 - R_1 = M_1 a_1 \qquad 3\text{-}76a$$

$$F_2 - R_2 = M_2 a_2 \qquad 3\text{-}76b$$

Equation 3-76 can be rewritten as:

$$a_1 = F_1/M_1 + R_2/M_1 - R_1/M_1 \qquad 3\text{-}77a$$

$$a_2 = F_2/M_2 - R_2/M_2 \qquad 3\text{-}77b$$

The integration procedures described for a single-degree-of-freedom system can also be applied to two-degrees-of-freedom systems. In the average acceleration procedure, if the equations are placed in the same form as Equation 3-61, i.e., if the acceleration at time t are written in terms of displacements and velocities at time t - Δt, then two equations are obtained which must be

solved simultaneously for a_1 and a_2. In the other numerical integration procedure, the recurrence formula (Equation 3-72) applies to each of the two displacements independently.

3-19.2.3. Damping

The effects of damping are hardly ever considered in blast design because of the following reasons:

(1) Damping has very little effect on the first peak of response which is usually the only cycle of response that is of interest.
(2) The energy dissipated through plastic deformation is much greater than that dissipated by normal structural damping.
(3) Ignoring damping is a conservative approach.

If damping has to be considered in an analysis, however, it should be expressed as some percentage of critical damping. For free vibration, this is the amount of damping that would remove all vibration from the system and allow it to return to its neutral position. Critical damping is expressed as

$$C_{cr} = 2\ kM \qquad 3\text{-}78$$

where k = stiffness of the system

M = mass of system

The damping coefficient, c, in Equations 3-61 and 3-67 is expressed as a percentage of critical damping, C_{cr}. For steel structures, c should be taken as $0.05C_{cr}$ and $0.01\ C_{cr}$ for reinforced concrete structures.

3-19.3. Design Charts for Idealized Loadings

3-19.3.1. General

The response of single-degree-of-freedom systems subjected to idealized blast loadings is presented in the form of non-dimensional curves. In order to utilize these response charts, both the blast loads (pressure - time history) and the resistance-deflection curve of the structural system are idealized to linear or bilinear functions. Methods for computing these idealized blast loads are given in Chapter 2 while the methods for computing the resistance-deflection functions as well as converting the actual system to an elastic or elasto-plastic single-degree-of-freedom system have been presented in previous sections of this chapter.

The response of a structural system subjected to a dynamic load is defined in terms of its maximum deflection X_m and the time tm to reach this maximum deflection. The dynamic load is defined by its peak value P and duration T while the single-degree-of-freedom system is defined in terms of its ultimate resistance r_u, elastic deflection X_E and natural period TN. Response charts relate the dynamic properties of the blast load (P and T) to those of the element (r, X, T_N), that is, X_m/X_E and t_m/T are plotted as a function of r_u/P and T/T_N.

Response charts have been prepared for simplified loads as well as for the more complex bilinear loadings. The simplified loadings include triangular,

rectangular, step load with finite rise time, triangular with rise time and sinusoidal pulse. The idealized triangular loading is utilized in the analyses of acceptor structures. These structures are subjected to the effects of unconfined explosions, such as free-air or surface bursts or partially confined explosions in donor structures which are fully vented. On the other hand, idealized instantaneously applied or gradually applied flat top loads are usually encountered in the design of roof elements of acceptor structures. These structures are subjected to very long duration loads produced by very large explosive quantities. The triangular loading with a rise time is similar to the previously mentioned triangular load except that it is an equivalent loading produced by the blast traversing an element. The sinusoidal loadings is usually associated with the vibrational type of load rather than blast induced input. The bilinear loading is utilized in the analysis of containment structures which allow partial venting of an explosion and in the analysis of acceptor structures where reflected pressures clear rapidly around the structure.

The effects of damping have not been included in the preparation of the response charts. In the design of the blast resistant structures, the first peak of response is usually the only cycle of response that is of interest since the maximum resistance and deflection is attained in that cycle. Damping has very little effect on this first peak and consequently, neglecting damping has negligible effects on maximum response calculations.

3-19.3.2. Maximum Response Of Linear Elastic System To Simplified Loads

To obtain the response of a linear elastic system, it is convenient to consider the concept of the dynamic load factor. This factor is defined as the ratio of the maximum dynamic deflection to the deflection which would have resulted from the static application of the peak load P, which is used in specifying the load-time variation. Thus the dynamic load factor (DLF) is given by:

$$DLF = X_m / X_s \qquad 3\text{-}79a$$

where X_s = static deflection or, in other words, the displacement produced in the system when the peak load is applied statically.

X_m = maximum dynamic deflection

Since deflections, spring forces, and stresses in an elastic system are all proportional, the dynamic load factor may be applied to any of these to determine the ratio of dynamic to static effects. Therefore, the dynamic load factor may be considered as the ratio of the maximum resistance attained to the peak load or:

$$DLF = r/p \qquad 3\text{-}79b$$

where r = maximum dynamic resistance
p = peak load used in specifying the load-time variation.

For a linear elastic system subjected to a simplified dynamic load, the maximum response is defined by the dynamic load factor, DLF and maximum response time, t_m. The dynamic load factor and time ratio t_m/T are plotted

versus the time ratio T/T_N for a triangular load, rectangular load, step load with finite rise time (T_r), triangular load with rise time, and sinusoidal pulse in Figures 3-49 through 3-53.

In many structural problems only the maximum value of the DLF is of interest. For the most prevalent load case, namely, the triangular load as well as the rectangular and step load with rise time, the maximum value of the DLF is 2. This immediately indicates that all maximum displacements, forces, and stresses due to the dynamic load are twice the value that would be obtained from a static analysis for the maximum load P.

The above response charts apply for elastic systems. However, the charts can be applied to the entire elasto-plastic range if the actual resistance-deflection curve (two step system, three step system, etc.) is replaced by the equivalent elastic system where the equivalent elastic stiffness K_E and the equivalent elastic deflection X_E are obtained according to previously explained procedures.

In a typical design example, the pressure-time loading is calculated and idealized to one of the simplified loads defined by P and T or T_r. A structural member is assumed and its corresponding dynamic properties are calculated. For a completely elastic response, the values of r_e and T_N are calculated while for a response in the elasto-plastic range, r_u, X_E and T_N are obtained. It should be noted that for a response in the elasto-plastic range, the value of T_N is calculated using the effective mass which is an average of the elastic and elasto-plastic values. Knowing the ratio of T/T_N the dynamic load factor (DLF) and the time ratio can be read from the appropriate figures. The maximum resistance r attained by the structural member is calculated from the DLF and the response time is obtained from the time ratio. If the resistance r is greater than r_e for a completely elastic response in the elasto-plastic range, then the analysis is not valid and the procedure is repeated. The maximum deflection is obtained from the resistance r and the stiffness K_e or K_E.

3-19.3.3. Maximum Plastic Response Of An Elasto-Plastic System To Simplified Loads

An elasto-plastic system may have an elastic or plastic response depending upon the magnitude of the blast load. If the response is elastic, that is, the member attains a resistance r which is less than its ultimate resistance r_u, then the charts of the preceding section are used. The response charts presented in this section are only for the plastic response of members where the ultimate resistance r_u is attained.

The maximum plastic response of an elasto-plastic system subjected to a blast load is defined by the maximum deflection, X_m it attains and the time, t_m it takes to reach this deflection. The blast load is defined by its peak value P and duration T while the singe-degree-of-freedom system is defined by its ultimate resistance r_u, elastic deflection X_E and natural period T_N. A non-dimensional response chart is constructed by plotting the ductility ratio X_m/X_E and the time ratio t_m/T as a function of r_u/P and T/T_N. Response charts are given for a triangular load, rectangular load, step load with finite rise time T_r and triangular load with rise time in Figures 3-54 through 3-61. It should be noted that for the step load with finite rise time, the load is

defined by the rise time T_r and, consequently, the response curves are plotted using T_r rather than T.

In a typical example, the pressure-time loading is calculated and idealized to one of the simplified loads defined by either P and T or P and T_r. A structural member is assumed and its corresponding dynamic properties (r_u, X_E, T_N) are calculated. Knowing the ratios of r_u/P and T/T_N (or T_r/T_N), the ductility ratio X_m/X_E and the time ratio t_m/T can be read from the appropriate figures. The maximum deflection X_m and response time tm can readily be calculated. If the ductility ratio X_m/X_E or the maximum deflection X_m and corresponding response time t_m are unsatisfactory, the procedure is repeated.

It should be noted that the value of the natural period of vibration T_N used in conjunction with the response charts varies according to the magnitude of the ductility ratio X_m/X_E. For small plastic deformations (X_m/X_E less than 5), the calculations of T_N is based on an average of the equivalent elastic and plastic masses. Whereas, for larger plastic deformations (X_m/X_E greater than 5), the equivalent plastic mass is used to obtain T_N.

3-19.3.4. Maximum Plastic Response Of An Elasto-Plastic System to Idealized Bilinear Loads.

Response charts have been prepared for bilinear loads in much the same manner as for simplified loads. However, four parameters are required to define the bilinear loading rather than two parameters which are required for the simplified loads. These additional parameters greatly increase the number of charts required for the rapid prediction of the dynamic response of an elasto-plastic system. However, the computational procedures remain comparatively simple.

A bilinear load is illustrated in Figure 3-62c. Four parameters are required to define this load shape, namely:

P = peak pressure of shock load (primary pulse)

C_1P = peak pressure of gas load (secondary pulse)

T = duration of shock load

C_2T = duration of gas load

It can be seen from Figure 3-62c that the value of C_1 will always be less than 1 while the value of C_2 will always be greater than 1.

Response charts for the bilinear load are prepared in the same way as the simplified loads except that each chart is prepared for a given value of C_1 and C_2. The ductility ratio X_m/X_E versus T/T_N is plotted on each chart for various values of P/r_u, t_m/T_N and t_E/T (where t_E is the time to reach the maximum elastic deflection x_E). Therefore, each chart contains three families of curves. In addition, each chart contains one, two or three boundaries which are formed by symbols. These boundaries delineate regions of each chart where certain approximations are preferable to chart interpolation. These approximations involve modification of the bilinear load for the various regions. The loads considered for each of the regions are given in Figure 3-62 while the boundary for the various regions are defined in Figure 3-63.

Numerous response charts are required for bilinear loads. Table 3-15 lists the figure numbers of the response charts prepared for the selected values of C_1 and C_2. These response charts are presented in Figures 3-64 through 3-266.

To use the response charts, the first step is to enter Table 3-15 with the required values of C_1 and C_2. Locate the points in the table with coordinates C_1 and C_2. The number in the box containing the point is the appropriate figure number to use to solve the problem. If the point is not located in a box having a number, the two or, more frequently, four numbers bracketing the point are the appropriate figure numbers to use. Interpolation for the required values of C_1 and C_2 must be performed. A graphical and mathematical interpolation procedure is presented in subsequent sections.

In a typical design, a structural member is assumed and the idealized resistance function defined by r_u, X_E and K_E can be determined along with the natural period. As previously explained for simplified loads; the equivalent mass used to calculated T_N varies according to the amount of plastic deformation. Knowing the ratio of P/r_u and T/T_N, note if the intersection point corresponding to these parameters, is located in region A,B,C or D on the response chart(s) for the required values of C_1 and C_2. The boundaries for these regions are represented by a line of asterisks, solid circles, and solid squares, as illustrated in Figure 3-63.

The final step in obtaining the solution depends on which region of the response chart(s) is applicable. These regions were established to reduce the amount of calculations required for a solution by eliminating, where possible, interpolation between charts. Except for one of the four regions, the actual bilinear blast load is replaced by a simplified load. Solution of the response for these simplified loads will predict a solution which is within 10 percent of the exact solution. Of course, the exact solution of the response for the structural member in these three regions can be obtained by using the required response charts and interpolating, where required, between charts.

3-19.3.4.1. Region A

This region is defined as the area to the left of the solid circles on the response charts. If a chart does not have a line of solid circles, then region A does not exist. Figures 3-221, 3-222 and 3-223 illustrate this case.

In region A the maximum dynamic response depends primarily upon the total impulse in the blast loading (area under the pressure-time curve). The actual pressure-time distribution does not significantly affect the maximum dynamic response because in these regions the durations T and C_2T are small in comparison to the response time, t_m of the structural member. In this region the response charts are not used and a solution is obtained by considering the modified loading shown in Figure 3-62a. This load shape yields the following equations:

$$\frac{X_m}{X_E} = \frac{1}{2} + \frac{\pi^2}{2}\left[\left[\frac{P}{r_u}\right]\left[\frac{T}{T_n}\right] F\right]^2 \qquad 3\text{-}80$$

and

$$\frac{t_m}{T_n} = \left[\frac{1}{2}\right] F \left[\frac{P}{r_u}\right]\left[\frac{T}{T_n}\right] \qquad 3\text{-}81$$

where

$$F = C_2 + \frac{C_2\,[1-C_1][1-C_2]}{C_2 - C_1} \qquad 3\text{-}82$$

3-19.3.4.2. Region B

This region is defined as the area in the chart to the left of the asterisks. If a chart has no line of asterisks, then region B does not exist. Figure 3-65 illustrates the case where region B does not exist.

In region B the maximum dynamic response depends primarily upon the gas load which is described by C_1P and C_2T. The shock load described by P and T is neglected. This load condition is shown in Figure 3-62b. Therefore the solution is obtained from consideration of a single triangular load. The dynamic response is obtained from Figure 3-64 which like Figures 3-54 and 3-55 is for a triangular load and will yield the same results. When using Figure 3-64 it must be realized that the P and T used in the chart are actually C_1P and C_2T, respectively. In a typical design, enter Figure 3-64 with the normalized parameters, C_1P/r_u and C_2T/T_N, and read the solution, X_m/X_E, t_m/T_N, and t_E/C_2T.

Figure 3-63 depicts region B as the area between the line of solid circles and the line of asterisks. It should be understood that the solution technique associated with region B (i.e., neglect the shock load and use Figure 3-64) applies everywhere to the left of the line of asterisks, including region A. In other words, two solution techniques are available in region A.

3-19.3.4.3. Region D

This region is defined as the area in the charts to the right of the line of solid squares. If a chart has no line of solid squares, then region D does not exist. Figure 3-69 illustrates the case where region D does not exist.

In region D the maximum dynamic response depends primarily upon the shock load which is described by P and T. The gas load described by C_1P and C_2T is neglected. This load condition is shown in Figure 3-62d. Therefore, the solution is obtained from consideration of a single triangular load. Similar to region B, the dynamic response is obtained from Figure 3-64 which is for a triangular load. Unlike region B, the parameters, P and T which describe the load are used in the figure. Therefore, in a typical design, enter Figure 3-64 with the normalized parameters P/r_u and T/T_N, and read the solution, X_m/X_E, t_m/T_N and t_E/T.

3-19.3.4.4. Region C

This is the region in the charts which do not meet the definitions of regions A, B and D. In most charts, region C is the area to the left of the line of

solid squares and to the right of the line of asterisks, as illustrated in Figure 3-63. Region C does not exist in some charts, such as Figure 3-97 which have over lapping regions A and D.

In region C, both the shock and gas load must be considered. Replacement of the actual bilinear load with a simplified load, as done for the other regions, will yield an incorrect solution. Therefore, in this region the response charts must be used. If the required values of C_1 and/or C_2 do not correspond to the response chart values, interpolation between response charts will be required to obtain a solution. In a few cases one or two response charts are needed, however, in general four response charts are required for a solution.

3-19.3.4.5. Response Chart Interpolation

Interpolation between four response charts will usually be required for region C. For regions A, B, or D, if conditions warrant an exact solution rather than the approximate solution usually used in these regions, interpolation between charts may be required. Either a graphical or mathematical interpolation procedure may be employed. The method selected depends upon personal choice. A brief description of each procedure is presented below and an example of each is given in Appendix A.

Graphical interpolation requires a sheet of log-log graph paper. A convenient size is 2 x 1 cycle with the single-cycle axis representing C_1 and C_2, and the two-cycle axis representing the desired parameter (X_m/X_E, t_m/T_N or t_E/T), called Y for ease of presentation. The appropriate figures to be used for a solution are obtained form Table 3-15 for the required values of C_1 and C_2. The procedure will illustrate the interpolation between four figures since this is by far the usual case. For the values of P/r_u and T/T_N corresponding to the structural system selected, determine the desired parameter Y for each of the four figures. Organize a table in the same format as Table 3-16 and enter each figure number and corresponding value of C_1, C_2 and Y.

In the table, C_{11} and C_{21} are the values of C_1 and C_2, respectively, from Figure 1. Likewise, C_{12} and C_{22} are the values of C_1 and C_2, respectively from Figure 2, etc. The symbol Y_1, is the desired parameter, such as X_m/X_E, which is read from Figure 1. The symbol Y_2 is the value read from Figure 2, etc. The interpolation is first performed for the required value of C_1 and then for the required value of C_2. That is, with C_{21} constant, graphically interpolate on the log-log paper between points (Y_1, C_{11}) and (Y_2, C_{12}) to find Y_a corresponding to C_1 and C_{21}, as shown on Figure 3-267. Similarly, with C_{23} constant, graphically interpolate between (Y_3, C_{13}) and (Y_4, C_{14}) to find Y_b corresponding to C_1 and C_{23}, also shown in Figure 3-267. The values of Y_a and Y_b are recorded in Table 3-16. Finally, with C_1 constant, graphically interpolate on the log-log paper between (Y_a, C_{21}) and (Y_b, C_{23}) to find Y corresponding to the required C_1 and C_2, as shown on Figure 3-267. The values of Y is the solution. Since there are three parameters to define the response of a structural, namely, X_m/X_E, t_m/T_N and t_E/T, the interpolation procedure is repeated three times, once for each parameter.

Mathematical interpolation requires the same initial steps as graphical interpolation. That is, the appropriate figures to be used for a solution are obtained from Table 3-15 and the required parameters are determined and

entered into Table 3-16. Logarithmic equations are used to obtain the values of Y_a, Y_b and Y. The value of $\ln Y_a$ is obtained from:

$$\ln Y_a = \ln Y_1 + \frac{\ln(Y_2 / Y_1) \ln(C_1 / C_{11})}{\ln(C_{12} / C_{11})} \qquad 3\text{-}83$$

and the value of $\ln Y_b$ is obtained from:

$$\ln Y_b = \ln Y_3 + \frac{\ln(Y_4 / Y_3) \ln(C_1 / C_{13})}{\ln(C_{14} / C_{13})} \qquad 3\text{-}84$$

Using the values of $\ln Y_a$ and $\ln Y_b$, the value of $\ln Y$ is obtained from:

$$\ln Y = \ln Y_a + \frac{(\ln Y_b - \ln Y_a) \ln(C_2 / C_{21})}{\ln(C_{23} / C_{21})} \qquad 3\text{-}85$$

The desired parameter Y is then obtained from:

$$Y = e^{\ln Y} \qquad 3\text{-}86a$$

The above equations use natural logarithms. Common logarithms can be used to solve the above equations and then solve for Y using:

$$Y = 10^{\log Y} \qquad 3\text{-}86b$$

It should be noted that if C_2 is represented by a response chart, then only two charts will be involved, and only Equation 3-83 will apply.

3-19.3.4.6. Accuracy

The prediction error is less than 10 percent for the approximate solutions obtained in regions A, B and D. This is true provided the recommended procedures are employed, that is, the actual load is replaced by the approximate loads as shown on Figure 3-62 and the solution is obtained using the equations provided for region A and using Figure 3-64 for regions B and D.

Exact solutions are obtained from the response charts if the required values of C_1 and C_2 correspond to those given in the charts. This is true for all four regions. Errors result from interpolation between the response charts. The prediction error in X_m/X_E for region C, where interpolation between charts is required, is less than 10 percent provided response charts bounded by the dashed or solid lines on Table 3-15 are not used. The prediction error in X_m/X_E will range from 55 to 100 percent for solutions in region C, if the point (C_1, C_2) lies in the area bounded by the solid line in Table 3-15, and will range from 10 to 55 percent for the area bounded by the dashed line. If the solution involves charts from both sides of either the dashed or solid lines, the prediction error will range from 10 to 55 percent. The large interpolation error for these charts result from the big change in X_m/X_E for a small change in P/r_u which is peculiar to this chart.

It should be noted that the large errors described above will always be on the high side, that is, the predicted value of X_m/X_E will always be greater than the exact value. Hence, a conservative design will always result. In addition, it should be noted that the prediction error in t_m/T_N is about half the error in X_m/X_E.

While the errors produced from interpolation between the charts in Table 3-15 bounded by the dashed and solid lines is large, the area in which they apply is small. As can be seen, region C is rather small on these charts. It is for points in this small area where interpolation must be performed. For the remaining areas (A, B and D), the approximate solutions may be used rather than interpolation. These approximate solutions will result in a error of less than 10 percent.

Solutions involving $0.920 < C_1 < 1.00$ and $C_2 \geq 100$ can result in very large errors if interpolating procedures are employed. In this region, the dynamic response is primarily due to the gas load. Therefore, Figure 3-64 is used to obtain X_m/X_E for the gas load. However, this value is too low and should be increased by 20 percent. The value of t_m/T_N corresponding to the increased value of X_m/X_E is then obtained from Figure 3-64.

3-19.3.5. Determination of Rebound

In the design of elements which respond to the pressure only and pressure-time relationship, the element must be designed to resist the negative deflection or rebound which can occur after maximum positive deflection has been reached. The ratio of the required unit rebound resistance to the ultimate unit resistance r/r_u, such that the element will remain elastic during rebound is presented in Figure 3-268 for a single-degree-of-freedom system subjected to a triangular loading function. Entering with ratios X_m/X_E and t/T_N previously determined for design, the required unit rebound resistance r- can be read in terms of the originally designed ultimate unit resistance r_u. To obtain the rebound resistance for an element subjected to another form of load other than the triangular loading function, a time-history analysis such as the one described in Section 3-19 has to be performed.

It may be noted that if the loading is applied in a relatively short time compared to the natural period of vibration of the system, the required rebound resistance can be equal to the resistance in the initial design direction. When the loading is applied for a relatively long time, the maximum deflection is reached when the positive forces are still large and the rebound resistance is reduced.

3-20. Elements Which Respond to Impulse

3-20.1. General

When an element responds to the impulse, the maximum response depends upon the area under the pressure time curve (impulse of blast loading). The magnitude and time variation of the pressure are not important. The response charts presented in Section 3-19, which are based on pressure-time relationship are therefore not required for these problems. Instead, the element resistance required to limit the maximum deflection to a specific value is obtained through the use of a semigraphical method of analysis.

Consider the pressure-time and resistance-time functions shown in Figure 3-269. The resistance curve depicted is for a two-way element with a resistance-deflection function having a post-ultimate range. From Newton's equation of motion it can be shown that the summation of the areas (considering area A as positive and area B as negative) under the load-time curves up to any time t_a divided by the corresponding effective masses is equal to the instantaneous velocity of that time:

$$v_a = \int_0^{t_a} \frac{(f-r)\,dt}{m_e} \qquad 3\text{-}87$$

The displacement at time t_a is found by multiplying each differential area divided by the appropriate effective mass by its distance to t_a and summing the values algebraically:

$$X_a = \int_0^{t_a} \frac{(f-r)}{m_e} \left[t_a - t\right] dt \qquad 3\text{-}88$$

In each range the mass is the effective plastic mass:

Time Interval	Resistance	Effective Mass
$0 \le t \le t_1$	r_u	$m_u = [K_{LM}]\, m_u$
$t_1 \le t \le t_m$	r_{up}	$m_{up} = [K_{LM}]\, m_{up}$

Time t_1 is the time at which the partial failure deflection X_1 occurs, and time t_m is the time at which maximum deflection X_m is reached ($X_m < X_u$).

For an element to be in equilibrium at its maximum deflection, its impulse capacity must be numerically equal to the impulse of the applied blast load. With the use of the foregoing equations, the expressions which define the motion and capacity of elements subjected to impulse type loads, can be defined. These expressions are presented for both large and limited deflection criteria. This criteria varies for the different materials used in protective design. The criteria for each material is obtained from the chapter that describes the design procedures for that material.

Case 1 - large deflections. Utilizing Equation 3-88 and by taking moments of the areas under the pressure-time and resistance-time curves (Figure 3-269) about time t_m, assuming that the unit blast impulse i_b is applied instantaneously at time t=0, and that time to reach yield t_y is also close to zero the expression for the maximum deflection is

$$X_m = \frac{i_b\, t_m}{m_u} - \frac{r_u\, t_1\, [t_m - t_1/2]}{m_u} - \frac{r_{up}\, [t_m - t_1]}{2m_{up}} [t_m - t_1] \qquad 3\text{-}89$$

If moments of the areas are taken about t_1, then the deflection at partial failure X_1, is

$$X_1 = \frac{i_b\, t_1}{m_u} - \frac{r_u\, t_1^2}{2m_u} \qquad 3\text{-}90$$

Using Equation 3-87 and summing the areas of t_m and recognizing that the instantaneous velocity at t_m equals zero.

$$\frac{i_b}{m_u} - \frac{r_u\, t_1}{m_u} - \frac{r_{up}\, [t_m - t_1]}{m_{up}} = 0 \qquad 3\text{-}91$$

Solution of the above three simultaneous equations is accomplished by solving Equation 3-91 for t_m and substituting this expression into Equation 3-89, and solving Equation 3-90 for t_1 and substituting this expression into the modified Equation 3-89. After continuing and rearranging terms, the general response equation becomes

$$\frac{i_b^2}{2m_u} = r_u x_1 + \frac{m_u}{m_{up}} r_{up}\, (x_m - x_1) \qquad 3\text{-}92$$

The left side of this equation is simply the initial kinetic energy resulting from the applied blast impulse and the right side is the modified potential energy of the element. The modification is required since the above analysis requires the use of two equivalent dynamic systems (before and after time t_1). The modification factor m_u/m_{up} equates the two dynamic systems. If the effective mass in each range was the same, $m_u/m_{u}p$ would equal one and the right side of the expression would be $r_u X_m$ which is the potential energy.

For one-way elements which do not exhibit the post-ultimate resistance range, or for two-way panels where the maximum deflection X_m is less than X_1, Equation 3-92 becomes

$$\frac{i_b^2}{2m_u} = r_u X_m \qquad 3\text{-}93$$

The above solutions are valid only for what is considered large deflection design since the variation of resistance with deflection in the elasto-plastic range has been ignored. This limitation is based on the assumption that the time to reach yield t_y and the duration of the impulse t_o are small in comparison to t_m.

Case 2 - limited deflections. For elements which respond to the impulse with limited deflections where the time to reach maximum deflection t_m is greater than three times the duration t_o of the load, but where the support rotations are equal to or less than the established criteria, the elasto-plastic range behavior of the element must be accounted for in determining the overall

response of the element to the applied blast load. For this case, Equation 3-92 becomes

$$\frac{i_b^2}{2m_a} = \frac{r_u X_E}{2} + \frac{m_a}{m_u} r_u[X_m - X_E] \qquad 3\text{-}94$$

where m_a is the average of the effective elastic and plastic masses and X_E the equivalent deflection.

When the response time t_m of an element is less than three times the load duration t_o, the element will respond to the pressure pulse rather than to the impulse alone. In this case the response of the element may be obtained through the use of a response chart considering a fictitious pressure pulse as outlined in Chapter 2. However, if the element's maximum deflection is greater than given in the response charts (ductility ratio X_m/X_E greater than 100), the response of the element may be obtained through use of the semi-graphical method of analysis as outlined in this paragraph considering the fictitious pressure pulse. It should be noted that the resistance time relationship used in the analysis to express the element's response should include the elasto-plastic region.

3-20.2. Determination of Time to Reach Maximum Deflection

The time t_m for each of the cases covered previously can be determined by applying Equations 3-87 and 3-88 to the particular problem. The resulting equations are as follows:

Case 1 - large deflections.

A. $X_1 < X_m \leq X_u$

$$t_m = \frac{i_b}{r_u} + \left[\frac{m_{up}}{m_u r_{up}} - \frac{1}{r_u}\right]\left[i_b^2 - 2m_u r_u X_1\right]^{1/2} \qquad 3\text{-}95$$

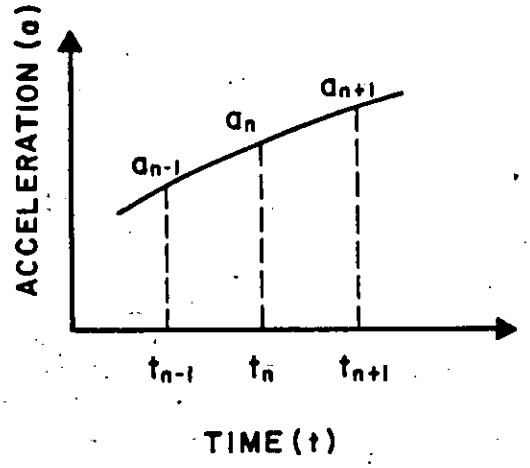
B. $X_m \leq X_1$

$$t_m = i_b / r_u$$

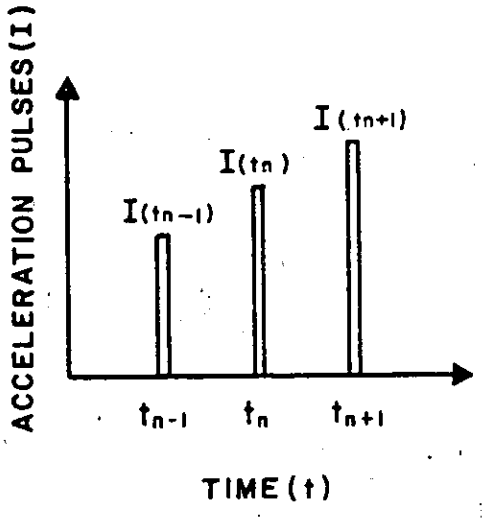
Case 2 - limited deflections.

Since the variation of resistance with time is not known in the elasto-plastic range, t_m can only be determined approximately by assuming a linear variation of resistance with time.

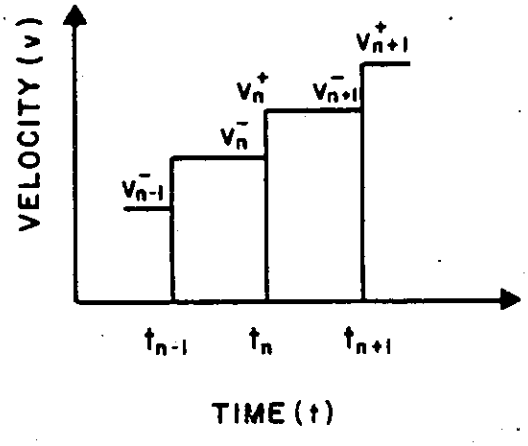
$$t_{m(approx)} = \frac{i_b}{r_u}\left[3 - \frac{m_u}{2m_a}\right] + \frac{1}{r_u}\left[\frac{m_u}{2m_a} - 1\right]\left[9i_b^2 - 6m_a r_u X_E\right]^{1/2} \qquad 3\text{-}97$$



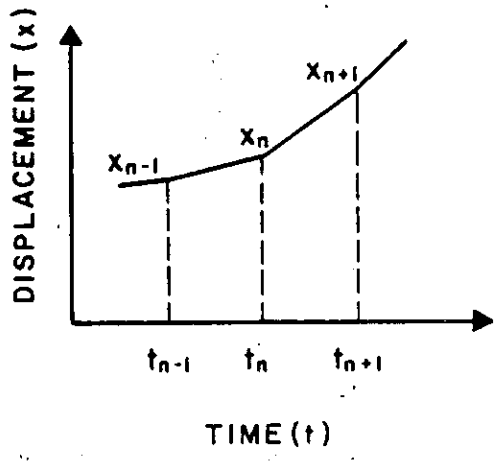
(a) GIVEN ACCELERATION CURVE



(b) ACCELERATION PULSES TO REPLACE THE GIVEN ACCELERATION CURVE



(c) VELOCITY



(d) DISPLACEMENT

Figure 3-45 Acceleration-impulse extrapolation method

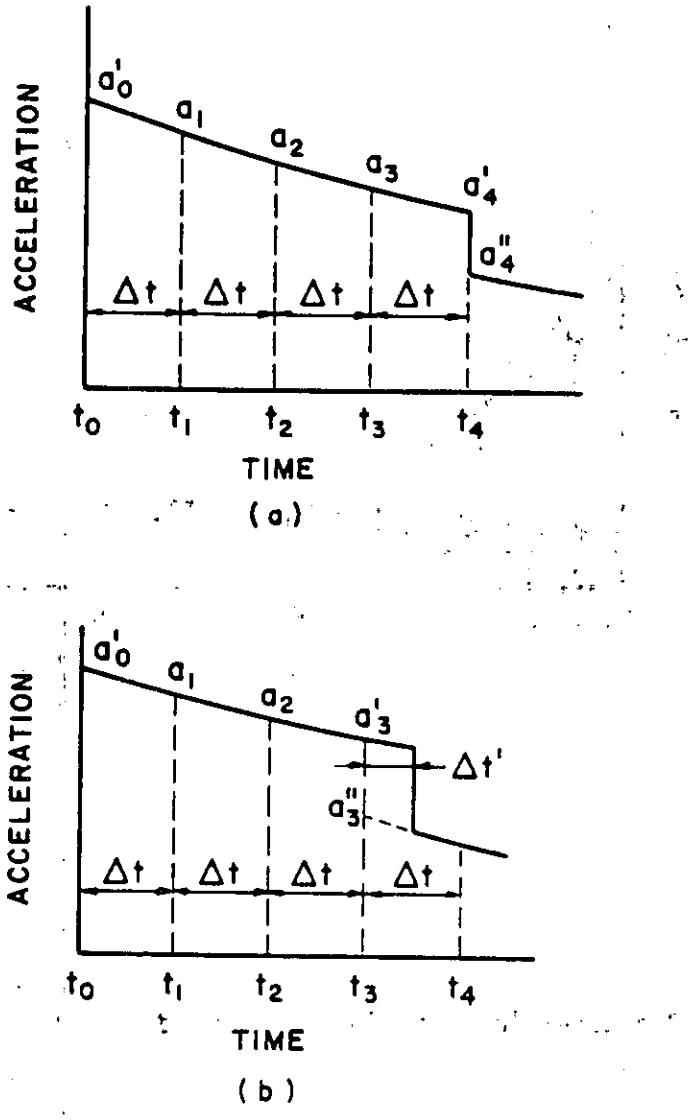


Figure 3-46 Discontinuities in the acceleration curve

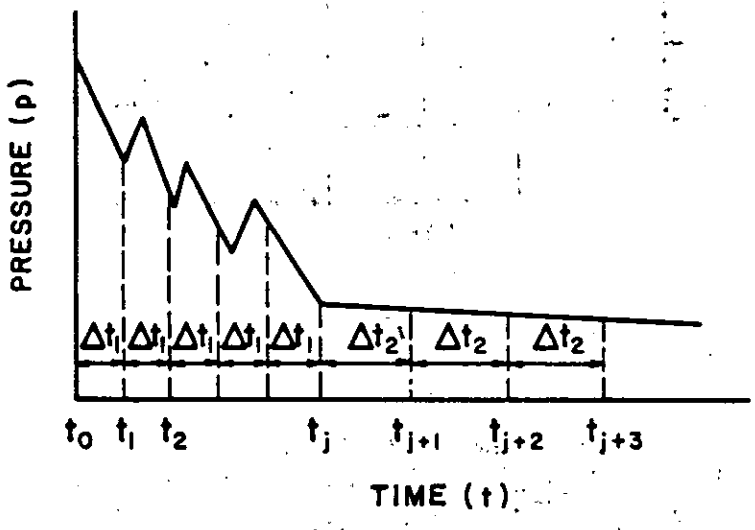


Figure 3-47 Pressure-time function with two different time intervals

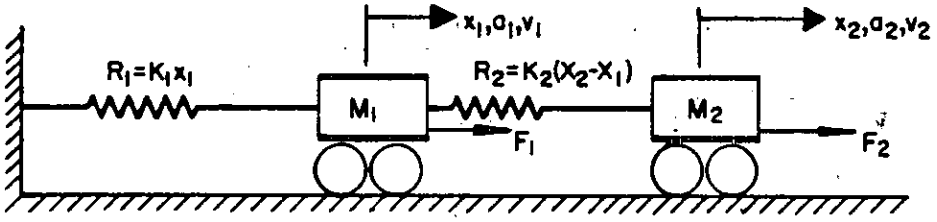
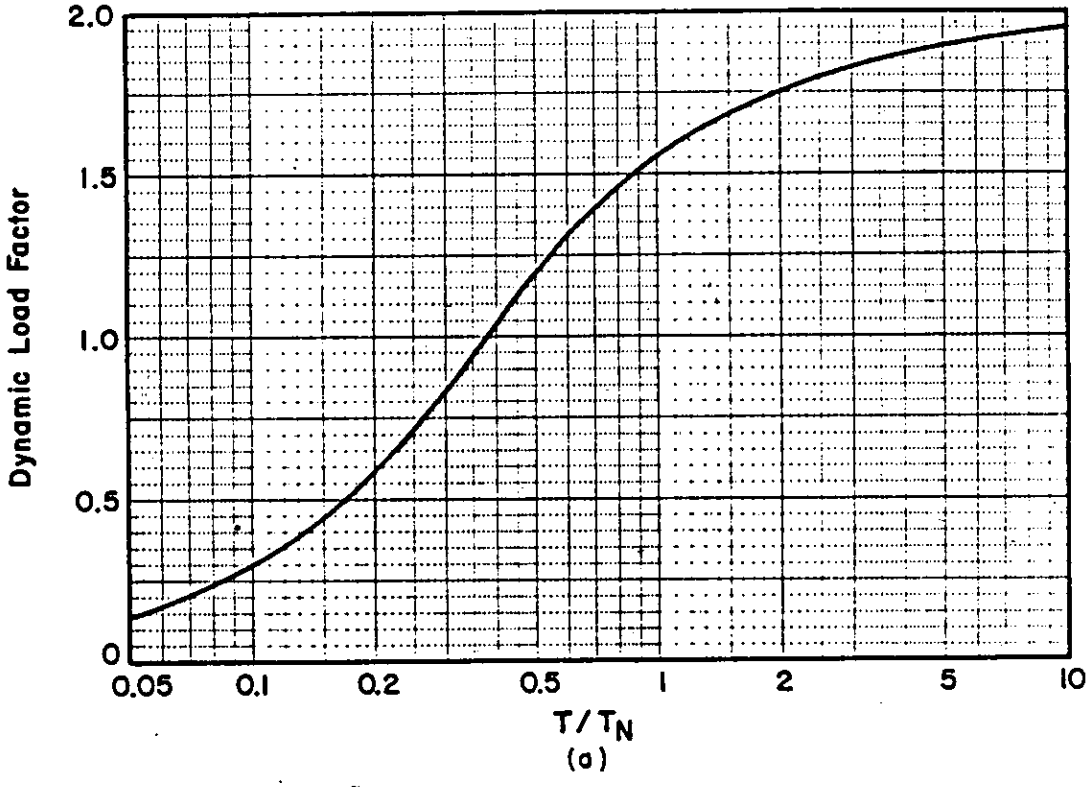


Figure 3-48 A two-degrees-of-freedom system



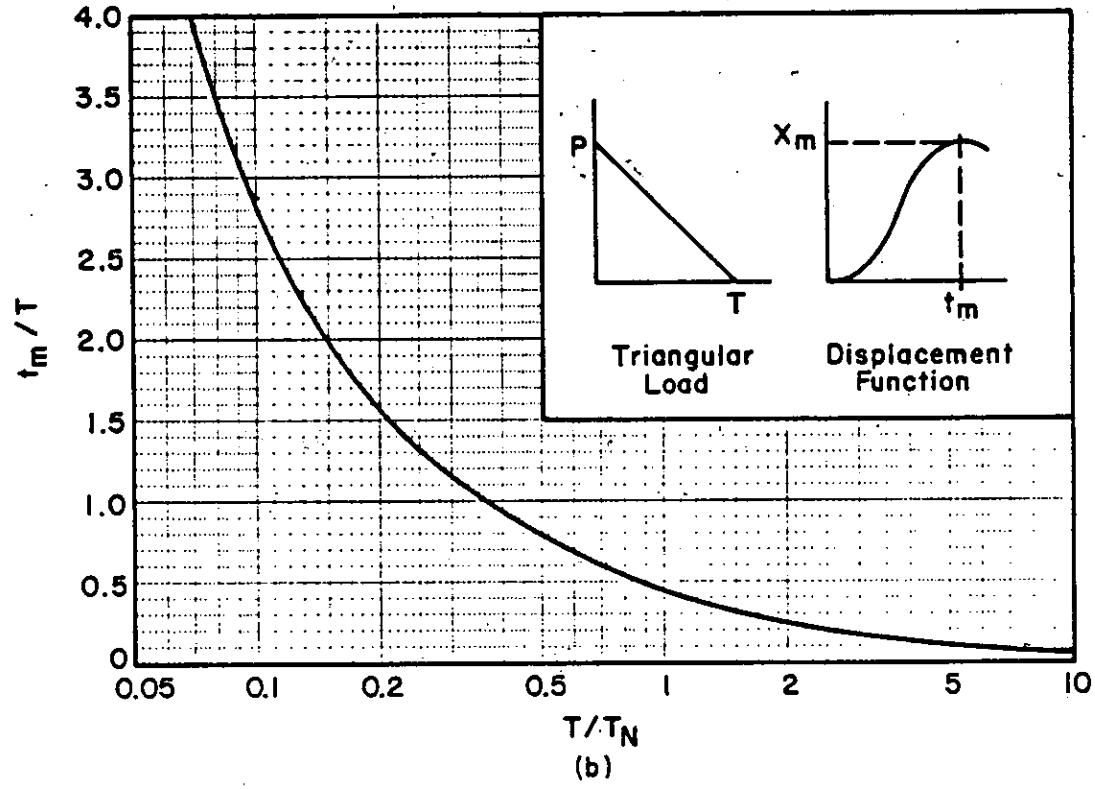


Figure 3-49 Maximum response of elastic one-degree-of-freedom system for triangular load

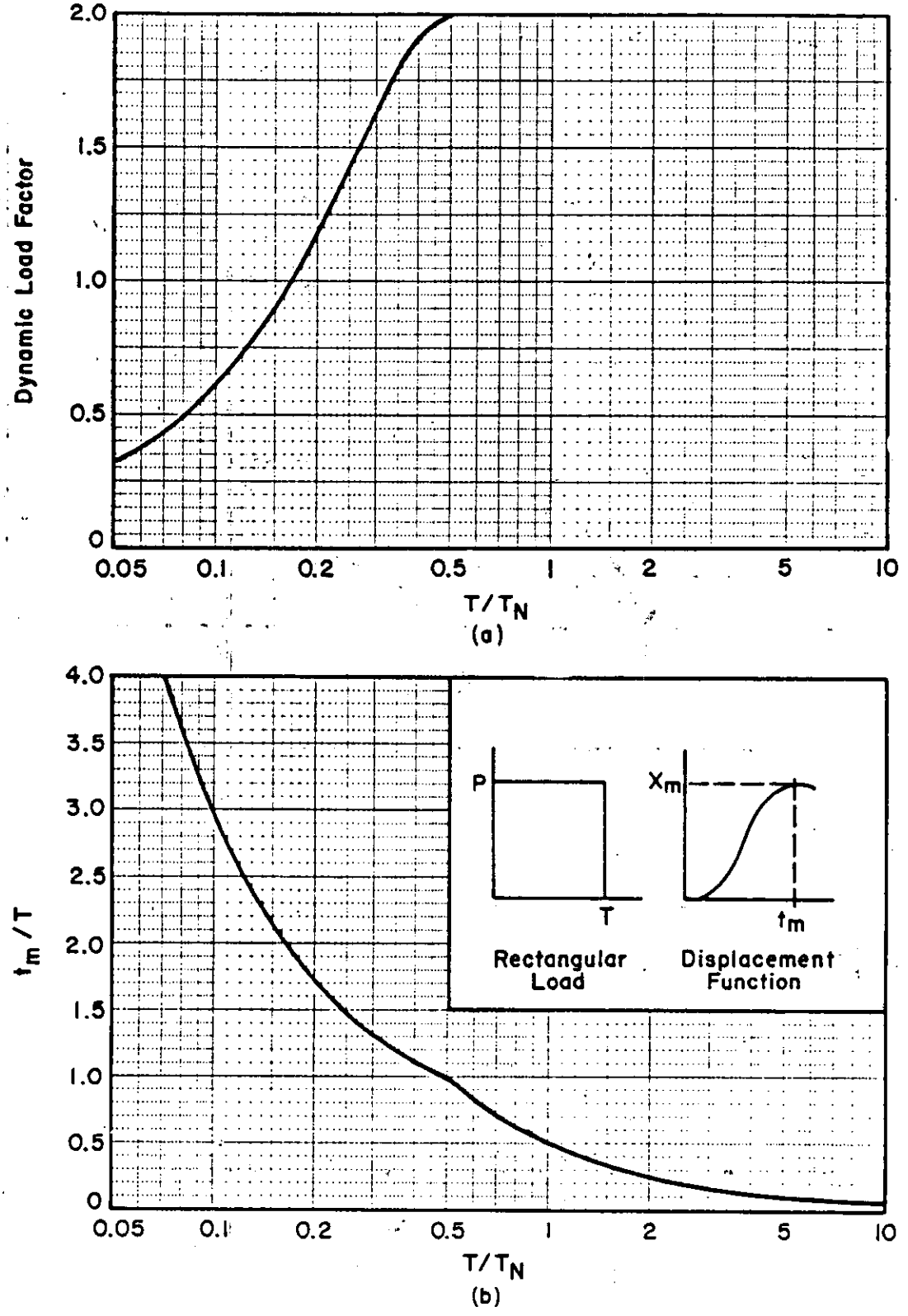


Figure 3-50 Maximum response of elastic, one-degree-of-freedom system for rectangular load

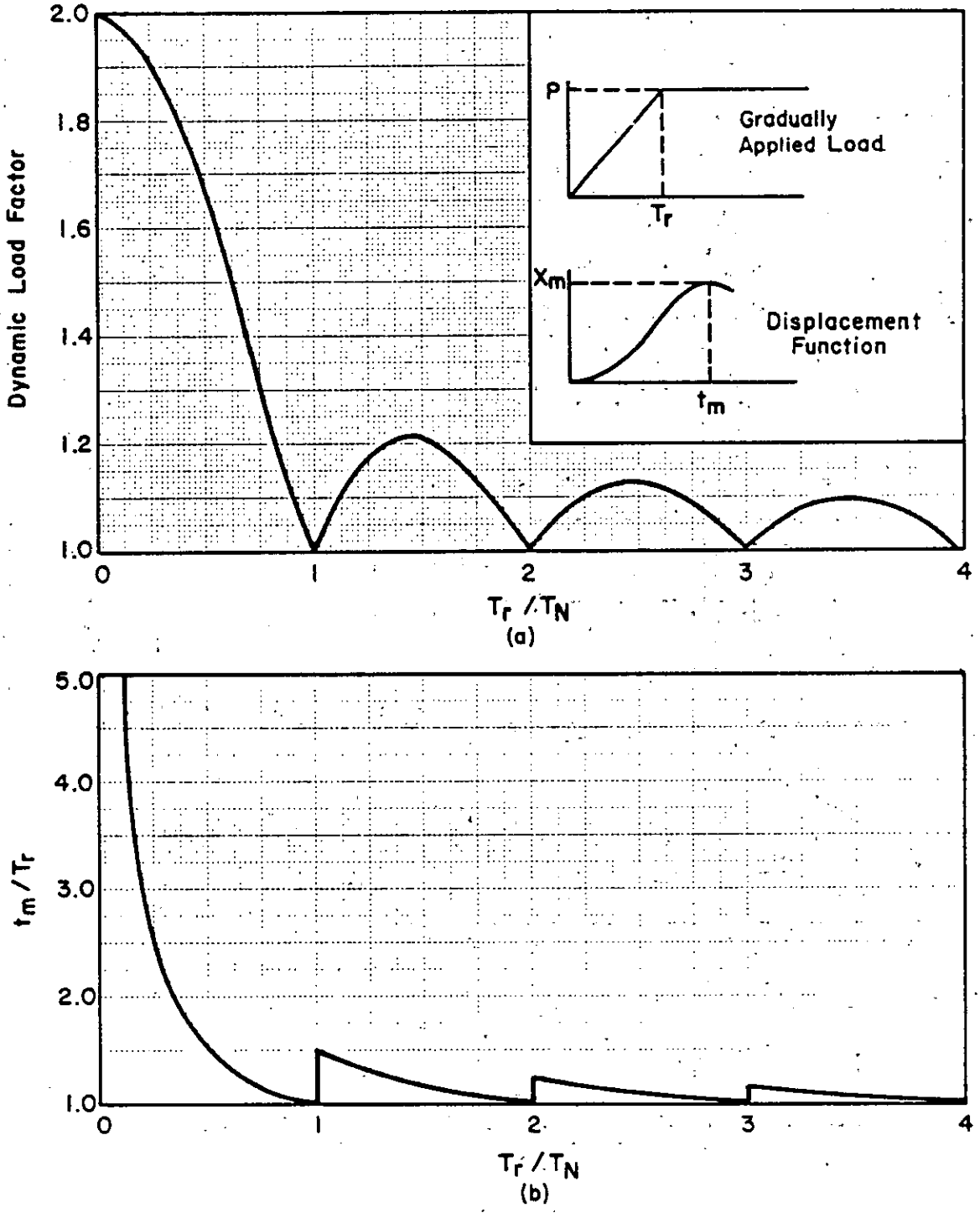


Figure 3-51 Maximum response of elastic, one-degree-of-freedom system for gradually applied load

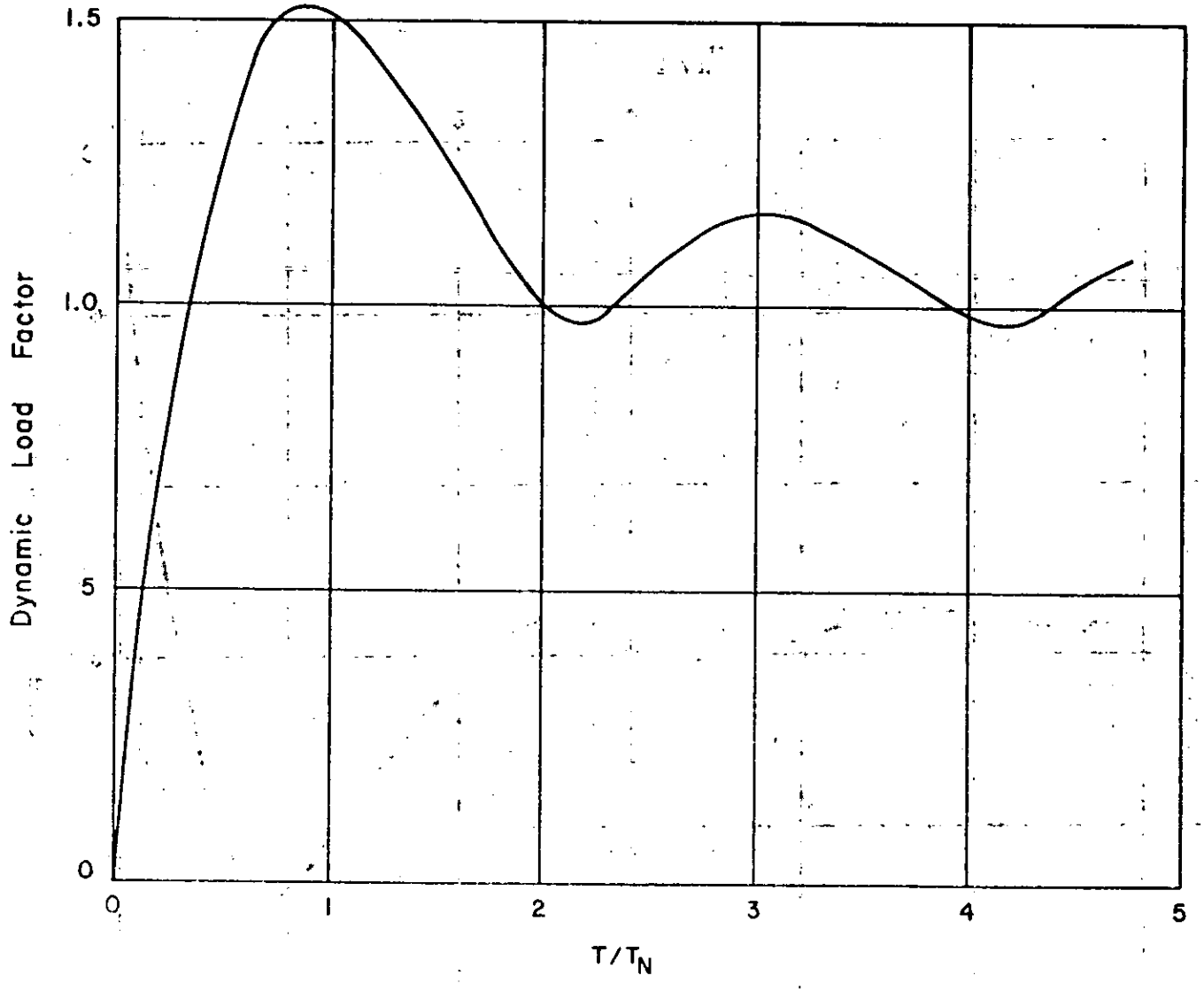


Figure 3-52 Maximum response of elastic one-degree-of-freedom system for triangular pulse load

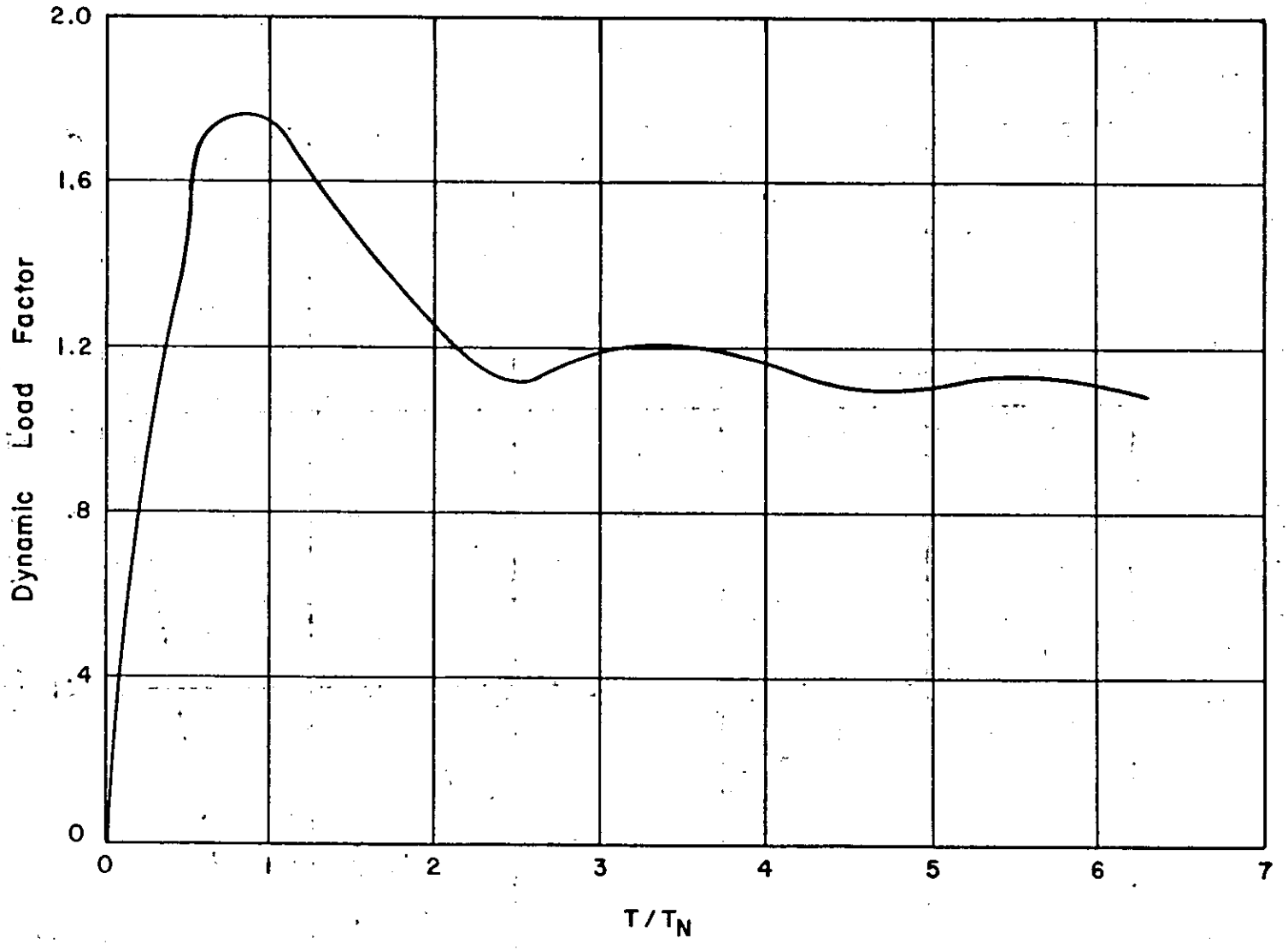


Figure 3-53 Maximum response of elastic one-degree-of-freedom system for sinusoidal pulse load

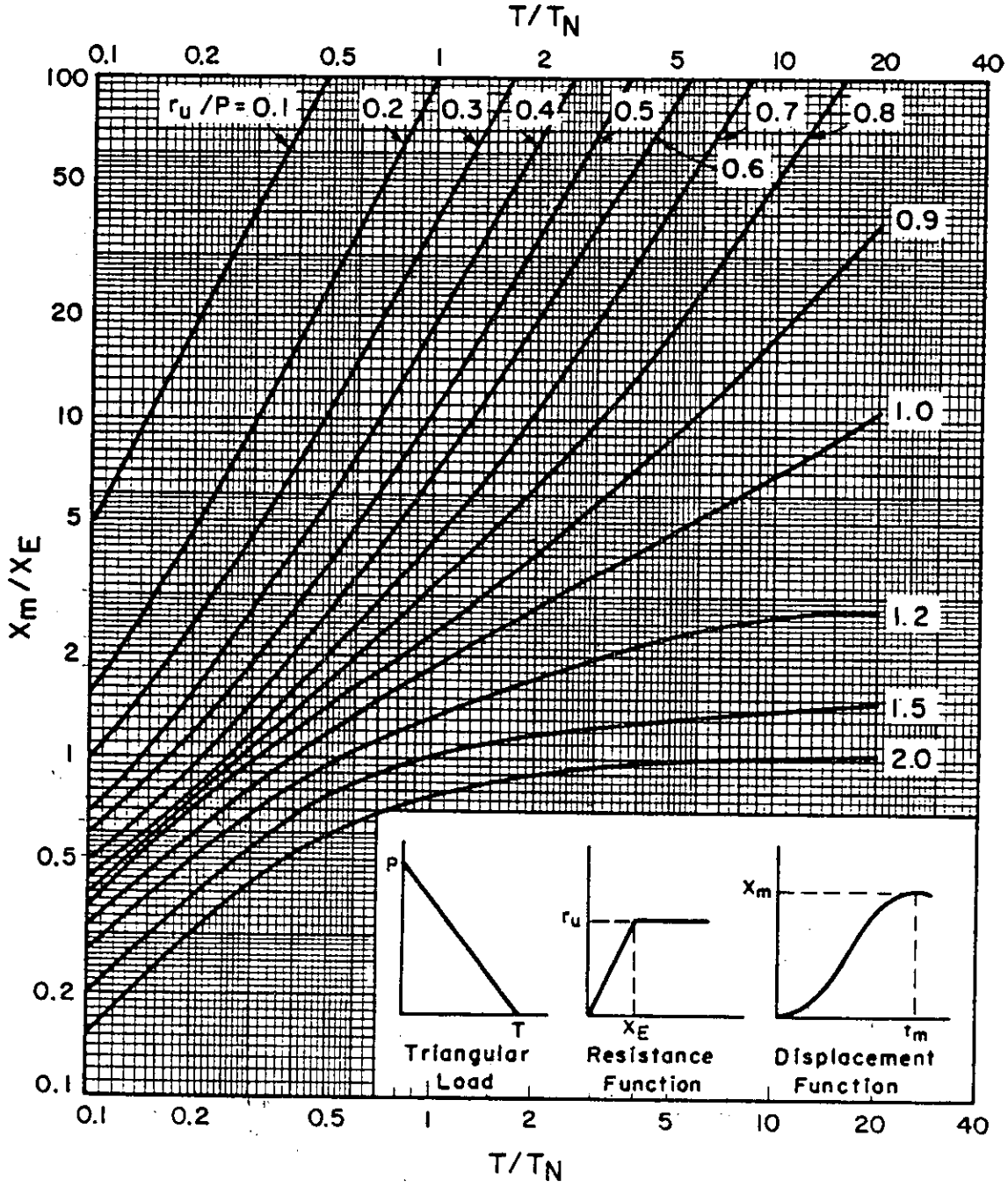


Figure 3-54 Maximum deflection of elasto-plastic, one-degree-of-freedom system for triangular load

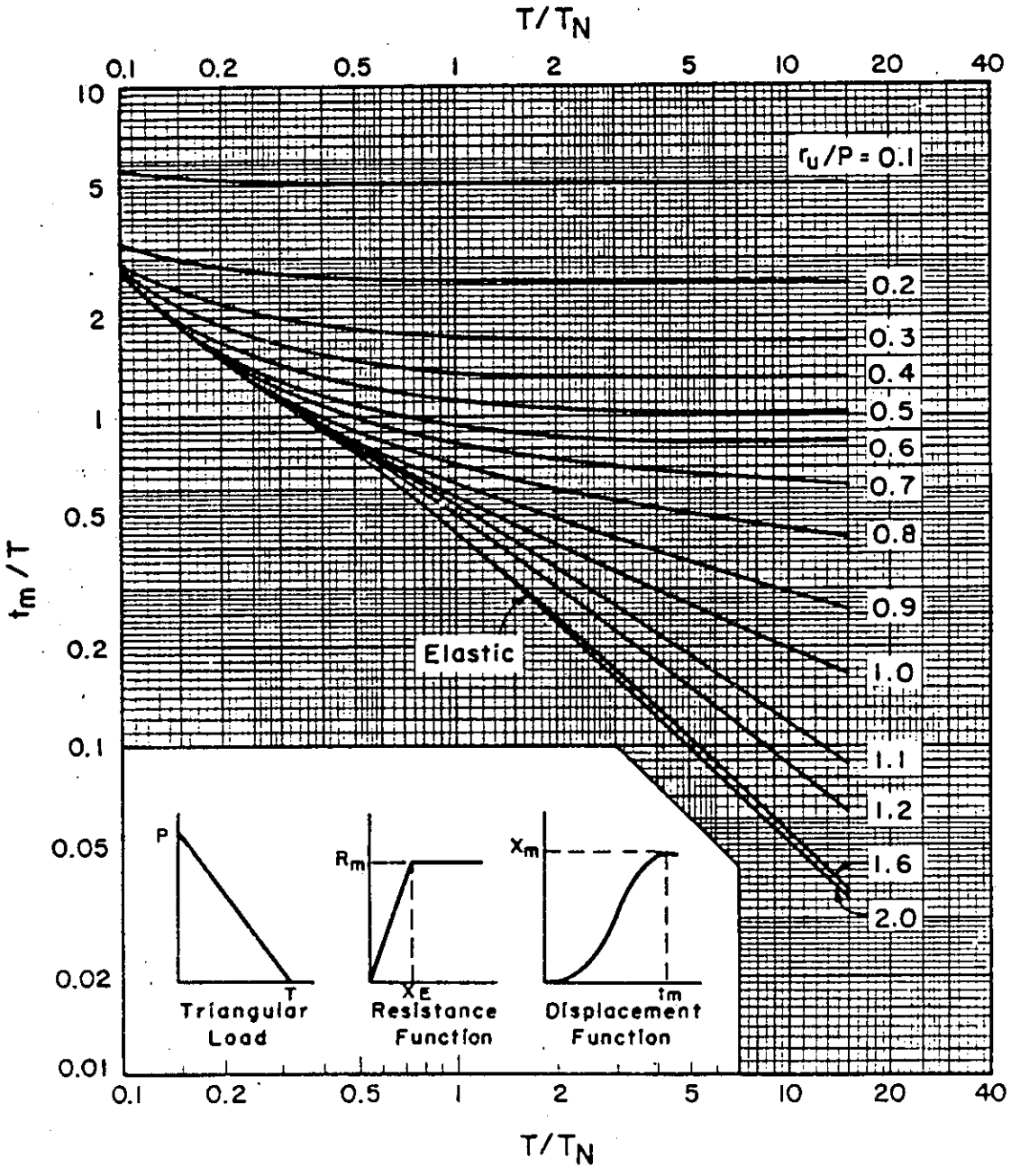


Figure 3-55 Maximum response time of elasto-plastic, one-degree-of-freedom system for triangular load

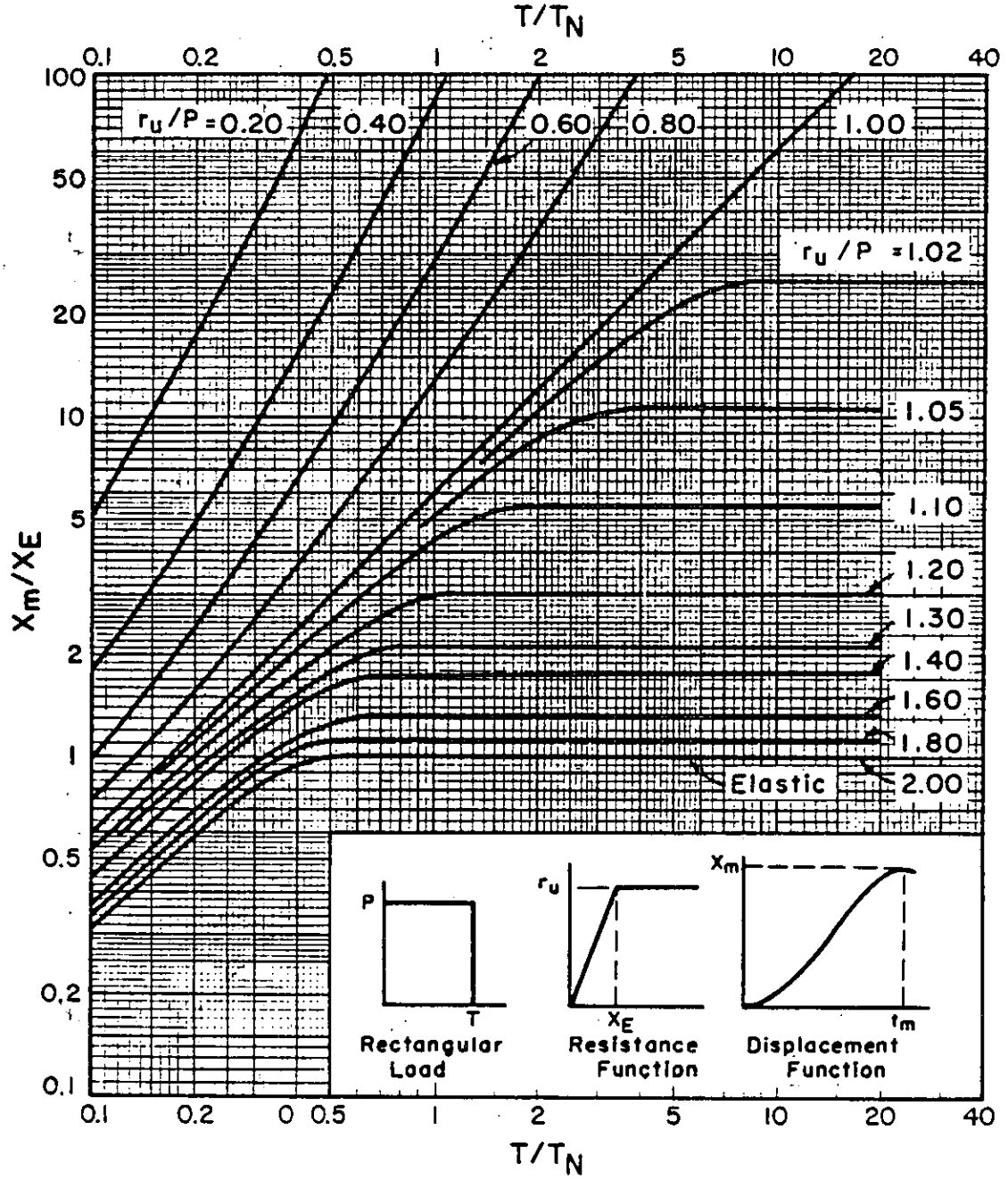


Figure 3-56 Maximum deflection of elasto-plastic, one-degree-of-freedom system for rectangular load

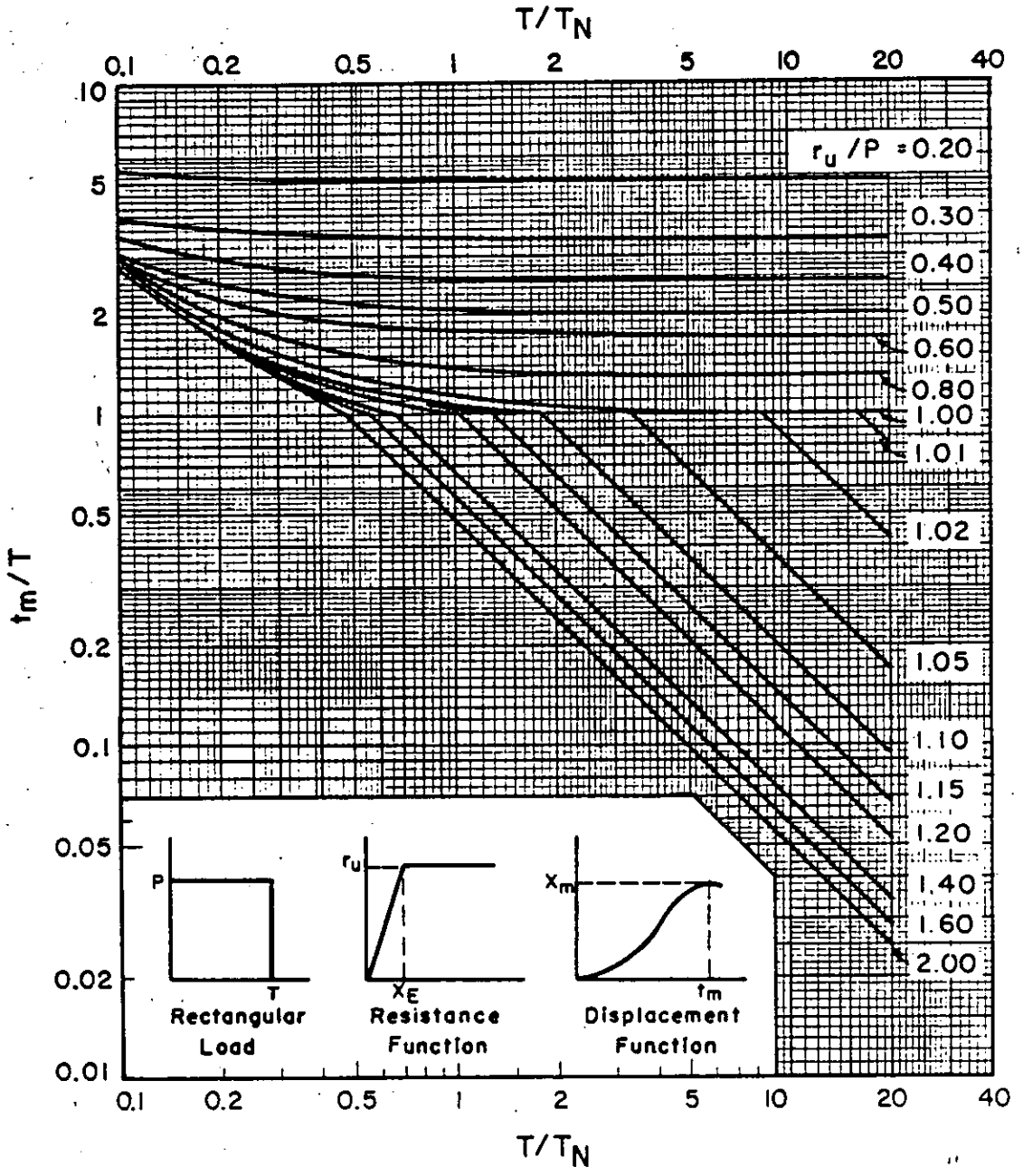


Figure 3-57 Maximum response time of elasto-plastic, one-degree-of-freedom for rectangular load

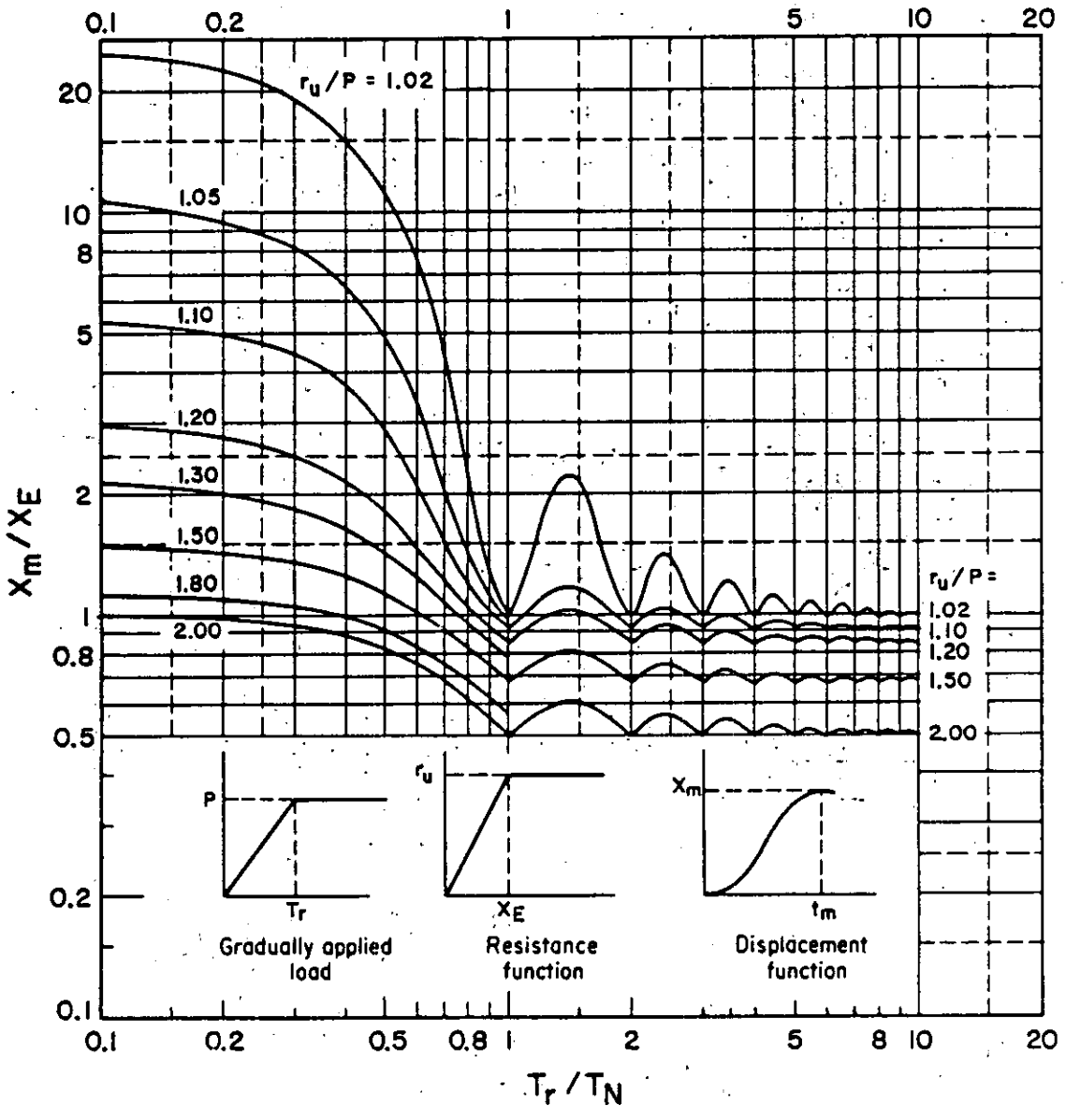


Figure 3-58 Maximum deflection of elasto-plastic, one-degree-of-freedom system for gradually applied load

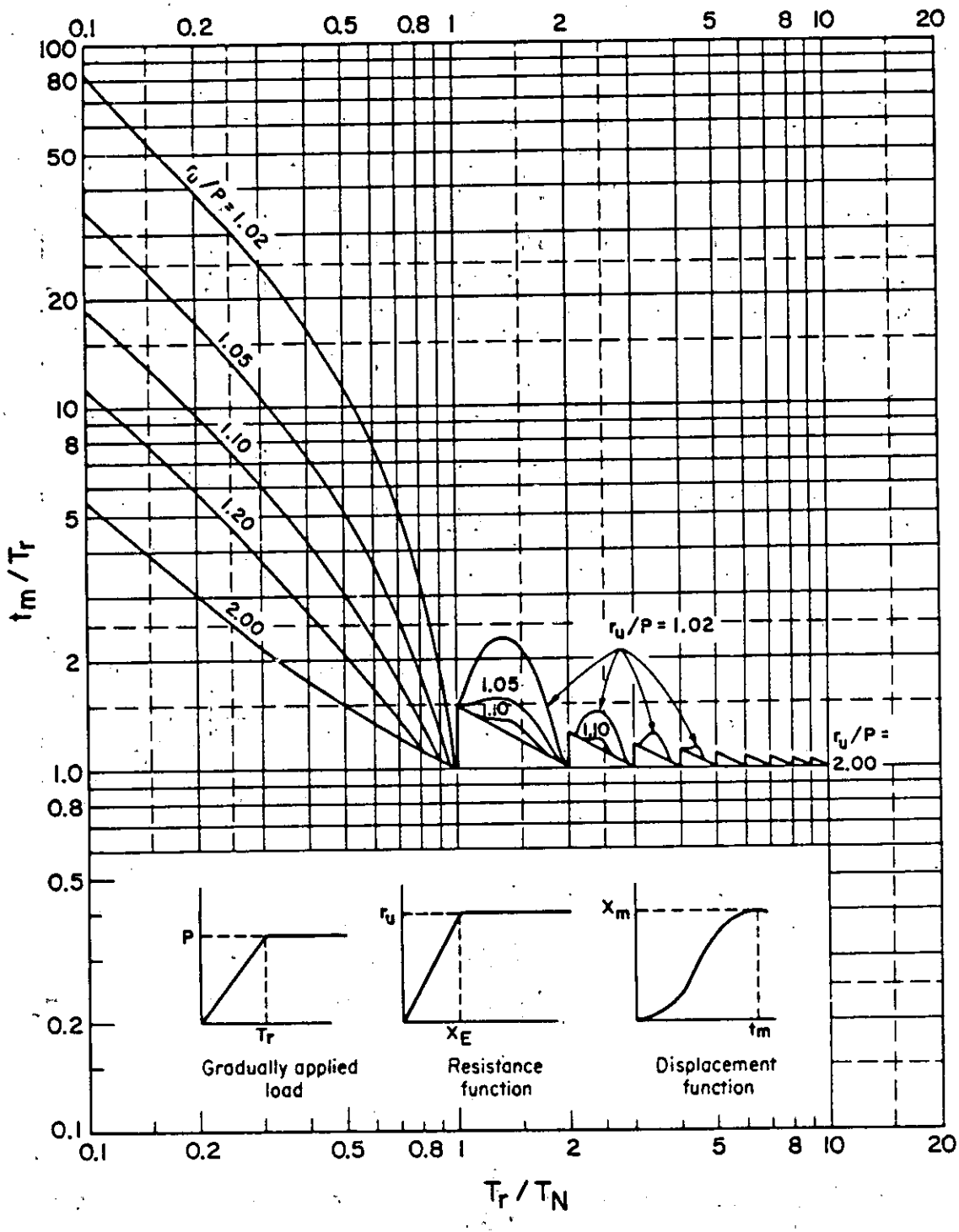


Figure 3-59 Maximum response time of elasto-plastic, one-degree-of-freedom system for gradually applied load

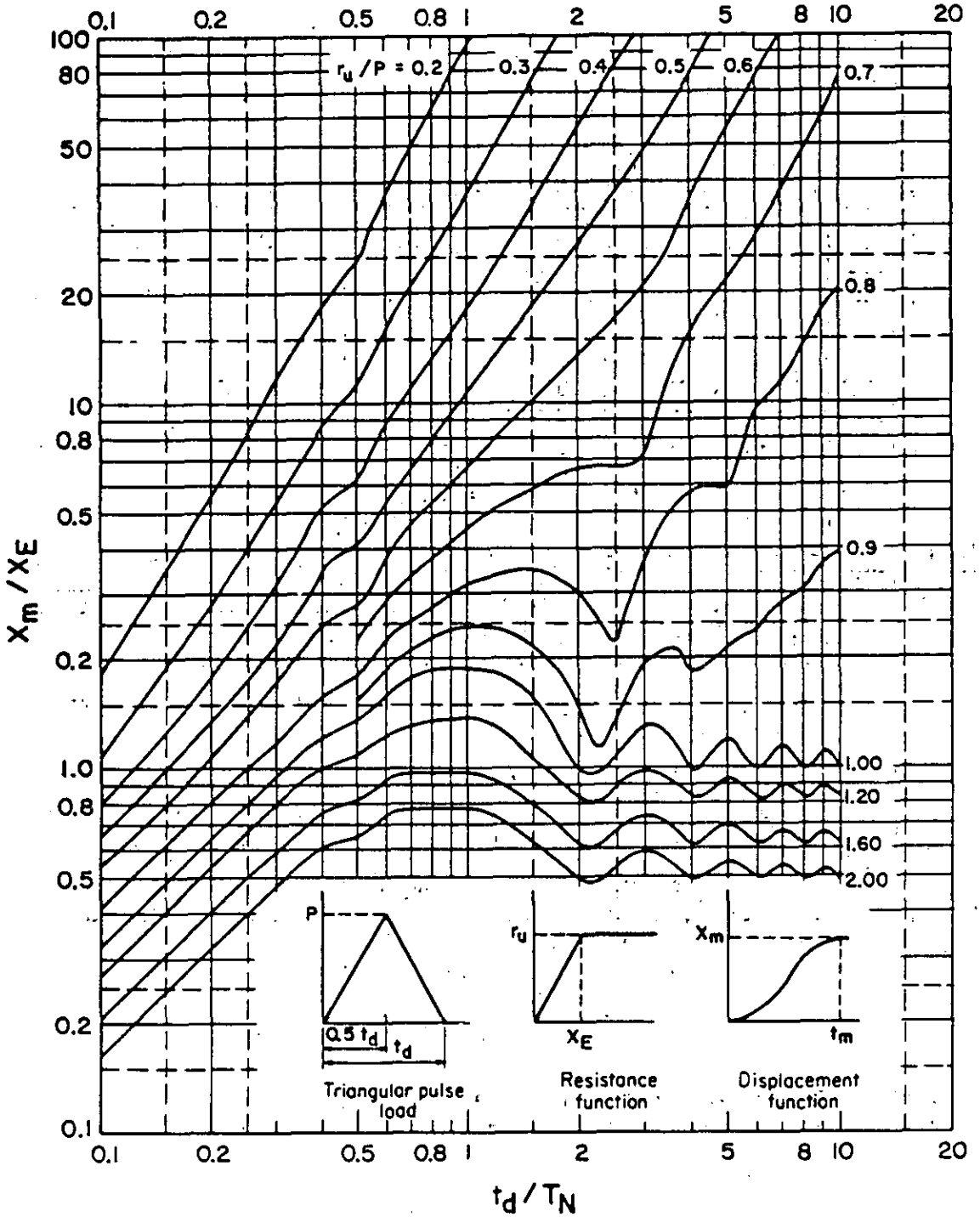


Figure 3-60 Maximum deflection of elasto-plastic, one-degree-of-freedom system for triangular pulse load

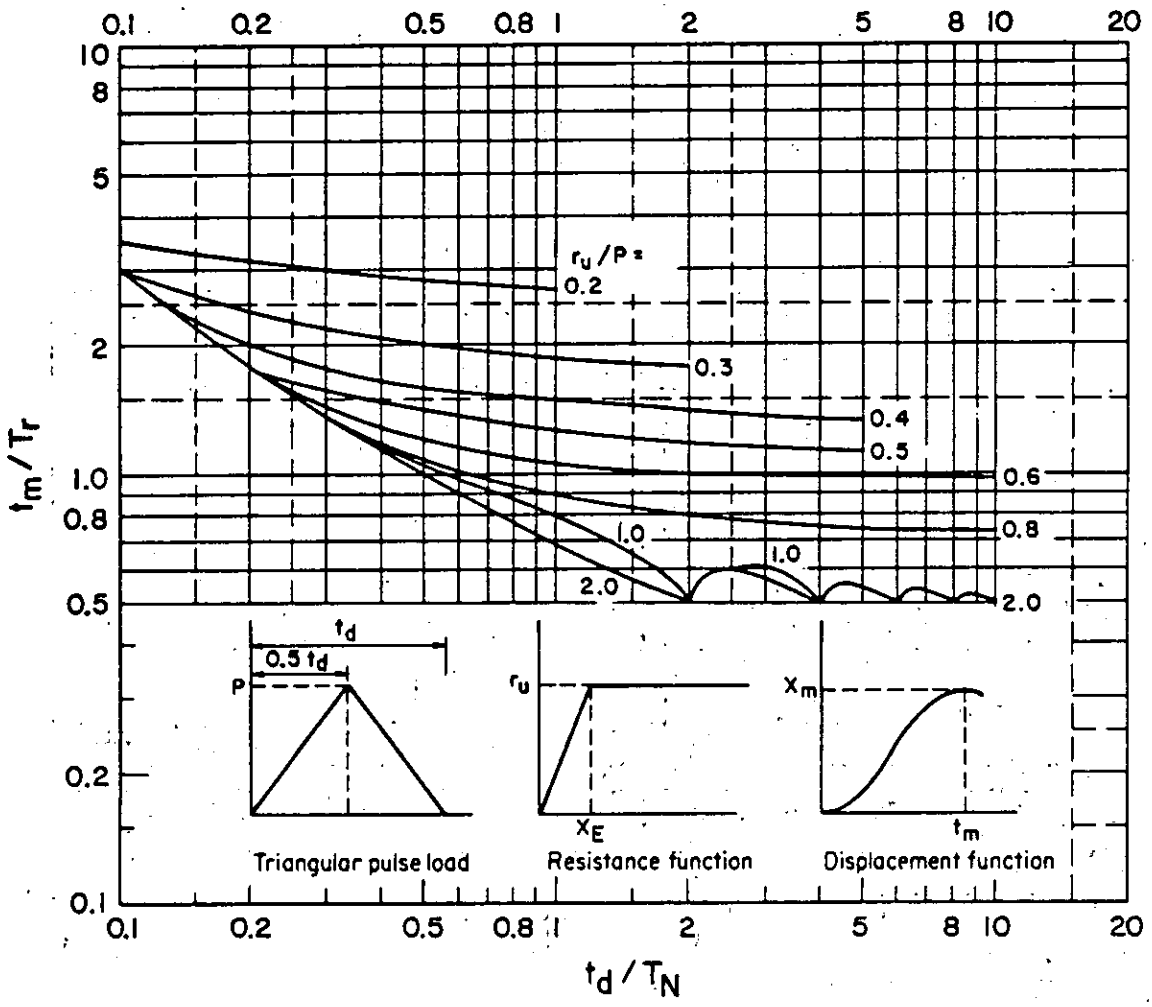
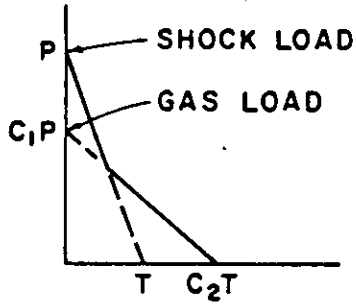
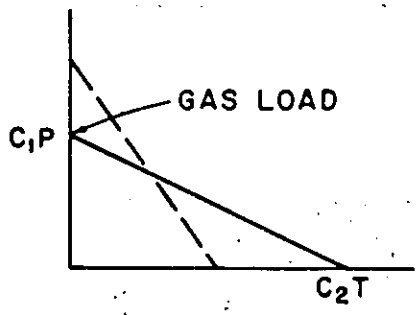


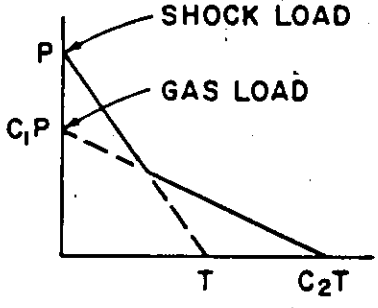
Figure 3-61 Maximum response time of elasto-plastic, one-degree-of-freedom system for triangular pulse load



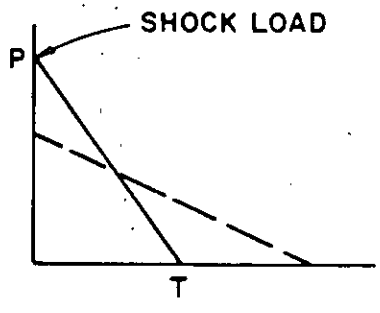
REGION A : NEGLECT CHARTS
USE EQUATIONS 3-80 AND 3-81



REGION B : NEGLECT SHOCK LOAD
USE FIGURE 3-64



REGION C: BOTH SHOCK AND GAS LOADS ARE SIGNIFICANT USE APPROPRIATE FIGURES AND INTERPOLATE.



REGION D : NEGLECT GAS LOAD
USE FIGURE 3-64

Figure 3-62 Various bilinear triangular loads

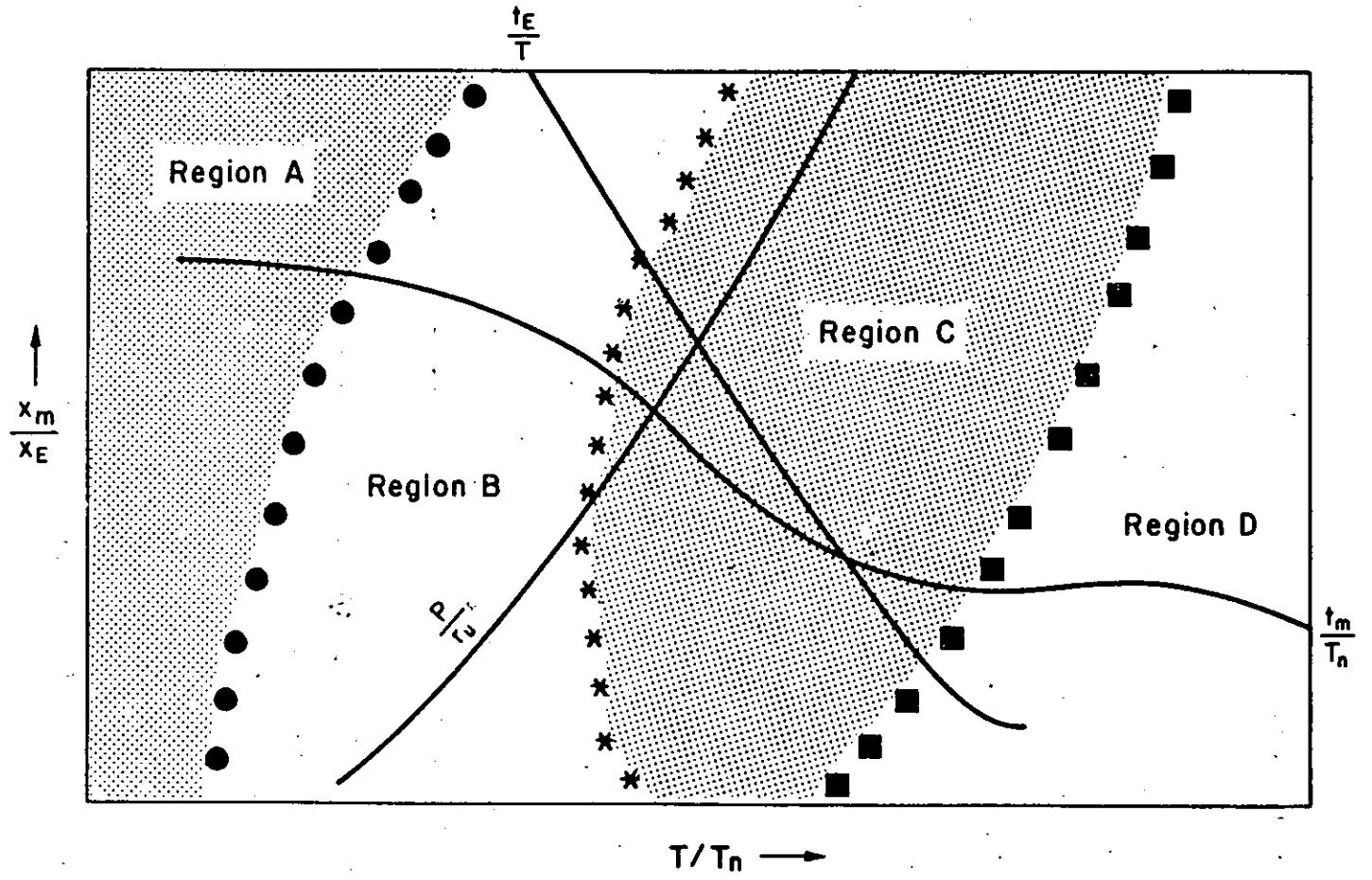


Figure 3-63 Regions of figures 3-64 through 3-266, labeling of axis and curves.

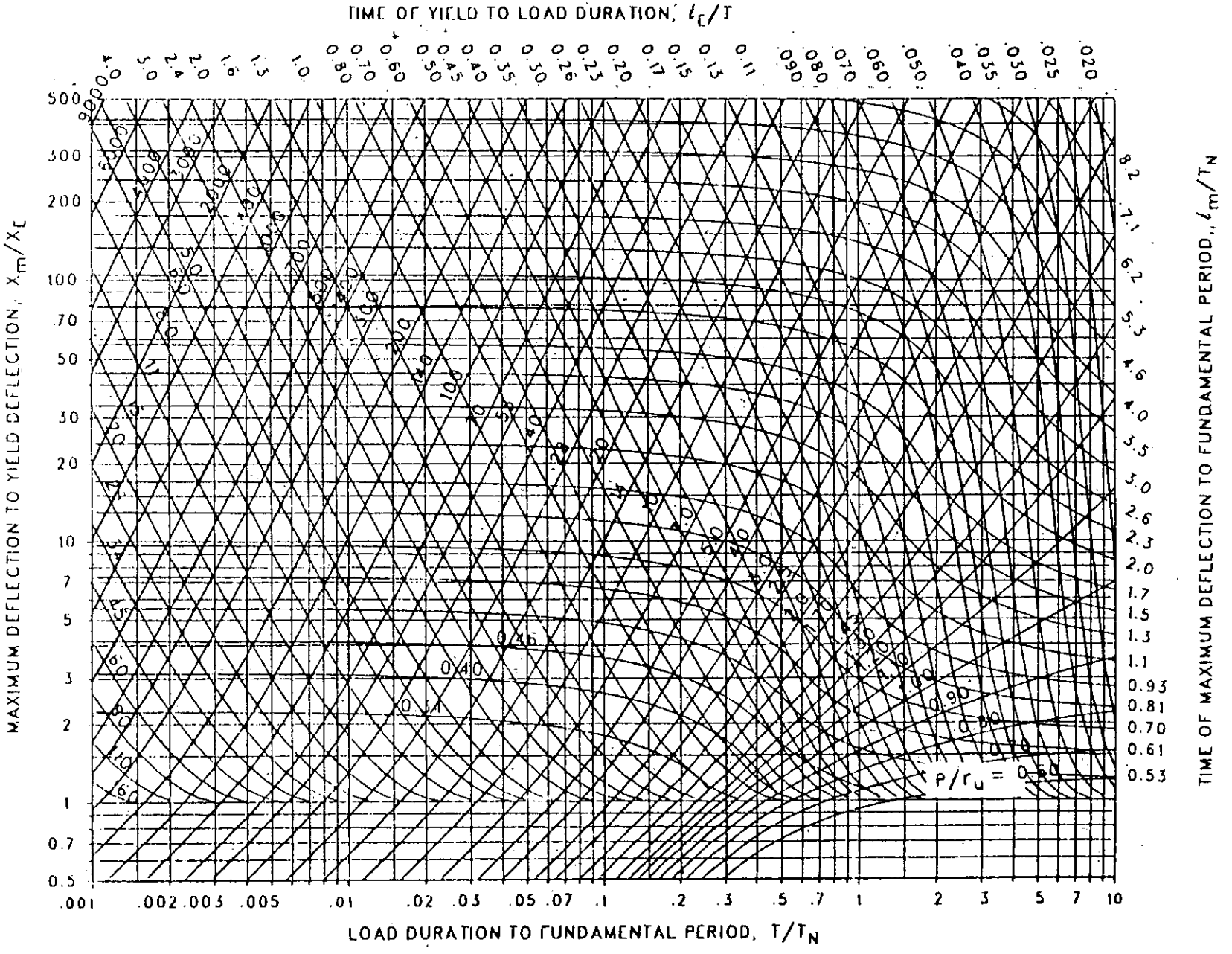


Figure 3-64a Maximum response of elasto-plastic, one-degree-of-freedom system for bilinear-triangular pulse (C_1 = 1.000, C_2 = 1.0)

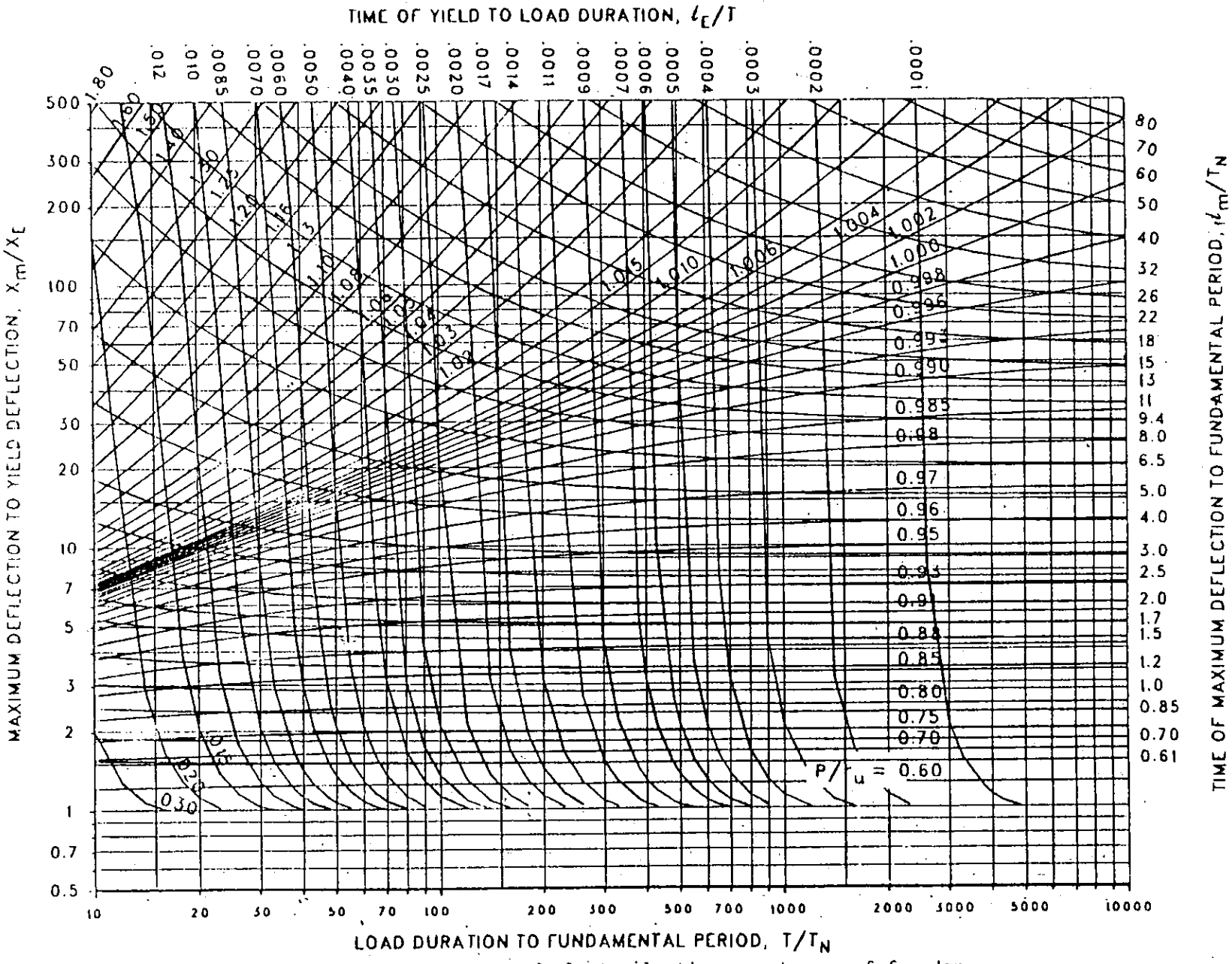


Figure 3-64b Maximum response of elasto-plastic, one-degree-of-freedom system for bilinear-triangular pulse (C_1 = 1.000, C_2 = 1.0) (cont.)

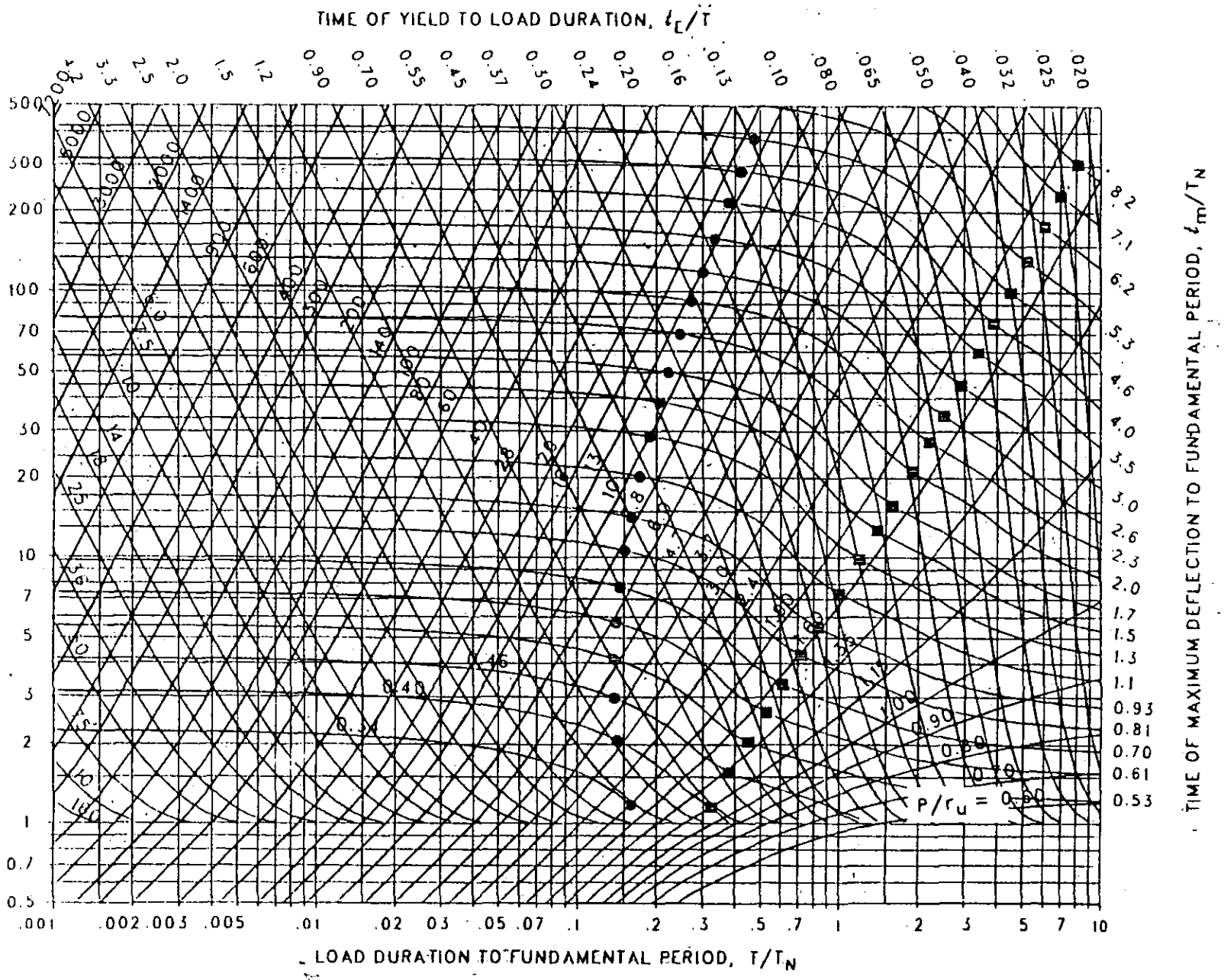


Figure 3-65 Maximum response of elasto-plastic, one-degree-of-freedom system for bilinear-triangular pulse ($C_1 = 0.681$, $C_2 = 1.7$)

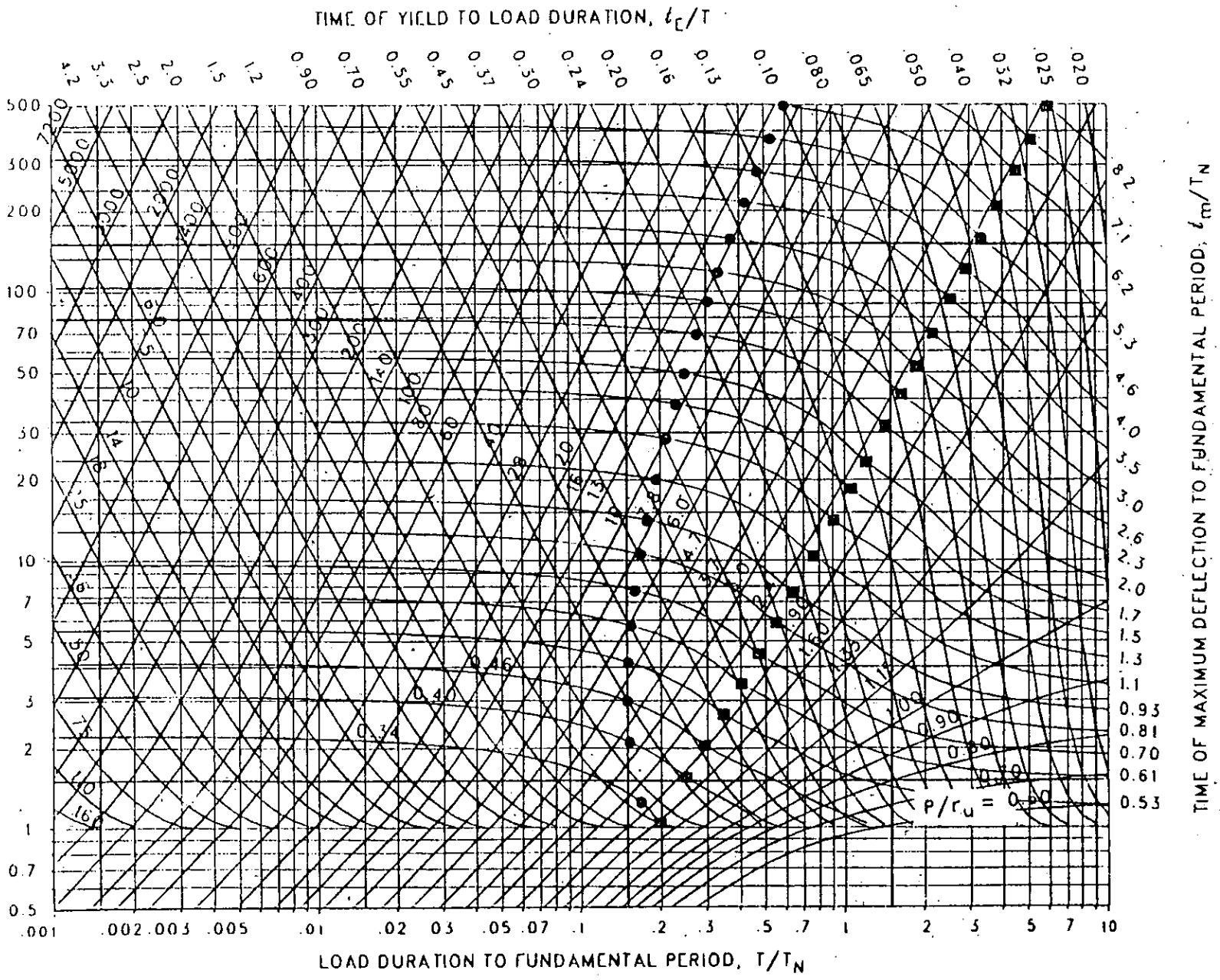


Figure 3-66 Maximum response of elasto-plastic, one-degree-of-freedom system for bilinear-triangular pulse ($C_1 = 0.464$, $C_2 = 1.7$)

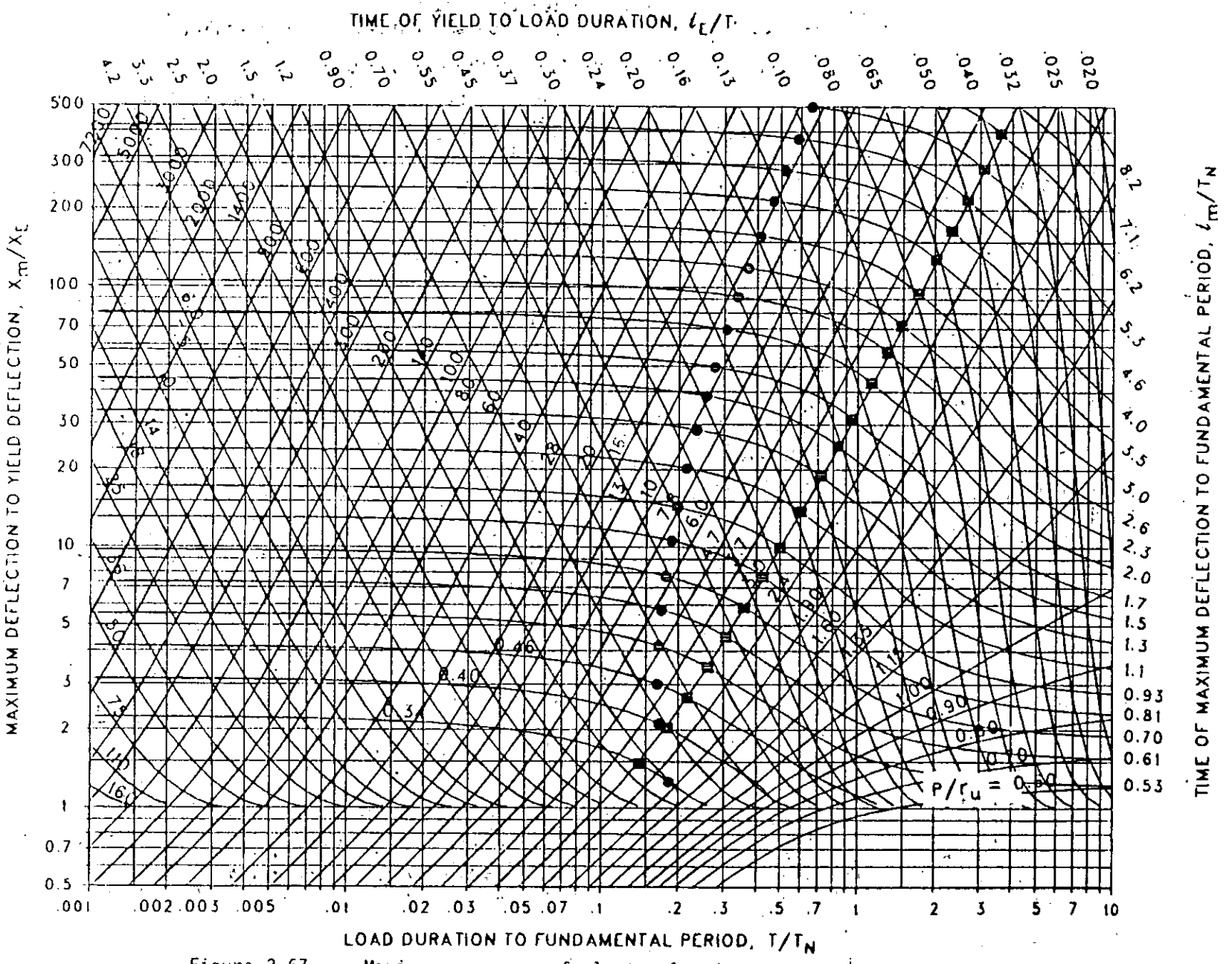


Figure 3-67 Maximum response of elasto-plastic, one-degree-of-freedom system for bilinear-triangular pulse ($C_1 = 0.316$, $C_2 = 1.7$)

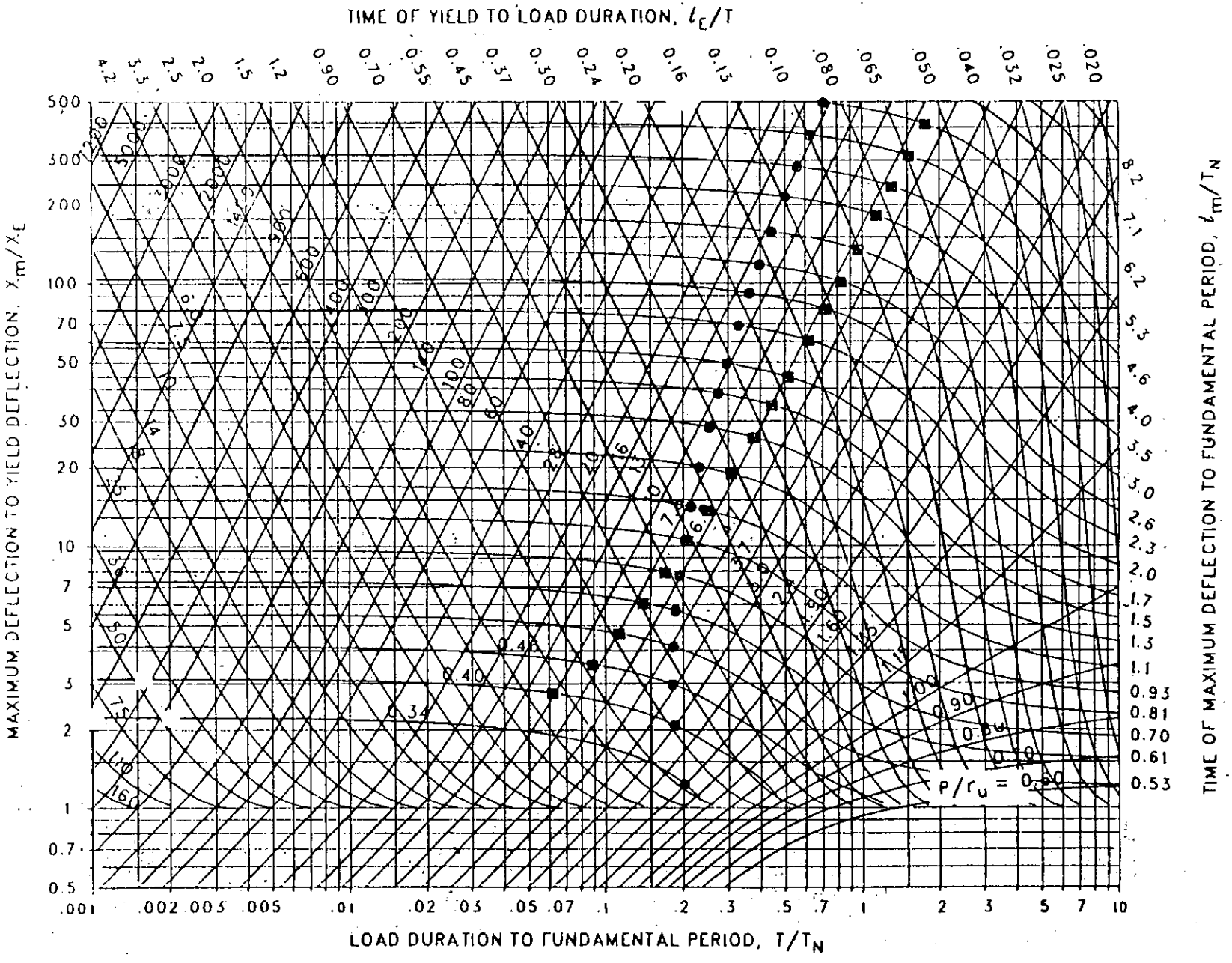


Figure 3-68 Maximum response of elasto-plastic, one-degree-of-freedom system for bilinear-triangular pulse ($C_1 = 1.215$, $C_2 = 1.7$)

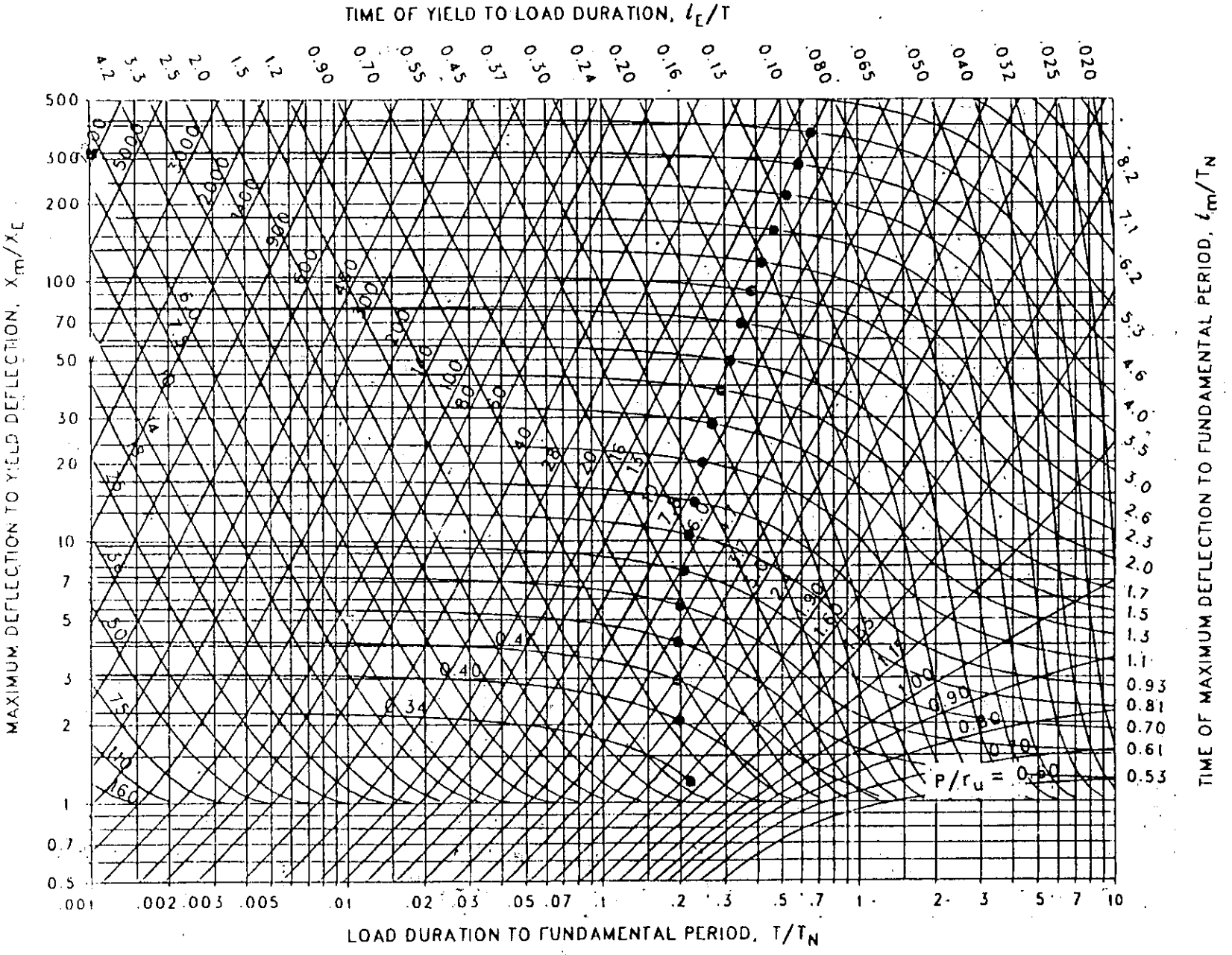


Figure 3-69 Maximum response of elasto-plastic, one-degree-of-freedom system for bilinear-triangular pulse (C_1 = 0.147, C_2 = 1.7)

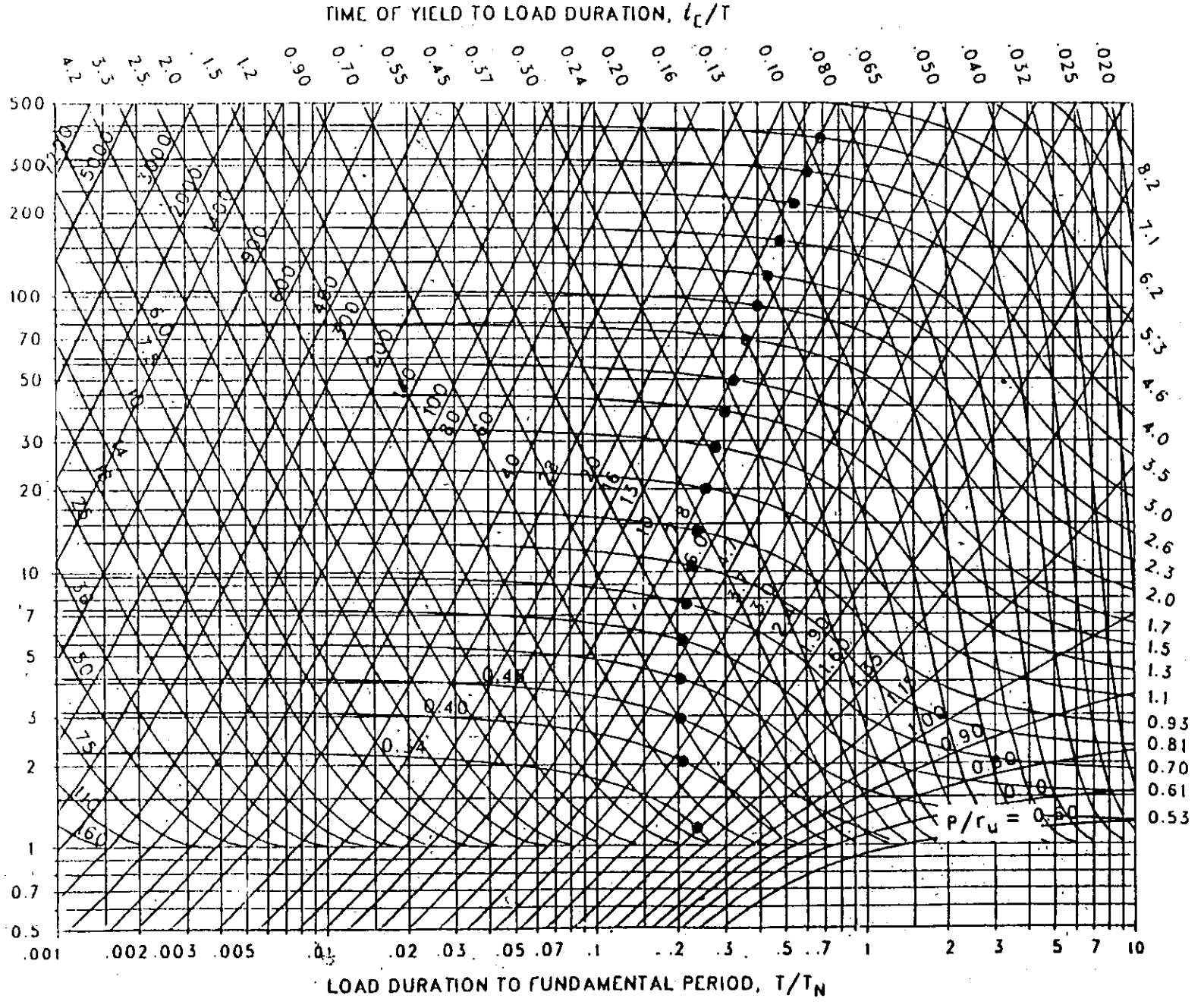


Figure 3-70 Maximum response of elasto-plastic, one-degree-of-freedom system for bilinear-triangular pulse ($C_1 = 0.100$, $C_2 = 1.7$)

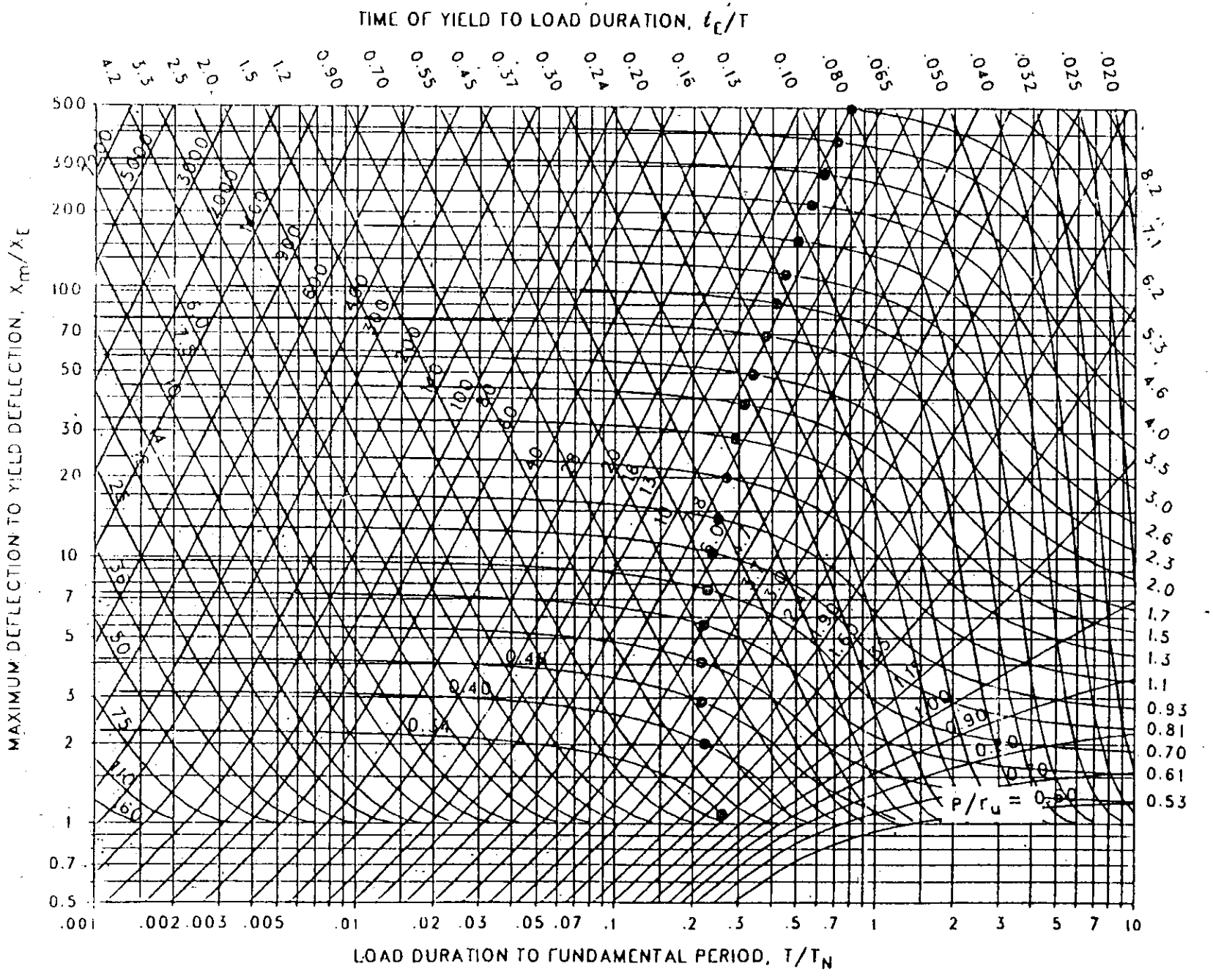


Figure 3-71 Maximum response of elasto-plastic, one-degree-of-freedom system for bilinear-triangular pulse ($C_1 = 0.056$, $C_2 = 1.7$)

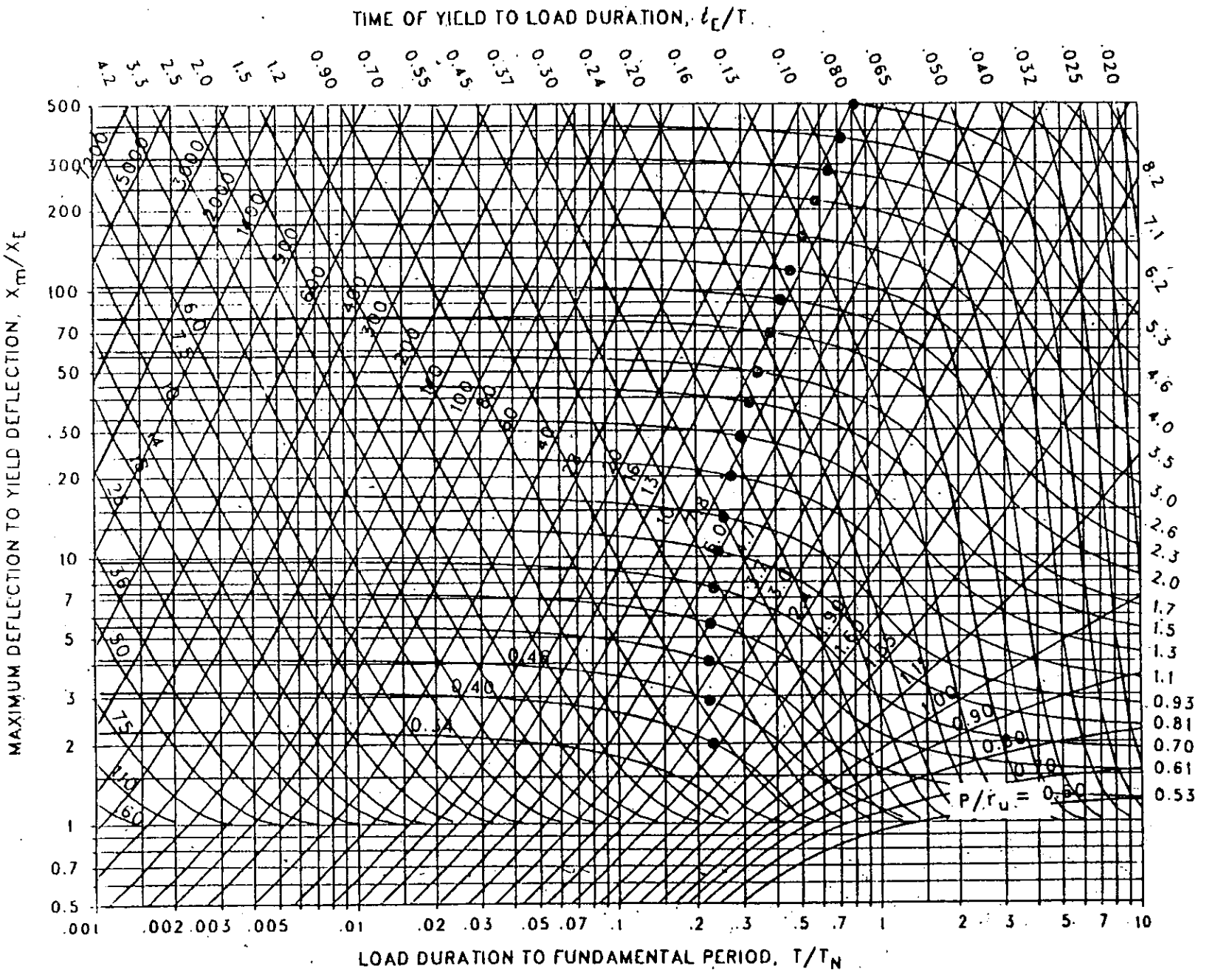


Figure 3-72 Maximum response of elasto-plastic, one-degree-of-freedom system for bilinear-triangular pulse (C_1 = 0.032, C_2 = 1.7)

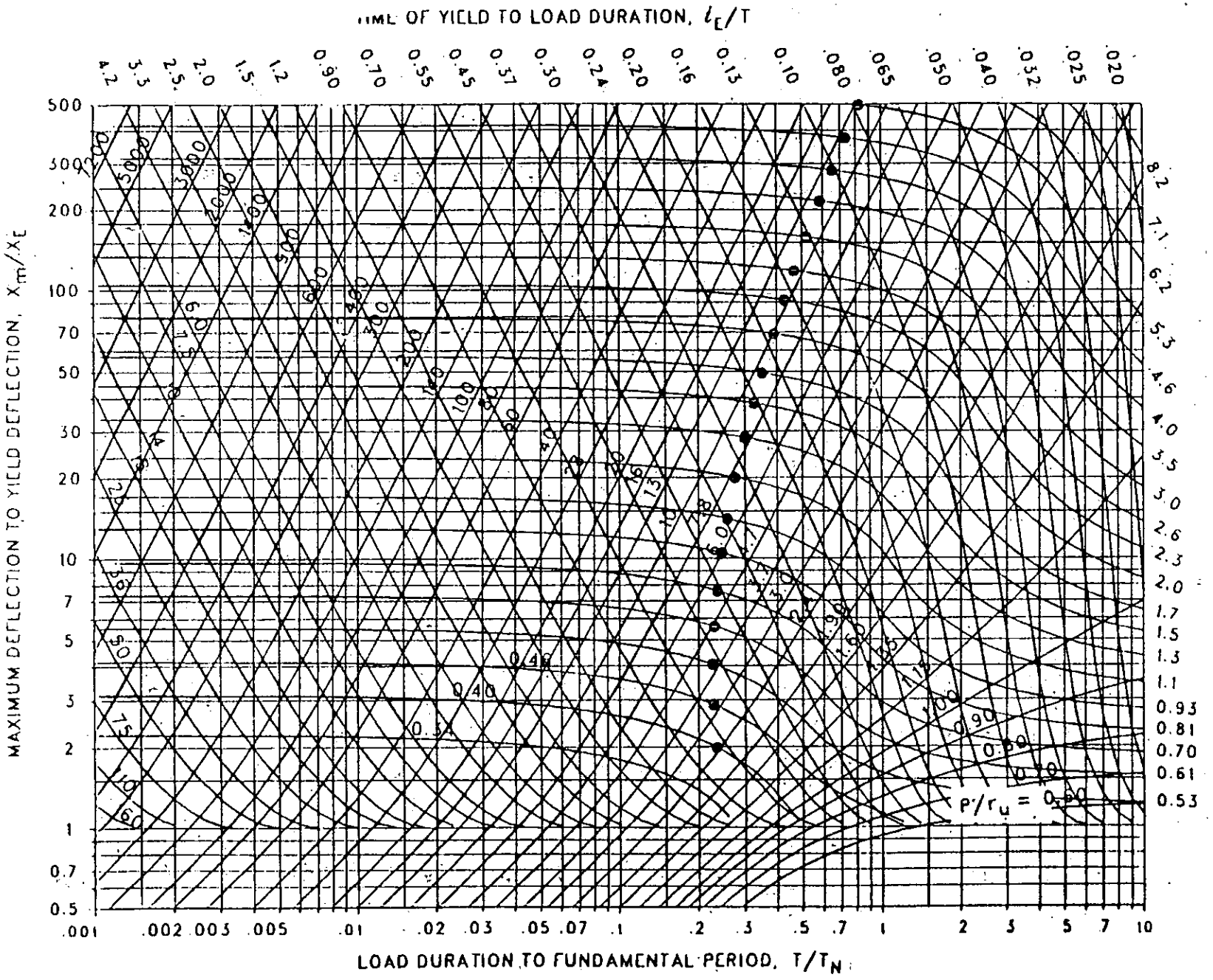


Figure 3-73 Maximum response of elasto-plastic, one-degree-of-freedom system for bilinear-triangular pulse ($C_1 = 0.018$, $C_2 = 1.7$)

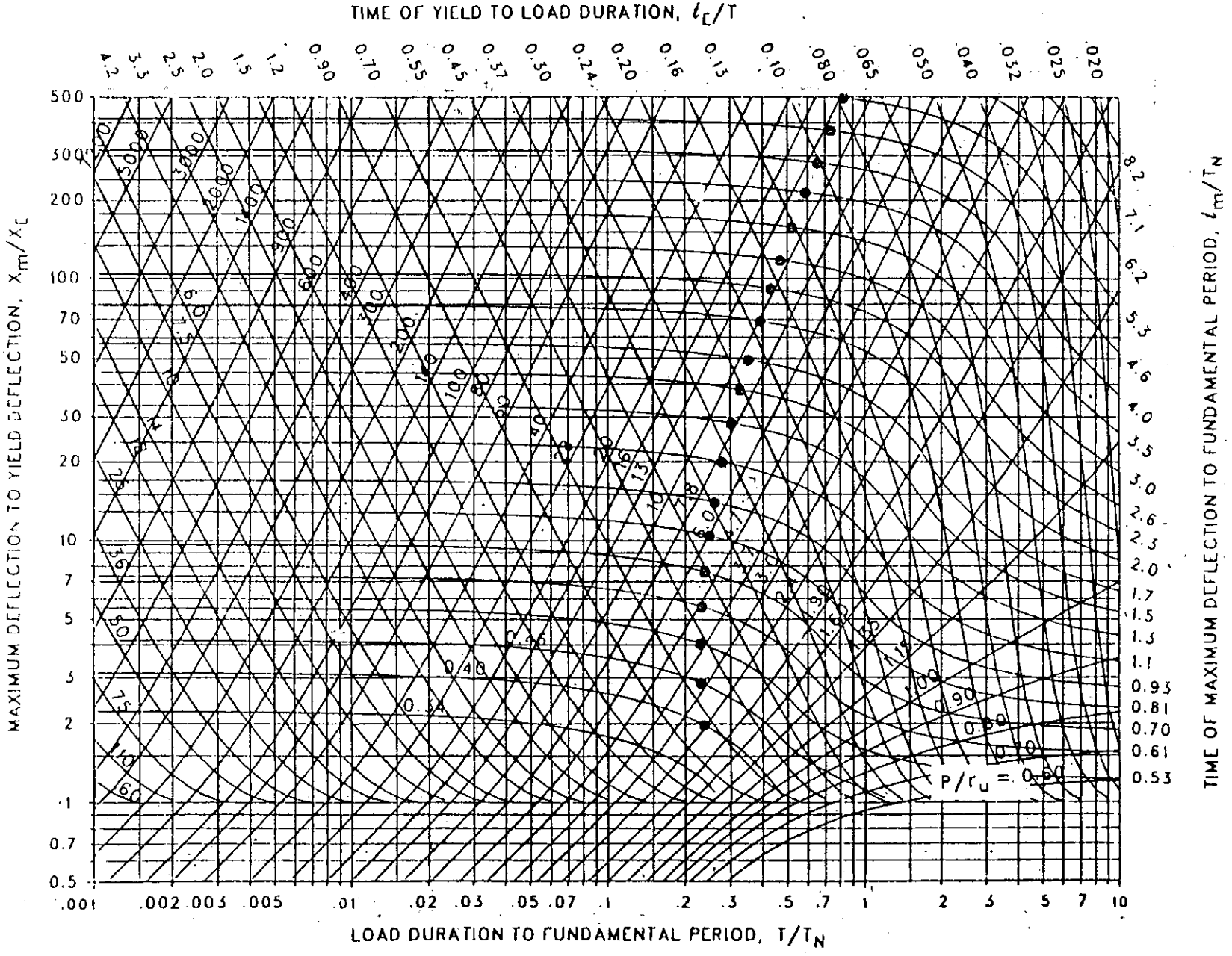


Figure 3-74 Maximum response of elasto-plastic, one-degree-of-freedom system for bilinear-triangular pulse ($C_1 = 0.010$, $C_2 = 1.7$)

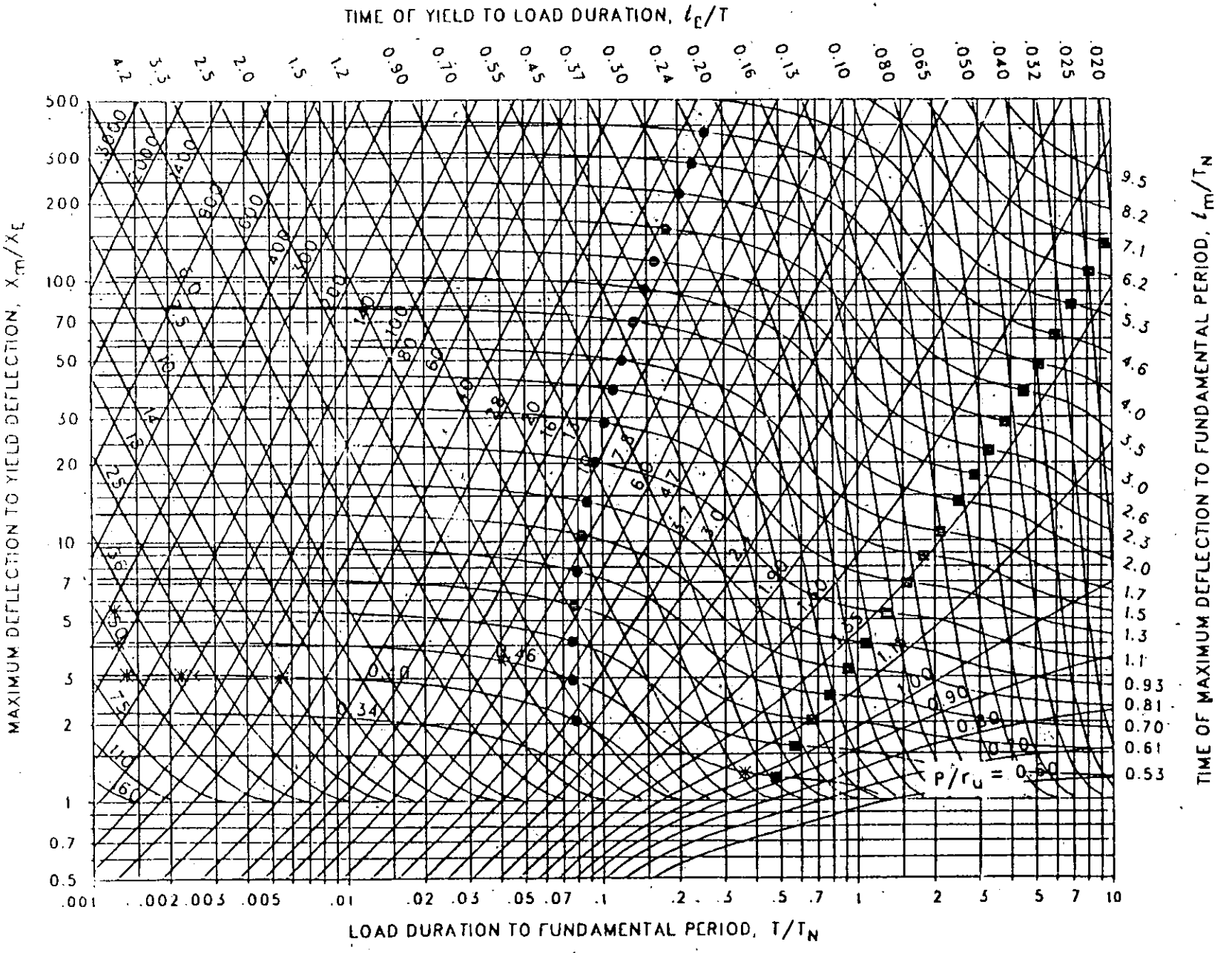


Figure 3-75 Maximum response of elasto-plastic, one-degree-of-freedom system for bilinear-triangular pulse ($C_1 = 0.681$, $C_2 = 3.0$)

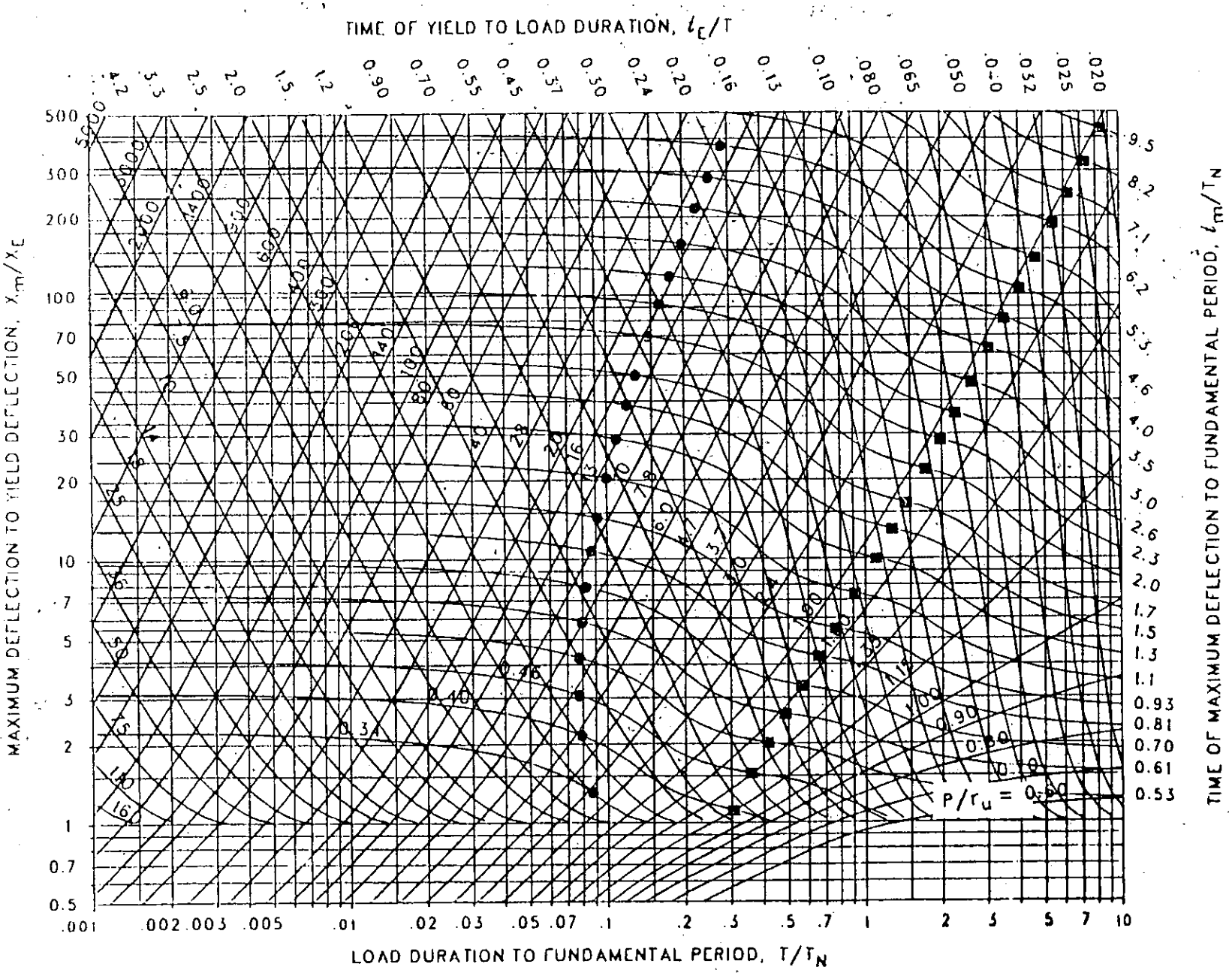


Figure 3-76 Maximum response of elasto-plastic, one-degree-of-freedom system for bilinear-triangular pulse ($C_1 = 0.464$, $C_2 = 3.0$)

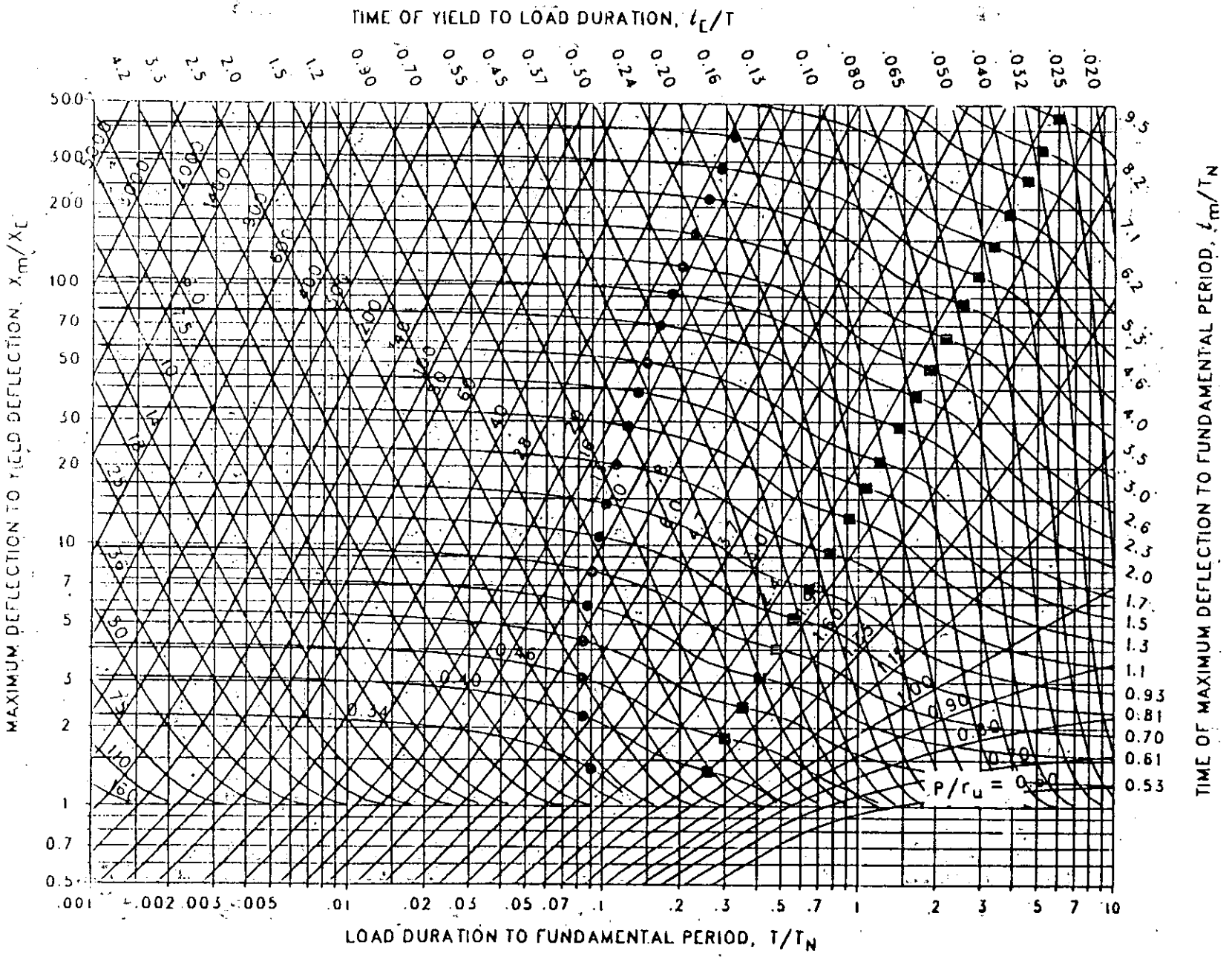


Figure 3-77 Maximum response of elasto-plastic, one-degree-of-freedom system for bilinear-triangular pulse ($C_1 = 0.316$, $C_2 = 3.0$)

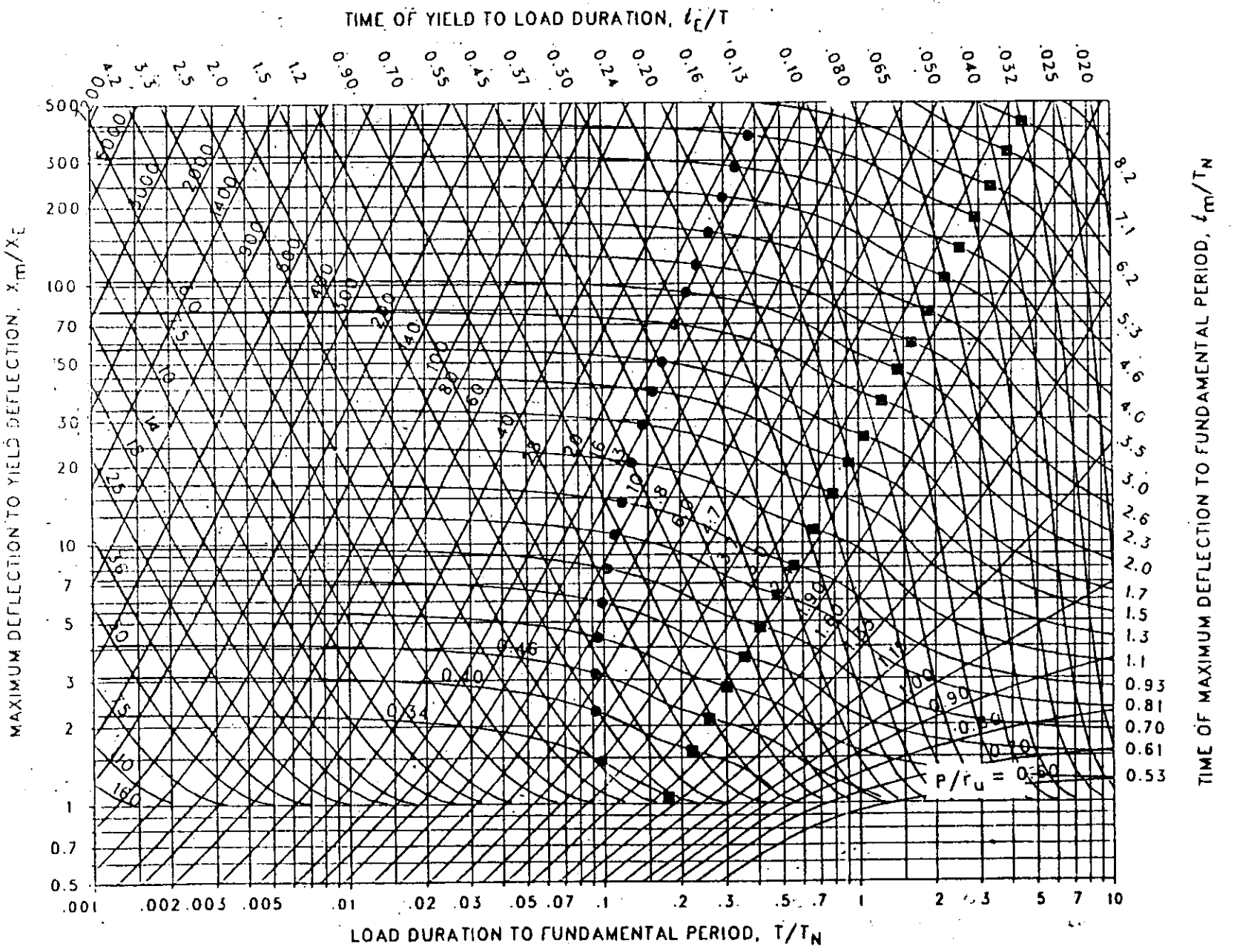


Figure 3-78 Maximum response of elasto-plastic, one-degree-of-freedom system for bilinear-triangular pulse ($C_1 = 1.215$, $C_2 = 3.0$)

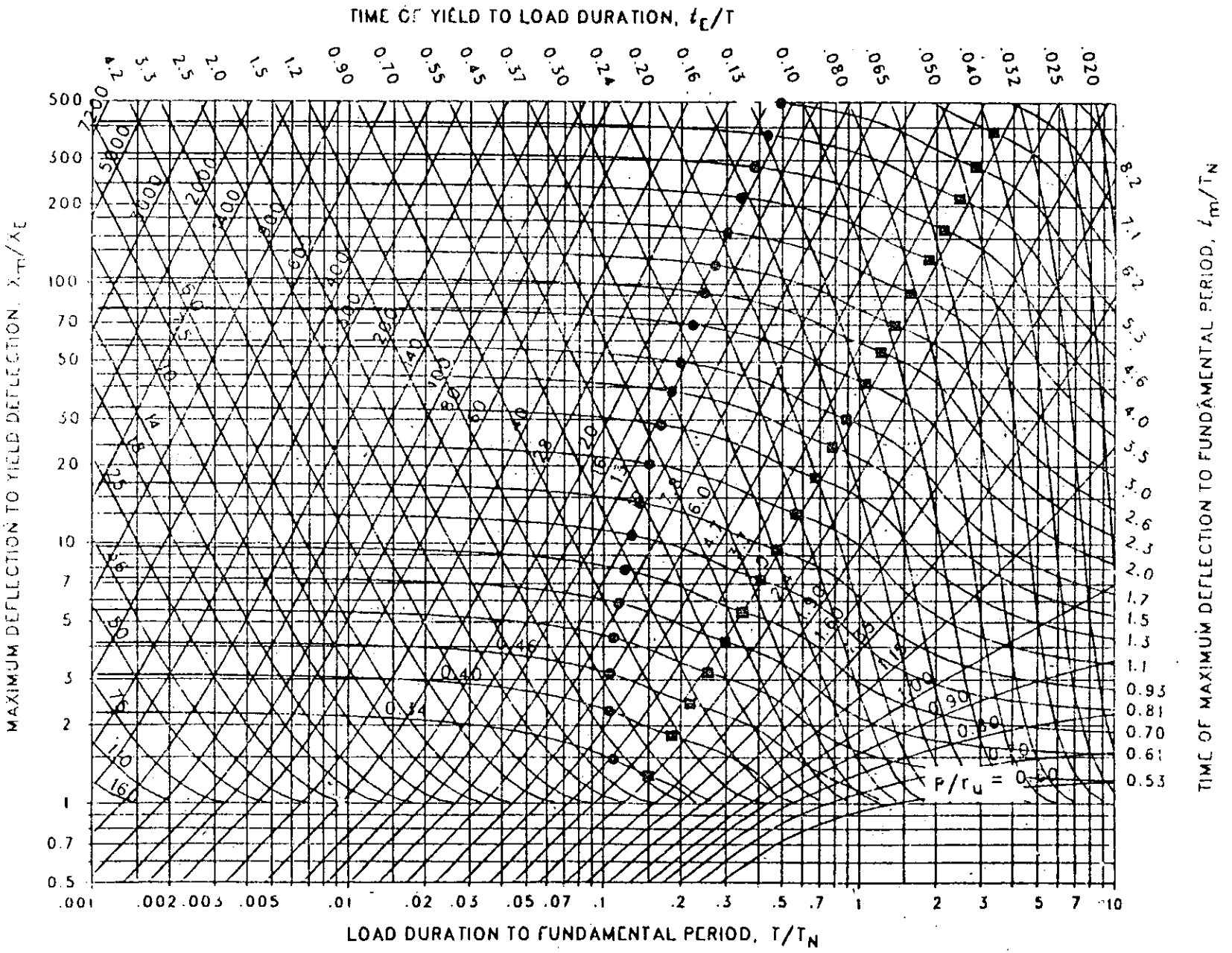


Figure 3-79 Maximum response of elasto-plastic, one-degree-of-freedom system for bilinear-triangular pulse ($C_1 = 0.147$, $C_2 = 3.0$)

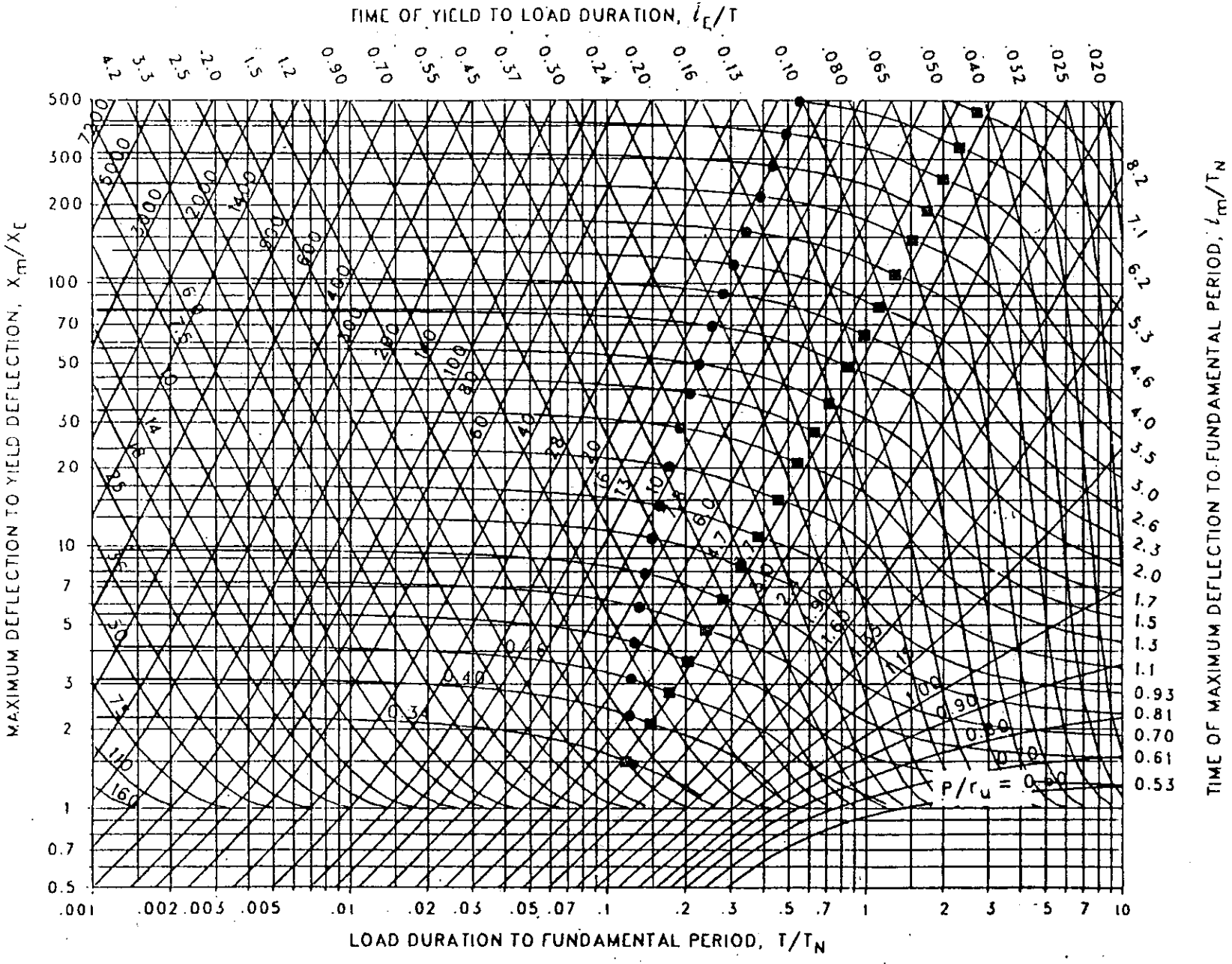


Figure 3-80 Maximum response of elasto-plastic, one-degree-of-freedom system for bilinear-triangular pulse ($C_1 = 0.100$, $C_2 = 3.0$)

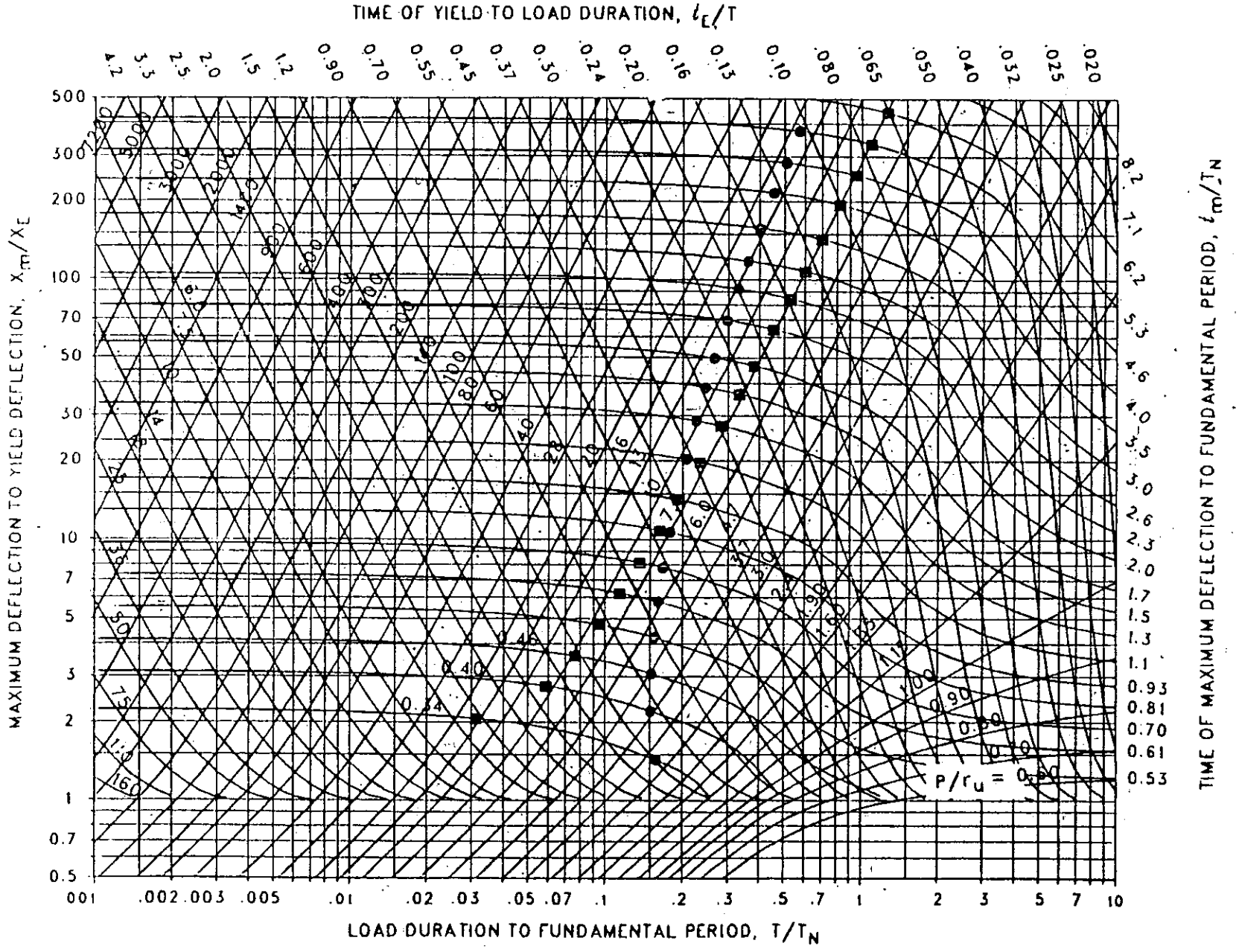


Figure 3-81 Maximum response of elasto-plastic, one-degree-of-freedom system for bilinear-triangular pulse ($C_1 = 0.056$, $C_2 = 3.0$)

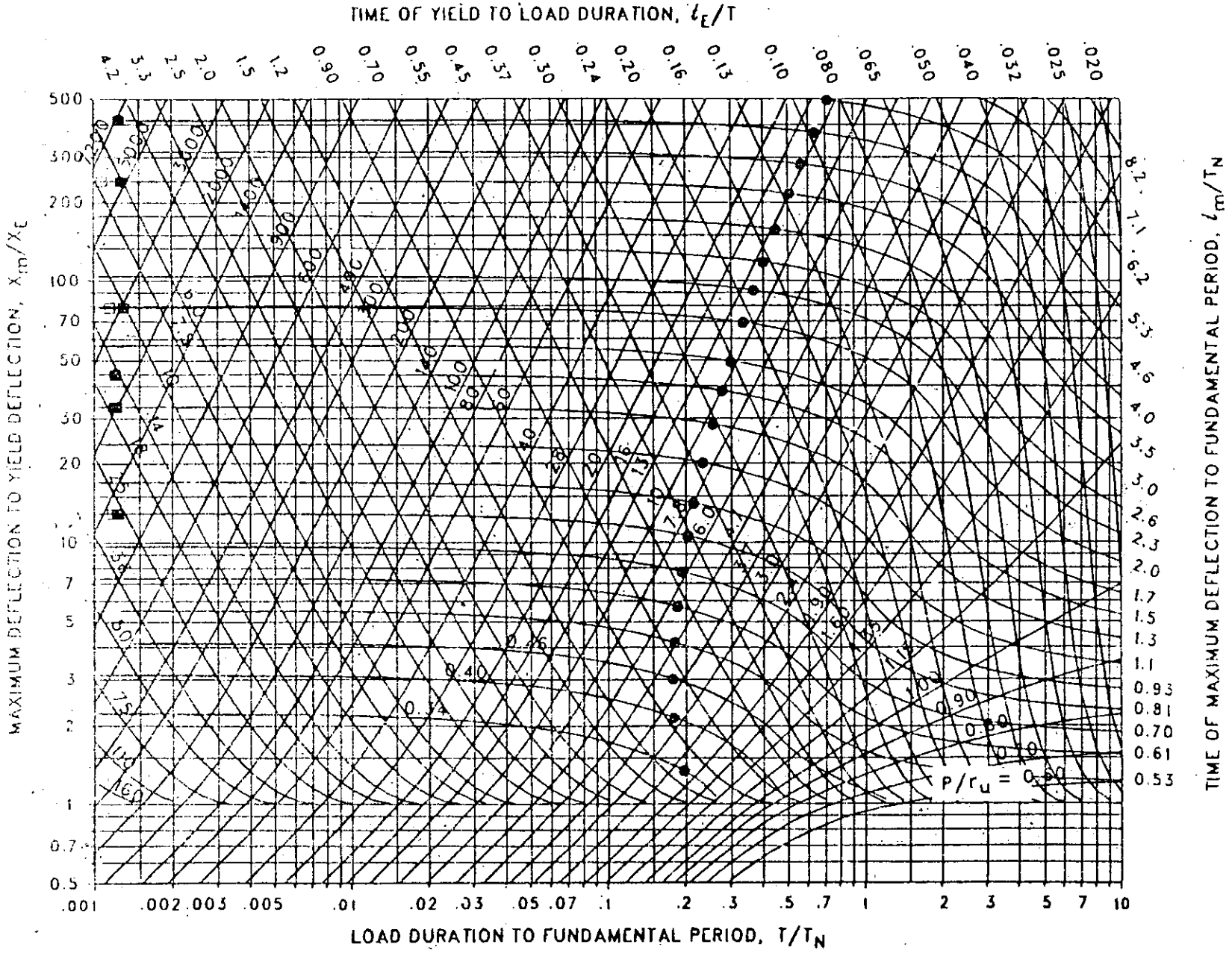


Figure 3-82 Maximum response of elasto-plastic, one-degree-of-freedom system for bilinear-triangular pulse ($C_1 = 0.032$, $C_2 = 3.0$)

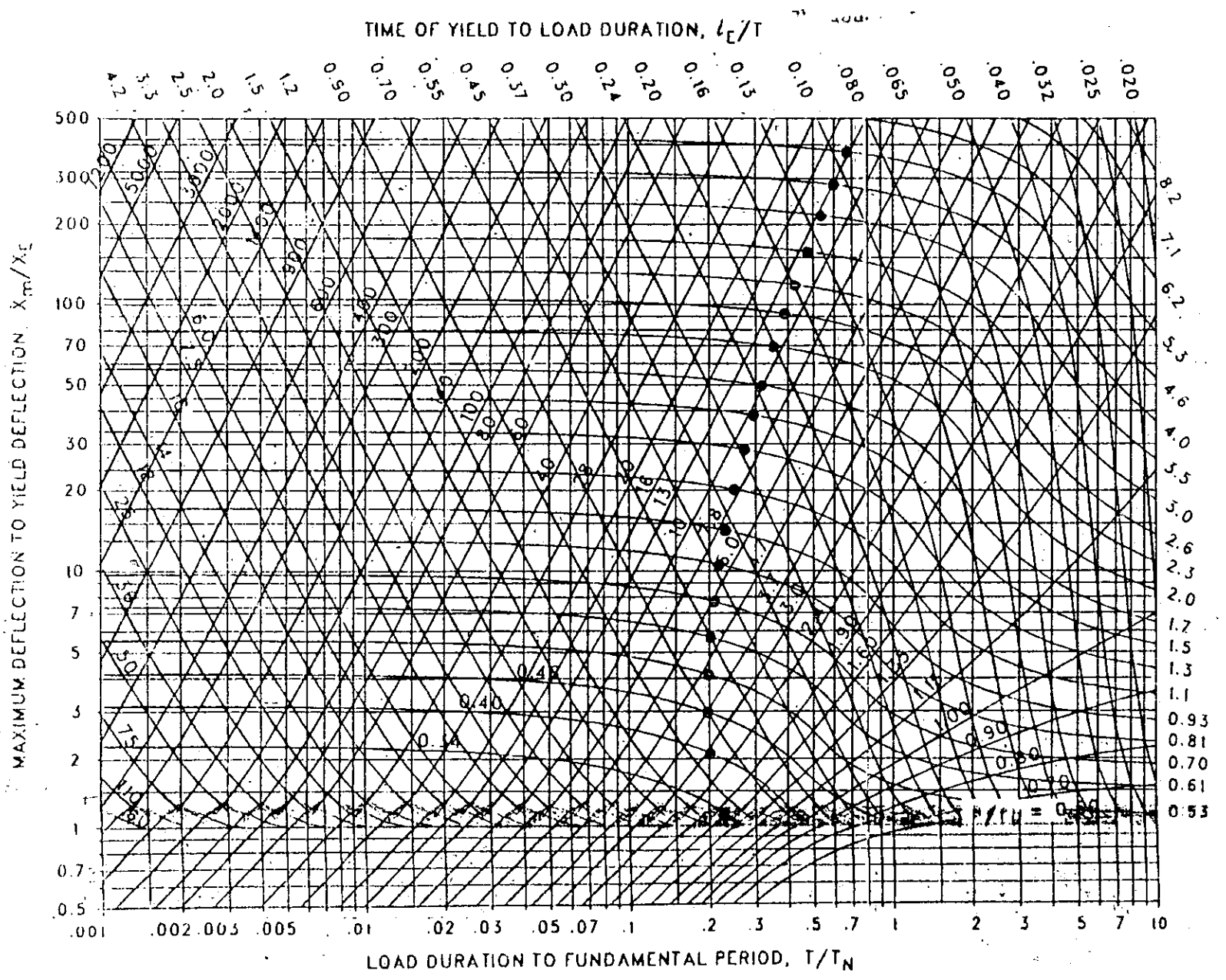


Figure 3-83 Maximum response of elasto-plastic, one-degree-of-freedom system for bilinear-triangular pulse ($C_1 = 0.018$, $C_2 = 3.0$)

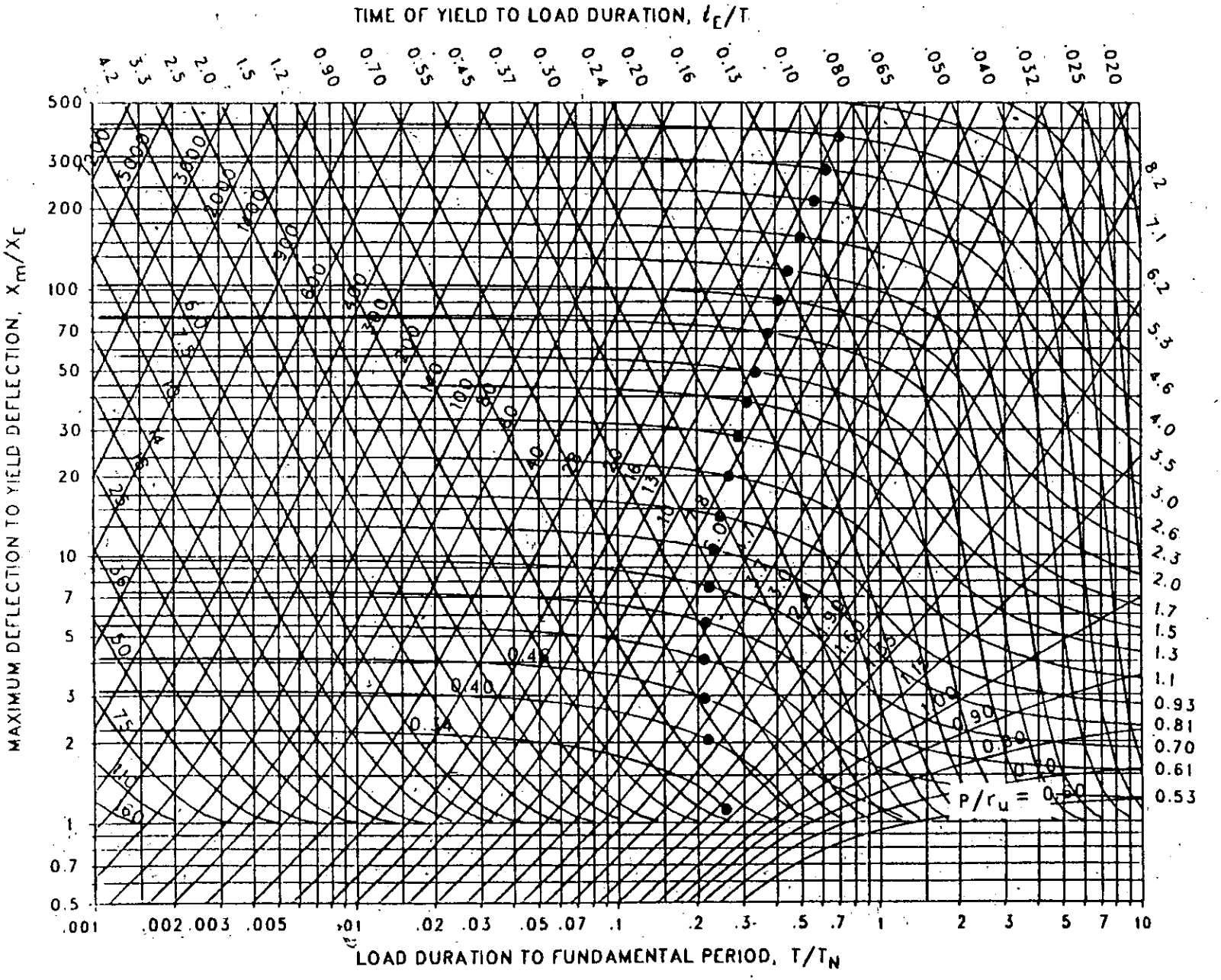


Figure 3-84 Maximum response of elasto-plastic, one-degree-of-freedom system for bilinear-triangular pulse ($C_1 = 0.010$, $C_2 = 3.0$)

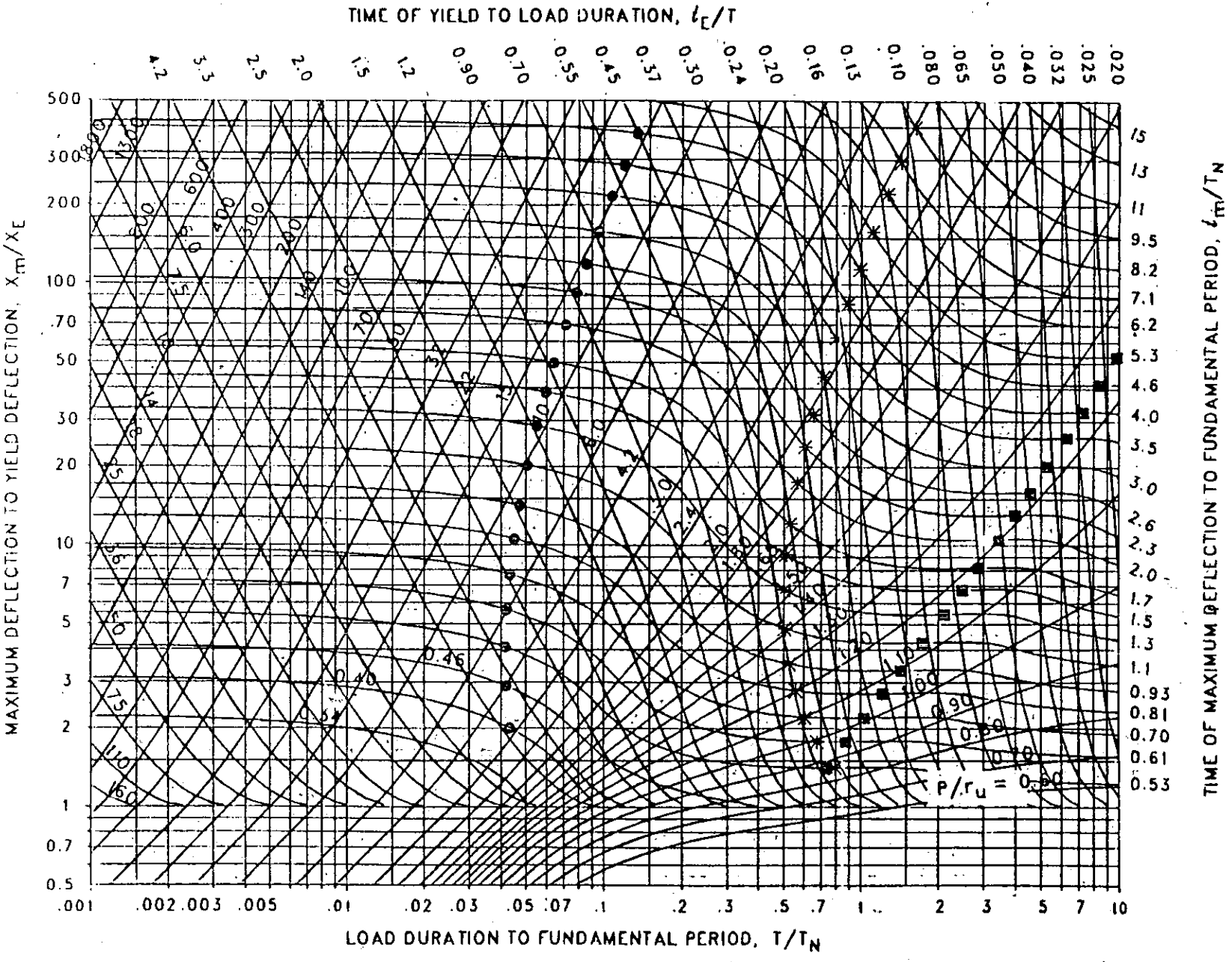


Figure 3-85 Maximum response of elasto-plastic, one-degree-of-freedom system for bilinear-triangular pulse ($C_1 = 0.750$, $C_2 = 5.5$)

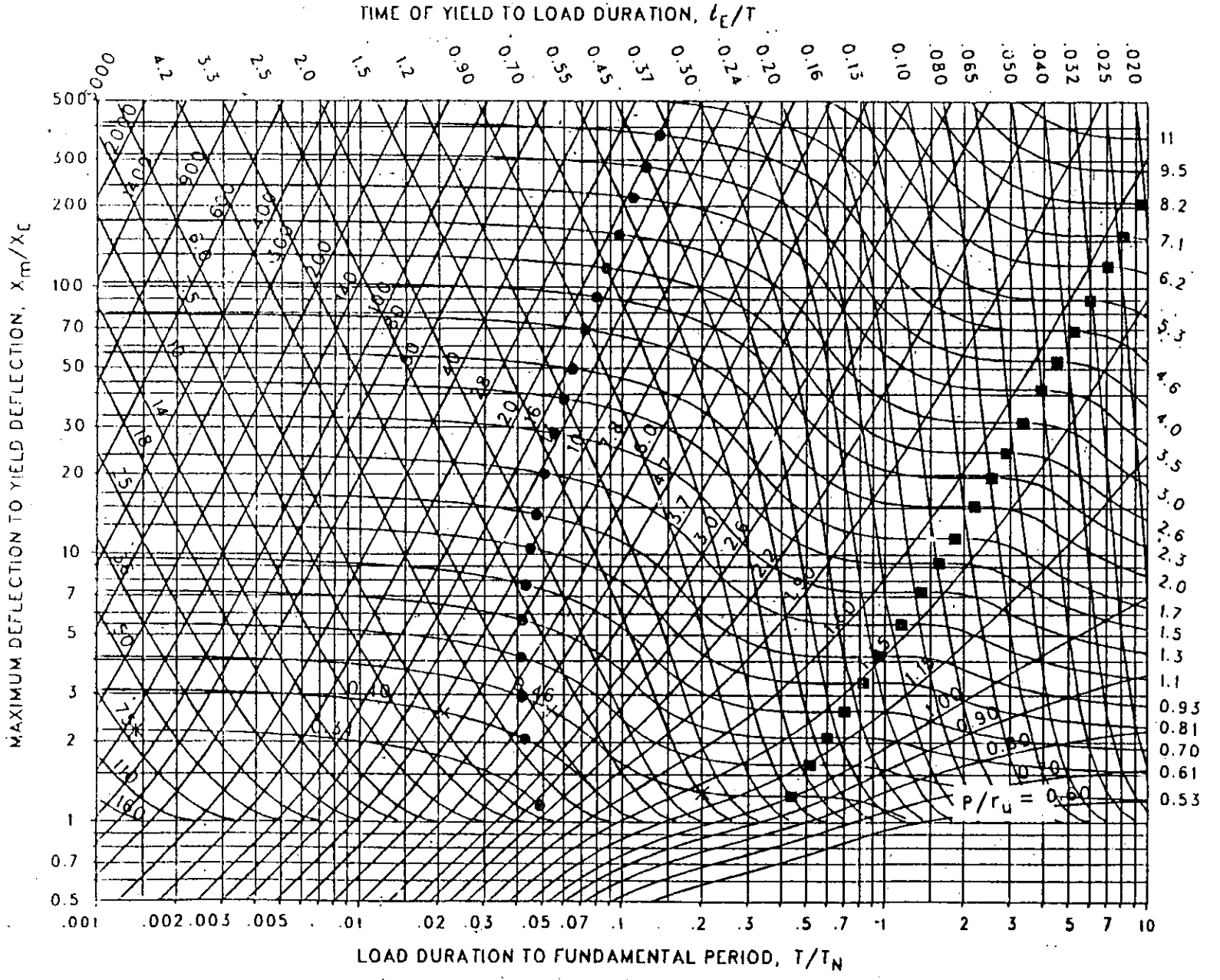


Figure 3-86 Maximum response of elasto-plastic, one-degree-of-freedom system for bilinear-triangular pulse ($C_1 = 0.562$, $C_2 = 5.5$)

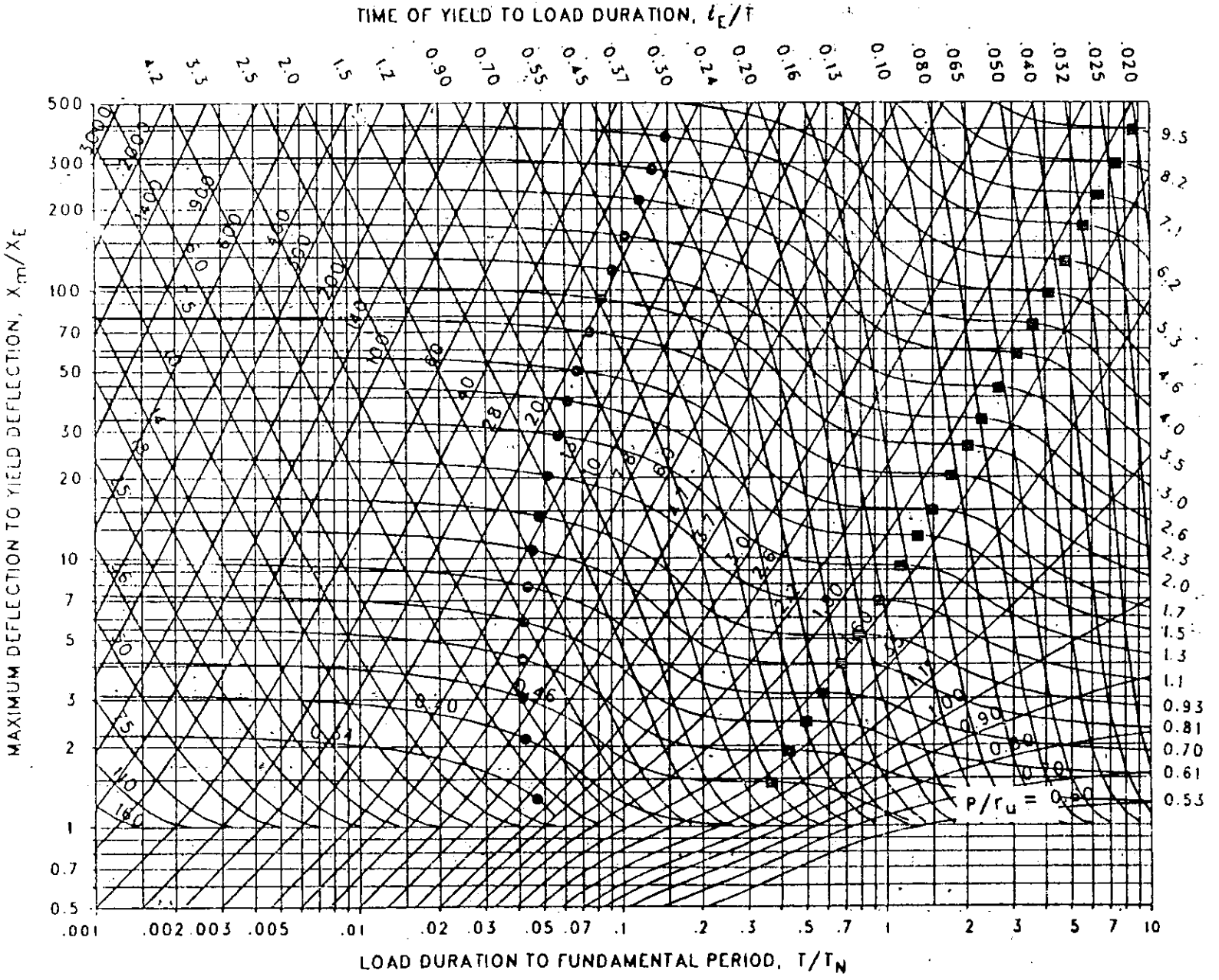


Figure 3-87 Maximum response of elasto-plastic, one-degree-of-freedom system for bilinear-triangular pulse ($C_1 = 0.422$, $C_2 = 5.5$)

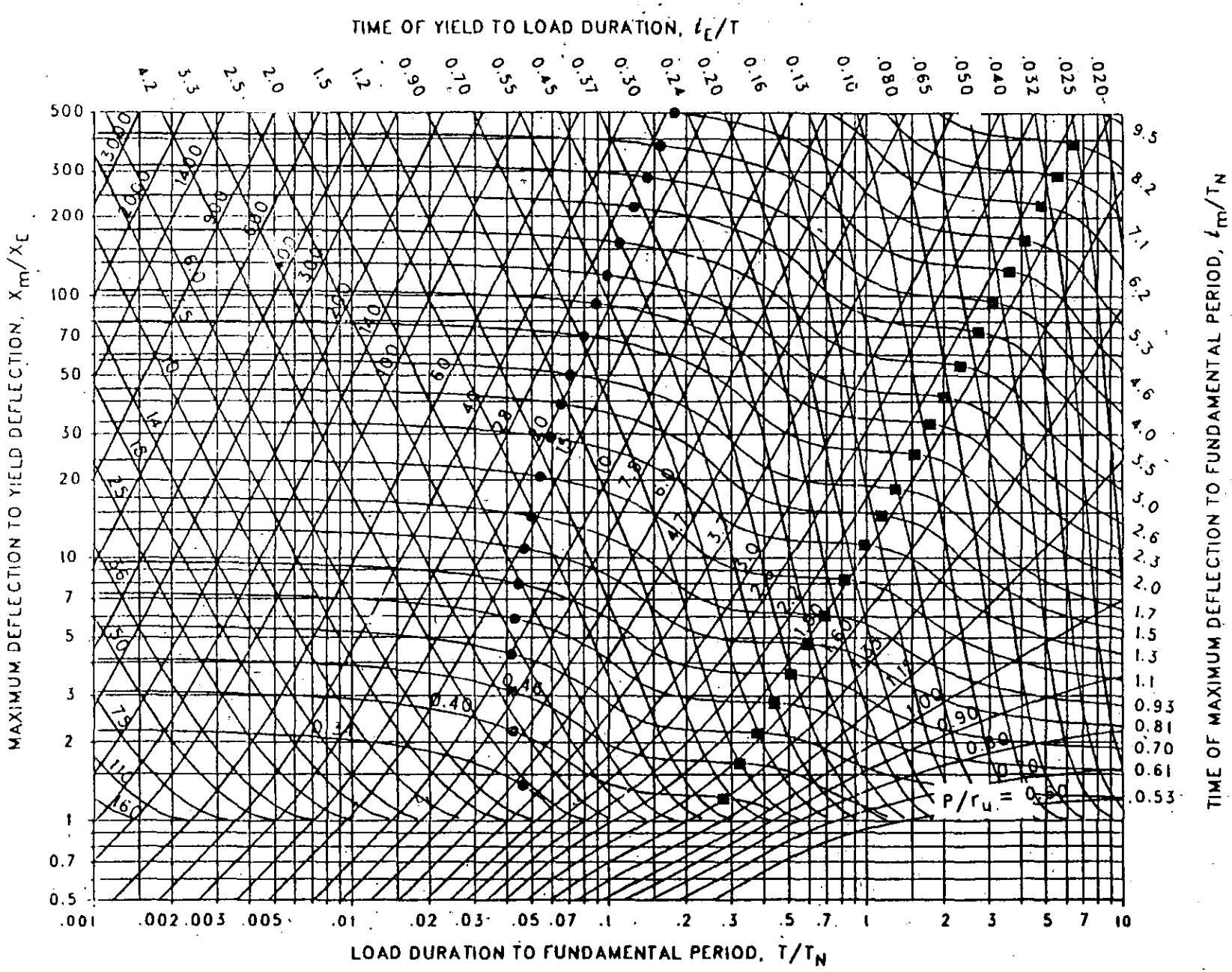


Figure 3-88 Maximum response of elasto-plastic, one-degree-of-freedom system for bilinear-triangular pulse ($C_1 = 0.316$, $C_2 = 5.5$)

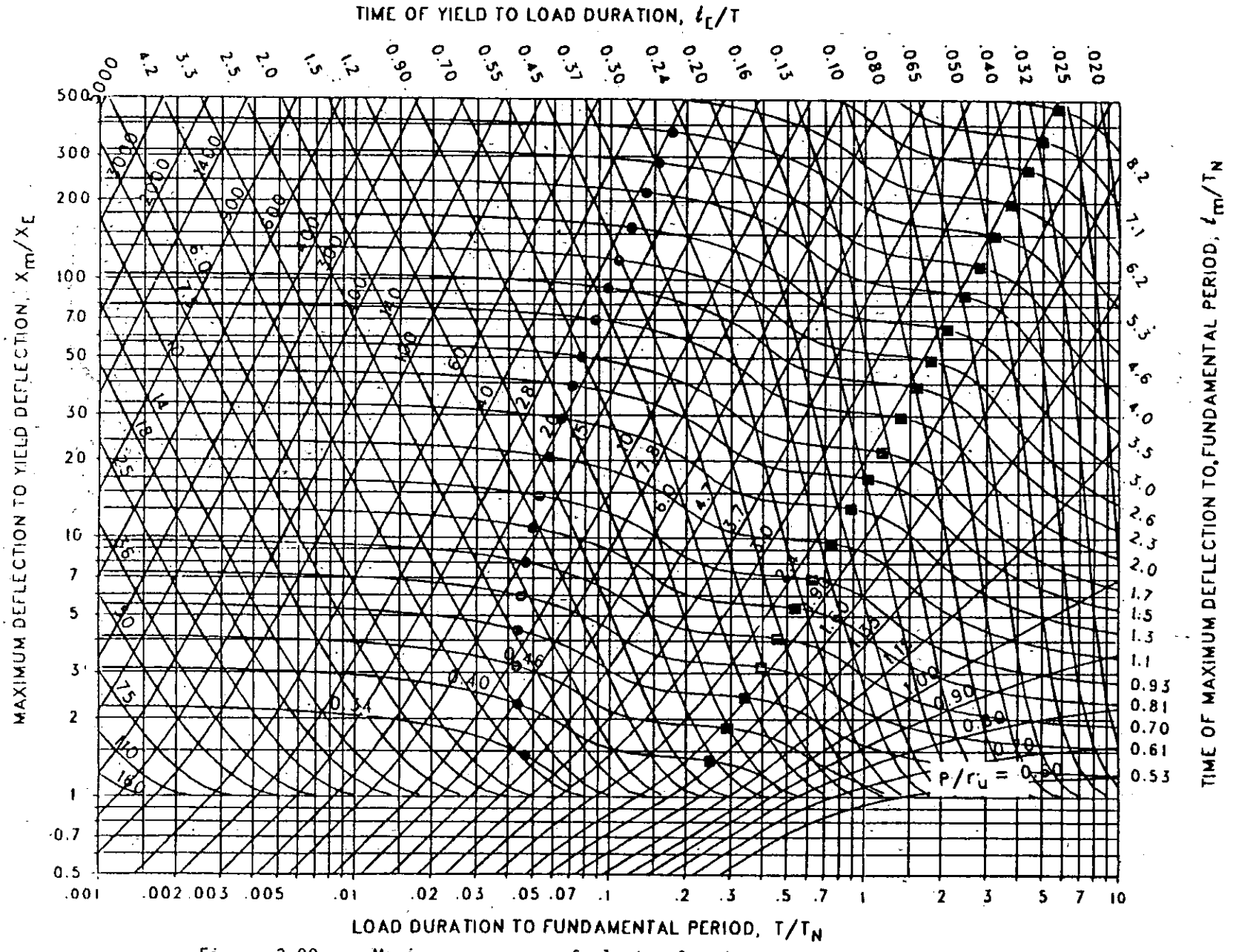


Figure 3-89 Maximum response of elasto-plastic, one-degree-of-freedom system for bilinear-triangular pulse ($C_1 = 0.237$, $C_2 = 5.5$)

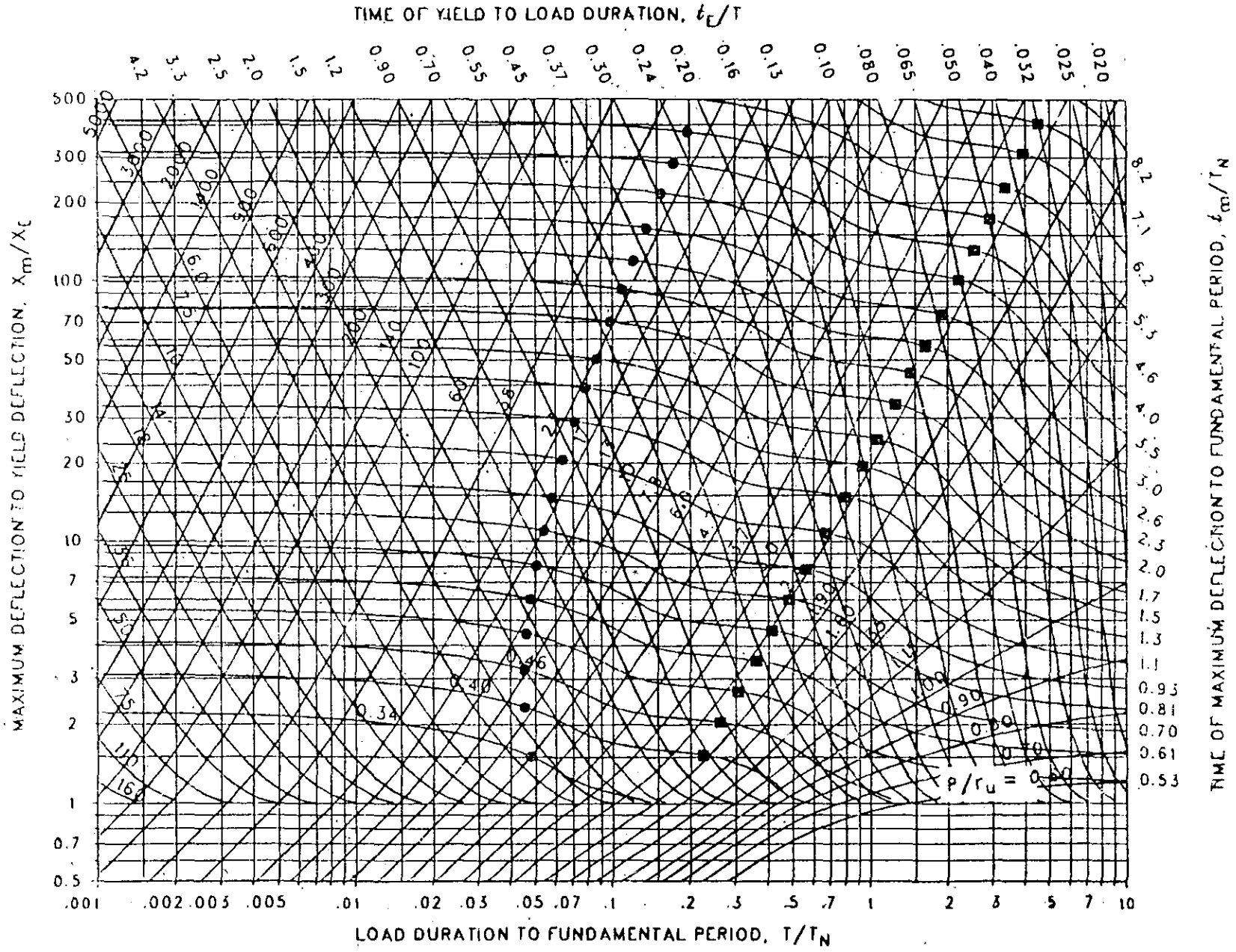


Figure 3-90 Maximum response of elasto-plastic, one-degree-of-freedom system for bilinear-triangular pulse ($C_1 = 0.178$, $C_2 = 5.5$)

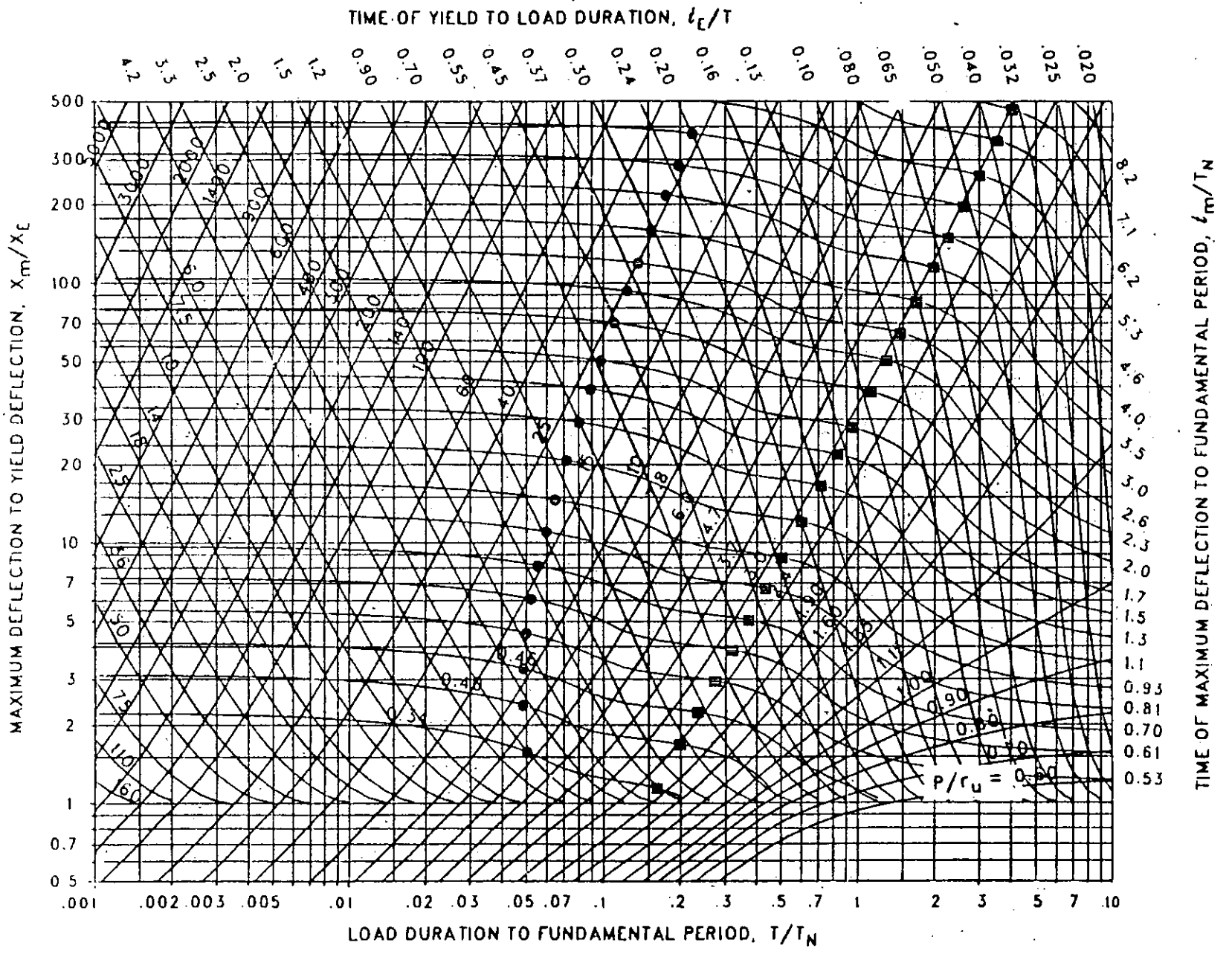


Figure 3-91 Maximum response of elasto-plastic, one-degree-of-freedom system for bilinear-triangular pulse ($C_1 = 0.133$, $C_2 = 5.5$)

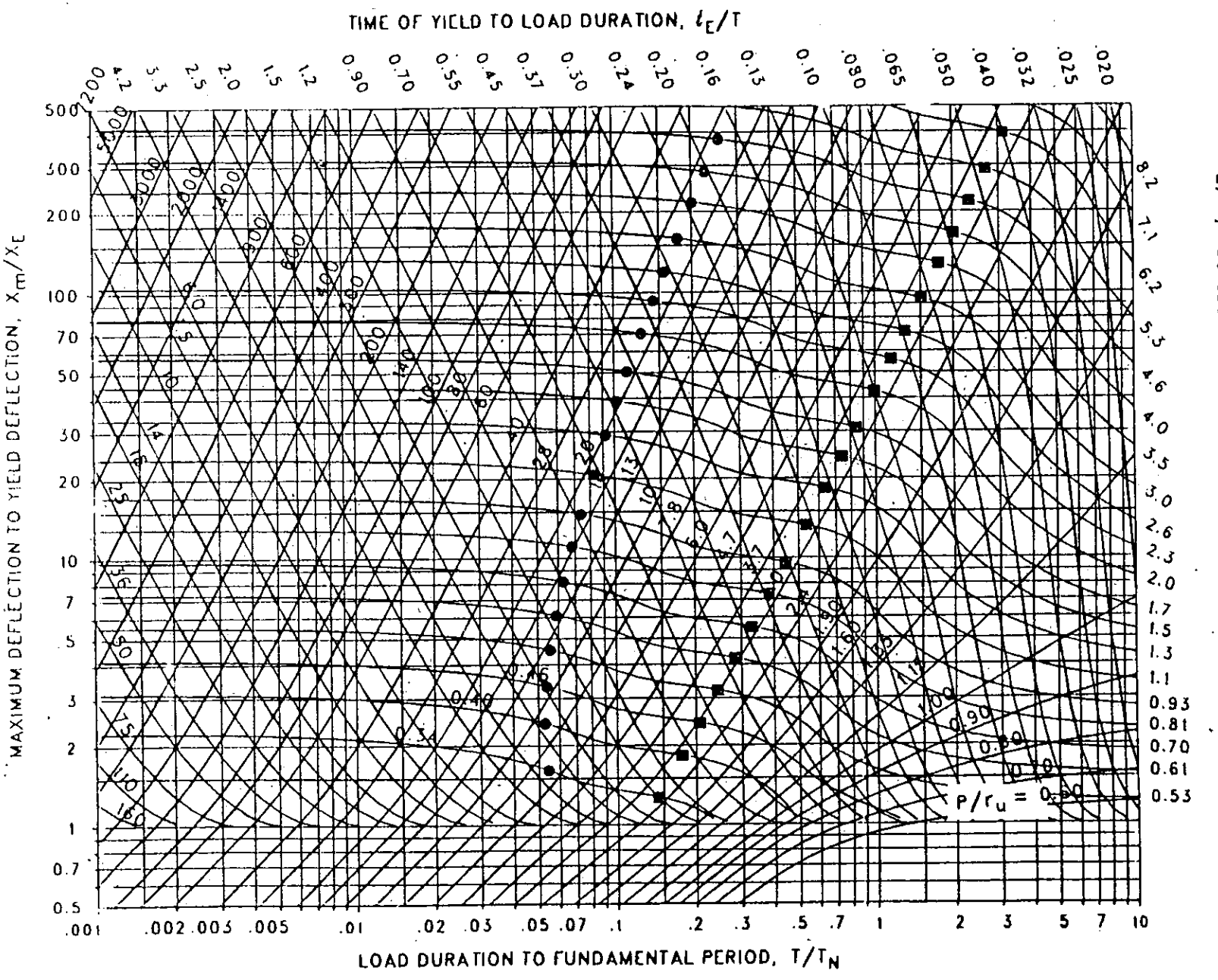


Figure 3-92 Maximum response of elasto-plastic, one-degree-of-freedom system for bilinear-triangular pulse ($C_1 = 0.100$, $C_2 = 5.5$)

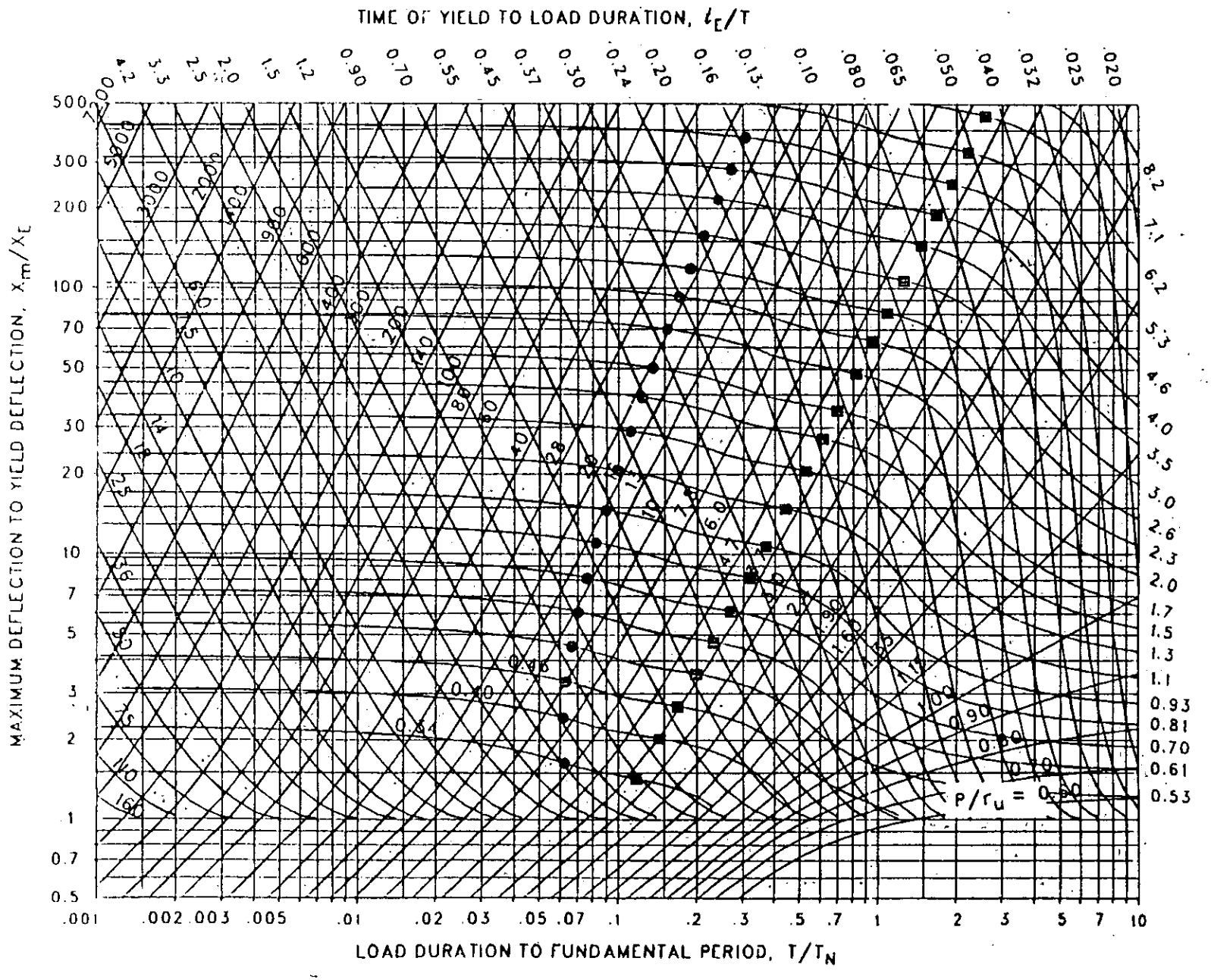


Figure 3-93 Maximum response of elasto-plastic, one-degree-of-freedom system for bilinear-triangular pulse ($C_1 = 0.068$, $C_2 = 5.5$)

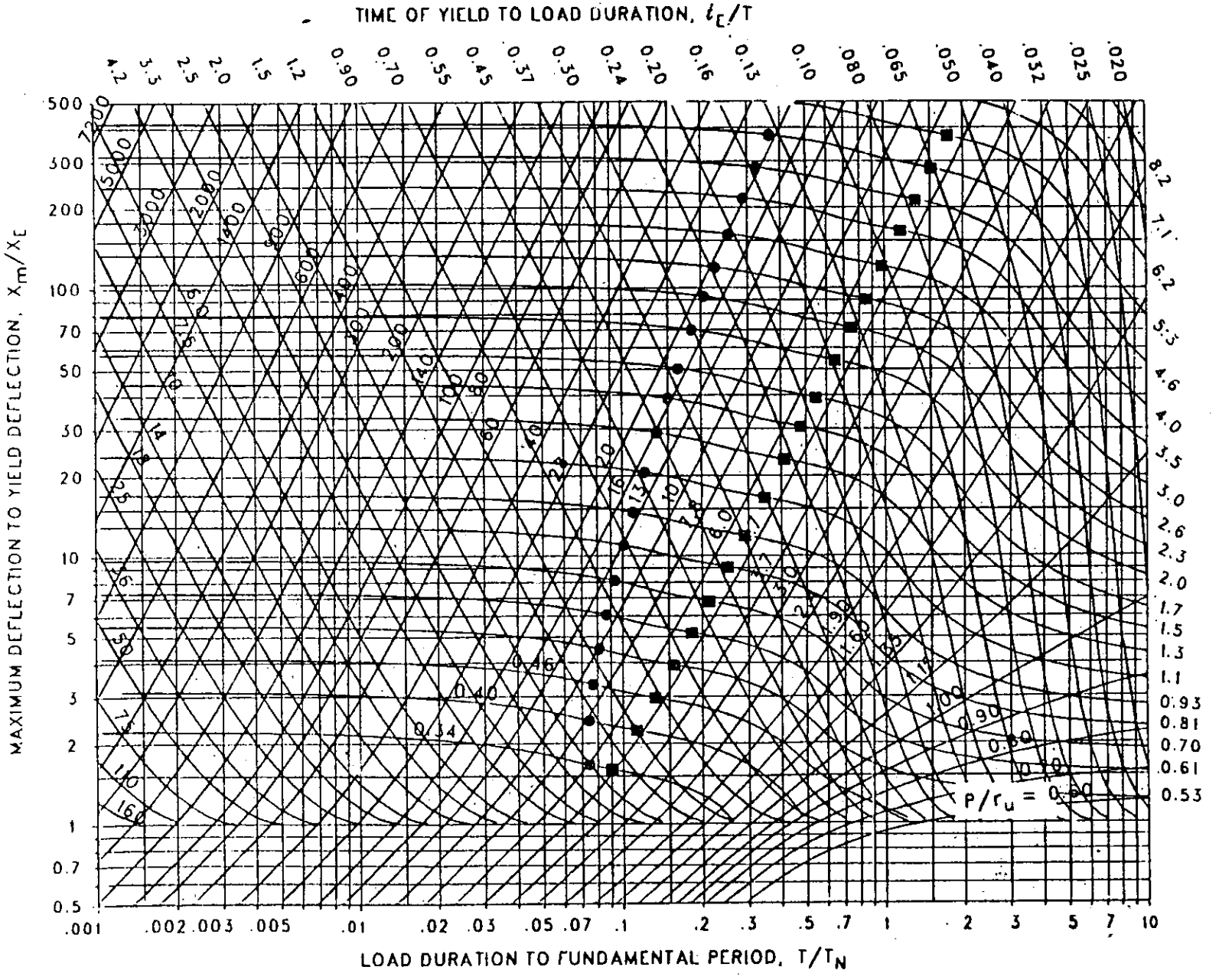


Figure 3-94 Maximum response of elasto-plastic, one-degree-of-freedom system for bilinear-triangular pulse (C_1 = 0.046, C_2 = 5.5)

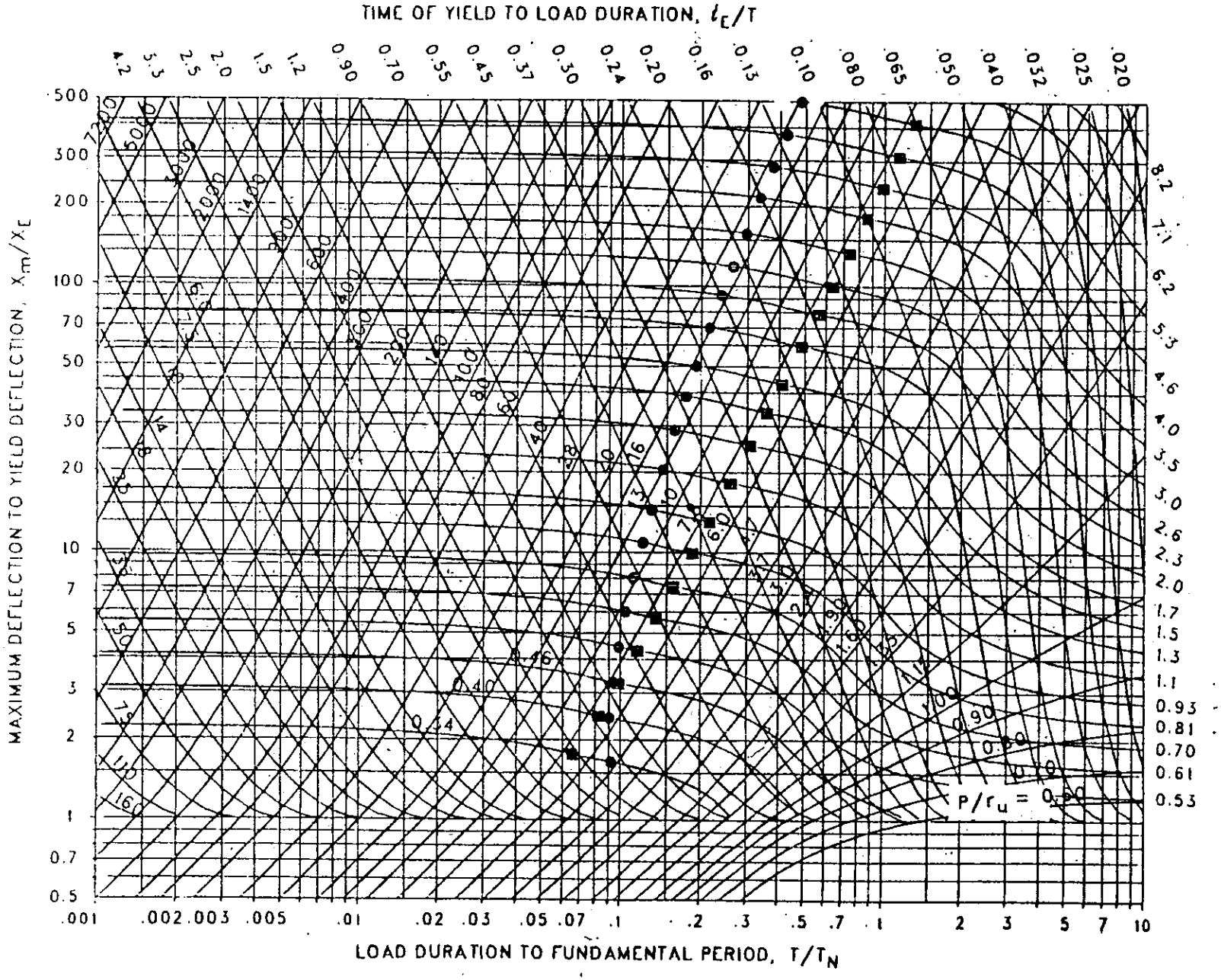


Figure 3-95 Maximum response of elasto-plastic, one-degree-of-freedom system for bilinear-triangular pulse ($C_1 = 0.032$, $C_2 = 5.5$)

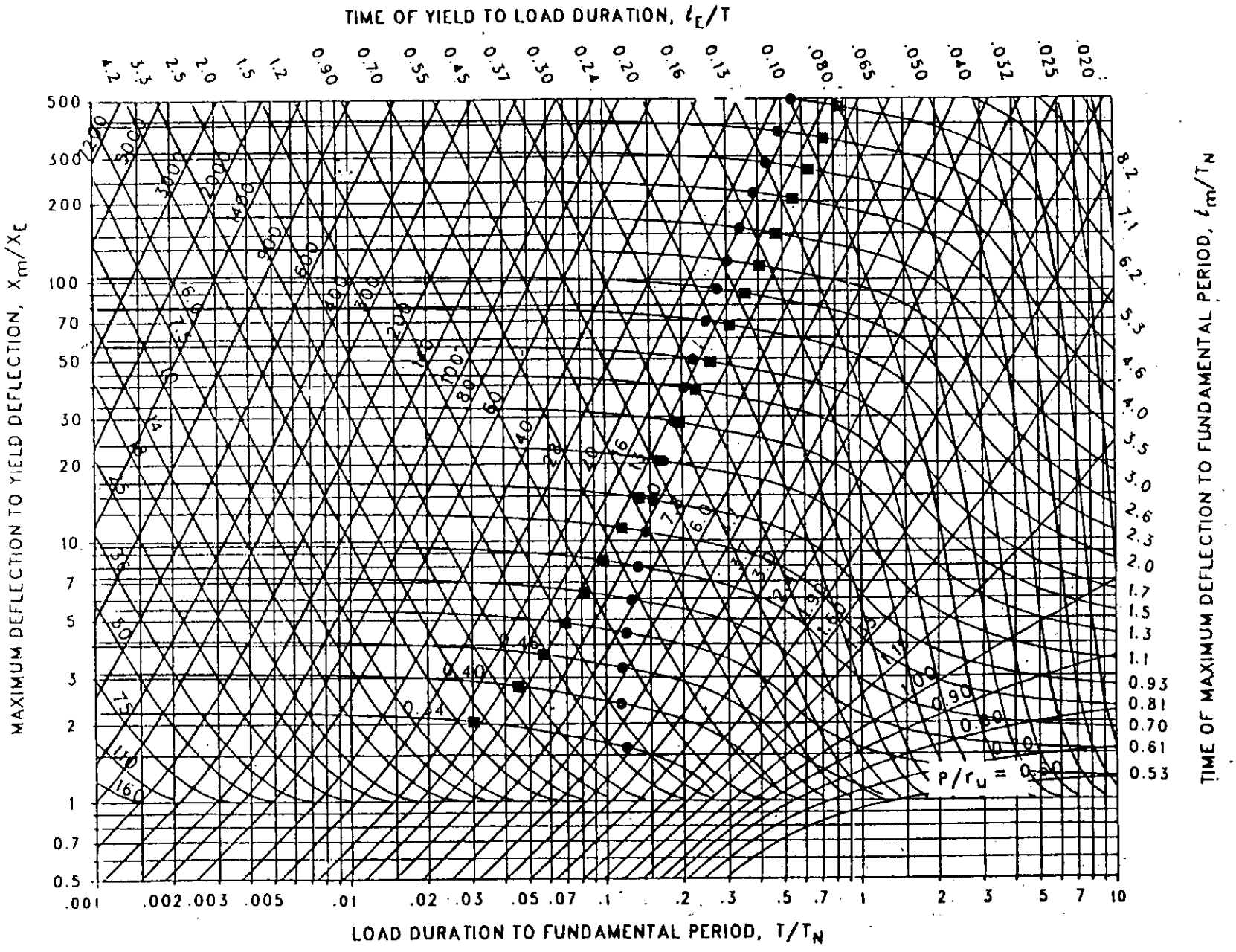


Figure 3-96 Maximum response of elasto-plastic, one-degree-of-freedom system for bilinear-triangular pulse (C_1 = 0.022, C_2 = 5:5)

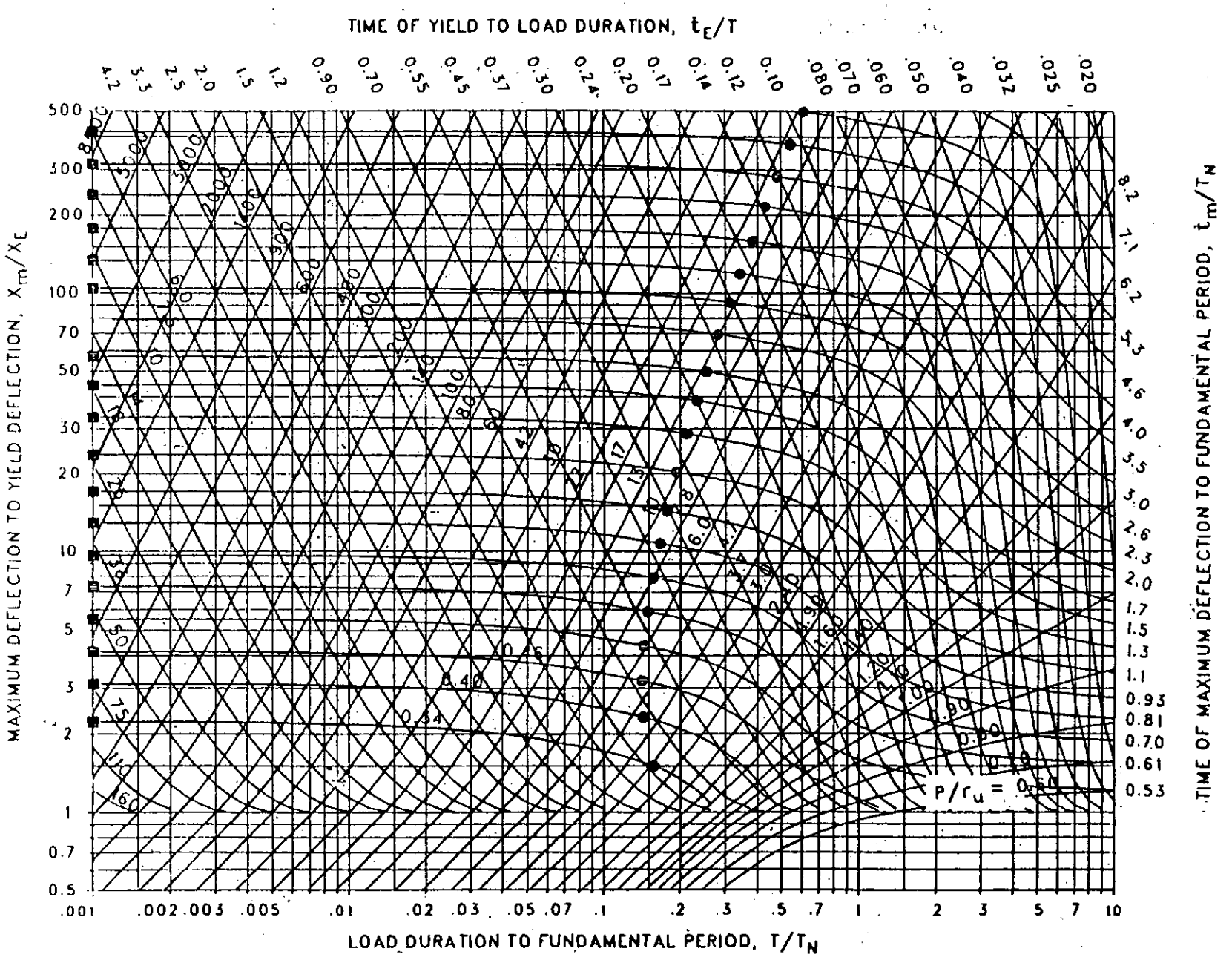


Figure 3-97 Maximum response of elasto-plastic, one-degree-of-freedom system for bilinear-triangular pulse (C_1 = 0.015, C_2 = .6)

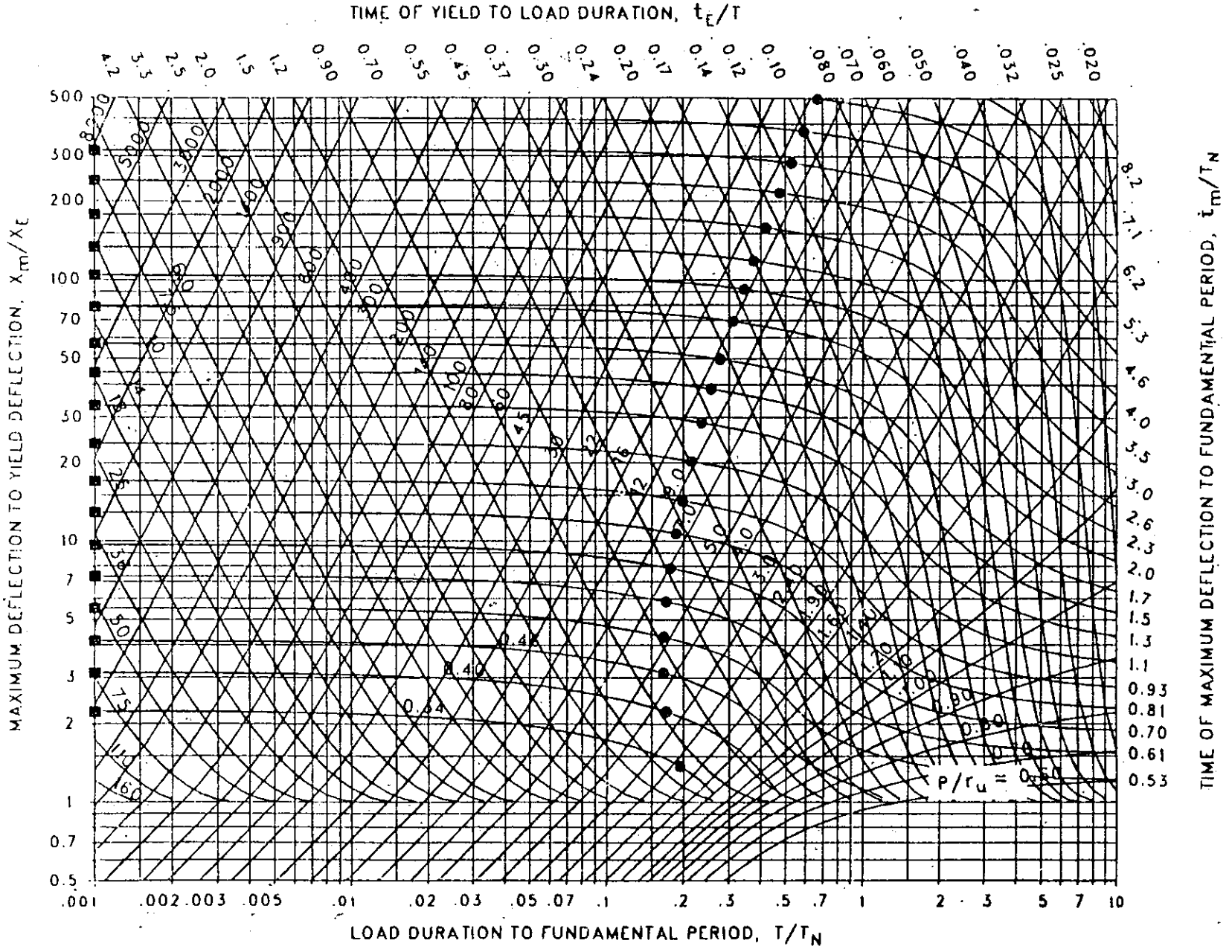


Figure 3-98 Maximum response of elasto-plastic, one-degree-of-freedom system for bilinear-triangular pulse (C_1 = 0.010, C_2 = 6)

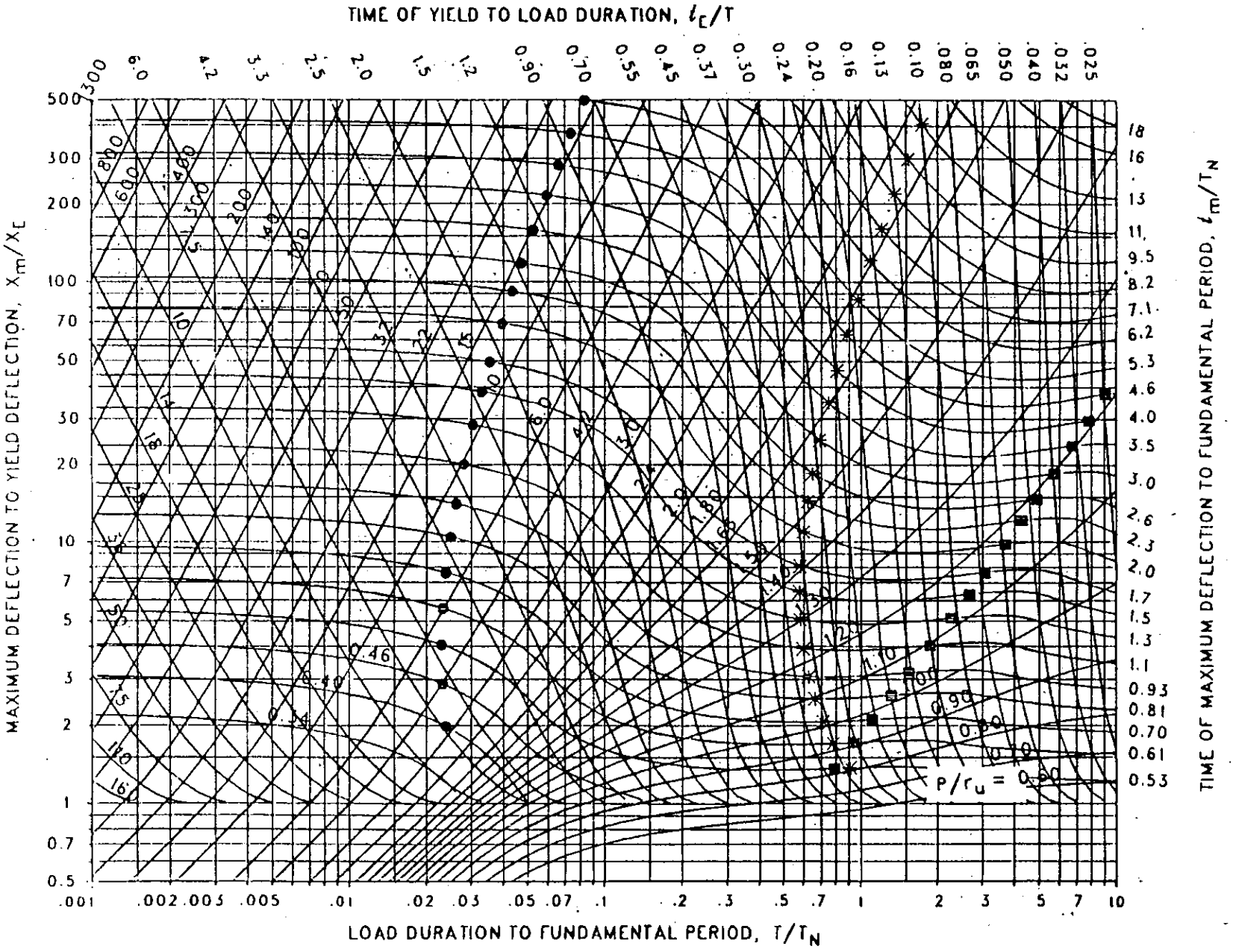


Figure 3-99 Maximum response of elasto-plastic, one-degree-of-freedom system for bilinear-triangular pulse ($C_1 = 0.750$, $C_2 = 10$)

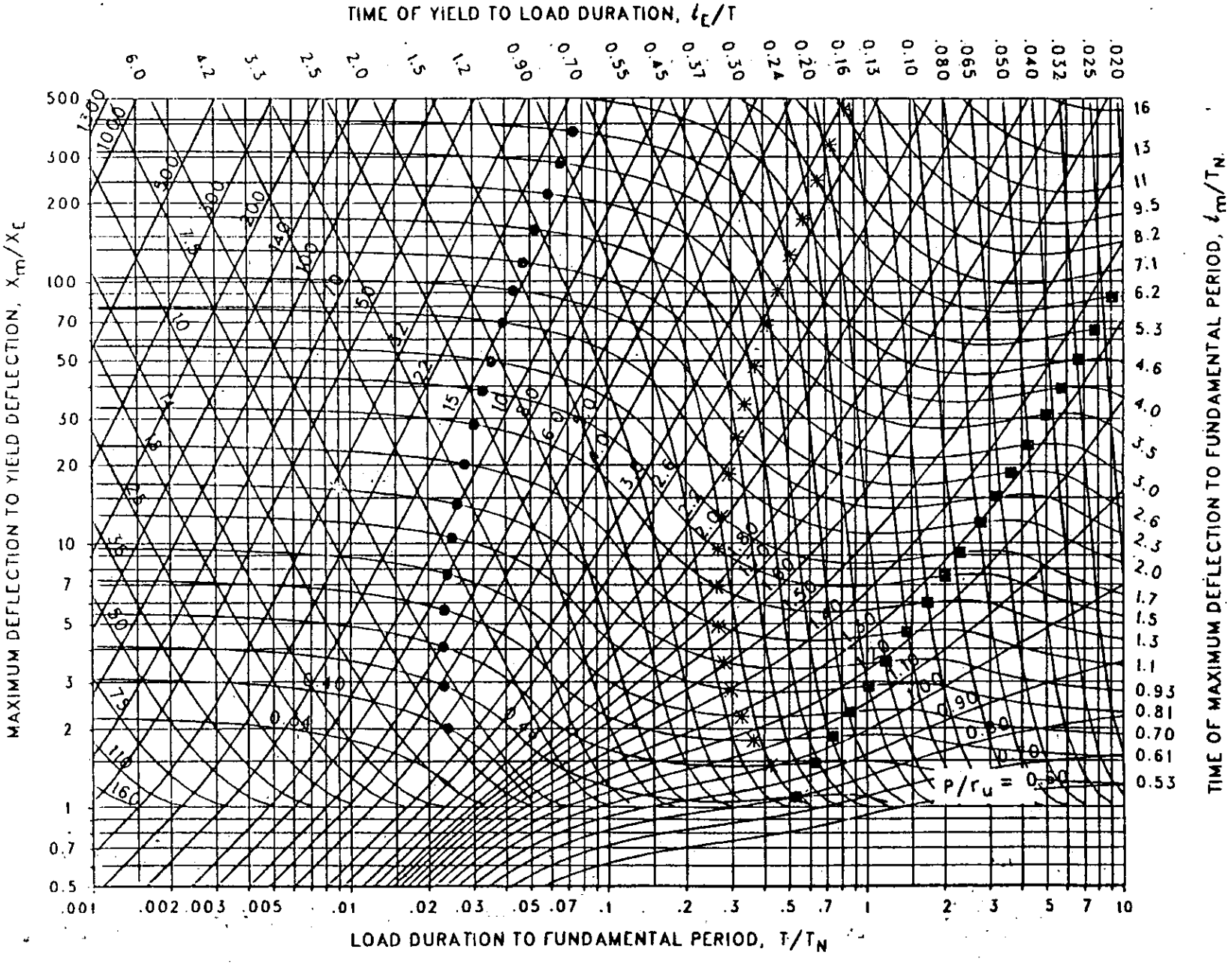


Figure 3-100 Maximum response of elasto-plastic, one-degree-of-freedom system for bilinear-triangular pulse ($C_1 = 0.648$, $C_2 = 10$)

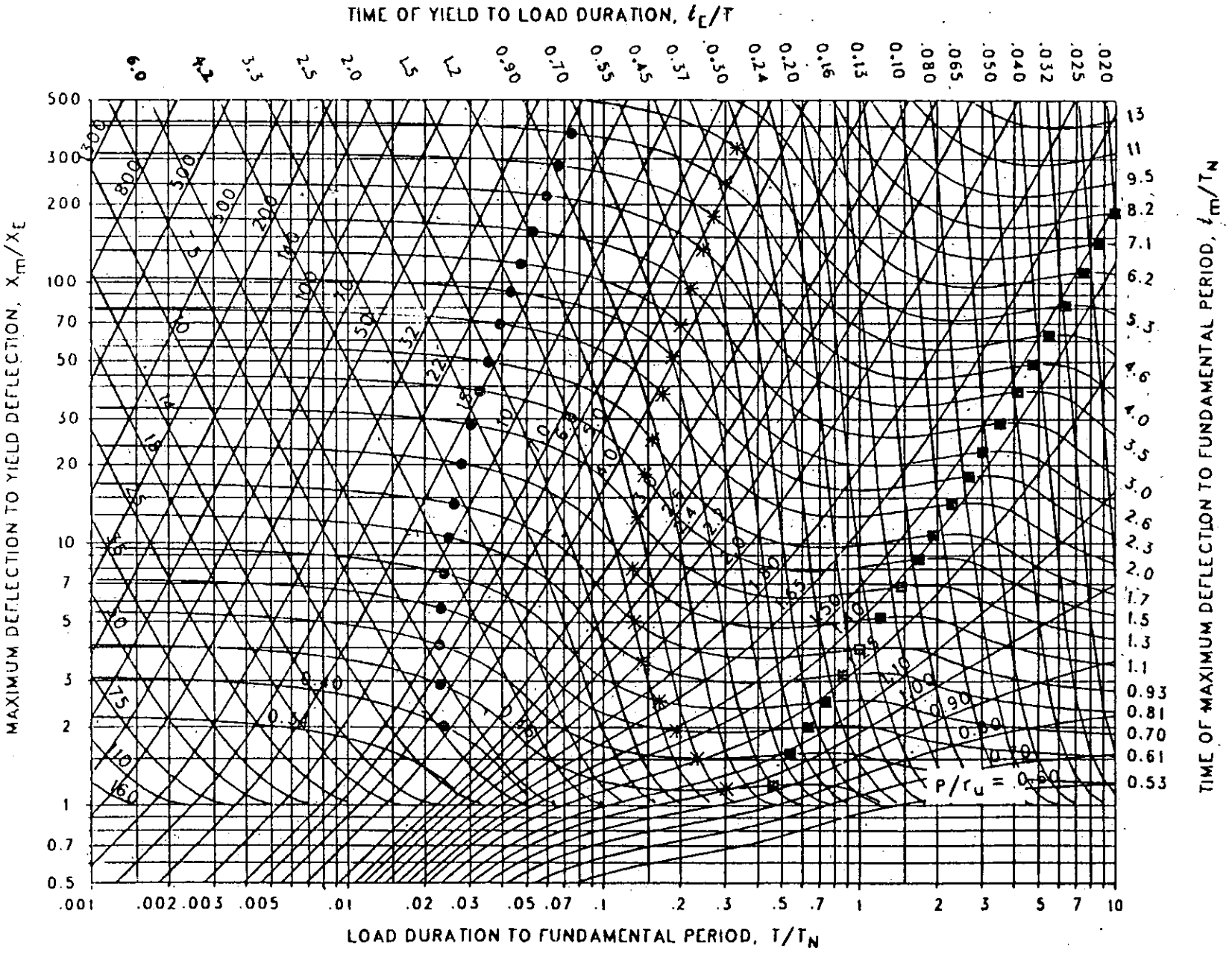


Figure 3-101 Maximum response of elasto-plastic, one-degree-of-freedom system for bilinear-triangular pulse ($C_1 = 0.562$, $C_2 = 10$)

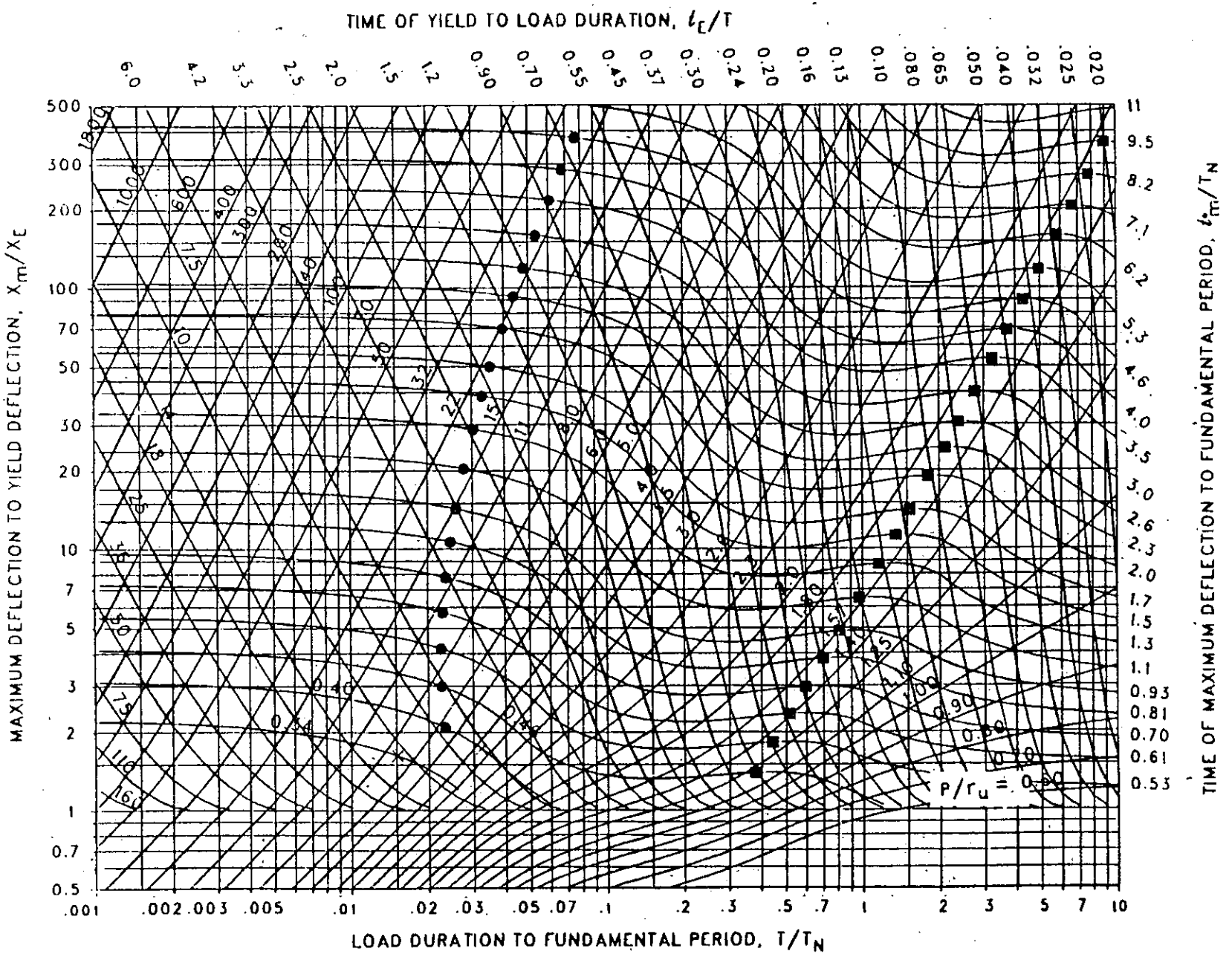


Figure 3-102 Maximum response of elasto-plastic, one-degree-of-freedom system for bilinear-triangular pulse ($C_1 = 0.422$, $C_2 = 10$)

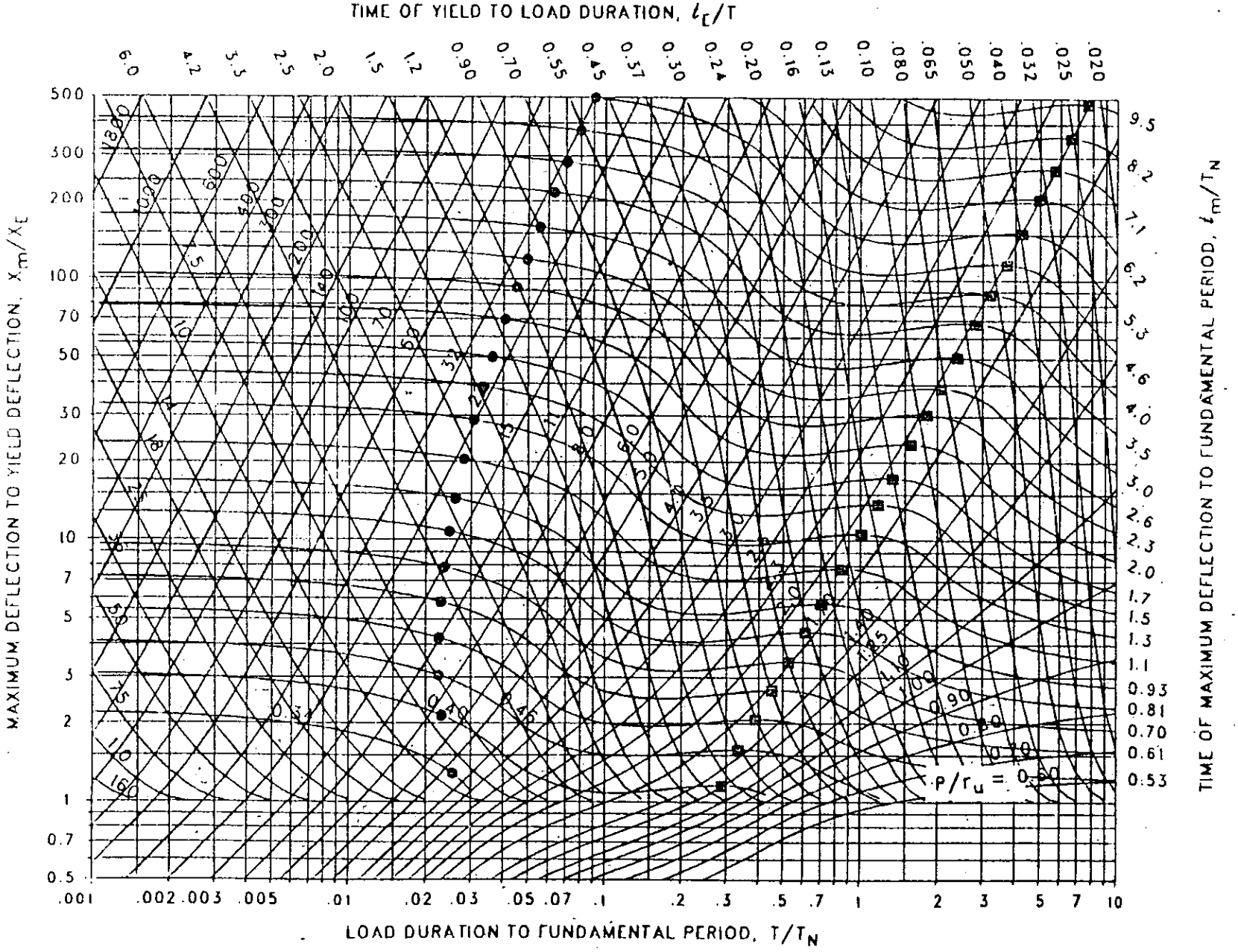


Figure 3-103 Maximum response of elasto-plastic, one-degree-of-freedom system for bilinear-triangular pulse ($C_1 = 0.316$, $C_2 = 10$)

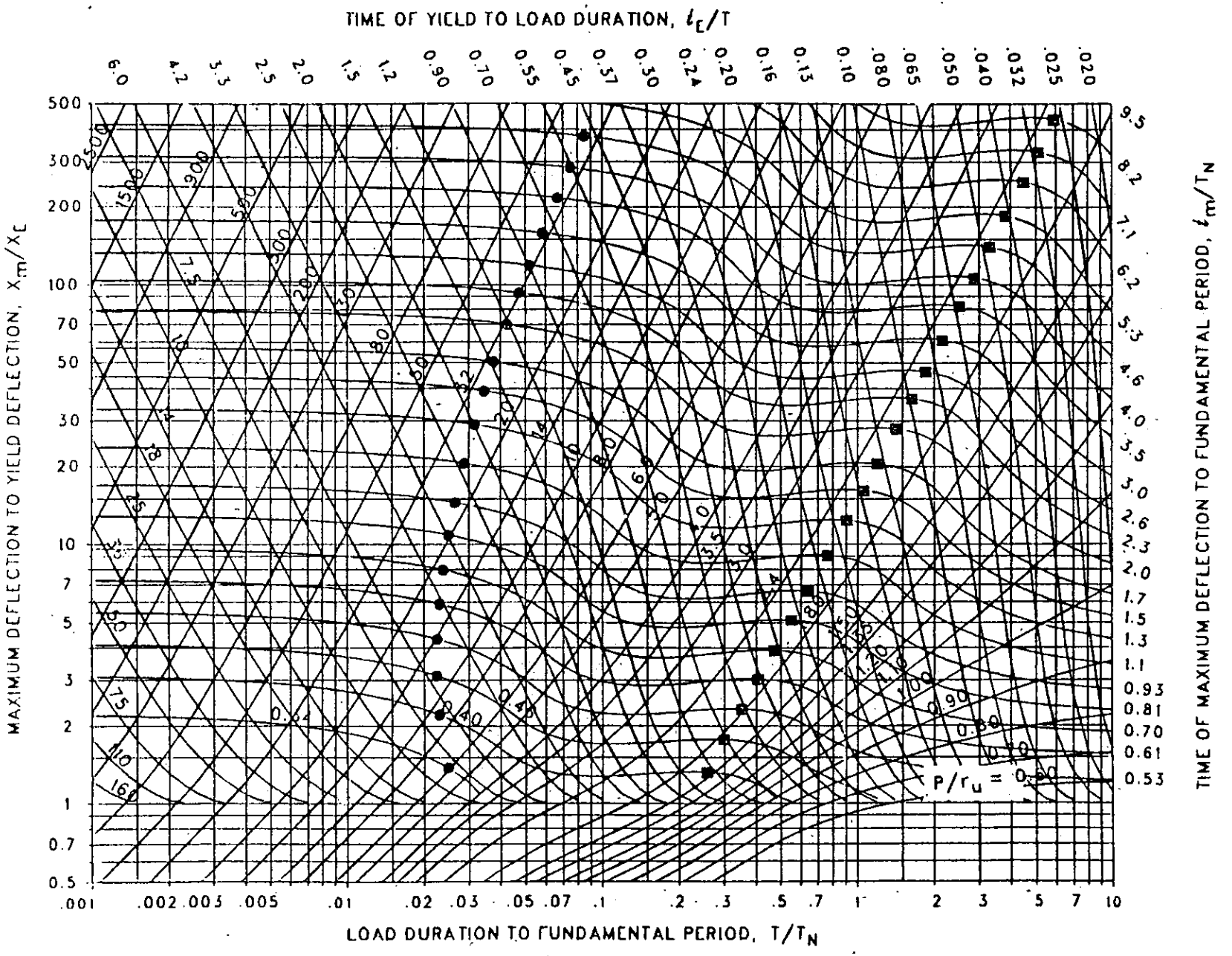


Figure 3-104 Maximum response of elasto-plastic, one-degree-of-freedom system for bilinear-triangular pulse ($C_1 = 0.237$, $C_2 = 10$)

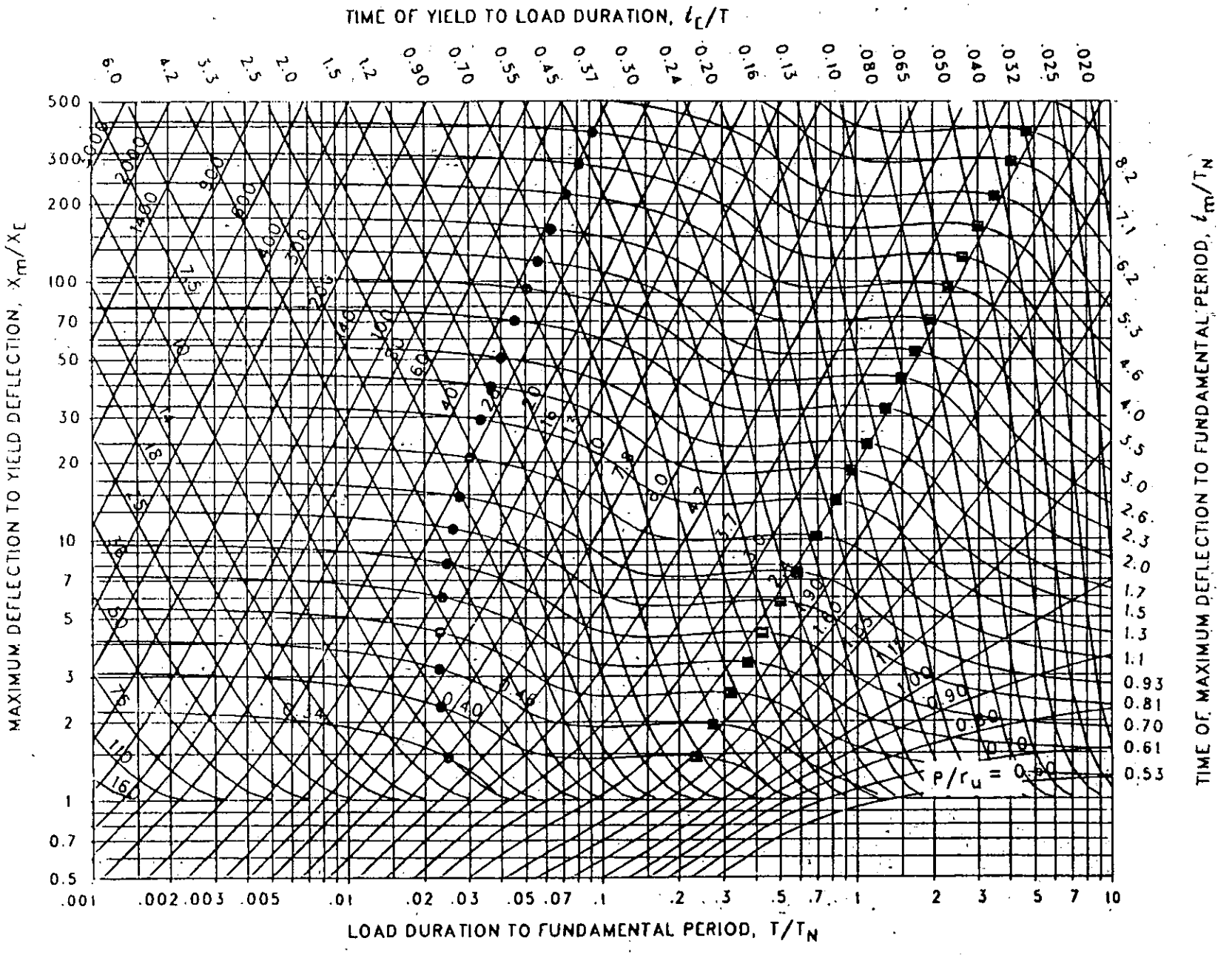


Figure 3-105 Maximum response of elasto-plastic, one-degree-of-freedom system for bilinear-triangular pulse ($C_1 = 0.178$, $C_2 = 10$)

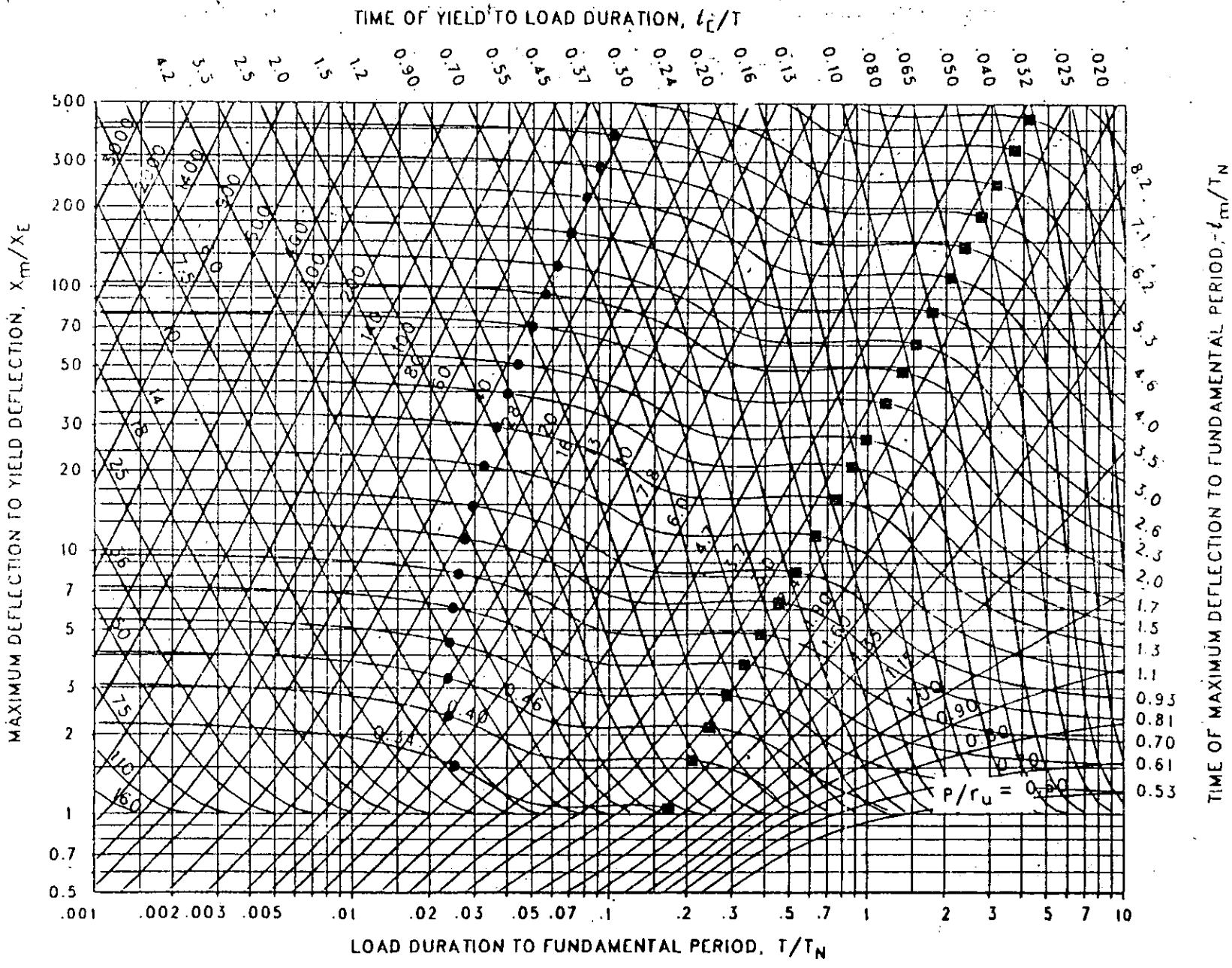


Figure 3-106 Maximum response of elasto-plastic, one-degree-of-freedom system for bilinear-triangular pulse ($C_1 = 0.133$, $C_2 = 10$)

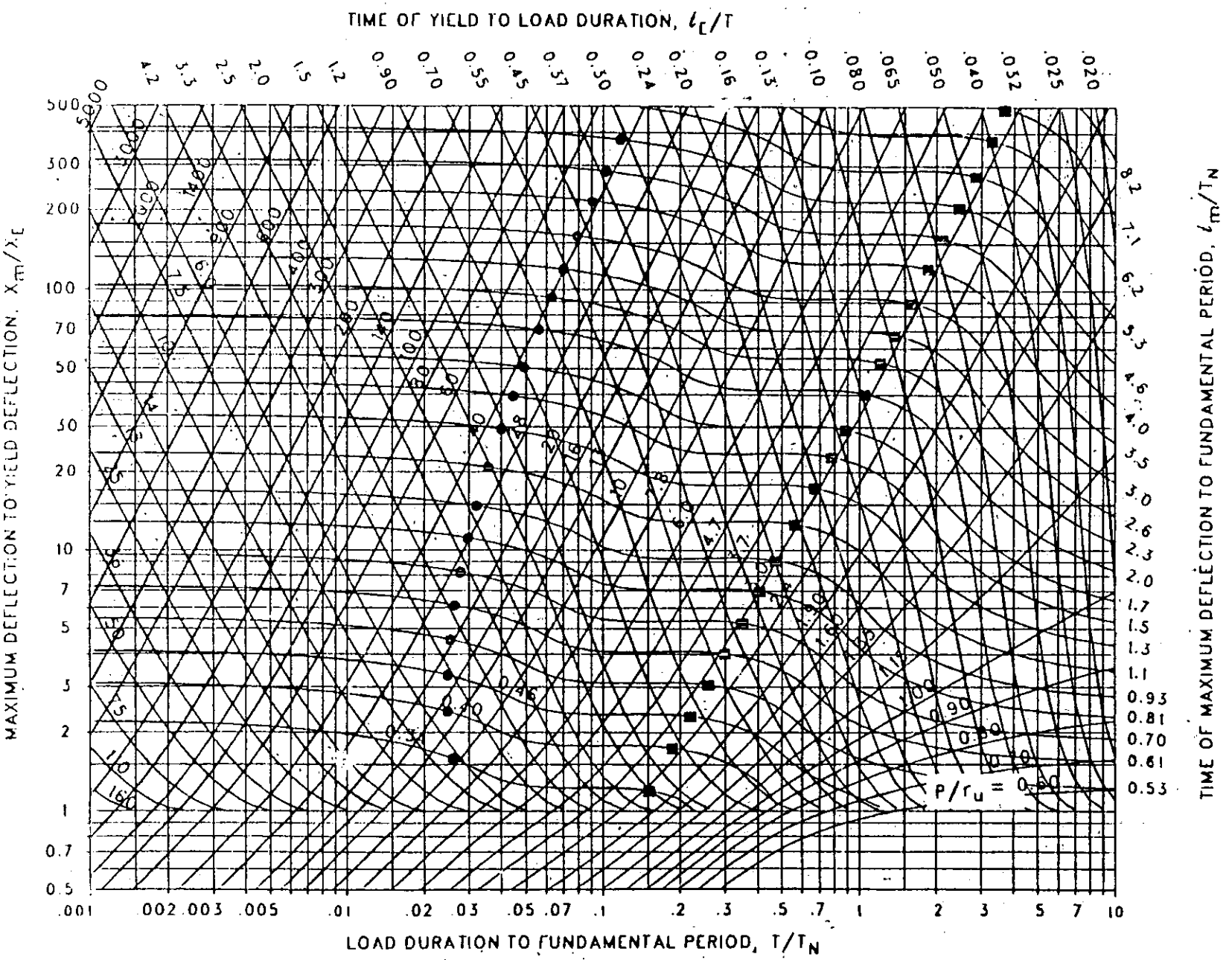


Figure 3-107 Maximum response of elasto-plastic, one-degree-of-freedom system for bilinear-triangular pulse ($C_1 = 0.100$, $C_2 = 10$)

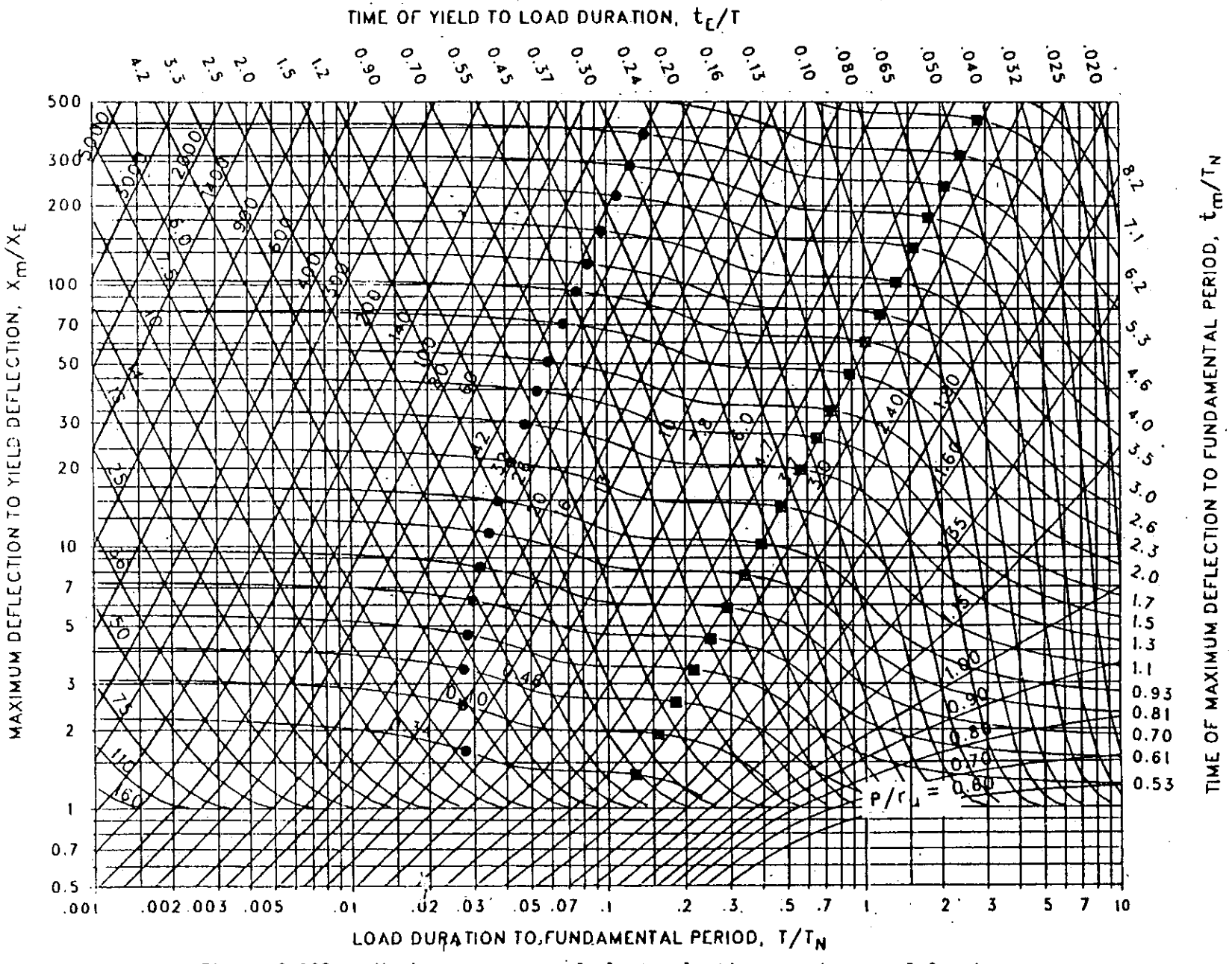


Figure 3-108 Maximum response of elasto-plastic, one-degree-of-freedom system for bilinear-triangular pulse ($C_1 = 0.068$, $C_2 = 10$)

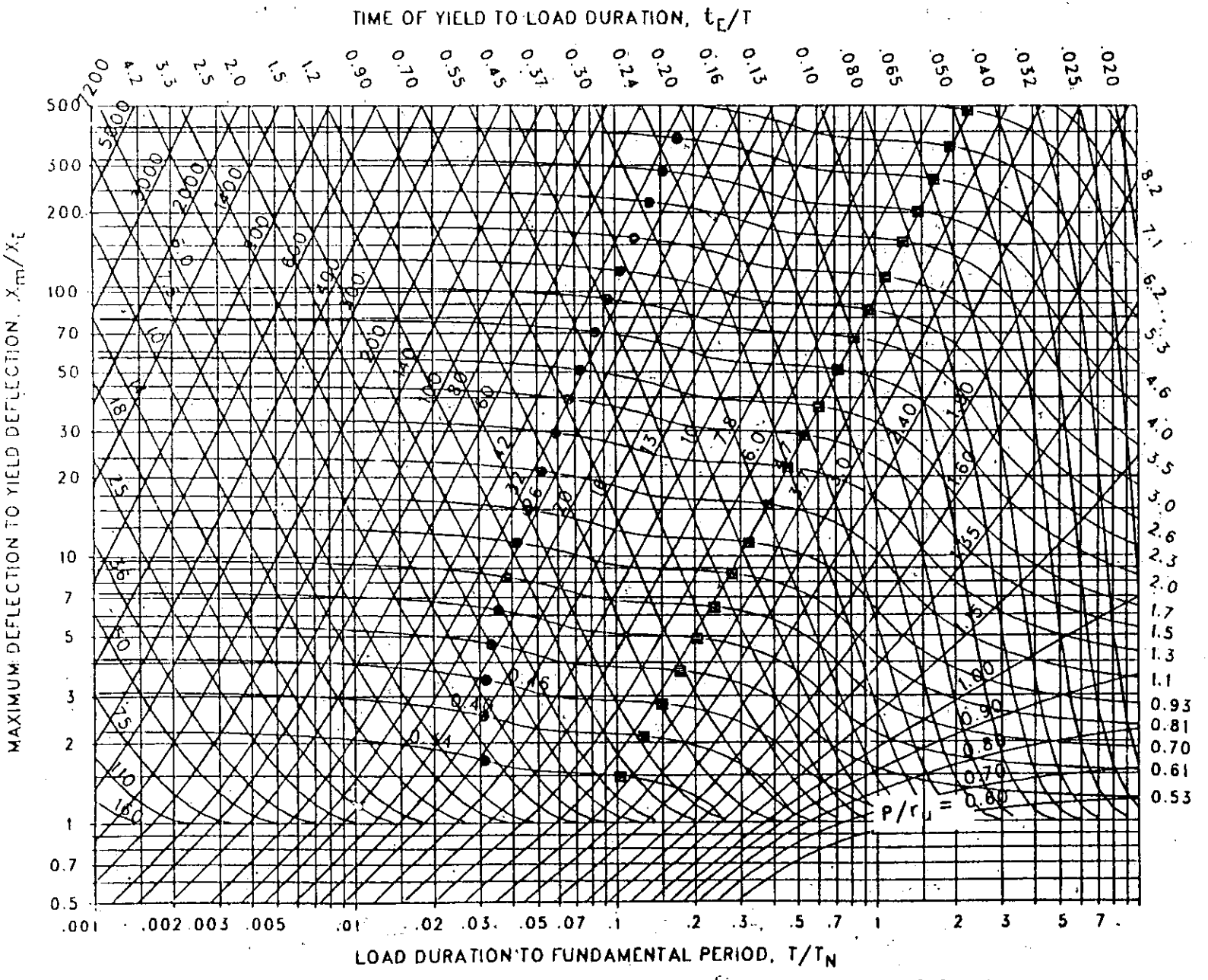


Figure 3-109 Maximum response of elasto-plastic, one-degree-of-freedom system for bilinear-triangular pulse (C_1 = 0.046, C_2 = 10)

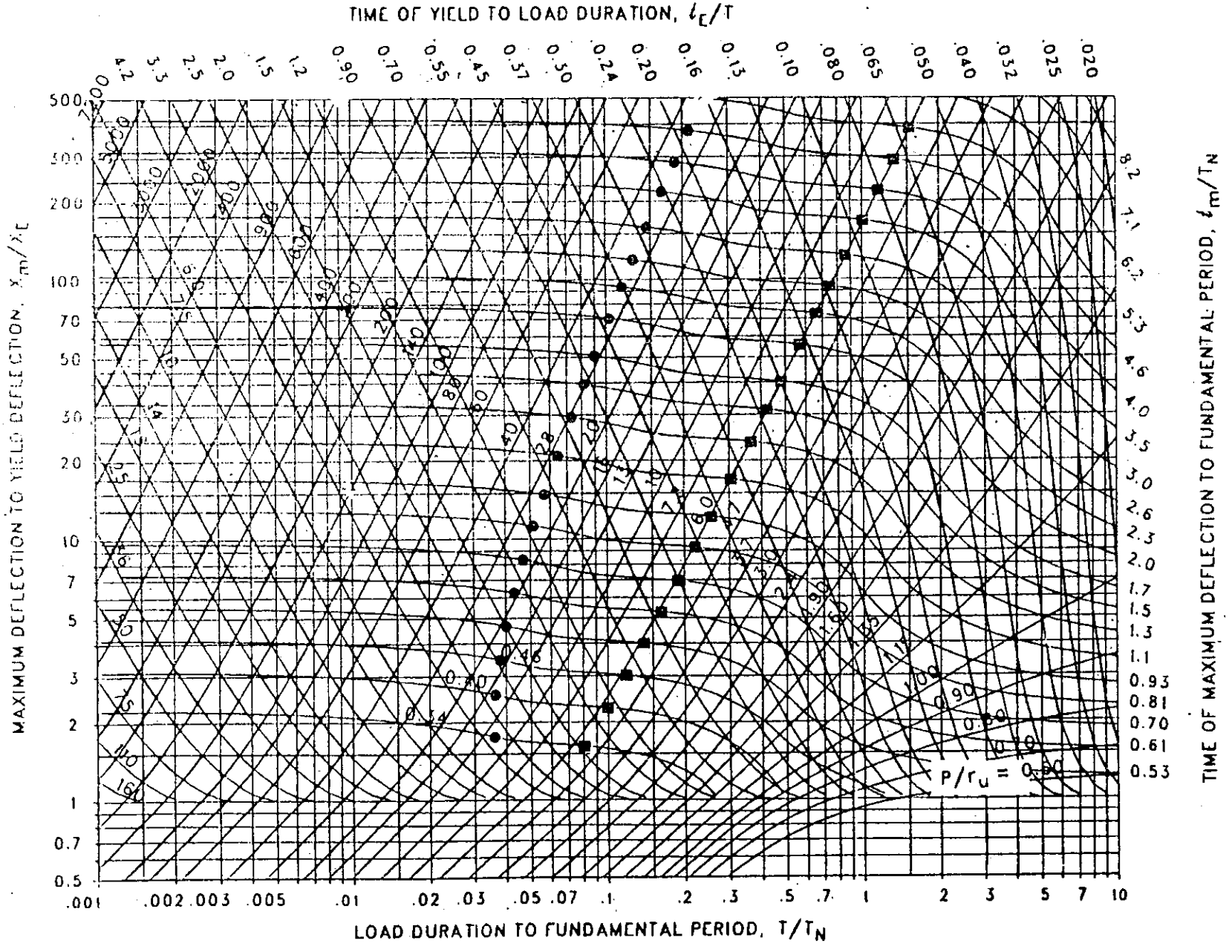


Figure 3-110 · Maximum response of elasto-plastic, one-degree-of-freedom system for bilinear-triangular pulse ($C_1 = 0.032$, $C_2 = 10$)

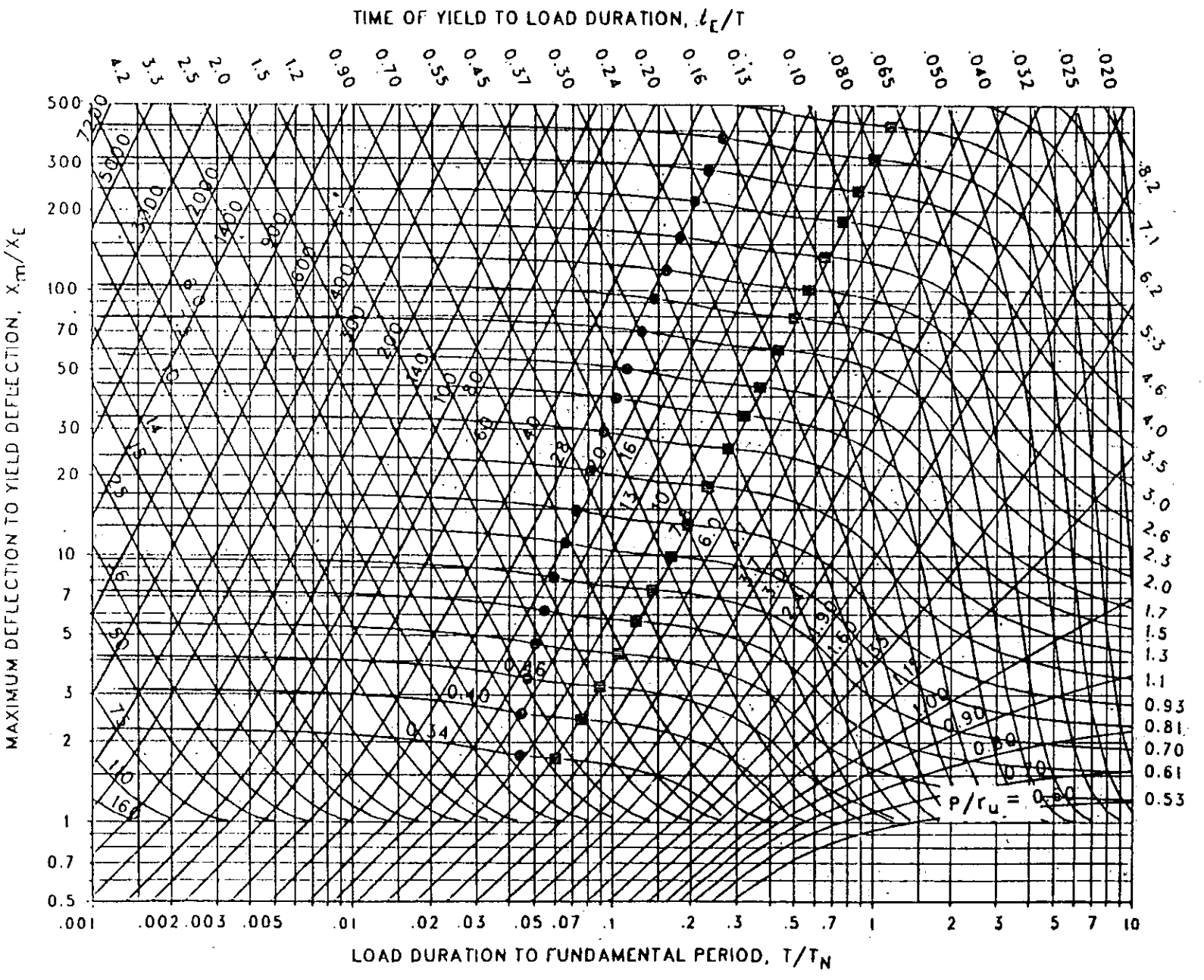


Figure 3-111 Maximum response of elasto-plastic, one-degree-of-freedom system for bilinear-triangular pulse ($C_1 = 0.022$, $C_2 = 10$)

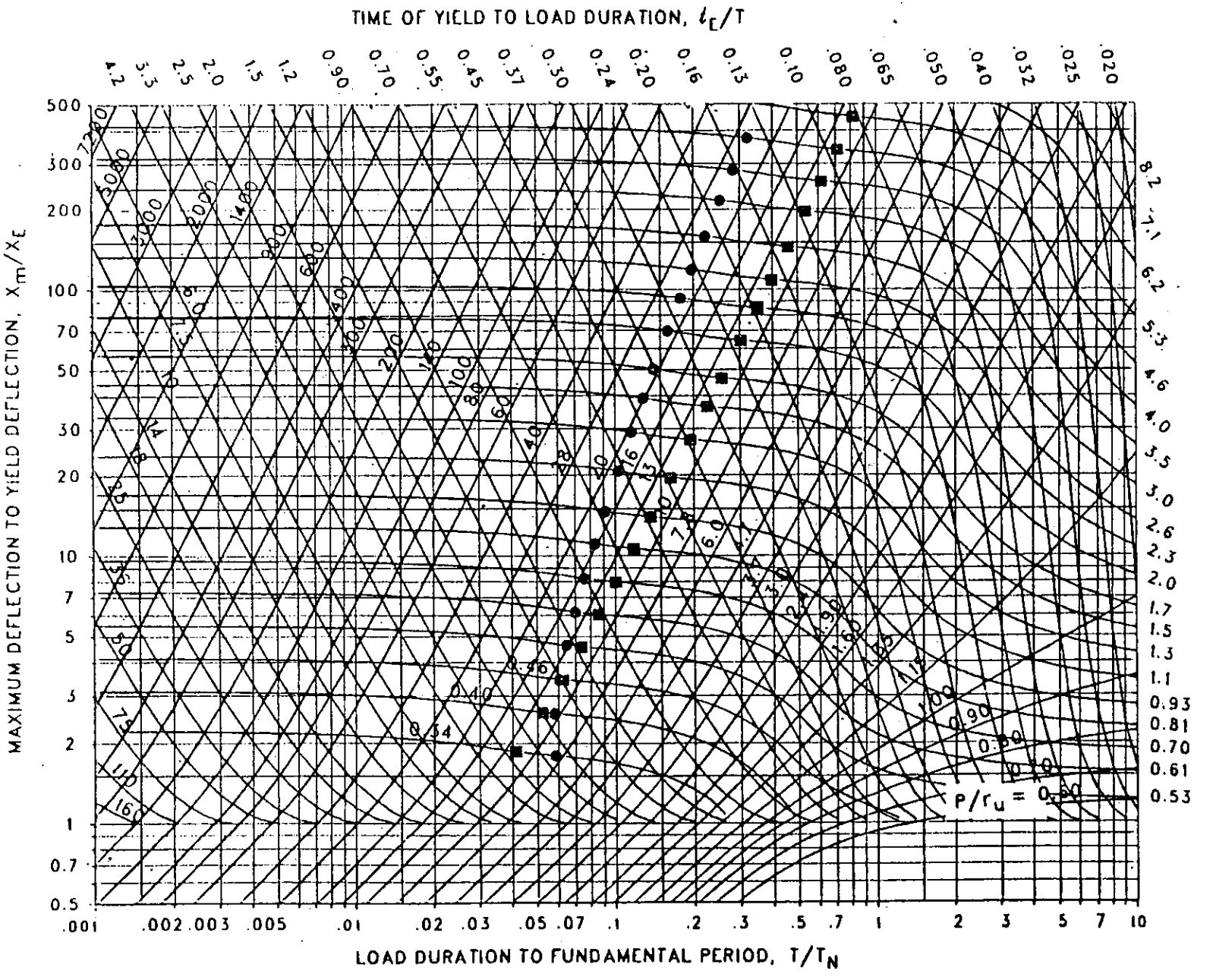


Figure 3-112 Maximum response of elasto-plastic, one-degree-of-freedom system for bilinear-triangular pulse ($C_1 = 0.015$, $C_2 = 10$)

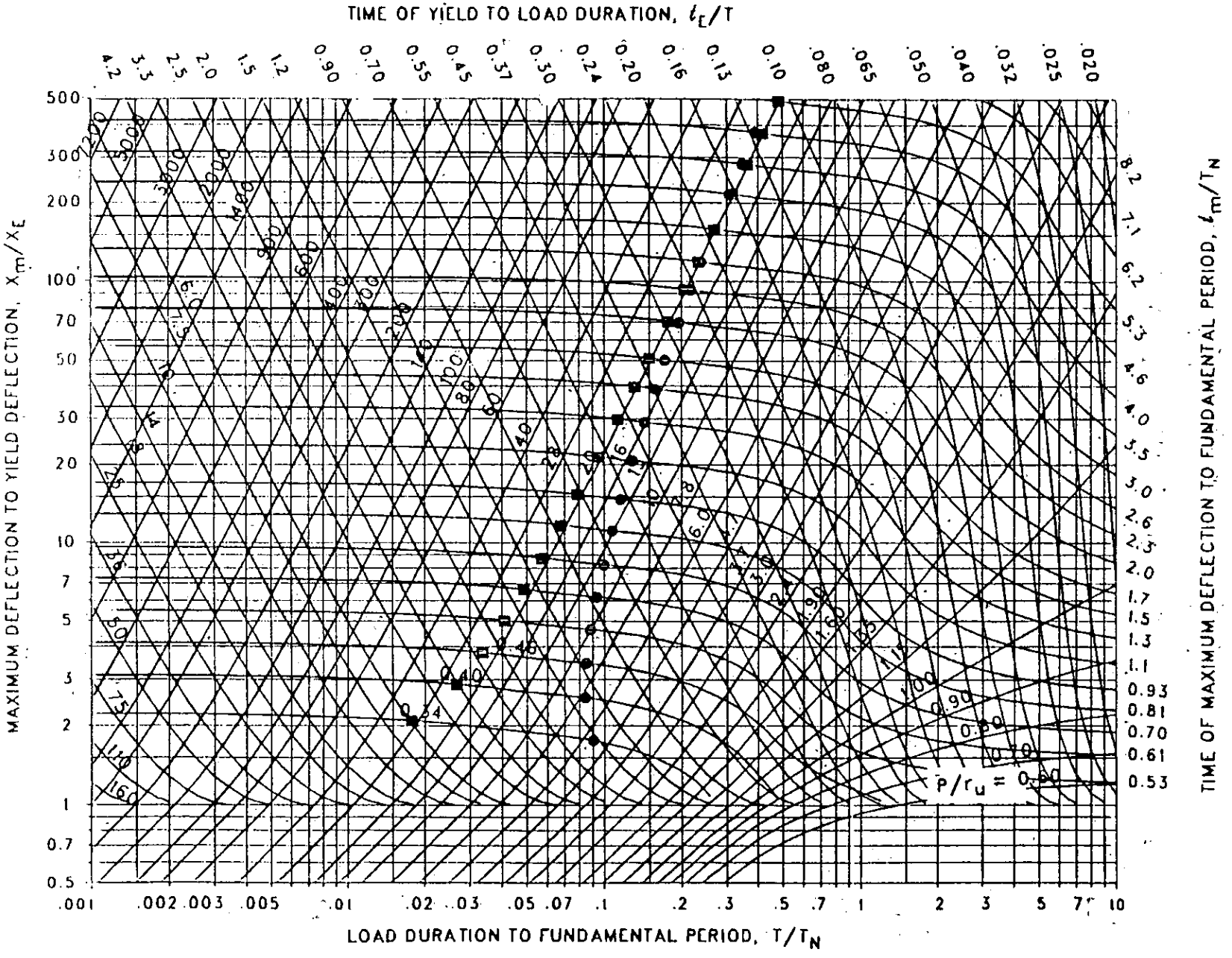


Figure 3-113 Maximum response of elasto-plastic, one-degree-of-freedom system for bilinear-triangular pulse (C_1 = 0.010, C_2 = 10)

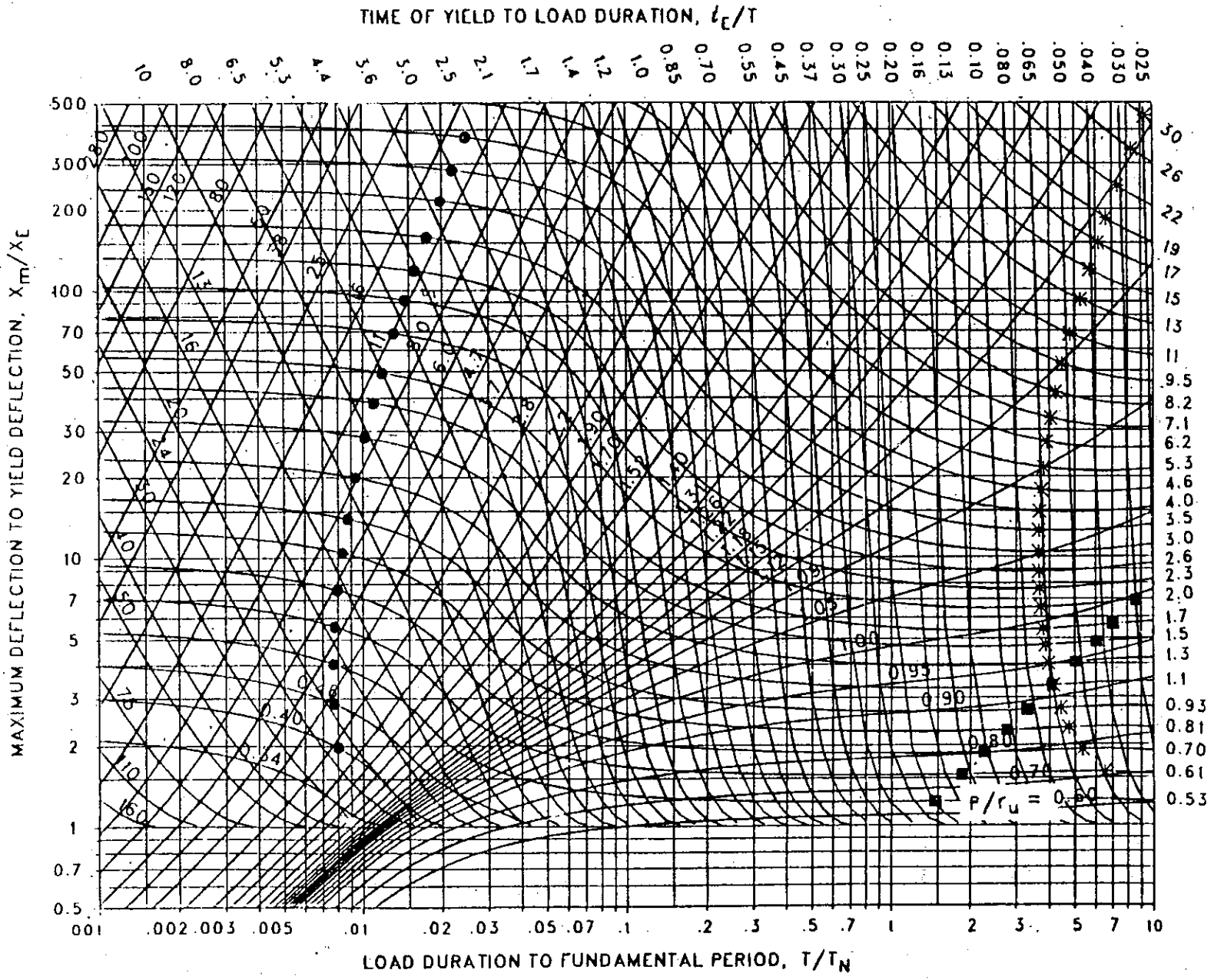


Figure 3-114 Maximum response of elasto-plastic, one-degree-of-freedom system for bilinear-triangular pulse ($C_1 = 0.909$, $C_2 = 30$)

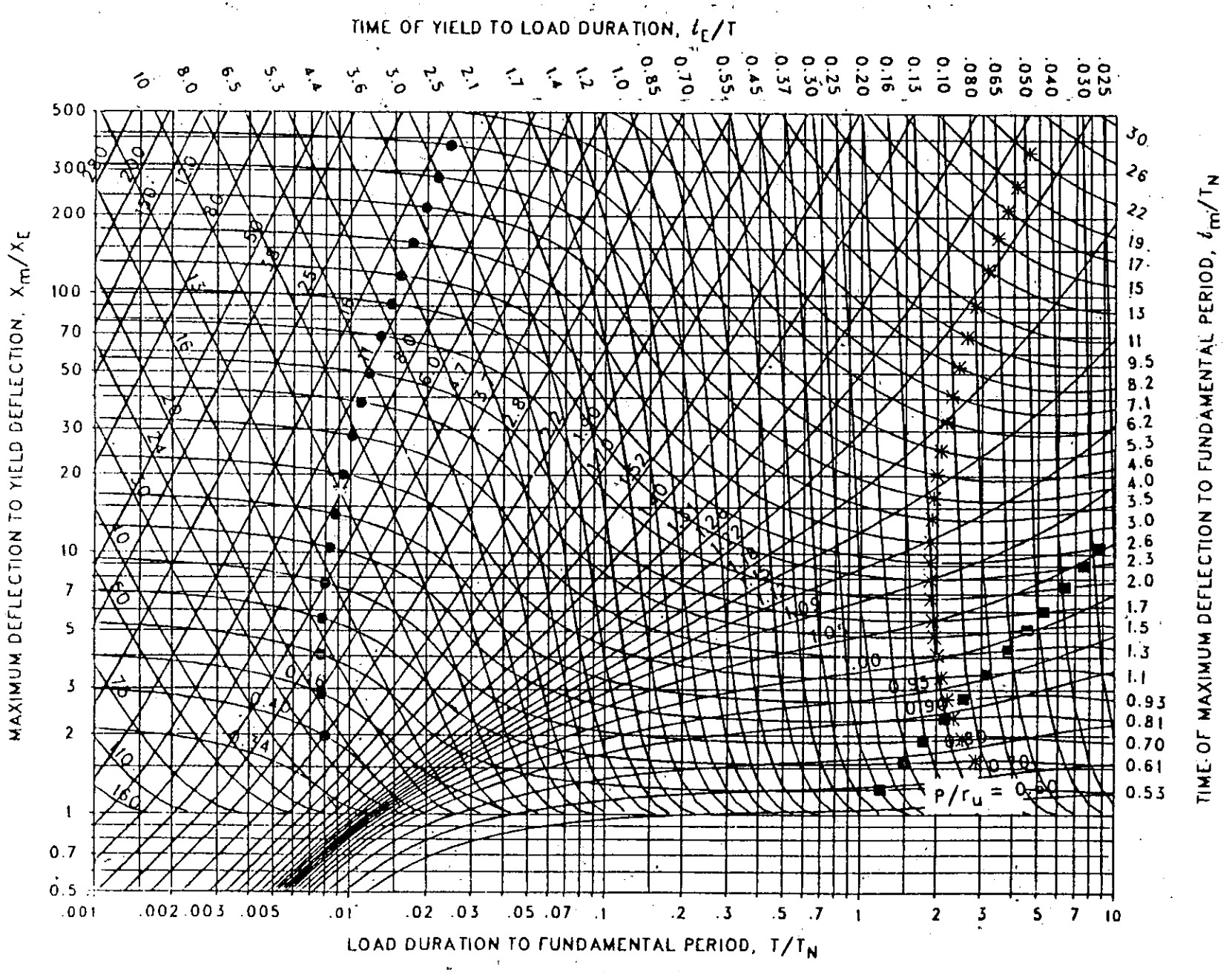


Figure 3-115 Maximum response of elasto-plastic, one-degree-of-freedom system for bilinear-triangular pulse (C_1 = 0.866, C_2 = 30)

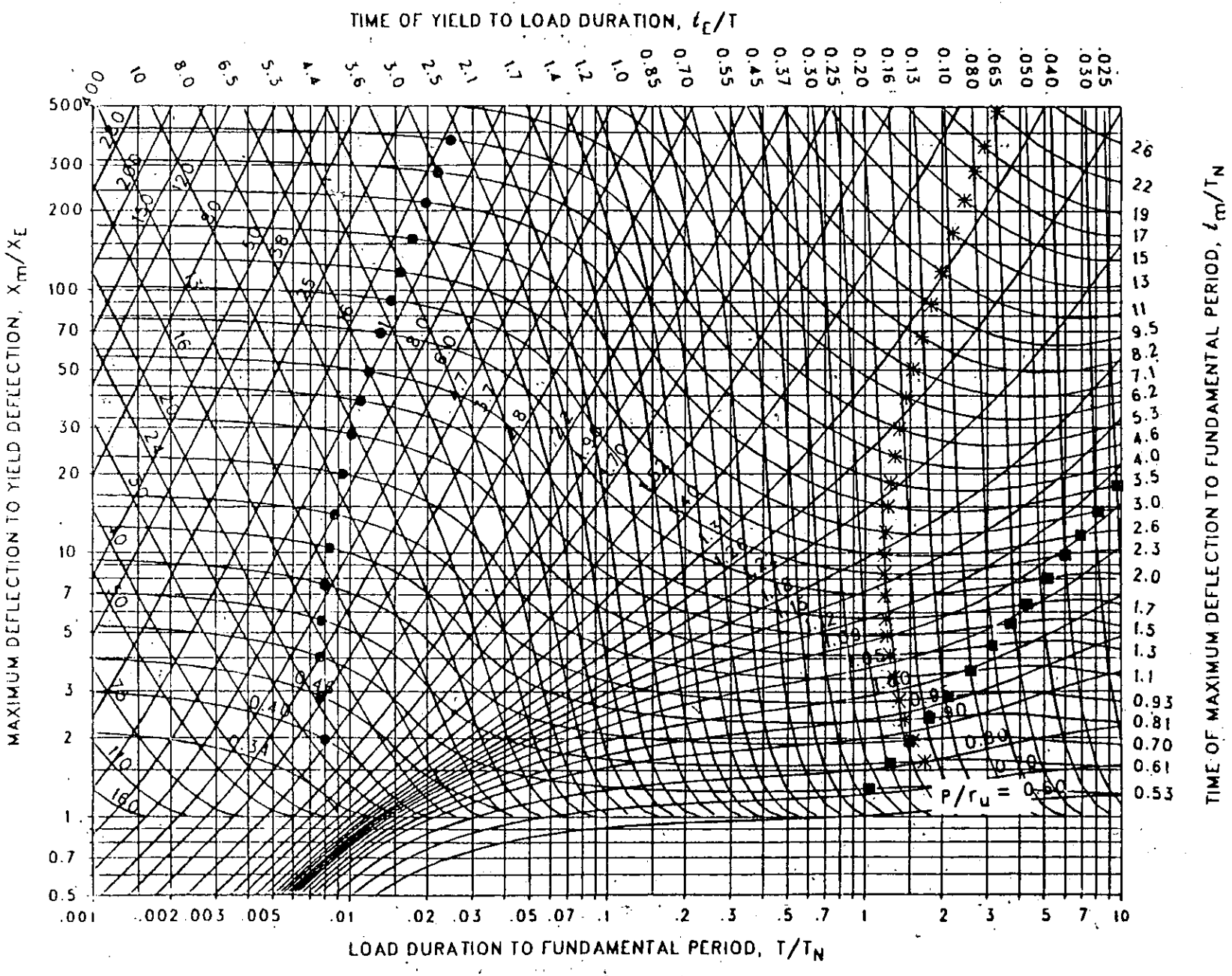


Figure 3-116 Maximum response of elasto-plastic, one-degree-of-freedom system for bilinear-triangular pulse ($C_1 = 0.825$, $C_2 = 30$)

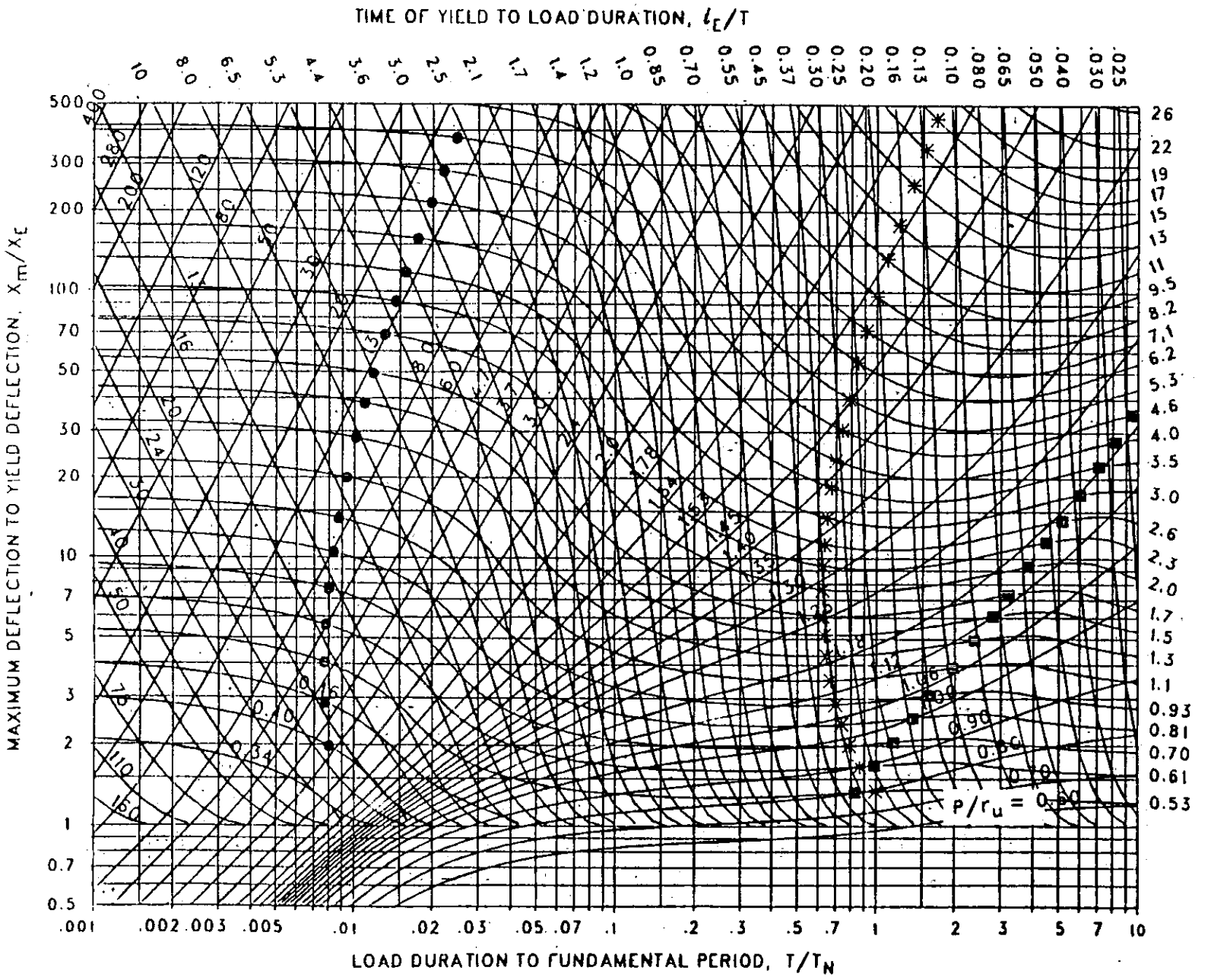


Figure 3-117 Maximum response of elasto-plastic, one-degree-of-freedom system for bilinear-triangular pulse ($C_1 = 0.750$, $C_2 = 30$)

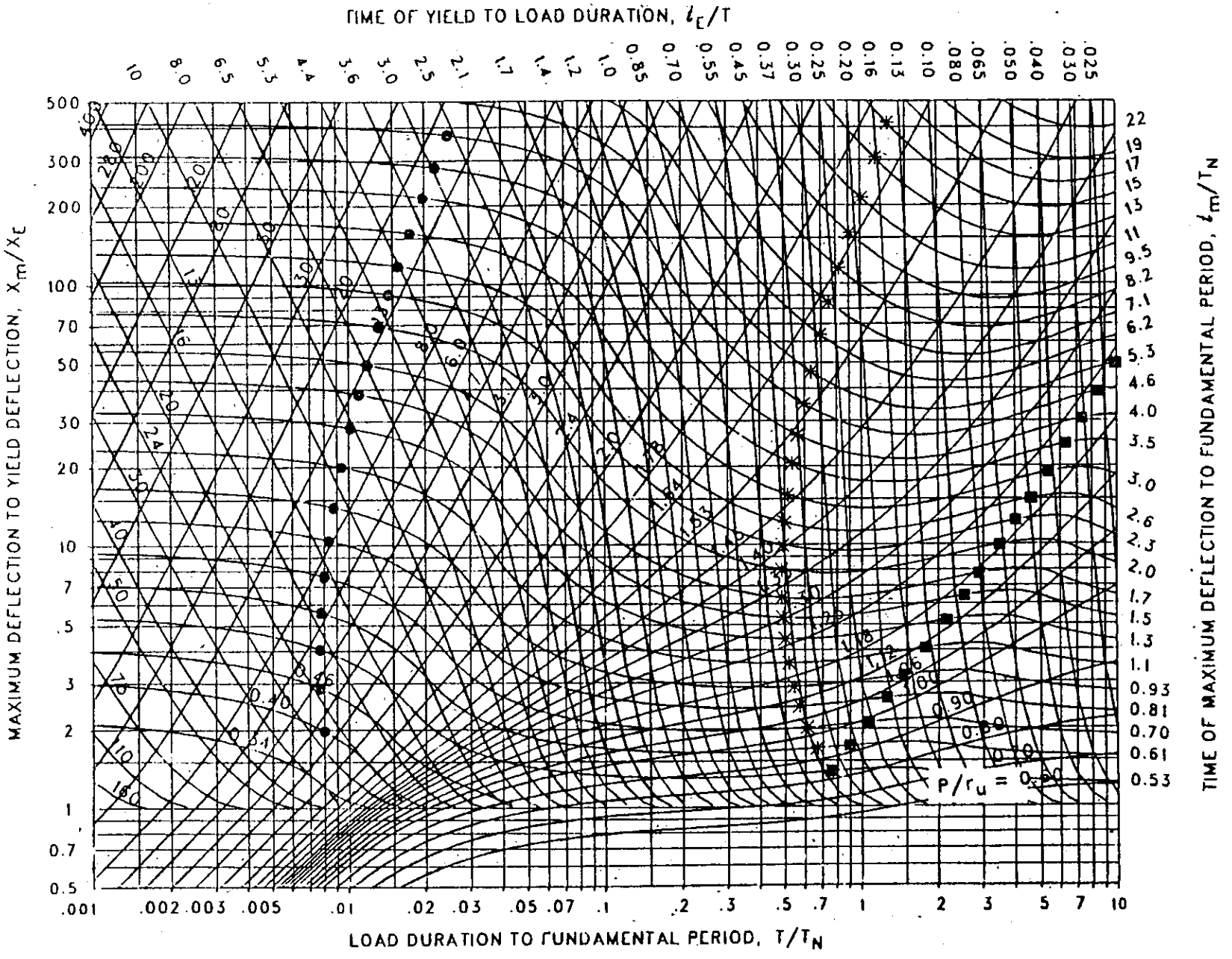


Figure 3-118 Maximum response of elasto-plastic, one-degree-of-freedom system for bilinear-triangular pulse (C_1 = 0.715, C_2 = 30)

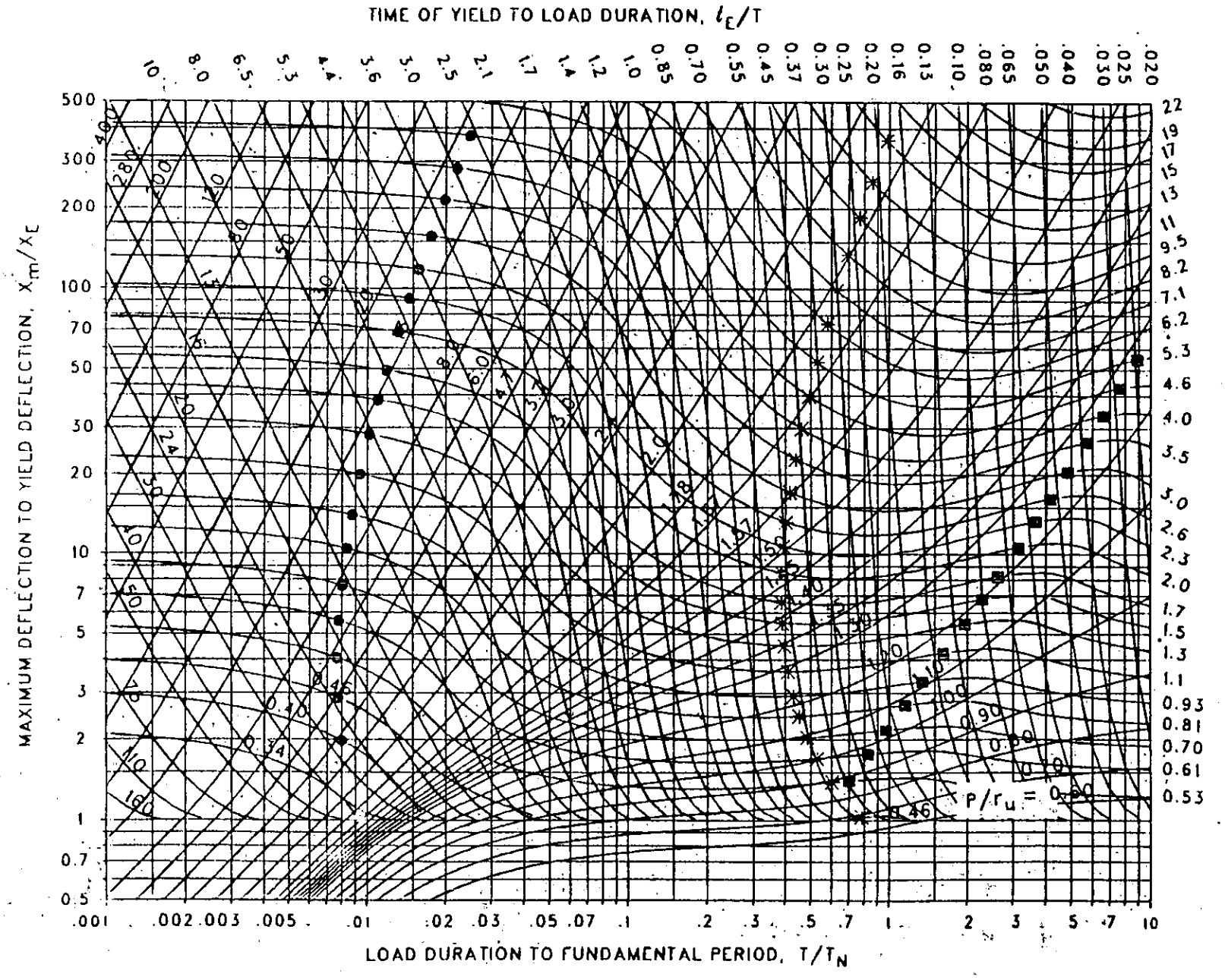


Figure 3-119 Maximum response of elasto-plastic, one-degree-of-freedom system for bilinear-triangular pulse ($C_1 = 0.681$, $C_2 = 30$)

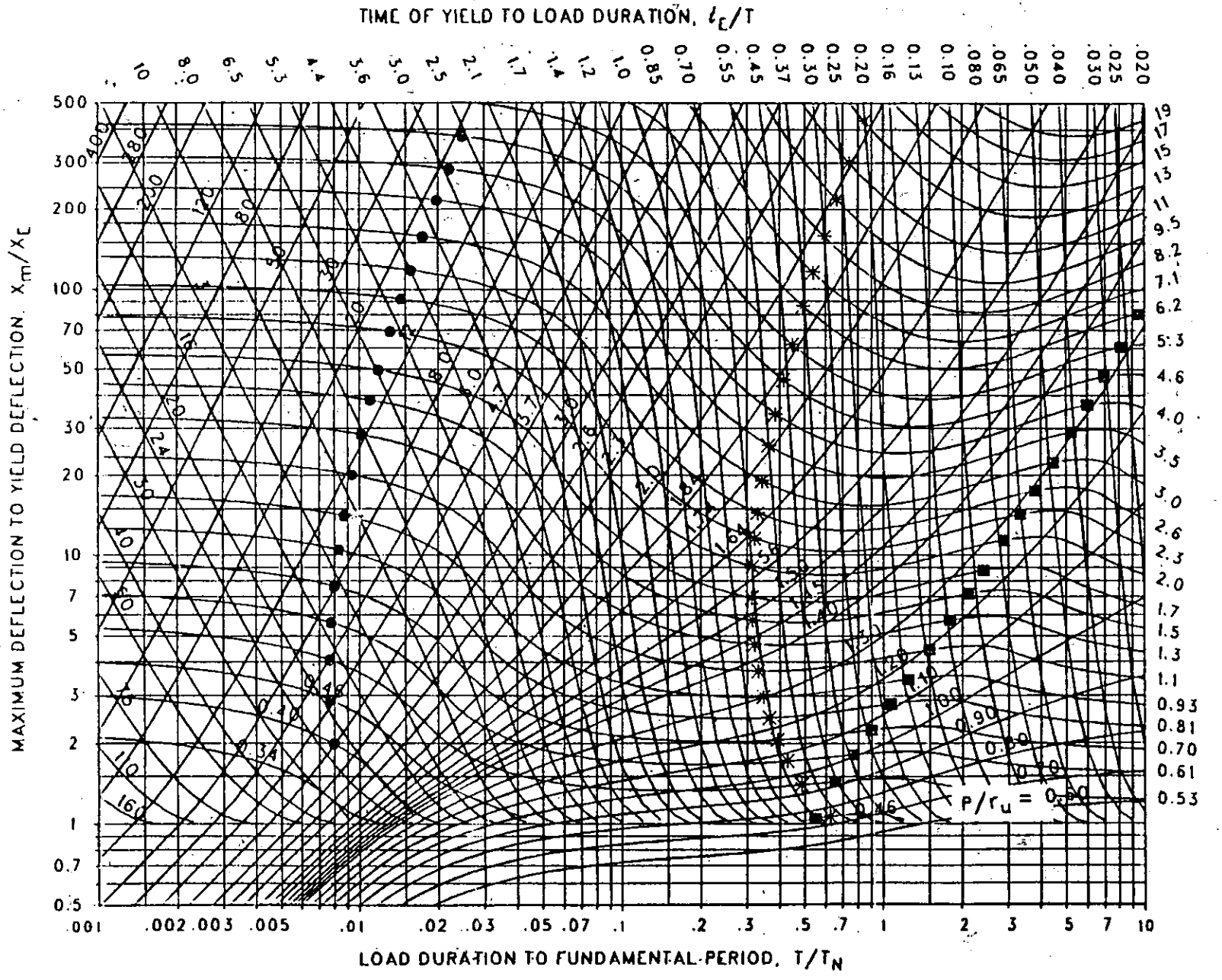


Figure 3-120 Maximum response of elasto-plastic, one-degree-of-freedom system for bilinear-triangular pulse ($C_1 = 0.648$, $C_2 = 30$)

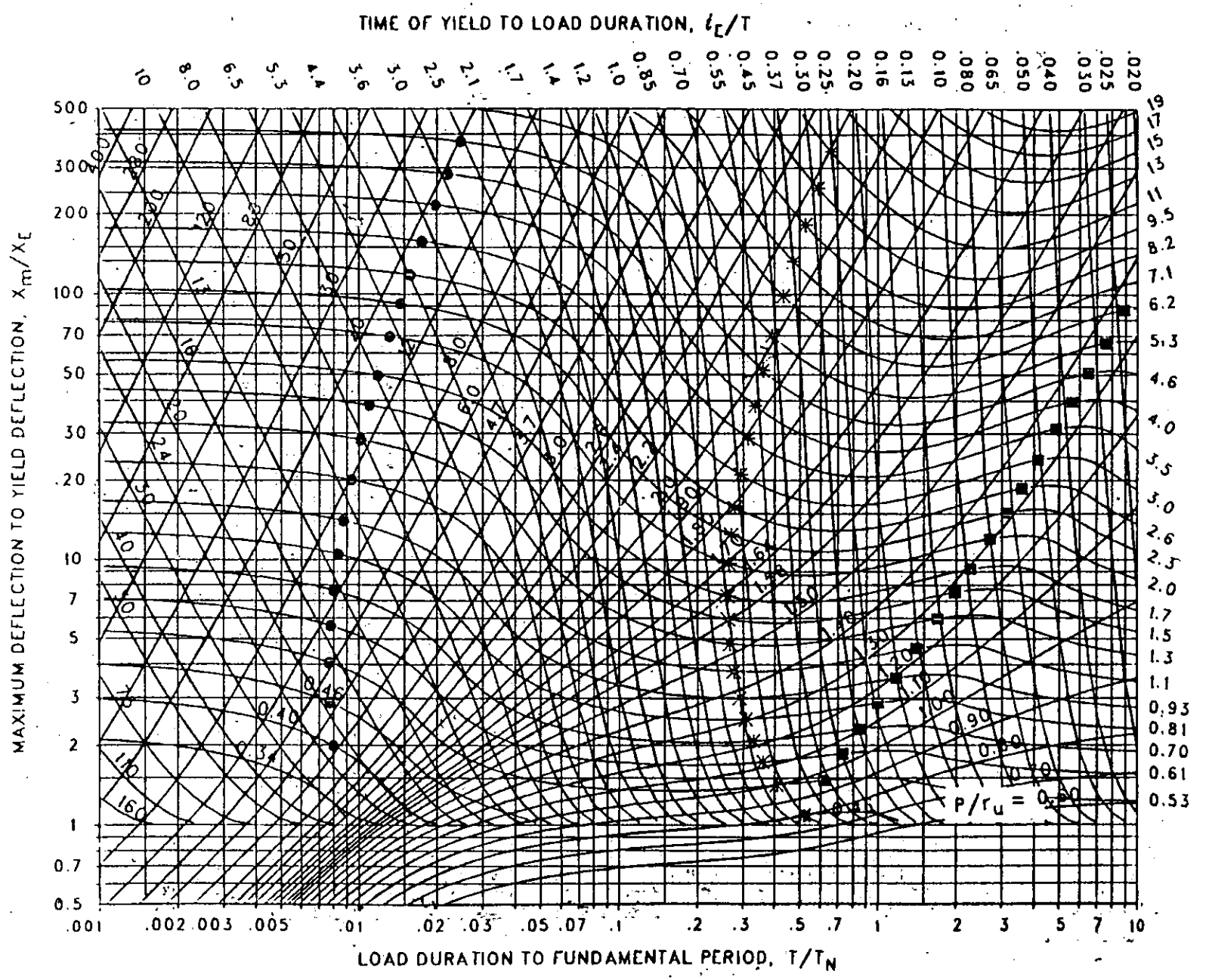


Figure 3-121 Maximum response of elasto-plastic, one-degree-of-freedom system for bilinear-triangular pulse ($C_1 = 0.619$, $C_2 = 30$)

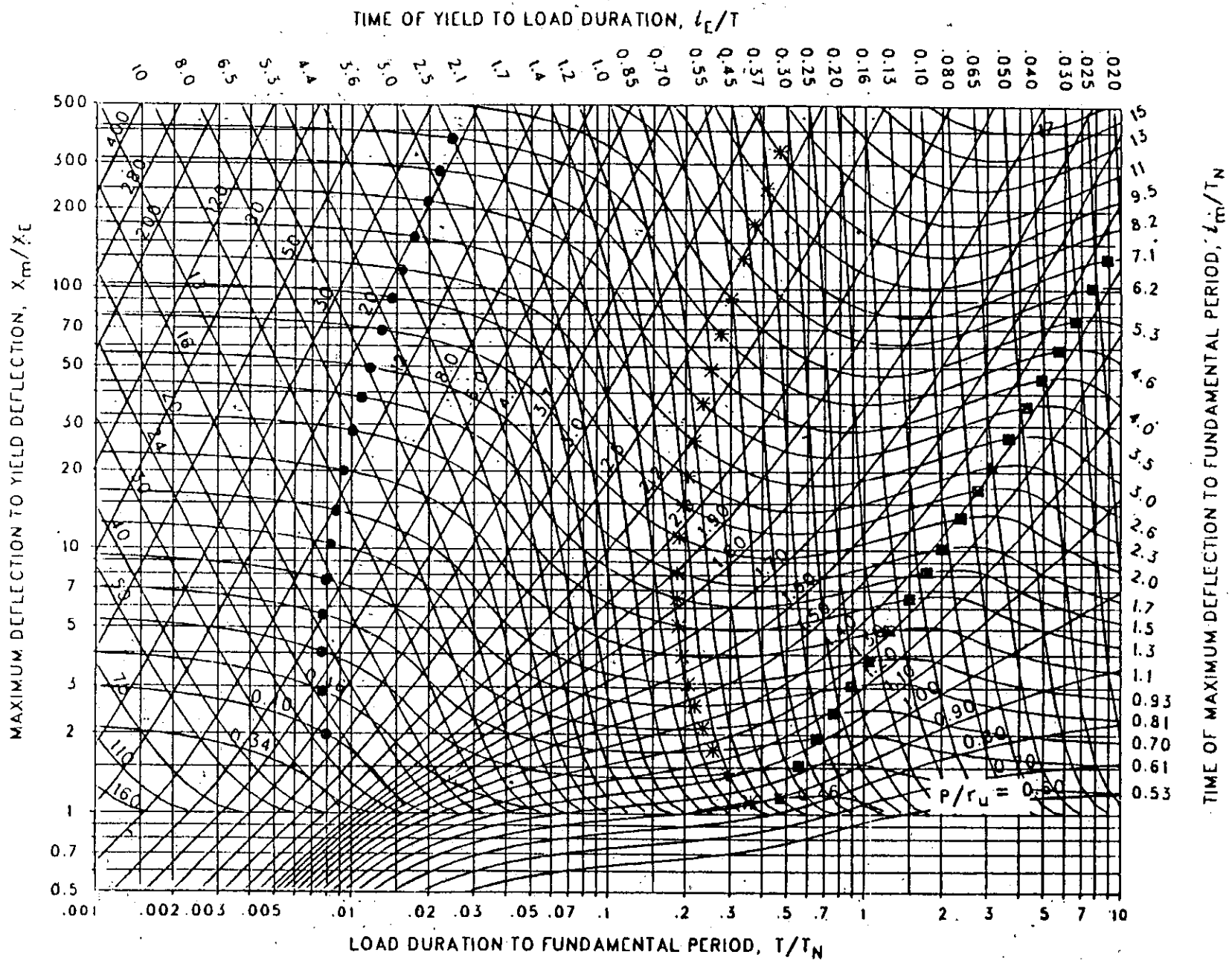


Figure 3-122 Maximum response of elasto-plastic, one-degree-of-freedom system for bilinear-triangular pulse ($C_1 = 0.562$, $C_2 = 30$)

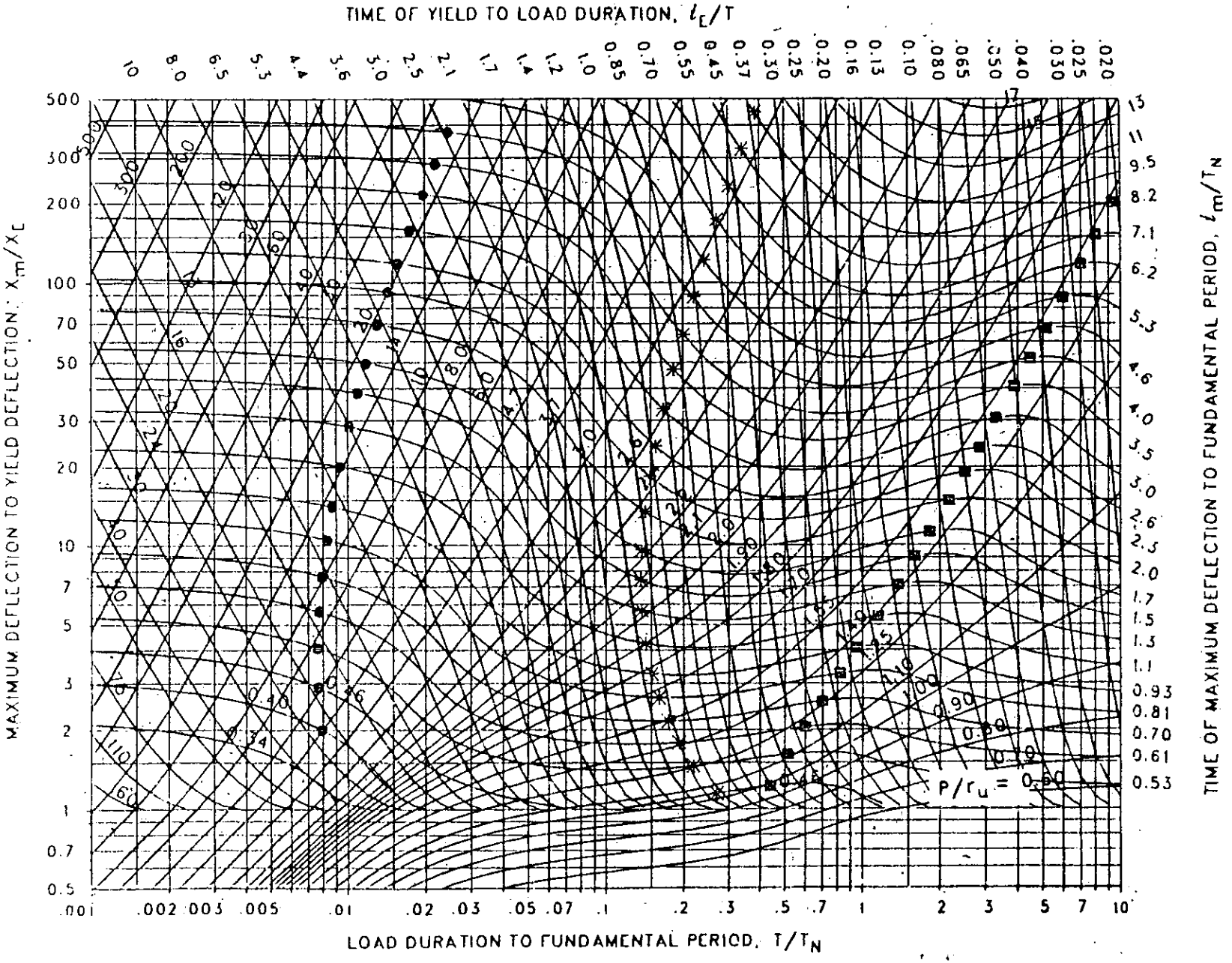


Figure 3-123 Maximum response of elasto-plastic, one-degree-of-freedom system for bilinear-triangular pulse ($C_1 = 0.511$, $C_2 = 30$)

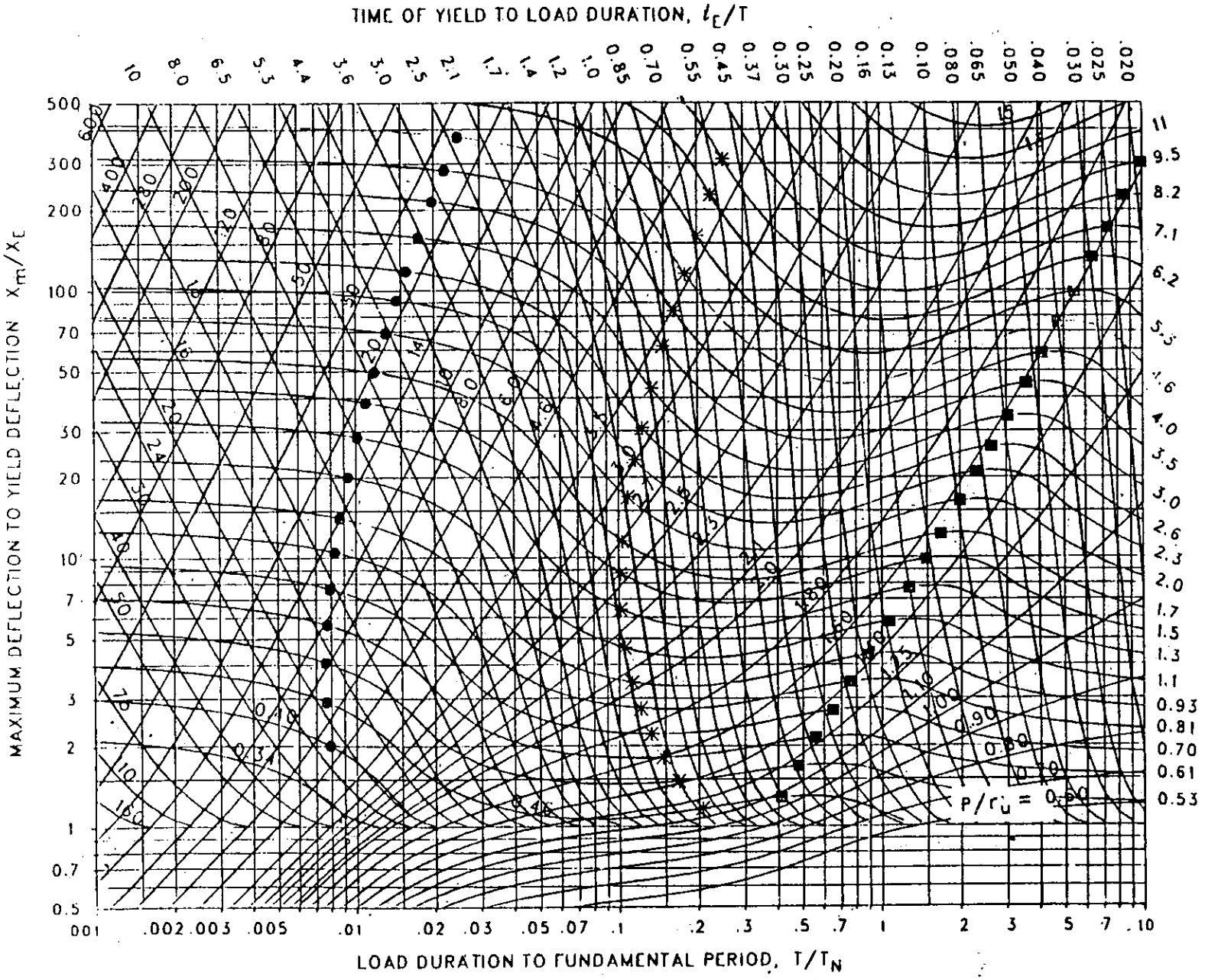


Figure 3-124 Maximum response of elasto-plastic, one-degree-of-freedom system for bilinear-triangular pulse (C_1 = 0.464, C_2 = 30)

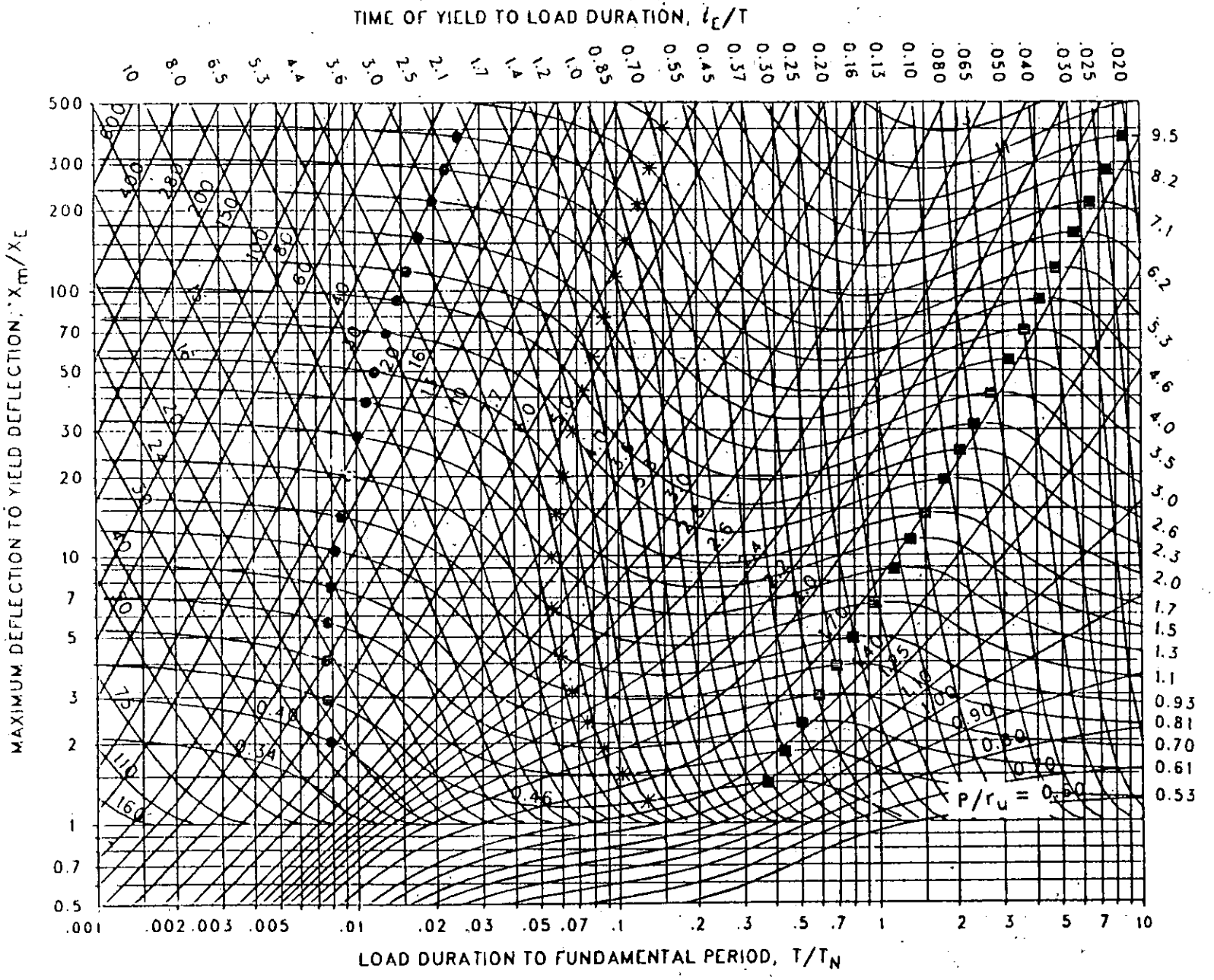


Figure 3-125 Maximum response of elasto-plastic, one-degree-of-freedom system for bilinear-triangular pulse ($C_1 = 0.383$, $C_2 = 30$)

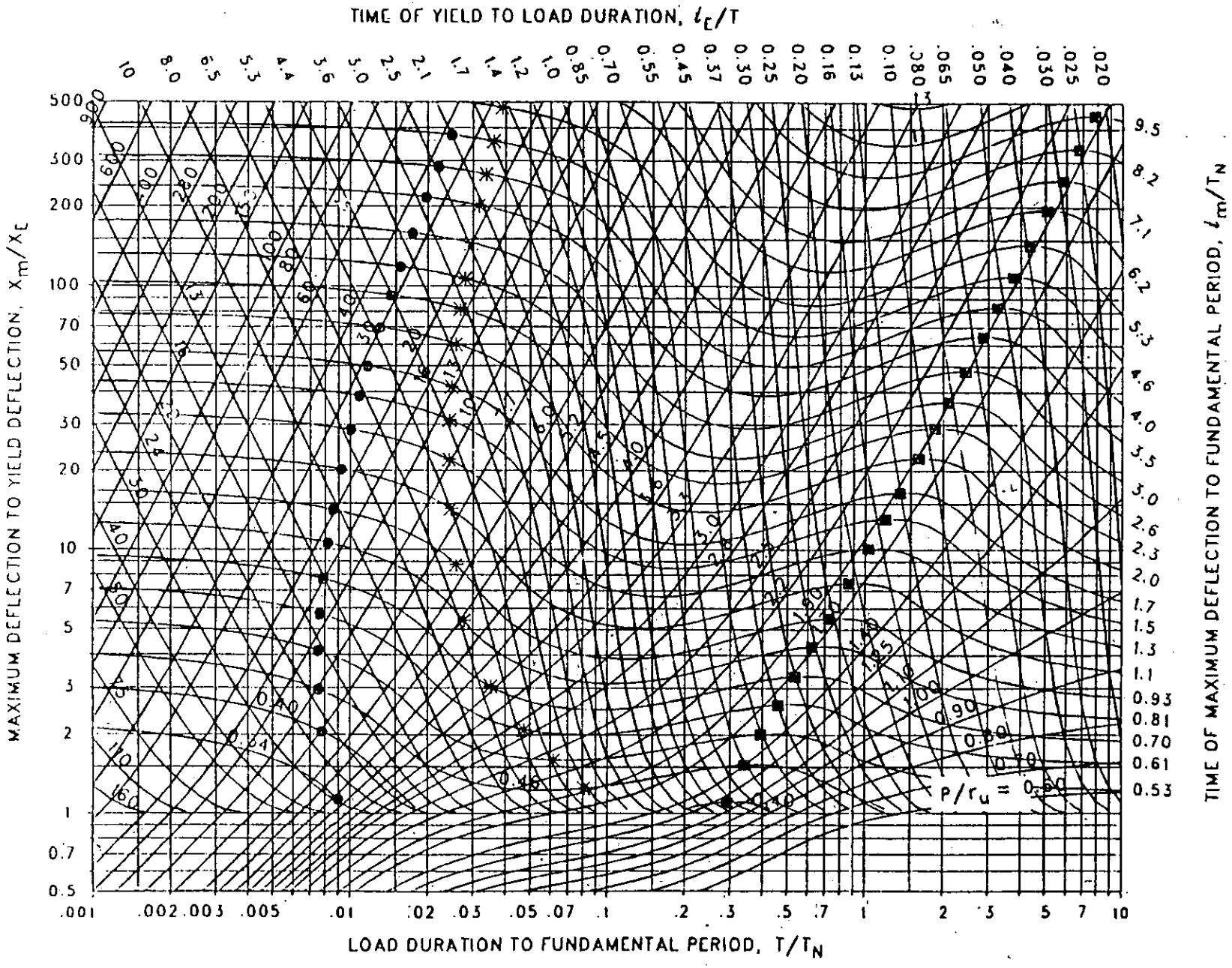


Figure 3-126 Maximum response of elasto-plastic, one-degree-of-freedom system for bilinear-triangular pulse ($C_1 = 0.316$, $C_2 = 30$)

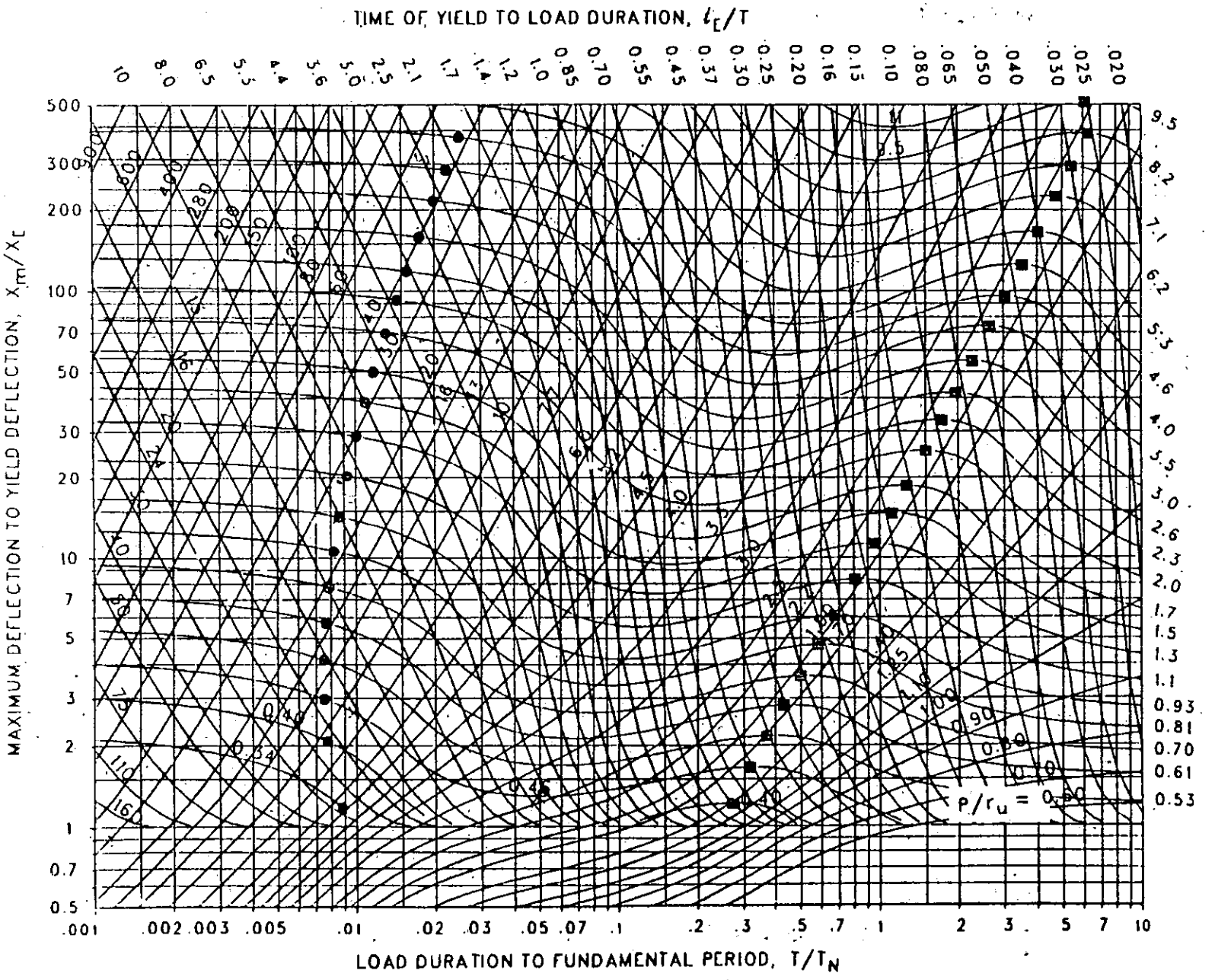


Figure 3-127 Maximum response of elasto-plastic, one-degree-of-freedom system for bilinear-triangular pulse ($C_1 = 0.261$, $C_2 = 30$)

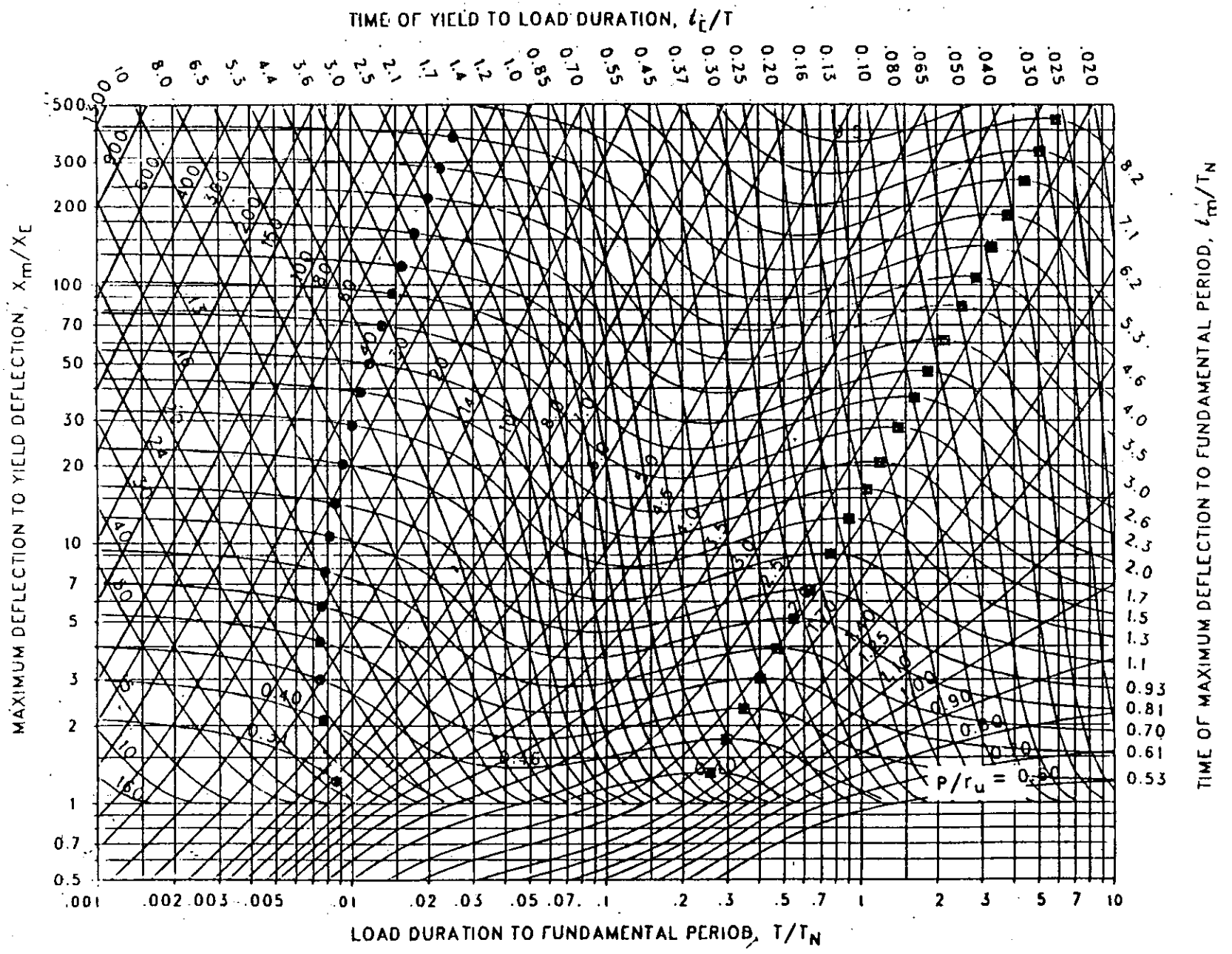


Figure 3-128 Maximum response of elasto-plastic, one-degree-of-freedom system for bilinear-triangular pulse ($C_1 = 0.215$, $C_2 = 30$)

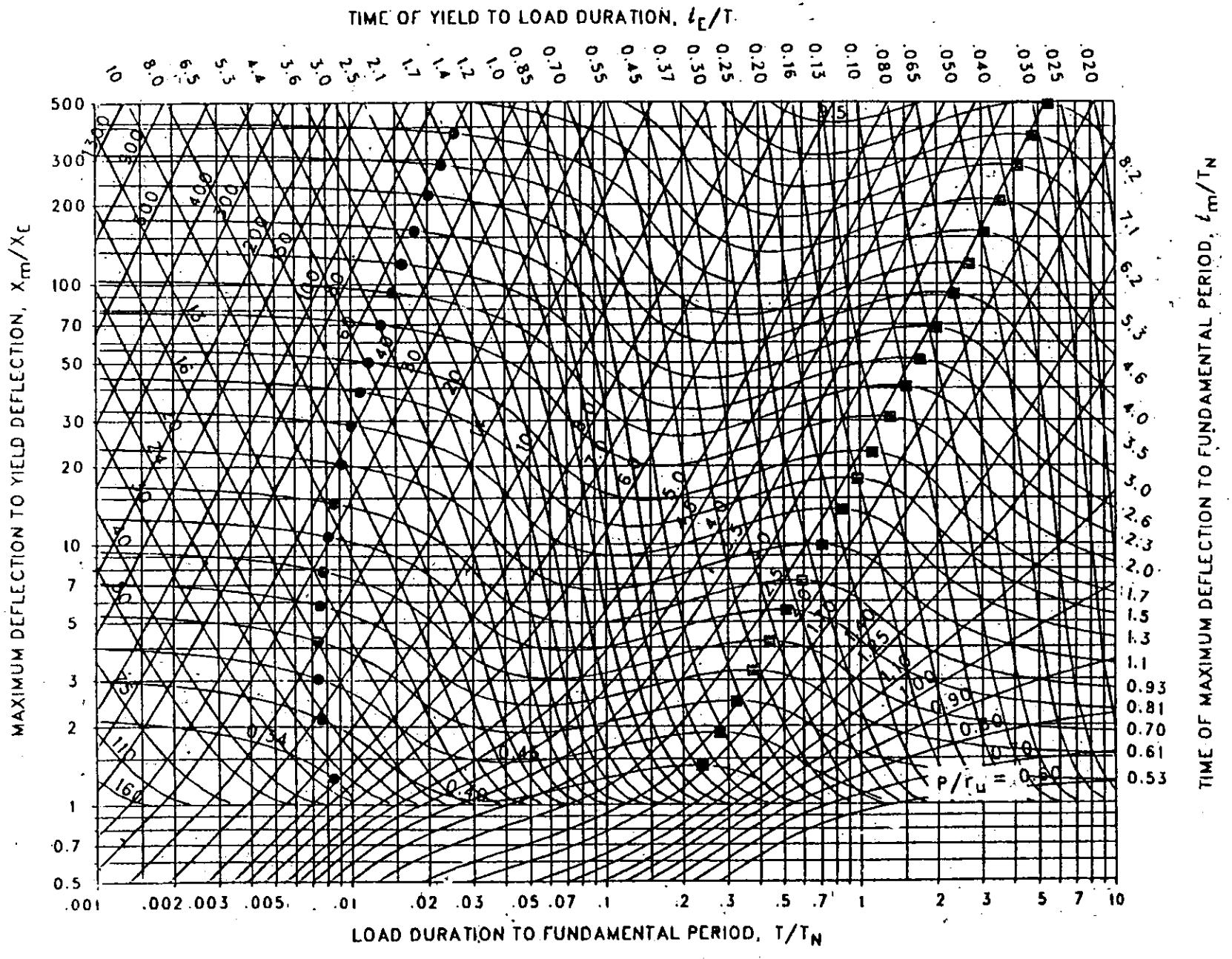


Figure 3-129 Maximum response of elasto-plastic, one-degree-of-freedom system for bilinear-triangular pulse ($C_1 = 0.178$, $C_2 = 30$)

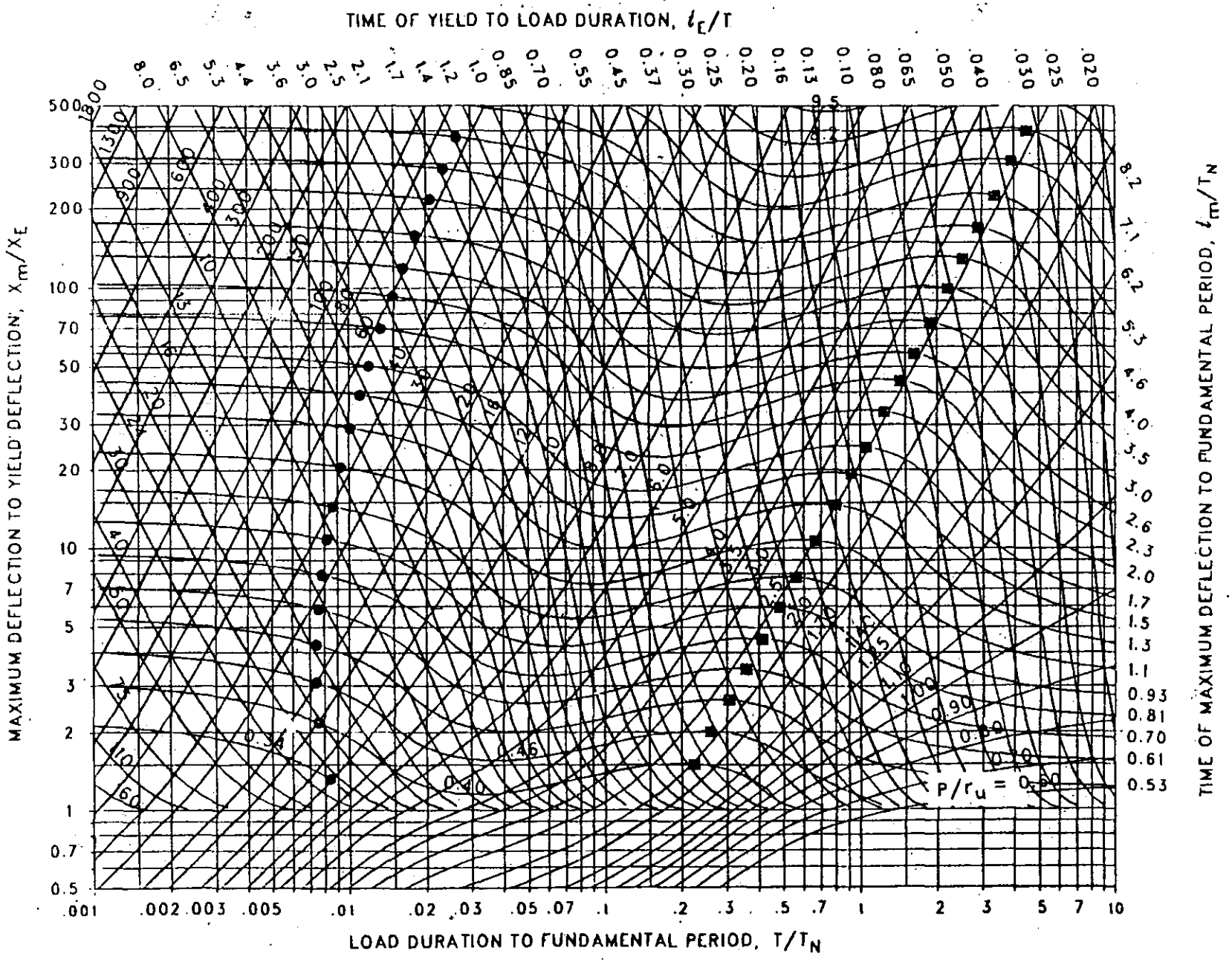


Figure 3-130 Maximum response of elasto-plastic, one-degree-of-freedom system for bilinear-triangular pulse ($C_1 = 0.147$, $C_2 = 30$)

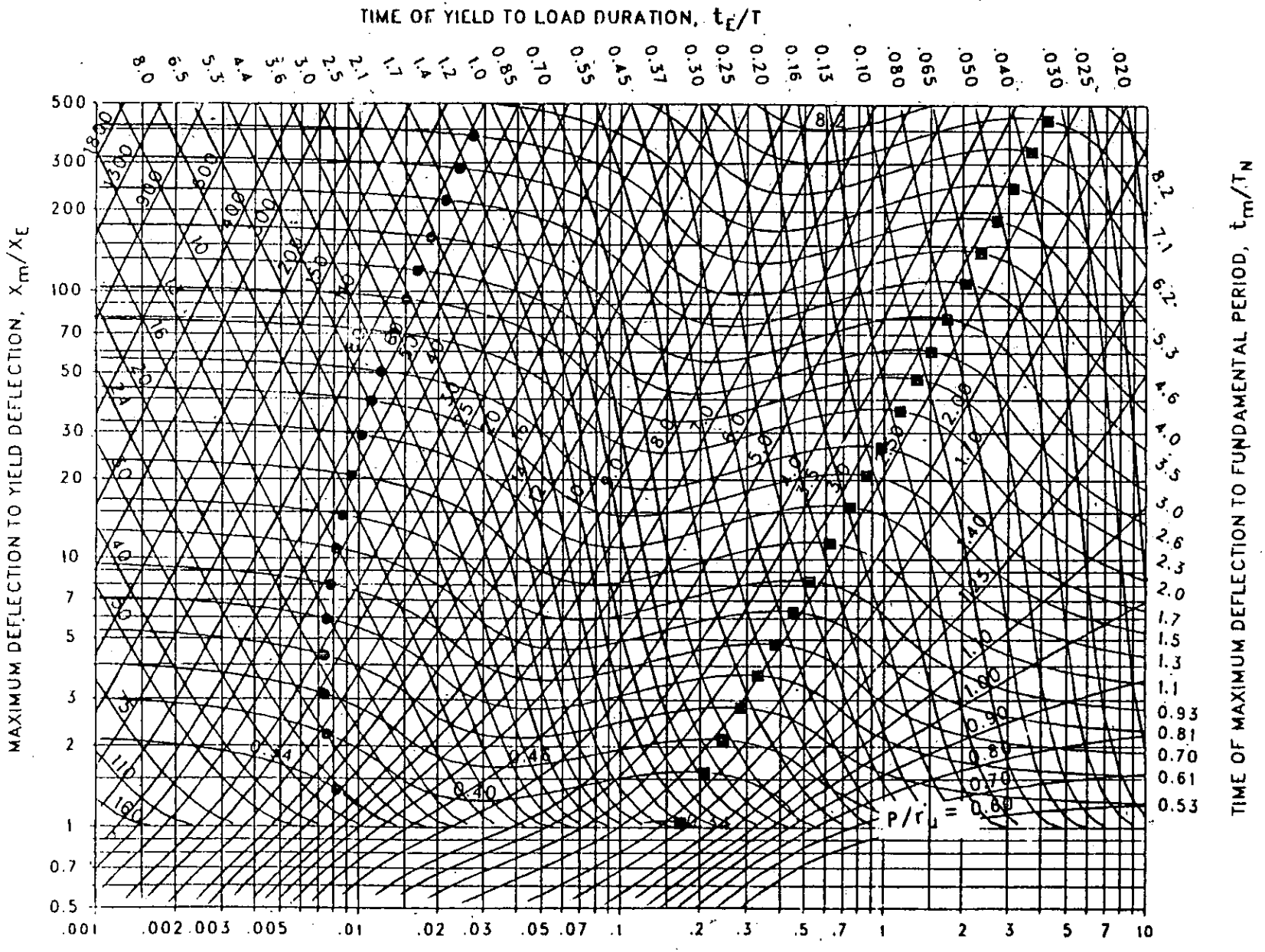


Figure 3-131 Maximum response of elasto-plastic, one-degree-of-freedom system for bilinear-triangular pulse ($C_1 = 0.121$, $C_2 = 30$)

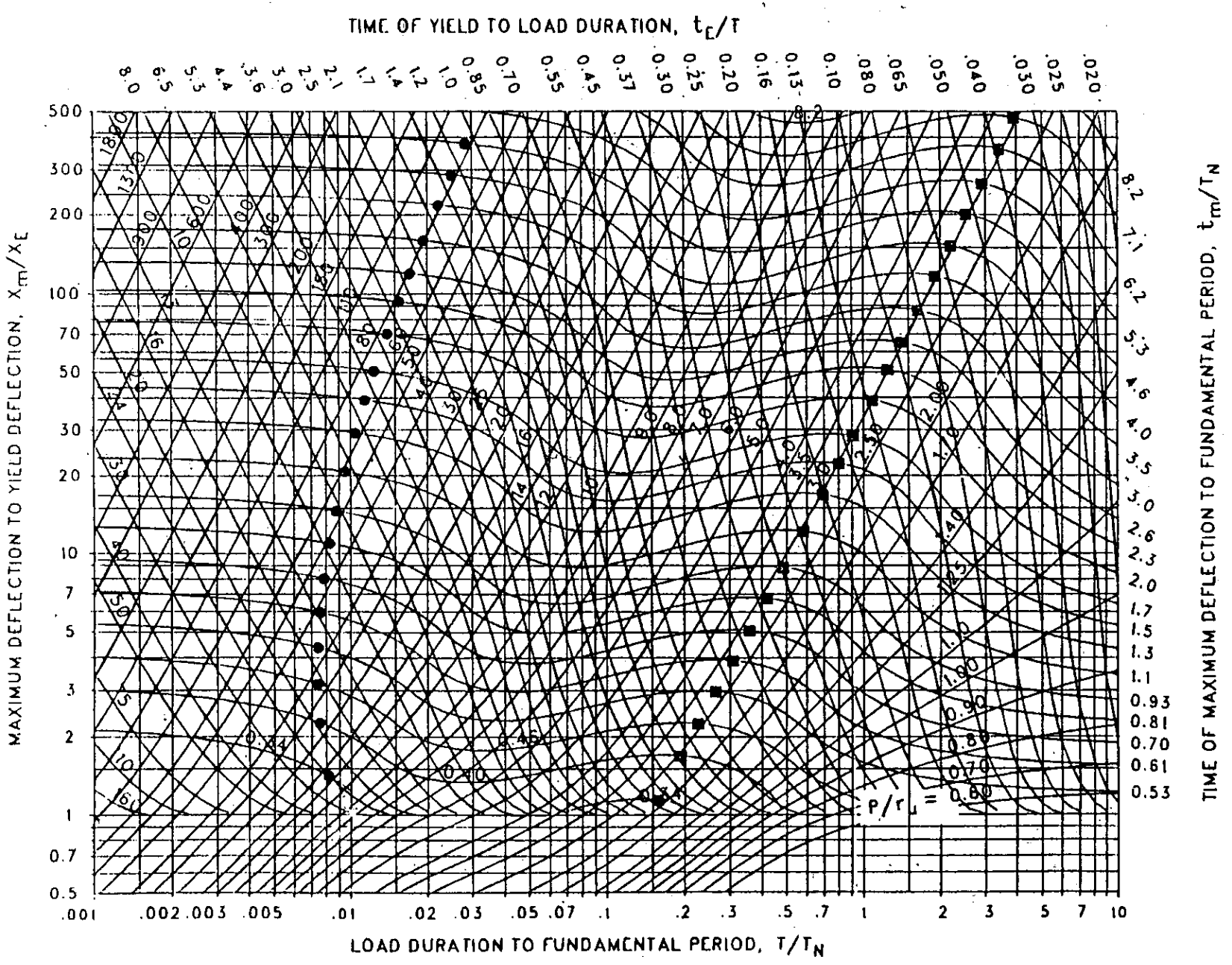


Figure 3-132 Maximum response of elasto-plastic, one-degree-of-freedom system for bilinear-triangular pulse (C_1 = 0.100, C_2 = 30)

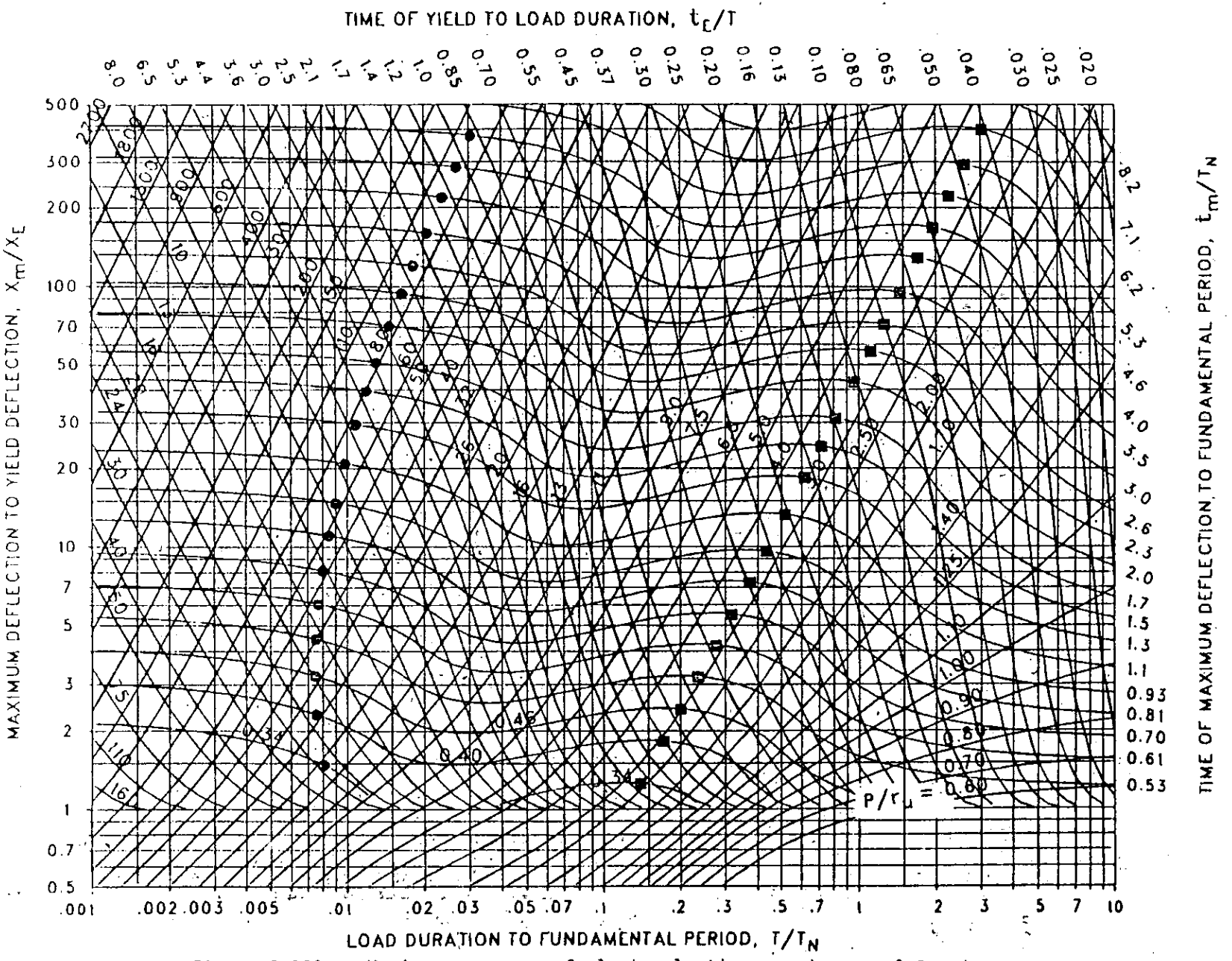


Figure 3-133 Maximum response of elasto-plastic, one-degree-of-freedom system for bilinear-triangular pulse ($C_1 = 0.075$, $C_2 = 30$)

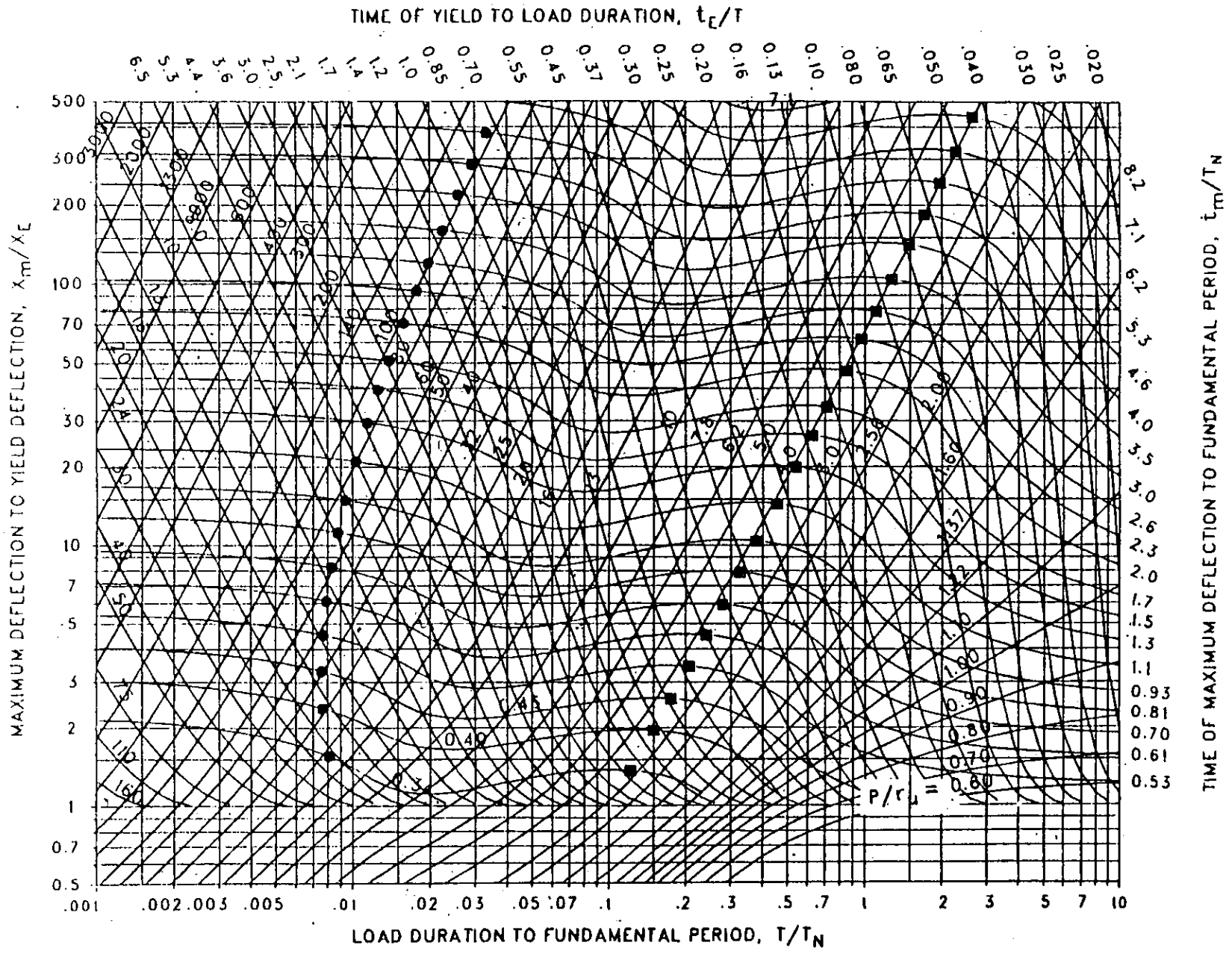


Figure 3-134 Maximum response of elasto-plastic, one-degree-of-freedom system for bilinear-triangular pulse ($C_1 = 0.056$, $C_2 = 30$)

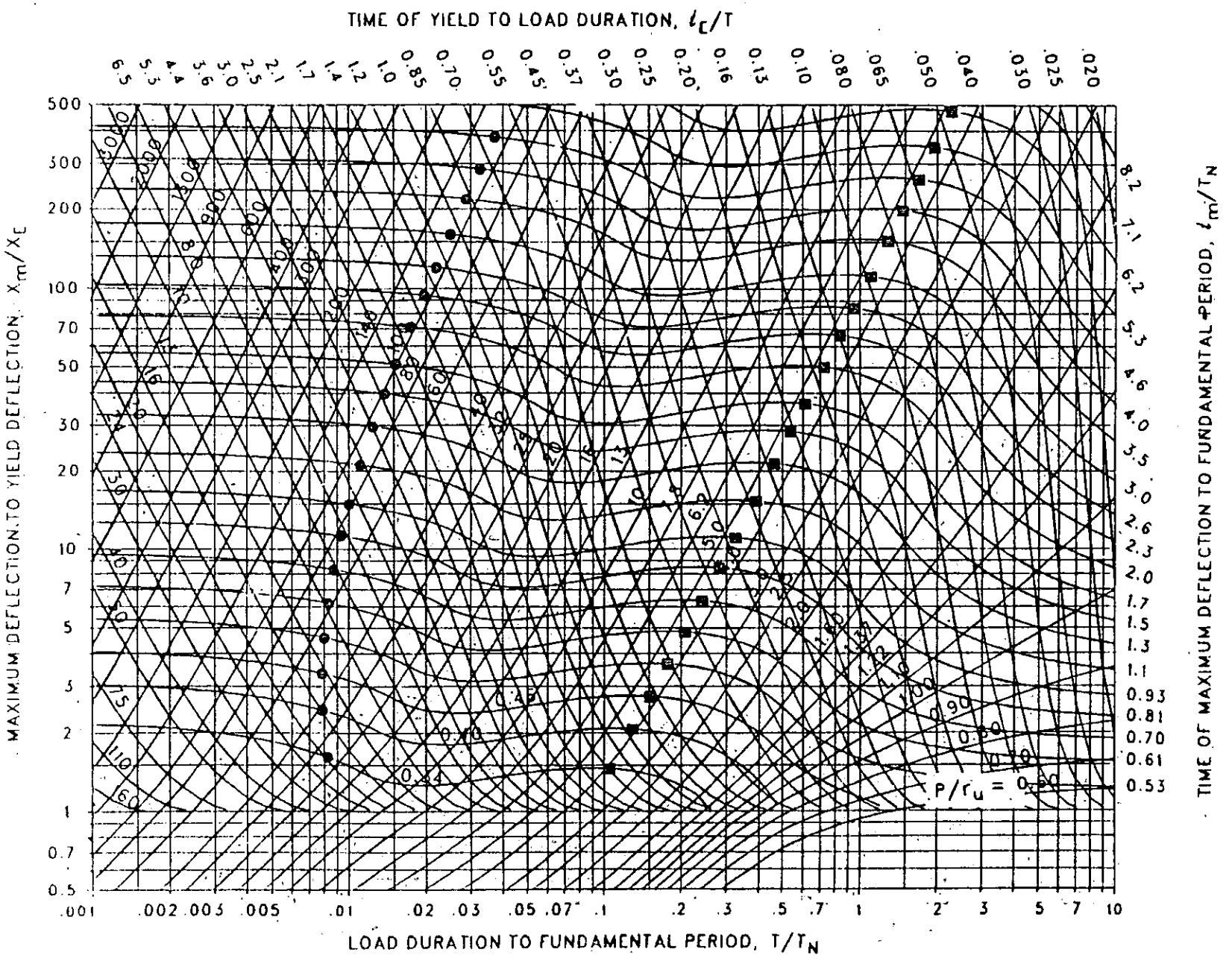


Figure 3-135 Maximum response of elasto-plastic, one-degree-of-freedom system for bilinear-triangular pulse ($C_1 = 0.042$, $C_2 = 30$)

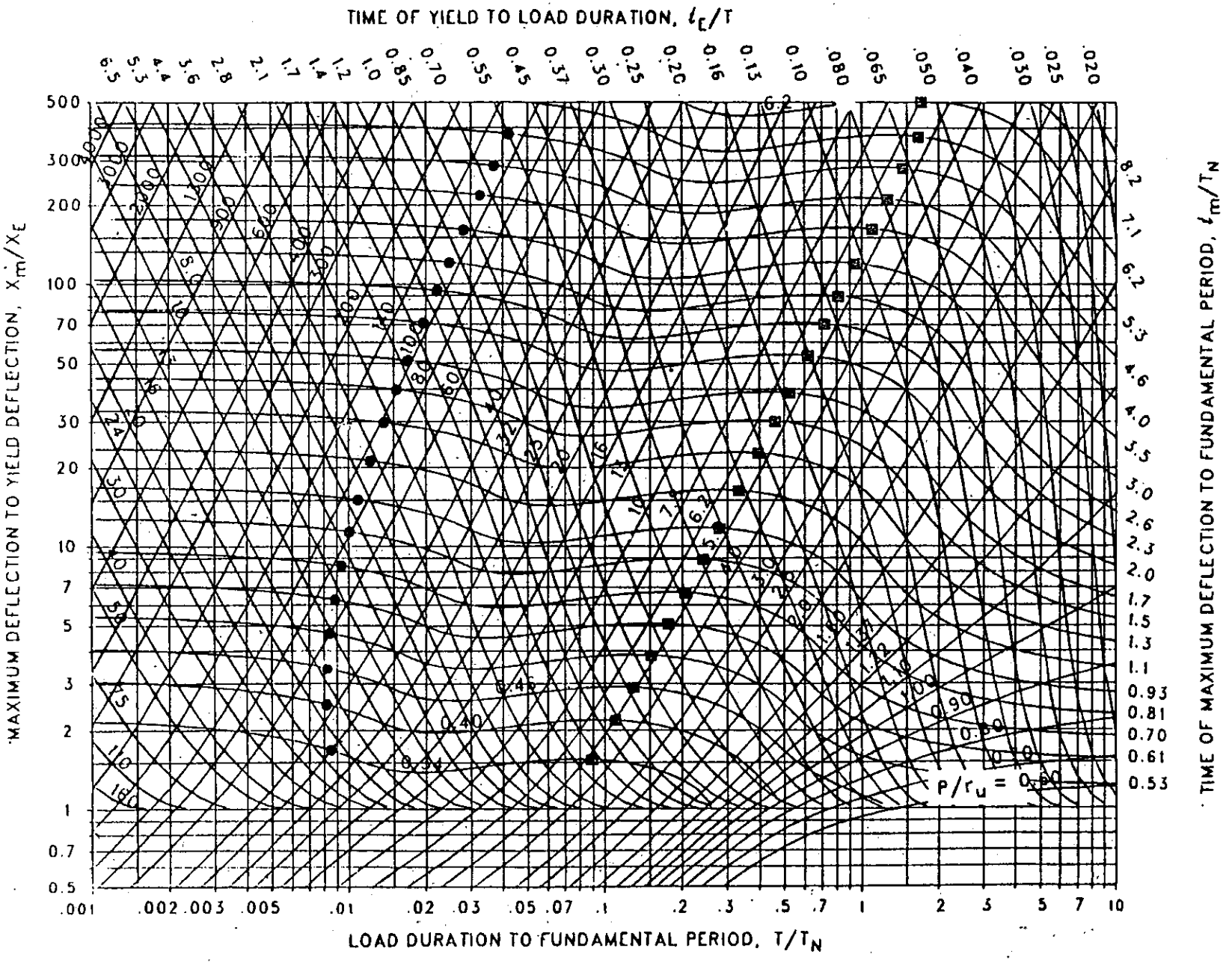


Figure 3-136 Maximum response of elasto-plastic, one-degree-of-freedom system for bilinear-triangular pulse ($C_1 = 0.032$, $C_2 = 30$)

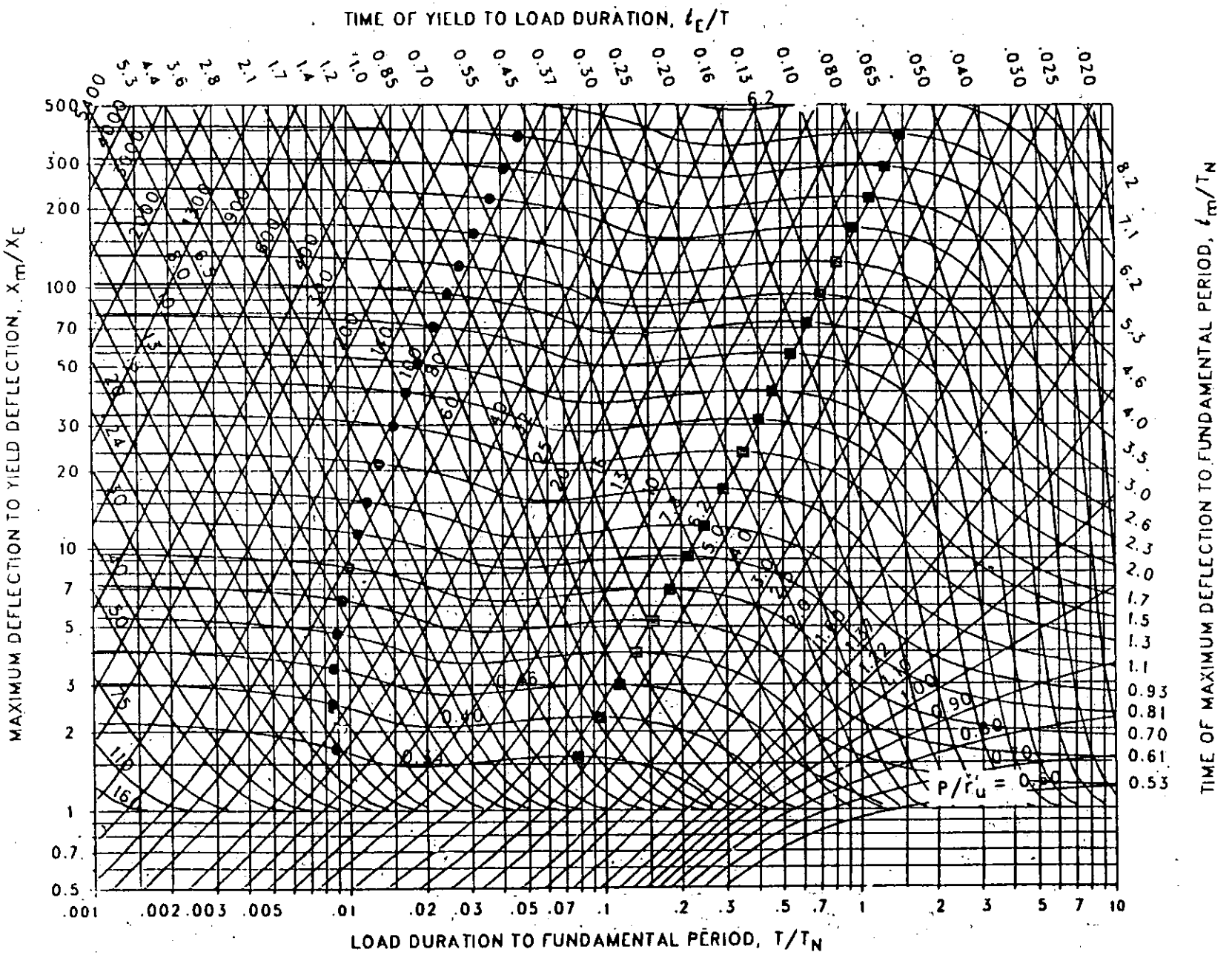


Figure 3-137 Maximum response of elasto-plastic, one-degree-of-freedom system for bilinear-triangular pulse (C_1 = 0.026, C_2 = 30)

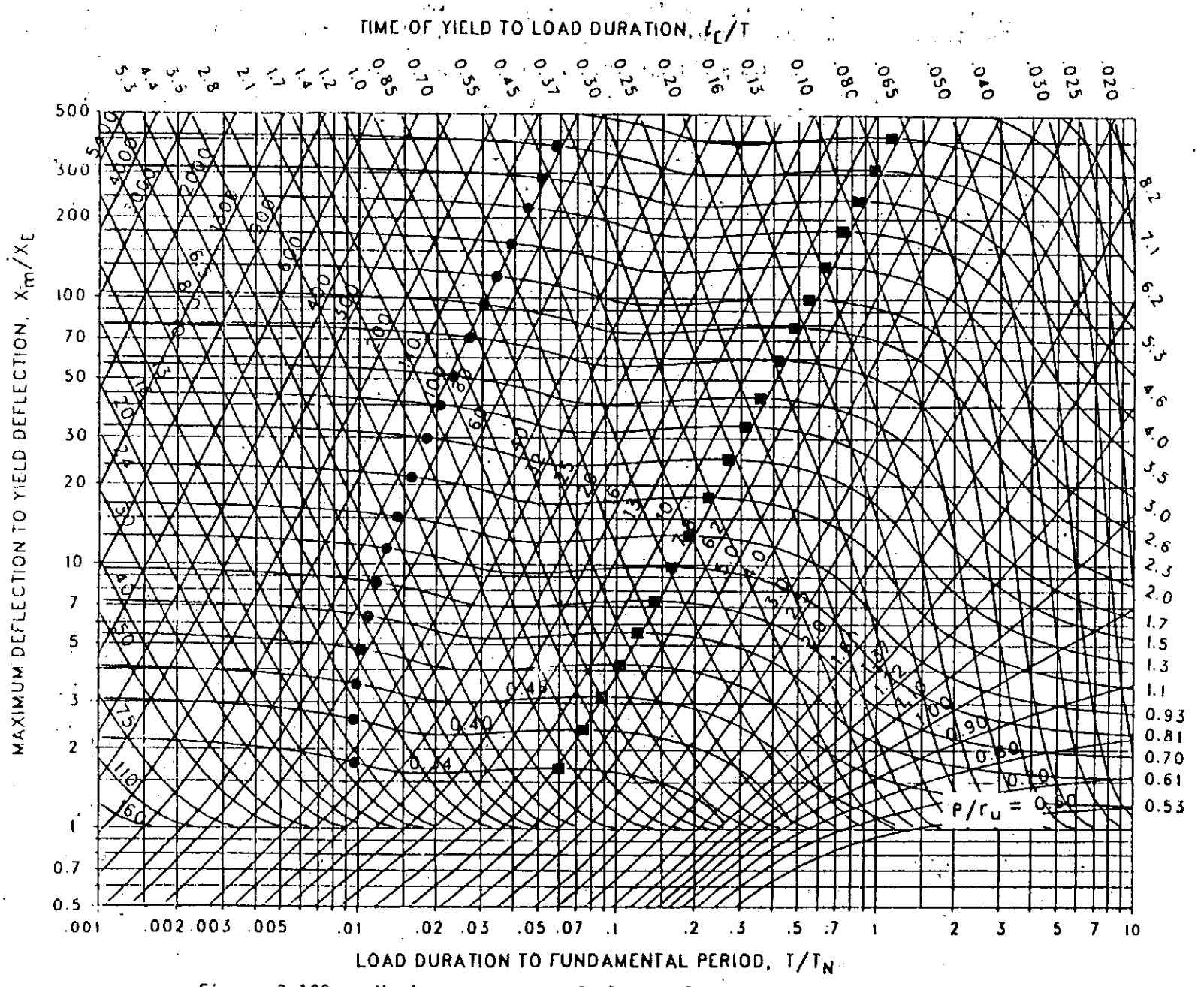


Figure 3-138 Maximum response of elasto-plastic, one-degree-of-freedom system for bilinear-triangular pulse ($C_1 = 0.018$, $C_2 = 30$)

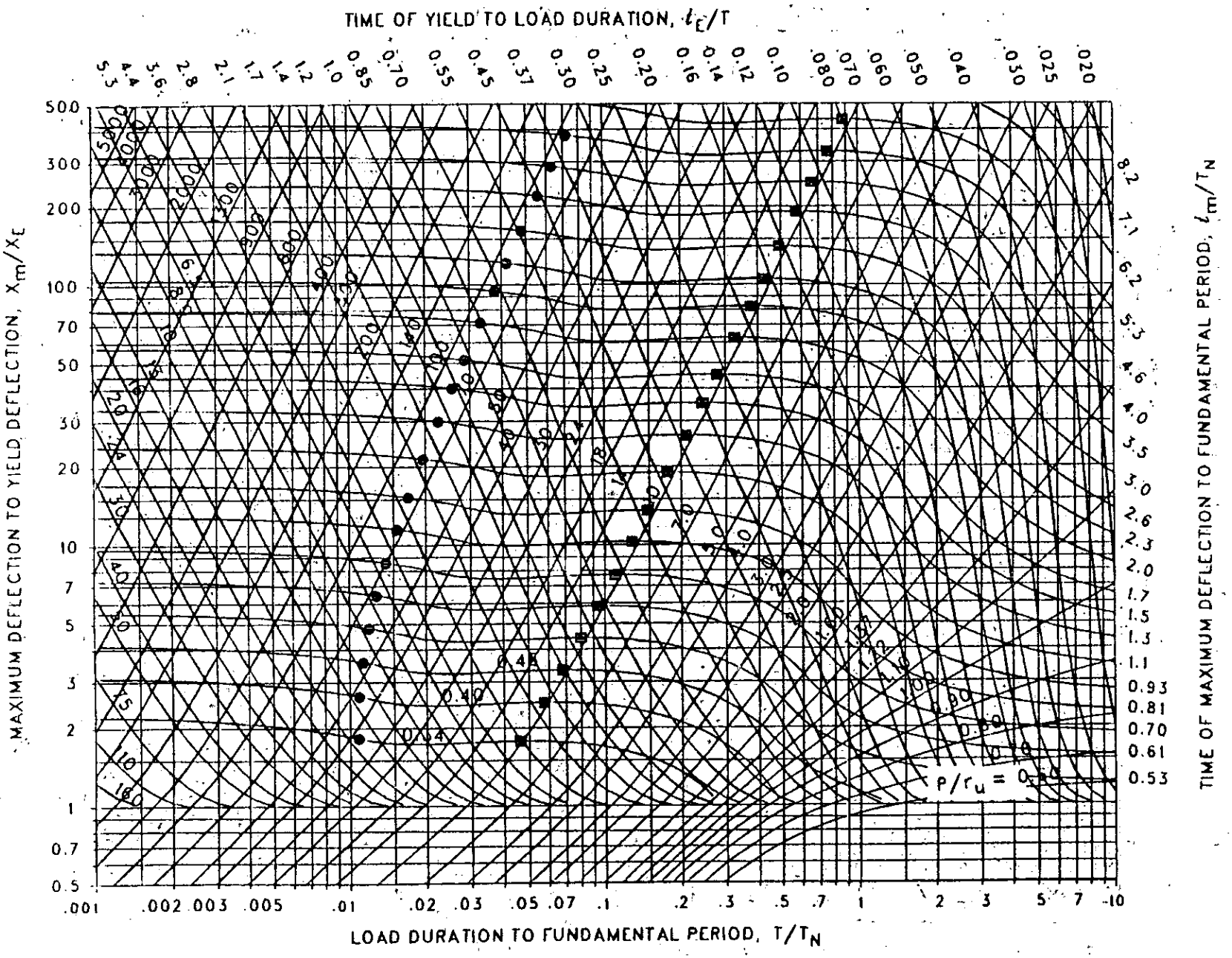


Figure 3-139 Maximum response of elasto-plastic, one-degree-of-freedom system for bilinear-triangular pulse ($C_1 = 0.013$, $C_2 = 30$)

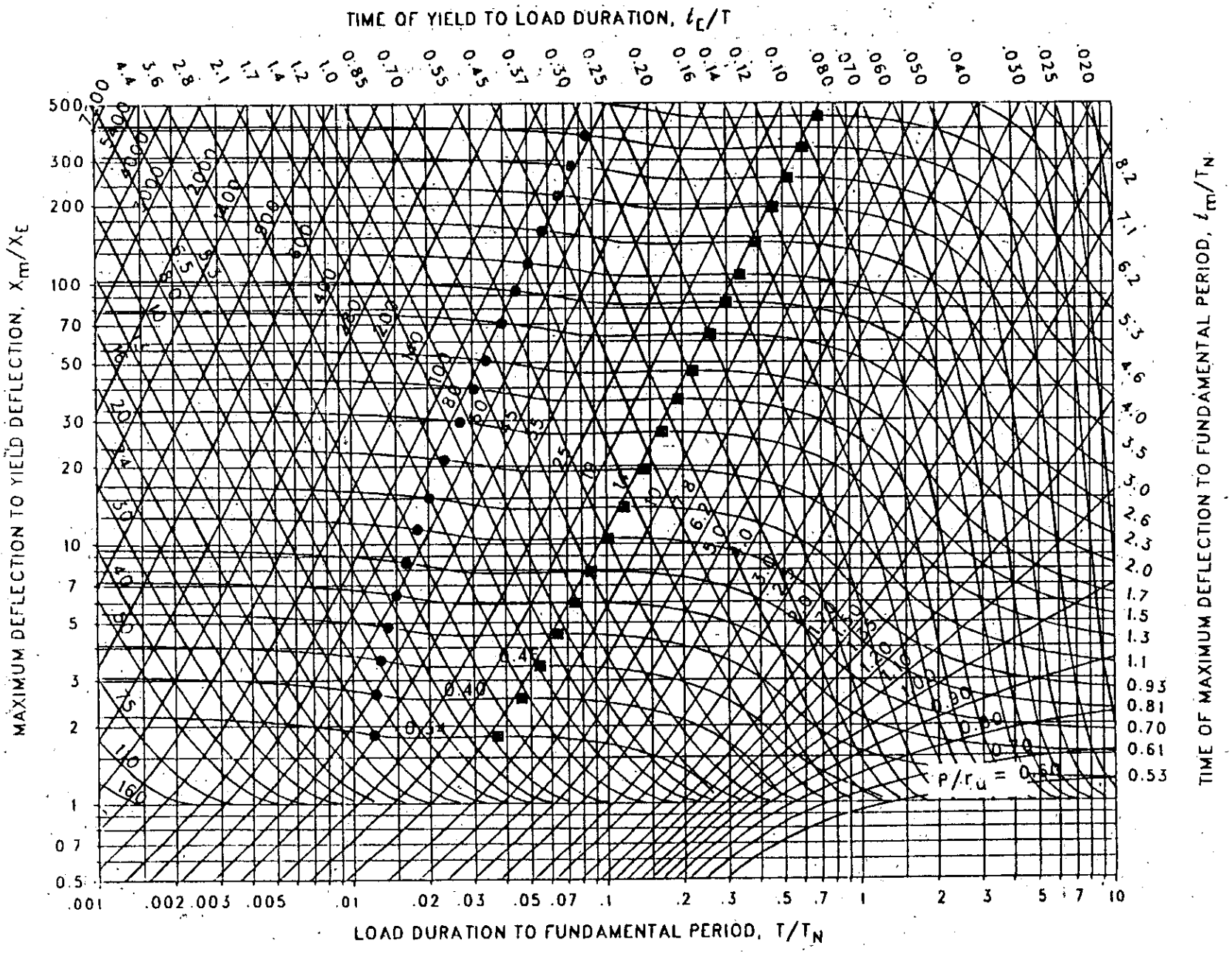


Figure 3-140 Maximum response of elasto-plastic, one-degree-of-freedom system for bilinear-triangular pulse (C_1 = 0.010, C_2 = 30)

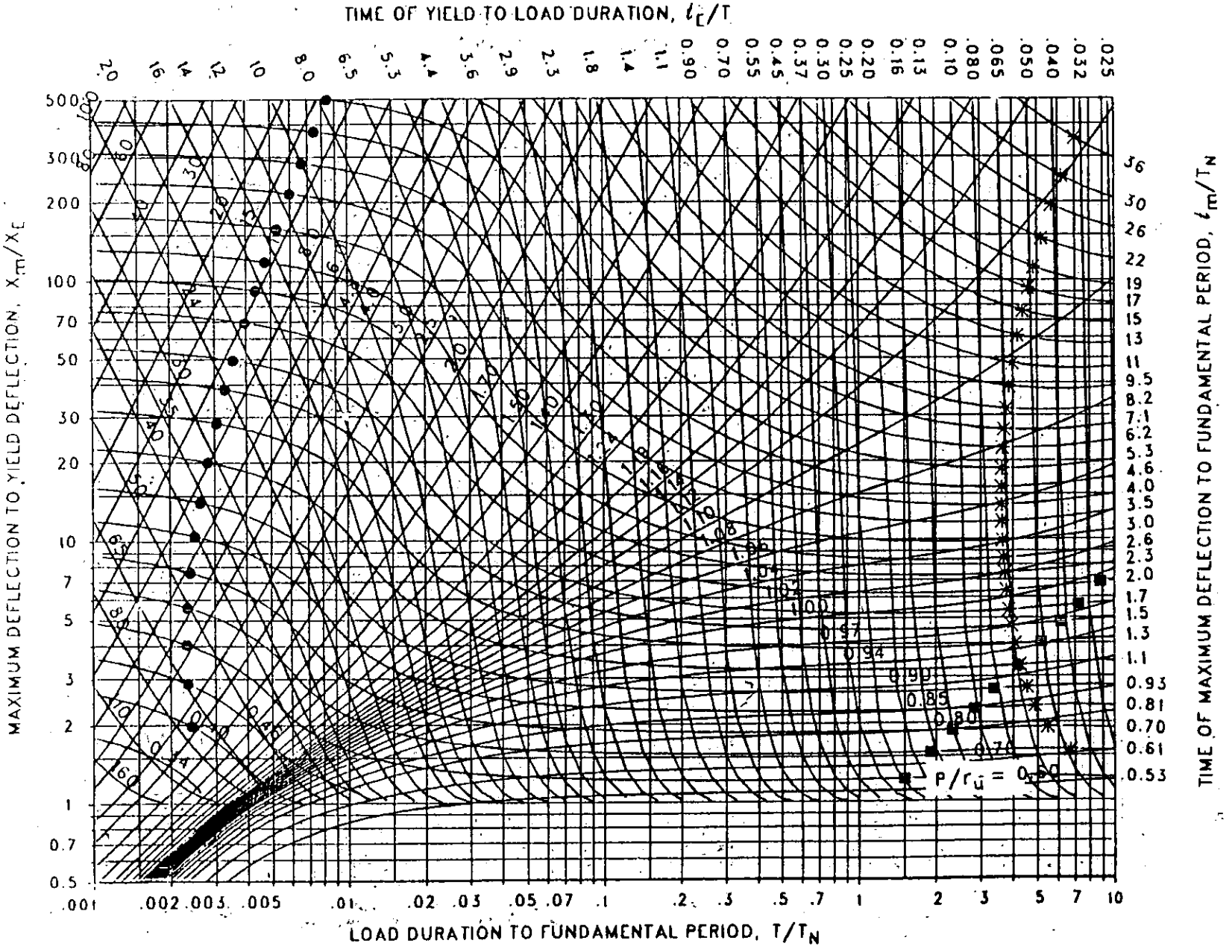


Figure 3-141 Maximum response of elasto-plastic, one-degree-of-freedom system for bilinear-triangular pulse (C_1 = 0.909, C_2 = 100.)

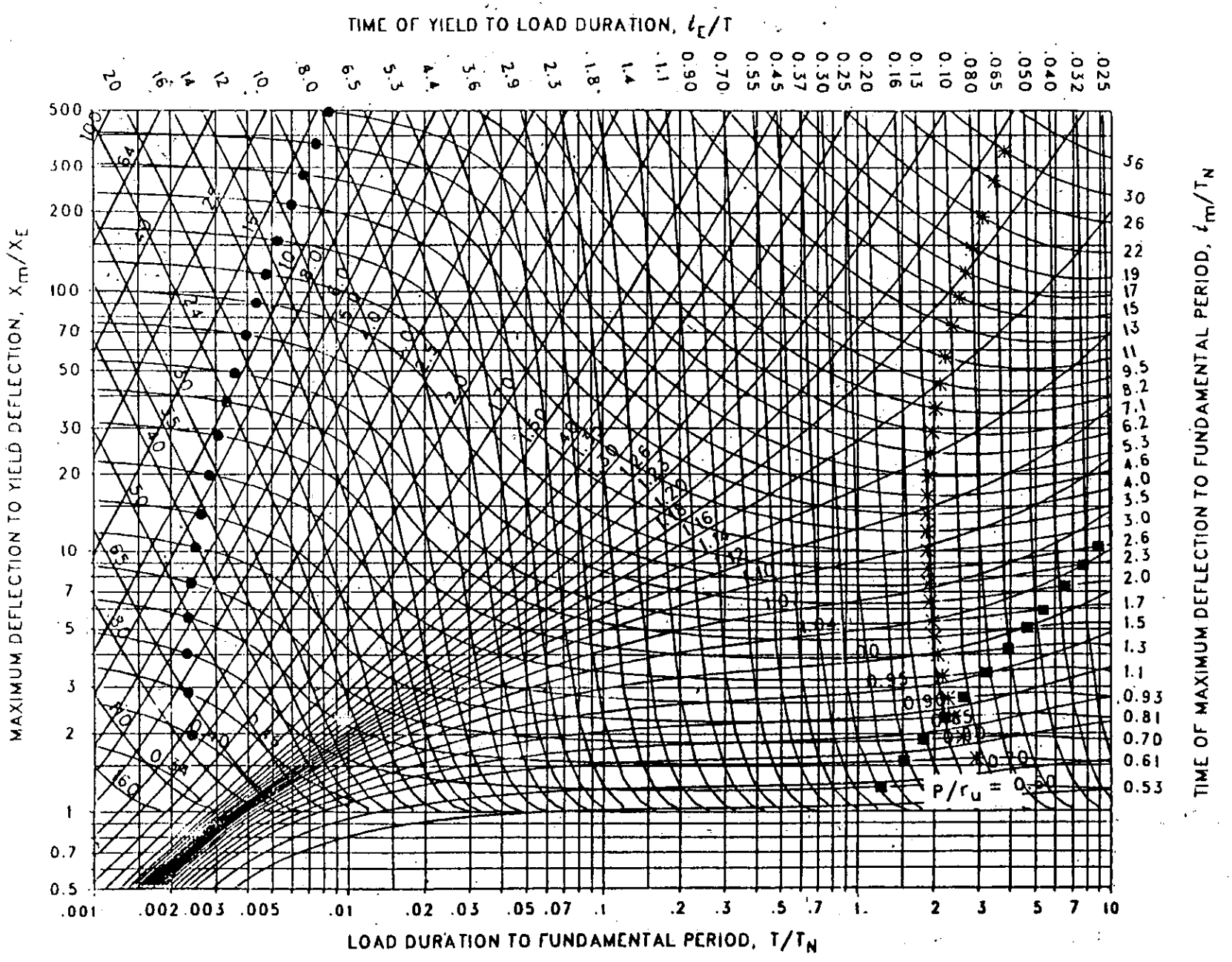


Figure 3-142 Maximum response of elasto-plastic, one-degree-of-freedom system for bilinear-triangular pulse (C_1 = 0.866, C_2 = 100.)

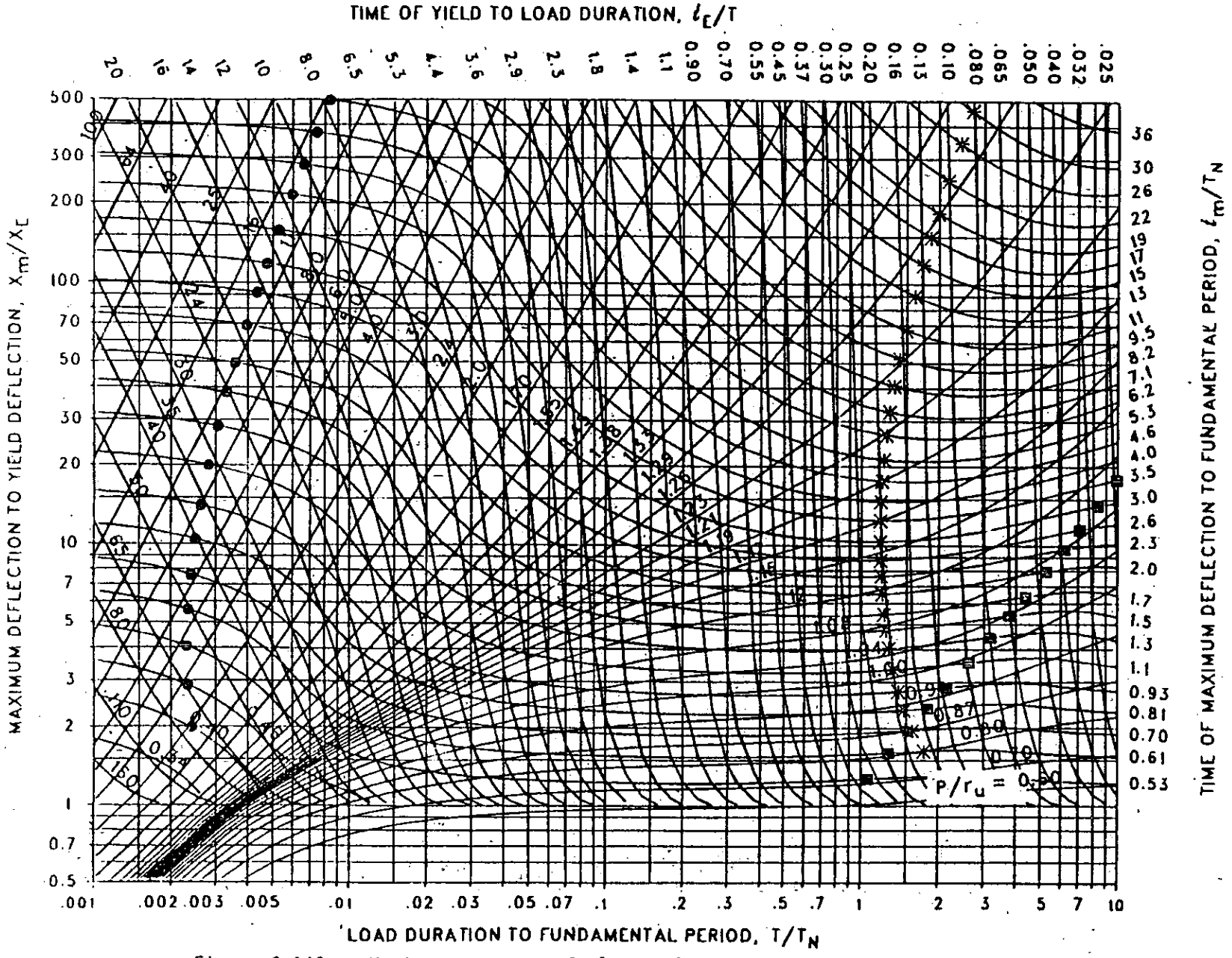


Figure 3-143 Maximum response of elasto-plastic, one-degree-of-freedom system for bilinear-triangular pulse ($C_1 = 0.825$, $C_2 = 100.$)

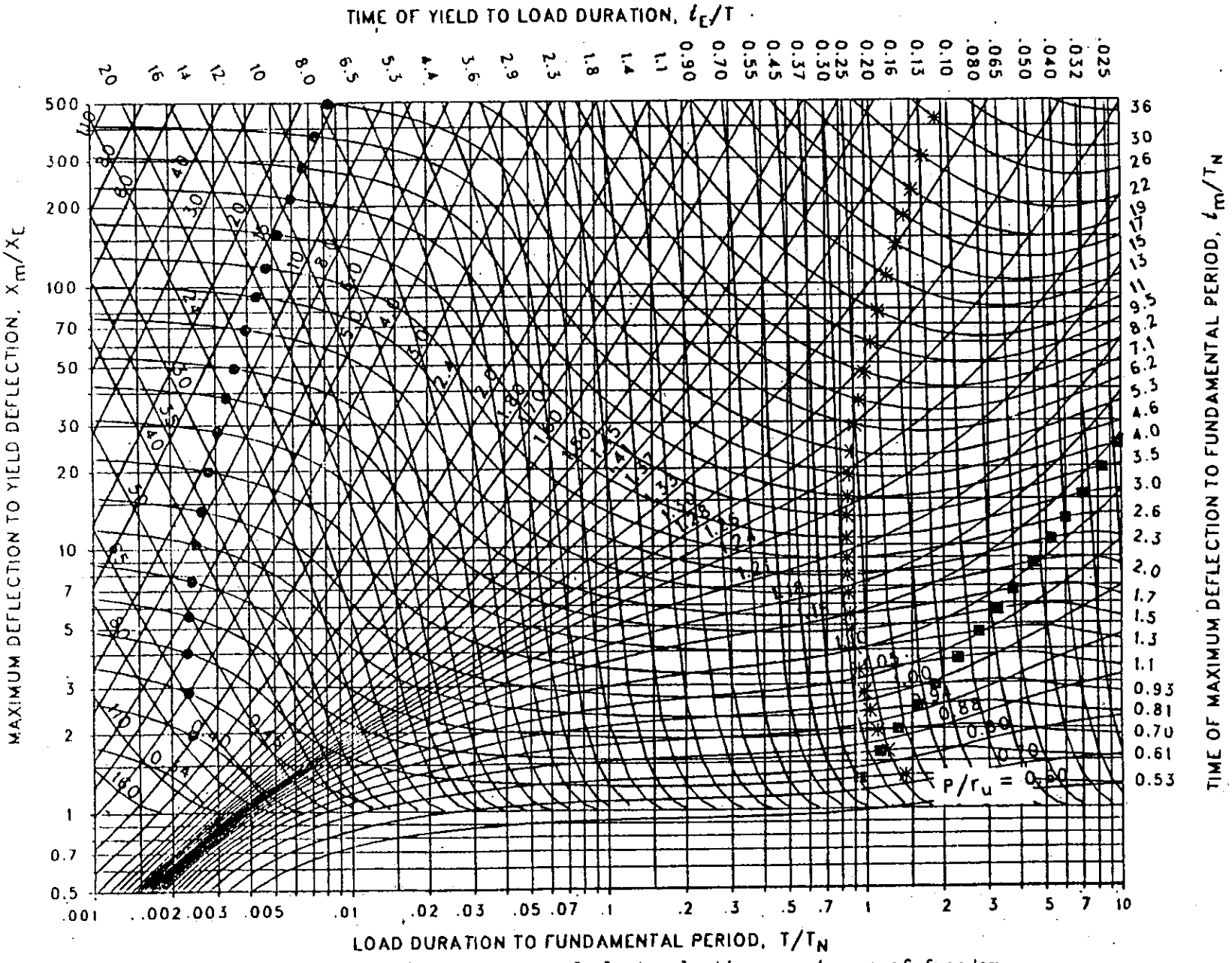


Figure 3-144 Maximum response of elasto-plastic, one-degree-of-freedom system for bilinear-triangular pulse ($C_1 = 0.787$, $C_2 = 100.$)

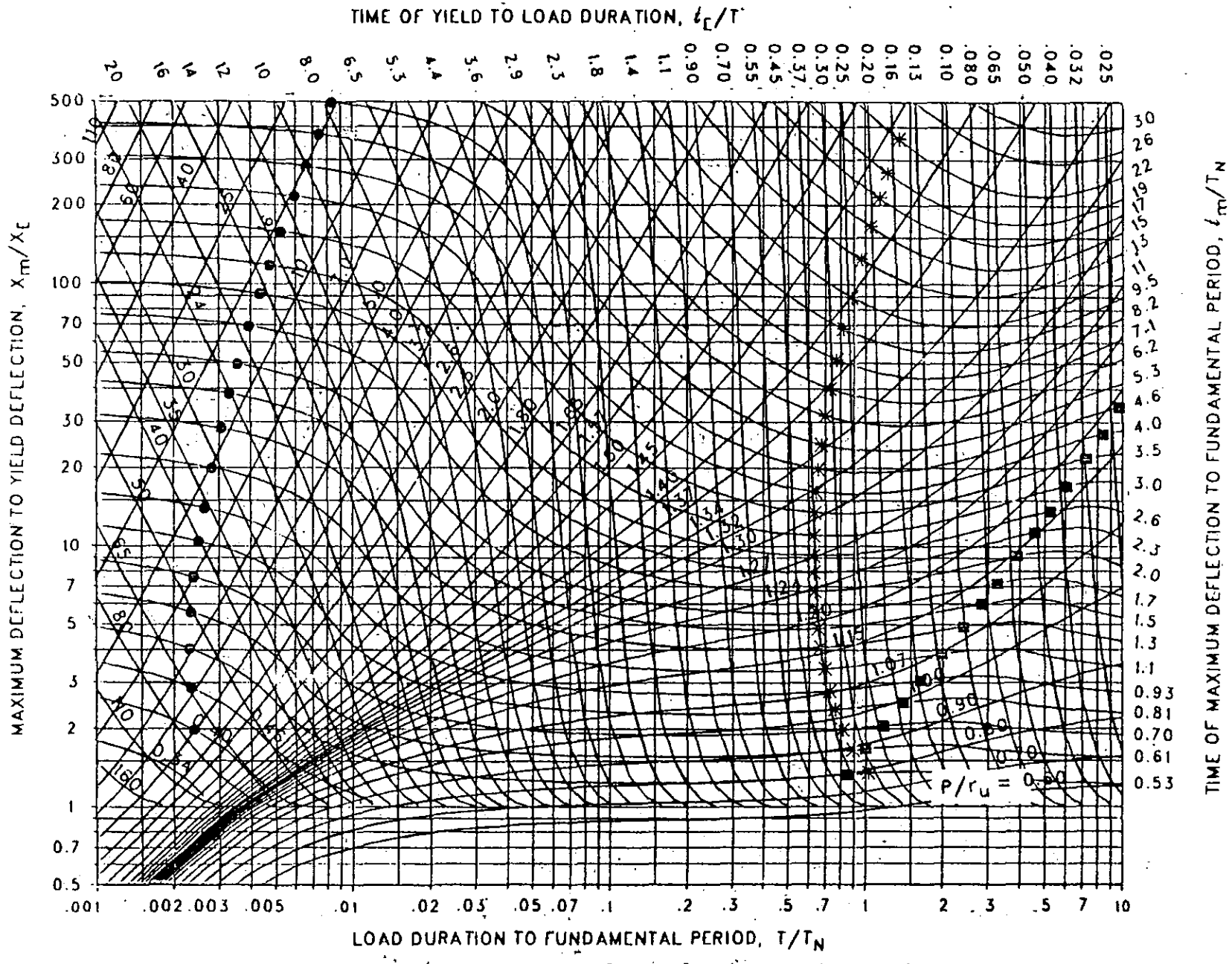


Figure 3-145 Maximum response or elasto-plastic, one-degree-of-freedom system for bilinear-triangular pulse (C_1 = 0.750, C_2 = 100.)

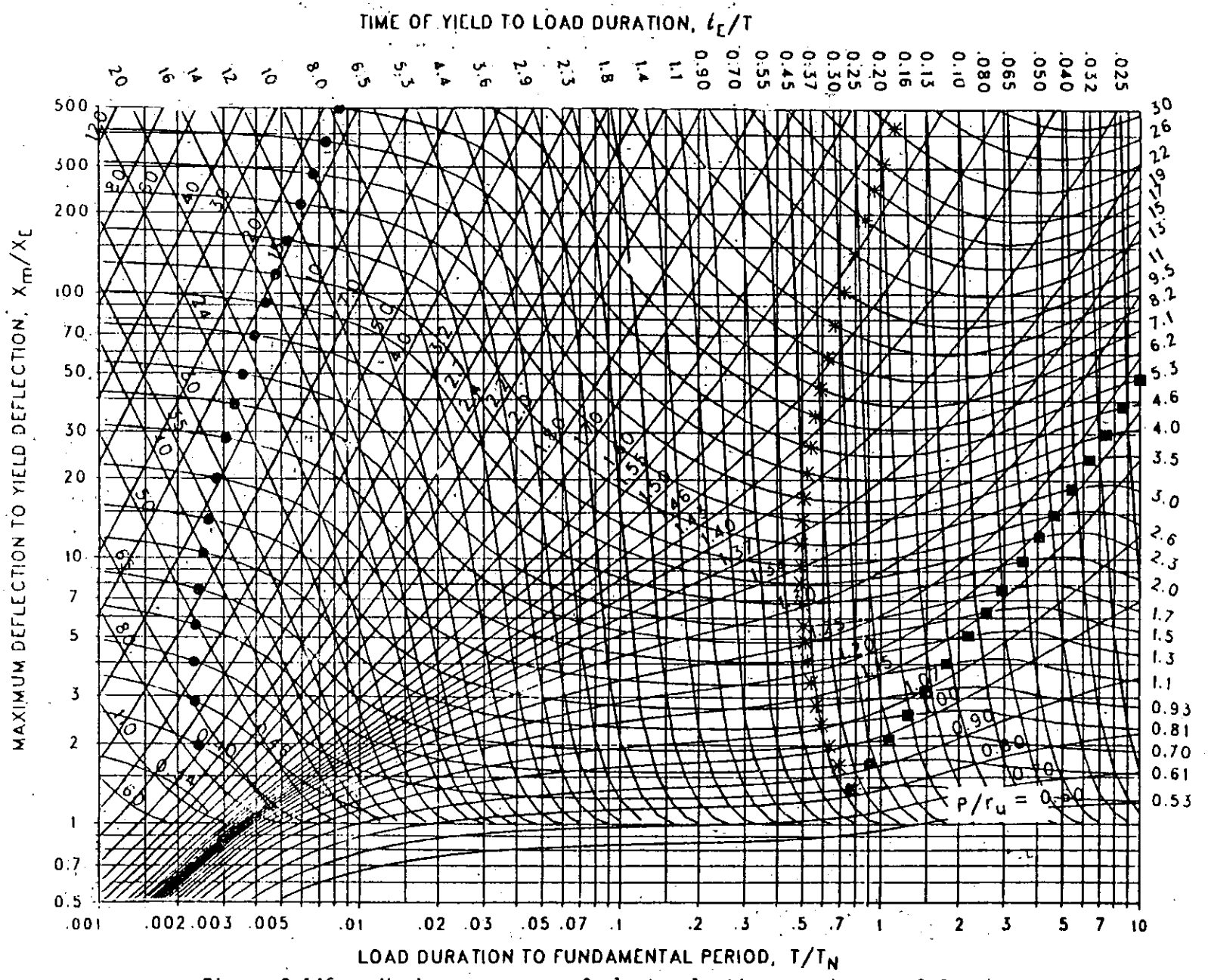


Figure 3-146 Maximum response of elasto-plastic, one-degree-of-freedom system for bilinear-triangular pulse (C_1 = 0.715, C_2 = 100.)

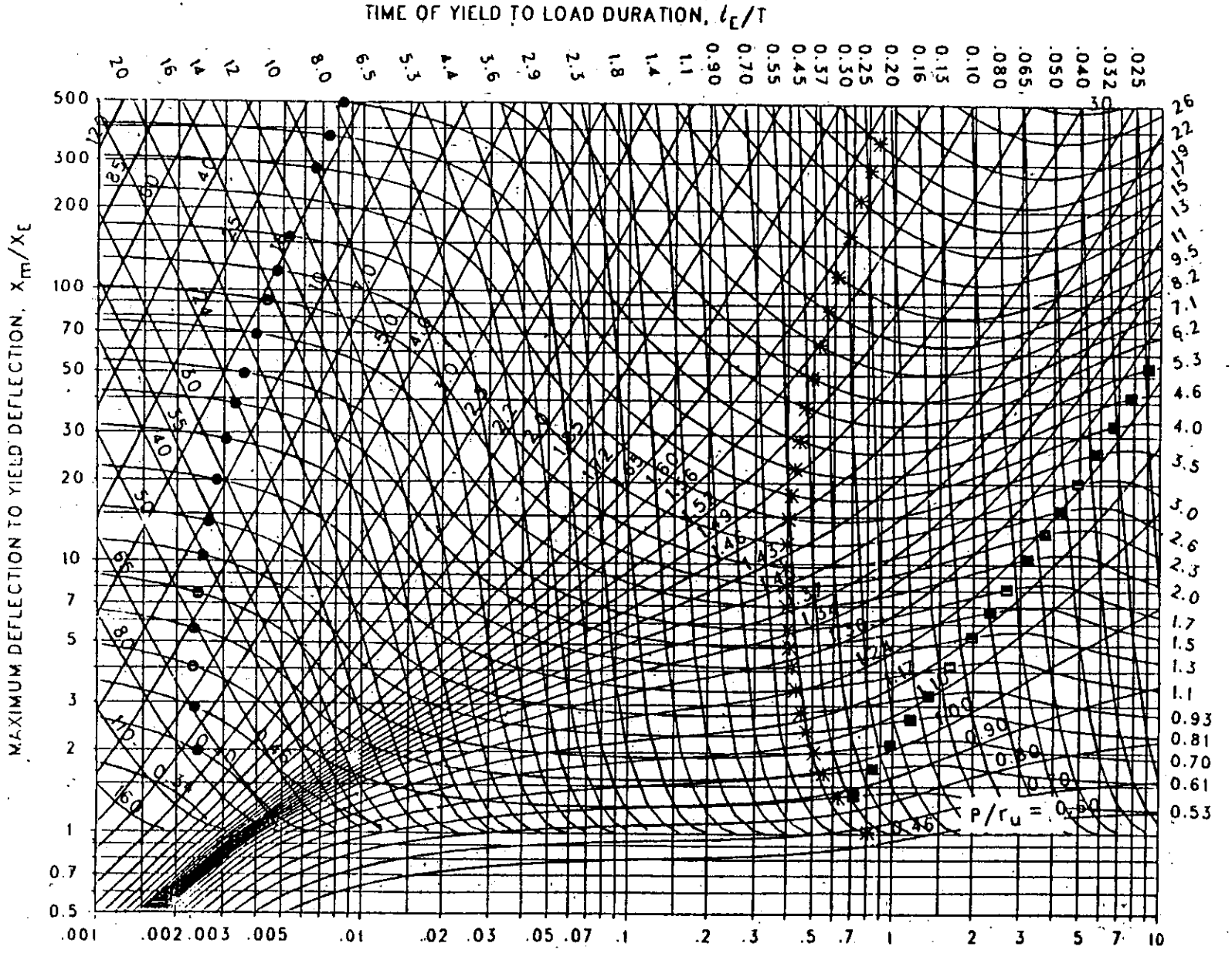


Figure 3-147 Maximum response of elasto-plastic, one-degree-of-freedom system for bilinear-triangular pulse (C_1 = 0.681, C_2 = 100.)

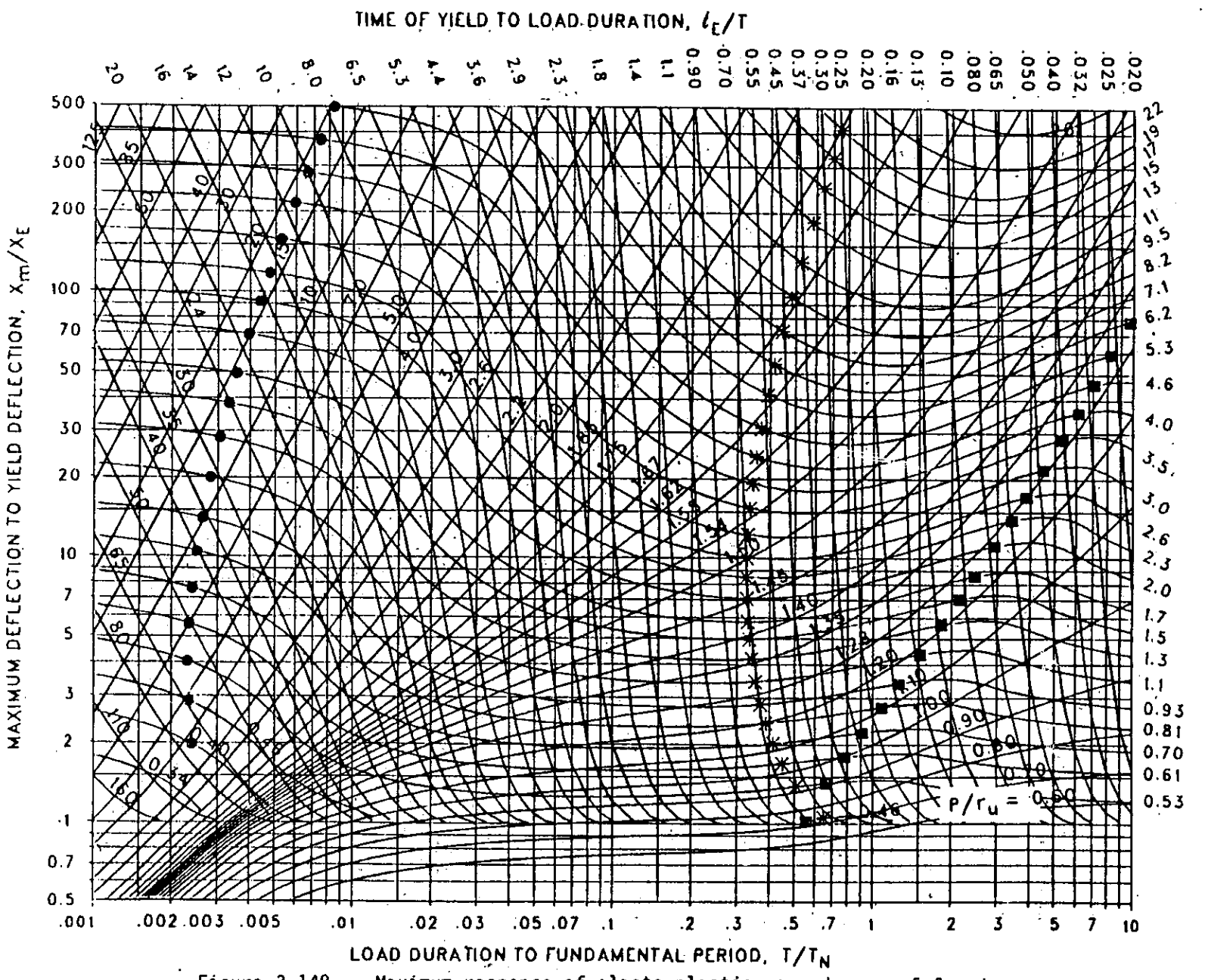


Figure 3-148 Maximum response of elasto-plastic, one-degree-of-freedom system for bilinear-triangular pulse ($C_1 = 0.648$, $C_2 = 100.$)

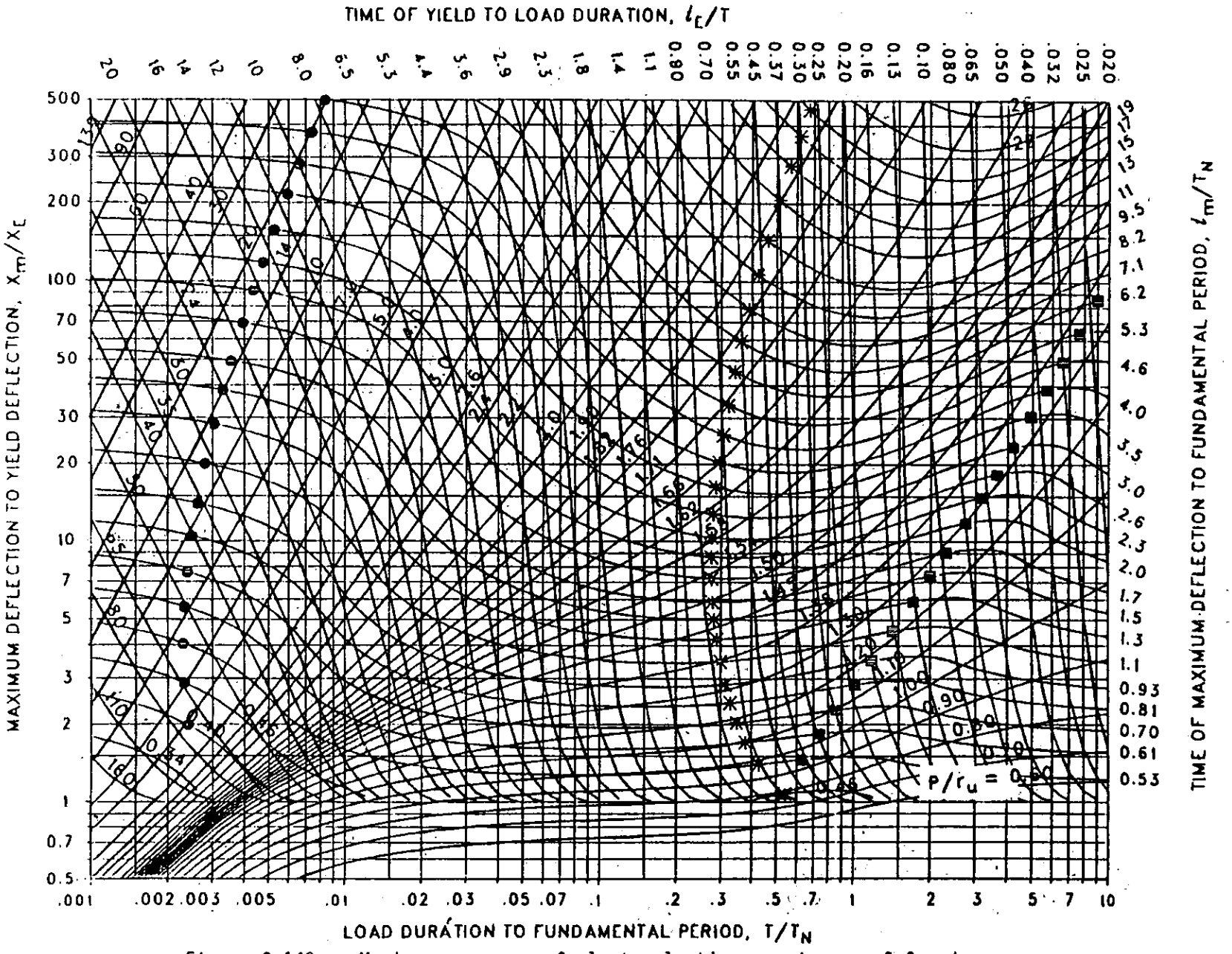


Figure 3-149 Maximum response of elasto-plastic, one-degree-of-freedom system for bilinear-triangular pulse ($C_1 = 0.619$, $C_2 = 100.$)

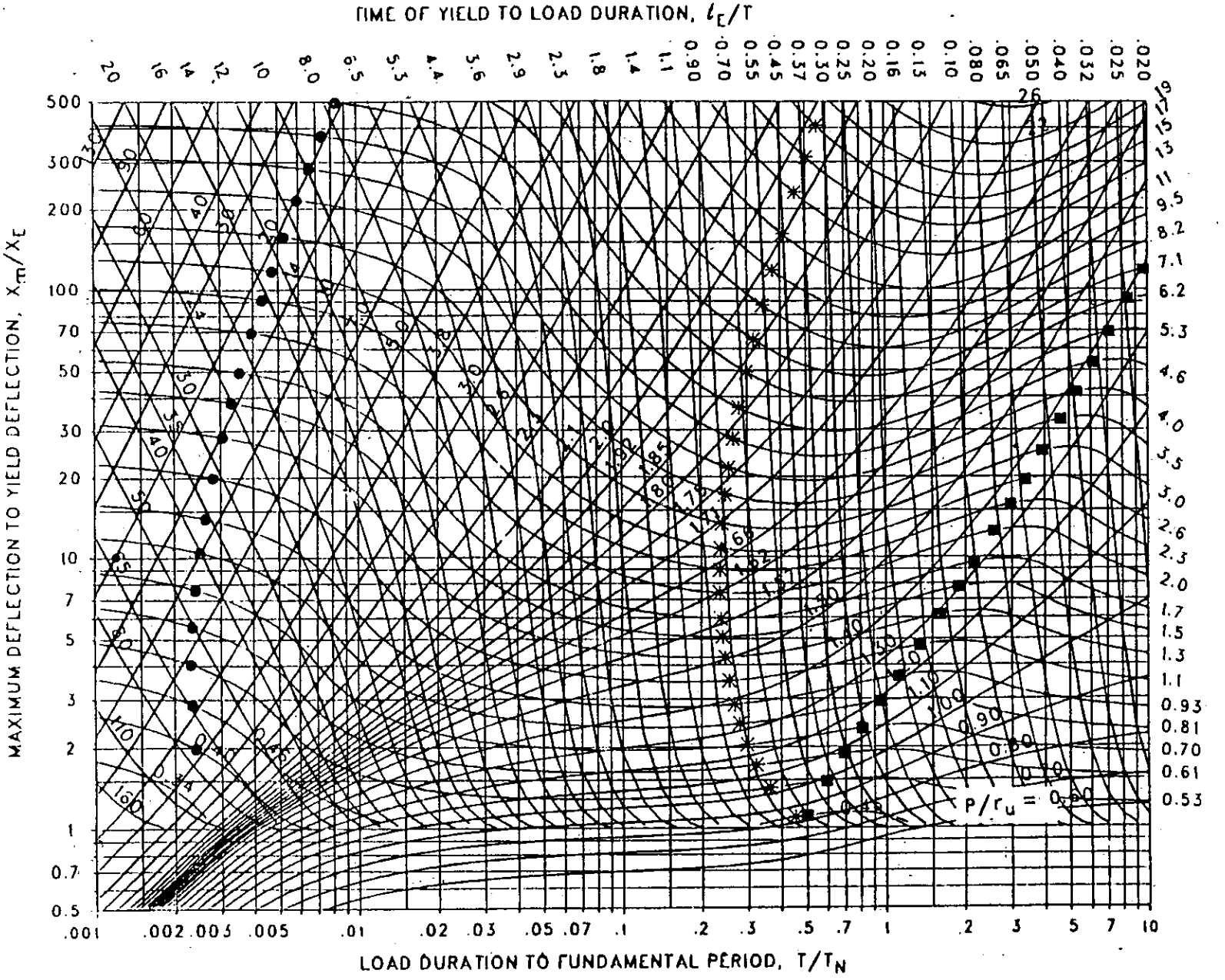


Figure 3-150 Maximum response of elasto-plastic, one-degree-of-freedom system for bilinear-triangular pulse (C_1 = 0.590, C_2 = 100.)

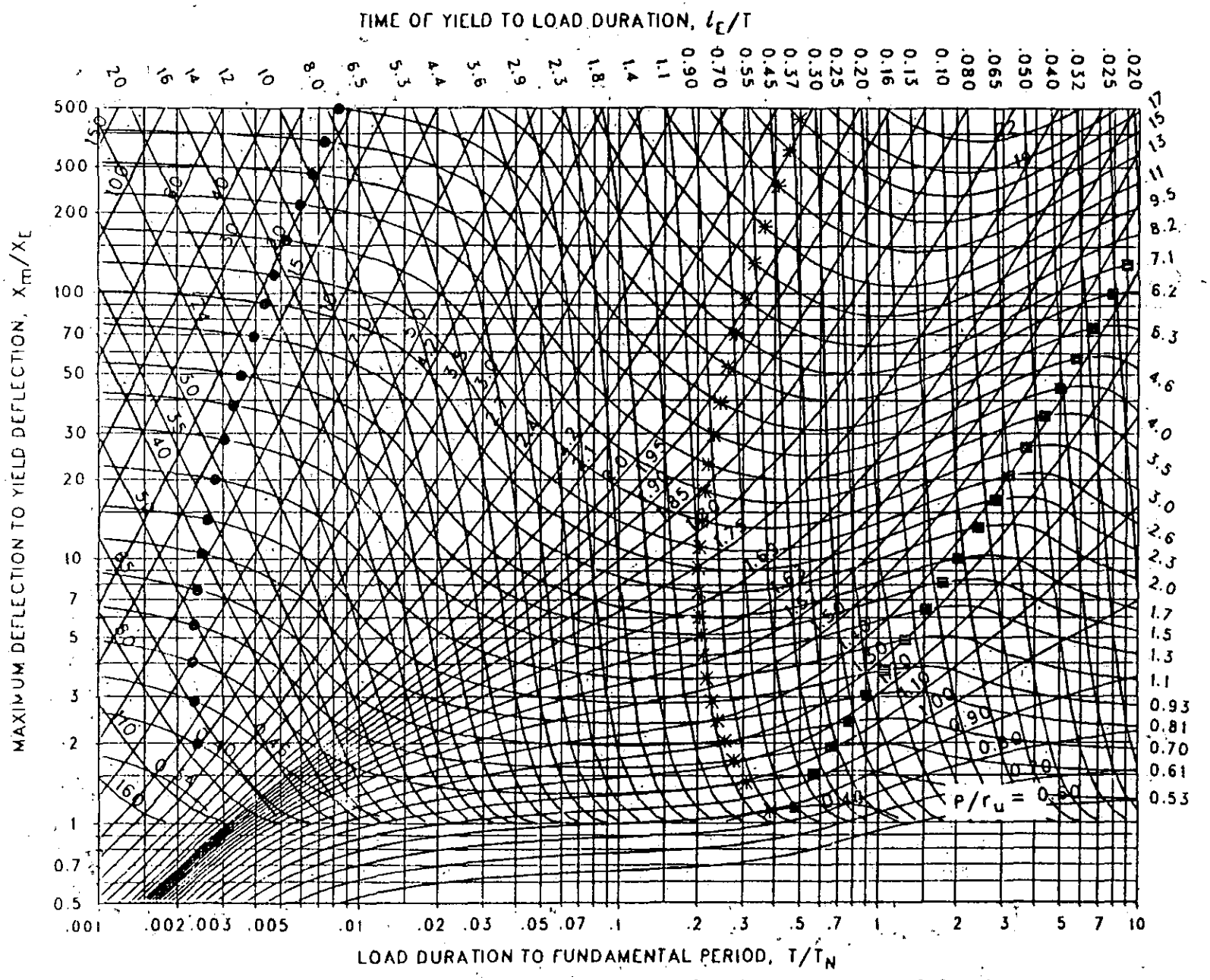


Figure 3-151 Maximum response of elasto-plastic, one-degree-of-freedom system for bilinear-triangular pulse ($C_1 = 0.562$, $C_2 = 100.$)

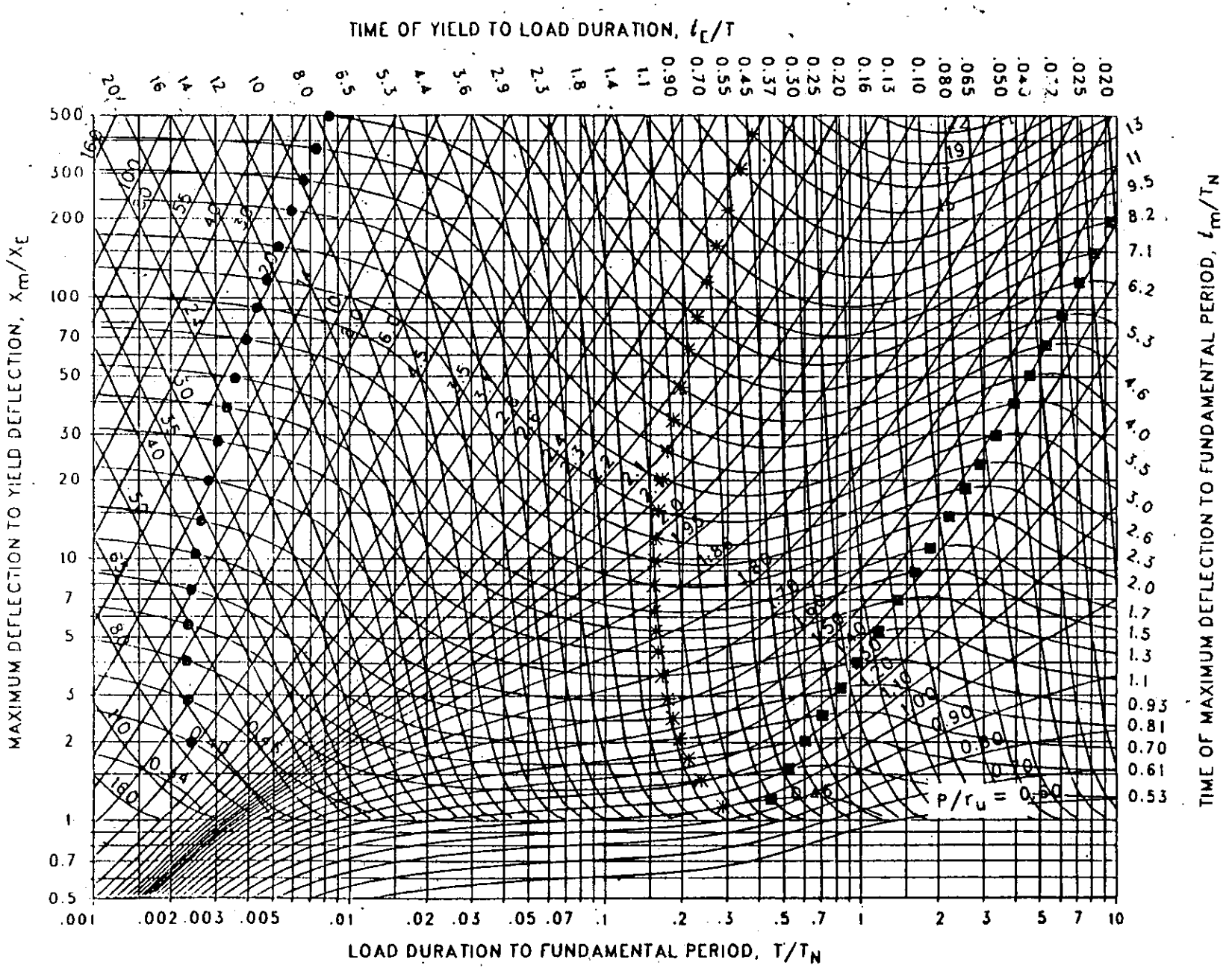


Figure 3-152 Maximum response of elasto-plastic, one-degree-of-freedom system for bilinear-triangular pulse ($C_1 = 0.511$, $C_2 = 100.$)

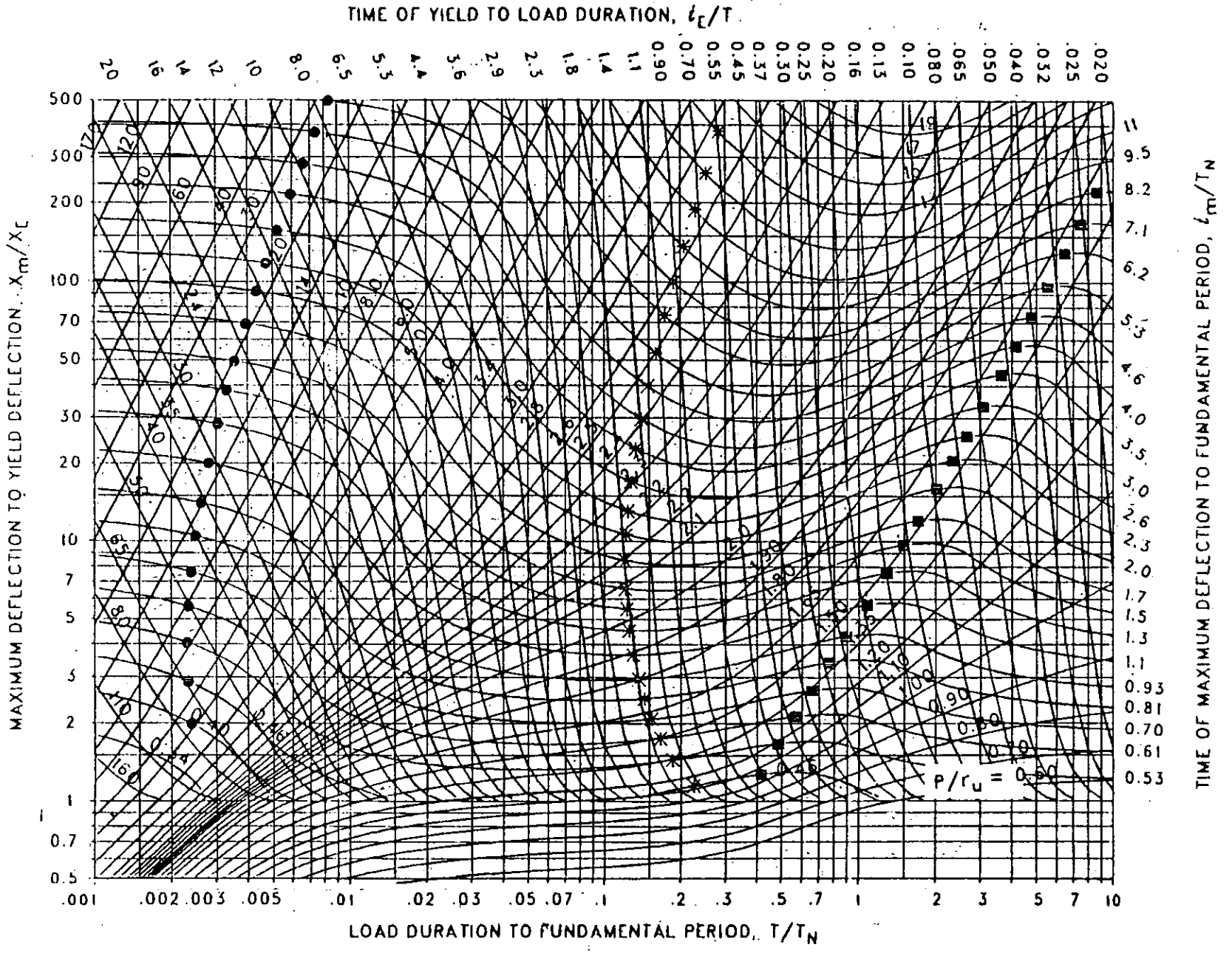


Figure 3-153 Maximum response of elasto-plastic, one-degree-of-freedom system for bilinear-triangular pulse (C_1 = 0.464, C_2 = 100.)

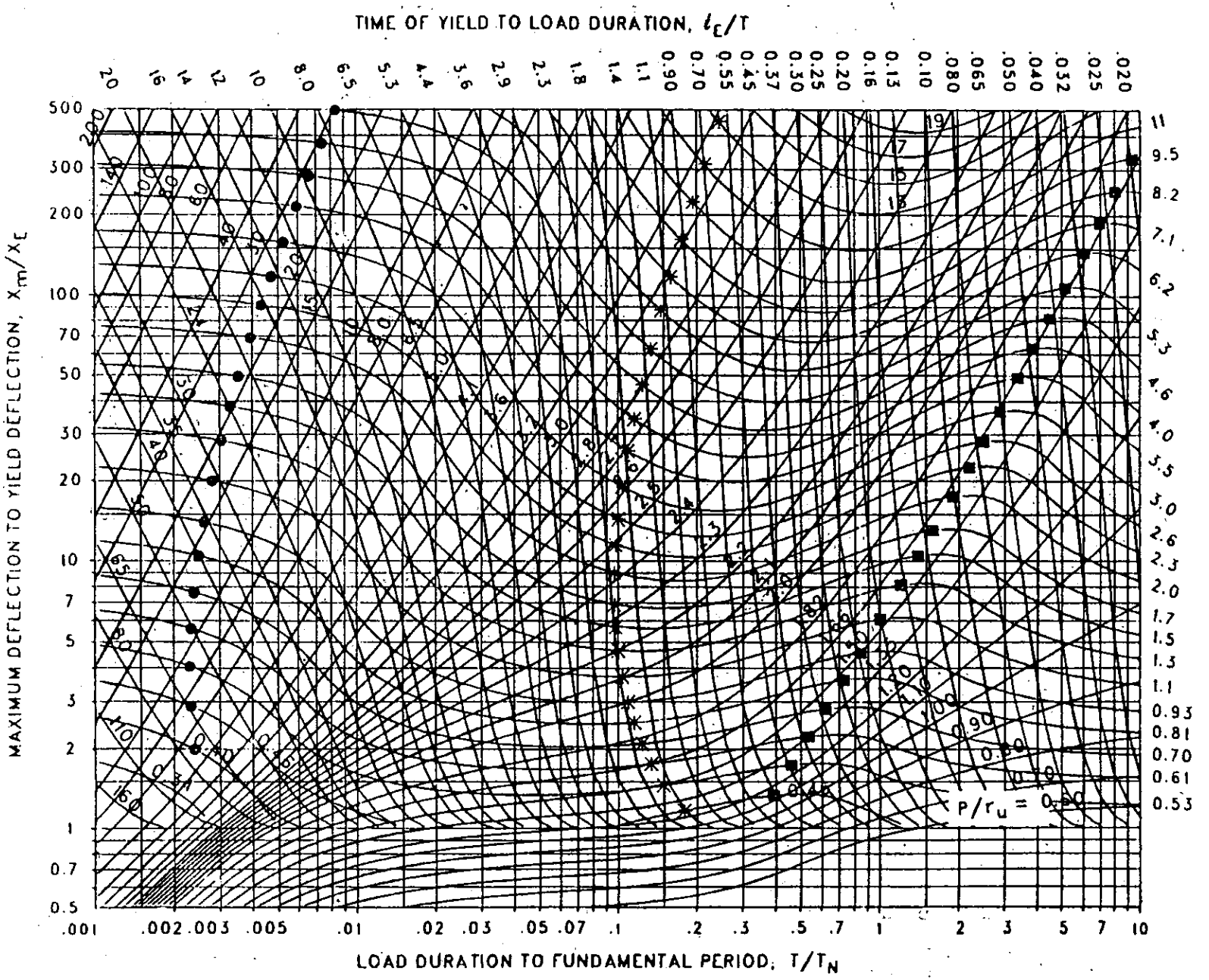


Figure 3-154 Maximum response of elasto-plastic, one-degree-of-freedom system for bilinear-triangular pulse (C_1 = 0.422, C_2 = 100.)

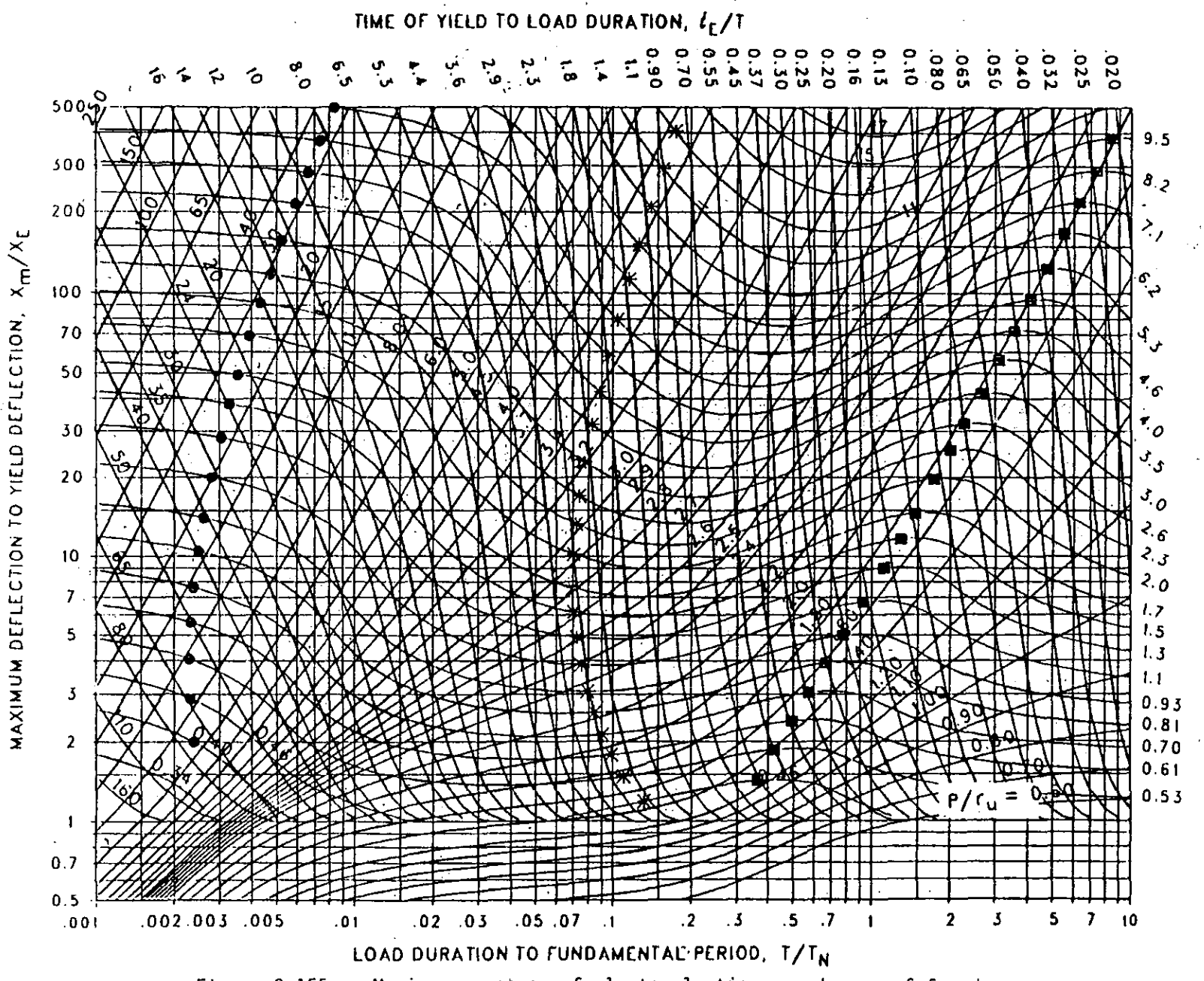


Figure 3-155 Maximum response of elasto-plastic, one-degree-of-freedom system for bilinear-triangular pulse (C_1 = 0.365, C_2 = 100.)

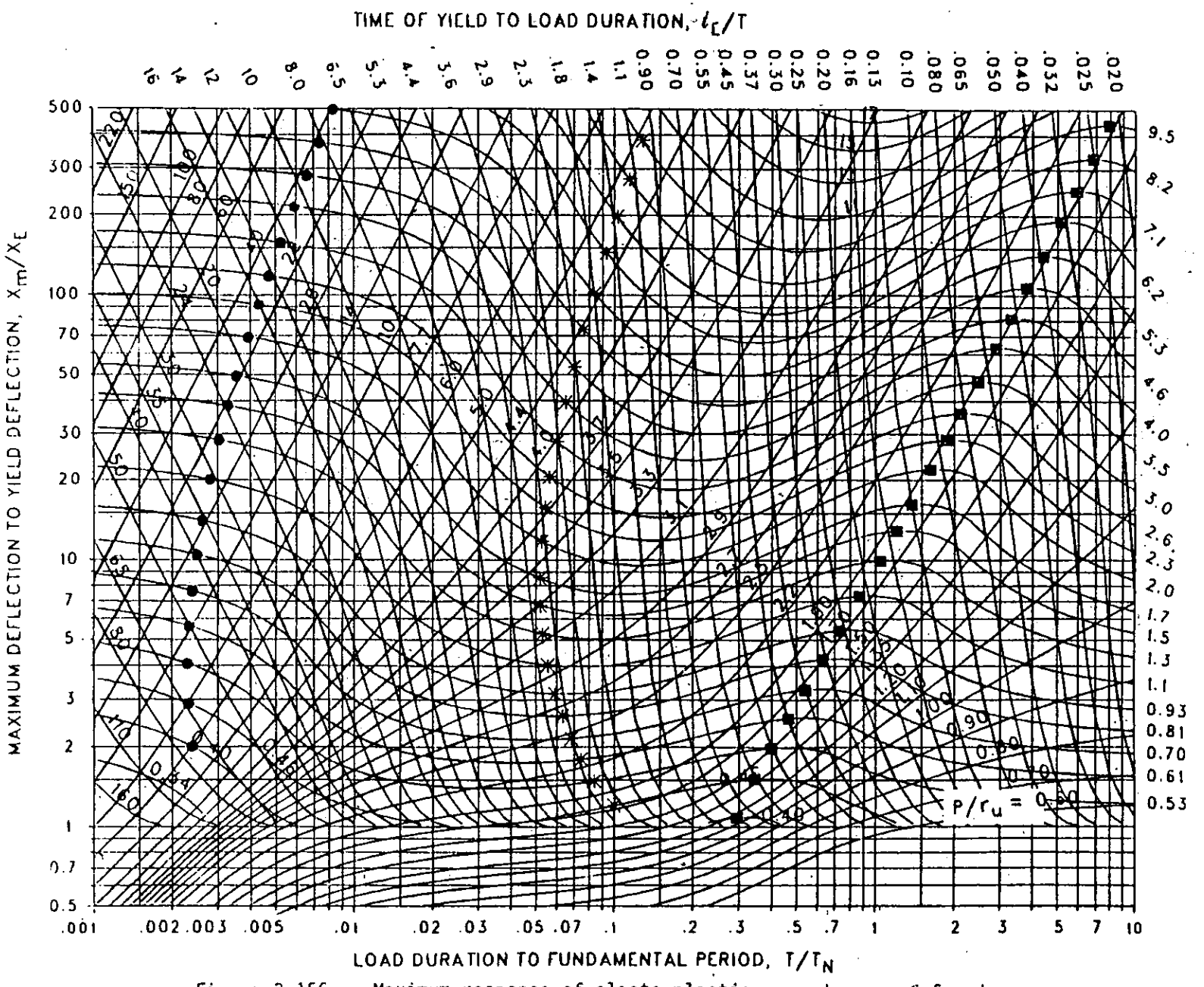


Figure 3-156 Maximum response of elasto-plastic, one-degree-of-freedom system for bilinear-triangular pulse ($C_1 = 0.316$, $C_2 = 100.$)

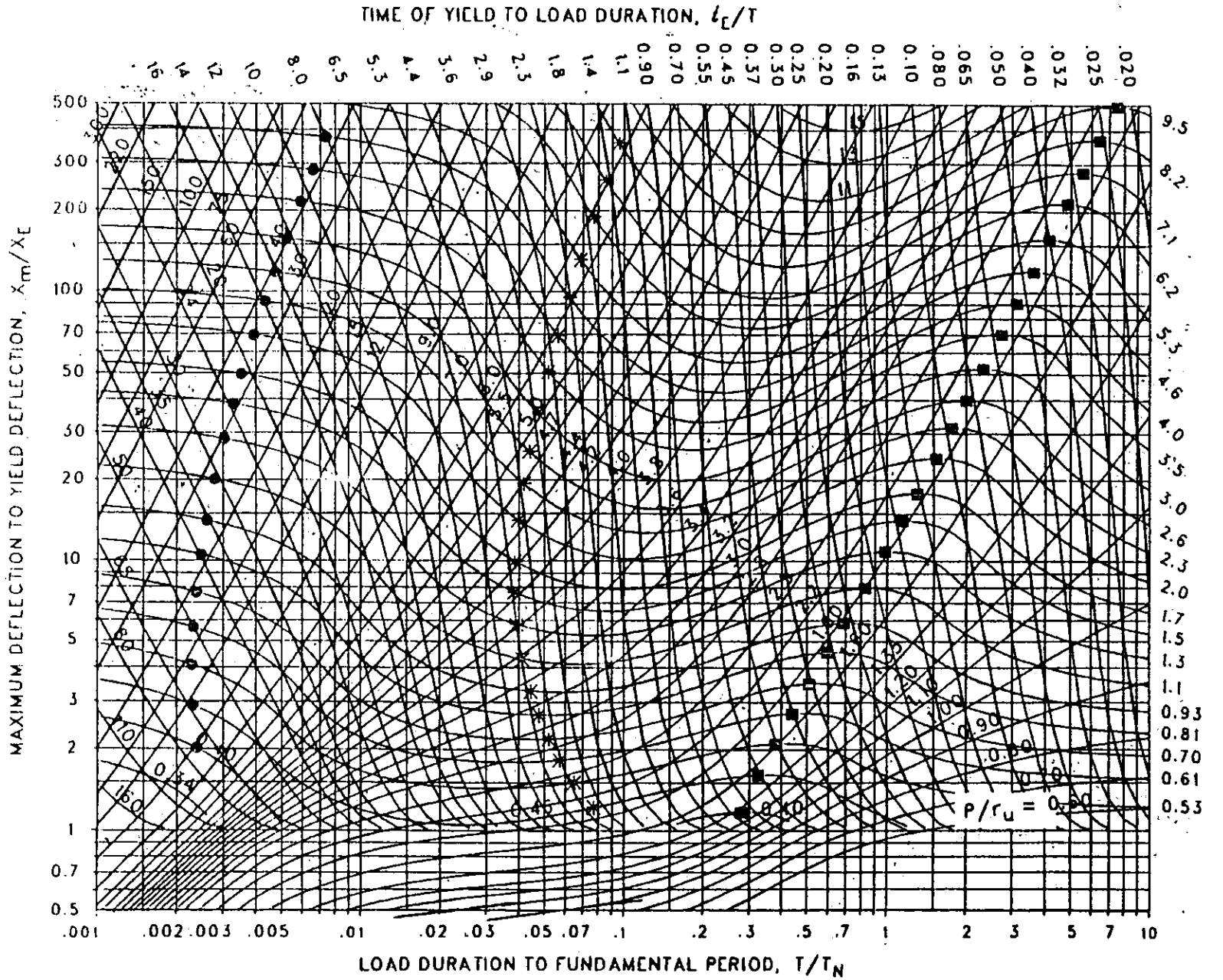


Figure 3-157 Maximum response of elasto-plastic, one-degree-of-freedom system for bilinear-triangular pulse ($C_1 = 0.274$, $C_2 = 100.$)

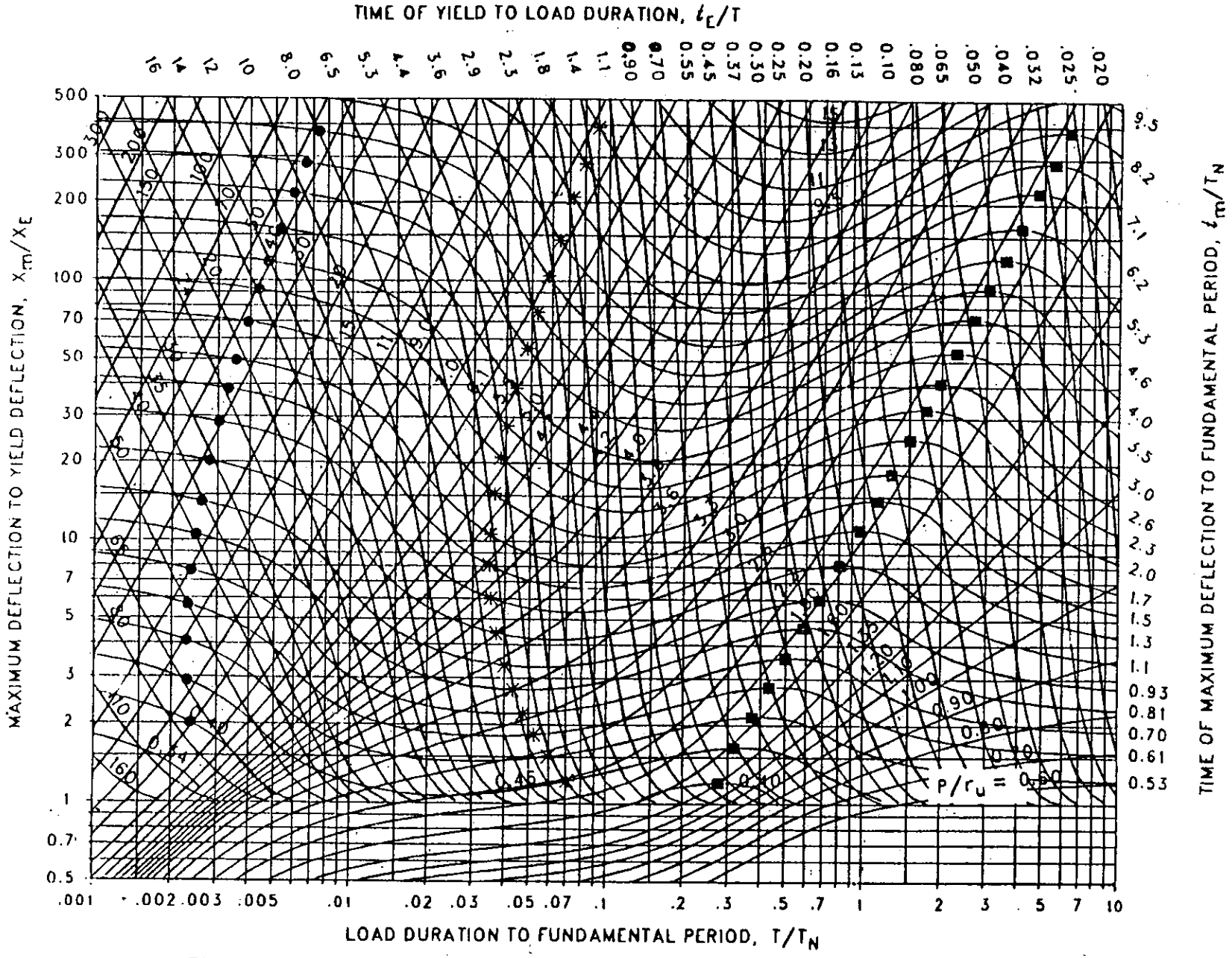


Figure 3-158 Maximum response of elasto-plastic, one-degree-of-freedom system for bilinear-triangular pulse (C_1 = 0.261, C_2 = 100.)

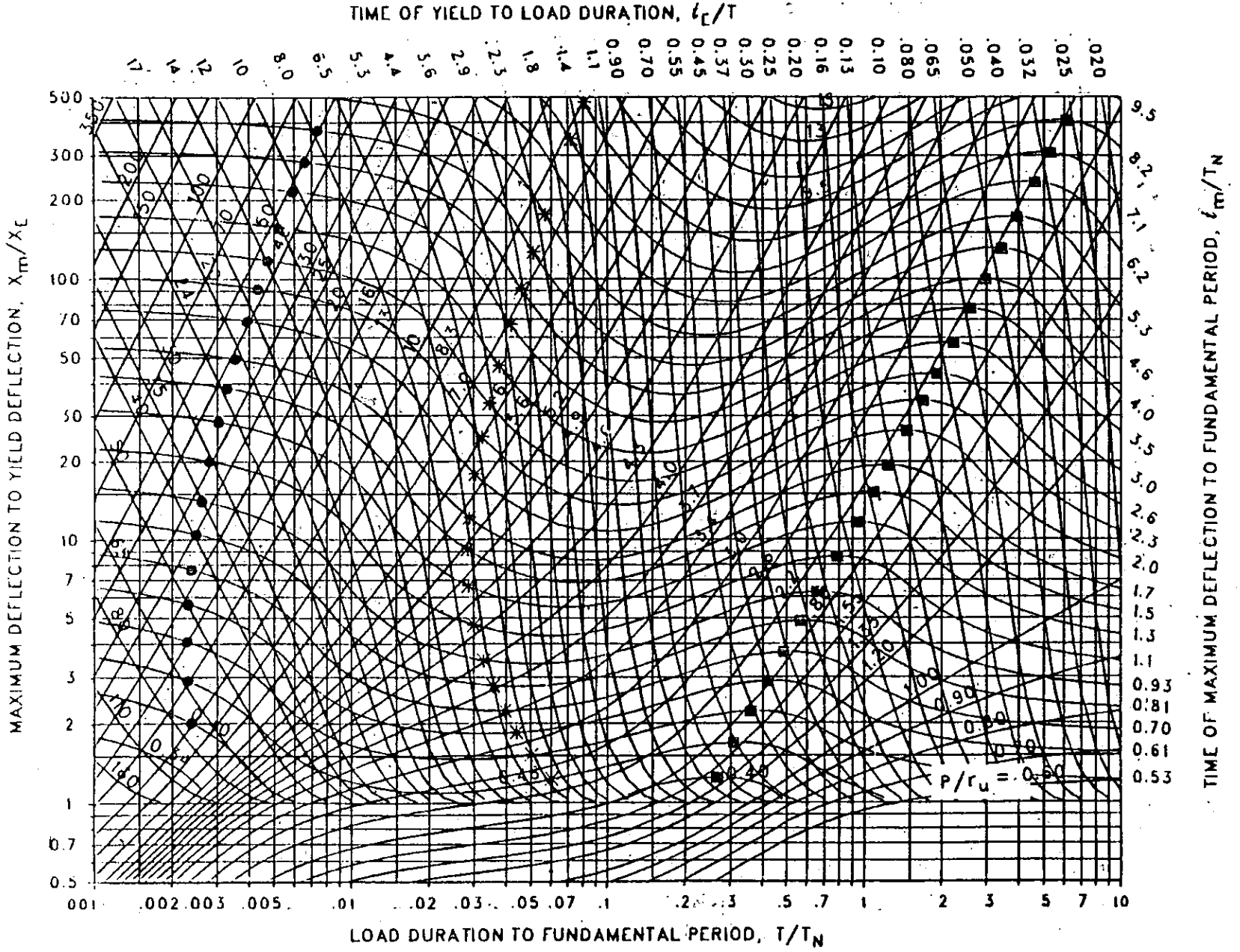


Figure 3-159 Maximum response of elasto-plastic, one-degree-of-freedom system for bilinear-triangular pulse (C_1 = 0.237, C_2 = 100.)

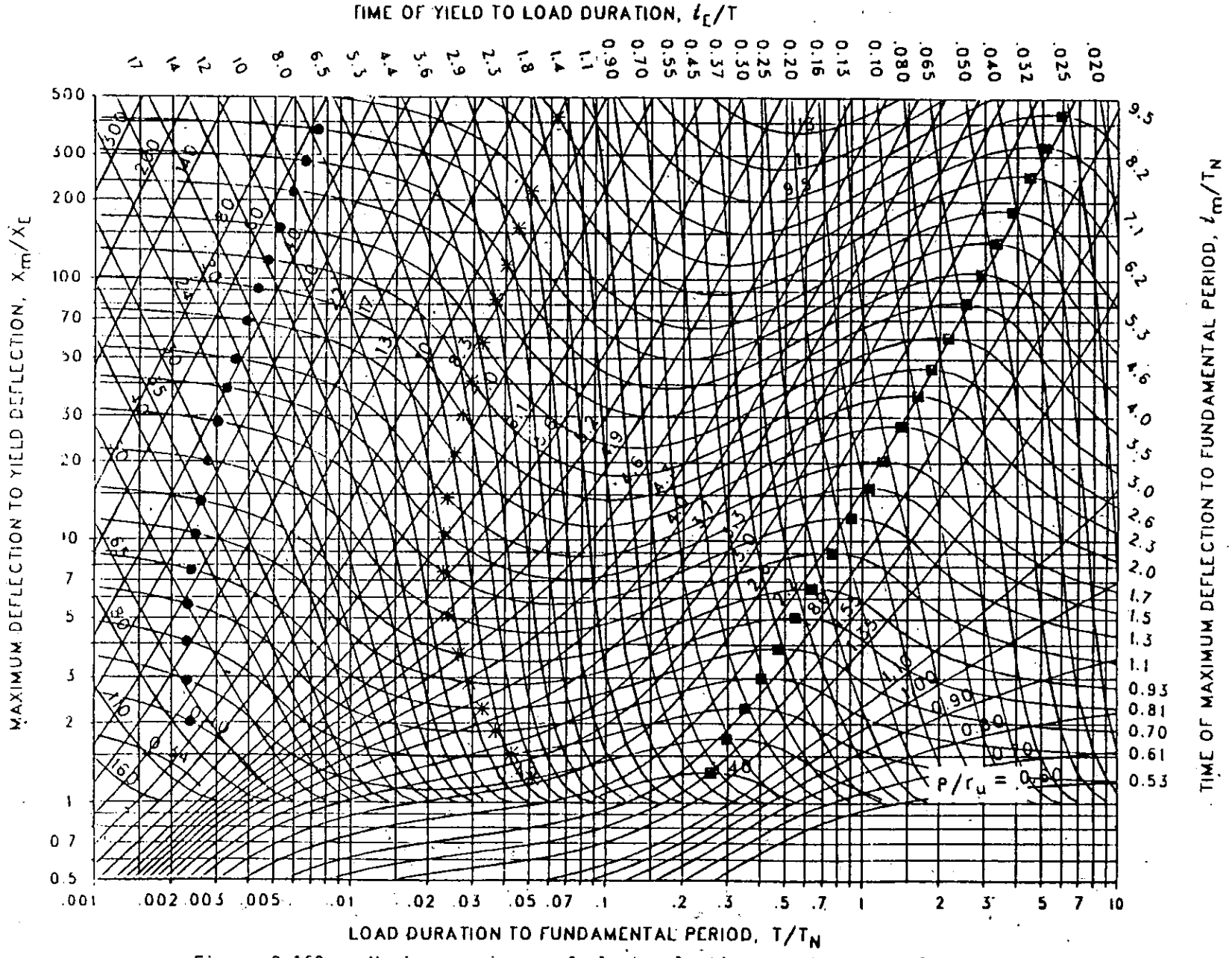


Figure 3-160 Maximum response of elasto-plastic, one-degree-of-freedom system for bilinear-triangular pulse (C_1 = 0.215, C_2 = 100.)

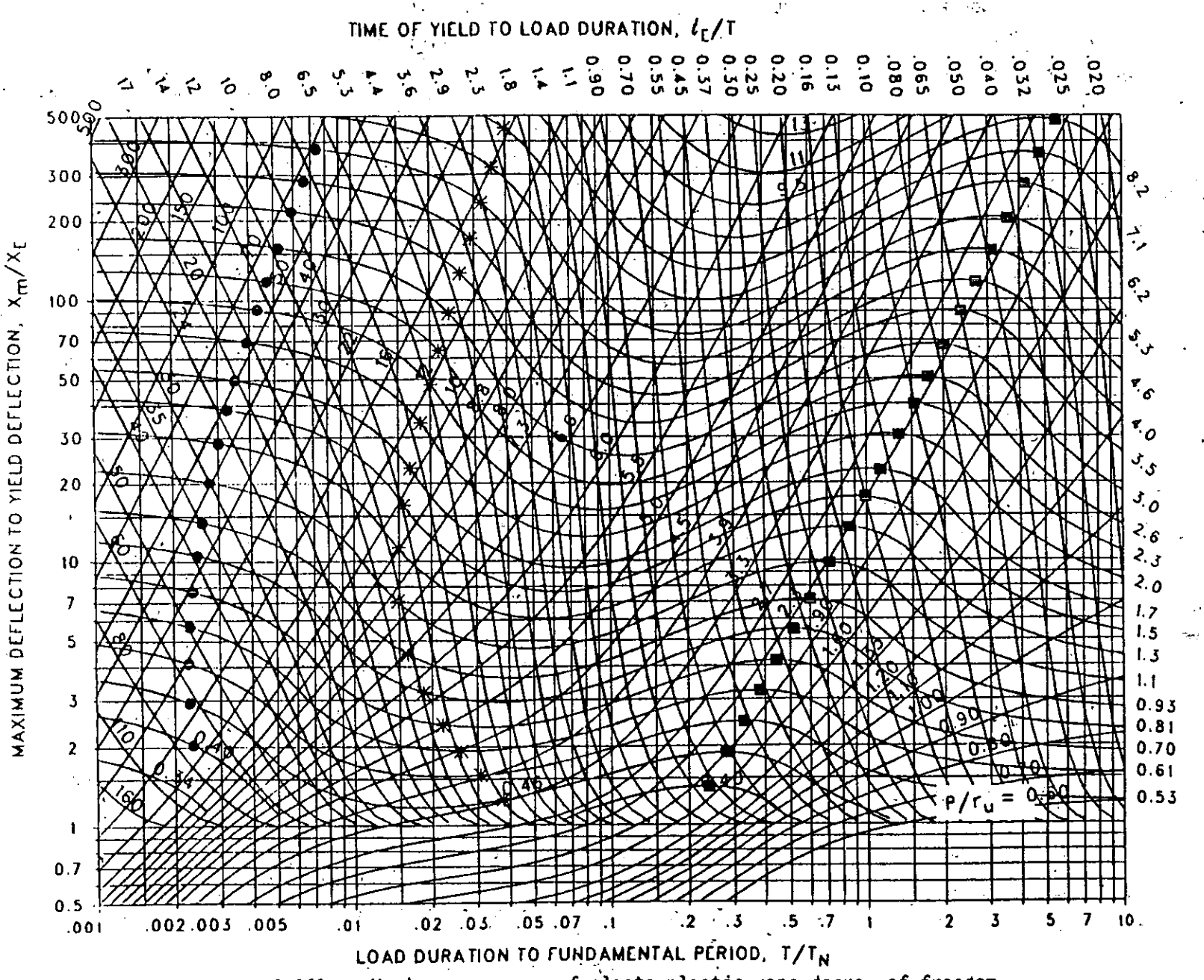


Figure 3-161 Maximum response of elasto-plastic, one-degree-of-freedom system for bilinear-triangular pulse (C_1 = 0.178, C_2 = 100.)

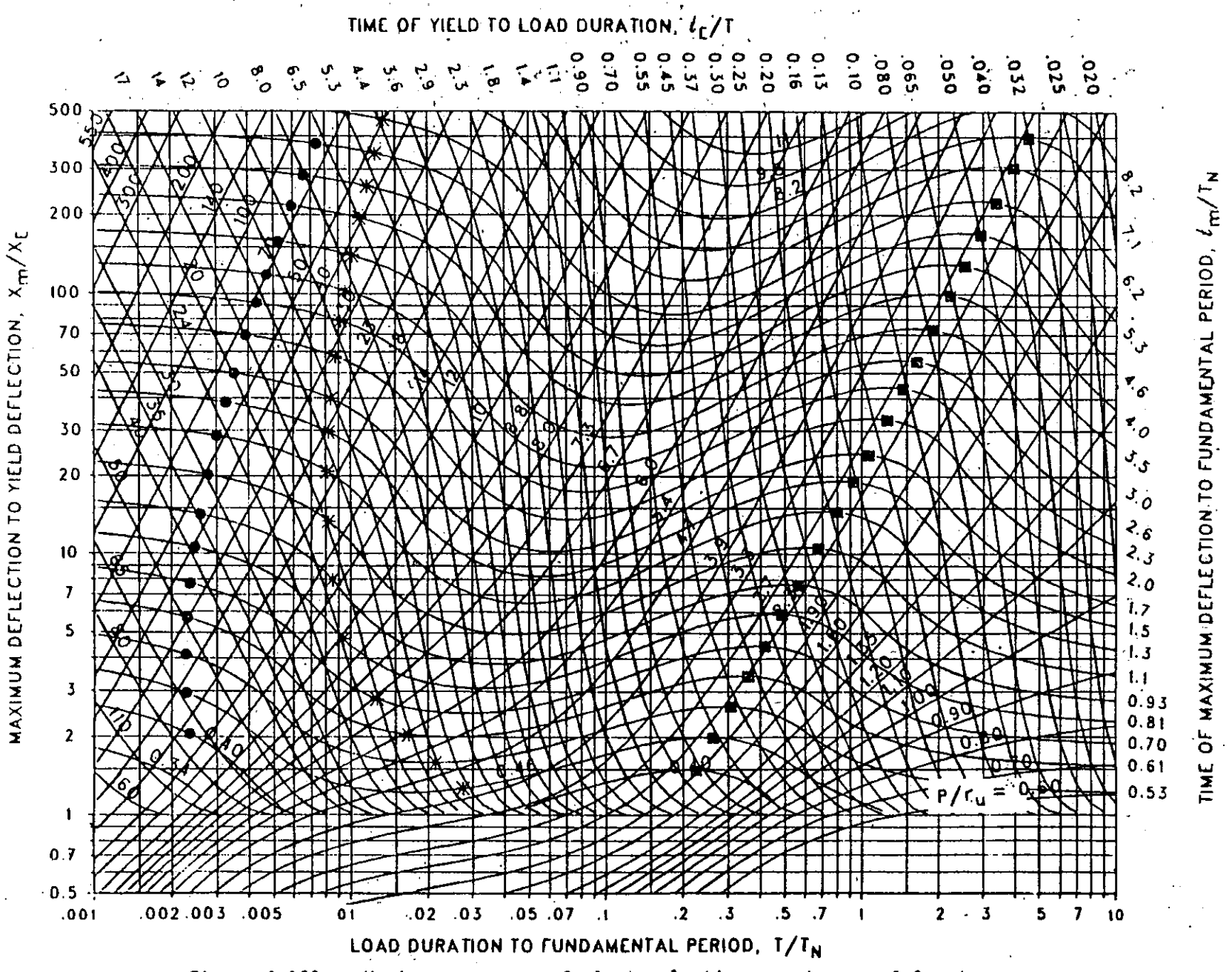


Figure 3-162 Maximum response of elasto-plastic, one-degree-of-freedom system for bilinear-triangular pulse ($C_1 = 0.147$, $C_2 = 100.$)

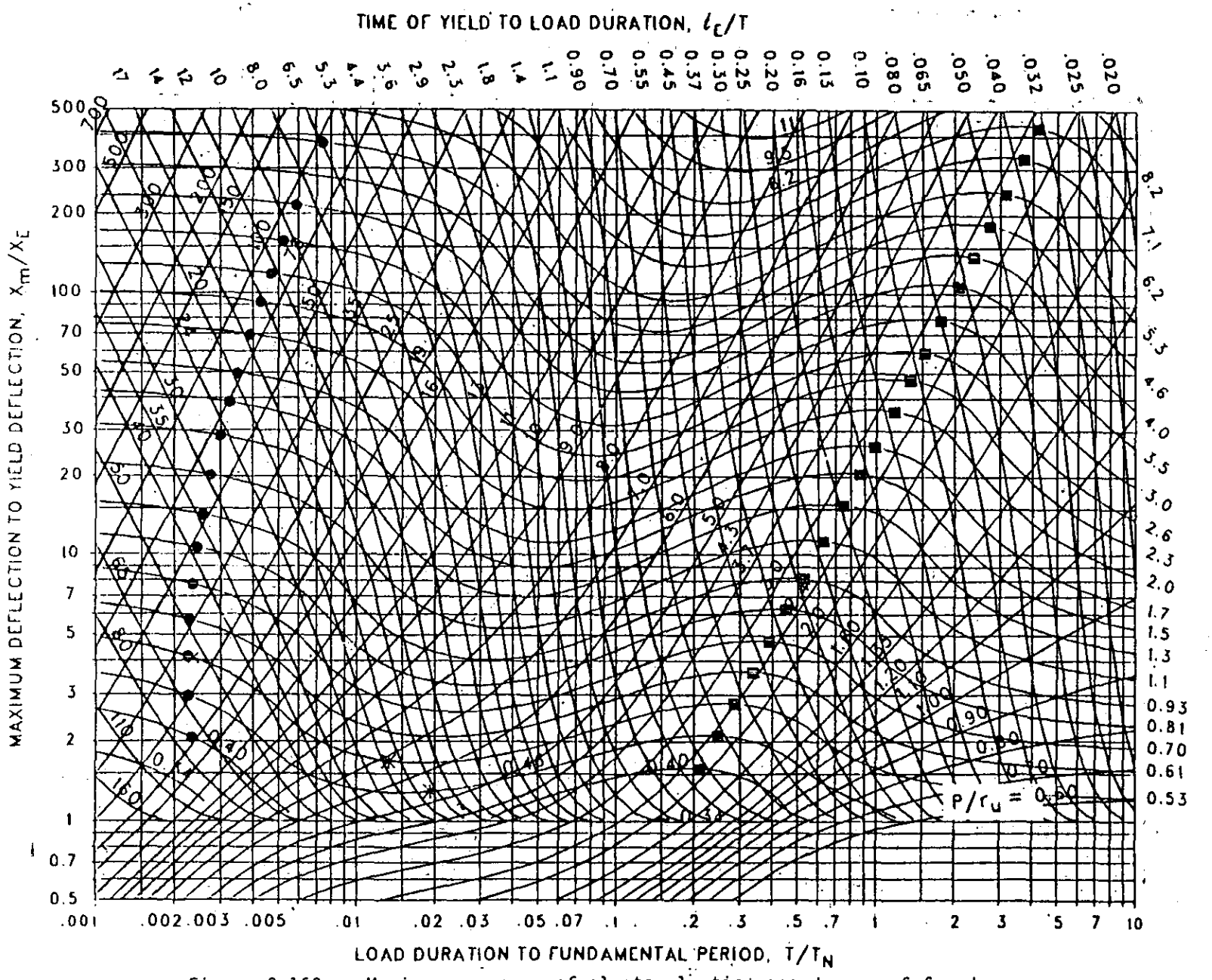


Figure 3-163 Maximum response of elasto-plastic, one-degree-of-freedom system for bilinear-triangular pulse ($C_1 = 0.121$, $C_2 = 100.$)

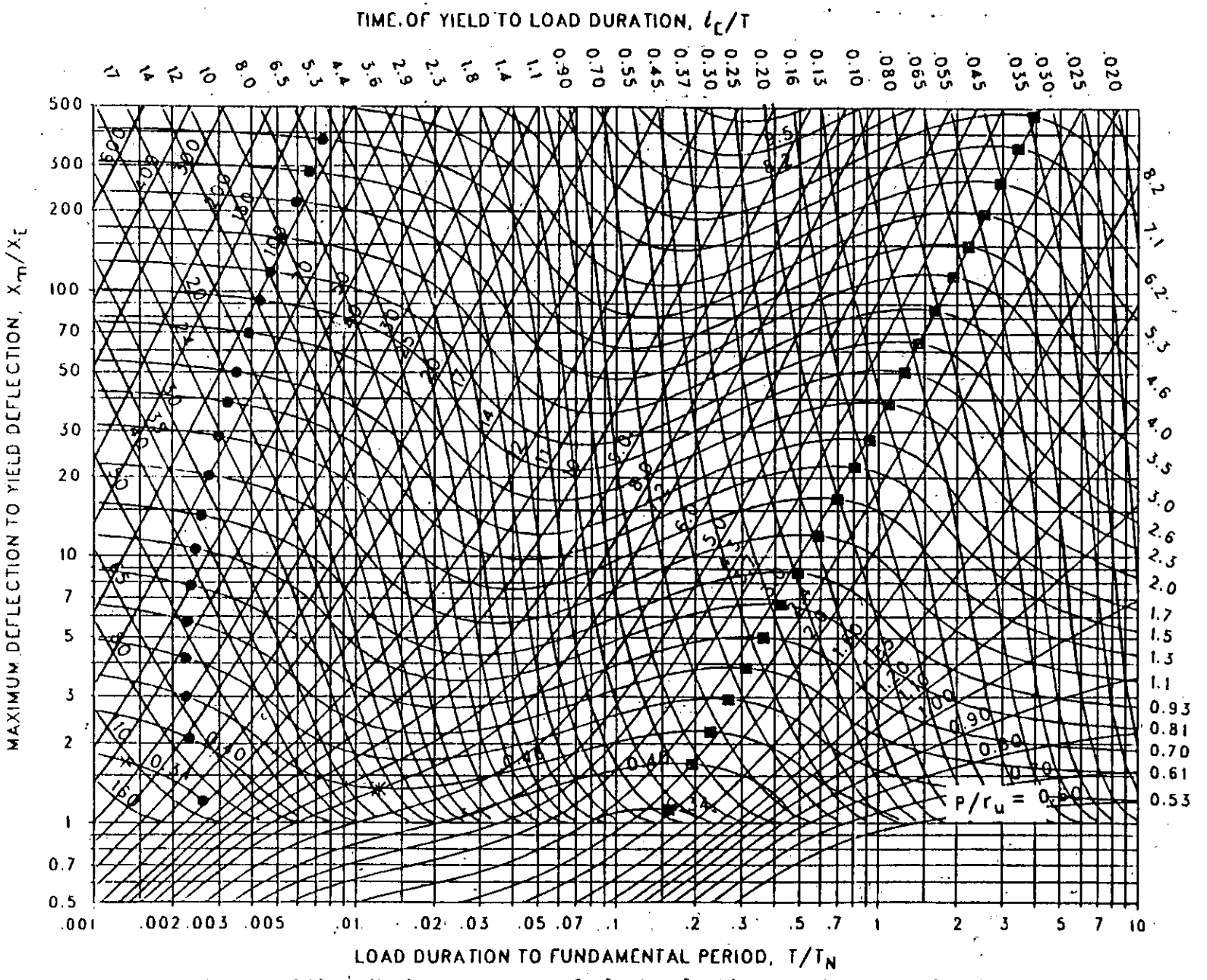


Figure 3-164 Maximum response of elasto-plastic, one-degree-of-freedom system for bilinear-triangular pulse ($C_1 = 0.100$, $C_2 = 100.$)

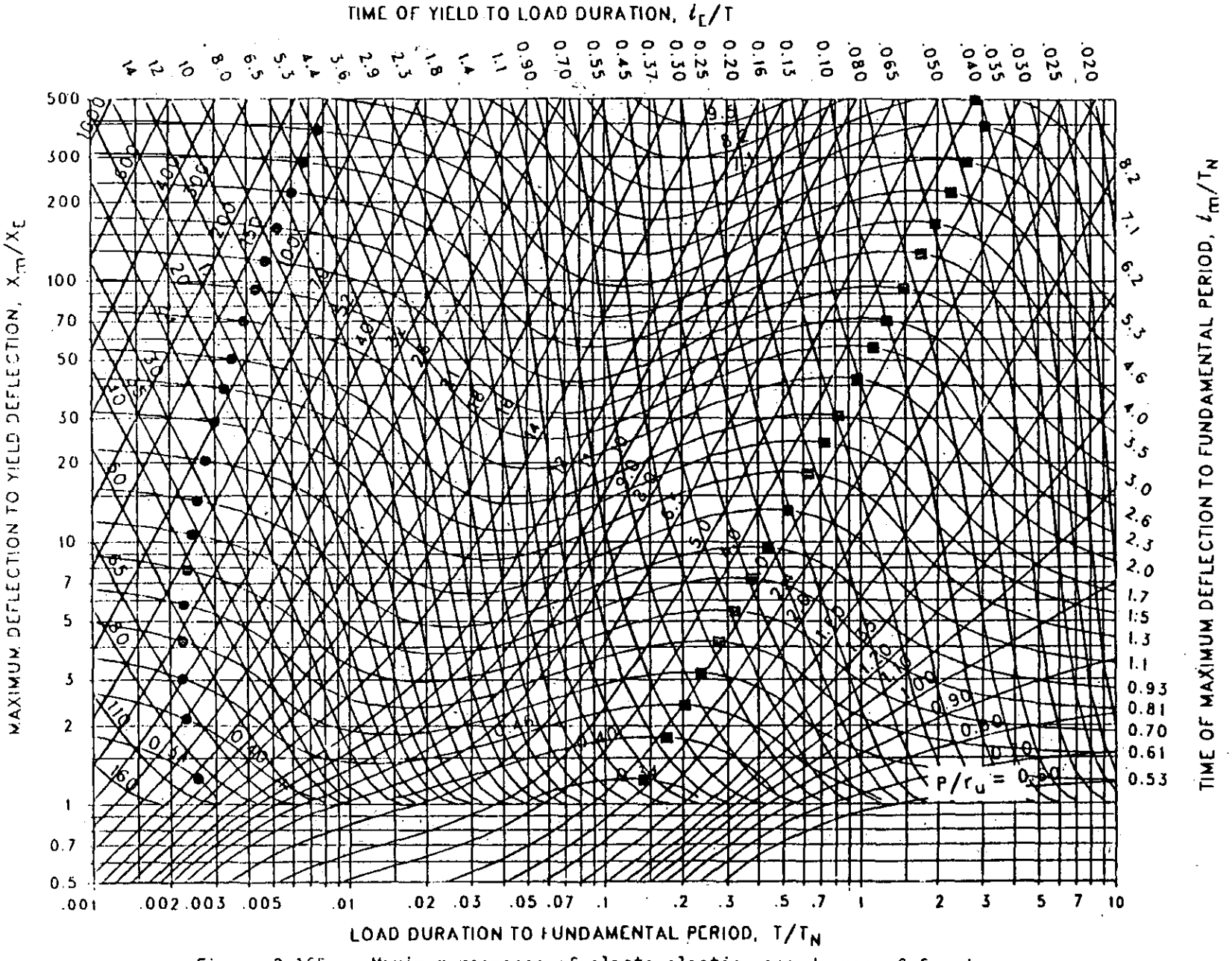


Figure 3-165 Maximum response of elasto-plastic, one-degree-of-freedom system for bilinear-triangular pulse (C_1 = 0.075, C_2 = 100.)

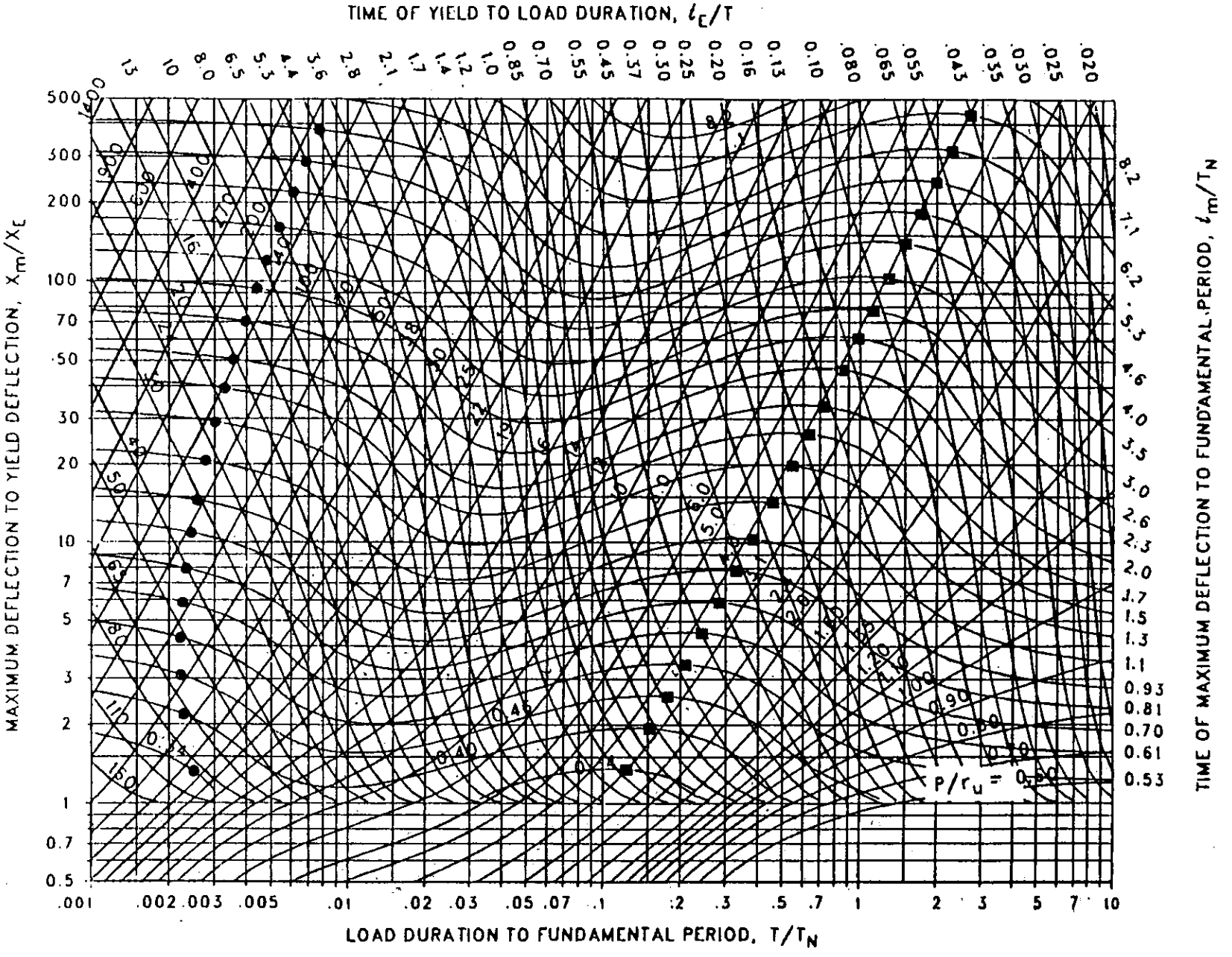


Figure 3-166 Maximum response of elasto-plastic, one-degree-of-freedom system for bilinear-triangular pulse (C_1 = 0.056, C_2 = 100.)

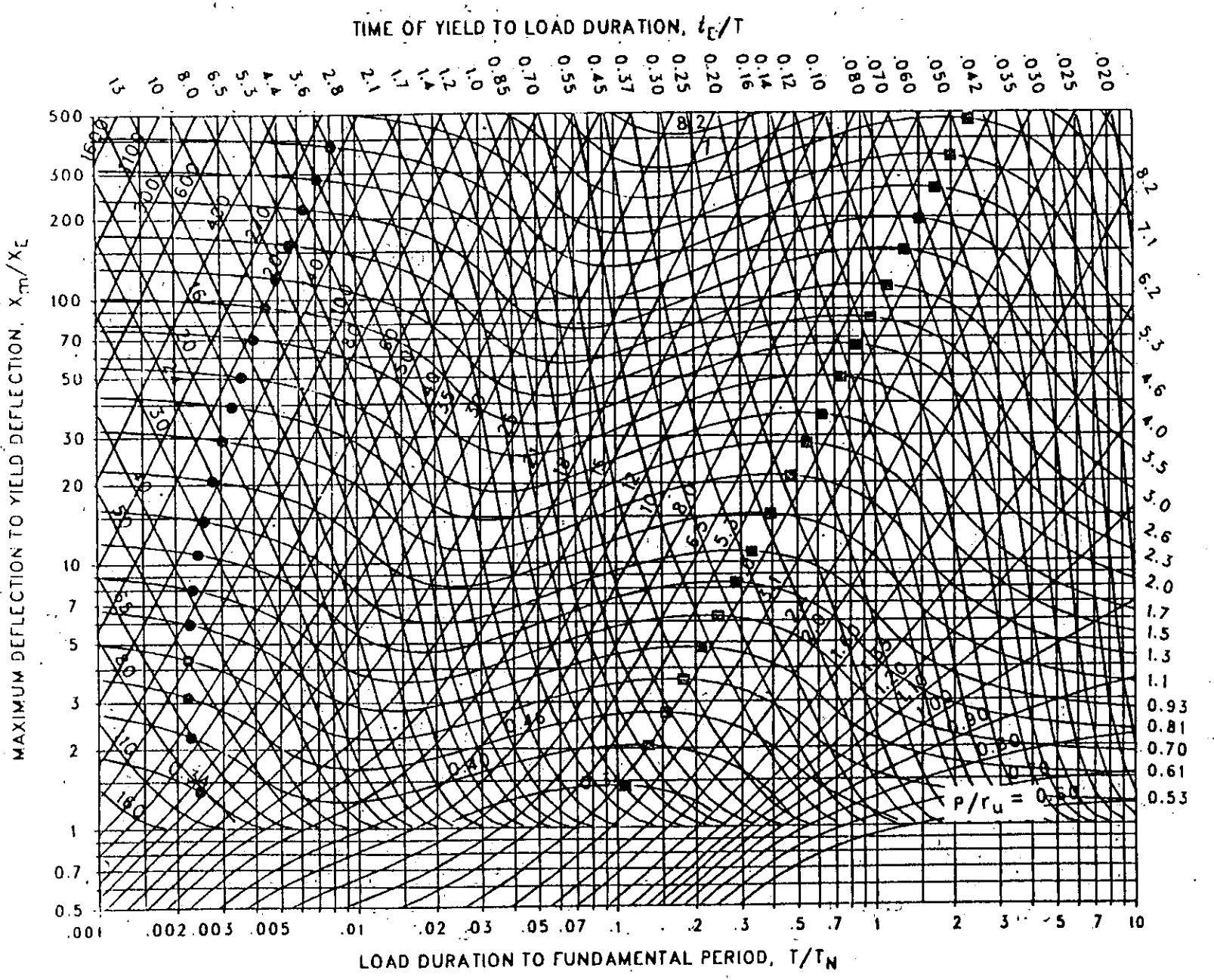


Figure 3-167 Maximum response of elasto-plastic, one-degree-of-freedom system for bilinear-triangular pulse (C_1 = 0.042, C_2 = 100.)

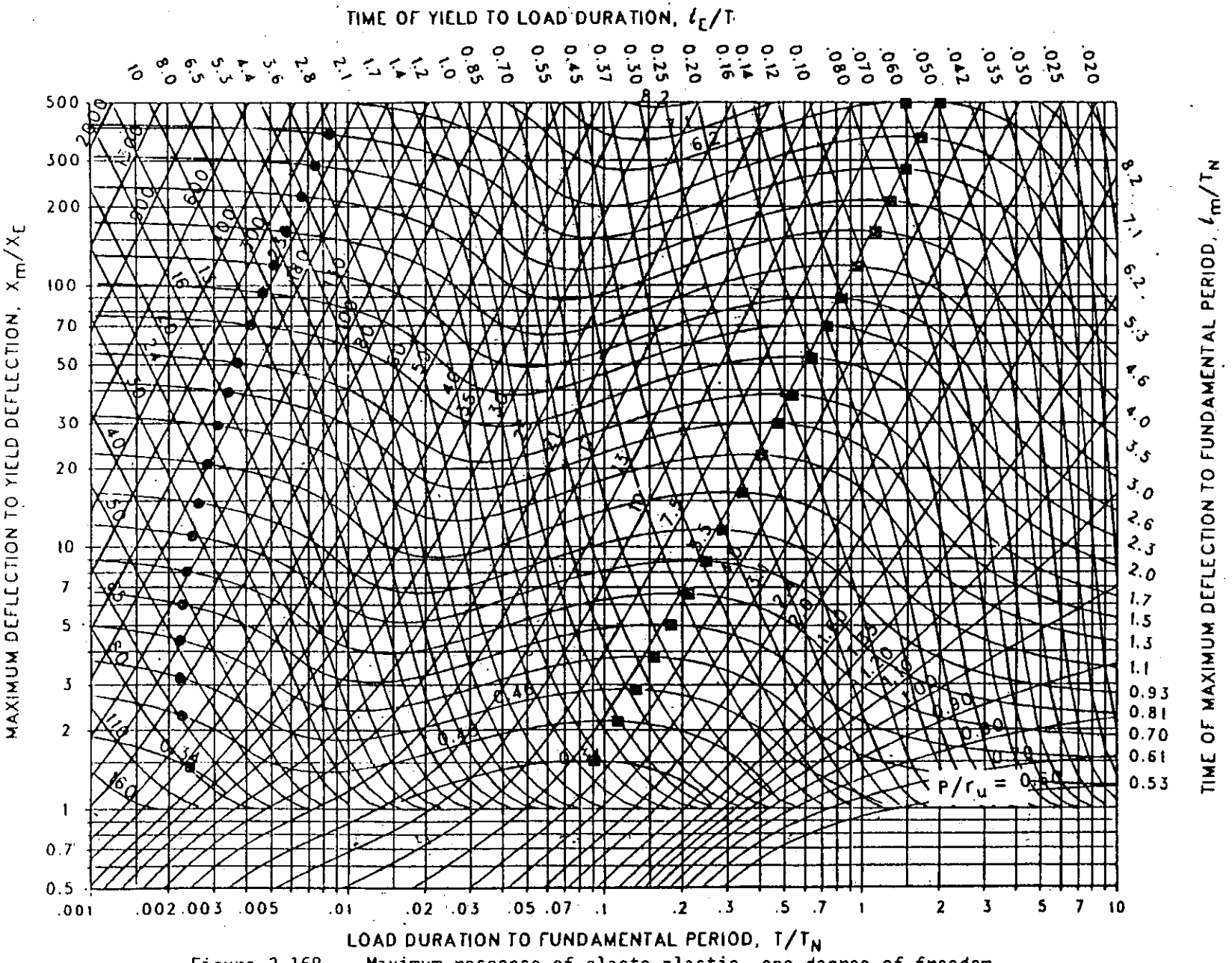


Figure 3-168 Maximum response of elasto-plastic, one-degree-of-freedom system for bilinear-triangular pulse ($C_1 = 0.032$, $C_2 = 100.$)

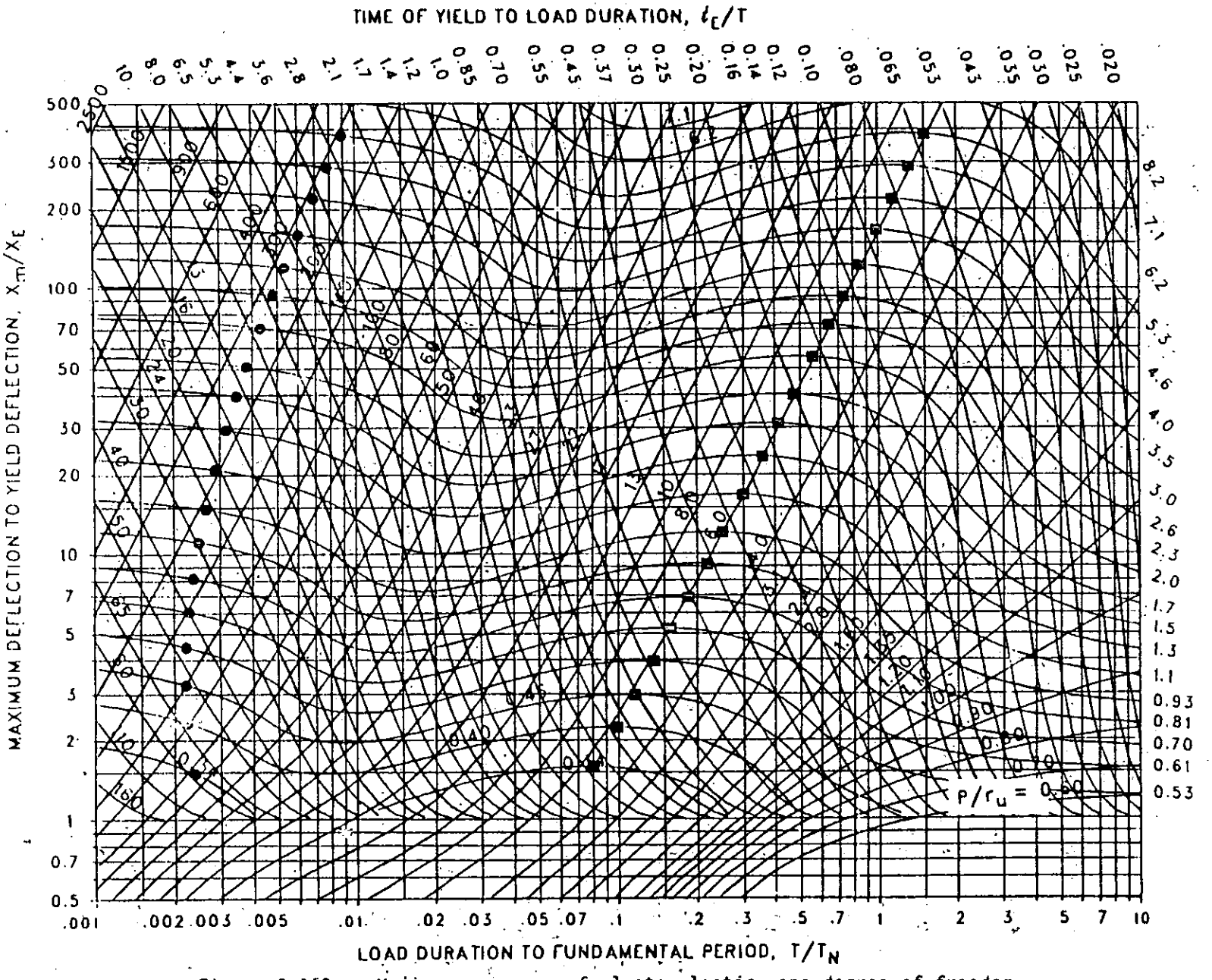


Figure 3-169 Maximum response of elasto-plastic, one-degree-of-freedom system for bilinear-triangular pulse ($C_1 = 0.026$, $C_2 = 100.$)

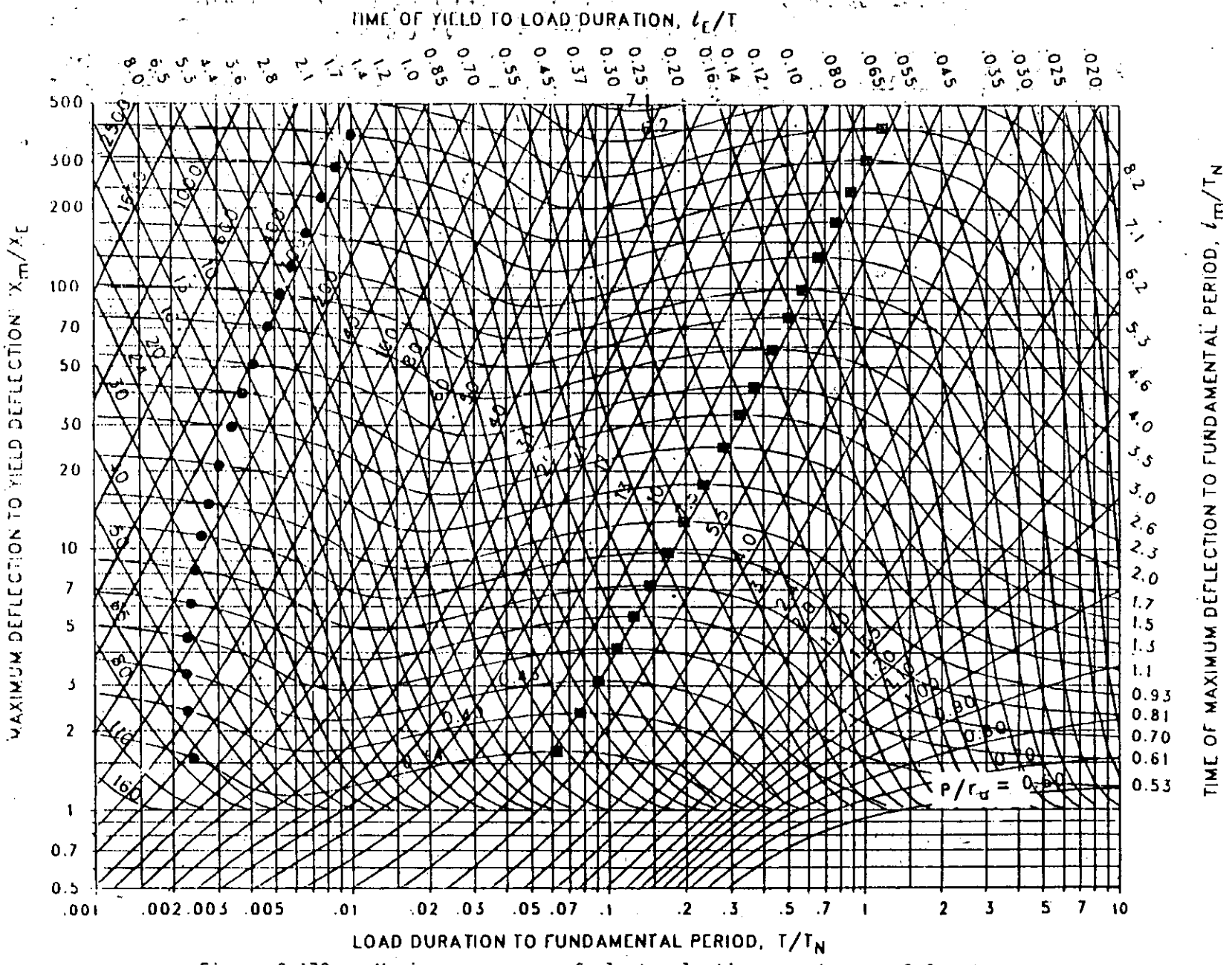


Figure 3-170 Maximum response of elasto-plastic, one-degree-of-freedom system for bilinear-triangular pulse ($C_1 = 0.018$, $C_2 = 100.$)

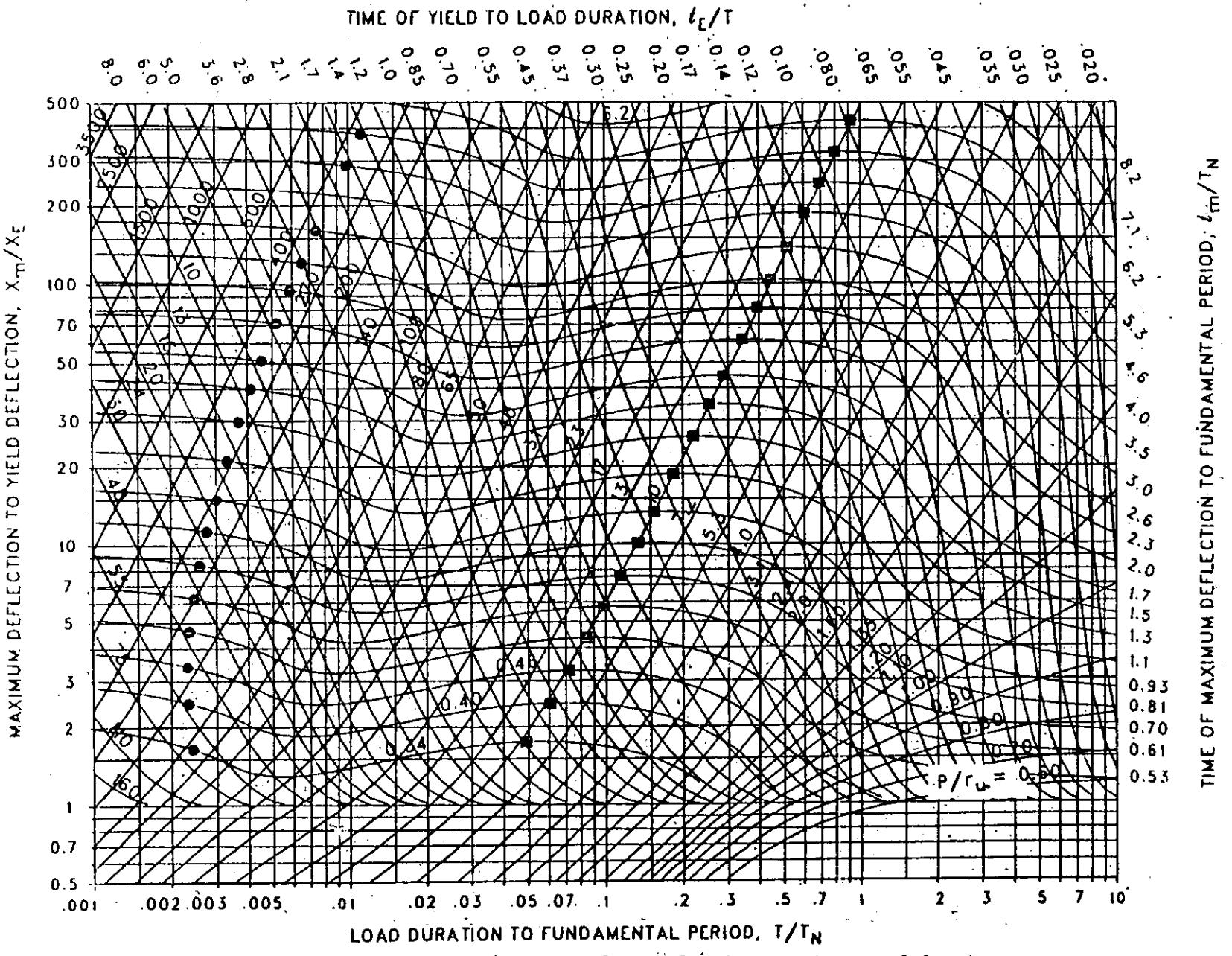


Figure 3-171 Maximum response of elasto-plastic, one-degree-of-freedom system for bilinear-triangular pulse ($C_1 = 0.013$, $C_2 = 100.$)

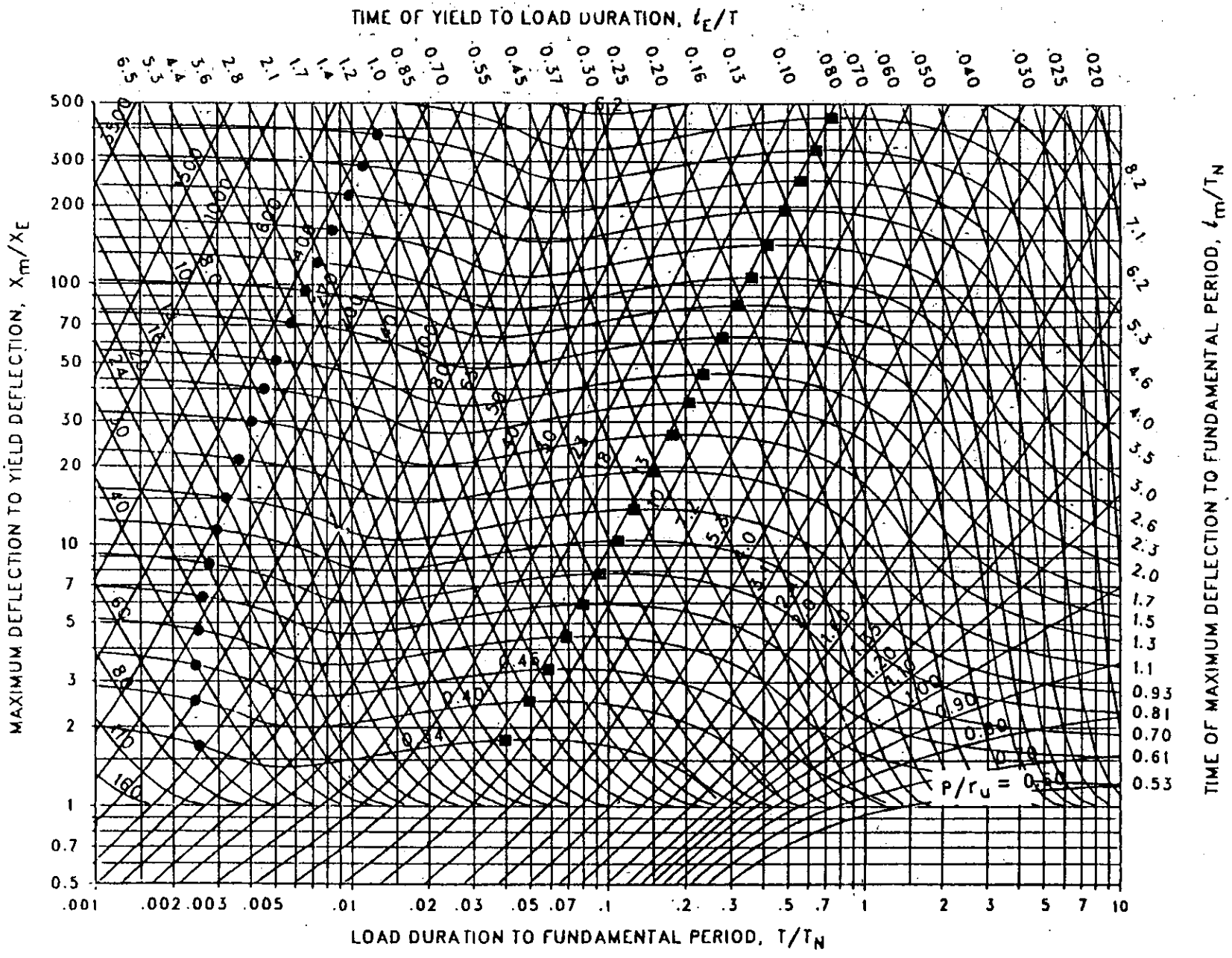


Figure 3-172 Maximum response of elasto-plastic, one-degree-of-freedom system for bilinear-triangular pulse ($C_1 = 0.010$, $C_2 = 100.$)

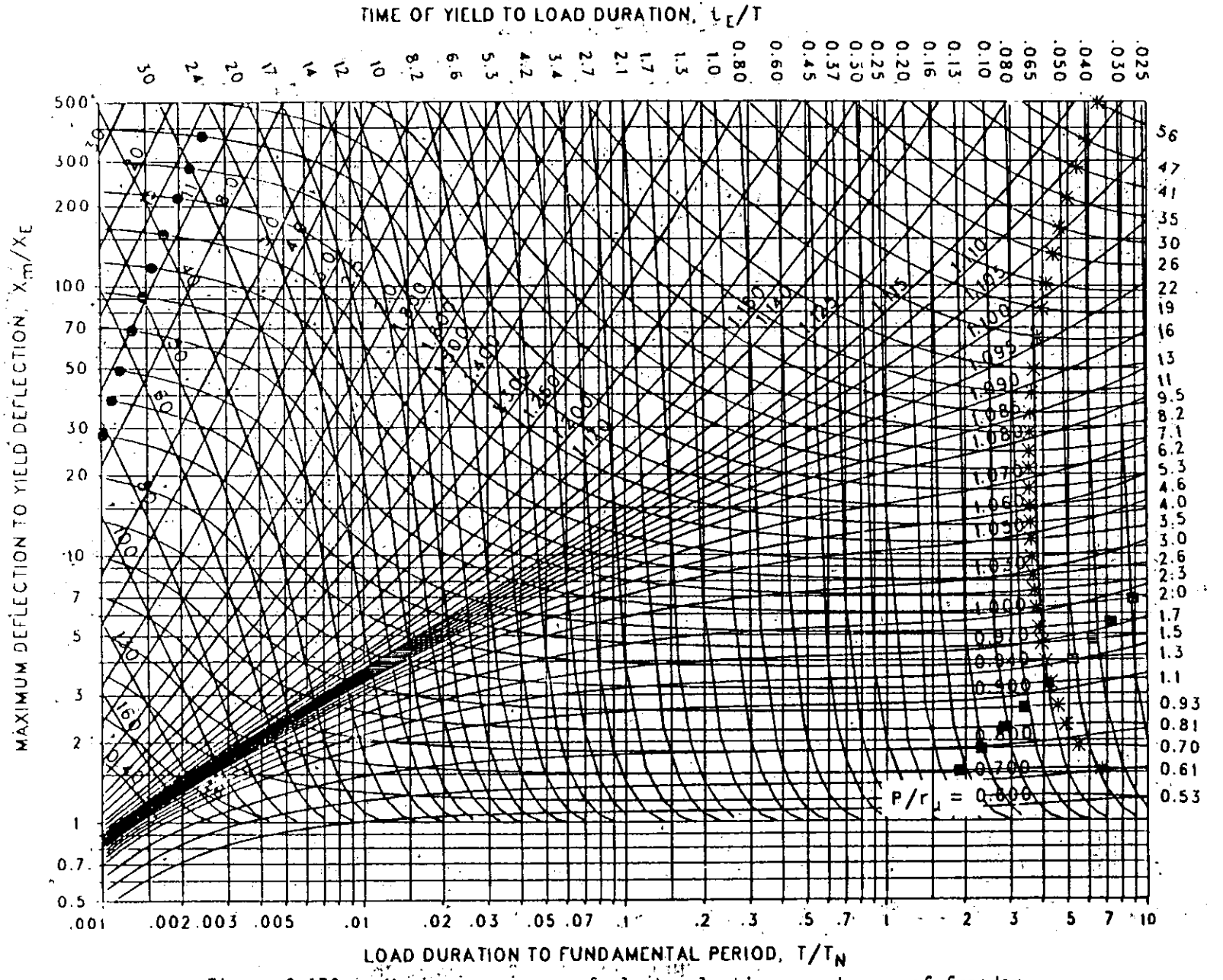


Figure 3-173 Maximum response of elasto-plastic, one-degree-of-freedom system for bilinear-triangular pulse ($C_1 = 0.909$, $C_2 = 300.$)

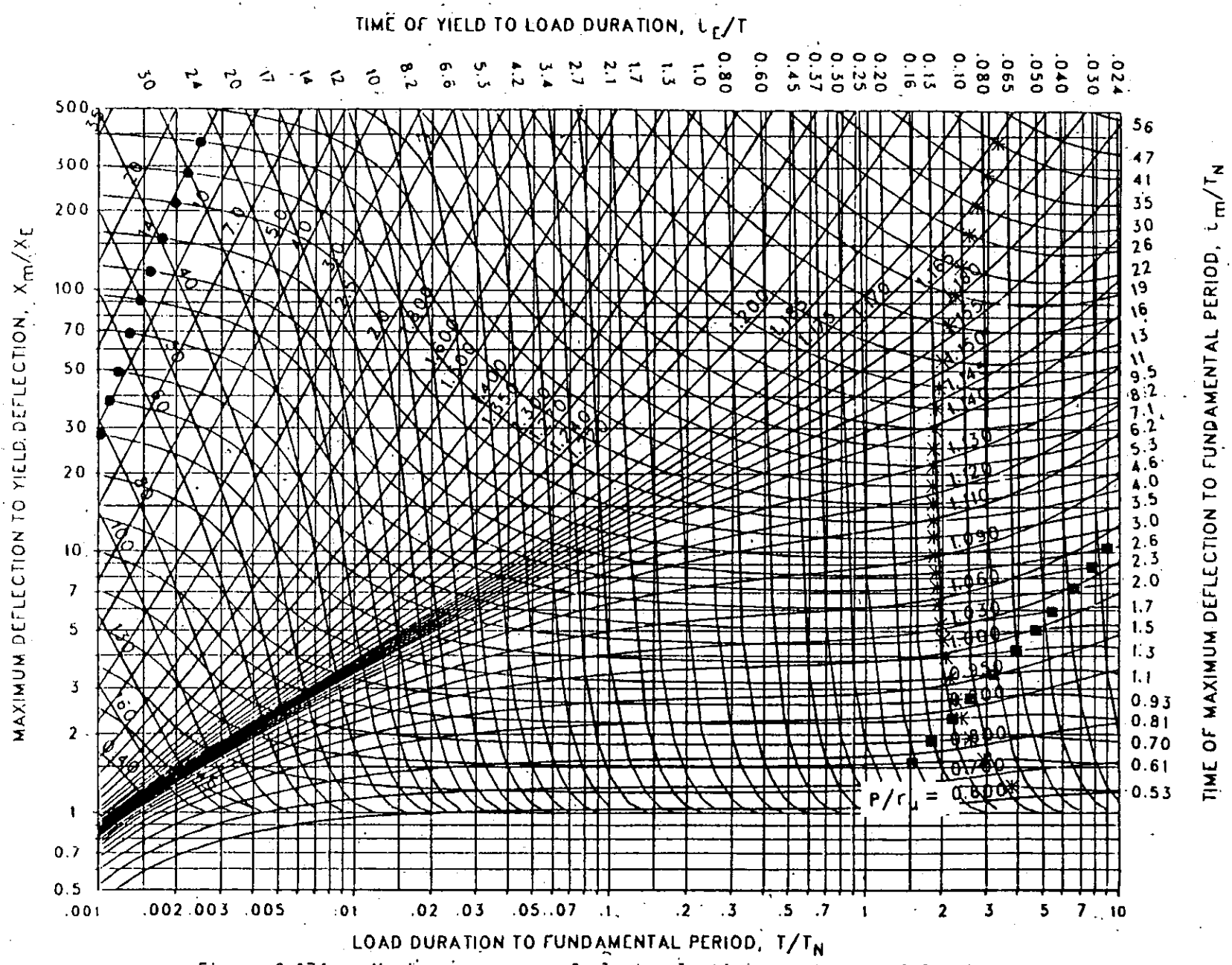


Figure 3-174 Maximum response of elasto-plastic, one-degree-of-freedom system for bilinear-triangular pulse ($C_1 = 0.866$, $C_2 = 300.$)

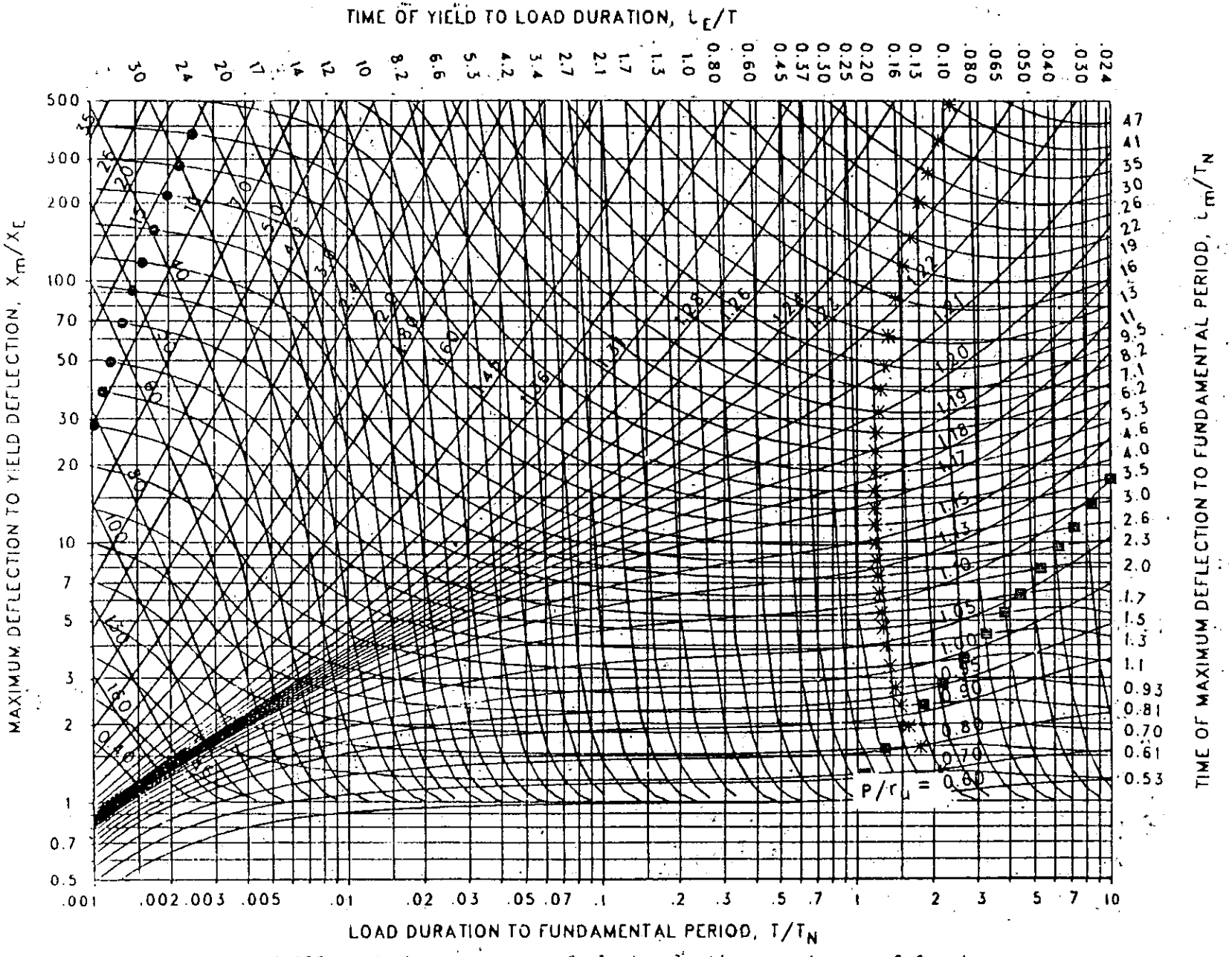


Figure 3-175 Maximum response of elasto-plastic, one-degree-of-freedom system for bilinear-triangular pulse ($C_1 = 0.825$, $C_2 = 300.$)

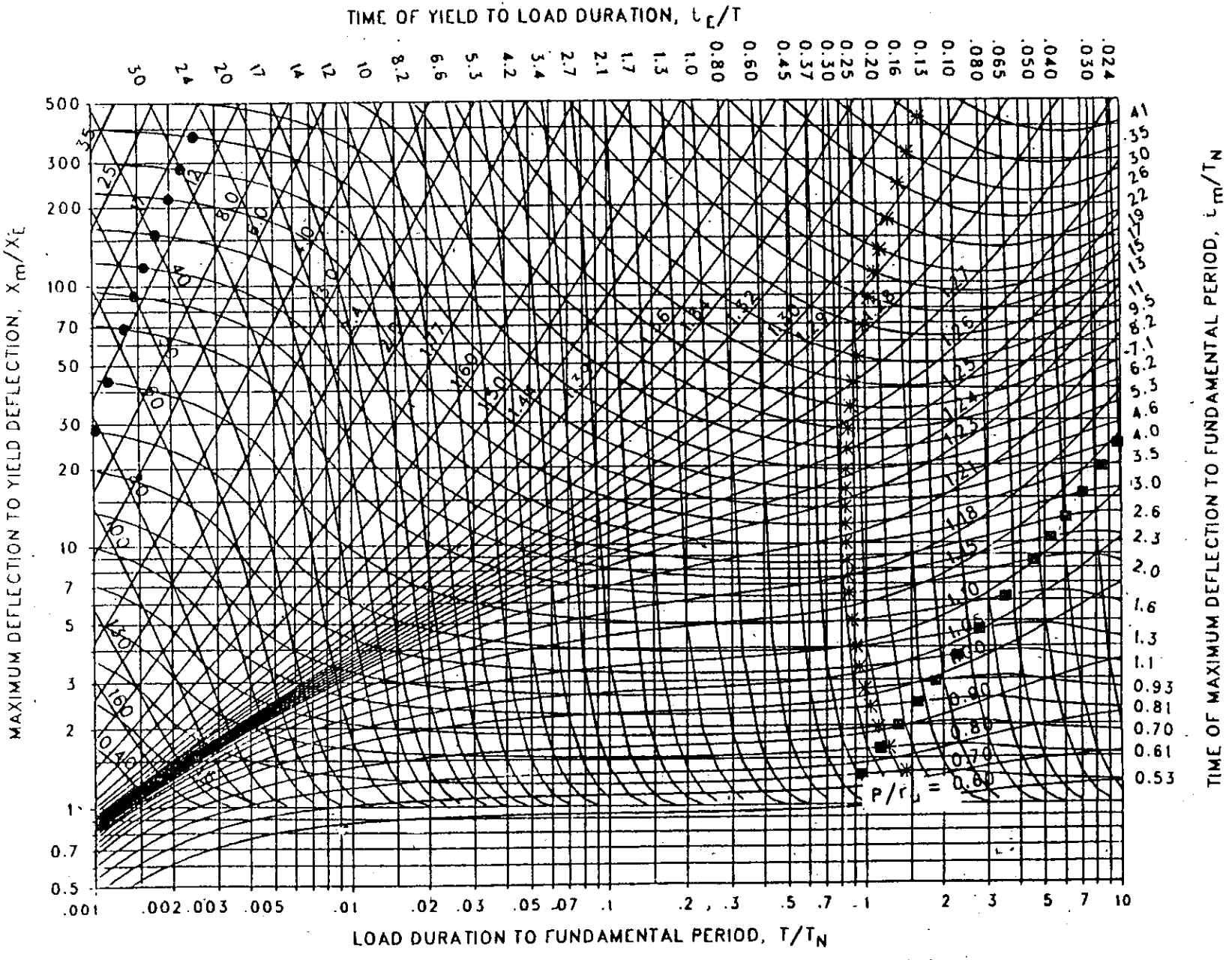


Figure 3-176 Maximum response of elasto-plastic, one-degree-of-freedom system for bilinear-triangular pulse ($C_1 = 0.787$, $C_2 = 300.$)

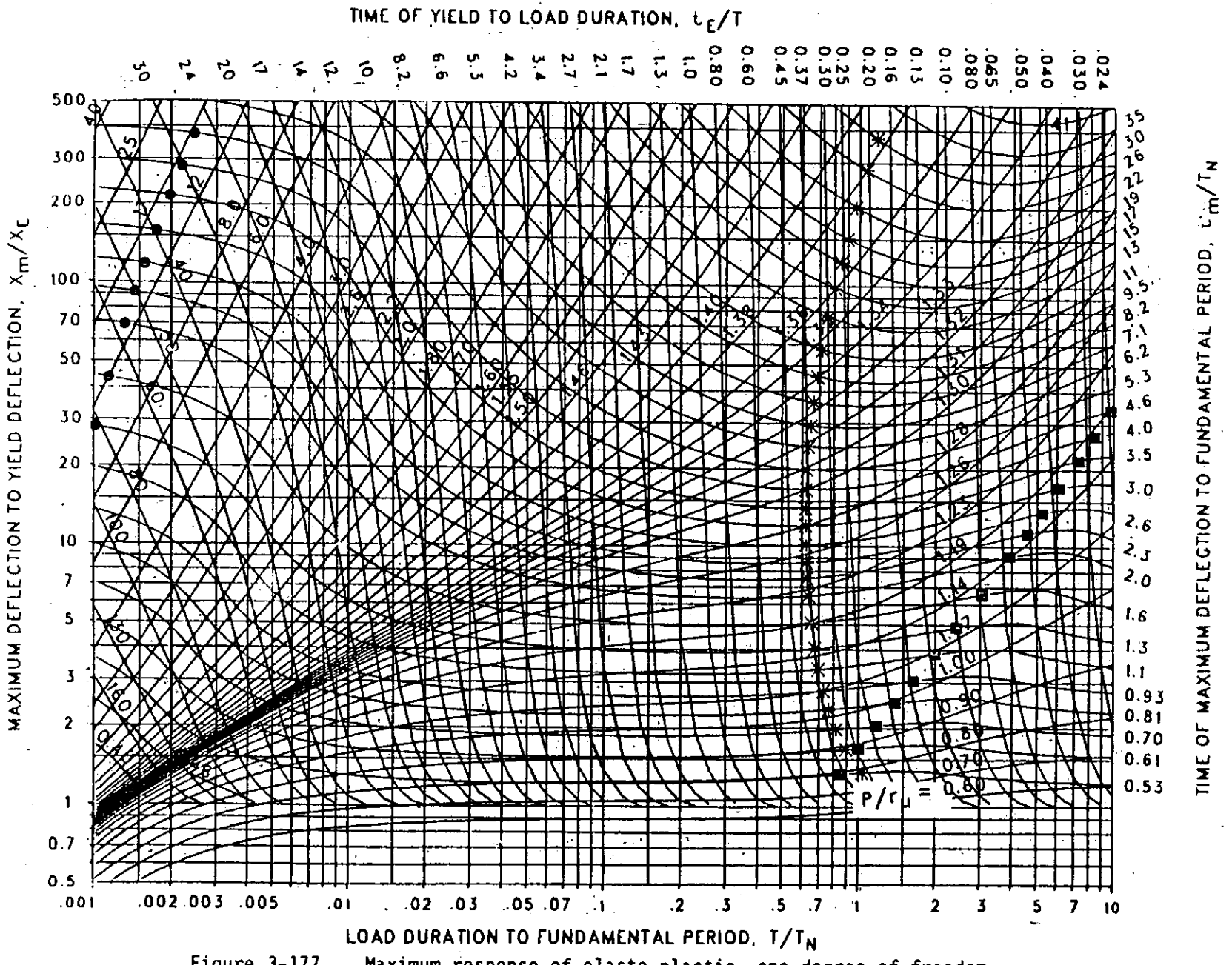


Figure 3-177 Maximum response of elasto-plastic, one-degree-of-freedom system for bilinear-triangular pulse ($C_1 = 0.750$, $C_2 = 300.$)

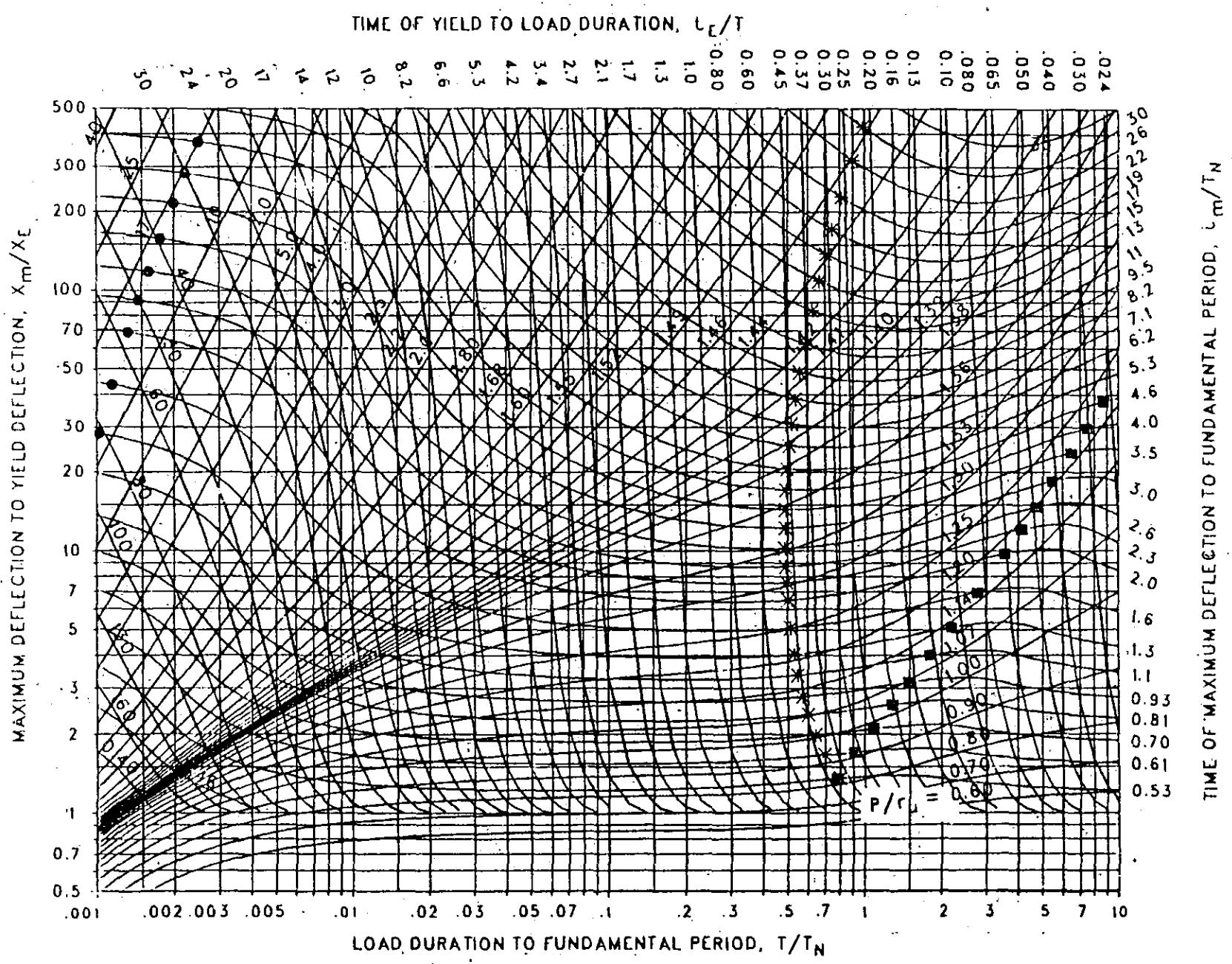


Figure 3-178 Maximum response of elasto-plastic, one-degree-of-freedom system for bilinear-triangular pulse (C_1 = 0.715, C_2 = 300.)

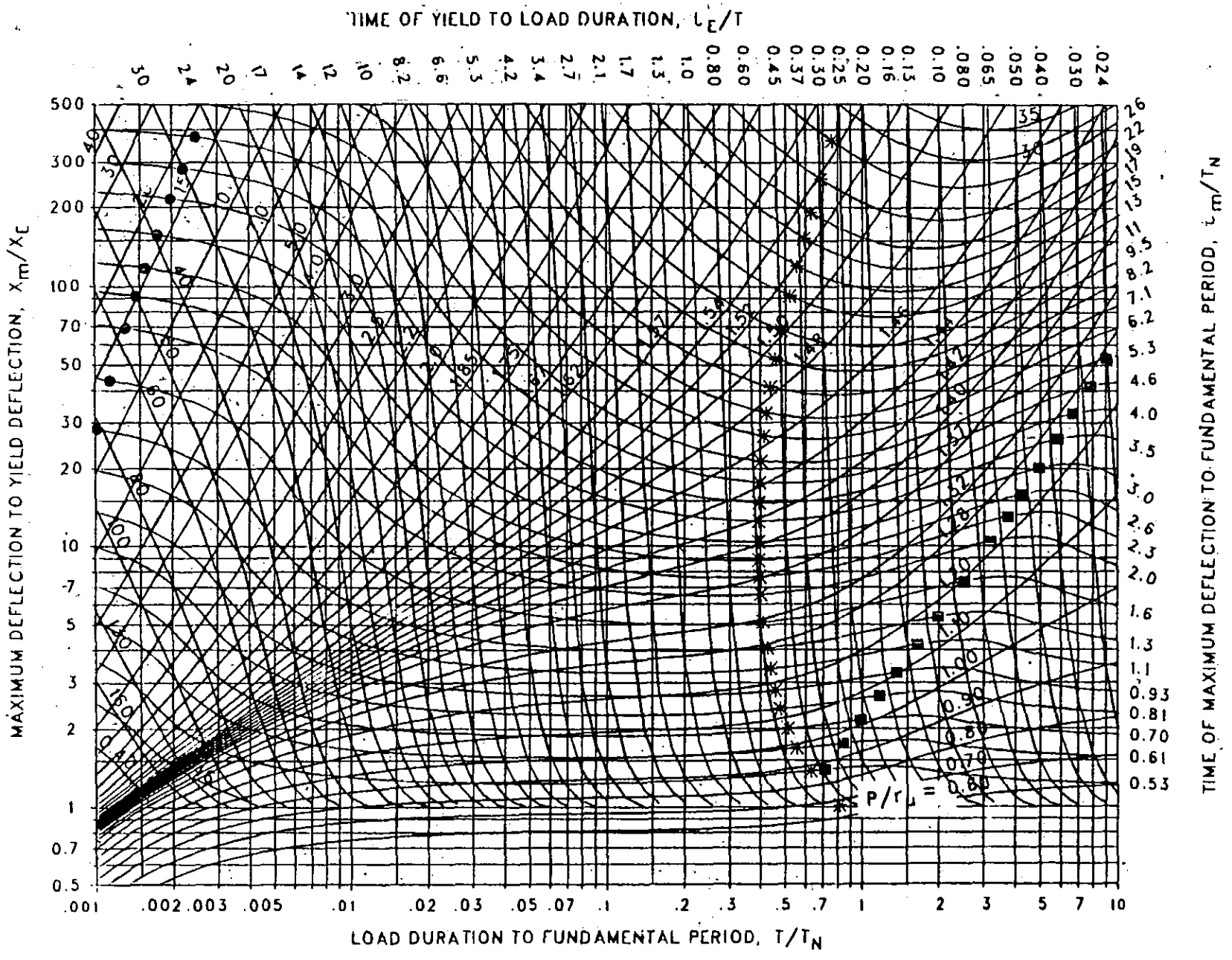


Figure 3-179 Maximum response of elasto-plastic, one-degree-of-freedom system for bilinear-triangular pulse (C_1 = 0.681, C_2 = 300.)

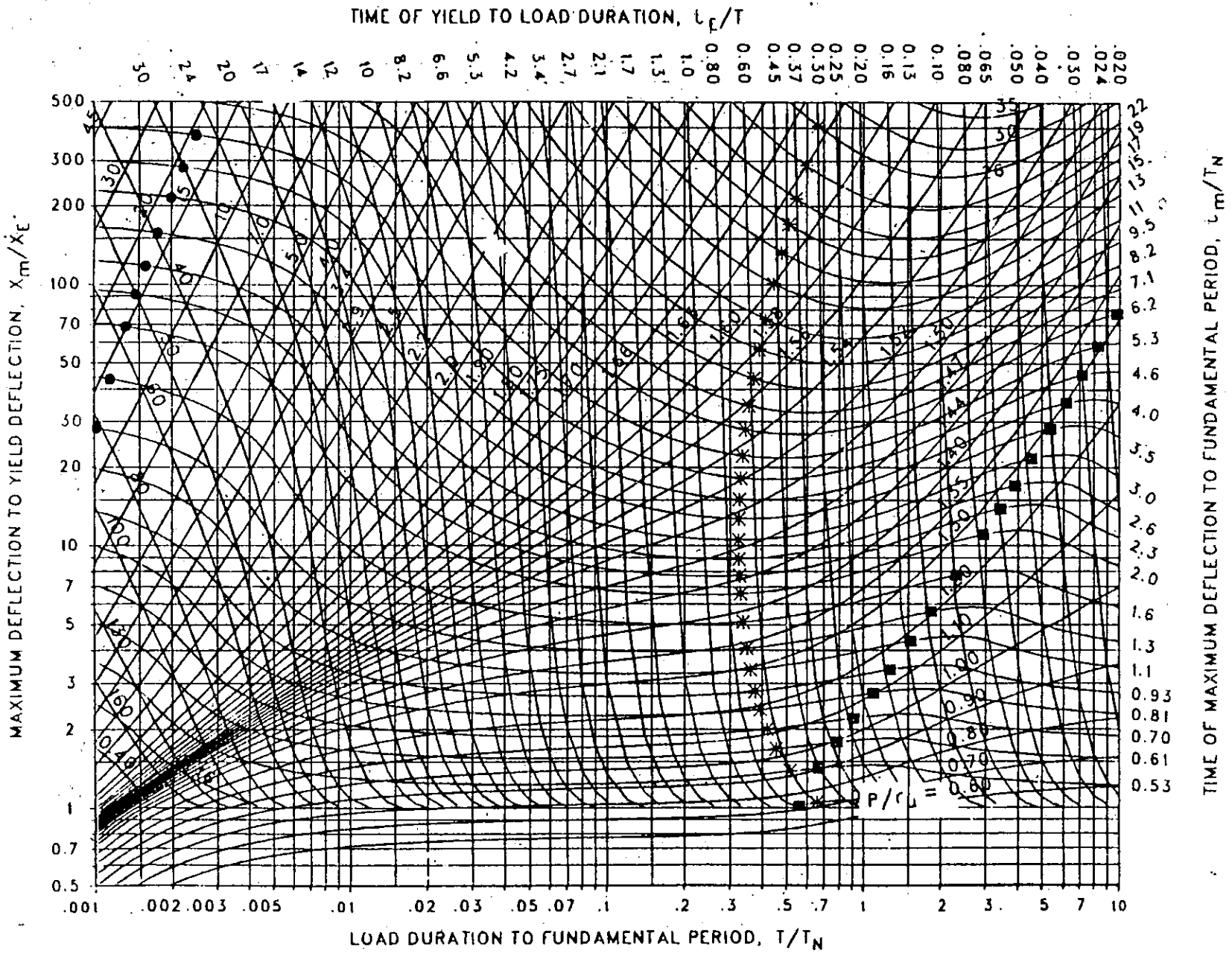


Figure 3-180 Maximum response of elasto-plastic, one-degree-of-freedom system for bilinear-triangular pulse ($C_1 = 0.648$, $C_2 = 300.$)

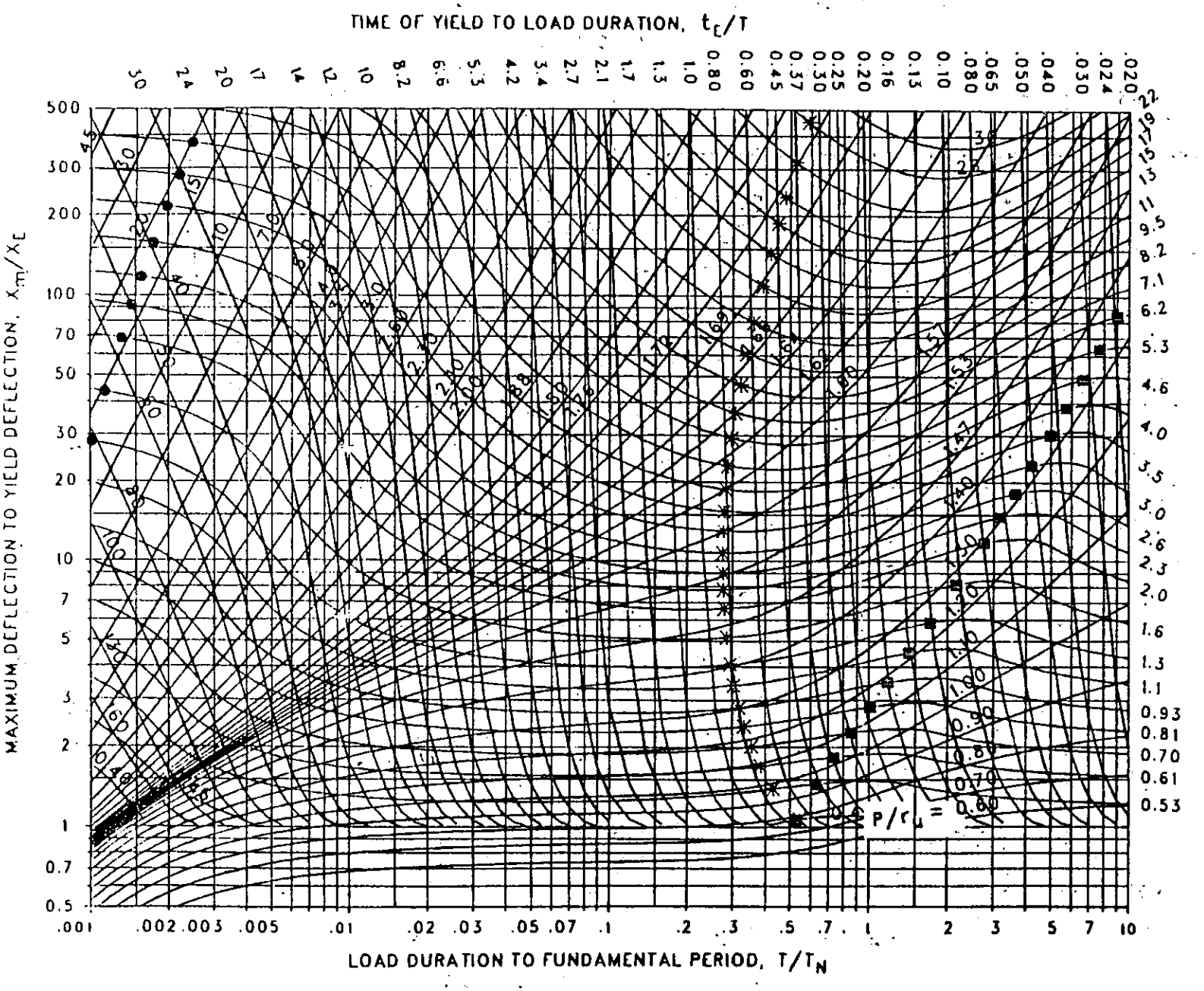


Figure 3-181 Maximum response of elasto-plastic, one-degree-of-freedom system for bilinear-triangular pulse (C_1 = 0.619, C_2 = 300.)

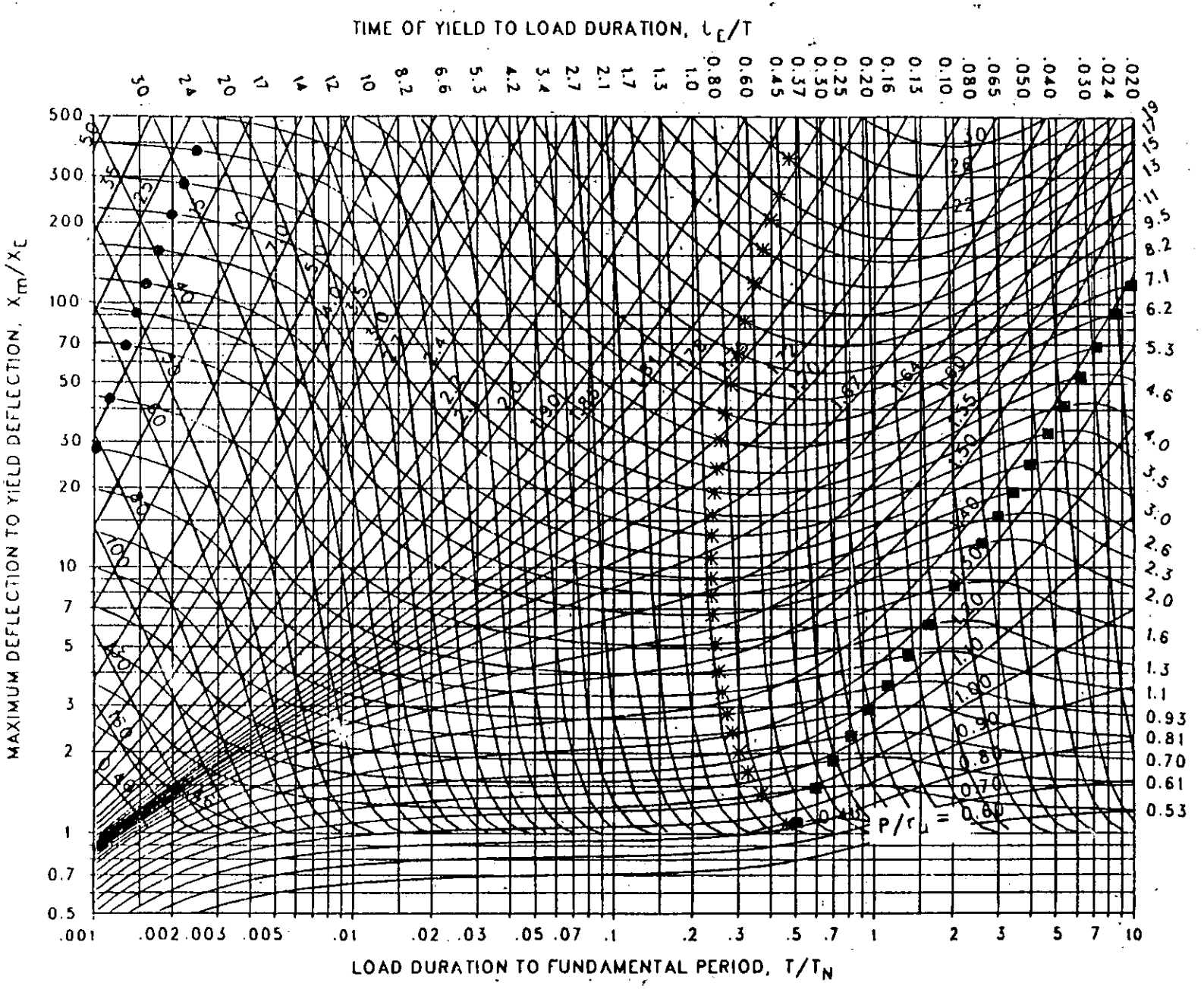


Figure 3-182 Maximum response of elasto-plastic, one-degree-of-freedom system for bilinear-triangular pulse ($C_1 = 0.590$, $C_2 = 300.$)

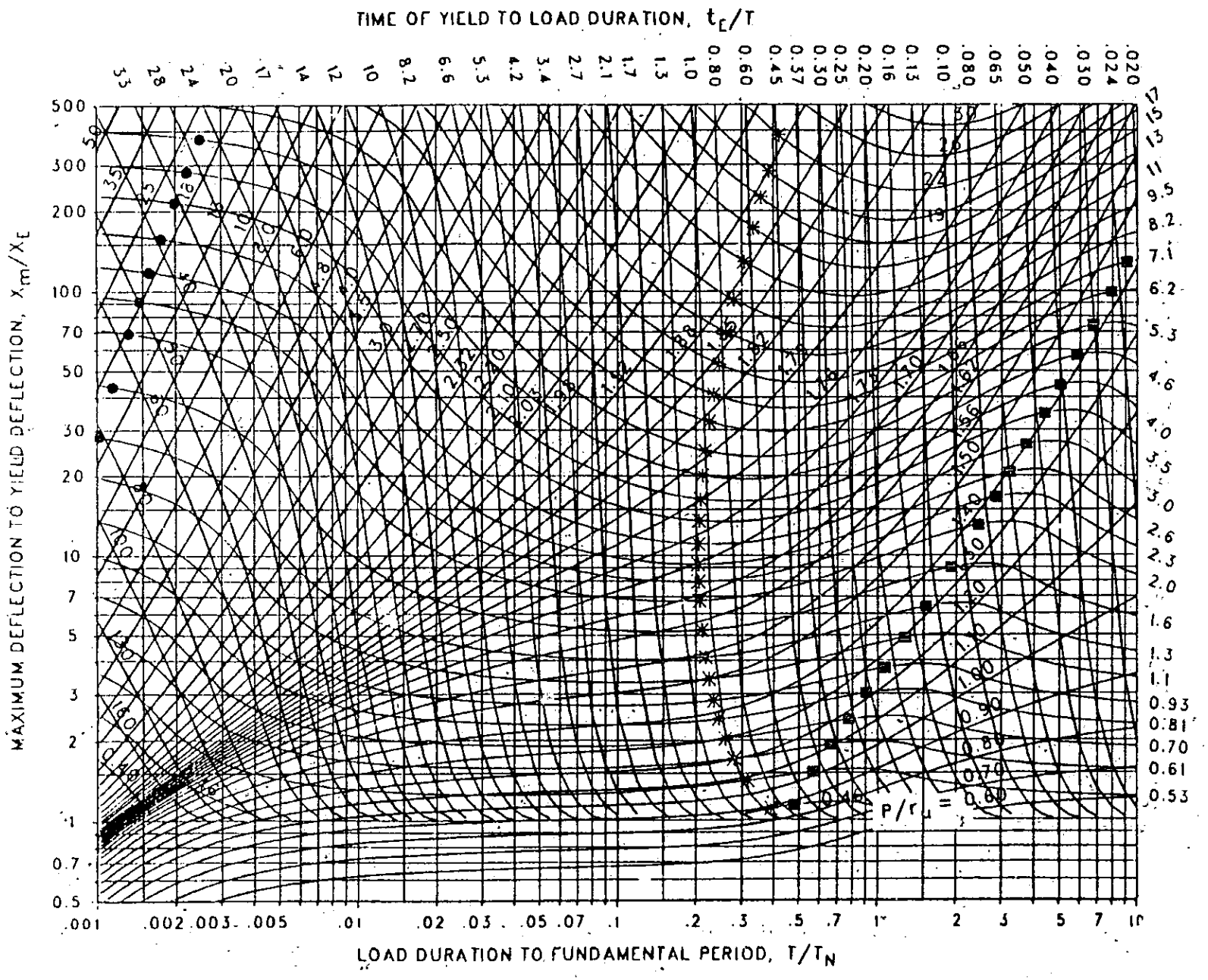


Figure 3-183 Maximum response of elasto-plastic, one-degree-of-freedom system for bilinear-triangular pulse (C_1 = 0.562, C_2 = 300.)

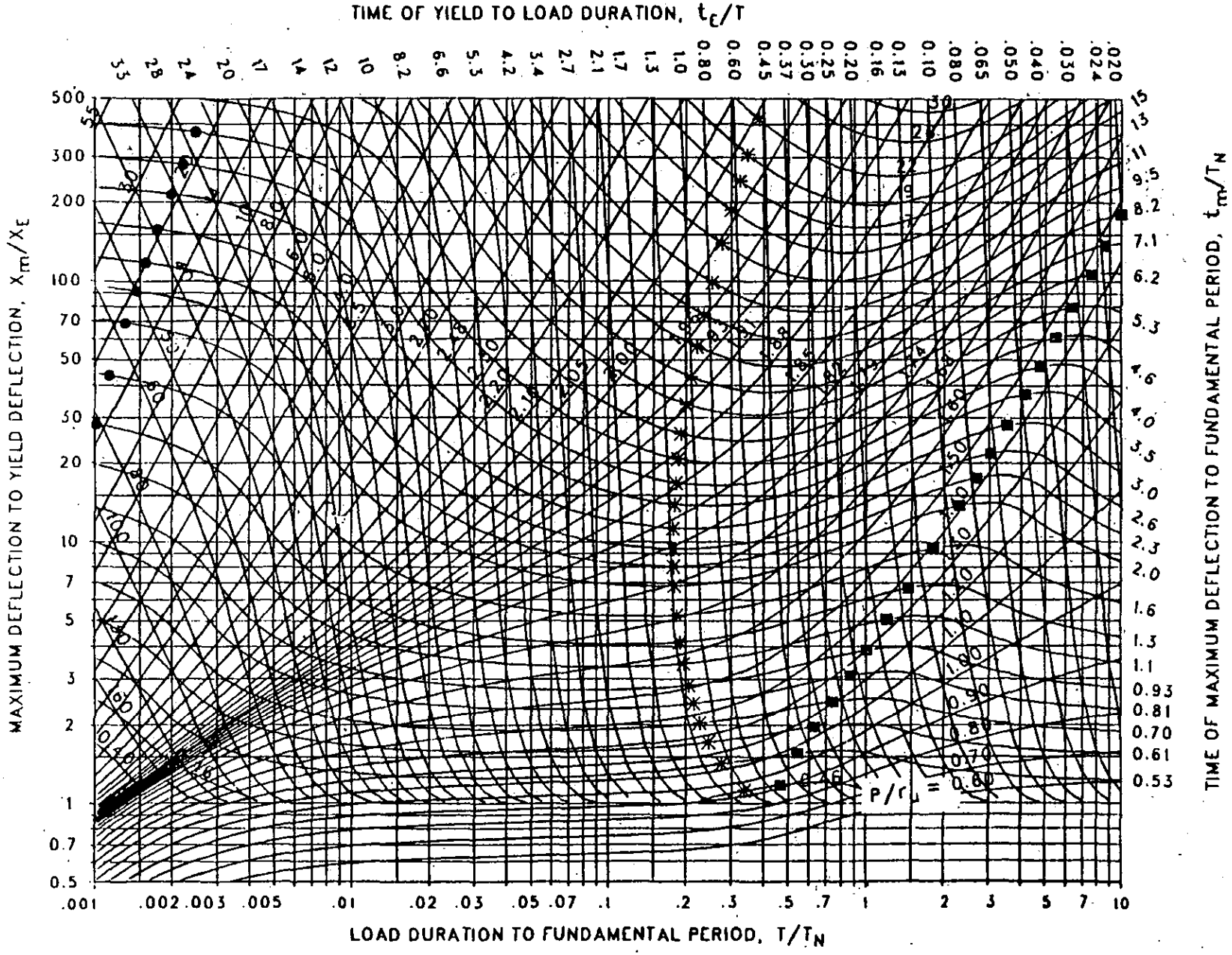


Figure 3-184 Maximum response of elasto-plastic, one-degree-of-freedom system for bilinear-triangular pulse ($C_1 = 0.536$, $C_2 = 300.$)

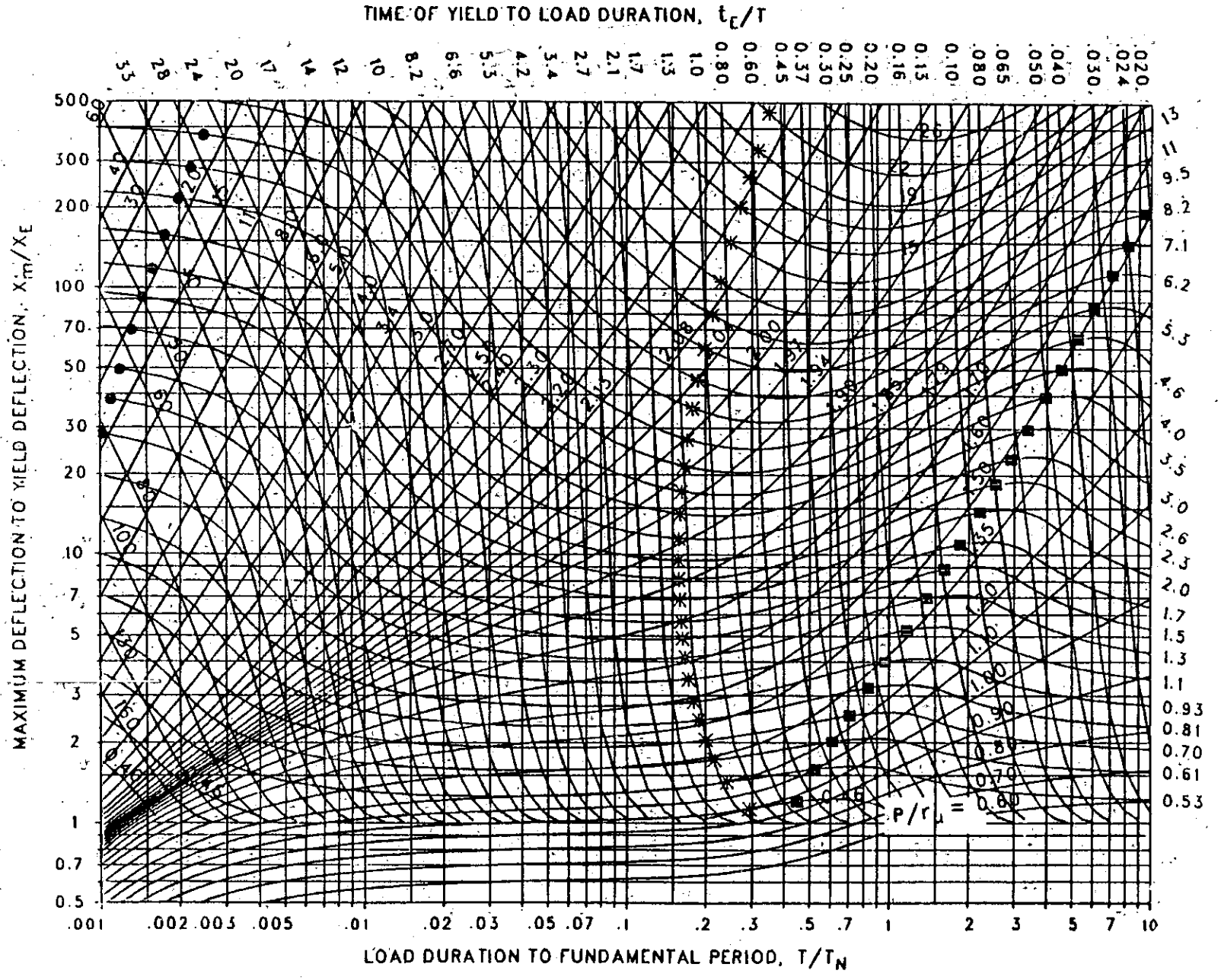


Figure 3-185 Maximum response of elasto-plastic, one-degree-of-freedom system for bilinear-triangular pulse ($C_1 = 0.511$, $C_2 = 300.$)

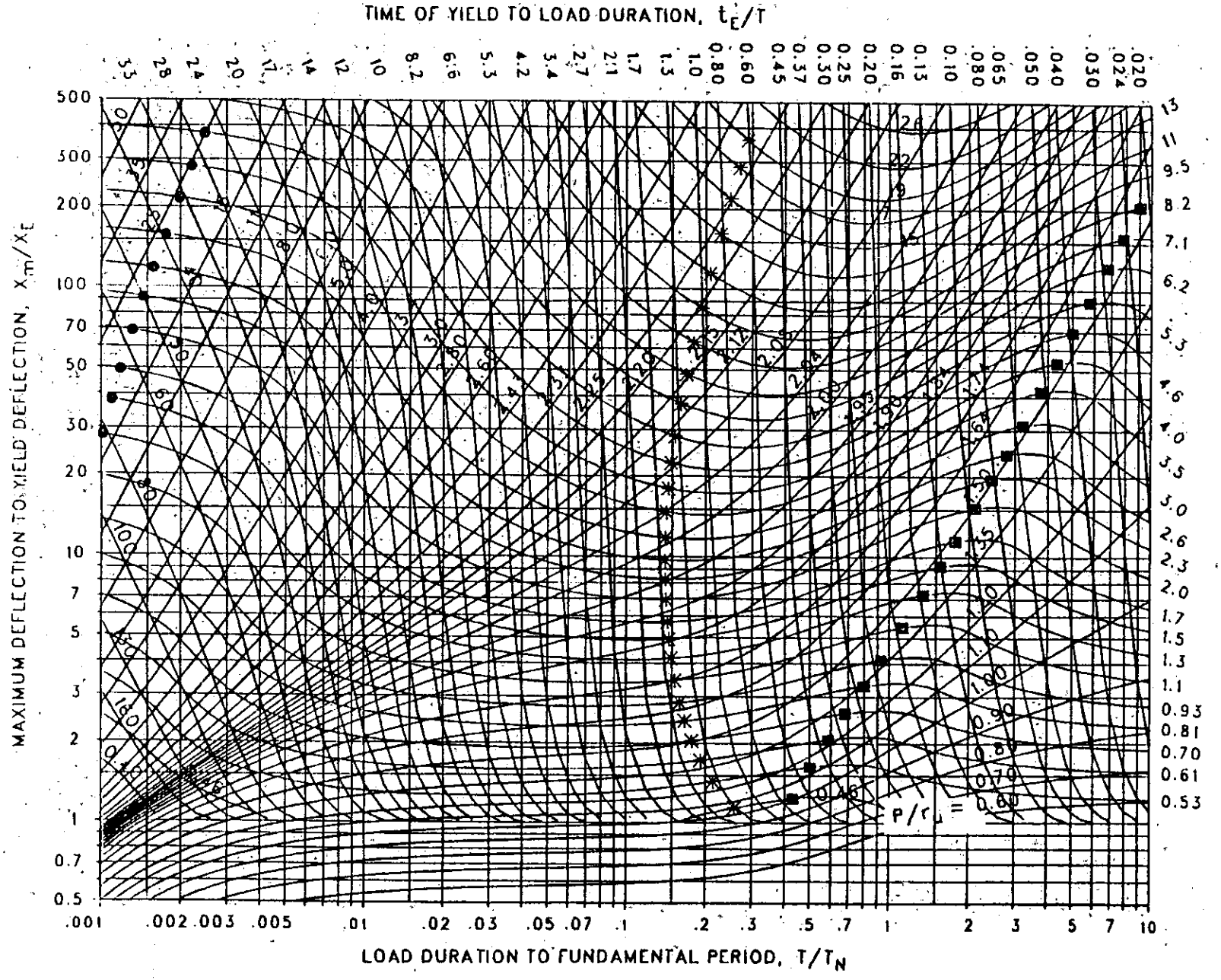


Figure 3-186 Maximum response of elasto-plastic, one-degree-of-freedom system for bilinear-triangular pulse (C_1 = 0.487, C_2 = 300.)

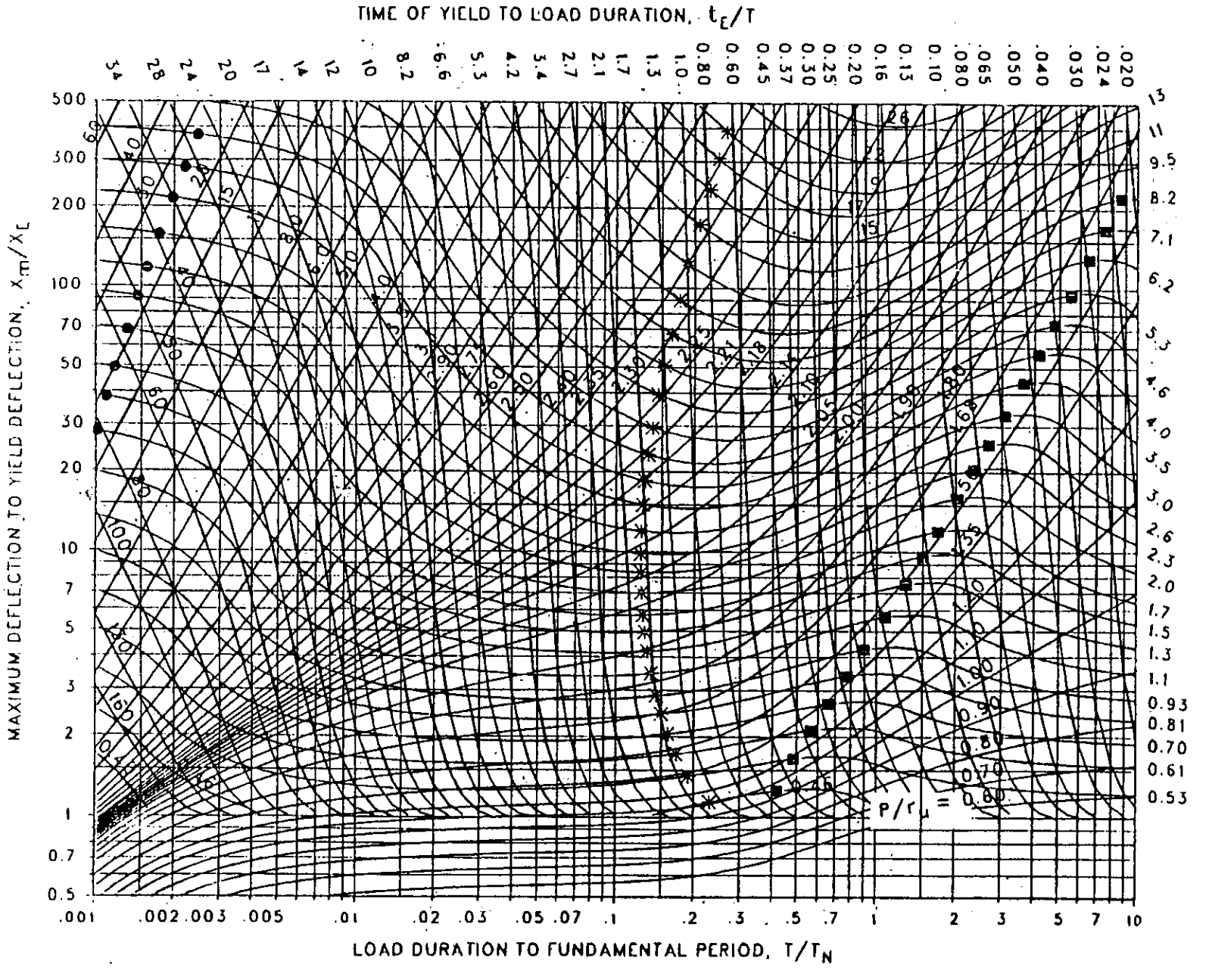


Figure 3-187 Maximum response of elasto-plastic, one-degree-of-freedom system for bilinear-triangular pulse ($C_1 = 0.464$, $C_2 = 300.$)

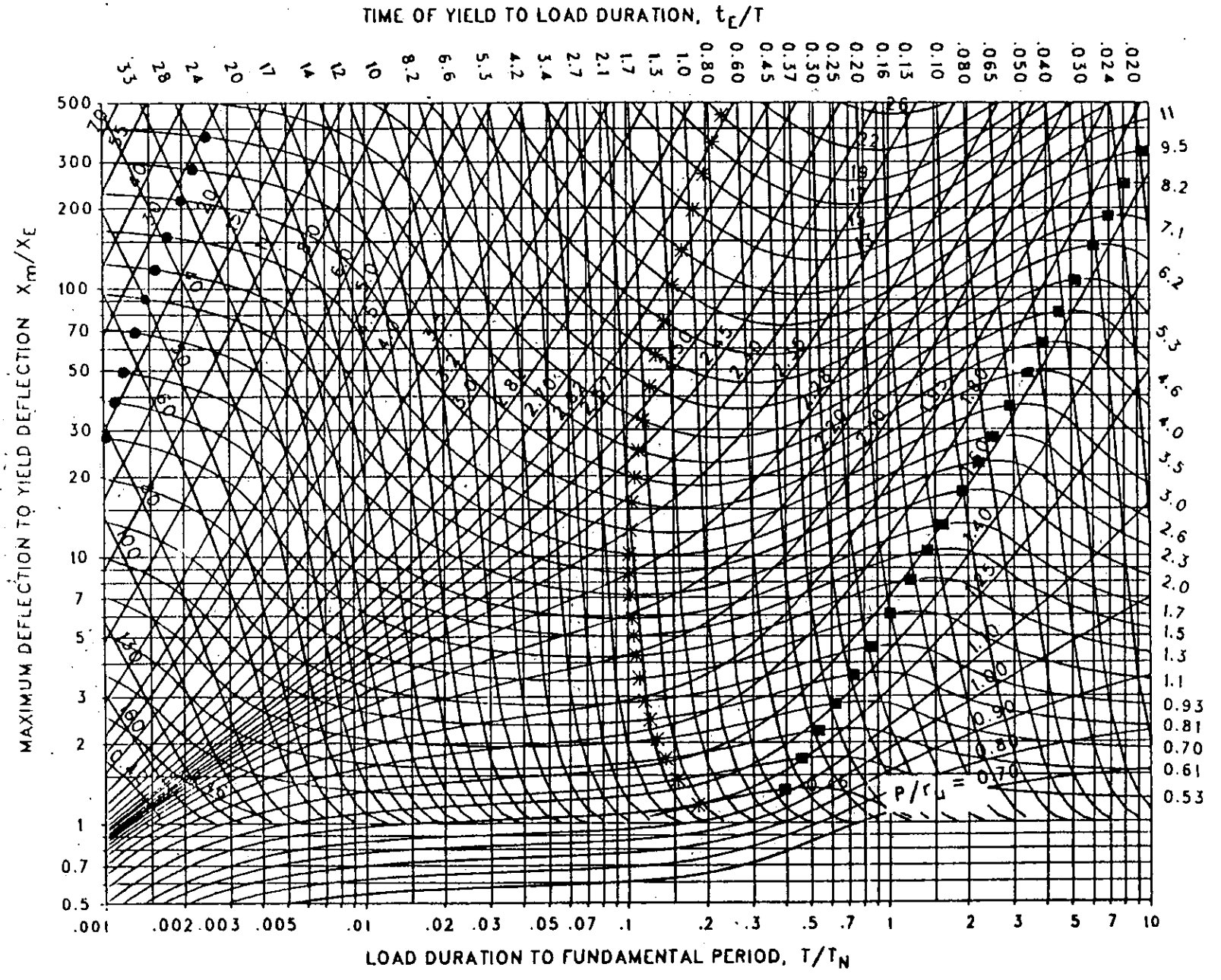


Figure 3-188 Maximum response of elasto-plastic, one-degree-of-freedom system for bilinear-triangular pulse (C_1 = 0.422, C_2 = 300.)

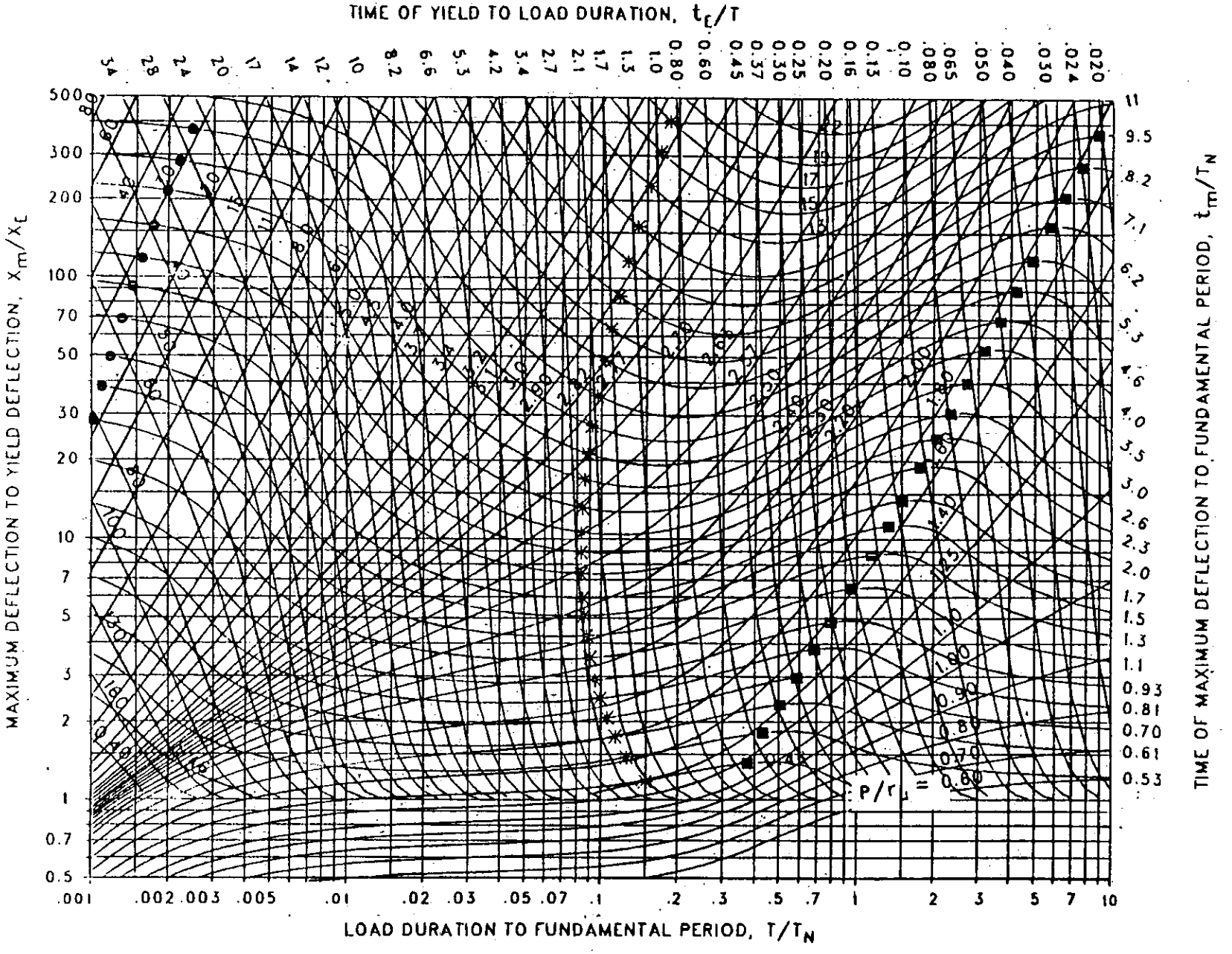


Figure 3-189 Maximum response of elasto-plastic, one-degree-of-freedom system for bilinear-triangular pulse (C_1 = 0.383, C_2 = 300.)

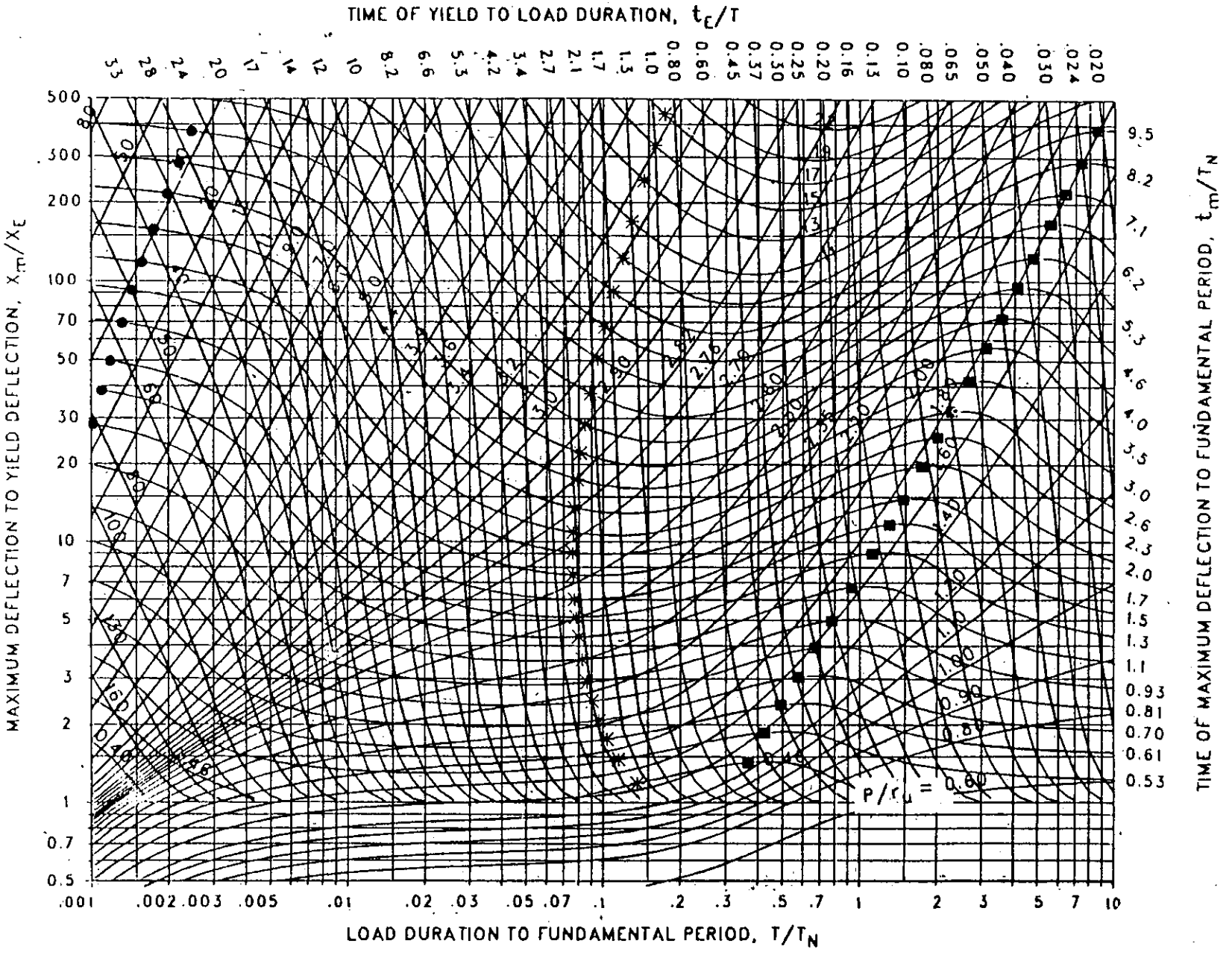


Figure 3-190 Maximum response of elasto-plastic, one-degree-of-freedom system for bilinear-triangular pulse (C_1 = 0.365, C_2 = 300.)

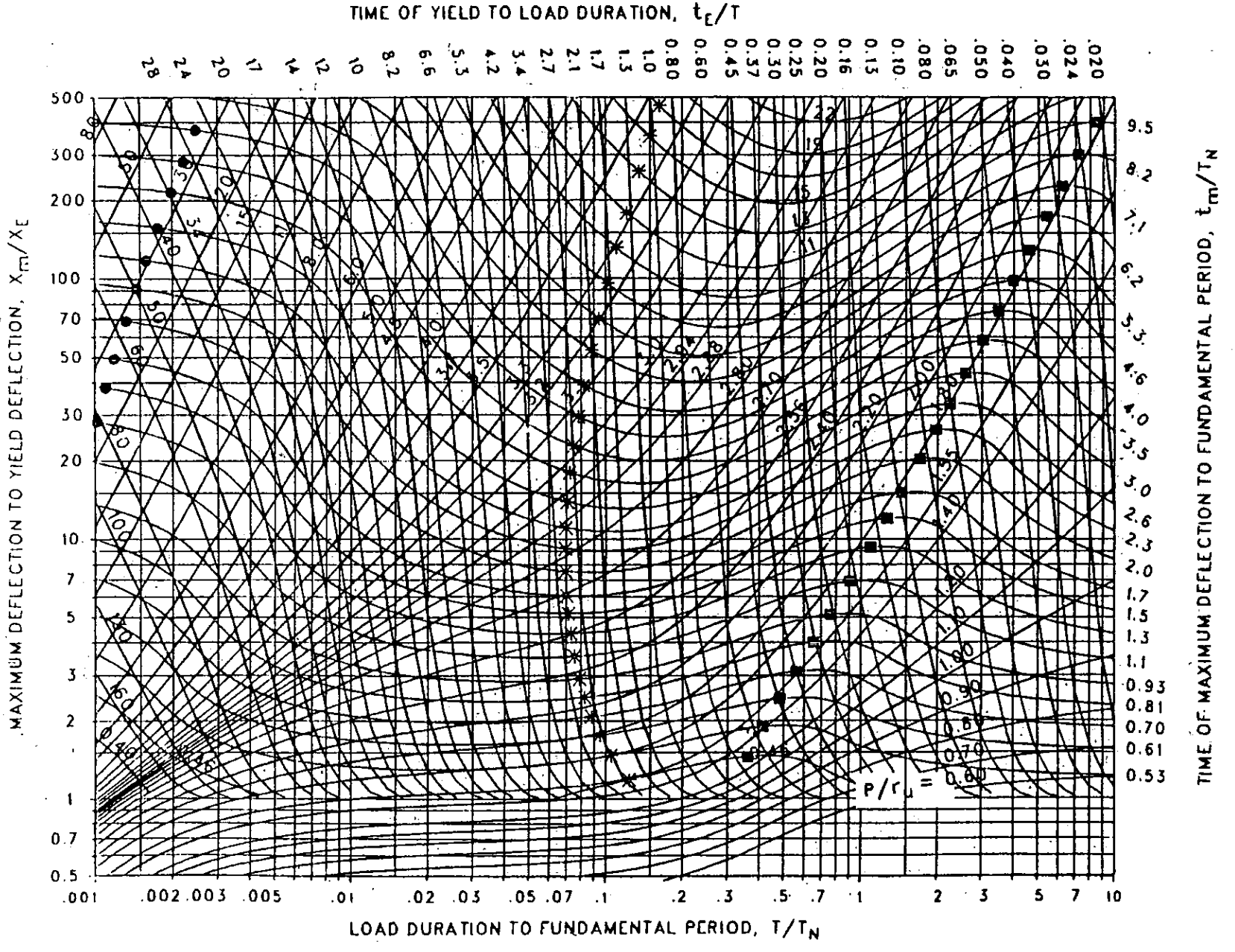


Figure 3-191 Maximum response of elasto-plastic, one-degree-of-freedom system for bilinear-triangular pulse ($C_1 = 0.348$, $C_2 = 300.$)

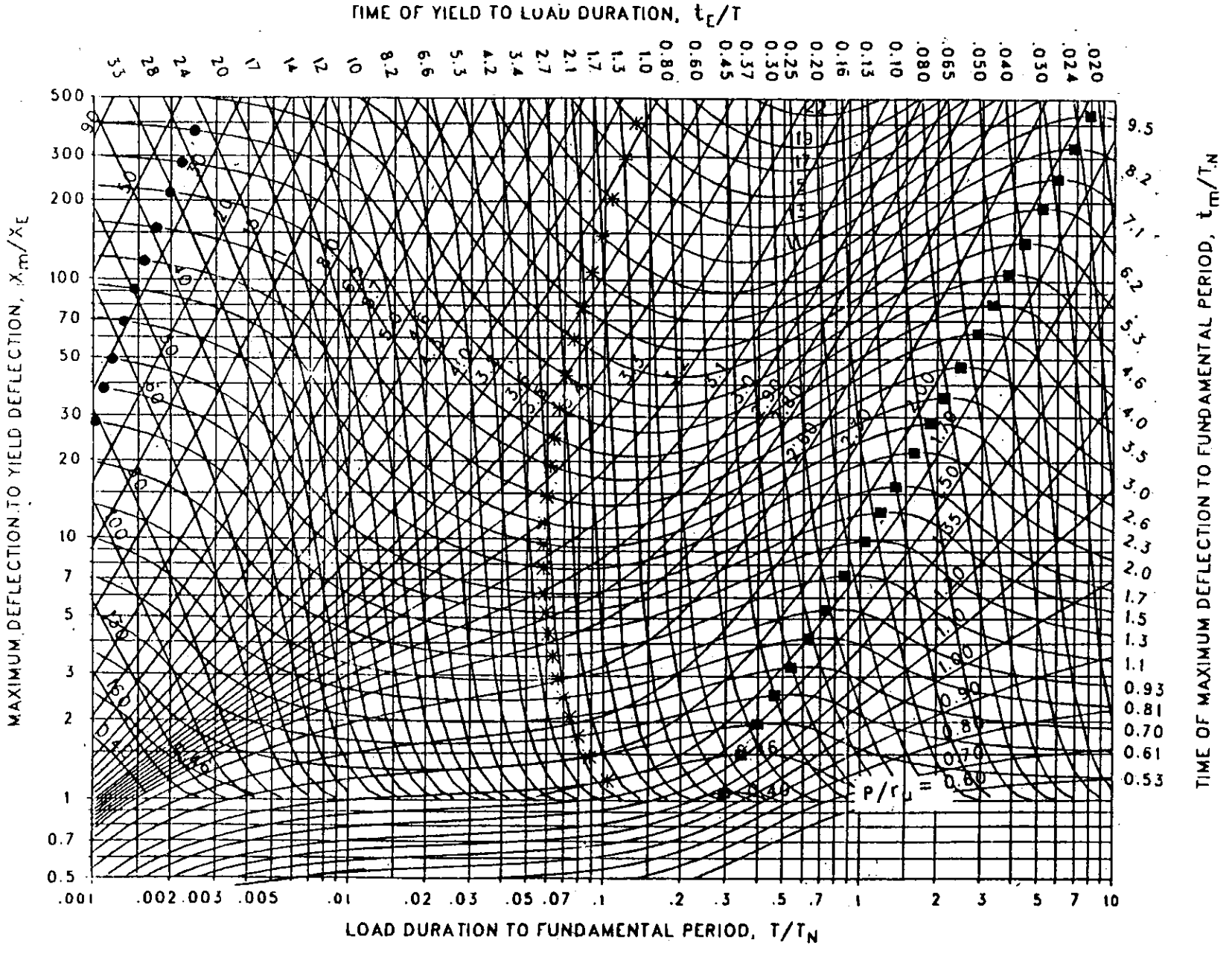


Figure 3-192 Maximum response of elasto-plastic, one-degree-of-freedom system for bilinear-triangular pulse (C_1 = 0.316, C_2 = 300.)

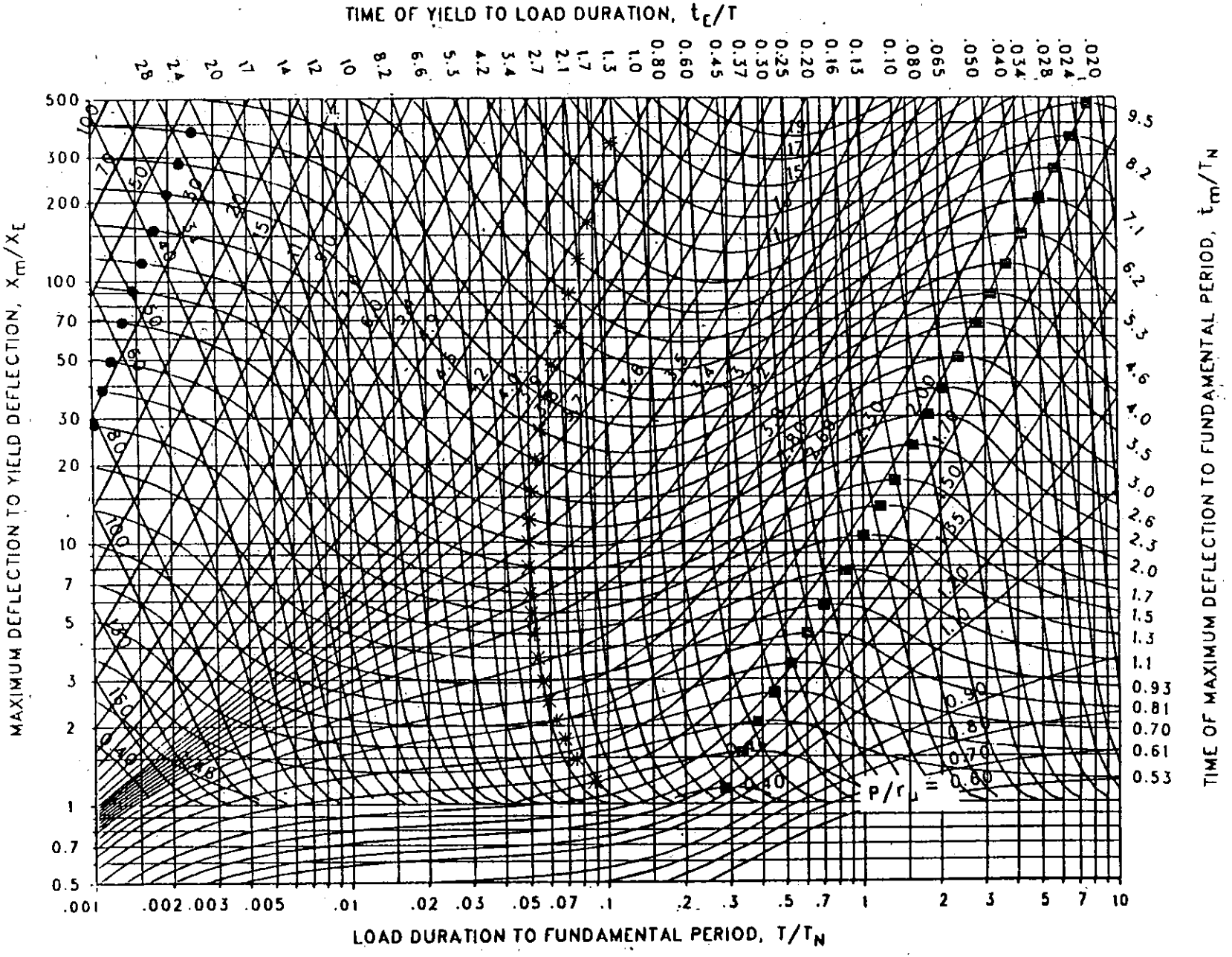


Figure 3-193 Maximum response of elasto-plastic, one-degree-of-freedom system for bilinear-triangular pulse (C_1 = 0.287, C_2 = 300.)

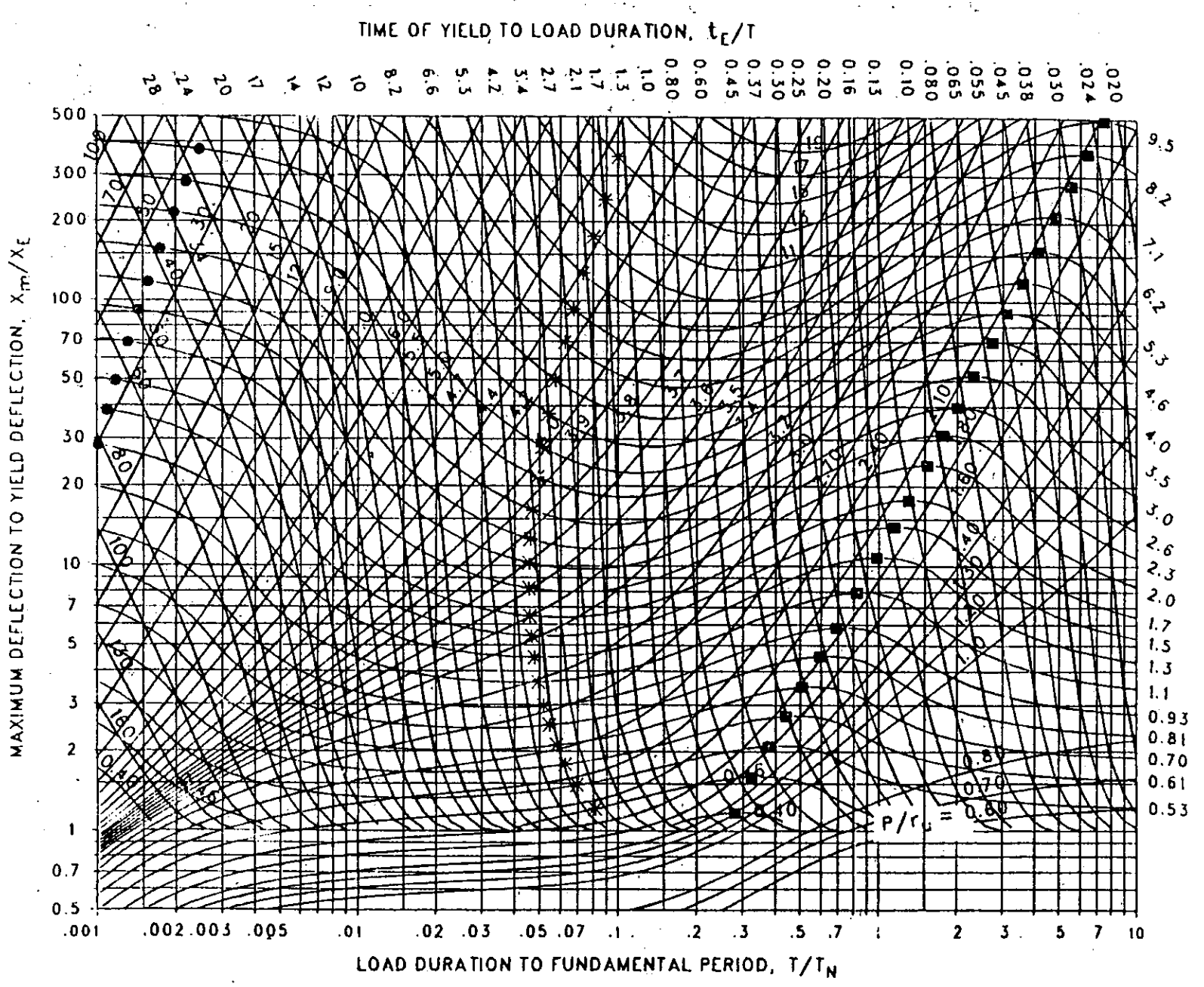


Figure 3-194 Maximum response of elasto-plastic, one-degree-of-freedom system for bilinear-triangular pulse (C_1 = 0.274, C_2 = 300.)

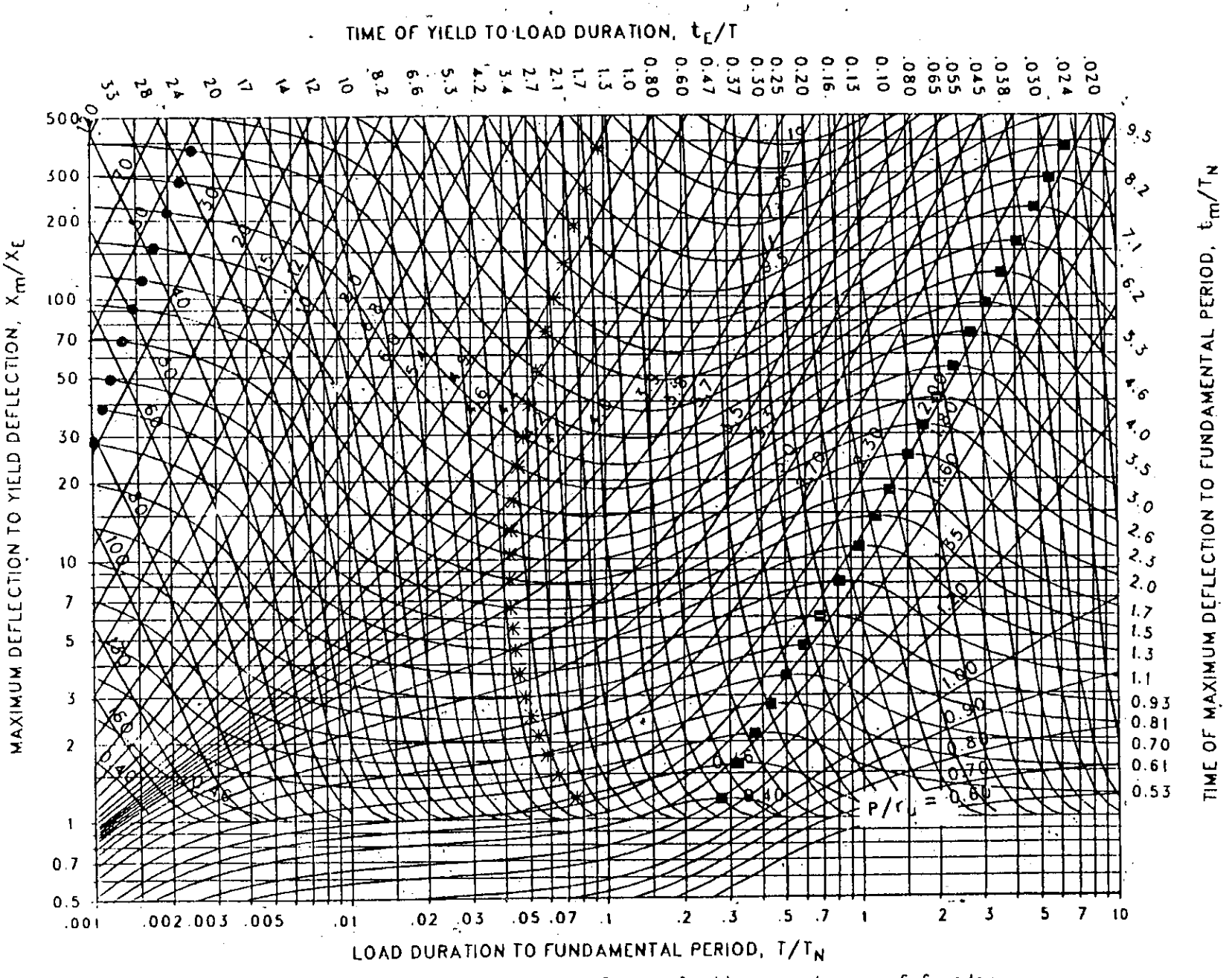


Figure 3-195 Maximum response of elasto-plastic, one-degree-of-freedom system for bilinear-triangular pulse (C_1 = 0.261, C_2 = 300.)

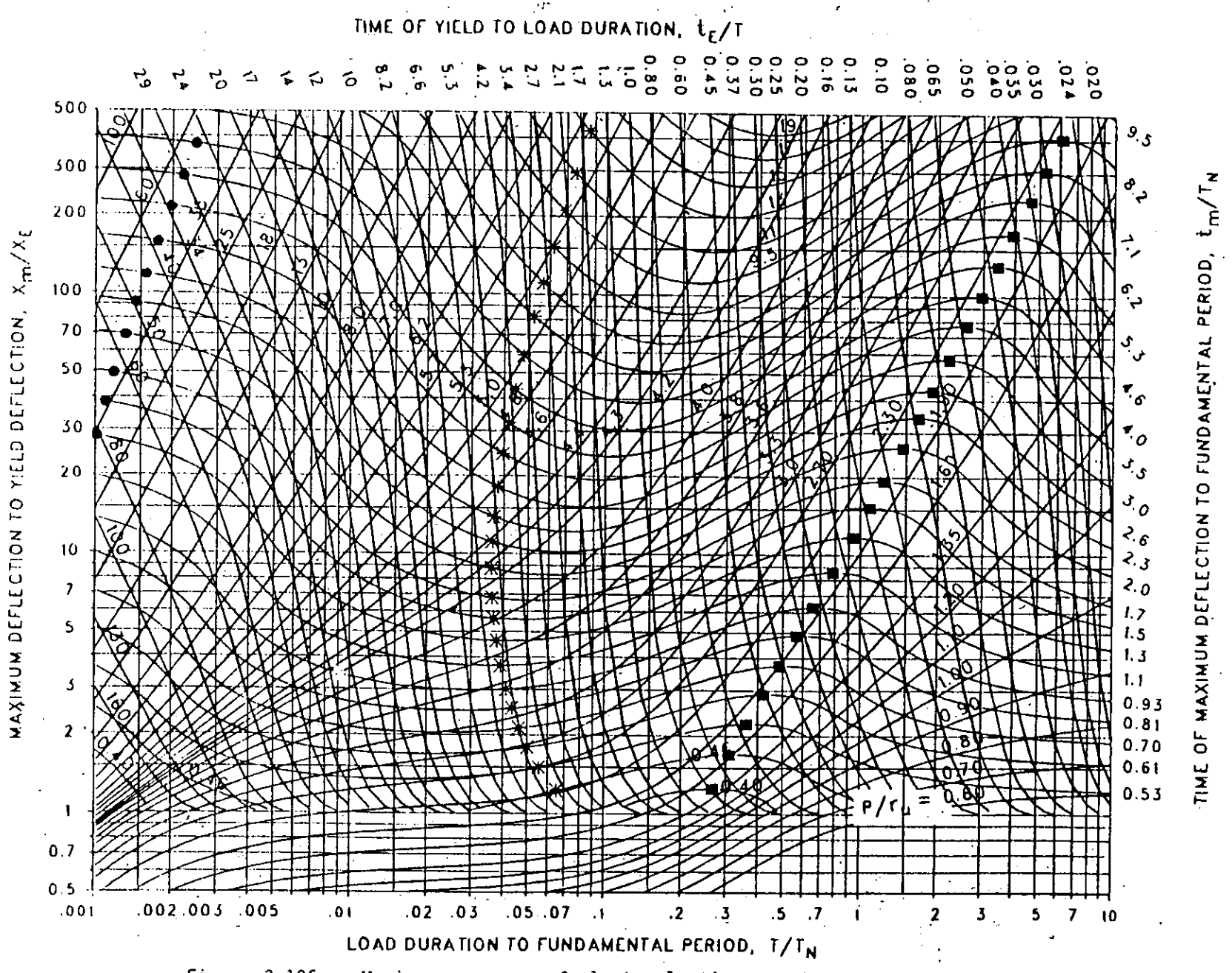


Figure 3-196 Maximum response of elasto-plastic, one-degree-of-freedom system for bilinear-triangular pulse (C_1 = 0.237, C_2 = 300.)

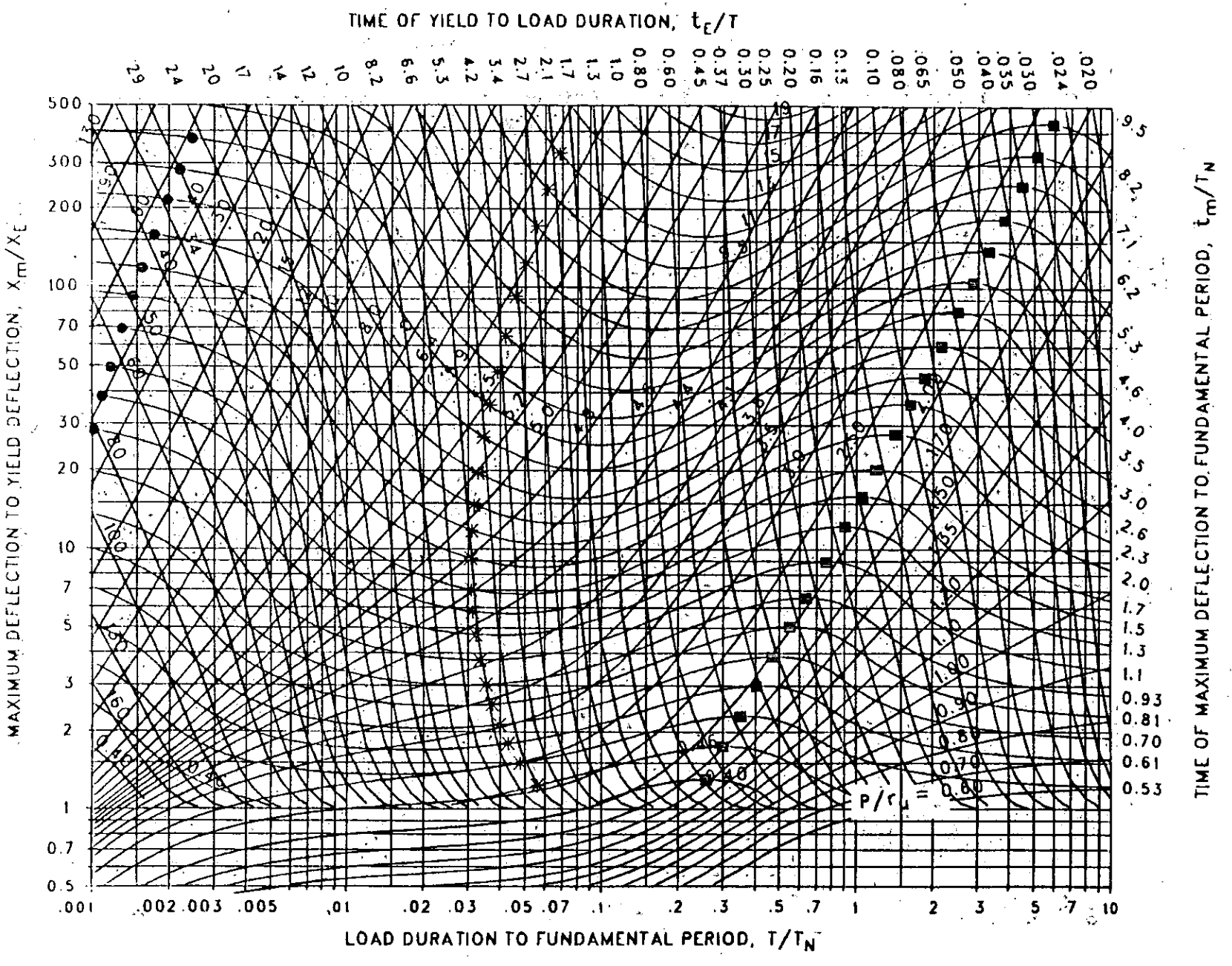


Figure 3-197 Maximum response of elasto-plastic, one-degree-of-freedom system for bilinear-triangular pulse ($C_1 = 0.215$, $C_2 = 300.$)

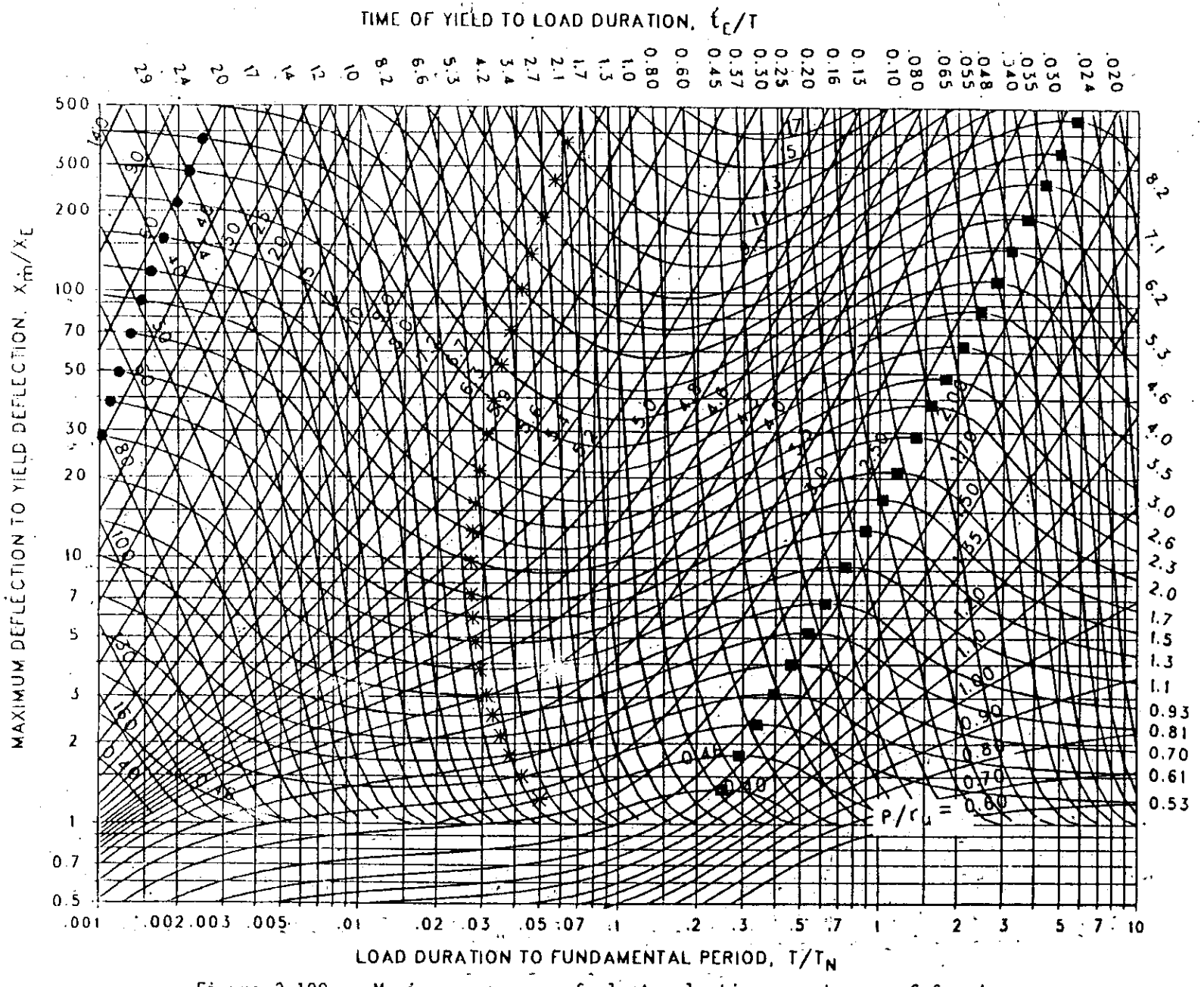


Figure 3-198 Maximum response of elasto-plastic, one-degree-of-freedom system for bilinear-triangular pulse (C_1 = 0.198, C_2 = 300.)

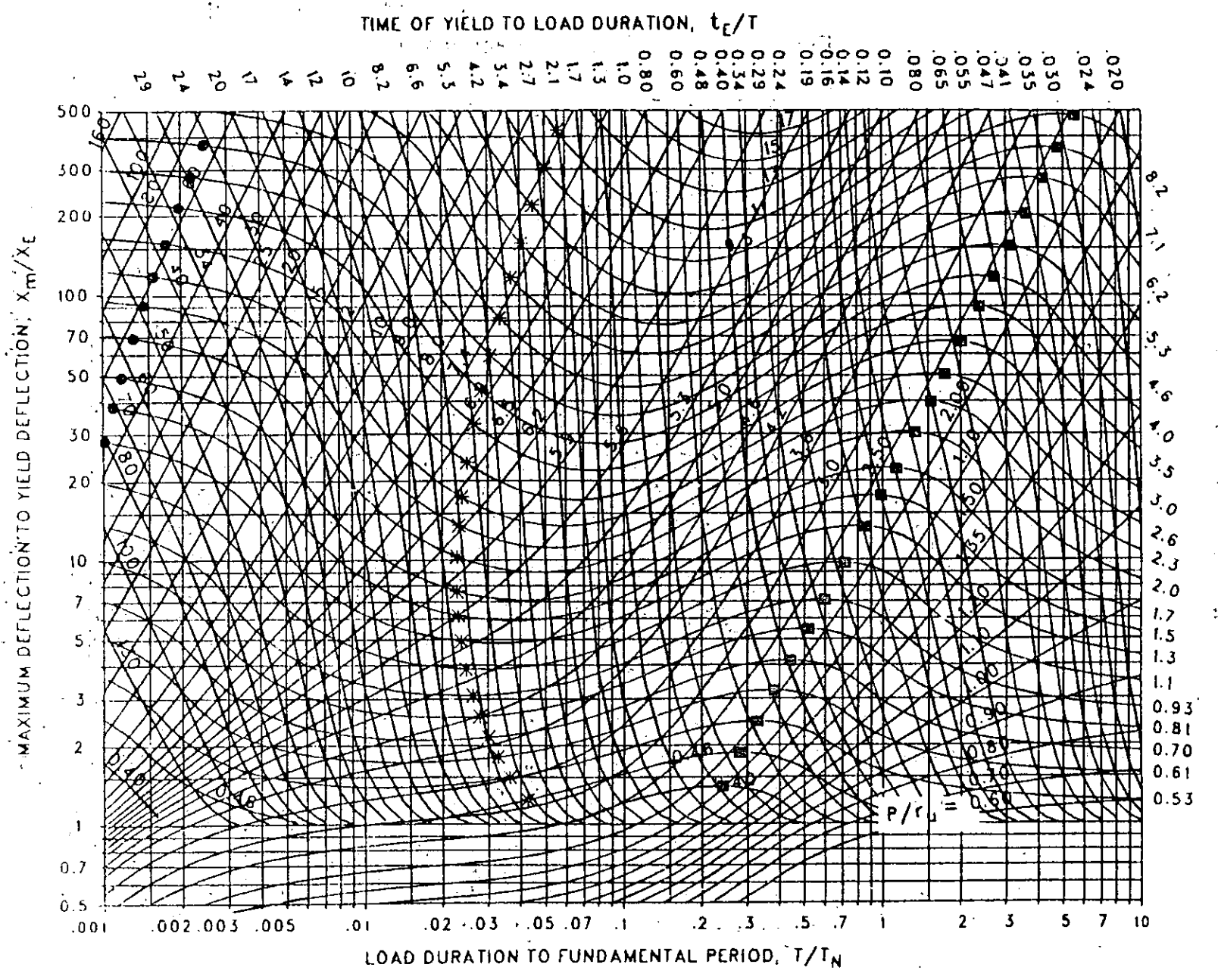


Figure 3-199 Maximum response of elasto-plastic, one-degree-of-freedom system for bilinear-triangular pulse ($C_1 = 0.178$, $C_2 = 300.$)

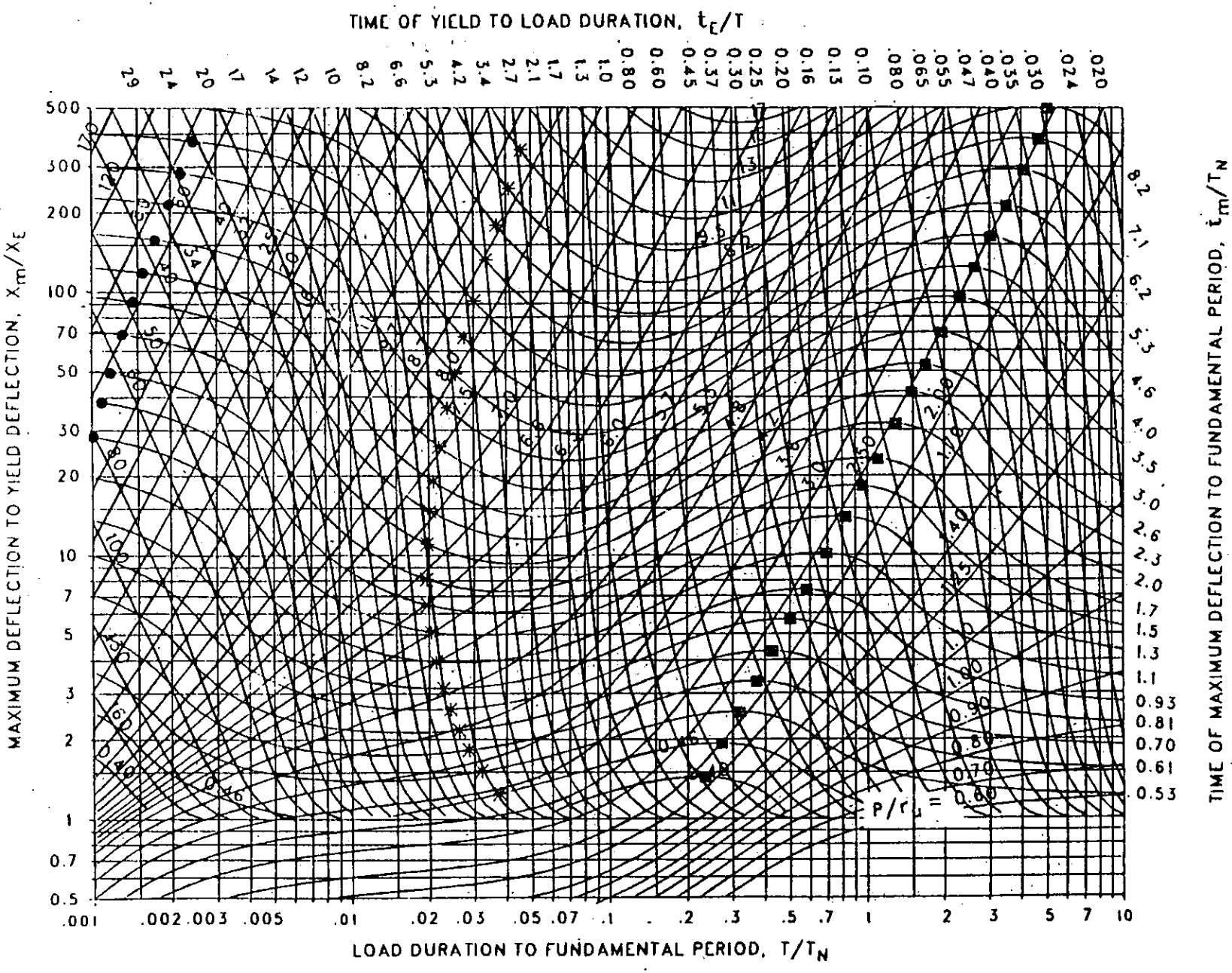


Figure 3-200 Maximum response of elasto-plastic, one-degree-of-freedom system for bilinear-triangular pulse ($C_1 = 0.162$, $C_2 = 300.$)

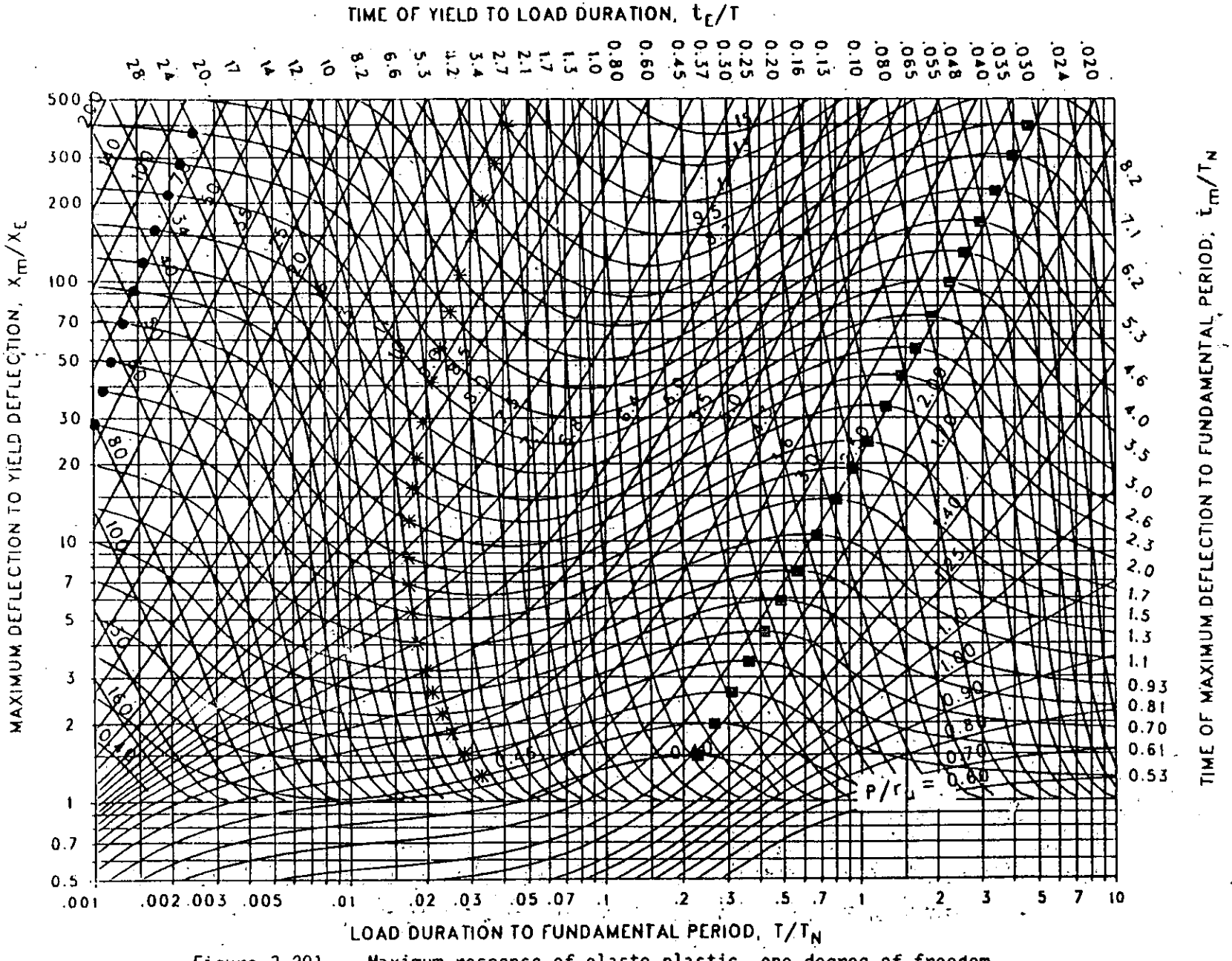


Figure 3-201 Maximum response of elasto-plastic, one-degree-of-freedom system for bilinear-triangular pulse ($C_1 = 0.147$, $C_2 = 300.$)

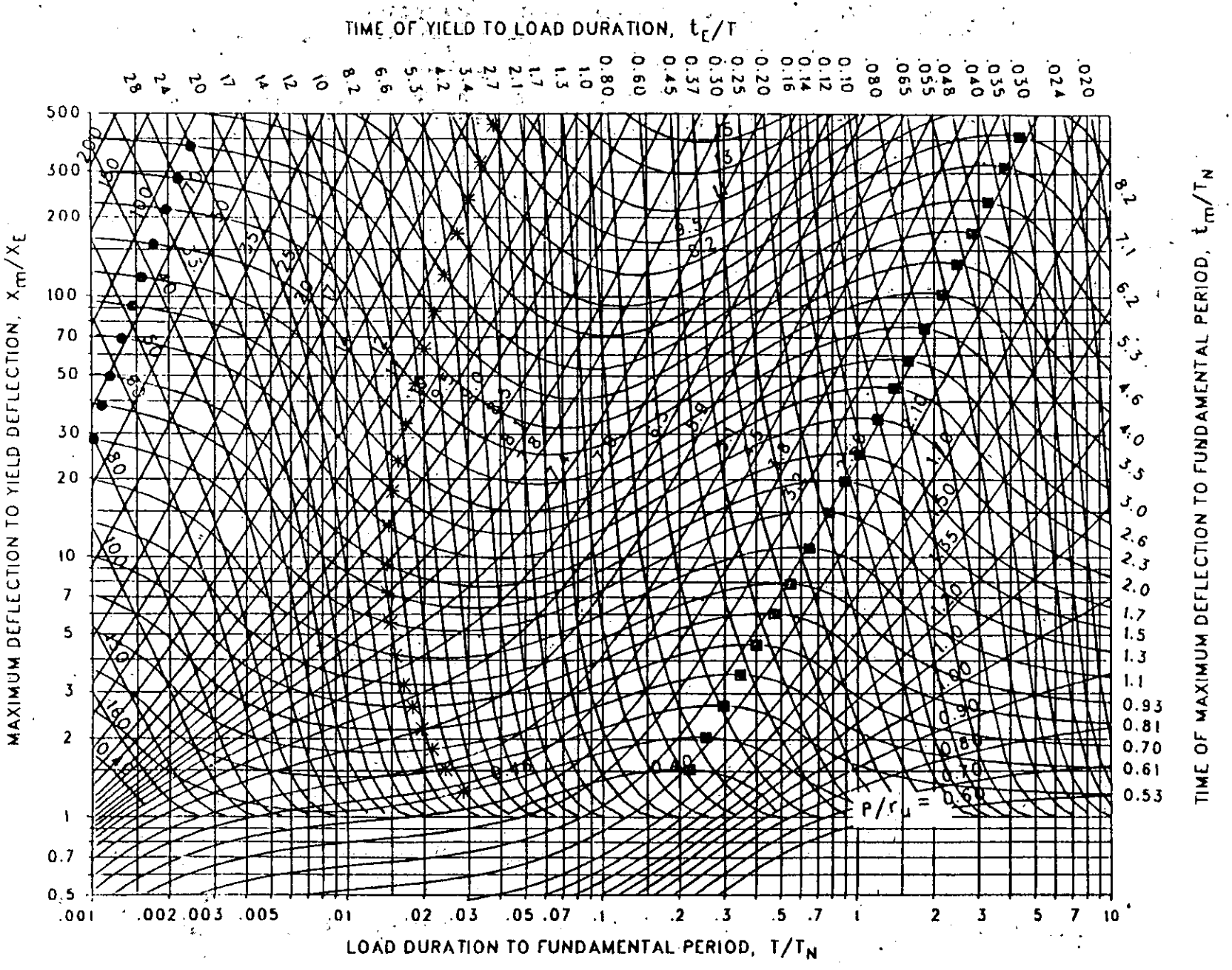


Figure 3-202 Maximum response of elasto-plastic, one-degree-of-freedom system for bilinear-triangular pulse ($C_1 = 0.133$, $C_2 = 300.$)

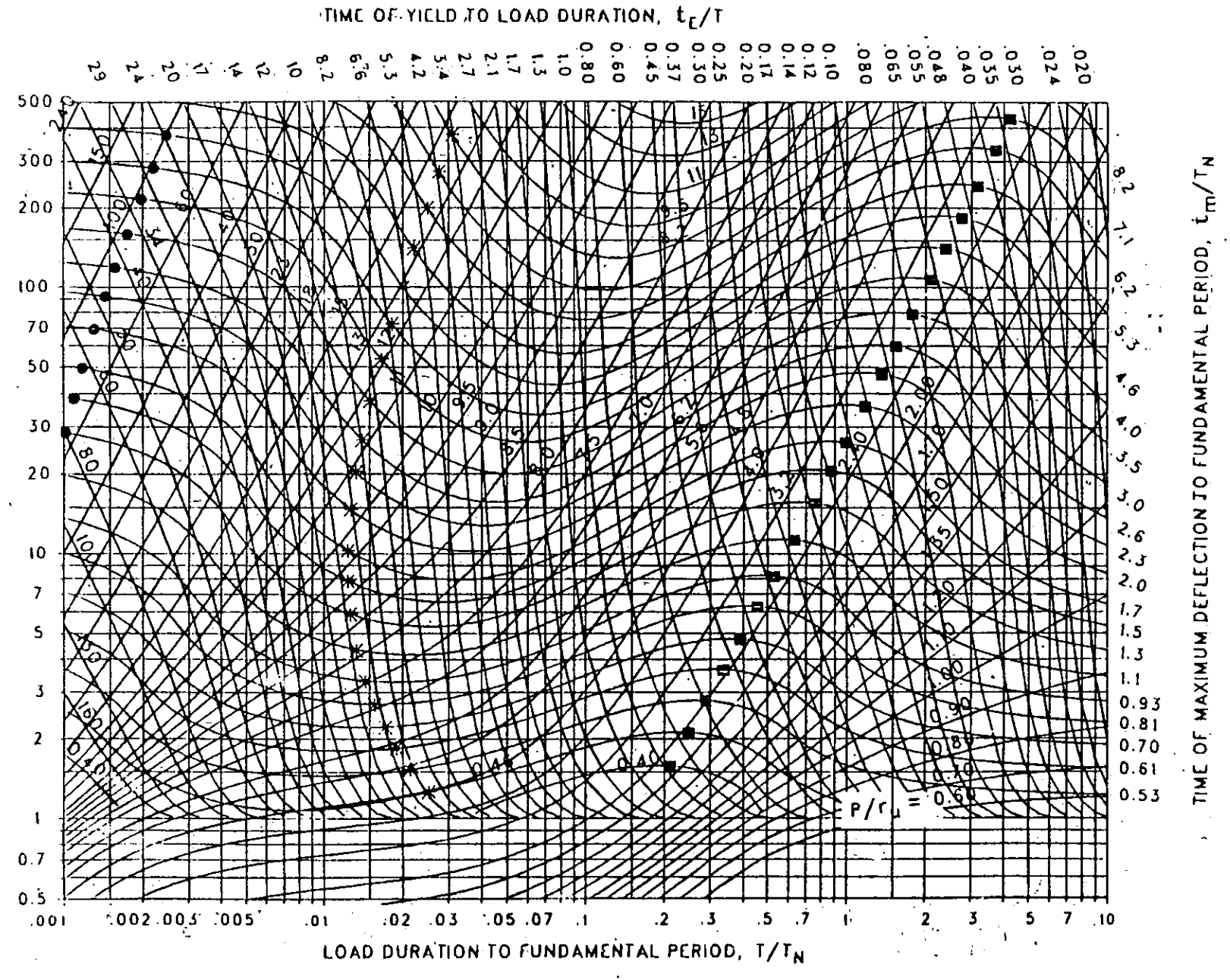


Figure 3-203 Maximum response of elasto-plastic, one-degree-of-freedom system for bilinear-triangular pulse ($C_1 = 0.121$, $C_2 = 300.$)

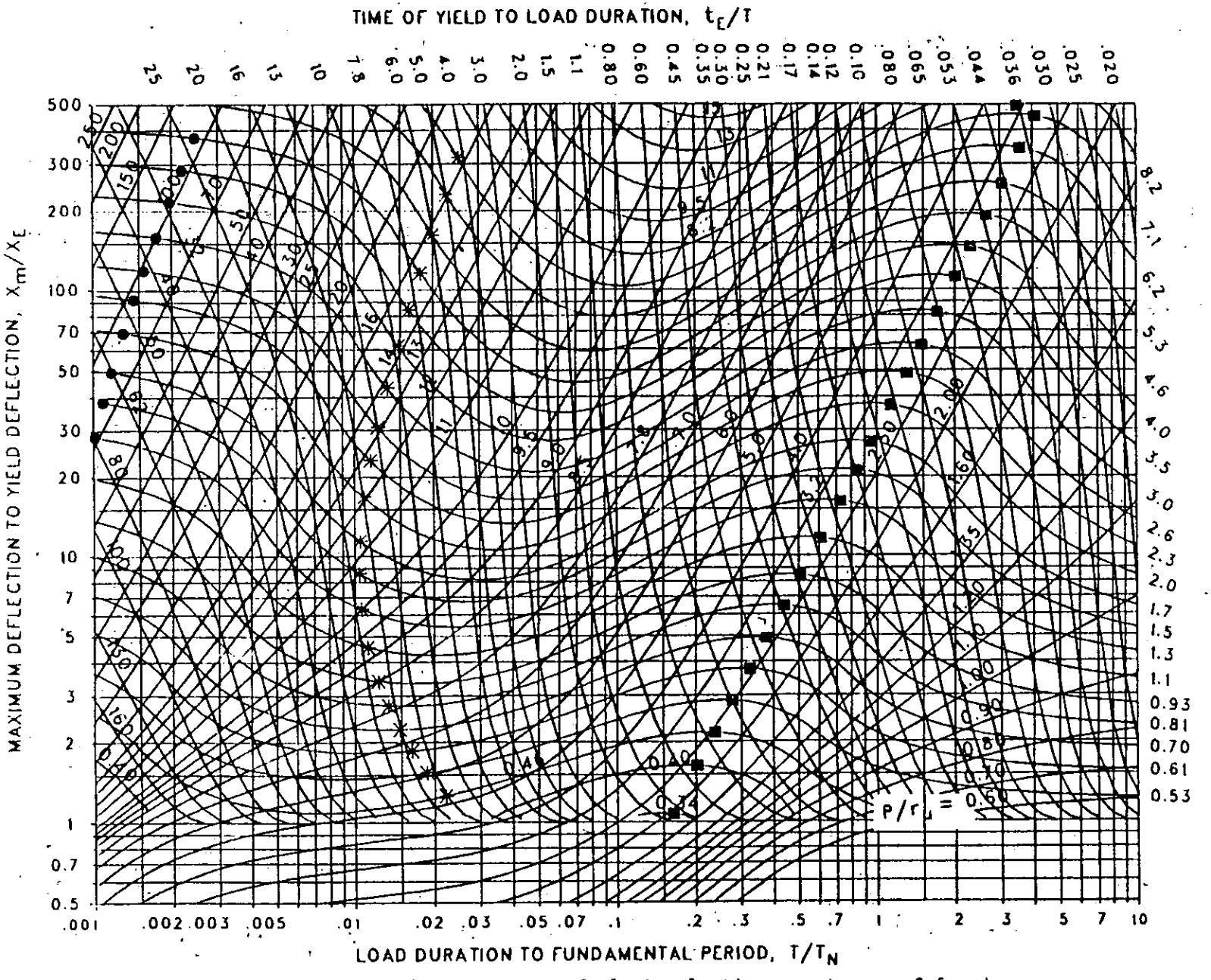


Figure 3-204 Maximum response of elasto-plastic, one-degree-of-freedom system for bilinear-triangular pulse ($C_1 = 0.110$, $C_2 = 300.$)

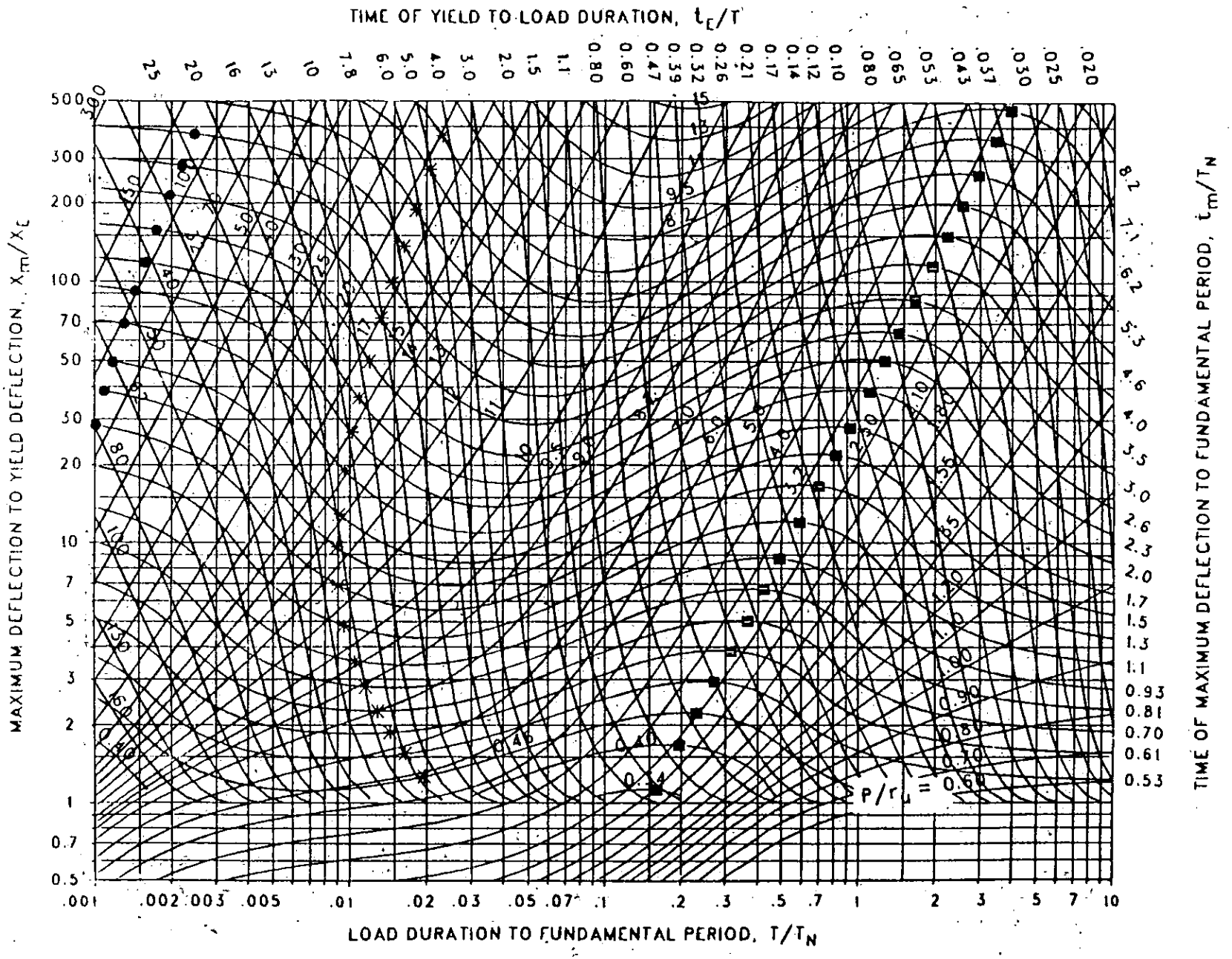


Figure 3-205 Maximum response of elasto-plastic, one-degree-of-freedom system for bilinear-triangular pulse ($C_1 = 0.100$, $C_2 = 300.$)

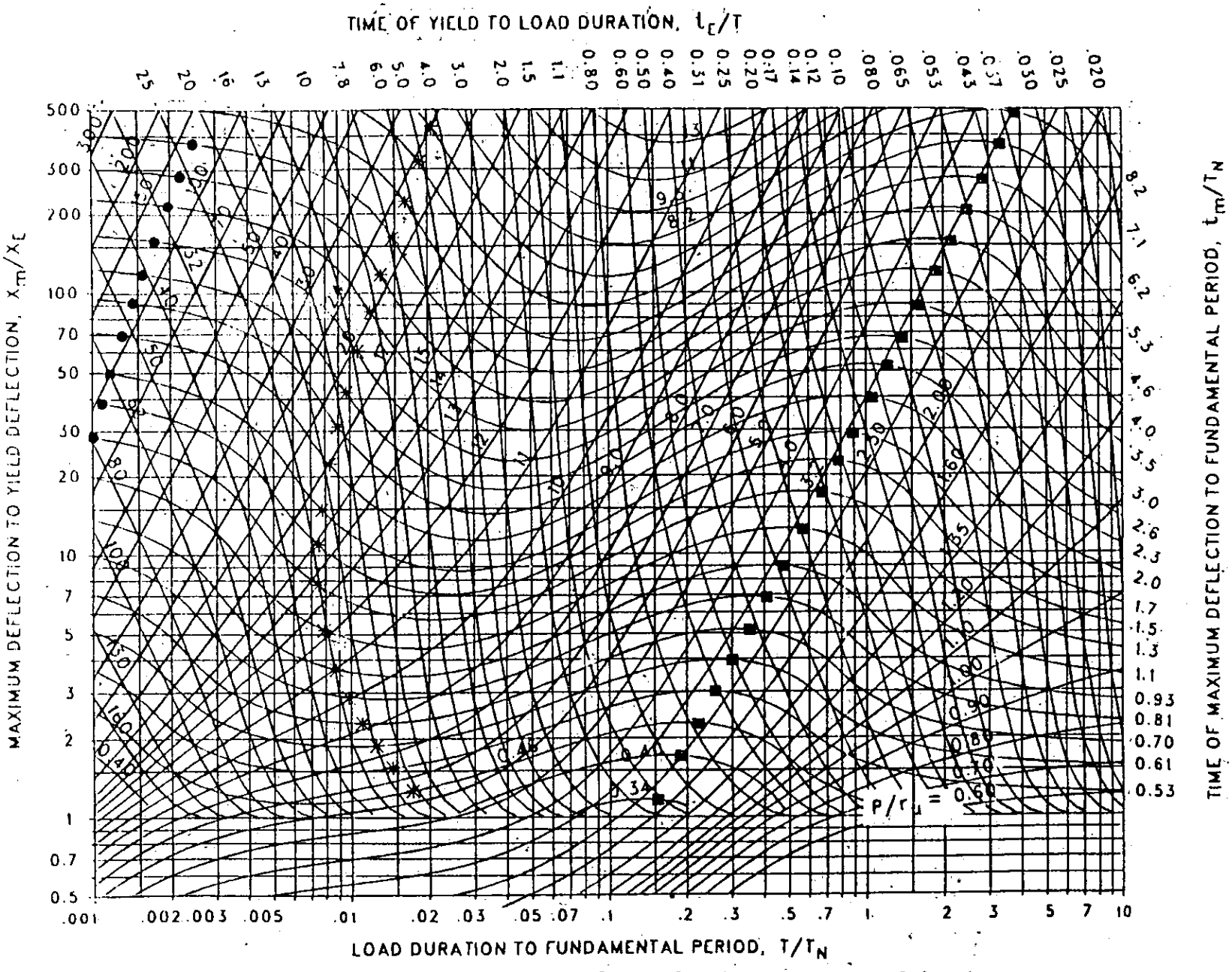


Figure 3-206 Maximum response of elasto-plastic, one-degree-of-freedom system for bilinear-triangular pulse ($C_1 = 0.091$, $C_2 = 300.$)

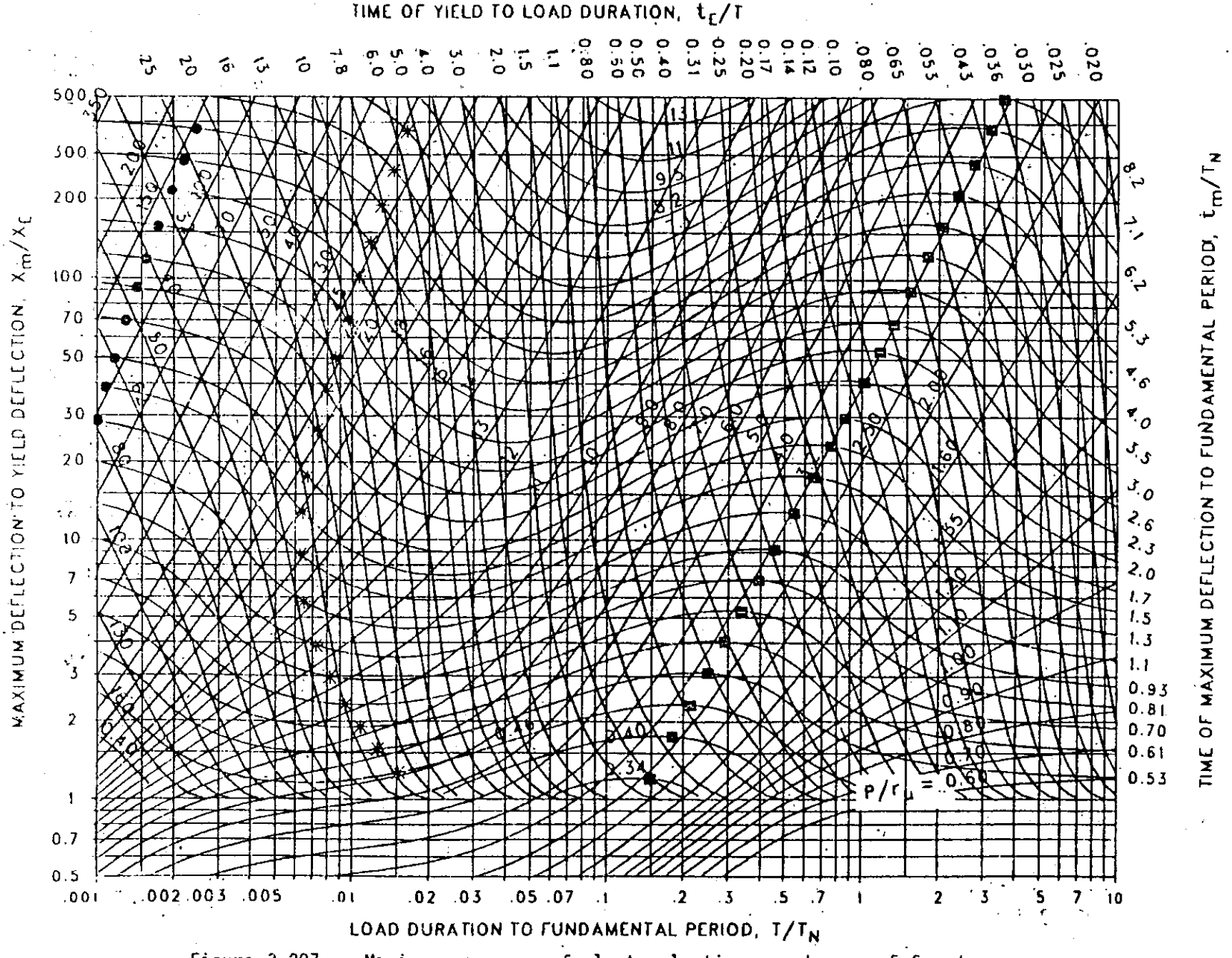


Figure 3-207 Maximum response of elasto-plastic, one-degree-of-freedom system for bilinear-triangular pulse ($C_1 = 0.083$, $C_2 = 300.$)

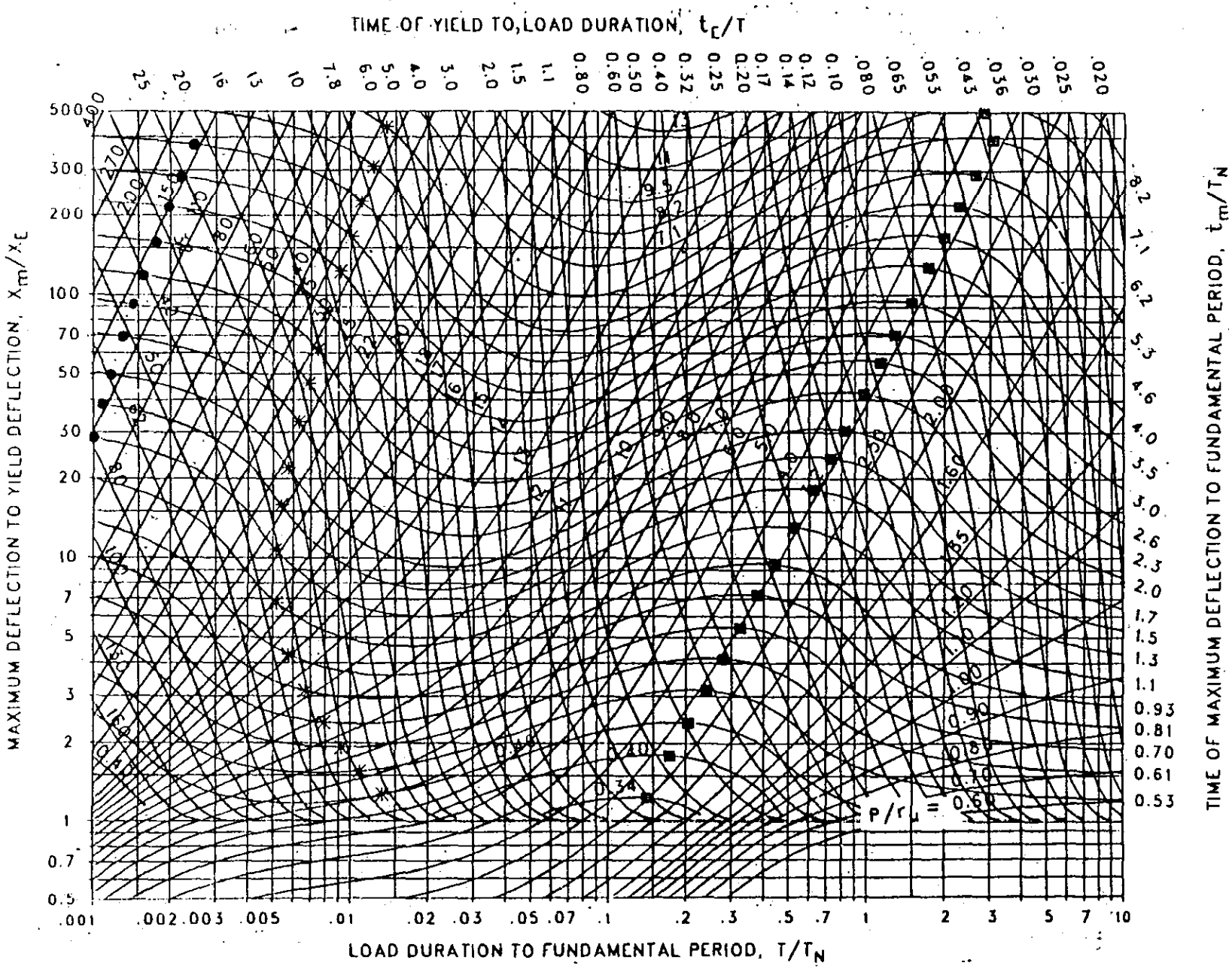


Figure 3-208 Maximum response of elasto-plastic, one-degree-of-freedom system for bilinear-triangular pulse (C_1 = 0.075, C_2 = 300.)

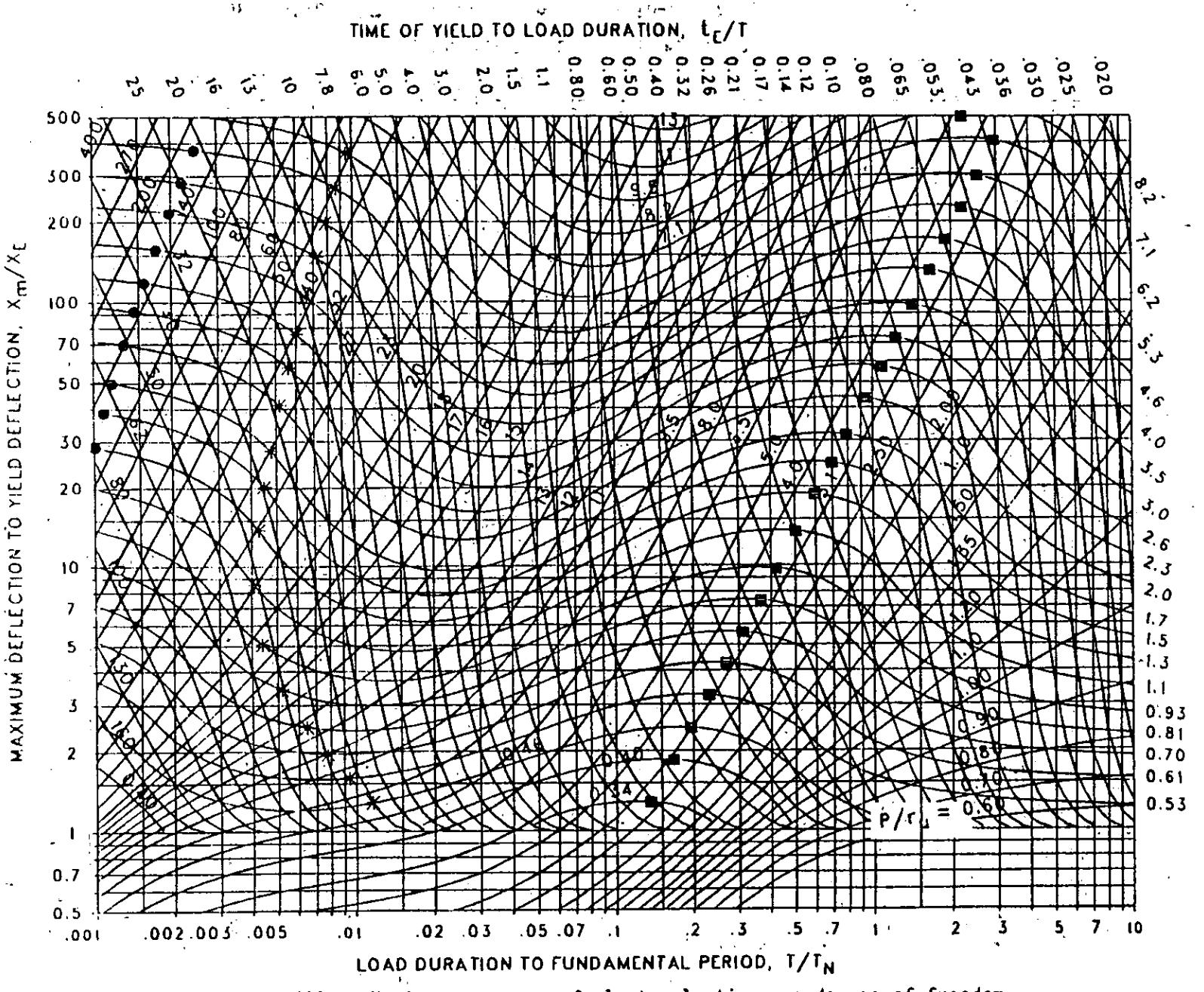


Figure 3-209 Maximum response of elasto-plastic, one-degree-of-freedom system for bilinear-triangular pulse (C_1 = 0.068, C_2 = 300.)

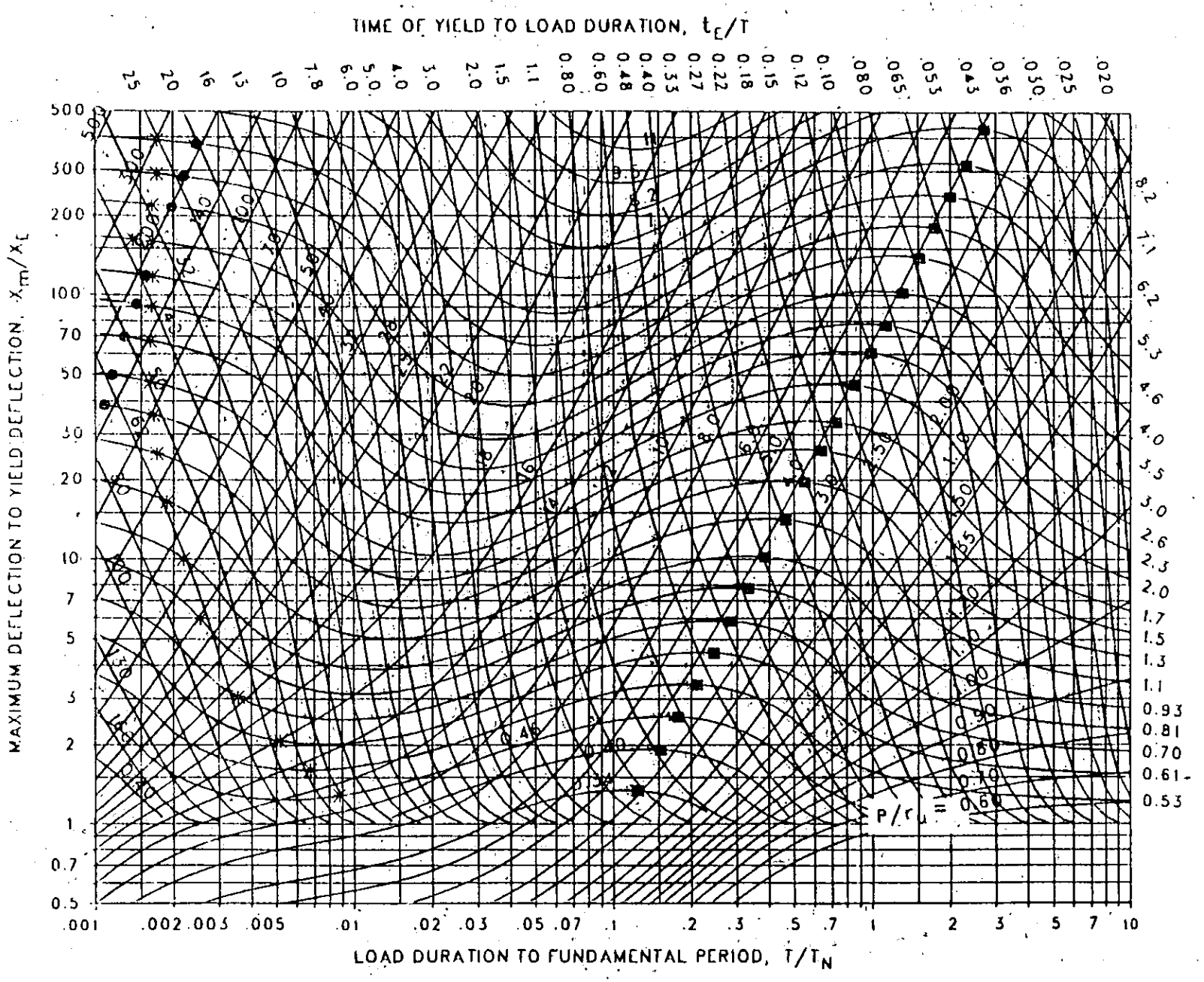


Figure 3-210 Maximum response of elasto-plastic, one-degree-of-freedom system for bilinear-triangular pulse (C_1 = 0.056, C_2 = 300.)

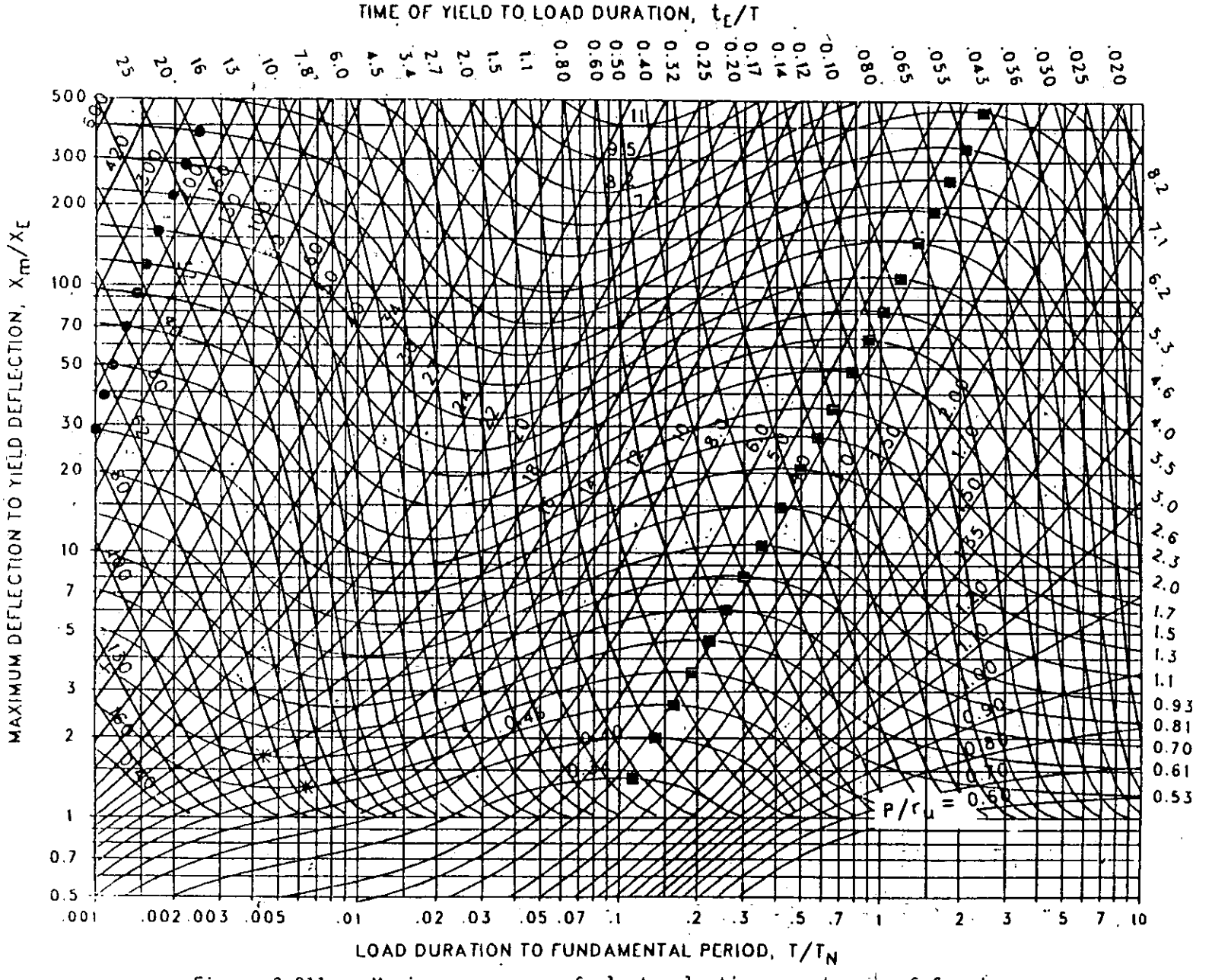


Figure 3-211 Maximum response of elasto-plastic, one-degree-of-freedom system for bilinear-triangular pulse ($C_1 = 0.046$, $C_2 = 300.$)

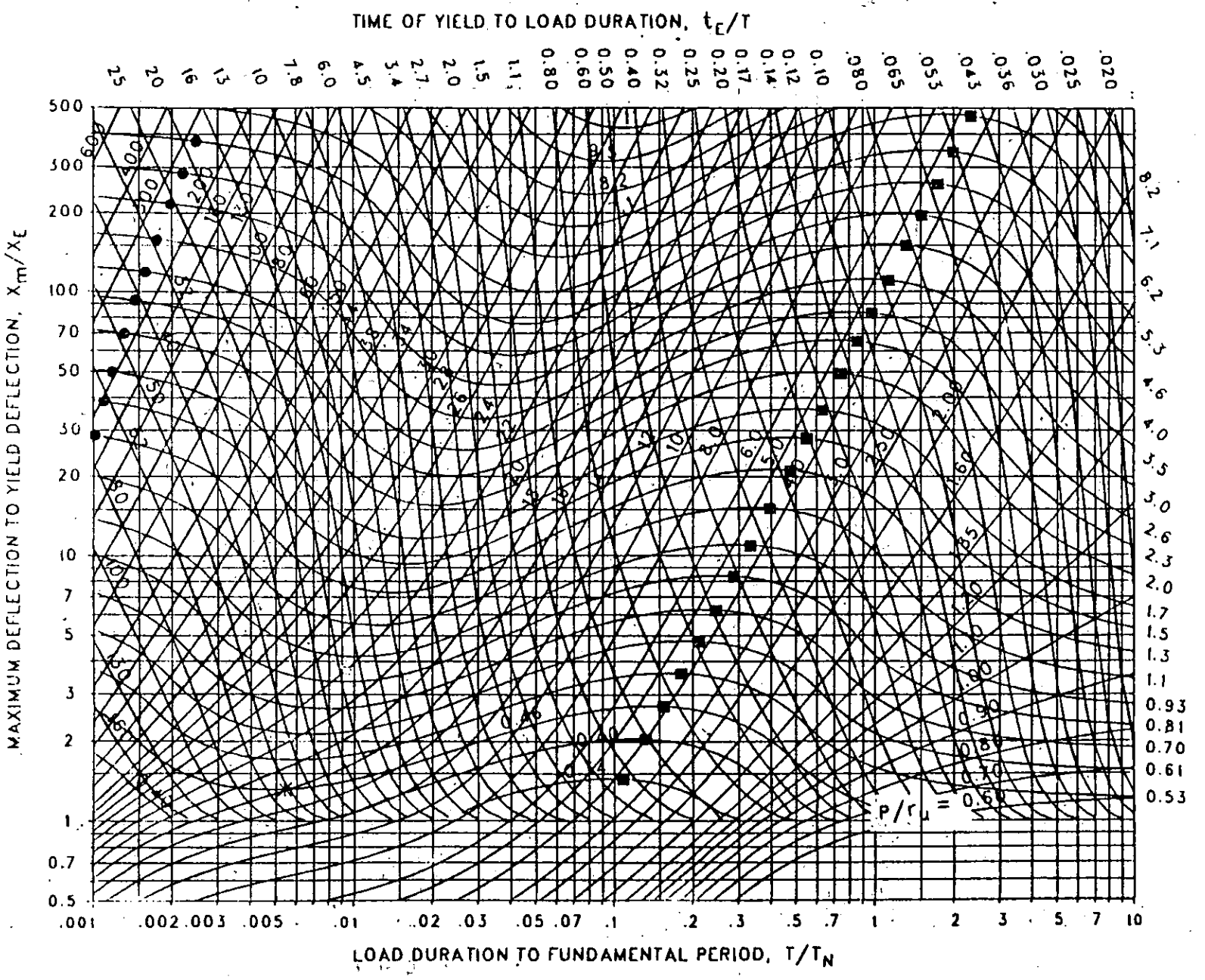


Figure 3-212 Maximum response of elasto-plastic, one-degree-of-freedom system for bilinear-triangular pulse ($C_1 = 0.042$, $C_2 = 300.$)

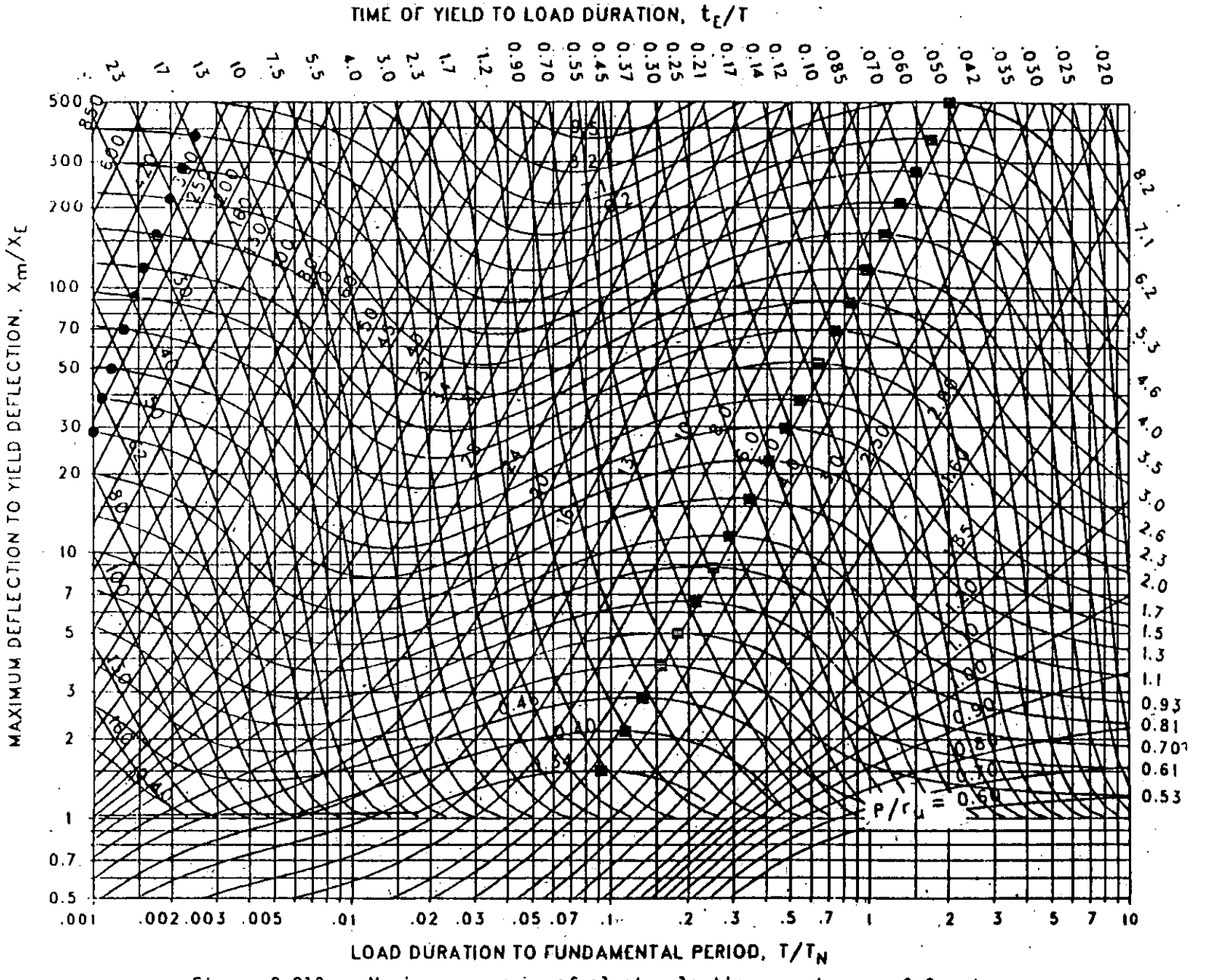


Figure 3-213 Maximum response of elasto-plastic, one-degree-of-freedom system for bilinear-triangular pulse ($C_1 = 0.032$, $C_2 = 300.$)

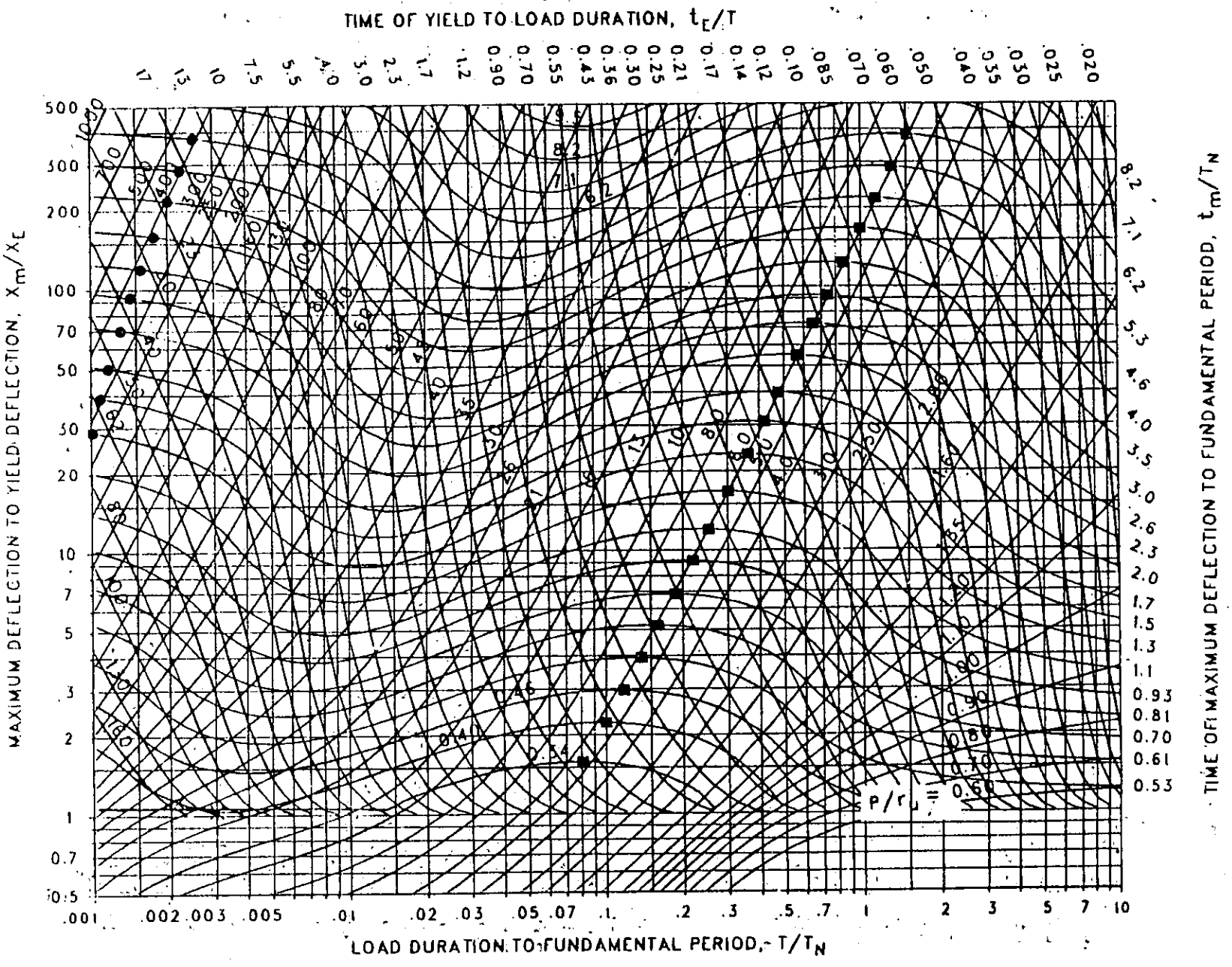


Figure 3-214 Maximum response of elasto-plastic, one-degree-of-freedom system for bilinear-triangular pulse ($C_1 = 0.026$, $C_2 = 300.$)

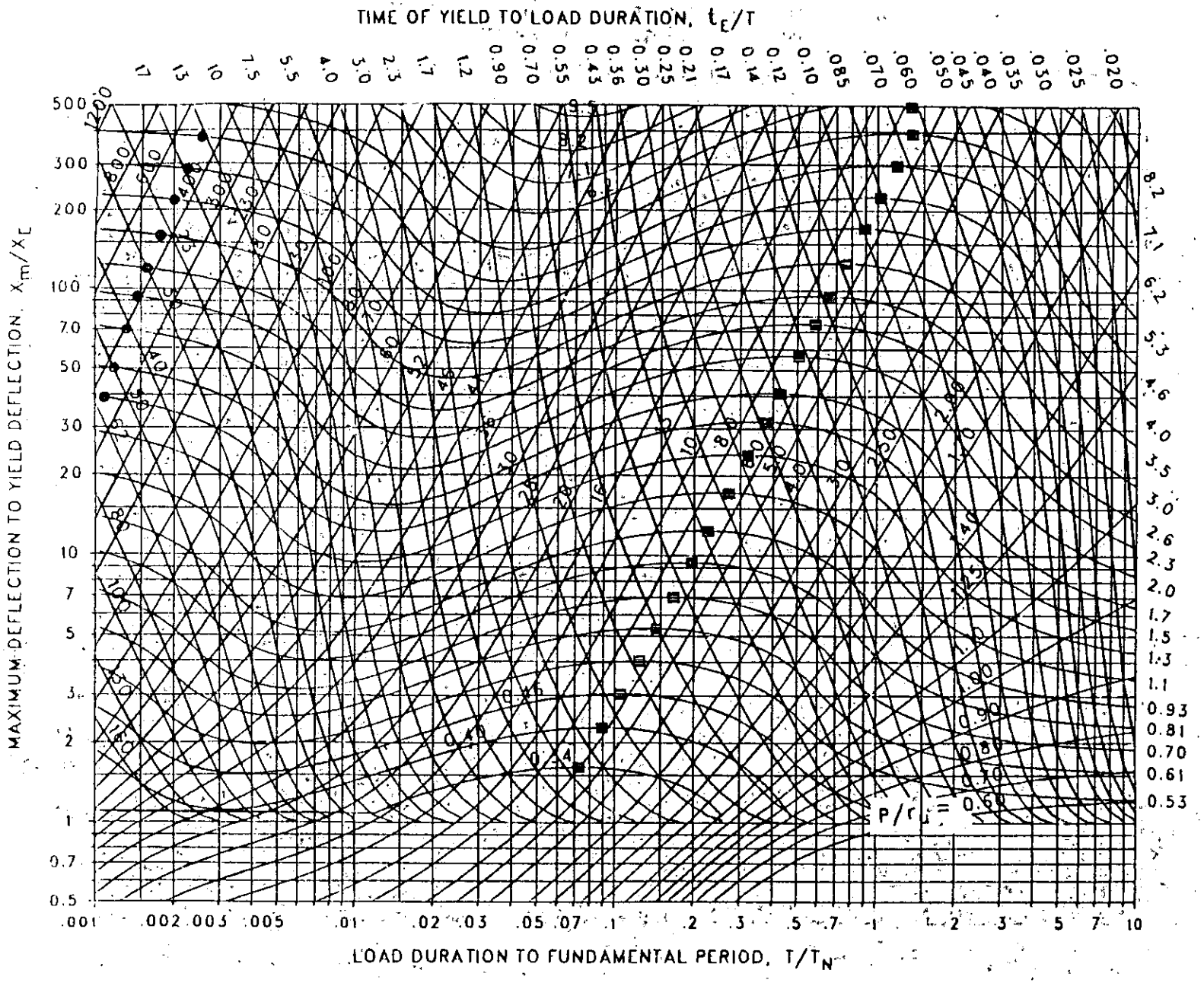


Figure 3-215 Maximum response of elasto-plastic, one-degree-of-freedom system for bilinear-triangular pulse (C_1 = 0.022, C_2 = 300.)

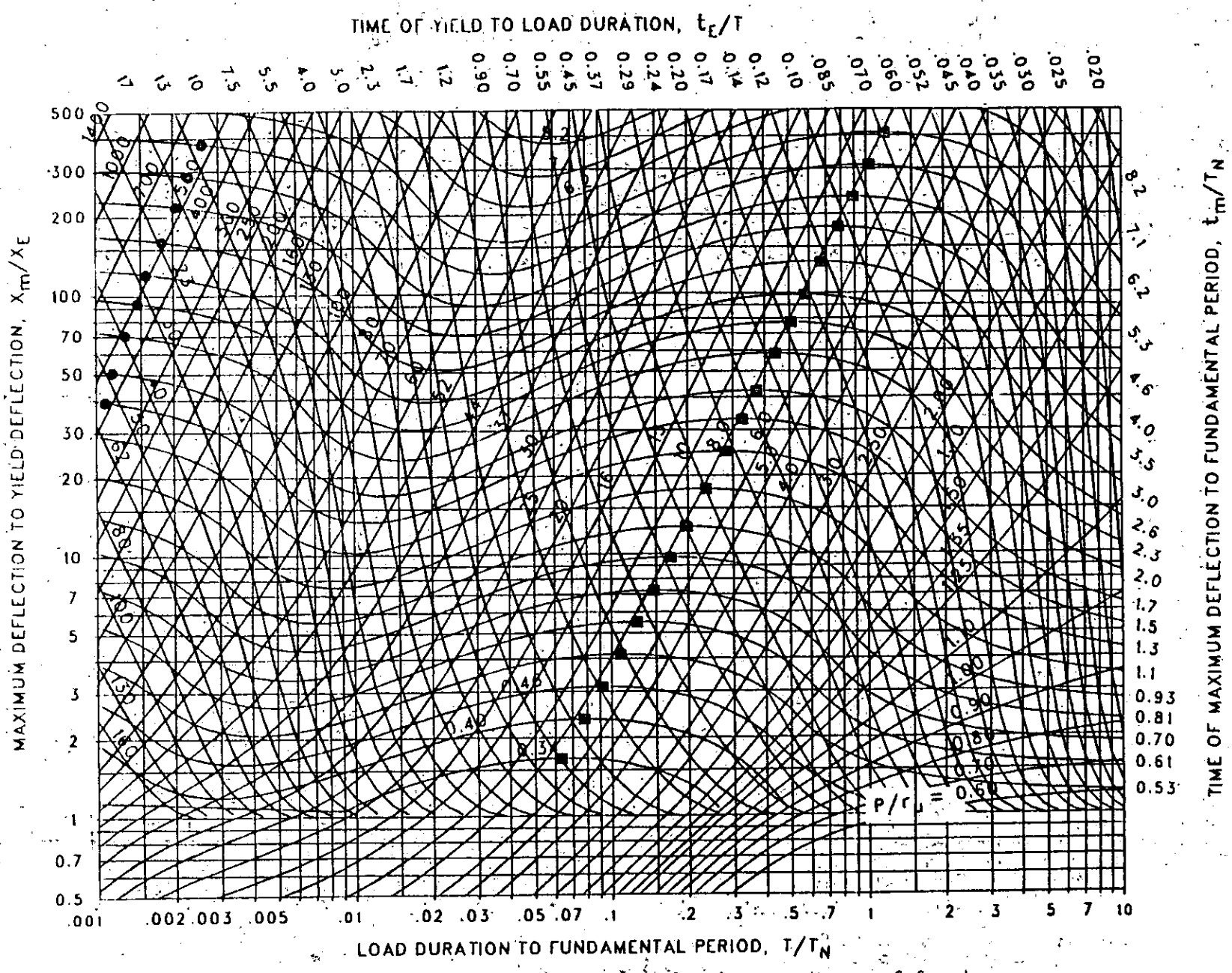


Figure 3-216 Maximum response of elasto-plastic, one-degree-of-freedom system for bilinear-triangular pulse (C_1 = 0.018, C_2 = 300.)

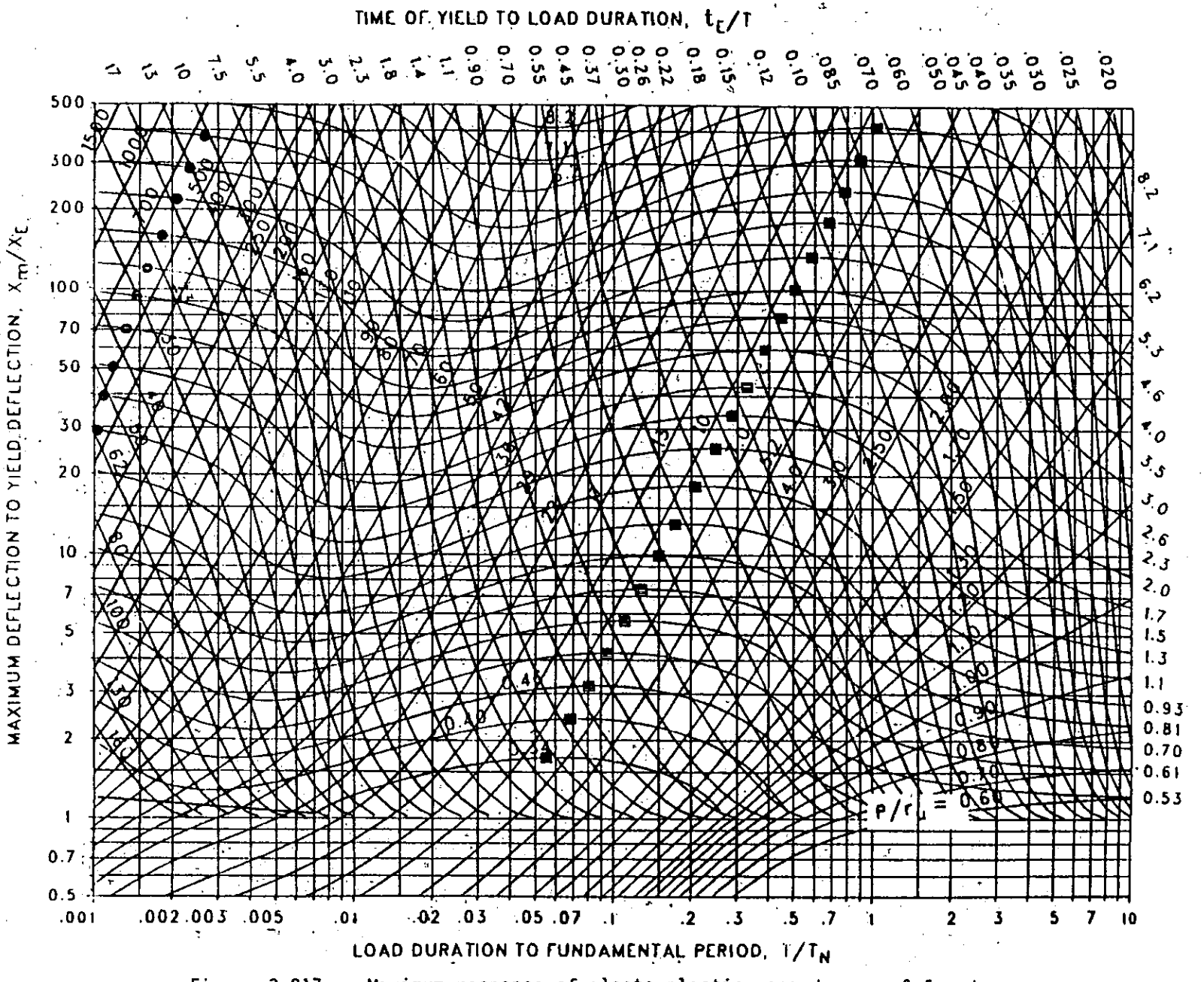


Figure 3-217 Maximum response of elasto-plastic, one-degree-of-freedom system for bilinear-triangular pulse ($C_1 = 0.015$, $C_2 = 300.$)

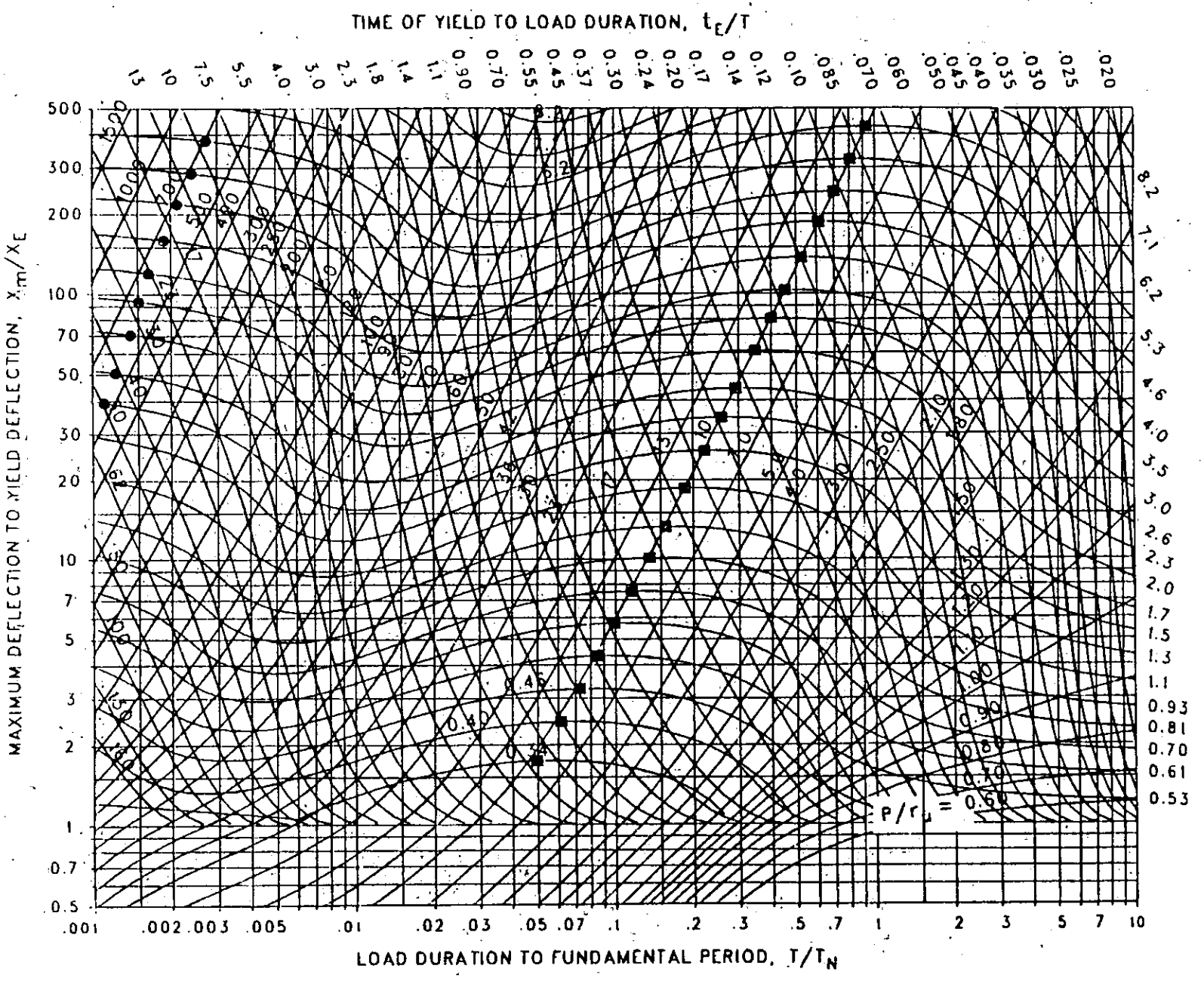


Figure 3-218 Maximum response of elasto-plastic, one-degree-of-freedom system for bilinear-triangular pulse (C_1 = 0.013, C_2 = 300.)

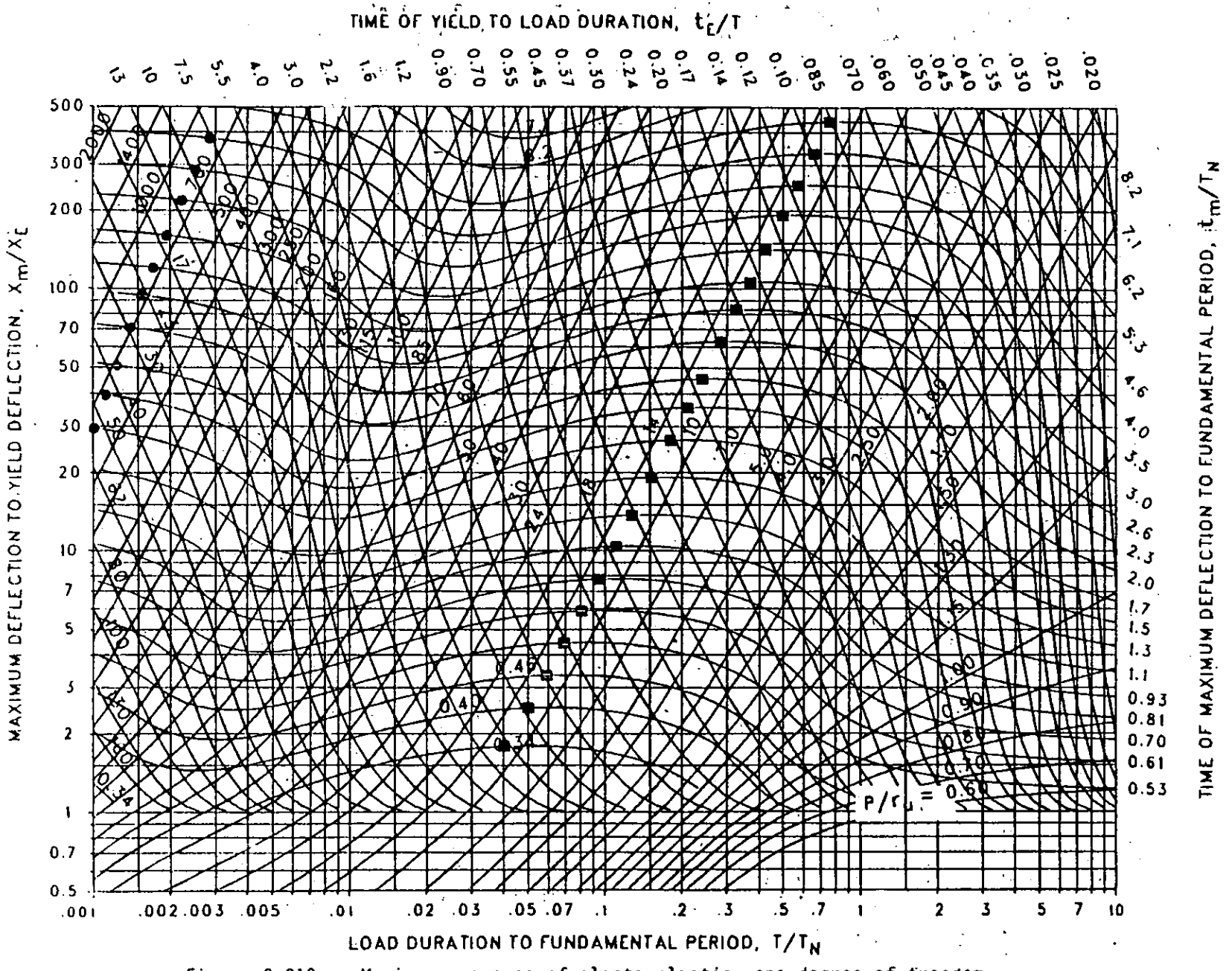


Figure 3-219 Maximum response of elasto-plastic, one-degree-of-freedom system for bilinear-triangular pulse ($C_1 = 0.010$, $C_2 = 300.$)

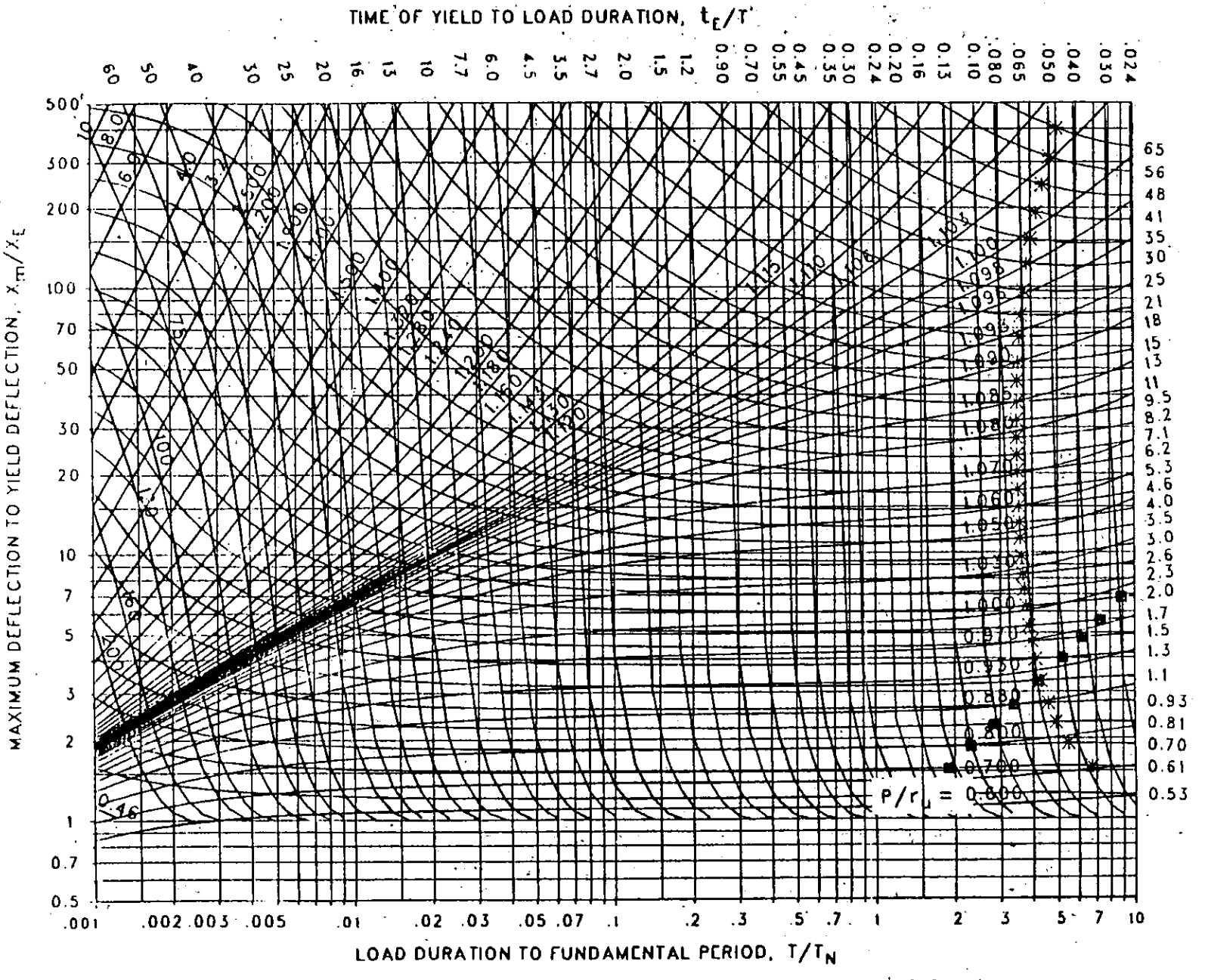


Figure 3-220 Maximum response of elasto-plastic, one-degree-of-freedom system for bilinear-triangular pulse ($C_1 = 0.909$, $C_2 = 1000.$)

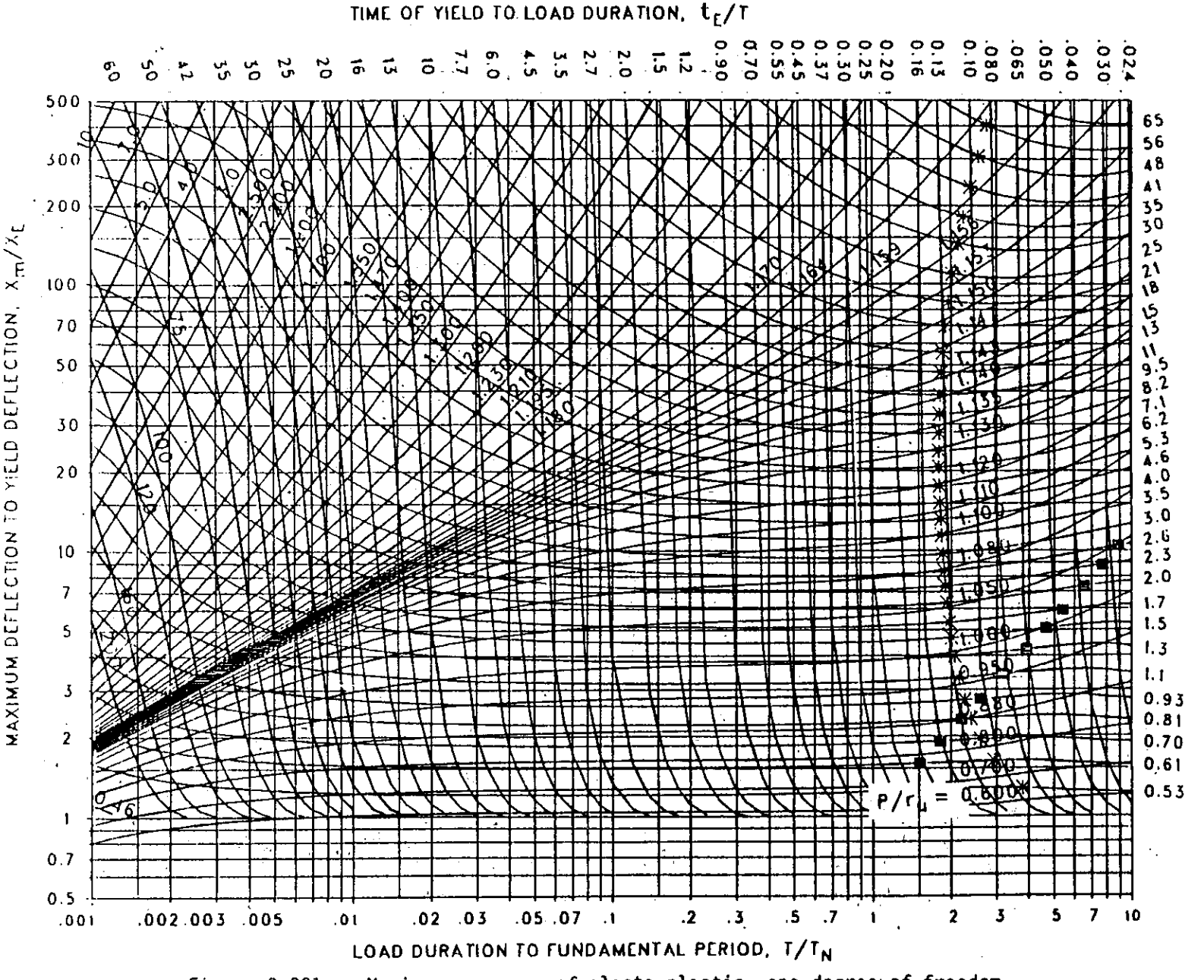


Figure 3-221 Maximum response of elasto-plastic, one-degree-of-freedom system for bilinear-triangular pulse ($C_1 = 0.866$, $C_2 = 1000.$)

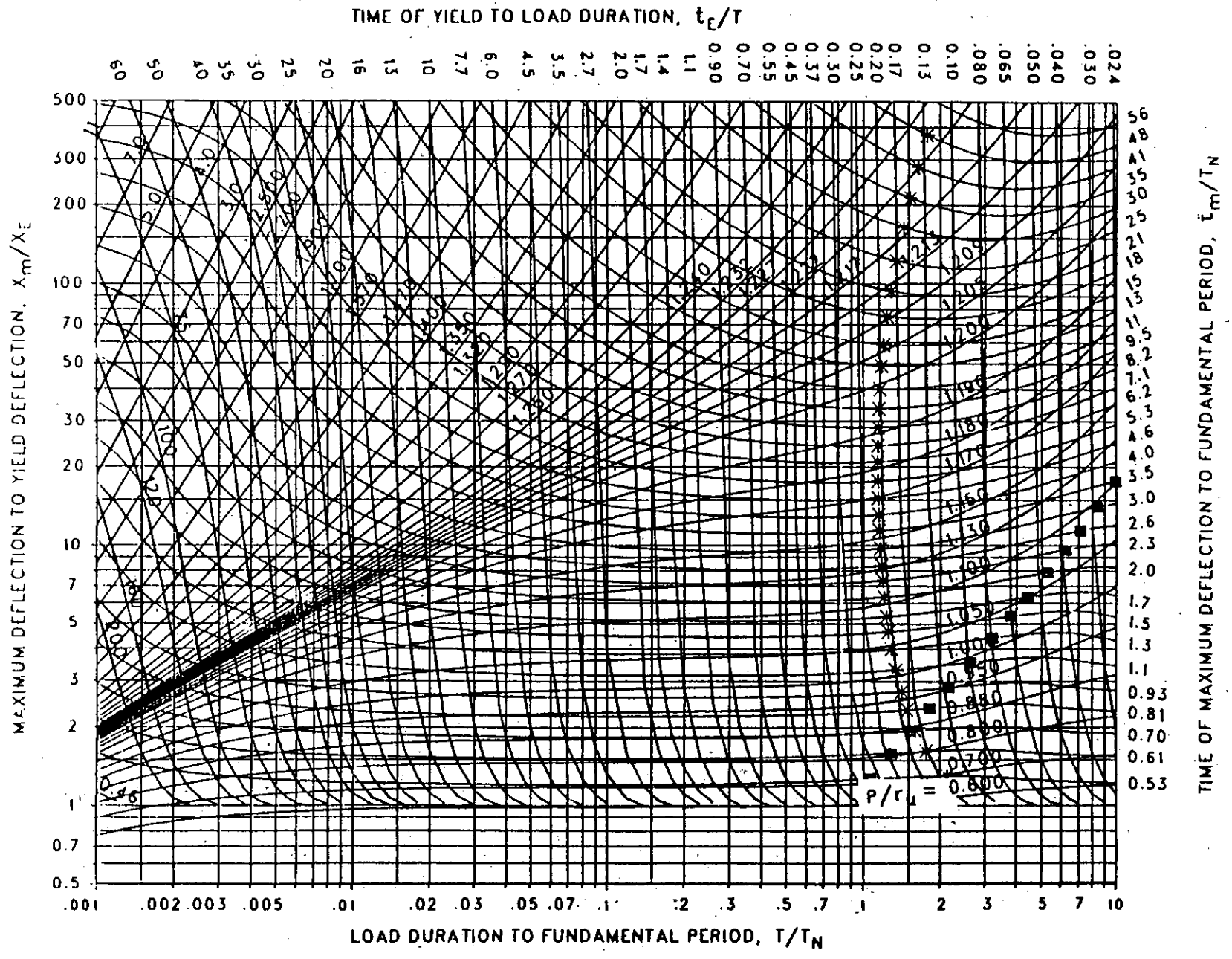


Figure 3-222 Maximum response of elasto-plastic, one-degree-of-freedom system for bilinear-triangular pulse (C_1 = 0.825, C_2 = 1000.)

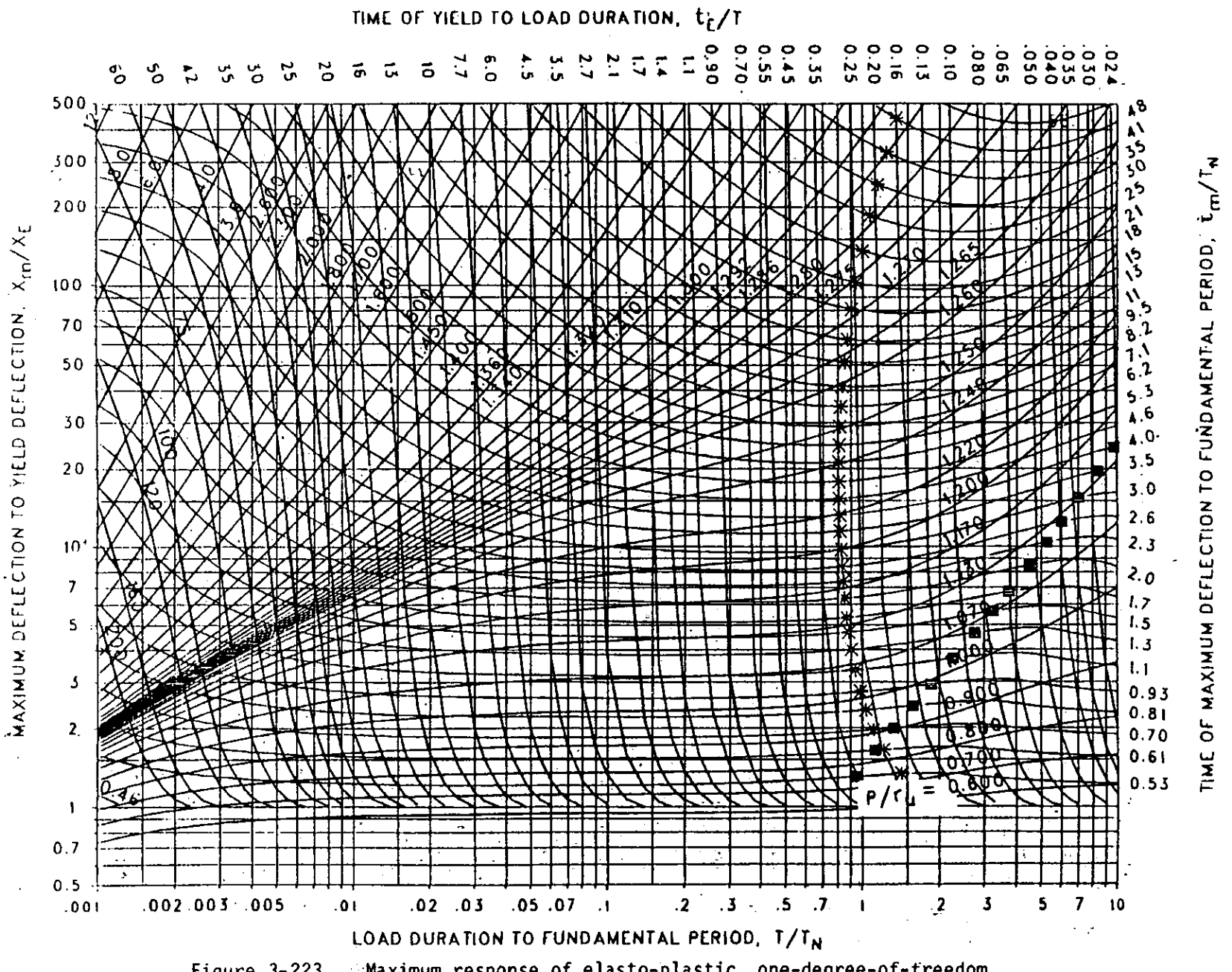


Figure 3-223 Maximum response of elasto-plastic, one-degree-of-freedom system for bilinear-triangular pulse (C_1 = 0.787, C_2 = 1000.)

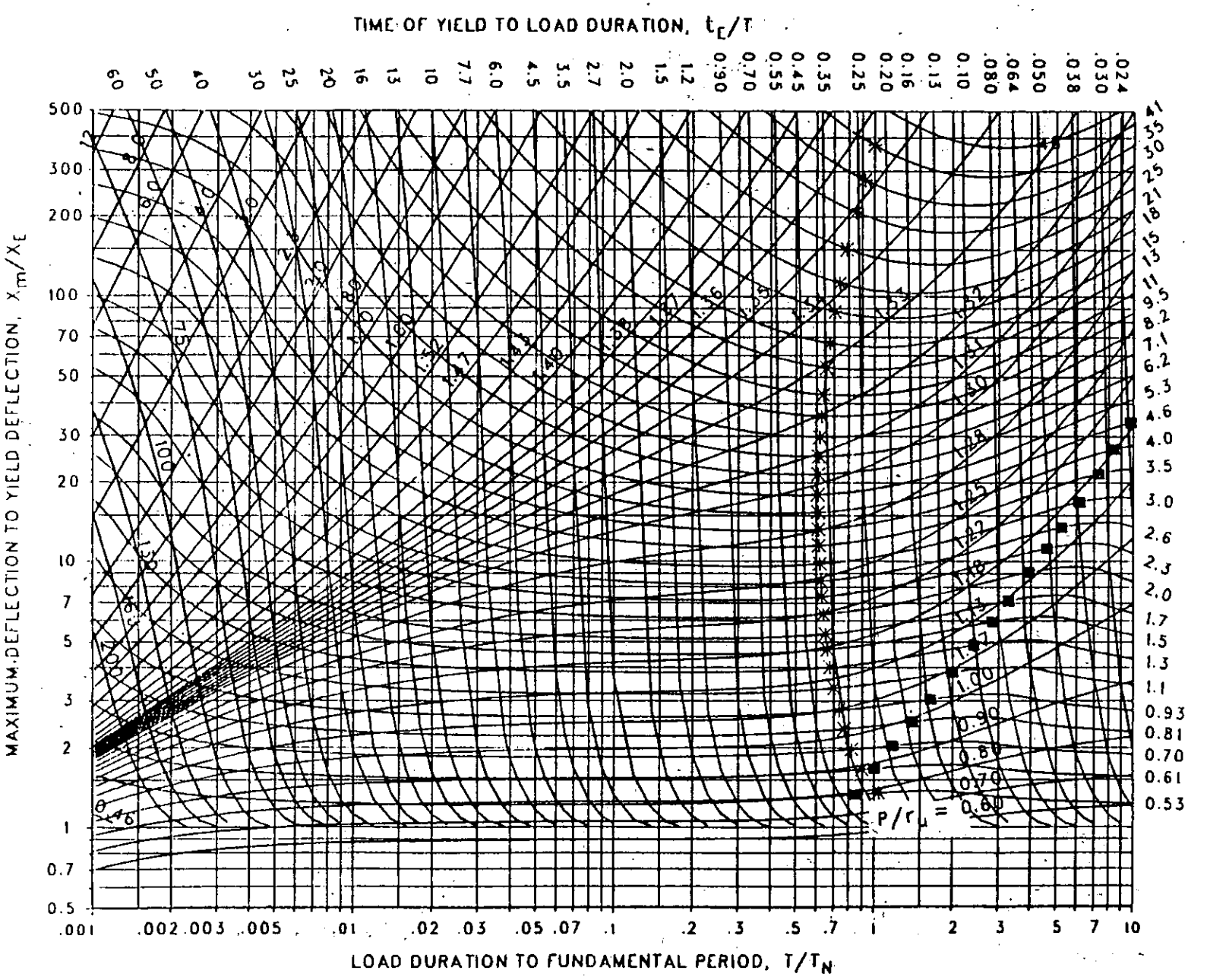


Figure 3-224 Maximum response of elasto-plastic, one-degree-of-freedom system for bilinear-triangular pulse ($C_1 = 0.750$, $C_2 = 1000.$)

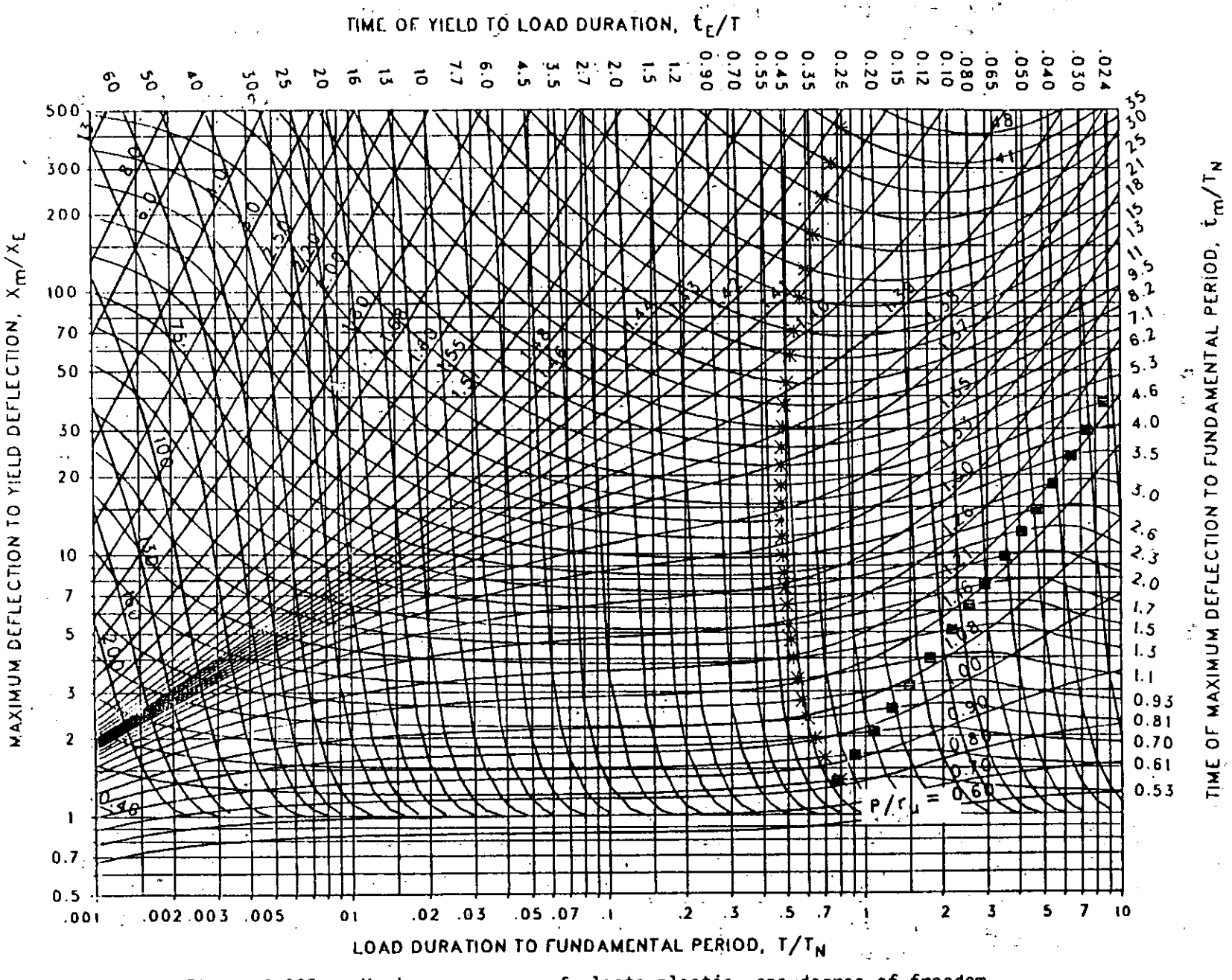


Figure 3-225 Maximum response of elasto-plastic, one-degree-of-freedom system for bilinear-triangular pulse (C_1 = 0.715, C_2 = 1000.)

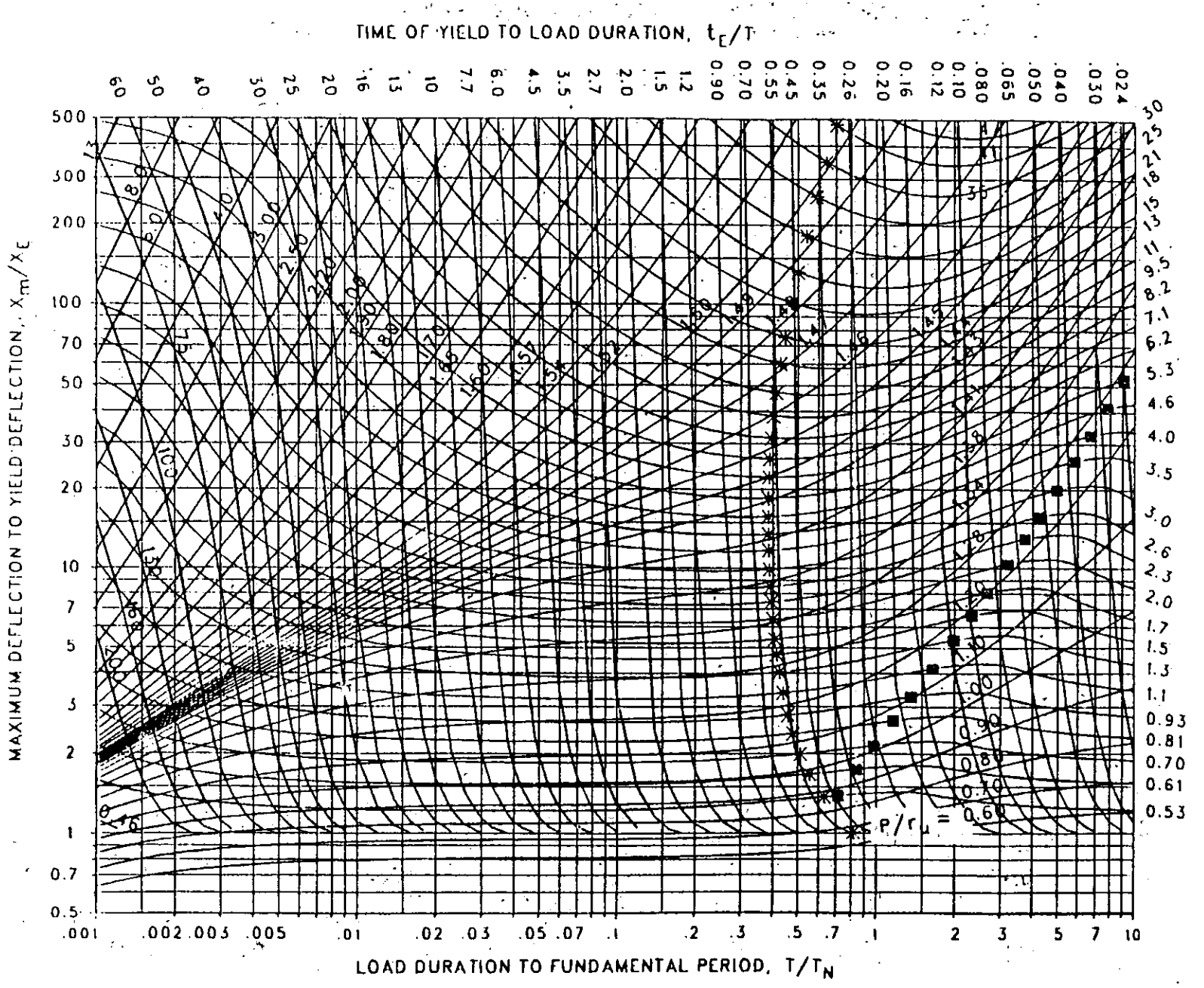


Figure 3-226 Maximum response of elasto-plastic, one-degree-of-freedom system for bilinear-triangular pulse (C_1 = 0.681, C_2 = 1000.)

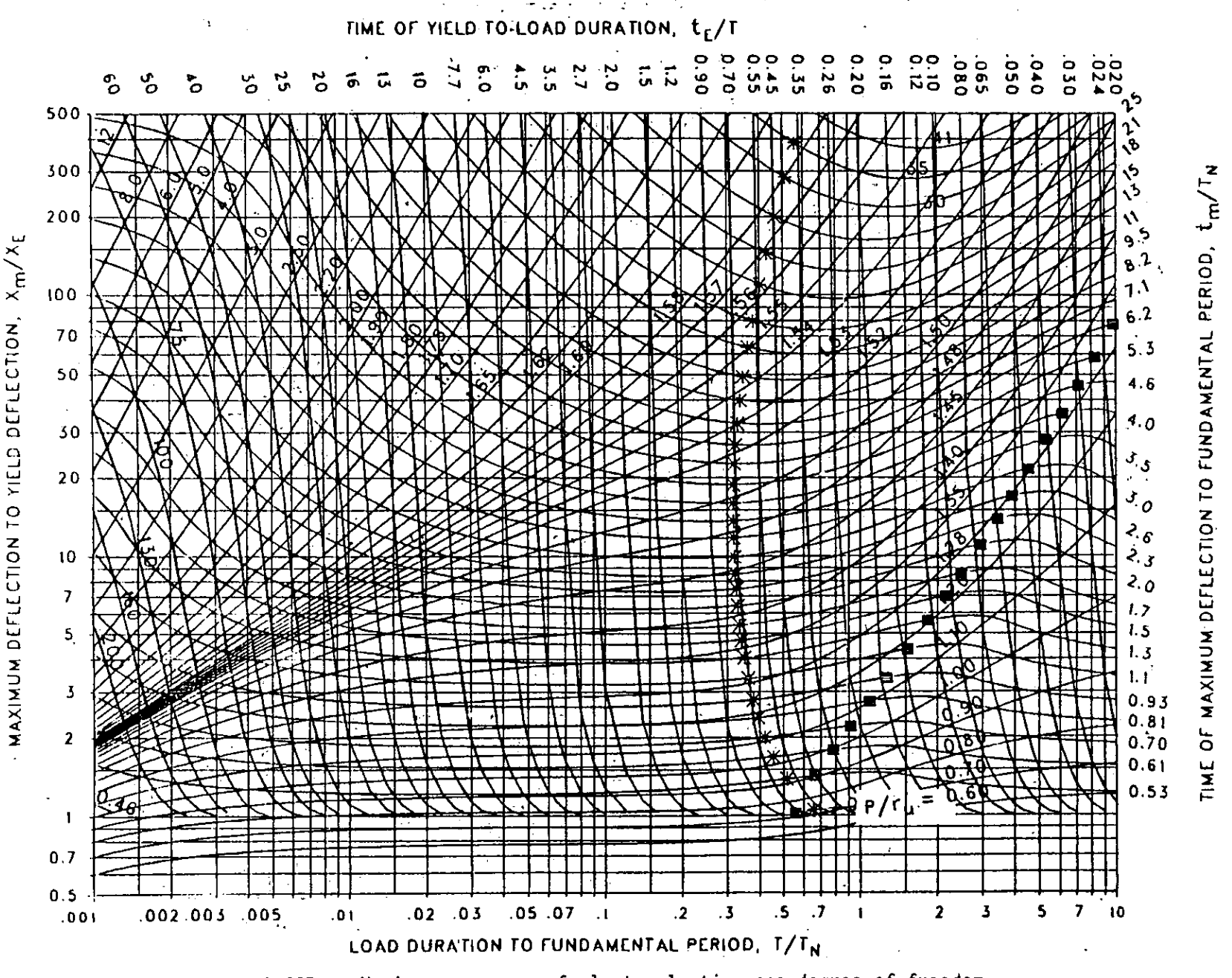


Figure 3-227 Maximum response of elasto-plastic, one-degree-of-freedom system for bilinear-triangular pulse (C_1 = 0.648, C_2 = 1000.)

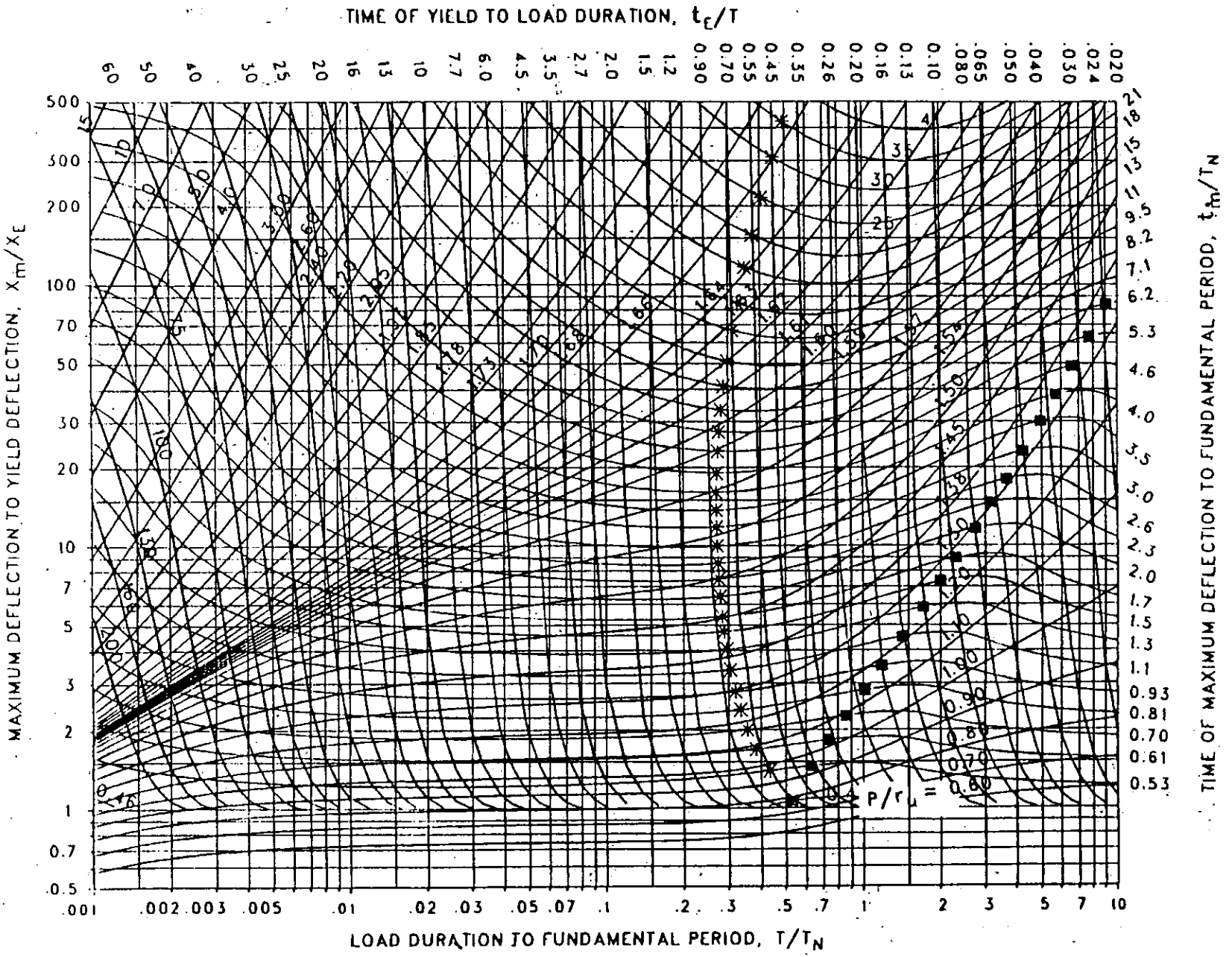


Figure 3-228 Maximum response of elasto-plastic, one-degree-of-freedom system for bilinear-triangular pulse (C_1 = 0.619, C_2 = 1000.)

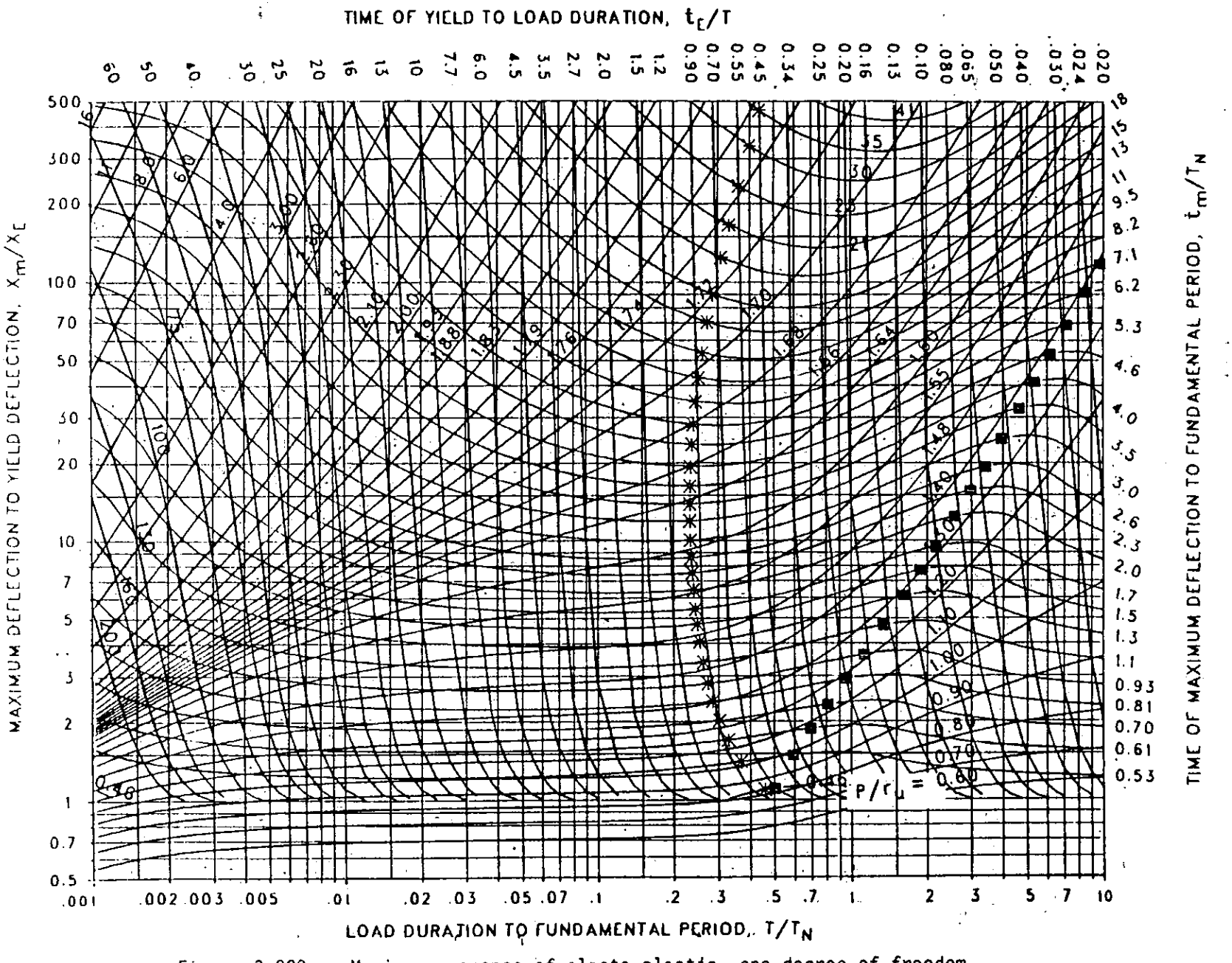


Figure 3-229 Maximum response of elasto-plastic, one-degree-of-freedom system for bilinear-triangular pulse (C_1 = 0.590, C_2 = 1000.)

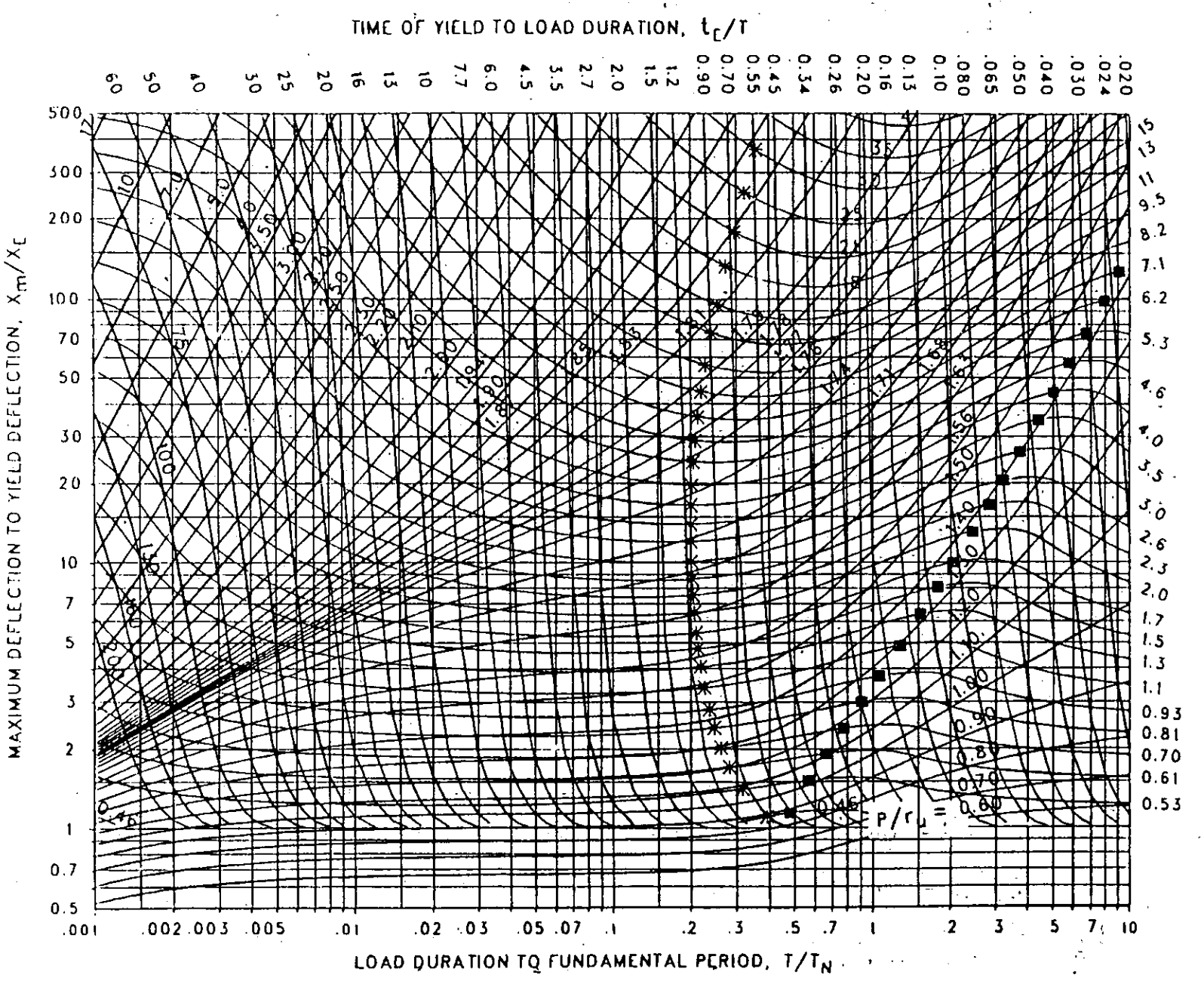


Figure 3-230 Maximum response of elasto-plastic, one-degree-of-freedom system for bilinear-triangular pulse ($C_1 = 0.562$, $C_2 = 1000.$)

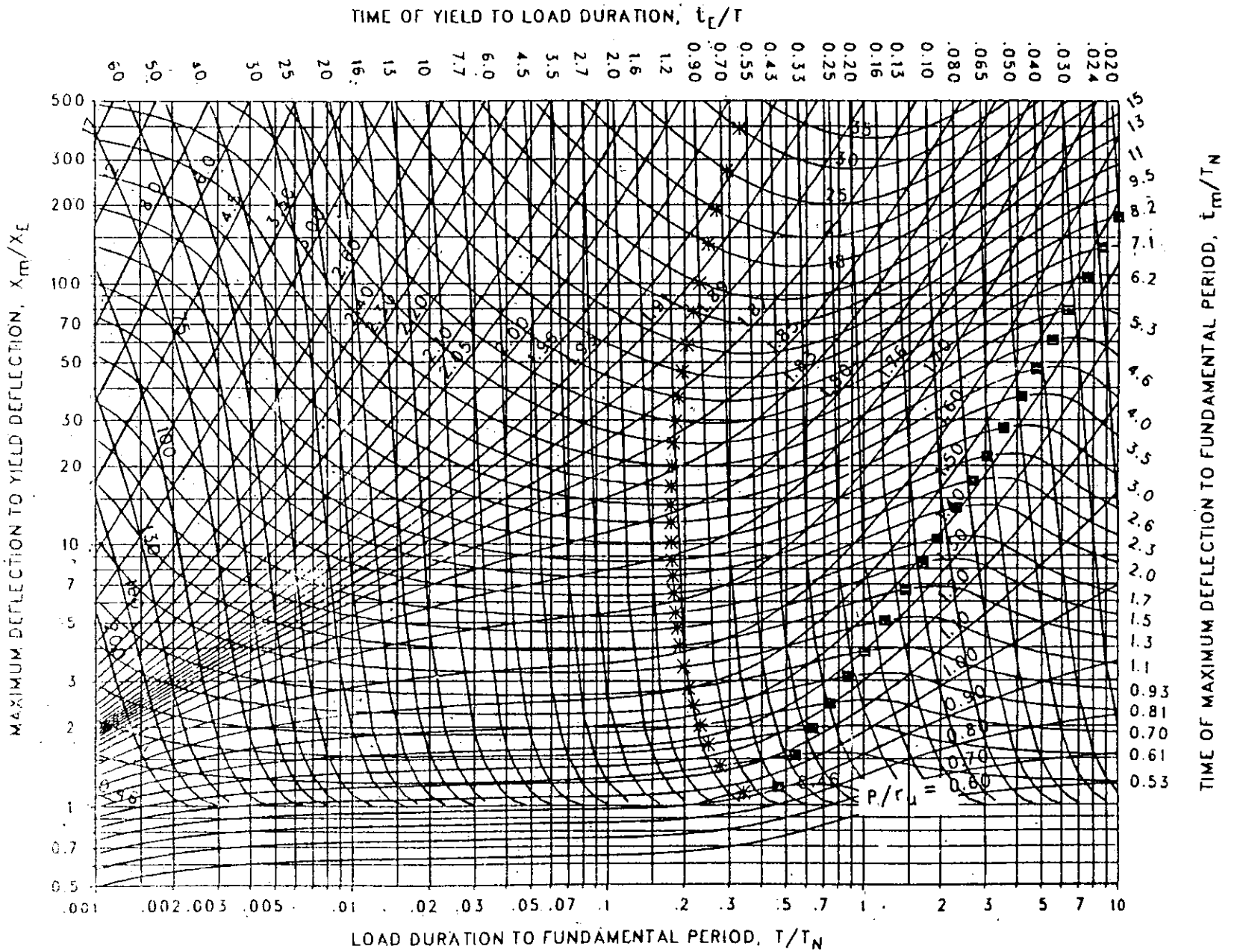


Figure 3-231 Maximum response of elasto-plastic, one-degree-of-freedom system for bilinear-triangular pulse (C_1 = 0.536, C_2 = 1000.)

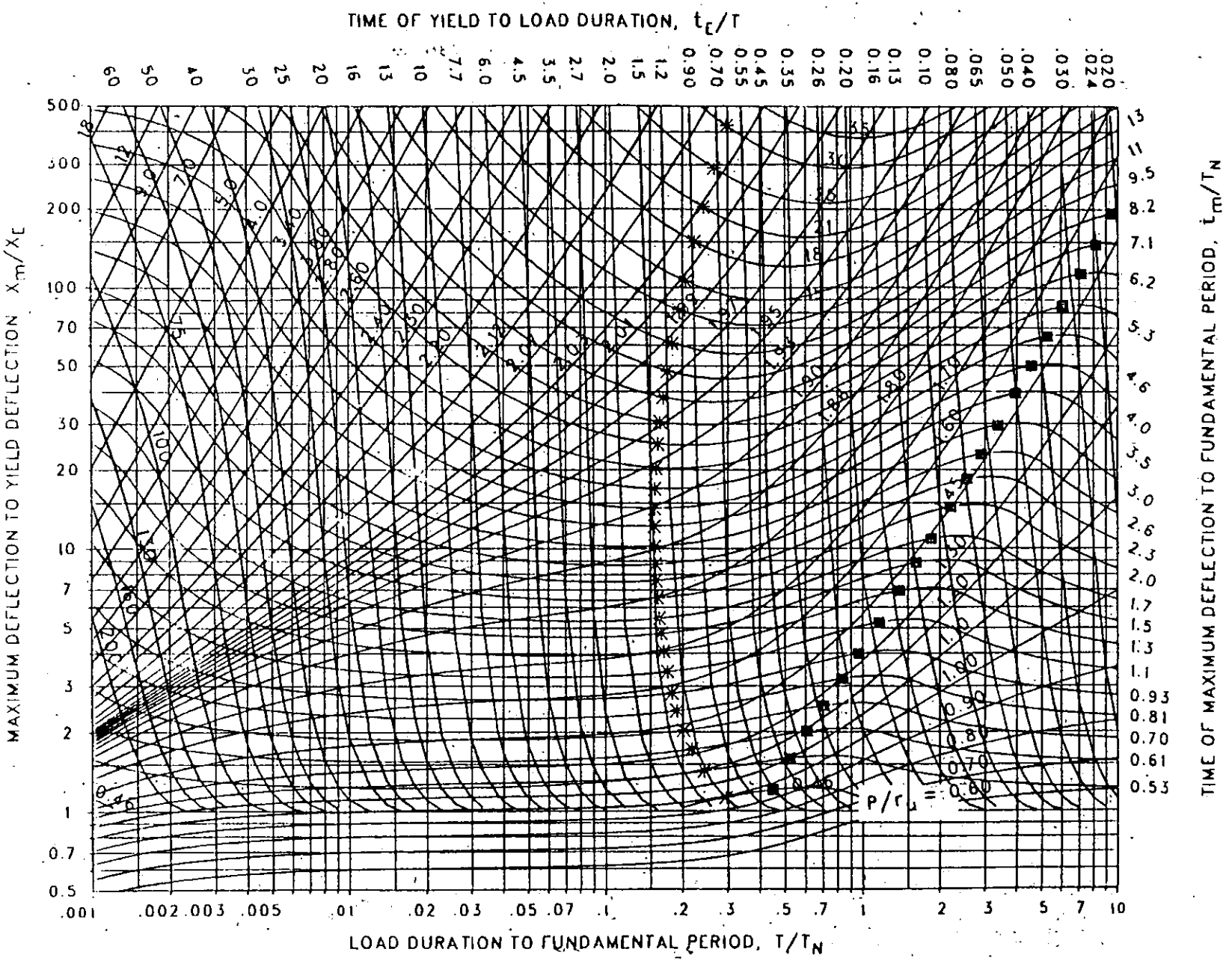


Figure 3-232 Maximum response of elasto-plastic, one-degree-of-freedom system for bilinear-triangular pulse ($C_1 = 0.511$, $C_2 = 1000.$)

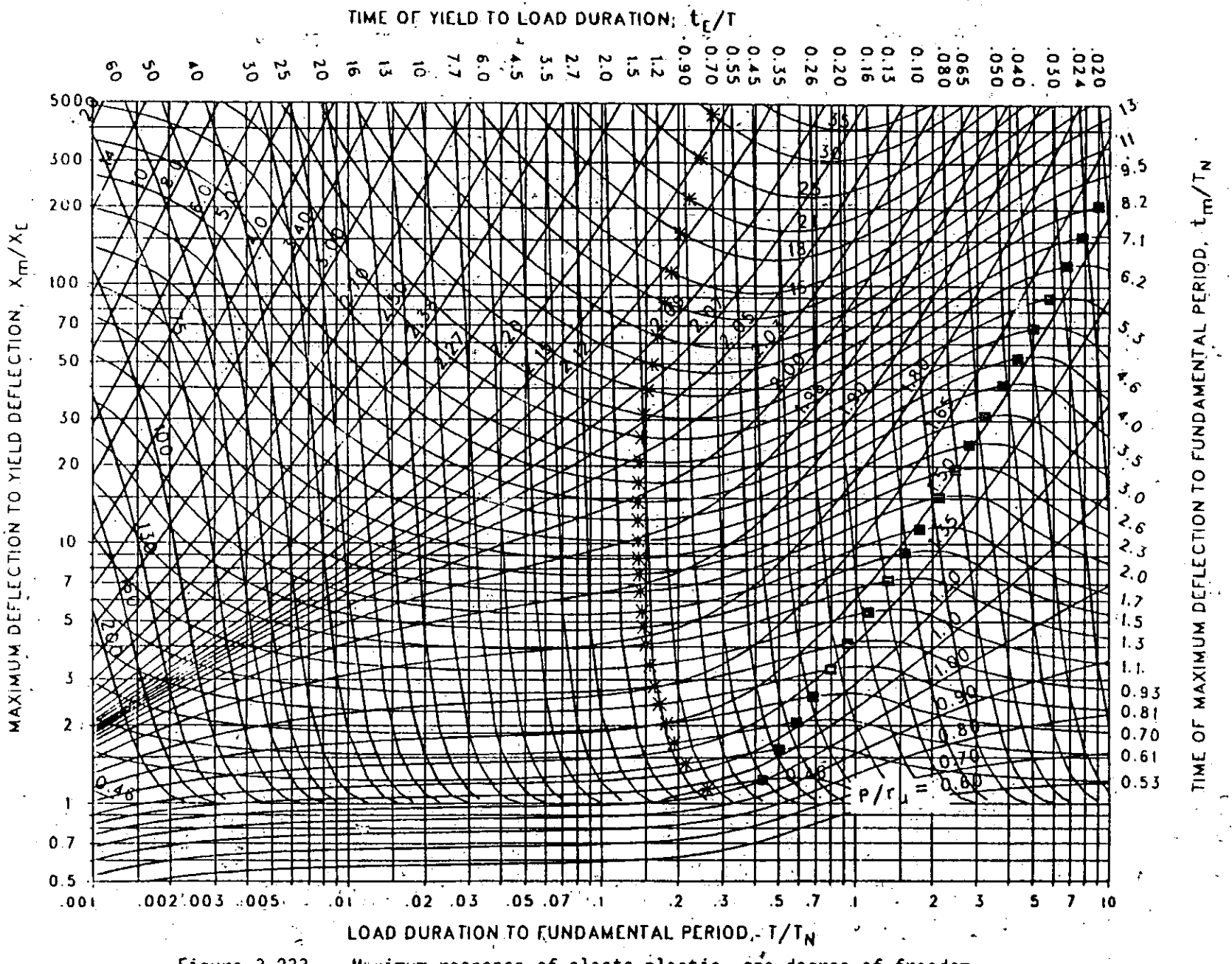


Figure 3-233 Maximum response of elasto-plastic, one-degree-of-freedom system for bilinear-triangular pulse (C_1 = 0.487, C_2 = 1000.)

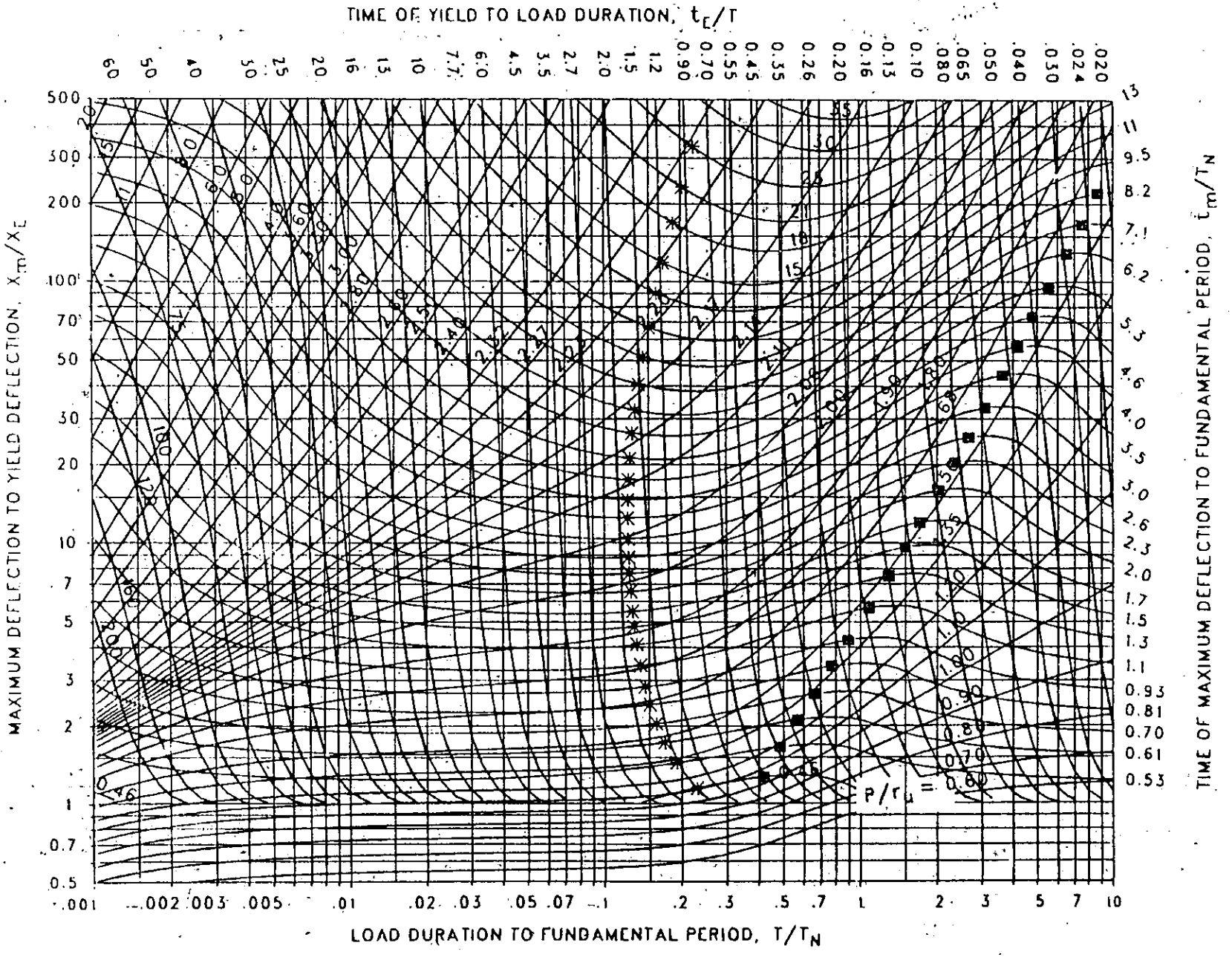


Figure 3-234 Maximum response of elasto-plastic, one-degree-of-freedom system for bilinear-triangular pulse (C_1 = 0.464, C_2 = 1000.)

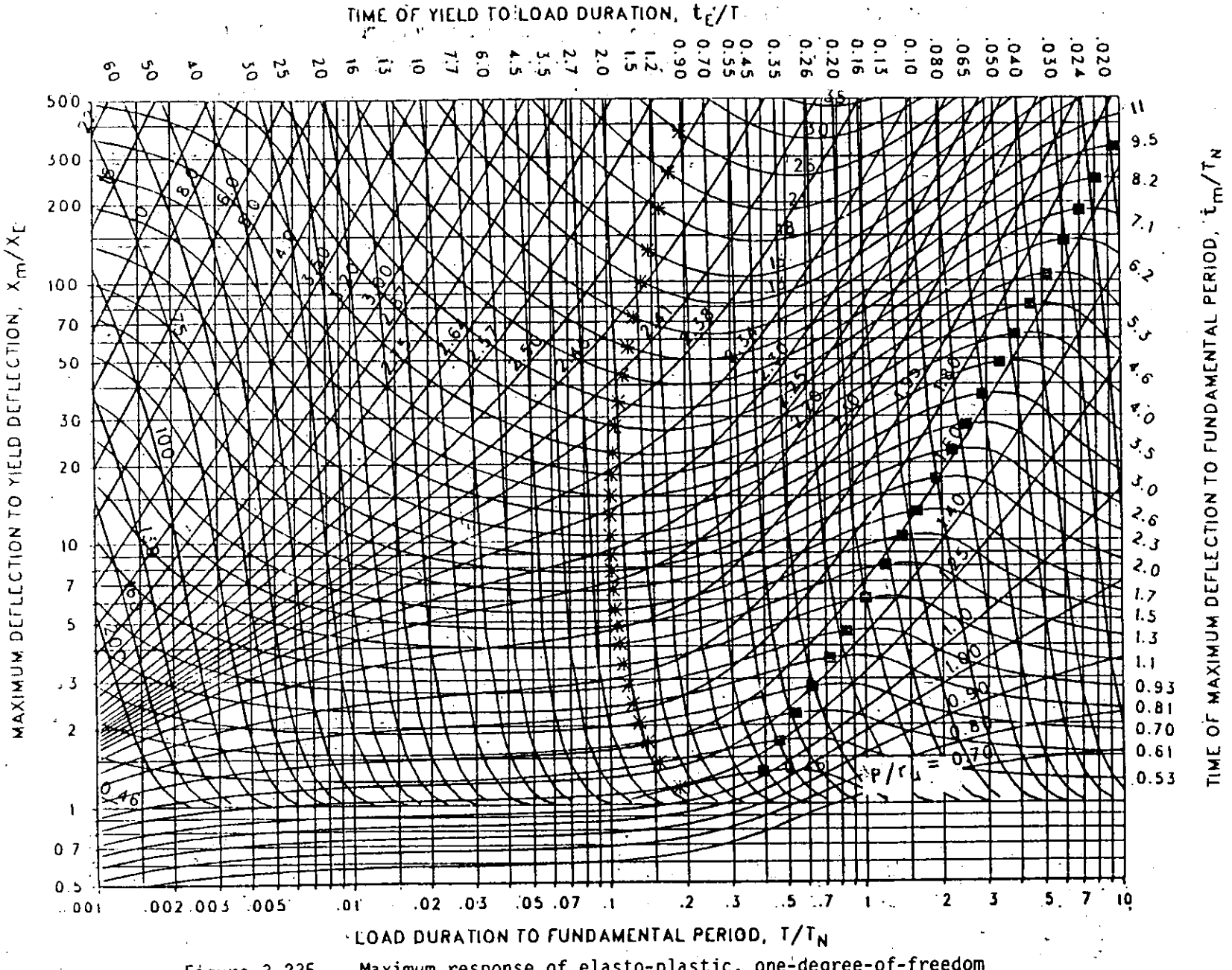


Figure 3-235 Maximum response of elasto-plastic, one-degree-of-freedom system for bilinear-triangular pulse ($C_1 = 0.422$, $C_2 = 1000.$)

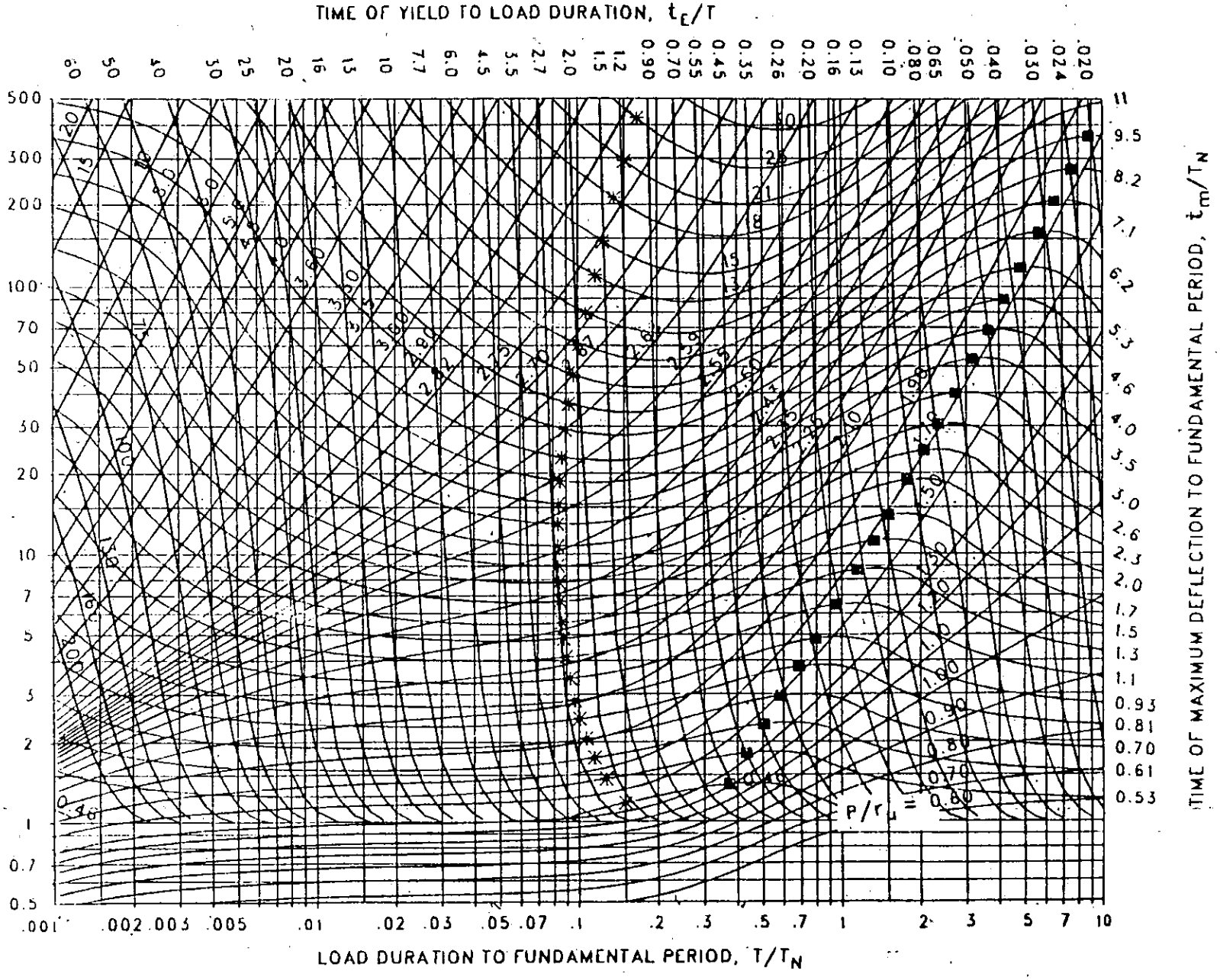


Figure 3-236 Maximum response of elasto-plastic, one-degree-of-freedom system for bilinear-triangular pulse (C_1 = 0.383, C_2 = 1000.)

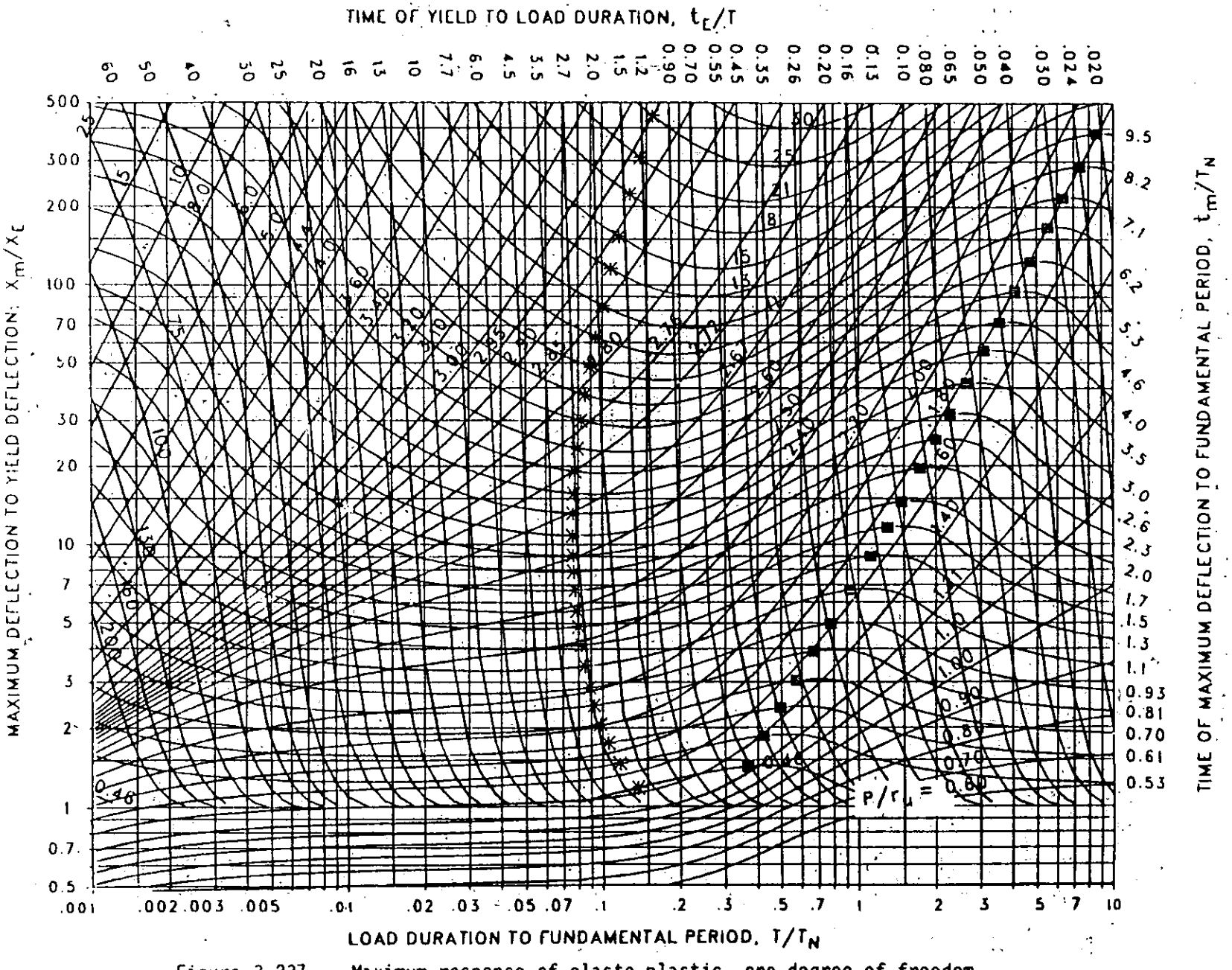


Figure 3-237 Maximum response of elasto-plastic, one-degree-of-freedom system for bilinear-triangular pulse ($C_1 = 0.365$, $C_2 = 1000.$)

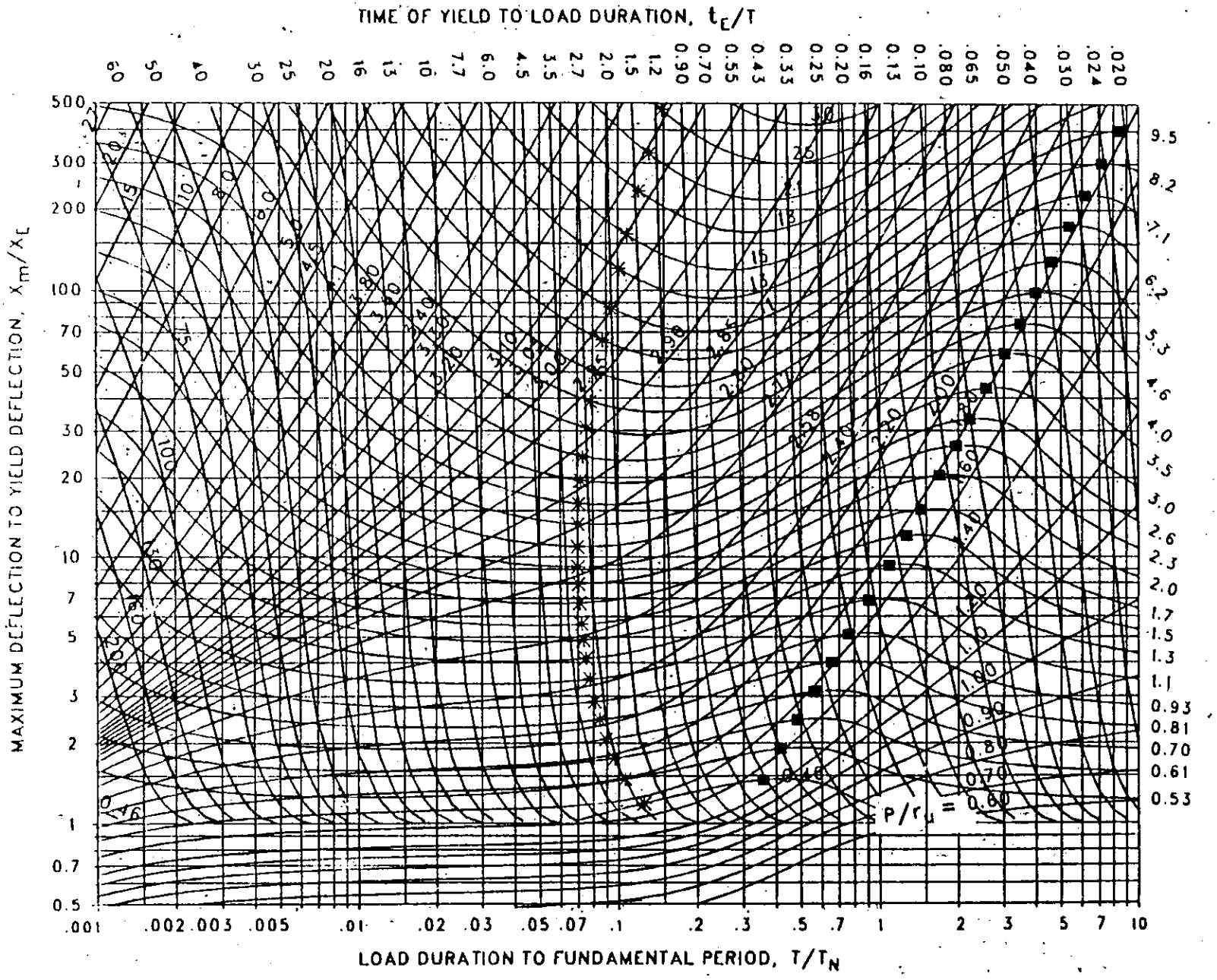


Figure 3-238 Maximum response of elasto-plastic, one-degree-of-freedom system for bilinear-triangular pulse ($C_1 = 0.348$, $C_2 = 1000.$)

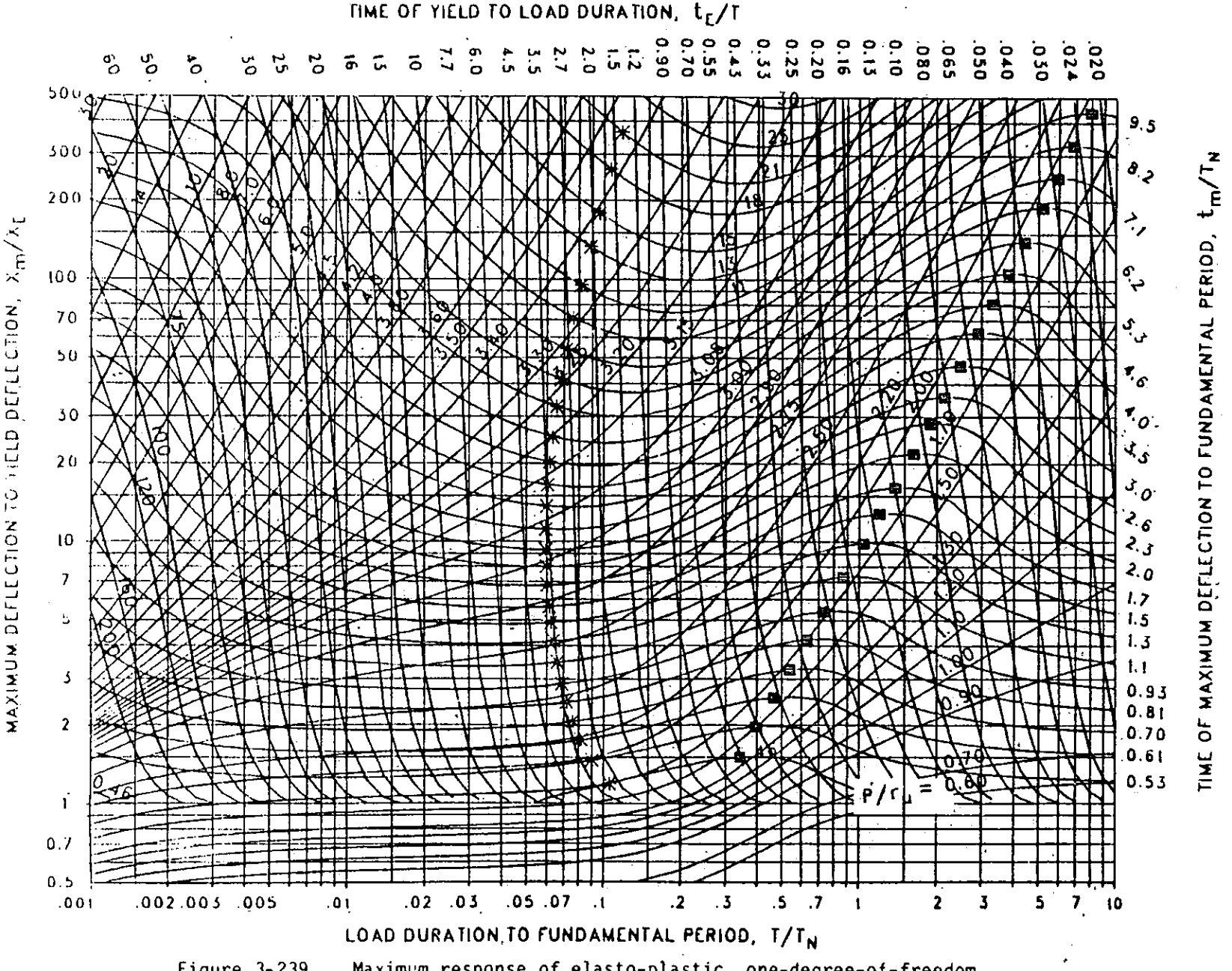


Figure 3-239 Maximum response of elasto-plastic, one-degree-of-freedom system for bilinear-triangular pulse (C_1 = 0.316, C_2 = 1000.)

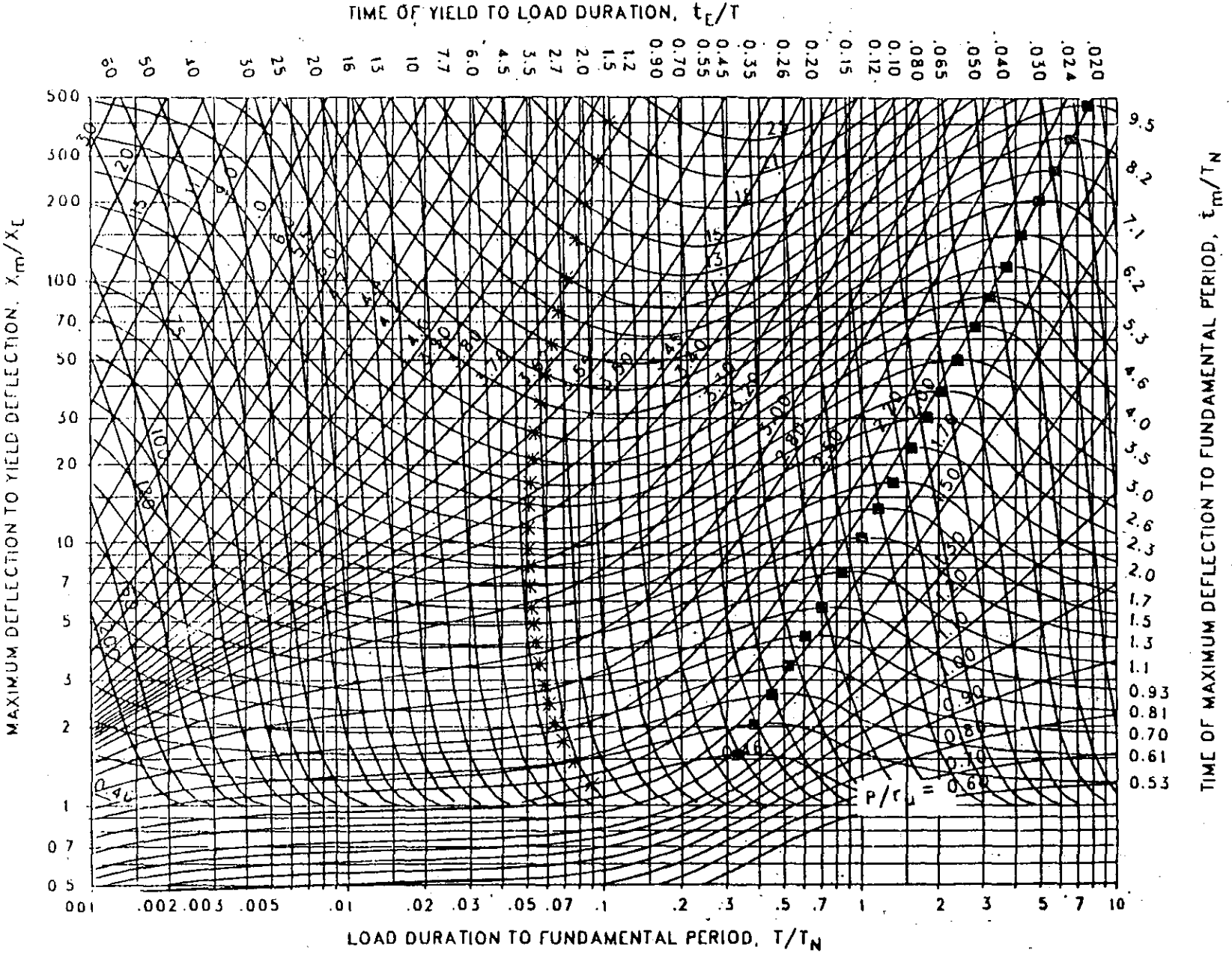


Figure 3-240 Maximum response of elasto-plastic, one-degree-of-freedom system for bilinear-triangular pulse ($C_1 = 0.287$, $C_2 = 1000.$)

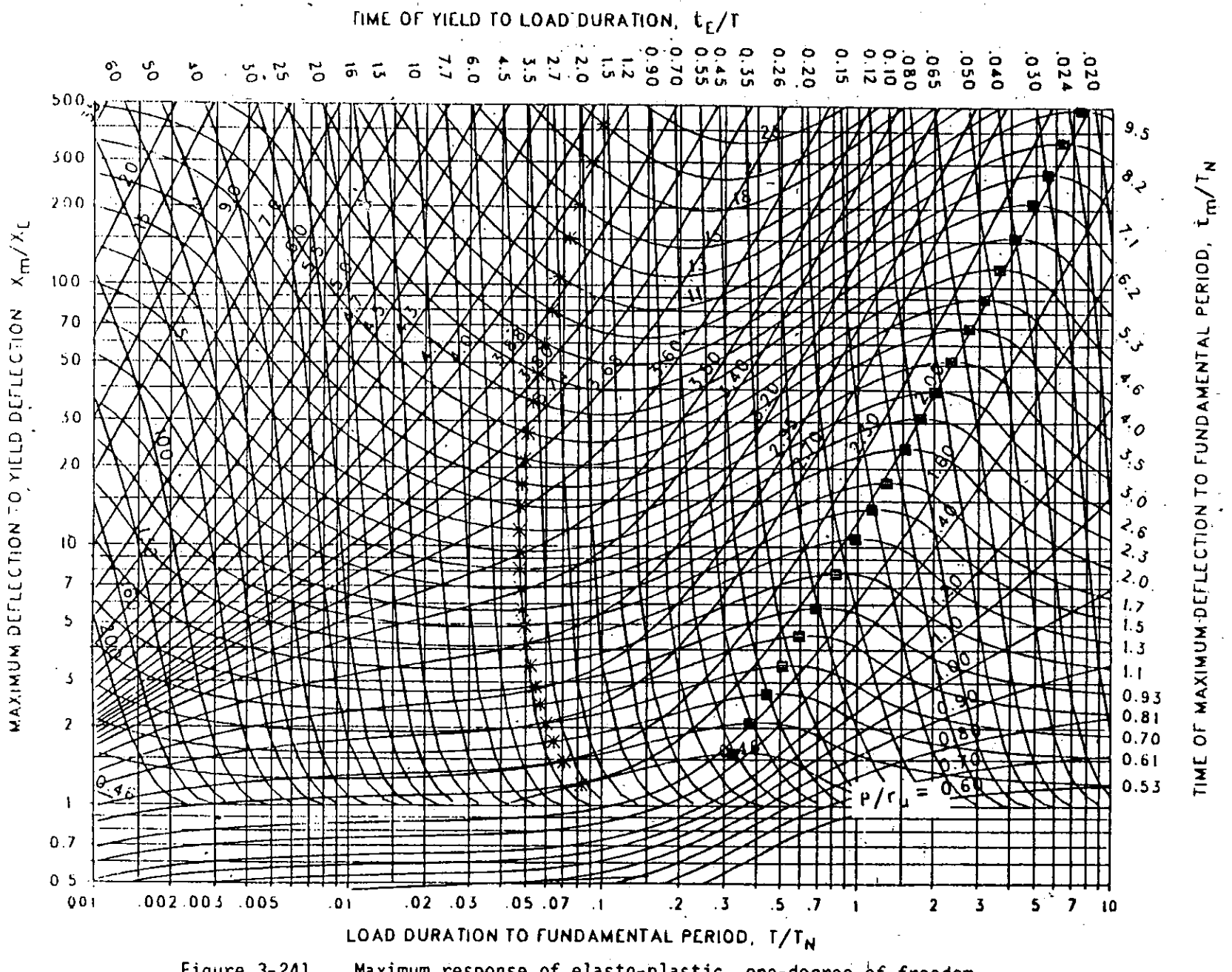


Figure 3-241 Maximum response of elasto-plastic, one-degree-of-freedom system for bilinear-triangular pulse (C_1 = 0.274, C_2 = 1000.)

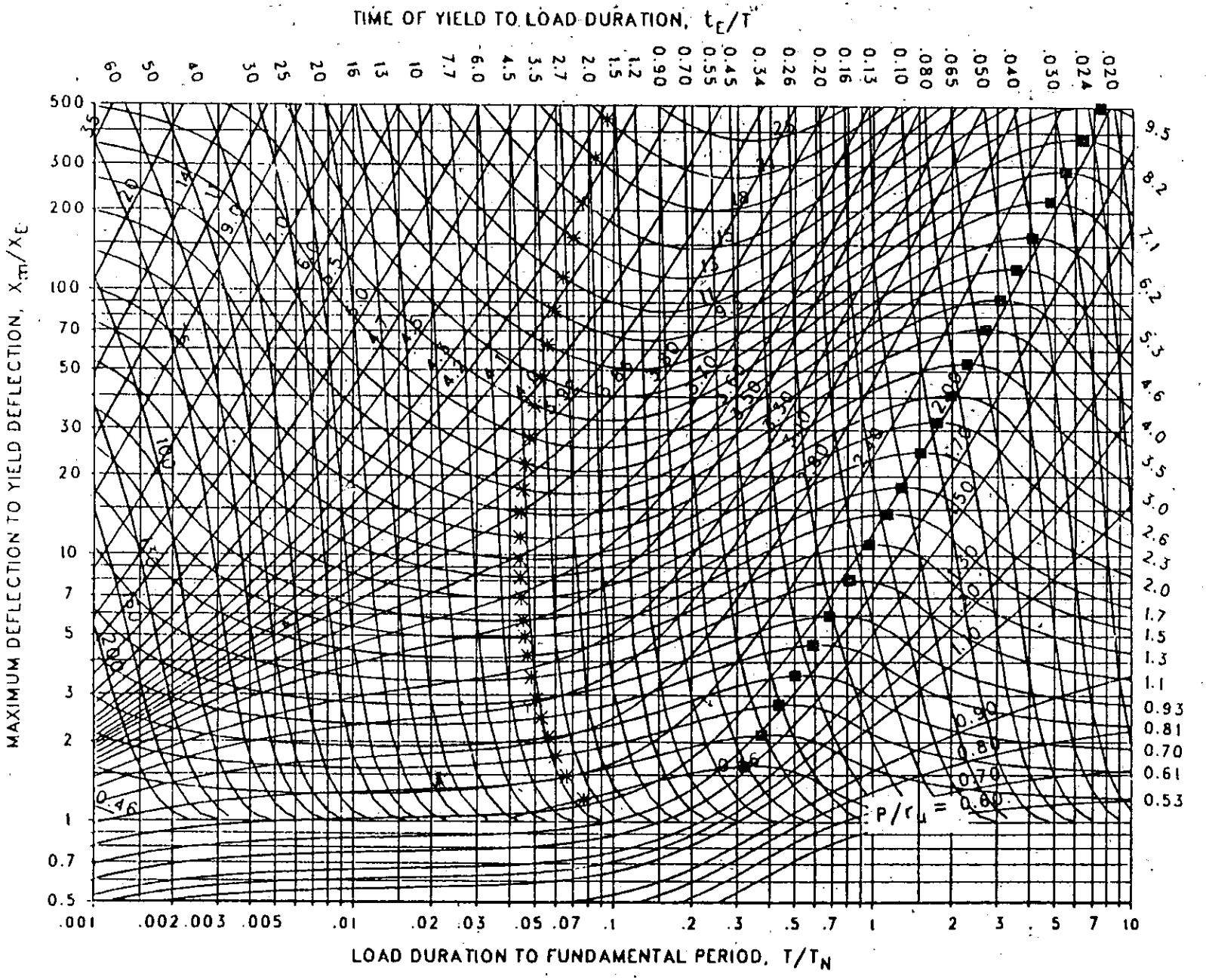


Figure 3-242 Maximum response of elasto-plastic, one-degree-of-freedom system for bilinear-triangular pulse (C_1 = 0.261, C_2 = 1000.)

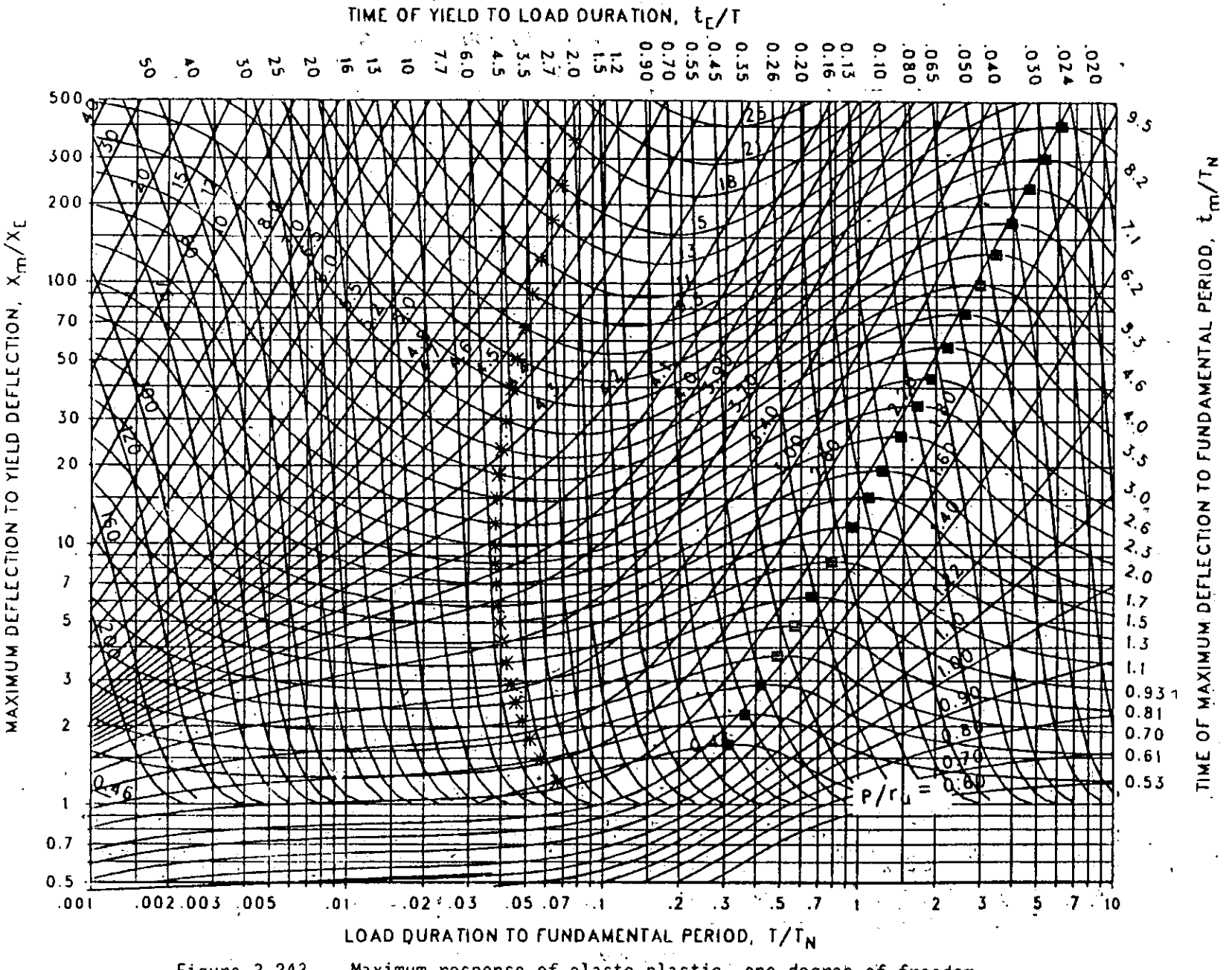


Figure 3-243 Maximum response of elasto-plastic, one-degree-of-freedom system for bilinear-triangular pulse (C_1 = 0.237, C_2 = 1000.)

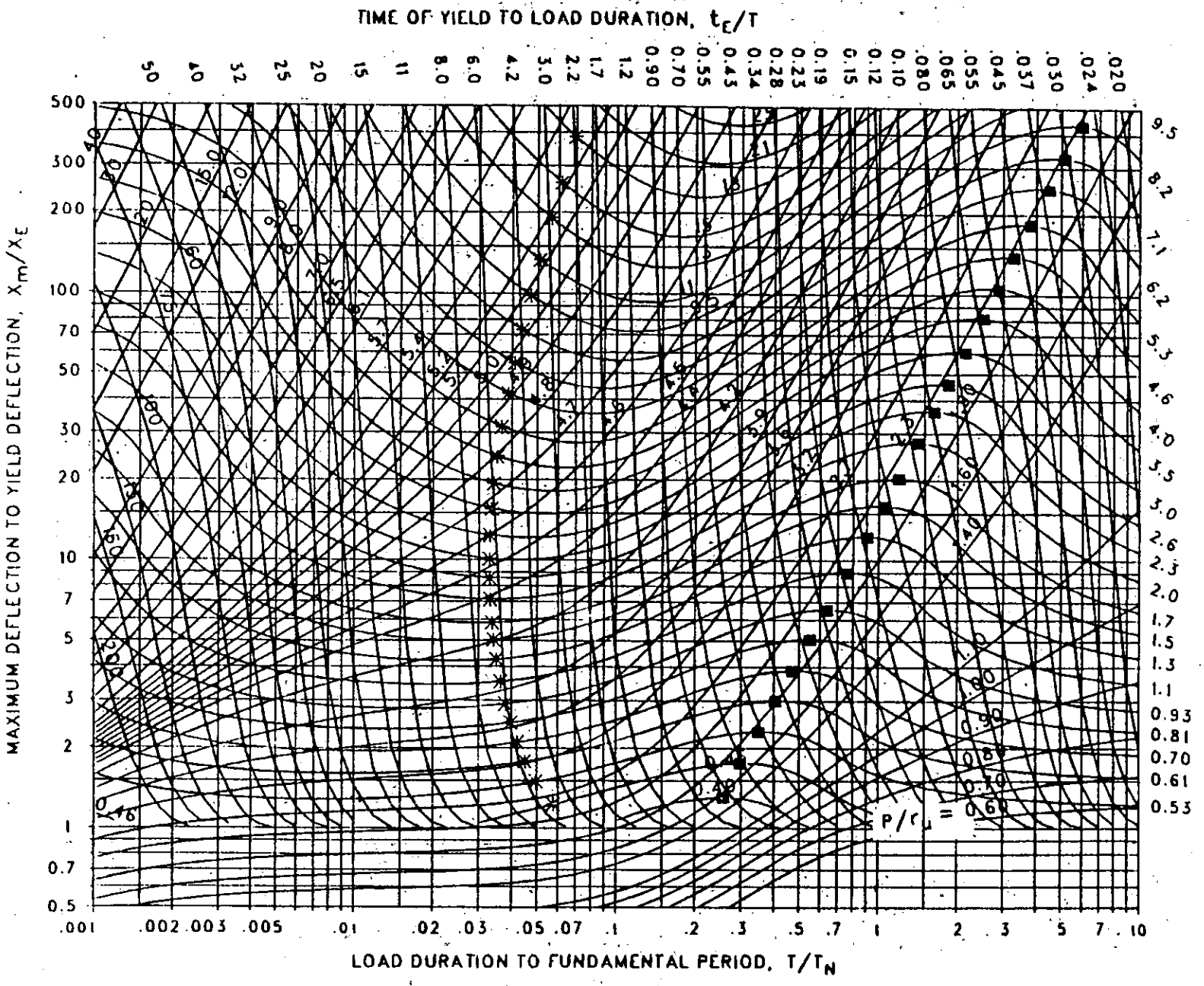


Figure 3-244 Maximum response of elasto-plastic, one-degree-of-freedom system for bilinear-triangular pulse ($C_1 = 0.215$, $C_2 = 1000.$)

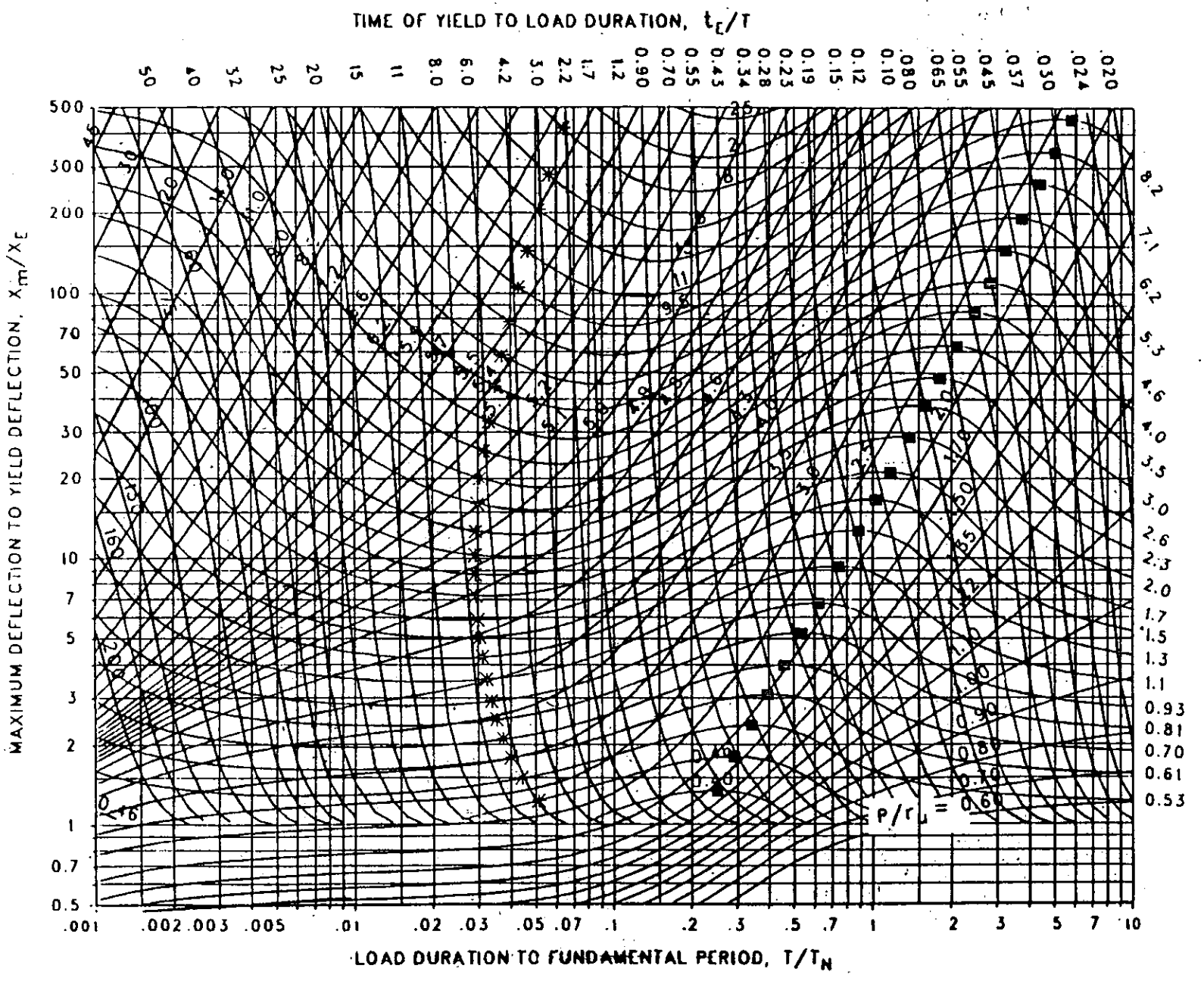


Figure 3-245 Maximum response of elasto-plastic, one-degree-of-freedom system for bilinear-triangular pulse (C_1 = 0.198, C_2 = 1000.)

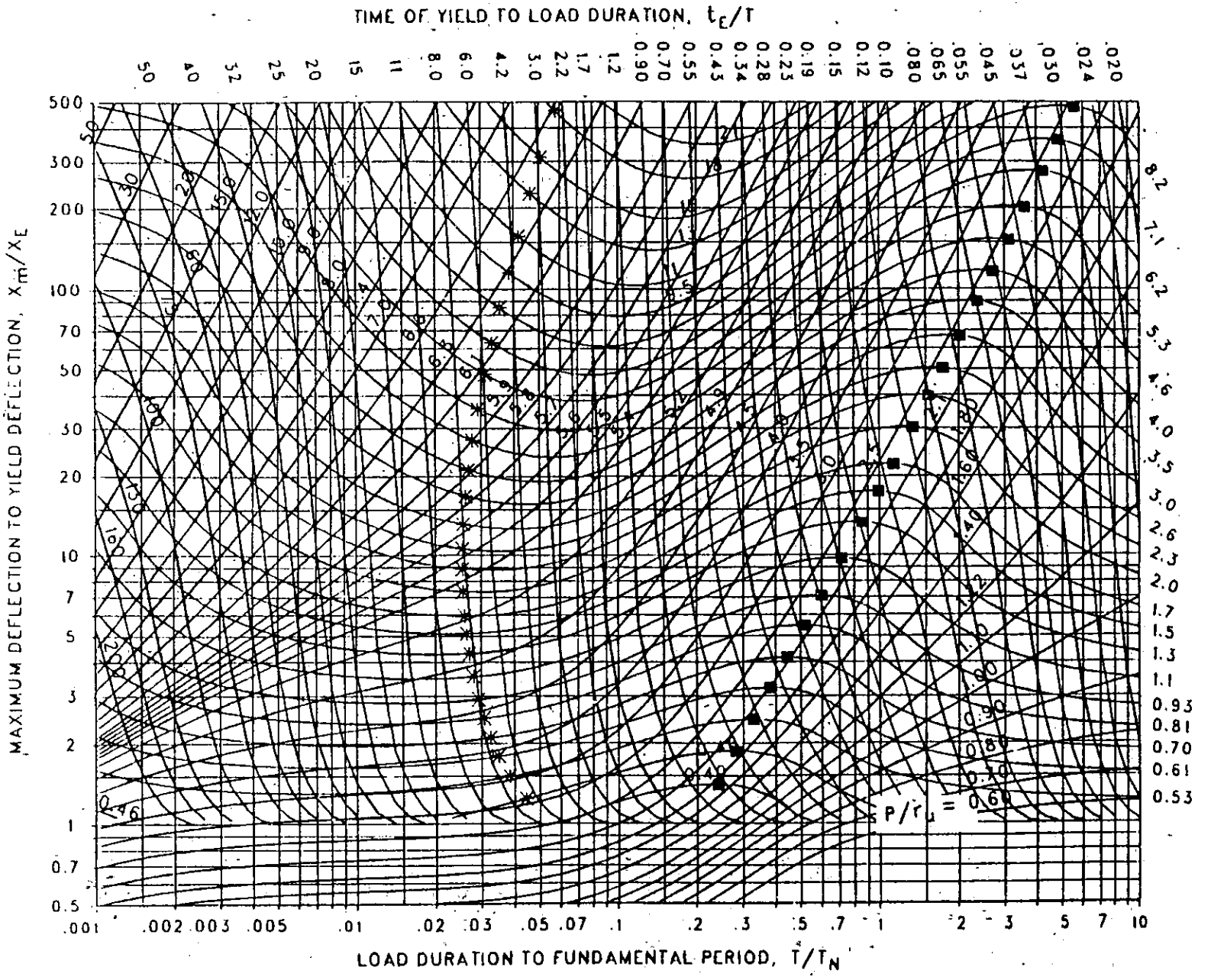


Figure 3-246 Maximum response of elasto-plastic, one-degree-of-freedom system for bilinear-triangular pulse ($C_1 = 0.178$, $C_2 = 1000.$)

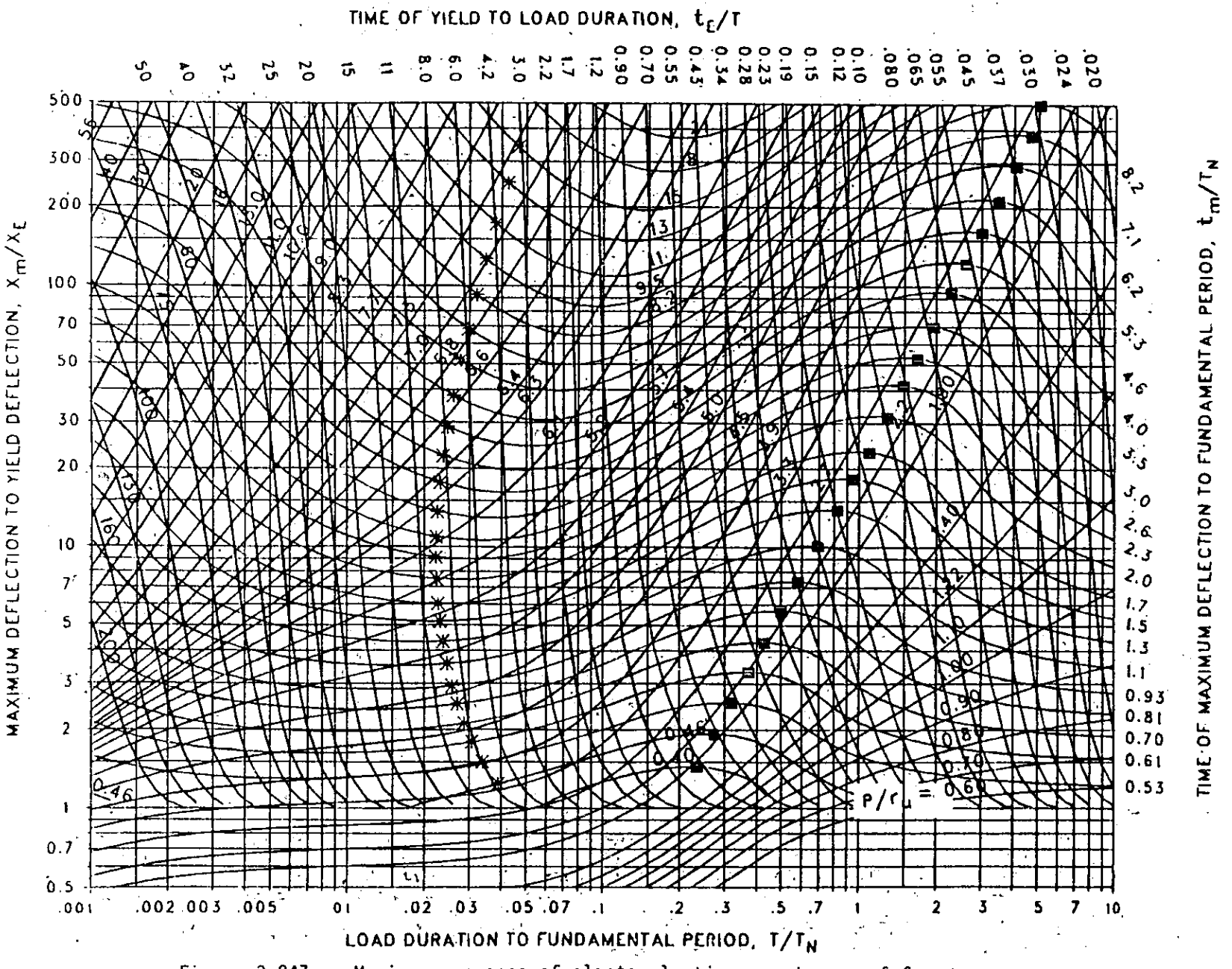


Figure 3-247 Maximum response of elasto-plastic, one-degree-of-freedom system for bilinear-triangular pulse (C_1 = 0.162, C_2 = 1000.)

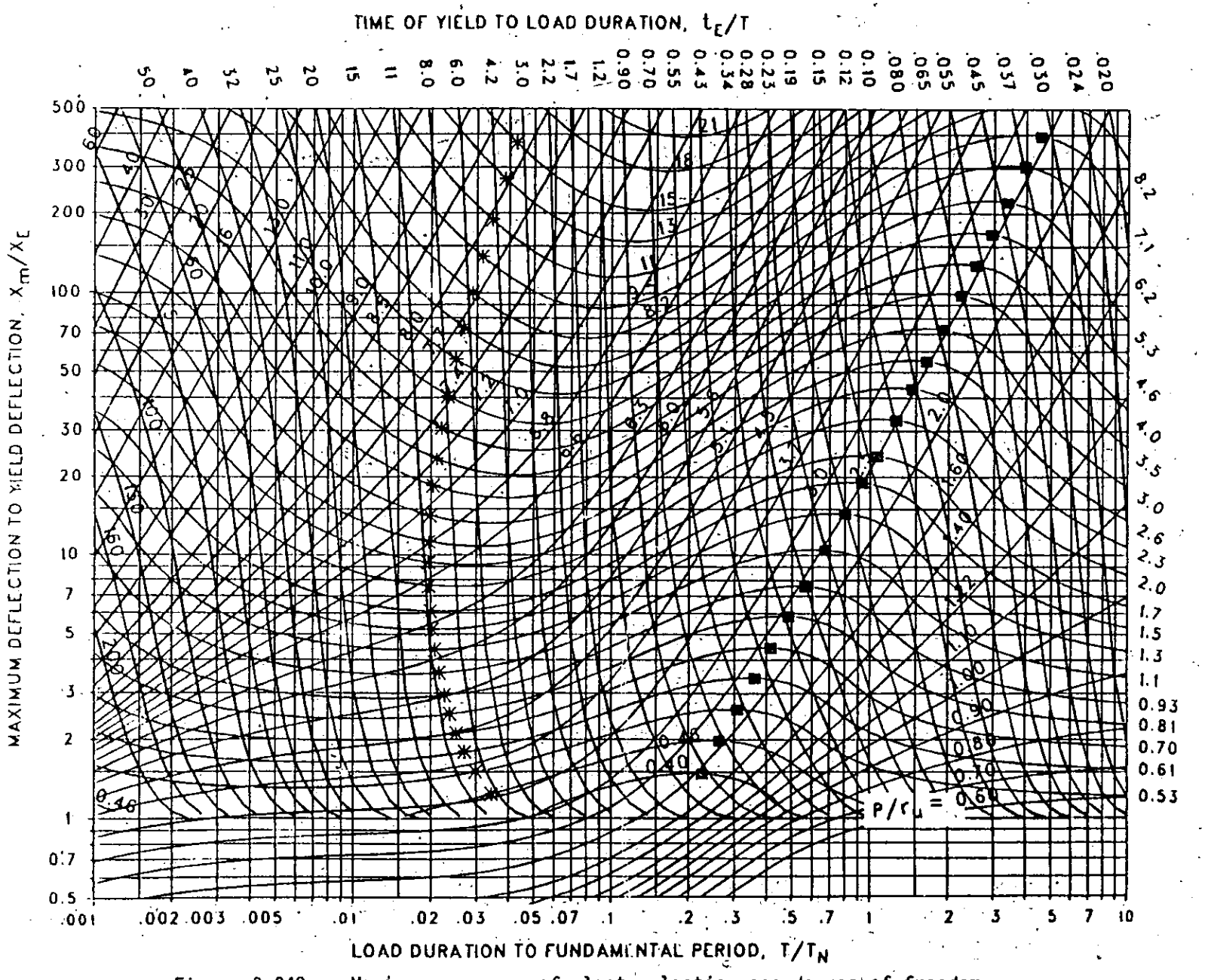


Figure 3-248 Maximum response of elasto-plastic, one-degree-of-freedom system for bilinear-triangular pulse ($C_1 = 0.147$, $C_2 = 1000.$)

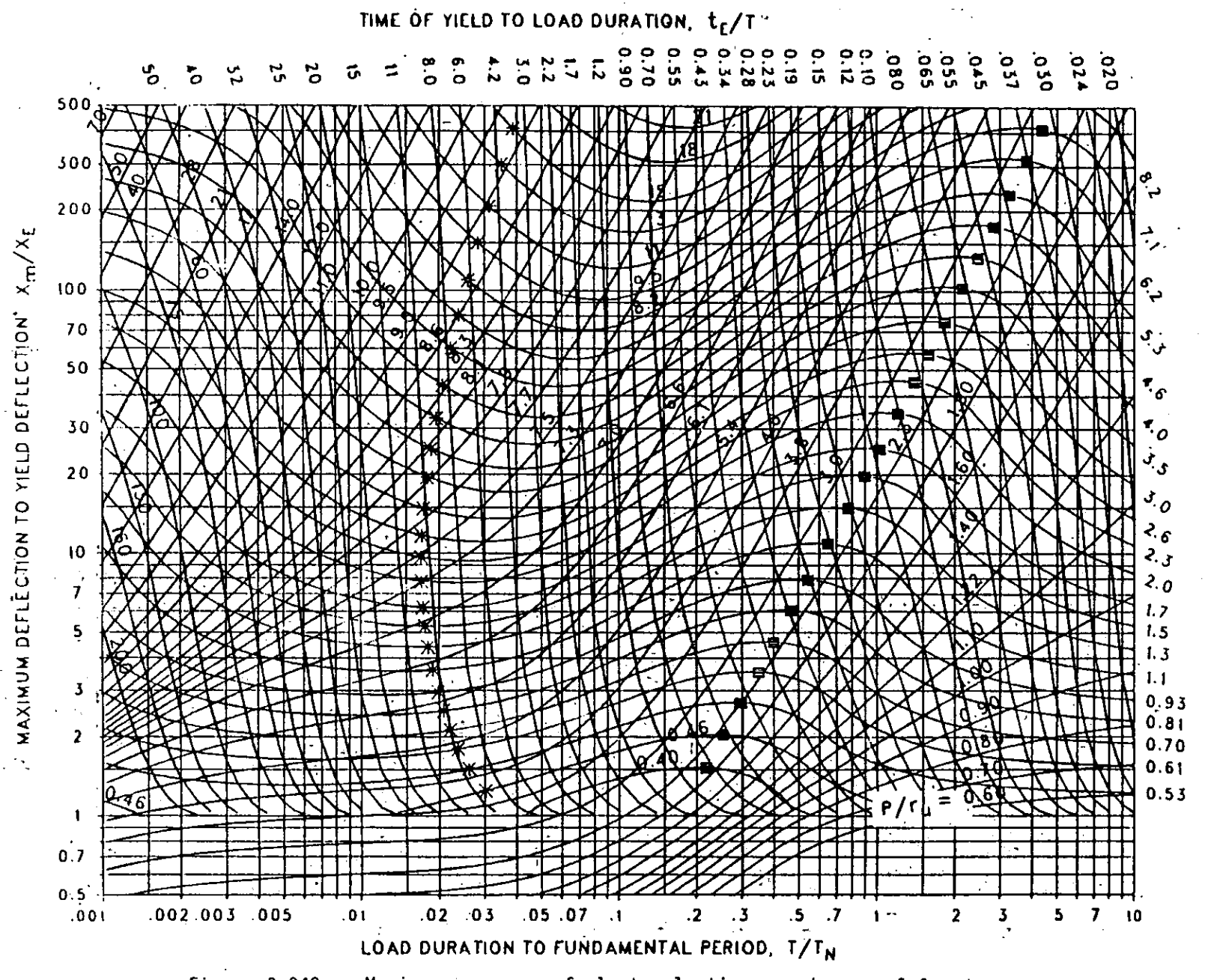


Figure 3-249 Maximum response of elasto-plastic, one-degree-of-freedom system for bilinear-triangular pulse ($C_1 = 0.133$, $C_2 = 1000.$)

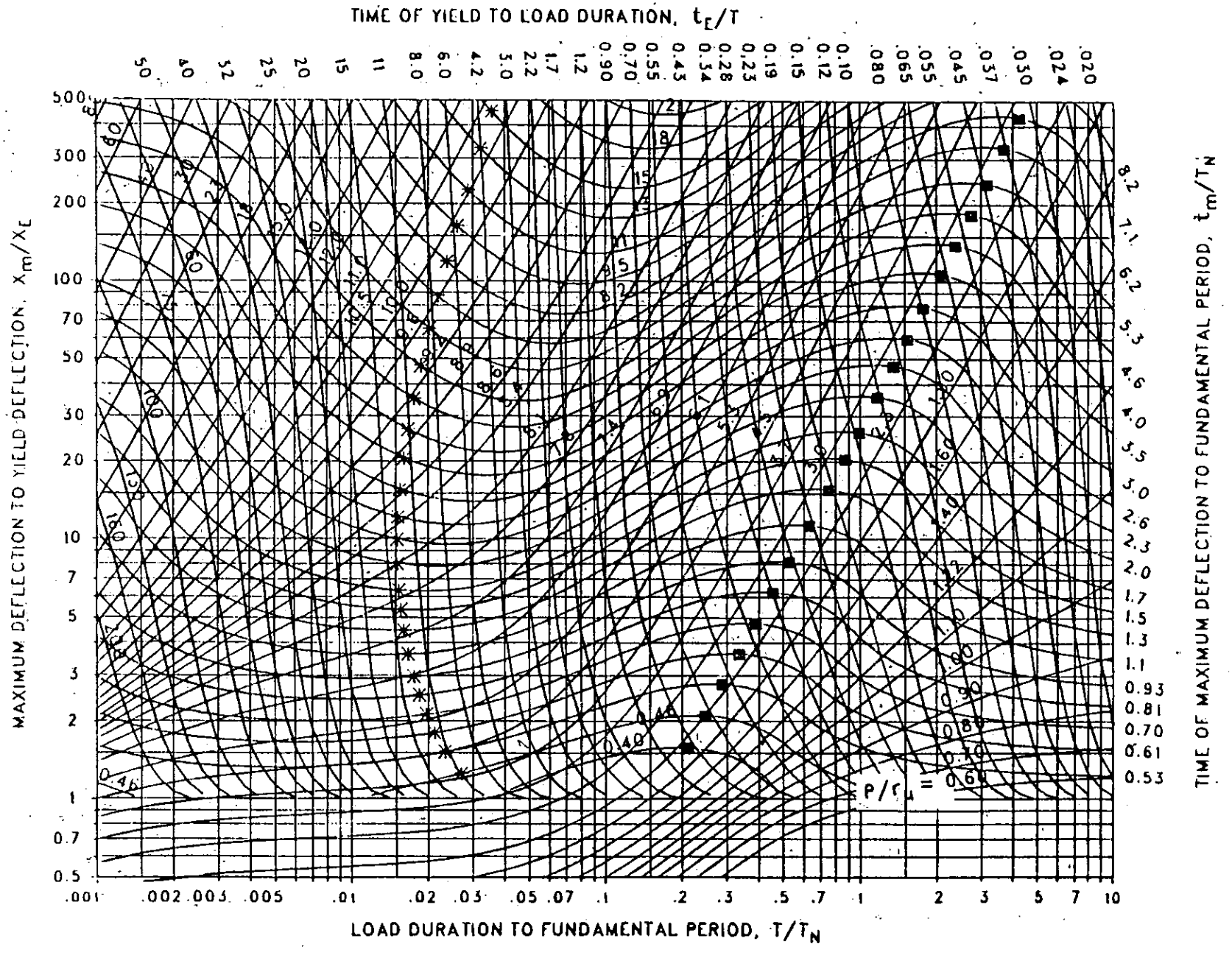


Figure 3-250 Maximum response of elasto-plastic, one-degree-of-freedom system for bilinear-triangular pulse ($C_1 = 0.121$, $C_2 = 1000.$)

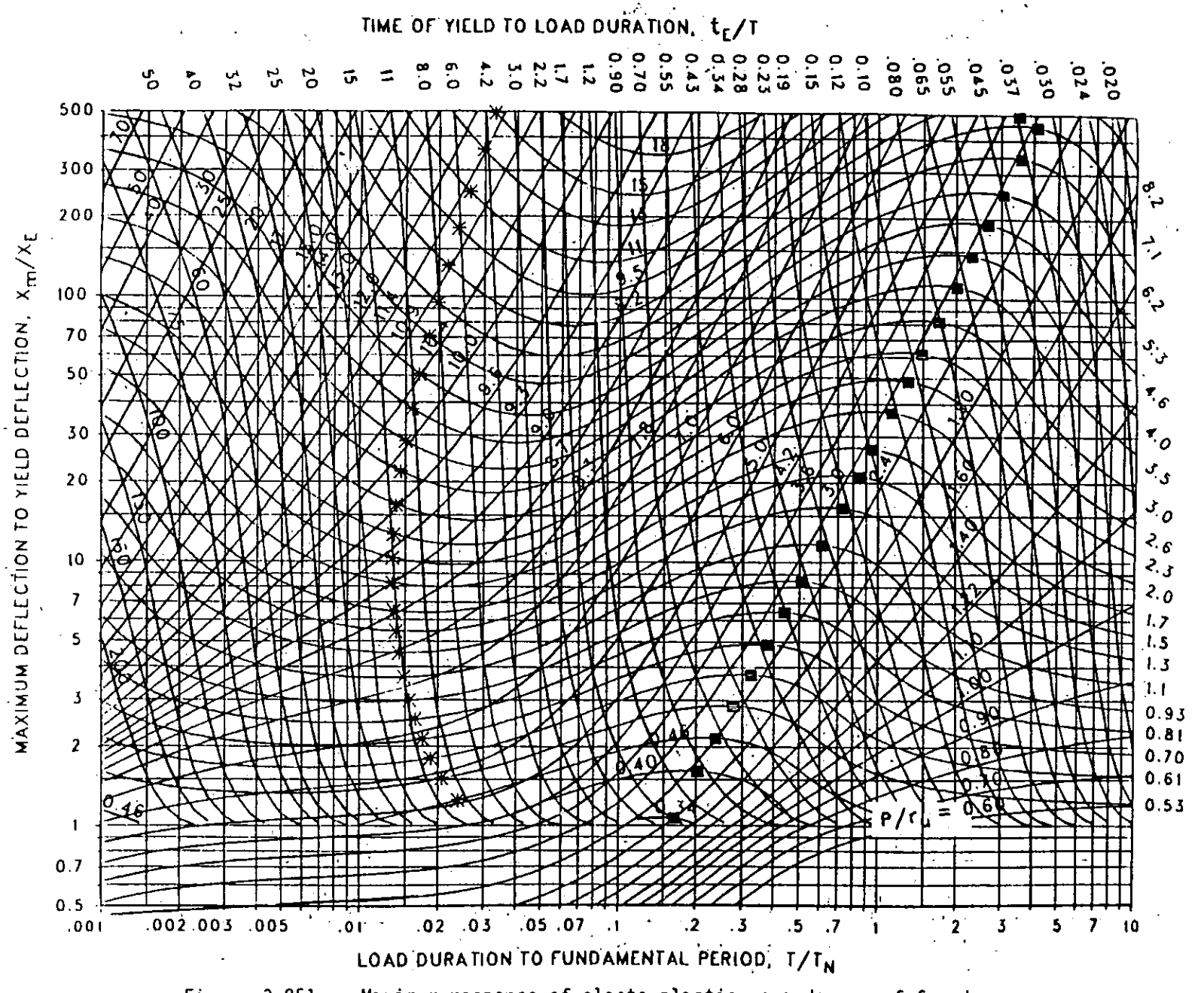


Figure 3-251 Maximum response of elasto-plastic, one-degree-of-freedom system for bilinear-triangular pulse ($C_1 = 0.110$, $C_2 = 1000.$)

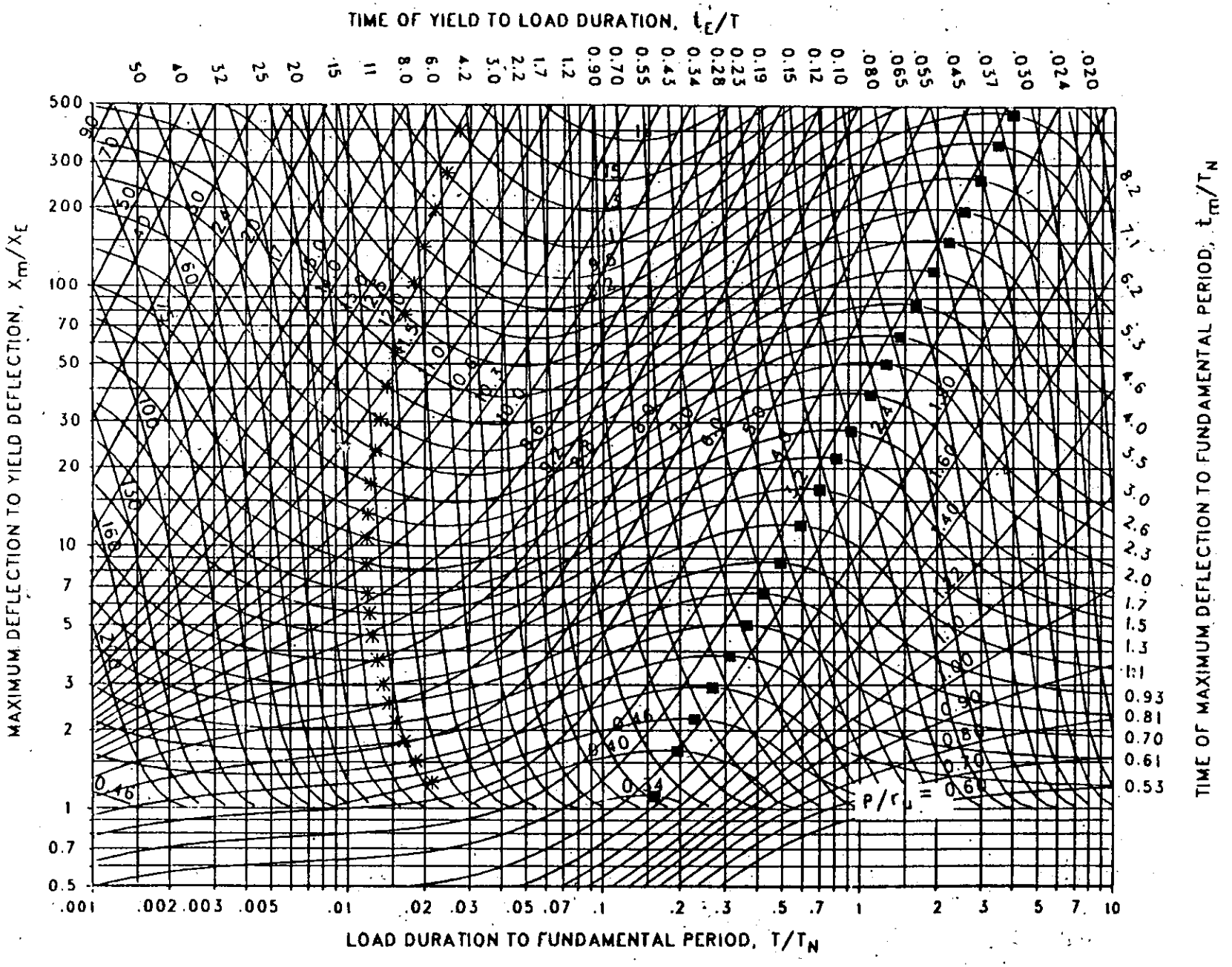


Figure 3-252 Maximum response of elasto-plastic, one-degree-of-freedom system for bilinear-triangular pulse (C_1 = 0.100, C_2 = 1000.)

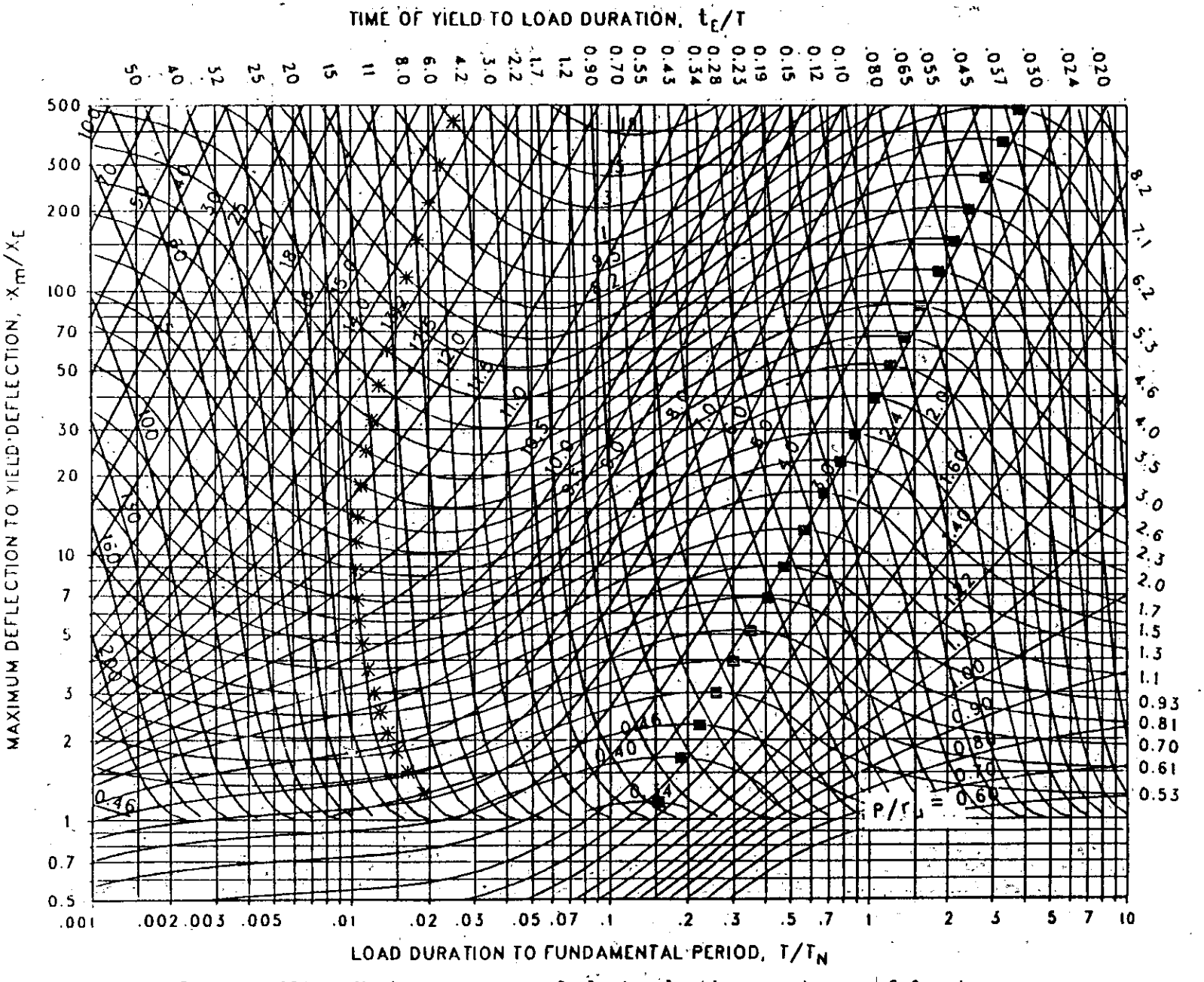


Figure 3-253 Maximum response of elasto-plastic, one-degree-of-freedom system for bilinear-triangular pulse ($C_1 = 0.091$, $C_2 = 1000.$)

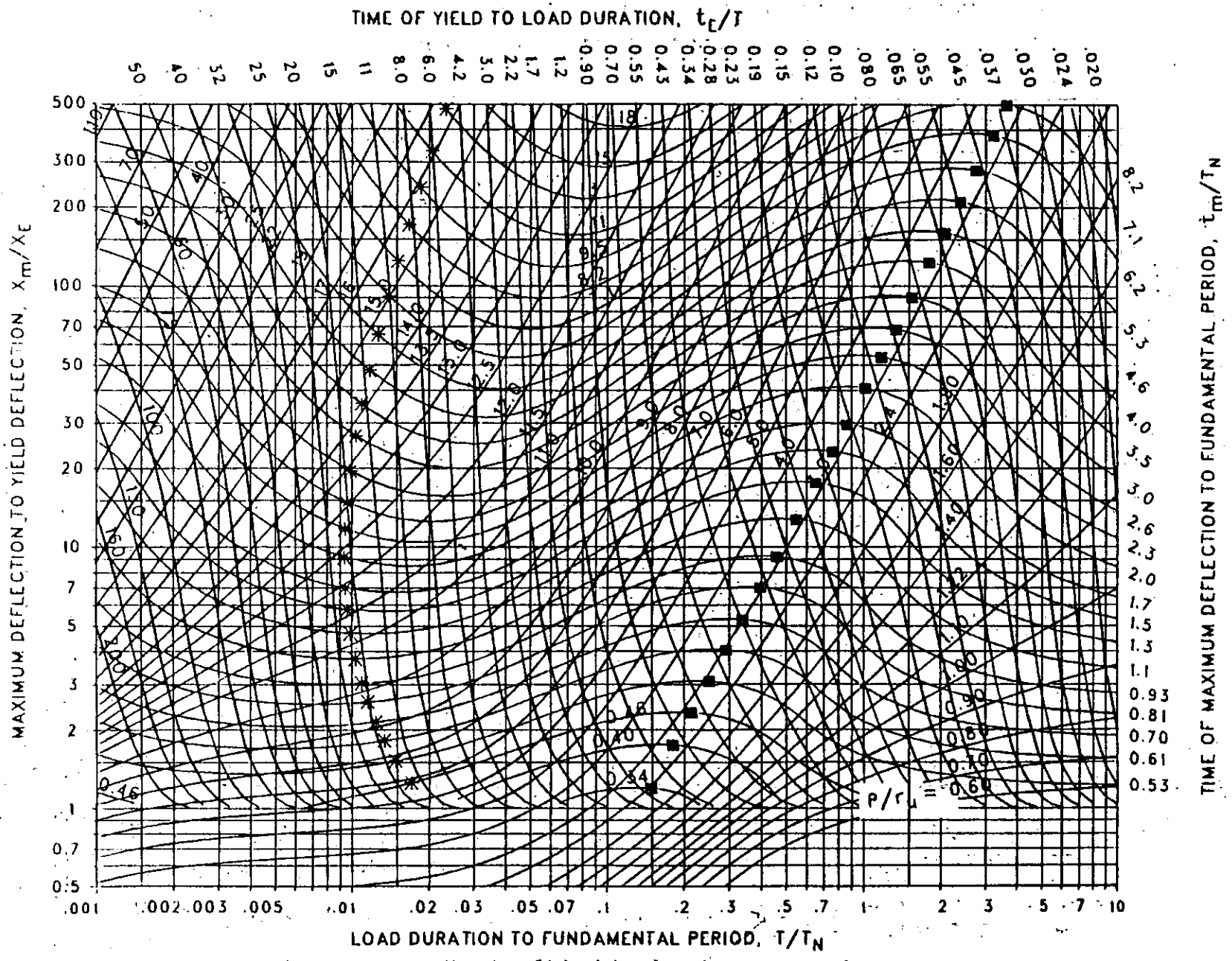


Figure 3-254 Maximum response of elasto-plastic, one-degree-of-freedom system for bilinear-triangular pulse ($C_1 = 0.083$, $C_2 = 1000.$)

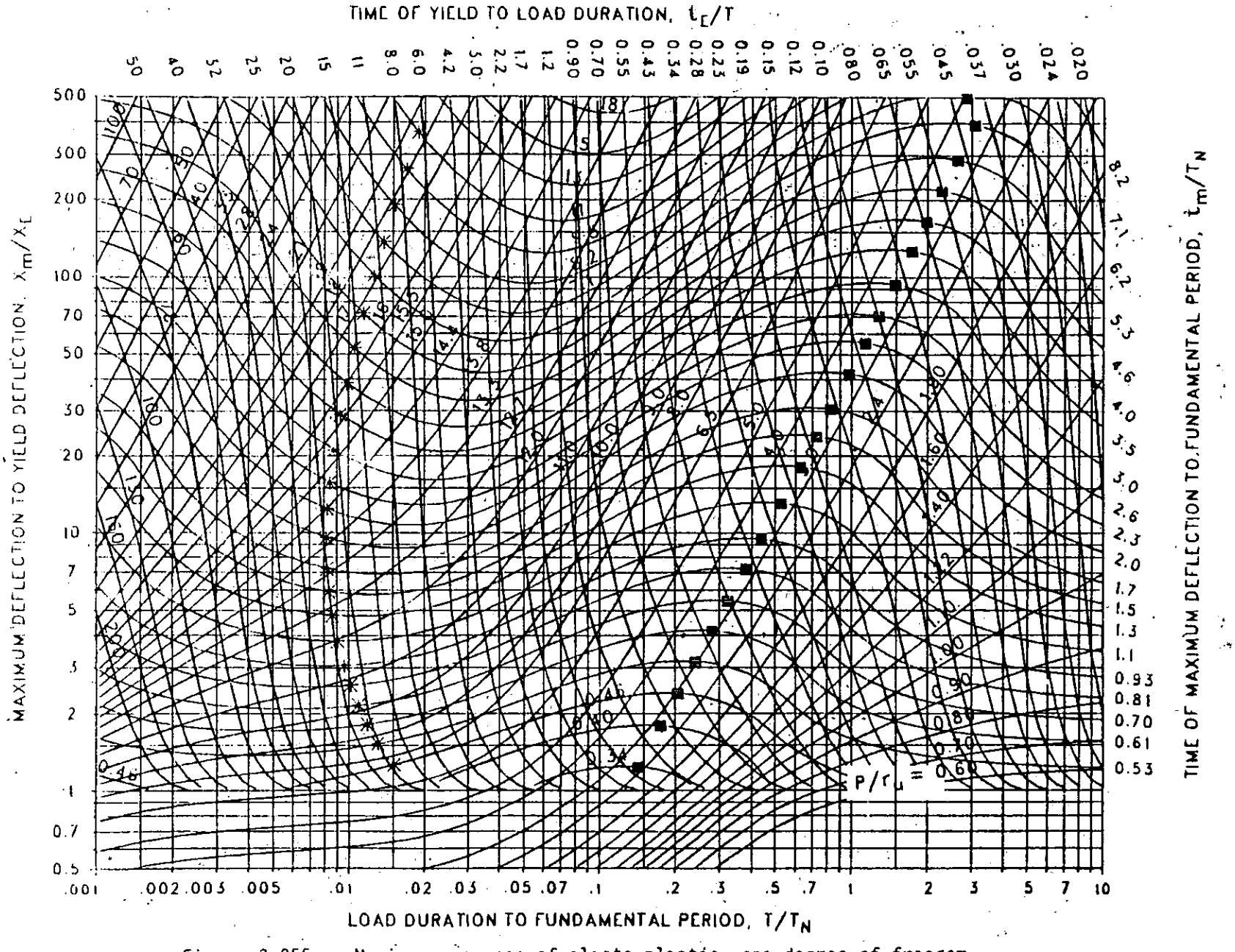


Figure 3-255 Maximum response of elasto-plastic, one-degree-of-freedom system for bilinear-triangular pulse (C_1 = 0.075, C_2 = 1000.)

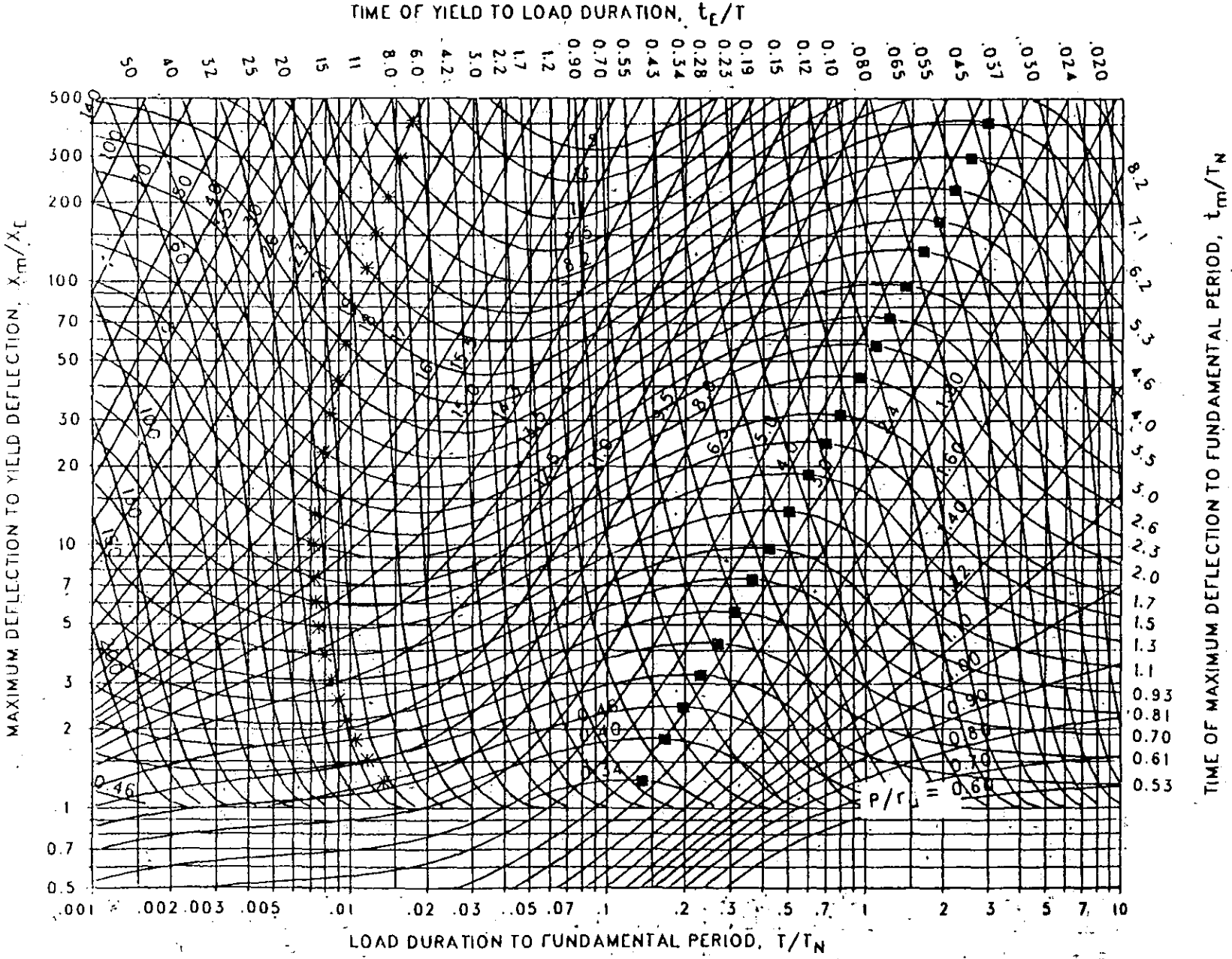


Figure 3-256 Maximum response of elasto-plastic, one-degree-of-freedom system for bilinear-triangular pulse ($C_1 = 0.068$, $C_2 = 1000.$)

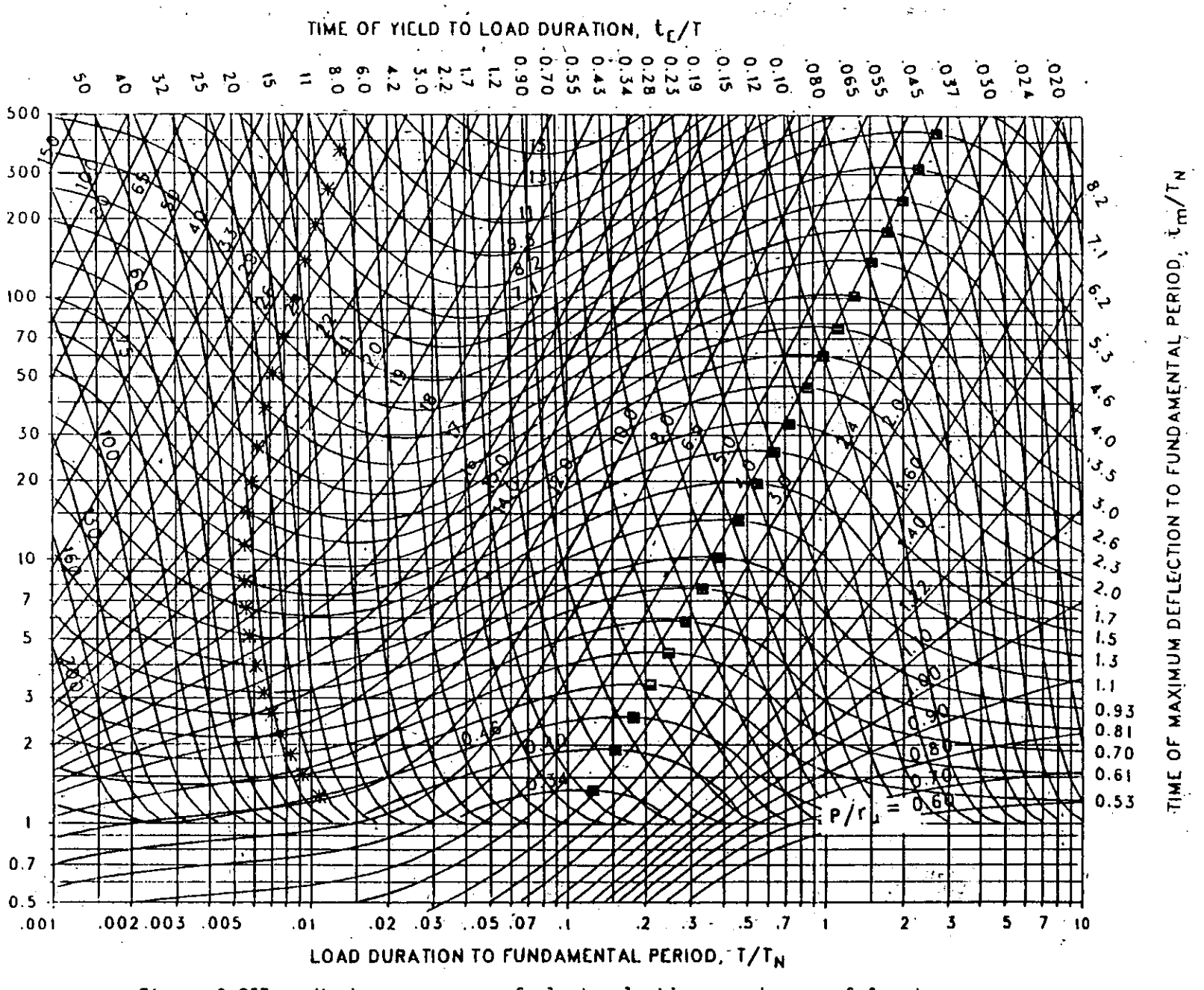


Figure 3-257 Maximum response of elasto-plastic, one-degree-of-freedom system for bilinear-triangular pulse ($C_1 = 0.056$, $C_2 = 1000$.)

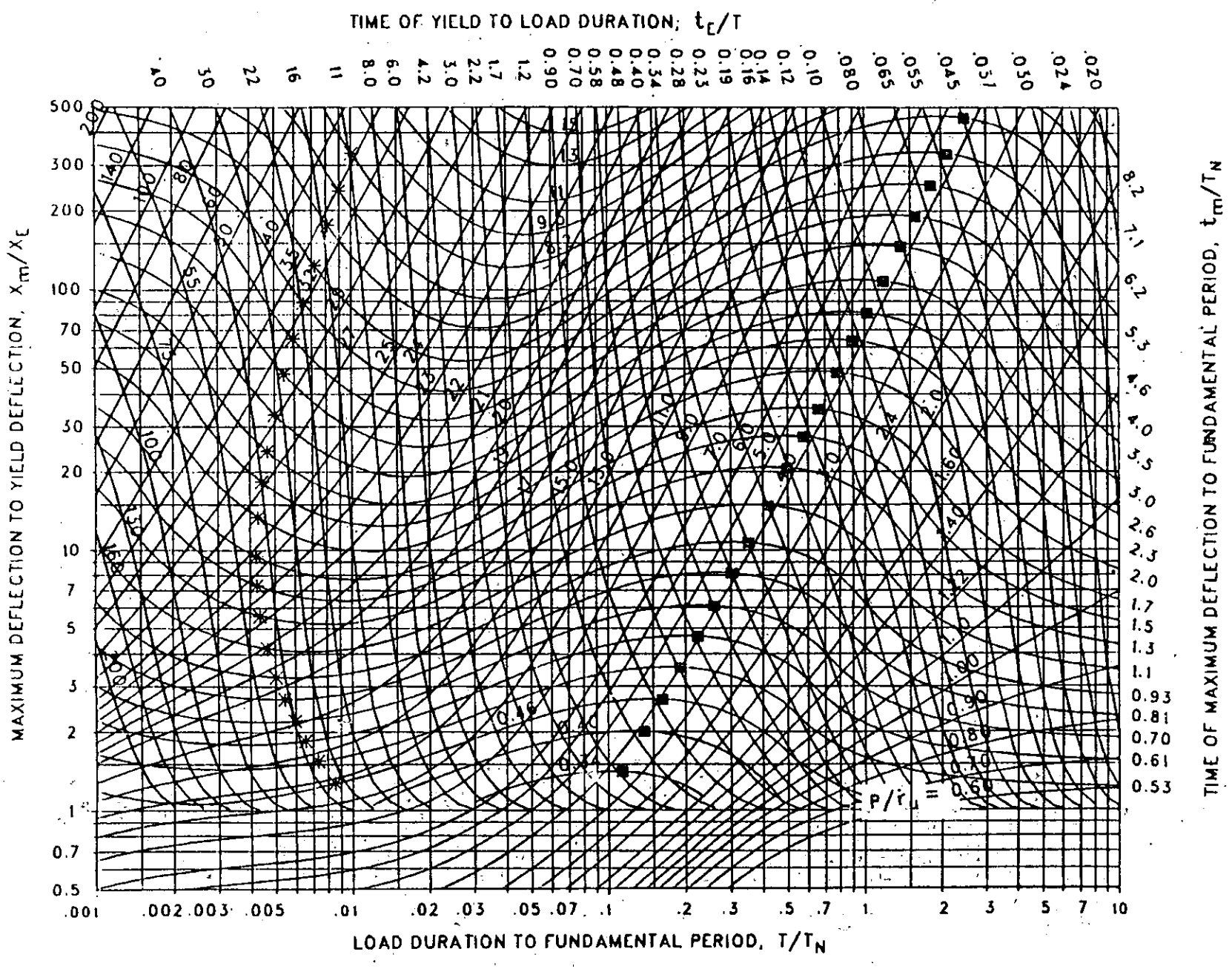


Figure 3-258 Maximum response of elasto-plastic, one-degree-of-freedom system for bilinear-triangular pulse ($C_1 = 0.046$, $C_2 = 1000.$)

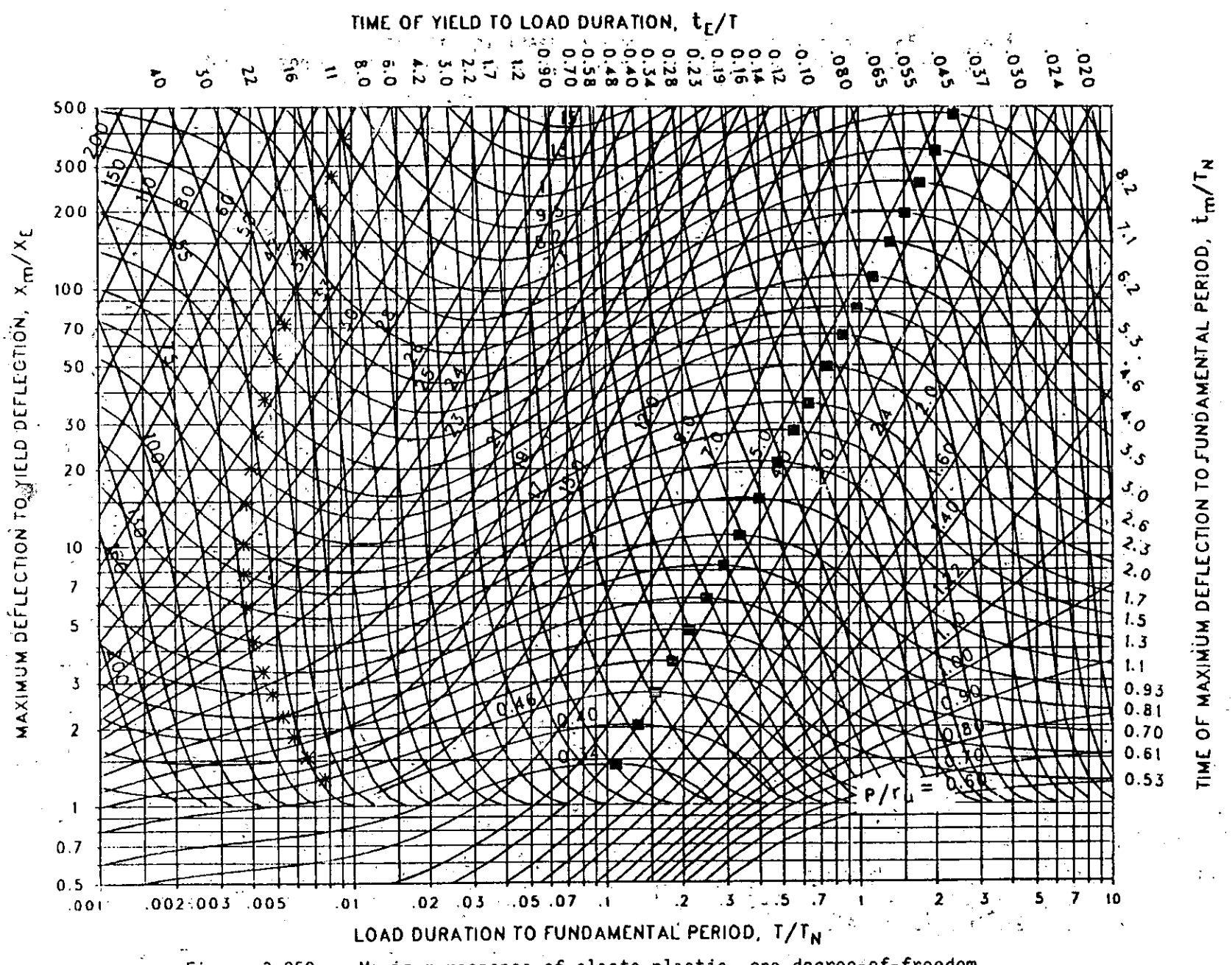


Figure 3-259 Maximum response of elasto-plastic, one-degree-of-freedom system for bilinear-triangular pulse (C_1 = 0.042, C_2 = 1000.)

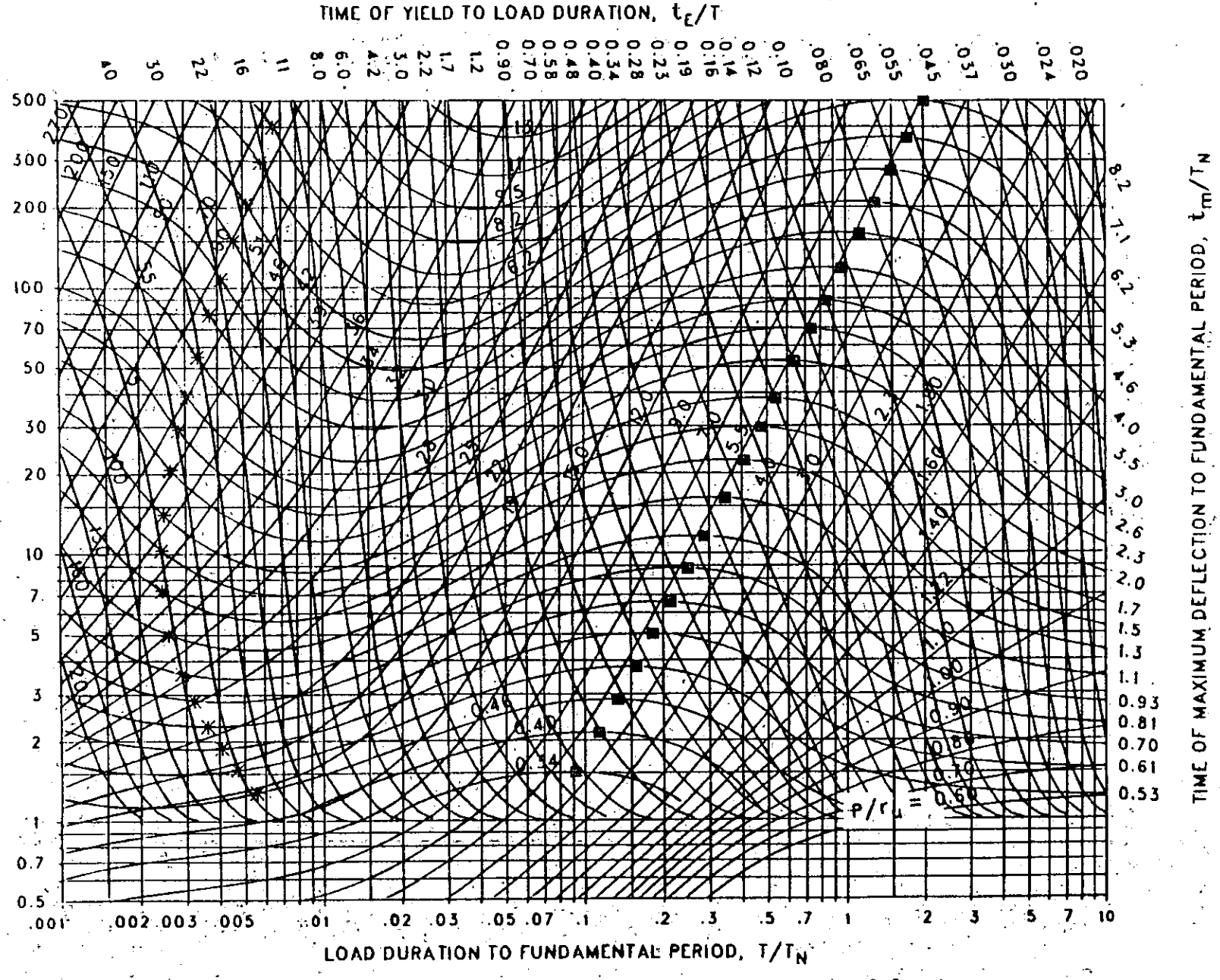


Figure 3-260 Maximum response of elasto-plastic, one-degree-of-freedom system for bilinear-triangular pulse ($C_1 = 0.032$, $C_2 = 1000.$)

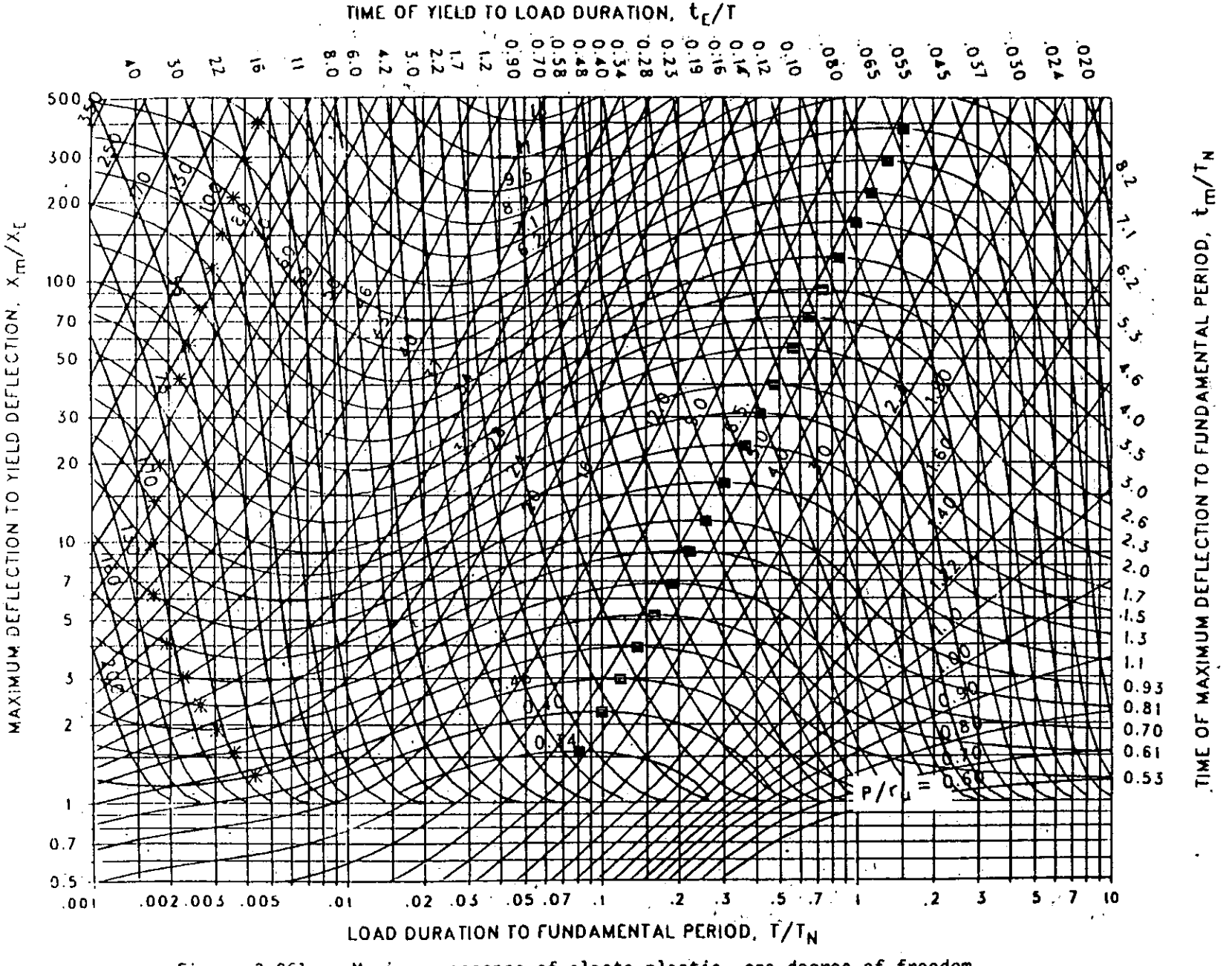


Figure 3-261 Maximum response of elasto-plastic, one-degree-of-freedom system for bilinear-triangular pulse ($C_1 = 0.026$, $C_2 = 1000.$)

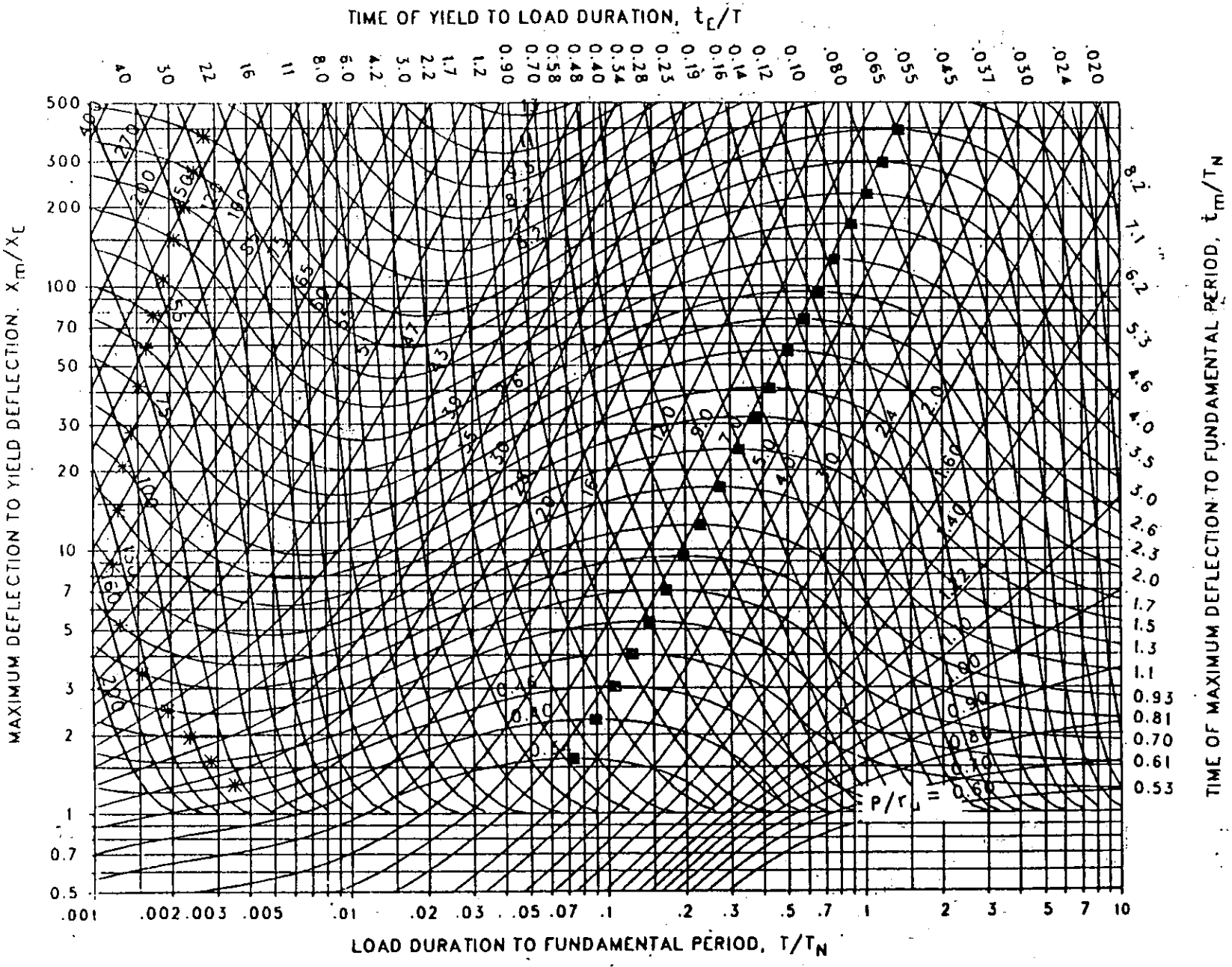


Figure 3-262 Maximum response of elasto-plastic, one-degree-of-freedom system for bilinear-triangular pulse (C_1 = 0.022, C_2 = 1000.)

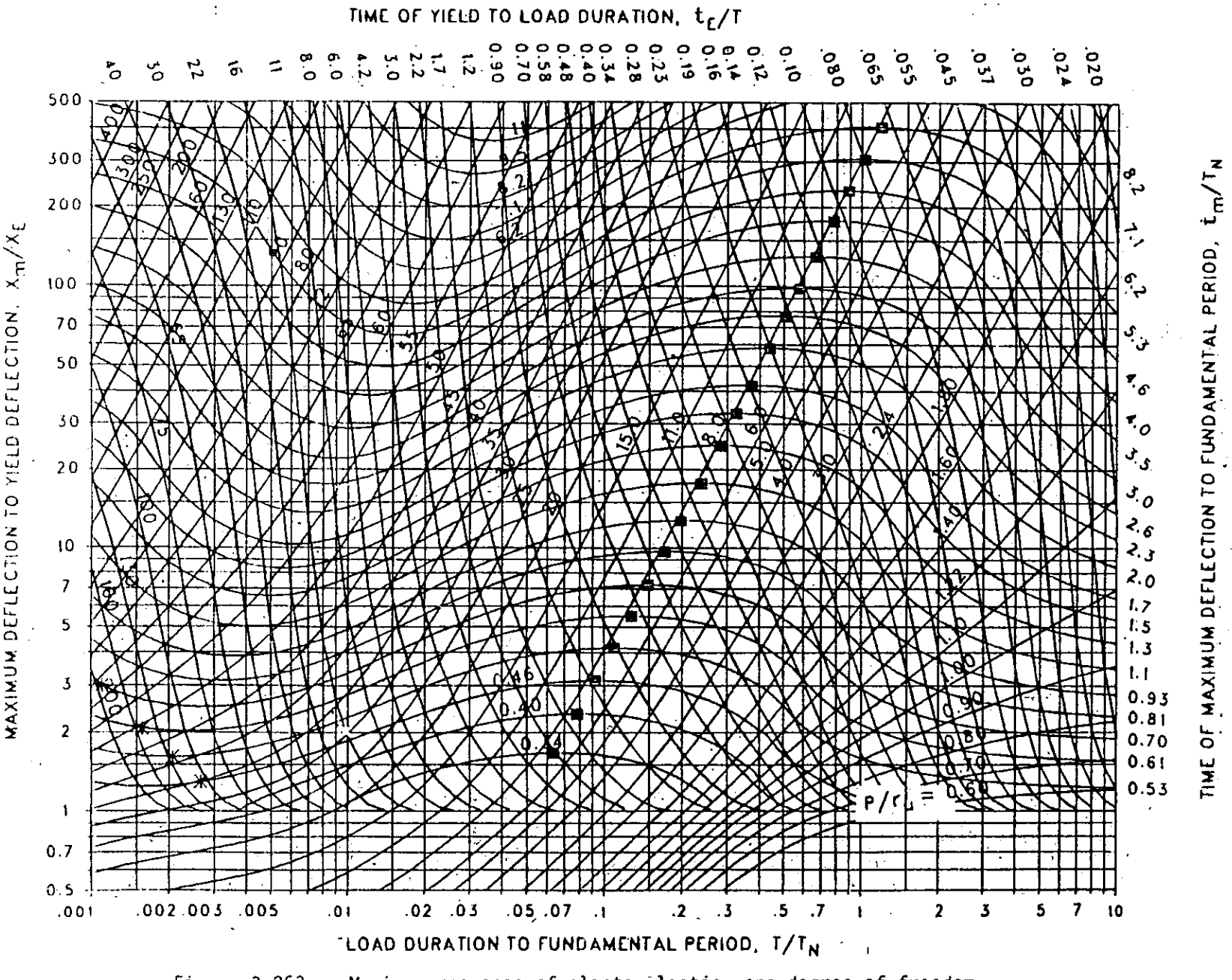


Figure 3-263 Maximum response of elasto-plastic, one-degree-of-freedom system for bilinear-triangular pulse (C_1 = 0.018, C_2 = 1000.)

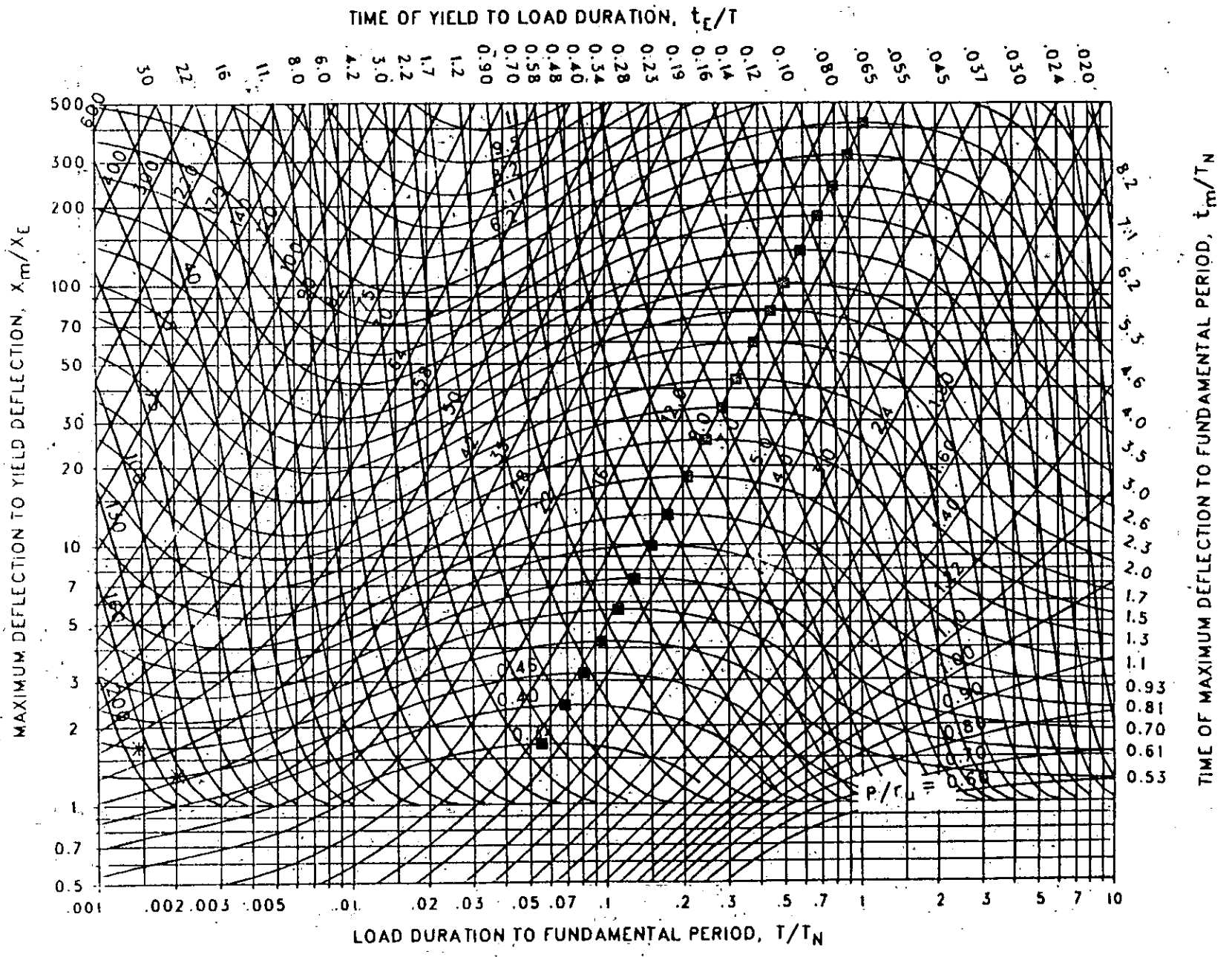


Figure 3-264 Maximum response of elasto-plastic, one-degree-of-freedom system for bilinear-triangular pulse (C_1 = 0.015, C_2 = 1000.)

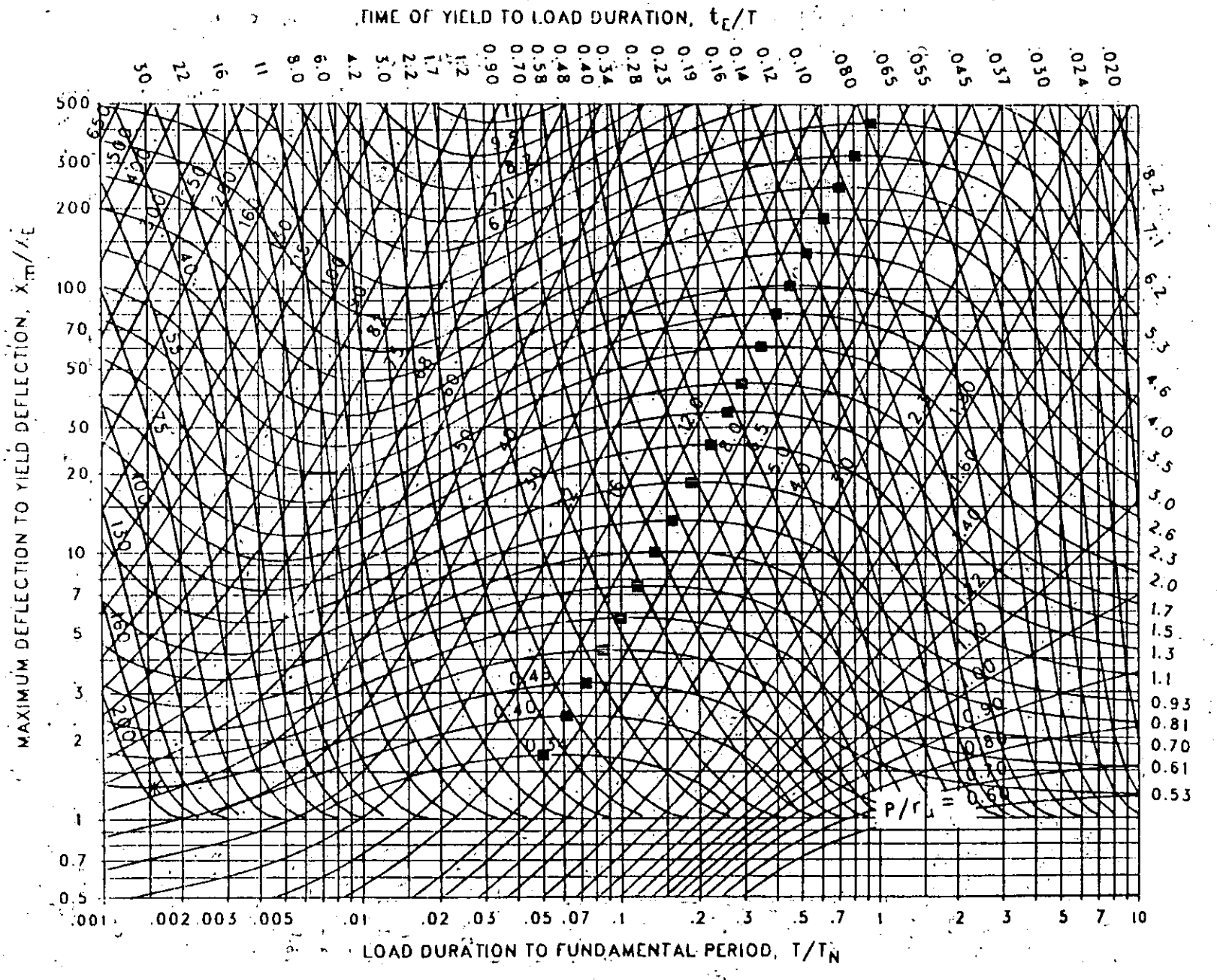


Figure 3-265 Maximum response of elasto-plastic, one-degree-of-freedom system for bilinear-triangular pulse (C_1 = 0.013, C_2 = 1000.)

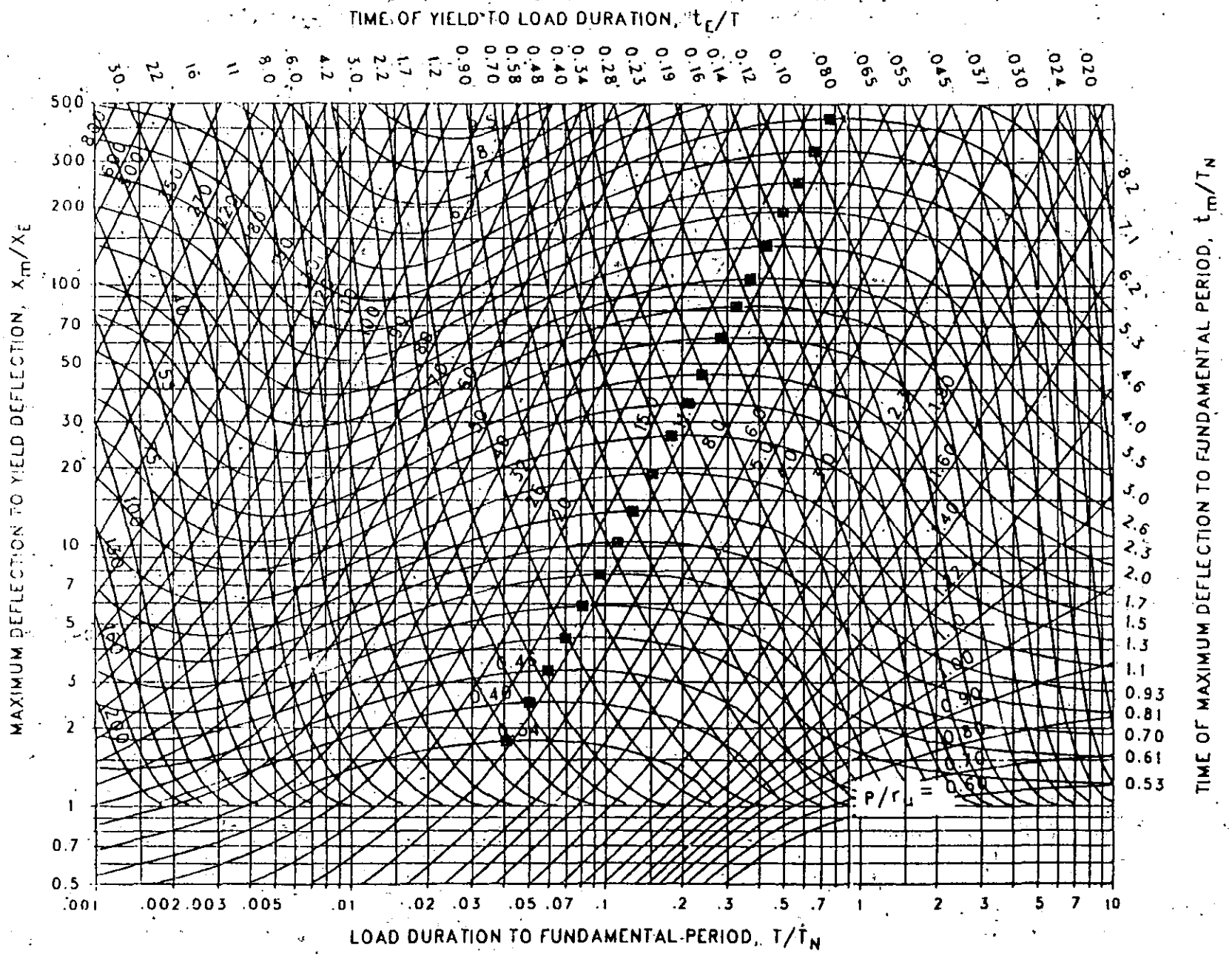


Figure 3-266 Maximum response of elasto-plastic, one-degree-of-freedom system for bilinear-triangular pulse (C_1 = 0.010, C_2 = 1000.)

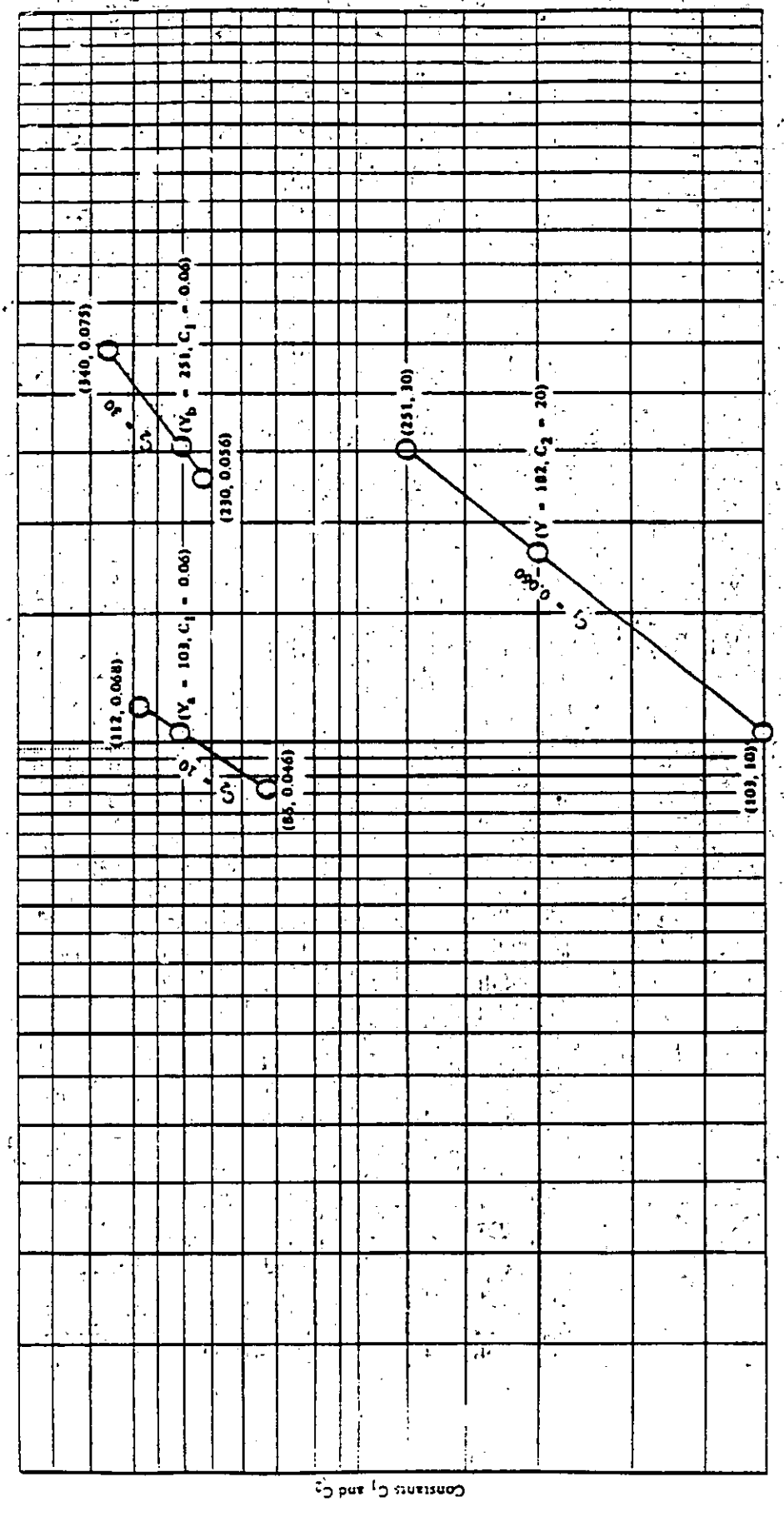


Figure 3-267 Graphical interpolation

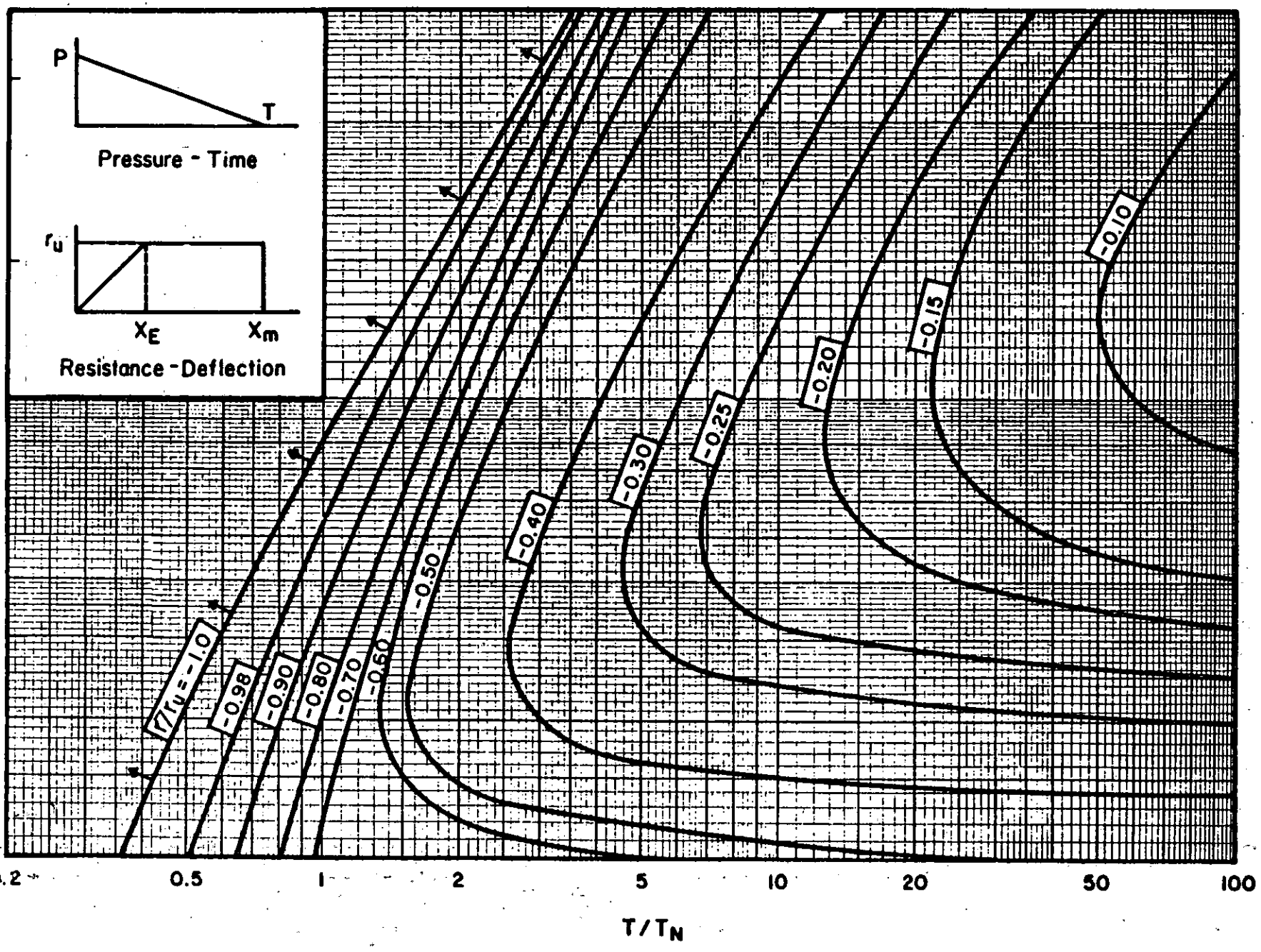


Figure 3-268 Elastic rebound of simple spring-mass system

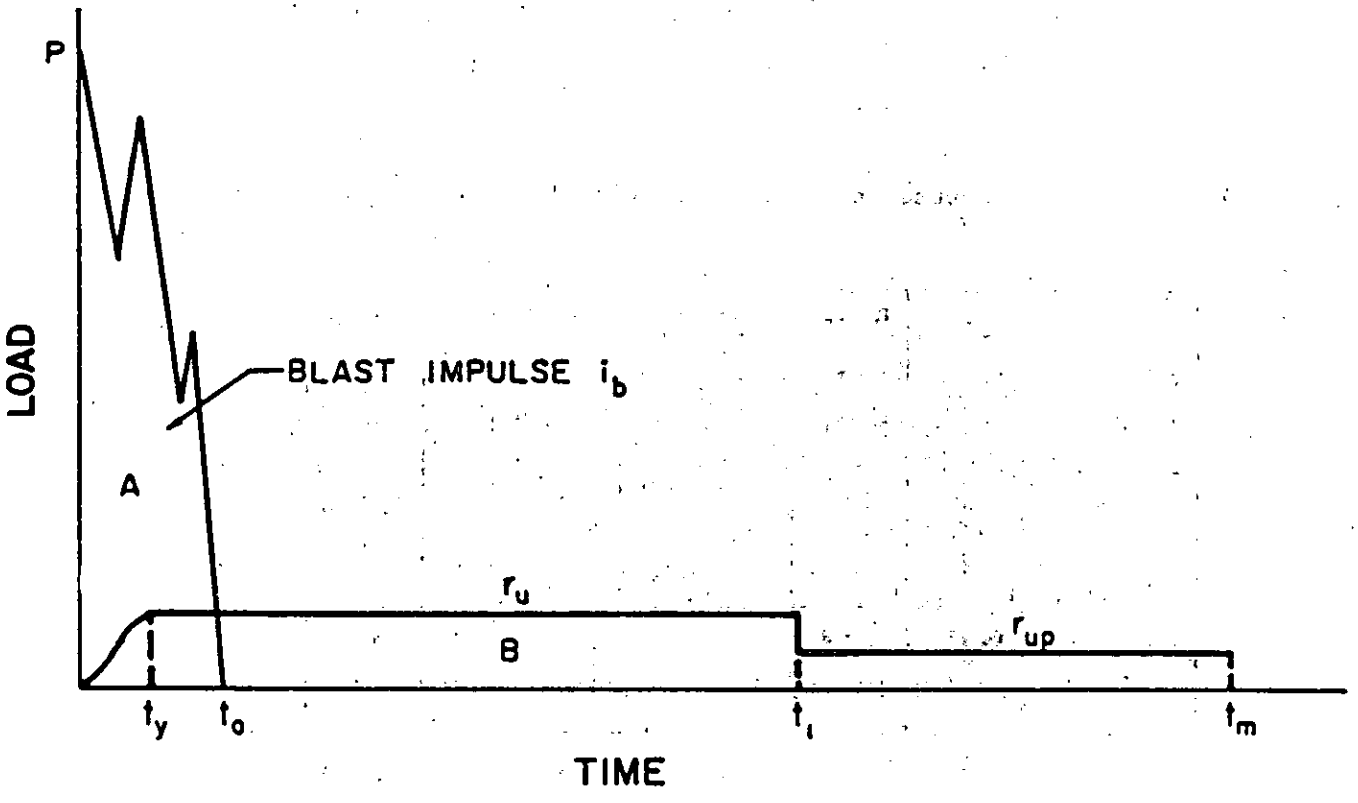


Figure 3-269 Pressure-time and resistance-time curves for elements which respond to impulse

Table 3-14 Details of computation by acceleration impulse extrapolation method

n	t	P_n	R_n	$P_n - R_n$	$a_n = (P_n - R_n)/m$	$a_n(\Delta t)^2$	$2X_n$	X_{n-1}	X_{n+1}
0	0	P_0	R_0	$P_0 - R_0$	a_0	$a_0(\Delta t_1)^2$	0	0	X_1
1	Δt_1	P_1	R_1	$P_1 - R_1$	a_1	$a_1(\Delta t_1)^2$	$2X_1$	0	X_2
2	$2(\Delta t_1)$	P_2	R_2	$P_2 - R_2$	a_2	$a_2(\Delta t_1)^2$	$2X_2$	X_1	X_3
.									
.									
j-1	$(j-1)\Delta t_1$	P_{j-1}	R_{j-1}	$P_{j-1} - R_{j-1}$	a_{j-1}	$a_{j-1}(\Delta t_1)^2$	$2X_{j-1}$	X_{j-2}	X_j
j	$j\Delta t_1$	P_j	R_j	$P_j - R_j$	a_j	$a_j(\Delta t_1)^2$	$2X_j$	X_{j-1}	X_{j+1}
j+1	$j(\Delta t_1) + \Delta t_2$	P_{j+1}	R_{j+1}	$P_{j+1} - R_{j+1}$	a_{j+1}	$a_{j+1}(\Delta t_1)^2$	$2X_{j+1}$	X_{j-1}	X_{j+2}

Table 3-15 Figure numbers corresponding to various combinations of C_1 and C_2

C1 \ C2	1.00	1.70	3.00	5.50	10.0	30.0	100.	300	1000
1.000	3-64	3-64	3-64	3-64	3-64	3-64	3-64	3-64	3-64
0.909						3-114	3-141	3-173	3-220
0.866						3-115	3-142	3-174	3-221
0.825						3-116	3-143	3-175	3-222
0.787							3-144	3-176	3-223
0.750				3-85	3-99	3-117	3-145	3-177	3-224
0.715						3-118	3-146	3-178	3-225
0.681	3-64	3-65	3-75			3-119	3-147	3-179	3-226
0.648					3-100	3-120	3-148	3-180	3-227
0.619						3-121	3-149	3-181	3-228
0.590							3-150	3-182	3-229
0.562				3-86	3-101	3-122	3-151	3-183	3-230
0.536								3-184	3-231
0.511						3-123	3-152	3-185	3-232
0.487								3-186	3-233
0.464	3-64	3-66	3-76			3-124	3-153	3-187	3-234
0.422				3-87	3-102		3-154	3-188	3-235
0.383						3-125		3-189	3-236
0.365							3-155	3-190	3-237
0.348								3-191	3-238
0.316	3-64	3-67	3-77	3-88	3-103	3-126	3-156	3-192	3-239
0.287								3-193	3-240
0.274							3-157	3-194	3-241
0.261						3-127	3-158	3-195	3-242
0.237				3-89	3-104		3-159	3-196	3-243
0.215	3-64	3-68	3-78			3-128	3-160	3-197	3-244
0.198								3-198	3-245
0.178				3-90	3-105	3-129	3-161	3-199	3-246
0.162								3-200	3-247
0.147	3-64	3-69	3-79			3-130	3-162	3-201	3-248
0.133				3-91	3-106			3-202	3-249
0.121						3-131	3-163	3-203	3-250
0.110								3-204	3-251
0.100	3-64	3-70	3-80	3-92	3-107	3-132	3-164	3-205	3-252
0.091								3-206	3-253
0.083								3-207	3-254
0.075						3-133	3-165	3-208	3-255
0.068				3-93	3-108			3-209	3-256
0.056	3-64	3-71	3-81			3-134	3-166	3-210	3-257
0.046				3-94	3-109			3-211	3-258
0.042						3-135	3-167	3-212	3-259
0.032	3-64	3-72	3-82	3-95	3-110	3-136	3-168	3-213	3-260
0.026						3-137	3-169	3-214	3-261
0.022				3-96	3-111			3-215	3-262
0.018	3-64	3-73	3-83			3-138	3-170	3-216	3-263
0.015				3-97	3-112			3-217	3-264
0.013						3-139	3-171	3-218	3-265
0.010	3-64	3-74	3-84	3-98	3-113	3-140	3-172	3-219	3-266

Table 3-16 Response Chart Interpolation

Figure Number	C_1	C_2	Desired Parameter
1	C_{11}	C_{21}	Y_1
	C_1	C_{21}	
2	C_{12}	$C_{22} - C_{21}$	Y_2
	C_1	C_2	
			Y_a
3	C_{13}	C_{23}	Y_3
	C_1	C_{23}	
4	C_{14}	$C_{24} - C_{23}$	Y_4
			Y_b
			Y

APPENDIX 3A

ILLUSTRATIVE EXAMPLES

Problem 3A-1(A) Ultimate Unit Resistance

Problem: Determine the ultimate unit resistance of a two-way structural element using (1) general solution and (2) charts.

Procedure: Part (a) - General Solution

Step 1. Establish design parameters.

Step 2. Assume yield line locations in terms of x and/or y considering support conditions, presence of openings, etc.

Step 3. Determine negative and positive moment capacities of sections crossed by assumed yield lines.

Step 4. Establish distribution of moments across negative and assumed yield lines, considering corner effects and those of openings.

Step 5. Determine the ultimate unit resistance for each sector in terms of x and/or y considering free body diagram of the sectors (fig. 3-3). Summation of the moments about the axis of rotation (support) of the sector yields equation 3-3.

Step 6. Equate the ultimate unit resistance of the sectors and solve for the yield line location x and/or y.

Step 7. With known yield line location, solve for ultimate unit resistance of the element, using equations obtained in Step 6.

Note: For complex problems (three or more different sectors) the solution for the ultimate unit resistance is most easily accomplished through a trial-and-error procedure by determining r_u for each sector for a given (assumed) yield line location and adjusting the yield lines until the several values of r_u agree to within a few percent.

Procedure: Part (b) - Chart Solution

Step 1. Same as in step 1 of part a.

Step 2. Same as in step 2 of part a.

Step 3. Determine the negative and positive ultimate moment capacities in vertical and horizontal directions.

Step 4. For given support conditions (and value of x_2/x_1 in the case of an element with three edges supported and fourth free), use the appropriate chart (figs. 3-4 through 3-20) to obtain yield line location ratios x/L or y/H for value of quantity obtained in step 4.. Then calculate x or y.

Step 5. Using the appropriate equation from table 3-2, determine the ultimate unit resistance of the element.

Example 3A-1 Ultimate Resistance

Required: Ultimate unit resistance of two-way structural steel element shown below using (1) general solution and (2) charts.

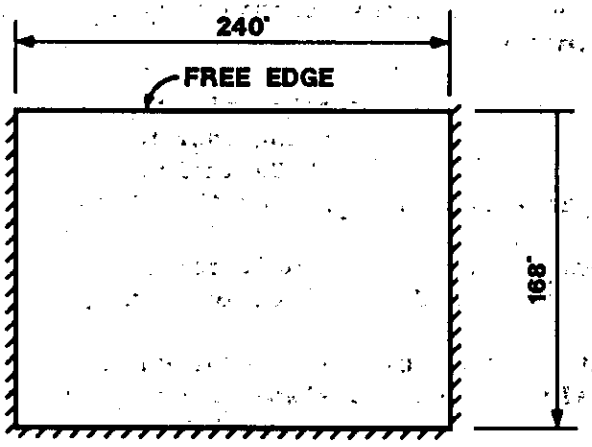


Figure 3A-1

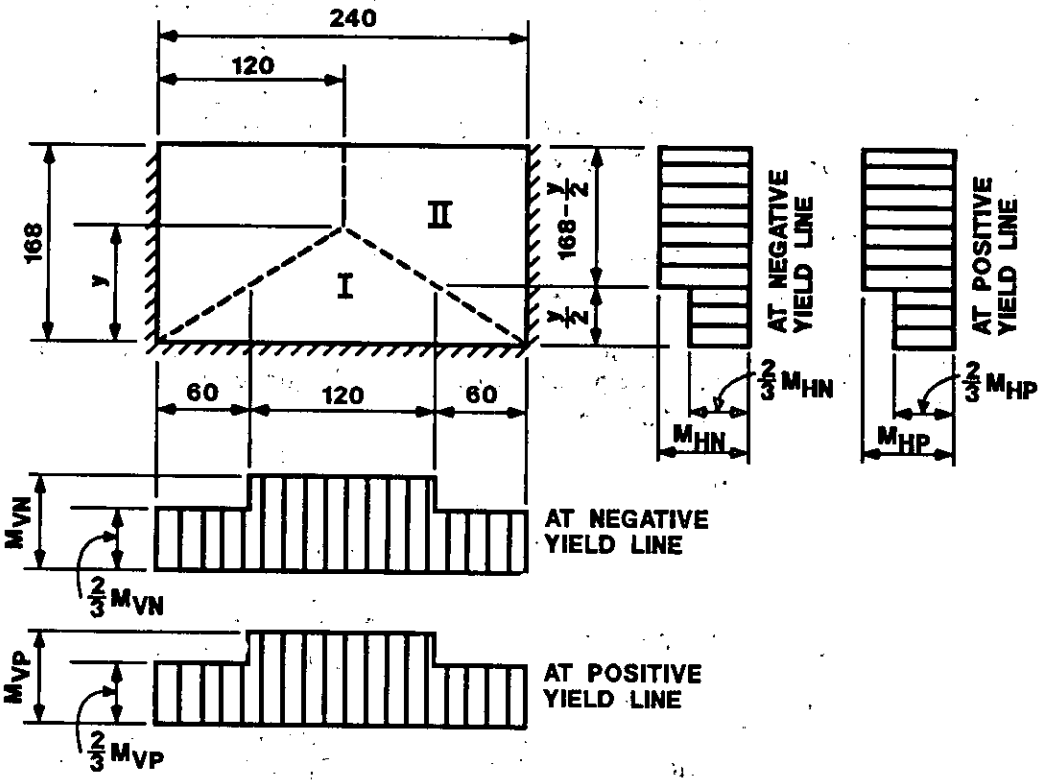
(Solution: Part (a) - General Solution)

Step 1. Given:

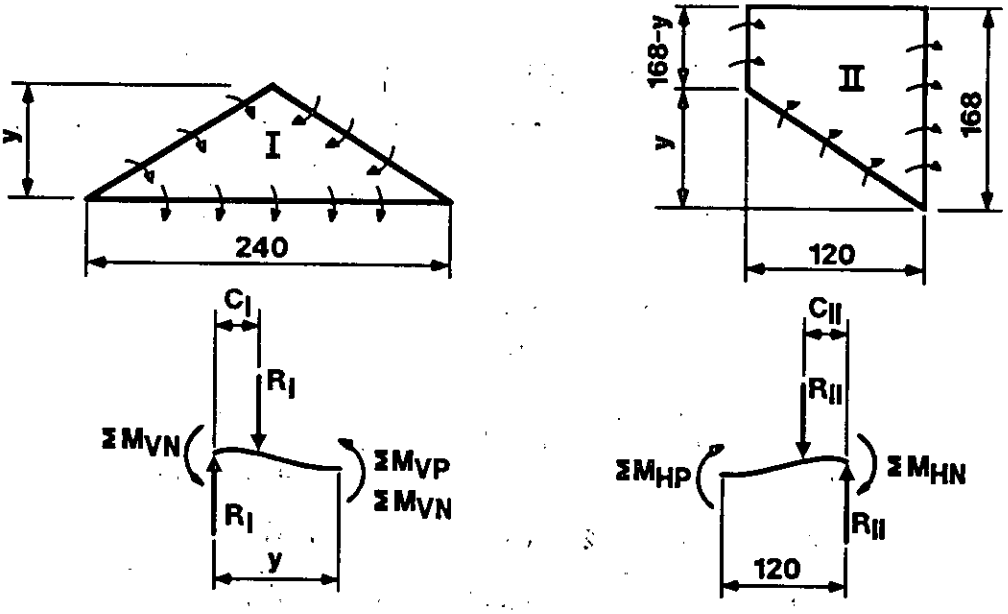
(a) L = 240 in H = 168 in
(b) Fixed on three sides and free at the fourth

Step 2. Assume yield line location (fig. 3A - 2)

Step 3. The negative and positive moment capacities in both the horizontal and vertical directions are determined from the properties of the material. For this example, it will be assumed that the moment capacities are equal to M = 20,000 inlbs/in.



a) ASSUMED YIELD LINES AND DISTRIBUTION OF MOMENTS



b) FREE-BODY DIAGRAMS FOR INDIVIDUAL SECTORS

Figure 3A-2

$M_{HN} = M_{HP} = M_{VN} = M_{VP} = 20{,}000$ in lbs/in.

Step 4. For distribution of moments across negative and assumed positive lines, see figure 3A - 2(a).

Step 5. The ultimate unit resistance of each sector is obtained by taking the summation of the moments about its axis of rotation (supports) so that

$$\Sigma M_N + \Sigma M_P = Rc = r_u Ac$$

a. Sector I (fig. 5A - 2)

$$\Sigma M_{VN} + \Sigma M_{VP} = 120(20{,}000) + 2(2/3)(20{,}000)(60) + 120(20{,}000) + 2(2/3)(20{,}000)(60) = 8.0\times10^6 \text{ in-lbs.}$$

$$r_u Ac = r_u \left[\frac{240(y)}{2}\right]\left[\frac{y}{3}\right] = 40\, r_u y^2$$

therefore,

$$r_u = 400(20{,}000)/40y^2 = 0.2\times10^6 / y^2$$

b. Sector II (fig. 3A - 2)

$$\Sigma M_{HN} + \Sigma M_{HP} = (168-y/2)(20{,}000) + 2/3(20{,}000)(y/2) + (20{,}000)(168-y/2) + 2/3(20{,}000)(y/2)$$

$$= 336(20{,}000) - y/3(20{,}000)$$

$$r_u Ac = r_u\left[\frac{120(168+168-y)}{2}\right]\left[\frac{120[168+2(168-y)}{3}\right] / (168+168-y)$$

$$= 4{,}800 r_u(252-y)$$

therefore,

$$r_u = \frac{336(20{,}000) - y/3(20{,}000)}{4800\,(252-y)}$$

Step 6. Equate the ultimate unit resistance of the sectors.

$$\frac{10(20{,}000)}{y^2} = \frac{336(20{,}000) - y/3(20{,}000)}{4800(252-y)}$$

Simplifying:

$$y^3 - 1008y^2 - 144000y + 36288000 = 0$$

and the desired root is: $y = 137.6$ ins.

Step 7. The ultimate unit resistance is obtained by substituting the value of y into either equation obtained in step 5, both of which yield:

$$r_u = (20,000)/(137.6)^2 = 10.6 \text{ psi}$$

Solution: Part (b) - Chart Solution

Note:

Element conforms to the requirements of section 3-8 since it is fixed on three sides and free on the remaining side and has uniform thickness in the horizontal and vertical directions.

Step 1. Same as step 1 in part a.

Step 2. For illustrative purposes, a different yield pattern (fig. 3A-3) will be assumed.

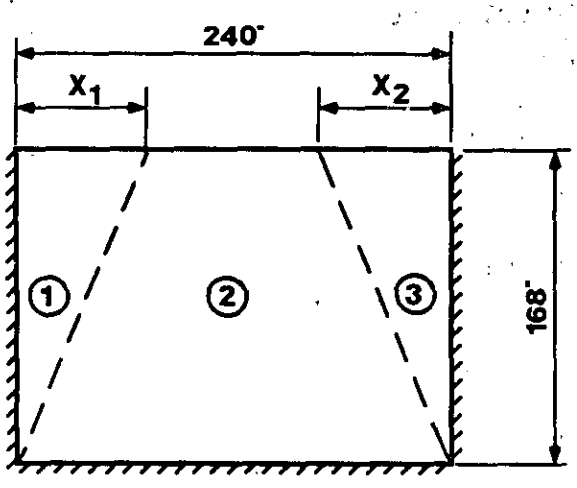


Figure 3A-3

Step 3. For ultimate moment capacities, see step 3 of part a

Step 4. For three sides fixed and the fourth free, calculate the parameter.

$$X_2/X_1=[(M_{HN3} + M_{HP})/(M_{HN1} + M_{HP})]^{1/2} = [(20,000)(2)/(20,000)(2)]^{1/2} = 1.0$$

From figure 3-11, $(X_2/X_1 = 1.0)$ calculate the parameters:

$$L/H[M_{VP}/(M_{HN1} + M_{HP})] = 240/168[20,000/(2)(20,000)]^{1/2} = 1.01$$

and

$$\frac{M_{VP}}{M_{VN2}} = \frac{20,000}{20,000} = 1.0$$

Read yield line location

X_1/L exceeds the maximum possible value of 0.5 therefore, assumed yield line pattern is wrong. Assume alternate yield line pattern as shown in figure 3A-2.

From figure 3-16 calculate the following parameters:

$$\frac{L}{H} = \frac{(M_{VN3} + M_{VP})^{1/2}}{(M_{HN2} + M_{HP})^{1/2} + (M_{HN1} + M_{HP})^{1/2}}$$

$$= \frac{240}{168}\left[\frac{(20,000+20,000)^{1/2}}{(20,000+20,000)^{1/2} + (20,000+20,000)^{1/2}}\right] = 0.71$$

and

$$X/L = \left[(M_{HN1} + M_{HP}) / (M_{HN2} + M_{HP})\right]^{1/2} / 1 + \left[M_{HN1} + M_{HP})/(M_{HN2} + M_{HP})\right]^{1/2}$$

$$= \left[40,000/40,000\right]^{1/2} / 1 + \left[40,000/40,000\right]^{1/2} = 1/2$$

from figure 3-16 read of yield line location:

$y/H = 0.82$; $y = 0.8(168) = 137.6$ in

$X/L = 0.50$; $X = 0.5(240) = 120.0$ in

Step 5. From table 3-2

NOTE: Both equations given in the table for each edge condition and yield line location, will provide identical values of r_u.

$$r_u = \frac{5(M_{VN} + M_{VP})}{y^2} = \frac{5(20,000+20,000)}{137.6^2} = (0.00055)20,000 = 10.5 \text{ psi}$$

Example 3A-1(B) Ultimate Unit Resistance

Required: Ultimate unit resistance of the element considered in example 3A-1(A) except there is an opening as shown in figure 3A-4.

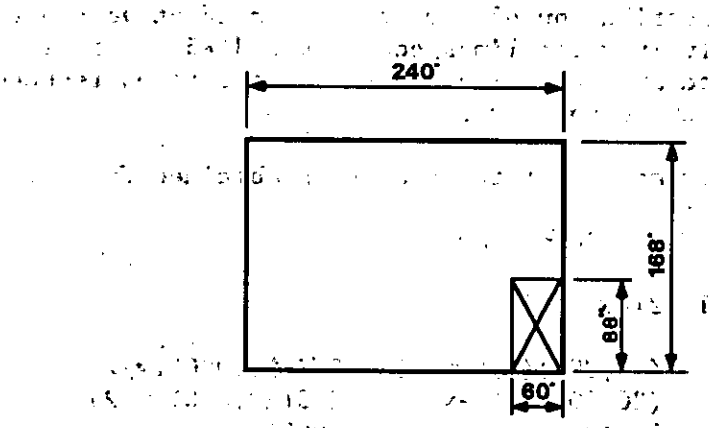


Figure 3A-4

Solution:

Step 1. Given:
(a) L = 240" H = 168" Two additional free edges are formed due to the presence of the opening.

Step 2. Assumed yield line location is shown in figrue 3A-5 (three different sectors are formed).

Step 3. Same as step 3 of Example 3A-1(A), part a.

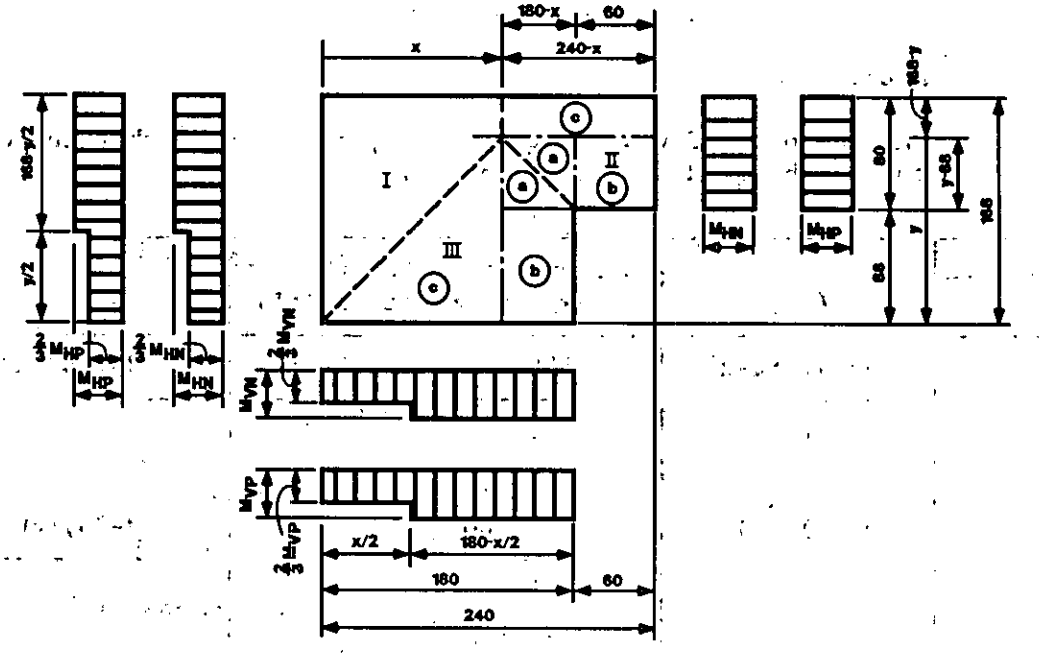


Figure 3A-5

Step 4. For distribution of moments across negative and assumed positively yield lines see figure 3A-5. (Since opening is located at lower right corner, there is no reduced moment capacity in this area.)

Step 5. The ultimate unit resistance is obtained from:

$$\Sigma M_N + \Sigma M_p = Rc = r_u Ac$$

a. Sector 1 (fig. 3A-5)

$$\Sigma M_{HN} + \Sigma M_{HP} = (20,000)(168-y/2) + 2/3(20,000)(y/2) + (20,000)(168-y/2) + 2/3(20,000)(y/2)$$
$$= 336(20,000) - y/3(20,000)$$
$$= (336-y/3)(20,000)$$

$$r_u Ac = r_u[x(168+168-y)/2]\ [x(168+2(168-y))/3(168+168-y)]$$
$$= r_u x^2(252-y)/3$$

therefore,

$$r_u = \frac{(1008-y)(20,000)}{x^2(252-y)}$$

b. Sector II (fig. 5A-5)

$$\Sigma M_{HN} + \Sigma M_{HP} = (20,000)(80) + (20,000)(80)$$
$$= 160(20,000)$$

Note:

The sector is divided into parts a, b, and c so that the centriod may be obtained (see table below).

Portion of Sector	Area (A')	Distance from Centroid to axis of rotation (c')	A'c'
a	$\frac{(y-88)(180-x)}{2}$	$\frac{(180-x)}{3} + 60 = \frac{360-x}{3}$	$\frac{(y-88)(180-x)(360-x)}{6}$
b	$(y-88)(60)$	$\frac{60}{2}$	$\frac{(y-88)(60)^2}{2}$
c	$(168-y)(240-x)$	$\frac{(240-x)}{2}$	$\frac{(168-y)(240-x)^2}{2}$

$$Ac = \Sigma A'c' = \frac{(y-88)(180-x)(360-x)}{6} + \frac{(y-88)(60)^2}{2} + \frac{(168-y)(240-x)^2}{2}$$

$$= 1/2\frac{(y-88)^2}{3}[(180-x)(360-x) + 10800] + (168-y)(240-x)^2$$

$$r_u = \frac{(\Sigma M_{HN} + \Sigma M_{HP})}{Ac}$$

$$= \frac{6,400,000}{\frac{(y-88)^2}{3}[(180-x)(360-x) + 10,800] + (168-y)(240-x)^2}$$

c. Sector III (fig. 3A-5)

$$\Sigma M_{vn} + \Sigma M_{vp} = (20,000)(180-x/2) + 2/3(20,000)(x/2) + (20,000)(180-x/2) + 2/3(20,000)(x/2)$$
$$= 360(20,000) - (20,000)x/3$$

Portion of Sector	Area (A')	Distance from Centroid to axis of rotation (c')	A'c'
a	$\frac{(180-x)(y-88)}{2}$	$\frac{(y-88)}{3} + 88 = \frac{y+176}{3}$	$\frac{(180-x)(y-88)(y+176)}{6}$
b	$(180-x)(88)$	$\frac{88}{2}$	$\frac{(180-x)(88)^2}{2}$
c	$\frac{xy}{2}$	$\frac{y}{3}$	$\frac{xy^2}{6}$

$$Ac = \Sigma A'c' = (y-88)(180-x)(y+176)/6 + (180-x)(88)^2/2 + xy^2/6$$
$$= 1/6\,(180-x)[(y-88)(y+176)+23,232] + xy^2$$

$$r_u = \frac{\Sigma M_{HN} + \Sigma M_{HP}}{Ac}$$

$$= \frac{(2160-2x)(20,000)}{(180-x)[(y-88)(y+176)+23,232]+xy^2}$$

Step 6. Due to the complexity of obtaining a direct solution for ultimate unit resistance, a trial-and-error solution will be used (see table below):

x	y	r_I	r_{II}	r_{III}
125	130	9.21	7.67	9.33
125	135	9.55	7.92	8.77
125	140	9.92	8.19	8.25
125	145	10.32	8.48	7.78
125	150	10.77	8.79	7.35
130	130	8.52	8.29	9.50
130	135	8.83	8.55	8.92
131	135	8.70	8.68	8.85

Therefore:

$x = 131$ ins
$y = 135$ ins
$r_u = 8.68$ psi

Problem 3A-2 Resistance - Deflection Function

Problem: Determine the actual and equivalent resistance deflection function in the elasto-plastic region for a two-way structural element.

Procedure:

Step 1. Establish design parameters
- a. Geometry of element.
- b. Support conditions

Step 2. Determine ultimate positive and negative moment capacities.

Step 3. Determine static properties:
- a. Modules of elasticity for the element.
- b. Moment of inertia of the element.

Step 4. Establish points of interest and their ultimate moment capacities (fig. 3-23)

Step 5. Compute properties at first yield.
- a. Location of first yield
- b. Resistance at first yield r_e
- c. Moments at remaining points consistent with r_e
- d. Maximum deflection at first yield.

Step 6. Compute properties at second yield
- a. Remaining moment capacity at other points
- b. Location of second yield.
- c. Change in unit resistance Δr between first and second yield.
- d. Unit resistance at second yield r_{ep}.
- e. Moment at remaining point consistent with r_{ep}.

f. Change in maximum deflection.
g. Total maximum deflection.

Note:

An element with unsymmetrical support conditions may exhibit three or four support yields. Therefore, repeat Step 6 as many times as necessary to obtain properties at the various yield points.

Step 7. Compute properties at final yield (ultimate unit resistance)

a. Ultimate unit resistance.
b. Change in resistance between ultimate unit resistance and resistance at prior yield.
c. Change in maximum deflection (for elements supported on two, three, or four sides, use stiffness obtained from figure 3-26, 3-30 and 3-36, respectively).
d. Total maximum deflection.

Step 8. Draw the actual resistance-deflection curve (fig. 3-39).

Step 9. Calculate equivalent maximum elastic deflection of the element.

Example: 3A-2 Resistance-Deflection Function

Required: The actual and equivalent resistance-deflection function (curve) in the elasto-plastic region for the two-way structural steel element.

Solution:

Step 1. Given:

a. L = 240 in. H = 168 in.
b. Fixed on three sides and free at the fourth.

Step 2. Same as step 3 of example 3A-1(A), part a.

Step 3. Static properties.

a. Modulus of elasticity, E_s for steel

$E_s = 29 \times 10^6$ psi

b. Considering a 1-inch strip (b = 1 inch)

Assume I = 144 in^4

Step 4. For points of interest, see figure 3A-6.

Step 5. Properties at first yield.

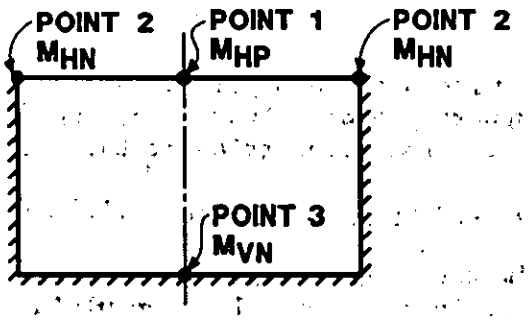


Figure 3A-6

From figure 3-27 for H/L = 0.7

$\beta_1 = 0.077 \qquad \beta_2 = 0.160 \qquad \beta_3 = 0.115$

$\gamma_1 = 0.012 \qquad \nu = 0.3$

a. $M_{HP} = M_{HN} = M_{VP} = M_{VN} = 20{,}000$ in-lbs/in

$M_P = \beta r H^2$

$r = M/\beta H^2$

$r_1 = 20{,}000/[(0.077)(168)^2] = 9.20$ psi

$r_2 = 20{,}000/[(0.160)(168)^2] = 4.43$ psi

$r_3 = 20{,}000/[(0.115)(168)^2] = 6.16$ psi

First yield at point 2 (smallest r)

b. $r_e = 4.43$ psi

c. M_P (Point 1) $= (0.077)(4.43)(168)^2 = 9{,}627$ in-lbs/in

M_N (Point 3) $= (0.115)(4.43)(168)^2 = 14{,}379$ in-lbs/in

d. $D = EI/b(1-\nu^2)$

$= 29 \times 10^6 \times 144/1[1-(0.3)^2] = 45.9 \times 10^8$ in-lbs

$X_e = \gamma_1 r_e H^4/D = (0.0120)(4.43)(168)^4/43(10^8) = 0.0092$ in

Step 6. Properties at second yield.

After first yield element assumes a simple-simple-fixed-free stiffness, therefore from figure 3-29 for H/L = 0.7.

$\beta_1 = 0.120$ $\beta_3 = 0.220$

$\gamma_1 = 0.045$ $\nu = 0.3$

a. M_p (Point 1) = M_{HP} - M_p (at r_e)

= 20,000 - 9627 = 10373 in-lbs/in

M_N (Point 3) = M_{VN} - M_p (at r_e)

= 20,000 - 14,379 = 5621 in-lbs/in

b. M_p (Point 1) = 10373 in-lbs/in = $\beta_1 \Delta r H^2$

$\Delta r = 10373/(0.120)(168)^2 = 3.06$ psi

M_n (Point 3) = 5,621 in-lbs/in = $\beta_3 \Delta r H^2$

$\Delta r = 5,621/[(0.220)(168)^2] = 0.90$ psi

Second yield at Point 3 (smaller Δr)

c. $\Delta r = 0.90$ psi

d. $r_{ep} = r_e + \Delta r = 4.43 + 0.90 = 5.33$ psi

e. M_p (Point 1) = $0.120(0.90)(168)^2$

= 3.048 in-lbs/in

f. $D = EI/b(1-\nu^2) = (29)(10^6)(144)/1[1-(0.3)^2]$

= 45.9×10^8 in-lbs/in

$\Delta x = \gamma_1 \Delta r H^4/D = 0.030(0.90)(168)^4/45.9(10)^8$

= 0.0047 in

g. $X_{ep} = X_e + \Delta X = 0.0092 + 0.0047 = 0.014$ in

Step 7. Properties at final yield (ultimate unit resistance). After second yield element assumes a simple-simple-simple-free stiffness, therefore from figure 3-30 for H/L = 0.7.

$\gamma_1 = 0.045$ $\nu = 0.3$

a. $r_u = 10.6$ psi (part a, example 3A-1(A))

b. $\Delta r = r_u - r_{ep} = 10.6 - 5.33 = 5.27$ psi

c. $D = EI/b(1-\nu^2) = 29(10^6)(144)/1[1-(0.3)^2]$

$= 45.9 \times 10^8$ in-lbs

$\Delta x = \gamma_1 r H^4 / D = (0.045)(5.27)(168)^4/45.9 \times 10^8$

$= 0.041$ in

d. $X_p = X_{ep} + \Delta X = 0.014 + 0.041 = 0.055$ in

Step 8. For actual resistance-deflection curve, see figure 3A-7.

Step 9. $X_E = X_e(r_{ep}/r_u) + X_{ep}[1-(r_e/r_u)] + X_p[1-(r_{ep}/r_u)]$ Equation 3-35

$X_E = 0.0092(5.33/10.6) + 0.014\ [1-(4.43/10.6)]$

$+ 0.055[1-(5.33/10.6)]$

$= 0.00463 + 0.0081 + 0.0273$

$= 0.040$ in

The equivalent resistance-deflection curve is shown in figure 3A-7.

Problem 3A-3 Dynamic Design Factors For A One Way Element

Problem: Determine the plastic load, mass and load-mass factors for a one-way element.

Procedure:

Step 1. Establish design parameters.

Step 2. Determine deflected shape.

a. geometry of element
b. support conditions
c. type of load and mass

Step 3. Determine maximum deflection

Step 4. Determine deflection function

a. For distributed load and/or continuous mass determine the deflection at any point.

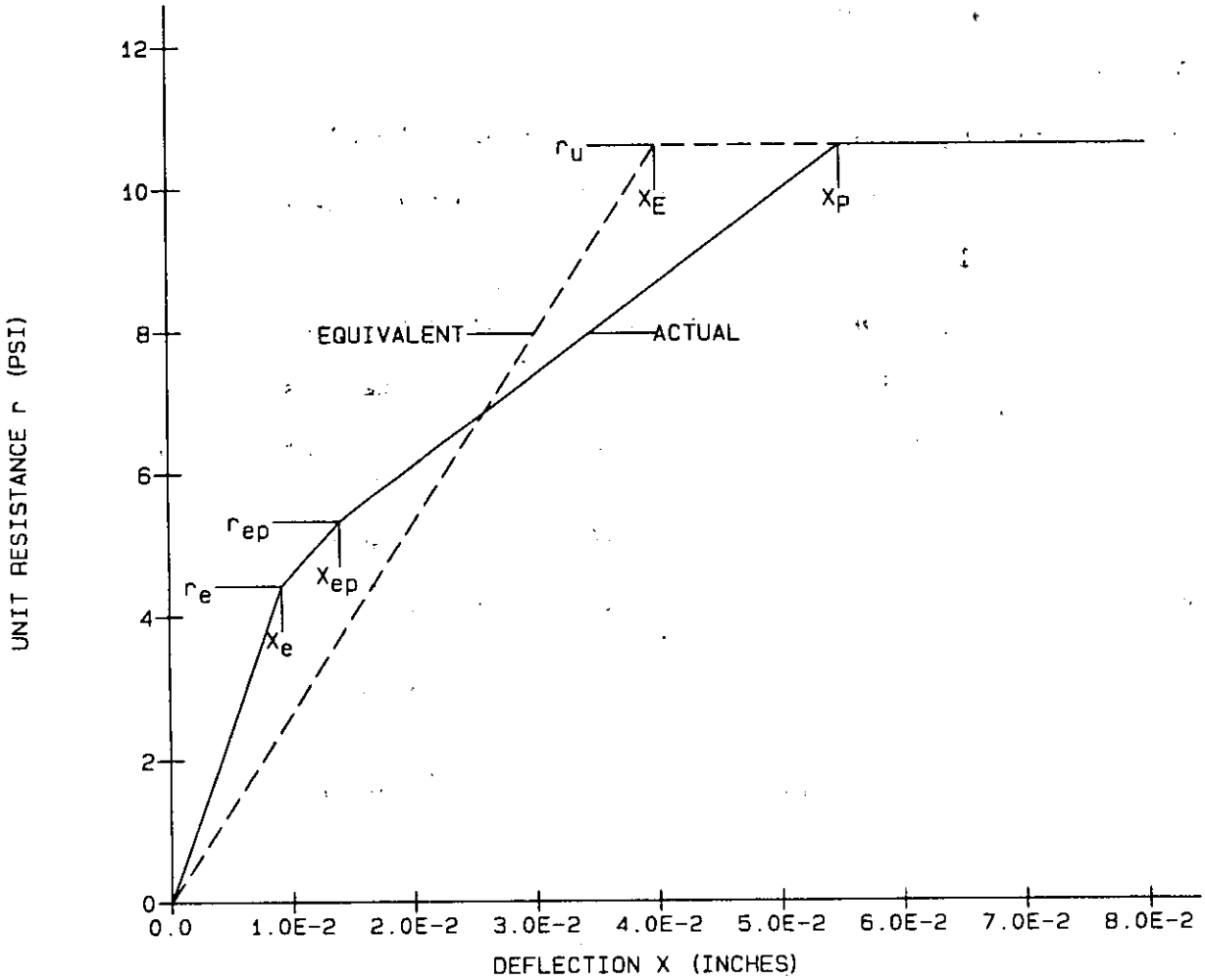

UNIT RESISTANCE r (PSI)
12
10
8
6
4
2
0
r_u
X_E
X_P
EQUIVALENT
ACTUAL
r_{ep}
X_{ep}
r_e
X_e
0.0
1.0E-2
2.0E-2
3.0E-2
4.0E-2
5.0E-2
6.0E-2
7.0E-2
8.0E-2
DEFLECTION X (INCHES)

Figure 3A-7

b. For concentrated loads and concentrated mass determine the deflection at the load.

Step 5. Calculate the shape function

a. For distributed load and/or continuous mass calculate $\phi(x)$, equation 3-43.

b. For concentrated load and concentrated mass calculate ϕ_r, equation 3-46.

Step 6. Calculate the load factor, K_L.

a. Use equations 3-41 and 3-42 for a distributed load.

b. Use equations 3-41 and 3-45 for a concentrated load

Step 7. Calculate the mass factor, K_M.

a. Use equations 3-47 and 3-48 for a continuous mass

b. Use equations 3-44 and 3-49 for concentrated mass

Step 8. Calculate the load-mass factor K_{LM}, from equation 3-53.

Example 3A-3(A) Dynamic Design Factors For A One-Way Element

Required: The load, mass and load-mass factors for a structural steel beam in the elastic range, with a distributed load.

Solution:

Step 1: Given structural steel beam shown in figure 3A-8

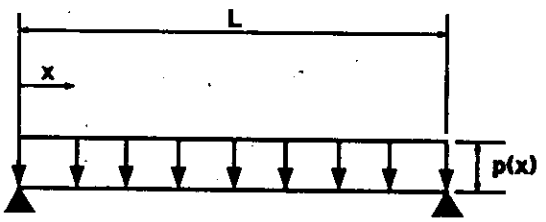


Figure 3A-8

a. L = 120 in.
b. Simply supported on both edges
c. p(x) = 2,000 lb/in
   m(x) = 0.0055(lb-s^2/in^4)/in

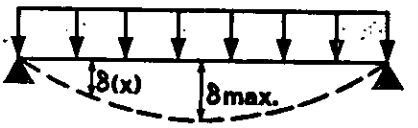


Figure 3A-9

Step 2: Assumed deflected shape for elastic range is shown in figure 3A-9

Step 3: The maximum deflection at the center is

$$\delta_{max} = \frac{5p(x)L^4}{384\ EI}$$

Step 4: Determine deflection function

$$\delta(x) = \frac{p(x)}{24EI}\ (L^3 - 2Lx^2 + x^3)$$

Step 5: Calculate the shape function using equation 3-43

$$\phi = \frac{\delta(x)}{\delta_{max}} = \frac{p(x)x}{24EI}\ (L^3 - 2Lx^2 + x^3)\ \frac{384EI}{5p(x)L^4}$$

$$= \frac{16}{5L^4}\ (L^3x - 2Lx^3 + x^4)$$

Step 6: a. Using equation 3-42, determine equivalent force

$$F_E = \int_0^L p(x)\phi(x)dx = \int_0^{120} (2{,}000\ \text{lb/in})\ \frac{16}{5L^4}\ (L^3x - 2Lx^3 + x^4)dx$$

$$= \frac{6{,}400}{L^4}\left[\frac{L^3x^2}{2} - \frac{2Lx^4}{4} + \frac{x^5}{5}\right]_0^{120} = 1{,}280L$$

$= 153{,}600$ lb.

b. From equation 3-41, find the load factor

$$K_L = \frac{F_E}{F} = \frac{153{,}600\ \text{lb.}}{(2{,}000\ \text{lb/in} \times 120\ \text{in.})}$$

$K_L = 0.64$ in the elastic range

Step 7: a. Find the equivalent mass from equation 3-48

$$M_E = \int_0^L m(x)\phi(x)^2 dx = .0055 \frac{256}{25L^8} \int_0^{120} (L^3x - 2Lx^3 + x^4)^2 \, dx$$

$$= \frac{1.408}{25L^8} \int_0^{120} (L^6x^2 - 4L^4x^4 + 2L^3x^5 + 4L^2x^6 - 4Lx^7 + x^8)dx$$

$$= \frac{1.408}{25L^8} \left[\frac{L^6x^3}{3} - \frac{4L^4x^5}{5} + \frac{2L^3x^6}{6} + \frac{4L^2x^7}{7} - \frac{4Lx^8}{8} + \frac{x^9}{9} \right]_0^{120}$$

$= .00277L$

$= 0.3325 \text{ lb}^2 \text{- s}^3/\text{in}$

b. From equation 3-47, calculate the mass factor

$$K_M = \frac{M_E}{M} = \frac{0.3325 \text{ lb - s}^2/\text{in}^3}{(0.0055 \text{ lb - s}^2/\text{in}^4 \text{ x } 120 \text{ in})}$$

$K_M = 0.50$ in the elastic range

Step 8: Calculate the load-mass factor as defined by equation 3-51

$K_{LM} = K_M/K_L$

$= 0.50/0.64$

$K_{LM} = 0.78$ in the elastic range

Example 3A-3(B) Dynamic Design Factors For A One-Way Element

Required: The load, mass and load-mass factors for a structural steel beam in the plastic range with a distributed load.

Solution:

Step 1. Given the structural steel beam shown in figure 3A-8

a. L = 120 in.
b. Simply-supported on both ends
c. p(x) = 2,000 lb/in
d. m(x) = 0.0055 (lb - s^2/in^4)/in

Step 2. Assume deflected shape for the plastic range is shown in figure 3A-10

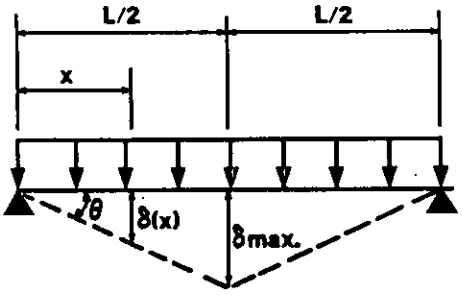


Figure 3A-10

Step 3. Determine maximum deflection

$$\delta_{max} = (L/2)\tan\Theta$$

Step 4. Determine the deflection at any point.

$$\delta(x) = x\tan\Theta \qquad x < L/2$$

Step 5. Calculate the shape function, equation 3-43

$$\phi(x) = \frac{\delta(x)}{\delta_{max}} = \frac{x\tan\Theta}{(L/2)\tan\Theta}$$

$$= 2x/L \quad x < L/2$$

Step 6:

a. Find F_E using equation 3-42.

$$F_E = \int_0^L p(x)\phi(x)dx = 2\int_0^{60} 2{,}000 \text{ lb/in})(2x/L)dx$$

$$= 4{,}000 \text{ lb/in} \left[x^2/L \right]_0^{60}$$

$$= 120{,}000 \text{ lb}$$

b. From equation 3-41

$$K_L = \frac{F_E}{F} = \frac{120{,}000 \text{ lb.}}{(2{,}000 \text{ lb/in})\ 120 \text{ in}}$$

$K_L = 0.5$ in the plastic range

Step 7:

a. Use equation 3-48 to find the equivalent mass

$$M_E = \int_0^L m(x)\phi^2(x)dx = 2\int_0^{60} (0.0055)(4\ x^2/L^2)dx$$

$$= 0.044 \left[\frac{x^3}{3L^2} \right]_0^{60}$$

$$= 0.22 \text{ lb - s}^2/\text{in}^3$$

b. As defined by equation 3-47

$$K_M = \frac{M_E}{M} = \frac{0.22 \text{ lb} - s^2/\text{in}^3}{(0.0055 \text{ lb} - s^2/\text{in}^4)120 \text{ in}}$$

$K_M = 0.33$ in the plastic range

Step 8. Calculate K_{LM} using equation 3-53

$$K_{LM} = K_M/K_L$$

$$= 0.33/0.5$$

$K_{LM} = 0.66$ in the plastic range

Example 3A-3(C) Dynamic Design Factors For A One-Way Element

Required: The load, mass and load-mass factors for a structural steel beam in the elastic range, with a concentrated load.

Solution:

Step 1: Given structural steel beam shown in figure 3A-11

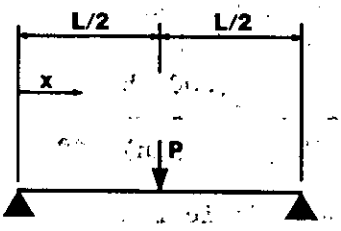


Figure 3A-11

a. L = 120 in.
b. Simply supported on both sides
c. F = 240 kips

$m(x) = 0.0055(\text{lb} - s^2/\text{in}^4)/\text{in}.$

Step 2: Assume deflected shape for elastic range is shown in figure 3A-12

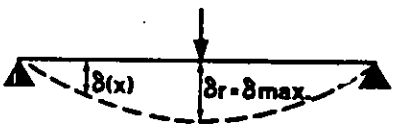


Figure 3A-12

Step 3: Determine maximum deflection

$$\delta_{max} = \frac{PL^3}{48EI}$$

Step 4: Determine deflection functions

a. for continuous mass,

$$\delta(x) = \frac{Px}{48EI}(3L^2 - 4x^2)$$

b. for concentrated load

$$\delta_r = \frac{PL^3}{48EI}$$

Step 5: Calculate shape functions

a. for continuous mass use equation 3-43

$$\phi(x) = \frac{\delta(x)}{\delta_{max}} = \frac{Px(3L^3 - 4x^2)}{48EI} \quad \frac{48EI}{PL^3}$$

$$= (3L^2x - 4x^3)/L^3$$

b. for concentrated load, use equation 3-46

$$\phi_r = \frac{PL^3}{48EI} \quad \frac{48EI}{PL^3}$$

$$= 1.0$$

Step 6:

a. Find equivalent force from equation 3-45

$$F_E = \sum^{i} F_r\phi_r = Pxl = 240 \text{ kips}$$

b. Using equation 3-41, calculate the load factor

$$K_L = \frac{F_E}{F} = \frac{240 \text{ kips}}{240 \text{ kips}}$$

$K_L = 1.0$ for the elastic range

Step 7: a. Equation 3-48 gives the equivalent mass.

$$M_E = \int_0^L m(x)\phi^2(x)\,dx = \int_0^{120} \frac{120\ (0.0055)}{L^6}\,(9L^4x^2 - 24L^2x^4 + 16x^6)dx$$

$$= \frac{0.0055}{L^6}\left[\,3L^4\,x^3 - \frac{24L^2\,x^5}{5} + \frac{16x^7}{7}\,\right]_0^{120}$$

$$= 0.0027L$$

$$= 0.32 \text{lb} \cdot s^2/in^3$$

b. From equation 3-47, calculate the mass factor

$$K_M = \frac{M_E}{M} = \frac{0.32 \text{lb} \cdot s^2/in^3}{(0.0055 \text{lb} \cdot s^2/in^4 \times 120 in)}$$

$K_M = 0.49$ in the elastic range

Step 8: Calculate the load-mass factor, from equation 3-53

$$K_{LM} = K_M/K_L$$

$$= 0.49/1.0$$

$K_{LM} = 0.49$ for the elastic range

Example 3A-3(D) Dynamic Design Factors For A One-Way Element

Required: Determine the load, mass and the load-mass factors for a structural steel beam, in the plastic range, with a concentrated load.

Solution:

Step 1. Given structural steel beams shown in figure 3A-11.

a. L = 120 in

b. Simply-supported at both edges

c. F = 240 kips

$m(x) = 0.0055\ (lb - s^2/in^4)/in$

Step 2. Assumed deflected shape for the plastic range is shown in figure 3A-13

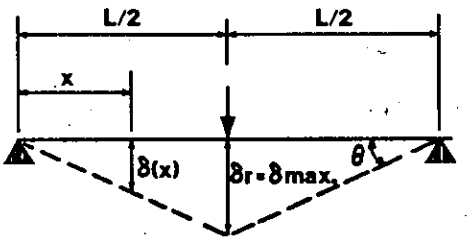


Figure 3A-13

Step 3: Determine maximum deflection

$$\delta_{max} = (L/2)\tan\theta$$

Step 4: Determine deflection function.

a. for continuous mass

$$\delta(x) = x\tan\theta \qquad x < L/2$$

b. for a concentrated load

$$\delta_r = (L/2)\tan\theta$$

Step 5: Calculate shape factors using

a. equation 3-43 for continuous mass

$$\phi(x) = \frac{\delta(x)}{\delta_{max}} = \frac{x\tan\theta}{(L/2)\tan\phi}$$

$$= 2x/L \qquad x < L/2$$

b. equation 3-46 for concentrated load

$$\phi_r = \frac{\delta_r}{\delta_{max}} = \frac{(L/2)\tan\theta}{(L/2)\tan\theta}$$

$$= 1.0$$

Step 6: a. The equivalent force is found using equation 3-45

$$F_E = \sum_{r=1}^{i} F_r\phi_r = Px_1 = 240 \text{ kips}$$

b. Equation 3-41 gives the load factor

$$K_L = \frac{F_E}{F} = \frac{240 \text{ kips}}{240 \text{ kips}}$$

$K_L = 1.0$ for plastic range

Step 7: a. The equivalent mass is found using equation 3-48

$$M_E = \int_0^L m(x)\phi^2(x)dx = 2\int_0^{60} (0.0055)(4\ x^2/L^2)dx$$

$$= 0.044 \left[\frac{x^3}{3L^2} \right]_0^{60} = 0.22 \text{ lb - s}^2/\text{in}^3$$

b. Solve for K_M using equation 3-47

$$K_M = \frac{M_E}{M} = \frac{0.22 \text{ lb - s}^2/\text{in}^3}{(0.0055 \text{ lb - s}^2/\text{in}^4)120 \text{ in}}$$

$K_M = 0.33$ in the plastic range

Step 8: From equation 3-53, calculate K_{LM}

$$K_{LM} = K_M/K_L$$

$= 0.33$ in the plastic range

Problem 3A-4 Plastic Load-Mass Factor

Problem: Determine the plastic load-mass factor K_{LM} for a two-way element using (1) general solution and (2) chart solution.

Note: The determination of the plastic load-mass factor follows the calculations for the ultimate resistance, hence the structural configuration and the location of the plastic yield lines will be known.

Procedure: Part (a) - **General Solution**

Step 1. See part a, problem 3A-1 for the structural configuration and location of plastic yield lines. Denote sectors formed by yield lines.

Step 2. Determine the load-mass factors properties I, c, and L' for all sectors.
Step 3. Determine the factor I/cL' for all sectors.
Step 4. Calculate the total area of the element.
Step 5. With values obtained above, calculate the plastic load-mass factor for the element using equation 3-57.

Note: In the above problem, an element of uniform thickness was considered. For non-uniform elements, the load-mass factor is calculated using equation 3-53 where the mass of the individual sectors must be considered.

Procedure: Part (b) - Chart Solution

Step 1. See part b, problem 3A-1 for structural configuration and location of plastic yield lines in terms of x/L or y/H.

Step 2. For known value of X/L or y/H and support condition, determine the load-mass factor for the element from figure 3-44.

Note: Chart solution may be used only if the element conforms to the requirements listed in section 3-17.3

Example 3A-4 Plastic Load-Mass Factor

Required: Plastic load-mass factor for the element considered in example 3A-1(A) using (1) general solution and (2) chart solution.

Solution: Part (a) - General Solution

Step 1. Given structural configuration and location of yield lines shown below (see part a, example 3A-1(A)) in figure 3A-14.

L = 240 in
H = 168 in
X = 120 in
y = 137.6 in
T_c = constant

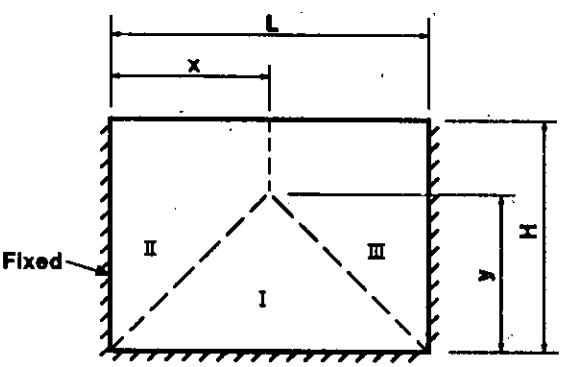


Figure 3A-14

Step 2. Load-mass factor properties.

a. Sector 1.

$L' = y = 137.6$ in

$c = y/3 = 137.6/3$

$I = L(L'^3)/12 = 240(137.6)^3/12.$

b. Sector II.

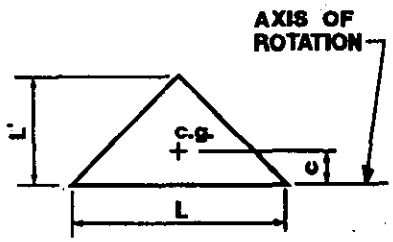


Figure 3A-15

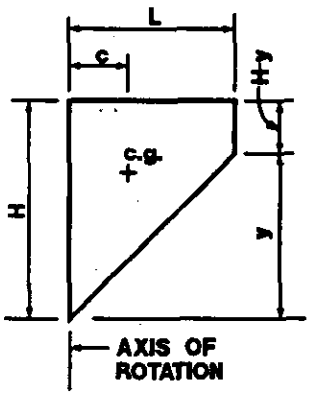


Figure 3A-16

$L' = x = 120$ in

$H - y = 168 - 137.6 = 30.4$ in

$$c = \frac{L'[H + 2(H-y)]}{3[H + (H-y)]} = \frac{120[168 + 2(30.4)]}{3(168 + 30.4)}$$

$$c = 120(0.384)$$

$$I = \frac{(H-y)(L')^3}{3} + \frac{y(L')^3}{12}$$

$$= \frac{30.4(120)^3}{3} + \frac{137.6(120)^3}{12} = 21.60(120)^3$$

Step 3. Calculate factor I/cL' for each sector:

Sector I. $\dfrac{I}{cL'} = \dfrac{240(137.6)^3 / 12}{(133.4/3)(133.4)} = 8{,}256 \text{ in}^2$

Sector II. $\dfrac{I}{cL'} = \dfrac{21.60(120)^3}{(0.390 \times 120)(120)} = 6{,}646 \text{ in}^2$

Sector III. $\dfrac{I}{cL'} = 6{,}646 \text{ in}^2$

Step 4. Area of panel

$A = LH = 240(168) = 40{,}320 \text{ in}^2$

Step 5. Load-mass factor

$$K_{LM} = \frac{I/cL'}{A} \qquad \text{(eq. 6-14)}$$

$$K_{LM} = \frac{8,256 + 2(6,646)}{40,320} = 0.534$$

Solution: Part (b) - Chart Solution

Step 1. Given: Panel fixed on 3 edges, 1 free and y/H = 0.803 (see part b, example 3A-1(A)).

Step 2. From figure 3-44, read load-mass factor

$K_{LM} = 0.543$

Problem 3A-5 Response of a Single-Degree-of Freedom System subject to Dynamic Load

Problem: Determine the maximum response and the corresponding time it occurs of a single-degree-of-freedom system subjected to dynamic load using (a) numerical methods and (b) design charts.

Procedure: Part (a) - Numerical Methods

Step 1. Establish dimensional parameters of the system.

Step 2. Determine the natural period of vibration and integration time interval.

Step 3. Construct a table similar to table 3-14 of section 3-19.2. Note:For the first interval n=1, Equation 3-59 is used and subsequent intervals, the recurrence formula (eqn. 3-56) is used.

Procedure: Part (b) - Chart solution

Step 1. Same as step 1 of example 3A-5, part a.

Step 2. Determine the non-dimensional parameters.

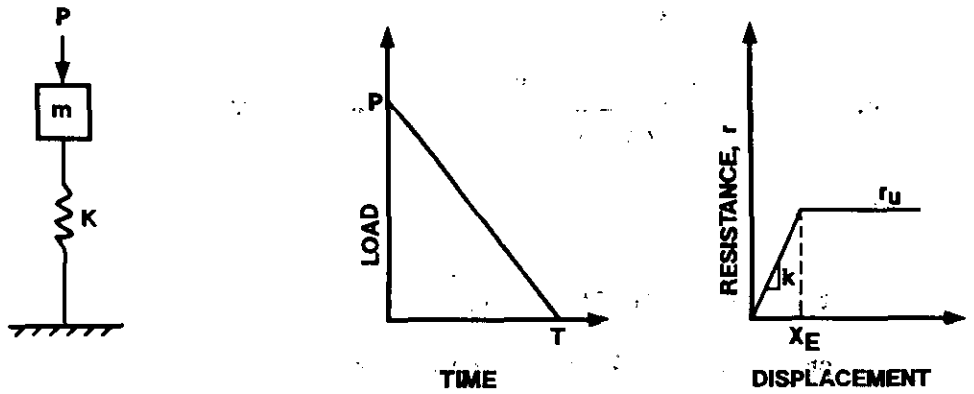
Step 3. Determine the ratio of the maximum displacement to the elastic displacement X_m/X_E and the ratio of the time at which this maximum displacement occurs to the duration of the blast load.

Example 3A-5 Maximum Response of Single-Degree-of-Freedom System Subjected to a Triangular Load.

Required: The maximum response and the time it occurs, of a single-degree-of-freedom system subjected to blast loads, using (a) numerical methods and (b) design charts.

Solution: Part (a) - Numerical Methods

Step 1. Given:



(a) Single-Degree-of-Freedom System **(b) External Load** **(c) Resistance Function**

Figure 3A-17

$m = 2.5$ Kips-sec^2/ft
$K = 9{,}860$ Kips/ft
$r_u = 750$ Kips
$X_E = 0.076$ ft
$T = 0.10$ sec
$P = 1000$ Kips

Step 2. Natural period of vibration and integration time interval.

$$T_N = 2\pi\,[m/K]^{1/2} = 2\pi\,[2.5/9{,}860]^{1/2} = 0.10 \text{ sec}$$

$$t = T_N/10 = 0.01 \text{ sec}$$

Step 3. Construct table as shown below.

1	2	3	4	5	6	7	8	9	10
n	t (sec)	P_n Kips	R_n (Kips)	P_n-R_n (Kips)	$A_n=(P_n-R_n/m$ (ft/sec^2)	$a_n(\Delta t)^2$ (ft)	$2X_n$ (ft)	X_{n-1} (ft)	X_{n+1} (ft)
0	0	1000	0	1000	400	0.040	0.0	0.0	0.020
1	0.01	900	197.200	702.800	281.120	0.028112	0.0400	0.0	0.068112
2	0.02	800	671.684	128.426	51.366	0.05137	0.13622	0.020	0.121357
3	0.03	700	750	-50.0	-20.0	-0.00200	0.242714	0.06811	0.17261
4	0.04	600	750	-150.0	-60.0	-0.00600	0.34522	0.121357	0.21786
5	0.05	500	750	-250.0	-100.0	-0.0100	0.43673	0.17261	0.25312
6	0.06	40	750	-350.0	-140.0	-0.0140	0.050623	0.21786	0.27437
7	0.07	300	750	-450.0	-180.0	-0.0180	0.54874	0.25312	0.27762
8	0.08	200	750	-550.0	-220.0	-0.0220	0.55525	0.27437	0.25880
9	0.09								

Note: $P_n = f(t_n) = 1000\ [1-n(\Delta t/T)]$

$$R_n = \begin{cases} KX_n \text{ for } X_n < X_e \\ r_u = 750 \text{ for } X_n > X_e \end{cases}$$

$$X_{n+1} = 2X_n - X_{n-1} + a_n\ (\Delta t)^2$$

Note:

For n=0, X_{n+1} (Column 10) $= X_{0+1} = X_1 = (1/2)a_0(\Delta t)^2$

$= (1/2)(0.040)$

$= 0.02$ ft

For n=1, $2X_n$ (Column 8)$= 2X_1 = 2[(1/2)a_0(\Delta t)^2]$

$= 2(0.02) = 0.04$ ft

X_{n-1} (Column 9) $= X_0 = 0.0$

X_{n+1} (Column 10) $= X_2 = 2X_1 - X_0 + a_1(\Delta t)^2$

$= 2(0.02) - 0 + 0.02811$

$= 0.06811$ ft

For n=2, $2X_n$ (Column 8)$= 2X_2 = 2(0.06811)$

$= 0.13622$ ft.

X_{n-1} (Column 9) $= X_1 = 0.02$ ft.

X_{n+1} (Column 10) $= X_3 = 2X_2 - X_1 + a_2 (\Delta t)^2$

$= (2)(0.06811) - 0.02 + 0.005137$

$= 0.121357$ ft.

For n=3, 4,..., repeat the above procedure.

Solution: Part (b) - Design Charts

Step 1. Same as step 1 of example 3A-5, part a

Step 2. Non-dimensional parameters

a. Natural period of vibration, T_n

$$T_n = 2\pi[m/K]^{1/2} = 2\pi[2.5/9,860]^{1/2} = 0.10 \text{ sec}$$

b. Ratio of duration of blast load T to natural period T_N

$$T/T_N = 0.10/0.10 = 1.0$$

c. Ratio of peak resistance r_u to peak load P

$$r_u/P = 750/1000 = 0.75$$

Step 3. Using the ratios calculated in step 2 and figures 3-54 and 3-55, determine the value of X_m/X_E and t_m/T_N.

For $T/T_N = 1$ and $r_u/P = 0.75$

$X_m/X_E = 3.7$ from figure 3-54

$t_m/T = 0.77$ from figure 3-55

Step 4. Determine X_m and t_m

$X_m/X_E = 3.7$

$X_m = (3.7)X_E = (3.7(r_u/K_E)$

$= (3.7)(750/9,860) = 0.28144$ ft.

$t_m/T = 0.77$

$t_m = (0.77)T = 0.77(0.10) = 0.077$ sec

Problem 3A-6 Maximum Response of a Single-Degree-of-Freedom System to Bilinear Blast Loads

Problem: Determine X_m/X_E, t_m/T_N and t_E/T (when applicable) for a single-degree-of-freedom system subject to various bilinear blast loads.

Procedure: Part (a) - **Solution in Region D**

Step 1. Establish normalized parameters

Step 2. Enter table 3-15 with the given C parameters and determine which figures have to be used.

Step 3. Enter each of the figures determined in step 2, with the given values of the other two parameters and determine the region where the intersection points are located.

Step 4. Based on the region where the intersection points are located,
enter the appropriate figure and find X_m/X_E, t_m/T_N and t_E/T.

Procedure: Part (b) - **Solution in Region C - Graphical Interpolation.**

Step 1. Same as step 1 in part a.

Step 2. Same as step 2 in part a.

Step 3. Same as step 3 in part a.

Step 4. Set up a table as shown in table 3A-1. Post each figure number and the corresponding values of C_1 and C_2, leaving a space between each line of information. Post in the spaces the appropriate values of C_1 and C_2 needed for interpolation. Enter each of the figures determined in Step 2 with the given parameters and find the values of X_m/X_E. Post these values in table 3A-1.

Step 5. Use log-log graph paper to plot the points obtained in Step 4. Post these values in table 3A-1, using linear interpolation where necessary.

Step 6. Plot on log-log graph paper the points which represent (X_m/X_E, C_2) for the given value of C. Use linear interpolation to find X_m/X_E for given value of C_2.

Procedure: Part (c) - **Solution in Region C - Mathematical Interpolation**

Step 1. Same as step 1 in part a.

Step 2. Same as step 2 in part a.

Step 3. Same as step 3 in part a.

Step 4. Same as step 4 in part b.

Step 5. Solve for $\ln Y_a$ and $\ln Y_b$ using equations 3-83 and 3-84.

Step 6. Solve for $\ln Y$ using equation 3-85.

Step 7. Solve for Y using equation 3-86.

Example 3A-6 Maximum Response of a Single-Degree-of-Freedom System to Bilinear Blast Loads

Required: Determine X_m/X_E, t_m/T_N and t_E/T (when applicable) for a single-degree-of-freedom system subject to various bilinear blast loads.

Solution: **Part (a) - Solution in Region D**

Step 1. Given: $P/r_u = 1.0$

$T/T_N = 3.0$

$C_1 = 0.66$

$C_2 = 50$

Step 2. Enter table 3-15 with C_1, = 0.66 and C_2 = 50. Note figures 3-119, 3-120, 3-147, and 3-148 apply.

Step 3. Enter each of the figures determined in step 2, with P/r_u = 1.0 and T/T_N = 3.0. Note that the intersection point is located to the right of the line of solid squares, defined as region D. In region D, the maximum dynamic response depends only on the shock load described by P/r_u and T/T_N; the gas load described by C_1P/r_u and C_2T/T_n does not influence the maximum dynamic response. Consequently, figures 3-64a and 3-64b for a single triangular load pulse apply. Enter figure 3-64a with P/r_u = 1.0 and T/T_N = 3.0 and find X_m/X_E = 3.55, t_m/T_N = 0.98, t_E/T = 0.086.

Solution: **Part (b) - Solution in Region C - Graphical Interpolation**

Step 1. Given: $P/r_u = 32$

$T/T_N = 0.10$

$C_1 = 0.06$

$C_2 = 20$

Step 2. Enter table 3-15 with C_1 = 0.06 and C_2 = 20. Note figures 3- 108, 3-109, 3-133 and 3-134 apply.

Step 3. Enter each of these figures with $P/r_u = 32$ and $T/T_n = 0.10$. Note that the intersection point is not located in regions A, B or D. Therefore the intersection points lie in region C and interpolation between charts is required to obtain a solution.

Step 4. Set up table as shown in table 3A-1 below. Post each chart number and the corresponding values of C_1 and C_2 leaving a space between each line of information. Post in the spaces the appropriate values of C_1 and C_2 needed for interpolation. Enter figure 3-108 with $P/r_u = 32$ and $T/T_N = 0.10$ and find $X_m/X_E = 112$. Post this value in the table. Enter figure 3-109 with $P/r_u = 32$ and $T/T_N = 0.10$ and find $X_m/X_E = 86$. Post this value in the table. Repeat this process for figures 3-133 and 3-134, and post values for X_m/X_E in the table.

Step 5. Use log-log graph paper to plot the points (112,0.068) and (86,0.046) which represent (X_m/X_E, C_1) for $C_2 = 10$ as shown in figure 3-267. Use straight-line interpolation to find $X_m/X_E = 103$ for $C_1 = 0.060$. Post this value in the table. Repeat this process for $C_2 = 30$, and find $X_m/X_E = 251$ for $C_1 = 0.06$ as shown in figure 3-267.

Step 6. Plot on log-log graph paper the points (103,10) and (251,30) which represent X_m/X_E, C_2) for C_1, = 0.060. Use straight-line interpolation for finding $X_m/X_E = 182$ for $C_2 = 50$ as shown in figure 3-267. Thus the solution is $X_m/X_E = 182$.

Table 3A-1

Figure No.	C_1	C_2	X_m/X_E		
3-108	0.068		112		
	0.060	10	--	103	
3-109	0.046	10	86		
	0.060	20	--		182
3-133	0.075	30	340		
	0.060	30	--	251	
3-134	0.056	30	230		

Solution: Part (c) - Solution in region C - Mathematical Interpolation

Step 1. Same as step 1 of part (b).

Step 2. Same as step 2 of part (b).

Step 3. Same as step 3 of part (b).

Step 4. Same as step 4 of part (b).

Step 5. Using equation 3-83 and 3-84, find $\ln Y_a$ and $\ln Y_b$.

$$\ln Y_a = \ln Y_1 + \frac{\ln[Y_2/Y_1]\,\ln[C_1/C_{11}]}{\ln[C_{12}/C_{11}]}$$

$$= \ln 112 + \frac{\ln(86/112)\ln(0.060/0.068)}{\ln(0.046/0.068)}$$

$$\ln Y_a = 4.6339$$

$$\ln Y_b = \ln Y_3 + \frac{\ln[Y_4/Y_3]\,\ln[C_1/C_{13}]}{\ln[C_{14}/C_{13}]}$$

$$= \ln 340 + \frac{\ln(230/340)\ln(0.06/0.075)}{\ln(0.056/0.075)}$$

$$\ln Y_b = 5.5304$$

Step 6. Find lnY from equation 3-85

$$\ln Y = \ln Y_a + \frac{(\ln Y_b - \ln Y_a)\ln(C_2/C_{21})}{\ln(C_{23}/C_{21})}$$

$$= 4.6339 + \frac{(5.5304 - 4.639)\ln(20/10)}{\ln(30/10)}$$

$$\ln Y = 5.1995$$

Step 7. Solve for Y using equation 3-86

$$Y = e^{\ln Y}$$

$$= e^{5.1995}$$

$$Y = 181$$

APPENDIX 3B

LIST OF SYMBOLS

a	(1) acceleration (in./ms^2) (2) depth of equivalent rectangular stress block (in.)
A	area (in.^{2})
A_a	area of diagonal bars at the support within a width b (in.^{2})
A_o	area of openings (ft^2)
A_s	area of tension reinforcement within a width b (in.^{2})
A'_s	area of compression reinforcement within a width b (in.^{2})
A_{sH}	area of flexural reinforcement within a width b in the horizontal direction on each face (in.^{2})*
A_{sV}	area of flexural reinforcement within a width b in the vertical direction on each face (in.^{2})*
A_v	total area of stirrups or lacing reinforcement in tension within a distance, s_s or s_1 and a width b_s or b_1 (in.^{2}).
A_I, A_{II}	area of sector 1 and II, respectively (in.^{2})
b	(1) width of compression face of flexural member (in.) (2) width of concrete strip in which the direct shear stresses at the supports are resisted by diagonal bars (in.)
b_s	width of concrete strip in which the diagonal tension stresses are resisted by stirrups of area A_v (in.)
b_1	width of concrete strip in which the diagonal tension stresses are resisted by lacing of area A_v (in.)
B	constant defined in pargraph
c	(1) distance from the resultant applied load to the axis of rotation (in.) (2) damping coefficient
c_I, c_{II}	distance from the resultant applied load to the axis of rotation for sectors I and II, respectively (in.)
c_s	dilatational velocity of concrete (ft/sec)
C	shear coefficient
C_{cr}	critical damping

* See note at end of symbols

C_d	shear coefficient for ultimate shear stress of one-way elements
C_f	post-failure fragment coefficient (lb^2-$ms^4/in.^8$)
$C_{r\alpha}$	peak reflected pressure coefficient at angle of incidence α
C_s	shear coefficient for ultimate support shear for one-way elements
C_{sH}	shear coefficient for ultimate support shear in horizontal direction for two-way elements*
C_{sV}	shear coefficient for ultimate support shear in vertical direction for two-way elements*
C_D	drag coefficient
C_Dq	drag pressure (psi)
C_Dq_o	peak drag pressure (psi)
C_E	equivalent load factor
C_H	shear coefficient for ultimate shear stress in horizontal direction for two-way elements*
C_L	leakage pressure coefficient
C_M	maximum shear coefficient
C_u	impulse coefficient at deflection X_u (psi-$ms^2/in.^2$)
C_u'	impulse coefficient at deflection X_m (psi-$ms^2/in.^2$)
C_v	shear coefficient for ultimate shear stress in vertical direction for two-way elements*
C_1	(1) impulse coefficient at deflection X_1 (psi-$ms^2/in.^2$) (2) parameter defined in figure (3) ratio of gas load to shock load
C_1'	impulse coefficient at deflection X_m (psi-$ms^2/in.^2$)
C_2	ratio of gas load duration to shock load duration
d	distance from extreme compression fiber to centroid of tension reinforcement (in.)
d'	distance from extreme compression fiber to centroid of compression reinforcement (in.)
d_c	distance between the centroids of the compression and tension reinforcement (in.)

* See note at end of symbols

d_e	distance from support and equal to distance d or d_c (in.)
d_i	inside diameter of cylindrical explosive container (in.)
d_l	distance between center lines of adjacent lacing bends measured normal to flexural reinforcement (in.)
d_{co}	diameter of steel core (in.)
d_l	diameter of cylindrical portion of primary fragment (in.)
D	(1) unit flexural rigidity (lb-in.) (2) location of shock front for maximum stress (ft) (3) minimum magazine separation distance (ft)
D_o	nominal diameter of reinforcing bar (in.)
D_E	equivalent loaded width of structure for non-planar wave front (ft)
DIF	dynamic increase factor
DLF	dynamic load factor
e	base of natural logarithms and equal to 2.71828...
$(2E')^{1/2}$	Gurney Energy Constant (ft/sec)
E	modulus of elasticity
E_c	modulus of elasticity of concrete (psi)
E_s	modulus of elasticity of reinforcement (psi)
f	unit external force (psi)
f'_c	static ultimate compressive strength of concrete at 28 days (psi)
f'_{dc}	dynamic ultimate compressive strength of concrete (psi)
f_{ds}	dynamic design stress for reinforcement (psi)
f_{du}	dynamic ultimate stress of reinforcement (psi)
f_{dy}	dynamic yield stress of reinforcement (psi)
f_s	static design stress for reinforcement (a function of f_y, f_u and θ) (psi)
f_u	static ultimate stress of reinforcement (psi)
f_y	static yield stress of reinforcement (psi)

F	(1) total external force (lbs) (2) coefficient for moment of inertia of cracked section (3) function of C_2 and C_1 for bilinear triangular load
F_o	force in the reinforcing bars (lbs)
F_E	equivalent external force (lbs)
g	variable defined in table 4-3
h	charge location parameter (ft)
H	(1) span height (in.) (2) distance between reflecting surface(s) and/or free edge(s) in vertical direction (ft)
H_c	height of charge above ground (ft)
$\bar{H}_c$	scaled height of charge above ground ($ft/lb^{1/3}$)
H_s	height of structure (ft)
H_T	scaled height of triple point ($ft/lb^{1/3}$)
i	unit positive impulse (psi-ms)
i^-	unit negative impulse (psi-ms)
$\bar{i}_a$	sum of scaled unit blast impulse capacity of receiver panel and scaled unit blast impulse attenuated through concrete and sand in a composite element ($psi\text{-}ms/lb^{1/3}$)
i_b	unit blast impulse (psi-ms)
$\bar{i}_b$	scaled unit blast impulse ($psi\text{-}ms/lb^{1/3}$)
$\bar{i}_{bt}$	total scaled unit blast impulse capacity of composite element ($psi\text{-}ms/lb^{1/3}$)
$\bar{i}_{ba}$	scaled unit blast impulse capacity of receiver panel of composite element ($psi\text{-}ms/lb^{1/3}$)
$\bar{i}_{bd}$	scaled unit blast impulse capacity of donor panel of composite element ($psi\text{-}ms/lb^{1/3}$)
i_e	unit excess blast impulse (psi-ms)
i_r	unit positive normal reflected impulse (psi-ms)
i_r^-	unit negative normal reflected impulse (psi-ms)
i_s	unit positive incident impulse (psi-ms)
i_s^-	unit negative incident impulse (psi-ms)

* See note at end of symbols

I	moment of inertia (in.^{4})
I_a	average of gross and cracked moments of inertia of width b (in.^{4})
I_c	moment of inertia of cracked concrete section of width b (in.^{4})
I_g	moment of inertia of gross concrete section of width b (in.^{4})
I_m	mass moment of inertia (lb-ms^2-in.)
j	ratio of distance between centroids of compression and tension forces to the depth d
k	constant defined in paragraph
K	(1) unit stiffness (psi-in for slabs) (lb/in/in for beams) (2) constant defined in paragraph
K_e	elastic unit stiffness (psi/in for slabs) (lb/in/in for beams)
K_{ep}	elasto-plastic unit stiffness (psi-in for slabs) (psi for beams)
K_E	equivalent elastic unit stiffness (psi-in for slabs) (psi for beams)
K_L	load factor
K_{LM}	load-mass factor
$(K_{LM})_u$	load-mass factor in the ultimate range
$(K_{LM})_{up}$	load-mass factor in the post-ultimate range
K_M	mass factor
K_R	resistance factor
K_1	factor defined in paragraph
KE	kinetic energy
l	charge location parameter (ft)
l_p	spacing of same type of lacing bar (in.)
L	(1) span length (in.) except in chapter 4 (ft)* (2) distance between reflecting surface(s) and/or free edge(s) in horizontal direction (ft)
L_1	length of lacing bar required in distance s_1 (in.)

L_o	embedment length of reinforcing bars (in.)
L_w	wave length of positive pressure phase (ft)
L_w^-	wave length of negative pressure phase (ft)
L_{wb}, L_{wd}	wave length of positive pressure phase at points b and d, respectively (ft)
L_l	total length of sector of element normal to axis of rotation (in.)
m	unit mass (psi-ms^2/in.)
m_a	average of the effective elastic and plastic unit masses (psi-ms^2/in.)
m_e	effective unit mass (psi-ms^2/in.)
m_u	effective unit mass in the ultimate range (psi-ms^2/in.)
m_{up}	effective unit mass in the post-ultimate range (psi-ms^2/in.)
M	(1) unit bending moment (in-lbs/in.) (2) total mass (lb-ms^2/in.)
M_e	effective total mass (lb-ms^2/in.)
M_u	ultimate unit resisting moment (in-lbs/in.)
M_c	moment of concentrated loads about line of rotation of sector (in.-lbs)
M_A	fragment distribution parameter
M_E	equivalent total mass (lb-ms^2/in.)
M_{HN}	ultimate unit negative moment capacity in horizontal direction (in.-lbs/in.)*
M_{HP}	ultimate unit positive moment capacity in horizontal direction (in.-lbs/in.)*
M_N	ultimate unit negative moment capacity at supports (in.-lbs/in.)
M_P	ultimate unit positive moment capacity at midspan (in.-lbs/in.)
M_{VN}	ultimate unit negative moment capacity in vertical direction (in.-lbs/in.)*
M_{VP}	ultimate unit positive moment capacity in vertical direction (in.-lbs/in.)*

* See note at end of symbols

n	(1) modular ratio (2) number of time intervals
N	number of adjacent reflecting surfaces
N_f	number of primary fragments larger than W_f
p	reinforcement ratio equal to $\frac{A_s}{bd}$ or $\frac{A_s}{bd_c}$
p'	reinforcement ratio equal to $\frac{A_s'}{bd}$ or $\frac{A_s'}{bd_c}$
p_b	reinforcement ratio producing balanced conditions at ultimate strength
p_m	mean pressure in a partially vented chamber (psi)
p_{mo}	Peak mean pressure in a partially vented chamber (psi)
p_H	reinforcement ratio in horizontal direction on each face*
p_T	reinforcement ratio equal to $p_H + p_v$
p_v	reinforcement ratio in vertical direction on each face*
$p(x)$	distributed load per unit length
P	(1) pressure (psi) (2) concentrated load (lbs)
P^-	negative pressure (psi)
P_i	interior pressure within structure (psi).
ΔP_i	interior pressure increment (psi)
P_f	fictitious peak pressure (psi)
P_o	peak pressure (psi)
P_r	peak positive normal reflected pressure (psi)
P_r^-	peak negative normal reflected pressure (psi)
$P_{r\alpha}$	peak reflected pressure at angle of incidence α (psi)
P_s	positive incident pressure (psi)
P_{sb}, P_{se}	positive incident pressure at points b and e, respectively (psi)

* See note at end of symbols

P_{so}	peak positive incident pressure (psi)
P_{so}^-	peak negative incident pressure
$P_{sob}, P_{sod}, P_{soe}$	peak positive incident pressure at points b, d, and e, respectively (psi)
q	dynamic pressure (psi)
q_b, q_e	dynamic pressure at points b and e, respectively (psi)
q_o	peak dynamic pressure (psi)
q_{ob}, q_{oe}	peak dynamic pressure at points b and e, respectively (psi)
r	(1) unit resistance (psi) (2) radius of spherical TNT (density equals 95 lb/ft^3 charge (ft))
r^-	unit rebound resistance (psi)
Δr	change in unit resistance (psi)
r_e	elastic unit resistance
r_{ep}	elasto-plastic unit resistance (psi)
r_u	ultimate unit resistance (psi, for slabs) (lb/in for beams)
r_{up}	post-ultimate unit resistant (psi)
r_l	radius of hemispherical portion of. primary fragment (in.)
R	(1) total internal resistance (lbs) (2) slant distance (ft)
R_f	distance traveled by primary fragment (ft)
R_l	radius of lacing bend (in.)
R_A	normal distance (ft)
R_E	equivalent total internal resistance (lbs)
R_G	ground distance (ft)
R_u	total ultimate resistance
R_I, R_{II}	total internal resistance of sectors I and II, respectively (lbs)
s_s	spacing of stirrups in the direction parallel to the longitudinal reinforcement (in.)

* See note at end of symbols

s_l	spacing of lacing in the direction parallel to the longitudinal reinforcement (in.)
S	height of front wall or one-half its width, whichever is smaller (ft)
SE	strain energy
t	time (ms)
Δt	time increment (ms)
t_a	any time (ms)
t_b, t_e, t_f	time of arrival of blast wave at points b, e, and f, respectively (ms)
t_c	(1) clearing time for reflected pressures (ms) (2) container thickness of explosive charges (in.)
t_d	rise time (ms)
t_E	time to reach maximum elastic deflection
t_m	time at which maximum deflection occurs (ms)
t_o	duration of positive phase of blast pressure (ms)
t_o^-	duration of negative phase of blast pressure (ms)
t_{of}	fictitious positive phase pressure duration (ms)
t_{of}^-	fictitious negative phase pressure duration (ms)
t_r	fictitious reflected pressure duration (ms)
t_u	time at which ultimate deflection occurs (ms)
t_y	time to reach yield (ms)
t_A	time of arrival of blast wave (ms)
t_1	time at which partial failure occurs (ms)
T	duration of equivalent triangular loading function (ms)
T_c	thickness of concrete section (in.)
T_c	scaled thickness of concrete section ($ft/lb^{1/3}$)
T_N	effective natural period of vibration (ms)
T_r	rise time (ms)
T_s	thickness of sand fill (in.)

* See note at end of symbols

T_s	scaled thickness of sand fill ($ft/lb^{1/3}$)
u	particle velocity (ft/ms)
u_u	ultimate flexural or anchorage bond stress (psi)
U	shock front velocity (ft/ms)
v	velocity (in./ms)
v_a	instantaneous velocity at any time (in./ms)
v_b	boundary velocity for primary fragments (ft/sec)
v_c	ultimate shear stress permitted on an unreinforced web (psi)
v_f	maximum post-failure fragment velocity (in./ms)
v_f(avg.)	average post-failure fragment velocity (in./ms)
v_i	velocity at incipient failure deflection (in./ms)
v_o	initial velocity of primary fragment (ft/sec)
v_r	residual velocity of primary fragment after perforation (ft/sec)
v_s	striking velocity of primary fragment (ft/sec)
v_u	ultimate shear stress (psi)
v_{uH}	ultimate shear stress at distance d_e from the horizontal support (psi)*
v_{uV}	ultimate shear stress at distance d_e from the vertical support (psi)*
V	volume of partially vented chamber (ft^3)
V_d	ultimate direct shear capacity of the concrete of width b (lbs)
V_{dH}	shear at distance d_e from the vertical support on a unit width (lbs./in.)*
V_{dV}	shear at distance d_e from the horizontal support on a unit width (lbs/in.)*
V_o	volume of structure (ft^3)
V_s	shear at the support on a unit width (lbs/in)*
V_{sH}	shear at the vertical support on a unit width (lbs/in.)*

V_{sV}	shear at the horizontal support on a unit width (lbs/in.)*
V_u	total shear on a width b (lbs)
w	weight density of concrete (lbs/ft^3)
w_s	weight density of sand (lbs/ft^3)
W	charge weight (lbs)
W_c	total weight of explosive containers (lbs)
W_f	weight of primary fragment (oz)
W_{co}	total weight of steel core (lbs)
W_{c1}, W_{c2}	total weight of plates 1 and 2, respectively (lbs)
W_s	width of structure (ft)
WD	work done
x	yield line location in horizontal direction (in.)*
X	deflection (in.)
X_a	any deflection (in.)
X_e	elastic deflection (in.)
X_{ep}	elasto-plastic deflection (in.)
X_f	maximum penetration into concrete of armor-piercing fragments (in.)
X_f'	maximum penetration into concrete of fragments other than armor-piercing (in.)
X_m	maximum transient deflection (in.)
X_p	plastic deflection (in.)
X_s	(1) maximum penetration into sand of armor-piercing fragments (in.) (2) static deflection
X_u	ultimate deflection (in.)
X_E	equivalent elastic deflection (in.)
X_1	partial failure deflection (in.)
y	yield line location in vertical direction (in.)*

* See note at end of symbols

Z	scaled slant distance ($ft/lb^{1/3}$)
Z_A	scaled normal distance ($ft/lb^{1/3}$)
Z_G	scaled ground distance ($ft/lb^{1/3}$)
α	(1) angle formed by the plane of stirrups, lacing, or diagonal reinforcement and the plane of the longitudinal reinforcement (deg)
α	(2) angle of incidence of the pressure front (deg)
β	(1) coefficient for determining elastic and elasto-plastic resistances
	(2) particular support rotation angle.(deg)
γ	coefficient for determining elastic and elasto-plastic deflections
γ	deflections increase in support rotation angle after partial failure (deg)
θ	support rotation angle (deg)
θ	angular acceleration (rad/ms^2)
θ_{max}	maximum support rotation angle (deg)
θ_H	horizontal rotation angle (deg)*
θ_V	vertical rotation angle (deg)*
Σo	effective perimeter of reinforcing bars (in.)
ΣM	summation of moments (in.-lbs)
ΣM_N	sum of the ultimate unit resisting moments acting along the negative yield lines (in.-lbs)
ΣM_P	sum of the ultimate unit resisting.moments acting along the positive yield lines (in.-lbs)
μ	ductility factor
ν	Poisson's ratio
ϕ	(1) capacity reduction factor (2) bar diameter (in.)
ϕ_r	assumed shape function for concentrated loads
$\phi(x)$	assumed shape function for distributed loads

* See note at end of symbols

———	free edge
═══	simple support
///////	fixed support
XXXXXXX	either fixed, restrained, or simple support

* Note. This symbol was developed for two-way elements which are used as walls. When roof slabs or other horizontal elements are under consideration, this symbol will also be applicable if the element is treated as being rotated into a vertical position.

APPENDIX 3C

BIBLIOGRAPHY

1. Blast Resistant Design, NAVFAC Design Manual 2.8, Department of the Navy, Naval Facilities Engineering Command, Alexandria, VA 22332, April 1982.

2. Design of Structures to Resist Nuclear Weapons Effects, ASCE Manual of Engineering Practice, No. 42, American Society of Civil Engineers, New York, NY, 1961. (1983 Edition under preparation)

3. Designing Facilities to Resist Nuclear Weapons Effects, Structures, TM5-858-3, Headquarters, Department of the Army, Washington, DC.

4. Structures to Resist the Effects of Accidental Explosions, Technical Manual TM5-1300, Navy Publication NAVFAC P-397, Air Force Manual AFM 88-22, Department of the Army, the Navy, and the Air Force, Washington, DC, June 1969.

5. Crawford, R. E., et al, The Air Force Manual for Design and Analysis of Hardened Structures, AFWL-TR-74-102, Air Force Weapons Laboratory, Kirtland Air Force Base, New Mexico, 87117.

6. Healey, J., et at, Design of Steel Structures to Resist the Effects of HE Explosions, by Ammann and Whitney, Consulting Engineers, New York, NY, Technical Report 4837, Picatinny Arsenal, Dover, NJ, August 1975.

7. Hopkins, J., Charts for Predicting Response of a Simple Spring-Mass System to a Bilinear Blast Load, Technical Note N-1669, Naval Civil Engineering Laboratory, Port Hueneme, CA, April 1983.

8. Stea, W., et al, Nonlinear Analysis of Frame Structures Subjected to Blast Overpressures, by Ammann and Whitney, Consulting Engineers, New York, NY, Contractor report ARLCD-CR-77008, U.S. Army Armament Research and Development Command, Large Caliber Weapon Systems Laboratory, Dover, NJ, May 1977.

9. Stea, W. Weissman, S., and Dobbs, N., Overturning and Sliding Analysis of Reinforced Concrete Protective Structures, by Ammann and Whitney, consulting Engineers, New York, NY, Technical Report 4921, Picatinny Arsenal, Dover, NJ, February 1976.

10. Javornicky, J. and Van Amerongen, C., Tables for the Analysis of Plates, Slabs and Diaphragms Based on the Elastic Theory, Bauverlag GmbH., Wiesbaden/Germany (2nd Edition 1971).

11. Roark, R.J. and Young, W. C., Formulas for Stress and Strain, McGraw Hill, New York (5th Edition 1975).

12. Cohen, E. and Dobbs, N., Design Procedures and Details for Reinforced Concrete Structures Utilized in Explosive Storage and Manufacturing Facilities, Ammann and Whitney, Consulting Engineers, New York, NY, Annals of the New York Academy of Sciences, Conference on Prevention of and Protection against Accidental Explosion of Munitions, Fuels and Other Hazardous Mixtures, Volume 152, Art. 1, October 1968.

CHAPTER 4. REINFORCED CONCRETE DESIGN

CHAPTER 4

REINFORCED CONCRETE DESIGN

INTRODUCTION

4-1. Purpose

The purpose of this manual is to present methods of design for protective construction used in facilities for development, testing, production, storage, maintenance, modification, inspection, demilitarization, and disposal of explosive materials.

4-2. Objective

The primary objectives are to establish design procedures and construction techniques whereby propagation of explosion (from one structure or part of a structure to another) or mass detonation can be prevented and to provide protection for personnel and valuable equipment.

The secondary objectives are to:

(1) Establish the blast load parameters required for design of protective structures.
(2) Provide methods for calculating the dynamic response of structural elements including reinforced concrete, and structural steel.
(3) Establish construction details and procedures necessary to afford the required strength to resist the applied blast loads.
(4) Establish guidelines for siting explosive facilities to obtain maximum cost effectiveness in both the planning and structural arrangements, providing closures, and preventing damage to interior portions of structures because of structural motion, shock, and fragment perforation.

4-3. Background

For the first 60 years of the 20th century, criteria and methods based upon results of catastrophic events were used for the design of explosive facilities. The criteria and methods did not include a detailed or reliable quantitative basis for assessing the degree of protection afforded by the protective facility. In the late 1960's quantitative procedures were set forth in the first edition of the present manual, "Structures to Resist the Effects of Accidental Explosions". This manual was based on extensive research and development programs which permitted a more reliable approach to current and future design requirements. Since the original publication of this manual, more extensive testing and development programs have taken place. This additional research included work with materials other than reinforced concrete which was the principal construction material referenced in the initial version of the manual.

Modern methods for the manufacture and storage of explosive materials, which include many exotic chemicals, fuels, and propellants, require less space for a given quantity of explosive material than was previously needed. Such concentration of explosives increases the possibility of the propagation of accidental explosions. (One accidental explosion causing the detonation of

other explosive materials.) It is evident that a requirement for more accurate design techniques is essential. This manual describes rational design methods to provide the required structural protection.

These design methods account for the close-in effects of a detonation including the high pressures and the nonuniformity of blast loading on protective structures or barriers. These methods also account for intermediate and far-range effects for the design of structures located away from the explosion. The dynamic response of structures, constructed of various materials, or combination of materials, can be calculated, and details are given to provide the strength and ductility required by the design. The design approach is directed primarily toward protective structures subjected to the effects of a high explosive detonation. However, this approach is general, and it is applicable to the design of other explosive environments as well as other explosive materials as mentioned above.

The design techniques set forth in this manual are based upon the results of numerous full- and small-scale structural response and explosive effects tests of various materials conducted in conjunction with the development of this manual and/or related projects.

4-4. Scope

It is not the intent of this manual to establish safety criteria. Applicable documents should be consulted for this purpose. Response predictions for personnel and equipment are included for information.

In this manual an effort is made to cover the more probable design situations. However, sufficient general information on protective design techniques has been included in order that application of the basic theory can be made to situations other than those which were fully considered.

This manual is applicable to the design of protective structures subjected to the effects associated with high explosive detonations. For these design situations, the manual will apply for explosive quantities less than 25,000 pounds for close-in effects. However, this manual is also applicable to other situations such as far- or intermediate-range effects. For these latter cases the design procedures are applicable for explosive quantities in the order of 500,000 pounds which is the maximum quantity of high explosive approved for aboveground storage facilities in the Department of Defense manual, "Ammunition and Explosives Safety Standards", DOD 6055.9-STD. Since tests were primarily directed toward the response of structural steel and reinforced concrete elements to blast overpressures, this manual concentrates on design procedures and techniques for these materials. However, this does not imply that concrete and steel are the only useful materials for protective construction. Tests to establish the response of wood, brick blocks, and plastics, as well as the blast attenuating and mass effects of soil are contemplated. The results of these tests may require, at a later date, the supplementation of these design methods for these and other materials.

Other manuals are available to design protective structures against the effects of high explosive or nuclear detonations. The procedures in these manuals will quite often complement this manual and should be consulted for specific applications.

Computer programs, which are consistent with procedures and techniques contained in the manual, have been approved by the appropriate representative of the US Army, the US Navy, the US Air Force and the Department of Defense Explosives Safety Board (DDESB). These programs are available through the following repositories:

(1) Department of the Army
Commander and Director
U.S. Army Engineer
Waterways Experiment Station
Post Office Box 631
Vicksburg, Mississippi 39180-0631
Attn: WESKA

(2) Department of the Navy
Commanding Officer
Naval Civil Engineering Laboratory
Port Hueneme, California 93043
Attn: Code L51

(3) Department of the Air Force
Aerospace Structures
Information and Analysis Center
Wright Patterson Air Force Base
Ohio 45433
Attn: AFFDL/FBR

If any modifications to these programs are required, they will be submitted for review by DDESB and the above services. Upon concurrence of the revisions, the necessary changes will be made and notification of the changes will be made by the individual repositories.

4-5. Format

This manual is subdivided into six specific chapters dealing with various aspects of design. The titles of these chapters are as follows:

Chapter 1	Introduction
Chapter 2	Blast, Fragment, and Shock Loads
Chapter 3	Principles of Dynamic Analysis
Chapter 4	Reinforced Concrete Design
Chapter 5	Structural Steel Design
Chapter 6	Special Considerations in Explosive Facility Design

When applicable, illustrative examples are included in the Appendices.

Commonly accepted symbols are used as much as possible. However, protective design involves many different scientific and engineering fields, and, therefore, no attempt is made to standardize completely all the symbols used. Each symbol is defined where it is first used, and in the list of symbols at the end of each chapter.

CHAPTER CONTENTS

4-6. General

This chapter is concerned with the design of above ground blast resistant concrete structures. Procedures are presented to obtain the dynamic strength of the various structural components of concrete structures. Except for the particular case of the design of laced reinforced concrete elements, the dynamic analysis of the structural components is presented in Chapter 3.

The dynamic strengths of both the concrete and reinforcement under various stress conditions are given for the applicable design range and the allowable deflection range. Using these strengths, the ultimate dynamic capacity of various concrete elements are given. These capacities include the ultimate moment capacity for various possible cross-section types, ultimate shear capacity as a measure of diagonal tension as well as ultimate direct shear and punching shear, torsion capacity of beams, and the development of the reinforcement through bond with the concrete.

This chapter contains procedures for the design of non-laced (conventional reinforcement) and laced concrete slabs and walls as well as procedures for the design of flat slabs, beams and columns. Procedures are presented for the design of laced and non-laced slabs and beams for close-in effects whereas procedures for the design of non-laced and flat slabs, beams and columns are given for far range effects. It is not economical to use laced slabs for far range effects. Design procedures are given for the flexural response of one- and two-way non-laced slabs, beams and flat slabs which undergo limited deflections. Procedures are also given for large deflections of these elements when they undergo tensile membrane action. Laced reinforced slabs are designed for flexural action for both limited and large deflections. Lastly, the design of columns is presented for elastic or, at best, slight plastic action.

The above design procedures are concerned with the ductile response of structural elements. Procedures are also given for the brittle mode response of concrete elements. The occurrence of both spalling and scabbing of the concrete as well as protection against their effects is treated. In addition, procedures are presented for post-failure fragment design of laced concrete walls and slabs. The resistance of concrete elements to primary fragment impact is considered. For the primary fragments determined in Chapter 2, methods are presented to determine if a fragment is embedded in or perforates a concrete wall. If embedment occurs, the depth of penetration is determined and the occurrence of spalling of the far face can be evaluated. If perforation occurs, the residual velocity of the fragment is determined.

Required construction details and procedures for conventionally reinforced and laced reinforced concrete structures is the last item discussed in the chapter. Conformance to these details will insure a ductile response of the structure to the applied dynamic loads.

BASIS FOR STRUCTURAL DESIGN

4-7. General

Explosive storage and operating facilities are designed to provide a predetermined level of protection against the hazards of accidental explosions. The type of protective structure depends upon both the donor and acceptor systems. The donor system (amount, type and location of the potentially detonating explosives) produces the damaging output while the acceptor system (personnel, equipment, and "acceptor" explosives) requires a level of protection. The protective structure or structural elements are designed to shield against or attenuate the hazardous effects to levels which are tolerable to the acceptor system.

Protective concrete structures are classified as either shelters or barriers. Shelters enclose the receiver system and are generally located far from a potential explosion. Barriers, on the other hand, generally enclose the donor system and, consequently, are located close to the potential explosion. A shelter is a fully enclosed structure which is designed to prevent its contents (acceptor system) from being subjected to the direct effects of blast pressures and fragments. A barrier may be either a fully enclosed structure (containment structure) or an open structure (barricade or cubicle type structure in which one or more surfaces are frangible or open to the atmosphere). Barriers are generally designed to resist close-in detonations. Their purpose is to prevent acceptor explosives, and to a lesser extent, personnel and equipment from being subjected to primary fragment impact and to attenuate blast pressures in accordance with the structural configuration of the barrier.

4-8. Modes of Structural Behavior

The response of a concrete element can be expressed in terms of two modes of structural behavior; ductile and brittle. In the ductile mode of response the element may attain large inelastic deflections without complete collapse. While, in the brittle mode, partial failure or total collapse of the element occurs. The selected behavior of an element for a particular design is governed by: (1) the magnitude and duration of the blast output, (2) the occurrence of primary fragments, and (3) the function of the protective structure, i.e., shelter or barrier depending upon the protection level required.

4-9. Structural Behavior of Reinforced Concrete

4-9.1. General

When a reinforced concrete element is dynamically loaded, the element deflects until such time that: (1) the strain energy of the element is developed sufficiently to balance the kinetic energy produced by the blast load and the element comes to rest, or (2) fragmentation of the concrete occurs resulting in either partial or total collapse of the element. The maximum deflection attainable is a function of the span of the element, the depth of the element, and the type, amount, and details of the reinforcement used in a particular design.

The resistance-deflection curve shown in Figure 4-1 demonstrates the flexural action of a reinforced concrete element. When the element is first loaded, the resistance ideally increases linearly with deflection until yielding of the reinforcement is first initiated. As the element continues to deflect, all the reinforcing steel yields and the resistance is constant with increasing deflection. Within this yield range at a deflection corresponding to 2 degrees support rotation, the compression concrete crushes. For elements without shear reinforcement, this crushing of the concrete results in failure of the element. For elements with shear reinforcement (single leg stirrups shown in Figure 4-2 or lacing shown in Figure 4-3) which properly tie the flexural reinforcement, the crushing of the concrete results in a slight loss of capacity since the compressive force is transferred to the compression reinforcement. As the element is further deflected, the reinforcement enters into its strain hardening region, and the resistance increases with increasing deflection. Single leg stirrups will restrain the compression reinforcement for a short time into its strain hardening region. At four (4) degrees support rotation, the element loses its structural integrity and fails. On the other hand, lacing through its truss action will restrain the reinforcement through its entire strain hardening region until tension failure of the reinforcement occurs at 12 degrees support rotation.

Sufficient shear capacity must be afforded by the concrete alone or in combination with shear reinforcement in order to develop the flexural capacity of an element (Figure 4-1). An abrupt shear failure can occur at any time during the flexural response if the flexural capacity exceeds the shear capacity of the element.

4-9.2. Ductile Mode of Behavior in the Far Design Range

In the far design range, the distribution of the applied blast load is fairly uniform and the deflections required to absorb the loading are comparatively small. Conventionally reinforced (i.e., non-laced) concrete elements with comparatively minor changes to standard reinforcing details are perfectly adequate to resist such loads. While laced reinforcement could be used, it would be extremely uneconomical to do so.

The flexural response of non-laced reinforced concrete elements is demonstrated through the resistance-deflection curve of Figure 4-1. For elements without shear reinforcement, the ultimate deflection is limited to deflections corresponding to 2 degrees support rotation whereas elements with shear reinforcement are capable of attaining 4 degrees support rotation. For ease of construction, single leg stirrups (Figure 4-2) are used as shear reinforcement in slabs and walls. This type of reinforcement is capable of providing shear resistance as well as the necessary restraint of the flexural reinforcement to enable the slab to achieve this increased deflection.

A conventionally reinforced slab may attain substantially larger deflections than those corresponding to 4 degrees support rotations . These increased deflections are possible only if the element has sufficient lateral restraint to develop in-plane forces. The resistance-deflection curve of Figure 4-4 illustrates the structural response of an element having lateral restraint. Initially, the element behaves essentially as a flexural member. If the lateral restraint prevents small motions, in-plane compressive forces are developed. Under flexural action, the capacity is constant with increasing deflection until the compression concrete crushes. As the deflection in-

creases further and the load carried by the slab decreases, membrane action in the slab is developed. The slab carries load by the reinforcement net acting as a plastic tensile membrane. The capacity of the element increases with increasing deflection until the reinforcement fails in tension.

4-9.3. Ductile Mode of Behavior in the Close-in Design Range

Close-in detonations produce nonuniform, high intensity blast load. Extremely high-pressure concentrations are developed which, in turn, can produce local (punching) failure of an element. To maintain the structural integrity of elements subjected to these loads and to permit the large deflections necessary to balance the kinetic energy produced, lacing reinforcement has been developed.

Lacing reinforcement is shown in Figure 4-3 while a typical laced wall is shown in Figure 4-5. A laced element is reinforced symmetrically, i.e., the compression reinforcement is the same as the tension reinforcement. The straight flexural reinforcing bars on each face of the element and the intervening concrete are tied together by the truss action of continuous bent diagonal bars. This system of lacing contributes to the integrity of the protective element in the following ways:

(1) Ductility of the flexural reinforcement, including the strain hardening region, is fully developed.
(2) Integrity of the concrete between the two layers of flexural reinforcement is maintained despite massive cracking.
(3) Compression reinforcement is restrained from buckling.
(4) High shear stresses at the supports are resisted.
(5) Local shear failure produced by the high intensity of the peak blast pressures is prevented.
(6) Quantity and velocity of post-failure fragments produced during the brittle mode of behavior are reduced.

The flexural response of a laced reinforced concrete element is illustrated by the entire resistance-deflection curve shown in Figure 4-1. The lacing permits the element to attain large deflections and fully develop the reinforcement through its strain hardening region. The maximum deflection of a laced element corresponds to 12 degrees support rotation.

Single leg stirrups contribute to the integrity of a protective element in much the same way as lacing, however, the stirrups are less effective at the closer explosive separation distances. The explosive charge must be located further away from an element containing stirrups than a laced element. In addition, the maximum deflection of an element with single leg stirrups is limited to 4 degrees support rotation under flexural action or 8 degrees under tension membrane action. If the charge location permits and reduced support rotations are required, elements with single leg stirrups may prove more economical than laced elements.

4-9.4. Brittle Mode of Behavior

The brittle behavior of reinforced concrete is composed of three types of concrete failure: direct spalling, scabbing and post-failure fragments. Direct spalling consists of the dynamic disengagement of the concrete cover over the flexural reinforcement due to high intensity blast pressures.

Scabbing also consists of the disengagement of the concrete cover over the flexural reinforcement, however, scabbing is due to the element attaining large deflections. Finally post-failure fragments are the result of the collapse of an element and are usually the more serious. Post-failure fragments are generally large in number and/or size with substantial velocities which can result in propagation of explosion. Spalling and scabbing are usually only of concern in those protective structures where personnel, equipment, or sensitive explosives require protection. Controlled post-failure fragments are only permitted where the acceptor system consists of relatively insensitive explosives.

The two types of spalling, direct spalling and scabbing, occur during the ductile mode of behavior. Because direct spalling is dependent upon the transmission of shock pressures, fragments formed from this type of spalling are produced immediately after the blast pressures strike the wall. Scabbing, on the other hand, occurs during the later stages of the flexural (ductile mode) action of the element. Both types of spalls affect the capacity of the element to resist the applied blast load.

Post-failure fragments are the result of a flexural failure of an element. The failure characteristics of laced and unlaced elements differ significantly. The size of failed sections of laced element is fixed by the location of the yield lines. The element fails at the yield lines and the section between yield lines remain intact. Consequently, failure of a laced element consists of a few large sections (Figure 4-6). On the other hand, failure of an unlaced element is a result of a loss of structural integrity and the fragments take the form of concrete rubble (Figure 4-7). The velocity of the post failure fragments from both laced and unlaced elements is a function of the amount of blast overload. However, tests have indicated that the fragment velocities of laced elements are as low as 30 percent of the maximum velocity of the rubble formed from similarly loaded unlaced elements.

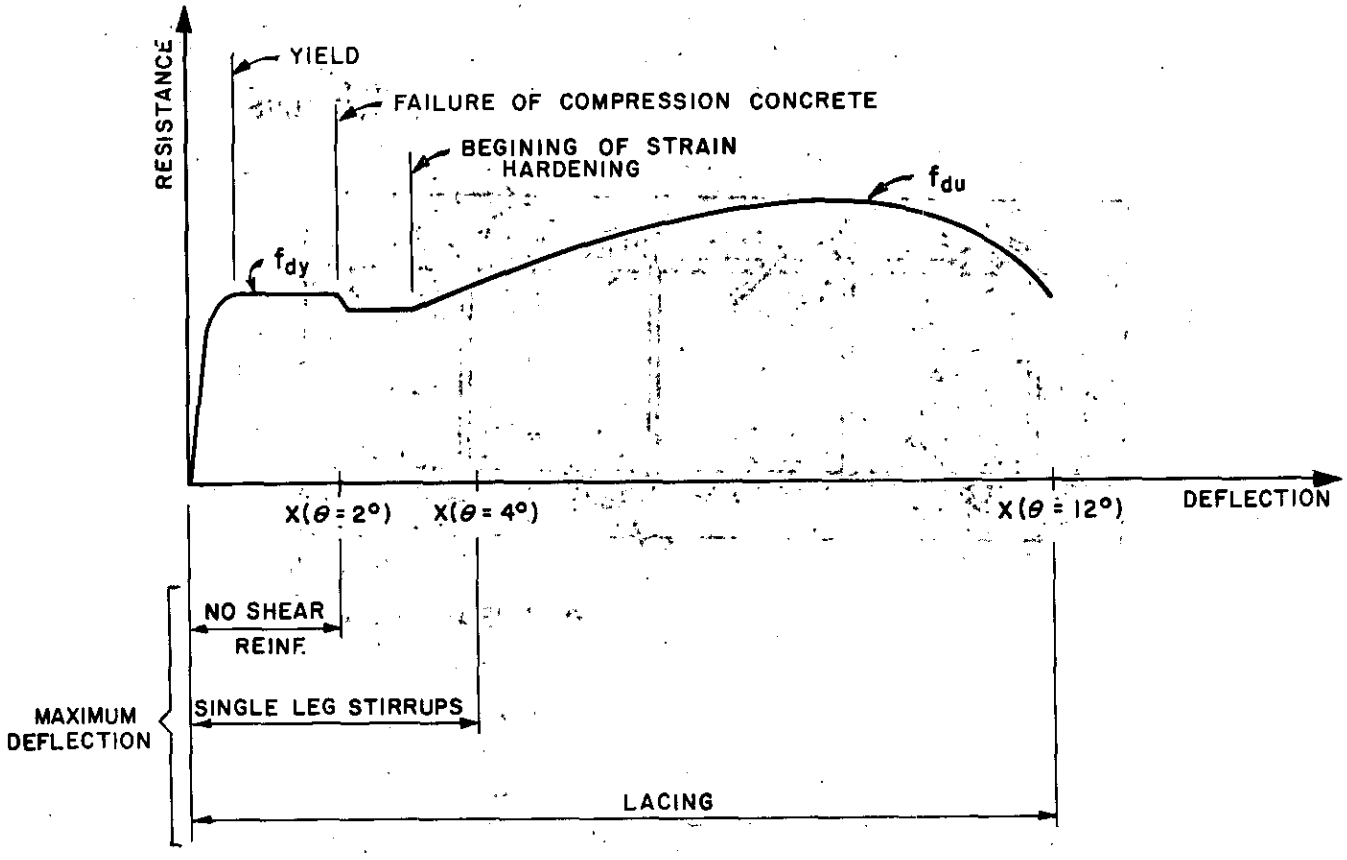


Figure 4-1 Typical resistance-deflection curve for flexural response of concrete elements

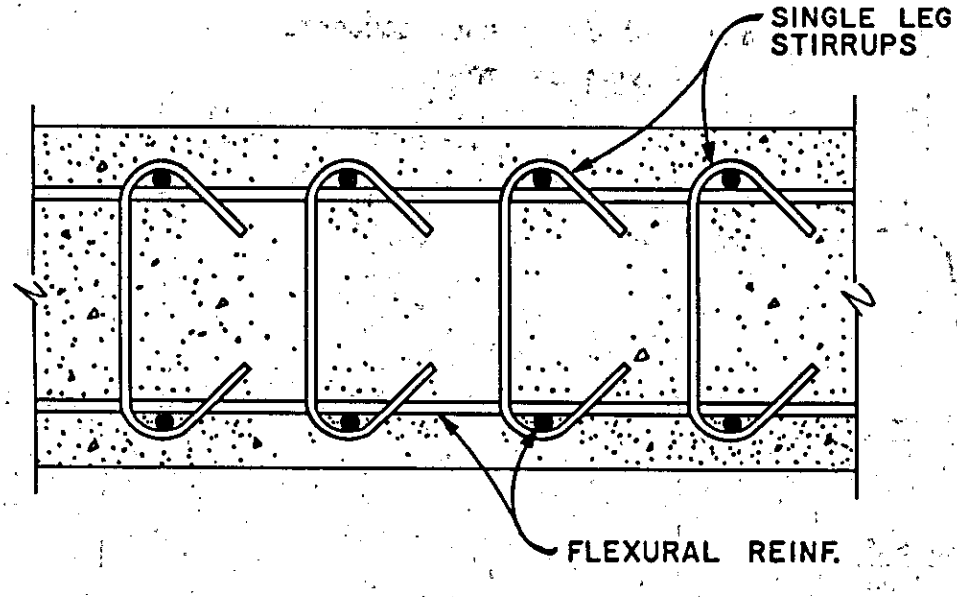


Figure 4-2 Element reinforced with single leg stirrups

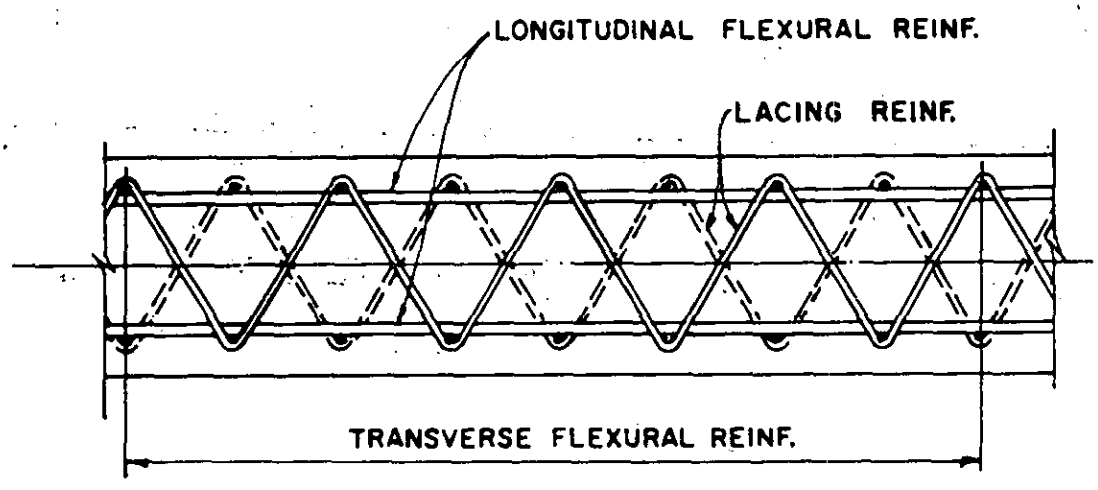


Figure 4-3 Lacing reinforcement

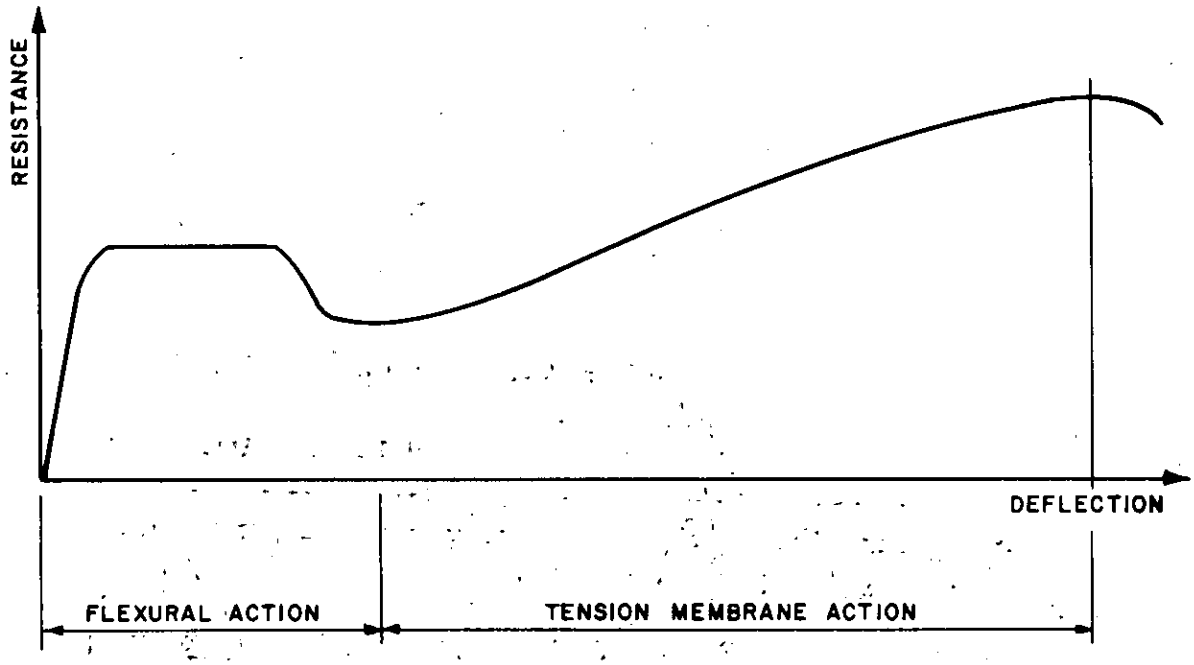


Figure 4-4 Typical resistance-deflection curve for tension membrane response of concrete

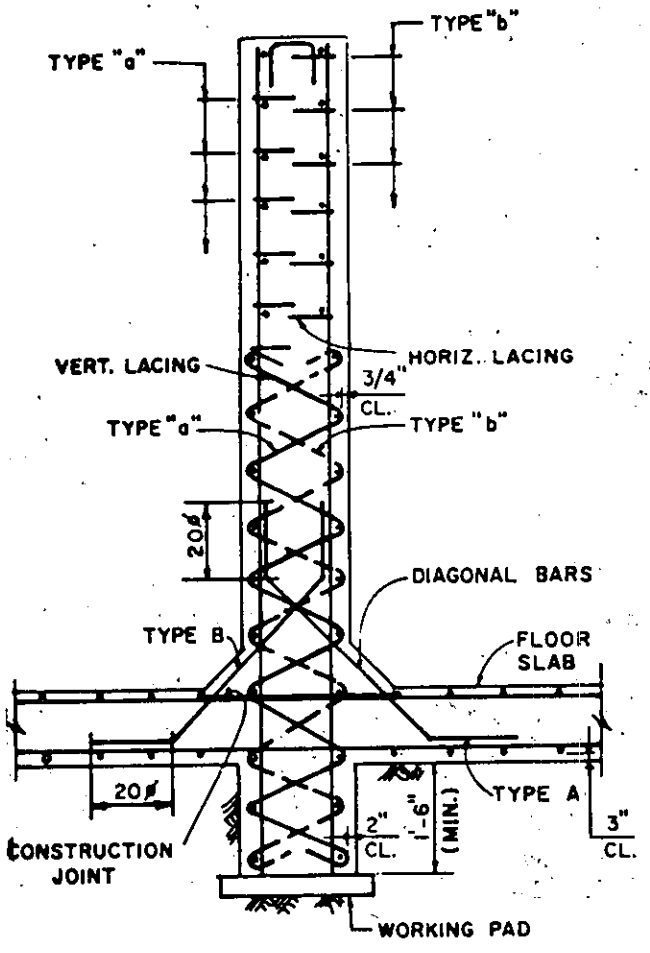


Figure 4-5 Typical laced wall



Figure 4-6 Failure of a laced element



Figure 4-7 Failure of an unlaced element

DYNAMIC STRENGTH OF MATERIALS

4-10. Introduction

A structural element subjected to a blast loading exhibits a higher strength than a similar element subjected to a static loading. This increase in strength for both the concrete and reinforcement is attributed to the rapid rates of strain that occur in dynamically loaded members. These increased stresses or dynamic strengths are used to calculate the element's dynamic resistance to the applied blast load. Thus, the dynamic ultimate resistance of an element subjected to a blast load is greater than its static ultimate resistance.

Both the concrete and reinforcing steel exhibit greater strength under rapid strain rates. The higher the strain rate, the higher the compressive strength of concrete and the higher the yield and ultimate strength of the reinforcement.

This phenomenon is accounted for in the design of a blast resistant structure by using dynamic stresses to calculate the dynamic ultimate resistance of the reinforced concrete members.

4-11. Stress-Strain Curve

Typical stress-strain curves for concrete and reinforcing steel are shown in Figure 4-8. The solid curves represent the stress-strain relationship for the materials when tested at the strain and loading rates specified in ASTM Standards. At a higher strain rate, their strength is greater, as illustrated by the dashed curves. Definitions of the symbols used in Figure 4-8 are as follows:

f'_c = static ultimate compressive strength of concrete

f'_{dc} = dynamic ultimate compressive strength of concrete

f_y = static yield stress of reinforcing steel

f_{dy} = dynamic yield stress of reinforcing steel

f_u = static ultimate stress of reinforcing steel

f_{du} = dynamic ultimate stress of reinforcing steel

E_s = modulus of elasticity for reinforcing steel

E_c = secant modulus of elasticity of concrete

ϵ_u = rupture strain

From the standpoint of structural behavior and design, the most important effect of strain rate is the increased yield and ultimate strengths of the reinforcement and the compressive strength of the concrete. For typical strain rates encountered in reinforced concrete elements subjected to blast loads, the increase in the yield strength of the steel and the compressive strength of the concrete is substantial. The ultimate strength of the

reinforcement is much less sensitive to the strain rate. The increase in the ultimate strength is slight and the strain at which this stress occurs is slightly reduced. There is essentially no change with strain rate in the modulus of elasticity and rupture strain of the steel. In the case of concrete, as the strain rate increases the scant modulus of elasticity increases slightly, and the strain at maximum stress and rupture remain nearly constant.

4-12. Allowable Material Strengths

4-12.1. General

The behavior of a structural element subjected to a blast loading depends upon the ultimate strength and ductility of the materials from which it is constructed. The required strength of a ductile element is considerably less than that necessary for a brittle element to resist the same applied loading. A ductile element maintains its peak or near-peak strength through large plastic strains whereas a brittle element fails abruptly with little energy absorbed in the plastic range. Reinforced concrete with well tied and anchored ductile reinforcement can be classified as a ductile material.

4-12.2. Reinforcement

Reinforcing steel, designated by the American Society for Testing and Materials (ASTM) as A 615, Grade 60, is considered to have adequate ductility in sizes up to No. 11 bars. The large No. 14 bars also have the desired ductility, but their usage is somewhat restricted due to their special requirements of spacing and anchorage. No. 18 bars are not recommended for use in blast resistant structures. For all reinforcement, ductility is reduced at bends, lapped splices, mechanical splices, etc., and location of these anchorages near points of maximum stress is undesirable and should be avoided.

Reinforcing steel having a minimum yield of 75,000 psi can be produced having chemical properties similar to ASTM A 615, Grade 60. However, production of this steel requires a special order to be placed in which large quantities of individual bar sizes (in the order of 200 tons per bar size) must be ordered. It is recommended that for these high strength bars only straight lengths of bars be utilized, splicing of bars be avoided and application of this reinforcement be limited to members designated to attain an elastic response or a slightly plastic response (X_m/X_E less than or equal to 3).

It is desirable to know the stress-strain relationship for the reinforcement being utilized in order to calculate the ultimate resistance of an element. This information is not usually available; however, minimum values of the yield stress f_y and the ultimate tensile stress f_u are required by ASTM Standards. For ASTM A 615, Grade 60 reinforcement, the minimum yield and ultimate stresses are 60,000 psi and 90,000 psi, respectively. Review of numerous mill test reports for this steel indicate yield stresses at least 10 percent greater than the ASTM minimum, and ultimate stresses at least equal to but not much greater than the ASTM minimum. Therefore it is recommended that for design purposes, the minimum ASTM yield stress be increased by 10 percent while the minimum ASTM ultimate stress be used without any increase. So that, the recommended design values for ASTM A 615, Grade 60 reinforcement, are:

$$f_y = 66{,}000 \text{ psi}$$

and

$$f_u = 90{,}000 \text{ psi}$$

4-12.3. Concrete

Even though the magnitude of the concrete strength is only significant in the calculation of the ultimate strength of elements with support rotations less than 2 degrees, its effects on the behavior of elements with both small and large support rotations are of equal importance. The shear capacity of an element is dependent upon the magnitude of the concrete strength. For elements with small support rotations (less than 2 degrees), the use of higher strength concrete may eliminate the need for shear reinforcement; while for elements requiring shear reinforcement, the amount of reinforcement is reduced as the concrete strength is increased. For elements with large support rotations (2 to 12 degrees), the cracking and crushing of the concrete associated with the larger rotations is less severe when higher strength concrete is employed. Therefore, the strength of the concrete used in a blast resistant structure may be selected to suit the particular design requirements of the structure. However, under no circumstances should the concrete strength f'_c be less than 3,000 psi. It is recommended that 4,000 psi strength concrete be used in all blast resistant structures regardless of the magnitude of the blast load and deflection criteria.

4-13. Dynamic Design Stresses for Reinforced Concrete

4-13.1. General

Ductility is a significant parameter influencing the dynamic response and behavior of reinforced concrete members subjected to blast loadings. The importance of ductility increases as the duration of the blast load decreases relative to the natural period of the member. In general, to safely withstand a blast load, the required ultimate resistance decreases with increasing ductility of the member. In fact, the ultimate resistance required of ductile members is considerably less than that required for brittle members which fail abruptly with little energy absorbed in the plastic range of behavior.

A ductile member is one that develops plastic hinges in regions of maximum moment by first yielding of the tension reinforcement followed by crushing of the concrete. This behavior is typical of under-reinforced concrete sections. A section can be designed to be very ductile by maintaining an under-reinforced section, adding compression reinforcement, and utilizing lacing bars to prevent buckling of the compression reinforcement. For a laced section, the reinforcement is stressed through its entire strain-hardening region, that is, the steel reaches its ultimate stress f_{du} and fails at its rupture strain ϵ_u. In a flexural member, the straining of the reinforcement, and consequently its stress, is expressed in terms of its angular support rotations.

4-13.2. Dynamic Increase Factor

The dynamic increase factor, DIF, is equal to the ratio of the dynamic stress to the static stress, e.g., f_{dy}/f_y, f_{du}/f_u and f'_{dc}/f'_c. The DIF depends upon the rate of strain of the element, increasing as the strain rate increases. The design curves for the DIF for the unconfined compressive strength of concrete and for the yield stress of ASTM A 615, Grade 60, reinforcing steel, are

given in Figure 4-9 and 4-10, respectively. The curves were derived from test data having a maximum strain rate of 10×10^{-3} in./in./msec. for concrete and 2.1×10^{-3} in./in./msec. for steel. Values taken from these design curves are conservative estimates of DIF and safe for design purposes.

Values of DIF have been established for design of members in the far design range as well as for members in the close-in design range. These design values of DIF are given in Table 4-1. Because of the increased magnitude of the blast loads and subsequent increase in the strain rate, the dynamic increase factors for elements subjected to a close-in detonation are higher than those for elements subjected to an explosion located far from the element.

The design values of DIF presented in Table 4-1 vary not only for the design ranges and type of material but also with the state of stress (bending, diagonal tension, direct shear, bond, and compression) in the material. The values for f_{dy}/f_y and f'_{dc}/f'_c for reinforced concrete members in bending assume the strain rates in the reinforcement and concrete are 0.0001 in./in./ msec. for the far design range and 0.0003 in./in./ msec. in the close-in design range. For members in compression (columns). these strain rates are 0.0002 in./in./msec. and 0.0005 in./in./msec. The lower strain rates in compression (compared to bending) account for the fact that slabs, beams and girders "filter" the dynamic effects of the blast load. Thus, the dynamic load reaching columns is typically a fast "static" load (long rise time of load) which results in lower strain rates in columns. These strain rates and the corresponding values of DIF in Table 4-1 are considered safe values for design purposes.

Available data is not sufficient to permit the construction of a design curve for the DIF for the ultimate stress of ASTM A 615 Grade 60 reinforcing steel. However, it is known that the increase in the ultimate strength of the steel is small and, therefore, not a significant factor in the design of reinforced concrete members. A nominal value of the DIF is given in Table 4-1.

The listed values of DIF for shear (diagonal tension and direct shear) and bond are more conservative than for bending or compression. This conservatism is justified by the need to prevent brittle shear and bond failure and to account for uncertainties in the design process for shear and bond.

A more accurate estimate of the DIF may be obtained utilizing the DIF design curve for concrete and steel given in Figure 4-9 and 4-10, respectively. The increase in capacity of flexural elements is primarily a function of the rate of strain or the reinforcement, in particular, the time to reach yield, t_E, of the reinforcing steel. The average rate of strain for both the concrete and steel may be obtained considering the strain in the materials at yield and the time to reach yield. The member is first designed (procedures given in subsequent sections) using the DIF values given in Table 4-1. The time to reach yield, t_E, is then calculated using the response charts presented in Chapter 2. For the value t_E, the average strain rate in the materials can be obtained. The average strain rate in the concrete (based on f'_{dc} being reached at $\epsilon_c = 9{,}992$ in./in.) is:

$$\epsilon'_c = 0.002 / t_E \qquad 4\text{-}1$$

while the average strain rate in the reinforcement is:

$$\epsilon'_s = f_{dy} / E_s t_E \qquad 4\text{-}2$$

where

ϵ'_c = average strain rate for concrete

ϵ'_s = average strain rate for reinforcement

t_E = time to yield the reinforcement

For the strain rates obtained from Equations 4-1 and 4-2, the actual DIF is obtained for the concrete and reinforcement from Figure 4-9 and 4-10, respectively. If the difference between the calculated DIF values and the design values of Table 4-1 are small, then the correct values of DIF are those calculated. If the difference is large, the calculated values of DIF are used as new estimates and the process is repeated until the differences between the "estimated" and "calculated" values of DIF are small. The process converges very rapidly and, in most cases, the second iteration of the process converges on the proper values of DIF.

In most cases, the values of DIF obtained from Table 4-1 are satisfactory for design and the determination of the actual DIF values is unwarranted. However, the DIF values can significantly effect the final design of certain members, and the extra calculations required to obtain the actual DIF values are fully warranted. These include deep members, members subjected to impulse-type blast loads and members designed to sustain large deflections. The actual DIF values (usually higher than the design values of Table 4-1) result in a more realistic estimate of the ultimate flexural resistance and, therefore, the maximum shear and bond stresses which must be resisted by the member.

For the elasto-plastic or plastic design of concrete elements, an equivalent elastic curve is considered rather than the actual elasto-plastic resistance-deflection function. The time to reach yield t_E is computed based on this curve using the equivalent elastic deflection X_E and stiffness K_E. Actually, the reinforcement along the supports yield in less time than t_E whereas the reinforcement at mid-span yields at a time greater than t_E. These differences are compensating errors. Therefore, the time to reach yield t_E for the equivalent curve when used in Equations 4-1 and 4-2 produces an accurate average DIF for the concrete and reinforcement at the critical sections throughout a reinforced concrete element.

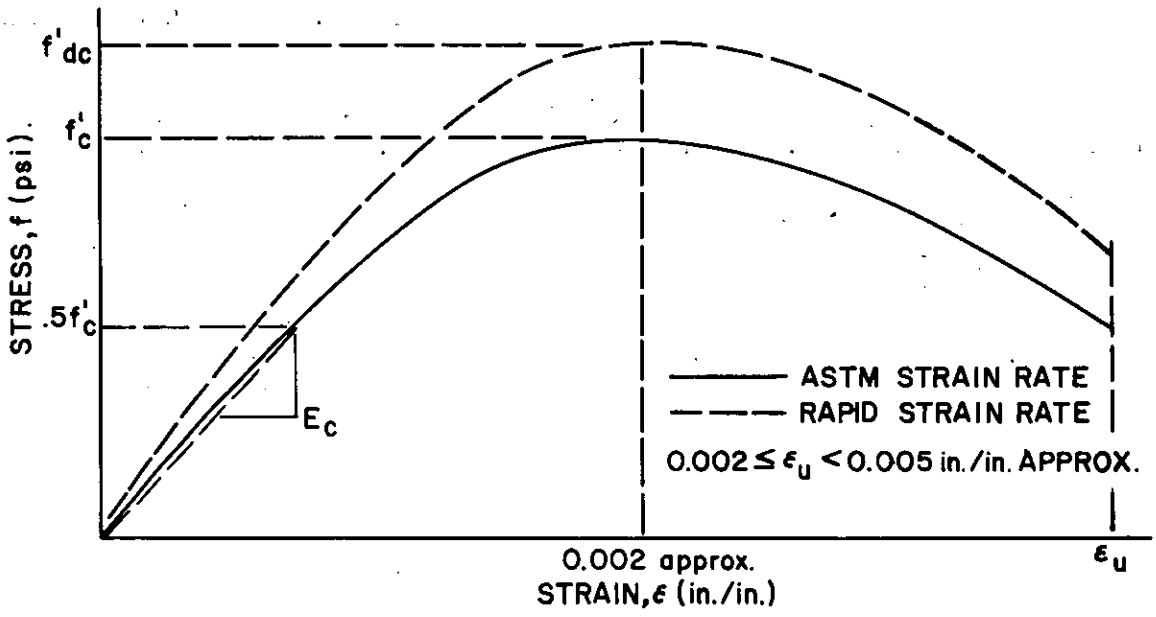
4-13.3. Dynamic Design Stresses.

The magnitude of stresses produced in the reinforcement of an element responding in the elastic range can be related directly to the strains. However, in the plastic range the stresses cannot be related directly to the strains. An estimate of the average stress over portions of the plastic range can be made by relating this average stress to the deflection of the element. The deflection is defined in terms of the angular rotation at the supports. The average dynamic stress is expressed as a function of the dynamic yield stress f_{dy} and the dynamic ultimate stress f_{du}.

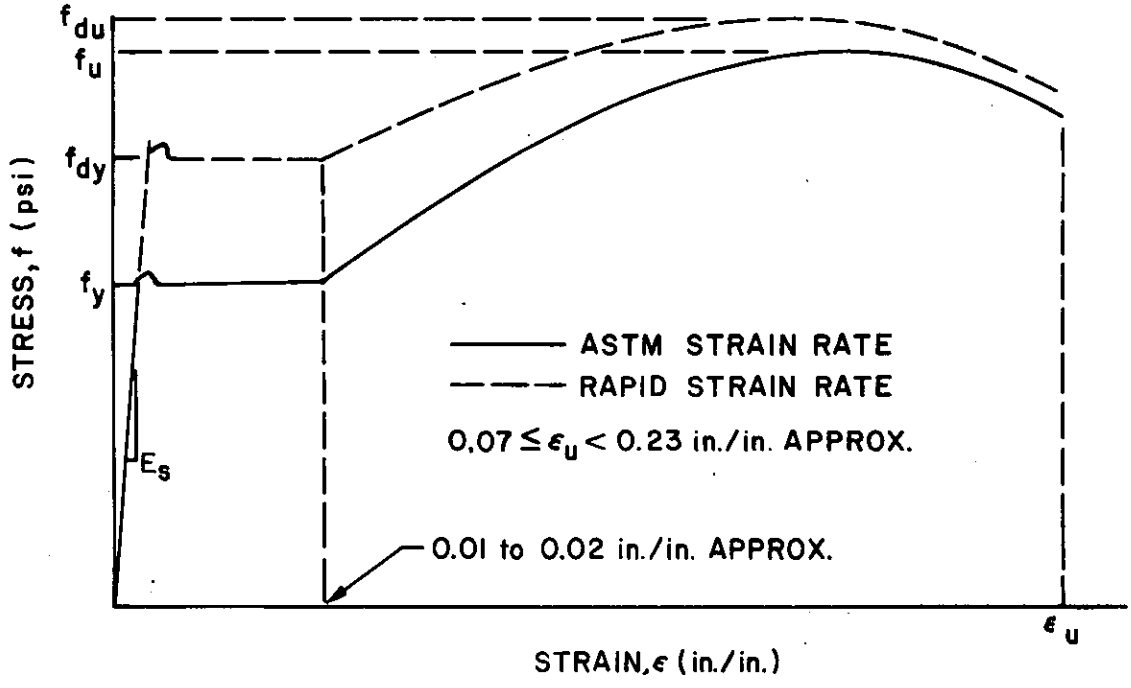
Criteria for the dynamic stresses to be used in the plastic design of ductile reinforced concrete elements are presented in Table 4-2. The dynamic design stress is expressed in terms of f_{dy}, f_{du}, and f'_{dc}. The value of these terms

is determined by multiplying the appropriate static design stress by the appropriate value of the DIF (Table 4-1), so that:

$$f_{(dynamic)} = DIF \times f_{(static)} \qquad 4\text{-}3$$



(a) STRESS-STRAIN CURVE FOR CONCRETE



(b) STRESS-STRAIN CURVE FOR STEEL

Figure 4-8 Typical stress-strain curves for concrete and reinforcing steel

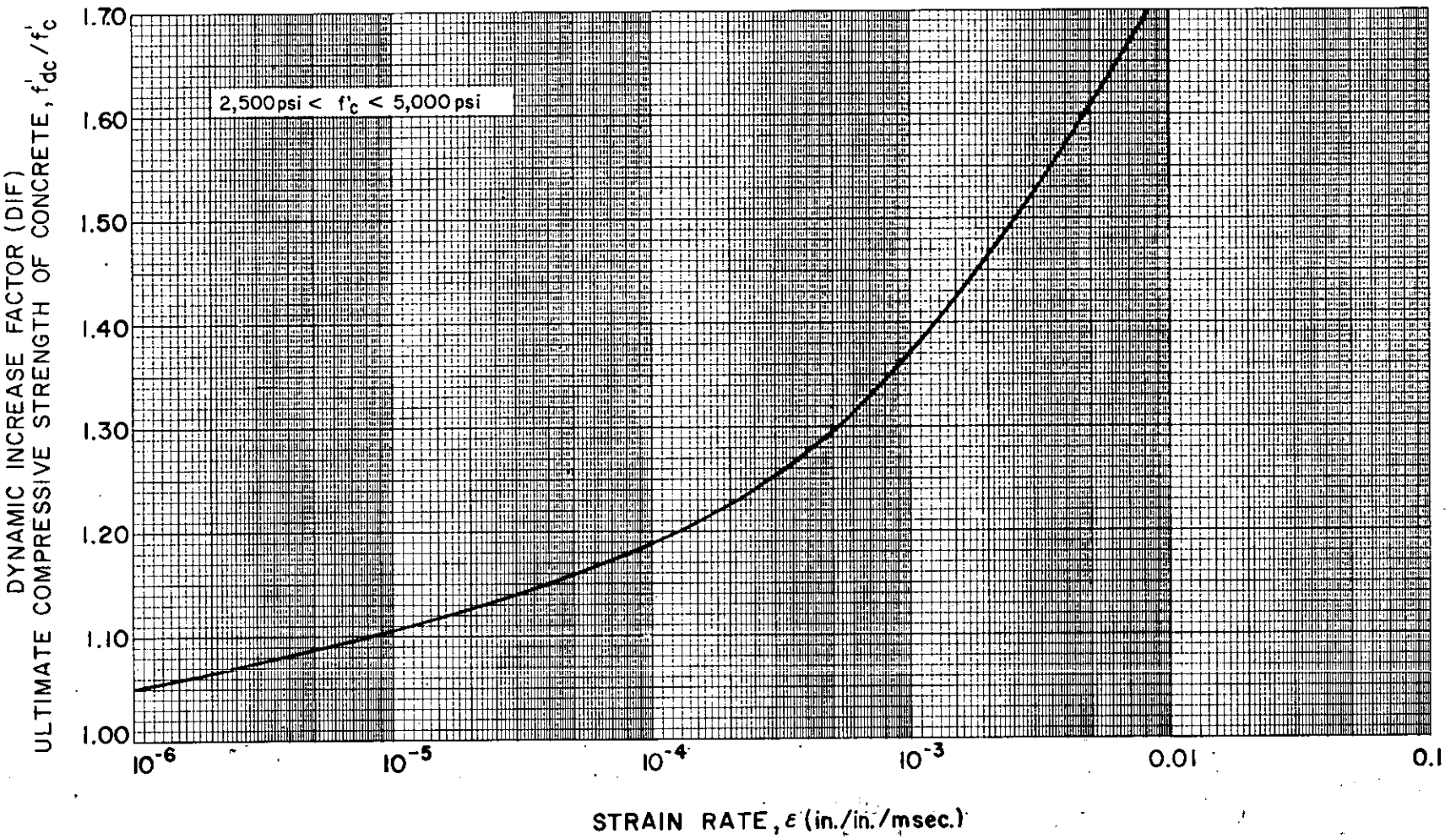


Figure 4-9 Design curve for DIF for ultimate compressive strength of concrete

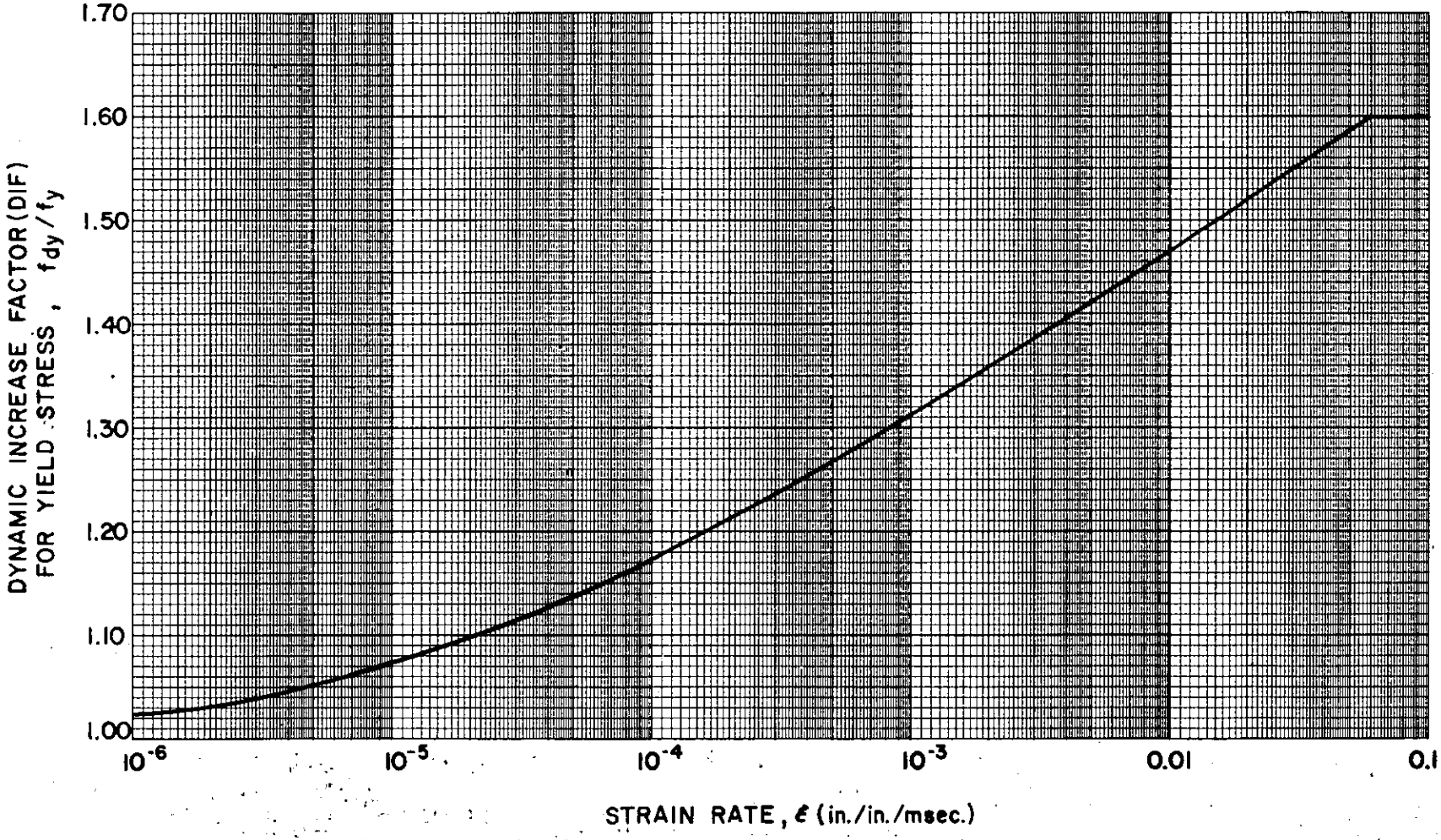


Figure 4-10 Design curve for DIF for yield stress of ASTM A 615 grade 60 reinforcing steel

Table 4-1 Dynamic Increase Factor (DIF) for Design of Reinforced Concrete Elements

TYPE OF STRESS	FAR DESIGN RANGE			CLOSE-IN DESIGN RANGE		
	Reinforcing Bars		Concrete	Reinforcing Bars		Concrete
	f_{dy}/f_y	f_{du}/f_u	f'_{dc}/f'_c	f_{dy}/f_y	f_{du}/f_u	f'_{dc}/f'_c
Bending	1.17	1.05	1.19	1.23	1.05	1.25
Diagonal Tension	1.00	——	1.00	1.10	1.00	1.00
Direct Shear	1.10	1.00	1.10	1.10	1.00	1.10
Bond	1.17	1.05	1.00	1.23	1.05	1.00
Compression	1.10	——	1.12	1.13	——	1.16

Table 4-2 Dynamic Design Stresses for Design of Reinforced Concrete Elements

TYPE OF STRESS	TYPE OF REINFORCEMENT	MAXIMUM SUPPORT ROTATION, θ_m (DEGREES)	DYNAMIC DESIGN STRESS	
			REINFORCEMENT, f_{ds}	CONCRETE, f_{dc}
Bending	Tension and Compression	$0 < \theta_m \leq 2$	f_{dy} (1)	f'_{dc}
		$2 < \theta_m \leq 5$	$f_{dy} + (f_{du} - f_{dy})/4$	(2)
		$5 < \theta_m \leq 12$	$(f_{dy}+f_{du})/2$	(2)
Diagonal Tension	Stirrups	$0 < \theta_m \leq 2$	f_{dy}	f'_{dc}
		$2 < \theta_m \leq 5$	f_{dy}	f'_{dc}
		$5 < \theta_m \leq 12$	f_{dy}	f'_{dc}
Diagonal Tension	Lacing	$0 < \theta_m \leq 2$	f_{dy}	f'_{dc}
		$2 < \theta_m \leq 5$	$f_{dy} + (f_{du}-f_{dy})/4$	f'_{dc}
		$5 < \theta_m \leq 12$	$(f_{dy} + f_{du})/2$	f'_{dc}
Direct Shear	Diagonal Bars	$0 < \theta_m \leq 2$	f_{dy}	f'_{dc}
		$2 < \theta_m \leq 5$	$f_{dy} + (f_{du}-f_{dy})/4$	(3)
		$5 < \theta_m \leq 12$	$(f_{dy} + f_{du})/2$	(3)
Compression	Column	(4)	f_{dy}	f'_{dc}

(1) Tension reinforcement only.
(2) Concrete crushed and not effective in resisting moment.
(3) Concrete is considered not effective and shear is resisted by the reinforcement only.
(4) Capacity is not a function of support rotation.

STATIC PROPERTIES

4-14. Modulus of Elasticity

4-14.1. Concrete

The modulus of elasticity of concrete E_c is equal to:

$$E_c = w_c^{1.5}\ 33\ (f'_c)^{1/2} \qquad 4\text{-}4$$

for values of w_c between 90 and 155 lbs/ft^3 where w_c is the unit weight of concrete and normally equal to 150 lbs/ft^3.

4-14.2. Reinforcing Steel

The modulus of elasticity of reinforcing steel E_s is:

$$E_s = 29 \times 10^6 \text{ psi} \qquad 4\text{-}5$$

4-14.3. Modular Ratio

The modular ratio n is:

$$n = E_s/E_c \qquad 4\text{-}6$$

and may be taken as the nearest whole number.

4-15. Moment of Inertia

The determination of the deflection of a reinforced concrete member in the elastic and elasto-plastic ranges is complicated by the fact that the effective moment of inertia of the cross section along the element changes continually as cracking progresses. It is further complicated by the fact that the modulus of elasticity of the concrete changes as the stress increases. It is recommended that the computation of deflections throughout this volume be based upon empirical relations determined from test data.

The average moment of inertia I_a should be used in all deflection calculations and is given by:

$$I_a = \frac{I_g + I_c}{2} \qquad 4\text{-}7$$

For the design of beams, the entire cross-section is considered, so that

$$I_g = \frac{bT_c^3}{12} \qquad 4\text{-}8a$$

and

$$I_c = Fbd^3 \qquad 4\text{-}8b$$

For the design of slabs, a unit width of the cross-section is considered, so that

$$I_g = \frac{T_c^3}{12} \qquad 4\text{-}9a$$

and:

$$I_c = Fd^3 \qquad 4\text{-}9b$$

where:

I_a = average moment of inertia of concrete cross section

I_g = moment of inertia of the gross concrete cross section (neglecting all reinforcing steel)

I_c = moment of inertia of cracked concrete cross section

b = width of beam

T_c = thickness of gross concrete cross section

F = coefficient given in Figures 4-11 and 4-12

d = distance from extreme compression fiber to centroid of tension reinforcement

The moment of inertia of the cracked concrete section considers the compression concrete area and steel areas transformed into equivalent concrete areas and is computed about the centroid of the transformed section. The coefficient F varies as the modular ratio n and the amount of reinforcement in the section. For sections with tension reinforcement only, the coefficient F is given in Figure 4-11 while for sections with equal reinforcement on opposite faces, the coefficient F is given in Figure 4-12.

The variation in the cracked moment of inertia obtained from Figure 4-11 and 4-12 is insignificant for low reinforcement ratios. The variation increases for the larger ratios. Consequently, for the comparatively low reinforcement ratios normally used in slab elements either chart may be used with negligible error. For the higher reinforcement ratios normally used for beams, Figure 4-12 must be used for equally reinforced sections whereas a weighted average from Figure 4-11 and 4-12 may be used for sections where the compression steel is less than the tension steel.

For one-way members the reinforcement ratio p used to obtain the factor F should be an average of the tension steel at the supports and midspan. Also, the effective depth d used to compute the cracked moment of inertia I_c should be an average of the effective depth at the supports and midspan. However, for two-way members, the aspect ratio must be considered in the calculation of the cracked moment of inertia. Average values for the reinforcement ratio p and effective depth d should be used to obtain the cracked moment of inertia in each direction and cracked moment of the member is then obtained from:

$$I_c = \frac{I_{cV}L + I_{cH}H}{L + H} \qquad 4\text{-}10$$

where:

I_{cV} = cracked moment of inertia in vertical direction

I_{cH} = cracked moment of inertia in horizontal direction

L = span length

H = span height

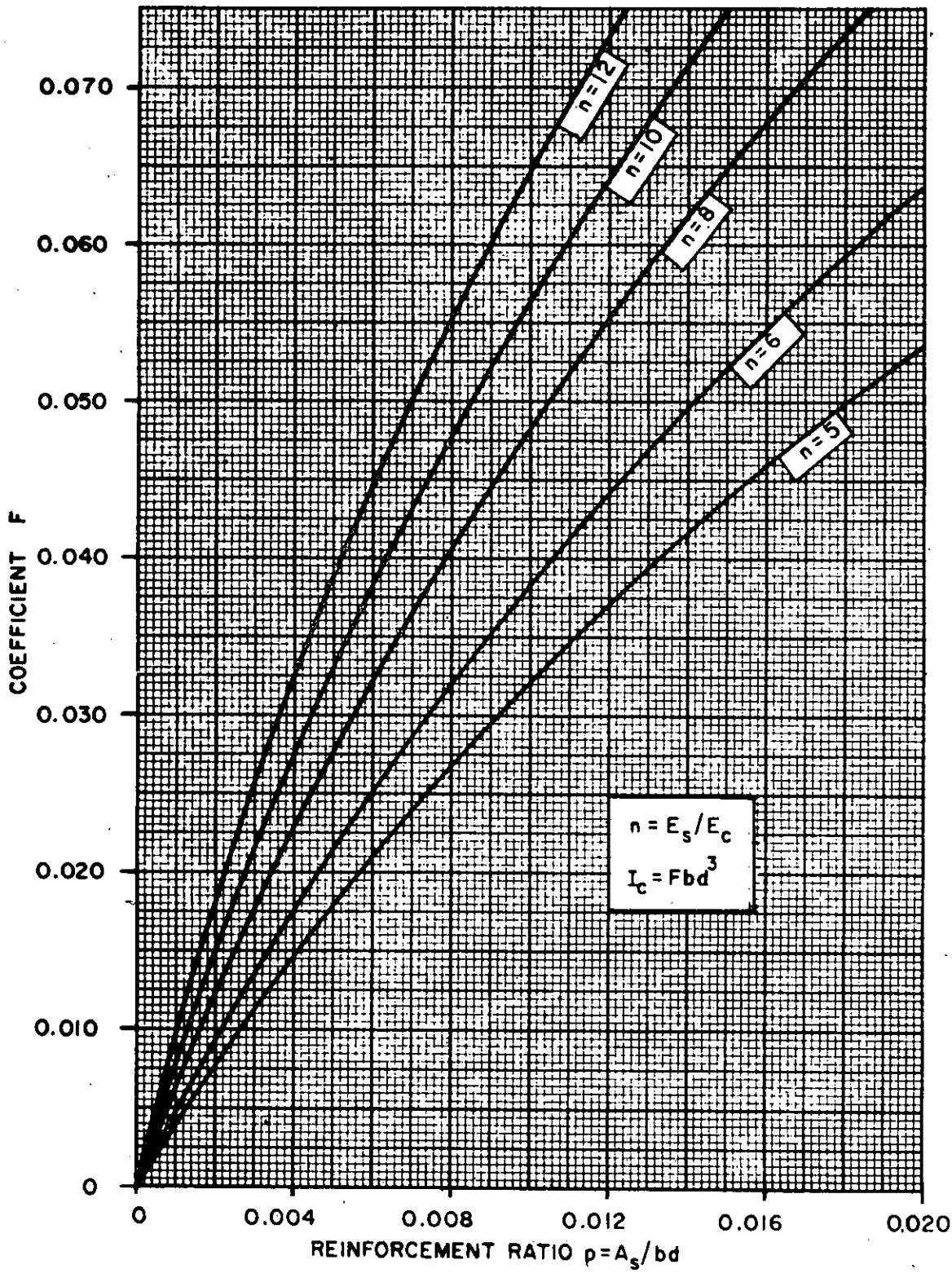


Figure 4-11 Coefficient for moment of inertia of cracked sections with tension reinforcement only

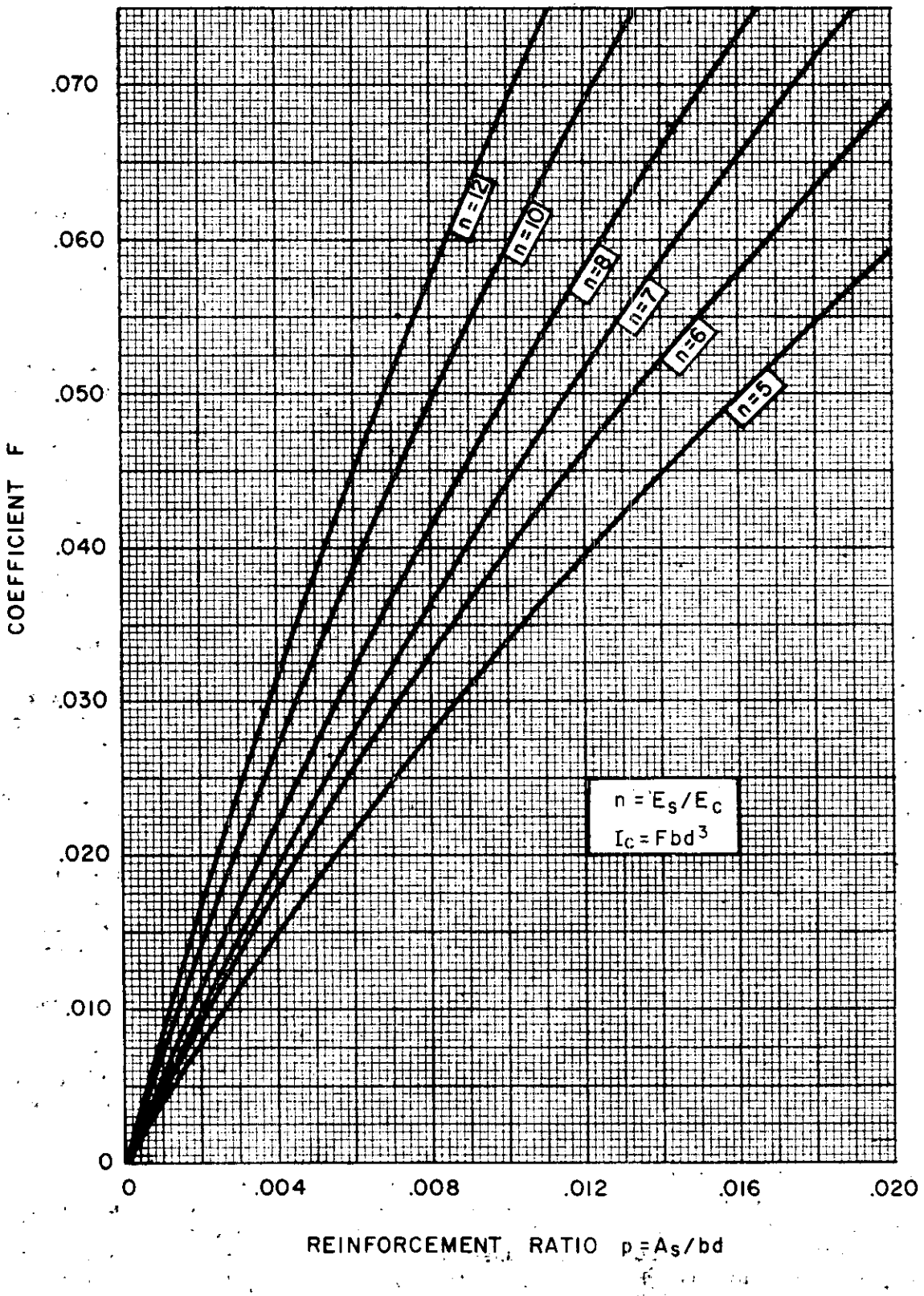


Figure 4-12 Coefficient for moment of inertia of cracked sections with equal reinforcement on opposite faces

ULTIMATE DYNAMIC STRENGTH OF SLABS

4-16. Introduction

Depending upon the magnitudes of the blast output and permissible deformations, one of three types of reinforced concrete cross sections (Figure 4-13) can be utilized in the design or analysis of blast resistant concrete slabs:

a. type I - The concrete is effective in resisting moment. The concrete cover over the reinforcement on both surfaces of the element remains intact.

b. type II - The concrete is crushed and not effective in resisting moment. Compression reinforcement equal to the tension reinforcement is required to resist moment. The concrete cover over the reinforcement on both surfaces of the element remains intact.

c. type III - The concrete cover over the reinforcement on both surfaces of the element is completely disengaged. Equal tension and compression reinforcement which is properly tied together is required to resist moment.

Elements designed using the full cross section (type I) are usually encountered in those structures or portions of structures designed to resist the blast output at the far design range. This type of cross section is utilized in elements with maximum deflections corresponding to support rotations less than 2 degrees. Maximum strength of an element is obtained from a type I cross section. Type I elements may be reinforced on either one or both faces. However, due to rebound forces, reinforcement is required on both faces of an element.

Crushing of the concrete cover over the compression reinforcement is exhibited in elements which undergo support rotations greater than 2 degrees. This failure results in a transfer of the compression stresses from the concrete to the compression reinforcement which, in turn, results in a loss of strength.

Sufficient compression reinforcement must be available to fully develop the tension steel (tension and compression reinforcement must be equal). Elements which sustain crushing of the concrete without any disengagement of the concrete cover are encountered in structures at the far design range when the maximum deflection conforms to support rotations greater than 2 degrees but less than 5 degrees.

Although the ultimate strength of elements with type III cross sections is no less than that of elements with type II cross sections, the overall capacity to resist the blast output is reduced. The spalling of the concrete cover over both layers of reinforcement, caused by either the direction transmission of high pressures through the element at the close-in range or large deflections at the far range, produces a loss of capacity due to the reduction in the concrete mass. A more detailed treatment of the phenomena of crushing and spalling is presented in subsequent sections of this chapter.

The ultimate dynamic strength of reinforced concrete sections may be calculated in accordance with the ultimate strength design methods of the American Concrete Institute Standard Building Code Requirements for Reinforced Concrete (hereafter referred to as the ACI Building Code). The capacity reduction factor 0 which has been established for conventional static load conditions is omitted for the determination of ultimate dynamic strength. Safety or reliability of the protective structure is inherent in the establishment of the magnitude of the blast output for the donor charge, and in the criteria specified for deflection, support rotation, or fragment velocity. Other permissible departures from the criteria for static or gas pressure loadings are described below.

Although certain formulae for elements constructed with conventional weight concrete are given in the following paragraphs of this chapter, more detailed information and design aids are given in the bibliography. Because tests have not yet been conducted to determine the response of lightweight concrete elements designed for close-in and far design ranges, the pertinent formulae for this type of concrete are not included in the manual. However, lightweight concrete may be utilized for structures designed for low pressures (less than 10 psi); but the reduction in mass from conventional weight concrete must be accounted for in the design to maintain the blast resistant capacity of the structure.

4-17. Ultimate Moment Capacity

4-17.1. Cross Section Type I

The ultimate unit resisting moment M_u of a rectangular section of width b with tension reinforcement only is given by:

$$M_u = (A_s f_{ds}/b)[d - (a/2)] \qquad 4\text{-}11$$

in which:

$$a = A_s f_{ds}/0.85\ b\ f'_{dc} \qquad 4\text{-}12$$

where:

A_s = area of tension reinforcement within the width b

f_{ds} = dynamic design stress for reinforcement

d = distance from extreme compression fiber to centroid of tension reinforcement

a = depth of equivalent rectangular stress block

b = width of compression face

f'_{dc} = dynamic ultimate compressive strength of concrete

The reinforcement ratio p is defined as:

$$p = A_s/bd \qquad 4\text{-}13$$

To insure against sudden compression failures, the reinforcement ratio p must not exceed 0.75 of the ratio p_b which produces balanced conditions at ultimate strength and is given by:

$$p_b = (0.85K_1 f'_{dc}/f_{ds})[87{,}000/(87{,}000 + f_{ds})] \qquad 4\text{-}14$$

where:

K_1 = 0.85 for f'_{dc} up to 4,000 psi and is reduced 0.05 for each 1,000 psi in excess of 4,000 psi.

For a rectangular section of width b with compression reinforcement, the ultimate unit resisting moment is:

$$M_u = [(A'_s)f_{ds}/b][d - (a/2)] + (A'_s f_{ds}/b)(d - d') \qquad 4\text{-}15$$

in which:

$$a = (A_s - A'_s) f_{ds}/0.85b f'_{dc} \qquad 4\text{-}16$$

where:

A'_s = area of compression reinforcement within the width b

d' = distance from extreme compression fiber to centroid of compression reinforcement

a = depth of equivalent rectangular stress block

The reinforcement ratio p' is:

$$p' = A'_s/b \qquad 4\text{-}17$$

Equation 4-15 is valid only when the compression steel reaches the value f_{ds} at ultimate strength, and this condition is satisfied when:

$$p - p' \geq 0.85K_1(f'_{dc}d'/f_{ds}d)[87{,}000/(87{,}000 - f_{ds})] \qquad 4\text{-}18$$

If p - p' is less than the value given by Equation 4-18 or when compression steel is neglected, the calculated ultimate unit resisting moment should not exceed that given by Equation 4-11. The quantity p - p' must not exceed 0.75 of the value of p_b given in Equation 4-14.

4-17.2. Cross Section Types II and III

The ultimate unit resisting moment of type II and type III rectangular sections of width b is:

$$M_u = A_s f_{ds} d_c/b \qquad 4\text{-}19$$

where:

A_s = area of tension or compression reinforcement within the width b

d_c = distance between the centroids of the compression and the tension reinforcement

The reinforcement ratios p and p' are equal to:

$$p_s = p'_c = A_s/bd \qquad 4\text{-}20$$

The above moment capacity can only be obtained when the areas of the tension and compression reinforcement are equal. In addition, this reinforcement must be properly restrained so as to maintain the integrity of the element when large deflections are encountered.

4-17.3. Minimum Flexural Reinforcement

To insure proper structural behavior under both conventional and blast loadings, a minimum amount of flexural reinforcement is required. This quantity of reinforcement insures that the moment capacity of the reinforced section is greater than that corresponding to the plain concrete section computed from its modulus of rupture. Failure of a plain concrete section is quite sudden. Also, this minimum reinforcement prevents excessive cracking and deformations under conventional loadings.

The minimum reinforcement required for slabs is somewhat less than that required for beams, since an overload would be distributed laterally and sudden failure would be less likely. The minimum reinforcement ratio for dynamic design of slabs is given in Table 4-3. However, this quantity of reinforcement must also satisfy static design requirements. Except for blast loads in the order of magnitude of static loads, the minimum requirements for dynamic loads will control. In cases where minimum requirements for static conditions control, the quantity of reinforcement must be at least 1.33 times the quantity required by static analysis or 0.0018 times the gross concrete area, whichever is less.

Concrete sections with tension reinforcement only are not permitted. For type I sections, compression reinforcement equal to at least one half the required tension reinforcement must be provided. This reinforcement is required to resist the ever present rebound forces. Depending upon the magnitude of these rebound forces, the compression reinforcement required may be greater than one half the tension reinforcement and substantially greater than the minimum quantity given in Table 4-3. For type II and III cross sections, the compression reinforcement is always equal to the tension reinforcement.

4-18. Ultimate Shear (Diagonal Tension) Capacity

4-18.1. Ultimate Shear Stress

The ultimate shear stress v_u, as a measure of diagonal tension, is computed for type I sections from:

$$v_u = V_u/bd \qquad 4\text{-}21$$

and for type II and III sections from:

$$v_u = V_u/bd_c \qquad 4\text{-}22$$

where V_u is the total shear on a width b at either the face of the support, or at the section a distance d (type I) or d_c (types II or III) from the face of the support. For the latter case, the shear at sections between the face of the support and the section d or d_c away need not be considered critical.

For laced elements, the shear stress is always calculated at d_c from the face of the support (or haunch) since the lacing and required diagonal bars provide sufficient corner reinforcement. For unlaced elements, the shear stress is calculated at d from the face of the support for those members that cause compression in their supports (Fig. 4-14a). This provision should not be applied for those members that cause tension in their supports (Fig. 4-14b). For this case, the ultimate shear stress should be calculated at the face of the support. In addition, the shear within the connection should be investigated and special corner reinforcement should be provided.

The ultimate shear stress v_u must not exceed $10\ (f'_{dc})^{\frac{1}{2}}$ in sections using stirrups. The thickness of such sections must be increased and/or the quantity of flexural reinforcement reduced in order to bring the value of v_u within tolerable limits. In sections using lacing, there is no restriction on v_u because of the continuity provided by this type of shear reinforcement. However, for large shear stresses the area of the lacing bars required may become impractical.

4-18.2. Shear Capacity of Unreinforced Concrete

The shear stress permitted on an unreinforced web of a member subjected to flexure only is limited to:

$$v_c = [1.9(f'_{dc})^{1/2} + 2500p] <= 3.5(f'_{dc})^{1/2} \qquad 4\text{-}23$$

where p is the reinforcement ratio of the tension requirement at the support. For the computation of the reinforcement ratio, d is used for type I sections and d_c for type II and III sections. For members subjected to significant axial tension, the shear stress permitted on an unreinforced web is limited to:

$$v_c = 2(1 + N_u/500A_g)\ (f'_{dc})^{1/2} \geq 0 \qquad 4\text{-}24$$

while for significant axial compression:

$$v_c = 2(1 + N_u/2000A_g)(f'_{dc})^{1/2} \qquad 4\text{-}25$$

where:

N_u = axial load normal to the cross section

A_g = gross area of the cross section

The axial load N_u must occur simultaneously with the total shear V_u on the section in order to apply Equations 4-24 and 4-25.

The value of N_u shall be taken as positive for compression and negative for tension. The simplified dynamic analysis normally performed is not sufficient to accurately determine the time variations between the desired forces and

moments from which N_u and V_u are obtained. Unless a time-history analyses is performed, any apparent strength increases due to loading combinations are unreliable. Therefore, it is recommended that the increased shear capacity due to compressive axial loads be neglected and, by the same reasoning, the reduced capacity due to tension forces be included. Both assumptions are conservative.

4-18.3. Design of Shear Reinforcement

Whenever the ultimate shear stress v_u exceeds the shear capacity v_c of the concrete, shear reinforcement must be provided to carry the excess. This shear reinforcement can be either stirrups or lacing, depending upon the magnitudes of the blast loading and support rotation permitted. Stirrups can be used only for elements designed to attain small deflections under flexural behavior. Lacing can also be used for elements designed to attain small deflections; however, lacing must be used for elements designed to attain large deflections. Therefore, stirrups may be used for elements with a type I, II, or III cross section as long as the element is designed to attain small deflections. An exception to this deflection criteria is for the particular case of slabs subjected to tension membrane action. Here the slab can attain large deflections. Lacing may be used for type II and III cross sections designed for either small or large deflections. It would be grossly unwarranted to use lacing for a type I cross section.

The required area of stirrups is calculated from:

$$A_v = [(v_u - v_c)b_s s_s]/\phi f_{ds} \qquad 4\text{-}26$$

while the required area of lacing reinforcement is:

$$A_v = \frac{[(v_u - v_c)\, b_1 s_1]}{\phi f_{ds}(\sin\alpha + \cos\alpha)} \qquad 4\text{-}27$$

where:

A_v = total area of stirrups or lacing reinforcement in tension within a width b_s or b_1, and a distance s_s or s_1

$v_u - v_c$ = excess shear stress

b_s = width of concrete strip in which the diagonal tension stresses are resisted by stirrups of area A_v

b_1 = width of concrete strip in which the diagonal tension stresses are resisted by lacing of area A_v

s_s = spacing of stirrups in the direction parallel to the longitudinal reinforcement

s_1 = spacing of lacing in the direction parallel to the longitudinal reinforcement

ϕ = capacity reduction factor equal to 0.85

α = angle formed by the plane of the lacing and the plane of the longitudinal reinforcement.

The angle of inclination α of the lacing bars is given by

$$\cos \alpha = \frac{-2B(1-B) \pm \{[2B(1-B)]^2 - 4[(1-B)^2 + A^2][B^2 - A^2]\}^{1/2}}{2[(1-B)^2 + A^2]} \qquad 4\text{-}28$$

in which

$$A = s_1/d_1 \qquad 4\text{-}29a$$

$$B = \frac{2R_1 + d_b}{d_1} \qquad 4\text{-}29b$$

where

d_1 = distance between centerlines of lacing bends measured normal flexural reinforcement

R_1 = radius of bend in lacing bars (min $R_1 = 4d_b$)

d_b = nominal diameter of reinforcing bar

A typical section of a lacing bar illustrating the terms used in the above equation, is shown in Figure 4-15. To facilitate the design of lacing bars, the angle α can be determined from Figure 4-15.

4-18.4. Minimum Shear Reinforcement

In order to develop the full flexural capacity of a slab, a premature shear failure must be prevented. Shear reinforcement must be provided to resist shear stresses in excess of the capacity of the concrete. However, except for slabs having a type I cross section or subjected to tension-membrane action in the far design range, minimum shear reinforcement must always be provided to insure the full development of the flexural reinforcement and enable the slab to attain large deflections.

Stirrups or lacing must conform to the following limitations to insure a proper distribution of shear reinforcement throughout the element and, in specific cases, to provide a minimum quantity of shear reinforcement.

1. The minimum design stress (excess shear stress $v_u - v_c$) used to calculate the required amount of shear reinforcement, must conform to the limitations of Table 4-4.

2. When stirrups or lacing reinforcement is required, the area A_v should not be less than $0.0015\ b_s\ s_s$ for stirrups or $0.0015\ b_1 s_1$ for lacing.

3. When stirrups or lacing are provided, the required area A_v is determined at the critical section and this quantity of reinforcement must be uniformly distributed throughout the element.

4. Single leg stirrups should be used for slabs. At least one stirrup must be located at each bar intersection.

5. A lacing bar is bent from a single reinforcing bar. In one direction, the lacing must be continuous across the slab between opposite supports. In all cases, the lacing must be carried past the face of the support and securely anchored within the support.

6. The maximum spacing of stirrups s_s is limited to d/2 for Type I cross sections and $d_c/2$ for Type II and III sections, but not greater than 24 inches.

7. The maximum spacing of lacing s_l is limited to d_c or 24 inches, whichever is smaller.

The spacing of stirrups and lacing is a function of the flexural bar spacing. Consequently, the above limitations for shear reinforcement should be considered in selecting the flexural bar spacing. Once selected, the flexural bar spacing may have to be altered to suit the above limitations.

4-19. Direct Shear Capacity

4-19.1. General

Direct shear failure of a member is characterized by the rapid propagation of a vertical crack through the depth of the member. This crack is usually located at the supports where the maximum shear stresses occur. Failure of this type is possible even in members reinforced for diagonal tension.

Diagonal bars are required at slab supports to prevent direct shear failure: when the design support rotation exceeds 2° (unless the slab is simply supported as given in section 4-19.2); when the design support rotation is ≤ 2° but the direct shear capacity of the concrete is insufficient; or when the section is in tension (as in containment cells). Diagonal reinforcement consists of inclined bars which extend from the support into the slab element.

4-19.2. Direct Shear Capacity of Concrete

If the design support rotation, θ, is greater than 2° ($\theta > 2°$), or if a section (with any support rotation) is in net tension, then the ultimate direct shear capacity of the concrete, V_d, is zero and diagonal bars are required to take all direct shear.

If the design support rotation, θ, is less than or equal to 2° ($\theta \leq 2°$), or if the section, with any rotation θ, is simply supported (total moment capacity of adjoining elements at the support must be significantly less than the moment capacity of the section being checked for direct shear), then the ultimate direct shear force, V_d, that can be resisted by the concrete in a slab is:

$$V_d = 0.18 f'_{dc} bd \qquad 4\text{-}30$$

4-19.3. Design of Diagonal Bars

The required area of diagonal bars is determined from:

$$A_d = (V_s b - V_d)/(f_{ds}\sin(\alpha)) \qquad 4\text{-}31$$

where:

$V_d = 0.18\, f'_{dc}\, bd.$ ($\theta \leq 2°$ or simple supports),

or $V_d = 0$ ($\theta > 2°$ or section in tension).

and A_d = total area of diagonal bars at the support within a width b

V_s = shear at the support of unit width b

α = angle formed by the plane of the diagonal reinforcement and the longitudinal reinforcement.

4-20. Punching Shear

4-20.1. Ultimate Punching Shear Stress

When a flat slab is supported on a column or a column rests on a two-way slab, failure occurs around and against the concentrated load, punching out a pyramid of concrete from the slab. The ultimate shear stress v_u, as a measure of punching shear, is computed from:

$$v_u = N_u/b_o d_e \qquad 4\text{-}32$$

where:

N_u = the total concentrated axial load or reaction

b_o = failure perimeter located at a distance d/2 from the concentrated load or reaction area

d_e = either d or d_c depending on the type of cross section

4-20.2. Punching Shear Capacity of Concrete

The shear stress permitted for punching shear is limited to:

$$v_c = 4(f'_{dc})^{1/2} \qquad 4\text{-}33$$

Equation 4-33 applies to circular columns and to rectangular columns with aspect ratios no greater than 2. For rectangular areas with aspect ratios greater than 2, the allowable value of v_c should be reduced according to the ACI provisions (not listed in this text).

Shear reinforcement is not permitted to increase the punching shear capacity of a slab. If the ultimate shear stress v_u is greater than the stress permitted for punching shear v_c, the slab thickness must be increased. In flat slab design, the use of a drop panel to increase slab thickness, and/or a

column capital to increase failure perimeter, may be employed to prevent punching shear failure. If a drop panel is used, punching shear must be checked at the perimeter of the drop panel, as well as at the top of the column.

4-21. Development of Reinforcement

4-21.1. General

In order to fully develop the flexural and/or axial load capacity of a concrete slab or wall, the full strength of the reinforcement must be realized. At any section along the length of a member, the tensile or compressive force in the reinforcement must be developed on each side of the section by proper embedment length, splices (lapped or mechanical), end anchorage, or for tension only, hooks. At a point of peak stress, this development length or anchorage is necessary on both sides of the point; on one side to transfer stress into and on the other side to transfer stress out of the reinforcing bar.

The types and locations of reinforcement anchorages are severely restricted for blast resistant structures. These restrictions are necessary to insure that the structure acts in a ductile manner. Typical details for both conventionally reinforced and laced reinforced concrete elements are given in latter sections dealing with construction details. Conformance to these details greatly simplifies the calculation of development lengths. The required development lengths to be used in conjunction with the required typical details are given below.

While conformance to the typical details given is mandatory, certain conditions may preclude their use. For these unusual conditions, the required anchorages are calculated according to the procedures given in the ACI Building Code. The basic development length is first calculated and then modified based on the construction details employed to obtain the required end anchorage or splice length. This procedure is outlined in Sections 4-21.4 through 4-21.7. However, it must be repeated that the typical details given must be followed and any deviation from these restrictions and requirements must be carefully considered to insure proper structural behavior.

4-21.2 Provisions for Conventionally Reinforced Concrete Elements

Typical details for conventionally reinforced (non-laced) concrete elements are given in subsequent sections. These details locate splices in reinforcement at points of low stress. This permits the minimum length of lap splices, as well as the development length for end anchorages, to be given by

$$l_d = 40\ d_b \qquad 4\text{-}34$$

where

l_d = development length

d_b = diameter of reinforcing bar

The value of l_d shall not be less than 24 inches. Equation 4-34 applies for end anchorage of #14 bars and smaller, and for lap splices of #11 bars and smaller since lap splices of #14 bars are not permitted.

Lap splices of reinforcement must not be located at critical sections. Rather, they must be located in regions of low stress (inflection points) where the area of reinforcement provided is more than twice the area of reinforcement required by analysis. In addition, not more than one-half of the reinforcement may be spliced at one location. The splice of adjacent bars must be staggered at least the required lap length of the bars since overlap of splices of adjacent bars is not desirable. Under these conditions, the required minimum length of lap splices is given in Equation 4-34. If it is impractical to locate splices at the inflection points, then the length of the splice must be calculated according to the provisions of Section 4-21.4.

Typical details for intersecting walls and slab/wall intersections avoid the use of end anchorage of the primary reinforcement. Rather, the reinforcement is anchored by continuing it through the support and bending it into the intersecting wall or slab. This reinforcement is then lap spliced with the reinforcement in the intersecting wall.

4-21.3 Provisions for Laced Reinforced Concrete Elements

Tests of laced elements have indicated that if continuity of the lacing and flexural reinforcement is maintained throughout the element, the required development length for end anchorage as well as the minimum length of lap splices is given by Equation 4-34, but not less than 24 inches. This equation applies for end anchorage of #14 bars and smaller, and for lap lengths of #11 bars and smaller since lap splices of #14 bars are not permitted.

Required construction details and procedures for laced reinforced concrete elements are given in subsequent sections. These details must be followed to insure the full development of both the concrete and reinforcement well into the range of plastic action of the materials. The use of Equation 4-34 to obtain the required development lengths of the reinforcement is predicated on the use of these details.

The typical details for laced reinforced concrete elements require that the reinforcement (flexural as well as lacing bars) must not be spliced at critical sections but rather must be spliced in regions of low stress (inflection points) where the area of reinforcement provided is more than twice the area of reinforcement required by analysis. In addition, not more than one-quarter of the reinforcement may be spliced at one location. The splice of adjacent bars must be staggered at least the required lap length of the bars since overlap of splices of adjacent bars is not desirable.

Specific end anchorage details are required for laced reinforced concrete walls and slabs to enable the reinforcement to attain its ultimate strength. The preferred method of end anchorage is through the use of wall extensions since this method presents the least construction problems. If architectural requirements do not permit the use of wall extensions, the reinforcement is anchored by continuing it through the support and bending it into the intersecting wall or slab. In this latter case, the reinforcement is developed by a combination of anchorage and lap splice. In either case, the lacing extending into the supports provides the necessary confinement which permits the use of Equation 4-34.

4-21.4. Development Length for Reinforcement in Tension

The basic development length for #11 bars and smaller which are in tension is given by:

$$l_d = 0.04\ A_b f a_{ds}/(f'_{dc})^{1/2} \qquad 4\text{-}35a$$

but not less than:

$$l_d = 0.0004 d_b\ f_{ds} \qquad 4\text{-}35b$$

where:

l_d = basic development length

A_b = area of reinforcing bar

d_b = diameter of reinforcing bar

The basic development length for #14 bars in tension is given by:

$$l_d = 0.085\ f_{ds}/(f'_{dc})^{1/2} \qquad 4\text{-}36$$

The use of #18 bars is not permitted by this manual.

For top reinforcement, that is, horizontal reinforcement so placed that more than 12 inches of concrete is cast in the slab below the reinforcement, the basic development length must be multiplied by 1.40. This provision applies to horizontal slabs only. Walls with multiple runs of horizontal bars plus vertical bars are not effected by this provision. In addition, the basic development length of all bars may be multiplied by 0.80 if the bars are spaced laterally at least six (6) inches on center. In no case shall the development length be less than 24 inches nor 40 times the diameter of the reinforcing bar.

4-21.5 Development Length for Reinforcement in Compression

The basic development length for bars in compression is given by:

$$l_d = 0.02\ d_b\ f_{ds}/(f'_{dc})^{1/2} \qquad 4\text{-}37a$$

but not less than:

$$l_d = 0.0003\ d_b\ f_{ds} \qquad 4\text{-}37b$$

The development length for compression is not modified for top bars nor lateral bar spacing. In no case shall the development length used be less than twelve (12) inches.

Under dynamic load conditions, members are subject to load reversal or rebound. Reinforcement subject to compressive forces under the primary load may be subject to tensile forces under rebound. Consideration must be given to this stress reversal, since the development length of bars in compression is less than the development length of bars in tension.

4-21.6. Development Length of Hooked Bars

The basic development length for bars in tension which terminate in a standard 90-degree or 180-degree hook is given by:

$$l_{dh} = 0.02\, d_b\, f_{ds}/(f'_{dc})^{1/2} \qquad 4\text{-}38$$

but not less than $8d_b$ or 6 inches, whichever is greater. The development length for a hooked bar l_{dh} is measured from the critical section along the length of the bar to the end of the hook. That is, the length l_{dh} includes the straight length of the bar between the critical section and point of tangency of the hook, the bend radius and one bar diameter. The required hook geometry as specified in the ACI Building Code is given in Figure 4-16.

In the development of hooked bars, no distinction is made between top bars and other bars. However, since hooked bars are especially susceptible to concrete splitting failure if the concrete cover is small, the above equation takes into account the effect of minimum concrete cover. For #11 bar and smaller with the cover not less than 2-½ inches, and for a 90-degree hook, with cover on the bar extension beyond the hook not less than 2 inches, the development length l_{dh} may be multiplied by 0.7.

Hooks are not to be considered effective in developing bars in compression. However, in the design of members subjected to dynamic loads, rebound or load reversal must be considered. That is, under the primary loading, reinforcement is subjected to tensile forces and anchored utilizing a standard hook, but this same hooked reinforcement may be subjected to compressive forces under rebound. Therefore, the straight portion of the hooked bar must be sufficient to develop this compressive force. For those cases where 100 percent rebound is encountered, the straight portion of a hooked bar must be equal to the development length for bars in compression.

4-21.7. Lap Splices of Reinforcement

In blast resistant structures, reinforcing bars may be lap-spliced using only contact lap splices; noncontact lap splices are not permitted. Lap splices shall not be used for reinforcing bars larger than #11 bars. If #14 bars are used, they must be continuous.

Lap splices of adjacent parallel reinforcing bars must be staggered by at least the length of the lap. The minimum length of lap for tension lap splices depends upon the location of the splice. For blast resistant structures, it is strongly recommended that splices be located in regions of low stress, where the area of reinforcement provided is at least twice that required. In such cases, the length of the lap is equal to the basic development length l_d for bars in tension as given by Equation 4-35 or 4-36 and modified, if applicable, for top bars and/or lateral spacing of the bars. In other design situations where the lap splice is not located in regions of low stress, the lap length is equal to 1.3 times the modified development length, l_d.

The minimum length of lap for compression lap splices is equal to the basic development length l_d for bars in compression as given by Equation 4-37. However, due to the occurrence of load reversal, it is recommended that the

length of lap splices be based in tension unless it can be shown that the reinforcement will always be in compression.

4-21.8. Mechanical Splices of Reinforcement

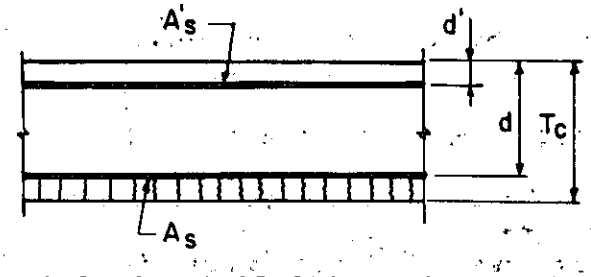
Mechanical devices may be used for end anchorage and splices in reinforcement. These devices must be capable of developing the ultimate dynamic tensile strength of the reinforcement without reducing its ductility. Tests showing the adequacy of such devices under dynamic conditions must be performed before these devices are deemed acceptable for use in hardened structures.

4-21.9. Welding of Reinforcement

Welding of reinforcement is to be avoided in blast resistant structures since it results in a reduction of the ultimate strength and ductility of the reinforcing steel. In those cases where welding is absolutely essential, it may be necessary to obtain special reinforcement manufactured with controlled chemical properties. Tests showing the adequacy of the combination of weld and reinforcing steel under dynamic conditions must be performed to demonstrate that this welding does not reduce the ultimate strength and ductility of the reinforcing steel. In lieu of these tests, welding is permitted if the stress in the reinforcement is maintained at a level less than 90 percent of the yield stress.

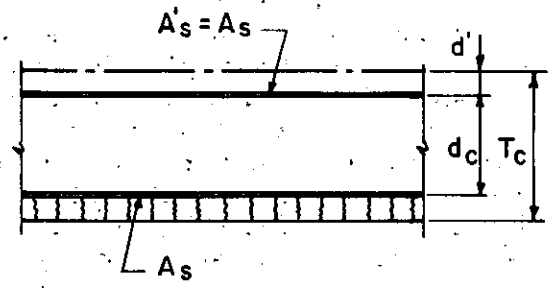
4-21.10. Bundled Reinforcing Bars

The use of bundled bars may be required for unusual conditions. However, their use is not desirable and should be avoided where possible. A 3 bar bundle should be the maximum bundle employed. The development length and lap splice length of individual bars within a bundle shall be that of the individual bar increased 20 percent for a 2 bar bundle and 33 percent for a 3 bar bundle. In addition, splices of the individual bars within a bundle should be staggered. That is, only one bar of the bundle should be spliced at a given location.



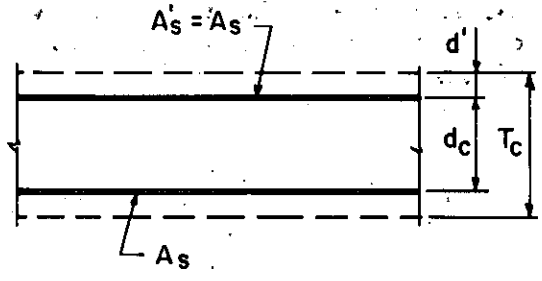
NO CRUSHING OR SPALLING

TYPE I



CRUSHING

TYPE II



SPALLING

TYPE III

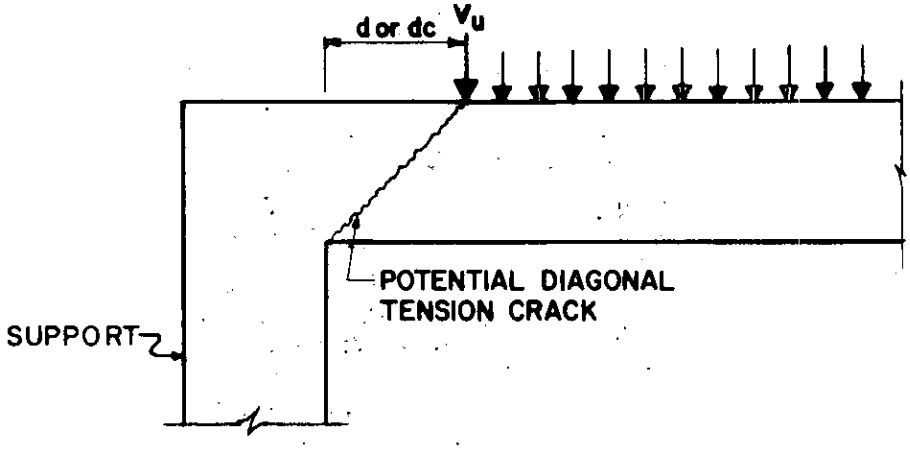
LEGEND:

CRACKING

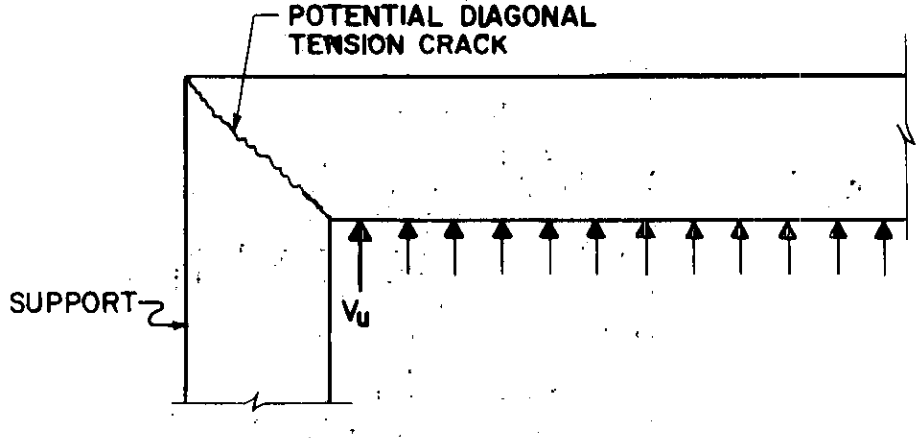
CRUSHING

DISENGAGEMENT

Figure 4-13 Typical reinforced concrete cross sections



a. CRITICAL SECTION AT d or d_c FROM FACE OF SUPPORT.



b. CRITICAL SECTION AT FACE OF SUPPORT

Figure 4-14 Location of critical sections for diagonal tension

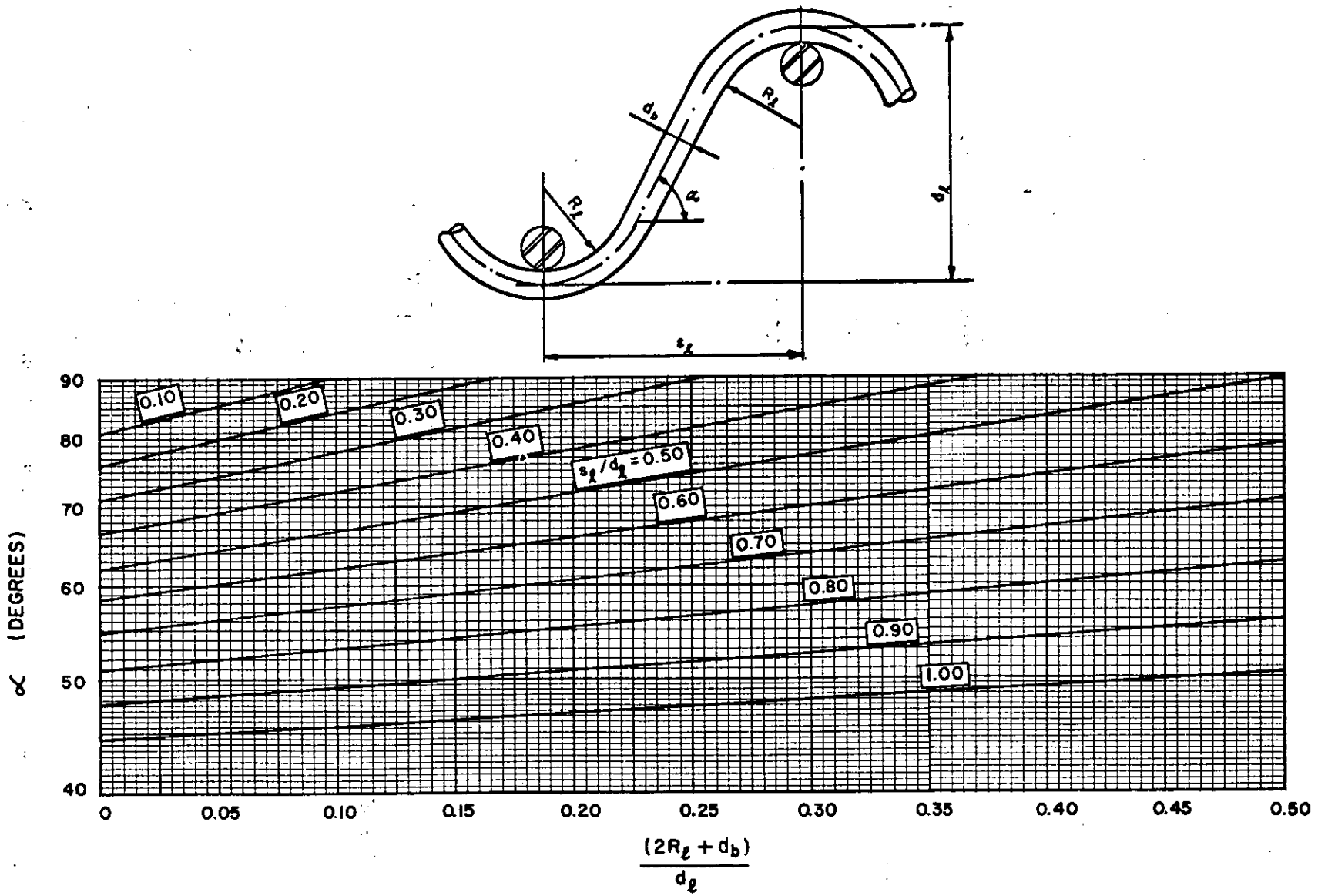


Figure 4-15 Angle of inclination of lacing bars

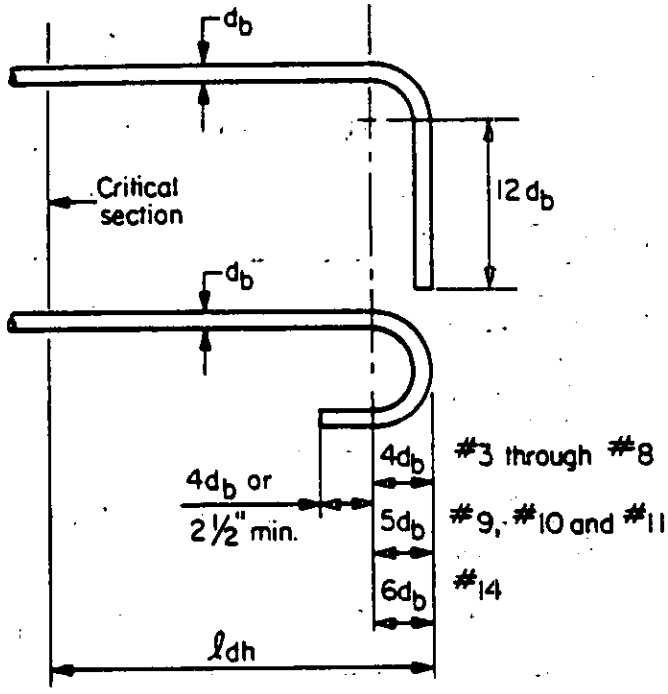


Figure 4-16 Geometry for standard hooked reinforcement

Table 4-3 **Minimum Area of Flexural Reinforcement**

Cross-Section	Reinforcement	One-Way Slabs	Two-Way Slabs
Type I	Main Direction	$A_s = 0.0015bd$ $A'_s = 0.0010bd$	$A_s = 0.0015bd$ $A'_s = 0.0010bd$
	Secondary Direction	$A_s = 0.0010bd$ $A'_s = 0.0010bd$	$A_s = 0.0015bd$ $A'_s = 0.0010bd$
Type II and Type III	Main Direction	$A_s = A'_s = 0.0015bd_c$	$A_s = A'_s = 0.0015bd_c$
	Secondary Direction	$A_s = A'_s = 0.0015bd_c$*	$A_s = A'_s = 0.0015bd_c$*

* but not less than $A_s/4$ used in the main direction

Table 4-4 Minimum Design Shear Stresses for Slabs

Design Range	Type of Cross-Section	Type of Structural Action	Type of Shear Reinforcement	Excess Shear Stress $v_u - v_c$		
				$v_u \leq v_c$	$v_c < v_u \leq 1.85v_c$	$v_u > 1.85v_c$
FAR	Type I	Flexure	Stirrups	0	$v_u - v_c$	$v_u - v_c$
	Type II	Flexure	Stirrups	$0.85v_c$	$0.85v_c$	$v_u - v_c$
	Type II & Type III	Tension Membrane	Stirrups	0	$v_u - v_c$	$v_u - v_c$
CLOSE-IN	Type II & Type III	Flexure or Tension Membrane	Stirrups or Lacing	$0.85v_c$	$0.85v_c$	$v_u - v_c$

DESIGN OF NON-LACED REINFORCED SLABS

4-22. Introduction

Conventional reinforced concrete elements are for the purpose of this manual, members without lacing. These non-laced elements make up the bulk of protective concrete construction. They are generally used to withstand the blast and fragment effects associated with the far design range but may also be designed to resist the effects associated with the close-in design range. In the latter case, the distance between the center of the explosive charge and the element must not be less than that corresponding to a scaled distance Z equal to 1.0. Laced elements are required for scaled distances less than 1.0. Non-laced elements may be designed to attain small or large deflections depending upon the protection requirements of the acceptor system.

A non-laced element designed for far range effects may attain deflections corresponding to support rotations up to 2 degrees under flexural action. Single leg stirrups are not required to attain this deflection. However, shear reinforcement is required if the shear capacity of the concrete is not sufficient to develop the ultimate flexural strength. A type I cross-section provides the ultimate moment capacity. The flexural action of a non-laced element may be increased to 4 degrees support rotation if single leg stirrups are provided to restrain the compression reinforcement. In this deflection range, a type II cross-section provides the ultimate moment capacity and mass to resist motion.

Single leg stirrups must be provided when a non-laced element is designed to resist close-in effects. The shear reinforcement must be provided to prevent local punching shear failure. When the explosive charge is located at scaled distances less than 1.0, a laced rather than a non-laced element must be employed. For scaled distances greater than 1.0 but less than 3.0, single leg stirrups must be provided, while for scaled distances greater than 3.0, shear reinforcement should be used only if required by analysis. With single leg stirrups, the member may attain deflections corresponding to support rotations up to 4 degrees under flexural action. A type I and II cross-section provides the ultimate moment capacity and mass to resist motion for elements designed for 2 and 4 degrees support rotation, respectively. If spalling occurs then a type III cross-section would be available. In addition, a non-laced element designed for small deflections in the close-in design range is not reusable and, therefore, cannot sustain multiple incidents.

A non-laced reinforced element may be designed to attain large deflections, that is, deflections corresponding to incipient failure. These increased deflections are possible only if the element has sufficient lateral restraint to develop in-plane forces. The element may be designed for both the close-in and far design range. A type III cross-section provides the ultimate moment capacity and mass to resist motion.

The design of non-laced reinforced elements subjected to a dynamic load involves an iterative (trial and error) design procedure. An element is assumed and its adequacy is verified through a dynamic analysis. The basic data required to determine the ultimate strength of the reinforced concrete section has been presented in previous sections. Procedures to determine the resistance-deflection function used for design, the dynamic properties of the

section, and the dynamic analysis required to determine an element's response is presented in Chapter 3. This section contains additional data needed to establish the resistance-deflection curve for design as well as procedures to design the element for shear.

The interrelationship between the various parameters involved in the design of non-laced elements is readily described with the use of the idealized resistance-deflection curve shown in Figure 4-17.

4-23. Distribution of Flexural Reinforcement

4-23.1. General

A prime factor in the design of any facility is construction economy. Construction costs are divided between labor and material costs. Labor cost is further divided into shop and field work, with field labor being generally the more costly. Labor cost can account for as mush as 70% of the cost of blast resistant reinforced concrete. Proper selection of concrete thickness and reinforcement steel will result in a design which optimizes the structural resistance and minimizes required construction materials. Subsequent sections will discuss procedures to optimize the required materials. The designer must then evaluate the issue of constructability. Factors such as standardization of rebar sizes, spacing, congestion, steel erection and concrete placement difficulties. These considerations may require that the initial design, optimized for material quantities, be modified. Such a modification may actually increase the cost of materials while reducing the overall construction cost by reducing labor intensive activities. In addition, improved constructability greatly reduces the risk of quality control problems during construction.

4-23.2. Optimum Reinforcement Distribution

For a given total amount of flexural reinforcement and a given concrete thickness, the dynamic capacity of an element varies with the amount of reinforcement placed in the vertical direction to the amount in the horizontal direction. For a given support condition and aspect ratio L/H, the ideal distribution of the reinforcement will result in the most efficient use of the reinforcement by producing the greatest blast capacity.

The optimum distribution of the reinforcement for a two-way element is that distribution which results in positive yield lines that bisect the 90 degree angle at the corners of the element (45 degree yield lines). For two-way elements there are numerous combinations of support conditions with various moment capacities due either to quantity of reinforcement provided or degree of edge restraint as well as various positive moment capacities again due to variations in the quantity of reinforcement provided. Due to these variations in possible moment capacities, the ratio of the vertical to horizontal reinforcement cannot be expressed as a function of the aspect ratio L/H for different support conditions. Figures 3-4 through 3-20 must be used to determine the moment capacities which will result in a "45 degree yield line". The reinforcement can then be selected from these moment capacities.

In some design cases, it may not be possible to furnish the optimum distribution of reinforcement in a particular element. One such case would be where the optimum distribution violates the maximum or minimum ratio of the vertical

to horizontal reinforcement A_{sV}/A_{sH} of 4.0 and 0.25, respectively. A second situation would arise when the optimum distribution requires less than minimum reinforcement in one direction. The most common case would result from the structural configuration of the building in which support moments may not be fully developed (restrained support rather than fully fixed) or from the need of maintaining continuous reinforcement from adjacent elements. In these and other situations where the optimum distribution of the reinforcement cannot be provided, the reinforcement should be furnished to give a distribution as close as the situation allows to the optimum distribution to maintain an economical design.

4-23.3. Optimum Total Percentage of Reinforcement

The relationship between the quantity of reinforcement to the quantity of concrete which results in the minimum cost of an element may be expressed as a total percentage of reinforcement. This total percentage of reinforcement p_T is defined as

$$p_T = p_V + p_H \qquad 4\text{-}39$$

where p_V and p_H are the average percentages of reinforcement on one face of the element in the vertical and horizontal directions, respectively. Based on the average costs of concrete and steel, the optimum percentage for a nonlaced reinforced element using single leg stirrups has been determined to be between 0.6 and 0.8 percent with 0.7 a reasonable design value. For elements which do not contain shear reinforcement, the optimum percentage would be somewhat higher. For large projects, a detailed cost analysis should be performed to obtain a more economical design.

In some design cases, it may be desirable to reduce the concrete thickness below low the optimum thickness. A small increase in cost (10 percent) would be incurred by increasing the value of p_T to one percent. Beyond one percent, the cost increase would be more rapid. However, except for very thin elements, it may be impractical to furnish such large quantities of reinforcement. In fact, in thick walls it may be impractical to even furnish the optimum percentage.

Unless single leg stirrups are required for other than shear capacity such as for close-in effects or to extend flexural action in the far design range from 2 to 4 degrees support rotation, it is more economical to design non-laced elements without shear reinforcement. In this case, the total percentage of reinforcement must be limited so that the ultimate resistance of the element does not produce shear stresses in excess of the concrete capacity.

4-24. Flexural Design for Small Deflections

The design range for small deflections may be divided into two regions; elements with support rotations less than 2 degrees (limited deflections) and support rotations between 2 and 4 degrees. Except for stirrup requirements and the type of cross-section available to resist moment, the design procedure is the same.

In the flexural design of a non-laced reinforced concrete slab, the optimum distribution of the flexural reinforcement must first be determined. A 45 degree yield line pattern is assumed and, based on the support conditions and

aspect ratio, the ratio of the vertical to horizontal moment capacities are determined from the yield line location figures of Chapter 3.

Reinforcing bars and a concrete thickness are next chosen such that the distribution of reinforcement is as close as possible to that determined above and such that the total reinforcement ratio p_T is approximately 0.7 for elements utilizing stirrups. For those elements not utilizing shear reinforcement p_T is minimized so that the shear capacity of the concrete is not exceeded. Using the equations of previous sections (eq. 4-11 for type I cross sections, eq. 4-19 for type II or III cross-sections) the moment capacities are computed. The moment capacities are required to calculate the ultimate unit resistance r_u and the equivalent elastic deflection X_E . These parameters along with the natural period of vibration T_N define the equivalent single-degree-of-freedom system of the slab, and are discussed in detail in Chapter 3.

A dynamic analysis (see Section 4-26) is then performed to check that the slab meets the response criteria. Lastly, the shear capacity is checked (Section 4-27). If the slab does not meet the response criteria or fails in shear (or is greatly overdesigned) a new concrete section is assumed and the entire design procedure is repeated.

4-25. Design for Large Deflections

4-25.1. Introduction

Design of non-laced reinforced concrete elements without shear reinforcement (single leg stirrups) for support rotations greater than 2 degrees or elements with single leg stirrups for support rotations greater than 4 degrees depends on their capacity to act as a tensile membrane. Lateral restraint of the element must be provided to achieve this action. Thus, if lateral restraint does not exist, tensile membrane action is not developed and the element reaches incipient failure at 2 degrees (4 degrees if adequate single leg stirrups are provided) support rotation. However, if lateral restraint exists, deflection of the element induces membrane action and in-plane forces. These in-plane forces provide the means for the element to continue to develop substantial resistance up to maximum support rotations of approximately 12 degrees.

4-25.2. Lateral Restraint

Adequate lateral restraint of the reinforcement is mandatory in order for the element to develop and the designer to utilize the benefits of tensile membrane behavior. Sufficient lateral restraint is provided if the reinforcement is adequately anchored into adjacent supporting members capable of resisting the lateral force induced by tensile membrane action.

Tensile membrane behavior should not be considered in the design process unless full external lateral restraint is provided in the span directions shown in Table 4-5. Full external lateral restraint means that adjacent members can effectively resist a total lateral force equivalent to the ultimate strength of all continuous reinforcement in the element passing the boundary identified by the arrows in Table 4-5. External lateral restraint is not required for elements supported on four edges provided the aspect ratio L/H is not less than one-half nor greater than 2. Within this range of L/H,

the inherent lateral restraint provided by the element's own compression ring around its boundary is sufficient lateral restraint to develop tensile membrane behavior.

4-25.3. Resistance-Deflection Curve

A typical resistance-deflection curve for laterally restrained elements is shown in Figure 4-18. The initial portion of the curve is due primarily to flexural action. If the lateral restraint prevents small motions, in-plane compressive forces are developed. The increased capacity due to these forces is neglected and is not shown in Figure 4-18. The ultimate flexural resistance is maintained until 2 degrees support rotation is produced. At this support rotation, the concrete begins to crush and the element loses flexural capacity. If adequate single leg stirrups were provided, the flexural action would be extended to 4 degrees. However, due to the presence of continuous reinforcement and adequate lateral restraint, tensile membrane action is developed. The resistance due to this action increases with increasing deflection up to incipient failure at approximately 12 degrees support rotation. The tensile membrane resistance is shown as the dashed line in Figure 4-18.

In order to simplify the design calculations, the resistance is assumed to be due to flexural action throughout the entire range of behavior. To approximate the energy absorbed under the actual resistance-deflection curve, the deflection of the idealized curve is limited to 8 degrees support rotation. Design for this maximum deflection would produce incipient failure conditions. Using this equivalent design curve, deflections between 2 degrees (or 4 degrees if single leg stirrups are provided) and incipient failure cannot be accurately predicted.

For the design of a non-laced laterally restrained element for 8 degrees support rotation, a type III cross-section is used to compute the ultimate moment capacity of the section as well as to provide the mass to resist motion. The stress in the reinforcement f_{ds} would be equal to that corresponding to support rotations $5 \geq \theta_m \geq 12$ given in Table 4-2. At every section throughout the element, the tension and compression reinforcement must be continuous in the restrained direction(s) in order to develop the tensile membrane action which is discussed in detail below.

4-25.4. Ultimate Tensile Membrane Capacity

As can be seen in Figure 4-18, the tensile membrane resistance of an element is a function of the element's deflection. It is also a function of the span length and the amount of continuous reinforcement. The tensile membrane resistance, r_T of a laterally restrained element at a deflection, X, is expressed as:

For one-way elements

$$r_T = X \left[\frac{8T_y}{L_y^2}\right] \qquad 4\text{-}40$$

For two-way elements

$$r_T = \frac{1.5\, X\pi^3 T_y / L_y^2}{4 \sum_{n=1,3,5} \left[\frac{1}{n^3}(-1)^{(n-1)/2} \left[1 - \frac{1}{\cosh\left[\frac{n\pi L_x}{2L_y} \left[\frac{T_y}{T_x} \right]^{1/2} \right]} \right] \right]} \qquad 4\text{-}41$$

in which

$$T_y = (A_s)_y f_{ds} \qquad 4\text{-}42$$

and

$$T_x = (A_s)_x f_{ds} \qquad 4\text{-}43$$

where

r_T = tensile membrane resistance

X = deflection of element

L_y = clear span in short direction

L_x = clear span in long direction

T_y = force in the continuous reinforcement in the short direction

T_x = force in the continuous reinforcement in the long direction

$(A_s)_y$ = continuous reinforcement in the short direction

$(A_s)_x$ = continuous reinforcement in the long direction

Even though the capacity of a laterally restrained element is based on flexural action, adequate tensile membrane capacity must be provided. That is, sufficient continuous reinforcement must be provided so that the tensile membrane resistance r_T corresponding to 8 degrees support rotation must be greater than the flexural resistance r_u. The deflection is computed as a function of the yield line locations (shortest sector length). The force in the continuous reinforcement is calculated using the dynamic design stress f_{ds} corresponding to 8 degrees support rotation (Table 4-2).

4-25.5. Flexural Design

Since the actual tensile membrane resistance deflection curve is replaced with an equivalent flexural curve, the design of a non-laced element for large deflections is greatly simplified. The design is performed in a similar manner as for small deflections. However, sufficient continuous reinforcement must be provided to develop the required tensile membrane resistance. Where

external restrain is required, the support must withstand the lateral forces T_y and T_x as given in Equations 4-42, and 4-43, respectively.

4-26. Dynamic Analysis

4-26.1. Design for Shock Load

The dynamic analysis of a slab is accomplished by first representing it as a single-degree-of-freedom system and then finding the response of that system when subject to a blast load. The equivalent single-degree-of-freedom system is defined in terms of its ultimate resistance r_u, equivalent elastic deflection X_E and natural period of vibration T_N. The ultimate unit resistance is calculated from the equations of Chapter 3 for the moment capacities determined according to the previous sections. The procedures and parameters necessary to obtain the equivalent elastic deflection and natural period of vibration can also be found in Chapter 3.

For elements subjected to dead loads in the same direction as the blast loads (for example a roof or retaining wall exposed to an exterior explosion) the resistance available to withstand the blast load is reduced. An approximation of the resistance available is

$$r_{avail} = r_u - r_{DL}\left[\frac{f_{ds}}{f_{dy}}\right] \qquad 4\text{-}44$$

where

r_{avail} = dynamic resistance available

r_{DL} = uniform dead load

Chapter 2 describes procedures for determining the dynamic load which is defined by its peak value P and duration T. For the ratios P/r_u and T/T_N, the ductility ratio X_m/X_E and t_m/T can be obtained from the response charts of Chapter 3. These values, X_m which is the maximum deflection, and t_m, the time to reach the maximum deflection, define the dynamic response of the element.

The effective mass and the stiffness used in computing the natural period of vibration T_N depends on the type of cross section and loadmass factor used, both of which depend on the range of the maximum deflection. When the deflections are small (less than 4 degrees) a type I or type II cross section is used. The mass is calculated using the entire thickness of the concrete element T_c. The spalling that occurs when an element acts under tensile membrane behavior or which may occur due to close-in effects requires the use of a type III cross section to resist moment. Since the concrete cover over the flexural reinforcement is completely disengaged, the mass is calculated based on the distance between the centroids of the compression and tension reinforcement.

When designing for completely elastic behavior, the elastic stiffness is used while, in other cases, the equivalent elasto-plastic stiffness K_E is used. The elastic value of the load-mass factor K_{LM} is used for the elastic range while, in the elasto-plastic range, the load-mass factor is the average of the elastic and elasto-plastic values. For small plastic deformations, the value of K_{LM} is equal to the average of the equivalent elastic value and the plastic

value. The plastic value of K_{LM} is used for slabs designed for large plastic deformations.

Due to the large number of variables involved in the design of non-laced reinforced elements, design equations have not been developed. However, design equations have been developed for laced elements subjected to impulse loads and are presented in subsequent sections of this chapter. Use of these procedures for the design of non-laced elements subjected to impulse load will result in a variety of errors depending upon support conditions, thickness of the concrete section, quantity and distribution of the flexural reinforcement, etc. However, these procedures may be used to obtain a trial section which then may be analyzed as described above.

4-26.2. Design for Rebound

Elements must be designed to resist rebound, that is, the damped elastic or elasto-plastic harmonic motion which occurs after the maximum positive displacement X_m has been attained. When an element reaches X_m, the resistance is at a maximum, the velocity is zero, and its deceleration is a maximum. The element will vibrate about the blast load curve (positive and/or negative phase) and/or the zero line (dead load for roofs) depending on the time to reach maximum deflection t_m and the duration of the blast load T.

Usually only those elements with a type I cross-section will require additional reinforcement to resist rebound. Additional reinforcement is not required for type II and III cross-sections since these sections have equal reinforcement on opposite faces and the maximum possible rebound resistance is equal to the ultimate (positive) resistance. However, the supports for all types of cross sections , including the anchorage of the reinforcement (compression reinforcement under positive phase loading is subjected to tension forces under rebound conditions) must be investigated for rebound (negative) reactions. Also, it should be noted that the support conditions for rebound are not always the same as for the positive load.

The negative resistance r^-, attained by an element when subjected to a triangular pressure-time load, is obtained from figure 3-268 of Chapter 3. Entering the figure with the ratios of X_m/X_E and T/T_N, previously determined for the positive phase of design, the ratio of the required rebound resistance to the ultimate resistance r^-/r_u is obtained. The element must be reinforced to withstand this rebound resistance r^- to insure that the slab will remain elastic during rebound. However, in some cases, negative plastic deformations are permissible.

The tension reinforcement provided to withstand rebound forces is added to what is the compression zone during the initial loading phase. To obtain this reinforcement, the element is essentially designed for a negative load equal to the calculated value of r^-. However, in no case shall the rebound reinforcement be less than one-half of the positive phase reinforcement. The moment capacities and the rebound resistance capacity are calculated using the same equations previously presented. Note that while dead load reduces the available resistance for the dynamic loading, this load increases the available resistance for rebound.

4-27. Design for Shear

4-27.1. General

The ultimate shear V_u at any section of a flexural element is a function of its geometry, yield line location and unit resistance r. For one-way or two-way elements the ultimate shear is developed when the resistance reaches the ultimate unit value r_u. In the design of a concrete element, there are two critical locations where shear must be considered. The ultimate shear stress v_u is calculated at a distance d or d_c from the supports to check the diagonal tension stress and to provide shear reinforcement (stirrups) is necessary. The direct shear force or the ultimate support shear V_s is calculated at the face of the support to determine the required quantity of diagonal bars.

4-27.2. Ultimate Shear Stress at d_e from the Support

4-27.2.1. One-Way Elements

The ultimate shear stresses v_u at a distance d_e from the support are given in Table 4-6 for one-way elements. Depending upon the cross section type being considered, d_e can represent either d or d_c. For those cases where an element does not reach its ultimate resistance r_u is replaced by the actual resistance r attained by the element. For those members whose loading causes tension in their supports, the ultimate shear stress is calculated at the face of the support. For those cases, the ultimate support shear V is calculated as explained in the next section. This shear is then divided by the effective cross-sectional area (bd or bd_c) of the element to obtain the ultimate shear stress.

4-27.2.2. Two-Way Elements

For two-way elements the ultimate shear stress must be calculated at each support. The shears acting at each section are calculated using the yield line procedure outlined in Chapter 3 for the determination of the ultimate resistance r_u. Because of the higher stiffness at the corners, the shear along any section parallel to the support varies. The full shear stress V acts along the supports except in the corners where only 2/3 of the shear stress is used (Fig. 4-19). Since the shear is zero along the yield lines, the total shear at any section of the sector is equal to the resistance r_u times the area between the section being considered and the positive yield lines.

To illustrate this procedure, consider a two-way element, fixed on three sides and free on the fourth, with the yield line pattern as shown in Figure 4-19. For the triangular sector I, the shear V_{dV} and shear stress v_{uV} at distance d_e from the support is

$$\frac{2}{3} V_{dv} \left(\frac{L'}{4} - \frac{d_e L}{2y} + \frac{L}{4} - \frac{d_e L}{2y}\right) + V_{dv}\left(\frac{L}{2}\right) \qquad 4\text{-}45a$$

$$= r_u \left(\frac{y - d_e}{2}\right)\left(L - \frac{d_e L}{y}\right)$$

$$V_{dv} = \frac{3r_u y\ (1 - d_e/y\ )^2}{(5 - 4\ d_e/y\ )} \qquad 4\text{-}45b$$

and since the shear stress v_u is equal to V/bd_e and b equals one inch

$$v_{uv} = \frac{3r_u\ (1 - d_e/y\ )^2}{\frac{d_e}{y}\ (5 - 4\ d_e/y\ )} \qquad 4\text{-}46$$

For the trapezoidal sector II

$$\frac{2}{3} V_{dH} \left(\frac{y}{2} - \frac{2d_e y}{L}\right) + V_{dH} \left(H - \frac{y}{2}\right)$$

$$= r_u \left(\frac{L}{2} - d_e\right) \frac{1}{2} \left(H - y + H - \frac{2d_e y}{L}\right) \qquad 4\text{-}47a$$

$$V_{dh} = \frac{3r_u(L - 2\ d_e) \left[2H - y - \frac{2d_e y}{L}\right]}{2 \left[6H - y - \frac{8d_e y}{L}\right]} \qquad 4\text{-}47b$$

$$v_{uH} = \frac{3r_u \left(1 - \frac{2d_e}{L}\right) \left(2 - \frac{y}{H} - \frac{2d_e y}{LH}\right)}{2\frac{d_e}{L} \left(6 - \frac{y}{H} - \frac{8d_e y}{LH}\right)} \qquad 4\text{-}48$$

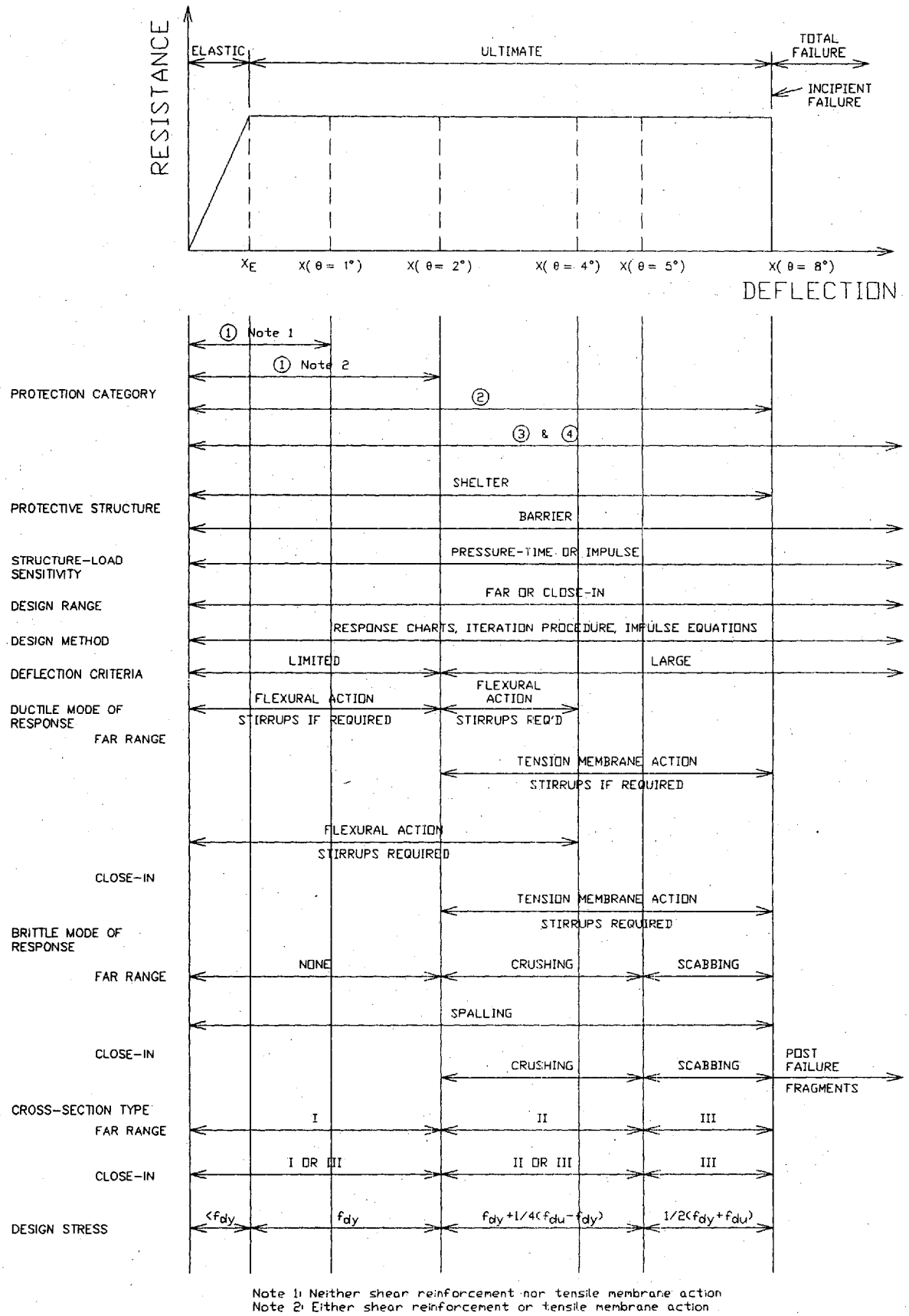
Values of the ultimate shear stresses v_{uH} and v_{uV} at a distance d_e from the support for several two-way elements are given in Table 4-7. As stated above, d_e represents either d or d_c, depending upon the type of cross section being considered. The ultimate shear stress is calculated at the face of the support for those members whose loading condition causes tension in their supports. For these cases, the ultimate support shear V is calculated as explained in the next section. This shear is then divided by the effective cross-sectional area (bd or bd_c) of the element to obtain the ultimate shear stress v.

For the situations where the ultimate resistance of an element is not attained, the maximum shear stress is less than the ultimate value. However, the distribution of the shear stresses is assumed to be the same and, there-

fore, the shear stresses can be calculated from the equation of Table 4-7 by replacing r_u with the actual resistance attained (r_e, r_{ep}, etc.).

4-27.3. Ultimate Support Shear

See Chapter 3, for procedures used to calculate the ultimate shears of both one-way and two-way elements.



Note 1: Neither shear reinforcement nor tensile membrane action
Note 2: Either shear reinforcement or tensile membrane action

Figure 4-17 Relationship between design parameters for unlaced elements

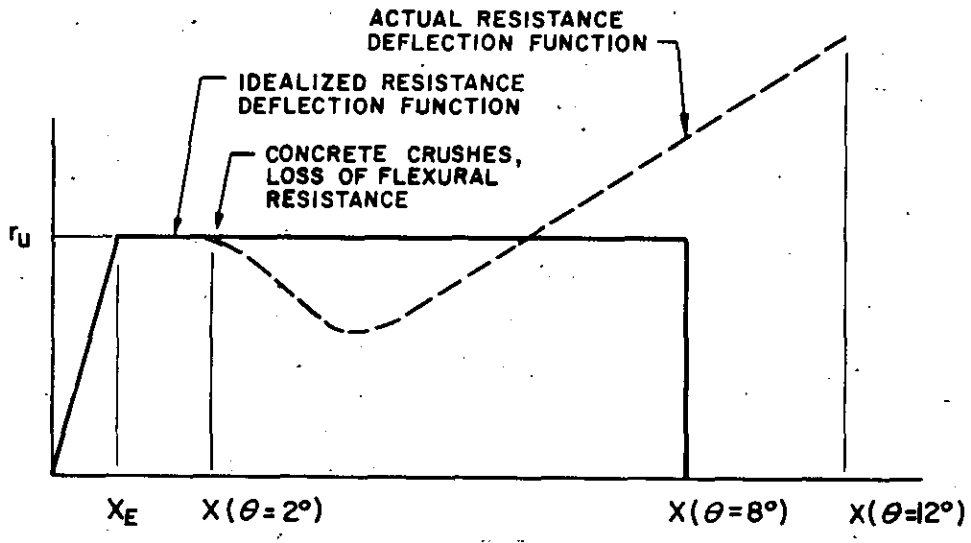


Figure 4-18 Idealized resistance-deflection curve for large deflections

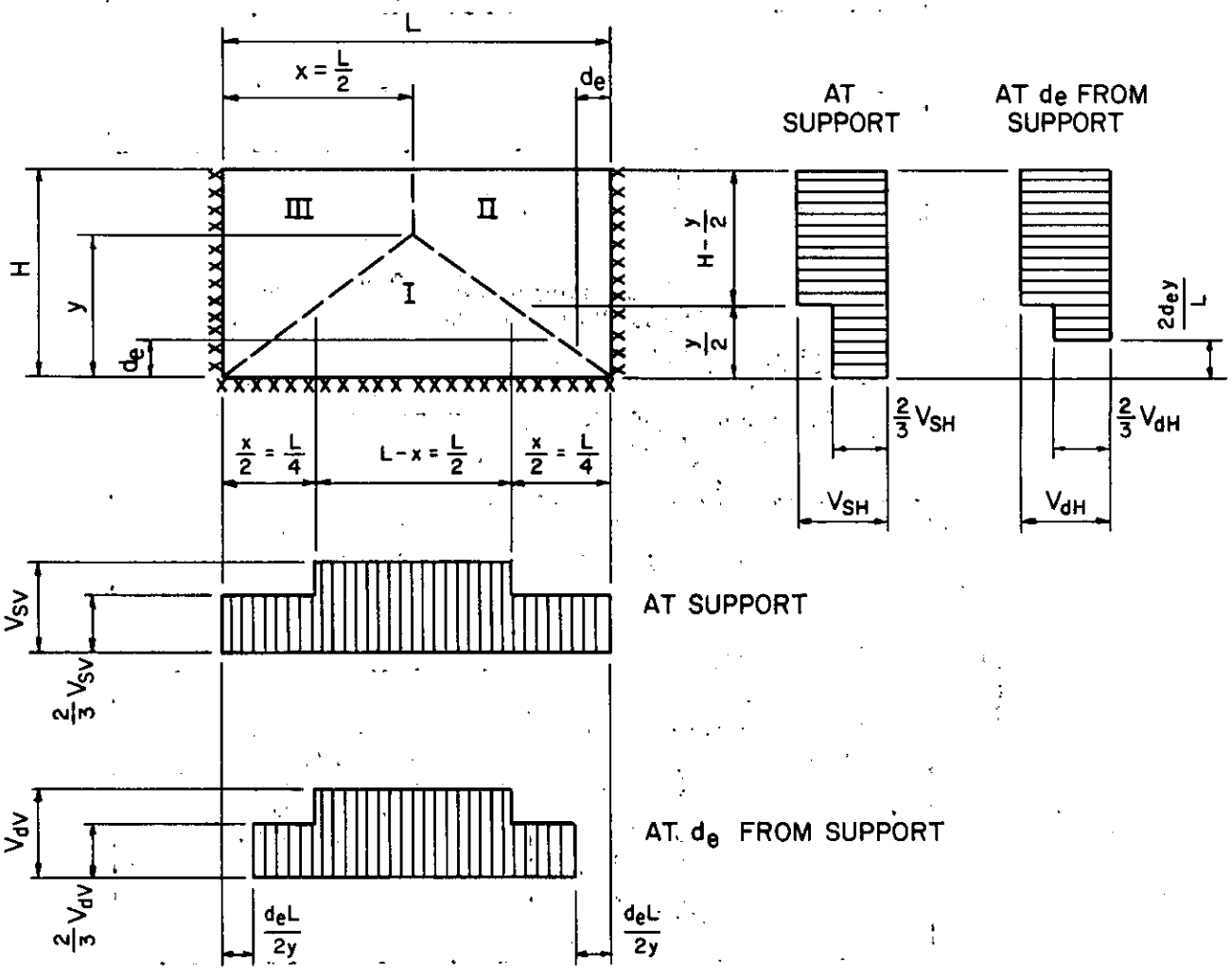
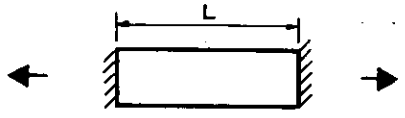
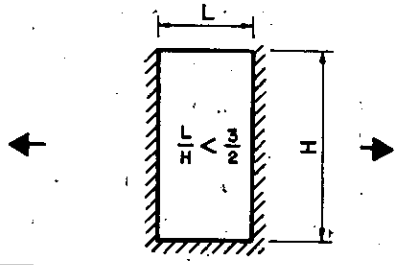
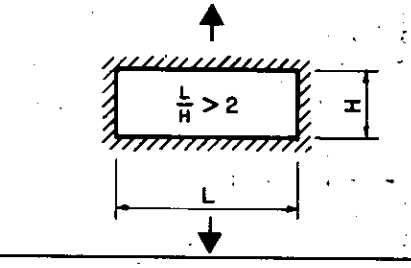
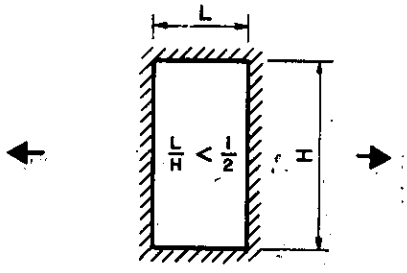
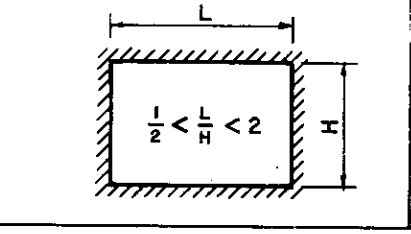


Figure 4-19. Determination of ultimate shears

Table 4-5 Restraint and Aspect Ratio Requirements for Tension Membrane Behavior

Edge Support Conditions	External Lateral Restraint Requirements
	Opposite edges
	Opposite edges
	Opposite edges short direction
	Opposite edges short direction
	None required

← Indicates direction of external lateral restraint which must be resisted by adjacent member

Table 4-6 Ultimate Shear Stress at Distance d_e from Face of Support for One-Way Elements

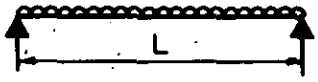
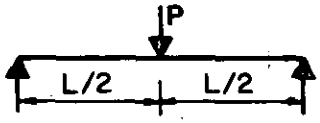
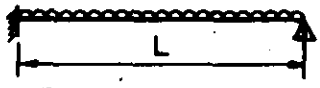
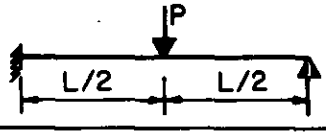
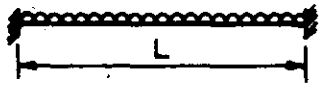
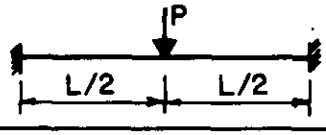
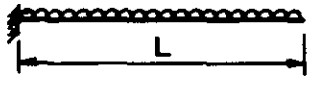
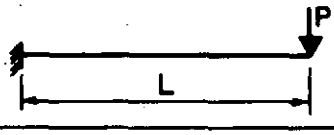
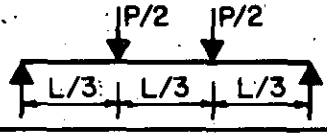
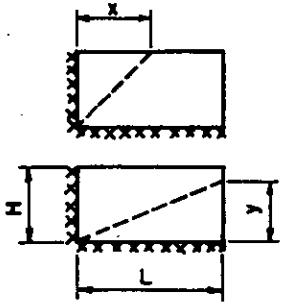
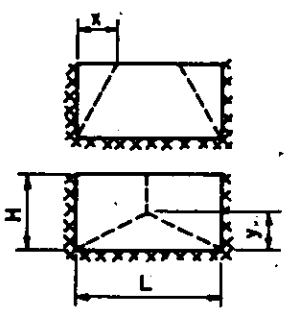
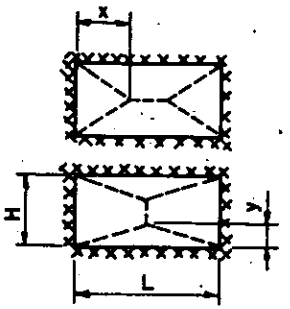
Edge Conditions and Loading Diagrams	ULTIMATE SHEAR STRESS V_u
	$\frac{r_u\left(\frac{L}{2}-d_e\right)}{d_e}$
	$\frac{R_u}{2d_e}$
	LEFT SUPPORT $r_u\left(\frac{5L}{8}-d_e\right)/d_e$ RIGHT SUPPORT $r_u\left(\frac{3L}{8}-d_e\right)/d_e$
	LEFT SUPPORT $\frac{11R_u}{16d_e}$ RIGHT SUPPORT $\frac{5R_u}{16d_e}$
	$\frac{r_u\left(\frac{L}{2}-d_e\right)}{d_e}$
	$\frac{R_u}{2d_e}$
	$\frac{r_u\left(L-d_e\right)}{d_e}$
	$\frac{R_u}{d_e}$
	$\frac{R_u}{2d_e}$

Table 4-7 Ultimate Shear Stress at Distance d_e from Face of Support for Two-Way Elements

Edge conditions	Yield line location	Limits	Ultimate horisontal shear stress v_{uH}	Limits	Ultimate vertical shear stress v_{uV}
Two adjacent edges fixed and two edges free		$0 \le d_e/x \le \frac{1}{2}$	$\frac{3r_u(1-d_e/x)^2}{d_e/x(5-4d_e/x)}$	$0 \le d_e/H \le \frac{1}{2}$	$\frac{3r_u(1-d_e/H)(2-x/L-d_ex/HL)}{d_e/H(6-x/L-4d_ex/HL)}$
		$\frac{1}{2} \le d_e/x \le 1$	$\frac{r_u(1-d_e/x)}{2(d_e/x)}$	$\frac{1}{2} \le d_e/H \le 1$	$\frac{r_u(1-d_e/H)(2-x/L-d_ex/HL)}{2d_e/H(1-d_ex/HL)}$
		$0 \le d_e/L \le \frac{1}{2}$	$\frac{3r_u(1-d_e/L)(2-y/H-d_ey/LH)}{d_e/L(6-y/H-4d_ey/LH)}$	$0 \le d_e/y \le \frac{1}{2}$	$\frac{3r_u(1-d_e/y)^2}{d_e/y(5-4d_e/y)}$
		$\frac{1}{2} \le d_e/L \le 1$	$\frac{r_u(1-d_e/L)(2-y/H-d_ey/LH)}{2d_e/L(1-d_ey/LH)}$	$\frac{1}{2} \le d_e/y \le 1$	$\frac{r_u(1-d_e/y)}{2d_e/y}$
Three edges fixed and one edge free		$0 \le d_e/x \le \frac{1}{2}$	$\frac{3r_u(1-d_e/x)^2}{d_e/x(5-4d_e/x)}$	$0 \le d_e/H \le \frac{1}{2}$	$\frac{3r_u(1-d_e/H)(1-x/L-d_ex/HL)}{d_e/H(3-x/L-4d_ex/HL)}$
		$\frac{1}{2} \le d_e/x \le 1$	$\frac{r_u(1-d_e/x)}{2(d_e/x)}$	$\frac{1}{2} \le d_e/H \le 1$	$\frac{r_u(1-d_e/H)(1-x/L-d_ex/HL)}{d_e/H(1-2d_ex/HL)}$
		$0 \le d_e/L \le \frac{1}{2}$	$\frac{3r_u(1-2d_e/L)(2-y/H-2d_ey/LH)}{2d_e/L(6-y/H-8d_ey/LH)}$	$0 \le d_e/y \le \frac{1}{2}$	$\frac{3r_u(1-d_e/y)^2}{d_e/y(5-4d_e/y)}$
		$\frac{1}{2} \le d_e/L \le \frac{1}{2}$	$\frac{r_u(1-2d_e/L)(2-y/H-2d_ey/LH)}{4d_e/L(1-2d_ey/LH)}$	$\frac{1}{2} \le d_e/y \le 1$	$\frac{r_u(1-d_e/y)}{2d_e/y}$
Four edges fixed		$0 \le d_e/x \le \frac{1}{2}$	$\frac{3r_u(1-d_e/x)^2}{d_e/x(5-4d_e/x)}$	$0 \le d_e/H \le \frac{1}{2}$	$\frac{3r_u(\frac{1}{2}-d_e/H)(1-x/L-2d_ex/HL)}{d_e/H(3-x/L-8d_ex/HL)}$
		$\frac{1}{2} \le d_e/x \le 1$	$\frac{r_u(1-d_e/x)}{2d_e/x}$	$\frac{1}{2} \le d_e/H \le \frac{1}{2}$	$\frac{r_u(\frac{1}{2}-d_e/H)(1-x/L-2d_ex/HL)}{d_e/H(1-4d_ex/HL)}$
		$0 \le d_e/L \le \frac{1}{2}$	$\frac{3r_u(\frac{1}{2}-d_e/L)(1-y/H-2d_ey/LH)}{d_e/L(3-y/H-8d_ey/LH)}$	$0 \le d_e/y \le \frac{1}{2}$	$\frac{3r_u(1-d_e/y)^2}{d_e/y(5-4d_e/y)}$
		$\frac{1}{2} \le d_e/L \le \frac{1}{2}$	$\frac{r_u(\frac{1}{2}-d_e/L)(1-y/H-2d_ey/LH)}{d_e/L(1-4d_ey/LH)}$	$\frac{1}{2} \le d_e/y \le 1$	$\frac{r_u(1-d_e/y)}{2d_e/y}$

DESIGN OF FLAT SLABS

4-28. Introduction

The typical unhardened flat slab structure consists of a two-way slab supported by columns. Except for edge beams which may be used at the exterior edge of the slab, beams and girders are not used to transfer the loads into the columns. In this case, the columns tend to punch upward through the slab. There are several methods that can be used to prevent this; the upper end of the column can be enlarged creating a column capital, a drop panel can be added by thickening the slab in the vicinity of the column, or both a column capital and a drop panel may be used.

Hardened flat slab structures may be designed to withstand the effects associated with a far range explosion. The flat slab of a hardened structure is similar to an unhardened slab but for a hardened flat slab structure, the exterior supports must be shear walls which are monolithic with the roof. The shear walls transmit the lateral loads to the foundations. Due to the stiffness of the walls, there is negligible sidesway in the columns and hence no induced moments due to lateral loads. Shear walls may also replace a row of interior columns if additional stiffness is required. Earth cover may or may not be used for hardened flat slab structures.

A portion of a typical hardened flat slab structure is shown in Figure 4-20. As depicted, there are generally four different panels to be considered, interior, corner and two exterior, each of which has a different stiffness. The exterior panels are designated as short and long span panels which refers to the length of the span between the columns and the exterior wall. In the typical flat slab, the reinforcement would be distributed according to elastic theory. The elastic distribution of the flexural stresses is approximated by the methods presented in the ACI Building Code. The static design must meet all of the criteria of the code as well as of all applicable local codes.

However, for blast resistant structures, certain design criteria are more restrictive than those given in the ACI Building Code. To ensure two-way action in the slab, the aspect ratio L/H of each panel must be greater than 1 but less than 2. While the ACI code permits unequal span lengths and offset columns, it is strongly recommended that offset columns not be used and the variation in span lengths be limited to 10 percent. Columns and column capitals may have either a round or square cross section, but round columns and capitals are preferred to avoid shear stress concentrations. It is also recommended that haunches be provided at the shear walls.

Flat slabs may be designed to attain limited or large deflections depending upon the magnitude and duration of the applied blast load and the level of protection required by the acceptor system. Under flexural action alone, the slab may attain deflections corresponding to 2 degrees support rotation. The flexural action may be extended to 4 degrees rotation if single leg stirrups are added to restrain the flexural reinforcement. If sufficient continuous flexural reinforcement is provided, the slab may attain 8 degrees support rotation through tension membrane action. Unless required for shear, single leg stirrups are not required for the slab to achieve support rotations less than 2 degrees nor tension membrane action. The stress in the reinforcement as well as the type of cross section used to determine the ultimate moment capacity of the reinforced concrete is a function of the maximum deflection.

The basic data required for determining the ultimate strength of the reinforced concrete, including the ultimate moment capacity and the ultimate shear capacity, have been presented in previous sections. Procedures for performing the dynamic analysis are presented in Chapter 3. Only modifications and additions relating to flat slabs are presented in this section. The interrelationship between the various parameters involved in the design of flat slabs is readily described with the use of the idealized resistance-deflection curve shown in Figure 4-21.

4-29. Distribution of Flexural Reinforcement

4-29.1. General

For a two-way slab continuously supported on its edges, the flexural stresses are distributed uniformly across the entire slab (except for the reduced stresses at the corners). The flexural stresses in a flat slab supported by walls and columns are distributed from one panel to the next depending on the relative stiffness of the supports and the spans of the panels. Flat slabs also distribute the flexural stresses transversely, concentrating the stresses in the vicinity of the column. A uniform distribution of reinforcement would result in a failure due to local "fan" yield lines around the columns at a relatively low resistance. By concentrating the reinforcement over the columns, a higher ultimate resistance is obtained.

An elastic distribution of reinforcement is required in the design procedure presented in this Manual. This distribution will insure the formation of a predictable collapse mechanism. Local failures around the columns, and one-or two-way folding (local one-way action) will be prevented. With an elastic distribution of reinforcement, the yield lines form simultaneously across the entire slab. In addition, the design will be more economical and cracking under service loads will be minimized.

4-29.2 Elastic Distribution of Moments According to the ACI Building Code

Procedures outlined in the ACI Building Code are employed to determine the elastic distribution of the reinforcement (and hence of the moments). The Code presents two design methods, namely the Direct Design Method and the Equivalent Frame Method. The Equivalent Frame Method may be used for all flat slab configurations whereas the Direct Design Method can only be used for three or more spans. Since the Direct Design Method requires fewer calculations, it is the preferred method and is discussed in detail in this section.

For the typical flat slabs with continuous exterior walls and $L/H > 1$, the column strips are $H/2$ in width in each direction. A wall strip is parallel and adjacent to an exterior wall and its width is $H/4$. The remaining portions of the slab are called middle strips.

Using the Direct Design Method as given in Chapter 13 of ACI 318-77 the moments are distributed taking into account the relative flexural and torsional stiffnesses of the wall, slab and beams. Assuming there are no beams or interior shear walls, the ratio of the flexural stiffness of the beam section to the slab section α , is zero. The torsional resistance of a concrete wall monolithic with the slab is very large and, therefore, the torsional stiffness ratio of the wall to the slab β_t may be assumed to be greater than 2.5.

The ratio of the flexural stiffness of the exterior wall and the flexural stiffness of the slab is defined as:

$$\alpha_{ec} = \frac{(4E_cI_w)/\ H_w}{(4E_cI_s)/\ l_s} \qquad 4\text{-}49$$

where

α_{ec} = ratio of the flexural stiffness of the exterior wall to slab

I_w = gross moment of inertia of wall

I_s = gross moment of inertia of slab

H_w = height of wall

l_s = span of flat slab panel

In direction H, Equation 4-49 becomes

$$\alpha_{ecH} = \frac{T_w^{\ 3}\ H}{T_s^{\ 3}\ H_w} \qquad 4\text{-}50$$

and in direction L

$$\alpha_{ecL} = \frac{T_w^{\ 3}\ L}{T_s^{\ 3}\ H_w} \qquad 4\text{-}51$$

where

T_w = thickness of wall

H = short span of flat slab panel

T_s = thickness of flat slab

L = long span of flat slab panel

The unit column and midstrip moments are proportioned from the total span moments. The distributions percentages for a flat slab with equal spans in each direction is as follows (see Fig. 4-22):

For Direction H:

$$m_1^{-} = 0.65\ \alpha'_{ecH}\ M_{OH}\ /L \qquad 4\text{-}52$$

$$m_2^{+} = 0.40\ (0.63 - 0.28\ \alpha'_{ecH})\ M_{OH}\ /(L - H/2) \qquad 4\text{-}53$$

$$m_3^{-} = 0.25\ (0.75 - 0.10\ \alpha'_{ecH})\ M_{OH}\ /(L-H/2) \qquad 4\text{-}54$$

$$m_4^{-} = 0.25\ (0.65)\ M_{OH}\ /(L-H/2) \qquad 4\text{-}55$$

$$m_5^+ = 0.40\ (0.35)\ M_{OH}\ /(L-H/2) \qquad 4\text{-}56$$

$$m_6^+ = 0.60\ (0.63 - 0.28\ \alpha'_{ecH})\ M_{OH}\ /(H/2) \qquad 4\text{-}57$$

$$m_7^- = 0.75\ (0.75 - 0.10\ \alpha'_{ecH})\ M_{OH}\ /(H/2) \qquad 4\text{-}58$$

$$m_8^- = 0.75\ (0.65)\ M_{OH}\ /(H/2) \qquad 4\text{-}59$$

$$m_9^+ = 0.60\ (0.35)\ M_{OH}\ /(H/2) \qquad 4\text{-}60$$

in which

$$M_{OH} = \frac{wL(H-c)^2}{8} \qquad 4\text{-}61$$

and

$$\alpha'_{ecH} = \frac{1}{1 + (1/\alpha_{ecH})} \qquad 4\text{-}62$$

M_{OH} = total panel moment for direction H

w = applied uniform load

c = width of column capital

For Direction L:

$$m_{10}^- = 0.65\ \alpha'_{ecL} M_{OL}\ /H \qquad 4\text{-}63$$

$$m_{11}^+ = 0.40\ (0.63 - 0.28\ \alpha'_{ecL})\ M_{OL}\ /(H/2) \qquad 4\text{-}64$$

$$m_{12}^- = 0.25\ (0.75 - 0.10\ \alpha'_{ecL})\ M_{OL}\ /(H/2) \qquad 4\text{-}65$$

$$m_{13}^- = 0.25\ (0.65)\ M_{OL}\ /(H/2) \qquad 4\text{-}66$$

$$m_{14}^+ = 0.40\ (0.35)\ M_{OL}\ /(H/2) \qquad 4\text{-}67$$

$$m_{15}^+ = 0.60\ (0.63 - 0.28\ \alpha'_{ecL})\ M_{OL}\ /(H/2) \qquad 4\text{-}68$$

$$m_{16}^- = 0.75\ (0.75 - 0.10\ \alpha'_{ecL})\ M_{OL}\ /(H/2) \qquad 4\text{-}69$$

$$m_{17}^- = 0.75\ (0.65)\ M_{OL}\ /(H/2) \qquad 4\text{-}70$$

$$m_{18}^+ = 0.60\ (0.35)\ M_{OL}\ /(H/2) \qquad 4\text{-}71$$

in which

$$M_{OL} = \frac{wH\ (L-c)^2}{8} \qquad 4\text{-}72$$

and

$$\alpha'_{ecL} = \frac{1}{1 + (1/\alpha_{ecL})} \qquad 4\text{-}73$$

where M_{OL} is the total panel moment for direction L.

For the wall strips in both directions the same reinforcement as in the adjacent middle strips is used. At the column, the larger of the two negative moments is chosen and the positive moment can then be adjusted up to 10 percent so that the total panel moments remain unchanged.

4-29.3 Design for Small Deflections

The resistance-deflection function for flat slabs with small deflections is shown in Figure 4-23a. With an elastic distribution of reinforcement all the yield lines form simultaneously and the slab remains elastic until it reaches its ultimate resistance. Since for small deflections the concrete remains effective in resisting stress, a type I cross section is used to compute the ultimate moment capacities. The slab may undergo a maximum support rotation of 2 degrees at which point the concrete crushes. Shear reinforcement is generally not required for flat slabs, but must be provided if required by analysis. If properly designed, single leg stirrups are provided, the flexural action of the slab may be extended to 4 degrees support rotation. While stirrups may be furnished to resist shear or to extend flexural action, it is usually more cost effective to design flat slabs without shear reinforcement.

4-29.4. Design for Large Deflections

Due to the geometric limitations (aspect ratio L/H of each panel must be greater than 1 but less than 2) imposed on flat slabs designed for blast loads, sufficient lateral restraint is available to develop in-plane forces and induce tension membrane action. This tension membrane action provides the means for the slab to attain deflections corresponding to a maximum support rotation in excess of 12 degrees. Continuous reinforcement must be provided to resist these in-plane tension forces.

A typical resistance-deflection curve for the flat slabs up to incipient failure is shown in Figure 4-23b. The initial portion of the curve is due primarily to flexural action. At 2 degrees support rotation, the concrete begins to crush and the slab loses flexural capacity. However, due to the presence of continuous reinforcement, tension membrane action is mobilized. The resistance due to this action increases with increasing deflection up to incipient failure at approximately 12 degrees support rotation. The tension membrane action is shown as the dashed line in Figure 4-23b.

In order to simplify the design calculations, the resistance is assumed to be equal to the flexural action throughout the entire range of behavior. To approximate the energy absorbed under the actual resistance-deflection curve, the deflection of the equivalent curve is limited to 8 degrees support rotation. This deflection would produce incipient failure conditions. Using this equivalent design curve, deflections between 2 degrees and incipient failure cannot be accurately predicted.

A type II or III cross section is used to compute the ultimate moment capacity of a flat slab designed for large deflections. At every section throughout the slab, tension and compression reinforcement must be continuous in order to develop the tension membrane action (tension membrane capacity is discussed in detail below). It should be noted that in addition to the above requirements

for the reinforcement, an elastic distribution of reinforcement must still be maintained.

Shear reinforcement is only provided when required by analysis. If the concrete can resist the shear stresses, shear reinforcement is not required for flexural action (deflections less than 2 degrees) nor for tension membrane action (deflections between 2 and 8 degrees). However, shear reinforcement, in the form of single leg stirrups, does allow the slab to rotate up to 4 degrees under flexural action. There are two design situations where single leg stirrups are desirable when designing for rotations between 2 and 4 degrees: (1) the slab is incapable of developing adequate tension membrane action and (2) the maximum deflection must be accurately predicted (which cannot be done utilizing tension membrane action). In all other design situations, it is usually more economical to eliminate single leg stirrups by increasing the slab thickness (to increase shear capacity) and/or by increasing the amount of continuous reinforcement (to develop adequate tension membrane capacity).

4-29.5. Minimum Reinforcement

To ensure proper structural behavior under dynamic loads and also to minimize excessive deformations under conventional loads, the minimum area of reinforcement must be at least equal to that specified in Table 4-3. With an elastic distribution of reinforcement in a flat slab, the minimum reinforcement generally will occur only in the center of the midstrip and/or in the wall strip. It is important to also check the static requirements for minimum reinforcement. Where static conditions control, the area of reinforcement must be at least equal to 0.0018 times the gross area of concrete or 1.33 times the area required by static loading conditions, whichever is less. Unless the blast loads are in the same order of magnitude as the static loads, this criteria does not control.

Although the spacing of the flexural reinforcement must not exceed two times the slab thickness nor 18 inches, the preferred spacing is 12 inches or less.

There is no minimum shear reinforcement requirement for flat slabs. Shear reinforcement is only provided when required by analysis. However, when a slab is designed to undergo flexural response with support rotations between 2 and 4 degrees (i.e., where tension membrane action is not considered). stirrups are required. The minimum area of the stirrups is given in Table 4-4.

4-30. Dynamic Analysis

4-30.1. General

The dynamic analysis of a structural element is accomplished by first representing the structural element as a single-degree-of-freedom system and then finding the response of that system when subject to a blast load. Chapter 3 presents procedures, figures and response charts for determining the dynamically equivalent system and its response. However, certain parameters of a flat slab, such as the ultimate resistance and the elastic deflections, cannot be calculated using the methods of Chapter 3. Methods for calculating those parameters are presented below.

4-30.2. Ultimate Flexural Resistance

4-30.2.1. General

The ultimate resistance r_u of a flat slab is a function of the strength, amount and distribution of the reinforcement, the thickness and strength of the concrete and the aspect ratios of the panels. The ultimate resistance is obtained using a yield line analysis. Since in-plane compression forces and tension membrane forces are not considered, the ultimate resistance determined from a yield line analysis will generally be lower than the actual resistance.

The first step in finding the ultimate resistance is to assume a yield line pattern consistent with the support conditions and the distribution of the reinforcement. The pattern will contain one or more unknown dimensions which locate the yield lines. The correct solution is the one which gives the lowest value of the ultimate resistance. Figure 4-24 shows the yield line pattern that will form in a multi-panel flat slab with an elastic distribution of reinforcement. The roof-slab interactions must be designed to insure that the perimeter yield lines form in the roof slab and not in the wall. The yield lines at the columns are assumed to form at the face of the column capitals.

The ultimate resistance can be found from the yield line pattern using either the equilibrium method or the virtual work method, both of which have been discussed in Chapter 3. The equilibrium method is one that has been employed in previous examples but, in the case of flat slabs, requires the introduction of nodal forces which are not always readily determined. The virtual work method though more difficult to solve algebraically, does not require the calculations of the nodal forces. Consequently, the virtual work method is the easier method to apply to flat slabs and is the method detailed below.

The virtual work method does not predict the correct yield line pattern but rather gives the minimum resistance of an assumed yield line pattern. If the distribution of reinforcement is not elastic and/or the span lengths are not approximately equal, the minimum resistance found by the virtual work method may not be the ultimate resistance. In these cases, local failures are possible. It is strongly recommended that these design situations be avoided. In the rare instances where they cannot be avoided, the nodal forces must be calculated and the equilibrium method used to predict the correct yield line pattern.

4-30.2.2. Virtual Work Method

In the virtual work method, equations for the external and internal work are written in terms of the unit resistance r_u, the moment capacities and the geometry. The expression for the external work is set equal to that for the internal work, and the resulting equation is solved for the minimum value of r_u and the associated failure mechanism.

A point within the slab boundaries is given a small displacement in the direction of the load. The resulting deflections and rotations of all of the slab segments are determined in terms of the displacement and the slab segment dimensions. Work will be done by the external loads and by the internal reactions along the yield lines.

The external work done by r_u is:

$$W = \Sigma\, r_u A\Delta \qquad 4\text{-}74$$

where:

W = external work
A = area of the sector
Δ = deflection of the sector's centroid

The internal work done by the reactions at the yield lines is due only to the bending moments since the support reactions do not undergo any displacement and the work done by the shear forces (nodal forces) is zero when summed over the entire slab.

The internal work is:

$$E = \Sigma\, m\theta l \qquad 4\text{-}75$$

where

E = internal work
m = ultimate unit moment
θ = relative rotation about yield line
l = length of the yield line

In terms of the moments and rotations in the principal reinforcement directions x and y:

$$E = \Sigma\, m_x \theta_x l_y + \Sigma\, m_y \theta_y l_x \qquad 4\text{-}76$$

Equating the external and internal work, W = E

$$\Sigma\, r_u A\Delta = \Sigma\, m_x \theta_x l_y + \Sigma\, m_y \theta_y l_x \qquad 4\text{-}77$$

Particular attention must be paid to the negative moment capacities of the yield lines radiating from the column capitals when determining E. Top bar cut-offs, if present, will reduce the moment capacity on the part of the yield line furthest from the column. In addition, corner effects must be considered where the two walls intersect. That is, as a result of the increased stiffness at the corners, the ultimate moment of the reinforcement is reduced to 2/3 of its capacity over a length equal to ½ the length of the positive yield line.

To illustrate the application of Equation 4-77, consider the flat slab shown in Figure 4-25. This flat slab is the roof of a square structure with one central column, and is symmetrical about the x and y axes.

Note that Sectors I and III, and Sectors II and IV are identical because of symmetry. To simplify calculations, each sector has been resolved into a rectangle and a triangle. The external work for each sector is:

$$W_I = W_{III} = r_u x(L - x)\,(\Delta/2) + r_u x(x/2)\,(\Delta/3) \qquad 4\text{-}78$$

$$W_{II} = W_{IV} = r_u c(L - x - c)(\Delta/2)$$

$$+ r_u (L - x - c)[(L - x - c)/2](2\Delta/3) \qquad 4\text{-}79$$

Substituting L = 4l and summing

$$\Sigma W = 2 (r_u \Delta/6)(32\, l^2 - 4lx + cx - 4cl - c^2) \qquad 4\text{-}80$$

where

c = width of column capital
L = length of panel
x = horizontal location of the yield line
l = width of ½ of the column strip
Δ = maximum deflection of slab

The internal work for each sector is:

$$E_I = E_{III} = \left[\frac{2}{3} m \frac{x}{2} + m \left(L - \frac{x}{2}\right) \right] \theta_A$$

$$+ \left[\frac{2}{3} (2m) \frac{x}{2} + 2m\left(3l - \frac{x}{2}\right) + 3ml\right]\theta_A \qquad 4\text{-}81$$

$$E_{II} = E_{IV} = [3ml + 2m(L - x - l)]\theta_B$$

$$+ [4.5ml + 1.5ml\ (L - x - l)]\theta_B \qquad 4\text{-}82$$

Substituting L = 4l, $\theta_A = \Delta/x$ and $\theta_B = \Delta/(L - x - c)$

$$\Sigma E = 2\Delta m \left[\frac{13\ l}{x} - \frac{1}{2} + \frac{18\ l - 3.5x}{4l - x - c}\right] \qquad 4\text{-}83$$

Equating W = E and solving for r_u

$$r_u = \frac{6m \left[\frac{13l}{x} - \frac{1}{2} + \frac{18l - 3.5x}{4l - x - c} \right]}{\left[32l^2 - 4lx + cx - 4cl - c^2 \right]} \qquad 4\text{-}84$$

with x as the only unknown. The minimum value of r_u is readily determined by trial and error.

A complete design example is presented in Appendix 4A.

In general, the virtual work equation will contain more than one unknown, and it will be correspondingly more difficult to obtain the minimum ultimate resistance. However, a trial and error process rapidly converges on the correct solution.

A trial and error procedure to solve for the minimum value of the resistance function (r_u/M_o for a preliminary design and r_u for a final design) with two unknown yield line locations, x and y, can be accomplished as follows:

1. Start with both yield lines located close to the centerline of the respective middle strips.

2. Vary x, holding y constant, in the direction which minimizes the resistance function until it begins to increase.

3. Hold x constant and vary y in the minimum direction until the resistance function begins to increase.

4. Once this minimum point is achieved, shift each yield line to either side of the minimum location to check that a further refinement of the yield line is not necessary to minimize the resistance function.

It should be noted that if the yield line should shift out of the middle strip, a new resistance function equation must be written and the procedure then repeated since the magnitude of the unit moments acting on the yield lines would change.

4-30.2.3. Effect of Column Capitals and Drop Panels

Although column capitals and drop panels are primarily used to prevent shear failures, they have a significant effect on the ultimate resistance. The addition of a column capital or revision of the size of the capital changes the clear span of a flat slab and requires the re-evaluation of a slab's ultimate resistance.

Drop panels increase the ultimate resistance by increasing the depth of the section and thus the moment capacity in the vicinity of the column. This effect can be countered by decreasing the amount of reinforcement to maintain the same moment capacity. If the drop panel is used to increase the negative moment capacity, it must extend at least 1/6 of the center-to-center span length in each direction. The width of the drop panel may be up to 20 percent larger than the column strip. When the drop panel is larger than the column strip, the percentage of reinforcement calculated for the column strip shall be provided throughout the drop panel. Additional reinforcement must be provided in the bottom of the drop panel to prevent it from scabbing and becoming hazardous debris. For a type II cross section, the reinforcement in the drop panel is the same as the negative reinforcement over the column. Only ½ the amount of the negative reinforcement is required in a drop panel for a type I cross section.

4-30.3. Ultimate Tension Membrane Capacity

When the support rotation of a flat slab reaches 2 degrees, the concrete begins to crush and flexural action is no longer possible. However, the slab is capable of sustaining large rotations due to tension membrane action. As previously explained, the actual resistance-deflection curve describing the tension membrane action has been replaced with an equivalent curve which considers flexural action only (Fig. 4-23b). Using this idealized curve,

incipient failure is taken to occur at 8 degrees which corresponds to an actual support rotation of approximately 12 degrees.

It can be seen from Figure 4-23b, that the tension membrane resistance is a function of the deflection. It is also a function of the span length and the amount of the continuous reinforcement. Data is not presently available to obtain the tension membrane capacity of a flat slab. However, an approximation may be made using the equation developed for two-way slabs. Therefore, the tension membrane capacity, r_T, of a flat slab is given by:

$$r_T = \frac{1.5X\pi^3 T_H / L_H^2}{4 \sum_{n=1,3,5} \left[\frac{1}{n^3} (-1)^{(n-1)/2} \left[1 - \frac{1}{\cosh \left[\frac{n\pi L_L}{2L_H} \left[\frac{T_H}{T_L} \right]^{1/2} \right]} \right] \right]} \qquad 4\text{-}85$$

where

r_T = tension membrane resistance

X = deflection of slab

L_H = clear span in short direction

L_L = clear span in long direction

T_H = force in the continuous reinforcement in short span direction

T_L = force in the continuous reinforcement in long span direction

Although the capacity of a flat slab is based on flexural action, adequate tension membrane capacity must be provided. That is, r_T corresponding to 8 degrees support rotation must be greater than the flexural resistance r_u when designing for large deflections. The deflection is computed as a function of the yield line locations (shortest sector length). The force in the continuous reinforcement is calculated using the dynamic design stress corresponding to 8 degrees (Table 4-2). The clear span L_H and L_L are calculated as the clear distance between the faces of the supports (face of the column if no column capital is used, face of the column capital, face of the wall if no haunch is used or the face of haunch).

4-30.4. Elastic Deflections

The elastic deflection of various points on an interior panel of a flat slab are given by the general equation

$$X_e = \frac{C r_u L^4 (1 - \nu^2)}{E_c I_a} \qquad 4\text{-}86$$

where

X_e = elastic deflection

C = deflection coefficient from Table 4-8

L = long span of panel

ν = poisson's ration = 0.167

I_a = average of the cracked and gross moment of inertia of the concrete slab

The deflection coefficient varies with the panel aspect ratio L/H, the ratio of the support size to the span C/L and the location within the panel. The values of the deflection coefficient given in Table 4-8 are based on a finite difference method and are given for the center of the panel C_C and the midpoints of the long and short sides, C_L and C_S, respectively.

The deflection for the interior panel is determined by using C_C in the above expression. For the long and short span panels and the corner panel (Fig. 4-20). No simplified solution for the center deflections are currently available. Generally, the deflections for the corner panels will be smaller than the deflection of the interior panel because of the restraining effects of the exterior walls. These deflections can be approximated by using the following expressions:

Long Span Panel	$C = C_C - C_S/2$	4-87
Short Span Panel	$C = C_C - C_L/2$	4-88
Corner Panel	$C = C_C - C_S/2 - C_L/2$	4-89

where the values of C_C, C_S and C_L are those for the interior panel from Table 4-8.

The dynamic response of a flat slab is more sensitive to the elastic stiffness when the maximum allowable deflection is small. The possible error diminishes with increasing allowable maximum deflection.

4-30.5. Load-Mass Factors

4-30.5.1. Elastic Range

No data is currently available to determine the loadmass factor, K_{LM}, of a flat slab in the elastic range of behavior. It is, therefore, recommended that the values listed in the table of the load-mass factors for two-way elements be used (Chapter 3). The slab should be considered as fixed on all four edges with the appropriate L/H ratio. Since an average value of the elastic and plastic load-mass factor is used in determining the natural period of vibration, the possible error incurred will diminish with increasing allowable maximum deflection.

4-30.5.2. Plastic Range

The load-mass factor on the plastic range is determined using the procedure outlined for two-way elements in Chapter 3. The supports for the individual sectors are at the face of the exterior walls (or haunches, if present) or at the face of the column capitals. Flat slabs without drop panels have a uniform thickness and the equation for determining the load-mass factor may be expressed in terms of the area moment of inertia and the area of the individual sectors. For flat slabs with drop panels, the equations must be expressed in terms of the mass moment of inertia and the non-uniform mass of the individual sectors to account for the non-uniform slab thickness.

4-30.6. Dynamic Response

The equivalent single-degree-of-freedom system of the flat slab is defined in terms of its ultimate resistance r_u, elastic deflection X_E and its natural period of vibration T_N. The procedure for determining the value of T_N has been presented in Chapter 3 while the calculation of r_u and X_E has been presented above. The resistance deflection curve used in the dynamic analysis is shown in Figure 4-26. The resistance available to withstand the blast loads must be reduced by the dead loads. An approximation of the resistance available is

$$r_{avail} = r_u - r_{DL} \left(\frac{f_{ds}}{f_y}\right) \qquad 4\text{-}90$$

where

r_{avail} = dynamic resistance available

r_{DL} = uniform dead load

The total deflection of the flat slab includes deflections due to dead load X_{DL} and blast X_m, so that the maximum support rotation θ_m is given by

$$\theta_m = \tan^{-1} \left(\frac{X_m + X_{DL}}{L_s}\right) \qquad 4\text{-}91$$

where L_s is the length of the shortest sector.

The blast load is defined in terms of its peak pressure P and its duration T which are determined from Chapter 2. Chapter 3 contains the procedures to determine the dynamic response of a slab which include the maximum dynamic deflection X_m and the time to reach that deflection t_m. It must be remembered that using the equivalent resistance-deflection curve to include tension membrane action, deflections between 2 degrees and incipient failure cannot be accurately predicted.

The required rebound resistance of the flat slab is calculated in accordance with Chapter 3 and the reinforcement necessary to attain this capacity must be provided. Note that while the dead load reduces the available resistance for the dynamic loading, this load increases the available resistance for rebound.

4-31. Dynamic Design

4-31.1. Flexural Capacity

The ultimate moment capacity of a flat slab is usually based upon a type I or type III cross section depending on the magnitude of the maximum allowable deflection. The distribution of reinforcement is critical in flat slab design. The actual moment capacity provided must be as close as possible to the unit moments required for an elastic distribution of stresses. The quantity of flexural reinforcement which is made continuous provides the tension membrane resistance.

If the amount of continuous reinforcement provided is inadequate for tension membrane action, care must be taken in furnishing additional reinforcement. Any additional reinforcement must be placed to maintain the elastic distribution of reinforcement and the new moment capacities and ultimate resistance must be re-evaluated. The ultimate moment capacity will not be altered if the additional reinforcement is provided by increasing the compression reinforcement.

4-31.2. Shear Capacity

Unlike continuously supported two-way slabs where shear stresses are "checked" after the flexural design is completed, the design for shear of a flat slab must be considered during the flexural design. Due to the nature of the support system, flat slabs will usually generate large shear stresses. Flat slabs with high percentages of flexural reinforcement and/or long spans should be avoided.

The shear forces acting at a support are a function of the tributary area of the sectors formed by the yield lines. The shears at the columns should be checked first, since design for these forces can drastically effect the flexural design of the slab. Two types of shear action must be considered; punching shear along a truncated cone around the column and beam shear across the width of the yield lines. These conditions are illustrated in Figure 4-27.

Shears at the columns may require the use of column capitals and/or drop panels. Punching shear can occur around the periphery of the columns or column capitals and drop panels. The critical section is taken at $d_e/2$ from the face of the support. The total load is calculated based on the area enclosed by the positive yield lines and is then distributed uniformly along the critical perimeter. Figure 4-27a illustrates the critical sections for punching shear. Beam shear, as a measure of diagonal tension, is taken as one-way action between supports where the width of the beam is taken as the spacing between the positive yield lines. The critical section is taken as d_e away from the face of the column or column capital and from the face of the drop panel (Fig. 4-27b). The total load is uniformly distributed along the critical section.

The slab at the exterior walls must be evaluated for diagonal tension capacity. Due to the assumed uniform distribution of load at the exterior walls, a unit width of loaded area may be considered between the positive yield line and the critical section. The critical section is taken at d_e from the face of the exterior wall or, if a haunch is used, from the face of the haunch.

The ultimate shear capacity of slabs has been previously presented. Using these procedures, the capacity of the slab is evaluated at the locations

described above. If required, stirrups may be furnished. However, it is more cost effective to revise the design to incorporate the use of column capitals, drop panels and/or increased slab thickness to reduce shear stresses. As previously stated, the use of stirrups is mandatory in the flexural design of flat slabs between 2 and 4 degrees support rotation.

Diagonal bars must be provided at the face of all supports due to the cracking caused by the plastic moments formed. For slabs designed for small support rotations, minimum diagonal bars must be furnished. However, for slabs designed for large support rotations where the cracking at the supports is severe, diagonal bars must be designed to resist the total support shear but not less than the minimum required. The diagonal bars furnished at the column supports should extend from the slab into the column. In slabs where shear stresses are high, it may be impractical to place the required diagonal bars.

If column capitals were not initially used, their addition would reduce the required quantity of diagonal bars. In the case where column capitals are furnished, at least one-half of the diagonal bars should extend into the column with the remainder cut-off in the column capital. Procedures for the design of diagonal bars have been previously presented while the required construction details are illustrated in subsequent sections.

4-31.3. Columns

The interior columns of a flat slab/shear wall structure are not subjected to lateral loads nor the moments they induce. These columns are designed to resist the axial loads and unbalanced shears generated by the ultimate resistance of the flat slab. The axial load and moments at the top of the column are obtained from the flat slab shear forces acting on the perimeter of the column capital plus the load on the tributary area of the column capital. As can be seen from Figure 4-28, the axial load is:

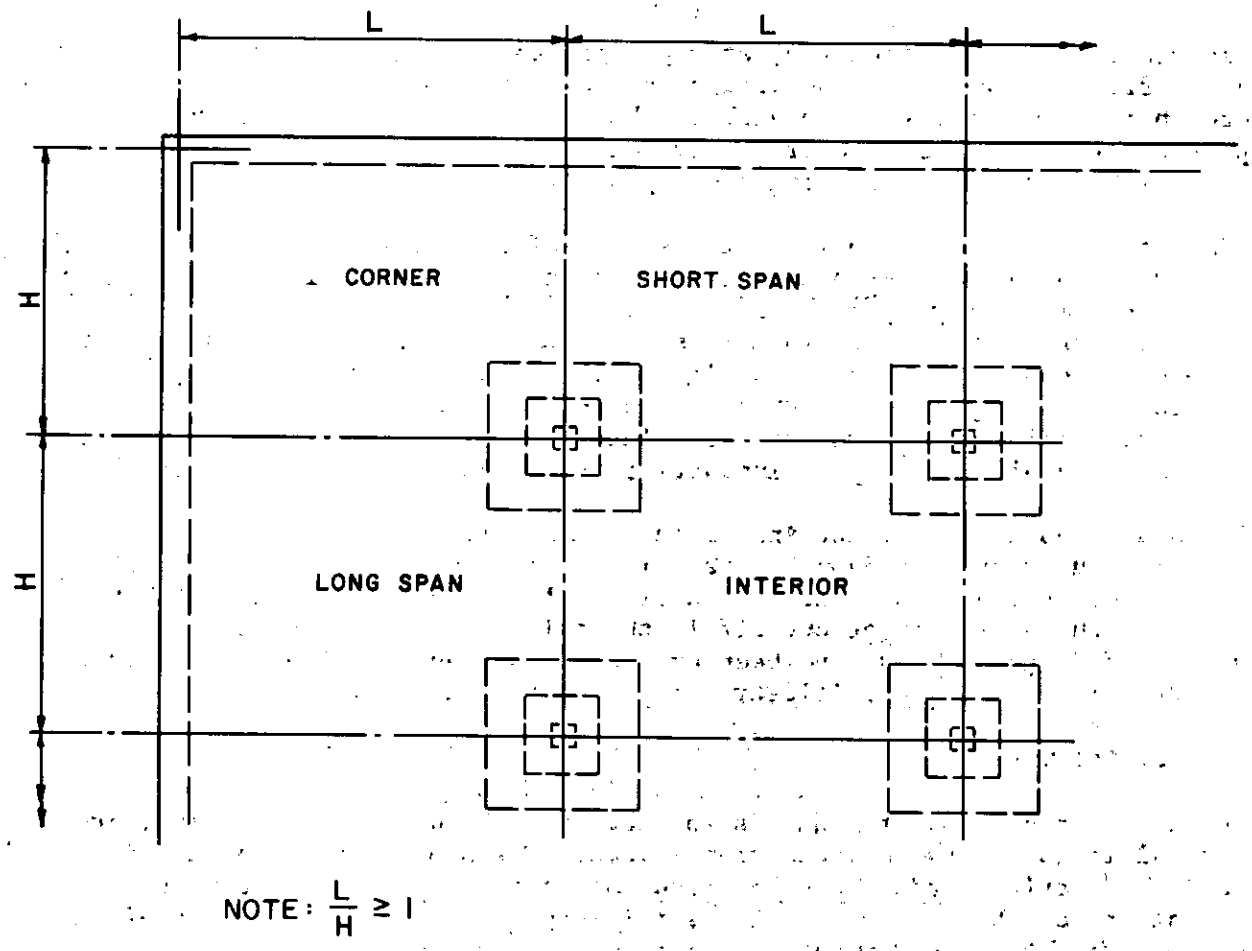
$$P = r_u \Sigma A + r_u c^2 \qquad 4\text{-}92$$

and the unbalanced moments are:

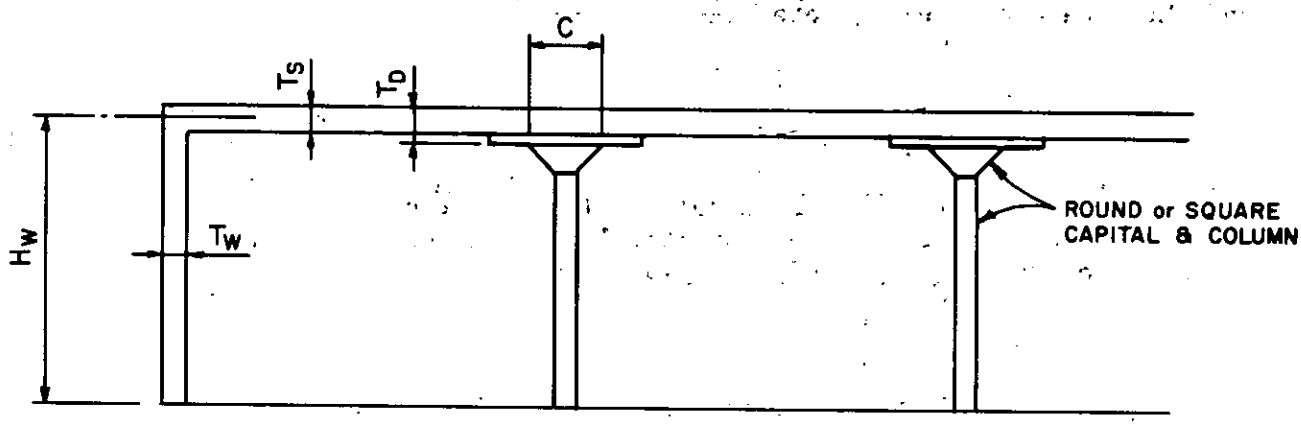
$$M_x = (V_4 - V_2)(c/2) \qquad 4\text{-}93$$

$$M_y = (V_1 - V_3)(c/2) \qquad 4\text{-}94$$

The procedures for the design of columns is presented in Section 4-49. When using these procedures, the unsupported length of the column is from the top of the floor to the bottom of the column capital.



PLAN



SECTION

Figure 4-20 Typical flat slab structure

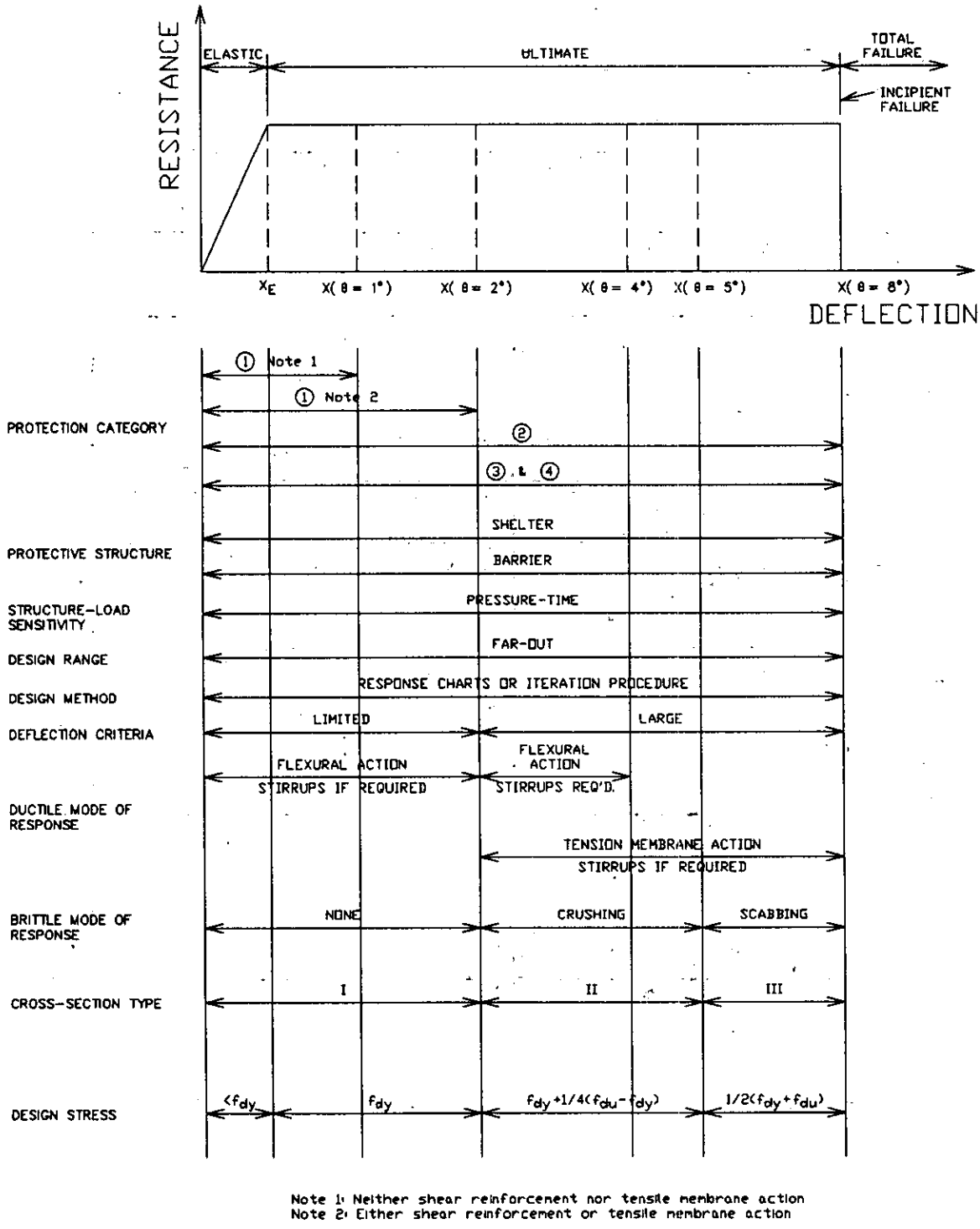
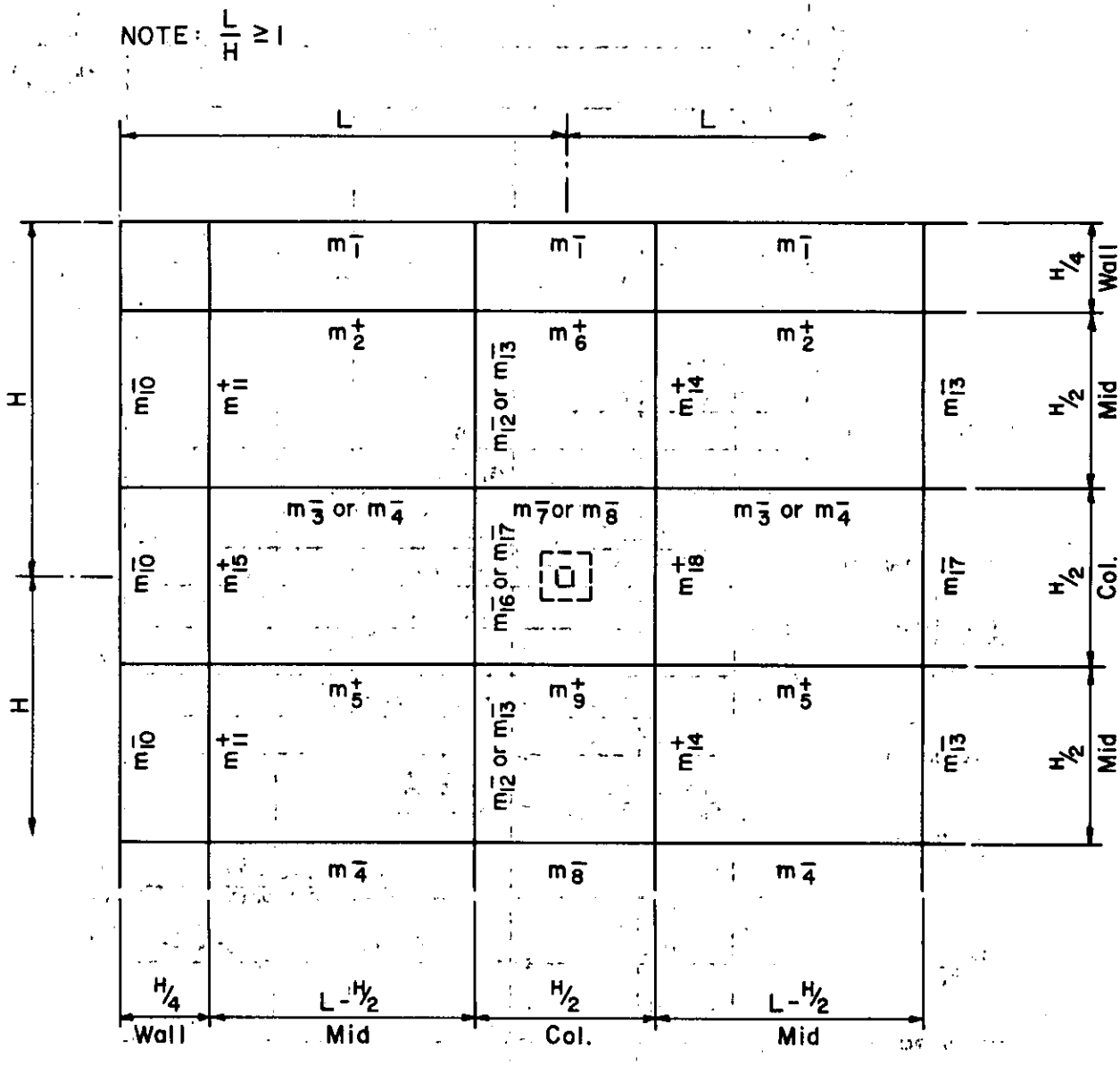
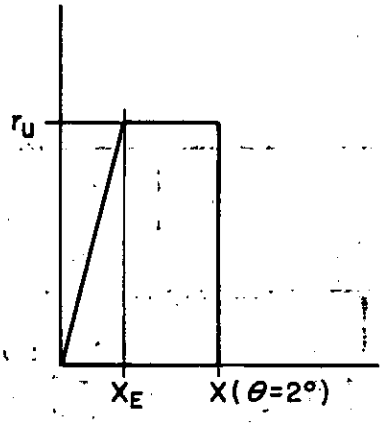


Figure 4-21 Relationship between design parameters for flat slabs

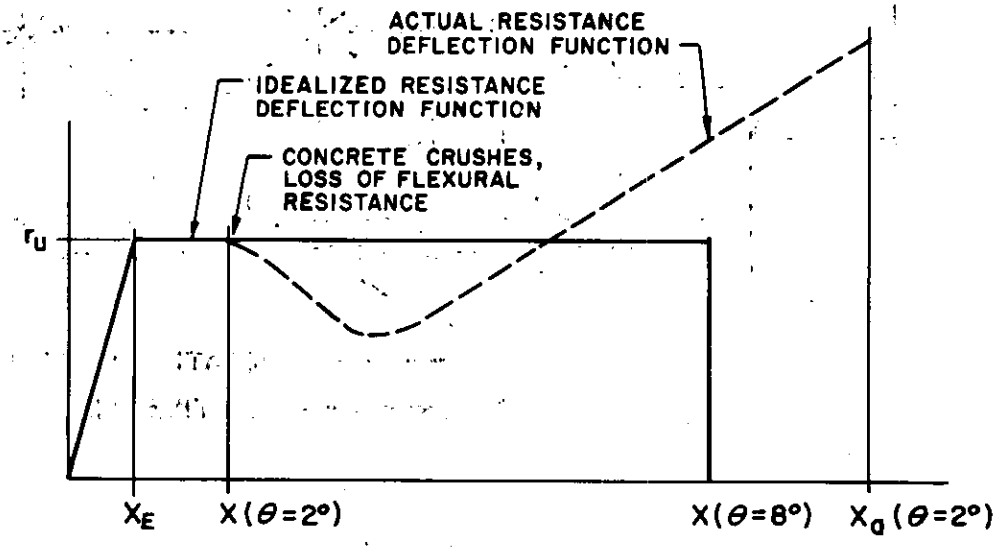


PLAN

Figure 4-22 Unit moments



a) Small Deflection



b) Large Deflection

Figure 4-23 Typical resistance-deflection functions for flat slabs

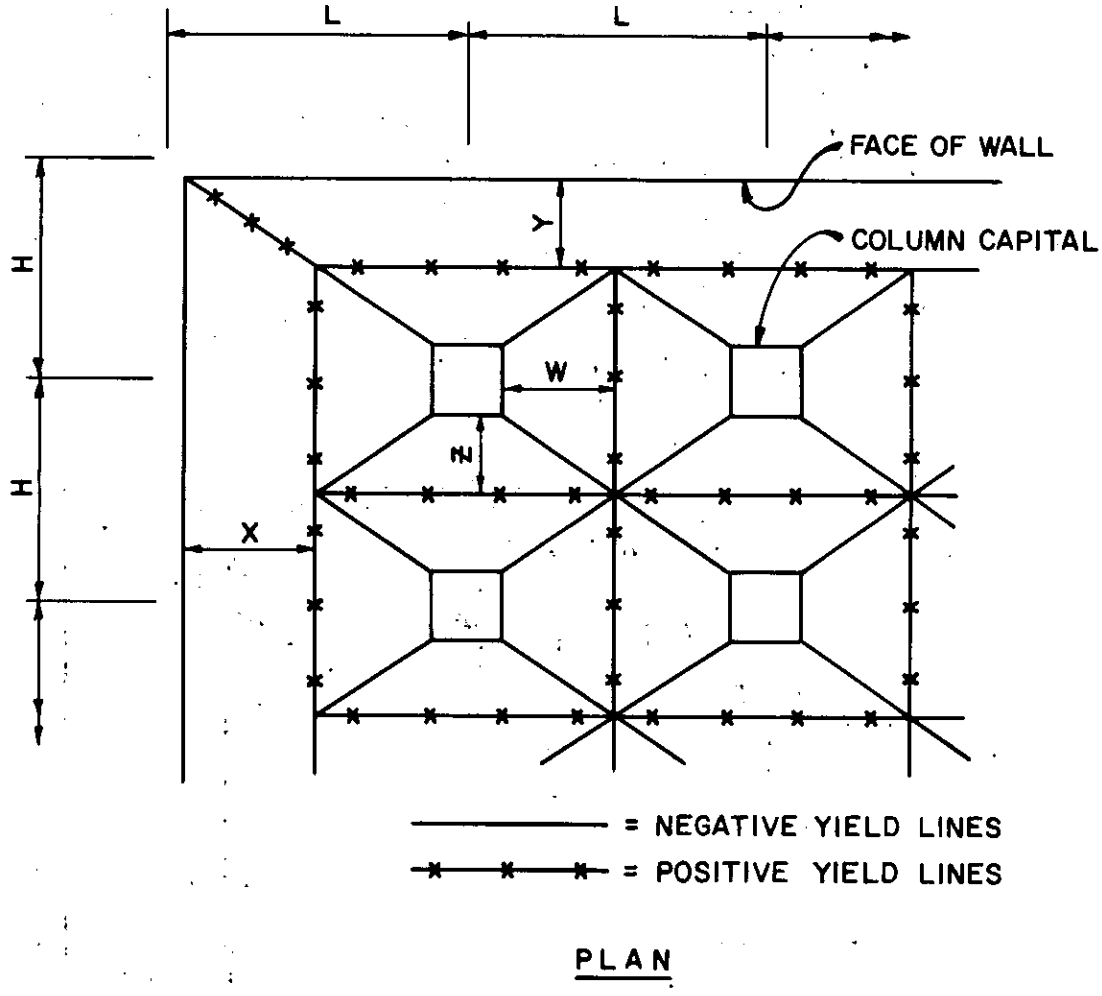
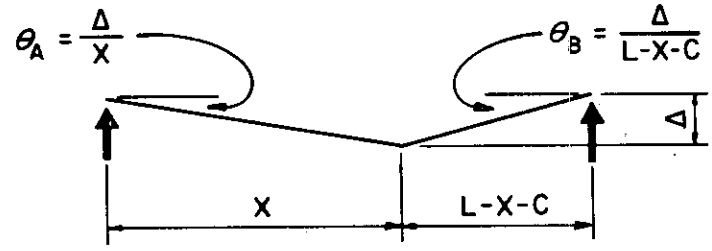
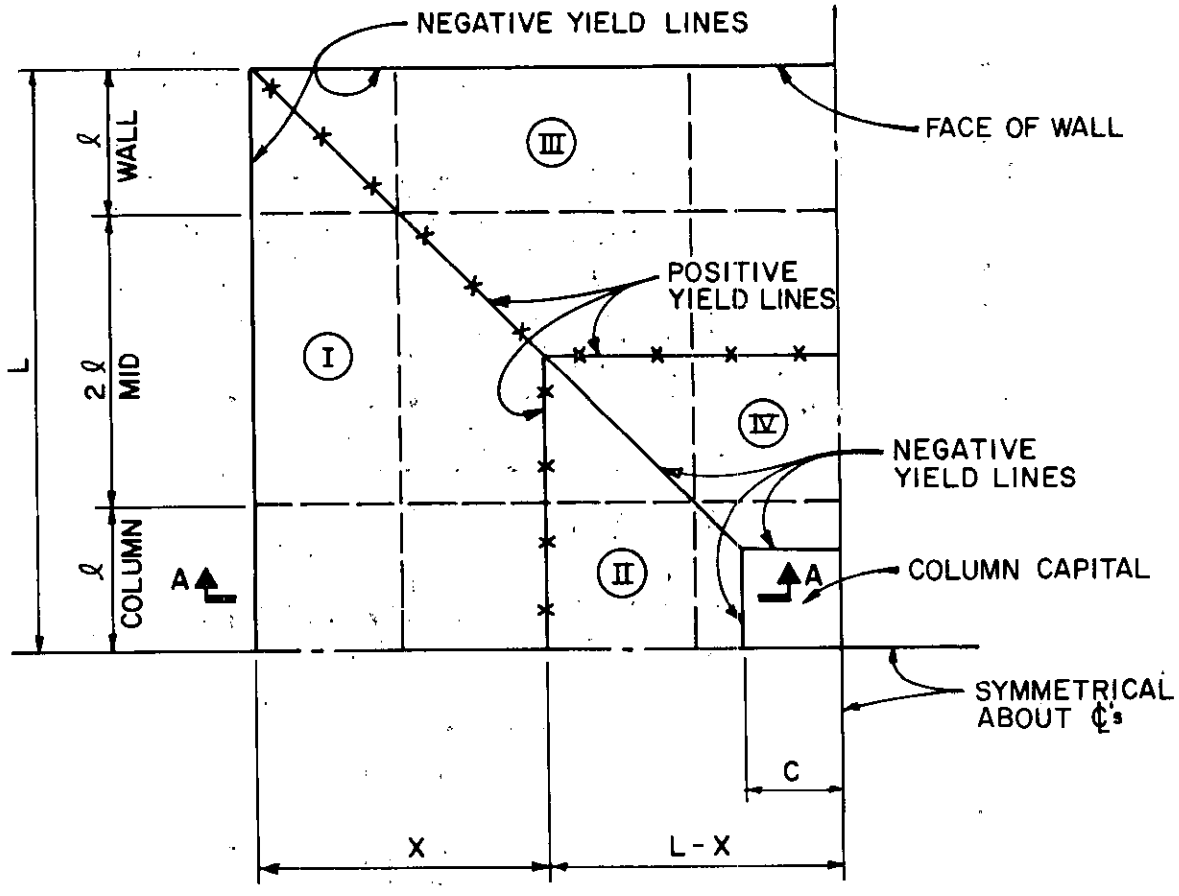


Figure 4-24 Yield line pattern for multi-panel flat slab



SECTION A-A



PLAN

UNIT MOMENT CAPACITIES:

	EXT. NEG.	POS.	INT. NEG.
WALL STRIP	m*	2m*	1.5m
MID STRIP	m*	2m*	1.5m
COLUMN STRIP	m	3m	4.5m

* 2/3 OF MOMENT CAPACITY EFFECTIVE AT CORNERS

Figure 4-25 Quarter panel of flat slab

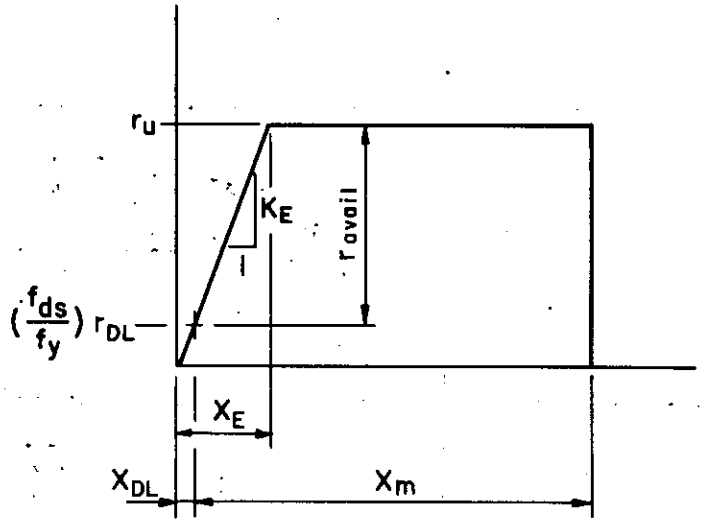
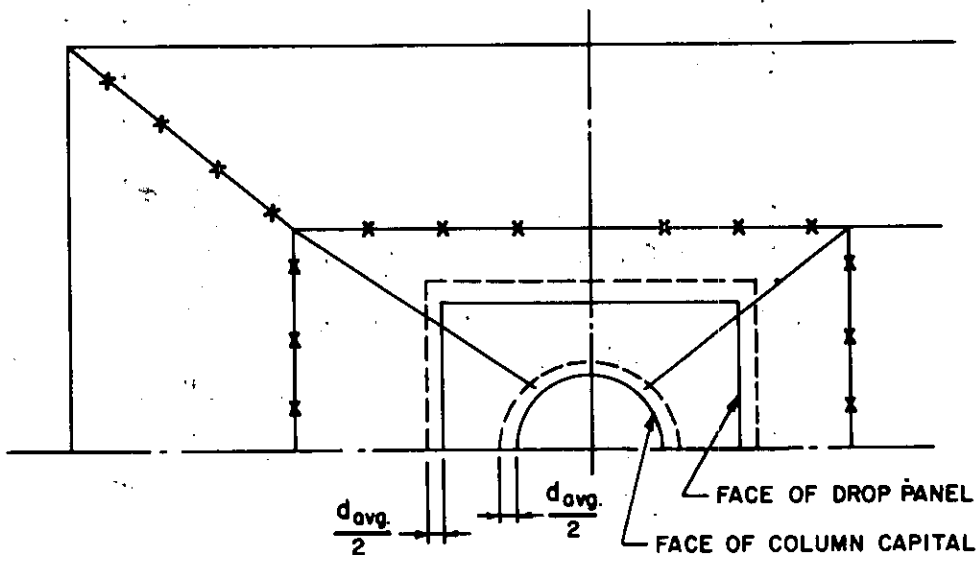
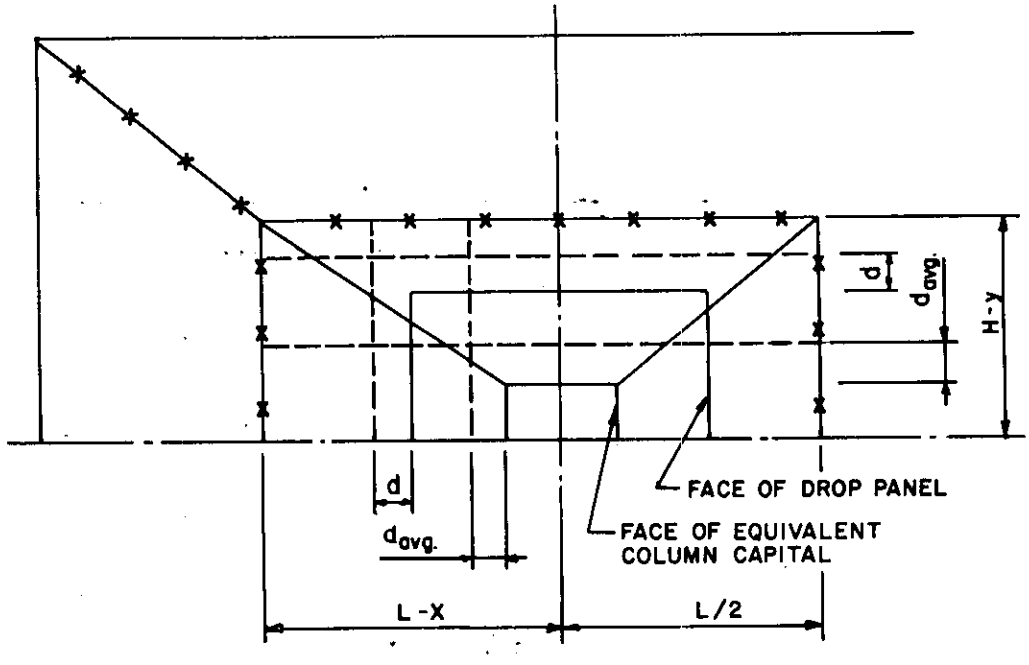


Figure 4-26 Dynamic resistance-deflection curve

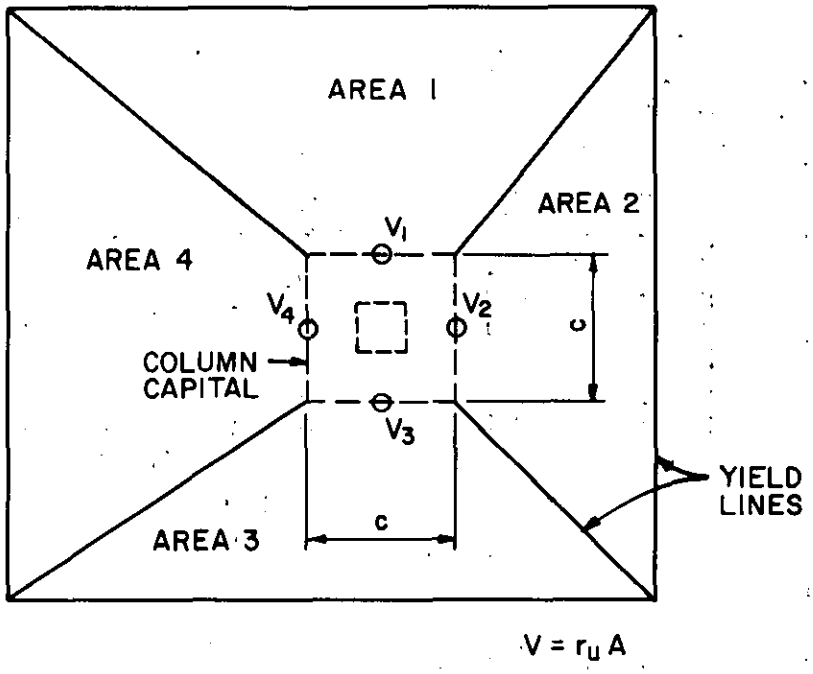


a. PUNCHING SHEAR

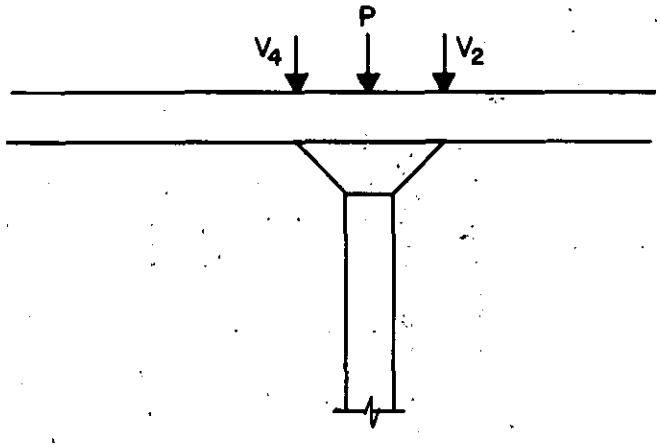


b. BEAM SHEAR

Figure 4-27 Critical locations for shear stresses



ROOF PLAN



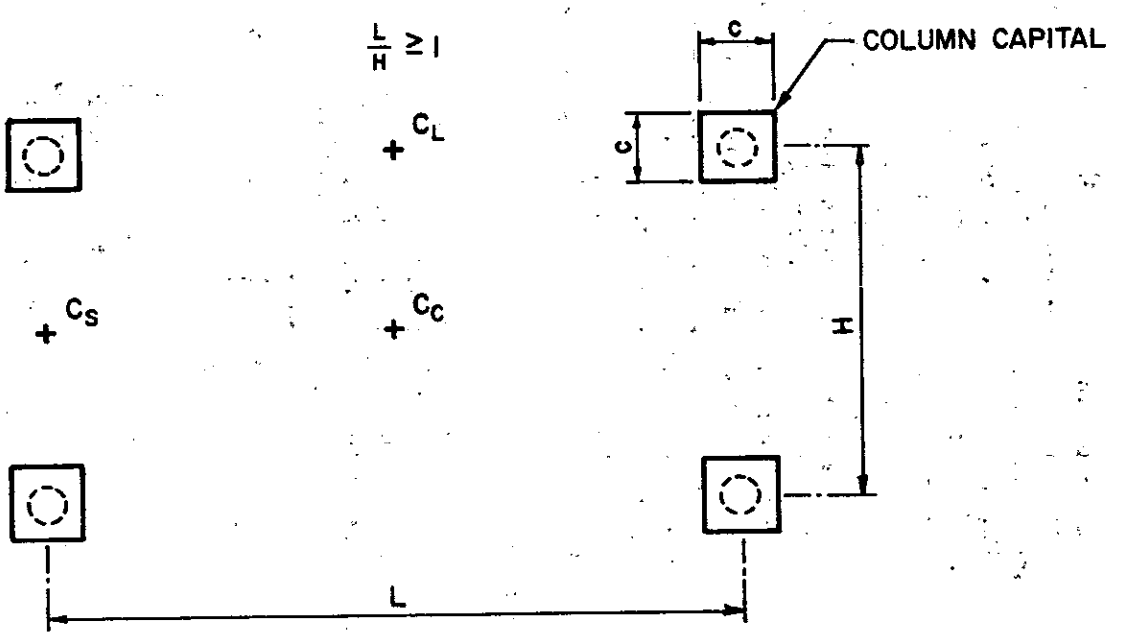
COLUMN. ELEVATION

Figure 4-28 Typical column loads

Table 4-8 Deflection Coefficients for Interior Panels of Flat Slabs

	Center of Panel C_C				Midspan of Long Side C_L				Midspan of Short Side C_S			
c/L L/H	0	0.1	0.2	0.3*	0	0.1	0.2	0.3*	0	0.1	0.2	0.3*
1.00	0.00581	0.00441	0.00289	0.00200	0.00435	0.00304	0.00173	0.00100	0.00435	0.00304	0.00173	0.00100
1.25	0.00420	0.0301	0.00189	0.00120	0.0378	0.00262	0.00155	0.00085	0.00230	0.00131	0.00057	0.00020
1.67	0.00327	0.00234	0.00143	0.00080	0.00321	0.00228	0.00137	0.00075	0.00099	0.00040	0.00008	0.00005
2.00	0.00301	0.00216	0.00129	0.00071	0.00299	0.00214	0.00127	0.00069	0.00058	0.00018	0.00004	

* Values for c/L = 0.3 are extrapolated



DESIGN OF LACED ELEMENTS

4-32. Introduction

The detonation of an explosive charge close to a barrier produces a non-uniform, high intensity blast load which acts on the barrier for a comparatively short period of time. The concept of lacing reinforcement (Fig. 4-4 and 4-5) has been developed for use in protective structures subjected to such loads. Lacing maintains the structural integrity of a barrier and permits it to attain large plastic deflections.

Extremely high pressure concentrations are caused by close-in detonations. These concentrations can produce local (punching) failure of an element. However, with the use of lacing, the high shears produced in the vicinity of these pressure concentrations are transferred to other areas of the element where the applied blast loads are less severe. In effect, the lacing tends to spread out the effects of the non-uniformity of the loading and permits the use of an average blast load over the entire surface area of the element. In addition, lacing is required in those elements where large deflections are desirable. In these cases, the lacing not only resists the high shears produced but also maintains the integrity of the severely cracked concrete between the tension and compression reinforcement during the latter stages of deflection.

The primary use of laced elements is to resist the effects of explosive charges located close to barriers. The minimum separation distance between the charge and the laced element is given in Section 2-14.2.1 of Chapter 2. It should be emphasized that these separation distances are the minimum clear distance from the surface of the charge to the surface of the laced element. The normal scaled distances R_A (center of charge to surface of barrier) corresponding to these minimum clear separation distances are equal to approximately 0.25 $ft/lb^{1/3}$.

A laced element may be designed for limited deflections (less than 5 degrees support rotation), large deflections (up to 12 degrees support rotation) or controlled post-failure fragments depending upon the protection requirements of the receiver system. The stresses developed in the reinforcement is a function of the deflection attained by the element. The type of cross-section which determines the ultimate moment capacity of the reinforced section is also a function of the deflection but, more importantly, is a function of the elements brittle mode response. High intensity blast pressures cause direct spalling during the initial phase of an element's response. Therefore, a type III cross-section will usually be available to provide moment capacity as well as the available mass to resist motion.

Single leg stirrups may be somewhat more economical than lacing as shear reinforcement. However, in many design situations, the use of lacing reinforcement is mandatory. When explosives are located at scaled distances less than 1.0, lacing must be used; single leg stirrups are not effective for such close charge locations. Also, the blast capacity of laced elements are greater than corresponding (same concrete thickness and quantity of reinforcement) elements with single leg stirrups. Laced elements may attain deflections corresponding to 12 degrees support rotation whereas elements with single leg stirrups are designed for a maximum rotation of 8 degrees. These non-laced elements must develop tension membrane action in order to develop

this large support rotation. If support conditions do not permit tension membrane action, lacing reinforcement must be used to achieve large deflections.

The design of concrete elements subjected to blast loads involves an iterative (trial and error) design procedure in which the element is assumed and then its adequacy is verified through a dynamic analysis (Chapter 3). The design of laced elements for limited deflections is performed in much the same manner. However, the design of laced elements for large deflections has unique features which permit the formulation of design equations. Since a laced element is subjected to very short duration blast loads, the actual pressure-time relationship of the load need not be considered. In fact, the actual duration of the load need not be considered at all. The load may be taken as an impulse (area under the pressure-time curve), that is, the entire load is applied instantaneously to the element. This assumption results in an insignificant error since the time for the element to reach the maximum deflection is large in comparison to the actual duration of the load. Secondly, the elastic portion of the element's resistance-deflection curve need not be considered. This assumption will also result in a negligible error since the plastic portion of the curve is many times that of the elastic portion. Lastly, laced elements must be symmetrically reinforced which greatly simplifies the expressions for an element's capacity. These features permit the formulation of design equations and design charts which are used to design laced elements for large deflections and for the preliminary design of laced elements for limited deflections.

This section includes the design of laced elements for ductile mode response. The brittle mode of response including the occurrence of spalling and the design for controlled post-failure fragments are presented in subsequent sections. The interrelationship of the parameters involved in the design of laced elements is illustrated in the idealized resistance-deflection curve shown in Figure 4-29.

4-33. Flexural Design for Large Deflections

4-33.1. General

The basic equations for the analysis of the impulse capacity of an element were derived in Chapter 3. For a two-way element which exhibits a post-ultimate resistance range and is designed for large deflections, the response is:

$$\frac{i_b^2}{2m_u} = r_u X_1 + \frac{m_u}{m_{up}} r_{up} (X_m - X_1) \qquad 4\text{-}95$$

The response equation for a one-way element, or a two-way element which does not exhibit a post-ultimate resistance range is:

$$\frac{i_b^2}{2m_u} = r_u X_m \qquad 4\text{-}96$$

i_b = applied blast impulse load

m_u, m_{up} - effective unit mass in the ultimate and post-ultimate ranges, respectively

r_u, r_{up} - unit resistances in the ultimate and post-ultimate ranges, respectively

X_1 - deflection at partial failure

X_m - maximum deflection

The above equations give the impulse capacity of a given structural element. Use of such equations for design purposes is not practical since the procedure would involve a tedious trial and error design.

4-33.2. Impulse Coefficients

Equations suitable for design are obtained by substituting the general expressions from Chapter 3 for the effective masses (m_u and m_{up}), the ultimate resistances (r_u and r_{up}) and maximum deflections (X_1, and X_u) into Equations 4-95 and 4-96 The resulting equations take the form:

$$\frac{i_b^2 H}{p_H d_c^3 f_{ds}} = C \qquad 4\text{-}97$$

H - height of the element

p_H - horizontal reinforcement ratio

d_c - distance from the centroid of the compression reinforcement to the centroid of the tension reinforcement

f_{ds} - dynamic design strength of the steel

C - impulse coefficient

To illustrate the method used to obtain the impulse coefficients, consider a two-way element (roof slab or wall) fixed on two adjacent edges and free on the other two. The yield line location is defined by y and $L < y < H$. The solution desired is for incipient failure (deflection X_u) of a spalled section (cross section type III).

From Chapter 3 the equations for the resistances, deflections and effective masses for this two-way element are as follows:

1. Ultimate unit resistance

$$r_u = \frac{5\,(M_{VN} + M_{VP})}{y^2} \qquad \text{(Table 3-2)}$$

where

$$M_{VN} = M_{VP} = \frac{A_s\, f_{ds}\, d_c}{b} = p_V f_{ds}\, d_c^2 \qquad \text{(eqs. 4-18 and 4-19)}$$

and p_V is defined as the vertical reinforcement ratio on each face.

2. Post-ultimate unit resistance

$$r_{up} = \frac{(M_{VN} + M_{VP})}{H^2} \qquad \text{(Table 3-4)}$$

3. Partial failure deflection

$$X_1 = L \tan 12° \qquad \text{(Table 3-6)}$$

4. Ultimate deflection

$$X_u = y\tan 12° + (H - y) \tan \gamma \qquad \text{(Table 3-6)}$$

where

$$\gamma = 12° - \tan^{-1}\left[\frac{\tan 12°}{y/L}\right]$$

5. Effective unit mass in the ultimate range

$$m_u = (K_{LM})_u \, m$$

$(K_{LM})_u$ is from figure 3-44

$$m = \frac{d_c}{1728}\left[\frac{150}{386 \cdot (10^{-6})}\right] = 225 d_c$$

6. Effective unit mass in the post-ultimate range

$$m_{up} = (K_{LM})_{up} \, m = (2/3) \, m$$

the units used are:

y, L, H, d_c, b, X_1, X_u	inches
i_b	psi-ms
M_{VN}, M_{VP}	in.-lbs/in.
f_{ds}, r_u, r_{up}	psi
A_s	$in.^2$
m , m_u, m_{up}	$psi\text{-}ms^2/in.$

Substituting into Equation 4-95

$$i_b^2 = 2 \text{ X } 225 d_c \, (K_{LM})_u \left[\frac{10 p_V d_c^2 f_{ds}}{y^2}\right] L \tan 12° \; +$$

$$\frac{(K_{LM})_u}{0.66}\left[\frac{2p_V\, d_c^2 f_{ds}}{H^2}\right]\left[Y\tan 12° + (H - y)\tan\gamma - L\tan 12°\right] \quad 4\text{-}98a$$

Factoring

$$i_b^2 = 2(225d_c)p_V d_c^2 f_{ds}\tan 12°\left[\frac{10(K_{LM})_u L}{y^2} + \frac{3(K_{LM})_u^2}{H^2}\right.$$

$$\left.(y - L + \frac{(H - y)\tan\gamma}{\tan 12°})\right] \quad 4\text{-}98b$$

Dividing each side by p_H the horizontal reinforcement ratio, and rearranging

$$\frac{i_b^2 H}{p_H d_c^3 f_{ds}} = 450\left(\frac{p_V}{p_H}\right)\tan 12°\left[\frac{10(K_{LM})_u\,(L/H)}{(y/H)^2} + \right.$$

$$\left.3(K_{LM})_u^2\left[\frac{Y}{H} - \frac{L}{H} + \left(1 - \frac{Y}{H}\right)\frac{\tan\gamma}{\tan 12°}\right]\right] \quad 4\text{-}98c$$

$$\frac{i_b^2 H}{p_H\, d_c^3 f_{ds}} = 287\left(\frac{p_V}{p_H}\right)\frac{3.33(K_{LM})_u(L/H)}{(y/H)^2} +$$

$$4.70\,(K_{LM})_u\left[\frac{Y}{H} - \frac{L}{H} + 4.70\left(1 - \frac{Y}{H}\right)\tan\gamma\right] \quad 4\text{-}99$$

where

$$\gamma = 12° - \tan^{-1}\left(\frac{0.2126}{y/L}\right) \quad 4\text{-}100$$

The solution for partial failure (deflection X_1,) for the above two-way element is obtained in a similar manner. Substituting the general expressions for partial failure into Equation 4-96 yields:

$$\frac{i_b^2 H}{p_H d_c^3 f_{ds}} = 957\left(\frac{p_V}{p_H}\right)(K_{LM})_u\frac{(L/H)}{(y/H)^2} \quad 4\text{-}101$$

Equations 4-99 and 4-101 can be rewritten as:

$$\frac{i_b^2 H}{p_H\, d_c^3 f_{ds}} = C_1 \quad 4\text{-}102$$

$$\frac{i_b^2 H}{p_H d_c^3 f_{ds}} = C_u \qquad 4\text{-}103$$

where the right-hand side of the equation is designated as the impulse coefficient. The impulse coefficient C_u is used for incipient failure design (maximum deflection equals X_u) whereas C_l is for partial failure design (maximum deflection equals X_l). These impulse coefficients are a proportional measure of the impulse capacity under the resistance-deflection curve up to the maximum deflection.

Expressions for the impulse coefficients of elements with various support conditions and yield line locations have been derived as above. Equations for C_l and C_u for two-way elements are given in Table 4-9 and Table 4-10, respectively. For one-way elements which do not exhibit the secondary resistance range ($X_l - X_u$), the coefficient C_l is equal to C_u. In addition, for a given support condition, C_u for a one-way element is a constant value. Table 4-11 gives the values of C_u for one-way elements.

4-33.3. Design Equations for Deflections X_l and X_u

For design purposes, Equations 4-102 and 4-103 can be rewritten as:

$$p_H d_c^3 = \frac{i_b^2 H}{C_l f_{ds}} \qquad 4\text{-}104$$

$$p_H d_c^3 = \frac{i_b^2 H}{C_u f_{ds}} \qquad 4\text{-}105$$

For a two-way element C_l and C_u are functions of support conditions, aspect ratio, yield line location, reinforcement ratios and the load-mass factors. It was shown in Chapter 3 the $(K_{LM})_u$ for a two-way element varies with the yield line location ratio y/H or x/L. Furthermore, it was shown that yield line location ratio is a function of the span ratio L/H and the moment ratio $[(M_{VN} + M_{VP})/(M_{HN} + M_{HP})]$. Since the cross sections used for large deflection design are equally reinforced on each face, the moment ratio is, in effect, the ratio of the reinforcement ratio p_V/p_H. Thus it can be seen that the impulse coefficients are solely functions of L/H and p_V/p_H for a given support condition.

To facilitate the design procedure, charts have been constructed for the impulse coefficients C_l and C_u for two-way elements as a function of p_V/p_H and L/H. These curves for various support conditions are given in Figures 4-30 through 4-32 for C_l and Figures 4-33 through 4-35 for C_u. For one-way elements C_u is a constant (see Table 4-11).

4-33.4. Optimum Reinforcement

A prime factor in the design of any facility is construction economy. Proper selection of section sizes and reinforcing steel will result in a design having optimum capacity and minimum cost. See discussion in paragraph 4-23.1.

To determine the optimum design of any particular two-way structural element, consideration must be given to the following:

1. There is an ideal distribution of flexural reinforcement, defined by the reinforcement ratio p_V/p_H, which is independent of section depth. This ratio will yield the maximum blast impulse capacity for a given total amount of flexural reinforcement p_T.

2. There is an ideal relationship between the quantity of reinforcement to the quantity of concrete which will result in the minimum cost of an element. This relationship is defined by the total percentage of reinforcement in one face of an element. This total percentage p_T is the sum of the vertical and horizontal reinforcement ratios, p_V and p_H, respectively.

4-33.4.1. Optimum Reinforcement Distribution

The blast impulse capacity of an element varies with the distribution of the reinforcement even though the total amount of reinforcement and the concrete thickness remains the same. This optimum reinforcement ratio varies for different support conditions as a function of the aspect ratio L/H. In addition, the optimum ratio is different for partial failure and incipient failure design.

To illustrate the determination of the optimum reinforcement distribution ratio p_V/p_H, consider a two-way panel fixed on three sides. The panel has an aspect ratio L/H equal to 3 and a total percentage of reinforcement p_T equal to 1 percent. For various values of p_V/p_H, the impulse capacity can be determined for both partial and incipient failure design from Figures 4-31 and 434, respectively.

If $(i_b{}^2H)/(d_c{}^3f_{ds}$ is plotted versus p_Vp_H the resulting curves are shown in Figure 4-36. The ideal p_V/p_H occurs at the maximum value of $i_b{}^2H/d_c{}^3f_{ds}$ and is indicated on the illustration as 1.58 for incipient failure and 1.93 for partial failure design. Increasing or decreasing the total amount of steel p_T, will shift the curves up or down but not effect the optimum p_V/p_H ratio. This optimum p_V/p_H ratio for other L/H ratios and support conditions are determined from similarly constructed curves.

The optimum values of p_V/p_H for various support conditions are plotted as a function of the aspect ratio. Figure 4-37 gives the optimum reinforcement for partial failure design, while Figure 4-38 gives the optimum ratio for incipient failure design.

The optimum reinforcement ratio for partial failure design always results in positive yield lines which bisect the 90 degree angle at the corners of the element (45 degree yield lines) for all support conditions. Consequently, all supports reach the maximum rotation of 12 degrees simultaneously and they are all on the verge of failure. Therefore, the optimum condition for partial failure is a particular case of incipient failure. This condition is evident from the common point on Figure 4-36. It can also be seen from this figure that at p_V/p_H ratios other than the common point, partial failure design is more conservative than incipient failure design which includes the post ultimate range. The optimum p_V/p_H ratio for partial failure design maximizes the impulse capacity up to X_1 leaving no reserve capacity (post ultimate

range). Therefore, at this ratio, the capacity is numerically equal to that for incipient failure design. While there is no quantitative advantage to optimum partial failure design over incipient failure design, there is a qualitative advantage. The elements remain intact since all supports are on the verge of failure as opposed to optimum incipient failure where some supports have failed and the remaining supports are on the verge of failure. In this latter case, there is unknown secondary cracking which is not accounted for in the design.

As previously explained, incipient failure design includes the capacity from two-way action of an element up to partial failure X_1, and the capacity of one-way action up to incipient failure X_u. Except as explained below, the optimum reinforcement ratio for incipient failure design results from maximizing the capacity due to one-way action after partial failure (post-ultimate range). The resulting optimum reinforcement ratios for incipient failure design produce various yield line configurations depending upon the support conditions. For four edges fixed, the optimum reinforcement ratio is 0.25 and 4.0 for aspect ratios less than and greater than one, respectively. This distribution maximizes the post ultimate one-way action in the shorter direction. For two edges fixed, the increase in capacity due to cantilever action in the post ultimate range is less than the decrease in capacity of the ultimate range. Thus, for these elements, the capacity cannot be increased above that for partial failure, and the optimum ratio for incipient failure design is the same as for partial failure design (45 degree yield lines). For three edges fixed, the post ultimate range capacity is due to either cantilever action in the vertical direction or fixed-fixed beam action in the horizontal direction. In regions where the post ultimate range consists of cantilever action (L/H ratio in the immediate vicinity of 2 and L/H ratio greater than 4) the optimum ratio is the same as for partial failure. For L/H ratios less than 1.5, the post ultimate range consists of fixed-fixed beam action and, therefore, the optimum ratio is equal to 0.25. Between these L/H regions, neither behavior dominates and the resulting optimum p_V/p_H ratios maximizes the combination of ultimate and post ultimate range capacities.

4-33.4.2. Optimum Total Percentage of Reinforcement

The optimum total percentage of reinforcement p_T gives the relationship between the quantity of reinforcement to the quantity of concrete which results in the minimum cost of an element. The total percentage of reinforcement in one face of the element is defined as:

$$p_T = p_V + p_H \qquad 4\text{-}106$$

The optimum percentage of reinforcement depends upon the relative costs of the concrete and reinforcing steel. Based on the average costs of concrete and steel, the optimum percentage of reinforcement p_T has been determined to be between 0.6 and 0.8 percent, with 0.7 being a reasonable value to be used for design. However, for large projects, a detailed cost analysis may result in a more economical design.

In the usual design situation, the optimum p_V/p_H ratio is first determined based on the support conditions and aspect ratio. Knowing this ratio, C_1 or C_u is determined and along with the given values of i_b H, f_{ds}, Equation 4-104 or 4-105 results in:

$$p_H d_c^3 = \text{constant} \qquad 4\text{-}107$$

With the known values of p_V/p_H and the optimum total percentage of reinforcement equal to 0.7, the required quantity of horizontal reinforcement p_H is calculated. The required thickness of the element is then calculated from Equation 4-107.

In some design cases, it may be desirable to reduce the concrete thickness below the optimum thickness. The quantity of reinforcement in excess of the optimum p_T must be provided to obtain the necessary impulse capacity. The cost increase is small for total percentages of steel in the vicinity of the optimum value of p_T. In fact, the use of p_T equal to 1 percent will result in a cost increase of less than 10 percent. Beyond 1 percent reinforcement, the cost increase is more rapid. However, except for very thin elements, the use of reinforcement in excess of 1 percent is impractical since the required details cannot be maintained with such large quantities of reinforcing steel. For thick walls providing even the optimum p_T of 0.7 percent may be impractical and p_T may have to be reduced to as low as 0.3 percent (minimum reinforcement of 0.15 percent in each direction) in order to permit placement of the reinforcing steel. The total reinforcement p_T may also be less than optimum if a minimum concrete thickness is required to prevent fragment penetration. When the minimum quantity of reinforcement is provided whether for strength or to satisfy minimum requirements, the resulting cost may be far in excess of optimum.

In some cases of incipient failure design, the optimum reinforcement ratio p_V/p_H is equal to 0.25 or 4.0. However, in most cases, it is impractical to provide four times as much reinforcement in one direction as in the other direction. Since the minimum required percentage of reinforcement in a given direction is 0.15, the orthogonal direction would require 0.6 percent for a total percentage of 0.75. Although this percentage is approximately equal to the optimum percentage of 0.7. it may still be impractical in all but thin walls. Consequently, in such design situations, a trade off between optimum reinforcement ratio p_V/p_H and the optimum total percentage reinforcement p_T must be made for an economical design.

4-33.5 Design Equation for Deflections Less than X_1 or X_u

For certain conditions, it is sometimes desired to design a structural element for maximum deflections other than partial failure deflection X_1 or incipient failure deflection X_u. For those cases, the impulse coefficients can be scaled relative to the deflections.

For a maximum deflection X_m in the deflection range $X_1 < X_m < X_u$, Equation 4-107 becomes

$$p_H d_c^3 = \frac{i_b^2 H}{C'_u f_{ds}} \qquad 4\text{-}108$$

where

$$C'_u = C_1 + \frac{X_m - X_1}{X_u - X_1}(C_u - C_1) \qquad 4\text{-}109$$

For a maximum deflection corresponding to a support rotation greater than 5 degrees, but less than X_1, Equation 4-108 becomes

$$p_H \, d_c^3 = \frac{i_b^2 H}{C'_1 f_{ds}} \qquad 4\text{-}110$$

where

$$C'_1 = \left(\frac{X_m}{X_1}\right) C_1 \qquad 4\text{-}111$$

The optimum p_V/p_H ratio for a given element is a constant for any deflection less than partial failure deflection X_1, and is determined from Figure 4-37. In the deflection range $X_1 < X_m < X_u$ the optimum p_V/p_H ratio varies with the maximum deflection. However, for design purposes, the values from Figure 4-38 for incipient failure may be used.

4-33.6. Design Equations for Unspalled Cross Sections

The impulse coefficients derived above may also be used for type II or unspalled cross sections. However, the general form of the equation is slightly modified to account for the change in the physical properties of the cross section. For a type II cross section, the full thickness of concrete element is included in calculating the effective mass. Thus, the design equations for the impulse coefficients of unspalled sections take the form:

$$p_H \, T_c \, d_c^2 = \frac{i_b^2 H}{C_1 \, f_{ds}} \qquad 4\text{-}112$$

$$p_H \, T_c \, d_c^2 = \frac{i_b^2 H}{C_u \, f_{ds}} \qquad 4\text{-}113$$

where T_c is the total thickness of the concrete section.

The optimum reinforcement ratios and the impulse coefficients are the same for spalled and unspalled cross sections . The design procedure for unspalled cross sections is very similar to the procedure described in Section 4-33.4.2. The total thickness of concrete T_c can be expressed in terms of d_c by approximating the value of d'. The value of d' can be estimated by determining the required concrete cover and assuming the reinforcing bar sizes.

4-34. Flexural Design for Limited Deflections

In the design of elements for large deflections, only the plastic range behavior of the element was considered, since the capacity due to elasto-plastic behavior is relatively small. For elements where support rotations are limited to 5 degrees or less, the elasto-plastic range is a significant portion of the element's total capacity as well as of its deflected shape. Therefore, it must be included in the determination of the response of such elements.

The blast impulse capacity of an element whose maximum deflection is less than or equal to 5 degrees was given in Chapter 3 as

$$\frac{i_b^2 H}{2m_a} = \frac{r_u X_E}{2} + \frac{m_a}{m_u} r_u (X_m - X_E) \qquad 4\text{-}114$$

where

m_a = average of the effective elastic and plastic unit masses

X_E = equivalent elastic deflection

This is an equation which is suitable for analysis rather than design. Impulse coefficients could theoretically be derived in a similar manner as that for large deflections. However, the equivalent elastic deflection cannot be defined by a mathematical expression making the determination of impulse coefficients for the various support conditions impractical.

The design of an element subjected to an impulse load (short duration pressure-time load) for limited deflections is accomplished using a trial and error procedure. An element would be assumed (concrete thickness and reinforcement) and its response determined from the response charts of Chapter 3. A preliminary estimate of the size of the element can be obtained using the equations for partial failure design where the impulse coefficient is modified for reduced rotations according to Equation 4-110. It should be noted that this preliminary design will underestimate the required element.

The above procedure would be used for laced elements designed for support rotations less than 5 degrees. However, if an element is designed for support rotations less than 2 degrees and single leg stirrups are used in place of lacing reinforcement, the above preliminary estimate of the size of the element may not be used. Since the position of the flexural reinforcement is not altered for single leg stirrups, an average d_c may not be used. Two values of d_c must be determined; one for the vertical reinforcement and second for the horizontal reinforcement. Therefore, the capacity of the element (flexural and shear capacity) must be determined according to the procedures for conventional reinforced slabs.

4-35 Design for Shear

4-35.1. General

After the flexural design of an element has been completed, the required quantity of shear reinforcement must be determined. This shear reinforcement insures that the desired flexural behavior in the ductile mode will be attained. The design of the lacing reinforcement has been discussed in previous sections. This section is concerned with the determination of the shear stresses and forces to be used in the design equations.

Shear coefficients can be derived in a manner similar to that used to derive the impulse coefficients above. The equations for support shear given in Chapter 3 and for the ultimate shear stress given in Section 4-27 show that the shear reinforcement is a function of the resistance of the element and not of the applied load. The shear forces and stresses vary as the ultimate unit resistance, the geometry and yield line locations of the element, and the section depth. If r_u is evaluated and substituted into these shear expres-

sions, it can be shown that the ultimate support shear V_s can be represented as an equation in the general form

$$V_s = C \frac{pd_c^2 f_{ds}}{L} \qquad 4\text{-}115$$

and the ultimate shear stress at distance d_c from the support as

$$v_u = Cpf_{ds} \qquad 4\text{-}116$$

where

C = shear coefficient

p = flexural reinforcement ratio

f_{ds} = dynamic design stress of the flexural reinforcement

The shear coefficient is different for each case and also different for one-way and two-way elements. Specific values are indicated in the following paragraphs of this section.

4-35.2. Ultimate Shear Stress

4-35.2.1. One-Way Elements

The ultimate shear stress v_u at distance d_c from the support for a one-way element is

$$v_u = C_d p f_{ds} \qquad 4\text{-}117$$

where C_d is the shear coefficient and a function of the ratio of d_c/L. Values of C_d are shown in Table 4-12.

4-35.2.2. Two-Way Elements

The ultimate shear stress V_{uH} in the horizontal direction (along side H) at a distance d_c from the support for a two-way element is given as

$$v_{uH} = C_H p_H f_{ds} \qquad 4\text{-}118$$

and in the vertical direction (along side L) as

$$v_{uV} = C_V p_V f_{ds} \qquad 4\text{-}119$$

where C_H and C_V are the horizontal and vertical shear coefficients, respectively. The shear coefficients, given in Table 4-13, vary as d_c/x or d_c/y for the triangular sectors and as x/L and d_c/H or y/H and d_c/L for the trapezoidal sectors. The solution for the shear coefficients is presented graphically in Figures 4-39 through 4-52.

The shear coefficients for the triangular sectors, can be read directly from either Figure 4-39 or 4-40, since the yield line location is the only variable involved. Plotting the shear coefficients for the trapezoidal sectors for a particular support condition yields a family of curves. That is, the shear

coefficient is plotted versus d_c/L for various values of y/H (or d_c/H for various values of x/L). The maximum value of the shear coefficient is different for each curve of y/H or x/L and occurs at various values of d_c/L or d_c/H. Therefore, these family of curves overlap and accurate interpolation between curves is difficult.

Using a method of coordinate transformation, the family of curves has been reduced to a set of curves with a common maximum point defined (using the horizontal shear coefficient as an example) by $C_H/C_M = 1$ and $(d_c/L)/(d_c/L)_M = 1$. The quantities C_M and $(d_c/L)_M$ represent the coordinates of the maximum point on the original family of curves for y/H and x/L. The left-hand portions of the curves become identical, and accurate interpolation in the right-hand portion is now possible. This transformation results in two figures to define the shear coefficient for a particular support condition and yield line pattern.

The above sets of curves are presented in Figures 4-41 through 4-52. When using these curves, the shear parameter curve for the applicable support condition is entered first with the value of x/L or y/H to determine C_M and $(d_c/H)_M$ or $(d_c/L)_M$. The second curve is then used to determine C_H or C_V.

It should be noted that when designing two-way panels for incipient failure, the shear stresses in the post-ultimate range must also be checked using the equations for one-way elements.

4-35.3. Ultimate Support Shears

4-35.3.1. One-Way element

The ultimate support shear V_s for a one-way element is

$$V_s = C_s \frac{p\, d_c^2 f_{ds}}{L} \qquad 4\text{-}120$$

where C_s is the shear coefficient and is a constant for a given support condition. Values of C_s for several one-way elements are given in Table 4-14.

4-35.3.2. Two-Way Elements

For a two-way element, the ultimate support shear V_{sH} in the horizontal direction (along side H) is represented as

$$V_{sH} = C_s \frac{p_H\, d_c^2 f_{ds}}{L} \qquad 4\text{-}121$$

and V_{sV}, in the vertical direction (along side L) is

$$V_{sV} = C_{sV} \frac{p_V\, d_c^2\, f_{ds}}{H}$$

where C_{sH} and C_{sv} are the horizontal and vertical shear coefficients, respectively. For a given support condition, these coefficients vary as the yield

line location ratios x/L or y/H. The shear coefficients are listed in Table 4-15 and for the trapezoidal sectors only are plotted in Figures 4-53 through 4-56 for various support conditions.

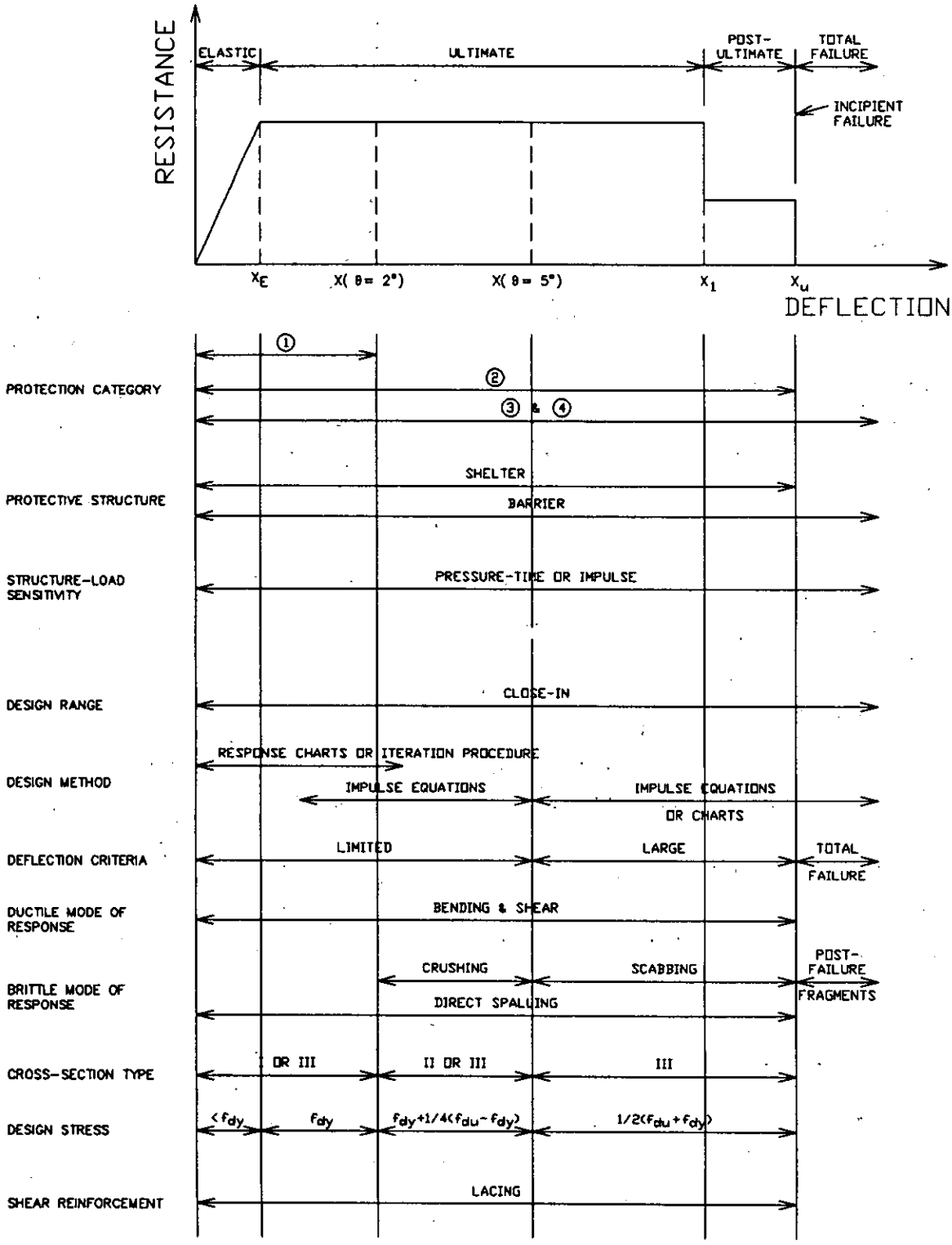


Figure 4-29 Relationship between design parameters for laced elements

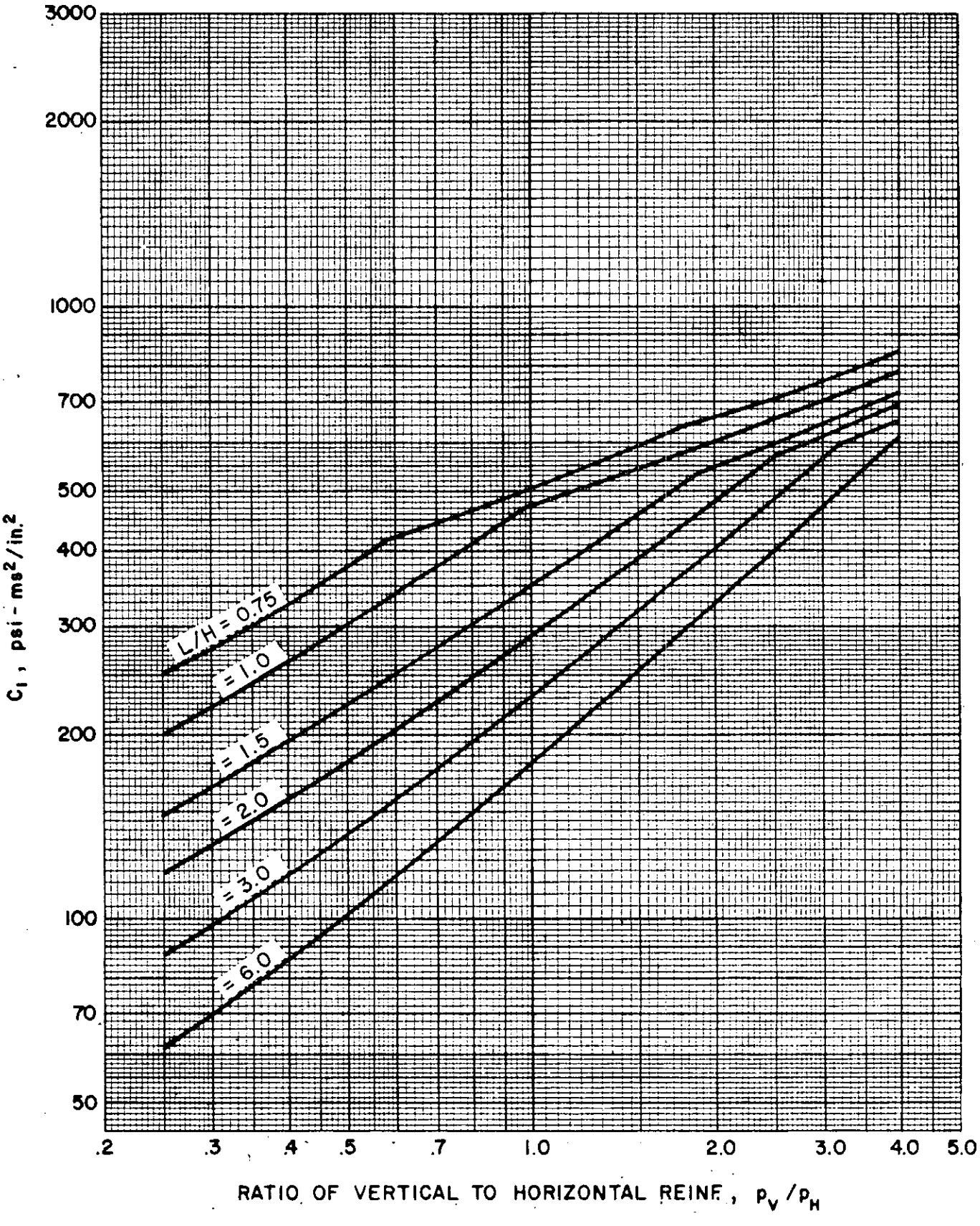


Figure 4-30 Impulse coefficient C_1 for an element with two adjacent edges fixed and two edges free

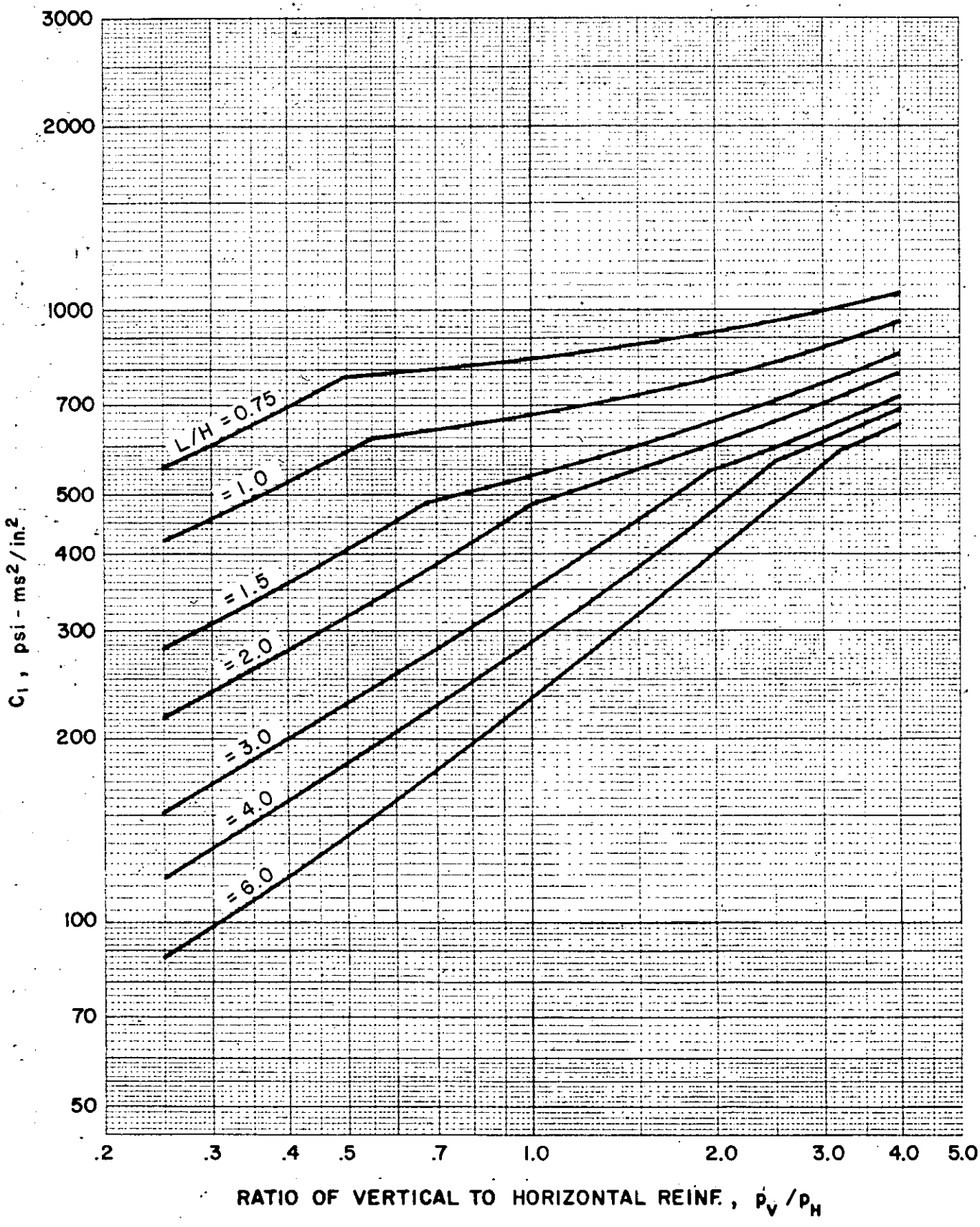


Figure 4-31 Impulse coefficient C_1 for an element with three edges fixed and one edge free

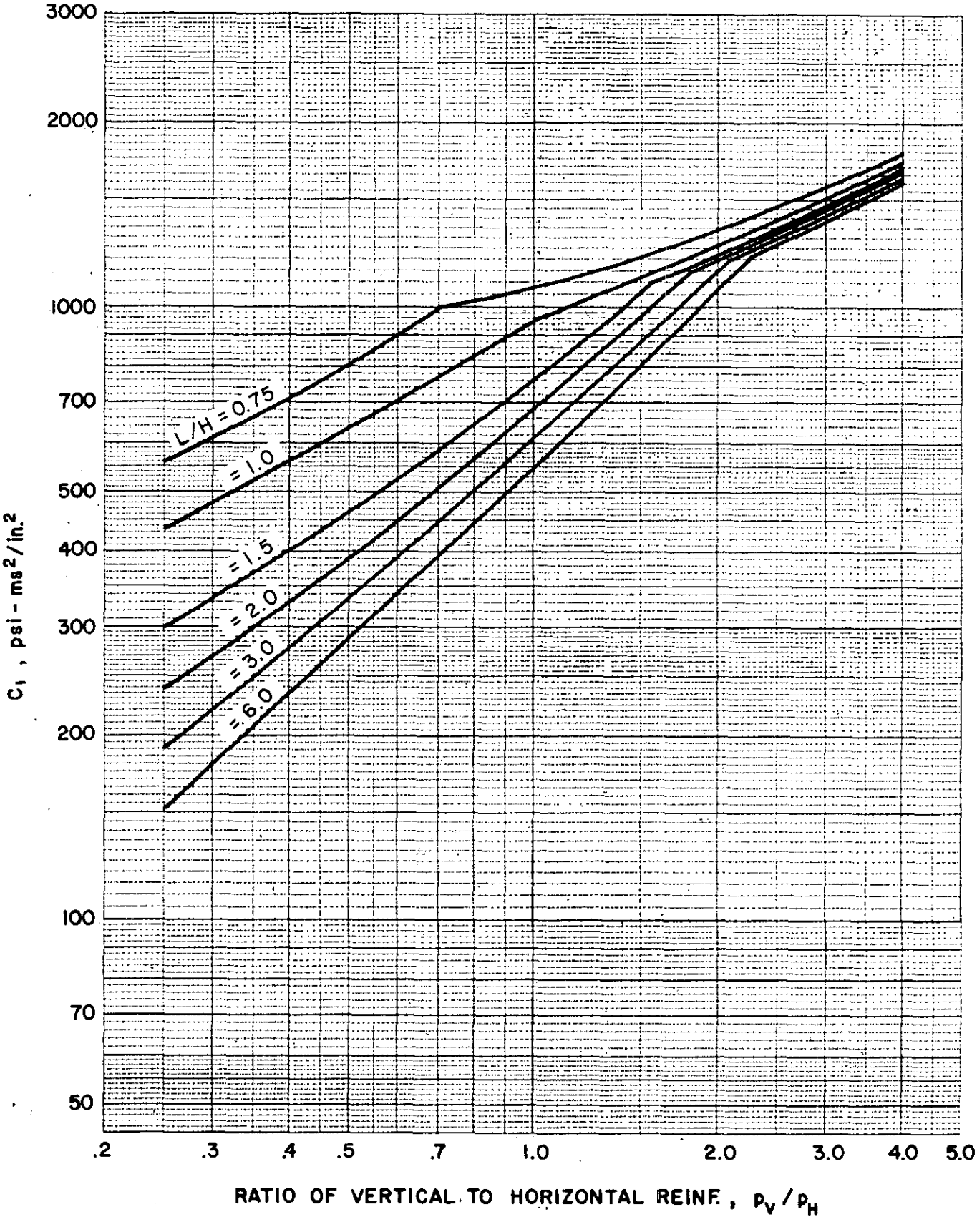


Figure 4-32 Impulse coefficient C_1 for an element with four edges fixed

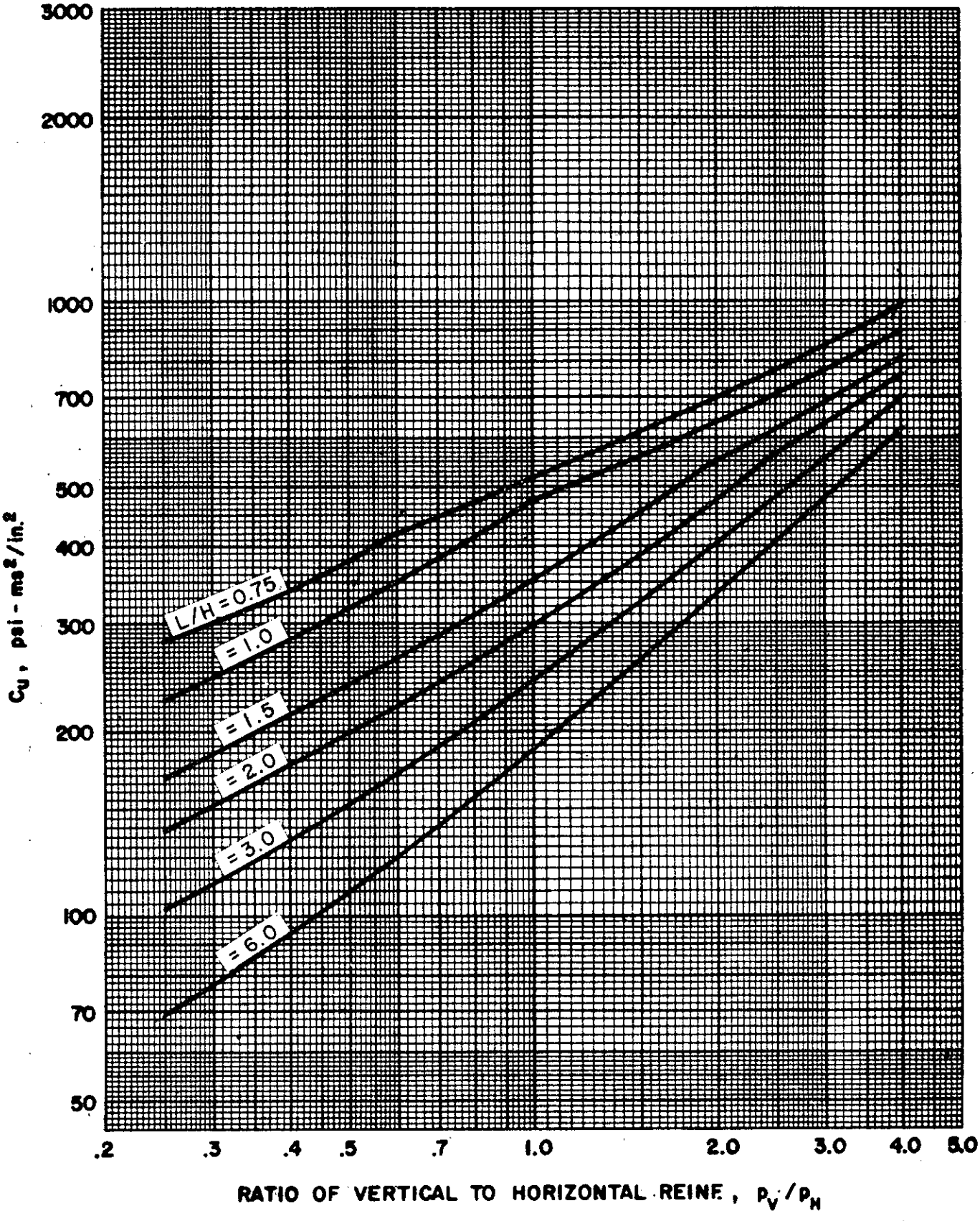


Figure 4-33 Impulse coefficient C_u for an element with two adjacent edges fixed and two edges free

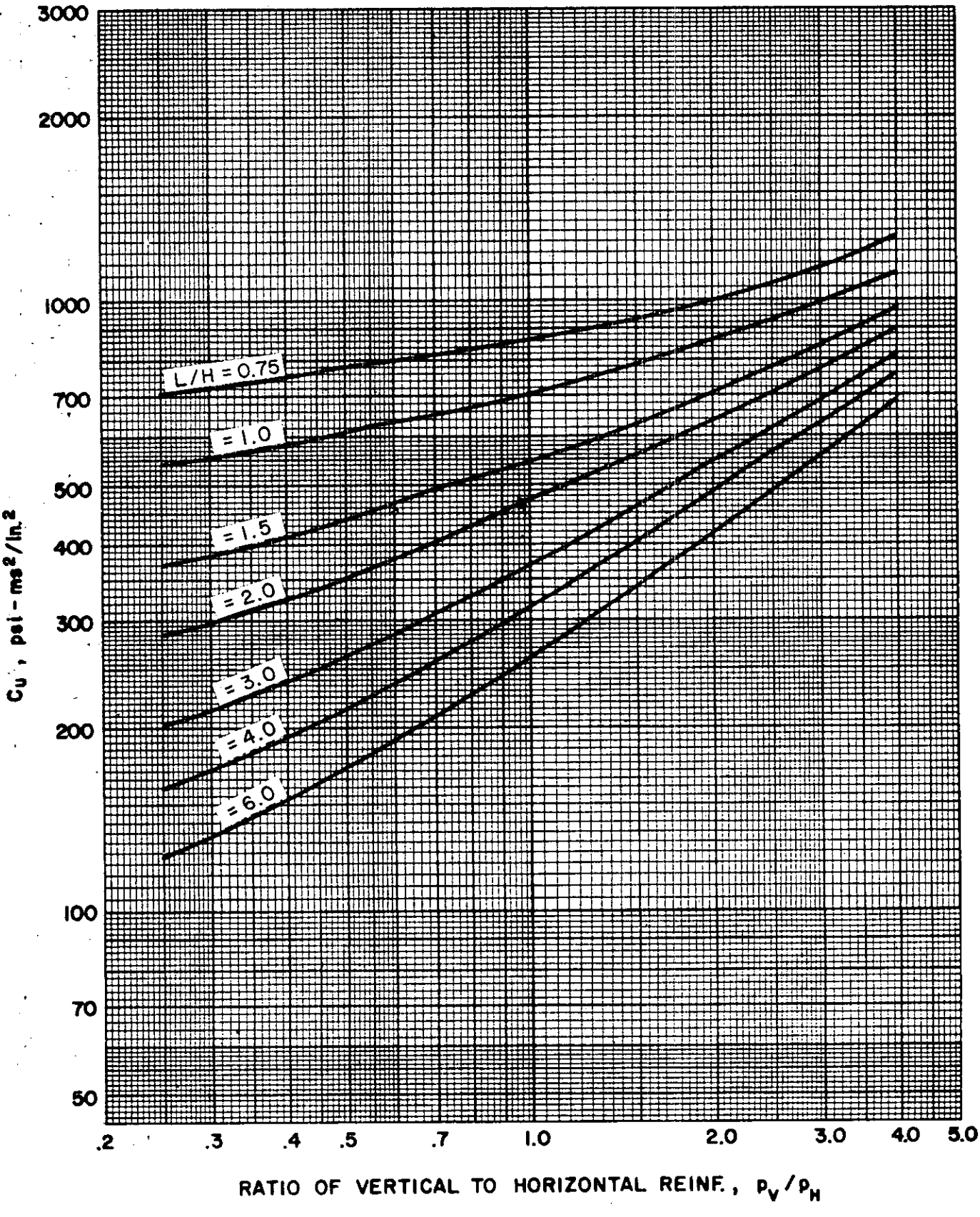


Figure 4-34 Impulse coefficient C_u for an element with three edges fixed and one edge free

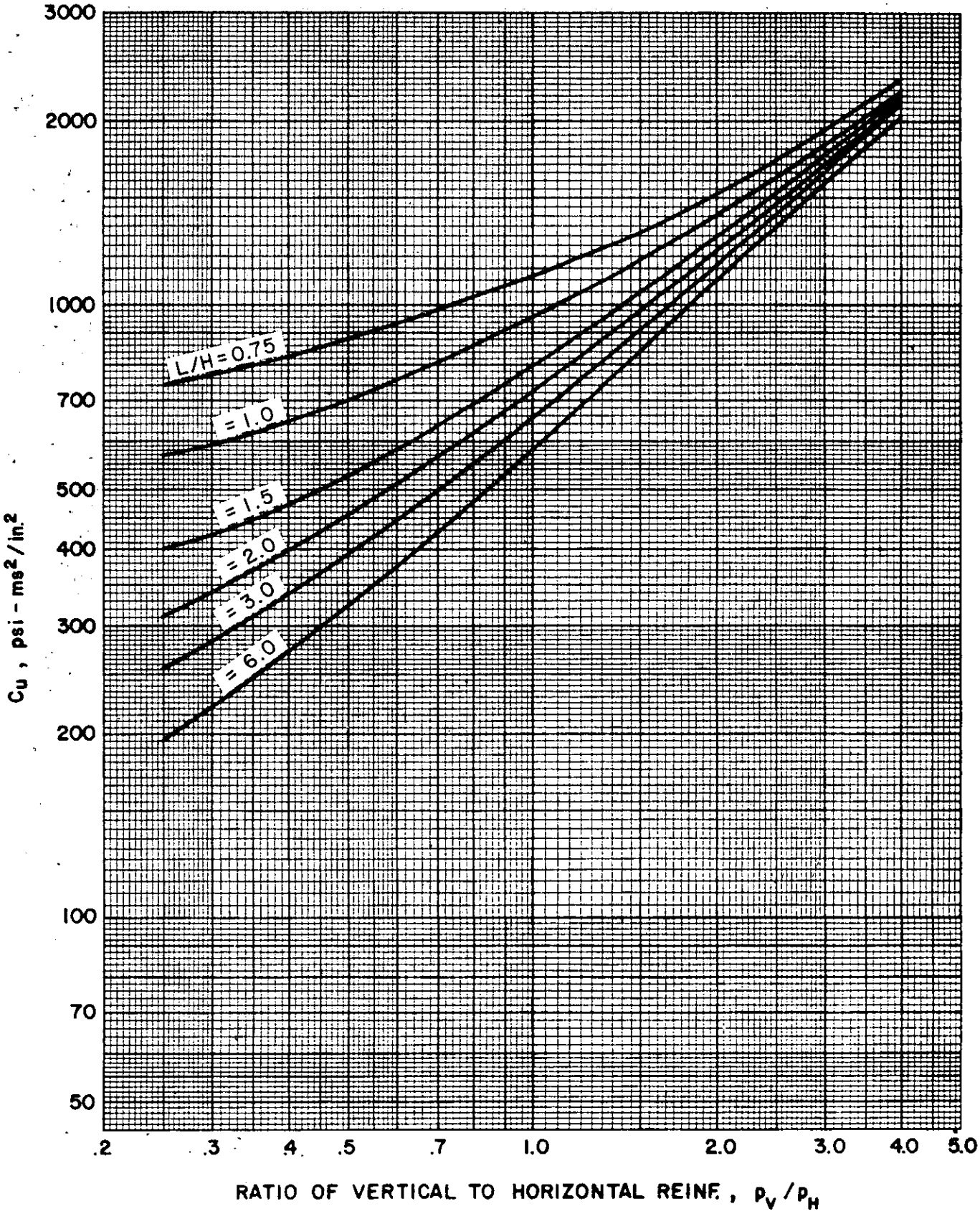


Figure 4-35 Impulse coefficient C_u for an element with four edges fixed

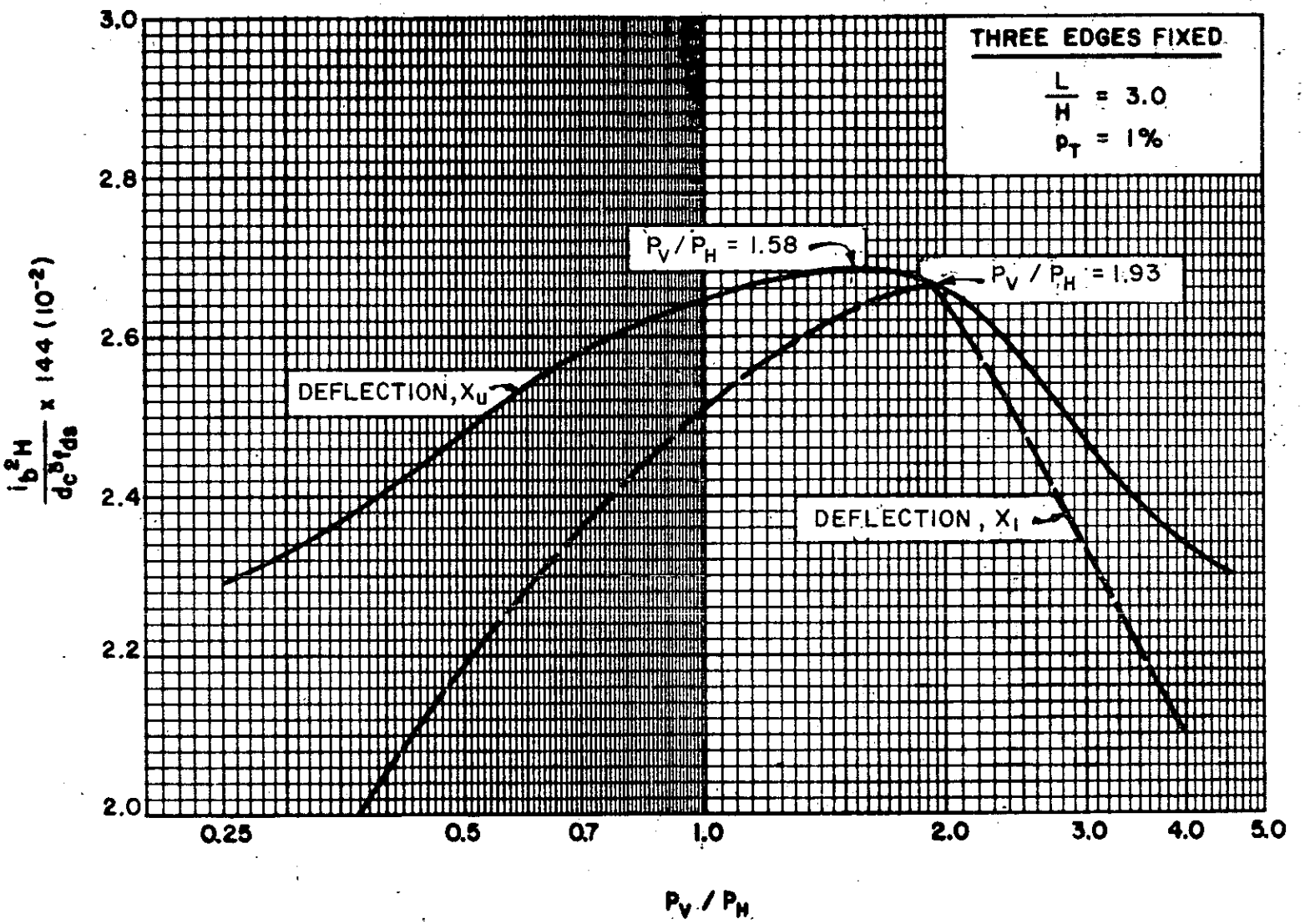


Figure 4-36 Determination of optimum ratio of p_V/p_H for maximum impulse capacity

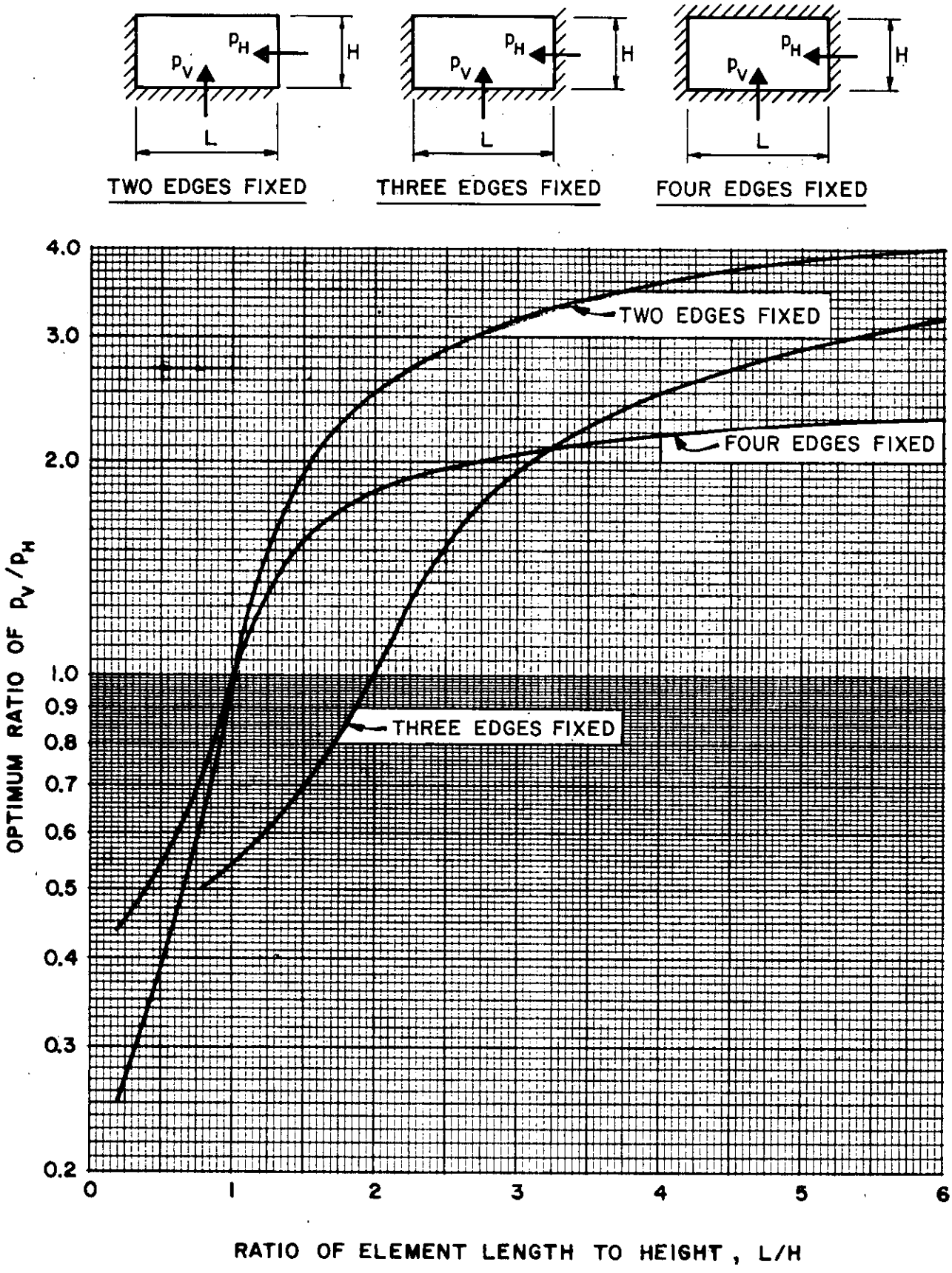


Figure 4-37 Optimum ratio of p_V/p_H for maximum capacity at partial failure deflection, X_1

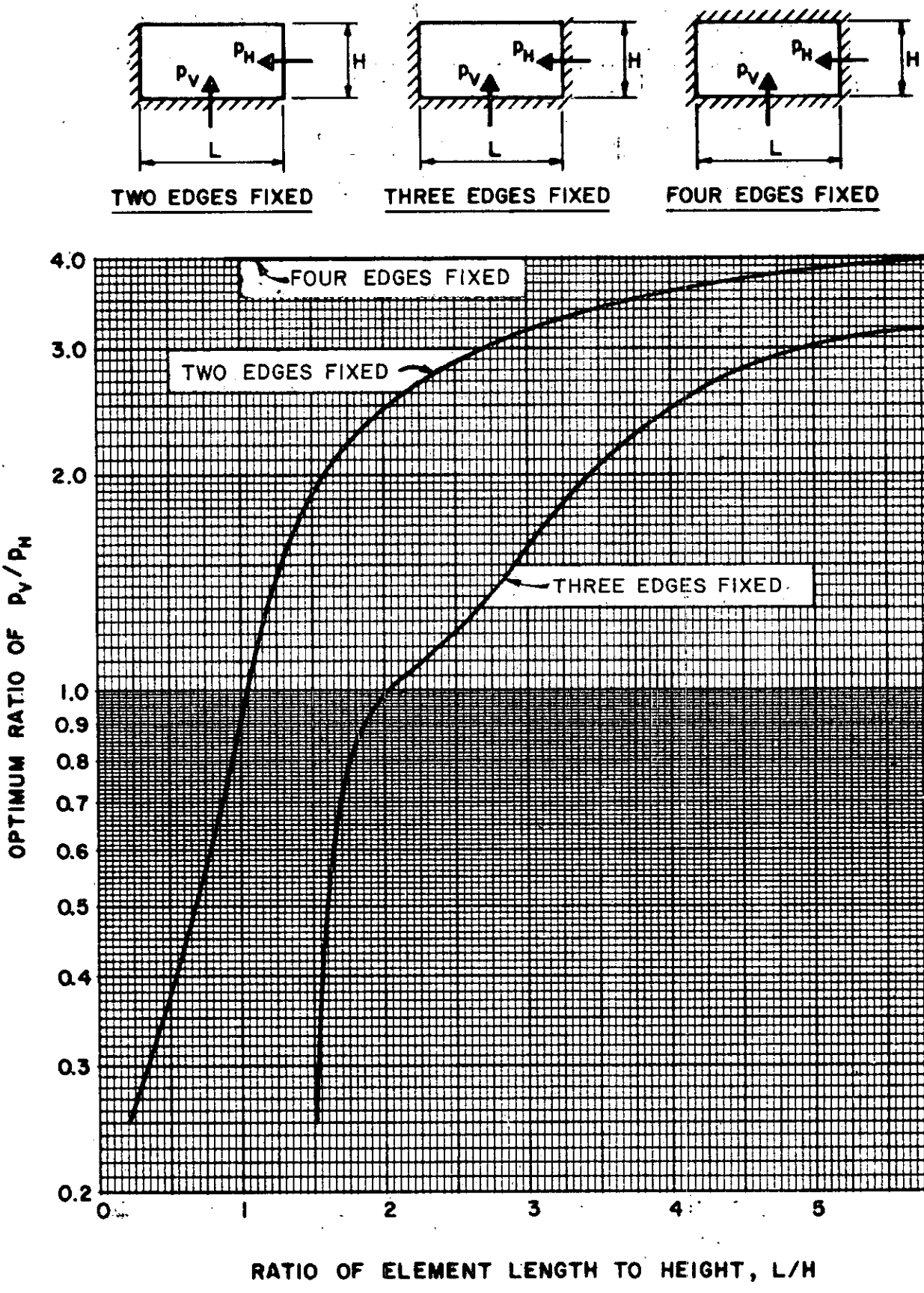


Figure 4-38 Optimum ratio of p_V/p_H for maximum capacity at incipient failure, X_u

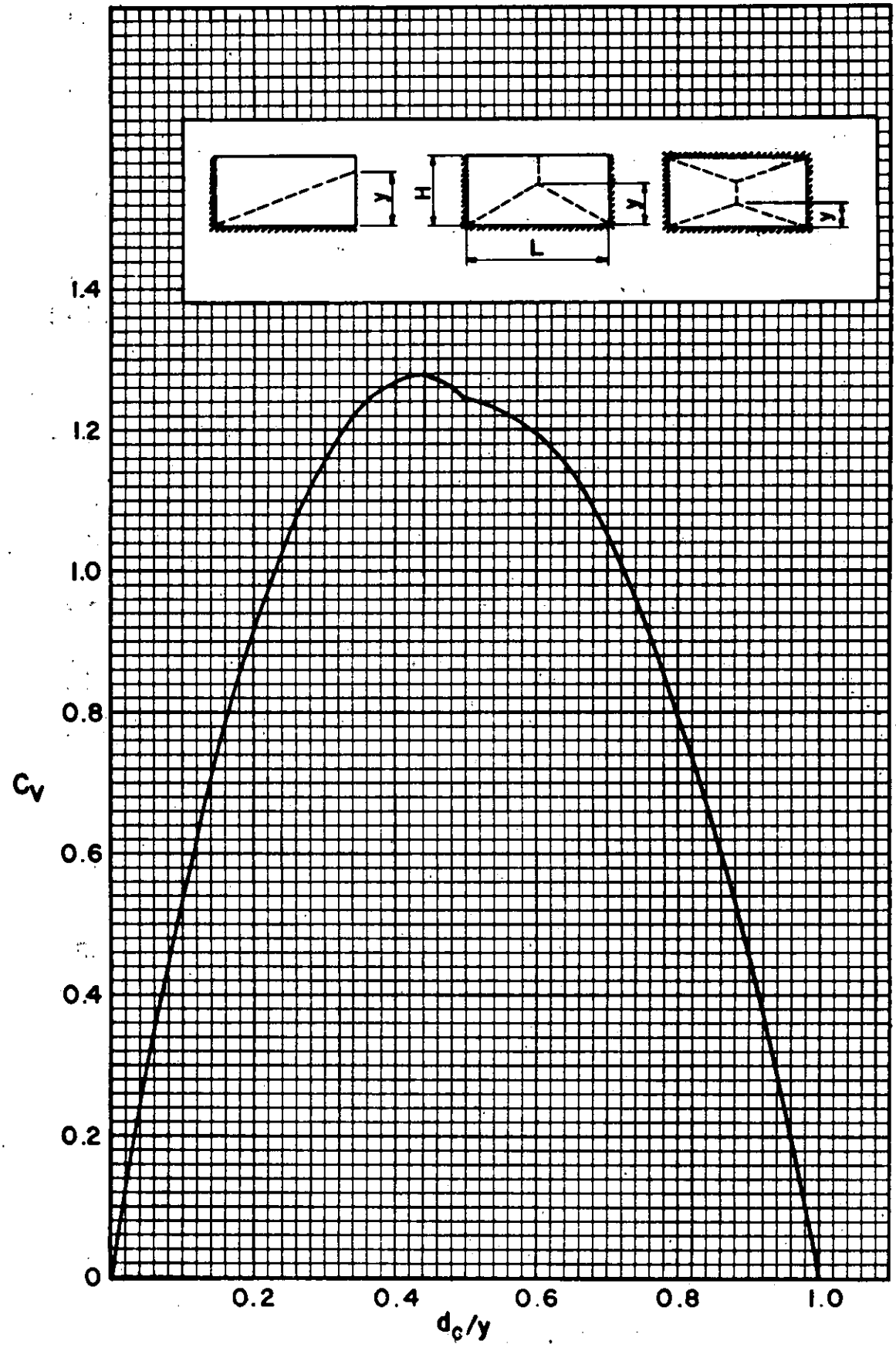


Figure 4-39 Vertical shear coefficients for ultimate shear stress at distance d_c from the support (cross section type II and III)

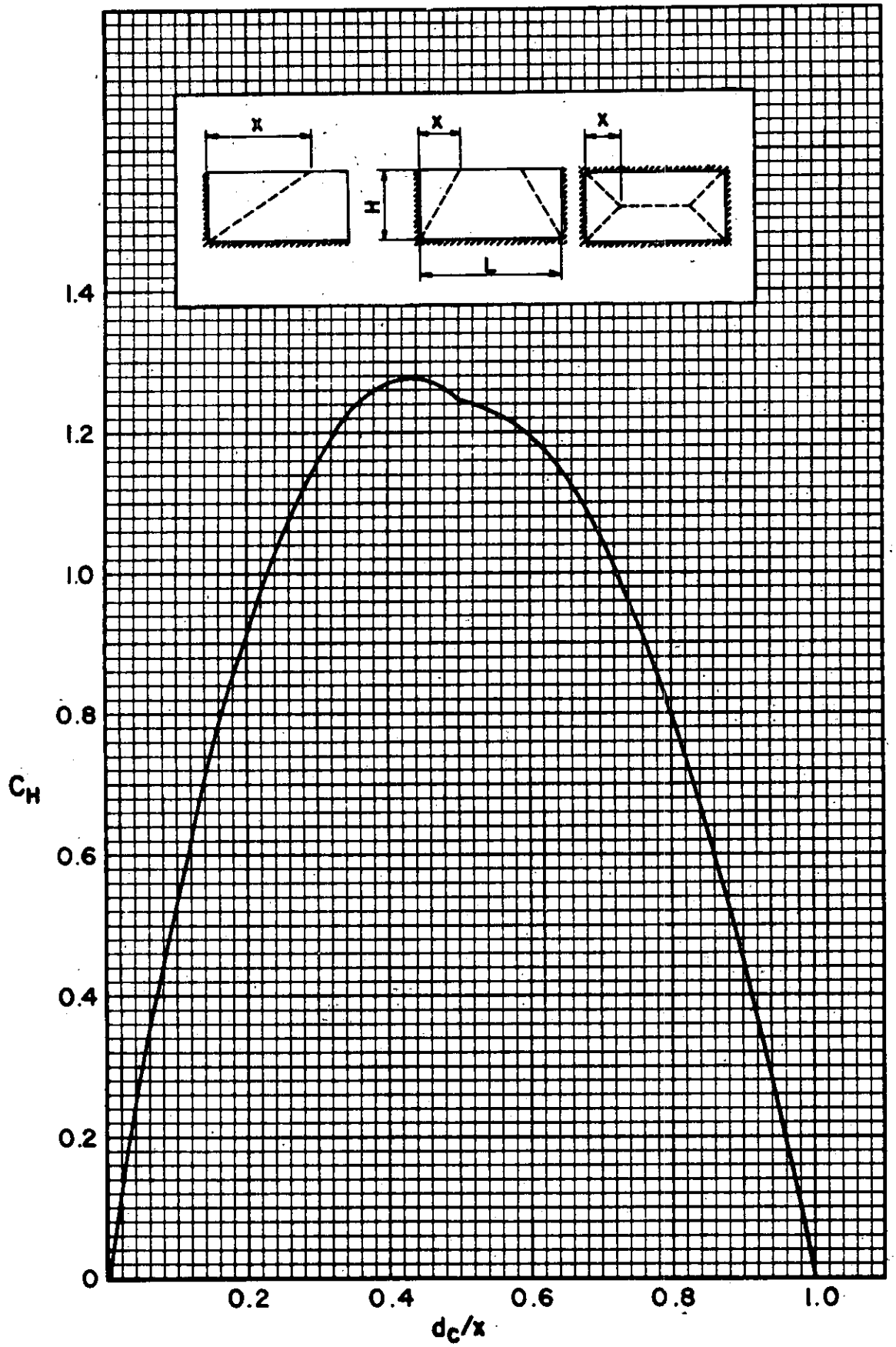


Figure 4-40 Horizontal shear coefficients for ultimate shear stress at distance d_c from the support (cross section type II and III)

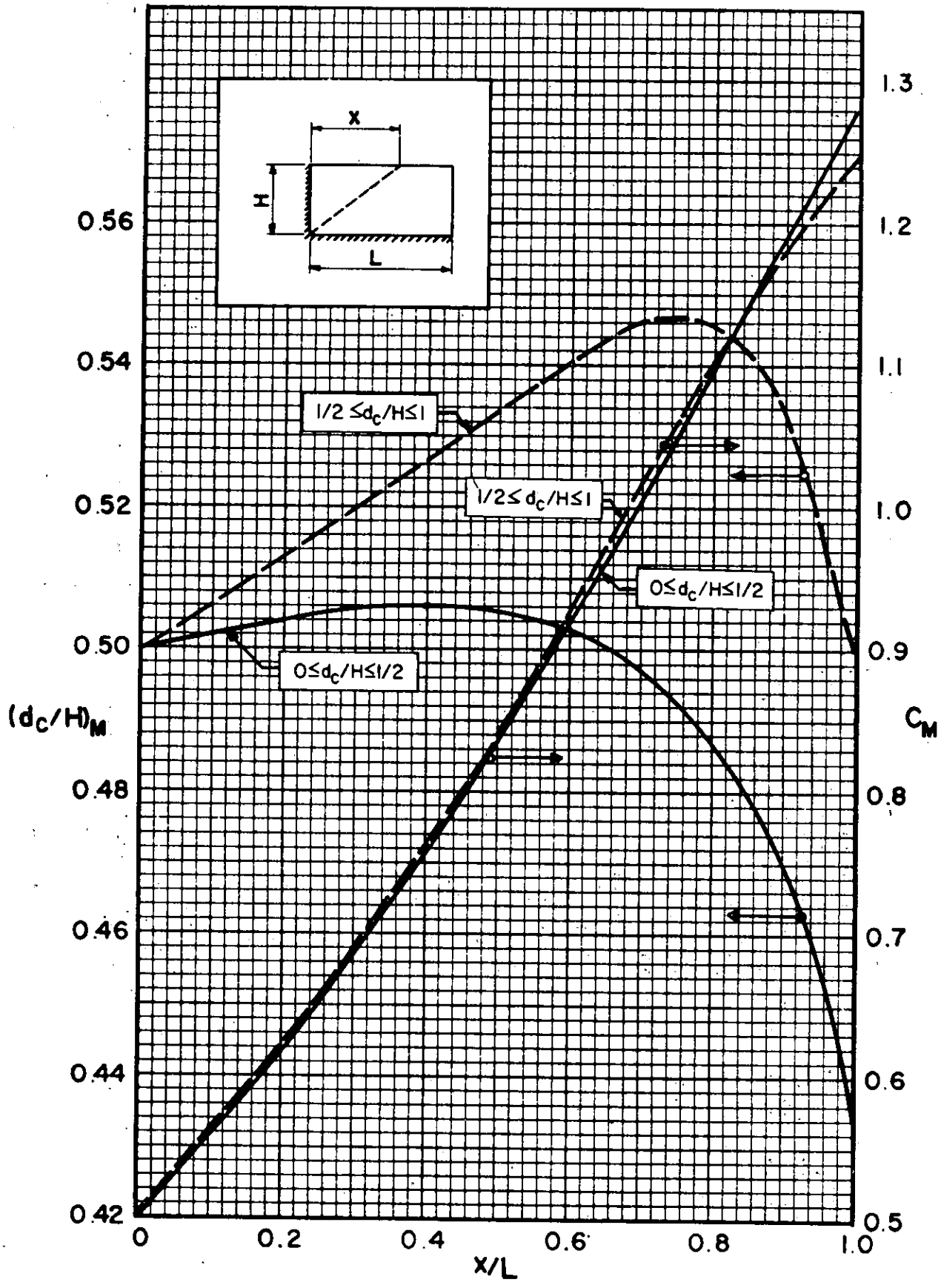


Figure 4-41 Vertical shear parameters for ultimate shear stress at distance d_c from the support (cross section type II and III)

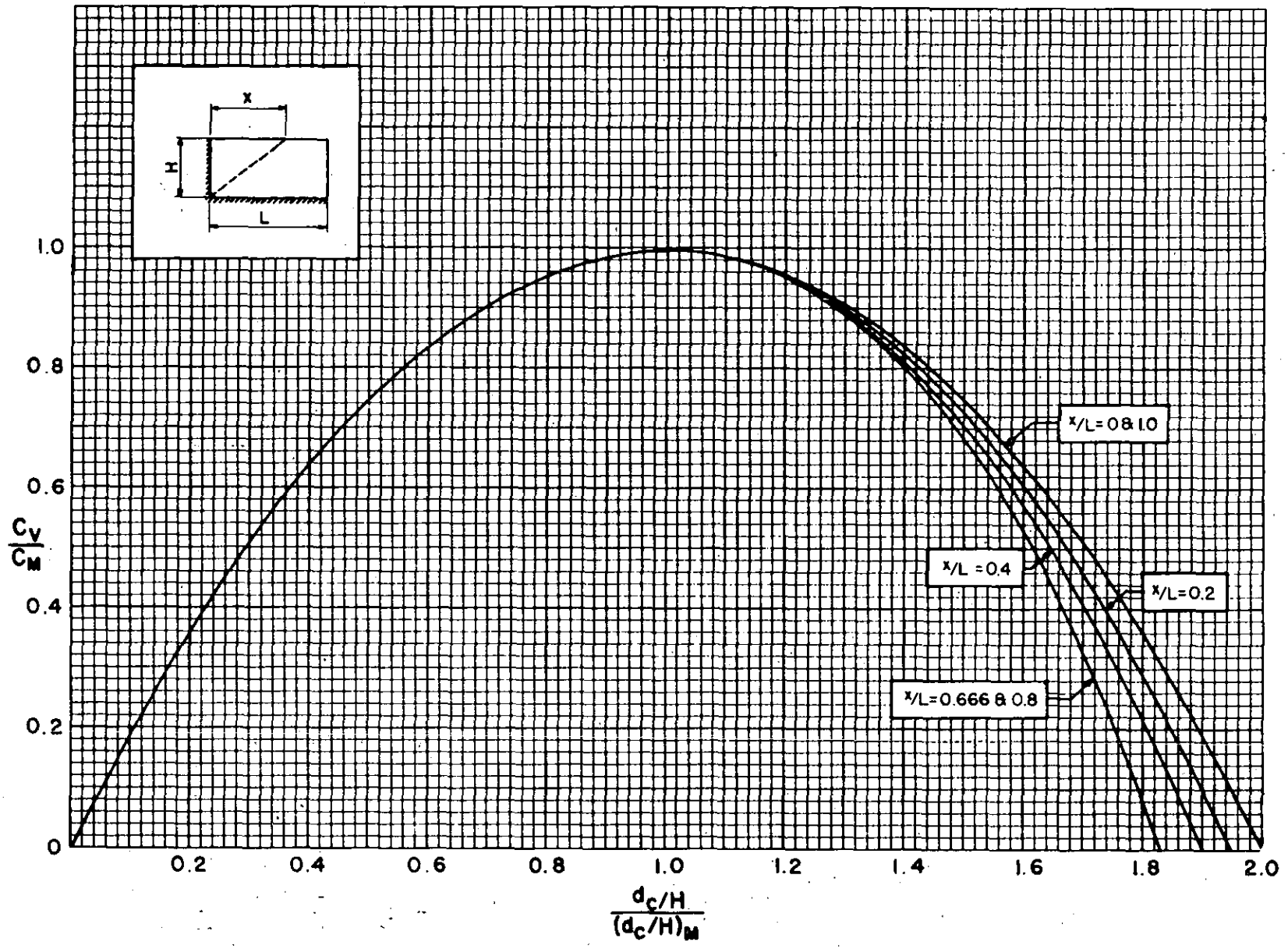


Figure 4-42 Vertical shear coefficient ratios for ultimate shear stress at distance d_c from support (cross section type II and III)

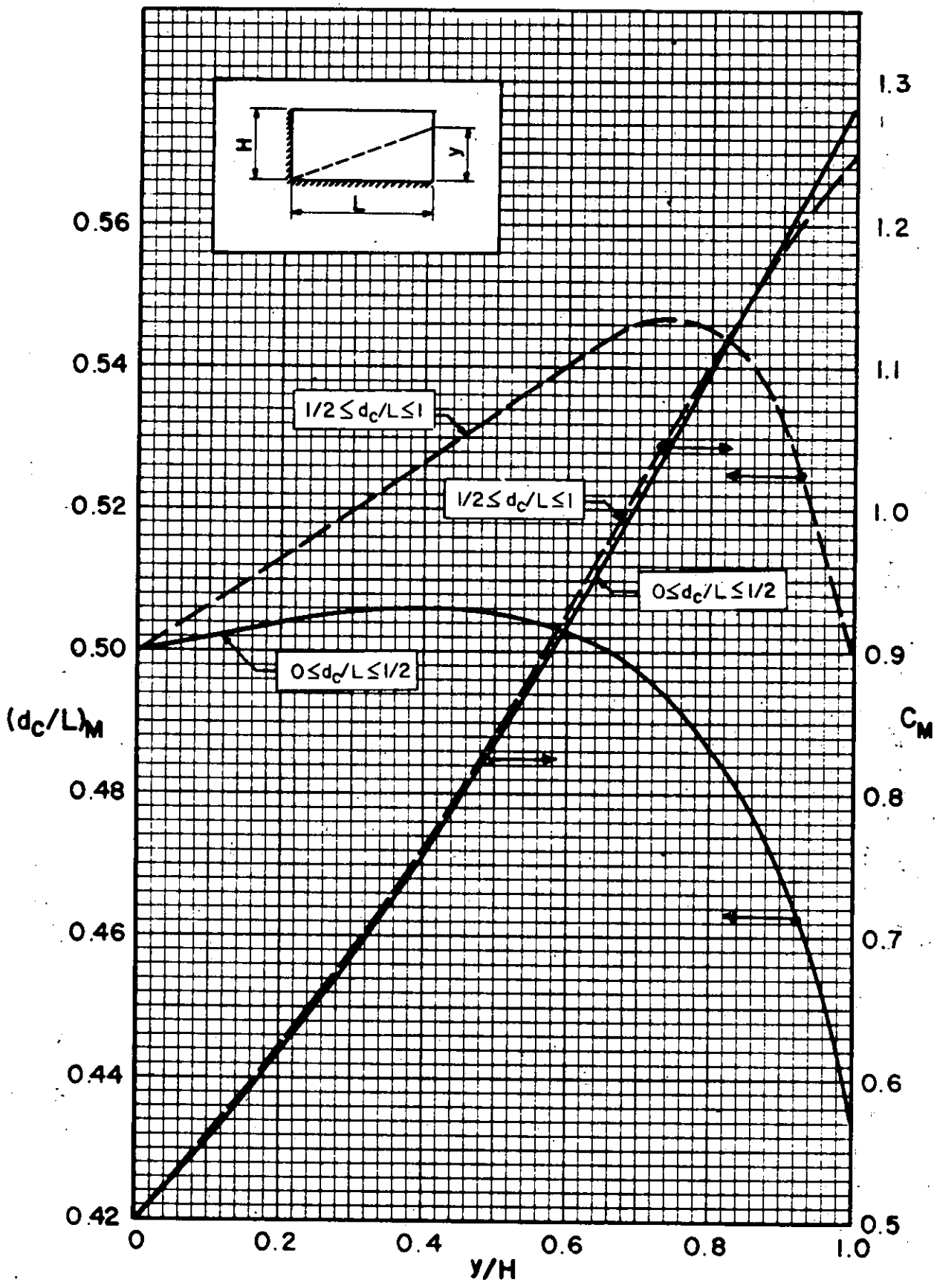


Figure 4-43 Horizontal shear parameters for ultimate shear stress at distance d_c from the support (cross section type II and III)

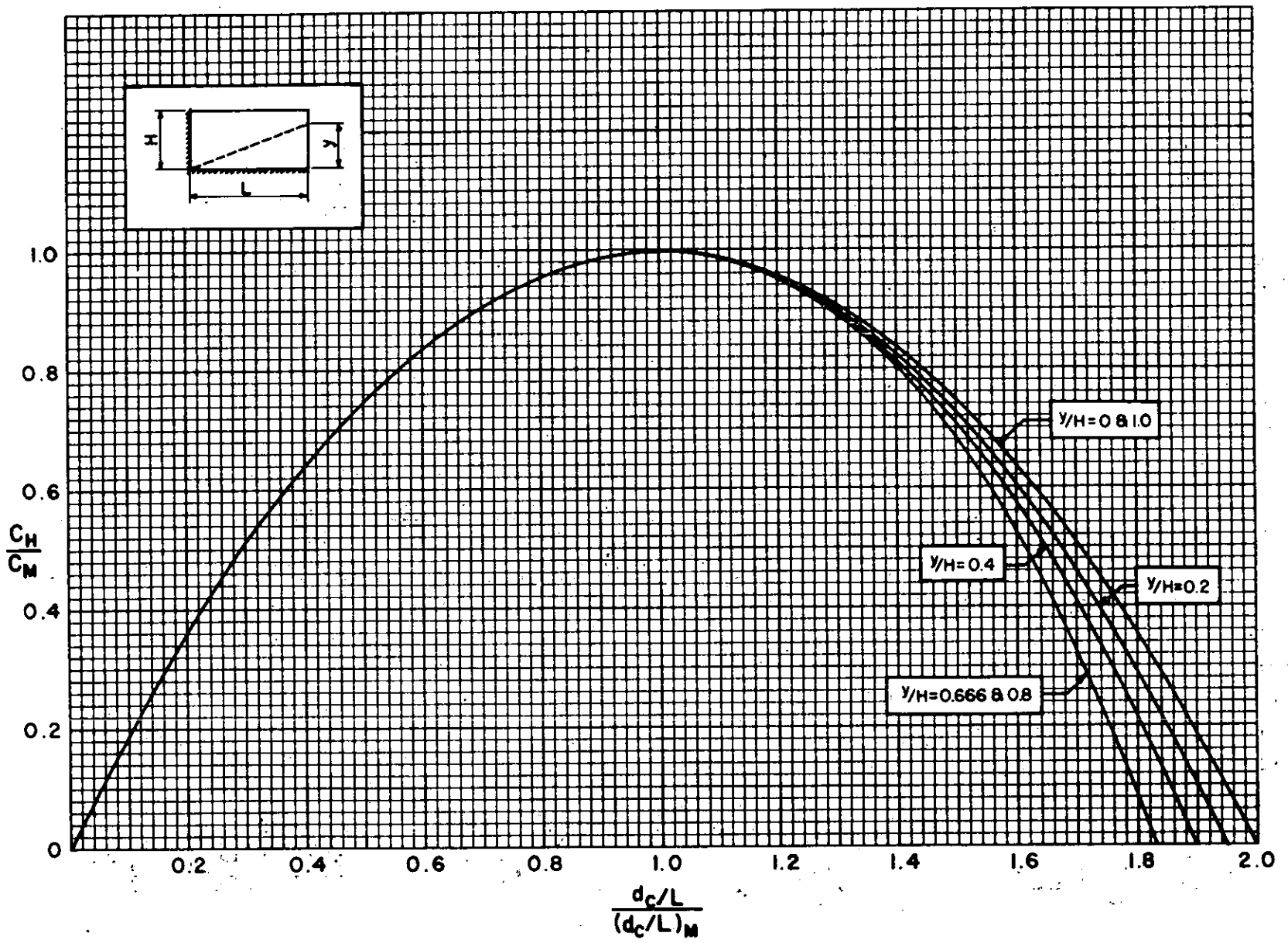


Figure 4-44 Horizontal shear coefficient ratios for ultimate shear stress at distance d_C from the support (cross section type II and III)

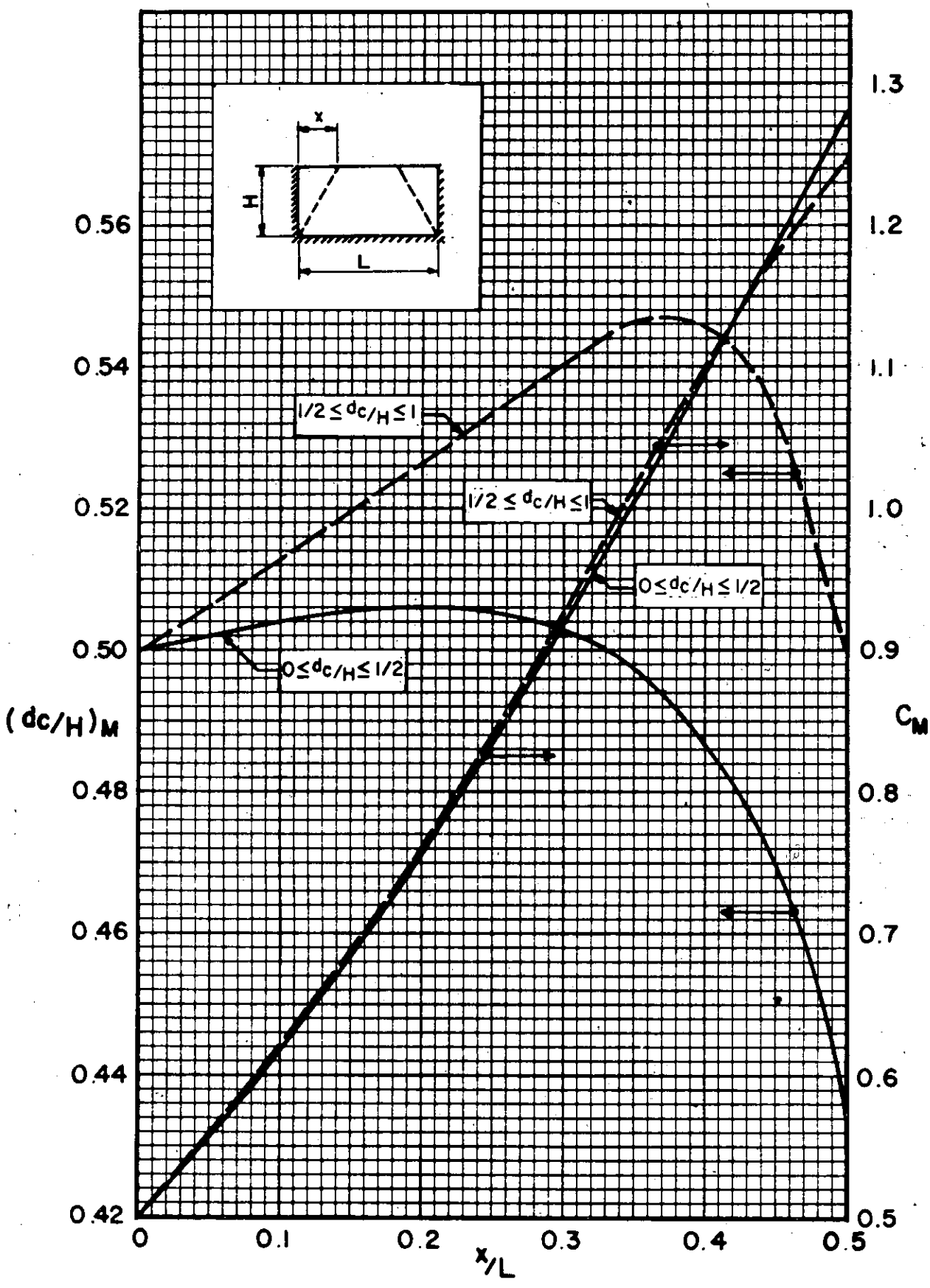


Figure 4-45 Vertical shear parameters for ultimate shear stress at distance d_c from the support (cross section type II and III)

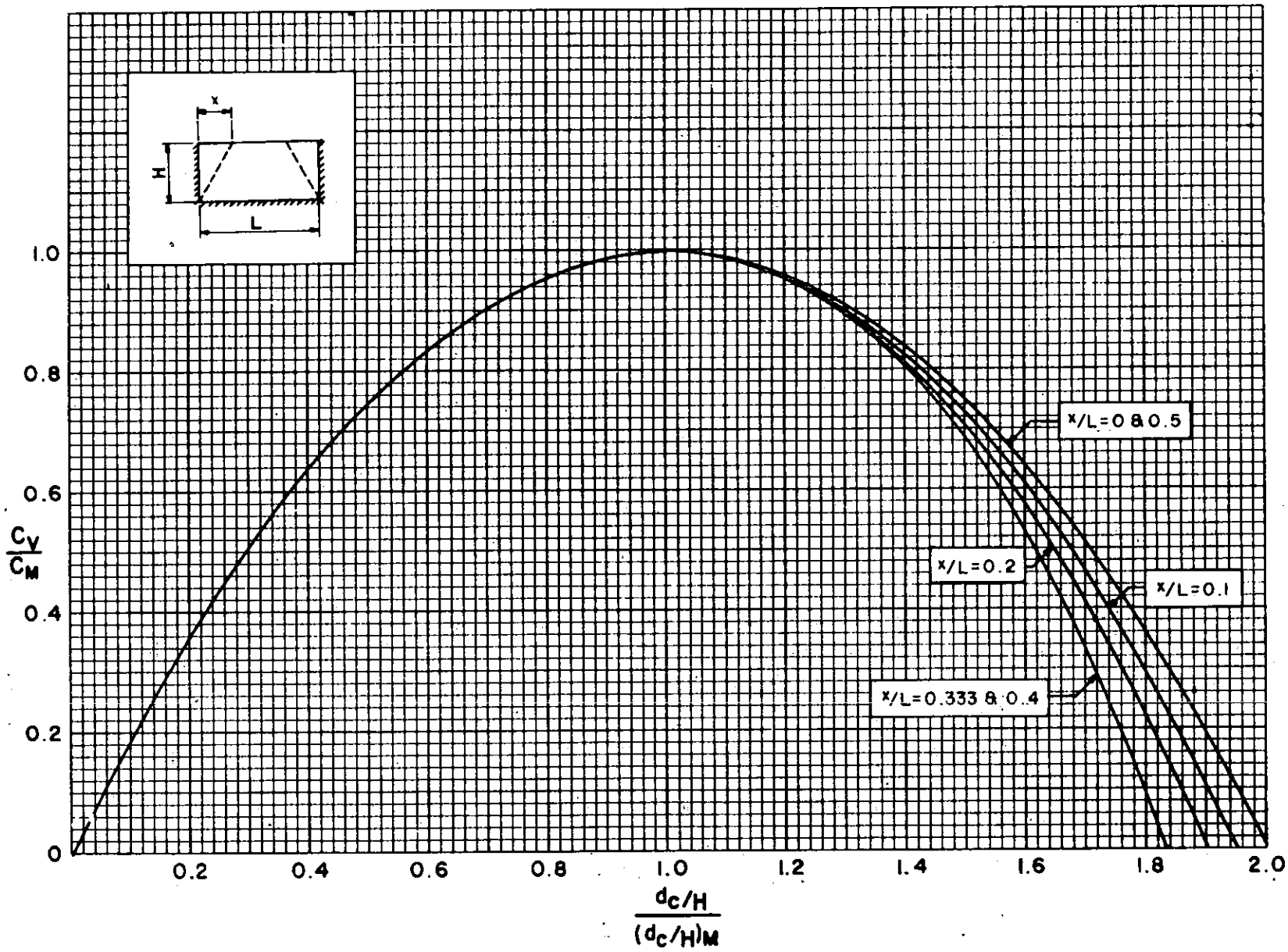


Figure 4-46 Vertical shear coefficient ratios for ultimate shear stress at distance d_c from the support (cross section type II and III)

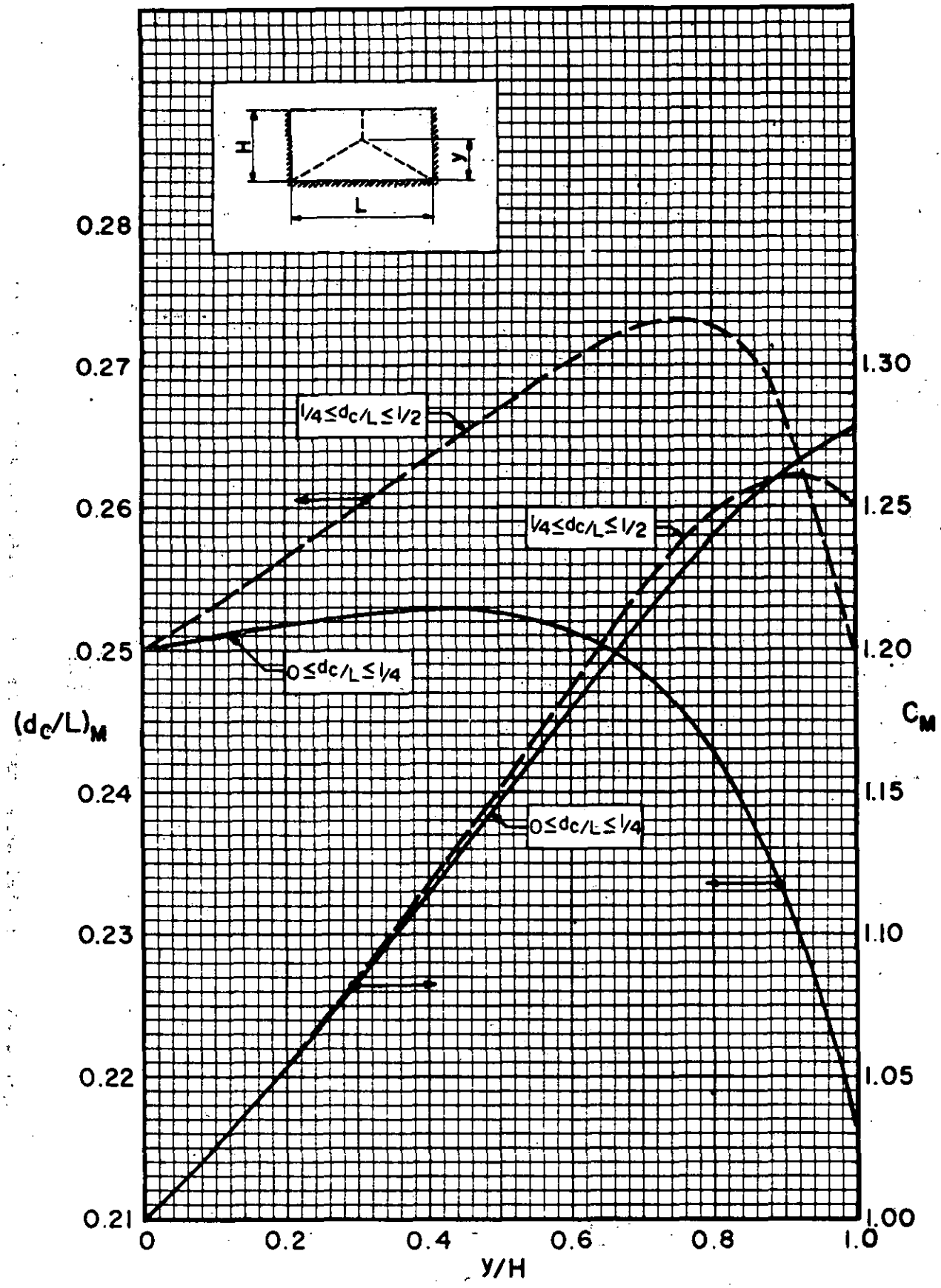


Figure 4-47 Horizontal shear parameters for ultimate shear stress at distance d_c from the support (cross section type II and III)

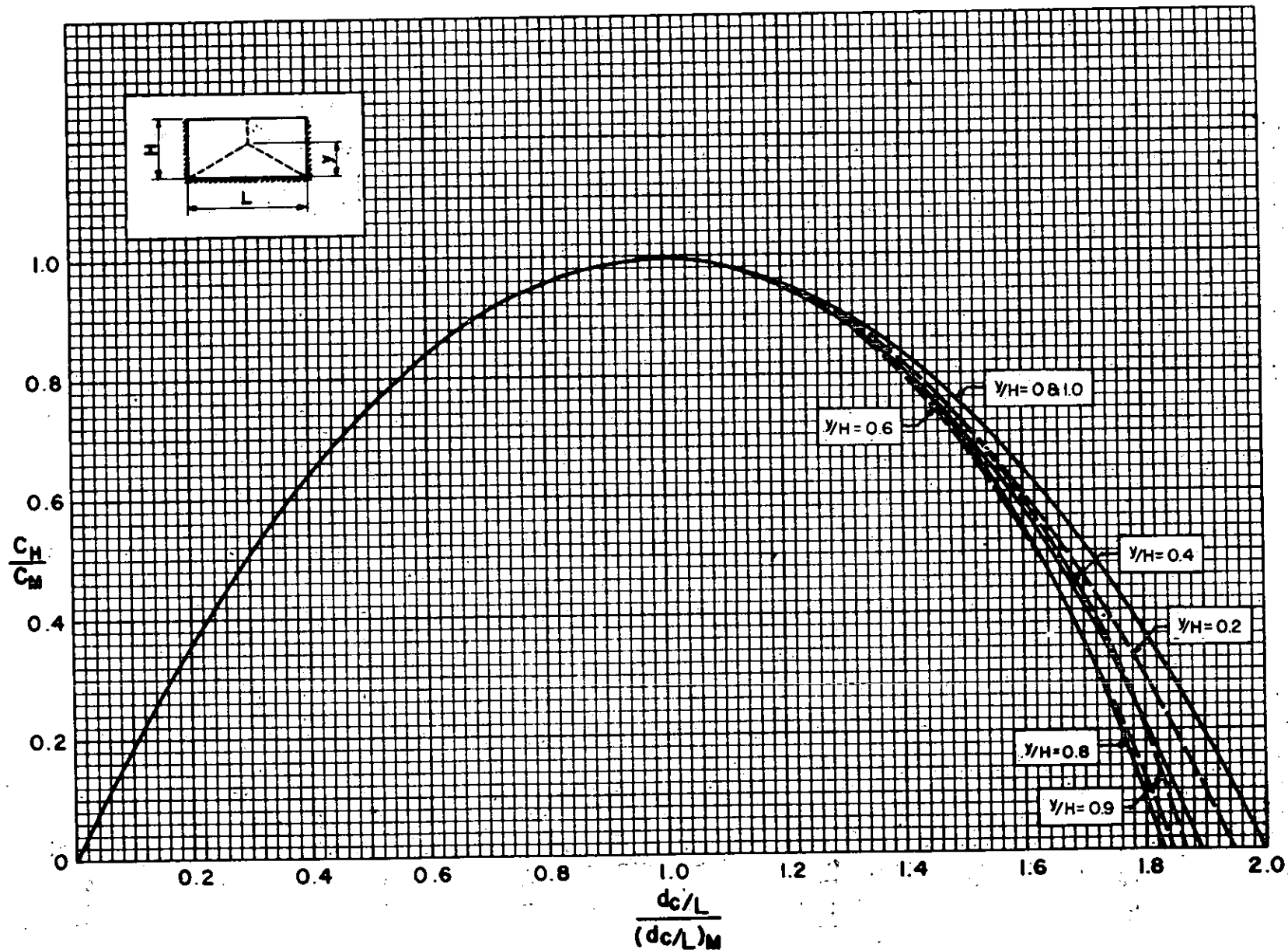


Figure 4-48 Horizontal shear coefficient ratios for ultimate shear stress at distance d_c from the support (cross section type II and III)

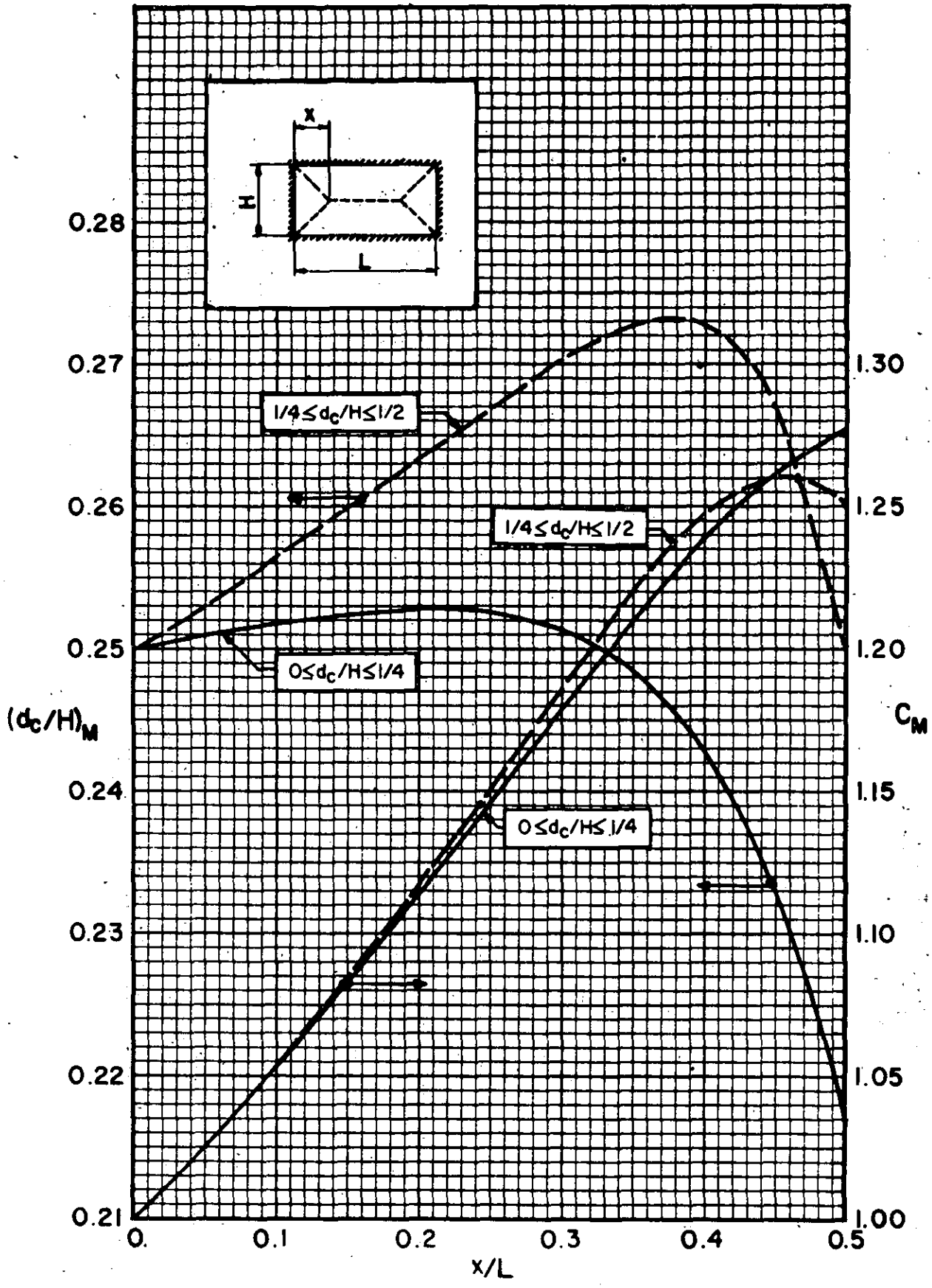


Figure 4-49 Vertical shear parameters for ultimate shear stress at distance d_c from the support (cross section type II and III)

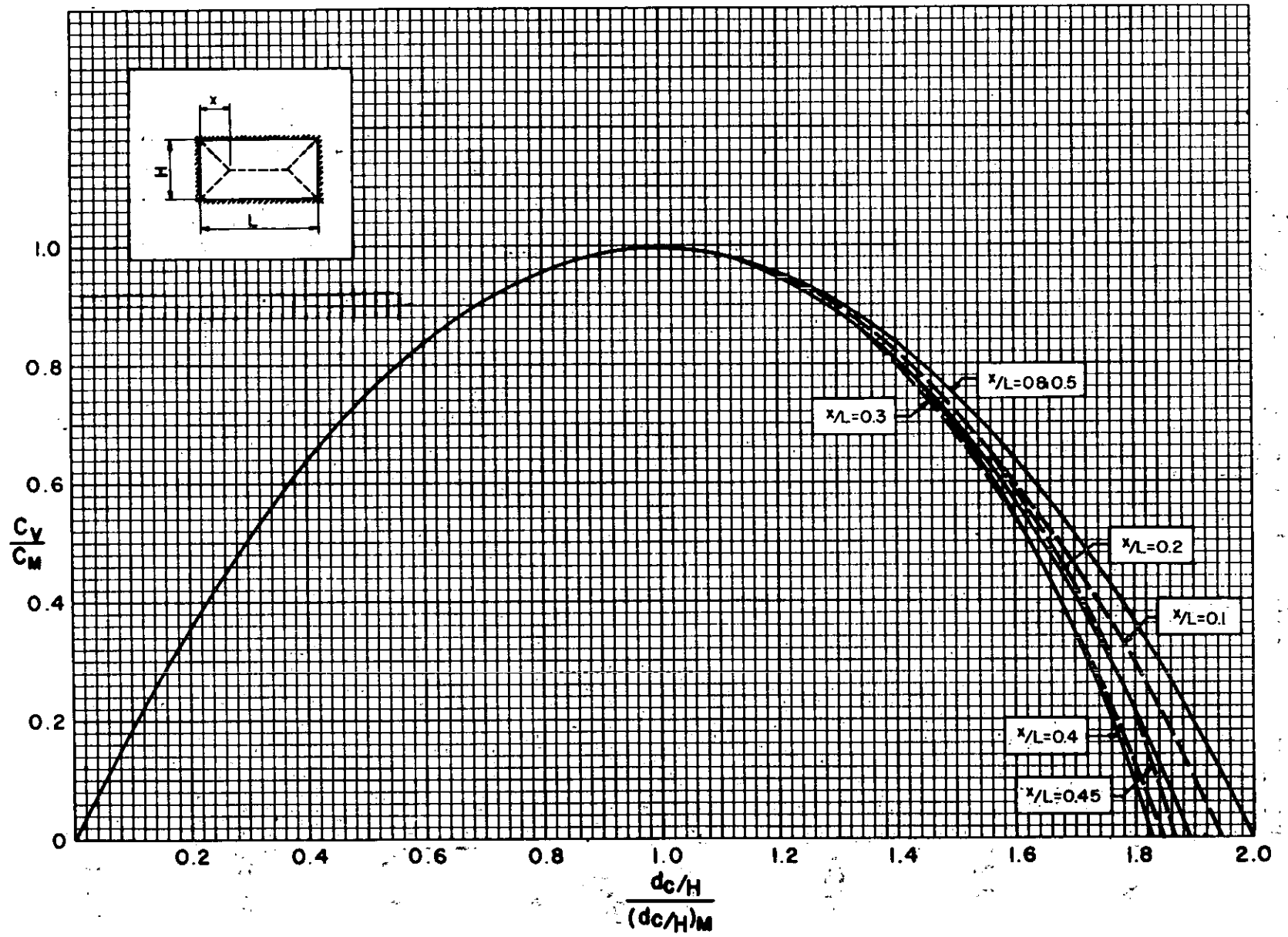


Figure 4-50 Vertical shear coefficient ratios for ultimate shear stress at distance d_c from the support (cross section type II and III)

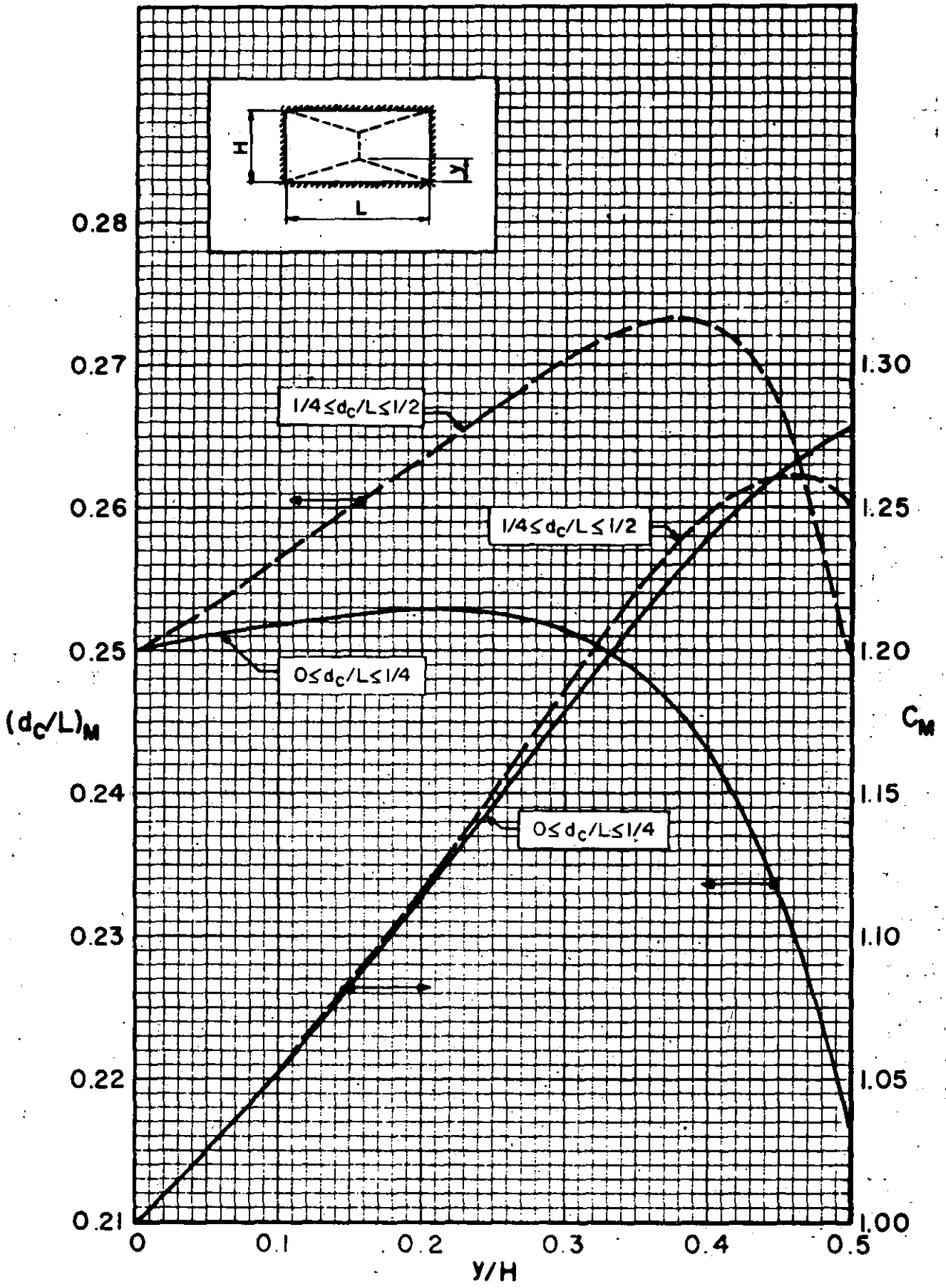


Figure 4-51 Horizontal shear parameters for ultimate shear stress at distance d_c from the support (cross section type II and III)

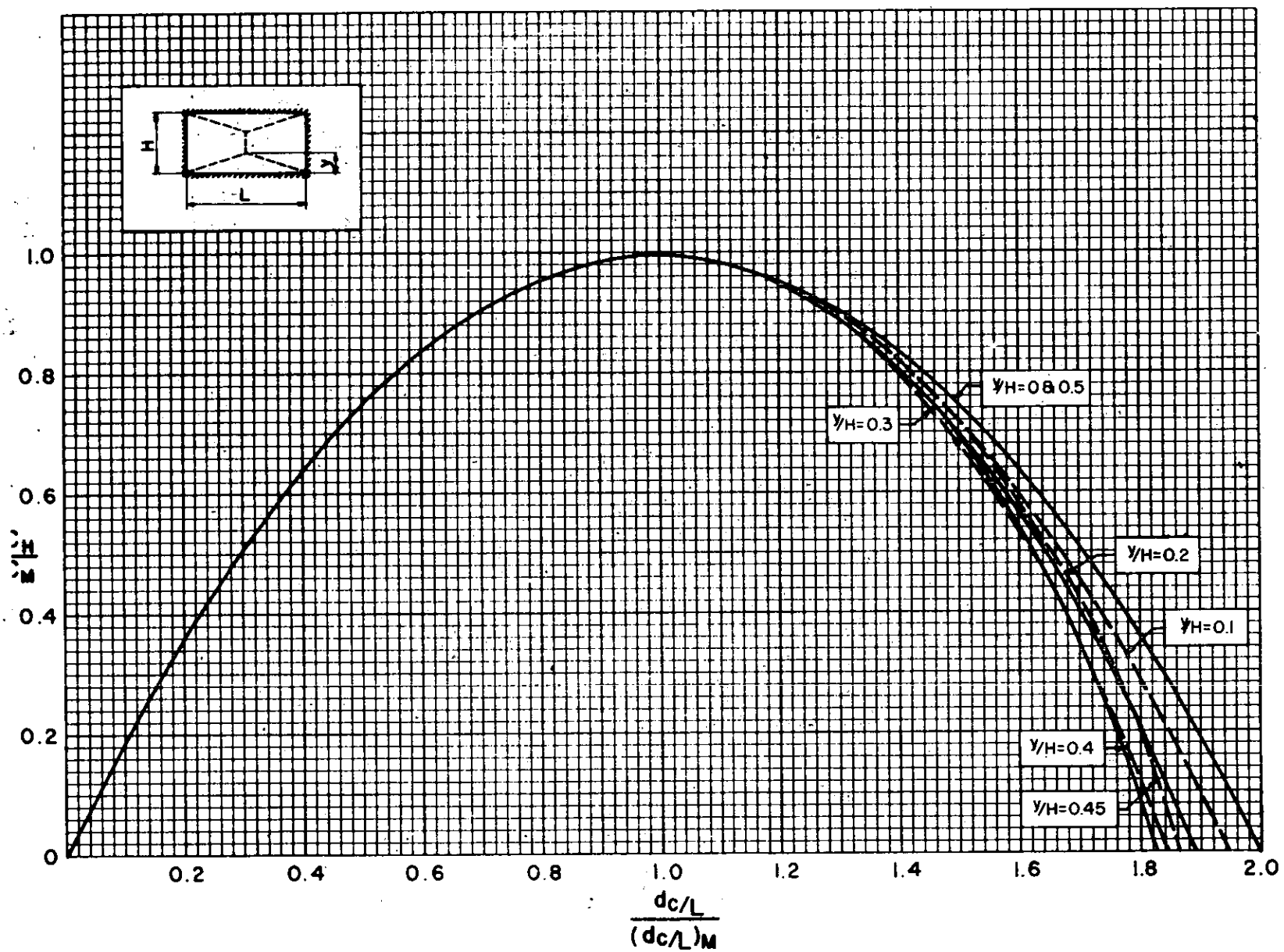


Figure 4-52 Horizontal shear coefficient ratios for ultimate shear stress at distance d_c from the support (cross section type II and III)

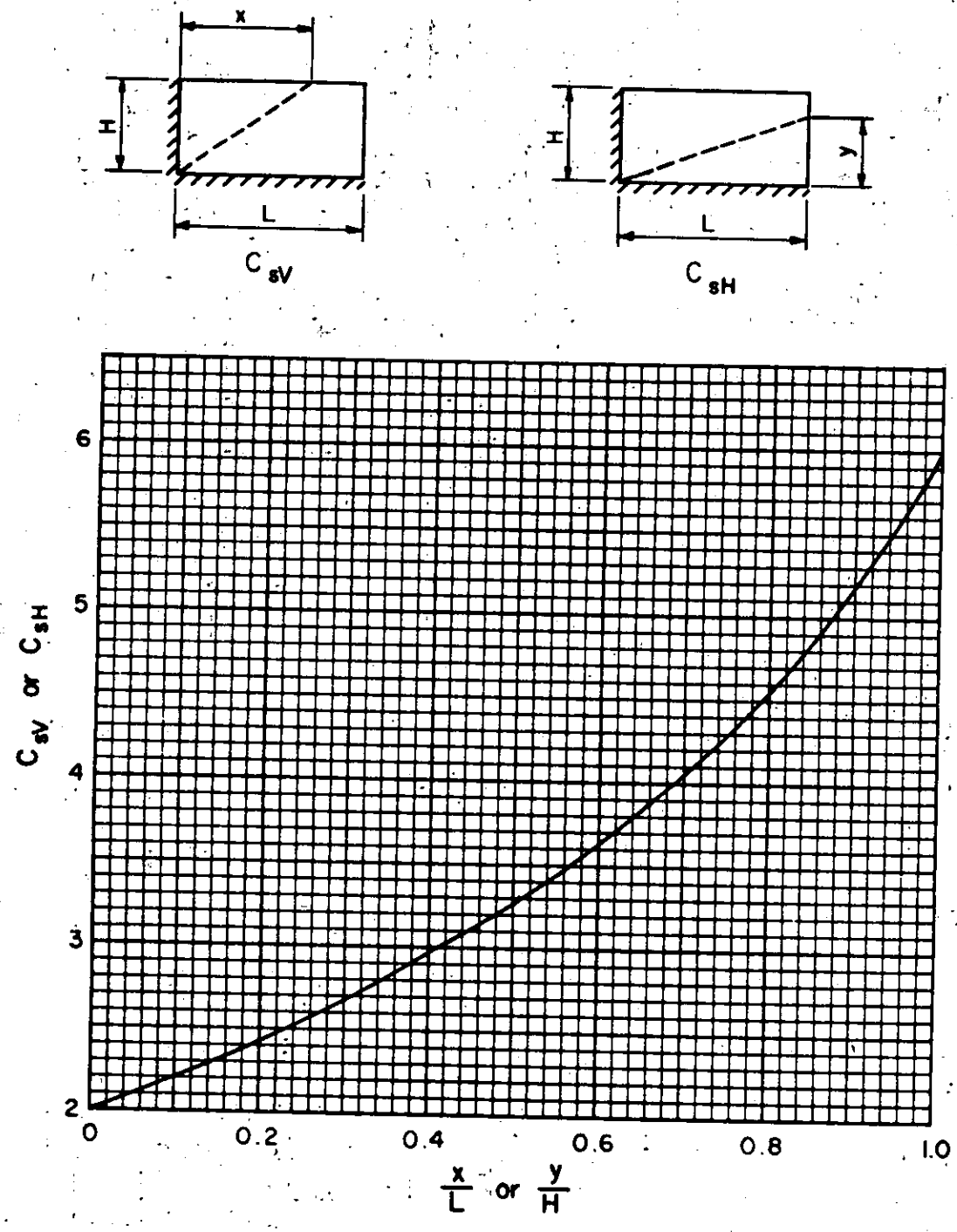


Figure 4-53 Shear coefficients for ultimate support shear (cross section type II and III)

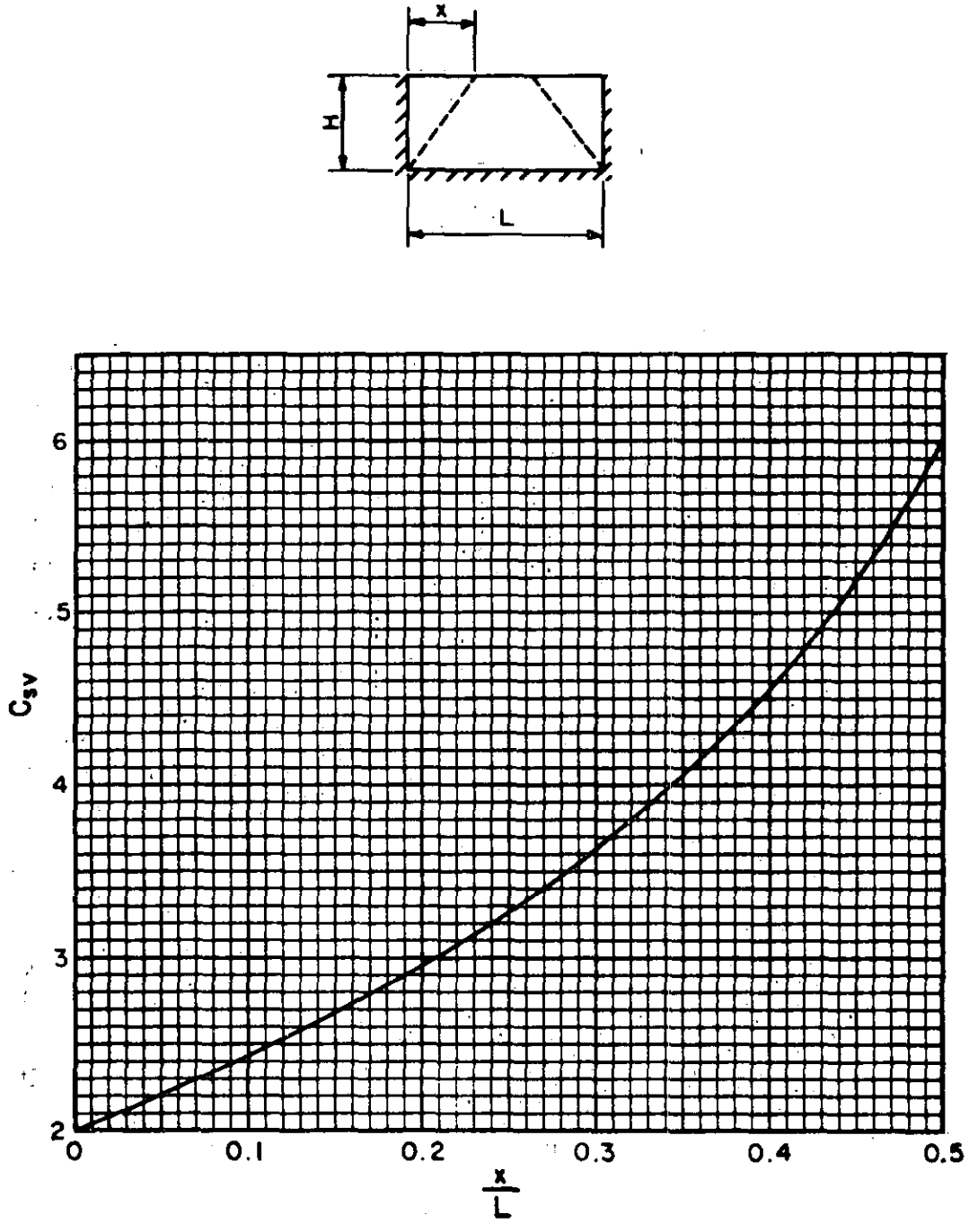


Figure 4-54 Shear coefficients for ultimate support shear (cross section type II and III)

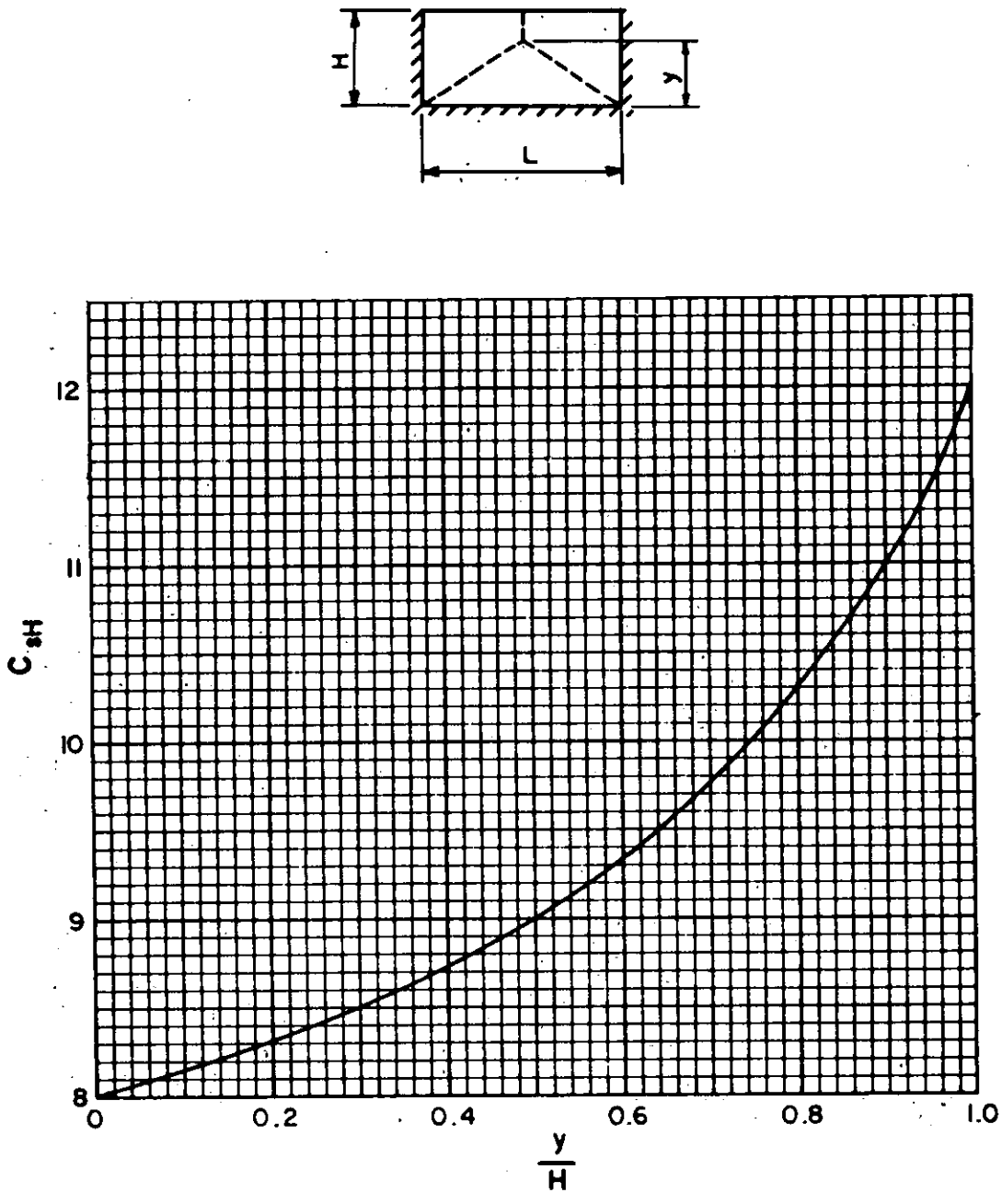


Figure 4-55 Shear coefficients for ultimate support shear (cross section type II and III)

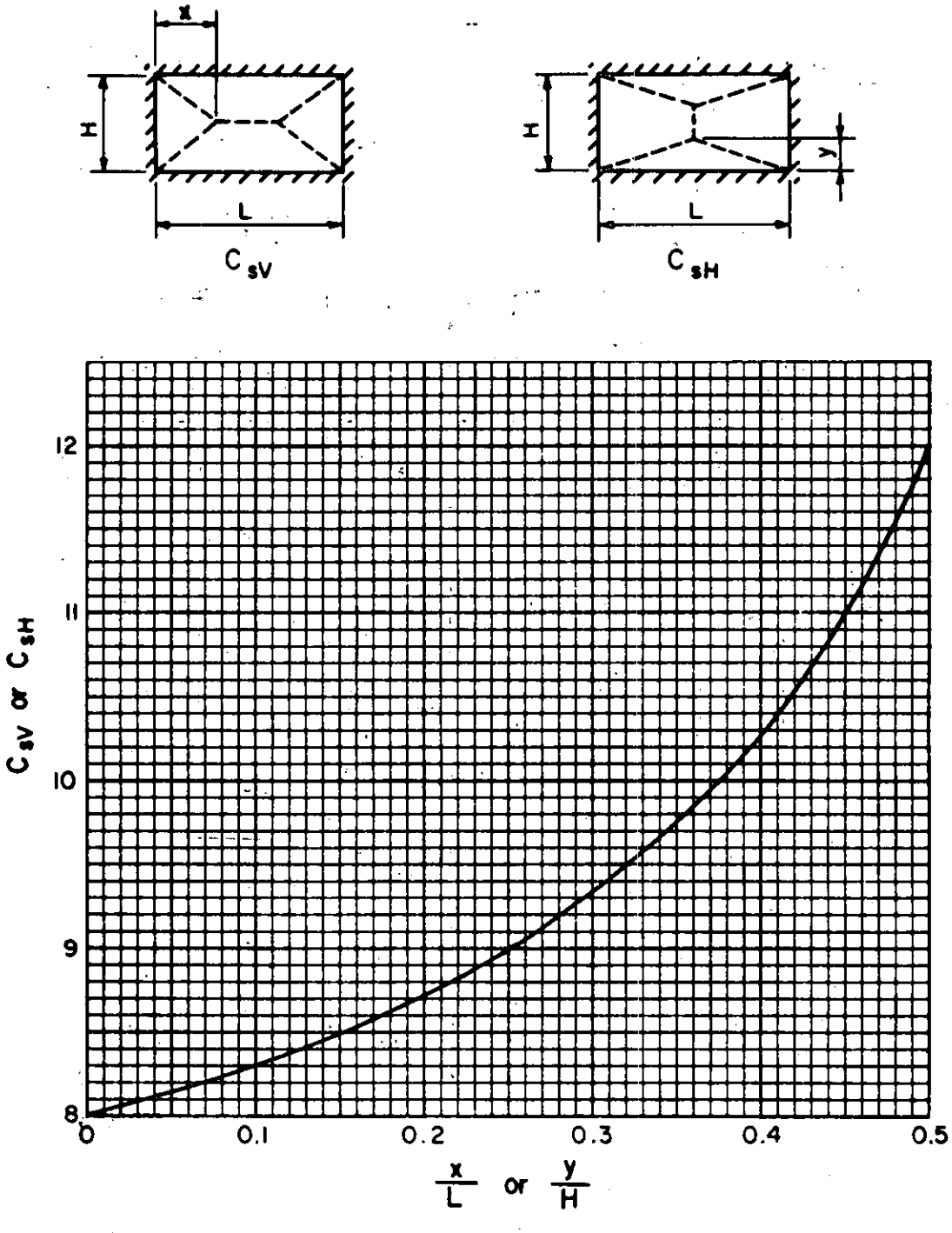


Figure 4-56 Shear coefficients for ultimate support shear (cross section type II and III)

Table 4-9 Impulse Coefficient C_1 for Two-Way Elements

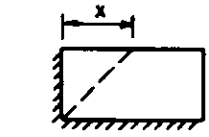
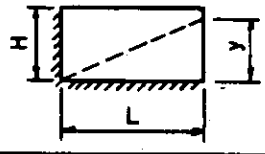
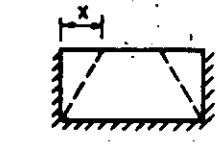
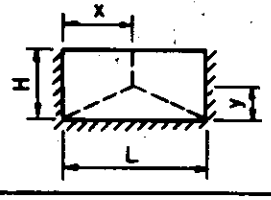
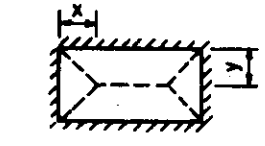
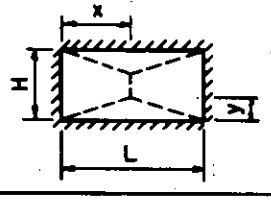
Edge Conditions	Yield Line Locations	Limits	Impulse Coefficient, C_1
Two adjacent edges supported and two edges free		$0 \le x/H \le 1$	$957\ \frac{(K_{LM})_u}{(x/H)}$
		$H \le x \le L$	$957\ \frac{(K_{LM})_u}{(x/H)^2}$
		$0 \le y/L \le 1$	$957\ \frac{(K_{LM})_u (p_V/p_H)}{(y/H)}$
		$L \le y \le H$	$957\ \frac{(K_{LM})_u (p_V/p_H)(L/H)}{(y/H)^2}$
Three edges supported and one edge free		$0 \le x/H \le 1$	$957\ \frac{(K_{LM})_u}{(x/H)}$
		$H \le x \le L/2$	$957\ \frac{(K_{LM})_u}{(x/H)^2}$
		$0 \le y/L \le \frac{1}{2}$	$957\ \frac{(K_{LM})_u (p_V/p_H)}{(y/H)}$
		$L/2 \le y \le H$	$478\ \frac{(K_{LM})_u (p_V/p_H)(L/H)}{(y/H)^2}$
Four edges supported		$0 \le x/H \le \frac{1}{2}$	$957\ \frac{(K_{LM})_u}{(x/H)}$
		$H/2 \le x \le L/2$	$478\ \frac{(K_{LM})_u}{(x/H)^2}$
		$0 \le y/L \le \frac{1}{2}$	$957\ \frac{(K_{LM})_u (p_V/p_H)}{(y/H)^2}$
		$L/2 \le y \le H/2$	$478\ \frac{(K_{LM})_u (p_V/p_H)(L/H)}{(y/H)^2}$

Table 4-10 Impulse Coefficient C_u for Two-Way Elements

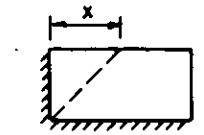
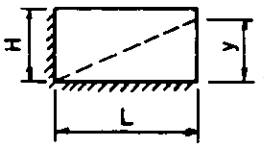
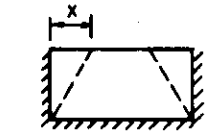
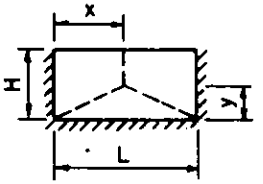
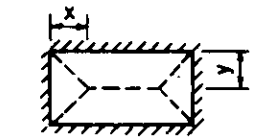
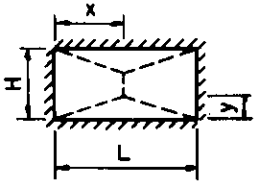
Edge Conditions	Yield Line Locations	Limits	Impulse Coefficient, C_u
Two adjacent edges supported and two edges free		$0 \le x/H \le 1$	$287\left[\frac{3.333(K_{LM})_u}{x/H}+(K_{LM})_u^2(p_V/p_H)(1-x/H)\right]$
		$H \le x \le L$	$287\left[\frac{3.333(K_{LM})_u}{(x/H)^2}+(K_{LM})_u^2\left(\frac{x/H-1}{(L/H)^2}+\frac{4.705(L/H-x/H)\tan\lambda}{(L/H)^2}\right)\right]$ Where, $\lambda=12°-\tan^{-1}\left(\frac{0.2126}{x/H}\right)$
		$0 \le y/L \le 1$	$287\left[\frac{3.333(K_{LM})_u(p_V/p_H)}{y/H}+\frac{(K_{LM})_u^2(L/H-y/H)}{(L/H)^2}\right]$
		$L \le y \le H$	$287\,(p_V/p_H)\left[\frac{3.333(K_{LM})_u(L/H)}{(y/H)^2}+(K_{LM})_u^2(y/H-L/H+4.705(1-y/H)\tan\lambda)\right]$ Where, $\lambda=12°-\tan^{-1}\left(\frac{0.2126}{y/L}\right)$
Three edges supported and one edge free		$0 \le x/H \le 1$	$287\left[\frac{3.333(K_{LM})_u}{x/H}+(K_{LM})_u^2(p_V/p_H)(1-x/H)\right]$
		$H \le x \le L/2$	$1148\left[\frac{0.833(K_{LM})_u}{(x/H)^2}+2(K_{LM})_u^2\left(\frac{x/H-1}{(L/H)^2}+\frac{4.705(L/2H-x/H)\tan\lambda}{(L/H)^2}\right)\right]$ Where, $\lambda=12°-\tan^{-1}\left(\frac{0.2126}{x/H}\right)$
		$0 \le y/L \le \frac{1}{2}$	$717\left[\frac{1.333(K_{LM})_u(p_V/p_H)}{y/H}+3.2(K_{LM})_u^2\frac{(L/2H-y/H)}{(L/H)^2}\right]$
		$L/2 \le y \le H$	$287\,(p_V/p_H)\left[\frac{1.667(K_{LM})_u(L/H)}{(y/H)^2}+(K_{LM})_u^2(y/H-L/2H+4.705(1-y/H)\tan\lambda)\right]$ Where, $\lambda=12°-\tan^{-1}\left(\frac{0.2126}{2y/L}\right)$
Four edges supported		$0 \le x/H \le \frac{1}{2}$	$1148\left[\frac{0.833(K_{LM})_u}{x/H}+(K_{LM})_u^2(p_V/p_H)\left(1-2\frac{x}{H}\right)\right]$
		$H/2 \le x \le L/2$	$1148\left[\frac{0.417(K_{LM})_u}{(x/H)^2}+2(K_{LM})_u^2\left(\frac{x/H-\frac{1}{2}}{(L/H)^2}+\frac{4.705(L/2H-x/H)\tan\lambda}{(L/H)^2}\right)\right]$ Where, $\lambda=12°-\tan^{-1}\left(\frac{0.2126}{2x/H}\right)$
		$0 \le y/L \le \frac{1}{2}$	$1148\left[\frac{0.833(K_{LM})_u(p_V/p_H)}{y/H}+(K_{LM})_u^2\frac{(L/H-2y/H)}{(L/H)^2}\right]$
		$L/2 \le y \le H/2$	$1148\,(p_V/p_H)\left[\frac{0.417(K_{LM})_u(L/H)}{(y/H)^2}+(K_{LM})_u^2(2y/H-L/H+4.705(1-2y/H)\tan\lambda)\right]$ Where, $\lambda=12°-\tan^{-1}\left(\frac{0.2126}{2y/L}\right)$

Table 4-11 Impulse Coefficient C_u for One-Way Elements

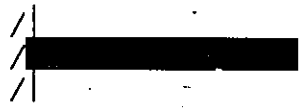
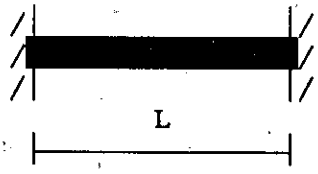
EDGE CONDITIONS	IMPULSE COEFFICIENTS C_u
CANTILEVER 	127
FIXED SUPPORTS 	510

Table 4-12 Shear Coefficients for Ultimate Shear Stress at Distance d_c from the Support for One-Way Elements (Cross Section Type II and III)

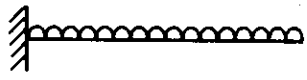
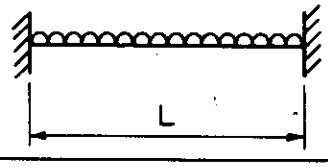
EDGE CONDITIONS	ULTIMATE SHEAR STRESS COEFFICIENTS C_d
CANTILEVER 	$2(\frac{d_c}{L})(1-\frac{d_c}{L})$
FIXED SUPPORTS 	$16(\frac{d_c}{L})(\frac{1}{2}-\frac{d_c}{L})$

Table 4-13 Shear Coefficients for Ultimate Shear Stress at Distance d_c from the Support for Two-Way Elements (Cross Section Type II and III)

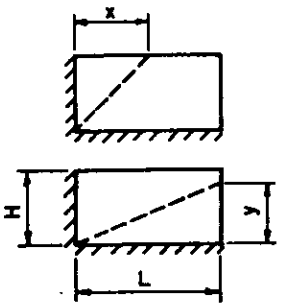
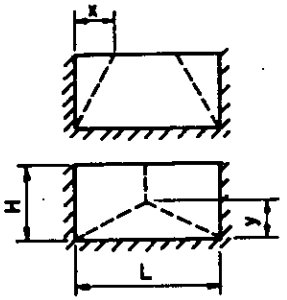
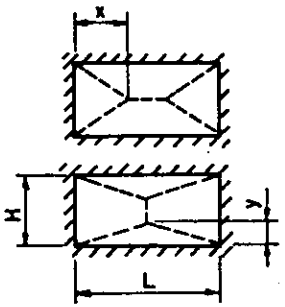
Edge conditions	Yield line location	Limits	Horisontal ultimate shear stress coefficient C_H	Limits	Vertical ultimate shear stress coefficient C_V
Two adjacent edges fixed and two edges free		$0 \le d_c/x \le \frac{1}{2}$	$\frac{30(d_c/x)(1-d_c/x)^3}{(5-4d_c/x)}$	$0 \le d_c/H \le \frac{1}{2}$	$\frac{6(d_c/H)(3+2x/L)(1-d_c/H)(2-x/L-d_cx/HL)}{(3-2x/L)(6-x/L-4d_cx/HL)}$
		$\frac{1}{2} \le d_c/x \le 1$	$5(d_c/x)(1-d_c/x)$	$\frac{1}{2} \le d_c/H \le 1$	$\frac{(d_c/H)(3+2x/L)(1-d_c/H)(2-x/L-d_cx/HL)}{(3-2x/L)(1-d_cx/HL)}$
		$0 \le d_c/L \le \frac{1}{2}$	$\frac{6(d_c/L)(3+2y/H)(1-d_c/L)(2-y/H-d_cy/LH)}{(3-2y/H)(6-y/H-d_cy/LH)}$	$0 \le d_c/y \le \frac{1}{2}$	$\frac{30(d_c/y)(1-d_c/y)^3}{(5-4d_c/y)}$
		$\frac{1}{2} \le d_c/L \le 1$	$\frac{(d_c/L)(3+2y/H)(1-d_c/L)(2-y/H-d_cy/LH)}{(3-2y/H)(1-d_cy/LH)}$	$\frac{1}{2} \le d_c/y \le 1$	$5(d_c/y)(1-d_c/y)$
Three edges fixed and one edge free		$0 \le d_c/x \le \frac{1}{2}$	$\frac{30(d_c/x)(1-d_c/x)^3}{(5-4d_c/x)}$	$0 \le d_c/H \le \frac{1}{2}$	$\frac{6(d_c/H)(3+4x/L)(1-d_c/H)(1-x/L-d_cx/HL)}{(3-4x/L)(3-x/L-4d_cx/HL)}$
		$\frac{1}{2} \le d_c/x \le 1$	$5(d_c/x)(1-d_c/x)$	$\frac{1}{2} \le d_c/H \le 1$	$\frac{2(d_c/H)(3+4x/L)(1-d_c/H)(1-x/L-d_cx/HL)}{(3-4x/L)(1-2d_cx/HL)}$
		$0 \le d_c/L \le \frac{1}{2}$	$\frac{12(d_c/L)(6-y/H)(1-2d_c/L)(2-y/H-2d_cy/LH)}{(3-2y/H)(6-y/H-8d_cy/LH)}$	$0 \le d_c/y \le \frac{1}{2}$	$\frac{30(d_c/y)(1-d_c/y)^3}{(5-4d_c/y)}$
		$\frac{1}{2} \le d_c/L \le 1$	$\frac{2(d_c/L)(6-y/H)(1-2d_c/L)(2-y/H-2d_cy/LH)}{(3-2y/H)(1-2d_cy/LH)}$	$\frac{1}{2} \le d_c/y \le 1$	$5(d_c/y)(1-d_c/y)$
Four edges fixed		$0 \le d_c/x \le \frac{1}{2}$	$\frac{30(d_c/x)(1-d_c/x)^3}{(5-4d_c/x)}$	$0 \le d_c/H \le \frac{1}{2}$	$\frac{24(d_c/H)(3-x/L)(1-2d_c/H)(1-x/L-2d_cx/HL)}{(3-4x/L)(3-x/L-8d_cx/HL)}$
		$\frac{1}{2} \le d_c/x \le 1$	$5(d_c/x)(1-d_c/x)$	$\frac{1}{2} \le d_c/H \le 1$	$\frac{8(d_c/H)(3-x/L)(1-2d_c/H)(1-x/L-2d_cx/HL)}{(3-4x/L)(1-4d_cx/HL)}$
		$0 \le d_c/L \le \frac{1}{2}$	$\frac{24(d_c/L)(3-y/H)(1-2d_c/L)(1-y/H-2d_cy/LH)}{(3-4y/H)(3-y/H-8d_cy/LH)}$	$0 \le d_c/y \le \frac{1}{2}$	$\frac{30(d_c/y)(1-d_c/y)^3}{(5-4d_c/y)}$
		$\frac{1}{2} \le d_c/L \le 1$	$\frac{8(d_c/L)(3-y/H)(1-2d_c/L)(1-y/H-2d_cy/LH)}{(3-4y/H)(1-4d_cy/LH)}$	$\frac{1}{2} \le d_c/y \le 1$	$5(d_c/y)(1-d_c/y)$

Table 4-14 Shear Coefficients for Ultimate Support Shear for One-Way Elements (Cross Section Type II and III)

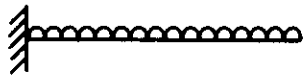
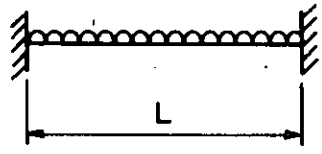
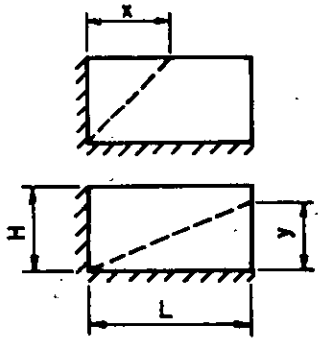
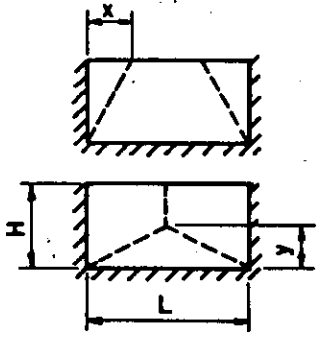
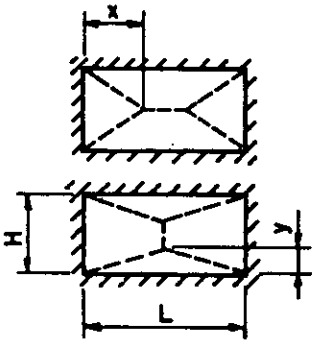
EDGE CONDITIONS	ULTIMATE SUPPORT SHEAR COEFFICIENTS C_s
CANTILEVER 	2
FIXED SUPPORTS 	8

Table 4-15 Shear Coefficients for Ultimate Support Shear for Two-Way Elements (Cross Section Type II and III)

Edge conditions	Yield line location	Horizontal ultimate support shear coefficient C_{uH}	Vertical ultimate support shear coefficient C_{uV}
Two adjacent edges fixed and two edges free		$\frac{6}{x/L}$ $\frac{6(2-y/H)(3+2y/H)}{(6-y/H)(3-2y/H)}$	$\frac{6(2-x/L)(3+2x/L)}{(6-x/L)(3-2x/L)}$ $\frac{6}{y/H}$
Three edges fixed and one edge free		$\frac{6}{x/L}$ $\frac{12(2-y/H)}{(3-2y/H)}$	$\frac{6(1-x/L)(3+4x/L)}{(3-x/L)(3-4x/L)}$ $\frac{6}{y/H}$
Four edges fixed		$\frac{6}{x/L}$ $\frac{24(1-y/H)}{(3-4y/H)}$	$\frac{24(1-x/L)}{(3-4x/L)}$ $\frac{6}{y/H}$

4-36. Composite Construction

4-36.1. General

Composite elements are composed of two concrete panels (donor and acceptor) separated by a sand-filled cavity. They have characteristics which are useful in the blast resistant design of structures located close-in to a detonation. For a large quantity of explosives, replacing a single concrete panel with a composite element can result in a considerable cost savings. It is not usually cost effective to use a composite element for smaller quantities of explosives where a single concrete panel would be three feet thick or less. Where a single concrete panel would be between three and five feet thick, a detailed cost analysis is required to determine whether or not a composite element would be more cost effective.

Composite walls are generally used as barricades to prevent propagation of explosion between large quantities of explosives. These structures are usually designed for incipient failure. Composite elements may be designed to provide higher degrees of protection, but the massive walls (greater than 5 feet thick) that make composite elements cost effective are generally not required in such cases. If the maximum support rotation is limited to 4 degrees or less, and a composite element is shown to be cost effective, single leg stirrups may be used instead of lacing reinforcement. Walls using single leg stirrups are somewhat more economical than laced walls.

Composite elements can also be useful for reducing the hazard due to direct spalling. Spalled fragments from the donor panel are trapped in the sand fill and, therefore, are of no concern. Spalling of the acceptor panel can be eliminated by maintaining the required minimum thickness and maximum density of the sand fill given in Section 4-56.2.

The mechanisms by which composite elements resist the blast pressures are (1) the strength and ductility of the concrete panels and (2) the blast attenuating ability of the sand fill. The attenuation of the blast by the sand is accomplished by (1) the increased mass it affords to the concrete portions of the wall, (2) the increased distance the blast wave must travel due to the increased wall thickness produced by the sand (dispersion of blast wave) and (3) the blast energy absorbed by the displacement and compression of the sand particles.

4-36.2. Blast Attenuation Ability of Sand Fill

The method for calculating the impulse capacity of composite elements is similar to that for single laced concrete elements except that the blast attenuating ability of the sand must be included in the calculation. The blast wave attenuation is partly due to the increased mass of the slab. When computing the impulse capacity of each concrete panel, the total effective mass includes both the mass of the concrete and the mass of one-half of the sand. This increased mass is taken into account by multiplying the impulse coefficients for spalled sections, by

$$\left[\frac{(T_c + d_c)}{2} + \left(\frac{w_s}{w_c}\right)\left(\frac{T_s}{2}\right) \right] / d_c \qquad 4\text{-}123$$

or for unspalled sections by

$$\left[T_c + \frac{w_s}{w_c}\left(\frac{T_s}{2}\right) \right] / T_c \qquad 4\text{-}124$$

where

w_s = weight density of sand

w_c = weight density of concrete

T_s = thickness of sand fill

The attenuating ability of the sand due to blast wave dispersion and energy absorption is a function of the thickness and density of the sand, the impulse capacity of the concrete panels and the quantity of explosive. Figures 4-57 and 4-58 have been developed to predict the impulse capacity of the concrete element for a sand density equal to 85 pcf and 100 pcf, respectively. These figures are based on identical donor and acceptor panels. The effect of the quantity of explosive is taken into account through the use of "scaled" parameters which are defined as follows:

$$\bar{T}_c = \frac{T_c}{12W^{1/3}} \qquad 4\text{-}125$$

$$\bar{T}_s = \frac{T_s}{12W^{1/3}} \qquad 4\text{-}126$$

$$\bar{i}_{ba} = \frac{i_{ba}}{W^{1/3}} \qquad 4\text{-}127$$

$$\bar{i}_a = \frac{i_a}{W^{1/3}} \qquad 4\text{-}128$$

where

$\bar{T}_c$ = scaled thickness of concrete panel

W = weight of explosive charge

$\bar{T}_s$ = scaled thickness of sand

$\bar{i}_{ba}$ = scaled blast impulse which can be resisted by acceptor panel

i_{ba} = blast impulse capacity of acceptor panel

$\bar{i}_a$ = sum of scaled blast impulse resisted by the acceptor panel and the scaled blast impulse absorbed by the sand

i_a = sum of blast impulse capacity of the acceptor panel and the blast impulse absorbed by the sand

Explosion response slab tests have indicated that the density of the sand fill affects the amount of blast energy absorbed by the sand displacement, i.e., the higher the initial sand density, the smaller amount of blast energy absorbed. Also, it was observed in the above response tests that for a unit weight of sand equal to 100 pcf, the deflection of the donor panel is approximately equal in magnitude to the deflection of the acceptor panel. On the other hand, with a unit weight of sand fill equal to 85 pcf, it was observed that the deflection of the donor panel usually was significantly larger than that of the acceptor panel. This latter phenomenon was caused by the fact that, with the lower density, the sand had more voids and, therefore, more room for movement of the sand particles. This sand movement in turn permitted larger displacements of the donor panel before the near solid state of the sand occurred.

Based on the above information, it can be seen that if near equal displacement of the donor and receiver panels are desired, then a unit weight of sand fill equal to 100 pcf should be used. A variation of the displacement of donor and receiver panels can be achieved using a unit weight of sand equal to 85 pcf, but the actual variation cannot be predicted.

Since the impulse capacity of composite elements is a function of the density of the sand, it is important to prevent the sand from compacting due to its own weight and/or water drainage. Several possible methods for maintaining the proper sand density are discussed in subsequent sections concerned with construction details of composite elements.

4-36.3. Procedure for Design of Composite Elements

The design of composite elements is a trial and error procedure. By using Figures 4-56 and 4-57 and the impulse coefficients of previous sections, the calculations are greatly simplified. The donor and acceptor slabs are identical making it necessary to design only one wall. The depth of the sand fill is usually equal to the total thickness of the two concrete panels. Using the procedures in the previous sections, each panel is designed to have a blast impulse capacity slightly less than half the required. This includes the increase in capacity due to the additional mass of the sand (Equations 4-123 and 4-124). It should be noted that the design is based on the assumption that both panels will attain the same deflection. If the density of the sand fill is 85 pcf, this will not be true. The donor panel will probably have a larger deflection than the acceptor panel. Since the actual deflection of each panel cannot be predicted, it must be assumed that the design deflection is an average of the two.

With the blast impulse capacity of the two concrete panels, Figure 4-56 or 4-57 is used to determine the total blast capacity of the composite element. The following procedure illustrates the use of these figures.

1. Using the given charge weight calculate the scaled thickness of the concrete panel and the sand, $\bar{T}_c$ and $\bar{T}_s$, respectively.

2. Calculate the scaled impulse capacity which can be resisted by the donor panel $\bar{i}_{bd}$ and the acceptor panel $\bar{i}_{ba}$.

3. Using either Figure 4-56 or 4-57

   a) Enter the ordinate at value of $\bar{i}_{ba}$.

   b) Proceed horizontally from $\bar{i}_{ba}$ to $\bar{T}_s$.

   c) Proceed vertically from $\bar{T}_s$ to $\bar{T}_c$.

   d) Proceed horizontally from $\bar{T}_c$ to $\bar{i}_a$ (the sum of the scaled unit blast impulse resisted by the acceptor panel and the scaled unit impulse absorbed by the sand).

4. Calculate the summations of $\bar{i}_{bd}$ and $\bar{i}_a$ to get the total unit impulse which can be resisted by the composite wall $\bar{i}_{bt}$.

5. Determine the scaled unit blast impulse $\bar{i}_b$ acting on the composite element.

6. Compare $\bar{i}_{bt}$ and $\bar{i}_b$. If the blast impulse which can be resisted by the composite element is not greater than or equal to the impulse produced by the blast then the impulse capacity of the walls should be increased and/or the thickness of the sand increased.

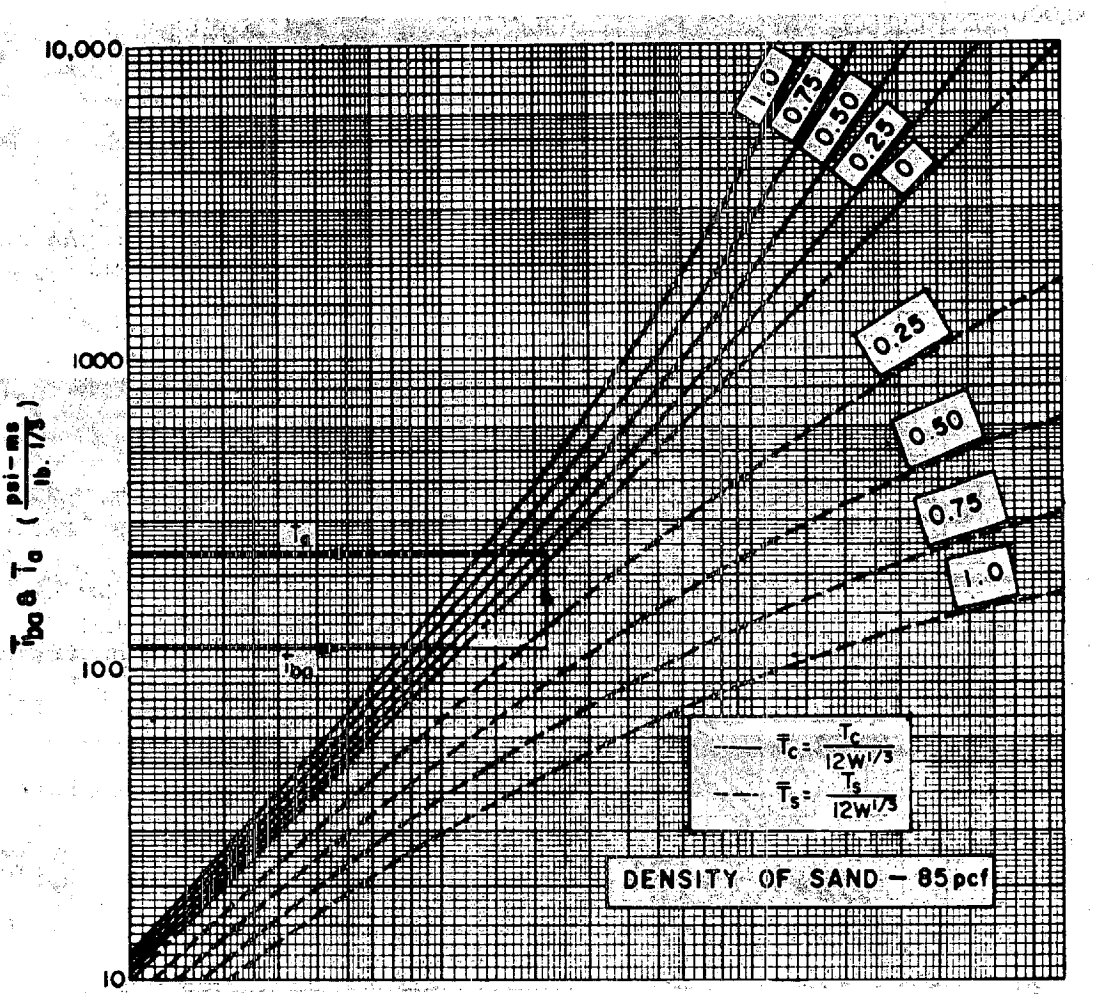


Figure 4-57 Attenuation of blast impulse in sand and concrete, w_s= 85 pcf

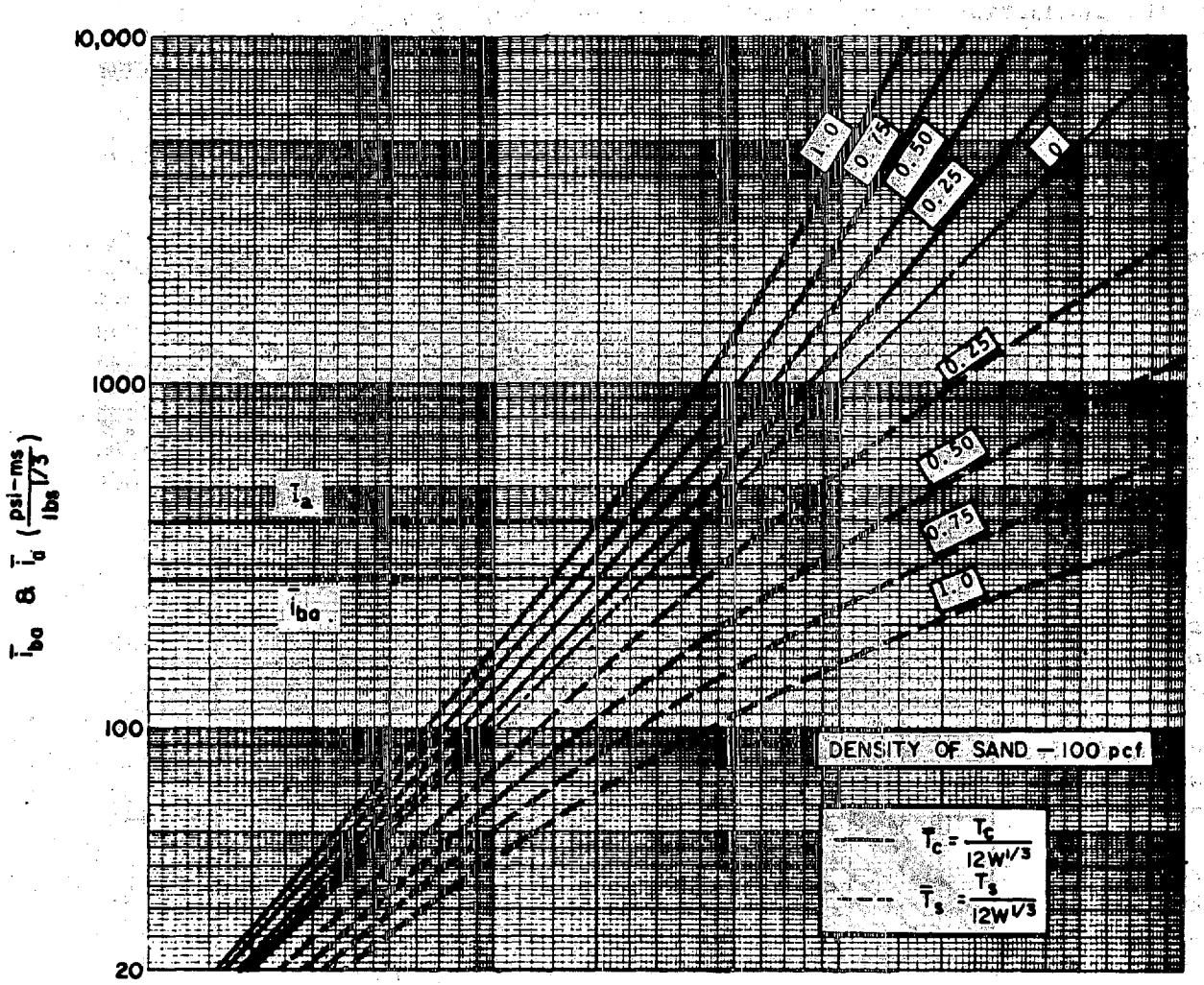


Figure 4-58 Attenuation of blast impulse in sand and concrete, w_s= 100 pcf

ULTIMATE DYNAMIC STRENGTH OF REINFORCED CONCRETE BEAMS

4-37 Introduction

Blast resistant concrete buildings subjected to external blast pressures are generally shear wall structures rather than rigid frame structures. Shear wall structures respond to lateral loads in a somewhat different manner than rigid frame structures; the basic difference being the manner in which the lateral loads are transferred to the foundation. In rigid frame structures the lateral loads are transmitted to the foundation through bending of the columns. Whereas, in shear wall structures, the lateral forces are transmitted to the foundation through both bending and shearing action of the shear walls. Shear walls are inherently strong and will resist large lateral forces. Consequently, shear wall structures are inherently capable of resisting blast loads and can be designed to resist substantially large blast loads whereas rigid frame structures cannot be economically designed to resist significant blast loads.

In shear wall structures, beams and columns are usually provided between shear walls to carry the vertical loads including blast loads on the roof and not to transmit lateral loads to the foundation. For example, blast loads applied to the front wall of a two-story shear wall structure are transmitted through the roof and intermediate floor slabs to the shear walls (perpendicular walls) and thus to the foundation. The front wall spans vertically between the foundation, the floor, and the roof slab. The upper floor and roof slabs act as deep beams, and in turn, transmit the front wall reactions to the shear walls. The roof and floor beams are not subjected to significant axial loads due to the diaphragm action of the slabs.

The design of beams as presented in the following sections applies to beams in shear wall type structures rather than rigid frame structures. The design procedure presented is for transverse loads only; axial loads are not considered. However, the procedure includes the design for torsion. The design of beams is similar to the design of slabs as described in sections 4-13 through 4-18. The most significant and yet not very important difference in the design procedure is that in the case of a slab the calculations are based on a unit area, whereas, for a beam, they are based on a unit length of beam.

Beams may be designed to attain limited or large deflections in the same manner as non-laced slabs. However, unlike non-laced slabs which in some cases do not require shear reinforcement (single leg stirrups), shear reinforcement in the form of closed ties must always be provided in beams. Under flexural action, a beam may attain deflections corresponding to 2 degrees support rotation with a type I cross-section to provide the ultimate moment capacity. The flexural action may be extended to 4 degrees support rotation if equal tension and compression reinforcement is furnished. A type II or III cross-section provides the ultimate moment capacity and the required closed ties restrain the compression reinforcement. If sufficient lateral restraint is provided, the beam may attain 8 degrees support rotation under tension membrane action. The above support rotations are incipient failure conditions for the structural configurations described.

Beams are primary support members and, as such, are generally not permitted to attain large plastic deformations. For personnel protection, the maximum

deflection is limited to a support rotation of 2.0 degrees. Structures intended to protect equipment and/or explosives may be designed for deflections up to incipient failure conditions.

Beams are generally employed in structures designed to resist the effects associated with far range explosions. In these structures, beams are usually used in the roof as primary support members and as secondary support members such as pilasters around door openings. To a far lesser extent, beams are designed to resist the effects of close-in detonations in containment type structures. In these cases, they are generally used as secondary support members such as pilasters around door openings. Large tensile forces are induced in containment type structures and, therefore, these structures lend themselves to tension membrane action when the applicable design criteria permits large deformations.

The interrelationship between the various parameters involved in the design of beams is readily described with the use of the idealized resistance-deflection curve shown in Figure 4-59.

4-38. Ultimate Moment Capacity

4-38.1. Tension Reinforcement Only

The ultimate dynamic resisting moment Mu of a rectangular beam section of width b with tension reinforcement only (type I) is given by:

$$M_u = A_s f_{ds} (d - a/2) \qquad 4\text{-}129$$

and:

$$a = \frac{A_s f_{ds}}{0.85b f'_{dc}} \qquad 4\text{-}130$$

where:

M_u = ultimate moment capacity

A_s = total area of tension reinforcement within the beam

f_{ds} = dynamic design stress of reinforcement

d = distance from extreme compression fiber to centroid of tension reinforcement

a = depth of equivalent rectangular stress block

b = width of beam

f'_{dc} = dynamic ultimate compressive strength of concrete

The reinforcement ratio p is defined as:

$$p = \frac{A_s}{bd} \qquad 4\text{-}131$$

and to insure against sudden compression failures, the reinforcement ratio p must not exceed 0.75 of the ratio p_b which produces balanced conditions at ultimate strength and is given by:

$$p_b = \left[\frac{0.85K_1 f'_{dc}}{f_{ds}} \right] \left[\frac{87,000}{87,000 + f_{ds}} \right] \qquad 4\text{-}132$$

where:

K_1 = 0.85 for f'_{dc} up to 4,000 psi and is reduced by 0.05 for each 1,000 psi in excess of 4,000 psi

4-38.2. Tension and Compression Reinforcement

The ultimate dynamic resisting moment M_u of a rectangular beam section of width b with compression reinforcement is given by:

$$M_u = (A_s - A'_s) f_{ds} (d - a/2) + A'_s f_{ds} (d - d') \qquad 4\text{-}133$$

and:

$$a = \frac{(A_s - A'_s) f_{ds}}{0.85 b f'_{dc}} \qquad 4\text{-}134$$

where:

A'_s = total area of compression reinforcement within the beam

d' = distance from extreme compression fiber to centroid of compression reinforcement

The compression reinforcement ratio p' is defined as:

$$p' = \frac{A'_s}{bd} \qquad 4\text{-}135$$

Equation 4-133 is valid only when the compression reinforcement yields at ultimate strength. This condition is satisfied when:

$$p - p' \leq 0.85 K_1 \left[\frac{f'_{dc} d'}{f_{ds} d} \right] \left[\frac{87,000}{87,000 - f_{ds}} \right] \qquad 4\text{-}136$$

In addition, the quantity p-p' must not exceed 0.75 of the value of p_b given in Equation 4-132 in order to insure against sudden compression failures. If p-p' is less than the value given by Equation 4-136, the ultimate resisting moment should not exceed the value given by Equation 4-129.

For the design of concrete beams subjected to far range blast loads which are to attain support rotations of 2 degrees or less, it is recommended that the ultimate resisting moment be computed using Equation 4-129 even though a

considerable amount of compression reinforcement is required to resist rebound loads. It should be noted that a large amount of compression steel that does not yield due to the linear strain variation across the depth of the section, has a negligible effect on the total capacity.

For type II or III cross-sections, the ultimate resisting moment M_u of a rectangular beam section of width b is given by:

$$M_u = A_s f_{ds} d_c \qquad 4\text{-}137$$

where

A_s = area of tension or compression reinforcement within the width b

d_c = distance between the centroids of the compression and the tension reinforcement

The above moment capacity can only be obtained when the areas of the tension and compression reinforcement are equal. In addition, the support rotation must be greater than 2 degrees except for close-in designs where direct spalling may occur and result in a type III.

4-38.3. Minimum Flexural Reinforcement

To insure proper structural behavior under both conventional and blast loadings, a minimum amount of flexural reinforcement is required. The minimum reinforcement required for beams is somewhat greater than that required for slabs since an overload load in a slab would be distributed laterally and a sudden failure will be less likely. The minimum required quantity of reinforcement is given by:

$$p = 200/f_y \qquad 4\text{-}138$$

which, for 60,000 psi yield strength steel, is equal to a reinforcement ratio of 0.0033. This minimum reinforcement ratio applies to the tension steel at mid-span of simply supported beams and to the tension steel at the supports and mid-span of fixed-end beams.

Concrete beams with tension reinforcement only are not permitted. Compression reinforcement, at least equal to one-half the required tension reinforcement, must be provided. This reinforcement is required to resist the ever present rebound forces. Depending upon the magnitude of these rebound forces, the required compression reinforcement may equal the tension reinforcement.

4-39. Ultimate Shear (Diagonal Tension) Capacity

4-39.1.. Ultimate Shear Stress

The nominal shear stress vu, as a measure of diagonal tension, is computed from:

$$v_u = \frac{V_u}{bd} \qquad 4\text{-}139$$

where:

v_u = nominal shear stress

V_u = total shear at critical section

The critical section is taken at a distance d from the face of the support for those members that cause compression in their supports. The shear at sections between the face of the support and the section d therefrom need not be considered critical. For those members that cause tension in their supports, the critical section is at the face of the supports.

4-39.2. Shear Capacity of Unreinforced Concrete

The shear stress permitted on an unreinforced web of a beam subjected to flexure only is limited to:

$$v_c = \left[1.9\ f'_{dc}{}^{1/2} + 2{,}500\ p\right] \leq 3.5\ f'_{dc}{}^{1/2} \qquad 4\text{-}140$$

where:

v_c = maximum shear capacity of an unreinforced web

p = reinforcement ratio of the tension reinforcement at the support

4-39.3. Design of Shear Reinforcement

Whenever the nominal shear stress vu exceeds the shear capacity vc of the concrete, shear reinforcement must be provided to carry the excess. Closed ties placed perpendicular to the flexural reinforcement must be used to furnish the additional shear capacity. Open stirrups, either single or double leg, are not permitted. The required area of shear reinforcement is calculated using:

$$A_v = \left[\frac{(v_u - v_c)\ b\ s_s}{\phi\ f_{dy}}\right] \qquad 4\text{-}141$$

where:

A_v = total area of stirrups

$v_u - v_c$ = excess shear stress

s_s = spacing of stirrups in the direction parallel to the longitudinal reinforcement

ϕ = capacity reduction factor equal to 0.85

4-39.4. Minimum Shear Reinforcement

In order to insure the full development of the flexural reinforcement in a beam, a premature shear failure must be prevented. The following limitations must be considered in the design of closed ties:

1. The design shear stress (excess shear stress $v_u - v_c$) used in Equation 4-140 shall be equal to or greater than the shear

capacity of unreinforced concrete v_c as obtained from equation 4-139.

2. The nominal shear stress v_u must not exceed 10 $(f'_{dc})^{1/2}$.

3. The area A_v of closed ties should not be less than $0.0015\ bs_s$.

4. The required area A_v of closed ties shall be determined at the critical section and this quantity and spacing of reinforcement shall be used throughout the entire member.

5. The maximum spacing of closed ties is limited to d/2 when $v_u - v_c$ is less than $4\ (f'_{dc})^{1/2}$ or 24 inches, whichever is smaller. When $v_u - v_c$ is greater than $4\ (f'_{dc})^{1/2}$ the maximum spacing is limited to d/4.

4-40. Direct Shear

Direct shear failure of a member is characterized by the rapid propagation of a vertical crack through the depth of the member. This crack is usually located at the supports where the maximum shear stresses occur. Failure of this type is possible even in members reinforced for diagonal tension.

Diagonal bars are required at supports to prevent direct shear failure: when the design support rotation exceeds 2° (unless the beam is simply supported), when the design support rotation is ≤ 2° but the direct shear capacity of the concrete is insufficient, or when the section is in tension. Diagonal reinforcement consists of inclined bars which extend from the support into the beam.

Diagonal bars are not typically recommended in beams. Therefore, beams should be designed for small rotations and with an adequate cross-sectional area for the direct shear capacity of the concrete, V_d, to exceed the ultimate direct shear force, V_s.

If the design support rotation, θ, is less than or equal to 2° ($\theta \leq 2°$), or if the section, with any rotation θ, is simply supported (total moment capacity of adjoining elements at the support must be significantly less than the moment capacity of the section being checked for direct shear), then the ultimate direct shear force, V_d, that can be resisted by the concrete in a slab is given by Equation 4-30.

If the design support rotation, θ, is greater than 2° ($\theta > 2°$), or if a section (with any support rotation) is in net tension, then the ultimate direct shear capacity of the concrete, V_d, is zero and diagonal bars are required to take all direct shear.

If diagonal bars must be used, the required cross-sectional area is:

$$A_d = (V_s b - V_d)/(f_{ds}\sin(\alpha)) \qquad 4\text{-}142$$

where:

$V_d = 0.18\ f'_{dc}\ bd.$ ($\theta \leq 2°$ or simple supports),

or $V_d = 0$ ($\theta > 2°$ or section in tension).

and A_d = total area of diagonal bars at the support within a width b

V_s = shear at the support of unit width b

α = angle formed by the plane of the diagonal reinforcement and the longitudinal reinforcement.

4-41. Ultimate Torsion Capacity

4-41.1. General

In addition to the flexural effects considered above, concrete beams may be subjected to torsional moments. Torsion rarely occurs alone in reinforced concrete beams. It is present more often in combination with transverse shear and bending. Torsion may be a primary influence but more frequently it is a secondary effect. If neglected, torsional stresses can cause distress or failure.

Torsion is encountered in beams that are unsymmetrically loaded. Beams are subject to twist if the slabs on each side are not the same span or if they have different loads. Severe torsion will result on beams that are essentially loaded from one side. This condition exists for beams around an opening in a roof slab and for pilasters around a door opening.

The design for torsion presented in this Section is limited to rectangular sections. For a beam-slab system subjected to conventional loading conditions, a portion of the slab will assist the beam in resisting torsional moments. However, in blast resistant design, a plastic hinge is usually formed in the slab at the beam and, consequently, the slab is not effective in resisting torsional moments.

4-41.2. Ultimate Torsional Stress

The nominal torsional stress in a rectangular beam in the vertical direction (along h) is given by:

$$v_{(tu)V} = \frac{3T_u}{b^2 h} \qquad 4\text{-}143$$

and the nominal torsional stress in the horizontal direction (along b) is given by:

$$v_{(tu)H} = \frac{3\,T_u}{bh^2} \qquad 4\text{-}144$$

where:

v_{tu} = nominal torsional stress

T_u = total torsional moment at critical section

b = width of beam

h = overall depth of beam

The critical section for torsion is taken at the same location as diagonal tension. It should be noted that the torsion stress in the vertical face of the beam (along h) is maximum when b is less than h whereas the torsion stress along the horizontal face of the beam (along b) is maximum when b is greater than h.

4-41.3 Capacity of Unreinforced Concrete for Combined Shear and Torsion

For a beam subjected to combined shear (diagonal tension) and torsion, the shear stress and the torsion stress permitted on an unreinforced section are reduced by the presence of the other. The shear stress permitted on an unreinforced web is limited to:

$$v_c = \frac{2\,(f'_{dc})^{1/2}}{\left[1 + \left[\frac{v_{tu}}{1.2v_u}\right]^2\right]^{1/2}} \qquad 4\text{-}145$$

while the torsion stress taken by the concrete of the same section is limited to:

$$v_{tc} = \frac{2.4\,(f'_{dc})^{1/2}}{\left[1 + \left[\frac{1.2v_u}{v_{tu}}\right]^2\right]^{1/2}} \qquad 4\text{-}146$$

where:

v_c = maximum shear capacity of an unreinforced web

v_{tc} = maximum torsion capacity of an unreinforced web

v_u = nominal shear stress

v_{tu} = nominal torsion stress in the direction of v_u

It should be noted that the shear stress permitted on an unreinforced web of a beam subjected to shear only is given by Equation 4-139. Whereas, the torsion stress permitted on an unreinforced web of a beam subjected to torsion only is given by:

$$v_{tc} = 2.4\,(f'_{dc})^{1/2} \qquad 4\text{-}147$$

Whenever the nominal shear stress vu exceeds the shear capacity vc of the concrete, shear reinforcement must be provided to carry the excess. This quantity of shear reinforcement is calculated using Equation 4-140 except the

value of vc shall be obtained from Equation 4-144 which includes the effects of torsion.

4-41.4. Design of Torsion Reinforcement

4-41.4.1. Design of Closed Ties

Whenever the nominal torsion stress vtu exceeds the maximum torsion capacity of the concrete, torsion reinforcement in the shape of closed ties, shall be provided to carry the excess. The required area of the vertical leg of the closed ties is given by:

$$A_{(t)V} = \frac{(v_{(tu)V} - v_{tc}) \; b^2 hs}{3\phi \; \alpha_t \; b_t \; h_t \; f_{dy}} \qquad 4\text{-}148$$

and the required area of the horizontal leg of the closed ties is given by:

$$A_{(t)H} = \frac{(v_{(tu)H} - v_{tc}) \; bh^2 s}{3\phi \; \alpha_t \; b_t \; h_t \; f_{dy}} \qquad 4\text{-}149$$

in which:

$$\alpha_t = 0.66 + 0.33 \; (h_t/b_t) \leq 1.50 \text{ for } h_t \geq b_t \qquad 4\text{-}150a$$

$$\alpha_t = 0.66 + 0.33 \; (b_t/h_t) \leq 1.50 \text{ for } h_t \geq b_t \qquad 4\text{-}150b$$

where:

A_t = area of one leg of a closed stirrup resisting torsion within a distance s

s = spacing of torsion reinforcement in a direction parallel to the longitudinal reinforcement

ϕ = capacity reduction factor equal to 0.85

b_t = center-to-center dimension of a closed rectangular tie along b

h_t = center-to-center dimension of a closed rectangular tie along h

The size of the closed tie provided to resist torsion must be the greater of that required for the vertical (along h) and horizontal (along b) directions. For the case of b less than h, the torsion stress in the vertical direction is maximum and the horizontal direction need not be considered. However, for b greater than h, the torsion stress in the horizontal direction is maximum. In this case the required At for the vertical and horizontal directions must be obtained and the greater value used to select the closed stirrup. It should be noted that in the horizontal direction a beam, in shear wall type structures, is not subjected to lateral shear (slab resists lateral loads) and the

value of v_{tc} used in Equation 4-148 is calculated from Equation 4-146 which does not include the effect of shear.

When torsion reinforcement is required, it must be provided in addition to reinforcement required to resist shear. The closed ties required for torsion may be combined with those required for shear. However, the area furnished must be the sum of the individually required areas and the most restrictive requirements for spacing and placement must be met. Figure 4-60 shows several ways to arrange web reinforcement. For low torsion and shear, it is convenient to combine shear and torsional web reinforcement in the form of a single closed stirrup whose area is equal to $A_t + A_v/2$. For high torsion and shear, it would be economical to provide torsional and shear reinforcement separately. Torsional web reinforcement consists of closed stirrups along the periphery, while the shear web reinforcement is in the form of closed stirrups distributed along the width of the member. For very high torsion, two closed stirrups along the periphery may be used. The combined area of the stirrups must equal At and they must be located as close as possible to each other, i.e., the minimum separation of the flexural reinforcement. In computing the required area of stirrups using Equation 4-147, the value of bt should be equal to the average center-to-center dimension of the closed stirrups as shown in Figure 4-60.

4-41.4.2. Design of Longitudinal Reinforcement

In addition to closed stirrups, longitudinal reinforcement must be provided to resist the longitudinal tension caused by the torsion. The required area of longitudinal bars Al shall be computed by:

$$A_l = 2A_t \left[\frac{b_t + h_t}{s}\right] \qquad 4\text{-}151a$$

or by:

$$A_l = \left[\frac{400bs}{f_{dy}} \frac{v_{tu}}{v_{tu} + v_u} - 2A_t\right] \left[\frac{b_t + h_t}{s}\right] \qquad 4\text{-}151b$$

whichever is greater. When using Equation 4-151b, the value of $2A_t$ shall be greater than or equal to $50\ bs/f_{dy}$. It should be noted that Equation 4-151a requires the volume of longitudinal reinforcement to be equal to the volume of the web reinforcement required by Equation 4-147 or 4-148 unless a greater amount of longitudinal reinforcement is required to satisfy the minimum requirements of Equation 4-151b.

Longitudinal bars should be uniformly distributed around the perimeter of the cross section with a spacing not exceeding 12 inches. At least one longitudinal bar should be placed in each corner of the closed stirrups. A typical arrangement of longitudinal bars is shown in Figure 4-60 where torsional longitudinal bars that are located in the flexural tension zone and flexural compression zone may be combined with the flexural steel.

The addition of torsional and flexural longitudinal reinforcement in the flexural compression zone is not reasonable. It is illogical to add torsional steel that is in tension to the flexural steel that is in compression. This method of adding torsional steel to flexural steel regardless of whether the latter is in tension or in compression is adopted purely for simplicity. For blast resistant design, flexural reinforcement added but not included in the calculation of the ultimate resistance could cause a shear failure. The actual ultimate resistance could be significantly greater than the calculated ultimate resistance for which the shear reinforcement is provided. Therefore, torsional longitudinal reinforcement cannot be indiscriminately placed but rather must be placed only where required.

In the design of a beam subjected to both flexure and torsion, torsional longitudinal reinforcement is first assumed to be uniformly distributed around the perimeter of the beam. The reinforcement required along the vertical face of the beam will always be provided. However, in the flexural compression zone, the reinforcement that should be used is the greater of the flexural compression steel (rebound reinforcement) or the torsional steel. In terms of the typical arrangement of reinforcement in Figure 4-60, either A'_s or A_l is used, whichever is greater, as the design steel area in the flexural compression zone. For the tension zone at the mid span of a uniformly loaded beam the torsional stress is zero and torsional longitudinal reinforcement is not added. Conversely, the tension zone at the supports is the location of peak torsional stresses and longitudinal torsional reinforcement must be added to the flexural steel.

4-41.5. Minimum Torsion Reinforcement

In the design of closed ties for beams subjected to both shear and torsion, the following limitations must be considered:

1. The minimum quantity of closed ties provided in a beam subjected to both shear and torsion shall not be less than that required for a beam subjected to shear alone.

2. The maximum nominal shear stress v_u must not exceed $10\ (f'_{dc})^{1/2}$

3. The maximum nominal torsion stress v_{tu} shall not exceed

$$\frac{12\ (f'_{dc})^{1/2}}{\left[1 + \left[(1.2\ v_u)\ /\ (v_{tu})\right]^2\right]^{1/2}}$$

4. The required spacing of closed stirrups shall not exceed $(b_t + h_t)/4$ or 12 inches nor the maximum spacing required for closed ties in beams subjected to shear only.

5. The required areas A_v and A_t shall be determined at the critical section and this quantity and spacing of reinforcement shall be used throughout the entire beam.

6. To insure the full development of the ties, they shall be closed using 135-degree hooks.

4-42. Flexural Design

4-42.1. Introduction

The flexural design of beams is very similar to the design of non-laced concrete slabs. The main difference is that in the case of a slab the calculations are performed based on a unit area, whereas for a beam, they are based on a unit length of beam. In addition, since beams are one-way members, the distribution of mutually perpendicular reinforcement does not have to be considered.

4-42.2. Small Deflections

The design range for small deflections may be divided into two regions; beams with support rotations less than 2 degrees (limited deflections) and support rotations between 2 and 4 degrees. Except for the type of cross-section available to resist moment, the design procedure is the same.

A concrete section and reinforcement are assumed. Using the equations of section 4-38 (Equation 4-129 for type I cross-sections, Equation 4-137 for type II and III cross-sections) the moment capacities of the trial section is computed. The moment capacities are required to calculate the ultimate unit resistance r_u and the equivalent elastic deflection X_E. These parameters, along with the natural period of vibration T_n, define the equivalent single-degree-of-freedom system of the beam, and are discussed in detail in Chapter 3.

A dynamic analysis (see section 4-43) is performed to check if the beam meets the allowable deflection criteria. Finally, the assumed section is designed for shear and torsion, if applicable. If the beam does not meet the allowable response criteria, the required shear reinforcement is excessive, or the beam is overdesigned, a new concrete section is selected and the entire design procedure is repeated.

4-42.3. Large Deflections

4-42.3.1. Introduction

Design of reinforced concrete beams for support rotations greater than 4 degrees depends on their ability to act as a tensile membrane. Lateral restraint of the beam must be provided to achieve this action. Thus, if lateral restraint does not exist, tensile membrane action is not developed and the beam reaches incipient failure at 4 degrees support rotation. However, if lateral restraint exists, deflection of the beam induces membrane action and axial forces. These axial tension forces provide the means for the beam to continue to develop substantial resistance up to maximum support rotations of approximately 12 degrees.

4-42.3.2. Lateral Restraint

Adequate lateral restraint of the reinforcement is mandatory in order for the beam to develop and the designer to utilize the benefits of tensile membrane

behavior. Sufficient lateral restraint is provided if the reinforcement is adequately anchored into adjacent supporting members capable of resisting the axial forces induced by tensile membrane action.

Tensile membrane behavior should not be considered in the design process unless full external lateral restraint is provided. Full lateral restraint means that adjacent members can effectively resist a total lateral force equivalent to the ultimate strength of all continuous reinforcement in the beam. This external resistance is more difficult to realize for beams than for slabs due to the concentration of the end reactions.

4-42.3.3. Resistance - Deflection Curve

The resistance-deflection curve for a beam is the same as that for a slab which is shown in Figure 4-18. The initial portion of the curve is primarily due to flexural action (increased capacity due to possible compression forces is not shown). At 4 degrees support rotation, the beam loses flexural capacity. However, due to the presence of continuous reinforcement and adequate lateral restraint, tensile membrane action developed. The resistance due to this action increases with increasing deflection up to incipient failure at approximately 12 degrees support rotation.

In order to simplify the design calculations, the resistance is assumed to be due to flexural action throughout the entire range of behavior (same procedure for slab calculations). To approximate the energy absorbed under the actual resistance-deflection curve, the maximum support of the idealized is limited to 8 degrees. Design for this deflection would produce incipient failure conditions.

For the design of a laterally restrained beam for 8 degrees support rotation, a type III cross-section is used to compute the ultimate moment capacity of the section as well as to provide the mass to resist motion. The stress in the reinforcement f_{ds} would be equal to that corresponding to support rotations $5 \leq \theta_m \leq 12$ given in Table 4-2. At every section throughout the beam, the tension and compression reinforcement must be continuous in order to develop the tensile membrane action discussed below.

4-42.3.4. Ultimate Tensile Membrane Capacity

As can be seen in Figure 4-18, tensile membrane resistance is a function of deflection. It is also a function of the span length and the amount of continuous reinforcement. The tensile membrane resistance rt of a laterally restrained beam at a deflection X is expressed as:

$$r_T = X \left[\frac{8T}{L^2} \right] \qquad 4\text{-}152$$

in which

$$T = A_{sc} f_{dy} \qquad 4\text{-}153$$

where

r_t = tensile membrane resistance

X = deflection of the beam

T = force in the continuous reinforcement

L = clear span

A_{sc} = total area of continuous reinforcement

Even though the capacity of a laterally restrained beam is based on flexural action, adequate tensile membrane capacity must be provided, that is, sufficient continuous reinforcement must be provided so that the tensile membrane resistance r_t corresponding to 8 degrees support rotation must be greater than the flexural resistance r_u. The deflection is computed as a function of the plastic hinge locations. The force in the continuous reinforcement is calculated using the dynamic design stress f_{ds} corresponding to 8 degrees support rotation (Table 4-2).

4-42.3.5. Flexural Design

Since the actual tensile membrane resistance-deflection curve is replaced with an equivalent flexural curve, the design of a beam for large deflections is greatly simplified. The design is performed in a similar manner as for small deflections. However, sufficient continuous reinforcement must be provided to develop the required tensile membrane resistance. This reinforcement must be fully anchored in the lateral supports. Care must be taken to ensure that the lateral supports are capable of resisting the lateral force T as given in Equation 4-153.

4-43. Dynamic Analysis

4-43.1. Design for Shock Load

When a concrete slab supported by beams is subjected to a blast load, the slab and beams act together to resist the load. The beam-slab system is actually a two-mass system and should be treated as such. However, a reasonable design can be achieved by considering the slab and beams separately. That is, the slab and beams are transformed into single-degree-of-freedom systems completely independent of each other and are analyzed separately. The dynamic analysis of slabs is treated extensively in previous sections.

The equivalent single-degree-of-freedom system of any structural element is defined in terms of its ultimate unit resistance, r_u, equivalent elastic deflection X_E and natural period of vibration T_N. The ultimate unit resistance is obtained from the table for one-way elements in Chapter 3 for the moment capacity given above. The procedures and parameters necessary to obtain the equivalent elastic deflection and natural period are also obtained from Chapter 3.

Chapter 2 describes procedures for determining the dynamic load which is defined by its peak value P and duration T. For the ratios P/r_u and T/T_N the ductility ratio X_m/X_E and t_m/T can be obtained from the response charts of Chapter 3. These values X_m, which is the maximum deflection, and t_m, the time to reach the maximum deflection define the dynamic response of the beam.

A beam is designed to resist the blast load acting over the tributary area supported by the beam. Therefore, the peak value of the blast load P is the product of the unit peak blast pressure times the spacing of the beams, and has the unit of pounds per inch.

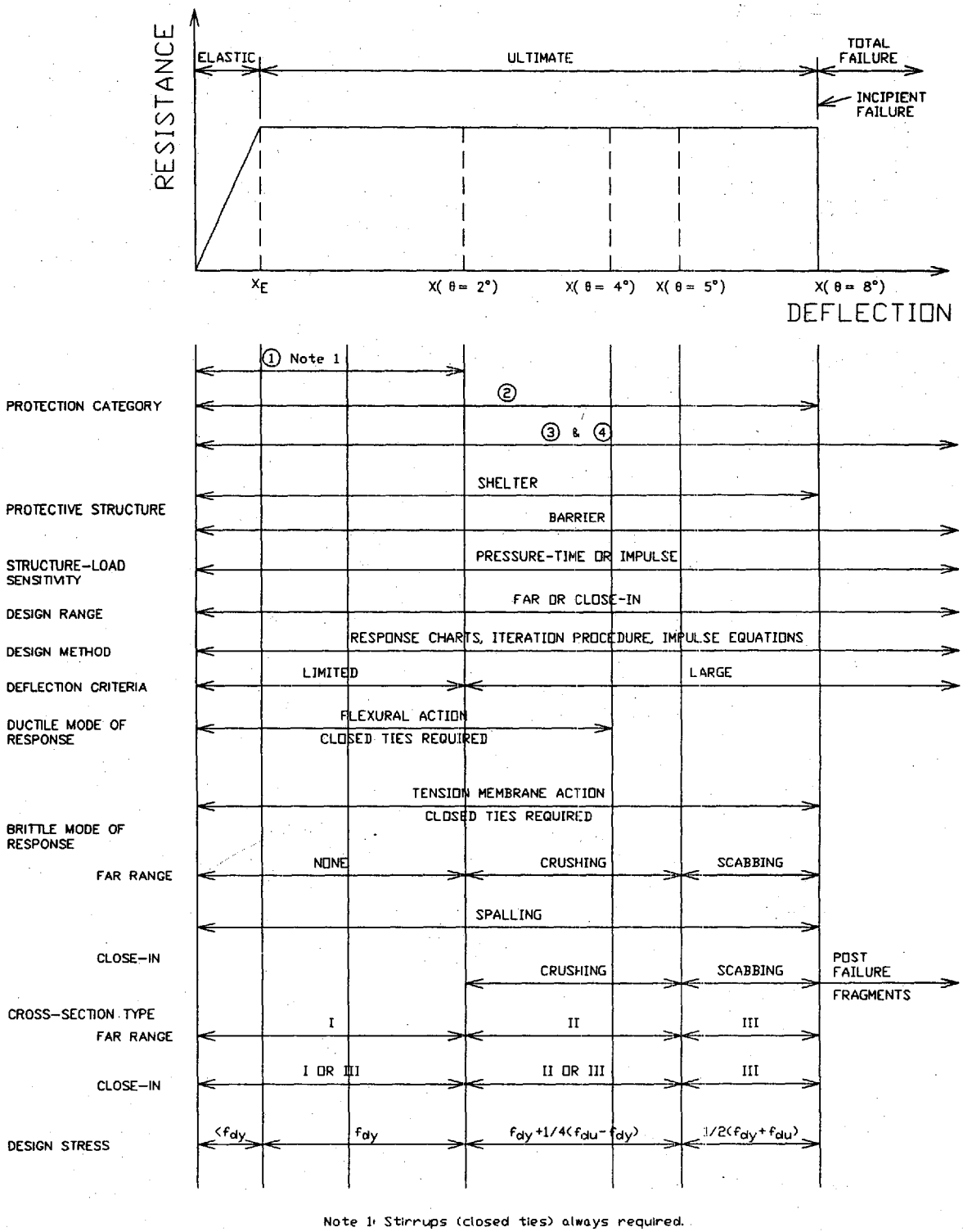
In addition to the short term effect of the blast load, a beam must be able to withstand the long term effect of the resistance of the element(s) being supported by the beam when the response time of the element(s) is equal to or greater than the duration of the blast load. To insure against premature failure, the ultimate resistance of the beam must be greater than the reaction of the supported element (slab, wall, blast door, etc.) applied to the beam as a static load.

In the case of a supported slab, the slab does, in fact, act with the beam; a portion of the mass of the slab acts with the mass of the beam to resist the dynamic load. It is, therefore, recommended that 20 percent of the mass of the slab (or blast door, wall, etc.) on each side of the beam be added to the actual mass of the beam. This increased mass is then used to compute the natural period of vibration T_N of the beam. It should be noted that in the calculation of T_N the values used for the effective mass and stiffness of the beam depends upon the allowable maximum deflection. When designing for completely elastic behavior, the elastic stiffness is used while, in other cases, the equivalent elasto-plastic stiffness K_E is used. The elastic value of the effective mass is used for the elastic range while, in the elasto-plastic range, the effective mass is the average of the elastic and elasto-plastic values. For small plastic deformations, the value of the effective mass is equal to the average of the equivalent elastic value and the plastic value while for large plastic deformations, the effective mass is equal to the plastic value.

4-43.2. Design for Rebound

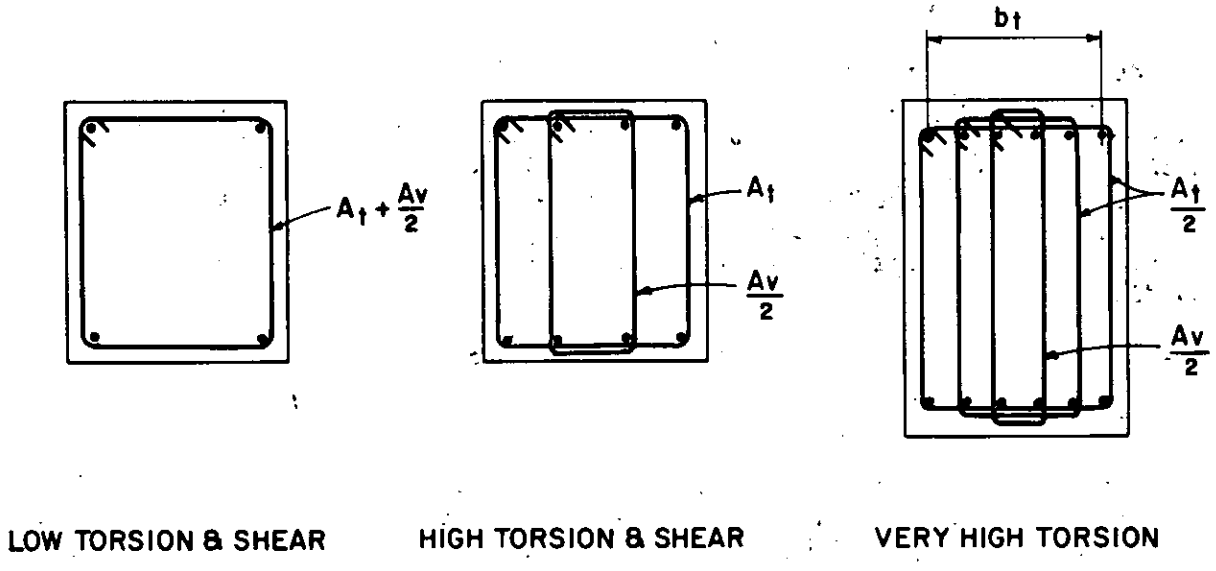
The beam must be designed to resist the negative deflection or rebound which occurs after the maximum positive deflection has been reached. The negative resistance r^-, attained by the beam when subjected to a triangular pressure-time load, is obtained from figure 3-268 in Chapter 3. Entering the figure with the ratios of X_m/X_E and T/T_N, previously determined for the positive phase of design, the ratio of the required rebound resistance to the ultimate resistance r^-/r_u is obtained. The beam must be reinforced to withstand this rebound resistance r^- to insure that the beam will remain elastic during rebound.

The tension reinforcement provided to withstand rebound forces is added to what is needed for the compression zone during the initial loading phase. To obtain this reinforcement, the beam is essentially designed for a negative load equal to the calculated value of r^-. However, in no case shall the rebound reinforcement be less than one-half of the positive phase reinforcement. The moment capacities and the rebound resistance capacity are calculated using the same equations previously presented.

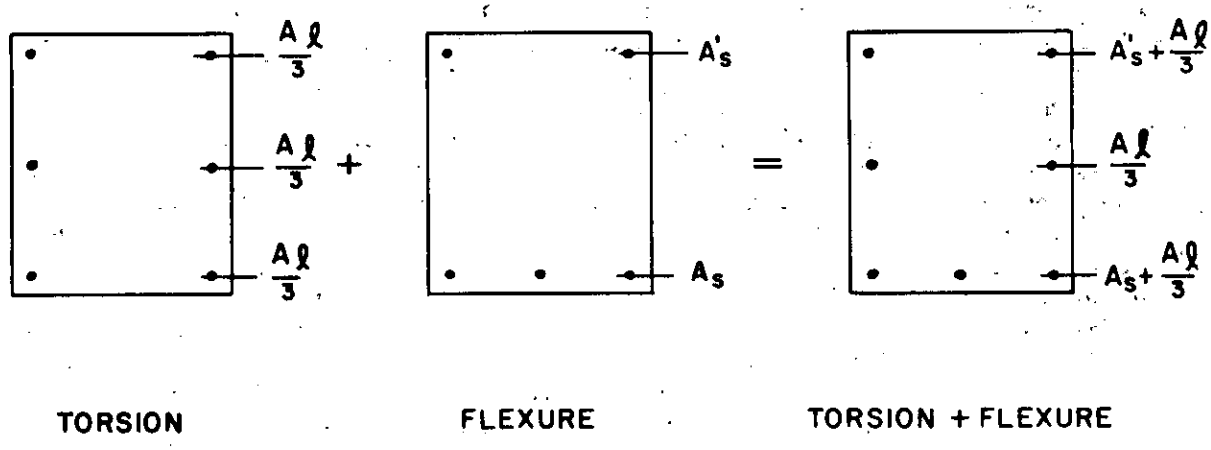


Note 1: Stirrups (closed ties) always required.

Figure 4-59 Relationship between design parameters for beams



(a) Arrangement of Shear and Torsional Web Reinforcement



(b) Arrangement of Torsional and Flexural Longitudinal Steel

Figure 4-60 Arrangement of reinforcement for combined flexure and torsion

DYNAMIC DESIGN OF INTERIOR COLUMNS

4-44. Introduction

The design of columns is limited to those in shear wall type structures where the lateral loads are transmitted through the floor and roof slabs to the exterior (and interior, if required) shear walls. Due to the extreme stiffness of the shear walls, there is negligible sidesway in the interior columns and, hence, no induced moments due to lateral loads. Therefore, interior columns are axially loaded members not subjected to the effects of lateral load. However, significant moments can result from unsymmetrical loading conditions.

4-45. Strength of Compression Members (P-M Curve)

4-45.1. General

The capacity of a short compression member is based primarily on the strength of its cross section. The behavior of the member encompasses that of both a beam and a column. The degree to which either behavior predominates depends upon the relative magnitudes of the axial load and moment. The capacity of be the column can be determined by constructing an interaction diagram as shown in Figure 4-61. This curve is a plot of the column axial load capacity versus the moment it can simultaneously withstand. Points on this diagram are calculated to satisfy both stress and strain compatibility. A single curve would be constructed for a given cross section with a specified quantity of reinforcement. The plot of a given loading condition that falls within the area represents a loading combination that the column can support, whereas, a plot that falls outside the interaction curve represents a failure combination. Three points of the interaction diagram are used to define the behavior of compression members under combined axial and flexural loads. These points are: (1) pure compression (P_o, M = 0), (2) pure flexure (P = 0, M_o), and, (3) balanced conditions (P_b, M_b). The eccentricity of the design axial load for the condition of pure compression is zero. However, under actual conditions, pure axial loads will rarely, if ever, exist. Therefore, the maximum axial load is limited by a minimum eccentricity, e_{min}. At balanced conditions, the eccentricity is defined as e_b while the eccentricity at pure flexure is infinity. The strength of a section is controlled by compression when the design eccentricity $e = M_u/P_u$, is smaller than the eccentricity under balanced conditions. The strength of the section is controlled by tension when the design eccentricity is greater than that for balanced conditions.

4-45.2. Pure Compression

The ultimate dynamic strength of a short reinforced concrete column subjected to pure axial load (no bending moments) is given by:

$$P_o = 0.85\, f'_{dc}(A_g - A_{st}) + A_{st}\, f_{dy} \qquad 4\text{-}154$$

where:

P_o = maximum axial load

A_g = gross area of section

A_{st} = total area of reinforcing steel

A member subjected to pure axial compression is a hypothetical situation since all columns are subjected to some moment due to actual load conditions. All tied and spiral columns must be designed for a minimum load eccentricity. This minimum design situation is presented in a subsequent section.

4-45.3. Pure Flexure

An interior column of a shear wall type structure cannot be subjected to pure flexure under normal design conditions. For the purpose of plotting a P-M curve, the criteria presented for beams is used.

4-45.4. Balanced Conditions

A balanced strain condition for a column subjected to a dynamic load is achieved when the concrete reaches its limiting strain of 0.003 in/in simultaneously with the tension steel reaching its dynamic yield stress f_{dy}. This condition occurs under the action of the balanced load P_b and the corresponding balanced moment M_b. At balanced conditions, the eccentricity of the load is defined as e_b, and is given by:

$$e_b = M_b/P_b \qquad 4\text{-}155$$

The actual values of the balanced load and corresponding balanced moment are generally not required. The balanced eccentricity is the important parameter since a comparison of the actual eccentricity to the balanced eccentricity distinguishes whether the strength of the section is controlled by tension or compression. The comparison of the actual eccentricity to the balanced eccentricity dictates the choice of the appropriate equation for calculating the ultimate axial load capacity, P_u.

Approximate expressions have been derived for the balanced eccentricity for both rectangular and circular members. These expressions are sufficiently accurate for design purposes. For a rectangular tied column with equal reinforcement on opposite faces (Fig. 4-62a). the balanced eccentricity is given by:

$$e_b = 0.20h + (1.54mA_s)/b \qquad 4\text{-}156$$

and:

$$m = (f_{dy})/(0.85\ f'_{dc}) \qquad 4\text{-}157$$

where:

e_b = balanced eccentricity

h = depth of rectangular section

b = width of rectangular section

A_s = area of reinforcement on one face of the section

For a circular section with spiral reinforcement (Fig. 4-62b), the balanced eccentricity is given by:

$$e_b = (0.24 + 0.39\ p_T m)\ D \qquad 4\text{-}158$$

and:

$$p_T = A_{st}/A_g \qquad 4\text{-}159$$

where:

p_T = total percentage of reinforcement

A_{st} = total area of reinforcement

A_g = gross area of circular section

D = overall diameter of circular section

4-45.5. Compression Controls

When the ultimate eccentric load P_u exceeds the balanced value P_b, or when the eccentricity e is less than the balanced value e_b, the member acts more as a column than as a beam. Failure of the section is initiated by crushing of the concrete. When the concrete reaches its ultimate strain, the tension steel has not reached its yield point and may actually be in compression rather than tension. The ultimate eccentric load at a given eccentricity e less than e_b may be obtained by considering the actual strain variation as the unknown and using the principles of statics. However, equations have been developed which approximate the capacity of the column. These approximate procedures are adequate for design purposes.

For a rectangular tied column with equal reinforcement on opposite faces (Fig. 4-62a), the ultimate axial load capacity at a given eccentricity is approximated by:

$$P_u = \frac{A_s f_{dy}}{[e/(2d-h)] + 0.5} + \frac{bh f'_{dc}}{(3he/d^2) + 1.18} \qquad 4\text{-}160$$

where:

P_u = ultimate axial load at actual eccentricity e

e = actual eccentricity of applied load

A_s = area of reinforcement on one face of the section

d = distance from extreme compression fiber to centroid of tension reinforcement

h = depth of rectangular section

b = width of rectangular section

For a circular section with spiral reinforcement, the ultimate axial load capacity at a given eccentricity is approximated by:

$$P_u = \left[\frac{A_{st}\ f_{dy}}{\frac{3e}{D_s} + 1.0}\right] + \left[\frac{A_g\ f'_{dc}}{\frac{9.6D_e}{(0.8D + 0.67\ D_s)^2} + 1.18}\right] \qquad 4\text{-}161$$

where:

A_{st} = total area of uniformly distributed longitudinal reinforcement

A_g = gross area of circular section

D = overall diameter of circular section

D_s = diameter of the circle through centers of reinforcement arranged in a circular pattern

4-45.6. Tension Controls

When the ultimate eccentric load P_u is less than the balance value P_b or when the eccentricity e is greater than the balanced value e_b, the member acts more as a beam than as a column. Failure of the section is initiated by yielding of the tension steel. The ultimate eccentric load at a given eccentricity e greater than e_b may be obtained by considering the actual strain variation as the unknown and using the principles of statics.

However, again, equations have been developed to approximate the capacity of the column. It should be pointed out that while tension controls are a possible design situation it is not an usual condition for interior columns of a shear wall type structure.

For a rectangular tied column with equal reinforcement on opposite faces (Fig. 4-62a), the ultimate axial load capacity at a given eccentricity is approximated by:

$$P_u = 0.85\, f'_{dc}\, bd \left[1-p - \frac{e'}{d} + \left[\frac{(1-e')^2}{d} + 2p_s \left[(m-1)\left(2 - \frac{h}{d}\right) + \frac{e'}{d} \right] \right]^{1/2} \right] \qquad 4\text{-}162$$

in which:

$$p_s = A_s / bd \qquad 4\text{-}163$$

$$e' = e + d - (h/2) \qquad 4\text{-}164$$

$$m = f_{dy} / (0.85\, f'_{dc}) \qquad 4\text{-}165$$

where:

p = percentage of reinforcement on one face of section

e' = eccentricity of axial load at the end of member measured from the centroid of the tension reinforcement

For a circular section with spiral reinforcement (Fig. 4-62b), the ultimate axial load capacity at a given eccentricity is approximated by:

$$P_u = 0.85\, f'_{dc} D^2 \left[\left[\left(\frac{0.85e}{D} - 0.38 \right)^2 + \frac{P_T m D_s}{2.5\, D} \right]^{1/2} - \left(\frac{0.85e}{D} - 0.38 \right) \right] \qquad 4\text{-}166$$

where:

P_T = total percentage of reinforcement and is defined in Equation 4-159

4-46. Slenderness Effects

4-46.1. General

The preceding section discussed the capacity of short compression members. The strength of these members is based primarily on their cross section. The effects of buckling and lateral deflection on the strength of these short members are small enough to be neglected. Such members are not in danger of buckling prior to achieving their ultimate strength based on the properties of the cross section. Further, the lateral deflections of short compression members subjected to bending moments are small, thus contributing little secondary bending moment (axial load P multiplied by lateral deflection). These buckling and deflection effects reduce the ultimate strength of a compression member below the value given in the preceding section for short columns.

In the design of columns for blast resistant buildings, the use of short columns is preferred. The cross section is selected for the given height and support conditions of the column in accordance with criteria presented below for short columns. If the short column cross section results in a capacity much greater than required, the dimensions may be reduced to achieve an economical design. However, slenderness effects must be evaluated to insure an adequate design. It should be noted that for shear wall type structures, the interior columns are not subjected to sidesway deflections since lateral loads are resisted by the stiff shear walls. Consequently, slenderness effects due to buckling and secondary bending moments (Pü) are the only effects that must be considered.

4-46.2. Slenderness Ratio

The unsupported length L_u of a compression member is taken as the clear distance between floor slabs, beams, or other members capable of providing lateral support for the compression member. Where column capitals or haunches are present, the unsupported length is measured to the lower extremity of capital or haunch in the plane considered.

The effective length of a column kL_u is actually the equivalent length of a pin ended column. For a column with pin ends the effective length is equal to the actual unsupported length (k = 1.0). Where translation of the column at both ends is adequately prevented (braced column), the effective length of the column is the distance between points of inflection (k less than 1.0). It is recommended that for the design of columns in shear wall type structures the effective length factor k may be taken as 0.9 for columns that are definitely restrained by beams and girders at the top and bottom. For all other cases k shall be taken as 1.0 unless analysis shows that a lower value may be used.

For columns braced against sidesway, the effects of slenderness may be neglected when:

$$\frac{kL_u}{r} < 34 - 12\frac{M_1}{M_2} \qquad 4\text{-}167$$

where:

k = effective length factor

L_u = unsupported length of column

r = radius of gyration of cross section of column (r = 0.3h for tied columns and 0.25D for circular columns)

M_1 = value of smaller end moment on column, positive if member is bent in single curvature and negative in double curvature

M_2 = value of larger end moment on column

In lieu of a more accurate analysis, the value of M_1/M_2 may conservatively be taken equal to 1.0. Therefore, in the design of columns the effect of slenderness may be neglected when:

$$\frac{kL_u}{r} \leq 22 \qquad 4\text{-}168$$

The use of slender columns is not permitted in order to avoid stability problems. Consequently, the slenderness ratio must be limited to a maximum value of 50.

4-46.3. Moment Magnification

Slenderness effects due to buckling and secondary bending moments must be considered in the design of columns whose slenderness ratio is greater than that given by Equation 4-167. The reduction in the ultimate strength of a slender column is accounted for in the design procedure by increasing the design moment. The cross section and/or reinforcement is thereby increased above that required for a short column.

A column braced against sidesway is designed for the applied axial load P and a magnified moment M defined by:

$$M = \delta M_2 \qquad 4\text{-}169$$

in which:

$$\delta = \frac{C_m}{1 - \frac{P}{P_c}} \qquad 4\text{-}170$$

where:

M = design moment

δ = moment magnifier

M_2 = value of larger end moment on column

C_m = equivalent moment correction factor defined by equation 4-171

M_1 = value of smaller end moment on column

P = design axial load

P_c = critical axial load causing buckling defined by equation 4-172

The value of the moment magnifier δ shall not be taken less than 1.0.

For columns braced against sidesway and not subjected to transverse loads between supports, i.e. interior columns of shear wall type structures, the equivalent moment factor C_m may be taken as:

$$C_m = 0.6 + 0.4\, M_1 / M_2 \qquad 4\text{-}171$$

The value of C_m may not under any circumstances be taken less than 0.4. In lieu of a more accurate analysis, the value of M_1/M_2 may conservatively be taken equal to 1.0. Therefore, in the design of interior columns, C_m may be taken as 1.0.

The critical axial load that causes a column to buckle is given by:

$$P_c = \frac{\pi^2\, EI}{(kL_u)^2} \qquad 4\text{-}172$$

In order to apply Equation 4-172, a realistic value of EI must be obtained for the section at buckling. An approximate expression for EI at the time of buckling is given by:

$$EI = \frac{E_c\, I_a}{1.5} \qquad 4\text{-}173$$

in which:

$$I_a = \frac{I_g + I_c}{2} \qquad 4\text{-}174$$

and:

$$I_c = Fbd^3 \qquad 4\text{-}175$$

where:

I_a = average moment of inertia of section

I_g = moment of inertia of gross concrete section about centroidal axis, neglecting reinforcement

I_c = moment of inertia of cracked concrete section with equal reinforcement on opposite faces

F = coefficient given in Figure 4-5

4-47. Dynamic Analysis

Columns are not subjected to the blast loading directly. Rather, the load that a column must resist is transmitted through the roof slab, beams and girders. These members "filter" the dynamic effects of the blast load. Thus, in buildings designed to obtain plastic deformations, the dynamic load reaching the columns is typically a fast "static" load, that is, a flat top pressure time load with a relatively long rise time.

The roof members and columns act together to resist the applied blast load. However, a reasonable design can be achieved by considering the column separately from the roof members. The response (resistance-time function) of the roof members to the blast load is taken as the applied dynamic load acting on the columns.

Columns are subjected to an actual axial load (with associated eccentricity) equal to the ultimate resistance of the appropriate roof members acting over the tributary area supported by the column. It is recommended for design of columns the ultimate axial load be equal to 1.2 times the actual axial load. This increase insures that the maximum response of the column will be limited to a ductility ratio (X_m/X_e) of 3.0 or less. If the rise time of the load (time to reach yield for the appropriate roof members) divided by the natural period of the column is small (approximately 0.1), the maximum ductility is limited to 3.0. Whereas, if the time ratio is equal to 1.0 or greater, the column will remain elastic. For the usual design cases, the ratio of the rise time to the natural period will be in the vicinity of 1.0. Therefore, the columns will remain elastic or, at best, sustain slight plastic action.

In some instances, buildings may be designed to remain completely elastic. In these cases, the actual axial load that the column must resist is equal to the maximum actual response of the roof members framing into the column. This response and, therefore, the maximum load on the column, can be no more than two times the blast load.

4-48. Design of Tied Columns

4-48.1. General

Interior columns are not usually subjected to excessive bending moments since sidesway is eliminated by the shear walls. However, significant moments about both axes can result from unsymmetrical loading conditions. These moments may be due to unequal spacing between columns or to time phasing of the applied loads. As a result of the complex load conditions, the columns must be proportioned considering bending about both the x and y axes simultaneously.

One method of analysis is to use the basic principles of equilibrium with the acceptable ultimate strength assumptions. This method essentially involves a trial and error process for obtaining the position of an inclined neutral axis. This method is sufficiently complex so that no formula may be developed for practical use.

An approximate design method has been developed which gives satisfactory results for biaxial bending. The equation is in the form of an interaction formula which for design purposes can be written in the form:

$$\frac{1}{P_u} = \frac{1}{P_x} + \frac{1}{P_y} - \frac{1}{P_o}$$

where:

P_u = ultimate load for biaxial bending with eccentricities e_x and e_y

P_x = ultimate load when eccentricity e_x is present ($e_y = 0$)

P_y = ultimate load when eccentricity e_y is present ($e_x = 0$)

P_o = ultimate load for a concentrically loaded column ($e_x = e_y = 0$)

Equation 4-176 is valid provided P_u is equal to or greater than $0.10\ P_o$. The usual design cases for interior columns satisfy this limitation. The equation is not reliable where biaxial bending is prevalent and is accompanied by an axial force smaller than $0.10\ P_o$. In the case of strongly prevalent bending, failure is initiated by yielding of the steel (tension controls region of P-M curve). In this range it is safe and satisfactorily accurate to neglect the axial force entirely and to calculate the section for biaxial bending only.

This procedure is conservative since the addition of axial load in the tension controls region increases the moment capacity. It should be mentioned that the tension controls case would be unusual and, if possible, should be avoided in the design.

Reinforcement must be provided on all four faces of a tied column with the reinforcement on opposite faces of the column equal. In applying Equation 4-176 to the design of tied columns, the values of P_x and P_y are obtained from Equation 4-160 and 4-162 for the regions where compression and tension control the design, respectively. The equations are for rectangular columns with equal reinforcement on the faces of the column parallel to the axis of

bending. Consequently, in the calculation of P_x and P_y, the reinforcement perpendicular to the axis of bending is neglected. Conversely, the total quantity of reinforcement provided on all four faces of the column is used to calculate P_o from Equation 4-154. Calculation of P_x, P_y and P_o in the manner described will yield a conservative value of P_u from Equation 4-176.

4-48.2. Minimum Eccentricity

Due to the possible complex load conditions that can result in blast design, all tied columns shall be designed for biaxial bending. If computations show that there are no moments at the ends of the column or that the computed eccentricity of the axial load is less than 0.1h, the column must be designed for a minimum eccentricity equal to 0.1h. The value of h is the depth of the column in the bending direction considered. The minimum eccentricity shall apply to bending in both the x and y directions, simultaneously.

4-48.3. Longitudinal Reinforcement Requirements

To insure proper behavior of a tied column, the longitudinal reinforcement must meet certain restrictions. The area of longitudinal reinforcement shall not be less than 0.01 nor more than 0.04 times the gross area of the section. A minimum of 4 reinforcing bars shall be provided. The size of the longitudinal reinforcing bars shall not be less than #6 nor larger than #11. The use of #14 and #18 bars as well as the use of bundled bars are not recommended due to problems associated with the development and anchorage of such bars. To permit proper placement of the concrete, the minimum clear distance between longitudinal bars shall not be less than 1.5 times the nominal diameter of the longitudinal bars nor 1.5 inches.

4-48.4. Closed Ties Requirements

Lateral ties must enclose all longitudinal bars in compression to insure their full development. These ties must conform to the following:

1. The ties shall be at least #3 bars for longitudinal bars #8 or smaller and at least #4 bars for #9 longitudinal bars or greater.

2. To insure the full development of the ties they shall be closed using 135-degree hooks. The use of 90-degree bends is not recommended.

3. The vertical spacing of the ties shall not exceed 16 longitudinal bar diameters, 48 tie diameters or ½ of the least dimension of the column section.

4. The ties shall be located vertically not more than ½ the tie spacing above the top of footing or slab and not more than ½ the tie spacing below the lowest horizontal reinforcement in a slab or drop panel. Where beams frame into a column, the ties may be terminated not more than 3 inches below the lowest reinforcement in the shallowest of the beams.

5. The ties shall be arranged such that every corner and alternate longitudinal bar shall have lateral support provided by the corner of a tie with an included angle of not more than 135 degrees and

no bar shall be farther than 6 inches clear on each side along the tie from such a laterally supported bar.

The above requirements for the lateral ties is to insure against buckling of the longitudinal reinforcement in compression. However, if the section is subjected to large shear or torsional stresses, the closed ties must be increased in accordance with the provisions established for beams (see section 4-39).

4-49. Design of Spiral Columns

4-49.1. General

Spiral columns may be subjected to significant bending moments about both axes and should, therefore, be designed for biaxial bending. However, due to the uniform distribution of the longitudinal reinforcement in the form of a circle, the bending moment (or eccentricities) in each direction can be resolved into a resultant bending moment (or eccentricity). The column can then be designed for uniaxial bending using Equations 4-161 and 4-166 for the regions where compression and tension control the design, respectively.

4-49.2. Minimum Eccentricity

Since spiral columns show greater toughness than tied columns, particularly when eccentricities are small, the minimum eccentricity for spiral columns is given as 0.05D in each direction rather than 0.1h in each direction for tied columns. The resultant minimum eccentricity for a spiral column is then equal to 0.0707D. Therefore, if computations show that there are no moments at the ends of a column or that the computed resultant eccentricity of the axial load is less than 0.0707D, the column must be designed for a resultant minimum eccentricity of 0.0707D.

4-49.3. Longitudinal Reinforcement Requirements

To insure proper behavior of a spiral reinforced column, the longitudinal reinforcement must meet the same restrictions given for tied columns concerning minimum and maximum area of reinforcement, smallest and largest reinforcing bars permissible and the minimum clear spacing between bars. The only difference is that for spiral columns the minimum number of longitudinal bars shall not be less than 6 bars.

4-49.4. Spiral Reinforcing Requirements

Continuous spiral reinforcing must enclose all longitudinal bars in compression to insure their full development. The required area of spiral reinforcement A_{sp} is given by:

$$A_{sp} = 0.1125\ s\ D_{sp} \left[\frac{D^2}{D_{sp}^2} - 1 \right] \frac{f'_{dc}}{f_{dy}} \qquad 4\text{-}177$$

where:

A_{sp} = area of spiral reinforcement

s = pitch of spiral

D = overall diameter of circular section

D_{sp} = diameter of the spiral measured through the centerline of the spiral bar

The spiral reinforcement must conform to the following:

1. Spiral column reinforcement shall consist of evenly spaced continuous spirals composed of continuous #3 bars or larger. Circular bars are not permitted.

2. The clear spacing between spiral shall not exceed 3 inches nor be less than 1 inch.

3. Anchorage of spiral reinforcement shall be provided by 1-½ extra turns of spiral bar at each end.

4. Splices in spiral reinforcement shall be lap splices equal to 1-½ turns of spiral bar.

5. Spirals shall extend from top of footing or slab to level of lowest horizontal reinforcement in members supported above.

6. In columns with capitals, spirals shall extend to a level at which the diameter or width of capital is two times that of the column.

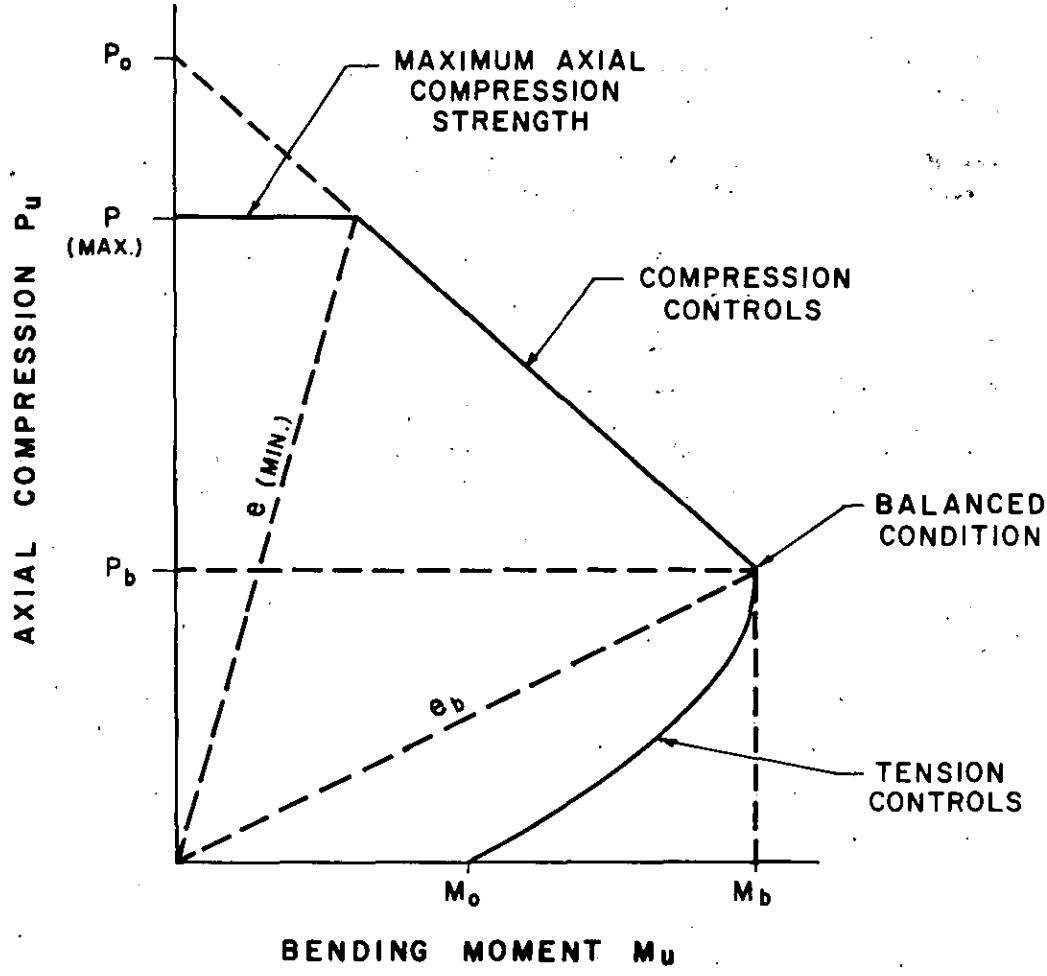
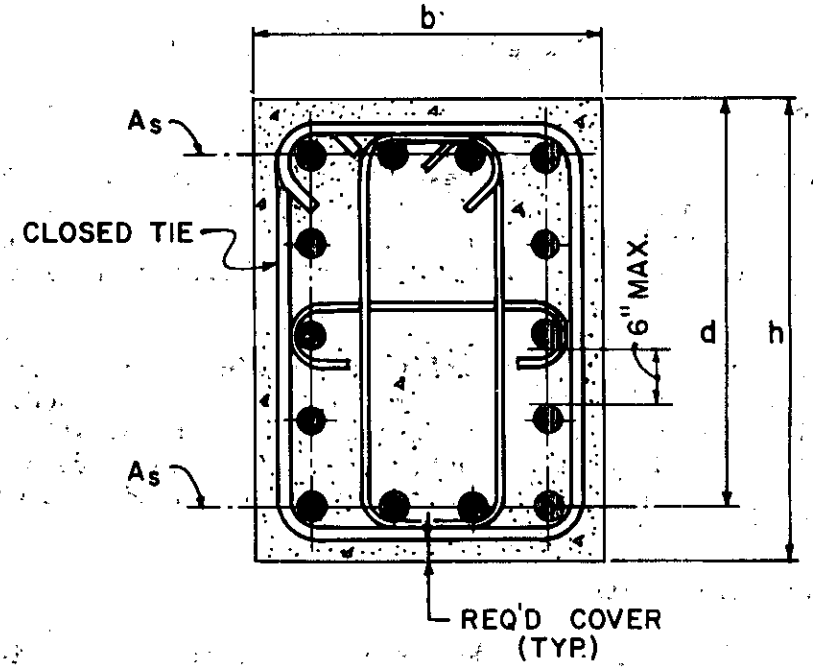
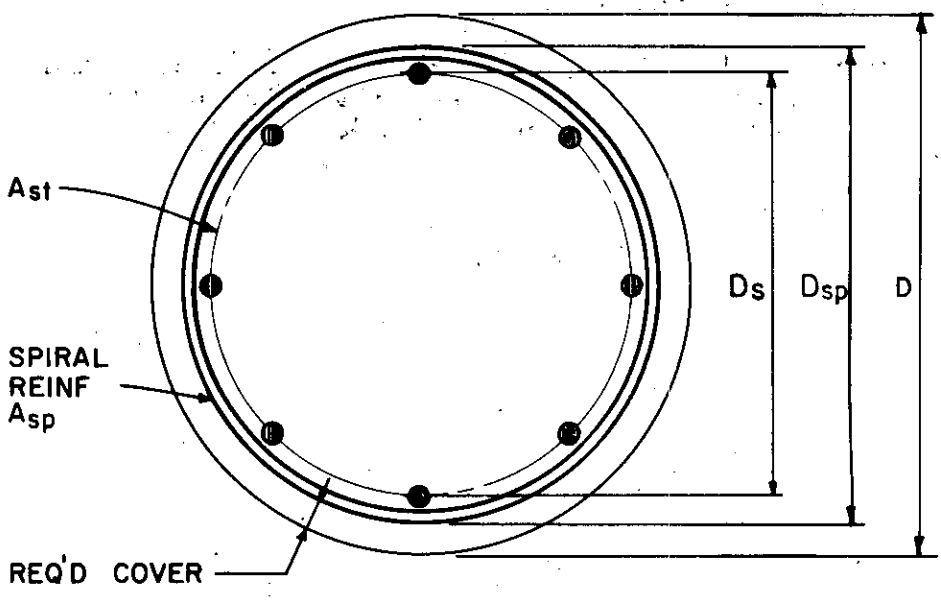


Figure 4-61 Column interaction diagram



a) RECTANGULAR SECTION WITH EQUAL REINFORCEMENT ON OPPOSITE FACES



b) CIRCULAR SECTION WITH UNIFORMLY DISTRIBUTED REINFORCEMENT

Figure 4-62 Typical interior column sections

DYNAMIC DESIGN OF EXTERIOR COLUMNS

4-50. Introduction

Exterior columns may be required for severe loading conditions. These columns could be monolithic with the exterior walls and as such would be subjected to both axial and transverse loading. The axial load results from the direct transfer of floor and roof beam reactions while the transverse load is due to the direct impact of the blast load.

The use of exterior columns would normally be restricted to use in framed structures to transfer roof and floor beam reactions to the foundation. Normally, only tied columns would be used since they are compatible with the placement of wall and beam reinforcement. Exterior columns are not normally required for flat slab structures since roof and floor loads are uniformly transmitted to the exterior walls.

4-51. Design of Exterior Columns

Exterior columns are generally designed as beam elements. The axial load on these columns may be significant, but usually the effect of the transverse load is greater. The column will usually be in the tension controls region (e greater than e_b) of the P-M curve (Fig. 4-61) where the addition of axial load increases the moment capacity of the member.

Consequently, the design of an exterior column as a beam, where the axial load is neglected, is conservative.

Since an exterior column is a primary member which is subjected to an axial load, it is not permitted to attain large plastic deformations. Therefore, the lateral deflection of exterior columns must be limited to a maximum ductility (X_m/X_E) of 3.

STRUCTURAL ANALYSIS AND DESIGN FOR BRITTLE MODE RESPONSE

4-52. Introduction

The response of a structural element in the brittle mode consists of that structural behavior which is associated with either partial or total failure of the element and is characterized by two types of concrete fragmentation: (1) spalling (either direct spalling or scabbing) which is the dynamic disengagement of the surface of the element, and (2) post-failure fragmentation which is associated with structural collapse.

Spalling is usually of concern only for those acceptor systems where personnel, valuable equipment and/or extremely sensitive explosives require protection. Where the acceptor system consists of relatively insensitive explosives so that fragment impact will not result in propagation of explosion or mass detonation, then post-failure fragmentation can be considered in the design. For this latter case, even though the velocity of the spalls can be greater than the velocity of the post-failure fragments, the effects of spalling can be neglected because of the smaller masses involved. Post-failure fragmentation cannot be permitted when personnel are being protected.

4-53. Direct Spalling

Direct spalling of a concrete element (Fig. 4-63) is the result of a tension failure in the concrete normal to its free surface and is caused by the shock pressures of an impinging blast wave being transmitted through the element.

When a shock front strikes the donor surface of a concrete element, compression stresses are transmitted from the air to the element. This stress disturbance propagates through the element in the form of a compression wave, and upon reaching the rear (acceptor) free surface, is reflected as a tension wave identical in shape and magnitude to the compression wave. During the return passage, if the tension stresses in the reflected wave exceed the stresses in the compression wave plus the tensile capacity of the concrete, the material will fracture with that part of the element between the rear free surface and the plane of failure being displaced from the remainder of the element. A portion of the stress wave is trapped in the failed section and contributes to its velocity. The part of the stress wave which remains within the main section continues to propagate with additional reflections and concrete fractures until its magnitude is reduced to that level below which spalling does not occur.

Direct spalling generally results in the formation of small concrete fragments. The size of the fragments is attributed to the nonuniformity of the shock wave (close-in effects) and the further distortions of the wave during its propagation through the element (nonhomogeneous material, nonelastic effects, etc.). Localized failures occur under the action of both flexural and shear stresses resulting in the rupture of the mortar binding the stone aggregate together. The failure zone propagates across the concrete surface forming a large number of comparatively small concrete fragments. The thickness of concrete between the rear (acceptor) surface of the element and the centroid of the rear face reinforcement is the usual depth of concrete dynamically disengaged from the element. Although the concrete between the layers of reinforcement may be cracked to some extent, it is confined by the flexural and lacing reinforcement, thus preventing its disengagement.

The size of the surface area which spalls depends upon the magnitude and duration of the applied blast loads striking and subsequently being transmitted through the element, in addition to the size and shape of the element itself. For long cantilever-type barricades, only a portion of the wall will usually spall, since the magnitudes of the applied blast pressures decrease rapidly along its length, while for cubicle-type structures, the entire wall surface will usually spall because of the amplification of the blast pressures due to their multiple reflections within the structures.

A wide range of velocities exists for spalled fragments. The initial velocity at which spalled fragments leave a structural element has been found to be low (50 feet per second or less). However, concrete elements subjected to the close-in effects of a detonation are generally accelerating before or soon after spalling takes place. This accelerated motion of the element in turn accelerates spalled fragments. The fragment velocities produced by these acceleration effects may be as high as several hundred feet per second. For analytical purposes, an upper limit for the velocities of direct spalled fragments from elements sensitive to impulse may be taken as the initial velocity of the element which is also assumed to be the maximum velocity. However, for elements which respond to the pressure only or pressure-time relationship, an evaluation of the resistance-time and pressure-time curves must be performed to obtain the maximum fragment velocity. The procedures and equations that are necessary to determine the above velocities are contained in Section 4-58.

4-54. Scabbing

Scabbing of reinforced concrete elements (Fig. 4-64) is the end result of a tension failure in the concrete normal to its free surface and is associated with large deflections. In the later stages of the ductile response mode of a reinforced concrete element, extremely large deflections are developed producing large strains in the flexural reinforcement and, consequently, severe cracking and/or crushing of the concrete perpendicular to the free surfaces. Because the tension and compression strains are highest at the surface and since the lacing reinforcement in the later stages of deflection confines the concrete between the layers of flexural reinforcement, damage to the concrete is more severe at the exterior of the reinforcement than between the layers. The applied loads having long since passed, the element is in a stage of deceleration at these large deflections. Therefore, the velocities of scabbed fragments, which are equal to the velocity of the element at $\theta = 5°$ (start of scabbing), are lower than the velocities of accelerated direct spalled fragments. However, the velocities of scabbed fragments also may be in the order of several hundred feet per second. Refer to Section 4-58 to determine the velocity of the element at a support rotation of five degrees.

4-55. Prediction of Concrete Spalling

As previously explained, direct spalling is due to a compression wave traveling through a concrete element, reaching the back face and being reflected as a tension wave. Spalling occurs when the tension is greater than the tensile strength of the concrete. Spalling will occur:

for: $\dfrac{Vi_r}{T_c\ P_r} \leq 1.0$ when $\dfrac{P_r}{\sigma_u} \geq 1.0$ 4-178

or for:

$$\frac{Vi_r}{T_c P_r} \leq 1.0 \quad \text{when} \quad \frac{P_r}{\sigma_u} \frac{T_c P_r}{Vi_r} \geq 1.0 \qquad 4\text{-}179$$

where:

$$\sigma_u = 0.1 f'_c \qquad 4\text{-}180$$

$$V = (E_c/\rho)^{1/2} \qquad 4\text{-}181$$

and:

P_r = peak normal reflected pressure

σ_u = tensile strength of concrete

V = velocity of compression wave through concrete

i_r = normal reflected impulse

T_c = thickness of concrete element

f'_c = static compressive strength of concrete

E_c = modulus of elasticity of concrete

ρ = mass density of concrete

Equations 4-178 and 4-179 are shown graphically in Figure 4-65. Use of this figure predicts the incidence of spalling, that is, whether or not spalling will occur at the point on the element which is subjected to the peak normal reflected pressure P_r and impulse i_r.

If spalling is predicted, the spalled area cannot be calculated from the above data. However, the spalled area may be qualitatively estimated by considering the distance of the plotted point above the line on Figure 4-65. The greater the distance above the line, the larger the spalled area is likely to be. In addition, if the average reflected pressure P_b and impulse i_b are substituted for P_r and i_r respectively, and spalling is still predicted, then the spalled area will likely include the major portion, if not all, of the element's surface.

If a concrete element is subjected to side-on pressures only, Figure 4-65 may still be used to predict the occurrence of spalling. In this case, the peak reflected pressure P_r and impulse i_r are replaced with peak side-on pressure P_{so} and impulse i_s, respectively.

4-56. Minimization of Effects of Spalling and Scabbing

If it is determined that concrete spall due to blast loading will occur (using the procedures outlined in the preceding Section), or that scabbing will occur

due to large deflections (>5°), then there are several procedures which can be utilized to minimize its effects.

4-56.1. Design parameters

The occurrence of direct spalling can be eliminated by an adjustment of the charge location, i.e., if an explosive charge is placed at a sufficient distance away from the surface of an element, the magnitude of the blast pressures striking the element will be less than those which will cause tension failure of the concrete. Large adjustments of the donor charge location in a design for the sole purpose of preventing direct spalling is usually not economically feasible.

Although sufficient separation distance between a detonation and an element prevents direct spalling, its effect in reducing scabbing is negligible. A reduction of scabbing is accomplished by limiting the magnitude of the maximum deflection of the element. By reducing this deflection, the strains in the concrete and reinforcement are lowered to a level where tensile failure of the concrete and subsequent scabbed fragment formation is prevented. Scaled tests have indicated that scabbing does not occur when deflections are limited to values less than those corresponding to support rotations of no larger than five degrees. To maintain the same response of the element, the resistance-mass product of the element must be increased proportionally to the decrease in deflection, and this capacity (resistance and/or mass) increase results in an increased construction cost.

4-56.2. Composite Construction

Direct spalling and scabbing can be eliminated through the use of composite elements composed of two concrete panels (donor and acceptor) separated by a sand-filled cavity. Spalling of the donor panel is not generally of concern since resulting fragments enter and are trapped in the sand fill. On the other hand, spalling of the receiver panel will endanger the acceptor system. By maintaining certain design parameters, both direct spalling and scabbing of the receiver panel can be prevented.

To prevent the occurrence of direct spalling, the high peak blast pressures applied to the donor panel of a composite element must be attenuated by the sand fill. This attenuating capability of the sand is attained by providing: (1) a thickness of the sand fill at least equal to twice the thickness of the donor panel where the panel thickness is predicated upon the required strength to resist the applied loads, (2) for one-way elements a ratio of the cavity thickness to span length not less than 0.25 for cantilevers and 0.05 for elements fixed on two opposite sides shall be used, and for two-way elements each direction (span) shall be considered separately as shown above and the larger cavity thickness used, and (3) the sand density shall not be greater than 85 pounds per cubic foot. Since scabbing is eliminated by limiting the element's deflection, scabbing of composite elements is prevented by limiting the deflection of the acceptor panel to the support rotation previously cited.

Figure 4-66 illustrates the use of composite construction to prevent spalling. The magnitude of the donor panel deflection was such that the panel was near incipient failure, the panel experiencing the effects of both direct spalling and scabbing. On the other hand, the deflection of the acceptor panel has been limited and, therefore, had only minor cracking. Direct spalled or

scabbed fragments were not formed on the exterior surface of the acceptor panel.

The use of composite barriers for the sole purpose of eliminating spalling is not usually economically feasible. However, if the magnitude of the applied blast loads warrant the use of composite construction, then the elimination of spalling can be achieved at a slight increase in cost by conforming to the previously stated element configurations and response.

4-56.3. Fragment Shields

4-56.3.1. General

Fragment shields are composed of steel plates or other structural material which can be attached to, or placed a short distance from, a protective barrier (fig. 4-67). Unlike the other methods, the use of shields does not reduce or deter the formation of spalled fragments but rather confines and prevents them from striking the acceptor system.

4-56.3.2. Attached Fragment Shield

If the permissible maximum deflection of a barrier is relatively small, then steel plates, blast mats, or other similar material attached rigidly to the barrier may be used to confine the concrete fragments, thus preventing their ejection from the barrier (Fig. 4-67a). It is recommended that for rigidly attached shields the deflection be limited to a five-degree support rotation to prevent failure of the shield and its connections as a result of excessive straining.

The velocity of spalled fragments due to the transmission of air blast is small. However, spalling occurs during the initial response of the element. Since the element is in motion when spalling occurs, the spalled fragments are actually being pushed by the concrete element. After the element reaches maximum velocity, the element and the attached shield decelerate due to the flexural resistance of the concrete element. The attached shield, therefore, decelerates the spalled fragments which are confined between the shield and the unspalled portion of the concrete. The maximum deceleration of the element and, consequently, of the confined spall fragments is given by:

$$a = r_u/m_u \qquad 4\text{-}182$$

where:

a = deceleration of the structural element

r_u = ultimate unit resistance of concrete element

m_u = effective unit mass of the concrete element in the plastic range

The force acting on the shield is due to the inertial force of the fragments. Thus, the required resistance of the fragment shield must be equal to this inertial force or:

$$r_{fs} = m_{sp}\, a \qquad 4\text{-}183$$

where:

r_{fs} = ultimate unit resistance of fragment shield

m_{sp} = mass of the spalled fragments

When calculating the mass of the spalled fragments the actual mass of the disengaged concrete is used. It is assumed that all the concrete from the rear face of the element to the centroid of the rear face reinforcement disengages. Thus, the spall thickness for a laced section is:

$$d_{sp} = (T_c - d_c)/2 \qquad 4\text{-}184$$

where:

d_{sp} = depth of spalled concrete

T_c = thickness of the concrete element

d_c = average distance between the centroids of the compression and tension reinforcement

An attached fragment shield usually consists of a flat or corrugated steel plate spanning between angles or channels. The angles or channels act as beams spanning between anchor bolts. The anchor bolts connect the plate and beams to the unspalled portion of the concrete. To insure that they do not fail due to concrete pull-out, the anchor bolts are hooked around the flexural reinforcement as shown in Figure 4-68. If the required resistance of the fragment shield is small, the fragment shield may be considered a two-way spanning member without the supporting beams. In such cases, the shield is designed as a flat slab with the anchor bolts supporting it at multiples of the flexural bar intersections. For larger resistances, the plate thickness would become excessive and the design uneconomical.

4-56.3.3. Separated Fragment Shield

If the barrier is permitted to attain large deflections (greater than five-degree support rotation) then the shields must be separated from the barrier. This separation distance should be sufficient to eliminate the possibility of impact between the deflecting barrier and shield. Fragment shields, separated from the main protective elements and affording protection against spalled fragments from the walls and/or roof, are shown in Figure 4-67b. The shield may consist of structural steel, reinforced concrete, wood, etc., and must be designed to resist the impact and penetration of the spalled fragments as well as the overall motion of the main protective structure and any leakage pressure which may occur.

To design a separated shield, the mass and velocity of the spalled fragments must be determined. As an approximation, an average velocity for all spalled fragments can be utilized. The average velocity of the spalled fragments is taken as equal to the maximum velocity of the element (single-degree-of-freedom system) so that:

$$v = i_b/m_u \qquad 4\text{-}185$$

where:

v = average velocity of spalled fragments

i_b = blast impulse

m_u = effective unit mass of the concrete element in the plastic range

The impulse imparted to the fragment shield by the spalled fragments is equal to their momentum or:

$$i_{fs} = m_{sp} V \qquad 4\text{-}186$$

where:

i_{fs} = required impulse capacity of the fragment shield.

m_{sp} = mass of the spalled fragments (Section 4-56.3.2)

The shield is designed to resist this impulse, i_{fs}.

The cost of separated shields may be somewhat more expensive than shields attached directly to the barrier. However, the cost reduction achieved by permitting the larger barrier deflections may offset the increased cost of the separated shield.

4-57. Post-Failure Concrete Fragments

When a reinforced concrete element is substantially overloaded by the blast output, the element fails and concrete fragments (post failure) are formed and displaced at high velocities. The type of failure as well as the size and number of the fragments depends upon whether the element has laced or unlaced reinforcement.

Failure of an unlaced element (Fig. 4-69) is characterized by the dispersal of concrete fragments formed by the cracking and displacement of the concrete between the donor and acceptor layers of the reinforcement. With increased deflections, these compression forces tend to buckle the reinforcement outward thereby initiating the rapid disintegration of the element.

Laced concrete elements exhibit a different type of failure from unlaced elements, the failure being characterized by reinforcement failures occurring at points of maximum flexural stress (plastic hinges) with the sections of the element between the points of failure remaining essentially intact. When fracture due to excessive straining of the tension reinforcement occurs at the positive yield lines, some small concrete fragments will be formed at the acceptor side of the barrier. Quite often, if the overload is not too severe, the compression reinforcement at the hinge points does not fail and thereby prevents total disengagement of the sections between the hinges (Fig. 4-70). In cubicle type structures where continuous laced and flexural reinforcement is used throughout, failure is sometimes initiated at the positive yield lines where flexural and lacing reinforcement fail, while at the supports, only the tension reinforcement fails. The intact sections between the failure points rotate with the compression reinforcement at the supports, acting as the mechanical hinges of an analogous swinging door (Fig. 4-71). The compression reinforcement at the supports, serving as hinges, produces rotational rather than translational motion of the failed sections, and energy which would ordinarily result in translational velocities is transferred to sections of the structure adjacent to the failed element. In other situations, where

there is a larger overloading of the element, the failed sections of the laced element are completely disengaged and displaced from the structure. The translational velocities of these sections are usually less than the maximum velocity of the element at incipient failure.

4-58. Post-Failure Impulse Capacity

4-58.1. General

Elements which protect non-sensitive explosives may be designed for controlled post-failure fragments with a substantial cost savings. These elements fail completely, but detonation is prevented by limiting the mass and velocity of the fragments. Barriers and shelters which will protect personnel, equipment and/or sensitive explosives cannot be designed for post-failure criteria. Procedures are presented below for determining the post-failure impulse capacity of laced elements.

4-58.2. Laced Elements

4-58.2.1. General

The idealized curves of Figure 4-72 illustrate the response of an impulse-sensitive two-way element when the applied blast impulse load is larger than it flexural impulse capacity (area under the resistance-time curve, Fig. 4-72a). The assumptions made in these curves are the same as those for impulse-sensitive systems whose response is less than or equal to incipient failure (Vol. III) namely: (1) the element prior to being loaded is at rest, and (2) the duration of the applied blast load and the time to reach to yield are small in comparison to the time to reach the ultimate deflection. In Figure 4-72 the duration of the applied blast load and time to reach yield have been taken as equal to zero so that the element will respond and reach its maximum velocity instantaneously (i.e., at $t_o = 0$, $v_o = i_b/m_u$).

When the element is designed to remain intact (equal to or less than incipient failure conditions), its velocity at time tu (deflection X_u) is equal to zero. However, if the element is overloaded, then the velocity just prior to failure is a finite value, the magnitude of which depends upon: (1) the magnitude of the overload, (2) the magnitude of the flexural capacity, and (3) mass of the element.

When laced elements are overloaded, failure occurs at the hinge lines and the element breaks into a small number of large sections. The magnitude of the velocity of each sector at failure varies from a maximum at the point of maximum deflection to zero at the supports. The variation of the fragment velocity across a section produces tumbling. This tumbling action may result in an acceptor charge which is located close to the barrier being stuck by that portion of a failed sector traveling at the highest velocity. If the acceptor charge is located at a considerable distance from the barrier, the velocity of the fragments should be taken as the translational velocity. The translational velocity is approximately equal to the average velocity of the sector before failure (the average momentum of the element before failure is equal to the average momentum after failure).

The analytical relationship which describes the response of a laced element, both in its flexural and post-failure ranges of action, is obtained through a

semigraphical solution of Newton's equation of motion similar to that described for incipient failure design in Chapter 3.

If the areas under the pressure-time and resistance-time curves (Fig. 4-72a) are considered to be positive and negative, respectively, and the velocity of the system before the onset of the load is zero, the summation of the areas at any time divided by the appropriate effective mass for each range is equal to the instantaneous velocity at that time. The velocity vi at the incipient failure deflection X_u (time, t_u) may be expressed as:

$$v_i = \frac{i_b}{m_u} - \frac{r_u\, t_1}{m_u} - \frac{r_{up}\,(t_u - t_1)}{m_{up}} \qquad 4\text{-}187$$

where the values of i_b, r_u, t_1 and t_u are defined in Figure 4-72 and m_u and m_{up} are the effective masses of the single-degree-of-freedom system in the various flexural ranges (ultimate and post-ultimate) of the two-way element. The acceptor charge is assumed to be close to the barrier, so that the maximum velocity of the fragment after failure v_f is equal to the maximum velocity of the element at incipient failure v_i.

The expression for the deflection at any time may be found by multiplying each differential area (between the time t_o and the time in question), divided by the appropriate effective mass, by the time which is defined by the distance between the centroid of the area and the time in question, and adding these values algebraically. Using this procedure and the expression for the deflection at partial failure (initial failure of a two-way element) the deflection at time t_1 is:

$$X_1 = \frac{i_b\, t_1}{m_u} - \frac{r_u\, t_1^2}{2m_u} \qquad 4\text{-}188$$

while the equation for the deflection at incipient failure at t_u is given by:

$$X_u = \frac{i_b\, t_u}{m_u} - \frac{r_u\, t_1}{m_u}\left[t_u - \frac{t_1}{2}\right] - \frac{r_{up}\,(t_u - t_1)^2}{2m_{up}} \qquad 4\text{-}189$$

4-58.2.2. Post-Failure Impulse Capacity

The expression for the blast overload impulse capacity of a two-way element includes both the flexural capacity and the post-failure fragment momentum portion of the element's response. Solving Equations 4-187 through 4-189 simultaneously gives the expression for the blast overload impulse capacity. For a two-way element the resulting equation is:

$$\frac{i_b^2}{2m_u} = r_u X_1 + \left[\frac{m_u}{m_{up}}\right] r_{up}\,(X_u - X_1) + \frac{m_u\, v_f^2}{2} \qquad 4\text{-}190$$

For a one-way element or a two-way element which does not exhibit a post-ultimate range, the blast overload impulse capacity is:

$$\frac{i_b^2}{2m_u} = r_u X_u + \frac{m_u v_f^2}{2} \qquad 4\text{-}191$$

4-58.2.3. Response Time

The response time is the time at which the elements reach the ultimate deflection X_u, and failure occurs. The expression for the response time t_u is found by solving Equations 4-187 and 4-188 simultaneously. The response time for a two-way element is:

$$t_u = \frac{i_b}{m_u} + \left[\frac{m_{up}}{m_u r_{up}} - \frac{1}{r_u} \right] \left[i_b^2 - 2m_u r_u X_1 \right]^{1/2} - \frac{m_u}{r_{up}} v_f \qquad 4\text{-}192$$

The response time of a one-way element or for a two-way element which does not exhibit a post-ultimate range is:

$$t_u = \frac{i_b}{r_u} - \left[\frac{m_u}{r_u} \right] v_f \qquad 4\text{-}193$$

4-58.2.4. Design Equations

The basic equations for the analysis of the blast impulse capacity of an element are given above. However, the form of these equations is not suitable for design purposes. The use of these equations would require a tedious trial-and-error solution. Design equations can be derived in the same manner as for elements designed for incipient failure or less (see Sect. 4-33).

If Equations 4-190 and 4-191 are compared with Equations 4-95 and 4-96, it may be seen that except for the right-hand term in each of the above equations, the corresponding analytical expressions are the same if X_u is substituted for X_m The additional term in the above equations is the kinetic energy of the fragments after failure. Because of this similarity, Equations 4-190 and 4-191 may be expressed in a form which will be a function of the impulse coefficients (section 4-33), the geometry of the element, applied blast impulse and a post-failure fragment coefficient. The resulting equation is:

$$i_b^2 = C_u \left[\frac{p_H d_c^3 f_{ds}}{H} \right] + C_f d_c^2 v_f^2 \qquad 4\text{-}194$$

where

i_b = applied unit blast impulse

p_H = reinforcement ratio in the horizontal direction

d_c = distance between centroids of the compression and tension reinforcement

f_{ds} = dynamic design stress for the reinforcement

H = span height

v_f = maximum velocity of the post-failure fragments

C_u = impulse coefficient for ultimate deflection X_u

C_f = post-failure fragment coefficient

Equation 4-194 is applicable to both one-way and two-way elements which are uniformly loaded. Values of C_u can be found in Section 4-33. The post-failure fragment coefficient takes into account the variation in the effective mass. It is a function of the element's horizontal and vertical reinforcement ratios, aspect ratio and boundary conditions. To facilitate the design procedure, values of the post-failure fragment coefficient C_f have been plotted in Figures 4-73, 4-74 and 4-75 for two-way elements supported on two adjacent edges, three edges and four edges respectively. For one-way elements, the value of coefficient C_f is a constant (C_f = 22,500).

4-58.2.5. Optimum Reinforcement

The optimum arrangement of the flexural reinforcement in two-way elements designed for post-failure fragments will not necessarily be the same as that for similar elements which are designed for incipient failure damage or less. The optimum ratio of the vertical to horizontal reinforcement p_v/p_H will be a function of the amount of the blast impulse absorbed through the flexural action of the element in comparison to that which contributes to the momentum of post-failure fragments. Unlike incipient failure design, the optimum ratio will vary with a variation in the depth of the element. As discussed earlier, the optimum depth of an element and total amount of reinforcement p_T is a function of the relative costs of concrete and reinforcing steel. In a given situation, the designer must establish, through a trial and error design procedure and a cost analysis, the optimum depth, reinforcement ratio p_v/p_H and total amount of reinforcement p_T.

For very large projects. this type of detailed analysis may result significant cost benefits, but for most projects using the values of p_v/p_H and p_T recommended for incipient failure design will yield an economical design.

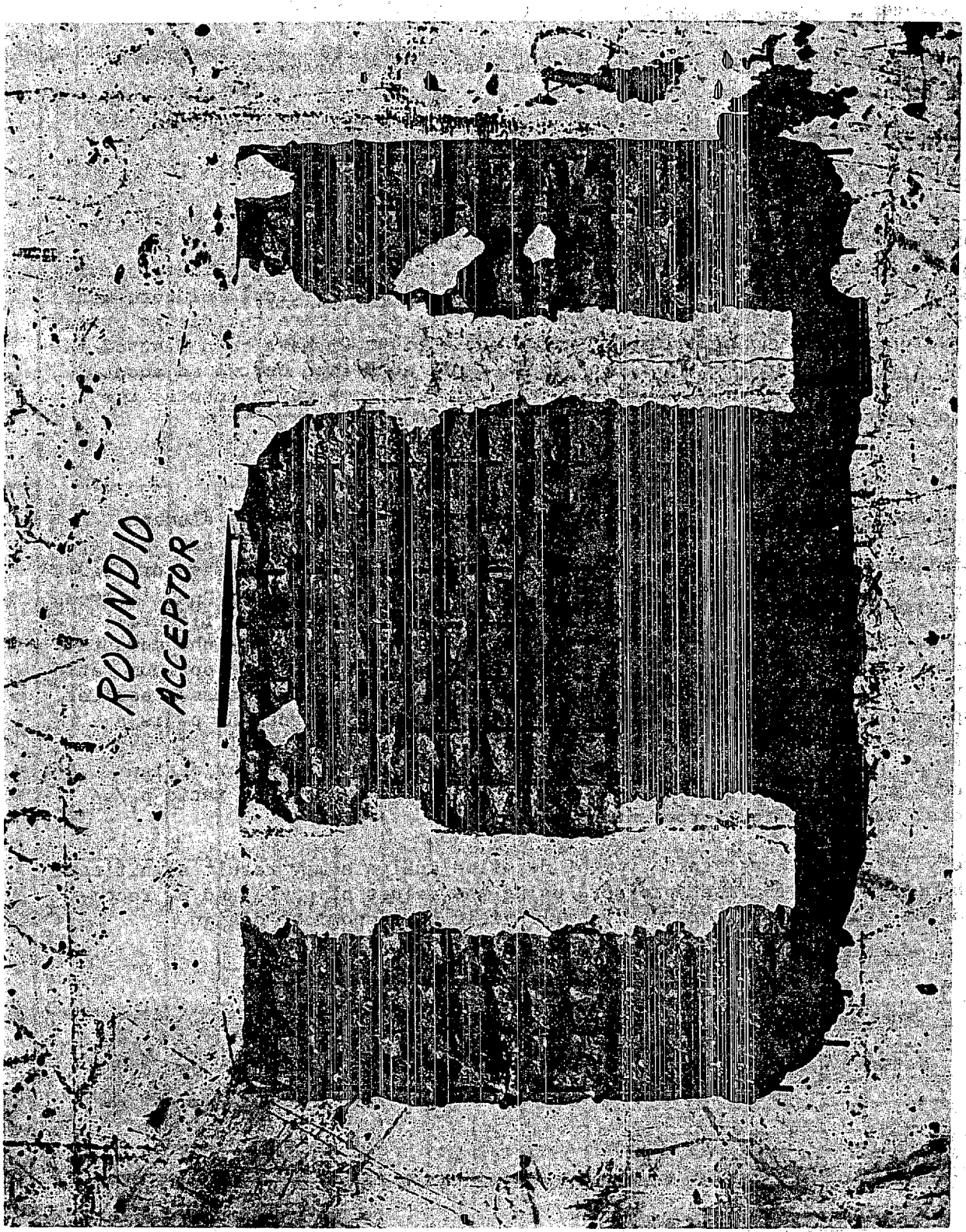


Figure 4-63 Direct spalled element

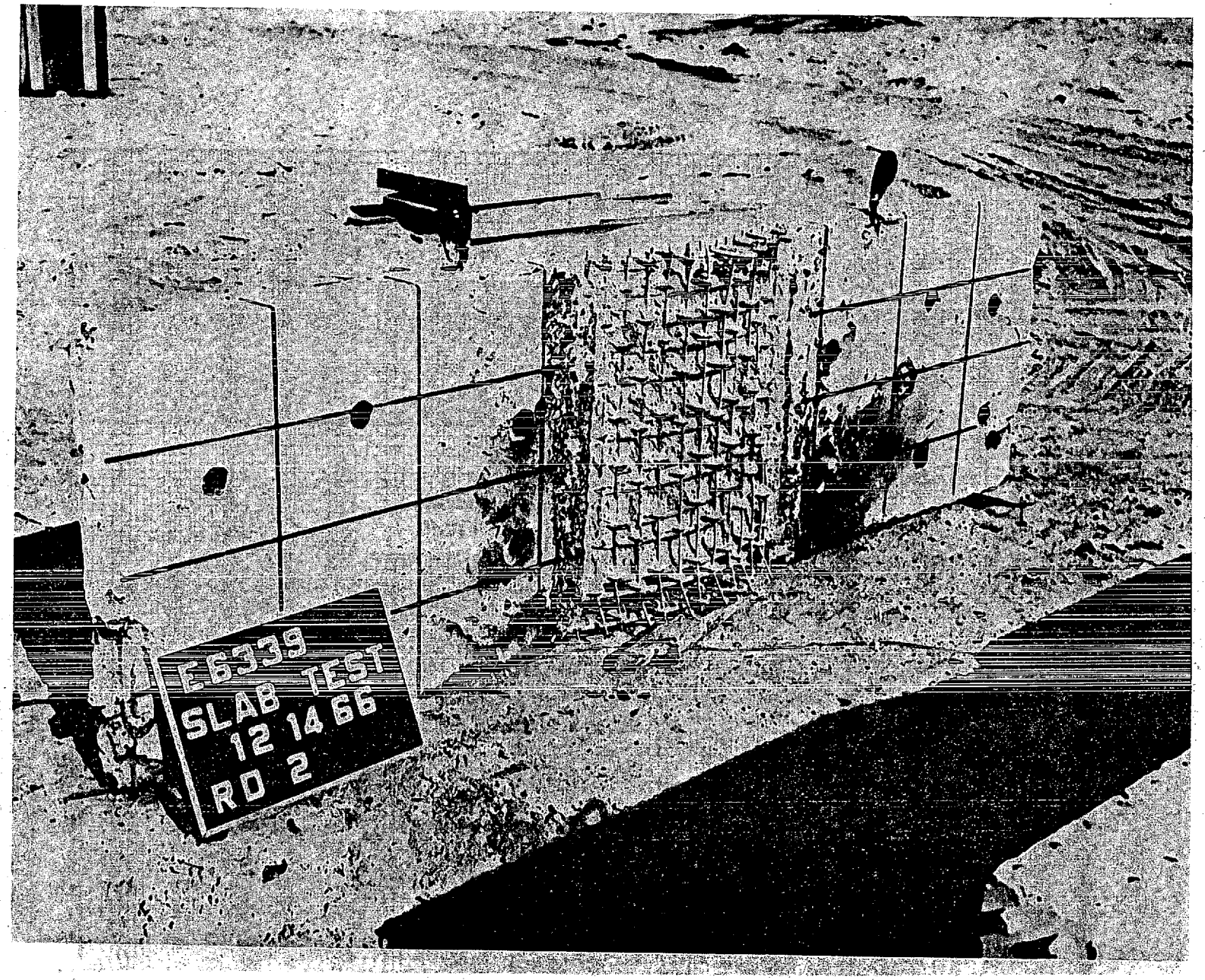


Figure 4-64 Scabbed element

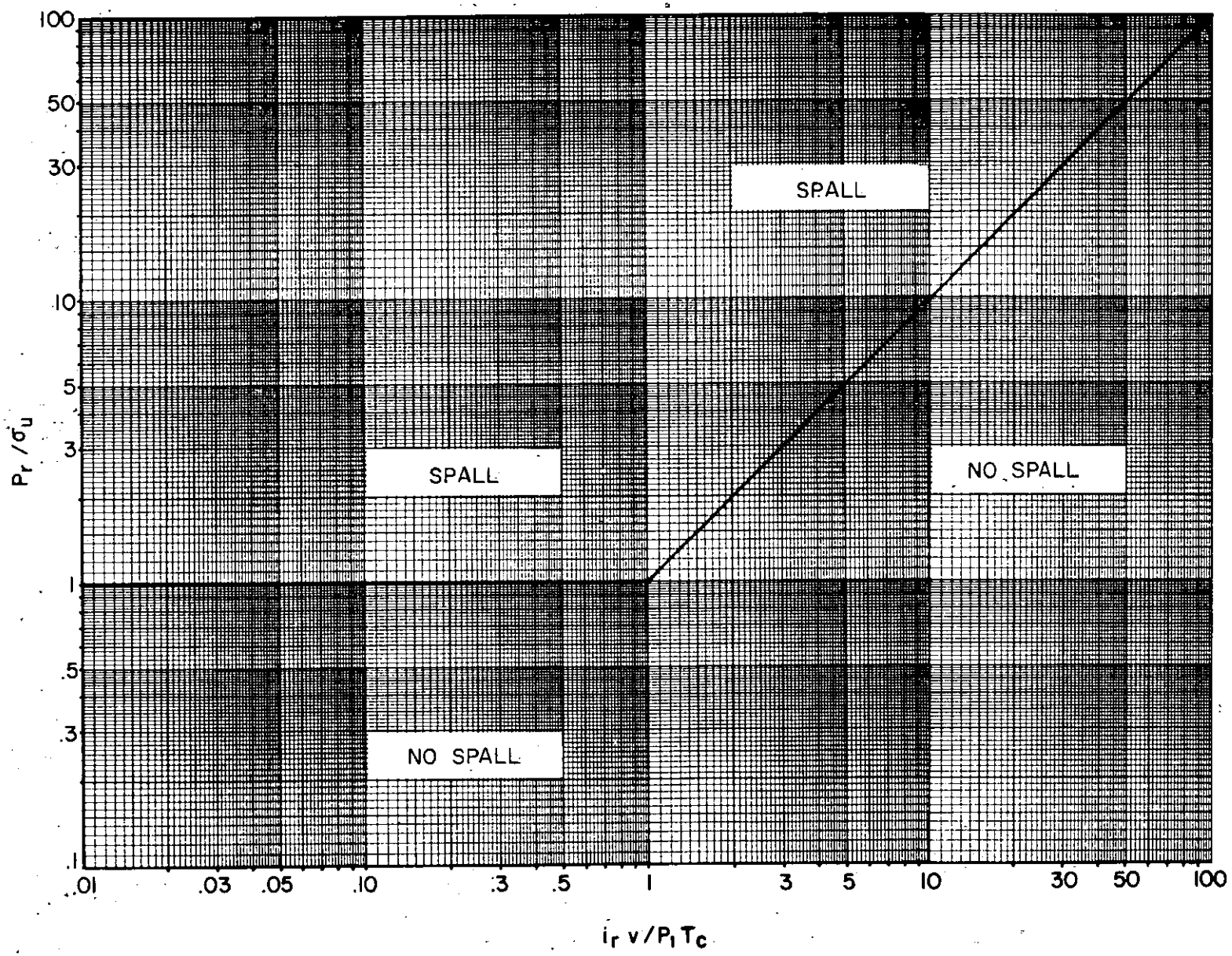


Figure 4-65 Spall threshold for blast waves loading walls

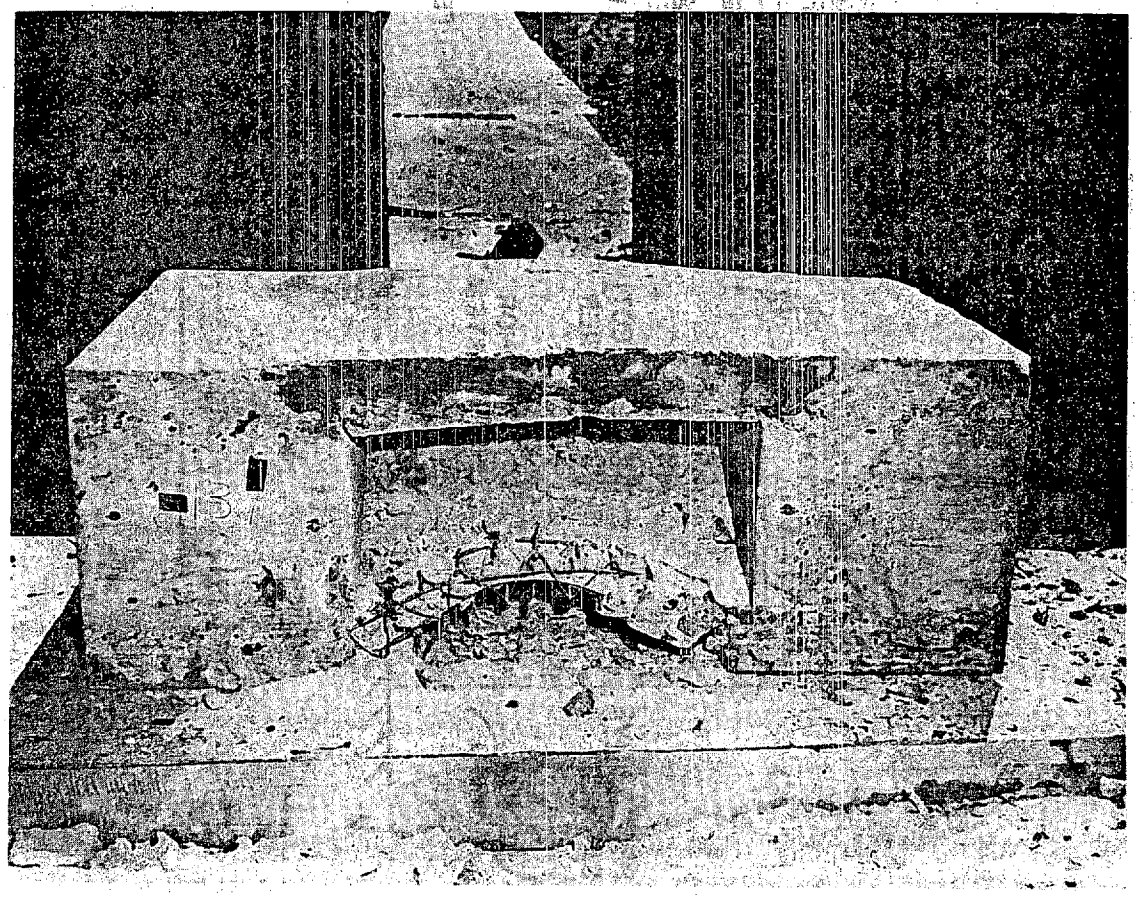


Figure 4-66 Unspalled acceptor panel of composite panel

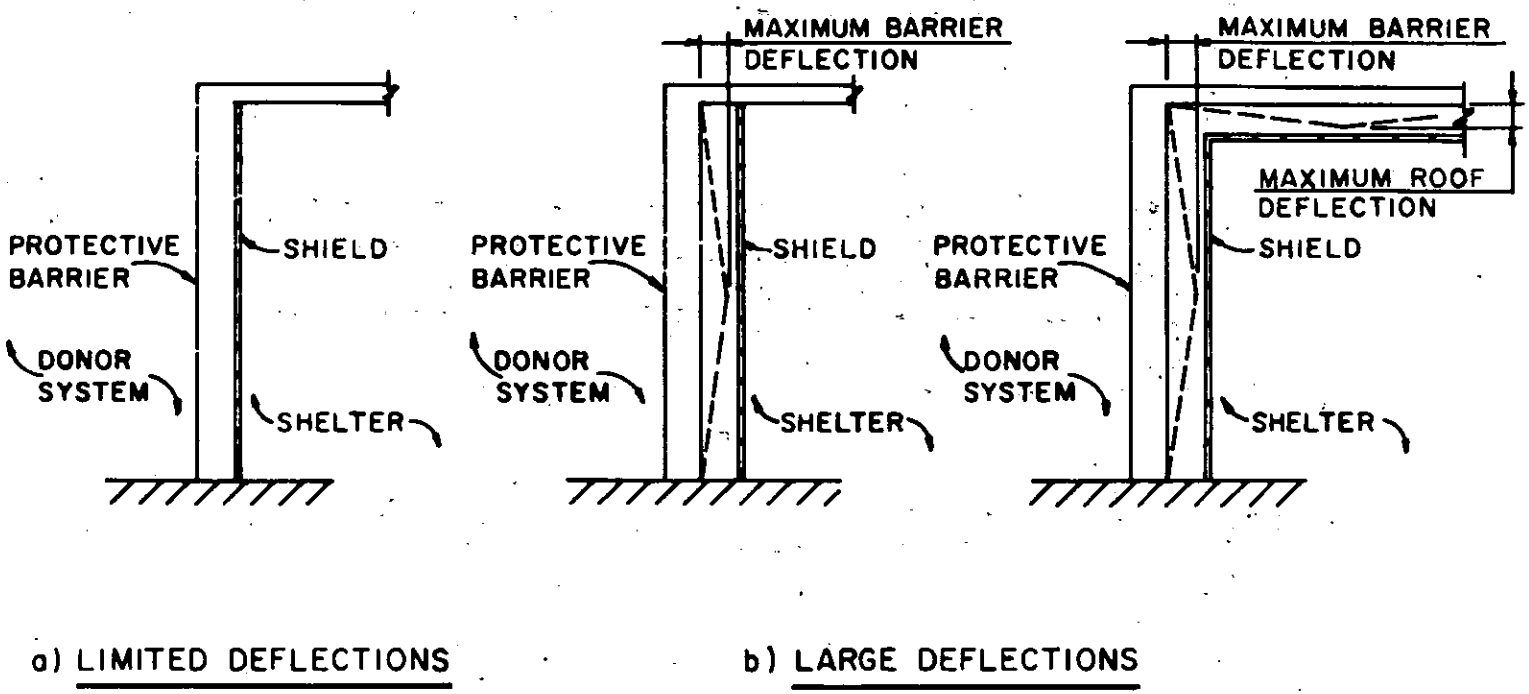


Figure 4-67 Sheilding systems for protection against concrete fragments

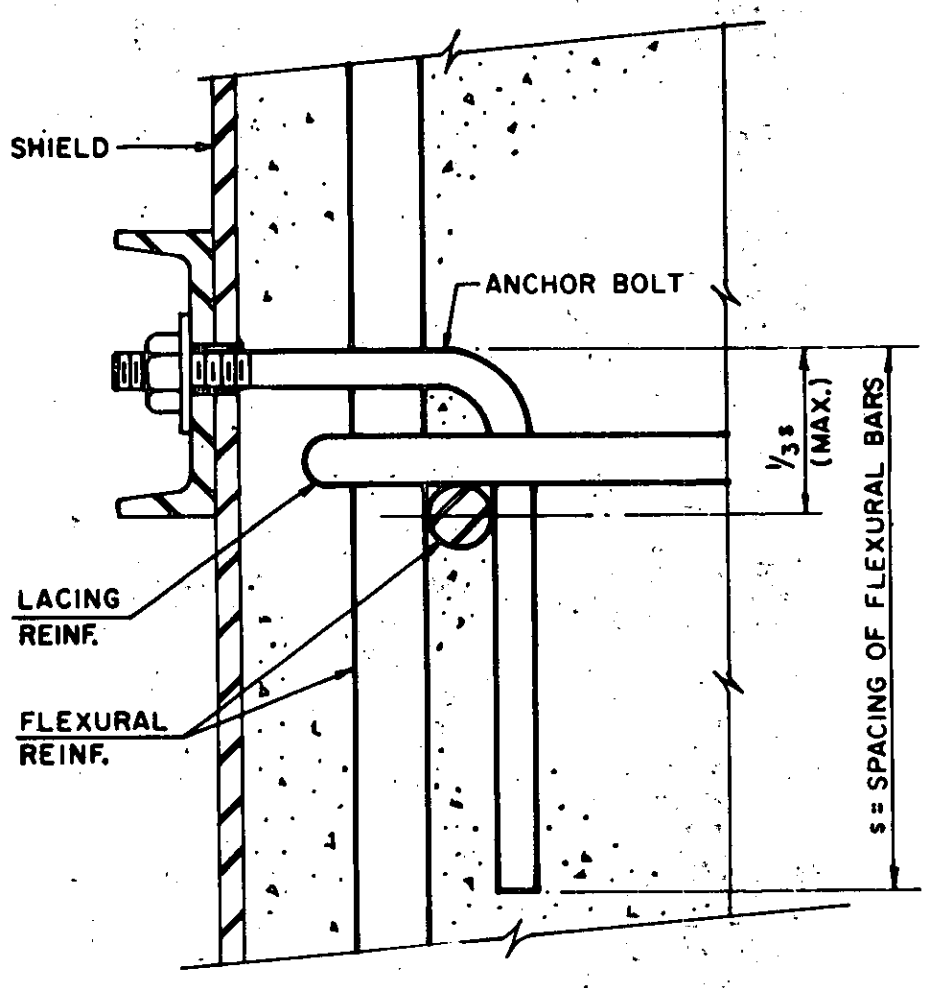


Figure 4-68 Rigid attachment of fragment shield to barrier



Figure 4-69 Failure of an unlaced element

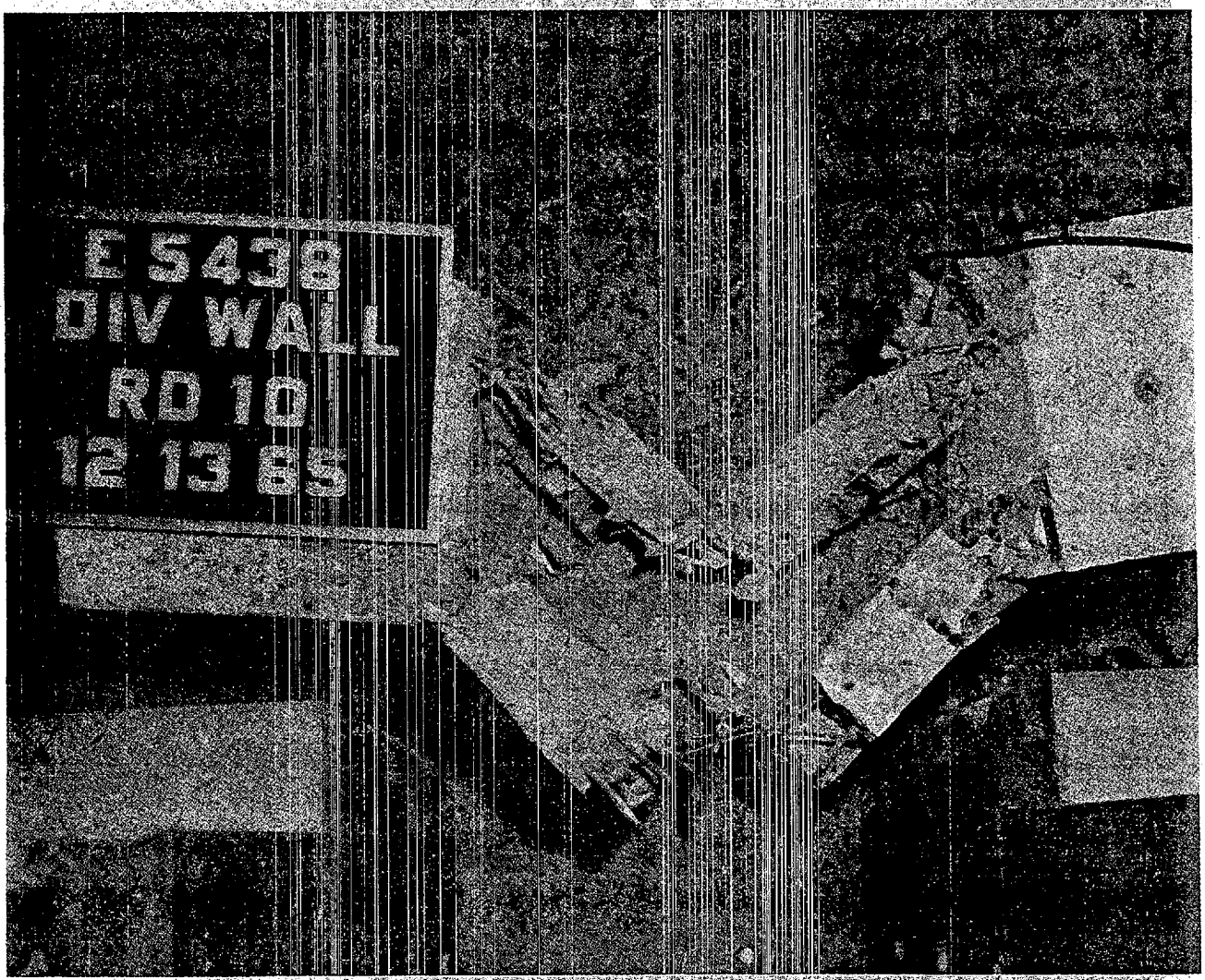


Figure 4-70. Failure at plastic hinges of laced elements.

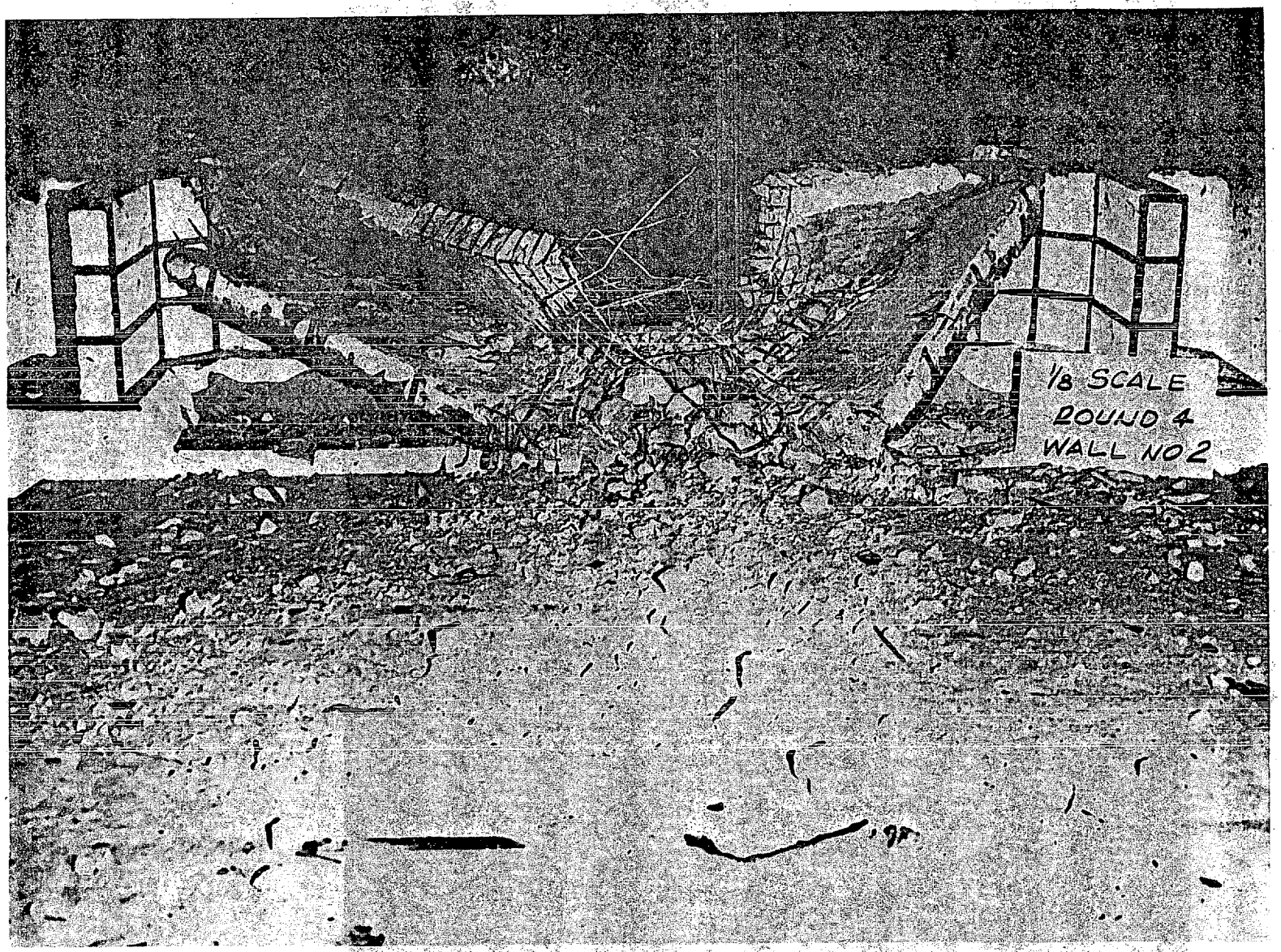
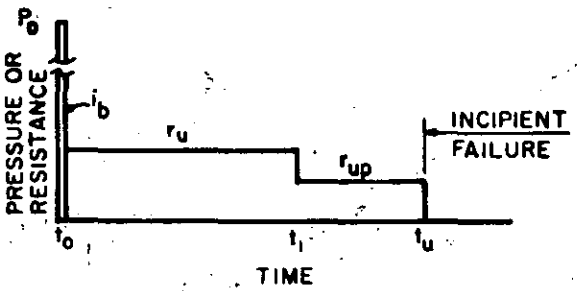
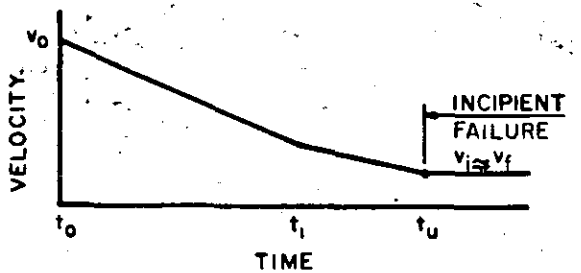


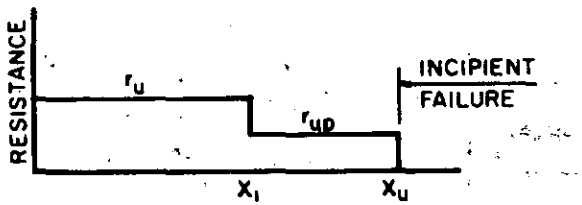
Figure 4-71 Backwall failure of cubicle with laced reinforcement



a) IDEALIZED PRESSURE - TIME AND RESISTANCE - TIME CURVES



b) IDEALIZED VELOCITY - TIME CURVE



C) IDEALIZED RESISTANCE - DEFLECTION CURVE

i_b = unit blast impulse
r_u = ultimate unit resistance
r_{up} = post-ultimate unit resistance
t_o = duration of positive phase of blast pressure
t_1 = time at which partial failure occurs
t_u = time at which ultimate deflection occurs
v_f = post-failure fragment velocity
v_i = velocity of element at incipient failure
v_o = initial velocity of element
X_1 = partial failure deflection
X_u = ultimate deflection

Figure 4-72 Idealized curves for determination of post-failure fragment velocities

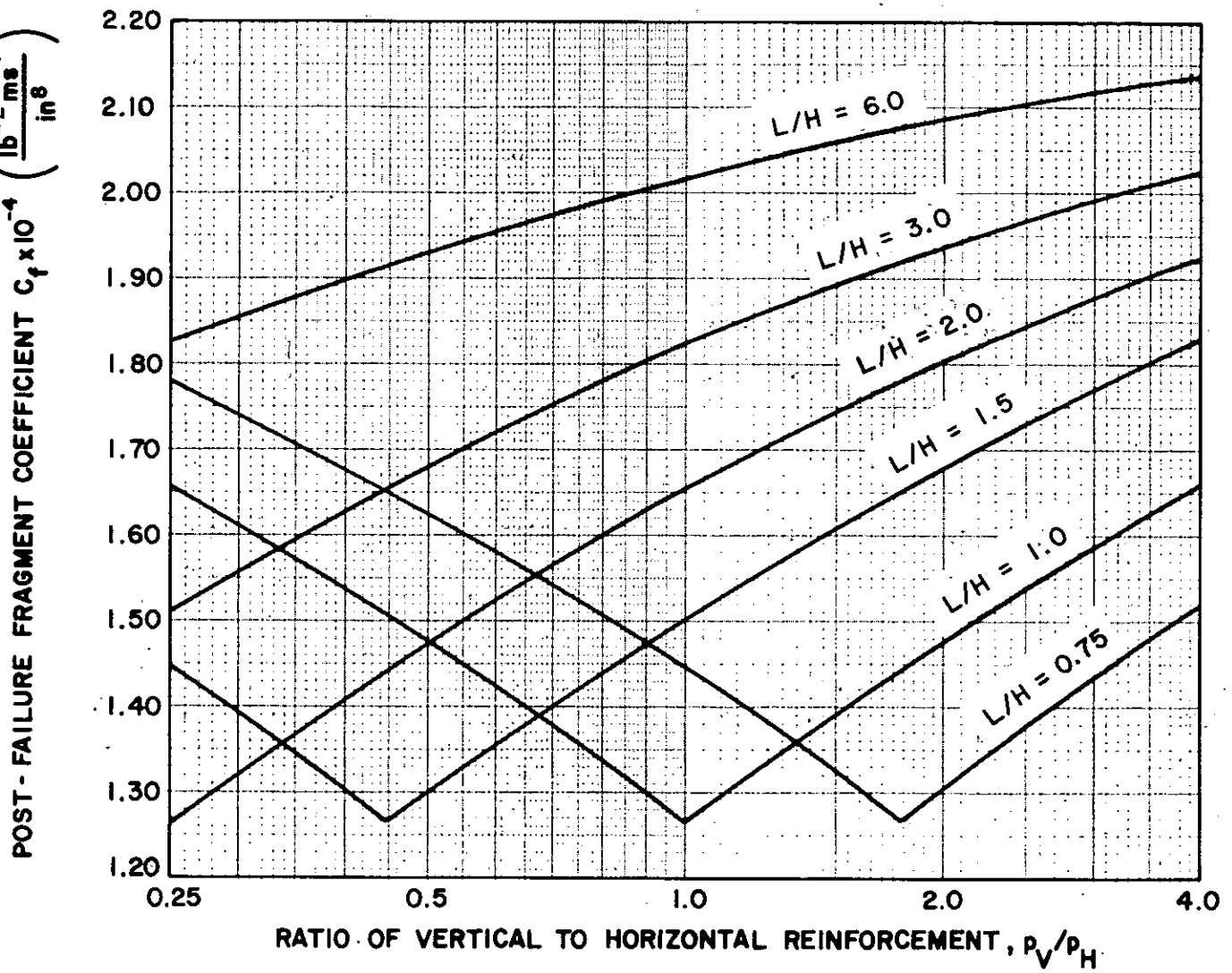


Figure 4-73 Post-failure coefficient C_f for an element fixed on two adjacent edges and two edges free

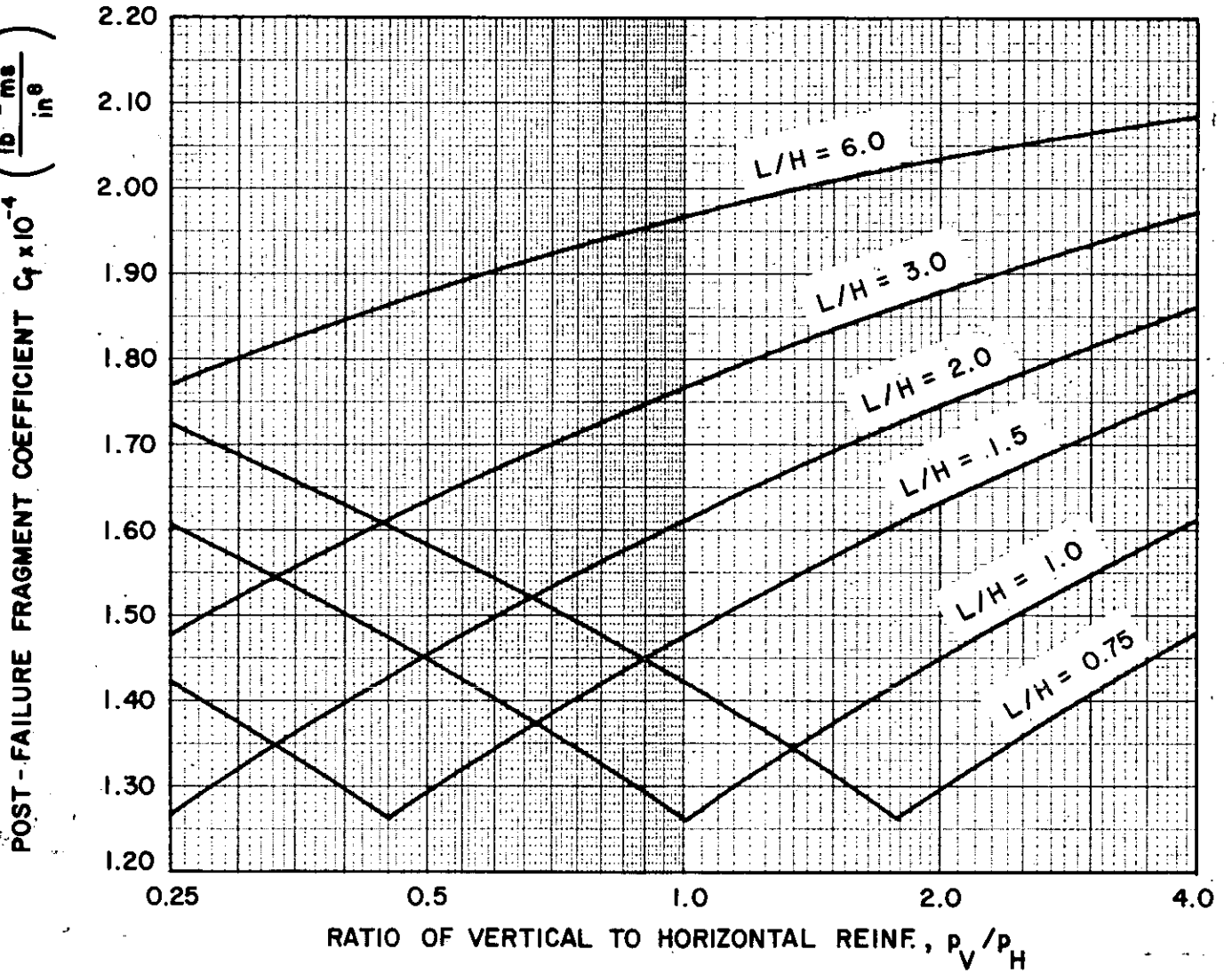


Figure 4-74 Post-failure coefficient C_f for an element fixed on three edges and one edge free

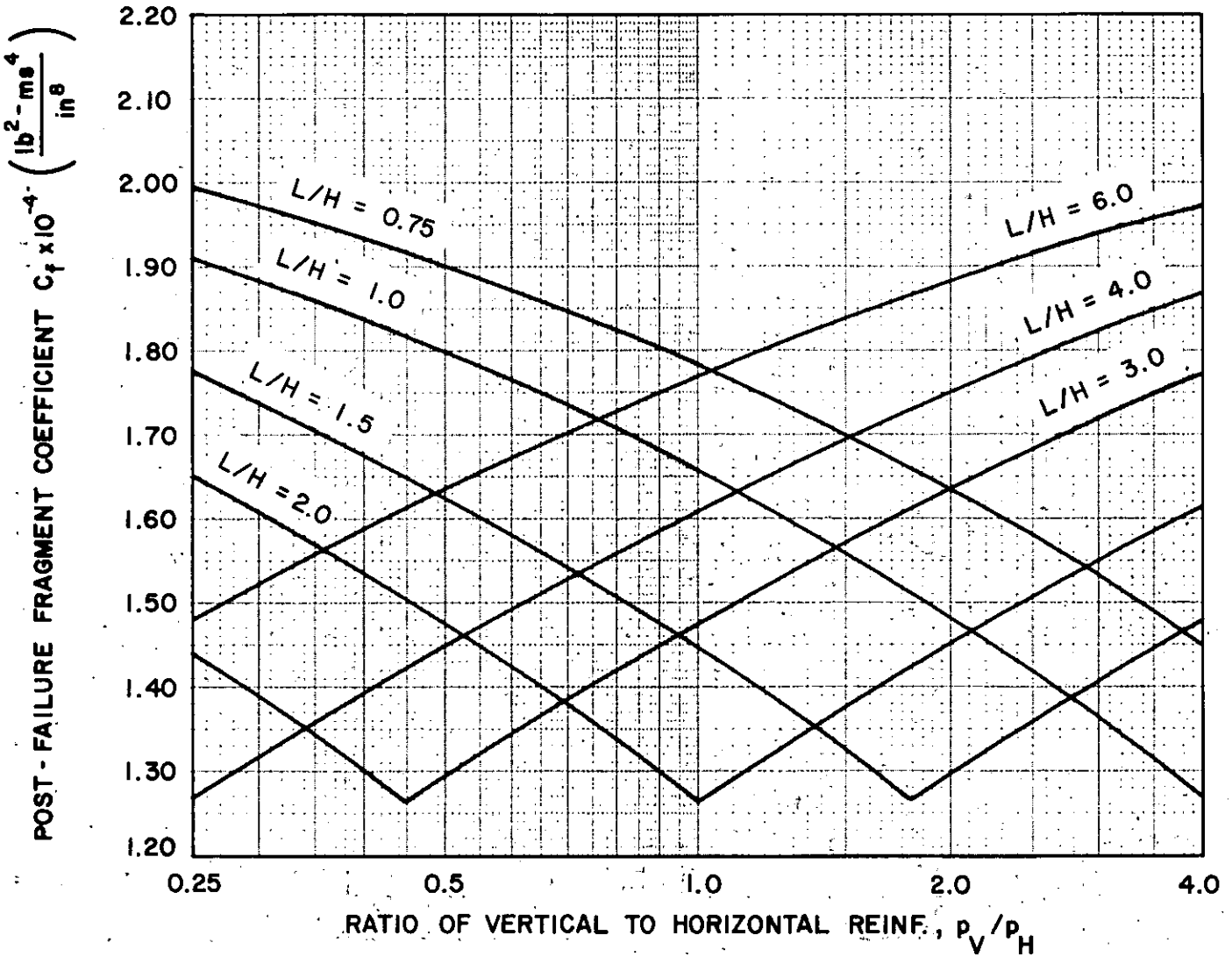


Figure 4-75 Post-failure coefficient C_f for an element fixed on four edges

STRUCTURAL BEHAVIOR TO PRIMARY FRAGMENT IMPACT

4-59. Introduction

4-59.1. Fragment Characteristics

Detonation of cased explosives results in the formation of primary fragments due to the shattering of the casing. These fragments are usually small in size and initially travel at velocities in the order of thousands of feet per second. Upon contact with a barrier, the fragments will either pass through (perforate), be embedded in (penetrate with or without spalling), or be deflected by the barrier. The resulting effect is dependent on the interaction of the following factors: (1) the magnitude of the initial velocity, (2) the distance between the explosion and the barrier, (3) the angle at which the fragment strikes the barrier (angle of obliquity), and (4) the physical properties of the fragment (mass, shape and material strength) and the barrier (concrete strength and thickness).

4-59.2. Velocity and Impact Limitations

This section deals with the situation where a fragment with given properties strikes a barrier element with a known velocity and where the angle of obliquity between the trajectory path of the fragment and a normal to the surface of the barrier is zero degrees (normal impact). The striking velocity of the fragment is assumed equal to its initial velocity for a detonation in close proximity to the element or is determined according to the procedure in Chapter 2 for cases where the fragment travels a distance greater than 20 feet.

4-60. Fragment Impact on Concrete

4-60.1.. General

When a primary fragment strikes a concrete barrier, penetration resisting pressures, in the order of thousands of psi, act on the cross-sectional area of the fragment. For a given mass of the fragment, as the striking velocity is increased, the resisting pressures also increase, while for an increase in the cross-sectional area of the fragment, the resisting pressures decrease. If the fragment can withstand these pressures acting on its frontal surface, then the amount of penetration will be governed by its mass, shape, and striking velocity. On the other hand, if the fragment deforms under the applied loads, then the resisting pressures in the concrete become effective over an increased cross-sectional area, thereby reducing the possible penetration for a given available kinetic energy of the fragment. Generally, larger penetrations may be expected with less ductile metals such as fragments from armor piercing casings.

As a fragment impinges on a wall surface, a section of the wall adjacent to the point of impact spalls, forming a crater around the impact area (Fig. 4-76). This crater is conical in shape but irregular. As the striking velocity of the fragment increases, the size of the crater also increases. At small velocities, the increase in the crater size for a given velocity increment is more rapid than at higher velocities in the order of several thousand feet per second. At a striking velocity of approximately 1,000 feet per second or less, the fragment does not usually penetrate beyond the depth of the crater,

while for larger velocities, the fragment penetrates beyond the front of the crater and either lodges within or passes through the barrier.
A crater similar to that formed on the front face of the barrier is also produced on the back side if the kinetic energy of the fragment upon impact is sufficient to produce excessive tensile stresses in the concrete. As in the case of the front-face crater the size of the crater on the back face increases with an increase in striking velocity of a particular fragment. The back-face crater is generally wider and shallower than the front-face crater, though again the surface of the crater is irregular. Quite often, the kinetic energy afforded by the striking fragment is only sufficient to dislodge the concrete on the exterior side of the rear face reinforcement. In this case, only spalling will occur. As the striking velocity is increased beyond the limit to cause spalling, the penetration of the fragment into the slab increases more and more until perforation is attained.

4-60.2. Penetration by Armor-Piercing Fragments

A certain amount of experimental data, which is analogous to primary fragment penetration, has been accumulated in connection with projects to determine the effects of bombs and projectile impact on concrete structures. This data has been analyzed in order to develop relationships for the amount of fragment penetration into concrete elements in terms of the physical properties of both the metal fragment and the concrete. A general expression for the maximum penetration into a massive concrete slab (i.e. a slab with infinite thickness) by an armor-piercing fragment has been obtained as follows:

$$X_f = 4.0 \times 10^{-3} (KND)^{0.5} d^{1.1} v_s^{0.9} \quad \text{for } X_f \le 2d, \qquad 4\text{-}195$$

$$X_f = 4.0 \times 10^{-6} KND\, d^{1.2} v_s^{1.8} + d \quad \text{for } X_f > 2d \qquad 4\text{-}196$$

and

$$K = 12.91/(f'_c)^{1/2} \qquad 4\text{-}197$$

where:

X_f = penetration by armor-piercing steel fragments

K = penetrability constant

N = nose shape factor as defined in Figure 4-77

D = caliber density as defined in Figure 4-77

d = fragment diameter

v_s = striking velocity

For the standard primary fragment and concrete strength f'_c equal to 4,000 psi, Equations 4-195 and 4-196 reduce to the following equations in terms of fragment diameter (in) and the striking velocity v_s (fps):

$$X_f = 2.86 \times 10^{-3} d^{1.1} v_s^{0.9} \quad \text{for } X_f \le 2d \qquad 4\text{-}198$$

$$X_f = 2.04 \times 10^{-6} d^{1.2} v_s^{1.8} + d \quad \text{for } X_f > 2d \qquad 4\text{-}199$$

Equations 4-198 and 4-199 can also be expressed in terms of fragment weight (standard shape) as:

$$X_f = 1.92 \times 10^{-3} W_f^{0.37} v_s^{0.9} \quad \text{for } X_f \leq 2d \qquad 4\text{-}200$$

$$X_f = 1.32 \times 10^{-6} W_f^{0.4} v_s^{1.8} + 0.695 W_f^{0.33} \quad \text{for } X_f > 2d \qquad 4\text{-}201$$

Figure 4-78 is a plot of the maximum penetration of a standard fragment through 4,000 psi concrete for various fragment weights and striking velocities.

Maximum penetration of fragments in concrete of strengths other than 4,000 psi, may be calculated using the values of X_f from Equation 4-200, 4-201 or Figure 4-78 and the following equation:

$$X'_f = X_f \left[\frac{4{,}000}{f'_c} \right]^{1/2} \qquad 4\text{-}202$$

where:

X_f = maximum penetration into 4,000 psi concrete

X'_f = maximum penetration into concrete with compressive strength equal to f'_c

In addition to the weight and striking velocity of a primary fragment, its shape will also affect the resulting penetration. The sharper the leading edge of a fragment, the greater the distance traveled through the concrete. The shape indicated in Figure 4-77 is not necessarily the most critical. When the container of an explosive shatters, it is statistically probable that some of the resulting fragments will have a sharper shape than the standard bullet shape assumed in this manual. However, the number of these fragments is usually very small in comparison to the total number formed, and the probability that these sharper fragments will have normal penetrations though the concrete is low. In most instances, the majority of the primary fragments will have a more blunt shape than that shown. Therefore, for design purposes, the normal penetrations defined for a bullet-shaped fragment can usually be assumed as critical.

4-60.3. Penetration of Fragments Other than Armor-Piercing

To estimate the concrete penetration of metal fragments other than armor-piercing, a procedure has been developed where the concrete penetrating capabilities of armor-piercing fragments have been related to those of other metal fragments. This relationship is expressed in terms of relative metal hardness (the ability of the metal to resist deformation) and density, and is represented by the constant in Equation 4-203.

$$X'_f = k X_f \qquad 4\text{-}203$$

where:

X'_f = maximum penetration in concrete of metal fragments other than armor-piercing fragments

k = constant depending on the casing metal, from Table 4-16

X_f = maximum penetration of armor-piercing fragment

It should be noted that X_f is calculated from Equation 4-200, 4-201 or Figure 4-78 if f'_c = 4,000 psi, and from Equation 4-202 when X_f is modified for concrete strengths other than 4,000 psi.

4-60.4. Perforation of Concrete

Quite often the magnitude of the initial kinetic energy of primary fragments will be large enough to produce perforation of the concrete. The depth of penetration X_f of a fragment into massive concrete is less than into a wall of finite thickness due to the high resisting stresses afforded by the massive concrete. Consequently, the concrete thickness required to prevent perforation is always greater than the depth of penetration X_f into massive concrete. The minimum thickness of concrete required to prevent perforation can be expressed in terms of the equivalent depth of penetration into massive concrete and the fragment size according to the following relationship:

$$T_{pf} = 1.13\, X_f\, d^{0.1} + 1.311\, d \qquad 4\text{-}204$$

where:

T_{pf} = minimum thickness of concrete to prevent perforation by a given fragment

X_f = depth of penetration corrected for concrete strength and fragment material

Fragments which perforate a concrete element will have a residual velocity which may endanger the receiver system. The magnitude of this velocity may be approximated from the expression which defines the velocity of the fragment at any time as it penetrates the concrete.

For cases where X_f is less than 2d:

$$v_r / v_s = \left[1 - (T_c / T_{pf})^2 \right]^{0.555} \qquad 4\text{-}205$$

and for cases where X_f is greater than 2d:

$$v_r / v_s = \left[1 - (T_c / T_{pf}) \right]^{0.555} \qquad 4\text{-}206$$

where:

T_c = thickness of the concrete, less than or equal to T_{pf}

v_r = residual velocity of fragment as it leaves the element

Plots of v_r / v_s against T_c / T_{pf} according to Equations 4-205 and 4-206 are presented in Figures 4-79 and 4-80, respectively.

4-60.5. Spalling due to Fragment Impact

When a primary fragment traveling at a high velocity strikes the donor surface of a concrete barrier, large compression stresses are produced in the vicinity of the point of impact. These stresses form a compression wave which travels from the impact point, expanding spherically until it reaches the back face element. At this free surface, the compression wave is reflected (reversed in direction and changed from a compression wave to a tension wave). When the stresses in the resulting tension wave exceed the tensile capacity of the concrete, spalling of the concrete at the receiver surface occurs. The spalling forms a crater on the receiver surface. This crater does not usually penetrate beyond the reinforcement at the receiver surface.

The occurrence of spalling is a function of the fragment penetration; i.e., the fragment must penetrate a barrier element to such a depth that sufficiently large stresses are formed at the receiver surface to produce spalling. If the thickness of the element is increased above the critical thickness at which spalling occurs for a particular fragment, then the spalling is eliminated. On the other hand, concrete spalling always occurs with fragment perforation. The minimum thickness of concrete barrier required to prevent spalling due to penetration of a given fragment can be expressed in terms of the fragment penetration into massive concrete and the fragment diameter:

$$T_{sp} = 1.215\, X_f\, d^{0.1} + 2.12d \qquad 4\text{-}207$$

where:

T_{sp} = minimum concrete thickness to prevent spalling

X_f = depth of penetration corrected for concrete strength and fragment material

The secondary fragment velocities associated with spalling resulting from fragment impact are usually small (less than 5 fps). However, when blast pressures are also involved, the magnitude of the resulting velocities can be quite large. The secondary concrete fragments are accelerated by the motion of the barrier resulting in possible fragment velocities up to several hundred feet per second.

Because of the potentially large secondary fragment velocities associated with primary fragment impact, full protection is usually required for personnel, valuable equipment, and sensitive explosives. This protection may be accomplished either by providing sufficient concrete thickness to eliminate spalling or by other mechanical means used to minimize the effects of spalling resulting from blast pressures as described in section 4-56. The required concrete thickness to eliminate spalling caused by primary fragment impact may be obtained from Equation 4-207.

4-61. Fragment Impact on Composite Construction

4-61.1. General To evaluate the effect of primary fragments on composite (concrete-sand-concrete) barriers, the penetration of the fragment through both the concrete and sand must be considered. For damage to be sustained at

the rear of a composite barrier a fragment must first perforate both the donor concrete panel and the sand, and then penetrate or perforate the receiver panel. If the fragment penetrates only part of the way through the receiver panel, then spalling may or may not occur, depending on the panel thickness. Obviously, fragment perforation of the receiver panel indicates perforation of the entire barrier.

4-61.2. Penetration of Composite Barriers

To determine the degree of damage at the receiver side, the penetration of the fragment in each section of the barrier must be investigated in sequence. Starting with the striking velocity and the weight of the primary fragment, the donor concrete section is first analyzed to determine whether or not perforation of that section occurs. If the calculations indicate that the fragment will stop within this section, then no damage will be sustained by the remainder of the barrier. On the other hand, if perforation does occur in the forward (donor) section, then the fragment penetration through the sand must be investigated.

The amount of the penetration through the sand depends upon the magnitude of the residual velocity as the fragment leaves the rear of the donor panel. This residual velocity is determined from Figures 4-79 and 4-80 utilizing the striking velocity, the thickness of the donor panel, and the theoretical maximum fragment penetration obtained from Figure 4-78.

The maximum penetration through massive sand is obtained from Equation 4-208, using the residual velocity calculated above as the striking velocity of the fragment on the surface of the sand.

$$X_s = 1.188\ Dd\ \ln\left(1 + 2.16 \times 10^{-3}\ v_s^2\right) \qquad 4\text{-}208$$

where:

X_s = penetration of the fragment into the sand

Substituting the caliber density D for a standard shape (Fig. 4-77), Equation 4-208 becomes:

$$X_s = 3.53d\ \ln\left(1 + 2.16 \times 10^{-3}\ v_s^2\right) \qquad 4\text{-}209$$

A plot of Equation 4-209 for a range of fragment weights and striking properties is shown in Figure 4-81. If the penetration in the sand is found to be less than the thickness of the sand layer, no damage is sustained at the rear surface of the barrier. In case of perforation, the penetration of the fragment into the rear section (receiver) of the barrier is governed by the residual velocity as the fragment leaves the sand. This residual velocity is calculated in a manner similar to that used for computing the residual velocity for the donor panel, except that the fragment penetration and striking velocity are those associated with movement of the fragment through the sand, that is:

$$v_r / v_s = \left[1 - T_s / X_s\right]^{0.555} \qquad 4\text{-}210$$

where:

T_s = actual thickness of the sand layer

Figure 4-80 can be used to calculate the residual velocity of a fragment perforating the sand layer.

Similar to the fragment penetration through the donor panel and sand, penetration of the fragment through the receiver panel is a function of the magnitude of the fragment velocity as the fragment strikes the forward surface of the panel. This velocity is equal to the residual velocity as the fragment leaves the sand. Once the penetration in the receiver panel is known, then the damage sustained at the rear of the composite barrier can be defined in terms of either spalling or fragment perforation.

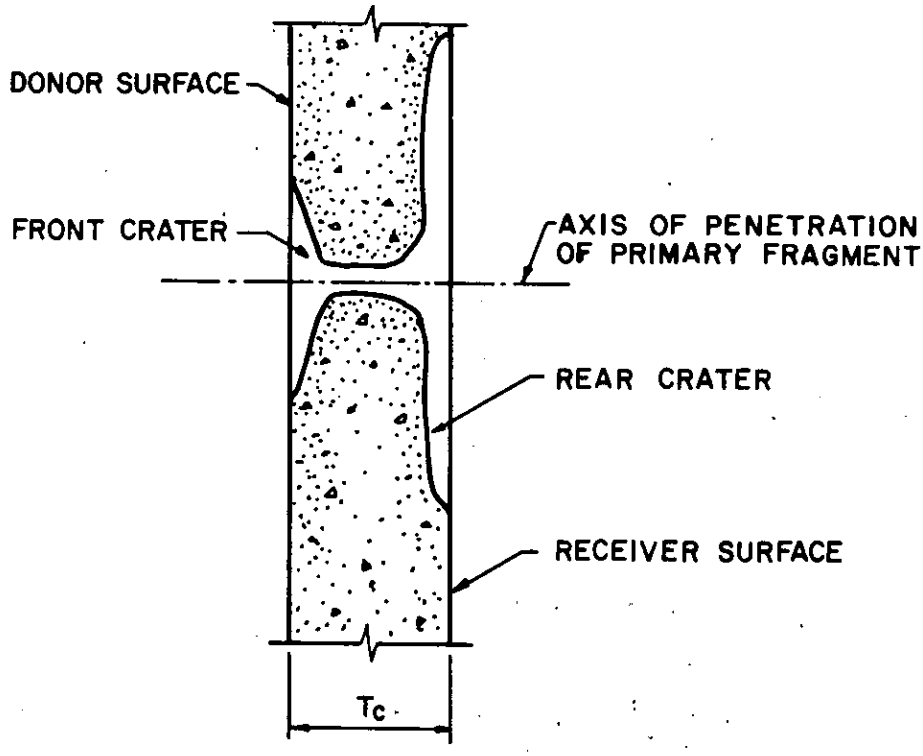
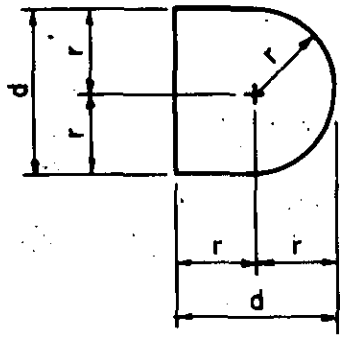


Figure 4-76 Perforation and spalling of concrete due to primary fragments



d = DIAMETER OF CYLINDRICAL PORTION OF FRAGMENT

r = RADIUS OF HEMISPHERICAL PORTION OF FRAGMENT

$r = \frac{d}{2}$

D = CALIBER DENSITY, W_f / d^3 = 2.976 oz./in.^{3}

W_f = FRAGMENT WEIGHT

N = NOSE SHAPE FACTOR = $0.72 + 0.25 \sqrt{n - 0.25} = 0.845$

n = CALIBER RADIUS OF THE TANGENT OGIVE OF THE FRAGMENT NOSE = r/d

Figure 4-77 Shape of standard primary fragments

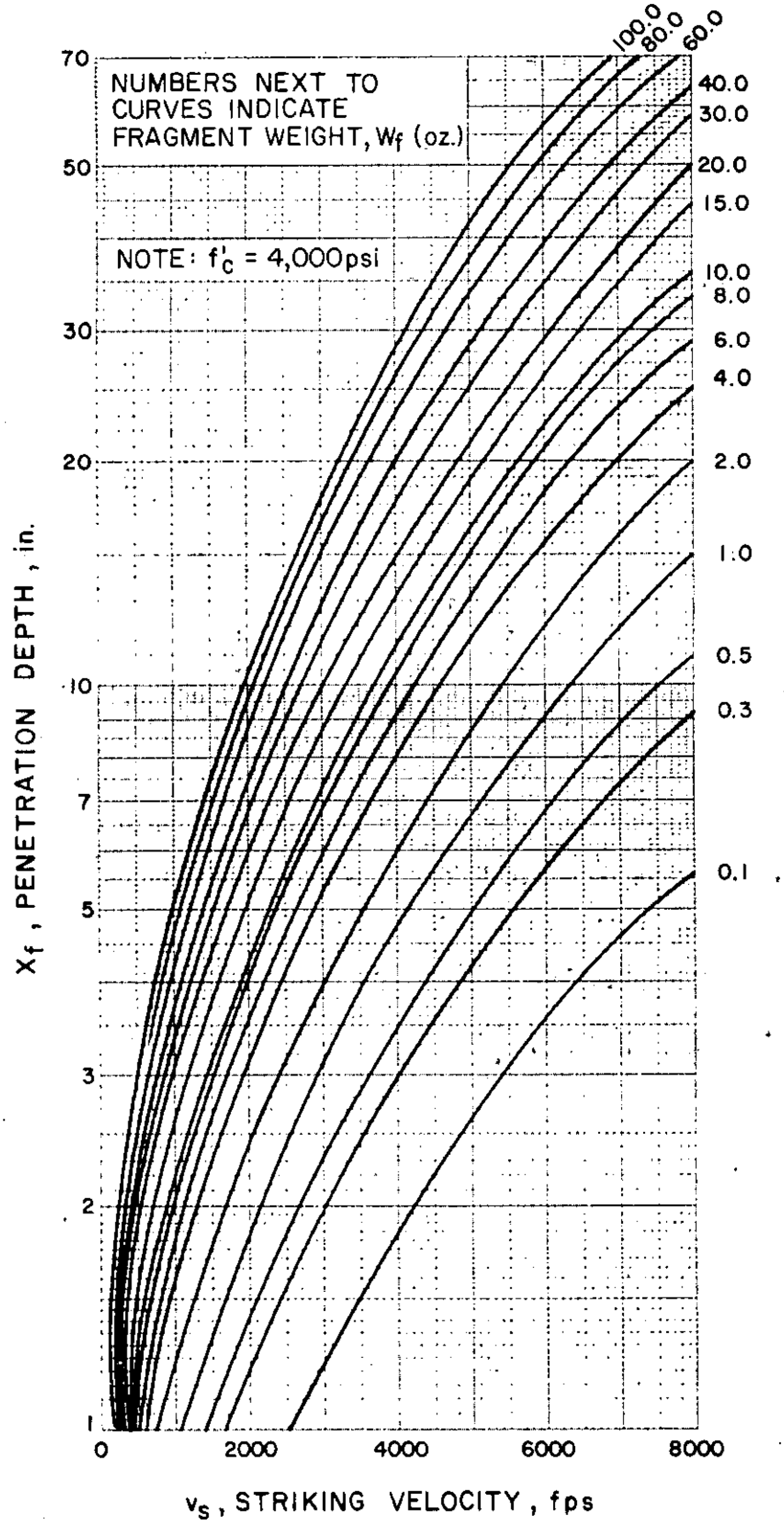


Figure 4-78 Concrete penetration chart for armor-piercing steel fragments

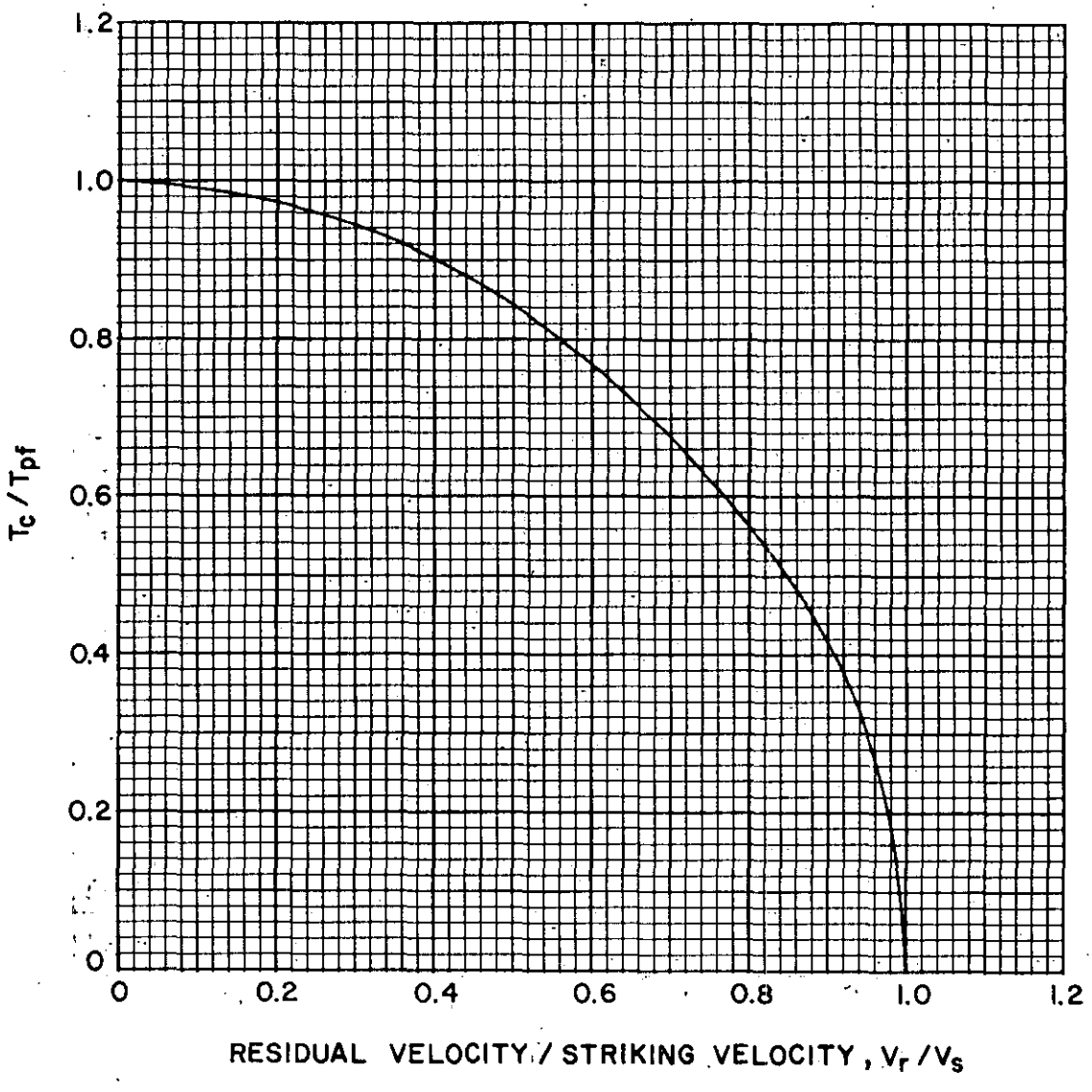


Figure 4-79 Residual fragment velocity upon perforation of concrete barriers (for cases where x < 2d)

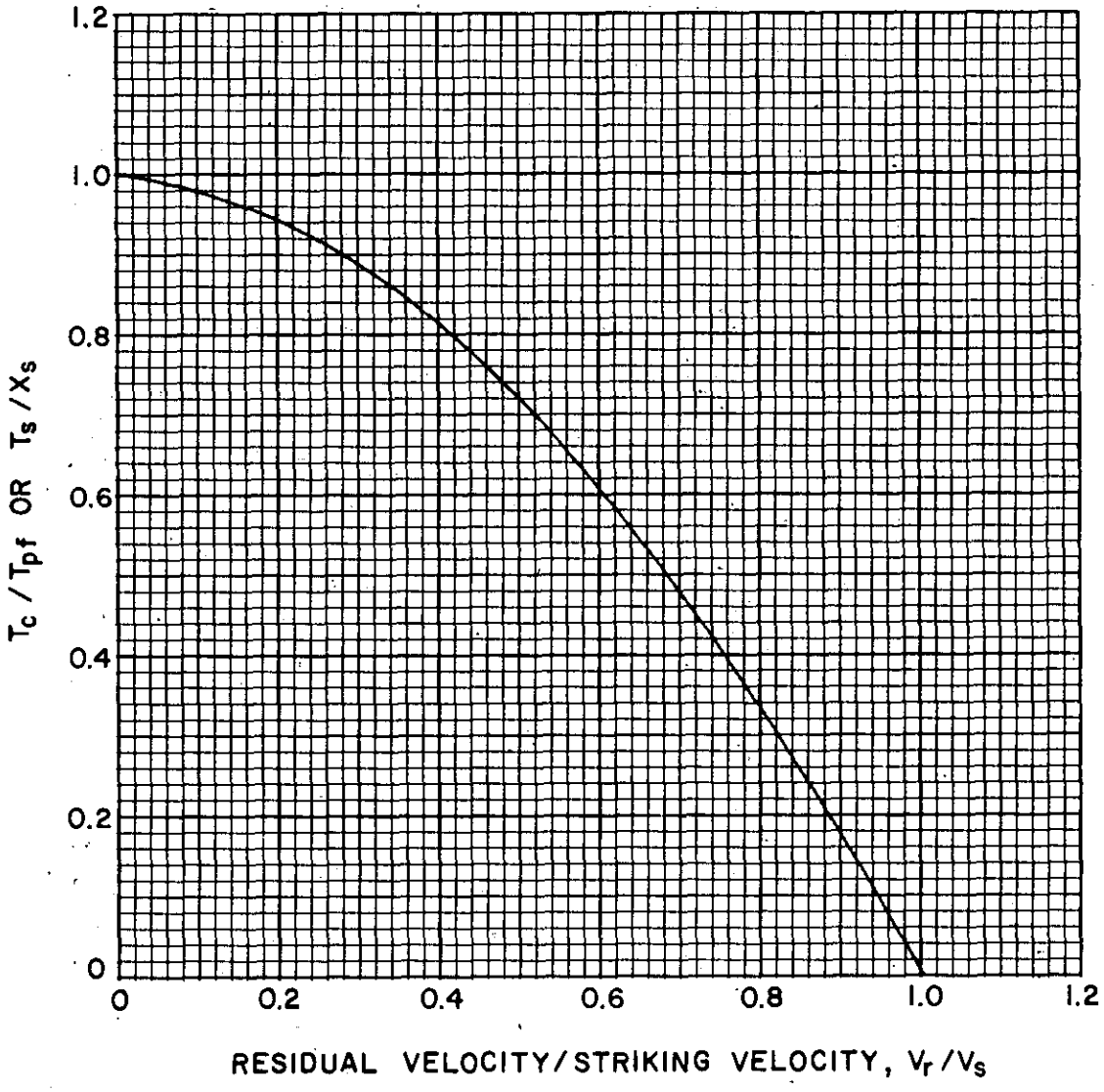


Figure 4-80 Residual fragment velocity upon perforation of :
(1) Concrete barriers (for cases where x > 2d)
(2) sand layers

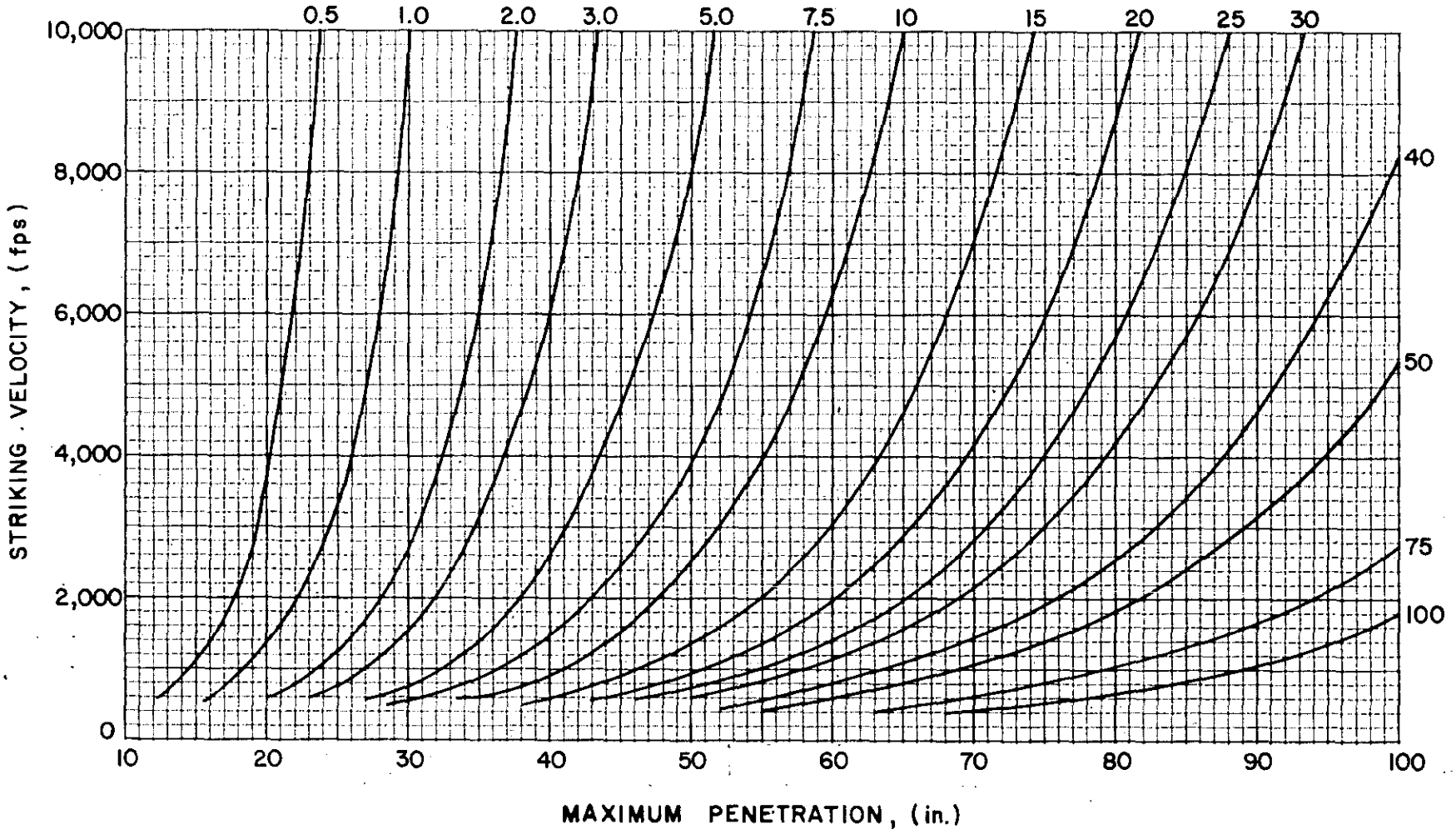


Figure 4-81 Depth of penetration into sand by standard primary fragments

Table 4-16 Relative Penetrability Coefficients for Various Missile Materials

Type of Metal	Constant k
Armor-piercing steel	1.00
Mild steel	0.70
Lead	0.50
Aluminum	0.15

CONSTRUCTION DETAILS AND PROCEDURES

4-62. Introduction

A major portion of the detailing and construction procedures required for structures designed to resist blast pressures is the same as required for structures designed conventionally. However, some differences do exist and neglecting them would result in an unsafe situation, since the structure would not act as assumed in the design. These sections describe the differences in construction. Particular attention is directed towards the construction of structures subjected to close-in blast effects (elements reinforced with lacing or single leg stirrups) but the construction of conventionally reinforced elements, flat slabs and composite elements is also discussed.

Although the construction of blast resistant structures is similar to conventional structures, some changes in the fabrication and construction procedures are required to insure full development of both the concrete and the reinforcement well into the range of plastic action of the various elements. Since these changes primarily affect the reinforcement rather than the concrete, the major portion of the following discussion pertains to reinforcing steel details. Typical details are presented to illustrate detailing procedures and design considerations. These details may not be applicable to all design situations, and may have to be modified by the engineers within the guidelines given below.

4-63. Concrete

The dynamic characteristics and high magnitude of the applied blast load require the strength of the concrete used in blast resistant construction to be higher than that required for conventional construction. Because of the flexural action of blast resistant elements while large deflections are required and the high pressures associated with blast loadings, it is recommended that a minimum concrete strength of 4,000 psi be used.

The properties and testing of the concrete materials (cement, aggregate, water) used in blast resistant concrete construction are the same as those normally used and should conform to the standards specified in the ACI Building Code. High early-strength Portland cement (type III) may be used. To minimize the effects of spalling, it is recommended that the size of the aggregate used be not greater than 1 inch. This limitation of the aggregate size also facilitates the placement of the concrete, particularly where the cover over the reinforcement is held to a minimum. In all cases, the minimum concrete cover should conform to that specified in the ACI Building Code and, wherever possible, should also be the maximum thickness of the concrete cover.

Because of the large amounts of flexural reinforcement and, in laced elements, the presence of lacing reinforcement, the concrete slump used is usually larger than that permitted for conventional construction. A concrete slump of 4 to 6 inches is recommended for laced elements to insure that concrete voids do not occur.

Wherever possible, both horizontal and vertical construction joints should be avoided. A wall whose height is equal to or less than 10 feet usually can be poured without a horizontal joint. On the other hand, good construction

techniques and economy may require the use of horizontal joints for higher walls. These joints should be located at points of low stress intensity. A more detailed discussion of joint locations is given later in sections.

4-64. Flexural Reinforcement

The flexural reinforcement used in blast resistant construction should be designated as ASTM A 615, Grade 60. Slabs must be reinforced in two mutually perpendicular directions. In all elements, the reinforcement should be continuous in any direction. All flexural reinforcement should consist of straight bars, and bends in the reinforcing within the span of an element should be avoided. However, the reinforcement may be bent well within the element's supports when additional anchorage is required.

The spacing of flexural bars is governed by the required area of the reinforcing steel, the selected bar size and, as discussed later, the spacing required to achieve a working and economical arrangement of lacing reinforcement and single leg stirrups. In general, flexural bars should be spaced fairly close together to insure that the cracked concrete between the layers of reinforcement will not be dislodged from the element. Tests have indicated that a maximum spacing of approximately 15 inches will insure confinement of the concrete.

Because of their reduced ductility, reinforcing steel larger than No. 14 bars (No. 18) should not be used as flexural reinforcement in blast resistant elements. Also, the size of the flexural steel should be at least equal to a No. 4 bar. Where necessary, the area of steel normally furnished by the special large bars should be provided by bundling smaller bars. However, the use of these bundled bars should be limited to one direction only, for any laced element. If bundled bars are used in an element whose main span is between two opposite supports, then all bars of each bundle should be continuous across the full span. On the other hand, if the main span is between a support and a free edge, then bundled bars may be cut off at points of reduced stress. At least one bar in each bundle should be continuous across the full span. For two-way elements these cutoffs must be located beyond the positive yield line with sufficient anchorage to develop the bars.

Continuous reinforcement should be used in blast resistant elements, but in many cases, this is a physical impossibility. Therefore, splicing of the reinforcement is necessary. Splices should be located in regions of reduced stress and their number held to a minimum by using the longest reinforcing bars practical (bars 60 feet in length are generally available throughout the country). Tests have indicated that the preferable method of splicing flexural reinforcement in laced concrete elements is by lapping the reinforcing bars. The length of each lap should be at least equal to 40 diameters of the larger of the two bars spliced, but not less than 2 feet (usually the same size bars will be spliced). In addition, splices of adjacent parallel bars should be staggered to prevent the formation of a plane of weakness. Figure 4-82 illustrates typical splicing patterns for both single and bundled bars used in the close-in design range.

In conventionally reinforced (non-laced) concrete elements used in the far design range, a two bar splice pattern is used. The length of the lap splices must be calculated to ensure full development of the reinforcement. If the splices occur in regions of low stress, the length of the lap is taken as 40

bar diameters. Lap splices of No. 14 bars are not permitted in either laced or non-laced concrete elements.

Mechanical splices may also be used, but they must be capable of developing the ultimate strength of the reinforcement without reducing its ductility. If the bar deformations have to be removed in the preparation of these splices, grinding rather than heat should be employed since heat can alter the chemical properties thereby changing the physical properties of the steel and possibly reducing the capacity of the element. Welding of the reinforcement should be prohibited unless it can be determined that the combination of weld and reinforcement steel will not result in a reduction of the ultimate strength and ductility. In those cases where welding is absolutely essential, it may be necessary to obtain special reinforcement manufactured with controlled chemical properties.

4-65. Construction Details for "Far Range" Design

4-65.1. General

Unlaced reinforced concrete elements are generally used in those facilities designed to resist explosive output at the far design range. The facilities generally consist of shelter-type structures.

Blast resistant structures utilizing unlaced reinforced concrete construction will only differ from conventional construction insofar as the increased magnitude and reversibility of applied loads are concerned. These differences are reflected in the details of the blast resistant structure. An increase in the amount of reinforcement is required to resist the large dynamic loads. Also, the reinforcement at both surfaces of an element must be detailed to prevent failure due to rebound stresses.

In general, conventionally reinforced elements are limited to deflections corresponding to support rotations of 2 degrees or less. However, elements designed for far range effects are capable of attaining deflections up to 4 degrees through the use of single leg stirrups and up to 8 degrees by developing tension membrane action. Elements subject to close-in effects require stirrups and are limited to 2 degrees support rotations. Details are presented below for elements designed for limited deflections, elements acting under tension membrane action and columns. For elements subjected to low and intermediate pressure and reinforced with stirrups, the details given below may be used without modification. However, details for elements with stirrups and subject to high pressures are discussed in the following section.

4-65.2. Elements Designed for Limited Deflections

Construction and detailing of unlaced, blast resistant structures is very similar to conventional structures. The major difference is the method of anchoring the reinforcement. A typical section through a non-laced wall is shown in Figure 4-83. At the roof-wall intersection, the exterior wall reinforcement is continued through the regions of high stress and lap spliced with the roof reinforcement in the vicinity of the point of inflection. Thus, the reinforcement is not actually anchored but rather developed. The interior reinforcement of both wall and roof is terminated with a standard hook in order to be effective in resisting rebound tension forces. However, this reinforcement will be in compression during the initial phase of loading and

therefore, the straight portion of the bar must be sufficient to develop the reinforcement in compression.

The bottom floor slab reinforcement is extended through the floor-wall intersection into the wall in the same manner as the roof-wall intersection. Again the reinforcement is developed into the wall. The vertical wall reinforcement is supported on the floor slab rather than supported above the floor slab on the reinforcement. Figure 4-83 illustrates a building with a slab-on-grade foundation. Figure 4-84 illustrates several alternative arrangements.

A horizontal section through the intersection through two discontinuous walls (Fig. 4-85) would reveal details very similar to those shown for the roof-wall intersection. The number of splices used would depend on the length of each wall.

Wherever possible, continuous reinforcement should be used. Lap slices may be used when necessary but their number should be held to a minimum and they must be located in regions of reduced stress. To prevent the formation of a plane of weakness, splices on adjacent parallel bars must be staggered. In addition, the splice pattern for the reinforcement on opposite faces of an element should not be in the same location. Figures 4-86 and 4-87 illustrate preferred splice locations for a two-way slab and a multi-span slab respectively.

4-65.3. Elements Designed for Large Deflections

Unlaced concrete slabs are capable of attaining deflections up to 8 degrees support rotation through the development of tension membrane action. Construction details are basically the same whether the slab attains large or small deflections, however, there are two important exceptions. At large deflections, tension membrane action produces large tensile strains in both tension and "compression" reinforcement. Therefore, all anchorage lengths and lap splice lengths must be calculated for the design stress f_{ds} and all the reinforcement is in tension. The second difference in detailing concerns the location of splices. Although splices should still be located in regions of low flexural stress, they will be located in regions of high tensile stress when the element attains its full tension membrane capacity. The length of the lap splice must, therefore, be increased to 1.3 times the modified development length given in Section 4-21.4 of a reinforcing bar in tension.

4-65.4. Column Details

Columns are generally required in blast resistant, shear wall structures. Their details differ little from those used in conventional structures. Both round, spiral reinforced columns and rectangular, tied columns can be used, but one or the other is preferred for a given design situation. Details of the reinforcement and formwork of rectangular columns are compatible with beam details and, therefore, are recommended for beam-slab roof systems. Round columns should be used for flat slab roofs.

Figure 4-88 illustrates a typical section through a circular column with a capital supporting a flat slab. A round column prevents stress concentrations that may cause local failures. The column capital, although not required, is preferred since it simplifies the placement of the diagonal bars as well as decreasing shear stresses. All diagonal bars should extend into the column.

If, however, the number and/or size of the diagonal bars do not permit all the bars to extend into the column, up to half the bars may be cut off in the capital as shown. Lateral reinforcement of a circular column consists of spiral reinforcement beginning at the top of the floor slab and extending to the underside of the drop panel or the underside of the roof slab if no drop panel is used. Within the column capital, No. 4 hoop reinforcement at 6 inches on center must enclose the diagonal bars.

In a beam-slab system, beam reinforcement does not permit the addition of diagonal bars at the top of the column. Therefore, the beams themselves must be able to provide adequate shear strength. Closed ties provide lateral support of the longitudinal reinforcement in rectangular columns. The ties must start not more than ½ tie spacing above the top of the floor slab and end not more than 3 inches below the lowest reinforcement in the shallowest beam. The ties must be arranged so that every corner and alternate longitudinal bar has the lateral support provided by the corner of a tie having an included angle no more than 135 degrees. In addition, no longitudinal bar shall be farther than 6 inches clear on either side from such a laterally supported bar.

The column footing illustrated in Figure 4-88 is the same for both rectangular and circular columns. Dowels anchor the column into its footing. Since there is little or no moment at the bottom of the column, splices need not be staggered as they are in a wall. The splice should be able to fully develop the reinforcement in tension in order to resist rebound tension forces. Within the column, no splices of the longitudinal reinforcement are permitted. Continuous reinforcement should not be a problem as blast resistant structures are limited to one and two-story buildings.

4-66. Construction Details for "Close-In Design"

4-66.1. General

Laced reinforced concrete elements are usually used in those facilities which are designed to resist the explosive output of close-in detonations (high-intensity pressures with short durations). The functional requirements of these facilities (storage and/or manufacture of explosives) normally dictate the use of one-story concrete buildings with austere architecture. Basically, these structures consist of a series of interconnecting structural elements (walls, floor slabs, and/or roofs) forming several compartments or cubicles. Because of this cubicle arrangement, the walls separating the individual areas are the predominant element used in laced construction and are the most critical component in the design. However, in some cases, the roof and/or floor slab can be of equal importance.

Single leg stirrups may replace lacing bars when the scaled normal distance between the charge and the element is equal to or greater than 1.0 ft/lbs$^{1/3}$. However, the maximum allowable support rotation for elements with single leg stirrups is less than for laced elements. Single leg stirrups are more economical to fabricate and slightly more economical to place during construction. Unlike laced reinforcement which requires that the position of the flexural reinforcement be changed to suit the horizontal and vertical lacing, the position of the flexural reinforcement remains constant for single leg stirrups. The stirrups are tied around the outer bars whether they are

horizontal or vertical. Details for flexural reinforcement, splice location and length, etc., are the same for single leg stirrups and laced reinforcement.

4-66.2. Laced Elements

4-66.2.1. Lacing Reinforcement

All flexural reinforcing bars must be tied with continuous diagonal lacing bars (Fig. 4-89). At any particular section of an element, the longitudinal or main tension and compression reinforcement is placed to the interior of the transverse or secondary flexural reinforcing steel around which the diagonal lacing bars are bent.

Lacing reinforcement must be fabricated without the formation of excessive stress concentrations at the bends. The bending should be performed without the use of heat, and in no case should the radius of the pin used to bend the lacing be less than four times the diameter of the bar. Figure 4-90 illustrates the typical lacing bends used with both single and bundled flexural bars.

The amount of lacing reinforcement required in an element depends upon the element's capacity (quantity and distribution of flexural reinforcement, thickness of the element, and the type and number of supports) while the size of the lacing bars is a function of the required area and spacing. The maximum and minimum size of the lacing bars should be No. 8 and No. 3 bars, respectively. However, the preferred maximum size of lacing bar is No. 6. Several lacing schemes have been developed (Fig. 4-91) which avoid excessive stress concentrations as a result of large angular bends , provide adequate restraint against buckling of the compression reinforcement, and make use of the most efficient arrangement of the lacing reinforcement (lacing making an angle of 45 degrees with the longitudinal reinforcement is most efficient). In these schemes, the transverse flexural reinforcement may or may not be tied at every intersection with a longitudinal bar. However, a grid system is established whereby bar intersections are tied within a distance s_1 or 2 feet, whichever is less. The choice of the scheme to be used depends upon the flexural bar spacing and the thickness of the element so that the angle α is approximately equal to, but never less than, 45 degrees. Although not tying every transverse flexural bar results in a large lacing bar size, the total cost of the lacing may be reduced since the size of the lacing bend associated with an increase in the spacing s_1 reduces the overall length of the bar and the number of bends required to cover a given longitudinal distance.

An additional cost saving in the fabrication of the lacing may be realized by utilizing the equipment that is used to bend the steel bars for open web steel joists. However, when detailing the flexural and lacing reinforcement and the concrete wall thickness, consideration must be given to the physical capabilities (size of bend and bar, depth of lacing, etc.) of the equipment. Alteration of bar joist equipment to meet the requirements of a design is not usually practical with respect to both time and cost.

The placement of the lacing depends upon the distribution of the flexural reinforcement and the number and type of supports. Lacing is always placed perpendicular to the element's supports to resist diagonal tension stresses. Because of the nonuniformity of the blast loads associated with close-in detonations, continuous lacing across the span length should be used to

distribute the loads. Except for cantilever elements, lacing in one-way elements is placed in the direction of and continuous across the span. Cantilever elements require lacing in two directions. Discontinuous lacing is located perpendicular and adjacent to the support while continuous lacing is placed across the full width of the element in direction parallel and adjacent to the free edge located opposite the element's support. For two-way elements, diagonal tension stresses must be resisted in two directions. Because of interference, lacing can only be continuous in one direction, which in general is in the direction of the longest span. Figure 4-92 illustrates the location of the lacing used in a cantilever wall as well as in several two-way elements. For two-way elements, the location of the lacing is not affected by the type of supports. Therefore, the supports indicated in Figure 4-92 can be simple, restrained, or fully fixed.

Similar to the flexural reinforcement, lacing will usually require splices. Tests have indicated that the preferable way of splicing lacing is by lapping the bars. The lap length which is measured along the bars should be at least equal to that required for a full tension slice (40-bar diameters). However, the lacing should also be bent around a minimum of three flexural bars. The splices of adjacent lacing bars should be staggered to avoid forming a plane of weakness in the element, and the slices should be located in regions of low stress (away from the supports and positive yield lines). Typical details for the splicing of lacing bars are presented in Figure 4-93. Wherever possible, welding of lacing bars should be avoided and is only permitted while the full development of the ultimate strength can be assured without any reduction in strength or ductility.

The location of the splices is determined from the distance along the length of the element which can be covered by a given length of lacing bar (usually 60 feet). The expression for the actual length of lacing bar L_1 required to cover the length s_1 is a function of the flexural bar spacing and the geometry of the lacing and is given in Figure 4-94.

4-66.2.2. Corner Details

Because of the magnitude of the blast loads associated with close-in detonations and their amplification at corners, the use of concrete haunches has been found to be a satisfactory method of maintaining the integrity of these sections of a structure. All corners should be reinforced with diagonal bars to transfer the high shear forces from the element to its support and to assist in maintaining the integrity of the intersection. Diagonal bars should be used in elements both with and without haunches. Reinforcement details for corners are shown in conjunction with wall intersections in the following section.

4-66.2.3. Walls

Figure 4-95 illustrates the detailing procedure for a typical laced wall. The wall is free at the top, supported at its sides by other walls (not shown), and at its base by the floor slab. It has vertical lacing which is continuous from the bottom of the wall to approximately midheight. In the upper half of the wall, the horizontal lacing reinforcement is continuous over the full length of the wall and anchored in the side supports. It should be noted that the horizontal flexural steel in the lower half of the wall is located at the exterior of the vertical reinforcement, while in the upper half of the wall it

is at the interior. This arrangement is necessary for the placement of the lacing so that the lacing can provide full confinement of both the flexural steel and the concrete separating the two layers of reinforcement. If spalling is critical, its effects may be minimized by reducing the concrete cover over the reinforcement in the upper half of the wall. The addition of U-bars at the top of the free edge also minimizes the formation of concrete fragments from this area. Reducing the concrete cover is not cost effective and, therefore, if spalling is not critical, the wall should have a constant thickness.

A portion of the wall should extend below the floor slab a distance no less than that required to anchor the flexural reinforcement (40-bar diameters) and in no case less than 1 foot - 6 inches. In addition to providing anchorage for the vertical reinforcement, the portion of the wall below the floor slab assists in resisting sliding of the structure by developing the passive pressure of the soil adjacent to the wall.

The working pad at the base of the wall provides the support required for the erection of the wall reinforcement and also affords protection for the reinforcement after construction is completed. It should be noted that in the example illustrated in Figure 4-95 the cover over the reinforcement in the portion of the wall above the floor slab is specified as 3/4 inch (minimum reinforcement cover required by the ACI Building Code for concrete not exposed to the weather), while below the floor slab it is specified as 2 inches (minimum cover required by ACI Building Code for concrete in contact with the ground after removal of the forms). The increased cover below the floor slab is achieved by increasing the wall thickness rather than bending the reinforcement.

Diagonal bars are provided at the intersection of the floor slab and wall. These bars transfer the high shear forces from the base of the wall through the haunch and into the floor slab. Section C-C, Figure 4-95 indicates the location of the diagonal bars relative to the lacing reinforcement.

Details of the reinforcement at wall intersections are similar to those at the intersection of the wall and floor slab. Figures 4-96 through 4-98 illustrate these details for the intersection of two continuous walls, one continuous and one discontinuous wall, and two discontinuous walls, respectively. In all cases, both the flexural and lacing reinforcement are fully anchored by being made continuous through the intersection (a distance of at least 40 bar diameters). In discontinuous walls, the wall must be extended a distance sufficient to anchor all reinforcement but not less than 1 foot-6 inches. This extension (or extensions) aids in resisting both the overturning of the structure and the tension force produced in the walls (discussed further in subsequent sections). Diagonal bars have been provided at all intersections to transfer the support shears and to maintain the integrity of the section. Where discontinuous walls are encountered, only one diagonal bar is effective for the continuous wall of Figure 4-97 and for both discontinuous walls of Figure 4-98. For these cases, bundled diagonal bars (2 bars maximum) may have to be used.

If wall extensions are not permitted due to architectural or other criteria, the reinforcement is anchored by bending it within the corner (figs. 4-99 and 4-100). However, the distance from the face of the support to the end of the hook must be at least 20 bar diameters. A standard hook may be used if; (1)

the total distance from the face of the support to the end of the bar (including the hook) is 40 bar diameters and (2) the length of the hook is at least 12 inches. The use of hooks may cause problems in the placement of the lacing reinforcement and is discussed in conjunction with the sequence of construction below.

In addition to flexural reinforcement, the walls of containment structures may require the addition of tension reinforcement. This reinforcement is placed at the mid-depth of the wall and has the same spacing as the flexural reinforcement. It may be required in the vertical and/or horizontal directions. The reinforcement is anchored at wall intersections in the same manner as the flexural reinforcement. Vertical tension reinforcement usually does not require splices. However, if the horizontal tension reinforcement requires splicing, the splice (lap, mechanical, weld) and pattern should be same as the flexural reinforcement. Of course, the tension steel should never be spliced at the same location as the flexural reinforcement.

4-66.2.4. Floors Slabs

Floor slabs on grade must provide sufficient capacity to fully develop the wall reinforcement. If sufficient resistance is provided by the soil, slabs poured on grade usually do not require lacing nor other shear reinforcement; although lacing reinforcement is always required in slabs exposed to multiple detonations. Soil strata having enough bearing capacity to support the dead load of the structure can be considered to provide the support required by the slab. Before placement of the slab, the top 6 inches of the subgrade should be compacted to 95 percent of maximum density in accordance with ASTM Standard D1557.

Piles are used to support a structure where the bearing capacity of the soil is inadequate. The piles are placed under the walls and the floor must span between them. Lacing or single leg stirrups must be provided. The reactions of the slab are transferred to the portion of the wall below the floor slab which acts as a beam spanning between piles.

In addition to flexural reinforcement, floor slabs may require tension reinforcement located at mid-depth of the slab. Tension forces are discussed in conjunction with single and multi-cubicle structures.

4-66.2.5. Roof Slabs

Roof slabs are similar to walls since they are usually supported only at their periphery and require the addition of lacing to distribute and resist the applied blast loads. In those facilities where the explosion occurs within a structure, the blast pressures acting on the interior surface of a nonfrangible roof causes tension stresses in the walls which require the addition of tension reinforcement above that needed for bending. Tension forces are discussed in conjunction with single and multi-cubicle structures.

4-66.3. Elements Reinforced with Single Leg Stirrups

4-66.3.1. Single Leg Stirrups

A single leg stirrup consists of a straight bar with a hook of at least 135 degrees at each end. Hooks shall conform to the ACI Building Code. At any

particular section of an element, the longitudinal flexural reinforcement is placed to the interior of the transverse reinforcement and the stirrups are bent around the transverse reinforcement (Fig. 4-101).

The required quantity of single leg stirrups is calculated in the same manner as lacing. They are a function of the element's flexural capacity while size rebar used is a function of the required area and spacing of the stirrups. The maximum and minimum size of stirrup bars are No. 8 and No. 3, respectively, while the spacing between stirrups is limited to a maximum of d/2 or $d_c/2$ for type I and type II or III, respectively.

The preferable placement of single-leg stirrups is at every flexural bar intersection. However, the transverse flexural reinforcement does not have to be tied at every intersection with a longitudinal bar. A grid system may be established whereby alternate bar intersections in one or both directions are tied within a distance not greater than 2 feet. The choice of the three possible schemes depends upon the quantity of flexural reinforcement, the spacing of the flexural bars and the thickness of the concrete element. For thick, lightly reinforced elements, stirrups may be furnished at alternate bar intersections, whereas for thin and/or heavily reinforced elements, stirrups will be required at every bar intersection. For those cites where large stirrups are required at every flexural bar intersection, the bar size used may be reduced by furnishing two stirrups at each flexural bar intersection. In this situation, a stirrup is provided at each side of longitudinal bar.

Single leg stirrups must be distributed throughout an element. Unlike shear reinforcement in conventionally loaded elements, the stirrups cannot be reduced in regions of low shear stress. The size of the stirrups is determined for the high stress areas and, because of the non-uniformity of the blast loads associated with close-in detonations, this size stirrup is placed across the span length to distribute the loads. For two-way elements, diagonal tension stresses must be resisted in two directions. The size of stirrup determined for each direction is placed to the same extent as the lacing shown in Figure 4-92. However, the distribution does not apply for cantilever elements since they are one-way elements requiring only one stirrup size which is uniformly distributed throughout.

4-66.3.2. Corner Details

Corner details for elements with single leg stirrups are the same as for laced elements. Concrete haunches, reinforced with diagonal bars, should be used at all corners. For those cases where compelling operational requirements prohibit the use of haunches, diagonal bars must still be placed at these corners. In addition to diagonal bars, closed ties must be placed at all corners (fig. 4-102) to assist in maintaining the integrity of the intersection. The tie should be the same size as the stirrups but not less than a No. 4 bar. The spacing of the ties should be the same as the flexural reinforcement.

4-66.3.3. Walls

The detailing procedure for a wall with single leg stirrups is similar to a laced wall. Figure 4-103 illustrates the detailing procedure for a typical wall with single leg stirrups. This wall is the same as the wall shown in Figure 4-95 except that stirrups are used rather than lacing. These are only

two differences between the two walls. First, there is no need to alter the position of the horizontal flexural reinforcement for the placement of stirrups. The horizontal reinforcement is in the main direction (assumed for wall illustrated) and, therefore, this steel is placed exterior of the vertical reinforcement for the entire height of the wall. Second, closed ties are placed at the wall and floor slab intersection to assist in maintaining the integrity of the section. The common requirements for both walls include the addition of U-bars, diagonal bars, concrete haunches, increased cover over the reinforcement below the floor slab by increasing the wall thickness, shear reinforcement (stirrups or lacing) in the wall extension below the floor slab, and the preferred use of a working pad.

Details of the reinforcement at wall intersections are similar to those at the intersection of the wall and floor slab. The requirements for anchorage of the flexural reinforcement and diagonal bars at wall intersections are exactly the same as laced walls (fig. 4-96 through 4-100). The placement of the single leg stirrups and the required closed ties are shown in Figure 4-102. Similar to laced walls, the use of wall extensions is the preferred method of reinforcement anchorage at discontinuous walls.

4-66.3.4. Floor Slabs

The floor slab must provide sufficient capacity to fully develop the wall reinforcement. The requirements are the same as a floor slab for laced walls.

4-66.3.5. Roof Slabs

Roof slabs are similar to walls since they are usually supported only at their periphery and require the addition of single leg stirrups to distribute and resist the applied blast loads. For interior explosions, the roof causes tension forces in the walls. Tension reinforcement is discussed in conjunction with single and multi-cubicle structures.

4-67. Composite Construction

Composite construction is primarily used for barricades and consists of two concrete panels separated by sand fill (Fig. 4-104). Details of each panel are similar to those described for single laced walls (or walls reinforced with single leg stirrups).

The concrete panels may be supported at the base either by the floor slabs or a concrete pedestal. When the pedestal is used, reinforcement across the base of both panels terminates in the floor slab and provides a monolithic connection between the two panels. The floor reinforcement serves as the monolithic connection when pedestals are not used.

The upper portion of the wall may either be open or solid. Open sections are usually used when the upper edge of the wall is unsupported; the solid section is used when an external tie system is used to restrain the motion and provide support for the top of the wall. The solid section must be reinforced to resist torsion and bending induced by the ties and the panels.

The impulse capacity of composite walls is a function of the density of the sand fill. The sand will be compacted after construction due to its own weight and/or by water drainage when the wall is exposed to the weather. The

sand fill must be continuously maintained at the level stipulated in the design by mechanical means which will allow periodic rearrangement of the sand fill. Clay pipe or other similar material may be placed in the wall cavity with the sand so that when the wall is loaded the clay pipe will be crushed by the impact of the donor panel, thereby providing space within the wall cavity into which the compacted sand may flow, hence reducing its density. If possible, the sand should be protected from the elements by sealing the top of the cavity.

4-68. Single and Multicubicle Structures

In single-cell structures (Fig. 4-105) unbalanced force (support reactions) exist at all element intersections (walls, and floor and wall intersections) and must be resisted by tension force produced in the support elements. In addition to the reinforcement required to resist flexural and shear stresses, tension reinforcement, distributed along the centerline of the elements, is required. Horizontal tension reinforcement in the side wall and floor slab (parallel to the side walls) is required to resist the vertical and horizontal reactions of the back wall, while horizontal steel in the back wall and floor slab (parallel to the back wall) resists the tension force produced by the side wall reactions.

These unbalanced forces are transmitted to the structure's foundation and, depending upon their magnitude, the size and configuration of the structure and the subgrade conditions, the structure may be subject to both translational and vertical rotational motions. Translation of the structure is resisted by the extension of the walls below the floor slab (shear key) and the friction developed between the floor slab and subgrade, whereas rotation is resisted by the mass of the structure with assistance from the blast load acting on the floor slab of the donor cell. The stability of the structure can be substantially increased by the extension of the walls and floor slab as illustrated in Figure 4-105b. This extension of the walls and floor slab (1) increases the resistance of the structure to overturning (rotation), (2) increases the rigidity of the structure, (3) reduces the effects of the unbalanced wall moments which cause twisting of the corners, (4) reduces the required thickness and/or reinforcement in the floor slab (moment capacity of the floor slab extension must be developed by bearing on the subgrade). and (5) eliminates the need to anchor the reinforcement by bending at the corners which would ordinarily hinder the placement of the concrete.

End cells of multicubicle arrangements also require the addition of tension reinforcement to resist unbalanced blast loads acting on the end walls. The interior cells do not require this additional reinforcement since the mass and base friction of adjoining cells provide the restraint to resist the lateral forces. Two possible multicubicle arrangements are shown in Figure 4-106. In both arrangements the back walls of the cells are continuous, whereas the side walls between the adjoining cells are either continuous or discontinuous. The type of cell arrangement (either one of those shown in Figure 4-106 or a combination of both arrangements) used in a particular design depends primarily upon the functional requirements of the facility and the economy involved. However, there are certain structural features which should be considered in the final selection of either structural arrangement. The horizontal reinforcement (flexural and lacing) in the side walls may be placed continuous across the back wall of scheme a, whereas with scheme b, the side wall horizontal reinforcement must be bent and anchored in the back wall. This latter

arrangement can result in congestion of the horizontal reinforcement at the wall intersections. On the other hand, by offsetting the side walls at each side of the back wall, the span length of the back wall between adjacent side walls is reduced thereby reducing the required strength (concrete thickness and/or reinforcement) of the back wall.

In general, continuous walls usually require constant concrete thickness and horizontal reinforcement. However, where economy can be achieved, it may be desirable to reduce the thickness and reinforcement of the continuous wall of one cell in comparison to those of adjoining cells. This reduction should only be made between the supports in order that a constant moment capacity can be maintained across the length of the reduced element. This capacity reduction requires the horizontal reinforcement to be sliced at the supports, and extreme caution should be exercised in the detailing of the splices.

4-69. Sequence of Construction

Although the construction procedure for all blast resistant concrete elements is similar, each structure must be evaluated to determine the specific sequence of construction which is most appropriate for the particular situation. This evaluation should consider: (1) type and location of shear reinforcement (single leg stirrups, horizontal and vertical lacing). (2) location of reinforcement splices, (3) erection sequence of the reinforcement (flexural and shear), (4) location of horizontal construction joints and (5) pouring sequence of concrete.

To illustrate the construction of a laced concrete structure, consider the recommended construction procedure for the cubicle structure shown in Figure 4-105 b. A vertical section through any wall is similar to the wall described in Figure 4-95. Figure 4-107 illustrates the pouring sequence for the following procedure.

1. Fabricate the reinforcement as indicated on the drawings.

2. Pour a working pad.

3. Erect vertical flexural reinforcement, vertical lacing and vertical diagonal bars in all walls. Thread horizontal flexural bars between vertical lacing and vertical flexural bars up to the top of the floor slab. Also place reinforcement for the floor slab.

4. Adjust reinforcement to required positions and complete second pour to the top of the floor slab. As an alternative, place sufficient horizontal lacing (as described in step 7) to insure proper positioning of the vertical flexural reinforcement and then complete second pour. Additional horizontal flexural bars may be placed beyond the limit of the pour to help stabilize the reinforcement.

5. Thread horizontal flexural bars between the vertical lacing and vertical flexural bars beyond the limit of the third pour. Adjust reinforcement and complete the third pour.

6. Thread the remainder of the horizontal flexural bars up to the top of the vertical lacing.

7. Place horizontal flexural and lacing reinforcement and diagonal bars between the top of the vertical lacing and the top of the wall. Placement of the horizontal flexural and horizontal lacing reinforcement is accomplished by lowering this reinforcement over the vertical reinforcement. At wall intersections the proper sequence is to first lower diagonal bars, type a. Then in the north-south walls lower horizontal lacing bar type b, place horizontal flexural reinforcement and lower opposing lacing bar type a. Repeat this sequence with the reinforcement in the east-west walls and complete this individual layer of reinforcement by placing the horizontal diagonal bars type b. The entire sequence is repeated for the remaining reinforcement.

8. Add U bars at the top of the wall and adjust reinforcement to required positions. Pour remainder of the wall.

The above procedure is for the cubicle structure of Figure 4-105 b, where wall extensions are provided at the corners. For the case where wall extensions are not used (Fig. 4-105 a), the horizontal reinforcement must utilize a 90 degree hook for anchorage (Fig. 4-100). The horizontal flexural reinforcement for the side walls requires a 90 degree hook at one end. Therefore, the reinforcement must be threaded between the vertical lacing and vertical flexural bars from behind the back wall. If the back wall was close to an existing structure, the horizontal reinforcement could not be threaded. The horizontal flexural reinforcement in the back wall requires a 90 degree hook at each end which would prohibit threading the bars. To place this steel, the bars would have to be spliced so that they could be threaded through the back wall from each side wall. The use of splices is not desirable and should be avoided, making the use of wall extensions preferable.

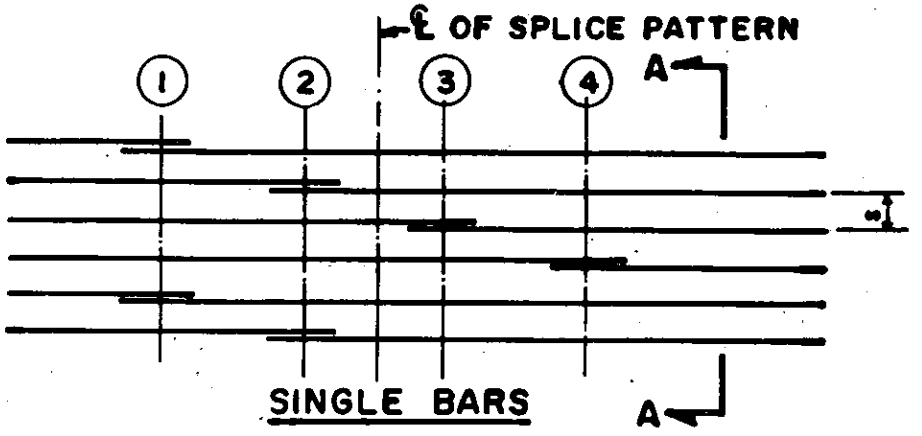
The construction procedure for an element reinforced with single leg stirrups is similar, but not quite as complex as laced elements. The single leg stirrups should be lowered into position if the vertical flexural reinforcing bars are exterior of the horizontal bars. However, if the horizontal bars are exterior of the vertical bars (Fig. 4-103). the horizontal bars should be threaded between the stirrups and vertical bars. Again, as for laced elements, the reinforcement of intersecting walls and the diagonal bars must be placed in sequence.

The use of construction joints (both vertical and horizontal) should be avoided wherever possible since all joints are a potential plane of weakness. However, joints in large structures cannot be avoided because good practice for placement of concrete and/or economy requires their use. All joints should be located in regions of low stress intensity, and, if possible, for laced elements, vertical joints should be situated in areas where horizontal lacing is located, and horizontal joints should be situated in areas where vertical lacing is located. However, vertical joints are difficult to form in laced construction. In most cases, vertical joints are not used, and a certain height of all walls is poured simultaneously. In addition, concrete surfaces should be roughened at all joints.

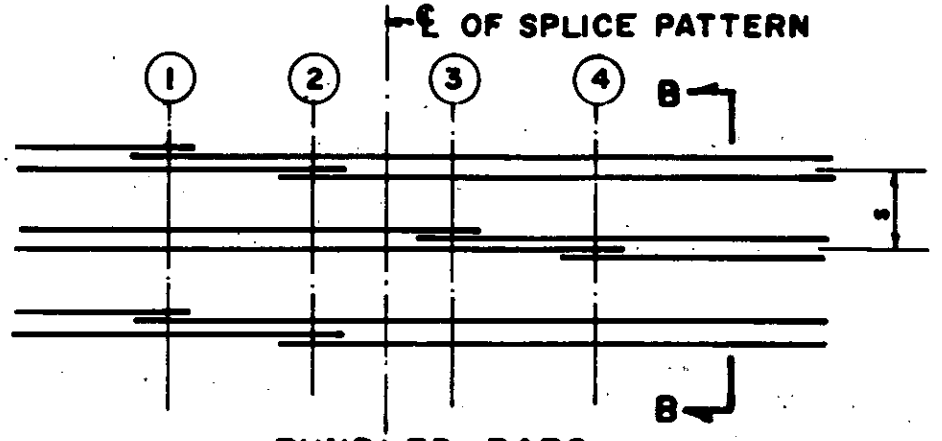
The above construction procedure required the use of two horizontal construction joints. The joint located at the floor slab is generally used in all blast resistant structures while the second joint in the upper section of the wall should only be used if the height of the wall warrants it. The use of

vertical construction joints is generally required for multicubicle arrangements. Walls (intersecting walls must be poured simultaneously) and corresponding floor slabs should be poured in checkerboard fashion to guard against joint separation due to shrinkage and temperature variations. To maintain a minimum rate of pour, multiple pouring crews may have to be used, and pumping of concrete; rather than the use of tremies, may be required for high walls.

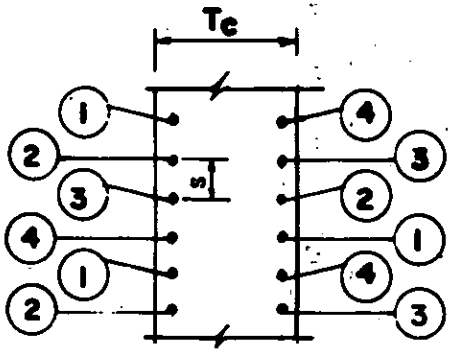
Expansion joints are generally not required for laced concrete elements due to the presence of relatively large amounts of reinforcement. However, their use should be considered for long buildings and/or structures subjected to extreme temperature changes.



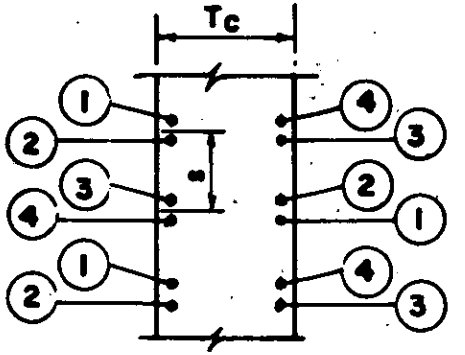
SINGLE BARS



BUNDLED BARS



SECTION A-A



SECTION B-B

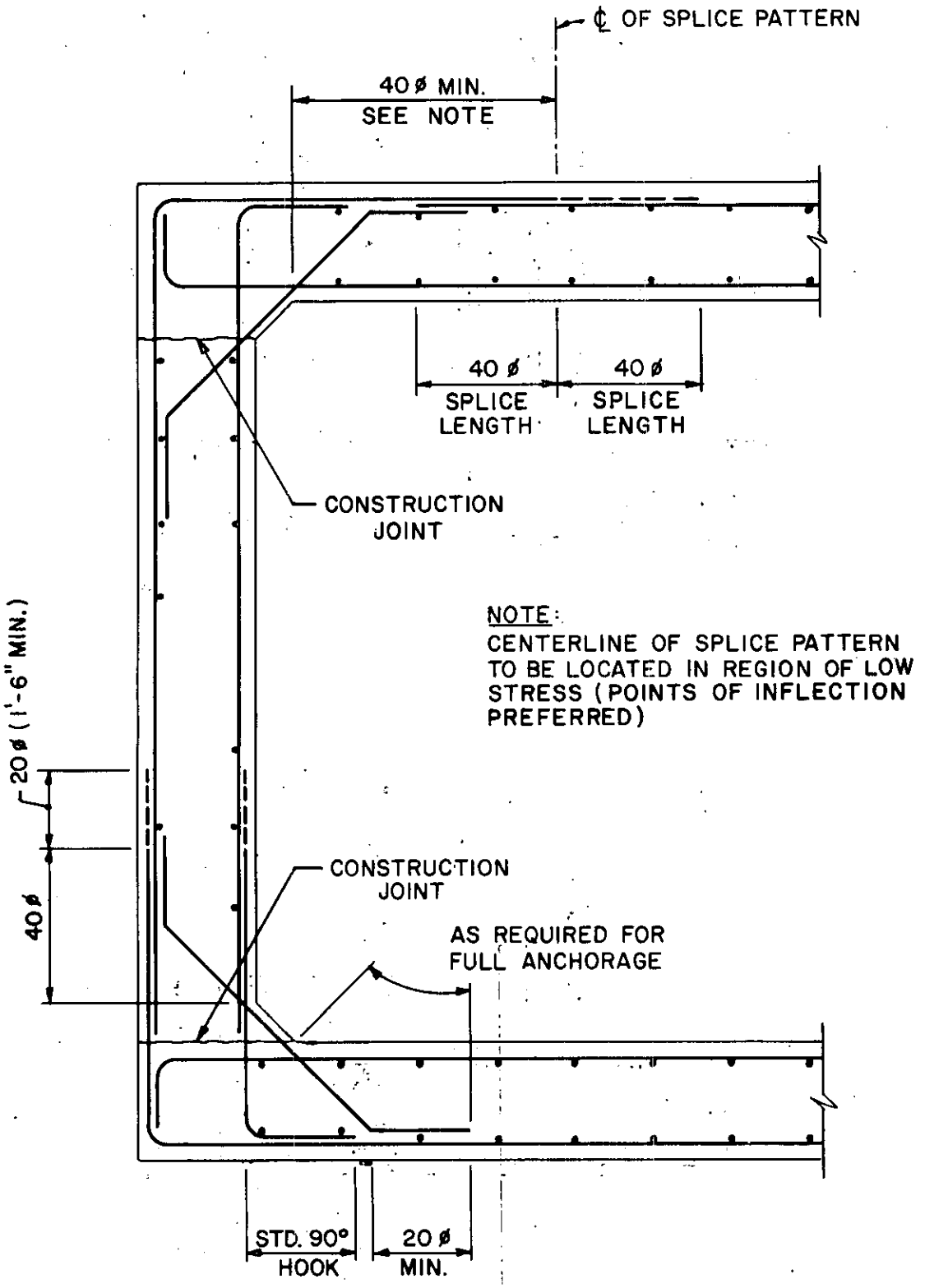


Figure 4-83 Typical section through conventionally reinforced concrete wall

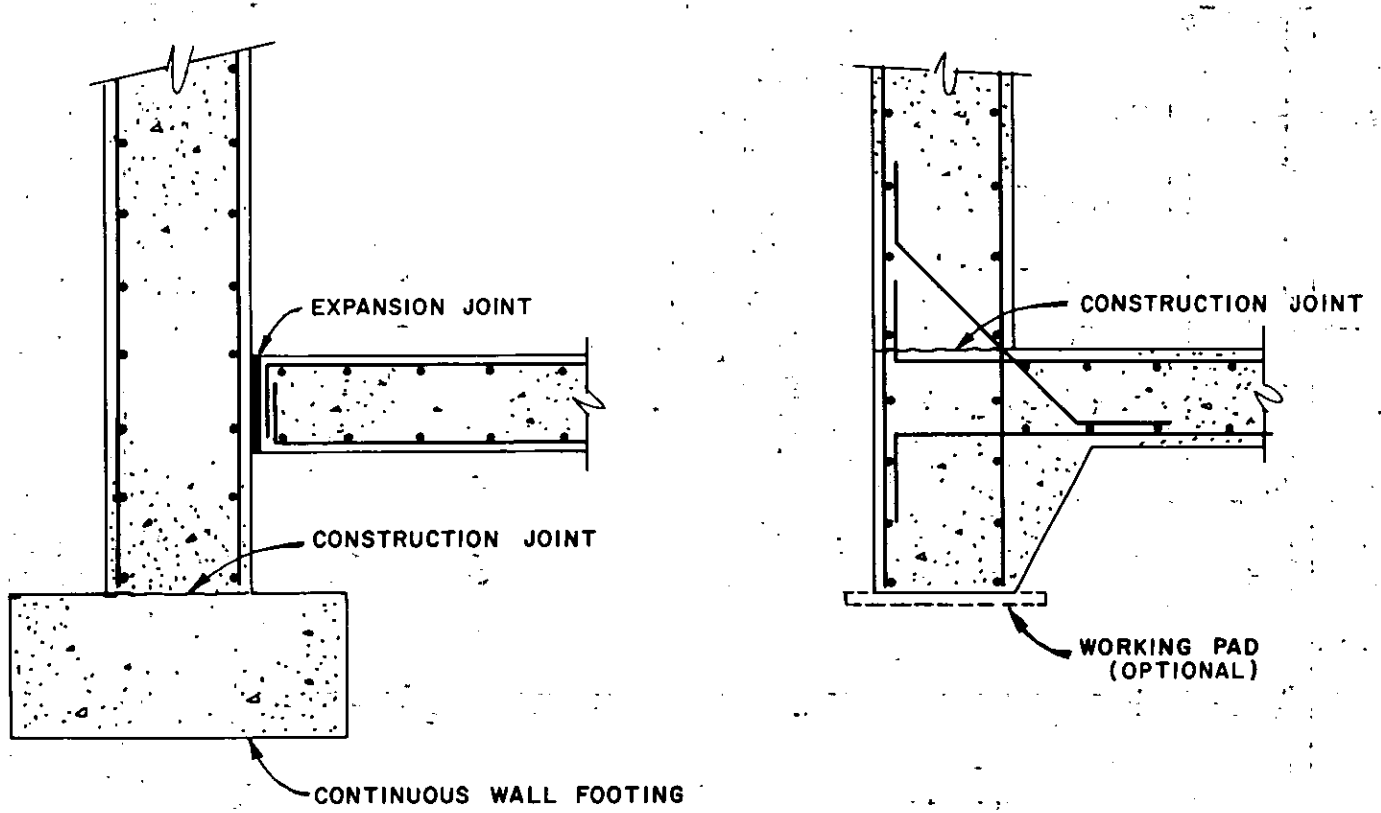


Figure 4-84 Floor slab-wall intersections

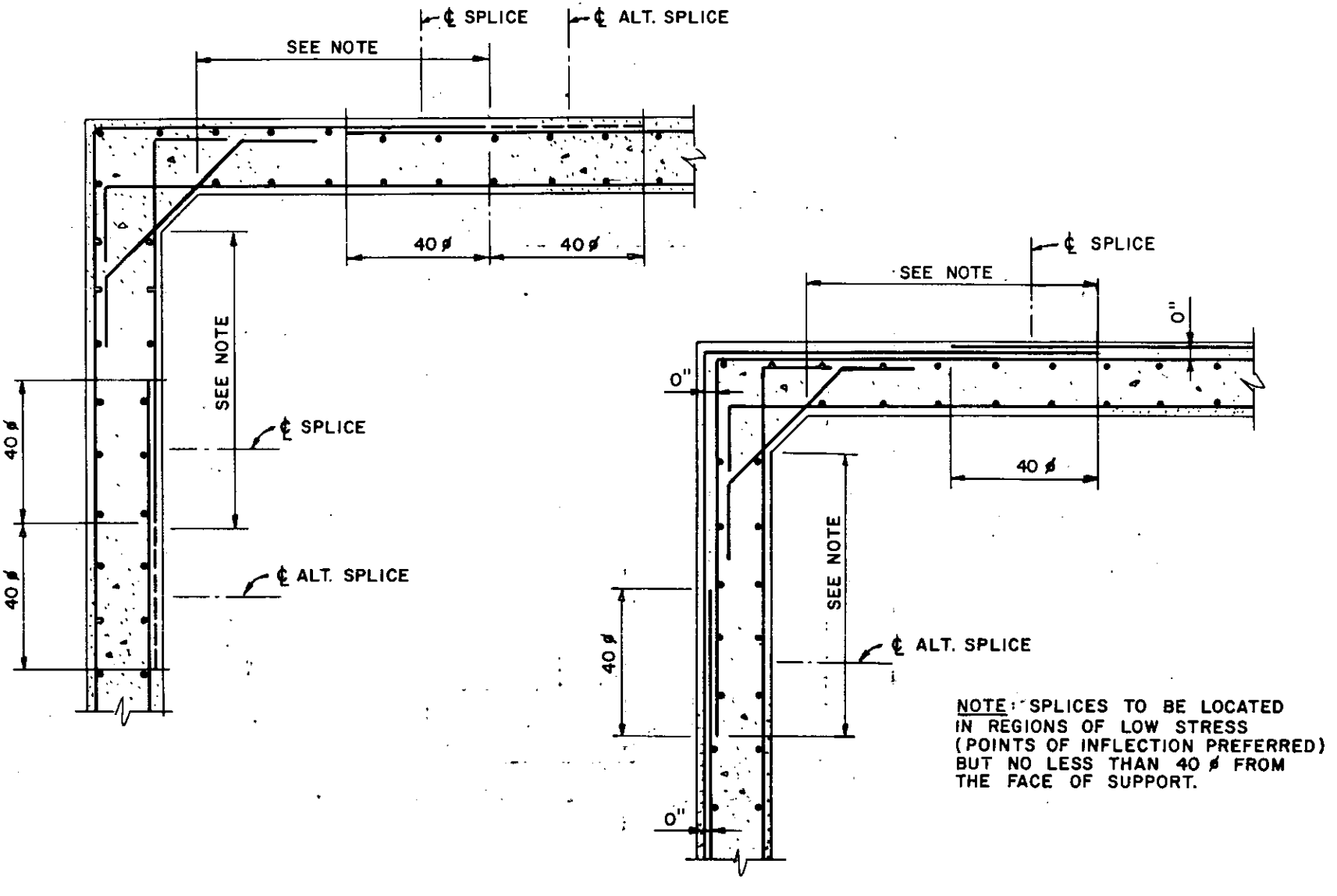


Figure 4-85 Typical horizontal corner details of conventionally reinforced concrete walls

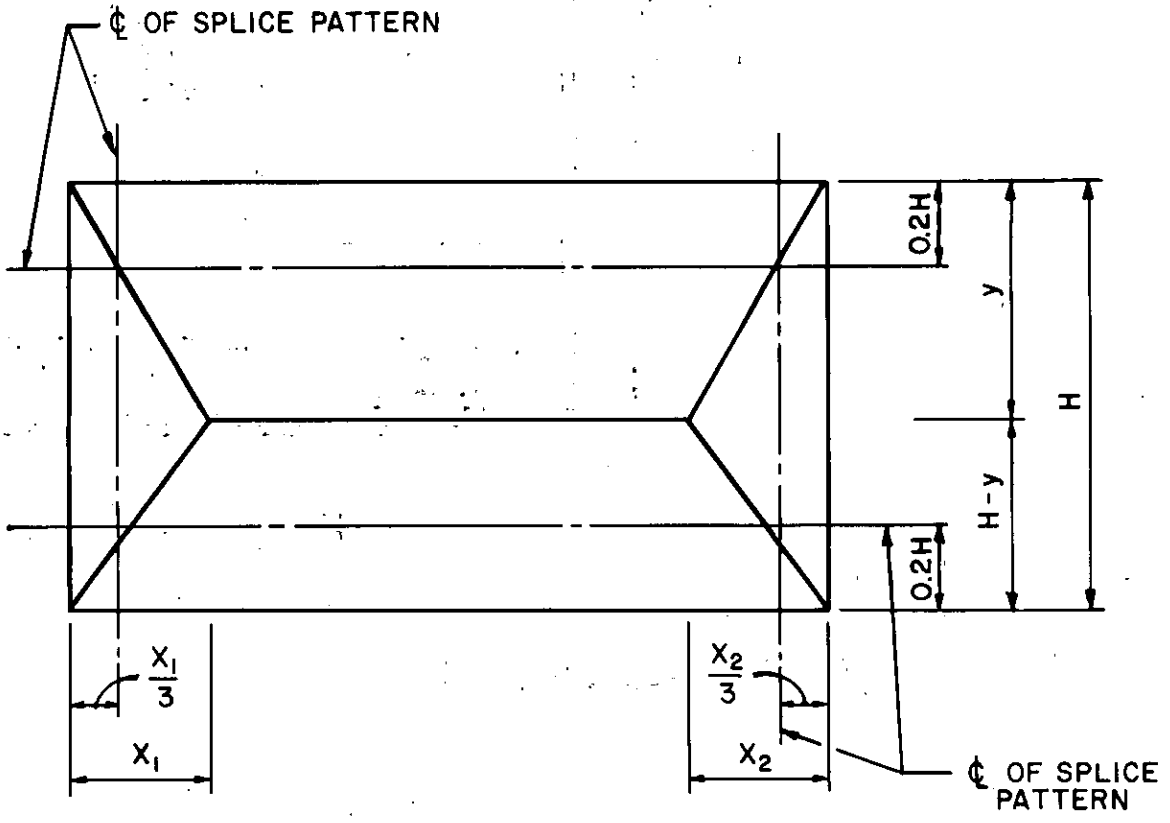
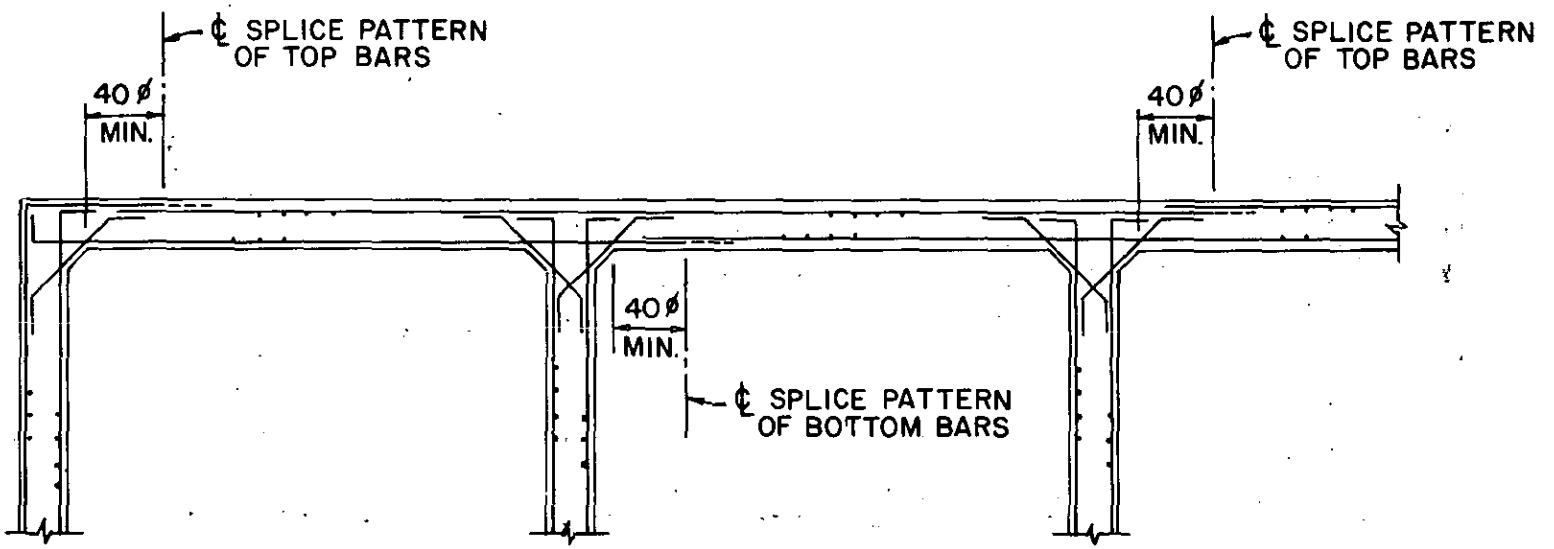


Figure 4-86 Preferred location of lap splices for a two-way element fixed on four edges



NOTE: ℄'s OF SPLICE PATTERNS TO BE LOCATED IN REGION OF LOW STRESS (POINTS OF INFLECTION PREFERRED)

Figure 4-87 Splice locations for multi-span slab

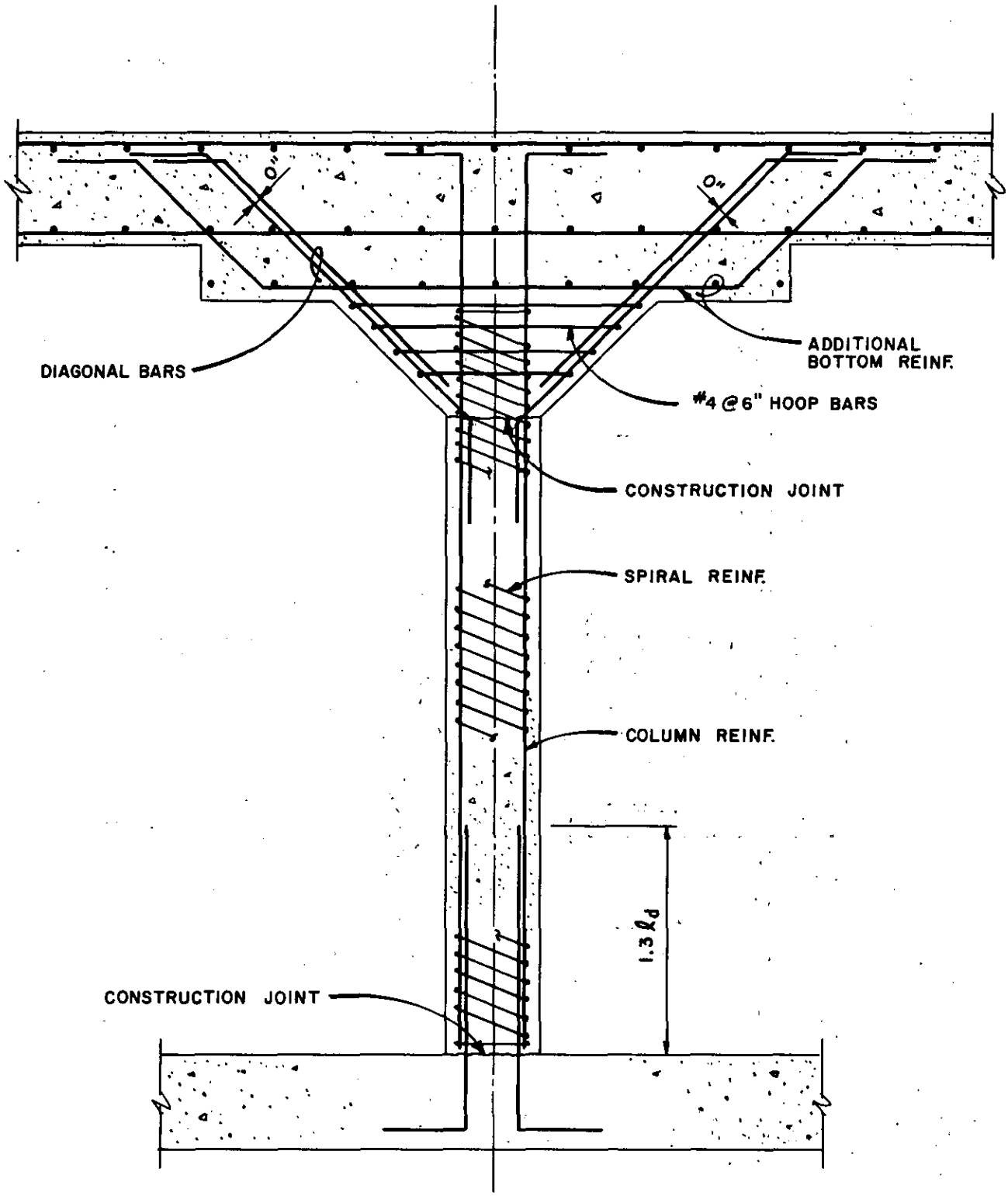


Figure 4-88 Section through column of flat slab

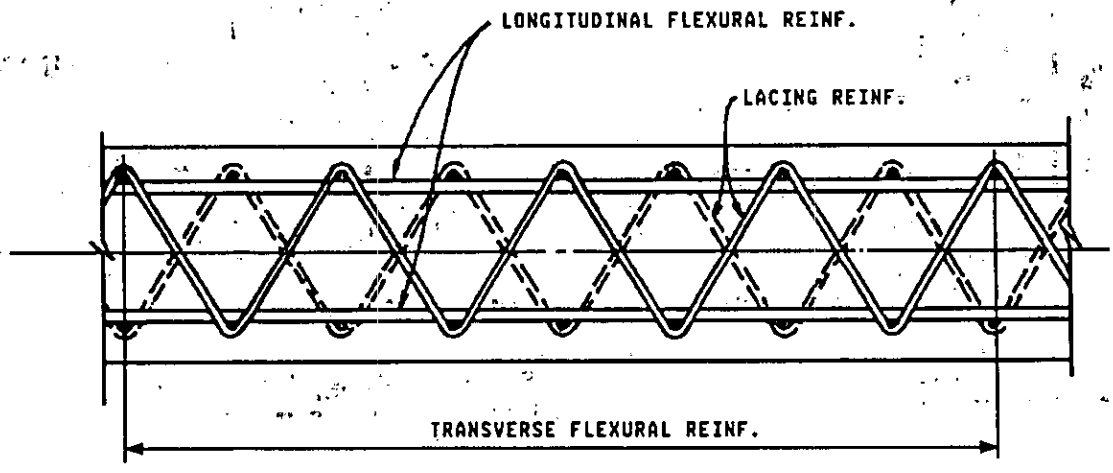


Figure 4-89 Laced reinforced element

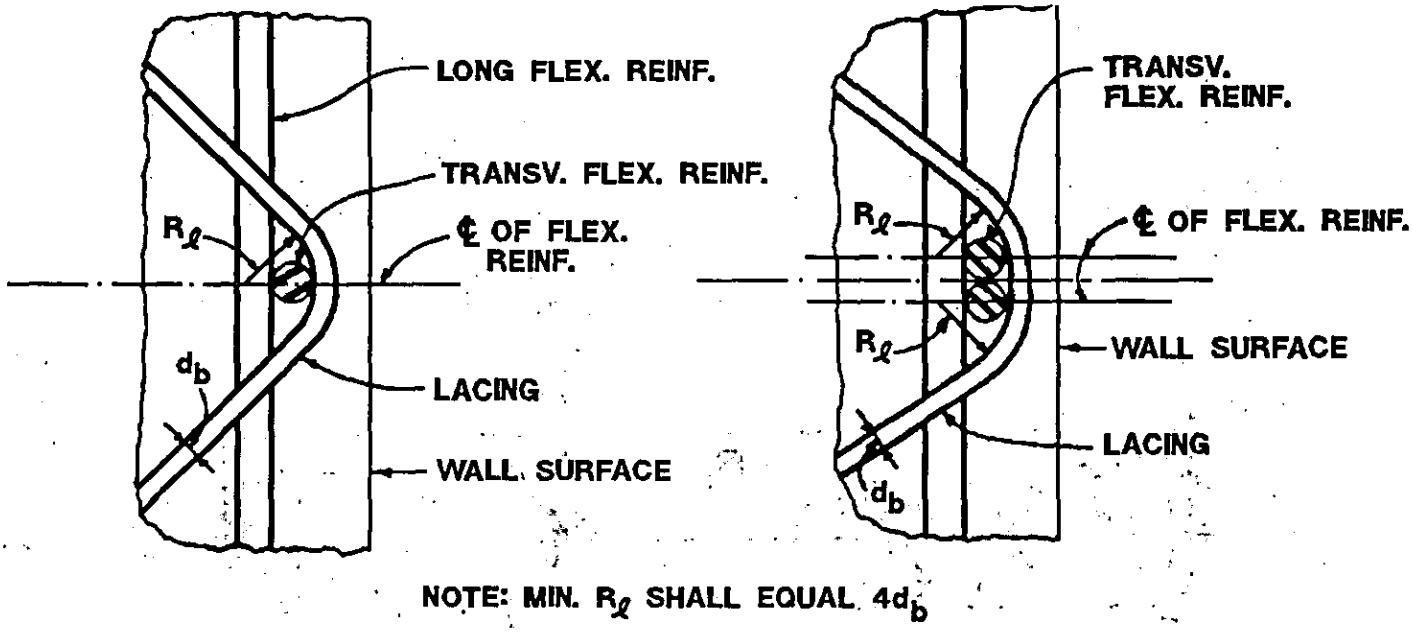


Figure 4-90 Typical lacing bend details

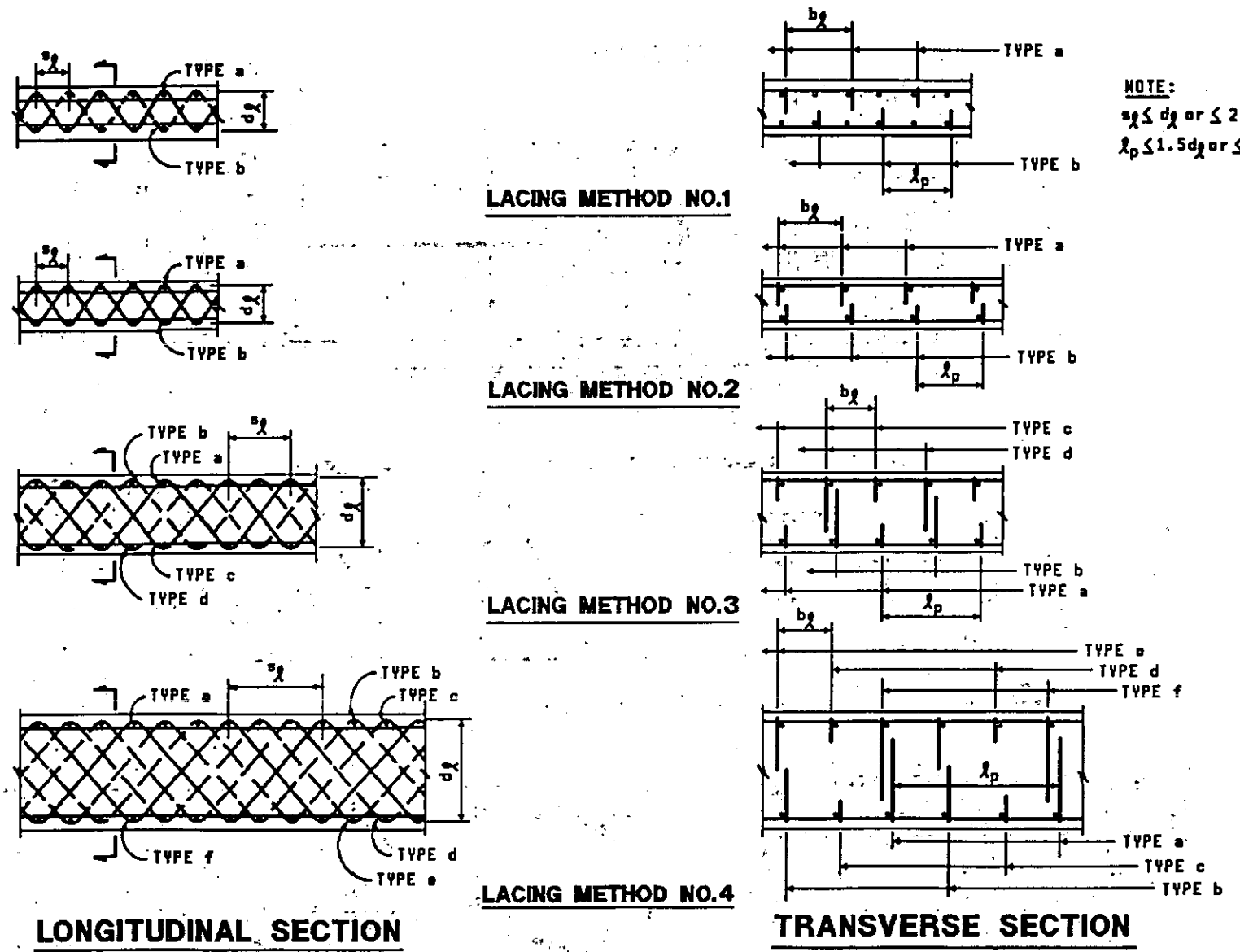


Figure 4-91 Typical methods of lacing

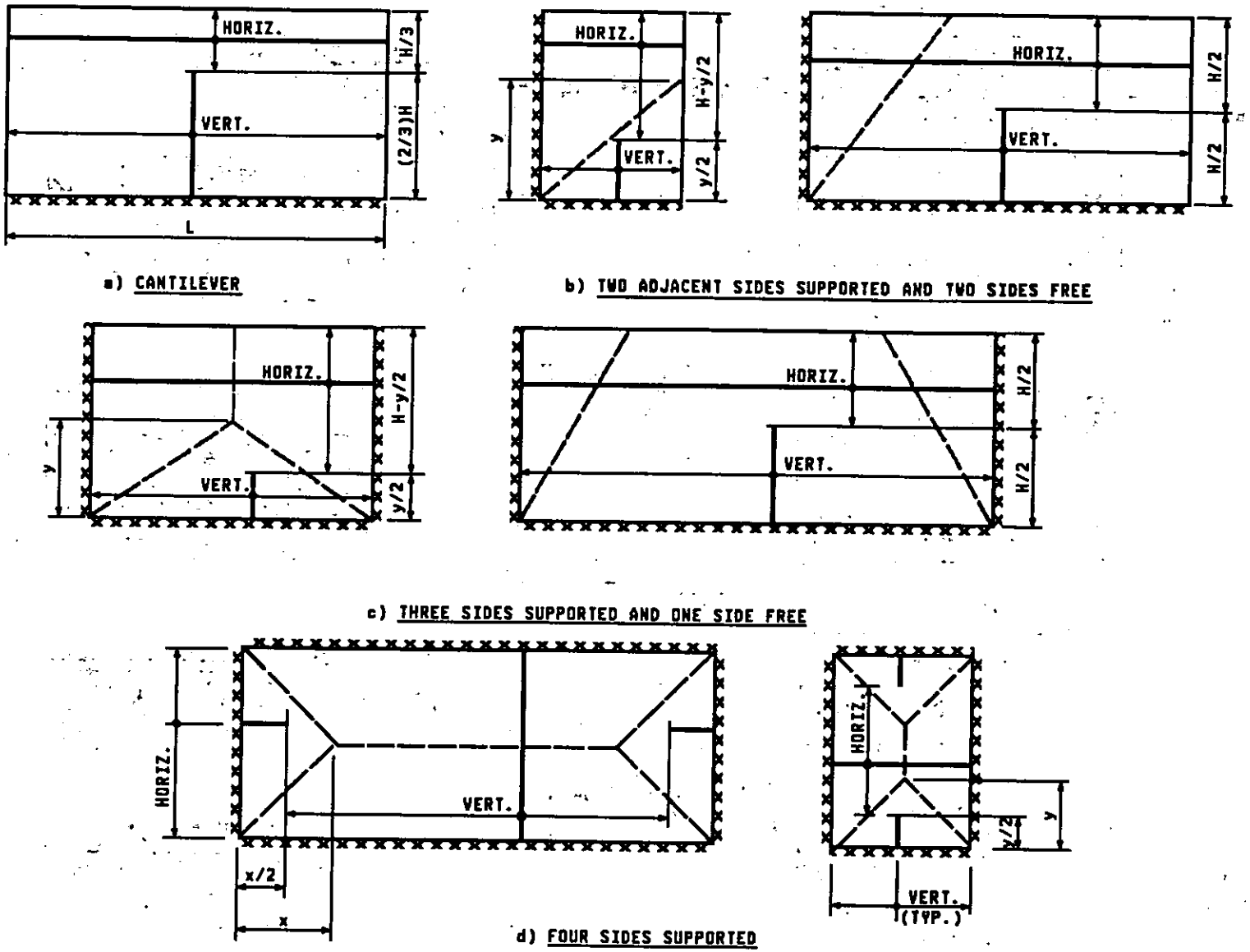


Figure 4-92 Typical location of continuous and discontinuous lacing

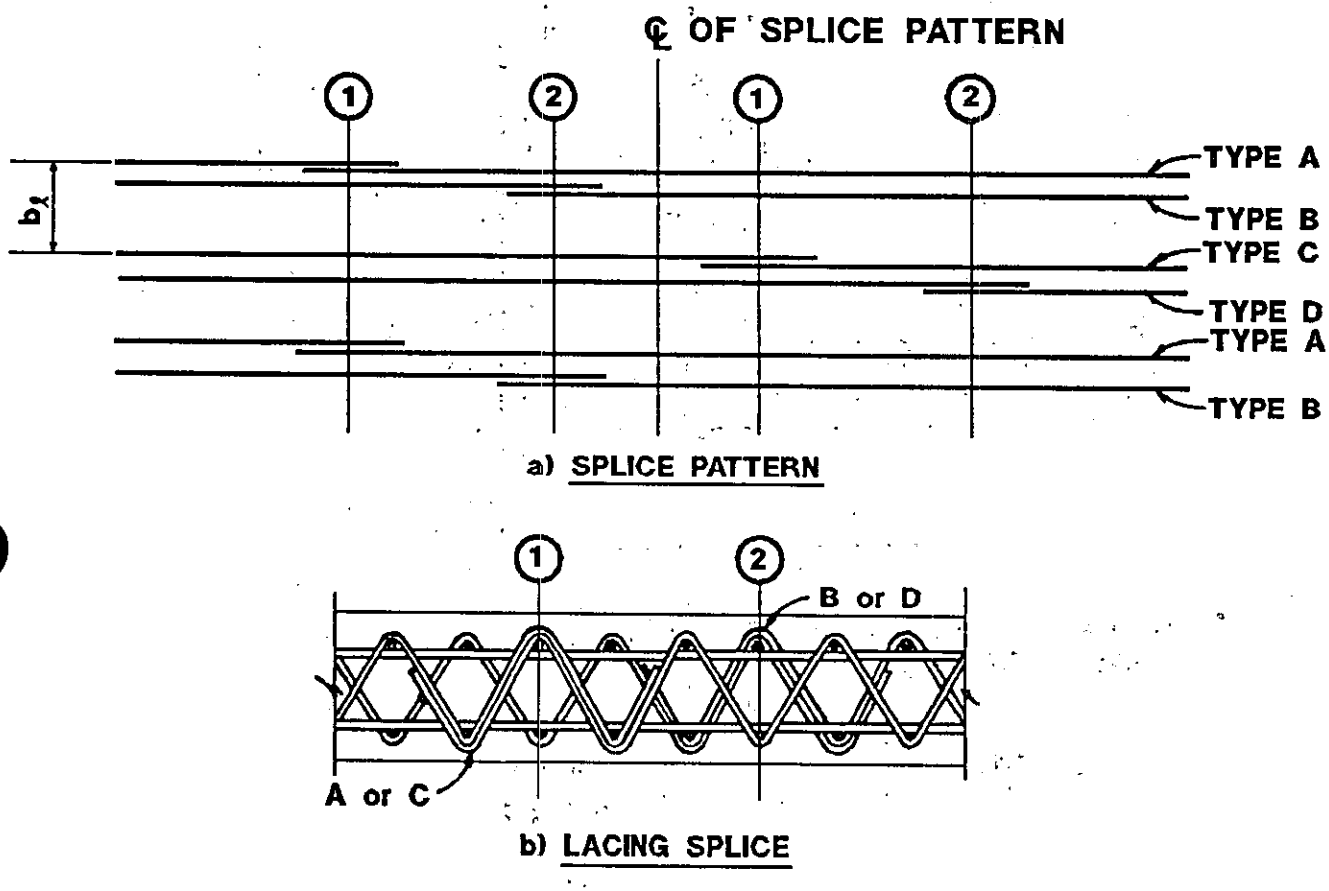
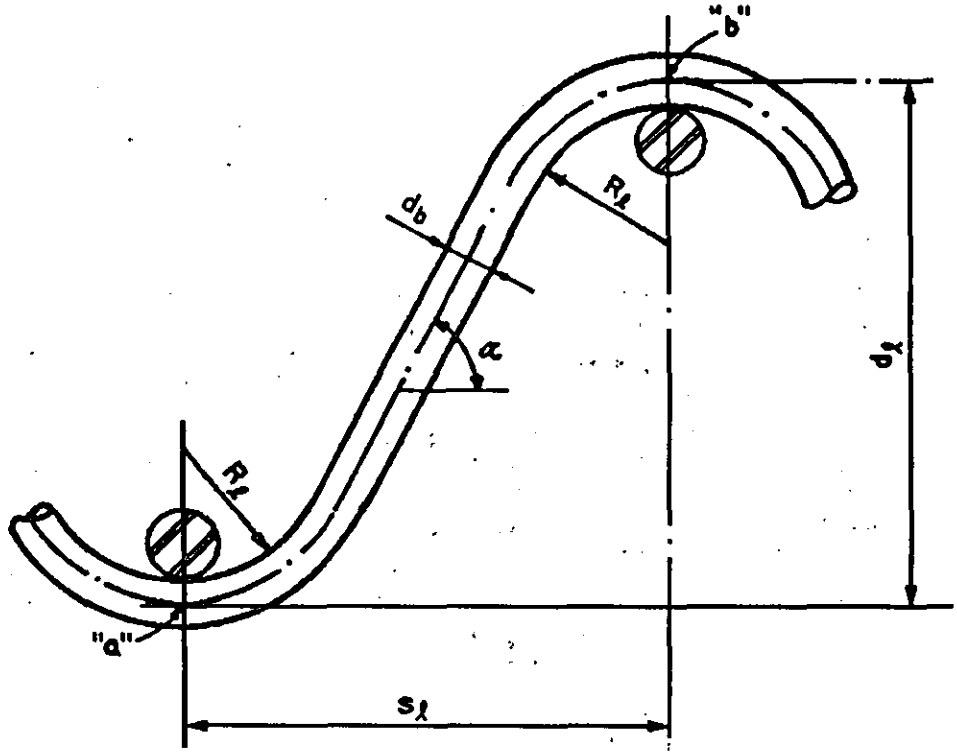


Figure 4-93 Typical details for splicing of lacing bars



NOTE: L_ℓ IS MEASURED ALONG CENTER LINE OF LACING BAR BETWEEN POINTS "a" AND "b"

$$L_\ell = \frac{s_\ell - (2R_\ell + d_b)\text{SIN}\,\alpha}{\text{COS}\,\alpha} + \pi(2R_\ell + d_b)\left(\frac{\alpha}{180}\right)$$

$$\text{COS}\,\alpha = \frac{-2B(1-B) \pm \sqrt{[2B(1-B)]^2 - 4[(1-B)^2 + A^2][B^2 - A^2]}}{2[(1-B)^2 + A^2]}$$

$$A = s_\ell / d_\ell \quad \text{AND} \quad B = \frac{2R_\ell + d_b}{d_\ell}$$

Figure 4-94 Length of lacing bars

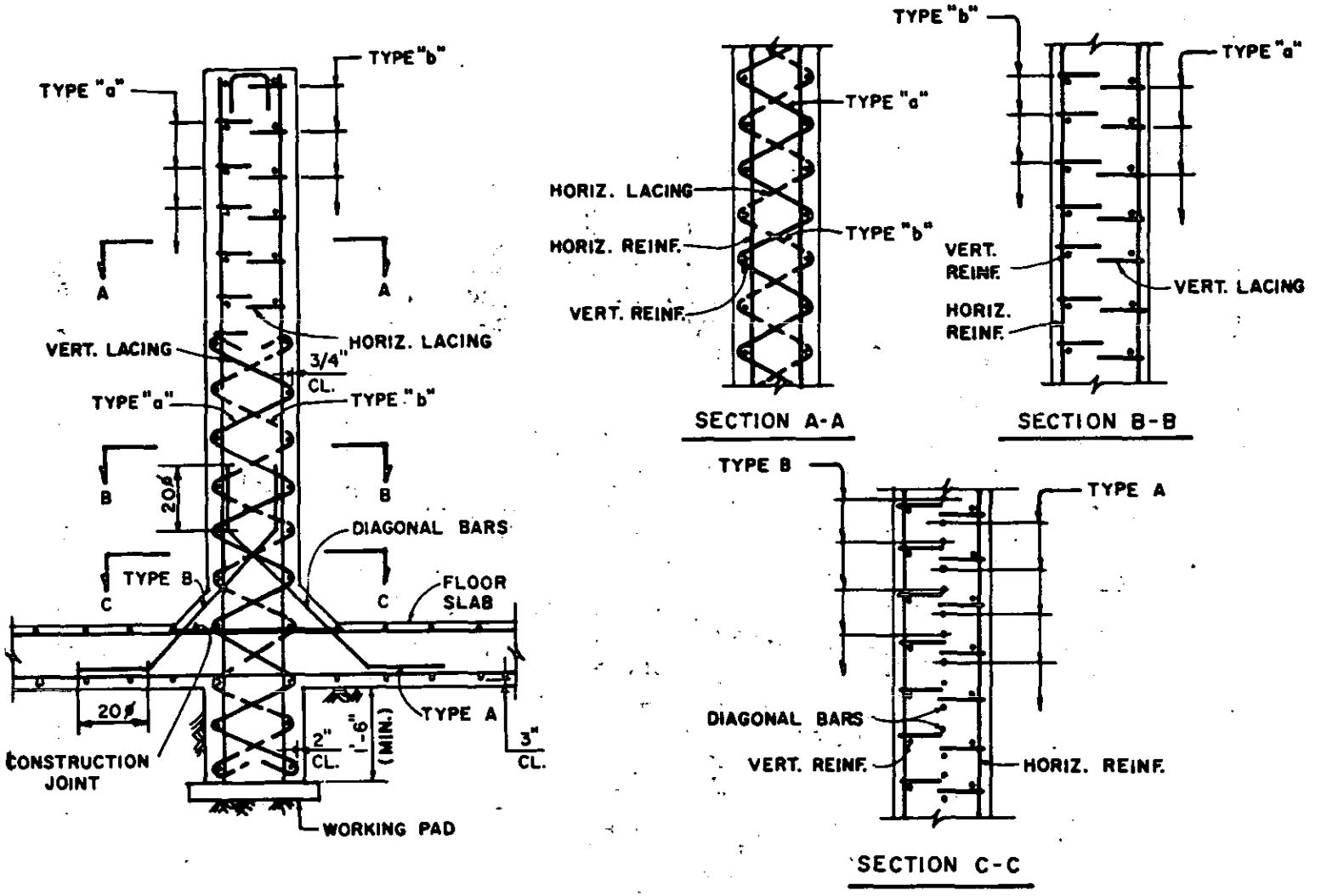


Figure 4-95 Reinforcement details of laced concrete walls

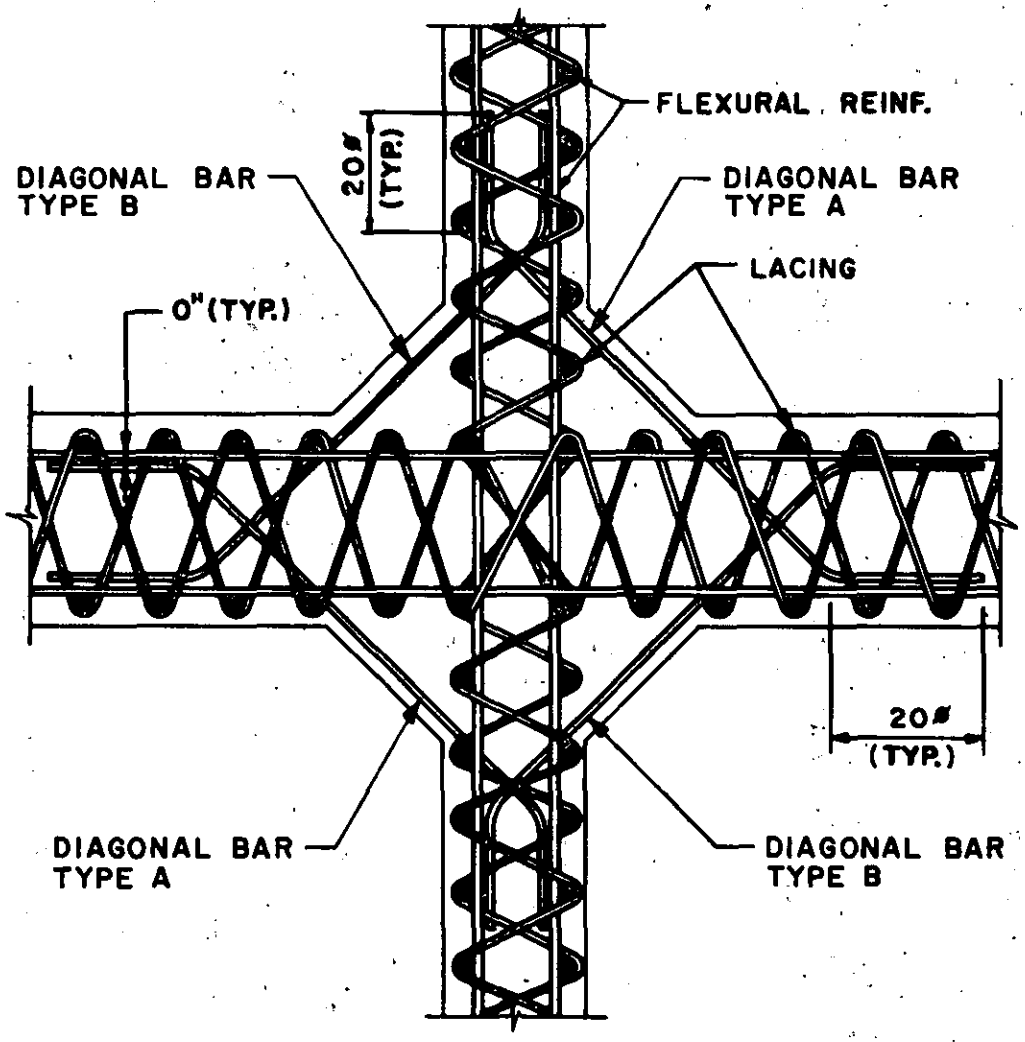


Figure 4-96 Typical detail at intersection of two continuous laced walls

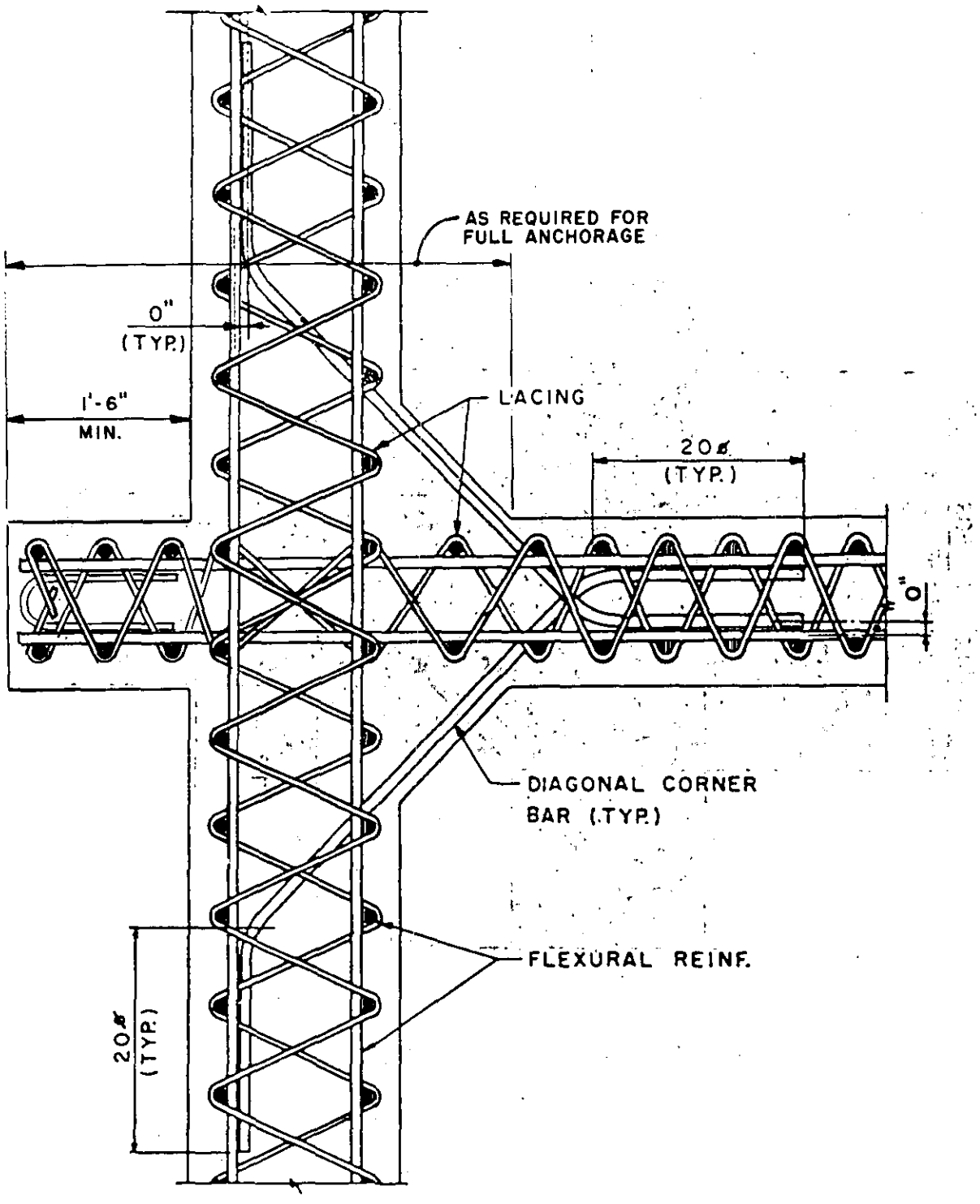


Figure 4-97 Typical detail at intersection of continuous and discontinuous laced walls

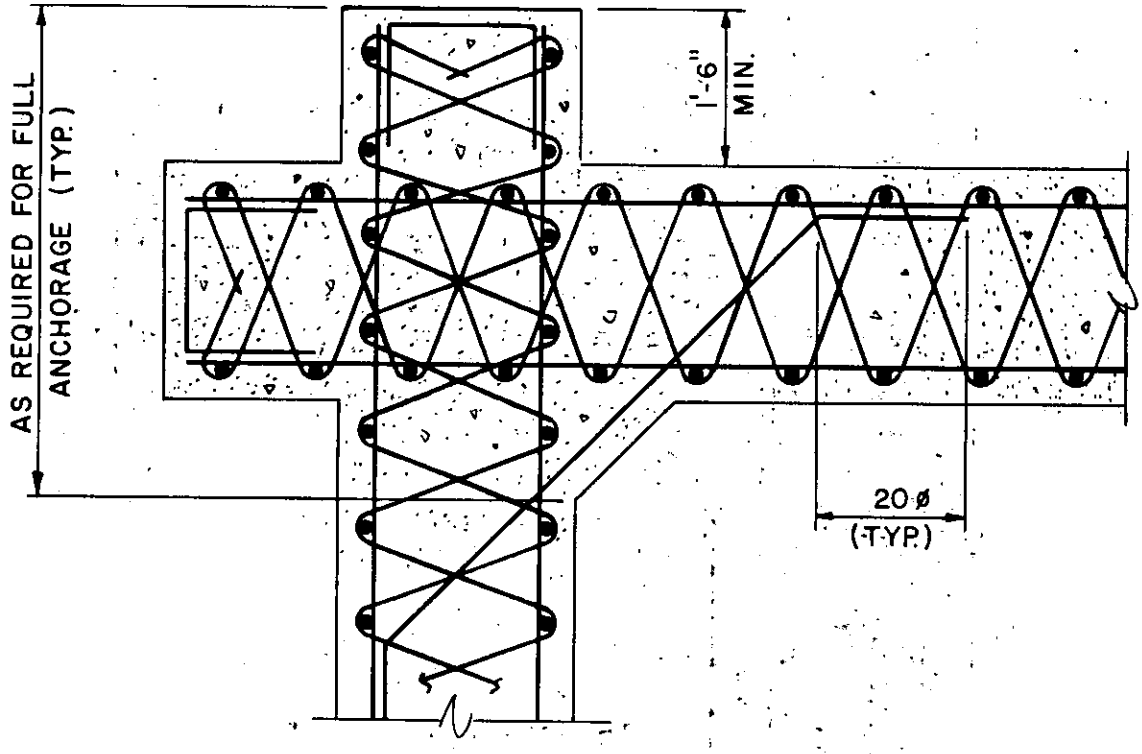


Figure 4-98 Typical detail at corner of laced walls

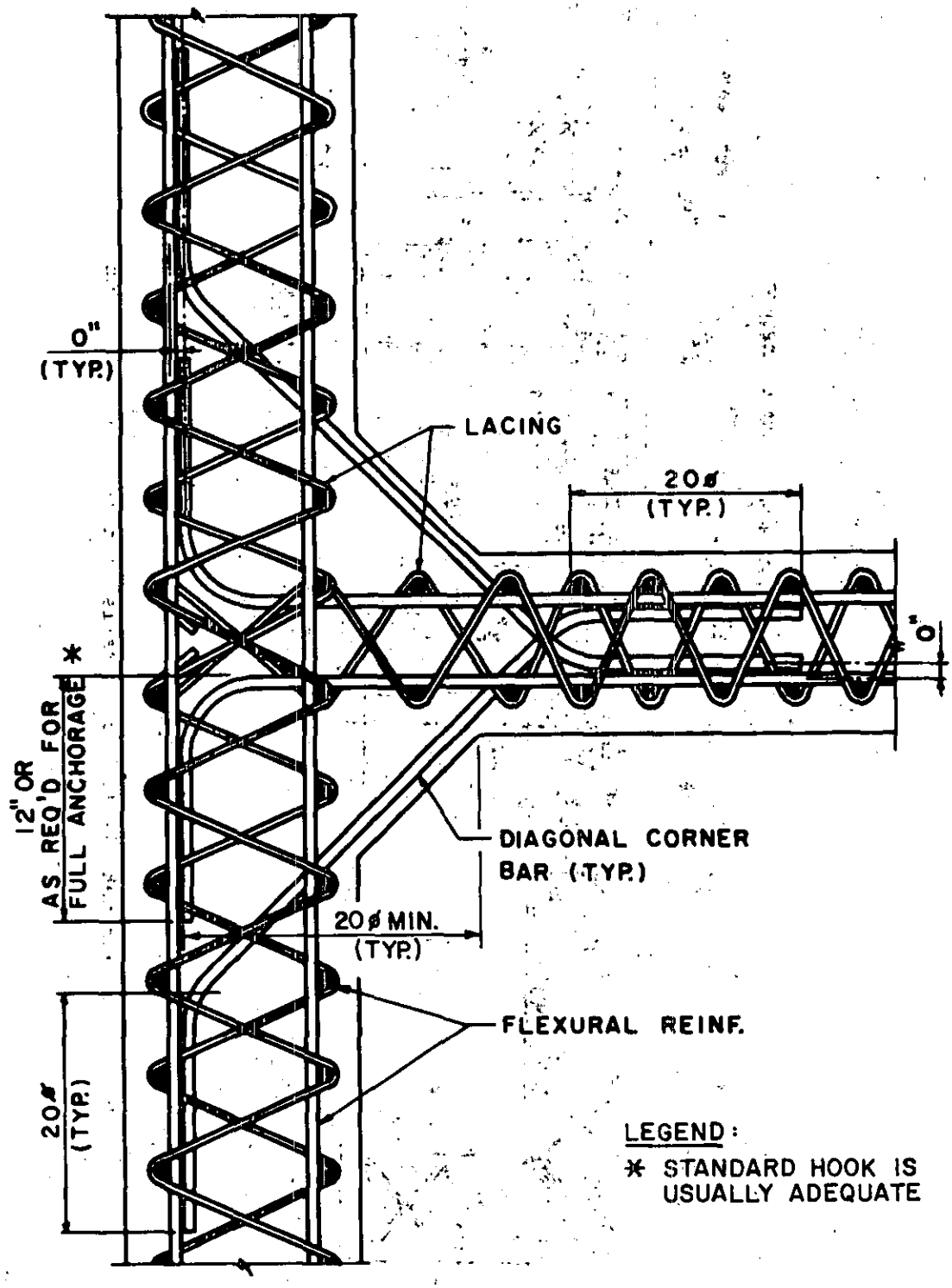


Figure 4-99 Intersection of continuous and discontinuous laced walls without wall extensions

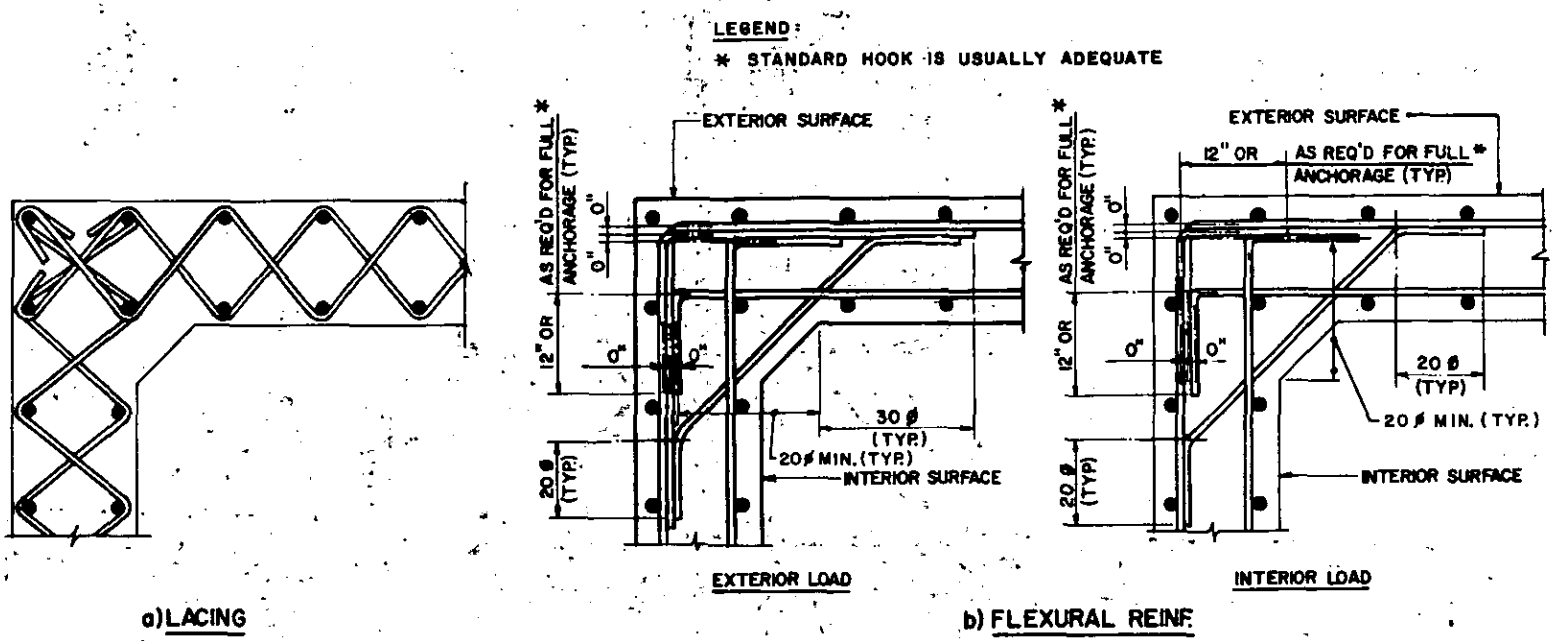


Figure 4-100 Corner details for laced walls without wall extensions

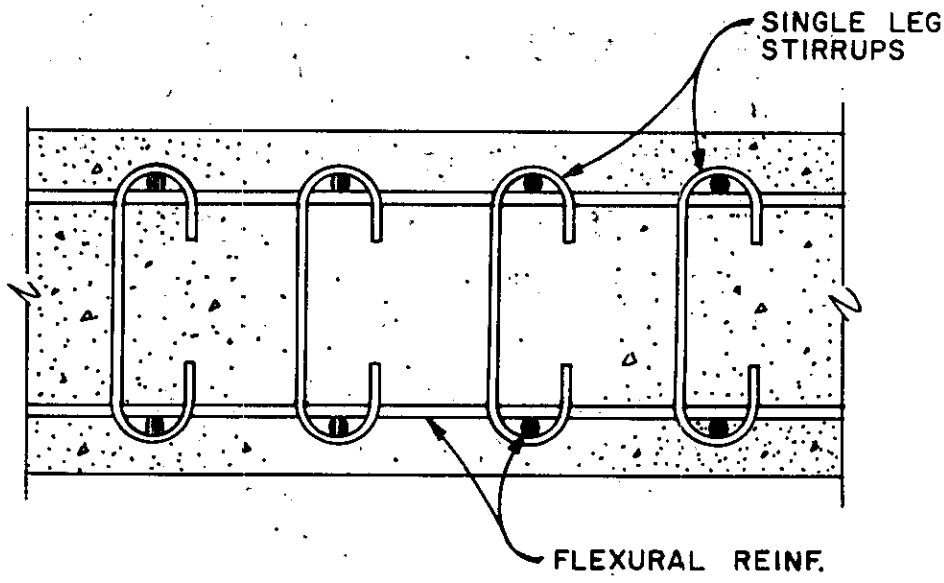


Figure 4-101 Element reinforced with single leg stirrups

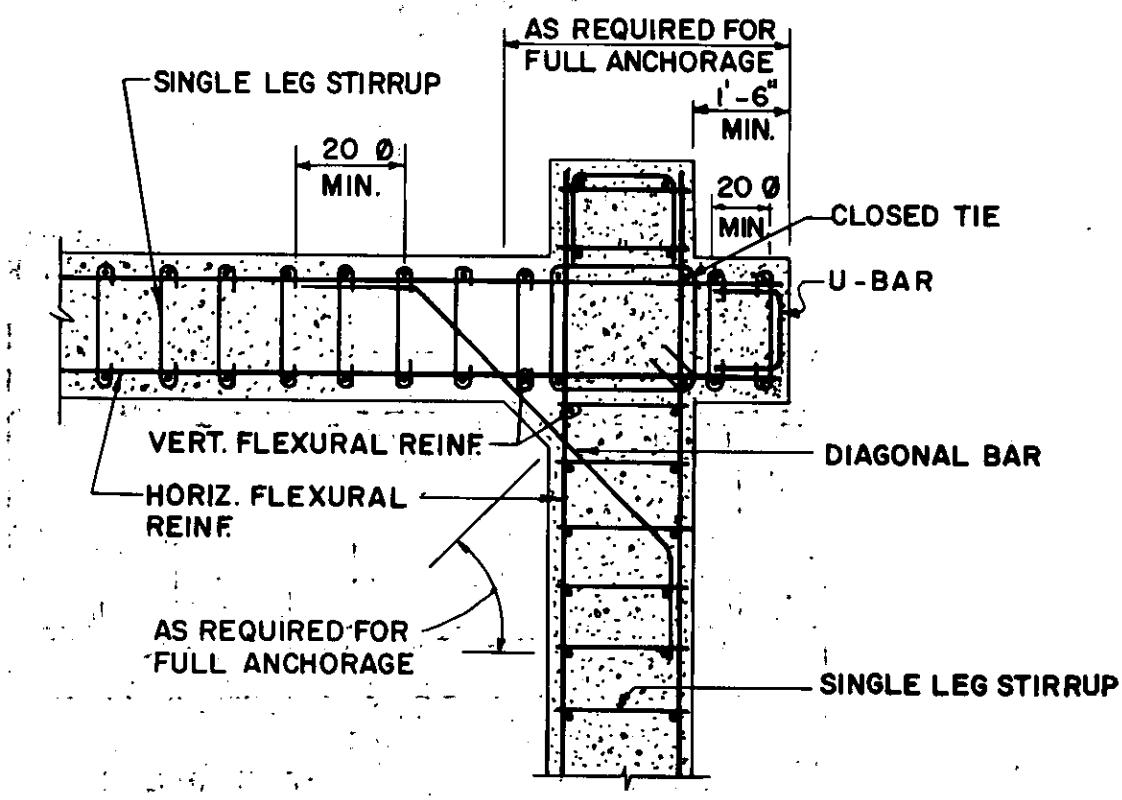


Figure 4-102 Typical detail at corner for walls reinforced with single leg stirrups

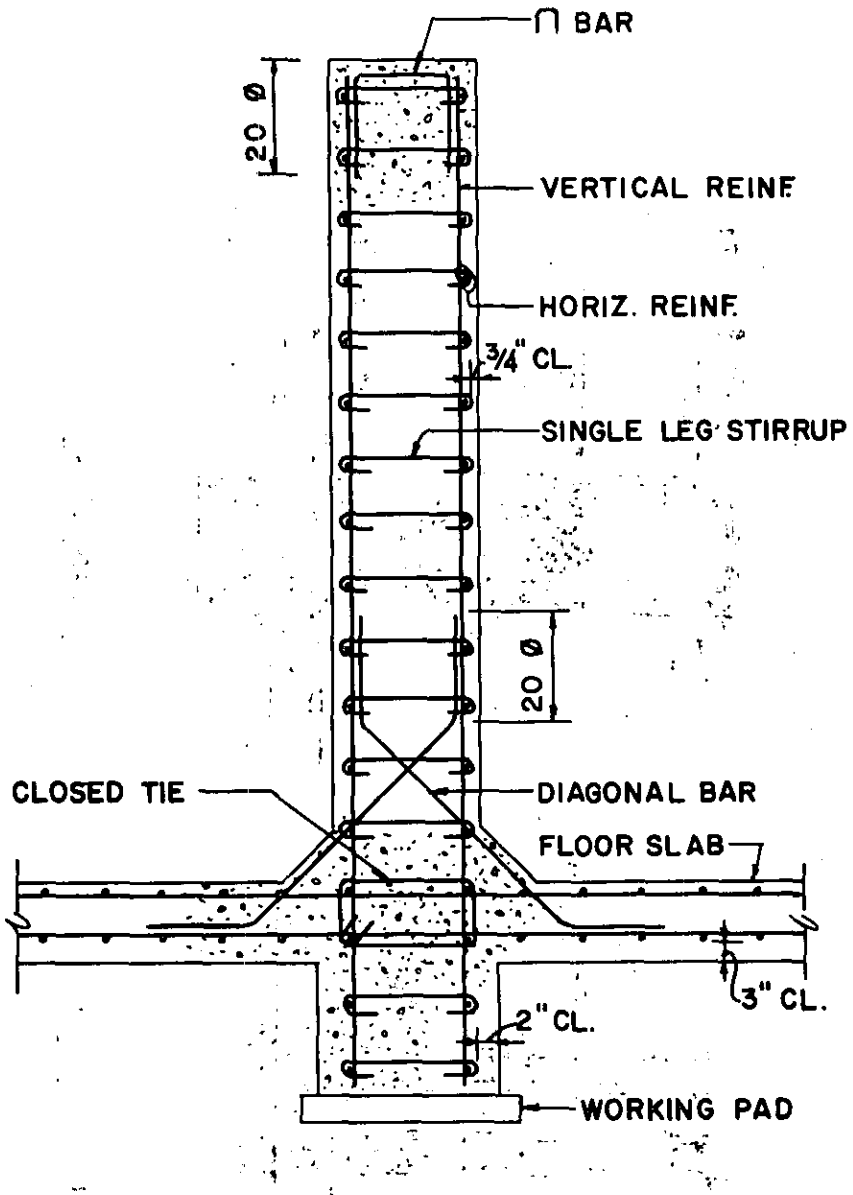


Figure 4-103 Reinforcement detail of wall with single leg stirrups

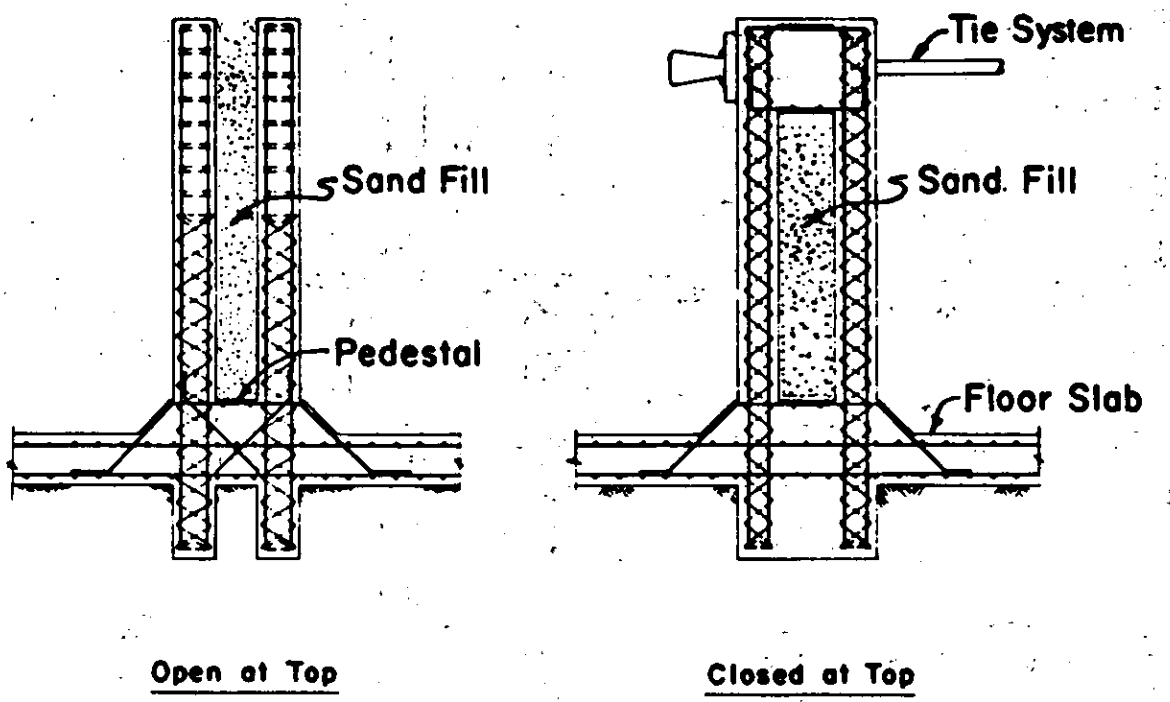
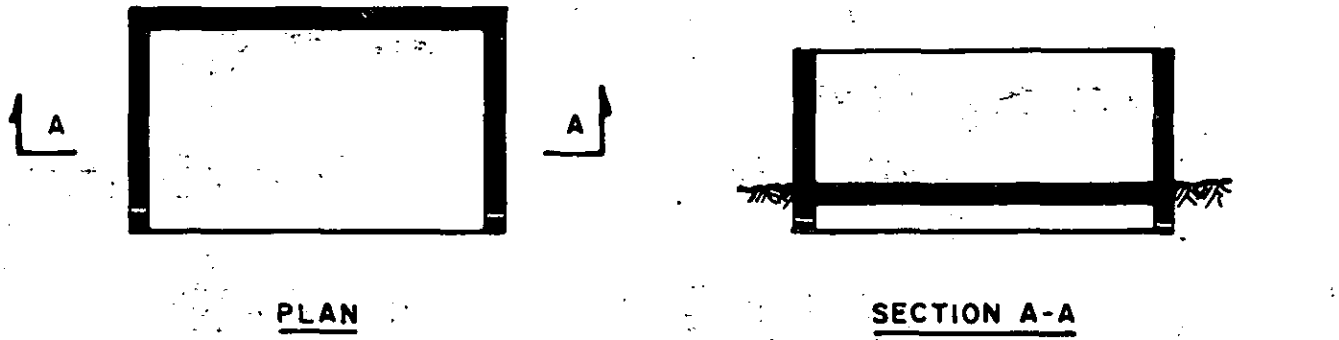
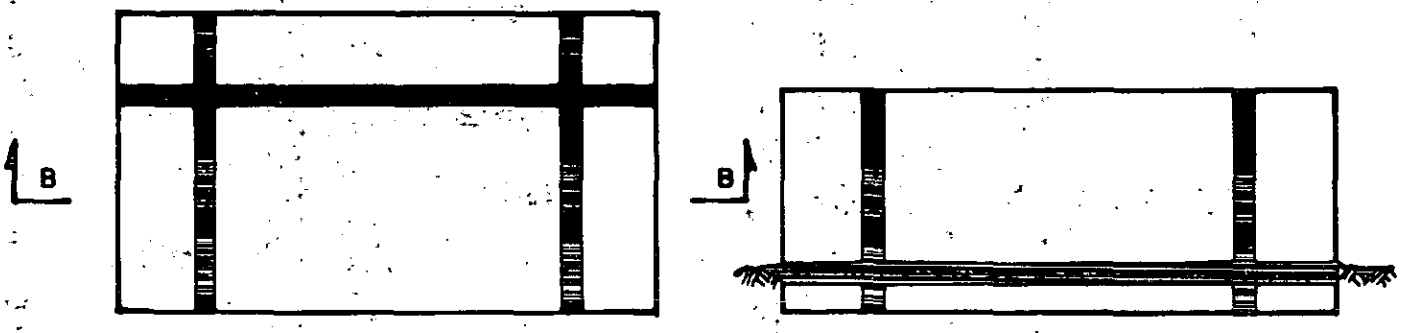


Figure 4-104 Typical composite wall details

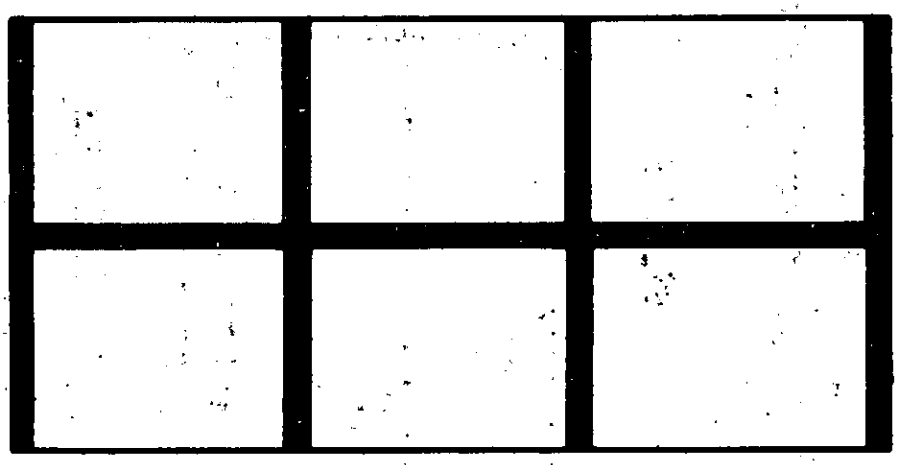


a) DISCONTINUOUS WALL CONSTRUCTION

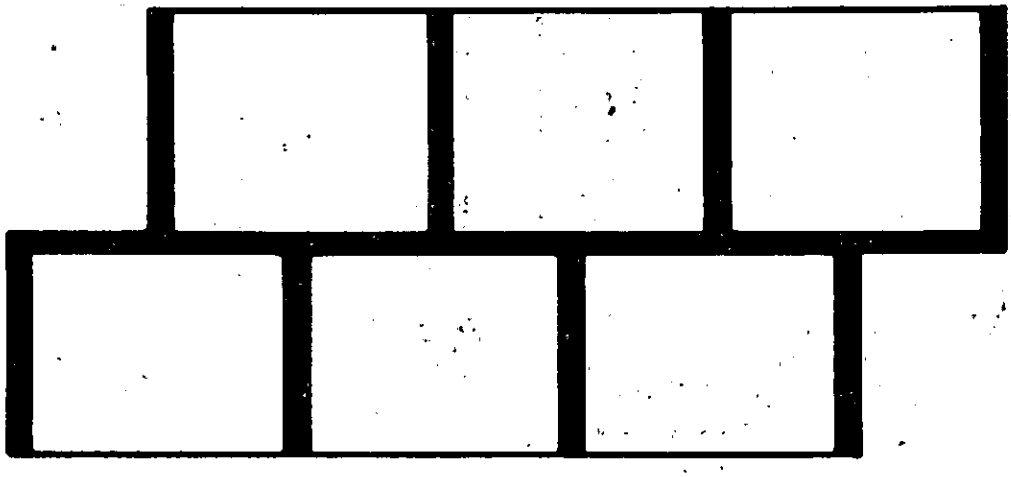


b) CONTINUOUS WALL CONSTRUCTION

Figure 4-105 Typical single-cell structures



SCHEME a) CONTINUOUS SIDE WALL CONSTRUCTION



SCHEME b) DISCONTINUOUS SIDE WALL CONSTRUCTION

Figure 4-106 Typical multicubicle structures

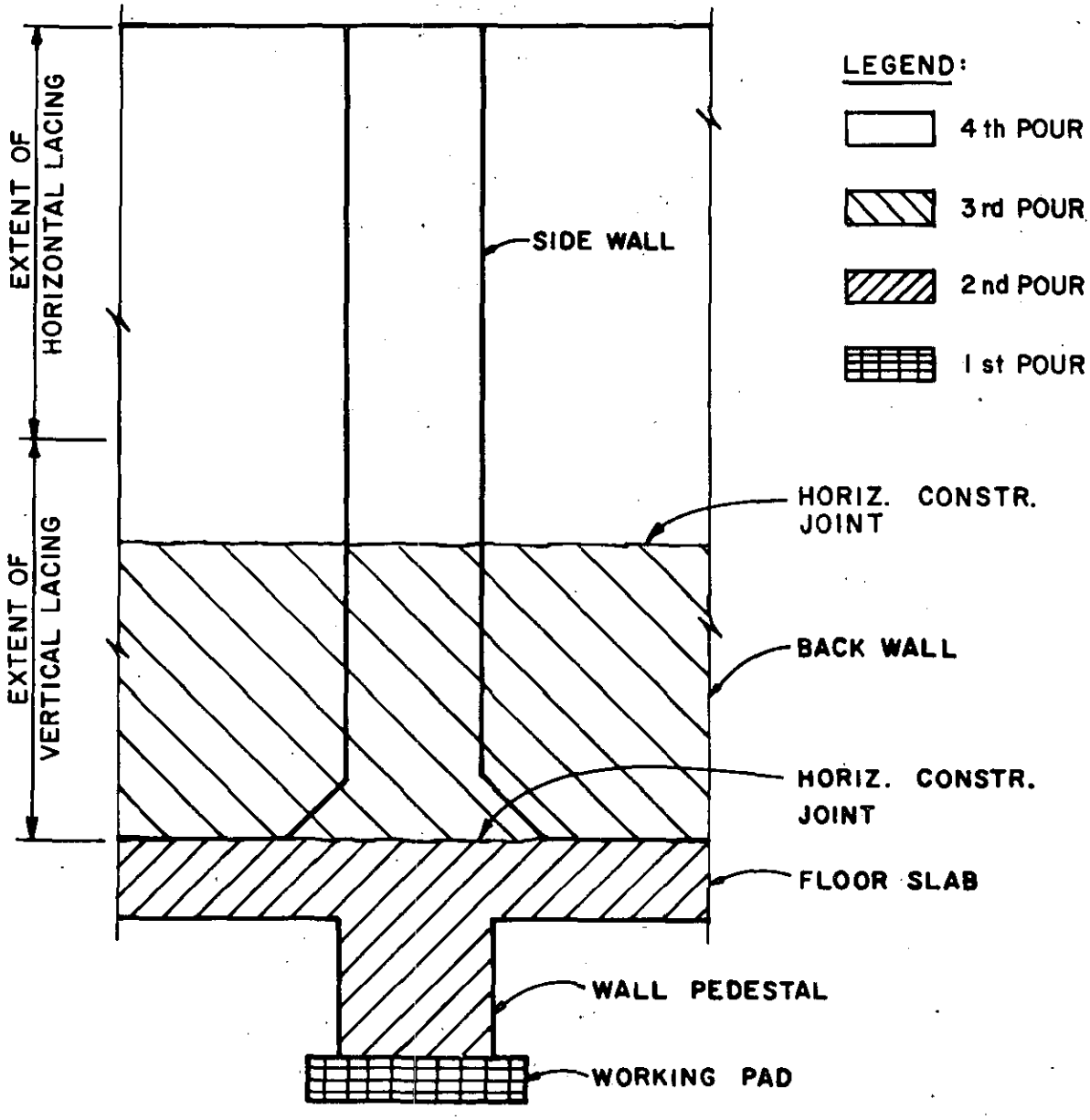


Figure 4-107 Pouring sequence

APPENDIX 4A

ILLUSTRATIVE EXAMPLES

Problem 4A-1. Elements Designed for the Pressure-Time Relationship

Problem: Design an element which responds to the pressure-time relationship.

Note:
Steps 5, 8, 10 through 18, 22 and 23 are specific for two-way elements, however, references are given defining similar procedures for one-way elements.

Procedure:

Step 1. Establish design parameters:

a. Blast loads including pressure-time relationship (Chapter 2).
b. Deflection criteria.
c. Structural configuration including geometry and support conditions.
d. Type of section available to resist blast, Type I, II or III depending upon the occurrence of spalling and/or crushing of the concrete cover.

Step 2. Select cross section of element including thickness and concrete cover over reinforcement. Also determine static stresses of concrete and reinforcing steel (Section 4-12).

Step 3. Determine dynamic increase factors for both concrete and reinforcement from table 4-1. Using the above DIF and the static stresses of step 2, calculate the dynamic strength of materials.

Step 4. Determine the dynamic design stresses using table 4-2 and the results from step 3.

Step 5. Assume vertical and horizontal reinforcement bars to yield the optimum steel distribution. The steel distribution is optimum when the resulting yield lines make an angle of 45 degrees with supports.

Step 6. Calculate d_e (d or d_c, depending upon type of cross section available to resist blast) for both the positive and negative moments in both vertical and horizontal directions. Determine reinforcing ratios. Also check for minimum steel ratios from table 4-3.

Step 7. Using the area of reinforcement, the value of d_e from step 6, and the dynamic design stresses of step 4, calculate the moment capacity (Section 4-17) of both the positive and negative reinforcement.

Note: Steps 8, 10 through 18 are required to determine the actual and equivalent resistance-deflection curves for two-way elements. To obtain these curves for one-way elements, see problem 4A-6.

Step 8. Using the equations of table 3-2 or table 3-3 and the moment capacities of step 7. calculate the ultimate resistance in the plastic range.

Step 9. Using equation 4-4, the static concrete stress of step 2, and unit weight for concrete equal to 150 psf, calculate the modulus of elasticity for concrete. With the above modulus for concrete and that for steel (eq. 4-5) and equation 4-6, calculate the modular ratio.

Step 10. With the use of equation 4-9a and the assumed concrete thickness of step 2, calculate the gross moment of inertia of the concrete. Using the value of d_e for the negative and positive reinforcement of step 6, calculate an average value of d_e. Also calculate an average percent of positive and negative reinforcement using the above d_e and the area of reinforcement of step 6 in both vertical and horizontal directions. With the values of p (average) and figure 4-11 or 4-12, determine the values of the constants F and calculate the moment of inertia of a cracked section with equation 49b in both directions. Calculate the average cracked moment of inertia for the element using equation 4-10, and also, the average moment of inertia of the element from equation 4-7.

Step 11. Using equation 3-33, and the modulus of elasticity of step 9 and the moment of inertia of step 10, calculate the unit flexural rigidity.

Step 12. Establish points of interest and their ultimate moment capacities (fig. 3-23).

Step 13. Compute properties of first yield.

a. Location of first yield.
b. Resistance at first yield r_e.
c. Moments at remaining points consistent with r_e.
d. Maximum deflection at first yield.

Step 14. Compute properties at second yield.

a. Remaining moment capacity at other points.
b. Location of second yield.
c. Change in unit resistance Δr, between first and second yield.
d. Unit resistance at second yield r_{ep}.
e. Moment at remaining points consistent with r_{ep}.
f. Change in maximum deflection.
g. Total maximum deflection.

Note:

An element with unsymmetrical support conditions may exhibit three or four support yields. Therefore, repeat step 14 as many times as necessary to obtain properties at various yield points.

Step 15. Compute properties at final yield (ultimate unit resistance).

a. Ultimate unit resistance.

b. Change in resistance between ultimate unit resistance and resistance at prior yield.

c. Change in maximum deflection (for elements supported on two, three or four edges, use stiffness obtained from figure 3-26, 3-30 and 3-36, respectively).

d. Total maximum deflection.

Step 16. Draw the actual resistance-deflection curve (fig. 3-39).

Step 17. Calculate equivalent maximum elastic deflection of the element.

Step 18. Calculate the equivalent elastic unit stiffness K_E from equation 3-36.

Step 19. Determine the load-mass factor K_{LM} for the elastic, elasto-plastic and plastic ranges from table 3-13 and figure 3-44. The average load mass factor is obtained by taking the average K_{LM} for the elastic and elasto-plastic ranges and averaging this value with the K_{LM} of the plastic range. In addition, calculate the unit mass of the element (account for reduced concrete thickness if spalling is anticipated) and multiply this unit mass by K_{LM} for the element to obtain the effective unit mass of the element.

Note:

For one-way elements, use table 3-12 to determine the average load mass factor.

Step 20. Using the effective mass of step 19 and the equivalent stiffness, calculate the natural period of vibration T_N from equation 3-60.

Step 21. Determine the response chart parameters:

a. Peak pressure P (step 1).

b. Peak resistance r_u (step 8).

c. Duration of load T (step 1).

d. Natural period of vibration T_N (step 20).

Also calculate the ratios of peak pressure P to peak resistance r_u and duration T to period T_N. Using these ratios and the response charts of Chapter 3, determine the value of X_m/X_E and t_m/T_N. Compute the value of X_m and compare it to the maximum permissible deflection of step 1, and if found satisfactory, proceed to step 22. If comparison is unsatisfactory, repeat steps 2 to step 21. In addition, compute the value of t_m/t_o from t_m/T_N and T/T_N and assuming that $T = t_o$, determine whether or not correct procedure has been used; for elements to respond to the pressure-time relationship, $0.1 < t_m/t_o < 3$.

Step 22. Using the ultimate resistance of step 8, the value of d_e of step 6 and equations of table 4-7, calculate the ultimate diagonal tension shear stresses at distance d_e from each support. Also calculate the shear capacity of the element from equation 4-23. If the capacity is greater than that produced by the load, shear reinforcement is not required. However, if the shear produced by the load is greater than the capacity, then shear reinforcement must be added to resist the excess.

Note:

For one-way elements, use table 4-6 to establish diagonal tension shear stress.

Step 23. Using the equations of table 3-10 or 3-11 and the ultimate resistance of step 8, calculate the shear at the supports. Determine required area of diagonal bars using equation 4-30. However, if section type I is used, then the minimum diagonal bars must be provided (eq. 4-31).

Note:

For one-way elements, use table 3-9 to calculate the shear at the supports.

Example 4A-1, Elements Designed for the Pressure-Time Relationship

Required: Design a wall which spans in two directions and is fully restrained at all supports for a given blast load.

Solution:

Step 1. Given:

a. Pressure-time loading (fig. 4A-1).

b. Maximum deflection equal to 3 times elastic deflection.

c. L = 180 in., H = 144 in. and fixed on four sides (fig. 4A-1).

d. Type I cross section.

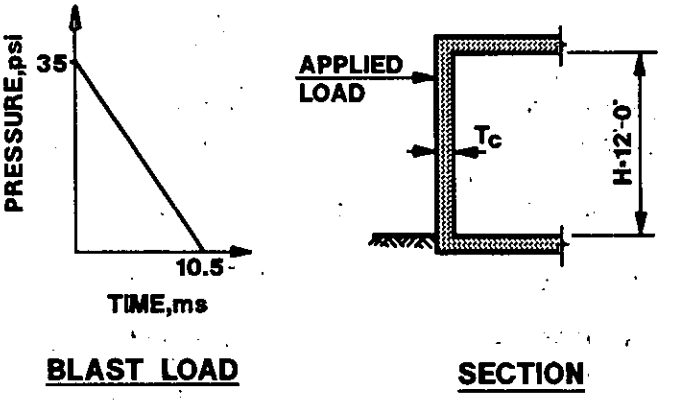
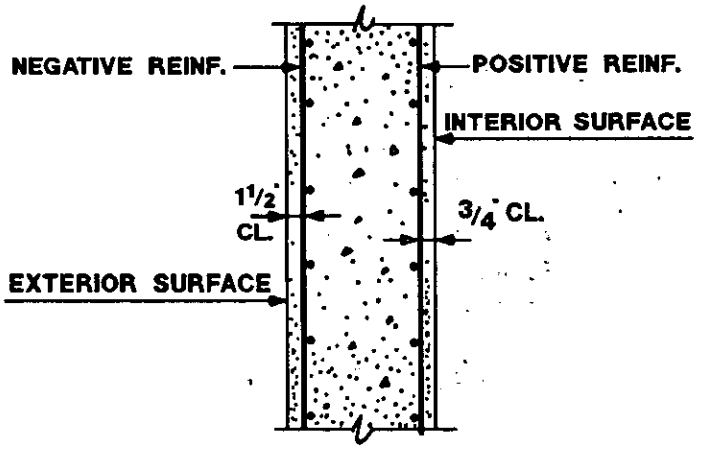


Figure 4A-1

Step 2. Select cross section of element and static stress of reinforcement and concrete (fig. 4A-2).



f'_c = 4,000 psi

f_y = 66,000 psi

Assume T_c = 12 in. and concrete cover as shown.

Figure 4A-2

Step 3. Determine dynamic stresses.

a. Dynamic increase factors - DIF (table 4-1).

Concrete:

Bending	- 1.19
Diagonal tension	- 1.00

Reinforcement:

Bending	- 1.17
Diagonal tension	- 1.00
Direct shear	- 1.10

b. Dynamic strength of materials

Concrete (f'_{dc}):

Compression	- 1.19 (4,000) = 4,760 psi
Diagonal tension	- 1.00 (4,000) = 4,000 psi

Reinforcement (f_{dv}):

Bending	- 1.17 (66,000) = 77,200 psi
Diagonal tension	- 1.00 (66,000) = 66,000 psi
Direct shear	- 1.10 (66,000) = 72,600 psi

Step 4. Dynamic design stresses from table 4-2.

Concrete (f'_{dc}):

Compression	- 4,760 psi
Diagonal tension	- 4,000 psi

Reinforcement ($f_{ds} = f_{dy}$):

Bending	- 77,200 psi
Diagonal tension	- 66,000 psi
Direct shear	- 72,600 psi

Step 5. In order to obtain optimum steel ratio p_V/p_H, set $x = H/2$ to have 45 degrees yield lines.

$$\frac{x}{L} = \frac{H}{2L} = \frac{144}{2 \times 180} = 0.40$$

From figure 3-17,

$$\frac{L}{H}\left[\frac{M_{VN} \quad M_{VP}}{M_{HN} + M_{HP}}\right]^{\frac{1}{2}} = 1.43$$

Therefore,

$$\frac{M_{VN} + M_{VP}}{M_{HN} + M_{HP}} = \left[\frac{1.43 \times 144}{180}\right]^2 = 1.31$$

Try No. 4 bars at 10 in. o.c. in vertical direction, and No. 4 bars at 12 in. o.c. in horizontal direction.

Step 6. Calculate d_c and steel ratios for each direction, minimum reinforcement ratio is equal to 0.15 percent.

Vertical:

Vertical reinforcement bars are No. 4 at 10 in. o.c. from step 5.

$$A_{sV} = .20 \times 12/10 = 0.24 \text{ in}^2/\text{ft}$$

Negative moment $d_v = 12 - 1.5 - 0.25 = 10.25$ in

Positive moment $d_v = 12 - 0.75 - 0.25 = 11.0$ in

$$\rho_V = \frac{A_{sV}}{bd_V} = \frac{0.24}{12 \times 11.0} = 0.00182 > 0.0015 \text{ O.K.}$$

Horizontal:

Horizontal reinforcement bars are No. 4 at 12 in. o.c. from step 5.

$$A_{sH} = .20 \times 12/12 = 0.20 \text{ in}^2/\text{ft}$$

Negative moment $d_H = 10.25 - 0.25 - 0.25 = 9.75$ in

Positive moment $d_H = 11.0 - 0.25 - 0.25 = 10.5$ in

$$\rho_H = \frac{A_{sH}}{bd_H} = \frac{.20}{12 \times 10.5} = 0.00158 > 0.0015 \text{ O.K.}$$

Step 7. Calculate moment capacity of both positive and negative reinforcement in both directions.

a. Depth of equivalent rectangular stress blocks.

$$a = \frac{A_s f_{ds}}{.85 \, bf'_{dc}} \qquad \text{(eq. 4-12)}$$

$$a_V = \frac{.24 \times 77{,}200}{.85 \times 12 \times 4760} = .382 \text{ in}$$

$$a_H = \frac{.20 \times 77{,}200}{.85 \times 12 \times 4760} = .318 \text{ in}$$

b. Moment capacity (eq. 4-11).

$$M_u = \frac{A_s f_{ds}}{b} \quad (d - a/2)$$

vertical negative $M_{VN} = \dfrac{0.24\ (77{,}200)(10.25 - .382/2)}{12} = 15531$ in-lbs/in

vertical positive $M_{VP} = \dfrac{0.24\ (77{,}200)\ (11.0 - .382/2)}{12} = 16689$ in-lbs/in

$M_{HN} = \dfrac{0.20\ (77{,}200)\ (9.75 - .318/2)}{12} = 12340$ in-lbs/in

$M_{HP} = \dfrac{0.20\ (77{,}200)\ (10.5 - .318/2)}{12} = 13305$ in-lbs/in

Step 8. Determine ultimate resistance of the element.

$$\frac{L}{H}\left[\frac{M_{VN} + M_{VP}}{M_{HN} + M_{HP}}\right]^{\frac{1}{2}} = \frac{180}{144}\left[\frac{15531 + 16689}{12340 + 13305}\right]^{\frac{1}{2}} = 1.40 \approx 1.43 \text{ (step 5)}$$

From figure 3-17,

$$\frac{x}{L} = .405$$

$$x = .405 \times 180 = 72.9 \text{ in}$$

Ultimate resistance (table 3-2).

$$r_u = \frac{5\ (M_{HN} + M_{HP})}{x^2} = \frac{5(12{,}340 + 13{,}305)}{(72.9)^2} = 24.13 \text{ psi}$$

Step 9. Determine modulus of elasticity and modular ratio.

a. Concrete (eq. 4-4)

$$E_c = w^{1.5} \ 33 \ (f'_c)^{1/2} = (150)^{1.5} \ (33)(4000)^{1/2}$$

$$= 3.83 \times 10^6 \text{ psi}$$

b. Steel (eq. 4-5)

$$E_s = 29 \times 10^6 \text{ psi}$$

c. $$n = \frac{E_s}{E_c} = \frac{29 \times 10^6}{3.83 \times 10^6} = 7.56 \qquad \text{(eq. 4-6)}$$

Step 10. Determine average moment of inertia for an inch strip.

a. Gross moment of inertia (eq. 4-9a)

$$I_g = \frac{T_c^3}{12} = \frac{12^3}{12} = 144 \text{ in}^4/\text{in}$$

b. Moment of inertia of cracked section (eq. 4-9b).

Vertical direction:

$$d_{(avg)} = \frac{10.25 + 11.0}{2} = 10.625 \text{ in}$$

$$\rho_{(avg)} = \frac{A_s}{bd_{(avg)}} = \frac{0.24}{12(10.625)} = 0.00188$$

$\therefore F = 0.0102$ (fig. 4-12)

$$I_{cV} = Fd_{(avg)}^3 = .0102 \times (10.625)^3 = 12.2 \text{ in}^4/\text{in}$$

Horizontal direction:

$$d_{(avg)} = \frac{9.75 + 10.50}{2} = 10.125 \text{ in}$$

$$P_{(avg)} = \frac{.20}{12\ (10.125)} = .00165$$

$\therefore F = 0.0092$

$$I_{cH} = .0092 \times (10.125)^3 = 9.5\ in^4/in$$

c. Average moment of inertia of cracked section.

$$I_c = \frac{LI_{cV} + HI_{cH}}{L + H} \qquad \text{(eq. 4-10)}$$

$$I_c = \frac{(180 \times 12.2) + (144 \times 9.5)}{180 + 144} = 11.0\ in_4/in$$

d. Average moment of inertia (eq. 4-7).

$$I_a = \frac{I_g + I_c}{2} = \frac{144.0 + 11.0}{2} = 77.5\ in^4/in$$

Step 11. Calculate unit flexural rigidity.

$$D = \frac{E_c I_a}{1-\nu^2} \qquad \text{(eq. 3-33)}$$

Use $\nu = .167$ for concrete

Therefore,

$$D = \frac{(3.83 \times 10^6)\ 77.5}{1-(.167)^2} = 305.34 \times 10^6\ \text{in-lbs}$$

Step 12. For points of interest, see figure 4A-3.

Step 13. Properties at first yield.

From figure 3-33 of Chapter 3 for H/L = 0.80

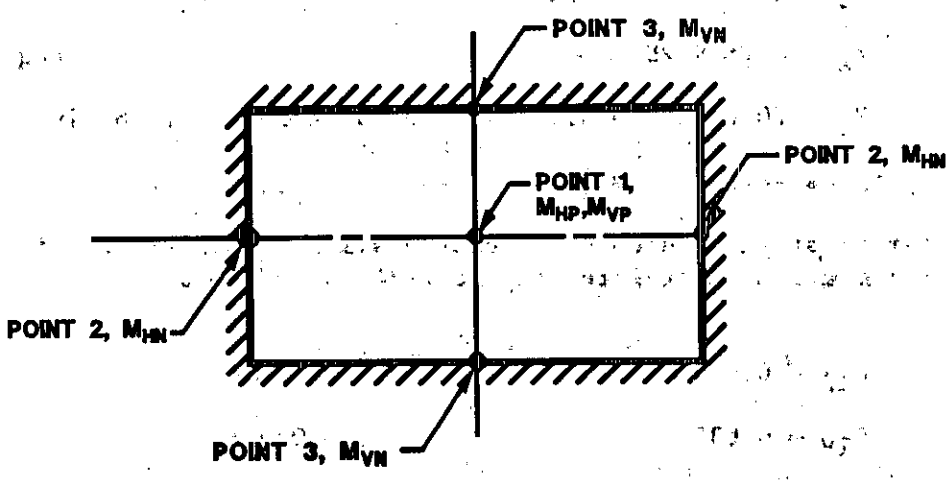


Figure 4A-3

$\beta_{1H} = 0.023$ $\beta_2 = 0.056$

$\beta_{1V} = 0.031$ $\beta_3 = 0.068$

$\gamma_1 = 0.0018$

a. $M_{Hp} = 13.305$ in-lbs/in $M_{HN} = 12,340$ in-lbs/in

$M_{Vp} = 16,689$ in-lbs/in $M_{VN} = 15,531$ in-lbs/in

$$M = \beta r H^2 \quad \therefore r = \frac{M}{\beta H^2} \qquad \text{(eq. 3-25)}$$

$r_{1H} = 13,305/[0.023(144)^2] = 27.90$ psi

$r_{1V} = 16,689/[0.031\ (144)^2] = 25.96$ psi

$r_2 = 12,340/[0.056(144)^2] = 10.63$ psi

$r_3 = 15,531/[0.068(144)^2] = 11.01$ psi

First yield at point 2 (smallest r).

b. $r_e = 10.63$ psi

c. $M_{1H} = (0.023)(10.63)(144)^2 = 5,070$ in-lbs/in

$M_{1V} = (0.031)(10.63)(144)^2 = 6,833$ in-lbs/in

$M_3 = (0.068)(10.63)(144)^2 = 14,989$ in-lbs/in

d. $X_e = \gamma_1 r_e H^4/D$ (eq. 3-32)

$X_e = (0.0018)(10.63)(144)^4/305.34 \times 10^6 = 0.0269$ in

Step 14. Properties at second yield.

After first yield element assumes a simple-simple-fixed-fixed configuration, therefore, figure 3-34 for H/L = 0.80.

$\beta_{1H} = 0.020$

$\beta_{1V} = 0.039$ $\beta_3 = 0.076$

$\gamma_1 = 0.0022$

a. $M_{1H} = M_{HP} - M_{1H}$ (at r_e) $= 13,305 - 5,070 = 8,235$ in-lbs/in

$M_{1V} = M_{VP} - M_{1V}$ (at r_e) $= 16,689 - 6,833 = 9,856$ in-lbs/in

$M_3 = M_{VN} - M_3$ (at r_e) $= 15,531 - 14,989 = 542$ in-lbs/in

b. $\Delta r = \dfrac{M}{\beta H^2}$

$\Delta r_{1H} = 8,235/[0.020(144)^2] = 19.86$ psi

$\Delta r_{1V} = 9,856/[0.039(144)^2] = 12.19$ psi

$\Delta r_3 = 542/[0.076(144)^2] = 0.34$ psi

Second yield at point 3 (smaller Δr)

c. $\Delta r = 0.34$ psi

d. $r_{ep} = r_e + \Delta r = 10.63 + .34 = 10.97$ psi (eq. 3-26)

e. $M_{1H} = (.020)(0.34)(144)^2 + 5,070 = 5,211$ in-lbs/in

$M_{1V} = (0.039)(0.34)(144)^2 + 6,833 = 7,108$ in-lbs/in

f. $\Delta X = \gamma_1 \Delta r H^4/D$

$\Delta X = (0.0022)(0.34)(144)^4/305.34 \times 10^6 = 0.0011$ in

g. $X_{ep} = X_e + \Delta X = 0.0269 + 0.0011 = .028$ in

Step 15. Properties at final yield (ultimate unit resistance). After second yield element assumes a simple-simple-simple-simple configuration, therefore, from figure 3.36 for H/L = 0.80.

$\gamma_1 = 0.0054$

a. $r_u = 24.13$ psi (from step 8)

b. $\Delta r = r_u - r_{ep} = 24.13 - 10.97 = 13.16$ psi

c. $\Delta X = \gamma_1 \Delta r H^4/D$

$\Delta X = (0.0054)(13.16)(144)^4/305.34 \times 10^6 = 0.100$ in

d. $X_p = X_{ep} + \Delta X = 0.028 + 0.100 = 0.128$ in

Step 16. For actual resistance deflection curve, see figure 4A-4.

Step 17. Equivalent elastic deflection from equation 3-35.

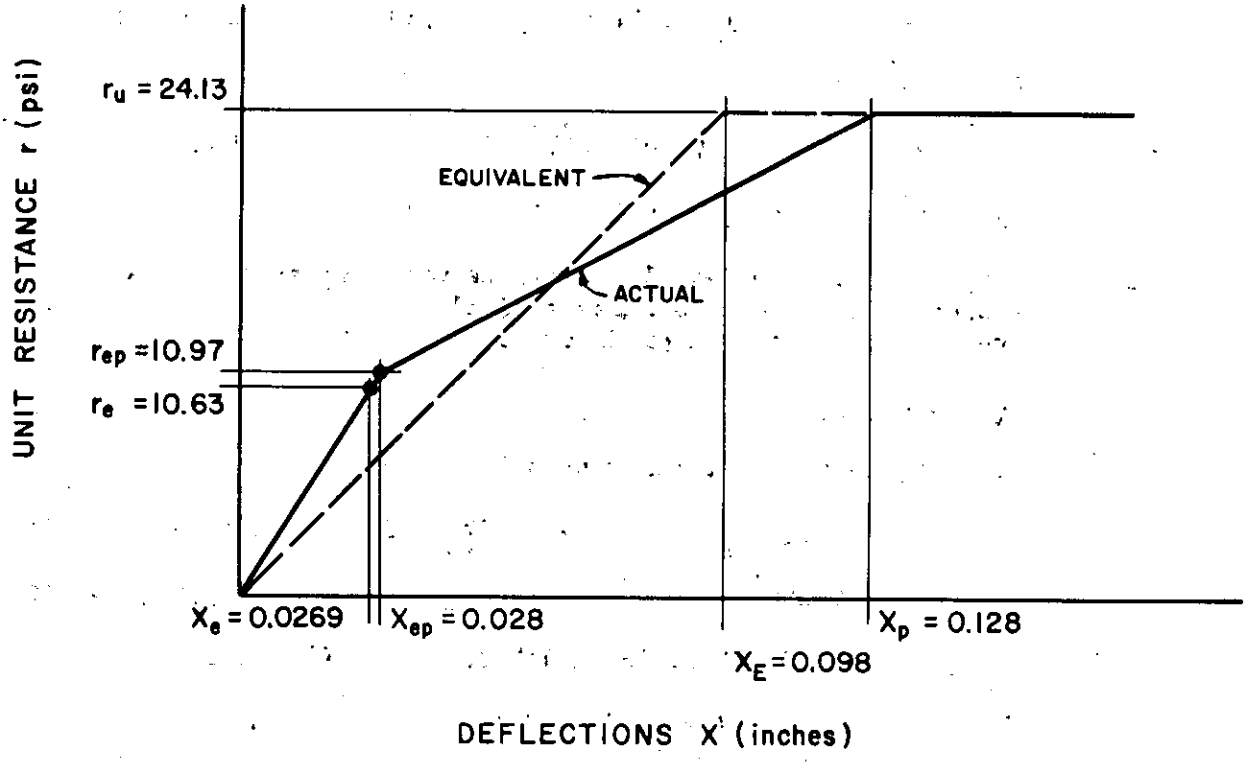

UNIT RESISTANCE r (psi)
r_u = 24.13
EQUIVALENT
ACTUAL
r_{ep} = 10.97
r_e = 10.63
X_e = 0.0269
X_{ep} = 0.028
X_E = 0.098
X_p = 0.128
DEFLECTIONS X (inches)

FIGURE 4A-4

$$X_E = X_e(r_{ep}/r_u) + X_{ep}[1 - (r_e/r_u)] + X_p[1 - (r_{ep}/r_u)]$$

$$X_E = 0.0269\ (10.97/24.13) + 0.028\ [1 - (10.63/24.13]$$

$$+ 0.128\ [1 - (10.97/24.13)] = 0.098 \text{ in}$$

The equivalent resistance-deflection curve is shown in figure 4A-4.

Step 18. Calculate equivalent elastic stiffness.

$$K_E = \frac{r_u}{X_E} = \frac{24.13}{0.098} = 246.2 \text{ psi/in} \qquad \text{(eq. 3-36)}$$

Step 19. Calculate effective mass of element.

a. Load mass factors (table 3-13 and fig. 3-44).

$L/H = 1.25$ $x/L = .405$

Elastic range - $K_{LM} = .61 + .16\ (1.25-1) = .65$

Elasto-plastic range:

two simple edges - $K_{LM} = .62 + .16(1.25-1) = .66$

four simple edges - $K_{LM} = .63 + .16(1.25-1) = .67$

Plastic range - $K_{LM} = .54$

$$K_{LM}\text{(avg. elastic and elasto-plastic)} = \frac{.65 + .66 + .67}{3} = .66$$

$$K_{LM}\text{ (avg. elastic and plastic)} = \frac{.66 + .54}{2} = .60$$

b. Unit mass of element.

$$m = \frac{wT_c}{g} = \frac{150 \text{ X } (1) \text{ X } 10^6}{32.2\ (1728)} = 2{,}700 \text{ psi - ms}_2\text{/in}$$

c. Effective unit mass of element.

$$m_e = K_{LM} m = .60\ (2,700) = 1,620\ \text{psi-ms}^2/\text{in}$$

Step 20. Calculate natural period of vibration.

$$T_N = 2\pi \left[\frac{m_e}{K_E}\right]^{\frac{1}{2}} \qquad \text{(eq. 3-60)}$$

$$T_N = 2(3.14) \left[\frac{1,620}{246.2}\right]^{\frac{1}{2}} = 16.1\ \text{ms}$$

Step 21. Determine response chart parameters (fig. 3-64a).

Peak pressure $P = 35$ psi (step 1)

Peak resistance $r_u = 24.13$ psi (step 8)

Duration $T = 10.5$ ms (step 1)

Period of vibration $T_N = 16.1$ ms (step 20)

$P/r_u = 35/24.13 = 1.45$ $T/T_N = 10.5/16.1 = 0.65$

From figure 3-64a:

$X_m/X_E = 2.8 < 3$ (step 1)

∴ Use assumed section

$t_m/T_N = 0.60$ (fig. 3-64a)

$$t_m/t_o = t_m/T = \frac{t_m/T_N}{T/T_N} = \frac{0.60}{0.65} = 0.923$$

The correct procedure has been used since $t_m/t_o = 0.923$ is within the range, $0.1 < t_m/t_o < 3$.

Step 22. Check diagonal tension at d_e distance from support.

a. Ultimate shear stress (table 4-7).

$$V_{uH} = \frac{3r_u\ (1 - d_e/x)^2}{d_e/x\ (5 - 4d_e/x)} \quad \text{where } d_e = d_H \text{ (of negative moment)}$$

$$V_{uH} = \frac{3 \text{ X } 24.13 \ (1 - 9.75/72.9)^2}{(9.75/72.9) \ [5 - 4 \ (9.75/72.9)]} = 91.0 \text{ psi}$$

$$V_{uV} = \frac{3r_u \ (0.5 - d_e/H)(1 - x/L - 2 \ d_e x/HL)}{d_e/H(3 - x/L - 8 \ d_e x/HL)}$$

where $d_e = d_v$ (of negative moment)

$$V_{uV} = \frac{3 * 24.13(.5 - 10.25/144)(1 - .405 - 2*.405*10.25/144)}{(10.25/144)(3 - .405 - 8*.405*10.25/144)}$$

$= 99.1$ psi

b. Allowable shear stress (eq. 4-23).

$$v_c = [1.9 \ (f'_{dc})^{1/2} + 2{,}500 \ p] \leq 3.50 \ (f'_c)^{1/2} = 221.4 \text{ psi}$$

where p is the steel ratio at support

$$v_{cH} = 1.9 \ (4{,}000)^{1/2} + \left[\frac{2{,}500 \ (0.20)}{12 \ (9.75)} \right] = 124.4 \text{ psi} > 91.0 \text{ psi}$$

$$v_{cV} = 1.9 \ (4{,}000)^{1/2} + \left[\frac{2{,}500 \ (0.24)}{12 \ (10.25)} \right] = 125.0 \text{ psi} > 99.1 \text{ psi}$$

∴ No stirrups required

Step 23. Determine minimum area of the diagonal bars (cross section type I).

$$A_d = v_c \ bd/f_{ds} \sin\alpha \qquad \text{(eq. 4-31)}$$

where d is equal to d_e at support.

Using $\alpha = 45°$,

$$A_{dH} = 124.4 \ (12 \text{ X } 9.75)/72{,}600 \ (0.707) = .283 \text{ in}^2/\text{ft}$$

$$A_{dV} = 125.0 \ (12 \text{ X } 10.25)/72{,}600 \ (0.707) = .300 \text{ in}^2/\text{ft}$$

use #5 diagonal bars @ 12"

Problem 4A-2. Preliminary Flat Slab Design for Large Deflection

Problem: Design a flat slab for large deflections.

Procedure:

Step 1. Establish design parameters:

a. Blast loads including pressure-time relationship (Chapter 2).
b. Deflection criteria.
c. Structural configuration including geometry and support conditions.
d. Type of section available to resist blast, type I, II or III depending upon the occurrence of spalling and/or crushing of the concrete cover.

Step 2. Select cross section of the slab and the column or column capital. Include concrete cover over reinforcement and maximum size of the reinforcing bars in the flat slab. Also determine allowable static stresses of concrete and reinforcing steel (Section 4-12).

Step 3. Determine dynamic increase factors for both concrete and reinforcement from table 4-1. Using the above DIF and the allowable static stresses of step 2, calculate the dynamic strength of materials.

Step 4. Determine the dynamic design stresses using table 4-2 and the results from step 3.

Step 5. Determine the ratio of the flexural stiffness of the wall to slab in both directions using equations 4-50, 4-51, 4-62 and 4-73.

Step 6. Proportion total span moments to unit column and midstrip moments in both directions using equations 4-52 through 4-60 and 4-63 through 4-71.

Note:
Use equivalent frame method for the direction(s) with only two spans.

Step 7. Adjust unbalanced negative unit moment at column and midstrip in both directions of the roof. Correct the corresponding positive moments to maintain the same total span moments.

Step 8. Calculate total external work done by r_u from equation 4-74 using yield line patterns similar to figure 4-24. Use uniform deflection (Δ) for all positive yield lines.

Step 9. Calculate total internal work done using equation 4-76 and the unit moments determined in steps 6 and 8.

Step 10. Equate the total external work to the internal work (equation 4-77). Solve the resulting equation for the ratio of r_u/M_{oH}. Use equations 4-61 and 4-72 to substitute M_{oL} with M_{oH}.

Step 11. Determine the minimum value of r_u/M_{oH} by trial and error procedure. Vary the assumed value of one of the yield location variables while assuming a constant value for the rest to find the minimum r_u/M_{oH}. Repeat until all yield line location variables are established (X, Y, W and Z). The last step will yield the final minimum value of r_u/M_{oH} to be used in the following steps.

Step 12. Calculate the load-mass factor for the flat slab using the procedure outlined in Chapter 3, for two-way elements. Use equation 3-59 for the slab sectors with no drop panel and equation 3-58 for the slab sectors with drop panel.

Step 13. Calculate effective unit mass of the slab using the larger d_e of the assumed slab section from step 2 and equation 3-54.

Step 14. Calculate the maximum deflection of the flat slab using the shortest sector length (L_s).

Step 15. Determine the required unit resistance (r_{avail} in equation 4-90) to resist the given impulse loading (Chapter 2) and the values from steps 13 and 14. Check that the correct procedure was used.

Step 16. Determine the uniform dead load of the flat slab and calculate the ultimate resistance of the slab (r_u) from equation 4-90.

Step 17. Determine the required total panel moments in each direction using the ultimate resistance from step 16, the minimum value of r_u/M_{oH} from step 11 and the ratio of M_{oL} to M_{oH} established in step 10.

Step 18. Calculate the minimum required unit moments in each direction from step 6 or 7 using the values of M_{oL} and M_{oH} from step 17.

Step 19. Calculate the minimum moment capacity of the slab section in each direction by choosing reinforcing bars. These capacities should be equal to or slightly larger than the corresponding moments from step 18. Also check for minimum reinforcing ratios from table 4-3.

Step 20. Determine provided resistance in each direction by using the ratios provided to required unit moments from steps 18 and 19. Find the average of these values to establish the unit resistance of the flat slab.

Step 21. Determine ultimate tension membrane capacity of the flat slab using equation 4-85. Find the average of continuous steel in the

mid and column strip using: unit moment ratios from step 6 or 7 and step 19. Use f_{ds} for bending from step 4 in calculating unit tension forces in the continuous reinforcement, in each span direction.

Step 22. Calculate diagonal tension stresses at d_e distance from the edge of wall supports according to Section 4-31.2 in both directions. Determine concrete capacity in diagonal tension from equation 4-23 using the ratios of unit moments from steps 6 or 7 and the reinforcing ratios from step 19. If the diagonal tension stresses are larger than the concrete capacity, single leg stirrups should be used or a drop panel be added along the wall in lieu of a change in flat slab cross section. If drop panels are used, the diagonal shear stress at d_e distance from the edge of wall drop panel must also be checked.

Step 23. Check punching shear $d_e/2$ distance out and around the column or column capital. Use the load area between positive yield lines minus the area supported by column or its capital. If the shear stress is larger than $4(f'_c)^{\frac{1}{2}}$, use a column drop panel and check the punching shear with the new thickness of the slab over the column.

Step 24. Determine the size of column drop panel by checking punching shear $d_e/2$ distance out and around the drop panel.

Step 25. Check one-way diagonal shear stress between positive yield lines d_e distance out from the column drop panel in each direction. Use equation 4-23 to find concrete capacity. Increase column drop panel size if required or use single leg shear stirrups according to Section 4-18.3.

Step 26. Check one-way diagonal shear stress between positive yield lines for an average d_e distance out from the column capital similar to step 25. Average d_e is based on the width of the drop panel to the total width. Increase column drop panel width or thickness if required.

Step 27. Assume preliminary reinforcement for the flat slab using unit moment ratios from step 6 and 7, M_{oL} and M_{oH} from step 17 and equation 4-19 with the slab thicknesses established throughout this procedure. Calculate all actual unit moment capacities.

Note:

Check the actual flat slab resistance using unit moments from step 27 and the established sizes and thicknesses of drop panels. Repeat steps 8 to 27 for the actual values in each direction. Also provide diagonal bars at wall and column according to sections 4-19 and 4-31.2.

Example 4A-2. Preliminary Flat Slab Design for Large Deflection

Required: Design of a flat slab with three equal spans in each direction for large deflections.

Solution:

Step 1. Given:

a. P = 96 psi, T = 15 ms and triangular loading.

b. Maximum support rotation of 8 degrees.

c. L = H = 240 in., continuous walls all around 207 in. high and 21 in. thick.

d. Type III cross section.

Step 2. Assume:

a. T_c = 15 in. thickness of flat slab.

b. D = 45 in. diameter of column capital.

c. Concrete cover: outside 2 in.
inside 3/4 in.

d. d = 3/4 in. largest bar diameter.

e. f'_c = 4,000 psi compressive strength of concrete.

f. f_y = 66,000 psi yield stress of reinforcing bars.

g. f_u = 90,000 psi ultimate stress of reinforcing bars.

Step 3. Determine dynamic stresses.

a. Dynamic increase factors. DIF (table 4-1).

Concrete:
Diagonal tension - 1.00

Reinforcement:
Bending, yield stress - 1.17

Bending, ultimate stress - 1.05

Direct shear yield stress - 1.10

Direct shear ultimate stress - 1.00

b. Dynamic strength of materials.

Concrete:

Diagonal tension (f'_c) - 1.00 (4,000) = 4,000 psi

Reinforcement:

Bending (f_{dv}) - 1.17 X 66,000 = 77,220 psi

Bending (f_{du}) - 1.05 X 90,000 = 94,500 psi

Direct shear (f_{dv}) - 1.10 X 66,000 = 72,600 psi

Direct shear (f_{du}) - 1.00 X 90,000 = 90,000 psi

Step 4. Dynamic design stresses from table 4-2.

Concrete (f'_c):

Diagonal tension - 4,000 psi

Reinforcement (f_{ds}):

$f_{ds} = (f_{dy} + f_{du})/2$

Bending - 85,860 psi

Direct shear - 81,300 psi

Note:
Since the structure is symmetrical in both directions, the calculations will be done only in one direction in steps 5 through 9, 12, 17 through 22, 25 and 26.

Step 5. Determine the ratio of the flexural stiffness of the wall to the roof slab.

$$\alpha_{ecH} = \frac{T_w^3 H}{T_s^3 H_w} = \frac{21^3 * 240}{15^3 * 207} = 3.18 \qquad \text{(eq. 4-50)}$$

$$\alpha'_{ecH} = \frac{1}{1+1/\alpha_{ecH}} = \frac{1}{1 + 1/3.18} = 0.76 \qquad \text{(eq. 4-62)}$$

Step 6. Calculate unit moments using equations 4-52 through 4-60. See figure 4A-5 for locations.

$m^-_1 = 0.65\ \alpha'_{ecH}\ M_{oH}/L = 0.65\ (0.76)\ M_{oH}/240 = (0.494)\ M_{oH}/240$

$m^{+}_{2} = 0.40\ (0.63 - 0.28\ \alpha'_{ecH})\ M_{oH}/(L - H/2)$

$= 0.40(0.63 - 0.28 \times 0.76)\ M_{oH}/(240 - 240/2) = (0.334)\ M_{oH}/240$

$m^{-}_{3} = 3.25\ (0.75 - 0.10\ \alpha'_{ecH})\ M_{oH}/(L - H/2)$

$= 0.25(0.75 - 0.10 \times 0.76)\ M_{oH}/(240 - 240/2) = (0.337)\ M_{oH}/240$

$m^{-}_{4} = 0.25\ (0.65) M_{oH}/(L - H/2)$

$= 0.25 \times 0.65\ M_{oH}/(240 - 240/2) = (0.325) M_{oH}/240$

$m^{+}_{5} = 0.40\ (0.35) M_{oH}/(L - H/2)$

$= 0.40 \times 0.35\ M_{oH}/(240 - 240/2) = (0.280) M_{oH}/240$

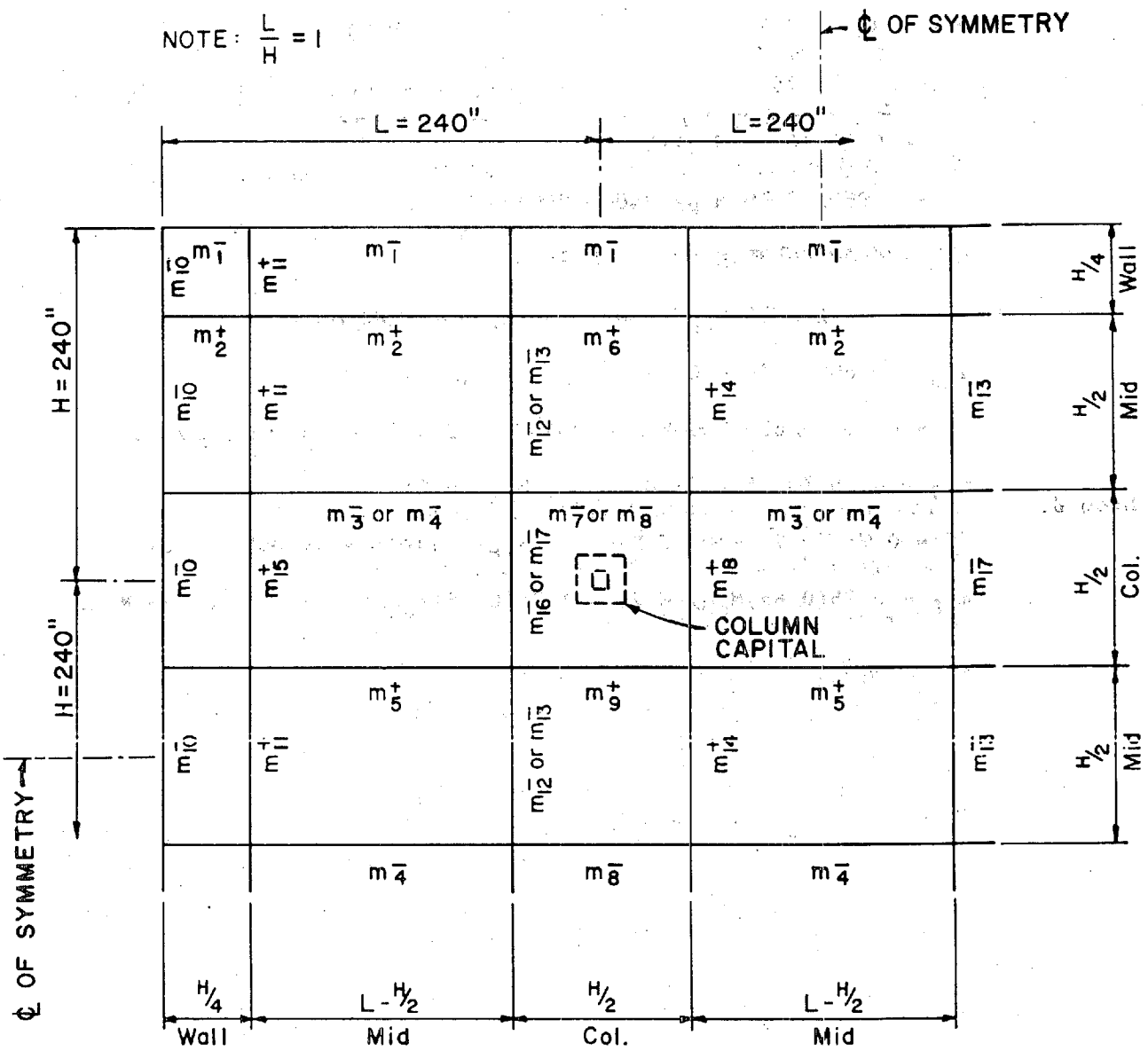
$m^{+}_{6} = 0.60\ (0.63 - 0.28\ \alpha'_{ecH})\ M_{oH}/(H/2)$

$= 0.60\ (0.63 - 0.28 \times 0.76)\ M_{oH}/(240/2) = (0.501) M_{oH}/240$

$m^{-}_{7} = 0.75\ (0.75 - 0.10\ \alpha'_{ecH})\ M_{oH}/(H/2)$

$= 0.75\ (0.75 - 0.10 \times 0.76)\ M_{oH}/(240/2) = (1.011) M_{oH}/240$

$m^{-}_{8} = 0.75(0.65) M_{oH}/(H/2) = 0.75(0.65) M_{oH}/(240/2) = (0.975) M_{oH}/240$



PLAN

FIGURE 4A-5

$m^-_9 = 0.60\ (0.35)M_{oH}/(H/2) = 0.60\ (0.35)M_{oH}/240/2 = (0.420)M_{oH}/240$

Step 7. a. Balance the negative unit moment over the column and midstrip.

$m^-_3 > m^-_4 \therefore m^-_3 = m^-_4 = (0.337)\ M_{oH}/240$

$m^-_7 > m^-_8 \therefore m^-_7 = m^-_8 = (1.011)\ M_{oH}/240$

b. Adjust the corresponding positive unit moment in order to keep total panel moments equal.

Adjusted $m^+_5 = m^+_5 - 2(m^-_3 - m^-_4)$

$\therefore\ m^+_5 = [0.280 - 2(0.337 - 0.325)]M_{oH}/240 = (0.256)\ M_{oH}/240$

Adjusted $m^+_9 = m^+_9\ \ 2(m^-_7 - m^-_8)$

$\therefore\ m^+_9 = [0.420 - 2\ (1.011 - 0.975)]M_{oH}/240 = (0.348)M_{oH}/240$

Step 8. Calculate total external work for an assumed deflection of Δ. Use one quarter of the roof slab due to symmetry in both directions. See figure 4A-6 for yield lines and sectors.

Equivalent square column capital, C X C.

$$C = \left[\frac{\pi D^2}{4}\right] = \left[\frac{\pi(45)^2}{4}\right]^{1/2} = 39.9 \text{ in.} \quad \text{say } 40 \text{ X } 40 \text{ in.}$$

$$W_I = W_{IV} = r_u \left[\left(\frac{3L}{2} - X \right) (X)\frac{\Delta}{2} + \left(\frac{X^2}{2}\right) \frac{\Delta}{3} \right]$$

$$= r_u \left[\left(\frac{3 \text{ X } 240}{2} - X\right) (X)\ \frac{\Delta}{2} + \left(\frac{X^2}{2}\right) \frac{\Delta}{3} \right]$$

$$W_{II} = W_V = r_u\left[C\left[H - C/2 - X\right]\frac{\Delta}{2} + \frac{1}{2}\left[\frac{3L}{2} - X - C\right]\left[H - \frac{C}{2} - X\right]\left[\frac{2\Delta}{3}\right]\right]$$

$$= r_u\left[40\left(240 - \frac{40}{2} - X\right)\frac{\Delta}{2} + \frac{1}{2}\left(\frac{3*240}{2} - X - 40\right)\left(240 - \frac{40}{2} - X\right)\left(\frac{2\Delta}{3}\right)\right]$$

$$W_{III} = W_{VI} = r_u\left[\frac{C}{2}(H - C)\frac{\Delta}{2} + \frac{1}{2}\left(\frac{3L}{2} - X - C\right)\left(\frac{H - C}{2}\right)\left(\frac{2\Delta}{3}\right)\right]$$

$$= r_u\left[\frac{40}{2}(240 - 40)\frac{\Delta}{2} + \frac{1}{2}\left[\frac{(3)(240)}{2} - X - 40\right]\left(\frac{240 - 40}{2}\right)\left(\frac{2\Delta}{3}\right)\right]$$

From equation 4-74.

$$W = \Sigma\, r_u A\Delta$$

$$W = \sum_{i=I}^{VI} W_i = \frac{r_u\Delta}{3}(243200 - 320X)$$

Step 9. Calculate total internal work for the assumed deflection of Δ. Use one quarter of the roof slab due to symmetry in both directions. See figure 4A-6 for angles of rotation.

$$\theta_{1H} = \theta_{1V} = \frac{\Delta}{X}$$

$$\theta_{2H} = \theta_{2H} = \frac{\Delta}{H - C/2 - X} = \frac{\Delta}{240 - 40/2 - X} = \frac{\Delta}{220 - X}$$

$$\theta_{3H} = \theta_{3V} = \frac{\Delta}{(H - C)/2} = \frac{\Delta}{(240 - 40)/2} = \frac{\Delta}{100}$$

Assume $0 < X < 3H/4 = 180$ in.

$$E_I = E_{IV} = m^-{}_1\theta_{1H}\left(\frac{3L - X}{2}\right) + \frac{2}{3}m^-{}_1\theta_{1H}\left(\frac{X}{2}\right)$$

$$+ m^+{}_6\theta_{1H}\left(\frac{L}{2}\right) + m^+{}_2\theta_{1H}\left(L - \frac{X}{2}\right) + \frac{2}{3}m^+{}_2\theta_{1H}\left(\frac{X}{2}\right)$$

$$= \frac{M_{oH}\,\Delta}{(2)\,(240)\,X}\left[0.494\left[3\,(240) - X/3\right] + 0.501\,(240) + 0.334\left[2\,(240) - X/3\right]\right]$$

$$E_{II} = E_V = m^{+}{}_6\theta_{2H}\left(\frac{L}{2}\right) + m^{+}{}_2\theta_{2H}(L - X) + m^{-}{}_7\theta_{2H}\left(\frac{L}{2}\right) + m^{-}{}_3\theta_{2H}(L - X)$$

$$= \frac{M_{oH}}{(2)\,(240)} \times \frac{\Delta}{220 - X}\left[(0.501 + 1.011)\,240 + 2\,(0.334 + 0.337)\,(240 - X)\right]$$

$$E_{III} = E_{VI} = m^{+}{}_9\theta_{3H}\left(\frac{L}{2}\right) + m^{+}{}_5\theta_{3H}(L-X) + m^{-}{}_7\theta_{3H}\left(\frac{L}{2}\right) + m^{-}{}_3\theta_{3H}(L-X)$$

$$= \frac{M_{oH}}{(2)(240)} \times \frac{\Delta}{100}\left[(0.348 + 1.011)\,240 + 2\,(0.256 + 0.337)\,(240 - X)\right]$$

From equation 4-75.

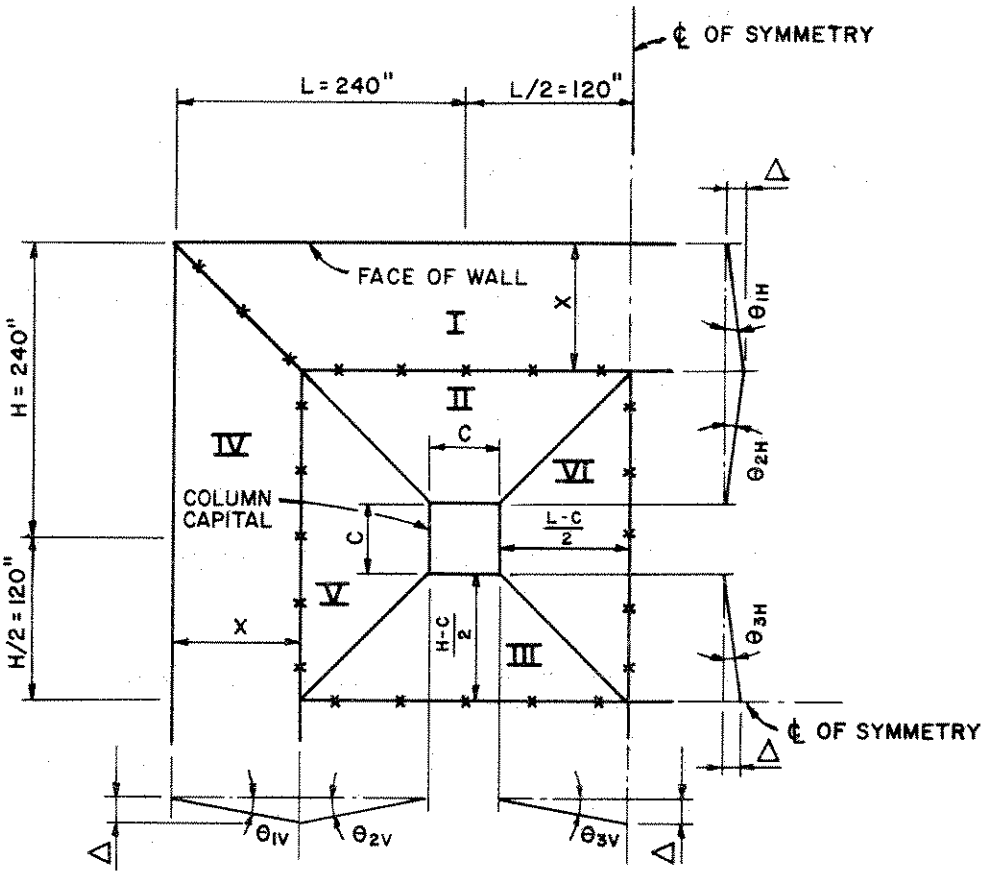
$$E = \Sigma\, m\, \theta l$$

$$E = \sum_{i=I}^{VI} E_i = \frac{M_{oH}\,\Delta\,[\,139972.8 + 1331.76X - 9.7832X^2 + 0.01186X^3\,]}{240X\,(220 - X)}$$

Step 10. Set the external work equal to the internal work and solve the equation for the ratios of r_u/M_{oH}.

$$W = E$$

$$\frac{r_u\Delta}{3}\,(243200 - 320X) = \frac{M_{oH}\Delta[139972.8 + 1331.76X - 9.7832X^2 + 0.01186X^3]}{240X\,(220 - X)}$$



LEGEND:

——— = NEGATIVE YIELD LINES

-*-*-*- = POSITIVE YIELD LINES

PLAN

FIGURE 4A-6

$$\therefore \frac{r_u}{M_{oH}} = \frac{139972.8 + 1331.76\,X - 9.7832X^2 + 0.01186X^3}{80X\,(220 - X)(243200 - 320X)}$$

Step 11. Minimize value of r_u/M_{oH} using the equation from step 10 by assuming various values for X to locate the yield line locations.

X (in)	r_u/M_{oH} (psi/in-lbs)	
110	913.212×10^{-9}	
115	911.686×10^{-9}	
120	912.445×10^{-9}	
116	911.654×10^{-9}	*minimum
117	911.713×10^{-9}	

Step 12. Calculate plastic load mass factor for the flat slab. See Section 4-30.5 and figure 4A-6.

$$\left(\frac{I}{cL_1}\right)_I - \left(\frac{I}{cL_2}\right)_{IV} = \frac{2}{3}\left(\frac{3L}{2} - X + \frac{1}{2}\left(\frac{X^2}{2}\right)\right) = \frac{2}{3}(116)\left(\frac{(3)(240)}{2} - 116\right) + \frac{1}{2}\left(\frac{116^2}{28}\right)$$

$$\left(\frac{I}{cL_1}\right)_{II} - \left(\frac{I}{cL_1}\right)_V = \frac{2}{3}C\left(H - \frac{C}{2} - X\right) + \frac{3}{4}\left(H - \frac{C}{2} - X\right)\left[\frac{3L}{2} - C - X\right]/2$$

$$= \frac{2}{3}(40)\left(240 - \frac{40}{2} - 116\right)$$

$$+ \frac{3}{4}\left(240 - \frac{40}{2} - 116\right)\left[\frac{3 \times 240}{2} - 40 - 116\right]/2$$

$$\left(\frac{I}{cL_1}\right)_{III} - \left(\frac{I}{cL_1}\right)_{VI} = \frac{2}{3}C\,(H - C)/2 + \frac{3}{4}(H - C)\left[\frac{3L}{2} - C - X\right]/4$$

$$= \frac{2}{3}(40)\left[240 - 40\right]/2$$

$$+ \frac{3}{4}(240 - 40)\left[\frac{3 \times 240}{2} - 40 - 116\right]/4$$

$$\sum_{i=I}^{VI} \left(\frac{I}{CL_1}\right)_i = 86558.67 \text{ in}^2$$

$$A_I = A_{IV} = \frac{X}{2}(3L - X) = \frac{116}{2}(3 \times 240 - 116)$$

$$A_{II} = A_V = (H - \frac{C}{2} - X)\left[\frac{3L}{2} + C - X\right]/2$$

$$= (240 - \frac{40}{2} - 116)\left[\frac{3 \times 240}{2} + 40 - 116\right]/4$$

$$A_{III} = A_{VI} = (H - C)\left[\frac{3L}{2} + C - X\right]/4$$

$$= (240 - 40)\left[\frac{3 \times 240}{2} + 40 - 116\right]/4$$

$$\sum_{i=I}^{VI} A_i = 128{,}000.0 \text{ in}^2$$

$$K_{LM} = \frac{\sum \left(\frac{I}{CL_1}\right)_i}{\sum A_i} = \frac{86558.67}{128{,}000.0} = 0.676 \qquad \text{(eq. 3-59)}$$

Step 13. Calculate the unit mass of the slab.

$$d_c = 15 - 2 - .75 - (2 \times .75)/2 = 11.5 \text{ in.}$$

$$m = \frac{W}{g} = \frac{11.5 \times 150 \times 1000^2}{12 \times 32.2 \times 1728} = 2583.5 \text{ psi-ms}^2/\text{in}$$

Determine effective unit mass from equation 3-54.

$$m_e = K_{LM} \times m = .676 \times 2583.5 = 1746.4 \text{ psi-ms}^2/\text{in}$$

Step 14. Find maximum deflection using shortest sector length.

$$L_s = \left(\frac{H - C}{2}\right) = \frac{240 - 40}{2} = 100. \text{ in}$$

$$X_m = L_s \tan \theta_{max} = 100 \times \tan 8 = 14.05 \text{ in.}$$

Step 15. Determine impulse load and required resistance for blast.

$$i_b = PT/2 = (96.0 \times 15.0) / 2 = 720.0 \text{ psi-ms}$$

$$\frac{i_b^2}{2m_u} = r X_m \qquad \text{(eq. 3-93)}$$

$$\therefore r = \frac{720.0^2}{2 \times 1746.4 \times 14.05} = 10.56 \text{ psi} = r_{avail}$$

Check for correct procedure.

$$t_m = \frac{i_b}{r} = \frac{720}{10.56} = 68.2 \text{ ms}$$

$$t_m/T = 68.2 / 15 = 4.55 > 3 \quad \text{O.K. (section 3-20)}$$

Step 16. Calculate uniform dead load of slab and the required ultimate resistance. Assume 150 psf concrete.

$$r_{DL} = 15/12 \times 150/12^2 = 1.30 \text{ psi}$$

$$r_{avail} = r_u - \frac{f_{ds}}{f_{dy}} r_{DL} \qquad \text{(eq. 4-90)}$$

$$\text{Required } r_u = 10.56 + \left(\frac{85,860}{66,000}\right) 1.30 = 12.25 \text{ psi}$$

Step 17. Calculate required panel moment using the required r_u from step 16 and the r_u/M_{oH} from step 11.

$$\text{Required } M_{oH} = (r_u)/\left(\frac{r_u}{M_{oH}}\right) = \frac{12.25}{911.654 \times 10^{-9}} = 13{,}437{,}115 \text{ in-lbs}$$

Step 18. Calculate the minimum required unit moments from step 7.

$$\text{Minimum unit moment} = m^+_5 = \frac{.256\ M_{oH}}{240}$$

$$\therefore m^+_5 = \frac{.256 \times 13{,}437{,}115}{240} = 14333 \text{ in-lbs/in}$$

Step 19. Calculate actual moment capacity at m^+_5, assume No. 4 reinforcing bars 12 in. o.c.

$$d_e \text{ in H direction} = d_H = 15 - 2 - .75 - 2 \times .75^* + 2 \times \frac{.5}{2} = 11.25 \text{ in}$$

$$d_e \text{ in L direction} = d_V = 15 - 2 - .75 - 2 \times .75^* - 2 \times \frac{.5}{2} = 10.25 \text{ in}$$

* Assumed No. 6 reinforcing in step 2.

$$M_u = \frac{A_s\ f_{ds}\ d_c}{b} \qquad \text{(eq. 4-19)}$$

$$M^+_{14} = \frac{.2 \times 85{,}860 \times 11.25}{12} = 16099 \text{ in-lb/in} > 14333 \text{ O.K.}$$

$$M^+_5 = \frac{.2 \times 85{,}860 \times 10.25}{12} = 14668 \text{ in-lbs/in} > 14333 \text{ O.K.}$$

$$p = \frac{A_s}{bd_e} \qquad \text{(eq. 4-13)}$$

$$p_{m^+14} = \frac{.20}{12 \times 11.25} = .0015 = .0015 \quad \text{O.K.}$$

$$P_{m^+5} = \frac{.20}{12 \text{ X } 10.25} = .0016 > .0015 \qquad \text{O.K.}$$

Step 20. Calculate the provided unit resistance of the flat slab.

$$r_u \text{ (provided)} = r_e \text{ (required)} \text{ X } \frac{\text{m (unit moment provided)}}{\text{m (unit moment required)}}$$

$$(r_u)_{m14} = 12.25 \text{ X } \frac{16099}{14333} = 13.76 \text{ psi}$$

$$(r_u)_{m5} = 12.25 \text{ X } \frac{14668}{14333} = 12.54 \text{ psi}$$

$$r_u = \frac{(r_u)_{m14} + (r_u)_{m5}}{2} = \frac{13.76 + 12.54}{2} = 13.15 \text{ psi} > 12.25 \text{ o.k.}$$

Step 21. Estimate minimum area of continuous steel in column strip using unit moment ratios from step 7.

$$(A_s)_{m9} = \frac{m^+_9}{m^+_5} \text{ X } (A_s)_{m5} = \frac{.348 \frac{M_{oH}}{240}}{.256 \frac{M_{oH}}{240}} \text{ X } (0.20) = .27 \text{ in}^2/\text{ft}$$

Calculate the average unit tension force in continuous steel.

$$T_L = \frac{(A_s)_{m5} \, H/2 + (A_s)_{m9} \, (L - H/2)}{b \text{ X } L} \text{ X } f_{ds} \text{ X } 2$$

$$= \frac{.20 \text{ X } 240/2 + .27 \text{ X } (240 - 240/2)}{12 \text{ X } 240} \text{ X } 85{,}860 \text{ X } 2 = 3.362 \text{ lbs/in}$$

Calculate tension membrane resistance from equation 4-85.

$$r_T = \frac{\pi^3 \; 1.5 \text{ X } T_H/L_H^2}{4 \sum_{n=1,3,5} \left(\frac{1}{n^3} (-1)^{(n-1)/2} \left[1 - \frac{1}{\cosh \left[\frac{n\pi L_L}{2L_H} \left[\frac{T_H}{T_L} \right]^{\frac{1}{2}} \right]} \right] \right)}$$

$$H_L = H - C = 240 - 40 = 200 \text{ in}$$

$$r_T = \frac{\pi^3 \ 1.5 \ X \ 14.05 \ X \ 3{,}363 \ / \ 200^2}{4 \sum_{n=1,3,5} \left(\frac{1}{n^3} (-1)^{(n-1)/2} \left[1 - \frac{1}{\cosh\left[\frac{n\pi(200)}{2(200)} \left[\frac{3{,}363}{3{,}363} \right]^{\frac{1}{2}} \right]} \right] \right)}$$

$$r_T = \frac{\pi^3 \ X \ 1.5 \ X \ 14.05 \ X \ 3{,}363}{4 \ X \ (200)^2 \ (.6015 - .0364 + .0080)} = 23.97 \text{ psi} > 13.15 \text{ psi O.K.}$$

Step 22. Calculate diagonal tension stresses at d_e distance from the edge of wall supports according to section 4-31.2 in both directions.

$$r_u \ X \ \text{Area (Sector I)} = V_V \left(\frac{3L - X}{2} \right) + \frac{2}{3} V_V \frac{X}{2}$$

$$13.15 \left(\frac{3 \ X \ 240 - 116}{2} \right) 116 = V_V \left(\frac{3 \ X \ 240 - 116}{2} \right) + \frac{2}{3} V_V \frac{116}{2}$$

$$\therefore V_V = \frac{460670.8}{340.67} = 1352.3 \text{ lbs/in}$$

Total diagonal shear load in L direction.

$$V_{uV} = V_V \left(\frac{3L - X}{2} \right) + \frac{2}{3} V_V \left(\frac{X}{2} - d_V \right)$$

$$= 1352.3 \left[\frac{3 \ X \ 240 - 116}{2} + \frac{2}{3} X \left[\frac{116}{2} - 10.25 \right] \right] = 451{,}443 \text{ lbs.}$$

Diagonal shear stress in L direction.

$$v_{uV} = \frac{V_{uV}}{(\frac{3L}{2} - d)\, d_V} = \frac{451,443}{(\frac{3 \times 240}{2} - 10.25)\ 10.25} = 125.9 \text{ psi}$$

Estimate reinforcing ratio at support using the ratio of unit moments.

$$r_{ml} = r_{m5} \left(\frac{ml}{m5}\right) = .0016 \left(\frac{.494 \frac{M_{oH}}{240}}{.256 \frac{M_{oH}}{240}}\right) = .0031$$

Calculate diagonal shear capacity of concrete.

$$v_c = 1.9 (f'_c)^{1/2} + 2500\ p \qquad \text{(eq. 4-23)}$$

$$v_{cV} = 1.9 (4000)^{1/2} + 2500 (0.0031) = 127.9 \text{ psi} > 125.9 \text{ psi}$$

∴ No stirrups or wall drop panel required.

Note:
Diagonal shear at d_e distance from the H direction wall will be less than the one in L direction due to symmetry and larger d_e in H direction. Calculation is not required.

Step 23. Check punching shear around column capital.

Use average d_e.

$$d_{avg} = \frac{d + d}{2} = \frac{10.25 + 11.25}{2} = 10.75 \text{ in}$$

Diameter of punching. $D_p = D + d_{avg} = 45 + 10.75 = 55.75$ in.

Find area between positive yield lines minus column capacity.

$$\text{Area} = \left[\frac{3L}{2} - X\right]^2 - \frac{\pi D_p^2}{4} = \left[\frac{3 \times 240}{2} - 116\right]^2 - \frac{\pi \times 55.75^2}{4}$$

$$= 57095 \text{ in}^2$$

$$v\ (\text{punching}) = \frac{r_u \times \text{Area}}{\pi\ D_p\ d_{avg}} = \frac{13.15 \times 57095}{\pi \times 55.75 \times 10.75} = 398.8 \text{ psi}$$

$$v_c = 4\ (f'_c)^{1/2} = 4\ (4000)^{1/2} = 253.0 \text{ psi} < 398.8 \text{ psi}$$

∴ Need drop panel, assume 6 in.

d_{avg} (revised) = 10.75 + 6 = 16.75 in.

D_p (revised) = 45 + 16.75 = 61.75 in.

$$\text{Area (revised)} = \left[\frac{3 \times 240}{2} - 116\right]^2 - \frac{\pi \times 61.75^2}{4} = 5641 \text{ in}^2$$

$$V\ (\text{punching}) = \frac{13.15 \times 56541}{\pi \times 61.75 \times 16.75} = 228.8 \text{ psi} < 253.0 \quad \text{O.K.}$$

Step 24. Assume 63 X 63 in. drop panel. Check punching shear.

Punching Length = $l_p = l + d_{avg} = 63 + 10.75 = 73.75$ in

$$\text{Area} = \left[\frac{3L}{2} - X\right]^2 - l_p^2 = \left[\frac{3 \times 240}{2} - 116\right]^2 - 73.752^2 = 54097 \text{ in}^2$$

$$v\ (\text{punching}) = \frac{r_u\ \text{Area}}{4\ l_p\ d_{avg}} = \frac{13.15 \times 54097}{4 \times 73.75 \times 10.75} = 224.3 \text{ psi} < 253.0 \text{ psi}$$

Step 25. Check one-way diagonal shear d_e distance away from column drop panel and between positive yield lines.

$$\text{Width in L direction} = \frac{3L}{2} - X = \frac{3 \times 240}{2} - 116 = 244 \text{ in.}$$

$$\text{Area in L direction} = \text{Width}\ (H - X - \frac{1}{2} - d_v)$$

$$= 244\ (240 - 116 - \frac{63}{2} - 10.75) = 19947\ in^2$$

$$v = \frac{r_u\ Area}{d_v\ \ Width} = \frac{13.15\ X\ 19947}{10.75\ X\ 244} = 100.\ psi < v_c^{1/2} \qquad O.K.$$

Note:
Diagonal shear in H direction will be less than the one in L direction due to symmetry and larger d_e in H direction. Calculation is not required.

Step 26. Check one-way diagonal shear at an average d distance away from column capital and between positive yield lines.

$$(Width)_L = 244\ in \quad (step\ 25)$$

$$d_{avg} = d_v + (\frac{1}{width})\ X\ drop\ panel\ depth$$

$$d_{avg} = 10.25 + \frac{63}{244}\ X\ 6 = 11.80\ in$$

$$Area\ in\ L\ direction = Width\ (H - X - \frac{C}{2} - d_{avg})$$

$$= 244\ (240 - 116 - \frac{40}{2} - 11.80) = 22496.8\ in^2$$

$$v = \frac{r_u\ Area}{d_{avg}\ Width} = \frac{13.15\ X\ 22496.8}{11.80\ X\ 244} = 102.7\ psi < v_c \qquad O.K.$$

Note:
Diagonal shear in H direction will be less than the one in L direction due to symmetry and larger d_e in H direction. Calculation is not required.

Step 27. Calculate all remaining required moments similar to step 18. Assume reinforcing bars for each, and determine actual provided unit moment capacities similar to step 19.

Problem 4A-3, Elements Designed for Impulse-Large Deflections

Problem: Design an element subjected to an impulse load for a large deflection.

Procedure:

Step 1. Establish design parameters:

a. Impulse load and duration (Chapter 2).

b. Deflection criteria.

c. Geometry of element.

d. Support conditions.

e. Type of section available to resist blast, type II or III depending upon the occurrence of spalling.

f. Materials to be used and corresponding static design strengths.

g. Dynamic increase factors (table 4-1).

Step 2. Determine dynamic yield strength and dynamic ultimate strength of reinforcement.

Step 3. Determine dynamic design stress for the reinforcement according to the deflection range (support rotation) required by the desired protection level (table 4-2).

Step 4. Determine optimum distribution of the reinforcement according to the deflection range considered (sect. 4-33.4 and figs. 4-37 and 4-38). Step not necessary for one-way elements.

Step 5. Establish design equation for deflection range considered and type of section (type II or III) available.

Step 6. Determine impulse coefficient C_l and/or C_u for optimum p_V/p_H ratio and L/H ratio.

Note:
If the desired deflection X_m is not equal to X_l or X_u, determine yield line location (figs. 3-4 through 3-20) for optimum p_V/p_H ratio and L/H ratio and calculate X_m, X_l, and, if necessary, X_u (table 3-5 or 3-6).

Step 7. Substitute known parameters into equation of step 5 to obtain relationship between p_H and d_c.

Step 8. Assume value of d_c and calculate p_H and from optimum p_V/p_H calculate p_V. Select bar sizes and spacings necessary to furnish required reinforcement (see Sect. for limitations).

Step 9. For actual distribution of flexural reinforcement, establish yield line location (figs. 3-4 through 3-20).

Note:

$$\frac{L}{H}\left[\frac{M_{VN}+M_{VP}}{M_{HN}+M_{HP}}\right]^{1/2}=\frac{L}{H}\left[\frac{p_V}{p_H}\right]^{1/2}=\frac{L}{H}\left[\frac{A_{sV}}{A_{sH}}\right]^{1/2}$$

since:

$$M_N = M_P = p\, d_c^{\,2}\, f_{ds} = \frac{A_s}{b}\, d_c\, f_{ds}$$

Step 10. Determine the ultimate shear stress at distance d_c from the support in both the vertical (v_{uV} from eq. 4-119) and horizontal (v_{uH} from eq. 4-118) directions where the coefficients C_V and C_H are determined from figures 4-39 through 4-52 (see sect. 4-35.2 for an explanation of the figures and parameters involved).

Step 11. Determine the shear capacity v_c of the concrete in both the vertical and horizontal directions (use eq. 4-21).

Step 12. Select lacing method to be used (fig. 4-91). (Note: Lacing making an angle of 45° with longitudinal reinforcement is most efficient.)

Step 13. Determine the required lacing bar sizes for both the vertical and horizontal directions from equation 4-26 where the parameters b_1 and s_1 are determined from the lacing method used (fig. 4-91), and the angle of inclination of the lacing bars α is obtained from figure 4-15. The lacing bar size d_b must be assumed in order to compute d_1 and R_1.

(Note: See sect. 4-18.3 for limitations imposed upon the design of the lacing).

Step 14. Determine required thickness T_c for assumed, d_c, selected flexural and lacing bar sizes, and required concrete cover. Adjust T_c to the nearest whole inch and calculate the actual d_c.

Step 15. Check flexural capacity based on either impulse or deflection. Generally, lacing bar sizes do not have to be checked since they are not usually affected by a small change in d_c.

a. Check of impulse. Compute actual impulse capacity of the element using the equation determined in step 5 and compare with anticipated blast load, Repeat design (from step 8 on) if capacity is less than required.

b. Check of deflection. Compute actual maximum deflection of the element using equation determined in step 5 and compare with deflection permitted by design criteria. Repeat design (from step 8 on) if actual deflection is greater than that permitted.

Step 16. Determine whether correct procedure has been used by first computing the response time of the element t_m (time to reach maximum deflection) from equation 3-95 or 3-96, depending on the deflection range considered in the design, and then compare response time t_m with duration of load t_o. For elements to be designed for impulse, $t_m > 3\ t_o$.

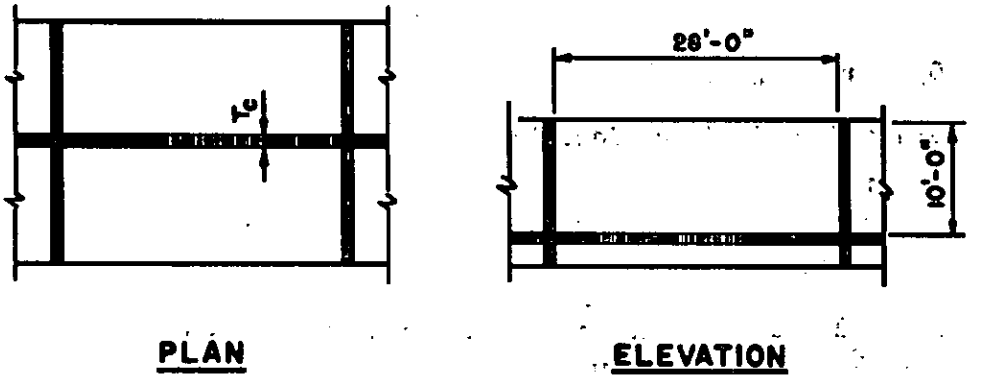
Step 17. Determine the ultimate support shear in both the vertical (V_{sV} from eq. 4-122) and horizontal (V_{sH} from eq. 4-121) directions. The coefficients C_{sV} and C_{sH} are determined from table 4-15 and figures 4-53 through 4-56 (see sect. 4-35.3 for an explanation of the figures and parameters involved).

Step 18. Determine the required diagonal bar sizes for the vertical and horizontal (intersecting elements may control) directions from equation 4-30. Diagonal bars should have the same spacing as the flexural reinforcement (fig. 4-95).

Note:
To obtain the most economical design repeat the above steps for several wall thicknesses and compare costs. Percentages of reinforcement may be used to reduce the amount of calculations. In determining the required quantities of reinforcement, lapping of the bars should be considered.

Example 4A-3, Elements Designed for Impulse-Large Deflections

Required: Design the back wall of the interior cell (fig. 4A-7) of a multicubicle structure for incipient failure.



PLAN ELEVATION

Figure 4A-7

Solution:

Step 1. Given:

a. i_b = 3,200 psi-ms and t_o = 5 ms

b. Incipient failure

c. L = 336 in, H = 120 in

d. Fixed on three edges and one edge free

e. Type III cross section

f. Reinforcement f_y = 66,000 psi and f_u = 90,000 psi

concrete f'_c = 4,000 psi

g. For reinforcement DIF = 1.23 for dynamic yield stress

DIF = 1.05 for ultimate dynamic stress

Step 2. Dynamic Strength of Materials

f_{dy} = DIF f_y = 1.23 x 66,000 = 81,180 psi

f_{du} = DIF f_u = 1.05 x 90,000 = 94,500 psi

Step 3. Dynamic Design Stress, from table 4-2.

$$f_{ds} = \frac{(f_{dy} + f_{du})}{2} = \frac{(81,180 + 94,500)}{2} = 87,840 \text{ psi}$$

Step 4. From figure 4-38 for $\frac{L}{H} = \frac{336}{120} = 2.8$ and 3 edges fixed,

Optimum: $p_V/p_H = 1.41$

Step 5. Since $X_m = X_u$ (incipient failure):

$$\frac{i_b^2 H}{p_H d_c^3 f_{ds}} = C_u \qquad \text{(eq. 4-103)}$$

Step 6. L/H = 2.8 is not plotted on figure 4-34, therefore must interpolate for optimum p_v/p_H.

For $p_V/p_H = 1.41$	
L/H	C_u
1.5	613.0
2.0	544.0
3.0	444.0
4.0	387.0

From figure 4A-8, $C_u = 461.0$.

Step 7.

$$p_H d_c^3 = \frac{i_b^2 H}{C_u f_{ds}}$$

$$p_H d_c^3 = \frac{(3,200)^2 (120)}{(461.0) (87,840)} = 30.3$$

Step 8. Assume $d_c = 21$ in:

$$p_H = \frac{30.3}{d_c^3} = \frac{30.3}{(21)^3} = 0.00327$$

$$p_V = \frac{p_V}{p_H} (p_H) = 1.41 (0.00327) = 0.00461$$

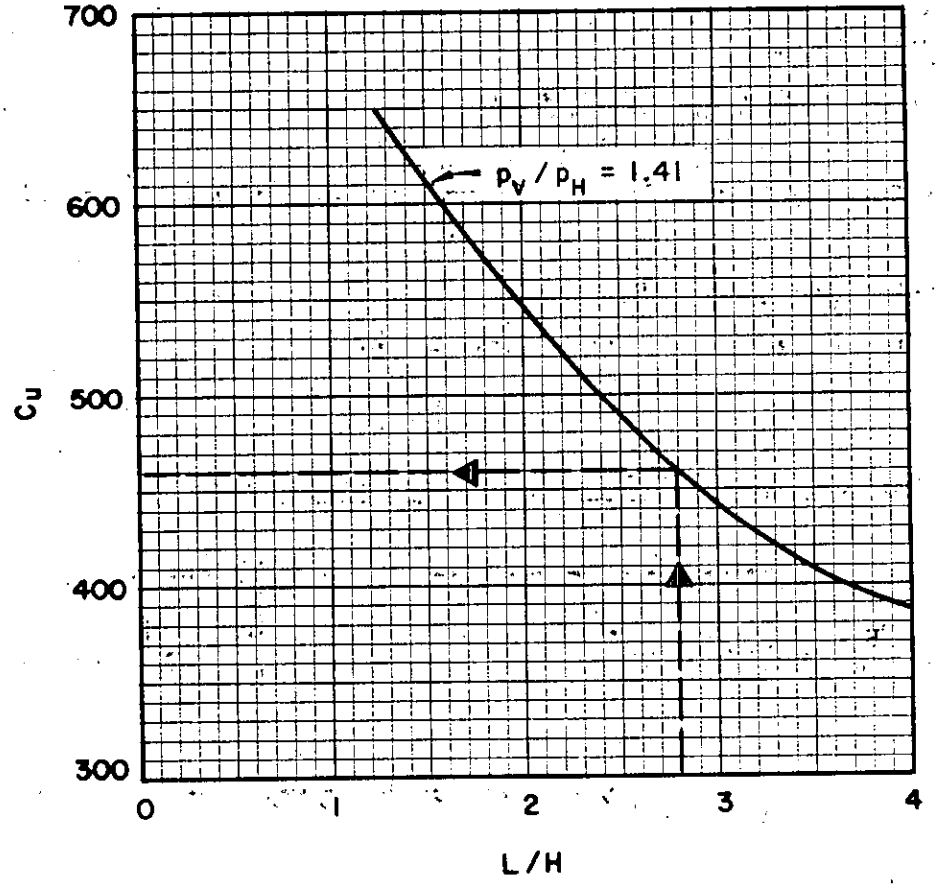


FIGURE 4A-8

A_{sH} = 0.00327 (12) (21) = 0.82 in^2/ft - Use #8 @ 11 (A_s = 0.86)

A_{sV} = 0.00461 (12) (21) = 1.16 in^2/ft - Use #9 @ 10 (A_s = 1.20)

Step 9. Yield line location.

Actual:

$$\frac{P_V}{2p_H} = \frac{A_{sV}}{2A_{sH}} = \frac{1.20}{2 \times 0.86} = 0.698$$

From figure 3-11 for $\frac{L}{H}\left[\frac{A_{sV}}{A_{sH}}\right]^{1/2} = 2.8\ (0.698)^{1/2} = 2.34$

and M_{vp}/M_{vN2} = 1.00

x/L = 0.385, x = 0.385 (336) = 129 in

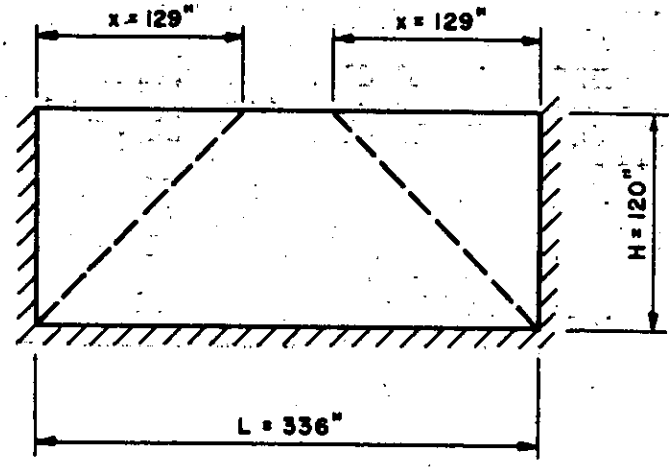


Figure 4A-9

Step 10. Ultimate shear stress at distance d_c from support.

a. Vertical Direction (along L):

For:

$$\frac{d_c}{H} = \frac{21}{120} = 0.175 \text{ and } x/L = 0.385$$

From figure 4-45:

$$\left(\frac{d_c}{H}\right)_M = 0.49 \quad \text{and} \quad C_M = 1.07$$

For:

$$\frac{d_c/H}{(d_c/H)_M} = \frac{0.175}{0.49} = 0.357$$

From figure 4-46:

$$\frac{C_V}{C_M} = 0.58$$

Therefore:

$$C_V = 1.07\ (0.58) = 0.62$$

$$P_V = \frac{A_{sV}}{b\ d_c} = \frac{1.20}{12(21)} = 0.00476$$

so that:

$$v_{uV} = C_V\ P_V\ f_{ds} \qquad \text{(eq. 4-119)}$$

$$= 0.62\ (0.00476)\ (87{,}840)$$

$$= 259 \text{ psi}$$

b. Horizontal Direction (along H)

For:

$$\frac{d_c}{x} = \frac{21}{129} = 0.163$$

From figure 4-40:

$$C_H = 0.81$$

$$P_H = \frac{A_{sH}}{b\ d_c} = \frac{0.86}{12(21)} = 0.00341$$

so that:

$$v_{uH} = C_H\, p_H\, f_{ds} \qquad \text{(eq. 4-118)}$$

$$= 0.81\ (0.00341)\ (87{,}840)$$

$$= 243 \text{ psi}$$

Step 11. Shear Capacity of Concrete (eq. 4-23)

a. Vertical Direction

$$v_c = (1.9\ (f'_c)^{1/2} + 2{,}500\ p_V)$$

$$= [1.9\ (4{,}000)^{1/2} + 2{,}500\ (0.00476)]$$

$$= 129 \text{ psi}$$

b. Horizontal Direction

$$v_c = (1.9\ (f'_c)^{1/2} + 2{,}500\ p_H)$$

$$= [1.9\ (4{,}000)^{1/2} + 2{,}500\ (0.00341)]$$

$$= 132 \text{ psi}$$

Step 12. Use lacing method No. 3 (see fig. 4-91).

Step 13. Lacing bar sizes:

a. Vertical Lacing Bars

$b_1 = 10$ in $\quad s_1 = 22$ in

Assume No. 6 Bars,

$$d_b = 0.75 \text{ in}$$

$$d_1 = 21 + 1.13 + 2.00 + 0.75$$

$$= 24.88 \text{ in.}$$

$$\text{Min } R_p = 4d_b$$

For:

$$\frac{s_1}{d_1} = \frac{22}{24.88} = 0.884 \qquad \text{(eq. 4-28)}$$

$$\frac{2\,R_1 + d_b}{d_1} = \frac{9\,d_b}{d_1} = \frac{9\,(0.75)}{24.88} = 0.271 \qquad \text{(eq. 4-29)}$$

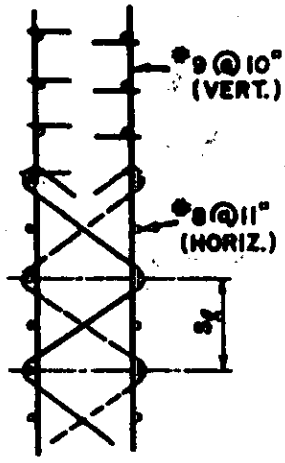


Figure 4A-10

From figure 4-15:

$\alpha = 53.0°$

For shear:

$f_{dy} = 1.10 \times 66{,}000 = 72{,}600$ psi

$f_{du} = 1.00 \times 90{,}000 = 90{,}000$ psi

$f_{ds} = (72{,}600 + 90{,}000)/2 = 81{,}300$ psi

$$A_v = \frac{(v_{uV} - v_c)\, b_1\, s_1}{\phi\, f_{ds}\, (\sin\alpha + \cos\alpha)} \qquad \text{(eq. 4-26)}$$

$$= \frac{(259 - 132)\,(10)\,(22)}{0.85\,(81{,}300)\,(0.799 + 0.602)}$$

$= 0.289$ in^2

Min $A_v = 0.0015\, b_1\, s_1$

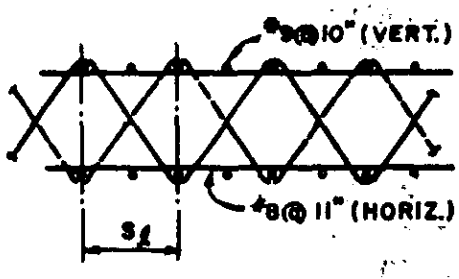
$= 0.0015\,(10)\,(22)$

$= 0.330$ in^2

Use No. 6 bars:

$(A = 0.44 \text{ in}^2)$

b. Horizontal Lacing:



$b_1 = 11$ in $s_1 = 20$ in

Figure 4A-11

Assume No. 6 Bars:

$d_b = 0.75$ in

$d_1 = 21.0 + 1.13 + 0.75 = 22.88$ in

Min. $R_1 = 4\ d_b$

For:

$$\frac{s_1}{d_1} = \frac{20}{22.88} = 0.874 \qquad \text{(eq. 4-28)}$$

$$\frac{2\ R_1 + d_b}{d_1} = \frac{9\ d_b}{d_1} = \frac{9\ (0.75)}{22.88} = 0.295 \qquad \text{(eq. 4-29)}$$

From figure 4-15:

$\alpha = 53.5°$

$$A_H = \frac{(v_{uH} - v_c)\ b_1\ s_1}{\phi\ f_{ds}\ (\sin \alpha + \cos \alpha)\ s_1} \qquad \text{(eq. 4-26)}$$

$$= \frac{(243 - 129)\ (11)\ (20)}{0.85\ (81{,}300)\ (0.804 + 0.595)}$$

$$= 0.259 \text{ in}^2$$

Min. $A_v = 0.0015\ b_1\ s_1$

$= 0.0015\ (11)\ (20)$

$= 0.330\ in^2$

Use No. 6 bars:

$(A = 0.44\ in^2)$

Step 14. Actual d_c depends upon vertical lacing.

Cover	- 2 x 0.75	= 1.50
Lacing	- 2 x 0.75	= 1.50
Horizontal	- 2 x 1.00	= 2.00
Vertical	- 1.13	= 1.13
		6.13 in

$T_c = d_c + 6.13 = 21 + 6.13$

$= 27.13$ in $\therefore$ Use 27 in

Actual $d_c = 27 - 6.13 = 20.87$ in

Step 15. Check capacity.

a. Actual impulse capacity.

For:

$$\frac{P_V}{P_H} = 1.40 \approx 1.41, \quad C_u = 461.0 \qquad \text{(fig. 4-34)}$$

For:

$$d_c = 20.87 \text{ in}, \quad P_H = \frac{0.86}{12(20.87)} = 0.00343$$

$$i_b = \frac{P_H\ d_c^3\ f_{ds}\ C_u}{H}$$

$$= \frac{0.00343(20.87)^3\ (87{,}840)\ (461.0)}{(120)}$$

$$i_b = 3244 \text{ psi-ms} > i_b = 3{,}200 \text{ psi-ms}$$

b. Actual maximum deflection.

For:

$$\frac{P_V}{P_H} = 1.40, \; C_1 = 452.0 \qquad \text{(fig. 4-31)}$$

Note: Interpolation for C_1 not shown.

$$C_u = 461.0$$

From table 3-6 for $x > H$:

$$X_1 = H \tan 12° = 120\,(0.2125) = 25.5 \text{ in}$$

$$X_u = x \tan \theta_{max} + \left(\frac{L}{2} - x\right) \tan\left[\theta_{max} - \tan^{-1}\frac{(\tan \theta_{max})}{x/H}\right]$$

$$= (129) \tan 12 + (168-129) \tan\left[12 - \tan^{-1}\left[\frac{\tan 12}{129/120}\right]\right]$$

$$= 27.42 + 0.56 = 27.98 \text{ in.}$$

From Step 5:

$$\frac{i_b^2 H}{P_H d_c^3 f_{ds}} = C_1 + (C_u - C_1)\left[\frac{X_m - X_1}{X_u - X_1}\right]$$

$$\frac{(3200)^2\,(120)}{0.00343(20.87)^3(87{,}840)} =$$

$$452.0 + (461.0 - 452.0)\left[\frac{X_m - 25.5}{27.98 - 25.5}\right]$$

From which: $X_m = 24.58 \text{ in} < X_1$

Note:
Since the deflection X_m is less than X_1, the above solution ($X_m = 24.58$) is incorrect because the equation used is for

the deflection range $X_1 \leq X_m \leq X_u$. Therefore, an equation for the deflection range $0 \leq X_m \leq X_1$ must be used to obtain the correct solution.

From Section 4-33.5 for Type III cross sections and valid for deflection range:

$$0 \leq X_m \leq X_1$$

$$\frac{i_b^2 H}{p_H d_c^3 f_{ds}} = C_1 \left(\frac{X_m}{X_1} \right)$$

$$X_m = \frac{i_b^2 H X_1}{p_H d_c^3 f_{ds} C_1}$$

$$= \frac{(3200)^2 (120) (25.5)}{(0.00343) (20.87)^3 (87,840) 452.0}$$

$$X_m = 25.3 \text{ in}$$

Note:
The element is slightly over-designed. To obtain a more economical design, the amount of flexural reinforcement may be reduced.

Step 16. The response time of the element is obtained from:

$$t_m = \frac{i_b}{r_u} \qquad \text{(eq. 3-96)}$$

where:

$$r_u = \frac{5 (M_{HN} + M_{HP})}{x^2} \qquad \text{(table 3-2)}$$

but:

$$M_{HN} = M_{HP} = \frac{A_{sH} f_{ds} d_c}{b}$$

$$= \frac{0.86\ (87,840)\ (20.87)}{12}$$

$$= 131,380 \text{ in-lbs/in}$$

therefore:

$$r_u = \frac{5\ (2)\ (131,380)}{(129)^2} = 78.9 \text{ psi}$$

so that:

$$t_m = \frac{i_b}{r_u} = \frac{3,200}{78.9} = 40.6 \text{ ms}$$

$$\frac{t_m}{t_o} = \frac{40.6}{5} = 8.12$$

The correct procedure has been used since:

$$\frac{t_m}{t_o} > 3$$

Step 17. Ultimate support shear.

a. Vertical Direction (along L):

From figure 4-54, for:

$x/L = 0.385$

$C_{sV} = 4.40$

$$V_{sV} = \frac{C_{sV}\ p_V\ d_c^2\ f_{ds}}{H} \qquad \text{(eq. 4-122)}$$

$$= \frac{4.40\ (1.20)\ (20.87)^2\ (87,840)}{12\ (20.87)\ (120)}$$

$$= 6720 \text{ lbs/in}$$

b. Horizontal Direction (along H):

From table 4-15:

$$C_{sH} = \frac{6}{(x/L)} = \frac{6}{0.385} = 15.6$$

$$V_{sH} = \frac{C_{sH}\, P_H\, d_c^2\, f_{ds}}{L} \qquad \text{(eq. 4-121)}$$

$$= \frac{15.6\ (0.00343)\ (20.87)^2\ (87{,}840)}{336}$$

$$= 6{,}090 \text{ lbs/in}$$

Step 18. Diagonal bar sizes.

Note:
Place bars on a 45° angle.

$$\therefore \sin \alpha = 0.707$$

a. Vertical Direction (at floor slab):

$$A_d = \frac{V_{sV}\, b}{f_{ds} \sin \alpha} = \frac{6{,}720\ (10)}{81{,}300\ (0.707)} = 1.17 \text{ in}^2 \qquad \text{(eq. 4-30)}$$

Required area of bar:

$$\frac{A_d}{2} = 0.58 \text{ in}^2$$

Use No. 8 @ 10.

b. Horizontal Direction (at wall intersections):

$$A_d = \frac{V_{sH}\, b}{f_{ds} \sin \alpha} = \frac{6{,}090\ (11)}{81{,}300\ (0.707)} = 1.16 \text{ in}^2 \qquad \text{(eq. 4-30)}$$

Required area of bar:

$$\frac{A_d}{2} = 0.58 \text{ in}^2$$

Use No. 8 @ 11.

Problem 4A-4, Elements Designed for Impulse-Limited Deflections

Problem: Design an element which responds to the impulse loading of a close-in detonation.

Procedure:

Step 1. Establish design parameters:

a. Blast loads including pressure-time relationship (Chapter 2).

b. Deflection criteria.

c. Structural configuration including geometry and support conditions.

d. Type of cross section available depending upon the occurrence of spalling and/or crushing of the concrete cover.

Step 2. Select cross section of element including thickness and concrete cover over the reinforcement. Also determine the static design stresses of concrete and reinforcing steel (Section 4-12).

Step 3. Determine dynamic increase factors for both concrete and reinforcement from table 4-1. Using the above DIF's and the static design stresses of step 2, calculate the dynamic strength of materials.

Step 4. Determine the dynamic design stresses using table 4-2 and the results from step 3.

Step 5. Assume vertical and horizontal reinforcement bars to yield the optimum steel ratio. The steel ratio is optimum when the resulting yield lines make an angle of 45 degrees with the supports.

Step 6. Calculate d_e (d or d_c depending upon the type of cross section available to resist the blast load) for both the positive and negative moments in both the vertical and horizontal directions. Determine the reinforcing ratios. Also check for the minimum steel ratios from table 4-3.

Step 7. Using the area of reinforcement and the value of de from step 6, and the dynamic design stress of step 4, calculate the moment capacity (Sect. 4-17) of both the positive and negative reinforcement. Also calculate the p_V/p_H ratio and compare to the optimum steel ratio from step 5.

Step 8. Establish values of K_E, X_E and r_u similar to the procedures of problem 4A-1, steps 8 to 18.

Step 9. Determine the load-mass factor K_{LM}, for elastic, elasto-plastic and plastic ranges from table 3-13 and figure 3-44. The average load mass factor is obtained by taking the average K_{LM} for the elastic

and elasto-plastic ranges and averaging this value with the K_{LM} of the plastic range. In addition, calculate the unit mass of the element (account for reduced concrete thickness if spalling is anticipated) and multiply this unit mass by K_{LM} for the element to obtain the effective unit mass of the element.

Step 10. Using the effective mass of step 9 and the equivalent stiffness of step 8, calculate the natural period of vibration T_N from equation 3-60.

Step 11. Determine the response chart parameters:

a. Peak pressure P (step 1).

b. Peak resistance r_u (step 8).

c. Duration of load T (step 1).

d. Natural period of vibration T_N (step 10).

Also calculate the ratios of peak pressure P to peak resistance r_u and duration T to period of vibration T_N. Using these ratios and the response charts of Chapter 3, determine the value of X_m/X_E. Compute the value of X_m.

Step 12. Determine the support rotation corresponding to the value of X_m from step 11 using the equations of table 3-6. Compare this value to maximum permissible support rotation of step 1, and if found to be satisfactory, proceed to step 13. If comparison is unsatisfactory, repeat steps 2 to 12.

Step 13. Using the ultimate resistance of step 8, the values of d_e of step 6 and the equations of table 4-6 or 4-7 (table 3-10 or 3-11 if shear at support is required), calculate the ultimate diagonal tension shear stress at a distance d_e from each support (or at each support). Also, calculate the shear capacity of the concrete from equation 4-23. If the capacity of the concrete is greater than that produced by the load, minimum shear reinforcement must be used. However, if the shear produced by the load is greater than the capacity of the concrete, then shear reinforcement in excess of the minimum required must be provided. Also check for maximum spacing of shear reinforcement.

Step 14. Using the equations of table 3-9, 3-10 or 3-11 and the ultimate resistance of step 8, calculate the shear at the supports. Determine the required area of diagonal bars using equation 4-30. However, if section type I is used, then the minimum diagonal bars must be provided.

Example 4A-4, Elements Designed for Impulse-Limited Deflections

Required: Design the side wall of cubicle with no roof or front wall and subject to the effects of a detonation of an explosive within the cubicle.

Solution:

Step 1: Given:

a. Pressure-time loading (fig. 4A-12).

b. Maximum support rotation equal to 2 degrees.

c. L = 180 in., H = 144 in. and fixed on two sides (fig. 4A-12).

d. Type III cross section.

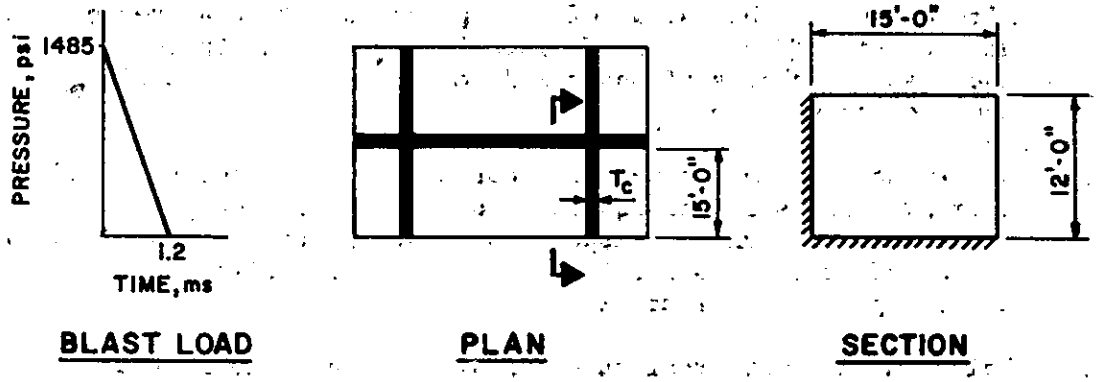


Figure 4A-12

Step 2. Select element thickness and static stress of reinforcement and concrete (fig 4A-13).

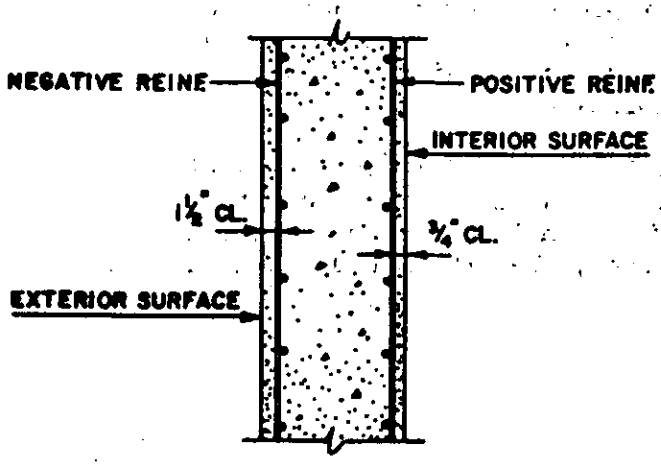


Figure 4A-13

f'_c = 4,000 psi

f_y = 66,000 psi

Assume T_c = 22 in. and concrete cover is as shown in figure 4A-13.

Step 3. Determine dynamic stresses.

a. Dynamic increase factors, DIF (from table 4-1).

Concrete:

Diagonal Tension - 1.00

Reinforcement:

Bending - 1.23

Diagonal Tension - 1.10

Direct Shear - 1.10

b. Dynamic strength of materials.

Concrete (f'_{dc}):

Diagonal Tension 1.00 (4,000) = 4,000 psi

Reinforcement (f_{dy}):

Bending 1.23 (66,000) = 81,180 psi

Diagonal Tension 1.10 (66,000) = 72,600 psi

Direct Shear 1.10 (66,000) = 72,600 psi

Step 4. Dynamic design stress from table 4-2.

Concrete (f'_{dc}):

Diagonal Tension - 4,000 psi

Reinforcement ($f_{ds} = f_{dy}$ for $0 < 2$)

Bending - 81,180 psi

Diagonal Tension - 72,600 psi

Direct Shear - 72,600 psi

Step 5. Determine the optimum steel ratio p_v/p_H. Set x = H to obtain 45 degree yield lines.

$$\frac{x}{L} = \frac{H}{L} = \frac{144}{180} = 0.80$$

From figure 3-4,

$$\frac{L}{H}\left(\frac{M_{VP}}{M_{HN}+M_{HP}}\right) = 1.08$$

Therefore,

$$\frac{M_{VP}}{M_{HN}+M_{HP}} = \left[\frac{1.08 \times 144}{180}\right]^2 = 0.75$$

or

$$M_{VP}/M_{HN} = 1.50$$

Try No. 7 bars at 8 in. o.c. in the vertical direction and No. 6 bars at 8 in. o.c. in the horizontal direction.

Step 6. Calculate d_c and the steel ratios for each direction.

Assume No. 3 stirrups.

$d_{cV} = 22 - (2 \times 0.375) - 0.75 - 1.5 - (2 \times 0.875/2) = 18.125$ in.

$d_{cH} = 18.125 - (2 \times 0.875/2) - (2 \times 0.75/2) = 16.50$ in.

$$P_V = \frac{A_{sV}}{bd_{cV}} = \frac{0.60}{8 \times 18.125} = 0.0041 > 0.0015 \text{ minimum}$$

$$P_H = \frac{A_{sH}}{bd_{cH}} = \frac{0.44}{8 \times 16.50} = 0.0033 > 0.0015 \text{ minimum}$$

Step 7. Calculate the moment capacity of both the positive and negative reinforcement in both directions (eq. 4-19).

$$M_u = \frac{A_s f_{ds} d_c}{b}$$

$$M_{VN} = M_{VP} = \frac{0.60\ (81{,}180)(18.125)}{8} = 110{,}354 \text{ in-lbs/in}$$

$$M_{HN} = M_{HP} = \frac{0.44\ (81{,}180)(16.50)}{8} = 73{,}671 \text{ in-lbs/in}$$

$M_{VN}/M_{HN} = 110{,}354/73{,}671 \approx 1.5 = 1.5$ from step 5 o.k.

Step 8. Using the procedure in example 4A-1, steps 8 through 18 and the moment capacities from step 7. establish the values of K_E, X_E and r_u.

K_E = 36.7 psi/in.

X_E = 0.968 in.

r_u = 35.53 psi

Step 9. Calculate the effective mass of the element.

a. Load mass factors (table 3-13 and fig. 3-44)

x/L = 0.80

elastic range K_{LM} = 0.65

elasto-plastic range:

one simple edge K_{LM} = 0.66

two simple edges K_{LM} = 0.66

plastic range K_{LM} = 0.54

K_{LM} (average elastic and elasto-plastic values)

$$= \frac{0.65 + 0.66 + 0.66}{3} = 0.66$$

K_{LM} (average elastic and plastic values)

$$= \frac{0.66 + 0.54}{2} = 0.60$$

b. Unit mass of element:

Using the larger d_c as the thickness of the element.

Due to spalling (Type III cross section) available thickness equals

$T_c = d_c = 18.125$ in.

$$m = \frac{w_c d_c}{g} = \frac{150\ (18.125)\ 10^6}{32.2 \times 12 \times 1728} = 4{,}072\ \text{psi-ms}^2/\text{in}$$

c. Effective unit mass of element:

$$m_e = K_{LM} m = 0.60\ (4,072) = 2,443\ \text{psi-ms}^2/\text{in}$$

Step 10. Calculate the natural period of vibration.

$$T_N = 2\pi\ (m_e/K_E)^{1/2} \qquad \text{(eq. 3-60)}$$

$$T_N = 2\ (3.14)\ (2443/36.7)^{1/2} = 51.2\ \text{ms}$$

Step 11. Determine maximum response of element.

a. Response chart parameters:

Peak pressure, P = 1485 psi (step 1)

Peak resistance, r_u = 35.53 psi (step 8)

Duration of blast load, T = 1.2 ms (step 1)

Period of vibration T_N = 51.2 ms (step 6)

$P/r_u = 1485/35.53 = 41.8$

$T/T_N = 1.2/51.2 = 0.023$

b. From figure 3-64a:

$X_m/X_E = 5.0$

$X_m = 5.0 \times 0.968 = 4.84$ in

Step 12. Check support rotation (table 3-6).

Since x = H = 144 in. and $0 < X_m < X_1$

$X_m = x \tan \theta_H$

$\tan \theta_H = 4.84/144$

$\theta_H = 1.93° < 2°$ assumed section is O.K.

Step 13. Check diagonal tension at supports (internal loading).

a. Calculate ultimate shear stresses at support by dividing the values of the support shear from table 3-10 by their respective d_c.

$$V_{sH} = 3r_u x/5 = 3 \times 35.53 \times 144/5 = 3{,}070 \text{ lb/in}$$

$$V_{sV} = \frac{3r_u H \left(2 - \frac{X}{L}\right)}{\left(6 - \frac{x}{L}\right)} = \frac{3\,(35.53)\,144\,(2 - 0.80)}{(6 - 0.80)} = 3{,}542 \text{ lb/in}$$

$$v_{uH} = V_{sH}/d_{cH} = 3{,}070/16.50 = 186.1 \text{ psi}$$

$$v_{uV} = V_{sV}/d_{cV} = 3{,}542/18.125 = 195.4 \text{ psi}$$

b. Allowable shear stresses (eq. 4-23)

$$v_c = 1.9\,(f'_c)^{1/2} + 2500\,p \leq 3.5\,(f'_c)^{1/2} = 221.4 \text{ psi}$$

where p is the steel ratio at the support.

$$v_{cH} = 1.9\,(4000)^{1/2} + 2500\,(0.0033) = 128.4 \text{ psi} < 221.4 \text{ psi}$$

$$v_{cV} = 1.9\,(4000)^{1/2} + 2500\,(0.0041) = 130.4 \text{ psi} < 221.4 \text{ psi}$$

c. Required area of single leg stirrups.

$$A_V = \frac{(V_u - V_c)bs}{0.85\,(f'_{ds})} \qquad \text{(eq. 4-26)}$$

$$v_{uH} - v_{cH} = 186.1 - 128.4 = 57.7 < 0.85v_{cH} = 108.8 \text{ psi}$$

Use $0.85\,v_{cH}$ as minimum.

$v_{uV} - v_{cV} = 195.4 - 130.4 = 65.0 < 0.85 v_{cV} = 110.8$ psi

Use 0.85 v_{cV} as minimum.

Tie every reinforcing bar intersection, therefore,

$b = s = 8$ in. $< d_c/2$ (maximum spacing) O.K.

$$A_{vH} = \frac{108.8 \times 8 \times 8}{0.85 \times 72{,}600} = 0.11 \text{ in}^2$$

minimum $A_v = 0.0015\ bs = 0.10\ \text{in}^2 < 0.11$ O.K.

$$A_{vV} = \frac{110.8 \times 8 \times 8}{0.85 \times 72{,}600} = 0.11 \text{ in}^2$$

minimum $A_v = 0.0015\ bs = 0.10\ \text{in}^2 < 0.11$ O.K.

The area of No. 3 bar is 0.11 in^2, so bar assumed in step 6 is O.K.

Step 14. Determine required area of diagonal bars using the values of the shear at the support from step 13.

$$A_d = \frac{V_s b}{f_{ds} \sin \alpha} \qquad \text{(eq. 4-30)}$$

Assume diagonal bars are inclined at 45 degrees.

$$A_{dH} = \frac{3.070 \times 8}{72{,}600 \times 0.707} = 0.48 \text{ in}^2 \text{ at 8 in. o.c.}$$

$$A_{dV} = \frac{3{,}542 \times 8}{72{,}600 \times 0.707} = 0.55 \text{ in}^2 \text{ at 8 in. o.c.}$$

Use No. 7 bars ($A_b = 0.60\ \text{in}^2$) at 8 in. o.c. at both supports

Problem 4A-5. Elements Designed for Impulse-Composite Construction

Problem: Design a composite (concrete-sand-concrete) wall to resist a given blast output for incipient failure.

Procedure:

Step 1. Establish design parameters.

a. Structure configuration.

b. Charge weight.

c. Blast impulse load (Chapter 2).

d. Thicknesses of concrete and sand portions of wall.

e. Blast impulse resisted by concrete panels.

f. Density of concrete and sand.

Step 2. Determine scaled thicknesses of concrete and sand using:

$$\bar{T}_c = T_c/W^{1/3} \text{ and } \bar{T}_s = T_s/W^{1/3}$$

Step 3. Determine scaled blast impulse resisted by each concrete panel using:

$$\bar{i}_{bd} = i_{bd}/W^{1/3} \text{ (donor panel)}$$

$$\bar{i}_{ba} = i_{ba}/W^{1/3} \text{ (acceptor panel)}$$

Step 4. Correct scaled blast impulse resisted by concrete (Step. 3.) to account for the increased mass produced by the sand and the reduction of the concrete mass produced by spalling and scabbing of the concrete panels using:

$$\text{(Corr.)} \quad \bar{i}_{bd} = \bar{i}_{bd} \left[\frac{\frac{T_c + d_c}{2} + \left(\frac{w_s}{w_c}\right)\left(\frac{T_s}{2}\right)}{d_c} \right]^{\frac{1}{2}}$$

$$\text{(Corr.)} \quad \bar{i}_{ba} = \bar{i}_{ba} \left[\frac{\frac{T_c + d_c}{2} + \left(\frac{w_s}{w_c}\right)\left(\frac{T_s}{2}\right)}{d_c} \right]^{\frac{1}{2}}$$

Step 5. Determine scaled blast impulse attenuated by acceptor panel and the sand $\bar{i}_a$ from figure 4-57 or 4-58, for w_s equal to 85 and 100 pcf., respectively.

Step 6. Calculate total impulse resisted by the wall using:

$$\bar{i}_{bt} = \bar{i}_a + \bar{i}_{bd}$$

Step 7. Compare blast impulse which is resisted by wall to that of the applied blast loads.

Example 4A-5, Elements Designed for Impulse-Composite Construction

Required: Design the composite wall shown below for incipient failure conditions.

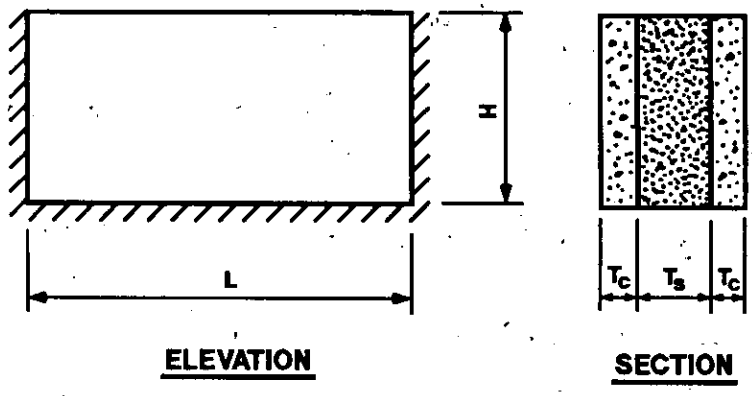


Figure 4A-14

Step 1. Given:

a. Structural configuration as shown in figure 4A-14.

b. W = 1,000 lbs.

c. i_b = 4,800 psi-ms (Chapter 2).

d. T_c = 1 ft, T_s = 2 ft, and d_c = 0.833 ft.

e. $i_{bd} = i_{ba}$ = 1,500 psi-ms (sect. 4-33).

f. w_c = 150 pcf and w_s = 100 pcf.

Step 2. Scaled thicknesses of concrete and sand:

$$\bar{T}_c = T_c/W^{1/3} = 1/(1000)^{1/3} = 0.1 \text{ ft/lb}^{1/3} \qquad \text{(eq. 4-125)}$$

$$\bar{T}_s = T_s/W^{1/3} = 2/(1000)^{1/3} = 0.2 \text{ ft/lb}^{1/3} \qquad \text{(eq. 4-126)}$$

Step 3. Scaled blast impulse resisted by individual concrete panels.

$$\bar{i}_{bd} = \bar{i}_{ba} = \frac{1500}{(1000)^{1/3}} = 150 \text{ psi-ms/lb} \qquad \text{(eq. 4-127)}$$

Step 4. Correction of scaled impulse resisted by concrete panel used in composite walls.

$$\text{(Corr.)}\ \bar{i}_{bd} = \bar{i}_{bd}\left[\frac{\frac{T_c + d_c}{2} + \left(\frac{w_s}{w_c}\right)\left(\frac{T_s}{2}\right)}{d_c}\right]^{\frac{1}{2}}$$

$$= 150\left[\frac{\frac{1.0 + 0.833}{2} + \frac{100}{150}\left(\frac{2}{2}\right)}{0.833}\right]^{\frac{1}{2}}$$

$$= 207 \text{ psi-ms/lb}^{1/3} = \bar{i}_{ba} \text{ (corr.)}$$

Step 5. Scaled blast impulse attenuated by acceptor panel and sand.

$$\bar{i}_a = 280 \text{ psi-ms/lb} \qquad \text{(fig. 4-58)}$$

Step 6. Total scaled blast impulse resisted by wall.

$$\bar{i}_{bt} = \bar{i}_a + \bar{i}_{bd} = 280 + 207 = 487 \text{ psi-ms/lb}^{1/3}$$

Step 7. Comparison of wall capacity and applied blast load.

$$\bar{i}_{bt} = 487 \approx \bar{i}_b = 480 \text{ psi-ms/lb}^{1/3} \qquad \text{O.K.}$$

Problem 4A-6, Design of a Beam in Flexure

Problem: Design an interior beam of a roof subjected to an overhead blast load.

Solution:

Step 1. Establish design parameters:

a. Structural configuration.

b. Pressure-time loading.

c. Maximum allowable support rotation.

d. Material properties

Step 2. From table 4-1, determine the dynamic increase factors, DIF. For the deflection criteria given in Step 1c, find the equation for the dynamic design stress from table 4-2. Using the DIF and the material properties from Step 1d, calculate the dynamic design stresses.

Step 3. Assuming reinforcing steel and concrete cover, calculate the distance from the extreme compression fiber to the centroid of the tension reinforcement, d.

Step 4. Calculate the reinforcement ratio of the steel assumed in Step 3. Check that this ratio is greater than the minimum reinforcement required by equation 4-137 but less than the maximum reinforcement permitted by equation 4-132.

Step 5. Using equations 4-129 and 4-130, the dynamic design stresses from Step 2, and the value of d from Step 3. calculate the ultimate moment capacity of the beam.

Step 6. Compute the ultimate unit resistance of the beam using the moment capacity of Step 4 and an equation from table 3-1.

Step 7. Calculate the modulus of elasticity of concrete E_c and steel E_s (equations 4-4 and 4-5, respectively) and the modular ratio n (equation 4-6). Determine the average moment of inertia I_a of the beam according to Section 4-15.

Step 8. From table 3-8, find the correct equation for the equivalent elastic stiffness K_E. Evaluate this equation using the values of E_c and I_a from Step 7.

Step 9. With the ultimate resistance from Step 6 and the stiffness K_E from Step 8, use equation 3-36 to calculate the equivalent elastic deflection X_E.

Step 10. Find the values for the load-mass factor K_{LM} in the elastic, elasto-plastic and plastic ranges from table 3-12. Average these values according to Section 3-17.4 to determine the value of K_{LM} to be used in design.

Step 11. Determine the natural period of vibration T_N using equation 3-60, K_{LM} from Step 10, K_E from Step 8 and the mass of the beam. The mass includes 20 percent of the adjacent slabs.

Step 12. Calculate the non-dimensional parameters T/T_N and r_u/P. Using the appropriate response chart by Chapter 3 determine the ductility ratio, μ.

Step 13. Compute the maximum deflection X_m using the ductility ratio from Step 12 and X_E from Step 9. Calculate the support rotation corresponding to X_m using an equation from table 3-5. Compare this rotation with the maximum allowable rotation of Step 1c.

Step 14. Verify that the ultimate support shear V_s given in table 3-9 does not exceed the maximum shear permitted by equation 4-142. If it does, the size of the beam must be increased and Steps 2 through 13 repeated.

Step 15. Calculate the diagonal tension stress v_u from equation 4-139 and check that it does not exceed $10(f_{dc}')^{1/2}$.

Step 16. Using the dynamic concrete strength f_{dc}' from Step 2 and equation 4-140, calculate the shear capacity of the unreinforced web, v_c.

Step 17. Design the shear reinforcement using equation 4-140, and the excess shear stress $(v_u - v_c)$ or the shear capacity of concrete v_c' whichever is greater.

Step 18. Check that the shear reinforcement meets the minimum area and maximum spacing requirements of Section 4-39.4.

Step 19. With T/T_N and X_m/X_E from Step 12, enter figure 3-268 and read the required resistance of the beam in rebound.

Step 20. Repeat Steps 3 through 6 to satisfy the required rebound resistance.

Example 4A-6, Design of a Beam in Flexure

Required: Design of an interior of a roof beam subjected to an overhead blast load.

Solution:

Step 1. Given:

a. Structural configuration is shown in figure 4A-15a.

b. Pressure-time loading is shown figure 4A-15c.

c. Maximum support rotation of one degree.

d. Yield stress of reinforcing steel, f_y = 66,000 psi

Concrete compressive strength, f'_c = 4,000 psi

Weight of concrete, w = 150 lbs/ft^3

Step 2. a. Dynamic increase factors from table 4-1 for intermediate and low pressure range.

Reinforcing steel	- bending, DIF	= 1.17
	- direct shear, DIF	= 1.10
Concrete	- compression, DIF	= 1.19
	- direct shear, DIF	= 1.10
	- diagonal tension, DIF	= 1.00

b. From table 4-2, for $\theta_m \leq 2°$:

$$f_{ds} = f_{dy}$$

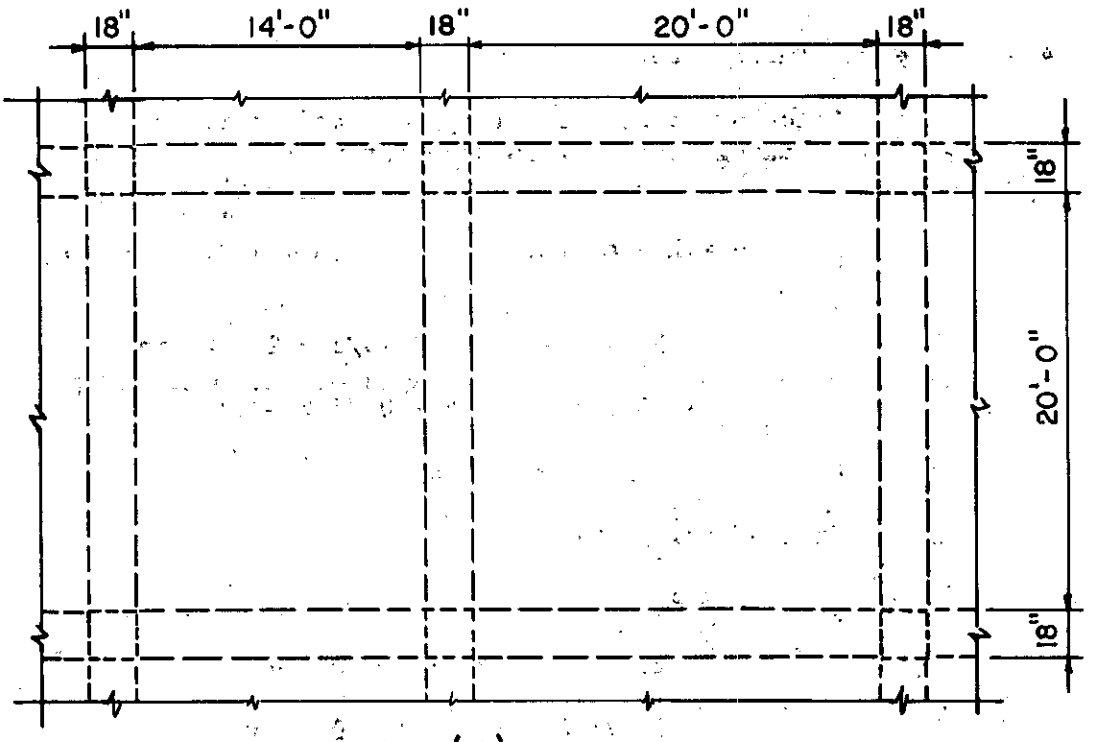
c. Dynamic design stresses from equation 4-3.

Reinforcing steel	- bending	f_{dy}	= 1.17 x 66,000 = 77,220 psi
	- diagonal tension	f_{dy}	= 1.00 x 66,000 = 66,000 psi
Concrete	- compression	f'_{dc}	= 1.19 x 4,000 = 4,760 psi
	- direct shear	f'_{dc}	= 1.10 x 4,000 = 4,400 psi
	- diagonal tension	f_{dy}	= 1.00 x 4,000 = 4,000 psi

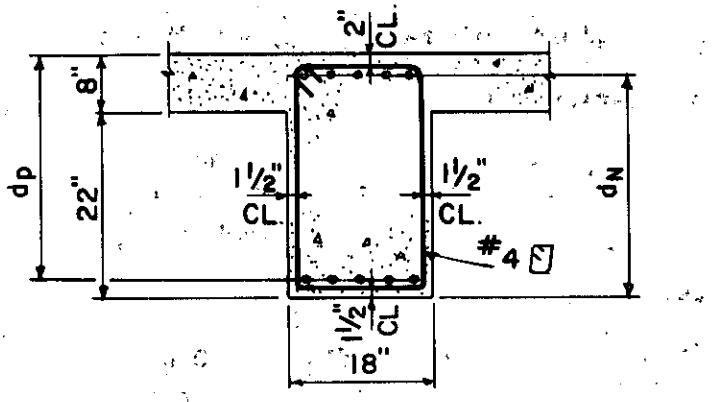
Step 3. Assume 5 No. 6 bars for bending:

A_s = 5 x .44 = 2.20 in^2

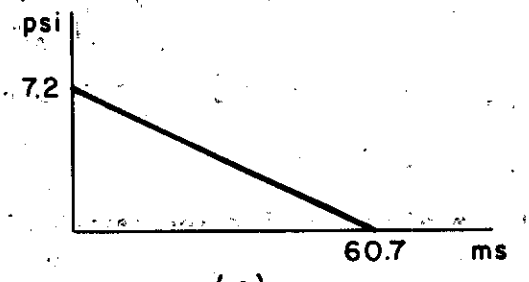
For concrete cover and beam sections see figure 4A-15b.



(a)



(b)



(c)

FIGURE 4A-15

Step 4. Check reinforcement requirements:

a. Calculate d negative (support) and positive (mid-span) for checking bending reinforcement ratios.

$$d = h - d' \text{ (cover)} - \phi \text{ ' (tie)} \frac{\phi}{2} \text{ (Bending Bar)}$$

$$d_N = 30 - 2 - 0.5 - 0.75/2 = 27.125 \text{ in}$$

$$d_p = 30 - 1.5 - 0.5 - 0.75/2 = 27.625 \text{ in}$$

b. Calculate reinforcement ratio:

From equation 4-131,

$$p = A_s/bd$$

$$p_N = 2.2/(18 \times 27.125) = 0.0045$$

$$p_p = 2.2/(18 \times 27.615) = 0.0044$$

c. Maximum reinforcement:

Maximum reinforcing ratio $p_{max} = 0.75 \times p_b$

From equation 4-132;

$$p_b = \frac{0.85K_1 f'_{dc}}{f_{dy}} * \frac{87,000}{87,000 + f_{dy}}$$

where:

$$K_1 = 0.85 - \frac{0.05 (f'_{dc} - 4,000)}{1,000} = 0.812$$

$$p_b = \frac{0.85 \times 0.812 \times 4760}{77,220} * \left(\frac{87,000}{87,000 + 77,220}\right) = 0.0225$$

$$p_{max} = 0.75 \times 0.0225 = 0.0169 > p_N = 0.0045 \text{ and}$$

$$p_p = 0.0044 \text{ O.K.}$$

d. Check for minimum reinforcing ratio using equation 4-138

$$p_{min} = 200 / f_y$$

$$p_{min} = \frac{200}{60,000} = 0.0033 < p_N = 0.0045 \text{ O.K.}$$

$$< p_p = 0.0044 \text{ O.K.}$$

Step 5. Moment capacity of the beam using equations 4-129 and 4-130 is:

$$M_u = A_s \ f_{dy} \ (d-a/2)$$

where:

$$a = \frac{A_s \ f_{dy}}{0.85b \ f'_{dc}}$$

$$a = \frac{2.20 \times 77,220}{0.85 \times 18 \times 4,760} = 2.333 \text{ in}$$

at support:

$$M_N = 2.20 \times 77,220 \times (27.125 - 2.333/2)$$

$$= 4,409,934 \text{ in-lbs}$$

at mid-span:

$$M_p = 2.20 \times 77,220 \times (27.625 - 2.333/2)$$

$$= 4,494,876 \text{ in-lbs}$$

Step 6. From table 3-1, ultimate resistance of a uniformly loaded beam with fixed ends is:

$$r_u = \frac{8 \ (M_N + M_p)}{L^2}$$

$$r_u = \frac{8 \ (4,409,934 + 4,494,934)}{240^2} = 1,236.79 \text{ lbs/in}$$

Step 7. From Section 4-15, calculate average moment of inertia of the beam section.

a. Concrete modulus of elasticity (eq. 4-4):

$$E_c = w^{1.5} \times 33 \times (f'_c)^{1/2}$$

$$E_c = 150^{1.5} \times 33 \times (4{,}000)^{1/2} = 3.8 \times 10^6 \text{ psi}$$

b. Steel modulus of elasticity (eq. 4-5):

$$E_s = 29 \times 10^6 \text{ psi}$$

c. Modular ratio (eq. 4-6):

$$n = \frac{E_s}{E_c}$$

$$n = \frac{29 \times 10^6}{3.8 \times 10^6} = 7.6$$

d. From figure 4-11 and having n, p_N and p_p, the coefficients for moment of inertia of cracked sections are:

$$F_N = 0.0235 \text{ at support}$$

$$F_p = 0.0230 \text{ at mid-span}$$

Cracked moment of inertia from equation 4-8b is:

$$I_c = Fbd^3$$

$$I_{cN} = 0.0235 \times 18 \times 27.125^3 = 8{,}442 \text{ in}^4$$

$$I_{cp} = 0.0230 \times 18 \times 27.625^3 = 8{,}728 \text{ in}^4$$

Average:

$$I_c = (I_{cN} + I_{cp}) / 2$$

$$I_c = \frac{8{,}442 + 8{,}728}{} = 8{,}585 \text{ in}^4$$

e. Gross moment of inertia (eq. 4-8):

$$I_g = \frac{bh^3}{12}$$

$$I_g = \frac{18 \times 30^3}{12} = 40{,}500 \text{ in}^4$$

f. Average moment of inertia of the beams from equation 4-7:

$$I_a = \frac{I_g + I_c}{2}$$

$$I_a = \frac{40{,}500 + 8{,}585}{2} = 24{,}542.5 \text{ in}^4$$

Step 8. From table 3-8, K_E of a uniformly loaded beam with fixed ends is:

$$K_E = \frac{307\ E_c\ I_a}{L^4}$$

$$K_E = \frac{307 \times 3.8 \times 10^6 \times 24{,}542.5}{240^4}$$

$$= 8{,}629.70 \text{ lbs/in/in}$$

Step 9. Equivalent elastic deflection from equation 3-36 is:

$$X_E = \frac{r_u}{K_E} = \frac{1{,}236.79}{8{,}629.70} = 0.1433 \text{ in}$$

Step 10. Load-mass factor from table 3-12 for a plastic range of a uniformly loaded beam with fixed ends is:

K_{LM} - elastic = 0.77
- elasto-plastic = 0.78
- plastic = 0.66

K_{LM} for plastic mode deflections; from Section 3-17.4 from Chapter 3:

$$K_{LM} = \left[\left[\frac{0.77 + 0.78}{2} \right] + 0.66 \right] / 2 = 0.72$$

Step 11. Natural period of the beam from equation 3-60 is:

$$T_N = 2\pi \, (K_{LM} \, m/K_E)^{1/2}$$

Where m is the mass of the beam plus 20% of the slabs span perpendicular to the beam:

$$m = w/g$$

$$m = (30 \times 18 + 2 \times 8 \times 102 \times 0.20) \times \frac{150}{12^3} \times \frac{1{,}000^2}{32.2 \times 12}$$

$$= 194{,}638.50 \text{ lbs-ms}^2/\text{in/in}$$

$$T_n = 2\pi \left[\frac{0.72 \times 194{,}638.50}{8{,}629.70}\right]^{\frac{1}{2}} = 25.3 \text{ ms}$$

Step 12. Find μ, ductility ratio from figure 3-54.

From Step 1:

$$T/T_N = 60.7/25.3 = 2.40$$

$$P = (18 + 84 + 120) \times 7.2$$

$$= 1{,}598.40 \text{ lbs/in}$$

$$r_u/P = \frac{1{,}236.79}{1{,}598.40} = 0.77$$

$$\mu = 9.0$$

Step 13. From table 3-5 support rotation is:

$$X_m = \frac{L \tan \theta}{2}$$

$$X_m = \mu \times X_E$$

$$X_m = 9.0 \times 0.1433 = 1.29 \text{ in}$$

$$\tan \Theta = \frac{2 \times 1.29}{240} = 0.01075$$

$$\Theta = 0.620 \leq 1° \quad \text{O.K.}$$

Step 14. Direct Shear from table 3-9 is:

$$V_s = \frac{r_u L}{2}$$

$$V_s = \frac{1236.79 \times 240}{2} = 148{,}415 \text{ lbs}$$

Section capacity in direct shear from equation 4-142:

$$V_d = 0.18 f'_{dc} bd$$

$$V_d = 0.18 \times 4{,}400 \times 18 \times 27.125$$

$$= 386{,}694 \text{ lbs} > V_s = 148{,}415 \quad \text{O.K.}$$

Step 15. Diagonal tension stress from equation 4-139:

$$v_u = \frac{V_u}{bd} \leq 10 (f'_c)^{1/2}$$

Total shear d distance from the face of support:

$$V_u = (L/2 - d)\, r_u$$

$$= \left(\frac{240}{2} - 27.125\right) 1236.79 = 114{,}867 \text{ lb}$$

$$V_u = \frac{114867}{18 \times 27.125} = 235.2 \text{ psi}$$

$$10 (f'_{dc})^{1/2} = 10 \times (4{,}000)^{1/2}$$

$$= 632.5 \text{ psi} > 235.2 \text{ psi} \quad \text{O.K.}$$

Step 16. Unreinforced web shear capacity using equation 4-140 is:

$$v_c = [1.9 (f'_{dc})^{1/2} + 2{,}500\, p]$$

$$< 3.5 (f'_{dc})^{1/2}$$

$$v_c = [1.9\ (4,000)^{1/2} + 2,500 \times 0.0045]$$

$$= 131.4 \text{ psi}$$

$$3.5\ (f'_{dc})^{1/2} = 3.5 \times (4,000)^{1/2}$$

$$= 221.4 \text{ psi} > 131.4 \text{ psi}\quad \text{O.K.}$$

Step 17. Area of web reinforcing from equation 4-141:

$$A_v = [(v_u - v_c) \times b \times s_s] / \phi \times f_{dy};\quad v_u - v_c \geq v_c$$

$$v_u - v_c = 235.2 - 131.4 = 104 < v_c \text{ use } v_c$$

Assume:

$$s_s = 9 \text{ in}$$

$$A_v = 131.4 \times 18 \times 9/(0.85 \times 66,000)$$

$$= 0.38 \text{ in } /9 \text{ in}^2$$

Use No. 4 tie:

$$A_v = 0.40 \text{ in}^2$$

Step 18. Minimum tie reinforcing area:

$$A_v \text{ (min)} = 0.0015\ bs_s$$

$$A_v \text{ (min)} = 0.0015 \times 18 \times 9$$

$$= 0.24 \text{ in}^2 < 0.40 \text{ in}^2 \quad \text{O.K.}$$

Maximum tie spacing:

$$4(f'_{dc})^{1/2} = 4 \times (4,000)^{1/2}$$

$$= 253 \text{ psi} > v_c = 131 \text{ psi}$$

$$> v_u - v_c = 104 \text{ psi}$$

$$s_{max} = d/2$$

$$s_{max} = 27.125 / 2 = 13.56 \text{ in} > 9 \text{ in} \quad \text{O.K.}$$

Step 19. Determine required resistance for rebound r^- from figure 3-268:

$$r^-/r_u = 0.50 \text{ for } T/T_N = 2.40 \text{ and } X_m/X_E = 9.0$$

Required:

$$r^- = 0.50 \times 1236.79 = 618.4 \text{ lbs/in}$$

Step 20. Repeat Steps 3 to 6:

Assume:

$A^-_s = 1.64 \text{ in}^2$, 2 No. 7 + 1 No. 6

p^-_N at support $= 0.0033 = 200/f_y$

p^-_p at mid-span $= 0.0034 > 200/f_y$

N^-_N at support $= 3{,}388{,}275$ in-lbs

M^-_p at mid-span $= 3{,}324{,}954$ in-lbs

$r^- = 932.4$ lbs/in

> 618.4 lbs/in O.K.

Problem 4A-7, Design of a Beam Subject to Torsion

Problem: Design a beam for a uniformly distributed torsional load.

Procedure:

Step 1. Design the beam and adjacent slabs in flexure for the applied blast load.

Step 2. Calculate the unbalanced slab support shears, V_T using the ultimate resistance of the slabs from Step 1.

$$V_T = \frac{r_{u1} L_1}{2} + \frac{r_{u2} L_2}{2}$$

Using the unbalanced slab support shears, compute the torsional load at d distance from the face of the support from:

$$T_u = \left(\frac{L}{2} - d\right) \frac{b}{2} (V_T)$$

Step 3. Using the torsional load from Step 2, compute the nominal torsional stress in the vertical direction from equation 4-143 and in the horizontal direction from equation 4-144. Verify that the torsional stresses do not exceed the maximum stress permitted in Sec. 4-41.5.

Note:
If the height of the beam is greater than width, the horizontal torsional stresses will not be critical and may be ignored.

Step 4. Determine the shear and torsional capacity of an unreinforced web, v_c and v_{tc}, from equations 4-145 and 4-146 or 4-147, the torsional stress from Step 3 and the shear stress from step 1.

Step 5. Find the excess shear stress $(v_u - v_c)$ where the nominal shear stress v_u is from Step 1, and the shear capacity of the unreinforced web v_c is from Step 4. Using the excess shear stress and equation 4-141, determine the area of web reinforcing for shear.

Step 6. With torsional capacity of the concrete from Step 4, the torsional stresses from Step 3, and equations 4-148 and 4-149, calculate the area of web reinforcement for torsion in the vertical and, if required, in the horizontal directions.

Step 7. Add the area of shear reinforcement from Step 5 and the area of torsion reinforcement in the vertical direction, and compare with the area of torsion reinforcement required in the horizontal direction. The larger of the two values will control for the design of the closed ties. (If height of beam is greater than width, see note at Step 3.)

Step 8. Check minimum area and maximum spacing requirements of ties according to section 4-41.5.

Step 9. Calculate the required area of longitudinal torsion reinforcement from equations 4-151a and 4-151b, the torsional stress from Step 3 and the torsion capacity of concrete from Step 4.

Step 10. Determine the distribution of flexural and longitudinal steel at the supports and at the midsection.

Example 4A-7, Design of Beam in Torsion

Required: Design of beam in example 4A-6, for torsional load due to unequal spans of adjacent slab.

Solution:

Step 1. Given:

a. Beam designed for flexure in example 4A-6 where:

$L = 240$ in

$d = 27.125$ in; $b = 18$ in

$v_u = 235.2$ psi

b. Slabs designed for flexure where:

$r_{u1} = 15.0$ psi $L_1 = 14$ ft $= 168$ in

$r_{u2} = 7.85$ psi $L_2 = 20$ ft $= 240$ in

Step 2. Calculate torsional load.

a. Unbalanced slab support shears:

$$V_T = \frac{r_{u1} L_1}{2} - \frac{r_{u2} L_2}{2}$$

$$= \frac{15(168)}{2} - \frac{7.85(240)}{2} = 320 \text{ lb/in}$$

b. Torsional load at d from the support:

$$T_u = \left(\frac{L}{2} - d\right) \frac{b}{2} \left(V_T\right)_T$$

$$= \left(\frac{240}{2} - 27.125\right) \times \frac{18}{2} \times 320 = 267{,}480 \text{ in-lb}$$

Step 3. Maximum torsional stress:

Since $h > b$, the torsional stress in the vertical direction is not critical and will be ignored.

a. Torsional stress:

$$v_{(tu)V} = \frac{3T_u}{b^2 h} \qquad \text{(eq. 4-143)}$$

$$= \frac{3 \times 267{,}480}{18^2 \times 30} = 82.5 \text{ psi}$$

b. Shear stress: $v_u = 235.2$ psi

c. Check maximum allowable torsional stress.

$$\max v_{tu} = \frac{12(f'_{dc})^{1/2}}{\left[1 + \left[\frac{1.2\ v_u}{v_{tu}}\right]^2\right]^{\frac{1}{2}}}$$

$$= \frac{12 \times (4000)^{1/2}}{\left[1 + \left[\frac{1.2 \times 235.2}{82.5}\right]^2\right]^{\frac{1}{2}}} = 212.9 > 82.5 \text{ O.K.}$$

Step 4. Find shear and torsional capacity of unreinforced web.

a. Shear capacity:

$$v_c = \frac{2\ (f'_{dc})^{1/2}}{\left[1 + \left[\frac{v_{tu}}{1.2 \times v_u}\right]^2\right]^{\frac{1}{2}}} \qquad \text{(eq. 4-145)}$$

$$v_c = \frac{2 \times (4000)^{1/2}}{\left[1 + \left[\frac{82.5}{1.2 \times 235.2}\right]^2\right]^{\frac{1}{2}}} = 121.4 \text{ psi}$$

b. Torsional capacity:

$$v_{tc} = \frac{2.4\ (f'_{dc})^{1/2}}{\left[1 + \left[\frac{1.2 v_u}{v_{tu}}\right]^2\right]^{\frac{1}{2}}} \qquad \text{(eq. 4-146)}$$

howdy

$$v_{tc} = \frac{2.4 \times (4{,}000)^{1/2}}{\left[1 \left[\frac{1.2 \times 235.2}{82.5}\right]^2\right]^{\frac{1}{2}}}$$

$$= 42.6 \text{ psi (Vertical Face)}$$

Step 5. Area of web reinforcing for shear using equation 4-141:

$$A_v = (v_u - v_c) \times b \times s/(\phi f_{dy})$$

Assume s = 12 in.

$$A_v = (235.2 - 121.4) \times 18 \times 12/(0.85 \times 66{,}000)$$

$$= 0.438 \text{ in}^2/\text{ft}$$

Step 6. Web reinforcing for torsional stress using equation 4-148:

$$A_t = \frac{(v_{tu} - v_{tc})^2 b \, hs}{3 \phi \, \alpha_t \, b_t \, h_t \, f_{dy}} \quad \text{Vertical}$$

where:

$$\alpha_t = 0.66 + 0.33 \frac{h_t}{b_t} \leq 1.50$$

$h_t = 30.0 - 2.0 - 1.5 - (2 \times 0.5/2) = 26$ in

See figure 4A-15.

$b_t = 18.0 - 1.5 - 1.5 - (2 \times 0.5/2) = 14.5$ in

See figure 4A-15.

$$\alpha_t = 0.66 + 0.33 \times \frac{26}{14.5} = 1.25 < 1.50 \quad \text{O.K.}$$

$$A_t = \frac{(82.5 - 42.6)\ 18^2 \times 30 \times 12}{3 \times 0.85 \times 1.25 \times 14.5 \times 26 \times 66{,}000}$$

$$= 0.059\ \text{in}^2/\text{ft}$$

Step 7. Total web reinforcement:

$$A_t + A_v/2 = 0.059 + 0.438/2 = 0.278\ \text{in}^2/\text{ft/Leg}$$

Use No. 4 ties @ 8 in = 0.300 in^2/ft/Leg.

Step 8. Minimum torsion reinforcement (sect. 4-41.5):

a. Minimum tie reinforcing area:

A_v (min) = A_v shear alone from example 4A-6

Use No. 4 ties @ 9 in.

$$A_v\ (\text{min}) = \frac{0.38}{2} \times \frac{12}{9}$$

$$= 0.253\ \text{in}^2/\text{ft/Leg} < 0.300\ \text{in}^2/\text{ft/Leg} \quad \text{O.K.}$$

b. Maximum spacing:

$$s_{max} = \frac{h_t + b_t}{4}$$

$$s_{max} = \frac{26 + 14.5}{4}$$

$$= 10.125\ \text{in} > 7\ \text{in} \quad \text{O.K.}$$

Step 9. Required area of longitudinal steel is the greater of the two values from equations 4-151a or 4-151b.

$$A_l = 2A_t \times \frac{b_t + h_t}{s}$$

$$A_l = 2 \times 0.06 \times \frac{14.5 + 26.0}{12} = 0.40 \text{ in}^2$$

or:

$$A_l = \left[\frac{400 \times b \times s}{f_{dy}} \frac{v_{tu}}{v_{tu} + v_u} - 2A_t \right] \times \frac{b_t + h_t}{s}$$

where:

$$2A_t = \frac{50bs}{f_{dy}}$$

$$\frac{50bs}{f_{dy}} = \frac{50 \times 18 \times 12}{66,000} = 0.16 \text{ in}^2/\text{ft } 2A_t$$

$$A_l = \left[\frac{400 \times 18 \times 12}{66,000} \frac{(82.5)}{82.5 + 235.2} - 0.12 \right]$$

$$\times \frac{14.5 + 26.0}{12} = 0.74 \text{ in}^2$$

Step 10. Distribute A_l, A_s, and A_s' as follows (see fig. 4A-16):

Distribute A_l equally between four corners of the beam and one on each face of depth, a total of six locations to satisfy maximum spacing of 12 inches.

$$A_l/6 = 0.74/6 = 0.12 \text{ in}^2$$

Vertical Face:

One (1) No. 4 bar

$= 0.20 \text{ in}^2 > 0.12$ O.K.

Horizontal Face at Top:

Support = 2.20 (bending) + 2 x 0.12 (torsion)

= 2.44 in^2

Two (2) No. 7 at corners + three (3) No. 6

= 2.52 in^2 O.K.

Midspan = 1.64 (rebound)

Two (2) No. 7 at corners + one (1) No. 6

= 1.64 in^2 O.K.

Horizontal Face at Bottom:

Support = Greater of rebound (1.64 in^2)
or torsion (2 x 0.12)

Two (2) No. 7 at corners + one (1) No. 6

= 1.64 in^2 O.K.

Midspan = 2.20 (bending)

Two (2) No. 7 at corners + one (1) No. 6 + two (2) No. 5

= 2.26 in^2 > 2.20 O.K.

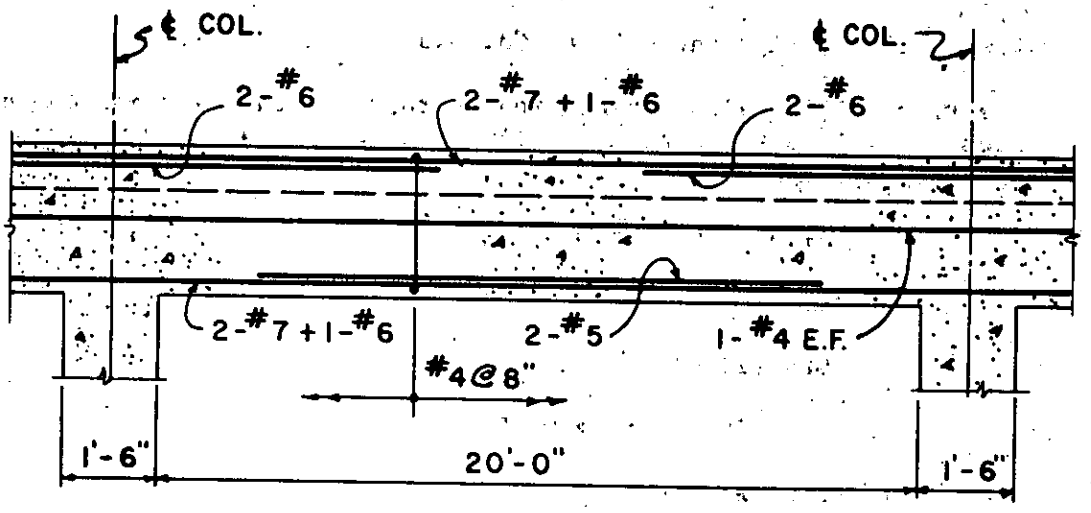


Figure 4A-16

Problem 4A-8, Column Design

Problem: Design an interior column of a one-story structure with shear walls.

Procedure:

Step 1. Establish design parameters:

a. End conditions of column.

b. Clear height of column.

c. Dynamic loads from roof.

d. Static material properties.

Step 2. Find equivalent static loads on the column by increasing the dynamic loads 20 percent (sect. 4-47).

Step 3. From table 4-1, determine the dynamic increase factors, DIF. Using the DIF, the material properties from Step 1d and equation 4-3, calculate the dynamic design strength of the concrete and the reinforcement.

Step 4. Assume a column section and reinforcing steel.

Step 5. Calculate the slenderness ratio of the column section assumed in Step 4, using either equation 4-167 or 4-168. If the slenderness ratio is less than 22, slenderness effects may be neglected. If it is greater than 22 and less than 50, the moment magnifier must be calculated from equation 4-170 and the moments increased according to equation 4-169. The column section must be increased if the slenderness ratio is greater than 50.

Step 6. Divide the moment by the axial load to obtain the design eccentricity in both directions. Verify that the design eccentricities are greater than the minimum eccentricity of 0.1h for a tied column and 0.0707D for a spiral column.

Step 7. Compute the balanced eccentricity e_b of the column using equation 4-156 or 4-158 (for a rectangular and circular column, respectively), the dynamic material properties from Step 3, and the section properties from Step 4. Compare the balanced eccentricity with the design eccentricity from Step 6. Determine if the column failure is controlled by compressive strength of the concrete ($e_b > e$) or tensile strength of reinforcement ($e_b < e$).

Step 8. Calculate the ultimate axial load capacity, at the actual eccentricity, in both directions. If compression controls use equation 4-160 or 4-161. If tension controls use equation 4-162 or 4-166.

Step 9. Using equation 4-154, compute the pure axial load capacity of the section.

Step 10. Compute the ultimate capacity of the column section, using the load capacities at the actual eccentricities from Step 8, the pure axial load capacity from Step 9, and equation 4-176. Verify that the ultimate load capacity is greater than the equivalent static load from Step 2.

Step 11. Provide ties according to section 4-48.4 for a tied column, or section 4-49.4 for a spiral reinforced column.

Example 4A-8, Column Design

Required: Design of a rectangular, tied interior column.

Solution:

Step 1. Given:

a. Both ends of column fixed

b. Clear height of column, $l = 120$ in

c. Axial load 491,000 lbs

Moment about x-axis, 2,946,000 in-lbs
No calculated moment about y-axis

d. Reinforcing steel, $f_y = 66{,}000$ psi

Concrete, $f'_c = 4{,}000$ psi

Step 2. Equivalent static loads.

a. Axial load

$P = 491{,}000 \times 1.2 = 589{,}200$ lbs

b. Moment about x-axis

$M_x = 2{,}946{,}000 \times 1.2 = 3{,}535{,}200$ in-lbs

c. Moment about y-axis

$M_y = 0$ in-lbs

Step 3. Dynamic material strengths:

a. Reinforcing Steel.

$f_{dy} = f_y \times DIF$

f_{dy} = 66,000 x 1.10 = 72,600 psi

b. Concrete.

$f'_{dc} = f'_c \times DIF$

f'_{dc} = 4,000 x 1.12 = 4,480 psi

Step 4. Use an 18" x 18" column section with 12 No. 7 reinforcing bars (see fig. 4A-17).

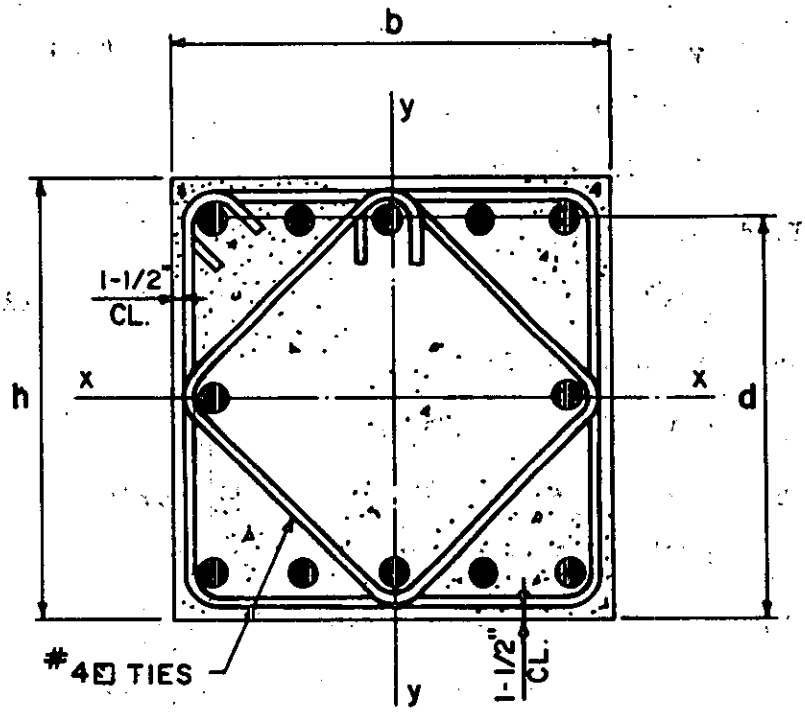


Figure 4A-17

Step 5. Radius of gyration for rectangular section is equal to 0.3 of depth.

$r_x = r_y = 0.3 \times 18 = 5.4$ in

From section 4-46:

$k = 0.9$

$$\frac{kl}{r} = \frac{0.9 \times 120}{5.4} = 20 < 22 \qquad \text{(eq. 4-168)}$$

Therefore slenderness effects may be neglected.

Step 6. Minimum eccentricity in both directions,

$e_{min} = 0.1 \times 18 = 1.8$ in

$e_x = M_x/P = 3,535,200/589,200 = 6$ in > 1.8 in O.K.

$e_y = M_y/P = 0/589,200 = 0 < 1.8$, use 1.8 in.

Step 7. Balanced eccentricity:

a. From figure 4A-17,

$d_x = d_y = 18 - 1.5 - 0.5 - 0.875/2 = 15.56$ in

$A_{sx} = 4 \times 0.6 = 2.40$ in^2

$A_{sy} = 2 \times 0.6 = 1.20$ in^2

b. Find value of m,

$m = f_{dy}/(0.85\ f'_{dc}) = 72,600/(0.85 \times 4,480) = 19.06$

c. Using equation 4-156,

$e_b = 0.20\ h + 1.54_s\ A\ m/b$

$e_{bx} = 0.20 \times 18 + (1.54 \times 2.40 \times 19.06)/18$

$= 7.51$ in > 6 in, compression controls

$e_{by} = 0.20 \times 18 + (1.54 \times 1.2 \times 19.06)/18$

$= 5.56$ in > 1.8 in, compression controls

Step 8. Axial load from equation 4-160:

$$P_u = \frac{A_s\ f_{dy}}{e/(2d - h) + 0.5} + \frac{bhf'_{dc}}{3he/d^2 + 1.18}$$

a. When only eccentricity e_x is present:

$$P_x = \frac{2.4 \times 72,600}{6/(2 \times 15.56 - 18) + 0.5} + \frac{18 \times 18\ 4,480}{3 \times 18\ 6/(15.56)^2 + 1.18}$$

$= 758,417$ lbs

b. When only eccentricity e_y is present:

$$P_y = \frac{1.2 \times 72{,}600}{1.8/(2 \times 15.56 - 18) + 0.5} + \frac{18 \times 18 \times 4{,}480}{3 \times 18 \times 1.8/(15.56)^2 + 1.18} = 1{,}054{,}557 \text{ lbs}$$

Step 9. Compute pure axial load capacity from equation 4-154.

$$P_o = 0.85 f'_{dc} (A_g - A_{st}) + A_{st} f_{dy}$$

$$A_g = 18 \times 18 = 324 \text{ in}^2$$

$$A_{st} = 12 \times 0.6 = 7.2 \text{ in}^2$$

$$P_o = 0.85 \times 4480 (324 - 7.2) + 7.2 \times 72{,}600$$

$$= 1{,}729{,}094 \text{ lbs}$$

Step 10. Ultimate capacity of the column from equation 4-176:

$$\frac{1}{P_u} = \frac{1}{P_x} + \frac{1}{P_y} - \frac{1}{P_o}$$

$$\frac{1}{P_u} = \frac{1}{758{,}417} + \frac{1}{1{,}054{,}557} - \frac{1}{1{,}729{,}094} = \frac{1}{592{,}254} \text{ 1/lbs}$$

$P_u = 592{,}254$ lbs > 589,200 O.K.

Step 11. Provide ties, according to section 4-48.4.

For #7 longitudinal bars, use #3 ties.

$s \leq 16\phi$ (longitudinal bars) = 16 x 0.875 = 14 in

and:

$s \leq 48\phi$ (ties) = 48 x 0.375 = 18 in

and:

$s \leq h/2$ = 9 in

Use two (2) #3 ties at 9 inches arranged as shown in figure 4A-17.

Problem 4A-9, Brittle Mode, Post-Failure Fragments

Problem: Design an element, which responds to blast impulse, for controlled post-failure fragments.

Procedure:

Step 1. Establish design parameters:

a. Impulse load and duration (Chapter 2).

b. Maximum average velocity of post-failure fragments v_f as required by receiver sensitivity.

c. Geometry of element.

d. Support conditions.

e. Materials to be used and corresponding static design strengths.

f. Dynamic increase factors (table 4-1).

Step 2. Determine dynamic yield strength and ultimate strength of reinforcement from equation 4-3.

Step 3. Determine the dynamic design stress for the flexural reinforcement according to the deflection range (support rotation) from table 4-2.

Step 4. Substitute known quantities of i_b (step 1a), f_{ds} (step 3), H (step 1c), and v_f (step 1b) into equation 4-194.

Step 5. Obtain optimum ratio of vertical to horizontal reinforcement p_v/p_H for a given wall thickness T_c:

a. Assume a value of d_c and substitute it into the equation obtained in step 4.

b. Read optimum: p_v/p_H ratio from figure 4-38.

Note:
For one-way elements, the ratio of the main to secondary reinforcement is always 4 to 1 unless minimum conditions govern (table 43). Obtain C_u from table 4-11 for the given support condition. C_f is always equal to 22,500 (Sect. 4-58)

Step 6. For the optimum p_V/p_H ratio, determine C_u (from figure 4-33, 4-34 or 4-35) and C_f (from figure 4-73, 4-74 or 4-75). Calculate p_v and p_H. Select bar sizes and spacings necessary to furnish the required reinforcement ratios.

Step 7. Determine the required lacing and diagonal bars. (Procedure is exactly the same as that for elements designed for the ductile mode for incipient failure or less. See problem 4A-3.)

Step 8. Determine the required T_c for the assumed d_c selected flexural and lacing bar sizes and required concrete cover. Adjust T_c to the nearest whole inch and calculate the actual d_c.

Step 9. Check flexural capacity of the element based on either blast impulse of post-failure fragment velocity. Generally, lacing bar sizes do not have to be checked since they are not usually affected by a small change in d_c.

a. Compute the actual impulse capacity of the element using equation 4-194 and compare with the anticipated blast load. Repeat design (from step 5 on) if the capacity is less than that required.

b. Compute the actual post-failure fragment velocity using equation 4-194 and compare with the value permitted by the acceptor sensitivity. Repeat design (from step 5 on) if the actual velocity is greater than that permitted.

Step 10. Determine whether the correct design procedure has been utilized by first computing the response time of the element t_u (time to reach ultimate deflection) from equation 4-192 or 4-193. Then compare the response time t_u with the duration of the blast load t_o. For elements that respond to impulse loading $t_u/t_o > 3$.

Note:
To obtain the most economical design, repeat steps 5 through 10 for several wall thicknesses and compare their costs. Percentages of reinforcement can be used to reduce the amount of calculations. In determining the required quantities of reinforcement, the length of the lap splice should be considered.

Example 4A-9, Brittle Mode, Post-Failure Fragments

Required: Design the back wall of an interior cell (fig. 4A-18) of a multicubicle structure for controlled post-failure fragments.

Solution:

Step 1. Given:

a. i_b = 4800 psi-ms, and t_o = 1.0 ms.

b. v_f = 100 fps = 1.2 in/ms.

c. L = 360 in., H = 120 in.

d. Fixed on three edges and one edge free.

e. Reinforcing bars; f_y = 66,000 psi and f_u = 90,000 psi

Concrete, f'_c = 4,000 psi

f. For reinforcement, DIF = 1.23 for yield stress

DIF = 1.05 for ultimate stress.

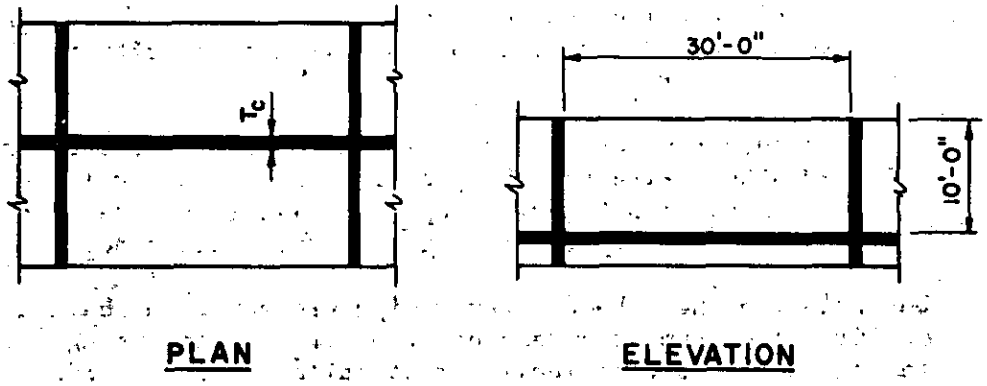


Figure 4A-18

Step 2. Dynamic strength of materials.

f_{dy} = DIF f_y = 1.23 X 66,000 = 81,180 psi

f_{du} = DIF f_u = 1.05 X 90,000 = 94,500 psi

Step 3. Dynamic design stress from table 4-2.

$$f_{ds} = \frac{f_{dy} + f_{du}}{2} = \frac{81,180 + 94,500}{2} = 87,840 \text{ psi}$$

Step 4. Substitute known quantities into equation 4-194.

$$i_b^2 = C_u \left[\frac{p_H d_c^3 f_{ds}}{H} \right] + C_f d_c^2 v_f^2$$

$$4800^2 = \frac{C_u p_H d_c^3 (87,840)}{120} + C_f d_c^2 (1.2)^2$$

$$23.04 \times 10^6 = 732 \; C_u p_H d_c^3 + 1.44 \; C_f d_c^2$$

Step 5. Optimum reinforcement ratio.

a. Assume $d_c = 21$ in. and substitute into equation 4-194.

$$23.04 \times 10^6 = 732 \; C_u p_H (21)^3 + 1.44 \; C_f (21)^2$$

Therefore:

$$p_H = \frac{23.04 \times 10^6 - 635 \; C_f}{6.78 \times 10^6 \; C_u}$$

b. Read optimum p_V/p_H value from figure 4-38 for $L/H = 3$.

$$p_V/p_H = 1.58$$

Step 6. For optimum $p_V/p_H = 1.58$

From figure 4-34, $C_u = 477$

From figure 4-74, $C_f = 1.583 \times 10^4$

$$p_H = \frac{[23.04 \times 10^6 - 635 \; (1.583 \times 10^4)]}{(6.78 \times 10^6)(477)} = 0.00402$$

$$p_V = 1.58 \; p_H = 1.58 \; (0.00402) = 0.00635$$

$$A_{sH} = 0.00402 \; (12) \; (21) = 1.013 \; in^2/ft.,$$

use #8 @ 9 in. (A_s = 1.05 in^2)

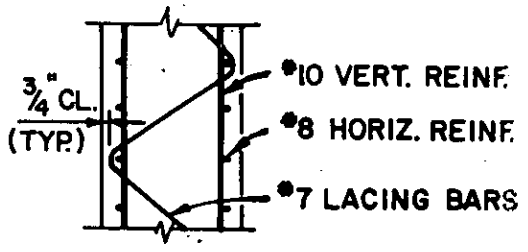
A_{sV} = 0.00635 (12) (21) = 1.60 $in^2/ft.$,

use #10 @ 9 in. (A_s = 1.69 in^2)

$$\text{Actual } \frac{P_V}{P_H} = \frac{A_{sV}}{A_{sH}} = \frac{1.69}{1.05} = 1.610$$

Step 7. Using lacing method No. 3, No. 7 vertical lacing bars are required. (Calculations are not shown since they are similar to those presented in example 4A-3 for incipient failure design. Also, the remainder of the design for shear will not be shown.)

Step 8. The actual d_c depends upon the details of the base of the wall (region of vertical lacing).



cover	= 2 X 0.75	= 1.50
lacing	= 2 X 0.875	= 1.75
horizontal bars	= 2 X 1.00	= 2.00
vertical bars	= 1.27	= 1.27
		6.52 in.

Figure 4A-19

$T_c = d_c + 6.52 = 27.52$ in., use 28 in.

actual $d_c = 28 - 6.52 = 21.48$ in.

Step 9. Actual capacity of element.

a. Actual impulse capacity.

For $p_V/p_H = 1.610$, $C_u = 481$

and $C_f = 1.588 \times 10^4$

$d_c = 21.48$ in. $\quad p_H = \dfrac{1.05}{12\ (21.48)} = 0.00407$

$$i_c^2 = C_u \left[\frac{p_H\ d_c^3\ f_{ds}}{H}\right] + C_f\ d_c^2\ v_f^2$$

$$i_c^2 = 481 \left[\frac{(0.00407)\ (21.48)^3\ (87,840)}{120}\right]$$

$$+ (1.588 \times 10^4)\ (21.48)^2\ (1.2)^2$$

$$i_c^2 = 24.75 \times 10^6$$

$i_c = 4,975$ psi-ms $> i_b = 4,800$ psi-ms O.K.

b. Actual post-failure fragment velocity.

$$i_b^2 = C_u \left[\frac{p_H\ d_c^3\ f_{ds}}{H}\right] + C_f\ d_c^2 v_f^2$$

$$4,800^2 = 481 \quad \frac{0.00407\ (21.48)^3\ (87,840)}{120}$$

$$+ (1.588 \times 10^4)\ (21.48)^2\ v_f^2$$

$v_f = 1.10$ in/ms $= 92$ fps $<$ 100 fps O.K.

Step 10. Response time of element t_u:

$M_{VN2} = M_{VP}$ and $M_{HN1} = M_{HN1} = M_{HN3} = M_{HP}$

$$M_{HP} = A_{sH}\, f_{ds}(d_c/b) = \frac{(1.05)\,(87{,}840)\,(21.48)}{12}$$

$$= 165{,}095 \text{ in-lbs/in}$$

$$M_{VP} = A_{sV}\, f_{ds}\, d_c/b = \frac{(1.69)\,(87{,}840)\,(21.48)}{12}$$

$$= 265{,}725 \text{ in-lbs/in}$$

$x_2/x_1 = 1.0$ (symmetrical yield lines)

$$\frac{L}{H}\left[\frac{M_{VP}}{M_{HN1} + M_{HP}}\right]^{\frac{1}{2}} = \frac{360}{120}\left[\frac{26{,}725}{2 \text{ X } 165{,}095}\right]^{\frac{1}{2}} = 2.69$$

$$\frac{M_{VP}}{M_{VN2}} = \frac{265{,}725}{265{,}725} = 1.0$$

From figure 3-11,

$x_1/L = 0.358$

$x_1 = x_2 = 0.358\ (360) = 128.88$

$$r_u = \frac{5(M_{HN1} + M_{HP})}{x_1^2} \quad \text{for } x_1 < L/2 \qquad \text{(table 3-2)}$$

$$r_u = \frac{5\ (2 \text{ X } 165{,}095)}{120^2} = 99.4 \text{ psi}$$

$m = 225 d_c = 225\ (21.48) = 4833\ psi\text{-}ms^2/in$

$(K_{LM})_u = 0.557$ (fig. 3-44)

$m_u = 0.557\ (4833) = 2692\ psi\text{-}ms^2/in$

$x_1 = 128.88 > H = 120$

∴ Vertical supports fail first and the post-ultimate range resistance is:

$$r_{up} = \frac{8\ (M_{HN1} + M_{HP})}{L^2} = \frac{8\ (2 \times 165{,}095)}{360^2} = 20.4\ psi$$

$m_{up} = 0.66 \times 4833 = 3{,}190\ psi\text{-}ms^2/in$

$X_1 = H \tan\theta_{max} = 12 \times \tan 12° = 25.51\ in.$ (table 3-6)

Use equation 4-192 for t_u.

$$t_u = \frac{i_b}{m_u} + \left[\frac{m_{up}}{m_{up}\, r_{up}} - \frac{1}{r_u}\right]\left[i_b^2 - 2 m_u r_u X_1\right]^{\frac{1}{2}} - \left[\frac{m_u}{r_{up}}\right] V_f$$

$$t_u = \frac{4{,}800}{2{,}692} + \left[\frac{3190}{2692 \times 20.4} - \frac{1}{99.4}\right]\left[4800^2 - 2 \times 2692 \times 99.4 \times 25.51\right]^{\frac{1}{2}}$$

$$\left(\frac{2692}{20.4}\right) 1.1 = 3.78\ ms$$

$\frac{t_u}{t_o} = 3.78 / 1.0 = 3.78 > 3$ ∴ correct procedure has been used

Problem 4A-10, Maximum Fragment Penetration

Problem: Determine the maximum penetration of a primary metal fragment into a concrete wall and determine if perforation occurs.

Procedure:

Step 1. Establish design parameters:

a. Type of fragment

b. Weight W_f and diameter d of fragment

c. Fragment striking velocity v_s

d. Thickness T_c and the ultimate compressive strength f'_c of concrete wall

Step 2. Determine the maximum penetration X_f from figure 4-78 (or equation 4-200 or 4-201) for the values of W_f and v_s in step 1. X_f is the maximum penetration of an armor-piercing steel fragment into 4,000 psi concrete.

Step 3. To determine the depth of penetration into concrete with ultimate strength other than 4,000 psi, use X_f from step 2, the concrete strength from step 1d and equation 4-202:

$$X'_f = X_f \, (4000/f'_c)^{1/2}$$

Step 4. To obtain the maximum penetration into concrete by metal fragments other than those of armor-piercing fragments use the penetration from step 3, the penetrability coefficient k from table 4-16 and equation 4-203.

$$X'_f = k \, X_f$$

Step 5. Calculate the limiting thickness of concrete at which perforation will occur from equation 4-204.

$$T_{pf} = 1.13 \, X \, d^{0.1} + 1.311 \, d$$

Where applicable, replace X_f with X'_f from step 3 or 4. If T_{pf} is less than T_c embedment will occur; if T_{pf} is greater than T_c the fragment will perforate the wall.

Example 4A-10, Maximum Fragment Penetration

Required: Maximum penetration of a primary fragment into a concrete wall; determine if perforation occurs.

Solution:

Step 1. Given:

a. Type of fragment: mild steel

b. Primary fragment weight: W_f = 30 ounces

Primary fragment diameter: d = 2.15 inches

c. Striking velocity: v_s = 3,500 fps

d. Thickness of wall: T_c = 18 inches

Ultimate concrete compressive strength: f'_c = 4,000 psi

Step 2. Maximum penetration:

For:

$$W_f = 30 \text{ oz and } v_s = 3{,}500 \text{ fps}$$

$$X_f = 14.5 \text{ inches from figure 4-78}$$

or from equation 4-199

$$X_f = 2.04 \times 10^{-6} \, d^{1.2} \, v_s^{1.8} + d \geq 2 \, d$$

$$= 2.04 \times 10^{-6} \, (2.15)^{1.2} \, (3500)^{1.8} + 2.15$$

$$= 14.4 \text{ inches}$$

$$X_f \geq 2 \, d = 2 \times 2.15 = 4.30 \quad \text{O.K.}$$

Step 3. Concrete strength adjustment (eq. 4-202)

$$X'_f = X_f \, (4000/f'_c)^{1/2}$$

$$= 14.5 \times 1 = 14.5 \text{ in.}$$

Step 4. Fragment material adjustment:

a. $k = 0.70$ (table 4-16)

b. $X'_f = kX_f$ (eq. 4-203)

$$= 0.7 \times 14.5 = 10.15 \text{ in}$$

Step 5. Calculate minimum thickness to prevent perforation.

$$T_{pf} = 1.13 \, X'_f \, d^{0.1} + 1.311 \, d \quad \text{(eq. 4-204)}$$

$$= 1.13 \, (10.15) \, (2.15)^{0.1} + 1.311 \, (2.15)$$

$T_{pf} = 15.20$ inches ≤ 18 in

Since T_{pf} is less than T_c the fragment does not perforate the slab.

Problem 4A-11, Determination of the Occurrence and Effects of Perforation

Problem: Determine the residual velocity of a primary fragment if it perforates a concrete wall.

Procedure:

Step 1. Determine the type, weight W_f, and striking velocity v_s of the primary fragment. Also, the thickness of the concrete wall T_c and the ultimate compressive stress f'_c of the concrete must be known.

Step 2. Proceed through steps 2, 3, 4, and 5 of Problem 4A-10. If T_{pf} is greater than T_c, perforation will occur.

Step 3. If perforation is not indicated by the calculations in step 2 then discontinue the analysis. If perforation does result, then compute the value of T_c/T_{pf}.

Step 4. Utilizing the value of T_c/T_{pf}, obtain v_r/v_s from figure 4-79 or 4-80.

Step 5. With the values of v_s and v_r/v_s of Steps 1 and 4, calculate the residual velocity v_r.

Example 4A-11, Determination of the Occurrence and Effects of Perforation

Required: Residual velocity of a primary fragment if it perforates a concrete wall.

Solution:

Step 1. Given:

a. Type of metal: mild steel

b. Primary fragment weight: W_f = 20 ounces

c. Primary fragment diameter: d = 1.89 inches

d. Striking velocity: v_s = 4,700 fps

e. Thickness of wall: T_c = 12 inches

f. Ultimate concrete compressive stress: f'_c = 4,500 psi

Step 2. For given conditions:

$$X_f = 19.75 \text{ inches} \qquad \text{(fig. 4-78)}$$

Actual maximum penetration:

$$X'_f = 19.75\ (4000/4500)^{1/2} \qquad \text{(eq. 4-202)}$$

$$= 18.6 \text{ inches}$$

$$k = 0.70 \qquad \text{(table 4-16)}$$

$$X'_f = 0.7\ (18.6) = 13.0 \text{ inches} \qquad \text{(eq. 4-203)}$$

Since T_{pf} is greater than X'_f, and X'_f (13.0 inches) already exceeds the wall thickness (12 inches), perforation will occur. It is necessary to determine T_{pf} (eq. 4-204) in order to calculate the residual fragment velocity. Hence:

$$T_{pf} = 1.13\ (13.0)\ (1.89)^{0.1} + 1.311\ (1.89)$$

$$= 15.6 + 2.5 = 18.1 \text{ inches}$$

Step 3. $T_c/T_{pf} = 12.0/18.1 = 0.663$

Step 4. Since the given conditions correspond to a case where:

$$X_f > 2d,$$

determine:

$$v_r/v_s$$

for: $T_c/T_{pf} = 0.663$ from figure 4-80.

Obtain:

$$v_r/v_s = 0.55$$

Step 5. $v_r = 0.55\ v_s$

$$= 0.55\ (4,700) = 2,585 \text{ fps}$$

Problem 4A-12, Determination of the Occurrence of Spalling

Problem: To determine if spalling of a concrete wall occurs if there is no perforation by the primary fragment.

Procedure:

Step 1. Determine the type, weight W_f and striking velocity v_s of the primary fragment. Also, the thickness of the concrete wall and the ultimate compressive stress of the concrete f'_c must be known.

Step 2. Proceed through Steps 2, 3, 4, and 5 of Problem 4A-10.

Step 3. If embedment of the fragment occurs, compute the limiting concrete thickness at which spalling will occur according to:

$$T_{sp} = 1.215\ X_f\ d^{0.1} + 2.12\ d \qquad \text{(eq. 4-207)}$$

If T_{sp} is greater than T_c, spalling will occur.

Example 4A-12, Determination of the Occurrence of Spalling

Required: Determine if spalling of a concrete wall occurs due to penetration by a primary fragment.

Solution:

Step 1. Given:

a. Type of metal: armor-piercing steel

b. Primary fragment weight: $W_f = 40$ ounces

c. Primary fragment diameter: 2.38 inches

d. Striking velocity: $v_s = 3{,}000$ fps

e. Thickness of wall: $T_c = 19$ inches

f. Ultimate concrete compressive stress: $f'_c = 5{,}000$ psi

Step 2. For given conditions:

$X_f = 12.8$ inches (fig. 4-78)

$X'_f = 12.8\ (4000/5000)^2$ (eq. 4-202)

$= 11.5$ in.

$k = 1.00$ (table 4-16)

$X'_f = X_f$

Then:

$T_{pf} = 1.13\ (11.5)\ (2.38)^{0.1}$ (eq. 4-204)

$+ 1.311\ (2.38)$

$= 14.2 + 3.1 = 17.3$ inches

Since T_c is greater than 17.3 inches, embedment occurs.

Step 3. Determine minimum concrete thickness to prevent spalling from equation 4-207:

$$T_{sp} = 1.215\ (11.5)\ (2.38)^{0.1} + 2.12\ (2.38)$$

$$= 20.3 \text{ inches}$$

Since T_{sp} is greater than 19 inches, spalling will occur.

Problem 4A-13. Determination of the Effects of a Primary Fragment on a Composite Wall

Problem: Determine the maximum penetration by a primary fragment into a composite wall and the resulting effects on the donor panel, sand layer and acceptor panel.

Procedure:

Step 1. Determine the type, weight W_f, and striking velocity v_s of the primary fragment. Also, the thicknesses of the concrete donor panel T_c (donor), the sand layer T_s, and the concrete receiver panel T_c (acceptor) and the ultimate compressive stress f'_c of the concrete must be known.

Step 2. Proceed through Steps 2, 3, 4, and 5 of Problem 4A-10.

If embedment of the fragment in the donor panel occurs, perform Step 3 of Problem 4A-12 to determine if spalling takes place.

If perforation of the donor panel occurs, compute:

$$T_c \text{ (donor)} / T_{pf}$$

and perform Steps 4 and 5 of Problem 4A-11 to find the residual velocity v_r.

Step 3. Utilizing v_r (donor) as the v_s of the sand layer and W_f, obtain X_s from figure 4-81.

If X_s is less than T_s, the fragment is embedded in the sand layer and the analysis is discontinued.

If X_s is greater than T_s, perforation of the sand occurs.

Step 4. Compute T_s/X_s if perforation results. Use this value and figure

4-80 to obtain v_r/v_s of the sand layer.

Calculate v_r(sand).

Step 5. Utilizing v_r(sand) as the v_s of the acceptor wall and W_f, obtain X_f (acceptor) from figure 4-78.

Proceed through Steps 3 and 4 of Problem 4A-10, if necessary.

If embedment of the fragment in the acceptor panel occurs, perform Step 3 of Problem 4A-12 to determine if spalling takes place.

If perforation of the acceptor wall occurs, compute T_c (acceptor) and perform Steps 4 and 5 of Problem 4A-11 to find v_r.

Example 4A-13. Determination of the Effects of a Primary Fragment on a Composite Wall

Required: Maximum penetration by a primary fragment into a composite wall and the resulting effects on the donor panel, sand layer and the acceptor panel.

Solution:

Step 1. Given:

a. Type of metal: armor-piercing steel

b. Primary fragment weight: W_f = 20 ounces

c. Primary fragment diameter: d = 1.89 inches

d. Striking velocity: v_s = 4,200 fps

e. Thicknesses:

T_c (donor) = 12 inches

T_s = 24 inches

T_c (acceptor) = 12 inches

f. Ultimate concrete compressive stress:

f'_c = 5,000 psi

Step 2. For given conditions:

X_f = 16.5 inches (fig. 4-78)

$X'_f = 16.5\ (4000/5000)^2$ (eq. 4-202)

= 14.7 inches

k = 1.00 (table 4-16)

$X'_f = X_f$

Since X'_f is greater than 12 inches, perforation of the donor panel will certainly occur. T_{pf} must be calculated in order to determine the residual velocity of the fragment.

$T_{pf} = 1.13\ (14.7)\ (1.89)^{0.1} + 1.311\ (1.89)$

$= 17.7 + 2.5 = 20.2$ inches

$T_c/T_{pf} = 12/20.2 = 0.594$

Since X_{pf} is greater than 2d, $v_r/v_s = 0.61$ from figure 4-80.

v_r (donor) = 0.61 (4,200) = 2,562 fps

Step 3. For:

v_s (sand) = 2,562 fps, (fig. 4-81)

X_s = 64.0 inches

Since T_s is less than 64.0 inches, perforation of the sand layer will occur.

Step 4. $T_s/X_s = 24/64.0 = 0.375$

from figure 4-80

$v_r/v_s = 0.77$

Step 5. v_r (sand) = 0.77 v_s

$v_r = 0.77\ (2,562) = 1,970$ fps

Step 6. For:

v_s (acceptor) = 1,970 fps

X_f (acceptor) = 5.6 inches (fig. 4-78)

$X'_f = 5.6\ (4000/5000)^{1/2}$ (eq. 4-202)

$= 5.0$ inches

$k = 1.00$ (table 4-16)

$X'_f = X_f$

$T_{pf} = 1.13\ (5.0)\ (1.89)^{0.1}$ (eq. 4-204)

$+ 1.311\ (1.89)$

$= 6.0 + 2.5 = 8.5$ inches

Since T_{pf} is less than T_c (acceptor), the fragment is embedded in the receiver panel. Calculate T_{sp} to determine if spalling occurs:

$T_{sp} = 1.215\ (5.0)\ (1.89)^{0.1}$ (eq. 4-207)

$+ 2.12\ (1.89)$

$= 6.5 + 4.0 = 10.5$ inches

Since T_{sp} is less than T_c (acceptor), spalling will not occur.

APPENDIX 4B

LIST OF SYMBOLS

a (1) acceleration (in./ms^2)
(2) depth of equivalent rectangular stress block (in.)
(3) long span of a panel (in.)

a_o velocity of sold in air (ft./sec.)

a_x acceleration in x direction (in./ms^2)

a_y acceleration in y direction (in./ms^2)

A (1) area (in.^{2})
(2) explosive composition factor (oz.$^{1/2}$in.$^{-3/2}$)

A_a area of diagonal bars at the support within a width b (in.^{2})

A_b area of reinforcing bar (in.^{2})

A_d (1) door area (in.^{2})
(2) area of diagonal bars at the support within a width b (in.^{2})

A_D drag area (in.^{2})

A_f net area of wall excluding openings (ft.^{2})

A_g area of gross section (in.^{2})

A_H maximum horizontal acceleration of the ground surface (g's)

A_l area of longitudinal torsion reinforcement (in.^{2})

A_L lift area (in.^{2})

A_n (1) net area of section (in.^{2})
(2) area of individual wall subdivision (ft.^{2})

A_o area of openings (ft.^{2})

A_{ps} area of prestressed reinforcement (in.^{2})

A_s area of tension reinforcement within a width b (in.^{2})

A'_s area of compression reinforcement within a width b (in.^{2})

A_s^- area of rebound reinforcement (in.^{2})

A_{sH} area of flexural reinforcement within a width b in the horizontal direction on each face (in.^{2})*

A_{sp} area of spiral reinforcement (in.^{2})

* See note at end of symbols

A_{st} total area of reinforcing steel (in.^{2})

A_{sV} area of flexural reinforcement within a width b in the vertical direction on each face (in.^{2})*

A_t area of one leg of a closed tie resisting torsion within a distance s (in.^{2})

A_v total area of stirrups or lacing reinforcement in tension within a distance, s_s or s_l and a width b_s or b_l (in.^{2})

A_V maximum vertical acceleration of the ground surface (g's)

A_w area of wall (ft.^{2})

A_I, A_{II} area of sector I and II, respectively (in.^{2})

b (1) width of compression face of flexural member (in.)
(2) width of concrete strip in which the direct shear stresses at the supports are resisted by diagonal bars (in.)
(3) short span of a panel (in.)

b_f width of fragment (in.)

b_s width of concrete strip in which the diagonal tension stresses are resisted by stirrups of area A_v (in.)

b_l width of concrete strip in which the diagonal tension stresses are resisted by lacing of area A_v (in.)

b_o failure perimeter for punching shear (in.)

b_t center-to-center dimension of a closed rectangular tie along b (in.)

B explosive constant defined in table 2-7 (oz.$^{1/2}$in.$^{7/6}$)

c (1) distance from the resultant applied load to the axis of rotation (in.)
(2) damping coefficient
(3) width of column capital (in.)

c_I, c_{II} distance from the resultant applied load to the axis of rotation for sectors I and II, respectively (in.)

c_s dilatational velocity of concrete (ft./sec.)

C (1) shear coefficient
(2) deflection coefficient for flat slabs

C_C deflection coefficient for the center of interior panel of flat slab

* See note at end of symbols

C_{cr} critical damping

C_d shear coefficient for ultimate shear stress of one-way elements

C_D drag coefficient

C_{Dq} drag pressure (psi)

C_{Dq_o} peak drag pressure (psi)

C_E equivalent load factor

C_f post-failure fragment coefficient ($lb.^2\ ms^4/in.^8$)

C_H shear coefficient for ultimate shear stress in horizontal direction for two-way elements*

C_L (1) leakage pressure coefficient from figure 2-235
(2) deflection coefficient for midpoint of long side of interior flat slab panel
(3) lift coefficient

C_M maximum shear coefficient

C_m equivalent moment correction factor

C_p compression wave seismic velocity in the soil from Table 2-10 (in./sec.)

C_r sound velocity in reflected region from figure 2-192 (ft./ms)

C_R force coefficient for shear at the corners of a window frame

$C_{r\alpha}$ Peak reflected pressure coefficient at angle of incidence α

C_s shear coefficient for ultimate support shear for one-way elements

C_{sH} shear coefficient for ultimate support shear in horizontal direction for two-way elements*

C_{sV} shear coefficient for ultimate support shear in vertical direction for two-way elements*

C_S deflection coefficient for midpoint of short side of interior flat slab panel

C_u impulse coefficient at deflection X_u ($psi\text{-}ms^2/in.^2$)

C'_u impulse coefficient at deflection X_m ($psi\text{-}ms^2/in.^2$)

C_v shear coefficient for ultimate shear stress in vertical direction for two-way elements*

* See note at end of symbols

C_x shear coefficient for the ultimate shear along the long side of window frame

C_y shear coefficient for the ultimate shear along the short side of window frame

C_L confidence level

C_1 (1) impulse coefficient at deflection X_1 (psi-ms^2/in.^{2})
(2) ratio of gas load to shock load

C'_1 impulse coefficient at deflection X_m (psi-ms^2/in.^{2})

C_2 ratio of gas load duration to shock load duration

d (1) distance from extreme compression fiber to centroid of tension reinforcement (in.)
(2) diameter (in.)
(3) fragment diameter (in.)

d' distance from extreme compression fiber to centroid of compression reinforcement (in.)

d_b diameter of reinforcing bar (in.)

d_c distance between the centroids of the compression and tension reinforcement (in.)

d_{cH} distance between the centroids of the horizontal compression and tension reinforcement (in.)

d_{co} diameter of steel core (in.)

d_{cV} distance between the centroids of the vertical compression and tension reinforcement (in.)

d_e distance from support and equal to distance d or d_c (in.)

d_i average inside diameter of explosive casing (in.)

d'_i adjusted inside diameter of casing (in.)

d_l distance between center lines of adjacent lacing bends measured normal to flexural reinforcement (in.)

d_p distance from extreme compression fiber to centroid of prestressed reinforcement (in.)

d_{sp} depth of spalled concrete (in.)

d_1 diameter of cylindrical portion of primary fragment (in.)

D (1) unit flexural rigidity (lb-in.)
(2) location of shock front for maximum stress (ft.)
(3) minimum magazine separation distance (ft.)
(4) caliber density ($lb/in.^3$)
(5) overall diameter of circular section (in.)
(6) damping force (lb.)
(7) displacement of mass from shock load (in.)

D_E equivalent loaded width of structure for non-planar wave front (ft.)

D_H maximum horizontal displacement of the ground surface (in.)

DIF dynamic increase factor

D_s diameter of the circle through centers of reinforcement arranged in a circular pattern (in.)

D_{sp} diameter of the spiral measured through the centerline of the spiral bar (in.)

DLF dynamic load factor

D_V maximum vertical displacement of the ground surface (in.)

e (1) base of natural logarithms and equal to 2.71828...
(2) distance from centroid of section to centroid of pre-stressed reinforcement (in.)
(3) actual eccentricity of load (in.)

e_b balanced eccentricity (in.)

$(2E')^{1/2}$ Gurney Energy Constant (ft./sec.)

E (1) modulus of elasticity
(2) internal work (in.-lbs.)

E_c modulus of elasticity of concrete (psi)

E_m modulus of elasticity of masonry units (psi)

E_s modulus of elasticity of reinforcement (psi)

f (1) unit external force (psi)
(2) frequency of vibration (cps)

f'_c static ultimate compressive strength of concrete at 28 days (psi)

f'_{dc} dynamic ultimate compressive strength of concrete (psi)

f'_{dm} dynamic ultimate compressive strength of masonry units (psi)

f_{ds} dynamic design stress for reinforcement (a function of f_y, f_u, and Θ) (psi)

f_{du} dynamic ultimate stress of reinforcement (psi)

f_{dy} dynamic yield stress of reinforcement (psi)

f'_m static ultimate compressive strength of masonry units (psi)

f_n natural frequency of vibration (cps)

f_{ps} average stress in the prestressed reinforcement at ultimate load (psi)

f_{pu} specified tensile strength of prestressing tendon (psi)

f_{py} yield stress of prestressing tendon corresponding to a 1 percent elongation (psi)

f_r reflection factor

f_s static design stress for reinforcement (psi)

f_{se} effective stress in prestressed reinforcement after allowances for all prestress losses (psi)

f_u static ultimate stress of reinforcement (psi)

f_y static yield stress of reinforcement (psi)

F (1) total external force (lbs.)
(2) coefficient for moment of inertia of cracked section
(3) function of C_2 and C_1 for bilinear triangular load

F_o force in the reinforcing bars (lbs.)

F_E equivalent external force (lbs.)

F_D Drag force (lbs.)

F_F frictional force (lbs.)

F_L lift force (lbs.)

F_N vertical load supported by foundation (lbs.)

g acceleration due to gravity (32.2 ft./sec.^{2})

G shear modulus (psi)

h (1) charge location parameter (ft.)
(2) height of masonry wall

h_n average clearing distance for individual areas of openings from Section 2-15.4.2

h_t center-to-center dimension of a closed rectangular tie along h (in.)

h' clear height between floor slab and roof slab

H (1) span height (in.)*
(2) distance between reflecting surface(s) and/or free edge(s) in vertical direction (ft.)
(3) minimum transverse dimension of mean presented area of object (ft.)

H_c height of charge above ground (ft.)

H_s height of structure (ft.)

H_T height of triple point (ft.)

H_w height of wall (ft.)

H^c heat of combustion (ft.-lb./lb.)

H^d heat of detonation (ft.-lb./lb.)

i unit positive impulse (psi-ms)

i_a sum of blast impulse capacity of the receiver panel and the least impulse absorbed by the sand (psi-ms)

i_{ba} blast impulse capacity of receiver panel (psi-ms)

i^- unit negative impulse (psi-ms)

$\bar{i}_a$ sum of scaled unit blast impulse capacity of receiver panel and scaled unit blast impulse attenuated through concrete and sand in a composite element (psi-ms/lb.$^{1/3}$)

i_b unit blast impulse (psi-ms)

$\bar{i}_b$ scaled unit blast impulse (psi-ms/lb.$^{1/3}$)

$\bar{i}_{ba}$ scaled unit blast impulse capacity of receiver panel of composite element (psi-ms/lb.$^{1/3}$)

$\bar{i}_{bd}$ scaled unit blast impulse capacity of donor panel of composite element (psi-ms/lb.$^{1/3}$)

$\bar{i}_{bt}$ total scaled unit blast impulse capacity of composite element (psi-ms/lb.$^{1/3}$)

i_c impulse capacity of an element (psi-ms)

i_d total drag and diffraction impulse (psi-ms)

i_e unit excess blast impulse (psi-ms)

i_{fs} required impulse capacity of fragment shield (psi-ms)

* See note at end of symbols

i_g gas impulse (psi-ms)

i_r unit positive normal reflected impulse (psi-ms)

i_r^- unit negative normal reflected impulse (psi-ms)

$i_{r\alpha}$ peak reflected impulse at angle of incidence α (psi-ms)

i_s unit positive incident impulse (psi-ms)

i_s^- unit negative incident impulse (psi-ms)

i_{st} impulse consumed by fragment support connection (psi-ms)

I (1) moment of inertia ($in.^4$/in. for slabs) ($in.^4$ for beams)
(2) total impulse applied to fragment

I_a average of gross and cracked moments of inertia ($in.^4$/in. for slabs) ($in.^4$ for beams)

I_c moment of inertia of cracked concrete section ($in.^4$/in. for slabs) ($in.^4$ for beams)

I_{ch} moment of inertia of cracked concrete section in horizontal direction ($in.^4$/in.)*

I_{cV} moment of inertia of cracked concrete section in vertical direction ($in.^4$/in.)*

I_g moment of inertia of gross concrete section ($in.^4$/in. for slabs) ($in.^4$ for beams)

I_m mass moment of inertia (lb.-ms^2-in.)

I_n moment of inertia of net section of masonry unit ($in.^4$)

I_s gross moment of inertia of slab ($in.^4$/in.)

I_{st} impulse consumed by the fragment support connection (psi-ms)

I_w gross moment of inertia of wall ($in.^4$/in.)

j ratio of distance between centroids of compression and tension forces to the depth d

k (1) constant depending on the casing metal
(2) effective length factor

k_v velocity decay coefficient

K (1) unit stiffness (psi/in. for slabs) (lb./in./in. for beams) (lb./in. for springs)
(2) constant defined in paragraph 2-18.2

* See note at end of symbols

K_e elastic unit stiffness (psi/in. for slabs) (lb./in./in. for beams)

K_{ep} elasto-plastic unit stiffness (psi/in. for slabs) (lb./in./in. for beams)

K_E (1) equivalent elastic unit stiffness (psi/in. for slabs) (lb./in./in. for beams)
(2) equivalent spring constant (lb./in.)

K_L load factor

K_{LM} load-mass factor

$(K_{LM})_u$ load-mass factor in the ultimate range

$(K_{LM})_{up}$ load-mass factor in the post-ultimate range

K_M mass factor

K_R resistance factor

KE kinetic energy

l charge location parameter (ft.)
(1) length of the yield line (in.)
(2) width of ½ of the column strip (in.)

l_d basic development length of reinforcing bar (in.)

l_{dh} development length of hooked bar (in.)

l_c length of cylindrical explosive (in.)

l_p spacing of same type of lacing bar (in.)

l_s span of flat slab panel (in.)

L (1) span length (in.)*
(2) distance between reflecting surface(s) and/or free edge(s) in horizontal direction (ft.)

L_{cyl} length of cylinder (in.)

L_f length of fragment (in.)

L_H clear span in short direction (in.)

L_l length of lacing bar required in distance s_l (in.)

L_L clear span in long direction (in.)

L_o embedment length of reinforcing bars (in.)

* See note at end of symbols

L_s length of shaft (in.)

L_u unsupported length of column (in.)

L_w wave length of positive pressure phase (ft.)

L_w^- wave length of negative pressure phase (ft.)

L_x clear span in long direction (in.)

L_y clear span in short direction (in.)

L_{wb}, L_{wd} wave length of positive pressure phase at points b and d, respectively (ft.)

L_1 total length of sector of element normal to axis of rotation (in.)

m (1) unit mass (psi-ms^2/in. for slabs) [beams, (lb./in-ms^2)/in.]
(2) ultimate unit moment (in.-lbs./in.)
(3) mass of fragment (lbs.-ms^2/in.)

m_a average of the effective elastic and plastic unit masses (psi-ms^2/in. for slabs) [beams, (lb./in-ms^2)/in]

m_e effective unit mass (psi-ms^2/in. for slabs) [beams, (lb/in-ms^2)/in]

m_{sp} mass of spalled fragments (psi-ms^2/in.)

m_u effective unit mass in the ultimate range (psi-ms^2/in. for slabs) [beams, (lb/in-ms^2]/in.]

m_{up} effective unit mass in the post-ultimate range (psi-ms^2/in.)

M (1) unit bending moment (in.-lbs./in. for slabs) (in.-lbs. for beams)
(2) total mass (lb.-ms^2/in.)
(3) design moment (in.-lbs.)

M_e effective total mass (lb.-ms^2/in.)

M_u ultimate unit resisting moment (in.-lbs./in.^{2} for slabs) (in.-lbs. for beams)

M_u^- ultimate unit rebound moment (in.-lbs./in. for slabs) (in.-lbs. for beams)

M_c moment of concentrated loads about line of rotation of sector (in.-lbs.)

M_A fragment distribution factor

M_E equivalent total mass (lb.-ms^2/in.)

M_{HN} ultimate unit negative moment capacity in horizontal direction (in.-lbs./in.)*

M_{HP} ultimate unit positive moment capacity in horizontal direction (in.-lbs./in.)*

M_{OH}, M_{OL} total panel moment for direction H and L respectively (in.-lbs.)

M_N ultimate unit negative moment capacity at supports (in.-lbs./in. for slabs) (in.-lbs. for beams)

M_P ultimate unit positive moment capacity at midspan (in.-lbs./in. for slabs) (in.-lbs. for beams)

M_{VN} ultimate unit negative moment capacity in vertical direction (in.-lbs./in.)*

M_{VP} ultimate unit positive moment capacity in vertical direction (in.-lbs./in.)*

M_1 value of smaller end moment on column

M_2 value of larger end moment on column

n (1) modular ratio
(2) number of time intervals
(3) number of glass pane tests
(4) caliber radius of the tangent ogive of fragment nose

N (1) number of adjacent reflecting surfaces
(2) nose shape factor

N_f number of primary fragments larger than W_f

N_u axial load normal to the cross section

N_T total number of fragments

p reinforcement ratio equal to A_s/bd or A_s/bd_c

p' reinforceaent ratio equal to A'_s/ bd or A'_s/ bd_c

p_b reinforcement ratio producing balanced conditions at ultimate strength

p_o ambient atmospheric pressure (psi)

p_p prestressed reinforcement ratio equal to A_{ps}/bd_p

p_m mean pressure in a partially vented chamber (psi)

p_{mo} peak mean pressure in a partially vented chamber (psi)

* See note at end of symbols

p_r average peak reflected pressure (psi)

p_H reinforcement ratio in horizontal direction on each face*

p_T total reinforcement ratio equal to $p_H + p_V$

p_V reinforcement ratio in vertical direction on each face*

$p(x)$ distributed load per unit length

P (1) pressure (psi)
(2) concentrated load (lbs.)

P^- negative pressure (psi)

P_c critical axial load causing buckling (lbs.)

P_g maximum gas pressure (psi)

P_i interior pressure within structure (psi)

ΔP_i interior pressure increment (psi)

P_f fictitious peak pressure (psi)

P_{max} maximum average pressure acting on interior face of wall (psi)

P_o (1) peak pressure (psi)
(2) maximum axial load (lbs.)
(3) atmospheric pressure (psi)

P_r peak positive normal reflected pressure (psi)

P_r^- peak negative normal reflected pressure (psi)

$P_{r\alpha}$ peak reflected pressure at angle of incidence α (psi)

P_{RIB} maximum average pressure on backwall (psi)

P_s positive incident pressure (psi)

P_{sb}, P_{se} positive incident pressure at points b and e, respectively (psi)

P_{so} peak positive incident pressure (psi)

P_{so} peak negative incident pressure (psi)

P_{sob}, P_{sod}, P_{soe} peak positive incident pressure at points b, d, and e, respectively (psi)

P_u ultimate axial load at actual eccentricity e (lbs.)

P_x ultimate load when eccentricity e_x

* See note at end of symbols

P_y ultimate load when eccentricity e_y is present (lbs.)

q dynamic pressure (psi)

q_b, q_e dynamic pressure at points b and e, respectively (psi)

q_o peak dynamic pressure (psi)

q_{ob}, q_{oe} peak dynamic pressure at points b and e, respectively (psi)

r (1) unit resistance (psi)
(2) radius of spherical TNT [density equals 95 lb./ft.^{3}] charge (ft.)
(3) radius of gyration of cross section of column (in.)

$\bar{r}$ unit rebound resistance (psi, for slabs) (lb./in. for beams)

r_{avail} dynamic resistance available (psi)

Δr change in unit resistance (psi, for slabs) (lb./in. for beams)

r_d radius from center of impulse load to center of door rotation (in.)

r_{DL} uniform dead load (psi)

r_e elastic unit resistance (psi, for slabs) (lb./in. for beams)

r_{ep} elasto-plastic unit resistance (psi, for slabs) (lb./in. for beams)

r_{fs} ultimate unit resistance of fragment shield (psi)

r_s radius of shaft (in.)

r_T tension membrane resistance (psi)

r_u ultimate unit resistance (psi, for slabs) (lb./in. for beams)

r_{up} post-ultimate unit resistance (psi)

r_1 radius of hemispherical portion of primary fragment (in.)

R (1) total internal resistance (lbs.)
(2) slant distance (ft.)
(3) ratio of S/G
(4) standoff distance (ft.)

R_{eff} effective radius (ft.)

R_f (1) distance traveled by primary fragment (ft.)
(2) distance from center of detonation (ft.)

R_g uplift force at corners of window frame (lbs.)

R_l radius of lacing bend (in.)

R_t target radius (ft.)

R_A normal distance (ft.)

R_E equivalent total internal resistance (lbs.)

R_G ground distance (ft.)

R_u total ultimate resistance (lb.)

R_I, R_{II} total internal resistance of sectors I and II, respectively (lbs.)

s (1) sample standard deviation
(2) spacing of torsion reinforcement in a direction parallel to the longitudinal reinforcement (in.)
(3) pitch of spiral (in.)

s_s spacing of stirrups in the direction parallel to the longitudinal reinforcement (in.)

s_l spacing of lacing in the direction parallel to the longitudinal reinforcement (in.)

S height of front wall or one-half its width, whichever is smaller (ft.)

S' weighted average clearing distance with openings (ft.)

SE strain energy

t time (ms)

Δt time increment (ms)

t_a any time (ms)

t_b, t_e, t_f time of arrival of blast wave at points b, e, and f, respectively (ms)

t_c (1) clearing time for reflected pressures (ms)
(2) average casing thickness of explosive charges (in.)

t'_c (1) adjusted casing thickness (in.)
(2) Clearing time for reflected pressures adjusted for wall openings (ms)

t_d rise time (ms)

t_E time to reach maximum elastic deflection (ms)

t_g fictitious gas duration (ms)

t_m time at which maximum deflection occurs (ms)

t_o duration of positive phase of blast pressure (ms)

t_o^- duration of negative phase of blast pressure (ms)

t_{of} fictitious positive phase pressure duration (ms)

t_{of}^- fictitious negative phase pressure duration (ms)

t_r fictitious reflected pressure duration (ms)

t_u time at which ultimate deflection occurs (ms)

t_y time to reach yield (ms)

t_A time of arrival of blast wave (ms)

t_{AG} time of arrival of ground shock (ms)

t_l time at which partial failure occurs (ms)

T (1) duration of equivalent triangular loading function (ms)
(2) thickness of masonry wall (in.)
(3) toughness of material (psi-in./in.)

T_c thickness of concrete section (in.)

$\bar{T}_c$ scaled thickness of concrete section (ft./lb.$^{1/3}$)

T_g thickness of glass (in.)

T_H force in the continuous reinforcement in the short span direction (lbs.)

T_i angular impulse load (lb.-ms-in.)

T_L force in the continuous reinforcement in the long span direction (lbs.)

T_N effective natural period of vibration (ms)

T_{pf} minimum thickness of concrete to prevent perforation by a given fragment (in.)

T_r rise time (ms)

T_s (1) thickness of sand fill (in.)
(2) thickness of slab (in.)

T_{sp} minimum concrete thickness to prevent spalling (in.)

$\bar{T}_s$ scaled thickness of sand fill (ft./lb.$^{1/3}$)

T_u total torsional moment at critical section (in.-lbs.)

T_w thickness of wall (in.)

T_y force of the continuous reinforcement in the short direction (lbs.)

u particle velocity (ft./ms)

u_u ultimate flexural or anchorage bond stress (psi)

U shock front velocity (ft./ms)

U_s strain energy

v velocity (in./ms)

v_a instantaneous velocity at any time (in./ms)

v_b boundary velocity for primary fragments (ft./sec.)

v_c ultimate shear stress permitted on an unreinforced web (psi)

v_f maximum post-failure fragment velocity (in./ms)

$v_{f(avg.)}$ average post-failure fragaent velocity (in./ms)

v_i velocity at incipient failure deflection (in./ms)

v_o initial velocity of primary fragaent (ft./sec.)

v_r residual velocity of primary fragment after perforation (ft./sec.)

v_s striking velocity of primary fragment (ft./sec.)

v_{tc} maximum torsion capacity of an unreinforced web (psi)

v_{tu} nominal torsion stress in the direction of v_u (psi)

v_u ultimate shear stress (psi)

v_{uH} ultimate shear stress at distance d_e from the horizontal support (psi)*

v_{uV} ultimate shear stress at distance d_e from the vertical support (psi)*

v_x velocity in x direction (in./ms.)

v_y velocity in y direction (in./ms.)

V (1) volume of partially vented chamber ($ft.^3$)
(2) velocity of compression wave through concrete (in./sec.)
(3) velocity of mass under shock load (in./sec.)

* See note at end of symbols

V_d ultimate direct shear capacity of the concrete of width b (lbs.)

V_{dH} shear at distance d_e from the vertical support on a unit width (lbs./in.)*

V_{dV} shear at distance d_e from the horizontal support on a unit width (lbs./in.)*

V_f free volume ($ft.^3$)

V_H maximum horizontal velocity of the ground surface (in./sec.)

V_o volume of structure ($ft.^3$)

V_s shear at the support (lb./in., for panels) (lbs. for beam)

V_{sH} shear at the vertical support on a unit width (lbs./in.)*

V_{sV} shear at the horizontal support on a unit width (lbs./in.)*

V_u total shear on a width b (lbs.)

V_V maximum vertical velocity of the ground surface (in./sec.)

V_x unit shear along the long side of window frame (lb./in.)

V_y unit shear along the short side of window frame, (lbs./in.)

w applied uniform load ($lbs.-in.^2$)

w_c (1) unit weight (psi, for panels) (lb./in. for beam)
(2) weight density of concrete ($lbs./ft.^3$)

w_s weight density of sand ($lbs./ft.^3$)

W (1) design charge weight (lbs.)
(2) external work (in.-lbs.)
(3) width of wall (ft.)

W_A weight of fluid (lbs.)

W_{ACT} actual quantity of explosives (lbs.)

W_c total weight of explosive containers (lbs.)

W_E effective charge weight (lbs.)

W_{E_g} effective charge weight for gas pressure (lb.)

W_{EXP} weight of explosive in question (lbs.)

W_f weight of primary fragment (oz.)

* See note at end of symbols

$\bar{W}_f$ average fragment weight (oz.)

W_F weight of frangible element (lb./ft.^{2})

W_{CI} weight of inner casing (lbs.)

W_{co} total weight of steel core (lbs.)

W_{CO} weight of outer casing (lbs.)

W_{c1}, W_{c2} total weight of plates 1 and 2, respectively (lbs.)

W_s width of structure (ft.)

WD work done

x yield line location in horizontal direction (in.)*

X (1) deflection (in.)
(2) distance from front of object to location of largest cross section to plane of shock front (ft.)

X_a any deflection (in.)

X_c lateral deflection to which a masonry wall develops no resistance (in.)

X_{DL} deflection due to dead load (in.)

X_e elastic deflection (in.)

X_E equivalent elastic deflection (in.)

X_{ep} elasto-plastic deflection (in.)

X_f maximum penetration into concrete of armor-piercing fragments (in.)

X_f' maximum penetration into concrete of fragments other than armor-piercing (in.)

X_m maximum transient deflection (in.)

X_p plastic deflection (in.)

X_s (1) maximum penetration into sand of armor-piercing fragments (in.)
(2) static deflection (in.)

X_u ultimate deflection (in.)

* See note at end of symbols

X_1 (1) partial failure deflection (in.)
(2) deflection at maximum ultimate resistance of masonry wall (in.)

y yield line location in vertical direction (in.)*

y_t distance from the top of section to centroid (in.)

Z scaled slant distance (ft./lb.$^{1/3}$)

Z_A scaled normal distance (ft./lb.$^{1/3}$)

Z_G scaled ground distance (ft./lb.$^{1/3}$)

α (1) angle formed by the plane of stirrups, lacing, or diagonal reinforcement and the plane of the longitudinal reinforcement (deg)
(2) angle of incidence of the pressure front (deg)
(3) acceptance coefficient
(4) trajectory angle (deg.)

α_{ec} ratio of flexural stiffness of exterior wall to flat slab

α_{ecH}, α_{ecL} ratio of flexural stiffness of exterior wall to slab in direction H and L respectively

β (1) coefficient for determining elastic and elasto-plastic resistances
(2) particular support rotation angle (deg)
(3) rejection coefficient
(4) target shape factor from figure 2-212

β_1 factor equal to 0.85 for concrete strengths up to 4,000 psi and is reduced by 0.05 for each 1,000 psi in excess of 4,000 psi

γ coefficient for determining elastic and elasto-plastic deflections

γ_p factor for type of prestressing tendon

δ moment magnifier

δ_n clearing factor

Δ deflection at sector's displacement (in.)

$\dot{\epsilon}'_c$ average strain rate for concrete (in./in./ms)

ϵ_m unit strain in mortar (in./in.)

$\dot{\epsilon}'_s$ average strain rate for reinforcement (in./in./ms)

ϵ_u rupture strain (in./in./ms)

* See note at end of symbols

θ (1) support rotation angle (deg)
(2) angular acceleration (rad/ms^2)

θ_{max} maximum support rotation angle (deg)

θ_H horizontal rotation angle (deg)*

θ_V vertical rotation angle (deg)*

λ increase in support rotation angle after partial failure (deg)

μ (1) ductility factor
(2) coefficient of friction

ν Poisson's ratio

ρ (1) mass density (lbs.-ms.^{2}/in.^{4})
(2) density of air behind shock front (lbs/ft.^{3})

ρ_a density of air (oz./in.^{3})

ρ_c density of casing (oz./in.^{3})

ρ_f mass density of fragment (oz./in.^{3})

ρ_o mass density of medium (lb.-ms.^{2}/in.^{4})

σ_u fracture strength of concrete (psi)

Σ_o effective perimeter of reinforcing bars (in.)

ΣM summation of moments (in.-lbs.)

ΣM_N sum of the ultimate unit resisting moments acting along the negative yield lines (in.-lbs.)

ΣM_p sum of the ultimate unit resisting moments acting along the positive yield lines (in.-lbs.)

τ_s maximum shear stress in the shaft (psi)

ϕ (1) capacity reduction factor
(2) bar diameter (in.)
(3) TNT conversion factor

ϕ_r assumed shape function for concentrated loads

$\phi(x)$ assumed shape function for distributed loads free edge

ω angular velocity (rad./ms)

* See note at end of symbols

═══	simple support
///////	fixed support
XXXXXXX	either fixed, restrained, or simple support

* Note. This symbol was developed for two-way elements which are used as walls. When roof slabs or other horizontal elements are under consideration, this symbol will also be applicable if the element is treated as being rotated into a vertical position.

APPENDIX 4C

BIBLIOGRAPHY

1. American Concrete Institute, Design Handbook, Volume 1 - Beams, One-Way Slabs, Brackets, Footings, and Pile Caps, in accordance with the Strength Design Method of ACI 318-83. Publication SP-17(84). ACI Committee 340, American Concrete Institute, Detroit, MI, 1984.
2. American Concrete Institute, Design Handbook, Volume 2 - Columns, in accordance with the Strength Design Method of ACI 318-83, Publication SP-17A(85), ACI Committee 340, American Concrete Institute, Detroit, MI, 1985.
3. American Concrete Institute, Design Handbook, Volume 2 - Columns, Publication SP-17A, ACI Committee 340, American Concrete Institute, Detroit, MI, 1978.
4. American Concrete Institute Standard Building Code Requirements for Reinforced Concrete, ACI Committee 318-77. American Concrete Institute, Detroit, MI, August, 1979.
5. American Concrete Institute Standard Building Code Requirements for Reinforced Concrete, ACI Committee 318-83, American Concrete Institute, Detroit, MI, November 1983.
6. Design Criteria for Deflection Capacity of Conventionally Reinforced Concrete Slabs, an investigation conducted by Construction Technology Laboratories, Structural Analytical Section, 5420 Old Orchard Road, Skokie, Illinois 60077, for Civil Engineering Laboratory, Naval Construction Battalion Center, Port Hueneme, CA, sponsored by Naval Facilities Engineering Command, Phase I - State-of-the-Art Report, CR 80.026, October 1980, Phase-1I - Design and Construction Requirements, CR 80.027, October 1980, Phase III - Summary of Design Criteria and Design and Construction Details - Design Examples, CR 80.028, October 1980.
7. Design Manual, AEC Test Structures , Volumes II and III, by Holmes and Narver, Inc., under Contract AT (29-2)-20, for U.S. Atomic Energy Commission, Albuquerque Operations Office, Albuquerque, NM, December 1961.
8. Design of Structures to Resist Nuclear Weapons Effects, ASCE Manual of Engineering Practice No. 42, American Society of Civil Engineers, New York, NY, 1961.
9. Design of Structures to Resist the Effects of Nuclear Weapons, Department of the Army Technical Manual TM 5-856-2, 3 and 4, Washington, D.C.
10. Dynamic Tests of Concrete Reinforcing Steels, Technical Report R 394, U.S. Naval Civil Engineering Laboratory, Port Hueneme, CA, September 1965.
11. Effects of Impact and Explosion, Volume 1, Office of Scientific Research and Development, National Defense Research Committee, Washington, D.C., 1946 (Confidential).
12. Fundamentals of Protective Design (Non-Nuclear), Department of the Army, Technical Manual TM 5-855-1, Washington, D.C., July 1965.
13. Impact Design Criteria for Blockhouses Subjected to Abortive Launch Environments, Technical Publication PMR-TR-70-2, Mechanics Research, Inc., for the Pacific Missile Range, Point Mugu, CA, July 1970.
14. Industrial Engineering Study to Establish Safety Design Criteria for Use in Engineering of Explosive Facilities and Operations, by Ammann & Whitney Consulting Engineers, New York, NY, under Contract DA-28-017-501-ORD-3889, for Process Engineering Branch, A.P.M.E.D., Picatinny Arsenal, Dover, NJ, April 1963.
15. Manual of Standard Practice for Detailing Reinforced Concrete Structures, ACI Committee 315-65, American Concrete Institute, Detroit, MI, 1965.

16. Non-Nuclear Weapons Effects on Protective Structures (U). Technical Report No. AFWL-TR-69-57, (SECRET), Mechanics Research, Inc., for the Air Force Weapons Laboratory, Kirtland Air Force Base, NM, September 1969.
17. Strength and Behavior of Laced Reinforced Concrete Slabs Under Static and Dynamic Load, Technical Report R620, prepared by Naval Civil Engineering Laboratory, Port Hueneme, California, Sponsored by Department of the Army, Picatinny Arsenal, April 1969.
18. Summary of One-Third Scale Slab Tests and Scaled Bay Structure Tests, by Ammann & Whitney, Consulting Engineers, New York, NY, under Contract DA-28-017-AMC-423(A) for Picatinny Arsenal, Dover, NJ, March 1969.
19. Ultimate Strength Design Handbook, Volume No. 1, Special Publication No. 17. ACI Committee 340, American Concrete Institute, Detroit, MI, 1967.
20. Ultimate Strength Design of Reinforced Concrete Columns, Publication SP-7, Interim Report of ACI Committee 340, American Concrete Institute, Detroit, MI, 1964.
21. U.S. Army Engineer Waterways Experiment Station, Technical Report N-72-10, Design and Testing of a Blast-Resistant Reinforced Concrete Slab System, Criswell, M.E., Vicksburg, MS, 1972.
22. Amirian, A., Dobbs, N. and Dede, M., Technical Approach for Structural Design Procedures for a Family of Horseshoe-Shaped MTC (Phase I), prepared for Naval Civil Engineering Laboratory, Port Hueneme, CA by Ammann and Whitney, Consulting Engineers, New York, N.Y., August 1985.
23. Ayvazian, H. and DeDe, M., Development of Preliminary Designs for NAVFAC MTCs and Preparation of Construction Cost Estimates, prepared for Naval Civil Engineering Laboratory, Port Hueneme, CA by Ammann and Whitney, Consulting Engineers, New York, N.Y., Draft.
24. Ball, J. W., Baylot, J.T. and Kiger, S.A., Kirtland Underground Munitions Storage Complex Model Designs, Construction, and Test Data, Technical Report SL-84-14, prepared by Structures Laboratory, Department of the Army, Waterways Experiment Station, Corps of Engineers, P.O. Box 631, Vicksburg, Mississippi 39180-0631, for Defense Nuclear Agency, Washington, D.C. 20305, Under DNA Subtask B990AXRE, Work Unit 0004 and Subtask B99QAXRD, Work Unit 0013, "Advanced Design Explosive Tests," September 1984.
25. Baylot, J.T., Kiger, S.A. and Ball, J.W., Structural Design of Blast-Containment Facilities, Abstract for the Twenty-First Explosive Safety Seminar, prepared by U.S. Army Engineer Waterways Experiment Station, Vicksburg, Mississippi, August 1984.
26. Baylot, J.T., Vulnerability of an Underground Weapon Storage Facility, Technical Report SL-84-16, prepared by Structures Laboratory, Department of the Army, Waterways Experiment Station, Corps. of Engineers, P.O. Box 631, Vicksburg, Mississippi 39180-0631, for Defense Nuclear Agency, Washington, DC 20305, Under Subtask A99QAXFC, Work Unit 00046, September 1984.
27. Bergstrom, P., et al., Hard-Structures Munitions -Phase I: Warehead (U), AFATL-TR-67-13, Volume III (AD-379, 468), (SECRET), Chamberlain Corporation, February 1967.
28. Beth, R. A., Final Report on Concrete Penetration, Report No. A-388, National Defense Research Committee, Office of Scientific Research and Development, March 1946.
29. Beth, R. A. and Stipe, J. G., Penetration and Explosion Tests on Concrete Slabs, Report I: Data, Interim Report No. 20, Committee on Passive Protection Against Bombing, National Research Council, January 1943.

30. Branson, D., Deformation of Concrete Structures, McGraw-Hill, Inc., New York, NY, 1977.
31. Brown, J. W., Response of Selected Materials to High-Speed Fragment Impact, U.S. Army Engineer Waterways Experiment Station, Vicksburg, MS, 1970.
32. Cohen, E. and Dobbs, N., Design Procedures and Details for Reinforced Concrete Structures Utilized in Explosive Storage and Manufacturing Facilities, Ammann & Whitney, Consulting Engineers, New York, NY, Annals of the New York Academy of Sciences, Conference on Prevention of and Protection Against Accidental Explosion of Munitions , Fuels and Other Hazardous Mixtures, Volume 152, Art. 1, October 1968.
33. Cohen, E. and Dobbs, N., Models for Determining the Response of Reinforced Concrete Structures to Blast Loads, Ammann & Whitney, Consulting Engineers, New York, NY, Annals of the New York Academy of Sciences, Conference on Prevention of and Protection Against Accidental Explosion of Munitions, Fuels and Other Hazardous Mixtures, Volume 152, Art. 1, October 1968.
34. Cohen, E. and Dobbs, N., Supporting Studies to Establish Safety Design Criteria for Storage and Processing of Explosive Materials - Interim Report No. 1, Summary of One-Third Scale Reinforced Concrete Slab Tests, Technical Memorandum C-1, by Ammann & Whitney, Consulting Engineers, New York, NY, under Contract: DA-28-017-AMC-423(A) for Picatinny Arsenal, Dover, NJ, June 1965.
35. Coltharp, D.R., Vitayaudom, K.P. and Kiger, S.A., NATO Semihardened Facility Design Criteria Improvement, Final Report, prepared by Engineering and Services Laboratory, Air Force Engineering and Services Center, Tyndall Air Force Base, Florida 32403. June 1985.
36. Criswell, M.E., Design and Testing of a Blast-Resistant Reinforced Concrete Slab System, Technical Report N-72-10, Conducted by U.S. Army Engineer Waterways Experiment Station, Weapons Effects Laboratory, Vicksburg, Mississippi, sponsored by Defense Civil Preparedness Agency, Work Order No. DAH C20-68-W-0192, Work Unit 1127E, November 1972.
37. Dede, M. and Amirian, A., Test Plan to Verify Failure Criteria for Conventionally Reinforced Concrete Slabs, prepared for Naval Civil Engineering Laboratory, Port Hueneme, California, by Ammann and Whitney, Consulting Engineers, New York, N.Y., April 1985.
38. Doyle, J. M., Klein, M. J. and Shah, H., Design of Missile Resistant Concrete Panels, Preprints of the 2nd International Conference on Structural Mechanics in Reactor Technology, Vol. 4, Commission of the European Communities, Brussels, 1973, Paper No. J 3/3.
39. Fisher, E. M., Explosion Effects Data Sheets, Report 2986, U.S. Naval Ordnance Laboratory, Silver Spring, MD, 1955.
40. Getchell, J.V. and Kiger, S.A., Vulnerability of Shallow-Burried Flat-Roof Structures, Technical Report SL-80-7, prepared by Structures Laboratory, U.S. Army Engineer Waterways Experiment Station, P.O. Box 631, Vicksburg, Mississippi 39180, for Defense Nuclear Agency, Washington, D.C. 20305 and Office, Chief of Engineers, U.S. Army, Washington, D.C. 20314, under DNA Subtask Y99QAXSC062, Work Unit 42, and Subtask H191AXSX337, Work Unit 02, and OCE R&D Project 4A762719AT40, Task AO, Work Unit 008, Report 2, Foam HEST 4, October 1980, Report 3, Foam HEST 5, February 1981, Report 4, Foam HEST 3 and 6, December 1981 and Report 5, Foam HEST 7, February 1982.
41. Gewaltney, R. C., Missile Generation and Protection in Light-Water-Cooled Power Reactor Plants, Nuclear Safety, 10(4): July-August 1969.

42. Giere, A. C., Calculating Fragment Penetration and Velocity Data for Use in Vulnerability Studies, NAVORD Report 6621, U.S. Naval Nuclear Evaluation Unit, Albuquerque, NM, October 1959.
43. Hoffman, P. R., McMath, R. R. and Migotsky, E., Projectile Penetration Studies AFWL Technical Report No. WL-TR-64-102, Avco Corporation for the Air Force Weapons Laboratory, Kirtland Air Force Base, NM, December 1964.
44. Ingraham, J. M. and Abbott, K. N., Feasibility Study of Laminated Metallic Armor (U), AMRA TR 63-30, (CONFIDENTIAL), U.S. Army Materials Research Agency, Watertown, MA, December 1963.
45. Iqbal, M. and Derecho, A., Design Criteria for Deflection Capacity of Conventionally Reinforced Concrete Slabs, Phase I - State-of-the-Art Report, Report No. CR 80.026, Naval Civil Engineering Laboratory, Port Hueneme, CA, October 1980.
46. Johnson, C. and Moseley, J.W., Preliminary Warhead Terminal Ballistic Handbook, Part 1: Terminal Ballistic Effects, NAVWEPS Report No. 7673, U.S. Naval Weapons Laboratory, Dahlgren, VA, March 1964.
47. Keenan, W. A., Strength and Behavior of Laced Reinforced Concrete Slabs Under Static and Dynamic Load, Technical Report R-620, U.S. Naval Civil Engineering Laboratory, Port Hueneme, CA, April 1969.
48. Keenan, W., Tancreto, J., Meyers, G., Johnson, F., Hopkins, J., Nickerson, H. and Armstrong, W., NCEL Products Supporting DOD Revision of NAVFAC P397, Technical Memorandum 2591TM, prepared by Naval Civil Engineering Laboratory, Port Hueneme, California 93043, Program No.: Y0995-01-003-201, Sponsored by Naval Facilities Engineering Command, Alexandria, Virginia 22332, March 1983.
49. Kiger, S.A. and Albritton, G.E., Response of Burried Hardened Box Structures to the Effects of Localized Explosions, Technical Report SL-80-1, prepared by Structures Laboratory, U.S. Army Engineer Waterways Experiment Station, P.O. Box 631, Vicksburg. Mississippi 39180, for Defense Nuclear Agency, Washington, D.C. 20305 and Office, Chief of Engineers, U.S. Army, Washington, D.C. 20314, under DNA Subtask Y99QAXSC062, Work Unit 04, and OCE R&D Project 4A762719AT40, Task A1, Work Unit 027, March 1980.
50. Kymer, J. R., Penetration Performance of Arrow Type Projectiles, Report R1814, U.S. Army Frankford Arsenal, Philadelphia, PA, May 1966.
51. Liu, T.C., Strength Design of Reinforced Concrete Hydraulic Structures, Preliminary Strength Design Criteria, Technical Report SL-80-4, Report 1 of a series, prepared by Structures Laboratory, U.S. Army Engineer Waterways Experiment Station, P.O. Box 631, Vicksburg, Mississippi 39180, for Office, Chief of Engineers, U.S. Army, Washington, D.C. 20314, under CWIS 31623. July 1980.
52. Mascianica, F. S., Summary of Terminal Ballistic Data on Lightweight Armor Materials (U), AMMRC TR 69-17, (CONFIDENTIAL), U.S. Army Materials and Mechanics Research Center, Watertown, MA, July 1969.
53. Nara, H. R. and Denington, R. J. Ricochet and Penetration of Steel Spheres in Clay and Sand Soils, TM-E7, AD-059 883, Case Institute of Technology, Project DOAN BROOK, October 1954.
54. Newmark, N. M. and Haltiwanger, J. D., Air Force Design Manual, Principles and Practices for Design of Hardened Structures, Technical Documentary Report No. AFSWC-TDR-62-138, by Department of Civil Engineering. University of Illinois, Urbana, Illinois, under Contract AF29 (601)-2390 for Research Directorate, Air Force Special Weapons Center, Air Force Systems Command, Kirtland Air Force Base, NM, December 1962.

55. Park, R. and Gamble, W. L., Reinforced Concrete Slabs, John Wiley & Sons, New York, NY, 1980.
56. Pecone, G., Design of Flat Slabs Subjected to Blast Loads, prepared for Northern Division, Naval Facilities Engineering Command, U.S. Naval Base, Philadelphia, PA, by Ammann and Whitney, Consulting Engineers, New York, N.Y., Contract No. N 62472-76-C-1148, June 1982.
57. Recht, R., et al., Application of Ballistic Perforation Mechanics to Target Vulnerability and Weapons Effectiveness Analysis (U), NWC TR 4333 (Confidential), Denver Research Institute for the Naval Weapons Center, China Lake, CA, October 1967.
58. Richey, H. M., Armed Services Explosives Safety Board Dividing Wall Program, Phase C, Tests 1 through 13. U.S. Naval Weapon Center, China Lake, CA, 1964 (Secret Restricted Data).
59. Rindner, R. M., Establishment of Safety Design Criteria for Use in Engineering of Explosive Facilities and Operations, Report No. 2, Detonation by Fragment Impact, Technical Report DB-TR: 6-59, Picatinny Arsenal, Dover, NJ, March 1959.
60. Robertson, H.P., Terminal Ballistics, Preliminary Report, Committee on Passive Protection Against Bombing, National Research Council, January 1941.
61. Rohani, B., Fragment and Projectile Penetration Resistance of Soils: Report 2, High-Velocity Fragment Penetration into Laboratory-Prepared Soil Targets, Miscellaneous Paper S-71-12, U.S. Army Engineer Waterways Experiment Station, Vicksburg, MS, June 1973.
62. Stipe, J. G., et al., Ballistic Tests on Small Concrete Slabs, Interim Report No. 28, Committee on Fortification Design, National Research Council, June 1944.
63. Schumacher, R.N., Kingery, C.N. and Ewing, Jr., W.O., Airblast and Structural Response Testing of a 1/4 Scale Category 1 Suppressive Shield, BRL Memorandum Report No. 2623, by U.S.A. Ballistic Research Laboratories, Aberdeen Proving Ground, Maryland, May 1976.
64. Schwartz, A., et. al., Establishment of Safety Design Criteria for Use in Engineering of Explosive Facilities and Operations, Report No. 6, Test of One-Tenth Scale Bay Structure, Technical Report 3439, by Picatinny Arsenal, Dover, NJ, and Ammann & Whitney, Consulting Engineers, New York, NY, under Contract DA-28-017-AMC-423(A), July 1966.
65. Takayahagi, T. and Derecho, A., Design Criteria for Deflection Capacity of Conventionally Reinforced Concrete Slabs, Phase III - Summary of Design Criteria and Construction Details - Design Examples Report No. CR 80.028, Naval Civil Engineering Laboratory, Port Hueneme, CA, October 1980.
66. Takayanagi, T., Derecho, A. and Iqbal, M., Design Criteria for Deflection Capacity of Conventionally Reinforced Concrete Slabs, Phase II - Design and Construction Requirements, Report No. CR 80.027, Naval Civil Engineering Laboratory, Port Hueneme, CA, October 1980.
67. Tancreto, J., Design Criteria for Deflection Capacity of Conventionally Reinforced Concrete Slabs, Naval Civil Engineering Laboratory, Special Project 1311 SP, Port Hueneme, CA, 1980.
68. Thomas, L.H., Computing the Effect of Distance on Damage by Fragments, Report No. 468, Ballistic Research Laboratories, Aberdeen Proving Ground, MD, May 1944.
69. Timoshenko, S. and Woinowsky-Krieger, S., Theory of Plates and Shells, McGraw-Hill Book Co., New York, NY, 1959.

70. Vanderbilt, M., Sozen, M. and Seiss, C., Deflections of Multiple-Panel Reinforced Concrete Floor Slabs, Journal of the Structural Division, Proceedings of the American Society of Civil Engineers, August 1965.
71. Vargas's, L. M., Hokanson, J. C. and Rinder, R. M., Explosive Fragmentation of Dividing Walls, by Southwest Research Institute, San Antonio, TX, Contractor Report ARLCD-CR-81018, U.S. Army Armament Research and Development Command, Large Caliber Weapons Systems Laboratory, Dover, NJ, July 1981.
72. Wachtell, S., Comparison of Blast Response-Scaled vs. Full-Size Concrete Structures, Picatinny Arsenal, Dover, NJ, Annals of the New York Academy of Sciences, Conference on Prevention of and Protection Against Accidental Explosions of Munitions, Fuels and Other Hazardous Mixtures , Volume 152, Art. 1, October 1968.
73. Wang, Chu-Kia and Salmon, Charles G., Reinforced Concrete Design, Intext Educational Publishers, New York, NY, 1973.
74. Whitney, C. S., Plastic Theory of Reinforced Concrete Design, Transactions of the American Society of Civil Engineers, Vol. 107, ASCE, New York, NY, 1942.
75. Whitney, C. S. and Cohen, E., Guide for Ultimate Strength Design of Reinforced Concrete, Ammann & Whitney, Consulting Engineers, New York, NY, Journal of the American Concrete Institute, November 1956.
76. Whitney, C. S., et. al., Design of Blast-Resistant Construction for Atomic Explosions, Ammann & Whitney, Consulting Engineers, New York, NY, Journal of the American Concrete Institute, March 1955.
77. Wood, R. W., Plastic and Elastic Design of Slabs and Plates, The Ronald Press Company, New York, NY, 1961.

CHAPTER 5. STRUCTURAL STEEL DESIGN

CHAPTER 5

STRUCTURAL STEEL DESIGN

INTRODUCTION

5-1. Purpose

The purpose of this manual is to present methods of design for protective construction used in facilities for development, testing, production, storage, maintenance, modification, inspection, demilitarization, and disposal of explosive materials.

5-2. Objective

The primary objectives are to establish design procedures and construction techniques whereby propagation of explosion (from one structure or part of a structure to another) or mass detonation can be prevented and to provide protection for personnel and valuable equipment.

The secondary objectives are to:

(1) Establish the blast load parameters required for design of protective structures.
(2) Provide methods for calculating the dynamic response of structural elements including reinforced concrete, and structural steel.
(3) Establish construction details and procedures necessary to afford the required strength to resist the applied blast loads.
(4) Establish guidelines for siting explosive facilities to obtain maximum cost effectiveness in both the planning and structural arrangements, providing closures, and preventing damage to interior portions of structures because of structural motion, shock, and fragment perforation.

5-3. Background

For the first 60 years of the 20th century, criteria and methods based upon results of catastrophic events were used for the design of explosive facilities. The criteria and methods did not include a detailed or reliable quantitative basis for assessing the degree of protection afforded by the protective facility. In the late 1960's quantitative procedures were set forth in the first edition of the present manual, "Structures to Resist the Effects of Accidental Explosions". This manual was based on extensive research and development programs which permitted a more reliable approach to current and future design requirements. Since the original publication of this manual, more extensive testing and development programs have taken place. This additional research included work with materials other than reinforced concrete which was the principal construction material referenced in the initial version of the manual.

Modern methods for the manufacture and storage of explosive materials, which include many exotic chemicals, fuels, and propellants, require less space for a given quantity of explosive material than was previously needed. Such concentration of explosives increases the possibility of the propagation of accidental explosions. (One accidental explosion causing the detonation of

other explosive materials.) It is evident that a requirement for more accurate design techniques is essential. This manual describes rational design methods to provide the required structural protection.

These design methods account for the close-in effects of a detonation including the high pressures and the nonuniformity of blast loading on protective structures or barriers. These methods also account for intermediate and far-range effects for the design of structures located away from the explosion. The dynamic response of structures, constructed of various materials, or combination of materials, can be calculated, and details are given to provide the strength and ductility required by the design. The design approach is directed primarily toward protective structures subjected to the effects of a high explosive detonation. However, this approach is general, and it is applicable to the design of other explosive environments as well as other explosive materials as mentioned above.

The design techniques set forth in this manual are based upon the results of numerous full- and small-scale structural response and explosive effects tests of various materials conducted in conjunction with the development of this manual and/or related projects.

5-4. Scope

It is not the intent of this manual to establish safety criteria. Applicable documents should be consulted for this purpose. Response predictions for personnel and equipment are included for information.

In this manual an effort is made to cover the more probable design situations. However, sufficient general information on protective design techniques has been included in order that application of the basic theory can be made to situations other than those which were fully considered.

This manual is applicable to the design of protective structures subjected to the effects associated with high explosive detonations. For these design situations, the manual will apply for explosive quantities less than 25,000 pounds for close-in effects. However, this manual is also applicable to other situations such as far- or intermediate-range effects. For these latter cases the design procedures are applicable for explosive quantities in the order of 500,000 pounds which is the maximum quantity of high explosive approved for aboveground storage facilities in the Department of Defense manual, "Ammunition and Explosives Safety Standards", DOD 6055.9-STD. Since tests were primarily directed toward the response of structural steel and reinforced concrete elements to blast overpressures, this manual concentrates on design procedures and techniques for these materials. However, this does not imply that concrete and steel are the only useful materials for protective construction. Tests to establish the response of wood, brick blocks, and plastics, as well as the blast attenuating and mass effects of soil are contemplated. The results of these tests may require, at a later date, the supplementation of these design methods for these and other materials.

Other manuals are available to design protective structures against the effects of high explosive or nuclear detonations. The procedures in these manuals will quite often complement this manual and should be consulted for specific applications.

Computer programs, which are consistent with procedures and techniques contained in the manual, have been approved by the appropriate representative of the US Army, the US Navy, the US Air Force and the Department of Defense Explosives Safety Board (DDESB). These programs are available through the following repositories:

(1) Department of the Army
Commander and Director
U.S. Army Engineer
Waterways Experiment Station
Post Office Box 631
Vicksburg, Mississippi 39180-0631
Attn: WESKA

(2) Department of the Navy
Commanding Officer
Naval Civil Engineering Laboratory
Port Hueneme, California 93043
Attn: Code L51

(3) Department of the Air Force
Aerospace Structures
Information and Analysis Center
Wright Patterson Air Force Base
Ohio 45433
Attn: AFFDL/FBR

If any modifications to these programs are required, they will be submitted for review by DDESB and the above services. Upon concurrence of the revisions, the necessary changes will be made and notification of the changes will be made by the individual repositories.

5-5. Format

This manual is subdivided into six specific chapters dealing with various aspects of design. The titles of these chapters are as follows:

Chapter 1	Introduction
Chapter 2	Blast, Fragment, and Shock Loads
Chapter 3	Principles of Dynamic Analysis
Chapter 4	Reinforced Concrete Design
Chapter 5	Structural Steel Design
Chapter 6	Special Considerations in Explosive Facility Design

When applicable, illustrative examples are included in the Appendices.

Commonly accepted symbols are used as much as possible. However, protective design involves many different scientific and engineering fields, and, therefore, no attempt is made to standardize completely all the symbols used. Each symbol is defined where it is first used, and in the list of symbols at the end of each chapter.

CHAPTER CONTENTS

5-6. General

This chapter contains procedures and guidelines for the design of blast-resistant steel structures and steel elements. Light construction and steel framed acceptor structures provide an adequate form of protection in a pressure range of 10 psi or less. However, if fragments are present, light-gage construction may only be partially appropriate. The use of structural steel frames in combination with precast concrete roof and wall panels (Chapter VI) will provide a measure of fragment protection at lower pressure ranges. Containment structures or steel elements of containment structures, such as blast doors, ventilation closures, fragments shields, etc. can be designed for almost any pressure range. This chapter covers detailed procedures and design techniques for the blast-resistant design of steel elements and structures subjected to short-duration, high-intensity blast loading. Provisions for inelastic, blast-resistant design will be consistent with conventional static plastic design procedures. Steel elements such as beams, beam columns, open-web joists, plates and cold-formed steel panels are considered. In addition, the design of steel structures such as rigid frames, and braced frames are presented as they relate to blast-resistant design. Special considerations for blast doors, penetration of fragments into steel, and unsymmetrical bending are also presented.

STEEL STRUCTURES IN PROTECTIVE DESIGN

5-7. Differences Between Steel and Concrete Structures in Protective Design

Qualitative differences between steel and concrete protective structures are summarized below:

(1) In close-in high-impulse design situations where a containment structure is utilized, a massive reinforced concrete structure, rather than a steel structure, is generally employed in order to limit deflections and to offer protection against the effects of primary and secondary fragments. However, elements of containment structures such as blast doors, ventilation closures, etc., are generally designed using structural steel. Fragment protection is usually accomplished by increasing the element thickness to resist fragment penetration or by providing supplementary fragment protection. In some cases, structural steel can be used in the design of containment cells. However, explosive charge weights are generally low, thereby preventing brittle modes of failure (Section 5-18.3) due to high pressure intensity.

(2) Structural steel shapes are considerably more slender, both in terms of the overall structure and the components of a typical member cross section. As a result, the effect of overall and local instability upon the ultimate capacity is an important consideration in steel design. Moreover, in most cases, plate elements and structures will sustain large deformations in comparison to those of more rigid concrete elements.

(3) The amount of rebound in concrete structures is considerably reduced by internal damping (cracking) and is essentially eliminated in cases where large deformations or incipient failure are permitted to occur. In structural steel, however, a larger response in rebound, up to 100 percent, can be obtained for a combination of short duration load and a relatively flexible element. As a result, steel structures require that special provisions be made to account for extreme responses of comparable magnitude in both directions.

(4) The treatment of stress interaction is more of a consideration in steel shapes since each element of the cross section must be considered subject to a state of combined stresses. In reinforced concrete, the provision of separate steel reinforcement for flexure, shear and torsion enables the designer to consider these stresses as being carried by more or less independent systems.

(5) Special care must be taken in steel design to provide for connection integrity up to the point of maximum response. For example, in order to avoid premature brittle fracture in welded connections, the welding characteristics of the particular grade of steel must be considered and the introduction of any stress concentrations at joints and notches in main elements must be avoided.

(6) If fragments are involved, special care must be given to brittle modes of failure as they affect construction methods. For example, fragment penetration depth may govern the thickness of a steel plate.

5-8. Economy of Design of Protective Structures in the Inelastic Range

The economy of facility design generally requires that blast-resistant structures be designed to perform in the inelastic response range during an accident. In order to ensure the structure's integrity throughout such severe conditions, the facility designer must be cognizant of the various possible failure modes and their inter-relationships. The limiting design values are dictated by the attainment of inelastic deflections and rotations without complete collapse. The amount of inelastic deformation is dependent not only upon the ductility characteristics of the material, but also upon the intended use of the structure following an accident as well as the protection required. In order for the structure to maintain such large deformations, steps must be taken to prevent premature failure by either brittle fracture or instability (local or overall). Guidelines and criteria for dealing with these effects are presented in the body of this chapter.

5-9. Applications of Steel Elements and Structures In Protective Design

The design procedures and applications of this chapter are directed toward steel acceptor- and donor-type structures.

Acceptor-type structures are removed from the immediate vicinity of the detonation. These include typical frame structures with beams, columns and beam-columns composed of standard structural shapes, and built-up sections. In many cases, the relatively low blast pressures suggest the use of standard building components such as open-web joists, prefabricated wall panels and roof decking detailed as required to carry the full magnitude of the dynamic loads. Another economical application can be the use of entire pre-engineered buildings, strengthened locally, to adapt their designs to low blast pressures (up to 2 psi) with short duration. For guidelines on the blast evaluation of pre-engineered buildings, see "Special Provisions for Pre-engineered Buildings", Chapter VI.

Donor-type structures, which are located in the immediate vicinity of the detonation may include steel containment cells or steel components of reinforced concrete containment structures such as blast doors or ventilation and electrical closure plates. In some cases, the use of suppressive shielding to control or confine the hazardous blast, fragment, and flame effects of detonations may be an economically feasible alternative. A brief review of suppressive shield design and criteria is outlined in Section 6-23 to 6-26 of Chapter VI. The high blast pressures encountered in these structures suggest the use of large plates or built-up sections with relatively high resistances. In some instances, fragment impact or pressure leakage is permitted.

5-10. Application of Dynamic Analysis

The first step in a dynamic design entails the development of a trial design considering facility requirements, available materials, and economy with members sized by a simple preliminary procedure. The next step involves the performance of a dynamic analysis to determine the response of the trial

design to the blast and the comparison of the maximum response with the deformation limits specified in this chapter. The final design is then determined by achieving an economical balance between stiffness and resistance such that the calculated response under the blast loading lies within the limiting values dictated by the operational requirements of the facility.

The dynamic response calculation involves either a single-degree-of-freedom analysis using the response charts in Chapter 3, or, in more complex structures, a multi-degree-of-freedom analysis using available dynamic elasto-plastic frame programs.

A single-degree-of-freedom analysis may be performed for the design analysis of either a given structural element or of an element for which a preliminary design has been performed according to procedures given in this chapter. Since this type of dynamic analysis is described fully with accompanying charts and tables in Chapter 3, it will not be duplicated herein. In principle, the structure or structural element is characterized by an idealized, bilinear, elasto-plastic resistance function and the loading is treated as an idealized triangular (or bilinear) pulse with zero rise time (Chapter 3). Response charts are presented in Chapter 3 for determining the ratio of the maximum response to the elastic response and the time to reach maximum response for the initial response. The equations presented for the dynamic reactions are also applicable to this chapter.

Multi-degree-of-freedom, nonlinear dynamic analyses of braced, and unbraced rigid frames can be performed using programs available through the repositories listed in Section 5-4 and through the reports listed in the bibliography at the end of this chapter.

PROPERTIES OF STRUCTURAL STEEL

5-11. General

Structural steel is known to be a strong and ductile building material. The significant engineering properties of steel are strength expressed in terms of yield stress and ultimate tensile strength, ductility expressed in terms of percent elongation at rupture, and rigidity expressed in terms of modulus of elasticity. This section covers the mechanical properties of structural steel subjected to static loading and dynamic loading. Recommended dynamic design stresses for bending and shear are then derived. Structural steels that are admissible in plastic design are listed.

5-12. Mechanical Properties

5-12.1. Mechanical Properties Under Static Loading; Static Design Stresses

Structural steel generally can be considered as exhibiting a linear stress-strain relationship up to the proportional limit, which is either close to or identical to the yield point. Beyond the yield point, it can stretch substantially without appreciable increase in stress, the amount of elongation reaching 10 to 15 times that needed to reach yield, a range that is termed "the yield plateau". Beyond that range, strain hardening occurs, i.e., additional elongation is associated with an increase in stress. After reaching a maximum nominal stress called "the tensile strength", a drop in the nominal stress accompanies further elongation and precedes fracture at an elongation (at rupture) amounting to 20 to 30 percent of the specimen's original length (see Figure 5-1). It is this ability of structural steel to undergo sizable permanent (plastic) deformations before fracturing, i.e., its ductility, that makes steel a construction material with the required properties for blast resistant design.

Some high strength structural steels do not exhibit a sharp, well defined yield plateau, but rather show continuous yielding with a curved stress-strain relation. For those steels, it is generally accepted to define a quantity analogous to the yield point, called "the yield stress", as that stress which would produce a permanent strain of 0.2 percent or a total unit elongation of 0.4 to 0.5 percent. Although such steels usually have a higher yield stress than those steels which exhibit definite yield and tensile stresses, their elongation at rupture is generally smaller. Therefore, they should be used with caution when large ductilities are a prerequisite of design.

Blast-resistant design is commonly associated with plastic design since protective structures are generally designed with the assumption that economy can be achieved when plastic deformations are permitted. The steels to be used should at least meet the requirements of the American Institute of Steel Construction (AISC) Specification in regard to the adequacy for plastic design.

Since the average yield stress for structural steels having a specified minimum yield stress of 50 ksi or less is generally higher than the specified minimum, it is recommended that the minimum design yield stress, as specified by the AISC specification, be increased by 10 percent. That is, the average yield stress to be used in a blast resistant design shall be 1.1 times the minimum yield stress for these steels. This increase, which is referred to as

the increase factor (a), should not be applied to high strength steels since the average increase may be less than 5 percent.

The minimum yield stress, f_y, and the tensile stress, f_u, (minimum) for structural steel shapes and plates which conform to the American Society for Testing and Materials (ASTM) Specification are listed in Table 5-1. All are admissible in plastic design except for ASTM A514 which exhibits the smallest reserve in ductility since the minimum tensile stress is only 10 percent higher than the minimum yield stress. However, elastic dynamic design may require the use of this steel or its boiler plate equivalent, as in ASTM A517.

5-12.2. Mechanical Properties Under Dynamic Loading, Dynamic Increase Factors

The effects of rapid loading on the mechanical behavior of structural steel have been observed and measured in uniaxial tensile stress tests. Under rapidly applied loads, the rate of strain increases and this has a marked influence on the mechanical properties of structural steel.

Considering the mechanical properties under static loading as a basis, the effects of increasing strain rates are illustrated in Figure 5-1 and can be summarized as follows:

(1) The yield point increases substantially to the dynamic yield stress value. This effect is termed the dynamic increase factor for yield stress.
(2) The modulus of elasticity in general will remain insensitive to the rate of loading.
(3) The ultimate tensile strength increases slightly. However, the percentage increase is less than that for the yield stress. This effect is termed the dynamic increase factor for ultimate stress.
(4) The elongation at rupture either remains unchanged or is slightly reduced due to increased strain rate.

In actual members subjected to blast loading, the dynamic effects resulting from the rapid strain rates may be expressed as a function of the time to reach yielding. In this case, the mechanical behavior depends on both the loading regime and the response of the system which determines the dynamic effect felt by the particular material.

For members made of ASTM A36 and A514 steels, studies have been made to determine the percentage increase in the yield stress as a function of strain rate. Design curves for the dynamic increase factors (DIF) for yield stresses of A36 and A514 structural steel are illustrated in Figure 5-2. Even though ASTM A514 is not recommended for plastic design, the curve in Figure 5-2 may be used for dynamic elastic design.

The strain rate, assumed to be a constant from zero strain to yielding, may be determined according to Equation 5-1:

$$\dot{\epsilon} = f_{ds}/E_s t_E \qquad 5\text{-}1$$

where

$\dot{\epsilon}$ = average strain rate in the elastic range of the steel (in/in/sec)

t_E = time to yield (sec)

f_{ds} = dynamic design stress (Section 5-13)

Dynamic increase factors for yield stresses in various pressure levels in the bending, tension, and compression modes are listed in Table 5-2. The values for bending assume a strain rate of 0.10 in/in/sec in the low design pressure range and 0.30 in/in/sec in the high pressure design range. For tension and compression members, the DIF values assume the strain rates are 0.02 in/in/sec in the low design pressure range and 0.05 in/in/sec in the high design pressure range. Lower strain rates are selected for the tension and compression members since they are likely to carry the reaction of a beam or girder which may exhibit a significant rise time, thereby increasing the time to reach yield in the tension or compression mode.

On the basis of the above, the dynamic increase factors for yield stresses summarized in Table 5-2 are recommended for use in dynamic design. However, a more accurate representation may be derived using Figure 5-2 once the strain rate has been determined.

Steel protective structures and members are generally not designed for excessive deflections, that is, deflections associated with elongations well into the strain-hardening region (see Figure 5-1). However, situations arise where excessive deflections may be tolerated and will not lead to structural failure or collapse. In this case, the ultimate stresses and associated dynamic increase factors for ultimate stresses must be considered. Table 5-3 lists the dynamic increase factors for ultimate stresses of steels. Unlike the dynamic increase factors for yield stress, these values are independent of the pressure ranges.

5-13. Recommended Dynamic Design Stresses

5-13.1. General

The yield point of steel under uniaxial tensile stress is generally used as a base to determine yield stresses under other loading states namely, bending, shear and compression, or tension. The design stresses are also functions of the average strength increase factor, a, and the dynamic increase factor, c.

5-13.2. Dynamic Design Stress for Ductility Ratio $\mu \leq 10$

To determine the plastic strength of a section under dynamic loading, the appropriate dynamic yield stress, f_{dy}, must be used. For a ductility ratio (see Section 5-16.3) $\mu \leq 10$, the dynamic design stress, f_{ds}, is equal to the dynamic yield stress, f_{dy}. In general terms, the dynamic yield stress, f_{dy}, shall be equal to the product of the dynamic increase factor, c, the average yield strength increase factor, a, (see Section 5-12.1) and the specified minimum yield stress of the steel. The dynamic design stress, f_{ds}, for bending, tension, and compression shall be:

$$f_{ds} = f_{dy} = c \times a \times f_y \qquad 5\text{-}2$$

where

f_{dy} = dynamic yield stress

c = dynamic increase factor on the yield stress (Figure 5-2 or Table 5-2)

a = average strength increase factor (= 1.1 for steels with a specified minimum yield stress of 50 ksi or less; = 1.0 otherwise)

f_y = static yield stress from Table 5-1

5-13.3. Dynamic Design Stress for Ductility Ratio, $\mu > 10$

Where excessive deflections or ductility ratios may be tolerated, the dynamic design stress can be increased to account for deformations in the strain-hardening region. In this case, for $\mu > 10$, the dynamic design stress, f_{ds}, becomes

$$f_{ds} = f_{dy} + (f_{du} - f_{dy})/4 \qquad 5\text{-}3$$

where:

f_{dy} = dynamic yield stress from Equation 5-2

f_{du} = dynamic ultimate stress equal to the product of f_u from Table 5-1 and the value of c from Table 5-3 or Figure 5-2

It should be noted that the average strength increase factor, a, does not apply to f_{du}.

5-13.4. Dynamic Design Stress for Shear

The dynamic design stress for shear shall be:

$$f_{dv} = 0.55\ f_{ds} \qquad 5\text{-}4$$

where f_{ds} is from Equation 5-2 or 5-3.

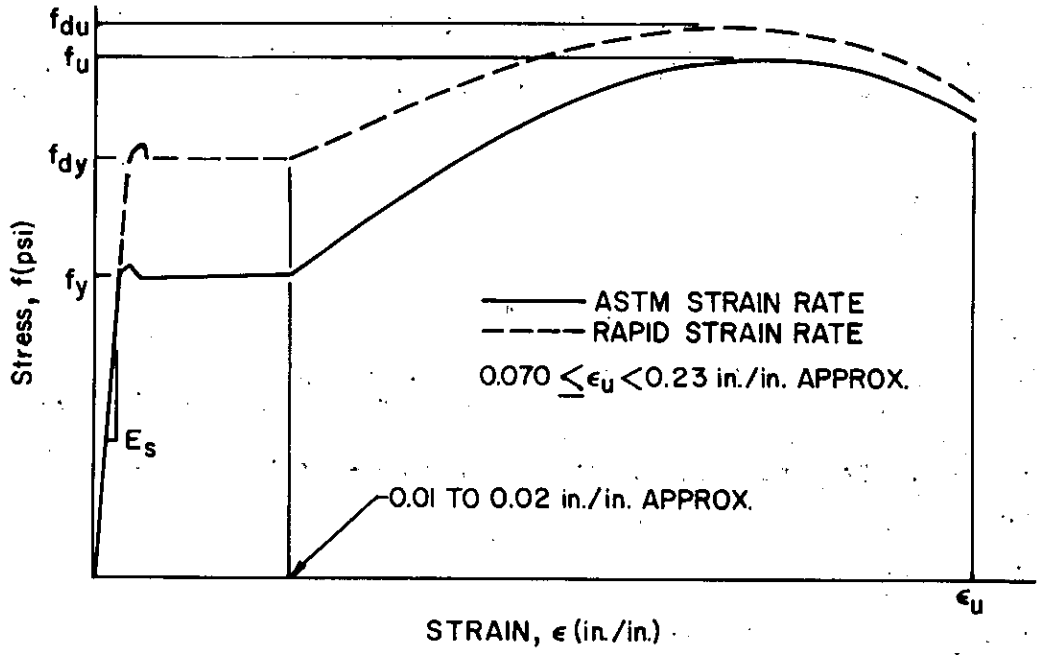


Figure 5-1 Typical stress-strain curves for steel

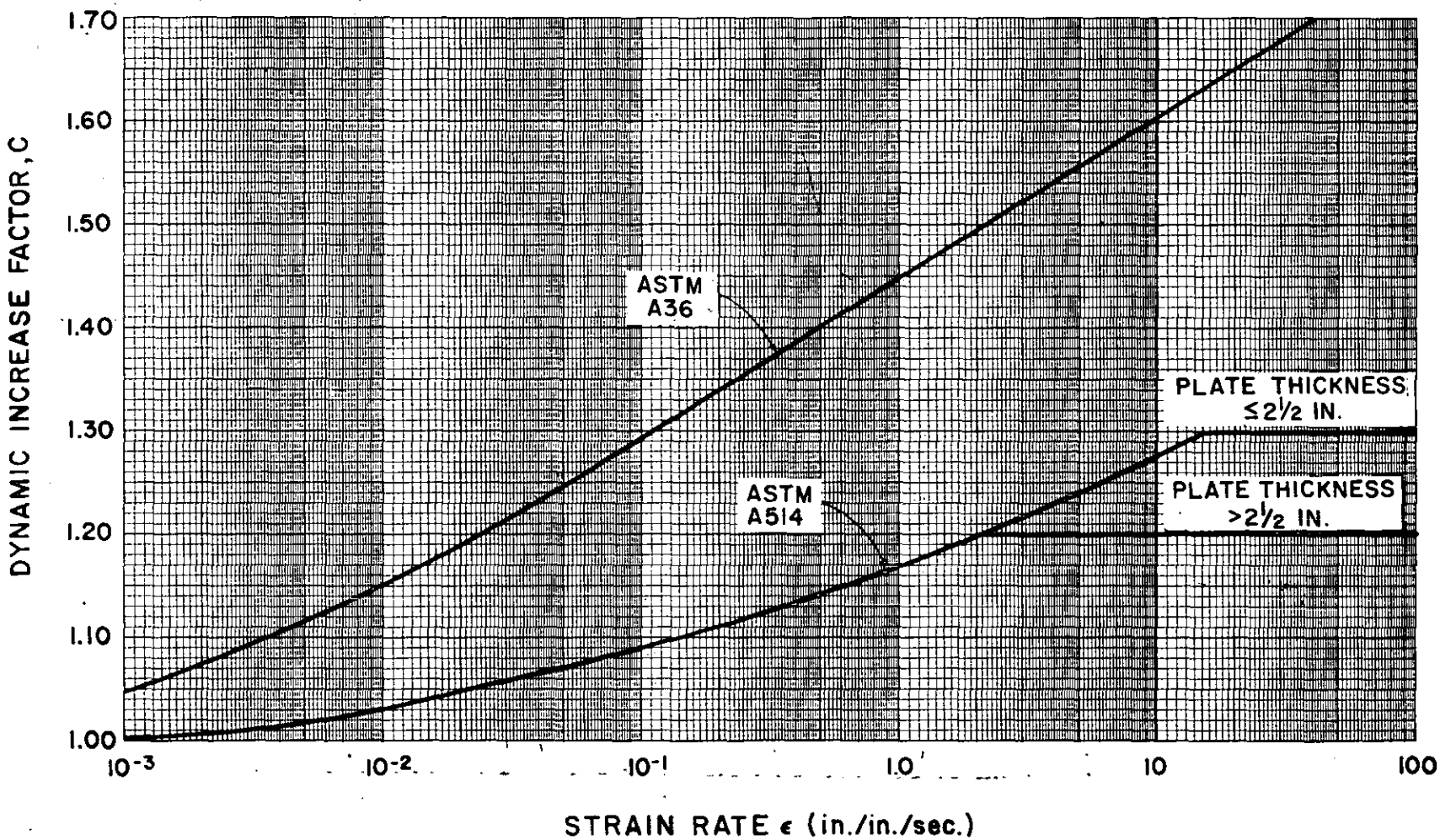


Figure 5-2 Dynamic increase factors for yield stresses at various strain rates for ASTM A-36 and A-514 steels

Table 5-1 Static Design Stresses for Materials

Material (ASTM)	f_y min (ksi)	f_u min (ksi)
A36	36	58
A529	42	60
A441	40	60
	42	63
	46	67
	50	70
A572	42	60
	50	65
	60	75
	65	80
A242	42	63
	46	67
	50	70
A588	42	63
	46	67
	50	70
A514	90	100
	100	110

Table 5-2 Dynamic Increase Factor, c, for Yield Stress of Structural Steels

Material	Bending		Tension or Compression	
	Low Pressure ($\dot{\epsilon}$ = 0.10 in/in/sec)	High Pressure ($\dot{\epsilon}$ = 0.30)	Low Pressure ($\dot{\epsilon}$ = 0.02)	High Pressure ($\dot{\epsilon}$ = 0.05)
A36	1.29	1.36	1.19	1.24
A588	1.19*	1.24*	1.12*	1.15*
A514	1.09	1.12	1.05	1.07

*Estimated

Table 5-3 Dynamic Increase Factor, c, for Ultimate Stress of Structural Steels

Material	c
A36	1.10
A588	1.05*
A514	1.00

*Estimated

DYNAMIC RESPONSE OF STEEL STRUCTURES IN THE PLASTIC RANGE

5-14. Plastic Behavior of Steel Structures

Although plastic behavior is not generally permissible under service loading conditions, it is quite appropriate for design when the structure is subjected to a severe blast loading only once or at most a few times during its existence. Under blast pressures, it will usually be uneconomical to design a structure to remain elastic and, as a result, plastic behavior is normally anticipated in order to utilize more fully the energy-absorbing capacity of blast-resistant structures. Plastic design for flexure is based on the assumption that the structure or member resistance is fully developed with the formation of near totally plastified sections at the most highly stressed locations. For economical design, the structure should be proportioned to assure its ductile behavior up to the limit of its load-carrying capacity. The structure or structural element can attain its full plastic capacity provided that premature impairment of strength due to secondary effects, such as brittle fracture or instability, does not occur.

Structural resistance is determined on the basis of plastic design concepts, taking into account dynamic yield strength values. The design proceeds with the basic objective that the computed deformations of either the individual members or the structure as a whole, due to the anticipated blast loading, should be limited to prescribed maximum values consistent with safety and the desired post accident condition.

5-15. Relationship Between Structure Function and Deformations

5-15.1. General

Deformation criteria are specified in detail for two categories of structures, namely, acceptor-type structures in the low pressure range and structures in the high pressure range which may either be acceptor- or donor-type. A description of the two categories of structures follow.

5-15.2. Acceptor-type Structures in the Low Pressure Ranges

The maximum deformations to be specified in this category are consistent with maintaining structural integrity into the plastic range while providing safety for personnel and equipment. The type of structure generally associated with this design category may be constructed of one or two stories with braced or rigid frames. Main members consisting of columns and main beams should be fabricated from hot rolled steel while secondary members, consisting of purlins or girts which span the frame members, can be hot-rolled I-shapes and channels or cold-formed Z-shapes and channels. The structure skin shall consist of cold-formed siding and decking spanning between the wall girts or roof purlins.

5-15.3. Acceptor- or Donor-type Structures in the High Pressure Range

The deformation criteria specified in this category cover the severe conditions associated with structures located close-in to a blast. In cases where the design objective is the containment of an explosion the deformations should be limited. In other cases where prevention of explosion propagation or of missile generation is required, the structure may be allowed to approach

incipient failure, and deformations well into the strain hardening region may be permitted for energy absorption. In general, plate elements and curved plate-type structures fall under these categories.

5-16. Deformation Criteria

5-16.1. General

The deformation criteria presented in this chapter will be consistent with designing the structure for one accident. However, if it is desirable for a structure to sustain two or three "incidents" in its lifetime, the designer may limit design deformations so that, in its post accident condition, the structure is suitable for repair and reuse.

The deformation criteria for beams (including purlins, spandrels and girts) are presented in Section 5-16.5. The criteria for frames, including sidesway, are presented in Section 5-16.6 and that for plates are given in Section 5-16.7. Special consideration is given to the deformation criteria for open-web joists (Section 5-33) and cold-formed metal decking (Section 5-34). Deformation criteria are summarized in Section 5-35.

5-16.2. Structural Response Quantities

In order to restrict damage to a structure or element which is subjected to the effects of accidental explosion, limiting values must be assigned to appropriate response quantities. Generally speaking, two different types of values are specified, namely, limits on the level of inelastic dynamic response and limits on the maximum deflections and rotations.

For elements which can be represented as single-degree-of-freedom systems such as beams, floor and wall panels, open-web joists, and plates, the appropriate quantities are taken as the maximum ductility ratio and the maximum rotation at an end support.

For systems such as frame structures which can be represented by multi-degree-of-freedom systems, the appropriate quantities are taken as the sidesway deflection and individual frame member rotations.

5-16.3. Ductility Ratio, μ

Following the development in Chapter 3 of this manual, the ductility ratio, μ, is defined as the ratio of the maximum deflection (X_m) to the equivalent elastic deflection (X_E) corresponding to the development of the limiting resistance on the bilinear resistance diagram for the element. Thus, a ductility ratio of 3 corresponds to a maximum dynamic response three times the equivalent elastic response.

In the case of individual beam elements, ductility ratios as high as 20 can be achieved provided that sufficient bracing exists. Subsequent sections of this chapter cover bracing requirements for beam elements. In the case of plate elements, ductility ratios are important insomuch as the higher ductility ratios permit the use of higher design stresses.

Support rotations, as discussed in the next paragraph, provide the basis for beam and plate design. For a beam element, the ductility ratio must be

checked to determine whether the specified rotation can be reached without premature buckling of the member. A similar provision shall apply to plates even though they may undergo larger ductility ratios in the absence of premature buckling.

5-16.4. Support Rotation, θ

The end rotation, θ, and the associated maximum deflection, X_m, for a beam are illustrated in Figure 5-3. As shown, θ is the angle between the chord joining the supports and the point on the element where the deflection is a maximum.

5-16.5. Limiting Deformations for Beams

A steel beam element may be designed to attain large deflections corresponding to 12 degrees support rotation. To assure the integrity of the beam element, it must be adequately braced to permit this high level of ductile behavior. In no case, however, shall the ductility ratio exceed 20.

A limiting support rotation of 2 degrees, and a limiting ductility ratio of 10 (whichever governs) are specified as reasonable estimates of the absolute magnitude of the beam deformation where safety for personnel and equipment is required. These deformations are consistent with maintaining structural integrity into the plastic range. Adequate bracing shall be present to assure the corresponding level of ductile behavior.

The interrelationship between the various parameters involved in the design of beams is readily described in the idealized resistance-deflection curve shown in Figure 5-4. In the figure, the values shown for the ductility ratio, μ, and the support rotation θ, are arbitrary. For example, the deflection corresponding to a 2-degree support rotation can be greater than that corresponding to a ductility ratio of 10.

5-16.6. Application of Deformation Criteria to a Frame Structure

In the detailed analysis of a frame structure, representation of the response by a single quantity is not possible. This fact combined with the wide range and time-varying nature of the end conditions of the individual frame members makes the concept of ductility ratio intractable. Hence, for this case, the response quantities referred to in the criteria are the sidesway deflection of each story and the end rotation, θ, of the individual members with reference to a chord joining the member ends, as illustrated in Figure 5-3. In addition, in lieu of a ductility ratio criterion, the amount of inelastic deformation is restricted by means of a limitation on the individual member rotation. For members which are not loaded between their ends, such as an interior column, θ is zero and only the sidesway criteria must be considered. The maximum member end rotation, as shown in Figure 5-3, shall be 2 degrees. The maximum sidesway deflection is limited to 1/25 of the story height.

These response quantities, sidesway deflection, and end rotation are part of the required output of various computer programs which perform an inelastic, multi-degree-of-freedom analysis of frame structures. These programs are available through the repositories listed in Section 5-4 and several reports listed in the bibliography at the end of this chapter. The designer can use the output of these programs to check the sidesway deflection of each story and the maximum rotation of each member.

5-16.7. Limiting Deformations for Plates

Plates and plate-type structures can undergo large deformations with regard to support rotations and ductility ratios. The effect of overall and local instability upon the ultimate capacity is considerably more important to structural steel shapes than to plates. Depending upon the functional requirements for a plate, the following deformation criteria should be considered in the design of a plate:

(1) Large deflections at or close to incipient failure.

(2) Moderate deflections where the structure is designed to sustain two or three "incidents" before being nonreusable.

(3) Limited deflections where performance of the structure is critical during the blast as in the case of a blast door designed to contain pressure and/or fire leakage.

(4) Elastic deflections where the structure must not sustain permanent deflections, as in the case of an explosives test chamber.

This is a partial list of design considerations for plates. It can be seen that the designer must establish deformation criteria based on the function of the plate or plate system.

A plate or plate-type structure may undergo a support rotation, as illustrated in Figure 3-22 of Chapter 3, of 12 degrees. The corresponding allowable ductility ratio shall not exceed 20. It should be noted that higher design stresses can be utilized when the ductility ratio exceeds 10 (See Section 5-13.3).

A limiting support rotation of 2 degrees is specified as a reasonable estimate of the absolute magnitude of the plate support rotation where safety for personnel and equipment in an acceptor-type structure is required. As in the deformation criteria for beams, the ductility ratio shall not exceed 10.

Two edge conditions may govern the deformation of plates in the plastic region. The first occurs when opposite edges are not built-in. In this case, elastic plate deflection theory and yield-line theory apply. The second involves tension-membrane action which occurs when at least two opposite edges are clamped. In this case, tensile-membrane action can occur before the plate element reaches a support rotation of 12 degrees. Tensile-membrane action of built-in plates is not covered in this chapter. However, the designer can utilize yield-line theory for limited plate deflection problems.

The interrelationship between the various parameters involved in the design of plates is readily described in the idealized resistance-deflection curve shown in Figure 5-5. The figure shows the values for the ductility ratio, μ, and the support rotation, θ, are arbitrary. For example, the deflection corresponding to a 2-degree support rotation can be greater than that corresponding to a ductility ratio of 10.

5-17. Rebound

Another aspect of dynamic design of steel structures subjected to blast loadings is the occurrence of rebound. Unlike the conditions prevailing in reinforced concrete structures where rebound considerations may not be of primary concern, steel structures will be subjected to relatively large stress reversals caused by rebound and will require lateral bracing of unstayed compression flanges which were formerly in tension. Rebound is more critical for elements supporting light dead loads and subjected to blast pressures of short duration. It is also a primary concern in the design of reversal bolts for blast doors.

5-18. Secondary Modes of Failure

5-18.1. General

In the process of designing for the plastic or ductile mode of failure, it is important to follow certain provisions in order to avoid premature failure of the structure, i.e., to ensure that the structure can develop its full plastic resistance.

These secondary modes of failure can be grouped in two main categories:

(1) Instability modes of failure

(2) Brittle modes of failure

5-18.2. Instability Modes of Failure

In this category, the problem of structural instability at two levels is of concern, namely, overall buckling of the structural system as a whole, and buckling of the component elements.

Overall buckling of framed structures can occur in two essentially different manners. In the first case, the load and the structure are symmetric; deformations remain also symmetric up to a critical value of the load for which a sudden change in configuration will produce instant anti-symmetry, large sidesway and displacement, and eventually a failure by collapse if not by excessive deformations. This type of instability can also occur in the elastic domain before substantial deformation or any plastification has taken place. It is called "instability by bifurcation".

In the second case, the loading or the structure or both are nonsymmetric. With the application of the load, sidesway develops progressively. In such cases, the vertical loads acting through the sidesway displacements, commonly called "the P-Δ effect", create second order bending moments that magnify the deformation. Because of rapidly increasing displacements, plastic hinges form, thereby decreasing the rigidity of the structure and causing more sidesway. This type of instability is related to a continuous deterioration of the stiffness leading to an early failure by either a collapse mechanism or excessive sidesway.

Frame instability need not be explicitly considered in the plastic design of one- and two-story unbraced frames provided that the individual columns and girders are designed according to the beam-column criteria of Section 5-37.

For frames greater than two stories, bracing is normally required according to the AISC provisions for plastic design in order to ensure the overall stability of the structure. However, if an inelastic dynamic frame analysis is performed to determine the complete time-history of the structural response to the blast loading, including the P-Δ effects, it may be established, in particular cases, that lateral bracing is not necessary in a frame greater than two stories. As mentioned previously, computer programs which perform an inelastic, multi-degree-of-freedom analysis of frame structures may be employed for such an analysis.

Buckling of an element in the structure (e.g., a beam, girder, or column) can occur under certain loading and end conditions. Instability is of two types, namely, buckling of the member as a whole (e.g., lateral torsional buckling) and local buckling at certain sections, including flange buckling and web crippling.

Provisions for plastic design of beams and columns are presented in a separate section of this chapter.

5-18.3. Brittle Modes of Failure

Under dynamic loading, there is an enhanced possibility that brittle fracture can develop under certain conditions. Since this type of failure is sudden in nature and difficult to predict, it is very important to diminish the risk of such premature failure.

The complexity of the brittle fracture phenomena precludes a complete quantitative definition. As a result, it is impossible to establish simple rules for design. Brittle fracture will be associated with a loss in flexural resistance.

Brittle fractures are caused by a combination of adverse circumstances that may include a few, some, or all of the following:

(1) Local stress concentrations and residual stresses

(2) Poor welding

(3) The use of a notch sensitive steel

(4) Shock loading or rapid strain rate

(5) Low temperatures

(6) Decreased ductility due to strain aging

(7) The existence of a plane strain condition causing a state of triaxial tension stresses, especially in thick gusset plates, thick webs and in the vicinity of welds

(8) Inappropriate use of some forms of connections

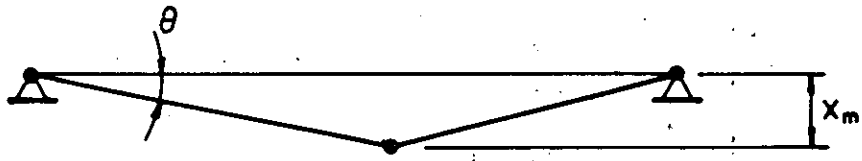
The problem of brittle fracture is closely related to the detailing of connections, a topic that will be treated in a separate section of this chapter.

However, there are certain general guidelines to follow in order to minimize the danger of brittle fracture:

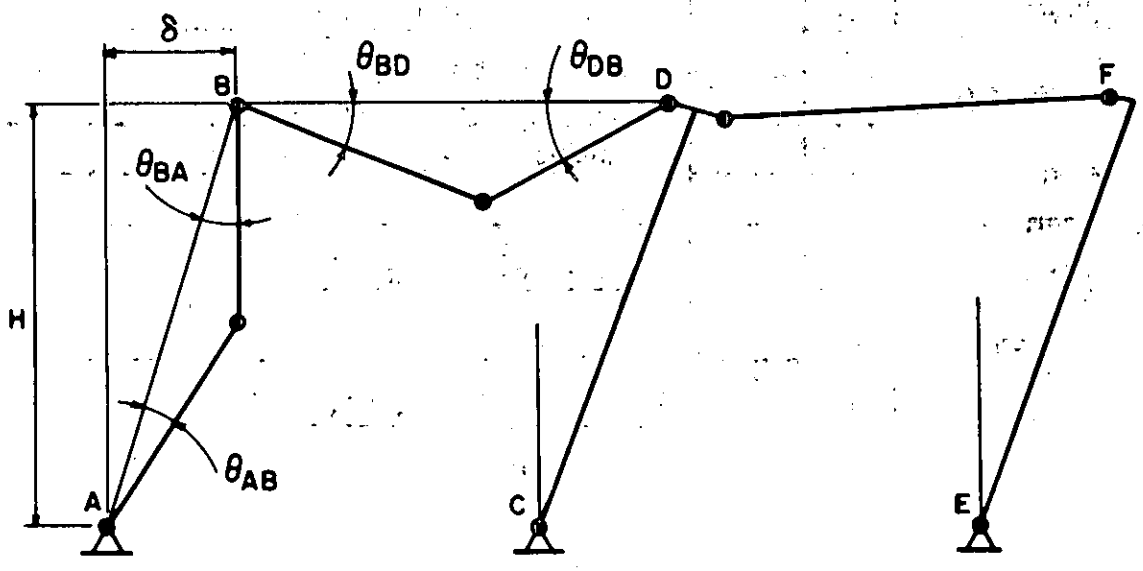
(1) Steel material must be selected to conform with the condition anticipated in service.

(2) Fabrication and workmanship should meet high standards, e.g., sheared edges and notches should be avoided, and material that has been severely cold-worked should be removed.

(3) Proportioning and detailing of connections should be such that free movement of the base material is permitted, stress concentrations and triaxial stress conditions are avoided, and adequate ductility is provided.



BEAM, SLAB OR PANEL



FRAME

Figure 5-3 Member end rotations for beams and frames

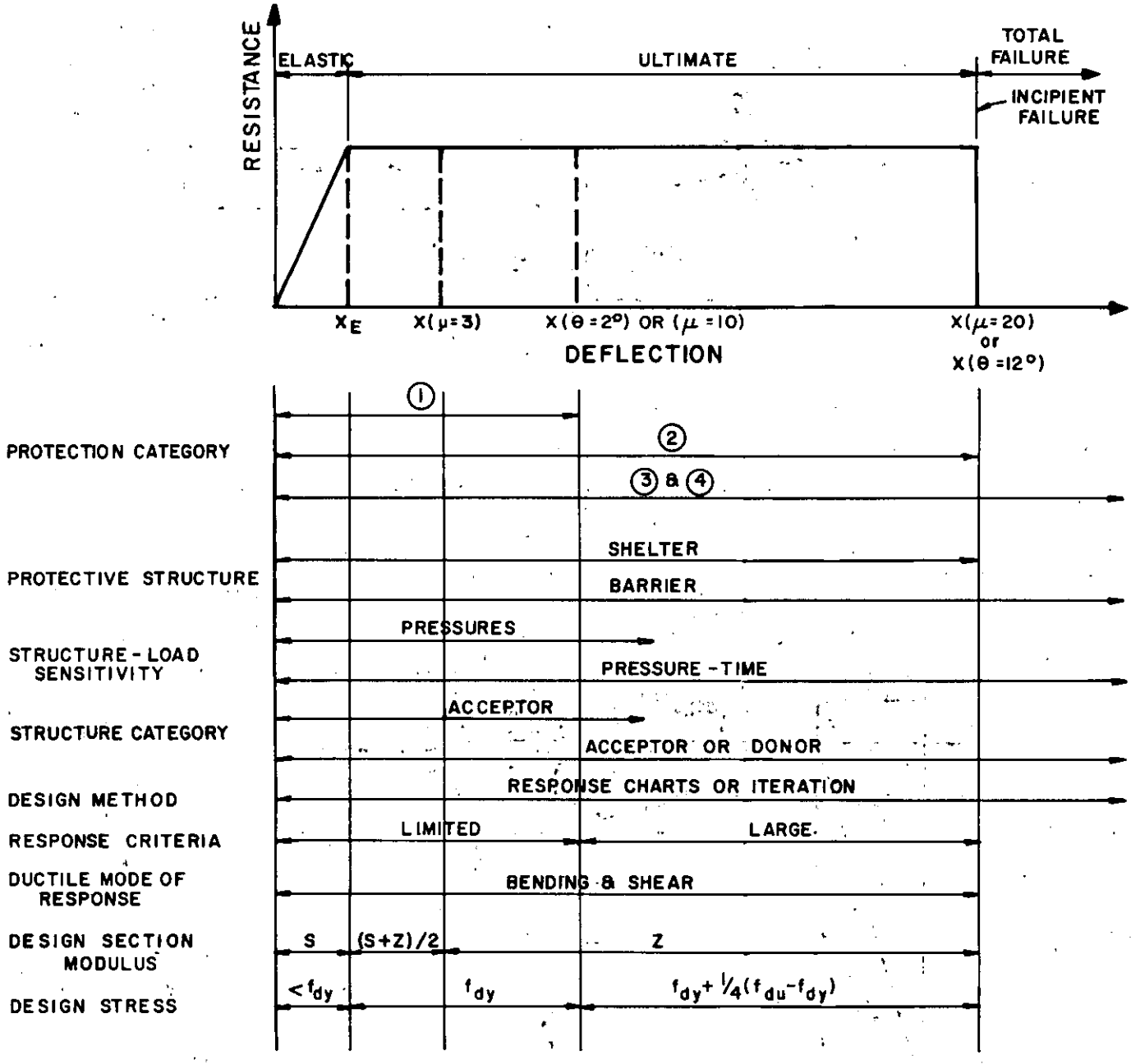


Figure 5-4 Relationships between design parameters for beams

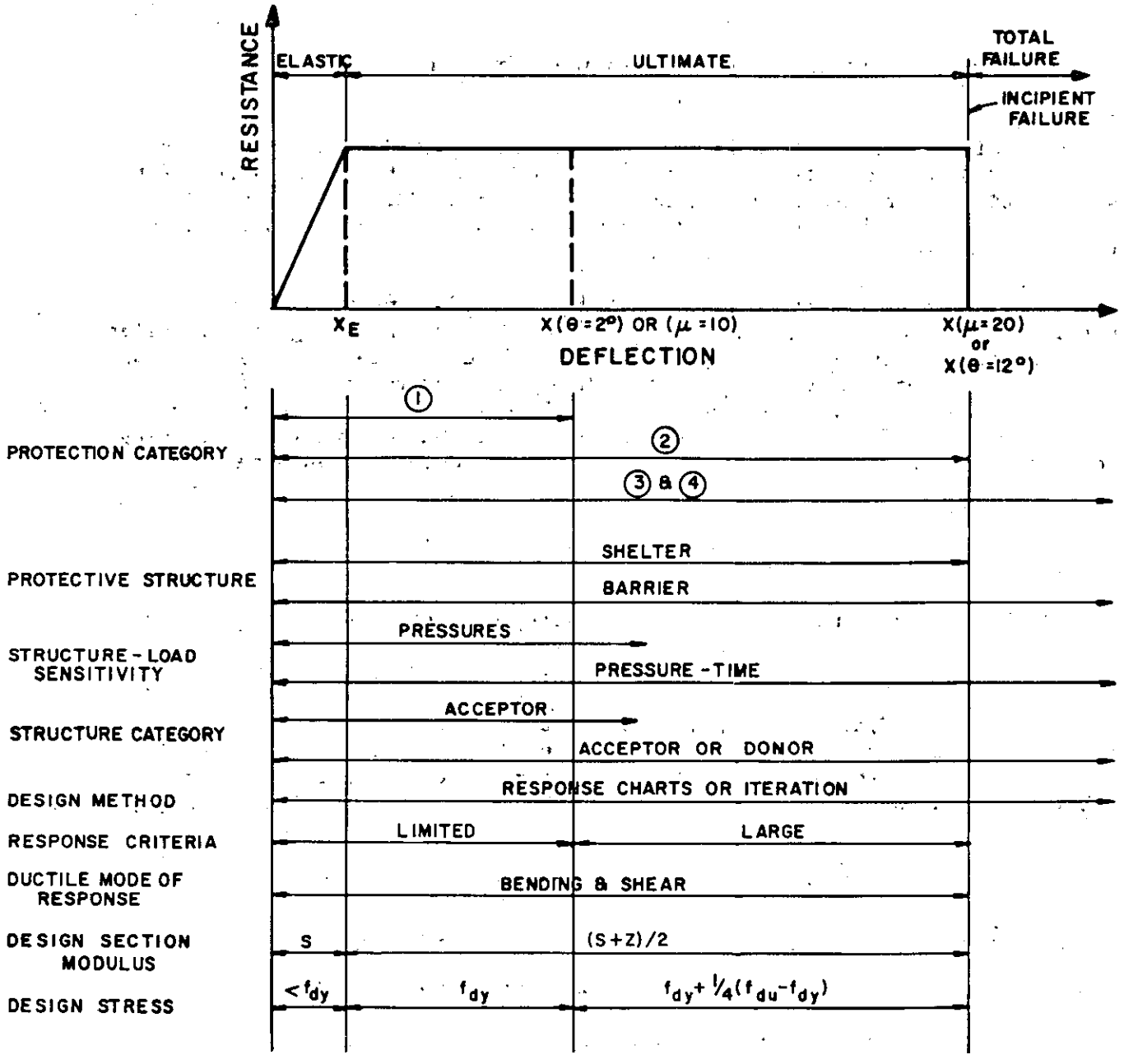


Figure 5-5 Relationships between design parameters for plates

DESIGN OF SINGLE SPAN AND CONTINUOUS BEAMS

5-19. General

The emphasis in this section is on the dynamic plastic design of structural steel beams. Design data have been derived from the static provisions of the AISC Specification with necessary modifications and additions for blast design. It should be noted that all provisions on plastic design in the AISC Specification apply, except as modified in this chapter.

The calculation of the dynamic flexural capacity of beams is described in detail. The necessary information is presented for determining the equivalent bilinear resistance-deflection functions used in evaluating the basic flexural response of beams. Also presented are the supplementary considerations of adequate shear capacity and local and overall stability which are necessary for the process of hinge formation, moment redistribution and inelastic hinge rotation to proceed to the development of a full collapse mechanism.

5-20. Dynamic Flexural Capacity

5-20.1. General

The ultimate dynamic moment resisting capacity of a steel beam is given by

$$M_{pu} = f_{ds} Z \qquad 5\text{-}5$$

where f_{ds} is the dynamic design stress (as described in Section 5-13) of the material and Z is the plastic section modulus. The plastic section modulus can be calculated as the sum of the static moments of the fully yielded elements of the equal cross section areas above and below the neutral axis, i.e.:

$$Z = A_c m_1 + A_t m_2 \qquad 5\text{-}6$$

Note: $A_c m_1 = A_t m_2$ for a doubly-symmetric section

where A_c = area of cross section in compression

A_t = area of cross section in tension

m_1 = distance from neutral axis to the centroid of the area in compression

m_2 = distance from neutral axis to the centroid of the area in tension

For standard I-shaped sections (S, W, and M shapes), the plastic section modulus is approximately 1.15 times the elastic modulus for strong axis bending and may be obtained from standard manuals on structural steel design.

It is generally assumed that a fully plastic section offers no additional resistance to load. However, additional resistance due to strain hardening of the material is present as the deformation continues beyond the yield level of the beam. In the analysis of structural steel beams, it is assumed that the plastic hinge formation is concentrated at a section. Actually, the plastic region extends over a certain length that depends on the type of loading

(concentrated or distributed) on the magnitude of the deformation, and on the shape factor of the cross section. The extent of the plastic hinge has no substantial influence on the ultimate capacity; it has, however, an influence on the final magnitude of the deflection. For all practical purposes, the assumption of a concentrated plastic hinge is adequate.

In blast design, although strains well into the strain-hardening range may be tolerated, the corresponding additional resistance is generally not sufficient to warrant analytical consideration since excessive support rotation and/or ductility ratios of beams, which are susceptible to local flange or lateral torsional buckling, are not recommended.

5-20.2. Moment-curvature Relationship for Beams

Figure 5-6 shows the stress distribution at various stages of deformation for a plastic hinge section. Theoretically, the beam bends elastically until the outer fiber stress reaches f_{ds} and the yield moment designated by M_y is attained (Figure 5-6a). As the moment increases above M_y, the yield stress progresses inward from the outer fibers of the section towards the neutral axis as shown in Figure 5-6b. As the moment approaches the fully plastic moment, a rectangular stress distribution as shown in Figure 5-6c is approached. The ratio between the fully plastic moment to the yield moment is the shape factor, f, for the section, i.e., the ratio between the plastic and elastic section modulii.

A representative moment-curvature relationship for a simply-supported steel beam is shown in Figure 5-7. The behavior is elastic until the yield moment My is reached. With further increase in load, the curvature increases at a greater rate as the fully plastic moment value, M_2, is approached. Following the attainment of M_2, the curvature increases significantly, with only a small increase in moment capacity.

For design purposes, a bilinear representation of the moment-curvature relationship is employed as shown by the dashed lines in Figure 5-7. For beams with a moderate design ductility ratio ($\mu \leq 3$), the design moment $M_p = M_1$. For beams with a larger design ductility ratio ($\mu > 3$), the design moment $M_p = M_2$.

5-20.3. Design Plastic Moment, M_p

The equivalent plastic design moment shall be computed as follows:

For beams with ductility ratios less than or equal to 3:

$$M_p = f_{ds} (S + Z)/2 \qquad 5\text{-}7$$

where S and Z are the elastic and plastic section modulii, respectively. For beams with ductility ratios greater than 3 and beam columns:

$$M_p = f_{ds}Z \qquad 5\text{-}8$$

Equation 5-7 is consistent with test results for beams with moderate ductilities. For beams which are allowed to undergo large ductilities, Equation 5-8, based upon full plastification of the section, is considered reasonable for design purposes.

It is important to note that the above pertains to beams which are supported against buckling. Design provisions for guarding against local and overall buckling of beams during plastic deformation are discussed in Sections 5-24, 5-25, and 5-26.

5-21. Resistance and Stiffness Functions

5-21.1. General

The single-degree-of-freedom analysis which serves as the basis for the flexural response calculation requires that the equivalent stiffness and ultimate resistance be defined for both single-span beams and continuous beams. The ultimate resistance values correspond to developing a full collapse mechanism in each case. The equivalent stiffnesses correspond to load-deflection relationships that have been idealized as bilinear functions with initial slopes so defined that the areas under the idealized load deflection diagrams are equal to the areas under the actual diagrams at the point of inception of fully plastic behavior of the beam. This concept is covered in Section 3-13 of Chapter 3.

5-21.2. Single-span Beams

Formulas for determining the stiffness and resistance for one-way steel beam elements are presented in Tables 3-1 and 3-8 of Chapter 3. The values of M in Table 3-1 represents the plastic design moment, M_p. For example, the value of r_u for the fixed-simple, uniformly loaded beam becomes $r_u = 12\ M_p/L^2$.

5-21.3. Multi-span Beams

The beam relationships for defining the bilinear resistance function for multi-span continuous beams under uniform loading are summarized below. These expressions are predicated upon the formation of a three-hinge mechanism in each span. Maximum economy normally dictates that the span lengths and/or member sizes be adjusted such that a mechanism forms simultaneously in all spans.

It must be noted that the development of a mechanism in a particular span of a continuous beam assumes compatible stiffness properties at the end supports. If the ratio of the length of the adjacent spans to the span being considered is excessive (say, greater than three). it may not be possible to reach the limit load without the beam failing by excessive deflection.

For uniformly distributed loading on equal spans or spans which do not differ in length by more than 20 percent, the following relationships can be used to define the bilinear resistance function:

Two-span continuous beam:

$$R_u = r_u bL = 12\ M_p/L \qquad 5\text{-}9$$

$$K_E = 163\ EI/L^3 \qquad 5\text{-}10$$

Exterior span of continuous beams with three or more spans:

$$R_u = r_u bL = 11.7 M_p/L \qquad 5\text{-}11$$

$$K_E = 143EI/L^3 \qquad 5\text{-}12$$

Interior span of continuous beam with three or more spans:

$$R_u = r_u bL = 16.0M_p/L \qquad 5\text{-}13$$

$$K_E = 300EI/L^3 \qquad 5\text{-}14$$

For design situations which do not meet the required conditions, the bilinear resistance function may be developed by the application of the basic procedures of plastic analysis.

5-22. Design for Flexure

5-22.1. General

The design of a structure to resist the blast of an accidental explosion consists essentially of the determination of the structural resistance required to limit calculated deflections to within the prescribed maximum values as outlined in Section 5-35. In general, the resistance and deflection may be computed on the basis of flexure provided that the shear capacity of the web is not exceeded. Elastic shearing deformations of steel members are negligible as long as the depth to span ratio is less than about 0.2 and hence, a flexural analysis is normally sufficient for establishing maximum deflections.

5-22.2. Response Charts

Dynamic response charts for one-degree-of-freedom systems in the elastic or elasto-plastic range under various dynamic loads are given in Chapter 3. To use the charts, the effective natural period of vibration of a structural steel beam must be determined. The procedures for determining the natural period of vibration for one-way elements are outlined in Section 3-17.4 of Chapter 3. Equation 5-15 can be used to determine the natural period of vibration for any system for which the total effective mass, M_e, and equivalent elastic stiffness, K_E are known:

$$T_N = 2\pi (M_e / K_E)^{1/2} \qquad 5\text{-}15$$

5-22.3. Preliminary Dynamic Load Factors

For preliminary flexural design of beams situated in low pressure range, it is suggested that an equivalent static ultimate resistance equal to the peak blast pressure be used for those beams designed for 2 degrees support rotation. For large support rotations, a preliminary dynamic load factor of 0.5 is recommended. Since the duration of the loading for low pressure range will generally be the same or longer than the period of vibration of the structure, revisions to this preliminary design from a dynamic analysis will usually not be substantial. However, for structures where the loading environment pressure is such that the load duration is short as compared with the period of vibration of the structure, this procedure may result in a substantial overestimate of the required resistance.

5-22.4. Additional Considerations in Flexural Design

Once a dynamic analysis is performed on the single span or continuous beam, the deformations must be checked with the limitations set in the criteria. The provisions for local buckling, web crippling and lateral bracing must be met. The deformation criteria for beam elements including purlins, spandrels and girts are summarized in Section 5-35.

The rebound behavior of the structure must not be overlooked. The information required for calculating the elastic rebound of structures is contained in Figure 3-268 of Chapter 3. The provisions for local buckling and lateral bracing, as outlined in subsequent sections of this chapter, shall apply in the design for rebound.

5-23. Design for Shear

Shearing forces are of significance in plastic design primarily because of their possible influence on the plastic moment capacity of a steel member. At points where large bending moments and shear forces exist, the assumption of an ideal elasto-plastic stress-strain relationship indicates that during the progressive formation of a plastic hinge, there is a reduction of the web area available for shear. This reduced area could result in an initiation of shear yielding and possibly reduce the moment capacity.

However, it has been found experimentally that I-shaped sections achieve their fully plastic moment capacity provided that the average shear stress over the full web area is less than the yield stress in shear. This result can basically be attributed to the fact that I-shaped sections carry moment predominantly through the flanges and shear predominantly through the web. Other contributing factors include the beneficial effects of strain hardening and the fact that combinations of high shear and high moment generally occur at locations where the moment gradient is steep.

The yield capacity of steel beams in shear is given by:

$$V_p = f_{dv} A_w \qquad 5\text{-}16$$

where V_p is the shear capacity, f_{dv} is the dynamic yield stress in shear of the steel (Equation 5-4), and A_w is the area of the web. For I-shaped beams and similar flexural members with thin webs, only the web area between flange plates should be used in calculating A_w.

For several particular load and support conditions, equations for the support shears, V, for one-way elements are given in Table 3-9 of Chapter 3. As discussed above, as long as the acting shear V does not exceed V_p, I-shaped sections can be considered capable of achieving their full plastic moment. If V is greater than V_p, the web area of the chosen section is inadequate and either the web must be strengthened or a different section should be selected.

However, for cases where the web is being relied upon to carry a significant portion of the moment capacity of the section, such as rectangular cross section beams or built-up sections, the influence of shear on the available moment capacity must be considered as treated in Section 5-31.

5-24. Local Buckling

In order to ensure that a steel beam will attain fully plastic behavior and attain the desired ductility at plastic hinge locations, it is necessary that the elements of the beam section meet minimum thickness requirements sufficient to prevent a local buckling failure. Adopting the plastic design requirements of the AISC Specification, the width-thickness ratio for flanges of rolled I- and W-shapes and similar built-up single web shapes that would be subjected to compression involving plastic hinge rotation shall not exceed the following values:

f_y (ksi)	$b_f/2t_f$
36	8.5
42	8.0
45	7.4
50	7.0
55	6.6
60	6.3
65	6.0

where f_y is the specified minimum static yield stress for the steel (Table 5-1), b_f is the flange width, and t_f is the flange thickness.

The width-thickness ratio of similarly compressed flange plates in box sections and cover plates shall not exceed $190/(f_y)^{1/2}$. For this purpose, the width of a cover plate shall be taken as the distance between longitudinal lines of connecting rivets, high-strength bolts, or welds.

The depth-thickness ratio of webs of members subjected to plastic bending shall not exceed the value given by Equation 5-17 or 5-18 as applicable.

$$\frac{d}{t_w} = \frac{412}{f_y}\left[1 - 1.4\frac{P}{P_y}\right] \quad \text{when} \quad \frac{P}{P_y} \leq 0.27 \qquad 5\text{-}17$$

$$\frac{d}{t_w} = \frac{257}{f_y} \quad \text{when} \quad \frac{P}{P_y} > 0.27 \qquad 5\text{-}18$$

where

P = the applied compressive load

P_y = the plastic axial load equal to the cross-sectional area times the specified minimum static yield stress, f_y

These equations which are applicable to local buckling under dynamic loading have been adopted from the AISC provisions for static loading. However, since the actual process of buckling takes a finite period of time, the member must accelerate laterally and the mass of the member provides an inertial force retarding this acceleration. For this reason, loads that might otherwise cause failure may be applied to the members for very short durations if they

are removed before the buckling has occurred. Hence, it is appropriate and conservative to apply the criteria developed for static loads to the case of dynamic loading of relatively short duration.

These requirements on cross section geometry should be adhered to in the design of all members for blast loading. However, in the event that it is necessary to evaluate the load-carrying capacity of an existing structural member which does not meet these provisions, the ultimate capacity should be reduced in accordance with the recommendations made in the Commentary and Appendix C of the AISC Specification.

5-25. Web Crippling

Since concentrated loads and reactions along a short length of flange are carried by compressive stresses in the web of the supporting member, local yielding may occur followed by crippling or crumpling of the web. Stiffeners bearing against the flanges at load points and fastened to the web are usually employed in such situations to provide a gradual transfer of these forces to the web.

Provisions for web stiffeners, as given in Section 1.15.5 of the AISC Specification, should be used in dynamic design. In applying these provisions, f_y should be taken equal to the specified static yield strength of the steel.

5-26. Lateral Bracing

5-26.1. General

Lateral bracing support is often provided by floor beams, joists or purlins which frame into the member to be braced. The unbraced lengths (l_{cr}, as defined in Sections 5-26.2 and 5-26.3) are either fixed by the spacing of the purlins and girts or by the spacing of supplementary bracing.

When the compression flange is securely connected to steel decking or siding, this will constitute adequate lateral bracing in most cases. In addition, inflection points (points of contraflexure) can be considered as braced points.

Members built into a masonry wall and having their web perpendicular to this wall can be assumed to be laterally supported with respect to their weak axis of bending. In addition, points of contraflexure can be considered as braced points, if necessary.

Members subjected to bending about their strong axis may be susceptible to lateral-torsional buckling in the direction of the weak axis if their compression flange is not laterally braced. Therefore, in order for a plastically designed member to reach its collapse mechanism, lateral supports must be provided at the plastic hinge locations and at a certain distance from the hinge location. Rebound, which constitutes stress reversals, is an important consideration for lateral bracing support.

5-26.2. Requirements for Members with $\mu \leq 3$

Since members with the design ductility ratios less than or equal to three undergo moderate amounts of plastic deformation, the bracing requirements are somewhat less stringent.

For this case, the following relationship may be used:

$$1/r_T = \left[(102 \times 10^3 C_b)/f_{ds}\right]^{1/2} \qquad 5\text{-}19$$

where

l = distance between cross sections braced against twist or lateral displacement of the compression flange

r_T = radius of gyration of a section comprising the compression flange plus one-third of the compression web area taken about an axis in the plane of the web

C_b = bending coefficient defined in Section 1.5.1.4.5 of the AISC Specification

5-26.3. Requirements for Members with $\mu > 3$

In order to develop the full plastic moment, M_p for members with design ductility ratios greater than three, the distance from the brace at the hinge location to the adjacent braced points should not be greater than l_{cr} as determined from either Equation 5-20 or 5-21, as applicable:

$$\beta \frac{l_{cr}}{r_y} = \frac{1375}{f_{ds}} + 25 \text{ when } 1.0 \geq \frac{M}{M_p} > -0.5 \qquad 5\text{-}20$$

$$\beta \frac{l_{cr}}{r_y} = \frac{1375}{f_{ds}} \text{ when } -0.5 \geq \frac{M}{M_p} \geq -1.0 \qquad 5\text{-}21$$

where

r_y = the radius of gyration of the member about its weak axis

M = the lesser of the moments at the ends of the unbraced segment

M/M_p = the end moment ratio. The moment ratio is positive when the segment is bent in reverse curvature and negative when bent in single curvature.

β = critical length correction factor (See Figure 5-8)

The critical length correction factor, β, accounts for the fact that the required spacing of bracing, l_{cr}, decreases with increased ductility ratio. For example, for a particular member with $r_y = 2$ in. and $f_{ds} = 51$ ksi and using the equation for $M/M_p = 0$, we get $l_{cr} = 71.7$ in. for $\mu = 6$ and $l_{cr} = 39.7$ in. for $\mu = 20$.

5-26.4. Requirements for Elements Subjected to Rebound

The bracing requirements for nonyielded segments of members and the bracing requirements for members in rebound can be determined from the following relationship:

$$f = 1.67 \left[2/3 - \frac{f_{ds} \, (l/r_T)^2}{1530 \times 10^3 \, C_b} \right] f_{ds} \qquad 5\text{-}22$$

where

f = the maximum bending stress in the member, and in no case greater than f_{ds}

When f equals f_{ds}, this equation reduces to the l/r_T requirement of Equation 5-19.

5-26.5. Requirements for Bracing Members

In order to function adequately, the bracing member must meet certain minimum requirements on axial strength and axial stiffness. These requirements are quite minimal in relation to the properties of typical framing members.

Lateral braces should be welded or securely bolted to the compression flange and, in addition, a vertical stiffener should generally be provided at bracing points where concentrated vertical loads are also being transferred. Plastic hinge locations within uniformly loaded spans do not generally require a stiffener. Examples of lateral bracing details are presented in Figure 5-9.

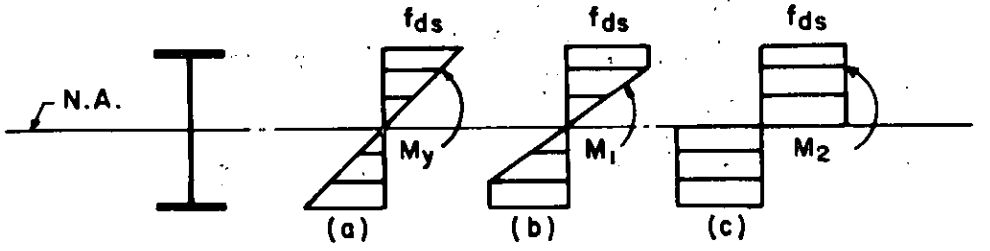


Figure 5-6 Theoretical stress distribution for pure bending at various stages of dynamic loading

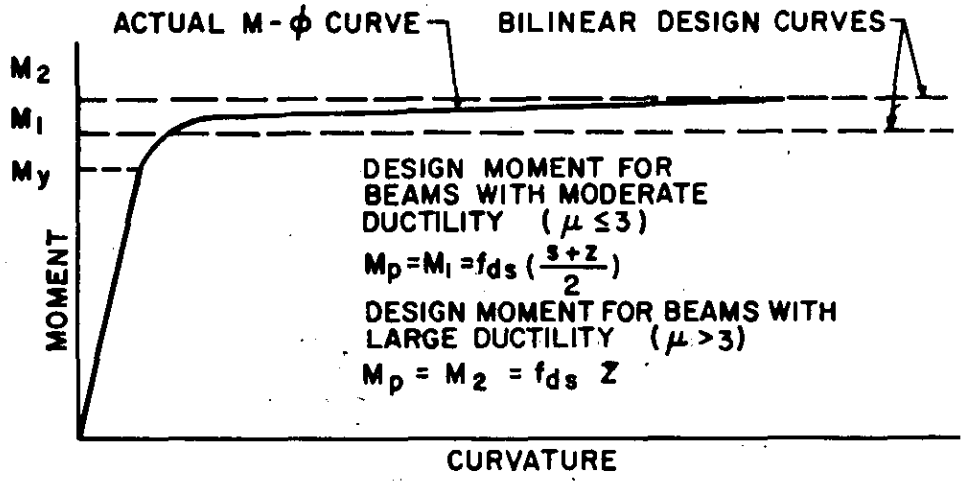


Figure 5-7 Moment-curvature diagram for simple-supported, dynamically loaded, I-shaped beams

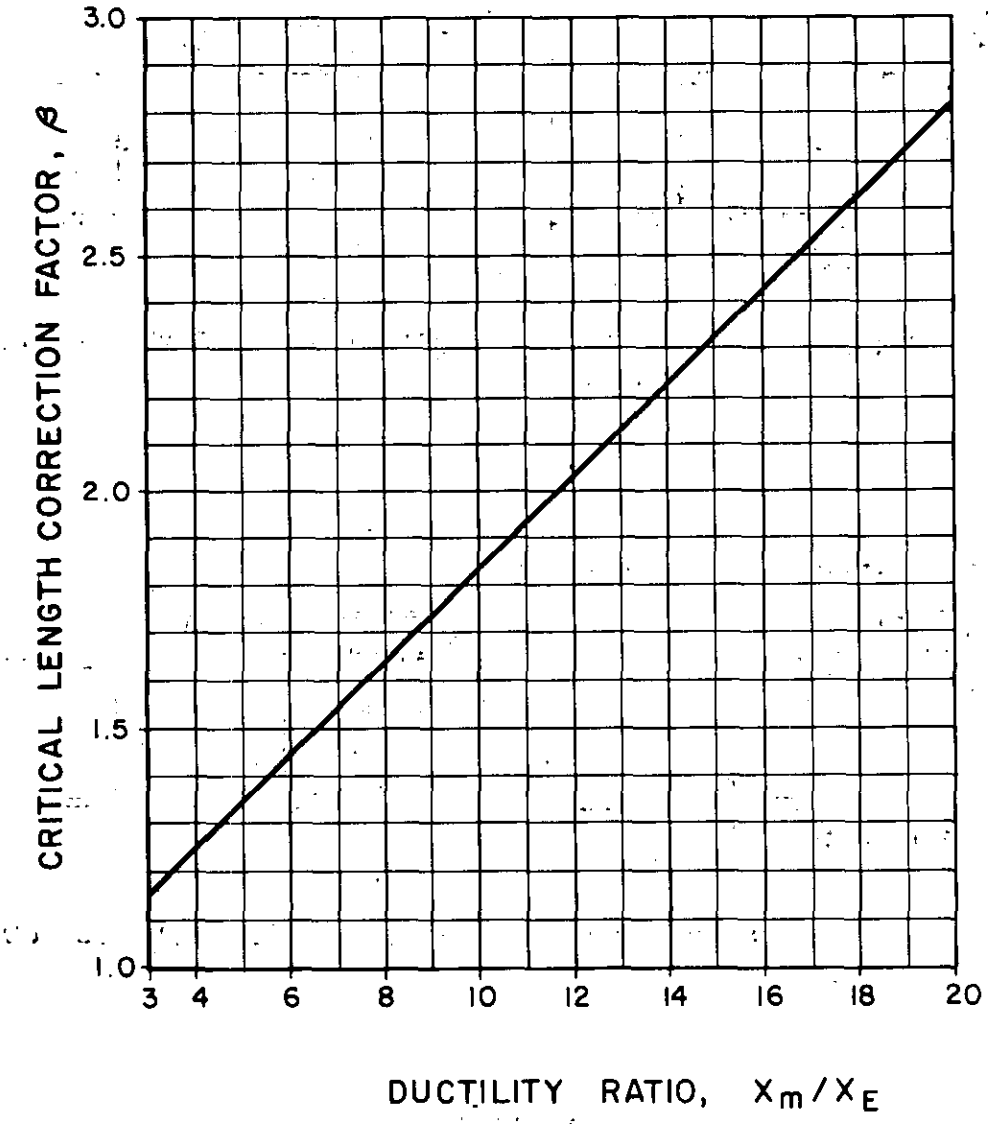
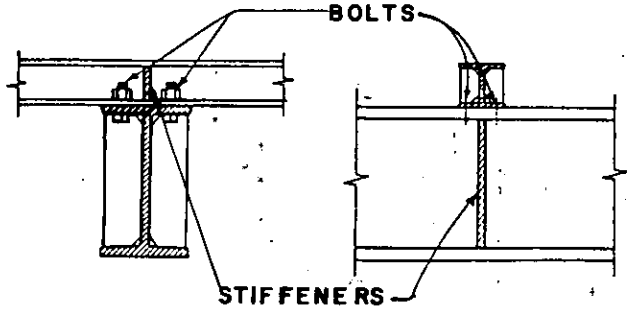
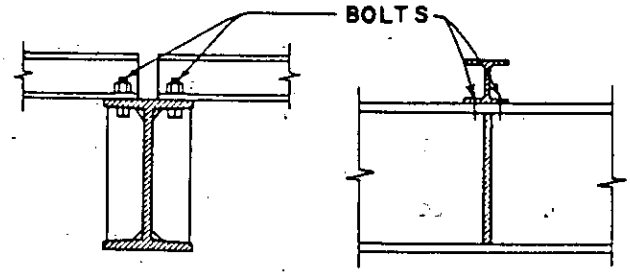


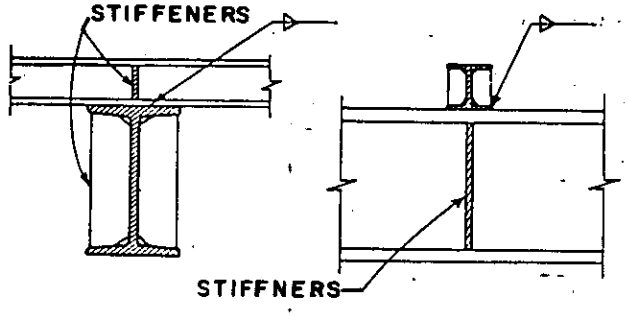
Figure 5-8 Values of β for use in equations 5-20 and 5-21



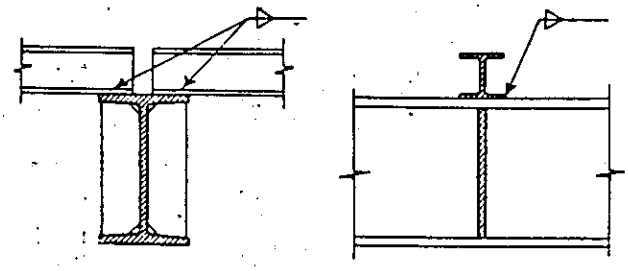
BOLTED CONTINUOUS CONNECTION



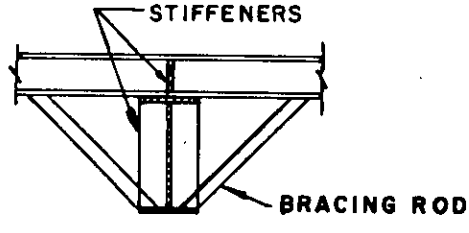
BOLTED DISCONTINUOUS CONNECTION



WELDED CONTINUOUS CONNECTION



WELDED DISCONTINUOUS CONNECTION



TIED BOTTOM FLANGE CONNECTION

Figure 5-9 Typical lateral bracing details

DESIGN OF PLATES

5-27. General

The emphasis in this section is on the dynamic plastic design of plates. As in the case for simply supported and continuous beams, design data have been derived from the static provisions of the AISC Specification with necessary modifications and additions for blast design.

This section covers the dynamic flexural capacity of plates, as well as the necessary information for determining the equivalent bilinear resistance-deflection functions used in evaluating the flexural response of plates. Also presented is the supplementary consideration of adequate shear capacity at negative yield lines.

5-28. Dynamic Flexural Capacity

As is the case for standard I-shaped sections, the ultimate dynamic moment-resisting capacity of a steel plate is a function of the elastic and plastic modulii and the dynamic design stress. For plates or rectangular cross section beams, the plastic section modulus is 1.5 times the elastic section modulus.

A representative moment-curvature relationship for a simply-supported steel plate is shown in Figure 5-10. The behavior is elastic until a curvature corresponding to the yield moment M_y is reached. With further increase in load, the curvature increases at a greater rate as the fully plastic moment value, M_2, is approached. Following the attainment of M_2, the curvature increases while the moment remains constant.

For plates and rectangular cross section beams, M_2 is 50 percent greater than M_y, and the nature of the transition from yield to the fully plastic condition depends upon the plate geometry and end conditions. It is recommended that a capacity midway between M_y and M_2 be used to define the plastic design moment, M_p (M_1 in Figure 5-11), for plates and rectangular cross section beams. Therefore, for plates with any ductility ratio, Equation 5-7 applies.

5-29. Resistance and Stiffness Functions

Procedures for determining stiffness and resistance factors for one- and two-way plate elements are outlined in Chapter 3. These factors are based upon elastic deflection theory and the yield-line method, and are appropriate for defining the stiffness and ultimate load-carrying capacity of ductile structural steel plates. In applying these factors to steel plates, the modulus of elasticity should be taken equal to 29,600,000 psi. For two-way isotropic steel plates, the ultimate unit positive and negative moments are equal in all directions; i.e.

$$M_{vn} = M_{vp} = M_{hn} = M_{hp} = M_p$$

where M_p is defined by Equation 5-7 and the remaining values are ultimate unit moment capacities as defined in Section 3-9.3 of Chapter 3. Since the stiffness factors were derived for plates with equal stiffness properties in each direction, they are not applicable to the case of orthotropic steel plates,

such as stiffened plates, which have different stiffness properties in each direction.

5-30. Design for Flexure

The procedure for the flexural design of a steel plate is essentially the same as the design of a beam. As for beams, it is suggested that preliminary dynamic load factors listed in Table 5-4 be used for plate structures. With the stiffness and resistance factors from Section 5-29 and taking into account the influence of shear on the available plate moment capacity as defined in Section 5-31, the dynamic response and rebound for a given blast loading may be determined from the response charts in Chapter 3. It should be noted that for $\mu > 10$, the dynamic design stress, incorporating the dynamic ultimate stress, f_{du}, may be used (see Equation 5-2).

5-31. Design for Shear

In the design of rectangular plates, the effect of simultaneous high moment and high shear at negative yield lines upon the plastic strength of the plate may be significant. In such cases, the following interaction formula describes the effect of the support shear, V, upon the available moment capacity, M:

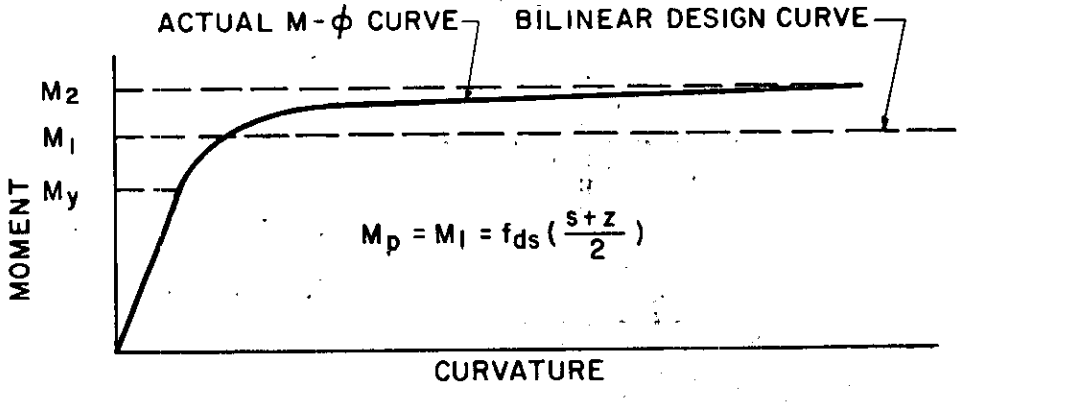
$$M/M_p = 1 - (V/V_p)^4 \qquad 5\text{-}23$$

where M_p is the fully plastic moment capacity in the absence of shear calculated from Equation 5-7, and V_p is the ultimate shear capacity in the absence of bending determined from Equation 5-16 where the web area, A_w, is taken equal to the total cross sectional area at the support.

For two-way elements, values for the ultimate support shears which are applicable to steel plates are presented in Table 3-10 of Chapter 3.

It should be noted that, due to the inter-relationship between the support shear, V, the unit ultimate flexural resistance, r_u, of the two-way element, and the fully plastic moment resistance, M_p, the determination of the resistance of steel plates considering Equation 5-23, is not a simple calculation. Fortunately, the number of instances when negative yield lines with support shears are encountered for steel plates will be limited. Moreover, in most applications, the V/V_p ratio is such that the available moment capacity is at least equal to the plastic design moment for plates (Equation 5-7).

It is recommended that for a V/V_p ratio on negative yield lines less than 0.67, the plastic design moment for plates, as determined from Equation 5-7, should be used in design. However, if V/V_p is greater than 0.67, the influence of shear on the available moment capacity must be accounted for by means of Equation 5-23.



NOTE: SEE FIGURE 5-7 FOR M_y, M_1 AND M_2

Figure 5-10 Moment-curvature diagram for dynamically loaded plates and rectangular cross-section beams

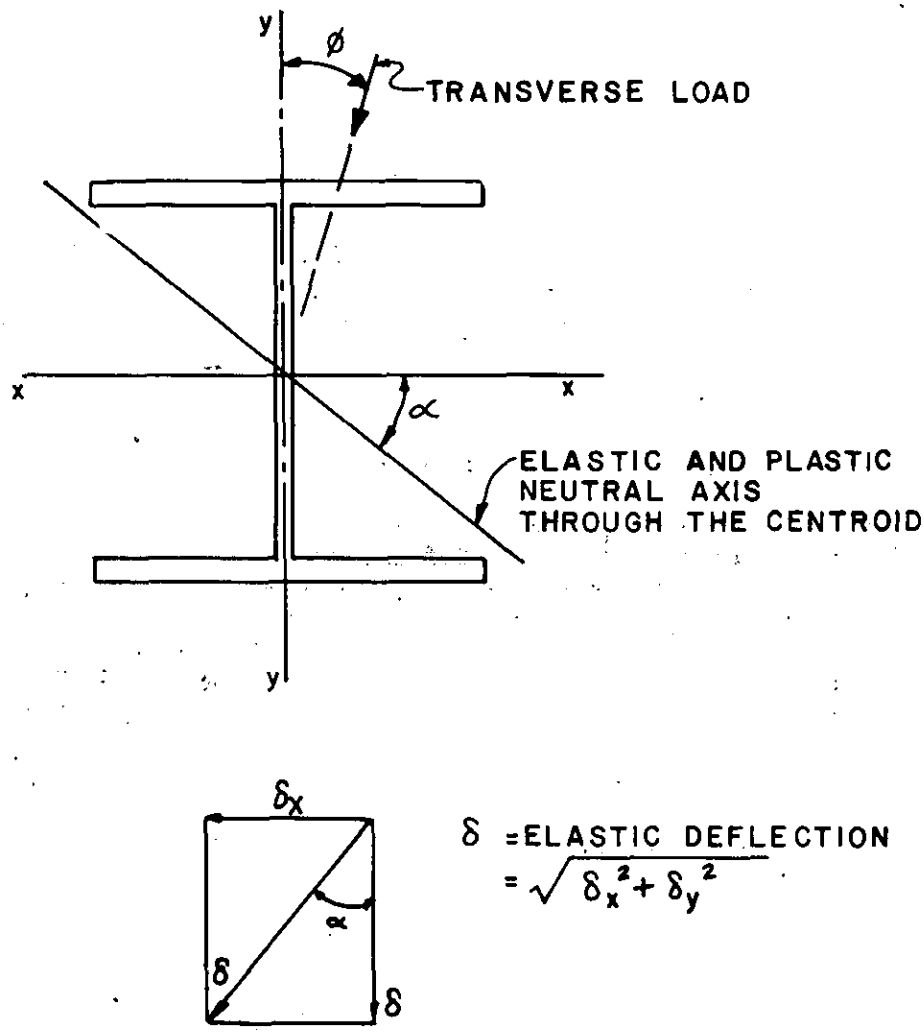


Figure 5-11 Biaxial bending of a doubly-symmetric section

Table 5-4 Preliminary Dynamic Load Factors for Plates

Deflection Magnitude	Deformation*		DLF
	θ max	μ max	
Small	2	5	1.0
Moderate	4	10	0.8
Large	12	20	0.6

* Whichever governs

SPECIAL CONSIDERATIONS, BEAMS

5-32. Unsymmetrical Bending

5-32.1. General

In blast design, the number of situations where unsymmetrical bending occurs is limited and where encountered, it can be treated without serious economic penalty. Due to the fact that blast overpressure loads act normal to the surfaces of a structure, the use of doubly-symmetric cross sections for purlins and girts (e.g., hot-rolled S- and W-sections or cold-formed channels used back-to-back) is generally recommended. In such cases, the deformation criteria for flexural members in Section 5-22 apply.

Unsymmetrical bending occurs when flexural members are subjected to transverse loads acting in a plane other than a principal plane. With this type of loading, the following are applicable:

(1) The member's neutral axis is not perpendicular to the plane of loading.

(2) Stresses cannot in general be calculated by means of the simple bending formula (M_c/I).

(3) The bending deflection does not coincide with the plane of loading but is perpendicular to the inclined neutral axis.

(4) If the plane of loads does not pass through the shear center of the cross section, bending is also accompanied by twisting.

Doubly-symmetric S, W, and box sections acting as individual beam elements and subjected to biaxial bending, i.e., unsymmetrical bending without torsion, can be treated using the procedures outlined in the following sections.

5-32.2. Elastic and Plastic Section Modulus

The inclination of the elastic and plastic neutral axis through the centroid of the section can be calculated directly from the following relationship (see Figure 5-11):

$$\tan \alpha = (I_x / I_y) \tan \phi \qquad 5\text{-}24$$

where α = angle between the horizontal principal plane and the neutral axis

ϕ = angle between the plane of the load and the vertical principal plane

and x and y refer to the horizontal and vertical principal axes of the cross-section.

The equivalent elastic section modulus may be evaluated from the following equation:

$$S = (S_x S_y)/(S_y \cos \phi + S_x \sin \phi) \qquad 5\text{-}25$$

where S_x = elastic section modulus about the x-axis

S_y = elastic section modulus about the y-axis

The plastic section modulus can be calculated using Equation 5-6. With these values of the elastic and plastic section modulii, the design plastic moment capacity can be determined from Equation 5-7.

5-32.3. Equivalent Elastic Stiffness

In order to define the stiffness and bilinear resistance function, it is necessary to determine the elastic deflection of the beam. This deflection may be calculated by resolving the load into components acting in the principal planes of the cross section. The elastic deflection, δ, is calculated as the resultant of the deflections determined by simple bending calculations in each direction (see Figure 5-11). The equivalent elastic deflection on the bilinear resistance function X_E, may then be determined by assuming that the elastic stiffness is valid up to the development of the design plastic moment capacity, M_p.

5-32.4. Lateral Bracing and Recommended Design Criteria

The bracing requirements of Section 5-26 may not be totally adequate to permit a biaxially loaded section to deflect into the inelastic range without premature failure. However, for lack of data, the provisions of Section 5-26 on lateral bracing may be used if the total member end rotation corresponding to the total deflection due to the inclined load is limited to 2 degrees. In addition, the actual details of support conditions and/or bracing provided to such members by the other primary and secondary members of the frame must be carefully checked to ensure that the proper conditions exist to permit deflections in the inelastic range.

5-32.5. Torsion and Unsymmetrical Bending

The inelastic behavior of sections subjected to unsymmetrical bending, with twisting, is not totally known at present. Consequently, the use of sections with the resultant load not passing through the shear center is not recommended in plastic design of blast-resistant structures, unless torsional constraints are provided for the elements. In actual installations, however, the torsional constraint offered to a purlin or girt by the flexural rigidity of the floor, roof, or wall panels to which it is attached may force the secondary member to deflect in the plane of loading with little or no torsional effects. Under such conditions or when some other means of bracing is provided to prevent torsional rotation in both the loading and rebound phases of the response, such unsymmetrically loaded members may be capable of performing well in the plastic range. However, because of the limited data presently available, there is insufficient basis for providing practical design guidelines in this area. Hence, if a case involving unsymmetrical bending with torsion cannot be prevented in design, the maximum ductility ratio should be limited to 1.0.

Furthermore, special precautions may have to be taken to restrict the torsional-flexural distortions that can develop under unsymmetrical loading, thereby reducing the flexural capacity of the member.

5-33. Steel Joists and Joist Girders (Open-web Steel Joists)

Open-web joists are commonly used as load-carrying members for the direct support of roof and floor deck in buildings. The design of joists for conventional loads is covered by the "Standard Specifications, Load Tables and Weight Tables for Steel Joists and Joist Girders", adopted by the Steel Joist Institute. For blast design, all the provisions of this Specification are in force, except as modified herein.

These joists are manufactured using either hot-rolled or cold-formed steel. H-Series joists are composed of 50-ksi steel in the chord members and either 36-ksi or 50-ksi steel for the web sections. LH Series, DLH Series and joist girders are composed of joist chords or web sections with a yield strength of at least 36 ksi, but not greater than 50 ksi.

Standard load tables are available for simply supported, uniformly loaded joists supporting a deck and so constructed that the top chord is braced against lateral buckling. These tables indicate that the capacity of a particular joist may be governed by either flexural or shear (maximum end reaction) considerations. As discussed previously, it is preferable in blast applications to select a member whose capacity is controlled by flexure rather than shear, which may cause abrupt failure.

The tabulated loads include a check on the bottom chord as an axially loaded tensile member and the design of the top chord as a column or beam column. The width-thickness ratios of the unstiffened or stiffened elements of the cross section are also limited to values specified in the Standard Specifications.

The dynamic ultimate capacity of open-web joists may be taken equal to 1.7 a x c times the load given in the joist tables. This value represents the safety factor of 1.7 multiplied by a dynamic increase factor, c, and the average strength increase factor, a (see Section 5-12).

The adequacy of the section in rebound must be evaluated. Upon calculating the required resistance in rebound, r^-/r_u, using the rebound chart in Chapter 3 (Figure 3-268), the lower chord must be checked as a column or beam column. If the bottom chord of a standard joist is not adequate in rebound, the chord must be strengthened either by reducing the unbraced length or by increasing the chord area. The top chord must be checked as an axial tensile member, but in most circumstances, it will be adequate.

The bridging members required by the joist specification should be checked for both the initial and rebound phase of the response to verify that they satisfy the required spacing of compression flange bracing for lateral buckling.

The joist tables indicate that the design of some joists is governed by shear, that is, failure of the web bar members in tension or compression near the supports. In such cases, the ductility ratio for the joist should not exceed unity. In addition, the joist members near the support should be investigated for the worst combination of slenderness ratio and axial load under load reversal.

For hot-rolled members not limited by shear considerations, design ductility ratios up to the values specified in Section 5-35 can be used. The design

ductility ratio of joists with light gauge chord members should be limited to 1.0.

The top and bottom chords should be symmetrical about a vertical axis. If double angles or bars are used as chord members, the components of each chord should be fastened together so as to act as a single member.

SPECIAL CONSIDERATIONS, COLD-FORMED STEEL PANELS

5-34. Blast Resistant Design of Cold-Formed Steel Panels

5-34.1. General

Recent studies on cold-formed panels have shown that the effective width relationships for cold-formed light gauge elements under dynamic loading do not differ significantly from the static relationships. Consequently, the recommendations presently contained in the AISI Specifications are used as the basis for establishing the special provisions needed for the design of cold-formed panels subjected to blast loads. Some of the formulas of the Specification have been extended to comply with ultimate load conditions and to permit limited performance in the inelastic range.

Two main modes of failure can be recognized, one governed by bending and the other by shear. In the case of continuous members, the interaction of the two influences plays a major role in determining the behavior and the ultimate capacity. Due to the relatively thin webs encountered in cold-formed members, special attention must also be paid to crippling problems. Basically, the design will be dictated by the capacity in flexure but subject to the constraints imposed by shear resistance and local stability.

5-34.2. Resistance in Flexure

The material properties of the steel used in the production of cold-formed steel panels conforms to ASTM A446. This standard covers three grades (a, b, and c) depending on the yield point. Most commonly, panels are made of steel complying with the requirements of grade a, with a minimum yield point of 33 ksi and an elongation of rupture of 20 percent for a 2-inch gauge length. However, it is generally known that the yield stress of the material used in the manufacture of cold-formed panels generally exceeds the specified minimum yield stress by a significant margin; therefore, it is recommended that a design minimum yield stress of 40 ksi (corresponding to an average strength increase factor of a = 1.21) be used unless the actual yield stress of the material is known. For grades b and c which exhibit higher minimum yield points, an average strength increase factor of 1.21 is also recommended.

In calculating the dynamic yield stress of cold-formed steel panels, it is recommended that a dynamic increase factor, c, of 1.1 be applied irrespective of actual strain rate and, consequently, the value of the dynamic design stress to be used is

$$f_{ds} = a \times c \times f_y = 1.21 \times 1.1 \times f_y = 1.33\ f_y \qquad 5\text{-}26$$

and hence, f_{ds} equals 44 ksi for the particular case of f_y = 33 ksi.

Ultimate design procedures, combined with the effective width concept, are used in evaluating the strength of cold-formed light gauge elements. Thus, a characteristic feature of cold-formed elements is the variation of their section properties with the intensity of the load. As the load increases beyond the level corresponding to the occurrence of local buckling, the effective area of the compression flange is reduced; as a result, the neutral axis moves toward the tension flange with the effective properties of the cross section such as A (area), I (moment of inertia) and S (section modulus),

decreasing with load increase. The properties of the panels, as tabulated by the manufacturer, are related to different stress levels. The value of S referred to that of the effective section modulus at ultimate and the value of I related to a service stress level of 20 ksi. In the case of panels fabricated from hat sections and a flat sheet, two section modulii are tabulated, S^+ and S^-, referring to the effective section modulus for positive and negative moments, respectively. Consequently, the following ultimate moment capacities are obtained:

$$M_{up} = f_{ds} S^+ \qquad 5\text{-}27$$

$$M_{un} = f_{ds} S^- \qquad 5\text{-}28$$

where M_{up} = ultimate positive moment capacity for a 1-foot width of panel

M_{un} = ultimate negative moment capacity for a 1-foot width of panel

It should be noted that in cases where tabulated section properties are not available, the required properties may be calculated based upon the relationships in the AISI Design Specification.

As for any single-span flexural element, the panel may be subjected to different end conditions, either simply supported or fixed. The fixed-fixed condition is seldom found in practice since this situation is difficult to achieve in actual installations. The simply fixed condition is found because of symmetry in each span of a two-span continuous panel. For multi-span members (three or more), the response is governed by that of the first span which is generally characterized by a simply supported condition at one support and a partial moment restraint at the other. Three typical cases can, therefore, be considered:

(1) Simply supported at both ends (single span).

(2) Simply supported at one end and fixed at the other (two equal span continuous member).

(3) Simply supported at one end and partially fixed at the other (first span of an equally spaced multi-span element).

The resistance of the panel is a function of both the strength of the section and the maximum moment in the member.

The ability of the panel to sustain yielding of its cross section produces significant moment re-distribution in the continuous member which results in an increase of the resistance of the panel.

The behavior of cold-formed steel sections in flexure is nonlinear as shown in Figure 5-12. To simulate the bilinear approximation to the resistancedeflection curve, a factor of 0.9 is applied to the peak resistance. Therefore, for design purposes, the recommended resistance formula for a simply supported, single-span panel is given by:

$$r_u = 0.9 \times 8\, M_{up}/L^2 = 7.2\, M_{up}/L^2 \qquad 5\text{-}29$$

where r_u is the resistance per unit length of panel, and L is the clear or effective span length.

The recommended resistance formula for a simply-fixed, single-span panel or first span of an equally spaced continuous panel is given by:

$$r_u = 0.9 \times 4 (M_{un} + 2M_{up})/L^2 = 3.6 (M_{un} + 2M_{up})/L^2 \qquad 5\text{-}30$$

5-34.3. Equivalent Elastic Deflection

As previously mentioned, the behavior of cold-formed sections in flexure is nonlinear as shown in Figure 5-12. A bilinear approximation of the resistance-deflection curve is assumed for design. The equivalent elastic deflection X_E is obtained by using the following equation:

$$X_E = (\beta r_u L^4)/EI_{20} \qquad 5\text{-}31$$

where β is a constant which depends on the support conditions and whose values are as follows:

$\beta = 0.0130$ for a simply supported element

$\beta = 0.0062$ for simply fixed or continuous elements

I_{20} is defined as the effective moment of inertia of the section at a service stress of 20 ksi. The value of I_{20} is generally tabulated as a section property of the panel. The value of r_u is obtained from Equation 5-29 or 5-30

5-34.4. Design for Flexure

When performing a one-degree-of-freedom analysis of the panel's behavior, the properties of the equivalent system can be evaluated by using a load-mass factor, $K_{LM} = 0.74$, which is an average value applicable to all support conditions. The natural period of vibration for the equivalent single-degree system is thus obtained by substituting into Equation 5-15:

$$T_N = 2\pi (0.74\ mL/K_E)^{1/2} \qquad 5\text{-}32$$

where m = w/g is the unit mass of the panel

K_E = $r_u L/X_E$ is the equivalent elastic stiffness of the system

5-34.5. Recommended Ductility Ratios

Figure 5-12 illustrates the nonlinear character of the resistance-deflection curve and the recommended bilinear approximation. The initial slope of the actual curve is fairly linear until it enters a range of marked nonlinearity and, finally, a point of instability. However, excessive deflections cause the decking to act as a membrane in tension (solid curve) and, consequently, a certain level of stability sets in. It should be noted that, in order to use the procedure outlined in this section, care must be taken to adequately connect the ends of the decking so that it can achieve the desired level of tension-membrane action. A discussion of connectors at end panels is presented in Section 5-48. When tension-membrane action is not present, increased

deflection will result in a significant dropoff in resistance as illustrated by the dotted curve in Figure 5-12.

Two limits of deformation are assigned, depending on end-anchorage condition of the panel. For panels having nominal end anchorage, that is, where tension-membrane action is minimal, the maximum deflection of the panel is X_o, as illustrated in Figure 5-12, and is defined by:

$$X_o = 1.75\ X_E \qquad 5\text{-}33$$

For panels with sufficient end anchorage to permit tension-membrane action, the maximum deflection of the panel is X_m, as illustrated in Figure 5-12, and is defined by:

$$X_m = 6.0\ X_E \qquad 5\text{-}34$$

5-34.6. Recommended Support Rotations

In order to restrict the magnitude of rotation at the supports, limitations are placed on the maximum deflections X_o and X_m as follows:

For elements where tension-membrane action is not present:

$$X_o = L/92 \text{ or } \theta_{max} = 1.25 \text{ degrees} \qquad 5\text{-}35$$

For elements where tension-membrane action is present:

$$X_m = L/92 \text{ or } \theta_{max} = 4 \text{ degrees} \qquad 5\text{-}36$$

5-34.7. Rebound

Appropriate dynamic response charts for one-degree-of-freedom systems in the elastic or elasto-plastic range under various dynamic loads are given in Chapter 3. The problem of rebound should be considered in the design of decking due to the different section properties of the panel, depending on whether the hat section or the flat sheet is in compression. Figure 5-13 presents the maximum elastic resistance in rebound as a function of T/T_N. While the behavior of the panel in rebound does not often control, the designer should be aware of the problem; in any event, there is a need for providing connections capable of resisting uplift or pull-out forces due to load reversal in rebound.

5-34.8. Resistance in Shear

Webs with h/t in excess of 60 are in common use among cold-formed members and the fabrication process makes it impractical to use stiffeners. The design web stresses must, therefore, be limited to ensure adequate stability without the aid of stiffeners, thereby preventing premature local web failure and the accompanying loss of load-carrying capacity.

The possibility of web buckling due to bending stresses exists and the critical bending stress is given by Equation 5-37:

$$f_{cr} = 640{,}000/(h/t)^2 \leq f_y \qquad 5\text{-}37$$

By equating f_{cr} to 32 ksi, which is a stress close to the yielding of the material, a value h/t = 141 is obtained. Since it is known that webs do not actually fail at these theoretical buckling stresses due to the development of post-buckling strength, it can be safely assumed that webs with $h/t \leq 150$ will not be susceptible to flexural buckling. Moreover, since the AISI recommendations prescribe a limit of h/t = 150 for unstiffened webs, this type of web instability need not be considered in the design.

Panels are generally manufactured in geometrical proportions which preclude web-shear problems when used for recommended spans and minimum support-bearing lengths of 2 to 3 inches. In blast design, however, because of the greater intensity of the loading, the increase in required flexural resistance of the panels requires shorter spans.

In most cases, the shear capacity of a web is dictated by instability due to either

(1) Simple shear stresses
(2) Combined bending and shearing stresses

For the case of simple shear stresses, as encountered at end supports, it is important to distinguish three ranges of behavior depending on the magnitude of h/t. For large values of h/t, the maximum shear stress is dictated by elastic buckling in shear and for intermediate h/t values, the inelastic buckling of the web governs; whereas for very small values of h/t, local buckling will not occur and failure will be caused by yielding produced by shear stresses. This point is illustrated in Figure 5-14 for f_{ds} = 44 ksi. The provisions of the AISI Specification in this area are based on a safety factor ranging from 1.44 to 1.67 depending upon h/t. For blast-resistant design, the recommended design stresses for simple shear are based on an extension of the AISI provisions to comply with ultimate load conditions. The specific equations for use in design for f_{ds} = 44, 66 and 88 ksi are summarized in Tables 5-5a, 5-6a, and 5-7a, respectively.

At the interior supports of continuous panels, high bending moments combined with large shear forces are present, and webs must be checked for buckling due to these forces. The interaction formula presented in the AISI Specification is given in terms of the allowable stresses rather than critical stresses which produce buckling. In order to adapt this interaction formula to ultimate load conditions, the problem of inelastic buckling under combined stresses has been considered in the development of the recommended design data.

In order to minimize the amount and complexity of design calculations, the allowable dynamic design shear stresses at the interior support of a continuous member have been computed for different depth-thickness ratios for f_{ds} = 44, 66, and 88 ksi, and tabulated in Tables 5-5b, 5-6b, and 5-7b, respectively.

5-34.9. Web Crippling

In addition to shear problems, concentrated loads or reactions at panel supports, applied over relatively short lengths, can produce load intensities that can cripple unstiffened thin webs. The problem of web crippling is rather complicated for theoretical analysis because it involves the following:

(1) Nonuniform stress distribution under the applied load and the adjacent portions of the web

(2) Elastic and inelastic stability of the web element

(3) Local yielding in the intermediate region of load application

(4) The bending produced by the eccentric load (or reaction) when it is applied on the bearing flange at a distance beyond the curved transition of the web

The AISI recommendations have been developed by relating extensive experimental data to service loads with a safety factor of 2.2 which was established taking into account the scatter in the data. For blast design of cold-formed panels, it is recommended that the AISI values be multiplied by a factor of 1.50 in order to relate the crippling loads to ultimate conditions with sufficient provisions for scatter in test data.

For those sections that provide a high degree of restraint against rotation of their webs, the ultimate crippling loads are given as follows:

Allowable ultimate end support reaction

$$Q_u = 1.5\ f_{ds} t^2\ [4.44 + 0.558\ (N/t)^{1/2}] \qquad 5\text{-}38$$

Allowable ultimate interior support reaction

$$Q_u = 1.5\ f_{ds} t^2\ [6.66 + 1.446\ (N/t)^{1/2}] \qquad 5\text{-}39$$

where Q_u = ultimate support reaction

f_{ds} = dynamic design stress

N = bearing length (in.)

t = web thickness (in)

The charts in figures 5-15 and 5-16 present the variation of Q_u as a function of the web thickness for bearing lengths from 1 to 5 inches for f_{ds} = 44 ksi for end and interior supports, respectively. It should be noted that the values reported in the charts relate to one web only, the total ultimate reaction being obtained by multiplying Q_u by the number of webs in the panel.

For design, the maximum shear forces and dynamic reactions are computed as a function of the maximum resistance in flexure. The ultimate load-carrying capacity of the webs of the panel must then be compared with these forces. As a general comment, the shear capacity is controlled for simply supported elements and by the allowable design shear stresses at the interior supports for continuous panels.

In addition, it can be shown that the resistance in shear governs only in cases of relatively very short spans. If a design is controlled by shear resistance, it is recommended that another panel be selected since a flexural failure mode is generally preferred.

5-35 Summary of Deformation Criteria for Structural Elements

Deformation criteria are summarized in Table 5-8 for frames, beams and other structural elements including cold-formed steel panels, open-web joists and plates.

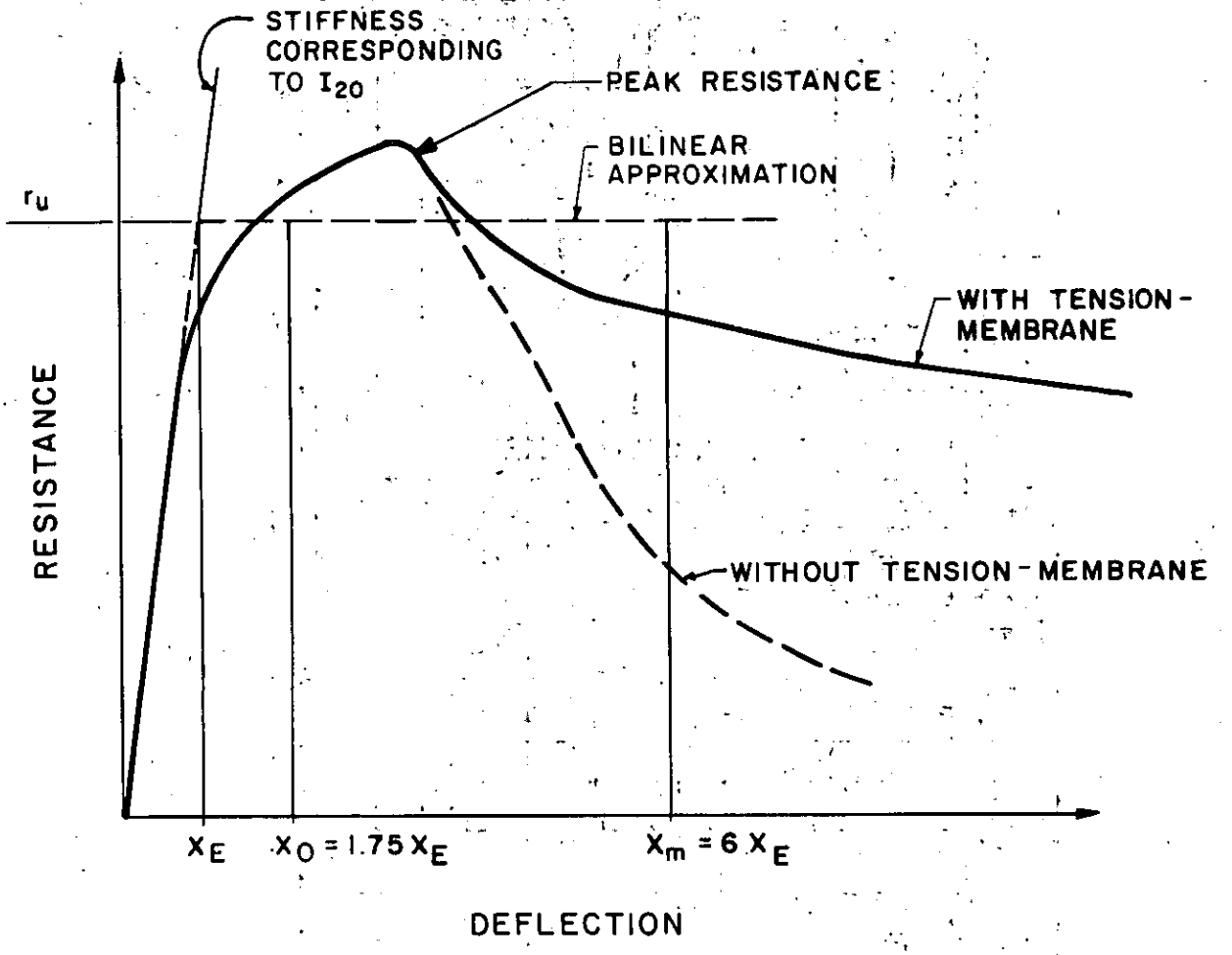


Figure 5-12 Resistance-deflection curve for a typical cold-formed section

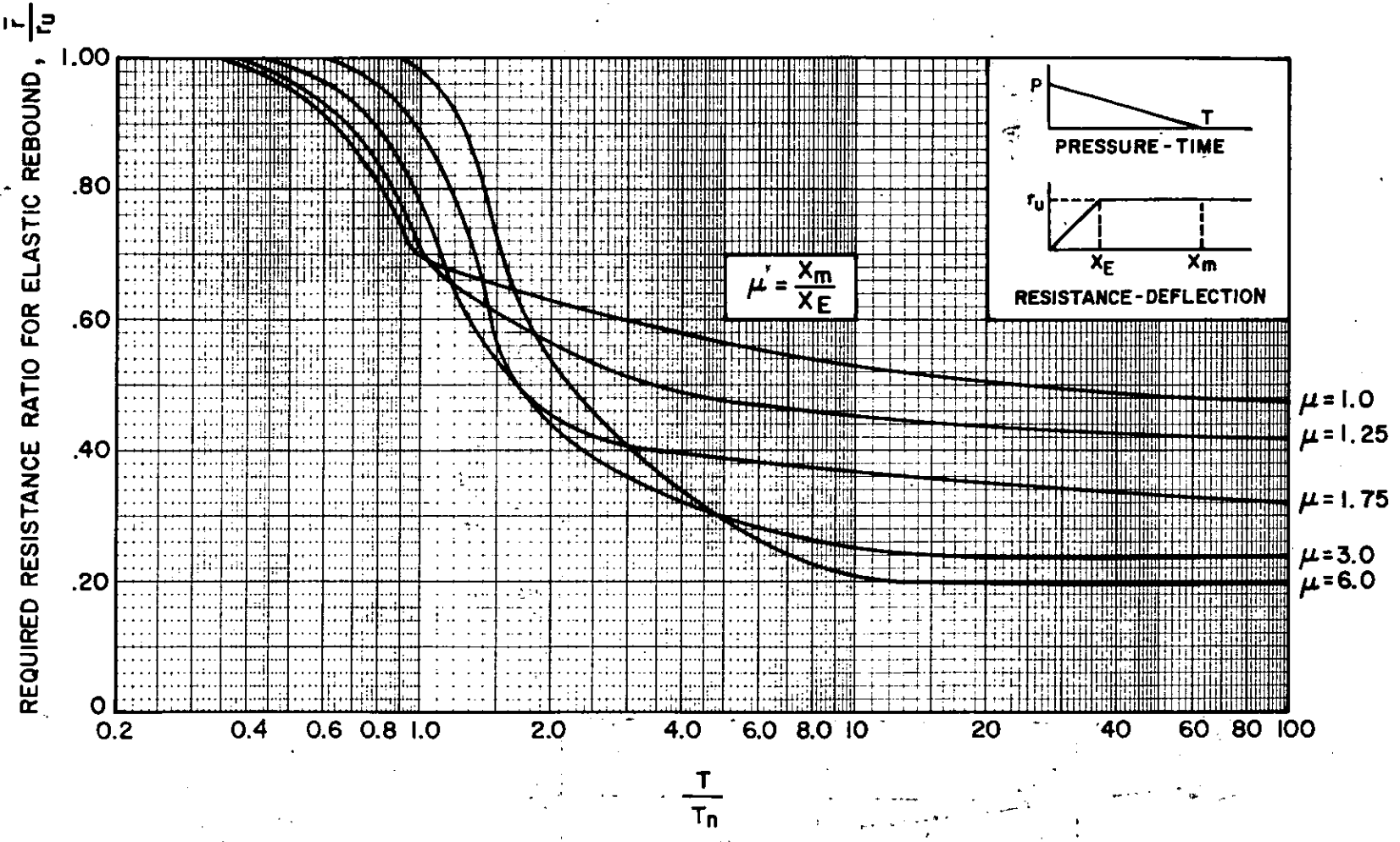


Figure 5-13 Elastic rebound of single-degree-of-freedom system

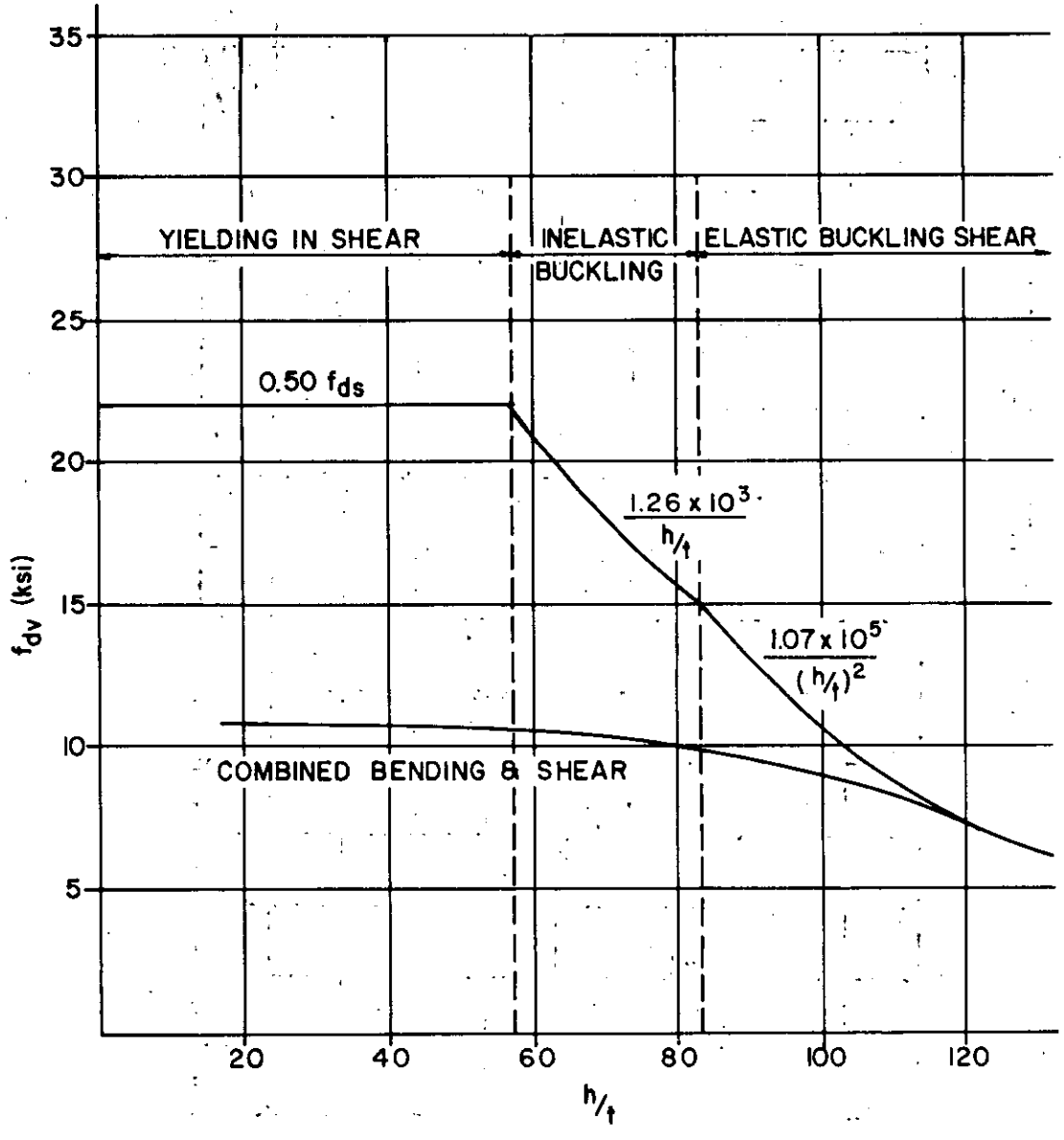


Figure 5-14 Allowable dynamic (design) shear stresses for webs of cold-formed members (f_{ds} = 44 ksi)

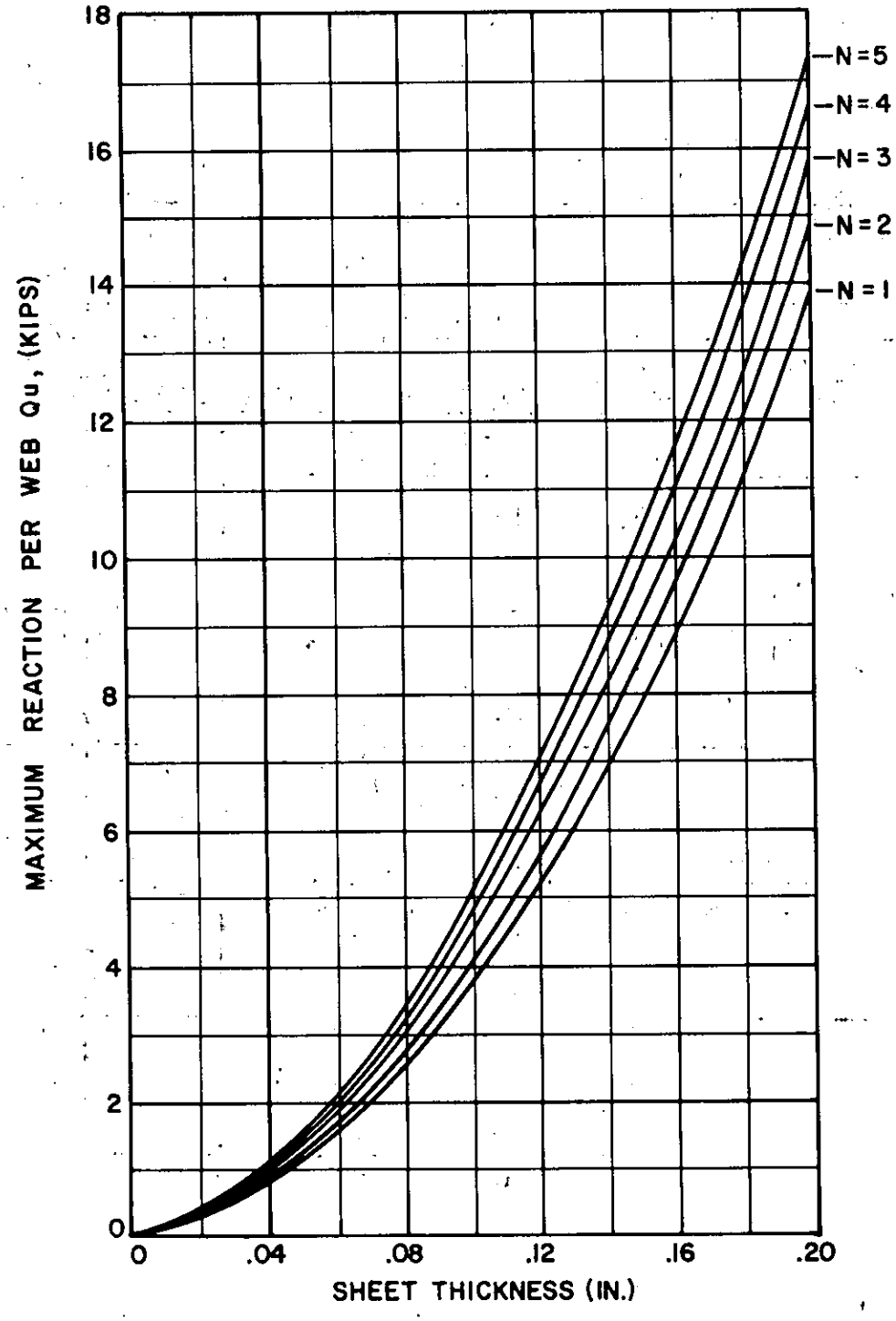


Figure 5-15. Maximum end support reaction for cold-formed steel sections (f_{ds} = 44 ksi)

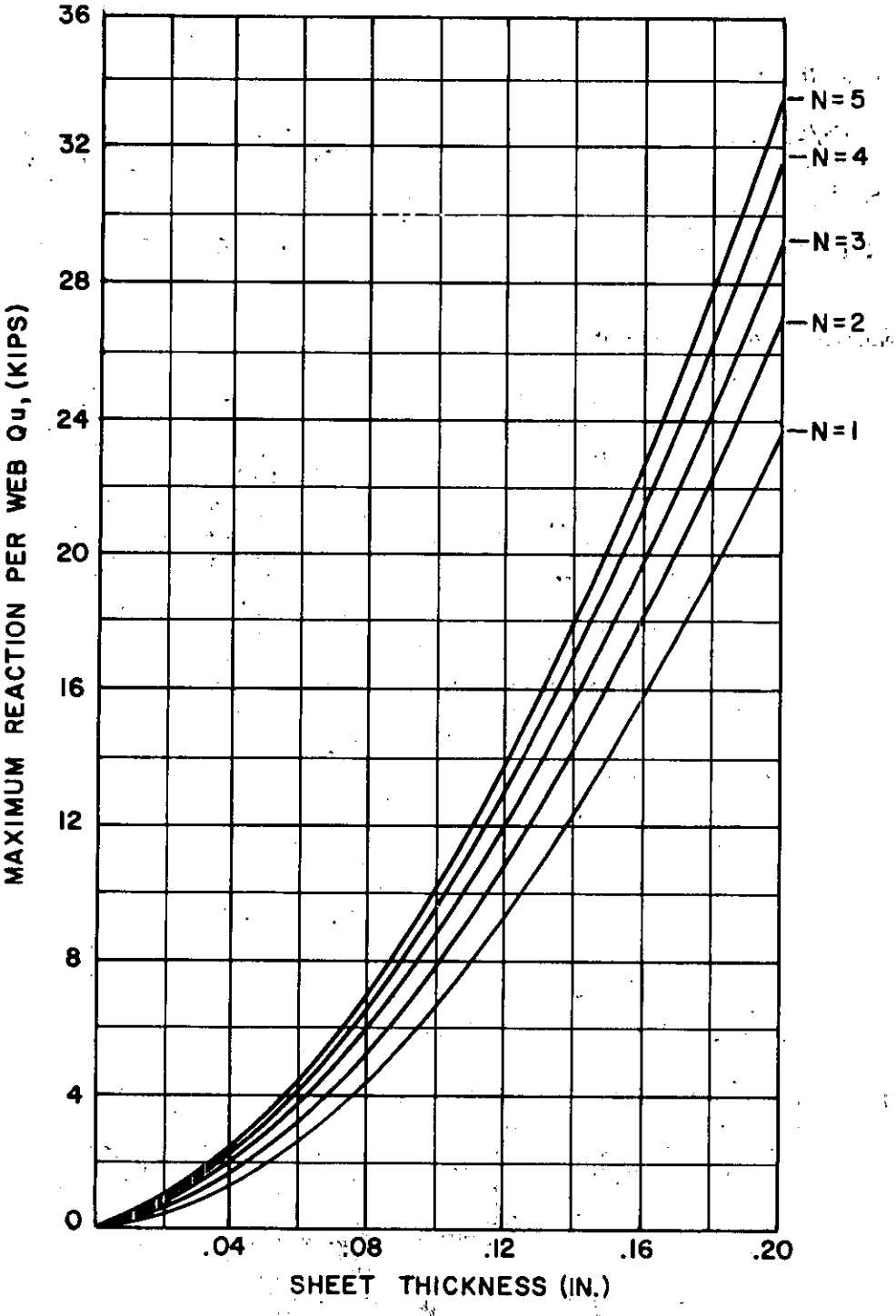


Figure 5-16 Maximum interior support reaction for cold-formed steel sections (f_{ds} = 44 ksi).

Table 5-5 Dynamic Design Shear Stress for Webs of Cold-formed Members (f_{ds} = 44 ksi)

(a) Simple Shear

$(h/t) \leq 57$	$f_{dv} = 0.50\ f_{ds} \leq 22.0$ ksi
$57 < (h/t) \leq 83$	$f_{dv} = 1.26 \times 10^3 / (h/t)$
$83 < (h/t) \leq 150$	$f_{dv} = 1.07 \times 10^5 / (h/t)$

(b) Combined Bending and Shear

(h/t)	f_{dv} (ksi)
20	10.94
30	10.84
40	10.72
50	10.57
60	10.42
70	10.22
80	9.94
90	9.62
100	9.00
110	8.25
120	7.43

Table 5-6. Dynamic Design Shear Stress for Webs of Cold-formed Members (f_{ds} = 66 ksi)

(a) Simple Shear

$(h/t) \leq 47$	$f_{dv} = 0.50\ f_{ds} \leq 33$ ksi
$47 < (h/t) \leq 67$	$f_{dv} = 1.54 \times 10^3/(h/t)$
$67 < (h/t) \leq 150$	$f_{dv} = 1.07 \times 10^5/(h/t)$

(b) Combined Bending and Shear

(h/t)	f_{dv} (ksi)
20	16.41
30	16.23
40	16.02
50	15.75
60	15.00
70	14.20
80	13.00
90	11.75
100	10.40
110	8.75
120	7.43

Table 5-7 Dynamic Design Shear Stress for Webs of Cold-formed Members (f_{ds} = 88 ksi)

(a) Simple Shear

$(h/t) \leq 41$	$f_{dv} = 0.50\ f_{ds} \leq 44$ ksi
$41 < (h/t) \leq 58$	$f_{dv} = 1.78 \times 10^3/(h/t)$
$58 < (h/t) \leq 150$	$f_{dv} = 1.07 \times 10^5/(h/t)$

(b) Combined Bending and Shear

(h/t)	f_{dv}(ksi)
20	21.60
30	21.00
40	20.00
50	18.80
60	17.50
70	16.00
80	14.30
90	12.50
100	10.75
110	8.84
120	7.43

Table 5-8 Summary of Deformation Criteria

Element	Highest level of Protection (Category No.) *	Additional Specifications	Deformation Type **	Maximum Deformation
Beams, purlins, spandrels or girts	1		θ μ	2° 10
	2		θ μ	12° 20
Frame structures	1		δ θ †	H/25 2°
Cold-formed steel floor and wall panels	1	Without tension-membrane action	θ μ	1.25° 1.75
		With tension-membrane action	θ μ	4° 6
Open-web joists	1		θ μ	2° 4
		Joists controlled by maximum end reaction	θ μ	1° 1
Plates	1		θ μ	2° 10
	2		θ μ	12° 20

θ = maximum member end rotation (degrees) measured from the chord joining the member ends.

δ = relative sidesway deflection between stories.

H = story height.

μ = ductility ratio (X_m/X_E)

* as defined in Chapter 1.
** whichever governs.
† individual frame member.

SPECIAL CONSIDERATIONS; BLAST DOORS

5-36. Blast Door Design

5-36.1. General

This section outlines procedures for the design of steel blast doors. Analytical procedures for the design of the individual elements of the blast door plate have been presented in earlier sections of this chapter. In addition to the door plate, door frames and anchorage, reversal bolts, gaskets and door operators are discussed. Blast doors are categorized by their functional requirements and method of opening.

5-36.2. Functions and Methods of Opening

5-36.2.1. Functional Requirements

Blast doors may be designed to contain an accidental explosion from within a structure so as to prevent pressure and fireball leakage and fragment propagation. Blast doors may also be designed to protect personnel and/or equipment from the effects of external blast loads. In this case, a limited amount of blast pressures may be permitted to leak into the protected area. In most cases, blast doors may be designed to protect the contents of a structure, thereby negating propagation when explosives are contained within the shelter.

5-36.2.2. Method of Opening

Blast doors may be grouped based on their method of opening, such as: (a) single leaf, (b) double leaf, (c) vertical lift, and (d) horizontal sliding.

5-36.3. Design Considerations

5-36.3.1. General

The design of a blast door is intrinsically related to its function during and/or after an explosion. Design considerations include whether or not the door should sustain permanent deflections, whether rebound mechanisms or fragment protection is required, and whether pressure leakage be tolerated. Finally, the design pressure range may dictate the type of door construction that is to be used, including solid steel plate or built-up doors.

5-36.3.2. Deflections

As stated in Section 5-16.7, plates can sustain a support rotation of 12 degrees without failing. This is applicable to blast doors providing that the resulting plate deflection does not collapse the door by pushing it through the opening. However, deflections may have to be limited if the mechanism used to open the door after an explosion is required to function. In addition, if a blast door is designed with a gasket so as to fully or nearly contain the pressure and fireball effects of an explosion, then deflections should be limited in order to ensure satisfactory performance of the gasket.

5-36.3.3. Rebound Mechanisms

Steel doors will be subjected to relatively large stress reversals caused by rebound. Blast doors may have to transfer these reversal loads by means of retracting pins or "reversal bolts." These heads can be mounted on any edge (sides, top, or bottom) of a doorplate. Reversal bolts can be designed as an integral part of the panic hardware assembly or, if tapered, they can be utilized in compressing the gasket around a periphery. The magnitude of the rebound force acting on the blast doors is discussed later.

5-36.3.4. Fragment Protection

A plate-type blast door, or the plate(s) of a built-up blast door may be sized to prevent fragment penetration. However, when the blast door is subjected to large blast loads and fragments, a supplementary fragment shield may be necessary since the combined effects of the fragments and pressures may cause premature door failure due to the notching effects produced by the fragments. Procedures for predicting the characteristics of primary fragments such as impact, velocity, and size of fragment are presented in Chapter 2. Methods for determining the depth of penetration of fragments into steel are given in Section 5-49.

5-36.3.5. Leakage Protection (gaskets)

Blast doors may be designed to partly or fully contain the pressure and fireball effects of an explosion in which case gaskets may have to be utilized around the edge if a door or its opening. A sample of a gasket is illustrated in Figure 5-17. This gasket will have to be compressed by means of a hydraulic operator which is capable of overcoming a force of 125 pounds per linear inch of the gasket. This gasket is made of neoprene conforming to the material callouts in Note 2 of Figure 5-17.

5-36.3.6. Type of Construction

Blast doors are formed from either solid steel plate or built-up steel construction.

Solid steel plate doors are usually used for the high pressure ranges (50 psi or greater) and where the door span is relatively short. Depending on plate thicknesses, these doors may be used when fragment impact is critical. These plates can range in thickness of 1-inch or greater. For thick plates, connections using high strength bolts or socket head cap screws are recommended in lieu of welding. However, the use of bolts or screws must preclude the passage of leakage pressures into or out of the structure depending on its use.

Built-up doors are used usually for the low pressure range and where long spans are encountered. A typical built-up blast door may consist of a peripheral frame made from steel channels with horizontal channels serving as intermediate supports for the interior and/or exterior steel cover plates. The pressure loads must be transferred to the channels via the plate. Concrete or some other material may be placed between the plates in order to add mass to the door or increase its fragment resistance capabilities.

5-36.4. Examples of Blast Door Designs

5-36.4.1. General

In order to illustrate the relationship between the function of a blast door and its design considerations, four examples are presented in the following section. Table 5-9 lists the design requirements of each of the above door examples.

5-36.4.2. Door Type A (Figure 5-18)

This blast door is designed to protect personnel and equipment from external blast pressures resulting from an accidental explosion. The door opening measures 8-feet high by 8-feet wide. It is a built-up double-leaf door consisting primarily of an exterior plate and a thinner interior plate both welded to a grid formed by steel tubes. Support rotations of each element (plate, channel, tube) have been limited to 2 degrees in order to assure successful operation of the panic hardware at the door interior. The direct blast load is transferred from the exterior plate to tubular members which form the door grid. The grid then transfers the loads to the door frame at the center of the opening through a set of pins attached to the top and bottom of the center mullions of the grid. At the exterior, the loads are transferred to the frame through the hinges which are attached to the exterior mullions and the frame. The reversal loads are also transferred by the pins and by the built-up door hinges. The center pins are also operated by the panic hardware assembly.

5-36.4.3. Door Type B (Figure 5-19)

This blast door is designed to prevent propagation from an accidental explosion into an explosives storage area. It is a built-up, sliding door protecting an opening 11-feet high by 16-feet wide, consisting of an exterior plate and a thinner interior plate. These plates are welded to vertical S-shapes which are spaced at 15-inch intervals. This door is designed to act as a one-way member, spanning vertically. Since flange buckling of the S-shapes is prohibited in the presence of the outer and inner plates acting as braces, the composite beam-plate arrangement is designed for a support rotation of 12 degrees. The yield capacity of the webs of the S-shapes in shear (Equation 5-16), as well as web crippling (Section 5-25), had to be considered in the design. This door has not been designed to resist reversal or rebound forces.

5-36.4.4. Door Type C (Figure 5-20)

This single-leaf blast door is designed as part of a containment cell which is used in the repeated testing of explosives. The door opening measures 4-feet 6-inches wide by 7-feet 6-inches high. It is the only door, in these samples, designed elastically since it is subjected to repeated blast loads. It consists primarily of a thick steel door plate protected from test fragments by a mild steel fragment shield. It is designed as a simply-supported (four sides) plate for direct internal loads and as a one-way element spanning the door width for rebound loads. It is equipped with a neoprene gasket around the periphery (Figure 5-17) as well as a series of six reversal bolts designed to transfer the rebound load into the door frame. The large thickness of the door plate warrants the use of high-strength, socket head cap screws in lieu

of welding to connect the plate to the reversal bolt housing as well as to the fragment shield.

5-36.4.5. Door Type D (Figure 5-21)

This single-leaf blast door is designed as part of a containment structure which is used to protect nearby personnel and structures in the event of an accidental explosion. The door opening measures 4-feet wide by 7-feet high. It is designed as simply-supported on four sides for direct load and as a one-way element spanning the door width for rebound loads. It is equipped with a neoprene gasket around the periphery and a series of six reversal bolts which transfer the rebound load to the door frame. The reversal bolt housing and bearing blocks are welded to the door plate. Excessive deflections of the door plate under blast loading would hamper the sealing capacity of the gasket. Consequently, the door plate design rotation is limited to 2 degrees.

5-36.4.6. Other Types of Doors

Another type of blast door design is a steel arch or "bow" door. The tension arch door requires compression ties to develop the compression reactions from the arch. The compression arch door requires tension members to develop the tension reactions from the arch. These doors are illustrated in Figure 5-42.

5-36.5. Blast Door Rebound

Plate or element rebound can be determined for a single-degree-of-freedom system subjected to a triangular pulse (see Figure 5-13). However, when a system is subjected to a bilinear load, only a rigorous, step-by-step dynamic analysis can determine the percentage of elastic rebound. In lieu of a rigorous analysis, a method of determining the upper bound on the rebound force is presented here.

Three possible rebound scenarios are discussed. Figure 5-22 is helpful in describing each case.

(a) Case I - Gas load not present ($P_{gas} = 0$). In this case, the required rebound resistance is obtained from Figure 5-13.

(b) Case II - $t_m \leq t_i$ In this case, the required rebound resistance is again obtained from Figure 5-10. This procedure, however, can overestimate the rebound load.

(c) Case III - $t_m > t_i$ Figure 5-22 illustrates the case whereby the time to reach the peak response, t_m, is greater than the point where the gas load begins to act (t_i). Assuming that the gas pressure can be considered constant over a period of time, it will act to lower the required rebound resistance since the resistance time curve will oscillate about the gas pressure time curve. In this case, the upper bound for the required rebound resistance is:

$$\bar{r} = r_u - P_{gas} \qquad 5\text{-}40$$

However, in all three cases, it is recommended that the required rebound resistance be at least equal to 50 percent of the peak positive door response.

5-36.6. Methods of Design

5-36.6.1. General

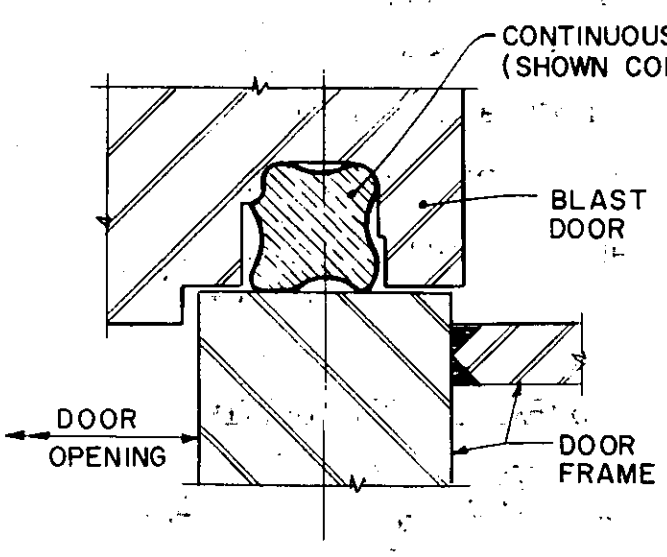
Techniques used for the design of two types of blast doors will be demonstrated. The first technique is used for the door illustrated in Figure 5-18 while the second is used for the door shown in Figure 5-21. Detailed procedures for the design of plate and beam elements, as well as the related design criteria, are presented in earlier section of this chapter and numerical examples are presented in Appendix A.

5-36.6.2. Built-up Door

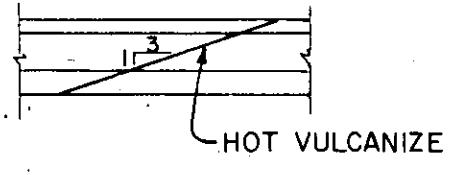
The built-up steel door shown in Figure 5-18 is constructed by welding the steel plates to the steel tubular grid (fillet welded to the exterior plate and plug-welded to the interior plate). The heavy exterior plate is designed as a continuous member supported by the tubes. The horizontal tubes, in turn, are designed as simply supported members, transferring load to the vertical tubes. The interior tubes are also designed as simply supported elements which transfer the direct and rebound loads to the pins while the side tubes transfer the direct load to the door frame proper and rebound loads to the hinges. The exterior tubes are also designed as simply supported elements with the supports located at the hinges.

5-36.6.3. Solid Steel Plate Door

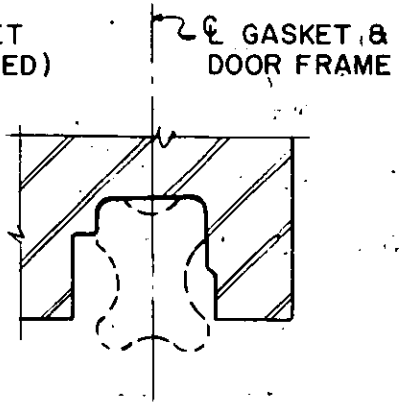
The steel plate of the blast door shown in Figure 5-21 is initially sized for blast pressures since no high speed fragments will be generated in the facility. The plate is sized for blast loading, considering the plate to be simply supported on four edges. The direct load is transferred to the four sides of the door frame. In rebound, the plate acts as a simple beam spanning the width of the door opening. The rebound force is transferred to the six reversal bolts and then into the door frame. The door frame, as illustrated in Figure 5-19, consists of two units; the first unit is imbedded into the concrete and the second unit is attached to the first one. This arrangement allows the first frame to be installed in the concrete wall prior to the fabrication of the door. After the door construction is completed, the subframe is attached to the embedded frame and, thus, the door installation is completed.



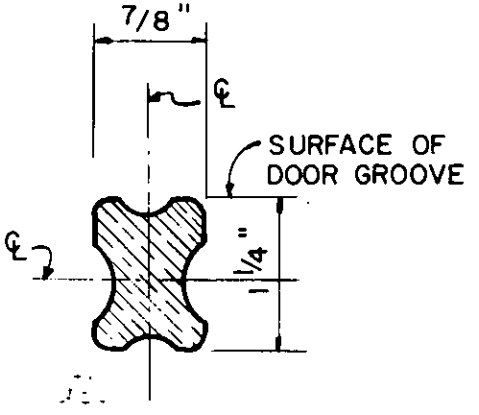
DETAIL
(TYPICAL AROUND
PERIPHERY OF DOOR)



GASKET SPLICE



DOOR GROOVE

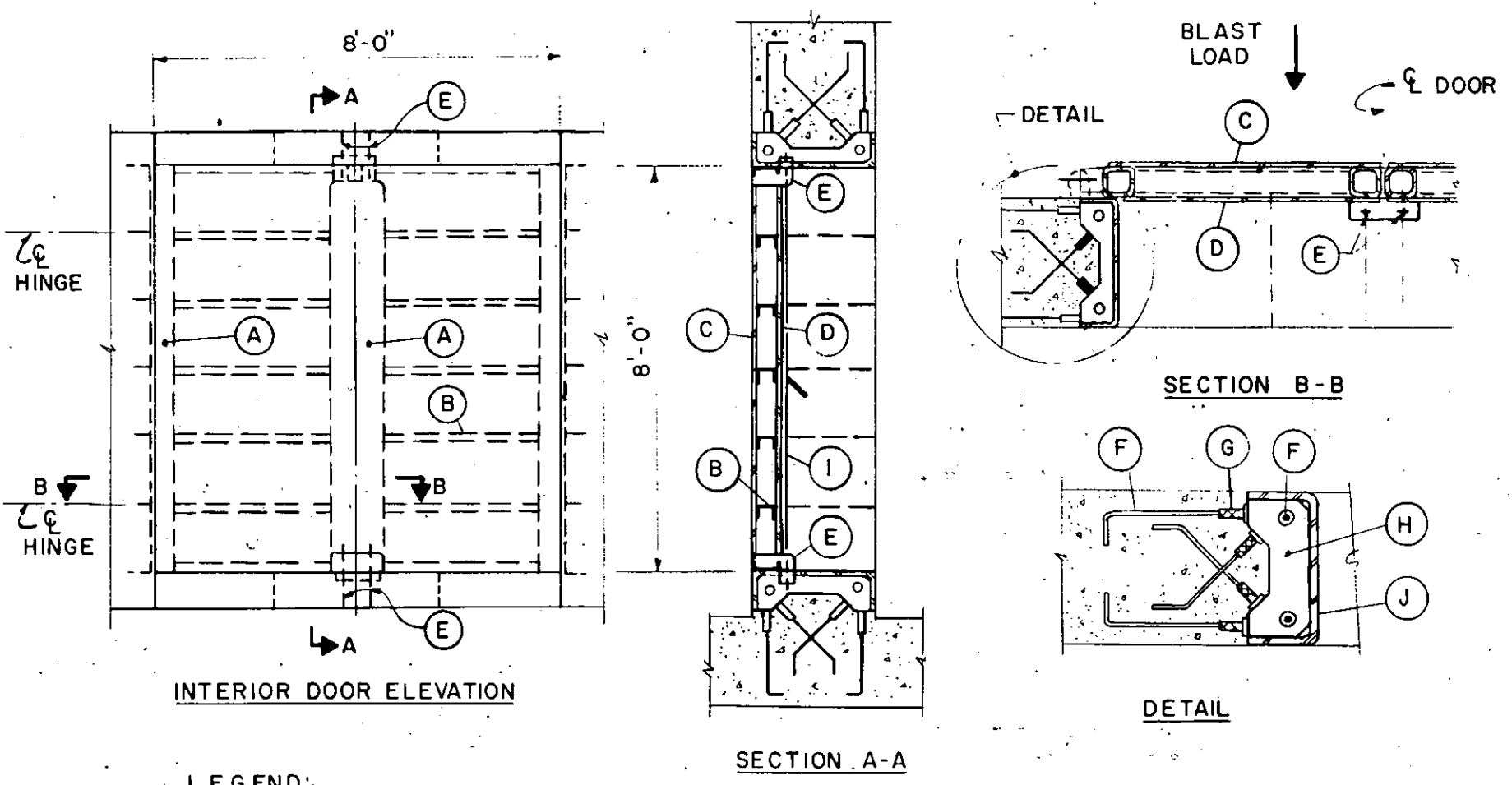


GASKET

NOTES FOR GROOVE & GASKET

1. ALL SURFACES OF DOOR GROOVE SHALL BE MACHINED TO 125 MICROINCHES AND SHALL NOT BE PAINTED.
2. GASKETS FOR ALL DOORS SHALL MEET THE SPECIFICATION REQUIREMENTS AS PER ASTM D 2000-77a AND AS INDICATED IN THE FOLLOWING LINE CALL OUT; 2BC 520 A14 B14 C12 F17.
3. THE FORCE REQUIRED TO CLOSE DOOR IS APPROXIMATELY 125 POUNDS PER LINEAR INCH OF GASKET.

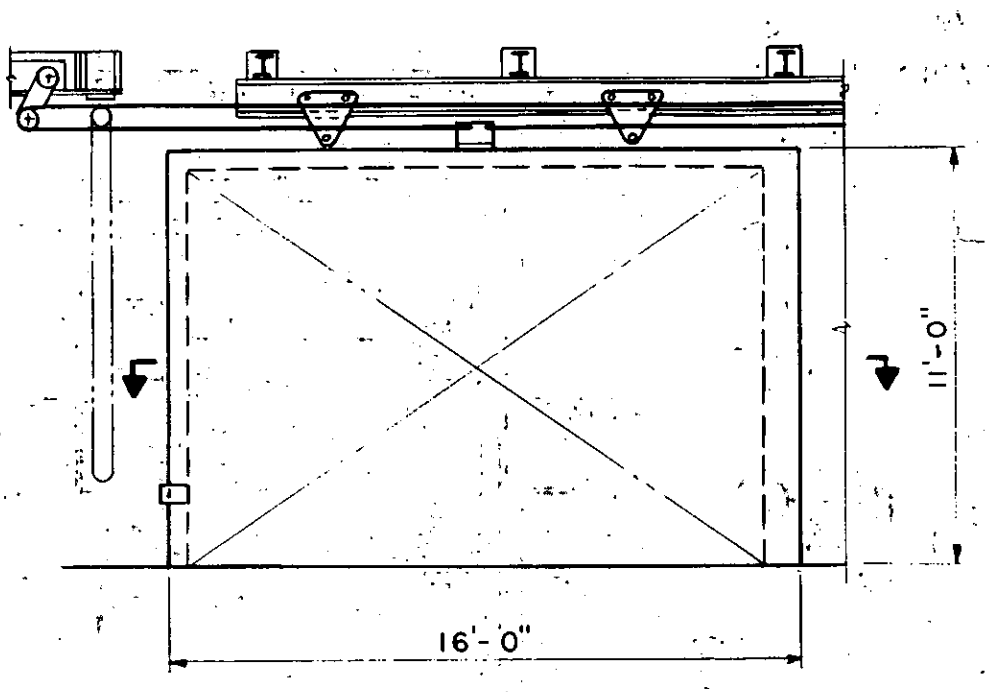
Figure 5-17 Gasket detail for blast door



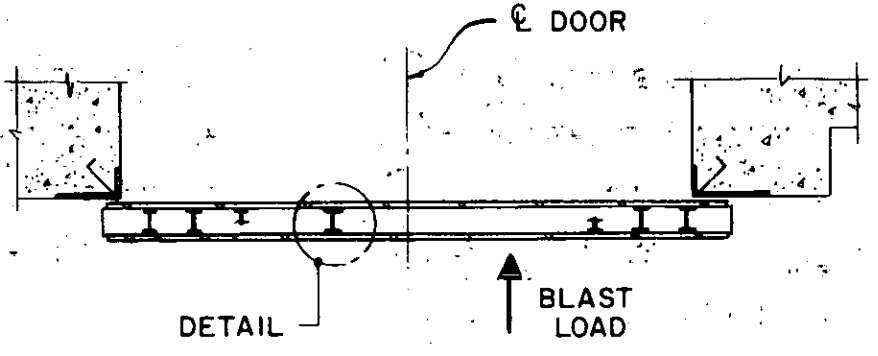
LEGEND:

- (A) - STRUCTURAL TUBE
- (B) - CHANNEL
- (C) - EXTERIOR PLATE
- (D) - INTERIOR PLATE
- (E) - PINS FOR LOAD TRANSFER AND PANIC HARDWARE
- (F) - REINFORCING BAR
- (G) - MECHANICAL ANCHOR
- (H) - STIFFENER PLATE
- (J) - BENT DOOR FRAME PLATE
- (I) - PANIC HARDWARE

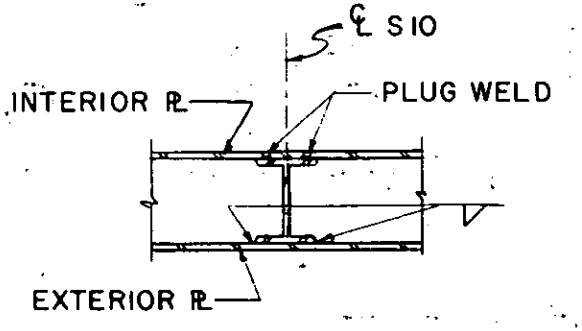
Figure 5-18 Built-up double-leaf blast door with frame built into concrete



EXTERIOR FACE OF SLIDING DOOR



SECTION



DETAIL

Figure 5-19 Horizontal sliding blast door

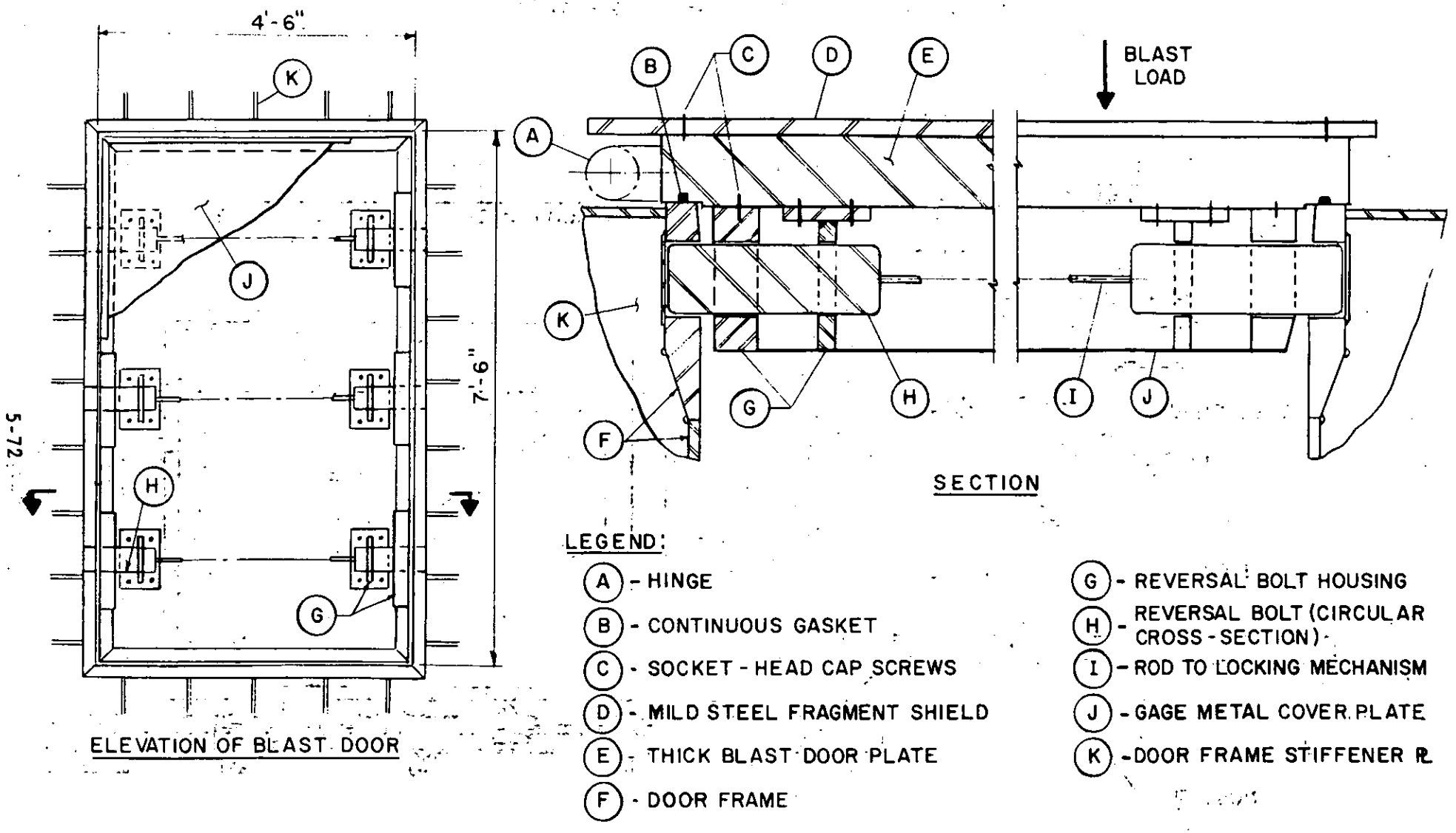
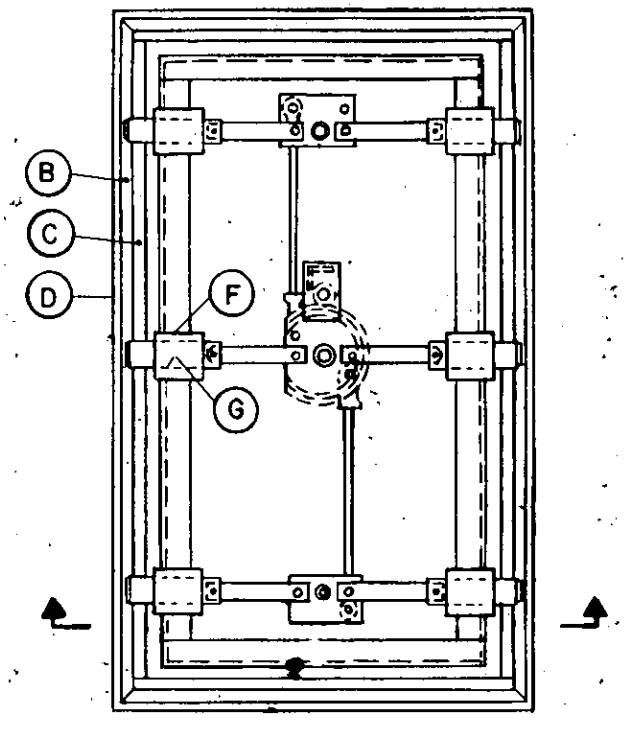
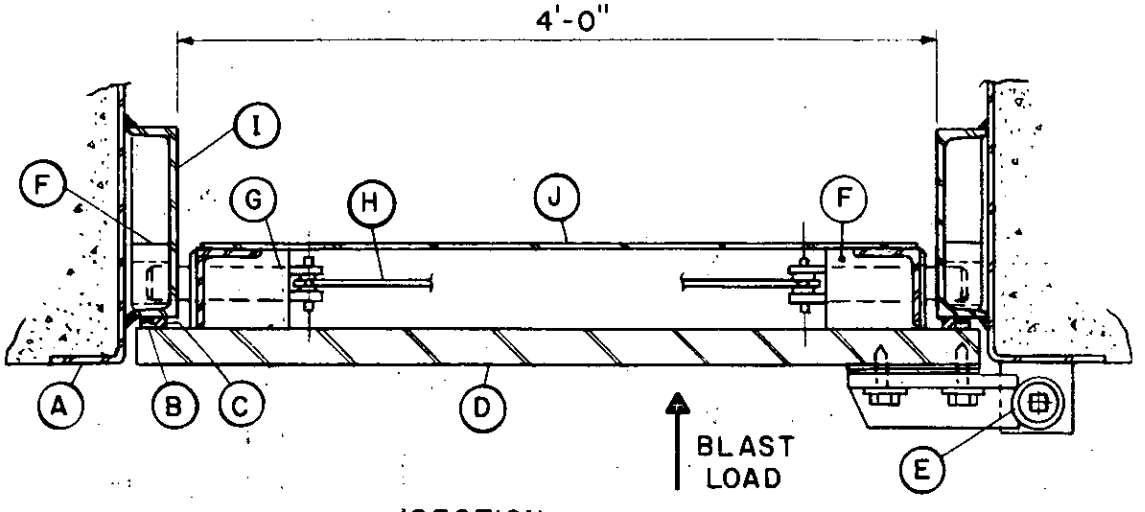


Figure 5-20 Single-leaf blast door with fragment shield (very high pressure)



ELEVATION OF BLAST DOOR

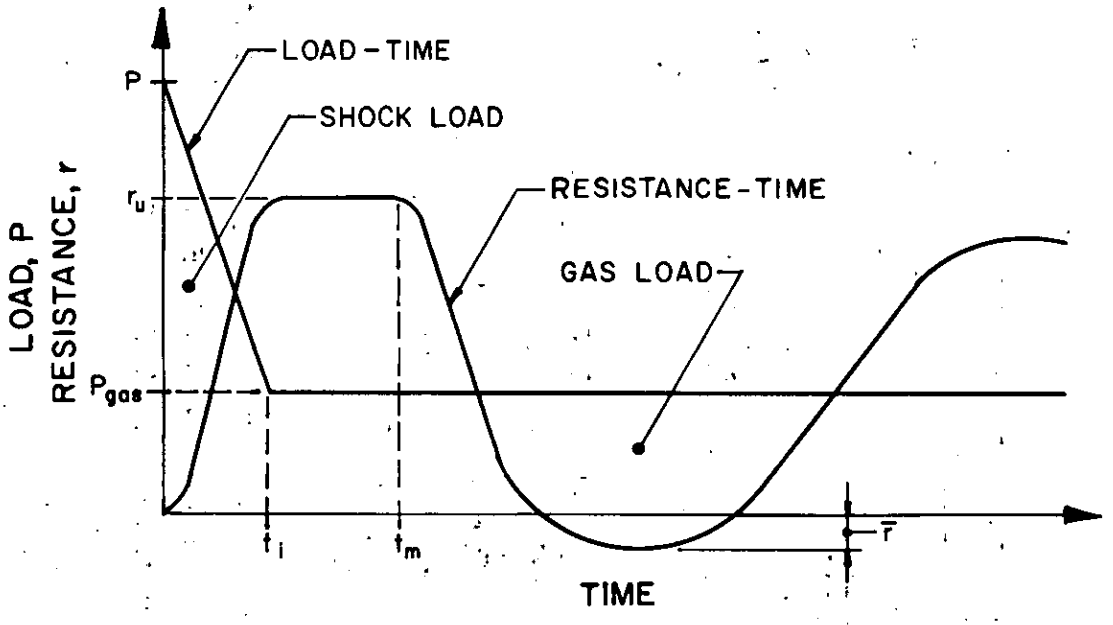


SECTION

LEGEND:

- (A) - STEEL FRAME EMBEDDED IN CONCRETE.
- (B) - CONTINUOUS GASKET
- (C) - BEARING BLOCK
- (D) - BLAST DOOR PLATE
- (E) - DOOR HINGE
- (F) - REVERSAL BOLT HOUSING
- (G) - REVERSAL BOLT
- (H) - BAR CONNECTED TO CLOSURE MECHANISM
- (I) - STEEL FRAME EQUIPPED WITH BLAST DOOR
- (J) - LIGHT GAGE COVER PLATE

Figure 5-21 Single-leaf blast door (high pressure)



P = PEAK LOAD
P_{gas} = GAS PRESSURE
r_u = PEAK POSITIVE RESPONSE
$\bar{r}$ = REQUIRED REBOUND RESISTANCE
t_i = TIME AT WHICH SHOCK AND GAS LOADS INTERSECT
t_m = TIME TO REACH MAXIMUM RESPONSE

Figure 5-22 Bilinear blast load and single-degree-of-freedom response for determining rebound resistance

Table 5-9 Design Requirements for Sample Blast Doors

Door Description			Design Requirements								
			Permanent Deflections			Rebound Mechanisms		Fragment Protection		Level of Leakage Protection Required	
Door	Figure	Method of Opening	None	Limited	Large	Yes	No	Yes	No	Low	High
A	5-18	Double-Leaf		X		X			X	X	
B	5-19	Sliding			X		X		X	X	
C	5-20	Single-Leaf	X			X		X			X
D	5-21	Single-Leaf		X		X		X			X

COLUMNS AND BEAM COLUMNS

5-37. Plastic Design Criteria

5-37.1. General

The design criteria for columns and beam columns must account for their behavior not only as individual members but also as members of the overall frame structure. Depending on the nature of the loading, several design cases may be encountered. Listed below are the necessary equations for the dynamic design of steel columns and beam columns.

5-37.2. In-plane Loads

In the plane of bending of compression members which would develop a plastic hinge at ultimate loading, the slenderness ratio l/r shall not exceed the constant (C_c) defined as:

$$C_c = (2\pi^2 E/f_{ds})^{1/2} \qquad 5\text{-}41$$

where, E = modulus of elasticity of steel (psi)

f_{ds} = dynamic design stress (see Section 5-13)

The ultimate strength of an axially loaded compression member shall be taken as:

$$P_u = 1.7AF_a \qquad 5\text{-}42$$

where A = gross area of member,

$$F_a = \frac{(1 - (Kl/r)^2 / 2C_c^2)\, f_{ds}}{5/3 + 3(Kl/r)/8C_c - (Kl/r)^3 / 8C_c^3}, \text{ and} \qquad 5\text{-}43$$

Kl/r = largest effective slenderness ratio listed in Table 5-10 or 5-11

5-37.3. Combined Axial Loads and Biaxial Bending

Members subject to combined axial load and biaxial bending moment should be proportioned so as to satisfy the following set of interaction formulas:

$$P/P_u + C_{mx}M_x /(1 - P/P_{ex})M_{mx} + C_{my}M_y /(1 - P/P_{ey})M_y \leq 1.0 \qquad 5\text{-}44$$

$$P/P_p + M_x /1.18M_{px} + M_y /1.18M_{py} \leq 1.0 \text{ for } P/P_p \geq 0.15 \qquad 5\text{-}45$$

or $$M_x /M_{px} + M_y /M_{py} \leq 1.0 \text{ for } P/P_p < 0.15 \qquad 5\text{-}46$$

where M_x, M_y = maximum applied moments about the x- and y-axes

P = applied axial load

$P_{ex} = 23/12AF'_{ex}$

$P_{ey} = 23/12Af'_{ey}$

$F'_{ex} = 12\pi^2E/[23(Kl_b/r_x)^2]$

$F'_{ey} = 12\pi^2E/[23(Kl_b/r_y)^2]$

l_b = actual unbraced length in the plane of bending

r_x, r_y = corresponding radii of gyration

$P_p = Af_{ds}$

C_{mx}, C_{my} = coefficients applied to bending term in interaction formula and dependent upon column curvature caused by applied moments (AISC Specification, Section 1.6.1)

M_{px}, M_{py} = plastic bending capacities about x and y axes

($M_{px} = Z_xf_{ds}$, $M_{py} = Z_yf_{ds}$)

M_{mx}, M_{my} = moments that can be resisted by the member in the absence of axial load.

For columns braced in the weak direction, $M_{mx} = M_{px}$ and $M_{my} = M_{py}$.

When columns are unbraced in the weak direction:

$$M_{mx} = [1.07 - (1/r_y)\ (f_{ds})^{1/2}/3160]\ M_{px} \leq M_{px} \qquad 5\text{-}47$$

$$M_{my} = [1.07 - (1/r_x)\ (f_{ds})^{1/2}/3160]\ M_{py} \leq M_{py} \qquad 5\text{-}48$$

Subscripts x and y indicate the axis of bending about which a particular design property applies. Also, columns may be considered braced in the weak direction when the provisions of Section 5-26 are satisfied. In addition, beam columns should also satisfy the requirements of Section 5-23.

5-38. Effective Length Ratios for Beam-columns

The basis for determining the effective lengths of beam columns for use in the calculation of P_u, P_{ex}, M_{mx}, and M_{my} in plastic design is outlined below.

For plastically designed braced and unbraced planar frames which are supported against displacement normal to their planes, the effective length ratios in Tables 5-10 and 5-11 shall apply.

Table 5-10 corresponds to bending about the strong axis of a member, while Table 5-11 corresponds to bending about the weak axis. In each case, l is the distance between points of lateral support corresponding to r_x or r_y, as applicable. The effective length factor, K, in the plane of bending shall be governed by the provisions of Section 5-40.

For columns subjected to biaxial bending, the effective lengths given in Tables 5-10 and 5-11 apply for bending about the respective axes, except that P_u for unbraced frames shall be based on the larger of the ratios Kl/r_x or

Kl/r_y. In addition, the larger of the slenderness ratios, l/r_x or l/r_y, shall not exceed C_c.

5-39. Effective Length Factor, K

In plastic design, it is usually sufficiently accurate to use the K factors from Table C1.8.1 of the AISC Manual (reproduced here as Table 5-12) for the condition closest to that in question rather than to refer to the alignment chart (Figure C.1.8.2 of AISC Manual). It is permissible to interpolate between different conditions in Table 5-12 using engineering judgment. In general, a design value of K equal to 1.5 is conservative for the columns of unbraced frames when the base of the column is assumed pinned, since conventional column base details will usually provide partial rotational restraint at the column base. For girders of unbraced frames, a design K value of 0.75 is recommended.

Table 5-10 Effective Length Ratios for Beam Columns (Webs of members in the plane of the frame; i.e., bending about the strong axis)

Braced Planar Frames*	One-and Two-Story Unbraced Planar Frames*
P_u Use larger ratio, l/r_y or l/r_x	Use larger ratio, l/r_y or Kl/r_x
P_{ex} Use l/r_x	Use Kl/r_x
M_{mx} Use l/r_y	Use l/r_y

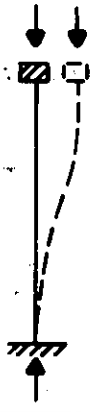
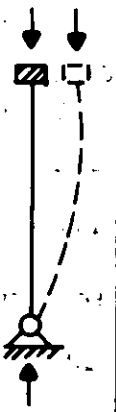
* l/r_x shall not exceed C_c.

Table 5-11 Effective Length Ratios for Beam Columns (Flanges of members in the plane of the frame; i.e., bending about the weak axis)

Braced Planar Frames*	One- and Two-Story Unbraced Planar Frames*
P_u Use larger ratio, l/r_y or l/r_x	Use larger ratio, l/r_x or Kl/r_y
P_{ey} Use l/r_y	Use Kl/r_y
M_{my} Use l/r_x	Use l/r_x

* l/r_y shall not exceed C_c.

Table 5-12 Effective Length Factors for Columns and Beam-columns

	(a)	(b)	(c)	(d)	(e)	(f)
Buckled shape of column is shown by dashed line.						
Theoretical K value.	0.5	0.7	1.0	1.0	2.0	2.0
Recommended design value when ideal conditions are approximated.	0.65	0.80	1.2	1.0	2.10	2.0
End condition code.		Rotation fixed and translation fixed. Rotation free and translation fixed. Rotation fixed and translation free. Rotation free and translation free.				

FRAME DESIGN

5-40. General

The dynamic plastic design of frames for blast resistant structures is oriented toward industrial building applications common to ammunition manufacturing and storage facilities, i.e., relatively low, single-story, multi-bay structures. This treatment applies principally to acceptor structures subjected to relatively low blast overpressures.

The design of blast resistant frames is characterized by (a) simultaneous application of vertical and horizontal pressure-time loadings with peak pressures considerably in excess of conventional loads, (b) design criteria permitting inelastic local and overall dynamic structural deformations (deflections and rotations), and (c) design requirements dictated by the operational needs of the facility and the need for reusability with minor repair work after an incident must be considered.

Rigid frame construction is recommended in the design of blast resistant structures since this system provides open interior space combined with substantial resistance to lateral forces. In addition, this type of construction possesses inherent energy absorption capability due to the successive development of plastic hinges up to the ultimate capacity of the structure. However, where the interior since and wall opening requirements permit, it may be as effective to provide bracing.

The particular objective in this section is to provide rational procedures for efficiently performing the preliminary design of blast resistant frames. Rigid frames as well as frames with supplementary bracing and with rigid or nonrigid connections are considered. In both cases, preliminary dynamic load factors are provided for establishing equivalent static loads for both the local and overall frame mechanism. Based upon the mechanism method, as employed in static plastic design, estimates are made for the required plastic bending capacities as well as approximate values for the axial loads and shears in the frame members. The dynamic deflections and rotations in the sidesway and local beam mechanism modes are estimated based upon single degree-of-freedom analyses. The design criteria and the procedures established for the design of individual members previously discussed apply for this preliminary design procedure.

In order to confirm that a trial design meets the recommended deformation criteria of Table 5-8 and to verify the adequacy of the member sizes established on the basis of estimated dynamic forces and moments, a rigorous frame analysis should be performed. This analysis should consider the moments produced by the axial load deflection P-delta effects) in determining the sizes of individual elements. Several computer programs are available through the repositories listed in Section 5-4. These programs have the capability of performing a multi-degree-of-freedom, nonlinear, dynamic analysis of braced and unbraced, rigid and nonrigid frames of one or more story structures.

5-41. Trial Design of Single-Story Rigid Frames

5-41.1. Collapse Mechanisms

General expressions for the possible collapse mechanism of single-story rigid frames are presented in Table 5-13 for pinned and fixed base frames subjected to combined vertical and horizontal blast loads.

The objective of this trial design is to proportion the frame members such that the governing mechanism represents an economical solution. For a particular frame, the ratio of horizontal to vertical peak loading denoted by α is influenced by the horizontal frame plan of the structure and is determined as follows:

$$\alpha = q_h / q_v \qquad 5\text{-}49$$

where

$q_v = p_v b_v$ = peak vertical load on rigid frame

$q_h = p_h b_h$ = peak horizontal load on rigid frame

p_v = blast overpressure on roof

p_h = reflected blast pressure on front wall

b_v = tributary width for vertical loading

b_h = tributary width for horizontal loading

The orientation of the roof purlins with respect to the blast load directions are shown in Figure 5-23. The value of α will usually lie in the range from about 1.8 to 2.5 when the direction of the blast load is perpendicular to the roof purlins. In this case, the roof purlins are supported by the frame and the tributary width is the same for the horizontal and vertical load. The value of α is much higher when the direction of the blast load is parallel to the roof purlins. In this case, the roof purlins are not supported by the girder of the frame and the tributary width of the vertical loading (b_v = purlin spacing) is much smaller than the tributary width of the horizontal loading (b_h = frame spacing).

It is assumed in this procedure that the plastic bending capacity of the roof girder, M_p, is constant for all bays. The capacity of the exterior and interior columns are taken as CM_p and C_1M_p, respectively. Since the exterior column is generally subjected to reflected pressures, it is recommended that a value of C greater than 1.0 be selected. In analyzing a given frame with certain member properties, the controlling mechanism is the one with the lowest resistance. In design, however, the load is fixed and the required design plastic moment is the largest M_p value obtained from all possible mechanisms. For that purpose, C and C_1 should be selected so as to minimize the value of the maximum required M_p from among all possible mechanisms. After a few trials, it will become obvious which choice of C and C_1 tends to minimize the largest value of M_p.

5-41.2. Dynamic Deflections and Rotations

It will normally be more economical to proportion the members so that the controlling failure mechanism is a combined mechanism rather than a beam mechanism. The mechanism having the least resistance constitutes an acceptable mode of failure provided that the magnitudes of the maximum deflections and rotations do not exceed the maximum values recommended in Table 5-8.

5-41.3. Dynamic Load Factors

To obtain initial estimates of the required mechanism resistance, the dynamic load factors listed in this section may be used to obtain equivalent static loads for the indicated mechanisms. These load factors are necessarily approximate and make no distinction for different end conditions. However, they are expected to result in reasonable estimates of the required resistance for a trial design. Once the trial member sizes are established, then the natural period and deflection of the frame can be calculated.

It is recommended that the DLF for a beam collapse mechanism be equal to 1.25 while that for a panel or combined collapse mechanism be equal to 0.625. The DLF for a frame is lower than that for a beam mechanism, since the natural period of vibration in the sidesway mode will normally be much greater than the natural periods of vibration of the individual elements.

5-41.4. Loads in Frame Members

Estimates of the peak axial forces in the girders and the peak shears in the columns are obtained from Figure 5-24. In applying the values of Figure 5-24, the equivalent horizontal static load shall be computed using the dynamic load factor for a panel or combined sidesway mechanism.

Preliminary values of the peak axial loads in the columns and the peak shears in the girders may be computed by multiplying the equivalent vertical static load by the roof tributary area. Since the axial loads in the columns are due to the reaction from the roof girders, the equivalent static vertical load should be computed using the dynamic load factor for the beam mechanism.

5-41.5. Sizing of Frame Members

Each member in a frame under the action of horizontal and vertical blast loads is subjected to combined bending moments and axial loads. However, the phasing between critical values of the axial force and bending moment cannot be established using a simplified analysis. Therefore, it is recommended that the peak axial loads and moments obtained from Figure 5-24 be assumed to act concurrently for the purpose of trial beam-column design. The overall resistance of the frame depends upon the ultimate strength of the members acting as beam-columns.

When an exterior frame of a building is positioned such that the shock front is parallel to frame, the loadings on each end of the building are equal and sideways action will only occur in the direction of the shock wave propagation. Frame action will also be in one direction, in the direction of the sidesway. If the blast wave impinges on a building from a quartering direction, then the columns and girders in the exterior frames are subjected to biaxial bending due to the simultaneous loads acting on the various faces of

the structure. This action will also cause sidesway in both directions of the structure. The interior girders will usually be subjected to bending in one direction only. However, interior columns may be subjected to either uniaxial or biaxial bending, depending upon the column connections to the girder system. In such cases, the moments and forces can be calculated by analyzing the response of the frame in each direction and superimposing the respective moments and forces acting on the individual elements. This approach is generally conservative since it assumes that the peak values of the forces in one direction occur simultaneously throughout the three-dimensional structure.

Having estimated the maximum values of the forces and moments throughout the frame, the preliminary sizing of the members can be performed using the criteria previously presented for beams and columns.

5-41.6. Stiffness and Deflection

The stiffness factor K for single-story rectangular frames subjected to uniform horizontal loading is defined in Table 5-14. Considering an equivalent single degree-of-freedom system, the sidesway natural period of this frame is

$$T_N = 2\pi(m_e/KK_L)^{1/2} \qquad 5\text{-}50$$

where K_L is a load factor that modifies K, the frame stiffness, due to a uniform load, so that the product KK_L is the equivalent stiffness due to a unit load applied at the equivalent lumped mass m_e.

The load factor is given by

$$K_L = 0.55\ (1 - 0.25\beta) \qquad 5\text{-}51$$

where β is the base fixity factor and is equal to zero and one for pinned base and fixed base frames, respectively.

The equivalent mass m_e to be used in calculating the period of a sidesway mode consists of the total roof mass plus one-third of the column and wall masses. Since all of these masses are considered to be concentrated at the roof level, the mass factor, K_M, is equal to one.

The limiting resistance R_u is given by

$$R_u = \alpha wH \qquad 5\text{-}52$$

where w is equal to the equivalent static uniform load based on the dynamic load factor for a panel or combined sidesway mechanism.

The equivalent elastic deflection X_E corresponding to R_u is

$$X_E = R_u / K_E \qquad 5\text{-}53$$

Knowing the sidesway resistance R_u and the sidesway natural period of vibration T_n, the ductility ratio (μ) for the sidesway deflection of the frame can be computed using the dynamic response charts (Chapter 3). The maximum deflection X_m is then calculated from

$$X_m = \mu X_E \qquad 5\text{-}54$$

where

μ = ductility ratio in sidesway

5-42. Trial Design of Single-Story Frames with Supplementary Bracing

5-42.1. General

Frames with supplementary bracing can consist of (a) rigid frames in one direction and bracing in the other direction, (b) braced frames in two directions with rigid connections, and (c) braced frames in two directions with pinned connections. Most braced frames utilize pinned connections.

5-42.2. Collapse Mechanisms

The possible collapse mechanisms of single-story frames with diagonal tension bracing (X-bracing) are presented in Tables 5-15 and 5-16 for pinned-base frames with rigid and nonrigid girder-to-column connections, respectively. In these tables, the cross sectional area of the tension brace is denoted by A_b, the dynamic design stress for the bracing member is f_{ds}, and the number of braced bays is denoted by the parameter m. In each case, the ultimate capacity of the frame is expressed in terms of the equivalent static load and the member ultimate strength (either M_p or $A_b f_{ds}$). In developing these expressions in the tables, the same assumptions were made as for rigid frames, i.e., M_p for the roof girder is constant for all bays, the bay width L is constant, and the column moment capacity coefficient C is greater than 1.0.

For rigid frames with tension bracing, it is necessary to vary C, C_1, and A_b in order to achieve an economical design. When nonrigid girder-to column connections are used, C and C_1 drop out of the resistance function for the sidesway mechanism and the area of the bracing can be calculated directly.

5-42.3. Bracing Ductility Ratio

Tension brace members are not expected to remain elastic under the blast loading. Therefore, it is necessary to determine if this yielding will be excessive when the system is permitted to deflect to the limits of the design criteria previously given.

The ductility ratio associated with tension yielding of the bracing is defined as the maximum strain in the brace divided by its yield strain. Assuming small deflections and neglecting axial deformations in the girders and columns, the ductility ratio is given by

$$\mu = \delta\ (\cos^2\gamma)\ E/Lf_{ds} \qquad 5\text{-}55$$

where

μ = ductility ratio

δ = sidesway deflection, inches

γ = vertical angle between the bracing and a horizontal plane

L = bay width, inches

From the deflection criteria, the sidesway deflection is limited to H/25. The ductility ratio can be expressed further as

$$\mu = (H/25L)(\cos^2\gamma)(E/f_{ds}) \qquad 5\text{-}56$$

5-42.4. Dynamic Load Factor

The dynamic load factors listed in Section 5-41.3 may also be used as a rational starting point for a preliminary design of a braced frame. In general, the sidesway stiffness of braced frames is greater than unbraced frames and the corresponding panel or sidesway dynamic load factor may also be greater. However, since these dynamic load factors are necessarily approximate and serve only as a starting point for a preliminary design, refinements to these factors for frames with supplementary diagonal braces are not warranted.

5-42.5. Loads in Frame Members

Estimates of the peak axial loads in the girders and the peak shears in the columns of a braced rigid frame are obtained from Figure 5-25. It should be noted that the shear in the blastward column and the axial load in the exterior girder are the same as the rigid frame shown in Figure 5-24. The shears in the interior columns V2 are not affected by the braces while the axial loads in the interior girders P are reduced by the horizontal components of the force in the brace F_H. If a bay is not braced, then the value of F_H must be set equal to zero when calculating the axial load in the girder of the next braced bay. To avoid an error, horizontal equilibrium should be checked using the formula:

$$R_u = V1 + nV2 + mF_H \qquad 5\text{-}57$$

where

R_u, V1, V2 and F_H are defined in Figure 5-25

n = number of bays

m = number of braced bays

In addition, the value of M_p used in Figure 5-25 is simply the design plastic moment obtained from the controlling panel or combined mechanism.

An estimate of the peak loads for braced frames with nonrigid girder to column connections may be obtained using Figure 5-25. However, the value of M_p must be set equal to zero. For such cases, the entire horizontal load is taken by the exterior column and bracing. There is no shear force in the interior columns.

Preliminary values of the peak axial loads in the columns and the peak shears in the girders are obtained in the same manner as rigid frames. However, in computing the axial loads in the columns, the vertical components of the forces in the tension braces must be added to the vertical shear in the roof girders. The vertical component of the force in the brace is given by

$$F_v = A_b f_{ds} \sin\gamma \qquad 5\text{-}58$$

The reactions from the braces will also affect the load on the foundation of the frame; therefore, the design of the footings must include these loads.

5-42.6. Stiffness and Deflection

The equations for determining the sidesway natural period of vibration and the deflection at yield for braced frames are similar to that of rigid frames. The primary difference is the inclusion of the horizontal stiffness (K_b) provided by tension bracing. The equations for the natural period and elastic deflection are as follows:

natural period of vibration

$$T_N = 2\pi \left[m_e / KK_L + K_b)\right]^{1/2} \qquad 5\text{-}59$$

and the equivalent elastic deflection is

$$X_E = R_u / (KK_L + K_b) \qquad 5\text{-}60$$

The horizontal stiffness of the tension bracing is given by

$$K_b = (nA_bE \cos^3\gamma)/L \qquad 5\text{-}61$$

and other values have been defined previously. It may be noted that for braced frames with nonrigid girder-to-column connections, the value of the frame stiffness (K) is equal to zero.

5-42.7. Slenderness Requirements for Diagonal Braces

The slenderness ratio of the bracing should be less than 300 to prevent vibration and "slapping". This design condition can be expressed as

$$r_b \geq L_b / 300 \qquad 5\text{-}62$$

where r_b = minimum radius of gyration of the bracing member

L_b = length between points of support

Even though a compression brace is not considered effective in providing resistance, the tension and compression braces should be connected where they cross. In this manner, L_b for each brace may be taken equal to half of its total length.

5-42.8. Sizing of Frame Members

Estimating the maximum forces and moments in frames with supplementary bracing is similar to the procedures described for rigid frames. However, the procedure is slightly more involved since it is necessary to assume a value for the brace area in addition to the assumptions for the coefficients C and C_1. For frames with nonrigid connections, C and C_1 do not appear in the resistance formula for a sidesway mechanism and A_b can be determined directly. In selecting a trial value of A_b for frames with rigid connections, the minimum brace size is controlled by slenderness requirements. In addition, in each particular application, there will be a limiting value of A_b beyond which there will be no substantial weight savings in the frame members since there

are maximum slenderness requirements for the frame members. In general, values of A_b of about 2 square inches will result in a substantial increase in the overall resistance for frames with rigid connections. Hence, an assumed brace area in this range is recommended as a starting point. The design of the beams and columns of the frames follow the procedures previously presented.

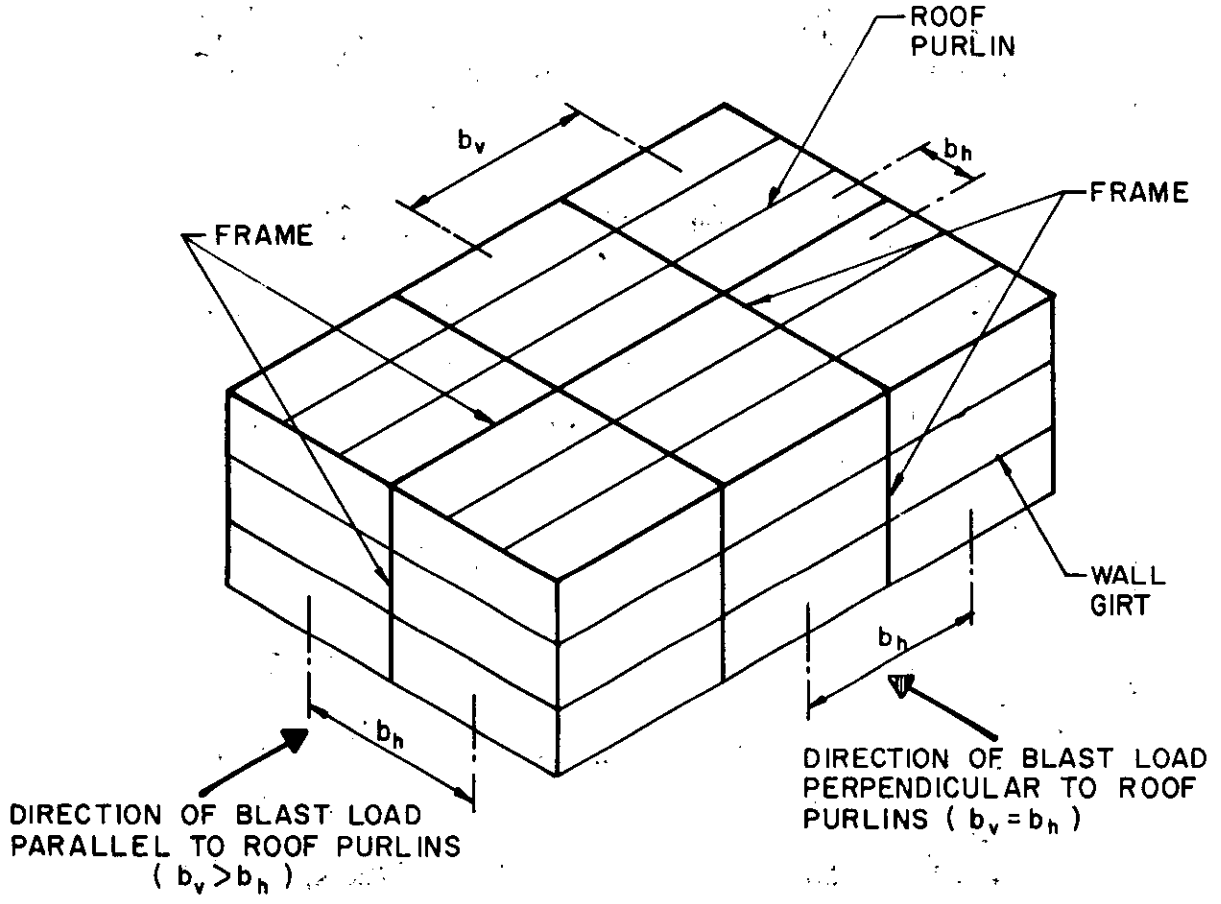
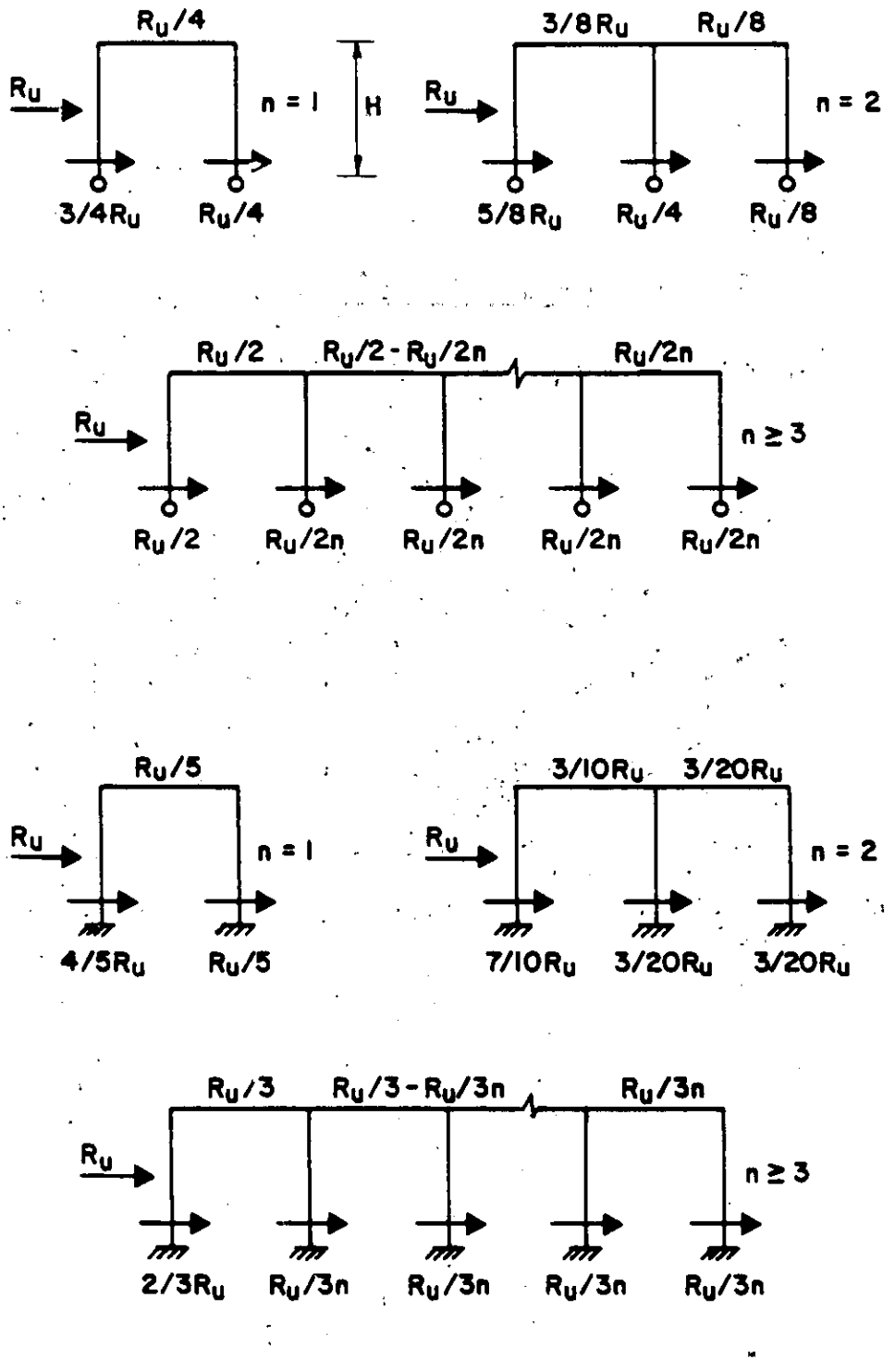


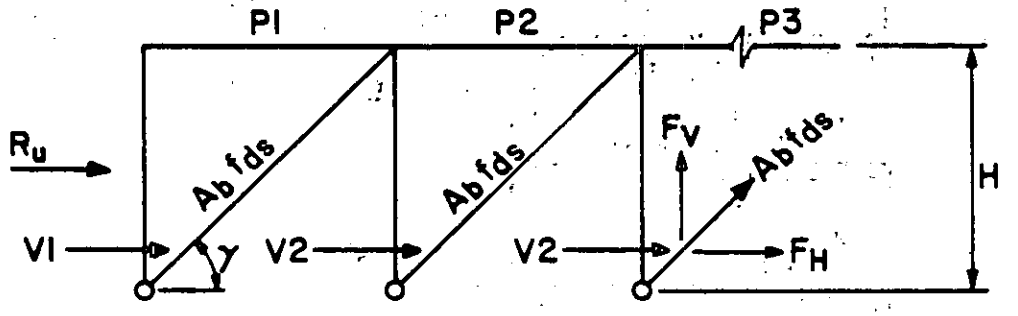
Figure 5-23 Orientation of roof purlins with respect to blast load direction for frame blast loading



n = NUMBER OF BAYS

$R_u = awH$ = EQUIVALENT HORIZONTAL STATIC LOAD

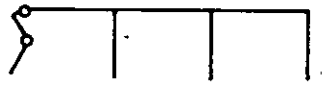
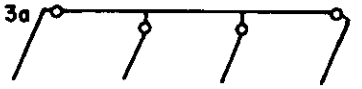
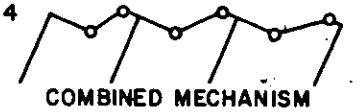
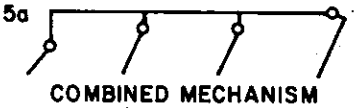
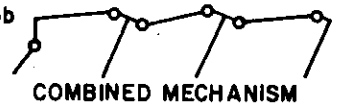
Figure 5-24 Estimates of peak shears and axial loads in rigid frames due to horizontal loads

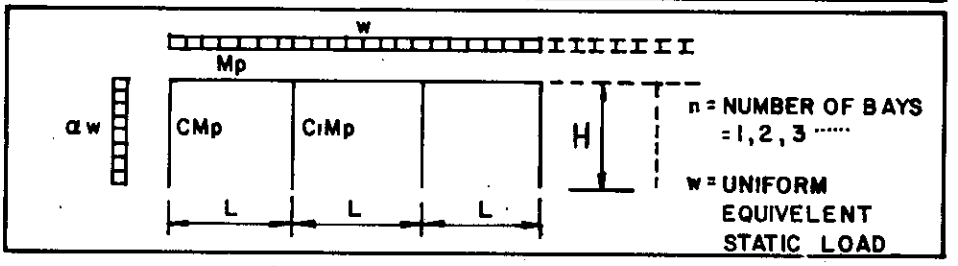


$$R_u = \alpha w H$$
$$V1 = R_u/2 + M_p/H$$
$$P1 = R_u/2 - M_p/H$$
$$P2 = P1 - V2 - F_H$$
$$F_H = A_b f_{ds} \cos\gamma$$
$$F_V = A_b f_{ds} \sin\gamma$$
$$V2 = R_u/2n - M_p/nH$$
$$P3 = P2 - V2 - F_H$$
$$P_n = P(n-1) - V2 - F_H$$

Figure 5-25 Estimates of peak shears and axial loads in braced frames due to horizontal loads

Table 5-13 Collapse Mechanisms for Rigid Frames with Fixed and Pinned Bases

COLLAPSE MECHANISM	PLASTIC MOMENT M_p	
	PINNED BASES	FIXED BASES
1  BEAM MECHANISM	$\frac{wL^2}{16}$	$\frac{wL^2}{16}$
2  BEAM MECHANISM	$\frac{\alpha w H^2}{4(2C+1)}$	$\frac{\alpha w H^2}{4(3C+1)}$
3a  PANEL MECHANISM	$\frac{\alpha w H^2}{2} \cdot \frac{1}{2+(n-1)C_1}$ $(C_1 \geq 2)^*$	$\frac{\alpha w H^2}{4} \cdot \frac{1}{1+(n-1)C_1+C}$ $(C_1 \geq 2)^*$
3b  PANEL MECHANISM	$\frac{\alpha w H^2}{4n}$ $(C_1 \geq 2)^*$	$\frac{\alpha w H^2}{2} \cdot \frac{1}{2(n+C)+(n-1)C_1}$ $(C_1 \geq 2)^*$
4  COMBINED MECHANISM	$\frac{w}{8n}(\alpha H^2+\frac{n}{2}L^2)$	$\frac{w}{2} \cdot \frac{\alpha H^2+\frac{n}{2}L^2}{2(2n+C)+(n-1)C_1}$
5a  COMBINED MECHANISM	$\frac{\frac{3}{8}\alpha w H^2}{C+\frac{1}{2}+\frac{C_1}{2}(n-1)}$ $(C_1 \geq 2)^*$	$\frac{\frac{3}{8}\alpha w H^2}{\frac{5}{2}C+(n-1)C_1+\frac{1}{2}}$ $(C_1 \geq 2)^*$
5b  COMBINED MECHANISM	$\frac{\frac{3}{8}\alpha w H^2}{C+(n-\frac{1}{2})}$ $(C_1 \geq 2)^*$	$\frac{\frac{3}{8}\alpha w H^2}{\frac{5}{2}C+(n-1)\frac{C_1}{2}+(n-\frac{1}{2})}$ $(C_1 \geq 2)^*$
6  COMBINED MECHANISM	$\frac{\frac{w}{8}[3\alpha H^2+(n-1)L^2]}{C+(2n-\frac{3}{2})}$	$\frac{\frac{w}{8}[3\alpha H^2+(n-1)L^2]}{\frac{5}{2}C+(n-1)\frac{C_1}{2}+(2n-\frac{3}{2})}$



* FOR $C_1 = 2$ HINGES FORM IN THE GIRDERS AND COLUMNS AT INTERIOR JOINTS.

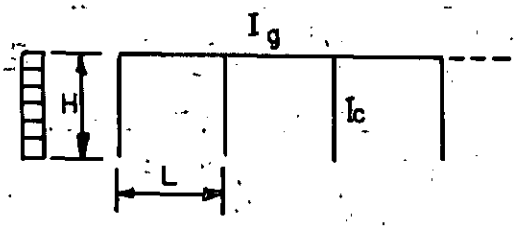
Table 5-14 Stiffness Factors for Single Story, Multi-bay Rigid Frames Subjected to Uniform Horizontal Loading

STIFFNESS FACTOR $K = \frac{E I_{ca}}{H^3} \cdot C_2 \cdot [1 + (0.7 - 0.1\beta)(n-1)]$

n = NUMBER OF BAYS

β = BASE FIXITY FACTOR†

$D = \frac{I_g / L}{I_{ca}\,(0.75 + 0.25\beta) / H}$



I_{ca} = AVERAGE COLUMN MOMENT OF INERTIA = $\sum I_c / (n+1)$

D	C_2		
	$\beta = 1.0$	$\beta = 0.5$*	$\beta = 0$
0.25	26.7	14.9	3.06
0.50	32.0	17.8	4.65
1.00	37.3	20.6	6.04

* VALUES OF C_2 ARE APPROXIMATE FOR THIS β

† β = 1.0 FOR FIXED BASE
= 0.0 FOR HINGED BASE

WHERE:

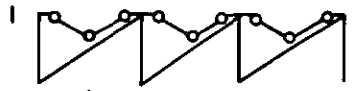
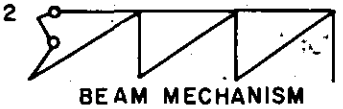
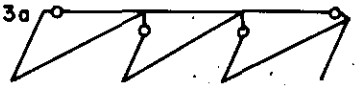
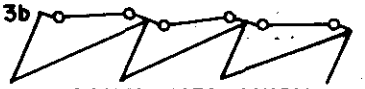
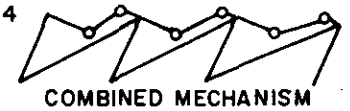
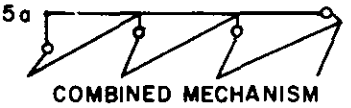
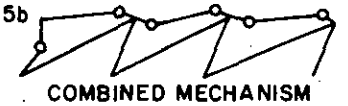
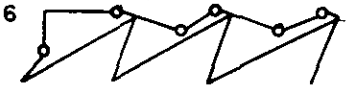
E = MODULUS OF ELASTICITY (PSI)

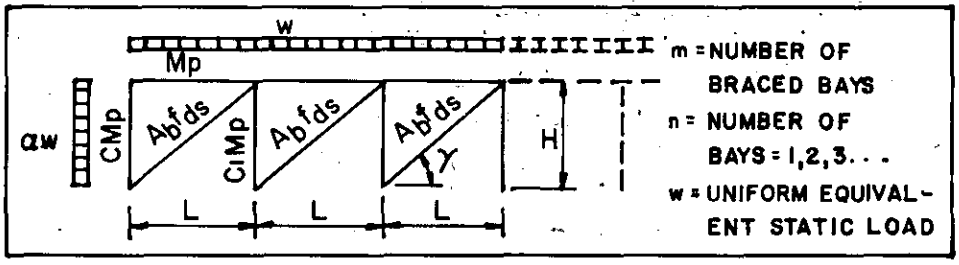
I_{ca}, I_g, I_c = MOMENT OF INERTIA (IN^4)

H = HEIGHT (FEET)

L = BAY LENGTH (FEET)

Table 5-15 Collapse Mechanisms for Rigid Frames with Supplementary Bracing and Pinned Bases

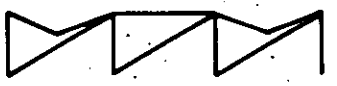
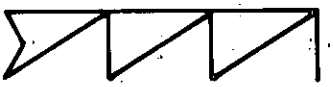
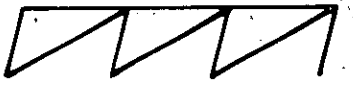
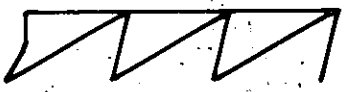
COLLAPSE MECHANISM	PLASTIC MOMENT M_p
1  BEAM MECHANISM	$\frac{wL^2}{16}$
2  BEAM MECHANISM	$\frac{\alpha w H^2}{4(2C+1)}$
3a  PANEL MECHANISM	$\left(\frac{\alpha w H^2}{2} - m A_b f_{ds} H \cos\gamma\right) \frac{1}{2+(n-1)C_1}$ $(C_1 \leq 2)^*$
3b  PANEL MECHANISM	$\frac{\alpha w H^2}{4n} - \frac{m A_b f_{ds} H \cos\gamma}{2n}$ $(C_1 \geq 2)^*$
4  COMBINED MECHANISM	$\frac{w}{8n}(\alpha H^2 + \frac{n}{2}L^2) - \frac{m A_b f_{ds} H \cos\gamma}{4n}$
5a  COMBINED MECHANISM	$\frac{\frac{3}{8}\alpha w H^2 - \frac{m}{2} A_b f_{ds} H \cos\gamma}{C + \frac{1}{2} + \frac{C_1}{2}(n-1)}$ $(C_1 \leq 2)^*$
5b  COMBINED MECHANISM	$\frac{\frac{3}{8}\alpha w H^2 - \frac{m}{2} A_b f_{ds} H \cos\gamma}{C + (n - \frac{1}{2})}$ $(C_1 \geq 2)^*$
6  COMBINED MECHANISM	$\frac{\frac{w}{8}[3\alpha H + (n-1)L] - \frac{m}{2} A_b f_{ds} H \cos\gamma}{C + (2n - \frac{3}{2})}$



m = NUMBER OF BRACED BAYS
n = NUMBER OF BAYS = 1,2,3...
w = UNIFORM EQUIVALENT STATIC LOAD

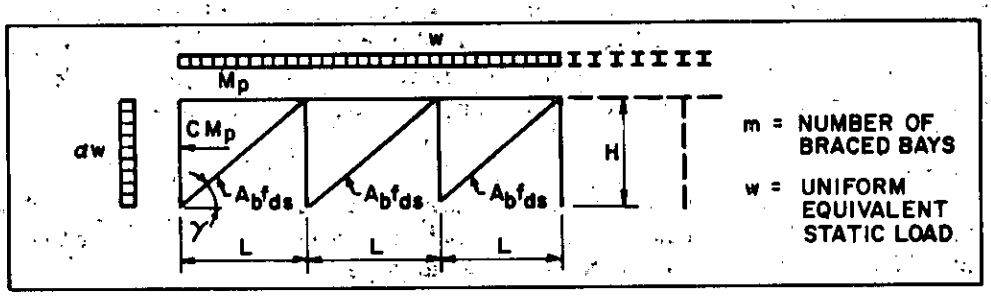
* FOR $C_1 = 2$ HINGES FORM IN THE GIRDERS AND COLUMNS AT INTERIOR JOINTS.

Table 5-16 Collapse Mechanisms for Frames with Supplementary Bracing, Non-rigid Girder-to-Column Connections and Pinned Bases

COLLAPSE MECHANISM	ULTIMATE CAPACITY	FRAMING TYPE
1.  BEAM MECHANISM EXTERIOR GIRDER	$M_p = wL^2/8$ $M_p = wL^2/12$ $M_p = wL^2/16$	(1) (2) (3)
2.  BEAM MECHANISM INTERIOR GIRDER	$M_p = wL^2/8$ $M_p = wL^2/16$	(1) (2) & (3)
3.  BEAM MECHANISM BLASTWARD COLUMN	$M_p = \alpha wH^2/8$ $M_p = \frac{\alpha wH^2}{4(2C+1)}$	(1) & (2) (3)
4.  PANEL MECHANISM	$A_b f_{ds} = \alpha wH/2m\cos\gamma$ $A_b f_{ds} = \frac{\alpha wH}{2m\cos\gamma} - \frac{2M_p}{mH\cos\gamma}$	(1) & (2) (3)
5.  COMBINED MECHANISM	$A_b f_{ds} = \frac{3\alpha wH}{4m\cos\gamma} - \frac{(2C+1)M_p}{mH\cos\gamma}$	(3)

GIRDER FRAMING TYPE:

(1) GIRDER SIMPLY SUPPORTED BETWEEN COLUMNS
(2) GIRDER CONTINUOUS OVER COLUMNS
(3) GIRDER CONTINUOUS OVER COLUMNS AND RIGIDLY CONNECTED TO EXTERIOR COLUMNS ONLY



CONNECTIONS

5-43. General

The connections in a steel structure designed in accordance with plastic design concepts must fulfill their function up to the ultimate load capacity of the structure. In order to allow the members to reach their full plastic moments, the connections must be capable of transferring moments, shears and axial loads with sufficient strength, proper stiffness and adequate rotation capacity.

Connections must be designed with consideration of economical fabrication and ease of erection. Connecting devices may be rivets, bolts, welds, screws or various combinations thereof.

5-44. Types of Connections

The various connection types generally encountered in steel structures can be classified as primary member connections, secondary member connections and panel attachments. Primary member connections are corner frame, beam-to-column, beam-to-girder and column base connections as well as splices. Secondary member connections are purlin-to-frame, girt-to-frame and bracing connections. Panel attachments are roof-to-floor panel and wall siding connections.

Primary member connections refer to those used in design and construction of the framing of primary members. They generally involve the attachment of hot-rolled sections to one another, either to create specific support conditions or to achieve continuity of a member or the structure. In that respect, connections used in framing may be classified into three groups, namely, rigid, flexible (nonrigid) and semirigid, depending upon their degree of restraint which is the ratio of the actual end moment that may be developed to the end moment in a fully fixed-ended beam. Approximately, the degree of restraint is generally considered as over 90 percent for rigid connections, between 20 to 90 percent for semirigid connections and below 20 percent for flexible connections.

It should be mentioned that the strength and rotation characteristics of semirigid connections are dependent upon the properties of the intermediate connection elements (angles, plates, tees) and thus, are subject to much variation. Since semirigid structural analyses are seldom undertaken due to their great complexity, no further details on semirigid connections will be given here.

Secondary member connections are used to fasten members such as purlins, girts or bracing members to the primary members of a frame, either directly or by means of auxiliary sections such as angles and tees.

Basic requirements for primary and secondary member connections, as well as general guidelines for proper design, are presented in Sections 5-45 and 5-46. In addition, dynamic design stresses to be used in the selection and sizing of fastening devices are given in Section 5-47.

Panel attachments are used to attach elements of the skin or outer shell of an installation as well as floor and wall panels to the supporting skeleton.

Connections of this type are distinguished by the fact that they fasten relatively thin sheet material to one another or to heavier rolled sections. Roof decks and wall siding have to withstand during their lifetime (apart from accidental blast loads) exposure to weather, uplift forces, buffeting and vibration due to winds, etc. For this reason, and because of their widespread use, special care should be taken in design to ensure their adequate behavior. Some basic requirements for panel connections are presented in Section 5-48.

5-45. Requirements for Main Framing Connections

The design requirements for frame connections may be illustrated by considering the behavior of a typical corner connection as shown in Figure 5-26. Two members are joined together without stiffening of the corner web. Assuming that the web thickness is insufficient, the behavior of the connection is represented by Curve 1 which shows that yielding due to shear force starts at a relatively low load. Even though the connection rotates past the required hinge rotation, the plastic moment M_p is not reached. In addition, the elastic deformations are also larger than those assumed by the theoretical design curve.

A second and different connection may behave as indicated by Curve 2. Although the elastic stiffness is satisfactory and the maximum capacity exceeds M_p, the connection failed before reaching the required hinge rotation and thus, is unsatisfactory.

These considerations indicate that connections must be designed for strength, stiffness and rotation capacity. They must transmit the required moment, shear and axial load, and develop the plastic moment M_p of the members.

Normally, an examination of a connection to see if it meets the requirements of stiffness will not be necessary. Compared to the total length of the member, the length of the connection is small, and, if the connection is slightly more flexible than the member which it joins, the general effect on the structural behavior is not great. Approximately, the average unit rotation of the connecting zone should not exceed that of an equivalent length of the members being joined.

Of equal importance with the strength of the connection is an adequate reserve of ductility after the plastic moment has been attained. Rotation capacity at plastic hinge locations is essential to the development of the full ultimate load capacity of the structure.

5-46. Design of Connections

It is not the intent of this section to present procedures and equations for the design of the various types of connections likely to be encountered in the blast-resistant design of a steel structure. Instead, the considerations necessary for a proper design will be outlined.

After completion of the dynamic analysis of the structure, the members are sized for the given loadings. The moments, shears, and axial loads at the connections are known. Full recognition must be given to the consideration of rebound or stress reversal in designing the connections. Additionally, in continuous structures, the maximum values of P, M, and V may not occur simultaneously and thus, several combinations may have to be considered.

With rigid connections such as a continuous column-girder intersection, the web area within the boundaries of the connection should meet the shear stress requirements of Section 5-23. If the web area is unsatisfactory, diagonal stiffeners or web doubler plates should be provided.

Stiffeners will normally be required to prevent web crippling and preserve flange continuity wherever flange-to-flange connections occur at columns in a continuous frame. Web crippling must also be checked at points of load application such as beam-girder intersections. In these cases, the requirements of Section 5-25 of this chapter and Sections 1.10.5 and 1.10.10 of the AISC Specification must be considered.

Since bolted joints will develop yield stresses only after slippage of the members has occurred, the use of friction-type bolted connections is not recommended.

5-47. Dynamic Design Stresses for Connections

In accordance with Section 2.8 of the AISC Specification, bolts, rivets and welds shall be proportioned to resist the maximum forces using stresses equal to 1.7 times those given in Part 1 of the Specification. Additionally, these stresses are increased by the dynamic increase factor specified in Section 5-12.2; hence,

$$f_d = 1.7cf_s \qquad 5\text{-}63$$

where f_d = the maximum dynamic design stress for connections

c = the dynamic increase factor Figure 5-2 or Table 5-2)

f_s = the allowable equivalent static design stress of the bolt, rivet, or weld

Rather than compiling new tables for maximum dynamic loads for the various types of connections, the designer will find it advantageous to divide the forces being considered by the factor 1.7c and then to refer to the allowable load tables in Part 1 of the AISC Specification.

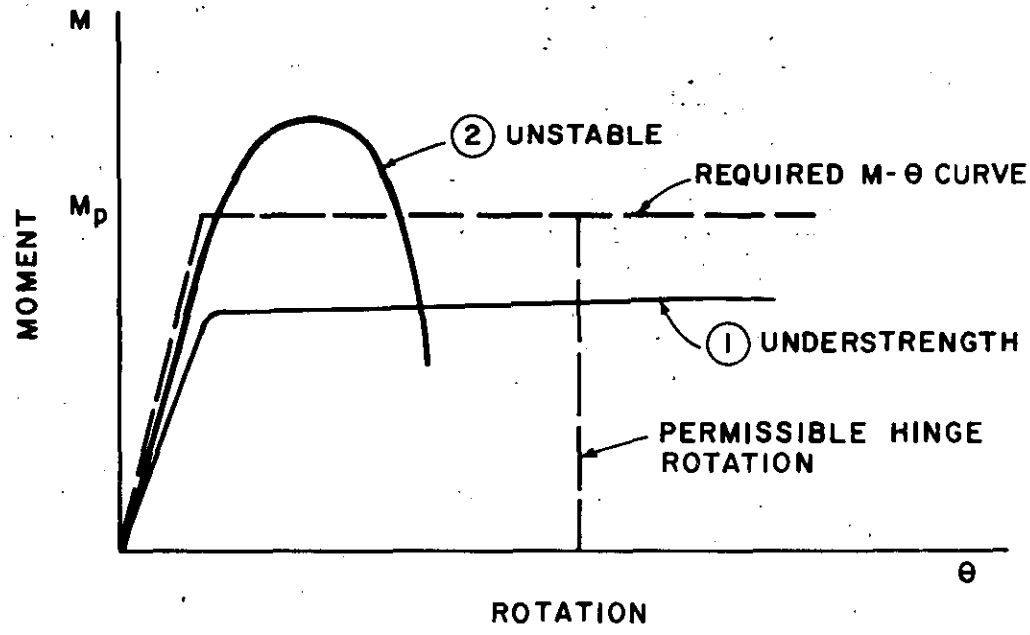
5-48. Requirements for Floor and Wall Panel Connections

Panel connections, in general, can be considered either panel-to-panel connections, or panel-to-supporting-frame connections. The former type involves the attachment of relatively light-gage materials to each other such that they act together as an integral unit. The latter type is generally used to attach sheet panels to heavier cross sections.

The most common type of fastener for decking and steel wall panels is the self-tapping screw with or without washer. Even for conventional design and regular wind loading, the screw fasteners have often been the source of local failure by tearing the sheeting material. It is evident that under blast loading and particularly on rebound, screw connectors will be even more vulnerable to this type of failure. Special care should be taken in design to reduce the probability of failure by using oversized washers and/or increased material thickness at the connection itself.

Due to the magnitude of forces involved, special types of connectors, as shown in Figure 5-27, will usually be necessary. These may consist of self-piercing, self-tapping screws of larger diameters with oversized washers, puddle welds or washer plug welds, threaded connectors fired into the elements to be attached, or threaded studs, welded to the supporting members, which fasten the panel by means of a special arrangement of bushing and nut.

Apart from fulfilling their function of cladding and load-resisting surfaces, by carrying loads perpendicular to their surface, floor, roof and wall, steel panels can, when adequately connected, develop substantial resistance to in-plane forces, acting as diaphragms contributing a great deal to the overall stiffness and stability of the structure. As a result, decking connections are, in many cases, subjected to a combination of shearing forces and pull-out forces. It is to be remembered also that after the panel has deflected under blast loading, the catenary action sustained by the flat sheet of the decking represents an important reserve capacity against total collapse. To allow for such catenary action to take place, connectors and especially end connectors should be made strong enough to withstand the membrane forces that develop.



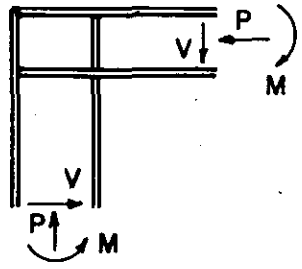


Figure 5-26 Corner connection behavior

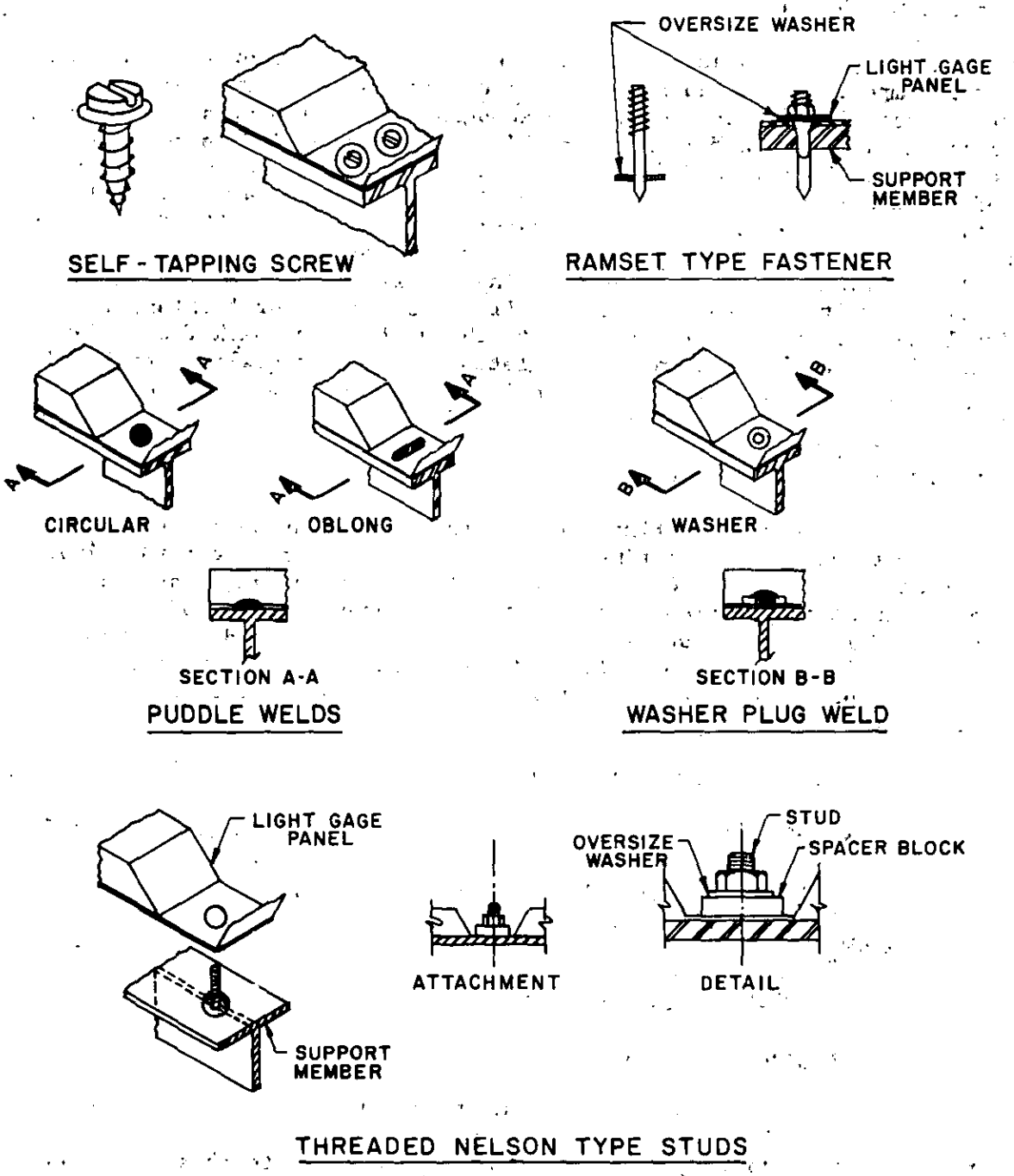


Figure 5-27 Typical connections for cold-formed steel panels

FRAGMENT PENETRATION

5-49. Penetration of Fragments into Steel

5-49.1. Failure Mechanisms

In deriving a prediction equation for the penetration and perforation of steel plates, it is important to recognize the failure mechanisms. The failure mode of primary concern in mild to medium hard homogeneous steel plates subjected to normal impact is ductile failure. In this mode, as the missile penetrates the plate, plastically deformed material is pushed aside and petals or lips are formed on both the front and back faces with no material being ejected from the plate. For plates with Brinell hardness values above 300, failure by "plugging" is a strong possibility. In this brittle mode of failure, a plug of material is formed ahead of the penetrating missile and is ejected from the back side of the plate. A third mode of failure is disking or flaking, in which circular disks or irregular flakes are thrown from the back face. This type of failure is mainly a concern with plates of inferior quality steel and should not, therefore, be a common problem in the design of protective structures.

5-49.2. Primary Fragment Penetration Equations

In protective design involving primary fragments, a penetration equation is required which yields reliable estimates corresponding to the standard primary fragment illustrated in figure 4-77 of Chapter 4. These design equations consider only normal penetration which is critical for the design of protective structures. These equations apply to penetration into mild steel and are conservative for plates with a Brinell hardness value above 150. Steel penetration equations in design for primary fragment impact are expressed in the following forms:

For AP steel fragments penetrating mild steel plates,

$$x = 0.30\, W_f^{0.33}\, V_s^{1.22} \qquad 5\text{-}64$$

and for mild steel fragments penetrating mild steel plates,

$$x = 0.21\, W_f^{0.33}\, V_s^{1.22} \qquad 5\text{-}65$$

where

x = depth of penetration (in.)

W_f = fragment weight (oz.)

V_s = striking velocity of fragment (kfps)

Charts for steel penetration by primary fragments according to these equations are presented in figures 5-28 and 5-29.

To estimate the penetration of metal fragments other than armor piercing, the procedures outlined in Section 4-60.3 of Chapter 4 are entirely applicable to steel plates.

5-49.3. Residual Velocity After Perforation of Steel Plate

The penetration equations presented in Section 5-49.2 may be used for predicting the occurrence of perforation of metallic barriers and for calculating the residual fragment velocity after perforation.

For normal impact of a steel fragment, with the shape illustrated in figure 4-77 of Chapter 4, the equation for residual velocity is

$$V_r / V_s = [1 - (V_x / V_s)^2]^{1/2} / (1 + t/d) \qquad 5\text{-}66$$

where V_r = residual velocity

V_s = striking velocity

V_x = critical perforation velocity for the fragment of impacting the plate of thickness t (see explanation below)

d = diameter of cylindrical portion of fragment (in.), as illustrated in figure 4-77 of Chapter 4

The value of V_x is determined from Figure 5-28 or 5-29 by substituting the plate thickness t for the penetration depth x and reading the corresponding value of striking velocity, V_s. This striking velocity becomes the critical perforation velocity, V_x. A plot of the residual velocity equation for a range of t/d ratios is presented in Figure 5-30.

Multiple plate penetration problems may be analyzed by the successive application of Equations 5-64 or 5-65 for predicting the depth of penetration and Equation 5-66 for calculating the residual velocity upon perforation of the plate. In addition, composite construction, consisting of concrete walls with attached spall plates, can be analyzed for fragment impact by tracing the motion of the fragment through each successive layer. The striking velocity of the fragment upon each intermediate layer is the residual fragment velocity after perforation of the previous layer. The conservative assumptions are made that the fragment remains intact during the penetration and that it does not deviate from a straight line path as it crosses the interface between the different media.

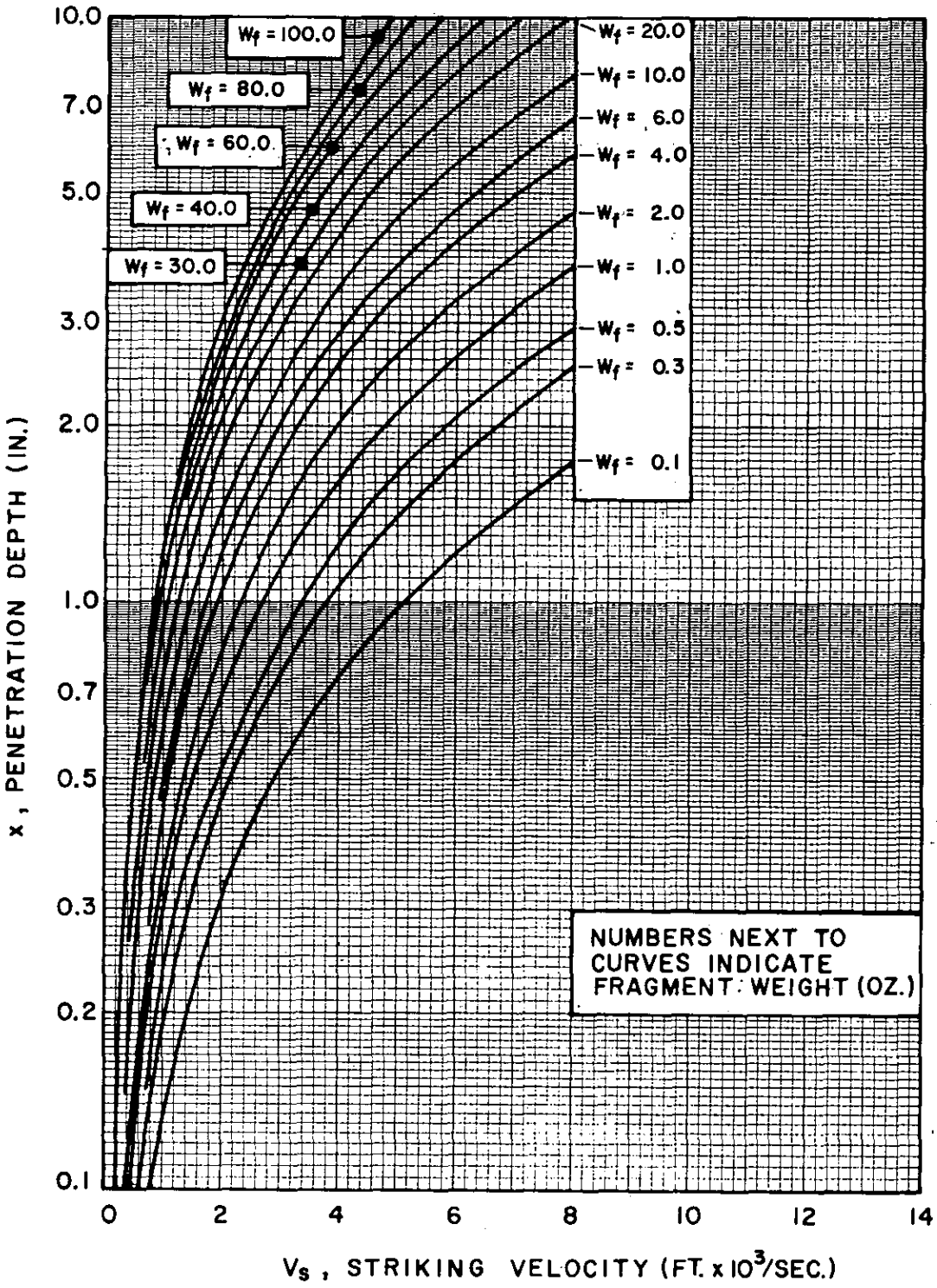


Figure 5-28 Steel penetration design chart - AP steel fragments penetrating mild steel plates

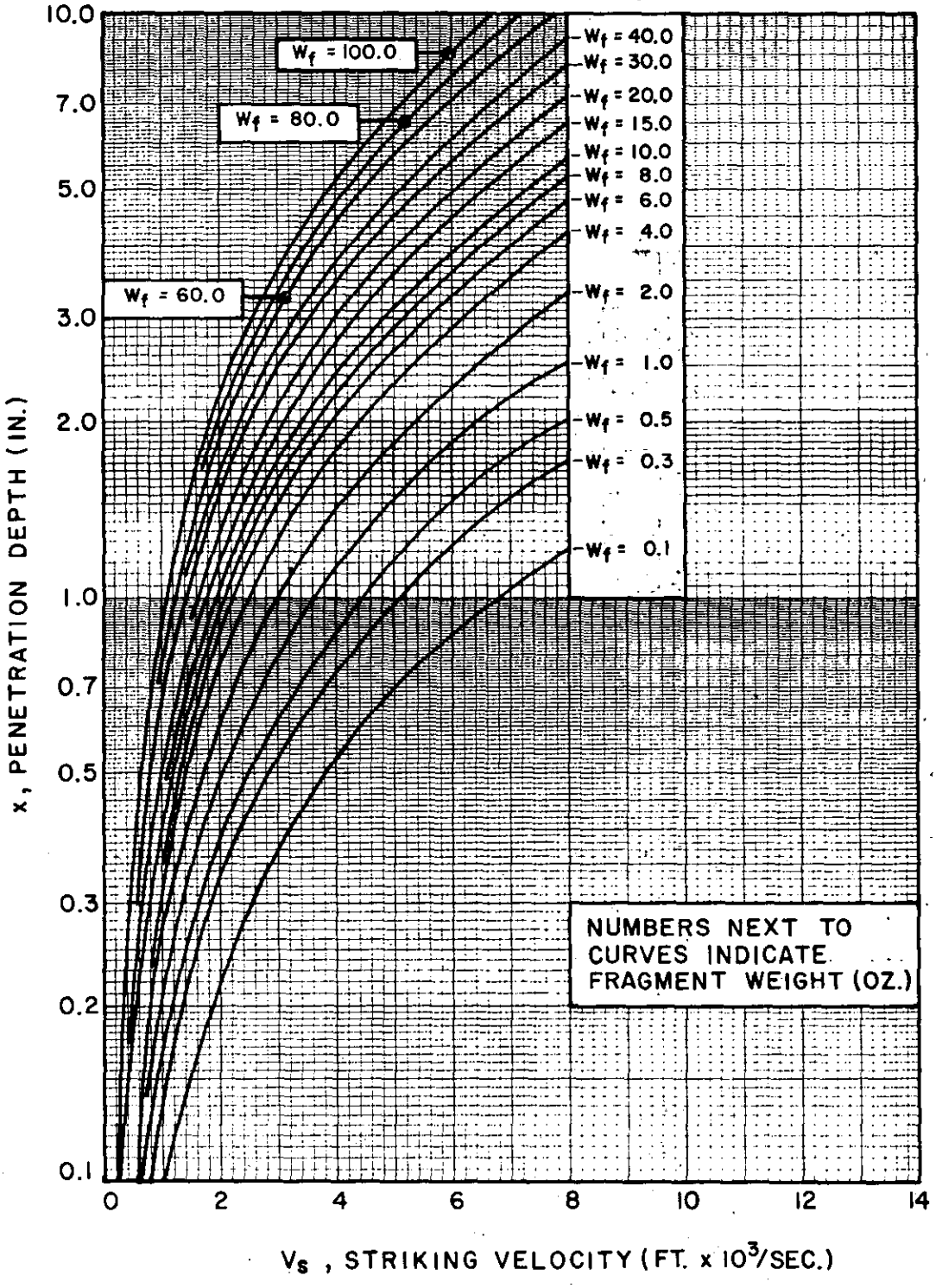


Figure 5-29 Steel penetration design chart - mild steel fragments penetrating mild steel plates

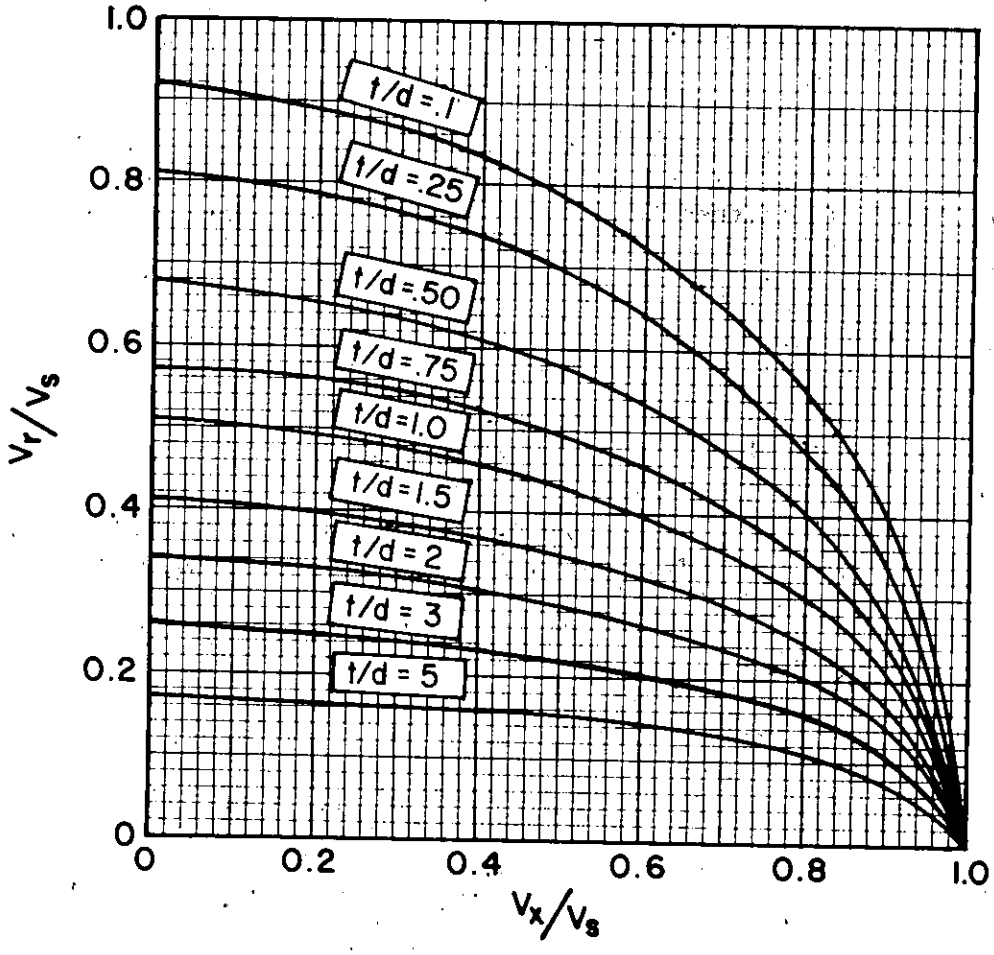


Figure 5-30 Residual fragment velocity upon perforation of steel barriers

TYPICAL DETAILS FOR BLAST-RESISTANT STEEL STRUCTURES

5-50. General

This section presents several examples of typical framing connections, structural details and blast doors used in industrial installations designed to resist accidental blast loadings. This section is intended to augment those details presented in prior sections of this chapter.

5-51. Steel Framed Buildings

Such buildings are often rectangular in plan, two or three bays wide and four or more bays long. Figure 5-31 shows an example of a typical framing plan for a single-story building designed to resist a pressure-time blast loading impinging on the structure at an angle with respect to its main axes. The structural system consists of an orthogonal network of rigid frames. The girders of the frames running parallel to the building length serve also as purlins and are placed, for ease of erection, on top of the frames spanning across the structure's width.

Figures 5-32 to 5-35 present typical framing details related to the general layout of Figure 5-31. As a rule, the columns are fabricated without splices, the plate covers and connection plates are shop welded to the columns, and all girder to column connections are field bolted. A channel is welded on top of the frame girders to cover the bolted connections and prevent (avoid) interference with the roof decking. All of the framing connections are designed to minimize stress concentrations and to avoid triaxial strains. They combine ductility with ease of fabrication.

5-52. Cold-formed, Light Gage Steel Panels

Figure 5-36 shows typical cross sections of cold-formed, light gage steel panels commonly used in industrial installations. The closed sections, which are composed of a corrugated hat section and a flat sheet, are used to resist blast pressures in the low pressure range, whereas the open hat section is recommended only for very low pressure situations as siding or roofing material. A typical vertical section illustrates the attachment of the steel paneling to the supporting members. Of particular interest is the detail at the corner between the exterior wall and the roof, which is designed to prevent peeling of the decking that may be caused by negative pressures at the roof edge.

Figure 5-37 gives some typical arrangements of welded connections for attaching cold-formed steel panels to their supporting elements. Type A refers to an intermediate support whereas Type B refers to an end support. It is recommended that the diameter of puddle welds be 3/4 of an inch minimum and should not exceed 1-1/2 inches because of space limitations in the panel valleys. For deeper panels, it is often necessary to provide two rows of puddle welds at the intermediate supports in order to resist the uplift forces in rebound. It should be noted that welds close to the hooked edge of the panel are recommended to prevent lifting of adjacent panels.

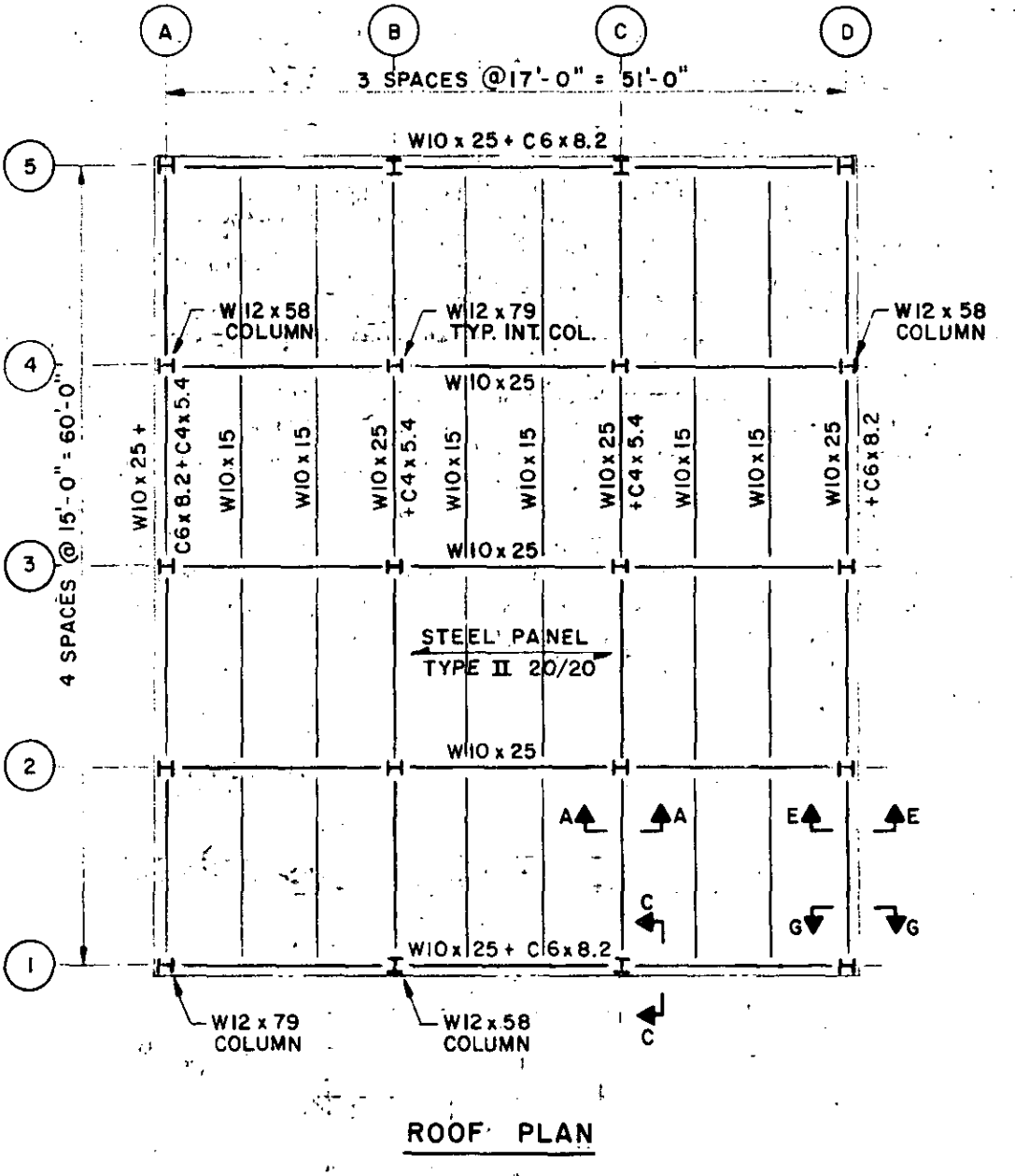
Figure 5-38 shows an arrangement of bolted connections for the attachment of cold-formed steel panels to the structural framing. The bolted connection consists of: a threaded stud resistance welded to the supporting member, a

square steel block with a concentric hold used as a spacer, and a washer and nut for fastening. Figure 5-39 presents a cross section of that connection with all the relevant details along with information pertaining to puddle welds.

5-53. Blast Doors

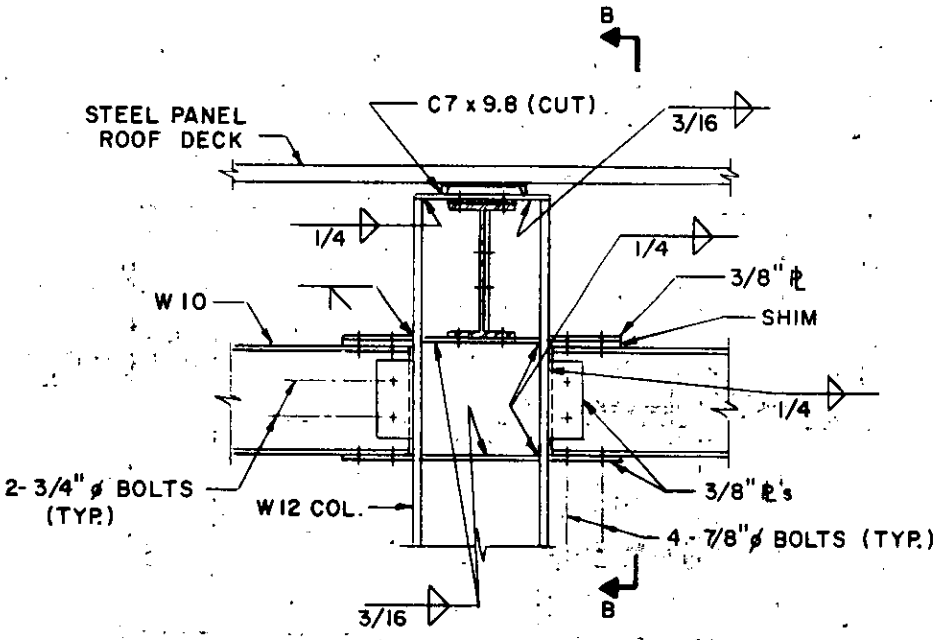
Figures 5-40 and 5-41 show details of single-leaf and double-leaf blast doors, respectively. Figure 5-40 presents a single-leaf door installed in a steel structure. The design is typical of doors intended to resist relatively low pressure levels. It is interesting to note that the door is furnished with its tubing frame to ensure proper fabrication and to provide adequate stiffness during erection. In Figure 5-41, the double-leaf door with its frame is installed in place and attached to the concrete structure. In both figures details of hinges, latches, anchors, and panic hardware are illustrated. It should be noted that the pins at the panic latch ends are made of aluminum in order to eliminate the danger of sparking, a hazard in ammunition facilities which might arise from steel-on-steel striking.

Figure 5-42 shows details of compression arch and tension arch doors. The tension arch door requires compression ties to develop the compression reactions for the arch and to prevent the door from being blown through the opening. The compression arch door requires a tension tie plate to develop the reactions and to prevent large distortions in the door that may bind it in place.

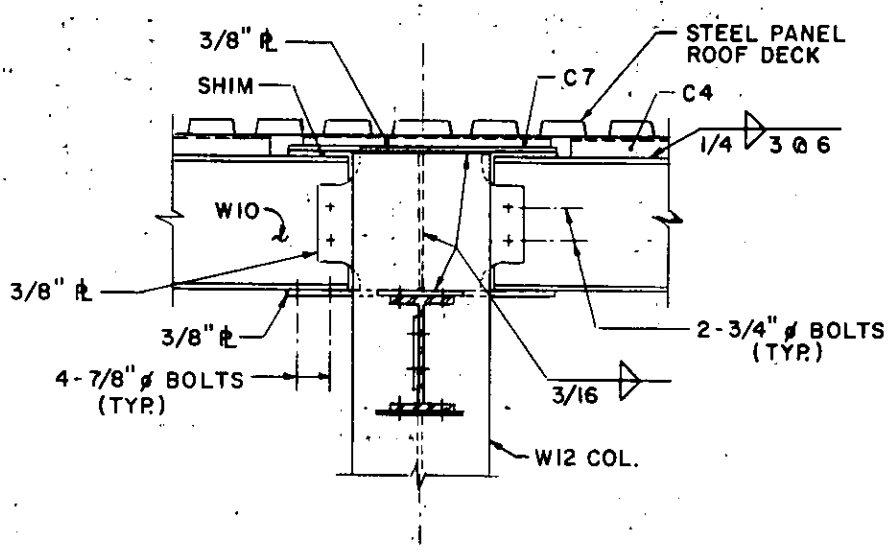


ROOF PLAN

Figure 5-31 Typical framing plan for a single-story blast-resistant steel structure

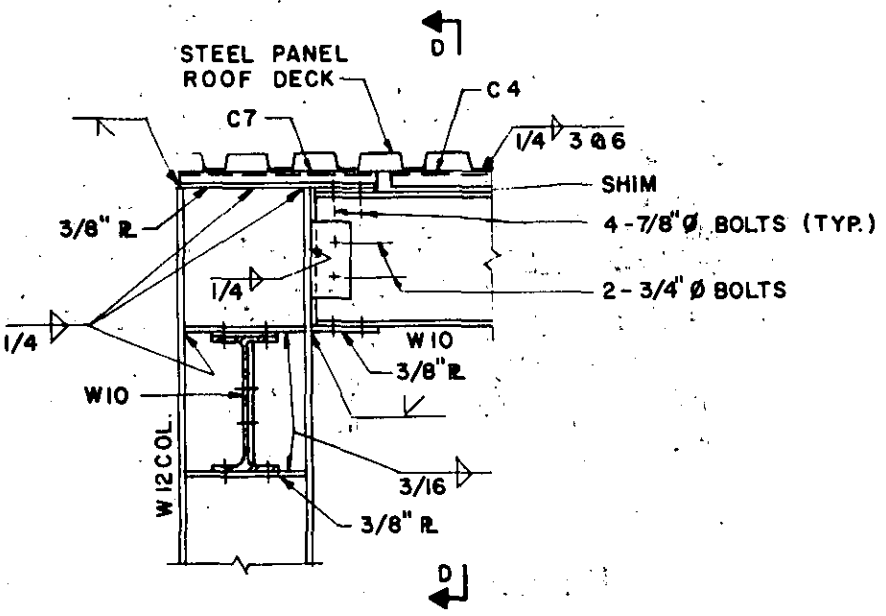


SECTION A-A

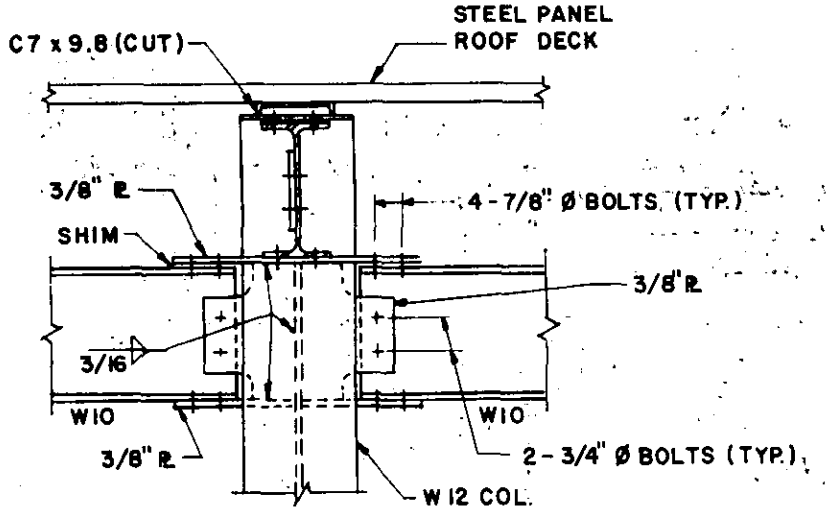


SECTION B-B

Figure 5-32 Typical framing detail at interior Column 2-C

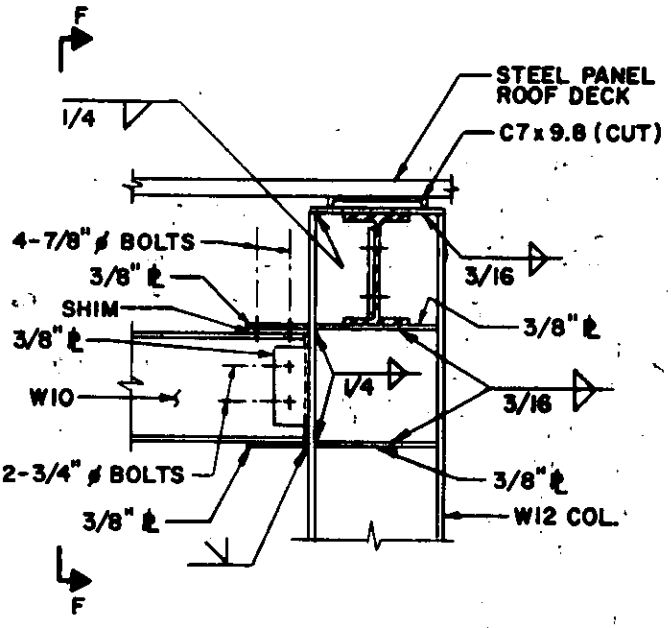


SECTION C-C

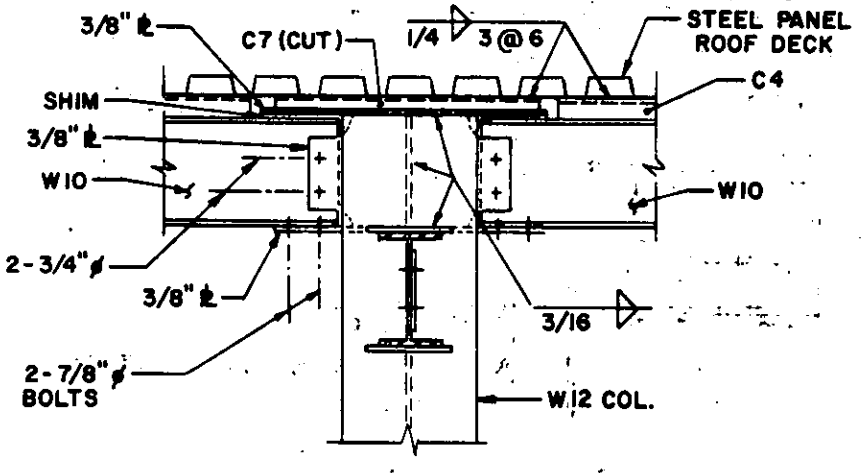


SECTION D-D

Figure 5-33 Typical framing detail at end Column 1-C



SECTION E-E



SECTION F-F

Figure 5-34. Typical framing detail at side column 2-D

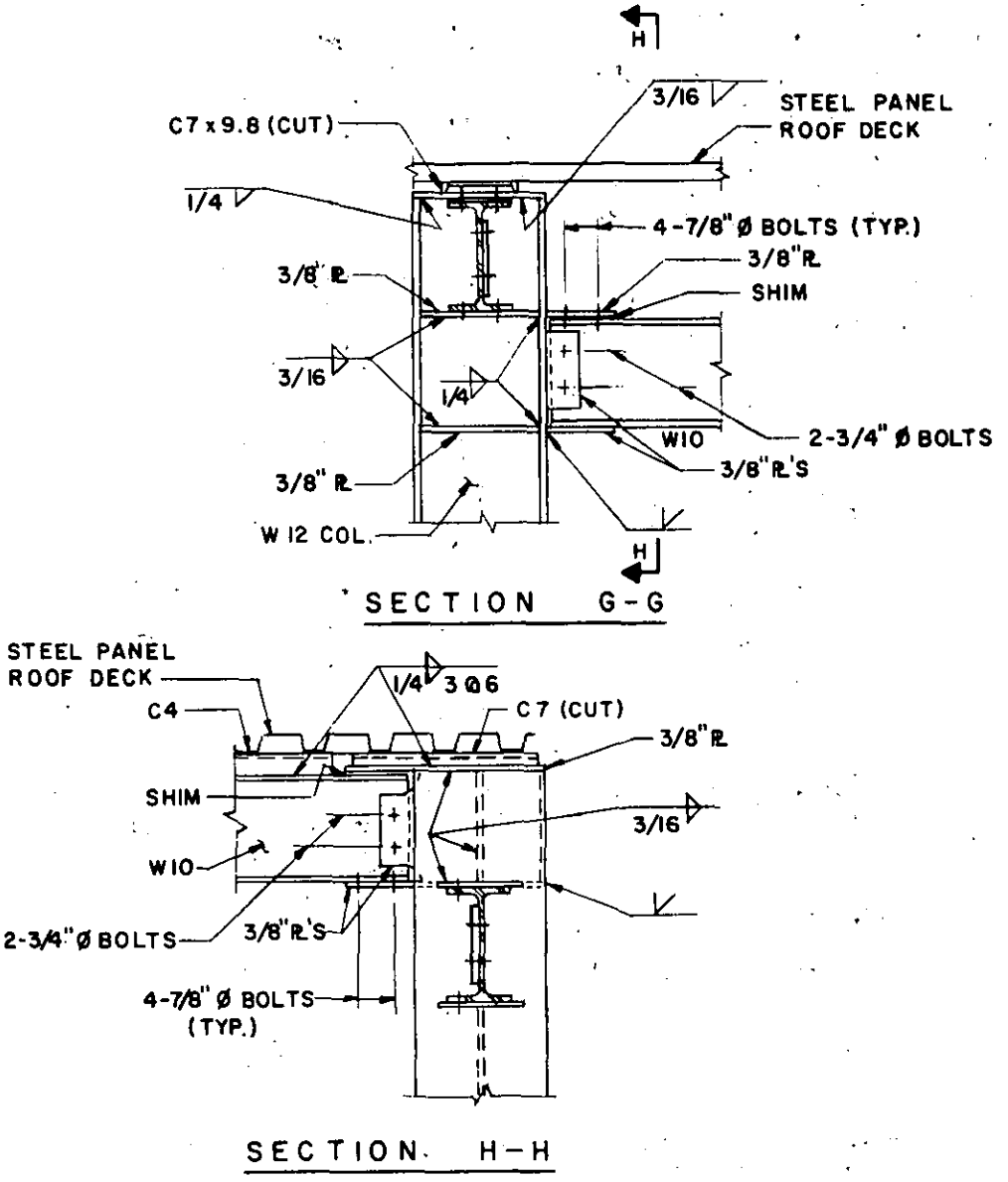


Figure 5-35 Typical framing detail at corner Column 1-D

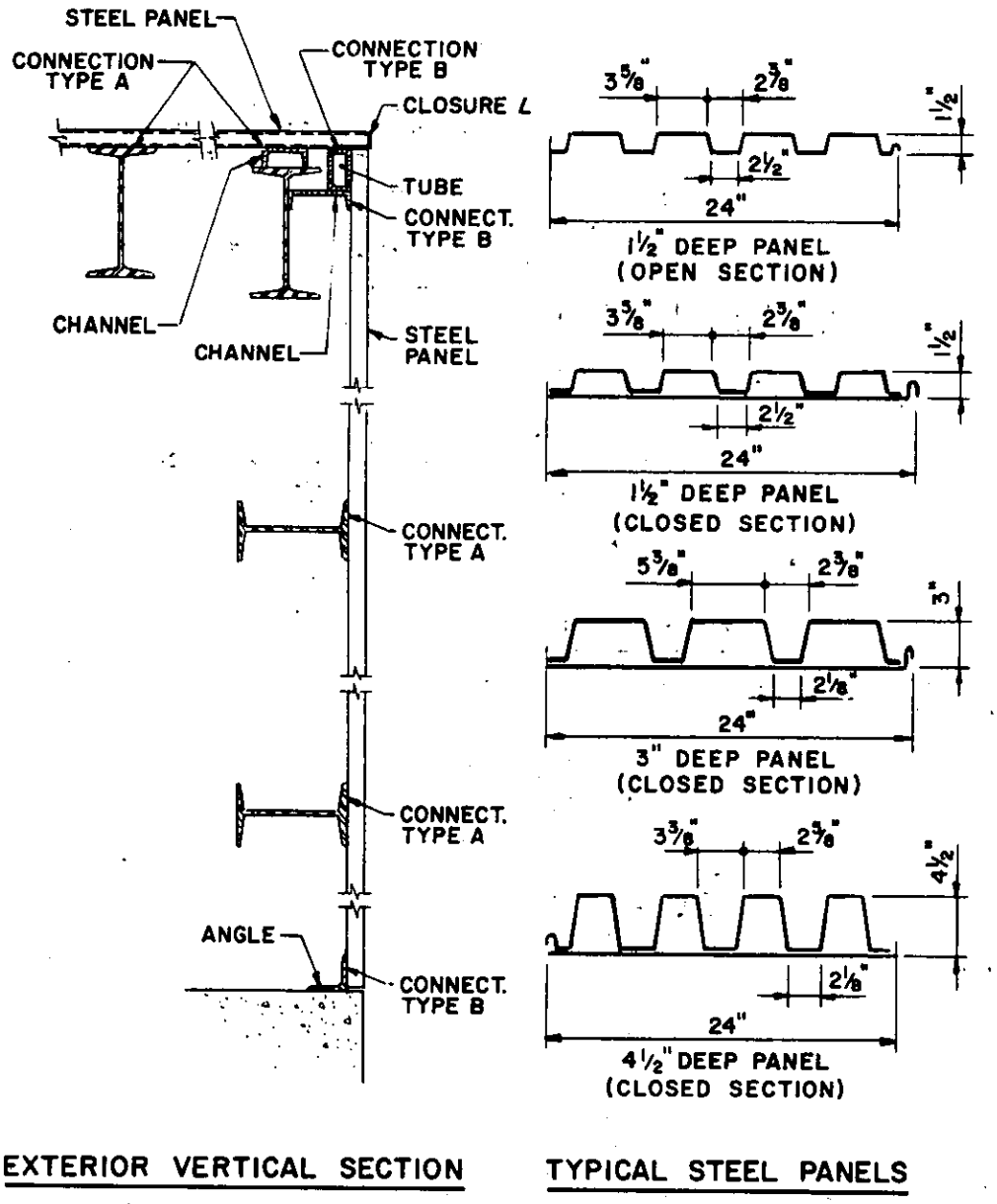


Figure 5-36 Typical details for cold-formed, light gage steel paneling

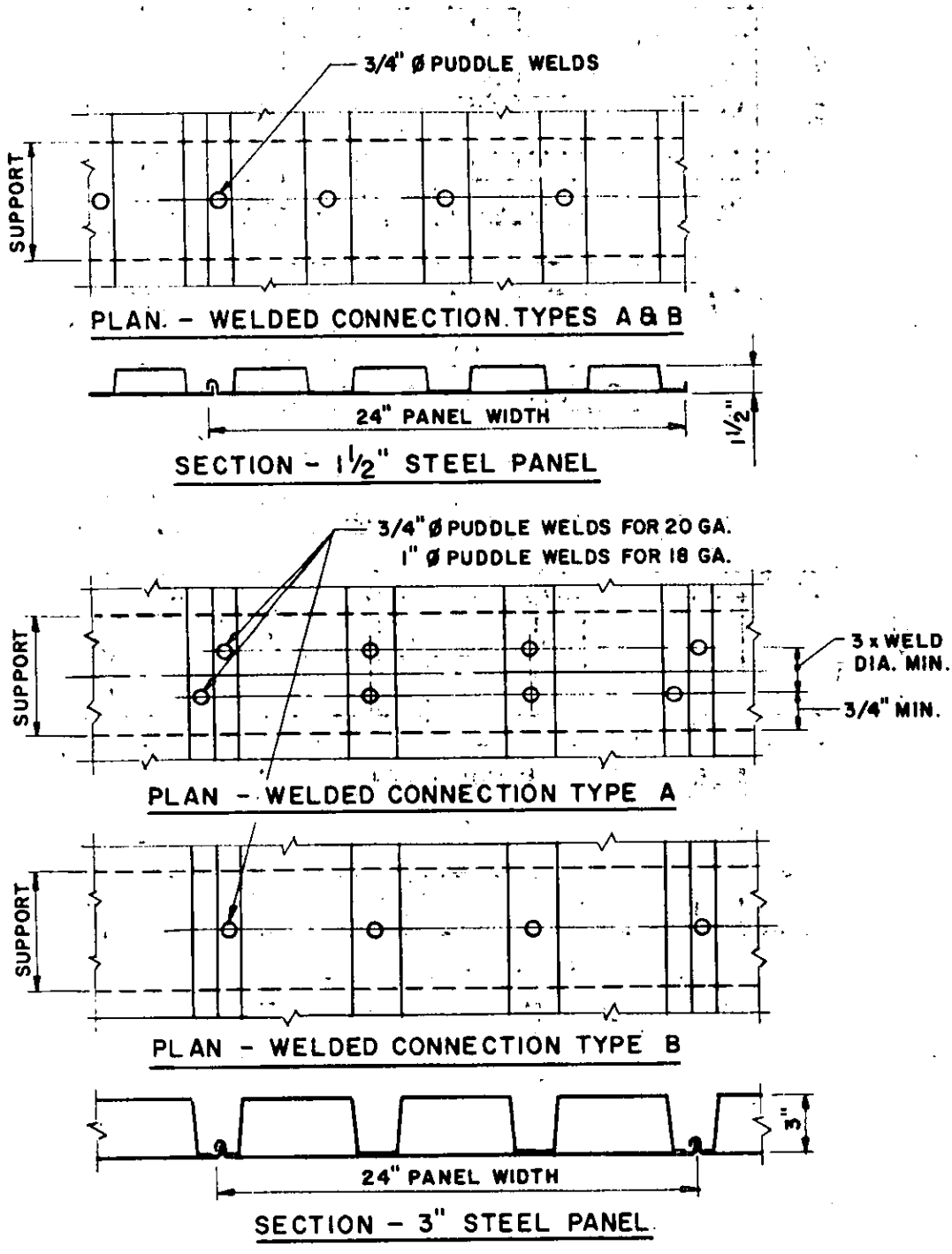


Figure 5-37 Typical welded connections for attaching cold-formed steel panels to supporting members

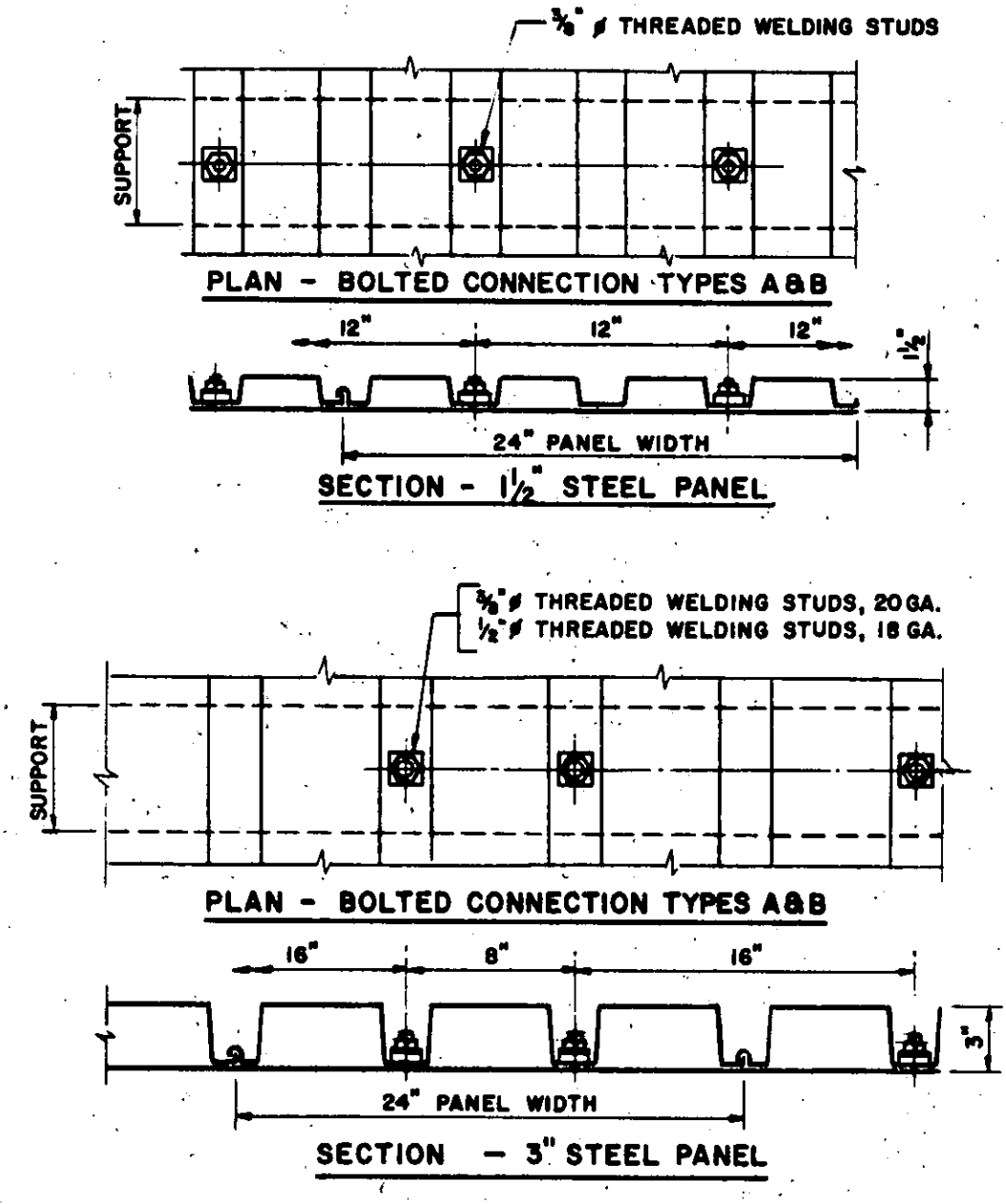
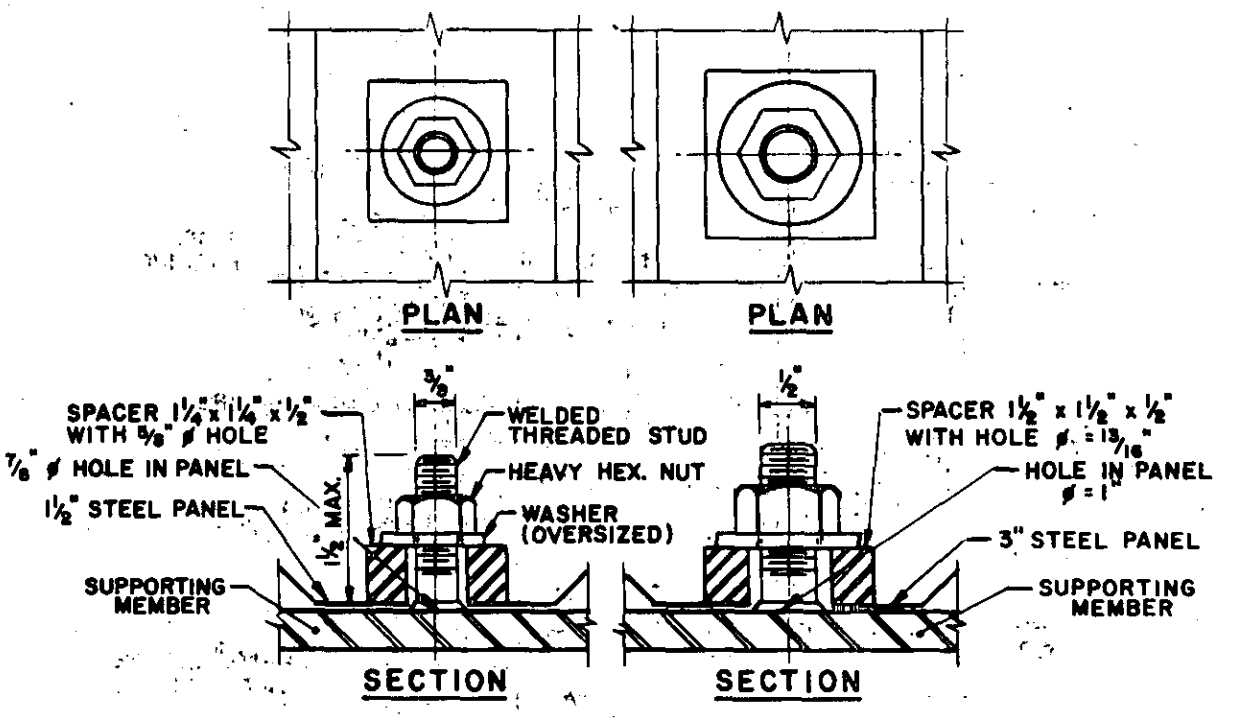
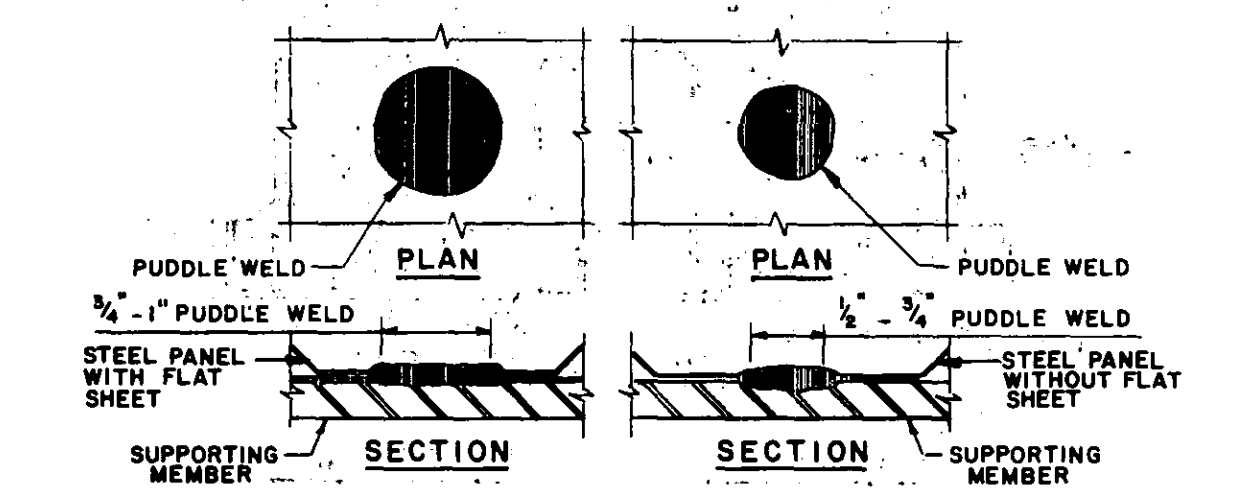


Figure 5-38 Typical bolted connections for attaching cold-formed steel panels to supporting members



TYPICAL BOLTED CONNECTION



TYPICAL WELDED CONNECTION

Figure 5-39 Details of typical fasteners for cold-formed steel panels

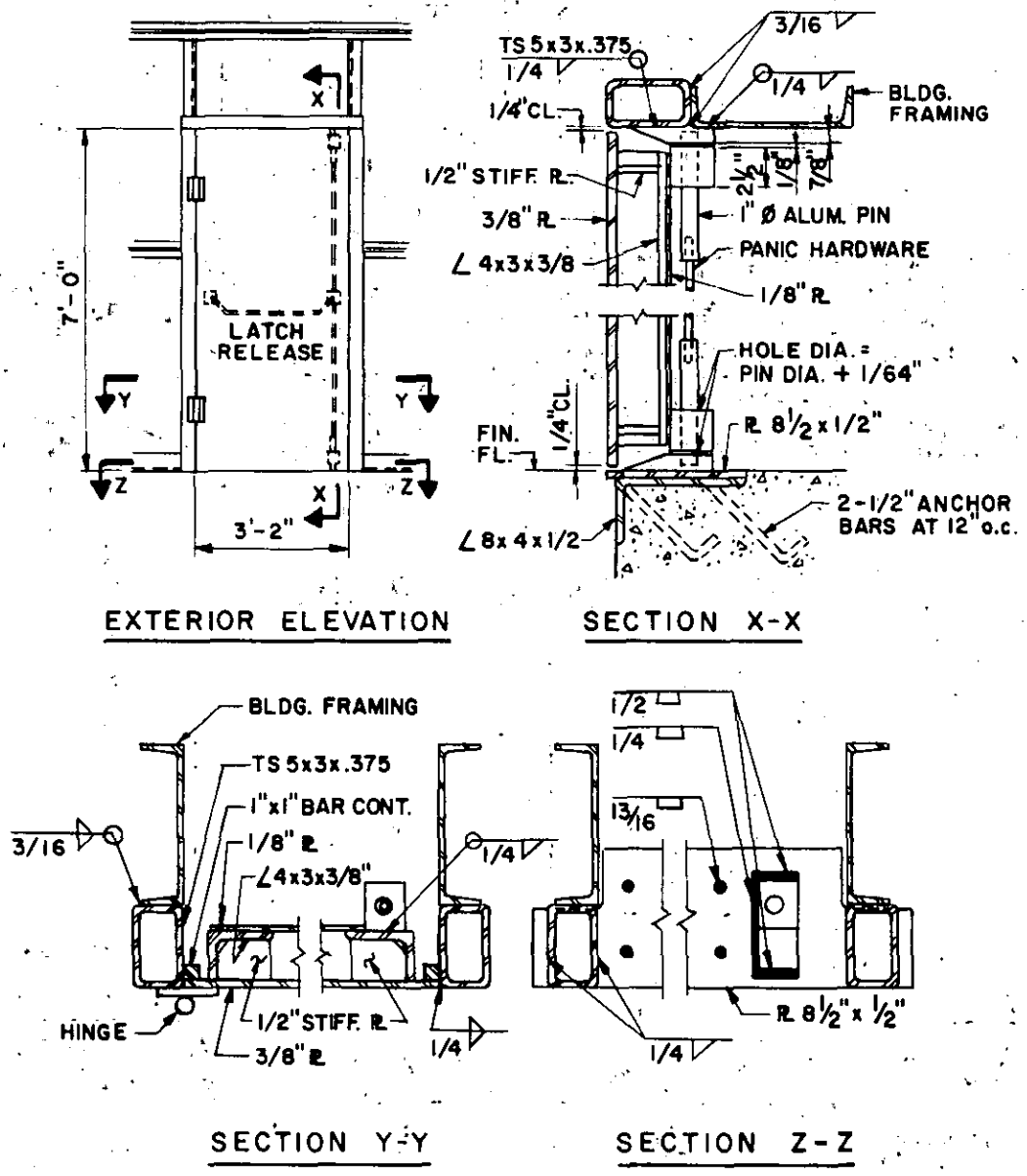


Figure 5-40 Single-leaf blast door installed in a steel structure

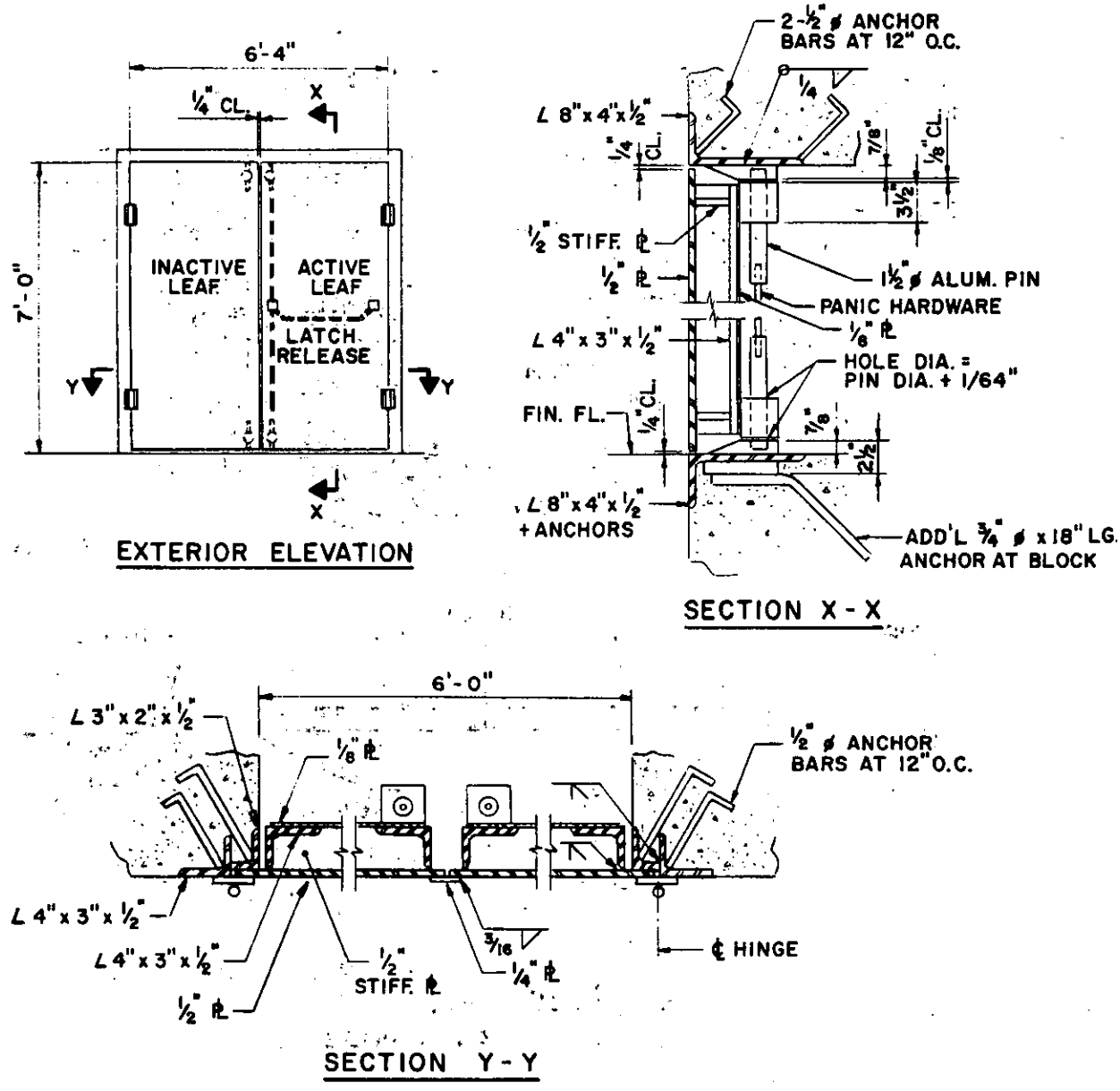
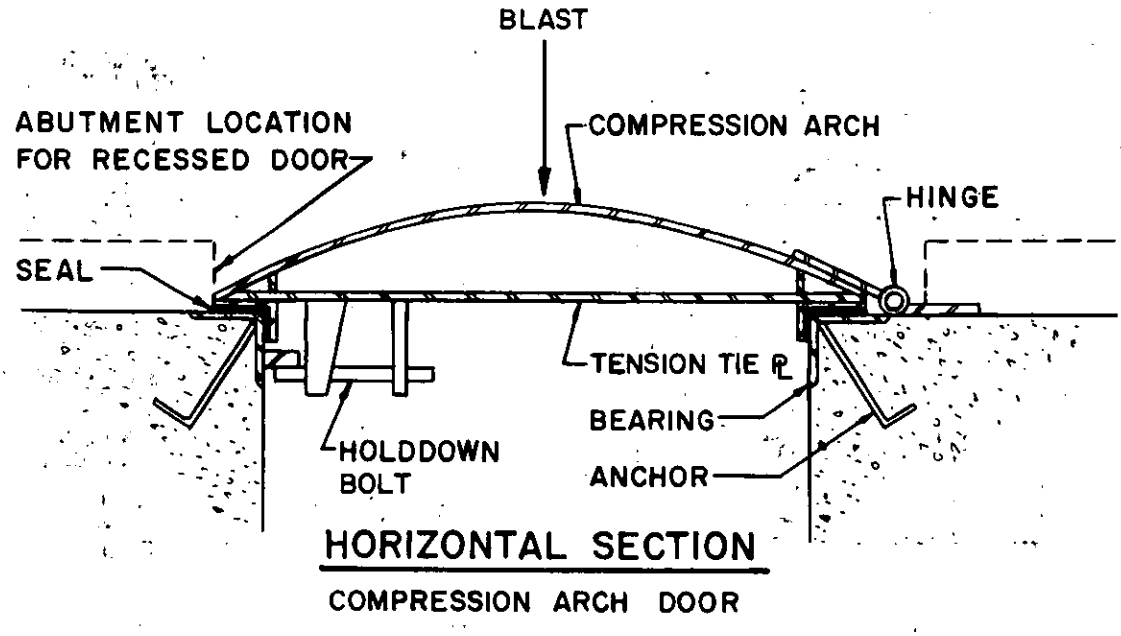


Figure 5-41 Double-leaf blast door installed in a concrete structure



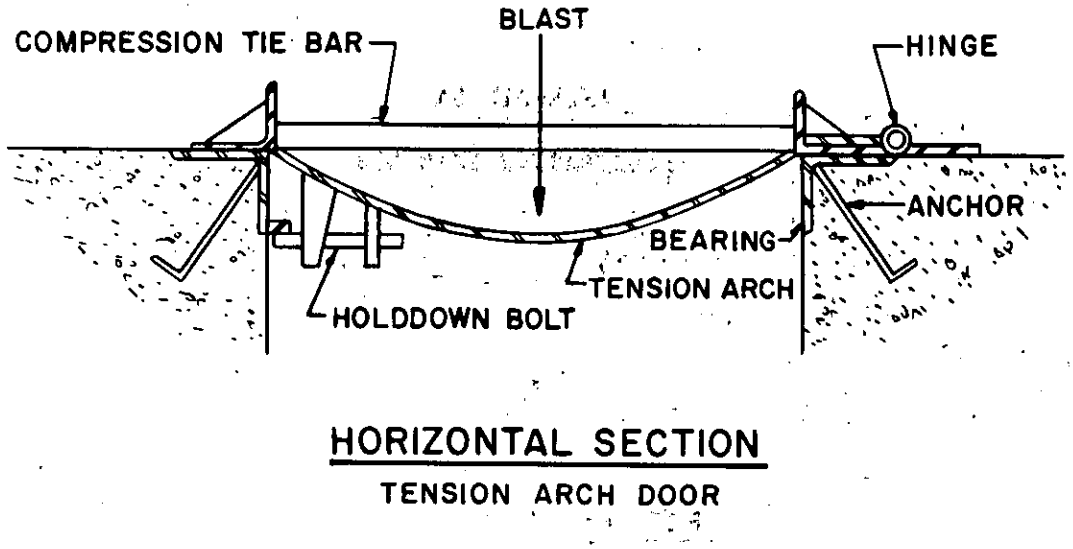


Figure 5-42 Compression-arch and tension-arch blast doors

APPENDIX 5A

ILLUSTRATIVE EXAMPLES

This appendix presents detailed design procedures and numerical examples on the following topics:

1. Flexural elements subjected to pressure-time loading
2. Lateral bracing requirements
3. Cold-formed steel panels
4. Columns and beam-columns
5. Open-web joists
6. Single-story rigid frames
7. Blast doors
8. Unsymmetrical bending

References are made to the appropriate sections of this chapter and to charts, tables, and equations from Chapter 3 "Principles of Dynamic Analysis".

Problem 5A-1 Design of Beams for Pressure-Time Loading

Problem: Design of a purlin or girt as a flexural member which responds to a pressure-time loading.

Procedure:

Step 1. Establish the design parameters:

a. Pressure-time load

b. Design criteria: Maximum support rotation, θ, depending on protection category.

c. Span length, L, beam spacing, b, and support conditions.

d. Properties and type of steel used, i.e., f_y and E.

Step 2. Determine the equivalent static load, w, using the following preliminary dynamic load factors as discussed in Section 5-22.3.

$$\text{DLF} = \begin{cases} 1.0 & \text{for } \theta = 2^\circ \\ 0.5 & \text{for } \theta = 12^\circ \end{cases}$$

Step 3. Using the appropriate resistance formula from Table 3-1 and the equivalent static load derived in Step 2, determine M_p.

Step 4. Select a member size using equation 5-7 or 5-8. Check the local buckling criteria of Section 5-24 for the member chosen.

Step 5. Determine the mass, m, including the weight of the decking over a distance center-to-center of purlins or girts, and the weight of the members.

Step 6. Calculate the equivalent mass M_e using Table 3-12 (Chapter 3).

Step 7. Determine the equivalent elastic stiffness K_E from Table 3.1.

Step 8. Calculate the natural period of vibration, T_N, using equation 5-15.

Step 9. Determine the total resistance, R_u, and peak pressure load, P. Enter appropriate chart in Section 3-19.3 with the ratios T/T_N and P/R_u and the values of C_1, and C_2 in order to establish the ductility ratio μ.

Step 10. Check the assumed DIF used in Step 4. Enter the response charts with the ratio T/T_N and μ and to determine t_E. Using equation 5-1, determine the strain rate. Using figure 5-2, determine the DIF and C. If there is a significant difference from that assumed, repeat Steps 4 through 9.

Step 11. Calculate the equivalent elastic deflection X_E as given by the equation

$$X_E = R_u/K_E$$

and establish the maximum deflection X_m given by

$$X_m = \mu X_E$$

Compute the corresponding member end rotation. Compare θ with the criteria summarized in Section 5-35.

$$\tan \theta = X_m/(L/2)$$

Step 12. Check for shear using equation 5-16 and Table 3-9.

Step 13. If a different member size is required, repeat Steps 2 through 12 by selecting a new dynamic load factor.

Example 5A-1 Design of a Beam for Pressure-Time Loading

Required: Design a simply supported beam for shear and flexure in a low pressure range where personnel protection is required.

Step 1. Given:

a. Pressure-time loading (Figure 5A-1)

b. Criteria: Personnel protection required. Support rotation limited to 2°.

c. Structural configuration (Figure 5A-1).

d. f_y = 36 ksi, E = 30 x 10^3 ksi, A36 steel

e. Compression flanged braced.

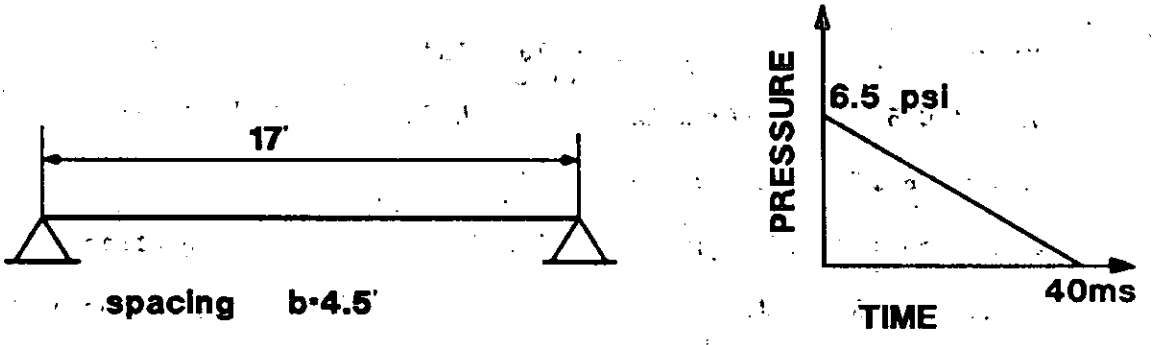


Figure 5A-1 Beam configuration and loading, Example 5A-1

Step 2. Determine the equivalent static load (i.e., required resistance). For this pressure range, the equivalent static load is assumed equal to the peak pressure (Section 5-22.3). The running load becomes:

$$w = 1.0 \times 6.5 \times 4.5 \times 144/1000 = 4.21 \text{ k/ft}$$

Step 3. Determine required M_p.

$$M_p = \frac{wL^2}{8} = \frac{4.21 \times 17^2}{8} = 152.1 \text{ k-ft} \qquad \text{(Table 3-1)}$$

Step 4. Select a member.

$$(S + Z) = \frac{2M_p}{f_{ds}} = \frac{2 \times 152.1 \times 12}{51.1} = 71.4 \text{ in}^3 \qquad \text{(Equation 5-7)}$$

where

$$f_{ds} = a \times c \times f_y = 1.1 \times 1.29 \times 36 = 51.1 \text{ ksi} \qquad \text{(Equation 5-2)}$$

where

a = 1.1 from Section 5-13.2

c = 1.29 corresponding to a DIF in the low pressure range (see Table 5-2)

Select W12 x 26, $S = 33.4\ in^3$ $I = 204\ in^4$

$Z = 37.2\ in^3$

$S + Z = 70.6\ in^3$

$M_p = (70.6 \times 51.1)/(2 \times 12) = 150.3$ k-ft

Check local buckling criteria.

$d/t_w = 53.1 < 412/(f_y)^{1/2} = 68.7$ O.K. (Equation 5-17)

$b_f/2t_f = 8.5$ O.K. (Section 5-24)

Step 5. Calculate M.

$$M = \frac{wL}{g} = \frac{[(4.5 \times 4.8) + 26]\ (17 \times 10^6)}{32.2 \times 1000} = 25{,}130\ (k\text{-}ms^2)/ft$$

Step 6. Calculate the effective mass, M_e, for a response in the elasto-plastic range.

$K_{LM} = (0.78 + 0.66)/2 = 0.72$ (Table 3-12)

$M_e = 0.72 \times 25{,}130 = 18{,}100$ k-ms^2/ft

Step 7. Determine K_E.

$$K^E = \frac{384\ EI}{5L^3} = \frac{384 \times 30 \times 10^3 \times 204}{5 \times 17^3 \times 144} = 664\ k/ft$$ (Table 3-8)

Step 8. Calculate T_N.

$T_N = 2\pi(M_e/K_E)^{1/2} = 2\pi(18{,}100/664)^{1/2}$ (Equation 5-15)

Step 9. Establish the ductility ratio μ and compare with the criteria.

$T/T_N = 40/32.8 = 1.22$

$$P = p \times L \times b = \frac{6.5 \times 17 \times 4.5 \times 144}{1000} = 71.6 \text{ kips}$$

$R_u = 8M_p/L = (8 \times 150.3)/17 = 70.7$ kips

$P/R_u = 71.6/70.7 = 1.01$

From figure 3-64a,

$\mu = X_m/X_E = 2.1$

At this point, the designer would check lateral bracing requirements. Sample problem 5A-2 outlines this procedure.

Step 10. Check the assumed DIF.

From Table 3-64a, for $P/R_u = 1.01$ and $T/T_N = 1.22$.

$t_E/T = 0.24$

$t_E = 0.24 \times 40 = 9.6$ ms

Find $\dot{\epsilon}$:

$\dot{\epsilon} = f_{ds}/E_s t_E = 51.1/30 \times 10^3 \times .0096 = 0.177$ in/in/sec (Equation 5-1)

From figure 5-2

DIF = 1.31 = 1.29 O.K.

Step 11. Determine X_E:

$X_E = R_u/K_E = (70.7 \times 12)/664 = 1.28$ inch

Find X_m:

$X_m = \mu X_E = 2.1 \times 1.28 = 2.69$ inches

Find end rotation, Θ.

$\tan \Theta = X_m/(L/2) = 2.69/(8.5 \times 12) = 0.0264$ (Table 3-5)

$\Theta = 1.52° < 2°$ O.K.

Step 12. Check shear.

Dynamic yield stress in shear

$f_{dv} = 0.55\ f_{ds} = 0.55 \times 51.1 = 28.1$ ksi (Equation 5-4)

Ultimate shear capacity

$V_p = f_{dv} \times A_w = 28.1 \times 0.23 \times 12 = 77.6$ kips (Equation 5-16)

Maximum support shear

$V_s = r_u \times L/2 = R_u/2 = 70.7/2 = 35.4$ kips (Table 3-9)

$V_p > V_s$ O.K.

Problem 5A-2 Spacing of Lateral Bracing

Problem: Investigate the adequacy of the lateral bracing specified for a flexural member.

The design procedure for determining the maximum permissible spacing of lateral bracing is essentially a trial and error procedure if the unbraced length is determined by the consideration of lateral torsional buckling only. However, in practical design, the unbraced length is usually fixed by the spacing of purlins and girts and then must be investigated for lateral torsional buckling.

Procedure:

Step 1. Establish design parameters.

a. Bending moment diagram obtained from a design analysis.

b. Unbraced length, 1, and radius of gyration of the member, r_y, about its weak axis.

c. Dynamic design strength, f_{ds}. (Section 5-13)

d. Design ductility ratio, μ, from a design analysis.

Step 2. From the moment diagram, find the end moment ratio, M/M_p, for each segment of the beam between points of bracing. (Note that the end moment ratio is positive when the segment is bent in reverse curvature and negative when bent in single curvature).

Step 3. Compute the maximum permissible unbraced length, l_{cr}, using equation 5-20 or 5-21, as applicable. Since the spacing of purlins and girts is usually uniform, the particular unbraced length that must be investigated in a design will be the one with the largest moment ratio. The spacing of bracing in nonyielded segments of a member should be checked against the requirements of Section 1.5.1.4.5a of the AISC Specification (see Section 5-26.3).

Step 4. The actual length of a segment being investigated should be less than or equal to l_{cr}.

Example 5A-2 Spacing of Lateral Bracing

Required: Investigate the unbraced lengths shown for the W10 x 39 beam in figure 5A-2.

Step 1. Given:

a. Bending moment diagram shown in figure 5A-2.

b. Unbraced length (each segment) = 36 inches
r_y = 1.98 inches

c. Dynamic design stress = 51.1 ksi

d. Design ductility ration, μ = 5.

Step 2. The moment ratio is -0.5 for segments BC and CD (single curvature) and 0.5 for segments AB and DE (double curvature).

Step 3. Determine the maximum permissible unbraced length. By inspection, equation 5-21 results in the lower value of l_{cr}.

$$\frac{\beta l_{cr}}{r_y} = \frac{1375}{f_{ds}}$$

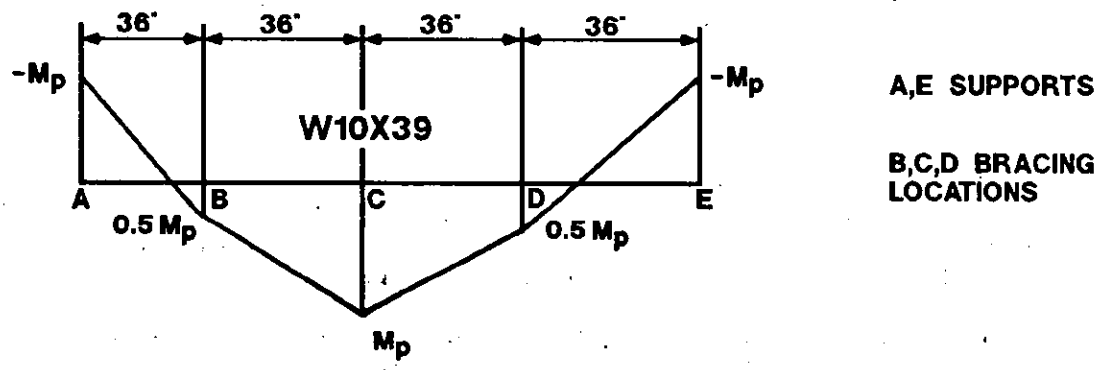


Figure 5A-2 Bending moment diagram, Example 5A-2

From figure 5-9 for $x_m/x_E = 5$, $\beta = 1.36$

$$\therefore \quad l_{cr} = \frac{1375 \times 1.98}{1.36 \times 51.1} = 39.2"$$

Step 4. Since the actual unbraced length is less than 39.2 inches, the spacing of the bracing is adequate.

Problem 5A-3 Design a Roof Deck as a Flexural Member which Responds to Pressure-Time Loading

Problem: Design of cold-formed, light gauge steel panels subjected to pressure-time loading.

Step 1. Establish the design parameters:

a. Pressure-time loading

b. Design criteria: Specify values of μ and θ depending upon whether tension-membrane action is present or not.

c. Span length and support conditions

d. Mechanical properties of steel

Step 2. Determine an equivalent uniformly distributed static load for a 1-ft width of panel, using the following preliminary dynamic load factors.

	Tension-membrane action not present	Tension-membrane action present
DLF	1.33	1.00

These load factors are based on an average value of $T/T_N = 10.0$ the recommended design ductility ratios. They are derived using figure 3-64 of Chapter 3.

Equivalent static load $w = DLF \times p \times b$, $b = 1$ ft

Step 3. Using the equivalent load derived in step 2, determine the ultimate moment capacity using equation 5-29 or 5-30 (assume positive and negative are the same).

Step 4. Determine required section moduli using equation 5-27 or 5-28.

Select a panel.

Step 5. Determine actual section properties of the panel:

S^+, S^-, I_{20}, w.

Step 6. Compute r_u, the maximum unit resistance per 1-ft width of panel using equation 5-29 or 5-30.

Step 7. Determine the equivalent elastic stiffness, $K_E = r_u L/X_E$, using equation 5-31.

Step 8. Compute the natural period of vibration.

$$T_N = 2\pi (0.74\ mL/K_E)^{1/2} \qquad \text{(Equation 5-32)}$$

Step 9. Calculate P/r_u and T/T_N. Enter figure 3-64 with the ratios P/r_u and T/T_N to establish the actual ductility ratio μ.

Compare μ with the criteria of step 1. If μ is larger than the criteria value, repeat steps 4 to 9.

Step 10. Compute the equivalent elastic deflection X_E using $X_E = r_u L/K_E$. Evaluate the maximum deflection, $X_m = \mu X_E$.

Determine the maximum panel end rotation.

$$\theta = \tan^{-1} [X_m/(L/2)]$$

Compare θ with the criteria of step 1. If θ is larger than specified in the criteria, select another panel and repeat steps 5 to 10.

Step 11. Check resistance in rebound using figure 5-13.

Step 12. Check panel for maximum resistance in shear by applying the criteria relative to:

a. Simple shear, Table 5-5a, 5-6a or 5-7a.

b. Combined bending and shear, Table 5-5b, 5-6b or 5-7b.

c. Web crippling, figures 5-15 or 5-16.

If the panel is inadequate in shear, select a new member and repeat steps 4 to 12.

Example 5A-3 Design a Roof Deck as a Flexural Member which Responds to Pressure-Time Loading

Required: Design a continubus cold-formed steel panel in a low pressure range.

Step 1. Given:

a. Pressure-time loading (figure 5A-3).

b. Criteria: (Tension-membrane action present)

maximum ductility ratio $\mu_{max} = 6$

maximum rotation $\theta_{max} = 4°$

c. Structural configuration figure 5A-3.

d. Steel A446, grade a

$E = 30 \times 10^6$ psi

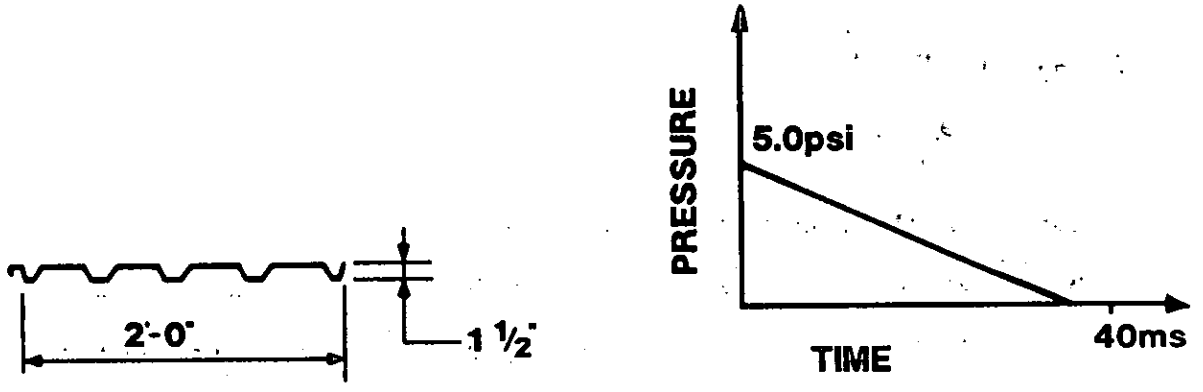
$f_{ds} = a \times c \times f_y = 1.21 \times 1.1 \times 33{,}000 = 44{,}000$ psi (Equation 5-26)

Step 2. Determine the equivalent static load.
Say DLF = 1.0

$w = DLF \times p \times b = 1.0 \times 5.0 \times 12 \times 12 = 720$ lb/ft

Step 3. Determine required ultimate moment capacities. For preliminary selection, assume

$M_{up} = M_{un} = wL^2/10.8 = 720 \times (4.5)^2/10.8 = 1{,}350$ lb-ft (Equation 5-30)



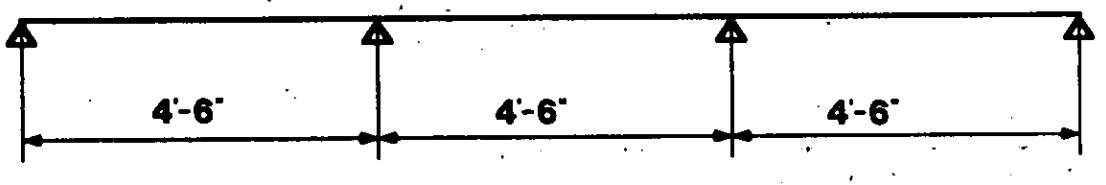


Figure 5A-3 Roof decking configuration and loading, Example 5A-3

Step 4. Determine required section moduli.

$S^+ = S^- = (1350 \times 12)/44{,}000 = 0.368 \text{ in}^3$

(Select Sec. 3-18, 1-1/2 inches deep)

Step 5. Determine actual section properties.

For manufacturer's guide:

$S^+ = 0.398 \text{ in}^3$

$S^- = 0.380 \text{ in}^3$

$I_{20} = 0.337 \text{ in}^4$

$w = 2.9 \text{ psf}$

Step 6. Compute maximum unit resistance r_u.

$M_{un} = (44{,}000 \times 0.398)/12 = 1{,}459 \text{ lb-ft}$ (Equation 5-27)

$M = (44{,}000 \times 0.380)/12 = 1{,}393 \text{ lb-ft}$ (Equation 5-28)

$$r_u = 3.6\,(M_{un} + 2M_{up})/L^2 = \frac{3.6}{4.5^2}\,(1{,}393 + 2 \times 1{,}459) = 766 \text{ lb/ft}$$

(Equation 5-30)

Step 7. Determine equivalent static stiffness.

$$K_E = \frac{r_u L}{X_E} = \frac{EI_{20} \times r_u \times L}{0.0062 \times r_u \times L^4} = \frac{EI_{20}}{0.0062\,L^3}$$ (Equation 5-31)

$$\frac{30^6 \times 10 \times 0.337}{0.0062\,(4.5^3) \times 144} = 124{,}260 \text{ lb/ft}$$

Step 8. Compute the natural period of vibration for the 1-ft width of panel.

$mL = w/g = (2.9 \times 10^6 \times 4.5)/32.2 = 4.05 \times 10^5 \text{ lb-ms}^2/\text{ft}$

$T_N = 2x[(0.74 \times 4.05 \times 105)/124{,}260]^{1/2} = 9.75$ msec

Step 9. Calculate P/r_u and T/T_N

$P = p \times b = 5.0 \times 12 \times 12 = 720$ lb/ft

$P/r_u = 720/766 = 0.94$

$T/T_N = 40/9.75 = 4.10$

Entering figure 3-64a with these values.

$X_m/X_E = 3.5 < 6$ O.K.

Step 10. Check maximum deflection and rotation.

$X_E = r_u L/K_E = 766 \times 4.5/124{,}260 = 0.028$ ft

$X_m = 3.5\ X_E = 0.098$ ft

$\theta = \tan^{-1}[X_m/(L/2)] = \tan^{-1}[0.098/2.25] = 2.5 < 4°$ O.K.

Step 11. Check resistance in rebound.

From figure 5-13, $\bar{r}/r = 0.33$; O.K. since available maximum elastic resistance in rebound is approximately equal to that under direct loading.

Step 12. Check resistance in shear.

a. Interior support (combined shear and bending). Determine dynamic shear capacity of a 1-ft width of panel:

$h = (1.500 - 2t)$ inches, $t = 0.048$ inch

$= 1.500 - 0.096 = 1.404$ inches

$h/t = 1.404/0.048 = 29.25 = 30$

f_{dv} = 10.84 ksi (Table 5-5)

Total web area for 1-ft width of panel:

$(8 \times h \times t)/2 = 4 \times 1.404 \times 0.048 = 0.270$ in^2

$V_u = 0.270 \times 10.84 = 2.92$ k = 2,922 lb

Determine maximum dynamic shear force:

The maximum shear at an interior support of a continuous panel using limit design is:

$V_{max} = 0.55\ r_u L = 0.55 \times 766 \times 4.5 = 1{,}896$ lb

= 1,896 lb < 2,922 lb O.K.

b. End support (simple shear)

Determine dynamic shear capacity of a 1-ft width of panel:

For $h/t \leq 57$, $f_{dv} = 0.50\ f_{ds} = 0.5 \times 44.0 = 22.0$ ksi (Table 5-5a)

$V_u = 0.270 \times 22{,}000 = 5{,}940$

Determine maximum dynamic shear force:

The maximum shear at an end support of a continuous panel using limit design is

$V_{max} = 0.45 \times r_u \times L = 0.45 \times 766 \times 4.5$

= 1,551 lb < 5,940 lb O.K.

c. Web crippling (4 webs per foot)

End support (N = 2-½ inches)

$Q_u = 1{,}200 \times 4 = 4{,}800$ lb > 1,551 O.K. (figure 5-15)

Interior support (N = 5 inches)

$Q_u = (2,400 \times 4)/2 = 4,800$ lb > 1,896 O.K. (figure 5-16)

Problem 5A-4 Design of Columns and Beam-Columns

Problem: Design a column or beam-column for axial load combined with bending about the strong axis.

Procedure:

Step 1. Establish design parameters.

a. Bending moment M, axial load P, and shear V are obtained from either a preliminary design analysis or a computer analysis.

b. Span length l and unbraced lengths l_x and l_y.

c. Properties of structural steel:

Minimum yield strength f_y

Dynamic increase factor c (Table 5-2)

Dynamic design strength f_{ds} (Equation 5-2)

Step 2. Select a preliminary member size with a section modulus S such that $S \geq M/f_{ds}$ and $b_f/2t_f$ complies with the structural steel being used (Section 5-24).

Step 3. Calculate P_y (Section 5-24) and the ratio P/P_y. Using either equation 5-17 or 5-18, determine the maximum allowable d/t_w ratio and compare it to that of the section chosen. If the allowable d/t_w ratio is less than that of the trial section, choose a new trial section.

Step 4. Check the shear capacity of the web. Determine the web area A_w (Section 5-23) and the allowable dynamic shear stress f_{dv} (equation 5-4). Calculate the web shear capacity V_p (equation 5-16) and compare to the design shear V. If inadequate, choose a new trial section and return to Step 3.

Step 5. Determine the radii of gyration, r_x and r_y, and plastic section modulus, Z, of the trial section from the AISC Handbook.

Step 6. Calculate the following quantities using the various design parameters:

a. Equivalent plastic resisting moment

$$M_p = f_{ds}Z \qquad \text{(Equation 5-8)}$$

b. Effective slenderness ratios Kl_x/r_x and Kl_y/r_y. For the effective length factor K, see Section 1.8 of the Commentary on the AISC Specification and Section 5-38.

c. Allowable axial stress F_a corresponding to the larger value of Kl/r.

d. Allowable moment M_m from equation 5-47 or 5-48.

e. F'_e and "Euler" buckling load P_e (Section 5-37.3).

f. Plastic axial load (Section 5-37.3) and ultimate axial load P_u (equation 5-42).

g. Coefficient C_m (Section 1.6.1 AISC Specification).

Step 7. Using the quantities obtained in Step 6 and the applied moment M and axial load P, check the interaction formulas (equations 5-44 and 5-45). Both formulas must be satisfied for the trial section to be adequate.

Example 5A-4 (a) Design of a Roof Girder as a Beam-Column

Required: Design a fixed-ended roof girder in a framed structure for combined bending and axial load in a low pressure range.

Step 1. Given:

a. Preliminary computer analysis gives the following values for design:

M_x = 115 ft-kips

M_y = 0

P = 53.5 kips

V = 15.1 kips

b. Span length l_x = 17'-0"

Unbraced lengths l_x = 17'-0" and l_y = 17'-0"

c. A36 structural steel

$f_y = 36$ ksi

$c = 1.29$ (Table 5-2)

$a = 1.1$ (Section 5-12.1)

$\therefore f_{ds} = c \times a \times f_y = 1.29 \times 1.1 \times 36 = 51.1$ ksi (Equation 5-2)

Step 2.

$S = M_x/f_{ds} = 115\ (12)/51.1 = 27.0\ in^3$

Try W 12 x 30 ($S = 38.6\ in^3$)

$A = 8.79\ in^2$ $d/t_w = 47.5$

$b_f/2t_f = 7.4 < 8.5$ O.K. (Section 5-24)

Step 3.

$P_y = Af_y = 8.79 \times 36 = 316$ kips (Section 5-24)

$P/P_y = 53.5/316 = 0.169 < 0.27$

$$d/t_w = \left[412/(f_y)^{1/2}\right]\left[1 - 1.4\ (P/P_y)\right]$$ (Equation 5-17)

$$= (412/(36)^{1/2})\ [1 - 1.4\ (0.169)] = 52.4 > 47.5$$ O.K.

Step 4.

$V_p = f_{dv} A_w$ (Equation 5-16)

$f_{dv} = 0.55\ f_{ds} = 0.55\ (51.1) = 28.1$ ksi (Equation 5-4)

$A_w = t_w(d - 2t_f) = 0.260\ [12.34 - 2\ (0.440)]$

$= 2.98\ in^2$ (Section 5-23)

$V_p = 28.1(2.98) = 83.7$ kips > 15.1 kips O.K.

Step 5. $r_x = 5.21$ in.

$r_y = 1.52$ in. (AISC Manual)

$Z = 43.1$ in^3

Step 6.

a. $M_{px} = f_{ds} \times Z_x = 51.1 \times 43.1 \times 1/12 = 183.5$ ft-kips (Equation 5-8)

b. $K = 0.75$ (Section 5-39)

$Kl_x/r_x = [0.75(17)12] / 5.21 = 29$

$Kl_y/r_y = [0.75(17)12] / 1.52 = 101$

c. $F_a = 12.85$ ksi for $Kl_y/r_y = 101$ and $f_y = 36$ ksi (Appendix A, AISC Specification)

$1.42(12.85) = 18.25$ ksi for $f_{ds} = 51.1$ ksi

d. $$M_{mx} = \left[1.07 - \frac{(l/r_y)(f_{ds})^{1/2}}{3,160}\right] M_{px} \leq M_{px}$$ (Equation 5-47)

$$= \left[1.07 - \frac{(204/1.52)\ (51.1)^{1/2}}{3,160}\right] 183.5 = 140.6 < 183.5 \text{ ft-kips}$$

e. $$F'_{ex} = \frac{12\pi^2 E}{23(Kl_b/r_x)^2} = \frac{12\pi^2(29,000)}{23(29)^2} = 177.6 \text{ ksi}$$ (Section 5-37.3)

$$P_{ex} = \frac{23AF'_{ex}}{12} = \frac{23(8.79)177.6}{12} = 2,992 \text{ kips}$$ (Section 5-37.3)

f. $P_p = f_{ds}A = 51.1(8.79) = 449$ kips (Section 5-37.3)

$$P_u = 1.7AF_a = 1.7(8.79)18.25 = 273 \text{ kips} \quad \text{(Equation 5-42)}$$

g. $C = 0.85$ (Section 1.6.1, AISC Specification)

Step 7.
$$\frac{P}{P_u} + \frac{C_{mx} M_x}{(1 - P/P_{ex})M_{mx}} + \frac{C_{my} M_y}{(1 - P/P_{ey})M_{my}} \leq 1 \quad \text{(Equation 5-44)}$$

$$= \frac{53.5}{273} + \frac{0.85(115)}{(1 - 53.5/2992)140.6} = 0.196 + 0.708 = 0.904 < 1 \quad \text{O.K.}$$

$$\frac{P}{P_p} + \frac{M_x}{1.18M_{px}} + \frac{M_y}{1.18M_{py}} \leq 1 \quad \text{(Equation 5-45)}$$

$$= \frac{53.5}{449} + \frac{115}{1.18(183.5)} = 0.119 + 0.531 = 0.650 < 1 \quad \text{O.K.}$$

Trial section meets the requirements of Section 5-37.3.

Example 5A-4 (b) Design of Column

Required: Design of an exterior fixed-pinned column in a framed structure for biaxial bending plus axial loads in a low pressure range.

Step 1. Given:

a. Preliminary design analysis of a particular column gives the following values at a critical section:

$M_x = 311$ ft-kips

$M_y = 34$ ft-kips

$P = 76$ kips

$V = 54$ kips

b. Span length $l = 17'\text{-}3"$

Unbraced lengths $l_x = 17'\text{-}3"$ and $l_y = 4'\text{-}0"$ (laterally supported by wall girts).

c. A36 structural steel

f_y = 36 ksi

c = 1.29 (Table 5-2)

a = 1.1 (Section 5-12.1)

$f_{ds} = a \times c \times f_y = 1.1 \times 1.29 \times 36 = 51.1$ ksi (Equation 5-2)

Step 2.

$S = M_x/f_{ds} = 311(12)/51.1 = 73.0$ in^3

Try W 14 x 68 ($S = 103$ in^3)

$A = 20.0$ in^2 $d/t_w = 33.8$

$b_f/2t_f = 7.0 < 8.5$ O.K. (Section 5-24)

Step 3.

$P_y = Af_y = 20.0(36) = 720$ kips (Section 5-24)

$P/P_y = 76/720 = 0.106 < 0.27$

$d/t_w = [412/(f_y)^{1/2}] [1 - 1.4(P/P_y)]$ (Equation 5-17)

$= [412/(36)^{1/2}] [1 - 1.4(0.106)] = 58.5 > 32.9$ O.K.

Step 4.

$V_p = f_{dv} A_w$ (Equation 5-16)

$f_{dv} = 0.55 f_{ds} = 0.55(51.1) = 28.1$ ksi (Equation 5-4)

$A_w = t_w(d - 2t_f) = 0.415 [14.04 - 2(0.720)] = 5.23$ in^2 (Section 5-23)

$V_p = 28.1(5.23) = 147$ kips > 54 kips O.K.

Step 5. $r_x = 6.01$ inches

$r_y = 2.46$ inches

$Z_x = 115$ in^3 (AISC Manual)

$Z_y = 36.9$ in^3

Step 6.

a. $M_p = f_{ds}Z$ (Equation 5-8)

$M_{px} = 51.1 \times 115 \times 1/12 = 490$ ft-kips

$M_{py} = 51.1 \times 36.9 \times 1/12 = 157$ ft-kips

b. Use K = 1.5 (Section 5-39)

$$\frac{Kl_x}{r_x} = \frac{1.5(17.25)12}{6.01} = 52$$

$$\frac{Kl_y}{r_y} = \frac{1.5(4.00)12}{2.46} = 29$$

c. $F_a = 18.17$ ksi for $Kl_x/r_x = 52$ and $f_y = 36$ ksi

$1.42(18.17) = 25.79$ ksi for $f_{ds} = 51.1$ ksi

$M_{mx} = M_{px} = 490$ ft-kips

d. $M_{my} = M_{py} = 157$ ft-kips (Section 5-37.3)

$$F'_{ex} = \frac{12\pi^2 E}{23(Kl_b/r_x)^2} = \frac{12\pi^2(29{,}000)}{23(52)^2} = 55.2 \text{ ksi}$$ (Section 5-37.3)

$$F'_{ex} = \frac{12\pi^2 E}{23(Kl_b/r_y)^2} = \frac{12\pi^2(29{,}000)}{23(29)^2} = 178 \text{ ksi}$$ (Section 537.3)

$$P_{ex} = \frac{23AF'_{ex}}{12} = \frac{23(20.0)55.2}{12} = 2{,}116 \text{ kips}$$

$$P_{ey} = \frac{23AF'_{ey}}{12} = \frac{23(20.0)178}{12} = 6{,}823 \text{ kips} \qquad \text{(Section 5-37.3)}$$

$$P_p = f_{ds}A = 51.1(20) = 1{,}022 \text{ kips}$$

$$P_u = 1.7AF_a = 1.7(20)25.79 = 877 \text{ kips}$$

$C_{mx} = C_{my} = 0.85$ (Section 1.6.1, AISC Specification)

Step 7.

$$\frac{P}{P_u} + \frac{C_{mx}M_x}{(1 - P/P_{ex})M_{mx}} + \frac{C_{my}M_y}{(1 - P/P_{ey})M_{my}} \leq 1 \qquad \text{(Equation 5-44)}$$

$$\frac{76}{877} + \frac{0.85(311)}{(1 - 76/2116)490} + \frac{0.85(34)}{(1 - 76/6{,}823)157} =$$

$0.087 + 0.560 + 0.186 = 0.833 < 1$ O.K.

$$P/P_p + M_x/(1.18M_{px}) + M_y/(1.18M_{py}) \leq 1 \qquad \text{(Equation 5-45)}$$

$76/1022 + 311/[1.18(490)] + 34/[1.18(157)] =$

$0.074 + 0.538 + 0.183 = 0.795 < 1$ O.K.

Trial section meets the requirements of Section 5-37.3

Problem 5A-5 Design of Open-Web Steel Joists

Problem: Analysis or design of an open-web joist subjected to a pressure-time loading.

Procedure:

Step 1. Establish design parameters.

a. Pressure-time curve

b. Clear span length and joist spacing

c. Minimum yield stress f_y for chord and web members

Dynamic increase factor, c. (Table 5-2)

d. Design ductility ratio μ and maximum end rotation, θ.

e. Determine whether joist design is controlled by maximum end reaction.

Step 2. Select a preliminary joist size as follows:

a. Assume a dynamic load factor (Section 5-22.3)

b. Compute equivalent static load on joist due to blast overpressure

w_1 = DLF x p x b
(Dead load of joist and decking not included)

c. Equivalent service live load on joist
$w_2 = w_1/1.7 \times a \times c$ (Section 5-33)

d. From "Standard Load Tables" adopted by the Steel Joist Institute, select a joist for the given span and the structural steel being used, with a safe service load (dead load of joist and decking excluded) equal to or greater than w_2. Check whether ultimate capacity of joist is controlled by flexure or by shear.

Step 3. Find the resistance of the joist by multiplying the safe service load by 1.7 x a x c (Section 5-33).

Step 4. Calculate the stiffness of the joist, K_E, using Table 3-8. Determine the equivalent elastic deflection X_E given by

$$X_E = r_u L/K_E$$

Step 5. Determine the effective mass using the weight of the joist with its tributary area of decking, and the corresponding load-mass factor given in Table 3-12 of Chapter 3.

Calculate the natural period of vibration, T_N.

Step 6. Follow procedure outlined in step 6a or 6b depending on whether the joist capacity is controlled by flexure or by shear.

Step 6a. Joist design controlled by flexure.

a. Find ductility ratio $\mu = X_m/X_E$ from the response charts in Chapter 3, using the values of T/T_N and P/r_u.

b. Check if the ductility ratio and maximum end rotation meet the criteria requirements outlined in Section 5-35.

If the above requirements are not satisfied, select another dynamic load factor and repeat Steps 2 to 5.

c. Check the selection of the dynamic increase factor used in Step 2c. Using the response charts, find t_E to determine the strain rate, ϵ in equation 5-1. Using figure 5-2, determine DIF. (If elastic response, use T/T_N and appropriate response charts to check DIF).

d. Check if the top chord meets the requirements for a beam-column (Section 5-37.3).

Step 6b. Joist design controlled by shear.

a. Find ductility ratio $\mu = X_m/X_E$ from the response charts in Chapter 3, using the values of T/T_N and P/r_u.

b. If $\mu \leq 1.0$, design is O.K.

If $\mu > 1.0$, assume a higher dynamic load factor and repeat Steps 2 to 5. Continue until $\mu \leq 1.0$. Check end rotation, θ, against design criteria.

c. Check the selection of the dynamic increase factor used in Step 2c, using the value of T/T_N and the appropriate elastic response chart in Section 3-19.3.

d. Since the capacity is controlled by maximum end reaction, it will generally not be necessary to check the top chord as a beam-column. However, when such a check is warranted, the procedure in Step 6a can be followed.

Step 7. Check the bottom chord for rebound.

a. Determine the required resistance, $\bar{r}$, for elastic behavior in rebound.

b. Compute the bending moment, M, and find the axial forces in top and bottom chords using $P = M/d$ where d is taken as the distance between the centroids of the top and bottom chord sections.

c. Determine the ultimate axial load capacity of the bottom chord considering the actual slenderness ratio of its elements.

$$P_u = 1.7AF_a$$

where F_a is defined in Section 5-37.3.

The value of F_a can be obtained by using either equation 5-43 or the tables in the AISC Specification which give allowable stresses for compression members. When using these tables, the yield stress should be taken equal to f_{ds}.

d. Check if $P_u > P$.

Determine bracing requirements.

Example 5A-5 (a) Design of an Open-Web Steel Joist

Required: Design a simply-supported open-web steel joist whose capacity is controlled by flexure.

Solution:
Step 1. Given:

a. Pressure-time loading [figure 5A-5 (a)]

b. Clear span = 50'-0"
Spacing of joists = 7'-0"
Weight of decking = 4 psf

c. Structural steel properties

Chords f_y = 50,000 psi

Web f_y = 36,000 psi

Dynamic increase factor (chords only).

c = 1.19 (Table 5-2, for A588)

Dynamic design stress; $f_{ds} = c \times a \times f_y$ (Equation 5-2)

Chords $f_{ds} = 1.19 \times 1.1 \times 50{,}000 = 65{,}450$ psi

d. Design criteria (Section 5-35)

Maximum ductility ratio: $\mu_{max} = 4.0$

Maximum end rotation: $\theta_{max} = 2°$

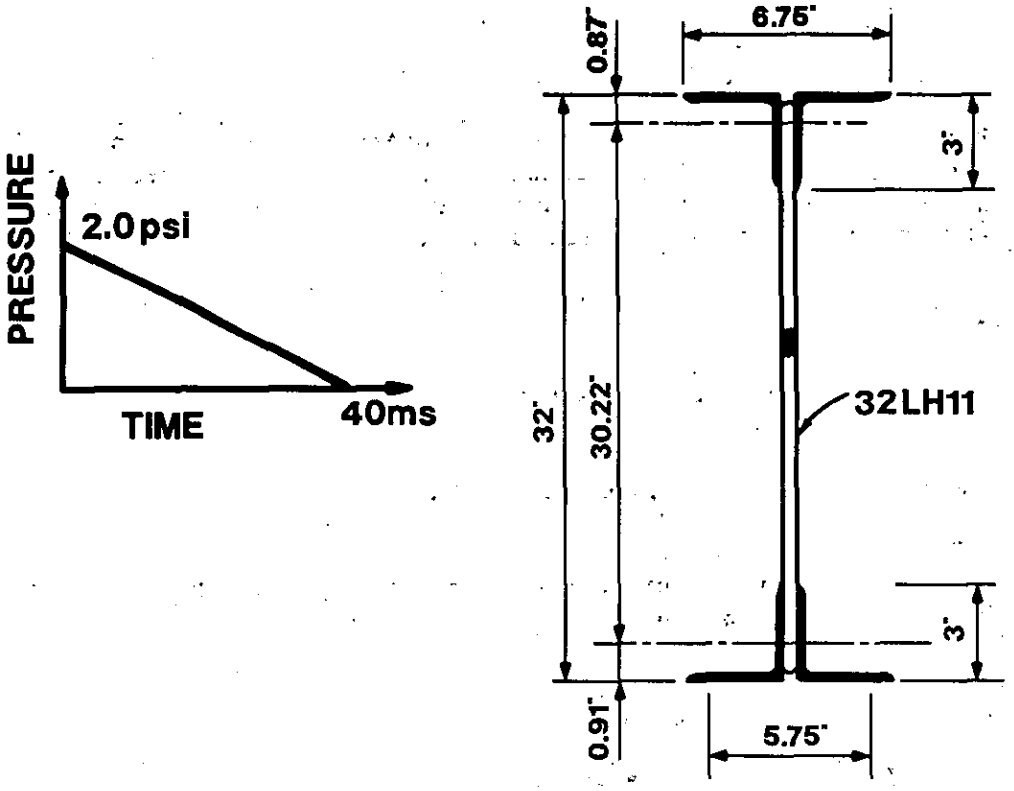


Figure 5A-5(a) Joist cross-section and loading, Example 5A-5(a)

Step 2. Selection of joist size

a. Assume a dynamic load factor. For preliminary design, a DLF = 1.0 is generally recommended. However, since the span is quite long in this case, a DLF of 0.62 is selected.

b. Equivalent static load on joist:

$w_1 = 0.62 \times 2.0 \times 144 \times 7.0 = 1,250$ lb/ft

c. Service live load on joist:

$w_2 = w_1/1.7 \times 1.19 \times 1.1 = 1,250/2.23 = 561$ lb/ft

d. Using the "Standard Specifications, Load Tables and Weight Tables" of the Steel Joist Institute, for a span of 50'-0", try 32LH11. Joist tables show that capacity is controlled by flexure.

Total load-carrying capacity (including dead load = 602 lb/ft).

Approximate weight of joist and decking

= 28 + (4 x 7) = 56 lb/ft

Total load-carrying capacity (excluding dead load = 602 - 56 = 546 lb/ft)

The following section properties refer to the selected joist 32LH11 [Figure 5A-5 (a)]:

Top Chord:
Two 3 x 3 x 5/16 angles

$A = 3.56\ in^2$

$r_x = 0.92$ in.

$r_y = 1.54$ in.

$I_x = 3.02\ in_4$

Bottom Chord:
Two 3 x 2-1/2 x 1/4 angles

$A = 2.62\ in^2$

$r_x = 0.945$ in.

$r_y = 1.28$ in.

$I_x = 2.35\ in^4$

I_{xx} for joist = $1,383.0\ in^4$

Panel length = 51 inches

Step 3. Resistance per unit length

$r_u = 1.7 \times 1.19 \times 1.1 \times 546 = 1215$ lb/ft (Section 5-33)

Step 4. $K_E = 384\ EI/5L^3 = \dfrac{384 \times 29 \times 10^6 \times 1,383}{5(12 \times 50)^3} = 14,260$ lb/in (Table 3-8)

$$X_E = r_u L/K_E = \frac{1,215 \times 50}{14,260} = 4.26 \text{ inches}$$

Step 5. Total mass of joist plus decking

$$M = \frac{56 \times 50 \times 10^6}{386} = 7.25 \times 10^6 \text{ lb-ms}^2/\text{in}$$

Total effective mass $M_e = K_{LM}M$

$K_{LM} = 0.5(0.78 + 0.66) = 0.72$ (Table 3-12)

$M_e = 0.72\ (7.25 \times 10^6) = 5.22 \times 10^6$ lb-ms^2/in

Natural period $T_N = 2\pi(M_e/K_E)^{1/2} = 2\pi(5{,}220{,}000/14{,}260)^{1/2} = 120.2$ ms

Behavior controlled by flexure. Use Step 6a.

Step 6a. a.

$$T/T_N = 40/120.2 = 0.332$$

$$P/r_u = \frac{2.0 \times 144 \times 7}{1{,}105} = 1.82$$

From figure 3-64a,

$$\mu = X_m/X_E = 2.3 < 4 \qquad \text{O.K.}$$

b.

$$X_m = 2.3 \times 3.87 = 8.9 \text{ inches}$$

$$\tan \Theta = X_m/(L/2) = 8.9/(25 \times 12) = 0.0297$$

$$\Theta = 1.7^\circ < 2^\circ \quad \text{O.K.}$$

c. Check selection of DIF.

From Table 3-64a, for $\mu = 2.3$ and $T/T_N = 0.33$

$t_E/T = 0.55$, $t_E = 0.55 \times 40 = 22$ ms

Find $\dot{\epsilon}$

$$\dot{\epsilon} = f_{ds}/E_s t_E = 65.45/30 \times 10^3 \times .022 = 0.099 \text{ in/in/sec}$$

(Equation 5-1)

From figure 5-2 (average of A36 and A514)

DIF = 1.18 ≈ 1.19 assumed O.K.

d. Check top chord as a beam column.

Maximum moment at mid-span

$$M = r_u L^2/8 = \frac{1{,}105 \times (50)^2 \times 12}{8 \times 1{,}000} = 4{,}144 \text{ in-kips}$$

Maximum axial load in chords

$P = M/d$

d = distance between centroids of top and bottom chords [see figure 5A-5 (a)]
= 30.22 inches

$P = 4{,}144/30.22 = 137.1$ kips

l = panel length = 51 inches

Slenderness ratio, $l/r_x = 51/0.92 = 55.4 < C_c$

where $C_c = (2\pi^2 E/f_{ds})^{1/2} = 95$ (Equation 5-41)

$F_a = 23.5$ ksi for $f_y = 50$ ksi
(Table 3-50, AISC Specification)

1.31 (23.5) = 30.8 ksi for $f_{ds} = 65{,}450$ psi

$P_u = 1.7AF_a = 1.7 \times 3.56 \times 30.8 = 186.4$ kips
(Equation 5-42)

Considering the first panel as a fixed, simply supported beam, the maximum moment in the panel is

$$M = r_u L^2/12 = \frac{1{,}105\ (51)^2}{12 \times 12 \times 1{,}000} = 19.96 \text{ in-kips}$$

The effective slenderness ratio of the top chord in the first panel is

$Kl_b/r_x = (1.0 \times 51)/0.92 = 55.4$

$$F'_{ex} = \frac{12\pi^2 E}{23(Kl_b/r_x)^2} = \frac{12\pi^2 \times 29{,}000}{23\ (55.4)^2} = 48.7 \text{ ksi}$$

$P_{ex} = (23/12)AF'_{ex} = 23/12 \times 3.56 \times 48.7 = 333$ kips

$(1 - P/P_{ex}) = (1.0 - 126.6/333) = 0.62$

To determine M_m, the plastic moment M_p is needed and the value of Z_x has to be computed. The neutral axis for a fully plastic section is located at a distance x from the flange.

$$3\bar{x} = (3 - 5/16)\ 5/16 + 3\ (5/16 - \bar{x})$$

$$= (43)\ 5/(16 \times 16) + 15/16 - 3\bar{x}$$

$\bar{x} = 455/(6 \times 256) = 0.296$ inch

The plastic section modulus, Z_x, is found to be

$$Z_x = 2\left[\frac{(0.296)^2}{2} \times 3 + (3.0 - 0.3125)\ \frac{(0.3125 - 0.296)^2}{2} + \frac{(3 - 0.296)^2}{2} \times 0.3125\right] = 0.263 + 0.0007 + 2.285 = 2.549 \text{ in}^3$$

$M_{px} = f_{ds}Z_x = 65.45 \times 2.549 = 166.8$ in-kips (Equation 5-8)

$$M_{mx} = \left[1.07 - \frac{(l/r_y)\ (f_{ds})^{1/2}}{3160}\right] M_{px} \leq M_{px} \quad \text{(Equation 5-37)}$$

where r_y is least radius of gyration = 0.92

$= [1.07 - (55.4/391)]\ 166.8 = 154.8$ in-kips

$C_m = 0.85$ (Section 1.6.1, AISC)

$P/P_u + C_m M/[(1 - P/P_{ex})M_{mx}] \leq 1.10$ (Equation 5-44)

$$\frac{137.1}{186.4} + \frac{0.85\ (19.96)}{0.62\ (154.8)} \leq 1.0 = 0.736 + 0.176 = 0.912 < 1.0 \text{ O.K.}$$

Step 7. Check bottom chord for rebound.

a. Calculate required resistance in rebound.

$T/T_N = 0.33$

From figure 5-13, 100% rebound

$\bar{r}/r_u = 1.0$

$\bar{r} = r_u = 1{,}105$ lb/ft

b. Moment and axial forces in rebound

$M = (\bar{r} \times L^2)/8 = 4{,}144$ in-kips

Maximum axial force in bottom chord

$P = M/d = 137.1$ kips (compression)

c. Ultimate axial load capacity

Stability in vertical direction (about x-axis)

$l = 51$ inches $r_x = 0.945$

$l/r = 51/0.945 = 54.0 < C_c$

where $C_c = [(2\pi^2 E)/f_{ds}]^{1/2} = 95$

$F_a = 23.72$ ksi for $f_y = 50$ ksi (Table 3-50, AISC Specification)

$1.31(23.72) = 31.1$ ksi for $f_{ds} = 65{,}450$ psi

$P_u = 1.7AF_a = 1.7 \times 2.62 \times 31.1 = 138.5$ kips

d. Check bracing requirements.

$P = 137{:}1 < P_u = 138.5$ O.K.

Adding a vertical member between panel joints of bottom chord would have been required had $P > P_u$. This additional bracing would have been needed in mid-span but may be spared at the joist ends.

Stability in the lateral direction (about y-axis)

$P_u = 137.1$ kips

$r_y = 1.28$ inches, $A = 2.62$ in^2

$F_a = P_u/(1.7 \times 1.31A) = 137.1/(1.7 \times 1.31 \times 2.62) = 23.5$ ksi

For a given $F_a = 23.5$, the corresponding slenderness ratio is

$l/r \approx 55$ (Table 3-50, AISC Specification)

Therefore, the maximum unbraced length in mid-span is

$l_b = 55 \times 1.28 = 70.4$ inches

Use lateral bracing at panel points, i.e., 51 inches at midspan. The unbraced length may be increased at joist ends, but not greater than specified for bridging requirements in the joist specification.

Example 5A-5 (b) Analysis of Existing Open-Web Steel Joist

Required: Analyze a simply supported, open-web steel joist whose capacity is controlled by shear.

Solution:

Step 1. Given:

a. Pressure-time loading [figure 5A-5 (b)]

Joist 22H11

b. Clear span = 32'-0"

Spacing of joists = 6'-0"

Weight of decking = 4 psf

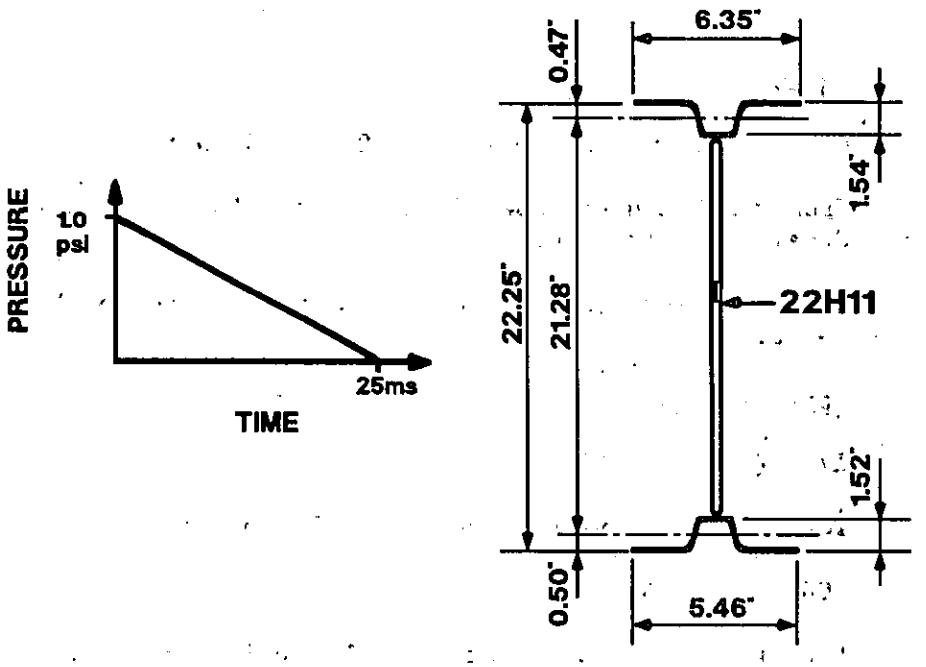


Figure 5A-5(b) Joist cross-section and loading, Example 5A-5(b)

c. Properties of structural steel:

Chords f_y = 50,000 psi

Web f_y = 36,000 psi

Dynamic increase factor (chords only) c = 1.19 (Table 5-2 for A588)

Dynamic design stress, $f_{ds} = c \times a \times f_y$

Chords $f_{ds} = 1.19 \times 1.1 \times 50{,}000 = 65{,}450$ psi

d. Design criteria (Section 5-35)

For members controlled by shear:

$\mu_{max} = 1.0$

$\theta_{max} = 1°$

Step 2. a. Assume the DLF = 1.25

b. Overpressure load on joist

$w_1 = 1.25 \times 1.0 \times 144 \times 6 = 1{,}080$ lb/ft

c. Equivalent service load

$w_2 = w_1/1.7 \times a \times c = 1{,}080/2.23 = 485$ lb/ft

d. From the "Standard Specifications and Load Tables" of the Steel Joist Institute:

Total load-carrying capacity (including dead load) = 506 lb/ft.

Approximate weight of joist plus decking =

17 + (6 x 4) = 41 lb/ft

Total load-carrying capacity (excluding dead load) =

506 - 41 = 465

From the steel joist catalog, the following are the section properties of Joist 22H11 [figure 5A-5 (b)]:

Panel length = 24 inches

Top Chord:

$A = 1.935$ in^2

$I_x = 0.455$ in^4

$r_x = 0.485$ in.

$r_y = 1.701$ in.

Bottom Chord:

$A = 1.575$ in^2

$I_x = 0.388$ in^4

$r_x = 0.497$ in.

$r_y = 1.469$ in.

I_{xx} for joist = 396.0 in^4

Step 3. Resistance per unit length

$r_u = 2.23 \times 465 = 1{,}035$ lb/ft

Step 4.

$$K_E = \frac{384EI}{5L^3} = \frac{384 \times 29 \times 10^6 \times 396}{5 \times (12 \times 32)^3} = 15{,}580 \text{ lb/in} \quad \text{(Table 3-8)}$$

$$X_E = r_u L/K_E = \frac{1{,}035 \times 32}{15{,}580} = 2.13 \text{ inches}$$

Step 5. Mass of joist plus decking

$$M = \frac{41 \times 32 \times 10^6}{386} = 3.4 \times 10^6 \text{ lb-ms}^2\text{/in}$$

Effective mass $M_e = K_{LM}M$

$= 0.78 \times 3.4 \times 10^6 = 2.65 \times 10^6$ lb-ms^{2}in

Natural period $T_N = 2\pi(M_e/K_E)^{1/2}$

$= 2\pi(2{,}650{,}000/15{,}580)^{1/2} = 81.8$ ms

Behavior controlled by shear. Use Step 6b of the procedure.

Step 6b.

a. $T/T_N = 25/81.8 = 0.305$

$$P/r_u = \frac{6 \times 144 \times 1.0}{1{,}035} = 0.835$$

b. From Figure 3-64a of Chapter 3:

$\mu = X_m/X_E < 1.0$; elastic, O.K.

$\tan \theta = X_m/(L/2)$

$= 2.13/(16.0 \times 12) = 0.0111$

$\theta = 0.64° < 1°$ O.K.

c. Check selection of DIF from figure 3-49 of Chapter 3, for $T/T_N = 0.305$, $t_m/T = 1.12$; $t_m = 1.12 \times 25 = 28$ ms

Find $\dot{\epsilon}$

$\dot{\epsilon} = f_{ds}/E_s t_e \quad (t_E = t_m)$ (Equation 5-1)

$= 65.45/30 \times 10^3 \times 0.028 = 0.078$ in/in/sec

From figure 5-2, (average of A36 and A514)

DIF = 1.18 = 1.19 assumed, O.K.

d. Check of top chord as a beam-column is not necessary.

Step 7. Check bottom chord in rebound.

a. For $\mu = 1$ and $T/T = 0.305$, rebound is 100% (Figure 5-13)

$\bar{r} = r_u$

b. Determine axial load in bottom chord, P = M/d.

For an elastic response, $\mu < 1.0$, where $T/T_N = 0.305$, the DLF = 0.87 (Figure 3-49)

Equivalent static load, w

$w = DLF \times b \times p = 0.87 \times 12 \times 12 \times 6 \times 1.0 = 751$ lb/ft

Maximum moment in rebound, $M = wL^2/8$

$M = [751 \times (32)^2/8]\ 12 = 1,155,000$ in-lb

$P = M/d = 1,155,000/21.28 = 54,300$ lb = 54.3 kips

c. Check bracing requirements.

(1) Vertical bracing of bottom chord:

Panel length = 24 inches

$r_x = 0.497, \quad r_y = 1.469, \quad A = 1.575$ in^2

$l/r_x = 24/0.497 = 48.3$

Allowable $P = 1.7 \times a \times c \times A \times F_a$

$= 1.7 \times 1.1 \times 1.19 \times 1.575 \times 24.6 = 86.2$ kips > 54.3 kips
(Table 3-50, AISC Specification)

No extra bracing required.

(2) Lateral bracing of bottom chord:

$P = 54.3$ kips, $A = 1.575$ in^2

$F_a = P/1.7A = 54.3/(1.7 \times 1.575 \times 1.1 \times 1.19) = 15.5$ ksi

For $f_y = 50$ ksi and $F_a = 15.5$ ksi

$l/r = 96$

$l = 96 \times 1.469 = 141$ inches
(Table 3-50, AISC Specification)

Therefore, use lateral bracing at every fifth panel point close to mid-span. The unbraced length may be increased at joist ends, but not greater than specified for bridging requirements in the joist specification.

Problem 5A-6 Design of Single-Story Rigid Frames for Pressure-Time Loading

Problem: Design a single-story, multi-bay rigid frame subjected to a pressure-time loading.

Procedure:

Step 1. Establish the ratio α between the design values of the horizontal and vertical blast loads.

Step 2. Using the recommended dynamic load factors presented in Section 5-41.3 establish the magnitude of the equivalent static load w for:

a. local mechanisms of the roof and blastward column

b. panel or combined mechanisms for the frame as a whole.

Step 3. Using the general expressions for the possible collapse mechanisms from Table 5-13 and the loads from Step 2, assume values of the moment capacity ratios C and C_1 and proceed to establish the required design plastic moment M_p considering all possible mechanisms. In order to obtain a reasonably economical design, it is desirable to select C and C_1 so that the least resistance (or the required value of M_p) corresponds to a combined mechanism. This will normally require several trials with assumed values of C and C_1.

Step 4. Calculate the axial loads and shears in all members using the approximate method of Section 5-41.4.

Step 5. Design each member as a beam-column using the ultimate strength design criteria of Sections 5-37.3, 38, and 39. A numerical example is presented in Section 5A-4.

Step 6. Using the moments of inertia from Step 5, calculate the sidesway natural period using Table 5-14 and Equations 5-50 and 5-51. Enter the response charts in Chapter 3 with the ratios of T/T_N and P/R_u. In this case, P/R_u is the reciprocal of the panel or sidesway mechanism dynamic load factor used in the trial design. Multiply the ductility ratio by the elastic deflection given by equation 5-53 and establish the peak deflection X_m from equation 5-54. Compare the maximum sidesway deflection X_m with the criteria of Section 5-35. Note that the sidesway deflection δ in Table 5-8 is X_m.

Step 7. Repeat the procedure of Step 6 for the local mechanisms of the roof and blastward column. The stiffness and natural period may be obtained from Table 3-8 of Chapter 3 and equation 5-15, respectively. The resistance of the roof girder and the blastward column may be obtained from Table 5-13 using the values of M_p and CM_p determined in Step 3. Compare the ductility ratio and rotation with the criteria of Section 5-35.

Step 8. a. If the deflection criteria for both sidesway and beam mechanisms are satisfied, then the member sizes from Step 5 constitute the results of this preliminary design. These members would then be used in a more rigorous dynamic frame analysis. Several computer programs are available through the repositories listed in Section 5-4.

b. If the deflection criterion for a sidesway mechanism is exceeded, then the resistance of all or most of the members should be increased.

c. If the deflection criterion for a beam mechanism of the front wall or roof girder is exceeded, then the resistance of the member in question should be increased. The member sizes to be used in a final analysis should be the greater of those determined from Steps 8b and 8c.

Example 5A-6 Design of a Rigid Frame for Pressure-Time Loading

Required: Design a four-bay, single-story, reusable, pinned-base rigid frame subjected to a pressure-time loading in its plane.

Given:

a. Pressure-time loading (Figure 5A-6)

b. Design criteria: It is required to design the frame structure for more than one incident. The deformation limits shall be half that permitted for personnel protection, that is:

$$\delta = H/50 \text{ and}$$

$$\theta_{max} = 1^\circ \text{ for individual members}$$

c. Structural configuration (figure 5A-6)

d. A36 steel

e. Roof purlins spanning perpendicular to frame ($b_v = b_n$, Figure 5-26)

f. Frame spacing, b = 17 ft

g. Uniform dead load of deck, excluding frame

Step 1. Determine α: (Section 5-41.1)

$b_h = b_v = 17$ ft

$q_h = 5.8 \times 17 \times 12 = 1{,}183$ lb/in

$q_v = 2.5 \times 17 \times 12 = 510$ lb/in

$\alpha = q_h/q_v = 2.32$

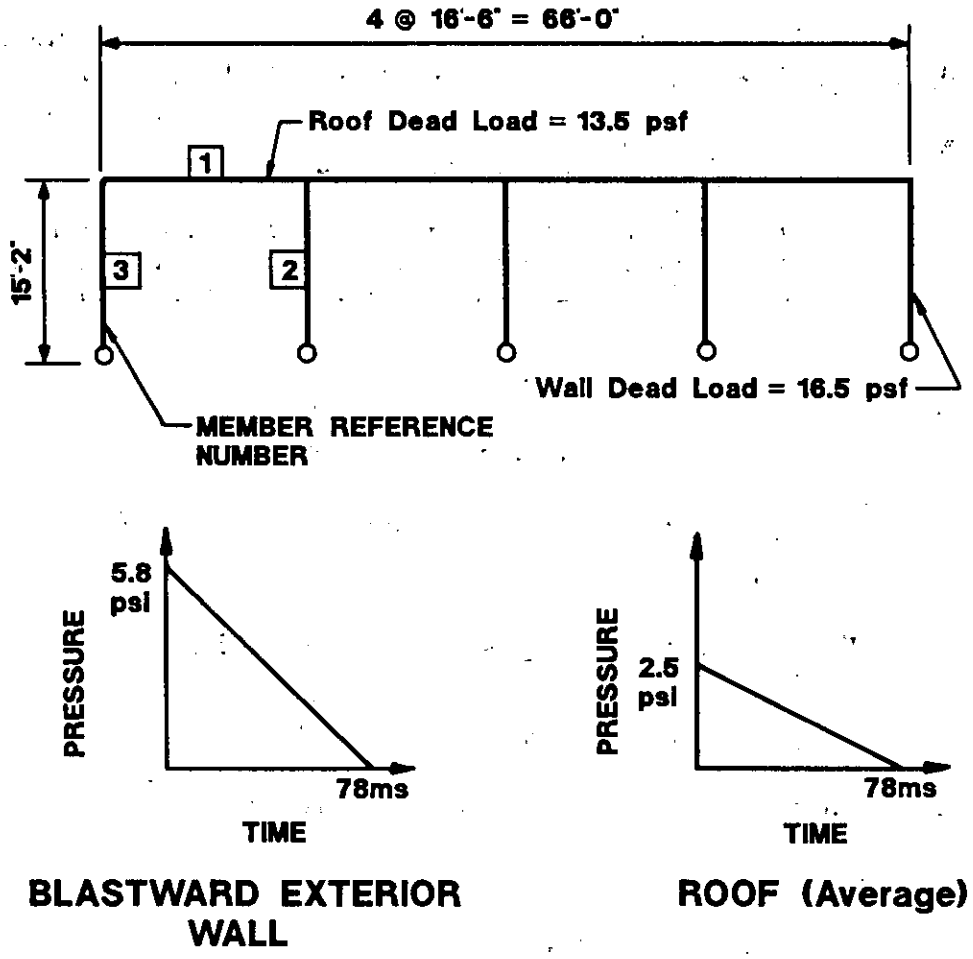


Figure 5A-6. Preliminary design of four-bay, single-story rigid frame, Example 5A-6

Step 2. Establish equivalent static loads (Section 5-41.3)

a. Local beam mechanism, $w = DLF \times q_v$.

$$w = \frac{1.25 \times 510 \times 12}{1{,}000} = 7.65 \text{ k/ft}$$

b. Panel or combined mechanism, $w = DLF \times q_h$

$$w = \frac{0.625 \times 510 \times 12}{1{,}000} = 3.83 \text{ k/ft}$$

Step 3. The required plastic moment capacities for the frame members are determined from Table 5-13 based upon rational assumptions for the moment capacity ratios C_1 and C. In general, the recommended starting values are C_1 equal to 2 and C greater than 2. From Table 5-13. for n = 4, $\alpha = 2.32$, H = 15.167 ft, L = 16.5 ft and pinned bases, values of C_1 and C were substituted and after a few trials, the following solution is obtained:

$$M_p = 130 \text{ kip-ft}, \quad C_1 = 2.0 \quad \text{and} \quad C = 3.5.$$

The various collapse mechanisms and the associated values of M_p are listed below:

Collapse Mechanism	w (k/ft)	M_p (k-ft)
1	7.65	130
2	7.65	128
3a, 3b	3.83	128
4	3.83	129
5a, 5b	3.83	110
6	3.83	116

The plastic design moments for the frame members are established as follows:

Girder, $M_p = 130$ k-ft

Interior column, $C_1 M_p = 260$ k-ft

Exterior column, $CM_p = 455$ k-ft

Step 4. a. Axial loads and shears due to horizontal blast pressure.

$w = 3.83$ k/ft

From figure 5-27, $R = \alpha wH = 2.32 \times 3.83 \times 15.167 = 135$ kips

1. Member 1, axial load

$P_1 = R/2 = 67$ kips

2. Member 2, shear force

$V_2 = R/2(4) = 135/8 = 16.8$ kips

3. Member 3, shear force

$V_3 = R/2 = 67$ kips

b. Axial loads and shears due to vertical blast pressure,

$w = 7.65$ k/ft

1. Member 1, shear force

$V_1 = w \times L/2 = 7.65 \times 16.5/2 = 63.1$ kips

2. Member 2, axial load

$P_2 = w \times L = 7.65 \times 16.5 = 126.2$ kips

3. Member 3, axial load

$P_3 = w \times L/2 = 63.1$ kips

Note:
The dead loads are small compared to the blast loads and are neglected in this step.

Step 5. The members are designed using the criteria of Sections 5-37.3, 5-38, and 5-39 with the following results:

Member	M_p (k-ft)	P (k)	V (k)	Use	I_x (in^4)
1	130	67.0	63.1	w12x35	285
2	260	126.2	16.8	w14x61	640
3	455	63.1	67.0	w14x74	796

Step 6. Determine the frame stiffness and sway deflection.

$$I_{ca} = \frac{(3 \times 640) + (2 \times 796)}{5} = 702 \text{ in}^4 \qquad \text{(Table 5-14)}$$

$$I_g = 285 \text{ in}^4$$

$$\beta = 0$$

$$D = \frac{I/L_g}{0.75 I_{ca}/H} = \frac{285/16.8}{(0.75)(702/15.167)} = 0.498 \qquad \text{(Table 5-14)}$$

$$C_2 = 4.65$$

$$K = \frac{EI_{ca} C_2}{H^3} [1 + (0.7 - 0.1\beta)(n-1)] \qquad \text{(Table 5-14)}$$

$$= \frac{(30)(10)^3 (702)(4.65)[1 + 0.7(3)]}{(15.167 \times 12)^3} = 50.2 \text{ k/in}$$

$$K_L = 0.55 (1 - 0.25\beta) = 0.55 \qquad \text{(Equation 5-51)}$$

Calculate dead weight, W:

$$W = b[(4Lw_{dr}) + (1/3)(Hw_{dw})] + (35 \times 66) + 1/3 (15.167)[(3 \times 61) + (2 \times 74)] = 20,548 \text{ lb}$$

$$m_e = W/g = 20,548/32.2 = 638 \text{ lb-sec}^2/\text{ft} = 638 \times 10^6 \text{ lb-ms}^2/\text{ft}$$

$$T_N = 2\pi[m_e/KK_L]^{1/2} \qquad \text{(Equation 5-50)}$$

$$= 2\pi[(638 \times 10^6)/(50.2 \times 12 \times 10^3 \times 0.55)]^{1/2} = 276 \text{ ms}$$

$$T/T_N = 78/276 = 0.283$$

$P/R_u = 1.6$

$\mu = X_m/X_E = 1.40$ (Figure 3-64a)

$$X_E = R_u/K_E = \alpha wH/K_E = \frac{2.32 \times 3.83 \times 15.167}{50.2} = 2.68 \text{ inches}$$

(Equation 5-52 and 5-53)

$X_m = \delta = 1.40 \times 2.68 = 3.75$ inches (Equation 5-54)

$\delta = 3.75/(15.167)\ (12)H = 0.0206H = H/48.5$

Step 7. Check deflection of possible local mechanisms.

a. Roof girder mechanism (investigate W12 x 35 from Step 5)

$T_N = 2\pi\ (m_e/K_E)^{1/2}$ (Equation 5-15)

$m_e = K_{LM} \times m$

For an elasto-plastic response, take the average load-mass factor for the plastic and elastic response, or:

$K_{LM} = (0.77 + 0.66)/2 = 0.715$ (Table 3-12)

$\therefore m = 0.715 \times W/g$

$w = (13.5 \times 17) + 36 = 265$ lb/ft

$W = w \times L = 265 \times 16.5 = 4372$ lb.

$m_E = 0.715 \times 4372/368 = 8.1$ lb-sec^2/in.

$K_E = 307\ EI/L^3$ (Table 3-8)

$$\therefore K = \frac{307\ (30)\ (10^6)\ (285)}{(16.5 \times 12)^3} = 332{,}000 \text{ lb/in.}$$

$\therefore T_N = 2\pi\ (8.1/332{,}000)^{1/2} \times 1{,}000$

$= 31.0$ ms

$T/T_N = 78/31.0 = 2.52$

$R_u = 16M_p/L = (16 \times 130)/16.5 = 126$ kips (Table 5-13)

$P = pbL = (2.5)(17)(144)(16.5)/1{,}000 = 101$ kips

$P/R_u = 101/126 = 0.80$

$\mu = X_m/X_E = 1.80$ (Figure 3-64a)

Check end rotation of girder.

$X_E = R_u/K_E = 126/332 = 0.380$ inch

$X_m = 1.80 \times 0.380 = 0.69$ inch

$X_m/(L/2) = 0.69/(8.25)(12) = 0.069 = \tan \theta$,

$\theta = 0.40° < 1°$ O.K.

b. Exterior column mechanism (investigate W14 x 74 from Step 5).

$$T_N = 2\pi (m_e/K_E)^{1/2}$$ (Equation 5-15)

$$m_e = K_{LM} \times m = \left[\frac{0.78 + 0.66}{2} \right] \frac{w}{g}$$ (Table 3-12)

$$= 0.72\ w/g$$

$w = (16.5 \times 17) + 74 = 354$ lb/ft

$W = 354 \times 15.167 = 5369$ lb

$M_e = 0.72\ (5369)/386 = 10.0$ lb-sec^2/in.

$K_E = 160\ EI/L^4$ (Table 3-8)

$$K_E = \frac{(160)(30)(10)(796)}{(182)^3} = 632{,}000 \text{ lb/in}$$

$$T_N = 2\pi(10.0/632,000)^{1/2} \times 1000 = 25.0 \text{ ms}$$

$$T/T_N = 78/25.0 = 3.12$$

$$R_u = \frac{4M_p(2C + 1)}{H} = \frac{4\ (130)\ [(2 \times 3.5) + 1]}{15.167} = 275 \text{ kips}$$

(Table 5-13)

$$P = (2.32)\ (7.65/1.25)\ (15.167) = 215 \text{ kips}$$

$$P/R_u = 215/275 = 0.78$$

$$\mu = X_m/X_E = 1.80$$ (Figure 3-64a)

Check end rotation of columns.

$$X_E = R_u/K = 275/632 = 0.435 \text{ inch}$$

$$X_m = 1.80 \times 0.435 = 0.78 \text{ inch}$$

$$X_m/(L/2) = 0.78/(7.58)\ (12) = 0.0086 = \tan \theta$$

$$\theta = 0.49° < 1° \quad \text{O.K.}$$

Step 8. The deflections of the local mechanisms are within the criteria. The sidesway deflection is acceptable.

Summary: The member sizes to be used in a computer analysis are as follows:

Member	Size
1	W12 x 35
2	W14 x 61
3	W14 x 74

Problem 5A-7 Design of Doors for Pressure-Time Loading

Problem: Design a steel-plate blast door subjected to a pressure-time loading.

Procedure:

Step 1. Establish the design parameters

a. Pressure-time load

b. Design criteria: Establish support rotation, θ_{max}, and whether seals and rebound mechanisms are required.

c. Structural configuration of the door including geometry and support conditions

d. Properties of steel used:

Minimum yield strength, f_y, for door components (Table 5-1)

Dynamic increase factor, c (Table 5-2)

Step 2. Select the thickness of the plate.

Step 3. Calculate the elastic section modulus, S, and the plastic section modulus, Z, of the plate.

Step 4. Calculate the design plastic moment, M_p, of the plate (equation 5-7).

Step 5. Compute the ultimate dynamic shear, V_p (equation 5-16).

Step 6. Calculate maximum support shear, V, using a dynamic load factor of 1.25 and determine V/V_p. If V/V_p is less than 0.67, use the plastic design moment as computed in Step 4 (Section 5-31). If V/V_p is greater than 0.67, use Equation 5-23 to calculate the effective M_p.

Step 7. Calculate the ultimate unit resistance of the section (Table 3-1), using the equivalent plastic moment as obtained in Step 4 and a dynamic load factor of 1.25.

Step 8. Determine the moment of inertia of the plate section.

Step 9. Compute the equivalent elastic unit stiffness, K_E, of the plate section (Table 3-8).

Step 10. Calculate the equivalent elastic deflection, X_E, of the plate as given by $X_E = r_u/K_E$.

Step 11. Determine the load-mass factor K_{LM} and compute the effective unit mass, m_e.

Step 12. Compute the natural period of vibration, T_N.

Step 13. Determine the door plate response using the values of P/r_u and T/T_N and the response charts of Chapter 3. Determine X_m/X_E and T_E.

Step 14. Determine the support rotation,

$$\text{Tan } \theta = (X_m) / (L/2)$$

Compare θ with the design criteria of step 1b.

Step 15. Determine the strain rate, ϵ, using equation 5-1. Determine the dynamic increase factor using figure 5-2 and compare with the DIF selected in Step 1d.

If the criteria of Step 1 is not satisfied, repeat Steps 2 to 15 with a new plate thickness.

Step 16. Design supporting flexural element considering composite action with the plate (if so constructed).

Step 17. Calculate elastic and plastic section moduli of the combined section.

Step 18. Follow the design procedure for a flexural element as described in Section 5A-1.

Example 5A-7 (a) Design of a Blast Door for Pressure-Time Loading

Required: Design a double-leaf, built-up door (6 ft by 8 ft) for the given pressure-time loading.

Step 1. Given:

a. Pressure-time loading (Figure 5A-7)

b. Design criteria: This door is to protect personnel from exterior loading. Leakage into the structure is permitted but the maximum end rotation of any member is limited to 2° since panic hardware must be operable after an accidental explosion.

c. Structural configuration (Figure 5A-7)

NOTE:
This type of door configuration is suitable for low-pressure range applications.

d. Steel used: A36

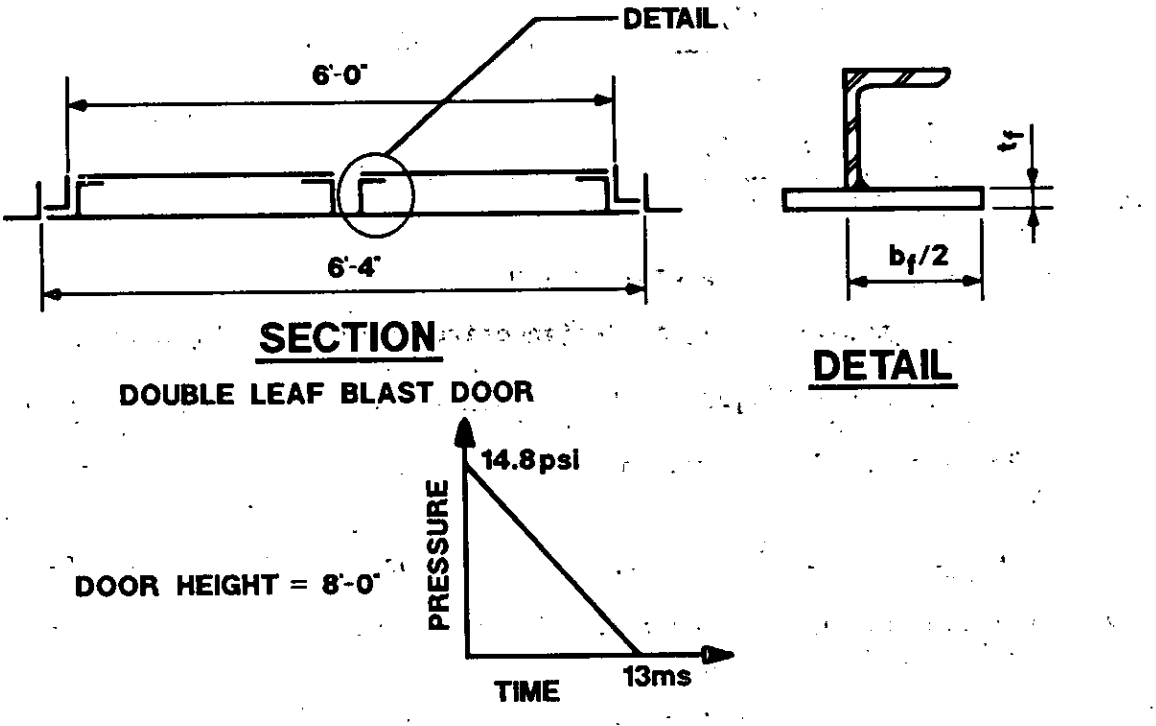


Figure 5A-7(a) Door configuration and loading, Example 5A-7(a)

Yield strength, f_y = 36 ksi (Table 5-1)

Dynamic increase factor, c = 1.29 (Table 5-2)

Average yield strength increase factor, a = 1.1 (Section 5-12.1)

Hence, the dynamic design stress,

f_{ds} = 1.1 x 1.29 x 36 = 51.1 ksi (Equation 5-2)

and the dynamic yield stress in shear,

$f_{dv} = 0.55\ f_{ds} = 0.55 \times 51.1 = 28.1$ ksi (Equation 5-4)

Step 2. Assume a plate thickness of 5/8 inch.

Step 3. Determine the elastic and plastic section moduli (per unit width).

$$S = \frac{bd^2}{6} = \frac{1 \times (5/8)^2}{6} = 6.515 \times 10^{-2} \text{ in}^3/\text{in}$$

$$Z = \frac{bd^2}{4} = \frac{1 \times (5/8)^2}{4} = 9.765 \times 10^{-2} \text{ in}^3/\text{in}$$

Step 4. Calculate the design plastic moment, M_p.

$$M_p = f_{ds} (S + Z)/2 = 51.1 [(6.515 \times 10^{-2}) + (9.765 \times 10^{-2})]/2 = 51.1 \times 8.14 \times 10^{-2} = 4.16 \text{ in-k/in} \quad \text{(Equation 5-7)}$$

Step 5. Calculate the dynamic ultimate shear capacity, V_p, for a 1-inch width.

$$V_p = f_{dv} A_w = 28.1 \times 1 \times 5/8 = 17.56 \text{ kips/in} \quad \text{(Equation 5-16)}$$

Step 6. Evaluate the support shear and check the plate capacity. Assume DLF = 1.25

$$V = \text{DLF} \times P \times L/2 = \frac{1.25 \times 14.8 \times 36 \times 1}{2} = 333 \text{ lb/in} = 0.333 \text{ kip/in}$$

$$V/V_p = 0.333/13.61 = 0.0245 < 0.67 \quad \text{(Section 5-31)}$$

No reduction in equivalent plastic moment is necessary.

NOTE:
When actual DLF is determined, reconsider Step 6.

Step 7. Calculate the ultimate unit resistance, r_u, (assuming the plate to be simply-supported at both ends).

$$r_u = 8M_p/L^2 = \frac{8 \times 4.16 \times 10^3}{(36)^2} = 25.7 \text{ psi} \quad \text{(Table 3-1)}$$

Step 8. Compute the moment of inertia, I, for a 1-inch width.

$$I = \frac{bd^3}{12} = \frac{1 \times (5/8)^3}{12} = 0.02035 \text{ in}^4/\text{in}$$

Step 9. Calculate the equivalent elastic stiffness, K_E.

$$K_E = 384EI/5bL^4 = \frac{384 \times 29 \times 106 \times .02035}{5 \times 1 \times (36)^4} = 27.0 \text{ psi/in}$$ (Table 3-8)

Step 10. Determine the equivalent elastic deflection, X_E.

$$X_E = r_u/K_E = 25.7/27.0 = 0.95 \text{ inch}$$

Step 11. Calculate the effective mass of element.

a. K_{LM} (average elastic and plastic)
$= (0.78 + 0.66)/2 = 0.72$

b. Unit mass of element, m

$$m = w/g = \frac{5/8 \times 1 \times 1 \times .490 \times 10^6}{1,728 \times 32.2 \times 12} = 458.0 \text{ psi-ms}^2/\text{in}$$

c. Effective unit of mass of element, m_e

$$m_e = K_{LM}m = 0.72 \times 458.0$$

$$= 330 \text{ psi-ms}^2/\text{in}$$

Step 12. Calculate the natural period of vibration, T_N.

$$T_N = 2\pi (330/27.0)^{1/2} = 22 \text{ ms}$$

Step 13. Determine the door response.

Peak overpressure $P = 14.8$ psi

Peak resistance $r_u = 25.7$ psi

Duration $T = 13.0$ ms

Natural period of vibration $T_N = 22$ ms

$P/r_u = 14.8/25.7 = 0.58$

$T/T_N = 13.0/22.0 = 0.59$

From Figure 3-64a of Chapter 3,

$X_m/X_E < 1$

Since the response is elastic, determine the DLF from Figure 3-49 of Chapter 3.

DLF = 1.3 for $T/T_N = 0.59$

Step 14. Determine the support rotation.

$$X_m = \frac{1.3 \times 14.8 \times 0.95}{25.7} = 0.713 \text{ inch}$$

$$\tan \theta = X_m/(L/2) = 0.713/(36/2) = 0.0396$$

$\theta = 2.27° > 2°$ N.G.

Step 15. Evaluate the selection of the dynamic increase factor.

Since this is an elastic response, use figure 3-49(b) of Chapter 3 to determine t_m. For $T/T_N = 0.59$, $t_m/T = 0.7$ and $t_m = 9.1$ ms. The strain rate is:

$$\dot{\epsilon} = f_{ds}/E_s t_E \qquad \text{(Equation 5-1)}$$

Since the response is elastic,

$$f_{ds} = 51.1 \times \frac{X_m}{X_E} = 51.1 \times \frac{0.713}{0.95} = 38.4 \text{ ksi}$$

and $t_E = t_m = 0.0091$ sec. Hence,

$$\dot{\epsilon} = 38.4/29.6 \times 10^3 \times 0.0091 = .142 \text{ in/in/sec}$$

Using figure 5-2, DIF = 1.31. The preliminary selection of DIF = 1.29 is acceptable.

Since the rotation criterion is not satisfied, change the thickness of the plate and repeat the procedure. Repeating these calculations, it can be shown that a 3/4-inch plate satisfies the requirements.

Step 16. Design of the supporting flexural element.

Assume an angle L4 x 3 x 1/2 and attached to the plate as shown in Figure 5A-7(b).

Determine the effective width of plate which acts in conjunction with the angle

$b_f/2t_f \leq 8.5$ (Section 5-24)

where $b_f/2$ is the half width of the outstanding flange or overhang and t_f is the thickness of the plate.

With t_f = 3/4 inch, $b_f/2 \leq 8.5 \times 3/4$, i.e., 6.38 inches

Use overhang of 6 inches.

Hence, the effective width = 6 + 2 = 8 inches. The angle together with plate is shown in Figure 5A-7(b).

Step 17. Calculate the elastic and plastic section moduli of the combined section.

Let $\bar{y}$ be the distance of c.g. of the combined section from the outside edge of the plate as shown in Figure 5A-7(b), therefore

$$\bar{y} = \frac{(8 \times 3/4 \times 3/8) + (4 + 3/4 - 1.33) \times 3.25}{(8 \times 3/4) + 3.25} = 1.445 \text{ inches}$$

Let y_p be the distance to the N.A. of the combined section for full plasticity.

$$y_p = \frac{1}{8 \times 2} [(8 \times 3/4) + 3.25] = 0.578 \text{ inch}$$

$$I = \frac{8 \times (3/4)^3}{12} + 8 \times 3/4 \times (1.45 - 3/8)^2$$

$$+ 5.05 + 3.25 (4 + 3/4 - 1.33 - 1.445)^2 = 24.881 \text{ in}^4$$

Hence, $S_{min} = 24.881/(4.75 - 1.445) = 7.54 \text{ in}^3$

$$Z = 8 (0.578)^2/2 + 8 (0.75 - 0.578)^2/2$$

$$+ 3.25 (4.75 - 1.33 - 0.578) = 10.69 \text{ in}^3$$

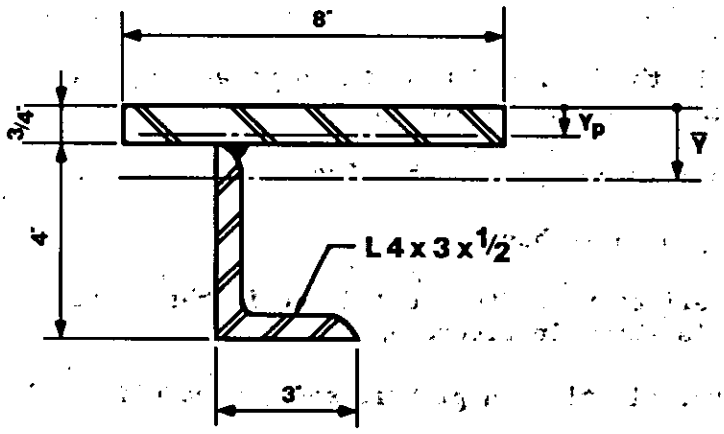


Figure 5A-7(b) Detail of composite angle/plate supporting element, Example 5A-7(b)

Step 18. Follow the design procedure for the composite element using steps 4 through 13. Calculate the design plastic moment M_p of the supporting flexural element.

$M_p = 51.1\ (7.54 + 10.69)/2 = 465.8$ in-kips (Equation 5-7)

Calculate the ultimate dynamic shear capacity, V_p.

$V_p = f_{dv}A_w = 28.1\ (4.0 - 1/2)\ 1/2 = 49.2$ kips (Equation 5-16)

Calculate support shear and check shear capacity.

$L = 8'\text{-}0" = 96$ inches

$V_p = (14.8 \times 36/2 \times 96)/2 = 12{,}790$ lb $= 12.79$ kips $< V$ O.K. (Section 5-23)

Calculate the ultimate unit resistance, r_u.

Assuming the angle to be simply supported at both ends:

$r_u = 8M_p/L^2 = (8 \times 465.8 \times 1{,}000)/(96)^2 = 405$ lb/in (Table 3-1)

Calculate the unit elastic stiffness, K_E.

$$K_E = 384EI/5L^4 = \frac{384 \times 29 \times 10^6 \times 24.881}{5 \times (96)^4} = 652.5 \text{ lb/in}^2$$ (Table 3-8)

Determine the equivalent elastic deflection, X_E.

$X_E = r_u/K_E = 405/652.5 = 0.620$ inch

Calculate the effective mass of the element.

$K_{LM} = 0.72$

$$w = \frac{11.1}{12} + \frac{3}{4} \times 18 \times \frac{490}{1{,}728} = (0.925 + 3.825) = 4.750 \text{ lb/in}$$

Effective unit mass of element,

$$m_e = 0.72 \times \frac{4.75 \times 10^6}{32.2 \times 12} = 0.89 \times 10^4 \text{ lb-ms}^2/\text{in}^2$$

Calculate the natural period of vibration, T_N.

$T_N = 2\pi[(89 \times 10^2)/652.5]^{1/2} = 23.2$ ms

Determine the response parameters. (Figure 3-64a)

Peak overpressure $P = 14.8 \times 36/2 = 266.5$ lb/in

Peak resistance $r_u = 405$ lb/in

Duration $T = 13.0$ ms

Natural period of vibration, $T_N = 23.2$ ms

$P/r_u = 266.5/405 = 0.658$

$T/T_N = 13/23.2 = 0.56$

From Figure 3-64a,

$$\mu = X_m/X_E < 1$$

From Figure 3-49 for $T/T_N = 0.56$,

DLF = 1.28

$$\text{Hence, } X_m = \frac{1.28 \times 14.8 \times 36/2}{652.5} = 0.522 \text{ in}$$

$$\tan \theta = X_m/(L/2) = 0.522/48 = 0.0109$$

$$\theta = 0.69° < 2° \qquad \text{O.K.}$$

Check stresses at the connecting point.

$$\sigma = My/I = 355 \times 10^3 \times (1.445 - 0.75)/24.881$$

$$= 9{,}900 \text{ psi } \left(M = \frac{X_m}{X_E} \times M_p = \frac{0.522}{0.62} \times 405 = 341\right)$$

$$\tau = VQ/Ib = \frac{12.79 \times 103 \times 8 \times 3/4 \times (1.445 - 0.75/2)}{24.881 \times 1/2} = 5{,}321 \text{ psi}$$

Effective stress at the section $= (\sigma^2 + \tau^2)^{1/2}$

$= 10^3 \times (9.9^2 + 5.321^2)^{1/2} = 11{,}239 \text{ psi} < 39.600 \text{ psi}$ O.K.

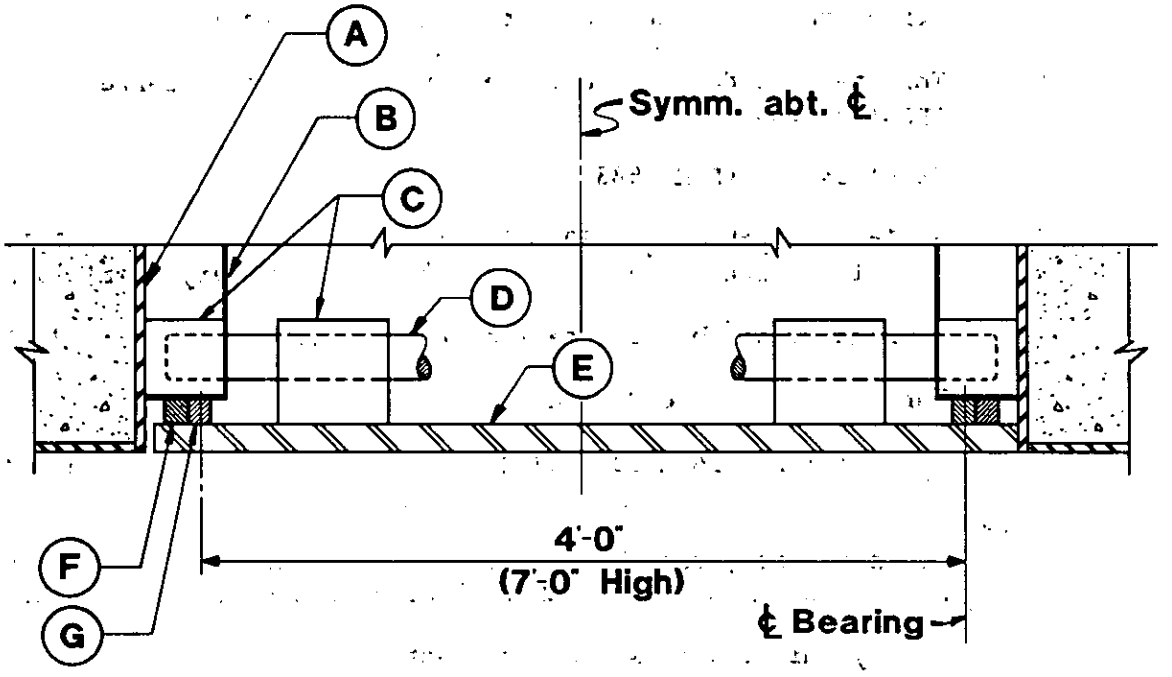
Example 5A-7 (b) Design of a Plate Blast Door for Pressure-Time Loading

Required: Design a single-leaf door (4 ft by 7 ft) for the given pressure-time loading.

Step 1. Given:

a. Pressure-time loading [figure 5A-7 (c)]

b. Design criteria: Door shall be designed to contain blast pressures from an internal explosion. Gasket and reversal



PLAN / SECTION

Legend:

A - Steel frame embedded in concrete
B - Steel sub-frame
C - Reversal bolt housing
D - Reversal bolt
E - Blast door plate
F - Continuous gasket
G - Continuous bearing block

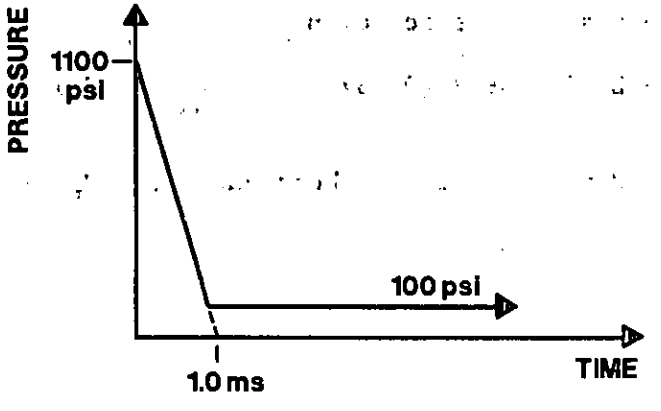


Figure 5A-7(c)Door configuration and loading, Example 5A-7(b)

mechanisms shall be provided. Support rotation shall be limited to 3°

c. Structural configuration [see figure 5A-7 (c)]

Note: This type of door is suitable for high pressure range applications.

d. Steel used: ASTM A588

Yield strength, f_y = 50 ksi (Table 5-1)
Dynamic increase factor, c = 1.24 (preliminary, Table 5-2)

Average strength increase factor, a = 1.1 (Section 5-12.1)

Hence, the dynamic design stress,

f_{ds} = 1.1 x 1.24 x 50 = 68.2 ksi (Equation 5-2)

Note:
It is assumed, for the limited design rotation of 3° , that $\mu < 10$, and, therefore, that equation 5-3 does not govern.

The dynamic design stress in shear

$f_{dv} = 0.55\ f_{ds} = 37.5$ ksi (Equation 5-4)

Step 2. Assume a plate thickness of 2 inches

Step 3. Determine the elastic and plastic section moduli (per unit width)

$$S = \frac{bd^2}{6} = \frac{1\ (2)^2}{6} = 0.667\ in^3/in$$

$$Z = \frac{bd^2}{4} = \frac{1\ (2)^2}{4} = 1.0\ in^3/in$$

Step 4. Calculate the design plastic moment, M_p

$M_p = f_{ds}\ (S + Z)/2 = 68.2\ (0.667 + 1.0)/2 = 56.8$ in-k/in (Equation 5-7)

Step 5. Calculate the dynamic ultimate shear capacity, V_p, for a 1-inch width.

$V_p = f_{dv}A_w = 37.5 \times 2 = 75.0$ kips/in (Equation 5-16)

Step 6. Evaluate the support shear and check the plate shear capacity.

Example 5A-7(b)

Assume DLF = 1.0 (Table 5-4)

For simplicity, assume the plate is a one-way member, hence:

$V = DLF \times P \times L/2 = 1.0 \times 1100 \times 48/2 = 26{,}400$ lb/in

$= 26.4$ kips/in

$V/V_p = 26.4/75. = 0.352 < 0.67$ (Section 5-31)

No reduction in equivalent plastic moment is necessary.

Step 7. Calculate the ultimate unit resistance, r_u.

For a plate, simply-supported on four sides (direct load)

$r_u = 5M_p/X^2$ (Table 3-2)

where $M_{HP} = M_p$ and $M_{HN} = 0$ and

$$\frac{X}{L} = 0.35 \quad \text{for} \quad \frac{L}{H} = 1.75$$ (Figure 3-17)

thus, $X = 0.35 \times 12 \times 7 = 29.4$ in

$r_u = 5 \times 56.8/(29.4)^2 = 329$ psi

Step 8. Compute the moment of inertia, I, for a 1-inch width

$$I = \frac{bd^3}{12} = \frac{1 \times 2^3}{12} = 0.667 \text{ in}^4/\text{in}$$

Step 9. Calculate the equivalent elastic stiffness, K_E

$K_E = r/x = D/\gamma H^4$ (Figure 3-36)

where

$\gamma = 0.0083$ (for H/L = 0.57)

$D = EI/b\ (1 - \nu^2)$ (Equation 3-33)

$D = 29.6 \times 10^6 \times 0.667/1\ (1 - .3^2) = 2.17 \times 10^7$

$K_E = 2.17 \times 10^7/0.0083 \times 48^4 = 492$ psi/in

Step 10. Determine the equivalent elastic deflection, X_E.

$X_E = r_u/K_E = 329/492 = 0.669$ in

Step 11. Calculate the effective mass of the element

a. K_{LM} (average elastic and plastic)

$= (0.78 + 0.66)/2 = 0.72$

b. Unit mass of element,

$$m = w/g = \frac{2 \times 1 \times 1 \times 490 \times 10^6}{1{,}728 \times 32.2 \times 12} = 1{,}468\ \frac{\text{psi-ms}^2}{\text{in}}$$

c. Effective unit mass of element, m_e

$$m_e = K_{LM} \times m = 0.72 \times 1{,}468 = 1{,}057\ \frac{\text{psi-ms}^2}{\text{in}}$$

Step 12. Calculate the natural period of vibration, T_N

$T_N = 2\pi\ (1{,}057/492)^{1/2} = 9.2$ ms

Step 13. Determine the door plate response for:

$P/r_u = 1100/329 = 3.34$

$T/T_N = 1.0/9.2 = 0.109$

$C_1 = 100/1100 = 0.091$ (Figure 3-62, Region C)

$C_2 > 1000$

Using Figure 3-253,

$X_m/X_E = 1.5$

$X_m = 1.5 \times 0.669 = 1.00$ in

Step 14. Determine the support rotation.

$\theta = \tan^{-1} (1/24) = 2.39° < 3°$

Step 15. Evaluate the selection of the dynamic increase factor.

$\dot{\epsilon} = f_{ds}/E_s t_E$ (Equation 5-1)

$t_E/T = 1.8$, $t_E = 1.8$ ms (Figure 3-253)

$\dot{\epsilon} = 68.2/29.6 \times 10^3 \times .0018 = 1.28$ in./in./sec.

DIF = 1.3 (figure 5-2, average of A36 and A514)

Initial selection of DIF = 1.24 is adequate.

Since the support rotation criteria has been satisfied and the preliminary selection of the DIF is acceptable, a 2 inch thick plate is used in design.

Steps 15 through 18 These steps are bypassed since the door plate has no stiffening elements.

Problem 5A-8 Design of Doubly Symmetric Beams Subjected to Inclined Pressure-Time Loading

Problem: Design a purlin or girt as a flexural member which is subjected to a transverse pressure-time load acting in a plane other than a principal plane.

Procedure:

Step 1. Establish the design parameters.

a. Pressure-time load

b. Angle of inclination of the load with respect to the vertical axis of the section

c. Design criteria: Maximum support rotation limited to 2°.

d. Member spacing, b

e. Type and properties of steel used:

Minimum yield strength for the section (Table 5-1)

Dynamic increase factor, c (Table 5-2)

Step 2. Preliminary sizing of the beam.

a. Determine the equivalent static load, w, using a preliminary dynamic load factor equal to 1.0.

$$\therefore w = 1.0 \times p \times b$$

b. Using the appropriate resistance formula from Table 3-1 and the equivalent static load derived in Step 2a, determine the required M_p.

c. Determine the required section properties using equation 5-7. Select a larger section since the member is subjected to unsymmetrical bending.

Note that for a load inclination of 10°, it is necessary to increase the required average section modulus, (1/2) (S + Z), by 40 percent.

Step 3. Check local buckling of the member (Section 5-24).

Step 4. Calculate the inclination of the neutral axis (equation 5-24).

Step 5. Calculate the elastic and plastic section moduli of the section (equation 5-25).

Step 6. Compute the design plastic moment, M_p, (equation 5-6).

Step 7. Calculate ultimate unit resistance, r_u, of the member.

Step 8. Calculate elastic deflection, δ (Section 5-32.3).

Step 9. Determine the equivalent elastic unit stiffness, K_E, of the beam section using δ from Step 8.

Step 10. Compute the equivalent elastic deflection, X_E, of the member as given by $X_E = r_u/K_E$.

Step 11. Determine the load-mass factor, K_{LM}, and obtain the effective unit mass, m_e, of the element.

Step 12. Evaluate the natural period of vibration, T_N.

Step 13. Determine the dynamic response of the beam. Evaluate P/r_u and T/T_N, using the response charts of Chapter 3 to obtain X_m/X_E and θ. Compare with criteria.

Step 14. Determine the ultimate dynamic shear capacity, V_p, (equation 5-16) and maximum support shear, V, using Table 3-9 of Chapter 3 and check adequacy.

Example 5A-8 Design an I-Shaped Beam for Unsymmetrical Bending Due to Inclined Pressure-Time Loading

Required: Design a simply-supported I-shaped beam subjected to a pressure-time loading acting at an angle of 10° with respect to the principal vertical plane of the beam. This beam is part of a structure designed to protect personnel.

Step 1. Given:

a. Pressure-time loading [figure 5A-8 (a)]

b. Design criteria: The structure is to be designed for more than one "shot." A maximum end rotation = 1°, is therefore assigned

c. Structural configuration [figure 5A-8(a)]

d. Steel used: A36

Yield strength, f_y = 36 ksi (Table 5-1)

Dynamic increase factor, c = 1.29 (Table 5-2)

Average yield strength increase factor, a = 1.1 (Section 5-12.1)

Dynamic design strength, f_{ds} = 1.1 x 1.29 x 36 = 51.1 ksi (equation 5-2)

Dynamic yielding stress in shear, f_{dv} = 0.55 f_{ds} = 0.55 x 51.1 = 28.1 ksi (equation 5-4)

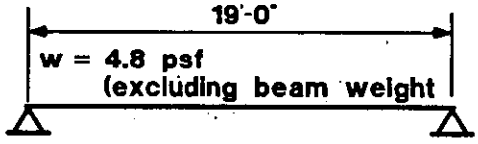
Modulus of elasticity, E = 29,000,000 psi

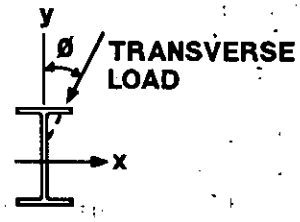
Step 2. Preliminary sizing of the member.

a. Determine equivalent static load.

Select DLF = 1.2 (Section 5-22.3)

w = 1.25 x 4.5 x 4.5 x 144/1,000 = 3.65 k/ft





Spacing: b = 4.5'

ø = 10°

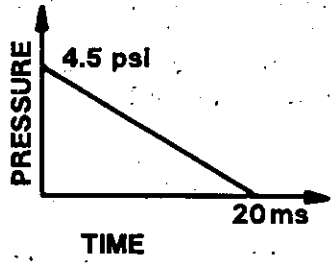


Figure 5A-8(a) Beam configuration and loading, Example 5A-8(a)

b. Determine minimum required M_p

$M_p = (wL^2)/8 = (3.65 \times 19^2)/8 = 165$ k-ft (Table 3-1)

c. Selection of a member.

For a load acting in the plane of the web,

$(S + Z) = 2M_p/f_{ds} = (2 \times 165 \times 12)/51.1$ (Equation 5-7)

$(S + Z) = 77.5$ in^3

$(S + Z)$ required $1.4 \times 77.5 = 109$ in^3

Try W14 x 38, $S_x = 54.6\ in^3$, $Z_x = 61.5\ in^3$

$(S + Z) = 116.1\ in^3$, $I_x = 385\ in^4$

$I_y = 26.7\ in^4$

Step 3. Check against local buckling.

For W14 x 38,

$d/t_w = 45.5 < (412 / (36)^{1/2})\ (1 - 1.4 \times P/P_y) = 68.66$ O.K. (Equation 5-17)

$b_f/2t_f = 6.6 < 8.5$ O.K. (Section 5-24)

Step 4. Inclination of elastic and plastic neutral axes with respect to the x-axis.

$\tan \alpha = (I_x/I_y) \tan \phi = (385/26.7) \tan 10° = 2.546$ (Equation 5-24)

$\alpha = 68.5°$

Calculate the equivalent elastic section modulus.

$S = (S_x S_y)/(S_y \cos \phi + S_x \sin \phi)$

$S_x = 54.6\ in^3$, $S_y = 7.88\ in^3$, $\phi = 10°$

$\sin 10° = 0.174$, $\cos 10° = 0.985$

$S = (54.6)\ (7.88)/(7.88 \times 0.985 + 54.7 \times 0.174) = 24.9\ in^3$

Step 5. Calculate the plastic section modulus, Z.

$Z = A_c m_1 + A_t m_2$ (Equation 5-6)

$A_c = A_t = A/2 = 11.2/2 = 5.6\ in^2$

Let $\bar{y}$ be the distance of the c.g. of the area of cross section in compression from origin as shown in Figure 5A-8 (b).

$$\bar{y} = \frac{1}{5.6}\left[6.770 \times 0.515 \times \left(\frac{14.10}{2} - \frac{0.515}{2}\right) + \frac{1}{2}(14.10 - 2 \times 0.515) \times 0.310 \times \frac{1}{2}\left(\frac{14.10}{2} - 0.515\right)\right] = 5.42 \text{ inches}$$

$$m_1 = m_2 = \bar{y} \sin \alpha = 5.42 \sin 68° 30' = 5.05 \text{ inches}$$

$$Z = 2A_c m_1 = 11.2 \times 5.05 = 56.5 \text{ in}^3$$

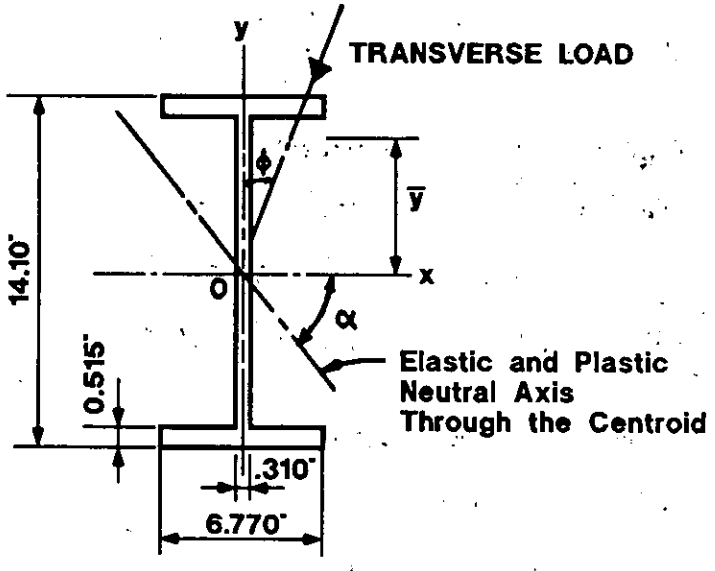


Figure 5A-8(b) Loading on beam section, Example 5A-8(b)

Step 6. Determine design plastic moment, M_p.

$$M_p = f_{ds}(S + Z)/2 = 51.1(24.9 + 56.5)/2 \qquad \text{(Equation 5-7)}$$

$= 51.1 \times 40.7 = 2{,}080$ in-kips

Step 7. Calculate ultimate unit resistance, r_u.

$$r_u = 8M_p/L^2 = (8)\ (2{,}080)\ (1{,}000)/(19 \times 12)^2 = 320 \text{ lb/in}$$

(Table 3-1)

Step 8. Compute elastic deflection, δ.

$$\delta = [(\delta_x^2 + \delta_y^2)]^{1/2}$$

(Section 5-32.3)

$$\delta_y = \frac{5w \cos\phi\ L^4}{384EI_x}$$

$$\delta_x = \frac{5w \sin\phi\ L^4}{384EI_y}$$

w = equivalent static load + dead load

$$= 2.92 + \frac{(4.8 \times 4.5) + 38}{1{,}000} \text{ kips/ft} = 2.94 \text{ kips/ft}$$

$$\delta = \left[\frac{[\ 5w\sin\phi L^4\ ]^2}{384EI_y} + \frac{[\ 5w\cos\phi L^4\ ]^2}{384EI_x} \right]^{1/2}$$

$$= \frac{5wL^4}{38{,}400E}\ [(0.652)^2 + (0.256)^2\ ]^{1/2} = 2.08 \text{ inches}$$

Step 9. Calculate the equivalent elastic unit stiffness, K_E.

$$K_E = w/\delta = \frac{2.94 \times 1{,}000 \times 1}{12 \times 2.085} = 117.8 \text{ lb/in}^2$$

(Get w from Step 8)

Step 10. Determine the equivalent elastic deflection, X_E.

$$X_E = r_u/K_E = 320/117.8 = 2.72 \text{ inches}$$

Step 11. Calculate the effective mass of the element, m_e.

a. Load-mass factor, K_{LM} (Table 3-12)

K_{LM} (average elastic and plastic)

$= (0.78 + 0.66)/2 = 0.72$

b. Unit mass of element, m

$$m = w/g = \frac{[(4.5 \times 4.8) + 38] \times 10^6}{32.2 \times 12 \times 12} = 1.286 \times 10^4 \text{ lb-ms}^2/\text{in}^2$$

c. Effective unit mass of element, m_e

$m_e = K_{LM}m = 0.72 \times 1.286 \times 10^4 = 0.93 \times 10^4 \text{ lb-ms}^2/\text{in}^2$

Step 12. Calculate the natural period of vibration, T_N.

$T_N = 2\pi [(93 \times 10^2)/117.8]^{1/2} = 55.8$ ms (Section 5-22.2)

Step 13. Determine the beam response.

Peak overpressure $P = 4.5 \times 4.5 \times 12 = 243$ lb/in

Peak resistance $r_u = 320$ lb/in

Duration $T = 20$ ms

Natural period of vibration, $T_N = 55.8$ ms

$P/r_u = 243/320 = 0.76$

$T/T_N = 20/55.8 = 0.358$

From figure 3-64a

$X_m/X_E < 1$

From figure 3-49, for $T/T_N = 0.358$,

DLF = 0.97

Hence, X_m = 0.97 x 4.5 x 4.5 x 12/117.8 = 2.0 in

Find end rotation, Θ.

tan $\Theta = X_m/(L/2) = 2.0/[(19 \times 12)/2] = 0.0175$

Θ = 1.0° O.K.

Step 14. Calculate the dynamic ultimate shear capacity, V_p, and check for adequacy.

$V_p = f_{dv}A_w = 28.1\ (14.10 - 2 \times 0.515)\ (0.310) = 113.9$ kips (Equation 5-16)

V = DLF x P x b x L/2

= 0.97 x 4.5 x 4.5 x 19 x 144/(2 x 1,000)

= 26.9 kips < 89.2 kips < V_p O.K. (Table 3-9)

APPENDIX 5B

LIST OF SYMBOLS

a yield stress increase factor

A Area of cross section (in^2)

A_b Area of bracing member (in^2)

A_c Area of cross section in compression (in^2)

A_t Area of cross section in tension (in^2)

A_w Web area (in^2)

b Width of tributary loaded area (ft)

b_f Flange width (in)

b_h Tributary width for horizontal loading (ft)

b_v Tributary width for vertical loading (ft)

c,DIF (1) Dynamic increase factor
c (2) Distance from neutral axis to extreme fiber of cross-section in flexure (in)

C, C_1 Coefficients indicating relative column to girder moment capacity (Section 5-42.1)

C_b Bending coefficient defined in Section 1.5.1.4.5 of the AISC Specification

C_c Column slenderness ratio indicating the transition from elastic to inelastic buckling

C_{mx}, C_{my} Coefficients applied to the bending terms in interaction formula (AISC Specification Section 1.6.1)

C_2 Coefficient in approximate expression for sidesway stiffness factor (Table 5-14)

D Coefficient indicating relative girder to column stiffness (Table 5-14)

DLF Dynamic load factor

d (1) Web depth (in)
(2) Diameter of cylindrical portion of fragment, in.

E Young's modulus of elasticity (psi)

f (1) Maximum bending stress (psi)
(2) Shape factor, S/Z

f_a Axial stress permitted in the absence of bending moment from Section 5-37.3 (psi)

f_b Bending stress permitted in the absence of axial force (psi)

f_{cr} Web buckling stress (psi)

f_d Maximum dynamic design stress for connections (psi)

f_{ds} Dynamic design stress for bending, tension and compression (psi)

f_{dv} Dynamic yielding shear stress (psi)

f_{dv} Dynamic ultimate stress (psi)

f_{dy} Dynamic yield stress (psi)

F'_{ex}, F'_{ey} Euler buckling stresses divided by safety factor (psi)

F_H Horizontal component of force in bracing member (lb)

F_s Allowable static design stress for connections (psi)

f_u Ultimate tensile stress (psi)

f_y Minimum static yield stress (psi)

g Acceleration due to gravity (386 in/sec^2)

H Story height (ft)

h Web depth for cold-formed, light gauge steel panel sections (in)

I Moment of inertia (in^4)

I_{ca} Average column moment of inertia for single-story multi-bay frame (in^4)

I_{20} Effective moment of inertia for cold-formed section at a service stress of 20 ksi (in^4 per foot width)

I_x Moment of inertia about the x-axis (in^4)

I_y Moment of inertia about the y-axis (in^4)

K (1) Effective length factor for a compression member
(2) Stiffness factor for rigid single-story, multi-bay frame from Table 5-14

K_b Horizontal stiffness of diagonal bracing (lb/ft)

K_E Equivalent elastic stiffness (lb/in or psi/in)

K_L Load factor

K_{LM} Load-mass factor

K_M Mass factor

L (1) Span length (ft or in)
(2) Frame bay width (ft)

l Distance between cross section braced against twist or lateral displacement of compression flange or distance between points of lateral support for beams or columns

l/r Slenderness ratio

l_b Actual unbraced length in the plane of bending (in)

l_{cr} Critical unbraced length (in)

M Total effective mass (lb-ms^2/in)

M_{mx}, M_{my} Moments about the x- and y-axis that can be resisted by member in the absence of axial load

M_p Design plastic moment capacity

M_1, M_2 Design plastic moment capacities (figures 5-6 and 5-10)

M_{px}, M_{py} Plastic bending moment capacities about the x- and y-axes

M_{pu} Ultimate dynamic moment capacity

M_{up} Ultimate positive moment capacity for unit width of panel

M_{un} Ultimate negative moment capacity for unit width of panel

M_y Moment corresponding to first yield

m (1) Unit mass of panel (psi-ms^2/in)
(2) Number of braced bays in multi-bay frame

m_e Effective unit mass (psi-ms^2/in)

m_1 Distance from plastic neutral axis to the centroid of the area in compression in a fully plastic section (in)

m_2 Distance from plastic neutral axis to the centroid of the area in tension in a fully plastic section (in)

N Bearing length at support for cold-formed steel panel (in)

n Number of bays in multi-bay frame

P (1) Applied compressive load (lb)

(2) Peak pressure of equivalent triangular loading function, (psi) [when used with r_u], or peak total blast load (lb) [when used with R_u].

P_{ex}, P_{ey} Euler buckling loads about the x- and y-axes

P_p Ultimate capacity for dynamic axial load, Af_{dy} (lb)

P_u Ultimate axial compressive load (lb)

P_y Ultimate capacity for static axial load Af_y (lb)

P_h Reflected blast pressure on front wall (psi)

P_v Blast overpressure on roof (psi)

Q_u Ultimate support capacity (lb)

q_h Peak horizontal load on rigid frame (lb/ft)

q_v Peak vertical load on rigid frame (lb/ft)

R Equivalent total horizontal static load on frame (lb)

R_u Ultimate total flexural resistance (lb)

r_b Radius of gyration of bracing member (in)

r_T Radius of gyration, equation 5-22 (in)

r_u Ultimate unit flexural resistance (psi)

r_x, r_y Radii of gyration about the x- and y-axes (in)

$\bar{r}$ Required resistance for elastic behavior in rebound (psi)

S Elastic section modulus (in^3)

S_x, S_y Elastic section modulus about the x- and y-axes (in^3)

S^+ Effective section modulus of cold-formed section for positive moments (in^3)

S^- Effective section modulus of cold-formed section for negative moments (in^3)

T Load duration (sec)

T_N Natural period of vibration (sec)

t (1) Thickness of plate element (in)
(2) Thickness of panel section (in)

t_E Time to yield (sec)

t_f Flange thickness (in)

t_m Time to maximum response (sec)

t_w Web thickness (in)

V Support shear (lb)

V Ultimate shear capacity (lb)

V_r Residual velocity of fragment (fps)

V_s Striking velocity of fragments, (fps)

V_x Critical perforation velocity of fragment (fps)

W Total weight (lb)

W_c Total concentrated load (lb)

W_E External work (lb-in)

W_f Fragment weight (oz.)

W_I Internal work (lb-in)

w (1) Flat width of plate element (in)
(2) Load per unit area (psi)
(3) Load per unit length (lb/ft)

X_o Deflection at design ductility ratio (figure 5-12)

X_E Equivalent elastic deflection (in)

X_m Maximum deflection (in)

x Depth of penetration of steel fragments (in)

Z Plastic section modulus (in^3)

Z_x, Z_y Plastic section moduli about the x- and y-axes (in^3)

α (1) Angle between the horizontal principal plane of the cross section and the neutral axis (deg)
(2) Ratio of horizontal to vertical loading on a frame

β (1) Base fixity factor (Table 5-14)
(2) Support condition coefficient (Section 5-34.3)
(3) Critical length for bracing correction factor (Section 5-26.3)

γ Angle between bracing member and a horizontal plane (deg)

δ (1) Total transverse elastic deflection (in)
(2) Lateral (sidesway) deflection (in)

ϵ Strain (in/in)

$\dot{\epsilon}$ Average strain rate (in/in/sec)

θ (1) Member end rotation (deg)
(2) Plastic hinge rotation (deg)

θ_{max} Maximum permitted member end rotation

μ Ductility ratio

μ_{max} Maximum permitted ductility ratio

ϕ Angle between the plane of the load and the vertical principal plane of the cross section (deg)

APPENDIX 5C

BIBLIOGRAPHY

1. Healey, J., et al., Design of Steel Structures to Resist the Effects of HE Explosions, by Ammann & Whitney, Consulting Engineers, New York, New York, Technical Report 4837, Picatinny Arsenal, Dover, New Jersey, August 1975.
2. Keenan, W., Tancreto, J., Meyers, G., Johnson, F., Hopkins, J., Nickerson, H. and Armstrong, W., NCEL Products Supporting DOD Revision of NAVFAC P-397, Program No. Y0995-01-003-201, Technical Memorandum 2591TM, sponsored by Naval Facilities Engineering Command, Alexandria, Virginia and Naval Civil Engineering Laboratory, Port Hueneme, California, March 1983.
3. Stea, W., Tseng, G. and Kossover, D., Nonlinear Analysis of Frame Structures Subjected to Blast Overpressures, by Ammann & Whitney, Consulting Engineers, New York, New York, Contractor Report ARLCD-CR-77008, U.S. Army Research and Development Command, Large Caliber Weapons Systems Laboratory, Dover, New Jersey, May 1977.
4. Stea, W., and Sock, F., Blast-resistant Capacities of Cold-formed Steel Panels, by Ammann & Whitney, Consulting Engineers, New York, New York, Contractor Report ARLCD-CR-81001, U.S. Army Research and Development Command, Large Caliber Weapon Systems Laboratory, Dover, New Jersey, May 1981.
5. Stea, W., Dobbs, N. and Weissman, S., Blast Capacity Evaluation of Pre-engineered Building, by Ammann & Whitney, Consulting Engineers, New York, New York, Contractor Report ARLCD-CR-79004, U.S. Army Research and Development Command, Large Caliber Weapons Laboratory, Dover, New Jersey, March 1979.
6. Healey, J., Weissman, S., Werner, H. and Dobbs, N., Primary Fragment Characteristics and Impact Effects on Protective Barriers, by Ammann & Whitney, Consulting Engineers, New York, New York, Technical Report 4903, Picatinny Arsenal, Dover, New Jersey, December 1975.
7. Manual of Steel Construction, Eighth Edition, American Institute of Steel Construction, New York, New York, 1980.
8. Specification for the Design, Fabrication and Erection of Structural Steel for Buildings and Commentary thereon, American Institute of Steel Construction, New York, New York, 1978.
9. Specification for the Design of Cold-Formed Steel Structural Members and Commentary thereon, American Iron and Steel Institute, New York, New York 1968.
10. Design of Structures to Resist the Effects of Atomic Weapons, Department of the Army Technical Manual TM 5-856-2, 3 and 4, Washington, D.C., August 1965.
11. Bleich, F., Buckling Strength of Metal Structures, McGraw-Hill, New York, 1952.
12. Newmark, N.M, and Haltiwanger, J.D., Principles and Practices for Design of Hardened Structures, Air Force Design Manual, Technical Documentary Report Number AFSWC, TDR-62-138, Air Force Special Weapons Center, Kirtland Air Force Base, New Mexico, December 1962.
13. Seely, F.B., and Smith, J.O., Advanced Mechanics of Materials, Second Edition, J. Wiley & Sons, New York, New York, 1961.
14. Bresler, B., et al., Design of Steel Structures, J. Wiley & Sons, New York, New York, 1968.
15. Johnston, B.G., ed., Guide to Design Criteria for Metal Compression Members, Second Edition, J. Wiley & Sons, New York, New York 1966.
16. McGuire, W., Steel Structures, Prentice Hall, Englewood, New Jersey, 1968.

17. Tall, L., et al., Structural Steel Design, Ronald Press, New York, New York, 1964.
18. Beedle, L.S., Plastic Design of Steel Frames, J. Wiley & Sons, New York, New York, 1958.
19. Hodge, P.G., Plastic Analysis of Structures, McGraw-Hill, New York, 1959.
20. Massonet, C.E., and Save, M.A., Plastic Analysis and Design, Blaisdell, New York, New York, 1965.
21. Plastic Design in Steel, A Guide and Commentary, Second Edition, Joint Committee of the Welding Research Council and the American Society of Civil Engineers, ASCE, 1971.

CHAPTER 6. SPECIAL CONSIDERATIONS IN EXPLOSIVE FACILITY DESIGN

CHAPTER 6

SPECIAL CONSIDERATIONS IN EXPLOSIVE FACILITY DESIGN

INTRODUCTION

6-1. Purpose

The purpose of this manual is to present methods of design for protective construction used in facilities for development, testing, production, storage, maintenance, modification, inspection, demilitarization, and disposal of explosive materials.

6-2. Objective

The primary objectives are to establish design procedures and construction techniques whereby propagation of explosion (from one structure or part of a structure to another) or mass detonation can be prevented and to provide protection for personnel and valuable equipment.

The secondary objectives are to:

(1) Establish the blast load parameters required for design of protective structures.
(2) Provide methods for calculating the dynamic response of structural elements including reinforced concrete, and structural steel.
(3) Establish construction details and procedures necessary to afford the required strength to resist the applied blast loads.
(4) Establish guidelines for siting explosive facilities to obtain maximum cost effectiveness in both the planning and structural arrangements, providing closures, and preventing damage to interior portions of structures because of structural motion, shock, and fragment perforation.

6-3. Background

For the first 60 years of the 20th century, criteria and methods based upon results of catastrophic events were used for the design of explosive facilities. The criteria and methods did not include a detailed or reliable quantitative basis for assessing the degree of protection afforded by the protective facility. In the late 1960's quantitative procedures were set forth in the first edition of the present manual, "Structures to Resist the Effects of Accidental Explosions". This manual was based on extensive research and development programs which permitted a more reliable approach to current and future design requirements. Since the original publication of this manual, more extensive testing and development programs have taken place. This additional research included work with materials other than reinforced concrete which was the principal construction material referenced in the initial version of the manual.

Modern methods for the manufacture and storage of explosive materials, which include many exotic chemicals, fuels, and propellants, require less space for a given quantity of explosive material than was previously needed. Such concentration of explosives increases the possibility of the propagation of accidental explosions. (One accidental explosion causing the detonation of

other explosive materials.) It is evident that a requirement for more accurate design techniques is essential. This manual describes rational design methods to provide the required structural protection.

These design methods account for the close-in effects of a detonation including the high pressures and the nonuniformity of blast loading on protective structures or barriers. These methods also account for intermediate and far-range effects for the design of structures located away from the explosion. The dynamic response of structures, constructed of various materials, or combination of materials, can be calculated, and details are given to provide the strength and ductility required by the design. The design approach is directed primarily toward protective structures subjected to the effects of a high explosive detonation. However, this approach is general, and it is applicable to the design of other explosive environments as well as other explosive materials as mentioned above.

The design techniques set forth in this manual are based upon the results of numerous full- and small-scale structural response and explosive effects tests of various materials conducted in conjunction with the development of this manual and/or related projects.

6-4. Scope

It is not the intent of this manual to establish safety criteria. Applicable documents should be consulted for this purpose. Response predictions for personnel and equipment are included for information.

In this manual an effort is made to cover the more probable design situations. However, sufficient general information on protective design techniques has been included in order that application of the basic theory can be made to situations other than those which were fully considered.

This manual is applicable to the design of protective structures subjected to the effects associated with high explosive detonations. For these design situations, the manual will apply for explosive quantities less than 25,000 pounds for close-in effects. However, this manual is also applicable to other situations such as far- or intermediate-range effects. For these latter cases the design procedures are applicable for explosive quantities in the order of 500,000 pounds which is the maximum quantity of high explosive approved for aboveground storage facilities in the Department of Defense manual, "Ammunition and Explosives Safety Standards", DOD 6055.9-STD. Since tests were primarily directed toward the response of structural steel and reinforced concrete elements to blast overpressures, this manual concentrates on design procedures and techniques for these materials. However, this does not imply that concrete and steel are the only useful materials for protective construction. Tests to establish the response of wood, brick blocks, and plastics, as well as the blast attenuating and mass effects of soil are contemplated. The results of these tests may require, at a later date, the supplementation of these design methods for these and other materials.

Other manuals are available to design protective structures against the effects of high explosive or nuclear detonations. The procedures in these manuals will quite often complement this manual and should be consulted for specific applications.

Computer programs, which are consistent with procedures and techniques contained in the manual, have been approved by the appropriate representative of the US Army, the US Navy, the US Air Force and the Department of Defense Explosives Safety Board (DDESB). These programs are available through the following repositories:

(1) Department of the Army
Commander and Director
U.S. Army Engineer
Waterways Experiment Station
Post Office Box 631
Vicksburg, Mississippi 39180-0631
Attn: WESKA

(2) Department of the Navy
Commanding Officer
Naval Civil Engineering Laboratory
Port Hueneme, California 93043
Attn: Code L51

(3) Department of the Air Force
Aerospace Structures
Information and Analysis Center
Wright Patterson Air Force Base
Ohio 45433
Attn: AFFDL/FBR

If any modifications to these programs are required, they will be submitted for review by DDESB and the above services. Upon concurrence of the revisions, the necessary changes will be made and notification of the changes will be made by the individual repositories.

6-5. Format

This manual is subdivided into six specific chapters dealing with various aspects of design. The titles of these chapters are as follows:

Chapter 1	Introduction
Chapter 2	Blast, Fragment, and Shock Loads
Chapter 3	Principles of Dynamic Analysis
Chapter 4	Reinforced Concrete Design
Chapter 5	Structural Steel Design
Chapter 6	Special Considerations in Explosive Facility Design

When applicable, illustrative examples are included in the Appendices.

Commonly accepted symbols are used as much as possible. However, protective design involves many different scientific and engineering fields, and, therefore, no attempt is made to standardize completely all the symbols used. Each symbol is defined where it is first used, and in the list of symbols at the end of each chapter.

CHAPTER CONTENTS

6-6. General

This chapter contains procedures for the design of blast resistant structures other than above ground, cast-in-place concrete or structural steel structures, as well as the design of other miscellaneous blast resistant components. Included herein is the design of reinforced and non-reinforced masonry walls, recast elements both prestressed and conventionally reinforced, pre-engineered buildings, suppressive shielding, blast resistant windows, underground structures, earth-covered arch-type magazines, blast valves and shock isolation systems.

MASONRY

6-7. Application

Masonry units are used primarily for wall construction. These units may be used for both exterior walls subjected to blast overpressures and interior walls subjected to inertial effects due to building motions. Basic variations in wall configurations may be related to the type of masonry unit such as brick, clay tile or solid and hollow concrete masonry units (CM), and the manner in which these units are laid (running bond, stack bond, etc.), the number of wythes of units (single or double), and the basic lateral load - carrying mechanism (reinforced or non-reinforced, one or two-way elements).

In addition to their inherent advantages with respect to fire protection, acoustical and thermal insulation, structural mass and resistance to flying debris, masonry walls when properly designed and detailed can provide economical resistance to relatively low blast pressures. However, the limitation on their application includes a limited capability for large deformations, reduced capacity in rebound due to tensile cracking in the primary phase of the response as well as the limitations on the amount and type of reinforcement which can be provided. Because of these limitations, masonry construction in this Manual is limited to concrete masonry unit (CM) walls placed in a running bond and with single or multiple wythes. However, because of the difficulty to achieve the required interaction between the individual wythes, the use of multiple wythes should be avoided.

Except for small structures (such as tool sheds, garage, etc.) where the floor area of the building is relatively small and interconnecting block walls can function as shear walls, masonry walls will usually require supplementary framing to transmit the lateral forces produced by the blast forces to the building foundation. Supplementary framing is generally classified into two categories (depending on the type of construction used); namely (1) flexible type supports such as structural steel framing, and (2) rigid supports including reinforced concrete frames or shear wall slab construction. The use of masonry walls in combination with structural steel frames is usually limited to incident over-pressures of 2 psi or less while masonry walls when supported by rigid supports may be designed to resist incident pressures as high as 10 psi. Figures 6-1 and 6-2 illustrate these masonry support systems.

Depending on the type of construction used, masonry walls may be classified into three categories: namely (1) cavity walls, (2) solid walls, and (3) a combination of cavity and solid walls. The cavity walls utilize hollow load - bearing concrete masonry units conforming to ASTM C90. Solid walls use solid load-bearing concrete masonry units conforming to ASTM C145 or hollow units whose cells and voids are filled with grout. The combined cavity and solid walls utilize the combination of hollow and solid units. Masonry walls may be subdivided further depending on the type of load-carrying mechanism desired: (1) joint reinforced masonry construction, (2) combined joint and cell reinforced masonry construction, and (3) non-reinforced masonry construction.

Joint reinforced masonry construction consists of single or multiple wythes walls and utilizes either hollow or solid masonry units. The joint reinforced wall construction utilizes commercially available cold drawn wire assemblies (see Figure 6-3), which are placed in the bed joints between the rows of the masonry units. Two types of reinforcement are available; truss and ladder

types. The truss reinforcement provides the more rigid system and, therefore, is recommended for use in blast resistance structures. In the event that double wythes are used, each wythe must be reinforced independently. The wythes must also be tied together using wire ties. Joint reinforced masonry construction is generally used in combination with flexible type supports. The cells of the units located at the wall supports must be filled with grout. Typical joint reinforced masonry construction is illustrated in Figure 6-4.

Combined joint and cell reinforcement masonry construction consists of single wythe walls which utilize both horizontal and vertical reinforcement. The horizontal reinforcement may consist either of the joint reinforcement previously discussed or reinforcing bars. Where reinforcing bars are used, special masonry units are used which permit the reinforcement to sit below the joint (Figure 6-5). The vertical reinforcement consists of reinforcing bars which are positioned in one or more of the masonry units cells. All cells, which contain reinforcing bars, must be filled with grout. Depending on the amount of reinforcement used, this type of construction may be used with either the flexible or rigid type support systems.

Non-reinforced masonry construction consists of single wythe of hollow or solid masonry units. This type of construction does not utilize reinforcement for strength but solely relies on the arching action of the masonry units formed by the wall deflection and support resistance (Figure 6-6). This form of construction is utilized with the rigid type support system and, in particular, the shear wall and slab construction system.

6-8. Design Criteria for Reinforced Masonry Walls

6-8.1. Static Capacity of Reinforced Masonry Units

Figure 6-7 illustrates typical shapes and sizes of concrete masonry units which are commercially available. Hollow masonry units shall conform to ASTM C90, Grade N. This grade is recommended for use in exterior below and above grade and for interior walls. The minimum dimensions of the components of hollow masonry units are given in Table 6-1.

The specific compressive strength (f'_m) for concrete masonry units may be taken as:

Type of Unit	Ultimate Strength (f'_m)
Hollow Units	1350 psi
Hollow Units filled with grout	1500 psi
Solid Units	1800 psi

while the modulus of elasticity (E_m) of masonry units is equal to:

$$E_m = 1000\ f'_m \qquad 6\text{-}1$$

The specific compressive strength and the modulus of elasticity of the mortar may be assumed to be equal to that of the unit.

Joint reinforcement shall conform to the requirements of ASTM A82 and, therefore, it will have a minimum ultimate (f_{un}) and yield (f_m) stresses equal to 80 ksi and 70 ksi respectively. Reinforcing bars shall conform to ASTM

A615 (Grade 60) and have minimum ultimate stress (f_{un}) of 90 ksi and minimum yield stress (f_m) of 60 ksi. The modulus of elasticity of the reinforcement is equal to 29,000,000 psi.

6-8.2 Dynamic Strength of Material

Since design for blast resistant structures is based on ultimate strength, the actual yield stresses of the material, rather than conventional design stresses or specific minimum yield stresses, are used for determining the plastic strengths of members. Further, under the rapid rates of straining that occur in structures loaded by blast forces, materials develop higher strengths than they do in the case of statically loaded members. In calculating the dynamic properties of concrete masonry construction it is recommended that the dynamic increase factor be applied to the static yield strengths of the various components as follows:

Concrete

Flexure	$1.19\ f'_m$
Shear	$1.00\ f'_m$
Compression	$1.12\ f'_m$

Reinforcement

Flexure	$1.17\ f_y$

6-8.3 Ultimate Strength of Reinforced Concrete Masonry Walls

The ultimate moment capacity of joint reinforced masonry construction may be conservatively estimated by utilizing the horizontal reinforcement only and neglecting the compressive strength afforded by the concrete. That is the reinforcement in one face will develop the tension forces while the steel in the opposite face resists the compression stresses. The ultimate moment relationship may be expressed for each horizontal joint of the wall as follows:

$$M_u = A_s f_{dy} d_c \qquad 6\text{-}2$$

where:

A_s = area of joint reinforcement at one face

f = dynamic yield strength of the joint reinforcement

d_c = distance between the centroids of the compression and tension reinforcement

M_u = ultimate moment capacity

On the contrary, the ultimate moment capacity of the cell reinforcement (vertical reinforcement) in a combined joint and cell reinforced masonry construction utilizes the concrete strength to resist the compression forces.

The method of calculating ultimate moment of the vertical reinforcement is the same as that presented in Chapter 4 of this manual which is similar to that presented in the American Concrete Institute Standard Building Code Requirements for Reinforced Concrete.

The ultimate shear stress in joint reinforced masonry walls is computed by the formula:

$$v_u = V_u / A_n \qquad 6\text{-}3$$

where:

v_u = unit shear stress

V_u = total applied design shear at $d_c/2$ from the support

A_n = net area of section

In all cases, joint reinforced masonry walls, which are designed to resist blast pressures, shall utilize shear reinforcement which shall be designed to carry the total shear stress. Shear reinforcement shall consist of; (1) bars or stirrups perpendicular to the longitudinal reinforcement, (2) longitudinal bars bent so that the axis or inclined portion of the bent bar makes an angle of 45 degrees or more with the axis of the longitudinal part of the bar; or (3) a combination of (1) and (2) above. The area of the shear reinforcement placed perpendicular to the flexural steel shall be computed by the formula:

$$A_v = \frac{v_u b s}{\phi f_m} \qquad 6\text{-}4$$

where:

A_v = area of shear reinforcement

b = unit width of wall

s = spacing between stirrups

f_m = yield stress of the shear reinforcement

ϕ = strength reduction factor equal to 0.85

When bent or inclined bars are used, the area of shear reinforcement shall be calculated using:

$$A_v = \frac{v_u\, bs}{\phi f_m\, (\sin \alpha + \cos \alpha)} \qquad 6\text{-}5$$

where:

α = angle between inclined stirrup and longitudinal axis of the member.

Shear reinforcement in walls shall be spaced so that every 45 degree line extending from mid depth ($d_c/2$) of a wall to the tension bars, crosses at least one line of shear reinforcement.

Cell reinforced masonry walls essentially consist of solid concrete elements. Therefore, the relationships, for reinforced concrete as presented in Chapter 4 of this manual may also be used to determine the ultimate shear stresses in cell reinforced masonry walls. Shear reinforcement for cell-reinforced walls may only be added to the horizontal joint similar to joint reinforced masonry walls.

6-8.4. Dynamic Analysis

The principles for dynamic analysis of the response of structural elements to blast loads are presented in Chapter 3 of this manual. These principles also apply to blast analyses of masonry walls. In order to perform these analyses, certain dynamic properties must be established as follows:

Load-mass factors, for masonry walls spanning in either one direction (joint reinforced masonry construction) or two directions (combined joint and cell reinforced masonry construction) are the same as those load-mass factors which are listed in Tables 3-12 and 3-13. The load-mass factors are applied to the actual mass of the wall. The weights of masonry wall can be determined based on the properties of hollow masonry units previously described and utilizing a concrete unit weight of 150 pounds per cubic foot. The values of the loadmass factors K_{LM}, will depend in part on the range of behavior of the wall; i.e., elastic, elasto-plastic, and plastic ranges. An average value of the elastic and elasto-plastic value of K_{LM} is used for the elasto-plastic range while an average value of the average K_{LM} for the elasto-plastic range and K_{LM} of the plastic range is used for the wall behavior in the plastic range.

The resistance-deflection function is illustrated in Figure 3-1. This figure illustrates the various ranges of behavior previously discussed and defines the relationship between the wall's resistances and deflections as well as presents the stiffness K in each range of behavior. It may be noted in Figure 3-1, that the elastic and elasto-plastic ranges of behavior have been idealized forming a bilinear (or trilinear) function. The equations for defining these functions are presented in Section 3-13.

The ultimate resistance r_u, of a wall varies; (1) as the distribution of the applied load, (2) geometry of the wall (length and width), (3) the amount and distribution of the reinforcement, and (4) the number and type of supports. The ultimate resistances of both one and two-way spanning walls are given in Section 3-9.

Recommended maximum deflection criteria for masonry walls subjected to blast loads is presented in Table 6-2. This table includes criteria for both reusable and non-reusable conditions as well as criteria for both one and two-way spanning walls.

When designing masonry walls for blast loads using response chart procedures of Chapter 3 the effective natural period of vibration is required. This effective period of vibration when related to the duration of the blast loading of given intensity and a given resistance of the masonry wall determines the maximum transient deflection X_m of the wall. The expression for the

natural period of vibration is presented in equation 3-60, where the effective unit mass m_e has been described previously and the equivalent unit stiffness K_E is obtained from the resistance-deflection function. The equivalent stiffness of one way beams is presented in Table 3-8. This table may be used for one way spanning walls except that a unit width shall be used. Methods for determining the stiffnesses and period of vibrations for two-way walls are presented in Sections 3-11 through 3-13. Determining the stiffness in the elastic and elasto-plastic range is complicated by the fact that the moment of inertia of the cross section along the masonry wall changes continually as cracking progresses, and further by the fact that the modulus of elasticity changes as the stress increases. It is recommended that computations for deflections and therefore, stiffnesses be based on average moments of inertia I_a as follows:

$$I_a = \frac{I_n + I_c}{2} \qquad 6\text{-}6$$

In Equation 6-6, I_n is the moment of inertia of the net section and I_c is the moment of inertia of the cracked section. For solid masonry units the value of I_n is replaced with the moment of inertia of the gross section. The values of I_n and I_g for hollow and solid masonry units used in joint reinforced masonry construction are listed in Table 6-3. The values of I_g for solid units may also be used for walls which utilize combined joint and cell masonry construction. The values of I_c for both hollow and solid masonry construction may be obtained using:

$$I_c = 0.005\ bd_c^3 \qquad 6\text{-}7$$

6-8.5. Rebound

Vibratory action of a masonry wall will result in negative deflections after the maximum positive deflection has been attained. This negative deflection is associated with negative forces which will require tension reinforcement to be positioned at the opposite side of the wall from the primary reinforcement. In addition, wall ties are required to assure that the wall is supported by the frame (Figure 6-8). The rebound forces are a function of the maximum resistance of the wall as well as the vibratory properties of the wall and the load duration. The maximum elastic rebound of a masonry wall may be obtained from Figure 3-268.

6-9. Non-Reinforced Masonry Walls

The resistance of non-reinforced masonry walls to lateral blast loads is a function of the wall deflection, mortar compression strength and the rigidity of the supports.

6-9.1. Rigid Supports

If the supports are completely rigid and the mortar's strength is known, a resistance function can be constructed in the following manner.

Both supports are assumed to be completely rigid and lateral motion of the top and bottom of the wall is prevented. An incompletely filled joint is assumed to exist at the top as shown in Figure 6-9a. Under the action of the blast

load the wall is assumed to crack at the center. Each half then rotates as a rigid body until the wall takes the position shown in Figure 6-9b. During the rotation the midpoint m has undergone a lateral motion X_c in which no resistance to motion will be developed in the wall, and the upper corner of the wall (point o) will be just touching the upper support. The magnitude of X_c can be found from the geometry of the wall in its deflected position:

$$\left[T - X_c\right]^2 = L^2 - \left[h/2 + (h' - h)/2\right]^2 \qquad 6\text{-}8$$

$$= L^2 - (h'/2)^2$$

where:

$$X_c = T - \left[L^2 - (h'/2)^2\right]^{1/2} \qquad 6\text{-}9$$

and

$$L = \left[(h/2)^2 + T^2\right]^{1/2} \qquad 6\text{-}10$$

All other symbols are shown in Figure 6-9.

For any further lateral motion of point m, compressive forces will occur at points m and o. These compressive forces form a couple that produces a resistance to the lateral load equal to:

$$r_u = 8M_u / h^2 \qquad 6\text{-}11$$

where all symbols have previously been defined. When point m deflects laterally to a line n-o (Figure 6-9c), the moment arm of the resisting couple will be reduced to zero and the wall will become unstable with no further resistance to deflection. In this position the diagonals o-m and m-n will be shortened by an amount:

$$L - h'/2 \qquad 6\text{-}12$$

The unit strain in the wall caused by the shortening will be:

$$\epsilon_m = (L - h'/2)/L \qquad 6\text{-}13$$

where:

ϵ_m = unit strain in the mortar

All the shortening is assumed to occur in the mortar joints and therefore:

$$f_m = E_n \epsilon_m \qquad 6\text{-}14$$

where:

E_n = modulus of elasticity of the mortar

f_m = compressive stress corresponding to the strain ϵ

In most cases f_m will be greater than the ultimate compressive strength of the mortar f'_m, and therefore cannot exist. Since for walls of normal height and thickness each half of the wall undergoes a small rotation to obtain the position shown in Figure 6-9c, the shortening of the diagonals o-m and m-n can be considered a linear function of the lateral displacement of point m. The deflection at maximum resistance X_1, at which a compressive stress f_m exists at points m, n and o can therefore be found from the following:

$$\frac{X_1 - X_c}{T - X_c} = \frac{f'_m}{f_m} = \frac{f'_m}{E_n \epsilon_m} \qquad 6\text{-}15a$$

or

$$X_1 = \frac{(T - X_c)\, f'_m}{(E_n \epsilon_m)} + X_c \qquad 6\text{-}15b$$

The resisting moment that is caused by a lateral deflection X_1 is found by assuming rectangular compression stress blocks to exist at the supports (points o and n) and at the center (point m) as shown in Figure 6-10a. The bearing width a is chosen so that the moment M_u is a maximum, that is, by differentiating M_u with respect to a and setting the derivative equal to zero, which for a solid masonry unit will result in:

$$a = 0.5\,(T - X_1) \qquad 6\text{-}16$$

and the corresponding ultimate moment and resistance (Figure 6-10b) are equal to:

$$M_u = 0.25\, f'_m \left[T - X_1\right]^2 \qquad 6\text{-}17$$

and

$$r_u = (2/h^2)\, f'_m \left[T - X_1\right]^2 \qquad 6\text{-}18$$

When the mid span deflection is greater than X_1 the expression for the resistance as a function of the displacement is:

$$r = (2/h^2) f'_m (T - X)^2 \qquad 6\text{-}19$$

As the deflection increases the resistance is reduced until r is equal to zero and maximum deflection X_m is reached (Figure 6-10b). Similar expressions can be derived for hollow masonry units. However, the maximum value of a can not exceed the thickness of the flange width.

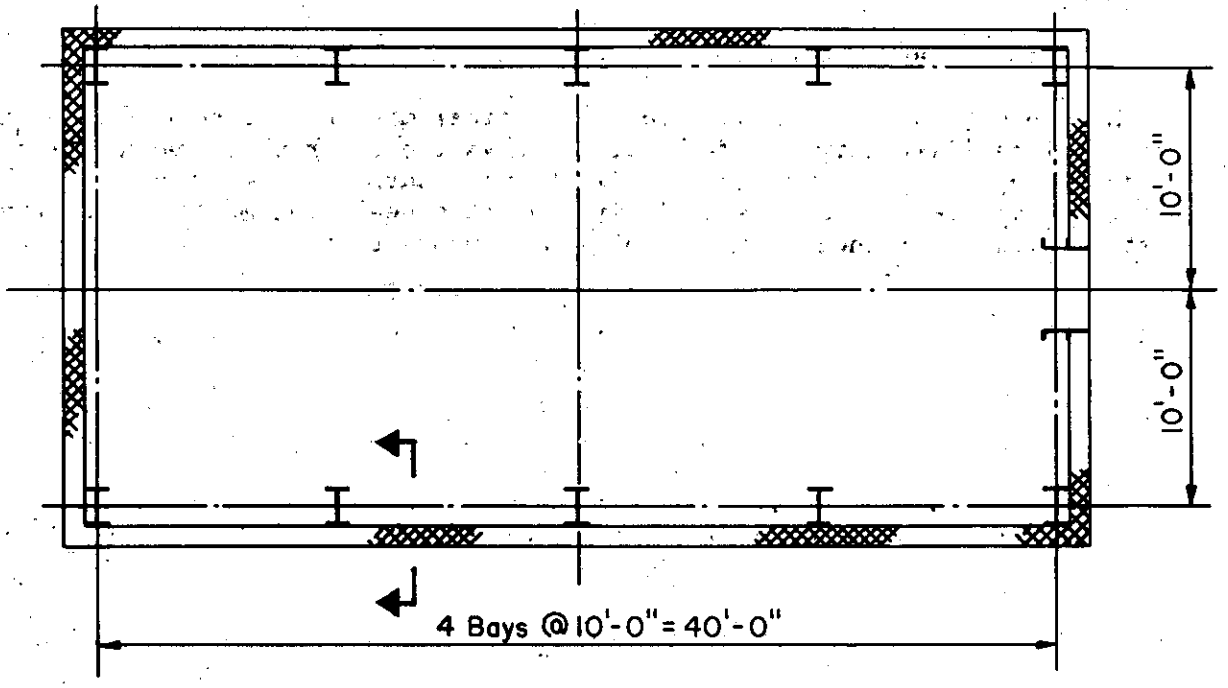
6-9.2. Non-rigid Supports

For the case where the wall is supported by elastic supports at the top and/or bottom, the resistance curve cannot be constructed based on the value of the compression force (af'_m) which is determined solely on geometry of the wall.

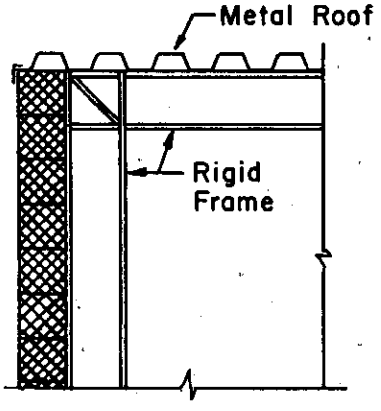
Instead the resistance curve is a function of the stiffness of the supports. Once the magnitude of the compression force is determined, equations similar to those derived for the case of the rigid supports can be used.

6-9.3. Simply Supported Walls

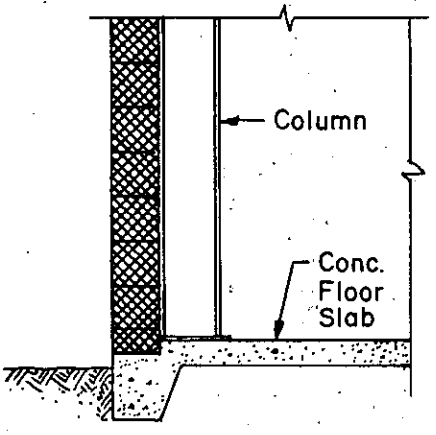
If the supports offer no resistance to vertical motion, the compression in the wall will be limited by the wall weight above the floor plus any roof load which may be carried by the wall. If the wall carries no vertical loads, then the wall must be analyzed as a simply supported beam, the maximum resisting moment being determined by the modulus of rupture of the mortar.



FLOOR PLAN

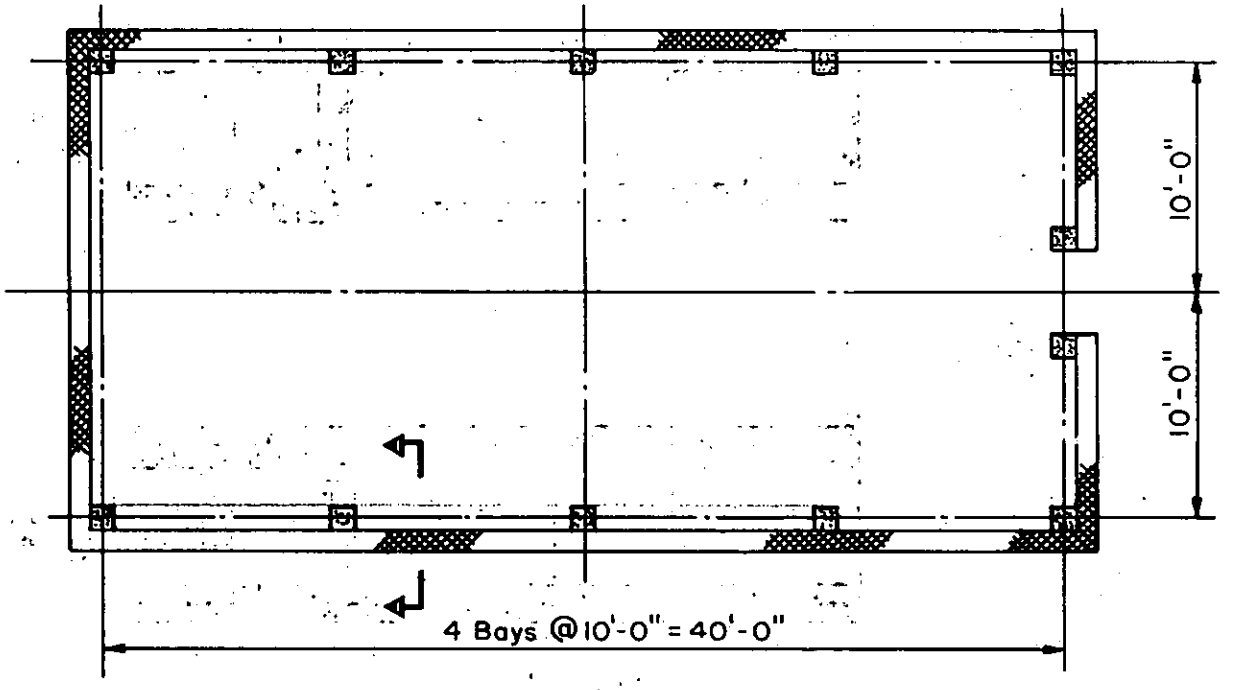


AT ROOF

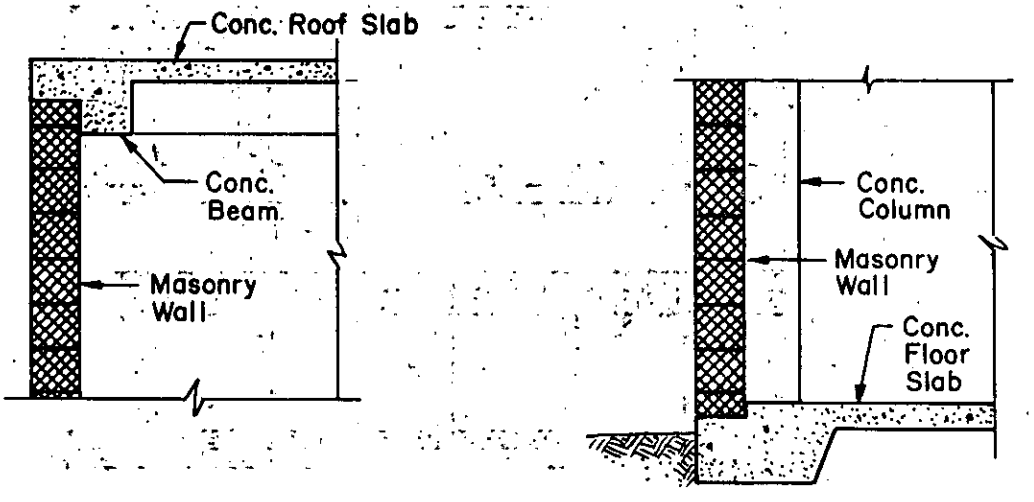


AT FLOOR

Figure 6-1 Masonry wall with flexible support



FLOOR PLAN



AT ROOF

AT FLOOR

Figure 6-2 Masonry wall with rigid support

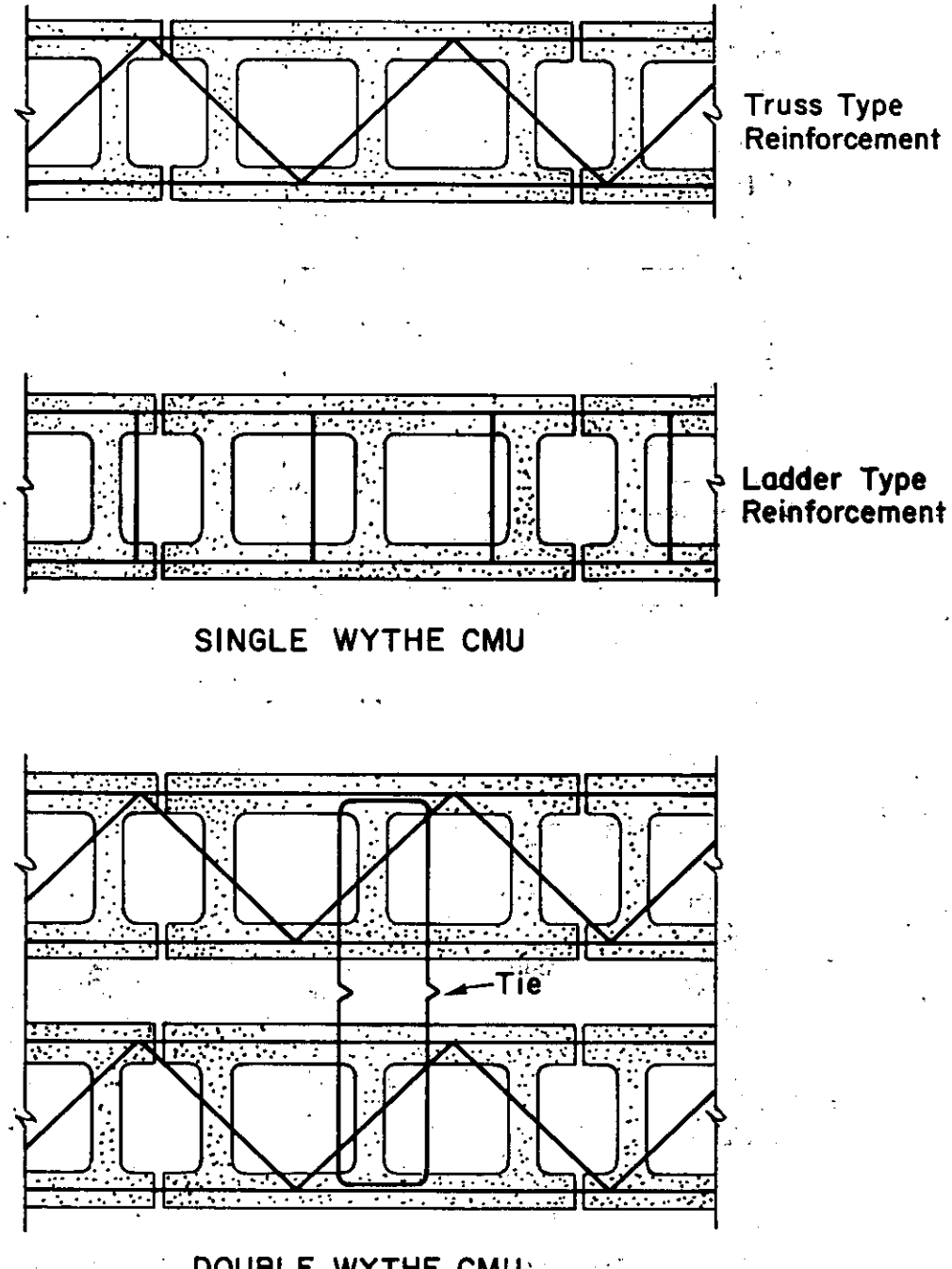
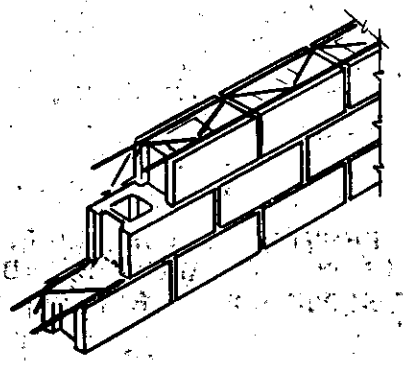
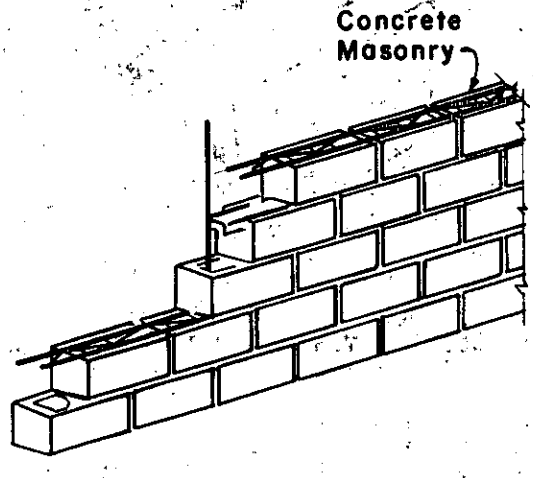


Figure 6-3 Concrete masonry walls



JOINT REINFORCED MASONRY CONSTRUCTION



COMBINED JOINT AND CELL REINFORCED
MASONRY CONSTRUCTION

Figure 6-4 Typical joint reinforced masonry construction

THE SPECIAL PROVISIONS FOR REINFORCEMENT PLACEMENT AS SHOWN, ARE AVAILABLE IN MANY OF THE BLOCK CONFIGURATIONS ILLUSTRATED IN FIG. 6-7.

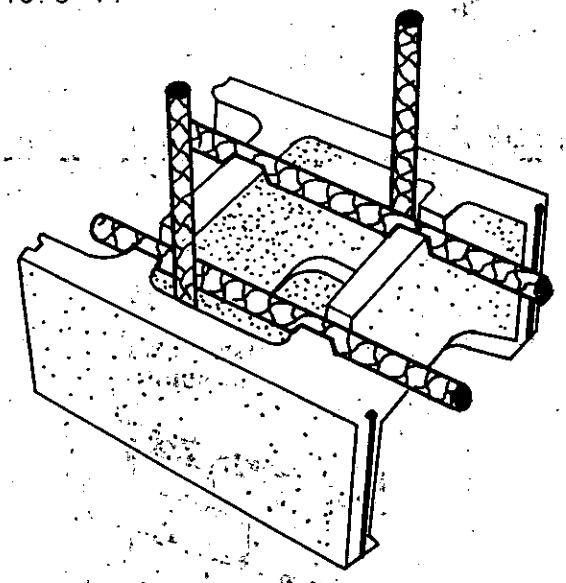


Figure 6-5 Special masonry unit for use with reinforcing bars

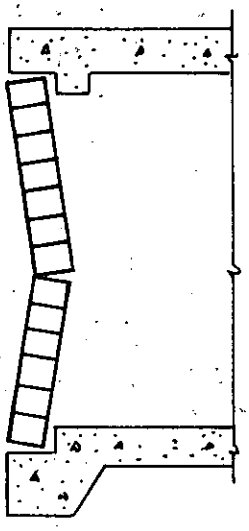


Figure 6-6 Arching action of non-reinforced masonry wall

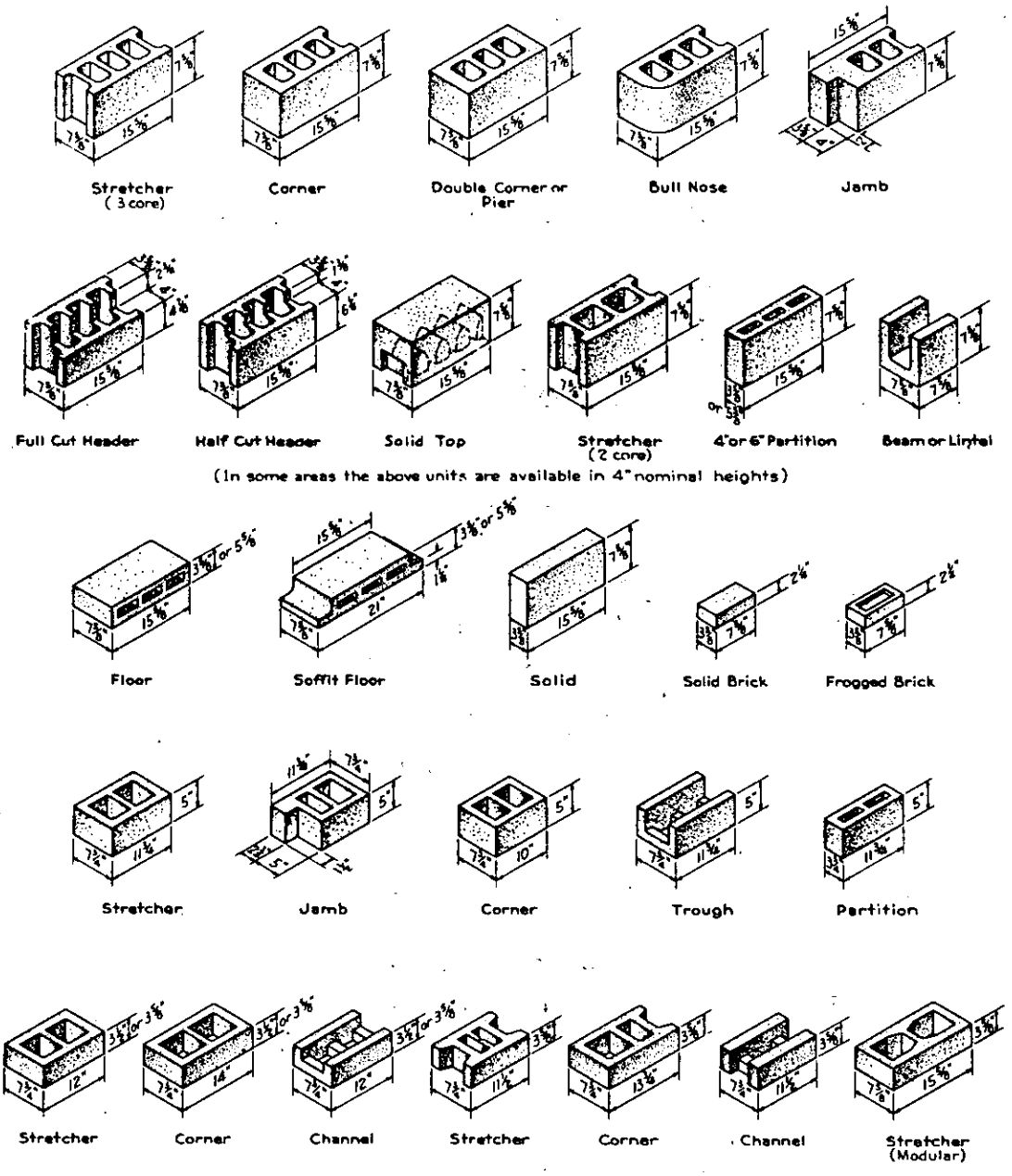
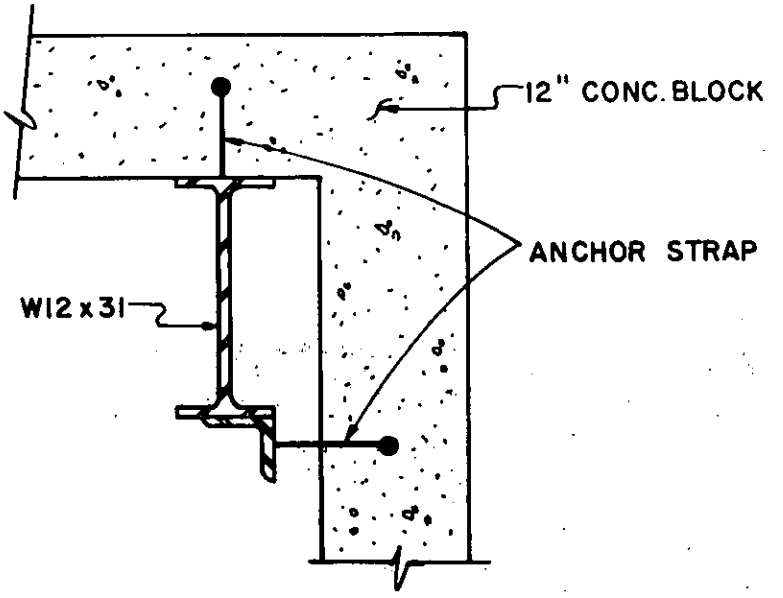
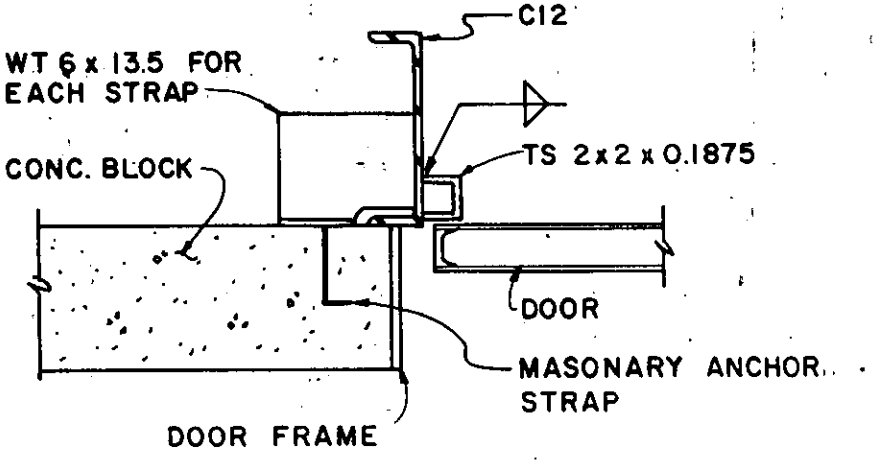


Figure 6-7 Typical concrete masonry units



(a) Masonry Anchor Straps at Corners



(b) Masonry Anchor Strap Detail at Door.

Figure 6-8 Connection details for rebound and/or negative overpressures

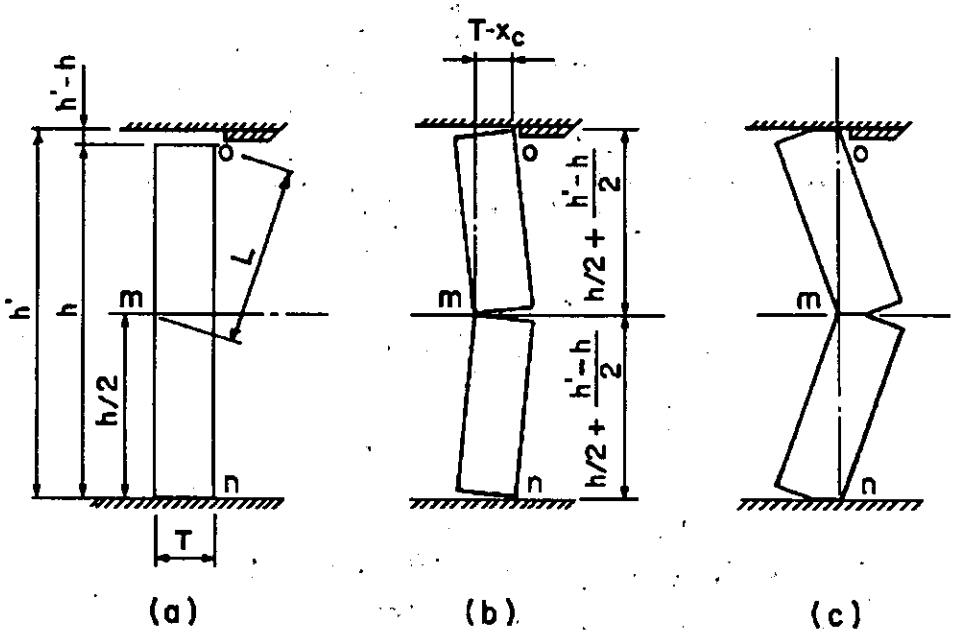
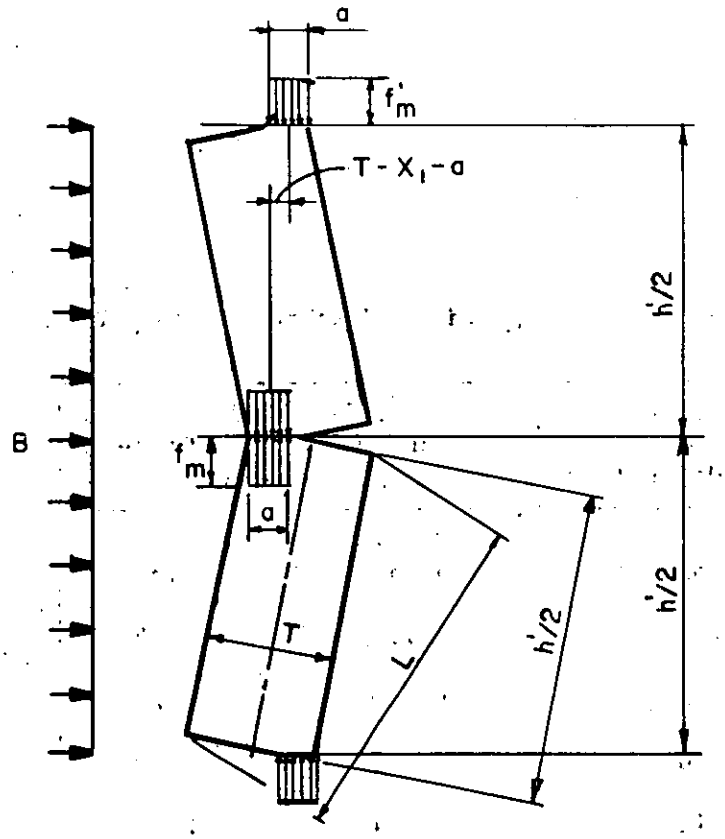
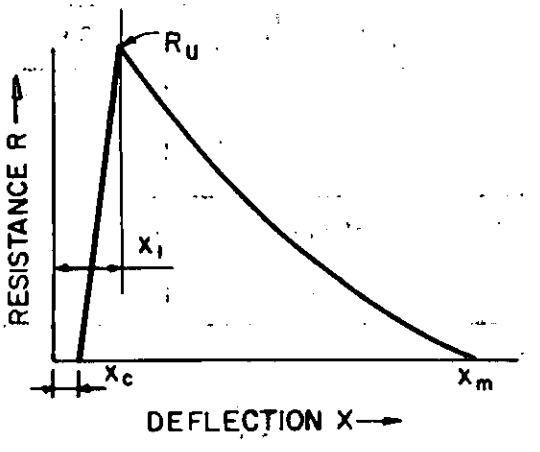


Figure 6-9 Deflection of non-reinforced masonry walls



(a)

ARCHING BEHAVIOR



(b)

RESISTANCE - DEFLECTION FUNCTION

Figure 6-10 Structural behavior of non-reinforced solid masonry panel with rigid supports

Table 6-1 Properties of Hollow Masonry Units

Nominal Width of Units (in)	Face-Shell Thickness (in)	Equiv. Web Thickness (in)
3 and 4	0.75	1.625
6	1.00	2.25
8	1.25	2.25
10	1.375	2.50
12	1.500	2.50

Table 6-2 Deflection Criteria for Masonry Walls

Wall Type	Support Type	Support Rotation
Reusable	One-way	0.5°
	Two-way	0.5°
Non-Reusable	One-way	1.0°
	Two-way	2.0°

Table 6-3 Moment of Inertia of Masonry Walls

Type of Unit	Width of Unit (in)	Moment of Inertia (in^4)/in
Hollow	3	2.0
	4	4.0
	6	12.7
	8	28.8
	10	51.6
	12	83.3
Solid	3	2.7
	4	5.3
	6	18.0
	8	42.7
	10	83.0
	12	144.0

PRECAST CONCRETE

6-10. Applications

Precast concrete construction can consist of either prestressed or conventionally reinforced members. Prestressing is advantageous in conventional construction, for members subjected to high flexural stresses such as long span or heavily loaded slabs and beams. Other advantages of precast concrete construction include: (1) completion time for precast construction will be significantly less than the required for cast-in-place concrete, (2) precast construction will provide protection against primary and secondary fragments not usually afforded by steel construction and (3) precast work is generally more economical than cast-in-place concrete construction especially when standard precast shapes can be used. The overriding disadvantage of precast construction is that the use of precast members is limited to buildings located at relatively low pressure levels of 1 to 2 psi. For slightly higher pressure levels, cast-in-place concrete or structural steel construction becomes the more economical means of construction. However, for even higher pressures, cast-in-place concrete is the only means available to economically withstand the applied load.

Precast structures are of the shear wall type, rigid frame structures being economically impractical (see the discussion of connections, Section 6-16 below). Conventionally designed precast structures may be multi-story, but for blast design it is recommended that they be limited to single story buildings. Some of the most common precast sections are shown in Figure 6-11. The single tee and double tee sections are used for wall panels and roof panels. All the other sections are beam and girder elements. In addition, a modified flat slab section will be used as a wall panel around door openings. All of the sections shown can be prestressed or conventionally reinforced. In general though, for blast design, beams and roof panels are prestressed, while columns and wall panels are not. For conventional design, prestressing wall panels and columns is advantageous in tall multi-story building, and thus of no benefit for blast resistant design which uses only single story buildings. In fact, in the design of a wall panel, the blast load is from the opposite direction of conventional loads and hence prestressing a wall panel decreases rather than increases the capacity of section.

6-11. Static Strength of Materials

6-11.1. Concrete

Generally the minimum compressive strength of the concrete, f_c, used in precast elements is 4000 to 5000 psi. High early-strength cement is usually used in prestressed elements to ensure adequate concrete strength is developed before the prestress is introduced.

6-11.2. Reinforcing Bars

Steel reinforcing bars are used for rebound and shear reinforcement in prestressed members as well as for flexural reinforcement in non-prestressed members. For use in blast design, bars designated by the American Society for Testing and Materials (ASTM) as A 615, grade 60, are recommended. As only small deflections are permitted in precast members, the reinforcement is not

stressed into its strain hardening region and thus the static design strength of the reinforcement is equal to its yield stress (f_m = 60,000 psi).

6-11.3. Welded Wire Fabric

Welded wire fabric, designated as A 185 by ASTM, is used to reinforce the flanges of tee and double tee sections. In conventional design welded wire fabric is sometimes used as shear reinforcement, but it is not used for blast design, which requires closed ties. The static design strength f_m, of welded wire fabric is equal to its yield stress, 65,000 psi.

6-11.4. Prestressing Tendons

There are several types of reinforcement that can be used in prestressing tendons. They are designated by ASTM as A 416, A 421 or A 722, with A 416, grade 250 or grade 270, being the most common. The high strength steel used in these types of reinforcement can only undergo a maximum elongation of 3.5 to 4 percent of the original length before the ultimate strength is reached. Furthermore, the high strength steel lacks a well defined yield point, but rather exhibits a slow continuous yielding with a curved stress-strain relationship until ultimate strength is developed (see Figure 6-12). ASTM specifies a fictitious yield stress f_{py}, corresponding to a 1 percent elongation. The minimum value of f_{py} depends on the ASTM designation, but it ranges from 80 to 90 percent of the ultimate strength, f_{pu}.

6-12. Dynamic Strength of Materials

Under the rapid rate of straining of blast loads, most materials develop higher strengths than they do when statically loaded. An exception, is the high strength steel used in prestressing tendons. Researchers have found that there was very little increase in the upper yield stress and ultimate tensile strengths of high strength steels under dynamic loading.

The dynamic design strength is obtained by multiplying the static design strength by the appropriate dynamic increase factor DIF, which is as follows:

(a)	Concrete:	Compression	DIF = 1.19
		Diagonal tension	DIF = 1.00
		Direct shear	DIF = 1.10
		Bond	DIF = 1.00
(b)	Non-prestressed Steel Reinforcement;		
		Flexure	DIF = 1.17
		Shear	DIF = 1.00
(c)	Welded Wire Fabric:		DIF = 1.10
(d)	Prestressed Reinforcement		DIF = 1.00

6-13. Ultimate Strength of Precast Elements

The ultimate strength of non-prestressed precast members is exactly the same as cast-in-place concrete members and as such is not repeated here. For the

ultimate strength of non-prestressed precast elements, see Chapter 4 of this manual.

6-13.1 Ultimate Dynamic Moment Capacity of Prestressed Beams

The ultimate dynamic moment capacity M_u of a prestressed rectangular beam (or of a flanged section where the thickness of the compression flange is greater than or equal to the depth of the equivalent rectangular stress block, a) is as follows:

$$M_u = A_{ps} f_{ps} (d_p - a/2) + A_s f_{dy} (d-a/2) \qquad 6\text{-}20$$

and

$$a = \frac{(A_{ps} f_{ps} + A_s f_{dy})}{.85 f'_{dc} b} \qquad 6\text{-}21$$

where:

M_u = ultimate moment capacity

A_{ps} = total area of prestress reinforcement

f_{ps} = average stress in the prestressed reinforcement at ultimate load

d_p = distance from extreme compression fiber to the centroid of the prestressed reinforcement

a = depth of equivalent rectangular stress block

A_s = total area of non-prestressed tension reinforcement

f_{dy} = dynamic design strength of non-prestressed reinforcement

d = distance from extreme compression fiber to the centroid of the non-prestressed reinforcement

f'_{dc} = dynamic compressive strength of concrete

b = width of the beam for a rectangular section or width of the compression flange for a flanged section

The average stress in the prestressed reinforcement at ultimate load f_{ps} must be determined from a trial-and-error stress-strain compatibility analysis. This may be tedious and difficult especially if the specific stress-strain curve of the steel being used is unavailable. In lieu of such a detailed analysis, the following equations may be used to obtain an appropriate value of f_{ps}:

For members with bonded prestressing tendons:

$$f_{ps} = f_{pu}\left[1 - \frac{\gamma_p}{\beta_1}\right]\left[p_p \frac{f_{pu}}{f'_{dc}} + \frac{df_{dy}}{d_p f'_{dc}}(p-p')\right] \qquad 6\text{-}22$$

and

$$p_p = A_{ps}/bd_p \qquad 6\text{-}23$$

$$p = A_s/bd \qquad 6\text{-}24$$

$$p' = A_s'/bd \qquad 6\text{-}25$$

where:

f_{pu} = specified tensile strength of prestressing tendon

γ_p = factor for type of prestressing tendon

= 0.40 for $f_{py}/f_{pu} \geq 0.80$

= 0.28 for $f_{py}/f_{pu} \geq 0.90$

f_{py} = "fictitious" yield stress of prestressing tendon corresponding to a 1 percent elongation

β_1 = 0.85 for f'_{dc} up to 4000 psi and is reduced 0.05 for each 1000 psi in excess of 4000 psi

p_p = prestressed reinforcement ratio

p = ratio of non-prestressed tension reinforcement

p' = ratio of compression reinforcement

A_s = total area of compression reinforcement

If any compression reinforcement is taken into account when calculating f_{ps} then the distance from the extreme compression fiber to the centroid of the compression reinforcement must be less than $0.15d_p$ and

$$p_p \frac{f_{pu}}{f'_{dc}} + \frac{df_{dy}}{d_p f'_{dc}}(p-p') \geq 0.17 \qquad 6\text{-}26$$

If there is no compression reinforcement and no non-prestressed tension reinforcement, Equation 6-22 becomes:

$$f_{ps} = f_{pu}\left[1 - \frac{\gamma_p}{\beta_1} p_p \frac{f_{pu}}{f'_{dc}}\right] \qquad 6\text{-}27$$

For members with unbonded prestressing tendons and a span-to-depth ratio less than or equal to 35:

$$f_{ps} = f_{se} + 10{,}000 + f'_{dc}/(100p_p) \leq f_{py} \qquad 6\text{-}28a$$

and

$$f_{ps} \leq f_{se} + 60{,}000 \qquad 6\text{-}28b$$

where:

f_{se} = effective stress in prestressed reinforcement after allowances for all prestress losses

For members with unbonded prestressing tendons and a span-to-depth ratio greater than 35:

$$f_{ps} = f_{se} + 10{,}000 + f'_{dc}/(300\ p_p) \leq f_{py} \qquad 6\text{-}29a$$

and

$$f_{ps} \leq f_{se} + 30{,}000 \qquad 6\text{-}29b$$

To insure against sudden compression failure the reinforcement ratios for a rectangular beam, or for a flanged section where the thickness of the compression flange is greater than or equal to the depth of the equivalent rectangular stress block will be such that:

$$\frac{p_p f_{ps}}{f'_{dc}} + \frac{df_{dy}}{d_p f'_{dc}}(p - p') \leq 0.36\beta_1 \qquad 6\text{-}30$$

When the thickness of the compression flange of a flanged section is less than the depth of the equivalent rectangular stress block, the reinforcement ratios will be such that

$$\frac{p_{pw}\ f_{ps}}{f'_{dc}} + \frac{df_{dy}}{d_p f'_{dc}}(p_w - p'_w) \leq 0.36\beta_1 \qquad 6\text{-}31$$

p_{pw}, p_w, p'_w = reinforcement ratios for flanged sections computed as for p_p, p and p' respectively except that b shall be the width of the web and the reinforcement area will be that required to develop the compressive strength of the web only.

6-13.2. Diagonal Tension and Direct Shear of Prestressed Elements

Under conventional service loads, prestressed elements remain almost entirely in compression, and hence are permitted a higher concrete shear stress than non-prestressed elements. However at ultimate loads the effect of prestress is lost and thus no increase in shear capacity is permitted. The shear capacity of a precast beam may be calculated using the equations of Chapter 4 of this manual. The loss of the effect of prestress also means that d is the actual distance to the prestressing tendon and is not limited to 0.8h as it is in the ACI code. It is obvious then that at the supports of an element with draped tendons, d and thus the shear capacity are greatly reduced. Draped tendons also make it difficult to properly anchor shear reinforcement at the supports, exactly where it is needed most. Thus it is recommended that only straight tendons be used for blast design.

6-14. Dynamic Analysis

The dynamic analysis of precast elements uses the procedures described in Chapter 3 of this manual.

Since precast elements are simply supported, the resistance-deflection curve is a one-step function (see Figure 3-39a). The ultimate unit resistance for various loading conditions is presented in Table 3-1. As precast structures are subject to low blast pressures, the dead load of the structures become significant, and must be taken into account.

The elastic stiffness of simply supported beams with various loading conditions is given in Table 3-7. In determining the stiffness, the effect of cracking is taken into account by using an average moment of inertia I_a, as follows:

$$I_a = (I_g + I_c)/2 \qquad 6\text{-}32$$

where:

I_g = moment of inertia of the gross section

I_c = moment of inertia of the cracked section

For non-prestressed elements, the cracked moment of inertia can be determined from Chapter 4. For prestressed elements the moment of inertia of the cracked section may be approximated by:

$$I_c = n\, A_{ps}\, d_p^2 \left[1 - (p_p)^{1/2} \right] \qquad 6\text{-}33$$

where n is the ratio of the modulus of elasticity of steel to concrete. The load-mass factors, used to convert the mass of the actual system to the equivalent mass, are given in Table 3-12 for prestressed elements the load-mass factor in the elastic range is used. An average of the elastic and plastic range load-mass factors is used in the design of non-prestressed elements.

The equivalent single-degree-of-freedom system is defined in terms of its ultimate resistance r_u, equivalent elastic deflection X_E, and natural period of vibration T_N. The dynamic load is defined by its peak pressure P and duration T. The figures given in Chapter 3 may be used to determine the response of an element in terms of its maximum deflection X_m, and the time to reach maximum deflection t_m.

Recommended maximum deflection criteria for precast elements is as follows:

(1) For prestressed flexural members:
$\theta_{max} \leq 2°$ or $\mu_{max} \leq 1$, whichever governs

(2) For non-prestressed flexural members
$\theta_{max} \leq 2°$ or $\mu_{max} \leq 3$, whichever governs

(3) For compression members
$\mu_{max} \leq 1.3$

where θ_{max} = maximum support ratio

μ_{max} = maximum ductility ratio

6-15. Rebound

Precast elements will vibrate under dynamic loads, causing negative deflections after the maximum deflection has been reached. The negative forces associated with these negative deflections may be predicted using Figure 3-268.

6-15.1. Non-prestressed elements

The design of non-prestressed precast elements for the effects of rebound is the same as for cast-in-place members. See Chapter 4 for a discussion of rebound effects in concrete elements.

6-15.2. Prestressed elements

In prestressed elements, non-prestressed reinforcement must be added to what is the compression zone during the loading phase to carry the tensile forces of the rebound phase. The rebound resistance will be determined from Figure 3-268, but in no case will it be less than one-half of the resistance available to resist the blast load.

The moment capacity of a precast element in rebound is as follows:

$$M_u^- = A_s^- f_{dy} (d^- - a^-/2) \qquad 6\text{-}34$$

where:

M_u^- = ultimate moment capacity in rebound

A_s^- = total area of rebound tension reinforcement

f_{dy} = dynamic design strength of reinforcement

d^- = distance from extreme compression fiber to the centroid of the rebound reinforcement

a^- = depth of the equivalent rectangular stress block

It is important to take into account the compression in the concrete due to prestressing and reduce the strength available for rebound. For a conservative design, it may be assumed that the compression in the concrete due to prestressing is the maximum permitted by the ACI code, i.e. $0.45\ f'_c$. Thus the concrete strength available for rebound is

$$0.85\ f'_{dc} - 0.45 f_c' = 0.85 f'_{dc} - 0.45 f'_{dc}/DIF = 0.47 f'_{dc} \qquad 6\text{-}35$$

A more detailed analysis may be performed to determine the actual concrete compression due to prestress. In either case the maximum amount of rebound reinforcement added will be

$$A_s^- \leq \left[\frac{(0.85 f'_{dc} - d_1)\beta}{f_{dy}}\right]\left[\frac{(87000 - nf)\ bd^-}{(87000 - nf + f_{dy})}\right] \qquad 6\text{-}36$$

where f is the compression in the concrete due to prestressing and all the other terms have been defined previously. If available concrete strength is assumed to be $0.47 f'_{dc}$, equation 6-36 becomes:

$$A_s^- \leq \frac{(0.47 f'_{dc}\beta_1)}{f_{dy}}\left[\frac{(87{,}000 - 0.378 n f'_{dc})\ bd^-}{(87000 - 0.378 n f'_{dc} + f_{dy})}\right] \qquad 6\text{-}37$$

6-16. Connections

6-16.1. General

One of the fundamental differences between a cast-in-place concrete structure and one consisting of precast elements is the nature of connections between members. For precast concrete structures, as in the case of steel structures, connections can be detailed to transmit gravity loads only, gravity and lateral loads, or moments in addition to these loads. In general though, connectors of precast members should be designed so that blast loads are transmitted to supporting members through simple beam action. Moment-resisting connections for blast resistant structures would have to be quite heavy and expensive because of the relatively large rotations, and hence induced stresses, permitted in blast design.

In the design of connections the capacity reduction factor ϕ, for shear and bearing stresses on concrete are as prescribed by ACI code, i.e. 0.85 and 0.7 respectively. No capacity reduction factor is used for moment calculations and no dynamic increase factors are used in determining the capacity of a connector. Capacity of the connection should be at least 10 percent greater than the reaction of the member being connected to account for the brittleness of the connection. In addition the failure mechanism should be controlled by tension or bending stress of the steel, and therefore the pullout strength of

the concrete and the strength of the welds should be greater than the steel strength.

The following connections are standard for use in blast design but they are not intended to exclude other connection details. Other details are possible but they must be able to transmit gravity and blast loads, rebound loads and lateral loads without inducing moments.

6-16.2. Column-to-Foundation Connection

The standard PCI column-to-foundation connection may be used for blast design without modification. However anchor bolts must be checked for tension due to rebound in order to prevent concrete pullout.

6-16.3. Roof Slab-to-Girder Connection

Figure 6-13 shows the connection detail of a roof panel (tee section) framing into a ledger beam. The bearing pads transmit gravity loads while preventing the formation of moment couples. The bent plate welded to the plate embedded in the flange of the tee transmits lateral loads but is soft enough to deform when the roof panel tries to rotate. The angle welded to the embedded plate in the web of the tee restricts the panel, through shear action, from lifting off the girder during the rebound loading. The effects of dimensional changes due to creep, shrinkage and relaxation of prestress should be considered in this type of connection.

6-16.4. Wall Panel-to-Roof Slab Connection

The basic concepts employed in the roof slab-to-girder connection apply to the wall panel-to-roof slab connection shown in Figure 6-14. The roof panel instead of bearing on the girder, bears on a corbel cast with the tee section. The angle that transmits lateral loads has been moved from the underside of the flange to the top of the flange to facilitate field welding.

6-16.5. Wall Panel-to-Foundation Connection

The wall panel In Figure 6-15 is attached to the foundation by means of angles welded to plates cast in both the wall panel and the foundation. It is essential to provide a method of attachment to the foundation that is capable of taking base shear in any direction, and also a method of levelling and aligning the wall panel. Non-shrinking grout is used to fill the gap between the panel and the foundation so as to transmit the loads to the foundation.

6-16.6. Panel Splice

Since precast structures are of the shear wall type, all horizontal blast loads are transferred by diaphragm action, through wall and roof slabs to the foundations. The typical panel splice shown in Figure 6-16 is used for transferring the horizontal loads between panels.

6-16.7. Reinforcement Around Door Openings

A standard double tee section cannot be used around a door opening. Instead a special panel must be fabricated to satisfy the requirements for the door

opening. The design of the reinforcement around the door opening and the door frame is discussed in Chapter 4.

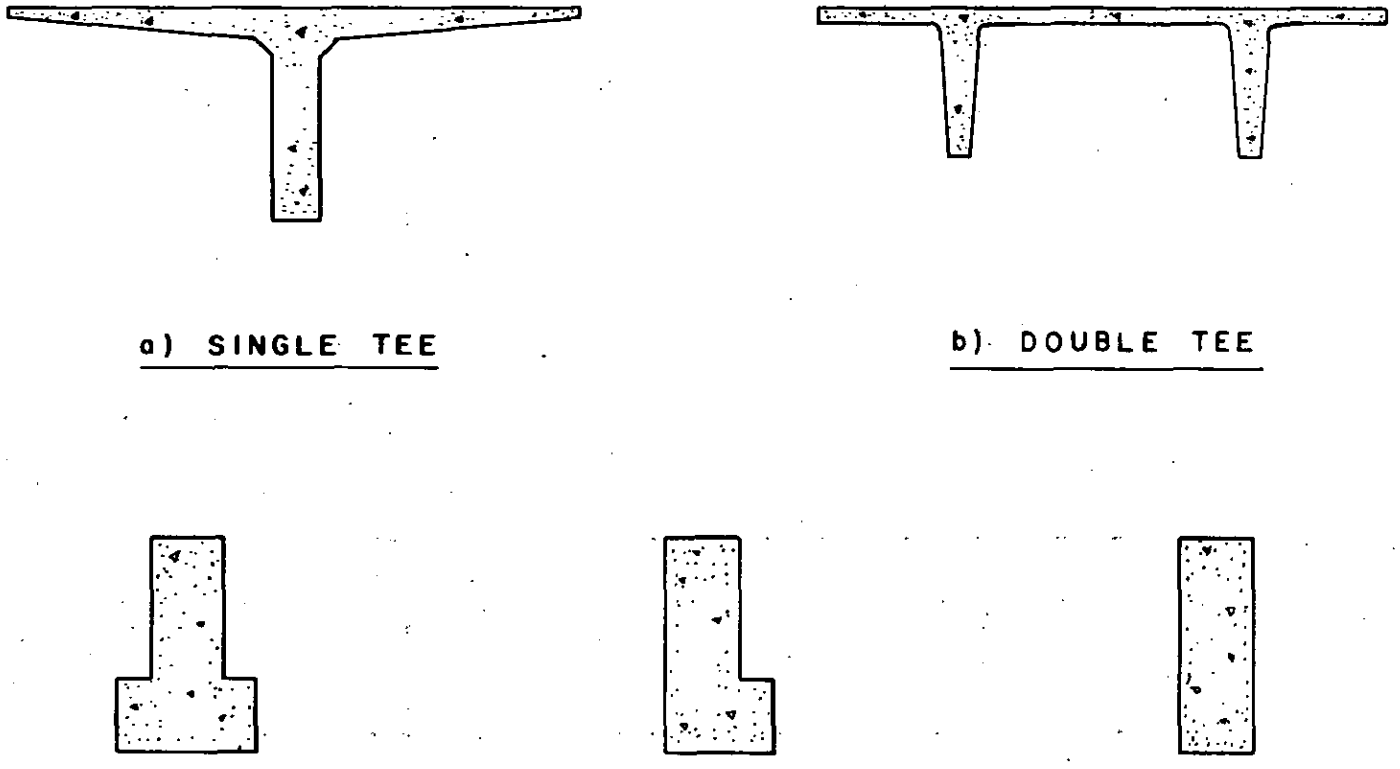


Figure 6-11 Common precast elements

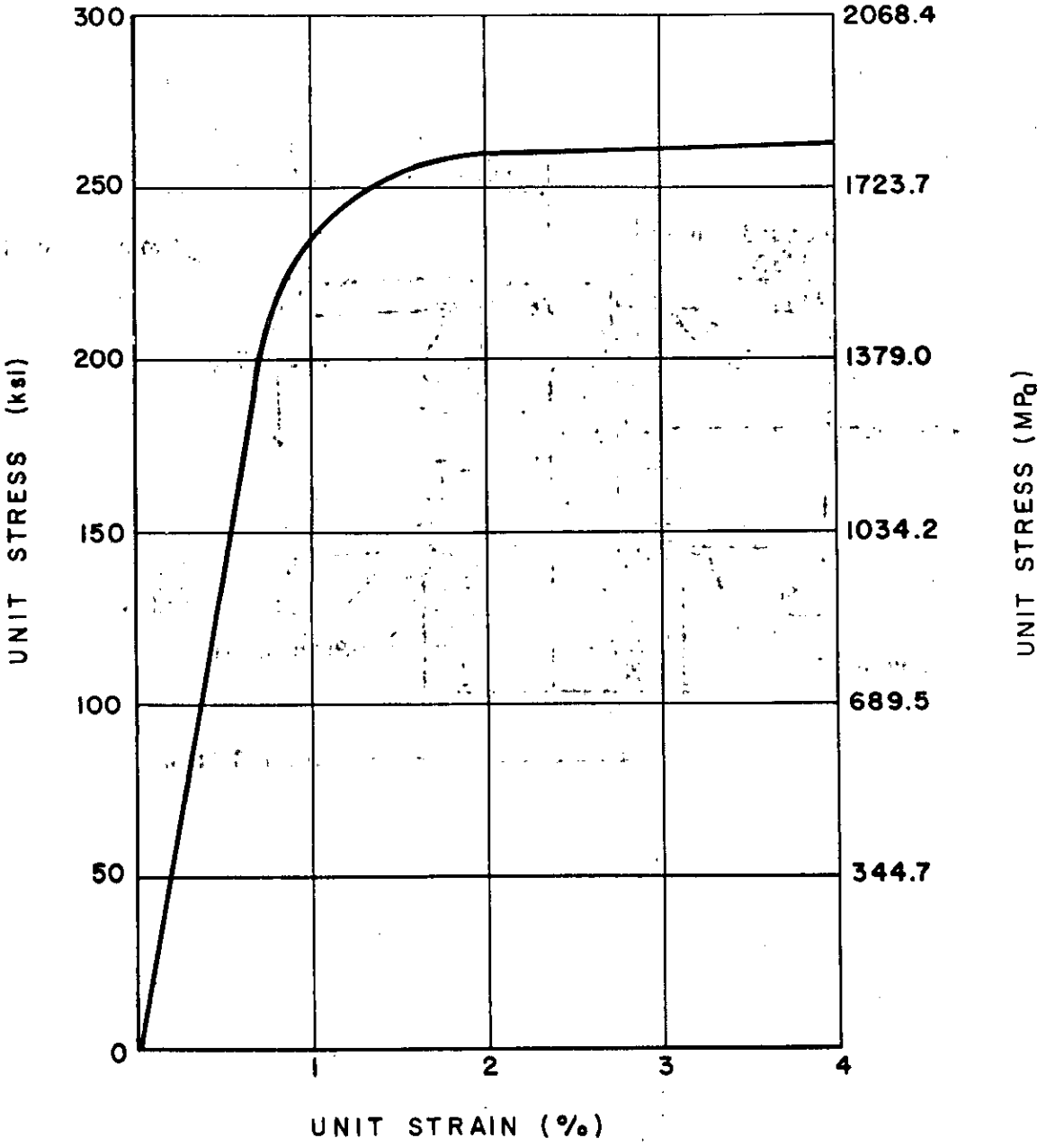


Figure 6-12 Typical stress-strain curve for high strength wire

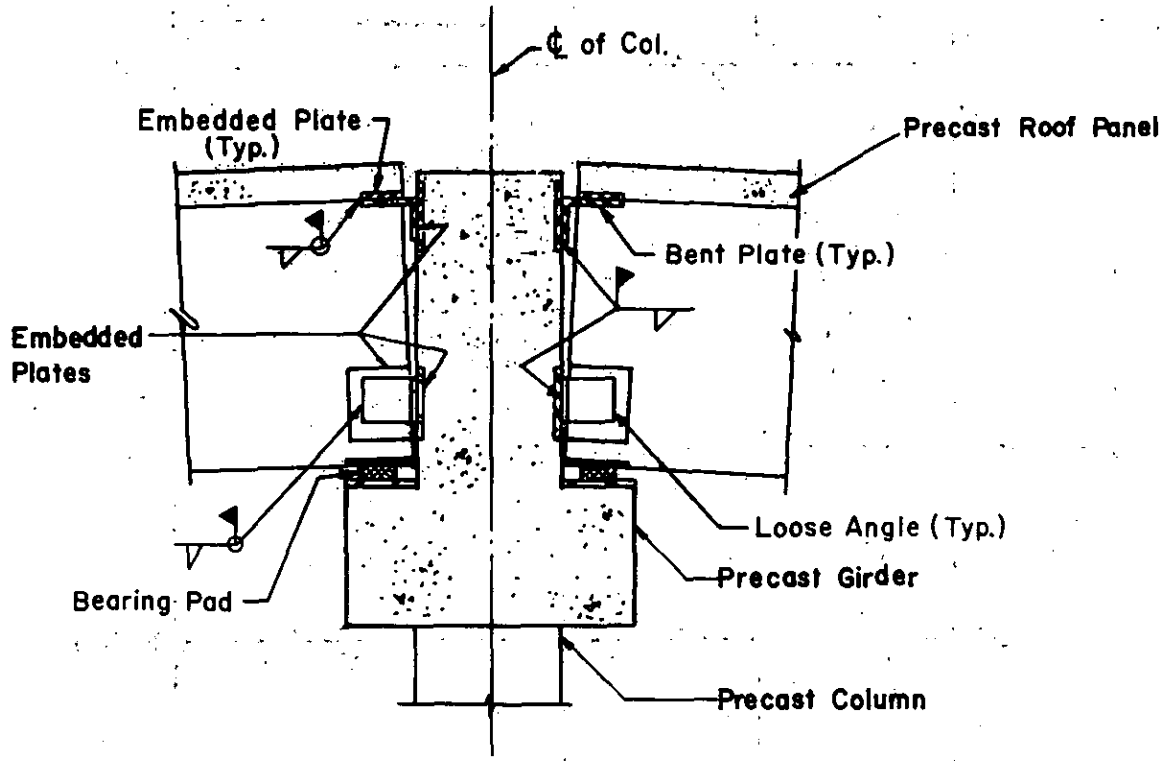


Figure 6-13 Roof slab-to-girder connection

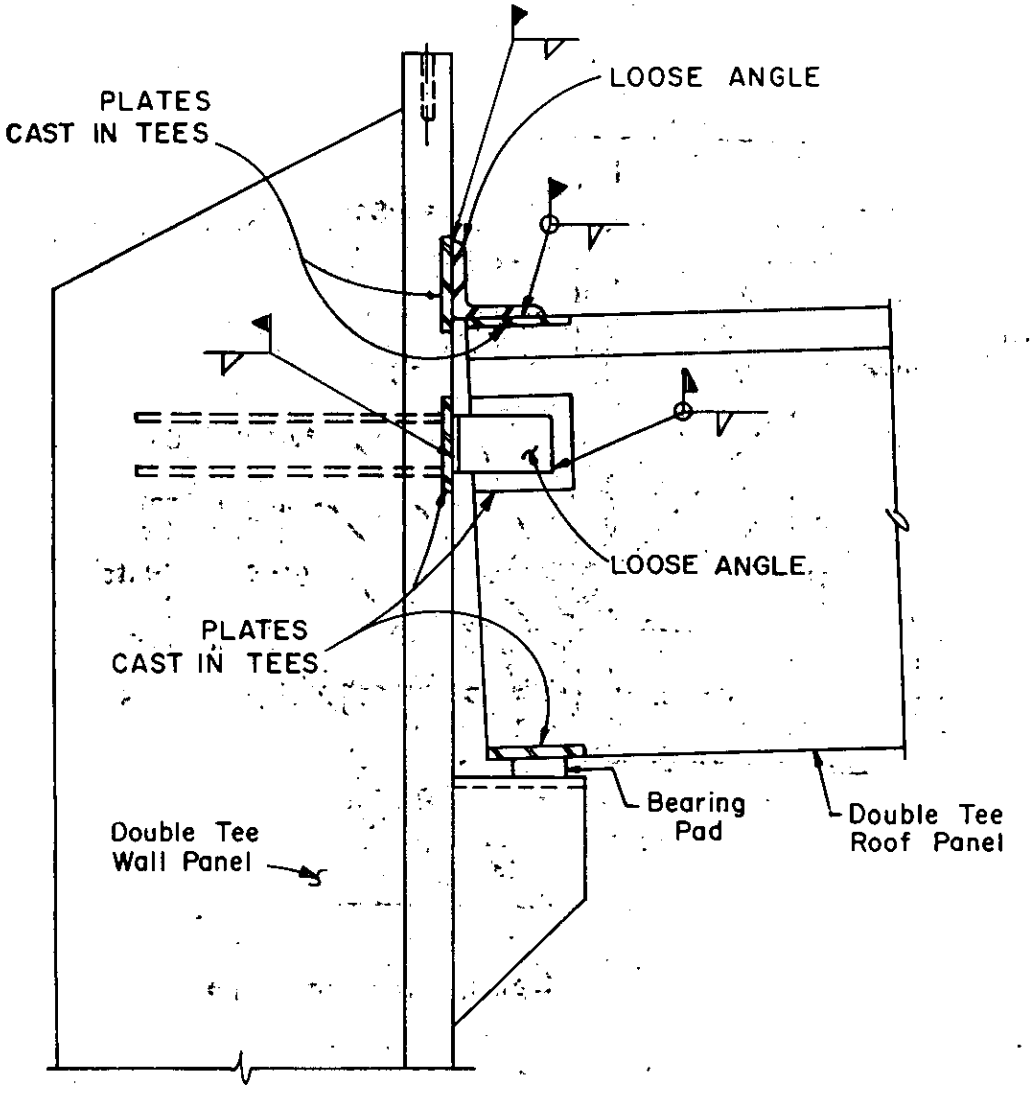


Figure 6-14 Typical wall panel-to-roof slab connection

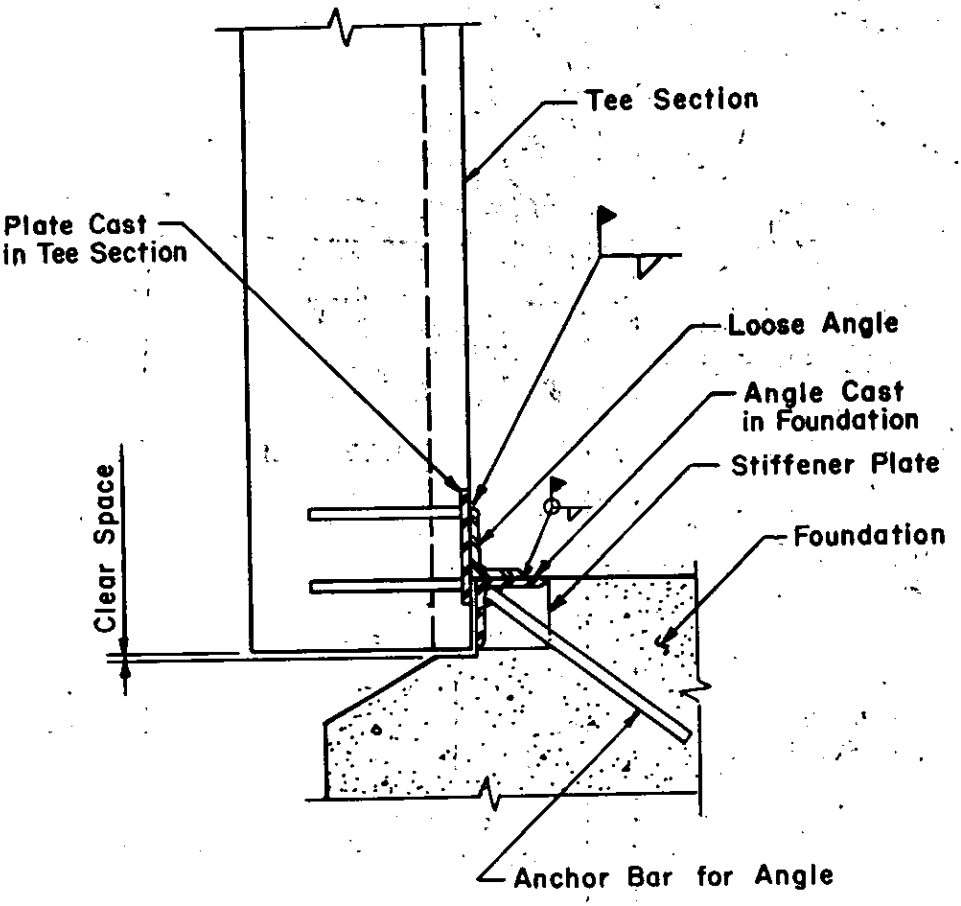


Figure 6-15 Wall panel-to-foundation connection

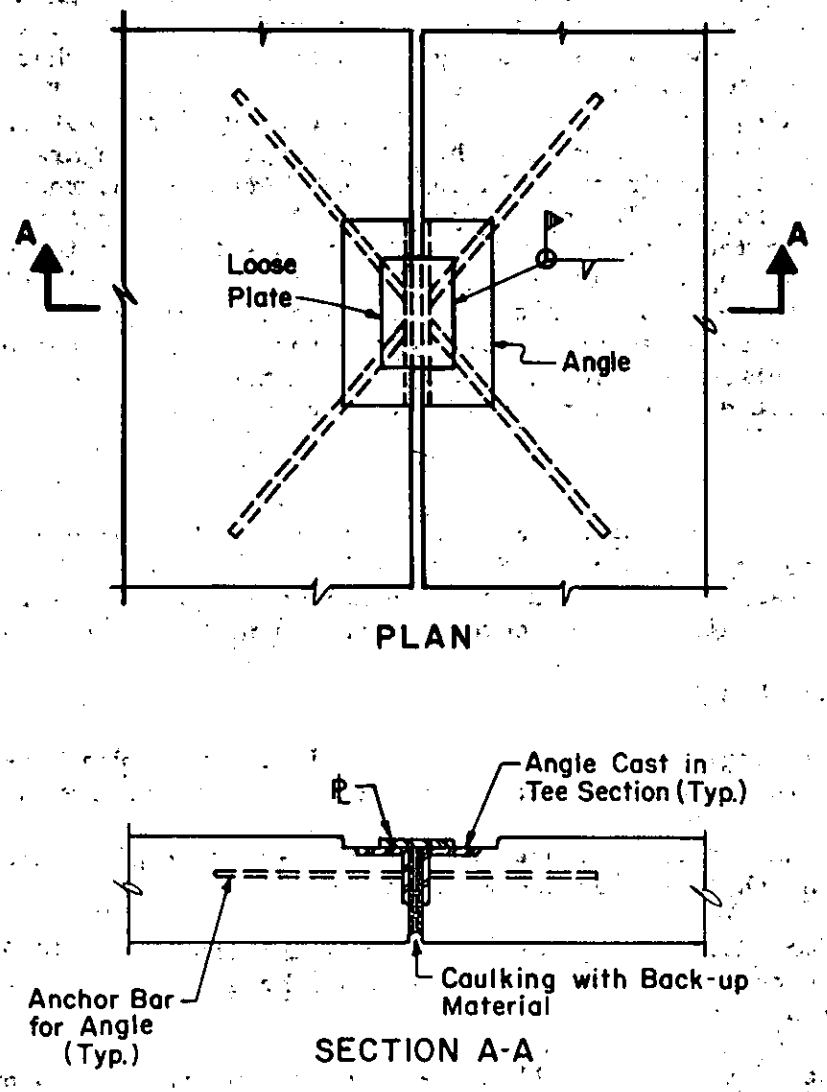


Figure 6-16 Typical panel splice

SPECIAL PROVISIONS FOR PRE-ENGINEERED BUILDING

6-17. General

Standard pre-engineered buildings are usually designed for conventional loads (live, snow, wind and/or seismic). Blast resistant pre-engineered buildings are also designed in the same manner as standard structures. However, the conventional loadings, which are used for the latter designs, are quite large to compensate for effects of blast loads. Further, as with standard buildings, pre-engineered structures, which are designed for blast, are designed elastically for the conventional loadings with the assumption that the structure will sustain plastic deformations due to the blast. The design approach will require a multi-stage process, including: preparation of general layouts and partial blast designs by the design engineer; preparation of the specifications, by the engineer including certain features as recommended herein; design of the building and preparation of shop drawings by the pre-engineered building manufacturers; and the final blast evaluation of the structure by design engineer utilizing the layouts on the previously mentioned shop drawings. At the completion of the analysis some slight modifications in building design may be necessary. However, if the following procedures are used, then the required modifications will be limited and in some cases eliminated for blast overpressures upward to 2 psi.

6-18. General Layout

The general layout of pre-engineered buildings is based on both operational and blast resistant requirements. Figure 6-17 illustrates a typical general layout of the pre-engineered building. The general requirements for structural steel, concrete, wall and roof coverings and connections are given below.

6-18.1. Structural Steel

In order for a pre-engineered building to sustain the required blast loading, structural steel layout must conform to the following requirements:

1. The maximum spacing between main transverse rigid frames (bay width) shall not exceed 20 feet.

2. The maximum spacing between column supports for rigid frames shall not exceed 20 feet while the overall height of frames shall be 30 feet or less.

3. Slope of the roof shall not exceed four horizontal to one vertical. However, the roof slope shall be as shallow as physically possible and be in compliance with the requirements of the Metal Building Manufacturers' Association.

4. Spacing between girts shall not exceed 4 feet while the space between purlins shall not be greater than 5 feet.

5. Primary members, including frames and other main load carrying members, shall consist of hot rolled structural steel shapes. The shapes must be doubly-symmetrical and have a constant depth. They may be wide-flange sections, I-sections, structural tubes, or

welded shapes built-up from hot rolled steel sheet, strips or plates. Secondary structural framing, such as girts, roof purlins, bridging, eave struts and other miscellaneous secondary framing, may consist of either hot rolled or cold-formed structural steel. All main secondary members (purlins, girts, etc.) shall be doubly-symmetrical sections of constant depth (e.g. wide flange, "I"-shaped, structural tubing).

6. Primary structural framing connections shall be either shop welded or bolted or field bolted assemblies. ASTM A 325 bolts with appropriate nuts and washers shall be used for connecting of all primary members; where as secondary members may use bolts conforming to ASTM A 307. A minimum of two bolts shall be used for each connection while bolts for primary and secondary members shall not be less than 3/4 and 1/2-inch in diameter, respectively.

7. Base plates for columns shall be rolled and set on grout bed of 1-inch minimum thickness. ASTM A 307 steel bolts shall be used to anchor all columns.

6-18.2. Foundations

Concrete floor and foundation slabs shall be monolithic in construction and shall be designed to transfer all horizontal and vertical loads from the pre-engineered superstructure to the foundation soil. Minimum slab thickness shall be 6 inches with edge beams thickened to meet local frost conditions.

6-18.3. Roof and Walls

Roof and wall coverings must meet the following requirements:

1. Roof and wall coverings shall conform to ASTM A 446, G 90, have a minimum depth of 1-1/2 inches corrugation and have a material thickness of 22 gauge.

2. Conventional side laps are not usually sufficient to resist the effects of blast loads. The construction details required to strengthen those joints depend upon the type of decking employed. Chapter 5 gives the required panel-to-panel attachments for various types of decking.

3. Insulation retainers or sub girts shall be designed to transmit all external loads (listed below) which act on the metal cover to the structural steel framing.

4. Roof and wall liners shall be a minimum of 24 gauge and shall be formed to prevent waviness, distortion or failure as a result of the impact by external loads.

6-18.4. Connections for Roof and Wall Coverings

The connections used in a blast resistant structure are especially critical. To ensure full development of structural steel and the roof and wall panels, connections must meet the following criteria:

1. Fasteners for connecting roof and wall coverings to structural steel supports shall be designed to support the external loads (listed below) and shall consist of either self-tapping screws, self-drilling and self-tapping screws, bolts and nuts, self-locking rivets, self-locking bolts, end welded studs, or welds. Fasteners of covering to structural steel shall be located at valleys of the covering and shall have a minimum of one fastener per valley.

2. Fasteners which do not provide positive locking such as self-tapping screws, etc. shall not be used at side laps and for fastening accessories to panels. At least one fastener for side laps shall be located in each valley and at a maximum spacing along the valley of 8 inches.

3. Self tapping screws shall not have a diameter smaller than a no. 14 screw while the minimum diameter of a self-drilling and self-tapping type shall be equal to or greater than a no. 12 screw. Automatic welded studs shall be shouldered type and have a shank diameter of at least 3/16 inch. Fasteners for use with power actuated tools shall have a shank diameter of not less than 1/2 inch. Blind rivets shall be stainless steel type and have a minimum diameter of 1/8 inch. Rivets shall be threaded stem type if used for other than fastening trim and if of the hollow type shall have closed ends. Bolts shall not be less than 1/4 inch in diameter and will be provided with suitable nuts and washers.

   If suction and/or rebound loads dictate, provide oversized washers with a maximum outside diameter of 2 inches or a 22 gauge thick metal strip along each valley.

6-19. Preparation of Partial Blast Analysis

A partial blast analysis of a pre-engineered building shall be performed by the design engineer. This analysis shall include the determination of the minimum size of the roof and wall panels which is included in the design specifications and the design of the building foundation and floor slab. The foundation and floor slab shall be designed monolithically and have a minimum thickness as previously stated. The slab shall be designed for a foundation load equal to either 1.3 times the yield capacity of the building roof equivalent blast load or the static roof and floor loads listed below. Quite often the foundation below the building columns must be thickened to distribute the column loads. For the blast analysis of the building foundation and floor slab, the dynamic capacity of the soil below the foundation slab can conservatively be assumed to be equal to twice the static soil capacity. The resistance of the roof of the building can be determined in accordance with the procedures given in Chapter 5. The front panel of the building is designed in the same manner as the roof panel. The blast loads for determining the capacities of the roof and wall panels can be determined from Chapter 2.

6-20. Pre-Engineered Building Design

Design of the pre-engineered building shall be performed by the pre-engineered building manufacturer using static loads and conventional stresses.

Conventional stresses are listed in "Specification for the Design, Fabrication and Erection of Structural Steel for Buildings with Commentary". Static design loads shall be as follows:

1. Floor live loads shall be as specified in the report titled "American National Standard Building Code Requirements for Minimum Design Loads in Buildings and Other Structures" (hereafter referred to as ANSI) but not less than 150 pounds per square foot.

2. Roof live loads shall be as specified ANSI.

3. Dead loads are based on the materials of construction.

4. Wind pressure shall be as computed in accordance with ANSI for exposure "C" and a wind speed of 100 miles per hour.

5. Seismic loads will be calculated according to the Uniform Building Code for the given area. If this load is greater than the computed wind pressure, than the seismic load will be substituted for wind load in all load combinations.

6. Auxiliary and collateral loads are all design loads not listed above and include suspended ceilings, insulation, electrical systems, mechanical systems, etc.

Combinations of design loads shall include the following (a) dead loads plus live loads; (b) dead loads plus wind loads, and (c) 75 percent of the sum of dead, live and wind loads.

6-21. Blast Evaluation of the Structure

Blast evaluation of the structure utilizing the shop drawings prepared in connection with the above design shall be performed by the design engineer. A dynamic analysis which describes the magnitude and direction of the elasto-plastic stresses developed in the main frames and secondary members as a result of the blast loads, shall be performed using the methods described in Chapter 5. This evaluation should be made at the time of the shop drawing review stage.

6-22. Recommended Specification for Pre-Engineered Buildings

Specifications for pre-engineered buildings shall be consistent with the recommended design changes set forth in the preceding Section. These example specifications are presented using the Construction Specification Institute (CSI) format and shall contain as a minimum the following:

1. APPLICABLE PUBLICATIONS. The following publications of the issues listed below, but referred to thereafter by basic designation only, form a part of this specification to the extent indicated by the reference thereto:

1.1 American Society of Testing and Materials (ASTM)

A 36 Structural Steel

A 307-80 Standard Specification for Carbon Steel Externally and Internally Threaded Standard Fasteners

A 325 Standard Specification for High Strength Bolts for Structural Steel Joint Including Suitable Nuts and Plain Hardened Washers

A 446 Specification for Steel Sheet, Zinc Coated (Galvanized) by the Hot-Dip Process, Physical (Structural) Quantity

A 501 Standard Specification for Hot-Formed Welded and Seamless Carbon Steel Structural Tubing

A 529 Standard Specification for Structural Steel with 42,000 psi Minimum Yield Point

A 570 Standard Specification for Hot-Rolled Carbon Steel Sheet and Strip, Structural Quality

A 572 Specification of High-Strength Low-Allow Columbium-Vanadium Steels of Structural Quality

1.2 American Iron and Steel Institute (AISI)

Specification for the Design of Cold-Formed Steel Structural Members and Commentary

1.3 American National Standards Institute (ANSI)

A58.1 Minimum Design Loads for Buildings and Other Structures

B18.22.1 Plain Washers

1.4 American Institute of Steel Construction (AISC)

Specification for the Design Fabrication and Erection of Structural Steel for Buildings with Commentary Research Council on Riveted and Bolted Structural Joints (RCRBSJ) Specification for Structural Joints Using ASTM A 325 or A 490 Bolts

1.5 American Welding Society (AWS)

D1.1 Structural Welding Code

1.6 Metal Building Manufacturers' Association (MBMA)

Metal Buildings Systems Manual

1.7 Uniform Building Code

2. GENERAL.

2.1 This section covers the manufacture and erection of pre-engineered metal structures. The structure manufacturer shall be regularly engaged in the fabrication of metal structures.

2.2 The structure shall include the rigid framing, which are spaced at a maximum of 20 feet on center, roof and wall covering, trim, closures, and accessories as indicated on the drawings. Minor alterations in dimensions shown on the drawings will be considered in order to comply with the manufacturer's standards building system, provided that all minimum clearances indicated on the drawings are maintained. Such changes shall be submitted for review and acceptance prior to fabrication.

2.3 Drawings shall indicate extent and general assembly details of the metal roofing and sidings. Members and connections not indicated on the drawings shall be designed by the Contractor in accordance with the manufacturer's standard details. The Contractor shall comply with the dimensions, profile limitations, gauges and fabrication details shown on the drawings. Modification of details will be permitted only when approved by the Owner. Should the modifications proposed by the Contractor be accepted by the Owner, the Contractor shall be fully responsible for any re-design and re-detailing of the building construction effected.

3. DEFINITIONS.

3.1 Low Rigid Frame. The building shall be single gable type with the roof slope not to exceed one on four.

3.2 Framing.

3.2.1 Primary Structural Framing. The primary structural framing includes the main transverse frames and other primary load carrying members and their fasteners.

3.2.2 Secondary Structural Framing. The secondary structural framing includes the girts, roof purlins, bridging, eave struts, and other miscellaneous secondary framing members and their fasteners.

3.2.3 Roof and Wall Covering. The roof and wall covering includes the exterior ribbed metal panel having a minimum depth of one and one-half inches, neoprene closure, fasteners and sealant.

3.3 Building Geometry.

3.3.1 Roof Slope. The roof of the building shall have a maximum slope not to exceed one on four.

3.3.2 Bay Spacing. The bay spacing shall not exceed 20 feet.

3.4 Column Shape. Main frame columns shall be doubly symmetrical members of constant depth; tapered columns will not be permitted.

3.5 Calculations. The Contractor shall submit for review complete design calculations for all work, sealed by a registered professional engineer.

4. STRUCTURAL DESIGN.

4.1 Structural Analysis. The structural analysis of the primary and secondary framing and covering shall be based on linear elastic behavior and shall accurately reflect the final configuration of the structure and all tributary design loadings.

4.2 Basic Design Loads.

4.2.1 Roof Live Load. Shall be applied to the horizontal roof projection. Roof live loads shall be:

0 to 200 square feet tributary area - 20 psf

200 to 600 square feet tributary area - linear variation 20 psf to 12 psf

over 600 square feet tributary area - 12 psf

4.2.2 Wind Pressure. Wind design loads shall be computed in accordance with ANSI A58.1 for exposure "C" and a basic wind speed of 100 miles per hour.

4.2.2.1 Typical Wind Loading. As shown on drawings (Figure 6-18).

4.2.2.2 Wind Loading at Building Corners. As shown on the drawings (Figure 6-18).

4.2.2.3 Wind Loading on Girts. As shown on drawings (Figure 6-18).

4.2.2.4 Wind Loading on Purlins and Roof Tributary Areas. As shown on drawings (Figure 6-18).

4.2.2.5 Wind Loading for Design of Overall Structure. As shown on drawings (Figure 6-18).

4.2.3 Auxiliary and Collateral Design Loads. Auxiliary and collateral design loads are those loads other than the basic design live, dead, and wind loads; which the building shall safely withstand, such as ceilings, insulation, electrical, mechanical, and plumbing systems, and building equipment and supports.

4.3 Application of Design Loads.

4.3.1 Roof Live Load and Dead Load. The roof live load (L), and dead load (D), shall be considered as a uniformly distributed loading acting vertically on the horizontal projection of the roof.

4.3.2 Snow Loads. application of 30 psf due to snow loads.

4.3.3 Wind Loads (W). Application of forces due to wind shall conform to the latest ANSI A58.1

4.3.4 Combination of Loads. The following combinations of loads shall be considered in the design of all members of the structure:

D + L
D + W
.75 (D + L + W)

4.4 Deflection Limitations.

4.4.1 Structural Framing. The primary and secondary framing members shall be so proportioned that their maximum calculated roof live load deflection does not exceed 1/120 of the span;

5. STRUCTURAL FRAMING.

5.1 General

5.1.1 All hot rolled structural shapes and structural tubing shall have a minimum yield point of 36,000 psi in conformance with ASTM A 36 or A 501. All hot rolled steel plate, strip and sheet used in the fabrication of welded assemblies shall conform to the requirements of ASTM A 529, A 572, Grade 42 or A 570 Grade "E" as applicable. All hot rolled sheet and strip used in the fabrication of cold-formed members shall conform to the requirements of ASTM A 570, Grade"E" having a minimum yield strength of 50,000 psi. Design of cold-formed members shall be in accordance with the AISI specifications.

5.1.2 The minimum thickness of framing members shall be:

Cold-formed secondary framing members	- 18 gauge
Pipe or tube columns	- 12 gauge
Webs of welded built-up members	- 1/8 inch
Flanges of welded built-up members	- 1/4 inch
Bracing rods	- 1/4 inch

5.1.3 All framing members shall be fabricated for bolted field assembly. Bolt holes shall be punched or drilled only. No burning-in of holes will be allowed. The faying surfaces of all bolted connections shall be smooth and free from burrs or distortions. Provide washers under head and nut of all bolts. Provide beveled washers to match sloping surfaces as required. Bolts shall be of type specified below. Members shall be straight and dimensionally accurate.

5.1.4 All welded connections shall be in conformance with the STRUCTURAL WELDING CODE D1.1 of the American Welding Society. The flange-to-web welds shall be one side continuous submerged arc fillet welds. Other welds shall be by the shielded arc process.

5.2 Primary Structural Framing.

5.2.1 The primary members shall be constructed of doubly-symmetrical, hot rolled structural steel shapes or doubly-symmetrical built-up

members of constant depth, welded from hot rolled steel sheet, strip or plates.

5.2.2 Compression flanges shall be laterally braced to withstand any combination of loading.

5.2.3 Bracing system shall be provided to adequately transmit all lateral forces on the building to the foundation.

5.2.4 All bolt connections of primary structural framing shall be made using high-strength zinc-plated (0.0003 bronze zinc plated) bolts, nuts, and washers conforming to ASTM A 325. Bolted connections shall have not less than two bolts. Bolts shall not be less than 3/4 inch diameter. Shop welds and field bolting are preferred. All field welds will require prior approval of the Owner. Installation of fasteners shall be by the turn-of-nut or load-indicating washer method in accordance with the specifications for structural joints of the Research Council on Riveted and Bolted Structural Joints.

5.3 Secondary members may be constructed of either hot rolled or cold-formed steel. Purlins and girts shall be doubly symmetrical sections of constant depth and they may be built-up, cold-formed or hot rolled structural shapes.

5.3.1 Maximum spacing of roof purlins and wall girts shall not exceed 5 feet.

5.3.2 Compression flanges of purlins and girts shall be laterally braced to withstand any combination of loading.

5.3.3 Supporting lugs shall be used to connect the purlins and girts to the primary framing. The lugs shall be designed to restrain the light gauge sections from tipping or warping at their supports. Each member shall be connected to each lug by a minimum of two fasteners.

5.3.4 Vertical wall members not subjected to axial load, e.g. vertical members at door openings, shall be constant depth sections. They may consist of hot rolled or cold-form steel. They shall be either built-up, cold-formed or hot rolled "C" or "I" shapes.

5.3.5 Fasteners for all secondary framing shall be a minimum of 1/2 inch diameter (0.003 zinc plated) bolts conforming to ASTM A 307. The fasteners shall be tightened to SNUG TIGHT condition. Plain washers shall conform to ANSI standard B18.22.1.

6. ANCHORAGE.

6.1 Anchorage. The building anchor bolts for both primary and secondary columns shall conform to ASTM A 307 steel and shall be designed to resist the column reactions produced by the specified design loading. The quantity, size and location of anchor bolts shall be specified and furnished by the building manufacturer. A minimum of two anchor bolts shall be used with each column.

6.2 Column Base Plates. Base plates for columns shall conform to ASTM A 36 and shall be set on a grout bed of 1 inch minimum thickness.

7. ROOF AND WALL COVERING.

7.1 Roof and wall panels shall conform to zinc-coated steel, ASTM A 446, G 90 coating designation. Minimum depth of each panel corrugation shall be 1-1/2 inches and shall have a minimum material thickness of 22 gauge. The minimum yield strength of panel material shall be 33,000 psi. Wall panels shall be applied with the longitudinal configurations in the vertical position. Roof panels shall be applied with the longitudinal configuration in direction of the roof slope. Side laps of roof and wall panels shall be fastened as shown on drawings. End laps, if required shall occur at structural steel supports and have a minimum length of 12 inches.

7.2 Insulation.

7.2.1 Semi-rigid insulation for the preformed roofing and siding shall be supplied and installed by the preformed roofing and siding manufacturer.

7.2.2 Insulation Retainers. Insulation retainers or sub girts shall be designed to transmit all external loads (wind, snow and live loads) acting on the metal panels to the structural steel framing. The retainers shall be capable of transmitting both the direct and suction loads.

7.3 Wall and Roof Liners. Wall and roof liners shall be a minimum of 24 gauge. All liners shall be formed or patterned to prevent waviness, distortion or failure as a result of the impact by external loads.

7.4 Fasteners. Fasteners for roof and wall panels shall be zinc-coated steel or corrosion-resisting steel. Exposed fasteners shall be gasketed or have gasketed washers of a material compatible with the covering to waterproof the fastener penetration. Gasketed portion of fasteners or washers shall be neoprene or other elastomeric material approximately 1/8 inch thick.

7.4.1 Type of Fasteners. Fasteners for connecting roof or wall panels to structural steel supports shall consist of self-tapping screws, self-drilling and self-tapping screws, bolts, end welded studs, and welds. Fasteners for panels which connect to structural supports shall be located in each valley of the panel and with a minimum of one fastener per valley while at end laps and plain ends, a minimum of two fasteners shall be used per valley. Fasteners shall not be located at panel crowns.

7.4.2 Fasteners which do not provide positive locking such as self-tapping screws or self-drilling and self-tapping screws shall not be used at side laps of panels and for fastening accessories to panels. Fasteners for side laps shall be located in each valley of the overlap and positioned a maximum of 8 inches on center.

7.4.3 Screws shall be not less than No. 14 diameter if self-tapping type and not less than No. 12 diameter if self-drilling and self-tapping type.

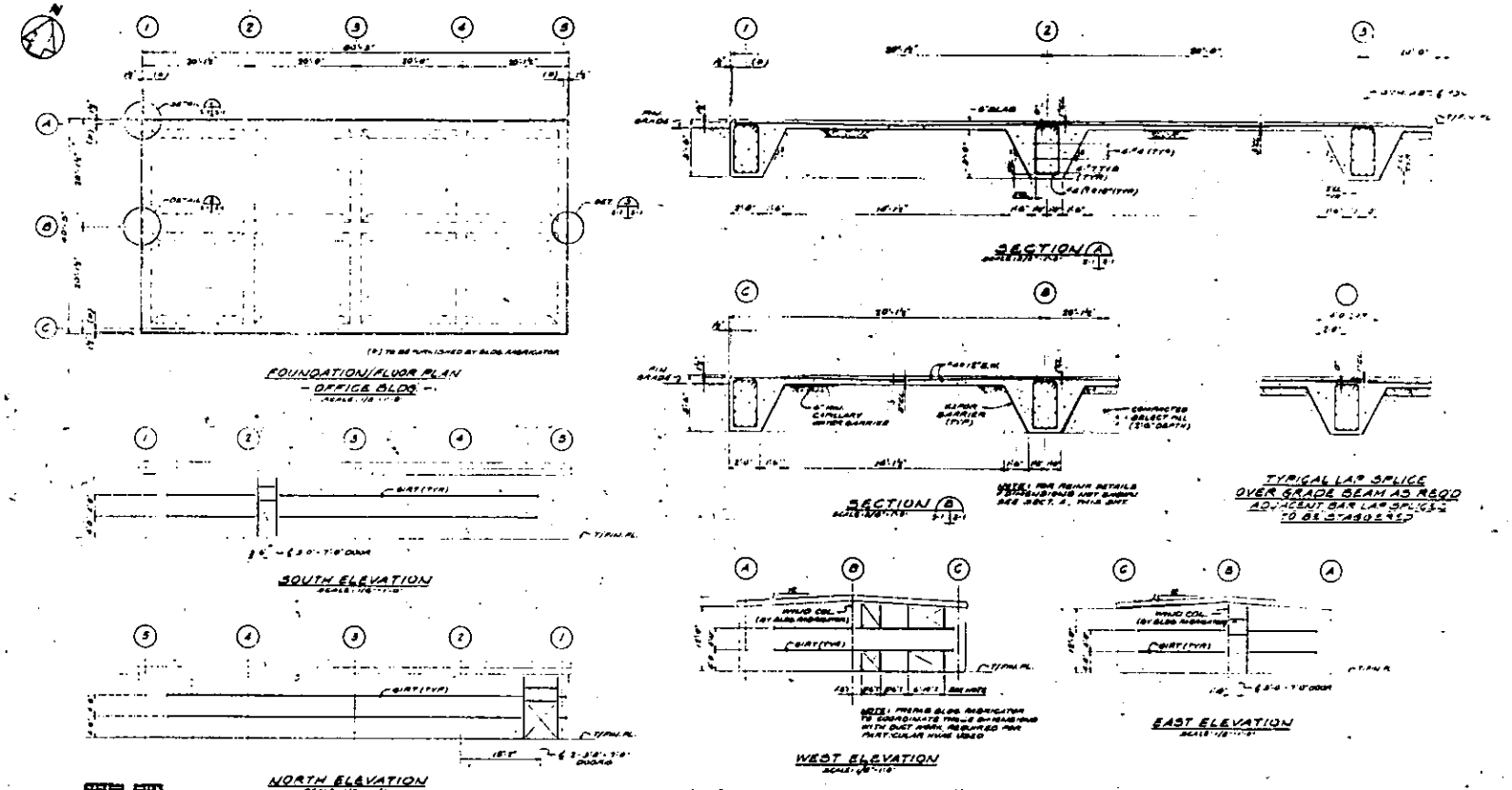
7.4.4 Automatic end-welded studs shall be shouldered type with a shank diameter of not less than 3/16 inch with cap and nut for holding the covering against the shoulder.

7.4.5 Fasteners for use with power actuated tools shall have a shank diameter of not less than 1/2 inch. Fasteners for securing wall panels shall have threaded studs for attaching approved nuts or caps.

7.4.6 Blind rivets shall be stainless steel with 1/8 inch nominal diameter shank. Rivets shall be threaded stem type if used for other than fastening of trim. Rivets with hollow stems shall have closed ends.

7.4.7 Bolts shall not be less than 1/4 inch diameter, shoulders or plain shank as required with proper nuts.

7.4.8 Provide oversize washers with an outside diameter of 1 inch at each fastener or a 22 gauge thick metal strip along each valley of the panel to negate pull-out of the panel around the fasteners.



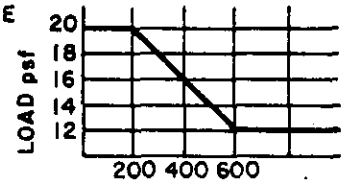
GENERAL NOTES

1. ALL CONCRETE SHALL HAVE A MINIMUM COMPRESSIVE STRENGTH OF f'_c = 4,000 psi AT 28 DAYS.
2. ALL REINFORCING BARS SHALL CONFORM TO SPECIFICATIONS FOR DEFORMED BILLET STEEL BARS FOR CONCRETE REINFORCEMENT, ASTM DESIGNATION A-615, GRADE 60, UNLESS NOTED OTHERWISE.
3. CONCRETE AGGREGATE SHALL HAVE A MAXIMUM SIZE OF 3/4 INCH.
4. MINIMUM AND MAXIMUM CONCRETE SLUMP SHALL BE 2 AND 3 INCHES, RESPECTIVELY, UNLESS NOTED OTHERWISE.
5. ALL REINFORCING BARS SHALL BE CONTINUOUS IN ANY ONE DIRECTION, EXCEPT WHERE OTHERWISE SHOWN ON DRAWINGS.
6. NO WELDING OF REINFORCING SHALL BE PERMITTED EXCEPT AS SHOWN ON DRAWINGS AND FOR BRAZING OR SPOT-WELDING AT ENDS OF REINFORCING BARS FOR GROUNDING.
7. SURFACES OF ALL JOINTS SHALL BE ROUGHENED BEFORE THE SET OF CONCRETE. SURFACES OF SET CONCRETE SHALL BE PREPARED BEFORE NEW POUR AS SPECIFIED IN THE ACI MANUAL OF CONCRETE INSPECTION, SP-2.
8. VERTICAL AND HORIZONTAL CONSTRUCTION JOINTS SHALL NOT BE PERMITTED, EXCEPT AS SHOWN ON DRAWINGS, OR WITH THE APPROVAL OF THE CONTRACTING OFFICER.
9. AT LEAST THE TOP 6 INCHES OF SUBGRADE SHALL BE COMPACTED TO 95% OF MAXIMUM DENSITY IN ACCORDANCE WITH ASTM STANDARD D-1557.
10. EXCEPT AS NOTED, ALL CONCRETE CONSTRUCTION, INCLUDING REINFORCEMENT DETAILING AND PLACEMENT, SHALL CONFORM TO THE MANUAL OF STANDARD PRACTICE FOR DETAILING REINFORCED CONCRETE STRUCTURES (ACI 315, LATEST EDITION), AND THE BUILDING CODE REQUIREMENTS FOR REINFORCED CONCRETE (ACI 318 AND COMMENTARY - LATEST EDITION).
11. THE STRUCTURAL STEEL CONSTRUCTION SHALL CONFORM TO THE AISC SPECIFICATIONS FOR DESIGN, FABRICATION AND ERECTION OF STRUCTURAL STEEL FOR BUILDINGS.
12. ALL PRIMARY STRUCTURAL STEEL SHAPES AND BASE PLATES SHALL CONFORM TO SPECIFICATIONS FOR STRUCTURAL STEEL, ASTM DESIGNATION A-36 (LATEST EDITION), UNLESS NOTED OTHERWISE. HIGH-STRENGTH BOLTING SHALL BE IN ACCORDANCE WITH THE RCBRSJ SPECIFICATION FOR STRUCTURAL JOINTS USING ASTM A-325 BOLTS AND SHALL HAVE A MINIMUM DIAMETER OF 3/4 INCHES.
13. ALL SECONDARY STRUCTURAL STEEL CONSISTING OF [illegible] SHEET OR STRIP USED FOR THE FABRICATION OF COLD-FORMED MEMBERS SHALL CONFORM TO ASTM A-570 GRADE E. DESIGN OF COLD-FORMED MEMBERS SHALL BE IN ACCORDANCE WITH AISI SPECIFICATIONS. STANDARD CARBON BOLTS CONFORMING TO ASTM A-307 SHALL BE USED FOR ASSEMBLING COLD-FORMED MEMBERS. MINIMUM DIAMETER OF BOLTS IS 1/2 INCH.
14. ALL WELDING OF STRUCTURAL STEEL SHALL CONFORM TO THE STANDARD SPECIFICATIONS FOR STRUCTURAL WELDING CODE AWS D1.1 (LATEST EDITION).
15. THE CONTRACTOR SHALL BE RESPONSIBLE FOR THE DESIGN OF ALL STRUCTURAL STEEL CONNECTIONS AND OTHER STRUCTURAL MEMBERS, NOT SHOWN ON THE DRAWINGS, IN ACCORDANCE WITH THE AISC SPECIFICATIONS. ALL FLEXURAL MEMBER CONNECTIONS SHALL BE DESIGNED FOR THE FULL SHEAR CAPACITY OF THE MEMBER. BOLTED CONNECTIONS SHALL NOT HAVE LESS THAN TWO (2) BOLTS.
16. SHOP DRAWINGS SHALL BE SUBMITTED FOR APPROVAL.

Figure 6-17 General layout of pre-engineered building

1. FLOOR LIVE LOAD: 150 psf

2. ROOF LIVE LOAD



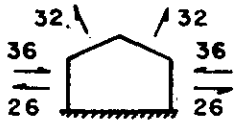
3. ROOF SNOW LOAD: 30 psf

4. DEAD LOAD: AS PER MATERIALS USED

5. WIND LOADS: WIND PARALLEL OR PERPENDICULAR TO ROOF RIDGE (BASED ON 100 mph WIND)

A. WINDWARD/LEEWARD AND ROOF PRESSURES (psf)

a. WHEN TRIBUTARY SUPPORT AREAS > 200 ft²



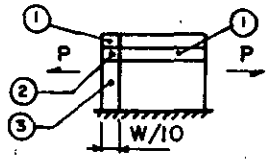
FOR DESIGN OF MAIN FRAMES AND OTHER INDIVIDUAL MEMBERS, USE VALUES SHOWN.

b. WHEN TRIBUTARY SUPPORT AREA ≤ 200 ft²



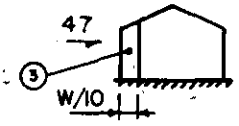
FOR DESIGN OF MAIN FRAMES, USE VALUES SHOWN FOR TRIBUTARY AREA > 200 ft². FOR DESIGN OF OTHER INDIVIDUAL MEMBERS, USE VALUES SHOWN

B. SIDEWALL PRESSURES (psf)



FOR DESIGN OF INDIVUAL MEMBERS:
WHEN TRIBUTARY SUPPORTED > 200 ft², USE P = 32
WHEN TRIBUTARY SUPPORTED ≤ 200 ft², USE P = 43

C. SIDESWAY PRESSURES (psf)



FOR DESIGN OF MAIN FRAMES FOR TRIBUTARY SUPPORTED AREAS, TA, LESS THAN, EQUAL TO, OR GREATER THAN, 200 ft²

D. LOCAL PRESSURES - SEE FIGURES IN 'B' AND 'C' FOR REGIONS OF APPLICATION

REGION 1 : 50 psf	SUCTION	FOR DESIGN OF DECKING
REGION 2 : 105 psf	SUCTION	CONNECTIONS AT REGIONS
REGION 3 : 42 psf	SUCTION	CITED

"W" IS LEAST WIDTH OF ENCLOSED AREA

NOTE: FIGURES DEPICT WIND PERPENDICULAR TO RIDGE. FOR WIND PARALLEL TO RIDGE, USE SAME VALUES.

6. LOADING COMBINATIONS:

A. D	WHERE
B. D + L	D = DEAD LOAD
C. D + W	L = LIVE LOAD
D. 0.75 (D + L + W)	W = WIND LOAD

Figure 6-18 Recommended pre-engineered building design loads

SUPPRESSIVE SHIELDING

6-23. General

This manual presents methods for the design and construction of conventional reinforced concrete and steel protective facilities which provide adequate safety for hazardous operations such as munitions loading, maintenance, renovation, or demilitarization. Such safety considerations include the utilization of conventional protective barriers, total containment construction, or the use of separation distances or isolation of the specific operation from other parts of the facility using appropriate quantity distance specifications. However, an alternative available to the designer of these facilities is the use of suppressive shielding as outlined in HNDM 1110-1-2, "Suppressive Shields Structural Design and Analysis Handbook,", 18 November 1977.

A suppressive shield is a vented steel enclosure which controls or confines the hazardous blast, fragment, and flame effects of detonations. Suppressive shielding may provide cost or safety effective alternatives to conventional facilities, depending upon the hazardous situation under study. HNDM 1110-1-2 presents procedures for design, analysis, quality control, and economic analysis of suppressive shields. In this section, a brief review of these procedures is presented. The reader should refer to HNDM 1110-1-2 for details necessary for design.

6-24. Application

Facility operations such as munitions loading, maintenance, modification, renovation, or demilitarization must be analyzed to determine which operations involve potentially catastrophic (CAT I or II, MIL STD 882A) hazards in the event of an inadvertent ignition or detonation. Where the hazard analysis shows such a potential, the facility design must provide adequate safety for those operations. The alternatives presented to the designer of the facility are varied and may include the utilization of conventional protective barricades with appropriate separation distances, reinforced concrete or steel structures, suppressive shields, or isolation of a particular operation from the rest of the facility by the appropriate quantity-distance. The decision as to which alternative system to use is based primarily on economic factors, provided all safety considerations are equal. The facility, availability of real estate, and equipment costs to include maintenance, operation, useful life, replacement, and modification or renovation must be analyzed for each alternative method of protection. Costs will be estimated and compared over the facility life to determine the most economical mode of protection.

A major factor which is paramount in the determination of which form of protection to use is the requirement for approval of the facility by the Department of Defense Explosives Safety Board. If the designer can, based on economic factors, adapt suppressive shields in the design and support the adaptation with proven accepted analytical techniques, he should begin development of a facility concept which employs suppressive shields using those shields which have been safety approved.

6-24.1. Safety Approved Suppressive Shields

There are eight suppressive shield design groups that have been developed to various stages of definition. These shield groups are summarized in Table 6-4 and illustrated schematically in Figure 6-19. Of the design groups illustrated, five had been safety approved by the Department of Defense Explosive Safety Board in 1977.

The five suppressive shield group designs approved by the DoD Explosive Safety Board (Groups 3, 4, 5, 6, and 81 mm) have been designed to meet the requirements for most applications to ammunition load, assembly, pack (LAP) in the Munitions Production Base Modernization and Expansion Program. However, specific shield requirements will vary with other applications and, even with LAP applications, design details will vary from plant to plant and between munitions or different operations on the line. It will, therefore, frequently be necessary to modify the approved shields to adapt them to the operation under consideration.

Chapter II and Appendix A of HNDM 1110-1-2 describes the safety approved shield group designs, provides guidance concerning acceptable modifications, recommends procedures for securing safety approval of new shield designs, and provides summary information on overall dimensions of the shield structure, charge capacity, rated overpressure, fragment stopping wall thickness, and type of construction of the five approved basic shield groups.

6-24.2. New Shield Design

In exceptional cases where a safety approved shield cannot be made to fit a desired application, a new shield can be designed. The guidance needed to design a new shield and the procedures for obtaining the safety approval for the new design are outlined in HNDM 1110-1-2.

6-24.2.1. Hazardous Environments

Considering that the hazardous environments normally associated with suppressive shielding involves explosives and/or explosive ordnance, Chapter III of HNDM 1110-1-2 presents information relative to internal and external air blast, fragmentation, and fireball phenomena. This information can be used in support of blast and fragment methods in this manual to determine venting requirements, air blast loads on the structure, and protection required to defeat fragments. Some graphs and prediction methods in Chapter 2 of this manual are taken directly from the suppressive shields manual.

6-24.2.2. Structural Behavior

Suppressive shields can be subjected to large, high pressure loads applied very rapidly. The allowance of inelastic behavior of the shield material structural elements enables much more efficient use of the structural material and does not impair the function of the shield provided, of course, that the inelastic behavior is maintained within acceptable limits.

The structural materials of primary interest in suppressive shielding are steel and reinforced concrete. Chapter IV of HNDM 1110-1-2 discusses the behavior and properties of these structural materials under static and dynamic loading. Additionally, ductility ratios as they apply to suppressive shield

application are covered. Some of the information provided will duplicate material in chapters of this manual. In case of a conflict, this manual takes precedence.

6-24.2.3. Structural Design and Analysis

Chapter V of HNDM 1110-1-2 describes techniques which are sufficiently accurate for preliminary designs in all cases, and in most cases, adequate for final designs. These methods deal primarily with the dynamic loadings imposed by internal explosions. The design methods supplement material presented in chapters of this manual. Again, in case of conflict, this manual takes precedence.

6-24.2.4. Structural Details

Each suppressive shield used for ammunition manufacturing and other hazardous operations will have specific requirements for utility penetrations, and doors for personnel, equipment, and products. Guidance on the provision of acceptable structural details such as these is presented in Chapter VI of HNDM 1110-1-2 along with information on structural details which have been successfully proof-tested.

6-24.2.5. Economic Analysis

The design of a facility entails the need to ascertain the most cost effective configuration from among a set of workable design alternatives. All will be designed to provide the desired level of reliability and safety, and the selection of one over another will be based primarily on dollar costs. The economic analysis of alternative facility design is a complex process unique to each facility. Chapter VII of HNDM 1110-1-2 illustrates the many factors that must be considered.

6-24.2.6. Assuring Structural Quality

In the design of suppressive shields, specifications for the quality of the basic material is paramount. The strength of welds and concrete components are also determining factors in the overall strength of the structure. Chapter VIII of HNDM 1110-1-2 provides the guidance which outlines a quality assurance program for suppressive shield design packages.

Included in Appendix A of HNDM 1110-1-2 is a detailed description of the safety approved suppressive shields and guidance concerning acceptable modifications. Copies of the fabrication drawings for each approved shield design are included along with direction for ordering full-size copies. Appendix B of that manual includes response charts for use in preliminary design. The charts are based on the combined short duration shock load and infinite duration quasi-static load, along with an undamped elastic-plastic responding structure.

6-25. Design Criteria

Design criteria for use of suppressive shields, or suppressive shielding panels, are very dependent on specific applications in protective structures. These criteria may include complete suppression of fragmentation effects, both primary and secondary; attenuation of blast overpressures and impulses to

specified levels of specific distances from the shield or shield panels; attenuation of fireball radiation; or even essentially complete suppression of all of these effects.

Suppressive shields may or may not present reasonable or cost effective solutions to specific design problems in protective structures. Generally, they have appeared attractive when fragment hazards are severe and when potentially explosive sources are rather concentrated. The safety-approved shields protect against effects as limited as small trays of detonators, and as severe as a large melt kettle in a HE melt-pour operation containing several thousand pounds of explosive. The designer should consider their use, and use the methods presented in HNDM 1110-1-2 to evaluate their efficacy, compared to other types of protective structures discussed in this manual.

No general design criteria can be given here because the criteria for different operations or plants, and available real estate, differ too widely. In each specific protection design contract, the AE should be provided with quite detailed design criteria, in addition to general regulations which fix safety criteria such as AMCR 385-100. Both the specific and more general criteria must be evaluated when deciding whether or not suppressive shields will be useful in the facility design.

6-26. Design Procedures

6-26.1. Space Requirements

Once the operation requiring suppressive shields has been identified, consideration must be given to the size and shape of the equipment needed to perform the operation and the work space required inside the shield. These factors necessarily provide the designer with an estimate of the size and shape of the shield required. Additionally, space available on the line or in the building will place limitations on the overall shield base dimensions and height.

6-26.2. Charge Parameters

A principal factor in the selection of a shield which will govern the shield requirements is the establishment of the charge parameters for any specific application. The charge parameters are: charge weight (W). shape, confinement, and composition; ratio of charge weight to shield internal chapter (W/V); and scaled distance (Z) from the charge to the nearest wall or roof of the shield. ($Z = R/W^{1/3}$), where R is the distance from the center of the charge to the nearest wall or roof in feet and W is the charge weight in pounds. These parameters for approved shield groups are summarized in Table 6-5. New shield designs can be developed for individual needs.

6-26.3. Fragment Parameters

Another key factor in the procedure a designer follows in the selection of an approved design or the design of a new concept is the suppression of primary and secondary fragments generated by the detonation of explosives or munitions. Much of the material in HNDM 1110-1-2 for fragment perforation of spaced plates has been adapted to Chapter 5 of this manual.

6-26.4. Structural Details

Suppressive shields used for ammunition manufacturing and other hazardous operations require provisions for gaining access to the operation being protected. Personnel must be able to enter the shield to accomplish routine and emergency maintenance and clean-up and other essential operations. An opening of sufficient size must be provided to enable the installation or removal of equipment in realistically large subassemblies. Openings for conveyors and chutes must also be provided and properly configured to prevent excessive pressure and fragments from escaping. Provisions must be made to provide all utilities and satisfy all environmental conditioning needs which may be essential to the operations inside the shield.

Utility penetrations, ventilating and air-conditioning ducts, and vacuum lines must not diminish the overall protective capability of the shield. They must not alter the basic mode of structural failure of the suppressive shield and should be small compared to the general size of the shield.

Operations that produce explosive dust may require the use of liners both inside and outside the shield to prevent the accumulation of dust within shield panels. With configurations such as the Group 5 shield, which is primarily designed for use with propellants or pyrotechnic materials, liners must not inhibit the venting characteristics of the shield.

Utility lines passing through suppressive shields are vulnerable to both air blast and fragment hazards. The air blast could push unprotected utility penetrations through the walls of the shield and create secondary fragments. Fragments from an accidental explosion could perforate the thin walls of an unprotected utility pipe and escape from the shield. To eliminate the threat of air blast and fragments, a protective box is used to cover the area where the utility lines pass through the shield wall. The box is configured to rest on the inside surface of the shield and is welded to the shield. The size of the wall penetrations is limited to that required for the utilities. Each pipe is bent at a right angle inside the shield within the protective box. The penetrations of the shield wall are reinforced with a sleeve or box section welded to the shield panel through which the utility line passes. The penetration box is designed to maintain the structural integrity of the shield area penetrated. A typical protective box design is shown in Figure 6-20.

The cover plate thickness is selected to stop the worst case fragment.

Typical penetrations for approved safety design suppressive shields are illustrated in Figures 6-21 and 6-22, and a vacuum line penetration is illustrated in Figure 6-23.

6-26.5. Access Penetrations

In the munitions plant environment, suppressive shields are designed to protect Category I or II hazardous operations as defined in MIL STD 882A. Remote operation may be required so personnel will not be inside the shield during operations. However, personnel access is required to allow for maintenance, repair, and inspection. Further, these doors must provide large openings to enable most equipment to be installed or removed in large subassemblies.

Access is also required for munitions components, explosives, and assembled munitions to pass through the suppressive shield. In the case of conveyor transporting systems, consideration must be given to the proper pass-through of the conveyor. Requirements for this type of access depend on the configuration of the munitions product, transporting pallets, and conveyors, as well as production rates and other factors unique to each operation. For these reasons, definition of specific design requirements is not possible.

6-26.5.1. Personnel Door

Three different types of doors have been developed for use in suppressive shields: sliding, hinged, and double leaf. The hinged door was designed to swing inward. This feature reduces the usable space inside the shield. A sliding door is preferred for personnel access to munitions operations. Figure 6-24 illustrates a typical sliding door. This type door is used with the Group 4, 5, and Milan 81 mm shields. The sliding door consists of an entire shield panel suspended from a monorail system. The panel is inside the shield and is not rigidly attached to the column members. Special consideration was given to the air gap between the door panel and the column to assure that excessive pressure leakage would not occur and that fragments could not pass through the gap.

The cylindrical Group 3 shield contains a two-leaf door, hinged at each side. It swings inward as shown in Figure 6-25. The door is curved to match the shield wall contour and is fabricated from S5 x 10 I-beams. Pressure loading restraint is provided by the door bearing on the external support rings of the shield at the top and bottom of the door. An external latch provides restraint during rebound of the door.

6-26.5.2. Product Door

Only one type of product door has been developed conceptually for use in suppressive shields. It is the rotary, three lobed configuration shown in Figure 6-26. The design procedure for this door is described to illustrate the type of analysis required. It can be used as a guide for analysis of similar alternate design concepts for product doors.

The air blast will most severely load the rotating product door when the munitions opening is coincident with the pocket in the rotary door. A non-overriding clutch prevents the door from counter-rotating. The angular impulsive load is:

$$T_i = i_r A_d r_d \qquad 6\text{-}38$$

where

T_i = angular impulsive load
i_r = reflected impulse
A_d = door area
r_d = radius from center of impulse load to the center of door rotation

Assuming the product door to be initially at rest, the rotational velocity imparted to the door is given by:

$$w_i = T_m / I \qquad 6\text{-}39$$

where

ω = angular velocity

I_m = mass moment of inertia of the door about shaft axis

The kinetic energy imparted to the door is given by:

$$KE = \frac{I_m \omega^2}{2} = \frac{T_i^2}{2I_m} \qquad 6\text{-}40$$

The strain energy absorbed by a circular shaft is given by:

$$U_s = \frac{\pi L_s}{4G}(r_s \tau_s)^2 \qquad 6\text{-}41$$

where

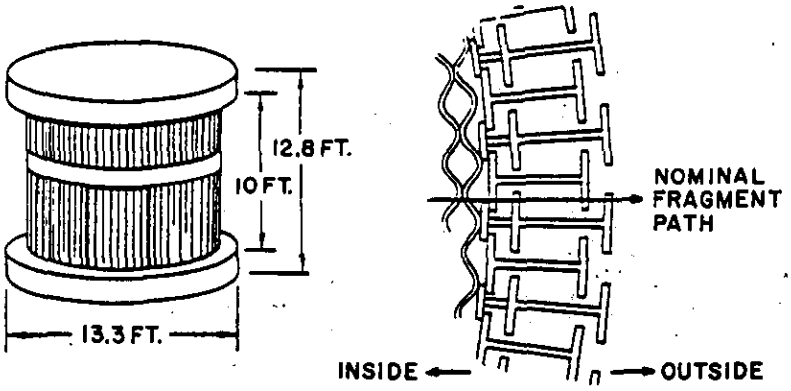
U_s = strain energy
L_s = length of the shaft
G = shear modulus of the shaft material
r_s = radius of the shaft
τ_s = maximum shear stress in the shaft

Equating the kinetic energy of the rotating door to the strain energy in the shaft and solving for the shear stress yields:

$$\tau_s = \frac{T_i}{r_s}\left[\frac{2G}{\pi I_m L_s}\right]^{1/2} \qquad 6\text{-}42$$

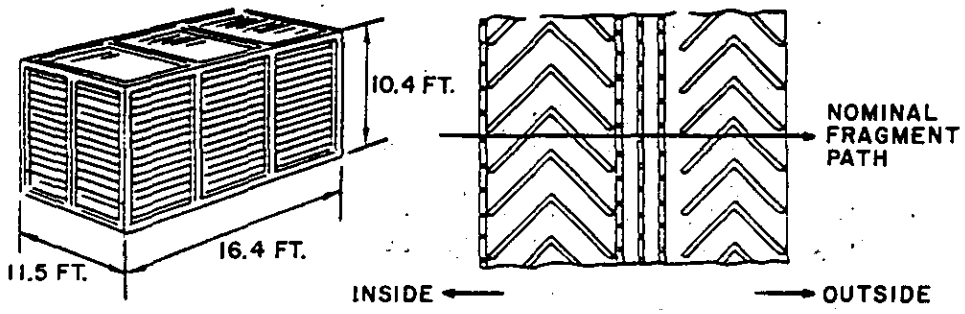
The computed shear stress in the shaft must be less than the dynamic shear stress of the shaft material, i.e.,:

$$s < 0.55\, f_{dy} \qquad 6\text{-}43$$

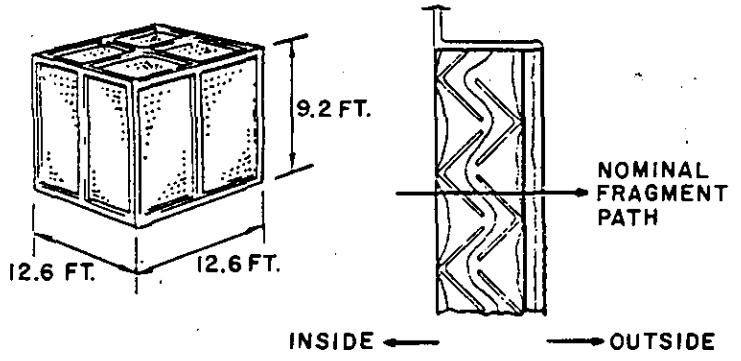


SUPPRESSIVE SHIELD GROUP 3

(GROUPS 1 & 2 ARE SIMILAR, BUT MUCH LARGER, AND HAVE THREE EXTERNAL RINGS)

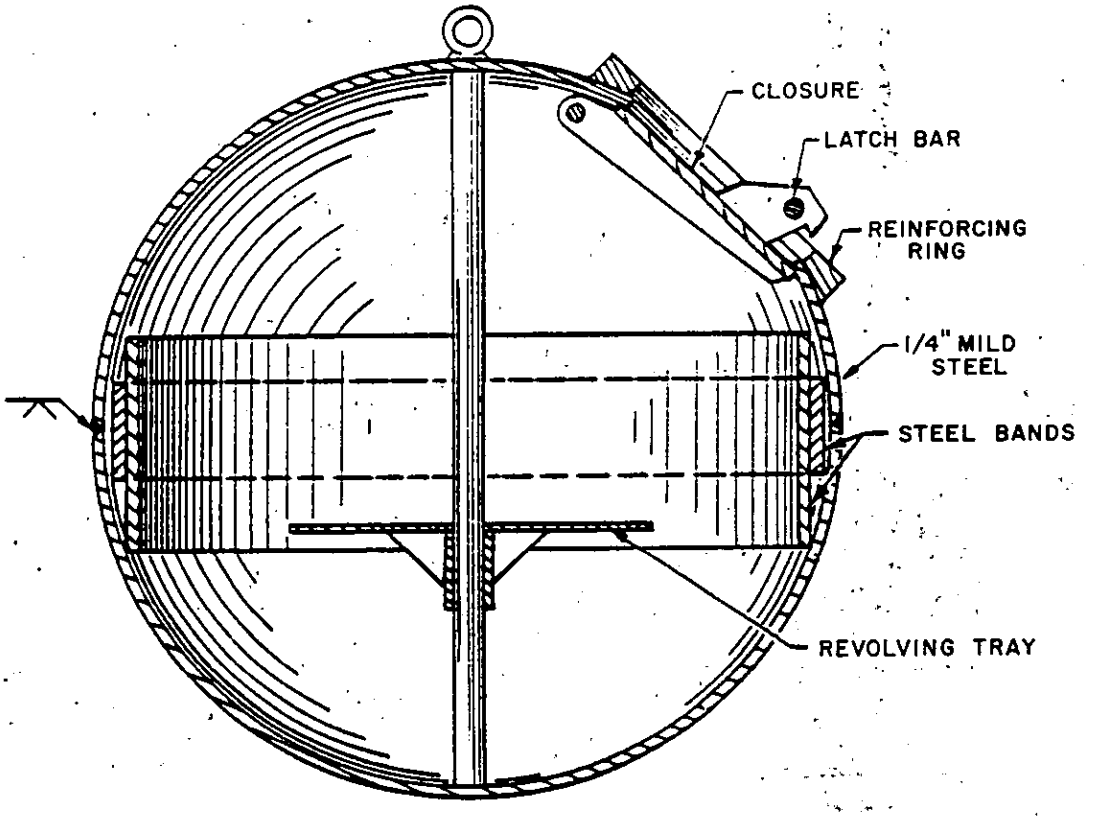


SUPPRESSIVE SHIELD GROUP 4

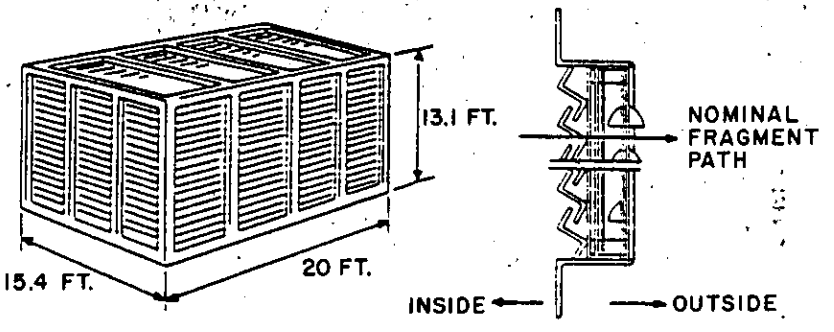


SUPPRESSIVE SHIELD GROUP 5

Figure 6-19a. General configuration of suppressive shield groups



SUPPRESSIVE SHIELD GROUP 6



SUPPRESSIVE SHIELD GROUP 81mm

Figure 6-19b General configuration of suppressive shield groups (continued)

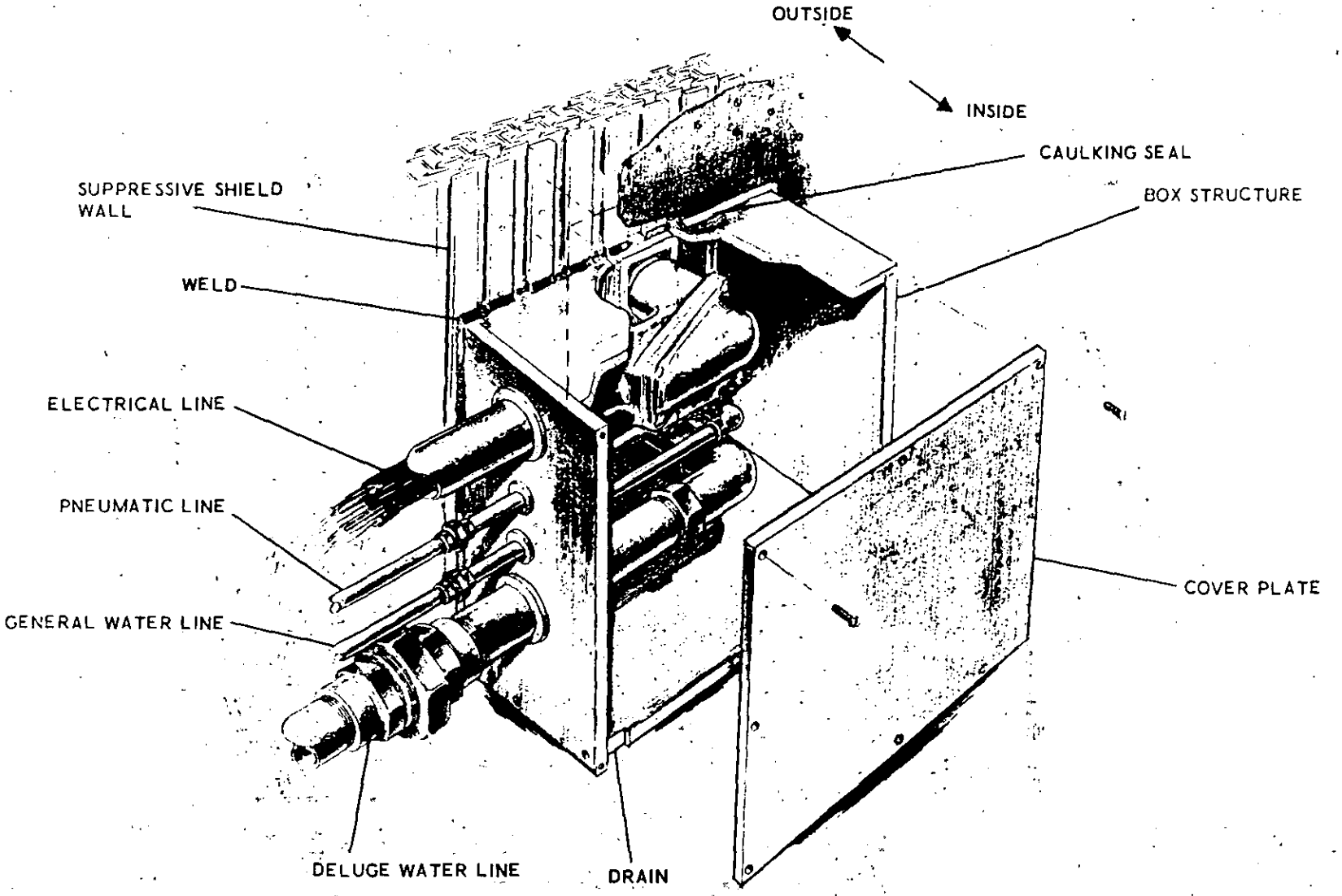


Figure 6-20 Typical utility penetration

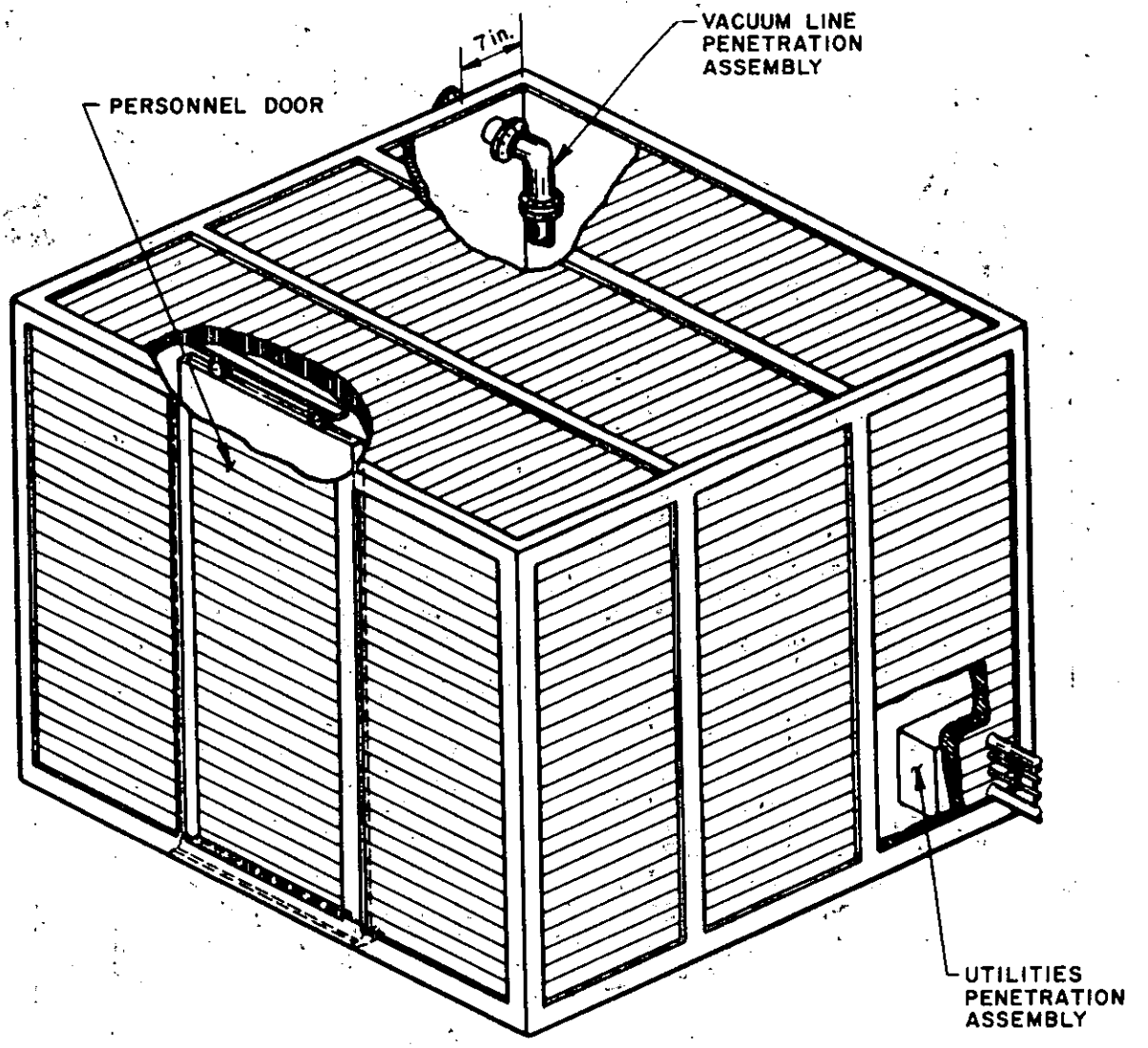


Figure 6-21 Typical location of utility penetration in shield groups 4, 5, and 81 mm

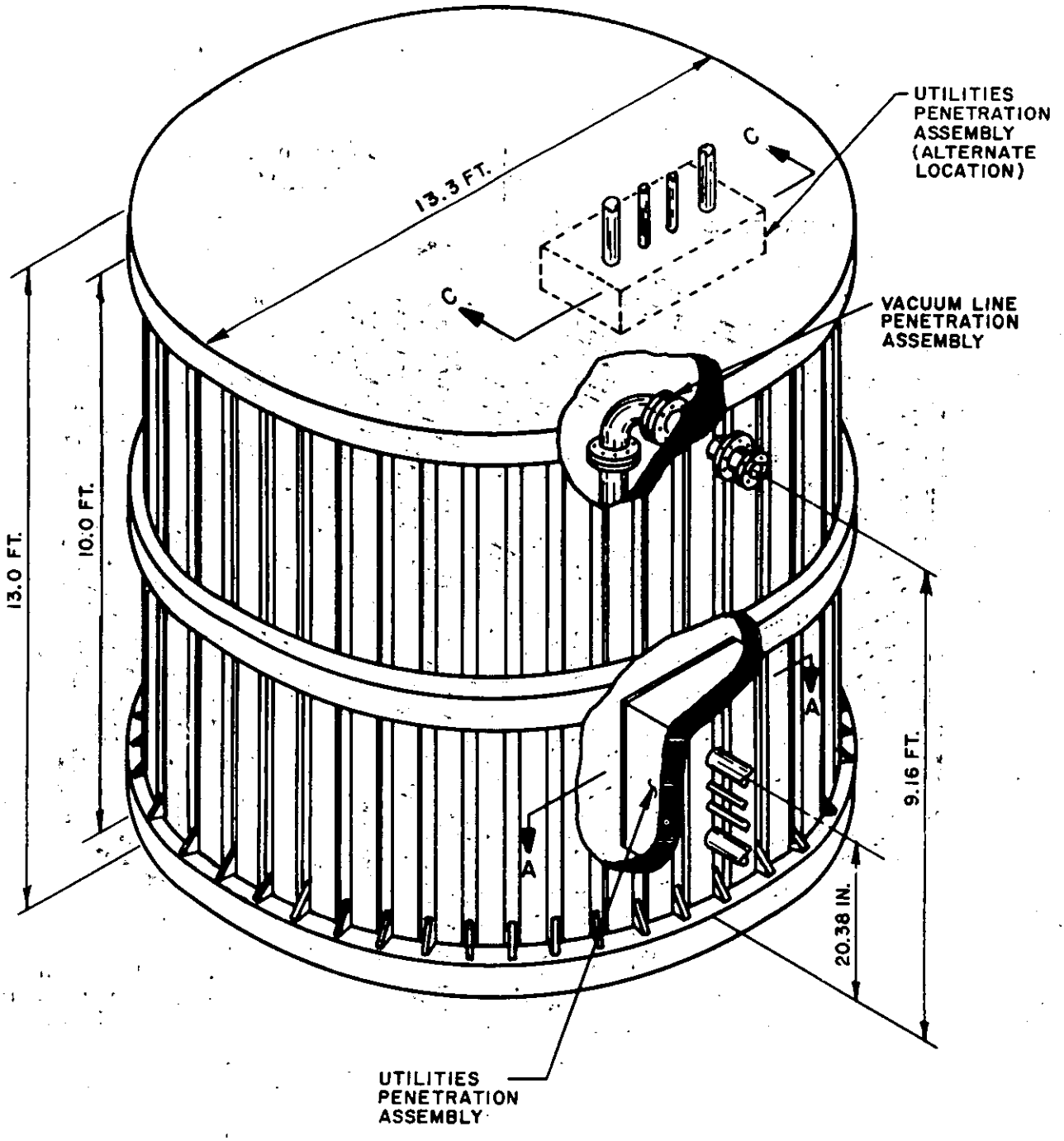


Figure 6-22 Typical location of utility penetrations in shield group 3

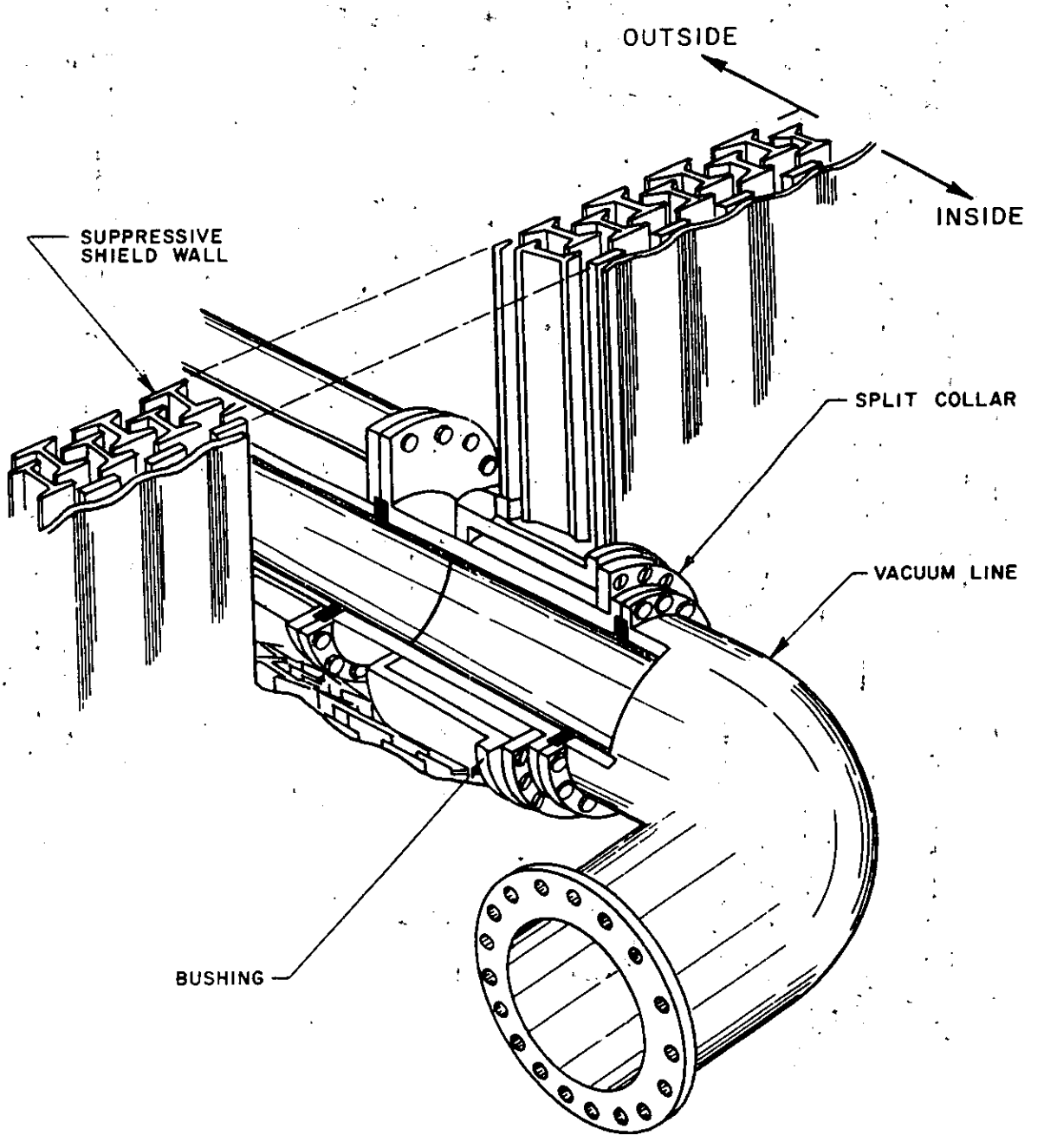


Figure 6-23 Typical vacuum line penetration

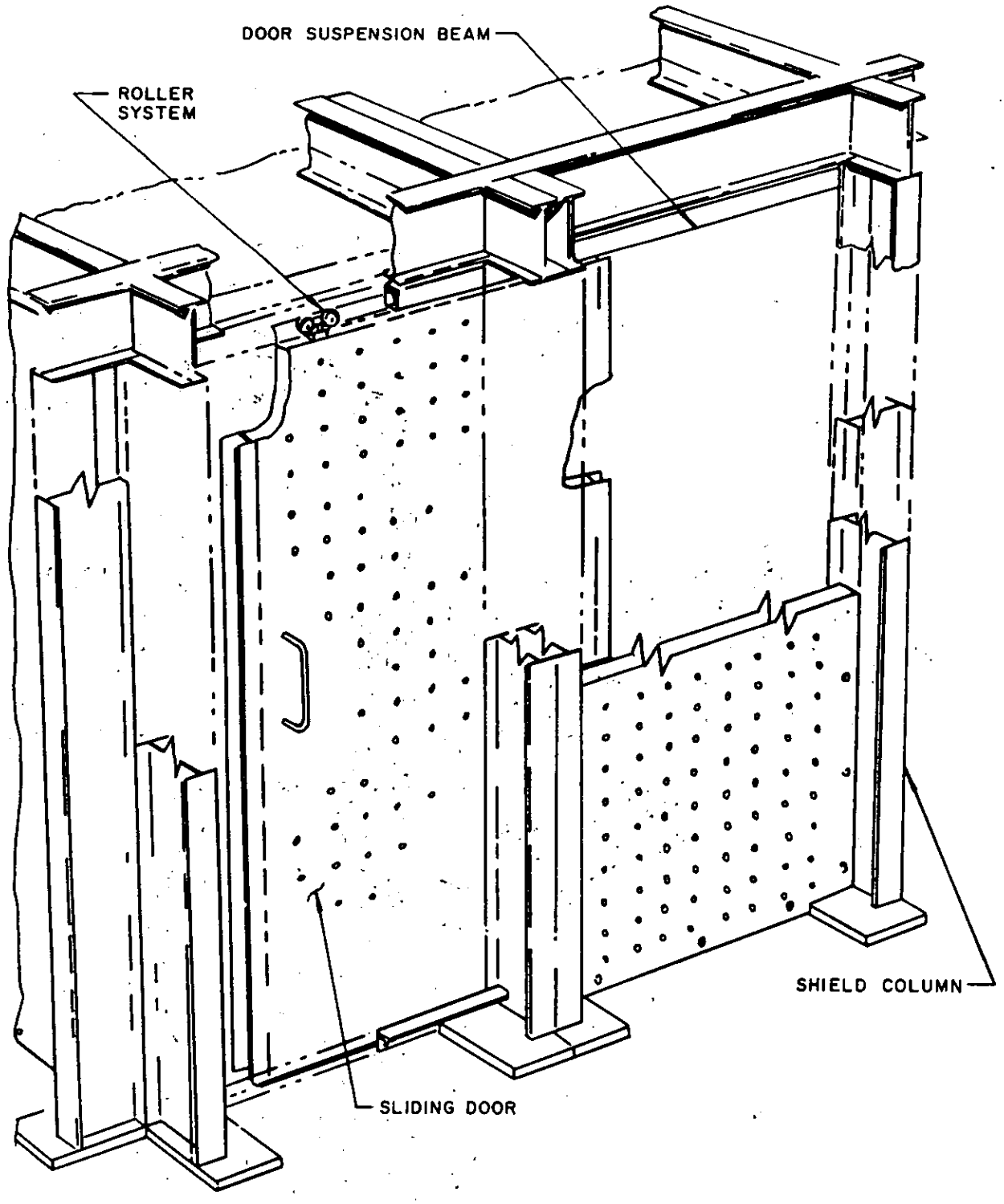


Figure 6-24 Sliding personnel door

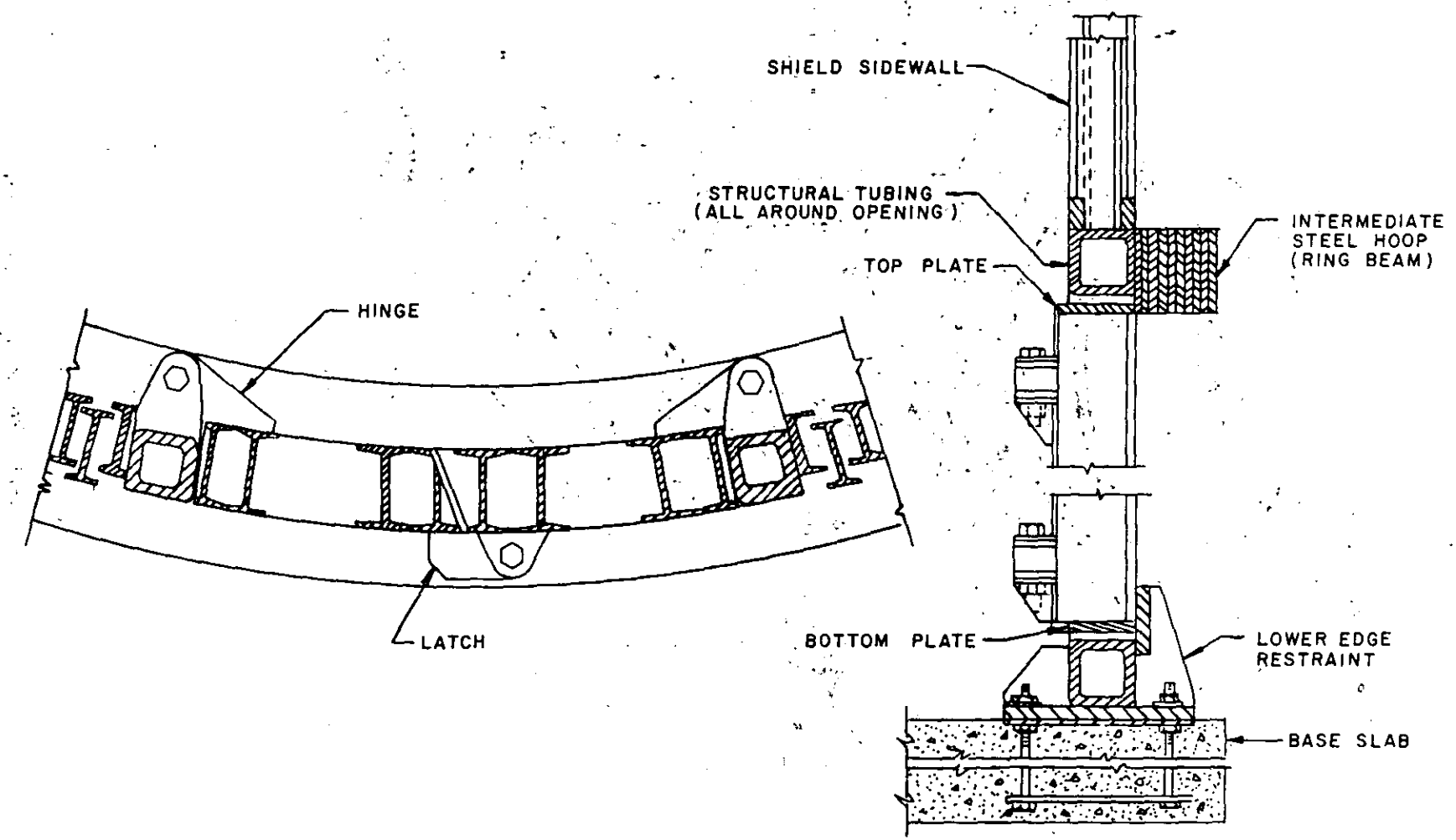


Figure 6-25 Door - group 3 shield

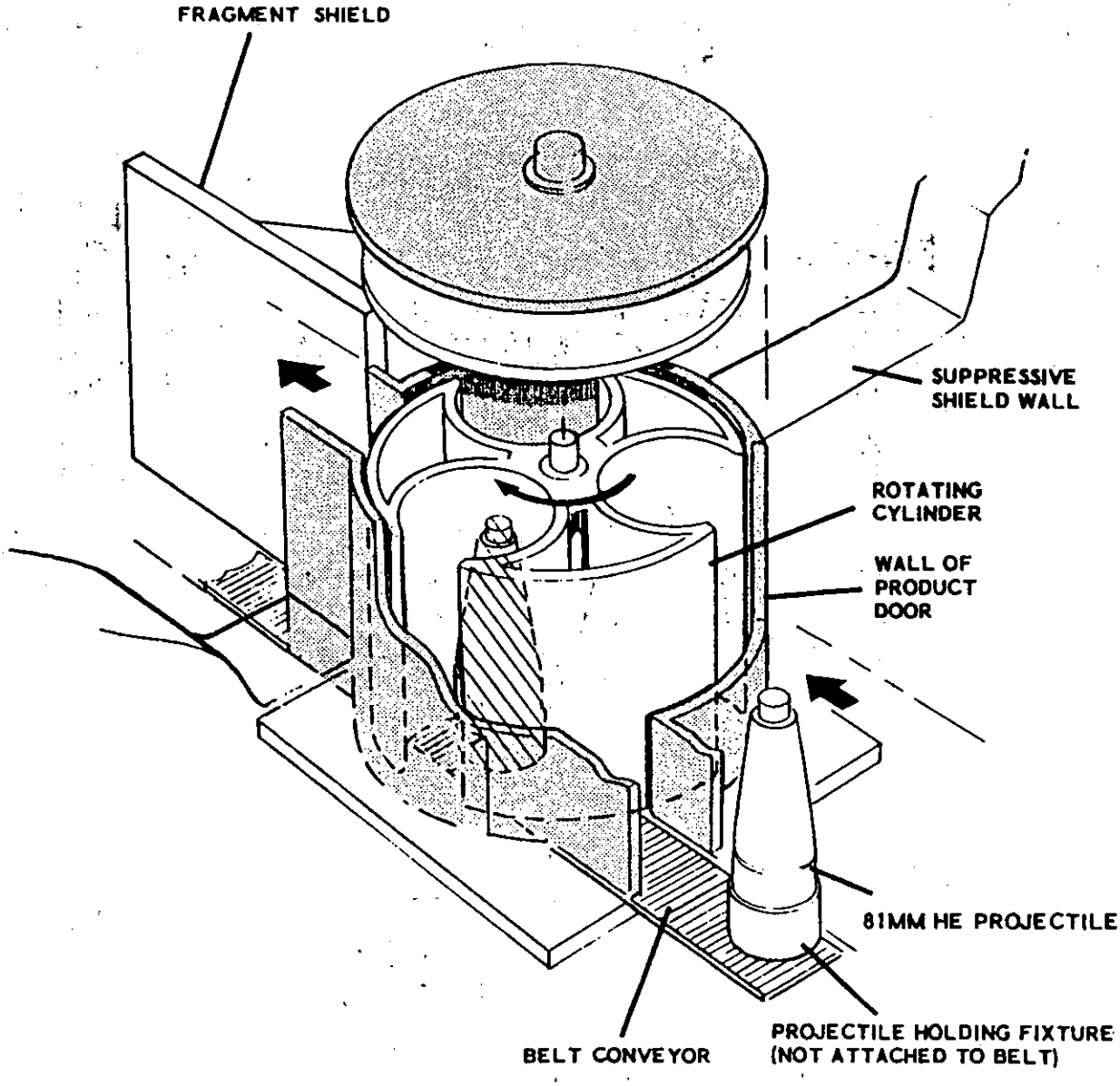


Figure 6-26 Rotating product door

Table 6-4 Summary of Suppressive Shield Groups

SHIELD GROUP	HAZARD PARAMETER		REPRESENTATIVE APPLICATIONS	LEVEL OF PROTECTION *
	BLAST	FRAGMENTATION		
1	High	Severe	Porcupine Melter (2000 lbs) plus two pour units 250 lbs each	Reduce blast pressure at intraline distance by 50 percent
2	High	Severe	HE Bulk (750 lb) Minute melter	Reduce blast pressure at intraline distance by 50 percent
3	High	Moderate	HE Bulk (37 lb) Detonators, fuses	Category I hazard 6.2 feet from shield
4	Medium	Severe	HE Bulk (91b) Processing rounds	Category I hazard 19 feet from shield
5	Low	Light	30 lb Illuminant Igniter slurry mixing HE processing (1.84 lb)	Category I hazard 3.7 feet from shield
6	Very High	Light	Laboratory, handling, and transportation	Category I hazard at 1 foot from shield
7	Medium	Moderate	Flame/fireball attenuation	Category I hazard at 5 feet from shield
81 mm	High	Moderate	81 mm mortar drill-and-face and/or cast-finishing operation	Category I hazard at 3 feet from shield

* All shield groups contain all fragments

Table 6-5 Charge Parameters for Safety Approved Shields

	MINIMUM Z ($ft/lb^{1/3}$)		
SHIELD GROUP	WALL	ROOF	MAXIMUM W/V (lb/ft^3)
3	1.63	1.45	0.04157
4	2.23	2.19	0.00762
5	4.14	6.79	0.00215
6A	1.01	N/A	0.22970
6B	1.22	N/A	0.13200
Prototype 81 mm *	3.62	3.21	0.00340
Milan 81 mm *	4.23	3.75	0.00280

* See Figure 6-19

BLAST RESISTANT WINDOWS

6-27. Introduction

Historical records of explosion effects demonstrate that blast-propelled glass fragments from failed windows are a major cause of injuries from accidental explosions. Also, failed window glazing often leads to additional injuries as blast pressure can enter interior building spaces and subject personnel to high pressure jetting, incident overpressure, secondary debris impact, and thrown body impact. These risks are heightened in modern facilities, which often have large areas of glass.

Guidelines are presented for both the design, evaluation, and certification of windows to safely survive a prescribed blast environment described by a triangular-shaped pressure-time curve. Window designs using monolithic (unlaminated) thermally tempered glass based on these guidelines can be expected to provide a probability of failure equivalent to that provided by current safety standards for safely resisting wind loads.

Guidelines are presented in the form of load criteria for the design of both the glass panes and framing system for the window. The criteria account for both the bending and membrane stresses and their effect on maximum principle stresses and the nonlinear behavior of glass panes. The criteria cover a broad range of design parameters for rectangular-shaped glass panes. Design charts are presented for monolithic thermally tempered glazing with blast overpressure capacity up to 100 psi, an aspect ratio of $1.00 \leq a/b \leq 4.00$, pane area $1.0 \leq ab \leq 25$ ft^2, and nominal glass thickness $1/4 \leq t \leq 3/4$ inches. An alternate method for blast capacity evaluation by calculation is also presented. This can be used to evaluate the blast capacity of glass when interpolation between charts is unadvisable, when design parameters are outside the limits of the chart, and to calculate rebound loads. Presently, the design criteria are for blast-resistant windows with thermally treated, monolithic tempered glass. Further research is required to extend these design criteria to laminated tempered glass.

6-28. Background

The design criteria cover monolithic tempered glass meeting the requirements of Federal Specifications DD-G-1403B and DDG-451d. Additionally, thermally tempered glass must meet the minimum fragment weight requirements of ANSI Z97.1-1984, Section 5.1.3(2).

Annealed glass is the most common form of glass available today. Depending on manufacturing techniques, it is also known as plate, float or sheet glass. During manufacture, it is cooled slowly. The process results in very little, if any, residual compressive surface stress. Consequently, annealed glass is of relatively low strength when compared to tempered glass. It has large variations in strength and fractures into dagger-shaped, razor-sharp fragments. For these reasons, annealed glass is not recommended for use in blast resistant windows.

Thermally tempered glass is the most readily available tempered glass on the market. It is manufactured from annealed glass by heating to a high uniform temperature and then applying controlled rapid cooling. As the internal temperature profile relaxes towards uniformity, internal stresses are created.

The outer layers, which cool and contract first, are set in compression, while internal layers are set in tension. As it is rare for flaws, which act as stress magnifiers, to exist in the interior of tempered glass sheets, the internal tensile stress is of relatively minimal consequence. As failure originates from tensile stresses exciting surface flaws in the glass, precompression permits a larger load to be carried before the net tensile strength of the tempered glass pane is exceeded. Tempered glass is typically four to five times stronger than annealed glass.

The fracture characteristics of tempered glass are superior to those of annealed glass. Due to the high strain energy stored by the prestress, tempered glass will eventually fracture into small cubical-shaped fragments instead of the razor-sharp, dagger-shaped fragments associated with the fracture of annealed glass. Breakage patterns of side and rear windows in American automobiles are a good example of the failure mode of thermally or heat-treated tempered glass.

Semi-tempered glass is often marketed as safety or heat-treated glass. However, it exhibits neither the dicing characteristics upon breakage nor the higher tensile strength associated with fully tempered glass, and, therefore, it is not recommended for blast resistant windows.

Another common glazing material is wire-reinforced glass, annealed glass with an embedded layer of wire mesh. Its only use is as a fire-resistant barrier. Wire glass has the fracture and low strength characteristics of annealed glass and, although the wire binds fragments, it contributes metal fragments as an additional hazard. Wire glass is never recommended for blast resistant windows.

6-29. Design Criteria for Glazing

6-29.1. Specified Glazing

The design of blast-resistant windows is currently restricted to heat-treated, fully-tempered glass in fixed or non-openable frames meeting both Federal Specification DD-G1403B and ANSI Z97.1-1984. Tempered glass meeting only DD-G-1403B may possess a surface precompression of only 10,000 psi. At this level of precompression, the fracture pattern is similar to annealed and semi-tempered glass. Tempered glass meeting the minimum fragment specifications of ANSI Z97.1-1984 (Section 5.1.3(2)) has a higher surface precompression level and tensile strength, which improves the capacity of blast-resistant windows and results in smaller, cubical-shaped fragments on failure.

Although thermally tempered glass exhibits the safest failure mode of any glass, failure under blast loading still presents a significant health hazard. Results from blast tests reveal that on failure, tempered glass fragments may be propelled in cohesive clumps that only fragment on impact into smaller rock-salt-shaped fragments. Even if the tempered glass initially breaks into small fragments, sufficient velocities may still be imparted by the blast loading to cause severe hazards to personnel. Because the expected geometry of glass fragments involve multiple, potentially sharp corners, a high probability of injury would result from application of the 58 ft-lb criterion for acceptable kinetic energy. Because of these hazards to personnel, blast-resistant glazing should be designed to survive expected loads.

6-29.2. Design Stresses

The design stress, the maximum principal tensile stress allowed for the glazing, f_{un}, is set at 16000 psi. This correlates with a probability of failure equal to or less than 0.001. The design stress for blast-resistant glazing is slightly higher than that commonly used in the design of one-minute wind loads, but, it is justified because of the expected, significantly shorter, duration of loading.

6-29.3. Dynamic Response to Blast Load

An analytical model was used to predict the blast load capacity of annealed and tempered glazings. Characteristic parameters of the model are illustrated in Figure 6-27.

The glazing is a rectangular, fully thermally tempered glass plate having a long dimension, a; a short dimension, b; a thickness, t; a poisson ratio, ν = 0.22; and an elastic modulus, $E = 1 \times 10^6$ psi. The plate is simply supported along all four edges, with no inplane and rotational restraints at the edges. The bending stiffness of the support elements is assumed to be infinite relative to the pane. Recent static and blast load tests indicate that the allowable frame member deflections of 1/264-th of the span will not significantly reduce pane resistance from that predicted for an infinitely stiff frame.

The blast pressure loading is described by a peak triangular-shaped pressure-time curve as shown in Figure 6-27. The blast pressure rises instantaneously to a peak blast pressure, B, and then decays linearly with a blast pressure duration, T. The pressure is uniformly distributed over the surface of the pane and applied normal to the pane.

The resistance function, r(X) (static uniform load, r as a function of center deflection, X) for the plate accounts for both bending and membrane stresses. The effects of membrane stresses produce a nonlinear stiffness of the resistance-deflection function (Figure 6-27). The design deflection, X_u, is defined as the center deflection where the maximum principle tensile stress at any point in the glass first reaches the design stress, f_{un}, of 16,000 psi. Typically, as the deflection of the plate exceeds a third of its thickness, the points of maximum stress will migrate from the center and toward the corners of the plate.

The model, illustrated in Figure 6-27, uses a single-degree-of-freedom system to simulate the dynamic response of the plate. To be conservative, no damping of the window pane is assumed. The model calculates the peak blast pressures required to exceed the prescribed probability of failure. The model assumes that failure occurs when the maximum deflection exceeds ten times the glazing thickness. This restricts solutions to the valid range of the Von Karmen plate equations while preventing edge disengagement of the plate.

6-29.4. Design Charts

Charts are presented in Figures 6-28 to 6-48 and Tables 6-6 to 6-12 for the design and evaluation of glazing to survive a prescribed blast loading with a probability of failure no greater than 0.001. The charts relate the peak blast overpressure capacity of thermally tempered glazing to all combinations

of the following design parameters: a/b = 1.00, 1.25, 1.50, 1.75 2.00, 3.00, and 4.00; $1.00 \leq ab \leq 25$ ft^2; $12 \leq b \leq 60$ inches; $2 \leq T \leq 1{,}000$ msec; and t = 1/4, 5/16, 3/8, 1/2, 5/8, and 3/4 inches (nominal). Thermally tempered glass up to 3/4 inch thick can easily be purchased in the United States. Thickness greater than 3/4 inch can only be obtained by lamination, but, research and blast load testing are required to develop approved designs for laminated glass.

The charts are based on the minimum thickness of fabricated glass allowed by Federal Specification DD-G-451d (see Table 6-7). They are created by numerically integrating the equations of motion of a single-degree-of-freedom system as modeled in Figure 6-27. A Wilson-Theta technique was employed with a time step corresponding limited to 1/25th of each of the five increasing linear resistances used to model the resistance function.

6-29.5. Alternate Design Procedure

Design procedures in this section can be used to evaluate the blast capacity of monolithic tempered glass when interpolation between charts is unadvisable, when design parameters are outside the limits of the chart, or to calculate rebound loads. It is recommended that the design charts be used for initial guesses of required glass thickness.

Procedures to calculate resistance, r_u, (Table 6-6) deflection, X_u, effective static resistance, r_{eff}, effective pane stiffness, K_e, and the period of vibration, T_N follow. The response charts can be used with these parameters to determine dynamic response. Table 6-11 reports the fundamental period of vibration and Table 6-12 reports the effective elastic, static resistance for most dimensions of glass panes. In many cases these values and the single equation in Step 10 below can be used to directly compute blast overpressure capacity.

Step 1. Determine if the glass pane will behave as a linearly responding plate under the design load. If the ratio of the short side of the plate, b, to its actual (not nominal) thickness is less than the maximum in the second column of Table 6-8, then simple formulas can be used for parameters needed to use the response charts. Only glass panes above and to the left of the steeped line in Table 6-6 will qualify. If the glass pane has a b/t-ratio less than that specified in Table 6-8, the glass will behave in a nonlinear manner with the membrane stresses induced by straining of the neutral plane or axis of the plate. Proceed to steps 2-9 to determine key parameters for this nonlinear plate behavior.

For glass plates that respond linearly, the design static resistance and the effective elastic resistance are:

$$r_{eff} = r_u = C_r(t/b)^2 \text{ psi} \qquad 6\text{-}44a$$

The center deflection is:

$$X_u = C_D\ (b^2/t) \qquad 6\text{-}44b$$

Coefficients for computing the effective resistance, C_r, and the center deflection, C_D, are listed in Table 6-8.

The fundamental period of vibration is :

$$T_N = C_T (b^2/t) \qquad 6\text{-}45$$

Coefficient C_T is reported in the last column of Table 6-8. Proceed to Step 10 to determine blast capacity.

Step 2 For nonlinear behavior with the b/t-ratio greater than specified in column 2 of Table 6-8, determine the nondimensional design stress, S_{SD}, as:

$$S_{ND} = 0.0183 (b/t)^2 \qquad 6\text{-}46$$

where: b = short span of glass measured between center lines of the gaskets (inches), and

t = actual thickness of glass, from Table 6-7 (inches)

For values of a/b greater than 4, use a/b = 4.

Step 3 Enter Figure 6-49 with the values of S_{ND} and a/b to determine the nondimensional design load, L_{ND}.

Step 4 Compute static design resistance as:

$$r_u = 876{,}000 (L_{ND})(t/b)^4 \text{ psi} \qquad 6\text{-}47$$

Use this value for frame design calculations other than those for rebound. Use r_{eff} defined in Step 7 for the rebound phase.

Step 5 Use a/b and L_{ND} in Figure 6-50 to obtain the nondimensional deflection, X/t. If X/t exceeds 10, use the value of L_{ND} corresponding to an X/t of 10 and recalculate r_u using Figure 6-49.

Step 6 Determine center deflection of the glass pane as:

$$X_u = (X/t)t, \text{ inches} \qquad 6\text{-}48$$

Step 7 Determine the effective elastic, static design resistance as:

$$r_{eff} = 0.4 (r_1 + r_2 + r_3 + r_4 + 0.5r_u) \text{ psi} \qquad 6\text{-}49$$

where: r_1 = resistance at 0.2 X_u
r_2 = resistance at 0.4 X_u
r_3 = resistance at 0.6 X_u
r_4 = resistance at 0.8 X_u
r_u obtained in Step 4
X_u obtained in Step 6

Figures 6-49 and 6-50 should be used for r_1 through r_4. The equivalent static design load is the resistance that a linearly responding plate would exhibit at the same strain energy as the nonlinearly responding plate at the design center deflection X_u. It is always less than r_u. By this technique, the linear response charts can be used with reasonable accuracy.

Step 8 Determine effective stiffness as:

$$K_E = r_{eff}/X_u, \text{ psi/in} \qquad 6\text{-}50$$

Step 9 Determine the fundamental period of vibration as:

$$T_N = 2\pi \, (K_{LM} \, m / K_E)^{1/2}, \text{ msec} \qquad 6\text{-}51$$

where: $K_{LM} = 0.63 + 0.16(a/b - 1)$ $\quad 1 \leq a/b \leq 2$
$K_{LM} = 0.79$ $\quad a/b \geq 2$

The unit mass, m, of the glass is:

$$m = 233t, \text{ lb-ms}^2/\text{in}^3$$

Step 10 Use Figure 3-49 of Chapter 3 with the ratio of load duration to period of vibration, T/T_N, to obtain the dynamic load factor, D_{LF}. The blast overpressure capacity of the glass pane is:

$$B = r_{eff}/D_{LF} \qquad 6\text{-}52$$

For T/T_N-ratios greater than 10, set D_{LF} equal to 2. For ratios less than 0.05, set D_{LF} equal to 0.3.

6-30. Design Criteria for Frames

6-30.1. Sealants, Gaskets, and Beads

All gaskets or beads must be at least 3/8 inch wide with a Shore "A" durometer hardness of 50 and conform to ASTM Specification C509-84 (Cellular Elastomeric Preformed Gasket Sealing Material). The bead and sealant must form a weather-proof seal.

6-30.2. Glazing Setting

Minimum frame edge clearances, face clearance, and bite (Figure 6-51) are specified in Table 6-7.

6-30.3. Frame Loads

The window frame must develop the static design strength, r_u of the glass pane (Table 6-6). Otherwise, failure will occur at less than the predicted blast pressure capacity of the window pane. This results from the frame deflections which induce higher principal tensile stresses in the pane, thus reducing the strain energy capacity available to resist the blast loading.

In addition to the load transferred to the frame by the glass, frame members must also resist the static design load, r_u, applied to all exposed members. Maximum allowable limits for frame design are:

1. Deflection: Relative displacements of frame members shall be the smallest of 1/264th of its span or 1/8 inch.

2. Stress: The maximum stress in any member shall not exceed $f_m/1.65$, where f_m is the yield stress of the members material.

3. Fasteners: The maximum stress in any fastener shall not exceed $f_m/2.00$.

The design loads for the glazing are based on large deflection theory, but the resulting design loads transferred to the frame are based on small deflection theory for normally loaded plates. Analysis indicates this approach to be considerably simpler and more conservative than using the frame loading based exclusively on large deflection plate behavior, characteristic of window panes. The effect of the static design load, r_u, applied directly to the exposed frame members of width, w, should also be considered.

The design load, r_u, produces a line shear, V_x, applied by the long side, a, equal to:

$$V_x = C_x r_u b \sin(\pi x/a) + r_u w, \text{ lb/in} \qquad 6\text{-}53$$

The design load, r_u, produces a line shear, V_y, applied by the short side, b, equal to:

$$V_y = C_y r_u b \sin(\pi y/a) + r_u w, \text{ lb/in} \qquad 6\text{-}54$$

The design load also produces a corner concentrated load, R, tending to uplift the corners of the window pane equal to:

$$R = C_R r_u b^2, \text{ lb} \qquad 6\text{-}55$$

Distribution of these forces are illustrated in Figure 6-52. Table 6-9 presents design coefficients, C_x, C_y, and C_R for practical aspect ratios. Linear interpolation can be used for aspect ratios not shown.

Although frames with mullions are included in the design criteria, it is recommended that single pane frames be used. Experience indicates that mullions complicate the design and reduce the reliability of blast-resistant frames. If mullions are used, the certification test must be conducted as the complexity of the mullion cross sections may cause some of the assumptions to be unconservative for local shear and stress concentrations. Also, economic analysis indicates that generally thicker glass will be more cost effective than the more complex mullion frame. If mullions are used, the loads from Equations 6-55 to 6-57 should be used to check the frame mullions and fasteners for compliance with deflection and stress criteria. Note that the design load for mullions is twice the load given by Equations 6-53 to 6-55 to account for the effects of two panes supported by a common mullion.

Special design considerations should be taken to assure that deflection of the building wall will not impose deflections on the frame greater than 1/264th of the length of the panes edge. When insufficient wall rigidity is provided, it is recommended that the frames be pinned at the corners to provide isolation from the walls rotation.

6-30.4. Rebound

Response to the dynamic loading will cause the window to rebound (outward deflection) after its initial positive (inward) deflection. The outward pane displacement and the stresses produced by the negative deflection must be safely resisted by the window while positive pressures act on the window. Otherwise, the window which safely resists stresses caused by inward deflections may fail in rebound while the positive pressure still acts. This can propel glass fragments into the structure. However, if the window fails in rebound during the negative phase of blast loading, glass fragments will be drawn away from the structure. Rebound will occur during the negative loading phase if the effective blast duration is no greater than one half of the natural period of vibration, T_N, of the glass pane. For $T \geq 10\ T_N$, significant rebound does not occur during the positive blast loading, so, for this situation, design for rebound is not required. For $0.5 \leq T/T_N \leq 10$, the frame must be designed for the peak negative pressure acting during the positive overpressure phase. Table 6-11 reports T_N for practical glass pane dimensions.

As the rebound chart, Figure 3-268 of Chapter 3, can be unconservative for predicting maximum rebound (for glass panes), dynamic analysis using numerical integration or a more conservative simplified analysis is required. In lieu of a numerical analysis, it is conservative to set the maximum rebound load, r^-, to the static design load, r_u. The resistance function for this analysis can be generated by the Alternate Design Procedure. If the pane has a b/t ratio less than specified in Table 6-8, the pane will behave as a linear plate and Equations 6-44 can be used to determine r_u, X_u, and the resistance function. If the pane has a b/t ratio larger than specified in Table 6-8, use Steps 2 through 7 to define the resistance function. The negative resistance function is a mirror image of the positive resistance function.

The portion of the frame outboard of the glass must resist the rebound load, r^-. Use Equations 6-53 to 6-55 to apply the rebound load to the frame members. In some design situations the resistance built into the member outboard of the glass to resist the corner concentrated force, R (Equation 6-55), during deflections of the pane inward will provide enough strength to resist rebound.

6-31. Acceptance Test Specification

Certification tests of the entire window assembly are required unless analysis demonstrates that the window design is consistent with the design criteria. All window assembly designs using mullions must be tested. The certification tests consist of applying static uniform loads on at least two sample window assemblies until failure occurs in either the glass or frame. Although at least two static uniform load failure tests are required, the acceptance criteria presented below encourages a larger number of test samples. All testing should be performed by an independent testing laboratory certified by the contracting officer.

6-31.1. Test Procedure - Window Assembly Test

The test windows (glass panes plus support frames) shall be identical in type, size, sealant, and construction to those furnished. The test frame assembly shall be secured to simulate the adjoining walls. Using either a vacuum or a

liquid-filled bladder, an increasing uniform load shall be applied to the entire window assembly (glass and frame) until failure occurs in either the glass or frame. Failure shall be defined as either breaking of glass or loss of frame resistance. The failure load shall be recorded to three significant figures. The load should be applied at a rate of 0.5 r_u per minute which corresponds to approximately one minute of significant stress duration until failure. Table 6-6 presents the static ultimate resistance of old tempered glass, correlated with a probability of failure, equal to 0.001 and a load duration of 1 second, whereas this criteria is for a load duration of 1 minute. This longer duration will weaken the glass by ceramic fatigue, but new glass should tend to be stronger than old glass. To account for these effects the certified static load capacity, r_s, of a glass pane is to be rated as:

$$r_s = 0.876\ r_u \qquad 6\text{-}56$$

6-31.2. Acceptance Criteria

The window assembly (frame and glazing) are considered acceptable when the arithmetic mean of all the samples tested, r, is such that:

$$\bar{r} \geq r_u + s\ \alpha \qquad 6\text{-}57$$

where

r_u = static ultimate resistance of the glass pane
s = sample standard deviation
α = acceptance coefficient

For n test samples, $\bar{r}$ is defined as:

$$\bar{r} = \frac{\sum_{i=1}^{n} r_i}{n} \qquad 6\text{-}58$$

where r_i is the recorded failure load of the i^{th} test sample. The standard sample deviation, s, is defined as:

$$s = \left[\frac{\sum_{i=1}^{n} \left[r_i - \bar{r} \right]^2}{(n-1)} \right]^{1/2} \qquad 6\text{-}59$$

The minimum value of the sample standard deviation, s, permitted to be employed in equation 6-47 is:

$$s_{min} = 0.145\ r_u \qquad 6\text{-}60$$

This assures a sample standard deviation which is no better than the ideal tempered glass in ideal frames.

The acceptance coefficient, α, is tabulated in Table 6-10 in terms of the number of samples tested.

The following equation is presented to aid in determining if additional test samples are justified. If:

$$\bar{r} \leq r_u + s\,\beta \qquad 6\text{-}61$$

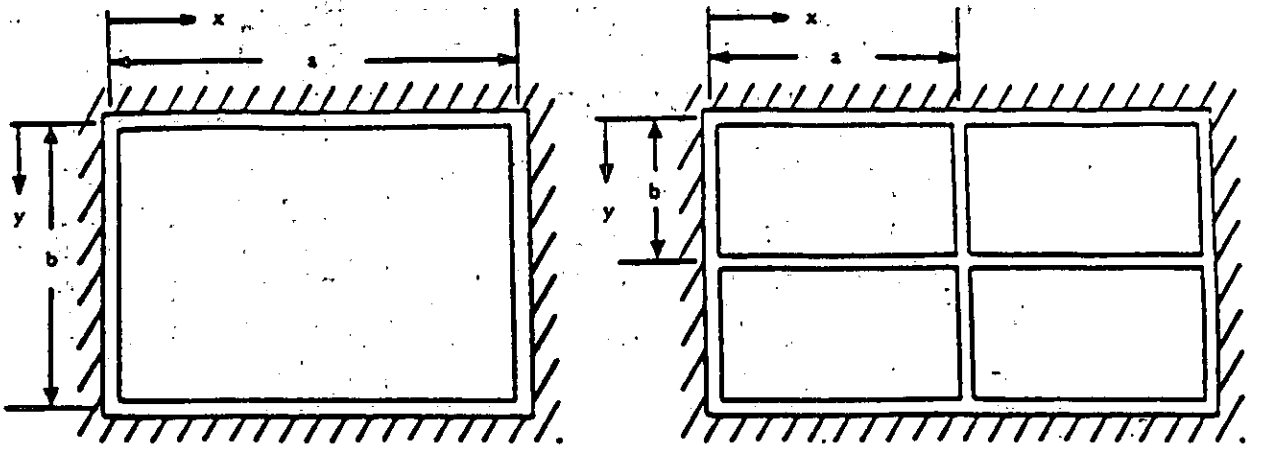
then with 90% confidence, the design will not prove to be adequate with additional testing. The rejection coefficient, β, is from Table 6-10.

6-31.3. Certification for Rebound

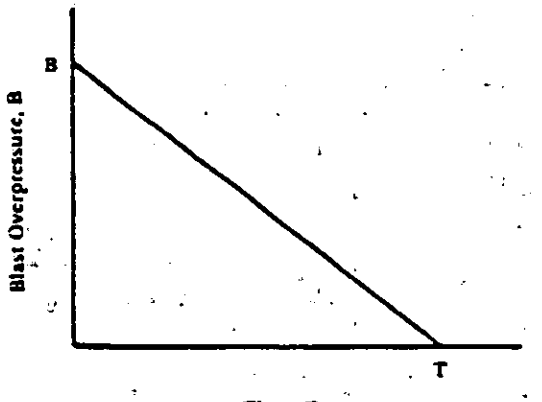
Acceptance testing shall be performed for rebound unless analysis demonstrates that the frame meets rebound criteria. All frames with mullions must be tested. Testing is performed with the load applied to the inboard surface of the window assembly. The equivalent static rebound load, $\bar{r}$, is substituted for the design load, r_u.

6-32. Installation Inspection

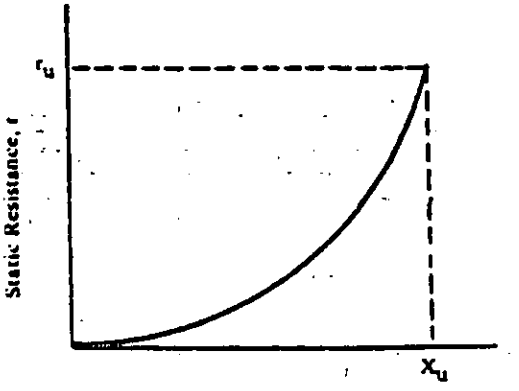
A survey of glazing failures due to wind load indicates that improper installation of setting blocks, gaskets, or lateral shims, or poor edge bite is a significant cause of the failures experienced.



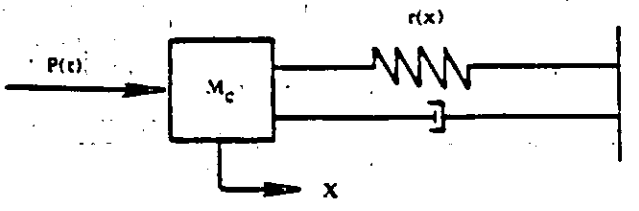
(a) Window pane geometry



(b) Blast loading



(c) Resistance of glass pane



(d) Dynamic response model

Figure 6-27 Characteristic parameters for glass pane, blast loading, resistance function and response model.

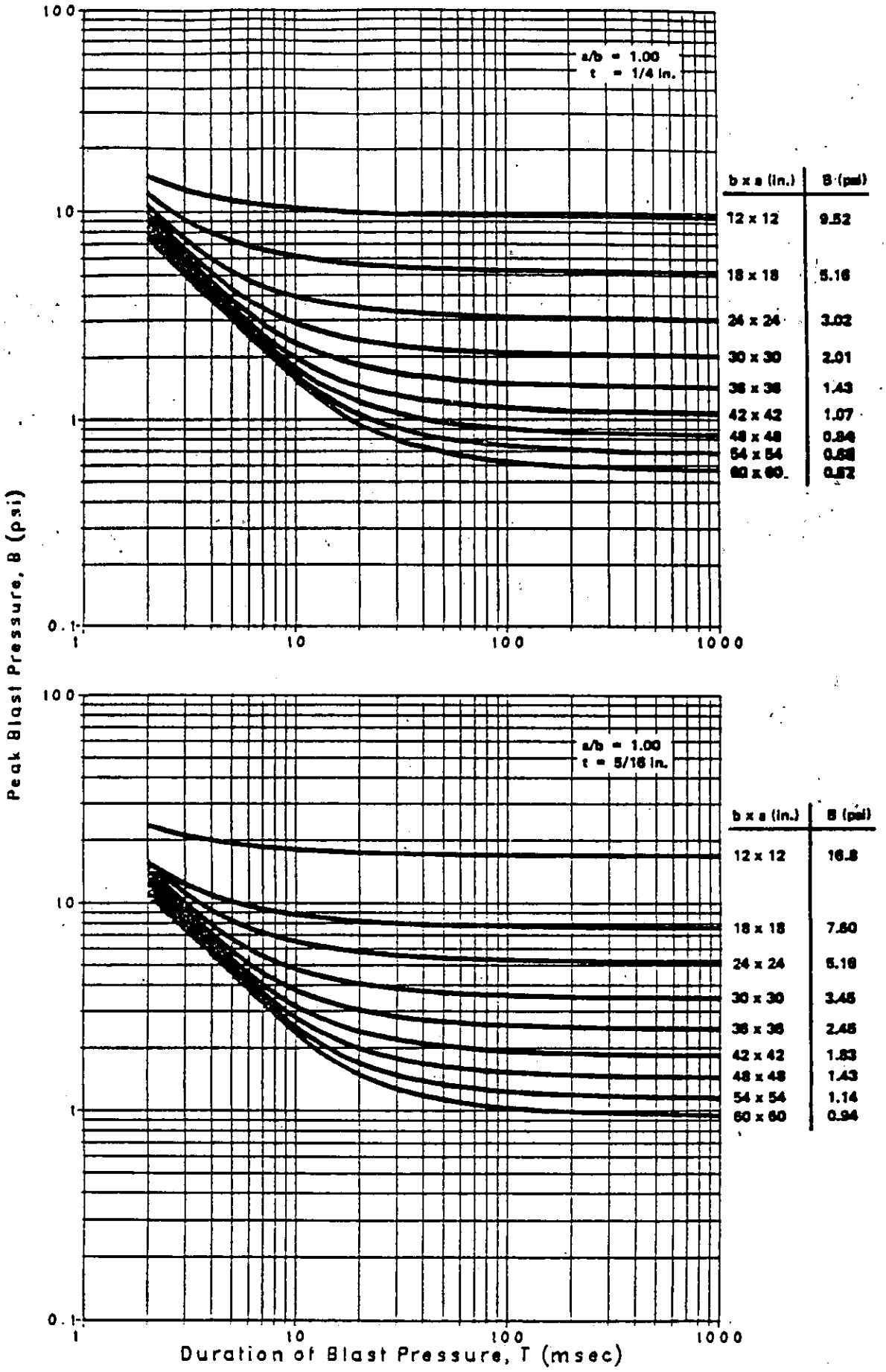


Figure 6-28 Peak blast pressure capacity for tempered glass panes: a/b = 1.00, t = 1/4 and 5/16 in.

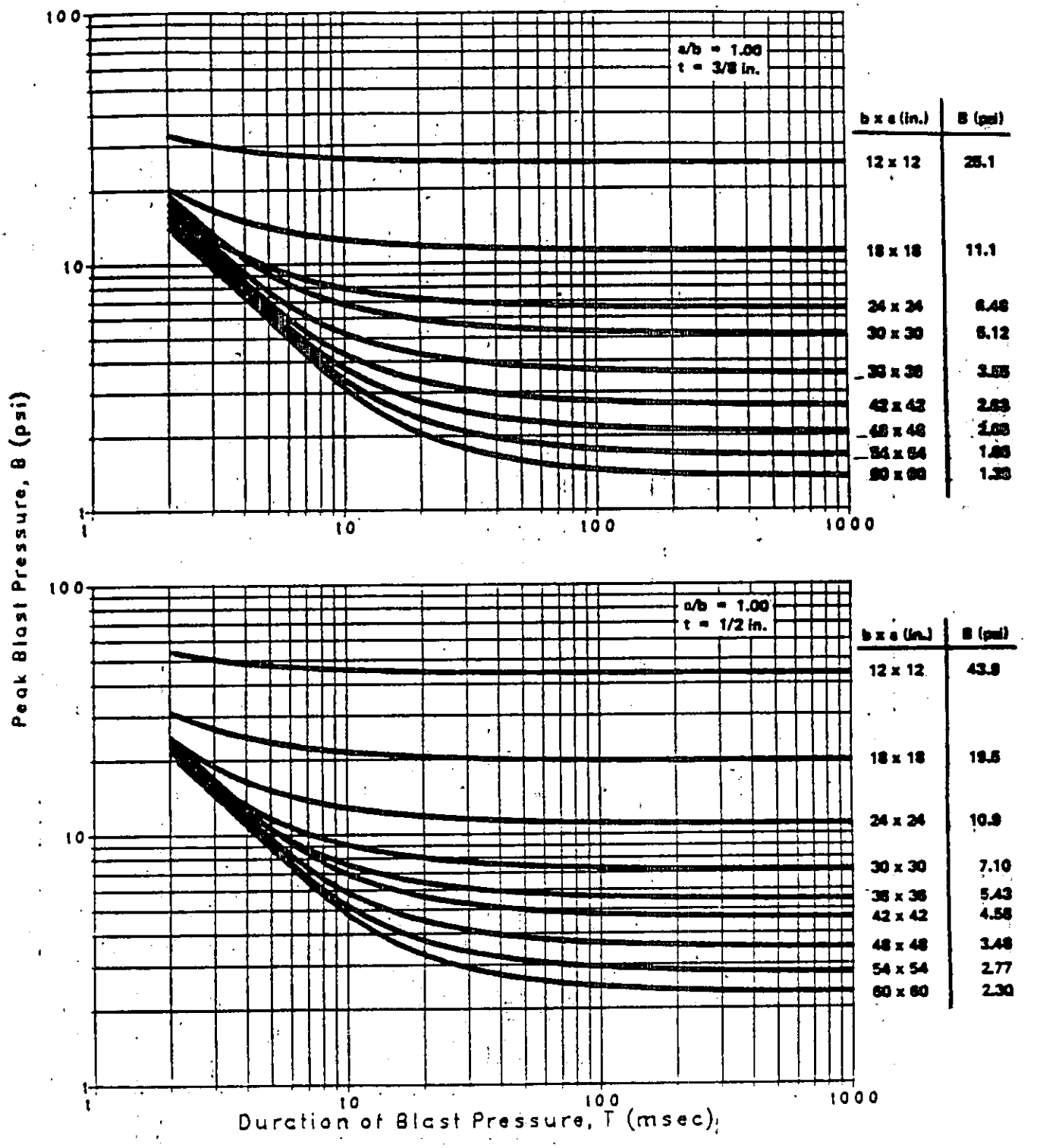


Figure 6-29 Peak blast pressure capacity for tempered glass panes: a/b = 1.00, t = 3/8 and 1/2 in.

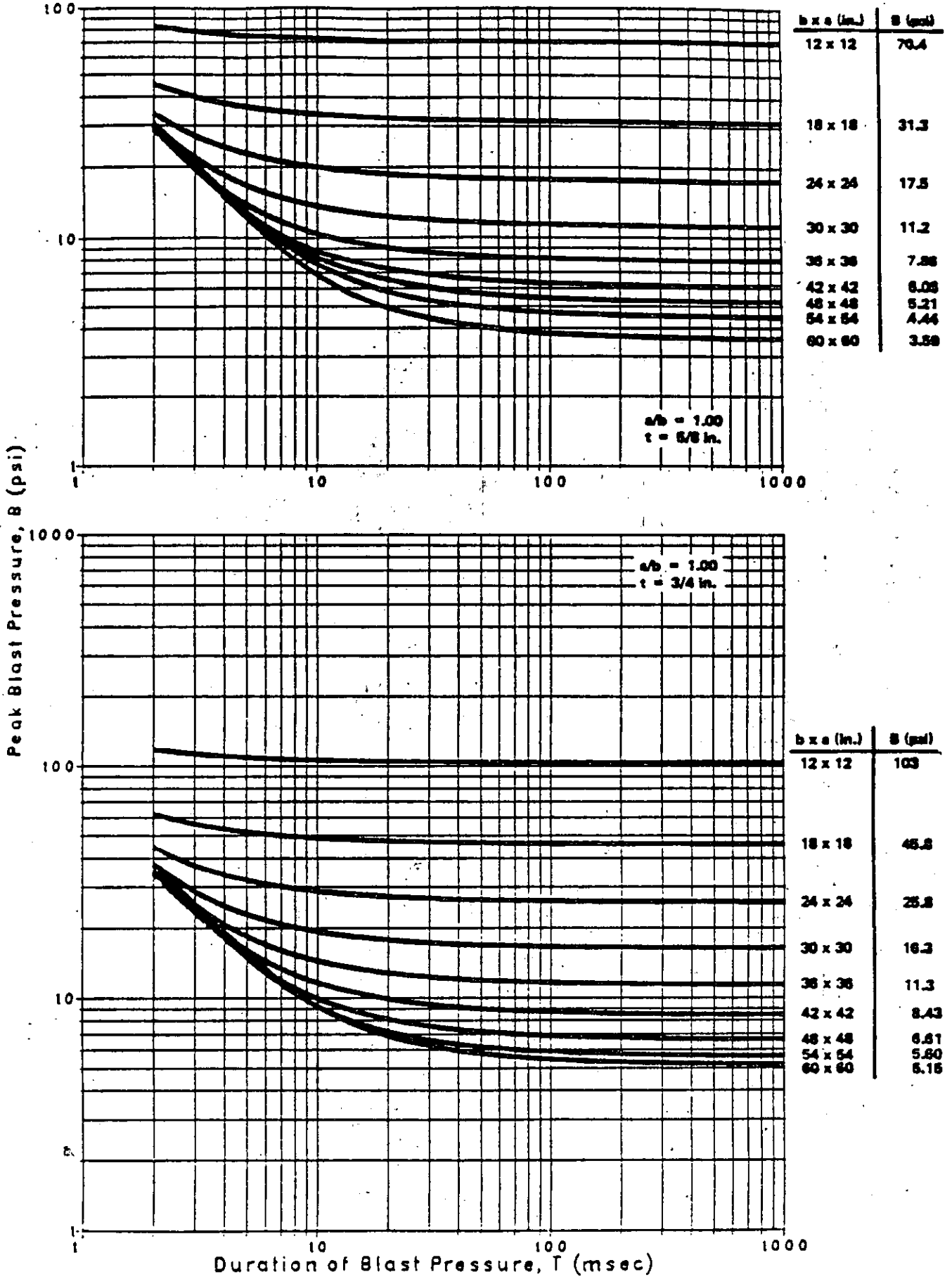


Figure 6–30 Peak blast pressure capacity for tempered glass panes: a/b = 1.00, t = 5/8 and 3/4 in.

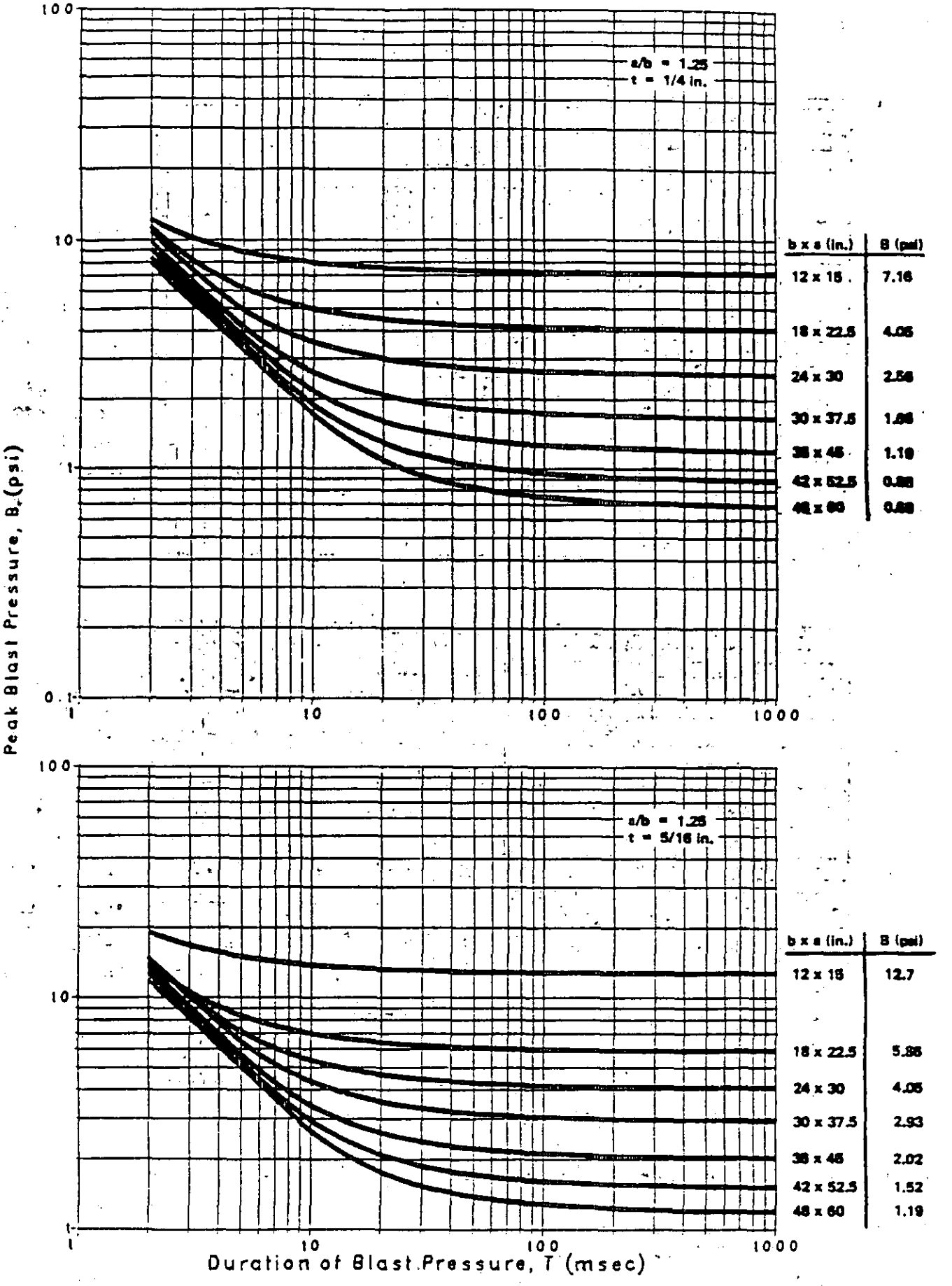


Figure 6-31 Peak blast pressure capacity for tempered glass panes: a/b = 1.25, t = 1/4 and 5/16 in.

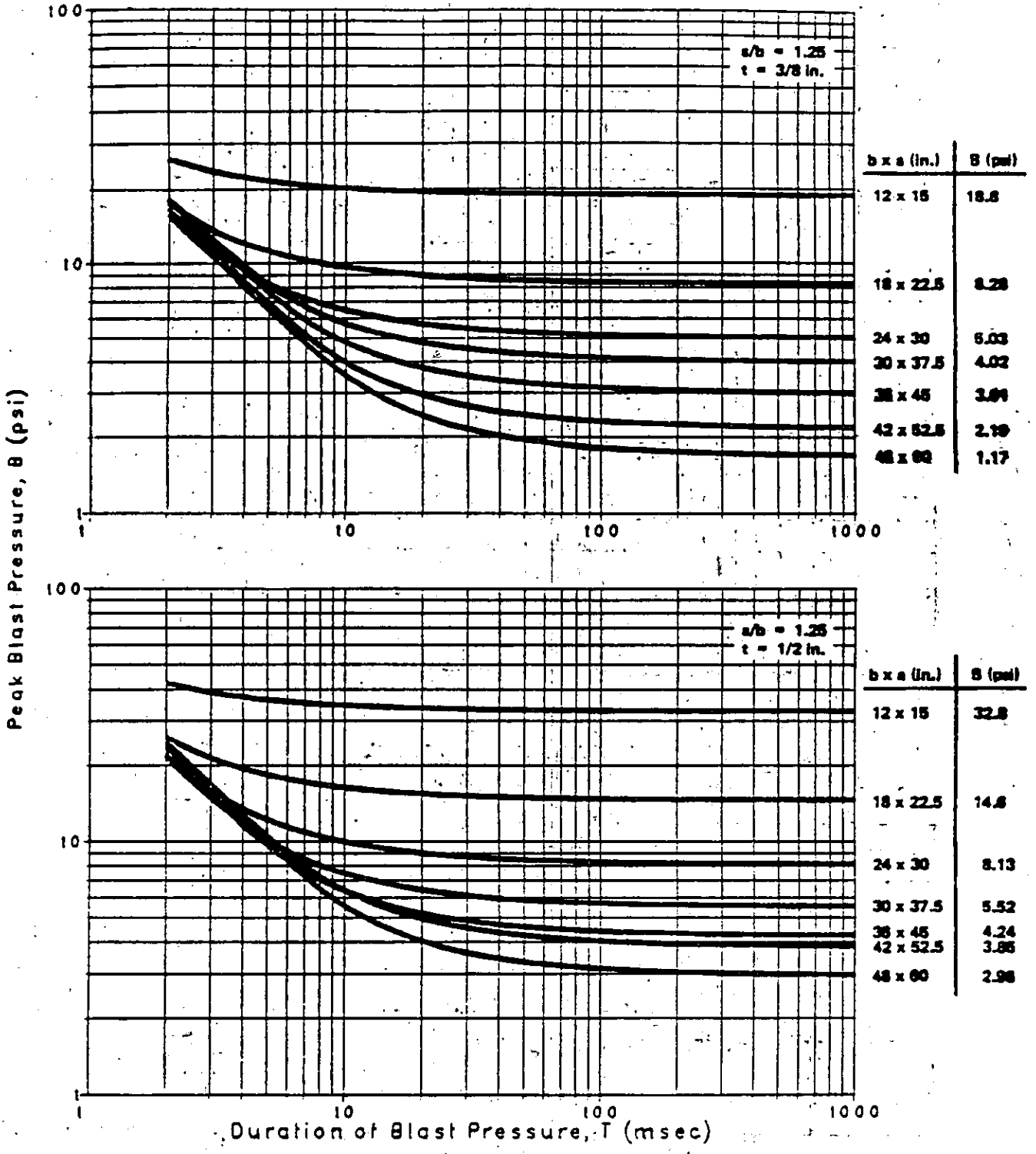


Figure 6-32 Peak blast pressure capacity for tempered glass panes: a/b = 1.25, t = 3/8 and 1/2 in.

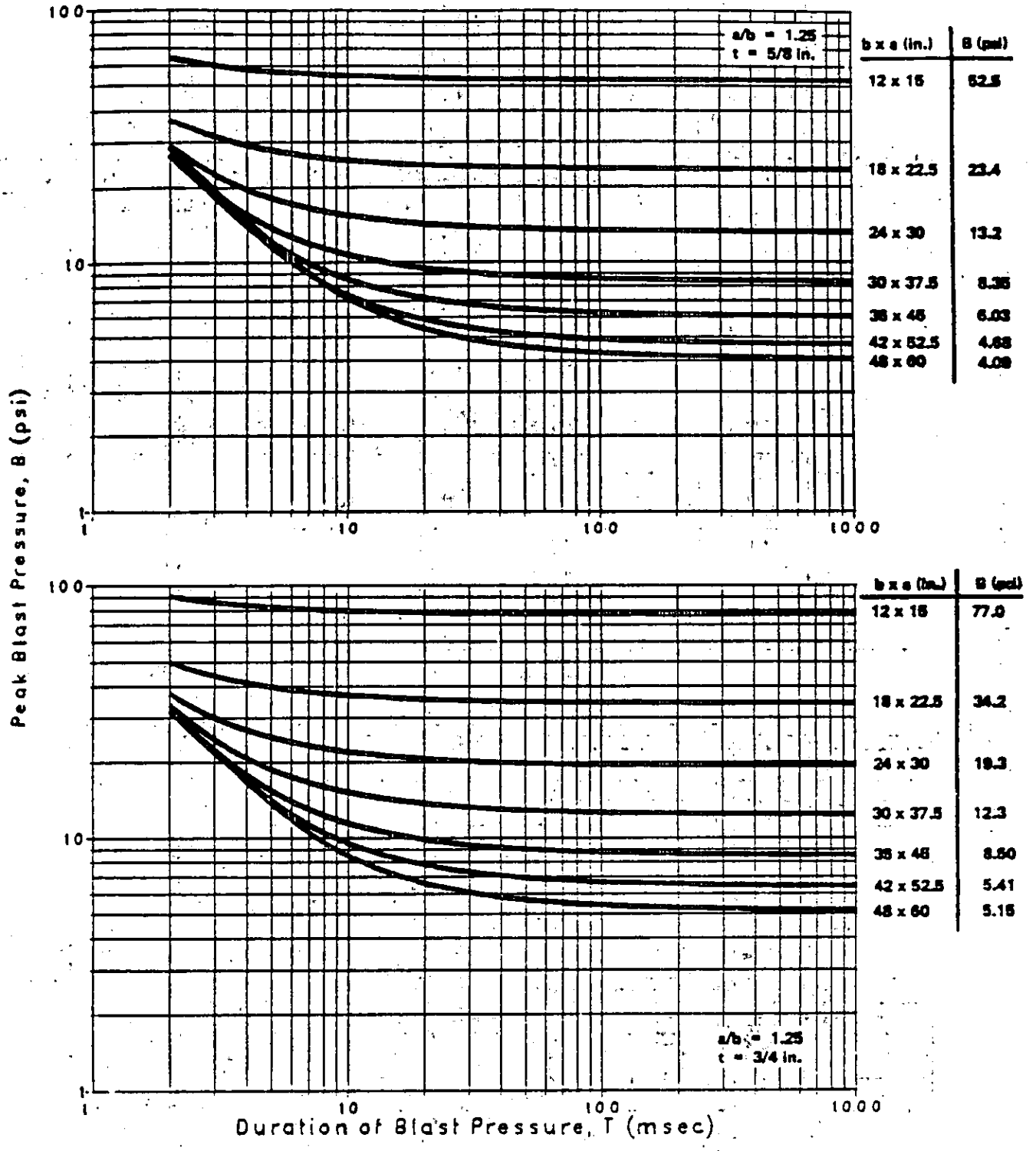


Figure 6–33 Peak blast pressure capacity for tempered glass panes: a/b = 1.25, t = 5/8 and 3/4 in.

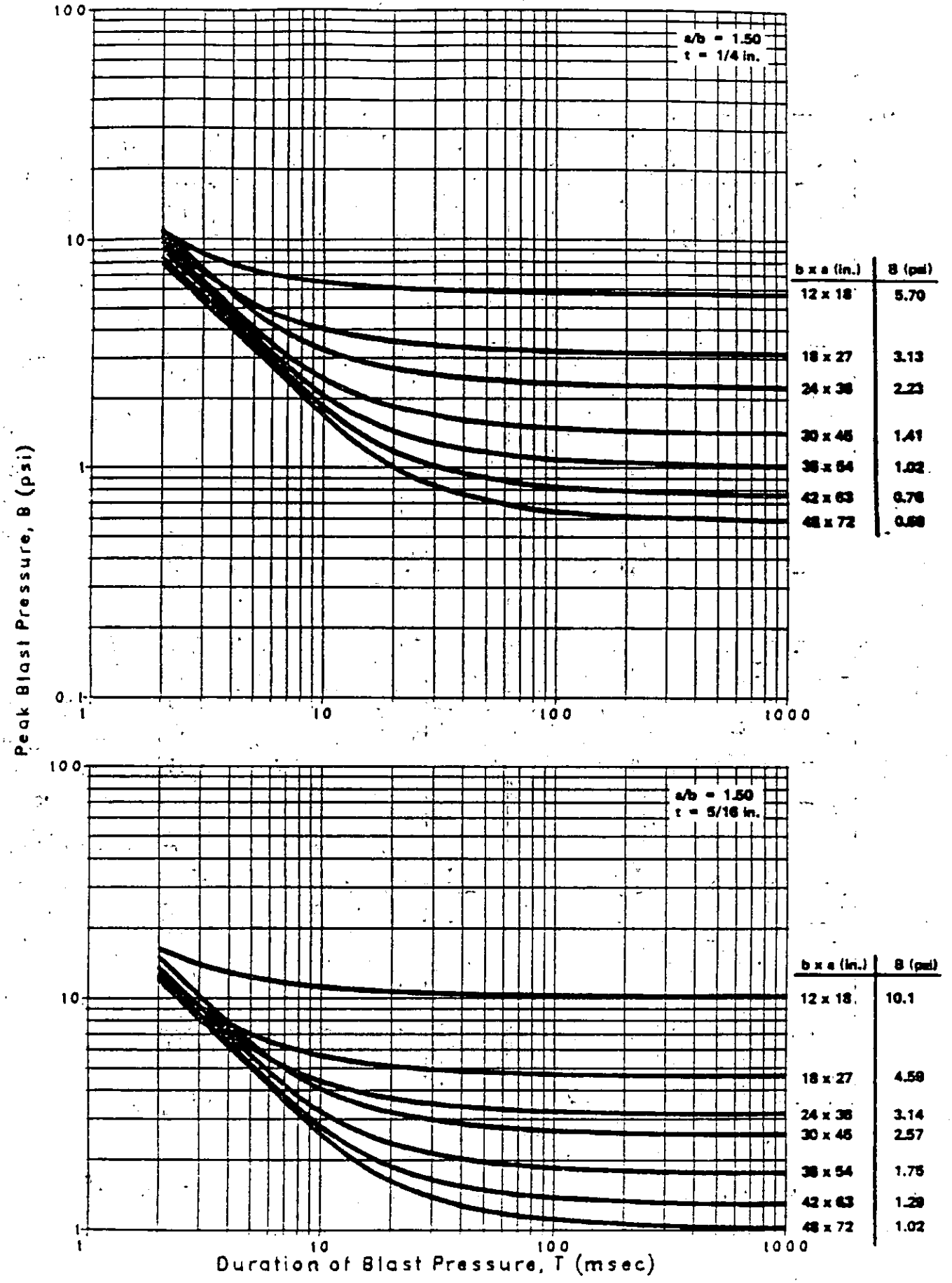


Figure 6-34 Peak blast pressure capacity for tempered glass panes: a/b = 1.50, t = 1/4 and 5/16 in.

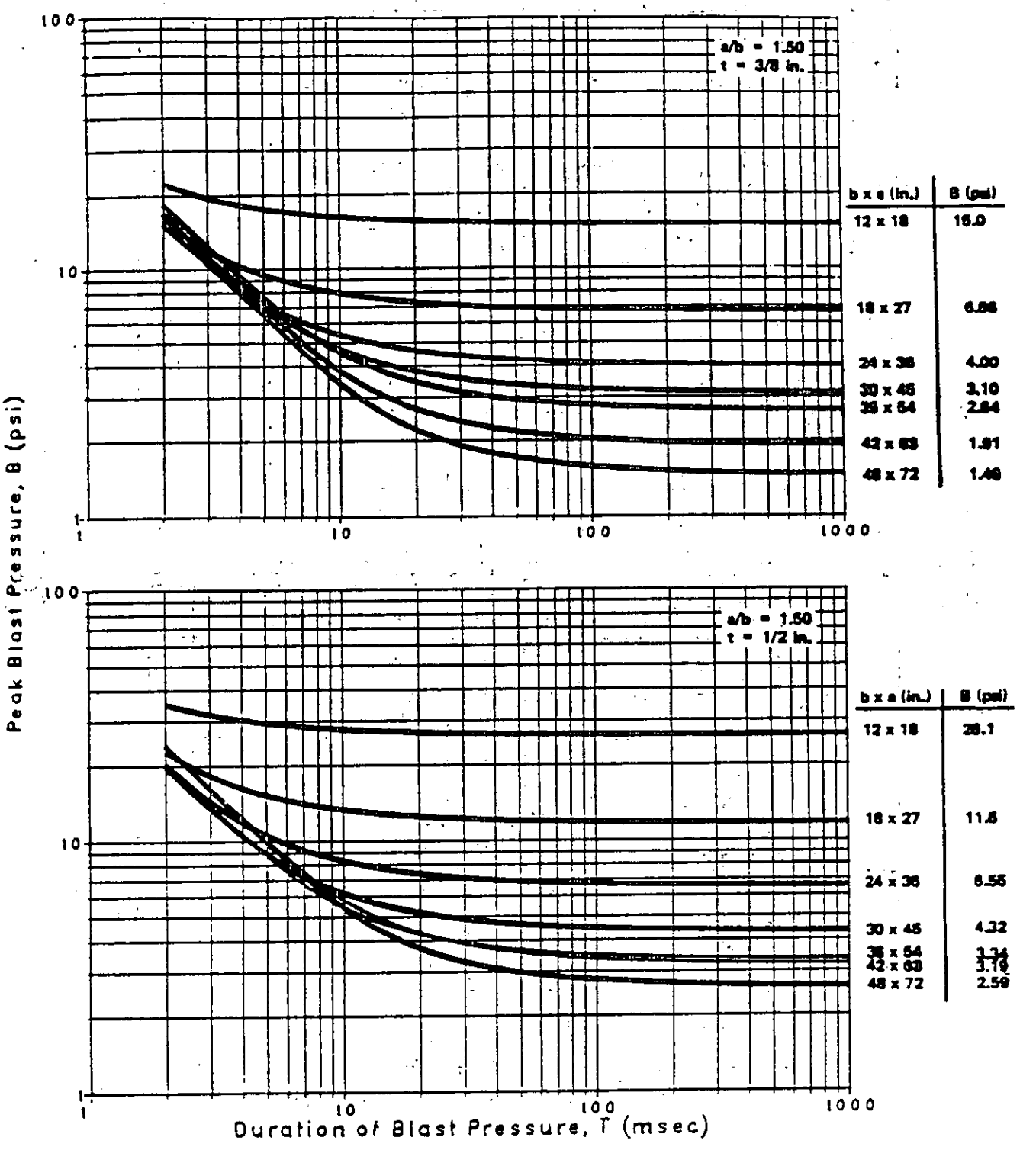


Figure 6-35 Peak blast pressure capacity for tempered glass panes: a/b = 1.50, t = 3/8 and 1/2 in.

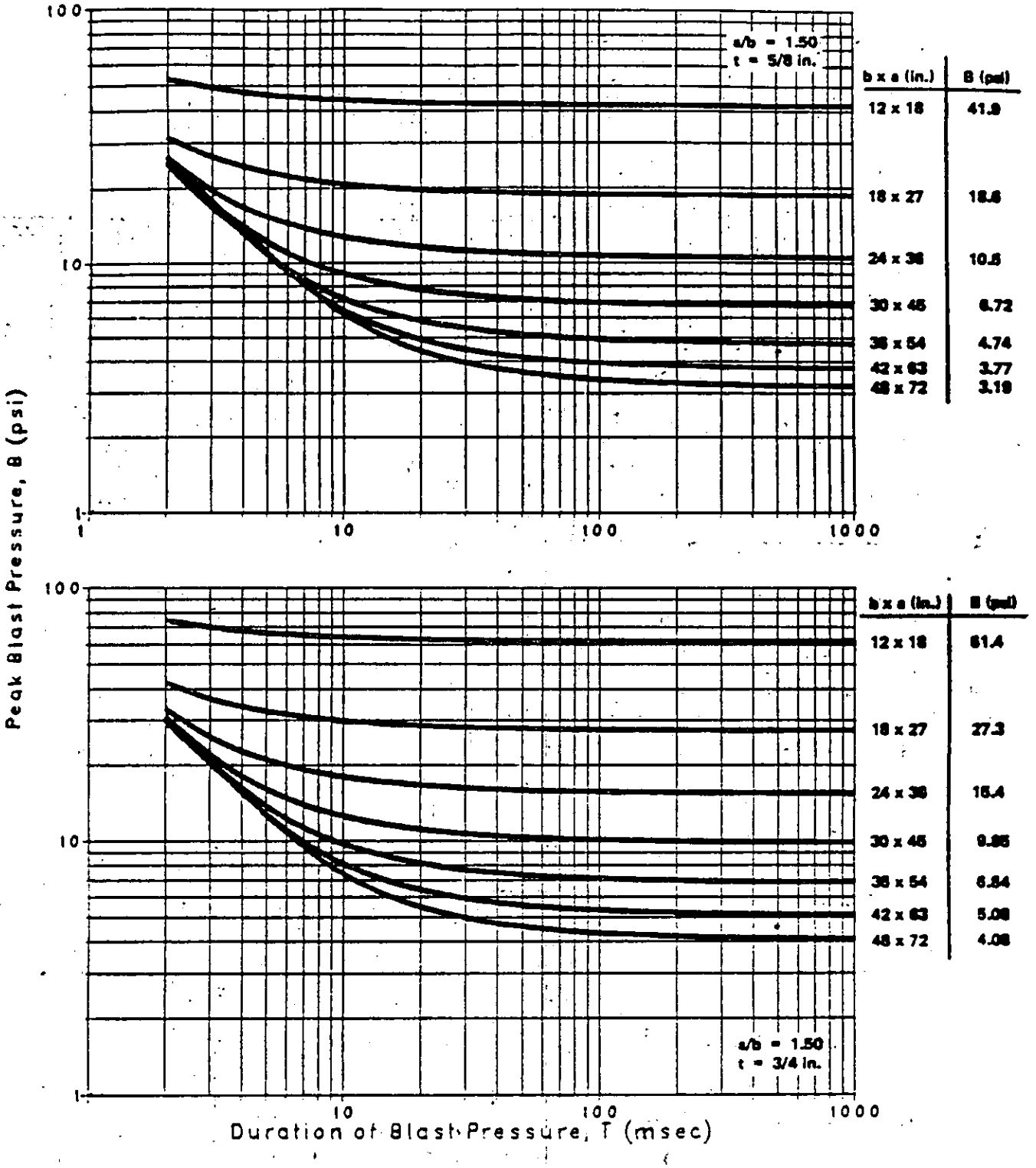


Figure 6-36 Peak blast pressure capacity for tempered glass panes: a/b = 1.50, t = 5/8 and 3/4 in.

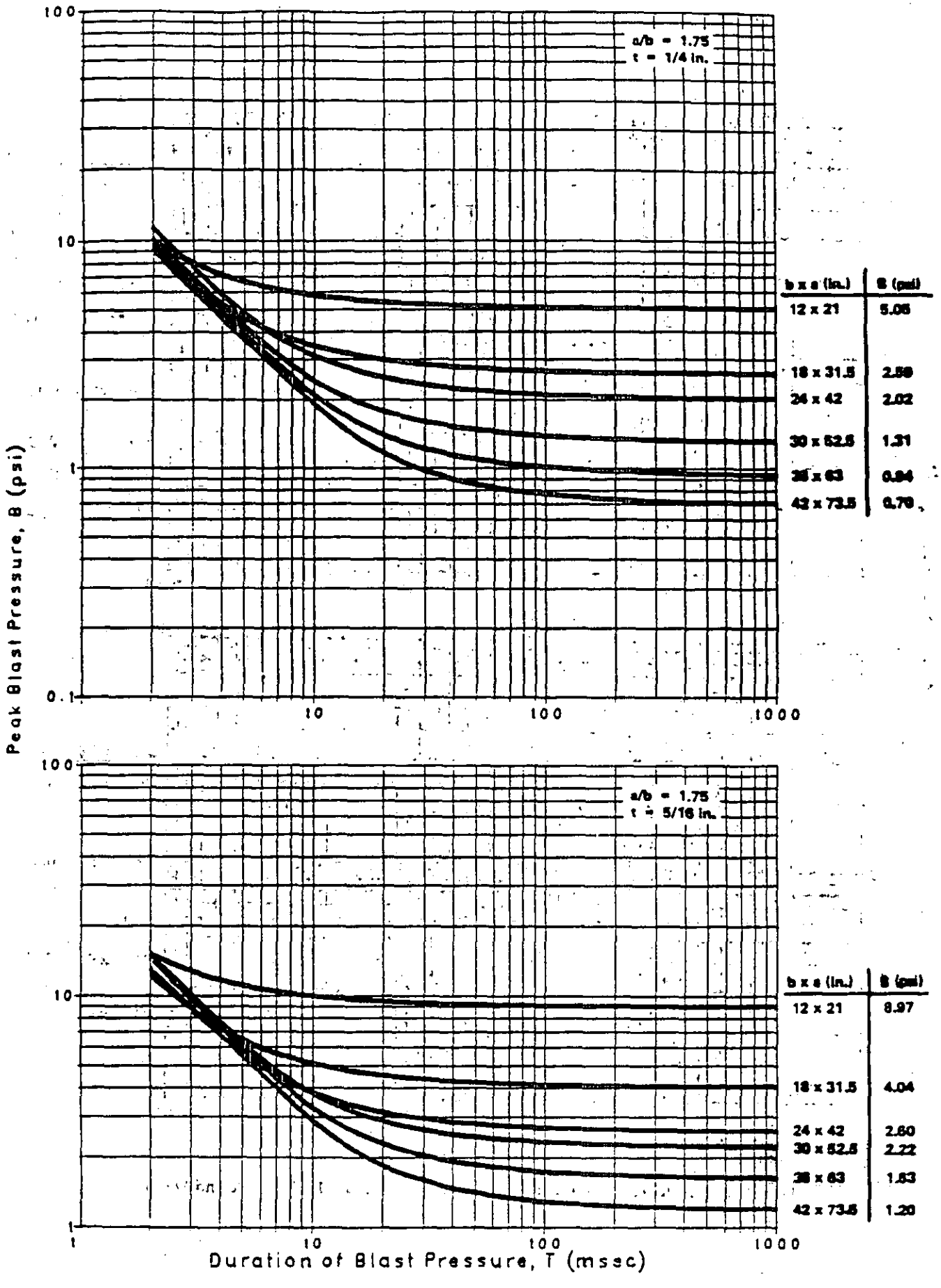


Figure 6-37 Peak blast pressure capacity for tempered glass panes: a/b = 1.75, t = 1/4 and 5/16 in.

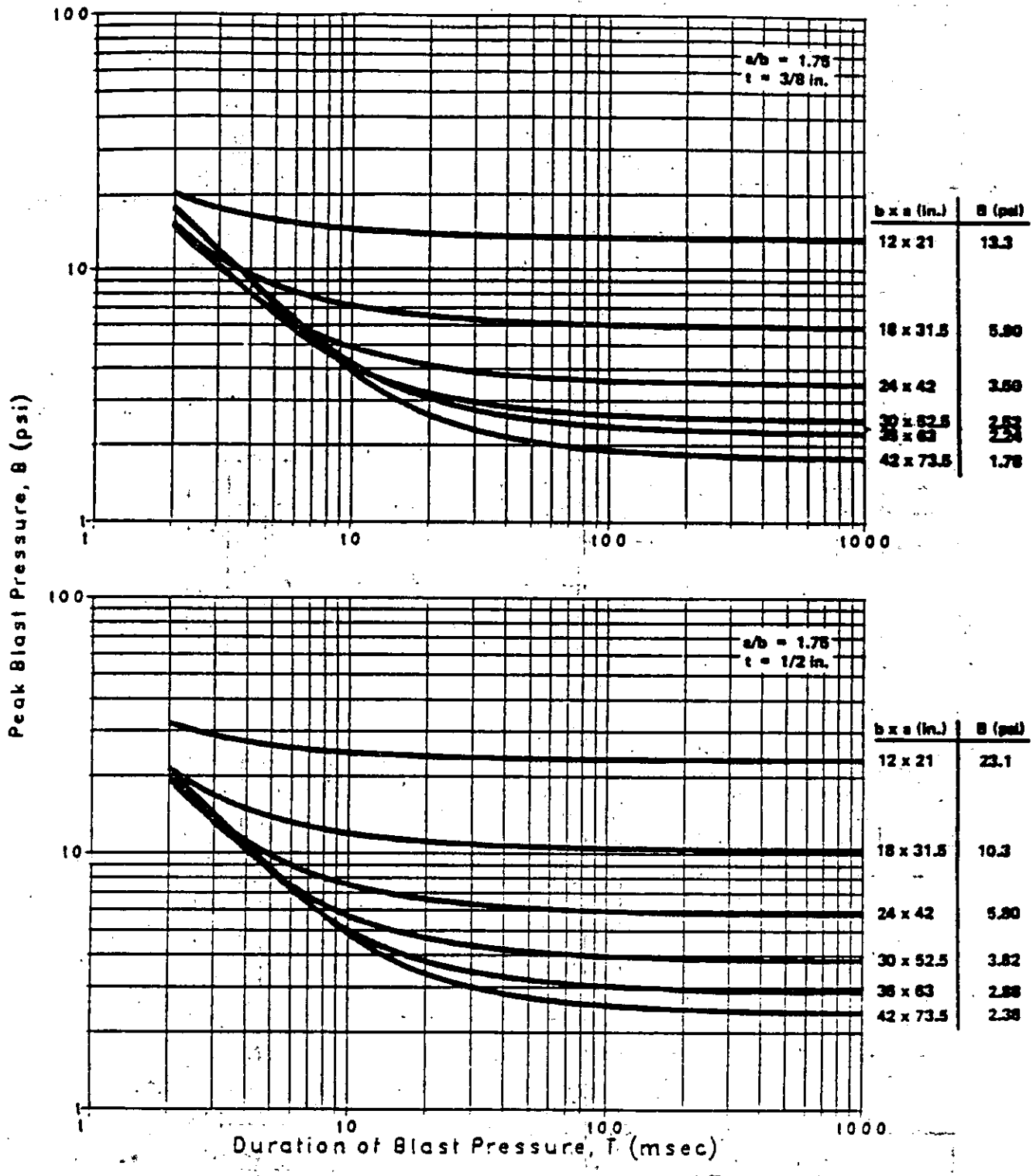


Figure 6-38 Peak blast pressure capacity for tempered glass panes: a/b = 1.75, t = 3/8 and 1/2 in.

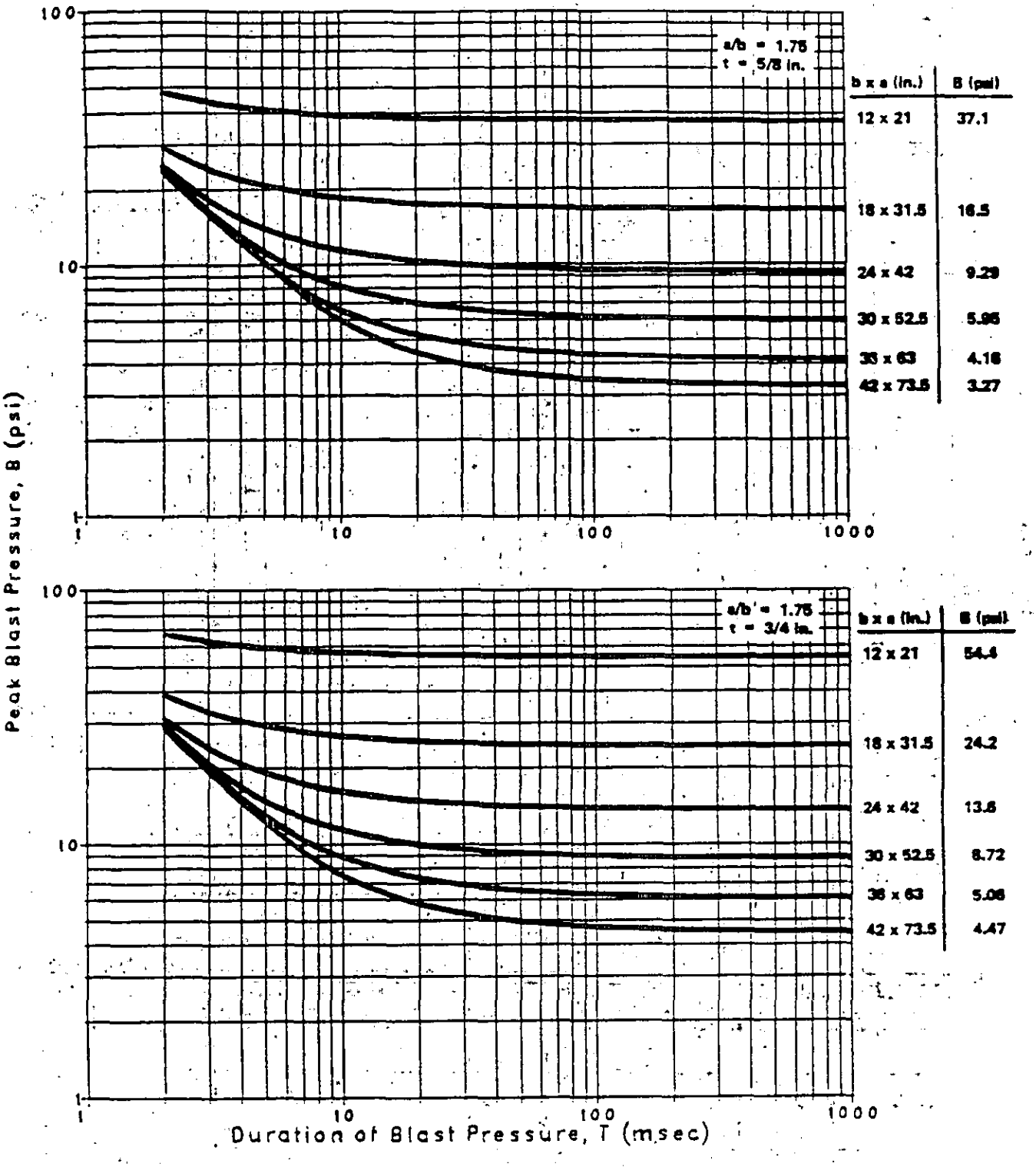


Figure 6-39 Peak blast pressure capacity for tempered glass panes: a/b = 1.75, t = 5/8 and 3/4 in.

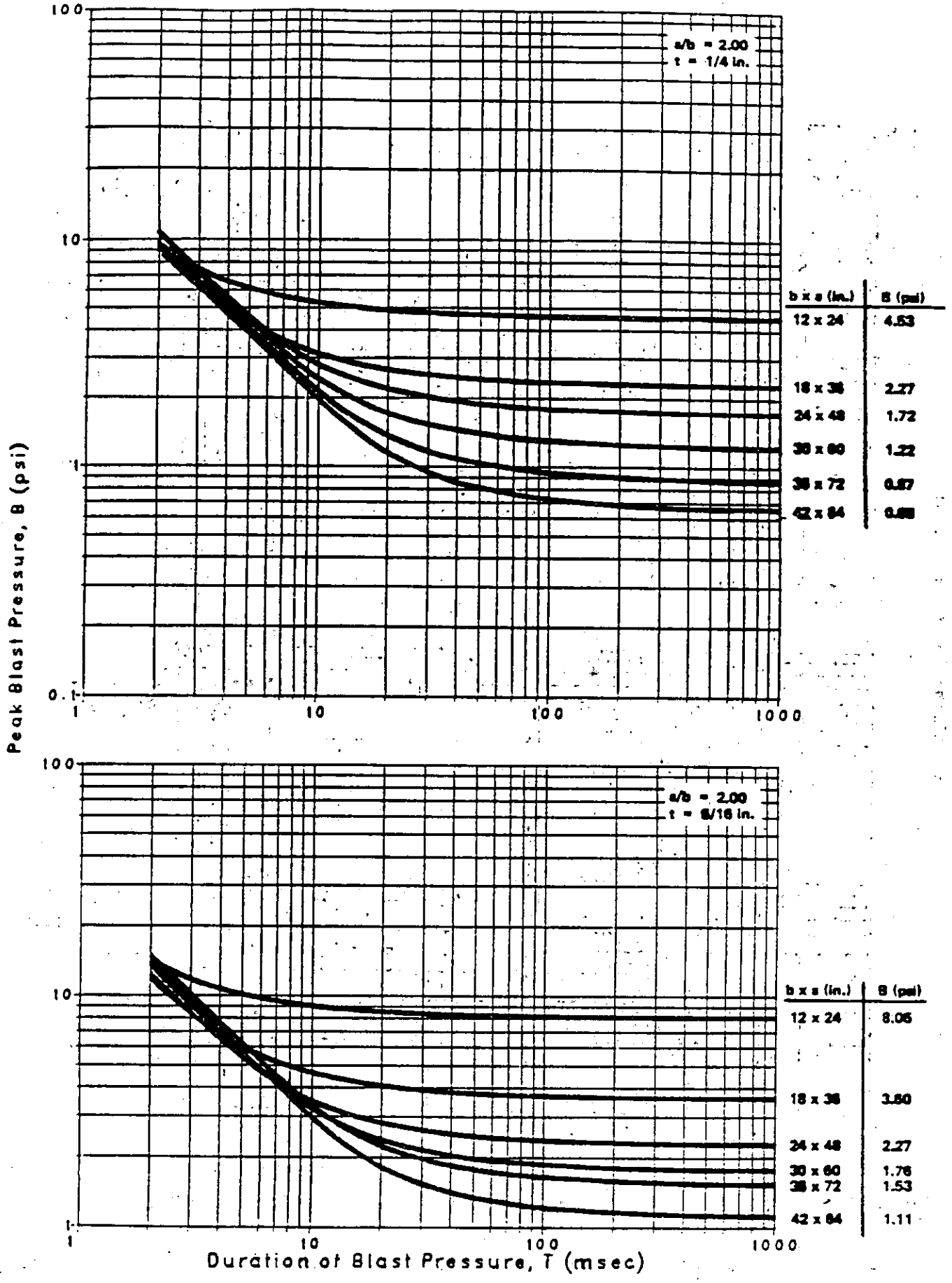


Figure 6–40 Peak blast pressure capacity for tempered glass panes: a/b = 2.00, t = 1/4 and 5/16 in.

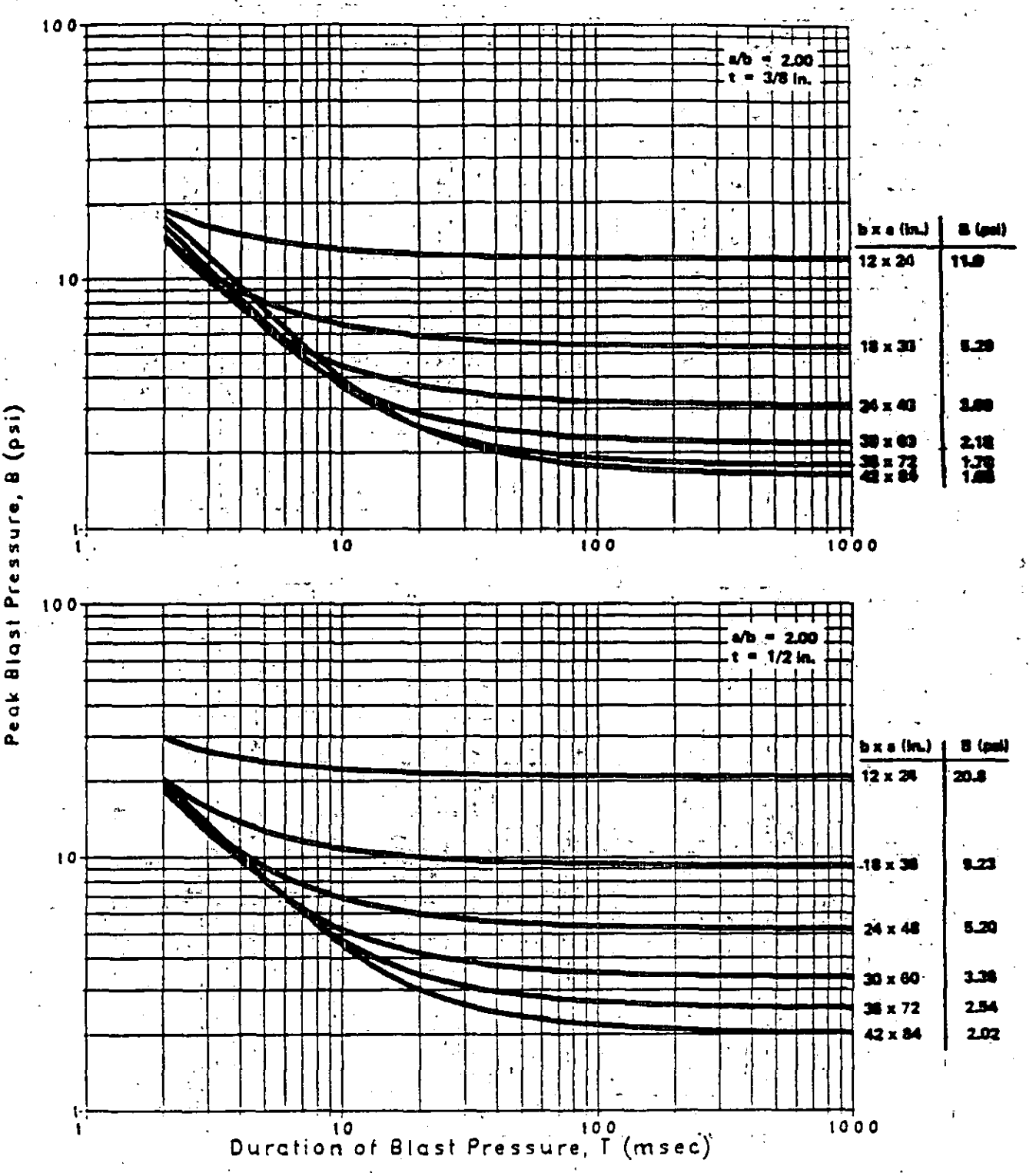


Figure 6-41 Peak blast pressure capacity for tempered glass panes: a/b = 2.00, t = 3/8 and 1/2 in.

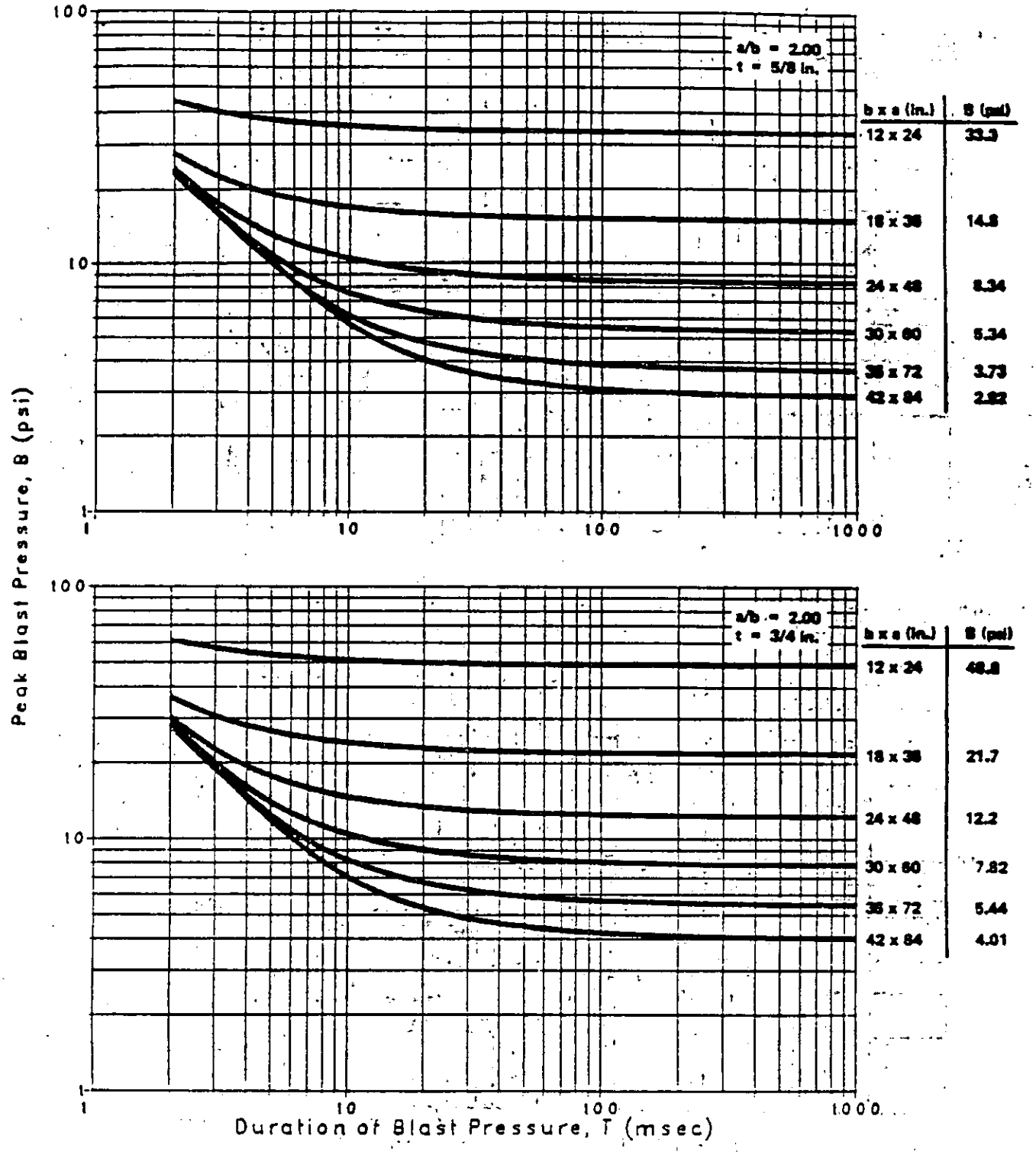


Figure 6-42

Peak blast pressure capacity for tempered glass panes: a/b = 2.00, t = 5/8 and 3/4 in.

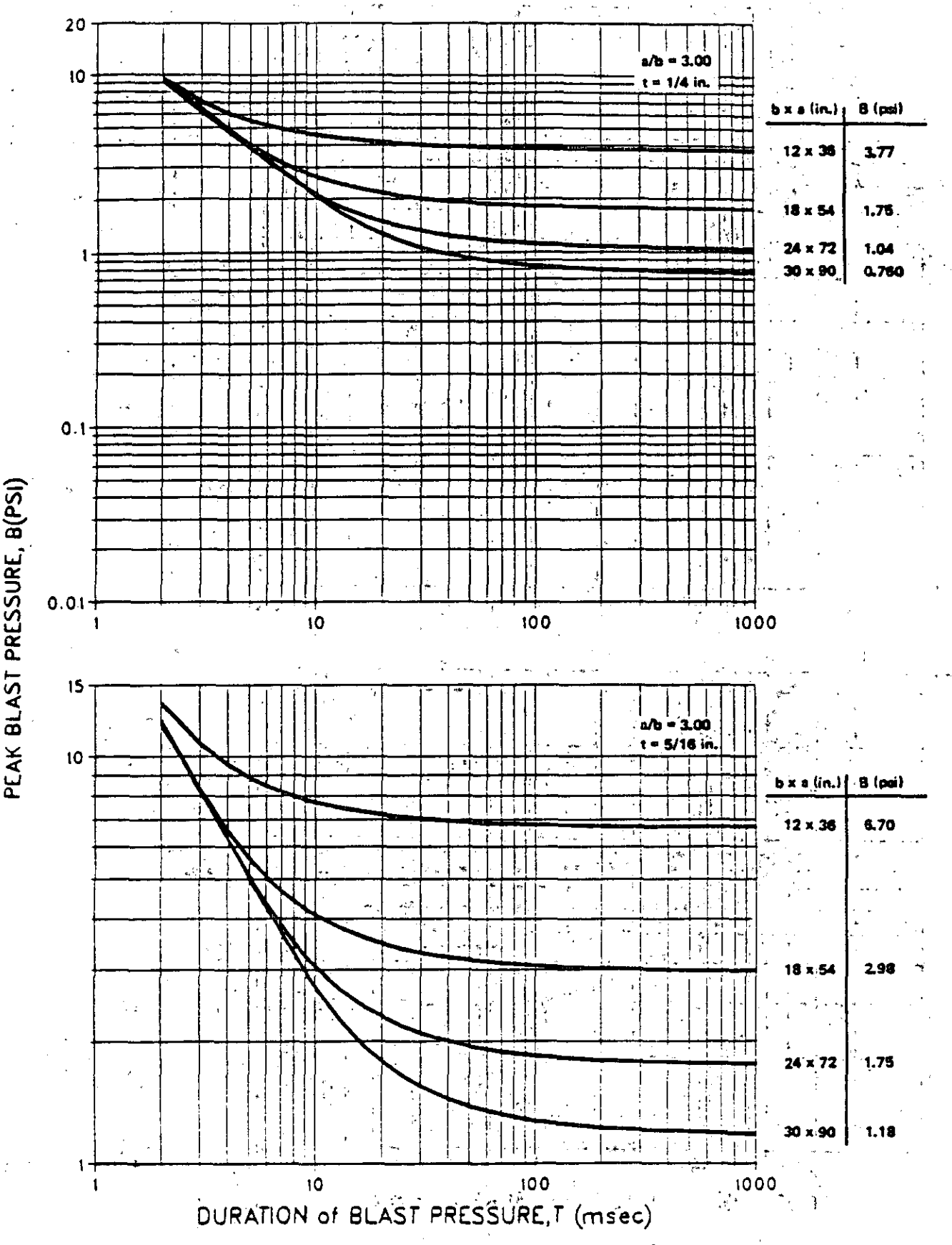


Figure 6-43 Peak blast pressure capacity for tempered glass panes: a/b = 3.00, t = 1/4 and 5/16 in.

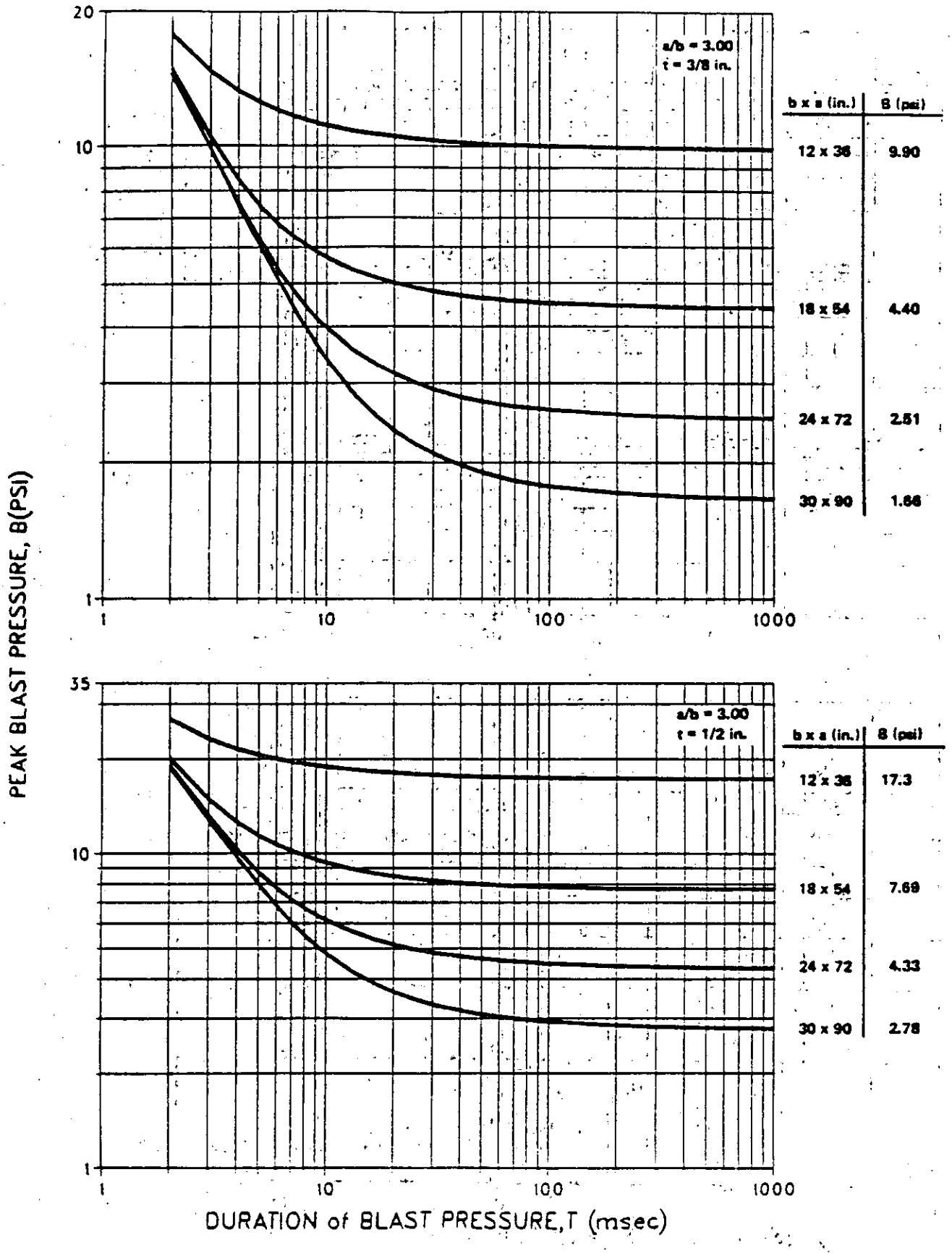


Figure 6-44 Peak blast pressure capacity for tempered glass panes: a/b = 3.00, t = 3/8 and 1/2 in.

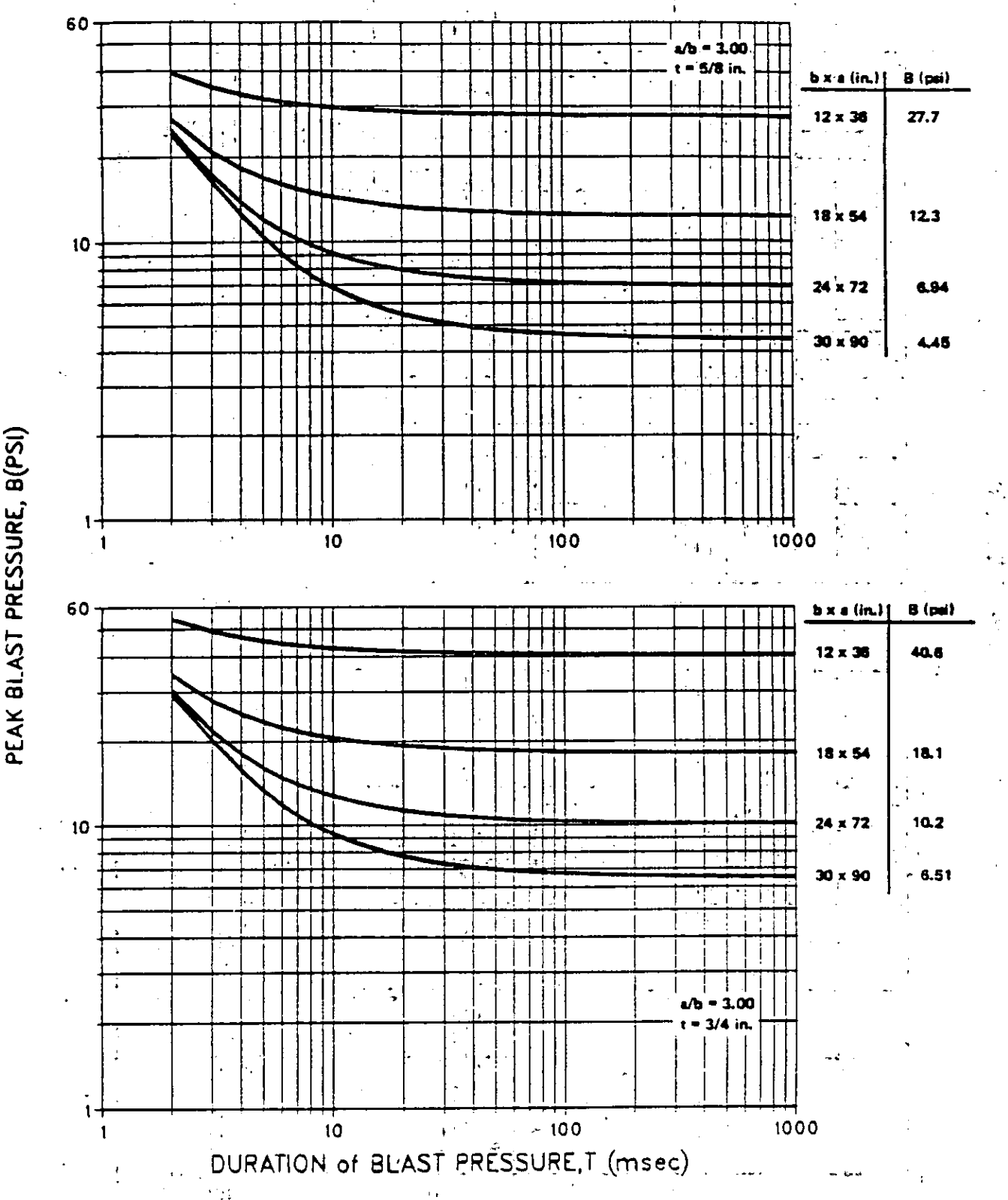


Figure 6–45 Peak blast pressure capacity for tempered glass panes: a/b = 3.00, t = 5/8 and 3/4 in.

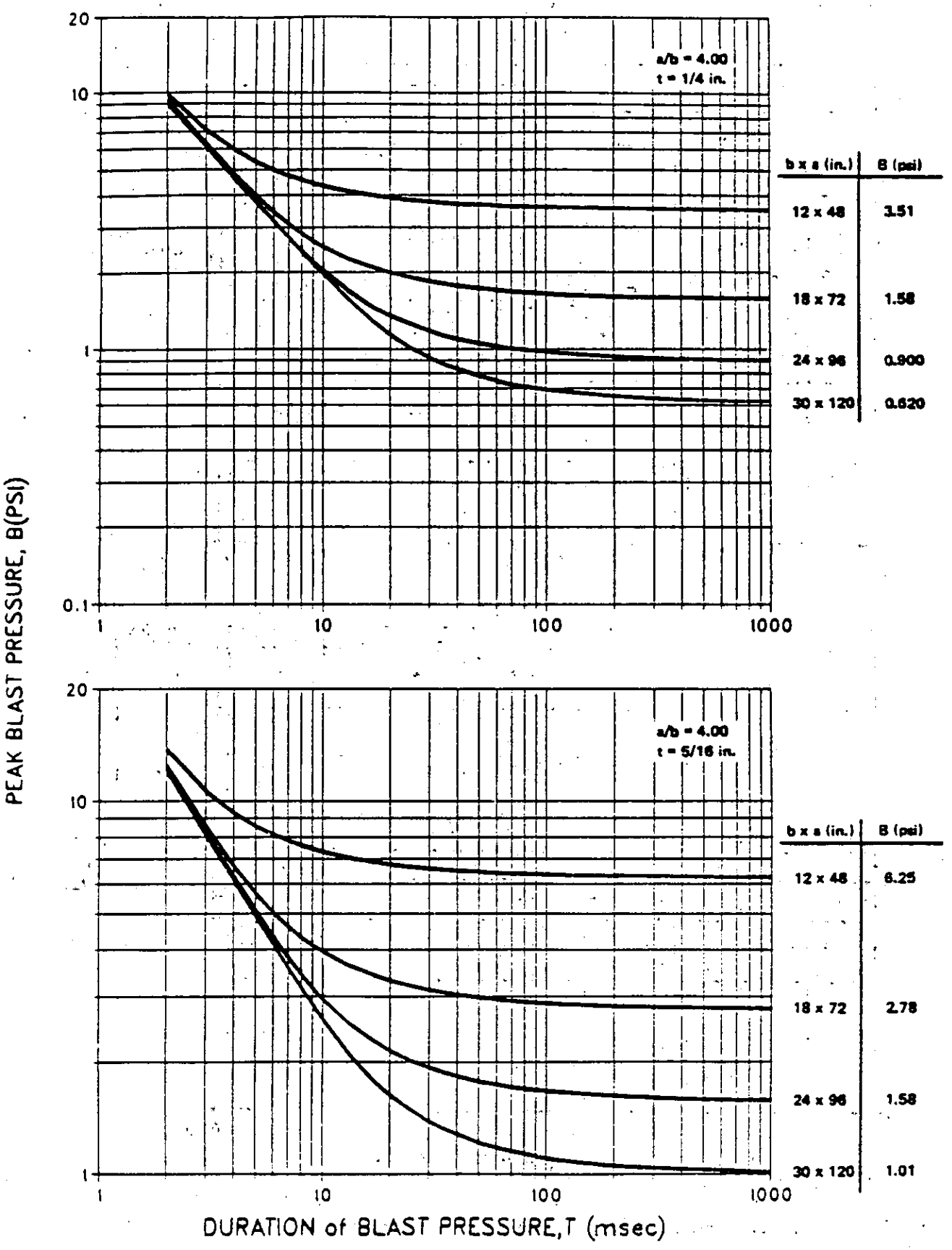


Figure 6–46 Peak blast pressure capacity for tempered glass panes: a/b = 4.00, t = 1/4 and 5/16 in.

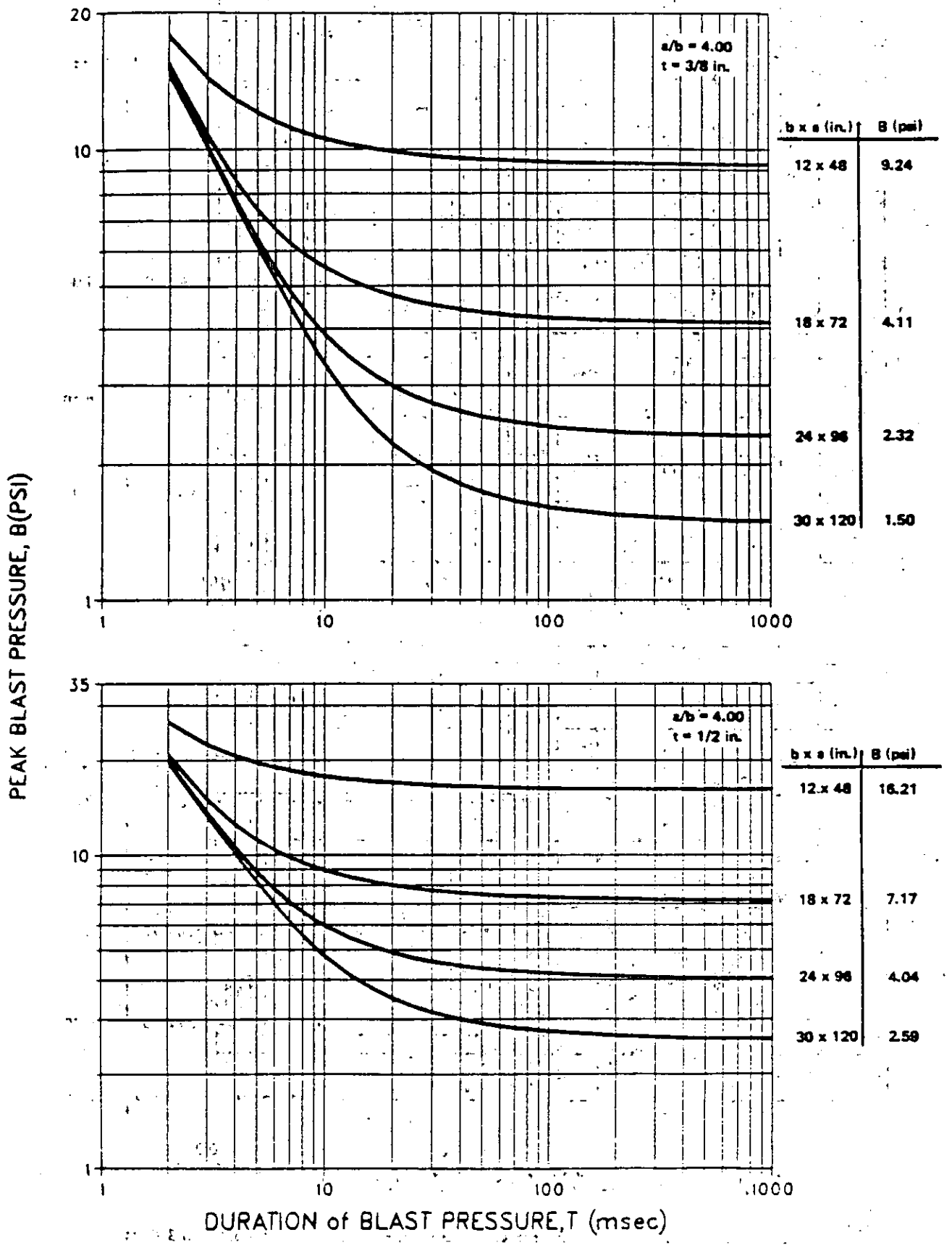


Figure 6-47 Peak blast pressure capacity for tempered glass panes: a/b = 4.00, t = 3/8 and 1/2 in.

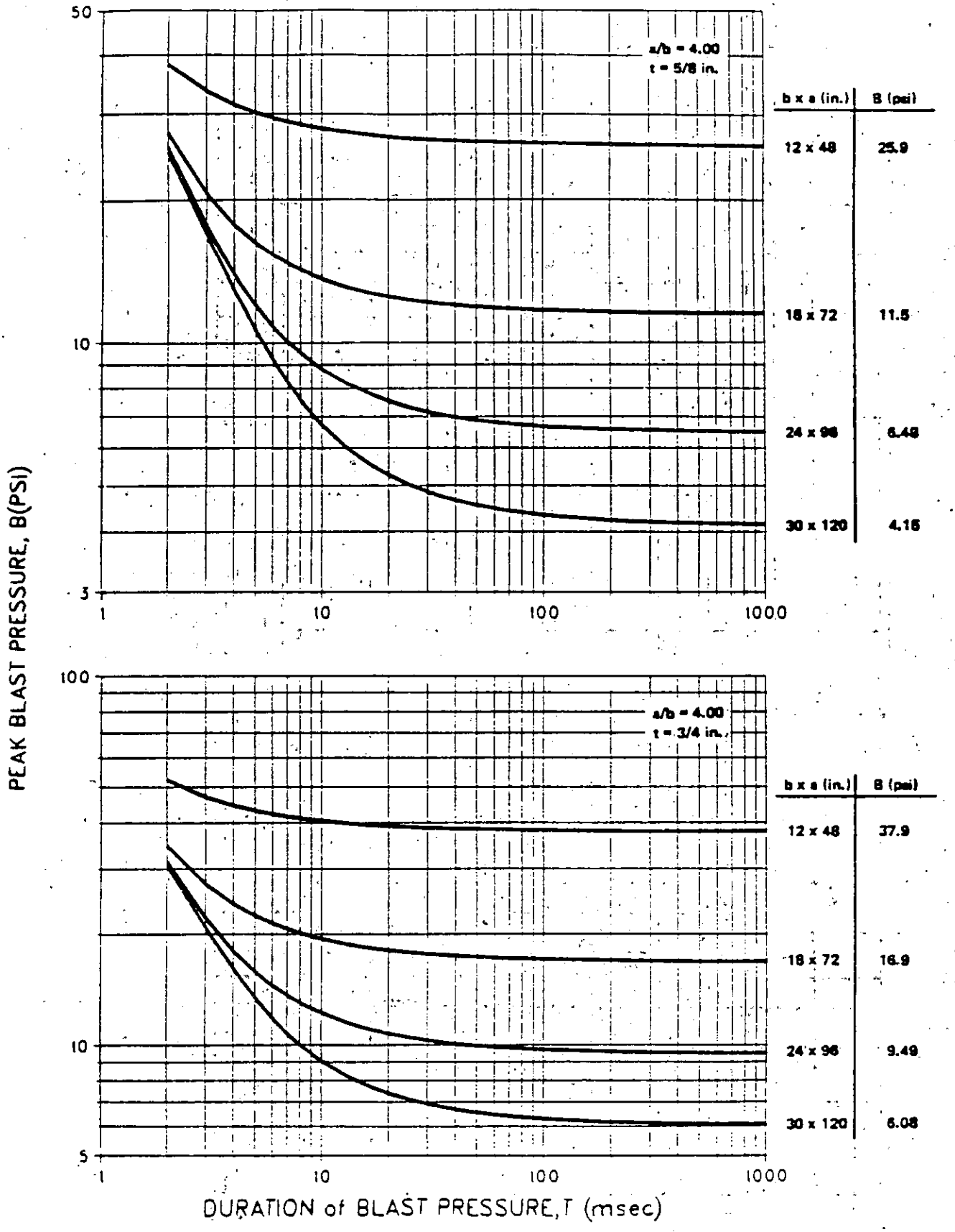


Figure 6-48 Peak blast pressure capacity for tempered glass panes: a/b = 4.00, t = 5/8 and 3/4 in.

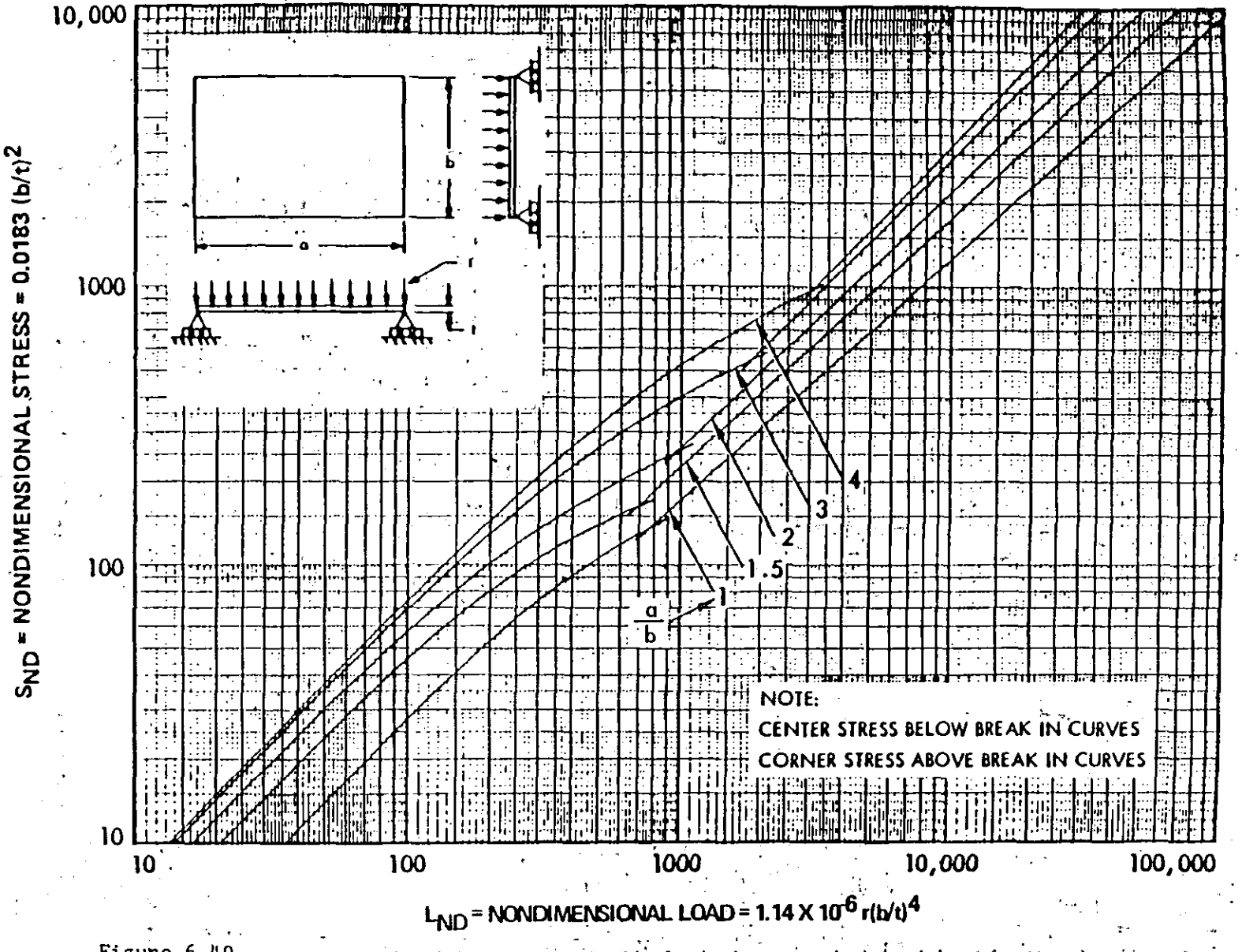


Figure 6-49 Nondimensional static load-stress relationships for simply supported tempered glass (after Moore).

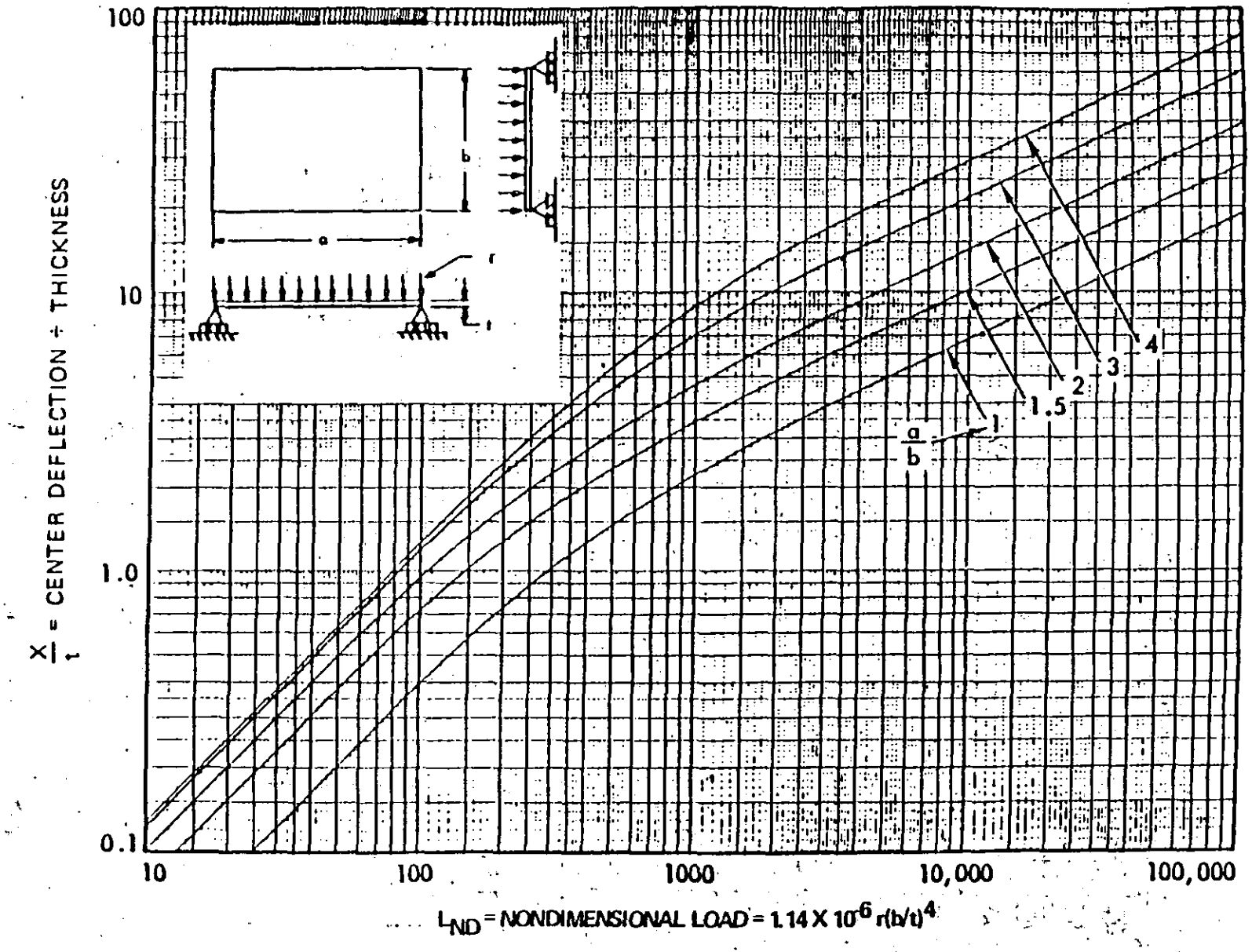


Figure 6–50 Nondimensional static load-crater deflection relationships for simply supported tempered glass (after Moore).

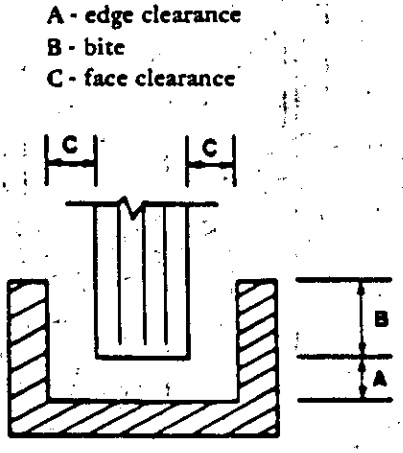


Figure 6-51 Edge, face, and bite requirements.

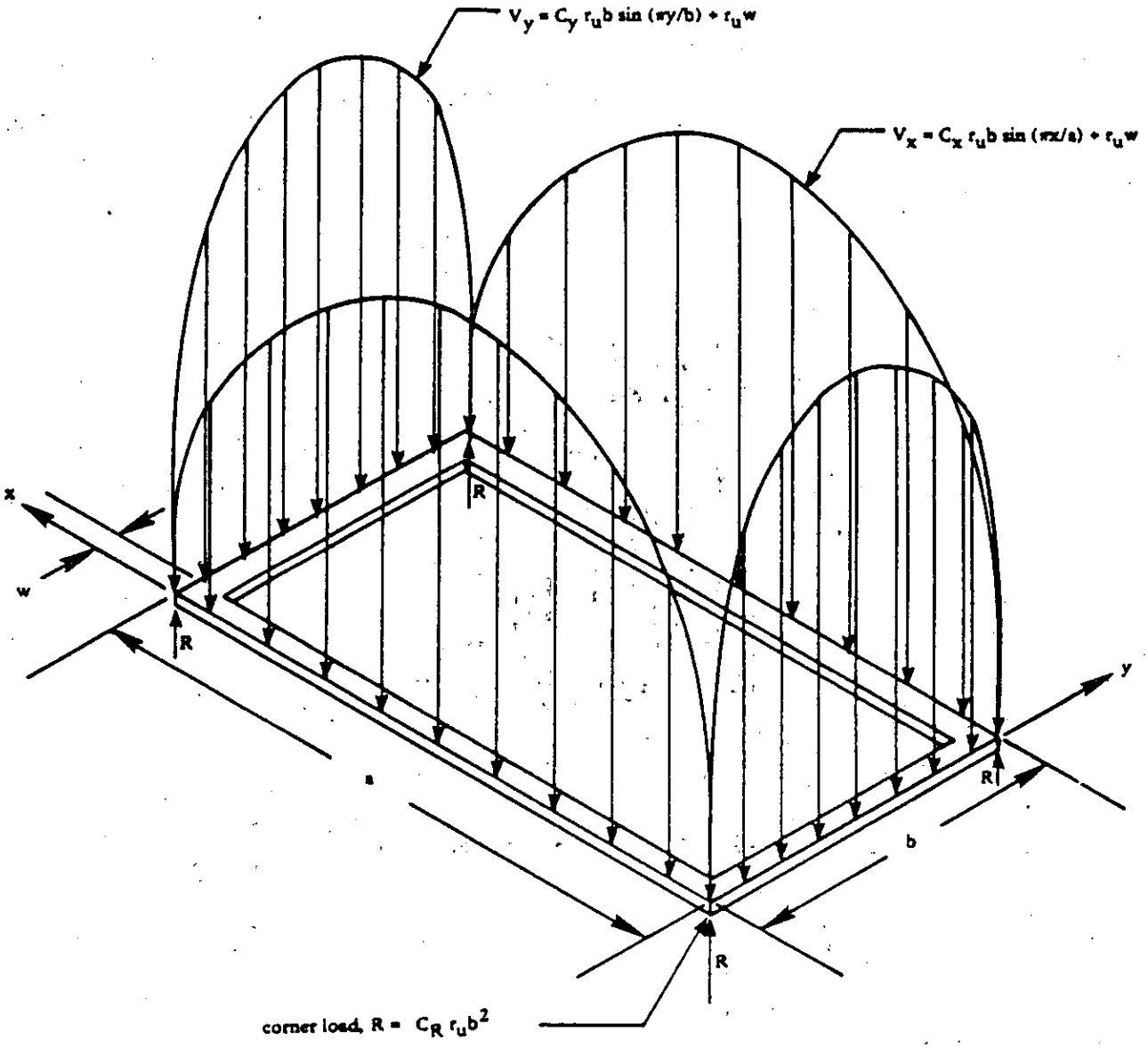


Figure 6-52 Distribution of lateral load transmitted by glass pane to the window frame.

Table 6-6 Static Design Strength r_u (psi), for Tempered Glass* [a = long dimension of glass pane (in.); b = short dimension of glass pane (in.)]

ASPECT RATIO = 1.00

Glass Size, b x a (in.)	Static Design Strength (psi) for a Window Thickness, t, of --					
	3/4 in.	5/8 in.	1/2 in.	3/8 in.	5/16 in.	1/4 in.
12x12	206	141	87.7	40.3	27.5	20.2
13x13	176	120	74.7	42.8	23.9	17.6
14x14	151	103	64.5	36.9	21.1	15.5
15x15	132	90.1	56.1	32.2	18.7	14.2
16x16	116	79.2	49.3	28.3	16.7	13.4
17x17	103	70.1	43.7	25.5	15.1	12.7
18x18	91.6	62.5	39.0	23.1	14.1	12.6
19x19	82.2	56.1	35.0	21.0	13.5	12.1
20x20	74.2	50.7	31.6	19.2	12.9	11.0
21x21	67.3	46.0	28.6	17.7	12.7	10.0
22x22	61.3	41.9	26.4	16.3	12.6	9.20
23x23	56.1	38.3	24.4	15.1	11.8	8.52
24x24	51.5	35.2	22.7	14.3	10.9	7.91
25x25	47.5	32.4	21.2	13.8	10.1	7.43
26x26	43.9	30.0	19.7	13.4	9.39	7.00
27x27	40.7	27.9	18.5	12.9	8.80	6.62
28x28	37.9	26.2	17.4	12.8	8.26	6.22
29x29	35.3	24.6	16.4	12.6	7.78	5.86
30x30	33.0	23.2	15.4	12.6	7.39	5.53
31x31	30.9	21.9	14.6	12.0	7.04	5.22
32x32	29.0	20.8	14.2	11.3	6.71	4.94
33x33	27.4	19.7	13.8	10.6	6.39	4.69
34x34	26.0	18.7	13.5	10.0	6.07	4.45
35x35	24.8	17.8	13.2	9.50	5.77	4.23
36x36	23.6	17.0	12.8	9.05	5.50	4.04
37x37	22.5	16.2	12.7	8.63	5.24	3.86
38x38	21.5	15.4	12.7	8.24	5.01	3.69
39x39	20.5	14.8	12.6	7.88	4.79	3.53
40x40	19.7	14.4	12.5	7.57	4.58	3.39
41x41	18.8	14.1	11.9	7.30	4.39	3.25
42x42	18.1	13.8	11.4	7.04	4.21	3.12
43x43	17.3	13.5	10.9	6.80	4.05	3.00
44x44	16.7	13.2	10.4	6.56	3.90	2.89
45x45	16.0	13.0	9.99	6.32	3.75	2.78
46x46	15.4	12.9	9.59	6.08	3.62	2.68
47x47	14.9	12.8	9.24	5.86	3.49	2.58
48x48	14.5	12.7	8.91	5.65	3.37	2.49
49x49	14.2	12.6	8.59	5.45	3.25	2.41
50x50	14.0	12.6	8.30	5.27	3.15	2.33
51x51	13.7	12.4	8.02	5.09	3.04	2.25
52x52	13.5	11.9	7.76	4.92	2.95	2.18
53x53	13.3	11.5	7.54	4.76	2.85	2.11
54x54	13.1	11.1	7.33	4.61	2.77	2.05
55x55	12.9	10.7	7.13	4.47	2.68	1.99
56x56	12.8	10.3	6.94	4.33	2.60	1.93
57x57	12.7	9.99	6.76	4.20	2.53	1.87
58x58	12.7	9.66	6.59	4.08	2.45	1.82
59x59	12.6	9.38	6.40	3.97	2.38	1.77
60x60	12.6	9.11	6.22	3.85	2.32	1.72

* Panes to the right and below the stepped dividing line behave according to large deflection plate theory.

(continued)

Table 6-6 Static Design Strength r_u (psi), for Tempered Glass* [a = long dimension of glass pane (in.); b = short dimension of glass pane (in.)] (Continued)

ASPECT RATIO = 1.25

Glass Size, b x a (in.)	Static Design Strength (psi) for a Window thickness, t, of -- 3/4 in.	5/8 in.	1/2 in.	3/8 in.	5/16 in.	1/4 in.
12x15	154	105	65.5	37.5	20.5	15.4
13x16.25	131	89.5	55.8	32.0	17.9	13.5
14x17.5	113	77.2	48.1	27.6	15.8	12.3
15x18.75	98.5	67.2	41.9	24.0	14.2	11.1
16x20	86.6	59.1	36.8	21.1	13.0	10.2
17x21.25	76.7	52.4	32.6	19.0	12.0	9.86
18x22.5	68.4	46.7	29.1	17.2	11.1	9.78
19x23.75	61.4	41.9	26.1	15.8	10.3	9.72
20x25	55.4	37.8	23.6	14.6	9.96	9.54
21x26.25	50.3	34.3	21.4	13.6	9.79	8.69
22x27.5	45.8	31.3	19.7	12.8	9.78	7.95
23x28.75	41.9	28.6	18.2	12.0	9.70	7.30
24x30	38.5	26.3	17.0	11.3	9.49	6.75
25x31.25	35.5	24.2	15.9	10.7	8.77	6.27
26x32.5	32.8	22.4	14.9	10.2	8.14	5.83
27x33.75	30.4	20.8	14.1	9.98	7.57	5.45
28x35	28.3	19.5	13.4	9.80	7.07	5.12
29x36.25	26.4	18.4	12.8	9.79	6.63	4.81
30x37.5	24.6	17.4	12.3	9.77	6.23	4.54
31x38.75	23.1	16.4	11.7	9.71	5.87	4.31
32x40	21.7	15.6	11.2	9.65	5.54	4.09
33x41.25	20.4	14.9	10.7	9.22	5.25	3.90
34x42.5	19.4	14.2	10.3	8.71	4.98	3.71
35x43.75	18.5	13.6	10.1	8.24	4.74	3.53
36x45	17.6	13.1	9.93	7.81	4.52	3.36
37x46.25	16.8	12.7	9.80	7.41	4.32	3.20
38x47.5	16.1	12.3	9.79	7.05	4.14	3.06
39x48.75	15.5	11.8	9.78	6.72	3.97	2.92
40x50	14.8	11.4	9.75	6.42	3.82	2.80
41x51.25	14.3	11.0	9.71	6.13	3.66	2.68
42x52.5	13.8	10.6	9.66	5.87	3.51	2.57
43x53.75	13.4	10.3	9.47	5.63	3.37	2.47
44x55	13.0	10.2	9.06	5.40	3.24	2.37
45x56.25	12.6	10.0	8.68	5.19	3.11	2.28
46x57.5	12.3	9.87	8.32	5.00	3.00	2.19
47x58.75	11.9	9.80	7.99	4.81	2.89	2.11
48x60	11.5	9.79	7.67	4.64	2.78	2.03
49x61.25	11.2	9.78	7.37	4.49	2.68	1.96
50x62.5	10.9	9.77	7.11	4.34	2.59	1.89
51x63.75	10.6	9.74	6.85	4.21	2.50	1.83
52x65	10.3	9.70	6.61	4.08	2.42	1.77
53x66.25	10.2	9.67	6.38	3.96	2.34	1.71

* Panes to the right and below the stepped dividing line behave according to large deflection plate theory.

(continued)

Table 6-6 Static Design Strength r_u (psi), for Tempered Glass* [a = long dimension of glass pane (in.); b = short dimension of glass pane (in.)] (Continued)

ASPECT RATIO = 1.50

Glass Size, b x a (in.)	Static Design Strength (psi) for a Window thickness, t, of -- 3/4 in.	5/8 in.	1/2 in.	3/8 in.	5/16 in.	1/4 in.
12x18	123	83.8	52.3	29.9	16.3	11.9
13x19.5	105	71.4	44.5	25.5	13.9	10.5
14x21	90.2	61.6	38.4	22.0	12.3	9.43
15x22.5	78.6	53.6	33.4	19.2	11.1	8.88
16x24	69.1	47.2	29.4	16.8	10.0	8.26
17x25.5	61.2	41.8	26.0	14.9	9.31	8.14
18x27	54.6	37.3	23.2	13.3	8.85	8.02
19x28.5	49.0	33.4	20.8	12.3	8.84	7.90
20x30	44.2	30.2	18.8	11.4	7.83	7.78
21x31.5	40.1	27.4	17.1	10.6	7.81	7.62
22x33	36.5	24.9	15.6	9.86	7.80	7.03
23x34.5	33.4	22.8	14.2	9.32	7.77	6.45
24x36	30.7	21.0	13.1	8.98	7.77	5.95
25x37.5	28.3	19.3	12.4	8.64	7.63	5.50
26x39	26.2	17.9	11.7	8.24	7.19	5.10
27x40.5	24.3	16.6	11.0	7.86	6.69	4.74
28x42	22.6	15.4	10.4	7.85	6.24	4.42
29x43.5	21.0	14.4	9.89	7.85	5.83	4.14
30x45	19.7	13.4	9.42	7.84	5.47	3.88
31x46.5	18.4	12.8	9.16	7.83	5.13	3.64
32x48	17.3	12.2	8.91	7.82	4.83	3.43
33x49.5	16.2	11.6	8.65	7.72	4.55	3.27
34x51	15.3	11.1	8.34	7.62	4.30	3.13
35x52.5	14.4	10.6	8.05	7.28	4.07	3.00
36x54	13.6	10.2	8.02	6.90	3.85	2.87
37x55.5	13.0	9.78	7.99	6.55	3.66	2.74
38x57	12.5	9.42	7.96	6.22	3.47	2.61
39x58.5	12.0	9.21	7.93	5.92	3.33	2.50
40x60	11.6	9.01	7.91	5.64	3.21	2.39
41x61.5	11.2	8.82	7.88	5.38	3.09	2.29
42x63	10.8	8.60	7.85	5.13	2.98	2.19
43x64.5	10.4	8.35	7.77	4.91	2.88	2.10
44x66	10.1	8.12	7.69	4.70	2.77	2.02
45x67.5	9.71	7.90	7.62	4.50	2.66	1.94
46x69	9.42	7.69	7.35	4.31	2.56	1.86
47x70.5	9.25	7.62	7.06	4.14	2.47	1.79
48x72	9.08	7.55	6.78	3.97	2.38	1.73

* Panes to the right and below the stepped dividing line behave according to large deflection plate theory.

(continued)

Table 6-6 Static Design Strength r_u (psi), for Tempered Glass* [a = long dimension of glass pane (in.); b = short dimension of glass pane (in.)] (Continued)

ASPECT RATIO = 1.75

Glass Size, b x a (in.)	Static Design Strength (psi) for a Window thickness, t, of -- 3/4 in.	5/8 in.	1/2 in.	3/8 in.	5/16 in.	1/4 in.
12x21	109	74.2	46.3	26.5	14.4	10.2
13x22.75	92.6	63.2	39.4	22.6	12.3	8.91
14x24.5	79.9	54.5	34.0	19.5	10.6	8.01
15x26.25	69.6	47.5	29.6	17.0	9.46	7.32
16x28	61.2	41.7	26.0	14.9	8.52	6.83
17x29.75	54.2	37.0	23.0	13.2	7.85	6.36
18x31.5	48.3	33.0	20.6	11.8	7.30	5.93
19x33.25	43.4	29.6	18.5	10.6	6.88	5.76
20x35	39.1	26.7	16.7	9.71	6.49	5.73
21x36.75	35.5	24.2	15.1	8.96	6.12	5.70
22x38.5	32.4	22.1	13.8	8.36	5.84	5.68
23x40.25	29.6	20.2	12.6	7.87	5.73	5.57
24x42	27.2	18.6	11.6	7.43	5.71	5.27
25x43.75	25.1	17.1	10.7	7.11	5.70	5.00
26x45.5	23.2	15.8	9.97	6.81	5.69	4.67
27x47.25	21.5	14.7	9.37	6.52	5.66	4.35
28x49	20.0	13.6	8.83	6.24	5.45	4.05
29x50.75	18.6	12.7	8.38	5.98	5.21	3.79
30x52.5	17.4	11.9	8.01	5.82	4.98	3.56
31x54.25	16.3	11.1	7.66	5.74	4.70	3.36
32x56	15.3	10.4	7.35	5.73	4.43	3.17
33x57.75	14.4	9.93	7.11	5.71	4.17	3.00
34x59.5	13.5	9.46	6.89	5.70	3.94	2.85
35x61.25	12.8	9.02	6.67	5.69	3.73	2.72
36x63	12.1	8.62	6.45	5.67	3.54	2.60
37x64.75	11.4	8.30	6.24	5.63	3.37	2.49
38x66.5	10.8	8.00	6.04	5.44	3.21	2.37
39x68.25	10.3	7.73	5.87	5.26	3.06	2.26
40x70	9.91	7.47	5.80	5.09	2.93	2.16
41x71.75	9.52	7.26	5.74	4.93	2.82	2.06
42x73.5	9.15	7.07	5.72	4.71	2.71	1.97
43x75.25	8.81	6.90	5.70	4.50	2.61	1.89
44x77	8.50	6.73	5.69	4.30	2.51	1.81
45x78.75	8.24	6.55	5.70	4.12	2.42	1.74

* Panes to the right and below the stepped dividing line behave according to large deflection plate theory.

(continued)

Table 6-6 Static Design Strength r_u (psi), for Tempered Glass* [a = long dimension of glass pane (in.); b = short dimension of glass pane (in.)] (Continued)

ASPECT RATIO = 2.00

Glass Size, b x a (in.)	Static Design Strength (psi) for a Window thickness, t, of -- 3/4 in.	5/8 in.	1/2 in.	3/8 in.	5/16 in.	1/4 in.
12x24	97.6	66.6	41.5	23.8	13.0	9.05
13x26	83.1	56.7	35.4	20.3	11.0	7.81
14x28	71.7	48.9	30.5	17.5	9.52	6.87
15x30	62.4	42.6	26.6	15.2	8.31	6.29
16x32	54.9	37.5	23.4	13.3	7.43	5.81
17x34	48.6	33.2	20.7	11.9	6.72	5.40
18x36	43.4	29.6	18.5	10.6	6.26	5.03
19x38	38.9	26.6	16.6	9.49	5.86	4.71
20x40	35.1	24.0	14.9	8.56	5.51	4.56
21x42	31.9	21.7	13.6	7.85	5.19	4.46
22x44	29.0	19.8	12.4	7.25	4.90	4.42
23x46	26.6	18.1	11.3	6.73	4.64	4.39
24x48	24.4	16.6	10.4	6.39	4.55	4.37
25x50	22.5	15.3	9.56	6.08	4.47	4.32
26x52	20.8	14.2	8.84	5.79	4.40	4.24
27x54	19.3	13.2	8.23	5.53	4.39	4.01
28x56	17.9	12.2	7.73	5.29	4.38	3.74
29x58	16.7	11.4	7.27	5.07	4.37	3.50
30x60	15.6	10.7	6.86	4.86	4.31	3.28
31x62	14.6	9.98	6.57	4.67	4.25	3.09
32x64	13.7	9.36	6.32	4.58	4.08	2.93
33x66	12.9	8.80	6.08	4.52	3.85	2.78
34x68	12.2	8.31	5.87	4.47	3.64	2.64
35x70	11.5	7.91	5.66	4.41	3.44	2.51
36x72	10.8	7.53	5.47	4.40	3.26	2.39
37x74	10.3	7.18	5.29	4.39	3.11	2.28
38x76	9.73	6.86	5.12	4.38	2.97	2.18
39x78	9.24	6.62	4.96	4.37	2.84	2.08
40x80	8.78	6.42	4.81	4.34	2.72	1.98
41x82	8.37	6.23	4.67	4.30	2.60	1.89
42x84	8.03	6.05	4.60	4.25	2.50	1.80

* Panes to the right and below the stepped dividing line behave according to large deflection plate theory.

(continued)

Table 6-6 Static Design Strength r_u (psi), for Tempered Glass* [a = long dimension of glass pane (in.); b = short dimension of glass pane (in.)] (Continued)

ASPECT RATIO = 3.00

Glass Size, b x a (in.)	Static Design Strength (psi) for a Window thickness, t, of -- 3/4 in.	5/8 in.	1/2 in.	3/8 in.	5/16 in.	1/4 in.
12x36	81.1	55.4	34.5	19.8	10.8	7.53
13x39	69.1	47.2	29.4	16.9	9.18	6.41
14x42	59.6	40.7	25.4	14.5	7.92	5.57
15x45	51.9	35.4	22.1	12.7	6.90	4.94
16x48	45.6	31.2	19.4	11.1	6.06	4.42
17x51	40.4	27.6	17.2	9.86	5.43	3.98
18x54	36.1	24.6	15.3	8.79	4.92	3.61
19x57	32.4	22.1	13.8	7.89	4.48	3.29
20x60	29.2	19.9	12.4	7.12	4.10	3.01
21x63	26.5	18.1	11.3	6.46	3.77	2.80
22x66	24.1	16.5	10.3	5.88	3.48	2.61
23x69	22.1	15.1	9.40	5.44	3.22	2.44
24x72	20.3	13.8	8.63	5.06	3.00	2.29
25x75	18.7	12.8	7.95	4.71	2.82	2.15
26x78	17.3	11.8	7.35	4.40	2.66	2.08
27x81	16.0	10.9	6.82	4.13	2.51	2.01
28x84	14.9	10.2	6.34	3.88	2.38	1.95
29x87	13.9	9.48	5.91	3.65	2.26	1.89
30x90	13.0	8.86	5.56	3.44	2.14	1.83
31x93	12.2	8.30	5.26	3.25	2.08	1.80
32x96	11.4	7.79	4.98	3.08	2.03	1.78
33x99	10.7	7.32	4.72	2.93	1.97	1.76
34x102	10.1	6.90	4.48	2.80	1.92	1.77

* Panes to the right and below the stepped dividing line behave according to large deflection plate theory.

Table 6-6 Static Design Strength r_u (psi), for Tempered Glass* [a = long dimension of glass pane (in.); b = short dimension of glass pane (in.)] (Continued)

ASPECT RATIO = 4.00

Glass Size, b x a (in.)	Static Design Strength (psi) for a Window thickness, t, of -- 3/4 in.	5/8 in.	1/2 in.	3/8 in.	5/16 in.	1/4 in.
12x48	75.7	51.7	32.2	18.5	10.1	7.02
13x52	64.5	44.0	27.5	15.7	8.57	5.99
14x56	55.6	38.0	23.7	13.6	7.39	5.16
15x60	48.5	33.1	20.6	11.8	6.43	4.52
16x64	42.6	29.1	18.1	10.4	5.66	3.99
17x68	37.7	25.8	16.1	9.20	5.01	3.56
18x72	33.7	23.0	14.3	8.20	4.49	3.19
19x76	30.2	20.6	12.9	7.36	4.05	2.87
20x80	27.3	18.6	11.6	6.65	3.67	2.60
21x84	24.7	16.9	10.5	6.03	3.34	2.37
22x88	22.5	15.4	9.59	5.49	3.06	2.18
23x92	20.6	14.1	8.77	5.03	2.81	2.02
24x96	18.9	12.9	8.05	4.63	2.59	1.88
25x100	17.5	11.9	7.42	4.28	2.39	1.76
26x104	16.1	11.0	6.86	3.97	2.23	1.66
27x108	15.0	10.2	6.36	3.70	2.09	1.57
28x112	13.9	9.49	5.92	3.45	1.96	1.49
29x116	13.0	8.85	5.52	3.22	1.84	1.41
30x120	12.1	8.27	5.15	3.02	1.75	1.34

* Panes to the right and below the stepped dividing line behave according to large deflection plate theory.

Table 6-7 Minimum Design Thickness, Clearances, and Bite Requirements

Glass Thickness (Nominal) in	mm	Actual Glass Thickness For Design, t (in)	"A" Minimum Edge Clearance (in)	"B" Nominal Bite (in)	"C" Minimum Face Clearance (in)
5/32	4.0	0.149	3/16	1/2	1/8
3/16	5.0	0.180	3/16	1/2	1/8
1/4	6.0	0.219	1/4	1/2	1/8
3/8	10.0	0.355	5/16	1/2	3/16
1/2	12.0	0.469	3/8	1/2	1/4
5/8	16.0	0.594	3/8	1/2	1/4
3/4	19.0	0.719	3/8	1/2	5/16

Table 6-8 **Maximum (b/t) Ratio for Linear Plate Behavior Under Blast Load and Coefficients for Resistance and Deflection and Fundamental Period of Simply Supported Glass Plates Based on Small Deflection Theory (No Tensile Membrane Behavior)**

Aspect Ratio, a/b	Maximum (b/t) Ratio	Design Coefficients		
		Design Resistance, C_r	Design Deflection, C_D	Fundamental Period of Vibration, C_T
1.0	53.6	5.79×10^{4}	2.58×10^{-4}	5.21×10^{-3}
1.2	59.0	4.42×10^{4}	2.72×10^{-4}	6.30×10^{-3}
1.4	63.9	3.68×10^{4}	2.83×10^{-4}	7.21×10^{-3}
1.5	66.2	3.36×10^{4}	2.88×10^{-4}	7.60×10^{-3}
1.6	67.9	3.22×10^{4}	2.91×10^{-4}	7.99×10^{-3}
1.8	71.3	2.91×10^{4}	2.98×10^{-4}	8.65×10^{-3}
2.0	74.7	2.72×10^{4}	3.02×10^{-4}	9.23×10^{-3}
3.0	84.3	2.32×10^{4}	3.12×10^{-4}	10.12×10^{-3}
4.0	89.4	2.24×10^{4}	3.15×10^{-4}	10.36×10^{-3}
∞	89.4	2.24×10^{4}	3.15×10^{-4}	10.44×10^{-3}

Table 6-9 Coefficients for Frame Loading

a/b	C_R	C_x	C_y
1.00	0.065	0.495	0.495
1.10	0.070	0.516	0.516
1.20	0.074	0.535	0.533
1.30	0.079	0.554	0.551
1.40	0.083	0.570	0.562
1.50	0.085	0.581	0.574
1.60	0.086	0.590	0.583
1.70	0.088	0.600	0.591
1.80	0.090	0.609	0.600
1.90	0.091	0.616	0.607
2.00	0.092	0.623	0.614
3.00	0.093	0.644	0.655
4.00	0.094	0.687	0.685

Table 6-10 Statistical Acceptance and Rejection Coefficients

Number of Window Assemblies n	Acceptance Coefficient α	Rejection Coefficient β
2	4.14	.546
3	3.05	.871
4	2.78	1.14
5	2.65	1.27
6	2.56	1.36
7	2.50	1.42
8	2.46	1.48
9	2.42	1.49
10	2.39	1.52
11	2.37	1.54
12	2.35	1.57
13	2.33	1.58
14	2.32	1.60
15	2.31	1.61
16	2.30	1.62
17	2.28	1.64
18	2.27	1.65
19	2.27	1.65
20	2.26	1.66
21	2.25	1.67
22	2.24	1.68
23	2.24	1.68
24	2.23	1.69
25	2.22	1.70
30	2.19	1.72
40	2.17	1.75
50	2.14	1.77

Table 6-11 Fundamental Period of Vibration, T_n, for Monolithic Tempered Glass

Aspect Ratio = 1.00

Glass Dimensions (in.)		Fundamental Period of Vibration (msec) for Window Thickness, t, of --					
b	a	3/4-in.	5/8-in.	1/2 in.	3/8 in.	5/16 in.	1/4 in.
12	12	1.05	1.27	1.61	2.13	2.83	3.38
13	13	1.23	1.49	1.89	2.50	3.29	3.93
14	14	1.43	1.73	2.19	2.89	3.76	4.50
15	15	1.64	1.99	2.52	3.30	4.39	5.09
16	16	1.87	2.26	2.87	3.72	4.95	5.68
17	17	2.11	2.55	3.23	4.17	5.53	6.27
18	18	2.37	2.86	3.63	4.63	6.12	6.84
19	19	2.64	3.19	4.02	5.10	6.71	7.42
20	20	2.92	3.54	4.43	5.77	7.30	8.08
21	21	3.22	3.90	4.86	6.32	7.89	8.76
22	22	3.53	4.28	5.30	6.89	8.44	9.45
23	23	3.86	4.68	5.75	7.48	9.06	10.2
24	24	4.21	5.07	6.23	8.07	9.72	10.9
25	25	4.56	5.47	6.70	8.65	10.4	11.6
26	26	4.94	5.89	7.40	9.25	11.1	12.3
27	27	5.32	6.33	7.94	9.84	11.8	13.1
28	28	5.72	6.77	8.50	10.4	12.5	13.8
29	29	6.12	7.23	9.07	11.0	13.2	14.6
30	30	6.52	7.70	9.65	11.5	14.0	15.3
31	31	6.93	8.17	10.3	12.2	14.7	16.1
32	32	7.36	8.64	10.8	12.8	15.4	16.9
33	33	7.80	9.41	11.4	13.5	16.1	17.8
34	34	8.24	9.95	12.0	14.2	16.9	18.6
35	35	8.70	10.5	12.6	14.9	17.7	19.4
36	36	9.17	11.1	13.2	15.6	18.4	20.2
37	37	9.64	11.6	13.8	16.3	19.2	21.0
38	38	10.1	12.2	14.3	17.0	20.0	21.9
39	39	11.0	12.8	14.9	17.7	20.9	22.8
40	40	11.4	13.4	15.5	18.5	21.7	23.6
41	41	12.0	14.0	16.1	19.2	22.5	24.5
42	42	12.5	14.6	16.8	19.9	23.3	25.4
43	43	13.1	15.2	17.4	20.6	24.1	26.3
44	44	13.6	15.8	18.1	21.3	25.0	27.2
45	45	14.2	16.4	18.8	22.1	25.8	28.1
46	46	14.8	16.9	19.5	22.8	26.7	29.0
47	47	15.4	17.5	20.2	23.6	27.5	30.8
48	48	16.0	18.1	20.9	24.4	28.4	31.7
49	49	16.6	18.7	21.6	25.2	29.3	32.6
50	50	17.2	19.2	22.3	26.0	30.2	33.5
51	51	17.7	19.8	23.0	26.8	31.1	34.4
52	52	18.3	20.4	23.8	27.6	32.0	35.4
53	53	19.0	21.1	24.5	28.4	32.9	35.4
54	54	19.5	21.8	25.2	29.2	33.7	36.3
55	55	20.1	22.4	26.0	30.0	34.6	37.3
56	56	20.7	23.1	26.7	30.8	35.5	38.2
57	57	21.3	23.8	27.4	31.6	36.4	39.2
58	58	21.8	24.5	28.1	32.5	37.3	40.1
59	59	22.4	25.2	28.8	33.3	38.2	41.1
60	60	23.0	25.9	29.6	34.1	39.2	42.1

Table 6-11 Fundamental Period of Vibration, T_n, for Monolithic Tempered Glass (Continued)

Aspect Ratio = 1.25

Glass Dimensions (in.)		Fundamental Period of Vibration (msec) for Window Thickness, t, of --					
b	a	3/4 in.	5/8 in.	1/2 in.	3/8 in.	5/16 in.	1/4 in.
12	15	1.40	1.69	2.14	2.83	3.82	4.39
13	16.25	1.64	1.99	2.52	3.32	4.41	5.04
14	17.5	1.90	2.30	2.92	3.85	5.03	5.99
15	18.75	2.18	2.64	3.35	4.42	5.68	6.77
16	20	2.49	3.01	3.81	5.03	6.61	7.57
17	21.25	2.81	3.40	4.30	5.61	7.36	8.34
18	22.5	3.15	3.81	4.82	6.21	8.14	9.08
19	23.75	3.50	4.24	5.37	6.83	8.94	9.82
20	25	3.88	4.70	5.95	7.48	9.72	10.6
21	26.25	4.28	5.18	6.56	8.12	10.5	11.5
22	27.5	4.70	5.69	7.14	9.19	11.2	12.4
23	28.75	5.14	6.22	7.73	9.95	12.0	13.3
24	30	5.59	6.77	8.34	10.7	12.7	14.3
25	31.25	6.07	7.34	8.96	11.5	13.6	15.2
26	32.5	6.56	7.94	9.60	12.3	14.5	16.2
27	33.75	7.08	8.56	10.3	13.1	15.5	17.2
28	35	7.61	9.13	10.9	13.9	16.4	18.2
29	36.25	8.16	9.71	12.1	14.6	17.3	19.2
30	37.5	8.74	10.3	12.9	15.3	18.3	20.2
31	38.75	9.33	11.0	13.6	16.1	19.3	21.2
32	40	9.94	11.6	14.4	16.8	20.3	22.3
33	41.25	10.5	12.2	15.2	17.7	21.3	23.3
34	42.5	11.1	12.9	16.0	18.6	22.3	24.4
35	43.75	11.7	13.5	16.8	19.5	23.3	25.5
36	45	12.3	14.8	17.6	20.4	24.3	26.6
37	46.25	12.9	15.5	18.3	21.3	25.3	27.7
38	47.5	13.5	16.3	19.1	22.3	26.3	28.8
39	48.75	14.2	17.0	19.8	23.2	27.4	29.9
40	50	14.8	17.8	20.5	24.2	28.4	31.0
41	51.25	15.5	18.6	21.3	25.1	29.5	32.2
42	52.5	16.1	19.4	22.0	26.1	30.6	33.4
43	53.75	16.8	20.2	22.8	27.1	31.7	34.6
44	55	18.2	21.0	23.7	28.1	32.8	35.7
45	56.25	18.9	21.8	24.6	29.1	33.9	37.0
46	57.5	19.7	22.5	25.5	30.1	35.0	38.2
47	58.75	20.5	23.3	26.4	31.1	36.2	39.4
48	60	21.2	24.0	27.4	32.1	37.3	40.6
49	61.25	22.0	24.8	28.3	33.1	38.5	41.8
50	62.5	22.8	25.5	29.2	34.1	39.6	43.1
51	63.75	23.6	26.2	30.2	35.2	40.8	44.3
52	65	24.4	27.0	31.1	36.2	42.0	45.6
53	66.25	25.2	27.8	32.1	37.2	43.2	46.8

Table 6-11 Fundamental Period of Vibration, T_n, for Monolithic Tempered Glass (Continued)

Aspect Ratio = 1.50

Glass Dimensions (in.)		Fundamental Period of Vibration (msec) for Window Thickness, t, of --					
b	a	3/4 in.	5/8 in.	1/2 in.	3/8 in.	5/16 in.	1/4 in.
12	18	1.59	1.92	2.43	3.22	4.36	5.09
13	19.5	1.86	2.26	2.86	3.78	5.12	5.83
14	21	2.16	2.62	3.31	4.38	5.84	6.61
15	22.5	2.48	3.00	3.80	5.03	6.56	7.79
16	24	2.82	3.42	4.33	5.72	7.32	8.70
17	25.5	3.19	3.86	4.89	6.46	8.09	9.63
18	27	3.57	4.33	5.48	7.23	9.37	10.5
19	28.5	3.98	4.82	6.10	7.93	10.3	11.3
20	30	4.41	5.34	6.76	8.65	11.2	12.1
21	31.5	4.86	5.89	7.46	9.40	12.1	13.0
22	33	5.34	6.46	8.18	10.2	13.0	14.1
23	34.5	5.83	7.06	8.94	10.9	13.8	15.1
24	36	6.35	7.69	9.71	12.4	14.6	16.2
25	37.5	6.89	8.34	10.4	13.3	15.5	17.3
26	39	7.46	9.02	11.1	14.2	16.5	18.4
27	40.5	8.04	9.73	11.9	15.1	17.6	19.6
28	42	8.65	10.5	12.6	16.0	18.6	20.7
29	43.5	9.28	11.2	13.4	16.9	19.7	21.9
30	45	9.93	12.0	14.2	17.8	20.8	23.1
31	46.5	10.6	12.7	14.9	18.5	21.9	24.3
32	48	11.3	13.4	16.6	19.3	23.1	25:5
33	49.5	12.0	14.1	17.5	20.2	24.2	26:7
34	51	12.8	14.9	18.4	21.1	25.4	27.8
35	52.5	13.5	15.6	19.3	22.1	26.6	29.0
36	54	14.3	16.4	20.2	23.2	27.8	30.3
37	55.5	15.0	17.2	21.2	24.3	28.9	31.5
38	57	15.7	18.0	22.1	25.3	30.2	32.8
39	58.5	16.4	18.7	22.9	26.4	31.3	34.1
40	60	17.2	20.5	23.8	27.5	32.5	35.4
41	61.5	17.9	21.4	24.5	28.6	33.7	36.7
42	63	18.6	22.3	25.3	29.7	34.9	38.1
43	64.5	19.4	23.2	26.2	30.8	36.1	39:4
44	66	20.2	24.2	27.1	32.0	37.4	40.8
45	67.5	21.0	25.1	28.0	33.1	38.7	42.2
46	69	21.7	26.0	29.0	34.3	40.0	43.6
47	70.5	22.4	26.9	30.0	35.5	41.3	45.0
48	72	24.5	27.8	31.1	36.7	42.6	46.4

Table 6-11 Fundamental Period of Vibration, T_n, for Monolithic Tempered Glass (Continued)

Aspect Ratio = 1.75

Glass Dimensions (in.)		Fundamental Period of Vibration (msec) for Window Thickness, t, of --					
b	a	3/4 in.	5/8 in.	1/2 in.	3/8 in.	5/16 in.	1/4 in.
12	21	1.69	2.04	2.59	3.42	4.63	5.52
13	22.75	1.98	2.40	3.04	4.01	5.44	6.37
14	24.5	2.30	2.78	3.52	4.65	6.30	7.27
15	26.25	2.64	3.19	4.04	5.34	7.15	8.20
16	28	3.00	3.63	4.60	6.08	8.02	9.52
17	29.75	3.39	4.10	5.19	6.86	8.93	10.6
18	31.5	3.80	4.60	5.82	7.69	9.85	11.7
19	33.25	4.23	5.12	6.49	8.57	11.2	12.8
20	35	4.69	5.68	7.19	9.41	12.3	13.8
21	36.75	5.17	6.26	7.92	10.3	13.4	14.8
22	38.5	5.67	6.87	8.70	11.2	14.5	15.8
23	40.25	6.20	7.51	9.51	12.1	15.6	16.8
24	42	6.75	8.17	10.4	13.0	16.6	18.0
25	43.75	7.33	8.87	11.2	13.9	17.6	19.1
26	45.5	7.92	9.59	12.1	15.5	18.6	20.3
27	47.25	8.54	10.3	12.9	16.6	19.6	21.6
28	49	9.19	11.1	13.8	17.7	20.7	22.9
29	50.75	9.86	11.9	14.7	18.8	21.8	24.2
30	52.5	10.6	12.8	15.6	19.8	23.0	25.5
31	54.25	11.3	13.6	16.5	20.9	24.2	26.9
32	56	12.0	14.5	17.5	22.0	25.4	28.2
33	57.75	12.8	15.4	18.3	22.9	26.7	29.6
34	59.5	13.6	16.2	20.1	23.9	28.0	30.9
35	61.25	14.4	17.1	21.2	24.9	29.4	32.3
36	63	15.2	17.9	22.3	25.9	30.7	33.6
37	64.75	16.1	18.8	23.3	27.0	32.0	35.0
38	66.5	16.9	19.8	24.4	28.1	33.4	36.5
39	68.25	17.8	20.7	25.5	29.3	34.7	38.0
40	70	18.6	21.6	26.6	30.4	36.1	39.5
41	71.75	19.5	22.5	27.7	31.5	37.4	40.9
42	73.5	20.3	24.4	28.7	32.8	38.8	42.5
43	75.25	21.2	25.4	29.7	34.0	40.2	44.0
44	77	22.1	26.5	30.7	35.3	41.6	45.5
45	78.75	23.0	27.6	31.7	36.6	43.0	47.1

Table 6-11 Fundamental Period of Vibration, T_n, for Monolithic Tempered Glass (Continued)

Aspect Ratio = 2.00

Glass Dimensions (in.)		Fundamental Period of Vibration (msec) for Window Thickness, t, of --					
b	a	3/4 in.	5/8 in.	1/2 in.	3/8 in.	5/16 in.	1/4 in.
12	24	1.78	2.16	2.73	3.61	4.89	5.85
13	26	2.09	2.53	3.21	4.24	5.74	6.82
14	28	2.43	2.94	3.72	4.91	6.66	7.84
15	30	2.78	3.37	4.27	5.64	7.63	8.89
16	32	3.17	3.83	4.86	6.42	8.61	9.96
17	34	3.58	4.33	5.48	7.24	9.64	11.4
18	36	4.01	4.85	6.15	8.12	10.7	12.7
19	38	4.47	5.41	6.85	9.05	11.8	13.9
20	40	4.95	5.99	7.59	10.0	13.3	15.2
21	42	5.46	6.61	8.37	11.09	14.5	16.4
22	44	5.99	7.25	9.18	12.0	15.7	17.6
23	46	6.55	7.92	10.0	13.0	17.0	18.8
24	48	7.13	8.63	10.9	14.1	18.3	19.9
25	50	7.73	9.36	11.9	15.2	19.5	21.1
26	52	8.37	10.1	12.8	16.2	20.7	22.2
27	54	9.02	10.9	13.8	17.9	21.9	23.5
28	56	9.70	11.7	14.8	19.1	23.0	24.9
29	58	10.4	12.6	15.8	20.3	24.1	26.4
30	60	11.1	13.5	16.8	21.6	25.3	27.9
31	62	11.9	14.4	17.8	22.9	26.4	29.3
32	64	12.7	15.3	18.9	24.1	27.7	30.8
33	66	13.5	16.3	20.0	25.3	29.1	32.3
34	68	14.3	17.3	21.17	26.6	30.5	33.8
35	70	15.2	18.3	22.1	27.8	32.0	35.3
36	72	16.0	19.2	24.0	28.9	33.5	36.8
37	74	16.9	20.3	25.2	30.1	35.0	38.4
38	76	17.9	21.3	26.5	31.2	36.5	40.0
39	78	18.8	22.3	27.7	32.4	37.9	41.6
40	80	19.8	23.4	29.0	33.5	39.4	43.2
41	82	20.8	24.5	30.3	34.7	40.9	44.9
42	84	21.7	25.6	31.5	35.8	42.4	46.6

Table 6-11 Fundamental Period of Vibration, T_n, for Monolithic Tempered Glass (Continued)

Aspect Ratio = 3.00

Glass Dimensions (in.)		Fundamental Period of Vibration (msec) for Window Thickness, t, of --					
b	a	3/4 in.	5/8 in.	1/2 in.	3/8 in.	5/16 in.	1/4 in.
12	36	2.02	2.45	3.10	4.10	5.55	6.64
13	39	2.37	2.87	3.64	4.81	6.51	7.79
14	42	2.75	3.33	4.22	5.58	7.55	9.02
15	45	3.16	3.83	4.84	6.40	8.67	10.3
16	48	3.60	4.35	5.51	7.28	9.87	11.6
17	51	4.06	4.91	6.22	8.22	11.1	13.1
18	54	4.55	5.51	6.98	9.22	12.4	14.5
19	57	5.07	6.14	7.77	10.3	13.7	16.4
20	60	5.62	6.80	8.61	11.4	15.1	18.1
21	63	6.19	7.50	9.50	12.6	16.6	19.8
22	66	6.80	8.23	10.4	13.8	18.1	21.6
23	69	7.43	8.99	11.4	15.0	20.1	23.4
24	72	8.09	9.79	12.4	16.3	21.7	25.3
25	75	8.78	10.6	13.5	17.6	23.5	27.2
26	78	9.49	11.5	14.6	19.0	25.3	29.1
27	81	10.2	12.4	15.7	20.4	27.1	31.0
28	84	11.0	13.3	16.9	21.8	28.9	32.9
29	87	11.8	14.3	18.1	23.3	30.8	34.9
30	90	12.6	15.3	19.3	24.8	32.8	36.8
31	93	13.5	16.3	20.6	26.9	34.7	38.7
32	96	14.4	17.4	21.9	28.6	36.5	40.5
33	99	15.3	18.5	23.2	30.3	38.4	42.3
34	102	16.2	19.7	24.6	32.0	40.4	44.1

Table 6-11 Fundamental Period of Vibration, T_n, for Monolithic Tempered Glass (Continued)

Aspect Ratio = 4.00

Glass Dimensions (in.)		Fundamental Period of Vibration (msec) for Window Thickness, t, of --					
b	a	3/4 in.	5/8 in.	1/2 in.	3/8 in.	5/16 in.	1/4 in.
12	48	2.09	2.53	3.21	4.24	5.75	6.87
13	52	2.46	2.97	3.77	4.98	6.74	8.07
14	56	2.85	3.45	4.37	5.77	7.82	9.36
15	60	3.27	3.96	5.02	6.63	8.98	10.7
16	64	3.72	4.51	5.71	7.54	10.2	12.2
17	68	4.20	5.09	6.44	8.51	11.5	13.7
18	72	4.71	5.70	7.22	9.54	12.9	15.3
19	76	5.25	6.35	8.05	10.6	14.3	17.0
20	80	5.82	7.04	8.92	11.8	15.9	18.9
21	84	6.41	7.76	9.83	13.1	17.4	20.8
22	88	7.04	8.52	10.8	14.3	19.1	22.8
23	92	7.69	9.31	11.8	15.6	20.8	24.8
24	96	8.37	10.1	12.8	16.9	22.8	26.9
25	100	9.09	11.0	13.9	18.3	24.7	29.1
26	104	9.83	11.9	15.1	19.8	26.6	31.3
27	108	10.6	12.8	16.3	21.3	28.6	33.5
28	112	11.4	13.8	17.5	22.9	30.7	35.8
29	116	12.2	14.8	18.8	24.5	32.8	38.2
30	120	13.1	15.8	20.1	26.2	35.0	40.6

Table 6-12 Effective Elastic Static Resistance, r_{eff}

Aspect Ratio = 1

Glass Dimensions (in.)		Effective Elastic Static Resistance (psi) for Glass Thickness, t, of --					
b	a	3/4 in.	5/8 in.	1/2 in.	3/8 in.	5/16 in.	1/4 in.
12	12	206.	140.	87.7	50.3	27.5	19.1
13	13	175.	119.	74.7	42.8	23.9	16.3
14	14	151.	103.	64.5	36.9	21.1	14.2
15	15	131.	90.1	56.1	32.2	17.5	12.7
16	16	115.	79.2	49.3	28.3	15.5	11.6
17	17	102.	70.1	43.7	25.5	13.8	10.7
18	18	91.6	62.5	39.0	23.1	12.6	10.3
19	19	82.2	56.1	35.0	21.0	11.7	9.75
20	20	74.2	50.7	31.6	18.0	11.0	8.76
21	21	67.3	46.0	28.6	16.4	10.4	7.93
22	22	61.3	41.9	26.4	15.1	10.2	7.20
23	23	56.1	38.3	24.4	13.9	9.51	6.57
24	24	51.5	35.2	22.7	12.9	8.71	6.01
25	25	47.5	32.4	21.2	12.2	8.01	5.56
26	26	43.9	23.0	18.6	11.5	7.39	5.19
27	27	40.7	27.9	17.3	11.0	6.83	4.87
28	28	37.9	26.2	16.2	10.5	6.33	4.55
29	29	35.3	24.6	15.1	10.3	5.89	4.25
30	30	33.0	23.2	14.2	10.2	5.53	3.98
31	31	30.9	21.9	13.4	9.61	5.22	3.74
32	32	29.0	20.8	12.8	9.00	4.95	3.51
33	33	27.4	18.5	12.2	8.45	4.68	3.31
34	34	26.0	17.5	11.7	7.95	4.42	3.14
35	35	24.8	16.6	11.3	7.49	4.18	2.98
36	36	23.6	15.7	10.9	7.06	3.96	2.82
37	37	22.5	14.9	10.5	6.67	3.75	2.67
38	38	21.5	14.2	10.4	6.31	3.57	2.54
39	39	19.4	13.5	10.3	5.98	3.39	2.42
40	40	18.5	13.0	10.1	5.70	3.24	2.30
41	41	17.6	12.6	9.59	5.45	3.09	2.19
42	42	16.8	12.1	9.12	5.22	2.96	2.09
43	43	16.1	11.7	8.69	5.02	2.83	2.00
44	44	15.4	11.4	8.29	4.83	2.70	1.92
45	45	14.8	11.1	7.92	4.63	2.59	1.84
46	46	14.2	10.8	7.57	4.43	2.48	1.77
47	47	13.6	10.5	7.24	4.25	2.38	1.70
48	48	13.2	10.4	6.93	4.08	2.29	1.64
49	49	12.8	10.3	6.64	3.92	2.20	1.58
50	50	12.4	10.2	6.37	3.77	2.11	1.52
51	51	12.1	9.96	6.11	3.63	2.04	1.47
52	52	11.7	9.56	5.87	3.50	1.96	1.42
53	53	11.4	9.19	5.67	3.37	1.90	1.38
54	54	11.2	8.84	5.48	3.26	1.83	1.33
55	55	10.9	8.52	5.30	3.15	1.77	1.29
56	56	10.7	8.21	5.14	3.05	1.72	1.25
57	57	10.5	7.92	4.99	2.95	1.66	1.21
58	58	10.4	7.64	4.85	2.85	1.61	1.17
59	59	10.3	7.40	4.70	2.76	1.56	1.14
60	60	10.2	7.10	4.55	2.67	1.52	1.11

Table 6-12 Effective Elastic Static Resistance, r_{eff} (Continued)

Aspect Ratio = 1.25

Glass Dimensions (in.)		Effective Elastic Static Resistance (psi) for Glass Thickness, t, of --					
b	a	3/4 in.	5/8 in.	1/2 in.	3/8 in.	5/16 in.	1/4 in.
12	15	154.	105.	65.5	37.5	20.5	15.2
13	16.25	131.	89.5	55.8	32.0	17.9	13.5
14	17.5	113.	77.2	48.1	27.6	15.8	11.0
15	18.75	98.5	67.2	41.9	24.0	14.2	9.84
16	20	86.6	59.1	36.8	21.1	11.9	8.91
17	21.25	76.7	52.4	32.6	19.0	10.8	8.36
18	22.5	68.4	46.7	29.1	17.2	9.79	8.12
19	23.75	61.4	41.9	26.1	15.8	8.99	7.86
20	25	55.4	37.8	23.6	14.6	8.50	7.49
21	26.25	50.3	34.3	21.4	13.6	8.19	6.73
22	27.5	45.8	31.3	19.7	11.6	8.07	6.11
23	28.75	41.9	28.6	18.2	10.8	7.79	5.57
24	30	38.5	26.3	17.0	10.1	7.44	5.09
25	31.25	35.5	24.2	15.9	9.40	6.81	4.68
26	32.5	32.8	22.4	14.9	8.89	6.27	4.31
27	33.75	30.4	20.8	14.1	8.53	5.79	4.00
28	35	28.3	19.5	13.4	8.25	5.37	3.73
29	36.25	26.4	18.4	11.7	8.14	4.99	3.49
30	37.5	24.6	17.4	11.0	8.04	4.65	3.28
31	38.75	23.1	16.4	10.4	7.82	4.34	3.09
32	40	21.7	15.6	9.91	7.62	4.07	2.92
33	41.25	20.4	14.9	9.41	7.21	3.84	2.76
34	42.5	19.4	14.2	8.99	6.75	3.62	2.61
35	43.75	18.5	13.6	8.70	6.35	3.43	2.47
36	45	17.6	12.0	8.45	5.99	3.26	2.34
37	46.25	16.8	11.5	8.25	5.66	3.10	2.22
38	47.5	16.1	11.0	8.16	5.35	2.96	2.12
39	48.75	15.5	10.6	8.09	5.07	2.82	2.01
40	50	14.8	10.1	7.98	4.81	2.69	1.91
41	51.25	14.3	9.72	7.81	4.57	2.57	1.82
42	52.5	13.8	9.34	7.66	4.34	2.45	1.74
43	53.75	13.4	9.01	7.43	4.14	2.34	1.66
44	55	11.8	8.78	7.06	3.96	2.25	1.59
45	56.25	11.4	8.57	6.72	3.79	2.16	1.52
46	57.5	11.0	8.38	6.42	3.63	2.07	1.46
47	58.75	10.6	8.24	6.14	3.49	1.98	1.40
48	60	10.3	8.17	5.88	3.36	1.90	1.34
49	61.25	9.93	8.11	5.63	3.23	1.83	1.29
50	62.5	9.60	8.06	5.39	3.12	1.76	1.25
51	63.75	9.29	7.93	5.18	3.01	1.69	1.20
52	65	9.02	7.80	4.97	2.90	1.63	1.16
53	66.25	8.82	7.68	4.78	2.80	1.57	1.12

Table 6-12 Effective Elastic Static Resistance, r_{eff} (Continued)

Aspect Ratio = 1.50

Glass Dimensions (in.)		Effective Elastic Static Resistance (psi) for Glass Thickness, t, of --					
b	a	3/4 in.	5/8 in.	1/2 in.	3/8 in.	5/16 in.	1/4 in.
12	18	123.	83.8	52.3	29.9	16.3	11.9
13	19.5	105.	71.4	44.5	25.5	13.9	10.5
14	21	90.2	61.6	38.4	22.0	12.3	9.43
15	22.5	78.6	53.6	33.4	19.2	11.1	7.86
16	24	69.1	47.2	29.4	16.8	10.1	7.16
17	25.5	61.2	41.8	26.0	14.9	9.31	6.56
18	27	54.6	37.3	23.2	13.3	7.83	6.25
19	28.5	49.0	33.4	20.8	12.3	7.24	6.30
20	30	44.2	30.2	18.8	11.4	6.71	6.23
21	31.5	40.1	27.4	17.1	10.6	6.37	5.91
22	33	36.5	24.9	15.6	9.86	6.16	5.36
23	34.5	33.4	22.8	14.23	9.32	6.35	4.86
24	36	30.7	21.0	13.1	7.99	6.21	4.44
25	37.5	28.3	19.3	12.4	7.56	5.94	4.08
26	39	26.2	17.9	11.7	7.13	5.51	3.75
27	40.5	24.3	16.6	11.0	6.75	5.06	3.47
28	42	22.6	15.4	10.4	6.46	4.68	3.21
29	43.5	21.0	14.4	9.89	6.28	4.35	2.99
30	45	19.7	13.4	9.42	6.18	4.05	2.79
31	46.5	18.4	12.8	9.16	6.33	3.78	2.61
32	48	17.3	12.2	7.90	6.32	3.54	2.45
33	49.5	16.2	11.6	7.57	6.11	3.32	2.33
34	51	15.3	11.1	7.24	5.92	3.12	2.21
35	52.5	14.4	10.6	6.94	5.59	2.93	2.10
36	54	13.6	10.2	6.66	5.24	2.77	2.00
37	55.5	13.0	9.78	6.46	4.94	2.62	1.90
38	57	12.5	9.42	6.32	4.67	2.49	1.81
39	58.5	12.0	9.21	6.20	4.42	2.38	1.72
40	60	11.6	8.03	6.22	4.19	2.28	1.64
41	61.5	11.2	7.78	6.33	3.98	2.18	1.57
42	63	10.8	7.52	6.36	3.78	2.09	1.49
43	64.5	10.4	7.26	6.20	3.60	2.01	1.42
44	66	10.1	7.02	6.05	3.43	1.92	1.36
45	67.5	9.71	6.79	5.91	3.27	1.84	1.30
46	69	9.42	6.57	5.65	3.13	1.77	1.25
47	70.5	9.25	6.45	5.39	2.99	1.70	1.20
48	72	8.12	6.33	5.14	2.86	1.63	1.15

Table 6-12 Effective Elastic Static Resistance, r_{eff} (Continued)

Aspect Ratio = 1.75

Glass Dimensions (in.)		Effective Elastic Static Resistance (psi) for Glass Thickness, t, of --					
b	a	3/4 in.	5/8 in.	1/2 in.	3/8 in.	5/16 in.	1/4 in.
12	21	109.	74.2	46.3	26.5	14.4	10.2
13	22.75	92.6	63.2	39.4	22.6	12.3	8.91
14	24.5	79.9	54.5	34.0	19.5	10.6	8.01
15	26.25	69.6	47.5	29.6	17.0	9.46	7.32
16	28	61.2	41.7	26.0	14.9	8.52	6.20
17	29.75	54.2	37.0	23.1	13.2	7.85	5.65
18	31.5	48.3	33.0	20.6	11.7	7.30	5.19
19	33.25	43.4	29.6	18.5	10.67	6.27	4.89
20	35	39.1	26.7	16.7	9.71	5.79	4.70
21	36.75	35.5	24.2	15.1	8.96	5.38	4.64
22	38.5	32.4	22.1	13.8	8.36	5.05	4.50
23	40.25	29.6	20.2	12.6	7.87	4.84	4.31
24	42	27.2	18.6	11.6	7.43	4.70	4.02
25	43.75	25.1	17.1	10.7	7.11	4.65	3.79
26	45.5	23.2	15.8	9.97	6.17	4.54	3.51
27	47.25	21.5	14.7	9.37	5.82	4.41	3.24
28	49	20.0	13.6	8.83	5.52	4.19	3.00
29	50.75	18.6	12.7	8.38	5.23	3.96	2.78
30	52.5	17.4	11.9	8.01	5.02	3.77	2.60
31	54.25	16.3	11.1	7.66	4.86	3.53	2.43
32	56	15.3	10.4	7.35	4.73	3.30	2.29
33	57.75	14.4	9.93	7.11	4.68	3.09	2.16
34	59.5	13.5	9.46	6.27	4.64	2.90	2.05
35	61.25	12.8	9.02	6.00	4.56	2.73	1.94
36	63	12.1	8.62	5.74	4.46	2.58	1.85
37	64.75	11.4	8.30	5.51	4.36	2.44	1.76
38	66.5	10.8	8.00	5.30	4.18	2.32	1.67
39	68.25	10.3	7.73	5.10	4.01	2.21	1.59
40	70	9.91	7.47	4.97	3.86	2.11	1.51
41	71.75	9.52	7.26	4.85	3.72	2.02	1.44
42	73.5	9.15	6.51	4.75	3.53	1.93	1.38
43	75.25	8.81	6.29	4.70	3.36	1.85	1.32
44	77	8.50	6.07	4.67	3.20	1.78	1.26
45	78.75	8.24	5.86	4.64	3.05	1.71	1.20

Table 6-12 Effective Elastic Static Resistance, r_{eff} (Continued)

Aspect Ratio = 2.00

Glass Dimensions (in.)		Effective Elastic Static Resistance (psi) for Glass Thickness, t, of --					
b	a	3/4 in.	5/8 in.	1/2 in.	3/8 in.	5/16 in.	1/4 in.
12	24	97.6	66.6	41.5	23.8	13.0	9.05
13	26	83.1	56.7	35.4	20.3	11.0	7.81
14	28	71.7	48.9	30.5	17.5	9.52	6.87
15	30	62.4	42.6	26.6	15.2	8.31	6.29
16	32	54.9	37.5	23.4	13.4	7.43	5.81
17	34	48.6	33.2	20.7	11.9	6.72	4.98
18	36	43.4	29.6	18.5	10.6	6.26	4.54
19	38	38.9	26.6	16.6	9.49	5.86	4.19
20	40	35.1	24.0	14.9	8.56	5.12	3.93
21	42	31.9	21.7	13.6	7.85	4.72	3.74
22	44	29.0	19.8	12.4	7.25	4.40	3.59
23	46	26.6	18.1	11.3	6.73	4.11	3.48
24	48	24.4	16.6	10.4	6.39	3.92	3.42
25	50	22.5	15.3	9.56	6.08	3.75	3.33
26	52	20.8	14.2	8.84	5.79	3.62	3.24
27	54	19.3	13.2	8.23	5.15	3.51	3.04
28	56	17.9	12.2	7.73	4.85	3.45	2.81
29	58	16.7	11.4	7.27	4.58	3.40	2.61
30	60	15.6	10.7	6.86	4.36	3.32	2.42
31	62	14.6	9.98	6.57	4.15	3.25	2.27
32	64	13.7	9.36	6.32	3.99	3.10	2.14
33	66	12.9	8.80	6.08	3.86	2.90	2.02
34	68	12.2	8.31	5.87	3.74	2.72	1.91
35	70	11.5	7.91	5.66	3.64	2.56	1.81
36	72	10.8	7.53	5.07	3.56	2.41	1.72
37	74	10.3	7.18	4.84	3.49	2.28	1.63
38	76	9.73	6.86	4.64	3.45	2.17	1.56
39	78	9.24	6.62	4.46	3.41	2.06	1.48
40	80	8.78	6.42	4.30	3.36	1.97	1.41
41	82	8.37	6.23	4.14	3.30	1.88	1.34
42	84	8.03	6.05	4.02	3.25	1.80	1.28

Table 6-12 Effective Elastic Static Resistance, r_{eff} (Continued)

Aspect Ratio = 3.00

Glass Dimensions (in.)		Effective Elastic Static Resistance (psi) for Glass Thickness, t, of --					
b	a	3/4 in.	5/8 in.	1/2 in.	3/8 in.	5/16 in.	1/4 in.
12	36	81.1	55.4	34.5	19.8	10.8	7.53
13	39	69.1	47.2	29.4	16.9	9.18	6.41
14	42	59.6	40.7	25.4	14.5	7.92	5.57
15	45	51.9	35.4	22.1	12.7	6.90	4.94
16	48	45.6	31.2	19.4	11.1	6.06	4.42
17	51	40.4	27.6	17.2	9.86	5.43	3.98
18	54	36.1	24.6	15.3	8.79	4.92	3.61
19	57	32.4	22.1	13.8	7.89	4.48	3.15
20	60	29.2	19.9	12.4	7.12	4.10	2.86
21	63	26.5	18.1	11.3	6.46	3.77	2.64
22	66	24.1	16.5	10.3	5.88	3.48	2.45
23	69	22.1	15.1	9.40	5.44	3.08	2.25
24	72	20.3	13.8	8.63	5.06	2.84	2.08
25	75	18.7	12.8	7.95	4.71	2.66	1.92
26	78	17.3	11.8	7.35	4.40	2.49	1.82
27	81	16.0	10.9	6.82	4.13	2.34	1.74
28	84	14.9	10.2	6.34	3.88	2.18	1.66
29	87	13.9	9.48	5.91	3.65	2.04	1.58
30	90	13.0	8.86	5.56	3.44	1.91	1.51
31	93	12.2	8.30	5.26	3.11	1.83	1.47
32	96	11.4	7.79	4.98	2.93	1.76	1.43
33	99	10.7	7.32	4.72	2.78	1.70	1.41
34	102	10.1	6.90	4.48	2.64	1.63	1.39

Table 6-12 Effective Elastic Static Resistance, r_{eff} (Continued)

Aspect Ratio = 4.00

Glass Dimensions (in.)		Effective Elastic Static Resistance (psi) for Glass Thickness, t, of --					
b	a	3/4 in.	5/8 in.	1/2 in.	3/8 in.	5/16 in.	1/4 in.
12	48	75.7	51.7	32.2	18.5	10.1	7.02
13	52	64.5	44.0	27.5	15.7	8.57	5.99
14	56	55.6	38.0	23.7	13.6	7.39	5.16
15	60	48.5	33.1	20.6	11.8	6.43	4.52
16	64	42.6	29.1	18.1	10.4	5.66	3.99
17	68	37.7	25.8	16.1	9.20	5.01	3.56
18	72	33.7	23.0	14.3	8.20	4.49	3.19
19	76	30.2	20.6	12.9	7.36	4.05	2.87
20	80	27.3	18.6	11.6	6.65	3.67	2.54
21	84	24.7	16.9	10.5	6.03	3.34	2.30
22	88	22.5	15.4	9.59	5.49	3.06	2.10
23	92	20.6	14.1	8.77	5.03	2.81	1.94
24	96	18.9	12.9	8.05	4.63	2.52	1.79
25	100	17.5	11.9	7.42	4.28	2.32	1.67
26	104	16.1	11.0	6.86	3.97	2.15	1.56
27	108	15.0	10.2	6.36	3.70	2.00	1.46
28	112	13.9	9.49	5.92	3.45	1.88	1.38
29	116	13.0	8.85	5.52	3.22	1.76	1.30
30	120	12.1	8.27	5.15	3.02	1.66	1.23

UNDERGROUND STRUCTURES

6-33. Introduction

Underground structures are not usually used for production and handling of explosives since access for both personnel and explosives is more difficult than for an aboveground structure. However, an explosion may result in severe hazards from which an aboveground structure can not provide adequate protection and a buried structure will be required. An example might be a manned control building at a test site which must be located very close to a high-hazard operation involving a relatively large quantity of explosives.

There is limited test data available to predict the pressures acting on an underground structure. What test data that is available was developed for use in the design of protective structures to resist the effects of an attack with conventional weapons. The results of this data and the design procedures developed from it are given in the technical manual, "Fundamentals of Protective Design for Conventional Weapons," TM 5-855-1. The data presented may be expanded to include the design of structures subjected to accidental explosions. The pertinent sections are briefly summarized below.

A typical underground structure used to resist conventional weapons attack is shown in Figure 6-53. The burster slab prevents a weapon from penetrating through the soil and detonating adjacent to the structure. A burster slab is not mandatory, but if it is not used the structure will have to be buried much deeper. The burster slab must extend far enough beyond the edge of the building to form at least a 45 degree angle with the bottom edge of the building. It may have to be extended further, though, if it is possible for a bomb to penetrate at a very shallow angle, travel beneath the burster slab and detonate adjacent to the structure (see Figure 6-53). Sand is used as backfill because materials with high volume of air-filled voids and low relative densities are poor transmitters of ground shock. In addition, sand resists penetration better than soil.

6-34. Design Loads for Underground Structures

6-34.1. General

The pressure-time relationships for roof panels and exterior walls are determined separately. For the roof panel, an overhead burst produces the most critical loading while for an exterior wall a sideburst is critical. A general description of the procedure for determining the peak pressures and their durations is given below. For a more detailed description, including the required equations, see TM 5-855-1.

The magnitude of the ground shock is affected by:

1. The size of the explosive charge and its distance from the structure;

2. The mechanical properties of the soil, rock, and/or concrete between the detonation point and the structure; and

3. The depth of penetration at the time of detonation.

The stresses and ground motions are greatly enhanced as the depth of the explosion increases. To account for this effect a coupling factor is used. The coupling factor is defined as the ratio of the ground shock magnitude from a near surface burst to that of a fully buried burst. A single coupling factor applies to all ground shock parameters and depends on the depth of the explosion and whether detonation occurs in soil, concrete or air.

6-34.2. Roof Loads

A typical roof load (shown in Figure 6-54) consists of a free-field pressure P_o and a reflected pressure P_r. The reflected pressure occurs when the free-field pressure impinges on the roof panel and is instantly increased to a higher pressure. The amount of increase is a function of the pressure in the free-field wave and the angle formed between the rigid surface and the plane of the pressure front. However, TM 5-855-1 suggests that an average reflection factor of 1.5 is reasonable.

The pressures on the roof of an underground structure are not uniform across the panel, especially if the depth of the explosion is shallow. However, in order to use a single-degree-of-freedom analysis, a uniform load is required and hence an average uniform pressure must be determined. TM 5-855-1 presents figures that give the ratio peak pressures at the center of a roof panel to the average pressure across the entire panel. This ratio is a function of the support conditions and aspect ratio of the panel and the height of the burst above the roof.

For the most severe roof load the explosive is positioned directly over the center of the panel. The average free-field and average reflected pressures are calculated as described above. The duration of the pressure pulse also varies across the roof panel and a fictitious average duration t_o must be determined. TM 5-855-1 recommends calculating the duration of the peak free-field pressure pulse at a point located one quarter of the way along the short span and at the center of the long span. This duration is then used as the average duration of the entire panel. The peak free-field pressure and impulse are calculated using equations given in TM 5-855-1. The duration is found by assuming a triangular pressure-time relationship. The duration of the average reflected pressure t_r is given in TM 5-855-1 as a function of either the thickness of the structural element or the distance to the nearest free edge of the structure. The smaller of the two numbers should be used in analysis.

6-34.3. Wall Loads

The design loads on an exterior wall are determined using the procedures described in Section 6-34.2 for roof loads. However, in addition to the pressure wave traveling directly from the explosion, the wall may be subject to a pressure wave reflected off the ground surface or burster slab and/or a pressure wave reflected off a lower rock layer or water table.

The parameters of each wave (average reflected pressure, average free-field pressure, durations and time of arrival) are determined separately using procedures very similar to those described in Section 6-34.2. The total pressure-time history is equal to the superposition of the three waves as shown in Figure 6-55. The superposition results in a very complicated load shape. The response charts of Chapter 3 are not applicable for such a shape,

therefore the load must be idealized. The actual load is transformed into a triangular load having the same total impulse (area under the actual load curve equal to the sum of the areas of the direct and reflected waves). The maximum pressure of the idealized load is equal to the maximum pressure of the actual load neglecting the short reflected peaks. The duration is then established as a function of the total impulse and maximum pressure (Figure 6-55). For an exact solution, the actual load curve is used in a single-degree-of-freedom computer program analysis or numerical analysis as given in Section 3-19.2.

6-35. Structural Design

6-35.1. Wall and Roof Slabs

The structural design of underground structures is very similar to the design of aboveground structures as described in Chapter 4. The effect of the soil is to modify the response of the structural components. The dead load of the soil reduces the resistance available to resist blast. At the same time a portion of the soil acts with the structural elements to increase the natural period of vibration. In the case of a wall, it is assumed that the mass of two (2) feet of soil acts with the mass of the wall. Whereas for a roof, the entire mass of the soil supported by the roof, or a depth of soil equal to one quarter of the roof span (short span for a two-way panel) whichever is smaller, is added to the mass of the roof.

The dynamic response of underground structures must obviously be limited to comparatively small deformations to prevent collapse of the structure due to earth loads. A protective structure subjected to conventional weapons attack should be designed for a ductility ratio of 5.0, as recommended by TM 5-855-1. This ratio may be increased to 10 if special provisions are taken. A maximum deflection corresponding to a support rotation of one (1) degree or a ductility ratio of 10.0 is permitted for underground structures subjected to accidental explosions.

Spalling is the ejection of material from the back face of a slab or beam. It results from high-intensity, close-in explosions. Fragment shields or backing plates, as shown in Figure 6-56, are of some value in protecting personnel and equipment. These steel plates must be securely anchored to the inside face of the concrete member. Tests have shown that the shock of a deep penetrating detonation to be enough to cause inadequate welds to fail over a large area, adding the whole steel plate to the concrete spall. A strongly attached plate adds about 10 percent to the perforation resistance of a concrete slab. For a further discussion of backing plates, see Chapter 4.

6-35.2. Burster Slab

For protective structures, a burster slab prevents a weapon from penetrating through the soil and detonating adjacent to the structure. Its thickness and length may have to be determined by a trial and error procedure in order to limit pressures on the structure to a given value. However, the minimum dimensions are shown in Figure 6-53. The minimum reinforcement is 0.1 percent in each face, in each direction or a total of 0.4 percent. In the design of structures subject to accidental explosions, the ground floor slab of the donor building serves a purpose similar to that of a burster slab. The floor slab helps to prevent fragment penetration and to attenuate the load.

6-36. Structure Motions

6-36.1. Shock Spectra

TM 5-855-1 gives equations for acceleration, velocity and displacements for underground structures. These simplified methods take into account the attenuation of the pressure wave as it transverses the structure. For a sideburst, the vertical acceleration, velocity and displacements are 20 percent of the horizontal values. The horizontal motions are uniform over the entire floor while vertical motions at the leading edge are twice those at midspan.

Once the peak in-structure acceleration, velocity and displacements have been determined an in-structure shock spectra can be developed using the principles of Chapter 2 of this manual.

6-36.2. Shock Isolation Systems

Chapter 1 presents the upper limits of the shock environment that personnel and equipment can tolerate. If the shock environment exceeds human tolerances and/or equipment "fragility levels" then shock isolation systems are required to protect personnel and sensitive equipment. Using the shock spectra developed as described above, shock isolation systems are designed as outlined in Sections 6-43 through 6-49.

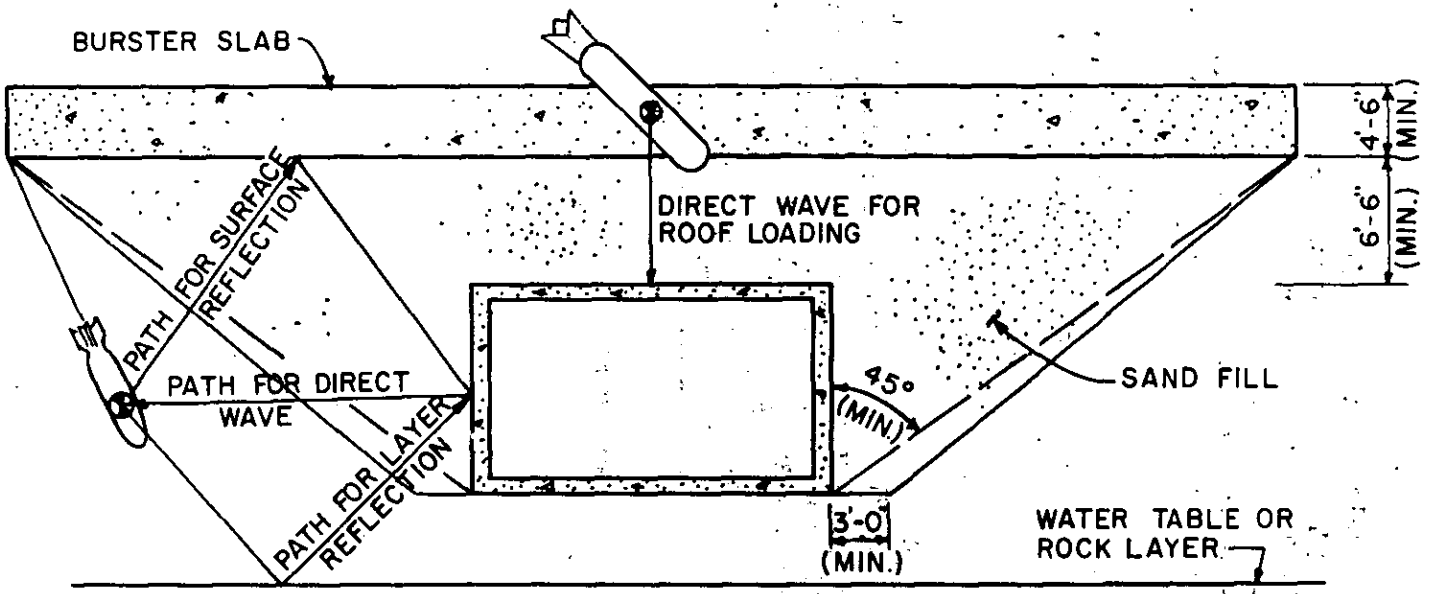


Figure 6-53 Geometry of a buried structure

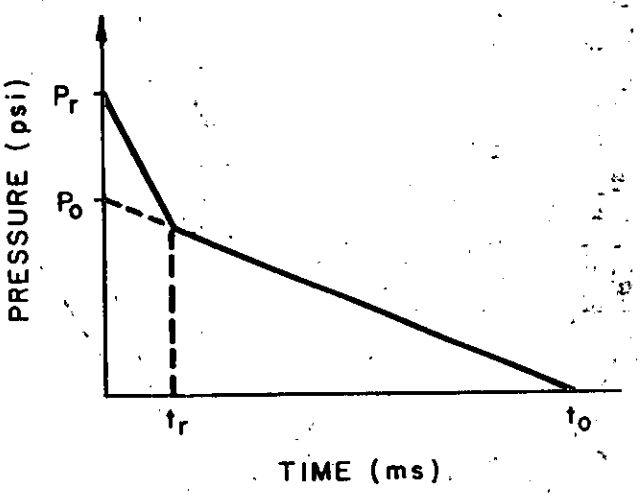


Figure 6-54 Typical roof panel load

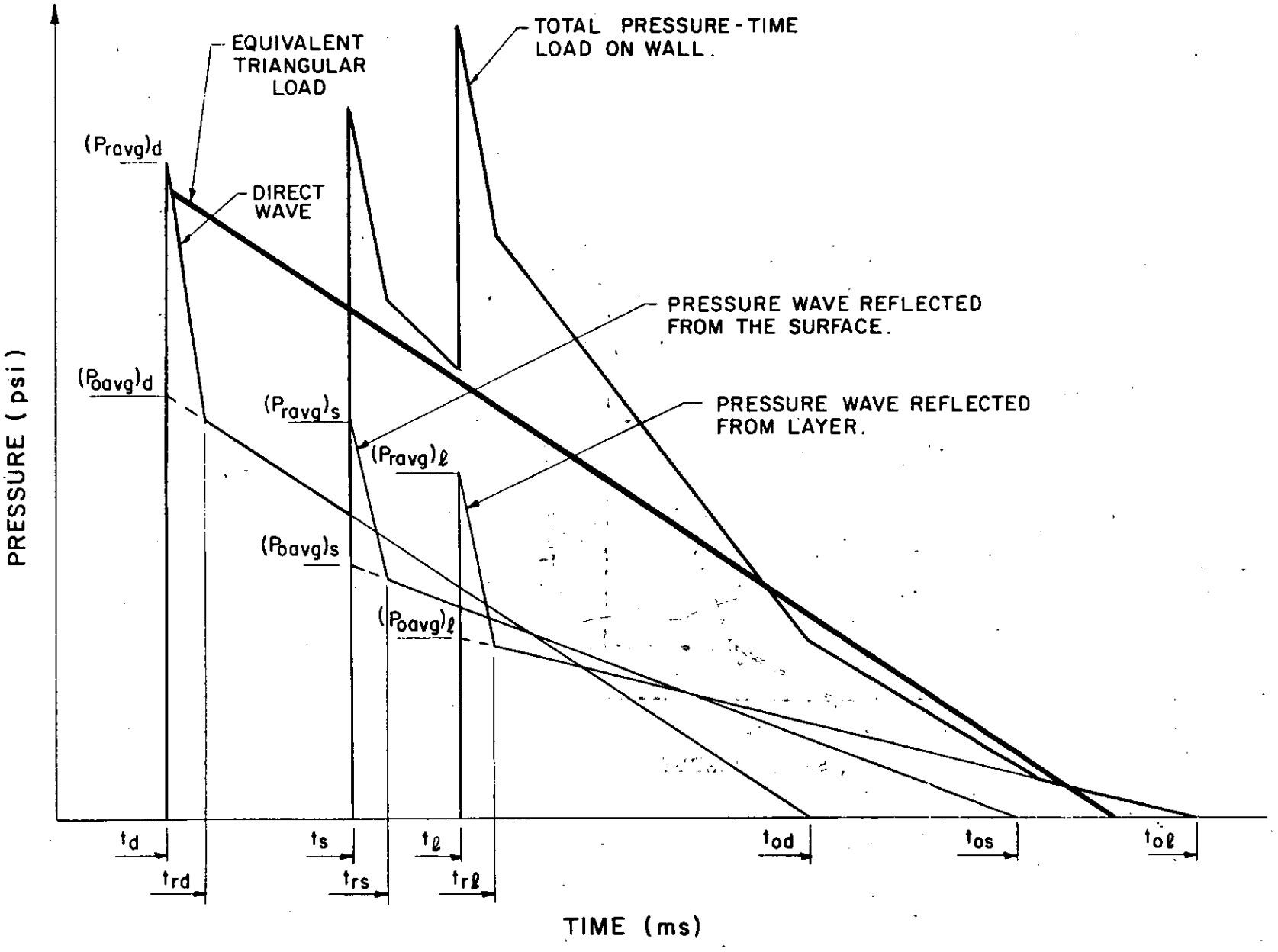
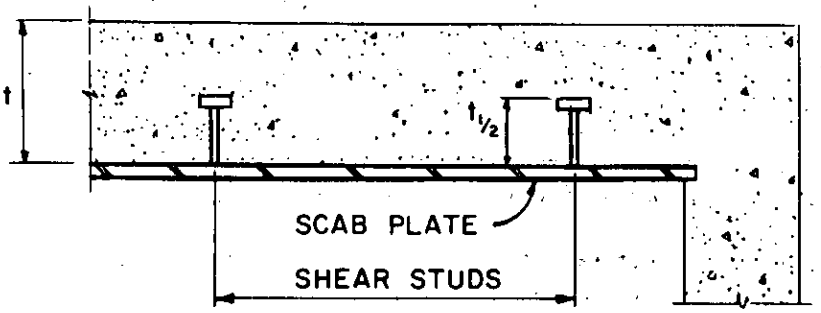
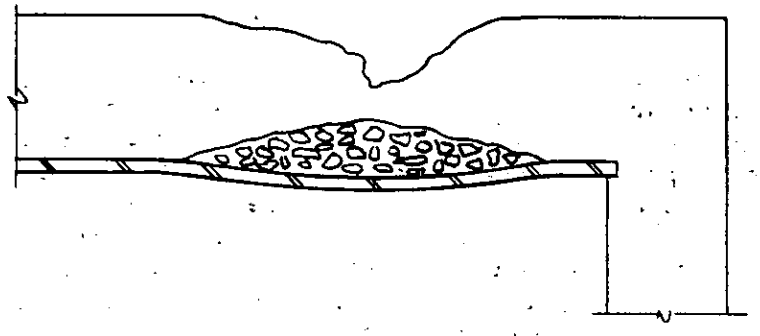


Figure 6-55 Contribution of three pressure waves on a wall





RETENTION OF SCAB MATERIAL

Figure 6-56 Spall plate

EARTH-COVERED ARCH-TYPE MAGAZINES

6-37. General

Certain types of earth-covered concrete-arch and steel-arch magazines have been approved and standardized for use by the Department of Defense Explosives Safety Board. These magazines provide definite advantages over other types of magazines. Among these advantages are:

1. Less real estate per magazine is required because of the decreased intermagazine separations permitted when approved magazines are used.

2. An almost infinite number of storage situations exists because magazines can be designed to any length.

3. Because of the reduced separation distances, less roads, fences, utilities, etc., are required.

Unlike the other structures discussed elsewhere in this manual, an earth-covered magazine is not designed to resist the damaging effects of its exploding contents. It is accepted that the magazine will be demolished if an internal explosion occurs. During such an incident, the inside of a large-span arch might experience initial blast pressures considerably in excess of 10,000 psi. Less than 100 psi could lift the arch completely out of the ground; therefore, the major portion of the protection is provided by the receiver magazines rather than the donor magazine.

Earth-covered magazines are utilized primarily to prevent propagation of explosion. These structures may also be used for operating buildings and can provide personnel protection. In such cases, separation distances greater than those required to prevent propagation of explosions will be necessary. In addition, a special evaluation of the structure is required. This evaluation must include the leakage of blast pressures into the protected area, the strength and attachment of easily damaged or lightly supported accessories which may become hazardous debris, the transmission of shock to personnel through the walls or floors, and overall movement of the magazines.

6-38. Description of Earth-Covered Arch-Type Magazines

A typical earth-covered arch-type magazine used for storing explosives has the following features:

1. A semicircular or oval arch constructed of reinforced concrete or corrugated steel used to form roof and sides.

2. A reinforced concrete floor slab, sloped for drainage.

3. A reinforced concrete rear wall.

4. A reinforced concrete headwall that extends at least 2-1/2 feet above the crown of the arch.

5. Reinforced concrete wingwalls on either side of the headwall. The wingwalls may slope to the ground or may adjoin wingwalls from adjacent

magazines. The wingwalls may be either monolithic or separated by expansion joints from the headwall.

6. Heavy steel doors in the headwall (either manually operated and/or motorized).

7. An optional gravity ventilation system.

8. Earth cover over the top, sides and rear of the structure. This cover must be at least 2 feet thick at the crown of the arch. The earth above the structure (within the spring line of each arch and between the head and rear walls) is sloped for drainage while beyond the outline of the structure the earth is sloped 2 horizontal to 1 vertical.

9. Its own built-in lightning protection and grounding systems.

A typical earth-covered steel arch magazine is illustrated in Figure 6-57.

6-39. Separation Distances of Standard Magazines

Numerous full scale tests of standard magazines have been performed over a period of several years. As a result magazine separation formulae have been established, which will prevent magazine-to-magazine propagation of explosions. All possible right angle arrangements have been considered, i.e., side-to-side, rear-to-rear, front-to-rear, etc. The standard magazines, which are at least equivalent in strength to those tested, are listed in the DoD Standard, "DoD Ammunition and Explosives Safety Standards, 6055.9-STD." The required separation distances, as a function of the quantity of explosives stored in the structure are also given in the DoD Standard. A possible magazine arrangement is shown in Figure 6-58.

6-40. Design

Protection of magazines adjacent to a donor magazine is accomplished by combining the following factors:

1. The intensity of the pressure front moving from the donor magazine to receiver magazines diminishes rapidly as the distance traveled increases.

2. The earth cover over and around the donor magazine provides some confinement and tends to directionalize the explosive force both upward and outward from the door end of the magazine.

3. The earth around and over receiver magazines resists fragment penetrations and provides mass to the arch to resist the blast pressures.

4. The arch of receiver magazines is capable of resisting blast loads considerably in excess of the dead loads normally imposed on it.

Design of presently used magazines is essentially conventional except for two features, which are doors and arch. The doors are designed to withstand the dynamic forces from an explosion in a nearby magazine if the siting is in accordance with Figure 6-58. However, they provide almost no resistance to the effects of an explosion within the magazine. Also, the capacity of the

doors to resist elastic rebound and negative phase pressures may be less than their capacity to resist positive phase pressures. Therefore, where personnel are concerned, all doors should be analyzed to determine their ultimate capacity to resist all the loadings involved. The arches used for the standard earth-covered magazines are the same as those used in the test structures to establish the required separation distances. These arches have not been dynamically designed for the blast loads and may be in excess of that required.

6-41. Construction

Effectiveness of earth-covered magazines is largely determined by the quality of construction. A few of the construction details that could be sources for problems in this type of structure are discussed below.

Moisture proofing of any earth-covered structure is usually difficult. This difficulty is increased with a steel-arch structure because of the many lineal feet of joints available for introducing moisture. For example, a large 26-by 80-foot magazine contains approximately 1,050 feet of edges. A sealant tape must be used that will not deteriorate or excessively deform under any anticipated environmental or structural condition.

Earthfill material should be clean, cohesive, and free from large stones. A minimum earth cover of two feet must be maintained. Surface preparation of the fill is usually required to prevent erosion of the 2-foot cover.

Restricting granular size of material reduces throwout of fragments in case of an accidental explosion and creates a more uniform energy absorbent over the top of the magazine.

Lightning protection is rather easily obtained in a steel-arch structure. All sections of steel-arch plate must be interconnected so that they become electrically continuous. In a concrete-arch magazine, the reinforcing steel must be interconnected. In effect, a "cage" is created about the magazine contents. Probably the most critical point for lightning protection is the optional ventilator stack which projects above the surrounding earth cover.

6-42. Non-Standard Magazines

Non-standard earth-covered magazines, that is magazines not listed in DoD Standard 6055.9-STD may also be used for explosive storage. However, if a "non-standard" earth-covered magazine or an aboveground magazine is used the separation distances must be increased. The DoD Standard 6055.9-STD includes the increased separation distances, as well as other criteria, for "non-standard" earth-covered and aboveground magazines.

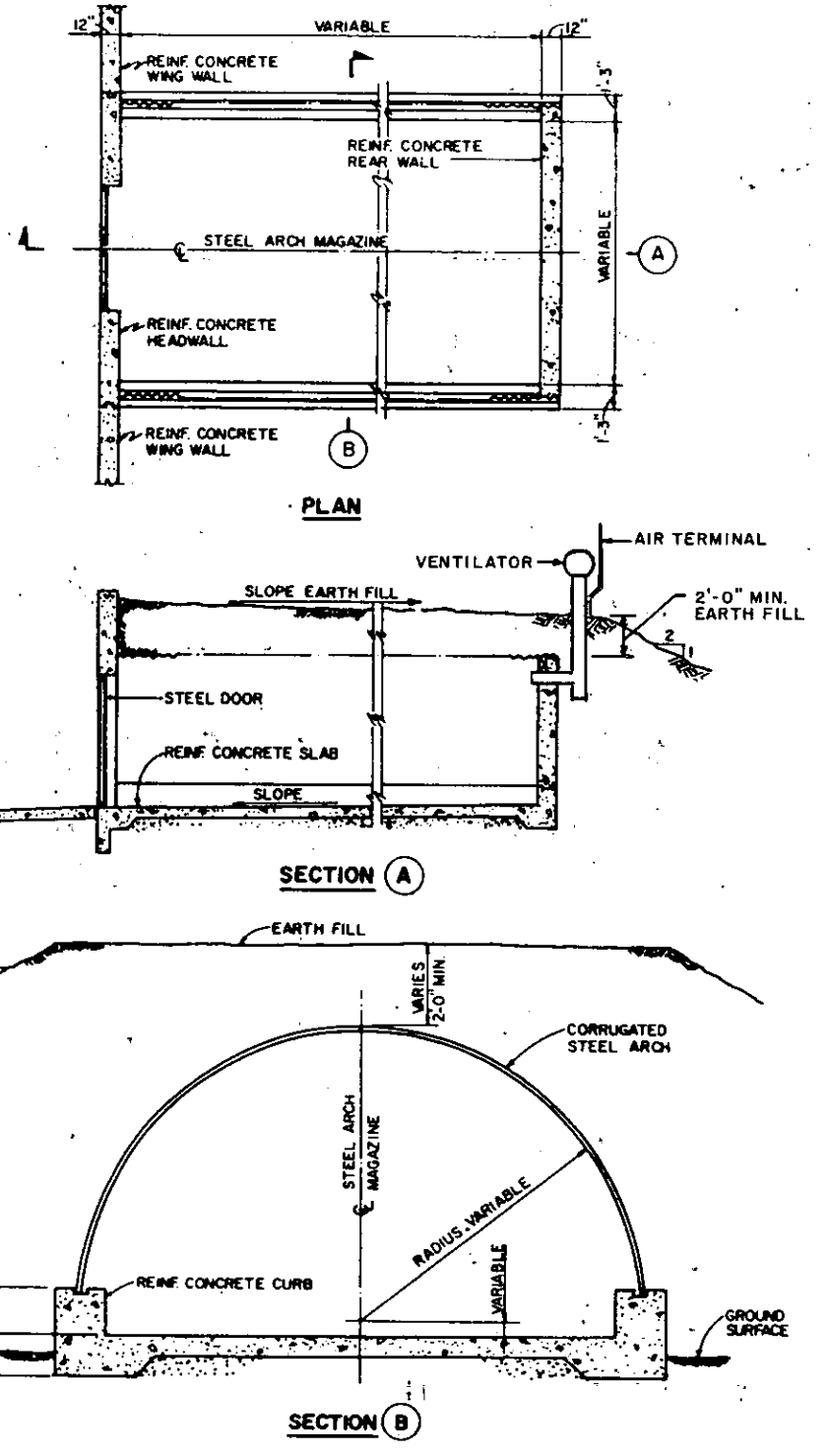
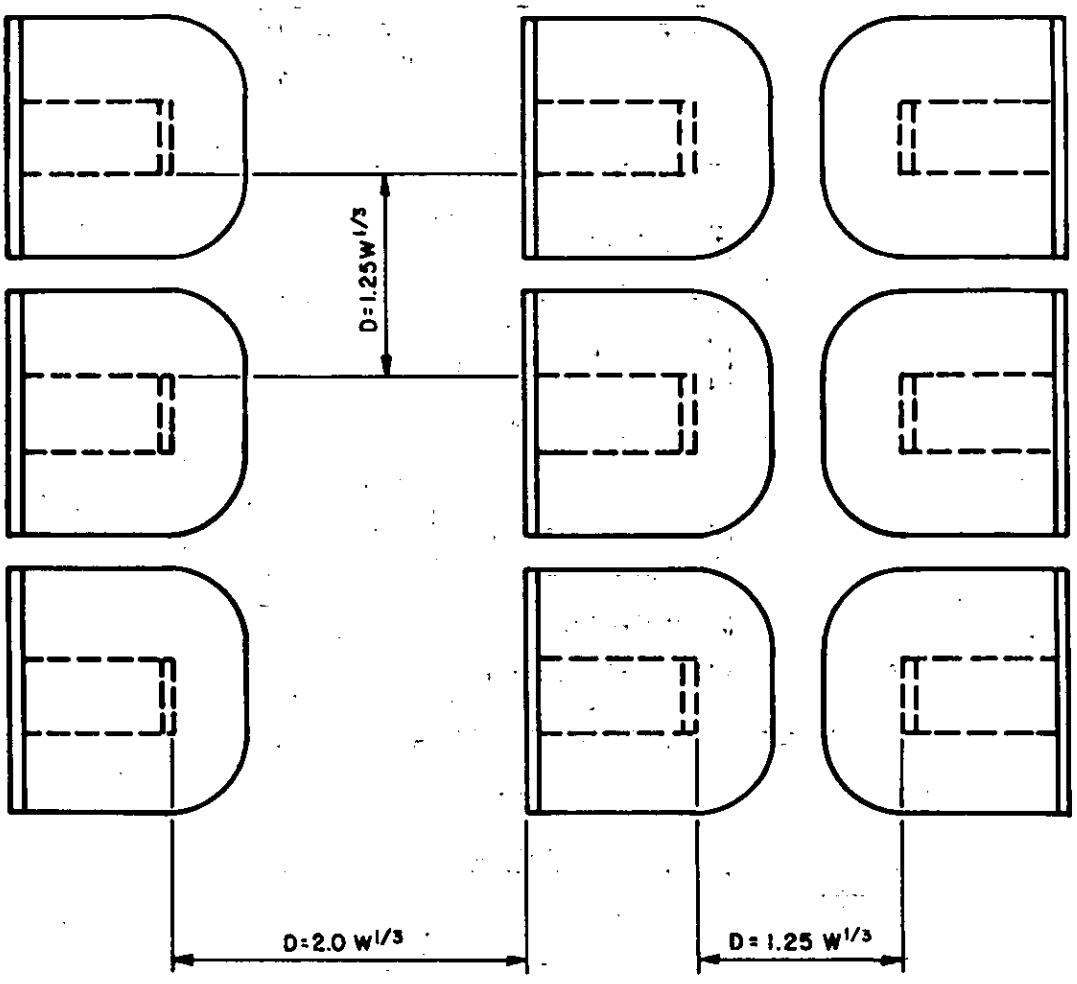


Figure 6–57 Typical earth-covered steel-arch magazine



HEADWALL

REAR WALL

EDGE OF EARTH COVER

EDGE OF ARCH

W = CHARGE WEIGHT

Figure 6–58 Minimum separation distances of standard magazines

BLAST VALVES

6-43. General

6-43.1. Applications

A prime concern of blast resistant structures is to restrict the flow of high pressures into or out of a structure. For donor structures pressures released may have to be restricted in order to limit pressures acting on adjacent structures to tolerable levels. Also, pressures leaking into acceptor structures must be limited to prevent pressure buildup beyond acceptable levels. In either case openings may have to be completely sealed to prevent the diffusion of contaminants.

The simplest, most economical way of limiting leakage pressure into or out of a protective structure is to restrict the number and size of air intake and exhaust openings. In a donor structure the leakage pressures may be further reduced by venting them through a stack. The stack increases the distance from the point of release of the pressure to the acceptor structure thereby attenuating the blast loading. Methods for predicting the pressures leaking out of a building and the pressure buildup within a building are discussed in Chapter 2. If the leakage pressure can not be reduced to acceptable levels or if contaminants are released during an explosion, the openings must be sealed with either blast valves or other protective closure device.

Blast valves may be either remote-actuated (closed mechanically by remote sensors) or blast-actuated (closed by the pressure wave itself). Both types can be non-latching or latching. A non-latching valve will open under negative pressures. A latching valve is one that can only be reopened manually. In addition, a blast-actuated valve can be double-acting. A double-acting valve will seal against the positive blast pressure, move in the opposite direction to seal against negative pressures and then reopen when pressures return to normal.

6-43.2. Remote-Actuated valves

Remote-actuated valves are dependent on external sensing devices which trigger the closure mechanism and close the valve before arrival of the blast wave. Actuating devices have been developed that are sensitive to the blast pressure of an explosion and react electrically to trigger protective closure systems. Other actuating devices sensitive to flash and thermal radiation are also available. The pressure sensing device is placed on a circumference at a predetermined radius from the valve (closer to ground zero) in order to compensate for time delays of electrical and mechanical control equipment and to permit valve closure before the blast arrives. Thermal sensors are designed to detect the characteristic pulse emitted by an explosion to prevent actuation by other sources such as lightning, fires, etc., which may occur with flash sensors. Remote-actuated valves present problems of protection against multibursts and button-up time for combustion-type equipment installed within the structure. In addition to problems of hardenability of the exposed sensor and suitability for multiburst operation, it is often necessary for sensors to initiate reopening of the valves as soon as dangerous pressures have subsided. In general, remote-actuated valves can not close fast enough to be effective during an H. E. explosion.

6-43.3. Blast-Actuated Valves

Self-acting blast-actuated valves, which close under the action of the blast pressure, overcome some of the disadvantages described above and present other factors to be considered. Since the valves are closed by pressure, they are not dependent upon sensing devices for operation. They can be automatically reopened after passage of the positive phase or latched closed during the negative phase if this is required. Double-acting valves automatically seal the opening during the negative phase. Since blast-actuated valves are closed by the blast, there is an inherent leakage problem to be considered due to the finite closing time. Although this is in the order of milliseconds for most valves, sufficient flow to cause damage may pass the port openings for certain valve designs and pressure levels. Effectiveness of closing at both high- and low-pressure ranges must be checked. The amount of blast entering depends on the closing time of the valve which, in turn, depends on the mass of the moving parts, disk diameter, and the distribution of pressures on both faces of the disk.

Ideally, a blast-actuated valve should possess the following characteristics: instantaneous closure or no leakage beyond the valve during and after closure, no rebound of moving parts, equal efficiency at all pressures below the design pressure, operational and structural reliability, minimum of moving parts, low-pressure drop through the valve at normal ventilation or combustion air flows, multiple detonation capability, durability, and easy maintenance.

Although instantaneous closure is not physically possible, the closing time can be reduced sufficiently to reduce the leakage to insignificant values. This may be accomplished by increasing the activating pressure-force-to-moving-mass ratio, decreasing the length of travel, permitting no deceleration during closure, and other methods.

6-43.4. Plenums

Blast valves, especially blast-actuated valves, will allow some pressure leakage. While the leakage pressure may not significantly increase the ambient pressure at some distance from the valve, there might be a "jetting effect" causing very high pressures in the immediate vicinity. A plenum may be used to protect against these high pressures. Two examples of plenums are, a plenum chamber and a plenum constructed of hardened duct work. A plenum chamber is a room where pressures attenuate by expansion. A hardened duct work plenum reduces the pressures by increasing the distance traveled (similar to the stack discussed in Section 6-43.1). For a donor structure, a plenum would only be necessary if contaminants are released during an explosion and the air must be filtered before being vented to the exterior. In that case, a plenum would be used to lower the pressures and prevent damage to the filters. A plenum in an acceptor structure would be used to prevent high leakage pressures from directly entering the building's air duct system and possibly causing local failure of the system.

Plenum chambers should be designed to avoid a buildup of interior pressure which would impede closing of the valve. The ratio of the area of the chamber cross section to that of the valve outlet should be preferably greater than 4:1 so as to diffuse leakage flow as quickly as possible. A chamber which has the prescribed necessary volume but has little change in area would act like a

tunnel wherein entering pressures would encounter little attenuation in the length provided.

6-43.5. Fragment Protection

To ensure that blast valves function properly, they must be protected from fragments that may perforate the valves or jam them in an open position. One of several methods of accomplishing the required protection is by offsetting the opening from the blast valve by means of a blast-resistant duct or tunnel which would prevent the propagation of fragments to the blast valve. Another method is to enclose the blast valve in a concrete chimney. Other methods include using a debris pit or steel shields or debris cover attached directly to the blast valves.

6-44. Types of Blast Valves

6-44.1. General

Various types of blast valves have been developed and many of them are available commercially from suppliers both here and overseas (see Table 6-13). For present designs, air flow rates from about 300 cfm to 35,000 cfm can be obtained. Some valve designs are available in more than one size and can be either blast or remote-actuated. The pressure loss across the valve at the rated air flow is, in most cases, less than one inch of water.

The maximum incident pressure capability of available valves is above 50 psi and generally at least 100 psi. For shelter purposes, these valves may be overdesigned since the protection level for many shelters will be less than 50 psi. Except for cost factors, using a 100-psi valve for a 10-psi shelter design should not necessarily present technical problems since a valve must operate at all pressures below the maximum design level.

The best type of actuation (blast or remote) depends partly on the design pressure as previously discussed with regard to reaction time and operational considerations. For long arrival times (low pressure). a remote-actuated device can close the valve before the blast arrival whereas leakage may occur for a blast-actuated valve. At a high pressure (short arrival time),the closing time for the remote-actuated valve may be longer than the arrival time.

6-44.2. Blast Shield

If it can be assumed that the ventilation system can be closed off during a hazardous operation and kept closed until there is no danger of further blast, a relatively simple structural closure (blast shield), such as a steel plate can be utilized. This type of closure is especially useful for an exterior opening which would only be opened periodically, such as maintenance facilities where the release of toxic fumes from within the structure is required.

6-44.3. Sand Filter

In shelters where normal operational air requirements are small, sand filters are useful in the attenuation of leakage pressures. With this type of filter the pressures continue to increase throughout the positive phase. Thus this

filter is good only for loads with a relatively short duration. A sketch of a 300-cfm sand filter is shown in Figure 6-59.

6-44.4. Blast Resistant Louvers

The blast resistant louver shown in Figure 6-60 is blast actuated and has a rated flow of 600 cfm at less than 1 inch water (gage) pressure drop. If a larger volume of air is required the louvers can be set into a frame and used in series (see Figure 6-61). Louvers can be used in acceptor structures subject up to 50 psi. A major drawback of the louvers is that there may be as much as 40 percent leakage across the valve, especially at lower pressures.

6-44.5. Poppet Valves

6-44.5.1. Applications

A poppet valve has many advantages. It has few moving parts which might need repair. It can be blast or remote-actuated, latching, non-latching, or double-acting and is available in sizes from 600 to 5,000 cfm. A blast-actuated poppet valve has a very fast closing time, approximately 20 milliseconds, making it the only valve that reacts fast enough to be used in a containment cell.

A typical blast-actuated poppet valve is shown in Figure 6-62. The valve consists of an actuating plate, a valve seat, a backing plate that supports the actuating plate, and a spring which holds the valve open during normal operations. The normal air flow is around the actuating plate. A blast load will compress the spring and move the actuating plate against the valve seat thereby sealing the opening. As the blast pressure moves the actuating plate, some pressure will flow around the plate while it is closing.

The leakage pressures can be completely prevented by using a valve similar to the one schematically illustrated in Figure 6-63. In this valve the normal air flow is around the actuating plate through a length of duct. When the valve is subjected to a blast load, the pressure starts moving the actuating plate while at the same time flowing through the duct. The length of the duct must be long enough to ensure that the time it takes the blast pressures to flow through the duct (delay path) will be longer than the time required for the actuating plate to seal the valve. As an alternate to the long duct, an expansion chamber may be used to delay the blast.

6-44.5.2 Recommended Specification for Poppet Valves

Presented below is an example specification for the design, testing and construction of a poppet valve, but it may be adapted for other types of blast valves. This example specification is presented using the Construction Specification Institute (CSI) format and shall contain as a minimum the following:

1. APPLICABLE PUBLICATIONS: Except as otherwise stated herein all materials and work furnished in accordance with this specification shall comply with the following codes and standards.

1.1 Federal Specification (Fed. Spec.)

TT-P-37D	Paint, Alkyd Resin; Exterior Trim, Deep Colors
TT-P-645A	Primer, Paint Zinc Chromate Alkyd Type
TT-P-86G	Paint, Red- Lead-Base, Ready Mixed

1.2 American Society for Testing and Materials (ASTM)

A 53-81a	Pipe, Steel Black, and Hot-Dipped, Zinc-Coated, Welded and Seamless
D 2000-80	Rubber Products in Automotive Applications, Classification System For
E-709-80	Magnetic Particle Examination

1.3 American Institute of Steel Construction (AISC)

Specification for the Design, Fabrication and Erection of Structural Steel for Buildings (Eighth Edition) with commentary

1.4 American Iron and Steel Institute (AISI)
304 17-7th

1.5 American Welding Society (AWS)
D.1.1 Structural Welding Code(latest edition)

2. SUBMITTALS: The following information shall be submitted for approval. Materials shall not be delivered to the site until approved shop drawings have been returned to the Contractor. Partial submittals, or submittals for less than the whole of any system made up of interdependent components will not be accepted. Submittals for manufactured items shall be manufacturer's descriptive literature, shop drawings, and catalog cuts that include the manufacturer's dimensions, capacity, specification reference, and all other information necessary to establish contract compliance.

2.1 Qualifications: The Contractor shall submit for approval, data to support the qualifications of the manufacturer and installer. A list of previously successfully completed jobs of a similar nature, indicating the name and address of the owner of the installation shall be included with the information.

2.2 Manufacturer's Data: Before executing any fabrication work, a completely marked and coordinated package of documents sufficient to assure full compliance with the drawings and specifications shall be submitted. The submittal shall include a complete technical evaluation of the capacity of each valve as described below. The drawings shall include: detailed fabrication and equipment drawings; assembly showing the complete installation, including methods for supporting the valves, subframes and frames; a listing

of all materials and material specifications; surface finishes; fabrication, assembly and installation tolerances; locking devices and locking device release mechanisms; and a detailed sequence for installation of valves and frames in conjunction with other phases of construction. Structural fabrication drawings shall conform to the requirements of AISC and welding shall conform to AWS. Assembly and installation shall be based on field established conditions and shall be fully coordinated with architectural, structural, and mechanical systems. All aspects of any work developed in connection with the development of these valves shall be fully documented and become the property of the Government.

2.2.1 Standard Compliance: Where equipment or materials are specified to conform to requirements of the standards of organizations such as ANSI, NFPA, UL, etc., which use a label or listing as a method of indicating compliance, proof of such conformance shall be submitted for approval. The label or listing of the specified organization will be acceptable evidence. In lieu of the label or listing, the Contractor shall submit a notarized certificate from a nationally recognized testing organization adequately equipped and competent to perform such services, and approved by the Contracting Officer stating that the items have been tested with the specified organization's methods and that the item conforms to the specified organization's standards.

2.3 Preliminary Hydraulic Characteristics: Prior to Construction, submit with shop drawings an estimate of the hydraulic characteristics of each valve, under actual operating conditions. Ratings shall be based on tests or test data. All necessary corrections and adjustments shall be clearly identified. Corrections shall be established for actual altitude and air flow directions as shown on the drawings as well as hydraulic effects produced by mounting and/or connection of the valve.

2.4 Tests and Test Reports: Except as noted otherwise, the testing requirements for materials stated herein or incorporated in referenced documents, will be waived, provided certified copies of reports of tests from approved laboratories performed on previously manufactured materials are submitted and approved. Test reports shall be accompanied by notarized certificates from the manufacturer certifying that the previously tested material is of the same type, quality and manufacture as that furnished for this project.

2.5 Blast pressure analysis calculations and/or results of approved tests shall be submitted, for both the blast valve and subframe, for approval and shall conform to the requirement of the paragraph entitled, BLAST VALVE TESTS. The calculations and/or test results shall include all components of the valves and subframe subjected to the blast pressures. Calculations are not required for the frame embedded in the concrete. This frame shall conform to that shown on the drawings. However, the fabrications of the blast valve and associated subframe and embedded frame shall be the responsibility of the blast valve manufacturer. This manufacturer shall also be responsible for installation of this equipment.

2.6 Qualification of Welders: Before assigning any welder to work covered by this section of the specification, the Contractor shall submit the names of the welders to be employed on the work together with certifica-

tion that each of these welders has passed the qualification test using procedures covered in AWS Standard D1.1.

2.7 Operational and Maintenance Manual: Operation and maintenance manuals shall be furnished by the Contractor. Complete manuals shall be furnished prior to the time of installation. The manual shall have a table of contents and shall be assembled to conform to the table of contents with tab sheets placed before instructions covering the subject.

2.8 Shop Test Reports: The Contractor shall furnish copies of shop inspection and test results of fabrication welding.

3. MATERIALS:

3.1 Structural steel pipe used for blast valve construction shall conform to ASTM A 53 seamless pipe.

3.2 All structural steel plate components of the valve shall consist of stainless steel and shall conform to AISI 304.

3.3 Spring type components shall consist of stainless steel and conform to AISI 17-7th, Condition C.

3.4 Blast Seal Material: Seals for blast valves shall conform to ASTM D 2000.

4. BLAST VALVE REQUIREMENTS: All blast valves shall be poppet type and shall have the following characteristics.

4.1 Pressure capacity: Each valve shall be capable of withstanding a sustained blast pressure of 100 psi as well as the impact force produced by the closing of the valve. The valve shall be designed to sustain elastic deformation when subjected to the above loads. The blast valve shall be capable of closing under a force of 15 pounds.

4.2 Temperature Capacity: Each valve shall be capable of satisfactory operation over a temperature range of 35° to 300° F.

4.3 Valve Actuation: Each valve shall be actuated by the blast overpressure. The valve shall be in the closed position 20 milliseconds after the onset of the blast front. The blast pressures are given on the drawings.

4.4 Valve Parameters: A minimum of 12-inch diameter blast valve shall be used. After the valve is closed by the blast overpressure, it shall remain in the closed position until manually opened. This shall require that the valve be equipped with a locking device which shall be located at the exterior side of the valve. A release mechanism for the locking devices shall be provided which shall be operated from a position immediately adjacent to the interior of the valve. Any penetration through the valve or the structure must be capable of being sealed against blast leakage through the penetration. The air flow capacity of the valves shall be 1500 SCFM (1710 ACFM) for the supply and return valves and 880 SCFM (1000 ACFM) for the exhaust valve. Total actual pressure drop across the valve with air movement in either direction shall not exceed one inch of water (gage). The valve and its operating parts shall be designed for a 20-year life and shall have an operating frequency of 10,000.

4.5 Blast Seals: Blast seals shall be provided between the face of each valve and subframe and between the subframe and the frame to provide a pressure tight condition. Seals shall be adjustable and easily replaceable. The seal shall be designed to be leakproof with a pressure differential across the seal of 100 psi.

4.5.1 Blast Seal Material: Seal material shall conform to ASTM D 2000. Four sets of blast seals shall be furnished with each valve. Three sets of the seals shall be packaged for long term storage.

4.5.2 Adhesive: Adhesive for blast seals shall be as recommended by the manufacturer of the seals. Sufficient adhesive shall be provided for installation of the packaged seals at a later date.

4.6 Field Removal: Blast valves shall have the capabilities of being completely field removed and disassembled.

5. FABRICATION:

5.1 Qualification of Manufacturer: The manufacture and installation of blast valves and frames shall be performed by the blast valve manufacturer who shall be fully responsible for valve operation. The manufacturer shall have complete facilities, equipment and technical personnel for the design, fabrication, installation and testing of complete blast valve assemblies.

5.2 General: The drawings indicate the location of the blast valves in the structure. The manufacturer shall carefully investigate the drawings and finished conditions affecting his work and shall design the units to meet the job condition and the dynamic loads. The blast valves shall be complete with gaskets, fasteners, anchors, mechanical operators, and all other equipment and accessories as required for complete installation.

5.3 Metalwork: Except as modified herein, fabrication shall be at a minimum, in accordance with the AISC Specification for the Design, Fabrication and Erection of Structural Steel for Buildings. Welding of steel shall be in accordance with the requirements for AWS Specification D1.1. A welding sequence to reduce distortion and locked-up stresses to a minimum shall be used. All welded units shall be stress relieved. All welded members shall be post weld straightened free of twist and wind. Fabricated steel shall be well formed to shape and size, with sharp lines and angles. Exposed welds shall be ground smooth. Exposed surface of work, in place, shall have a smooth finish. Where tight fits are required joints shall be milled to a close fit. Corner joint shall be coped or mitered, well formed, and in true alignment. Permanent connections for all assemblies and components, except those requiring removal for installation and maintenance, shall be welded. Each valve and subframe shall be removable from the embedded frame.

5.3.1 Machining: Parts and assemblies shall be machine finished wherever necessary to insure proper fit of the parts and the satisfactory performance of the valves.

5.3.2 Weld Details: The types of edge preparation used for welds shall be chosen by the manufacturer to be the most suitable for the joint and position of welding. Where required, all groove welds shall be complete penetration welds with complete joint fusion. Groove weld edge preparations

shall be accurately and neatly made. All full penetration groove joints shall be back-chipped and back welded where both sides are accessible. Where both sides are not accessible, backing strips not exposed to view may be left in place unless removal is required for clearance. Backing strip not removed shall be made continuous by welding ends and junctions.

5.3.3 Weld Tests: Inspection and tests of welds shall be as specified in AWS Specification D1.1. All welding shall be subjected to normal continuous inspection.

5.3.3.1 Nondestructive dye penetrator testing shall be performed for all welding in accordance with Method B of ASTM E 165 or ASTM E 709. Allowable defects shall conform to AWS Specification D1.1.

5.3.3.2 Penetration Welds: All full or partial penetration corners, tees and inaccessible butt joints shall be subjected to 100 percent ultrasonic examination. All penetration joints shall be considered to be tension joints. All tests shall be performed by a testing laboratory approved by the Contracting Officer. The testing laboratory shall be responsible for interpretation of the testing, which shall be certified and submitted in a written report for each test. In addition to the weld examination performed by the Contractor, the Contracting Officer reserves the right to perform independent examination of any welds at any time. The cost of all Government reexamination will be borne by the Government.

5.3.3.3 Correction of Defective Welds: Welds containing defects exceeding the allowable which have been revealed by the above testing shall be chipped or ground out for full depth and rewelded. This correction of the defected weld area and retest shall be at the Contractor's expense.

5.4 Metal Cleaning and Painting:

5.4.1 Cleaning: Except as modified herein, surfaces shall be cleaned to bare metal by an approved blasting process. Any surface that may be damaged by blasting shall be cleaned to bare metal by powered wire brushing or other mechanical means. Cleaned surfaces which become contaminated with rust, dirt, oil, grease, or other contaminants shall be washed with solvents until thoroughly clean.

5.4.2 Pretreatment: Except as modified herein, immediately after cleaning, steel surfaces shall be given a crystalline phosphate base coating; the phosphate base coating shall be applied only to blast cleaned, bare metal surfaces.

5.4.3 Priming: Treated surfaces shall be primed as soon as practicable after the pretreatment coating has dried. Except as modified herein, the primer shall be a coat of zinc chromate primer conforming to Fed. Spec. TT-P-645, or a coat of red lead paint, Type I or Type III conforming to Fed. Spec. TT-P-86G, applied to a minimum dry film thickness of 1.0 mil. Surfaces that will be concealed after construction and will require no overpainting for appearance may be primed with a coat of asphalt varnish, applied to a minimum dry film thickness of 1.0 mil. Damage to primed surfaces shall be repaired with the primer.

5.4.4 Painting: Shop painting shall be provided for all metalwork, except for non-ferrous metals and corrosion resistant metals and surfaces to be embedded in concrete. Surfaces to be welded shall not be coated within three inches of the weld, prior to welding. All machined surfaces in contact with outer surfaces and bearing surfaces shall not be painted. These surfaces shall be corrosion protected by the application of a corrosion preventive compound. Surfaces to receive adhesives for gaskets shall not be painted. Surfaces shall be thoroughly dry and clean when the paint is applied. No painting shall be done in freezing or wet weather except under cover; the temperature shall be above 45° F but not over 90° F. Paint shall be applied in a workmanlike manner and all joints and crevices shall be coated thoroughly. Surfaces which will be concealed or inaccessible after assembly shall be painted prior to assembly. Paint shall conform to Fed. Spec. TT-P37D.

6. BLAST VALVE TESTS:

6.1 Response Tests: The following static and dynamic response shall be performed to demonstrate the blast resistant capabilities of the blast value design. These tests shall be witnessed by the Contracting Officer.

6.1.1 Closure Time Test: Prior to shipment to the site, the Contractor shall perform a test to demonstrate that the closure of the blast valve will not exceed the 20 milliseconds specified. A suggested method for recording the valve closure is with the use of a high speed camera.

6.1.2 Static Pressure Test: Prior to shipment to the site, the Contractor shall perform a pneumatic test to demonstrate the static capacity of the blast valve design. The valve must sustain the pressure of 100 psi for a minimum of two hours. The total pressure loss during that period shall not exceed 1 psi.

6.1.3 Dynamic Pressure Test: Prior to shipment to the site, the Contractor shall perform a test to demonstrate the dynamic capacity of the blast valve design. This test shall simulate the combined effects of impact forces produced by the valve closure system and the blast load. This test may be replaced by design analyses which demonstrate that the head and frame of the valve shall have the capability to resist the stresses produced by the above forces. The blast load as indicated on the drawings shall be used for this analysis.

6.1.4 Blast Tests: If the effects of one or more of the above blast valve tests have been demonstrated by prior blast valve tests on similar valves, then the results of these tests shall be submitted for review; and the above test performances may not be required.

6.2 Test: After installation, a trip test shall be performed and demonstrated to the operating personnel.

6.3 Hydraulic Characteristics: Prior to shipment to the site, the Contractor shall perform a final test to establish the hydraulic characteristics of each valve and provide the necessary corrections and adjustments as stated previously.

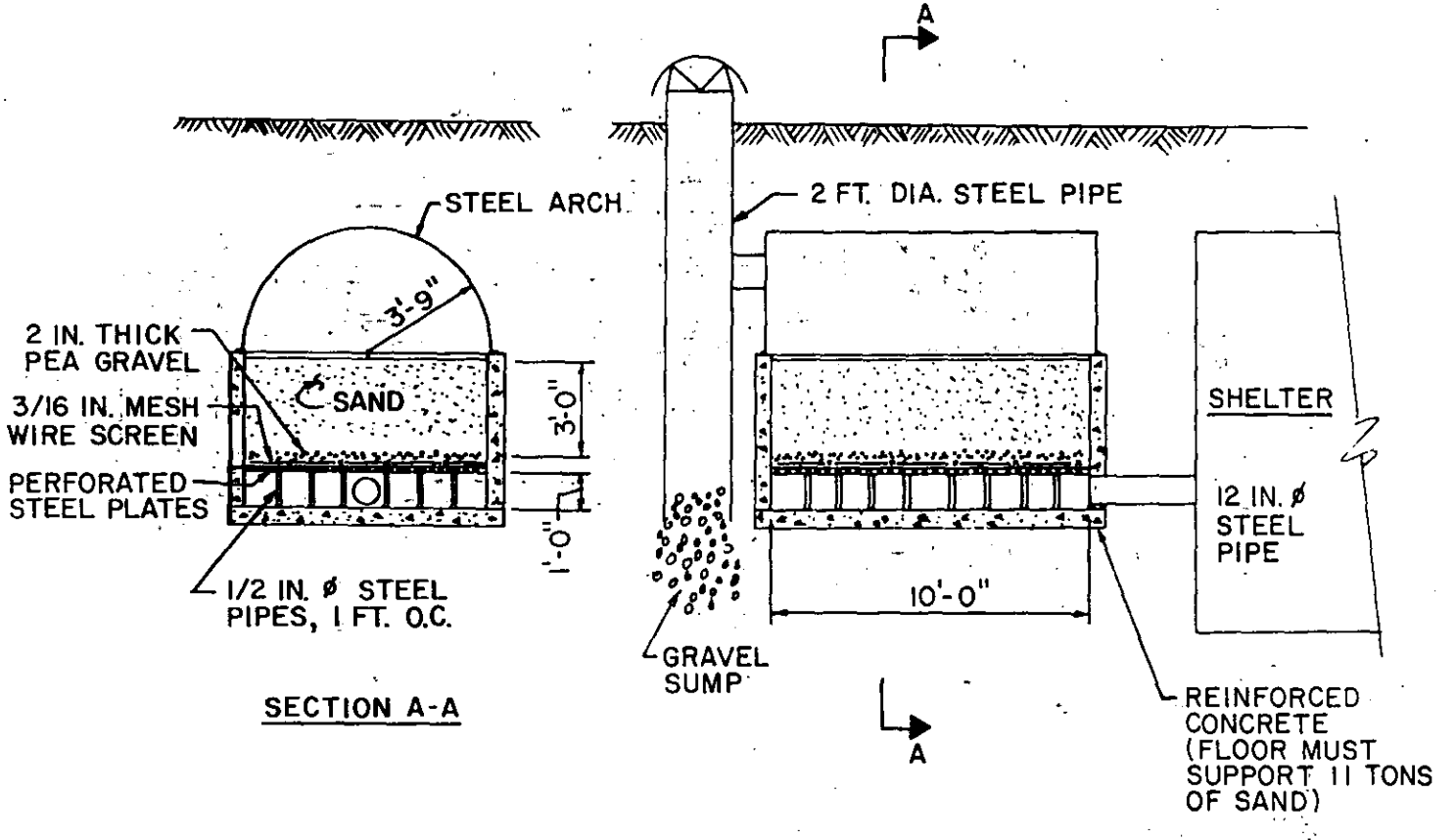


Figure 6-59 Sketch of 300 cfm sand filter

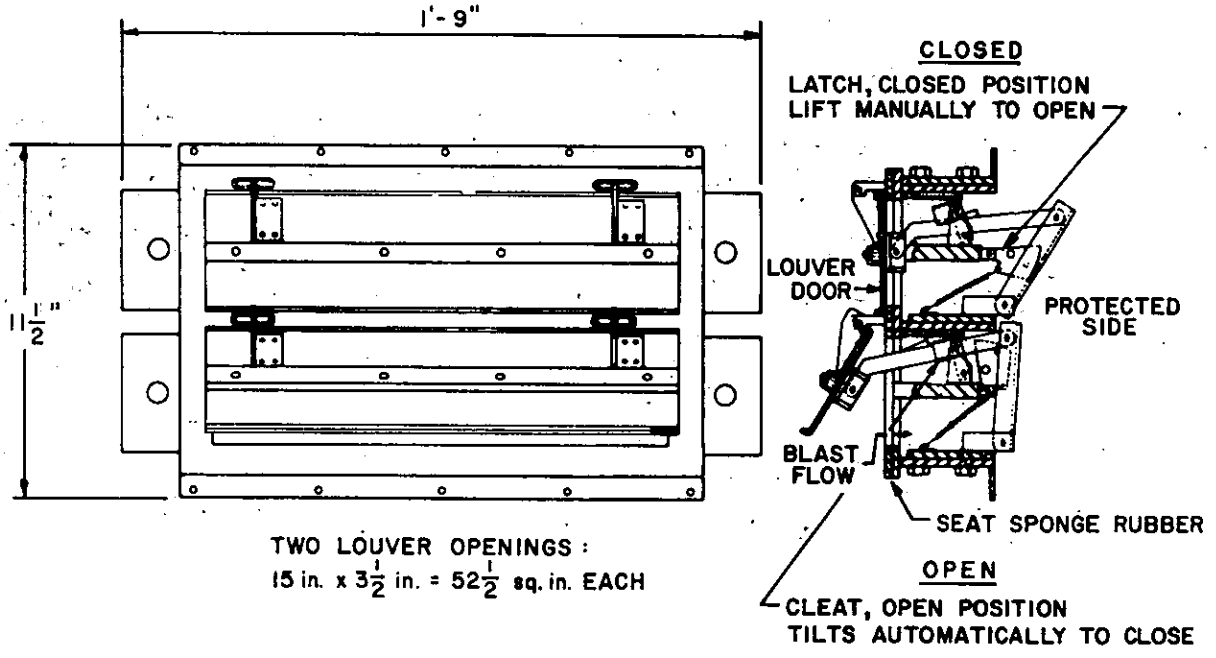


Figure 6-60 Blast-actuated louver

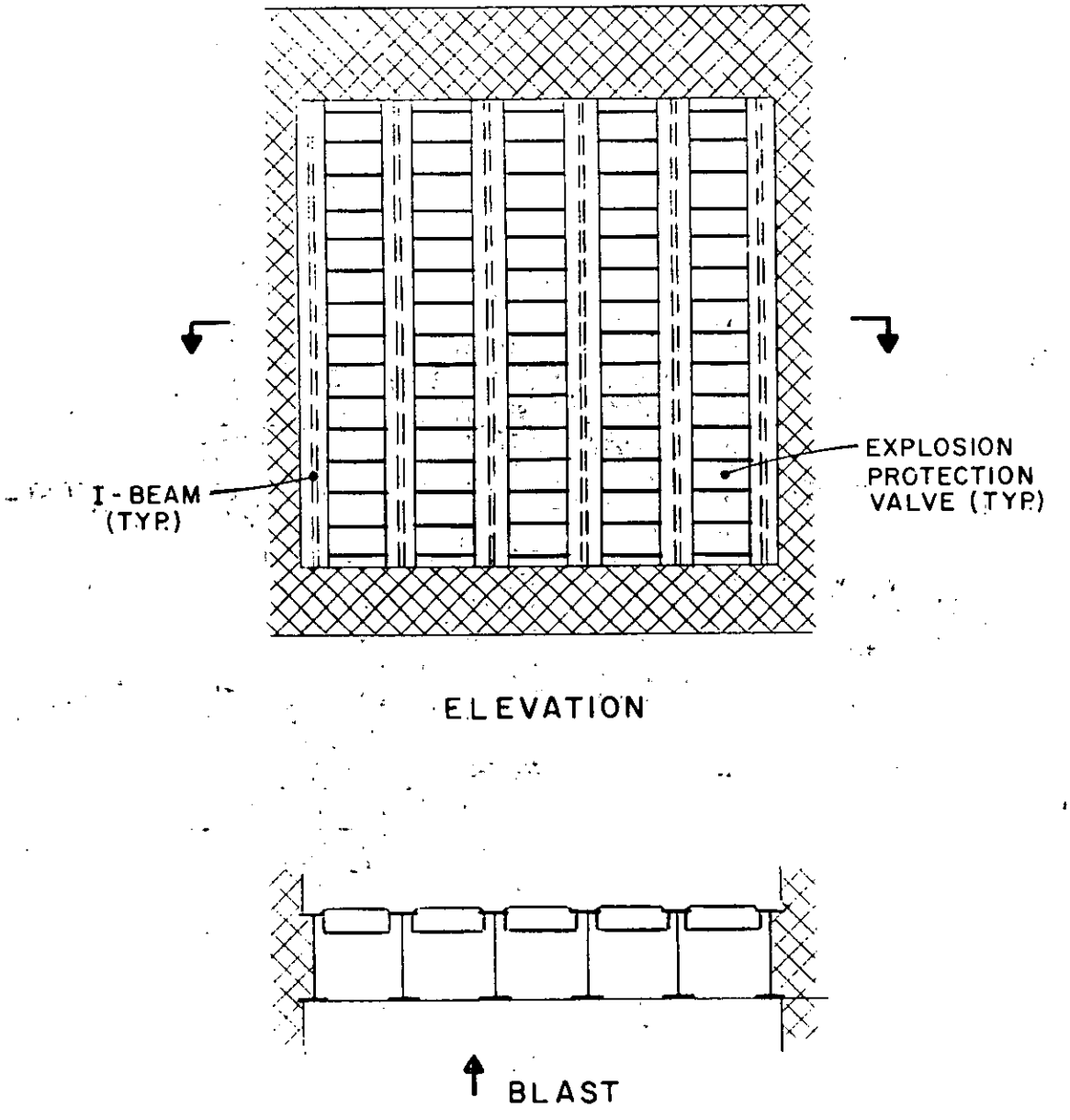


Figure 6-61 Arrangement of multiple louvers for a large volume of air

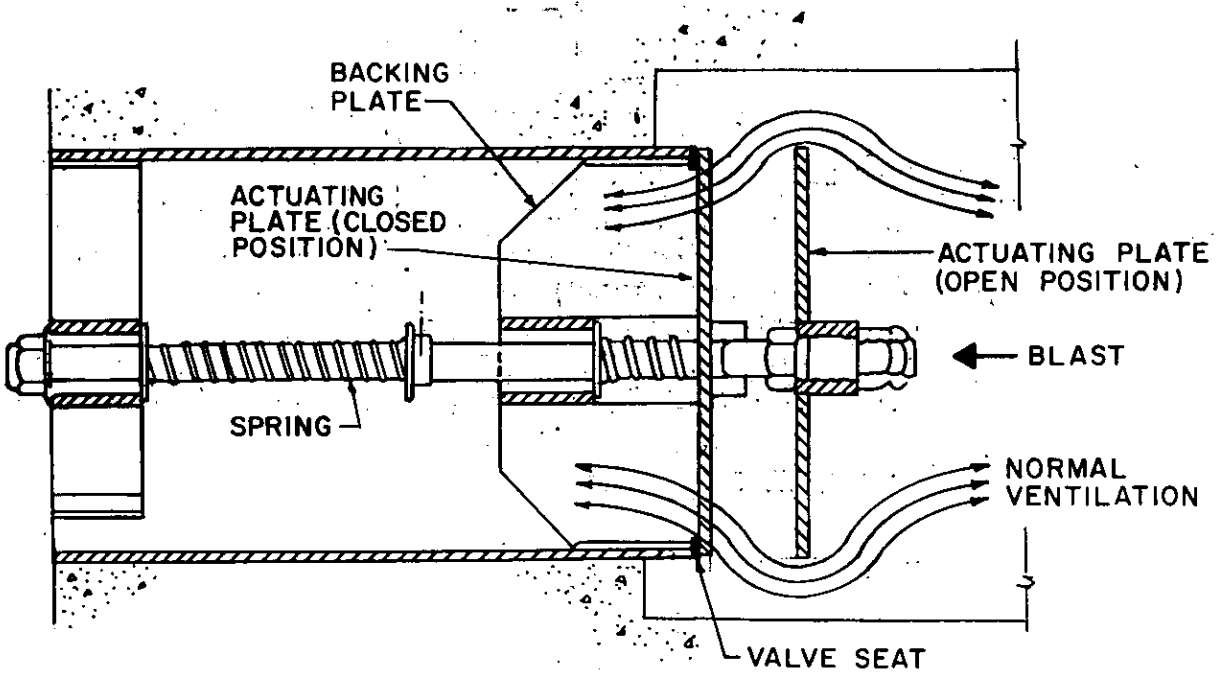


Figure 6-62 Typical blast-actuated poppet valve

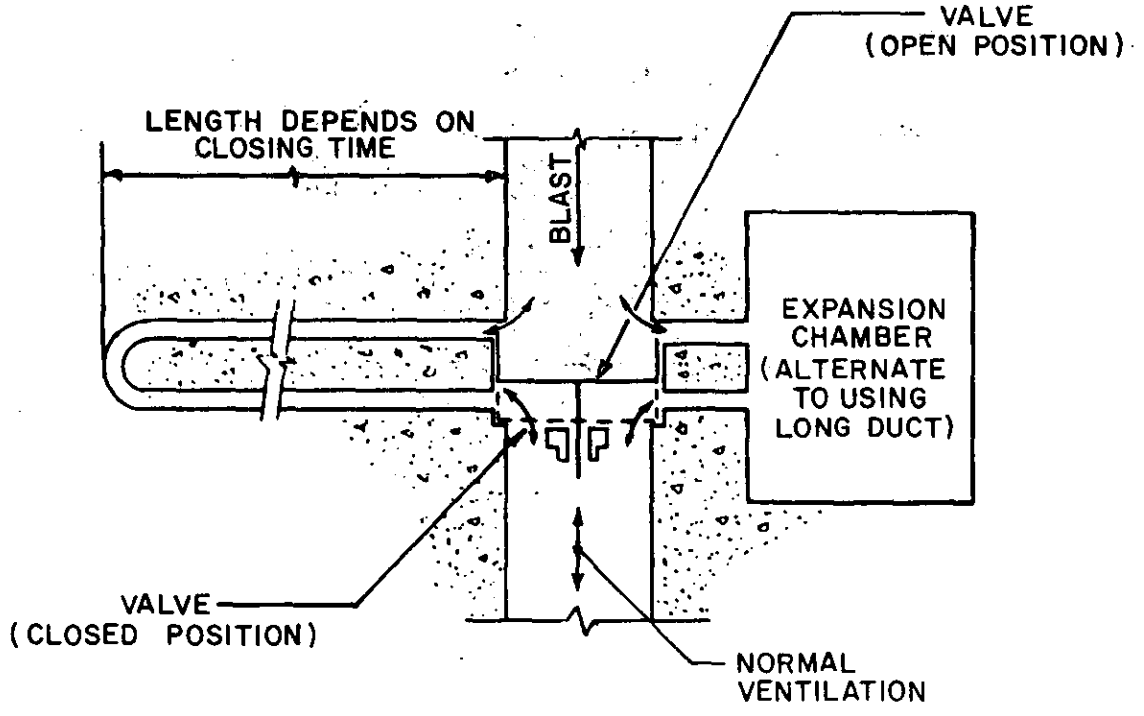


Figure 6-63. Time delay path

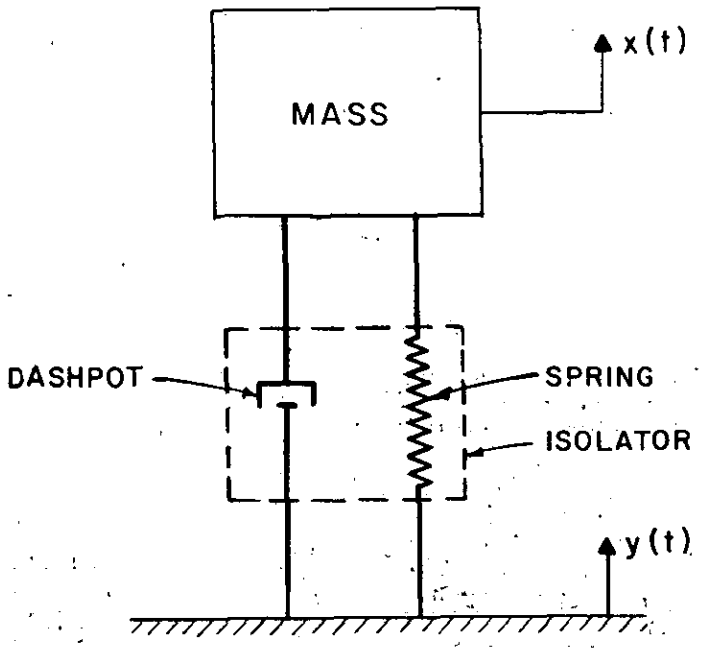


Figure 6-64 Idealized model of shock isolated mass

Table 6-13 Blast Valves

Name of Valve		Type (Actuated)	Blast Characteristics		Locking Mechanisms	Air Flow Rates (cfm)	Tested
			Pressure (psi)	Closing Time (ms)			
U.S. Army Chemical Corps M-1		Blast	100	*	Yes	300	Field
U.S. Army Chemical Corps E191R1		Blast	50	*	Yes	600	Shock tube and field
Office of Civil Defense	12"0	Blast and Remote	100	*	Yes	600	Field
	16"0		50	50	Yes	1,200	
	24"0		50	*	Yes	2,500	
Office of Corps of Engineers		Blast and Remote	*	20	Yes	5,000	Shock tube
Bureau of Yards and Docks		Remote	*	500	Yes	2,200 to 30,000	*
Temet USA, Inc.		Blast	100	20	Yes	2,250 to 3,700	Shock tube
Jaern and Plat	4"0		280	*		150	Field
	8"0					600	
	14"0					1,750	
Technical Facilities WS-107 A2		Remote	*	*		35,000	*
American Machine Foundry		Blast	100	*	Yes	80	*
Luwa		Blast	15 to 160	2	No	450	Shock tube
Suffield Experimental Stations		Blast	4 to 20	*		*	*
New Naval Civil Engineering Lab	Brechenridge	Blast	100	*	No	600	Compressed Air
	Bayles-Denny		5 to 100	*	No	180	
	Stephenson		5 to 104	*	No	125	
Artes Machinery (Sand Filtered)		Blast	100	*	No	300	Field

* Unknown

SHOCK ISOLATION SYSTEMS

6-45. Introduction

Previous sections have presented methods for the prediction of blast and fragment effects associated with the detonation of explosives and the design or analysis of structures to withstand these effects. In the design of shelters, an important part of the design process is to insure the survival of personnel and equipment. It is possible that the structure could withstand the air blast and ground shock effects but the contents be so severely damaged by structure motions that the facility could not accomplish its intended function. A similar problem is in the design of shelter type structures that houses sensitive explosives. These explosives must be protected from structure motions since these motions could result in initiation of the explosive. This section deals with the protection of vulnerable components from structure motions due to air blast and ground shock.

6-46. Objectives

The objective of shock isolation in protective design applications is to reduce the magnitude of motions transmitted by a vibrating structure to personnel or shock sensitive equipment. These motions must be attenuated to levels tolerable to personnel and to be various pieces of equipment used in the facility. A second consideration in some cases is to reduce the magnitude of motions transmitted by vibrating equipment to its supports. These latter motions can be significant for equipment mounted on shock-isolated platforms.

The general functional objectives of a shock isolation system are:

1. Reduce input motions to acceptable levels.
2. Minimize rattle space requirements consistent with system effectiveness and cost.
3. Minimize coupling of horizontal and vertical motions.
4. Accommodate a spectrum of inputs of uncertain waveforms.
5. Limit the number of cycles of motion of the isolated body.
6. Support the system under normal operating conditions without objectionable motions.
7. Maintain constant attitude under normal operating conditions.
8. Accommodate changes in load and load distribution.
9. Maintain system vibration characteristics over long periods of time.
10. Interface properly with other components or parts.
11. Require minimum maintenance

6-47. Structure Motions

Ground shock results from the energy which is imparted to the ground by an explosion. Some of this energy is transmitted through the air in the form of air-blast-induced ground shock and some is transmitted through the ground as direct-induced ground shock. Both of these forms of ground shock when imparted to a structure will cause the structure to move in both a vertical and horizontal direction. Movement of the structure imparts motions to items attached to the structure's interior. Motion of interior items is obtained from a response spectrum. This is a plot giving the maximum responses (in terms of displacement, velocity, and acceleration) of all possible linear single-degree-of-freedom systems which may be attached to the structure due to a given input motion. Therefore, having the spectra for the structure and given input motion, the maximum response of any item within the structure is obtained based on the natural frequency of the item. Methods for preparing response shock spectra are presented in Chapter 2 of this manual.

In addition to motion of the structure as a whole, the exterior walls and roof respond to the direct application of the blast load. Methods for calculating the response of these elements are given in Chapter 3 of this manual using the parameters given in Chapter 4 and 5 for concrete and steel, respectively. Maximum displacements, velocities, and accelerations of these elements can be determined in a straightforward manner. These quantities can be used to determine effects on items attached or located near walls or roofs.

6-48. Shock Tolerance of Personnel and Equipment

The requirement for shock isolation is based upon the shock tolerance of personnel and/or critical items of equipment contained within the protective structure. If the predicted shock input exceeds the shock tolerance of personnel, a shock isolation system is required. If the shock input exceeds the shock tolerance of equipment, the equipment can either be ruggedized to increase its shock tolerance or it can be shock isolated. There are practical limits to ruggedization and the costs may exceed those of an isolation system. If the input does not exceed the shock tolerance of the equipment, it can be hard-mounted to the structure.

6-48.1. Personnel

The effects of structural motions on personnel depend on the magnitude, duration, frequency, and direction of the motion, as well as their position at the time of the loading. The shock tolerance of personnel is presented in Chapter 1 of this manual.

6-48.2. Equipment

In many cases, the need for shock isolation of equipment must be established before detailed characteristics of the system components are established. Further, because of the constraints of procurement procedures, shock isolation systems must be designed and built prior to specific knowledge of the equipment to be installed. In such instances, the choice lies between specifying minimum acceptable shock tolerances for the new equipment or using whatever data is available for similar types of equipment.

The most practical means of determining the shock tolerance of a particular item of equipment is by testing. However, even experimental data can be of questionable value if the test input motion characteristics differ greatly from those that would actually be experienced by the equipment. Since testing of equipment may not be practical in many cases due to the amount of time allotted from the inception of a project to its completion, procurement procedures, and cost limitations, it is often necessary to rely on data obtained from shock tests of similar items. The shock capacity of various types of equipment is presented in Chapter 1 of this manual.

6-49. Shock Isolation Principles

6-49.1. General Concepts

A full treatment of the problem of shock isolation systems is not possible in this manual. The following discussion provides an introduction to the subject and presents some of the important characteristics of shock isolation systems.

In general, the analytical treatment of shock isolation systems is based upon the principles of dynamic analysis presented in Chapter 3. In most cases, the actual system can be represented by a simplified mathematical model consisting of a rigid mass connected by a spring and dash pot as shown in Figure 6-64. The figure represents the simplest case, that of a single-degree-of-freedom system restrained to move in only one direction. Actually, an isolation system would have at least six degrees of freedom, i.e., three displacements and three rotations. Under certain conditions, these six modes can be uncoupled and the system analyzed as six single-degree-of-freedom systems.

The single-degree-of-freedom system shown in Figure 6-64 can be used to illustrate the importance of some of the parameters affecting the effectiveness of shock isolation systems in general. The isolator is represented by the linear spring and viscous damping device enclosed within the dotted square. The suspended mass is taken to be a rigid body. It is assumed that the base of the system is subjected to a periodic sinusoidal motion whose frequency is f. The undamped natural frequency of the system is f_n and is given by:

$$f_n = \frac{1}{2\pi}\left[\frac{386.4\ K}{W}\right]^{1/2} \qquad 6\text{-}62$$

where

f_n = natural frequency of vibration

K = unit stiffness of spring

W = weight supported by spring

When the frequency of the disturbing motion f is small compared to the natural frequency f_n of the single-degree-of-freedom system, the displacement of the mass is approximately equal to the displacement of the base. When the frequency of the base motion is several times that of the system, the motion of the mass is a small fraction of the base motion. When the ratio of frequencies become large (20 to 30). the system can not respond to the base

motion to any significant degree. At frequency ratios near one, large motions of the mass are possible and the magnitude is strongly affected by the amount of damping in the system.

One obvious shock isolation approach is to use a low frequency suspension system so that the ratio of frequencies is always large. However, low frequency (referred to as soft) systems possess the undesirable characteristic of larger static and dynamic displacements and greater probability of coupling between modes of vibration. Although soft systems may be acceptable under some conditions, the obvious constraint that will preclude their use is a limit on the relative motion between the suspended mass and its supports or adjacent parts of the facility. This relative motion determines the amount of rattle space that must be provided to avoid impact between the mass and other fixed or moving parts of the facility.

The acceleration of the mass is a function of the forces applied to the mass by the spring and damping devices. In the case of a linear undamped spring, the force is a function of the relative displacement between the mass and its support. In viscous damping devices, the damping force is a function of the percent damping and the relative velocity between the mass and its supports. Acceleration limits for the critical items will impose restraints on spring stiffness and the amount of damping in the isolation system. In practice, a compromise combination of spring stiffness and damping is necessary to minimize input motions to the mass for a specified allowable rattle space or to minimize the rattle space required for specified allowable motions of the mass.

The need to avoid resonance (ratio of the frequency of the base motion to the natural frequency of the isolation system equal to one) is obvious. The structural motions resulting from an explosion are not steady-state sinusoidal in nature. However, these motions are of an oscillatory type and the displacement-frequency relationships discussed above are applicable.

A more detailed discussion of the effects of load duration, nonlinear springs, damping, and system frequency on response can be obtained from publications listed in the bibliography.

The basic objective in shock isolation is to select a combination of isolation system properties which will reduce the input motions to the desired level. In design, it is a straightforward process. System properties are assumed and an analysis is performed to determine its response to the input motions. If the shock tolerance and rattle space criteria are not satisfied, the system must be altered and the analysis repeated until the criteria are satisfied.

6-49.2. Single-Mass Dynamic Systems

A single mass system can have six degrees of freedom, that is, translation in three orthogonal axes and three rotations. The system can also be classified as coupled or uncoupled.

A coupled system is one in which forces or displacements in one mode will affect or cause a response in another mode. For example, a vertical displacement of a single rigid mass might also cause rotation of the mass. An uncoupled system, on the other hand, is one where forces or displacements in one mode do not generate a response in another mode. If the system is

completely uncoupled, base translations in any one of the three orthogonal directions will cause translations of the mass in that direction only. Similarly, a pure rotation of the base about any one of the three orthogonal principal inertia axes with their origin through the mass center, will cause only pure rotations of the body about that axis. The principal inertia axes are those about which the products of inertia vanish. The principal elastic axes of a resilient element (isolator) are those axes for which an unconstrained element will experience a displacement collinear with the direction of the applied force. If the principal elastic axes and the principal inertia axes of the shock isolation system coincide with the origin or point of intersection of both sets of axes at the center of gravity of the mass, the modes of vibration are uncoupled. Such a system is also referred to as a balanced system.

In Figure 6-65, if all the springs have the same elastic stiffness, the elastic center will be located at point A, which, in this case, is at the center of the individual springs. If the suspended mass is of uniform density, its center of gravity is also located at A, and the system is uncoupled for motion input through the springs. Some systems may be uncoupled only for motions in a particular direction. If point B in Figure 6-65 is the center of gravity of the mass, a horizontal motion in the direction parallel to the X-axis of the structure would cause only a horizontal motion of the mass. A vertical motion of the structure would cause both a vertical and rotational motion of the mass. In this case, the vertical and rotational modes are coupled. If the center of gravity were located at point C, then vertical, horizontal and rotational modes are coupled. If the characteristics of the mass and shock isolation system are such that the modes of vibration can be uncoupled, the system can be analyzed as a series of independent single-degree-of-freedom systems. The response of each of these systems can be determined on the basis of input motions and isolator properties in a direction parallel to or about one of the principal inertia axes. The response in each one of these modes can be summed in various ways to obtain the total response of the system. The sum of the maximum responses would neglect differences in phasing and should represent an upper limit of the actual motions. It is recommended that the square root of the sum of the squares of the maximums (root mean square values) be used to represent a realistic maximum response since it is unlikely that response will occur simultaneously in all modes. Superposition of modal response is appropriate for elastic systems only.

A dynamically balanced shock isolation system offers advantages other than a simplification of the computation effort. A balanced system results in reduced motions during oscillation. As a result of the absence of coupling of modes in a balanced system and the usually small, if any, rotational inputs to the system in protective construction applications, rotational motions of the shock isolated mass will be minimized. This is particularly important for large masses where small angles of rotation can result in large displacements at locations far from the center of gravity.

Because of the advantages of a dynamically balanced system, various approaches are taken to minimize coupling of modes. One criterion is that frequencies in the six modes should be separated sufficiently to avoid resonance between modes. Because of the importance of minimizing rotational modes of response, it is suggested that extremely low stiffnesses in these modes should be avoided. For the analysis of multiple degrees of freedom, single-mass systems

where the various modes of response are coupled, the modal method of analysis or numerical integration techniques can be utilized. The modal method of analysis requires solution of simultaneous equations of motion to determine characteristic shapes and frequencies of each mode and is limited to the elastic case. The numerical techniques do not require prediction of mode shapes and frequencies and will handle both elastic and inelastic response. If the dynamic system is also a multiple mass system, the above methods can be utilized to analyze the system. While an in-depth discussion is beyond the scope of this manual, a complete discussion of these methods can be found in publications listed in the bibliography.

6-49.3. Shock Isolation Arrangements

6-49.3.1. Individual versus Group Mounting

The two basic approaches to shock isolation in protective construction are to provide individually tailored systems for each component and to group together two or more items on a common platform. In the latter case, the system is selected to satisfy the requirements of the most critical item. In some cases, where the shock tolerance of the various items differs greatly, a combination of the two approaches may be the most effective solution. Although the relative location or size of some items may make individual mounts the more practical approach in certain cases, group mounting will generally be as reliable and the least costly solution.

Where personnel must be protected, a platform is the most practical solution. Except for extremely sensitive equipment, the shock tolerance of the personnel will govern the design of the system. The combination of personnel and equipment on the same platform will permit the personnel to move freely (however cautiously) between items of equipment. Where personnel are not required to be mobile, but rather may be able to remain seated while operating the equipment during hazardous periods, the shock tolerance of the personnel are greatly increased. This increased tolerance will reduce the shock isolation requirements while at the same time affording a higher degree of protection for personnel since they are protected from the unknown consequences of falling.

There are several advantages of group mounted systems. A group mounted system is less sensitive to variations in weights of individual items of equipment because of the larger combined weight of all items and the platform. With a number of items there is a greater flexibility of controlling the center of gravity of the total mass. In fact, ballast may be added to the platform to align the center of gravity with the principal axis to form a balanced system. A group mounted system generally requires less rattle space than several independently mounted items. Also, the interconnections between components is greatly simplified if they are all mounted on a single platform. Finally, an important advantage of group systems is cost. Individual mounts will require a large number of isolator units. Although larger, more costly, units are required for the group mounting system, fewer units are required and the cost per pound of supported load will be much lower.

6-49.3.2. Platform Characteristics

A platform for group mounted systems offers great flexibility in controlling the center of gravity of the supported masses to produce a balanced system where modes of vibration are uncoupled. Ballast may be securely anchored to the platform at locations which would move the center of gravity of the total mass to coincide with the elastic center of the isolation system. The determination of the weight and location of this ballast can be greatly simplified by uncoupling the effect of adding weight in the x and y directions of the principle elastic axes. This uncoupling can be accomplished by locating the ballast symmetrically about the x axis when moving the location of the center of gravity in the y direction. In this manner, the location of the center of gravity may be altered independently about the elastic center in the x and y directions. If for practical reasons the ballast cannot be located symmetrically about a principle axis, then the two directions must be considered simultaneously.

Providing additional ballast in excess of that required to balance the platform provides for future changes in equipment or the addition of new equipment without actually changing the isolation system. The springs will not require replacement nor will the structural members of the platform need to be increased in size. Additional equipment is placed on the platform and ballast is removed and/or relocated to balance the new equipment arrangement. To provide for future equipment changes, it is suggested that additional ballast equal to 25 percent of the weight of the equipment and the required ballast be distributed on the platform. The location of this ballast must not change the center of gravity of the existing balanced system. If future needs have been established, the platform and isolators would be designed for the future equipment. However, ballast would be provided to compensate for the weight of the future equipment and balance the system for the existing equipment.

The stiffness of the platform must be large enough to insure that the platform and associated group mounted equipment can be treated as a rigid body. This criterion is usually satisfied if the lowest natural frequency of any member of the platform is at least five (5) times the natural frequency of the spring mass system. When large, heavy items of equipment are involved, platforms meeting this stiffness criteria may not be practical. In such cases, the platform equipment configuration should be treated as a multi-mass system.

6-49.3.3. Isolator Arrangements

There are many ways to support a shock isolated item. Some desirable features have been discussed previously in connection with dynamically balanced systems. The isolators may be positioned in many ways. The more important factors affecting the selection of an isolator arrangement are:

1. The size, weight, shape and location of the center of gravity of the suspended mass;

2. The direction and magnitude of the input motions;

3. Rotation of the lines of action of the devices should be small over the full range of displacements of the system to avoid system nonlinearities;

4. Coupling of modes should be minimized;

5. Static and dynamic instability must be prevented;

6. It is desirable in most cases, and necessary in some, that the system return to its nominal position;

7. Space available for the isolation system; and type of isolation devices used.

Some of the more common isolator arrangements are shown in Figures 6-67 and 6-68. The systems shown are assumed to have the same arrangements of isolators in a plane through the center of gravity (c.g.) and perpendicular to the surface of the page. The dynamically balanced system (intersection of the elastic axes and the principal inertia axes located at point A) shown in Figure 6-65, is probably the least common of all suspension systems.

6-49.3.4. Base-Mounted Isolation Systems

In Figure 6-66a, the mass is supported on four (4) isolators. These isolators must provide horizontal, vertical and rotational stiffnesses in order for the system to be stable under all possible motions. There will be coupling between horizontal displacements and rotations about horizontal axes. This arrangement and that shown in Figure 6-66b are appropriate in those cases where there are no convenient supports for horizontal isolators.

The arrangement of Figure 6-66b is preferred since the line of action of the isolators can be directed towards the c.g. of the mass to allow decoupling of some modes. As in the case of Figure 6-66a, the isolators must possess adequate stiffness in axial and lateral directions to insure stability under static and dynamic conditions.

In Figure 6-66c, the isolators are oriented parallel to the three orthogonal system axes. This arrangement provides system stability even when the isolators possess only axial stiffness. If the c.g. of the suspended mass is located as shown, decoupling of modes is possible. While the lines of action of the isolators pass through the c.g. under static conditions, response of the system to base motions will obviously alter its geometry. When the line of action of the isolators is changed due to displacement of the mass relative to its supports, coupling of the modes of vibration will be introduced. The degree of coupling is affected by the magnitude of the displacements and the length of the isolators. Consequently, isolator properties and arrangement should be selected so as to minimize the effects of displacements.

6-49.3.5. Overhead Pendulum Systems Using Platforms

Two arrangements of overhead pendulum shock isolation devices using platforms to support the sensitive components are shown in Figure 6-67. In both cases, the center of gravity of the suspended mass is relatively low. These types of suspension systems have been used extensively in protective structures for various conditions including individual small and large items, multiple items of various sizes as well as a combination of personnel and equipment supported on various sized platforms. The overhead pendulum system normally uses swivel joints at the points of attachment so that the system may swing freely. Horizontal input motions cause the pendulum to swing. Gravity provides the

horizontal restoring force or stiffness. This force is a function of the total weight of the suspended mass. The natural frequency of vibration of the pendulum is a function of the length of the pendulum and is given by:

$$f_n = \frac{1}{2\pi}\left[\frac{386.4}{L}\right]^{1/2} \qquad 6\text{-}63$$

where

f_n = natural frequency of vibration
L = length of pendulum

Each pendulum arm includes an isolator which establishes the stiffness of the system in the vertical direction. These isolators can introduce nonlinearities and coupling between the pendulum and vertical spring modes. The system is linear for small angular displacements, that is, when the angular change θ of the pendulum arm from the vertical position is approximately equal to the sine of the angle ($\theta = \sin\theta$). The system can be considered uncoupled if the pendulum frequency is not near one half of the vertical spring frequency. If the pendulum frequency is in the vicinity of one half the vertical frequency, the interchange of energy between the modes can lead to pendulum motions greatly exceeding those predicted by linear assumptions.

In a shock spectra maximum displacements occur at low frequencies, maximum velocities at intermediate frequencies, and maximum accelerations at high frequencies. Since most pendulum systems have low natural frequencies, they are displacement sensitive. These systems attain maximum displacements and minimum accelerations. Consequently, they will normally require greater rattle space than other systems while at the same time providing maximum protection against horizontal accelerations at minimum costs. It should be realized that for explosions, maximum displacements are comparatively small and can be accommodated. One of the main advantages of overhead pendulum systems is that they do not require horizontal stiffness elements. Their attractiveness is greatly diminished in those cases requiring horizontal damping because of large motions.

The swivel joint attaching the pendulum arm to the platform determines the location of the horizontal elastic axis of the system. Figure 6-58b illustrates two ways of varying the point of attachment of the pendulum arm to the platform. The horizontal elastic axis is raised to coincide with the center of gravity of the suspended mass at the equilibrium position and help minimize coupling between modes of response. At the left side of the platform the isolator is contained in a housing rigidly attached to the platform. At the right side, a structural member is rigidly attached to the platform and the isolator is included in the pendulum arm. In addition to supporting personnel and equipment, overhead pendulum systems can be used to shock-isolate building utilities. Individual utility runs may be isolated or several different utilities may be supported on a single platform. A single platform may cover an entire room and all building services may be supported. They would include a hung ceiling, lighting fixtures, utility piping, HVAC ducts, electrical cables and process piping. Of course, flexible connections must be used when connecting the services to the building or equipment.

6-50. Shock Isolation Devices

6-50.1. Introduction

A fundamental element of every shock isolation system is some sort of energy storage or energy dissipative device. These devices must be capable of supporting the items to be isolated under static and dynamic conditions and, at the same time, prevent transmission of any harmful shock loads to the items. In most cases, the isolator must have elastic force-displacement characteristics so that the system will return to a nominal equilibrium position after the dynamic loads have been applied. The desirable features of these devices include:

1. The dynamic force-displacement relationship of the isolator should be predictable for all directions in which it is required to provide stiffness.

2. The isolator should have low mass in order to minimize transmission of high frequency motions to the supported mass.

3. The frequency of the isolator should remain constant with changes in load, that is, its stiffness should vary in direct proportion to the load it supports. This allows the system to remain dynamically balanced throughout changes in the position of the supported mass.

4. The static position of the isolator should be adjustable so that the system can be leveled and returned to its nominal position should the suspended load change.

5. The isolator should have high reliability, long service life and low cost.

The various types of isolators used in most protective construction applications possess these characteristics in varying degrees. Any real isolator has some mass, and in some applications, the mass can be quite large and must be considered in the final analysis. Nonlinear force-displacement characteristics are often accepted to gain some other advantage. In energy dissipative systems, it may be necessary to provide other means of restoring the system to its original position. In general, most devices are some compromise combination of the desirable features which best suit the particular design situation.

The inclusion of energy dissipative (damping) devices in the isolation system offers several significant advantages; that is, damping can:

1. Reduce the severity of output motion response;

2. Reduce the effect of coupling between modes, thus reducing rattle space requirements;

3. Restore the system to an equilibrium position more quickly;

4. Decrease the sensitivity of the system to variations in input motions.

Damping can be provided internally in some isolation devices such as in liquid springs, but must be added externally in others such as those systems using helical coil springs. Different types of damping offer advantages and disadvantages which must be evaluated in the design process. A damping device may be effective in attenuating low frequency components of input motions but can increase the severity of high frequency components. Also, a damping device could prevent the system from returning to its nominal equilibrium position. Thus, care must be exercised in either designing a system employing isolator devices possessing inherent damping characteristics or adding damping devices, if the isolation system is to perform properly.

There are numerous types of isolators which can be used to accomplish the shock isolating function. In the design of protective structures for explosions, the induced building motions are not usually severe and the maximum building displacements are relatively small. As a result, shock isolation systems using helical coil springs (Figure 6-68) are by far the most common system employed. The reasons for the extensive use of helical springs should be obvious from the discussion below. Other shock isolation devices which may also be used are presented, in less detail, below.

It should be noted that the protective design engineer does not furnish the design for the shock isolator. The engineer designs the shock isolation system to be used but does not design the isolators (in most cases, a helical coil spring). Rather, specifications are furnished which define the desired characteristics of the isolator. For a helical spring, the specifications may include some or all of the following: maximum load, maximum static deflection, maximum dynamic deflection, spring stiffness, maximum height, maximum diameter, and factors of safety regarding allowable stresses and bottoming of the spring. It must be realized that as the number of specified parameters increase, the options available to the spring manufacturer are decreased.

6-50.2. Helical Coil Springs

A helical coil spring is fabricated from bar stock or wire which is coiled into a helical form. Figure 6-68 illustrates several spring mounts.

The helical coil spring has numerous advantages and comparatively few disadvantages. The advantages are that the spring is not strain-rate sensitive, self-restoring after an applied load has been removed, resists both axial and lateral loads, linear spring rate and requires little or no maintenance. For most applications, the coil spring usually requires a larger space compared to other available shock isolators, and the spring cannot be adjusted to compensate for changes in loading conditions. If the weight of the supported object is changed, it is necessary to either change the spring or add additional springs. For most purposes, the helical coil spring can be considered to have zero damping. If damping is required, it must be provided by external means.

Helical coil springs may be used in either compression or extension. The extension springs are not subject to buckling and may offer a more convenient attachment arrangement. However, extension spring attachments are usually more costly and cause large stress concentrations at the point of attachment. For shock isolation applications, coil springs are generally used in compression. Buckling which can be a problem with compression springs, can be overcome by proper design or through the use of guides which are added either

internally or externally to the coils. The discussion below will be concerned primarily with compression springs unless otherwise stated.

Helical coil springs may be mounted in two ways, the ends are either clamped or hinged. In most shock isolation applications, the spring ends are clamped since this method greatly increases the force required to buckle the spring. If space is at a premium, the energy storage capacity may be increased by nesting the springs (placing one or more springs inside the outermost spring). When nesting springs, it is advisable to alternate the direction of coils to prevent the springs from becoming entangled.

Although permanent set may be acceptable in some instances, it is normally required that the system return to its original position after being loaded. This can be accomplished in various ways, but the most common approach in the case of helical coil springs is to prevent inelastic action of the spring.

Helical coil springs are capable of resisting lateral load. While it is possible to use springs in this application, care should be exercised. There are possible arrangements which avoid subjecting the springs to this type of loading.

While the actual design of the helical coil spring is done by the manufacturer, the engineer must be certain that the springs he is specifying can actually be obtained and the space he has allocated for the springs are sufficient. Therefore, preliminary spring sizes must be obtained by the engineer to suit his intended application. It is suggested that available manufacturer's data be used for this purpose.

6-50.3. Torsion Springs

Torsion springs provide resistance to torque applied to the spring. In shock isolation applications, the torque is usually the result of a load applied to a torsion lever which is part of the torsion spring system. A typical torsion spring shock isolation system is illustrated in Figure 6-69.

Since the axis of a torsion spring is normal to the direction of displacement, it can be used advantageously when space in the direction of displacement is limited. Torsion springs have linear spring rates, are not strain-rate sensitive, are self-restoring, and require little or no maintenance. Torsion springs can not be adjusted to compensate for changes in weight of shock isolation equipment, and damping must be provided by external means. The axial length of some types may preclude their use when space is limited.

There are three basic types of torsion springs; (1) torsion bars, (2) helical torsion springs, and (3) flat torsion springs. The type to be used will depend upon the space available and the capacity required. The torsion bar is normally used for light to heavy loads, the helical torsion spring for light to moderate loads, and the flat torsion spring for light loads. The torsion bar is the type most commonly found in protective structure applications and is most commonly used where large loads must be supported.

6-50.4. Pneumatic Springs

Pneumatic springs are springs whose action is due to the resiliency of compressed air. They are used in a manner similar to coil springs. The two

basic types are the pneumatic cylinder with single or compound air chambers and the pneumatic bellows. The pneumatic cylinder is shown schematically in Figure 6-70.

Pneumatic springs have the advantage of being adjustable to compensate for load changes. The spring rate can be made approximately linear over one range of deflection but will be highly nonlinear over another. They are quite versatile due to the variety of system characteristics which can be obtained by regulation of the air flow between the cylinder chamber and the reservoir tank. Some of the possible variations include:

1. Velocity-sensitive damping by a variable orifice between chamber and reservoir;

2. Displacement-sensitive damping by a variable orifice controlled by differential pressure between chamber and reservoir;

3. A nearly constant height maintained under slowly changing static load by increasing or decreasing the system air content using an external air supply and a displacement-sensitive servo-system controlling inlet and exhaust valves;

   A constant height under widely varying temperatures achieved by the same system described for maintaining a constant height.

The disadvantages of pneumatic springs include higher cost and more fragile construction. They have a limited life span in comparison to mechanical springs and must be maintained. Also these springs provide resistance for axial loads only.

6-50.5. Liquid Springs

A liquid spring consists of a cylinder, piston rod, and a high pressure seal around the piston rod. The cylinder is completely filled with a liquid, and as the piston is pushed into the cylinder, it compresses the liquid to very high pressures. The configurations of liquid springs are divided into three major classes according to the method of loading. The classes are simple compression, simple tension and compound compression-tension. Although they are loaded in different ways, all three types function as a result of compression of the liquid in the cylinders. Schematics of the tension and compression types are shown in Figure 6-71. The compound spring is merely a more complex mechanical combination of the two basic types. The tension type is the more common in protective construction applications. The cylinders are often fitted with ported heads to guide the piston and provide damping. Damping can also be provided through the addition of drag plates to the piston rods.

Liquid springs are very compact devices with high, nearly linear, spring rates. They can be adjusted to compensate for load changes, are self-restoring and can absorb larger amounts of energy. They are highly sensitive to changes in temperature and fluid volume changes. Because liquid springs normally operate at high pressures, high quality, close tolerance seals are required around the piston. Friction between the seal and piston provides appreciable damping and increases the spring rate from 2 to 5 percent. Liquid springs are high pressure vessels requiring high quality materials and pre-

cision machine work, and as a result, they are expensive. However, they are difficult to equal as compact energy absorption devices.

6-50.6. Other Devices

6-50.6.1. Introduction

The helical, torsion, pneumatic and liquid springs are the more common types of isolators for larger masses. There are other devices especially suited for particular applications and smaller loads. Some of these isolators are discussed below.

6-50.6.2. Belleville Springs

Belleville springs, also called Belleville washers or coned-disc springs, are essentially spring steel washers which have been formed into a slightly conical shape. A typical Belleville spring is illustrated in Figure 6-72.

The main advantage of Belleville springs over other types of springs is the ability to support large loads at small deflections with minimum space requirements in the direction of loading. They are useful in applications requiring limited shock attenuation and as back up systems to reduce shock in the event of bottoming of coil springs. They are relatively inexpensive and readily available in capacities up to 60,000 pounds. Changes in loading conditions are accommodated by the addition or removal of units.

6-50.6.3. Flat Springs

A flat spring is simply a steel beam or plate whose physical dimensions and support conditions are varied to provide the desired force displacement relationship. The two basic configurations are the simple spring with one element and leaf springs with multiple elements. Flat springs normally require only a limited amount of space in the direction of displacement and provide linear, non-strain-rate sensitive and self-restoring spring. They require little or no maintenance. Single element flat springs can be considered to have no damping while leaf springs will exhibit some damping due to the friction between individual elements.

6-50.6.4. Solid Elastomer Springs

Solid elastomer springs are made from rubberlike materials. They are often called shock mounts because of their wide use in shock isolation applications. They are normally used in medium to light duty applications and represent an economical solution to the isolation of small items of equipment. However, these springs will allow only small displacements. These springs are fabricated from a wide variety of natural and synthetic rubbers and compounds and in numerous sizes and shapes to satisfy a wide range of applications. Because of the range in capacity and characteristics of commercially available units, only in unusual cases is it necessary to design a unit.

In most applications, the solid elastomer spring will require little space and exhibits good weight to energy storage ratios. Use of these springs requires consideration of the operating environment. The desirable properties of some elastomers can be significantly degraded when exposed to low or high temperatures, sunlight, ozone, water or petroleum products.

The response of elastomeric springs is nonlinear in most applications because of the nonlinear stress-strain properties of elastomers. The springs are self-damping because of the viscoelastic properties of the elastomers. They are almost always in compression because of bonding limitations. These springs will only permit comparatively small displacements.

6-51. Hardmounted Systems

Some items of equipment do not require shock isolation because the predicted motions at their point of attachment to the supporting structure does not exceed their shock tolerance. Those items can normally be hardmounted to the supporting structure. A hardmount is a method of attachment which has not been specifically designed to provide a significant reduction in the input motions to the equipment. Since all methods of attachment exhibit some flexibility, there is no precise division between shock isolators and hardmounts. Both types of devices will modify input motions to some degree. However, the modification of input motions produced by hardmounts will generally be small while shock isolators can greatly affect these motions.

In contrast to shock isolation systems, hardmounted systems will normally exhibit natural frequencies much higher than those corresponding to the lower modes of vibration of the supporting structure. Although this characteristic offers the advantage of reduced rattlespace, it also provides for the more efficient transmission of higher frequency components of the support structure motion to the attached item. Thus, it would appear that a more exact structural analysis is required for hardmounted systems in order to include higher modes of vibration. In practice, the need for exact analyses is at least partially offset by higher factors of safety in mount design and equipment shock tolerance. However, such an approach can lead to unrealistic attachment designs. A more practical approach is to choose, or design, attachments which limits the fundamental frequency of the hardmounted system. A lower frequency system provides some attenuation of higher frequency input motions, and reduces the possibility of resonance with high frequency motions resulting from stress wave reflections within structural elements. Although the choice of a natural frequency will depend on the properties of the supporting structure and the hardmounted equipment, fundamental frequencies in the range of 10 to 1000 cycles per second are reasonable for most applications. The approach chosen for hardmount design is normally a combination of higher safety factors and the use of lower frequency systems. The design will be based upon considerations of cost, importance of the item supported, the size and weight of the item, and the consequence of failure of the attachment system.

The use of shock spectra to define the input motions of hardmount systems is considered adequate for final design of all simple hardmount systems of a non-critical nature. It is also considered adequate for preliminary design of critical systems and those whose representation as a single degree of freedom system is questionable. However, it is recommended that the final design be performed using a more exact dynamic analysis wherever practical.

6-52. Attachments

6-52.1. Introduction

In a shelter type structure subjected to air blast and ground shock effects, all interior contents must be firmly attached to the structure. This attach-

ment insures that the building contents will not be dislodged and become a source of injury to personnel or damage to critical equipment. The building contents would include not only equipment which is either shock isolated or hardmounted (attached directly to structure) but also the building utilities as well as interior partitions and hung ceilings. The building utilities would include all piping (such as process, potable water, sanitary, fire protection, etc.), HVAC ducts, electrical cables, light fixtures and electrical receptacles.

6-52.2. Design Loads

An object subjected to a shock loading produces an inertial force which acts through its center of gravity. The magnitude of this force is given by:

$$F = Wa$$

where

F = inertial force
W = Weight of object
a = acceleration in g's

Accelerations may be imparted to the object in one or more directions producing inertial forces in the respective directions. These inertial forces are resisted by the reactions developed at the object's supports. All inertial forces are assumed to be acting on the object concurrently. The support reactions are obtained by considering the static equilibrium of the system.

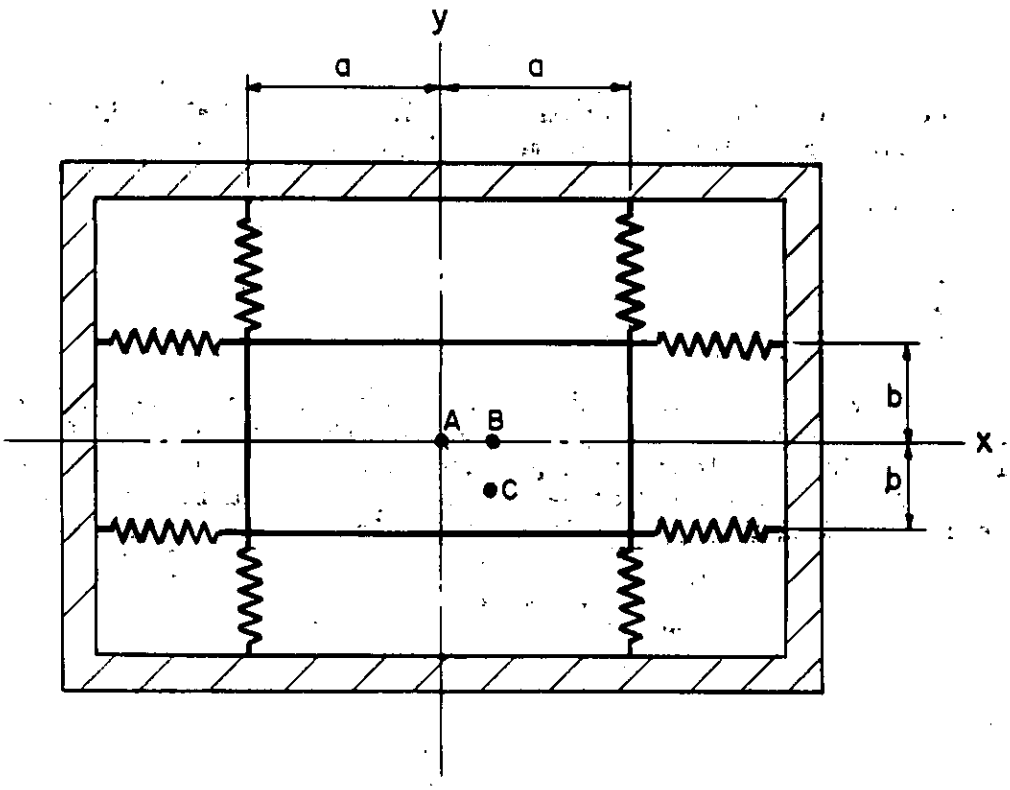


Figure 6-65 Shock isolation system

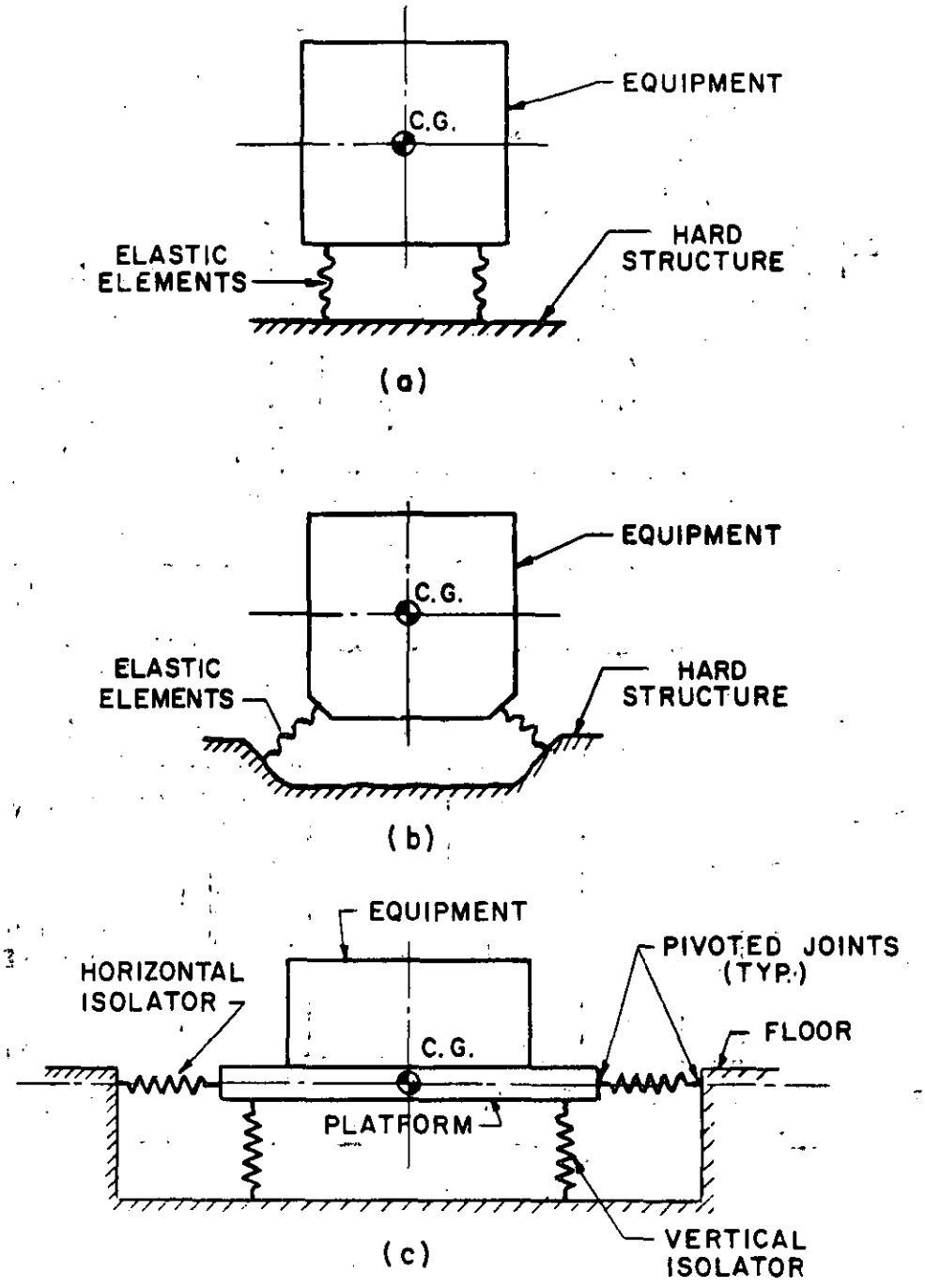


Figure 6-66 Base-mounted isolation systems configuraiton

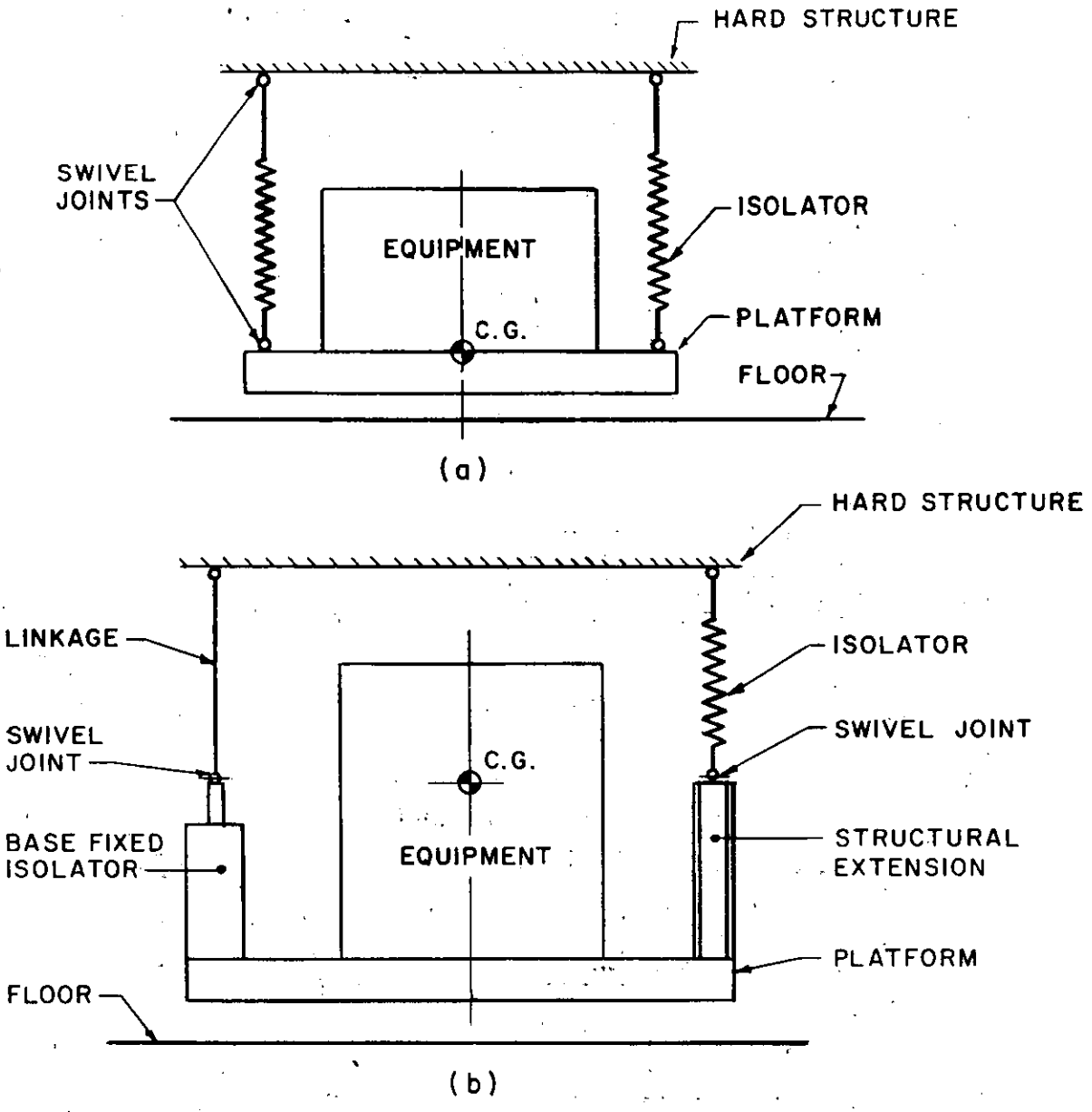
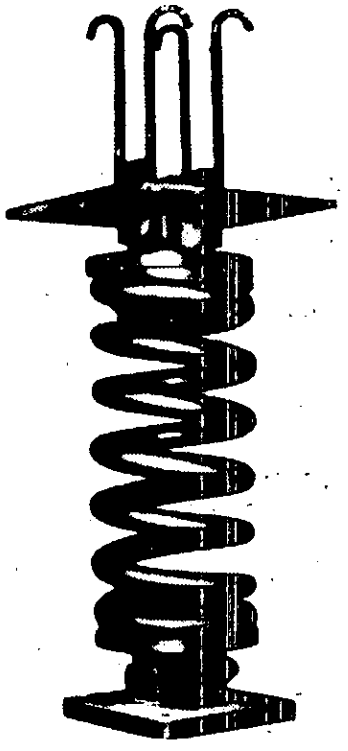
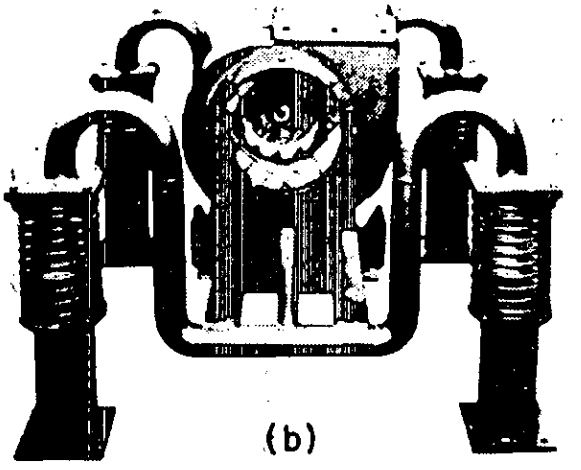


Figure 6-67 Overhead pendulum shock isolation systems using platforms



VERTICAL
SHOCK MOUNT



(b)

CENTER OF GRAVITY MOUNT PREVENTS
ROCKING UNDER SHOCK



HORIZONTAL SHOCK MOUNT

Figure 6-68 Helical compression spring mounts

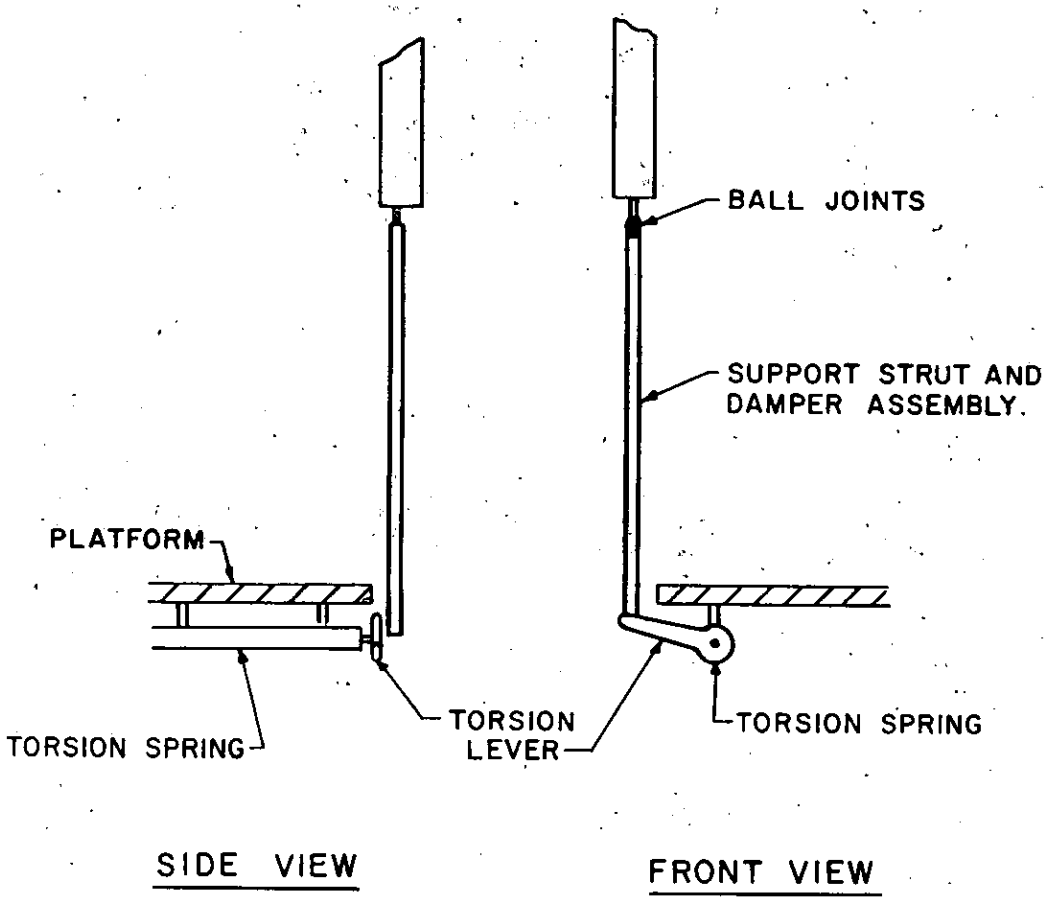


Figure 6-69 Typical torsion spring shock isolation system

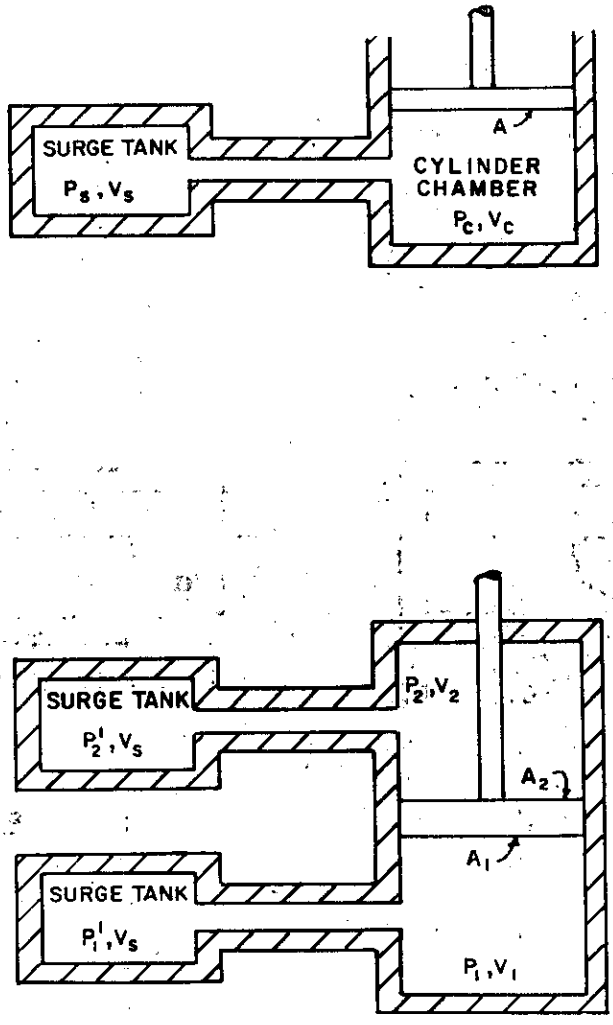


Figure 6-70 Schematic of single and double acting pneumatic cylinders

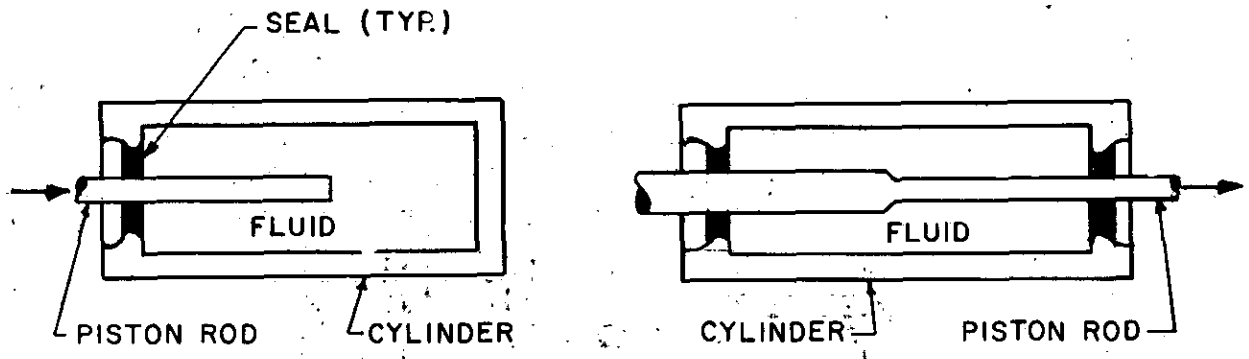
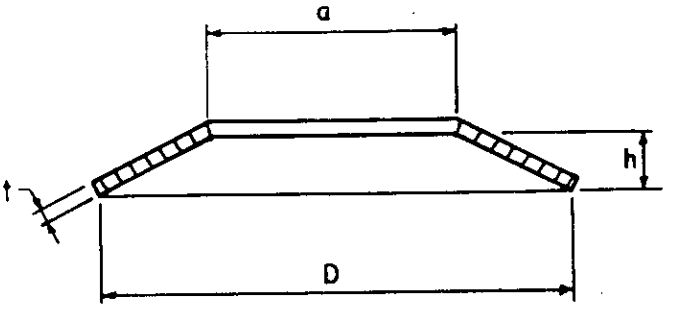
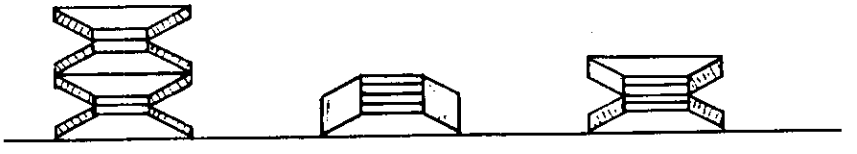


Figure 6-71 Schematic of liquid springs





(a) SERIES (b) PARALLEL (c) PARALLEL-SERIES

Figure 6-72 Belleville springs

APPENDIX 6A

ILLUSTRATIVE EXAMPLES

Problem 6A-1 Masonry Wall Design

Problem: Design a reinforced masonry wall for an exterior blast load.

Procedure:

Step 1. Establish design parameters:

a. Pressure-time loading.

b. Structural configuration including geometry, support conditions and type of wall (i.e. reusable or non-reusable).

Step 2. Select masonry unit size and the size and type of reinforcement. Assume the distance between the tension and compression reinforcement (d_c). Also determine the static design stresses for the masonry unit and the reinforcement (Section 6-8.1). The average yield stress of reinforcement is increased 10 percent.

Step 3. Calculate the dynamic design stress of the reinforcement, using the static stresses from Step 2 and the dynamic increase factors from Section 6-8.2. (For joint reinforced masonry construction the compressive strength of the concrete may be ignored. See Section 6-8.3).

Step 4. For the size and type of reinforcement selected in Step 2, calculate the area of reinforcement per unit width of the wall. Using the value of d_c from Step 2, the dynamic design strength from Step 3 and the area of reinforcement from above, determine the ultimate moment capacity of the wall (Eq. 6-2).

Step 5. Determine the ultimate resistance of the wall using the ultimate moment capacity of Step 4 and the equations of Table 3-1 (if the wall is a one-way spanning element) or Table 3-2 or 3-3 (if the wall spans two directions).

Step 6. From Table 6-3, find the moment of inertia of the net section I_n. Calculate the moment of inertia of the cracked section I_c, using Equation 6-7 and the value of d_c from Step 2. Determine the average moment of inertia, using the values of I_g and I_c from above and Equation 6-6.

Step 7. Calculate the modulus of elasticity of the masonry unit E_m from Equation 6-1 and the masonry unit strength of Step 2.

Step 8. If the wall spans one direction only, use the average moment of inertia from Step 6, the modulus of elasticity from Step 7 and the equations from Table 3-8, to find the equivalent elastic stiffness. For a two-way spanning wall, use the methods of Section 3-13 to calculate the equivalent elastic stiffness.

Step 9. Determine the equivalent elastic deflection using the ultimate resistance (Step 5), the equivalent stiffness (Step 8) and Equation 3-36.

Step 10. Find the load-mass factor K_{LM}, for the elastic, elasto-plastic and plastic ranges from Table 3-12 or 3-13. Average the values of K_{LM} for the elastic and elasto-plastic ranges. Average that value with the K_{LM} for the plastic range to find the value of K_{LM} to be used for the element. Calculate the unit mass of the masonry unit and multiply the unit mass by K_{LM} to obtain the effective unit mass of the wall.

Step 11. Calculate the natural period of vibration from Equation 3-60, the effective mass from Step 10 and the equivalent stiffness from Step 8.

Step 12. Determine response chart parameters:

a. Peak dynamic loading P (Step 1).
b. Ultimate resistance r_u (Step 5).
c. Duration of load T (Step 1).
d. Natural period of vibration T_N (Step 11).

Calculate the ratio of ultimate resistance to peak dynamic loading (r_u/P) and duration of load to natural period (T/T_N). Using these ratios and the appropriate figures (Figs. 3-54 through 3-266) determine the ductility ratio X_m/X_E.

Step 13. Compute the maximum deflection X_m by multiplying the ductility ratio by the elastic deflection of Step 9. From Table 3-5 (for a one-way spanning wall. For a two-way spanning wall use Table 3-6) and the value of X_m, find the maximum support rotation. Find the maximum rotation permitted from Table 6-2 and compare with the rotation calculated above. If rotation is larger than that permitted, repeat steps 1 through 13.

Step 14. Determine the ultimate shear stress at $d_c/2$ from the support. Using Equation 6-4 or 6-5, compute the area of shear reinforcement required for the above shear stress.

Step 15. Using X_m/X_E and T/T_N (both values from step 12) find the rebound resistance from Figure 3-268. With rebound resistance and the equations of Table 3-9, 3-10 or 3-11, calculate the rebound shear. Then compute the area of anchor reinforcing required using the rebound shear from above and the dynamic strength of the reinforcement from step 3.

Example 6A-1 Masonry Wall Design

Required: Design a joint reinforced masonry wall supported by steel columns for an exterior blast load.

Solution:

Step 1. Given:

a. Pressure-time loading (Fig. 6A-1).

b. Wall spans in one direction only, is rigidly supported at both ends, and has a clear span between columns of 150 inches. The wall is part of a reusable structure.

Step 2. Use 12" wide hollow concrete masonry units and ladder type reinforcing with No. 8 Gage side rods and No. 9 Gage cross rods 16" o.c. Assume d_c = 10" for this type of reinforcing. For hollow concrete masonry units the static compressive stress (f'_m) is 1350 psi. For joint reinforcement the yield stress of 70,000 psi is increased 10 percent to 77,000 psi.

Step 3. Calculate dynamic design stresses of the reinforcement:

a. Dynamic Increase factors

- flexure: 1.17
- shear: 1.00

b. Dynamic strengths

- flexure f_{dy} = 1.17 X 77,000 = 90,090 psi
- shear f_{dy} = 1.0 X 77,000 = 77,000 psi

Step 4. Determine the ultimate moment capacity of the wall.

a. Calculate the area of reinforcement per unit width of the wall.

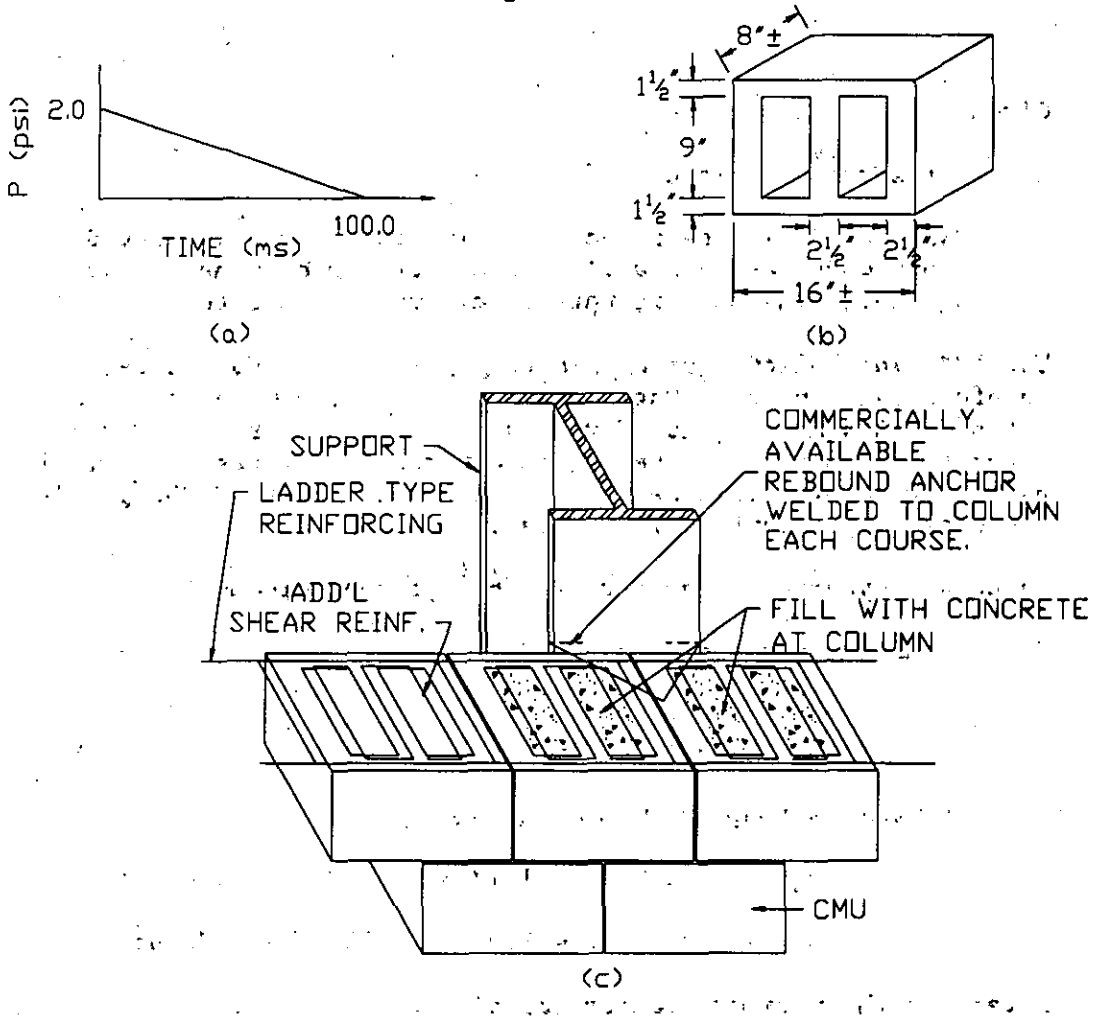
Use one layer of reinforcement between every masonry unit joint, therefore 8 inches o.c.

A_s = 0.0206/8 = 0.0026 in^2/in

b. Ultimate moment capacity (Eq. 6-2).

$M_u = A_s f_{dy} d_c$ = 0.0026 X 90,090 X 10 = 2342 in-lbs/in

Figure 6A-1


P (psi)
2.0
TIME (ms)
100.0
(a)
8"±
1½"
9"
1½"
2½"
2½"
16"±
(b)
SUPPORT
LADDER TYPE REINFORCING
ADD'L SHEAR REINF.
COMMERCIALLY AVAILABLE REBOUND ANCHOR WELDED TO COLUMN EACH COURSE.
FILL WITH CONCRETE AT COLUMN
CMU
(c)

Step 5. Calculate ultimate resistance (Table 3-1)

$$r_u = \frac{8(M_N + M_p)}{L^2}$$

$$= \frac{8(2342 + 2342)}{150^2}$$

$$= 1.66 \text{ psi}$$

Step 6. Find the average moment of inertia.

a. Moment of inertia of net section (Table 6-3).

For a 12 inch unit

$I_n = 83.3 \text{ in}^4/\text{in}$

b. Moment of inertia of cracked section (Eq. 6-7).

$I_c = 0.005 \times d_c^3 \times 6$

$= 0.005 \times 10^3 \times 12$

$= 5.0 \text{ in}^4/\text{in}$

c. Average moment of inertia (Eq. 6-6).

$I_a = (I_n + I_c) / 2$

$= (83.3 + 5.0) / 2$

$= 44.2 \text{ in}^4/\text{in}$

Step 7. Compute modulus of elasticity of the masonry unit (Eq. 6-1).

$E_m = 1000 f'_m$

$= 1000 \times 1350$

$= 1.35 \times 10^6 \text{ psi}$

Step 8. Determine the equivalent elastic stiffness (Table 3-8).

$K_E = (307 E_m I_a) / L^4$

$= (307 \times 1.35 \times 10^6 \times 44.2) / 150^4$

$= 36.19 \text{ psi/in}$

Step 9. Calculate the equivalent elastic deflection (Eq. 3-36).

$$X_E = r_u/K_E = 1.66/36.19 = 0.046 \text{ in}$$

Step 10. Calculate the effective unit mass of the wall.

a. Find the average load-mass factor K_{LM} (Table 3-12)

Elastic $K_{LM} = 0.77$

Elasto-plastic $K_{LM} = 0.78$

Plastic $K_{LM} = 0.66$

For limited plastic deflections

$$K_{LM} = [(0.77 + 0.78)/2 + 0.66]/2 = 0.72$$

b. Determine the unit mass of wall.

Using Table 6-1

$$W = \frac{[(16 \times 12) - 2(4.25 \times 9)]}{16} \times \frac{150 \text{ pcf}}{12^3} = 0.627 \text{ psi}$$

$$m = \frac{w}{g} = \frac{0.627}{32.2 \times 12 \times 10^{-6}} = 1622.7 \text{ psi-ms}^2 / \text{in}$$

c. Calculate effective unit mass.

$$m_e = K_{LM}\, m$$

$$= 0.72 \times 1622.7$$

$$= 1168.3 \text{ psi-ms}^2/\text{in}$$

Step 11. Determine the natural period of vibration (Eq. 3-60).

$$T_N = 2\pi (m_e/K_E)^{1/2}$$

$$= 2\pi (1168.3/36.19)^{1/2}$$

$$= 35.7 \text{ ms}$$

Step 12. Determine the response of the wall.

a. Calculate design chart parameters.

$T/T_N = 100.0/35.7 = 2.80$

$r_u/P = 1.66/2.0 = 0.83$

b. From Figure 3-54

$\mu = X_m / X_E = 8.0$

Step 13. Check support rotation.

a. Compute maximum deflection.

$X_m = \mu X_E$

$= 8.0 \times 0.046$

$= 0.368$ in

b. Calculate support rotation (Table 3-5)

$\theta = \tan^{-1}(2X_m/L)$

$= \tan^{-1}(2 \times 0.368/150)$

$= 0.28°$

c. Compare rotation with criteria.

From Table 6-2

$\theta = 0.5° > 0.28°$ O.K.

Step 14. Design shear reinforcement.

a. Calculate shear force $d_c/2$ from support.

$$V_u = \frac{ru\ (L-d_c)}{2}$$

$$= \frac{1.66(150-10)}{2}$$

$= 116.2$ lb/in

b. Find net area of section from Table 6-1.

A_n = 2b X Face thickness/b

= 2 X 8 X 1.5/8

= 3.0 in_2/in

c. Compute ultimate shear stress (Eq. 6-3)

$v_u = V_u/A_n$

$= \frac{116.2}{3.0} = 38.73$ psi

d. Find area of shear reinforcement required (Eq. 6-4)

Assume s = 4".

$A_v = \frac{v_u bs}{\Phi f_y}$

$= \frac{38.73 \text{ X } 8 \text{ X } 4}{0.85 \text{ X } 77,000}$

= 0.0189 in^2 Use No. 8 Gage

Use 3 legs of No. 8 gage wire at 4" o.c. between each cross rod.

Step 15. Design rebound anchor ties.

a. Find rebound resistance force.

$T/T_N = 2.8$

$X_m/X_E = 8.0$

From Figure 3-268

$r^-/r_u = 0.47$

$r^- = 0.47 \text{ X } 1.66$

= 0.78 psi

b. Calculate rebound shear at supports

$$V_r = \frac{r L}{2}$$

$$= \frac{0.78 \times 150}{2} = 58.5 \text{ lb/in}$$

c. Required area of anchor reinforcing

$$A_r = \frac{rV}{f_{dy}} = \frac{58.5}{90{,}090} = 0.00065 \text{ in}^2/\text{in}$$

Use one anchor between every masonry unit joint, therefore 8" o.c.

$$A_r = 0.00065 \times 8$$

$$= 0.0052 \text{ in}^2/\text{anchor}$$

Use 3/16" diameter triangular ties.

Problem 6A-2 Design of Prestressed Recast Element

Problem: Design a prestressed recast element for a given blast load.

Procedure:

Step 1. Establish design parameters:

a. Pressure-time loading.

b. Material strength.

c. Span length.

d. Static loads.

e. Deflection criteria.

Step 2. Select a standard recast section from the PCI Design Handbook or manufacturer's catalogs. Also select a standard strand pattern.

Step 3. Determine dynamic increase factors for concrete and reinforcement from paragraph 6-12. Increase the static design stress of the reinforcing bars and welded wire fabric 10 percent for the average yield stress. Calculate the dynamic design design stresses using the above DIF and the static stresses.

Step 4. From Chapter 4 and a unit weight of concrete equal to 150 pcf, calculate the modulus of elasticity for concrete. With the above modulus for concrete and those for reinforcing bars and prestressing tendons, calculate the modular ratio.

NOTE: If the section has a flange (e.g. a single or double tee section) it must be designed according to the principles of Chapter 4. The flange is a one-way, non-prestressed slab spanning between webs. The critical section is usually a cantilever.

Step 5. Calculate the properties of the section:

a. Gross area.

b. Gross moment of inertia.

c. Unit weight.

d. Distance from extreme compression fiber to the centroid of the prestressing tendon, d_p.

e. Area of prestressing tendons.

f. Prestressed reinforcement ratio (Eq. 6-23).

Step 6. Given the type of prestressing tendon, determine γ_p. Using the dynamic concrete stress from step 3, calculate β . Using Equation 6-27, 6-28 or 6-29 and the values of γ_p and β_1 from above, calculate the average stress in the prestressing tendon.

Step 7. With the reinforcement ratio from step 5e, the average stress in the prestressing tendon and the value of β_1 from step 6, and the dynamic strength of materials from step 3, check that reinforcement ratios are less than the maximum permitted by Equation 6-30 or 6-31.

Step 8. Using the area of reinforcement and the value of d_p from step 5, the dynamic stresses of step 3, and the average stress in the prestressing tendon from step 6, calculate the moment capacity of the element (eqs. 6-20 and 6-21).

Step 9. With the equations of Table 3-1 and the moment capacity of step 8, calculate the ultimate unit resistance. As recast buildings are only subject to low blast pressures, the static loads become significant. To determine the resistance available to resist the blast load, subtract the static dead and live loads from the ultimate unit resistance.

Step 10. Calculate the moment of inertia of the cracked section I_c, using Equation 6-33. the modular ratio from step 4 and the area of prestressing tendons, the value of d_p and the prestressed reinforcement ratio from step 5. Using this value of I_c and the gross moment of inertia of step 5b, find the average moment of inertia from Equation 6-32.

Step 11. Using the equations of Table 3-8, the modulus of elasticity for concrete from step 4 and the average moment of inertia from step 10, calculate the elastic stiffness of the section.

Step 12. Determine the load-mass factor K_{LM}, in the elastic range for the appropriate loading condition from Table 3-12. Also, calculate the unit mass of the section and multiply it by K_{LM} to obtain the effective unit mass of the element.

Step 13. With Equation 3-60, the effective mass from step 12 and the elastic stiffness from step 11, calculate the natural period of vibration T_N, of the section.

Step 14. Determine the response chart parameters:

a. Duration of load T (step 1).

b. Natural period of vibration T_N (step 13).

Calculate the ratio T/T_N and using this ratio, determine the dynamic load factor DLF from Figures 3-49 through 3-53. Section must remain elastic, and hence the actual resistance obtained by the element (which is equal to the peak dynamic load from step 1 multiplied by the DLF) must be less than the resistance available.

If the section does not remain elastic steps 1 through 14 must be repeated.

NOTE: For bilinear loads, calculate the ratio of the peak dynamic load P to the resistance available. Using P/r_u and the value of T/T_N calculated above, enter the appropriate response chart (Figs. 3-64 through 3-266) and find the ductility ratio X_m/X_E. For the section to remain elastic the ductility ratio must be less than or equal to one.

Step 15. Calculate the deflection of the element X_m by adding the dead and live loads (step 1), and the resistance obtained by the structure (step 14) and dividing by the elastic stiffness (step 11). Using the deflection and the equations of Table 3-5. determine the support rotation. Compare the rotation with deflection criteria of step 1e. If comparison is satisfactory continue with step 16. If comparison is not satisfactory repeat steps 1 through 15.

Step 16. Calculate the elastic deflection X_m from Equation 3-36, using the ultimate resistance of step 9 and the elastic stiffness of step 11. Then calculate the ductility ratio X_m/X_E using the value of X_m from step 15. With the ductility ratio and the ratio T/T_N from step 14, enter Figure 3-268 and find the percentage of rebound. Extrapolate if necessary.

Step 17. Find the required rebound resistance by multiplying the ultimate unit resistance by the ratio from step 16 and subtracting the dead load. In no case should the required rebound resistance be less than half the resistance available during the loading phase. With equations of Table 3-1 and the required rebound resistance, find the required rebound moment capacity.

Step 18. Calculate an approximate value of d^- and the amount of concrete strength available for rebound (Eq. 6-35). Assume a depth of the equivalent rectangular stress block and, by a trial and error method, using Equation 6-34 find the area of rebound reinforcement required. Check that the amount of reinforcement does not exceed the maximum permitted by Equation 6-36 or 6-37.

Step 19. Calculate the shear stress at d_p away from the support. Also calculate the allowable shear stress on an unreinforced web. using the dynamic design stress (step 16). Design the shear reinforcement.

Step 20. Calculate the shear at the support V_d from the equations of Table 3-9 and the value of the total load. Calculate the maximum allowable direct shear using the dynamic concrete strength.

Compare the allowable shear with V_d. If V_d is greater than the size of the section must be increased.

Step 21. Check if section is adequate for service loads using the PCI Design Handbook and the ACI Code.

Example 6A-2 Design of a Prestressed Recast Roof Panel

Required: Design a prestressed recast roof subject to an overhead blast load. Use a double tee section.

Solution:

Step 1. Given:

a. Pressure-time loading (Fig 6A-2).

b. Material strengths

Concrete: $f'_c = 5000$ psi

Prestressing Steel: $f_{pu} = 270{,}000$ psi

$f_{py}/f_{pu} = 0.85$

Welded Wire Fabric $f_y = 65{,}000$ psi

Reinforcing Bars $f_y = 60{,}000$ psi

c. Span length is 40 ft. = 480 in.

d. Live load is 15 psf

e. Maximum ductility ratio < 1.0

Maximum support rotation < 2°

Step 2. Select a double tee section and strand pattern.

Try 8DT24 (Fig. 6A-2)

Section properties from PCI Design Handbook:

$A = 401$ in^2 $y_t = 6.85$ in

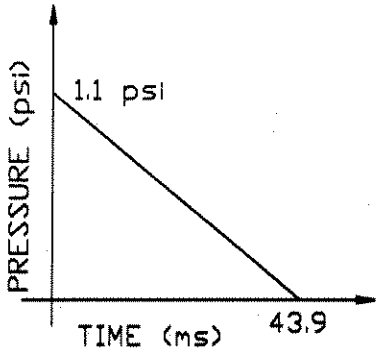
$I = 20{,}985$ in^2 $w = 418$ lb/ft.

Try strand pattern 48-S, two 1/2 inch diameter straight strands in each tee.

Area of each strand = 0.153 in^2

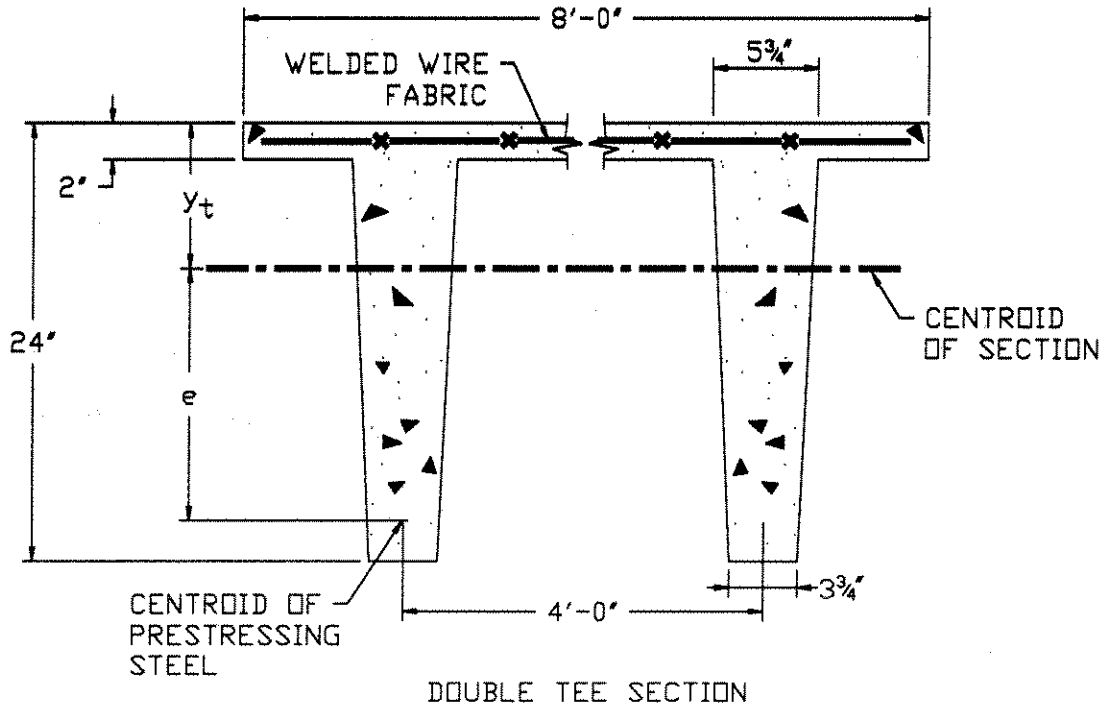
$e = 14.15$ in

Figure 6A-2



(a)

PRESSURE-TIME LOADING



DOUBLE TEE SECTION

(b)

Step 3. Determine design stresses.

a. Dynamic increase factors:

Concrete flexure:	1.19
Concrete diagonal tension:	1.00
Concrete direct shear:	1.10
Prestressing Steel:	1.00
Welding Wire Fabric:	1.10
Reinforcing Steel flexure:	1.17
Reinforcing Steel shear:	1.00

b. Dynamic strengths.

Concrete

- flexure: $f'_{dc} = 1.19 \times 5{,}000 = 5950$ psi
- diagonal tension: $f'_{dc} = 1.0 \times 5{,}000 = 5000$ psi
- direct shear: $f'_{dc} = 1.1 \times 5{,}000 = 5500$ psi

Prestressing Steel: $f_{dy} = 1.0 \times 270{,}000 = 270{,}000$ psi

Welded Wire Fabric: $f_{dy} = 1.10 \times 1.10 \times 65{,}000 = 78{,}650$ psi

Reinforcing Bars

- flexure: $f_{dy} = 1.17 \times 1.10 \times 60{,}000 = 77{,}220$ psi
- shear: $f_{dy} = 1.0 \times 1.10 \times 60{,}000 = 66{,}000$ psi

Step 4. Calculate modulus of elasticity and modular ratio.

a. Concrete

$$E_c = 33 w_c^{1.5} (f'_c)^{1/2}$$
$$= 33(150)^{1.5}(5000)^{1/2}$$
$$= 4.29 \times 10^6 \text{ psi}$$

b. Steel

$E_s = 29.0 \times 10^6$ psi

$$n = \frac{E_s}{E_c} = \frac{29.0 \times 10^6}{4.29 \times 10^6} = 6.76$$

NOTE: The flange is designed in accordance with the principles of Chapter 4. Considering the flange a one-way non-prestressed slab, the cantilever portion was found to be critical. In order to remain elastic the flange thickness must be increased to 3 inches. The reinforcement is two layers of welded wire fabric; 6 X 6 - W1.4 X W2.0 in the top and 6 X 6 - W1.4 X W1.4 in the bottom.

Step 5. Calculate the section properties of the double tee with a 3 inch flange.

a. new $A = 497$ in^2

b. new $y_t = 6.43$ in

new $I_g = 25180$ in^4

c. $w = 497 \times 150$ pcf$/12^3 = 43.1$ lb/in

d. $d_p = 7.85 + 14.15 = 22.0$ in

$A_{ps} = 4 \times 0.153 = 0.612$ in^2

f. Prestressed reinforcement ratio (Eq. 6-23)

$p_p = A_{ps}/bd_p = 0.612/(96 \times 22.0) = 0.000290$

Step 6. Determine the average stress in the prestressing tendon.

a. $f_{py}/f_{pu} = 0.85$ so $\gamma_p = 0.40$

b. $\beta_1 = 0.85 - 0.05(5950-4000)/1000 = 0.7525$

c. Average stress (Eq. 6-27)

$$f_{ps} = f_{pu}\left[1 - \frac{\gamma_p\, p_p\, f_{pu}}{\beta_1\, f'_{dc}}\right]$$

$$= 270{,}000\left[1 - \frac{0.40\ (0.000290 \times 270{,}000)}{(.7525)\ (5950)}\right]$$

$f_{ps} = 268{,}111$ psi

Step 7. Check maximum reinforcement ratio (Eq. 6-30).

$p_p f_{ps}/f'_{dc} \leq 0.36 \beta_1$

$p_p f_{ps}/f'_{dc} = 0.000290 \times 268{,}111/5950 = 0.0131$

$0.36 \beta_1 = 0.36 \times 0.7525 = 0.2709 > 0.0131$ O.K.

Step 8. Calculate moment capacity of beam.

From Equation 6-21

$$a = \frac{A_{ps} f_{ps}}{0.85 f'_{dc} b} = \frac{0.612 \times 268{,}111}{0.85 \times 5950 \times 96} = 0.34 \text{ in}$$

$c = a/\beta_1 = 0.34/0.7525 = 0.45 < 3.0$ in thick flange

Hence the neutral axis is within the flange and the section can be analyzed as a rectangular section. If the neutral axis had extended into the web, a strain compatibility analysis would be required.

From Equation 6-20

$M_u = A_{ps} f_{ps} (d_p - a/2)$

$= 0.612 \times 268.111 \ (22.0 - 0.34/2)$

$M_u = 3582$ k-in

Step 9. Find the resistance available to resist blast load.

a. Find the ultimate resistance (Table 3-1).

$r_u = 8M_u/L^2$

$= 8 \times 3582/480^2 = 0.124$ k/in

$= 124$ lbs/in

b. Resistance available for blast load

$r_{avail} = r_u - DL - LL$

$= 124 - 43.1 - (15 \text{ psf} \times 8 \text{ ft}/12)$

$= 124 - 43.1 - 10.0$

$= 70.9$ lb/in

Step 10. Determine the average moment of inertia.

a. Moment of inertia of cracked section (Eq. 6-33):

$$I_c = nA_{ps}d_p^2 \left[1-(p)^{1/2}\right]$$

$$= 6.76 \times 0.612(22.0)^2 \left[1-(0.00029)^{1/2}\right] = 1970 \text{ in}^4$$

b. Average moment of inertia (Eq. 6-32)

$$I_a = (I_g + I_c)/2$$

$$= (25180 + 1970)/2 = 13575 \text{ in}^4$$

Step 11. Using equations of Table 3-8, calculate the elastic stiffness.

$$K_E = \frac{384\ E_c\ I_a}{5L^4} = \frac{384 \times 4.29 \times 10^6 \times 13575}{5 \times 480^4}$$

$$= 84.25 \text{ lb/in/in}$$

Step 12. Calculate the effective mass

a. Load-mass factor (Table 3-12)

In the elastic range

$$K_{LM} = 0.78$$

b. Unit mass

$$m = w/g = 43.1/(32.2 \times 12)$$

$$= 0.1116 \text{ lb-s}^2/\text{in}^2$$

$$= 11.16 \times 10^4 \text{ lb-ms}^2/\text{in}^2$$

c. Effective mass

$$m_e = K_{LM}\ m$$

$$= 0.78 \times 11.16 \times 10^4$$

$$= 8.70 \times 10^4 \text{ lb-ms}^2/\text{in}^2$$

Step 13. Calculate the natural period of vibration (Eq. 3-60).

$$T_N = 2\pi\ (m_e/K_E)^{1/2}$$

$$= 2\pi\ (8.70 \times 10^4/84.25)^{1/2} = 201.9 \text{ ms}$$

Step 14. Determine response of beam.

T = duration of load = 43.9 ms (step 1a)

T_N = natural period = 201.9 ms (step 13)

T/T_N = 43.9/201.9 = 0.217

From Figure 3-49, DLF = 0.65

Actual resistance obtained r = DLF X P $\leq r_{avail}$

P = peak dynamic load

= 1.1 psi (step 1a)

r = 0.65 X (1.1 X 96)

= 68.4 lb/in < 70.9 lb/in (r_{avail}, step 9) O.K.

Step 15. Check rotation.

a. Total load on beam = (DLF X p) + DL + LL

= 68.4 + 43.1 + 10.0

= 121.5 lb/in

b. Maximum deflection:

X_m = (121.5 lb/in)/K_E

= 121.5/84.25

= 1.44 in

c. Support rotation (Table 3-5)

$\theta = \tan^{-1}(2X_m/L)$

$= \tan^{-1}(2 \times 1.44/480)$

= 0.34° < 2° O.K.

Step 16. Calculate percent of rebound:

a. Calculate elastic deflection (Eq. 3-36)

$X_E = r_u/K_E$

= 124/84.25

= 1.47 in

b. Calculate ductility ratio.

$\mu = X_m/X_E$

$= 1.44/1.47$

$= 0.98$

c. Find percent of rebound from Figure 3-268.

$X_m/X_E = 0.98$ and $T/T_N = 0.216$

$r^-/r = 1.0$

so, 100 percent rebound

Step 17. Determine required rebound moment capacity.

a. Required rebound resistance

$r_{req}^- = r^- - DL > r_{avail}/2$

$= 68.4 - 43.1$

$= 25.3$ lb/in

$r_{avail}/2 = 70.9/2 = 35.4 > 25.3$ lb/in

Use 35.4 lb/in or considering a single tee

$r_{req}^- = 17.7$ lb/in

b. Required moment capacity (Table 3-1).

$M_u^- = r_{req}^- L^2/8$

$= 17.7 \times 480^2/8$

$M_u^- = 509{,}760$ in-lb/stem

Step 18. Determine rebound reinforcement.

a. Approximate value of d^-

$d^- = h - cover - \Phi_{wire} - \Phi_{tie} - (\Phi_{bar}/2)$

$= 25 - 0.625 - 0.135 - 0.375 - 0.5/2$

$= 23.62$ in

b. Rebound concrete strength

$f = 0.47f'_{dc} = 0.47 \times 5950 = 2796.5$ psi

c. Required rebound reinforcement

Assume a = 2.0 in

$A_s^- = M_u^-/[f_{dy}(d^- - a/2]$ (Eq. 6-34)

$= 509,760/[77,220(23.62 - 2.0/2)] = 0.29 \text{ in}^2$

$$a = \frac{A_s^- f_{dy}}{(0.47f'_{dc})b}$$

$$= \frac{0.29 \text{ X } 77,220}{2796.5 \text{ X } 3.75} = 2.1 \text{ in} \approx 2.0 \text{ in} \quad \text{O.K.}$$

Use 2 No. 4 bars in each stem

$A_s^- = 0.40 \text{ in}^2$

d. Check maximum reinforcement (Eq. 6-36).

$$A_s \leq \frac{0.47f'_{dc}\beta_1}{f_{dy}}\left[\frac{87,000 - 0.378.n\, f'_{dc}}{(87.000 - 0.378nf'_{dc} + f_{dy})}\right] bd^-$$

$$= \frac{2796.5 \text{ X } 0.7525}{77,220}\left[\frac{87,000-0.378 \text{ X } 6.76 \text{ X } 5950}{(87.000-0.378.\text{X } 6.76 \text{ X } 5950 + 77,220)}\right]$$

$$\text{X } (3.75 \text{ X } 23.62)$$

$= 1.16 \text{ in}^2 > 0.40 \text{ in}^2$ O.K.

Step 19. Design the shear reinforcement.

Calculate shear at distance d_p from support.

$v_u = r(L/2 - d_p)/b_w d_p$

r = 121.5 lb/in (total load on beam, step 15a)

$v_u = 121.5 \ (480/2 - 22.0)/(2 \text{ X } 4.75 \text{ X } 22.0) = 127 \text{ psi}$

b. Maximum allowable shear stress.

$10 \ (f_{c'})^{1/2} = 10 \text{ X } (5000)^{1/2}$

= 707 psi > 127 psi O.K.

c. Allowable shear stress on unreinforced web.

$$v_c = 1.9(f'_c)^{1/2} + 2500p_p \leq 2.28(f'_c)^{1/2}$$

$$= 1.9(5000)^{1/2} + 2500 \frac{0.612}{(2 \times 4.75 \times 22)} = 142 \text{ psi}$$

$$2.28(f'_c)^{1/2} = 2.28(5000)^{1/2}$$

$$= 161 \text{ psi} > 142 \text{ psi} \quad \text{O.K.}$$

d. Excess shear.

$$v_u - v_c \leq v_c$$

$$v_u - v_c = 127 - 142 = -15 \text{ psi}$$

so, use v_c

e. Shear reinforcement.

Assume #3 closed ties

$$A_v = 2 \times 0.11 = 0.22 \text{ in}^2$$

$$s_s = \frac{A_v \Phi f_y}{v_c b} = \frac{.22 \times 0.85 \times 66{,}000}{142 \times 4.75}$$

$$= 18.3 \text{ in}$$

f. Check maximum spacing and minimum required reinforcement.

$$s \leq d_p/2 = 22.0/2 = 11.0 \text{ in.}$$

$$A_v \leq 0.0015bs_s$$

$$= 0.0015 \times 4.75 \times 11.0 \quad = 0.08 \text{ in}^2 > 0.22 \text{ in}^2$$

Shear reinforcement is thus #3 ties at 11 inches in both stems.

Step 20. Check direct shear.

a. Calculate shear at the support (Table 3-9)

$$V_d = rL/2$$

$$= 121.5 \times 480/2$$

$$= 29160 \text{ lbs}$$

b. Calculate allowable direct shear.

$V_d \leq 0.18\ f'_c\ bd$

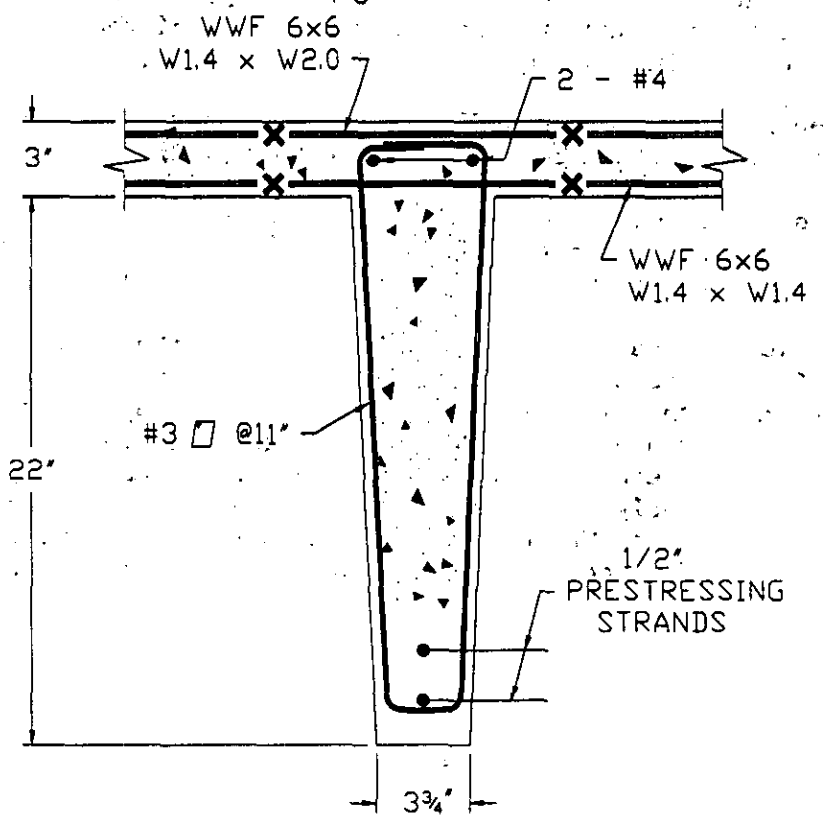
$= 0.18 \times 5{,}500 \times (2 \times 4.75) \times 22.0$

$= 206{,}910$ lbs $> 29{,}160$ lbs O.K.

Step 21. Check section for conventional loads.

This section as designed for blast loads is shown in Figure 6A-3. Using the PCI Design Handbook and the latest ACI code, the section must be checked to make sure it is adequate for service loads.

Figure 6A-3



Problem 6A-3 Design of Windows

Problem: Determine the minimum thickness of glazing to resist a given blast load, and the design loads for the framing.

Procedure:

Step 1. Establish design parameters:

a. Pressure-time loading.

b. Dimensions of pane(s).

c. Type of glazing.

Step 2. Calculate aspect ratio of pane.

Step 3. With the parameters of Steps 1 and 2, enter Figures 6-28 to 6-42 to determine which one applies. Using the peak pressure of the dynamic load, its duration and the dimensions of the pane, determine the minimum required glazing thickness.

NOTE: If given window geometry differs from chart parameters, interpolation as outlined in Section 6-28.4 may be required.

Step 4. Find the static ultimate resistance r_u of the glazing from Table 6-6 for the given aspect ratio, the short dimension and the thickness of the glazing (interpolate if required).

Step 5. From Table 6-9 and the aspect ratio determine the design coefficients C_R, C_X and C_Y for the window frame loading. With these coefficients, the dimensions of the pane from step 1b, the static ultimate resistance of step 4 and Equation 6-55, calculate the uplift force in each corner. Then using Equations 6-53 and 6-54 calculate the design loads along the long and short spans of the pane. Finally from Table 6-11, determine the fundamental period, T_N, and check for rebound requirements in accordance with Section 6-30.4

Example 6A-3 Design of Windows

Required: Find the minimum glazing thickness and the design loads on the frame of a non-openable window consisting of four equal size panes of glass.

Solution:

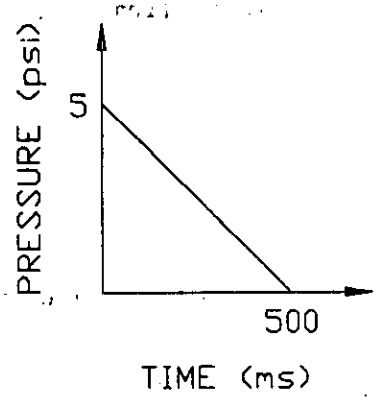
Step 1. Given:

a. Pressure-time loading (Fig. 6A-4)

b. Each pane is 37.5 inches long by 30 inches high.

c. The glazing is heat-treated tempered glass meeting Federal Specification DO-G-1403B and ANSI Z97.1-1984.

Figure 6A-4



Step 2. Calculate aspect ratio.

a/b = 37.5/30 = 1.25

Step 3. Determine minimum glazing thickness.

a. For a/b = 1.25 and tempered glass use Figure 6-33.

b. From Figure 6-33, t = 3/4 inch.

Step 4. Find static ultimate resistance r_u, (Table 6-6).

r_u = 24.6 psi

The window frame must be designed to safely support, without undue deflections, a static uniform load of 24.6 psi applied normal to both the glazing and the exposed frame members.

Step 5. Compute design loads on the window frame.

Note: The exposed surface width of the frame is 2 inches.

a. Determine design coefficients from Table 6-9, interpolating for a/b = 1.25.

$C_R = 0.077$

$C_x = 0.545$

$C_y = 0.543$

b. Calculate the unit shear along the long span of the frame (Eq. 6-53).

$V_x = C_x r_u b \sin(\pi x/a)$

$= 0.545 \times 24.6 \times 30 \sin(\pi x/37.5) + 24.6*2$

$= 402 \sin(\pi x/372.5) + 49.2$ lb/in

c. Calculate the unit shear along the short span of the frame (Eq. 6-54).

$V_y = C_y r_u b \sin(\pi y/b)$

$= 0.543 \times 24.6 \times 30 \sin(\pi y/30) + 24.6*2$

$= 400 \sin(\pi y/18) + 49.2$ lb/in

d. Calculate the uplift force at the corners of the panes (Eq. 6-55).

$$R = -C_R r_u b^2$$

$$= - 0.077 \times 24.6 \times 30^2$$

$$= - 1705 \text{ lbs.}$$

Distribution of the design load of the pane on the frame is shown in Figure 6-52.

e. From Table 6-11, $T_N = 8.74$ msec, $T/T_N = 1000/8.74 = 114$

Since $T/T_N = 114 \geq 10$, design for rebound is not necessary.

Problem 6A-4 Design of Shock Isolation System

Problem: Design an overhead pendulum shock isolation system using a platform for a given loading.

Step 1. Establish design parameters:

a. Structural configuration.
b. Magnitude and location of loads on platform.
c. Shock spectra for horizontal and vertical motion.
d. Maximum allowable motion.

Step 2. Compute member sizes of platform.

Step 3. Compute center of gravity of the loads (live and dead) on platform.

Step 4. Compute the elastic center of the spring supporting system.

Step 5. Determine the required weight and location of ballast to balance the system (i.e. to move the center of gravity of loads to coincide with the elastic center of the spring supporting system).

Step 6. Compute the total weight of the isolation system. Additional ballast equal to 25% of the weight of the equipment and ballast from Step 5 is added to provide for future changes in equipment. Also determine the equivalent uniform load equal to the total load divided by the area of the platform.

Step 7. Determine the natural frequency of the individual members of the platform (Using the equivalent uniform load computed in Step 6). The natural frequency is

$$f = \frac{9.87}{2\pi} \frac{EIg}{wL^4}$$

for a simply supported beam with a uniform load.

Step 8. Using the shock spectrum for vertical motion, determine the required frequency of the system that will reduce the input accelerations to the maximum allowable. In addition, determine the displacement at this frequency.

Step 9. Verify rigid body motion of the platform.

The natural frequency of the individual members of the platform should be at least 5 times greater than the natural frequency of the system for rigid body motion of the platform to occur.

To increase the frequency of the individual members, increase member sizes, and repeat Steps 3 through 7.

Step 10. Determine the natural frequency for horizontal motion (pendulum action) of the platform where

$$f_{\text{horizontal motion}} = 1/2\pi \cdot (386.4/L)^{1/2} \qquad (6\text{-}56)$$

where L is the suspended length.

Step 11. Verify that dynamic coupling will not occur between vertical and horizontal motions. According to Section 6-47.3.2 dynamic coupling will not occur if

$$f_{\text{horizontal motion}} < 1/2\, f_{\text{vertical motion}}$$

Step 12. From the shock spectra for horizontal motion, determine the maximum dynamic displacement, velocity and acceleration using the frequency computed in Step 10.

Verify that the maximum acceleration is less than the allowable.

Step 13. Compute the load in each spring.

$$\text{Load in each spring} = \frac{\text{Total Load}}{\text{Number of Springs}}$$

Step 14. Determine stiffness of springs to produce the required frequency of the system. Compute the static and maximum displacement. Using the static displacement and the load in each spring from Step 13, calculate the required spring stiffness K from,

$$K = \frac{\text{load in each spring}}{\text{static displacement}}$$

Or using the vertical frequency from Step 8, and the mass on each spring the stiffness can be calculated from

$$K = [2\pi\, f_{\text{vert}}]\, m^2$$

In addition, compute the travel of the spring according to Section 6-48.2, i.e.

$$\text{travel} = \frac{\text{Maximum displacement}}{0.85}$$

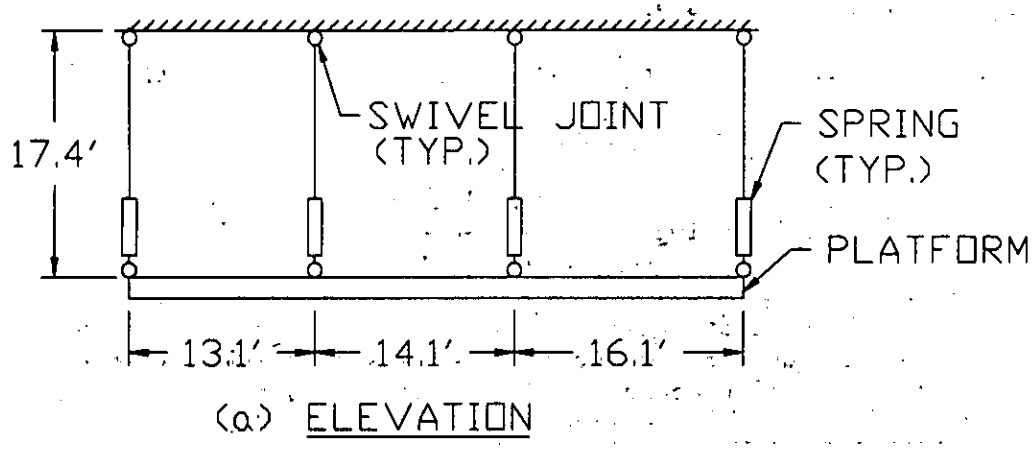
Example 6A-4 Design Shock Isolation System

Required: Design an overhead pendulum shock isolation system using a platform for a given loading.

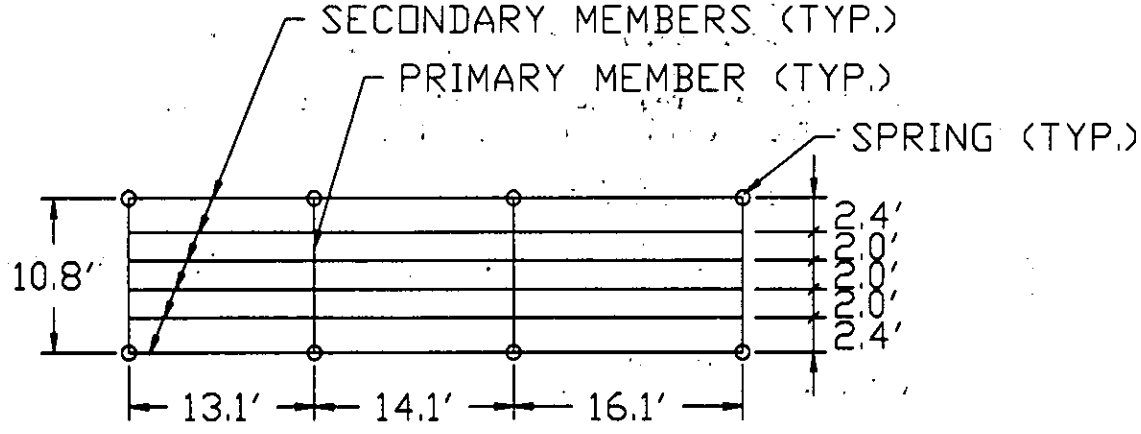
Step 1. Given:

a. Structural configuration shown in Figure 6A-5a and Figure 6A-5b.

Figure 6A-5



(a) ELEVATION



(b) PLATFORM (PLAN)

b. Magnitude and location of loads on platform (Figure 6A-6)

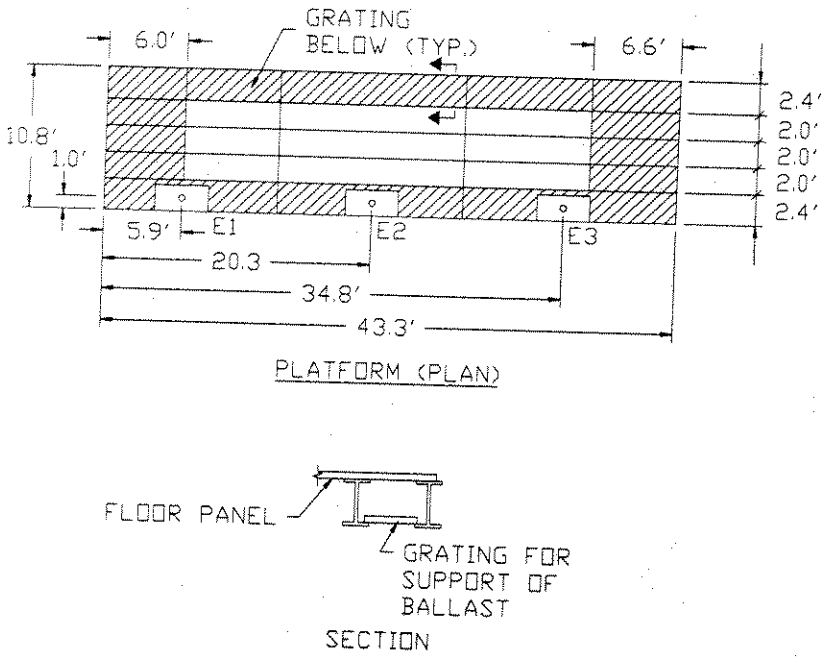
Equipment: E_1 = 4960 lbs.
E_2 = 4960 lbs.
E_3 = 4960 lbs.

Floor panel = 5.5 psf (covers the whole area of platform)

Grating = 7.2 psf

Live load = 150 psf

Figure 6A-6



c. Shock spectra for horizontal and vertical motions are given in Figure 6A-7a and 6A-5b, respectively.

d. Maximum allowable acceleration

Vertical Motion = 0.50g

Horizontal Motion = 0.75g

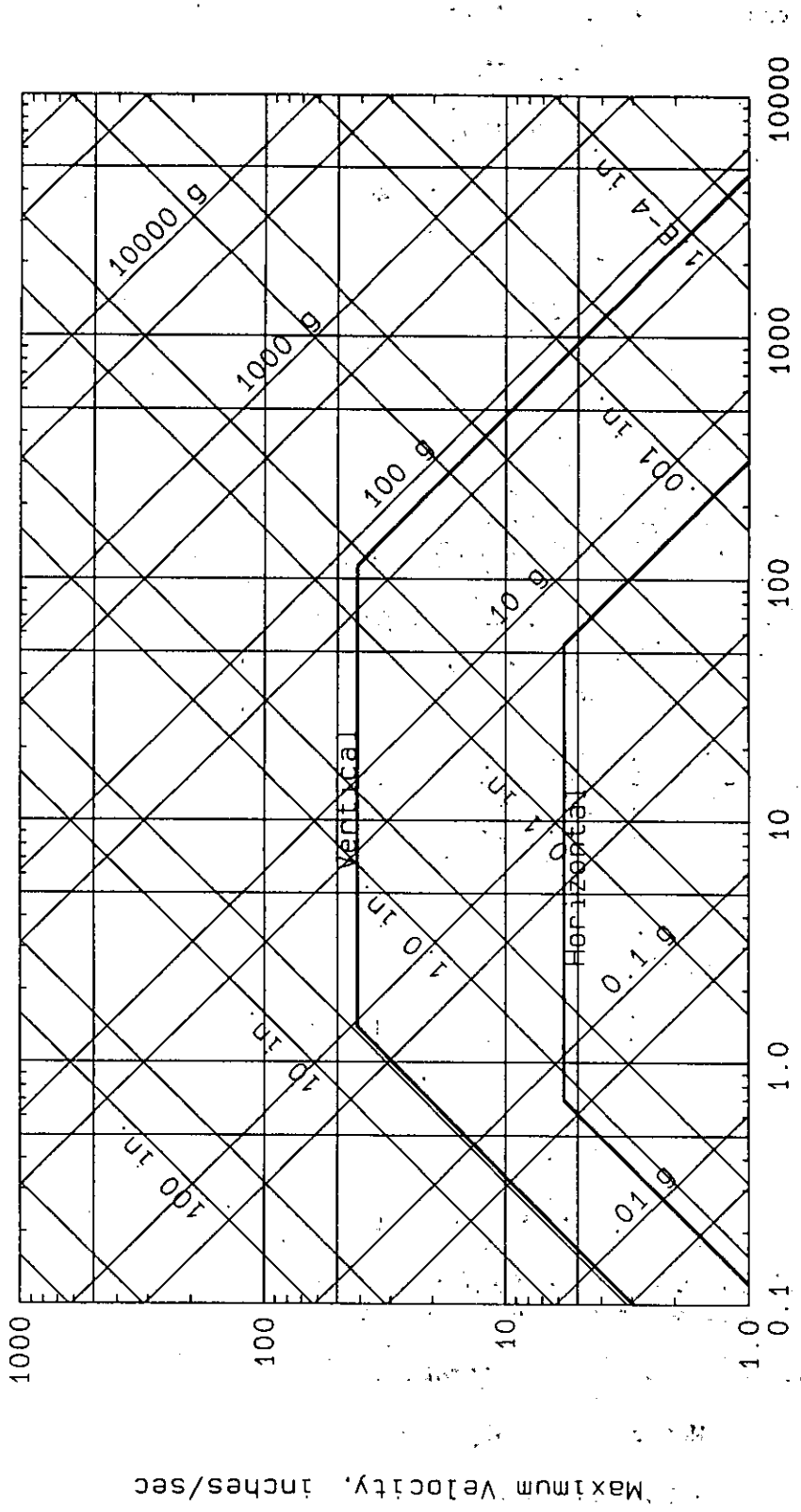

Maximum Velocity, inches/sec
1000
100
10
1.0
0.1
Frequency, cps
1.0
10
100
1000
10000
Vertical
Horizontal
10000 g
1000 g
100 g
10 g
1.0 g
0.1 g
0.01 g
400 in.
40 in.
4.0 in.
0.4 in.
0.04 in.

Figure 6A-7

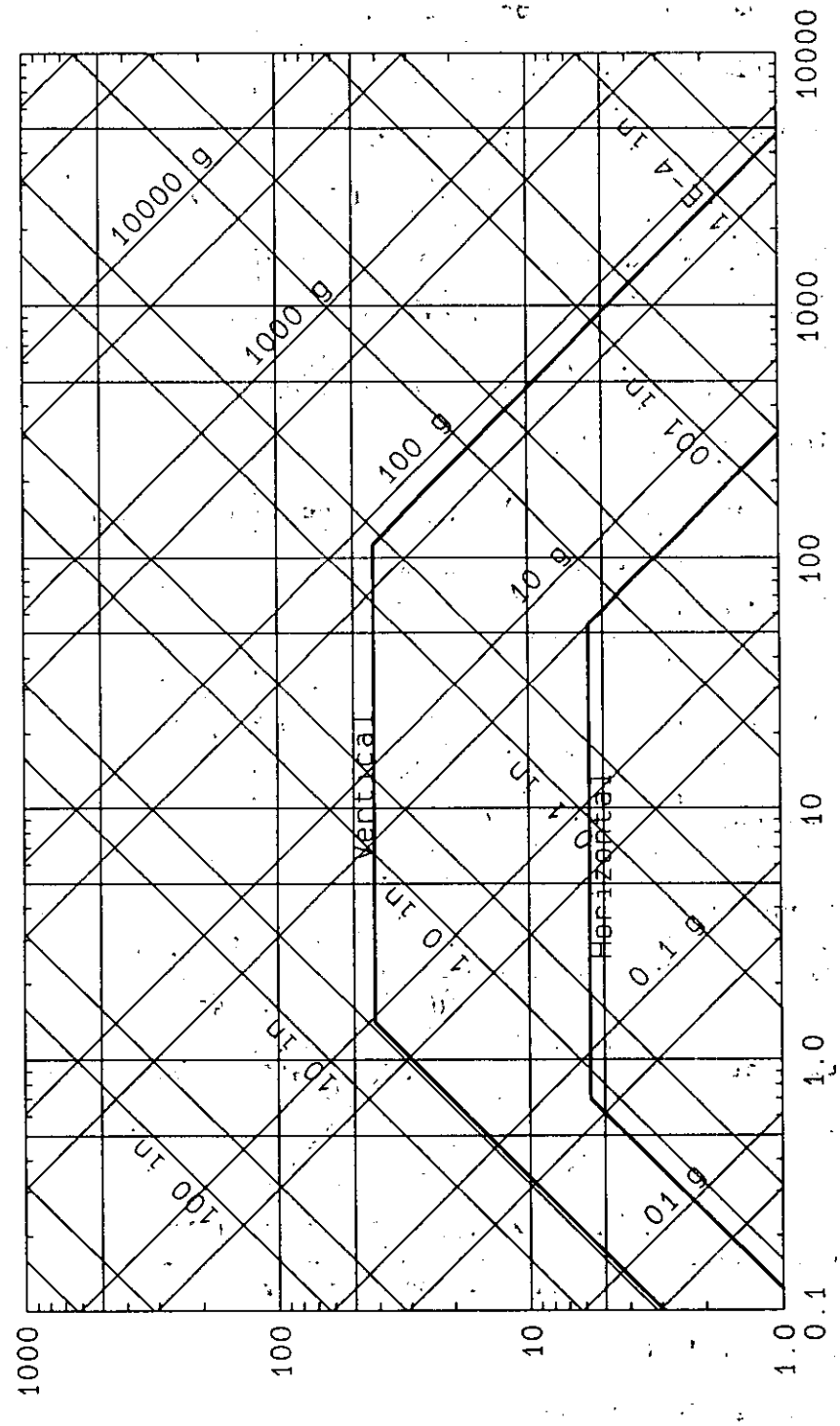

Maximum Velocity, inches/sec
1000
100
10
1.0
0.1
Frequency, cps
1.0
10
100
1000
10000
Vertical
Horizontal
10000 g
1000 g
100 g
10 g
1.0 g
0.1 g
100 in.
10 in.
1.0 in.
0.1 in.
0.01 in.
0.001 in.

Figure 6A-7.

Step 2. Member sizes

Design Loads:

Dead load = 20 psf (assume)

Live Load = 150 psf

Primary Member (a): - (See Fig. 6A-5a).

$w = 170 \times (7.05 + 8.05) = 2567$ lbs/ft.

Maximum Bending moment = $(wL^2)/8$ (at center)

$= (2567 \times 10.8^2) / 8$

$= 37427$ lb.-ft.

Using allowable stress design,

Allowable bending stress = 0.66_y (for compact shapes AISC).

$$\text{so, Required } S_x = \frac{\text{Maximum Bending Moment}}{\text{Allowable Bending Stress}}$$

$= (37427 \times 12) / (0.66 \times 36{,}000)$

$= 18.9 \text{ in}^3$

Try section W10 X 21,

$S_x = 21.5 \text{ in}^3 > 18.9 \text{ in}^3$ O.K.

Check deflection:

$$\text{Maximum allowable deflection} = \frac{L}{360} = \frac{10.8 \times 12}{360}$$

Maximum deflection = $(5WL^4) / 384EI$ (at center)

For W10 X 21,

$I = 107 \text{ in}^3$

$$\text{Maximum deflection} = \frac{5 \times (2567/12) \times (10.8 \times 12)^4}{384 \times 29{,}000 \times 10^3 \times 107}$$

$= 0.25 \text{ in} < 0.36 \text{ in.O.K.}$

so, Use W10 X 21 for all primary members.

Secondary Member (b): See Fig. 6A-5a.

$$w = 170\ (1.0 + 1.2) = 374\ \text{lb/ft}$$

Maximum Bending moment = $(wL^2)\ /\ 8$ (at center)

$$= (374 \times 16.1^2)/8 = 12118\ \text{lb.-ft.}$$

Using allowable stress design,

Allowable bending stress = $0.66\ F_y$ (for compact shapes, AISC).

$$\text{so, Required } S_x = \frac{12118 \times 12}{0.66 \times 36{,}000} = 6.12\ \text{in}^3$$

Try section W8 x 13,

$$S_x = 9.90\ \text{in}^3 > 6.12\ \text{in}^3 \quad \text{O.K.}$$

Check deflection:

$$\text{Maximum allowable deflection} = \frac{L}{360}$$

$$= \frac{16.1 \times 12}{360}$$

$$= 0.54\ \text{in.}$$

For W8 X 13, $I = 39.6\ \text{in}^4$

$$\text{Maximum deflection} = \frac{5WL^4}{384\ EI}$$

$$= \frac{5 \times (374/12) \times (16.1 \times 12)^4}{384 \times 29{,}000 \times 10^3 \times 39.6}$$

$$= 0.49 < 0.54 \quad \text{O.K.}$$

so, Use W8 X 13 for all secondary members.

NOTE: Members should be checked for concentrated equipment loads.

Step 3. Find center of gravity of the loads on the platform (see Figure 6A-8).

Item	Weight W_1 (lbs.)	X (ft.)	Y (ft.)	W_1X (lb. ft.)	W_1Y (lb. ft.)
$A_1A_2 \ldots A_6$	226.8	0.0	5.4	0.0	1224.7
$B_1B_2 \ldots B_6$	226.8	13.1	5.4	2971.1	1224.7
$C_1C_2 \ldots C_6$	226.8	27.2	5.4	6169.0	1224.7
$D_1D_2 \ldots D_6$	226.8	43.3	5.4	9820.4	1224.7
$A_1B_1C_1D_1$	562.9	21.65	10.8	12187.0	6079.3
$A_2B_2C_2D_2$	562.9	21.65	8.4	12187.0	4728.4
$A_3B_3C_3D_3$	562.9	21.65	6.4	12187.0	3602.6
$A_4B_4C_4D_4$	562.9	21.65	4.4	12187.0	2476.8
$A_5B_5C_5D_5$	562.9	21.65	2.4	12187.0	1351.0
$A_6B_6C_6D_6$	562.9	21.65	0.0	12187.0	0.0
E_1	4960.0	5.9	1.0	29264.0	4960.0
E_2	4960.0	20.3	1.0	100688.0	4960.0
E_3	4960.0	34.8	1.0	172608.0	4960.0
$A_1D_1D_2A_2$	748.2	21.65	9.6	16199.0	7183.0
$A_5D_5D_6A_6$	748.2	21.65	1.2	16199.0	897.8
$A_2G_{11}G_{12}A_5$	259.2	3.0	5.4	777.6	1400.0
$D_2D_5G_{14}G_{15}$	259.2	4.0	5.4	10368.0	1400.0
Floor Panel	2572.0	21.65	5.4	55684.0	13889.0
Σ	23751.4		Σ	493870.0	62786.7

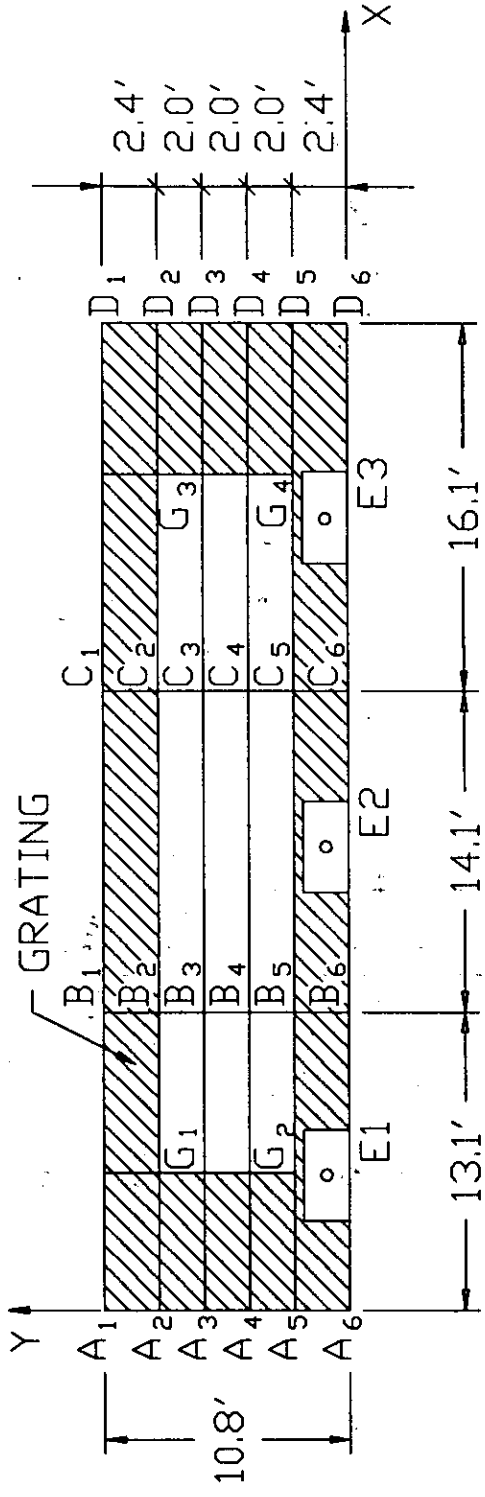

X
2.4'
2.0'
2.0'
2.0'
2.4'
D1 D2 D3 D4 D5 D6
C1 C2 C3 C4 C5 C6
G3 G4
E3
16.1'
B1 B2 B3 B4 B5 B6
GRATING
E2
14.1'
G1 G2
E1
13.1'
Y
A1 A2 A3 A4 A5 A6
10.8'

Figure 6A-8

Center of gravity of loads (dead + live) = $(\bar{X}_1, \bar{Y}_1)$

$$\text{Then, } \bar{X}_1 = \frac{\Sigma W_1 X}{\Sigma W_1}$$

$$= \frac{493870}{23751.4}$$

$$= 20.8 \text{ ft.}$$

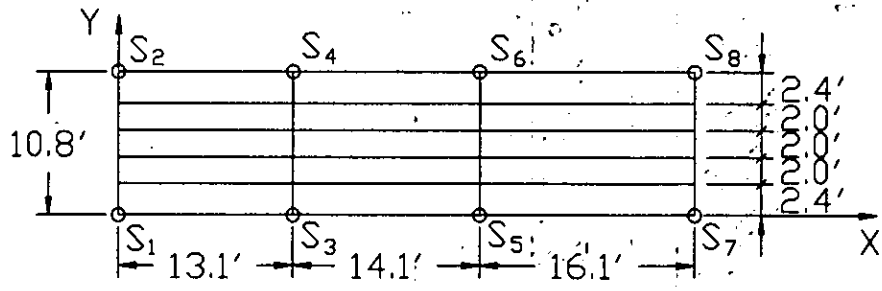
$$Y_1 = \frac{\Sigma W_1 Y}{\Sigma W_1}$$

$$= \frac{62786.7}{23751.4}$$

$$= 2.64 \text{ ft.}$$

Step 4. **Elastic center of the spring support system.**

Figure 6A-9



NOTE: All springs have the same stiffness

Spring No.	Force (W)	X (ft.)	Y (ft.)	WX	WY
S_1	P	0	0	0	0
S_2	P	0	10.8	0	10.8P
S_3	P	13.1	0	13.1P	0
S_4	P	13.1	10.8	13.1P	10.8P
S_5	P	27.2	0	27.2P	0
S_6	P	27.2	10.8	27.2P	10.8P
S_7	P	43.3	0	43.3P	0
S_8	P	43.3	10.8	43.3P	10.8P
Σ	8P		Σ	167.2P	43.2P

Elastic center of spring support system = $(\bar{X}_s, \bar{Y}_s)$.

$$\bar{X}_s = \frac{\Sigma WX}{\Sigma W}$$

$$= \frac{167.2P}{8P} = 20.9 \text{ ft.}$$

$$\bar{Y}_s = \frac{\Sigma WY}{\Sigma W}$$

$$= \frac{43.2P}{8P} = 5.4 \text{ ft.}$$

Step 5. Find the weight and location of ballast to balance the system (relocate the c.g. of the platform to coincide with the elastic center of the isolation system).

a. For the x direction - Try placing ballast at x = 30.3 ft., i.e. 4 feet from the right edge of the platform. The ballast is placed symmetrically about the x axis of the elastic center so as not to affect the location of the center of gravity in the y direction.

Weight of ballast = W_{BX}

$$\Sigma W_1 X + 39.3 W_{BX} = \bar{X}_s [\Sigma W_1 + W_{BX}]$$

$$493870 + 39.3 W_{BX} = 20.9(23751.4 + W_{BX})$$

$$W_{BX} = 2534.3/18.4 = 137.7 \text{ lbs.}$$

b. For the y direction - Try placing ballast at y = 9.6 feet, i.e. 1.2 feet from the top of the platform. The ballast is placed symmetrically about the y axis of the elastic center so as not to affect the location of the center of gravity in the x direction.

Weight of ballast = W_{BY}

$$\Sigma W_1 Y + 9.6 W_{BY} = \bar{Y}_s [\Sigma W_1 + W_{BY}]$$

$$62786.7 + 9.6 W_{BY} = 5.4(2375.1 + W_{BY})$$

$$W_{BY} = 65470.9/4.2 = 15588.3 \text{ lbs.}$$

c. Total ballast

$$W_B = W_{BX} + W_{BY} = 137.7 + 15588.3 = 15726 \text{ lbs.}$$

Step 6. Total load on the platform and equivalent uniform load.

a. Total load.

Dead Load:

Floor panel	=	2572 lbs.
Members	=	4284.6
Grating	=	2014.8
	Σ =	8871.4 lbs.

Live Load:

Equipment	=	14880 lbs.
Ballast	=	15726
Additional Ballast = 0.25(30606)	=	7651.6
Personnel (5 @ 150 lb.)	=	750
	Σ =	39007.5 lbs.

Total = 8871.4 + 39007.5
= 47878.9 lbs.

b. Equivalent uniform load

$$W = \frac{47878.9}{10.8 \times 43.3}$$

$$= 102.4 \text{ psf} \leq 170 \text{ psf} \qquad \text{O.K.}$$

Preliminary design of platform members is O.K. However, members supporting ballast must be checked as their actual load may be higher than the equivalent uniform load.

Step 7. Natural frequency of the individual members of the platform.

For a simply supported member with a uniform load,

$$\text{Natural frequency } f_n = \frac{9.87}{2\pi} \cdot \frac{EIg}{WL^4}$$

Primary Members (a): A portion of the adjacent slab acts with the beam. Add 20% of the mass of the slab on each side of the beam to the actual mass of the beam.

W10 X 21

$I = 107 \text{ in}^3.$

$L = 10.8 \times 12$

$= 129.6 \text{ inches}$

$b = 0.40(7.05 + 8.05)$

$= 6.04 \text{ feet}$

$g = 386.4 \text{ in/sec}^2$

$E = 29000 \times 10^3 \text{ psi.}$

w: (Use equivalent uniform load):

$\bar{w} = 102.4 \times 6.04$

$= 618.5 \text{ lb/ft}$

$= 51.54 \text{ lb/in}$

$$f_n = \frac{9.87}{2\pi}\left[\frac{29000 \times 10^3 \times 107 \times 386.4}{51.54 \times (29.6)^4}\right]^{\frac{1}{2}}$$

$$= 14.3 \text{ cps}$$

Secondary Members (b): Since the spacing of the secondary beams is less than 1/4 of the length of the beams the total mass of the slab act with the beam.

W 8 X 13 $I = 39.6 \text{ in}^4$

$L = 16.1 \times 12$

$= 193.2$ in.

$b = 2.2$ ft.

$w = 102.4 \times 2.2$

$= 225.3$ lb/ft

$= 18.78$ lb/in

$E = 29000 \times 10^3$ psi

$g = 386.4 \text{ in/sec}^2$

$$f_n = \frac{9.87}{2\pi}\left[\frac{29{,}000 \times 10^3 \times 39.6 \times 386.4}{18.78 \times (193.2)^4}\right]^{\frac{1}{2}}$$

$$= 6.5 \text{ cps}$$

Step 8. Required frequency of system to limit motions.

To limit the maximum acceleration of the system to 0.5g or less, choose the frequency of the system from Figure 6A-7b as

$f = 1$ cps

which produces a maximum acceleration of 0.4g and a maximum dynamic displacement of 4.7 inches.

Step 9. Verification of rigid body motion of platform.

$$f_{\text{individual member}} > 5 \times f_{\text{system}}$$

From Step 8.,

$$f_{\text{system}} = 1 \text{ cps}$$

From Step 7.,

$f_{\text{primary member}}$ = 14.2 cps > 5 cps O.K.

$f_{\text{secondary member}}$ = 6.5 cps > 5 cps O.K.

Therefore, platform is in rigid body motion.

Step 10. Natural frequency of platform for horizontal motion (i.e. pendulum type action).

Assume the center of gravity of supported mass is located at the top of the platform so that the length of the pendulum arm is 17.4 feet.

Frequency of platform for horizontal motion

$$f = 1/2\pi\ (386.4/L)^{1/2} \qquad (6\text{-}56)$$

$$= 0.22 \text{ cps}$$

Step 11. Check for dynamic coupling of vertical and horizontal motion.

From Step 8.,

$f_{\text{vertical motion}}$ = 1 cps

From Step 10.,

$f_{\text{horizontal motion}} = 0.22 \text{ cps} < 1/2\ f_{\text{vertical motion}} = 0.5 \text{ cps}$

Dynamic coupling will not occur.

Step 12. Maximum dynamic displacement, velocity and acceleration for horizontal motion.

From shock spectra for horizontal motion, (Fig.6A-7a) for f = 0.22 cps,

Maximum acceleration = 0.007g < 0.75g O.K.

Maximum velocity = 0.9 in/sec.

Maximum dynamic displacement = 1.3 in.

The maximum dynamic displacement is the required "rattle space" or the minimum horizontal clearance between the platform and the structure or anything attached to the structure.

Step 13. Load in each spring.

$$\text{Load in each spring} = \frac{\text{Total Load}}{\text{Number of Springs}}$$

$$= \frac{47878.9}{8}$$

$$= 5985 \text{ lbs.}$$

Step 14. Design the springs.

a. Static displacement

From Step 8.,

For a maximum acceleration of 0.48g the maximum dynamic displacement = 4.7 in.

so, Static displacement = 4.7/0.48

b. Stiffness of spring = 4.7/0.48

$$K = \frac{\text{Load in each spring}}{\text{Static displacement}}$$

$$= \frac{5985}{9.79} = 611.2 \text{ lb/in}$$

or

$$K = (2\pi f_{vert})^2 \, m$$

$$= (2\pi \times 1\text{cps})^2 (5985/386.4)$$

$$K = 611.5 \text{ lb/in}$$

c. Maximum travel of spring.

Maximum displacement = (static + dynamic) displacement

$$= 9.79 + 4.7$$

$$= 14.49 \text{ in}$$

From Section 6-48.2

$$\text{Travel of spring} = \frac{\text{maximum displacement}}{0.85}$$

$$= \frac{14.49}{0.85}$$

$$= 17.0 \text{ in.}$$

Thus the vertical rattle space (clearance) is 17.0 inches.

APPENDIX 6B

LIST OF SYMBOLS

a	(1) acceleration (in./ms^2) (2) depth of equivalent rectangular stress block (in.) (3) long span of a panel (in.)
A	area (in.^{2})
A_a	area of diagonal bars at the support within a width b (in.^{2})
A_d	door area (in.^{2})
A_g	area of gross section (in^2)
A_n	net area of section (in.^{2})
A_o	area of openings (ft^2)
A_{ps}	area of prestressed reinforcement (in.^{2})
A_s	area of tension reinforcement within a width b (in.^{2})
A'_s	area of compression reinforcement within a width b (in.^{2})
A_s^-	area of rebound reinforcement (in.^{2})
A_{sH}	area of flexural reinforcement within a width b in the horizontal direction on each face (in^2)*
A_{sV}	area of flexural reinforcement within a width b in the vertical direction on each face (in^2)*
A_v	total area of stirrups or lacing reinforcement in tension within a distance, s_s or s_1 and a width b_s or b_1 (in.^{2}).
A_I, A_{II}	area of sector I and II, respectively (in.^{2})
b	(1) width of compression face of flexural member (in.) (2) width of concrete strip in which the direct shear stresses at the supports are resisted by diagonal bars (in.) (3) short span of a panel (in.)
b_s	width of concrete strip in which the diagonal tension stresses are resisted by stirrups of area A_v (in.)
b_1	width of concrete strip in which the diagonal tension stresses are resisted by lacing of area A_v(in.)
B	(1) constant defined in paragraph. (2) peak blast overpressure capacity
C	shear coefficient

c	(1) distance from the resultant applied load to the axis of rotation (in.) (2) damping coefficient (3) distance from extreme compression fiber to neutral axis (in.)
c_I, c_{II}	distance from the resultant applied load to the axis of rotation for sectors I and II, respectively (in.)
C_{cr}	critical damping
C_d	shear coefficient for ultimate shear stress of one-way elements
C_D	(1) drag coefficient (2) coefficient for center deflection of glass
C_{Dq}	drag pressure (psi)
C_{Dq_o}	peak drag pressure (psi)
C_E	equivalent load factor
C_f	post-failure fragment coefficient (lb_2-ms_4/$in._8$)
C_H	shear coefficient for ultimate shear stress in horizontal direction for two-way elements*
C_L	leakage pressure coefficient
C_M	maximum shear coefficient
C_R	force coefficient for shear at the corners of a window frame
C_r	coefficient for effective resistance of glass
$C_{r\alpha}$	peak reflected pressure coefficient at angle of incidence α
c_s	dilatational velocity of concrete (ft/sec)
C_s	shear coefficient for ultimate support shear for one-way elements
C_{sH}	shear coefficient for ultimate support shear in horizontal direction for two-way elements*
C_{sV}	shear coefficient for ultimate support shear in vertical direction for two-way elements*
C_T	coefficient for period of vibration for glass
C_u	impulse coefficient at deflection X_u (psi-ms^2/$in.^2$)
C'_u	impulse coefficient at deflection X_m (psi-ms^2/$in.^2$)

* See note at end of symnbols

C_v	shear coefficient for ultimate shear stress in vertical direction for two-way elements*
C_x	shear coefficient for the ultimate shear along the long side of window frame
C_y	shear coefficient for the ultimate shear along the short side of window frame
C_1	(1) impulse coefficient at deflection X_1 (psi-ms^2/in.^{2}) (2) parameter defined in figure (3) ratio of gas load to shock load
C'_1	impulse coefficient at deflection X_m (psi-ms^2/in.^{2})
C_2	ratio of gas load duration to shock load duration
d	distance from extreme compression fiber to centroid of tension reinforcement (in.)
d'	distance from extreme compression fiber to centroid of compression reinforcement (in.)
d_c	distance between the centroids of the compression and tension reinforcement (in.)
d_{co}	diameter of steel core (in.)
d_e	distance from support and equal to distance d or d_c (in.)
d_i	inside diameter of cylindrical explosive container (in.)
d_l	distance between center lines of adjacent lacing bends measured normal to flexural reinforcement (in.)
d_p	distance from extreme compression fiber to centroid of prestressed reinforcement (in.)
d_1	diameter of cylindrical portion of primary fragment (in.)
D	(1) unit flexural rigidity (lb-in.) (2) location of shock front for maximum stress (ft) (3) minimum magazine separation distance (ft)
D_o	nominal diameter of reinforcing bar (in.)
D_E	equivalent loaded width of structure for non-planar wave front (ft)
DIF	dynamic increase factor
DLF	dynamic load factor

* See note at end of symnbols

e	(1) base of natural logarithms and equal to 2.71828... (2) distance from centroid of section to centroid of prestressed reinforcement (in.)
$(2E')^{1/2}$	Gurney Energy Constant (ft/sec)
E	modulus of elasticity
E_c	modulus of elasticity of concrete (psi)
E_m	modulus of elasticity of masonry units (psi)
E_s	modulus of elasticity of reinforcement (psi)
f	(1) unit external force (psi) (2) frequency of vibration (cps)
f'_c	static ultimate compressive strength of concrete at 28 days (psi)
f'_{dc}	dynamic ultimate compressive strength of concrete (psi)
f'_{dm}	dynamic ultimate compressive strength of masonry units (psi)
f_{ds}	dynamic design stress for reinforcement (psi)
f_{du}	dynamic ultimate stress of reinforcement (psi)
f_{dy}	dynamic yield stress of reinforcement (psi)
f'_m	static ultimate compressive strength of masonry units (psi)
f_n	natural frequency of vibration (cps)
f_{ps}	average stress in the prestressed reinforcement at ultimate load (psi)
f_{pu}	specified tensile strength of prestressing tendon (psi)
f_{py}	yield stress of prestressing tendon corresponding to a 1 percent elongation (psi)
f_s	static design stress for reinforcement (a function of f_y, f_u & ϕ (psi)
f_{se}	effective stress in prestressed reinforcement after allowances for all prestress losses (psi)
f_u	static ultimate stress of reinforcement (psi)
f_y	static yield stress of reinforcement (psi)
F	(1) total external force (lbs) (2) coefficient for moment of inertia of cracked section (3) function of C_2 & C_1 for bilinear triangular load

F_o force in the reinforcing bars (lbs)

F_E equivalent external force (lbs)

g (1) variable defined in table 4-3
(2) acceleration due to gravity (ft/sec^2)

G shear modulus (psi)

h (1) charge location parameter (ft)
(2) height of masonry wall

h' clear height between floor slab and roof slab

H (1) span height (in.)
(2) distance between reflecting surface(s) and/or free edge(s) in vertical direction (ft)

H_c height of charge above ground (ft)

H_c scaled height of charge above ground ($ft/lb^{1/3}$)

H_s height of structure (ft)

H_T scaled height of triple point ($ft/lb^{1/3}$)

i unit positive impulse (psi-ms)

i^- unit negative impulse (psi-ms)

$\bar{i}_a$ sum of scaled unit blast impulse capacity of receiver panel and scaled unit blast impulse attenuated through concrete and sand in a composite element ($psi\text{-}ms/lb^{1/3}$)

i_b unit blast impulse (psi-ms)

i_b scaled unit blast impulse ($psi\text{-}ms/lb^{1/3}$)

i_{bt} total scaled unit blast impulse capacity of composite element ($psi\text{-}ms/lb^{1/3}$)

$\bar{i}_{ba}$ scaled unit blast impulse capacity of receiver panel of composite element ($psi\text{-}ms/lb^{1/3}$)

$\bar{i}_{bd}$ scaled unit blast impulse capacity of donor panel of composite element ($psi\text{-}ms/lb^{1/3}$)

i_e unit excess blast impulse (psi-ms)

i_r unit positive normal reflected impulse (psi-ms)

i_r^- unit negative normal reflected impulse (psi-ms)

i_s unit positive incident impulse (psi-ms)

i_s^-	unit negative incident impulse (psi-ms)
I	moment of inertia ($in.^4$)
I_a	average of gross and cracked moments of inertia of width b ($in.^4$)
I_c	moment of inertia of cracked concrete section of width b ($in.^4$)
I_g	moment of inertia of gross concrete section of width b ($in.^4$)
I_m	mass moment of inertia ($lb\text{-}ms^2\text{-}in.$)
I_n	moment of inertia of net section of masonry unit ($in.^4$
j	ratio of distance between centroids of compression and tension forces to the depth d
k	constant defined in paragraph
K	(1) unit stiffness (psi-in for slabs) (lb/in/in for beams)(lb/in for springs) (2) constant defined in paragraph
K_e	elastic unit stiffness (psi/in for slabs) (lb/in/in for beams)
K_{ep}	elasto-plastic unit stiffness (psi-in for slabs) (psi for beams)
K_E	equivalent elastic unit stiffness (psi-in for slabs) (psi for beams) equivalent spring constant
K_L	load factor
K_{LM}	load-mass factor
$(K_{LM})_u$	load-mass factor in the ultimate range
$(K_{LM})_{up}$	load-mass factor in the post-ultimate range
K_M	mass factor
K_R	resistance factor
K_1	factor defined in paragraph
KE	kinetic energy
l	charge location parameter (ft)
l_p	spacing of same type of lacing bar (in.)

L	(1) span length (in.)* (2) distance between reflecting surface(s) and/or free edge(s) in horizontal direction (ft)
L_1	length of lacing bar required in distance s_1 (in.)
L_o	embedment length of reinforcing bars (in.)
L_s	length of shaft (in.)
L_w	wave length of positive pressure phase (ft)
L_w^-	wave length of negative pressure phase (ft)
L_{wb}, L_{wd}	wave length of positive pressure phase at points b and d, respectively (ft)
L_1	total length of sector of element normal to axis of rotation (in.)
m	unit mass (psi-ms^2/in.)
m_a	average of the effective elastic and plastic unit masses (psi-ms^2/in.)
m_e	effective unit mass (psi-ms^2/in.)
m_u	effective unit mass in the ultimate range (psi-ms^2/in.)
m_{up}	effective unit mass in the post-ultimate range (psi-ms^2/in.)
M	(1) unit bending moment (in-lbs/in.) (2) total mass (lb-ms^2/in.)
M_e	effective total mass (lb-ms^2/in.)
M_u	ultimate unit resisting moment (in-lbs/in.)
M_u^-	ultimate unit rebound moment (in-lbs/in.)
M_c	moment of concentrated loads about line of rotation of sector (in.-lbs)
M_A	fragment distribution parameter
M_E	equivalent total mass (lb-ms^2/in.)
M_{HN}	ultimate unit negative moment capacity in horizontal direction (in.-lbs/in.)*
M_{HP}	ultimate unit positive moment capacity in horizontal direction (in.-lbs/in.)*

* See note at end of symnbols

M_N	ultimate unit negative moment capacity at supports (in.-lbs/in.)
M_P	ultimate unit positive moment capacity at midspan (in.-lbs/in.)
M_{VN}	ultimate unit negative moment capacity in vertical direction (in.-lbs/in.)*
M_{VP}	ultimate unit positive moment capacity in vertical direction (in.-lbs/in.)*
n	(1) modular ratio (2) number of time intervals (3) number of glass pane tests
N	number of adjacent reflecting surfaces
N_f	number of primary fragments larger than W_f
p	reinforcement ratio equal to (A_s/bd) or (A_s/bd_c)
p'	reinforcement ratio equal to (A'_s/bd) or (A'_s/bd_c)
p_b	reinforcement ratio producing balanced conditions at ultimate strength
p_p	prestressed reinforcement ratio equal to A_{ps}/bd_p
p_m	mean pressure in a partially vented chamber (psi)
p_{mo}	peak mean pressure in a partially vented chamber (psi)
p_H	reinforcement ratio in horizontal direction on each face*
p_T	reinforcement ratio equal to $p_H + p_v$
p_v	reinforcement ratio in vertical direction on each face*
p(x)	distributed load per unit length
P	(1) pressure (psi) (2) concentrated load (lbs)
P^-	negative pressure (psi)
P_i	interior pressure within structure (psi)
P_i	interior pressure increment (psi)
P_f	fictitious peak pressure (psi)
P_o	peak pressure (psi)

* See note at end of symnbols

P_r	peak positive normal reflected pressure (psi)
P_r^-	peak negative normal reflected pressure (psi)
P_{ra}	peak reflected pressure at angle of incidence a (psi)
P_s	positive incident pressure (psi)
P_{sb}, P_{se}	positive incident pressure at points b and e, respectively (psi)
P_{so}	peak positive incident pressure (psi)
P_{so}^-	peak negative incident pressure
P_{sob}, P_{sod}, P_{soe}	peak positive incident pressure at points b, d, and e, respectively (psi)
P(F)	probability of failure of glass pane
q	dynamic pressure (psi)
q_b, q_e	dynamic pressure at points b and e, respectively (psi)
q_o	peak dynamic pressure (psi)
q_{ob}, q_{oe}	peak dynamic pressure at points b and e, respectively (psi)
r	(1) unit resistance (psi) (2) radius of spherical TNT (density equals 95 lb/ft^3 charge (ft))
r^-	unit rebound resistance (psi, for panels) (lb/in for beams)
Δr	change in unit resistance (psi, for panels) (lb/in for beams)
r_d	radius from center of impulse load to center of door rotation (in.)
r_e	elastic unit resistance (psi, for panels) (lb/in for beams)
r_{ep}	elasto-plastic unit resistance (psi, for panels) (lb/in for beams)
r_s	radius of shaft (in.)
r_u	ultimate unit resistance (psi, for panels) (lb/in for beams)
r_{up}	post-ultimate unit resistant (psi)
r_1	radius of hemispherical portion of primary fragment (in.)
R	(1) total internal resistance (lbs) (2) slant distance (ft)

R_f	distance traveled by primary fragment (ft)
R_g	uplift force at corners of window frame (lbs)
R_l	radius of lacing bend (in.)
R_A	normal distance (ft)
R_E	equivalent total internal resistance (lbs)
R_G	ground distance (ft)
R_u	total ultimate resistance
R_I, R_{II}	total internal resistance of sectors I and II, respectively (lbs)
s	sample standard deviation
s_s	spacing of stirrups in the direction parallel to the longitudinal reinforcement (in.)
s_l	spacing of lacing in the direction parallel to the longitudinal reinforcement (in.)
S	height of front wall or one-half its width, whichever is smaller (ft)
S_E	strain energy
t	time (ms)
Δt	time increment (ms)
t_a	any time (ms)
t_b, t_e, t_f	time of arrival of blast wave at points b, e, and f, respectively (ms)
t_c	(1) clearing time for reflected pressures (ms) (2) container thickness of explosive charges (in.)
t_d	rise time (ms)
t_E	time to reach maximum elastic deflection
t_m	time at which maximum deflection occurs (ms)
t_o	duration of positive phase of blast pressure (ms)
t_o^-	duration of negative phase of blast pressure (ms)
t_{of}	fictitious positive phase pressure duration (ms)
t_{of}^-	fictitious negative phase pressure duration (ms)

t_r	fictitious reflected pressure duration (ms)
t_u	time at which ultimate deflection occurs (ms)
t_y	time to reach yield (ms)
t_A	time of arrival of blast wave (ms)
t_1	time at which partial failure occurs (ms)
T	(1) duration of equivalent triangular loading function (ms) (2) thickness of masonry wall
T_c	thickness of concrete section (in.)
T_c	scaled thickness of concrete section ($ft/lb^{1/3}$)
T_g	thickness of glass (in.)
T_i	angular impulse load (lb-ms-in.)
T_N	effective natural period of vibration (ms)
T_r	rise time (ms)
T_s	thickness of sand fill (in.)
$\overline{T}_s$	scaled thickness of sand fill ($ft/lb^{1/3}$)
u	particle velocity (ft/ms)
u_u	ultimate flexural or anchorage bond stress (psi)
U	shock front velocity (ft/ms)
U_s	strain energy
v	velocity (in./ms)
v_a	instantaneous velocity at any time (in./ms)
v_b	boundary velocity for primary fragments (ft/sec)
v_c	ultimate shear stress permitted on an unreinforced web (psi)
v_f	maximum post-failure fragment velocity (in./ms)
v_f(avg.)	average post-failure fragment velocity (in./ms)
v_i	velocity at incipient failure deflection (in./ms)
v_o	initial velocity of primary fragment (ft/sec)
v_r	residual velocity of primary fragment after perforation (ft/sec)

v_s	striking velocity of primary fragment (ft/sec)
v_u	ultimate shear stress (psi)
v_{uH}	ultimate shear stress at distance d_e from the horizontal support(psi)*
v_{uV}	ultimate shear stress at distance de from the vertical support (psi)*
V	volume of partially vented chamber (ft^3)
V_d	ultimate direct shear capacity of the concrete of width b (lbs)
V_{dH}	shear at distance d_e from the vertical support on a unit width (lbs./in.)*
V_{dV}	shear at distance d_e from the horizontal support on a unit width (lbs/in.)*
V_o	volume of structure (ft^3).
V_s	shear at the support (lb/in, for panels) (lbs.for beam)
V_{sH}	shear at the vertical support on a unit width (lbs/in.)*
V_{sV}	shear at the horizontal support on a unit width (lbs/in.)*
V_u	total shear on a width b (lbs)
V_x	unit shear along the long side of window frame (lb/in.)
V_y	unit shear along the short side of window frame, (lbs/in.)
w	unit weight (psi, for panels) (lb/in for beam)
w_c	weight density of concrete (lbs/ft^3)
w_s	weight density of sand (lbs/ft^3)
W	(1) charge weight (lbs) (2) weight (lbs)
W_c	total weight of explosive containers (lbs)
W_f	weight of primary fragment (oz)
W_{co}	total weight of steel core (lbs)
W_{c1}, W_{c2}	total weight of plates 1 and 2, respectively (lbs)
W_s	width of structure (ft)

* See note at end of symnbols

WD	work done
x	yield line location in horizontal direction (in.)*
X	deflection (in.)
X_a	any deflection (in.)
X_c	lateral deflection to which a masonry wall develops no resistance (in.)
X_e	elastic deflection (in.)
X_{ep}	elasto-plastic deflection (in.)
X_f	maximum penetration into concrete of armor-piercing fragments (in.)
X'_f	maximum penetration into concrete of fragments other than armor-piercing (in.)
X_m	maximum transient deflection (in.)
X_p	plastic deflection (in.)
X_s	(1) maximum penetration into sand of armor-piercing fragments (in.) (2) static deflection
X_u	ultimate deflection (in.)
X_E	equivalent elastic deflection (in.)
X_1	(1) partial failure deflection (in.) (2) deflection at maximum ultimate resistance of masonry wall (in.)
y	yield line location in vertical direction (in.)*
y_t	distance from the top of section to centroid (in.)
Z	scaled slant distance ($ft/lb^{1/3}$)
Z_A	scaled normal distance ($ft/lb^{1/3}$)
Z_G	scaled ground distance ($ft/lb^{1/3}$)
α	(1) angle formed by the plane of stirrups, lacing, or diagonal reinforcement and the plane of the longitudinal reinforcement (deg) (2) angle of incidence of the pressure front (deg) (3) acceptance coefficient

* See note at end of symbols

β	(1) coefficient for determining elastic and elasto-plastic resistances (2) particular support rotation angle (deg) (3) rejection coefficient
β_1	factor equal to 0.85 for concrete strengths up to 4000 psi and is reduced by 0.05 for each 1,000 psi in excess of 4,000 psi
γ	coefficient for determining elastic and elasto-plastic deflections
γ_p	factor for type of prestressing tendon
ϵ_m	unit strain in mortar (in./in.)
Θ	support rotation angle (deg)
$\ddot{\Theta}$	angular acceleration (rad/ms^2)
Θ_{max}	maximum support rotation angle (deg)
Θ_H	horizontal rotation angle (deg)*
Θ_V	vertical rotation angle (deg)*
λ	increase in support rotation angle after partial failure (deg)
μ	ductility factor
ν	Poisson's ratio
Σ_o	effective perimeter of reinforcing bars (in.)
ΣM	summation of moments (in.-lbs)
ΣM_N	sum of the ultimate unit resisting moments acting along the negative yield lines (in.-lbs)
ΣM_p	sum of the ultimate unit resisting moments acting along the positive yield lines (in.-lbs)
τ_s	maximum shear stress in the shaft (psi)
ϕ	(1) capacity reduction factor (2) bar diameter (in.)
Φ_r	assumed shape function for concentrated loads
$\phi(x)$	assumed shape function for distributed loads free edge
ω	angular velocity (rad./ms)
———	simple support

* See note at end of symnbols

//////	fixed support
XXXXXX	either fixed, restrained, or simple support

* Note. This symbol was developed for two-way elements which are used as walls. When roof slabs or other horizontal elements are under consideration, this symbol will also be applicable if the element is treated as being rotated into a vertical position.

APPENDIX 6C

BIBLIOGRAPHY

Masonry

1. Design of Masonry Structures to Resist the Effects of HE Explosions, prepared by Ammann & Whitney, Consulting Engineers, New York, NY, for Picatinny Arsenal, Dover, NJ, 1976.
2. Gabrielsen, G., Wilton, C., and Kaplan, K., Response of Arching Walls and Debris from Interior Walls Caused by Blast Loading, URS 7030-23, URS Research Company, San Mateo, CA, February 1976.
3. McDowell, E., McKee, K., and Sevin, E., Arching Action Theory of Masonry Walls, Journal of the Structural Division, ASCE, Vol. 82, No. ST 2, March 1956.
4. Wilton, C., and Gabrielsen, B., Shock Tunnel Tests of Pre-Loaded and Arched Wall Panels, URS 7030-10, URS Research Company, San Mateo, CA. June 1973.

Precast Concrete

5. PCI Design Handbook Precast Prestressed Concrete, Prestressed Concrete Institute, Chicago, IL, 1978.
6. PCI Manual for Structural Design of Architectural Precast Concrete, Prestressed Concrete Institute, Chicago, IL.
7. PCI Manual on Design of Connections for Precast Prestressed Concrete, Prestressed Concrete Institute, Chicago, IL.
8. Lin, T. Y., Design of Prestressed Concrete Structures, John Wiley & Sons, New York, NY, July 1955.

Pre-Engineered Buildings

9. American National Standard Minimum Design Loads for Buildings and Other Structures, ANSI A58.1-1982, American National Standards Institute, New York, NY, March 1982.
10. Specification for the Design of Cold-Formed Steel Structural Members, American Iron and Steel Institute, New York, NY, 1968.
11. Specification for the Design, Fabrication and Erection of Structural Steel for Buildings, Manual of Steel Construction, American Institute of Steel Construction, New York, NY, 1969.
12. Uniform Building Code (1979 Edition), International Conference of Building Officials, Whittier, CA, 1979.
13. Healey, J. J., et al., Design of Steel Structures to Resist the Effects of HE Explosions, Technical Report 4837, Picatinny Arsenal, Dover, NJ, August 1975.
14. Stea, W., et al., Blast Capacity Evaluation of Pre-Engineered Building, Contractor Report ARLCD-CR-79004, U. S. Army Armament Research and Development Command, Dover, NJ, March 1979.
15. Stea, W., et al., Nonlinear Analysis of Frame Structures to Blast Overpressures, by Ammann & Whitney, Consulting Engineers, New York, NY, Contractor Report ARLCD-CR-77008, U.S. Army Armament Research and Development Command, Dover, NJ, May 1977.
16. Tseng, G., et al., Design Charts for Cold-Formed Steel Panels and Wide-Flange Beams Subjected to Blast Loads, Technical Report 4838, Picatinny Arsenal, Dover, NJ, August 1975.

Suppressive Shielding

17. Final Report Application of Suppressive Structure Concepts to Chemical Agent Munitions Demilitarization System (CAMDS), Report EA-FR-2B02, Edgewood Arsenal, Aberdeen Proving Ground, MD, June 27, 1973.

18. Shields Operational for Ammunition Operations, Criteria for Design of, and Tests for Acceptance, MIL STD 398, U.. S. Government Printing Office, Washington, D. C., November 5, 1976.
19. Study of Suppressive Structures Applications to an 81 mm Automated Assembly Facility, Report EA 1002, Edgewood Arsenal, Aberdeen Proving Ground, MD, April 16, 1973.
20. Suppressive Shielding, AAI Corporation, Cockeysville, MD, DAAA15-75-C-0120, U. S. Army Armament Research and Development Command, Chemical Systems Laboratory, Aberdeen Proving Ground, MD, April 1977.
21. Suppressive Shields Structural Design and Analysis Handbook, HNDM 1110-1-2, U. S. Army Corps of Engineers, Huntsville Division, Huntsville. AL, November 1977..
22. System Safety Program Requirements, MIL STD 882A, U. S. Government Printing Office, Washington, D. C., June 28, 1977.
23. Baker, W. E., et al., Design Study of a Suppressive Structure for a Melt Loading Operation, EM-CR-76043, Report No. 9, Edgewood Arsenal, Aberdeen Proving Ground, MD, December 1975.
24. Baker, W. E. and Oldham, G. A., Estimates of Blowdown of Quasi-Static Pressures in Vented Chambers, EM-CR-76029, Edgewood Arsenal, Aberdeen Proving Ground, MD, November 1975.
25. Baker, W. E. and Westine, P. S., Methods of Predicting Blast Loads Inside and Outside Suppressive Structures, EM-CR-76026, Report No. 5. Edgewood Arsenal, Aberdeen Proving Ground, MD, 1975.
26. Cox, P. A., et al., Analysis and Evaluation of Suppressive Shields, Edgewood Arsenal Contractor Report ARCFL-CR-77028, Report No. 10, Contract No. DAAA15-75-C-0083, Edgewood Arsenal, Aberdeen Proving Ground, MD; January 1978..
27. Dutton, S. R. and Katsanis, D. Computer-Aided Design of Suppressive Shields, EM-CR-76080, AAI Corporation, Baltimore, MD, Report for Edgewood Arsenal, Aberdeen Proving Ground, MD, June 1976.
28. Esparza, E. D., Estimating External Blast Loads from Suppressive Structures, Edgewood Arsenal Contract Report EM-CR-76030, Report No. 3, Edgewood Arsenal, Aberdeen Proving Ground, MD, November 1975.
29. Esparza, E. D., Baker, W. E., and Oldham, G. A., Blast Pressures Inside and Outside Suppressive Structures, Edgewood Arsenal Contractor Report EM-CR-76042, Report No. 8, Edgewood Arsenal, Aberdeen Proving Ground, MD, December 1975.
30. Gregory, F. H., Blast Loading Calculations and Structural Response Analyses of the 1/4-Scale Category I Suppressive Shield, BRL Report No. 2003, U. S. Army Ballistic Research Laboratory, Aberdeen Proving Ground, MD, August 1977.
31. Hubich, H. O. and Kachinski, R. L., Explosive Waste Removal Systems for Suppressive Shields, Edgewood Arsenal Contractor Report No. EM-CR76002, Edgewood Arsenal, Aberdeen Proving Ground, MD, August 1975.
32. Jezek, B. W., Suppressive Shielding for Hazardous Munitions Production Operations, Technical Report No. ARCSL-TR-77020, U. S. Army Armament Research and Development Command, Chemical Systems Laboratory, Aberdeen Proving Ground, MD, April 1977.
33. Kachinski, R. L., et al., Technical Feasibility of Suppressive Shields for Improved Hawk Launch Sites, Edgewood Arsenal Contractor Report No. EM-CR-76057. Edgewood Arsenal, Aberdeen Proving Ground, MD, February 1976.
34. Katsanis, D. J.. Safety Approval of Suppressive Shields, Edgewood Arsenal Technical Report No. EM-TR-76088, Edgewood Arsenal, Aberdeen Proving Ground, MD, August 1976.

35. Katsanis, D. J. and Jezek, B. W., Suppressive Shielding of Hazardous Ammunition Production Operations, Technical Report No. EM-TR-76015, Edgewood Arsenal, Aberdeen Proving Ground, MD, December 1975.

36. Kingery, C. N., Coulter, G., and Pearson, R., Venting of Pressure through Perforated Plates, Technical Report No. ARBRL-TR-02105, U. S. Army Ballistic Research Laboratory, Aberdeen Proving Ground, MD, September 1978.

37. Kingery, C. N., Pearson, R., and Coulter, G., Shock Wave Attenuation by Perforated Plates with Various Hole Sizes, BRL Memorandum Report No. 2757, U. S Army Materiel Development and Readiness Command, Alexandria, VA, June 1977.

38. Kingery, C. N., Schumacher, R., and Ewing, W., Internal Pressure from Explosions in Suppressive Shields, BRL Memorandum Report No. ARBRL-MR-02848, U. S. Army Armament Research and Development Command, Aberdeen Proving Ground, MD, June 1978.

39. Koger, D. M and McKown, G. L., Category 5 Suppressive Shield Test Report No. EM-TR-76001, Edgewood Arsenal, Aberdeen Proving Ground, MD, October 1975.

40. Kusher, A. S., et al., Recommended Design and Analysis Procedures for Suppressive Shield Structures, Technical Report No. NSWC/WOL/TR 76112, Naval Surface Weapons Center, White Oak Laboratory, White Oak, Silver Spring, MD, March 1977.

41. Nelson, K. P. Spherical Shields for the Containment of Explosions, Edgewood Arsenal Technical Report No. EM-TR-76096, Edgewood Arsenal, Aberdeen Proving Ground, MD, March 1977.

42. Nelson, K. P., The Economics of Applying Suppressive Shielding to the M483A1 Improved Conventional Munitions Loading, Assembling, and Packing Facility, Technical Report No. EM-TR-76087, Edgewood Arsenal, Aberdeen Proving Ground, MD, January 1977.

43. Oertel, F. H., Evaluation of Simple Models for the Attenuation of Shock Waves by Vented Plates, BRL Report No. 1906, U. S. Army Ballistic Research Laboratory, Aberdeen Proving Ground, MD, August 1976.

44. Pei, R., A Design Aid and Cost Estimate Model for Suppressive Shielding Structures, Department of Safety Engineering USAMC Intern Training Center, Report No. YTC-02-08-76-413, Red River Army Depot, Texarkana, TX, December 1975.

45. Ricchiazzi, A. J. and Barb, J. C., Test Results for 608 Gram Fragments against Category I Suppressive Structures, BRL Memorandum Report No. 2592, U. S. Army Ballistic Research Laboratory, Aberdeen Proving Ground, MD, February 1976.

46. Schroeder, F. J., et al., Engineering Design Guidelines, Drawings and Specifications for Support Engineering of Suppressive Shields, Edgewood Arsenal Contractor Report No. EM-CR-76097, Edgewood Arsenal, Aberdeen Proving Ground, MD, December 1976.

47. Schumacher, R. N., Air Blast and Structural Response Testing of a Prototype Category III Suppressive Shield, BRL Memorandum Report No. 2701, U. S. Army Ballistic Research Laboratory, Aberdeen Proving Ground, MD, November 1976.

48. Schumacher, R. N. and Ewing, W. O., Blast Attenuation Outside Cubical Enclosures Made Up of Selected Suppressive Structures Panel Configurations, BRL Memorandum Report No. 2537, U. S. Army Ballistic Research Laboratory, Aberdeen Proving Ground, MD, September 1975.

49. Schumacher, R. N., Kingery, C. N., and Ewing, W. O., Air Blast and Structural Response Testing of a 1/4-Scale Category I Suppressive

Shield, BRL Memorandum Report No. 2623. U. S. Army Ballistic Research Laboratory, Aberdeen Proving Ground, MD, May 1976.

50. Spencer, A. F. and McKivrigan, J. L., Preliminary Design Procedures for Suppressive Shields, Technical Report No. EM-TR-76089, Edgewood Arsenal, Aberdeen Proving Ground, MD, December 1976.
51. Westine, P. S. and Baker, W. E., Energy Solutions for Predicting Deformations in Blast-Loaded Structures, Edgewood Arsenal Contractor Report No. EM-CR-76027, Report No. 6, Edgewood Arsenal, Aberdeen Proving Ground, MD, November 1975.
52. Westine, P. S. and Cox, P. A., Additional Energy Solutions for Predicting Structural Deformations, Edgewood Arsenal Contractor Report No. EM-CR-76031, Report No. 4, Edgewood Arsenal, Aberdeen Proving Ground, MD. November 1975.
53. Westine, P. S. and Kineke, J. H., "Prediction of Constrained Secondary Fragment Velocities," The Shock and Vibration Bulletin, Part 2, Isolation and Damping, Impact, Blast, Bulletin 48, September 1978.

Blast Resistant Windows

54. Federal Specification Glass, Plate, Sheet, Figured (Float, Flat, for Glazing, Corrugated, Mirrors and Other Uses). General Service Administration, Federal Specification DD-G-451d, Washington, D. C., 1977.
55. Glass, Plate (Float), Sheet, Figured, and Spandrel (Heat Strengthened and Fully Tempered). General Service Administration, Federal Specification DD-G-1403B, Washington, D.. C., 1972.
56. A Method for Improving the Shatter Resistance of Window Glass, U. S. Army Picatinny Arsenal, National Bomb Data Center, General Information Bulletin 73-9, Dover, NJ, November 1973.
57. PPG Glass Thickness Recommendations to Meet Architect's Specified 1-Minute Wind Load, PPG Industries, Pittsburgh, PA, March 1981.
58. Safety Performance Specifications and Methods of Test for Safety Glazing Material Used in Buildings, American National Standards Institute, ANSI Z97.1-1975, New York, NY, 1975.
59. Structural Performance of Glass in Exterior Windows, Curtain Walls, and Doors under the Influence of Uniform Static Loads by Destructive Method, American Society for Testing Materials, ASTM Standard (draft). Draft of Proposed Standard by ASTM Committee E06.51, Philadelphia, PA, October 1982.
60. Anians, D., Experimental Study of Edge Displacements of Laterally Loaded Window Glass Plates, Institute for Disaster Research, Texas Technical University, Lubbock, TX, June 1980.
61. Beason, W. L., A Failure Prediction Model for Window Glass, Texas Technical University, NSF/RA 800231, Lubbock, TX, May 1980.
62. Beason, W. L., TAMU Glass Failure Prediction Model, Preliminary Report, Texas A&M University, College Station, TX, March 1982.
63. Beason, W. L., and Morgan, J. R., A Glass Failure Prediction Model, submitted for publication in the Journal of the Structural Division, American Society of Civil Engineers.
64. Levy, S., Bending of Rectangular Plates with Large Deflections, NACA Technical Note No.. 845. 1942.
65. Meyers, G. E., Interim Design Procedure for Blast-Hardened Window Panes, 567h Shock and Vibration Bulletin, Monterey, CA, October 1985.
66. Meyers, G. E., A Review of Adaptable Methodology for Development of a Design Procedure for Blast Hardened Windows, Naval Civil Engineering Laboratory, Special Report, Port Hueneme, CA, August 1982.

67. Moore, D. M., Proposed Method for Determining the Thickness of Glass in Solar Collector Panels, Jet Propulsion Laboratory, Publication 8034, Pasadena, CA, March 1980.
68. Moore, D. M., Thickness Sizing of Glass Plates Subjected to Pressure Loads, FSA Task Report No. 5101-291, Pasadena, CA, August 1982.
69. Timoshenko, S. and Woinowsky-Krieger, S., Theory of Plates and Shells, McGraw-Hill Book Company, New York, NY, 1959.
70. Vallabhan, C. V. G. and Wang, B. Y., Nonlinear Analysis of Rectangular Glass Plates by Finite Difference Method, Texas Technical University, Institute for Disaster Research, Lubbock, TX, June 1981.
71. Weissman, S., et al., Blast Capacity Evaluation of Glass Windows and Aluminum Window Frames, U. S. Army Armament Research and Development Command, ARLCO-CR-78016, Dover, NJ, June 1978..

Underground Structures

72. Fundamentals of Protective Design for Conventional Weapons, TM 5-8551, prepared by U. S. Army Engineer Waterways Experimental Station, Vicksburg, MS, November 1983 (Draft).
73. Arya, et al., Blast Capacity Evaluation of Below-Ground Structures, by Ammann & Whitney, Consulting Engineers, New York, NY, Contractor Report ARLCO-CR-77006, U. S. Army Armament Research and Development Command, Dover, NJ, May 1977.

Earth-Covered Arch-Type Magazine

74. DoD Ammunition and Explosives Safety Standards, Department of Defense Standard, 6055.9-STD
75. Flathou, W. J., et al., Blast Loading and Response of Underground Concrete-Arch Protective Structures WT-1420, U. S. Waterways Experiment Station, Jackson, MS, Operation Plumbbob, Project 3.1, Chief, Defense Atomic Support Agency, Washington, D. C.
76. Sound, A. R., Summary Report of Earth-Covered, Steel-Arch Magazine Tests, Technical Progress Report No. 401, U. S. Naval Weapon Center, China Lake, CA, July 1965.
77. Weals, F. H., Tests to Determine Separation Distances of Earth-Covered Magazines, U. S. Naval Weapon Center, China Lake, CA, Annals of the New York Academy of Sciences, Conference on Prevention of and Protection against Accidental Explosion of Munitions, Fuels and Other Hazardous Moistures, Volume 152, Art. 1, October 1968.

Blast Valves

78. Investigations Concerning Feasibility of Various Designs for a Blast Closure Device, by American Machine and Foundry Co., Chicago, IL, under Contract No. NBy-13030, for U. S. Navy, Bureau of Yards and Docks, Washington, D. C.
79. Shock Tube Test of Mosler Safe Company Blast Valve, BRL Information Memorandum No. 20, Explosion Kinetics Branch, Ballistic Research Laboratories, Aberdeen Proving Ground, MD, August 1959.
80. Shock Tube Test of Mosler Safe Company Blast Valve, Phase II, BRL Information Memorandum No. 25, Explosion Kinetics Branch, Ballistic Research Laboratories, Aberdeen Proving Ground, MD, August 1959.

81. Study of Blast-Closure Devices, AFSWC-TDR-62-10, by American Machine and Foundry Co., Chicago, IL for Air Force Special Weapons Center, Kirtland Air Force Base, NM, February 1962.
82. Allen, F. C. et al., Test and Evaluation of Anti-Blast Valves for Protective Ventilating Systems, WT-1460, Operation Plumbbob, Project 31.5, available from the Office of Technical Services, Department of Commerce, Washington, D. C.
83. Bayles, J. J., Development of the B-D Blast-Closure Valve, Technical Note No. N-546, U. S. Naval Civil Engineering Laboratory, Port Hueneme, CA, December 1963.
84. Bergman, S. and Staffors, B., Blast Tests on Rapid-Closing Anti-Blast Valves, Royal Swedish Fortification Administration, Stockholm, Sweden, November 1963.
85. Breckenridge, T. A., Preliminary Development and Tests of a Blast-Closure Valve, Technical Note No. N-460, U. S. Naval Civil Engineering Laboratory, Port Hueneme, CA, September 1962.
86. Chapler, R. S., Evaluation of Four Blast Closure Valves, Technical Report R 347, DASA-13.154, U. S. Naval Civil Engineering Laboratory, Port Hueneme, CA, January 1965 (Official Use Only).
87. Cohen, E., Blast Vulnerability of Deep Underground Facilities as Affected by Access and Ventilation Openings, Ammann & Whitney, Consulting Engineers, New York, NY, Proceedings of the Second Protective Construction Symposium, R-341, Volume I, The RAND Corporation, Santa Monica, CA, 1959.
88. Cohen, E. and Weissman, S., Blast Closure Systems, Ammann & Whitney, Consulting Engineers, New York, NY, Proceedings of the Symposium on Protective Structures for Civil Populations, Subcommittee on Protective Structures, Advisory Committee on Civil Defense, National Academy of Sciences and National Research Council, April 1965.
89. Hassman, M. and Cohen, E., Review of Blast Closure Systems, Ammann & Whitney, Consulting Engineers, New York, NY, 29th Symposium on Shock, Vibration and Associated Environments, Part III, Bulletin No. 29, U. S. Naval Research Laboratory, Washington, D. July 1961, available from the Office of Technical Services, Department of Commerce, Washington, D. C.
90. Hellberg, E. N., Performance of the Swedish Rapid-Closing Anti-Blast Valve, Technical Note No. 439, Task Y-F 008-10-11, U. S. Naval Civil Engineering Laboratory, Port Hueneme, CA, May 1962.
91. Jones, W. A., et al., A Simple Blast Valve, Suffield Technical Note No. 113, Suffield Experimental Station, Ralston, Alberta, Canada, Defense Research Board, Department of National Defense, Canada, DRB Project No. D89-16-01-09, February 1963.
92. Ort, F. G. and Mears, M. D., Development of the Closure, Protective Shelter, Anti-Blast, 600 cfm, E19R1, Technical Report CWLR-2269, Chemical Warfare Laboratories, U. S. Army Chemical Center, Edgewood, MD, January 1959.
93. Stephenson, J. M., Preliminary Tests of the Stephenson Valve, 2nd Report, Technical Note No. N-619. U. S. Naval Civil Engineering Laboratory, Port Hueneme, CA, July 1964.
94. Stephenson, J. M., Test of German Sand-Type Filter, Technical Report R263, U. S. Naval Civil Engineering Laboratory, Port Hueneme, CA, November 1963.

95. A Guide for the Design of Shock Isolation Systems for Underground Protective Structures AFSWC TDR 62-64, Air Force Special Weapons Center, Kirtland AFB, NM, December 1962.
96. Handbook of Mechanical Spring Design, Associated Spring Corporation, Bristol, CT, 1964.
97. Study of Shock Isolation for Hardened Structures, Department of the Army, Office of the Chief of Engineers, Washington, D. C. AD 639 303, June 1966.
98. Crawford, R. E. Higgins, C. J., and Bultmann, E.H., A Guide for the Design of Shock Isolation Systems for Ballistic Missile Defense Facilities, TR S-23, U.S. Army Construction Engineering Research Laboratory, Champaign, IL, August 1973.
99. Harris, C.M. and Crede, C.E., Shock and Vibration Handbook, McGraw-Hill Book Company, New York, NY, 1961.
100. Hirsch, A.E., Man's Response to Shock Motions, David Taylor Model Basin Report 1797. Washington, D.C. AD 4 36809, January 1964.
101. Platus, David L., et al., Investigation of Optimum Passive Shock Isolation Systems, AFWL-TR-72-148, Air Force Weapons Laboratory, Kirtland Air Force Base, NM, November 1972.
102. Saffell, H.R., Development of Standard Design Specifications and Techniques for Shock Isolation Systems, Document No. SAF-37, Vol. I, U.S. Army Engineer Division, Huntsville, AL, August 1971.
103. Shigley, J.E., Mechanical Engineering Design, McGraw-Hill Book Company, New York, NY, 1963.
104. Veletnor, A., Design Procedures for Shock Isolation System for Underground Protective Structures, RTD-TDR-63-3096, Vol. III, Air Force Weapons Laboratory, Kirtland Air Force Base, NM, January 1964.

By Order of the Secretaries of the Army, the Navy and the Air Force:

CARL E. VUONO
General, United States Army
Chief of Staff

Official:

THOMAS F. SIKORA
Brigadier General, United States Army
The Adjutant General

D. E. BOTTORFF
Rear Admiral, United States Navy
Commander, Naval Facilities Engineering Command

Official:

MERRILL A. McPEAK
General, USAF
Chief of Staff

Official:

EDWARD A. PARDINI, *Colonel, USAF*
Director of Information Management

DISTRIBUTION:

*U.S. Government Printing Office: 1993 — 342-074/72270